Talanta, Vol. 32, No. 1, pp. 1–6, 1985
Printed in Great Britain

0039-9140/85 $3.00 + 0.00
Pergamon Press Ltd

DETERMINATION OF THE RARE EARTHS, YTTRIUM AND SCANDIUM IN SILICATE ROCKS AND FOUR NEW GEOLOGICAL REFERENCE MATERIALS BY ELECTROTHERMAL ATOMIZATION FROM GRAPHITE AND TANTALUM SURFACES

J. G. SEN GUPTA
Geological Survey of Canada, Ottawa, Ontario, Canada

(*Received* 11 *April* 1984. *Revised* 15 *June* 1984. *Accepted* 1 *August* 1984)

Summary—An improved graphite furnace atomic-absorption method has been developed for the determination of Sc, Y and the rare-earth elements in silicate rocks and related materials. The method, which involves the separation of the lanthanides by ion-exchange followed by their determination by electrothermal atomization, with use of an automatic sampling device, is more rapid than a previous method based on separation by co-precipitation with calcium oxalate and hydrous ferric oxide followed by normal injection of the solution into the furnace. Greater sensitivity (~ 10–40-fold) for La, Ce, Pr, Gd, Tb and Lu is also achieved by using a tantalum foil-lined graphite furnace instead of a pyrolytically-coated furnace. Results obtained for five international reference rock samples, NIM-G, SCo-1, MAG-1, SDC-1 and BHVO-1, are compared with those obtained previously by the oxalate–hydrous oxide co-precipitation method and with other published values. Results are given for four new Canadian iron-formation reference materials, FeR-1 to FeR-4.

In previous work,[1–3] scandium, yttrium and the lanthanides in rocks were determined by graphite-furnace AAS involving manual injection of the sample solution after separation of the rare earths by double calcium oxalate and single hydrous ferric oxide co-precipitations. Because petrogenetic modelling requires the determination of traces of the rare-earth elements in various ultramafic and common rocks and rock-forming minerals, more rapid and sensitive methods are required for their determination, particularly the lighter lanthanide elements. Following the acquisition of a more modern graphite furnace coupled with an automatic sampling device, an attempt was made to expedite the determination of the rare earths by using this equipment and a faster separation procedure. Separation by extraction of the salicylate complexes into methyl isobutyl ketone[4] was tested but abandoned because of interferences in the separation of the phases. The ion-exchange procedure used earlier[5] was therefore investigated, but had to be modified. This paper describes the results and shows that greater sensitivity can be achieved for lanthanum, praseodymium, gadolinium, terbium and lutetium, as well as for cerium, by using a pyrolytically-coated graphite tube lined with tantalum foil.[6] Results obtained by this method for five international reference rock samples are compared with those obtained earlier[1–3] and with other published values. Results are also given for four new Canadian iron-formation reference materials, FeR-1, FeR-2, FeR-3 and FeR-4.

EXPERIMENTAL

Apparatus

The AAS equipment and ancillary apparatus was the same as that used for the cerium determination described earlier,[6] including the tantalum-lined furnace. The ion-exchange column was that used in the earlier work on lanthanides.[7] The AAS operating conditions are given in Tables 1–3.

Reagents

Stock 1000-ppm solutions of scandium, yttrium and the lanthanides were prepared and standardized as described earlier,[6,7] and diluted further with 0.1*M* nitric acid as required, to give working standards.

Standard mixtures, approximating the compositions of two international reference rocks GA (granite)[8,9] and SY-2 (syenite),[9,10] were prepared as described previously.[7] All reagents were of analytical reagent grade and demineralized water was used for the preparation of all solutions.

Procedures

Calibration solutions. Prepare three calibration solutions with concentrations corresponding to 0.05, 0.1 and 0.2 g of sample per ml by diluting appropriate volumes of the "GA" or "SY-2" standard mixtures (depending on the type of sample being analysed) to a known volume with 0.1*M* nitric acid.[7]

Preparation of solution for analysis. Depending on the rock type, decompose a 1–2 g sample and separate the lanthanides, yttrium and scandium by ion-exchange as described earlier,[7] to obtain "Solution A".

AAS determination. Transfer the calibration and sample solutions (Note 1) to plastic vials in the sample dispenser, then, using 20-μl portions of the sample solutions, measure

Table 1. Instrumental parameters

Element	Wavelength, *nm*	Hollow-cathode lamp	Current, *mA*	Spectral bandpass, *nm*
Sc	391.18	Westinghouse	5	0.2
Y	410.2	Westinghouse	5	0.5
La	550.13	Varian-Techtron	10	R*
Ce	567.0	Westinghouse	10	R*
Pr	495.1	Westinghouse	10	R*
Nd	492.45	Westinghouse	10	0.2 or R*
Sm	429.67	Westinghouse	10	0.2 or R*
Eu	459.4	Westinghouse	5	0.2
Gd	368.4	Westinghouse	10	0.2 or R*
Tb	432.7	Cathodeon	10	0.2 or R*
Dy	421.2	Westinghouse	10	0.2
Ho	410.4	Westinghouse	10	0.2
Er	400.8	Westinghouse	5	0.2
Tm	371.8	Varian	10	0.2
Yb	398.8	Westinghouse	5	0.5
Lu	336.0	Varian-Techtron	10	R*

*R = restricted 0.5 nm slit-width.

the absorbances of scandium, yttrium and the lanthanides (Note 2), with the appropriate graphite tubes and the instrumental conditions shown in Tables 1–3 (Notes 3–7). For calibration use 5, 10, 15 and 20 μl of a standard "GA" or "SY-2" solution, depending on the sample taken, plus sufficient 0.1*M* nitric acid to give a total volume of 20 μl. For interpretation use either the concentration read-out of the AAS instrument or individual calibration curves (Note 8).

Notes

1. Depending on the sensitivity, it is preferable to use sample solutions containing ~0.1 g of sample per ml, using a scale expansion of up to 10× (see under *Interferences* for details).

2. Because minor to trace amounts of some common elements retained on the resin and co-eluted with the rare earths by 6*M* hydrochloric acid (see under Discussion) interfere seriously with the determination of cerium by electrothermal atomization, this element should be determined by either of the following procedures.

(*a*) Using a 3-ml aliquot of Solution A, precipitate the rare-earth elements as described previously[12] as the hydrous oxides in the presence of SiO_2 (added as tetraethyl silicate),

Table 2. Operating parameters for the pyrolytically-coated graphite furnace

Element	Step number	Temperature, °C	Time, *sec*	Argon gas flow, *l./min*	Read
Sc, Y, Nd,	1	75	15	3	
Sm, Eu, Dy,	2	90	60	3	
Ho, Er, Tm	3	120	10	3	
and Yb	4	850	10	3	
	5	1800†	10§	3	
	6	1800†	2	0	
	7	2700‡	1.3	0	*
	8	2700‡	2	0	*
	9	2800‡	5	3	

†1400°C for Eu and Yb, 2200°C for Sm, Dy, Er and Tm, 2400°C for Ho.
§15 sec for Nd and Dy, 20 sec for Ho.
‡2200°C for Yb.

Table 3. Operating parameters for the tantalum foil-lined graphite furnace

Element	Step number	Temperature, °C	Time, *sec*	Argon gas flow, *l./min*	Read
La, Ce, Pr,	1	75	15	3	
Gd, Tb and	2	90	60	3	
Lu	3	120	60	3	
	4	850	10	3	
	5	1800†	10	3	
	6	1800†	2	0	
	7	2600	1.3	0	*
	8	2600	2	0	*
	9	2600	1	3	

†2000°C for Gd, 2200°C for Tb and Lu.

Al^{3+} and Fe^{3+}, ignite the precipitate to constant weight at 1200° and determine cerium by emission spectrography.

(*b*) Using a 6-ml aliquot of Solution A, co-precipitate the rare-earth elements once with calcium oxalate and once with hydrous ferric oxide as described previously.[1,2] Decompose the organic material by heating with concentrated nitric acid and 30% hydrogen peroxide and evaporating to dryness on a steam-bath, then dissolve the salts in 0.1*M* nitric acid, transfer the solution to a 5-ml standard flask and dilute to volume with the same acid solution. Use the resulting solution, or a diluted solution, for the determination of cerium by electrothermal atomization, with the operating parameters shown in Tables 1 and 3.

3. The sample dispenser capillary tip should be cleaned periodically with a tissue to prevent formation of a bubble and permit uninterrupted flow of liquid into the furnace during injection.

4. After about 50 firings of a new pyrolytically-coated graphite tube at the recommended temperatures (Table 2) the absorbances decrease because of the destruction or loss of some of the pyrolytic coating. The absorbances of the standards should therefore be checked at this stage and a correction factor applied if necessary.

5. After several firings, the tantalum foil may shift inside the graphite tube and block the hole because of expansion and contraction, so the alignment of the holes should be checked periodically to ensure the correct delivery of solution into the cavity.

6. The condition of the tantalum foil should be monitored by firing a standard after every 5 or 10 samples, and the foil changed when the performance begins to deteriorate (usually after about 40 firings). After about 80 firings the graphite tube and tantalum lining should be discarded.

7. The drying time recommended for the tantalum-lined furnace (Table 3) is suitable for up to 20 μl of solution. For >20 μl, use either a longer drying time at 120°, or multiple injections of 20-μl portions, each being dried before addition of the next.

8. It is recommended that two international reference rocks for which "usable values" for the rare-earth elements have been reported[9] should be run with every batch to check the recovery.

RESULTS AND DISCUSSION

Sensitivity

The manual for the GTA-95 gives sensitivities for dysprosium, erbium, europium and terbium but not for scandium, yttrium and the other lanthanides. Tests with a pyrolytically-coated graphite tube fired at 2700° showed that though the sensitivities for neodymium, yttrium, samarium, erbium, holmium, dysprosium, scandium, europium, thulium and ytterbium ranged from moderate to good, in that

Table 4. Sensitivities for Sc, Y and the lanthanides in pyrolytically-coated and tantalum foil-lined graphite furnaces

Element	Atomization temperature, °C	Sensitivity* Pyrolytically-coated furnace (PCF)	Ta-foil lined furnace (TaF)	Sensitivity enhancement factor (PCF/TaF) at 2600°C
Sc	2600	1.3×10^{-10}	1.2×10^{-11}	10.8
	2700	1.0×10^{-10}		
Y	2600	2.6×10^{-9}	2.8×10^{-10}	9.3
	2700	1.3×10^{-9}		
La	2600	4×10^{-8}	2×10^{-9}	20
	2700	2×10^{-8}		
Ce	2600	2×10^{-7}	5×10^{-9}†	40
	2700	0.8×10^{-7}		
Pr	2600	1.6×10^{-8}	1.5×10^{-9}	10.7
	2700	1×10^{-8}		
Nd	2600	3×10^{-9}	2×10^{-10}	15
	2700	1.5×10^{-9}		
Sm	2600	1×10^{-9}	7×10^{-11}	14.3
	2700	0.8×10^{-9}		
Eu	2600	5.5×10^{-11}	4×10^{-12}	13.8
	2700	3.4×10^{-11}		
Gd	2600	2.1×10^{-8}	7.3×10^{-10}	28.8
	2700	1.4×10^{-8}		
Tb	2600	6.4×10^{-9}	3.2×10^{-10}	20
	2700	4.1×10^{-9}		
Dy	2600	2×10^{-10}	2×10^{-11}	10
	2700	1.4×10^{-10}		
Ho	2600	5.5×10^{-10}	3.1×10^{-11}	17.7
	2700	2.8×10^{-10}		
Er	2600	4.4×10^{-10}	1.3×10^{-11}	33.8
	2700	2.8×10^{-10}		
Tm	2600	3.7×10^{-11}	4×10^{-12}	9.3
	2700	1.8×10^{-11}		
Yb	2600	3.3×10^{-12}	5.4×10^{-13}	6.1
	2700	2.5×10^{-12}		
Lu	2600	4.9×10^{-9}	1.4×10^{-10}	35
	2700	3.5×10^{-9}		

*Defined as the weight of the element in g which produces a change, compared with a pure solvent or blank, of 0.0044 absorbance unit.

†Value obtained previously.[6]

Table 5. Determination of Sc, Y and the rare-earth elements in international reference rocks (concentrations in *ppm*)

Element	NIM-G (Granite) This work	NIM-G (Granite) Other values	SCo-1 (Cody shale) This work*	SCo-1 (Cody shale) Other values	MAG-1 (Marine mud) This work*	MAG-1 (Marine mud) Other values	SDC-1 (Mica schist) This work*	SDC-1 (Mica schist) Other values	BHVO-1 (Hawaiian basalt) This work*	BHVO-1 (Hawaiian basalt) Other values
Sc	1	(1‡, 1§) # 0.48–9[a], 1?[b]	11	(10‡, 11¶, 9§) # 10.6 ± 0.9[c], 11?[b]	19	(17‡, 18¶,§) # 17 ± 2[c], 15?[b]	20	(17‡, 18¶,§) # 17 ± 2[c], 15?[b]	28	(32‡, 33¶, 36§) # 30 ± 2[c], 31[b]
Y	122	115‡,[d], 133§[e] 80–187[e], 145[b]	30	(24‡, 25§)[d] 26[c], 24?[b]	31	29§,[d], 27?[b] (25, 57)[c]	42	(40‡, 41§)[d] (44,70)[c], 42?[b]	27	(28‡, 27§)[d] 28 ± 2[c], 27?[b]
La	120	113¶,[d], 122§[e] 84–200[a], 105?[b]	31	(30¶, 29§)[d] 35 ± 10[c], 29?[b]	46	(48¶, 46§)[d] 46[c], 41?[b]	45	(45¶, 46§)[d] (42.2, 54.7)[c]	19	(18¶, 19§)[d] 16.7 ± 0.8[c], 17?[b]
Ce	200†	217§,[d], 200[b] 145–224[a]	69†	66§,[d], 63[b] 62 ± 6[c]	90†	90§,[d], 86?[b] 94 ± 7[c]	85†	92§,[d], 92[b] 104 ± 12[c]	49†	49§,[d], 39[b] 41 ± 4[c]
Pr	18	19¶,[d] (19, 19.8)[a]	7.5	7¶,[d] 5.43[c], 7.62[f]	10	10¶,[d] 8.73[c]	9.5	10¶,[d] 8.73[c]	7	6¶,[d] 5.6[c]
Nd	70	69§,[d], 68?[b] 43–83.4[a]	28	28¶,[d], 27[b] 26 ± 2[c]	41	(38‡, 42§)[d] 44 ± 3[c], 41[b]	39	(38‡, 42§)[d] 41 ± 6[c], 38[b]	29	(28‡, 26§)[d] 24 ± 6[c], 24[b]
Sm	16	16‡,[d], 16?[b] 14.6–21.5[a]	6	5.5‡,[d], 5.1?[b] 5.3 ± 0.4[c]	8.2	8.3‡,[d], 8.1?[b] 7.8 ± 0.9[c]	8	7.5‡,[d], 8.3?[b] 8 ± 2[c]	6	6‡,[d], 6.1[b] 6.1 ± 0.7[c]
Eu	0.5	0.4‡,[d], 0.4?[b] 0.31–2.2[a]	1.4	1.2‡,[d], 1.2?[b] 1.2 ± 0.2[c]	1.8	1.8‡,[d], 1.5?[b] 1.6 ± 0.2[c]	2	1.7‡,[d], 1.7[b] 1.8 ± 0.2[c]	2	2‡,[d], 2[b] 2.0 ± 0.4[c]
Gd	12.4	13¶,[d], 11?[g] 9.6–20[a]	5	4.7¶,[d], 4.2?[b] 5 ± 1[c]	6	7¶,[d], 6.6?[b] 7 ± 2[c]	7	7¶,[d], 7.2?[b] 1.7–9.9[c]	6.6	6.3¶,[d], 6[b] 7 ± 2[c]
Tb	3	2.5¶,[d], 3?[b] 1.9–3.5[a]	1	0.7¶,[d], 0.8?[b] 0.75 ± 0.04[c]	1	1¶,[d], 1?[b] 1.02 ± 0.05[c]	1.2	1.2¶,[d], 1.2?[b] 1.26 ± 0.08[c]	1	0.9¶,[d], 1?[b] 1.0 ± 0.2[c]
Dy	17	17‡,[d], 16[g] 15.4–17.2[a]	4.6	4.3‡,[d], 4.2?[b] 3.8[c], 5.7[h]	5.3	5‡,[d],5.02[f] 5.4[h]	7.5	7.3‡,[d] 7.8[h]	5	5.3‡,[d], 5?[b] 4.8 ± 0.2[c], 5.5[h]
Ho	4.6	4.4‡,[d], 3?[g] 3–5[a]	1	1¶,[d], 0.9?[b] 0.93[c]	1	1¶,[d] 1.12[f]	1.5	1.4¶,[d]	1	0.95¶,[d] 0.94[c]
Er	12	12‡,[d], 10?[g] 9.6–13.5[a]	3	2.5‡,[d], 2.5?[b] 2.5[c], 2.39[f]	2.8	2.8‡,[d] 3.16[f]	5	4‡,[d]	2.4	2.5‡,[d] 2.0 ± 0.3[c]
Tm	2	2¶,[d], 2?[g] 1.6–2.5[a]	0.5	0.4¶,[d], 0.5?[b] 0.35[c], 0.61[h]	0.45	0.4¶,[d] 0.44[c], 0.54[h]	0.7	0.6¶,[d], 0.7?[b] 0.72[c]	0.3	0.3¶,[d], 0.3[b] 0.31 ± 0.04[c]
Yb	15	13‡,[d], 14[b] 6.8–16[a]	2.7	(2.3‡, 2.5§)[d] 2.6 ± 0.3[c], 2.6[b]	2.7	(2.5‡, 2.7§)[d] 3.0 ± 0.3[c], 2.6[b]	4.2	(4‡, 4.2§)[d] 5 ± 1[c], 4.2[b]	2.4	(2‡, 2.2§)[d] 2.1 ± 0.5[c]
Lu	2	2¶,[d], 2?[b] 1.58–3.09[a]	0.3	0.32¶,[d] 0.37[c], 0.34[f]	0.4	0.4¶,[d] 0.4[c], 0.45[f]	0.5	0.5¶,[d] 0.49[c]	0.4	0.36¶,[d] 0.32[c]

*Preconcentrated by ion-exchange unless otherwise indicated.
†Preconcentrated by ion-exchange, followed by a single calcium oxalate and single hydrous ferric oxide co-precipitations.
‡Flame AAS value.
§Emission spectrographic value.
Sen Gupta.[2]
¶Graphite furnace AAS value.
[a]Reported in a compilation of data by Steele *et al.*[14]
[b]"Usable value" reported in a compilation of data by Abbey.[9]
[c]Reported in a compilation of data by Gladney and Goode.[15]
[d]Sen Gupta.[3]
[e]Sen Gupta (unpublished work).
[f]McLennan and Taylor (spark-source mass-spectrographic value).[16]
[g]"Usable value" reported in a compilation of data by Abbey.[13]

order, the sensitivities for lanthanum, cerium, praseodymium, gadolinium, terbium and lutetium were very poor. L'vov and Pelieva[11] had earlier reported increased sensitivities for 13 lanthanides without any marked memory effects when a tantalum foil liner was used inside an ordinary graphite tube, and a 40-fold increase in sensitivity had been obtained for cerium in the same way.[6] A tantalum foil-lined graphite furnace was therefore used in the present work for determination of lanthanum, cerium, praseodymium, gadolinium, terbium and lutetium. Scandium, yttrium and the other lanthanides were determinable with the pyrolytically-coated graphite furnace.

Interferences

Although there are no interelement interferences in determination of lanthanides by electrothermal atomization in the graphite furnace,[1] some common elements that are retained on the ion-exchange column and co-eluted with the rare earths cause positive errors. To ascertain the nature of these associated common elements (other than iron since it does not interfere[1,6]), an aliquot of Solution A was mixed with 5 mg of Fe^{3+} (to act as a carrier), the elements were precipitated as hydroxides and carbonates with ammonia and ammonium carbonate in presence of some filter pulp, and the precipitate was filtered off, washed and ignited to the oxides. A qualitative emission spectrographic analysis of this material for common elements (iron excepted) showed the presence of major amounts of calcium and traces of aluminium, magnesium, barium and strontium.

Tests showed that interferences from associated common elements could be eliminated by heating the sample at about 1800–2000° before atomization of the lanthanides (except cerium) at 2700° in a pyrolytically-coated graphite furnace or at 2600° in a tantalum foil-lined furnace. Tables 2 and 3 show the temperatures suitable for the elimination of these interferences, for each rare-earth element. To minimize these interference effects, it is also recommended that the sample taken should be such that the apparent sample concentration in the final solution is equivalent to not more than 0.1–0.2 g of sample per ml.

A temperature of about 1800° was found to be adequate for removal of the interferences after separation by double calcium oxalate and single hydrous ferric oxide co-precipitations[1,2] because, except for the small amount of iron added during the co-precipitation step, the final solution is relatively free of other elements. In the case of cerium, the elements retained on the ion-exchange column and co-eluted with the cerium cause severe interference at 567.0 nm, the most sensitive line. Consequently, it is necessary to separate cerium from these elements. This can be done after the ion-exchange separation, by co-precipitating cerium once with calcium oxalate and once with hydrous ferric oxide.[1,2]

Table 4 shows the sensitivities obtained for scandium and the lanthanides. At 2600° the tantalum-

Table 6. Determination of Sc, Y and the rare-earth elements in Canadian iron-formation reference materials (concentrations in *ppm*)

	FeR-1		FeR-2		FeR-3		FeR-4	
Element	This work*	Other values	This work*	Other values	This work*	Other values	This work*	Other values
Sc	0.9	0.7–1‡ 0.8?§	6	4–6.7‡ 6?§	0.6	(0.497, 0.58, 2)‡	1.5	1.29–2‡ 1.5?§
Y	17	11–46‡	18	12–19‡, 15?§	6	2–6‡, 6?§	9	4–10‡, 8?§
La	14	7–41‡ 12?§	16	12–26.4‡ 14?§	4	1.9–19‡ 2?§	10	5–25.6‡ 8?§
Ce	24†	(11, 21.4)‡	26†	11–32.1‡	8†	5‡	19†	7.33–14.48‡
Pr	3	—	3	—	1	—	2.5	—
Nd	10	—	12	15‡	4	—	10	—
Sm	2	1.64–1.85‡ 1.7?§	3	2.5–3.3‡ 2.6?§	0.9	0.52–0.67‡ 0.6?§	2.8	2.1–2.32‡ 2.2?§
Eu	3	0.76–3.1‡	1.3	1.1–1.32‡	0.3	0.18–0.24‡	0.8	0.61–0.77‡
Gd	2.3	1.5‡	2.3	2‡	0.8	0.3‡	1.6	1.1‡
Tb	0.4	(0.17, 0.43)‡	0.4	(0.32, 0.49)‡	0.14	—	0.2	(0.15, 0.35)‡
Dy	2.5	1.76‡	2.6	2.36‡	0.8	0.34‡	1.3	1.05‡
Ho	0.5	0.33‡	0.6	0.6‡	0.17	0.08‡	0.3	0.22‡
Er	1.4	—	1.6	—	0.4	—	0.8	—
Tm	0.2	—	0.25	—	0.1	—	0.05	—
Yb	1.2	0.98–1‡ 1?§	1.4	1.2–1.7‡ 1.3?§	0.25	0.19–0.36‡ 0.2?§	0.7	0.3–0.76‡ 0.5?§
Lu	0.2	0.12–2‡ 0.2?§	0.2	(0.23, 0.26)‡	<0.1	0.06–0.09‡	0.1	0.11–0.141‡

*Preconcentrated by ion-exchange unless otherwise indicated.
†Preconcentrated by ion-exchange followed by single calcium oxalate and single hydrous ferric oxide co-precipitations.
‡Reported in a compilation of data by Abbey *et al.*[18]
§"Usable value" reported by Abbey *et al.*[18]

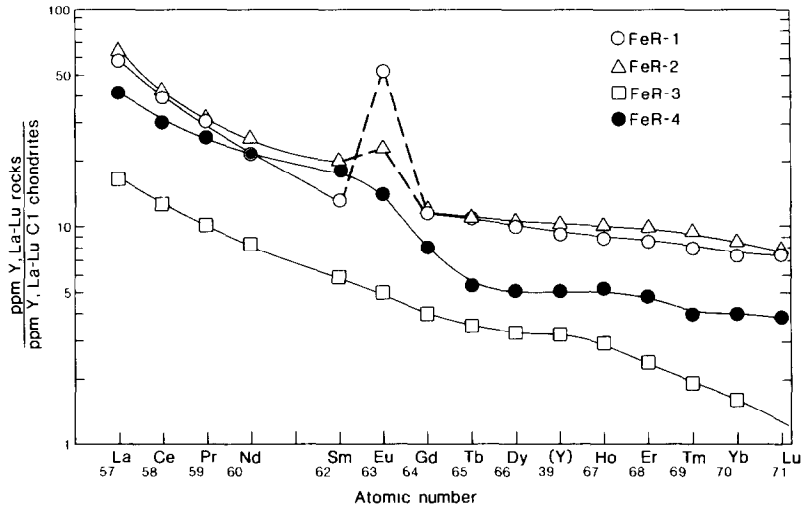

Fig. 1. Chondrite-normalized Y and REE patterns for Canadian iron-formation reference materials.

lined furnace gives considerably higher sensitivity than the pyrolytically-coated graphite furnace, particularly for lanthanum, cerium, neodymium, gadolinium, terbium, erbium and lutetium. Heating of the tantalum-lined furnace at 2700° is not recommended, because the lining deteriorates very rapidly under these conditions.

The method was tested with one South African and four U.S.G.S. reference rocks for which other values were available for comparison purposes, and applied to four new Canadian iron-formation reference materials. The results are given in Tables 5 and 6. Results for praseodymium, erbium and thulium in FeR-1 to FeR-4, for terbium in FeR-3 and for neodymium in FeR-1, FeR-3 and FeR-4 have not been reported previously.

The rare-earth element abundances of FeR-1 to FeR-4 are plotted (normalized to the values for Cl-chondrites of Evensen *et al.*[19]) in Fig. 1 against the atomic numbers. The yttrium abundance data were normalized to the chondritic abundance data of Haskin *et al.*[20] and the data points are plotted between those for dysprosium and holmium because of the similarity in properties and ionic radius for the three elements. From these plots, it is apparent that the lighter rare-earth elements are more fractionated than the heavier ones and, with the exception of the positive europium anomalies for FeR-1 and FeR-2, the shapes of the curves are generally smooth, which supports the accuracy of the data.

Acknowledgements—The author is indebted to Ryan A. Meeds for qualitative emission spectrographic examination of the impurities in the rare-earth concentrates of rocks obtained after ion-exchange separation, and to Elsie M. Donaldson of Canada Centre for Mineral and Energy Technology for critical reading of the manuscript.

REFERENCES

1. J. G. Sen Gupta, *Talanta*, 1981, **28**, 31.
2. *Idem*, *Anal. Chim. Acta*, 1982, **138**, 295.
3. *Idem*, *Geostds. Newsl.*, 1982, **6**, 241.
4. R. Keil, *Z. Anal. Chem.*, 1980, **303**, 188.
5. M. R. Hughson and J. G. Sen Gupta, *Am. Mineral.*, 1964, **49**, 937.
6. J. G. Sen Gupta, *Talanta*, 1984, **31**, 1045.
7. *Idem*, *ibid.*, 1984, **31**, 1053.
8. M. Roubault, H. De La Roche and K. Govindaraju, *Sci. de la Terre*, 1968, **13**, 379.
9. S. Abbey, *Geol. Surv. Can. Paper*, 1983, 83-15.
10. *Idem*, *Canada Centre for Mineral and Energy Technology Rept.*, 1979, 79-35.
11. B. V. L'vov and L. A. Pelieva, *Can. J. Spectrosc.*, 1978, **23**, 1.
12. J. G. Sen Gupta, *Geostds. Newsl.*, 1977, **1**, 149.
13. S. Abbey, *Geol. Surv. Can. Paper*, 1980, 80-14.
14. T. W. Steele, A. Wilson, R. Goudvis, P. J. Ellis and A. J. Radford, *Geostds. Newsl.*, 1978, **2**, 71.
15. E. S. Gladney and W. E. Goode, *ibid.*, 1981, **5**, 31.
16. S. M. McLennan and S. R. Taylor, *Chem. Geol.*, 1980, **29**, 333.
17. R. J. Rosenberg and R. Zilliacus, *Geostds. Newsl.*, 1980, **4**, 191.
18. S. Abbey, C. R. McLeod and W. Liang-Guo, *Geol. Surv. Can. Paper*, 1983, 83-19.
19. N. M. Evensen, P. J. Hamilton and R. K. O'Nions, *Geochim. Cosmochim. Acta*, 1978, **42**, 1199.
20. L. A. Haskin, M. A. Haskin, F. A. Frey and T. R. Wildeman, in *Origin and Distribution of the Elements*, L. H. Ahrens (ed.), p. 889. Pergamon Press, Oxford, 1968.

Talanta, Vol. 32, No. 1, pp. 7–10, 1985
Printed in Great Britain.

0039-9140/85 $3.00 + 0.00

THE MANGANESE(IV) OXIDE ELECTRODE AS A MANGANESE(II) SENSOR

DEREK MIDGLEY
Central Electricity Generating Board, Central Electricity Research Laboratories, Kelvin Avenue, Leatherhead, Surrey, England

DENNIS E. MULCAHY
South Australian Institute of Technology, The Levels, P.O. Box 1, Ingle Farm, South Australia 5098, Australia

(*Received* 13 *July* 1984. *Accepted* 27 *July* 1984)

Summary—Manganese(IV) oxide electrodes formed with a graphite/PTFE substrate are shown to have near-theoretical response to manganese(II) ions in pH-4 acetate medium and a sub-Nernstian response in 0.1*M* nitric acid medium. Lead and iron(III) ions interfere, and iron(II) ions even more so, but other bivalent transition metal ions have little effect. The main drawback of this type of electrode is its long response time (~20 min). Some attempts to use manganese(IV) oxide electrodes as the basis for phosphate electrodes by use of $MnHPO_4.3H_2O$ and $MnNH_4PO_4.H_2O$ are also described.

No manganese(II)-selective electrodes are commercially available and very few experimental electrodes have been reported[1–5]. Electrodes with heterogeneous membranes of either manganese(II) carbonate or manganese(II) hydrogen phosphate respond to manganese(II) ions, but unselectively.[6] An electrode with a sintered manganese(II) telluride–silver sulphide membrane[7] is reported to respond to manganese(II) ions with a sensitivity of 25 mV/pMn, and is selective relative to alkali-metal and alkaline-earth metal cations, but no other performance characteristics were described. More recently[8], a membrane consisting of an ion-exchange resin embedded in an epoxy resin matrix has been proposed for manganese(II) determinations.

Solid-state electrodes based on manganese(II) sulphide, analogous to those for copper, lead and cadmium, are not practicable, mainly because manganese(II) sulphide is soluble in acid solutions. Even in alkaline solutions, however, the useful range would be very small. From the solubility products[9] of manganese(II) sulphide ($pK_s = 12.6$) and manganese(II) hydroxide ($pK_s = 12.72$) and the protonation constants[9] of the sulphide ion, we calculate that hydroxide would displace sulphide from the precipitate at pH > 10. In the pH range 7–10, the range of free manganese concentrations available between dissolution of the manganese(II) sulphide and manganese(II) hydroxide precipitation is fairly small (Table 1) and the range of Nernstian response would be smaller still. These calculations neglect the further complication that in air-saturated solutions oxidation leading to the formation of manganese(IV) oxide, MnO_2, would occur.[10]

In view of this, it was decided to try an electrode based on manganese(IV) oxide. This material has been extensively studied[11–13] because of its use in dry storage batteries, but in many cases the mass ratio of manganese(IV) oxide to solution was high enough for the composition of the solution to be affected. The electrode in these studies usually consisted of a platinum electrode in a paste or suspension of manganese(IV) oxide particles: this is inconvenient for analytical applications since it involves either preparing a fresh electrode for each solution or prolonged washing if carry-over of one solution to the next is to be avoided. We have, therefore, applied manganese(IV) oxide to the surface of a Růžička "Selectrode",[14,15] since this arrangement enables a relatively small surface area to be repeatedly and conveniently presented to successive solutions and has already worked successfully with a lead(IV) oxide coating.[16] The most notable of the previous studies of the manganese(IV) oxide electrode in manganese(II) solutions are those by Covington and co-workers[17,18] and by Caudle *et al.*[19] We have also tested electrodes impregnated with mixtures of manganese(IV) oxide and sparingly soluble phosphate salts, as phosphate sensors.

Table 1. Calculated range of manganese(II) sulphide electrodes

pH	pMn_{max} (MnS saturation)	pMn_{min} [$Mn(OH)_2$ precipitation]
7	3.1	−1.3
7.5	3.5	−0.3
8	3.8	0.7
8.5	4.0	1.7
9	4.3	2.7
9.5	4.5	3.7
10	4.8	4.7

THEORY

Manganese(IV) oxide gives a redox reaction according to equation (1)

$$MnO_{2(s)} + 4H^+ + 2e^- \rightleftharpoons Mn^{2+}_{aq} + 4H_2O \quad (1)$$

for which the electrode potential is

$$E = E^\circ - 2k\,pH - k/2 \log\{Mn^{2+}\} \quad (2)$$

where $k(=2.303\ RT/F)$ is the Nernst slope factor for a one-electron change. It follows from equation (2) that the electrode is sensitive both to pH and to manganese(II) ions. Use of the electrode as a manganese sensor demands, therefore, that the pH of the solution should be rigorously controlled, especially as the electrode is four times as sensitive to pH as to $\log\{Mn^{2+}\}$.

The pH should be controlled by an acidic medium [to avoid the formation of manganese(II) hydroxide or hydroxo-complexes] which does not interact strongly with manganese ions. The media tested were 0.05*M* nitric acid and pH-4 acetate buffer. The stability constant of the manganese acetate complex[20] is $10^{1.4}$.

EXPERIMENTAL

Apparatus

The e.m.f. values were measured with a digital pH-meter reading to 0.1 mV and were displayed on a chart-recorder. A Techne C-100 thermocirculator was used to maintain the temperature of the solution and the electrodes at 25° in a water-jacketed glass vessel. Solutions were stirred by a magnetic stirrer bar.

Manganese(IV) oxide electrodes were prepared by impregnation of the PTFE-graphite substrate of a Radiometer F3012 "Selectrode".[14] The reference electrode was a Radiometer K701 double-junction calomel electrode, the outer sleeve of which was filled with whichever buffer solution was being used at the time, diluted to the same concentration as that in the test solution.

Reagents

The manganese(IV) oxide was Ventron "puratronic" grade (99.999% as metal).

A stock 0.01*M* manganese(II) solution was prepared from manganese(II) sulphate. Other standard manganese solutions were prepared from it by successive dilution.

Solutions for pH adjustment (added in 1:20 v/v ratio) were as follows: 1*M* nitric acid was prepared from a B.D.H. "Con-Vol" ampoule, and acetic acid–acetate buffer, pH 4.0, was prepared by dissolving 243 g of sodium acetate trihydrate in 400 ml of water, adding 480 g of glacial acetic acid and diluting to 1 litre.

Interference tests were made with solutions of sulphate [iron(II), copper(II), cobalt(II)] or nitrate [zinc, lead, nickel, mercury(II), iron(III)] salts.

For the phosphate tests, standard solutions were prepared from stock solutions of 0.1*M* potassium dihydrogen phosphate or 0.2*M* disodium hydrogen phosphate, the former being used in acidic media, the latter in alkaline media.

For solutions in the pH region 4–6, the acetate buffer solution was used, adjusted to the appropriate pH. For pH > 7 the alkaline phosphate solutions were adjusted to the desired pH by addition of 1*M* nitric acid.

Reagents were B.D.H. AnalaR grade unless otherwise specified. Water was distilled and then demineralized on a mixed-bed ion-exchange resin.

RESULTS

Calibration slope

The response in 0.05*M* nitric acid medium was non-linear and the slope in the 10^{-4}–10^{-3}*M* region was about −18 mV/pMn. In the pH-4 acetate medium, the response was almost Nernstian (between −28 and −29 mV/pMn at 25°) at concentrations above 10^{-4}*M*. Deviations from the Nernstian response were obvious below the 5×10^{-5}*M* level. Figure 1 shows the calibration graphs for both media.

Standard potential

The standard potential was calculated from equation (3)

$$E^\circ = E + \frac{k}{2}\log[Mn^{2+}] + \frac{k}{2}\log\alpha + \frac{k}{2}\log f_{Mn} + 2k\ pH + E_{ref} - E_j \quad (3)$$

where E_{ref} is the half-cell potential of the saturated calomel reference electrode, E_j is the liquid-junction potential calculated by means of the Henderson equation, f_{Mn} is the activity coefficient of the manganese(II) ion calculated by the Davies equation,[21] α is a term allowing for complexation with the acetate in the buffer medium and $[Mn^{2+}]$ is the total manganese concentration. The standard potential obtained from measurements in the pH-4 acetate medium was 1224 mV (the standard deviation for the mean of 12 results was 0.4 mV). This figure was obtained with electrodes less than 8 hr old. As the electrodes aged the apparent standard potential decreased by 1–2 mV/day. In these calculations, $k \log \alpha$ had the value −3.0 mV and E_j −0.02 mV. Literature values[17,18] for the standard potential are in the

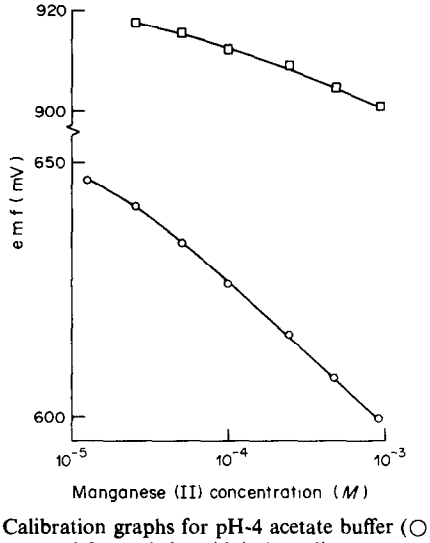

Fig. 1. Calibration graphs for pH-4 acetate buffer (○) and 0.01*M* nitric acid (□) media.

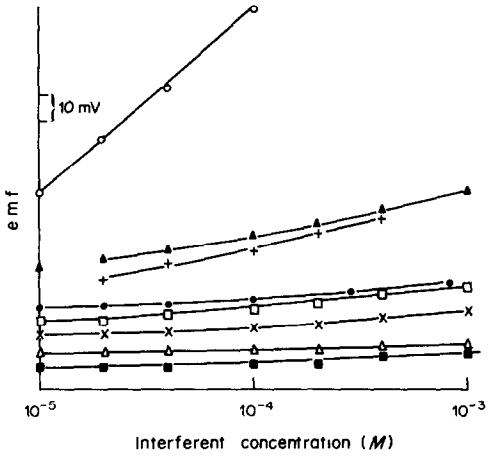

Fig. 2. Interferences in pH-4 acetate buffer medium, Fe^{2+}(○), Pb^{2+}(▲), Fe^{3+}(+), Hg^{2+}(×), Co^{2+}(□), Cu^{2+}(●), Zn^{2+}(△), Ni^{2+}(■).

range 1230–1240 mV with which our measurements are, therefore, in fairly good agreement.

Response time

The response of the manganese(IV) oxide electrode to an approximately twofold increase in concentration was complete within about 10 min in 0.05*M* nitric acid medium, but took 20–30 min in pH-4 acetate buffer, these times being obtained for gently stirred solutions in a beaker. When the electrode was placed in a flow-cell which also provided vigorous stirring at the electrode surface, shorter response times were observed, *e.g.*, equilibrium was reached in 15–20 min (including 3 min dead-time) for tenfold upward and downward changes in concentration.

Interferences

Figure 2 shows the response curves for various metal ions in the pH-4 acetate medium, where the manganese response was most nearly Nernstian; the e.m.f. values are displaced arbitrarily on the ordinate for the sake of clarity. Zinc, nickel, mercury(II) and copper(II) ions had little or no interfering effect at concentrations up to about 10^{-4} but at higher levels gave approximately linear responses of, respectively, −2.7, −4.1, −6.5 and −8.5 mV/decade. Cobalt(II) below $10^{-4}M$ had a more discernible effect and an almost linear response of about −8.5 mV/pCo over the range 10^{-4}–$10^{-3}M$. Iron(III) produced a significant effect: the curve in Fig. 2 represents an almost Nernstian response of about −25 mV/pFe(III), but this graph was constructed from readings taken arbitrarily about 1 hr after the change of concentration, since the potentials were still drifting slowly at that time. The response to lead ions was sub-Nernstian, at −18 mV/pPb. Iron(II) produced the largest effect: the sensitivity was about −115 mV/pFe(II) up to $10^{-4}M$, but this figure was also obtained from potentials recorded arbitrarily after 60 min because equilibrium potentials were not attained within that time.

Selectivity coefficients were determined by the separate solutions method for those ions giving an approximately Nernstian response, with the results shown in Table 2.

Compared with sulphide-based electrodes for transition metal ions, the manganese(IV) oxide electrode is notably tolerant of copper(II) and mercury(II) ions. Comparison with the lead(IV) oxide electrode for lead ions[16] shows very similar interference by zinc, nickel, copper and mercury and cobalt ions and the selectivity coefficient for lead ion with respect to the manganese(IV) oxide electrode is approximately the inverse of that for manganese(II) ion with respect to the lead(IV) oxide electrode. The likeliest explanation for these interferences is an ion-exchange mechanism. The much larger iron(II) interference is presumably brought about by reduction of manganese(IV) oxide, with a consequent release of manganese(II) ions.

DISCUSSION

Manganese (II) response

The results show that the manganese(IV) oxide electrode could be a useful manganese(II)-selective electrode, with a Nernstian response down to $5 \times 10^{-5}M$. The main practical problem is the slow response. The need for precise control of pH is a disadvantage, but this control differs little from the ionic strength adjustment procedures usually applied in measurements with ion-selective electrodes. The durability of the electrode was not specifically tested, but one application of manganese(IV) oxide lasted for at least 2 weeks, during which the standard potential decreased as described above.

The slow response is probably related to the mechanism elucidated by Caudle *et al.*,[19] in which the manganese(IV) oxide electrode does not respond directly to manganese(II) ions but only to hydrogen ions, with sensitivity of 59 mV/pH. Reactions (4) and (5) relate the manganese(II) ion concentration to the pH and hence to the electrode potential with respect to H^+, which, at equilibrium, conforms to that given by equation (1):

$$MnO_{2(s)} + Mn^{2+} + 2H_2O \rightleftharpoons 2MnOOH_{(s)} + 2H^+ \quad (4)$$

$$MnO_{2(s)} + H^+ + e^- \rightleftharpoons MnOOH_{(s)} \quad (5)$$

The formation of MnOOH implies changes in the (solid) membrane phase greater than expected with

Table 2. Selectivity coefficients for manganese(IV) oxide electrodes

Ion	Concentration range, M	Selectivity coefficient
Fe^{3+}	10^{-4}–4×10^{-4}	0.02
Pb^{2+}	10^{-4}–10^{-3}	~0.5

most ion-selective electrodes, unless these are subject to a major interference effect. In the light of the mechanism proposed above, the slow response is less surprising.

Since MnOOH would be expected to be formed first at the surface, changes in the composition of the solid phase would be expected to be slow and gradual, which is in accord with the observed slow changes in standard potential (1–2 mV/day).

Investigation of possible phosphate-selective electrodes

The grey modification of manganese hydrogen phosphate trihydrate[22] has a solubility product[23] of 1.4×10^{-13} and manganese ammonium phosphate[24] has a solubility of the order of $10^{-5}M$ in weakly acidic solutions of ammonium salts.[25] The manganese(IV) oxide electrode, in conjunction with one or other of these salts, was tested for response to phosphate. The tests were performed in two ways: electrodes impregnated with manganese(IV) oxide/phosphate salt mixtures were immersed in phosphate solutions, and electrodes impregnated with only manganese(IV) oxide were immersed in solutions saturated with a sparingly soluble phosphate. Solutions for use with manganese ammonium phosphate contained ammonium nitrate at $1M$ concentration. In no case was a response to phosphate obtained. At pH 8 the pink manganese ammonium phosphate turned white, presumably indicating hydroxide formation. At pH 4–6 (acetate buffer) the e.m.f. changed in the opposite direction to that expected from depression of the manganese concentration in equation (2) by the common ion effect of phosphate. Such e.m.f. changes were traced to small shifts in pH resulting from inadequate buffer capacity at the higher phosphate levels (up to $0.035M$). The manganese(IV) oxide electrode, therefore, appears not to be a suitable basis for a phosphate-selective electrode.

Acknowledgements—This work was done at the Central Electricity Research Laboratories and is published by permission of the Central Electricity Generating Board. D.E.M. thanks the South Australian Institute of Technology and C.E.R.L. for facilitating study leave.

REFERENCES

1. J. Koryta, *Anal. Chim. Acta*, 1972, **61**, 329.
2. *Idem, ibid.*, 1977, **91**, 1.
3. *Idem, ibid.*, 1979, **111**, 1.
4. *Idem, ibid.*, 1982, **139**, 1.
5. Y. Su, *Fenxi Huaxue*, 1983, **11**, 905.
6. E. B. Buchanan and J. L. Seago, *Anal. Chem.*, 1968, **40**, 517.
7. H. Hirata and K. Higashiyama, *Talanta*, 1972, **19**, 391.
8. U.S. Lal, M. C. Chattopadhyaya, M. C. Ghosh and A. K. Dey, *Indian Agric.*, 1982, 139; *Chem. Abstr.*, 1983, **99**, 15614w.
9. A. Ringbom, *Complexation in Analytical Chemistry*, Interscience, New York, 1963.
10. J. Kragten, *Atlas of Metal-Ligand Equilibria in Aqueous Solution*, p. 452. Horwood, Chichester, 1978.
11. W. C. Vosburgh, *J. Electrochem. Soc.*, 1959, **106**, 839.
12. A. Kozawa and R. J. Brodd (eds.), *Manganese Dioxide Symposium, Cleveland 1975*, Vol. 1, I.C. Sample Office, Cleveland, 1975.
13. B. Schumm, H. M. Joseph and A. Kozawa (eds.), *Manganese Dioxide Symposium, Tokyo 1980*, Vol. 2, I.C. MnO_2 Sample Office, Cleveland, 1981.
14. J. Růžička, C. G. Lamm and J. C. Tjell, *Anal. Chim. Acta*, 1972, **62**, 15.
15. D. Midgley and D. E. Mulcahy, *Ion-Selective Electrode Rev.*, 1983, **5**, 165.
16. D. Midgley, *Anal. Chim. Acta*, 1984, **159**, 63.
17. A. K. Covington, T. Cressey, B. G. Lever and H. R. Thirsk, *Trans. Faraday Soc.*, 1962, **58**, 1975.
18. J. Ambrose, A. K. Covington and H. R. Thirsk, *ibid.*, 1969, **65**, 1897.
19. J. Caudle, K. G. Summer and F. L. Tye, *J. Chem. Soc. Faraday I*, 1973, **69**, 885.
20. D. W. Archer and C. B. Monk, *J. Chem. Soc.*, 1964, 3117.
21. C. W. Davies, *Ion Association*, p. 41. Butterworths, London, 1962.
22. R. Klement and H. Haselbeck, *Z. Anorg. Allgem. Chem.*, 1964, **334**, 27.
23. M. V. Goloshchapov, B. A. Martynenko and T. N. Filatova, *Zh. Neorgan. Khim.*, 1966, **11**, 935.
24. J. W. Mellor, *A Comprehensive Treatise on Inorganic and Theoretical Chemistry*, Vol. 12, p. 452. Longmans, London, 1932.
25. G. S. Reddy and Y. K. Reddy, *Indian J. Chem.*, 1977, **15A**, 352.

Talanta, Vol. 32, No. 1, pp. 11–14, 1985
Printed in Great Britain

0039-9140/85 $3.00 + 0.00
Pergamon Press Ltd

GRAVIMETRIC AND SPECTROPHOTOMETRIC DETERMINATION OF PALLADIUM WITH 2,3,4-PENTANETRIONE TRIOXIME

J. CACHO, M. A. LACOMA and C. NERÍN*
Department of Analytical Chemistry, Faculty of Sciences, University of Zaragoza, Zaragoza, Spain

(*Received* 6 *October* 1982. *Revised* 12 *July* 1984. *Accepted* 27 *July* 1984)

Summary—A study of the use of 2,3,4-pentanetrione trioxime (PTT) in the gravimetric and spectrophotometric determination of palladium is reported. PTT has been applied to the determination of palladium in various synthetic and standard samples. The reagent has some advantages over dimethylglyoxime.

Vicinal α-dioximes have been used as analytical reagents for transition metals,[1] especially nickel and palladium, since Tschugaeff[2] discovered and outlined the selective properties of the dioximes at the beginning of the 20th century. Dimethylglyoxime (DMG) has been the most studied and most often used, but has the drawback of low solubility in water and hence a risk of precipitation in gravimetric procedures.

With the aim of eliminating this problem and studying the effect of an additional oxime group, the reagent 2,3,4-pentanetrione trioxime (PTT) has been prepared and applied to spectrophotometric determination of iron(II), and its analytical characteristics have been studied.[3] The presence of the third oxime group greatly increases the solubility in water, while leaving the analytical properties the same as those of DMG. The use of the reagent for determination of palladium has therefore been examined. It can be used both gravimetrically and spectrophotometrically.

EXPERIMENTAL

Reagents

All chemicals were of analytical-reagent grade. Stock solutions (0.1 and 7.5%) of PTT in water were prepared. The palladium solutions were prepared from palladium chloride and standardized with DMG. An acetic acid/sodium acetate buffer (pH 4.5–6.0) was prepared.

Synthesis of PTT

To 36 g of isonitrosoacetylacetone, add 50 g of hydroxylamine hydrochloride and 100 g of sodium acetate and dilute to 400 ml with distilled water. Heat at 70–80° for 2 hr. Cool, adjust to pH 7 with sodium hydroxide and extract with ether. Evaporate the extract.

Gravimetric procedures

Place a sample containing 25–50 mg of Pd in a beaker, adjust to pH 0.5–2 with hydrochloric acid and dilute to about 150 ml with distilled water, then heat on a water-bath at 80°. Add 50 ml of 7.5% PTT solution with continuous stirring, then digest on the water-bath for at least 30 min. Cool, then filter off the yellow precipitate and wash it with 100 ml of hydrochloric acid (1 + 100). Dry at 110–120°, cool and weigh. The conversion factor from $Pd(C_5H_8N_3O_3)_2$ to Pd is 0.2519.

Determination of Pd in palladinized active carbon. Ignite 250–500 mg of sample at 800°. Dissolve the residue in 10 ml of *aqua regia.* Evaporate almost to dryness and dilute with distilled water. Filter off and wash any residue, and transfer the filtrate to a 400-ml beaker, then determine the palladium as above.

Determination of Pd in Pd–$CaCO_3$ catalyst. Dissolve 250–500 mg of sample in 10 ml of concentrated hydrochloric acid and 1 ml of concentrated nitric acid. Evaporate almost to dryness and dilute with distilled water to 200 ml. Precipitate according to the method above.

Spectrophotometric procedure

Place an aliquot of sample, containing 10–50 μg of palladium, in a 100-ml separatory funnel, add 15 ml of 0.2*M* EDTA, 5 ml of 0.1% PTT solution, and 20 ml of acetate buffer (pH 4.5–6) and dilute to 50 ml with distilled water. Then add 10 ml of chloroform–butan-1-ol mixture (5:1 v/v) and shake the mixture vigorously for 1 min. Separate the layers, filter the organic layer through a Whatman No. 1 PS paper and measure its absorbance at 270 nm against a reagent blank prepared along with the sample.

If molybdenum is present, after the EDTA add sodium fluoride in at least 10-fold molar ratio to the molybdenum. If gold is present, after the EDTA add potassium thiocyanate solution (tolerance limit 500 mg of KSCN).

Determination of Pd in palladinized active carbon. Calcine a 60-mg sample at 800°, and treat the residue as described for the gravimetric method, but finally dilute to volume in a 1000-ml standard flask. Use a 5-ml aliquot for the spectrophotometric determination.

Determination of Pd in palladinized calcium carbonate. Treat a 120-mg sample as described for the gravimetric method, but finally dilute the solution and complete the determination as for the spectrophotometric analysis of palladinized active carbon.

RESULTS AND DISCUSSION

PTT is easily soluble in water, and the solution is stable at room temperature for at least a month. Its first dissociation constant is $pK_1 = 13.7$.[3] The order in which the protons are dissociated is not known. It appears to be a bidentate ligand with a convenient

*Present address: Departamento de Quimica, Escuela Técnica Superior de Ingenieros Industriales, Ciudad Universitaria, Zaragoza, Spain.

Table 1. NMR spectra of PTT and its Pd-complex

Sample	*ppm*	Integration	Assignment	Remarks
PTT	1.8	3	CH_3	sharp singlet
	1.9	3	CH_3	sharp singlet
	10.3	1	OH	sharp singlet
	11.5	2	OH	multiplet
Pd–PTT	2.0	3	CH_3	multiplet
	2.3	3	CH_3	multiplet
	11.85	1	OH	wide band
	13.35	1	OH	wide band

steric arrangement of its donor groups, and a conjugate system of π-electrons connected with the donor groups.

The Pd–PTT complex

Elemental analysis confirms the formula $Pd(PTT)_2$. The structure has been studied and compared with that of $Pd(DMG)_2$.[4]

The infrared spectrum of the complex shows three bands, at 1533, 1280 and 1140 cm^{-1}, which do not appear in the reagent spectrum. The band at 1533 cm^{-1} is attributed to the asymmetric C = N stretching vibration and the other two bands to N = O stretching modes.[5] Two other bands, at 820 and 780 cm^{-1}, are associated with the Pd–N stretching mode. The Ni–PTT complex was also prepared and its infrared spectrum obtained. New bands also appeared clearly at 1545, 1280 and 1168^{-1}. These considerations lead us to suppose that the chelation will be similar to that of Pd with DMG, which means that only two of the three oxime groups are involved.

Table 1 shows the data from the NMR spectra of PTT and its palladium complex. The characteristic peaks are displaced owing to formation of the complex.

The X-ray powder diffraction pattern shows a very strong peak at $2\theta = 9.19°$, the others peaks being irrelevant. We conclude that there is a layer-stacked structure similar to that of the $Pd(DMG)_2$ complex. The 2θ values for the characteristic peaks are 9.19°, 11.76°, 13.65°, 15.34°, 18.32°, 19.13°, 21.78°, 23.53°. The structure is still being worked out from the X-ray data, but it can be concluded that it could be that shown in Fig. 1.

The thermogravimetric curve for the complex (Fig. 2) shows that the complex is stable up to 180°. Sharp decreases occur at 230° and 290°. At above 410° a stable species appears, and at 800° palladium metal is obtained.

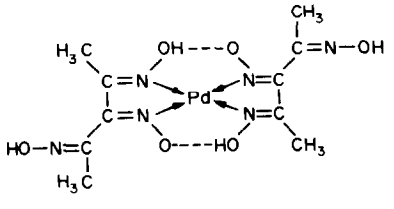

Fig. 1. Structure of the palladium complex.

Optimum precipitation conditions

The precipitate is slightly soluble in water (52 mg/l.), and should be washed with dilute acid. Various acids were examined and dilute hydrochloric acid (1 + 100) was found the most suitable (solubility of the precipitate 3.3 mg/l.). At least a 30-fold molar ratio of PTT to Pd is required for quantitative precipitation (Fig. 3). The precipitation can be done at any temperature from ambient up to 100°, and the optimum pH range is 0.5–2 (Fig. 4).

The most suitable amount of palladium for gravimetric determination is 25–50 mg (Fig. 4). The relative standard deviation for 35–45 mg of palladium is 0.1% (three levels, 10 determinations at each).

Spectrophotometric determination

The yellow Pd–PTT complex is soluble in alkaline medium, but the colour in this medium is unstable and cannot be used for a spectrophotometric determination. The precipitate obtained in acid medium,

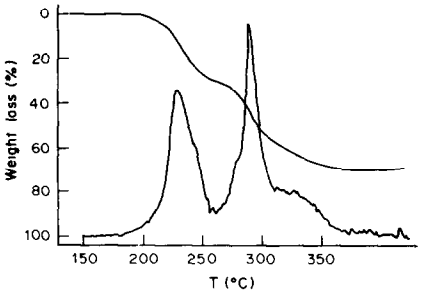

Fig. 2. Thermogravimetric and differential curves of $Pd(PTT)_2$ complex. Temperature increase 20°/min.

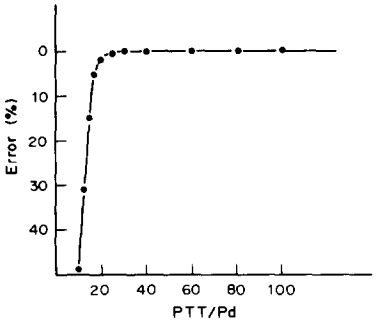

Fig. 3. Optimum PTT/Pd molar ratio for gravimetric determination of Pd.

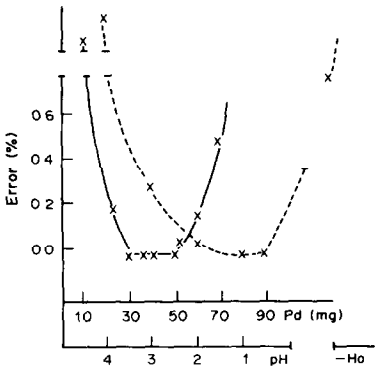

Fig. 4. Influence of pH (- - -) and amount of palladium (——) in the gravimetric determination of Pd.

unlike that obtained with DMG, is insoluble in chloroform, but easily dissolved in slightly more polar liquids, such as a chloroform–butan-1-ol (5:1 v/v) mixture or methyl isobutyl ketone (MIBK). In our study the mixed solvent was preferred, since the more polar solvents such as MIBK are capable of extracting the chloro-complexes of various metals, and these might produce interference in the determination of palladium.

The solvent mixture has minimum absorption at 245 nm. The absorption spectra of the reagent and its palladium-complex in the mixture are shown in Fig. 5. There is a shoulder in the spectrum of the complex at about 270 nm, whereas the absorbance of the reagent is small. At wavelengths longer than 310 nm the absorbance of the reagent is negligible.

The organic solutions of the reagent and its complex are stable for at least 1 month. Beer's law is obeyed up to at least 8 ppm of Pd in the organic phase. The molar absorptivity of the complex is 1.91×10^4 l.mole^{-1}.cm^{-1}.

Influence of pH on extraction of the reagent and its Pd-complex. A wavelength of 320 nm was used for measuring the complex, to avoid the absorbance of excess of the reagent extracted, and the PTT was measured at 230 nm (its wavelength of maximum absorption). The absorbance is practically constant for the complex over the pH range 1–6, and pH 4–5 for the reagent (Fig. 6). As the absorbance of the reagent is low at the wavelength (270 nm) used in the determination, a pH of 4.5–6 is recommended, in order to obtain better results in the removal of possible interferences by means of masking agents.

Extraction of PTT. The distribution coefficient and degree of extraction of the reagent were determined at pH 4.5–6, to establish the maximum amount of reagent permissible for the absorbance blank at 270 nm to be less than 0.2. The distribution coefficient was found by spectrophotometric determination of the PTT concentrations in the two phases after a single extraction, by the procedure given above. The average value of 6 determinations was $D = 0.102 \pm 0.005$ and the degree of extraction was $2.01 \pm 0.005\%$. Consequently, in the proposed method, the aqueous phase can contain a maximum of 6.6 mg of PTT.

In the pH range 4.5–6 the absorbance of the complex is constant if the molar ratio of PTT to Pd is 55:1. A ratio of 100:1 was chosen. It was found that the extraction of the complex was 100.0% complete in a single extraction for 20–50 μg of palladium.

Interferences

The selectivity was investigated by gravimetric determination of 29.44 mg of Pd and spectrophotometric determination of 35.3 μg of Pd in the presence of a number of other ions; the results are summarized in Table 2. Strong oxidants such as chromium(VI) interfere seriously in the gravimetric method. In the spectrophotometric method the interference of Cu, Ni, Fe, Pt, Co, V, Zr, Sn, La and Hg can be eliminated by adding EDTA, and that of Au by adding potassium thiocyanate. The interference of Mo can be eliminated by adding sodium fluoride in at least 10:1 molar ratio to the molybdenum, but only if the molar ratio of Mo to Pd is less than 100.

Fe(II) is oxidized to Fe(III) by dissolving the sample in *aqua regia*, and evaporating almost to dryness.

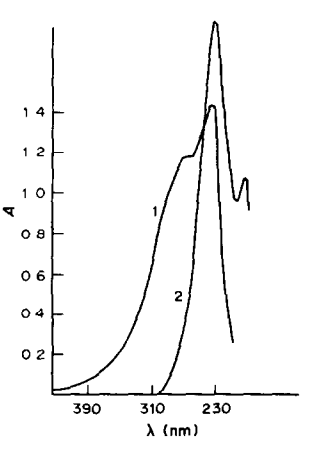

Fig. 5. Absorption spectra of PTT and its Pd complex in $CHCl_3$—butan-1-ol (5:1 %) mixture. $C_{DPTT} = 1.5 \times 10^{-4} M$; $C_{complex} = 6.2 \times 10^{-5} M$.

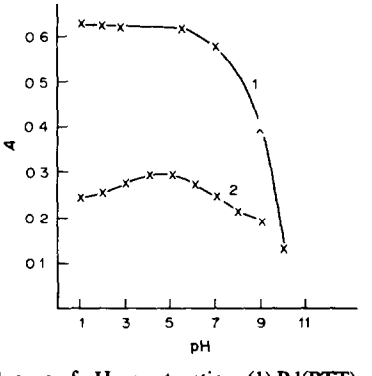

Fig. 6. Influence of pH on extraction. (1) $Pd(PTT)_2$ complex. $C_R = 1.25 \times 10^{-3} M$; $C_{Pd} = 2.0 \times 10^{-5} M$; $\lambda = 330$ nm. (2) PTT; $C_R = 1.25 \times 10^{-3} M$; $\lambda = 270$ nm.

Table 2. Effect of diverse ions in determination of 29.44 mg of Pd (gravimetric) and of 35.3 μg of Pd (spectrophotometric)

Ion added	Mole ratio, *ion/Pd*	Error, % Gravimetric	Error, % Spectrophotometric	Ion added	Mole ratio, *ion/Pd*	Error, % Gravimetric	Error, % Spectrophotometric
SO_3^{2-}	100		−29	Pt(IV)	1	−0.1	
I^-	100		−38		100		+14.3
Citrate	100	0.0	−14.5		100*		0.0
$C_2O_4^{2-}$	60	0.0		Fe(III)	100	−0.7	−43
	100		+12.7		100*		0.0
Tartrate	100		−18.2		1000*		+0.1
$S_2O_3^{2-}$	100		−52		5000*		+0.4
$S_2O_8^{2-}$	100		−4.0	Zn(II)	10	0.0	
SCN^-	100		0.0		100		−0.1
	10000		0.0	Au(III)	100		+61
PO_4^{3-}	100	−1.0	−1.6		100†		0.0
	1000		−5.6	Se(VI)	100		+0.07
IO_3^-	100		+67	As(V)	100		+0.2
EDTA	100		0.0	Te(VI)	100		−0.1
	10000		0.0	Ba(II)	100		0.0
CrO_4^{2-}	100		−53	Sr(II)	100		0.0
CN^-	100		−85	La(III)	100		−8.0
F^-	100		0.0		100*		+0.1
	1000		−4.6	Zr(IV)	1		+0.1
	10000		−23.0		100		−14.0
Al(III)	1	0.0			100*		0.0
	100		−0.1	Tl(I)	100		0.0
Cd(II)	1	0.0		Bi(III)	100		−0.1
	100		0.0	Sn(IV)	100		+4.7
Co(II)	1	+0.4			100*		+0.8
	100		+11.1	Pb(II)	100		0.0
	100*		0.0	NH_4^+	100		+0.07
Cr(III)	100		0.0	Mo(VI)	10	−6.0	
Ni(II)	100	0.0	+130		100		−9.7
	1000*		+0.4		100§		0.0
	10000*		+1.3	Hg(II)	1	−0.1	
Cu(II)	100	+1.0	+60		100		+4.7
	100*		0.0		100*		+0.4
	1000*		+0.1	Mn(II)	1	0.0	
	10000*		+1.3		100		−0.1
V(V)	1	−0.2		In(III)	100		+20.8
	100		−20.2		100*		+8.6
	100*		+0.8	Rh(III)	100		+8.1
W(VI)	100		−74		100*		+0.1
	100*		−53				

*EDTA added. †SCN^- added. §F^- added.

Table 3. Spectrophotometric determination of Pd in synthetic samples with PTT

Composition (%)	Pd found, %
Fe (24.93) + Co (24.93) + Cu (24.93) + Ni (24.93) + Pd (0.28)	0.27 g
Fe (16.64) + Co (16.64) + Ni (16.64) + Cu (16.64) + Mo (16.64) + V (16.64) + Pd (0.16)	0.16_1
Pt (16.64) + Rh (16.64) + Fe (16.64) + Co (16.64) + Ni (16.64) + Cu (16.64) + Pd (0.16)	0.16_0

Applications

Results for the determination of palladium in palladinized calcium carbonate and active carbon, and in synthetic mixtures are shown in Tables 3 and 4. The main advantages of PTT over DMG in the spectrophotometric method are the need for only one extraction, and the much higher sensitivity. In the gravimetric method PTT has the advantages of high solubility in water and a more favourable conversion factor.

Table 4. Determination of Pd with PTT and DMG in real samples

	Pd found, % Gravimetric PTT*	Gravimetric DMG†	Spectrophotometric PTT	Spectrophotometric DMG
Carbon/10% Pd			9.97	9.88
$CaCo_3$/5% Pd			4.99	5.01
Carbon/5% Pd	4.99	4.99		
$CaCO_3$/10% Pd	9.95	9.90		

*Mean of 5 determinations (s.d. 0.01).
†Mean of 3 determinations (s.d. 0.1).

REFERENCES

1. B. Egneus, *Talanta*, 1972, **19**, 1387.
2. L. Tschugaeff, *Z. Anorg. Allgem. Chem.*, 1905, **46**, 144.
3. J. L. Aznárez, J. R. Castillo and J. Cacho, *Rv. Acad. Ciencias Zaragoza*, 1976, **31**, 91.
4. D. Dyrssen, *Trans. Roy. Inst. Technol. Stockholm*, 1964, 220.
5. R. Blinc and D. Hadzi, *J. Chem. Soc.*, 1958, 4536.
6. D. W. Davis, *Talanta*, 1969, **16**, 1330.

Talanta, Vol. 32, No. 1, pp. 15–18, 1985
Printed in Great Britain.

0039-9140/85 $3.00 + 0.00

HOMOGENEOUS IMMUNOASSAY OF PHENOBARBITAL BY PHASE-RESOLVED FLUORESCENCE SPECTROSCOPY

FRANK V. BRIGHT and LINDA B. MCGOWN*
Department of Chemistry, Oklahoma State University, Stillwater, OK 74078, U.S.A.

(*Received* 11 *June* 1984. *Accepted* 27 *July* 1984)

Summary—A new technique for determination of phenobarbital by homogeneous fluoroimmunoassay is described. Simultaneous determination of free and antibody-bound fluorescein-labelled phenobarbital is accomplished by making phase-resolved fluorescence measurements, in which selectivity is provided by the difference between the fluorescence lifetimes of the two species, as well as by the difference in fluorescence intensities. The technique requires no specialized reagents other than those inherent in immunoassay (antibody, antigen and labelled antigen). Problems due to non-specific binding of labelled antigen to sample matrix components can be alleviated by addition of a relative excess of albumin.

Immunoassays are based on the competitive binding of an antibody (Ab) to its corresponding antigen (Ag) and to an appropriately labelled form of the antigen (Ag*):

$$Ag^* + Ag + Ab \rightleftharpoons Ag^*\text{–}Ab + Ag\text{–}Ab + Ag^* + Ag \quad (1)$$

The original immunoassays used radioactively-labelled antigens. However, in recent years, investigators have sought non-isotopic alternatives to radioimmunoassays (RIA). Fluoroimmunoassay (FIA), in which a fluorescent label is used in lieu of a radioisotope, has offered a promising alternative to RIA. In addition to providing good sensitivity and detection limits, FIA can be either heterogeneous (requiring separation of Ag* and Ag*–Ab) or homogeneous (no separation needed), whereas RIA is inherently heterogeneous.

The use of difference in fluorescence lifetimes for achieving selectivity in heterogeneous FIA, by means of single-photon counting time-resolved fluorescence has been described.[1] Homogeneous FIA based on fluorescence-lifetime selectivity has not, to our knowledge, been previously demonstrated. It has been shown that phase-resolved fluorescence spectroscopy (PRFS) can be used for simultaneous determination of a single species in two different biological microenvironments, on the basis of differences in fluorescence lifetime.[2] In the work described here, PRFS is similarly employed to determine free and antibody-bound labelled antigen simultaneously, thereby providing a homogeneous immunoassay. The phase-resolved fluoroimmunoassay (PRFIA) does not require any specialized reagents beyond those basic to immunoassay (Ab, Ag and Ag*).

Phenobarbital was chosen as a representative hapten analyte to demonstrate PRFIA. Clinical determinations of phenobarbital aid in drug-dosage monitoring and correct patient management as well as in diagnosis of drug abuse. Other homogeneous FIA techniques for phenobarbital have been described, which use fluorescence polarization[3] and a substrate-labelled enzymatic approach.[4]

*Author to whom correspondence should be directed.

THEORY

Phase-resolved fluorescence spectroscopy

The theory and instrumentation of PRFS have been described in detail elsewhere.[5–7] The technique is based on the phase-modulation method for the determination of fluorescence lifetimes, in which the sample is excited with sinusoidally modulated light having an angular modulation frequency $\omega = 2\pi f$, where f is the frequency of linear modulation. The time-dependent intensity of the excitation beam $E(t)$ is given by:

$$E(t) = E_0(1 + m_{ex}\sin\omega t) \quad (2)$$

where E_0 is the d.c. intensity contribution and m_{ex} is the degree of beam modulation (*i.e.* the ratio of a.c. amplitude to d.c. intensity). The resulting fluorescence emission, $F(t)$, of a single component with homogeneous exponential decay will be phase-shifted by an angle ϕ and appear as:

$$F(t) = F_0[1 + m_{ex}\cos\phi\,\sin(\omega t + \phi)] \quad (3)$$

where F_0 represents the d.c. component of the fluorescence intensity and $\cos\phi$ is the demodulation factor. For a solution containing two fluorophores, 1 and 2, a similar equation arises:

$$F(t) = F_{01}[1 + m_{ex}\cos\phi_1\sin(\omega t + \phi_1)] + F_{02}[1 + m_{ex}\cos\phi_2\sin(\omega t + \phi_2)] \quad (4)$$

In PRFS, the a.c. component of the fluorescence emission is observed with a phase-sensitive detector in which the fluorescence emission function, equation

(4), is multiplied by a constant function and then integrated. The resulting time-independent signal is proportional to the cosine of the difference between the phase-angles of the detector and the sample. The phase-sensitive fluorescence intensity at detector phase angle ϕ_D for a two-component system will be:

$$F(\phi_D) = F_{01} m_{ex} \cos\phi_1 \cos(\phi_D - \phi_1) + F_{02} m_{ex} \cos\phi_2 \cos(\phi_D - \phi_2) \quad (5)$$

Phase-resolved fluoroimmunoassay

PRFIA involves the use of phase-resolved measurements at a series of non-null ($\phi_D \neq \phi \pm 90°$) detector phase-angles, as has previously been described.[2,8,9] In this multiple phase-angle approach to FIA, a series of linear simultaneous equations is generated. The following equations are used for the determination of free and bound Ag* at n detector phase-angles:

$$\begin{aligned} I_{\phi 1}^{PRF} &= I_{\phi 1}^{F}(\text{free Ag*}) + I_{\phi 1}^{B}(\text{bound Ag*}) \\ &\cdot \\ &\cdot \\ &\cdot \\ I_{\phi n}^{PRF} &= I_{\phi n}^{F}(\text{free Ag*}) + I_{\phi n}^{B}(\text{bound Ag*}) \end{aligned} \quad (6)$$

where $I_{\phi i}^{PRF}$ is the phase-resolved fluorescence intensity (PRFI) of a solution, $I_{\phi i}^{F}$ is the PRFI of the solution containing only free Ag*, and $I_{\phi i}^{B}$ is the PRFI of the solution containing only bound Ag*, for the ith equation generated at $\phi_D = \phi_i$. This set of equations is valid only if the total cuvette concentration of Ag* (free + bound) is constant for all the solutions. The set can be represented in matrix form:

$$\begin{bmatrix} I_{\phi 1}^{F} & I_{\phi 1}^{B} \\ \cdot & \cdot \\ \cdot & \cdot \\ \cdot & \cdot \\ \cdot & \cdot \\ \cdot & \cdot \\ I_{\phi n}^{F} & I_{\phi n}^{B} \end{bmatrix} \begin{bmatrix} (\text{free Ag*}) \\ (\text{bound Ag*}) \end{bmatrix} = \begin{bmatrix} I_{\phi 1}^{PRF} \\ \cdot \\ \cdot \\ \cdot \\ \cdot \\ \cdot \\ I_{\phi n}^{PRF} \end{bmatrix} \quad (7)$$

If $n > 2$ the matrix is "solved" for the fractions of free and bound Ag* by using a Gauss–Newton iterative procedure which includes the constraint:

$$\%\text{free Ag*} + \%\text{bound Ag*} = 100\%\ \text{Ag*} \quad (8)$$

When $n = 1$, *e.g.*, for use of either a single ϕ_D or steady-state conditions, a square matrix is generated, where equation (8) provides the second equation. The matrix can be solved exactly by using Cramer's rule. The PRFIA calibration curve for phenobarbital is constructed by plotting the percentage of free Ag* *vs.* analyte concentration (Ag), followed by third-order polynomial fitting.

EXPERIMENTAL

Materials

Demineralized water was used for all preparations.

Me_2POPOP[1,4-bis(4-methyl-5-phenyloxazol-2-yl)benzene] (Aldrich) was used as a reference fluorophore for the fluorescence lifetime determinations.

Phosphate buffer (0.01M, pH 7.5) was prepared from NaH_2PO_4 and Na_2HPO_4 and contained 1% sodium chloride, and 0.1% sodium azide as a preservative.

The immunoassay reagents, including anti-phenobarbital antibody (Ab), fluorescein-labelled phenobarbital (Ag*), phenobarbital standard and test solutions (Ag), and IgG were purchased as a kit (American Diagnostics Inc., Newport Beach, CA) and used without further purification. Additional phenobarbital standard and test solutions were prepared by weighing the appropriate amount of phenobarbital (Sigma) and diluting with buffered human serum albumin ($10^{-4}M$). The kit standards and test solutions contained 0–80 μg of phenobarbital per ml. These solutions were subsequently diluted 1:101 with buffer before addition to the cuvette solutions.

Human serum albumin (HSA, 30 μM) was prepared by dissolving 201 mg of HSA (Sigma, fatty acid-free, prepared from fraction V, catalogue no. A-1887) in 100 ml of buffer.

Polyethylene disposable cuvettes (Precision Cells Inc.) were used for all fluorescence measurements.

All the cuvette solutions, including the blank, free Ag*, antibody-bound Ag*, standard Ag, and test Ag, are described in Table 1. Fluorescence intensities were all corrected to correspond to 3.000 ml total volume in the cuvette. The addition of a large concentration of HSA to all samples ensured that, if non-specific adsorption of "free" (non-Ab bound) Ag* were to occur, it would be uniform (*i.e.*, all free Ag* would be adsorbed) with all adsorption occurring at a primary site on the HSA. It is important that all non-Ab bound Ag* be in a single type of microenvironment to ensure a homogeneous fluorescence lifetime for the free Ag* component. For simplicity, and to be consistent with immu-

Table 1. Preparation of standard and test solutions

Solution	Buffered[d]	Immunoassay reagents HSA[e]	Ag*[e]	Ab[e]	Ag[c,e]	IgG[e]
Free Ag*	2.500	200	100	0	100	200
Bound Ag*	2.500	200	100	200	100	0
Std. (Ag)[a]	2.500	200	100	100	100	0
Test (Ag)[b]	2.500	200	100	100	100	0
Blank	2.500	200	0	200	100	0

[a]Standards corresponding to 0, 4.75, 9.37, 18.7, 37.4, and 74.8 μg/ml phenobarbital in the original, undiluted standards.

[b]Test solutions 1, 2, and 3 contained 7.03, 14.03, and 28.05 μg/ml phenobarbital, respectively, in original, undiluted solutions.

[c]Shows volume added of the 1:101 dilutions of the original standard or test solutions.

[d]ml added to cuvette.

[e]μl added to cuvette.

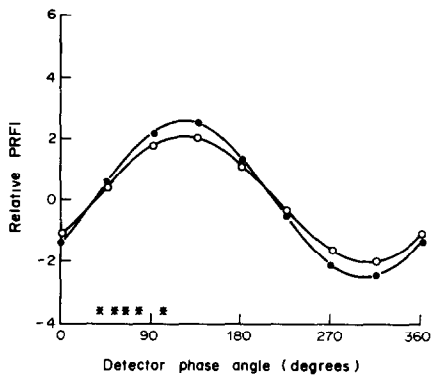

Fig. 1. Relative phase-resolved fluorescence intensity as a function of detector phase angle ϕ_D. Modulation frequency = 30 MHz. ○ Ab-bound Ag*; ● free Ag*. Phase angles used for multiple phase angle determinations are indicated by * (45.0, 58.5, 72.0, 85.5 and 117.0°).

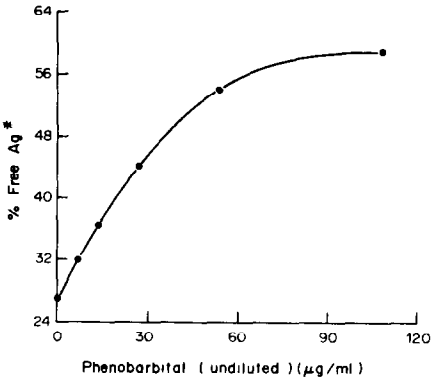

Fig. 2. Phenobarbital calibration curves obtained by using 5 detector phase angles (see Fig. 1).

noassay terminology, the non-Ab bound Ag* will be referred to as "free" Ag*, although it may actually be non-specifically adsorbed on albumin.

As seen in Table 1, the equivalent of ~1 μl of original, undiluted sample is used in 3.000 ml total cuvette volume. This 3000-fold dilution should minimize matrix interferences in the phenobarbital determinations.

Apparatus

All PRFS measurements were made with an SLM 4800S spectrofluorimeter (SLM Instruments, Inc.), with a 450-W xenon source, Hamamatsu R928 photomultiplier-tube detection, and a Glan-Thompson calcite prism polarizer (SLM) in the excitation beam, at 35° to the vertical.

Sample turret temperature was maintained at 20° for all measurements, by means of a Neslab constant-temperature bath (Neslab Instruments).

The excitation and emission monochromators were set at 490 and 520 nm, respectively (the maxima for fluorescein). The slits were set at 16, 0.5, 0.5, 8 and 8 nm resolution for the excitation monochromator entrance and exit, modulation tank exit, and emission monochromator entrance and exit, respectively.

PRFS measurements were all made at 30 MHz modulation frequency, in the delta-phase mode (a ratiometric mode) to minimize the effects of source-output fluctuations and excitation modulation drift. All solutions were measured first at one detector phase-angle (ϕ_D), and then the next, and so on, to eliminate irreproducibility due to resetting the detector phase-angle.

All measurements were made in triplicate, each measurement being the electronic average obtained by integration of 100 samplings during about 30 sec, performed internally by the SLM instrument.

An Apple IIe was used for computation, with programs written in BASIC.

RESULTS AND DISCUSSION

The plots of relative PRFI *vs.* ϕ_D for free and bound Ag* are shown in Fig. 1. The phase-angle difference between the two species corresponds to a fluorescence-lifetime difference of 100 psec. Fluorescence-lifetime (τ_f) determinations were made with Me_2POPOP as the reference fluorophore ($\tau_f = 1.45$ nsec),[10] and yielded 4.04 and 3.94 nsec for the lifetimes of free and bound Ag* respectively.

A typical PRFIA calibration curve generated by using 5 detector phase-angles is shown in Fig. 2.

The effect of the number of detector phase-angles on the accuracy of determinations of phenobarbital in the test solutions was studied. Calibration curves were generated and test solutions analysed for every possible combination of the *n* detector phase-angles, where *n* was varied from 1 to 5. Results for the best combination for each number of detector phase-angles are shown in Table 2. The results indicate that the accuracy is best when 3 detector phase-angles are used, but the magnitude of the errors is relatively large. The combination of 5 detector phase-angles provided good accuracy and the smallest average

Table 2. Error of determination[a]

Test solution	Number of detector phase angles[b] 5	4[c]	3[d]	2[e]	1[f]
1	1.0	5.4	−12.5	−16.9	−5.9
2	−0.4	1.8	2.3	9.6	−11.7
3	8.1	9.5	11.2	21.2	3.1
Ave. error	2.9	5.6	0.3	4.6	−4.8
Ave. |error|	3.2	5.6	8.7	15.9	6.9

[a]Relative error, %.
[b]Results for best case of all possible combinations.
[c]$\phi_D = 58.5°$, 72.0°, 85.5° and 117.0°.
[d]$\phi_D = 45.0°$, 58.5°, and 117.0°.
[e]$\phi_D = 45.0°$ and 58.5°.
[f]$\phi_D = 117.0°$.

error. These 5 detector phase-angles were therefore used for all subsequent studies. The lower accuracy obtained by using 5 angles instead of 3 was probably due to the relative redundancy of the data from the three fairly closely spaced angles 58.5, 72.0 and 85.5° (see Fig. 1), in which case any errors present in the data obtained at these angles outweigh the discriminatory advantage accruing from their use.

A relative standard deviation of 6.7% was found for a set of four calibration curves, normalized as described below, and obtained on a weekly basis (one per week). Each curve was normalized to the percentage of free Ag* found for the highest concentration standard (74.8 μg/ml). Normalization was used to minimize variations due to reagent degradation, which was found to cause a uniform decrease in the apparent values of percentage of free Ag*. Curves were compared by taking values at the 5 standard concentrations from each fitted curve and comparing these values with a "mean" calibration curve obtained by fitting all four sets of data simultaneously. The limit of detection for phenobarbital (defined as 3 times the standard deviation of the blank) was estimated to be 3 μg/ml in the original undiluted sample, corresponding to 1 ng/ml in the cuvette.

Calibration curves (normalized as described above) obtained by using heterogeneous FIA (by the procedure described in the Amerifluor kit) and PRFIA were compared. A correlation coefficient of 0.97 was obtained for the linear ($y = 1.18x - 0.11$) correlation plot.

A homogeneous steady-state quenching approach was also used, based on the difference between the steady-state fluorescence intensities for free and bound Ag*. The steady-state FIA method generated a square 2 × 2 matrix (see section on PRFIA theory, above). The values obtained for free Ag* were poorly correlated ($r = 0.6$) with the standard concentrations. The superior performance of the phase-resolved fluorescence intensity approach indicates the advantage of using fluorescence-lifetime selectivity in addition to selectivity based on fluorescence quenching.

CONCLUSIONS

This phase-resolved approach to homogeneous FIA, as demonstrated by the PRFIA for phenobarbital, offers several advantages. Greater discrimination between free and bound Ag* is achieved than that attainable in a determination based solely on steady-state intensity differences. Homogeneous immunoassay is accomplished without requiring additional specialized reagents (*e.g.*, enzymes, second labels, *etc.*). PRFIA is applicable to determination of antigen species regardless of their molecular weight (provided there is a sufficiently large change in fluorescence lifetime on antibody-binding of the labelled antigen), whereas polarization FIA depends on a large enough change in molecular volume on binding, and is generally best suited to the determination of smaller antigens (molecular weight $< 4 \times 10^4$).[11] In addition, problems due to nonspecific adsorption or binding to sample matrix components such as albumin can be minimized by the addition of an excess of binding reagent (*e.g.*, albumin), provided that there is a sufficient fluorescence-lifetime difference between the reagent-adsorbed and Ab-bound Ag*.

Acknowledgements—The authors wish to acknowledge support for this research from the Department of Health and Human Services, through a grant from the National Institute on Drug Abuse, No. R03 DA 03479. F. V. Bright also expresses gratitude for a Grant-in-Aid of Scientific Research from Sigma Xi, the Scientific Research Society (1983–84).

REFERENCES

1. K. Petterson, H. Siitari, I. Hemmila, E. Soini, T. Lovgren, V. Hanninen, P. Tanner and U. Stenman, *Clin. Chem.*, 1983, **29,** 60.
2. L. B. McGown, *Anal. Chim. Acta*, 1984, **157,** 327.
3. A. M. Sidki, M. Pourfarzaneh, F. J. Rowell and D. S. Smith, *Ther. Drug Monit.*, 1982, **4,** 397.
4. B. Fingerhut, R. Costano, Z. Chaudri and S. Rizvi, *ibid.*, 1982, **4,** 419.
5. T. V. Veselova, A. S. Cherkasov and V. I. Shirokov, *Opt. Spectrosc.*, 1970, **29,** 617.
6. J. R. Lakowicz, *Principles of Fluorescence Spectroscopy*, Chapter 4. Plenum Press, New York, 1983.
7. D. M. Jameson, E. Gratton and R. D. Hall, *App. Spectrosc. Rev.* 1984, **20,** 55.
8. F. V. Bright and L. B. McGown, *Anal. Chim. Acta*, 1984, **162,** 275.
9. L. B. McGown and F. V. Bright, *Anal. Chem.*, 1984, **56,** 2195.
10. J. R. Lakowicz, H. Cherek and A. Balter, *J. Biochem. Biophys. Meth.*, 1981, **5,** 131.
11. D. S. Smith, M. Hassan and R. D. Nargessi, in *Modern Fluorescence Spectroscopy*, Vol. 3, E. L. Wehry (ed.), p. 162. Plenum Press, New York, 1981.

Talanta, Vol. 32, No. 1, pp. 19—22, 1985
Printed in Great Britain.

0039-9140/85 $3.00 + 0.00

CHARACTERIZATION AND ELIMINATION OF THE INTERFERING EFFECTS OF FOREIGN SPECIES IN THE ATOMIC-ABSORPTION DETERMINATION OF IRON

A. M. ABDALLAH, M. M. EL-DEFRAWY and M. A. MOSTAFA
Department of Chemistry, Faculty of Science, Mansoura University, Mansoura, Egypt

A. B. SAKLA
Microanalytical Center, Faculty of Science, Cairo University, Dokki, Cairo, Egypt

(*Received* 28 *September* 1983. *Revised* 26 *June* 1984. *Accepted* 17 *July* 1984)

Summary—The inhibition-release titration method has been used to study interference effects in flame atomic-absorption determination of iron. Interferences from anions, cations and complexing agents with the atomic-absorption of iron when a stoichiometric air-acetylene flame is used, can be obviated by a preliminary treatment of the sample solution with sulphosalicylic acid to convert the iron into the same complex before aspiration, thus giving a constant environment for the iron in the flame processes.

Determinations of iron in a wide variety of materials by atomic-absorption spectrophotometry have been collated in the analytical literature.[1-3] Slavin[2] reported that the determination is almost free from interference when a stoichiometric air–acetylene flame is used. Another study by Thompson *et al.*[4] showed that in fuel-rich flames both Fe(II) and Fe(III) give non-linear calibration curves and that a fuel-lean flame is best with respect to linearity, but at sacrifice of sensitivity. However, different cations and anions are reported to affect the iron signal.[5] With measurement in the upper parts of the flame, 8-hydroxyquinoline has been used as a releasing agent to eliminate interference from Co, Ni and Cu in the atomic-absorption determination of iron[6] but is only applicable over a narrow range of interferent concentrations because of precipitation. In addition, the observation height* is a critical parameter. Black *et al.*[7] studied the use of volatile metal-chelate systems for the introduction of iron and other metals into an inductively coupled plasma, and this approach can be used in flame-based systems. Extraction procedures have been used to avoid interferences from a variety of matrices in determination of iron by AAS.[8-10]

EXPERIMENTAL

Reagents

Stock solutions of 3.6 m*M* Fe(III) (chloride), and Na, K, Ca, Ba, Cd, Zn, Co, Ni, Cu and Mn (chloride, nitrate and sulphate) were prepared from reagent-grade chemicals. Pt and Pd solutions were prepared from H_2PtCl_6 and K_2PdCl_4.

Apparatus

The atomic-absorption analysis was done with a Unicam SP 90A Series 2 atomic-absorption spectrophotometer, which incorporated a new HTA photo-tube. Air was supplied from a compressor, and acetylene was obtained from cylinders and passed through concentrated sulphuric acid and glass wool for purification. A continuous titration device[11] was attached to the instrument. Absorbance values were recorded with a single-pen recorder.

The instrumental parameters were: lamp current, 12 mA; wavelength, 248.3 nm; slit-width, 0.1 mm; observation height, 0.8 cm; air flow-rate, 5.0 l./min; fuel flow-rate, 1.4 l./min.

*The distance from the top of the burner to "grazing incidence position".

RESULTS AND DISCUSSION

Effect of anions

A series of almost neutral solutions was prepared, containing iron in 0.36 m*M* concentration and one of the anions in increasing amounts. The anions used were I^-, Br^-, NO_2^-, NO_3^-, Cl^-, ClO_4^-, SO_4^{2-} and PO_4^{3-}, added as the sodium or potassium salt. No interference from these foreign anions was found for up to 7.9, 12.5, 21.7, 16.1, 28.2, 10.1, 10.4 and 10.5 m*M* concentrations respectively.

Interfering effects of cations

The effect of various cations on the atomic-absorption of iron in presence of mineral acids was examined. Figure 1 shows that Na, K, Ca, Ba, Cd, Zn, Co, Ni, Cu and Mn chlorides in hydrochloric acid medium have insignificant effect on the absorption signal of iron up to 43.5, 25.6, 25, 7.3, 8.9, 15.3, 17, 17.5 and 18.2 m*M* for each cation respectively. A relative decrease of 20% in the iron signal was caused by the presence of 0.75m*M* Pt or Pd. A presumable cause for this depressive effect is that the ferric ions are stacked in the crystal lattices of H_2PtCl_6 and K_2PdCl_4 when the solvent has been evaporated in the flame, and are not completely released and atomized

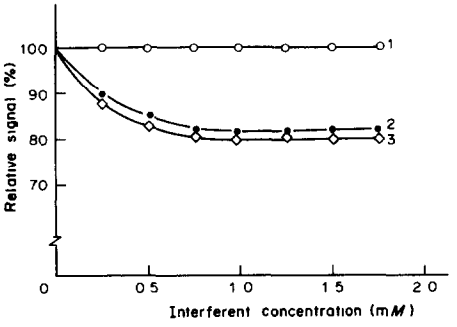

Fig. 1. Interference of some cations as chlorides on the signal from 0.36m*M* iron(III) chloride; (1) Na, K, Ca, Ba, Cd, Zn, Co, Ni, Cu and Mn; (2) Pt as H_2PtCl_6; (3) Pd as K_2PdCl_4.

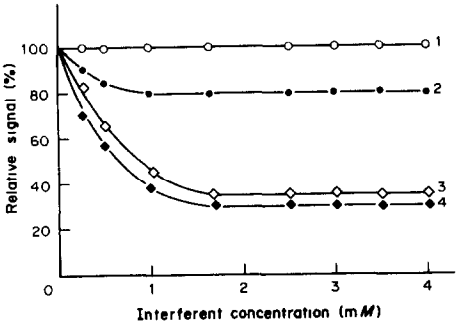

Fig. 2. Influence of some nitrates on the signal from 0.36m*M* iron(III) nitrate; (1) Na, K, Ca, Ba, Cd, Zn, Mn, Pt and Pd; (2) Cu; (3) Co; (4) Ni.

by the time measurement is made. However, the depressive effect totally disappears if the measurement is done in higher parts of the flame, where release and atomization have become complete.

The effect of the same cations was investigated in solutions containing nitric or sulphuric acid. Figures 2 and 3 show that under these conditions, Ni, Co and Cu are the only cations which cause significant depressive effect on the absorption of iron. This effect also disappears when the measurements are performed in the upper parts of the flame (1.5–2.0 cm burner height). Again, the effect can be attributed to retention of the iron by the matrix as a result of incomplete volatilization.

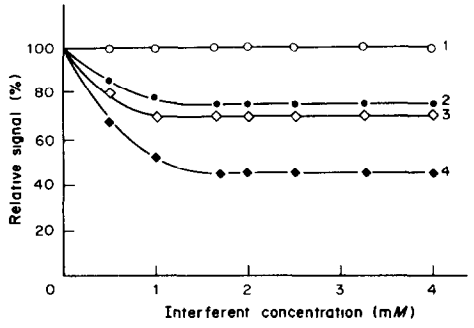

Fig. 3. Influence of some sulphates on the signal from 0.36m*M* iron(III) sulphate: (1) Na, K, Ca, Ba, Cd, Zn, Mn, Pt and Pd; (2) Co; (3) Cu; (4) Ni.

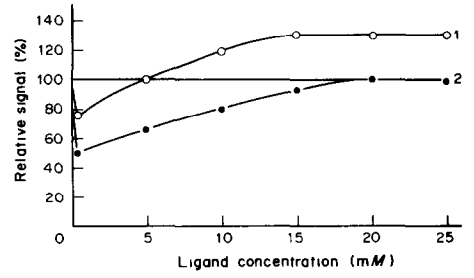

Fig. 4. Changes in the absorption signal from 0.36m*M* iron(III) chloride with increasing ligand concentration; (1) 4-aminosalicylic acid and (2) sulphosalicylic acid.

Effect of complexing agents

Figures 4 and 5 show the effect of some ligands that form iron complexes. The general trend shown by the graphs is to form stable 1:1 complexes with iron (as indicated by the position of the minimum in the iron signal). The stability of the Fe–N, Fe–O or Fe–S bonds left after combustion of the ligands determines the rate of release of iron atoms in the flame. As recently proposed,[12] the effect of ligands on the absorption of metals is principally dependent on the relative stability of the M–N, M–O or M–S bonds in the flame. When these bonds are strong enough, they produce molecular species as the dominant products in the flame and hence there is a depressive effect on the analyte signal. On the other hand, weak bonding

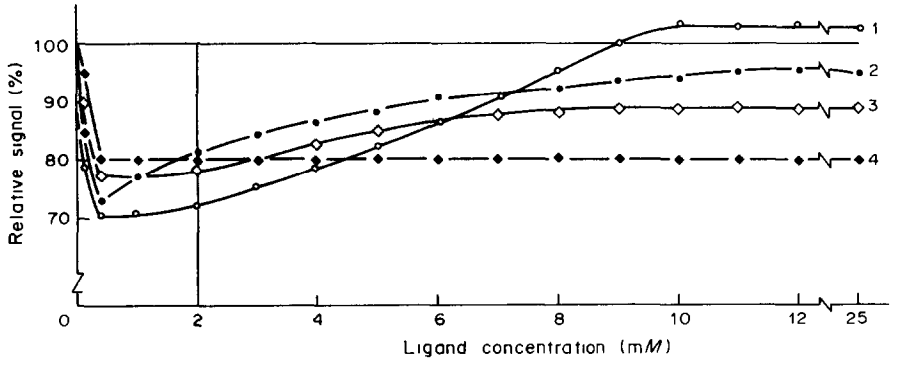

Fig. 5. Titration of 0.36m*M* iron(III) chloride with (1) EDTA, (2) DCTA, (3) NTA, (4) glycine.

Table 1. Interference (and its elimination) of a variety of organic compounds and inorganic salts, in the determination of 0.36m*M* iron

Substance added	Concentration, m*M*	Iron recovery, % Without treatment	With 30m*M* 4-aminosalicylic acid	With 20m*M* sulphosalicylic acid
EDTA	0.40	70	100	99
DCTA	0.40	73	100	100
NTA	0.40	77	98	99
glycine	0.40	80	100	99
n-butylamine	0.40	84	100	100
Cu (sulphate)	1.57	70	100	100
Ni (sulphate)	1.70	45	100	100
Co (sulphate)	1.70	75	100	100
Cu (nitrate)	1.75	80	98	100
Ni (nitrate)	1.70	30	96	100
Co (nitrate)	1.70	35	99	100
Pt (H_2PtCl_6)	0.51	85	100	100
Pd (K_2PdCl_4)	0.94	80	100	100

militates against formation of the molecular compounds and enhances the release of the analyte atoms. Naturally, there should be a sufficient concentration of the ligand to give the desired effect. This is clearly shown by Figs. 4 and 5, which indicate a levelling trend with increase in ligand concentration.

Elimination of interferences

Further investigation revealed that if a large enough excess of 4-aminosalicylic acid or sulphosalicylic acid (60–100 fold relative to iron) is present the absorption signal for iron becomes constant irrespective of the ligand concentration, and also the depressive effect of various complexing agents and metal salts is eliminated (Table 1). The large excess of added ligand presumably leads to essentially complete preferential formation of its iron complex, thus giving a fixed environment for the iron in the flame atomization process.

Since AAS determination of iron in some of its complexes, particularly those containing phenanthroline, bipyridyl and/or amino groups, gives incorrect and variable results,[13,14] an investigation was made of the distribution of iron atoms as a function of the observation height in the flame for different iron complexes. Figure 6 shows that there is a marked difference in the rates of production of free iron atoms in the lower parts of the flame, but the system rapidly reaches the same equilibrium with the flame species (at 2 cm above the burner top). Thus correct results should be obtainable whatever the iron species present in the solution, provided the measurement is made at a high enough position in the flame, but only at the expense of the sensitivity. The treatment of the iron complexes with sulphosalicylic

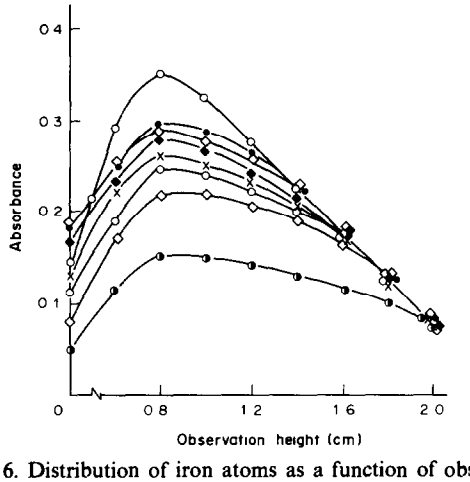

Fig. 6. Distribution of iron atoms as a function of observation height for different iron complexes (each solution 0.36m*M* iron); (○) $FeCl_3$, (●) $Fe(phen)_3.Hg(CN)_4$, (◇) $Fe(phen)_3.Hg(SCN)_4$, (◆) $Fe(bipy)_2.(CN)_2.Hg(CN)_2$, (×) $Fe(phen)_2.(CN)_2.NO_3.4H_2O$, (⊙) $Na_3Fe(CN)_5NH_3$, (◈) $Fe(C_5H_7O_2)_3$ and (◑) $Fe(bipy)_2.(CN)_2.NO_3$.

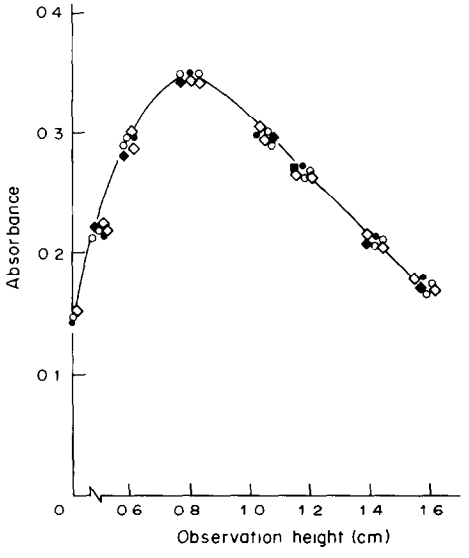

Fig. 7. Distribution of iron atoms as a function of the observation height for different iron complexes (each solution 0.36m*M* iron) in presence of 20m*M* sulphosalicylic acid: symbols as for Fig. 6.

Table 2. Determination of 0.36 m*M* iron in various complexes, in presence of 20 m*M* sulphosalicylic acid

	Iron recovery			
	Without sulphosalicylic acid,		With sulphosalicylic acid,	
	*m*M	%	*m*M	%
$Fe(C_5H_7O_2)_3$	0.23	65	0.35	98
$Fe(bipy)_2.(CN)_2.NO_3$	0.15	42	0.35	98
$Fe(phen)_2.(CN)_2.NO_3.4H_2O$	0.27	75	0.36	100
$Na_3Fe(CN)_5NH_3$	0.25	69	0.35	98
$Fe(phen)_3.Hg(CN)_4$	0.30	83	0.35	98
$Fe(phen)_3.Hg(SCN)_4$	0.30	83	0.36	100
$Fe(bipy)_2(CN)_2.Hg(CN)_2$	0.29	80	0.36	100

bipy = bipyridyl; phen = phenanthroline.

acid overcomes the depressive effect in the lower part of the flame, resulting in the iron signal being independent of the nature of the original complex present, though it still varies with the position in the flame (Fig. 7). This indicates that conversion into the iron sulphosalicylate complex takes place in solution, before the aspiration. Table 2 shows the effect of sulphosalicylic acid on the various interferences.

REFERENCES

1. W. T. Elwell and J. A. F. Gidley, *Atomic Absorption Spectrophotometry*, 2nd Ed., Pergamon Press, Oxford, 1966.
2. W. Slavin, *Atomic Absorption Spectroscopy*, Interscience, New York, 1969.
3. D. J. Halls and A. Townshend, *Anal. Chim. Acta*, 1966, **36**, 278.
4. K. C. Thomson and K. Wagstaff, *Analyst*, 1980, **105**, 641.
5. M. M. M. El-Defrawy, *Ph.D. Thesis*, Hungary, 1980.
6. J. M. Ottaway, D. T. Coker, W. B. Rowston and D. R. Bhattaral, *Analyst*, 1970, **95**, 567.
7. M. S. Black and R. F. Browner, *Anal. Chem.*, 1981, **53**, 249.
8. V. A. Orlova, T. M. Malyutina and T. I. Kirillova, *Ref. Zh. Metall.*, 1980, Abstr. No. 22G109 or 11K24 (same paper!)
9. B. Magnusson and S. Westerlund, *Anal. Chim. Acta*, 1981, **131**, 63.
10. O. Ichijo, *Bunseki Kagaku*, 1981, **30**, 477.
11. D. Stoijanovic, J. Bradshaw and J. D. Winefordner, *Anal. Chim. Acta*, 1978, **96**, 45.
12. M. A. Mostafa, *Ph.D. Thesis*, University of Mansoura, Egypt, 1983.
13. Analytical Laboratories of Talkha Fertilizers and Chemicals Plant, personal communication.
14. F. R. Hartlage, *Anal. Chim. Acta*, 1967, **39**, 273.

Talanta, Vol. 32, No. 1, pp. 23–26, 1985
Printed in Great Britain.

0039-9140/85 $3.00 + 0.00

MATRIX MODIFICATION FOR DETERMINATION OF SELENIUM IN GEOLOGICAL SAMPLES BY GRAPHITE-FURNACE ATOMIC-ABSORPTION SPECTROMETRY AFTER PRESEPARATION WITH THIOL COTTON FIBRE

SHAN XIAO-QUAN*
Institute of Environmental Chemistry, Academia Sinica, P.O. Box 934, Beijing, People's Republic of China

HU KAI-JING
Laboratory of Geological Bureau of Hunan Province, People's Republic of China

(*Received* 8 *September* 1983. *Accepted* 16 *July* 1984)

Summary—A graphite-furnace atomic-absorption method has been developed for the determination of selenium in geological samples at or below the μg/g level after decomposition of the sample with a mixture of perchloric, hydrofluoric and nitric acids and separation of selenium from the sample matrix with thiol cotton fibre. A few micrograms of palladium are added as a matrix modifier for the atomic-absorption determination. In the presence of palladium the charring temperature for selenium can be raised to 1100°, and the signal enhancement is greater than with other matrix modifiers reported in the literature.

The determination of selenium in geological materials at or below the μg/g level is important, as selenium is a geochemically interesting indicator for several types of mineral deposit,[1] and also presents a potential public health problem. The methods available for determining selenium in rocks and soils include solution spectrophotometry, flame atomic-absorption spectrometry (AAS) and d.c. arc emission spectrometry. However, these methods are interference-prone, have poor sensitivity and require a multistage process to complete the analysis. Although graphite-furnace atomic-absorption spectrometry offers sufficient sensitivity for the determination of selenium in geological materials at the μg/g level, serious interference problems are encountered, arising from the diverse and complicated nature of the matrices. It seems that preseparation is required. Sanzolone and Chao[2] have developed a method for the determination of selenium in the range 0.05–1000 μg/g. The sample was decomposed with a mixture of nitric, perchloric and hydrofluoric acids and heated with hydrochloric acid to reduce selenium(VI) to selenium(IV), which was then extracted into toluene from hydrochloric acid–hydrobromic acid medium containing iron. The toluene extract was injected into a carbon-rod atomizer, with nickel added as matrix modifier. In a previous paper[3] we reported a method for the determination of selenium in soil, based on digestion of the sample with a mixture of sulphuric and perchloric acids in the presence of ascorbic acid, followed by extraction of the resultant selenium(IV) with 1,2-diamino-4-nitrobenzene, and AAS determination in a zirconium-coated graphite tube. Recently, Kujirai *et al.*[4] have described a method for determining trace selenium in heat-resisting alloys by co-precipitation with arsenic, followed by graphite-furnace AAS with zinc as a matrix modifier to stabilize selenium during the charring step and thus enhance the sensitivity in the atomization step.

The present study describes a method for the determination of selenium in geological samples at or below the μg/g level by graphite-furnace AAS after separation with thiol cotton fibre (TCF). The samples are decomposed with a mixture of nitric, perchloric and hydrofluoric acids. Selenium(VI) in the sample solution is reduced to selenium(IV) by heating on a water-bath with 5*M* hydrochloric acid, and the selenium(IV) quantitatively absorbed on a column packed with TCF, and then desorbed by destruction of the thiol with a mixture of hydrochloric acid and nitric acid. Finally, the selenium(IV) is introduced into a heated graphite-atomizer along with palladium as a matrix modifier which allows the charring temperature for selenium to be raised to 1100° and gives greater enhancement than other matrix modifiers reported in the literature.

EXPERIMENTAL

Apparatus

A Perkin-Elmer model 380 atomic-absorption spectrometer equipped with a model HGA-400 graphite furnace and a Hitachi model 056 chart-recorder was used for the

*To whom correspondence should be addressed.

measurement of the selenium absorbance at 196.0 nm, under "argon stop" conditions. The band-width was set at 0.7 nm. The Perkin-Elmer electrodeless selenium discharge lamp was operated at 6 W. A 20-μl Eppendorf pipette with disposable polypropylene tips was used to introduce sample solutions into the graphite-tube atomizer. A deuterium background-corrector was used throughout.

Reagents

Selenium(IV) stock solution, 1000 μg/ml, was prepared by dissolving 0.1000 g of black elemental selenium in 2 ml of concentrated hydrochloric acid and 1 ml of concentrated nitric acid with gentle heating, and diluting to 100 ml with demineralized water. Other working selenium standard solutions were prepared by serial dilution from this stock solution with 0.1*M* hydrochloric acid.

Palladium and platinum solutions, 1000 μg/ml, were made by dissolving 0.100 g of palladium or platinum metal in a small volume of *aqua regia*, evaporating the solution on a water-bath nearly to dryness, taking up the residue with 10 ml of 0.1*M* hydrochloric acid and diluting to 100 ml with demineralized water.

Procedures

Preparation of thiol cotton fibre (TCF) and package of absorption column. Cotton cellulose (4 g) was soaked in a mixture of 28 g of thioglycollic acid, 15 g of acetic anhydride, 7 g of acetic acid and 0.1 g of sulphuric acid, and left standing for 4 days at 40°. It was then washed with demineralized water and dried under reduced pressure. The fibrous product contained 3–4% of thiol group. A 0.15-g amount of TCF was packed in the neck of a separatory funnel, the inner diameter and length of the neck being 6 mm and 8 cm, respectively. The absorption column was packed in this way to combine filtration of the sample solution with absorption of selenium(IV).

Sample decomposition. A 0.200-g sample was weighed into a 50-ml Teflon crucible, and 0.5 ml of demineralized water was added to moisten the sample thoroughly, followed by 1 ml of concentrated perchloric acid, 15 ml of hydrofluoric acid and 10 ml of nitric acid, in succession. The crucible was placed on a hot-plate, the surface temperature of which was raised from about 160° to 240° in 60 min and kept at the latter temperature until fumes of perchloric acid appeared. The crucible was then removed and cooled to room temperature. Then 30 ml of 5*M* hydrochloric acid were added and the crucible was covered with a watch-glass and heated on a boiling water-bath for 3 min, then cooled to room temperature.

Absorption and desorption of selenium(IV) and determination by graphite-furnace AAS. There was sometimes a precipitate left after the sample decomposition, and this was filtered off on a Millipore filter paper, the filtrate being passed into a TCF column prewashed twice with 5*M* hydrochloric acid; the crucible was rinsed with several 2–3 ml portions of 5*M* hydrochloric acid, the rinsings being passed through the filter paper and TCF column. The paper was washed several times with 5*M* hydrochloric acid and removed, then the TCF was carefully taken out of the column, squeezed dry and transfered to a graduated test-tube containing 1 ml of concentrated hydrochloric acid and *ca.* 0.05 ml of concentrated nitric acid. The tube was loosely stoppered with a glass stopper,[2] heated on a water-bath until the TCF was destroyed, then cooled to room temperature. The solution was diluted to 10 ml with demineralized water and shaken thoroughly, then let stand for a few minutes to allow the cotton fibre to settle out. Finally a 20-μl portion of supernatant solution was introduced into a graphite-tube atomizer, dried at 110° for 30 sec, charred at 1000° for 30 sec and atomized at 2100° for 5 sec at maximum power, and selenium absorbance measured under "argon stop" conditions. The graphite tube was then cleaned by firing at 2600° for 4 sec.

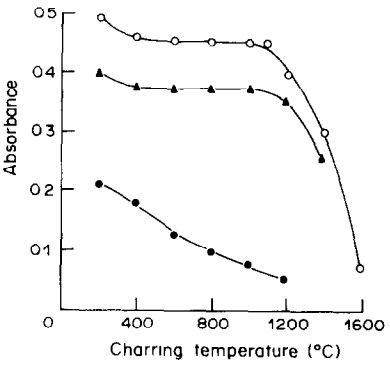

Fig. 1. Effect of charring temperature on the absorbance of selenium in the presence or absence of matrix modifiers: (●) 4 ng of Se in 1*M* HCl; (○) 4 ng of Se + 2 μg of Pd in 0.01*M* HCl; (▲) 4 ng of Se + 20 μg of Zn in 2.5*M* HNO_3.

RESULTS AND DISCUSSION

Stabilizing effect of palladium

It is well known that selenium is relatively volatile, so a certain loss may occur during the pre-atomization stages. To prevent such loss addition of various metal ions, such as nickel,[5] cobalt,[6] molybdenum,[7] lanthanum,[8] copper,[9] chromium[10] and zinc[4] has been recommended, as so-called matrix modifiers. We have found that palladium is the most effective matrix modifier for selenium. When palladium is present the charring temperature for selenium can be raised to 1100°, and the sensitivity is greater by a factor of 1.2 than that obtained by using zinc as matrix modifier (Fig. 1).

The stabilizing effect of palladium depends on the amount present. The absorbance for selenium increases over the range 0–1 μg of palladium and is constant for 1–3 μg (Fig. 2), so addition of 2 μg of palladium was selected as optimal.

Relationship between solution acidity and selenium absorbance

Since a mixture of concentrated hydrochloric and nitric acids is used for desorbing selenium(IV) from

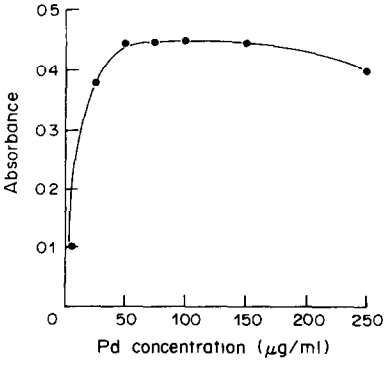

Fig. 2. Dependence of selenium absorbance on amount of palladium: 4 ng of Se + 20 μl of palladium solution of concentration shown (charring temperature 600°).

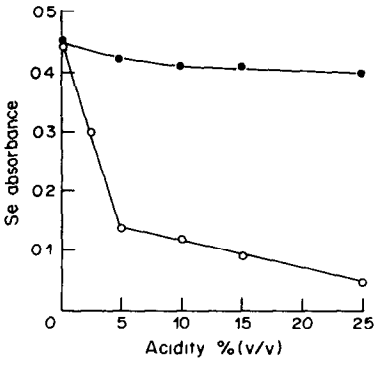

Fig. 3. Effect of acidity (volume percentage of concentrated acid in test solution) of selenium solution on absorbance in the presence of palladium: 4 ng of Se in HCl (●) or HNO_3 (○).

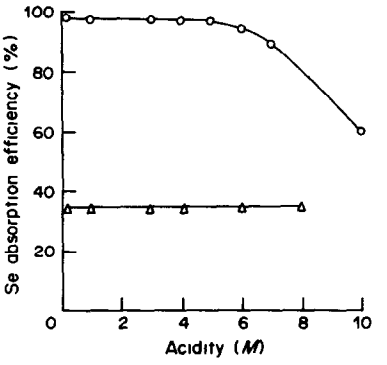

Fig. 4. Relationship between the absorption efficiency of selenium(IV) and selenium(VI) by TCF and the acidity of the sample solution: (○) 1 μg of Se(IV) in 30 ml of HCl; (△) 1 μg of Se(VI) in 30 ml of HCl.

the TCF, as described later, the sample solution which is introduced into the atomizer is highly acidic, so the relationship between solution acidity and selenium absorbance was examined. The results are shown in Fig. 3. The selenium absorbance is fairly constant with 10–25% v/v hydrochloric acid but strongly suppressed by nitric acid. A mixture of 10% v/v hydrochloric acid and 0.5% v/v nitric acid was therefore chosen as optimal for the measurement.

Sorption of selenium on thiol cotton fibre and desorption

Selenium is widely distributed in small amounts in geological materials, with an estimated crustal abundance of 0.05–0.075 μg/g.[11] Besides this problem of low concentration, there is that of the severe interferences encountered in the determination of selenium by graphite-furnace atomic-absorption spectrometry. Hence preseparation and/or concentration of selenium is a prerequisite for its accurate determination in ores and minerals. In the present study a TCF column was used for this purpose. The most important parameters affecting the sorption of selenium are its oxidation state, the acidity of the sample solution, and the amount of TCF used. To find the optimum conditions, an absorption column was packed as described in the procedure and used at a flow-rate of 0.05 ml/sec. Selenium(IV) solutions (30 ml) of various acidities were passed through the column and the selenium concentrations in the filtrate determined, and hence the absorption efficiency. The results are shown in Figs. 4 and 5. The absorption efficiency was found to be >95% over the range 0.5–6*M* hydrochloric acid. Selenium(VI) is not sorbed, but some of it can be reduced to selenium(IV) by the thiol group and sorbed when a selenium(VI) solution is passed through a TCF column, giving an apparent absorption efficiency of 35% for selenium(VI). Hence reduction of selenium(VI) to selenium(IV) is required, and can be obtained by boiling the sample solution with 5*M* hydrochloric acid for 3–5 min. The optimum amount of TCF is 0.15–0.20 g for sorption of 1 μg of selenium(IV) in 30 ml of aqueous solution. Less than 0.15 g is not sufficient, but if more than 0.20 g is used it is difficult to desorb all the selenium(IV). The absorption efficiency increases with volume of aqueous sample solution up to 20 ml and then levels off. The optimum conditions are therefore considered to be the use of 30 ml of 5*M* hydrochloric acid sample solution, and 0.15 g of TCF.

Various acid mixtures were tried for the desorption and a mixture of 1 ml of concentrated hydrochloric acid and 0.05 ml of nitric acid was found the most effective. The eluate was diluted to 10 ml to give the optimum acidity for measurement.

Permissible amounts of diverse ions

Because of the severe interferences encountered in the determination of selenium by graphite-furnace atomic-absorption spectrometry, a very selective extraction procedure was employed in our earlier method.[3] From the general composition of ore and mineral materials and the sample weights taken for analysis in this work, a realistic set of matrix com-

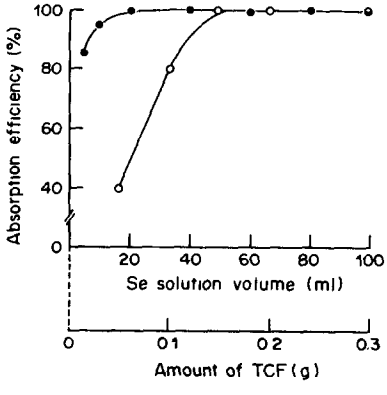

Fig. 5. Dependence of absorption efficiency of selenium(IV) on amount of TCF and volume of sample solution: (●) 0.15 g of TCF used for sorbing 1 μg of Se in various volumes of sample solution; (○) various amounts of TCF used for sorbing 1 μg of Se in 30 ml of sample solution.

Table 1. Recovery of selenium

Sample	Sample weight, *g*	Se in sample, *ng*	Se added, *ng*	Total Se found, *ng*	Recovery, %
Lead-zinc ore	0.100	22.5	62.5	85.7	101
Copper ore	0.100	24.9	62.5	87.4	100
Pyrite	0.050	213	250	453	96
Siderite	0.200	102	125	226	99
Stibnite	0.050	236	250	471	94

Table 2. Determination of selenium in geological samples

Sample	Selenium in sample, $\mu g/g$		
	This work*	DPP	Certified value
GSD-3	1.130		1.07 ± 0.14
GSD-5	0.350		0.363 ± 0.075
GSD-7	0.340		0.301 ± 0.057
Pyrite	5.64	5.00	
Limonite	3.57	3.71	
Lead-zinc ore	4.85	5.19	
Copper ore	6.88	7.00	
Soil	1.58	1.66	

*Average value of 3 replicate determinations.
GSD = Geochemical Standard Reference Drainage Sediment.
DPP = differential pulse polarography.

ponent levels was established for study, and it was found that for the determination of 1 μg of selenium in 30 ml of aqueous solution no interference was observed from 0.15 g of Ca, 0.1 g of Pb, Zn, K, Na and Mn, 45 mg of Mg, 40 mg of Fe, Al, Sb, Cu, 30 mg of W, 20 mg of Si, P, 10 mg of Ba, La, 6 mg of Hg, 4 mg of Ni, Mo and Th, 1 mg of Ag, Bi, Cd and Yb, 0.25 mg of As, 0.2 mg of F and 0.1 mg of Au.

Recovery

Various samples were spiked with known quantities of selenium before decomposition of the sample and the total selenium contents were determined and compared with the selenium content of the samples. Table 1 shows that good recovery was obtained.

Determination of selenium in ores and minerals

Although no pronounced interference effects occur and good recoveries are obtained by the recommended method, the standard-additions method was used. The results for some ore and mineral samples are summarized in Table 2, and a good agreement was achieved with the certified values. The relative standard deviation was found to be 7.4% for 9 replicate determinations of selenium in GSD-3 Geochemical Standard Reference Drainage Sediment, for which the certified selenium value is 1.07 ± 0.14 μg/g. It should be pointed out that this method can be employed for the determination of selenium in geological samples at or below the μg/g level.

REFERENCES

1. R. W. Boyle, *Geol. Surv. Can. Papers*, 1974, **74**, 45.
2. R. F. Sanzolone and T. T. Chao, *Analyst*, 1981, **106**, 647.
3. Shan Xiao-quan, Jin Long-zhu and Ni Zhe-ming, *At. Spectrosc.*, 1982, **3**, 41.
4. O. Kujirai, T. Kobayashi, K. Ide and E. Sudo, *Talanta*, 1983, **30**, 9.
5. R. D. Ediger, *At. Absorpt. Newsl.*, 1975, **14**, 127.
6. K. G. Brodie, *Am. Lab.*, 1977, **9**, No. 3, 73.
7. E. L. Henn, *Anal. Chem.*, 1975, **47**, 428.
8. T. M. Vickrey and M. S. Buren, *Anal. Lett.*, 1980, **13**, 1465.
9. T. Kamada, T. Shiraishi and Y. Yamamoto, *Talanta*, 1978, **25**, 15.
10. G. F. Kirkbright, S. Hsiao-chuan (Shan Xiao-quan) and R. D. Snook, *At. Spectrosc.*, 1980, **1**, 85.
11. H. W. Lakin and D. F. Davidson, *U.S. Geol. Surv. Prof. Papers*, 1973, No. 820, 573.

Talanta, Vol. 32, No. 1, pp 27–30, 1985
Printed in Great Britain

0039-9140/85 $3.00 + 0.00

PHOTOMETRIC COMPLEX-FORMATION TITRATION OF SUBMICROMOLE AMOUNTS OF URANIUM

J. KRAGTEN and W. OZINGA
Laboratory for Analytical Chemistry, University of Amsterdam, Nieuwe Achtergracht 166, 1018 WV Amsterdam, The Netherlands

(*Received* 28 *March* 1984. *Accepted* 30*th June* 1984)

Summary—With DTPA present in excess, small amounts of uranium (100–200 μg) can be reduced quantitatively to the quadrivalent state in a Jones reductor (5% amalgamated Zn powder, 50 mesh). The excess of DTPA is back-titrated photometrically with thorium, with Semi-Xylenol Orange as the indicator. The accuracy is ± 0.2 μg at the 200-μg level. Metals forming complexes with DTPA at pH 2 interfere.

In the determination of uranium, complexometry has so far found little use for a number of reasons. Uranyl ions form complexes with many reagents, such as acetate, sulphate, nitrate, ascorbic acid, *etc.*,[1] but those with the complexing agents DCTA, DTPA and EDTA are remarkably weak.[2] Low concentrations therefore cannot be determined and interference by other elements is rather strong. Moreover, weak 2:1 complexes are also formed, so the stoichiometry is variable.[2] The sexivalent state is hence regarded as rather unsuitable for complexometric determinations.[3]

Uranium(IV) forms stable complexes[4] in strict 1:1 stoichiometry with EDTA, DCTA and DTPA, but its complexometric determination has been of little importance so far, first because of a lack of accuracy and secondly because oxidimetric determination is the obvious choice if the uranium has been reduced to the quadrivalent state, since the oxidative titrations give the same or even greater accuracy and can be done in the presence of a much larger number of metals. Only at low uranium concentrations (10^{-5}–$10^{-4}M$) do the advantages of oxidimetry disappear. The potential jump becomes less pronounced and the reduction may partially proceed to the tervalent state,[5] which is unstable towards water and air. Aeration, recommended in most procedures,[1,5] does not always stop at the quadrivalent state. For macrodeterminations the procedure functions well, but generally the free U^{4+} ions are less easy to keep from decay at low concentrations.[6–8] We have therefore re-examined the possibilities for the complexometric determination of uranium(IV) at low concentrations (10^{-5}–$10^{-4}M$) with accurate analysis as our aim.

A crucial point is the reduction to the quadrivalent state and its preservation. Reducing agents, added in excess, theoretically have the advantage of keeping the element in the reduced state. Hydrazine and sodium tetrahydroborate were examined but did not give quantitative reduction; zinc, ascorbic acid and bisulphite[6–8] were rejected for the same reason. Sodium dithionite ($Na_2S_2O_4$) has been used by various authors.[8–10] Although it gives quantitative reduction it is less suitable because colloidal sulphur is formed at low pH and hydrolysis of U^{4+} occurs at low acidity. At the recommended pH of 3 an accuracy of 7 μg is claimed[9] in a direct photometric titration with EDTA. We tried to improve this by performing the reduction in the presence of EDTA in order to stabilize the U(IV) state and to protect it from hydrolysis, but the accuracy was hardly improved.

Use of reductor columns was tried as an alternative. A silver reductor[5] does not introduce impurities and was therefore considered first. The reduction potential of the silver reductor is

$$E = 0.22 + 0.059\text{pCl} \qquad (1)$$

Combining this with the redox reaction

$$UO_2^{2+} + 4H^+ + 2e \rightleftharpoons U^{4+} + H_2O \ (E^0 = 0.33\ \text{V}) \qquad (2)$$

and taking into account possible side-reactions of both UO_2^{2+} and U^{4+}, we can derive for the conditional equilibrium ratio

$$\log \frac{[UO_2']}{[U(IV)']} = -3.8 + 2\text{pCl} + 4\text{pH} - \log \alpha_{U(IV)} + \log \alpha_{UO_2} \qquad (3)$$

where the primes indicate conditional values.

It will be obvious that in the absence of complexing agents, the hydrochloric acid concentration should theoretically be higher than 1M. This agrees with practical experience that 4M acid must be used (at 60°).[11] We found incomplete reduction with 1M acid, presumably because of low reactivity at the silver surface covered with silver chloride. As high acidity leads to a high ionic strength, causing interference in the titrations or needing time-consuming evaporation to remove the excess of acid (with consequent risk of oxidation), this method is also less suitable. In the presence of EDTA and DTPA (we selected the latter for our experiments because of its much higher solubility in acid media[12]) reduction remains incomplete; at pH 1 the contribution of $\log \alpha_{U(IV)}$, is not

able to compensate for the effect of the term 4pH (Table 1). Neither EDTA nor DTPA is reduced by the silver reductor; nevertheless the reductor is unsuitable for quantitative reduction of uranium(VI) at moderate acidity.

The Jones reductor,[5,15,16] filled with amalgamated zinc, is more powerful and so can be applied at lower acid concentrations (0.01–0.1*M* hydrochloric acid). Both zinc and mercury can participate in the reduction process,[5] but which metal reacts preferentially depends on the substance to be reduced. Uranium(VI) is reduced only by zinc,[16] which leads to an increase of Zn^{2+} in solution and a decrease of metallic zinc at the amalgam surface. Moreover, although the mercury suppresses the evolution of hydrogen because of the large overpotential, gas formation is not negligible. All these processes together make the reduction potential approximately 0.70 V.[5] Combining this value with equation (2) we get

$$\log \frac{[UO_2^+]}{[U(IV)']} = -35 + 4\,pH - \log \alpha_{U(IV)} + \log \alpha_{UO_2} \quad (4)$$

Hence under all experimental conditions of interest, the reduction will theoretically be complete.

Uranium can also be reduced to the tervalent state according to

$$U^{4+} + e \rightleftharpoons U^{3+} \quad E^0 = -0.61\ V \quad (5)$$

With the Jones reductor we get

$$\log \frac{[U(IV)']}{[U(III)']} \approx -1.5 + \log \alpha_{U(IV)} - \log \alpha_{U(III)} \quad (6)$$

From Table 1 it will be obvious that in the region of interest (pH > 1) tervalent uranium will not be formed when DTPA is present in excess, and so aeration can be omitted.

In the presence of atmospheric oxygen (redox potential $E = 1.23–0.059\,pH$) uranium(VI) is the stable form ($\log [UO_2^+]/[U(IV)'] > 25$), but it is known that, even in the absence of ligands, oxidation of U(IV) by atmospheric oxygen proceeds so slowly that working under nitrogen is not necessary in macrodeterminations.[6–8,11,16] At low concentration levels, however, irregular results were observed, which is remarkable as a still lower reactivity should have been expected. The cause is indirectly oxygen, which is reduced to hydrogen peroxide in the column:[17]

$$Hg + O_2 + 2H^+ + 2Cl^- \rightarrow Hg_2Cl_2\downarrow + H_2O_2 \quad (7)$$

Although further reduction by the half-reaction $H_2O_2 + 2H^+ + 2e \rightleftharpoons 2H_2O$ has a standard potential of +1.77 V, this reaction is very slow in the reductor because the overpotential for reduction of H_2O_2 at a mercury surface is extremely high ($\simeq 2.5$ V).[17] Hence a steady-state peroxide concentration is built up. Prior deaeration reduces the production of peroxide insufficiently for accurate analysis.

The interference seems not to be simply due to the reoxidation of U^{4+} ions to uranyl ions. It is known that uranyl ions form complexes with hydrogen peroxide. Tridot[18] showed that at pH 0.5–3.5 uranyl ions can be quantitatively precipitated as uranyl peruranate. He states that any U(IV) is first oxidized and then precipitated as peruranate. This is important, because if H_2O_2 is formed in the column first, peruranate may pass in colloidal state through the column before its reduction occurs. It turns out that if DTPA is present in excess during the reduction, U(IV)—once formed—is transformed into its DTPA complex, which is not oxidized by any H_2O_2 formed in the column; no interference by hydrogen peroxide could be observed in our experiments.

It has been found experimentally, that aerial oxidation of the U(IV) in the effluent from the reductor is negligible; 20% oxidation to uranyl ions took place during exposure for a weekend.

It has been reported that oxidation of U(IV) is accelerated appreciably by ultraviolet radiation and direct sunlight.[1] On the other hand, methods have been proposed for the photochemical reduction of U(VI) to U(IV) in the presence of lactic acid, ethanol and other reducing agents.[19,29] Standing for 4 hr in moderate light conditions was found to lead to an

Table 1.

		pH					
	[DTPA] in excess, M	0	0.5	1.0	1.5	2.0	2.5
$\log \alpha_{U(IV)}$	10^{-4}	0	0.3	2.8	5.5	8.0	10.1
	10^{-5}	0	0	1.8	4.5	7.0	9 1
$\log \alpha_{U(III)}$	10^{-4}	0	0	0	0.7	3.0	5.1
	10^{-5}	0	0	0	0.1	2.0	4.1

From the stability constants[2] of the uranyl–DTPA complex and the small tendency for hydrolysis[13] it can be concluded that at moderate uranyl ion concentrations $\log \alpha_{UO_2} = 0$ below pH 3.5. For U(III) no reliable hydrolysis constants are known,[1] but if U(III) is regarded as comparable to lanthanides it can be assumed that hydrolysis is negligible below pH 4.[1] Hence $\log \alpha_{U(III)} = \log \alpha_{U(III)DTPA}$, which has been calculated from the data for protonation of DTPA: $\log \beta_1 = 10.46$, $\log \beta_2 = 18.87$, $\log \beta_3 = 23.01$, $\log \beta_4 = 25.71$, $\log \beta_5 = 27.79$, $\log \beta_6 = 29.01$ and $\log \beta_7 = 29.76$, and $\log K_{U(III)DTPA} = 25.1$.[14] For U(IV) $\log \alpha_{U(IV)}$ is given by $\log \alpha_{U(IV)} = \log \alpha_{U(IV)XDTPA)}$. The literature value[4] $\log K_{U(IV)DTPA} = 28.8$ has been corrected for the neglect of the DTPA protonation constants determined recently,[12] $\log \beta_6$ and β_7, the corrected value being $\log K = 30.1$.

error smaller than -0.1%. Within the experimental error ($\pm 0.1\%$) of the photometric back-titration with thorium [Semi-Xylenol Orange (SXO) as indicator] at pH 2, there was complete recovery of EDTA and DTPA passed through the Jones reductor. This implies first that no Hg^{2+} ions are released in the reduction, and secondly that zinc ions do not interfere in the titration. For each 10 ml of the eluent (0.1*M* hydrochloric acid) 10 μmoles of Zn^{2+} are found to be produced. It is important to use >99.9% pure zinc, as otherwise some of the impurities may interfere.

The procedure developed allows reduction of 150–260 μg of uranium in the presence of excess of DTPA, the surplus being back-titrated with thorium (SXO as indicator).

EXPERIMENTAL

The Jones reductor

Zinc powder (<99.9% pure, Merck) is sieved and the 0.18–0.60 mm fraction collected; a 15-g portion is etched in a 100-ml beaker by short exposure to 1*M* hydrochloric acid, then washed twice with water of "sub-boiling" quality. The wet powder is amalgamated by vigorous stirring with 25 ml of 0.1*M* hydrochloric acid in which 800 mg of mercury chloride have been dissolved. After 15 min the solution is decanted and the zinc washed thrice with sub-boiled water. This produces so-called 5% amalgamated zinc.

As mercury is not consumed during the reduction of U(VI) we thought that 1% amalgamated zinc (made by using 200 mg of mercuric chloride instead of 800 mg) might react faster because of the smaller diffusion distances through the mercury film. However, the reduction is less efficient, as evolution of hydrogen increases and tends to reduce the available mercury surface area by forming a protective gas film.

The amalgamated zinc is transferred into the column (0.8 × 6 cm) with 0.1*M* hydrochloric acid, Merck, Suprapur). The column should not be allowed to become dry. Before use it is filled with 0.1*M* hydrochloric acid and inverted to remove the hydrogen bubbles from between the grains. It is then washed with 0.1*M* hydrochloric acid to remove zinc ions and hydrogen peroxide. This pretreatment should be performed at least daily. The size of the amalgamated particles increases by coagulation, but the large internal surface of the zinc in each grain is increased sufficiently by the use of fine powder for exhaustion of the zinc atoms at the mercury surface not to occur, and the reduction is complete.

Reduction procedure

After pretreatment of the column about 1 ml of the acid is left above the amalgam and 0.005*M* DTPA (250 μl) is added to it from a microburette with a U-shaped tip which is immersed in the solution. On removal, the tip is washed with a few hundred μl of 0.1*M* hydrochloric acid. Then a 200-μl sample containing about 1 μmole of uranium (in 0.1*M* hydrochloric acid) is similarly introduced. Nitrogen gas is introduced through a Teflon microtube to mix the solution and expel atmospheric oxygen. The solution is then let flow through the column until its surface is just above the amalgam. The column is then rinsed with three 0.5-ml portions of 0.1*M* hydrochloric acid, and then with 15 ml of the acid in 3-ml portions. The flow-rate should not exceed about 2 ml/min.

Titration procedure

The eluent is caught directly in a 20-ml titration cell containing hexamine solution (at pH 7). The pH is adjusted to 2.0 with either hydrochloric acid or additional hexamine solution.

The pH-meter electrodes are rinsed with 0.01*M* hydrochloric acid. Then 250 μl of 0.06% SXO solution in acetone are added. The cell is placed in the spectrophotometer and the excess of DTPA is back-titrated with 0.005*M* thorium (adjusted to pH 2) at 530 nm. For accurate analysis, glassware calibration corrections have to be applied.

RESULTS AND DISCUSSION

At pH > 7.5 U(IV)–DTPA dissociates, forming either a precipitate or a soluble hydroxide[21] (Fig. 1). Once formed—for instance locally during neutralization with a strong base—these products will cause irregular results; some uranium will escape from analysis as DTPA will react only slowly with the $U(OH)_5^-$ ions, and precipitated $U(OH)_4$ is easily oxidized by air.[13,22] That is why the eluent is caught directly in the cell and neutralized with a hexamine buffer adjusted to pH 7.

Use of 0.01*M* hydrochloric acid medium in the reduction procedure causes large errors, presumably because it leads to local pH values far above 2 because of the reduction of protons to hydrogen.

SXO[23] has to be preferred to Xylenol Orange (XO) as the indicator. With XO systematic deviations occur at low concentrations because of the predominant formation of Th_2XO.[24] Thorium and SXO form only the ThSXO and $Th(SXO)_2$ complexes, with conditional constants $\log \beta_{11} = 6.85$ and $\log \beta_{12} = 11.4$ (pH = 2.00, I = 0.1, perchlorate medium).[25]

The conditions for photometric back-titrations[26] are amply fulfilled. The curvature of the L-shaped titration curve near the equivalence point agrees very well with the values for $\log \beta_{ThSXO}$, $\log K_{U(IV)DTPA}$ and the difference in stability constants of U(IV)DTPA and ThDTPA as mentioned by Piskunov *et al.*[4]

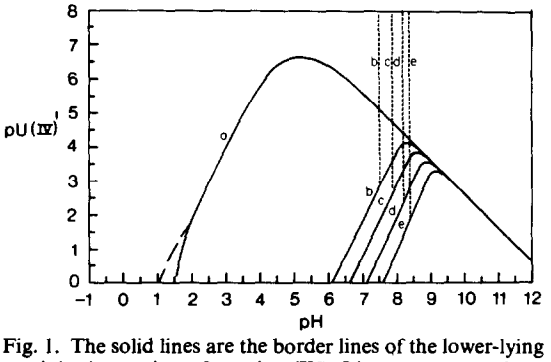

Fig. 1. The solid lines are the border lines of the lower-lying precipitation region of uranium(IV). Line a corresponds to uranium(IV) in the absence of complexing agents; lines b–e hold for the presence of DTPA in excess concentrations of 10^{-4}, 10^{-3}, 10^{-2} and $10^{-1}M$, respectively. The vertical dotted lines mark the region at high pH in which more than 1% of the original U(IV)DTPA is converted into the soluble hydroxide complex. The hydrolysis data for U(IV) used in constructing the diagram are $\log {}^*\beta_1 = -1.5$, $\log {}^*\beta_2 = -3.0$, $\log {}^*\beta_3 = -7.3$, $\log {}^*\beta_4 = -11.80$, $\log {}^*\beta_5 = -17.6$, $\log {}^*\beta^{15}{}_6 = -17.20$ and $\log {}^*K_{s0} = 5.0$.[21,22] The dashed line indicates the 1% border of polycomplex formation, but plays no role in our analysis.

($\Delta \log K = 2.1$). The procedure has been applied to several intermetallic compounds such as UCo_2, UFe_2 and UAl_2 with excellent results. Nickel interferes, as do all metals forming DTPA complexes at pH 2. Perchlorate does not interfere. Nitrate interferes strongly; nitric acid used for sample dissolution should be expelled with perchloric acid. For metallic uranium samples an error of 0.1% can be achieved if all the volumetric apparatus is calibrated. The DTPA can be standardized against high-purity metallic copper by photometric titration with TAR as the indicator. The thorium solution can be standardized against the DTPA solution and its titre need not be known quite so accurately.

REFERENCES

1. *Analytical Chemistry of Uranium*, P. N. Palei (ed.), Ann Arbor-Humphrey, London, 1970.
2. P. A. Overvoll and W. Lund, *Anal. Chim. Acta*, 1982, **143**, 153.
3. R. Přibil, *Applied Complexometry*, p. 117. Pergamon Press, Oxford, 1982.
4. E. M. Piskunov and A. G. Rykov, *Radiokhimiya*, 1972, **14**, 265.
5. I. M. Kolthoff, R. Belcher, V. A. Stenger and G. Matsuyama, *Volumetric Analysis*, Vol. III, p. 10. Interscience, London, 1957.
6. J. Korkisch, *Anal. Chim. Acta*, 1961, **24**, 306.
7. J. Kinnunen and B. Wennerstrand, *Chemist-Analyst*, 1957, **46**, 92.
8. B. Buděšínský, A. Bezděková and D. Vrzalová, *Collection Czech. Chem. Commun.*, 1962, **27**, 1528; *Anal. Abstr.*, 1963, **10**, 1011.
9. R. Keil, *Z. Anal. Chem.*, 1977, **283**, 357.
10. B. H. J. de Heer, Th. van der Plas and M. E. A. Hermans, *Anal. Chim. Acta*, 1965, **32**, 292.
11. C. L. Wilson and D. W. Wilson, *Comprehensive Analytical Chemistry*, Vol. 1c, p. 647. Elsevier, Amsterdam, 1962.
12. J. Kragten and L. G. Decnop-Weever, *Talanta*, 1983, **30**, 623.
13. J. Kragten, *ibid.*, 1977, **24**, 483.
14. A. I. Moskvin, *Radiokhimiya*, 1969, **11**, 458.
15. H. W. Stone and D. N. Hume, *Ind. Eng. Chem., Anal. Ed.*, 1939, **11**, 598.
16. J. H. Kennedy, *Anal. Chem.*, 1960, **32**, 150.
17. J. Lingane, *The Analytical Chemistry of Selected Metallic Elements*, p. 81. Reinhold, New York, 1966.
18. G. Tridot, *Compt. Rend.*, 1951, **232**, 1215.
19. G. G. Rao and V. P. Rao, *Anal. Chim. Acta*, 1956, **15**, 97.
20. G. G. Rao, V. P. Rao and N. Venkatama, *Z. Anal. Chem.*, 1956, **150**, 178.
21. C. F. Baes Jr. and R. E. Mesmer, *The Hydrolysis of Cations*, p. 176. Wiley, New York, 1976.
22. J. Kragten, *Atlas of Metal-Ligand Equilibria in Aqueous Solutions*, p. 34. Ellis Horwood, Chichester, 1978.
23. F. Smedes, L. G. Decnop-Weever, Nguyen Trong Uyen, J. Nieman and J. Kragten, *Talata*, 1983, **30**, 614.
24. J. Kragten, *Z. Anal. Chem.*, 1973, **246**, 356.
25. *Idem*, *Anal. Chim. Acta*, to be published.
26. *Idem*, *Talanta*, 1973, **20**, 937.

Talanta, Vol. 32, No. 1, pp. 31–33, 1985
Printed in Great Britain

0039-9140/85 $3.00 + 0.00

SHORT COMMUNICATIONS

A SIMPLE SPECTROPHOTOMETRIC METHOD FOR THE DETERMINATION OF NYLIDRIN HYDROCHLORIDE, ISOXSUPRINE HYDROCHLORIDE AND SALBUTAMOL SULPHATE IN PHARMACEUTICAL PREPARATIONS

R. T. SANE*, V. G. NAYAK and V. B. MALKAR
Department of Chemistry, Ramnarain Ruia College, Matunga, Bombay 400019, India

(*Received* 5 *April* 1982. *Revised* 20 *July* 1984. *Accepted* 14 *September* 1984)

Summary—A simple spectrophotometric method for the determination of nylidrin hydrochloride, isoxsuprine hydrochloride and salbutamol sulphate is described, based on measurement of the orange-yellow species produced when the drugs are coupled with diazotized benzocaine (*p*-aminoethyl benzoate) in trimethylamine medium. The method is applicable over the range 1–12 μg/ml for isoxsuprine hydrochloride and nylidrin hydrochloride and 1–8 μg/ml for salbutamol sulphate. The method is a modification of the Bratton–Marshall reaction and is simple, reproducible, accurate and more sensitive than those cited in the literature.

Nylidrin (buphenine) is a peripheral vasodilator and is incorporated in various pharmaceutical products. No colorimetric method for its determination has been reported but methods such as non-aqueous titration, gas chromatography and HPLC have been used.[1-3]

Isoxsuprine hydrochloride is an orally and parenterally active peripheral and cerebral vasodilator. In addition to adrenolytic action it has a direct relaxant effect on the smooth muscular tissue of the blood vessels and of the uterus. Several methods such as ultraviolet spectrophotometry, gas chromatography and HPLC coupled with colorimetry are cited in the literature for its determination.[1,3-6]

Salbutamol sulphate is a bronchodilator. Non-aqueous titration, ultraviolet spectrophotometry, colorimetry, stable-isotope dilution, fragmentation mass spectrometry, gas chromatography and NMR have been used for its determination.[4,7-14]

We have now developed a rapid, sensitive and general method for the determination of nylidrin hydrochloride, isoxsuprine hydrochloride and salbutamol sulphate, based on our observation that when coupled with diazotized benzocaine in trimethylamine solution these drugs yield an orange-yellow compound, the absorbance of which can be measured at 460 nm. The method is a modification of the Bratton–Marshall reaction, since the diazotization is done in a mixture of trichloroacetic acid and sulphuric acid. This method has wide applicability in the determination of nylidrin hydrochloride, isoxsuprine hydrochloride and salbutamol sulphate in pharmaceutical preparations.

*Author for correspondence.

EXPERIMENTAL

Reagents

Analytical grade chemicals were used throughout.

Benzocaine. A 2 mg/ml solution in 95% alcohol.

Acid mixture. A mixture of 86 ml of 15% trichloroacetic acid solution, 20 ml of 2*M* sulphuric acid and 94 ml of distilled water.

Sodium nitrite solution, 0.1%.

Trimethylamine solution, 40%.

Standard drug solutions

Standard isoxsuprine hydrochloride and nylidrine hydrochloride were checked for purity and strength according to the U.S.P. specifications, which they met. Standard salbutamol sulphate was checked for purity and strength according to the B.P. 1980 specifications and was found to meet those requirements.

Standard solutions were prepared by dissolving 25 mg of the drug (accurately weighed) and diluting to volume in a 250-ml standard flask to give a 100 μg/ml working standard solution.

Optimum reaction conditions

The optimum experimental conditions for the determination were established by systematic variation of reagent volumes. The results are summarized in Fig. 1.

General procedure

Into each of a series of 25-ml standard flasks pipette 1 ml of benzocaine solution, and add 1 ml of acid mixture and 2 ml of sodium nitrite solution. Let the flasks stand for 15 min, then add 2.5 ml of 95% ethanol to each. Next add portions of standard drug solutions ranging from 0.25 to 3 ml for nylidrin hydrochloride or isoxsuprine hydrochloride and from 0.25 to 2.00 ml for salbutamol sulphate, to

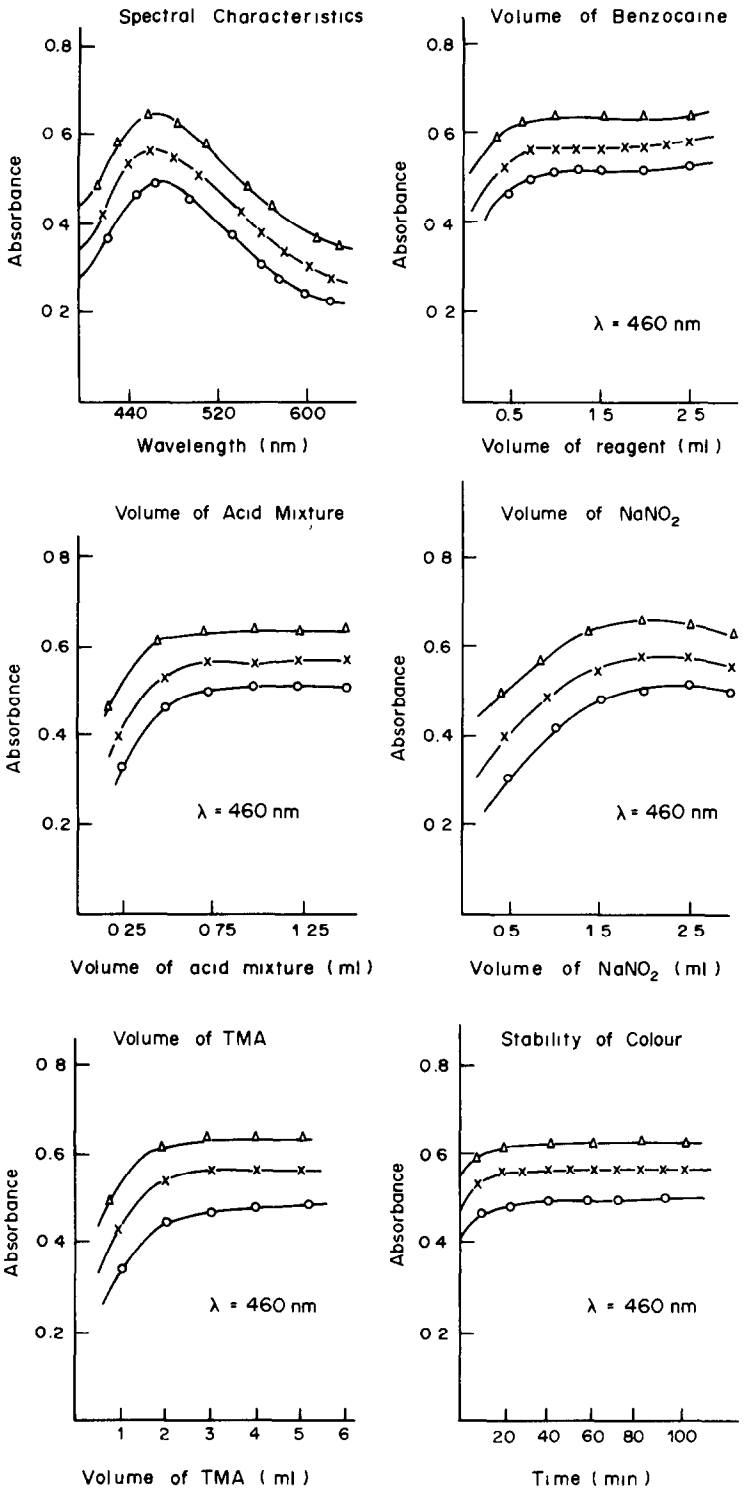

Fig. 1. Absorption spectra and optimization of conditions. × Nylidrin hydrochloride; ○ isoxsuprine hydrochloride; △ salputamol sulphate.

Table 1.

Drug	Product	Nominal content	Coefficient of variation, %	Nominal recovery, %	Molar absorptivity, 10^4 $l.mole^{-1}.cm^{-1}$
Nylidrin hydrochloride	Tablets	6 mg	1.5	100.2	3.36
	Injection	5 mg/ml	1.6	100.4	
Isoxsuprine hydrochloride	Tablets	10 mg	1.9	100.6	2.17
	Injections	5 mg/ml	1.5	99.0	
Salbutamol sulphate	Tablets	2 mg	1.8	100.1	2.30
	Tablets	4 mg	1.7	100.1	
	Syrup	2 mg/5 ml	2.3	100.1	

construct a calibration graph. Let the flasks stand for 5 min and finally add 3 ml of trimethylamine solution and dilute to the mark with distilled water. Measure the absorbances at 460 nm against a reagent blank prepared along with the standards. Analyse the test samples in the same way.

The calibration graphs are linear over the range 1–12 μg/ml for nylidrin hydrochloride and isoxsuprine hydrochloride and 1–8 μg/ml for salbutamol sulphate, in the final solution measured.

Application to pharmaceutical preparations

Tablets. Powder 20 tablets containing one or the other of nylidrin hydrochloride, isoxsuprine hydrochloride and salbutamol sulphate and mix. Weigh an amount of the powder equivalent to about 25 mg of drug and dissolve it and dilute the solution accurately to 250 ml with distilled water. Analyse the solution as detailed above.

Injections or syrups. Thoroughly mix the sample, pipette out a quantity corresponding to about 25 mg of drug and accurately dilute to 250 ml. Analyse the solution as described above.

Recovery experiments

To study the precision and accuracy of the method, a statistical study was undertaken. A fixed volume of sample solution was taken and standard drug solution was added at three different levels and the total amount of drug was determined. Each level was tested 7 times. The recovery was calculated by regression analysis. A standard additions graph gave the drug content of the sample. Results are given in Table 1.

RESULTS AND DISCUSSION

The pharmacopoeial methods described in the U.S.P. and B.P. for the determination of the three drugs require larger quantities of sample, whereas the present method needs less than 200–300 μg of the drugs (in the final solution).

The method is simple and rapid. The diazotization can be done at room temperature, and the excess of nitrite need not be removed. The colour development is complete within 30 min and the product is stable for at least 2 hr. There is no interference from the common excipients such as starch, talc *etc.* used as binding materials in tablet formulation. In the determination of salbutamol sulphate in syrups, the Tartrazine Yellow present does not interfere in the reaction. The recoveries range between 99 and 101% and the coefficients of variations are low. The method can be used for routine quality-control analysis of the drugs.

Acknowledgement—One of the authors (V. G. Nayak) is grateful to U.G.C., New Delhi, for the award of a Junior Research Fellowship.

REFERENCES

1. *United States Pharmacopeia*, 20th Rev., pp. 434, 562. Mack Printing Co., Easton, 1980.
2. H. Li and P. Cervoni, *J. Pharm. Sci.*, 1976, **65**, 1352.
3. F. Volpe, J. Zintel and D. Spiegel, *ibid.*, 1979, **68**, 1264.
4. *British Pharmacopoeia 1980*, Vol. II, pp. 394, 628, 781, 661, 819. HMSO, Cambridge, 1980.
5. R. Bryant, D. E. Mantle, D. L. Timma and D. S. Yoder, *J. Pharm. Sci.*, 1968, **57**, 658.
6. L. B. Hakes, T. C. Corby and B. J. Meakin, *J. Pharm. Pharmacol.*, 1979, **31**, (Suppl.), 25P.
7. A. A. M. Wahbi, H. Abdine, M. Korany and M. H. Abdel-Hay, *Assoc. Off. Anal. Chem.*, 1978, **61**, 1113.
8. S. Alba Dalgado and G. Lara Gonzalez, *Rev. Cubana Farm*, 1979, **13**, 141.
9. L. E. Martin, J. Rees and R. J. N. Tanner, *Adv. Mass. Spectrum. Biochem. Med.*, 1976, **I**, 475; *Anal. Abstr.*, 1976, **31**, 6A1.
10. L. E. Martin, J. Rees and R. J. N. Tanner, *Biomed. Mass Spectrom.*, 1976, **3**, 184.
11. R. T. Parfitt, G. H. Dewar and J. K. Kwakye, *J. Pharm. Pharmacol.*, 1978, **30** (Suppl.), 62P.
12. J. Eyem, *Adv. Mass Spectrom. B*, 1978, **7**, 1534.
13. D. M. Singbal and K. U. Sawant, *Indian Drugs*, 1981, **18**, 368.
14. R. T. Sane, C. H. Thombare, A. B. Ambardekar and A. Y. Sathe, *ibid.*, 1981, **19**, 195.

Talanta, Vol. 32, No 1, pp. 34–36, 1985
Printed in Great Britain

0039-9140/85 $3.00 + 0.00

APPLICATION OF ION-EXCHANGE REACTIONS BETWEEN MEMBRANES AND RESINS

JAMES A. COX* and NOBUYUKI TANAKA
Department of Chemistry and Biochemistry, Southern Illinois University, Carbondale, IL 62901, U.S.A.

(*Received* 13 *June* 1984. *Accepted* 2 *August* 1984)

Summary—The separation of a solution of an electrolyte from an ion-exchange resin by an ion-exchange membrane, where the charge sign of the fixed sites is the same, results in a process that is comparable to Donnan dialysis in its overall effect. That is, the counter-ions from the resin can be exchanged for ions of the same charge sign in the electrolyte. The reaction is demonstrated and the efficiency of the process evaluated by monitoring the metathesis of carbonic acid from sodium carbonate. An application of the metathesis of a non-electrolyte to a preconcentration method for ion chromatography is demonstrated.

Ion-exchange reactions are typically performed between solute ions and those held on a resin with fixed sites of the appropriate charge sign. In the present report we describe what is seemingly a direct exchange reaction between ions on a pair of ion-exchange materials. To our knowledge, such a reaction has not been previously described.

The process, dual ion-exchange, has potential application to both analytical and synthetic chemistry. In the format used, the separation of a resin slurry bath from an electrolyte solution by an ion-exchange membrane, the process is similar to Donnan dialysis; however, incursion of the counter-ion of the electrolyte, which is a limitation of Donnan dialysis because of the non-zero transport numbers for cations (anions) in anion (cation)-exchange membranes,[1-3] cannot occur. In many experimental procedures the ability of dual ion-exchange to introduce a prescribed ion into the sample without even trace level incursion of the counter-ion is desired. Dual ion-exchange has other merits. The change of concentration of an analyte ion in solution because of adsorption losses or sample volume change, which commonly occurs in conventional ion-exchange, is minimized. Only a small sample volume is therefore required. There is virtually no dead volume with this method.

EXPERIMENTAL

Apparatus

The dual ion-exchange apparatus consisted of the following: a Nafion 811 cation-exchange tubular membrane (DuPont Polymer Products, Wilmington, Delaware), 0.64 mm bore, 0.89 mm outer diameter, coiled on a holder made of glass rods; a slurry of 55 g of Dowex 50WX4 100/200 mesh cation-exchange resin, proton form, and 24 g of water, in a 100-ml beaker; a Model 375A tubing pump (Sage Instruments, Cambridge, Massachusetts) and a Nuova II hotplate/magnetic stirrer (Thermolyne Corp., Dubuque, Iowa). The system was assembled as shown in Fig. 1.

The cation-exchange resin was regenerated with 4*M* hydrochloric acid (3 volumes per volume of resin). It was subsequently rinsed with about 150 resin-volumes of water.

The initial clean-up step for a new portion of Nafion tubing consisted of passing 1*M* hydrochloric acid through the tubing for 1 hr, while the tubing was also immersed in 1*M* hydrochloric acid. A specific pretreatment of the Nafion tubing to set the initial ionic form was not necessary. Instead, the holder with the tubing was placed in the resin slurry; the ionic form of the membrane became the same as that of the resin slurry. Between samples, water was pumped through the tubing for at least 2 min. A plug of air was always injected before a sample was introduced, in order to eliminate dilution. In the experiments where the slurry was heated, some water was occasionally added to the slurry in order to compensate for evaporation loss.

The carbonate was determined by flow-injection analysis with conductimetric detection. A model 2010i ion-chromatograph (Dionex Corp., Sunnyvale, California) was used with the columns by-passed (*i.e.*, the injector was coupled directly to the detector with a length of tubing). Water was used as the carrier at a flow-rate of 0.3 ml/min. The conductivity was monitored and displayed on a Speed Servo II strip-chart recorder (Esterline Angus Instrument Co., Indianapolis, Indiana). Solutions of sodium carbonate were used as the sample. In the course of the dual ion-exchange process, the sodium carbonate is converted into carbonic acid, which rapidly decomposes into CO_2 and water.

The efficiency of the process was reported as "% metathesized" based on the change of carbonate concentration as the sample passed through the system. The concentration of carbonate after metathesis was determined by fitting the conductivity of the sample to a calibration curve prepared with standard solutions. The "% metathesized" was calculated as the percentage decrease in carbonate concentration.

In one experiment, nitrate was determined after Donnan dialysis into a mixed sodium bicarbonate/carbonate receiver and dual ion-exchange of the dialysate. Measurement was done by ion-chromatography performed in the conventional manner. The Donnan dialysis of nitrate was performed in a cylindrical cell with an R-1035 anion-exchange membrane 11.3 cm^2 in area (RAI Research Corporation, Hauppauge, New York), 5 ml of receiver electrolyte, 100 ml of sample and dialysis for 30 min. Details of the procedure are available elsewhere.[4]

All chemicals used were ACS reagent grade. Distilled water doubly-demineralized with Cole-Parmer research grade cartridges, was used

*To whom correspondence should be addressed.

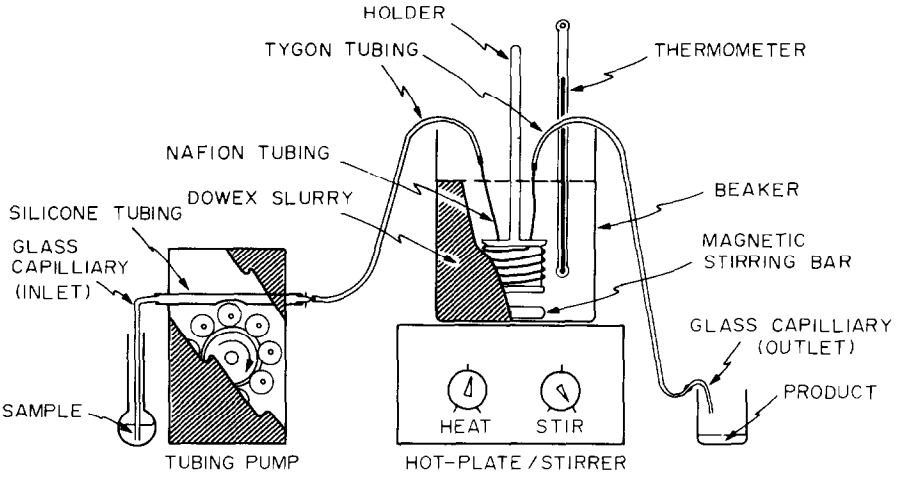

Fig. 1. Apparatus for dual ion-exchange metathesis.

RESULTS AND DISCUSSION

The general characteristics of the dual ion-exchange system were established in experiments performed under the following conditions: sample, 0.20*M* sodium carbonate; Nafion 811 cation-exchange tubing length, 2 m; resin slurry temperature, 75°; sample flow-rate, 0.29 ml/min. The sample was pumped through the Nafion tubing, which was immersed in the stirred, heated slurry. With 0.20*M* sodium carbonate as sample, there was 99.96% conversion into carbonic acid.

The flow-rate does not need to be carefully controlled to give reproducible results; at 0.58 ml/min the final carbonate concentration was $7.2 \times 10^{-5}M$ and $7.7 \times 10^{-5}M$ at a flow-rate of 0.29 ml/min. With shorter lengths of the cation-exchange tubing, the flow-rate is more critical; with a 0.20*M* carbonate sample, a slurry at 75° and 1 m of Nafion tubing, flow-rates of 0.17 and 0.29 ml/min yielded final carbonate concentrations of $1.3 \times 10^{-4}M$ and $6.5 \times 10^{-4}M$, respectively.

In other applications of tubular cation-exchange membranes, the use of either beads[5] or a filament[3,6] as packing material to decrease the dead volume was reported to improve the efficiency. With the dual ion-exchange system, the results shown in Table 1 were obtained. The volumes of the open tube, bead-packed tube and filament-packed tube were 0.46, 0.27 and 0.25 ml, respectively. The efficiency was not related to dead volume, and turbulence within the tubing apparently caused the increased efficiency. With the open tube the turbulence resulted from the decomposition of carbonic acid into CO_2 and water. The bead-packed Nafion tube was generally employed in subsequent experiments.

To establish the optimum operating parameters of the system, it is important to consider the electrolyte concentration of the sample. Table 2 summarizes the effects of temperature, flow-rate and concentration on the efficiency when 1 m of bead-packed tubing is used. The system can be operated at room temperature when the electrolyte concentration is below 0.1*M* and/or slow flow-rates are employed. Alternatively, a longer tube can be used.

The precision was determined by performing eight consecutive experiments at 76°. With 2 m of open Nafion tubing, a 0.1*M* sodium carbonate sample and a 0.29 ml/min flow-rate, the average residual carbonate was $7.5 \times 10^{-5}M$, with a relative standard deviation of 7.7%.

The lifetime of the slurry depends on its volume and the capacity of the ion-exchange resin. Under the reported conditions, the slurry produced carbonic

Table 1. Effect of reducing the dead volume of the Nafion tube, on the efficiency*

Packing	Flow-rate, *ml/min*	Final $[Na_2CO_3]$, M	Conversion, %
None	0.17	1.3×10^{-4}	99.9
Beads	0.17	9.0×10^{-5}	99.9
Filament	0.17	3.8×10^{-4}	99.6
None	0.29	6.5×10^{-4}	99.4
Beads	0.29	3.4×10^{-4}	99.7
Filament	0.29	4.0×10^{-3}	96.0

*Sample, 0.10*M* Na_2CO_3; temperature, 75°; tubing length, 1 m.

Table 2. Efficiency of dual ion-exchange as a function of temperature, flow rate and electrolyte concentration*

Initial $[Na_2CO_3]$, M	Temperature, °C	Flow-rate, *ml/min*	Final $[Na_2CO_3]$, M	Conversion, %
0.02	30	0.17	2.7×10^{-5}	99.9
0.10	30	0.17	9.0×10^{-5}	99.9
0.20	30	0.17	1.4×10^{-3}	99.3
0.20	52	0.17	8.0×10^{-5}	99.9
0.02	30	0.29	5.4×10^{-5}	99.7
0.10	30	0.29	3.4×10^{-4}	99.7
0.20	30	0.29	5.8×10^{-2}	71
0.20	52	0.29	9.0×10^{-5}	99.9
0.02	30	0.58	7.4×10^{-5}	99.6
0.10	30	0.58	3.2×10^{-2}	68
0.20	30	0.58	0.1	50
0.20	52	0.58	4.8×10^{-2}	76
0.20	75	0.58	6.5×10^{-5}	99.9

*Bead-packed Nafion tube, 1 m.

acid from 0.08 mole of sodium carbonate of exchange capacity (160 ml of 0.5*M* solution). This corresponded to utilization of 2.9 meq per gram of the wet resin; the stated capacity of the dry resin was 5.2 meq/g. Since the specific capacity of the wet resin must be lower than that of the dry, it was evident that a very high percentage of the available proton population was used before regeneration was necessary. Further, the residual carbonate peak was constant until this point was reached, so it was obvious when regeneration was necessary.

The dual ion-exchange process is not limited to carbonate samples. Comparable results are obtained for the conversion of sodium hydroxide into water, trisodium phosphate into phosphoric acid H_3PO_4 and sodium sulphite into sulphurous acid.

The analytical utility of the process is demonstrated by using Donnan dialysis as a preconcentration and matrix normalization technique[4,7–9] prior to ion-chromatography. Such a method has potential advantages over the use of a preconcentrator column,[10] but the Donnan dialysis receiver electrolyte, which must have at least 100 times the ionic strength of the sample, is not suitable for injection into an ion-chromatograph employing a conductivity detector.

A 0.50-mg/l. nitrate sample was Donnan-dialysed into a 0.04*M* sodium carbonate/0.16*M* sodium bicarbonate receiver electrolyte. The dialysate was subsequently passed through the dual ion-exchange system and diluted to 10 ml. The nitrate in the diluted sample was determined by ion-chromatography. The concentration found was 2.5 mg/l. corresponding to an enrichment factor of 5.0. The enrichment factor was independent of nitrate concentration and did not change when chloride, sulphate and/or phosphate were included in the initial sample. Other analytical applications of the dual ion-exchange system, such as a procedure to determine trace level impurities in selected electrolytes, are being investigated in our laboratory.

Acknowledgements—Although the research described in this article was funded in part by the United States Environmental Protection Agency under assistance agreement number CR-809397 to Southern Illinois University, it has not been subjected to the Agency's required peer and administrative review and therefore does not necessarily reflect the view of the Agency and no official endorsement should be inferred.

REFERENCES

1. H. L. Yeager, in *Perfluorinated Ionomer Membranes*, A. Eisenberg and H. L. Yeager (eds.), Ch. 4. American Chemical Society Symposium Series 180, Washington, D. C., 1982.
2. J. A. Cox, R. Gajek, G. R. Litwinski, J. Carnahan and W. Trochimczuk, *Anal. Chem.*, 1982, **54**, 1153.
3. P. K. Dasgupta, *ibid.*, 1984, **56**, 96.
4. G. L. Lundquist, G. Washinger and J. A. Cox, *ibid.*, 1975, **47**, 319.
5. T. S. Stevens, G. L. Jewett and R. A. Bredeweg, *ibid.*, 1982, **54**, 1206.
6. P. K. Dasgupta, *ibid.*, 1984, **56**, 103.
7. J. A. Cox and K. H. Cheng, *ibid.*, 1978, **50**, 601.
8. J. A. Cox and Z. Twardowski, *Anal. Chim. Acta*, 1980, **119**, 39.
9. N. Tanaka and J. A. Cox, *Pittsburgh Conference on Analytical Chemistry and Applied Spectroscopy*, Abstract 989, Atlantic City, New Jersey, 1983.
10. J. E. DiNunzio and M. Jubara, *Anal. Chem.*, 1983, **55**, 1013.

Talanta, Vol. 32, No. 1, pp. 37–40, 1985
Printed in Great Britain

0039-9140/85 $3.00 + 0.00

COMPUTER CONTROL OF MICROPROCESSOR-BASED INSTRUMENTS BY KEYPAD EMULATION

P. M. WIEGAND and S. R. CROUCH
Department of Chemistry, Michigan State University, East Lansing, Michigan 48824-1322, U.S.A.

(*Received* 11 *June* 1984. *Accepted* 31 *July* 1984)

Summary—A keypad emulation method for controlling microprocessor-based instruments by laboratory microcomputers is presented. It is applicable to instruments that use "polled" keypad arrays; the instrument can be controlled by the laboratory computer or operated independently by manual keypad entry. To illustrate the approach, a microprocessor-based HPLC solvent-delivery system was controlled by a laboratory microcomputer which synchronized and sequenced the entire HPLC experiment, including solvent delivery, valve control for column switching and back-flushing, data-acquisition, and data-processing.

Almost all scientific instruments on the market today are equipped with microprocessor control. The incorporation of microprocessors in modern instruments has greatly increased their versatility by making many of the instrument functions user-programmable, often by means of a simple keypad entry system. Despite this increased versatility, it is often desirable to control such instruments externally with a laboratory microcomputer for permanent program storage, for display purposes and for synchronization with other system components. Instrument manufacturers are beginning to recognize this need, and some newer instruments include ports for communicating with general-pupose laboratory computers. Often, however, communication ports are lacking or do not provide the same degree of flexibility as manual keypad entry.

In this paper we describe a general method for controlling microprocessor-based instruments with "polled" keypad arrays from an external laboratory computer. The method uses an integrated circuit (IC) multiplexer and an IC demultiplexer to simulate a keystroke by connecting the desired column of the array to the desired row under computer control. Keypad emulation utilizes fully the existing instrument circuitry, and allows the internal microprocessor to perform its built-in logic and error-checking functions. Manual keypad entry remains undisturbed. Additional advantages of the keypad emulation method are described below.

DESIGN CONSIDERATIONS

There are many approaches to interfacing laboratory microcomputers to microprocessor-based instruments. These range from the hardware interface (the laboratory computer has complete control over the hardware and blocks all control by the instrument) to the keypad emulator, which operates identically to manual keypad entry, except that the laboratory computer assumes control over the key closures.

The hardware interface has several disadvantages when an entire instrument must be controlled. First, the circuitry needed to drive the hardware is usually complex, and is likely to be redundant, since driver circuits should already be present in the instrument. Even if the existing driver circuitry is used, the interface still has the complex tasks of synchronization and inter-circuit signal transfer; interface construction requires detailed knowledge of the instrument design. A hardware interface is also difficult to implement without altering the original functions of the instrument. Simulation of the manual keypad entry system eliminates many of these disadvantages and provides several benefits, as discussed later.

The design of a keypad emulator for an instrument with discrete switches could be very complicated. However, the advent of TTL-based, microprocessor-controlled instrumentation has spawned the keypad array as a convenient, efficient means of entering parameters. These arrays have been used for some time in computer terminals as a simple way to encode a large number of keys with only 8 bits of code.[1–3] Design of a keypad emulator to simulate a keystroke in keypad array-based entry systems is relatively straightforward.

For use in a microprocessor-based instrument, a keypad array must have driver and receiver circuits as shown in Fig. 1. The driver circuit scans across the columns of the array, activating each column in turn by sending it a logic-level pulse. If a key is depressed, the pulse is transmitted along the proper row to the receiving circuit, where it is sensed and acted upon. By knowing the column that was activated and the row from which the pulse was received, the microprocessor can deduce which key was depressed. The keypad driver and receiver are often contained in a single IC as in the National Semiconductor MM5740.[4] The activating pulses are active-high in some implementations, but active-low in others. Whatever the specific logic of the driver circuitry, the general strategy for keypad emulation is the same.

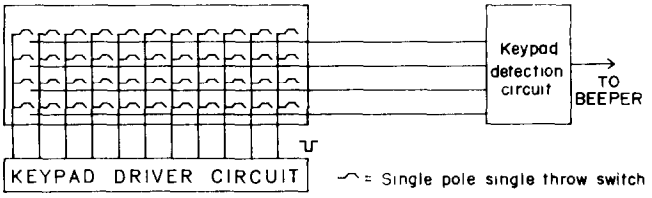

Fig. 1. Schematic of typical 11 × 4 keypad array.

The column selection is made by an IC multiplexer, and the row selection by an IC demultiplexer. Eight lines are sufficient to control a 16 × 8 array of keys: seven of the lines for coding purposes and one to gate the interface on and off. A simple 8-bit parallel input/output (PIO) port is thus sufficient for this size of array.

EXPERIMENTAL

Figure 2 shows the multidimensional chromatography system in which the keypad emulator was employed to allow a laboratory microcomputer[5] to control a Spectra-Physics SP8700 solvent-delivery system. The SP8700 contains a Z80 microprocessor and controls a proportioning valve and dual-piston reciprocating pump to produce HPLC mobile phases of the proper solvent mix and flow-rate. The laboratory microcomputer is based on the 8085 microprocessor; it sequences and controls the entire HPLC experiment. Software for the 8085 processor is loaded from an LSI 11/23 minicomputer (Digital Equipment Corporation), and raw data are sent back for high-level processing and graphics display.

The 11 × 4 keypad array used in the SP8700[6] is shown in Fig. 1. Although the array-driver and receiver circuits are not contained in a single IC, the basic operation is identical to that described above. The characteristics of the signals entering the array were obtained with an oscilloscope. The driver circuit was found to supply active-low pulses 85 μsec in duration. An entire scan cycle was completed in 2.420 msec.

Figure 3 shows the complete interface scheme. The multiplexer is a one-of-sixteen data selector (74150). The input line is chosen by the logic levels established at control inputs A–D. In this way, four PIO lines are used to select which keypad column is the input to the multiplexer. A fifth PIO line is used to gate the interface on and off by using the multiplexer "chip enable" input (E, active-low). When the multiplexer is enabled, the inverted column pulse is transmitted through a logic gate to the demultiplexer, which is a dual 2-line to 4-line decoder (74155). The chip can be used in several ways, but the implementation shown uses an inverting input to obtain the original pulse logic at the output. The A and B inputs are control lines. These are attached to two PIO lines which select the proper row to which the pulse is transmitted. The E input on the demultiplexer is an active-low enable input, tied to a single-pole, double-throw toggle switch which can be used to disable microcomputer control completely. Thus, only 7 of the 8 PIO lines are needed to control an array of this size.

The AND gates shown on the inputs to the receiving circuit allow for simultaneous manual keypad entry. The exclusive-OR gate shown between the multiplexer and demultiplexer acts as a selective inverter to ensure that all outputs of the demultiplexer are high when the multiplexer is disabled. Thus, low pulses arriving by either path are transmitted through the AND gates to the receiving circuit.

Although this implementation was designed for driver circuits that produce active-low pulses, the strategy for active-high pulses is similar. The scheme in Fig. 3 can be modified for active-high pulses by replacing the AND gates with OR gates and putting inverters on the demultiplexer outputs. A non-inverting input is then used on the demultiplexer to restore the original pulse logic after the inverters.

Although not essential to the operation of the interface, a method to verify entries was desired. Many microprocessor-based instruments provide an acknowledgement signal to inform the operator that an entry was valid. The SP8700 uses a beeper which is triggered by a short active-low TTL pulse. A monostable multivibrator (74121)

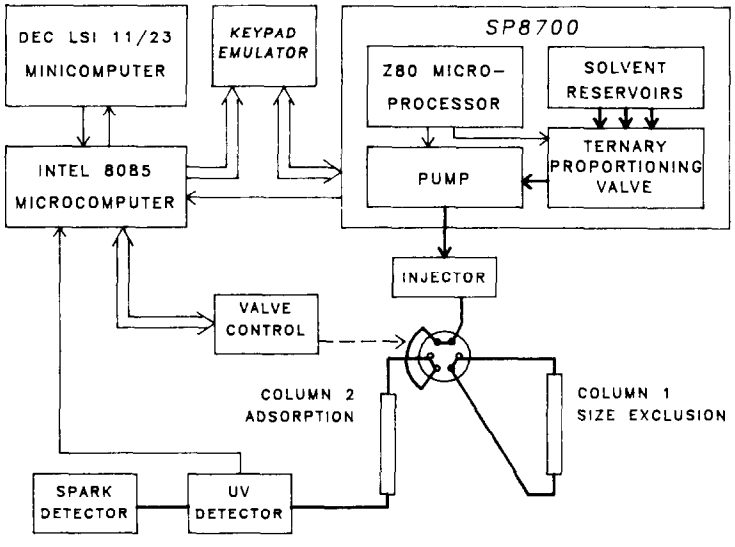

Fig. 2. Block diagram of experimental set-up.

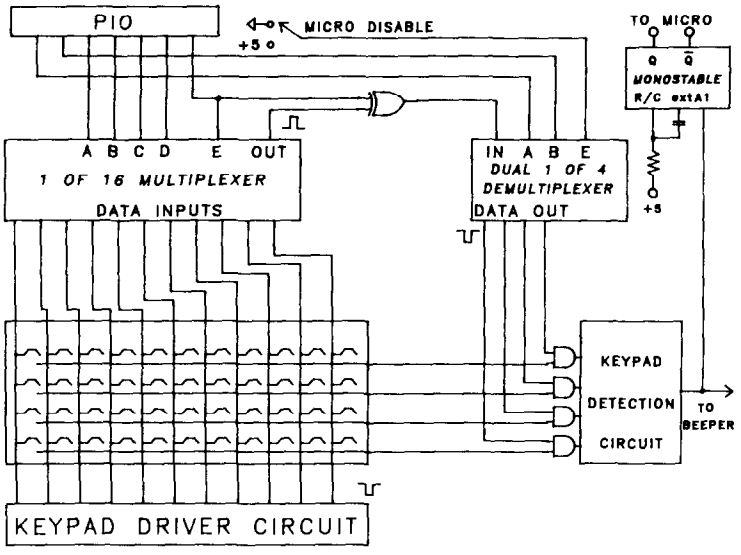

Fig. 3. Keypad array schematic including keypad emulator modification: multiplexer = 74150, demultiplexer = 74155, monostable multivibrator = 74121.

was added to convert the trigger pulse into a 13-msec active-high pulse appropriate for our laboratory microcomputer.

DISCUSSION

Figure 4 shows a simple flow-chart for operation of the keypad emulator. To simulate one keystroke, the microcomputer sends the control code for that key to the PIO port, with the control line to the multiplexer held low. For example, if the multiplexer code for the column is 0110 and the demultiplexer code for the row is 01, the binary word 0101100, or decimal 44, would be sent to the PIO port. This code is maintained at the PIO port for at least one complete array-scan cycle. If an acknowledgement is not being utilized, the emulator is disabled by sending a 1 to the port. The status of the other lines of the PIO is unimportant during the disable period. The microcomputer is then free to send the next control word, or to return to the calling routine.

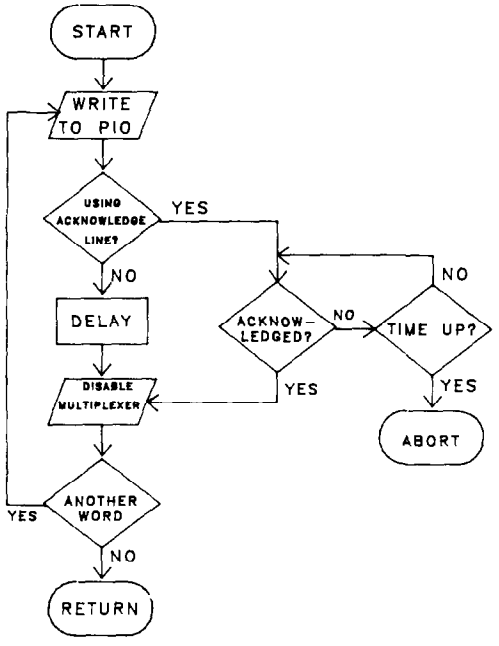

Fig. 4. Flow-chart for operation of keypad emulation system.

If an acknowledgement signal is being used, and the keystroke is not acknowledged within one scan period, the laboratory microcomputer can perform some other action. This lack of acknowledgement usually happens when invalid parameters are entered and discovered by the logic and error-checking routines of the instrument. The emulator itself has been 100% successful in simulating the proper keystroke.

CONCLUSIONS

The keypad emulation system described has been an invaluable addition to our laboratory. It has increased the capabilities of our HPLC system in three ways. (1) The system now has the ability to store a large number of experimental parameters permanently, on hard disk, floppy disk, or as hard copy; disk-stored parameters can be retrieved and re-entered at will. (2) The instrument clock and the laboratory microcomputer clock are synchronized. (3) A feedback loop can be established so that the parameters of the HPLC experiment can be altered on the basis of the chromatogram itself.

Since only simple PIO is required for operation, there are no restrictions on the choice of laboratory microcomputer or programming language. As already said, simultaneous manual operation is also possible, and no modifications are needed to convert from manual to computer operation. Some other advantages are the low cost and the need for only a few chips. By far the best feature, however, is that the

emulator operates independently of the rest of the instrument, so only a minimal knowledge of the instrument circuitry is necessary for implementation.

Acknowledgement—This work was partially supported by grant NAG3-93 from the National Aeronautics and Space Administration.

REFERENCES

1. H. V. Malmstadt, C. G. Enke and S. R. Crouch, *Electronics and Instrumentation for Scientists*, pp. 346–347. Benjamin/Cummings, Menlo Park, CA, 1981.
2. *Operations Manual* 595-2595-04 for the model H-19A video terminal, Heath Company, Benton Harbor, MI, 1981.
3. *Technical Manual* EK-VT100-TM for the model VT-100 terminal, Digital Equipment Corp., Cotton Road, Nashua, NH, 1981.
4. *MOS/LSI Databook*, pp. 10/2–10/9. National Semiconductor Corp., Santa Clara, CA, 1977.
5. B. Newcome and C. G. Enke, *Rev. Sci. Inst.*, in the press.
6. *SP8700 Solvent Delivery System Operating and Service Manual A0099-088*, Spectra-Physics, Santa Clara, CA, 1980.

Talanta, Vol. 32, No. 1, pp. 41–43, 1985
Printed in Great Britain.

0039-9140/85 $3.00 + 0.00

POSITIVE FEEDBACK COMPENSATION OF *iR*-DROP IN MODIFIED NORMAL PULSE POLAROGRAPHY OF SODIUM ION IN ACID SOLUTION

MINORU HARA
Faculty of Education, Toyama University, 3190 Gofuku Toyama-shi, Toyama 930, Japan

(*Received* 19 *March* 1984. *Accepted* 31 *July* 1984)

Summary—The well-defined polarographic wave for sodium, obtained by modified normal pulse polarography in which the polarographic current is sampled after the fall of each pulse, shifts to more negative potentials with decrease in the pH of the solution. The shift is attributed to the effect of the uncompensated resistance of the sample solution, and can be compensated by a positive feedback circuit.

It has been reported that well-defined polarograms for the five alkali metals and barium in acid solutions can be obtained by modified normal pulse polarography (MNPP),[1,2] the principle of which is represented schematically in Fig. 1. The negative-going potential pulses of duration T_2 are added to the fixed initial potential E_1 to give a pulse potential E_2 after a delay time of T_1 from the growth of a new drop from a dropping mercury electrode (DME). The pulses increase regularly in amplitude and are applied once per drop in the same manner as in normal pulse polarography. The polarographic current is integrated for 16.7 msec after a delay time of T_3 from the fall of the pulse. The average of the polarographic current over the integration period is plotted as ordinate and the pulse potential E_2 as abscissa. When E_1 is set at the potential where hydrogen ion is not reduced, as shown in Fig. 1, the anodic current measured during T_4 does not contain a hydrogen-wave component, because of its irreversibility. Therefore, even in 0.01*M* hydrochloric acid, the MNPP does not give a hydrogen wave but does give well-defined waves for the alkali metals and for barium. The half-wave potentials, however shift to more negative values with decrease in the pH of the sample solution.

Since it was presumed that the shift resulted from the uncompensated resistance between the working and reference electrodes, *iR*-drop compensation by use of a positive feedback circuit was investigated.

EXPERIMENTAL

Apparatus

A positive feedback circuit and a current-averaging circuit were added to the polarograph reported previously.[1] The block diagram of the system is shown in Fig. 2. An *iR*-drop compensation unit, Model 923 (Fuso Manufacturing), was employed as an *iR*-drop compensator. As shown in Fig. 2 (section within the broken line), the unit consists of a current follower with positive feedback and a differential amplifier similar to the one reported by Ohsaka and de Levie.[3] A 1-kΩ resistor was used as the negative feedback resistor to avoid saturation of the output of the current follower, because compensation is made impossible by saturation. The magnitude of positive feedback, α, was adjusted with a 5-kΩ potentiometer. With a fraction α of its output voltage fed back, the output voltage V_1 of the current follower is given by $V_1 = -iR_f/(1-\alpha)$, where i is the cathodic cell current and R_f is the resistance of negative feedback. The voltage of the working electrode is $V_1\alpha$ with respect to ground:

$$V_1\alpha = -iR_f\left(\frac{\alpha}{1-\alpha}\right)$$

If the quantity $R_f\{\alpha/(1-\alpha)\}$ is chosen equal to the uncompensated resistance R_u, the iR_u-drop is compensated. Since V_1 depends on the value of α, the current sensitivity also depends on the value of α. A differential amplifier, with gain of -1, is employed to make the current sensitivity independent of α, and the output voltage V_2 of the differential amplifier is given by

$$\begin{aligned} V_2 &= V_1\alpha - V_1 \\ &= -iR_f\left(\frac{\alpha}{1-\alpha} - \frac{1}{1-\alpha}\right) \\ &= iR_f. \end{aligned}$$

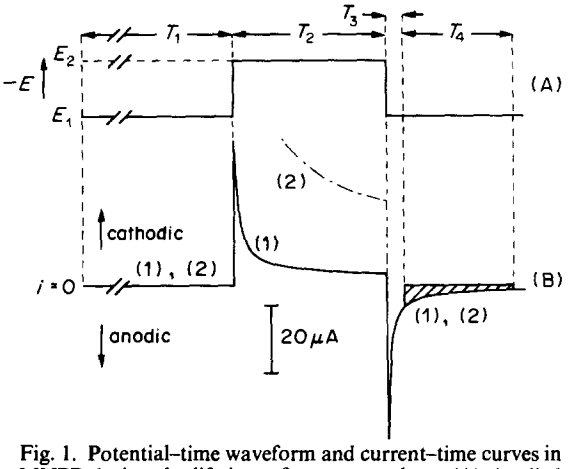

Fig. 1. Potential–time waveform and current–time curves in MNPP during the lifetime of a mercury drop. (A) Applied potential–time curve. (B) Current–time curves. $T_1 = 1.111$ sec, $T_2 = 23.2$ msec, $T_3 = 2.3$ msec, $T_4 = 16.7$ msec, $E_1 = -1.00$ V, $E_2 = -2.30$ V. (1) $4.33 \times 10^{-4}M$ NaCl, 0.1*M* Me_4NBr. (2) $4.33 \times 10^{-4}M$ NaCl, 0.001*M* HCl, 0.1*M* Me_4NBr.

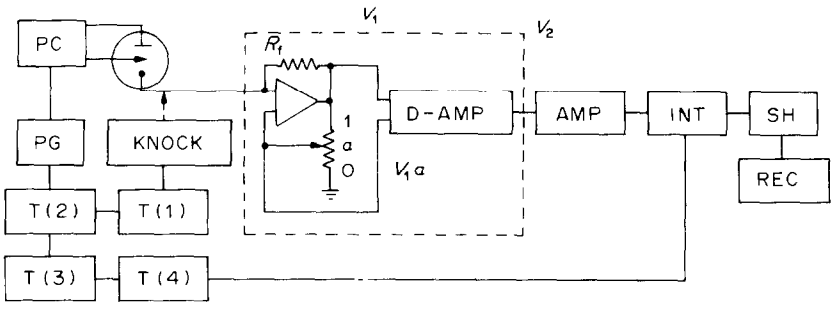

Fig. 2. Block diagram of the modified normal pulse polarograph. PC, potential controller; PG, pulse generator; KNOCK, DME knocker; D-AMP, differential amplifier; AMP, inverting voltage amplifier; INT, integrator; SH, sample-hold; REC, pen recorder. T(1), T(2), T(3) and T(4), timers which generate T_1, T_2, T_3 and 16.7 msec, respectively.

In order to record the average current, the anodic current was integrated for 16.7 msec, the period of one cycle of the a.c. mains, by an integrator circuit consisting of a MOSFET input type operational amplifier, μPC252 (Nihon Electric), and two MOSFETs, 3SK38A (Toshiba Electric). A DME containing an air-bubble[1] was used to suppress a.c. noise on the current–time curves. The mercury flow-rate was 0.422 mg/sec and the dropping period, τ, was controlled to 2.00 sec by a mechanical knocker. The remainder of the apparatus was identical with that reported previously.[1] The sample solutions were deaerated by passage of nitrogen through them for 15 min.

RESULTS AND DISCUSSION

Polarograms of $4.33 \times 10^{-4}M$ sodium in $0.01M$ hydrochloric acid/$0.1M$ tetramethylammonium bromide were measured with different values of α. Figure 3 shows two examples, for α-values of zero and 0.27. Their wave heights and slopes are equal, but the half-wave potential of curve 1 is 0.05 V more positive than that of curve 2 and is identical with that for a neutral solution. It is likely that the shift in the half-wave potential results from an iR-drop in the solution, associated with the large reduction current of the hydrogen ions.

In order to study the cause of the shift, the reduction current was measured throughout the duration of the pulse for various pulse potentials, and the results are shown in Fig. 4, in which the initial potential was −1.00 V in every case and the pulse potentials of curves 1, 2 and 3 were −2.00, −2.20 and −2.40 V respectively. In the uncompensated cases, the current plateaus appeared at the beginning of the curves. Under those conditions where a plateau appears in the reduction current–time curve, the normal pulse polarographic wave for hydrogen ion had a maximum wave. The potentiostat without iR-drop compensator can control only the potential differences between the working and the reference electrodes, and not the potential drop across the working electrode/solution interface.[4] When the cell current and/or the resistance of the solution becomes larger, the iR-drop between the working and reference electrodes cannot be neglected. The actual electrode potential deviates from the applied potential in proportion to the current.

On the other hand, the current–time curves with iR-drop compensation are simple, as can be seen in Fig. 4. Curve 4 in Fig. 4 represents three identical current–time curves for which the compensated pulse potentials are −2.00, −2.20 and −2.40 V. The log i *vs.* log t plot for curve 4 gives a straight line with slope

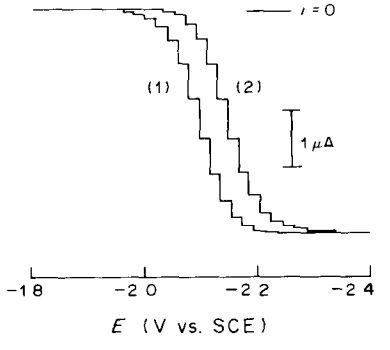

Fig. 3. Modified normal pulse polarograms for sodium. $4.33 \times 10^{-4}M$ NaCl, $0.01M$ HCl, $0.1M$ Me_4NBr. $E_1 = -1.00$ V; $T_1 = 1.111$ sec; $T_2 = 117.6$ msec; $T_3 = 2.3$ msec; α-value, (1) 0.27; (2) 0.00.

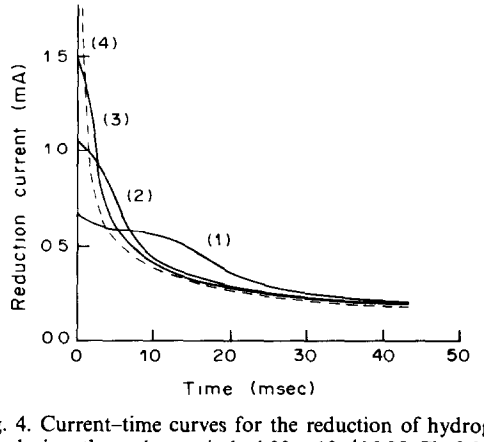

Fig. 4. Current–time curves for the reduction of hydrogen ion during the pulse period. $4.33 \times 10^{-4}M$ NaCl, $0.01M$ HCl, $0.1M$ Me_4NBr. $T_1 = 1.111$ sec; $E_1 = -1.00$ V; E_2, (1) −2.00 V (α = 0); (2) −2.20 V (α = 0); (3) −2.40 V (α = 0); (4) −2.00, −2.20, −2.40 V (α = 0.27).

Table 1. Effect of pulse duration T_2, concentrations of the supporting electrolyte and hydrochloric acid, and α-value on the half-wave potential of sodium; $4.33 \times 10^{-4}M$ NaCl, $E_1 = -1.00$ V, $T_1 = 1.111$ sec, $T_3 = 2.3$ msec

T_2 msec	Wave height at pH 5.6, μA	$E_{1/2}$, V vs. SCE					
		pH 5.6 (0.1M Me_4NBr)		pH 1.9 (0.1M Me_4NBr)		pH 1.9 (0.2M Me_4NBr)	
		α = 0.00	α = 0.30	α = 0.00	α = 0.27	α = 0.00	α = 0.18
5.8	1.21	−2.09	−2.09	−2.44	−2.14	−2.29	−2.14
11.7	1.72	−2.09	−2.09	−2.31	−2.12	−2.22	−2.12
23.2	2.26	−2.09	−2.09	−2.24	−2.11	−2.18	−2.10
57.3	3.07	−2.09	−2.09	−2.17	−2.10	−2.14	−2.10
117.6	3.71	−2.09	−2.09	−2.14	−2.09	−2.12	−2.09
240.0	4.45	−2.09	−2.09	−2.13	−2.09	−2.11	−2.09

equal to −0.53. Since this slope is approximately equal to −0.50, the theoretical slope for use of a stationary spherical electrode, it is supposed that the *iR*-drop is satisfactorily compensated in this system. If the α-value exceeded 0.27 then the potentiostat became unstable, and could not control the electrode potential because of oscillation of the amplifier. The optimum α-value in a particular cell system is selected as the maximum value which does not cause oscillation of the potentiostat.

The effects of pulse duration, concentrations of supporting electrolyte and hydrochloric acid, and α-value on the half-wave potential of sodium are summarized in Table 1. In the case of solutions at pH 5.6, the half-wave potential is constant regardless of pulse duration and α-value, but the wave height increases with pulse duration. Since the cell current decreases with time for any given potential, the difference between the applied and the actual potentials is largest at the beginning of the pulse, then decreases gradually with time. Therefore, the shorter the pulse duration T_2, the more significant is the effect of the *iR*-drop. In the solution at pH 1.9, the half-wave potential shifts to more negative values with decrease of pulse duration, even when α is 0.27. These shifts result from insufficient compensation. When the concentration of the supporting electrolyte is doubled, the shift in the uncompensated half-wave potential is less, since the increase of conductivity decreases the *iR*-drop, and adequate compensation can be achieved with a smaller α-value.

We conclude that the shift in the half-wave potential for sodium in acid solution is due to the *iR*-drop between the working electrode and the reference electrode. The *iR*-drop can be compensated satisfactorily by a positive feedback circuit.

REFERENCES

1. M. Hara and N. Nomura, *Bunseki Kagaku*, 1983, **32**, E185.
2. *Idem*, *Talanta*, 1984, **31**, 105.
3. T. Ohsaka and R. de Levie, *J. Electroanal. Chem.*, 1979, **99**, 255.
4. D. D. Macdonald, *Transient Techniques in Electrochemistry*, p. 30. Plenum Press, New York, 1977.

Talanta, Vol. 32, No. 1, pp. 44–46, 1985
Printed in Great Britain.

0039-9140/85 $3.00 + 0.00

REVERSED-PHASE PARTITION HIGH-PRESSURE LIQUID CHROMATOGRAPHY OF TRACE AMOUNTS OF INORGANIC AND ORGANIC MERCURY WITH SILVER DIETHYLDITHIOCARBAMATE

SADANOBU INOUE*, SUWARU HOSHI and MUTSUYA MATHUBARA
Department of Environmental Engineering, Kitami Institute of Technology, Kitami-shi, 090, Japan

(*Received* 24 *March* 1984. *Accepted* 27 *July* 1984)

Summary—Inorganic and organic mercury diethyldithiocarbamates have been separated by reversed-phase partition high-pressure liquid chromatography. The mercury chelates were formed by an exchange reaction with silver diethyldithiocarbamate in chloroform, in the presence of acetate buffer (pH 5.0). The inorganic and organic mercury chelates in the extract were separated within 30 min on a 3.9 × 300 mm μ-Bondapak C_{18} column. EDTA ($10^{-4}M$) in methanol–water mixture (78:22 v/v) was used as eluent at a flow-rate of 0.5 ml/min.

Recently, considerable attention has been paid to rapid and sensitive determination of trace amounts of inorganic and organic mercury in the environment. Trace amounts of inorganic mercury have been determined by flameless atomic-absorption spectrophotometry, and of organic mercury by gas chromatography. In the past ten years a few reports on the application of high-pressure liquid chromatography (HPLC) to determination of organic mercury have appeared.[1-3] MacCrehan *et al.* reported the use of liquid chromatography with differential pulse electrochemical detection,[1] and the separation of organic mercury compounds by reversed-phase chromatography of their 2-mercaptoethanol complexes.[2] Funasaka *et al.*[3] reported the high-speed liquid chromatographic separation of organic mercury compounds. In a previous paper,[4] the determination of inorganic and organic mercury by HPLC after extraction of diethyldithiocarbamate (DDTC) chelates was described, but many metal ions were extractable as their DDTC chelates and copper(II), nickel(II) and cobalt(II) interfered in the HPLC determination.

In the present paper, separations and simultaneous micro determinations of inorganic and organic mercury–DDTC chelates extracted by the following exchange reactions with silver–DDTC in chloroform from aqueous media by HPLC are described:

$$Hg^{2+} + 2Ag(DDTC) \rightarrow Hg(DDTC)_2 + 2Ag^+$$
$$RHg^+ + Ag(DDTC) \rightarrow RHg(DDTC) + Ag^+$$

where R = $-CH_3$, $-C_2H_5$ and $-C_6H_5$.

EXPERIMENTAL

Reagents

All chemicals used were of analytical-reagent grade.

Standard mercury(II) solution. Dissolve mercuric chloride in 0.01*M* hydrochloric acid to give a $3.75 \times 10^{-2}M$ stock solution, and standardize it by titration with EDTA.

Standard methylmercury solution. Dissolve methylmercuric chloride (purified by recrystallization from methanol) in distilled water to give a $3.75 \times 10^{-4}M$ stock solution.

Standard ethylmercury solution. Dissolve ethylmercuric chloride (purified by recrystallization from ethanol) in a small quantity of ethanol, and dilute with distilled water to give a $3.75 \times 10^{-4}M$ stock solution.

Standard phenylmercury solution. Dissolve phenylmercuric chloride in 0.1*M* sodium hydroxide to give a $3.75 \times 10^{-4}M$ stock solution. Dilute these stock solutions accurately before use.

Silver diethyldithiocarbamate solution. Dissolve silver diethyldithiocarbamate in chloroform to give a $7.5 \times 10^{-4}M$ solution.

Acetate buffer solution. Mix 0.1*M* acetic acid and 0.1*M* sodium acetate to obtain a buffer of pH 5.0.

Apparatus

A Hitachi model 635A HPLC instrument with a wavelength-tunable effluent-monitor set at 254 nm was used. A μ-Bondapak C_{18} column (3.9 × 300 mm, Waters Associates) was used. Inorganic and organic mercury compounds were extracted in 50-ml cylindrical glass vials fitted with polyethylene stoppers and plastic caps.

Procedure

Pipette aliquots of sample solutions containing up to 60, 65, 69 and 83 μg for inorganic mercury(II), methylmercury, ethylmercury and phenylmercury, respectively, into 25-ml standard flasks. Add 2.5 ml of acetate buffer (pH 5.0), dilute to 25 ml with distilled water and transfer to cylindrical glass vials. Shake with 10.0 ml of silver–DDTC solution in chloroform for 3 min. Separate the phases by centrifugation (1000 rpm, 10 min). Inject 25 μl of the chloroform layer by microsyringe into the HPLC column. Use $10^{-4}M$ EDTA in methanol–water mixture (78:22 v/v) as eluent, at a flow-rate of 0.5 ml/min.

RESULTS AND DISCUSSION

Extraction of inorganic and organic mercury with silver–DDTC

The effect of pH on the extraction was investigated

*To whom correspondence should be addressed.

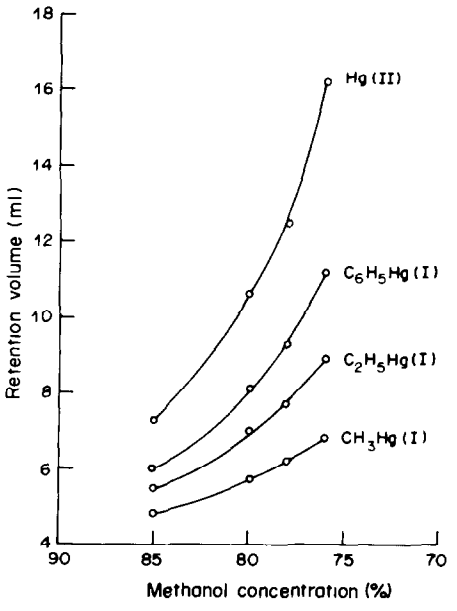

Fig. 1. Variation of retention volume with methanol concentration in the eluent. Column μ-Bondapak C_{18}; flow-rate 0.5 ml/min; wavelength 254 nm; injection volume 25 μl.

and the pH ranges for extraction were found to be from 5.1 to −0.3 for inorganic mercury(II), 5.2–0 for methylmercury, 5.2–2 for ethylmercury and 5.5–2.4 for phenylmercury. Lowering the silver–DDTC concentration to $3.0 \times 10^{-4} M$ had no effect. A pH of 5.0 (acetate buffer) was selected for the simultaneous extraction of inorganic and organic mercury. The DDTC chelates are $Hg(DDTC)_2$,[5] $RHg(DDTC)$[6] and Ag(DDTC),[5] and the wavelengths of the maximum absorbance in chloroform are 275 nm for the inorganic mercury(II) complex, 254 nm and 297 nm for the organomercurials and 273 nm for silver(I). Inorganic and organic mercury chelates in the eluent were detected at 254 nm.

Separation of inorganic and organic mercury–DDTC

Inorganic and organic mercury–DDTC chelates can be separated by HPLC, on a μ-Bondapak C_{18} column. The effect of methanol content and flow-rate of the eluent on the separation of the chelates was studied. The retention volumes of the chelates were found to increase with increasing concentration of water in the eluent but although good separations were achieved (Fig. 1), the peaks were broad. The most suitable eluent for the separation of the chelates was a 78:22 v/v methanol–water mixture. To avoid contamination with metal ions through contact between the eluent and the metal parts of the HPLC apparatus, $10^{-4} M$ EDTA was added to the eluent.[7] A flow-rate of 0.5 ml/min was most suitable for the separation. A typical separation is shown in Fig. 2. All four peaks are well resolved. The retention volumes are 6.2 ml for methylmercury, 7.7 ml for ethylmercury, 9.3 ml for phenylmercury and 12.5 ml for inorganic mercury(II). The elution order is the same as that observed by McCrehan *et al.*[2] for 2-mercaptoethanol chelates. The degree of interaction of the stationary phase with these chelates probably increases in the order

$$Hg(II) > C_6H_5Hg > C_2H_5Hg > CH_3Hg.$$

Calibration graph

The amounts of inorganic and organic mercury could be determined from the peak areas under the recorded elution curve (full-scale deflection = 0.04 absorbance). Calibration graphs were linear in the ranges 0–6.02 μg for inorganic mercury(II), 0–6.47 μg for methylmercury, 0–6.89 μg for ethylmercury and 0–8.33 μg for phenylmercury, per ml of chloroform solution. The detection limits were 8.8 ng for inorganic mercury(II), 9.5 ng for methylmercury, 13.8 ng for ethylmercury and 10.8 ng for phenylmercury. The coefficients of variation were 3.2% for inorganic mercury(II), 2.8% for methylmercury, 1.6% for ethylmercury and 3.6% for phenyl mercury for 10 measurements with 3.01 μg of inorganic mercury(II), 3.23 μg of methylmercury, 3.44 μg of ethylmercury and 4.16 μg of phenylmercury per ml of chloroform solution.

Interferences

The interference of several metal ions was studied. Mn(II), As(III), Sn(II), Ni(II), Cr(III), Fe(II), Fe(III),

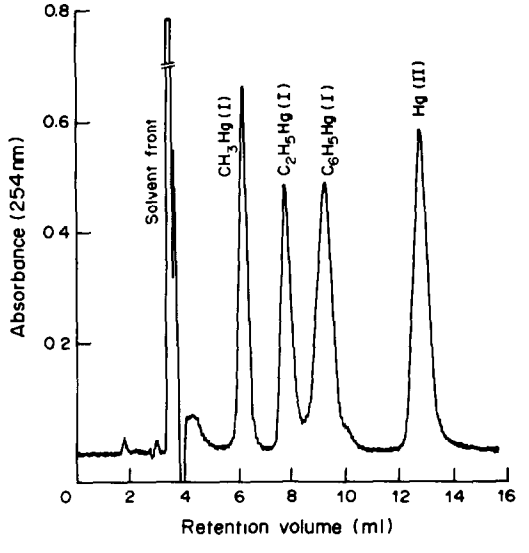

Fig. 2. Chromatogram of CH_3Hg, C_2H_5Hg, D_6H_5Hg and Hg(II) chelates of DDTC. Chelate concentration in chloroform (μg/ml): CH_3Hg 6.47, C_2H_5Hg 6.89, C_6H_5Hg 8.33, Hg(II) 6.02, Column μ-Bondapak C_{18} (3.9 mm × 300 mm); eluent methanol–water (78:22 v/v) containing $10^{-4} M$ EDTA; flow-rate 0.5 ml/min; injection volume 25 μl.

Co(II), Cd(II) and Zn(II) (1000 μg), Bi(III) (100 μg) and Pb(II) (20 μg) were not extracted under the experimental conditions described above. However, Pb(II) (100 μg) and Cu(II) (10 μg) were partially extracted, although the DDTC chelates of Cu(II), Pb(II) and Ag(I) were not eluted in the range of retention volumes of the mercury–DDTC chelates under the chromatographic conditions specified. From these results, this method is found to be free from interference from other metal ions and can be used for the simultaneous determination of trace amounts of inorganic and organic mercury.

REFERENCES

1. W. A. MacCrehan and R. A. Durst, *Anal. Chem.*, 1978, **50**, 2108.
2. W. A. MacCrehan, R. A. Durst and J. M. Bellama, *Anal. Lett.*, 1977, **10**, 1175.
3. W. Funasaka, T. Hanai and K. Fujimura, *J. Chromatogr. Sci.*, 1974, **12**, 517.
4. S. Inoue, S. Hoshi and M. Sasaki, *Bunseki Kagaku*, 1982, **31**, E243.
5. M. Yamazaki, M. Teranishi, R. Igarashi and J. Niwa, *Nippon Kagaku Kaishi*, 1980, No. 11, 1723.
6. H. Takehara, T. Takeshita and I. Hara, *Bunseki Kagaku*, 1966, **15**, 332.
7. H. Hoshino and T. Yotsuyanagi, *ibid.*, 1980, **29**, 807.

Talanta, Vol. 32, No. 1, pp. 47–48, 1985
Printed in Great Britain.

0039-9140/85 $3.00 + 0.00

THIN-LAYER CHROMATOGRAPHY OF THE MBTH DERIVATIVES OF SOME ALIPHATIC ALDEHYDES

V. CARUNCHIO, G. DE ANGELIS, A. M. GIRELLI and A. MESSINA
Department of Chemistry, University of Rome, 00185 Rome, Italy

(*Received* 12 *March* 1984. *Accepted* 18 *July* 1984)

Summary—A rapid, simple method for resolution and detection of mixtures of aliphatic aldehyde by thin-layer chromatography of their MBTH derivatives is proposed. Less than 1 mg/l. levels of each aldehyde in the original aqueous solution can be detected.

Techniques used for the separation and/or determination of various aldehydes (as such or as their derivatives) include thin-layer chromatography,[1–6] gas chromatography,[7–13] high-pressure liquid chromatography[14–21] and chemical-ionization mass spectrometry.[22] The aldehydes are usually separated and determined as the 2,4-dinitrophenylhydrazone (DNPH) derivatives, together with ketones, but the 3-methyl-2-benzothiazolinone hydrazone (MBTH) derivatives (which do not suffer from interference by ketones) have been proposed for thin-layer chromatography of aliphatic aldehydes on silica gel plates,[1,6] and for their spectrophotometric determination for routine environmental analysis.[23–27] However, the MBTH spectrophotometric method expresses the total aldehyde content empirically in terms of formaldehyde, because the products have almost identical wavelength of maximum absorption, but different molar absorptivities and rates of formation (Table 1).

We have therefore developed a thin-layer chromatographic method for separation of the MBTH derivatives formed in the presence of an oxidizing agent, with subsequent spectrophotometric determination.

EXPERIMENTAL

Reagents

All reagents were analytical grade. The aldehydes were Merck products.

3-Methyl-2-benzothiazolinone hydrazone hydrochloride (MBTH) solution, 0.050%. Stored at 5° (stable for one week), and filtered before use; the solution must not be coloured.

Oxidizing solution. An aqueous solution containing 1.0% $FeCl_3 \cdot 6H_2O$ and 1.6% sulphamic acid; it is stable for one month.

Procedure

Aldehyde–MBTH derivatives were prepared by addition of 10 ml of MBTH solution to 5 ml of aqueous aldehyde sample: 60 min later, 5 ml of oxidizing solution and 5 ml of water were added. After another 30 min 7.3 g of solid sodium chloride were added and the solution was shaken with 25 ml of chloroform in three portions (10, 10, 5 ml) and the combined extract was evaporated to 1 ml under reduced pressure at room temperature.

Silica gel TLC or HPTLC plates (Merck 60 F_{254}) were employed; 0.50-μl of the portions of the concentrated extracts were applied as streaks 1 cm apart, and 1 cm from the lower edge of the plate. Before the elution the chromatographic tank was equilibrated for 30 min with the eluent (benzene-ethanol 7:6 v/v) at room temperature. Ascending elution was run over a distance of about 3 cm.

After the chromatographic separation, accomplished in about 15 min, the spots were located by means of their

Table 1. Spectrophotometric characteristics of some aldehyde–MBTH derivatives in aqueous solution before addition of sodium chloride and extraction

Aldehyde	Colour	t,* *min*	λ_{max}, *nm*	ε, $10^4\ l \cdot mole^{-1} \cdot cm^{-1}$
Formaldehyde	blue	15	628	4.8_5
Acetaldehyde	blue	30	635	2.8_2
Propionaldehyde	blue	30	625	4.5_6
n-Butyraldehyde	blue	15	628	2.2_3
n-Valeraldehyde	blue	30	625	6.3_3
Acrolein	blue	30	625	4.1_4
Crotonaldehyde	blue	45	628	3.5_4
Glyoxal	yellow	30	625†	0.5_0

*Time needed to reach constant absorbance at room temperature after addition of oxidant.
†There is also a maximum at 450 nm.

Table 2. R_f values of oxidized aldehyde-MBTH derivatives

Aldehyde	R_f TLC	R_f HPTLC
Formaldehyde	0.19	0.37
Acetaldehyde	0.21	0.45
Propionaldehyde	0.28	0.53
n-Butyraldehyde	0.32	0.59
n-Valeraldehyde	0.37	0.65

colour or, better, by scanning at 628 nm with a densitometer.

RESULTS

Table 2 gives the R_f values for the TLC and HPTLC separation of the derivatives of some aliphatic aldehydes. Figure 1 shows the HPTLC chromatogram measured by densitometry.

The extraction with chloroform eliminates the background colour of iron from the chromatogram (since the iron is not extracted) and increases the sensitivity, as seen in Fig. 1, which refers to a concentration of 1 mg/l. of each aldehyde in the original aqueous sample (5 ml) and hence to about 2.5 ng of each aldehyde on the TLC plate.

This very small amount and the small volume (0.5 μl) of the organic solution spotted on the plate allow, especially in the HPTLC method, a very good separation, not previously achieved. The detection limit in the aqueous sample can be altered by changing the volumes of the sample taken and of the final organic solution. The resolution can be modified by changing the benzene/ethanol ratio. Complete separation has been achieved by a run of 3 cm, in 15 min: a longer elution does not increase the resolution. The proposed method is therefore more advantageous than the one based on chromatographic separation of the azine derivatives followed by spraying with the oxidizing-MBTH solution to form the coloured compounds, and those which involve precipitation of the derivatives (*e.g.*, the DNPH derivatives). The recovery of the aldehydes is complete: the aqueous solution does not absorb at 628 nm after the extraction. Hence the proposed chromatographic method, initially intended for the identification of the aldehydes present in order to improve the quantitative spectrophotometric analysis, could also be suitable for quantitative denitometic HPTLC determination provided proper standardizations are performed.

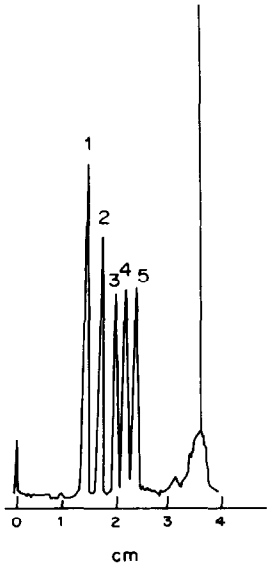

Fig. 1. Chromatogram of C_1—C_5 aliphatic aldehyde–MBTH derivatives on silica gel HPTLC plates: (1) formaldehyde, (2) acetaldehyde, (3) propionaldehyde, (4) n-butyraldehyde, (5) n-valeraldehyde. Eluent benzene–ethanol 7:6 v/v; λ = 628 nm; scan-rate 10 mm/min; chart-speed 10 mm/min. The initial weight of each aldehyde was 2.5 ng (see results).

Acknowledgement—This research was achieved with the financial support of the Project "Promozione della qualità dell'Ambiente" sponsored by Consiglio Nazionale delle Ricerche.

REFERENCES

1. F. C. Hunt, *J. Chromatog.*, 1968, **35,** 111.
2. Y. Suzuki, Y. Yamazaki and T. Takeuchi, *Bunseki Kagaku*, 1971, **20,** 1159; *Chem. Abstr.*, 1971, **75,** 147548s.
3. Y. Yamazaki, Y. Suzuki and T. Takeuchi, *ibid.*, 1972, **21,** 1223; *Chem. Abstr.*, 1973, **78,** 11275e.
4. J. C. Young, *J. Chromatog.*, 1977, **130,** 17.
5. N. M. Roscher and J. H. Onley, *ibid.*, 1977, **140,** 109.
6. G. De Angelis, A. M. Girelli and A. Messina, *IRSA, Metodi Analitici per le Acque (Notiziario)*, 1982, **2,** 49.
7. H. Kallio, R. R. Linko and J. Kaitaranta, *J. Chromatog.*, 1972, **65,** 355.
8. L. J. Papa and L. P. Turner, *J. Chromatog. Sci.*, 1972, **10,** 744.
9. A. Di Corcia, A. Liberti and R. Samperi, *Anal. Chem.*, 1973, **45,** 1228.
10. Y. Hoshika and Y. Takata, *J. Chromatog.*, 1976, **120,** 379.
11. Y. Hoshika and G. Muto, *ibid.*, 1978, **152,** 533.
12. A. Di Corcia, R. Samperi and C. Severini, *ibid.*, 1980, **198,** 347.
13. R. D. Cox and R. F. Earp, *Anal. Chem.*, 1982, **54,** 2265.
14. M. A. Carey and A. E. Persinger, *J. Chromatog. Sci.*, 1972, **10,** 537.
15. L. J. Papa and L. P. Turner, *ibid.*, 1972, **10,** 747.
16. S. Selim, *J. Chromatog.*, 1977, **136,** 271.
17. P. R. Demko, *ibid.*, 1979, **179,** 361.
18. K. Kuwata, M. Uebori and Y. Yamasaki, *J. Chromatog. Sci.*, 1979, **17,** 264.
19. K. Fung and D. Grosjean, *Anal. Chem.*, 1981, **53,** 168.
20. D. Grosjean, *Environ. Sci. Technol.*, 1982, **16,** 254.
21. K. Kuwata, M. Uebori, H. Yamasaki, Y. Kuge and Y. Kiso, *Anal. Chem.*, 1983, **55,** 2013.
22. T. Keough, *ibid.*, 1982, **54,** 2540.
23. E. Sawicki, T. R. Hauser, T. W. Stanley and W. Elbert, *ibid.*, 1961, **33,** 93.
24. E. Sawicki, T. R. Hauser and S. McPherson, *ibid.*, 1962, **34,** 1460.
25. T. R. Hauser and R. L. Cummins, *ibid.*, 1964, **36,** 679.
26. Istituto di Ricerca sulle Acque, *Metodi Analitici per le Acque: Aldeidi Alifatiche, Quad. Ist. Ric. Acque*, 11, Scheda E.015, 1978.
27. G. J. Nebel, *Anal. Chem.*, 1981, **53,** 1708.

Talanta, Vol. 32, No. 1, pp. 49–50, 1985
Printed in Great Britain.

0039-9140/85 $3.00 + 0.00

DETERMINATION OF IRON AND CYANIDE IN CYANOFERRATE COMPLEXES

NICOLETTA BURGER
Department of Chemistry and Biochemistry, Faculty of Medicine, University of Zagreb, 41000 Zagreb, Šalata 3, Yugoslavia

(*Received* 16 *May* 1984. *Accepted* 17 *July* 1984)

Summary—A simple method of destroying cyano-complexes and of analysing for both iron and cyanide in a single sample of a cyanoferrate complex is proposed.

It is well known that it is not possible to detect iron and cyanide in freshly prepared aqueous solutions of potassium hexacyanoferrate(II) at room temperature, because of stabilization of the complex anion by π-donor back-bonding between the metal ion and the ligands. Substitution of one or more of the cyanide ions by other ligands will result in changes in bonding and reactivity, but determination of iron and cyanide is still not possible without cleavage of the Fe–CN bonds.

Cleavage can be achieved by refluxing the complex with *aqua regia* or by Kjehldahl decomposition, and the iron determined by any convenient method, but the cyanide is destroyed and cannot be determined. Treatment with perchloric acid is often suggested, but for the iron determination the cyanide must be expelled as hydrocyanic acid by heating to fuming.[1] Ignition of the complex and determination of the iron as Fe_2O_3 is simple and useful, but again only if the cyanide is not to be determined. Distillation from phosphoric acid medium at reduced pressure gives low recovery of the cyanide, and so does a tartaric acid distillation method.[2] Refluxing with dilute sulphuric acid, in the presence of magnesium and mercuric chlorides, with passage of a current of air to transfer hydrogen cyanide into an absorption tube, seems to be satisfactory when applied to silver, zinc and nickel complex cyanides but not if applied to analysis of more stable cyano-complexes such as those of cobalt and iron.[2] Fusing finely ground complex cyano-compounds with sulphur at 300° permits determination of the cyanides but not of iron,[3] and decomposition of cyanoferrates with concentrated nitric acid produces ammonium salts, which can be determined by the Kjehldahl and Parnas methods.[4]

The methods of organic elemental analysis usually yield low results for the carbon and nitrogen contents (probably owing to the formation of stable carbides and nitrides with the central metal ion of the complex). However, during our investigations on oximatocyanoferrate(II) complexes,[5–7] we have found a simple possibility for cleaving cyanoferrates and determining both iron and cyanide in a single sample.

EXPERIMENTAL

Reagents

All reagents used were of analytical-reagent grade. Redistilled water was used throughout. The 0.4*M* acetate buffer, pH 3.5, was prepared by mixing 12.8 ml of 2*M* sodium acetate with 187.2 ml of 2*M* acetic acid and diluting with water to 1000 ml. A 0.0125*M* phenanthroline solution was prepared by dissolving 0.5406 g of 1,10-phenanthroline in 250 ml of 0.4*M* acetate buffer of pH 3.5. The 1% ascorbic acid solution used was always freshly prepared. A solution containing 100 μg of Hg^{2+} per ml was prepared by dissolving 0.0136 g of mercury(II) chloride in 100 ml of water.

$Na_2[Fe(CN)_5NO]\cdot 2H_2O$ (Kemika), $Na_3[Fe(CN)_5NH_3]\cdot 3H_2O$ (Touzart-Matignon), $K_3[Fe(CN)_6]$ and $K_4[Fe(CN)_6]\cdot 3H_2O$ (Merck) were obtained commercially.

Cleavage and analysis

Weigh 5–10 mg of sample into a three-necked round-bottomed flask and add 25 ml of a mixture of 10 ml of 0.0125*M* phenanthroline, 7 ml of acetate buffer, 7 ml of 1% ascorbic acid solution and 1 ml of mercury(II) chloride solution. Boil the mixture for 15–20 min under a nitrogen atmosphere. Use two Drechsel bottles, the first containing 100 ml of 2% sodium hydroxide and the second 100 ml of water, to collect the hydrogen cyanide produced. Mix the contents of the two bottles and titrate with 0.01*M* silver nitrate with potassium iodide as indicator. Transfer the contents of the reaction flask quantitatively into a 100-ml standard flask, dilute to volume and measure the absorbance of the ferroin at 510 nm against a reagent blank.

RESULTS AND DISCUSSION

The proposed method is based on earlier knowledge of the conditions under which potassium hexacyanoferrate(II) is totally decomposed into Fe^{2+} and CN^-,[8] namely an acidic medium, elevated temperature, and the presence of small amounts of Au^{3+}, Ag^+, Pt^{4+}, Pd^{2+}, Hg_2^{2+} or especially Hg^{2+}. Because the decomposition depends on successive displacement of cyanide ions to yield pentacyanoferrate(II), tetracyanoferrate(II) and so on, the same conditions can be applied for the cleavage of substituted cyanoferrate complexes. Ascorbic acid is added as

Table 1. Determination of iron and cyanides in cyanoferrate complexes

Complexes	Fe, %		CN^-, %		Mean recovery, %		No. of detns.
	Calc.	Found	Calc.	Found	Fe	CN^-	
$Na_2[Fe(CN)_5NO]\cdot 2H_2O$	18.75	19.1	43.67	43.3	101.9	99.2	13
$Na_3[Fe(CN)_5NH_3]\cdot 3H_2O$	17.14	17.3	39.92	39.6	100.9	99.2	5
$K_4[Fe(CN)_6]\cdot 3H_2O$	13.22	14.0*	36.96	38.5	105.9	104.2	5
$K_3[Fe(CN)_6]$	14.57	14.9	40.73	40.4	102.3	99.2	3

*Values of 13.8 and 14.2% had been obtained earlier by complexometry.

reductant to ensure that Fe^{2+} is the only oxidation state of iron present and to prevent already liberated iron(II) from bonding with the undestroyed hexacyanoferrate to form Prussian Blue. It also makes the method applicable to analysis of cyanoferrate(III) complexes. The colorimetric reagent is already present in the reaction mixture and immediately binds the liberated iron, the buffer ensures the correct acidity for both the displacement reaction and the ferroin formation (pH 3.5), and the Hg^{2+} acts as a catalyst. Results of analyses of some commercial samples of cyano-complexes are present in Table 1, and have good reproducibility. The potassium hexacyanoferrate(II) trihydrate was an old sample, and appears to have lost some of the water of crystallization. Sparingly soluble compounds cannot be analysed in this way, however.

Acknowledgement—The author is grateful to Professors V. Karas-Gašparec and Z. Gašparec for many counsels and instructions.

REFERENCES

1. R. Bastian, R. Weberling and F. Palilla, *Anal. Chem.*, 1956, **28,** 459.
2. F. J. Ludzack, W. A. Moore and C. C. Ruchhoft, *ibid.*, 1954, **26,** 1784.
3. S. K. Tobia, Y. A. Gawargious and M. F. El-Shahat, *Analyst*, 1974, **99,** 544.
4. E. Wasielewska and Z. Stasicka, *Bull. Acad. Pol. Sci., Ser. Sci. Chim.*, 1980, **28,** 149.
5. N. Burger and V. Karas-Gašparec, *Talanta*, 1977, **24,** 704.
6. *Idem, ibid.*, 1981, **28,** 323.
7. *Idem, ibid.*, 1984, **31,** 169.
8. V. Karas-Gašparec and T. Pinter, *Z. Phys. Chem. (Leipzig)*, 1962, **220,** 327.

Talanta, Vol. 32, No. 1, pp. 51–53, 1985
Printed in Great Britain.

0039-9140/85 $3.00 + 0.00

A NOVEL AND SENSITIVE SPOT-TEST FOR *m*-DINITROAROMATICS AND THEIR DERIVATIVES WITH SODIUM SULPHITE AND DIMETHYLSULPHOXIDE

SAEEDUZZAFAR QURESHI, PUSHKIN M. QURESHI* and SEEMA HAQUE
Department of Chemistry, Aligarh Muslim University, Aligarh 202001, India

(*Received* 27 *April* 1984. *Accepted* 17 *July* 1984)

Summary—Sodium sulphite has been used for a very sensitive characterization of *m*-dinitroaromatics and their derivatives, with dimethylsulphoxide as solvent.

The interaction of bases with polynitroaromatics is a fascinating field.[1–5] For quite some time we have been exploring the analytical potential of such reactions.[6–8] A significant and possible use of these reactions is for detection and determination of 2,4-dinitrophenyl (DNP) derivatives of amino-acids. Virtually all published tests for *m*-dinitroaromatics can, after suitable modification, be used for the determination of DNP derivatives.

However, because of the variation in the colours given by different *m*-dinitroaromatics, the tests cannot be used as general tests for the group identification of *m*-dinitroaromatics and the corresponding DNP derivatives. For example, we have re-investigated the reaction of sodium hydroxide with *m*-dinitroaromatics and their derivatives[8] and found that by a novel "alkali pellet spot-test", they can be detected at the nanogram level, and though the test is highly sensitive and useful for these compounds it is unlikely to be useful for DNP derivatives, because the colour produced depends on the substituents in the 1-position and hence the test is unlikely to be very characteristic of the 2,4-DNP group. It is therefore difficult to predict the effect of the substituent at the 1-position on the colour produced in this and related methods.

Though the reaction with sodium sulphite has been studied for a few polynitroaromatics, there has been no detailed investigation and as far as we are aware these reactions have not been used in organic analytical chemistry. An alternative test with sodium cyanide[8] is unattractive because of the poisonous nature of the reagent, and here again the colour produced is dependent on the substituent at the 1-position.

The analytical potential of sulphite has therefore been investigated. The test is more sensitive than all others except our recent method[8] but has the distinct advantage of appearing to be specific for the 2,4-DNP moiety and therefore usable as a characteristic and specific test for the detection of 2,4-DNP derivatives of amino-acids.

EXPERIMENTAL

Materials

Most nitroaromatics tested were Merck guaranteed reagents and used as received. Some were BDH laboratory-reagents grade and were recrystallized by standard procedures until the melting points were in agreement with literature values. The dimethylsulphoxide (DMSO) was a Baker "Analyzed" reagent. Merck acetone, BDH Analar dimethylformamide (DMF) and BDH sodium sulphite were used.

Procedures

(*a*) Transfer 1 μl of the test substance onto a white spot-plate, followed by 1 μl of a saturated sodium sulphite solution in conductivity water. Note the colour. Repeat with the addition of 1 μl of DMSO, acetone or DMF respectively. The colour of the product is deep or light violet in each case.

(*b*) Place a few resin beads (Amberlite IRA 400, Cl^- form) in the depression of a white spot-plate. Add 1 μl of the test substance, followed by the other reagents as described in method (*a*).

RESULTS

A number of other types of organic compounds were found not to interfere with the test. They included carbohydrates (xylose, starch, galactose, maltose, fructose, L(+)-arabinose, lactose, glucose, rhamnose, sucrose), acids (acetic, formic, tartaric, phthalic, pyrogallic, oxalic), alcohols (isopropyl, ethyl, methyl, 2-methylisopropyl, amyl, isoamyl), heterocyclic bases (pyridine, piperidine), aldehydes (formaldehyde, acetaldehyde, benzaldehyde, paraldehyde, *p*-chlorobenzaldehyde), ketones (acetophenone, cyclopentanone, cyclohexanone, propiophenone, benzophenone), hydrocarbons and their derivatives (benzene, xylene, *o*-dichlorobenzene, bromobenzene, toluene), ethers (diethyl anisole,

*Address for correspondence: Pushkin M. Qureshi, A-3 Professors' Bungalow, Medical College Enclave, A.M.U., Aligarh-202001 (U.P) India.

Table 1. Limits of detection, $\mu g/\mu l$

Compound	Solvent			Colour	Sensitivity relative to other tests
	Acetone	DMF	DMSO		
1-Chloro-2,4-dinitrobenzene	—(C) 0.2 (R)	0.8 (C) 0.2 (R)	0.6 (C) 0.1 (R)	(V)	200 (T) 10 (VD)
1-Fluoro-2,4-dinitrobenzene	—(C) 0.2 (R)	3 (C) 0.1 (R)	1.5 (C) 0.1 (R)	(V)	
2,4-Dinitroaniline	—(C) 4 (R)	—(C) 0.4 (R)	—(C) 0.2 (R)	(V)	
3,5-Dinitrobenzoic acid	—(C) —(R)	—(C) 0.8 (R)	—(C) 0.4 (R)	(OR)	12.5 (T) 2.5 (VD)
2,4-Dinitrotoluene	—(C) —(R)	—(C) 0.8 (R)	—(C) 0.4 (R)	(V)	5 (VD)
2,4-Dinitrophenylhydrazine	—(C) 4 (R)	—(C) 2 (R)	—(C) 1.6 (R)	(V)	
m-Dinitrobenzene	—(C) 1 (R)	0.8 (C) 0.1 (R)	0.4 (C) 0.1 (R)	(V)	12.5 (T) 12.5 (VD)
1:3:5-Trinitrobenzene	0.3 (C) 0.2 (R)	0.2 (C) 0.1 (R)	0.1 (C) 0.1 (R)	(RV)	12.5 (T) 12.5 (VD)
2,5,7-Trinitrofluorenone	0.1 (C) 0.1 (R)			(PV)	

Abbreviations—(C) Conventional spot-test; (R) Resin spot-test; (T) Tiwari *et al.*;[10] (VD) Verma and Dubey;[11] (V) violet; (OR) orange; (BV) blue violet; (PV) pink violet.

1,4-dioxan), amino-acids (DL-tryptophan, L-lysine, DL-phenylalamine, L-histidine), anilides (acetanilide, benzanilide), nitriles (aceto-, benzo-), amides (acetamide, benzamide), amines (trimethyl, triethyl, methyl, diethyl, aniline, diphenyl), phenols (phenol, *m*-cresol, resorcinol), chloroform, carbon tetrachloride, urea and thiourea.

The limit of detection for a number of nitrocompounds was determined and the results are summarized in Table 1.

DISCUSSION

Table 1 shows the resin spot-test to be much more sensitive than the conventional spot-test and DMSO seems to be the solvent of choice, in agreement with the solvent effect on anionic σ-complexes. An interesting feature was that compounds containing an electron-donor group, such as 2,4-dinitrotoluene, 2,4-dinitroaniline and 2,4-dinitrophenylhydrazine do not give a colour in the conventional spot-test but do on the resin. This is because the electron-donor group enhances the electron density within the ring, which is otherwise depleted by the two nitro-groups. In these cases the resin seems to play a specific role. With 2,4-dinitroaniline for example, the zwitterion canonical form in the tautomerism:

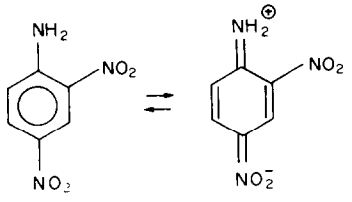

can react with hydroxide ion to give an anion:

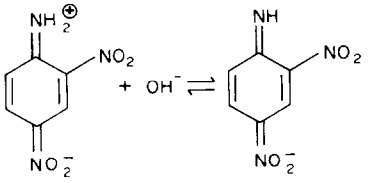

In the reaction with sulphite, however, addition seems more likely than proton loss, but because of the increased electron density within the ring (caused by the electron-donating amino group) anion addition can take place only with difficulty. However on the large positively charged matrix of the anion-exchanger the aniline loses much of its excess negative charge to the matrix, thereby facilitating anion addition and giving a positive test response on the resin surface.

Work reported by others[2,12] points to sulphite addition:

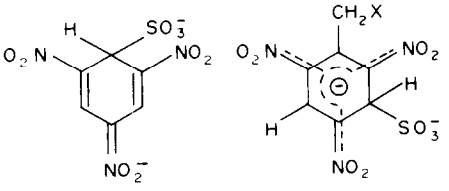

Since all the polynitroaromatics tested give a blue violet colour, the test seems to be independent of the substituent at the 1-position, and the colour seems specific for detection of the *m*-dinitroaromatic moiety.

Acknowledgements—The authors thank Professor Wasiur Rahman, Chairman, Department of Chemistry, for facilities, and C.S.I.R. (India) for financial assistance.

REFERENCES

1. M. R. Crampton, *Advan. Phys. Org. Chem.*, 1969, **7,** 211.
2. M. J. Strauss, *Chem. Rev.*, 1970, **70,** 667.
3. E. Buncel, A. R. Norris and K. E. Russell, *Quart. Rev. Chem.*, 1968, **22,** 123.
4. E. Buncel, M. R. Crampton, M. J. Strauss and F. Terrier, *Electron Deficient Aromatic- and Hetero-aromatic-Base Interactions*, Elsevier, Amsterdam, 1984.
5. R. Foster and C. A. Fyfe, *Rev. Pure. Appl. Chem.*, 1966, **161,** 61.
6. S. A. Nabi, A. Mohammad and P. M. Qureshi, *Talanta*, 1979, **26,** 1179.
7. M. Qureshi, S. A. Nabi, I. A. Khan and P. M. Qureshi, *ibid.*, 1982, **29,** 757.
8. S. A. Nabi, S. Haque and P. M. Qureshi, *Talanta*, 1983, **30,** 989.
9. J. A. Vinson and L. D. Pepper, *Anal. Biochem.*, 1977, **83,** 357.
10. R. D. Tiwari, G. Srivasta and J. P. Misra, *Analyst*, 1978, **103,** 651.
11. K. K. Verma and S. K. Dubey, *Talanta*, 1981, **28,** 485.
12. D. N. Brooke and M. R. Crampton, *J. Chem. Soc. Perkin II*, 1980, 1850.

Talanta, Vol. 32, No. 1, pp. 54–56, 1985
Printed in Great Britain

0039-9140/85 $3.00 + 0.00
Pergamon Press Ltd

2-[2-(5-CHLOROPYRIDYL)AZO]-5-DIMETHYLAMINOPHENOL AS INDICATOR FOR THE COMPLEXOMETRIC DETERMINATION OF ZINC

E. MARCHEVSKY, R. OLSINA and C. MARONE
Universidad Nacional de San Luis, Chacabuco y Pedernera, 5700-San Luis, Argentina

(*Received* 13 *October* 1983. *Revised* 4 *June* 1984. *Accepted* 16 *July* 1984)

Summary—2-[2-(5-Chloropyridyl)azo]-5-dimethylaminophenol (ClDMPAP) is proposed as a metallochromic indicator for zinc. The end-point colour change is from the violet-red of the zinc complex to the brownish-yellow of the indicator. The colour contrast is markedly greater than that for Erio-T.

Eriochrome Black T (Erio-T) is often used as a metallochromic indicator for complexometric determination of zinc,[1–3] but has some important deficiencies. Its solutions are unstable, and copper(II), cobalt(II), nickel(II) and aluminium(III) can interfere by blocking the indicator. Iron(III) and titanium(IV) also interfere. Cadmium(II) is co-titrated.

Use of PAN[4–6] and PAR[7] has therefore been recommended. Other pyridylazo reagents used in zinc titrations include 5-(2-pyridylazo)-2-monoethylamino-*p*-cresol,[8] 2-(2-pyridylazo)-4-methylphenol,[9] 5-(2-pyridylazo)-*p*-cresol,[10] and 2-[2-(5-bromo-2-pyridylazo)]-5-diethylamino-*m*-phenol.[9] All have in common a high colour contrast between the zinc complex and the free reagent, from violet-red to brownish-yellow, with a change of about 100 nm in the wavelength of the absorption maximum. The molar absorptivities (ε) are also high, *ca.* 1×10^{-5} $l.mole^{-1}.cm^{-1}$.

2-[2-(5-Chloropyridyl)azo]-5-dimethylaminophenol (ClDMPAP) is known[11] to react instantly with zinc in aqueous solutions buffered at pH 8.2–10.4, producing an intensely violet-red complex (ε is much greater than that for the zinc complexes listed above). The complex is stable for at least 5 days. The reagent is readily displaced from its zinc complex by EDTA and thus should be suitable as an indicator for EDTA titration of zinc.

EXPERIMENTAL

Reagents

Standard zinc solution (0.1000*M*). Prepared by dissolving the pure metal (6.537 g) with *ca.* 20 ml of hydrochloric acid (1 + 1) by gentle warming, cooling and dilution to volume in a standard flask with water.

EDTA solution, ca. *0.1*M. Standardized potentiometrically with the standard zinc solution[12] and further diluted as required.

5ClDMPAP. The reagent was synthesized according to Johnson and Florence.[13] A 0.05% solution in 95% ethanol was used as indicator. For spectrometric studies, solutions of the required molarity were prepared with 95% ethanol as solvent.

Ammonia–ammonium chloride buffer, ca. *0.1*M, *pH 8.5.* Ammonium chloride (4.55 g) was dissolved in a small volume of water and concentrated ammonia solution was added dropwise until pH 8.5 was reached. Final pH adjustment was made after dilution to nearly 1000 ml.

Aqueous Eriochrome Black T solution, ca. *0.05%*. Prepared immediately before use.

All other reagents, chemicals and standards were of analytical grade.

Apparatus

Spectrophotometric titrations were done in a cell constructed according to Sweetser and Bricker,[14] and the titrant was added from a Metrohm piston-burette.

Procedure

Take a 50-ml sample, make it slightly alkaline and finally adjust to pH 8.5 by adding 5 ml of ammonia–ammonium chloride buffer (the buffer capacity of the NH_4^+–NH_3 solution was enough to maintain this pH in the titration of 50 ml of zinc solution of concentration up to about 800 ppm). Add 60 ml of alcohol and 2 or 3 drops of indicator. Titrate with EDTA added at *ca.* 0.1 ml/min near the end-point. Typical results are summarized in Table 1.

Analysis of zinc insulin

In a 25–30 ml centrifuge tube, take 10.0 ml of the liquid sample. Add dilute hydrochloric acid (1 + 50) until a clear solution is obtained, and 6 ml of 10% trichloroacetic acid solution. Shake, then centrifuge for 5 min. Transfer the supernatant liquid to a 25-ml standard flask and dilute to the mark with water. Transfer 20 ml of the solution to the photometric titration cell and add 5 ml of ammonium chloride–ammonia buffer (pH 8.6), enough ethanol to give a final content of about 50% v/v, and 3 drops of 5ClDMPAP indicator, and titrate with EDTA.

Table 1. Changes in absorbance during the EDTA titration of zinc, with Erio-T and 5ClDMPAP as indicators

	Error, %	
Zn taken, *mg*	5ClDMPAP	Erio-T
0.813	1.0	1.5
3.250	0.06	0.1
8.14	0.03	0.1
16.28	0.02	0.08
40.69	0.006	0.09

RESULTS AND DISCUSSION

The spectral differences between Erio-T and 5ClDMPAP and their zinc complexes are shown in Fig. 1. 5ClDMPAP is clearly a very much more sensitive reagent, and the shift in the wavelength of maximum absorption on complexation is twice as great for 5ClDMPAP as for Erio-T, and gives a much bigger contrast in the colour change. The human eye is also more sensitive to the colour change for the 5ClDMPAP system. Graphical methods[15–17] were used to choose the optimum pH for the titration. The equilibrium constants required for construction of the graphs were obtained from the literature[18] or determined by us.[19] Results obtained by the method of Reilley and Schmid[15] are shown in Fig. 2. It can be seen that the pH range 5.5–9 is the most suitable; this was experimentally verified (Fig. 3). The curves in Fig. 4 correspond to spectrometric titrations with 5ClDMPAP. Curves for Erio-T are included for comparison.

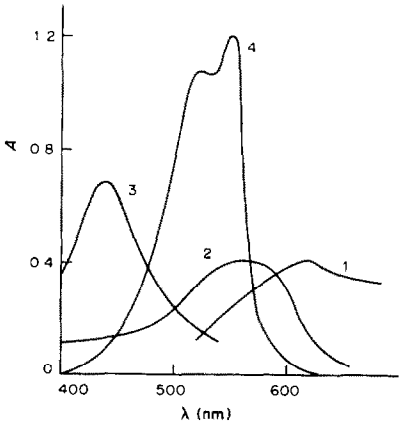

Fig. 1. Spectral curves of 5ClDMPAP and Erio-T and their zinc complexes, $C_{reag} = 2.0 \times 10^{-5} M$; $C_{Zn} = 6.2 \times 10^{-4} M$; (1) Erio-T; (2) Erio T–Zn complex; (3) 5ClDMPAP; (4) 5ClDMPAP–Zn complex.

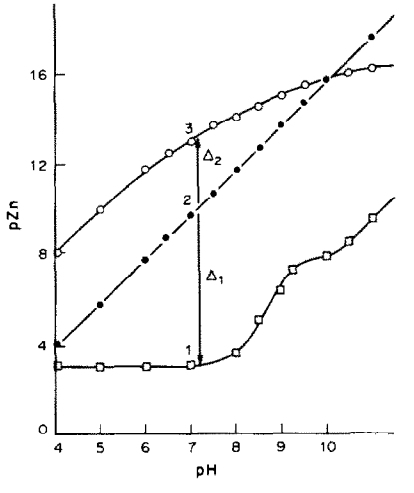

Fig. 2. The pZn data required for the method of Reilley and Schmid:[15]
(1) for the system Zn plus NH_4^+–NH_3 buffer;
(2) for 50% transformation of the indicator;
(3) for the system with EDTA added in 100% excess.

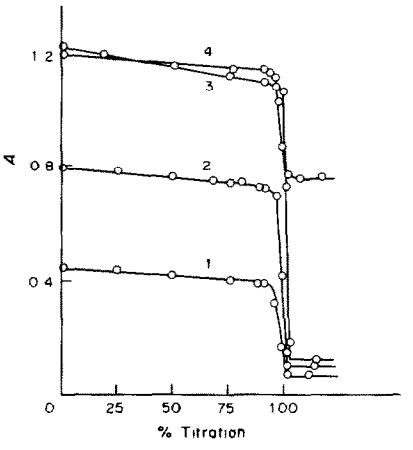

Fig. 3. Photometric titration: Effect of pH on the end-point. pH: (1) 4.5; (2) 5.6; (3) 7.2; (4) 8.5; (5) 9.0; (6) 10.8; (7) 12.

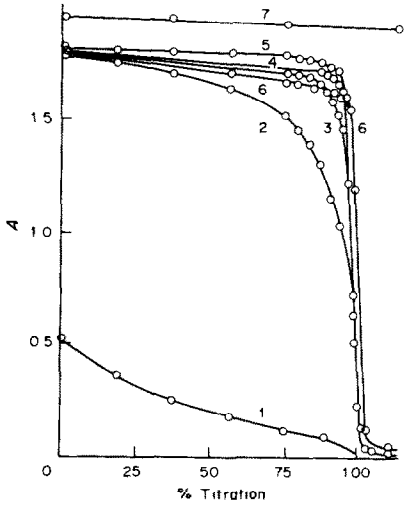

Fig. 4. Absorbances at λ_{max} of the zinc complex, in photometric, titration of zinc. [5ClDMPAP] = (1) $5 \times 10^{-6} M$; (2) $1 \times 10^{-5} M$; (3) $2 \times 10^{-5} M$; [Erio-T] = (4). $6 \times 10^{-5} M$.

Both indicators give the same location of the end-point, but the colour change is much sharper with 5ClDMPAP than with Erio-T. This is clearly shown by the change in absorbance (ΔA) on addition of 0.05-ml increments of EDTA in the vicinity of the end-point (Table 2).

Table 2. Comparison of results obtained with 5ClDMPAP and Erio-T in EDTA titration of zinc

	5ClDMPAP		Erio-T	
Titration, %	A_{550}	ΔA	A_{560}	ΔA
97.2	0.686	0.031	0.961	0.026
98.5	0.655	0.081	0.935	0.066
99.7	0.574	0.484	0.869	0.116
101.1	0.090	0.002	0.753	0.103
102.3	0.088	0.001	0.650	0.003
103.5	0.087		0.647	

Effect of ethanol content and ionic strength

Erio-T has the advantage that it can be used in purely aqueous solution, whereas 5ClDMPAP (which is insoluble in water) must be used in aqueous ethanolic medium. Hence the effect of the ethanol concentration was tested over the range 20–60% v/v. With <40% ethanol the reaction is slow, more time is required to stabilize the absorbance, and the end-point is sluggish. These effects are basically due to the low solubility of the zinc–5ClDMPAP complex. With 40–60% ethanol present these difficulties are overcome, but the relatively high ethanol content required limits the concentration of inorganic salts in the solution. The effect of ionic strength was tested on zinc solutions in 50% v/v ethanol–water medium by addition of sodium perchlorate, nitrate, chloride, sulphate and acetate. The most serious limitation is imposed by sulphate. At concentrations >0.2*M* sodium sulphate is not completely soluble in this medium and the dispersed solid makes it difficult to see the colour change at the end-point. For the other sodium salts tested this effect does not arise. With Erio-T in purely aqueous medium, the only effect was a slight diminution in ΔA at the end-point.

Effect of foreign ions

The ions which interfere were known from previous work,[11] the most serious being cadmium, copper, nickel, iron and cobalt, which also interfere in the complexometric titration. Nickel, copper and iron may be effectively dealt with by the cyanide–formaldehyde method (Table 3) but cadmium and cobalt cannot. Sodium, potassium, magnesium, barium, and strontium do not interfere in at least 100:1 w/w ratio to zinc. Calcium is tolerated at 25:1 ratio but iron and mercury are tolerated only in 5:1 ratio to zinc. Tolerance limits for most common anions were determined when the effect of ionic strength was studied, and found to be dictated by the solubility of the sodium salts in the alcoholic media used. Lead interferes but can be dealt with by the method used to eliminate its interference when Erio-T is used as indicator.[20]

Xylenol Orange shows an advantage over 5ClDMPAP in selectivity, mainly in the case of bismuth, thorium, scandium, lanthanum, lead, zinc and cadmium,[21] because it is used at pH < 6 (5ClDMPAP can be used in the pH range 5.5–9, with an appropriate buffer).

Table 3. Determination of zinc in binary samples; interferents were masked by the cyanide–formaldehyde method

Interferent	Zinc, *mg*		Ratio (w/w) of interferent to Zn
	Taken	Found	
Nickel	1.63	1.64	12.5
Copper	1.63	1.64	24.5
Iron	1.63	1.65	1.22

Applications

Analysis of a zinc insulin preparation (Lilly) gave a mean of 0.156 mg/ml by the present method (standard deviation 0.002 mg/ml), 0.157 (s.d. 0.0013) by a reference method,[22] and 0.154 (s.d. 0.0010) by AAS, for six replicates.

Synthetic brass samples corresponding to British Standards BCS 385 and BCS 344 were analysed by a modification of the recommended procedure (immediately after the pH was adjusted, 2 ml of 5% potassium cyanide solution followed by 4 ml of 5% formaldehyde solution were added). The zinc results were 38.4% (s.d. 0.02%) for BCS 385 (certified value 38.5%) and 30.8% (s.d. 0.02%) for BCS 344 (certified value 31.0%) for six replicates in each case.

Acknowledgements—The authors are gratefully indebted to SUBCYT for financial assistance, and Prof. Dr. J. A. Catoggio for helpful discussion.

REFERENCES

1. W. Biedermann and G. Schwarzenbach, *Chimia*, 1948, **2**, 1.
2. H. Flaschka, *Mikrochem. Mikrochim. Acta*, 1952, **39**, 38.
3. E. G. Brown and T. J. Hayes, *Anal. Chim. Acta*, 1953, **9**, 1.
4. H. Flaschka and H. Abdine, *Mikrochim. Acta*, 1956, 770.
5. K. L. Cheng, *Anal. Chem.*, 1948, **30**, 243.
6. I. Crişan and P. Tanase, *Rev. Chim. Bucharest*, 1968, **19**, 228.
7. M. Hniličková and L. Sommer, *Collection Czech. Chem. Commun.*, 1961, **26**, 2189.
8. S. I. Gusev and L. M. Shchurova, *Zh. Analit. Khim.*, 1971, **26**, 1740.
9. G. Nakawada and H. Wada, *Nippon Kagaku Zasshi*, 1962, **83**, 1098.
10. S. I. Gusev, E. M. Nikolaeva and E. A. Pirozhkova, *Zh. Analit. Khim.*, 1971, **26**, 1740.
11. E. Marchevsky, R. Olsina and C. Marone, *Anal. Asoc. Quím. Argentina*, 1984, **72**, 35.
12. C. N. Reilley, R. W. Schmid and D. W. Lamson, *Anal. Chem.*, 1958, **30**, 953.
13. D. A. Johnson and T. M. Florence, *Anal. Chim. Acta*, 1971, **53**, 73.
14. P. B. Sweetser and C. E. Bricker, *Anal. Chem.*, 1953, **25**, 253.
15. C. N. Reilley and R. W. Schmid, *ibid.*, 1959, **31**, 887.
16. E. Still and A. Ringbom, *Anal. Chim. Acta*, 1965, **33**, 50.
17. E. Still, *Acta Acad. Aboensis, Math. Phys.*, 1966, **26**, 6.
18. A. Ringbom, *Complexation in Analytical Chemistry*, Interscience, New York, 1963.
19. F. Ferretti, R. Olsina and C. Marone, *Anal. Asoc. Quím. Argentina*, 1978, **70**, 501.
20. H. Flaschka, *EDTA Titrations*, 2nd Ed., p. 102. Pergamon Press, Oxford, 1967.
21. J. Körbl, R. Přibil and A. Emr, *Collection Czechoslov. Chem. Commun.*, 1957, **22**, 961.
22. *U.S. Pharmacopeia*, 1975, p. 634.

Talanta, Vol. 32, No. 1, pp. 57–59, 1985
Printed in Great Britain

0039-9140/85 $3.00 + 0.00
Pergamon Press Ltd

THERMODESORPTIVE ANALYSIS OF GaAs AND ZnSe SURFACES

I. A. KIROVSKAYA*, G. M. ZELYEVA and A. V. YURYEVA
Omsk Polytechnical Institute, Omsk, USSR

(*Received* 12 *March* 1984. *Accepted* 16 *July* 1984)

Summary—This paper concerns thermodesorption analysis of the interaction of ammonia, hydrogen, carbon dioxide and a mixture of $H_2 + CO_2$ with GaAs and ZnSe surfaces, to determine the strength and concentration of acid surface centres. The mechanism of interaction of the gases and surfaces has been examined. This work was aimed at differentiating between the strengths of acid centres on GaAs and ZnSe semiconductor surfaces to obtain more information about the quantity of hydrogen and carbon dioxide adsorbed, their energy characteristics, the presence or absence of dissociation, and the nature of the CO_2 hydration.[1]

EXPERIMENTAL

For analysing surface acid–base properties, ammonia was used as the adsorbent probe. Thermodesorptive measurements were done with an apparatus similar to that described by Yakerson and Rozanov.[2] The desorption products were determined by gas chromatography and mass spectrometry, with programmed linear heating from 298 to 653 K at 10 K/min. The powdered samples were pressed into tablets at a pressure of 35 kg/m^2 and then conditioned at 673 K and 0.1 Pa pressure. The conditioned samples were then saturated with the gas under study (NH_3, H_2, CO_2, $H_2 + CO_2$) for 2 hr at the temperature of the experiment. The free gas was pumped out, and programmed heating of the reactor started, with simultaneous analysis of the desorption products. Helium was used as carrier gas. An MCh-1301, RMS-1 mass-spectrograph was used, with Pimonova's method.[3] The gases were obtained as described by Kirovskaya *et al.*[4]

RESULTS AND DISCUSSION

The thermochromatograms for ammonia desorption (Fig. 1) contain three peaks, one at 301–305 K, for both samples, the other two at 463 and 563 K for GaAs, and 433 and 533 K for ZnSe. These data indicate that ammonia is adsorbed on the semiconductor surfaces at three kinds of site, which differ in their activity. This is corroborated by the results of the thermodesorption curves, and the mass-spectrometric and infrared-spectrometric determination of the kinetics. By means of the approximately integrated Polani-Vigner equation[5] the desorption activation energy was calculated to be 12–21 kJ/mole for the low-temperature peak and 59–63 and 67–71 kJ/mole for the high-temperature peaks. At 301–305 K, the thermodesorption follows first-order kinetics, whereas at 353–503 K for GaAs and 363–573 K for ZnSe it follows second-order kinetics. These kinetic characteristics, combined with the results of the infrared spectroscopy, make it possible to state that at low temperature the ammonia is rapidly but feebly bound by residually adsorbed H_2O and OH-groups whereas at high temperatures the ammonia is co-ordinately bound to surface atoms,[7,8] with dissociation accompanying adsorption at the highest temperature. This is confirmed indirectly by the kinetic data and directly by the mass-spectral data (Fig. 2). The presence of small quantities of a species of mass number 18 seems to be due to water vapour in the gaseous ammonia used.

The difference in strength of the acid centres of the surfaces corresponds to the degree and temperature

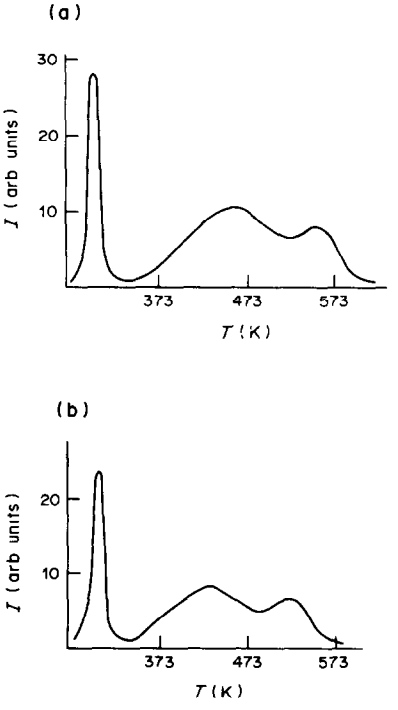

Fig. 1. Chromatograms of ammonia thermodesorption from GaAs (*a*) and ZnSe (*b*) surfaces.

*Author for correspondence.

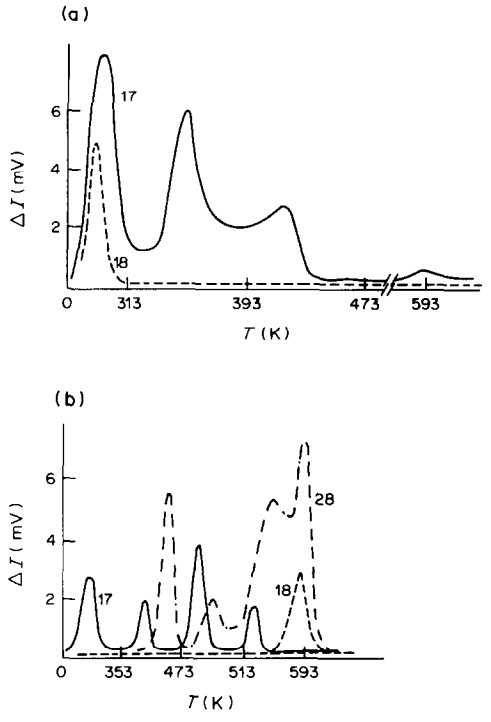

Fig. 2. Mass spectra of NH_3 desorption from GaAs (*a*) and ZnSe (*b*) surfaces.

of adsorption, the acid centres of ZnSe being weaker than those of GaAs.

Analysis of the adsorption characteristics of H_2 and CO_2 on ZnSe showed the following. The thermodesorptive chromatogram for H_2 (Fig. 3) has two distinct peaks at $T_{max_1} = 310$ K, $T_{max_2} = 338$ K, and a very broad and shallow one with $T_{max_3} = 523$ K. The three peaks correspond to three types of adsorption sites, differing in their bond strength. The first two types of site have activation energies of 19 and 25 kJ/mole respectively. That for the third type could not be identified because of the low intensity of the desorptive peak. At T_{max} desorption occurs by first-order kinetics, so at $T \leqslant 310$ K molecular adsorption prevails and at $T > 643$ K dissociative adsorption predominates. The comparatively low heat of chemical adsorption,[9] together with the secondary-ion mass spectra,[10] indicates that dissociation occurs on ZnSe and analogous surfaces at higher temperatures.

The thermodesorptive chromatogram of CO_2 has a very sharp peak at T_{max} about 336 K (Fig. 4), with 3 kJ/mole activation energy and first-order kinetics, *i.e.*, under these conditions weak non-dissociative adsorption of CO_2 takes place. The mass spectra[11] also indicate the absence of dissociation of adsorbed CO_2 on the ZnSe surface in the temperature interval examined. According to infrared spectroscopic

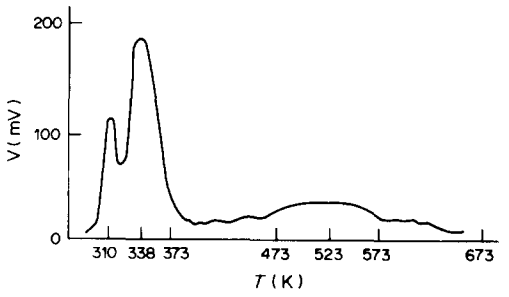

Fig. 3. Thermodesorption of H_2 from ZnSe surface.

examination[12] and the nature of the surface acid centres discussed above, CO_2 adsorption of this type should be due to formation of a linear donor–acceptor complex, without free molecular rotation, on the adsorbent surface ($\nu_{max} = 2380\ cm^{-1}$):

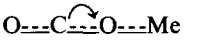

The mass-spectral examination of desorption of the $CO_2 + H_2$ mixture showed decreasing desorption at high temperatures and increasing yield of species with mass numbers 18 and 28 at $T > 423$ K. Taking the non-dissociative character of the CO_2 adsorption into account, the presence of CO_2 as well as H_2O in the desorbed phase is evidently due to interaction of the adsorbed CO_2 and H_2. As mentioned before,[1] such an interaction is accompanied by intermediate complex formation analogous to formation of adsorbed formic acid. The formic acid is relatively stable and is not decomposed at lower temperatures, but at higher temperatures (473–573 K) dissociates into CO and H_2O in the desorption process:

$$[HCOOH]^{+\delta} \rightarrow CO_{(gas)} + H_2O_{(gas)} + \delta^{\oplus *}$$

The lower desorption of water when the mixture is used, compared with that for hydrogen alone, also confirms that the carbon dioxide suppresses the hydrogen adsorption, as mentioned by us earlier.[4]

Thus the thermodesorptive examination of these semiconductor surfaces makes it possible to obtain some additional information about the surface acidity characteristics and some media interacting with

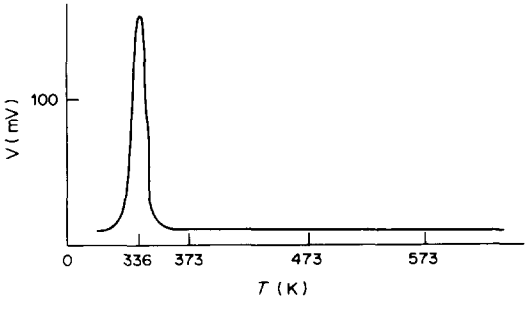

Fig. 4. Thermodesorption of CO_2 from ZnSe surface.

*$\delta^{\oplus}$ is an extra (effective) charge remaining on the surface.

them (H_2, CO_2, $H_2 + CO_2$). The latter information is most important in research into the physical chemistry of real diamond-like semiconductor surfaces.

REFERENCES

1. I. A. Kirovskaya, L. N. Pimenova, I. A. Votyakova and N. N. Sharangovich, *Russian J. Phys. Chem.*, 1978, **52,** 2356.
2. V. V. Yakerson and V. B. Rozanov, The investigation of the catalytic system by thermodesorption and gas chromatography methods, in *Itogi Nauki i Tehniki Series Physical Chemistry, Kinetics*, 1974, Vol. 3 (in Russian).
3. L. N. Pimenova, *Thesis*, Tomsk, 1975, p. 156 (in Russian).
4. I. A. Kirovskaya, L. N. Pimenova and V. N. Kryukov, *Russian J. Phys. Chem.*, 1974, **48,** 2825.
5. W. Kollen and A. W. Czanderna, *J. Colloid Interface Sci.*, 1972, **38,** 152.
6. A. V. Yuryeva, V. P. Vetrov and I. A. Kirovskaya, *The materials of the regional scientific and practical conference*, p. 72 (in Russian). Izd. TGU, Tomsk, 1977.
7. I. A. Kirovskaya, V. V. Limberova, N. I. Mercusheva and V. A. Prieditis, *Izd. Akad. Nauk* SSSR, *Ser. Inorganic Materials*, 1977, **13,** 1953.
8. I. A. Kirovskaya, V. V. Limberova, G. M. Zelyeva, Ph.E. Shakalov and L. A. Vlasova, *ibid.*, 1979, **15,** 1594.
9. L. G. Maidanovskaya and I. A. Kirovskaya, *Russian J. Phys. Chem.*, 1966, **40,** 606.
10. A. I. Chernitshov, I. A. Kirovskaya and A. N. Pushkaryeva, Rukopis N 2789/79, dep. 22.06.1979, Cherkassi (in Russian).
11. L. N. Pimenova and I. A. Kirovskaya, *Trudi TGU*, 1973, **249,** 63.
12. I. A. Kirovskaya and V. I. Bavrin, *ibid.*, 1973, **249,** 44.

Talanta, Vol. 32, No. 1, pp. 60–62, 1985
Printed in Great Britain.

0039-9140/85 $3.00 + 0.00

DIFFERENTIAL PULSE POLAROGRAPHY IN THE ALTERNATING PULSE MODE

CSABA URBANICZKY
Department of Analytical Chemistry, University of Uppsala, P.O. Box 531, S-751 21 Uppsala, Sweden

(*Received* 11 *June* 1984. *Accepted* 10 *July* 1984)

Summary—A polarographic two-drop pulse technique for trace analysis is described. By using a second pulse, in the opposite direction to the first one, on the second drop, a high current sensitivity is obtained, with a very flat background. The theoretical response for a reversible electrode process is presented together with experimental results for the reduction of Pb^{2+} in hydrochloric acid medium. It is shown that without enrichment determination of lead at concentrations as low as 71n*M* is possible with this technique.

Differential pulse polarography (DPP)[1,2] is a very useful electroanalytical technique, but it has the following disadvantages. At the dropping mercury electrode (DME) there is a charging current due to the continuous drop expansion, since the current is sampled at two different times during the life of a drop. Further, there is a contribution due to the potential-dependence of the differential capacity, since the current is measured at two different potentials. There is also a d.c. faradaic current contribution which leads to a positive distortion.[3] At the static mercury drop electrode (SMDE), on the other hand, there is a negative d.c. faradaic distortion.[4] Alternate-drop differential pulse polarography (ADDPP) compensates for these effects but the sensitivity is diminished.[5] In both DPP and ADDPP the potential at which the current peak appears is dependent on the magnitude of the applied potential pulses.

In this report a two-drop method is described, called differential pulse polarography in the alternating pulse mode (DPPAPM). This is a hybrid between ADDPP and differential normal-pulse voltammetry in the alternating pulse mode (DNPVAPM).[6] By using a second pulse in the opposite direction on the second drop, the following advantages are obtained: (1) higher current sensitivity than for ADDPP; (2) the potential at which the current peak appears is independent of the pulse amplitude; (3) the d.c. faradaic distortion current is absent: (4) the charging current is lower than it is in DPP and DNPVAPM.

EXPERIMENTAL

Apparatus

A Z-80 based personal computer, the Luxor ABC-80, was used to control the voltammetric instrumentation.[7-9] The potentiostat is of conventional addition design and employs National LF 356 Bi-FET operational amplifiers.

In this study the following settings were used throughout. The potential increments between the two drops were 2 mV and the step height of the applied potential pulses was 20 mV. The drop-time was 0.5 sec and pulses were applied during the last 40 msec. The current was sampled during the last 20 msec of each pulse. The time constants in the sample and hold circuits were 20 msec.

The polarograms were recorded on a Hewlett-Packard 9044A X–Y recorder.

Potential and time calibrations were performed with a Fluke 8050 A $4\frac{1}{2}$-digit digital multimeter and a Ballantine model 5500B timer/counter respectively.

Reagents

All chemicals were of analytical-reagent grade except the hydrochloric acid, which was of "Suprapur" grade. The hydrochloric acid concentration of the solutions was 10m*M*. Aliquots of a 4 m*M* stock solution of lead nitrate were diluted on the day of use to obtain working solutions. Distilled water was purified prior to use, with a Millipore Milli-Q filtration system. The mercury was purified before use.[10] Solutions were purged with water-saturated nitrogen before each scan.

Cell and electrodes

The cell, the SCE reference electrode (with a salt bridge) and the auxiliary electrode (a platinum wire) were conventional. The capillary used for the DME had a mercury flow-rate of 1.57 mg/sec and a drop-time of 5.36 sec on open circuit. Triton X-100 was added to give a final concentration of 10 ppm.

The temperature was kept at $25 \pm 0.5°$.

RESULTS AND DISCUSSION

In Fig. 1 the DPPAPM waveform is shown and the potential variables are defined. The potential on the first drop (α) is held at E_1^α and at the end of the drop-life, at time τ, a small potential pulse, ΔE, is added to obtain potential E_2^α during a time δ. The potential on the next drop (β) is held at E_1^β which has numerical value of $E_1^\alpha + 2\Delta E$, and at the end of the drop-life a small potential pulse is subtracted to obtain E_2^β with numerical value identical to E_2^α. Each consecutive pair of double pulses is similar, except that the scanned potential is incremented. The sampled currents are I_2^α and I_2^β and the differential current is monitored as a function of E_2.

For a reversible system, the current response for the DPPAPM waveform can be derived in a similar way as for ADDPP[5]. The current for a "pulsed drop"

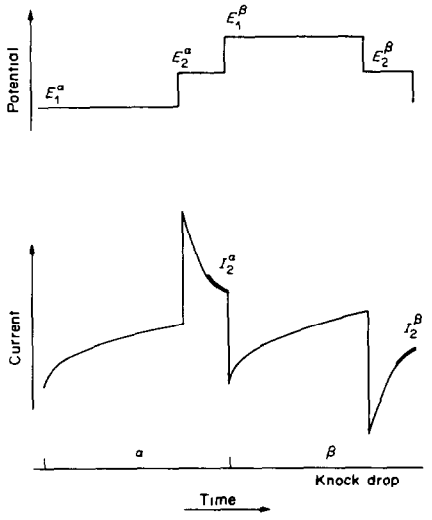

Fig. 1. Definitions of the potentials and the currents in differential pulse polarography in the alternate pulse mode. See the text for further information.

is [equation (16) in reference 5]:

$$I_2 = I_{F,DPP} + I_{Po}(E_1, \tau + \delta) + I_C(E_2, \tau + \delta) \quad (1)$$

where

$$I_{F,DPP} = nFkm^{2/3}C(\tau + \delta)^{2/3}(D/\pi\delta)^{1/2} \times \left[\frac{1}{1+\xi\Theta_2} - \frac{1}{1+\xi\Theta_1}\right] \quad (2)$$

$$\Theta = \exp[nF(E - E'_{1/2})/RT] \quad (3)$$

$E'_{1/2}$ is the reversible half-wave potential and the constant k has a numerical value of 0.8515 $cm^2/g^{2/3}$,

$$I_{Po} = (7D/3\pi)^{1/2}nFkm^{2/3}C(\tau + \delta)^{1/6}\left[\frac{1}{1+\xi\Theta_1}\right] \quad (4)$$

and

$$I_C = -(2/3)km^{2/3}Q(E_2)/(\tau + \delta)^{1/3} \quad (5)$$

Equation (4) is the Heyrovský–Ilkovič equation, and I_C is the charging current due to the drop growth. $Q(E)$ is the potential-dependent charge density on the electrode surface. All the other symbols are according to Bard and Faulkner.[11]

According to equation (1) the currents I_2^α and I_2^β are then

$$I_2^\alpha = I_{2,F,DPP}^\alpha + I_{2,Po}^\alpha(E_1^\alpha, \tau + \delta) + I_{2,C}^\alpha(E_2^\alpha, \tau + \delta) \quad (6)$$

$$I_2^\beta = I_{2,F,DPP}^\beta + I_{2,Po}^\beta(E_1^\beta, \tau + \delta) + I_{2,C}^\beta(E_2^\beta, \tau + \delta) \quad (7)$$

and the differential current sought is then

$$\Delta I = I_2^\alpha - I_2^\beta \quad (8)$$

The charging current, I_C, equation (5), is a function of only the potential and time. This component is absent at the SMDE, because the drop area is constant when the currents are sampled. At the DME the charging currents will be equal and can be cancelled. Since the currents are sampled at the same point of time in a drop-life, there is no d.c. faradaic distortion. After some algebraic manipulation

$$\Delta I = nFkm^{2/3}(\tau + \delta)^{2/3}(D/\pi\delta)^{1/2}C\{1 - [7\delta/3(\tau + \delta)]^{1/2}\}\left[\frac{1}{1+\xi\Theta_1^\alpha} - \frac{1}{1+\xi\Theta_1^\beta}\right] \quad (9)$$

is obtained. The same diminution factor as in ADDPP, $1 - [7\delta/3(\tau + \delta)]^{1/2}$, appears in this equation, but the last potential term is also a function of the applied second pulse and thus an improved current sensitivity is obtained. Equation (9) can be rewritten as

$$\Delta I = nFkm^{2/3}(\tau + \delta)^{2/3}(D/\pi\delta)^{1/2}C \times \{1 - [7\delta/3(\tau + \delta)]^{1/2}\} \times \frac{-\sinh(nF\Delta E/RT)}{\cosh(\ln\xi\Theta_2) + \cosh(nF\Delta E/RT)} \quad (10)$$

As in DNPVAPM, ΔI is symmetrical with respect to the peak potential in DPPAPM. The peak current, ΔI_S, is then

$$\Delta I_S = nFkm^{2/3}(\tau + \delta)^{2/3}D/\pi\delta)^{1/2}C \times \{1 - [7\delta/3(\tau + \delta)]^{1/2}\} \times \tanh(nF\Delta E/2RT) \quad (11)$$

Compared with DNPVAPM, the peak current for DPPAPM has a diminution factor in the same way as ADDPP has compared with DPP. From equation

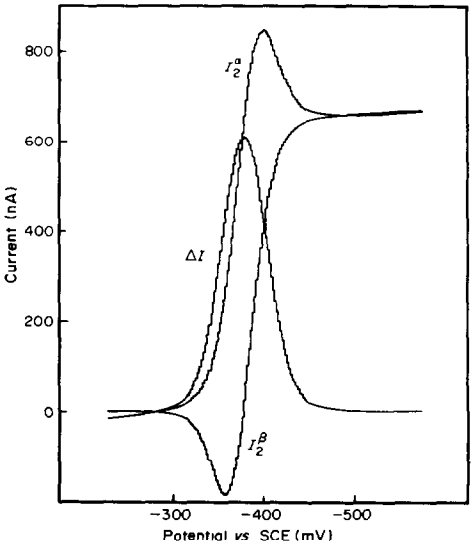

Fig. 2. The forward (I_2^α), the reverse (I_2^β) and the difference (ΔI) polarograms of 123 μM Pb^{2+} in acetate buffer.

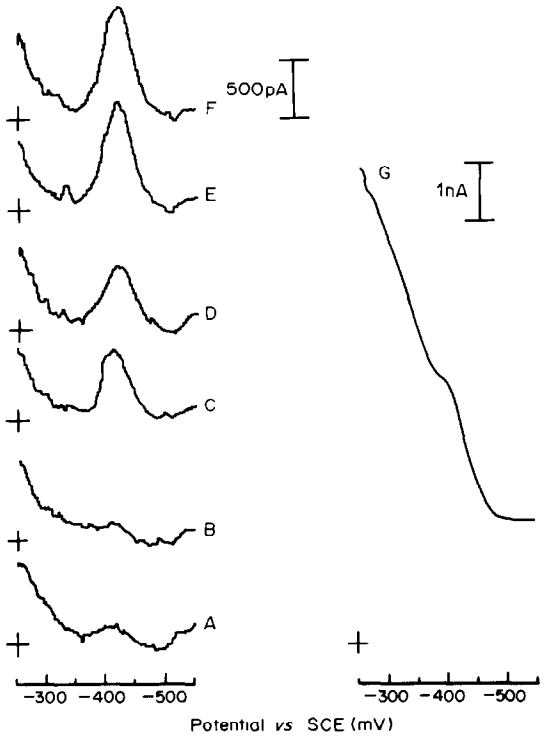

Fig. 3. DPPAPM (A–F) and DPP (G) polarograms of (A, B) 0, (C, D) 71 and (E–G) 142nM Pb^{2+}. The cross indicates zero current.

(10) the peak-width at half-height, $W_{1/2}$, is given by

$$W_{1/2} = \frac{2RT}{nF} \cosh^{-1}[2 + \cosh(nF\Delta E/RT)] \qquad (12)$$

The experimental behaviour of a reversible system is illustrated by reduction of Pb^{2+}. Figure 2 shows the experimental current responses from the forward (I_2^a) and reverse (I_2^β) potential pulses and that the difference polarogram (ΔI) gives a symmetrical peak. The current sensitivity, $\Delta I_C/C$, is 4.75, 2.78 and 5.00 mA.l.mole^{-1} for DPP, ADDPP and DPPAPM respectively. According to theory the quotients DPP/DPPAPM and ADDPP/DPPAPM are 1.00 and 0.57, which agree well with the experimental values of 0.95 and 0.56.

Curves A and B in Fig. 3 show that the charging current is considerably diminished when DPPAPM is used instead of DPP. Efforts to smooth the background further, included experiments with different ultraviolet-irradiated solutions. No improvement in background was obtained. In Fig. 3 it is also shown that determination of lead at concentrations down to $10^{-7}M$ is possible with DPPAPM at the DME when a drop-time of 0.5 sec is used. In the DPP voltamperogram the peak is hardly discernible.

REFERENCES

1. G. C. Barker and A. W. Gardner, *Z. Anal. Chem.*, 1960, **173,** 79.
2. E. P. Parry and R. A. Osteryoung, *Anal. Chem.*, 1965, **37,** 1634.
3. J. H. Christie and R. A. Osteryoung, *J. Electroanal. Chem.*, 1974, **49,** 301.
4. J. A. Anderson, A. M. Bond and R. D. Jones, *Anal. Chem.*, 1981, **53,** 1016.
5. J. H. Christie, L. L. Jackson and R. A. Osteryoung, *ibid.*, 1976, **48,** 242.
6. T. R. Brumleve, J. J. O'Dea, R. A. Osteryoung and J. Osteryoung, *ibid.*, 1981, **53,** 702.
7. C. Urbaniczky, *Voltammetric Instrumentation*, Part 1, UUIC A82/04, 1982.
8. *Idem*, *Voltammetric Instrumentation*, Part 2, UUIC A82/05, 1982.
9. *Idem*, *Voltammetric Instrumentation*, Part 3, UUIC A82/06, 1982.
10. G. C. Whitnack and R. Sasselli, *Anal. Chim. Acta*, 1969, **47,** 267.
11. A. J. Bard and L. R. Faulkner, *Electrochemical Methods*, Wiley, New York, 1980.

Talanta, Vol. 32, No. 1, pp. 63–65, 1985
Printed in Great Britain

0039-9140/85 $3.00 + 0.00
Pergamon Press Ltd

EXTRACTIVE-SPECTROPHOTOMETRIC DETERMINATION OF MOLYBDENUM AS AN ION-ASSOCIATION COMPLEX WITH THIOCYANATE AND ADOGEN

F. SALINAS, J. J. BERZAS NEVADO and M. I. ACEDO VALENZUELA
Department of Analytical Chemistry, Faculty of Sciences, University of Extremadura, Badajoz, Spain

(*Received* 12 *March* 1984. *Accepted* 30 *June* 1984)

Summary—A selective and sensitive method is described for the determination of trace amounts of molybdenum, based on its reaction with thiocyanate and its extraction (into toluene) as an ion-association complex formed with adogen (methyltrioctylammonium chloride). The molar absorptivity is 2.13×10^4 l.mole^{-1}.cm^{-1} at λ_{max} 467 nm. The method has been applied to molybdenum determination in steels.

The use of thiocyanate for the determination of molybdenum has been widely studied and a number of methods have been reported. The fundamental differences between these methods are the reducing agents and solvents used, and in recent years the use of mixed-ligand complexes or ion-association complexes. Stannous chloride is the reducing agent most commonly used,[1–8] but ascorbic acid is recommended[9–13] because it gives a high absorbance for the complex and its concentration is not critical. It has also been found that extraction of the molybdenum–thiocyanate complex is complete even in the absence of a reducing agent if the reaction mixture is shaken for at least 30 min.[12,13] However, the presence of a reducing agent is necessary to eliminate interference, such as that of Fe(III).

In this paper, we report a selective, sensitive and reproducible method for determination of molybdenum, based on reduction of Mo(VI) to Mo(V) with stannous chloride [in presence of Fe(II)] and then reaction with thiocyanate in hydrochloric acid media, formation of the Mo(V)–thiocyanate complex and its subsequent extraction into toluene with adogen.

EXPERIMENTAL

Reagents

Molybdenum(VI) solution. Prepared from sodium molybdate dihydrate and standardized gravimetrically. The working solution (Mo 11.6 μg/ml) was prepared by appropriate dilution.

Tin(II) solution. A 0.25*M* solution in 2*M* hydrochloric acid.

Adogen solution. A 0.5 g/l. solution in toluene.

Iron(II) solution. Freshly prepared by dissolving 1 g of $(NH_4)_2Fe(SO_4)_2.6H_2O$ in 100 ml of water.

Thiocyanate solution, 1M.

All solvents and reagents were of analytical grade.

Procedure

The sample solution, containing 2.5–50 μg of Mo, was placed in a 100-ml separatory funnel, then 6 ml of thiocyanate solution, 9.5 ml of 2*M* hydrochloric acid, 1 ml of iron(II) solution, and 0.5 ml of stannous chloride solution were added, followed by dilution to 50 ml with demineralized water. The mixture was then shaken with 10 ml of the toluene solution of adogen for 2 min. The toluene layer was collected 30 min later and dried over anhydrous sodium sulphate in a 50-ml beaker, and its absorbance was measured at 467 nm against adogen solution.

Determination of Mo in steel

A 0.1-g sample was dissolved in 5–7 ml of 70% perchloric acid and the solution evaporated to dryness. The residue was heated with 5 ml of concentrated hydrochloric acid and evaporated almost to dryness, then the mass was cooled, dissolved in 15–20 ml of 2*M* hydrochloric acid, and diluted to 100 ml with demineralized water. When perchloric acid was not satisfactory as the solvent, 10 ml of *aqua regia* were added and the mixture was heated to fumes of oxides of nitrogen. After the solution was cooled, 3–5 ml of sulphuric acid were added, the solution was evaporated to dryness and the dried mass was cooled and dissolved in 15–20 ml of 2*M* hydrochloric acid and diluted to 100 ml with demineralized water. An aliquot (containing not more than 5 mg of Fe) was taken in a 100-ml separatory funnel and molybdenum was then determined as described in the procedure above.

When the Mo content (in steel) is <0.1%, the standard-addition method is recommended.

RESULTS AND DISCUSSION

Spectral characteristics

The absorption spectrum of the ion-association complex in toluene is shown in Fig. 1. Adogen has negligible absorption at the wavelength of maximum absorption. The absorption peak of the complex (at 467 nm) corresponds to an Mo(V)–thiocyanate complex.[2]

Influence of reducing agents

Ascorbic acid and stannous chloride were tried as reducing agents. Ascorbic acid gives a high absorbance for the complex and the amount to be added is not critical when $[SCN^-] = 0.4M$ and $[HCl] = 2M$. Under these conditions the extraction (shaking for 2 min) is complete even in the absence of ascorbic acid. Stannous chloride [in the absence of Fe(II)]

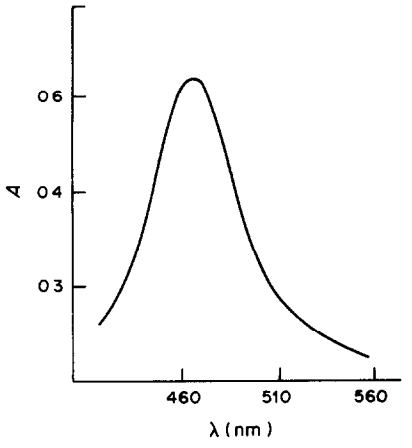

Fig. 1. Absorption spectrum of molybdenum–thiocyanate–adogen complex in toluene.

gives a lower absorbance and its concentration must be between 1×10^{-3} and $3.5 \times 10^{-3}M$ when $[SCN^-] = 0.1M$ and $[HCl] = 0.3M$. However, if iron(II) is present, stannous chloride gives a similar absorbance to that obtained with ascorbic acid. When stannous chloride is used, the absorbance can be measured against adogen solution, whereas when ascorbic acid is used, the absorbance must be measured against a reagent blank. Hence the stannous chloride/iron(II) system is preferred. The effect of the tin(II) concentration is shown in Fig. 2. The presence of iron(II) increases the extraction efficiency and makes the tin(II) concentration range less critical.

Effect of other variables

The extraction was found to be maximal at $[HCl] \geqslant 0.25M$ and 0.05–0.15M thiocyanate (Fig. 3); the adogen must have a concentration of at least 0.03%.

The presence of iron(II) increased the extraction of molybdenum. The absorbance was maximal and constant at $[Fe(II)] \geqslant 5$ ppm. A similar effect was observed when copper(II) was added, and the effect is not inhibited by the presence of EDTA or tartrate.

The absorbance was practically constant for aqueous/organic phase-volume ratios from 5:1 to 1:1. A shaking time of 2 min was sufficient for complete extraction. For low concentrations of molybdenum (1–2 ppm), the absorbance was constant for at least 6 hr, but for higher concentration (5 ppm) it was constant only for 15–60 min.

The order of addition of the reagents affects the absorbance (decreasing it), only when stannous chloride and molybdenum are mixed in the absence of thiocyanate.

Spectrophotometric characteristics

In the absence of iron(II), Beer's law is obeyed in the range 5–50 μg of Mo in the aqueous phase, and the molar absorptivity is 1.29×10^4 l.mole^{-1}.cm^{-1}. The relative error (95% confidence level) for 23 μg of Mo was $\pm 1.5\%$ (11 replicates). In presence of iron(II), Beer's law is obeyed in the range 2.5–50 μg of Mo in the aqueous phase, and the molar absorptivity is 2.13×10^4 l.mole^{-1}.cm^{-1}. The optimum range on the basis of a Ringbom plot is 10–40 μg of Mo. The relative error (95% confidence level) for 23 μg of Mo was $\pm 0.6\%$.

Composition of the complex

Different stoichiometries for Mo–thiocyanate complexes are given in the literature. We used the Job[14] and Yoe and Jones methods[15] and found the most probable composition of the ion-association complex to be 1:4:3, Mo–SCN–adogen, so the species extracted into toluene is probably $MoO_2(SCN)_4(ADG)_3$ where ADG is the trioctylmethylammonium ion. This stoichiometry agrees with that reported for the molybdenum–thiocyanate–tetrabutylammonium system.[16]

Interferences

The effect of other ions on the determination of 23 μg of Mo was examined. The tolerance limit was taken as the concentration that did not cause more than $\pm 2\%$ change in the absorbance. The results are summarized in Table 1.

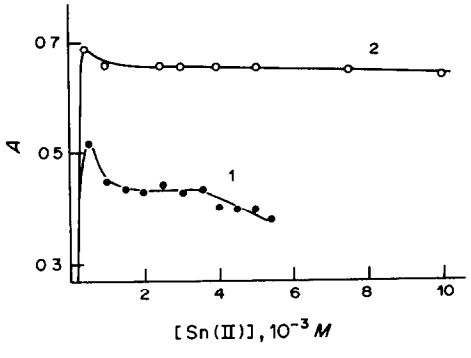

Fig. 2. Effect of Sn(II) concentration on the extraction of 29 μg of molybdenum: (1) in absence of iron(II); (2) in presence of 700 μg of Fe(II).

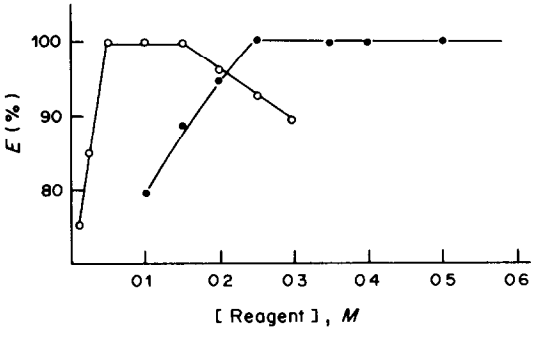

Fig. 3. Effect of thiocyanate and hydrochloric acid concentrations on the extraction of 35 μg of Mo: (○—○) % E *vs.* [SCN^-] (in 0.15M HCl); (●—●) % E *vs.* [HCl] (in 0.15M SCN^-).

Table 1. Interference of foreign ions in the determination of 23 μg of molybdenum

Ion added	Amount tolerated, *ppm*
sulphate, phosphate, EDTA, fluoride, Fe^{2+}	>1000
NH_4^+, K^+, Na^+, Li^+, Mg^{2+}, Ca^{2+}, Sr^{2+}, Ba^{2+} Fe^{3+}	150
V(V), Cu^{2+}, Bi^{3+}, Pb^{2+}, Cr^{3+}, As(V), Sb(III), Zr(IV), oxalate	100
Al^{3+}, Zn^{2+}, W(VI), U(VI), Mn^{2+}, Co^{2+}, Hg^{2+}, tartrate	50
Cd^{2+}, Ni^{2+}	25
Pd^{2+}	5

Table 2. Determination of molybdenum in steels

Sample	% composition certified	Mo certified, %	Mo found, %
BAS 33b	Cr(0.61), S(0.03), C(2.24)	0.40	0.41
	Si(2.00), P(0.11), Mn(0.64)		0.39
	Ni(2.24)		0.39
BAS 64b	C(0.90), Cr(4.55), V(1.99),	4.95	4.96
	W(7.05)		4.91
			4.94
BCS 261/1	$Cr(17.4_5)$, $Ni(13.1_0)$, $C(0.09_0)$	0.11	0.10
	Si(0.50), Mn(0.83), Nb(0.91)		0.11
	Cu(0.12)		0.12
BCS 432	Cr(0.21), Ni(0.24), Mn(1.10)	0.039	0.05
	Cu(0.16)		0.05
BCS 219/4	Cr(0.66), Ni(2.55), $C(0.31_5)$	0.58	0.60
	Mn(0.81), Cu(0.088)		0.62
BCS 406/1	Cr(2.10), Ni(1.52), C(0.23)	1.00	1.00
	Mn(0.61), Si(0.31), Cu(0.28)		1.00
			1.03

Table 3. Comparison of the proposed method with the existing thiocyanate methods

Method				
Reducing agent	Organic phase	ε, $l.mole^{-1}.cm^{-1}$	Applications	Reference
Sn^{2+}, Fe^{2+}	isoamyl alcohol	not stated	Soils	1
Sn^{2+}, Cu^{2+}, Fe^{3+} Tartaric acid	MIBK	1.04×10^4	Steels	4
Ascorbic acid	ethyl methyl ketone	8.0×10^3	Steels	11
Ascorbic acid	aminopyridines/benzene	$1.5–1.9 \times 10^4$	Steels, ores	12
Ascorbic acid	diarylbenzamidines/benzene	$1.65–1.85 \times 10^4$	Steels, ores	13
Sn^{2+}, Fe^{2+} (proposed method)	adogen/toluene	2.13×10^4	Steels	—

Applications

The validity of the method was tested with six alloy steels. The results are shown in Table 2. The method compares favourably with existing thiocyanate methods for determination of molybdenum. Our method is the most sensitive, as shown in Table 3.

REFERENCES

1. D. D. Perrin, *N.Z. J. Sci. Tech.*, 1946, **27A**, 396.
2. C. E. Crouthamel and C. E. Johnson, *Anal. Chem.*, 1954, **26**, 1284.
3. J. O. Hibbits, W. F. Davis, M. R. Menke and S. Kallmann, *Talanta*, 1960, **4**, 104.
4. J. O. Hibbits and R. T. Williams, *Anal. Chim. Acta*, 1962, **26**, 363.
5. H. Matsuo and S. Chaki, *Bunseki Kagaku*, 1967, **16**, 551.
6. A. A. Ponomareva, N. A. Agrinskaya and L. G. Anokhina, *Novye Metody Khim. Anal. Mater.*, 1971, 88.
7. S. P. Patil and V. M. Shinde, *Anal. Chim. Acta*, 1973, **67**, 473.
8. A. K. Bhadra and S. Banerjee, *Talanta*, 1973, **20**, 342.
9. A. I. Lazarev and V. I. Lazareva, *Zavodsk. Lab.*, 1958, **24**, 798.
10. I. Adamiec, *Chem. Anal. Warsaw*, 1966, **11**, 1175.
11. U. Madan and L. R. Kakkar, *Talanta*, 1982, **29**, 623.
12. K. S. Patel and R. K. Mishra, *ibid.*, 1982, **29**, 791.
13. K. S. Patel, R. M. Verma and R. K. Mishra, *Anal. Chem.*, 1982, **54**, 52.
14. P. Job, *Ann. Chim. Paris*, 1927, **9**, 114.
15. J. H. Yoe and A. L. Jones, *Ind. Eng. Chem., Anal. Ed.*, 1944, **16**, 111.
16. Yu. G. Eremin, E. F. Kolpikova and T. V. Rodionova, *Zh. Analit. Khim.*, 1976, **31**, 732.

Talanta, Vol 32, No. 1, pp. 66–67, 1985
Printed in Great Britain

0039-9140/85 $3.00 + 0.00
Pergamon Press Ltd

TITRIMETRIC DETERMINATION OF AMINOBENZOIC ACIDS

D. AMIN, F. M. EL-SAMMAN and H. ABDULAHED-MALALLA
Department of Chemistry, College of Science, University of Mosul, Mosul, Iraq

(*Received* 7 *November* 1983. *Revised* 14 *May* 1984. *Accepted* 19 *June* 1984)

Summary—A novel titrimetric method for determination of aminobenzoic acids is based on their reaction with excess of bromine to form *N*-bromo-2,4,6-tribromoaniline, which liberates an equivalent amount of iodine when treated with iodide. The method is applicable to the aminobenzoic acids in the range 0.1–5.0 mg, with a recovery ranging from 96 to 99.7% and a coefficient of variation of 0.2–2.0%, depending on the concentration level.

A method[1] based on bromine substitution has been used for determination of aminobenzoic acids, excess of bromine being back-titrated. A titrimetric[2] determination of as little as 2–30 mg has been reported for determination of aminobenzoic acids. The development of a sensitive, rapid and accurate titrimetric procedure based on the quantitative reaction of *o*-, *m*- and *p*-aminobenzoic acids with bromine was therefore undertaken.

The bromination of aromatic amines proceeds only at the unoccupied *ortho* and *para* positions on the ring. However, in the presence of a large excess of bromine the substitution goes further, to form *N*-bromo-2,4,6-tribromoaniline, which can be reacted with excess of iodide to liberate equivalent amounts of iodine which can be titrated with thiosulphate.

The suggested reactions are:

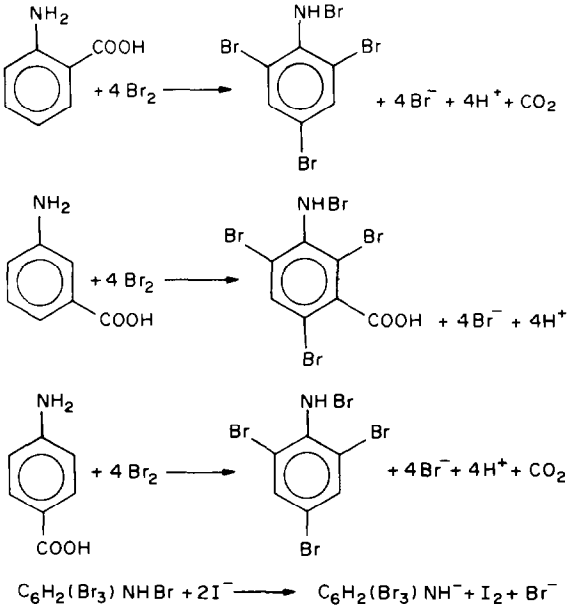

Scheme 1.

EXPERIMENTAL

Reagents

All chemicals used were of analytical grade, and distilled water was always used.

Aminobenzoic acid solutions. Aqueous solutions of each acid, with concentrations 0.1 and 1.0 mg/ml, were prepared in 0.04*M* sodium hydroxide.

Sodium thiosulphate solutions, 0.001 *and* 0.01*N*. Standardized against potassium iodate solutions of similar normality.

Solutions of bromine water (saturated) and formic acid (80%) were used.

Procedure

In a 50-ml conical flask, place a suitable volume (1–5 ml) of sample solution containing 0.1–5.0 mg of *o*-, *m*- or *p*-aminobenzoic acid, dilute with water to about 15 ml, then add about 3 ml of bromine water. Stopper the flask and shake it for 5 min. Remove the stopper, add about 1 ml of formic acid solution, shake for 1 min, then add 1 ml of concentrated phosphoric acid and about 0.5 g of potassium iodide. Let the flask stand for 10 min, with occasional shaking, then titrate the liberated iodine with 0.01*N* thiosulphate, with starch as indicator (for less than 2 mg of aminobenzoic acid, use 0.001*N* thiosulphate). Run a blank determination.

1 ml of 0.01*N* thiosulphate ≡ 0.6857 mg of aminobenzoic acid.

RESULTS AND DISCUSSION

The bromination of aminobenzoic acids normally proceeds at the unoccupied *ortho* and *para* positions, but preliminary studies confirmed that with a large excess of bromine the bromination goes further, to the amino group reacting to give the *N*-bromo derivative. Decarboxylation of the *o*- and *p*-isomers was confirmed by disappearance of the carboxylate band in the infrared spectrum.

The bromination is complete within 5 min; longer reaction time has no effect on the results. The complete bromination requires 2–3 ml of saturated bromine water, the excess of which is destroyed by addition of 1 ml of formic acid.

Reduction of the *N*-bromo-2,4,6-tribromoanilines requires about 0.5 g of potassium iodide and takes

Table 1. Determination of aminobenzoic acids (5 replicates)

Isomer	Weight, *mg*		Recovery, %	Coefficient of variation, %
	Taken	Mean found		
Ortho	0.100	0.096	96.0	1.7
	2.000	1.969	98.0	0.8
	5.000	4.952	99.0	0.4
Meta	0.100	0.098	98.0	1.1
	2.000	1.994	99.7	0.5
	5.000	4.960	99.2	0.2
Para	0.100	0.096	96.0	2.0
	2.000	1.978	98.9	0.8
	5.000	4.940	98.8	0.6

15–20 min. This time can be shortened to 10 min by adding about 1 ml of concentrated phosphoric acid. The blank is in the range 0.05–0.10 ml of 0.01*N* thiosulphate.

Compounds which can be brominated under the experimental conditions, *e.g.*, cresols,[3] toluidines[4] and phenols,[5] will interfere.

Table 1 shows the recoveries and the coefficient of variation for the compounds studied.

REFERENCES

1. S. Siggia and J. G. Hanna, *Quantitative Organic Analysis via Functional Groups*, p. 565. Interscience, New York, 1979.
2. F. M. Albert, V. Cimpa, M. Valeau and E. R. Jercan, *Rev. Roum. Chim.*, 1966, **11**, 1443.
3. D. Amin and K. Y. Saleem, *Intern. J. Environ. Anal. Chem.*, 1984, **17**, 3.
4. H. Abdulahed-Malalla, F. M. El-Samman and D. Amin, unpublished work.
5. D. Amin and W. A. Bashir, *Talanta*, 1984, **31**, 283.

Talanta, Vol. 32, No. 1, pp. 69–72, 1985
Printed in Great Britain.

0039-9140/85 $3.00 + 0.00

ANALYTICAL DATA

ARSENIC SPECIATION IN SOIL-PORE WATERS FROM MINERALIZED AND UNMINERALIZED AREAS OF SOUTH-WEST ENGLAND

STEPHEN J. HASWELL
Thames Polytechnic, Wellington Street, Woolwich, London SE18, England

PETER O'NEILL and KEITH C. C. BANCROFT
Plymouth Polytechnic, Drake Circus, Plymouth, Devon, England

(*Received* 1 *May* 1984. *Accepted* 27 *July* 1984)

Summary—Arsenate, arsenite and monomethylarsonic acid (MMAA) have been characterized in soil-pore waters extracted from soils in mineralized and unmineralized areas. Special attention has been paid to collection and storage of the samples. The dominant arsenic species in aerobic soils was arsenate, with small quantities of arsenite and MMAA in mineralized areas. In anaerobic soils arsenite was found to be the major soluble species. The analysis was done with an HPLC anion-exchange column combined with continuous-flow hydride-generation and atomic-absorption spectrometry. A preconcentration column was incorporated to increase the sensitivity.

Mineralization and past mining activities in South-West England have resulted in areas with above-average naturally occurring arsenic levels in the soil.[1] The high rainfall in the region results in waterlogging in many of these soils. The region thus lends itself to an investigation of the effects of mineralization and waterlogging on the soluble arsenic species found in these soils.

The chemical species of arsenic present in soil-pore waters will depend on the physical and chemical characteristics of the soil and the soil-pore water.[2] In aerobic soils, on which no arsenical herbicides have been used, arsenate is found to be the predominant species.[3,4] In waterlogged soils where reducing conditions occur the major species is reported to be arsenite.[5] The biomethylation of inorganic arsenic compounds[6,7] results in trace amounts of monomethylarsonic acid (MMAA) and dimethylarsinic acid (DMAA).[8,9] Takanatsu *et al.*[10] have also reported two unidentified organoarsenic compounds to be present in soil extracts.

In speciation studies a rapid reliable separative technique coupled with a suitable detection system is required. The samples should be analysed as soon as possible after collection, without use of sample-preservation techniques such as acidification which will modify the natural equilibria of the species present. The four arsenic species commonly reported to be present in soils, arsenate, arsenite, MMAA and DMAA, are all weak acids, the dissociation constants of which are quite different, and anion-exchange chromatography has been demonstrated to be a simple and efficient technique for their separation, with gravity column systems[11,12] and HPLC systems.[13] The greater control of eluent flow-rates, smaller sample and eluent volumes, and high resolving power of HPLC make it the separation technique of choice, and it is readily directly coupled to a detection system.

A popular method for determining low levels of reducible arsenic species involves the generation of arsine, followed by atomic-absorption detection.[8,14] The separation of arsenate, arsenite, MMAA and DMAA on a low-capacity anion-exchange HPLC column coupled to a graphite-furnace atomic-absorption spectrometer for arsenic detection has been demonstrated.[13] This method, however, does not give complete analysis of the eluate and has a sample analysis time of more than 30 min. Ricci *et al.*[8] have described an ion-chromatographic system, based on Dionex columns, which was coupled directly to a continuous arsine-generation system followed by atomization in a heated quartz-furnace and atomic-absorption determination (FAAS). The method used in the work reported here is based on HPLC anion-exchange chromatography with post-column continuous hydride-generation, followed by atomic-absorption measurement. The method takes 4 min for a single analysis and gives enhanced detection limits by the use of a preconcentration column.[15] The concentrations of arsenic species in soil-pore waters from mineralized and unmineralized soils are re-

ported in this paper. Special attention was paid to the collection and storage of the samples collected from reducing anaerobic waterlogged soils.

EXPERIMENTAL

Apparatus

A schematic diagram of the HPLC/FAAS continuous flow system for the determination of reducible arsenic is shown in Fig. 1. A Waters 6000A solvent-delivery system, and a Water U6K injection valve fitted with a 1-ml sample loop were attached to two anion-exchange columns in series. A peristaltic pump flow-rate of 1.6 ml/min and two borosilicate glass Auto-Analyser Y-pieces were used to entrain the hydrochloric acid (6*M*) and borohydride solution (4% solution in 0.1*M* sodium hydroxide) into the column eluate, flowing at 4 ml/min. Reduction took place in a short mixing coil and the arsine liberated was separated in a glass gas–liquid separator and subsequently flushed with nitrogen into a heated quartz tube mounted in the optical path of a Pye-Unicam SP9 spectrometer, with the detection wavelength adjusted to 193.6 nm. Samples (1 ml) were loaded onto the columns through the HPLC injector, with 10^{-4}% sulphuric acid as the eluent at a flow-rate of 4.0 ml/min. After loading, the eluent was switched from sulphuric acid to 0.01*M* ammonium carbonate (at the same flow-rate).

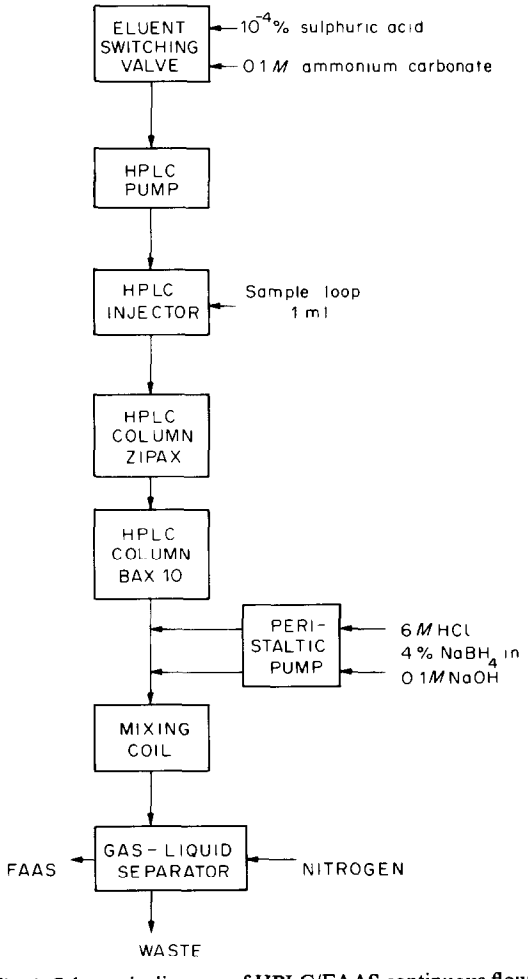

Fig. 1. Schematic diagram of HPLC/FAAS continuous flow system for the determination of arsenic.

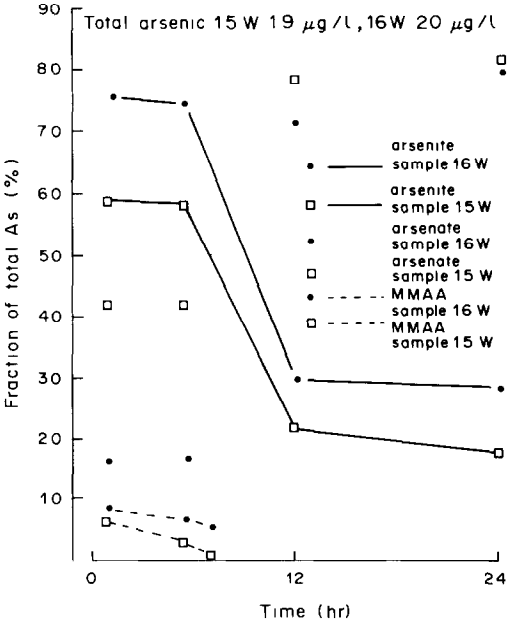

Fig. 2. Changes in arsenic species for samples filtered on site at time of collection and stored at room temperature in the light.

Chromatographic columns

A Zipax ion-exchange resin of mean particle size 40 μm, supplied by Dupont, was slurried into a stainless-steel Shandon 100 × 5 mm column. This column was attached in series to a second column containing a strong-base anion-exchange BAX10 resin, mean particle size 5 μm, supplied by Benson Co., which was slurried into a stainless-steel Shandon 250 × 5 mm column. The Zipax precolumn acted as a guard column and enabled a preconcentration step to be incorporated in the analysis; full details are given elsewhere.[15]

Reagents

Sulphuric acid, hydrochloric acid, ammonium carbonate, sodium borohydride, sodium hydroxide and the arsenic standards were all of analytical-reagent grade; the water used was demineralized and distilled.

Procedures

Aerobic soil-pore water extraction. Surface soil samples (0–10 cm depth) from the Dartington and Trusham series[16] were placed in 100-ml plastic centrifuge tubes and centrifuged on site (3000 rpm, 1000 *g* for 1 min) to extract a suitable volume of pore water (~0.5 ml). The pore water was drawn up into a plastic syringe and immediately filtered with a Whatman WCN filter (pore size 0.45 μm) in a Millipore Swinex apparatus, into an acid-washed vial, and the pH was taken. Arsenic determinations were made within 5 hr.

Anaerobic soil-pore water collection and sample storage. Soil-pore waters were collected from waterlogged soils of the Conway and Yeolland Park series[16] not directly affected by arsenic mineralization. These samples were treated in two ways: (*i*) filtered (0.45 μm filter) on site, and (*ii*) sealed unfiltered in an air-tight container and filtered (0.45 μm filter) just before analysis; both types of sample were stored in the light at room temperature. Figure 2 indicates that samples filtered on site may be stored for up to 5 hr with no apparent compositional changes, whereas losses of about 20% are observed for arsenite in unfiltered stored samples (Fig. 3) within the same time period. For samples treated by either method it was found that within 12 hr 90% of the arsenite was oxidized to arsenate, and both dimethylarsinic

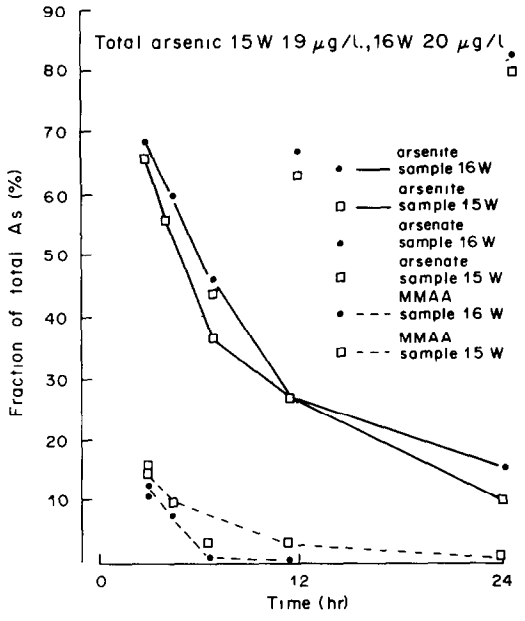

Fig. 3. Changes in arsenic species for samples not filtered on site, stored at room temperature in the light and filtered prior to analysis

acid and monomethylarsonic acid were partly lost from the system.

RESULTS AND DISCUSSION

Arsenic speciation in soil-pore waters from mineralized and unmineralized areas

Soil-pore waters were collected from mineralized, unmineralized, and unmineralized but waterlogged sites; the concentrations of arsenic species found are shown in Table 1.

In all the aerobic soils the predominant species (~90%) present in the soil-pore waters was found to be arsenate, in agreement with other published work.[3,4] From the *Eh*–pH diagram for arsenic,[2] the probability of finding arsenite in aerobic soils is greater at pH < 4.5 and in anaerobic soils at pH < 7. The pH of the soil-pore waters in this study was typically 4.1–5.3. Where mineralization had enhanced the soil arsenic-levels (samples 1M–8M) the presence of monomethylarsonic acid was observed. However, the range of arsenite in these samples was not noticeably different from that obtained for the unmineralized areas (samples 9U–14U). This suggests that there may be a threshold concentration of arsenite at which monomethylarsonic acid is microbially produced.[7] Samples 5M–8M, from a different mineralized area, have a range of arsenate levels similar to that of samples 1M–4M. Comparison of the samples containing the highest total levels of arsenic (samples 1M, 2M, 5M and 6M) indicates that samples 5M and 6M contain less monomethylarsonic acid than the other two do. This lower level of monomethylarsonic acid in samples 5M and 6M is accompanied by higher levels of arsenite; this relationship is also apparent in samples with intermediate total arsenic levels, namely 4M, 7M and 8M. Thus in samples with high arsenic levels the arsenite concentration may either be similar to those in samples with low arsenic levels, in which case monomethylarsonic acid will be present, or it may be 2–5 times the levels normally observed, in which case very little or no monomethylarsonic acid will be present.

The typical total levels of arsenic found in unmineralized aerobic soils (samples 9U–14U) are 16–56 μg/l., compared to 80–215 μg/l. for the mineralized soils discussed above. No monomethylarsonic acid was found in the samples from unmineralized areas except for one sample (10U), which was unusual in that the arsenite level was low.

Samples 15W and 16W were collected from anaerobic soils in an unmineralized area. The arsenite level

Table 1. Concentrations of arsenic species in soil-pore waters

Sample	pH	Arsenite, μg/l.	DMAA, μg/l.	MMAA, μg/l.	Arsenate, μg/l.	Sum of arsenic species, μg/l.	Total As, μg/l.
1M	3.9	3	ND	22	210	235	240
2M	4.2	2	ND	19	210	230	—
3M	5.0	2	ND	11	84	97	—
4M	5.3	8	ND	4	79	91	—
5M	4.1	6	ND	7	200	215	220
6M	4.0	7	ND	8	210	225	220
7M	4.9	11	ND	ND	80	91	93
8M	5.1	8	ND	ND	150	160	170
9U	5.7	2	ND	ND	35	37	40
10U	5.4	1	ND	1	34	36	—
11U	5.6	7	ND	ND	49	56	59
12U	5.5	2	ND	ND	44	46	45
13U	5.5	2	ND	ND	13	15	13
14U	5.5	1	ND	ND	15	16	15
15W	4.3	10	ND	1	8	19	17
16W	4.4	15	ND	2	3	20	22

ND, not detectable; M, mineralized soils; U, unmineralized soils; W, unmineralized waterlogged soils.

which represents 59 and 77% respectively of the total arsenic present, in contrast to the ~10% for aerobic soils, is in agreement with previously published results, which suggests that up to 80% of the total arsenic in anaerobic soils may be present as arsenite.[5] The chemical conditions in the aerobic and anaerobic environments suggest that the arsenite levels will be increased in the latter, owing to the chemical reducing conditions. Although microbial reduction of arsenate to arsenite has been reported,[7] at the negative redox potential found in anaerobic soils chemical reduction will override the microbial conversion of arsenate into arsenite. Though reduction of arsenate to arsenite is predominantly a chemically controlled reaction in both anaerobic and aerobic soils, methylation of arsenite to MMAA may be considered to be controlled by micro-organisms. No clear relationship between the arsenate, arsenite and MMAA levels is apparent from the results. As the MMAA levels increase, the levels of arsenite decrease, which may suggest that production of MMAA affects the residual arsenite levels in the soil. As indicated above the chemical conversion of arsenate into arsenite may preclude microbial activity, thus reducing the production of MMAA.

The complicated processes in the interconversion of arsenic species in soil systems depend primarily upon the *E*h–pH and the physicochemical factors affecting microbial activity. These processes pose a great problem to the analyst in the interpretation of experimental data.

CONCLUSIONS

This system of HPLC coupled with continuous-flow hydride generation and atomic-absorption measurement allows the rapid detection of reducible arsenic species at low concentrations in soil-pore waters. In aerobic soils the pore-water the main arsenic species is arsenate. Where mineralization and past mining activities have elevated the total soluble arsenic levels, arsenite and monomethylarsonic acid are also present. The arsenic species in anaerobic waterlogged soils are markedly different from those in aerobic soils, with arsenite predominant. Such samples should be filtered on site and analysed for arsenic species within 5 hr of collection.

REFERENCES

1. P. Colbourn, B. J. Alloway and I. Thornton, *Sci. Total Environ.*, 1975, **4,** 359.
2. J. F. Ferguson and J. Gavis, *J. Water Res.*, 1972, **6,** 1259.
3. A. J. Thompson and P. A. Thoresby, *Analyst*, 1977, **102,** 9.
4. E. K. Porter and P. J. Peterson, *Environ. Pollut.*, 1977, **14,** 255.
5. R. L. Duble, E. C. Holt and G. G. McBee, *Weed Sci.*, 1968, **16,** 421.
6. R. D. Wauchope and M. J. Yamamoto, *J. Environ. Qual.*, 1980, **4,** 597.
7. D. P. Cox, in *Arsenical Pesticides*, E. A. Woolson (ed.) p. 81. American Chemical Society, Washington DC, 1975.
8. G. R. Ricci, L. S. Shepard, G. Colovos and N. E. Hester, *Anal. Chem.*, 1981, **53,** 610.
9. M. Yamamoto, *Soil Sci. Soc. Am. Proc.* 1975, **39,** 859.
10. E. A. Woolson, *Weed Sci.*, 1977, **25,** 412.
11. J. Aggett and R. Kadwani, *Analyst*, 1983, **108,** 1495.
12. G. E. Pacey and J. A. Ford, *Talanta*, 1981, **28,** 935.
13. E. A. Woolson and N. Ahronson, *J. Assoc. Off. Anal. Chem.*, 1980, **63,** 523.
14. M. Thompson, B. Pahlavanpour and S. J. Walton, *Analyst*, 1978, **103,** 568.
15. C. T. Tye, S. J. Haswell, P. O'Neill and K. C. C. Bancroft, in preparation.
16. D. V. Hogan, *Soil Survey Record No. 44, Soils in Devon III*, Sheet SX47, Adlard, 1977.

Talanta, Vol. 32, No. 1, pp. 73–77, 1985
Printed in Great Britain.

0039-9140/85 $3.00 + 0.00

SPECTROPHOTOMETRIC AND POTENTIOMETRIC DETERMINATION OF THE PROTONATION CONSTANTS OF DITHIOCARBAZATES AND STUDIES ON SOME OF THEIR METALLIC CHELATES

A. IZQUIERDO
Department of Analytical Chemistry, University of Barcelona, Barcelona, Spain

J. GUASCH and F. X. RIUS
Department of Analytical Chemistry, University of Barcelona, Tarragona, Spain

(*Received* 22 *February* 1984. *Revised* 17 *April* 1984. *Accepted* 27 *July* 1984)

Summary—The protonation constants of 2-methyldithiocarbazate, 3,3-dimethyldithiocarbazate and 3-methyl-3-phenyldithiocarbazate, have been determined potentiometrically ($I = 1.00M$) and spectrophotometrically ($I = 0.01M$) at 25° in aqueous solution. The analytical properties of the reagents have been studied, and also the compositions of some of their insoluble metallic chelates.

Dithiocarbazates have been widely studied as potential substitutes for dithiocarbamates, which have found considerable application as surfactants, pharmaceuticals and very active fungicides, and in vulcanization processes. This has given rise to a number of papers dealing with their synthesis[1–4] and the study of their structural properties.[5–11] In contrast, their analytical properties have received little attention. 3-Phenyldithiocarbazate was proposed by Musil and Haas[12] for the gravimetric determination of Ag(I), Cu(II) and Pb(II) and by T'ien and Wang[13] for the colorimetric determination of Cu(II). Hydrazinium dithiocarbazate has been used in the photometric determination of V(V), Fe(II) and Fe(III) by Byr'ko *et al.*[14] and of Fe(II), Fe(III) and Co(II) by Haas *et al.*[15,16]

Because the substances containing the dithiocarbazate group are of interest as multidentate ligands, a systematic study of these compounds as analytical reagents has been undertaken in this laboratory. In this paper, the analytical properties of 2-methyldithiocarbazate (**I**), 3,3-dimethyldithiocarbazate (**II**) and 3-methyl-3-phenyldithiocarbazate (**III**) are described.

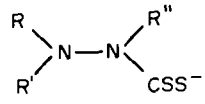

(I) $R = R' = H$; $R'' = CH_3$
(II) $R = R' = CH_3$; $R'' = H$
(III) $R = CH_3$; $R' = C_6H_5$; $R'' = H$

EXPERIMENTAL

Instruments

A Beckman 5260 spectrophotometer (1-cm cells) was used for spectrophotometric measurements. A Beckman 4260 infrared spectrophotometer (KBr discs) and a Perkin-Elmer R-24B NMR spectrophotometer were used. A Radiometer PHM-64 pH-meter along with a G-202B Radiometer glass electrode, an Ag/AgCl reference electrode prepared according to Brown[17] and a Wilhelm-type salt bridge[18] were used to measure pH values.

Reagents

Reagents (I) and (II) were obtained by the method of Anthoni *et al.*[4] by addition of CS_2 to the corresponding hydrazines in alkaline medium. Reagent (**III**) was synthesized by a modification of the method of Henriksen and Jensen.[3] A solution of 0.04 mole of CS_2 in 5 ml of dimethyl sulphoxide was added dropwise during 1 hr, at room temperature, to a suspension of 0.04 mole of sodium hydride (with 20% paraffin) in 15 ml of dry dimethyl sulphoxide containing 0.04 mole of 1-methyl-1-phenylhydrazine. The resulting solution was added to a mixture of 300 ml of acetone and diethyl ether (2:3) and allowed to stand for 24 hr at 4°. The white crystals obtained were filtered off by suction, washed with diethyl ether and recrystallized from chloroform (yield 24–30%). Melting points: (I) 178–179°, (II)128–129° and (III) 121–123°. Elemental analysis: (I) $H_2NN(CH_3)$ CSSK.$2H_2O$ requires 12.2% C, 4.6% H, 14.3% N, 32.7% S, 19.9% K; found 12.1% C, 4.3% H, 14.6% N, 31.8% S, 19.7% K. (II) $(CH_3)_2NNHCSSK.2H_2O$ requires 17.1% C, 5.3% H, 13.3% N, 30.5% S, 18.6% K; found 17.6% C, 4.9% H, 13.4% N, 29.9% S, 18.7% K. (III) (CH_3) (C_6H_5) NNHCSSNa.$2H_2O$ requires 37.5% C, 5.1% H, 10.9% N, 25.0% S, 9.0% Na; found 37.7% C, 5.0% H, 10.6% N, 25.8% S, 8.8% Na.

Because of the low stability of the solid dithiocarbazates in air (3–14% decomposition per day) they must be stored under nitrogen at 4°. They are then stable for at least 1 yr. Their purity was tested by the method of Clarke *et al.*,[19] originally devised for the analysis of dithiocarbamates. The substance is decomposed in strongly acidic medium and the

CS_2 evolved is collected in methanolic potassium hydroxide solution. Iodine titration of the xanthate thus formed showed, in all cases, the purity of the dithiocarbazates to be higher than 99%.

Protonation constants

The protonation constants were determined at $25 \pm 0.1°$ and $I = 0.01M$ by using the spectrophotometric method of Stenström and Goldsmith,[20] which makes use of the relationship between absorbance and pH; 1 ml of the aqueous $10^{-3}M$ dithiocarbazate solution was diluted to 50 ml with $0.01M$ buffer prepared as described by Perrin and Dempsey.[21] The pH and the absorbance at 273 nm (I), 267 nm (II) and 285 nm (III) were measured.

The potentiometric determination involved titration of alkaline solutions of the test substances (1.3×10^{-3}–$3.5 \times 10^{-3}M$) with $0.100M$ nitric acid at $I = 1.00M$, with potassium nitrate as ionic medium, at $25 \pm 0.1°$. Before and during the titration, a stream of pure nitrogen was continuously bubbled through the solutions. The potential of the following cell was measured:

Glass electrode (−)	Test solution: xM reagent, yM KOH, $(1-x-y)M$ KNO_3	$1.00M$ KNO_3	$0.01M$ KCl, $0.99M$ KNO_3, $AgCl_{(s)}$	Ag(+)

Beforehand, $0.10M$ nitric acid was titrated with $0.10M$ potassium hydroxide in the same cell. The Gran method[22] was used to determine $E^{\circ\prime}$ and E_j which relate the measured potential E to the hydrogen-ion concentration $[H^+]$ by means of the equation:

$$E(\text{mV}) = E^{\circ\prime} - 59.157 \log[H^+] + E_j$$

A known amount of reagent was added to the alkaline solution, then the mixture was titrated with nitric acid.

Chelation studies

The pH range over which complexation occurred, as indicated by colour and colour formation, was determined for each combination of metal ion and test substance by the technique established by Benedetti-Pichler.[23] The solubilities of the complexes in benzene, diethyl ether, chloroform, isoamyl alcohol and methyl isobutyl ketone were tested and absorption data (λ_{max}, ϵ) for buffered solutions of complexes were measured.

The insoluble metal chelates were prepared by reacting aqueous solutions of the metal ions with aqueous solutions of the dithiocarbazates in 1:4 mole ratio. The precipitates were filtered off, washed with water, ethanol and acetone and dried under reduced pressure over calcium chloride.

RESULTS AND DISCUSSION

The solubility values and the most significant infrared and NMR spectrophotometric data for the ligands are given in Table 1. The IR absorption peaks are assigned in accordance with earlier works.[1,3,4,6–9] These bands confirm the structure of the dithiocarbazates; thus, the addition of CS_2 to methylhydrazine takes place through the substituted nitrogen atom, giving rise to the appearance of the $-NH_2$ bending peak (1580–1645 cm^{-1}) in the spectrum of (I). This band does not appear in the spectra of (II) and (III) since the CS_2 is added to the primary nitrogen atom of 1,1-dimethylhydrazine and 1-methyl-1-phenylhydrazine. The NMR spectra recorded for D_2O solutions of the reagents with DSS as internal reference, give peaks similar to those reported previously.[10,11] The large shift corresponding to the methyl group of (II) ($\delta = 2.55$ ppm) relative to (III) ($\delta = 3.66$ ppm) is consistent with the presence of the neighbouring $-CSS^-$ group in the 2-methyldithiocarbazate.

The ultraviolet spectra of the reagents in some common solvents were measured (Table 2). A bathochromic shift of λ_{max} is observed for (I) and (II) as the polarity of the solvent decreases. This can be attributed to n–π^* transitions. The spectrum of (III) is more complicated, with the presence of overlapping bands corresponding to π–π^* aromatic ring transitions.

Table 1. Solubilities and infrared and NMR absorption peaks of the ligands

	Ligand		
	(I)	(II)	(III)
Solubility in water, *g/l.*	200	200	200
Solubility in ethanol, *g/l.*	17.1	6.5	8.3
Solubility in acetone, *g/l.*	3.5	2.0	1.8
Solubility in diethyl ether, *g/l.*	0.7	0.3	0.1
Solubility in benzene, *g/l.*	0.1	0.1	0.1
Solubility in hexane, *g/l.*	0.5	0.1	0.1
N–H stretch, cm^{-1}	3222–2928m	3210–2850m	3240–3100m
NH_2 bending, cm^{-1}	1635m	—	—
N–C stretch, cm^{-1}	1463m	1494s	1458m
CH_3 bending, cm^{-1}	1438m	1443m	1434m
H_3C–N stretch, cm^{-1}	1306s	1310s	1268m
N–N stretch, cm^{-1}	1012m	1000s	1005s
CSS^- stretch asymm, cm^{-1}	976s	974s	965s
CSS^- stretch symm, cm^{-1}	—	670m	694m
N^2–CH_3 protons (NMR), *ppm*	3.61	—	—
N^3–CH_3 protons (NMR), *ppm*	—	2.55	3.66
Aromatic protons (NMR), *ppm*	—	—	7.30

Table 2. Ultraviolet data for the ligands in common solvents

		(I)		(II)		(III)	
	Z values[24]	λ_{max}, nm	ϵ_{max}, $l.mole^{-1}.cm^{-1}$	λ_{max}, nm	ϵ_{max}, $l.mole^{-1}.cm^{-1}$	λ_{max}, nm	ϵ_{max}, $l.mole^{-1}.cm^{-1}$
Water	94.6	273	1.7×10^4	285	1.3×10^4	285	9.4×10^3
		228	1.0×10^4	252	9.6×10^3	255	9.4×10^3
Ethylene glycol	85.1	279.5	1.7×10^4	289.5	1.4×10^4	277	1.2×10^4
		—	—	252	7.4×10^3	263	1.3×10^4
Methyl alcohol	83.6	279.5	1.6×10^4	290	1.4×10^4	290	1.1×10^4
		231	8.7×10^3	252	9.0×10^3	253	1.0×10^4
Ethyl alcohol	79.6	281	1.7×10^4	291	1.5×10^4	292	1.2×10^4
		231	9.0×10^3	253	8.7×10^3	253	1.1×10^4
Isopropyl alcohol	76.3	282	1.7×10^4	291.5	1.5×10^4	289	8.9×10^3
		231	9.2×10^3	253.5	8.6×10^3	259	1.0×10^4

The stability of the reagents in aqueous solutions is pH-dependent. In neutral or alkaline media, the absorbance at λ_{max} decreases by about 15% in 24 hr, the sequence of stability being (II) > (III) > (I). In fairly acidic medium (pH < 2.5) all decompose rapidly with evolution of CS_2. This breakdown hinders the experimental determination of the absorbance of the protonated species in acidic media, as is required for the calculation of the equilibrium constants by the Stenström and Goldsmith method. Therefore, the Sommer method[25] was used, since it allows graphical determination of the values by solution of the equation:

$$A_R - A = A_R - A_{HR} - \frac{(A_R - A)}{[H^+]\,K_1^H}$$

where A_R and A_{HR} are the absorbances of the fully deprotonated and protonated reagents respectively, and K_1^H is the protonation constant. The resulting data have been optimized by the graphical method described by Rossotti and Rossotti[26] and McBryde.[27]

The values of the protonation constants determined fully coincide with those obtained by means of the least-squares program MINISPEF[28] (PDP 11/60 computer). Table 3 lists the values of the protonation constants of (I) and (II). Log K_1^H for (III) could not be determined because of interference from the absorbance of the 1-methyl-1-phenylhydrazine released on decomposition of (III) in acid. However, this constant, along with those for (I) and (II), was determined potentiometrically. The $E^{\circ\prime}$ and E_j values found in the Gran titration allowed determination of the protonation constant by use of the Bjerrum function,[29] $\bar{n}$,

$$\bar{n} = \frac{H_T - [H^+] + K_w/[H^+]}{R_T} = \frac{K_1^H[H^+]}{1 + K_1^H[H^+]}$$

which can be calculated experimentally from the pH of the solution, the total concentration of titratable hydrogen ion H_T and the total reagent concentration R_T. The constants were determined by use of the least-squares program MINIPOT.[30] The protonation constants are given in Table 3. The discrepancy between the spectrophotometric and potentiometric values is attributed to the difference in ionic strength.

The results obtained in the present work are not in accord with the overall ionization mechanism proposed for the hydrazinium dithiocarbazate by Byr'ko *et al.*,[14] who suggested

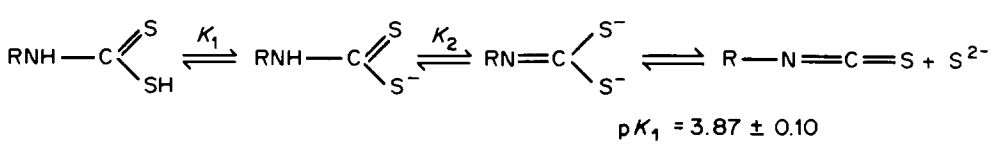

$pK_1 = 3.87 \pm 0.10$

$pK_2 = 8.90 \pm 0.10$

The fact that, in the present study, both potentiometrically and spectrophotometrically only a single protonation constant was observed, along with the absence of ionizable cations such the hydrazinium ion, provides strong evidence for a single acid–base equilibrium. This equilibrium, in a similar way to that proposed by Hulanicki[31] for the dithiocarbamates, could be represented by

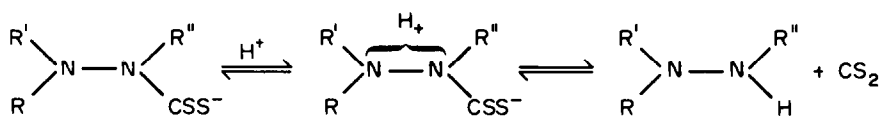

Table 3. Protonation constants of the reagents at 25 ± 0.1°C

Reagent	Spectrophotometrically ($I = 0.01M$) log K_1^H	Potentiometrically ($I = 1.00M$) log K_1^H
(I)	4.90 ± 0.07	5.42 ± 0.05
(II)	4.56 ± 0.02	4.73 ± 0.02
(III)	—	6.18 ± 0.03

This mechanism is consistent with the reported zwitterion structure of dithiocarbazic acid[1,7] and the indirect titration of the dithiocarbazates with iodine, where the presence of the CS_2 evolved in strongly acidic medium is required. On the other hand, the differences between constants for the different compounds show the influence of the substituents bound to the protonated N–N skeleton (the protonation of the CSS^- group would give rise to very similar values of the protonation constants, as occurs with xanthates and carboxydithioates[32]).

Table 4 gives the spectral characteristics of the soluble metal–reagent complexes, which have high absorptivities. The pH does not greatly influence the complex formation; this confirms that it is the N–N group rather than the CSS^- group that is protonated.

All three substances react very similarly with metal ions, although it is interesting to note the closer resemblance between (II) and (III). This behaviour can be attributed to the difference in structure of the complexes (Table 5). Reagents (II) and (III) give MS_4 type complexes, as previously reported by Battistoni *et al.*[7] Chelation occurs through both sulphur atoms, according to the structure:

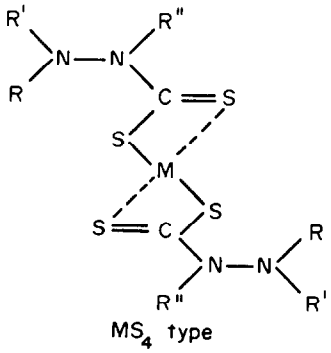

MS_4 type

The infrared spectra of the complexes studied show that the C–N stretching absorption (1525–1490 cm^{-1}) has been shifted to higher frequencies than for the

Table 4. Spectrophotometric characteristics of the complexes

Ligand	Metal ion	Optimum pH	λ, nm	ϵ, $l.mole^{-1}.cm^{-1}$
(I)	Tl(III)	2–7	320	2.4×10^4
(I)	Cu(II)	4–9	437	7.1×10^3
(I)	Fe(II)	4–9	317	7.6×10^3
(I)	Ni(II)	5–8	315	2.7×10^4
(I)	Bi(III)	7–10	358	1.2×10^4
(II)	Tl(III)	2–7	332	2.3×10^4
(II)	Cu(II)	9–12	600	1.2×10^4
(II)	Fe(II)	6–8	322	2.5×10^4
(II)	Fe(III)	4–8	338	6.6×10^3
(II)	Ni(II)	6–8	329	2.2×10^4
(III)	Cu(II)	7–9	455	1.2×10^4
(III)	Fe(II)	2–6	360	1.5×10^4
(III)	Fe(III)	5–10	351	7.6×10^3
(III)	Ni(II)	6–9	337	2.7×10^4
(III)	Co(II)	5–10	375	1.4×10^4

Table 5. Infrared data for the dithiocarbazato metal chelates

Compound*	Colour	Decomp. point, °C	$\delta_{(NH_2)}$	$\nu_{(C-N)}$	$\nu^{\S}_{(CSS-asym)}$	$\nu_{(CSS-sym)}$	Refs.
$Ag[NH_2N(CH_3)CS_2]$	yellow	125	1605	†	955(945)	577	
$Pb[NH_2N(CH_3)CS_2]_2$	white	140	1600		950(940)	580	
$Cu[NH_2N(CH_3)CS_2]_2$	brown	132	1597		970	567	
$Cd[NH_2N(CH_3)CS_2]_2$	white	154	1583		960(940)	573	
$Ni[NH_2N(CH_3)CS_2]_2$	red	185	1590		1010(1005)	564	2,7
$Bi[NH_2N(CH_3)CS_2]_3$	orange	93	1585		950(930)	576	
$Ag[(CH_3)_2NNHCS_2]$	white	164	—	1490	980	680	
$Pb[(CH_3)_2NNHCS_2]_2$	yellow	128	—	1495	977	675	
$Cu[(CH_3)_2NNHCS_2]_2$	green	119	—	1490	975	690	
$Cd[(CH_3)_2NNHCS_2]_2$	white	163	—	1512	970	685	
$Ni[(CH_3)_2NNHCS_2]_2$	green	190	—	1525	970	690	1,7
$Bi[(CH_3)_2NNHCS_2]_2$	yellow	154	—	1502	970	690	
$Cu[(C_6H_5)(CH_3)NNHCS_2]_2$	brown	235	—	1495	970	695	
$Ni[(C_6H_5)(CH_3)NNHCS_2]_2$	green	245	—	1492	970	690 7	

*These formulae were confirmed by elemental analysis.
†Overlapping band.
§Shoulders in brackets.

alkali-metal dithiocarbazates [1494 cm^{-1} (**II**) and 1498 cm^{-1} (**III**)] because of the important double bond C=N contribution in this type of chelate.[7,8] The antisymmetric and symmetric CSS^- stretching modes, absorbing at around 975 cm^{-1} and 685 cm^{-1} respectively, also confirm this kind of chelation as reported earlier for MS_4 chelates of nickel with 2-methyldithiocarbazate,[2,7] 3,3-dimethyldithiocarbazate[1,7] and 3-methyl-3-phenyldithiocarbazate.[7] In contrast reagent (**I**) forms MN_2S_2 type metal complexes, through the nitrogen and sulphur atoms:

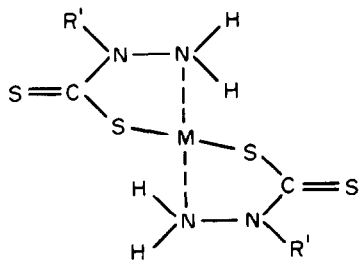

MN_2S_2 type

The C–N stretching vibration, with a smaller double bond contribution, overlaps in this case with neighbouring lower-frequency bands such as C–H (around 1440 cm^{-1}).[8] The chelates formed with reagent (**I**) all display NH_2 bonding peaks at lower frequencies (1605–1583 cm^{-1}), supporting the postulate of MN_2S_2 co-ordination.[7,8] Finally, the presence of a shoulder in the absorption peak assigned to the asymmetric CSS^- mode also confirms[7,8] the chelation through only one nitrogen and one sulphur atom.

REFERENCES

1. U. Anthoni, *Acta Chem. Scand.*, 1966, **20**, 2742, and references therein.
2. L. Cambi, E. D. Paglia, G. Bargigia and G. Crescentini, *Chim. Ind.*, 1966, **48**, 689.
3. L. Henriksen and O. R. Jensen, *Acta Chem. Scand.*, 1968, **22**, 3042.
4. U. Anthoni, B. M. Dahl, Ch. Larsen and P. H. Nielsen, *ibid.*, 1969, **23**, 1061.
5. A. Braibanti, L. Manotti, A. Tiripicchio and F. Lo Giudice, *Acta Cryst. Sec. B*, 1969, **25**, 93.
6. C. Battistoni, A. Monaci, G. Mattogno and F. Tarli, *Inorg. Nucl. Chem. Lett.*, 1971, **7**, 1081.
7. C. Battistoni, G. Mattogno, A. Monaci and F. Tarli, *J. Inorg. Nucl. Chem.*, 1971, **33**, 3815.
8. M. Akbar Alí, S. E. Livingstone and D. J. Phillips, *Inorg. Chim. Acta*, 1971, **5**, 119.
9. M. F. Iskander and L. El-Sayed, *J. Inorg. Nucl. Chem.*, 1971, **33**, 4253.
10. D. Gattegno and A. M. Giuliani, *Tetrahedron*, 1974, **30**, 701.
11. *Idem*, *J. Inorg. Nucl. Chem.*, 1974, **36**, 1553.
12. A. Musil and W. Haas, *Mikrochim. Acta*, 1958, 756.
13. Ping-Shih T'ien and K'uei Wang, *Sci. Sinica (Peking)*, 1957, **5**, 657; *Chem. Abstr.*, 1957, **51**, 17567.
14. V. M. Byr'ko, A. I. Busev, T. I. Tikhonova, N. V. Baibakova and L. I. Shepel, *Zh. Analit. Khim.*, 1975, **30**, 1885.
15. A. Musil and W. Haas, *Mikrochim. Acta*, 1959, 31.
16. W. Haas, *ibid.*, 1963, 274.
17. A. S. Brown, *J. Am. Chem. Soc.*, 1934, **56**, 646.
18. W. Forsling, S. Hietanen and L. G. Sillén, *Acta Chem. Scand.*, 1952, **6**, 601.
19. D. G. Clarke, H. Baum, E. L. Stanley and W. F. Hester, *Anal. Chem.*, 1951, **23**, 1842.
20. W. Stenström and N. Goldsmith, *J. Phys. Chem.*, 1926, **30**, 1683.
21. D. D. Perrin and B. Dempsey, *Buffers for pH and Metal Ion Control*, 4th Ed., Table 3.8 (pp. 44–7). Longmans, London, 1978.
22. G. Gran, *Analyst*, 1952, **77**, 661.
23. A. A. Benedetti-Pichler, *Microtechnique of Inorganic Analysis*, Wiley, New York, 1950.
24. E. M. Kosower, *J. Am. Chem. Soc.* 1958, **80**, 3253; 1958, **80**, 3261; 1958, **80**, 3267.
25. L. Sommer, *Folia Fac. Scienc. Nat. Univ. Purkynianae Brno*, 1964, **5**, 1.
26. F. J. C. Rossotti and H. Rossotti, *The Determination of Stability Constants*, McGraw-Hill, New York, 1961.
27. W. A. E. McBryde, *Talanta*, 1974, **21**, 979.
28. F. Gaizer and A. Puskás, *ibid.*, 1981, **28**, 925.
29. J. Bjerrum, *Metal Amine Formation in Aqueous Solution*, 2nd Ed., Haase, Copenhagen, 1957.
30. F. Gaizer and A. Puskas, *Talanta*, 1981, **28**, 565.
31. A. Hulanicki, *ibid.*, 1967, **14**, 1371.
32. L. G. Sillén and A. E. Martell, *Stability Constants of Metal-Ion Complexes*, 2nd Ed., Special Publication No. 17, The Chemical Society, London, 1964.

Talanta, Vol. 32, No. 1, pp. 78–80, 1985
Printed in Great Britain

0039-9140/85 $3.00 + 0.00
Pergamon Press Ltd

IONIC STRENGTH DEPENDENCE OF FORMATION CONSTANTS—V

PROTONATION CONSTANTS OF SOME NITROGEN-CONTAINING LIGANDS AT DIFFERENT TEMPERATURES AND IONIC STRENGTHS

PIER G. DANIELE,* CARMELO RIGANO† and SILVIO SAMMARTANO‡

*Istituto di Analisi Chimica Strumentale dell'Università, via Bidone 36, 10125 Torino, Italy
†Seminario Matematico dell'Università, viale A. Doria 6, 95125 Catania, Italy
‡Istituto di Chimica Analitica dell'Università, via dei Verdi, 98100 Messina, Italy

(*Received* 9 *May* 1984. *Accepted* 17 *July* 1984)

Summary—The protonation constants of 2,2′-bipyridyl, 1,10-phenanthroline, 1,3-diaminopropane, L-histidine and histamine have been determined potentiometrically, in the temperature range 10–40° and at ionic strengths ranging from 0.04 to 1 (potassium chloride). The dependence of the protonation constants on ionic strength is described by a simple general equation. The enthalpy changes for the protonation of the ligands have been calculated from the temperature dependence of the protonation constants.

In a series of papers[1-3] on the ionic strength dependence of formation constants we reported some interesting features of the function $\log K = f(I)$. In particular, (*a*) all the formation constants seem to follow the same trend as a function of ionic strength, if allowance is made for the different types of reaction stoichiometry and for the different charges of reagents and products and (*b*) there is a term in the equation $\log K = f(I)$ that is independent of the charges and accounts for the variations of the protonation constants of species that form cationic acids on protonation.

In order to elucidate the latter point we decided to investigate systematically cationic acids formed by protonation. Here we report a potentiometric study of the protonation of 2,2′-bipyridyl, 1,10-phenanthroline, 1,3-diaminopropane, L-histidine and histamine, at three temperatures (10°, 25°, 40°) and five ionic strengths (0.04, 0.1, 0.3, 0.6 and 1.0; KCl).

EXPERIMENTAL

Apparatus and procedures

The measurements were performed by potentiometric measurement of hydrogen-ion concentration with a model E600 Metrohm potentiometer equipped with Metrohm glass and silver/silver chloride electrodes. The glass electrode was calibrated (in $-\log[H^+]$ units) in the acid and alkaline region by titrating nitric acid (3–8 m*M*) with standard 1.000*M* carbonate-free potassium hydroxide, at the same ionic strength (adjusted with potassium chloride) as the solution under examination. The E° and pK_w values were calculated as reported elsewhere.[4] The ionic strength was adjusted by adding potassium chloride. This ionic medium was employed since interaction between potassium ions and the ligands concerned can be considered negligible.[2] The temperature (T°C) was kept constant by circulation of liquid from a model D1-G Haake thermocryostat. The titrant was delivered from a microsyringe (5000 divisions/ml). For each ligand five titrations were performed; the ligand concentration ranged from 3 to 6 m*M*; for each protonation step fifteen experimental points were used in the calculation.

Chemicals

2,2′-Bipyridyl, 1,10-phenanthroline, 1,3-diaminopropane, L-histidine monohydrochloride, histamine dihydrochloride and potassium chloride, all Fluka purissimum products, were used without further purification. The purity of the ligands, checked by acid–base titrations, was always >99% and was taken into account in the calculations. Nitric acid and potassium hydroxide stock solutions were prepared by diluting concentrated solutions (Merck ampoules).

Calculations

The protonation constants, expressed as

$$K_j^H = [H_jL]/([H][H_{j-1}L])$$

were calculated separately for each ionic strength by the program MINIQUAD 76A, modified in order to take into account the variation of ionic strength during the titrations;[5] the parameters defining the dependence on ionic strength were obtained from these values.

RESULTS AND DISCUSSION

The protonation constants of the ligands under study are collected in Table 1. The dependence of these values on ionic strength can be described by the general equation[1-3]

$$\log K^H(I) = \log K^H(I') - Az^*\left(\frac{\sqrt{I}}{1+B\sqrt{I}} - \frac{\sqrt{I'}}{1+B\sqrt{I'}}\right) + C(I-I') + D(I^{3/2} - I'^{3/2}) \quad (1)$$

where

$$A = 0.5115 + 8.885 \times 10^{-4}\,(T-25) + 2.953 \times 10^{-6}\,(T-25)^2$$

$$B = 1.489 + 8.772 \times 10^{-4}\,(T-25) + 4.693 \times 10^{-6}\,(T-25)^2;$$

Table 1. Protonation constants (log K^H)* at different temperatures and ionic strengths

Ligand	T, °C	Ionic strength 0.04	0.10	0.30	0.60	1.00
	$L + H^+ = [HL]^+$ (or $[HL] + H^+ = [H_2L]^+$), $z^* = 0$					
2,2'-Bipyridyl	10	4.52(3)	4.57(2)	4.65(1)	4.72(2)	4.86(2)
	25	4.38(1)	4.40(2)	4.46(2)	4.60(1)	4.68(2)
	40	4.27(2)	4.28(2)	4.34(2)	4.45(2)	4.50(1)
1,10-Phenanthroline	10	5.13(4)	5.14(4)	5.18(5)	5.22(5)	5.36(5)
	25	4.97(2)	4.97(3)	4.98(2)	5.10(3)	5.16(3)
	40	4.81(3)	4.81(2)	4.84(2)	4.93(2)	5.04(2)
1,3-Diaminopropane	10	11.19(3)	11.18(3)	11.23(2)	11.28(4)	11.37(3)
	25	10.59(2)	10.59(2)	10.64(2)	10.84(2)	10.85(2)
	40	10.10(2)	10.11(2)	10.12(2)	10.21(2)	10.31(2)
L-Histidine	10	6.27(2)	6.31(1)	6.34(2)	6.42(1)	6.51(2)
	25	5.99(2)	6.04(2)	6.08(2)	6.14(2)	6.23(2)
	40	5.75(1)	5.76(2)	5.82(1)	5.88(1)	5.94(2)
Histamine	10	10.22(2)	10.36(1)	10.39(2)	10.43(2)	10.52(2)
	25	9.80(1)	9.83(1)	9.85(1)	9.94(1)	10.02(1)
	40	9.31(3)	9.31(3)	9.33(3)	9.46(2)	9.51(2)
	$[HL]^+ + H^+ = [H_2L]^{2+}$ $z^* = -2$					
1,3-Diaminopropane	10	9.21(3)	9.27(2)	9.39(2)	9.47(3)	9.56(3)
	25	8.70(2)	8.79(3)	8.87(2)	9.04(2)	9.12(2)
	40	8.26(2)	8.32(2)	8.38(2)	8.54(2)	8.64(2)
Histamine	10	6.21(2)	6.39(1)	6.48(2)	6.60(1)	6.71(1)
	25	5.99(2)	6.07(1)	6.18(1)	6.29(1)	6.44(1)
	40	5.70(3)	5.77(1)	5.78(1)	6.03(2)	6.13(2)
	$L^- + H^+ = [HL]$ $z^* = 2$					
L-Histidine	10	9.52(2)	9.52(2)	9.53(1)	9.53(1)	9.58(2)
	25	9.08(1)	9.07(1)	9.08(2)	9.08(2)	9.14(1)
	40	8.75(1)	8.69(1)	8.69(1)	8.70(1)	8.72(1)

*The 95% confidence interval of the mean (C.I) is given in parentheses [*e.g.*, 4.52(3) = 4.52 ± 0.03], and was estimated by using the equation C.I. = $st/\sqrt{n}$, where s is the standard deviation of the mean value of log K_j^H (log K_j^H values were calculated separately for each titration), t is the Student-t value for $p = 0.95$, and n is the number of titration curves.

I and I' represent the actual and reference ionic strengths, respectively; $z^* = 2(1 - z - j)$ for the reaction $[H_{j-1}L]^{z+j-1} + H^+ = [H_jL]^{z+j}$ (z is the charge on L); C and D are parameters experimentally determined.

Considering that $A \simeq 0.5$ and $B \simeq 1.5$, equation (1) can be simplified, since small errors in A and B are absorbed in the linear term:[6]

$$\log K^H(I) = \log K^H(I') - z^*\left(\frac{\sqrt{I}}{2+3\sqrt{I}} - \frac{\sqrt{I'}}{2+3\sqrt{I'}}\right) + C(I - I') + D(I^{3/2} - I'^{3/2}) \quad (2)$$

The experimental values of C and D [equation (2)] are in general[1-3] a simple function of z^*:

$$C = c_0 + c_1 z^*, \quad D = dz^* \quad (3)$$

If $z^* = 0$ (for reactions involving uncharged ligands, such as $L + H^+ = [HL]^+$ or $[HL] + H^+ = [H_2L]^+$), substituting the values of C and D from equation (3) into equation (2) yields

$$\log K^H(I) = \log K^H(I') + c_0(I - I') \quad (4)$$

Over the temperature range used, for all the ligands considered the coefficient c_0 can be expressed as a function of temperature by

Table 2. Thermodynamic parameters for the protonation of the ligands under study, calculated for 25°C and $I = 0.25$; the 95% confidence interval is indicated by the figure in parentheses [*e.g.*, 6.10(3) = 6.10 ± 0.03]

Ligand	j	log K_j^H	$-\Delta G$, kcal/mole	$-\Delta H$, kcal/mole	ΔS, cal.mole^{-1}.deg^{-1}
2,2'-Bipyridyl	1	4.47(2)	6.10(3)	3.8(2)	8(1)
1,10-Phenanthroline	1	5.00(2)	6.82(3)	4.3(3)	9(2)
1,3-Diaminopropane	1	10.67(3)	14.55(4)	14.8(4)	−1(2)
	2	8.88(2)	12.11(3)	13.0(5)	−3(2)
L-Histidine	1	9.07(2)	12.37(3)	11.1(2)	4(1)
	2	6.07(1)	8.28(2)	7.2(2)	4(1)
Histamine	1	9.85(2)	13.44(3)	13.6(3)	−1(2)
	2	6.15(2)	8.39(3)	8.2(3)	1(2)

$$c_0 = 0.23 - 0.0013\ (T - 25) \qquad (5)$$

With the c_0 value calculated from equation (5), analysis of the data in Table 1 for reactions with $z^* \neq 0$ leads to the following values for c_1 and d [see equation (3)]:

T, °C	c_1	d
10	0.26	-0.18_5
25	0.23	-0.16_5
40	0.19	-0.13

(6)

If $\log K^{H}_{calcd}$ is the protonation constant ($z^* = 0$) calculated from equations (4) and (5), the mean deviation $\varepsilon = \log K^{H}_{exp} - \log K^{H}_{calcd}$ is:

$$\varepsilon = 0.05\,|\,I - 0.25\,| \qquad (7)$$

For the other protonation constants ($z^* \neq 0$) the mean deviation and the values of parameters c_1 and d, which define the dependence on ionic strength, are in agreement with our previous findings,[1] if allowance is made for the higher c_0 values found here.

The thermodynamic parameters ΔH and ΔS are collected in Table 2. These values can be considered to be in agreement with the literature values,[7] especially if it is taken into account that the protonation constants were determined at only three different temperatures.

REFERENCES

1. P. G. Daniele, C. Rigano and S. Sammartano, *Talanta*, 1983, **30**, 81.
2. *Idem*, *Transition Met. Chem.*, 1982, **7**, 109.
3. *Idem*, *Ann. Chim.* (*Rome*), 1983, **73**, 741.
4. P. Amico, P. G. Daniele, V. Cucinotta, E. Rizzarelli and S. Sammartano, *Inorg. Chim. Acta*, 1979, **36**, 1.
5. A. Sabatini, A. Vacca and P. Gans, *Talanta*, 1974, **21**, 53; P. Gans, A. Sabatini and A. Vacca, *Inorg. Chim. Acta*, 1976, **18**, 237; A. Vacca, personal communication; P. Amico, P. G. Daniele, C. Rigano and S. Sammartano, *Ann. Chim.* (*Rome*), 1982, **72**, 1.
6. P. G. Daniele, G. Ostacoli, C. Rigano and S. Sammartano, *Transition Met. Chem.*, in the press.
7. J. J. Christensen, L. D. Hansen and R. M. Izatt, *Handbook of Proton Ionization Heats and Related Thermodynamic Quantities*, Wiley, New York, 1976.

Talanta, Vol. 32, No. 1, pp. 81–82, 1985
Printed in Great Britain.

0039-9140/85 $3.00 + 0.00

CALCULATION OF THE Cu(II)–THIOSEMICARBAZONE COMPLEX FORMATION CONSTANTS BY A MODIFICATION OF THE DEFORD AND HUME METHOD APPLICABLE TO QUASI-REVERSIBLE AND IRREVERSIBLE PROCESSES

MANUEL ARGÜESO, M. DOLORES LUQUE DE CASTRO
and MIGUEL VALCÁRCEL
Department of Analytical Chemistry, Faculty of Sciences, University of Córdoba, Córdoba, Spain

(*Received* 27 *March* 1984. *Accepted* 16 *July* 1984)

Summary—Six cupric thiosemicarbazonates have been studied by differential pulse polarography and their formation constants calculated by the DeFord and Hume method and by a modification of this method applicable to quasi-reversible and irreversible processes. Comparison of the values found by both procedures shows the validity of the suggested modification.

Of the polarographic methods for calculation of complex formation constants, the one by DeFord and Hume[1] is undoubtedly the most widely used. In an earlier paper[2] we used this method, not in its original form but as the modification suggested by Heath and Hefter for differential pulse polarography (dpp)[3] with all its implicit approximations. An additional modification suggested by us involved taking into account not the theoretical number of electrons transferred but the product of the number of electrons and the transfer coefficient; the product was taken into account for each particular experiment and calculated in addition to I_p (peak intensity) and E_p (peak potential) by a computer program [F0(I)] based on applying a weighted least-squares method to the equation of the Tomes lines for a.c. polarography and dpp.[4] In the same paper[2] three computer programs for the calculation of the formation constants of chelates were suggested, and their applicability demonstrated for the cadmium–chloride,[3] cadmium–thiocyanate[5] and zinc–pyridine[4] systems. The suggested modification and programs have more recently been applied to the Bi(III)–azomethine 2-benzoylpyridine derivative systems,[6] which give irreversible reduction processes.

We now apply the modification and two of the programs to six Cu(II)–thiosemicarbazone systems.

EXPERIMENTAL

Apparatus

A Metrohm E-505 polarograph and E-506 recording system, with Ag/AgCl electrodes as reference and auxiliary electrodes, in conjunction with conventional dropping mercury and hanging drop electrodes. A Beckman 3500 pH-meter with combined calomel–glass electrode. An HP-85 microcomputer (32 kbyte).

Reagents

Acetone solutions ($5 \times 10^{-3} M$) of the thiosemicarbazones of the following carbonyl compounds: benzaldehyde (BAT), picolinaldehyde (PAT), 6-methylpicolinaldehyde (6-Me-PAT), biacetyl monoxime (BAMT), salicylaldehyde (SAT) and *p*-hydroxybenzaldehyde (pHBT). Aqueous solutions ($1.0 M$) of sodium perchlorate, potassium chlorate and potassium chloride, and $0.1 M$ tetramethylammonium bromide. Britton and Robinson buffers (pH 1–12). Gelatine solution (1%). Aqueous standardized copper(II) solution ($0.167 M$). More dilute solutions were prepared as required. All solvents were of analytical grade.

RESULTS AND DISCUSSION

The behaviour of the six systems is simultaneously discussed. Unless otherwise specified, the working conditions were as follows: initial potential, −0.2 V; scan-rate, 5 mV/sec; drop-time, 0.6 sec; pulse-amplitude, 50 mV; rate of mercury flow, 0.8083 mg/sec; height of the mercury head, 60 cm; temperature, 25°; [Cu(II)], $2 \times 10^{-4} M$; [ligand], $1.5 \times 10^{-3} M$.

The effect of type of supporting electrolyte was examined with sodium perchlorate, potassium chlorate, potassium chloride and tetramethylammonium bromide solutions. The concentration of organic solvent (acetone in all cases[7–9]) was below 4% for all the systems, since higher concentrations make the reduction processes more irreversible. Study of the effects of pH, temperature, drop-time and pulse amplitude showed that the processes were diffusion-controlled; the optimal values of these variables are summarized in Table 1.

The ligand concentration was changed between 50 and 100 times the cupric ion concentration for each thiosemicarbazone. The application of the F0(I) program allowed calculation of the $n\alpha$, I_p and E_p data

Table 1. Optimal values of variables

Ligand	Supporting electrolyte	pH
BAT	$NaClO_4$	11.0
PAT	KCl	9.7
6MePAT	KCl	10.6
BAMT	$NaClO_4$	11.5
SAT	KCl	11.5
pHBT	KCl	11.7

Temperature 25°, pulse amplitude 50 mV, drop-line 0.6 sec (except for 6 MePAT, for which it was 0.8 sec).

from each polarogram. The formation constants for each Cu(II)–thiosemicarbazone system were calculated by programs GIP II and FOW,[2] taking into account the theoretical number of electrons exchanged in the process ($n = 2$), that is, the Heath and Hefter modification,[3] (Table 2) and also taking into account[2] the product $n\alpha$ (Table 3).

The values of the formation constants obtained by our modification (Table 3) are all smaller than those found by the Heath and Hefter method because α was always < 1. The divergence between the values found by the two methods is a measurement of the irreversibility of the process.

The values of the formation constants for all the systems were very similar, except for the Cu(II)–PAT system. The great divergence in β values as well as in the number of formation constants obtained by both methods for the Cu–SAT and Cu–pHBT systems may be attributed to the marked degree of adsorption of the hydroxylic ligands on the electrode surface,[10] which dramatically disturbs their electrode behaviour.

In the Cu(II)–SAT system the occurrence of a ligand reduction which overlaps that of the complexed Cu(II) prevents the peak-width measurements necessary for calculating the $n\alpha$ values.

Once again the suitability of this modification for quasi and irreversible processes is emphasized.

REFERENCES

1. D. D. DeFord and D. N. Hume, *J. Am. Chem. Soc.*, 1951, **73**, 5321.
2. M. A. Gómez-Nieto, J. L. Cruz-Soto, M. D. Luque de Castro and M. Valcárcel, *Anal. Chim. Acta*, 1984, **156**, 77.
3. G. A. Heath and G. Hefter, *J. Electroanal. Chem.*, 1977, **84**, 295.
4. V. K. Sharman and J. N. Gaur, *ibid.*, 1965, **9**, 321.
5. K. Momoki H. Sato amd H. Ogawa, *Anal. Chem.*, 1967, **39**, 1072.
6. M. A. Gómez-Nieto, J. L. Cruz-Soto, M. D. Luque de Castro and M. Valcárcel, *Talanta*, 1984, **31**, 379.
7. M. Argüeso, M. D. Luque de Castro and M. Valcárcel, *Microchem. J.*, in the press.
8. *Idem*, *ibid.*, in the press.
9. *Idem*, *ibid.*, in the press.
10. F. Lázaro, M. D. Luque de Castro and M. Valcárcel, *ibid.*, in the press.

Table 2. Conditional formation constants of the Cu–thiosemicarbazone systems as calculated by the DeFord and Hume method

Ligand	β_1	β_2	β_3	Program
BAT	$(13.4 \pm 1.7) \times 10^{15}$	$(7.8 \pm 2.7) \times 10^{17}$	$(4.1 \pm 2.0) \times 10^{19}$	FOW
	$(11.3 \pm 1.2) \times 10^{15}$	$(22.3 \pm 4.8) \times 10^{16}$	$(3.6 \pm 0.3) \times 10^{19}$	PIG II
PAT	$(2.2 \pm 0.1) \times 10^{12}$	$(2.2 \pm 0.5) \times 10^{14}$	$(1.7 \pm 0.6) \times 10^{15}$	FOW
	$(21.0 \pm 1.0) \times 10^{11}$	$(18.5 \pm 2.0) \times 10^{13}$	$(14.5 \pm 1.7) \times 10^{14}$	PIG II
6MePAT	$(8.3 \pm 1.9) \times 10^{15}$	$(7.0 \pm 2.2) \times 10^{17}$	$(4.8 \pm 1.8) \times 10^{19}$	FOW
	$(10.1 \pm 2.0) \times 10^{15}$	$(7.1 \pm 1.0) \times 10^{16}$	$(4.5 \pm 0.4) \times 10^{18}$	PIG II
DAMT	$(4.9 \pm 3.0) \times 10^{15}$	$(2.2 \pm 0.3) \times 10^{18}$	$(19.2 \pm 2.2) \times 10^{19}$	FOW
	$(2.7 \pm 0.8) \times 10^{16}$	$(2.8 \pm 0.1) \times 10^{18}$	$(17.6 \pm 0.7) \times 10^{19}$	PIG II
SAT	$(1.3 \pm 0.1) \times 10^{16}$	$(5.4 \pm 0.7) \times 10^{18}$	$(1.8 \pm 0.4) \times 10^{21}$	FOW
	$(13.2 \pm 0.8) \times 10^{15}$	$(4.9 \pm 0.5) \times 10^{18}$	$(1.5 \pm 0.2) \times 10^{21}$	PIG II
pHBT	$(2.9 \pm 0.3) \times 10^{15}$	$(3.0 \pm 0.4) \times 10^{17}$	$(1.8 \pm 0.4) \times 10^{19}$	FOW
	$(3.5 \pm 0.3) \times 10^{15}$	$(2.6 \pm 0.2) \times 10^{17}$	$(1.6 \pm 0.1) \times 10^{19}$	PIG II

Table 3. Conditional formation constants of the Cu–thiosemicarbazone systems as calculated by the suggested modification

Ligand	β_1	β_2	β_3	Program
BAT	$(3.0 \pm 1.0) \times 10^{11}$	$(3.8 \pm 1.2) \times 10^{13}$	$(2.2 \pm 0.9) \times 10^{14}$	FOW
	$(4.4 \pm 0.4) \times 10^{11}$	$(3.3 \pm 0.2) \times 10^{13}$	$(2.0 \pm 0.1) \times 10^{14}$	PIG II
PAT	$(7.1 \pm 1.8) \times 10^{7}$	$(5.4 \pm 2.5) \times 10^{9}$	$(3.6 \pm 2.3) \times 10^{11}$	FOW
	$(7.0 \pm 1.5) \times 10^{7}$	$(4.6 \pm 1.1) \times 10^{9}$	$(3.1 \pm 0.7) \times 10^{11}$	PIG II
6MePAT	$(5.6 \pm 1.7) \times 10^{9}$	$(4.4 \pm 1.8) \times 10^{11}$	$(2.7 \pm 1.4) \times 10^{13}$	FOW
	$(6.7 \pm 1.5) \times 10^{9}$	$(4.1 \pm 0.7) \times 10^{11}$	$(2.4 \pm 0.3) \times 10^{13}$	PIG II
DAMT	$(1.6 \pm 0.9) \times 10^{11}$	$(6.5 \pm 0.7) \times 10^{13}$	$(5.4 \pm 0.5) \times 10^{15}$	FOW
	$(7.5 \pm 2.0) \times 10^{11}$	$(7.8 \pm 2.7) \times 10^{13}$	$(5.0 \pm 0.2) \times 10^{15}$	PIG II
SAT	—	—	—	FOW
	—	—	—	PIG II
pHABT	$(2.9 \pm 1.6) \times 10^{8}$	$(1.3 \pm 1.2) \times 10^{10}$	—	FOW
	$(2.7 \pm 0.9) \times 10^{8}$	$(1.0 \pm 0.2) \times 10^{10}$	$(5.5 \pm 0.7) \times 10^{11}$	PIG II

Talanta, Vol. 32, No. 1, pp. 83–85, 1985
Printed in Great Britain.

0039-9140/85 $3.00 + 0.00

FORMATION CONSTANTS FOR THE COMPLEXES OF ORTHOPHOSPHATE WITH MAGNESIUM AND HYDROGEN IONS

PETER W. LINDER and JOHN C. LITTLE
School of Chemical Sciences, University of Cape Town, Rondebosch 7700, South Africa

(*Received* 14 *June* 1984. *Accepted* 30 *June* 1984)

Summary—The system of orthophosphate, magnesium and hydrogen ions in aqueous solution at 25° and $I = 0.2M$ chloride has been characterized by means of glass-electrode potentiometry. Protonation constants for orthophosphate species and formation constants for the complexes $MgH_2PO_4^+$, $MgHPO_4$, $MgPO_4^-$ and $MgOH^+$ are reported.

We are currently developing a metal speciation model for urine along similar lines to our blood plasma model[1] and for this we require formation and protonation constants applicable to an ionic strength of $0.2M$ and a temperature of 37° for all the metal–ligand–proton complexes that can potentially be formed. The latter include complexes between magnesium, orthophosphate and hydrogen ions but the literature data[2–10] for this system cover ionic strengths sufficiently far removed from our requirements for us to be concerned about the reliability of applying theoretical corrections to the relevant constants. Furthermore, there is a variation in the range of magnesium complexes postulated, some authors[5–10] giving $MgHPO_4$ as the only one whereas others[3,4] include $MgPO_4^-$ and/or $MgH_2PO_4^+$. For these reasons, we decided to investigate the magnesium–phosphate–proton system further, at an ionic strength of $0.2M$ but at a temperature of 25°. This temperature was chosen in preference to 37° to avoid condensation problems inside the titration assembly and because it was considered that correction over as small a temperature range as 12° by using the van't Hoff equation and assuming constant enthalpies of reaction would not introduce errors of unacceptable magnitude for our urine model.

EXPERIMENTAL

Sodium hydroxide solutions ($0.1M$) were freshly prepared at frequent intervals, by dilution of the contents of Merck ampoules, under nitrogen, and standardized against potassium hydrogen phthalate (Merck). The $0.1M$ hydrochloric acid used was also prepared by use of Merck ampoules, and standardized with the sodium hydroxide solutions. Orthophosphoric acid solutions (0.01–$0.1M$) were prepared from the Merck concentrated acid and standardized with the sodium hydroxide solutions. Magnesium chloride solutions ($0.04M$) were prepared by dissolving high-purity magnesium ribbon (BDH) in hydrochloric acid after initial cleaning with the acid, washing with glass-distilled water and drying in a vacuum oven at 40°. The acid content of the magnesium chloride solutions was determined by titration with standardized sodium hydroxide. Sodium chloride solutions ($0.200M$) were prepared from Merck ampoules. All the solutions mentioned were prepared with boiled-out glass-distilled water. The sodium hydroxide, hydrochloric acid and orthophosphoric acid solutions were prepared with a total chloride concentration of $0.200M$, by addition of sodium chloride from Merck ampoules.

Equilibrium constants for the protonation of orthophosphate and the complexation of orthophosphate by magnesium were determined by potentiometric titrations in a Metrohm EA876-20 titration vessel maintained at 25°. The electrodes were Metrohm EA109 glass electrodes, and Metrohm EA404 calomel electrodes containing $5M$ sodium chloride as electrolyte. During the titrations, a purified nitrogen atmosphere was maintained in the titration vessel.

In the determination of the protonation constants, solutions containing orthophosphoric acid and sodium chloride were titrated with sodium hydroxide/chloride solution added from a Metrohm Dosimat E635 piston-burette controlled by a Metrohm Titroprocessor E636, which also measured and recorded the emf of the cell. The data obtained were used to calibrate the electrodes and determine the protonation constants simultaneously.

Three types of titration procedure were followed to investigate the complexation equilibria. Solutions containing orthophosphoric acid, magnesium chloride and sodium chloride were titrated with sodium hydroxide/chloride solution or a solution containing sodium hydroxide, orthophosphate and chloride. In the latter type of titration, the solutions were prepared in such a way that the orthophosphate concentration in the titration solution remained constant. In the third type of titration, the magnesium concentration was maintained at a constant level by titrating with solutions containing hydrochloric acid, magnesium chloride and sodium chloride. Concentration adjustments could be made before or during each titration by adding sodium chloride solution from a calibrated Metrohm E274-50 piston-burette.

The orthophosphate protonation constants and the electrode calibration parameters were determined by applying the MAGEC[11] and MINIQUAD[12] programs alternately to the relevant titration data, following the procedure described in reference 11. The complexation-titration data were processed initially by ZPLOT[13] in order to obtain formation curves and subsequently by MINIQUAD in order to obtain best-fitting chemical models and refined formation constants. The validity of the finally chosen chemical model and "best" formation constants was checked by supplying the latter as input to PSEUDOPLOT,[14] which generated theoretical formation curves. The degree of matching between the experimental and

theoretical formation curves gave a sound measure of the validity or accuracy of the chemical model.

As a further check, attempts were made to determine the formation constants by processing the constant-ligand and constant-metal titration data according to the method of Österberg,[15,16] but the conditions were found to be unsuitable

RESULTS AND DISCUSSION

Two protonation titrations were done with an initial orthophosphoric acid concentration of about 0.01*M* and two with an initial concentration of about 0.1*M*. Converging values were obtained for the electrode parameters and the protonation constants over a pH range of about 2–12. Satisfactory statistical fits between the parameters and the data were indicated by reasonable values obtained for the MAGEC objective function (0.016 cm^6), the MINIQUAD *R*-factor (0.0007) and χ^2 (23.7). Values found for the protonation constants, together with corresponding literature data, are presented in Table 1. Allowing for the variation in background medium and temperature, the agreement between our protonation constants and the literature data is acceptable. The value we find for the ionic product of water also appears to be acceptable.

Ten complexation titrations were done with initial conditions covering wide ranges of component concentration, namely 0.003–0.022*M* for orthophosphate and 0.002–0.008*M* for magnesium. Ligand to metal ratios ranged from 0.5:1 to 10:1. The pH ranged from 3 to 10. When MINIQUAD was applied in order to obtain consistent chemical models to explain the entire set of titrations, the data were divided into two groups, namely those for pH > 8 and for pH < 8. The first group was used to refine the constants for the species $MgPO_4^-$ and $MgOH^+$, and the second for $MgHPO_4$ and $MgH_2PO_4^+$. The equilibrium constants obtained, together with standard

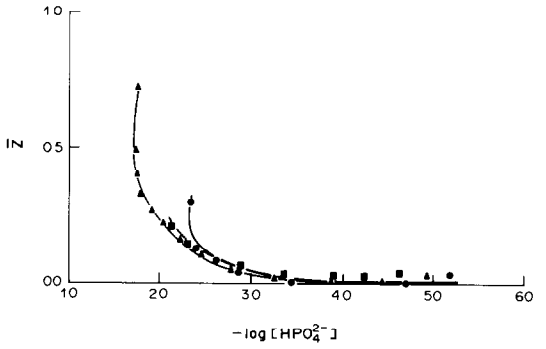

Fig. 1. PSEUDOPLOT curve calculated from the orthophosphate–proton and orthophosphate–magnesium formation constants in Table 1, plotted on a selection of the experimental formation values. Initial concentrations (m*M*) of orthophosphate and magnesium respectively were: 22.5 and 7.6 (▲); 11.3 and 2.1 (■); and 6.4 and 3.0 (●). ▲ = constant [orthophosphate] titration; ■ = constant [magnesium] titration.

deviations, the MINIQUAD *R*-factors, χ^2 values and corresponding literature data, are presented in Table 1. The *R* and χ^2 values indicate satisfactory fits of the data to the chemical model proposed and the corresponding formation constants. In Fig. 1, the individual points represent a selection of the formation function values (obtained from ZPLOT) plotted against the negative logarithm of the free HPO_4^{2-} concentration. Superimposed are theoretical formation curves generated by PSEUDOPLOT from the refined constants listed in Table 1. The good match between the curves and the points confirms the validity of the chemical model and the constants in Table 1. Figure 2 shows the species distribution for the magnesium–orthophosphate–proton system, computed from the constants in Table 1, for total concentrations of orthophosphate and magnesium both equal to 0.01*M*.

Table 1. Logarithms of formation constants (*K*) for proton and magnesium complexes of orthophosphate at 25° and $I = 0.2M$ [Cl^-]

Reaction	log *K*	*d*	*n*	*R*	χ^2	Literature data: log *K* (temp., *I*, [medium])[ref]
$H_2O \rightleftharpoons H^+ + OH^-$	−13.449	0.001	174	0.0007	23.7	−13.72 (25°, 0.1 [NaCl]).[17]
$H^+ + PO_4^{3-} \rightleftharpoons HPO_4^{2-}$	11.179	0.001	174	0.0007	23.7	11.30 (37°, 0.15 [KNO_3]).[2]
$H^+ + HPO_4^{2-} \rightleftharpoons H_2PO_4^-$	6.401	0.001	174	0.0007	23.7	6.70 (37°, 0.15 [KNO_3]),[2] 6.279 (25°, 3 [$NaClO_4$]).[3]
$H^+ + H_2PO_4^- \rightleftharpoons H_3PO_4$	1.684	0.002	174	0.0007	23.7	1.95 (37°, 0.15 [KNO_3]),[2] 1.879 (25°, 3 [$NaClO_4$]).[3]
$Mg^{2+} + PO_4^{3-} \rightleftharpoons MgPO_4^-$	3.13	0.01	109	0.0009	53	3.4 (37°, 0.15 [KNO_3]).[4]
$Mg^{2+} + HPO_4^{2-} \rightleftharpoons MgHPO_4$	1.94	0.08	387	0.0012	392	1.8 (37°, 0.15 [KNO_3]),[4] 1.42 (25°, 3 [$NaClO_4$]),[3] 2.5 (25°, 0),[5] 2.87 (38°, 0),[6] 1.52 (30°, 0.2 [KCl]),[7] 2.74 (30° 0),[8] 1.85 (25°, 0.2 [$(n\text{-}C_3H_7)_4N^+Cl^-$]),[9] 1.78 (15°, 0.1 [KCl]).[10]
$Mg^{2+} + H_2PO_4^- \rightleftharpoons MgH_2PO_4^+$	1.51	0.05	387	0.0012	392	0.60 (37°, 0.15 [KNO_3]),[4] 0.16 (25°, 3 [$NaClO_4$]).[3]
$Mg^{2+} + OH^- \rightleftharpoons MgOH^+$	3.07	0.04	47	0.0004	19	2.58 (25°, 0).[18]

H^+ represents the sum of all forms of hydrated protons; *d* = standard deviation of log *K*; *n* = number of observations; *R* = Hamilton *R*-factor, from MINIQUAD output; χ^2 indicates deviation (from normal distribution) of residuals in total concentrations from MINIQUAD output.

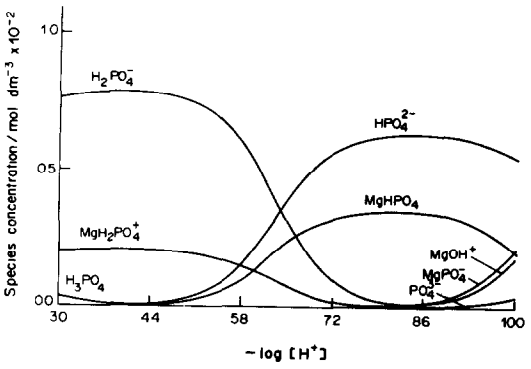

Fig. 2. Concentrations of the complexes present, as a function of $-\log[H^+]$ for the orthophosphate–magnesium–proton system when the total concentrations of orthophosphate and magnesium are both 10 m*M*.

The agreement between our constants for the magnesium complexes and the corresponding literature values is generally satisfactory, taking into consideration the differences in temperature and ionic background medium. The most commonly reported constant in the literature is for the species $MgHPO_4$.[5–10] Several of the authors concerned give this as the only magnesium complex, possibly because of the limited pH-range examined by these authors, and also because of the predominance of $MgHPO_4$, as illustrated in Fig. 2. In contrast, the reliability of our proposed model and constants is given weight by the good match, shown in Fig. 1, between the theoretical formation curves and the formation function points, even though the system is only weakly complexing and hence difficult to characterize quantitatively.

Attempts made to apply the method of Österberg[15,16] to the titrations with constant ligand but varying metal concentration and with constant metal but varying ligand concentration were not fruitful. This evidently stems from our inability to achieve, experimentally, the appropriate ranges of conditions required for application of the Österberg method.

Acknowledgements—Grateful acknowledgement is expressed to the University of Cape Town and the South African Council for Scientific and Industrial Research for generous grants. We also thank the University of Cape Town Computing Service for the smooth running of our programs on the Univac 1100/81.

REFERENCES

1. P. M. May, P. W. Linder and D. R. Williams, *J. Chem. Soc. Dalton Trans.*, 1977, 588.
2. C. W. Childs, *J. Phys. Chem.*, 1969, **73**, 2956.
3. J. Havel and E. Högfeldt, *Chemica Scripta*, 1974, **5**, 164.
4. C. W. Childs, *Inorg. Chem.*, 1970, **9**, 2465.
5. I. Greenwald, J. Redish and A. C. Kibrick, *J. Biol. Chem.*, 1940, **135**, 65.
6. H. Tabor and A. B. Hastings, *ibid.*, 1943, **148**, 627.
7. W. E. Trevelyan, P. F. E. Mann and J. S. Harrison, *Arch. Biochem. Biophys.*, 1952, **39**, 440.
8. H. B. Clarke, D. C. Cusworth and S. P. Datta, *Biochem. J.*, 1954, **58**, 146.
9. R. M. Smith and R. A. Alberty, *J. Am. Chem. Soc.*, 1956, **78**, 2376.
10. C. M. Frey and J. E. Stuehr, *ibid.*, 1972, **94**, 8898.
11. P. M. May, D. R. Williams, P. W. Linder and R. G. Torrington, *Talanta*, 1982, **29**, 249.
12. A. Sabatini, A. Vacca and P. Gans, *ibid.*, 1974, **21**, 53.
13. D. R. Williams, *J. Chem. Soc. Dalton Trans.*, 1973, 1064.
14. A. M. Corrie, G. K. R. Makar, M. L. D. Touche and D. R. Williams, *J. Chem. Soc. Dalton Trans.*, 1975, 105.
15. R. Österberg, *Acta Chem. Scand.*, 1960, **14**, 471.
16. *Idem*, *ibid.*, 1965, **19**, 1445.
17. E. Högfeldt, *Stability Constants of Metal-ion Complexes, Part A, Inorganic Ligands, IUPAC and Pergamon Press*, Oxford, 1982.
18. D. I. Stock and C. W. Davies, *J. Chem. Soc.*, 1938, 2093.

Talanta, Vol. 32, No 1, pp. 86–91, 1985
Printed in Great Britain.

0039-9140/85 $3.00 + 0.00

CHARACTERISTICS OF INDUSTRIAL DI(ALKYLPHENYL)DITHIOPHOSPHORIC ACIDS

Zs. WITTMANN, Z. DÉCSY and E. PUDMER
Hungarian Oil and Gas Research Institute, József Attila u. 34, H-8200 Veszprém, Hungary

(*Received* 26 *March* 1984. *Accepted* 30 *June* 1984)

Summary—Instrumental and classical methods have been used to characterize some industrial di(alkylphenyl)dithiophosphoric acids. The ^{31}P-NMR chemical shifts of di(nonylphenyl)dithiophosphoric acid and its derivatives are summarized.

Various dialkyldithiophosphoric acids and their derivatives have been investigated by several authors, and the NMR (^{31}P and ^{1}H), and infrared spectral data, pK values, methods of separation, *etc.*, have been given in the literature. Almost all the acids examined were dialkyldithiophosphoric acids with at most four carbon atoms in the alkyl chains. There are only a few data for di(alkylphenyl)dithiophosphoric acids.

In this paper, the identification and determination of the compounds formed during the production of industrial di(nonylphenyl)dithiophosphoric acid are described. All industrial di(nonylphenyl) dithiophosphoric acids contain similar compounds as impurities, sometimes only in traces. Products from a pilot plant were monitored to find several especially irregular samples containing various components in sufficient quantity for study.

EXPERIMENTAL

Mass spectrometry of di(nonylphenyl)dithiophosphoric acid samples

A high-resolution double-focusing mass spectrometer with Herzog–Mattauch geometry and equipped with a direct sample-inlet system was used at an ionization potential of 15 eV. The mass spectra of the various di(nonylphenyl)dithiophosphoric acids examined show the presence of several compounds characterized by molecular ions. Table 1 gives the data for the compounds identified.

Three main groups of compounds can be identified: alkylphenols, and various acids and neutral molecules containing phosphorus.

To find suitable analytical methods for determining the different groups of compounds, infrared and NMR (^{31}P and ^{1}H) spectrometry, potentiometric titration and classical methods were tried.

Infrared spectrometry

Infrared spectrometry is often used to examine dialkyldithiophosphoric acids, their derivatives and their metal salts. Nyquist,[1] Zimina,[2] and Mark and Van Wazer[3] have established the characteristic bands for the pure compounds.

The same groups in the different kinds of di(alkylphenyl)dithiophosphoric acids and their derivatives give similar infrared spectra. Therefore infrared spectrometry is not suitable for differentiating the individual compounds present in industrial di(nonylphenyl)dithiophosphoric acid samples. However, any alkylphenols present can be determined by infrared spectrometry, by means of the intensity of the ν_{O-H} band at 3620 cm^{-1} in carbon tetrachloride solution. Table 3 (see later) shows the alkylphenol content of some of the acids examined.

^{1}H-NMR spectrometry

The diazomethane derivatives of the acid compounds in industrial di(nonylphenyl)dithiophosphoric acid samples give characteristic NMR signals for S–CH_3 and O–CH_3, but as Kabachnik *et al.*[4] have pointed out, the products from dithiophosphoric acids are mixtures of isomers, and the thione–thiol equilibrium of the derivative is different from that for the parent acid. Hence use of ^{1}H-NMR spectrometry with these derivatives is not suitable for examining the composition of di(nonylphenyl)dithiophosphoric acid samples.

Potentiometric titration

Dialkylthiophosphoric acids exhibit a tautomeric equilibrium[5–7] as follows:

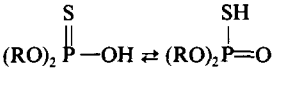

thione thiol

Kabachnik and co-workers[4,8] used potentiometric titration to study the tautomeric equilibrium of dialkyldithiophosphoric acids. Brazier and Elliott[9] titrated di(4-methylpentyl-2)dithiophosphoric acid. The titration curve showed two distinct inflections which could be attributed to the thione–thiol tautomerism

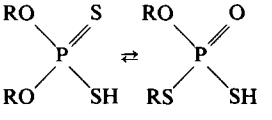

Di(nonylphenyl)dithiophosphoric acid samples were titrated in methanol with methanolic potassium hydroxide solution in our laboratory, and also gave two distinct inflections, from which the amount of the acids can be calculated (Table 3).

Kabachnik and co-workers[4,5] established that the tautomeric equilibrium of dialkyldithiophosphoric acids depends on the solvent used. In water the thiol form is dominant, and the thione in ethanol.

We have found that different industrial di(nonylphenyl)-dithiophosphoric acid samples of similar composition show

Table 1. Compounds in the di(nonylphenyl)dithiophosphoric acid samples examined

Number	Molecular weight	Name of compound	Formula
	206	Octylphenol	$C_8H_{17}—C_6H_4—OH$
	220	Nonylphenol	$C_9H_{19}—C_6H_4—OH$
	234	Decylphenol	$C_{10}H_{21}—C_6H_4—OH$
	346	Dinonylphenol	$(C_9H_{19})_2—C_6H_3—OH$
I	502	Di(nonylphenyl)phosphoric acid	$(C_9H_{19}—C_6H_4—O)_2P(O)OH$
II, III	518	Di(nonylphenyl)thiophosphoric acid	$(C_9H_{19}—C_6H_4—O)_2P(O)SH$; $(C_9H_{19}—C_6H_4—C_6H_4—O)_2P(S)OH$
IV	534	Di(nonylphenyl)dithiophosphoric acid	$(C_9H_{19}—C_6H_4—O)_2P(S)SH$
	660	(Dinonyl)phenyl(nonylphenyl)dithiophosphoric acid	$(C_9H_{19})_2—C_6H_3—O$ \ P(S)SH / $(C_9H_{19})—C_6H_4—O$
V	704	*O,O,O*-Tri(nonylphenyl)phosphate	$(C_9H_{19}—C_6H_4—O)_3P(O)$
VI	720	*O,O,O*-Tri(nonylphenyl)thiophosphate	$(C_9H_{19}—C_6H_4—O)_3P(S)$
	846	*O,O*-Di(nonylphenyl)-*O*-(dinonyl)phenylthiophosphate	$(C_9H_{19})_2—C_6H_3—O$ \ P(S) / $(C_9H_{19}—C_6H_4—O)_2$
VII	986	*O,O,O,O*-Tetra(nonylphenyl)pyrophosphate	$(C_9H_{19}—C_6H_4O)_2P(O)OP(O)(C_9H_{19}—C_6H_4O)_2$
VIII	1002	*O,O,O,O*-Tetra(nonylphenyl)thiopyrophosphate	$(C_9H_{19}—C_6H_2O)_2P(O)SP(O)(C_9H_{19}—C_6H_4O)_2$
IX	1018	*O,O,O,O*-Tetra(nonylphenyl)dithiopyrophosphate	$(C_9H_{19}—C_6H_4O)_2P(S)OP(S)(C_9H_{19}—C_6H_4O)_2$
X	1034	*O,O,O,O*-Tetra(nonylphenyl)trithiopyrophosphate	$(C_9H_{19}—C_6H_4O)_2P(S)SP(S)(C_9H_{19}—C_6H_4O)_2$
	1098	*O,O,O*-Tri(dinonylphenyl)thiophosphate	$((C_9H_{19})_2—C_6H_3—O)_3P(S)$

Table 2. NMR spectra of phosphorus compounds

Structure	Chemical shift, *ppm*	Reference and page no.	Number	Structure	Chemical shift, *ppm*	Reference and page no.
$(C_2H_5O)_2P(O)OH$	1.3	(14) 121 (15) 331	I	$(C_9H_{19}—C_6H_4—O)_2P(O)OH$	+1.1	—
$(C_2H_5O)_2P(O)SH$	−24.0	(16) 681 (15) 344	II	$(C_9H_{19}—C_6H_4—O)_2P(O)SH$	−30.6	—
$(C_2H_5O)_2P(S)OH$	—	—	III	$(C_9H_{19}—C_6H_4—O)_2P(S)OH$	−49.0	—
$(C_2H_5O)_2P(S)SH$	−85.7	(16) 588 (15) 373	IV	$(C_9H_{19}—C_6H_4—O)_2P(S)SH$	−78.7	—
$(C_2H_5O)_2P(O)ONa$	−3.8	(15) 331	Ia	$(C_9H_{19}—C_6H_4—O)_2P(O)ONa$	−2.1	—
$(C_2H_5O)_2P(O)SNa$	—	—	IIa	$(C_9H_{19}—C_6H_4—O)_2P(O)SNa$	−43.3	—
$(C_2H_5O)_2P(S)ONa$	−57	(15) 369	IIIa	$(C_6H_{19}—C_6H_4—O)_2P(S)ONa$	−51.7	—
$(C_2H_5O)_2P(S)SNH_4$	−110.5	(16) 588	IVa	$(C_9H_{19}—C_6H_4—O)_2P(S)SNa$	−107.1	—
C_2H_5C \ P(O)SNa / C_2H_5S	—	(15) 373		$C_9H_{19}—C_6H_4O$ \ P(O)SNa / $C_9H_{19}—C_6H_4S$	−90.3	—
$(C_2H_5O)_3P(O)$	−1.5	(14) 140	V	$(C_9H_{19}—C_6H_4—O)_3P(O)$	4.3	(14) 256
$(C_2H_5O)_2(C_2H_5S)P(O)$	−26.4	(15) 344	—	—	5.2	—
$(C_2H_5S)_2(C_2H_5O)P(O)$	−53.5	(15) 344	—	—	—	—
$(C_2H_5S)_3P(O)$	−61.3	(16) 787 (15) 345	—	—	—	—
$(C_2H_5O)_3P(S)$	−68	(14) 140	VI	$(C_9H_{19}—C_6H_4—O)_3P(S)$	−74.0 −72.1	(14) 256 —
$(C_2H_5S)_3P(S)$	−92.9	(16) 791				
$(C_2H_5O)_2P(O)OP(O)(C_2H_5O)_2$	11–16	(14) 262 (15) 331	VII	$(C_9H_{19}—C_6H_4—O)_2P(O)OP(O)(C_9H_{19}—C_6H_4O)_2$	8–10	—
$(C_2H_5O)_2P(O)SP(O)(C_2H_5O)_2$	—	—	VIII	$(C_9H_{19}—C_6H_4—O)_2P(O)SP(O)(C_9H_{19}—C_6H_4O)_2$	−41.2	—
$(C_2H_5O)_2P_\beta(S)OP_\alpha(O)(C_2H_5O)_2$	α −58.5 β −126.4 14.8 −54.0	(14) 262 (15) 330	—	—	—	—
$(C_2H_5O)_2P(S)OP(S)(C_2H_5O)_2$	−60.1 −14 −78	(14) 262 (15) 344	IX	$(C_9H_{19}—C_6H_4—O)_2P(S)OP(S)(C_9H_{19}—C_6H_4O)_2$	−59.0	—
$(C_2H_5O)_2P(S)SP(S)(C_2H_5O)_2$	−78.0 −78.4	(14) 262 (15) 373	X	$(C_9H_{19}—C_6H_4—O)_2P(S)SP(S)(C_9H_{19}—C_6H_4O)_2$	−78.2	—

*For convenience of identification, the suffix a denotes the sodium salt of the correspondingly numbered acid.

different tautomeric equilibria under the same conditions. This seems to show that the tautomerism can be affected by the preparation conditions.

Iodometric titration

Bode and Arnswald[10] determined the concentration of diethyldithiophosphoric acid by iodometric titration. This method is convenient for determining the acids containing a thiol group (Table 3).

Extraction method for determination of neutral molecules

The sample (about 1 g) was dissolved in 30 ml of petroleum ether (b.p. 40–70°). An equivalent amount of 2*M* sodium hydroxide in methanol was added and the sodium salt was extracted with 30 ml of water (methanol prevents foaming of the aqueous phase). The petroleum ether phase was washed three times with water and the ether was distilled off. The residue contained the neutral molecules. The purity of the ether phase and the absence of neutral molecules in the aqueous phase were checked by mass spectrometry. Table 3 shows the neutral-molecule content of some of the samples examined.

Dyrssen[11,12] established that the dimerization of di-n-butyl phosphate depends on the solvent used. In hydroxyl-containing solvents the dimerization is almost negligible. Potentiometric titration in methanol and extraction of the neutral molecules into petroleum ether does not result in dimerization of the acids (Table 3).

^{31}P-NMR spectrometry

The ^{31}P-NMR results are interesting and suitable for identifying several components of the di(nonylphenyl)-dithiophosphoric acids samples examined. The ^{31}P-NMR spectra were recorded at 8000 Hz on a commercial NMR spectrometer operating in the pulse–Fourier transform mode. The samples were diluted with deuterochloroform. All ^{31}P-NMR chemical shifts were referred to Merck reagent-grade 85% orthophosphoric acid as internal standard.

Figure 1 shows the ^{31}P-NMR spectra of one of the di(nonylphenyl)dithiophosphoric acid samples examined. Identification of the chemical shifts of the compounds was facilitated by separating the components of the acid sample by gel-permeation chromatography and using some general considerations.

Harris *et al.*[13] confirm that the magnitudes of the chemical shifts for $(RO)_2P(O)O^- \rightarrow (RO)_2P(O)S^-$ and $(RO)_2P(S)O^- \rightarrow (RO)_2P(S)S^-$ are similar for compounds containing these groups.

Most of the chemical shift data available refer only to diethyldithiophosphoric acid and its derivatives. These data were compared with the data for the compounds examined here. Table 2 shows the chemical shifts for diethyl-dithiophosphoric acid and di(nonylphenyl)dithiophosphoric acid and their derivatives. The data given without a literature reference were determined in our laboratory. As can be seen, structures that are similar but have different hydrocarbon moieties have chemical shifts of similar magnitude in their ^{31}P-NMR spectra.

The chemical shifts of the sodium salts of the acids and their derivatives were selected on the basis of the results of the chemical shifts measured on the aqueous phase containing the neutral molecules extracted as described above. The neutral molecules were identified by mass spectrometry. There are no chemical shift data in the literature for structure $(C_9H_{19}-C_6H_4-O)_2P(O)SP(O)(C_9H_{19}-C_6H_4-O)_2$ (VIII). The mass spectra showed a large amount of a compound with the same empirical formula as VIII in the extracted phase of some acid samples. The ^{31}P-NMR spectra contained only one unidentified peak of high intensity, which could therefore be assigned to this structure.

Table 3. Analysis of di(nonylphenyl)dithiophosphoric acid samples by different methods, % *w/w*

Sample	Acids: Alkylphenols IR	Alkylphenols GPC	Potentiometric titration	Iodometric titration (−SH)	^{31}P-NMR: From Na salt	^{31}P-NMR: From Acid	^{31}P-NMR: GPC	Neutral molecules: Extraction	Neutral molecules: ^{31}P-NMR	Neutral molecules: GPC
1	10.2	9.7	82.3	88.6	3.0 Ia 25.5 IIa 85.7 0.8 IIIa 60.2 IVa	I 1.0 II 2.3 III 22.7 IV 57.0	83.0	81.6	8.7	IX 3.6 VIII 4.2 7.8	6.9 (M* ~ 1000)
2	0.9	1	85.6	84.2	9.0 Ia 26.3 IIa 83.4 3.1 IIIa 57.1 IVa	I 2.5 II 7.0 III 20.3 IV 56.8	86.6	86.2	14.1	V 0.5 VI 0.2 VII 1.0 VIII 9.8 IX 1.1 X 0.8 13.4	~1 (M* ~ 780) 12.8 (M* ~ 1000)
3	0.6	1	88.5	81.7	7.0 Ia 24.3 IIa 79.4 12.3 IIIa 55.1 IVa	I 3.2 II 11.5 III 16.4 IV 56.1	87.2	85.7	12.5	VII 1.3 VIII 8.7 IX 1.1 X 0.5 11.6	10.7 (M* ~ 1000)

*M = estimated molecular weight.

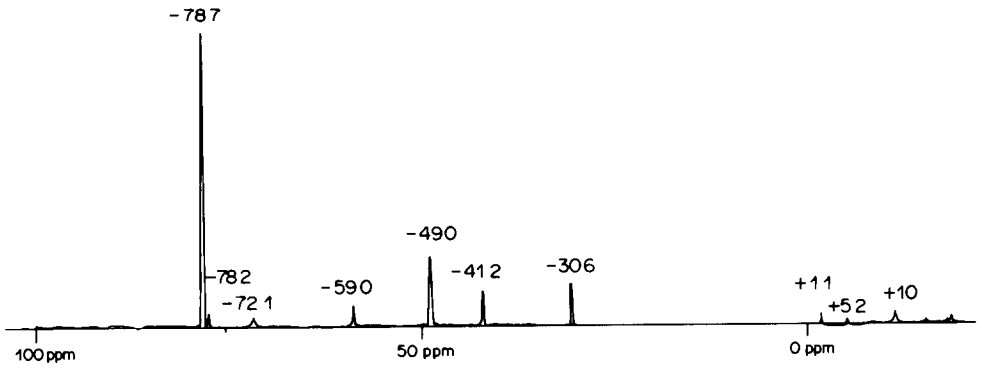

Fig. 1. ^{31}P-NMR spectrum of a di(nonylphenyl)dithiophosphoric acid sample.

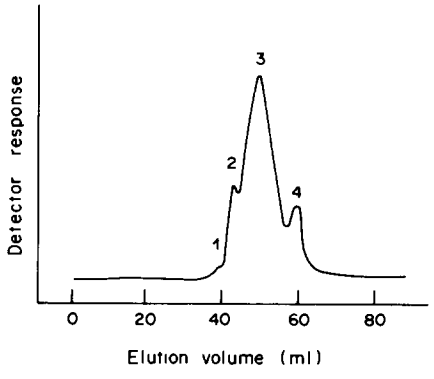

Fig. 2. Elution curve of a di(nonylphenyl)dithiophosphoric acid sample. 1 = tetra(nonylphenyl)pyrophosphates; 2 = tri-(nonylphenyl)phosphates; 3 = acids; 4 = alkylphenols.

Gel-permeation chromatography (GPC)

The alkylphenols, acids and neutral molecules in industrial di(nonylphenyl)dithiophosphoric acids can be determined by GPC. The functional groups of the acids are destroyed on the surface of the gel, so GPC is not directly usable, but the methyl derivatives obtained by reaction with diazomethane are suitable for separation. Although the derivatives are mixtures of isomers,[4] the molecular weights of the isomers are unchanged.

All separations were done on a 20-cm column (14 mm diameter) of 25–100 μm Sephadex LH-20. Dichloromethane–methanol mixture (9:1 v/v) was used as eluent at a flow-rate of 1.0 ml/min and a temperature of 25.0 ± 0.2°. A 3-mg sample reacted with diazomethane in dichloromethane was loaded on the column. The absorbance of the eluate was measured at 278 nm.

The neutral molecules were eluted first, followed by diazomethane derivatives of the acids and finally the diazomethane derivatives of the alkylphenols.

The elution volume is approximately a linear function of the logarithm of the molecular weight. Figure 2 shows the elution curve from an acid sample.

CONCLUSIONS

Table 3 shows the amounts of the components of some di(nonylphenyl)dithiophosphoric acid samples, found by different methods. The most information was given by ^{31}P-NMR spectrometry for the compounds containing phosphorus.

The phenols were determined by infrared spectrometry. The acid content of the samples was titrated potentiometrically and also measured on the basis of the peak intensities of the ^{31}P-NMR spectra.

Acids with an SH group were titrated iodometrically after formation of the sodium salts, and also determined directly from the ^{31}P-NMR spectra. These results are not in agreement, however, because the tautomeric equilibrium in alkaline solution is different from the equilibrium in the original acid sample. However, the amounts determined by ^{31}P-NMR spectrometry of the sodium salts show good agreement with the results of the iodometric titration.

The amounts of the neutral molecules determined by the extraction method are in agreement with the total amount of these molecules calculated from the ^{31}P-NMR spectra.

The total amounts of the groups of compounds in

Table 4. Reproducibility of methods for determination of components of a di(nonylphenyl)dithiophosphoric acid sample (mean ± s.d., % w/w)

Method	Alkylphenol	Acid	Neutral molecules
IR	10.2 ± 0.5	—	—
GPC	9.7 ± 0.5	81.6 ± 4.1	6.9 ± 0.4
Potentiometric titration	—	82.3 ± 1.6	—
Iodometric titration	—	83.0 ± 2.5	—
Extraction	—	—	8.7 ± 0.7
^{31}P-NMR	—	within	±5% relative for each components

industrial di(nonylphenyl)dithiophosphoric acids were determined by GPC; Table 3 shows the results.

Different industrial di(nonylphenyl)dithiophosphoric acid samples contain the detected components in different quantity. The methods described here are convenient for determining the components of any industrial di(nonylphenyl)dithiophosphoric acid sample.

The reproducibility of the analytical methods was tested by making 10 determinations of the components of an industrial di(nonylphenyl)dithiophosphoric acid; Table 4 shows the results.

Acknowledgement—The authors would like to thank Zs. Kovács who did the ^{31}P-NMR analyses.

REFERENCES

1. R. A. Nyquist, *Spectrochim. Acta*, 1969, **25A**, 47.
2. K. I. Zimina, G. G. Kotova, P. I. Sanin, V. V. Sher and G. N. Kuzmina, *Neftekhimia*, 1965, **5**, 629.
3. V. Mark and J. R. Van Wazer, *J. Org. Chem.*, 1964, **29**, 1006.
4. M. I. Kabachnik, S. T. Ioffe and T. A. Mastryukova, *J. Gen. Chem., U.S.S.R.*, 1955, **25**, 653.
5. M. I. Kabachnik and T. A. Mastryukova, *Zh. Obschch. Khim.*, 1955, **25**, 1924.
6. M. I. Kabachnik, T. A. Mastryukova, N. P. Radionova and E. M. Popov, *ibid.*, 1956, **26**, 120.
7. T. H. Handley, *Anal. Chem.*, 1963, **35**, 991.
8. M. I. Kabachnik and S. T. Ioffe, *Dokl. Akad. Nauk, U.S.S.R.*, 1953, **91**, 833.
9. A. D. Brazier and J. S. Elliott, *J. Inst. Petr.*, 1967, **53**, 63.
10. H. Bode and W. Arnswald, *Z. Anal. Chem.*, 1962, **185**, 99.
11. D. Dyrssen, *Acta Chem. Scand.*, 1957, **11**, 1771.
12. D. Dyrssen and Liem Djiet Hay, *ibid.*, 1960, **14**, 1091.
13. R. K. Harris, A. R. Katritzky, S. Musierowicz and B. Ternai, *J. Chem. Soc. (A)*, 1967, 37.
14. E. F. Mooney, *Annual Reports on NMR Spectroscopy*, Vol. 5B, Academic Press, New York, 1973.
15. M. M. Crutchfield, C. H. Dungan, J. H. Letcher, V. Mark and J. R. Van Wazer, *P^{31} Nuclear Magnetic Resonance*, Wiley, New York, 1967.
16. G. M. Kosolapoff and L. Maier, *Organic Phosphorus Compounds*, Vol. 7, Wiley, New York, 1976.

Talanta, Vol. 32, No. 1, pp. 93–94, 1985
Printed in Great Britain.

0039-9140/85 $3.00 + 0.00

ANNOTATION

OCCURRENCE OF CONSISTENT n*M* LEVELS OF PHOSPHATE IN DOUBLY DEMINERALIZED AND DEMINERALIZED-DISTILLED WATER*

VINCENT P. GUTSCHICK
Environmental Science Group, LS-6, Los Alamos National Laboratory, Los Alamos, NM 87545, U.S.A.

(*Received* 12 *May* 1984. *Accepted* 17 *July* 1984)

Summary—A double demineralization system and a demineralization-distillation system operated over several months consistently delivered water that was approximately 30 n*M* in phosphate, as determined by a molybdenum blue spectrophotometric method. Silicate and hydrolysed polyphosphate in the water, and contaminants in the analytical reagents, were eliminated as sources of error in the determination. Caution is suggested in preparing blanks and dilutions in analyses of samples of natural waters or plant nutrient solutions, when either of these types of purification system is used.

Recent studies of plant nutrition[1,2] and of dissolved nutrients in both fresh water[3] and sea-water[4] have established that the most frequently occurring and important range of phosphate concentration is below 1 μM (P < 31 μg/l.), and often below 0.1 μM. Various extractive spectrophotometric analytical methods[5,6] are in use for these water samples, as are double demineralization and demineralization–distillation systems to provide water for blanks, standards, and sample dilutions.

In the course of a current Los Alamos study of plant nutritional stress, it was found that phosphate blanks of either type of purified water routinely lay in the region of 50n*M* (P $\simeq$ 1.5 μg/l.). Such high blank values complicated the nutrient-level control and the uptake analyses in the plant nutrition experiment, which extended over several months. Contamination by trace phosphate in the analytical reagents was ruled out as the source of the error, when samples of plant nutrient solution inadvertently contaminated by a modest algal growth showed results equivalent to only 5n*M* phosphate. Several other possible sources for the high phosphate content of the other samples were eliminated, including desorption of phosphate from analytical equipment or storage containers, and photometric interference by silicate incompletely removed by the water purification systems. Phosphate appears to pass through the water purifiers in fairly consistent and significant traces, in monomeric form.

EXPERIMENTAL

Water purification

The double demineralization system consisted of a single Calgon mixed-bed resin in a 9-in. (23-cm) diameter steel vessel, followed by a Vaponics four-cartridge purifier (organic removal cartridge, two mixed-bed demineralizers, and a particulate filter). The specific resistance of the outflow from the Calgon resin and of the final outflow attained the theoretically limiting value of 18 MΩ (automatically corrected to 20°), within the resolution of the monitor. The demineralization–distillation system consisted of a similar Calgon mixed-bed resin, followed by a low flow-rate mixed-bed resin (Ion X Changer Research) and a Corning AG-3 all-glass still. The systems are thus typical of high-quality reagent-grade water supply systems.

Analytical methods

For sub-μM concentrations, a modification of the molybdenum blue method of Gibson *et al.*[5] (to be discussed in a future publication) was used. To a 1-litre sample were added 30 ml of concentrated hydrochloric acid, then 20 ml of molybdate reagent [50 g of $(NH_4)_6Mo7O_{24}\cdot 4H_2O$ per litre in 3.4 *N* hydrochloric acid], 2 ml of 1% potassium antimonyl tartrate solution, and 5 ml of 10% ascorbic acid solution, in that order. The solution was extracted successively with 30, 20 and 20 ml of methyl isobutyl ketone, with shaking for 10 min each time. The volumes of extract and the absorbances at 882 nm in a 1-cm cell were recorded and the sum of the three absorbance–volume (AV) products was calculated.

For higher concentrations of phosphate and silicate, as used during tests of silicate cross-reactivity, a scaled-down version of the method was used, with a 50-ml sample and a single extraction with 10 ml of the ketone.

All reagents were ACS analytical reagent grade, or better.

Samples

Samples of the water purifier outputs were taken directly in the analytical glassware used or stored for up to several weeks in bottles of either high- or low-density polyethylene. The bottles had been washed with phosphate-free detergent and hydrochloric acid and then rinsed seven or more times with the purified water. The plant nutrient solution samples were also taken in polyethylene bottles and then kept refrigerated for up to several months; most were acidified to pH 2 with sulphuric acid within 1 hr of collection in order to prevent loss of nitrate, which was also determined in the plant nutritional studies.

Calibration graphs for the analysis were constructed by sequential dilution of a weighed potassium dihydrogen

*Work performed under the auspices of the U.S. Department of Energy.

phosphate standard. The graphs were linear from 1μM down to 0.1μM phosphate or lower, with a standard deviation equivalent to 5nM.

RESULTS AND DISCUSSION

Fifteen blank samples from the two water purifiers obtained over a four-month period gave analytical readings in the range $\Sigma A_i V_i = 0.64$–1.69 ml, corresponding to phosphate concentrations of 47–125nM if it is assumed that the true blank value is zero. One other blank gave a reading corresponding to 15nM. The higher blank readings were attributed to residual phosphate on the molybdate reagent dispenser bottle; after a second filling of the bottle, no blank corresponded to a concentration above 75nM.

Three non-acidified but refrigerated samples of plant nutrient solution that showed algal contamination gave readings of $\Sigma A_i V_i = 0.07$–0.09 ml, corresponding to phosphate concentrations of 5–7nM. All properly preserved nutrient solution samples corresponded to 67nM concentration or above, with a single exception of 33nM.

It is known that properly adapted plants and algae can deplete phosphate down to a "compensation concentration" at least as low as 10nM.[1] This was taken to indicate that the algal-contaminated samples were close to a true blank, with the finite spectrophotometric reading attributable primarily to reagent contamination, and that measurable phosphate (or silicate) existed in both types of purified water. Phosphate contamination of the analytical glassware was eliminated as a possibility because the algal-contaminated low-reading samples were analysed in the same glassware. Similarly, phosphate contamination of the sample storage bottle was eliminated; also, direct delivery of purified water into the analytical apparatus gave very similar results to those from use of bottle-stored water for blanks.

Interference of silicate contaminants in the samples in the molybdenum blue analysis was a possible source of the blank reading, because at least one of the water purification systems used a glass holding tank, and because the Los Alamos County water input to the purifiers contains the equivalent of approximately 80 μg/ml SiO_2.[7] The performance of the Calgon demineralizers may reduce this to perhaps 20 ng/ml SiO_2 (300 nM). Extraction with ketones that are selective for phosphomolybdate relative to silicomolybdate[8] might decrease the spectrophotometric signal from this amount of silicate to that of the observed blank readings. In any case, polymeric silica, the form dominant in all the blanks and samples, is a much less significant interference than is monomeric silica. Indeed, both tap water and silica standards up to 30μM in concentration reacted negligibly. Even a 1-hr hydrolytic pretreatment with ammonia at pH 12 gave spectrophotometric results equivalent to a phosphate concentration only 2% of that of the silicate concentration. Furthermore, use of 1-butanol as extractant in order to favour extraction of silicomolybdate[8] gave results not significantly different from those obtained with methyl isobutyl ketone. Thus, the silica content of the blanks and samples could not explain the high blank readings obtained under the analytical conditions used.

It might be expected on chemical grounds that phosphate should be removed more efficiently than was observed. Polyphosphates are more likely than simple phosphates to penetrate the demineralizer resin beds. However, polyphosphates are unstable to hydrolysis and attain significant concentrations only when added intentionally and recently. The Los Alamos County water supply has no added polyphosphates for inhibiting pipe corrosion.

CONCLUSIONS

Double demineralization and demineralization–distillation water purification systems of two common types appear to pass phosphate at trace levels that can be significant in preparing and analysing plant nutrient solutions or in analysing natural water samples. For concentrations much below 1μM, corrections may often be necessary for dilution of samples below the standard volume of analysis and for calibrations and blanks, when these operations are done with such purified water. The use of separate anion- and cation-exchangers and the use of nuclear-grade resins may lower the phosphate contamination level, though probably not very near to a true zero (personal communication from resin manufacturers). The use of polyphosphates for pipe-corrosion inhibition in municipal water supplied to the purifiers may exacerbate the problem.

Acknowledgements—I thank Ed Cokal of Los Alamos for helpful discussions and criticisms. This work was supported by the U.S. Department of Energy, Division of Ecological Research.

REFERENCES

1. J. F. Loneragan and C. J. Asher, *Soil. Sci.*, 1967, **103,** 311.
2. H. Reisenauer, in *Environmental Biology*, P. L. Altman and D. S. Dittmer (eds.), p. 507. *Fed. Am. Soc. Exp. Biol.*, Bethesda, Md., 1966.
3. C. E. Boyd and L. W. Hess, *Ecology*, 1970, **51,** 296.
4. H. W. Harvey, *The Chemistry and Fertility of Sea Waters*. Cambridge Univ. Press, Cambridge, 1969.
5. A. R. Gibson, J. M. Bailey and D. J. Giltrap, *Commun. Soil Sci. Plant Anal.*, 1976, **7,** 427.
6. T. Fujinaga, T. Hori and Y. Kanada, *Bunseki Kagaku*, 1979, **28,** 222.
7. W. D. Purtymun, N. M. Becker and M. Maes, *Los Alamos Natl. Lab. Rept.* LA-9896-PR, 1984.
8. C. Wadelin and M. G. Mellon, *Anal. Chem.*, 1953, **25,** 1668.

Talanta, Vol. 32, No. 2, pp. 95–101, 1985
Printed in Great Britain.

0039-9140/85 $3.00 + 0.00

CALCULATION OF EQUILIBRIUM CONSTANTS FROM MULTIWAVELENGTH SPECTROSCOPIC DATA—I

MATHEMATICAL CONSIDERATIONS

HARALD GAMPP, MARCEL MAEDER, CHARLES J. MEYER and ANDREAS D. ZUBERBÜHLER
Institute of Inorganic Chemistry, University of Basel, CH-4056 Basel, Switzerland

(*Received* 19 *June* 1984. *Accepted* 20 *September* 1984)

Summary—Multiwavelength spectrophotometric and spectroscopic data in general contain considerably more information about complexation equilibria than potentiometric data do. With the construction of a fully automatic titration set-up built into a high-precision spectrophotometer, the problems related to the wider use of this method have shifted from the quality of the primary data to the complexity of their numerical treatment. Matrix algebra is used to show how these problems can be overcome. An algorithm is described for calculation of stability constants and absorption spectra, together with the associated standard errors, at a reasonable expense of computer time. Problems in finding the minimum in a multidimensional parameter space are reduced by elimination of the molar absorptivities from the algorithm for the iterative refinement. Numerical safety and speed of calculation are improved by use of analytical instead of numerical derivatives. The number of data to be fitted is decreased by principal-component analysis.

It is still a widespread belief that spectrophotometric data are inherently less precise than potentiometric, with standard errors of ± 0.003 units at best for single absorbance values.[1] Consequently most equilibrium constants are determined by means of potentiometric titrations, and only a few general programs are available at present for processing spectrophotometric data[2–4] (*cf.*[5–8] for reviews of the older literature).

Some time ago we developed a fully automatic titration set-up[9] which gives data with standard errors as low as $2–5 \times 10^{-4}$ absorbance units.[9,10] The spectrophotometric data from this unit have been shown to have a reproducibility similar to that of potentiometric titrations. In addition, spectrophotometric titrations have been found to be superior in discriminating between different models for a complexation equilibrium,[11,12] even for rather complicated systems.

Because of the availability of large quantities of high-quality data, a fast, reliable and user-friendly program for the numerical treatment was needed. Here we wish to describe the mathematical features which have been used to achieve this in our new program SPECFIT.[13]

In theory, any general non-linear least-squares program can be used for calculation of stability constants from spectrophotometric data obtained at a single wavelength. However, for all but the most simple equilibrium systems this straightforward approach does not really work and several problems have to be overcome.

(*i*) Even for data obtained at a single wavelength there are two adjustable parameters for each unknown species, *viz.* the stability constant and the molar absorptivity. Convergence properties tend to deteriorate rapidly with the number of parameters. This problem is overcome by the elimination of the molar absorptivities from the process of iterative refinement, effectively reducing the number of parameters to the number of unknown stability constants, as is the case with data from potentiometric titrations.

(*ii*) Because of the correlations between stability constants and molar absorptivities, and also between stability constants themselves, numerical difficulties can arise in the algorithm for the refinement of the stability constants (non-linear parameters). This can be eased by the use of analytical derivatives in the calculation of the Jacobian matrix, increasing not only numerical safety but also the speed of calculation.

(*iii*) In systems with more than two or three absorbing species it is unlikely that a single wavelength will be sufficient to differentiate between all the species. This is especially true for the electronic absorption spectra of transition metal complexes, which are often broad, rather unstructured, and strongly overlapping. Data from a large number of wavelengths should then be used, and factor analysis leads to a considerable reduction of the number of data points required to be subjected to the least-squares treatment.

In SPECFIT, the features described in (*i*)–(*iii*) are combined with the efficient Marquardt algorithm[14,15] to ensure convergence. Points (*i*)–(*iii*) will now be considered in turn. Matrix notation is used and schematic illustration is added whenever this is felt to be helpful. Most of the algorithms used in this paper have been described before in one form or another. Normally this was done in a highly abstract mathe-

matical way, out of the chemical context, and the different features have never been combined to give the complete picture. Here, we wish to describe the problems specifically for chemical equilibrium systems and in terms which should be understandable to the chemist with an elementary knowledge of matrix algebra and having some familiarity with equilibrium calculations.

SYMBOLS

Bold-face lower-case letters **v** represent column vectors $[v(1), \ldots, v(i), \ldots, v(I)]^t$ and upper case letters **M** general matrices with elements $M(i,j)$ consisting of J columns and I rows. $\mathbf{M}^t$ and $\mathbf{v}^t$ are transposes of **M** and **v**, respectively. Differentiation of vectors and matrices with respect to parameters **p** or a single variable p will be denoted by $D\mathbf{v}$ and $D\mathbf{M}$. The trace of a matrix will be indicated by tr(**M**). Appropriate subscripts, *e.g.*, $\mathbf{a}_{calc}$ or $D\mathbf{M}_p$ are added in cases of ambiguity. Dimensions of vectors and matrices are given in brackets.

a [K]	Analytical (total) concentrations, experimental values
$\mathbf{a}_{calc}$ [K]	Analytical (total) concentrations, calculated values
A [K, K]	Partial derivatives of $\mathbf{a}_{calc}$ with respect to **c**
α [K, J]	Stoichiometric coefficients
β [J]	Equilibrium constants, fixed or adjustable
c [K]	Actual concentrations of components
C [M, S]	Concentrations of absorbing species, identical with partial derivatives of **r** with respect to **e**
$\mathbf{C}_f$ [M, F]	Concentrations of absorbing species with fixed spectra
$\mathbf{C}_u$ [M, U]	Concentrations of absorbing species with unknown spectra
$\delta_{i,j}$	Kronecker delta, $\delta_{i,i} = 1$; $\delta_{i,j} = 0$ for $i \neq j$
e, $\hat{\mathbf{e}}$ [S]	Molar absorptivities at a single wavelength
$\hat{\mathbf{e}}_f$ [F]	Molar absorptivities of species with fixed spectra
$\hat{\mathbf{e}}_u$ [U]	Molar absorptivities of species with unknown spectra
f [M]	Elements of fitting (model) function
F	Number of species with fixed spectra
I	Identity matrix of appropriate dimensions
I	Number of significant eigenvectors in factor analysis
J [M, N]	Jacobian matrix, partial derivatives of **f** with respect to **p**
J	Number of species in solution
K	Number of components in equilibrium mixture
$\mathbf{L}_I$ [M, I]	Significant linear coefficients used in refinement
λ [I]	Significant eigenvalues
M [W, W]	$\mathbf{Y}^t\mathbf{Y}$, second-moment matrix of absorbances
M	Number of measurements (equilibrium mixtures)
N	Number of non-linear parameters (equilibrium constants)
p, $\Delta\mathbf{p}$ [N]	Non-linear parameters (equilibrium constants) with shifts
P [M, M]	Projector matrix
Q var	Hessian matrix of variable dimensions, *e.g.*, $\mathbf{C}^t\mathbf{C}$
r [M]	residuals, $\mathbf{f} - \mathbf{y}$
s [J]	Concentrations of species in a given mixture
S	Number of absorbing species
SQ	Sum of squares of residuals
T [U, U]	Upper triangular matrix
U [M, U]	Matrix with orthogonal columns, $\mathbf{U}^t\mathbf{U} = \mathbf{I}$
U	Number of species with unknown spectra
$\mathbf{V}_I$ [I, W]	Eigenvectors corresponding to significant eigenvalues λ
W	Number of wavelengths
y [M]	Experimental absorbances
$\mathbf{y}_u$ [M]	Absorbances due to species with unknown spectra

Note: **F**, **R**, **Y** and **E** are the multiwavelength analogues of **f**, **r**, **y** and **e**, dimensions [M,W] and [S, W], respectively. **L** and **V** are the hypothetical analogues of $\mathbf{L}_I$ and $\mathbf{V}_I$, assuming full rank of **Y**.

Standard non-linear least-squares method

Given a set of M measurements $\mathbf{y} = [y(1), \ldots, y(m), \ldots, y(M)]^t$, it is the goal of any least-squares calculation to find the elements of a fitting function, **f**, such that the length of the vector of residuals **r** (weighted if necessary) is minimized.

$$SQ = \mathbf{r}^t\,\mathbf{r} = (\mathbf{f} - \mathbf{y})^t(\mathbf{f} - \mathbf{y}) = \text{minimum} \qquad (1)$$

In the case of determination of stability constants from spectrophotometric data, the elements $\mathbf{f}(m)$ for a chemical model with a total of S absorbing species are obtained from Beer's law:

$$f(m) = \sum_{s=1}^{S} e(s)C(m,s) \quad \text{or} \quad \mathbf{f} = \mathbf{C}\,\mathbf{e} \qquad (2)$$

Here **e** contains the molar absorptivities of the S absorbing species and **C** is the matrix of concentrations of only the absorbing species. **C** can be calculated from the analytical concentrations of the components [ligand(s) and metal ion(s)], $\mathbf{a} = [a(1), \ldots, a(k), \ldots, a(K)]^t$, and the known or estimated set of stability constants β, see below. The molar absorptivities, **e**, are also, in general, unknowns and thus the minimum of SQ would have to be found in a parameter space of N (equilibrium constants) plus S (absorptivities) dimensions.

Elimination of linear parameters

The molar absorptivities (linear parameters) can, however, be replaced non-iteratively by their least-squares estimates $\hat{\mathbf{e}}$ for a given concentration matrix **C**:

$$\hat{\mathbf{e}} = (\mathbf{C}^t\,\mathbf{C})^{-1}\,\mathbf{C}^t\,\mathbf{y} \tag{3}$$

This possibility has been described for the numerical treatment of kinetic data, *e.g.*, the resolution of a sum of exponentials.[16] It is also used in SQUAD[2] and in ELORMA,[4] where a detailed description may be found. The main points are briefly summarized here. By making use of equation (3), the fitting function **f** and the vector of residuals **r** can be described as a function of the concentration matrix **C** or, indirectly, of the set of stability constants (non-linear parameters) β alone [equation (4)]. The dimensionality of the parameter space is thus reduced to the number of unknown equilibrium constants, N, as would be the case if data from potentiometric titrations were used.

$$\mathbf{r} = \mathbf{f} - \mathbf{y} = \mathbf{C}\,\hat{\mathbf{e}} - \mathbf{y} = \mathbf{C}\,(\mathbf{C}^t\,\mathbf{C})^{-1}\,\mathbf{C}^t\,\mathbf{y} - \mathbf{y} \tag{4}$$

As also discussed previously,[4] numerical safety can be significantly increased by decomposition of **C** into a matrix **U** with orthogonal columns, ($\mathbf{U}^t\,\mathbf{U} = \mathbf{I}$, **I** = identity matrix), and an upper triangular matrix **T**.

$$\mathbf{C} = \mathbf{U}\,\mathbf{T} \tag{5}$$

Then equation (4) can be transformed to give

$$\begin{aligned}\mathbf{r} &= \{\mathbf{U}\,\mathbf{T}\,[(\mathbf{U}\,\mathbf{T})^t\,\mathbf{U}\,\mathbf{T}]^{-1}\,(\mathbf{U}\,\mathbf{T})^t - \mathbf{I}\}\mathbf{y}\\ &= \{\mathbf{U}\,\mathbf{T}\,\mathbf{T}^{-1}\,(\mathbf{U}^t\,\mathbf{U})^{-1}\,(\mathbf{T}^t)^{-1}\,\mathbf{T}^t\,\mathbf{U}^t - \mathbf{I}\}\mathbf{y}\\ &= (\mathbf{U}\,\mathbf{U}^t - \mathbf{I})\mathbf{y}\end{aligned} \tag{6}$$

The use of equation (6) instead of equation (4) proved essential in ELORMA[4] when this program was implemented on a single-precision hobby computer, but equation (4) may be sufficient in SQUAD, which is written for a mainframe machine and makes use of the double precision facility. In fact, about half as many significant digits are lost by using equation (6) instead of equation (4),[17] so that single precision and (6) give similar performance to double precision and (4).

Parameter refinement with use of analytical derivatives

When the effective number of parameters $\mathbf{p} = [p(1), \ldots, p(n), \ldots, p(N)]^t$ has been reduced to that of the unknown equilibrium constants β, the next step in parameter refinement is compilation of the Jacobian matrix **J**, *i.e.* the partial derivatives of the elements of the fitting function with respect to the non-linear parameters, $J(m,n) = \partial f(m)/\partial p(n) = \partial r(m)/\partial p(n)$. Based on either equation (4) or (6) this is straightforward when numerical derivatives are used, as has also been discussed in the description of ELORMA.[4] Any of the standard procedures of least-squares refinement can be applied to the approximate Jacobian matrix **J** thus obtained, calculation of a shift vector $\Delta\mathbf{p}$ by solving the Gaussian normal equations (7) being the simplest possibility.

$$\Delta\mathbf{p} = -(\mathbf{J}^t\,\mathbf{J})^{-1}\,\mathbf{J}^t\,\mathbf{r} \tag{7}$$

However, whenever feasible, the use of analytical instead of numerical derivatives greatly increases numerical safety and in general decreases computation time. Analytical expressions for the Jacobian matrix **J** based on partial derivatives have been derived[18,19] in a highly sophisticated mathematical approach, on the assumption that **C** is a general matrix, with the only condition being the differentiability of its elements. Here, we describe the problem specifically for chemical equilibrium systems and in terms which should be understandable to the chemist. In addition, the description is as close as feasible to the algorithm used in SPECFIT.[13]

The differentiation of a product of matrices **A B** follows the normal rules of differentiation.

$$D(\mathbf{A}\,\mathbf{B}) = (D\mathbf{A})\mathbf{B} + \mathbf{A}(D\mathbf{B}) \tag{8}$$

We therefore obtain the nth column of the Jacobian matrix **J** by differentiation of the vector of residuals [equation (4)] with respect to the nth unknown non-linear parameter, $p(n)$ [equation (9)]:

$$D\mathbf{r}_n = D(\mathbf{C}\,\hat{\mathbf{e}}) = (D\mathbf{C})\hat{\mathbf{e}} + \mathbf{C}(D\hat{\mathbf{e}}) \tag{9}$$

For the calculation of $D\hat{\mathbf{e}}$ we need an algorithm for $D(\mathbf{C}^t\,\mathbf{C})^{-1}$. By abbreviating $\mathbf{C}^t\,\mathbf{C}$ to **Q** and again making use of equation (8) we obtain equations (10)–(12). Substitution into equation (3) gives equation (13) and then the final expression for $D\mathbf{r}_n$, equation (14).

$$\begin{aligned}D\mathbf{Q} = D(\mathbf{C}^t\,\mathbf{C}) &= D\mathbf{C}^t\,\mathbf{C} + \mathbf{C}^t\,D\mathbf{C}\\ &= D\mathbf{C}^t\,\mathbf{C} + (D\mathbf{C}^t\,\mathbf{C})^t\end{aligned} \tag{10}$$

$$D(\mathbf{Q}^{-1}\,\mathbf{Q}) = D(\mathbf{I}) = 0 = D\mathbf{Q}^{-1}\,\mathbf{Q} + \mathbf{Q}^{-1}\,D\mathbf{Q} \tag{11}$$

$$D\mathbf{Q}^{-1} = -\mathbf{Q}^{-1}\,D\mathbf{Q}\,\mathbf{Q}^{-1} \tag{12}$$

$$\begin{aligned}D\hat{\mathbf{e}} = D[(\mathbf{C}^t\,\mathbf{C})^{-1}\,\mathbf{C}^t\,\mathbf{y}] &= D\mathbf{Q}^{-1}\,\mathbf{C}^t\,\mathbf{y}\\ &\quad + \mathbf{Q}^{-1}\,D\mathbf{C}^t\,\mathbf{y}\\ &= -\mathbf{Q}^{-1}\,D\mathbf{Q}\,\mathbf{Q}^{-1}\,\mathbf{C}^t\,\mathbf{y}\\ &\quad + \mathbf{Q}^{-1}\,D\mathbf{C}^t\,\mathbf{y}\\ &= -\mathbf{Q}^{-1}\,D\mathbf{Q}\,\hat{\mathbf{e}} + \mathbf{Q}^{-1}\,D\mathbf{C}^t\,\mathbf{y}\end{aligned} \tag{13}$$

$$\begin{aligned}D\mathbf{r}_n &= D\mathbf{C}\,\hat{\mathbf{e}} - \mathbf{C}\,\mathbf{Q}^{-1}\,D\mathbf{Q}\,\hat{\mathbf{e}}\\ &\quad + \mathbf{C}\,\mathbf{Q}^{-1}\,D\mathbf{C}^t\,\mathbf{y} = D\mathbf{C}\,\hat{\mathbf{e}}\\ &\quad + \mathbf{C}\,\mathbf{Q}^{-1}\,(D\mathbf{C}^t\,\mathbf{y} - D\mathbf{Q}\,\hat{\mathbf{e}})\end{aligned} \tag{14}$$

The result [equation (14)] obtained so far is rather general and can be applied to any least-squares problem with a combination of linear and non-linear parameters, *i.e.*, a problem which can be described by an equation of type (4). Since $\mathbf{Q}^{-1}$, $D\mathbf{Q}$, and $\hat{\mathbf{e}}$ are simply functions of **C** (and **y**), all we need for the calculation of the vector of residuals, **r**, and the

Jacobian matrix **J**, is the knowledge of **C** and its derivative $D\mathbf{C}$ with elements $\partial C(m,s)/\partial p(n)$ (see below). For further reference we also note that **C** is identical with the partial derivative of **r** with respect to **e** and thus part of the total Jacobian matrix $\mathbf{J}_t$ which is obtained without elimination. Equally, **Q** would be part of the total Hessian $\mathbf{Q}_t = \mathbf{J}_t^t\,\mathbf{J}_t$ (see calculation of standard errors, below).

Inclusion of species with known spectra

Occasionally, the molar absorptivities of some of the complexes are already known from independent measurements and refinement is not desired. In this case, expressions analogous to equations (4) and (14) can be obtained for the residuals and the Jacobian matrix by subdividing **C** and $\hat{\mathbf{e}}$ into $\mathbf{C}_f$ and $\mathbf{C}_u$ for species with fixed or unknown absorptivities $\hat{\mathbf{e}}_f$ or $\hat{\mathbf{e}}_u$, respectively, followed by subtracting the contributions of $\mathbf{C}_f$ from **y**.

$$\mathbf{y}_u = \mathbf{y} - \mathbf{C}_f\,\hat{\mathbf{e}}_f \tag{15}$$

Equations (3) and (4) can then be transformed into (3a) and (4a), but for the calculation of the Jacobian matrix, we have to take into account that now $\mathbf{y}_u$ itself also is a function of the stability constants, $D\mathbf{y}_u = -D\mathbf{C}_f\,\hat{\mathbf{e}}_f$ [equation (14a)].

$$\hat{\mathbf{e}}_u = (\mathbf{C}_u^t\,\mathbf{C}_u)^{-1}\,\mathbf{C}_u^t\,\mathbf{y}_u = \mathbf{Q}_u^{-1}\,\mathbf{C}_u^t\,\mathbf{y}_u \tag{3a}$$

$$\begin{aligned}\mathbf{r}_u &= \mathbf{C}_u\,(\mathbf{C}_u^t\,\mathbf{C}_u)^{-1}\,\mathbf{C}_u^t\,\mathbf{y}_u - \mathbf{y}_u\\ &= \mathbf{C}_u\,\mathbf{Q}_u^{-1}\,\mathbf{C}_u^t\,\mathbf{y}_u - \mathbf{y}_u\\ &= \mathbf{C}_u\,\hat{\mathbf{e}}_u - \mathbf{y}_u\end{aligned} \tag{4a}$$

$$\begin{aligned}D\mathbf{r}_{u,n} &= D\mathbf{C}_u\,\hat{\mathbf{e}}_u + \mathbf{C}_u\,D\hat{\mathbf{e}}_u - D\mathbf{y}_u\\ &= D\mathbf{C}_u\,\hat{\mathbf{e}}_u + \mathbf{C}_u\,(D\mathbf{Q}_u^{-1}\,\mathbf{C}_u^t\,\mathbf{y}_u\\ &\quad + \mathbf{Q}_u^{-1}\,D\mathbf{C}_u^t\,\mathbf{y}_u + \mathbf{Q}_u^{-1}\,\mathbf{C}_u^t\,D\mathbf{y}_u)\\ &\quad + D\mathbf{C}_f\,\hat{\mathbf{e}}_f\\ &= D\mathbf{C}\,\hat{\mathbf{e}} + \mathbf{C}_u\,\mathbf{Q}_u^{-1}\,(D\mathbf{C}_u^t\,\mathbf{y}_u\\ &\quad - D\mathbf{Q}_u\,\hat{\mathbf{e}}_u - \mathbf{C}_u^t\,D\mathbf{C}_f\,\hat{\mathbf{e}}_f)\end{aligned} \tag{14a}$$

Obviously, $\mathbf{y}_u$ [equation (15)] has to be recalculated in each iterative cycle of parameter refinement, since $\mathbf{C}_f$ is also a function of the equilibrium constants.

Analytical derivatives of the species concentrations

For the calculation of stability constants from spectrophotometric data, $D\mathbf{C}$ consists of the partial derivatives of the concentrations of the absorbing species with respect to the equilibrium constants or, preferably,[20] their logarithms.

The use of analytical derivatives in the numerical treatment of solution equilibria was introduced by Bugaevsky *et al.*[21] More recently, this has been discussed for the treatment of potentiometric data[22] and incorporated into TITFIT[20] for the calculation of $\partial \mathrm{ml}_{calc}/\partial \ln \beta_{mlh}$, the partial derivatives of the amount of base consumed with respect to the logarithms of the equilibrium constants. In a somewhat analogous way $D\mathbf{C}$ can be obtained after calculation of all the species concentrations $\mathbf{s} = [s(1), \ldots, s(j), \ldots, s(J)]^t$ by the usual Newton–Raphson method.[23]

$$\begin{aligned}0 &= \mathbf{A}\,\Delta\mathbf{c} + \mathbf{a}_{calc} - \mathbf{a}\\ \Delta\mathbf{c} &= \mathbf{A}^{-1}(\mathbf{a} - \mathbf{a}_{calc});\ \mathbf{c}_{n+1} = \mathbf{c}_n + \Delta\mathbf{c}\end{aligned} \tag{16}$$

In equation (16), **a** contains the set of analytical (total) concentrations describing the chemical composition, **c** gives the actual free concentrations of the components, and $\Delta\mathbf{c}$ the corrections in the nth iterative cycle of refinement. The values in $\mathbf{a}_{calc} = [a(1)_{calc}, \ldots, a(k)_{calc}, \ldots, a(K)_{calc}]^t$ are the total concentrations calculated for a given set of equilibrium constants and component concentrations **c** [equation (17)] with the aid of the stoichiometric coefficients $\alpha(k,j)$, indicating the number of entities of component k contained in species j.

$$\begin{aligned}a(k)_{calc} &= \sum_{j=1}^{J} \alpha(k,j)\,s(j)\\ &= \sum_{j=1}^{J} \left\{\alpha(k,j)\,\beta(j)\,\prod_{i=1}^{K} c(i)^{\alpha(i,j)}\right\}\end{aligned} \tag{17}$$

The array **A** is made up finally from the partial derivatives of $\mathbf{a}_{calc}$ with respect to the component concentrations, $A(k,i) = \partial a(k)_{calc}/\partial c(i)$ and can readily be calculated from equation (17). Since the construction of **r** and **J** is actually done point by point, the subscript m is dropped for the present. It may be noted that one row of the concentrations of the absorbing species, **C**, and the concentrations of the components, **c**, are both subsets of **s**, and also that the non-linear parameters **p** are a subset of $\ln \boldsymbol{\beta}$.

After calculation of **s**, **c**, and **A** from equations (16) and (17), the elements of $D\mathbf{C} = \partial C(m,j)/\partial \delta p(n) = \partial s(j)/\partial \ln \beta(n)$ are obtained at little extra cost from equation (18):

$$\begin{aligned}\frac{\partial s(j)}{\partial \ln \beta(n)} &= \frac{\partial s(j)}{\partial \beta(n)}\,\beta(n) = s(j)\delta_{j,n}\\ &\quad + \sum_{k=1}^{K} \frac{\partial s(j)}{\partial c(k)}\,\frac{\partial c(k)}{\partial \ln \beta(n)}\end{aligned} \tag{18}$$

$$\partial s(j)/\partial c(k) = \alpha(k,j)s(j)/c(k) \tag{19}$$

In equation (18), $\delta_{j,n}$ is the Kronecker delta and the partial derivatives of the species concentrations with respect to the concentrations of the components [equation (19)] are already known from the Newton–Raphson procedure. The derivatives of the components with respect to $\ln \beta(n)$ are finally obtained by a simple matrix manipulation:

$$\begin{aligned}\frac{\partial a(k)_{calc}}{\partial \ln \beta(n)} &= 0 = \alpha(k,n)\,s(n)\\ &\quad + \sum_{i=1}^{K} \frac{\partial a(k)_{calc}}{\partial c(i)}\,\frac{\partial c(i)}{\partial \ln \beta(n)}\end{aligned}$$

or

$$\begin{aligned}D\mathbf{a}_{calc,n} &= 0 = \mathbf{s}_{\alpha,n} + \mathbf{A}\,D\mathbf{c}_n\\ D\mathbf{c}_n &= -\mathbf{A}^{-1}\,\mathbf{s}_{\alpha,n}\end{aligned} \tag{20}$$

The elements of $D\mathbf{C}$ are now obtained by simple substitution of the results from equations (19) and (20) into equation (18). It should be noted that the complete derivative of **C** with respect to the unknown parameters **p** is in fact a tensor with dimensions $M \times S \times N$ and that the derivatives with respect to all N parameters are obtained by making repetitive use of equations (18)–(20). With the knowledge of both **C** and $D\mathbf{C}$ we now obtain **r** and **J** from equations (4) and (14), so we are back to the standard situation of non-linear least-squares refinement. The elements of **J** can also be obtained by starting from equation (6), *i.e.*, after orthogonalization of **C**. However, this increases computing time and proved to be unnecessary when analytical instead of numerical derivatives were used. This possibility was therefore not included in the final version of SPECFIT.

Multiwavelength data—factor analysis

Data obtained at W different wavelengths are conveniently written as a matrix **Y** and the expression for the calculation of the residuals [equation (4)] is transformed into equation (21):

$$\mathbf{R} = \mathbf{F} - \mathbf{Y} = \mathbf{C}\,(\mathbf{C}^t\,\mathbf{C})^{-1}\,\mathbf{C}^t\,\mathbf{Y} - \mathbf{Y} = \mathbf{P}\,\mathbf{Y} \quad (21)$$

F, **R**, and **Y** are all matrices with M columns and W rows. The data can, however, be treated exactly as described by applying equations (4) and (14) [or (4a) and (14a)], by using successively the individual columns of **Y** in the place of **y**. For a given wavelength w, the residuals $\mathbf{r}_w$ and the Jacobian matrix $\mathbf{J}_w$ do not depend on corresponding elements from other wave lengths. Therefore, SQ as well as $\mathbf{J}^t\,\mathbf{J}$ and $\mathbf{J}^t\,\mathbf{r}$, which are needed for the iterative refinement, are all simply the sums of the corresponding elements obtained at the individual wavelengths, *cf.* equations (1), (4) and (14), respectively.

If, however, the number of wavelengths, W, is large compared to the number of absorbing species, S, the repetitive application of equations (1), (4) and (14) can become unnecessarily cumbersome. The demand on computer time can then be significantly reduced by applying the technique of factor analysis to **Y**.[24,25]

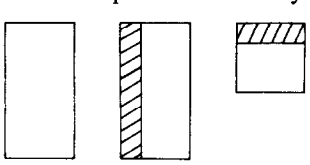

$$\mathbf{Y} \quad = \quad \mathbf{L} \qquad \mathbf{V} \qquad (22)$$

Since **V** is made up by the eigenvectors of **Y**, its rows are orthonormal, $\mathbf{V}\,\mathbf{V}^t = \mathbf{I}$. When equations (21) and (22) are combined, the sum of squares, SQ, can be written as:

$$SQ = \sum_{m=1}^{M}\sum_{w=1}^{W} R(m,w)^2 = \mathrm{tr}(\mathbf{R}^t\,\mathbf{R})$$
$$= \mathrm{tr}(\mathbf{R}\,\mathbf{R}^t) = \mathrm{tr}(\mathbf{P}\,\mathbf{Y}\,\mathbf{Y}^t\,\mathbf{P}^t)$$
$$= \mathrm{tr}(\mathbf{P}\,\mathbf{L}\,\mathbf{V}\,\mathbf{V}^t\,\mathbf{L}^t\,\mathbf{P}^t) = \mathrm{tr}(\mathbf{P}\,\mathbf{L}\,\mathbf{L}^t\,\mathbf{P}^t) \quad (23)$$

In other words, instead of calculating **R** from equation (21), we obtain the same SQ for a given **C** (and thus **P**) by using the linear coefficients **L** in place of the original data **Y**:

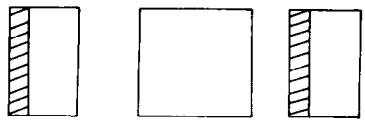

$$\mathbf{R} \quad = \quad \mathbf{P} \qquad \mathbf{L} \qquad (24)$$

Now, all the essential information concerning the data is contained in the first I (shaded) columns of **L**, that is, in $\mathbf{L}_I$. In fact, in the absence of experimental error, the rank of **Y** could not exceed the number of absorbing species, S, and at most S non-vanishing columns of **L** would be obtained. The right (unshaded) part of **L** thus contains only noise and does not have to be considered in the calculation. Therefore, the dimensions of **L** and **R** are reduced from $M \times W$ (typically $M \times 30$) to $M \times I$ (typically $M \times 5$) and the effect increases with the number of wavelengths included. The complete iterative refinement is now done on the reduced matrix $\mathbf{L}_I$ instead of on **Y**.

It may be noted that the number of columns I in $\mathbf{L}_I$ is neither uniquely defined nor very critical. As mentioned, experimental noise will increase the number of non-vanishing columns. On the other hand, spectra of some of the absorbing species may be essentially linear combinations of others, thus reducing the effective rank of **Y** to $I \leqslant S$.

Decomposition of **Y** into **L** and **V** can be accomplished in many ways. Practically all of them make use of the second-moment matrix **M**.

$$\mathbf{M} = \frac{1}{M}\,(\mathbf{Y}^t\,\mathbf{Y}) \quad (25)$$

In the present case, only a few eigenvectors with the largest I eigenvalues are needed, and the simple method of vector iteration[17] proves to be faster than general library routines which calculate all the eigenvectors of **M**. This technique yields the rows of **V** in decreasing order of the eigenvalues $\boldsymbol{\lambda} = [\lambda(1), \ldots, \lambda(i), \ldots, \lambda(I)]^t$.

Factor analysis also gives an indication of the number of relevant eigenvectors, I, or components in a given set of data, which is actually the most common application of factor analysis to chemical problems,[26–29] which can be made by comparing the estimated instrumental standard deviations of the absorbance measurements, SA with the residual errors of the decomposition, SD,[24] [equation (26)].

$$SD = \sqrt{\left[\mathrm{tr}(\mathbf{M}) - \sum_{i=1}^{I}\lambda(i)\right]/(W - I)} \quad (26)$$

We may assume that all relevant factors have been found if $SD \leqslant SA$.

The linear coefficients $\mathbf{L}_I$ which are needed in the iterative refinement are finally obtained from

$$\mathbf{L}_I = \mathbf{Y}\,\mathbf{V}_I^t \quad (27)$$

where $\mathbf{V}_I$ is the $I \times W$ matrix of I relevant eigenvectors. While the exact determination of I for the model-free deduction of the number of absorbing species[26–29] is by no means trivial and in many cases ambiguous, its choice for the present purpose of data reduction is uncritical. If I is made too small, some information may be lost, but the effect on the final values of the equilibrium constants is normally almost negligible. Too large values of I increase the computing time with little effect on the results. In addition, we note that the large $(M \times M)$ matrix $\mathbf{P}$ is never actually calculated. The residuals $\mathbf{R}_I$ and thus SQ are in fact obtained from

$$\mathbf{R}_I = \mathbf{C}\,(\mathbf{C}^t\,\mathbf{C})^{-1}\,\mathbf{C}^t\,\mathbf{L}_I - \mathbf{L}_I;\; SQ = \mathrm{tr}(\mathbf{R}_I^t\,\mathbf{R}_I) \quad (28)$$

which needs less computer space and time if done in the proper order.

In the case of strongly structured (*e.g.*, EPR[30]) spectra, it may be useful to obtain data at a rather large number of wavelengths, $W \gg M$. Then the second moment matrix $\mathbf{M}$ [equation (25)] with dimensions $W \times W$ may be unduly large and an alternative route for the calculation of $\mathbf{L}_I$ is preferable:

$$\mathbf{M}^* = \frac{1}{W}\,\mathbf{Y}\,\mathbf{Y}^t \quad (29)$$

$$\mathbf{L}_I = (\mathbf{V}_I^*)^t\,\mathbf{F};\; F(i,j) = \delta_{i,j}\,\sqrt{\lambda(i) \times W} \quad (30)$$

This method for calculation of $\mathbf{L}_I$ is somewhat simpler than the use of equations (25) and (27), and is therefore preferred whenever $W \geqslant M$.

Since equation (28) is identical in structure with equations (21) and (4), the calculations of SQ (1) and the Jacobian matrix (14), as well as the refinement of the equilibrium constants [equation (7)] proceeds exactly as with the original data. Fixed spectra $\hat{\mathbf{E}}_f$ are easily included, if they are first represented in the vector space spanned by the eigenvectors $\mathbf{V}$:

$$\hat{\mathbf{E}}_{f,V} = \hat{\mathbf{E}}^f\,\mathbf{V}^t \quad (31)$$

$\hat{\mathbf{E}}_f$ and $\hat{\mathbf{E}}_{f,V}$ are matrices with W and I columns, respectively. After this transformation, the columns of the Jacobian matrix may again be obtained from equation (14a) instead of (14), if some species with known spectra are present. In equation (28), the molar absorptivities $\hat{\mathbf{E}}^u$ of the absorbing species are not immediately available at the end of the iterative refinement. By analogy with equation (3a) they are, however, readily obtained from the original data and the previously calculated arrays $\mathbf{Q}_u^{-1}$ and $\mathbf{C}_u^t$ [equation (32)].

$$\hat{\mathbf{E}}_u = \mathbf{Q}_u^{-1}\,\mathbf{C}_u^t\,\mathbf{Y}_u \quad (32)$$

Estimation of standard errors

The standard errors of the refined parameters (and if desired the complete covariance matrix[15]) are obtained through equations (33) and (34), where $\mathbf{J}_t$ is the total Jacobian matrix with respect to both non-linear and linear parameters.

$$\mathbf{Q}_t = \mathbf{J}_t^t\,\mathbf{J}_t;\quad \mathbf{Q}_{I,t} = \mathbf{Q}_t^{-1} \quad (33)$$

$$\sigma(i) = \sqrt{Q_{I,t}\,(i,i)}\;\sigma(y) \quad (34)$$

The elements of $\mathbf{Q}_{I,t}$ can be obtained without first constructing $\mathbf{J}_t$ and $\mathbf{Q}_t$, however. Following ideas developed earlier,[31] we can subdivide $\mathbf{Q}_t$ and $\mathbf{Q}_{I,t}$ according to equation (35).

$$\mathbf{Q}_t = \begin{array}{|c|c|}\hline \mathbf{Q}_1 & \mathbf{Q}_3 \\ \hline \mathbf{Q}_3^t & \mathbf{Q}_2 \\ \hline \end{array}\;;\quad \mathbf{Q}_{I,t} = \begin{array}{|c|c|}\hline \mathbf{Q}_{I,1} & \mathbf{Q}_{I,3} \\ \hline \mathbf{Q}_{I,3}^t & \mathbf{Q}_{I,2} \\ \hline \end{array} \quad (35)$$

In equation (35), $\mathbf{Q}_1$ and $\mathbf{Q}_{I,1}$ refer only to the equilibrium constants, $\mathbf{Q}_2$ and $\mathbf{Q}_{I,2}$ belong only to the molar absorptivities, and $\mathbf{Q}_3$ and $\mathbf{Q}_{I,3}$ contain mixed terms. By applying the least-squares condition to both linear and non-linear parameters, the expressions (36)–(38) can be derived.[31]

$$\mathbf{Q}_{I,1} = (\mathbf{J}^t\,\mathbf{J})^{-1} \quad (36)$$

$$\mathbf{Q}_{I,3}^t = D\hat{\mathbf{e}}_p\,\mathbf{Q}_{I,1} \quad (37)$$

$$\mathbf{Q}_{I,2} = \mathbf{Q}_u^{-1} + \mathbf{Q}_{I,3}^t\,D\hat{\mathbf{e}}_p^t \quad (38)$$

In equation (36), $\mathbf{J}$ is the Jacobian matrix associated with the non-linear parameters after elimination of the linear ones. Thus $\mathbf{Q}_{I,1}$ is already known [equation (7)]. Equally, $\mathbf{Q}_u^{-1} = \mathbf{Q}_2^{-1} = (\mathbf{C}_u^t\,\mathbf{C}_u)^{-1}$ has been calculated before [equation (3a)]. Finally $D\hat{\mathbf{e}}_p$ is the matrix of partial derivatives of the molar absorptivities with respect to the N unknown equilibrium constants and thus consists of N columns of $D\hat{\mathbf{e}}$, [*cf.* equation (13)]. Therefore, all elements of $\mathbf{Q}_{I,t}$ are obtained at very little cost and the information available at the end of the refinement is identical to that obtained without elimination and without factor analysis.

CONCLUSIONS

By a combination of appropriate elementary matrix manipulations, the calculation of equilibrium constants from multiwavelength spectrophotometric data is greatly simplified. Equations (3) and (4) reduce the number of parameters in the iterative refinement to the number of unknown stability constants. The use of analytical derivatives [(14) and (18)] increases the numerical safety and speed of the calculation. Computer time and memory are saved by doing the iterative refinement in an orthogonal vector space spanned by the eigenvectors of the original absorbance matrix [equation (28)]. The standard errors of all parameters are readily obtained without ever calculating the full Jacobian matrix [equations (36)–(38)]. For the iterative refinement of the non-linear parameters, any modification to the solution of the Gaussian normal equations [equation (7)] may be applied, as in standard non-linear least-squares data reduction. A comprehensive computer program

SPECFIT which combines the ideas above with the efficient Marquardt algorithm[3,14,15,20] and is written in standard FORTRAN 77, will be described in a later paper.

Acknowledgement—This work was supported by the Swiss National Science Foundation (Grant No. 2.213-0.81).

REFERENCES

1. D. J. Leggett, S. L. Kelly, L. R. Shiue, Y. T. Wu, D. Chang and K. M. Kadish, *Talanta*, 1983, **30**, 579.
2. D. J. Leggett and W. A. E. McBryde, *Anal. Chem.*, 1975, **47**, 1065.
3. R. M. Alcock, F. R. Hartley and D. E. Rogers, *J. Chem. Soc. Dalton*, 1978, 115.
4. H. Gampp, M. Maeder and A. D. Zuberbühler, *Talanta*, 1980, **27**, 1037.
5. D. J. Leggett, *Am. Lab.*, 1982, **14**, No. 1, 29.
6. F. Gaizer, *Coord. Chem. Rev.*, 1979, **27**, 195.
7. W. A. E. McBryde, *Talanta*, 1974, **21**, 979.
8. P. Gans, *Coord. Chem. Rev.*, 1976, **19**, 99.
9. G. Hänisch, Th. A. Kaden and A. D. Zuberbühler, *Talanta*, 1979, **26**, 563.
10. A. D. Zuberbühler and Th. A. Kaden, *ibid.*, 1979, **26**, 1111.
11. M. Briellmann and A. D. Zuberbühler, *Helv. Chim. Acta*, 1982, **65**, 46.
12. H. Gampp, D. Haspra, M. Maeder and A. D. Zuberbühler, *Inorg. Chem.*, in the press.
13. H. Gampp, M. Maeder, C. J. Meyer and A. D. Zuberbühler, *Talanta*, submitted.
14. D. W. Marquardt, *J. Soc. Ind. Appl. Math.*, 1963, **11**, 431.
15. P. R. Bevington, *Data Reduction and Error Analysis for the Physical Sciences*, McGraw-Hill, New York, 1969.
16. W. H. Lawton and E. A. Sylvestre, *Technometrics*, 1971, **13**, 461.
17. H. R. Schwarz, H. Rutishauser and E. Stiefel, *Matrizennumerik*, Steuber, Stuttgart, 1972.
18. G. H. Golub and V. Pereyra, *SIAM J. Numer. Anal.*, 1973, **10**, 413.
19. D. A. Harville, *Technometrics*, 1973, **15**, 509.
20. A. D. Zuberbühler and Th. A. Kaden, *Talanta*, 1982, **29**, 201.
21. A. A. Bugaevsky and B. A. Dunai, *Zh. Analit. Khim.*, 1971, **26**, 205; A. A. Bugaevsky, L. E. Rudnaya and T. P. Mukhina, *ibid.*, 1972, **27**, 1675.
22. I. Nagypál, I. Páka and L. Zékány, *Talanta*, 1978, **25**, 549.
23. U. Hoffmann and H. Hofmann, *Einführung in die Optimierung*, Verlag Chemie, Weinheim, 1971.
24. J. J. Kankare, *Anal. Chem.*, 1970, **42**, 1322.
25. M. Maeder and H. Gampp, *Anal. Chim. Acta*, 1980, **122**, 303.
26. Z. Z. Hugus and A. A. El-Awady, *J. Phys. Chem.*, 1971, **75**, 2954.
27. S. Wold, *Technometrics*, 1978, **20**, 397.
28. R. N. Cochran and F. H. Horne, *Anal. Chem.*, 1977, **49**, 846.
29. E. R. Malinowsky, *ibid.*, 1977, **49**, 606.
30. H. Gampp, *Inorg. Chem.*, 1984, **23**, 1553.
31. F. S. G. Richards, *J. Roy. Stat. Soc.*, 1961, **23**, 469.

Talanta, Vol. 32, No. 2, pp. 103–109, 1985
Printed in Great Britain.

0039-9140/85 $3.00 + 0.00

SIMULTANEOUS DETERMINATION OF ARSENIC, SELENIUM, TIN AND MERCURY BY NON-DISPERSIVE ATOMIC FLUORESCENCE SPECTROMETRY*

A. D'ULIVO, R. FUOCO and P. PAPOFF
Istituto di Chimica Analitica Strumentale del C.N.R., Via Risorgimento, 35, 56100 Pisa, Italy

(*Received* 12 *March* 1984. *Revised* 29 *August* 1984. *Accepted* 14 *September* 1984)

Summary—A procedure is described for simultaneous determination of arsenic, selenium, tin and mercury in aqueous solution by non-dispersive atomic-fluorescence spectrometry. Radiofrequency-excited EDLs, 100% modulated in the kHz region, were used for atom excitation. Sodium tetrahydroborate was used as reductant and a hydrogen–argon miniflame as atomizer. In the optimized procedure, which uses 1 ml of sample, the limits of detection (three times the standard deviation of the blank) were 0.04, 0.08, 0.1 and 0.1 ng/ml for arsenic, selenium, tin and mercury respectively. The linear dynamic range was greater than three decades for all analytes and the precision was better than 7% (typically 3%) for concentrations ≥ 1 ng/ml. Results for mutual interference effects are reported. Copper, nickel, lead and cobalt interfered only with selenium (5 ng/ml), when present in at least 200-fold weight ratio to it. Using 5 ml of sample improved the limits of detection for selenium and arsenic (0.01 and 0.02 ng/ml respectively), but at the expense of greater interference. Recovery from spiked natural water samples was better than 95% at the ng/ml level, except for selenium in sea-water, when the recovery was only 85%. Determination of the four elements, including standard-addition and background measurements, requires about 10 min.

Non-dispersive atomic-fluorescence spectrometry (NDAFS) has proved to be superior to dispersive atomic-fluorescence and atomic-absorption spectrometry on account of its potential for simultaneous multielement analysis and its lower detection limit and larger dynamic range.[1–5]

In a previous paper,[6] describing a new instrument for simultaneous determination of elements by NDAFS, attention was mainly focused on the characteristics of the optical and electronic components and optimization of the signal to noise ratio (SNR). The present paper describes use of that instrument for simultaneous determination of arsenic, selenium, tin and mercury at sub-ng/ml levels, with sodium tetrahydroborate as reductant for generation of the volatile species measured.

EXPERIMENTAL

Apparatus

Radiofrequency-excited electrodeless discharge lamps (RFEDL) (Perkin-Elmer) were used in the four-channel excitation system.[6] Individual modulation of the RF power of each channel in the range 6–8 kHz allowed approximately 100% modulation of the light-beam, with a low (d.c.) background level.

An argon–hydrogen entrained air miniflame[7] was preferred because of its optical transparency and low noise as well as its chemical inertia and the absence of memory effects (which often occur with electrothermal atomizers[8]). The flame was supported on a glass tube (4 mm bore) and obtained, unless otherwise specified, with flow-rates of 0.35 l./min for hydrogen and 1.0 l./min for argon, the latter also serving as the carrier gas. Ball flowmeters (Sho-Rate 150, Brooks) were used to measure the flow-rates. The 70-ml reaction vessel was constructed as described by others.[7,9] Disposable micropipettes were used for adding the tetrahydroborate and for sample injection.

Reagents

As(III), Se(IV), Sn(IV) and Hg(II) stock solutions (1000 μg/ml) were prepared from pure As_2O_3, SeO_2, Sn and Hg. Working standards were prepared just before use. The sodium tetrahydroborate solution was stabilized with sodium hydroxide (0.1%) and filtered.[10] Erba RLE sodium tetrahydroborate (powder) was preferred because of its high purity and low cost. Merck "Suprapur" hydrochloric acid and sodium hydroxide were used.

Procedure

One ml of 2% sodium tetrahydroborate solution was placed in the reaction vessel and a disposable micropipette containing the sample (0.2–1.0 ml) was placed in the injector port. Argon was then passed through the reaction vessel until stable base-lines were obtained. The sample was then injected and the signals were recorded. For a sample volume of 5 ml, the procedure was modified. The sample was placed in the reaction vessel and stirred (magnetic stirrer) with argon passing through the vessel, then 1 ml of sodium tetrahydroborate solution was added through the injector port. The connecting tubing and the glass burner were conditioned with 3*M* hydrochloric acid before measurements, whenever determination of selenium was required.

*Presented in part at the "1° Convegno Incontri di Chimica Analitica dell'Ambiente", Genoa, Italy, 23–24 May 1983.

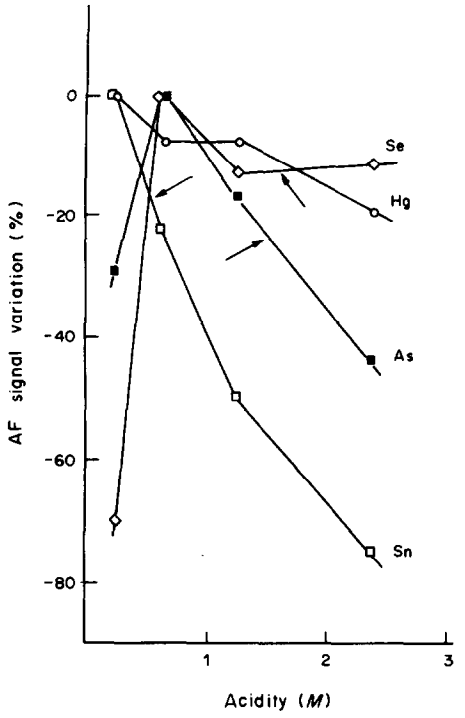

Fig. 1. Effect of sample acidity (HCl) on the atomic-fluorescence signals of arsenic, selenium, tin and mercury, each present at a concentration of 10 ng/ml. The arrows indicate the sample acidity proposed by Thompson and Thomerson.[9] Conditions: 1-ml sample, 1 ml of 2% $NaBH_4$ solution, observation height 15 mm, H_2 0.35 l./min, argon 1.0 l./min.

RESULTS AND DISCUSSION

Effect of gas flow-rates

In agreement with the findings of Tsujii and Kuga,[7] the hydrogen flow-rate was found to affect the SNR, depending on the acidity and volume of the solution injected into the reaction vessel. With 0.6*M* hydrochloric acid sample medium and different sample volumes, the best SNR was obtained with the following hydrogen flow-rates: 0.25 l./min for 0.2 and 0.5 ml samples, and 0.35 and 0.45 l./min for 1 and 5 ml samples respectively.

An argon flow-rate of 1.0 ± 0.2 l./min resulted in relatively large (7–9 sec) reproducible peak widths at half peak-height. It was therefore possible to use a relatively high time-constant (10 sec) at the output low-pass filter, with consequent gain in SNR.

Effect of acidity

Figure 1 shows, for each element, the effect of acidity on the signal peak heights. The arrows show the acid concentration giving maximal response, as obtained by Thompson and Thomerson[9] by AAS with a quartz furnace atomizer, other conditions being the same. For the elements for which the comparison is possible, the highest signals are reached at lower acidities in our procedure. This can be attributed to the fact that when the argon–hydrogen miniflame is used, the enhancement of the signal caused at increasing acidity by the increased rate of hydrogen production and faster stripping of volatile species, is offset by the change in geometry and stoichiometry of the flame, which decreases the degree of atomic excitation.

Anomalous behaviour was observed for selenium. If the glassware and tubing were not preconditioned, strong and reproducible signals were obtained only when the sample acid concentration was 1.2*M* hydrochloric acid. For instance, when successive 1-ml samples in 0.6*M* hydrochloric acid medium were injected, a progressive decrease in signal peak height was observed (Fig. 2). We attribute this to the relatively high acidity of hydrogen selenide ($K_a = 2.2 \times 10^{-4}$), resulting in its reacting along the walls of the transfer line with basic impurities resulting from decomposition of the sodium tetrahydroborate and carried away by the transport gas.

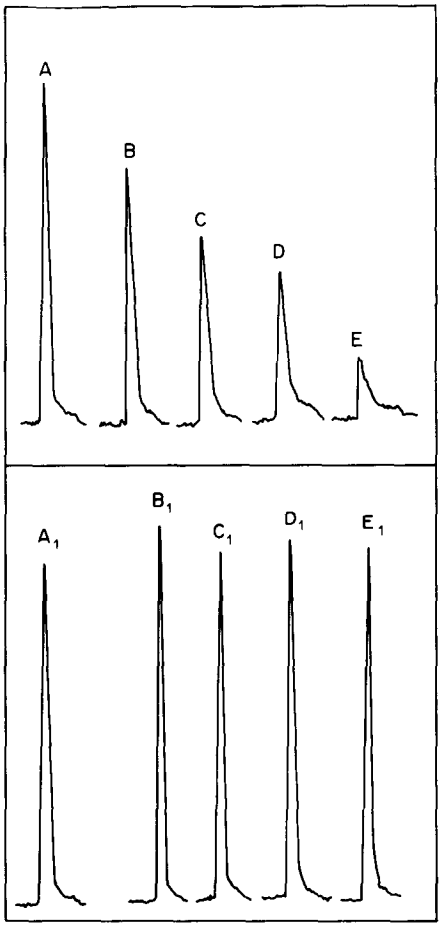

Fig. 2. Effect of acid preconditioning on the signal from 1 ml of 2-ng/ml selenium solution. Signals A–E were obtained with non-preconditioned apparatus, and signals A_1–E_1 with acid-preconditioned apparatus. Signals A and A_1 were obtained with 1.2*M* HCl sample medium. Signals B, C, D, E and B_1, C_1, D_1, E_1 were obtained with 0.6*M* HCl medium, injected straight after A and A_1 respectively. Other conditions: 1 ml of 2% $NaBH_4$ solution, H_2 0.35 l./min, argon 1.0 l./min, observation height 15 mm.

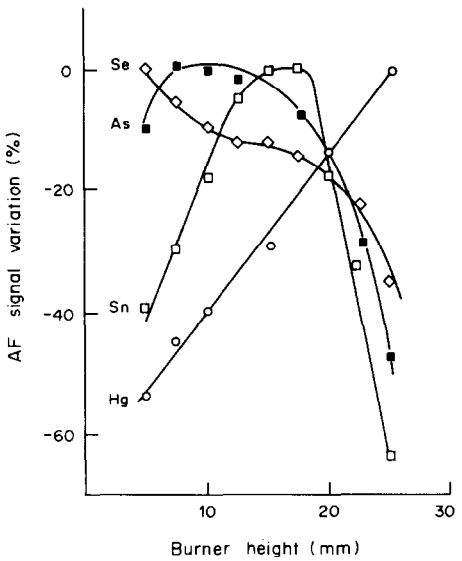

Fig. 3. Effect of observation height on atomic-fluorescence signal of arsenic, selenium, tin and mercury, each present at 10-ng/ml concentration. Conditions: 1 ml of sample in 0.6*M* HCl, 1 ml of 2% $NaBH_4$ solution, H_2 0.35 l./min, argon 1.0 l./min.

Preconditioning with 3*M* acid prevented this effect, and reproducible signals were obtained (Fig. 2) for several successive injections of sample.

For multielement determination, a sample acidity of 0.6*M* hydrochloric acid provides maximal sensitivity for arsenic and selenium and only a 10–20% loss in sensitivity for mercury and tin.

Effect of observation height

The optimum position for the optical path of the EDL light-beams is 15 mm above the burner top, which gives the highest sensitivity for arsenic and tin, and about 70 and 90% of maximum sensitivity for mercury and selenium respectively (Fig. 3).

Effect of amount of sodium tetrahydroborate

Figure 4 shows that the highest fluorescence signals were obtained for arsenic, mercury and selenium with 1 ml of 2% sodium tetrahydroborate solution. The signal for tin was 90% of the maximal value (reached with 1 ml of 4% sodium tetrahydroborate solution).

Effect of sample volume

The influence of sample volume on some of the performance characteristics is summarized in Table 1. Changing the sample volume changes the pH reached by the solution after the addition of tetrahydroborate (the change being biggest for the smallest sample volume), and the procedure must be changed when a 5-ml sample is used. The blank signal, S_B, is assumed to be due to the analyte present in the reagents. The detection limit C_L is taken as three times the standard deviation of the concentration in the blank, C_B. The peak-to-peak noise measured for the background near the signal, which is sometimes used for calculation of C_L in AFS, was practically devoid of meaning in this work, since the nature and size of the noise signal before and during the tetrahydroborate reaction were quite different.

Table 1 shows that the C_B values tended to decrease with increasing sample volume for all four elements, but with different patterns according to whether the impurities were mainly present in the acid or in the tetrahydroborate. In the case of selenium it is evident that the hydrochloric acid in the sample does not contribute to the size of C_B, since the product VC_B is fairly constant. The slope of the calibration graph would be expected to remain constant for constant yield of atomic events per unit volume of sample, *i.e.*, m/V should be constant. This was found to be approximately the case for arsenic over the whole sample volume range and for selenium in the 1–5 ml range, but for tin and mercury the yield decreased consistently with sample volume.

Since the decrease in detection limit when the sample volume is increased from 1.0 to 5 ml is very significant only for selenium, the use of 1 ml of sample is suggested, especially as interferences are higher with 5 ml of sample than with 1 ml, as will appear later.

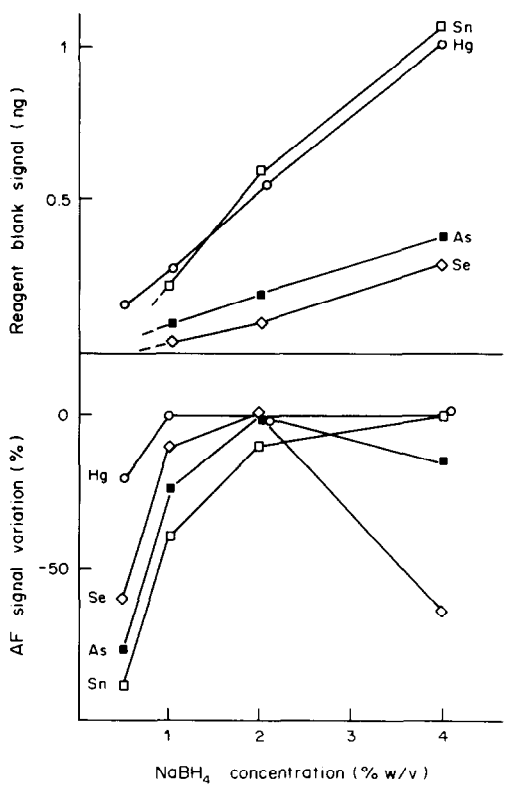

Fig. 4. Effect of concentration of $NaBH_4$ solution on blank signal and on atomic-fluorescence signal of arsenic, selenium, tin and mercury, each present at 10-ng/ml concentration. Conditions: 1 ml of sample in 0.6*M* HCl, 1 ml of $NaBH_4$ solution, H_2 0.35 l./min, argon 1.0 l./min, observation height 15 mm.

Table 1. Figures of merit: dependence on sample volume

Sample volume,	Arsenic					Selenium					Tin					Mercury				
V, *ml*	RSD_B	*m*	*m*/*V*	C_B	C_L	RSD_B	*m*	*m*/*V*	C_B	C_L	RSD_B	*m*	*m*/*V*	C_B	C_L	RSD_B	*m*	*m*/*V*	C_B	C_L
0.2	10.1	13	65	0.4	0.1_2	25	5	25	0.5	0.3_7	6.7	19	95	0.9	0.1_9	7.4	21	105	1.0	0.2_2
0.5	10.0	31	62	0.2	0.06	22.2	17	34	0.3	0.2_0	5.8	37	74	0.6	0.1_1	8.1	38	76	0.7	0.1_8
1.0	7.1	63	63	0.18	0.04	28.1	65	65	0.1	0.08	6.2	49	49	0.6	0.1_1	6.7	68	68	0.5	0.1_0
5.0	7.0	254	51	0.08	0.02	11.0	340	68	0.03	0.01	3.4	60	12	1.0	0.1_0	9.0	147	29	0.3	0.08

Conditions: 1 ml of 2% $NaBH_4$ solution, observation height 15 mm, Ar 1.0 l./min. For the different volumes of sample, see the relevant procedure in the text.
RSD_B = Relative standard deviation of blank signal (10 replicate measurements).
m = Slope of calibration curves (arbitrary units × ml/ng).
C_B = Apparent concentration of blank signal (ng/ml).
C_L = Limit of detection (ng/ml), taken as three times the standard deviation of the blank.

Table 2. Dynamic range and precision in single-element mode

	Dynamic range		Precision at various levels, *ng*/*ml*†			
Analyte	Upper limit *ng*/*ml*	Decades*	1.0	3.0	10.0	100
Arsenic	300	3.9	5.0	3.6	2.1	2.4
Selenium	450	3.8	7.0	7.2	5.9	2.8
Tin	400	3.6	4.8	3.5	3.2	2.0
Mercury	300	3.5	5.2	4.0	4.2	4.3

Conditions: 1 ml of sample in 0.6*M* HCl, 1 ml of 2% $NaBH_4$ solution, H_2 0.35 l./min, Ar 1.0 l./min, observation height 15 mm.
*Calculated as log ($C_{upper\ limit}/C_L$).
†Relative standard deviation on ten replicate measurements for each of the four levels.

Table 3. Mutual interelement effect on precision*

Analyte (1 ng/ml)	Precision†	Precision§ As	Se	Sn	Hg
Arsenic	5.0	—	5.1	4.1	5.0
Selenium	7.0	8.2	—	5.8	5.8
Tin	4.8	6.1	6.2	—	5.5
Mercury	5.2	7.3	4.8	6.2	—

*Conditions: as for Table 2.
†Relative standard deviation of ten replicate measurements in absence of interferent.
§Relative standard deviation of ten replicate measurements in presence of a 500 ng/ml concentration of interferent.

Dynamic range and precision

Table 2 shows that the precision was between 2 and 7% for all four elements at the 1-ng/ml level and improved with concentration, except for mercury, for which it was almost constant. The precision was unaffected by the presence of the other three elements in 500-fold w/w ratio to the analyte (Table 3) though there were some effects on signal height (Table 4, see below).

Interferences

In the preceding paper[6] the instrumental cross-talk was measured separately from chemical and optical effects and was calculated to be at least 68 dB.

Mutual interferences. Varying the sample volume but using a constant amount of sodium tetrahydroborate was found to affect the size of the interference effects, except for mercury (Table 4). Mercury is the only one of the four elements which does not form a hydride, so the interference probably arises in the hydride formation.

With 1 ml of sample, mercury interferes with the selenium signal only when present at concentrations higher than 5 μg/ml. Arsenic and tin present a peculiar mutual effect: the arsenic peak is enhanced by tin concentrations ≥ 0.5 μg/ml with maximal increase at tin ≥ 2 μg/ml. Arsenic affects the tin response with a similar but negative effect. The mutual arsenic–tin effect depends mainly on the concentration of the interferent and not on the concentration of analyte or the analyte/interferent concentration ratio (see Fig. 5). With 5 ml of sample, the effect of arsenic on the tin signal was the same as for 1 ml, but the effect of tin on the arsenic signal is evident at tin concentrations above 0.03 μg/ml. Mutual effects, not observed with 1 ml of sample, were found for the selenium–tin pair at interferent concentrations higher than 2 μg/ml and for the arsenic–selenium pair at interferent concentrations higher than 5 μg/ml.

Other interferences. Copper was considered as a typical example of an element which strongly interferes in the hydride generation of many elements.[8,11,12]

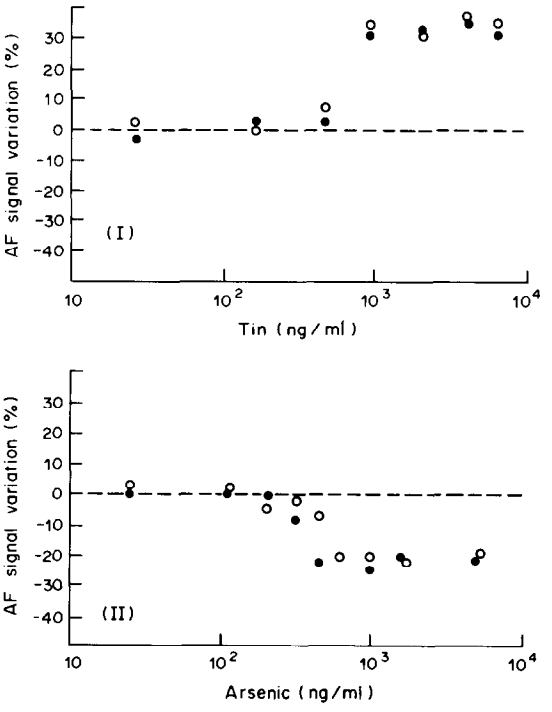

Fig. 5. (I). Interference effect of tin(IV) on arsenic signal for 1 ml of sample: As 25 ng/ml (●) and 250 ng/ml (○). (II). Interference effect of arsenic(III) on tin signal for 1 ml of sample: Sn 25 ng/ml (●) and 250 ng/ml (○).

Table 4. Mutual interelement interference effect on signal peak height

Analyte (5 ng/ml)	Change in peak height, %* 0.05 μg/ml As	Se	Sn	Hg	0.5 μg/ml As	Se	Sn	Hg	2.0 μg/ml As	Se	Sn	Hg	5.0 μg/ml As	Se	Sn	Hg
Arsenic†	—	0	0	0	—	0	+10	0	—	0	+30	0	—	0	+30	0
Arsenic§	—	0	+20	0	—	0	+45	0	—	−10	+45	0	—	−15	+35	0
Selenium†	0	—	0	0	0	—	0	0	0	—	0	0	0	—	0	+15
Selenium§	0	—	0	0	0	—	0	0	0	—	0	0	−15	—	−15	−10
Tin†	0	0	—	0	−20	0	—	0	−20	0	—	0	−20	0	—	0
Tin§	0	0	—	0	−20	0	—	0	−20	0	—	0	−25	−15	—	0
Mercury†	0	0	0	—	0	0	0	—	0	0	0	—	0	0	0	—
Mercury§	0	0	0	—	0	0	0	—	0	0	0	—	0	0	0	—

*Expressed as per cent change with respect to signal for each analyte in pure solution, for four interferent levels. Variations less than twice the s.d. were not taken into account.
†Sample volume 1 ml, 0.6*M* HCl. See text for procedure.
§Sample volume 5 ml, 0.6*M* HCl. See text for procedure.

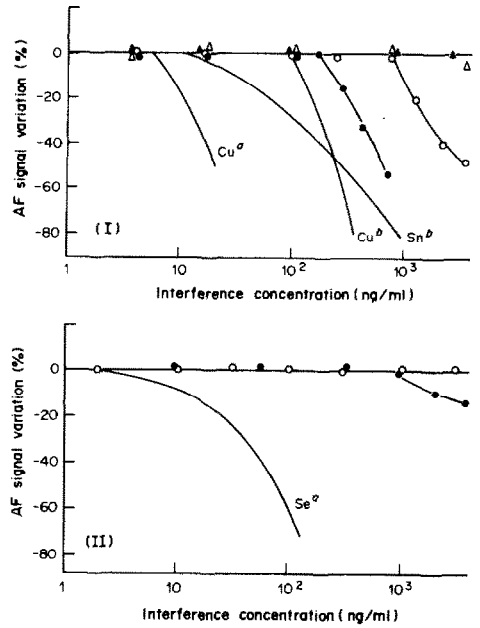

Fig. 6. (I). Interference effects on signal for selenium (5 ng/ml). Effect of copper(II) and tin(IV) as observed in present work: (○) copper, 1 ml of sample; (●) copper, 5 ml of sample; (▲) tin, 1 ml of sample; (△) tin, 5 ml of sample. Curves *a* and *b* refer to the effect of copper and tin on selenium (10 ng/ml) as observed by Welz and Melcher[7] (curve *a*) and Verlinden and Deelstra[12] (curve *b*).

(II). Interference effect of selenium(IV) on signal for arsenic (5 ng/ml) as observed in the present work with 1 ml (○) or 5 ml (●) of sample, and as observed by Welz and Melcher[7] (curve *a*).

With 1 ml of sample, each analyte at the 5-ng/ml level, and the copper concentration varied in the range 0.005–5 μg/ml, no interference with the signals of arsenic, tin and mercury was found. With selenium, copper did not interfere up to 1 μg/ml (Fig. 6). With 5 ml of sample and the same concentration of selenium, copper interfered at concentrations down to 0.2 μg/ml.

The effect of nickel, cobalt and lead (tested in the 0.005–5 μg/ml range) on the selenium signal for 1 ml of sample was then studied. It was found that nickel and cobalt exhibited the same behaviour as copper, whereas lead did not interfere.

Comparison with literature data

The interference effects could be compared with the literature only for arsenic and selenium, for which data obtained under similar experimental conditions were available.[8,11] The difference ih pattern from the literature data was essentially due to differences in the time elapsing between mixing of the reactants and stripping of the volatile hydrides from the cell, and to variation of the sample volume with constant tetrahydroborate volume. The interference threshold shifts towards higher interferent concentrations as the sample volume is decreased. It is the sample volume which is the more likely to play the decisive role. Decreasing the sample volume should increase the

Table 5. Simultaneous determination of As, Se, Sn and Hg in water samples

Sample	As added, *ng/ml*	As found, *ng/ml*	As recovery, %	Se added, *ng/ml*	Se found, *ng/ml*	Se recovery, %	Sn added, *ng/ml*	Sn found, *ng/ml*	Sn recovery, %	Hg added, *ng/ml*	Hg found, *ng/ml*	Hg recovery, %
Sea-water A	0	0.71		0	n.d.		0	n.d.		0	n.d.	
	1.0	1.70	98	1.0	0.87	87	2.0	1.9	95	2.0	1.9	95
B	0	1.10		0	n.d.		0	n.d.		0	n.d.	
	1.0	2.10	100	2.0	1.70	85	2.0	1.9	95	2.0	1.9	95
River water	0	1.23		0	n.d.		0	n.d.		0	n.d.	
	1.0	2.18	95	2.0	1.95	97	2.0	2.0	100	2.0	2.0	100
Tap water	0	0.18		0	n.d.		0	1.2		0	n.d.	
	1.0	1.18	100	2.0	1.93	96	2.0	3.2	100	2.0	2.0	100

With 5-ml samples, selenium was found only in the sea-water samples. The relevant concentrations for samples A and B were 0.02 and 0.07 ng/ml respectively.
All samples were filtered through a 0.45-μm filter, acidified to pH 2 with HCl and stored at 4°. Each measurement was repeated five times and the r.s.d. was always less than 10%.
Conditions: as for Table 2.

rapidity of mixing the sample and reagent solutions and give a higher reagent concentration, thus reducing the risk of incomplete analyte hydride formation on account of side-reactions with interferents. In this respect it is interesting that no mutual interference effects between arsenic, selenium and tin were reported in a study of their automatic continuous-flow hydride-generation, even at very high interferent concentrations.[13,14]

Application to water samples

The natural concentration levels[15–21] of mercury and tin in uncontaminated waters being lower than the detection limits, only selenium and arsenic can be determined in such samples without preconcentration. For potable or polluted waters the method can indicate whether the four elements are above or below the allowable limits. Depending on the analyte, the simultaneous determination may give speciation information, or only the total concentration. Under the experimental conditions used, inorganic arsenic and methylarsenic acids are reduced to the corresponding arsines, which give the same analytical response;[17,22] inorganic mercury, methylmercury, ethylmercury and phenylmercury are all reduced to mercury metal;[23] tin(II) and tin(IV) give the same response,[24] but some alkyltins found in natural waters cannot be quantitatively determined, owing to the high boiling point of the alkylstannanes generated by tetrahydroborate reduction.[20,21] Only selenium(IV) reacts with tetrahydroborate to give hydrogen selenide, and is practically the only form present in natural water.[25,26] If the presence of Se(VI) or Se(II) is suspected (as in polluted water) the sample must be chemically pretreated to transform all the selenium species into Se(IV).[27,28] Total selenium and tin must therefore be determined by single-mode procedures.[21,27,28] With the four-channel detector, the determination of arsenic, mercury, selenium and tin (including standard-addition and reagent background correction) requires about 10 min. This significant shortening of operation time allows replicate analysis of the same sample or analysis of a larger number of samples, with a consistent improvement of the statistical meaning of the analytical data. The accuracy of the method was tested by analysis of spiked samples. At the 1–2 ng/ml level the recovery was better than 95% except for selenium in sea-water, for which it was only 85% (Table 5). The relative standard deviation for five replicate measurements was better than 10%.

CONCLUSIONS

Arsenic, selenium, tin and mercury can be determined simultaneously at sub-ng/ml levels by non-dispersive atomic-fluorescence spectrometry combined with the vapour-generation technique with sodium tetrahydroborate as reductant. Sample volumes from 0.2 to 5 ml can be used. The lowest detection limit is obtained with 5 ml of sample for selenium and arsenic and either 1 or 5 ml of sample for mercury and tin. Except for determination of selenium and arsenic at concentrations near the detection limit, 1 ml of sample is to be preferred because the interferences are then minimal. The relative standard deviation is then less than 7% for each of the four analytes within their dynamic ranges and down to 1 ng/ml, regardless of the presence of high concentrations of the other three analytes. The linear dynamic ranges cover more than three orders of magnitude for all four analytes.

Acknowledgements—This work was supported by C.N.R. (Rome). One of the authors (P.P.) acknowledges assistance from the M.P.I.

REFERENCES

1. P. D. Warr, *Talanta*, 1970, **17**, 543.
2. T. J. Vickers, P. J. Slevin, V. I. Muscat and L. T. Farias, *Anal. Chem.*, 1972, **44**, 930.
3. T. S. West, *Analyst*, 1974, **99**, 886.
4. R. F. Browner, *ibid.*, 1974, **99**, 617.
5. N. Omenetto and J. D. Winefordner, *Prog. Anal. Atom. Spectrosc.*, 1979, **2**, 1.
6. A. D'Ulivo, C. Festa and P. Papoff, *Talanta*, 1983, **30**, 907.
7. K. Tsujii and K. Kuga, *Anal. Chim. Acta*, 1978, **97**, 51.
8. B. Welz and M. Melcher, *ibid.*, 1981, **131**, 17.
9. K. C. Thompson and D. R. Thomerson, *Analyst*, 1974, **99**, 595.
10. J. R. Knetchel and J. L. Fraser, *ibid.*, 1978, **103**, 104.
11. M. Verlinden and H. Deelstra, *Z. Anal. Chem.*, 1979, **296**, 253.
12. A. E. Smith, *Analyst*, 1975, **100**, 300.
13. F. D. Pierce and H. R. Brown, *Anal. Chem.*, 1977, **49**, 1417.
14. F. D. Pierce, T. C. Lamoreaux, H. R. Brown and R. S. Fraser, *Appl. Spectrosc.*, 1976, **30**, 38.
15. M. Dall'Aglio, *Wat. Anal. Bull.*, 1982, **7**, 163.
16. H. Robberecht and R. Van Grieken, *Talanta*, 1982, **29**, 823.
17. R. S. Braman, D. L. Johnson, C. C. Foreback, J. M. Ammons and J. L. Bricker, *Anal. Chem.*, 1977, **49**, 621.
18. A. Seritti, A. Petrosino, E. Morelli, R. Ferrara and C. Barghigiani, *Environ. Technol. Lett.*, 1982, **3**, 251.
19. J. Olafsson, *Mar. Chem.*, 1982, **11**, 129.
20. R. S. Braman and M. A. Thompkins, *Anal. Chem.*, 1979, **51**, 12.
21. V. F. Hodge, S. L. Seidel and E. D. Goldberg, *ibid.*, 1979, **51**, 1256.
22. J. S. Edmonds and K. A. Francesconi, *ibid.*, 1976, **48**, 2019.
23. J. Toffaletti and J. Savory, *ibid.*, 1975, **13**, 2091.
24. K. Tsujii and K. Kuga, *Anal. Chim. Acta*, 1978, **101**, 199.
25. Y. K. Chau and J. P. Riley, *ibid.*, 1965, **33**, 36.
26. F. Leutwein, *Handbook of Geochemistry*, K. H. Wedephol (ed.), p. 34-H, 2,3. Springer, Berlin, 1972.
27. J. M. Rankin, *Environ. Sci. Technol.*, 1973, **7**, 823.
28. G. A. Cutter, *Anal. Chim. Acta*, 1978, **98**, 59.

Talanta, Vol. 32, No. 2, pp. 111–114, 1985
Printed in Great Britain

0039-9140/85 $3.00 + 0.00
Pergamon Press Ltd

SEPARATION AND DETERMINATION OF ARSENIC(V) AND ARSENIC(III) IN SEA-WATER BY SOLVENT EXTRACTION AND ATOMIC-ABSORPTION SPECTROPHOTOMETRY BY THE HYDRIDE-GENERATION TECHNIQUE

SAMUEL A. AMANKWAH and JAMES L. FASCHING*
Department of Chemistry, University of Rhode Island, Kingston, RI 02881, U.S.A.

(*Received* 25 *October* 1983. *Revised* 7 *August* 1984. *Accepted* 14 *September* 1984)

Summary—Arsenic(V) and arsenic(III) in sea-water have been separated by complexing the arsenic(III) with ammonium pyrrolidinedithiocarbamate (APDC) in the range 4.0–4.5 and extracting the complex with chloroform. The organic phase is then wet-ashed with a 1:1 mixture of concentrated nitric acid and perchloric acid to get rid of all organics, and the arsenic(III) is determined by hydride generation and atomic-absorption spectrophotometry. Total arsenic is determined by first reducing arsenic(V) to arsenic(III) with potassium iodide and then applying the method used for arsenic(III). The arsenic(V) content is determined by difference. The low detection limit of 0.031 ng/ml and the high sensitivity and precision make the method suitable for analysis of open ocean waters.

Currently, four basic methods are used for the investigation of arsenic speciation: ion-exchange chromatography,[1–3] differential pulse polarography,[4] selective hydride evolution,[5,6] and solvent extraction followed by flame[7] or graphite-furnace[8] atomic-absorption spectrophotometry or neutron activation.[9]

Although the investigation of arsenic speciation by solvent extraction followed by graphite-furnace/atomic-absorption spectrophotometry gives good sensitivity, interference by trace elements in the sample matrix is a problem and tends to cause unreliable results, as has been observed in our laboratory.

Differential pulse polarography does not give the required detection limit for the determination of arsenic in sea-water.[4] Several attempts by us to repeat the experiments by Aggett and Aspell[5] involving selective hydride evolution did not prove successful.

The problem of interference can be solved by using a method based on solvent extraction, wet-ashing to eliminate organic interferences, and selective determination of arsenic(III) by the hydride-generation technique. Complexation with ammonium pyrrolidinedithiocarbamate (APDC) and extraction into chloroform is the preferred separation step. The optimum pH and reagent concentration, and the accuracy, precision, sensitivity and detection limits of the method have been determined.

EXPERIMENTAL

Apparatus

A Perkin–Elmer Model 403 atomic-absorption spectrophotometer equipped with an electrothermal quartz-cell furnace, a chart-recorder and an arsenic electrodeless discharge lamp powered by an 8-W supply was used for all analyses. The Perkin–Elmer MHS-10 mercury/hydride generation system was connected to the quartz cell through two traps containing calcium chloride to remove water vapour. The carrier gas was argon, and the flow-rate was regulated by a flowmeter. Figure 1 shows the assembly of the system.

The electrothermal quartz cell was 1.7 cm in diameter and 18.8 cm long, with open ends. Graphite sleeves were used for heat dissipation. A sufficient length (about 4 ft) of nichrome wire (diameter 0.0254 in., resistance 1 Ω/ft) was wound round the tube for a temperature of about 900° to be reached by resistance heating. To insulate the tube and maintain uniform temperature distribution round it, the tube was wrapped first with asbestos and then with fibre-glass cloth. Power to the resistance wire was supplied by a variable transformer.

Reagents

All solutions were prepared from analytical grade chemicals. Distilled demineralized water was used for making all solutions.

Standard arsenic(III) solution (1 mg/ml). Prepared by dissolving 1.322 g of primary standard As_2O_3 in 100 ml of alkaline solution.

Standard arsenic(V) solution (1 mg/ml). Prepared by dissolving 4.165 g of $Na_2HAsO_4 \cdot 7H_2O$ and diluting to 1000 ml.

Sodium borohydride solution (5%). Prepared by dissolving 5 g of sodium borohydride powder in 100 ml of demineralized water, followed by addition of 1 pellet of potassium hydroxide. The resulting turbid solution was filtered through a 0.45-μm membrane filter to obtain a clear solution. This solution was prepared once every two weeks, following the procedure of Bye[10] and of Knechtel and Fraser.[11]

Concentrated nitric acid and hydrochloric acid were redistilled in a Pyrex still before use. All cleaned Pyrex glass was assumed to be free from arsenic impurities.[12]

Synthetic sea-water. Prepared by dissolving 254.0 g of NaCl, 105.0 g of $MgCl_2 \cdot 6H_2O$, 39.1 g of Na_2SO_4, 11.0 g of $CaCl_2 \cdot 2H_2O$, 7.2 g of KCl, 2.03 g of $SrCl_2$, 0.27 g of H_3BO_3 and 19.2 g of $NaHCO_3$ in 10 litres of demineralized water.

Ammonium acetate buffer. pH 4.5. Equal volumes of 4*M* sodium acetate and 4*M* acetic acid were mixed.

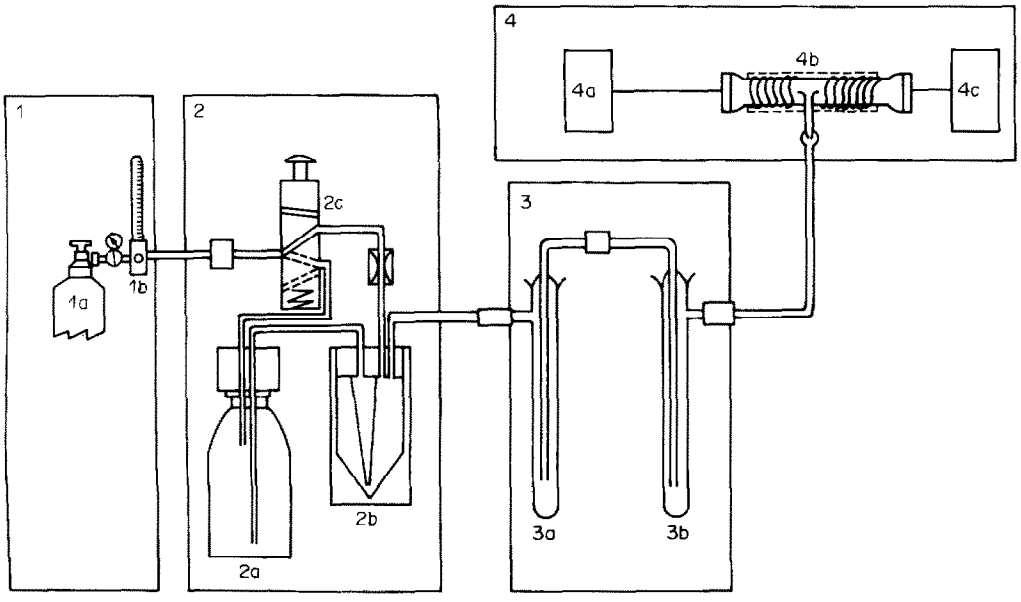

Fig. 1. Perkin–Elmer atomic-absorption spectrophotometric MHS-10 hydride-generation assembly: 1a, argon gas cylinder; 1b, flowmeter; 2, Perkin-Elmer MHS-10, 2a, sodium borohydride container; 2b, reaction vessel; 2c, plunger; 3a & b, contain calcium chloride pellets to remove water vapour; 4, Perkin-Elmer atomic-absorption spectrophotometer 403; 4a, arsenic electrodeless discharge lamp; 4b, electrothermal quartz-cell furnace; 4c, monochromators and detector.

Ammonium acetate buffer, pH 6.1. Concentrated ammonia solution (470 ml) was slowly added to 430 ml of glacial acetic acid, cooled in an ice-bath.

Atomic-absorption standards. Stock standards for lead (996 ppm), iron (1013 ppm), cobalt (998 ppm), zinc (1000 ppm), cadmium (1000 ppm), copper (1000 ppm), mercury (1000 ppm) and nickel (997 ppm) were obtained from Alpha Analytical Laboratories. These solutions were prepared from the chlorides except for the lead, nickel and mercury solutions, which were made from the nitrates. Each stock standard solution was diluted to the desired concentration before use.

Ammonium pyrrolidinedithiocarbamate (APDC) solution (1%). One g of APDC was dissolved in 100 ml of demineralized water, and the solution was filtered through a 0.45-μm membrane filter, then extracted with chloroform to purify it. The purified APDC solution was prepared as needed. The chloroform was used as received.

Procedure

All glassware was cleaned by washing several times with 4*M* nitric acid and then rinsed in demineralized water until the washings were neutral to litmus paper.

The synthetic sea-water was spiked with an appropriate concentration of arsenic(V) and arsenic(III).

Natural sea-water was collected from Narragansett Bay and filtered through a 0.45-μm membrane filter (Millipore) to remove any particulate matter. Analysis of the filter showed no retention of arsenic. The pH was lowered to 2 with hydrochloric acid and the solution stored in a polyethylene bottle (following the recommendation by Robertson[13]). It was assumed that the As(III)/As(V) ratio did not change at the pH value used. To study the two oxidation states of arsenic, a 10-litre sea-water sample (either synthetic or natural) was divided into two equal parts. To one aliquot about 100 g of potassium iodide was added to reduce all arsenic(V) to arsenic(III). The resulting solution was used for the total arsenic determination. The other aliquot was used for arsenic(III) determination.

A 300-ml sea-water (synthetic or natural) sample was placed in a 500-ml separatory funnel and brought to a pH within the range 4.0–4.5 with the ammonium acetate buffers. Ten ml of purified 1% APDC solution were then added, followed by 25 ml of chloroform. The mixture was shaken for 20 min on a horizontal mechanical shaker. After separation of the layers, the chloroform layer was drained into a 150-ml erlenmeyer flask. The aqueous layer was discarded. The chloroform layer was wet-ashed as follows. Ten ml of concentrated nitric acid and 10 ml of 70% perchloric acid were added, with some glass beads to prevent bumping and spattering, and the flask was fitted with a short-stemmed funnel. The mixture was boiled on a hot-plate until dense white fumes of perchloric acid were evolved. The flask was cooled, 10 ml of demineralized water were added, and the evaporation to dense white fumes of perchloric acid was repeated. The solution was then cooled to about 40°, and about 1 g of potassium iodide was added to reduce arsenic(V) to arsenic(III). The solution was made up to volume in a 50-ml standard flask with 1*M* hydrochloric acid. Arsenic(III) was then determined by the hydride-generation technique and atomic-absorption spectrophotometry with 15-ml portions of this solution, and the standard-addition method. The exact experimental procedure followed for the hydride generation procedure was that given in the manual for the Perkin-Elmer MHS-10 Mercury/Hydride system. Synthetic sea-water was used as the blank in all experiments.

RESULTS AND DISCUSSION

Effect of pH

The reaction between arsenic(III) and ammonium pyrrolidinedithiocarbamate is pH-dependent. The complex is extractable into organic solvents. Figure 2 shows the effect of pH on the complexation and extraction in the method developed, and indicates that the optimal pH-range is rather narrow, 4.5–4.6, but the pH range 4.0–4.5 gives adequate precision for the purpose.

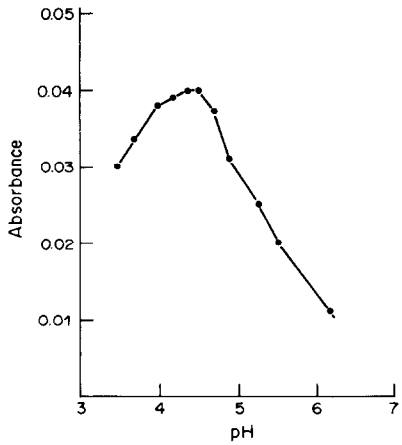

Fig. 2. Absorbance *vs.* pH of sample solution (in APDC preconcentration step).

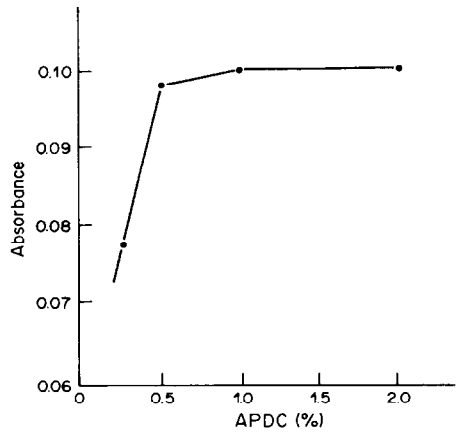

Fig. 3. Absorbance *vs.* APDC concentration.

Dependence of APDC concentration

Figure 3 shows the effect of APDC concentration on the efficiency of extraction of 50 ng of As(III) from 300 ml of synthetic sea-water at the optimum pH of 4.0–4.5. The extraction is constant and maximal when 10 ml of 1–2% APDC solution are used. Use of a 1% solution is recommended.

Sensitivity and detection limit

The sensitivity was obtained from the reciprocal of the mean slope of three graphs (plot of per cent absorption *vs.* concentration in ng/ml). The value of 0.140 ng/ml obtained (s.d. 0.006 ng/ml for triplicate analyses) is comparable to values reported for other methods involving the use of solvent extraction.[14]

The detection limit (D.L.) was determined from the relationship D.L. $= X \pm 3\ \sigma_{bl}$, according to Zief and Mitchell,[15] where X is the average value of ten determinations of the blank and σ_{bl} is the standard deviation.

The detection limit of 0.031 ng/ml (s.d. 0.005 ng/ml, triplicate analyses) is based on use of preconcentration to a volume of 50 ml, from which 10-ml aliquots are taken for the analysis. This value is very low and indicates that the method can be used for sea-water analysis.

Accuracy and precision

Tables 1 and 2 show the results for recovery and precision, obtained by the standard-addition method. Recoveries ranged from 95 to 106%. The precision data were obtained from analyses done on different days and the relative standard deviation of 0.6–0.8% shows the good reproducibility of the method.

Analysis of natural sea-water

The method was applied to the analysis of samples from Narragansett Bay. One sample was analysed on different days to assess the precision, and the results in Table 3 indicate that there was no change in the As(III)/As(V) ratio. The standard deviation for As(III) was the same as that for the synthetic sea-water samples, but that for As(V) was rather higher.

Interferences

Sea-water contains traces of metals such as Cu, Ni, Fe, Pb, Co, Zn, Cd and Hg. APDC forms complexes with all these elements[16] and they are therefore likely to be co-extracted and mineralized along with the arsenic. Severe interference by Cu and Ni in the hydride-generation determination of arsenic has also been reported.[17] The effect of traces of copper and nickel on the arsenic determination was therefore examined, and no interference was found from these species when present at below the 4-μg/ml level (Table 4). Since their concentration in sea-water is normally below 5 μg/ml,[1] they should not interfere in hydride-generation methods for arsenic, though they may be a problem in graphite-furnace analyses. No interference was found from Fe(III), Pb, Co(II), Zn, Cd and Hg(II) at the 1000 μg/ml level.

APDC and pyrrolidine were found to interfere

Table 1. Recovery of arsenic(III) and arsenic(V)

Sample	As(III) added, *ng*	As(V) added, *ng*	Total As(III + V) recovered, %	As(III) recovered, %	As(V) recovered, %
1	30	—	103.3	103.3	—
2	300	30	99.4	100.6	96.7
3	30	300	98.8	100.0	98.7
4	40	40	95.0	95.0	95.0
5	10	10	105.0	105.5	100.0

Table 2. Precision for arsenic(III) and arsenic(V) in synthetic sea-water for a 300 ml sample

Sample	As(III) added, *ng*	As(V) added, *ng*	As(III) found, *ng*	As(V) found, *ng*
1	150	150	148	146
2	150	150	146	145
3	150	150	148	148
4	150	150	148	147
		Mean	147.5	146.5
		Standard deviation	0.9	1.2
		RSD, %	0.6	0.8

Table 3. Precision of arsenic(III), arsenic(V) and total arsenic in natural sea-water for a 300 ml sample

Analysis	As(III) found, *ng*	Total As found, *ng*	As(V), *ng* (by difference)
1	15	144	129
2	14	140	126
3	15	145	130
4	16	140	124
Mean	15	142.3	127.3
Standard deviation	0.82	2.4	2.8
RSD, %	5.4	1.7	2.2

Table 4. Interference of Cu and Ni

Added ion concentration, *μg/ml*	As absorbance	
	Cu(II)	Ni(II)
0	0.880	0.877
1	0.875	0.870
2	0.875	0.867
3	0.874	0.865
4	0.874	0.867
5	0.594	0.560
10	—	0.440
100	—	0.165
200	0.484	—
1000	0.440	0.011

severely at trace levels. Besides being reduced to gaseous products by sodium borohydride, pyrrolidine complexes with arsenic to form an arsenic–amido derivative[18] if the arsenic is stripped from the As–APDC complex with concentrated nitric acid; since this derivative is more soluble in chloroform than in aqueous medium, much of the arsenic would be lost from the aqueous layer before its determination by hydride generation. Wet-ashing was therefore used to eliminate this problem.

CONCLUSIONS

The method has the following advantages. (*a*) The combination of wet–ashing and hydride generation makes the method free from interferences: (*b*) the detection limit of 0.031 ± 0.005 ng/ml is lower than values reported for other methods;[8,19,20] (*c*) twelve samples can be analysed per day, which makes the method economical for routine analysis of sea-water samples.

REFERENCES

1. L. R. Overby, S. F. Bocchieri and R. L. Frederickson, *J. Assoc. Off. Agr. Chem.*, 1965, **48,** 17.
2. J. A. Persson and K. Irgum, *Anal. Chim. Acta*, 1982, **138,** 111.
3. G. E. Pacey and J. A. Ford, *Talanta*, 1981, **28,** 935.
4. F. T. Henry and T. M. Thorpe, *Anal. Chem.*, 1980, **52,** 80.
5. J. Aggett and A. C. Aspell, *Analyst*, 1976, **101,** 341.
6. S. Nakashima, *ibid.*, 1979, **104,** 172.
7. F. Puttemans and D. L. Massart, *Anal. Chim. Acta*, 1982, **141,** 225.
8. T. Kamada, *Talanta*, 1976, **23, 835.**
9. S. Gohda, *Bull. Chem. Soc. Japan*, 1975, **48,** 1213.
10. R. Bye, *Talanta*, 1982, **29,** 797.
11. J. L. Fraser and J. R. Knechtel, *Analyst*, 1978, **103,** 104.
12. E. L. Wheeler, *Scientific Glassblowing*, pp. 10–23. Interscience, New York, 1958.
13. D. E. Robertson, *Anal. Chim. Acta*, 1968, **42,** 533.
14. K. S. Subramanian and J. C. Meranger, *ibid.*, 1981, **128,** 131.
15. M. Zief and J. W. Mitchell, *Contamination Control in Trace Element Analysis*, pp. 15–17. Wiley, New York, 1976.
16. K. Oikawa, *Trace Analysis of Atmospheric Samples*, pp. 84–106. Kodansha, Tokyo, 1977.
17. S. Nakashima, *Analyst*, 1978, **103,** 1031.
18. J. D. Smith, *Arsenic, Antimony and Bismuth*, in *Comprehensive Inorganic Chemistry*, pp. 596–598. Pergamon Press, Oxford, 1973.
19. W. H. Ficklin, *Talanta*, 1983, **30,** 371.
20. A. Hulanicki, *ibid.*, 1967, **14,** 1371.

Talanta, Vol. 32, No. 2, pp. 115–118, 1985
Printed in Great Britain.

0039-9140/85 $3.00 + 0.00

SPECTROPHOTOMETRIC DETERMINATION OF NITRATE AND NITRITE IN NATURAL WATER AND SEA-WATER

STANLEY J. BAJIC and BRUNO JASELSKIS
Department of Chemistry, Loyola University of Chicago, Chicago, IL 60626, U.S.A.

(*Received* 24 *February* 1984. *Revised* 31 *July* 1984. *Accepted* 14 *September* 1984)

Summary—Nitrate and nitrite in natural waters are determined spectrophotometrically by passage through an amalgamated zinc reductor at pH 3.4 into iron(III)–Ferrozine solution. Interference by high levels of nitrite is eliminated by treatment with azide. Levels as low as 0.2 μg/ml (expressed as nitrogen) can be determined with a precision of $\pm 3\%$.

Because the determination of nitrite and nitrate in natural and waste waters is of ecological importance, numerous analytical methods have been proposed and some are presented as either accepted or tentative methods in the publication of the American Public Health Association.[1] These methods, in general, can be classified as based on use of:

(*i*) direct spectrophotometric measurements in the ultraviolet;[2–6]

(*ii*) specific ion electrodes;[7–9]

(*iii*) spectrophotometric measurement involving use of brucine,[10–12] chromotropic acid,[13] Methylene Blue,[14] 2,4-xylenol,[15–17] or nitron;[1]

(*iv*) reduction of nitrate to nitrite, followed by diazotization and coupling to form a coloured dye;[18–21]

(*v*) reduction of nitrate and nitrite to ammonia.[22–25]

Nitrite in the presence of nitrate is determined spectrophotometrically by a diazotization reaction and formation of an azo dye.[26–28] It can also be determined by electrochemical methods.[29] In a similar manner nitrate can be reduced to nitrite and then determined electrochemically.[30,31] When small amounts of nitrite are accompanied by large amounts of nitrate the nitrite is determined first, then the nitrate is reduced by hydrazine or a cadmium reductor, the total of nitrate plus nitrite is determined, and the nitrate is obtained by difference. However, if there is more nitrite than nitrate, the latter can be determined only after elimination of the nitrite.

In this paper we present a rather simple colorimetric procedure for the determination of nitrate alone and in the presence of nitrite, involving reduction of nitrate and nitrite to hydroxylamine by the zinc amalgam reductor (Jones reductor) at pH 3.4 and reoxidation of the product with iron(III) in the presence of Ferrozine. Large amounts of nitrite are eliminated by a preferential reaction with sodium azide.[32]

EXPERIMENTAL

Apparatus

A Cary 14 spectrophotometer and a Corning Model XII pH-meter were used. The zinc amalgam reductor was prepared by treating analytical grade 20-mesh metallic zinc with acidified mercuric chloride by the procedure described by Kolthoff *et al.*[33] A shortened 50-ml burette was filled with enough amalgamated zinc to produce a 15-cm column. The reductor was copiously washed with water and then with the monochloroacetate–sodium chloride buffer solution. When not in use, the metal in the reductor was always kept covered with water. All glassware was washed with 6*M* hydrochloric acid and demineralized water.

Reagents

All chemicals were analytical or primary standard grade. Ferrozine, 3-(2-pyridyl)-5,6-diphenyl-1,2,4-triazine-*p,p'*-disulphonic acid disodium salt trihydrate (Aldrich), was used as a stock solution prepared by dissolving 2.55 g in 250 ml of demineralized water. An approximately 0.003*M* iron(III) stock solution was prepared by dissolving 0.363 g of reagent-grade ammonium ferric sulphate dodecahydrate in approximately 0.1*M* sulphuric acid and diluting with water to 250 ml. A stock 0.002*M* solution of sodium nitrite was prepared daily by dissolving exactly 69.0 mg of dry sodium nitrite in 500 ml of water; this corresponds to 28 μg/ml as nitrogen. Sodium nitrate solution was prepared by dissolving exactly 85.0 mg of sodium nitrate in 500 ml of water, corresponding to 28 μg/ml as nitrogen. Standard solutions were made by diluting the stock solutions.

A pH-3.2 buffer solution was prepared by dissolving 28.5 g of monochloroacetic acid in 900 ml of demineralized water, adjusting to pH 3.2 with concentrated sodium hydroxide solution, then diluting with water to 1 litre. An eluent solution was prepared by mixing 300 ml of this buffer with 100 ml of 1*M* sodium chloride.

A 0.4% aqueous sodium azide solution was prepared.

Procedures

Determination of nitrate or nitrite alone and in mixtures. Working nitrate and nitrite solutions were prepared by diluting 10 ml of the 0.002*M* stock solutions to 100 ml with demineralized water. Test solutions of nitrate or nitrite, alone or mixed, were prepared by taking from 1.0 to 10 ml of the working solutions and diluting to 100 ml with the eluent solution. The reductor column was prewashed with approximately 35 ml of the solution to be analysed, then filled with the solution, 20 ml of which were passed through

the column at a rate of 24–30 drops/min. Any gas bubbles produced were eliminated by tapping the burette. The eluent was collected in a 25-ml standard flask containing 2 ml of 0.003*M* iron(III) and 1.5 ml of 0.02*M* Ferrozine. The contents were diluted to the mark and the absorbance was measured at 562 nm after 15 min. A blank sample containing neither nitrate nor nitrite was prepared and treated in the same way as the test solution and all absorbance values were corrected for the blank absorbance.

Elimination of nitrite interference by treatment with azide. A sample containing nitrate and nitrite but no eluent buffer was transferred to a 100-ml standard flask. Then approximately 0.5 ml of 0.06*M* sodium azide was added followed by 0.05 ml of 1*M* sulphuric acid. The solution was stirred vigorously for 15 min. Hydrazoic acid was eliminated by passage of nitrogen for approximately 5 min. The solution was then diluted with the eluent buffer solution and analysed as for nitrate alone.

Determination of total nitrate and nitrite in natural waters. Natural or waste-waters were first filtered through a fine filter paper, then a 20-ml portion of the filtrate was transferred into a 25-ml standard flask containing Ferrozine and a small amount of ascorbic acid and buffer solution, to determine the amount of iron present. If the amount was small (commonly the case for Lake Michigan), then this absorbance was used as a blank correction in the nitrate and nitrite determination. Also 80 ml of the filtrate were placed in a 100-ml standard flask and diluted to volume with a buffer containing chloride. However, if the blank absorbance was high, the filtered water was passed through a strong acid cation-exchanger (Dowex 500-10 × 4; sodium form) the first 35 ml being used to precondition the ion-exchanger (and discarded) and the next 80 ml being collected in a 100-ml standard flask and diluted to the mark with the buffer solution containing chloride, and used for analysis. The Jones reductor was preconditioned with approximately 35 ml of the filtered and diluted solution and then a 20-ml portion of the effluent from the reductor was collected in a 25-ml standard flask containing 2 ml of iron(III) solution and 1.50 ml of Ferrozine solution, and diluted to the mark with demineralized water. The absorbance was then measured at 562 nm, and corrected for the reagent and iron blank as described above.

The amount of total nitrate plus nitrite in natural waters was also determined by the standard addition method. Two 80-ml samples of filtered natural water were taken. The first sample was directly diluted with the buffer solution to 100 ml, and 0.500 ml of 0.002*M* sodium nitrate was added to the second sample before the dilution with the buffer solution. Both samples were then passed through the Jones reductor and analysed as described above. The observed absorbances were corrected for the blank values and were used in the calculation of the total amount of nitrate plus nitrite nitrogen present in the original sample.

RESULTS

Synthetic samples containing nitrate and/or nitrite were first analysed for total nitrate plus nitrite and then, after the elimination of nitrite with azide, for nitrate. Results for an average of four determinations are summarized in Table 1. In each case blank absorbance values were determined in the presence and absence of azide.

Natural and synthetic sea-water samples were also analysed for total nitrate plus nitrite: the results are summarized in Table 2.

DISCUSSION

The method is based on hydroxylamine (resulting from initial reduction of nitrate or nitrite) reducing iron(III) to give the intensely coloured iron(II)–Ferrozine complex, the absorbance of which is proportional to the original amount of nitrate (or nitrite). The apparent molar absorptivity in terms of nitrate (or nitrite) is 4.21×10^4 l.mole^{-1}.cm^{-1}.

The reduction of nitrate and nitrite is affected significantly by the pH, as shown in Fig. 1. In the pH range 3.2–3.5 nitrate and nitrite are both reduced primarily to hydroxylamine and to some extent to ammonia. Hydroxylamine, in this determination, is oxidized by iron(III) to nitrous oxide, whereas ammonia is not oxidized. The amount of hydroxylamine produced decreases substantially at pH >4.5 and also at pH <2.7. At high pH, reduction of nitrate in particular is incomplete, and at low pH formation of ammonia is favoured. Thus, the pH must be kept between 3.2 and 3.5 and controlled to within ±0.1. In addition, it is advisable to add sodium chloride. This provides a higher ionic strength and gives more reproducible results.

Table 1. Determination of nitrate and nitrite in synthetic water samples*

Amount taken, 10^{-7} mole NO_3^-	Amount taken, 10^{-7} mole NO_2^-	Nitrogen taken, μg	Method†	Observed absorbance§	Total $NO_3^- + NO_2^-$ found, 10^{-7} mole‡	Nitrogen found,§ μg
0.00	0.00	0.00	—	0.120 ± 0.005	0.00	0.00
3.02	0.00	4.23	—	0.635 ± 0.008	3.06	4.28 ± 0.08
3.02	0.00	4.23	N_3^-	0.633 ± 0.008	3.05	4.26 ± 0.08
0.00	3.03	4.24	—	0.640 ± 0.008	3.09	4.32 ± 0.08
0.00	3.03	4.24	N_3^-	0.120 ± 0.005	0.00	0.00
0.40	3.03	4.80	—	0.700 ± 0.008	3.44	4.82 ± 0.08
0.40	3.03	4.80	N_3^-	0.193 ± 0.005	0.43	0.60 ± 0.04
1.01	2.02	4.24	—	0.640 ± 0.008	3.09	4.32 ± 0.08
1.01	2.02	4.24	N_3^-	0.295 ± 0.006	1.04	1.45 ± 0.05
2.02	1.01	4.24	—	0.640 ± 0.008	3.09	4.32 ± 0.08
2.02	1.01	4.24	N_3^-	0.470 ± 0.008	2.08	2.91 ± 0.07

*An appropriate aliquot of synthetic sample (in the concentration range $0.2–20 \times 10^{-5}M$) passed through the reductor is diluted to 25 ml.

†Removal of nitrite with azide.

§Average and standard deviation of four determinations.

‡Calculated from $25(A_{obs} - A_{blank})/4.21 \times 10^4$.

Table 2. Total nitrate and nitrite found in natural and synthetic sea-water*

Sample	Nitrogen added,† 10^{-7} mole	Observed absorbance	Amount found in the original sample	
			μmol/ml§	N, μg/ml
Reagent blank	0.00	0.090 ± 0.003	—	—
Lake Michigan (blank)	0.00	0.005 ± 0.001	—	—
Lake Michigan	0.00	0.525 ± 0.007	0.0161	0.226 ± 0.005
Lake Michigan	10.10	0.860 ± 0.008	0.0163	0.229 ± 0.005
Lagoon‡	0.00	0.155 ± 0.004	0.024	0.34 ± 0.010
Lagoon‡	80.80	0.425 ± 0.006	0.025	0.35 ± 0.010
Synthetic sea-water				
Blank	0.00	0.165 ± 0.004	—	—
Sample 1	10.40	0.512 ± 0.006	0.0103	0.14 + 0.005
Sample 2	5.20	0.338 ± 0.005	0.0052	0.73 ± 0.004

*An 80-ml portion of the lake water was diluted to 100 ml with a buffer solution and a 20-ml aliquot of this solution was passed through an amalgamated zinc reductor into a 25-ml standard flask.
†Amount of nitrate added to 80 ml of the water before the dilution to 100 ml.
§Calculated from $25(A_{obs} - A_{blank}) \times 100/4.21 \times 10^4 \times 80 \times$ aliquot volume (ml).
‡A 2.00-ml aliquot of the diluted lagoon water was taken for analysis.

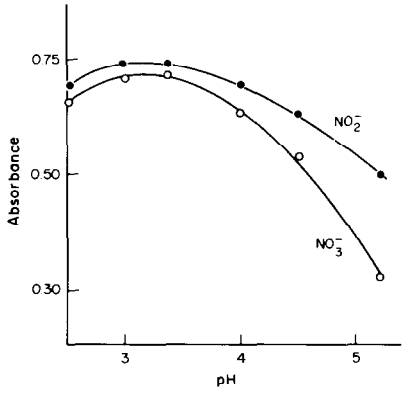

Fig. 1. Absorbance of iron(II)–Ferrozine after the reaction of iron(III) with the reduced products of nitrate and nitrite as a function of pH: nitrate concentration $1.60 \times 10^{-5}M$; nitrite concentration $1.63 \times 10^{-5}M$.

The degree of reduction depends also on the flow-rate through the reductor and on the length of the reductor. More ammonia is produced with a longer column than with a shorter one. Doubling the flow-rate through the reductor decreases the absorbance for nitrate (obtained at pH 3.3) by only approximately 3%. In general, the flow-rate is less critical for the pH range 3.2–3.5 than for higher pH values: between 1 and 1.2 ml/min is satisfactory. At higher pH the flow-rate has a greater effect on the amount of hydroxylamine produced. As shown in Fig. 1, nitrite is reduced somewhat faster than nitrate at pH 4, while in the pH range 3–3.5 nitrate is reduced as readily as nitrite. Also, in the optimum pH-range reduction of nitrate and nitrite is not affected by temperature variations of 20°, indicating that the reduction proceeds exclusively to hydroxylamine.

Nitrate in the presence of large amounts of nitrite is determined after the elimination of the nitrite with azide.[32] This reaction requires the pH to be less than 2.0 and is complete in less than 5 min. The excess of azide is eliminated as hydrazoic acid by passing a stream of nitrogen through the solution. Small amounts of hydrazoic acid remaining in solution do not interfere with the reduction of nitrate. The reduction of nitrite is ensured by adding an approximately 5–10-fold molar excess of azide. It is important, after elimination of hydrazoic acid, to adjust the pH before passing the solution through the reductor. The amount of nitrite is obtained by subtracting the nitrate value from the total amount of nitrate plus nitrite.

Interference by iron can be removed by passing the filtered solution through a cation-exchanger (in sodium form), but small amounts of iron can be tolerated if the sample absorbance is corrected for the absorbance of a blank obtained by running an equal volume of sample solution through the procedure, without reduction with the amalgamated zinc.

This method is particularly suitable for the determination of nitrate in the presence of large amounts of nitrite and of chloride, at levels as low as 0.1 ppm (when 1-cm cells are used) with a relative precision of better than 3%. The synthetic sea-water samples yielded consistently high blank values, which were primarily due to the nitrate impurities in the reagent grade sodium and potassium chlorides used for preparing the samples.

REFERENCES

1. *Standard Methods for the Analysis of Water and Wastewater*, 14th Ed., M. C. Rand, A. E. Greenberg, M. J. Taras and M. A. Franson (eds.), American Puolic Health Assoc., Washington, D.C., 1976.
2. R. C. Hoather, *Proc. Soc. Water Treat. Exam.*, 1953, **2**, 9.
3. R. C. Hoather and R. F. Rackman, *Analyst*, 1959, **84**, 549.
4. R. Bastian, *Anal. Chem.*, 1957, **29**, 1795.
5. R. Navone, *J. Am. Water Works Assoc.*, 1964, **56**, 781.
6. A. Otsuki, *Bunseki Kagaku*, 1981, **30**, 688.

7. D. Langmuir and R. L. Jacobson, *Environ. Sci. Technol.*, 1970, **4,** 835.
8. D. R. Keeney, B. H. Byrnes and J. J. Genson, *Analyst*, 1970, **95,** 383.
9. H. Hara, S. Okazaki and T. Fujinaga, *Bunseki Kagaku*, 1981, **30,** 86.
10. A. E. Greenberg, J. R. Rossum, N. Maskowitz and P. A. Villarruz, *J. Am. Water Works Assoc.*, 1958, **50,** 821.
11. D. Jenkins and L. L. Medsker, *Anal. Chem.*, 1964, **36,** 610.
12. G. H. Holty and H. S. Potworowski, *Environ. Sci. Technol.*, 1972, **6,** 835.
13. P. W. West and T. P. Ramachandran, *Anal. Chim. Acta*, 1966, **35,** 317.
14. H. Ciesielski, G. Sorgnet, M. Catone and P. Vancayzeele, *Analusis*, 1978, **6,** 38.
15. G. Norwitz, J. Farino and P. N. Keliher, *Anal. Chim. Acta*, 1979, **105,** 335.
16. G. Norwitz and P. N. Keliher, *ibid.*, 1979, **109,** 373.
17. *Idem, ibid.*, 1978, **98,** 323.
18. W. Werner, *Z. Anal. Chem.*, 1980, **304,** 117.
19. T. Ando and S. Ogata, *Nippon Dojo Hiryogaku Zasshi*, 1980, **51,** 48.
20. W. Davison and C. Woof, *Analyst*, 1978, **103,** 403.
21. A. Otsuki, *Anal. Chim. Acta*, 1978, **99,** 375.
22. M. S. Cresser, *Analyst*, 1977, **102,** 99.
23. F. W. Allerton, *ibid.*, 1947, **72,** 349.
24. J. M. Bremmer and D. R. Keeney, *Anal. Chem.*, 1965, **32,** 485.
25. W. H. Evans and J. G. Stevens, *J. Inst. Water Pollut. Control*, 1972, **71,** 98.
26. B. F. Rider and M. G. Mellon, *Ind. Eng. Chem., Anal. Ed.*, 1946, **18,** 96.
27. H. Barnes and A. R. Folkard, *Analyst*, 1951, **76,** 599.
28. L. Hainberger and J. Nozaki, *Mikrochim. Acta*, 1979 **II,** 187.
29. S. W. Boese, V. S. Archer and J. W. O'Laughlin, *Anal. Chem.*, 1977, **49,** 479.
30. D. C. Johnson, *Anal. Chim. Acta*, 1981, **130,** 295.
31. M. E. Bodini and D. T. Sawyer, *Anal. Chem.*, 1977, **49,** 485.
32. W. Seaman, A. R. Norton, W. J. Mader and J. J. Hugonet, *Ind. Eng. Chem., Anal. Ed.*, 1942, **14,** 420.
33. I. M. Kolthoff, E. B. Sandell, E. J. Meehan, and S. Bruckenstein, *Quantitative Chemical Analysis*, 4th Ed., p. 830. Macmillan, London, 1971.

Talanta, Vol. 32, No. 2, pp. 119–122, 1985
Printed in Great Britain.

0039-9140/85 $3.00 + 0.00

DETERMINATION OF SILVER IN DORE METAL BY WEIGHT TITRATION WITH EQUIVALENCE-POINT DETECTION BY DIFFERENTIAL ELECTROLYTIC POTENTIOMETRY

PABLO COFRE* and GEORGINA COPIA
Facultad de Química, Pontificia Universidad Católica de Chile, Vicuña Mackenna 4860, Santiago, Chile

(*Received* 25 *January* 1984. *Revised* 16 *July* 1984. *Accepted* 14 *September* 1984)

Summary—Use of weight titrimetry, with differential electrolytic potentiometry for detection of the equivalence point, instead of gravimetry, has been critically tested for the determination of silver in doré metal. The electrode response in the presence of possible interferences (Sb, As, Se, Cu, Ni, Fe, Pb and Co) was studied by voltammetry. Titration curves for six different samples were obtained and their differences from those for pure silver were interpreted. Positive errors were found to occur in the presence of 0.1% Fe(III) and Se(IV) but not in the presence of 1% Cu(II). The results obtained by gravimetry and weight titrimetry were compared. The imprecision of the proposed method was between 0.03 and 0.05% (relative standard deviation); that of gravimetry was between 0.05 and 0.08%. The absolute difference from the gravimetric results was between +0.05 and +0.08%. The time for analysis of one sample was between 60 and 80 min.

The doré metal obtained from the anodic sludges produced during the electrolytic refining of copper, obtained from the Chilean copper ore Chuquicamata, has a silver content of about 97–99% plus some other precious metals in small quantities. Its commercial value is mainly determined by its silver content.

The silver is currently determined gravimetrically by precipitation of silver chloride, with a precision of ±0.05%.[1] Although other gravimetric methods[2–4] could be used, all of them are time-consuming. Volumetric titration methods, although faster, do not provide the required precision.

Weight titrimetry[5] appears a possible alternative if a proper method for end-point location is chosen. Photometric, potentiometric and amperometric end-point detection, among others, have been reported,[6–8] but not applied to this system. We have demonstrated recently[9] that the combination of weight titrimetry with end-point location by differential electrolytic potentiometry can be applied successfully to the determination of silver in samples of pure silver and can replace the classical gravimetric method with advantage.

The purpose of the present work was to assess the validity of that method in analysis of doré metal samples, by study of possible interferences and comparison of the results with those of gravimetry.

EXPERIMENTAL

Apparatus

All the equipment used for the voltammetry[10] and weight titrations[9] has been described previously.

Reagents

All chemicals were of analytical reagent grade. Standard solutions were prepared as described by Smith and Parsons.[11] Samples of doré metal (six different batches) were purchased from Codelco-Chile, and spectrographically analysed by Centro de Investigación Minera y Metalurgica (CIMM). The determination of the copper and iron content was done by atomic-absorption spectrophotometry at the Centro de Servicio Externo in our Faculty. The determination of the selenium content was done by neutron-activation analysis at the Comisión Chilena de Energía Nuclear. The composition of the samples is shown in Table 1.

Procedure

Samples of doré metal (1 g for gravimetry and 0.5 g for weight titrimetry) were weighed to ±0.1 mg in 100-ml beakers. They were dissolved by adding 2 ml of nitric acid (1 + 1), covering with a watch-glass and heating on a hot-plate to eliminate nitrogen oxides. The insoluble metallic residue was filtered off with a medium porosity fritted-glass crucible, and washed with distilled water.

For the gravimetric determinations the ASTM E56-63 standard method was then followed.

For the gravimetric titrations, the filtrate and washings were combined in a 100-ml beaker, then concentrated by evaporation on a hot-plate to a final volume of 10–15 ml. Solid barium nitrate (2 g) was added and the solution titrated with standard potassium bromide solution. The concentration of the titrant was adjusted so that about 50 g would be needed for the titration.

The twin silver-electrodes, activated as previously described,[9] were immersed in the sample solution only when the titration was 95–98% complete. The titration was stopped when the first decrease in potential difference was observed.

RESULTS AND DISCUSSION

Voltammetry

The possible interference of the minor elements

*To whom correspondence should be addressed.

Table 1. Composition of doré metal samples (referred to solid samples)

Sample code	Spectrography, X-ray fluorescence†	Atomic absorption§, %	Neutron activation§, %
R-300*	*Au*, Ag, Al, As, B, Bi, Ca, Co, Cu, Fe, Mg, Mo, Na, P, Pb, Si, V, Pd, Ir	—	—
H-333	*Ag*, *Cu*, Al, As, Ca, Co, Fe, Mg, Mo, Na, Ni, Si, V, S	Cu 0.62 Fe 0.004	Se 0.003
H-337	*Ag*, Al, As, Au, Ca, Co, Cu, Fe, Mg, Mo, Na, Ni, Si, V, Pd, Zn, S	Cu 0.43 Fe 0.003	Se 0.005
H-338	*Ag*, *Cu*, Al, As, Au, Ca, Co, Fe, Mg, Mo, Na, Ni, Si, V, Ir	Cu 0.85 Fe 0.002	Se 0.007
H-339	*Ag*, *Cu*, Al, As, Au, Ca, Co, Fe, Mg, Mo, Na, Ni, Si, V, S	Cu 0.93 Fe 0.003	Se 0.002
H-340	*Ag*, Al, As, Au, Ca, Co, Cu, Fe, Mg, Mo, Na, Ni, Si, V, Pd, Zn, S	Cu 0.64 Fe 0.003	Se 0.008
H-341	*Ag*, *Cu*, Al, As, Au, Ca, Co, Fe, Mg, Mo, Na, Ni, Si, V, S, Pd, Zn	Cu 0.60 Fe 0.004	Se 0.022

Elements italicised: estimated content >0.1%.
*Insoluble residue after sample dissolution in HNO_3 (1 + 1).
†On solid samples.
§On solutions after sample attack and silver precipitation as AgCl.

present in doré metal, such as Sb, As, Se, Cu, Ni, Fe, Pb, Co, was studied by voltammetry. Results obtained are summarized in Fig. 1. Although all the species tested (except Co^{2+}, Ni^{2+} and Pb^{2+}) showed electrochemical activity, not all of them represent a potential hazard. They give reduction waves at particular electrode potentials, but the question is whether these electrochemical reactions actually occur at the silver electrode during the titration.

In our previous work,[9] we determined the range of electrode potentials of the anode and cathode in the end-point region of the titration. These are shown in Fig. 1 by the vertical dashed lines.

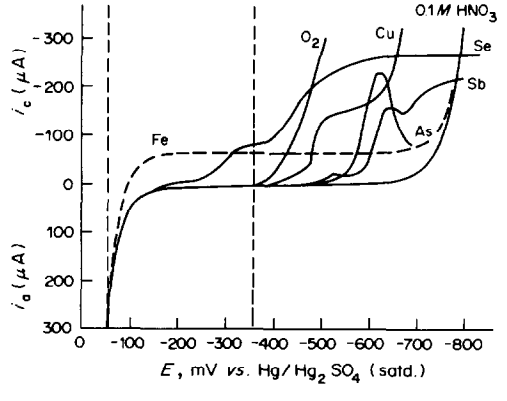

Fig. 1. Voltammetric behaviour of the silver electrode in the presence of different substances. Solution: 50 ml of 0.1*M* HNO_3 + *X* μl of 0.1*M* stock solution, as follows: *X* = 80 for As, Sb, Se; *X* = 100 for Cu, Fe, Ni, Co, Pb. For O_2, the solution was saturated with air.

If the impurities present in the solution are reduced at a potential more negative than −350 mV, there should be no interference with the indicator electrodes. This means there should be no interference by As(III), Sb(III) and Cu(II). Dissolved oxygen does not interfere either.[9]

The presence of Cu(II) has a slight effect on the electrode response well after the end-point, however. Reduction of Cu(II) at the silver cathode is possible, but this is expected to have no effect on the end-point location.

Se(IV) and Fe(III) were found to interfere severely. With both, a clear reduction wave was observed just between the potential limits indicated in Fig. 1. Se(IV) is reduced with consequent depositon of Se on the silver electrode. This is an irreversible reduction which interferes very severely with the electrode response, and the electrode is rapidly fouled.

Fe(III) is easily reduced at the silver cathode, introducing an imbalance between the twin indicator electrodes, which is greater the larger the polarizing current used. Silver ions generated at the anode would not be reduced at the cathode, but Fe(III) would be instead.

Titration curves

The results obtained by voltammetry encouraged us to study the titration curves for six different

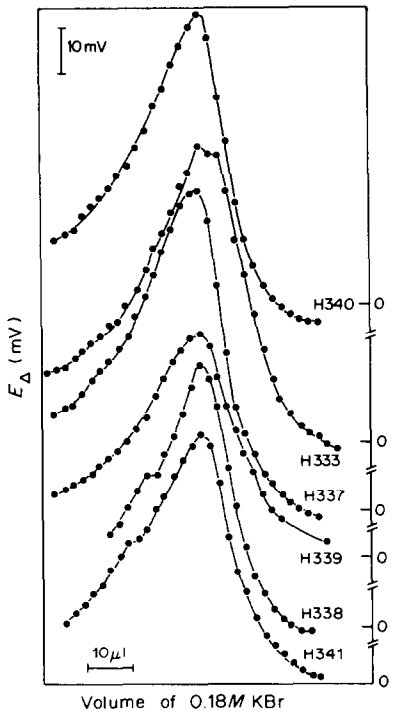

Fig. 2. Titration curves for samples of doré metal. Curves are vertically shifted for convenience. Polarizing current density: 2 μA/cm^2. Electrodes: silver wire, 0.5 cm^2 area.

samples of doré metal. The results obtained are shown in Fig. 2.

Two distinct differences from the curves obtained with pure silver[9] were found. The peaks have a broader base and the potential difference $\Delta E = E_{anode} - E_{cathode}$ becomes negative well after the end-point. Neither effect alters the width at half peak-height, which remains about 25μl, and neither has any influence on the end-point location. The end-point can be determined with the same precision as that for pure silver.[9]

The presence of Cu(II) in the solution was proved to be responsible for ΔE becoming negative after the end-point. Neither effect alters the width at half peak-height, which remains about 25 μl, and neither $Ag + Br^- \rightarrow AgBr + e^-$ would occur at a more negative potential than the cathodic reaction $Cu^{2+} + 2e^- \rightarrow Cu$.

The effect of Fe(III), Se(IV) and Cu(II) on the titration curves was studied separately. Synthetic samples of silver plus 0.1% of iron and selenium and 1% of copper were prepared. A dramatic reduction in peak height with slight positive shift of peak location was observed in the case of Fe(III) and Se(IV). Fortunately these two elements are present only at trace level in doré metal samples (see Table 1), so their effect is not expected to have any real importance. The titration curves shown in Fig. 2 confirm this. Cu(II) in the doré metals tested was always present in amounts large enough for the sample solutions to be pale blue before titration (see Table 1). Fortunately its effect is observed only well after the end-point, as predicted by voltammetry.

Weight titrations

Synthetic samples were first analysed by weight titrimetry in order to determine the effect of interference by Fe(III), Se(IV) and Cu(II). The results obtained, shown in Table 2, are the averages of five determinations (except for pure silver, for which ten determinations were done). It is clear that the presence of Fe and Se introduces only a small positive error when they are present at the 0.1% level (which is high for this type of material: real samples may contain these elements, but only at trace level). Cu(II) is definitely not an interference even at 1% level.

These results encouraged us to analyse real samples. We made ten determinations of silver by gravimetry and ten by weight titrimetry, on each of the six different samples of doré metal, in order to assess the reproducibility and accuracy of the proposed method. From the results, which are summarized in Table 3, we can conclude that the proposed method can be at least as good as gravimetry.

Five determinations were performed on each sample by two analysts, as indicated. There was a clear difference between the titrimetric and gravimetric results obtained by each analyst. Analyst A obtained a closer agreement than analyst B. If an F-test is applied to the sets of results produced by analyst A and B separately, the dispersion of results obtained by analyst B shows no significant difference between the two methods for the six samples analysed. However, the dispersion of the results obtained by analyst A shows a significant difference at the 95% confidence level for three of the six samples analysed (H337, H338, H340). If the whole set of ten determinations is considered, an F-test shows a significant difference between the two methods for three of the six samples analysed (this time H337, H339, H340). Nevertheless, it is clear that the dispersion of results obtained in our laboratory is less for the proposed method than for the classical gravimetry.

Table 2. Effect of interferences on the silver determination by weight titration; amount of Ag found

	Pure Ag*	Ag + 0.1% Fe(III)†	Ag + 0.1% Se(IV)†	Ag + 1% Cu(II)†
$\bar{X}$	99.95	100.04	100.03	99.94
S, %	0.04	0.03	0.03	0.04

*Average of ten determinations.
†Average of five determinations.

Table 3. Determination of silver in doré metal: comparison between gravimetry and weight titrimetry

Sample code		Gravimetry (G) Analyst*			Weight titrimetry (WT) Analyst*			Differences $\Delta\bar{X} = \bar{X}(WT) - \bar{X}(G)$		
		A	B	Total†	A	B	Total†	A	B	Total†
H-333	$\bar{X}$, %	98.86	98.79	98.82	98.86	98.91	98.88	0.00	+0.12	+0.06
	S, %	0.08	0.05	0.07	0.06	0.03	0.05			
H-337	$\bar{X}$, %	98.94	98.91	98.93	98.97	99.00	98.98	+0.03	+0.09	+0.05
	S, %	0.06	0.05	0.05	0.01	0.03	0.03			
H-338	$\bar{X}$, %	98.52	98.47	98.49	98.51	98.59	98.55	−0.01	+0.12	+0.06
	S, %	0.06	0.05	0.06	0.02	0.04	0.05			
H-339	$\bar{X}$, %	98.40	98.31	98.36	98.43	98.44	98.43	+0.03	+0.13	+0.07
	S, %	0.08	0.05	0.08	0.04	0.03	0.03			
H-340	$\bar{X}$, %	98.77	98.70	98.74	98.78	98.81	98.79	+0.01	+0.11	+0.05
	S, %	0.11	0.04	0.08	0.02	0.04	0.03			
H-341	$\bar{X}$, %	98.73	98.68	98.70	98.76	98.81	98.78	+0.03	+0.13	+0.08
	S, %	0.05	0.05	0.05	0.03	0.02	0.04			

*Set of five samples analysed by each analyst.
†Values for the whole set of ten samples.

If results given by gravimetry are accepted as correct and no previous calibration with reference material is used, the error of the proposed method is indicated in Table 3 as $\Delta\bar{X}$. Values are shown for both analysts separately and for the whole set of ten determinations. There is a clear positive error of 0.05–0.08% with the proposed method, because the end-point location requires a certain degree of overtitration. If a drop of titrant typically weighs 5 mg, and 50 g of titrant are needed, overtitration by one drop means an error of +0.01%. The higher results obtained by analyst B suggest a higher degree of overtitration. On the other hand the gravimetric results obtained by analyst B show a trend towards lower results. These two effects result in analyst A getting better agreement between the two methods than analyst B, but an F-test shows that analyst B's results should be more reliable than those of analyst A.

The only difficulty found with the proposed method was the need to introduce the indicator electrodes only when the titration is 95–98% complete. Otherwise they become coated with precipitate, which interferes with the electrode response. This degree of titration is easily judged by an experienced analyst from the amount of precipitate or turbidity observed after each titrant addition (made without stirring).

Another problem was the presence of insoluble metal residues from samples of doré metal. We tried to perform the titration with the residue present, but potential spikes developed each time a metallic particle struck the silver-wire electrodes (contact potentials). Although the titration was still possible if very gentle stirring was used, mixing of the solution was not good when a large quantity of precipitate was present. That is why we decided to filter the solutions and then concentrate them by evaporation, but these additional operations can increase the time for analysis of a single sample by 30–50 min, depending on the degree of dilution caused by washing the filter.

Finally, we mentioned in the previous paper[9] the possibility of automation. We now have to add, that anticipation of the end-point, which is needed for an automatic titration, can easily be achieved with this technique. All we have to do is to increase the polarizing current density by a factor of ten. The titration curves will broaden and fast addition of titrant be possible until the end-point region is reached. The titration can then be completed by decreasing the polarizing current density to the recommended value of 2 μA/cm^2. This implies that the problem of the electrode becoming covered with precipitate has to be solved in a different way, so that the twin silver electrodes can be introduced into the solution from the start.

Acknowledgement—This work was supported by the Dirección de Investigación de la Pontificia Universidad Católica de Chile, under Grant No 4/82.

REFERENCES

1. J. Hernández, CODELCO-CHILE, División Chuquicamata, 1979, personal communication.
2. B. V. Rao and D. R. Rao, *Indian J. Technol.*, 1979, **17**, 321.
3. F. Bosch Reig, J. Martínez Calatayad and R. M. Villanueva Camanas, *Afinidad*, 1979, **36**, 143.
4. W. W. White and C. R. Ranson, *Precious Met.* [*Proc. Intern. Precious Met. Inst. Conf.*], 5th, 1981 (Publ. 1982), 379.
5. B. Kratochvil and C. Maitra, *Am. Lab.*, 1983, **15**, No. 1, 22.
6. B. Kratochvil, E. J. Findlay and W. E. Harris, *J. Chem. Educ.*, 1973, **50**, 629.
7. R. Guevremont and B. Kratochvil, *Anal. Chem.*, 1978, **50**, 1945.
8. C. A. Seils Jr., R. J. Mayer and R. P. Larson, *ibid.*, 1963, **35**, 1673.
9. P. Cofré and G. Copia, *ibid.*, 1984, **56**, 589.
10. P. Cofré and A. Bustos, *J. Electroanal. Chem.*, 1983, **154**, 155.
11. B. W. Smith and M. L. Parsons, *J. Chem. Educ.*, 1973, **50**, 679.

Talanta, Vol. 32, No. 2, pp. 123–126, 1985
Printed in Great Britain.

0039-9140/85 $3.00 + 0.00

A SIMPLE THERMOMETRIC TECHNIQUE FOR REACTION-RATE DETERMINATION OF INORGANIC SPECIES, BASED ON THE IODIDE-CATALYSED CERIUM(IV)–ARSENIC(III) REACTION

F. GRASES, R. FORTEZA, J. G. MARCH and V. CERDA
Department of Analytical Chemistry, Faculty of Sciences, University of Palma de Mallorca, Spain

(*Received* 20 *December* 1983. *Revised* 30 *May* 1984. *Accepted* 14 *September* 1984)

Summary—A very simple reaction-rate thermometric technique is used for determination of iodide (5–20 ng/ml), based on its catalytic action on the cerium(IV)–arsenic(III) reaction, and for determination of mercury(II) (1.5–10 ng/ml) and silver(I) (2–10 ng/ml), based on their inhibitory effect on this reaction. The reaction is followed by measuring the rate of temperature increase. The method suffers from very few interferences and is applied to determination of iodide in biological and inorganic samples, and Hg(II) and Ag(I) in pharmaceutical products.

A common method for determination of traces of iodide is based on its catalysis of the redox reaction between cerium(IV) and arsenic(III), first studied in detail by Sandell and Kolthoff.[1,2]

The reaction has been applied to the determination of iodide in waters[3–7] and thyroid hormones,[8–10] and of inhibitors of the reaction, such as mercury and silver.[11,12] Osmium[12,13] and ruthenium[14] also catalyse the reaction and have been similarly determined. The reaction has been used as an indicator reaction in catalytic titrations.[15–19] The end-point can be detected spectrophotometrically, potentiometrically,[16,20] biamperometrically,[21] or thermometrically.[19] A flow enthalpimeter has been used to determine 0.01–10 μM iodide by measurement of the temperature rise in the Ce(IV)–As(III) system.[22,23] In the sense that the heat "pulse" detected by this method is the integral of the heat generated by the catalytic reaction in a specific time (determined by the flow characteristics) these were kinetics determinations, and in principle an initial-rate method was used. So far, however, measurements of the reaction rate do not seem to have been used as the determination technique. Generally, the principal advantages of reaction-rate methods (particularly the initial-rate method) are speed and precision. Very few examples of the use of calorimetry in reaction-rate methods for determination of inorganic species have been reported[24–26] and the method has been mainly used in biochemical analysis.[27,28]

EXPERIMENTAL

Reagents

Stock solutions included 0.1 M ceric ammonium sulphate in 1 M sulphuric acid, 0.1 M sodium arsenite in 1 M sulphuric acid, potassium iodide solution (iodide 0.983 g/l.), mercuric nitrate solution (mercury 0.972 g/l.) and silver nitrate solution (silver 0.960 g/l.).

Apparatus

The temperature-monitoring system consisted of a rapid-response thermistor, a Wheatstone bridge, and a recorder (Goerz, Servogor RE 511) (Fig. 1). The thermistor was sealed in glass and has a resistance of 100 kΩ at 25°. The e.m.f. for the Wheatstone bridge was supplied from a 7.85-V stabilized source. At the sensitivity setting used, the thermistor bridge yielded a temperature response of 60.6 mV/deg and full-scale deflection on the recorder was 2 mV (20 cm). This temperature-monitoring system is part of a thermometric titrator built according to the design of Lumbiarres *et al.*[29] An adiabatic cell (Fig. 1) was used. The solution in the cell was stirred with a magnetic stirrer. Rigid temperature control is essential.

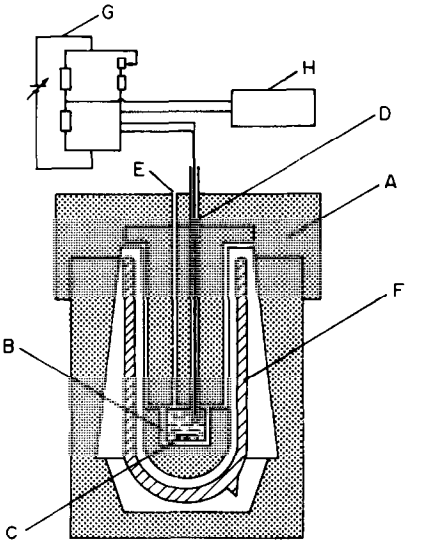

Fig. 1. Diagram of circuitry and apparatus used in reaction-rate thermometric analysis. A, polystyrene insulators; B, plastic beaker; C, magnetic stirrer; D, thermistor; E, Hole for pipette F, Dewar flask; G, Wheatstone bridge; H, recorder.

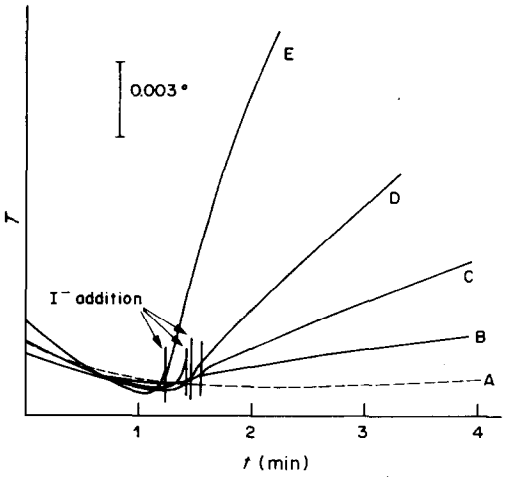

Fig. 2. Temperature–time curves for (A) 0, (B) 5, (C) 10, (D) 14 and (E) 20 ng/ml of iodide The recommended procedure was used.

Procedure

For iodide determination the following were placed in the cell compartment: 10 ml of 0.1*M* ceric sulphate, 10 ml of 0.1*M* sodium arsenite and enough sulphuric acid to give a concentration of 1*M* and a final volume of 50 ml. The recorder (chart speed 3 cm/min) was switched on. When the temperature–time curve was horizontal, the necessary volume of sample to give a final iodide concentration between 5 and 20 ng/ml was added. From the resulting curve, the rate of reaction was calculated by the initial-rate (tangent) method. All solutions were brought to 22° beforehand, in a thermostat.

To determine mercury(II) or silver, the same procedure was used, except that a suitable amount of the cation (75–500 ng for mercury, 100–500 ng for silver) was introduced before the sulphuric acid, and finally 1 μg of iodide was added.

RESULTS AND DISCUSSION

Examples of the temperature–time curves for determination of iodide are shown in Fig. 2. The slope of the curve should correspond to the temperature change due to catalytic reaction. To obtain rapid stabilization (horizontal temperature–time curves) before the addition of the iodide, all solutions must be brought to the same temperature (which must be the room temperature, so it is convenient to keep this as constant as possible). It has been found that the rate of initial thermal stabilization is remarkably favoured by eliminating the free air space above the solution in the inner part of the adiabatic cell (Fig. 1).

Minimal background is attained in the temperature–time curves by efficient stirring, and precise control of this variable is important.

Effect of reaction conditions

To optimize the conditions for determination of iodide, the effect of the sulphuric acid, arsenite and ceric sulphate concentrations on the reaction rate was studied (Figs. 3 and 4). The optimum concentrations are those at which the initial rate is maximal and the relative standard deviation minimal. These will be the concentrations at which the order of reaction with respect to these variables is as near zero as possible, since small variations in the concentrations will not affect the initial reaction rate. For this reason a sulphuric acid concentration of 1*M* and ceric sulphate and arsenite concentrations of 0.02*M* are considered optimum.

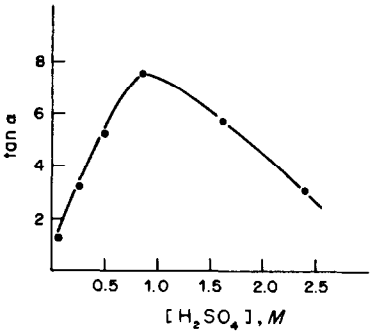

Fig. 3. Effect of sulphuric acid concentration on the initial rate: $[Ce(IV)] = 1 \times 10^{-2}M$, $[As(III)] = 1 \times 10^{-2}M$, $[I^-] = 70$ ng/ml.

Under these conditions, there was a linear relationship between the logarithm of the initial reaction rate and the iodide concentration in the range 5–20 ng/ml in the final solution. The reaction order for iodide, obtained from the corresponding logarithmic plot, was 3 ($v_0 = k[I^-]^3$ for $3.9 \times 10^{-8}M < [I^-] < 1.6 \times 10^{-7}M$).

Characteristics of the iodide determination

Owing to the shape of the temperature–time curves the initial-rate method was the only one applied for preparing the semi-logarithmic calibration graph (Fig. 5). The relative standard deviation was 1.1% ($n = 11, \alpha = 0.05$).

The selectivity has been examined, and the results in Table 1 show there are few interferences.

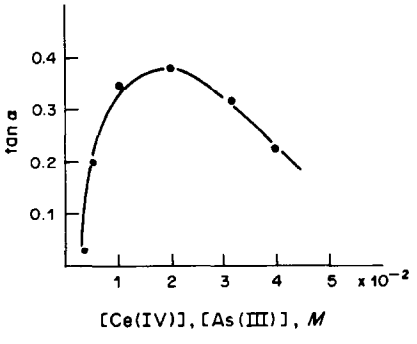

Fig. 4. Effect of As(III)–Ce(IV) concentrations on the initial rate: $[H_2SO_4] = 1M$, $[I^-] = 10$ ng/ml.

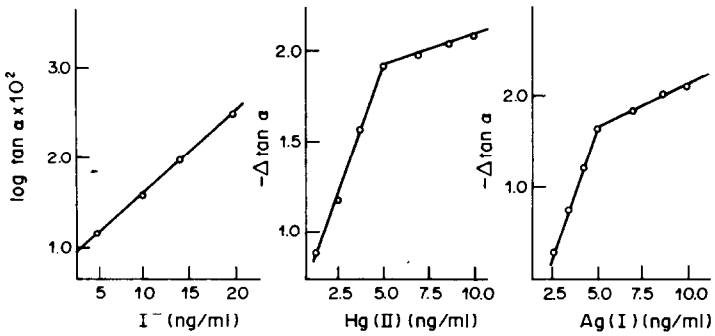

Fig. 5. Calibration graphs for I^-, Hg(II) and Ag(I).

Determination of mercury and silver

The inhibitory effect of mercury(II) and silver on the iodide catalysis of Ce(IV)/As(III) system has been used to develop reaction-rate methods for the determination of these cations. A fixed iodide concentration is used and the decrease in initial reaction-rate, caused by the presence of the inhibitor, is measured. As shown by Fig. 5, with an iodide concentration of 20 ng/ml the calibration graph is steep and linear for 1.5–10 ng/ml mercury and 2–10 ng/ml silver concentrations. The relative standard deviation for the 5-ng/ml level ($n = 11$, $\alpha = 0.05$) was 1.3% for mercury and 1.5% for silver.

Applications

To test the applicability of the proposed methods, they were applied to the determination of iodide in urine, sea-water and analytical-reagent grade sodium chloride, and of mercury(II) and silver in pharmaceutical products. In all instances, the standard-addition method was employed. The recovery was calculated by comparing the results obtained before and after the standard additions.

Iodide in urine was determined both before and after mineralization of the sample. The value obtained without mineralization was 7.0 μg/ml. To destroy organic matter and liberate the organically bound iodine the sample was evaporated to dryness on a hot-plate after addition of sodium carbonate, and then heated for 3 hr at 600° in a muffle furnace.[30] The cooled residue was dissolved in a minimum of 2*M* hydrochloric acid and diluted with water to the original sample volume. The value obtained was 13.6 μg/ml. These results were compared with those obtained by Acland's spectrophotometric method,[31] which uses As(III) and Ce(IV) as reagents and gave a value of 12.1 μg/ml for total iodide.

Iodide in sea-water was determined without previous treatment of the sample. The value obtained was 0.10 μg/ml. That found by the Acland method was 0.12 μg/ml.

The sodium chloride sample was dissolved in distilled water and the iodide determined. The value obtained was 0.0015% (reported maximum value, 0.0020% I^-).

Mercury was determined in a commercial pharmaceutical product (Resorpil, Reig Jofre) after dilution of the product with distilled water. The value obtained was 149 μg/ml (reported value, 150 μg/ml).

Silver was similarly determined in a commercial pharmaceutical product (Argentofenol, Bucca). The value found was 12.6% (reported value 12.7%).

Table 1. Concentrations of foreign ions tolerated (error ≤ 1.1%) for 20 ng/ml iodide

Ion added	Amount tolerated
Ca(II), Mg(II), Sr(II), Ba(II), Cd(II), Sn(II), Mo(VI), Co(II), Cu(II), Bi(III), V(V), Cr(III), Ni(II), Zn(II), Sb(III), Pb(II), Al(III), Cl^-, F^-, Br^-, CN^-, PO_4^{3-}, AcO^-, SCN^-	20* μg/ml
Mn(II)	2† μg/ml
Fe(III)	2§ μg/ml
IO_3^-	0.2† μg/ml
Hg(II)	1§ ng/ml
Ag(I)	1.5§ ng/ml

*Largest amount examined.
†Higher concentrations increase the initial rate.
§Higher concentrations decrease the initial rate.

REFERENCES

1. E. B. Sandell and I. M. Kolthoff, *J. Am. Chem. Soc.*, 1934, **56,** 1426.
2. *Idem*, *Mikrochim. Acta*, 1937, 9.
3. R. A. Barkley and T. Thompson, *Anal. Chem.*, 1960, **32,** 154.
4. H. Malmstadt and T. P. Hadjiioannou, *ibid.*, 1963, **35,** 2157.
5. M. Dubravcic, *Analyst*, 1955, **80,** 295.
6. G. Knapp and H. Spitzy, *Talanta*, 1969, **16,** 1353.
7. V. W. Truesdale and P. J. Smith, *Analyst*, 1975, **100,** 111.
8. R. D. Strickland and C. M. Maloney, *Anal. Chem.*, 1957, **29,** 1870.
9. G. Knapp and H. Leopold, *ibid.*, 1974, **46,** 719.
10. K. Müller, H. Skrube and H. Spitzy, *Mikrochim. Acta*, 1962, 1081.
11. H. Weisz, *Anal. Chim. Acta*, 1972, **60,** 385.
12. P. A. Rodriguez and H. L. Pardue, *Anal. Chem.*, 1969, **41,** 1376.
13. R. D. Sauerbrunn and E. B. Sandell, *Mikrochim. Acta*, 1953, 22.
14. C. Surasiti and E. B. Sandell, *Anal. Chim. Acta*, 1960, **22,** 261.
15. E. J. Greenhow, *Chem. Rev.*, 1977, **77,** 835.
16. T. P. Hadjiioannou, E. A. Piperaki and D. S. Papastathopoulos, *Anal. Chim. Acta*, 1974, **68,** 447.
17. K. C. Burton and H. M. N. H. Irving, *ibid.*, 1970, **52,** 441.
18. T. P. Hadjiioannou and M. M. Timotheu, *Mikrochim. Acta*, 1977, 61.
19. H. Weisz, T. Kiss and D. Klockow, *Z. Anal. Chem.*, 1969, **247,** 248.
20. H. Weisz, *Angew. Chem. Intern. Ed.*, **1976, 15,** 150.
21. H. Weisz and S. Pantel, *Anal. Chim. Acta*, 1972, **62,** 361.
22. J. M. Elvecrog and P. W. Carr, *ibid.*, 1980, **121,** 135.
23. R. S. Schifreen, C. S. Miller and P. W. Carr, *Anal. Chem.*, 1979, **51,** 278.
24. F. Grases, R. Forteza, J. G. March and V. Cerdá, *Anal. Chim. Acta*, 1984, **158,** 389.
25. F. Grases, J. G. March, R. Forteza and V. Cerdá, *Thermochim. Acta*, 1984, **73,** 181.
26. F. Grases, R. Forteza and J. G. March, *Analusis*, 1984, **12,** 194.
27. Ch. J. Martin and M. A. Marini, *CRC Crit. Rev. Anal. Chem.*, 1979, **8,** 221.
28. B. Z. Chowdhry, A. E. Beezer and E. J. Greenhow, *Talanta*, 1983, **30,** 209.
29. J. Lumbiarres, C. Mongay and V. Cerdá, *J. Thermal Anal.*, 1981, **22,** 275.
30. H. Varley, *Practical Clinical Biochemistry*, p. 423. Tecnos, Madrid, 1961.
31. J. J. D. Acland, *Biochem. J.*, 1957, **66,** 177.

Talanta, Vol. 32, No. 2, pp. 127–130, 1985
Printed in Great Britain.

0039-9140/85 $3.00 + 0.00

DETERMINATION OF SIMPLE AND COMPLEX IODIDES WITH FERRIC CHLORIDE—AN ALTERNATIVE TO THE ANDREWS TITRATION

M. CARTWRIGHT and A. A. WOOLF
School of Chemistry, University of Bath, Bath, England

(*Received* 18 *May* 1984. *Accepted* 2 *August* 1984)

Summary—The iodide content of simple and complex iodides can be extracted as iodine after dissolution of the sample with acidified ferric chloride solution. Most iodides can thus be decomposed in 3*M* hydrochloric acid medium. A suitable extraction flask is described. Information on the cation oxidation state can be obtained by titrating the released ferrous ions *in situ*. A precision of 0.2% for 1–5 mmoles of iodide is attainable.

During an investigation into the electrical properties of some simple and complex iodides we needed to confirm their stoichiometry and hence required a reasonably precise and widely applicable analytical method. The Andrews titrimetric method[1] was only partly suitable. The strongly acid conditions help to dissolve water-insoluble iodides, but the method becomes non-specific when the complex contains a cation that is oxidizable with iodate under the conditions used. We have therefore developed an alternative and specific method based on use of acidic ferric chloride solution as oxidant, followed by solvent extraction of the iodine formed. The iron(II) content of the extracted solution can also provide information on any cation oxidation.

EXPERIMENTAL

Apparatus

A standard (250-ml, B24 ground-glass neck) conical flask is modified by attaching a glass stopcock to the bottom (Fig. 1). A PTFE key is not recommended, because it obscures the phase interface during separation. (In effect the tap of a conical separating funnel is being shifted from the apex to the base and the funnel inverted.)

Reagents

$FeCl_3$ (0.1M). Dissolve 27 g of $FeCl_3 \cdot 6H_2O$ in the volume of concentrated hydrochloric acid corresponding to the acid molarity required, and dilute to 1 litre.

$Na_2S_2O_3$ (0.05M). Prepared by weight.[2]

$K_2Cr_2O_7$ (0.02M). Prepared by weight.

Extractants. Benzene–carbon tetrachloride, 60/40 v/v, and 50/50 v/v, or pure carbon tetrachloride.

Samples

Iodides not readily available were prepared from the elements or by precipitation. SnI_4 and AsI_3 were recrystallized from purified chloroform and vacuum-dried. SnI_2 and TiI_4 were purified by vacuum sublimation.

Procedure

By means of a long weighing tube (Fig. 1), place at the bottom of the extraction flask an amount of the solid iodide corresponding to not more than 5 mmoles of iodide. (If other oxidizable species are present, reduce the quantity correspondingly, *e.g.*, for SnI_2 the maximum quantity is 1.25 mmoles of SnI_2). Add 50 ml of 0.1*M* ferric chloride solution, stopper the flask and stir the mixture magnetically until the solid has dissolved and the iodine been liberated. Then add 25 ml of solvent and extract the iodine by moderate stirring. At this stage add a few drops of a dilute detergent solution to detach any solvent floating at the water–air interface and to enable water in the side-tube to be easily displaced. Hold a magnet under the flask to keep the internal magnet in place when the flask is tilted to fill the side-tube with the organic phase. Remove the stopper and run the lower organic layer into another conical flask containing about 50 ml of water. (The organic liquid in the capillary can be almost completely displaced, and the liquid remaining in the capillary runs back into the flask when that is uprighted.) Wash the capillary through with water before closing the tap. Perform three further extractions in the same way with 25-ml portions of solvent. Titrate the combined extracts with thiosulphate (starch as indicator) after adding some potassium iodide to help back-extraction. Titrate the

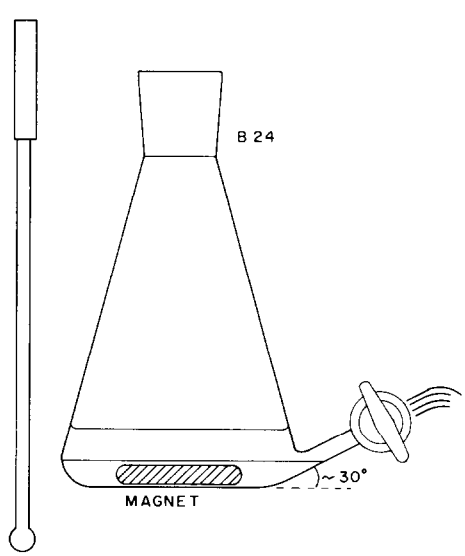

Fig. 1. Extraction flask and weighing tube.

Table 1. A comparison of the ferric chloride method with silver iodide gravimetry

Compound	[HCl], M	Sample taken, *mg*	Weight, *mg*, determined by		
			I_2 extraction	Fe^{2+} formation	AgI precipitation
KI	2.5	360.3	359.5	360.6	
	2.5	313.2	313.0	314.2	
	6	333.2	333.6		
	6	375.2	374.5		
	—	402.8			403.1
	—	413.3			413.6
CdI_2	3	389.4	383.9		
	3	321.4	317.4		
	4.5	324.2	323.5	324.7	
	6	397.5	398.1		
	—	582.5			581.2
	—	399.1			399.2
AsI_3	3	132.6	132.2		
	3	213.2	212.7		
	4.5	191.5	190.4		
	4.5	152.0	151.8	152.0	
	—	317.1			316.9
	—	251.1			250.6

iron(II) in the original flask with potassium dichromate after diluting to a hydrochloric acid concentration of about 1.5*M*.

RESULTS AND DISCUSSION

Distribution ratios, defined as the ratio of concentration of iodine extracted into the organic phase to concentration of residual iodine in the aqueous phase, were measured after each extraction in a few experiments. The solubility of iodine in hydrochloric acid, and in acidic metal chloride solutions, after equilibration for three days, was determined by taking weight aliquots of the filtrates, diluting with an equal volume of water and titrating with thiosulphate.

Some results are collected in Tables 1 and 2. For those in Table 1 the thiosulphate and dichromate titrations are equivalent since the cation in the salt is not oxidized. A direct comparison with conventional silver iodide gravimetry is possible with these water-soluble iodides.

The iodides in Table 2 are insoluble in water and some of the cations are oxidizable. Thus with a mole of $CuTiI_4$, four moles of Fe(II) arise from I^- oxidation, and two moles from the Cu(I)→Cu(II) and Ti(III)→Ti(IV) oxidations. The silver iodide estimation is included merely to show that even the extremely insoluble iodides can be handled at high acidities.

The relative efficiency of different extractants was examined. One consideration was that the efficiency of mixing of the phases with gentle stirring should be enhanced by minimizing the density difference between the phases. Another consideration was to increase the distribution ratio by changing the solvents. Mixtures of benzene and carbon tetrachloride

Table 2. Ferric chloride method for water-insoluble iodides

Compound	[HCl], M	Sample taken, *mg*	Weight, *mg*, determined by	
			I_2 extraction	Fe^{2+} formation
SnI_2	3	361.4	360.8	361.0
SnI_4	3	254.6	253.5	256.0
	3	251.9	251.3	
TiI_3	3	99.2	98.8	
		148.7	148.4	
TiI_4	3	246.2	247.0	
CuI	3	197.6	197.6	
	3	308.1	307.9	
HgI_2	10	159.5	160.7	
		220.6	220.0	
PbI_2*	3	441.3	443.1	
TlI	6	284.9	286.4	286.1
AgI†	10	200.0	199.4	
$CuTiI_4$§	3	206.3	206.1	205.8

*100 ml of oxidant used to keep $PbCl_2$ in solution.
†1.35 g of $HgCl_2$ added to dissolve AgI, and extraction for 20 hr.
§An independent copper determination by electro-deposition gave 10.20% (theory 10.26%).

Table 3. Iodine extraction and distribution data

Partition number	Degree of extraction of iodine, %									Distribution ratio (average) of expts. (1), (2), (3)
	CdI_2	AsI_3		KI		HgI_2				
	(1)	(2)	(3)	(4)	(5)	(6)	(7)	(8)	(9)	
1	88.6	86.7	88.9	84.6	90.3	19	31.9	35.0	44.2	14.7
2	98.2	97.7	98.4	97.4	98.8	29.7	45.7	65.4	70.3	10.5
3	99.6	99.6	99.7	99.5	99.8	32.2	49.6	92.2	96.8	8.6
4	100.0	100.0	100.0	100.0	100.0	33.2	51.4	91.0	99.8	—

(1), (2); (3) 0.1*M* $FeCl_3$, 4.5*M* HCl, C_6H_6/CCl_4 60/40
(4) 0.1*M* $FeCl_3$, 3*M* HCl, CCl_4
(5), (6) 0.1*M* $FeCl_3$, 3*M* HCl, C_6H_6/CCl_4 50/50
(7) 0.1*M* $FeCl_3$, 6*M* HCl, C_6H_6/CCl_4 50/50
(8) 0.25*M* $FeCl_3$, 10*M* HCl, CCl_4
(9) 0.25*M* $FeCl_3$, 10*M* HCl, C_6H_6/CCl_4 50/50

which had a density about 0.1 g/ml greater than that of the hydrochloric acid phase were chosen and these were more efficient than carbon tetrachloride alone in the first three partitions. Because four partitions were needed to complete the extraction there was no preference for use of the mixed solvent, except for mercuric iodide, for which more than four extractions were required if carbon tetrachloride was used alone.

Although not all iodides were examined, the scope of the method can be predicted from the general principles of periodicity. The iodides can be divided into three classes for analytical purposes. The water-soluble ionic iodides of Groups I, II and IIIB, which exist as the metal iodide or monomeric complexes such as MI^+, will behave like potassium or cadmium iodide. In these instances there is no advantage over the argentimetric or oxidimetric methods apart from specificity. A second class of more or less covalent iodides (*e.g.*, TiI_4, TiI_3, AsI_3, SnI_4, SnI_2) hydrolyses to give hydriodic acid and for this class, which covers Groups II-IV of the non-transition elements as well as transition elements from d^2 to about d^7, the ferric chloride method has definite advantages. First it can provide additional information on the oxidation states of the elements, and secondly it is possible to keep the iodides in solution with hydrochloric acid but not necessarily with the oxy-acids required in other methods. The water-insoluble iodides formed by some d^8 and d^9 transition metals constitute the third class of iodides. Apart from PdI_2 and AgI, which are the standard weighing forms anyway, these can be estimated conveniently by the ferric chloride method, though the difficulty increases with decrease in the solubility of the iodide. The method could obviously be extended to small quantities of iodides although the extractions would become more difficult as the Cl^-/I_2 ratio increased (see later discussion).

The combination of a suitable redox couple with a selective solvent extraction provides a general method specific for iodide. Previous methods used ferric chloride in sulphuric acid as the oxidant, followed by a steam distillation of the iodine,[3] or a stronger oxidant such as MnO_4^-, $Cr_2O_7^{2-}$, or MnO_2 followed by extraction of the liberated iodine into chloroform.[4] Insufficient details were given for the applications or accuracy of the methods to be assessed.

The basis of the method described is the selective oxidation of iodide by the ferric ion. The small difference in redox potential for the two reactions

$$Fe^{+3} + e \rightarrow Fe^{2+} \quad 0.77\ V$$

$$\tfrac{1}{2}I_2 + e \rightarrow I^- \quad 0.53\ V$$

gives an equilibrium constant of *ca.* 10^4 for the reaction

$$Fe^{3+} + I^- = Fe^{2+} + \tfrac{1}{2}I_2$$

Table 4. Solubilities of iodine in 2.86*M* hydrochloric acid containing metal chlorides, at 24.5°

Metal chloride (0.1*M*)	Solubility of iodine,* *mg/100 g of solution*	Change in solubility on salt addition, %
None	198, 192	—
$CrCl_3$	156	−20
$MnCl_2$	201	+3
$FeCl_3$	194	−0.5
$NiCl_2$	194	−0.5
$CuCl_2$	196	+0.5
$ZnCl_2$	165, 168	−15
$CdCl_2$	187, 187	−4
$HgCl_2$	52†, 321§	+65

*Solubility in water is 33.6 mg/100 g at 25°.
†By direct titration of diluted aqueous solution.
§By extraction into organic solvent before titration.

which means that the reaction is only about 99% complete unless the equilibrium is shifted to the right. When used for determination of ferric ion the reaction is brought to completion by making the iodide to iodine ratio large by use of a large excess of iodide and the removal of the liberated iodine by the titration with thiosulphate. In our method the equilibrium is shifted towards complete reaction by repeated extraction of the iodine into an organic phase. Solvent extraction prevents interference by some other species, such as sulphides, oxidized by the ferric ion. The decrease in redox potential for the iron(III)/iron(II) system by ferric ion complexing agents such as fluoride or EDTA is overcome by increasing the ferric chloride concentration.

Hydrochloric acid plays a key role in the method. It prevents hydrolysis of ferric chloride, increases the rate of dissolution of the less soluble iodides (Tables 2 and 3) and increases the solubility of iodine in aqueous media (Table 4), which prevents separation of solid iodine and loss by sublimation.

The solubility of iodine in 3*M* hydrochloric acid is about 6 times that in water, probably because of the formation of I_2Cl^-. The occurrence of this species can be inferred from previous analytical experience. Thus the solvent extraction of micro-amounts of iodine is inhibited by chlorides but not by sulphates,[5] iodine is retained on anion-exchange resins in the chloride form,[6] and the solubility of iodine in water goes through a maximum on addition of magnesium chloride.[7]

The di-iodochloride anion has been isolated in the salt $N(CH_3)_4^+ \cdot I_2Cl^-$, which slowly loses iodine at room temperature and rapidly disproportionates into the more stable ICl_2^- and I_3^- ions in acetonitrile solution.[8] The structure of I_2Cl^- is not known but is likely to resemble that of the I_2Br^- ion, in which the I–I and I–Br bonds are longer and weaker than in iodine or iodine bromide.

The formation constant for $I_2 + Cl^- \rightleftharpoons I_2Cl^-$ is likely to be of the same order as that of Br_2Cl^- (1.14) and much less than that of I_3^- (740 at 25°).[9] Hence it is understandable that the solubility of iodine increases with hydrochloric acid concentration, as the equilibrium is moved to the right. The decrease in distribution ratio as iodine is extracted also illustrates the effect of mass action as the Cl^-/I_2 ratio increases (Table 3). This would lead to more of the residual iodine being present as the complex ion in solution and to greater difficulty in extracting the whole of the iodine.

The metal ion can also affect the solubility and extractability of iodine and this is particularly noticeable for zinc, cadmium and mercury(II) (Table 4). For these chlorides the effects vary from an appreciable salting-out effect with zinc chloride to the large increase with mercuric chloride, which corresponds to an uptake of one I_2 molecule per 20 Hg^{2+} ions. It is possible that these effects are determined by the ternary metal–iodine–chloride interactions rather than the simple binary metal–halogen ones. Thus mercuric chloride, which in hydrochloric acid is predominantly complexed as $HgCl_3^-$ and $HgCl_4^{2-}$, could produce ions such as $[Cl_3HgCl \ldots I \ldots I]^{2-}$ or $[Cl_3Hg\,I \ldots I \ldots Cl]^{2-}$ in the presence of iodine. It is interesting to note that iodine can be extracted from mercuric chloride solutions in 3*M* hydrochloric acid but not from mercuric iodide solutions at the same acidity. In the latter solution formation of the most stable adduct[10] $[Cl_3Hg \ldots I \ldots I \ldots I]^{2-}$ could prevent oxidation and extraction (in view of the greater stability of I_3^- compared to that of I_2Cl^-).

REFERENCES

1. L. W. Andrews, *J. Am. Chem. Soc.*, 1903, **25,** 756.
2. A. A. Woolf, *Anal. Chem.*, 1982, **54,** 2134.
3. K. F. Shimizu and E. A. Kelly, *J. Am. Pharm. Assoc.*, 1942, **31,** 103.
4. S. W. Gorbatscheff and J. A. Kassatkina, *Z. Anorg. Chem.*, 1930, **191,** 104.
5. K. L. Maljaroff and W. B. Matskiewitsch (K. L. Malyarov and V. B. Matskyvich), *Mikrochemie*, 1933, **13,** 85.
6. C. Barraque and B. Trémillon, *Bull. Soc. Chim. France*, 1965, 1674.
7. J. C. Carter and C. R. Hoskins, *J. Chem. Soc.*, 1929, 580.
8. A. J. Popov and R. F. Swenson, *J. Am. Chem. Soc.*, 1955, **77,** 3724.
9. R. O. Bell and M. Pring, *J. Chem. Soc. (A)*, 1966, 1607.
10. V. I. Belevantsev, *Russ. J. Inorg. Chem.*, 1973, **18,** 1087.

Talanta, Vol. 32, No. 2, pp. 131–138, 1985
Printed in Great Britain.

0039-9140/85 $3.00 + 0.00

EFFECT OF ORGANIC COLLOIDS ON ASV SIGNALS OF Cd, Pb AND Cu

T. UGAPO and W. F. PICKERING
Department of Chemistry, University of Newcastle, N.S.W. 2308, Australia

(*Received* 10 *April* 1984. *Accepted* 14 *September* 1984)

Summary—The effect of organic colloids, such as humic and fulvic acids, on the ASV signals of Cd, Pb and Cu in acetate-buffer media has been investigated. Owing to their ability to adsorb metal ions, or form complexes (some sparingly soluble), the presence of the organic acids caused the magnitude of the signal peaks to decrease, the effect increasing with increase in organic acid:metal-ion ratio, and pH (from 5 to 8). Analysis before and after filtration through a 0.45-μm membrane indicated that most of the Cd retained was labile; in the Pb and Cu system less than half of the sorbed metal ion was labile, though a further fraction was displaced in the presence of Chelex 100 resin. The magnitude of the interference effect varied with the molarity of the medium and the presence of diverse anions (*e.g.*, chloride, bromide) in the system. Cu displayed the most anomalous behaviour, with the stripping peak tending to broaden and split, particularly in the presence of humic acids. This behaviour was enhanced when the contact time with the preformed Hg film before the deposition/stripping cycle was increased above 5–10 min. This effect has been attributed to reduction (and subsequent oxidation) of Cu–humate species adsorbed on the mercury film.

Colloidal particles are believed to play an important role in the movement and distribution of metal ions within an ecosystem.[1] Transport in streams is accompanied by redistribution between the aqueous and mobile solid phases, whilst flocculation of particulates (*e.g.*, in estuaries) promotes incorporation of the metals into the base sediments. Clarification of this role has been hindered, however, by the complexity of natural systems and limited understanding of many of the chemical equilibria involved.

Combination of anodic-stripping voltammetry with selective preliminary steps (such as membrane filtration, passage through a Chelex column and destruction of organic complexes) has been used to subdivide the metal-ion content of waters into several different categories, and it has been demonstrated, *inter alia*, that a significant fraction can be associated with colloidal organic matter.[2–7]

There are differing views, however, on the effect of organic compounds on ASV signals. For example, the addition of "fresh water" humic acid concentrate to synthetic sea-water was observed[8] to cause both enhancement and suppression of individual metal ion peaks (depending on the pH of the system) but there were no significant changes in the peak positions. With a different base electrolyte at pH 6.8, addition of humic acid was found to alter both peak height and position.[9] The size, shape and position of Cu, Pb and Cd peaks has been shown[8–13] to be sensitive to the presence of a wide range of organic species (including surfactants), and as with the humic acids, the changes induced tend to be random in nature.

The lability of metal ions associated with organic species has not been clearly resolved. This situation is complicated by the fact that bonding modes (*e.g.*, with humic acids) tend to vary with pH, relative concentrations and type of functional groups involved.[15,16] Extraction studies[17] indicate that a high proportion of the sorbed material is ion-exchangeable, and accordingly may be labile in ASV. The acid-soluble, lower molecular-weight, companion species, fulvic acid, is considered to form soluble metal complexes. The conditional formation constants reported vary with pH and the material used,[18–24] and under some conditions, sparingly soluble species have been isolated.[25,26] The apparent stabilities of the complexes formed when metal ions are added to natural waters are often similar to those quoted for metal fulvate complexes.[1]

In an attempt to provide additional basic information, the effect of both humic and fulvic acids on the ASV signals of Cd, Pb and Cu has been re-examined.

EXPERIMENTAL

Apparatus

An ESA Anodic Stripping Analyzer Model 2014, and a Rikandenki fast-response recorder (Model B-181 H) were used. Each of the four operating cells contained a wax-saturated graphite rod (precoated with a thin mercury film), a platinum counter-electrode and an Ag/AgCl reference electrode (S.R.E.) separated from the 5 ml of test solution by a porous Vicor® sheath. As the cell geometries differed slightly, all comparison studies were based on single-cell operation. A nitrogen flow (monitored by an in-line ball flowmeter) was used to remove dissolved oxygen and stir each test solution.

At the end of each working week, the existing thin mercury film was removed by gently stroking the polished electrode tip with the dampened edge of a tissue towel. A new film was then deposited overnight from a non-stirred solution containing 4 μmoles of mercury(II) chloride, at a cathode potential of -500 mV *vs.* the S.R.E. The electrode tips had geometric surface areas of 4.1 cm^2, hence this procedure yielded films having an average thickness of

around 145 nm. To compensate for mercury lost during the analytical sequences, at the end of each working day the film was augmented by plating out the metal present in 5.0 ml of $3.2 \times 10^{-4}M$ mercury(II) chloride. Control samples, run as part of each analytical sequence for comparison purposes, yielded Cd and Pb peaks which varied only marginally in size (4–5% R.S.D.) over the working week.

For a mixture containing 100 μg/l. each of Cd, Pb and Cu, the precision of five successive ASV scans was normally $<2\%$ R.S.D. for Cd and Pb and $<6\%$ R.S.D. for Cu. The poor reproducibility for Cu arose because the peak increased with each successive analytical cycle, a pattern of behaviour noted in other ASV studies.

Base solutions and particulates

Acidified 100-μg/ml stock solutions of metal ions (Cu, Cd, Pb) were prepared from the analytical grade salts, and diluted as required with demineralized water.

The base electrolyte used in most studies was $1M$ sodium acetate, adjusted to pH 5 by addition of acid. Metal ion impurities in this solution were reduced to a minimum by using an electrolytic reagent-cleaning system (ESA Model 2014P). In other study sequences, the pH of the base electrolyte was adjusted to 6.35 or 8.0, or the concentration was varied between 0.05 and $0.7M$. In other cases, salts (NaCl, NaF, KBr or K_2CO_3) were added at the $0.2M$ level. For comparison purposes, some studies were also made with sodium citrate as the base electrolyte.

The organic acid particles which were added to the test solutions varied in type from pure salicylic acid to technical grade "natural" products. The humic acids marketed by Fluka AG (HAI) and Aldrich (HAII) were widely studied. Both contained traces of Cu and Pb (corrected for by blank subtraction) and required pH > 8 for dissolution. At pH 5, the reported[14] sorptive capacities (mole/kg) are Cd^{2+}, 0.5 (0.25); Cu^{2+}, 0.8 (0.5); Pb^{2+}, 1.0 (0.7), the Aldrich values being given in brackets. Two other humic acids (THA-1 and THA-4), extracted from forest soils, had lower ash contents, and dissolved at pH > 6. The acid-soluble fulvic acid (molecular weight < 1000) was obtained from Contech Ltd., Ottowa.

ASV operating conditions

The ASV analytical cycle was based on a 5-min deaeration period (with a 40 ml/min nitrogen flow) and a 10-min electro-deposition, followed by a stripping scan at 50 mV/sec to cut-off at -50 mV. For simultaneous determination of Cu, Pb and Cd, the deposition potential used was -900 mV (acetate base) or -1.0 V (citrate base). Longer deaeration periods in the presence of the Hg film resulted in distorted Cu peaks.

Procedure

Each test solution (containing 5.0 ml of base solution and 100 μg/l. Cd, Pb and Cu) was subjected to five successive ASV deposition/stripping cycles, and mean values were calculated for peak current (i_p) and peak potential (E_p). Then 2 mg of finely divided solid were added to the cell and the procedure was repeated. Variations subsequently investigated included the effect of different weights of solid (0.5–10 mg), changes in the concentration of metal ion (20–100 μg/l.) or the concentration of electrolyte in the base solution (0.05–$1M$), and the presence of diverse anions ($0.2M$ Cl^-, Br^-, F^-, CO_3^{2-}) or chelating resin (6 mg of Chelex 100) or added $Hg(NO_3)_2$ (0.25–0.8 μmole).

To ascertain the total amount of sorption, one group of samples was filtered through 0.45-μm membranes before analysis of the filtrate by ASV. The Cd and Cu results were confirmed by atomic-absorption spectroscopy (AAS).

Cold vapour AAS was used to determine the mercury present in the acetate base solutions as a result of extended stirring of the solution in contact with the thin film electrode.

RESULTS AND DISCUSSION

Operational parameter effects

Numerous authors[27,28] have emphasised the importance of controlling the pH of the base electrolytes used in ASV studies, and for this investigation an acetate buffer system was selected because of the high lability[27] and relatively low stability[29] of metal acetato-complexes.

In this medium a cut-off potential of -50 mV yielded a clearly defined Cu peak but released only small amounts of Hg(II) into solution on standing (*e.g.*, 5.5 ng of Hg detected after 7 min, 11 μg after 25 min). The presence of 2 mg of humic acid (which strongly sorbs Hg^{2+})[30] increased the Hg found in solution to 10 μg (7 min) and 50 μg (25 min). Redeposition of this mercury in the next analytical cycle tends to provide the equivalent of an "*in situ*" film, a technique modification reported to yield enhanced peak currents.[11] With the conditions used in our investigation, the addition of 0.25, 0.5 and 0.8 μmole of Hg(II) to the test solution increased the Cu peak current by 60, 73 and 87%, respectively, and only part of this change can be attributed to thickening of the preformed (4 μmole) film. These additional amounts of mercury may have increased the metal volume (and hence the current) by 6, 12 and 20% and in fact, with 2 mg of humic acid present, the enhancement was of this order (11–19%).

Variations in film droplet size arising from partial dissolution and redeposition in repeated cycles provide a tenuous explanation for the continual increase in Cu stripping currents (noted by several authors.[11,13,31]) The humic acid result, on the other hand, suggests that sorbed Hg(II) has limited lability.

As the role of the supporting electrolyte is to reduce the solution resistance and vary the chemical form of the reducible species, dilution or composition changes affect both the plating and stripping stages and yield variations in ASV responses, such as those indicated in Fig. 1 and given in Table 1.

Dilution of the $1M$ pH-5 buffer solution (curves a, Fig. 1) led to anodic peak shifts and changes in peak current (particularly at $<0.2M$ CH_3COONa; with $<0.05M$ electrolyte the peaks became very broad and of minimal height). In a second series, varying amounts of sodium acetate were added to $0.2M$ acetic acid, yielding solutions having pH values between 3.8 and 5.5 (curves b). In these base solutions, the changes induced in peak size and position were relatively small (*e.g.*, ~ 30 mV) except with Cu and $<0.2M$ sodium acetate. Adding 2 mg of humic acid to these base solutions resulted in no significant shift in peak positions (curves c), but there were changes in stripping currents, attributable to metal-ion sorption by the solid, an effect which declined at pH < 4 as protons competed for the sorption sites.

It has been reported previously that Cu, Pb and Cd peak currents are almost independent of pH changes (between 4 and 7) when acetate base solutions are

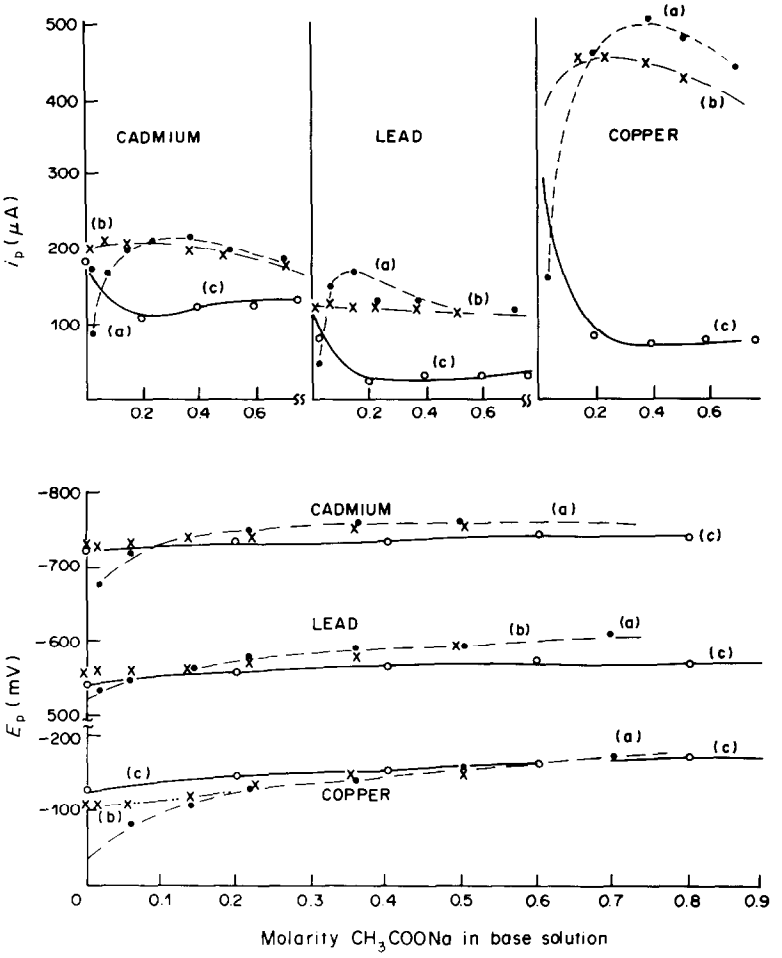

Fig. 1. Effect of base solution concentration on ASV peak size and position (100 μg/l, Cd^{2+}, Pb^{2+} and Cu^{2+}). (a) Dilution of buffer solution; NaOAc:HOAc = 5:1. (●). (b) 0.2*M* HOAc plus various NaOAc additions (×). (c) As in (b) plus 2 mg of humic acid (⊙).

Table 1. Effect of base solution (and humic acid) on ASV peaks (deposition potential −900 mV, 100 μg/l. M^{2+})

	Cadmium		Lead		Copper	
Base solution		+HA		+HA		+HA†
	A. Peak positions, *mV vs.* S.R.E.					
(1*M*) + (0.2*M*)						
NaOAc/HOAc (pH 5)	−793	−797	−636	−641	−193	−217*
+ K_2CO_3	−793	−793	−638	−641	−186	−200*
+ NaF	−790	−792	−636	−638	−186	−213*
+ NaCl	−799	−807	−647	−654	−292*	−356*
+ KBr	−809	−810	−636	−640	−359*	−365
Na_3cit + Hcit	−827*	−827	−693*	−705	−264*	−270
Na_3cit + KNO_3	−827*	−827	−684*	−685	−270*	−289
	B. Peak currents, *μA*					
NaOAc/HOAc (pH 5)	162	167	119	91*	161	67*
+ K_2CO_3	177	153*	131	89*	204	102*
+ NaF	174	137*	127	49*	256	91*
+ NaCl	122	113	109	55*	128	44*
+ KBr	169	155	117	81*	108*	102
Na_3cit + Hcit	4*	4	60	53	40	39
Na_3cit + KNO_3	12*	12	64	60	66	41

*Indicate major changes.
†Values for the cathodic component, companion peak ~100 mV more anodic.

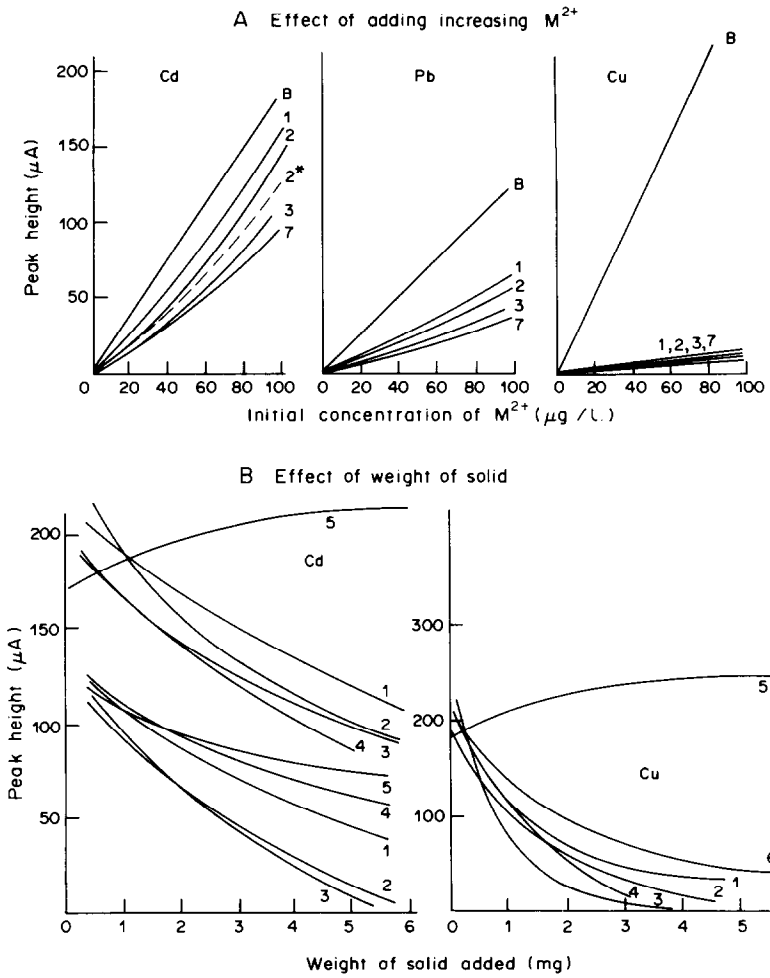

Fig. 2. Effect of M^{2+}:HA ratio on peak heights. A. 2 mg of HA, various initial M^{2+} concentrations. B. 100 μg/l. M^{2+}, various weights of solid added; base solution 1*M* NaOAc/HOAc, pH 5. 1, Fulvic acid; 2, HAII; 3, HAI; 4, THA-1; 5, salicyclic acid; 6, tannic acid; 7, THA-4; (2*, 3 mg of HAII—series A). B = blank (*i.e.*, no solid present).

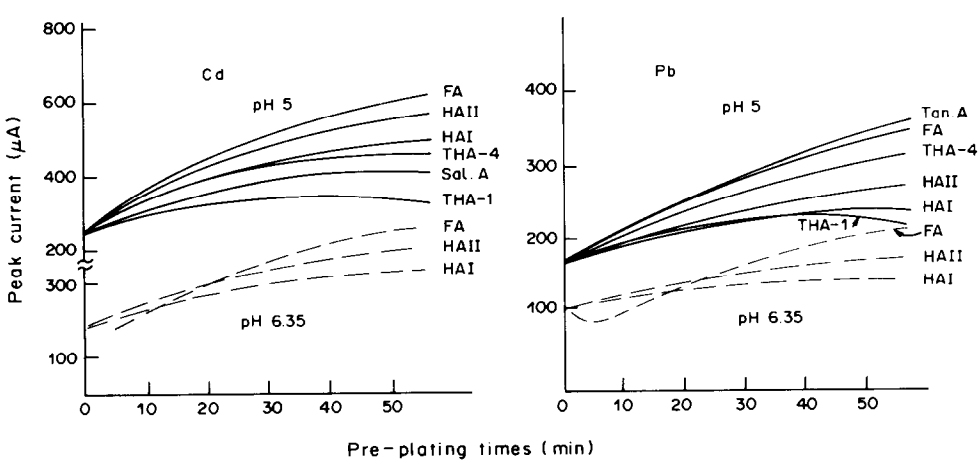

Fig. 3. Effect of pre-plating film-contact time and pH on the size of Cd and Pb ASV peaks in the presence of organic acids: 2 mg of solid acid, 5 ml of 1*M* NaOAc/HOAc buffer solution, 100 μg/l. M^{2+}, deposition at −900 mV. FA, fulvic acid; HAI and HAII, humic acids; THA-1 and THA-4, forest soil humic acids; Tan. A, tannic acid; Sal. A, salicylic acid.

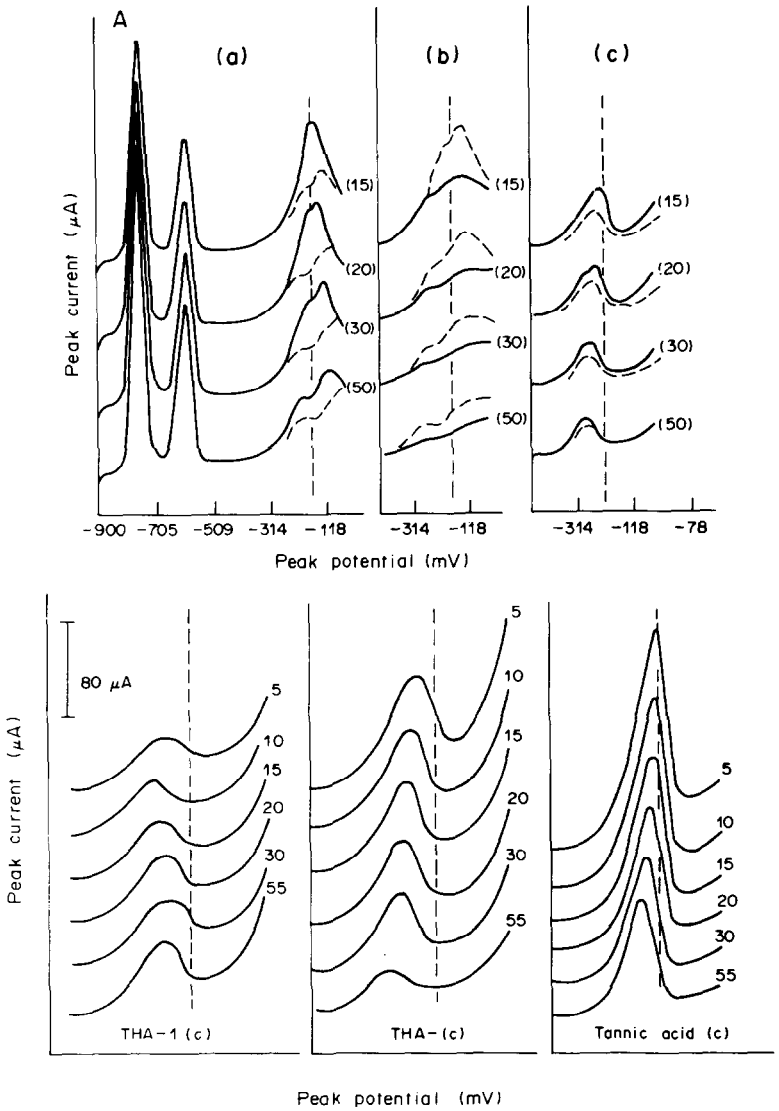

Fig. 4. Effect of pre-plating film-contact time and pH on the size of Cu ASV peaks in the presence of organic acids: 2 mg of solid acid, 100 μg/l. Cu^{2+}, deposition at −900 mV; 5 ml of buffer solution—(a) 1*M* NaOAc/HOAc, pH 5; (b) 1*M* NaOAc/HOAc, pH 6.35; (c) 1*M* NaOAc, 0.2*M* NaCl, pH 5. Contact time (min) in parentheses. Vertical dotted line—Cu peak position, organic acids absent. A. Influence of HAI (——) and HAII (---). B. Effect of part-soluble THA-1 and THA-4, and tannic acid.

used,[28,32] but several other studies[31,33-36] have indicated distinct pH effects, particularly at pH < 7. In our investigation, increasing the pH from 5 to 6.35 resulted in slight peak enhancement (< 10%) and small cathodic peak shifts (~8 mV, Cd, Pb; ~30 mV Cu). At pH 8, the extent of peak shifting doubled and current flows were suppressed (*ca.* 10% for Cd; 25% for Pb; 40% for Cu). With Cu, the plot indicated two partially resolved peaks, an effect which has been attributed[31,36,34] to adsorption of Cu(II) hydroxy compounds or the formation of some Cu(I) species. In the presence of humic acid (Table 1) this double peak became very low and broad, with almost complete loss of the larger peak (*i.e.*, E_p was similar to that for the more cathodic component). With Cd and Pb, the addition of organic acids at pH 8 resulted in little change in E_p, but significant depression of peak currents (~33% for Cd, ~66% for Pb). Adsorption of metal ions by humic acids increases with pH,[14] up to the point where dissolution begins, and this explains most of the observed peak changes.

Diverse anion effects

Cu signals are known[31,32,37] to be depressed by the presence of even low levels of chloride (*e.g.*, <0.05*M*), but the effect levels off at <0.1*M*, and inclusion of sodium chloride at the 0.2*M* level in acetate base solutions has been recommended. This

Table 2. Effect of filtration (0.45 μm) on ASV peak heights for metal ion–humic acid mixtures: 100 μg/l M^{2+}, 2 mg of solid humic acid; 5 ml of 1M NaOAc, pH 5 or pH 8 (values in parentheses)

	i_p, μA			Bonding of M^{2+} on solids, %	
Organic acid present	Suspension	Filtrate	Metal ion	Non-labile [Chelex] ASV	ASV Labile
Nil	154 (120)	144 (100)			
Fulvic	156 (116)	97 (62)	Cd	[5] 0 (3)	33 (35)
HAI	144 (80)	114 (64)		[10] 6 (33)	15 (3)
HAII	153 (76)	144 (56)		[0] 0 (37)	6 (9)
Nil	84 (70)	83 (47)			
Fulvic	69 (28)	43 (18)	Pb	[5] 17 (60)	31 (14)
HAI	55 (22)	43 (20)		[11] 34 (68)	14 (3)
HAII	65 (24)	44 (20)		[0] 22 (66)	22 (6)
Nil	164 (130)	165 (70)			
Fulvic	54; 49 (34)	50; 38 (18)	Cu*	[18] 37† (74)	10 (5)
HAI	33; 70 (40)	39; 47 (20)		[20] 38† (69)	10 (15)
HAII	33; 105 (29)	41; 59 (30)		[20] 15† (78)	24 (0)

*pH 5 dual peak, pH 8 broad peak.
†Based on sum of on peak heights.

excess of chloride swamps trace effects arising from chloride diffusing from the reference half-cell or introduced with the reagents, and it has been found to sharpen Cd and Pb peaks. All the previously described chloride effects were confirmed in our studies, *e.g.*, when the influence of diluted acetate/chloride base solutions was investigated. The effect of chloride on Cu behaviour has been attributed[32] to the existence of two poorly resolved dissolution processes, namely, $Cu + 2Cl^- \rightleftharpoons CuCl_2^- + e^-$, plus some oxidation to Cu(II) at a more positive potential, *i.e.*, $Cu + 3Cl^- \rightleftharpoons CuCl_3^- + 2e$. The stability of the chloro-complexes shifts the peak by ~100 mV; formation of the more stable bromo-species results in a greater shift (~170 mV). Discernible shoulders appear in the presence of both anions, but only in the case of Cl^- does the addition of some humic acid result in further cathodic shift (~65 mV) (Table 1).

The introduction of fluoride or carbonate ions had little effect on Cd, Pb or Cu peak positions, which confirmed the greater stability of the acetato–metal complexes in these mixtures. The addition of 2 mg of HAII resulted in no significant change in Cd or Pb peak positions, and with Cu the change was small (10–20 mV).

The major cathodic shifts observed for citrate base electrolyte solution are consistent with the citrate complexes of the three metal ions being more stable but less labile (smaller peaks) than other complexes examined in this study. The limited lability hindered uptake by humic acid particles (as shown by the small +HA effect). The peaks in citrate base solutions were reasonably broad, reflecting the ability of this ligand to form a sequence of complexes of varied stability,[29]

Sorption of organic compounds on the electrode can also result in peak broadening and lower i_p values, but this interpretation has been rejected since sorption is usually accompanied by anodic peak-shifts. In addition, i_p increased when the deposition potential was successively raised from −0.9 to −0.95, −1.0 and −1.1 V.

Sorption by suspended particles

The removal of metal ions from solution on the addition of fulvic or humic acids was clearly demonstrated when the cloudy test solutions were analysed before and after filtration through a 0.45-μm membrane (Table 2). The ASV readings were lower after filtration, which implies that part or all of the sorbed material was labile. With Cd and Pb there were only small shifts in E_p after the filtration, but with copper, both peaks shifted anodically (~20 and 30 mV). Carbon cup AAS analysis for Cd confirmed the filtrate analysis value (*i.e.*, no non-labile soluble complexes were identified). The acetate base interfered with Cu and Pb determinations by the carbon cup method, but confirmatory Cu solution levels were obtained by flame AAS (with maximum scale expansion).

The splitting of the Cu peak complicated calculation of the labile fraction, but the approximate values reported are consistent with the data derived from electrolyte displacement[17] and adsorption studies. Both Cu and Pb form sparingly soluble fulvates at around pH 5,[25] and the humic acids have a much greater affinity for Cu and Pb than for Cd.[14] The apparent high mobility of Cd associated with organic species present in natural waters has been noted previously.[6,38,39]

The loss on filtration of suspensions with a pH of 8 was greater than that for suspensions at pH 5, a change attributable to partial precipitation of metal hydroxy species, in addition to a higher degree of metal chelation with the organic acids.

When test solutions were equilibrated overnight with a mixture of 2 mg of organic acid and 6 mg of Chelex 100 resin, Cu was totally removed from solution, and the Cd and Pb values were halved. In the absence of humic acid, addition of Chelex removed 50% of the Cd, 60% of the Pb and 80% of the Cu present, and these values were used to calculate the fractions retained by the organic acid, from which were derived the apparent non-labile fractions, Chelex method ([] in Table 2). Comparison of these results with the ASV data indicates that about 20% of the Cu and Pb may be classified as moderately labile.

ASV studies provide only an indication of the lability of complexed or sorbed metal ions, since the peak currents recorded reflect both the experimental conditions chosen (*e.g.*, applied potential, system pH) and the type of bonding involved.

Another approach to stability studies involves adding increasing concentrations of metal ion to a fixed amount of ligand, or increasing amounts of ligand to a fixed amount of metal ion.

Figure 2(A) summarizes the ASV peak heights observed for test solutions of varied concentration, on addition of 2 mg of humic acid. It can be observed that the degree of current suppression varied with the metal ion involved and the organic acid used, and was in the order Cu > Pb > Cd.

This sequence was again evident when the weight of solid acid added was increased [Fig. 2(B)]. The addition of >3 mg of solid acid reduced the Cu ASV signals to near zero, with a small (5–10 mV) cathodic shift in peak position and the appearance of a more prominent shoulder. The change in E_p is attributed to a higher proportion of the copper being bound in non-labile complexes. If formation of a stable soluble complex were involved, a response similar to that obtained with salicylic acid would be expected.

The ability of humic acids to sorb metal ions strongly from their aqueous solutions at mg/l., concentration was demonstrated in an earlier study[14] which utilized AAS as the monitoring technique. The amount sorbed was found to vary with pH and the humic acid sample studied, with maximum removal of metal ion occurring within distinct pH regions (*e.g.*, pH 5.5–7 for Cu, Pb). The relative affinity order was Cu, Pb > Zn, Cd. Pb, and to a lesser extent Cu, Cd and Zn, have been found to form sparingly soluble metal fulvates[25] within narrow pH regions (*e.g.*, Pb, pH 5–7; Zn, pH 6.5–8).

In qualitative terms, these studies indicate that the three metal ions belong to different "lability" categories:

(*i*) strongly sorbed or bound, low lability—Cu;
(*ii*) firmly sorbed, intermediate lability—Pb;
(*iii*) weakly sorbed, high degree of lability—Cd.

Less predictable is the observation that adding <1 mg of organic acid leads to enhanced Cd and Pb peaks. Some surfactants also promote peak enhancement,[13] and it has been suggested[40] that in such systems electrostatic attraction between metal ions and adsorbed dipolar surfactant molecules may lead to acceleration of the discharge reaction at the electrode. Alternatively, the positive effects of dissolution of the mercury film in the presence of solids (discussed earlier) may exceed the sorption losses.

Mercury film effects

Enhancement of Cu and Pb peaks and formation of dual Cu peaks were also observed when the colloidal suspensions were left in contact with the MTFE for longer periods, prior to deposition and stripping analysis (*cf.* Figs. 3 and 4). These changes did not occur when the colloid–metal ion mixtures were retained in vials for various periods prior to transfer to the ASV cell, so the peak changes cannot be attributed to slow achievement of sorption equilibria, and must involve the mercury film.

With Cd and Pb, there were no changes in peak position but the peak height increased more or less linearly with the square root of the contact time (5–45 min). This time relationship implies that the slow step is probably a diffusion process. For example, gradual build up of an adsorbed organic layer could bring with it sorbed metal ions, leading to an elevated surface concentration and proportionately greater metal ion deposition. Alternatively, the film build-up may promote oxidation of the mercury, with redeposition in a more active form at the start of the deposition cycle. Disturbing the system, *e.g.*, by introducing a fresh base solution between the deposition and stripping cycles, led to much smaller current flows, which suggests that the film may consist of fine droplets of mercury, loosely attached to a more coherent base layer.

Peak sizes were also smaller when a pH of 6.35 was used (*cf.* Fig. 3), reflecting some change in bonding mode, but the contact time effect persisted. At both pH 5 and 6.35 the magnitude of the change varied with the type of organic material added (*cf.* Figs. 3 and 4) and the element being examined.

The behaviour of copper was far more anomalous. When a deposition potential of −800 mV was used, peak changes were relatively small, but when a voltage of −900 mV was applied (to ensure deposition of Cd) the peak characteristics became a definite function of film contact time (*cf.* Fig. 4).

A d.c. polarogram for an acetate base solution (pH 5) of copper (2 mg/l.) containing 10 mg of acid exhibited two distinct reduction steps. The first ($E_{1/2} \sim -60$ mV) matched the wave obtained in the absence of the organic solid. The slope of the second wave was more gradual, indicating an irreversible or kinetically controlled reduction process ($E_{1/2} \sim -900$ mV), most probably direct reduction of a copper–humate complex. The anodic shift of the $Cu(Hg) \rightarrow Cu^{2+}$ stripping peak with increased contact time thus probably indicates adsorption of organic matter on the electrode, whereas the cathodic

component of the dual peak possibly represents oxidation of Cu(I), present as a stable, poorly labile complex. Increasing the pH appears to increase the fraction of adsorbed copper present as a less labile chelate and so reduces the amount retained by electrostatic forces only, *i.e.*, the main contributor to i_p. Further investigations of the electrode phenomena are planned.

ANALYTICAL AND ENVIRONMENTAL ASPECTS

It has now been clearly established that both dissolved organic compounds and colloidal particles influence the size of the Cd, Pb and Cu ASV peaks and accordingly experimental conditions need to be carefully controlled if accurate data are to be recorded. Some of the inherent problems (*e.g.*, anion effects) can be minimized by proper selection of the base electrolyte, but others (*e.g.*, film contact-time effects, peak enhancements) require standardization of operating parameters and calibration by standard-additions. Separate determination of copper, at a much lower deposition potential, may be regarded as another wise precaution.

The study also emphasises the desirability of having an appreciation of the limitations of the technique and some knowledge of the system chemistry, before embarking on speciation studies. For example, it is standard practice to filter waters through a 0.45-μm membrane before analysing both filtrate and solid for total metal content, but omission of a third test, *viz.* analysing the water as collected (and thus determining the labile fraction attached to the isolated solids) may result in loss of evaluation of an important biologically active fraction. Similarly, analysing the filtrate by two techniques (*e.g.*, AAS and ASV) should readily allow the contribution of stable non-labile complexes to be assessed. The case for more detailed subdivision can then be based on this preliminary information.

The results of this ASV study also indicate that some of the published data on metal–organic acid complex stability may be in error because due allowance has not been made for the presence of sparingly soluble reaction products or sorption by colloidal particles.

An important environmental consideration is the high proportion of sorbed metal ion which is ASV-labile, and displaceable by electrolytes. The values determined by different approaches are not directly comparable, but each confirms that a portion of each colloidal particle load is destined to be conveyed directly to the sediments, while another fraction can be repeatedly cycled between phases. Preliminary studies have shown that a significant fraction of the metal ions sorbed by clays is also ASV-labile and that electrolytes displace ions from hydrous oxides (*e.g.*, MnOOH),[40] so ASV studies on unfiltered and filtered natural waters should provide interesting information on average overall lability or availability.

REFERENCES

1. B. T. Hart, *2nd Intern. Symp. on Interactions between Sediments and Freshwaters*, Kingston, 1981.
2. G. E. Batley and T. M. Florence, *Mar. Chem.*, 1976, **4**, 347.
3. G. E. Batley and D. Gardiner, *Estuarine Coastal Mar. Sci.*, 1978, **7**, 59.
4. D. Gardiner, *Water Res.*, 1974, **8**, 157.
5. K. K. Turekian, *Geochim. Cosmochim. Acta*, 1977, **41**, 1139.
6. T. M. Florence and G. E. Batley, *Crit. Rev. Anal. Chem.*, 1980, **9**, 219.
7. *Idem*, *Talanta*, 1977, **24**, 151.
8. P. Sagreb and W. Lund, *ibid.*, 1982, **29**, 457.
9. R. Ernst, H. E. Allen and K. H. Mancey, *Water Res.*, 1975, **9**, 969.
10. P. L. Brezonik, P. A. Brainer and W. Stumm, *ibid.*, 1976, **10**, 605.
11. G. E. Batley and T. M. Florence, *J. Electroanal. Chem.*, 1974, **55**, 23.
12. Z. Lukaszewski and M. K. Pawlak, *ibid.*, 1979, **103**, 225.
13. A. Beveridge and W. F. Pickering, *Water Res.*, 1984, **18**, 1119.
14. *Idem*, *Water, Air and Soil Pollut.*, 1980, **14**, 171.
15. H. Zurino, P. Peirano, M. Aguilera and E. Schalscha, *Soil Sci.*, 1975, **119**, 210.
16. F. J. Stevenson, *ibid.*, 1977, **123**, 10.
17. J. Slavek, J. Wold and W. F. Pickering, *Talanta*, 1982, **29**, 743.
18. V. Cheam and D. Gamble, *Can. J. Soil Sci.*, 1974, **54**, 413.
19. W. T. Bresnahan, C. L. Grant and J. H. Weber, *Anal. Chem.*, 1978, **50**, 1675.
20. F. L. Greter, J. Buffle and W. Haerdi, *J. Electroanal. Chem.*, 1979, **101**, 211 and 231.
21. G. Sposito, K. M. Holtzclaw and C. S. Le Vesque-Madore, *Soil Sci. Soc. Am. J.*, 1979, **43**, 1148.
22. M. S. Schuman and J. L. Cromer, *Environ. Sci. Technol.*, 1979, **13**, 543.
23. R. A. Saar and J. H. Weber, *ibid.*, 1980, **14**, 877.
24. J. Buffle, *Anal. Chim. Acta*, 1980, **118**, 29.
25. J. Slavek and W. F. Pickering, *Water, Air and Soil Pollut.*, 1981, **16**, 209.
26. M. Schnitzer and H. Kerdoff, *ibid.*, 1981, **15**, 97.
27. Y. K. Chau and Lum-Shue-Chan, *Water Res.*, 1973, **8**, 383.
28. I. Sinko and J. Doležal, *J. Electroanal. Chem.*, 1970, **25**, 299.
29. L. G. Sillén and A. E. Martell, *Stability Constants of Metal-ion Complexes*, Chemical Society Spec. Publns. 17 and 25, London, 1964 and 1971.
30. P. Thalabalasingham and W. F. Pickering, *Environ. Pollut. B*, in the press.
31. E. A. Schonberger and W. F. Pickering, *Talanta*, 1980, **27**, 11.
32. M. J. Pinchin and J. Newham, *Anal. Chim. Acta*, 1977, **90**, 91.
33. V. H. Lewin and M. J. Rowell, *Effluent Water Treat. J.*, 1973, **13**, 273.
34. A. Zurino and M. L. Healy, *Environ. Sci. Technol.*, 1972, **6**, 243.
35. T. M. Florence and G. E. Batley, *Talanta*, 1976, **23**, 179.
36. D. Jagner and L. Kryger, *Anal. Chim. Acta*, 1975, **80**, 255.
37. T. M. Florence and G. E. Batley, *J. Electroanal. Chem.*, 1977, **75**, 791.
38. P. Figura and B. McDuffie, *Anal. Chem.*, 1980, **52**, 1433.
39. D. P. H. Laxen and R. M. Harrison, *Water Res.*, 1981, **15**, 1053.
40. S. Krylov and I. F. Fishtik, *Electrokhimya*, 1981, **17**, 787.

Talanta, Vol. 32, No. 2, pp. 139–143, 1985
Printed in Great Britain.

0039-9140/85 $3.00 + 0.00

ANALYTICAL APPLICATIONS OF COPPER(II) AND COPPER(I) IN ACETONITRILE: POTENTIOMETRIC AND SPECTROPHOTOMETRIC DETERMINATION OF DITHIOCARBAMATES

B. C. VERMA*, SAROJ CHAUHAN, ANITA SOOD, D. K. SHARMA and H. S. SIDHU
Chemistry Department, Himachal Pradesh University, Shimla-171005, India

(*Received* 9 *January* 1984. *Accepted* 14 *September* 1984)

Summary—The use of copper(II) perchlorate and tetra-acetonitrilocopper(I) perchlorate (in acetonitrile) for the potentiometric and spectrophotometric determination of dithiocarbamates in acetonitrile medium is described. The proposed methods are simple, accurate and reliable and show promise of wide applicability. They are recommended for routine determination of dithiocarbamates. Their advantages over the carbon disulphide evolution method, commonly employed for the determination of these compounds, are discussed.

Dithiocarbamates find extensive use as agricultural fungicides and as vulcanization accelerators in the rubber industry. Because of the wide commercial importance of these compounds, their determination has received much attention. A variety of techniques has been used for the determination of these materials but the usual approach[1–6] involves hydrolysing them with hot mineral acids to the corresponding amines and carbon disulphide, either of which may be determined.

$$R_2N{-}\underset{\underset{S}{\|}}{C}{-}S^- + H^+ \rightarrow R_2NH + CS_2$$

Usually carbon disulphide is selected and measured either by the xanthate method (for macro/semimicro determination) or colorimetrically (for micro determination). The method in either case is tedious, and requires both special apparatus and careful control of experimental conditions if evolution of carbon disulphide is to be quantitative. There is, therefore, a need for a method which, besides being accurate and precise, should also be rapid. We have developed potentiometric and spectrophotometric methods that obviate the time-consuming degradation of the sample and the distillation step. These methods are based on oxidation of the dithiocarbamate with copper(II) perchlorate in acetonitrile. This system was chosen for the following reasons.

(*i*) Dithiocarbamates are easily oxidized to the corresponding thiuram disulphides **(I)**, but this is best done in non-aqueous medium, first because of the tendency of these compounds to undergo decomposition with acids[7,8] (which serve as the media for most conventional redox titrations) and secondly because of the interference[9,10] of the water-insoluble oxidation products **(I)** in neutral aqueous medium.

$$2RR'N{-}\underset{\underset{S}{\|}}{C}{-}S^- \rightarrow RR'N{-}\underset{\underset{S}{\|}}{C}{-}S{-}S{-}\underset{\underset{S}{\|}}{C}{-}NR'R + 2E^-$$

(I)

(R = alkyl group; R′ = hydrogen atom or alkyl group)

(*ii*) Acetonitrile, because of its high dielectric constant and resistance to oxidation and reduction, is a promising solvent for non-aqueous redox titrations.[11]

(*iii*) Copper(II) in acetonitrile is a powerful and stable oxidizing agent.[11,12]

The following observations were made.

(*i*) The potentiometric titrations show two well-defined breaks at copper(II):dithiocarbamate ratios of 0.5 and 1.0, corresponding to the oxidation mechanism:

$$4RR'N{-}\underset{\underset{S}{\|}}{C}{-}S^- + 2Cu^{2+} \rightarrow RR'N{-}\underset{\underset{S}{\|}}{C}{-}S{-}S{-}\underset{\underset{S}{\|}}{C}{-}NR'R + 2RR'N{-}\underset{\underset{S}{\|}}{C}{-}SCu$$

(I) **(II)**

$$2RR'N{-}\underset{\underset{S}{\|}}{C}{-}SCu + 2Cu^{2+} + 16CH_3CN \rightarrow RR'N{-}\underset{\underset{S}{\|}}{C}{-}S{-}S{-}\underset{\underset{S}{\|}}{C}{-}NR'R + 4[Cu(CH_3CN)_4^+]$$

(I)

(*ii*) The solution is initially colourless but becomes increasingly yellow [owing to the formation of cop-

*Author for correspondence.

per(I) dithiocarbamate] as the reagent is added, until a maximum is reached at a molar ratio of 0.5, then the colour starts decreasing again (thiuram disulphides are colourless) and finally becomes colourless, which substantiates the mechanism shown above.

These observations reveal that in acetonitrile medium, copper(II) and copper(I) salts could serve as useful reagents for the determination of dithiocarbamates. Consequently, we have been able to evolve simple, accurate and reliable methods, potentiometric and spectrophotometric, of wide applicability for the determination of dithiocarbamates with acetonitrile solutions of copper(II) perchlorate and tetraacetonitrilocopper(I) perchlorate as reagents. The most attractive feature of these reagents is their excellent stability. Copper(II) has a higher redox potential in acetonitrile than in aqueous medium because the copper(I) produced is stabilized by solvation[11-14] and is resistant to aerial oxidation and does not disproportionate. The conditional potential of the couple in acetonitrile is slightly higher than that of the hexanitratocerate couple in the same solvent.[13] The potentiometric titrations with tetraacetonitrilocopper(I) perchlorate as titrant are based on stoichiometric formation of the copper(I) dithiocarbamates.

$$RR'N-\underset{\underset{S}{\|}}{C}-S^- + Cu^+ \rightarrow RR'N-\underset{\underset{S}{\|}}{C}-SCu$$

To make the platinum electrode responsive to dithiocarbamate concentration, a drop of dilute iodine solution in acetonitrile is added to generate a trace of the corresponding thiuram disulphide.

$$2RR'N-\underset{\underset{S}{\|}}{C}-S^- + I_2 \rightarrow RR'N-\underset{\underset{S}{\|}}{C}-S-S-\underset{\underset{S}{\|}}{C}-NR'R + 2I^-$$

A sharp jump in potential is observed at the equivalence point at a 1:1 copper(I):dithiocarbamate ratio.

Photometric titration procedures have also been developed for the micro-determination of dithiocarbamates with either the copper(II) or copper(I) reagent. The titrations are monitored at 430 nm, the wavelength of maximum absorbance of copper(I) dithiocarbamates. With either reagent, the absorbance increases up to the end-point, then decreases in titrations with copper(II) and remains constant in those with copper(I).

For determination of traces of dithiocarbamates, the yellow colour resulting from their reaction with copper(I) perchlorate in acetonitrile can be measured; the colour develops immediately and is stable for at least 24 hr.

EXPERIMENTAL

Apparatus

Potentiometric titrations were performed with a bright platinum wire as indicator electrode and a modified calomel electrode (saturated methanolic potassium chloride used instead of aqueous solution) as reference.

Reagents

Acetonitrile. Distilled twice from phosphorus pentoxide (5 g/l.).

Dithiocarbamates. Sodium diethyldithiocarbamate was recrystallized before use. Sodium salts of n-propyl, n-butyl, sec-butyl, n-pentyl, dimethyl, di-n-propyl, di-n-butyl, di-n-pentyl and di-n-hexyl dithiocarbamic acids were prepared and purified by known methods.[15-18] Alkylammonium alkyl dithiocarbamates were prepared by the method of Anchutz[19] by mixing primary or secondary amines with carbon disulphide in dry ether. Monoalkylammonium monoalkyl dithiocarbamates ($RHN.CS.SNH_3R$ with R as methyl, n-propyl, n-butyl and n-pentyl) and dialkylammonium dialkyldithiocarbamates ($R_2N.CS.SNH_2R_2$ with R as methyl, n-propyl and n-butyl) were prepared and kept in a vacuum desiccator. The purity of each dithiocarbamate was checked by non-aqueous titration with iodine monobromide.[20]

Table 1. Potentiometric determination of dithiocarbamates with copper(II) perchlorate in acetonitrile

Dithiocarbamates	Mean and s.d. of 10 determinations	
	Amount found,* *mg*	Amount found,† *mg*
Sodium salts		
n-Propyl	3.98, 0.028	10.04, 0.082
n-Butyl	3.96, 0.032	9.94, 0.092
n-Pentyl	4.05, 0.029	10.08, 0.088
Dimethyl	3.98, 0.027	10.06, 0.076
Diethyl	3.97, 0.030	9.92, 0.062
Di-n-propyl	4.04, 0.031	10.10, 0.054
Di-n-butyl	3.99, 0.032	9.89, 0.062
Mono/dialkylammonium salts		
n-Propyl	4.04, 0.028	9.98, 0.058
n-Butyl	3.95, 0.029	9.96, 0.068
n-Pentyl	4.02, 0.032	10.00, 0.072
Dimethyl	4.00, 0.028	10.02, 0.082
Di-n-propyl	3.96, 0.032	9.98, 0.066
Di-n-butyl	3.98, 0.030	9.96, 0.058

*Amount taken, 4 mg.
†Amount taken, 10 mg.

Hydrated copper(II) perchlorate solution in acetonitrile (0.02 M). Prepared and standardized as described earlier.[21]

Tetra-acetonitrilocopper(I) perchlorate solution in acetonitrile (0.02 M). Solid $CuClO_4.4CH_3CN$ was prepared by a method similar to that reported by Hathaway *et al.*[22] To a solution of copper(II) perchlorate in acetonitrile, an excess of copper powder (99.9% pure) was added and the solution stirred vigorously. Complete reduction was indicated by the solution becoming colourless. The solution was then quickly filtered while hot. White crystals separated as the solution cooled and were recrystallized from anhydrous acetonitrile and dried under vacuum. Standard solutions were prepared by dissolving a little more than the calculated amount of the compound in acetonitrile and standardized by titration with ammonium hexanitratocerate(IV) in aqueous sulphuric acid with ferroin as indicator.

Procedures

Potentiometric titrations with copper(II) perchlorate. Aliquots of acetonitrile solutions of each dithiocarbamate are diluted to 30 ml with acetonitrile and titrated potentiometrically at room temperature (~25°) with the standard (0.02*M*) copper(II) perchlorate solution. The results as calculated on the basis of the first break for dialkyldithiocarbamates and the second break for monoalkyldithiocarbamates are given in Table 1. The potentiometric titration curves a and b (Fig. 1) are typical of the listed monoalkyldithiocarbamates and dialkyldithiocarbamates respectively.

Potentiometric titrations with tetra-acetonitrilocopper(I) perchlorate. The procedure is the same as that above except that a drop of 0.001*N* iodine solution in acetonitrile is added before the titration. The results are given in Table 2. Titration curve c (Fig. 1) is typical of the listed dithiocarbamates.

Photometric titrations. Aliquots of acetonitrile solutions of each dithiocarbamate are diluted to 8 ml with acetonitrile and titrated photometrically at 430 nm with copper(II) perchlorate solution in acetonitrile, with magnetic stirring. Dilution correction is applied and the titration curve plotted in the usual way. The results are recorded in Table 3 and a typical titration is represented by curve a in Fig. 2.

Alternatively, similar titrations are performed with copper(I) perchlorate in acetonitrile. The results are given in Table 4 and a typical titration is represented by curve b in Fig. 2.

Spectrophotometric determination. A suitable aliquot (0.1–2.0 ml) of dithiocarbamate solution in acetonitrile or chloroform is transferred to a 10-ml standard flask and diluted to between 8 and 9 ml with acetonitrile. Copper(I) perchlorate in acetonitrile (1 ml, 0.01*M*) is added and the solution diluted to the mark with acetonitrile. The absorbance at 430 nm is measured against a reagent blank. A calibration curve is constructed by taking standards through the same procedure. Working ranges and molar absorptivities are given in Tables 5 and 6 respectively.

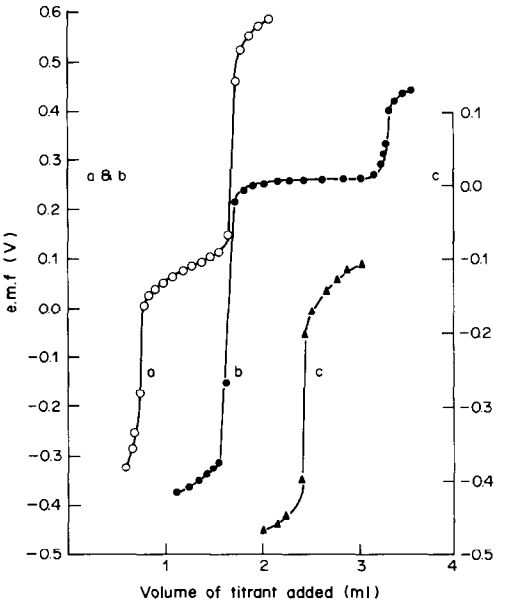

Fig. 1.

RESULTS AND DISCUSSION

Dithiocarbamates readily undergo decomposition with acids,[7,8] so oxidative determinations are notably lacking in the literature. The iodimetric method used in neutral aqueous medium suffers from difficulty in detection of the starch–iodine end-point in the presence of the thiuram disulphides which precipitate during the titration. Use of extraction of thiuram

Table 2. Potentiometric determination of dithiocarbamates with tetra-acetonitrilocopper(I) perchlorate in acetonitrile

Dithiocarbamates	Mean and s.d. of 10 determinations	
	Amount found* *mg*	Amount found† *mg*
Sodium salts		
n-Propyl	4.96, 0.028	12.02, 0.078
n-Butyl	4.98, 0.028	12.06, 0.064
Isobutyl	5.02, 0.032	12.08, 0.064
n-Pentyl	5.04, 0.026	11.98, 0.062
Dimethyl	4.98, 0.028	11.87, 0.080
Diethyl	4.95, 0.030	11.96, 0.072
Di-n-propyl	4.98, 0.031	11.90, 0.080
Di-n-butyl	5.05, 0.026	12.13, 0.068
Mono/dialkylammonium salts		
n-Propyl	4.98, 0.028	11.98, 0.062
n-Pentyl	4.96, 0.032	11.90, 0.064
Dimethyl	5.02, 0.030	12.12, 0.072
Di-n-propyl	5.04, 0.026	12.06, 0.070
Di-n-butyl	5.02, 0.028	11.95, 0.068

*Amount taken, 5 mg.
†Amount taken, 12 mg.

Table 3. Photometric titrations of dithiocarbamates with copper(II) perchlorate in acetonitrile

Dithiocarbamates	Mean and s.d. of 10 determinations: Amount found* mg	Amount found† mg
Sodium salts		
n-Propyl	0.301, 0.002	0.594, 0.004
n-Butyl	0.297, 0.001	0.602, 0.003
Isobutyl	0.298, 0.001	0.604, 0.003
n-Pentyl	0.302, 0.002	0.599, 0.005
Alkylammonium salts		
n-Propyl	0.300, 0.002	0.605, 0.004
n-Butyl	0.298, 0.001	0.593, 0.003
n-Pentyl	0.302, 0.002	0.602, 0.004

*Amount taken, 0.3 mg.
†Amount taken, 0.6 mg.

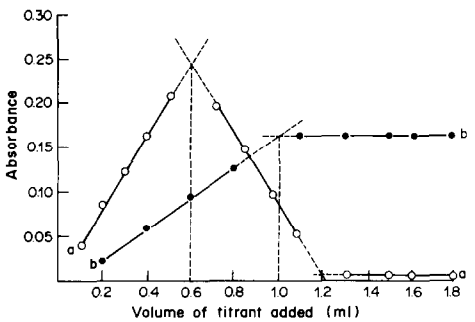

Fig. 2.

disulphides to overcome this difficulty[9,10] makes the method tedious. These problems can be avoided by use of non-aqueous redox titrimetry, and accurate and precise results obtained. The maximum relative standard deviation calculated from the pooled data of all the titrations performed with 4 and 10 mg of each dithiocarbamate with the copper(II) system was 0.7%. The same with 5 and 12 mg of each dithiocarbamate for copper(I) system was 0.6%. For photometric titrations, the relative standard deviations from the pooled data for all the titrations of 0.3 and 0.6 mg of each dithiocarbamate were 0.3% and 0.5% respectively for the first end-point of the

Table 5. Colorimetric determination of dithiocarbamates with tetra-acetonitrilocopper(I) perchlorate in acetonitrile; working range

Dithiocarbamates	Concentration range μg/ml
Sodium salts	
Dimethyl	0.8–12.6
Diethyl	1.0–12.0
Di-n-propyl	0.9–9.9
Di-n-butyl	0.6–8.4
Di-n-pentyl	0.5–10.0
Di-n-hexyl	0.4 ± 8.8
Dialkylammonium salts	
Dimethyl	1.0–10.0
Di-n-propyl	0.8–12.0
Di-n-butyl	0.6–8.4

Table 6. Molar absorptivities of copper(I) dialkyldithiocarbamates at 430 nm.

Compound	ϵ, $l.mole^{-1}.cm^{-1}$
Copper(I) dimethyldithiocarbamate	1.30×10^3
Copper(I) diethyldithiocarbamate	1.6×10^3
Copper(I) dipropyldithiocarbamate	1.7×10^3
Copper(I) dibutyldithiocarbamate	2.40×10^3
Copper(I) dipentyldithiocarbamate	2.60×10^3
Copper(I) dihexyldithiocarbamate	2.80×10^3

Table 4. Photometric titrations of dithiocarbamates with tetra-acetonitrilo-copper(I) perchlorate in acetonitrile

Dithiocarbamates	Mean and s.d. of 10 determinations: Amount found,* mg	Amount found,† mg
Sodium salts		
Dimethyl	0.396, 0.003	0.791, 0.006
Diethyl	0.400, 0.004	0.804, 0.007
Di-n-propyl	0.398, 0.002	0.805, 0.006
Di-n-butyl	0.404, 0.003	0.808, 0.005
Di-n-pentyl	0.399, 0.002	0.796, 0.005
Di-n-hexyl	0.400, 0.003	0.798, 0.006
Dialkylammonium salts		
Di-n-propyl	0.398, 0.002	0.798, 0.004
Di-n-butyl	0.404, 0.004	0.795, 0.008
Di-n-pentyl	0.401, 0.003	0.798, 0.018
Di-n-hexyl	0.398, 0.002	0.802, 0.005

*Amount taken, 0.4 mg.
†Amount taken, 0.8 mg.

copper(II) titrations and 0.8% for the copper(I) system (0.4 and 0.8 mg samples). For the spectrophotometric method, the relative standard deviation of the pooled data was 1.5% and the average error was +1.3%.

REFERENCES

1. J. H. Karchmer (ed.), *The Analytical Chemistry of Sulfur and its Compounds*, Part II, p. 629. Wiley-Interscience, New York, 1972.
2. G. D. Thorn and R. A. Ludwig, *The Dithiocarbamates and Related Compounds*, p. 143. Elsevier, New York, 1962.
3. E. E. Reid, *Organic Chemistry of Bivalent Sulfur*, Vol. IV, p. 227. Chemical Publishing Co., New York, 1962.
4. G. Zweig, *Analytical Methods for Pesticides, Plant Growth Regulators and Food Additives*, Vol. III, p. 74. Academic Press, New York, 1964.
5. R. Engst and W. Schnaak, *Residue Rev.*, 1974, **52,** 55.
6. D. G. Clarke, H. Baum, E. L. Stanley and W. F. Hester, *Anal. Chem.*, 1951, **23,** 1842.
7. M. L. Shankaranarayana and C. C. Patel, *ibid.*, 1964, **33,** 1398.
8. A. Hulanicki and L. Shishkova, *Talanta*, 1965, **12,** 485.
9. M. L. Shankaranarayana and C. C. Patel, *Z. Anal. Chem.*, 1961, **179,** 263.
10. R. C. Paul, N. C. Sharma, R. K. Chauhan and R. Parkash, *Indian J. Chem.*, 1972, **10,** 227.
11. B. Kratochvil, *Chem. in Canada*, 1968, **20,** 20.
12. *Idem*, *CRC Crit. Rev. Anal. Chem.*, 1971, **1,** 415.
13. *Idem*, *Rec. Chem. Prog.*, 1966, **27,** 262.
14. I. M. Kolthoff and J. F. Coetzee, *J. Am. Chem. Soc.*, 1957, **79,** 1182.
15. H. L. Klöpping and G. J. M. Van der Kerk, *Rec. Trav. Chim.*, 1951, **70,** 917.
16. J. Issoirie and L. Musso, *Mem. Poudres*, 1960, **42,** 427.
17. J. Emgene and J. Calabrelta, *J. Inorg. Chem.*, **4,** 973.
18. D. J. Halls, A. Townshend and P. Zuman, *Anal. Chim. Acta*, 1968, **40,** 459; 1968, **41,** 51.
19. R. Anchutz, *Ann.*, 1908, **359,** 202; *Chem. Ztg.*, 1910, **34,** 89.
20. B. C. Verma and S. Kumar, *Mikrochim. Acta*, 1976 **I,** 209.
21. *Idem*, *Talanta*, 1977, **29,** 694.
22. B. J. Hathaway, D. J. Holah and J. D. Postlethwaite, *J. Chem. Soc.*, 1961, 3215.

Talanta, Vol. 32, No. 2, pp. 145–147, 1985
Printed in Great Britain.

0039-9140/85 $3.00 + 0.00

SHORT COMMUNICATIONS

RUTHENIUM DETERMINATION IN SYNTHETIC PUREX WASTE SOLUTIONS BY AAS

W. HEINIG and K. MAUERSBERGER
Zentralinstitut für Isotopen- und Strahlenforschung der AdW der DDR, Permoserstr. 15, 7050 Leipzig, DDR

(*Received* 5 *September* 1984. *Accepted* 29 *September* 1984)

Summary—A method for the determination of ruthenium in synthetic Purex waste solutions by flame AAS is described. With the usual flames and a lanthanum buffer, only cerium interference in the air–acetylene flame need be considered under the conditions applied. Ruthenium nitrosyl nitrate, ruthenium(IV) hydroxychloride and alkaline ruthenate samples gave identical results, showing that the extraordinarily stable Ru–NO bond does not hinder atomization. The preparation and standardization of the ruthenium nitrosyl solutions, and the alkaline fusion, are briefly described.

Besides technetium, neptunium, and zirconium/niobium, ruthenium is one of the troublesome elements in the reprocessing of irradiated fuels. During the extraction of fuel solutions in nitric acid with TBP (Purex process) it is particularly the nitrate complexes of ruthenium nitrosyl that enter the organic phase and accompany uranium and plutonium. Problems arise from the diversity of existing ruthenium nitrosyl compounds, their different extraction coefficients and the sensitive equilibria between all the compounds.[1,2]

The elucidation of the extraction behaviour of all these species in nuclear fuel reprocessing, including ruthenium recovery from fission product solutions, requires efficient analytical methods for this element. Ruthenium in nuclear fuel solutions is usually determined radiometrically, by measurement of the gamma radiation of the nuclides ^{103}Ru and ^{106}Ru. However, depending on the intermediate storage time, much of the ruthenium activity may be lost[3] (Table 1). Therefore, conventional methods are also useful for low-activity samples, particularly for model experiments.

EXPERIMENTAL

Apparatus

All atomic-absorption measurements were done with a Carl Zeiss (Jena) AA spectrometer, type AAS 1N, equipped with a Beckman ruthenium hollow-cathode lamp. The lamp current was 10 mA, and the slits were set to give 0.12 nm spectral bandwidth. The air–acetylene flame (5-cm triple-slot burner) was used as well as a nitrous oxide–acetylene flame (5-cm single-slot burner). The instrument allows single and triple beam-passage through the flame, and it was shown that for ruthenium both modes are suitable, with either flame. The spectrophotometric determinations were done in 1-cm cells with a Carl Zeiss Specord.

Reagents

The powdery ruthenium metal used was 97.65% pure according to mass spectrometric analysis, and contained also 1.38% Pt and 0.66% Ir. All other reagents were of analytical grade. For AAS a lanthanum buffer was prepared by dissolution of 56.4 g of $La(NO_3)_3 . 6H_2O$ in 670 ml of 12*M* hydrochloric acid and dilution to 1000 ml.

Preparation and standardization of Ru solutions

The ruthenium nitrosyl nitrate solutions were prepared as described by Gorski and Foersterling.[4] Ruthenium metal was oxidized in three stages to RuO_2, K_2RuO_4, and RuO_4, respectively, and the last was absorbed in NO-saturated nitric acid. The ruthenium nitrosyl nitrate stock solutions were adjusted to 8*M* nitric acid concentration and kept under nitrogen in the dark. Their Ru content was determined gravimetrically according to Heinig and Foersterling.[5] Aliquots were evaporated to dryness and the residue reduced to the metal with hydrogen at 300° or, in a double determination, transformed into RuO_2 at 350°, weighed, and then reduced to the metal.

Ruthenium(IV) hydroxychloride solution was prepared by distilling ruthenium tetroxide into 6*M* hydrochloric acid. The ruthenium content was determined after Banks and O'Laughlin[6] by pipetting 4-ml aliquots into porcelain boats, carefully evaporating to dryness in an oven at 110° and reducing the residue to the metal with hydrogen at 300°. The

Table 1. Specific activity of fission ruthenium arising from ^{103}Ru and ^{106}Ru, depending on intermediate storage time for the thermal neutron fission of ^{235}U (thermal neutron flux: 2.5×10^{13} n.cm^{-2}.sec^{-1}, irradiation time: 3 years)

Storage time	Specific activity (*GBq/g Ru*)	Fraction of stable Ru isotopes, %
3 days	1.80×10^{4}	97.3
1 year	9.80×10^{2}	99.2
4 years	1.22×10^{2}	99.9
10 years	1.97×10^{0}	100

Table 2. Composition of the synthetic Purex waste solution

Species	Concn., g/l.	Species	Concn., g/l.
Ru^{3+}	0.49	Cr^{3+}	0.04
Sr^{2+}	0.17	Ni^{2+}	0.02
Zr^{4+}	0.70	U^{6+}	0.04
Mo^{6+}	0.62	Al^{3+}	0.002
Rh^{3+}	0.11	Ce^{3+}	0.54
Ba^{2+}	0.39	La^{3+}	0.28
Na^{+}	0.78	Sm^{3+}	1.55
Rb^{+}	0.07	Nd^{3+}	
Cs^{+}	0.78	Eu^{3+}	
Fe^{3+}	0.20	Y^{3+}	
Pd^{2+}	0.32		

ruthenium content of the stock solution was 2.80 ± 0.08 mg/ml.

Potassium ruthenate solution was prepared by heating 10 mg of Ru metal, 150 mg of potassium hydroxide and 50 mg of sodium peroxide at 550–570° in a nickel crucible for 1 hr, with further addition of another 100 mg of sodium peroxide, then dissolving the cooled melt in warm water and diluting accurately to 100 ml. The completeness of reaction was tested by measuring the absorbance of the orange-red K_2RuO_4 at the 465-nm absorption maximum.

The synthetic Purex waste solution was prepared according to Suess.[7] Its composition (Table 2) corresponded to a burn-up of 35,000 MWd/t and a 5-year intermediate storage time.

RESULTS AND DISCUSSION

All publications on ruthenium determination by flame AAS show that it is characterized by serious interferences and instabilities in all types of flames. In an air–acetylene flame most interferences can be controlled by using a copper/cadmium buffer according to Rowston and Ottaway.[8] Scarborough[9] eliminated strong disturbances caused by Mo, Pd, and Rh, by means of a massive addition of uranium. Montford and Cribbs[10] were also successful with uranium addition (except for interference by Ti), and so were Mallett *et al.*,[11] who also proposed use of vanadyl chloride. Heinemann[12] gave optimum analytical conditions for AAS determination of noble metals with maximum precision, but did not consider matrix phenomena. El-Defrawy *et al.*[13] successfully used cyanide solutions, and Harrington and Bramstedt[14] used a titanium buffer. Schwab and Hembree[15] examined ruthenium determination in nitric acid solutions of nuclear fuels and controlled instabilities by mixing samples with an equal volume of a buffer consisting of 0.13*M* lanthanum nitrate in 8*M* hydrochloric acid.

Table 3. Ru signal (air 730 l./hr; Ru 81.7 μg/ml) in presence of Ce^{3+}

$[Ce^{3+}]$, μg/ml	0	350	524	1050
C_2H_2: 130 l./hr*	0.225	0.223	0.223	0.212
C_2H_2: 140 l./hr†	0.0854	0.0833	0.0814	0.0747
C_2H_2: 100 l./hr†	0.117	0.117	0.117	0.113

*Triple beam-passage.
†Single beam-passage.

Lanthanum offers considerable enhancement in sensitivity, compensating for the dilution effect. Kolonina *et al.*[16] used lanthanum at lower concentrations.

Interference study

Each of the fission elements in the Purex waste solution was tested for interference in the ruthenium determination. The ruthenium absorbance was measured with and without the addition of each element listed in Table 2, at a concentration three times that in an average Purex solution. An additional comparison was made between a synthetic Purex solution and a pure ruthenium solution with precisely the same Ru concentration. To bring them into the linear range of the ruthenium calibration curve, samples were fivefold diluted with 4*M* nitric acid and then mixed with an equal volume of the lanthanum buffer.

Under these conditions, with the nitrous oxide–acetylene flame, none of the fission products caused an effect exceeding the experimental error of ±2%. The same was true for the air–acetylene flame except for cerium, which caused a significant depression, the magnitude of which depended on the flame stoichiometry and number of beam-passages, and increased with cerium/ruthenium ratio (Table 3). Furthermore, at a fixed Ce/Ru ratio, the relative depression depended on the absolute concentrations (Table 4), and on the oxidation state of the cerium.

Ruthenium determination

The air–acetylene flame gives good sensitivity but there is interference from cerium; however, this effect, which in practice amounts to −1%, can be easily compensated by adding cerium to the calibration solutions. Use of the nitrous oxide–acetylene flame is free from interferences but gives lower sensitivity (by a factor of 2.5) and a poorer signal to noise ratio; there is also a tendency for the single-slot burner to become blocked, owing to the high salt content.

Table 4. Concentration-dependent Ru absorbance depression (25.6-fold Ce excess; air, 730 l./hr; C_2H_2, 130 l./hr; triple beam-passage)

[Ru], μg/ml	15.3	30.6	61.2	122.5	245
A (no Ce)	0.055	0.107	0.190	0.378	0.722
[Ce], μg/ml	393	786	1570	3140	6284
A (Ce^{3+})	0.054	0.105	0.170	0.338	0.599
	(−1.8%)	(−1.9%)	(−10.5%)	(−10.6%)	(−17.0%)
A (Ce^{4+})	0.056	0.102	0.184	0.360	
	(+1.8%)	(−4.7%)	(−3.2%)	(−4.8%)	

Table 5. Results of some ruthenium determinations in several solutions

Solution	Taken, μg/ml	Found, μg/ml	
		AAS	Spectrophotometry
Ru(IV) hydroxychloride	28.0	27.8	—
Potassium ruthenate	19.5	19.0	19.2
	29.3	28.6	28.3
	39.1	39.0	37.9
	48.8	49.7	47.8
	58.6	58.5	57.5
Synthetic Purex waste solution	492	494	—
	492	501	—
	492	491	—
	492	495	—
	492	497	—
	492	488	—

All the ruthenium nitrosyl nitrate test samples were 4*M* in nitric acid, with a ruthenium concentration of 30–70 μg/ml, and were mixed with the lanthanum buffer. For the triple beam-passage in the air–acetylene flame a characteristic concentration of 1.7 μg/ml (for 1% absorption) and a detection limit of 0.1 μg/ml were found; for the nitrous oxide–acetylene flame the values were 4.4 and 0.35 μg/ml, respectively. The air–acetylene flame should also be preferred because of the better precision (r.s.d. 1.5%). Some results are shown in Table 5.

The ruthenium calibration standards (4*M* nitric acid) stored in borosilicate glass were found to be stable for months even without protection by a nitrogen atmosphere. The analysis of ruthenium(IV) hydroxychloride in 6*M* hydrochloric acid gave excellent agreement with the theoretical values. Furthermore, the determination is also possible, starting from alkaline ruthenate instead of nitrosyl nitrate solutions. To avoid systematic errors, the samples must be made 4*M* in nitric acid before the lanthanum addition. The analyte should be pipetted into nitric acid to avoid precipitation of ruthenium dioxide by local neutralization, and then the buffer is added.

The identical results from ruthenium nitrosyl, ruthenium chloride and ruthenate compounds prove that the atomization process in the flame is not influenced by the unusually strong Ru–NO bond.

REFERENCES

1. A. A. Siczek and M. J. Steindler, *At. En. Rev.*, 1978, **16,** 575.
2. G. G. Eichholz, *Prog. Nuclear Energy*, 1978, **2,** 29.
3. M. Roesseler, *ZfI-Mitt.*, 1984, **86,** 5.
4. B. Gorski and H.-U. Foersterling, *Isotopenpraxis*, 1984, **6,** 201.
5. W. Heinig and H.-U. Foersterling, *3rd Conf. Nucl. Anal. Meth., Dresden*, 1983, p. 293.
6. C. V. Banks and J. W. O'Laughlin, *Anal. Chem.*, 1957, **29,** 1412.
7. M. Suess, *Thesis*, Academy of Sciences of GDR, Leipzig, 1983.
8. W. B. Rowston and J. M. Ottaway, *Anal. Lett.*, 1970, **3,** 411.
9. J. M. Scarborough, *Anal. Chem.*, 1969, **41,** 250.
10. B. Montford and S. C. Cribbs, *Anal. Chim. Acta*, 1971, **53,** 101.
11. R. C. Mallett, D. C. G. Pearton, E. J. Ring and T. W. Steele, *Talanta*, 1972, **19,** 181.
12. W. Heinemann, *Z. Anal. Chem.*, 1976, **280,** 127.
13. M. M. M. El-Defrawy, J. Posta and M. T. Beck, *Anal. Chim. Acta*, 1978, **102,** 185.
14. D. E. Harrington and W. R. Bramstedt, *Talanta*, 1975, **22,** 411.
15. M. R. Schwab and N. H. Hembree, *At. Abs. Newsl.*, 1971, **10,** 15.
16. L. N. Kolonina, W. W. Nedler, W. M. Khokhrin and O. A. Zhiraeva, *Zh. Analit. Khim.*, 1979, **34,** 2374.

Talanta, Vol. 32, No. 2, pp. 148–149, 1985
Printed in Great Britain

0039-9140/85 $3.00 + 0.00
Pergamon Press Ltd

AN EXTRACTIVE SPECTROPHOTOMETRIC METHOD FOR THE DETERMINATION OF TETRAMISOLE HYDROCHLORIDE IN PHARMACEUTICAL PREPARATIONS

R. T. SANE, D. S. SAPRE and V. G. NAYAK
Department of Chemistry, Ramnarain Ruia College, Matunga, Bombay 400019, India

(*Received* 5 *April* 1982. *Revised* 20 *July* 1984. *Accepted* 14 *September* 1984)

Summary—A simple extractive photometric method for the determination of tetramisole hydrochloride in pharmaceutical preparations is described. The method uses the formation of coloured complexes of the drug with reagents such as Solochrome Dark Blue, Solochrome Black T, Bromocresol Purple, Bromothymol Blue, Bromophenol Blue and Bromocresol Green in an acidic buffer. The ion-pair complexes formed are quantitatively extracted into chloroform under the experimental conditions.

Tetramisole hydrochloride is an anthelmintic drug with antidepressant activity. Holbrook and Scales[1] have determined it in animal tissue extract polarographically. Mourot *et al.*[2] have determined it by HPLC in the routine analysis of veterinary anthelmintics. In the present communication an extractive spectrophotometric method for its determination is described. The method is rapid and sensitive. It is based on our observation that tetramisole hydrochloride forms ion-pair complexes in acidic buffer with dyestuffs such as Solochrome Dark Blue (SDB), Solochrome Black T (SBT), Bromocresol Purple (BCP), Bromothymol Blue (BTB), Bromophenol Blue (BPB) and Bromocresol Green (BCG) and these complexes are quantitatively extracted into chloroform under the reaction conditions used.

EXPERIMENTAL

Reagents

The dyestuffs were used as 0.08% solutions of BCP, BTB, BPB and BCG, a 0.2% solution of SDB and a 0.1% solution of SBT, all in distilled water; 1 ml of 0.1*M* sodium hydroxide was added to the SBT solution before its final dilution.

Buffer solutions were prepared by dissolving 10–20 g of potassium hydrogen phthalate (accurately weighed) in 1000 ml of distilled water, to give a solution of pH 4.01, portions of which were then adjusted with dilute hydrochloric acid or sodium hydroxide solution to pH 2.0, 2.5, 2.8, 3.5, 4.0 and 6.0.

The purity of the tetramisole hydrochloride used was checked by non-aqueous titration and found to meet the normal criteria for purity. Standard tetramisole hydrochloride solution (100 μg/ml) was prepared by accurately weighing 25 mg of the drug, dissolving it in distilled water and diluting to volume in a 250-ml standard flask.

Analytical grade chloroform was used.

Determination of optimum reaction conditions

The optimum conditions were established by a series of preliminary experiments, the results of which are summarized in Fig. 1.

General procedure

In each of a series of 125-ml separating funnels place 5 ml of buffer solution (pH as indicated in Table 1) and 5 ml of dye solution. To each funnel add an appropriate volume of working standard solution for construction of a calibration graph. Add 10 ml of chloroform when the dye is BCP, BTB, BPB or BCG and 25 ml when it is SDB or SBT. Shake the funnels vigorously for 2 min, then let them stand for clear separation of the phases. Measure the absorbance of the organic phase at 420 nm when BCP, BTB, BPB and BCG are used and 520 nm for SDB and SBT, against a reagent blank similarly prepared. The calibration graphs are linear over the concentration ranges given in Table 1. The colour is stable for at least 2 hr.

Application to pharmaceutical preparations

Weigh ten tablets accurately and grind them. Weigh a portion of the thoroughly mixed powder equivalent to 25 mg of the drug, dissolve it in distilled water and dilute the solution to volume in a 250-ml standard flask after filtration.

Table 1. Results of analysis for tetramisole hydrochloride

Reagent	pH	λ_{max}, *nm*	Beer's law range, *μg/ml*	Molar absorptivity, $10^3 l.mole^{-1}.cm^{-1}$	Recovery, %	Coefficient of variation, %
Solochrome Dark Blue	4.0	520	2–14	15.7	98.6	1.2
Solochrome Black T	2.0	520	2–16	13.2	100.4	1.4
Bromocresol Purple	6.0	420	5–50	3.9	99.9	1.6
Bromothymol Blue	2.8	420	2.5–20	10.1	98.7	1.4
Bromophenol Blue	2.5	420	2.5–10	23.1	99.1	1.2
Bromocresol Green	3.5	420	2.5–12.5	18.3	99.5	2.1

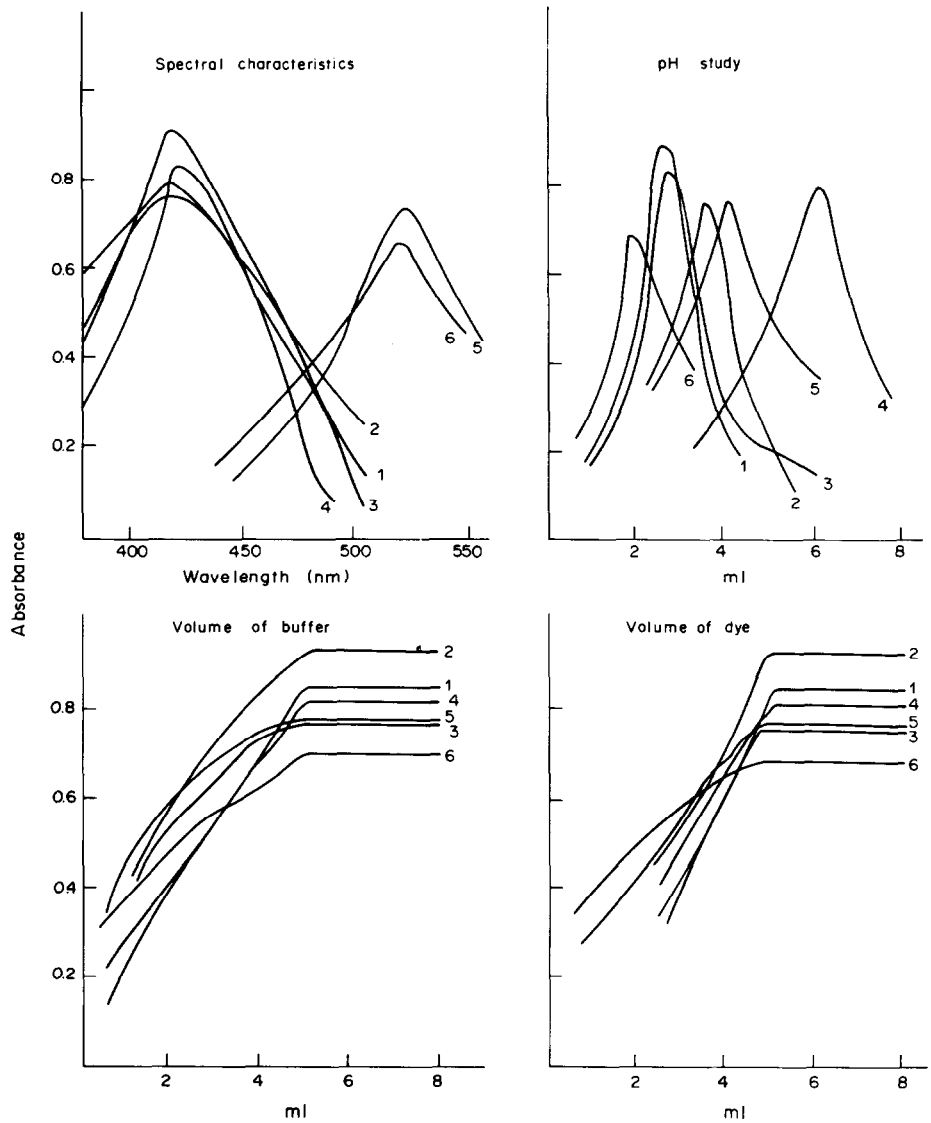

Fig. 1. Absorption spectra and optimization of conditions 1, BTB; 2 BPB; 3, BCG; 4, BCP; 5, SDB; 6, SBT.

Analyse the solution by the general procedure with an appropriate volume of sample solution.

Recovery

To study the precision and accuracy of the proposed method, a statistical study was made. Three series of fixed volumes of sample solution were taken and three different levels of standard drug solution were added, each level being repeated seven times. The total amount of the drug was determined by the proposed method. The recovery was calculated by regression analysis of the results.

A plot of the concentration of drug found against the concentration of drug added has an intercept which represents the concentration of the drug in the sample. Any deviation of the slope of the plot from unity indicates interference by a component of the pharmaceutical sample.

DISCUSSION

This is the first colorimetric method for the determination of tetramisole hydrochloride. It is simple, fast and sensitive and does not suffer interference from common excipients such as starch, talc, *etc.* There is no pharmacopoeial method described by the B.P., U.S.P. and I.P. for the determination of tetramisole hydrochloride in pharmaceutical formulations. The methods given in the literature[1,2] require mg quantities of the drug but the proposed method can be applied to a few hundred μg. The recoveries are between 98 and 100% and the coefficient of variation is 1–2% (Table 1). The proposed method can be successfully employed for the routine determination of tetramisole hydrochloride in pharmaceutical preparations.

Acknowledgements—The authors are grateful to Ethnor India Pvt. Ltd. for supply of the necessary reference standard and to Dr. V. G. Nayak for help and discussion.

REFERENCES

1. A. Holbrook and B. Scales, *Anal. Biochem.*, 1967, **18**, 46.
2. D. Mourot, B. Delepine, J. Boisseau and G. Gayot, *J. Pharm. Sci.*, 1979, **68**, 796.

Talanta, Vol. 32, No. 2, pp. 150–152, 1985
Printed in Great Britain.

0039-9140/85 $3.00 + 0.00

DETERMINATION OF NITRIC OXIDE BY BROMATE OXIDATION OF THE NITROSYL ETHYLENEDIAMINETETRA-ACETATOIRON(II) COMPLEX

SHUNICHI UCHIYAMA and GIICHI MUTO
Department of Environmental Engineering, Saitama Institute of Technology, 1690 Fusaiji, Okabe, Saitama, Japan

(*Received* 25 *August* 1982. *Revised* 16 *July* 1984. *Accepted* 14 *September* 1984)

Summary—A new spectrophotometric method for nitric oxide is proposed, based on formation of the nitrosyl-ethylenediaminetetra-acetatoiron(II) complex [Fe(II)NO–edta] by absorption of NO in Fe(II)edta solution and spectrophotometric determination of the NO_2^- produced by oxidation of the Fe(II)NO–edta complex by potassium bromate. The oxidation is easily performed completely and the absorption efficiency for 10.1–102.0 ppm NO (flow-rate, 100 ml/min) is nearly 100%. The detection limit is about 3 ppm for a sampling absorption time of 30 min.

Since the German patent was published in 1967,[1] it has been known that nitric oxide is effectively absorbed by a solution of the ethylenediaminetetra-acetatoiron(II) complex [Fe(II)edta] to form a nitrosyl-ethylenediaminetetra-acetatoiron(II) complex [Fe(II)NO–edta]. We have already proposed an indirect analytical method for NO in which the Fe(II)NO–edta complex is determined directly by spectrophotometry[2] and controlled potential coulometry[3] but the sensitivity is rather low and the absorption efficiency for low concentrations of NO was not examined.

We now report that the Fe(II)NO–edta complex can be oxidized by bromate to the Fe(III)edta complex and NO_2^-. This could form the basis for a more sensitive determination of the Fe(II)NO–edta complex and hence of NO by spectrophotometric determination of the NO_2^- produced by the oxidation. In the customary method,[4,5] nitric oxide has to be oxidized to NO_2 by oxidizing agents such as permanganate or ozone in a liquid–gas or a gas system, and the complete oxidation is rather difficult and time-consuming. Moreover, the "Saltzman factor" has to be used in calculating the amount of NO.

In contrast, in the method described here, the chemical conversion of the co-ordinated NO into NO_2^- is easily done in a liquid phase, and the Saltzman factor is not needed.

EXPERIMENTAL

Apparatus

A double-beam spectrophotometer (Hitachi Model 100-50) was used with 1-cm glass cells. The absorption system was made from two 200-ml Erlenmeyer flasks connected in series with Teflon tubing. A sintered-glass filter (porosity 3) and a gas flowmeter with needle valve were used to bubble NO through the absorbent at constant rate.

Reagents

Standard nitric oxide mixtures with nitrogen (10.1, 30.4, 70.2 and 102.0 ppm concentration) were obtained from Nihon Sanso.

The Saltzman colour-forming solution was that described by Fisher and Becknell.[5] All chemicals used were reagent grade.

Procedure

The appropriate weights of ferrous ammonium sulphate and ethylenediaminetetra-acetic acid needed to give 200 ml of a 0.01*M* solution of the complex were dissolved in 1*M* acetic acid–sodium acetate buffer (pH 4.0) purged with nitrogen. Then 1.00 ml of 2×10^{-3}–$2 \times 10^{-2}M$ sodium nitrite was added to this solution to give an Fe(II)NO–edta solution of concentration 1×10^{-5}–$1 \times 10^{-4}M$ by means of the reactions.

$$NO_2^- + \text{Fe(II)edta} + 2H^+ \rightarrow \text{Fe(III)edta} + NO + H_2O$$

$$NO + \text{Fe(II)edta} \rightarrow \text{Fe(II)NO–edta}$$

A 10-ml portion of this solution was treated with 4 ml of 0.01*M* potassium bromate for 5 min, the Fe(III)edta complex and NO_2^- being produced. Finally, 1 ml of this oxidized solution was reacted with 6 ml of Saltzman solution for 15 min, and the absorption spectrum was measured with a double-beam spectrophotometer. A calibration graph relating absorbance to amount of Fe(II)NO–edta complex, and hence of NO, was prepared.

To determine the absorption efficiency for NO, a standard gas mixture containing NO was bubbled into Fe(II)edta solution in the absorption system. The NO complex formed was oxidized, the colour reaction applied and the absorption efficiency calculated.

To investigate analysis of an NO and NO_2 mixture, a Teflon three-way stopcock was used to mix a gas containing 100 ppm of NO_2 (flowing at 40 ml/min) with the standard NO mixtures (flowing at 100 ml/min) to give a total flow-rate of 140 ml/min. The mixture of gases was bubbled first through Saltzman solution and then through Fe(II)edta solution, contained in absorption flasks connected in series. After the absorption, the Saltzman solution was diluted tenfold with additional Saltzman solution and the absorbance of this diluted solution was measured. The NO complex formed in the second flask was measured by the oxidation procedure already described.

RESULTS AND DISCUSSION

Oxidation and colour formation of the NO complex

The absorption spectra of $1 \times 10^{-3}M$ Fe(II)NO–edta complex (——) and of the solution

oxidized by bromate (---) are shown in Fig. 1. This result shows that the NO complex has two absorption peaks, at about 440 and 620 nm; a similar result has been reported by Ogura and Ozeki.[6] The oxidation destroys the NO complex completely, and only the spectrum of the Fe(III)edta complex is observed.

The absorption spectra of $5 \times 10^{-5}M$ NO complex solution and of the solution obtained by oxidation and reaction with Saltzman solution are shown in Fig. 2. The two peaks in the NO-complex spectrum could not be detected in this concentration range. The absorption spectrum of the coloured product has a maximum at 545 nm, in fair agreement with that obtained in the conventional Saltzman method. The molar absorptivity of this peak is about 100 times that of the NO complex at 620 nm, so the oxidative method is much more sensitive than direct spectrophotometric determination of the NO complex.

The effect of the volume of Saltzman solution added is shown in Fig. 3. Initially, the absorbance increases with amount of Saltzman solution, but then decreases with larger volumes because of dilution. The largest absorbance was obtained when 2 ml of Saltzman solution were added to 1 ml of oxidized solution, but the azo-dye was unstable if the total volume was less than 5 ml, so we chose to add 6 ml of Saltzman solution.

The stability of the absorbance (at 545 nm) as a function of bromate concentration used is shown in Fig. 4, for $0.01M$ Fe(II)edta concentration. When $0.01M$ bromate was used, the absorbance became constant within about 12 min, and was stable for a further 30 min, so this concentration was selected for use.

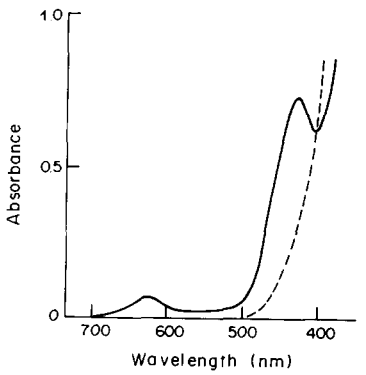

Fig. 1. Absorption spectra of $1 \times 10^{-3}M$ Fe(II)NO–edta complex solution (——) and the oxidized solution (---).

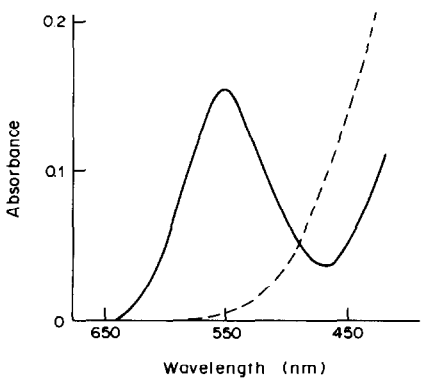

Fig. 2. Absorption spectra of $5 \times 10^{-5}M$ Fe(II)NO–edta complex solution (---) and the oxidized solution after colour development (——).

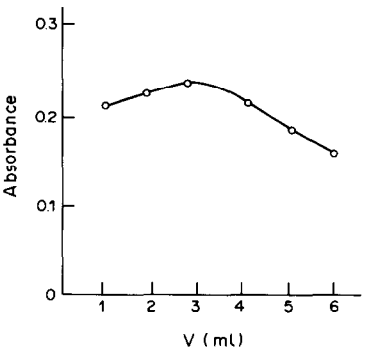

Fig. 3. Effect of the volume of added Saltzman solution on the absorbance of the coloured product from $5 \times 10^{-5}M$ Fe(II)NO–edta complex solution.

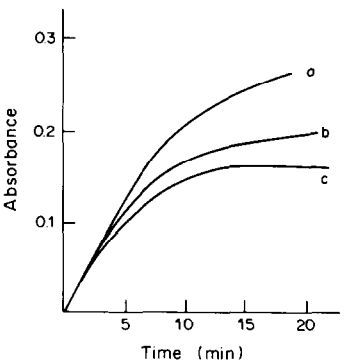

Fig. 4. Time-dependence of the absorbance of the coloured product from $5 \times 10^{-5}M$ Fe(II)NO–edta complex solution (at 545 nm) as a function of $KBrO_3$ concentration. [$KBrO_3$]: a, $0.1M$; b, $0.05M$; c, $0.01M$.

NO absorption

The calibration graph for the NO complex was linear over the Fe(II)NO–edta concentration range from 1×10^{-5} to $1 \times 10^{-4}M$, and was used to calculate the absorption efficiency for NO. The slope of this calibration curve was 35% lower than that in the conventional Saltzman method,[7] which suggests that the NO co-ordinated in the complex is oxidized to some other species besides NO_2^-, so the anion species obtained were determined by ion chromatography.[8] It was found that there was 65% conversion of NO into NO_2^- and 35% into NO_3^-, which accounts for the lower slope.

The effect of the concentration of Fe(II)edta complex is shown in Fig. 5. The absorbance becomes maximal and constant with an Fe(II)edta concentration above about $0.005M$.

Table 1 shows that NO was absorbed in the first absorption flask with 100% efficiency. The solution in the second absorption flask gave zero absorbance,

Table 1. Efficiency of absorption of NO by 0.01*M* Fe(II)edta during passage of 3 litres of sample gas at 100 ml/min

Concentration of NO gas, *ppm*	Absorbance	Absorption efficiency*, %	Coeff. of variation, %
10.1	0.024	100	4.3
30.4	0.073	100	4.0
70.2	0.166	99.4	1.3
102.0	0.243	99.6	3.1

*Mean of five results

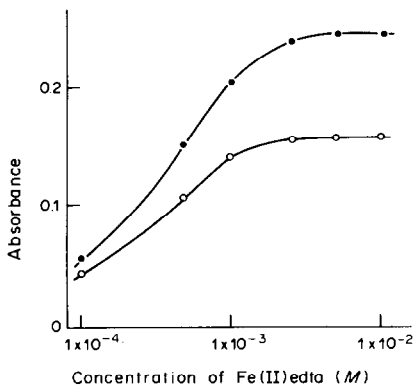

Fig. 5. Effect of the Fe(II)edta concentration in the absorbent, on the absorbance obtained: [NO] ●—102.0 ppm, ○—70.2 ppm; flow-rate, 100 ml/min.

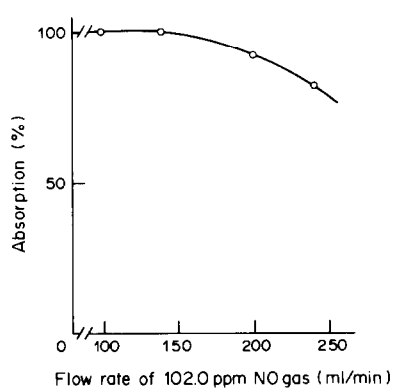

Fig. 6. Effect of sample flow-rate (102.0 ppm NO) on absorption efficiency.

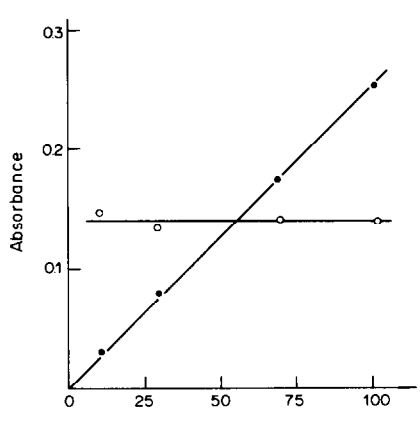

Fig. 7. Separative determination of NO and NO_2 in a mixture. ● NO (flow-rate 100 ml/min); ○ NO_2 (100 ppm, flow-rate 40 ml/min).

the second absorption flask gave zero absorbance, confirming complete absorption of NO in the first flask.

The effect of flow-rate on the absorption efficiency at the 102-ppm NO level is shown in Fig. 6. Absorption is complete if the flow-rate does not exceed about 130 ml/min.

From these results, it is seen that the method has the merits that NO can be completely absorbed and reproducibly (though not completely) oxidized to NO_2^-. The detection limit of the method is about 3 ppm for a sample size of about 3 litres of air; the analysis takes about an hour, half of this time being needed for sampling. No "Saltzman" type conversion factor is needed, since the fractional conversion of NO into NO_2^- is compensated for in the calibration procedure.

Nitrogen dioxide is also absorbed by the Fe(II)edta solution to form the Fe(II)NO–edta complex and NO_3^- in weakly acidic media,[9,10] so NO_2 might be expected to interfere in the determination of NO. However, NO_2 can be removed from its mixture with NO by selective absorption with Saltzman solution, and the NO then absorbed in Fe(II)edta solution. A series of mixtures of a fixed level of NO_2 and various concentrations of NO was analysed in this way, and gave the results shown in Fig. 7. The NO_2 gave practically constant absorbance on reaction with the Saltzman solution in the first flask, and the correct values were found for the NO collected in the second flask. Thus both oxides can be determined in the same sample.

Acknowledgements—We thank Mr. M. Komiya and Miss F. Takenouchi for their experimental assistance.

REFERENCES

1. *German Patent*, No. 1251900, 1967.
2. S. Uchiyama, K. Nozaki and G. Muto, *Bunseki Kagaku*, 1977, **26**, 219.
3. *Idem*, *ibid.*, 1977, **26**, 224.
4. B. E. Saltzman, *U.S. Pub. Health Rept.*, 999-AP-11, PC1-C7.
5. G. E. Fisher and D. E. Becknell, *Anal. Chem.*, 1972, **44**, 863.
6. K. Ogura and T. Ozeki, *J. Inorg. Nucl. Chem.*, 1981, **26**, 877.
7. B. E. Saltzman, *Anal. Chem.*, 1954, **26**, 1949.
8. H. Small, T. S. Stevens and W. C. Bauman, *ibid.*, 1975, **47**, 1801.
9. S. Uchiyama and G. Muto, *Bunseki Kagaku*, 1981, **30**, 251.
10. O. Hamamoto, S. Uchiyama, K. Nozaki and G. Muto, *ibid.*, 1979, **28**, 118.

Talanta, Vol. 32, No. 2, pp. 153–154, 1985
Printed in Great Britain

0039-9140/85 $3.00 + 0.00
Pergamon Press Ltd

COMPLEXOMETRIC DETERMINATION OF CITRIC ACID WITH COPPER

E. SZEKELY
Institute for Chemistry & Chemical Technology, The Institutes for Applied Research, Ben-Gurion University of the Negev, P.O. Box 1025, Beer-Sheva 84110, Israel

(*Received* 13 *April* 1984. *Revised* 14 *June* 1984. *Accepted* 14 *September* 1984)

Summary—A method is presented in which citrate is determined by complexation with excess of copper(II), followed by back-titration with EDTA. Small amounts of citrate can be determined by this method in the presence of large amounts of most organic acids present in natural products. Interfering reductants are removed by treatment with permanganate, amino-acids with nitrous acid, and metal ions with a cation-exchange resin. The indicator used for end-point detection is Szechromotrope, 4,4′-sulphonyl-bis(azobenzene) dichromotropic acid.

The use of 4,4′-sulphonyl-bis(azobenzene) dichromotropic acid as a metallochromic indicator for colorimetric and complexometric determination of small amounts of copper(II) was reported earlier.[1] This paper presents a method in which this indicator is used in the determination of citrate by addition of excess of copper(II) and back-titration with EDTA. Citric acid can be determined by this method with high precision in the presence of other acids if interfering amino-acids are removed by treatment with nitrous acid, reductants by treatment with permanganate, and metal ions by treatment with a cation-exchange resin.

The use of copper(II) for complexation and determination of citric acid has been reported before,[2–8] but our method has advantages of simplicity and reliability, can be performed without expensive instruments, and can also be used for micro-amounts of citrate.

The indicator was synthesized in our laboratory by diazotizing 4,4′-sulphonyldianiline and coupling it with chromotropic acid. It has been recommended as a reagent for the colorimetric determination of boron.[9] The indicator ($C_{32}H_{18}N_4O_{18}Na_4$) is a brownish-red powder, easily soluble in water to give a pink solution with molar absorptivity 5.8×10^4 $l.mole^{-1}.cm^{-1}$ at $\lambda_{max} = 538$ nm. A blue copper complex forms instantly at pH 6.8–7.6 (molar absorptivity 4.2×10^4 $l.mole^{-1}.cm^{-1}$ at $\lambda_{max} = 384$ nm). Aqueous solutions of the reagent and its complexes are stable. No blue colour develops with other uni-, bi- or tervalent metal ions. The reagent is commercially available under the trade name Szechromotrope, from Gammatest Ltd, Ben-Gurion University of the Negev, Beer-Sheva 84110, Israel.

EXPERIMENTAL

Reagents

Aqueous indicator solution, 0.1%.

Copper sulphate solution, 0.01M, *standardized by EDTA titration.*

Standard 0.01*M and* 0.001*M EDTA.*

Buffer solution. Ammonium chloride (1*M*)/sodium acetate (1*M*), adjusted to pH 7.5 with dilute ammonia solution or hydrochloric acid.

Tetra-amminocuprate(II) solution. Prepared by mixing 10 ml of 0.01*M* copper sulphate with 40 ml of the buffer.

Procedures

Detection and estimation. Transfer about 5 ml of water into a small flask or large test-tube, add 0.25 ml (5 drops) of amminocuprate solution and 1 drop of indicator solution and mix. Add nearly neutral sample solution slowly from a graduated pipette, continuously shaking the vessel until the colour changes from blue to violet, which corresponds to the presence of about 0.1 mg of citric acid in the volume of sample solution added. A colour change to pink indicates the presence of larger amounts of citric acid. Repeat the estimation with a more dilute sample solution if a colour change is observed after addition of only a few drops of sample. Interfering substances must be removed beforehand.

Determinations. (A) Transfer an amount of sample solution containing 1–8 mg of citric acid into an Erlenmeyer flask and dilute it to about 100 ml. Add exactly 5 ml of 0.01*M* copper sulphate, 2 drops of indicator solution, and if necessary 0.1*M* ammonia or hydrochloric acid until the colour turns blue (pH 6.8–7.6). Add 5 ml of buffer solution and titrate the excess of copper with 0.01*M* EDTA until the colour changes to pink.

(B) Transfer an aliquot of sample solution containing 0.2–3 mg of citric acid into an Erlenmeyer flask and dilute it to about 50 ml. Add exactly 2 ml of 0.01*M* copper sulphate, 1 drop of indicator solution, and if necessary 0.1*M* ammonia or hydrochloric acid until the colour becomes blue (pH 6.7–7.6). Add 2 ml of buffer solution and titrate the excess of copper with 0.001*M* EDTA until the colour changes to violet, then slowly until it becomes pink.

RESULTS AND DISCUSSION

Interferences

Only a few of the organic acids present in natural products interfere in the detection, estimation and determination of citrate ions by the procedures above. Up to 1000 ppm of tartaric, succinic, malic, hydroxyacetic, lactic, salicylic and quinic acids have no influence on the precision, nor do phosphoric or

nitric acids or univalent metal ions. Determinations performed in the presence of up to 5 g of glucose and up to 20 ml of ethanol in 100 ml of sample solution showed no bias. Interference by reducing acids such as ascorbic, oxalic, fumaric and sulphurous was prevented by the addition of 0.1*N* permanganate. Metal ions were removed by treatment with a cation-exchange resin. Interference from amino-acids was eliminated by addition of sodium or potassium nitrite to acidified solutions.

The reliability and precision were determined by repeated analysis. An accurately prepared 20-mg/ml citric acid stock solution was prepared with anhydrous citric acid dried at 110° to constant weight; a 10-ml aliquot of this solution was diluted, neutralized and made up to 200 ml: 1 ml ≡ 1 mg of citric acid. Various mixtures were also analysed.

Sample I. A 5-ml aliquot of the 1-mg/ml solution was diluted to about 100 ml and analysed by procedure (A). In 5 determinations an average of 2.40 ml of EDTA solution was used for titration of the excess of copper, with a maximum deviation of ±0.02 ml (0.8%). The amount of citric acid was calculated from citric acid = $(5 - a) \times 1.92$ mg where a = ml of 0.01*M* EDTA used (found: 4.99 mg).

A 5-ml aliquot of the 1-mg/ml solution was diluted accurately to 100 ml and a 10-ml portion of this solution was titrated with 0.001*M* EDTA by procedure (B). In 5 determinations an average of 17.40 ml of EDTA was used, with a maximal deviation of ±0.1 ml (0.6%). The amount of citric acid was calculated from citric acid = $(20 - a) \times 0.192$ mg = 0.499 mg.

Sample II. Citric acid, 0.02 g; malic acid, 0.50 g; tartaric acid, 1.00 g; glucose 10.0 g; ethanol, 20 ml; water to 100 ml. Samples of 10, 25, and 50 ml were taken. The 10-ml sample was diluted to about 50 ml, treated by procedure B, and titrated with 0.001*M* EDTA (14.9 ml). Citric acid found = 0.98 mg. The 25- and 50-ml samples were diluted to about 100 ml and titrated with 0.01*M* EDTA. Citric acid found = 2.53 mg (25-ml sample) and 4.90 mg (50 ml).

Sample III. Citric acid, 0.05 g; calcium chloride, 1.0 g; magnesium chloride, 0.50 g; urea, 5.0 g; water to 100 ml. A 50-ml portion was treated with Amberlite IR 120 cation-exchange resin, neutralized, and diluted to 100 ml. Three aliquots (25 ml each) were diluted to about 100 ml, treated by procedure A and titrated with 0.01*M* EDTA (1.76, 1.80 and 1.78 ml). Citric acid found = 6.18 mg, corresponding to 49.4 mg in 100 ml of sample III.

Sample IV. Citric acid, 0.50 g; ascorbic acid, 0.25 g; oxalic acid, 0.05 g; water to 100 ml. Ten ml were diluted to about 50 ml and 1 ml of 0.1*N* hydrochloric acid was added, and then 0.1*N* permanganate (dropwise). The excess of permanganate was removed by adding 1 drop of 0.1*N* thiosulphate. The solution was then treated with the cation-exchange resin, neutralized, and diluted to about 100 ml, treated by procedure A, and titrated with 0.01*M* EDTA (2.40, 2.42 and 2.42 ml). Citric acid found = 4.79 mg, corresponding to 0.479 g in sample IV.

Sample V. Citric acid, 0.50 g; lactic acid, 5.0 g; glutamic acid, 1.0 g; water to 100 m. To 25 ml of this solution 5 ml of concentrated hydrochloric acid and 0.5 g of sodium nitrite were added. The solution was mixed and heated to about 70° until no more gas was evolved. The neutralized solution was diluted to 100 ml. Three 5-ml aliquots of the sample solution were diluted to about 100 ml, treated by procedure A, and titrated with 0.01*M* EDTA (1.74, 1.72 and 1.74 ml). Citric acid found = 6.28 mg, corresponding to 0.502 g in sample V.

Though there are several indicators for complexometric determination of copper(II)[10] which can also be used in our method, the indicator recommended has several advantages. Murexide, though widely used, is less stable, the colour change from yellow to violet is less sensitive, and it is more difficult to maintain the desired pH. The nitrosochromotropic acid indicator[11,12] gives a colour change comparable to that of our indicator, but its solution, which has to be freshly prepared for each assay, is less stable. Also, two different pH ranges were recommended by the authors (pH 7.25–8.80 and 5.8–6.5), without explanation.

REFERENCES

1. E. Szekely, M. Flitman and M. Leon, *Proc. Israel Chem. Soc., 42nd Meeting*, 1972, 94.
2. G. Graffman, H. Domels and M. L. Strater, *Fetten, Seifen, Anstrich.*, 1974, **76,** 218.
3. M. Hamon, A. Hoppendt and M. Guernet, *Ann. Pharm. Franc.*, 1972, **30,** 595.
4. M. F. El-Taras and E. Pungor, *Anal. Chim. Acta*, 1976, **82,** 285.
5. A. Olin and B. Wallen, *ibid.*, 1983, **151,** 65.
6. A. Pierre and S. Braley, *Lait*, 1983, **63,** 623.
7. H. L. Nours, J. F. Le Meur and C. Bourgeois, *Sci. Aliments*, 1982, **2,** 483.
8. M. T. M. Zaki and R. Alquasmi, *Z. Anal. Chem.*, 1981, **306,** 400.
9. E. Szekely, *Proc. Annual Meeting Israel Chem. Soc.*, 41st Meeting, 1971, 13.
10. S. Schwarzenbach and H. Flaschka, *Complexometric Titrations*, 2nd Ed., Methuen, London, 1969.
11. C. S. Panda and T. S. Srivastava, *Z. Anal. Chem.*, 1962, **184,** 248.
12. A. B. Sen and T. S. Srivastava, *ibid.*, 1962, **187,** 401.

Talanta, Vol. 32, No. 2, pp. 155–157, 1985
Printed in Great Britain

0039-9140/85 $3.00 + 0.00
Pergamon Press Ltd

REVERSED-PHASE EXTRACTION CHROMATOGRAPHY OF GERMANIUM(IV) WITH TRIBUTYL PHOSPHATE ON SILICA GEL

S. N. BHOSALE and S. M. KHOPKAR
Department of Chemistry, Indian Institute of Technology, Powai, Bombay 400076, India

(*Received* 25 *April* 1984. *Accepted* 14 *September* 1984)

Summary—Germanium(IV) can be separated by reversed-phase extraction chromatography with TBP as stationary phase on a column of silica gel, with 6*M* hydrochloric acid as the mobile phase, and stripped with various eluents. Germanium can thus be separated (by selective extraction) from those elements which are not extractable with TBP, and (by selective stripping) from elements that *are* extractable.

Reversed-phase extraction chromatography offers a promising separation of germanium at tracer concentration from associated elements. Trioctylamine has been used as the stationary phase ("Corvic" as support) for separation of germanium from arsenic, indium, manganese, cobalt, copper and zinc.[1] Here we describe the use of tributyl phosphate as the stationary phase (on silica gel) for separation of germanium from iron, gallium, antimony and lead.

EXPERIMENTAL

Reagents

Stock germanium solution was prepared by fusing 1.27 g of pure germanium dioxide with an equal amount of sodium hydroxide in a platinum crucible, cooling, extracting with water, neutralizing, and diluting to 250 ml with water, standardized gravimetrically,[2] and diluted appropriately as required.

Gum arabic solution was prepared by dissolving 0.5 g of the powder in 50 ml of hot water.

Phenylfluorone solution was prepared by dissolving 0.03 g in 50 ml of ethanol and 5 ml of sulphuric acid (1 + 6).

Silica gel was rendered hydrophobic and coated with tributyl phosphate (TBP) as described earlier,[3] and a 2–3 g portion of the coated gel was slurried with 25 ml of distilled water and used to make a 6 × 0.8 cm column. The column was washed with 6*M* hydrochloric acid, pre-equilibrated with TBP.

RESULTS AND DISCUSSION

Germanium can be quantitatively extracted with 25% TBP in toluene from 3*M* hydrochloric acid containing 2*M* magnesium chloride as salting-out agent[4] and with pure TBP from 1.5*M* hydrochloric acid only in the presence of salting-out agent, but for the present extraction chromatographic study salting-out agents were not used. The retention of germanium on the column was measured for various concentrations of hydrochloric acid (1–6*M*) in the eluent. The retention increased with acid concentration, maximum extraction occurring from 5–6*M* hydrochloric acid. The degree of extraction was found to depend on the flow-rate of the mobile phase. Experiments with 4, 5 and 6*M* hydrochloric acid and flow-rates of 0.5, 1.0 and 2.0 ml/min showed that germanium was quantitatively retained from the 6*M* acid at a flow-rate of 0.5 ml/min (Fig. 1). The maximum uptake of germanium was also found to depend on the flow-rate (Table 1).

A portion of solution containing 64 μg of germanium was made 6*M* in hydrochloric acid and passed through the column at a flow-rate of 0.5 ml/min, then the germanium was stripped with an eluent, ten 2-ml fractions being collected and analysed spectrophotometrically with phenylfluorone,[5] with measurement at 510 nm. Hydrochloric acid

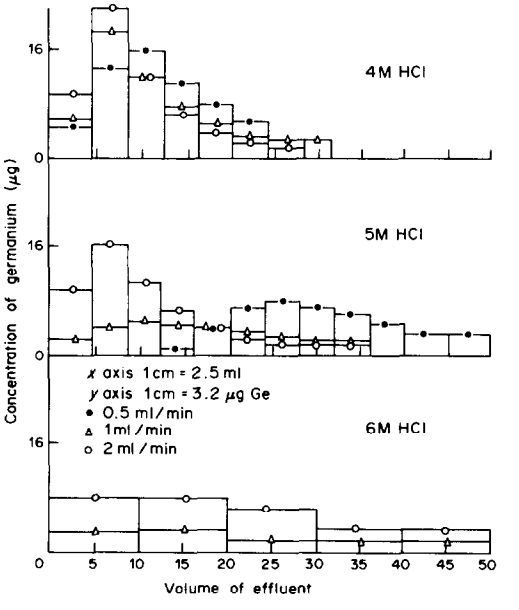

Fig. 1. Effect of flow-rate and eluent concentration on retention of Ge.

Table 1. Effect of flow-rate on column capacity (mobile phase 6*M* HCl)

Flow-rate, *ml/min*	Column capacity, *mg/g*
0.2	2.41
0.5	1.25
0.7	0.71
1.0	0.30

(0.001–3*M*), nitric acid (0.5–2*M*), sulphuric acid (0.5–2*M*), lithium chloride (0.2–1*M*) and water all gave quantitative elution (Table 2).

Separation of germanium from mixtures

Ions which are not extracted from 6*M* hydrochloric acid by TBP will pass through the column unsorbed, and germanium can be separated from them by retention on the column and then elution with 0.001*M* hydrochloric acid. Germanium can thus be separated from alkali and alkaline-earth metals, aluminium, yttrium, zirconium, vanadium(IV), chromium(III), manganese(II), cobalt, nickel, copper(II), zinc, bismuth and lead, by this technique, with 99.4–100% recovery.

Germanium can be separated from elements extractable by TBP from 6*M* hydrochloric acid by exploiting the differences in distribution coefficient at various concentrations of hydrochloric acid. Thus germanium can be separated from a mixture with thallium(III), chromium(VI) or mercury(II), by making the mixture 1*M* in hydrochloric acid before passing it through the column, where germanium is unextracted whereas the other species are retained and can subsequently be eluted with 0.1*M* hydrochloric acid containing 4% thiourea. Similarly germanium can be separated from gallium, iron(III), indium or antimony(III) by using 4*M* hydrochloric acid medium, the germanium again passing through.

Table 2. Elution of Ge(IV) (64 μg)

Eluent	Concentration, M	Peak elution volume, *ml*	Total volume, *ml*	Recovery, %
HCl	0.001	2	12	100.5
	0.5	2	15	100.2
	1.0	4	15	100.0
	2.0	4	30	100.1
	3.0	8	30	99.4
HNO_3	0.5	2	15	99.9
	1.0	4	15	99.6
	1.5	6	30	100.2
	2.0	6	30	100.2
H_2SO_4	0.5	2	16	99.8
	1.0	4	16	100.2
	1.5	4	16	100.1
	2.0	6	20	100.2
LiCl	0.2	2	12	100.2
	0.4	2	14	100.1
	0.6	4	16	101.1
	1.0	4	16	100.3
Water	—	2	10	100.1

Table 3. Separation of Ge(IV) from multicomponent mixtures

Mixture	Taken, μg	Found, μg	Bed height, *cm*	Flow-rate, *ml/min*	Eluent [HCl], M
Ge(IV)	64.3	64	6	1	3
Fe(III)	100.1	100			1
Cr(VI)	200.3	200			0.001
Ni/Bi	300.8	301	4	0.5	6
Ge(IV)	128.7	129			1
Cr(VI)	400.6	401			0.001
Co/Cr(III)	200.3	200	4	0.5	6
Ge(IV)	128.7	129			3
Fe(III)	510.3	511			0.5
V(IV)	300.6	301	4	0.5	5
Ge(IV)	64.3	64			2
Fe(III)	510.3	511			0.5
Al	70.3	70	5	0.5	6
Ge(IV)	64.3	64			3
Fe(III)	100.1	100			1
Cr(VI)	200.3	201			0.001

Separation from multicomponent mixtures

When a mixture of germanium, iron(III) and chromium(VI) in 3*M* hydrochloric acid is passed through the column, germanium comes out first, with no extraction. Iron(III) can then be eluted with 1*M* hydrochloric acid and finally chromium(VI) with 0.001*M* hydrochloric acid.

When a mixture of germanium with cobalt, chromium(III) and iron(III) in 6*M* hydrochloric acid is passed through the column, the cobalt or chromium(III) will pass through. Germanium can then be eluted with 3*M* hydrochloric acid, followed by elution of iron(III) with 0.5 or 1*M* hydrochloric acid.

These separation schemes can obviously be extended to cover mixtures of germanium with both the extractable and non-extractable groups of ions. Some results for analysis of some typical mixtures are shown in Table 3. The elements were determined either titrimetrically[6] or spectrophotometrically[5].

The separation of germanium from copper, zinc, gallium, lead and antimony is important as they are associated with it in various minerals. The proposed method is simple, rapid and selective. The total time required for separation and determination is just 3 hr. The results are reproducible within $\pm 1.1\%$. However, it was found impossible to separate germanium from cadmium (which is also associated with it in minerals).

Acknowledgement—We are thankful to the Council of Scientific and Industrial Research, New Delhi, India, for awarding a Senior Research Fellowship to one of the authors (S.N.B.).

REFERENCES

1. T. B. Pierce and W. M. Henry, *J. Chromatog.*, 1966, **23,** 457.
2. A. I. Vogel, *A Text Book of Quantitative Inorganic Analysis*, p. 653, Longmans, London, 1969.
3. S. N. Bhosale and S. M. Khopkar, *Talanta*, 1979, **26,** 889.
4. S. Kalyanraman and S. M. Khopkar, *Indian J. Chem.*, 1977, **15A,** 1031.
5. E. B. Sandell, *Colorimetric Determination of Trace Metals*, 3rd Ed., p. 489. Interscience, New York, 1959.
6. F. J. Welcher, *The Analytical Uses of Ethylenediamine Tetraacetic Acid*, Van Nostrand Reinhold, London, 1957.

Talanta, Vol. 32, No. 2, pp. 159–165, 1985
Printed in Great Britain.

0039-9140/85 $3.00 + 0.00

ANALYTICAL DATA

STUDIES ON FLUORESCEIN—II*

THE SOLUBILITY AND ACID DISSOCIATION CONSTANTS OF FLUORESCEIN IN WATER SOLUTION

HARVEY DIEHL and RICHARD MARKUSZEWSKI†
Department of Chemistry, Iowa State University, Ames, Iowa, 50011, U.S.A.

(*Received* 4 *April* 1984. *Accepted* 14 *September* 1984)

Summary—The solubility of yellow fluorescein and of red fluorescein as a function of pH has been measured in water at ionic strength 0.10. The pH of minimum solubility is the same for both, 3.28. The intrinsic solubility, defined as the solubility of the undissociated species, H_2Fl, and assumed to be constant and independent of pH, was calculated from the observed solubilities on the low-pH side of the minimum: $S_{i,yellow} = 3.80 \times 10^{-4} M$: $S_{i,red} = 1.45 \times 10^{-4} M$. The first dissociation constants were evaluated from the intrinsic solubilities and the observed solubilities on the low-pH side: both fluoresceins yielded the same value, $pK_{H_3Fl} = 2.13$. In using the observed solubilities on the high-pH side of the minimum to evaluate the intrinsic solubility and the second dissociation constant it was necessary to modify the existing theoretical approach by taking into account the presence of the fully dissociated anion. Appropriate mathematical treatments were devised to handle the more complex equations. Both fluoresceins yielded the same value for the second dissociation constant, $pK_{H_2Fl} = 4.44$. Both fluoresceins give the same yellow colour in saturated solution and the results just reported for the pH of minimum solubility and for the dissociation constants also indicate that for each of the three prototropic forms of fluorescein present in solution, H_3Fl^+, H_2Fl, and HFl^-, only one structure exists.

During 1980 we advanced structures for the three solid forms of fluorescein,[1] *viz.* for the colourless solid the lactone structure (**I**), for the red solid the *p*-quinonoid structure (**III**), and for the yellow solid a zwitterion structure with a positive charge distributed over the oxygen-bearing ring (**II**). We have now measured the solubilities of the yellow and red solids

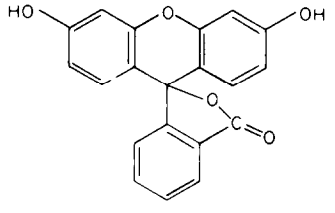

I Lactone structure, colourless form

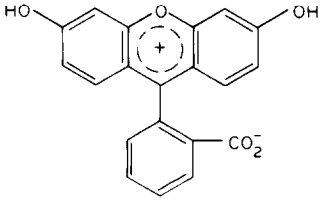

II Zwitterion structure, yellow form

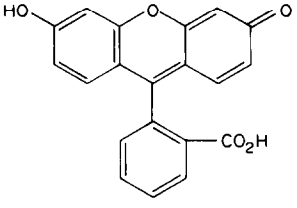

III *p*-Quinonoid structure, red form

as functions of pH. As pointed out in the earlier paper, the colourless lactone solid exists in solution only in dry organic non-polar solvents such as dioxan and, on contact with water, changes quickly to the yellow zwitterion form; it therefore plays no part in the present discussion.

Fluorescein is characterized by three acid dissociation constants. For clarity, and to emphasize the amphoteric nature of fluorescein, we have adopted the designation H_2Fl for fluorescein (the "free acid") and for the respective dissociation constants the symbols:

Reaction	*Constant*	
$H_3Fl^+ = H^+ + H_2Fl$	$K_{H_3Fl} = [H^+][H_2Fl]/[H_3Fl^+]$	(1)
$H_2Fl = H^+ + HFl^-$	$K_{H_2Fl} = [H^+][HFl^-]/[H_2Fl]$	(2)
$HFl^- = H^+ + Fl^{2-}$	$K_{HFl} = [H^+][Fl^{2-}]/[HFl^-]$	(3)

We have determined the first two of the three acid dissociation constants from data on the solubilities as a function of pH, for both the yellow and red solids, by a modification of the procedure of Krebs and Speakman.[2] The concentration of fluorescein in the various saturated solutions was determined by mea-

*Part I—*Talanta*, 1980, **27**, 937.
†Present address: Ames Laboratory, Iowa State University, Ames, Iowa 50011, U.S.A.

suring the fluorescence of an aliquot brought to pH 11.

As in the earlier paper, we worked with fluorescein prepared from diacetylfluorescein and verified the purity of the materials by titration with alkali; we thus avoided certain faults which adversely affected certain earlier studies.

EXPERIMENTAL

Materials

Diacetylfluorescein, yellow fluorescein and red fluorescein were prepared as described earlier.[1]

Buffers with pH-values in the range 1–6 were prepared from 0.10*M* hydrochloric acid, potassium hydrogen phthalate and potassium hydroxide. Dilutions were made with 0.10*M* potassium chloride to maintain the ionic strength. The pH of the buffer solutions was measured before and after saturation with the fluorescein, with a Corning Model 10 pH-meter, with a Beckman glass electrode and a saturated calomel electrode as reference electrode. The pH-meter was standardized with a standard buffer solution of pH 4.01, prepared from potassium hydrogen phthalate according to the NBS specification.

Preparation of calibration graphs

Highly purified yellow and red fluorescein were dried at 100–110° for 3 hr, and 100.0 mg of each were dissolved in, and diluted to exactly 1 litre with, 0.10*M* potassium hydroxide. Stock solutions containing 1.0 ppm of fluorescein were prepared by diluting 1.00 ml of these solutions to 100.0 ml with 0.10*M* potassium hydroxide. Volumes of 1, 3, 6, 10, 15 and 20 ml of these solutions were taken and diluted to 100.0 ml with 0.10*M* potassium hydroxide for fluorimetric measurement. The calibration curves for the yellow and red fluoresceins were identical.

Measurement of fluorescence

Relative fluorescence was measured with a Turner Model 110 Fluorometer. A Corning No. 5850 filter was used as a primary filter to isolate the blue portion of the excitation radiation. A combination of a Corning Yellow 2A-15 filter and a Wratten N. D. Filter 10 per cent 1.00 was used as the secondary filter. The calibration graphs were measured at three different sensitivity settings of the fluorometer. This, in combination with variations in the size of aliquots and final volumes, provided maximum accuracy.

Solubility measurements

Approximately 25 ml of each buffer solution was placed in a 600-ml plastic bottle provided with a screw cap. Into each bottle sufficient red or yellow fluorescein was added to ensure saturation of the resulting solution. Bottles and suspensions were then shaken mechanically for 72 hr at room temperature, 23.0 ± 0.5°. Each solution was subsequently filtered through a sintered-glass crucible, and the final pH was measured. A 5.00-ml aliquot of each solution was diluted to 100.0 ml with potassium hydroxide and the relative fluorescence of the solution was measured. The results are given in Table 1.

EVALUATION OF THE INTRINSIC SOLUBILITY OF THE YELLOW AND RED FLUORESCEINS

As will be seen on examination of Table 1 and Fig. 1, the solubilities of both the yellow and red forms of fluorescein exhibit a minimum at pH 3.28. The solubility increases on the low-pH side owing to protonation to form H_3Fl^+ [equation (1)] and on the high-pH side owing to dissociation to form HFl^- [equation (2)]. Such amphoteric behaviour is typical of zwitterions, and the dissociation constants can be evaluated from the solubility data by a method originated by Krebs and Speakman.[2]

The solubility of the free acid, the *intrinsic solubility*, S_i, is assumed to be constant and independent of pH:

$$S_i = [H_2Fl] \quad (4)$$

The solubility at any pH below the minimum is given by

$$S_j = [H_3Fl^+] + [H_2Fl] \quad (5)$$

and that at pH values above the minimum, S_h, is given by

$$S_h = [H_2Fl] + [HFl^-] \quad (6)$$

It is also assumed that over the pH range immediately above the minimum the concentration of Fl^{2-} is

Table 1. Solubility of yellow and red fluorescein as a function of pH; ionic strength 0.10

	Yellow fluorescein		Red fluorescein	
Initial pH of buffer	Final pH	Concentration, M	Final pH	Concentration, M
1.00	1.10	7.22×10^{-3}	1.05	2.41×10^{-3}
1.49	1.53	2.11×10^{-3}	1.51	6.92×10^{-4}
2.00	2.07	7.82×10^{-4}	2.05	2.59×10^{-4}
2.28	2.33	6.62×10^{-4}	2.35	2.50×10^{-4}
2.64	2.69	5.29×10^{-4}	2.65	1.87×10^{-4}
2.98	3.01	4.81×10^{-4}	3.01	1.69×10^{-4}
3.40	3.39	3.85×10^{-4}	3.43	1.50×10^{-4}
3.90	3.92	4.45×10^{-4}	3.92	1.62×10^{-4}
4.35	4.37	5.84×10^{-4}	4.36	2.17×10^{-4}
4.90	4.90	1.40×10^{-3}	4.90	5.06×10^{-4}
5.17	5.18	2.15×10^{-3}	—	—
5.35	5.34	3.31×10^{-3}	5.35	1.25×10^{-3}
5.55	5.53	4.72×10^{-3}	5.55	1.90×10^{-3}
6.04	6.03	1.80×10^{-2}	6.06	6.95×10^{-3}

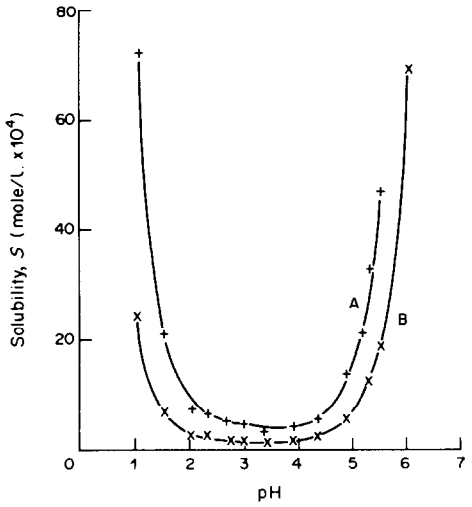

Fig. 1. Solubility of yellow fluorescein (curve A) and of red fluorescein (curve B) as a function of pH at 23°.

negligible (the validity of this assumption is examined below).

Combination of equations (1) and (4) yields

$$K_{H_3Fl} = [H^+]S_i/(S_j - S_i) \quad (7)$$

Rearrangement of equation (7) gives

$$S_j = S_i + [H^+]S_i/K_{H_3Fl} \quad (8)$$

and

$$-\log[(S_j/S_i) - 1] = -pK_{H_3Fl} + pH \quad (9)$$

According to equation (8) a plot of S_j *vs.* $[H^+]$ yields a straight line, the intercept of which at $[H^+] = 0$ is S_i. According to equation (9) the plot of $-\log[S_j/S_i) - 1]$ *vs.* pH yields a straight line of unit slope, the intercept of which is pK_{H_3Fl}.

Similarly, combination of equations (2) and (4) yields

$$K_{H_2Fl} = [H^+](S_h - S_i)/S_i \quad (10)$$

Rearrangement of equation (10) gives

$$S_h = S_i + K_{H_2Fl}S_i/[H^+] \quad (11)$$

or

$$\log[(S_h/S_i) - 1] = -pK_{H_2Fl} + pH \quad (12)$$

According to equation (11) a plot of S_h *vs.* $1/[H^+]$ yields a straight line, the intercept of which at $1/[H^+] = 0$ is S_i. According to equation (12) a plot of $\log[(S_h/S_i) - 1]$ *vs.* pH gives a straight line of unit slope, the intercept of which is $-pK_{H_2Fl}$.

Thus, the intrinsic solubility can be evaluated from two sets of data, on the low-pH side of the minimum, equation (8), and on the high-pH side, equation (11). For yellow fluorescein, the two approaches yielded somewhat different values, as shown in Table 2. Least-squares treatment of the 6 data points on the low-pH side yielded $S_j = 3.795 \times 10^{-4} + 0.0579[H^+]$ with R (correlation coefficient) = 0.997 (Fig. 2 curve A); hence $S_{i,yellow} = 3.80 \times 10^{-4}M$, and $K_{H_3Fl(yellow)} = 6.55 \times 10^{-3}$. For red fluorescein, the corresponding values were $S_j = 1.45 \times 10^{-4} + 0.0175[H^+]$, $R = 0.994$ (Fig. 1, curve B), $S_{i,red} = 1.45 \times 10^{-4}M$, and $K_{H_3Fl(red)} = 8.30 \times 10^{-3}$.

Least-squares treatment of the data on the high-pH side of the minimum, equation (11), yielded intercepts which varied with the number of data points used: $3.23 \times 10^{-4}M$ ($n = 4$), $3.49 \times 10^{-4}M$ ($n = 5$), $3.12 \times 10^{-4}M$ ($n = 6$), $3.22 \times 10^{-7}M$ ($n = 7$), $-0.347 \times 10^{-4}M$ ($n = 8$); although the successive plots (as n increased) were linear with high correlation coefficients (Fig. 3 curve A, for $n = 7$, for which least-squares gave $S_h = 3.22 \times 10^{-4} + 1.309 \times 10^{-9}/[H^+]$; $R = 0.9962$), only a likely average (disregarding

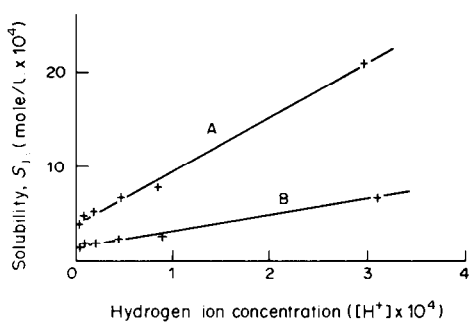

Fig. 2. Determination of the intrinsic solubility, S_i, of yellow fluorescein (curve A) and of red fluorescein (curve B) from solubility data on the low-pH side of the minimum solubility [equation (8)].

Table 2. Values for the intrinsic solubility, S_i, of yellow and red fluorescein (ionic strength 0.10)

Data used	Yellow fluorescein, 10^{-4}M	Red fluorescein, 10^{-4}M
Low-pH side of minimum: equation (8)	3.80	1.45
High-pH side of minimum: equation (11)*	3.27†	1.21†
equation (16)§		
first treatment*	3.42	1.24
second treatment*	3.48	1.30

*By least-squares treatment.
†Variable, depending on the number of data points included; see text.
§Correction made for the presence of Fl^{2-}.

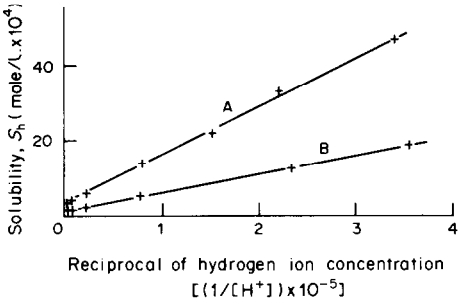

Fig. 3. Determination of the intrinsic solubility, S_i, of yellow fluorescein (curve A) and of red fluorescein (curve B) from solubility data on the high-pH side of the minimum solubility [equation (11)].

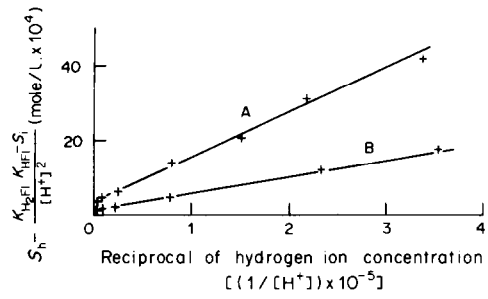

Fig. 4. Determination of the intrinsic solubility, S_i, of yellow fluorescein (curve A) and of red fluorescein (curve B) from solubility data on the high-pH side of the minimum solubility, with correction applied for the presence of Fl^{2-}; [equation (16), second approximation treatment].

$n = 8$) could be chosen: $S_{i,yellow} = 3.27 \times 10^{-4} M$ (Table 2). In general, the inclusion of the data at pH 6 (6.03 for yellow and 6.06 for red fluorescein) seriously distorted the results; it was suspected that at this pH (well above the pH, 5.5, at which the neutral form is completely dissociated) the systems did not conform to the assumptions made, so these data were not used in obtaining results by the unmodified Krebs and Speakman procedure.

For red fluorescein, corresponding treatment again yielded a value for the intercept which varied with the number of data included: $1.24 \times 10^{-4} M$ (4), $1.23 \times 10^{-4} M$ (5), $1.16 \times 10^{-4} M$ (6), $0.018 \times 10^{-14} M$ (7), *e.g.*, Fig. 2, curve B (for $n = 6$, for which least-squares gave $S_h = 1.16 \times 10^{-4} + 4.97 \times 10^{-9}/[H^+]$, $R = 0.99965$); again only a likely average (omitting the data for pH 6.06) could be chosen: $S_{i,red} = 1.21 \times 10^{-4} M$ (Table 2).

The variability and the drift in the values for the intrinsic solubilities obtained on the high-pH side of the minimum indicated that some additional factor was involved.

Since we knew from other work that the difference between the second and third dissociation constants is small (about 1.5–1.8 pK units) we realized that a significant amount of the doubly-charged anion must be present and of course increases with rising pH. The solubility on the high-pH side is then given by

$$S_h = [H_2Fl] + [HFl^-] + [Fl^{2-}] \qquad (13)$$

Introduction of equations (1)–(3) into (13) and assuming the solubility of the undissociated species to be constant and independent of pH, so that $[H_2Fl] = S_i$, gives

$$S_h = S_i\{1 + K_{H_2Fl}/[H^+] + K_{H_2Fl}K_{HFl}/[H^+]^2\} \qquad (14)$$

This is an awkward form for evaluation of S_i, and we adopted an approximation approach. The values best known at the time for the three constants in the third term within the braces were used to calculate the value of this term at each experimental pH, and this was applied as a correction to the solubility observed:

$$S_h - K_{H_2Fl}K_{HFl}S_i/[H^+]^2 = S_i + K_{H_2Fl}S_i/[H^+] \qquad (15)$$

For yellow fluorescein, the constants used in this treatment were p$K_{H_2Fl} = 4.73$, p$K_{HFl} = 6.36$, $S_{i,yellow} = 3.80 \times 10^{-4} M$. The correction was zero at the data points near the minimum but became significant at higher pH-values. The plots of $S_h - K_{H_2Fl}K_{HFl}S_i/[H^+]^2$ *vs.* $1/[H^+]$ were linear and led to an essentially constant value for the intrinsic solubility as the number of sets of data included was increased. The value obtained was $S_{i,yellow} = 3.42 \times 10^{-4} M$, Table 2. This value was then used in equation (12), as described in the next section, to obtain a new value for the second dissociation constant; this new value (p$K_{H_2Fl} = 4.52$) and the corrected S_i value were then used in a second approximation. The plot was linear (Fig. 3, curve A) and least-squares treatment yielded $S_h - K_{H_2Fl}K_{HFl}S_i/[H^+]^2 = 3.48 \times 10^{-4} + 1.198 \times 10^{-8}/[H^+]$, giving $S_{i,yellow} = 3.48 \times 10^{-4} M$, practically the same as that from the first approximation.

For red fluorescein, the constants used in the first approximation treatment were p$K_{H_2Fl} = 4.73$, p$K_{HFl} = 6.36$, $S_{i,red} = 1.16 \times 10^{-4} M$, and gave $S_{i,red} = 1.24 \times 10^{-4} M$ (Table 2). This value was used in equation (12) to obtain p$K_{H_2Fl} = 4.52$, and the second approximation treatment gave a linear plot (Fig. 4, curve

Table 3. Values for the dissociation constants, K_{H_3Fl} and K_{H_2Fl}, of yellow and of red fluorescein as determined from solubility data (ionic strength 0.10)

Constant	Yellow fluorescein	Red fluorescein
pK_{H_3Fl} low-pH side of minimum equation (9)[a]	2.15	2.11
pK_{H_2Fl} high-pH side of minimum equation (12)[b]	4.44[c,d]	4.42[e,d]
equation (18)	4.45[f]	4.43[f]

[a] By least-squares with slope forced to be equal to 1.000.
[b] From intercept on pH-axis.
[c] Including the data at pH 6.03.
[d] By least-squares; same value obtained by forcing slope to be 1.000.
[e] Including data point at pH 6.06.
[f] Slope of least-squares line was zero; direct averaging of the value on the ordinate of the plot gave: yellow fluorescein, pK 4.43, red fluorescein, pK 4.42.

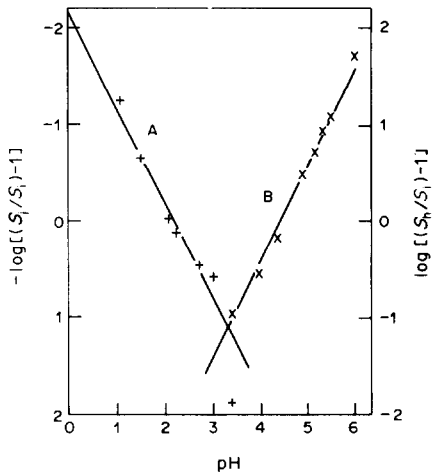

Fig. 5. Evaluation of the dissociation constants, K_{H_3Fl} and K_{H_2Fl}, of yellow fluorescein. Curve A, from solubility data on the low-pH side; $-\log[(S_j/S_i) - 1]$ *vs.* pH [equation (9)]; curve B, from solubility data on the high-pH side; $\log[(S_h/S_i) - 1]$ *vs.* pH [equation (12)]. For both straight lines the slope has been forced to be 1.000 in the least-squares treatment. The intersection point, pH 3.29, is the pH of minimum solubility.

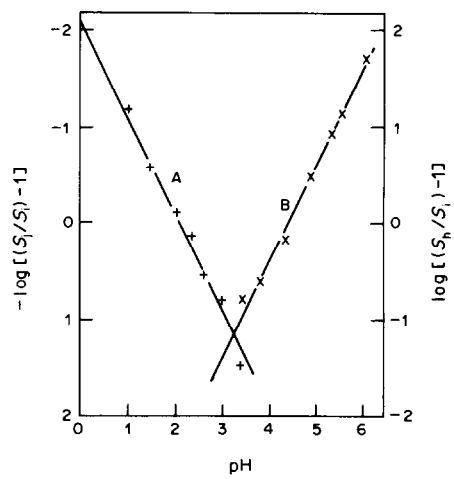

Fig. 6. Evaluation of the dissociation constants, K_{H_3Fl} and K_{H_2Fl}, of red fluorescein. Symbols and method as for Fig. 5. The point of intersection, pH 3.27, is the pH of minimum solubility.

B): $S_h - K_{H_2Fl}K_{HFl}\ S_i/[H^+]^2 = 1.30 \times 10^{-4} + 4.42 \times 10^{-9}/[H^+]$. Thus $S_{i,red} = 1.30 \times 10^{-4}M$ (Table 2) was again little changed from the first approximation.

EVALUATION OF THE FIRST AND SECOND DISSOCIATION CONSTANTS OF YELLOW AND RED FLUORESCEIN

To obtain values for the dissociation constants, it is convenient to place the two plots, $-\log[(S_j/S_i) - 1]$ *vs.* pH [equation (9)] and $\log[(S_h/S_i) - 1]$ *vs.* pH [equation (12)] on the same graph, as in Fig. 3 for yellow fluorescein and Fig. 4 for red fluorescein. The values obtained are given in Table 3.

For both fluoresceins, the values for the intrinsic solubility used in equation (9) were those found by evaluating the data on the low-pH side as described above: $S_{i,yellow} = 3.80 \times 10^{-4}M$; $S_{i,red} = 1.45 \times 10^{-4}M$. Least-squares treatment of data from equation (9) gave for both yellow fluorescein (Fig. 5, curve A) and red fluorescein (Fig. 6, curve A) straight lines of slope close to the theoretical value of one, and intercepts on the pH-axis which were not greatly changed by the number of sets of data included. We also used a least-squares treatment in which the slope was forced to be 1.000, and consider the values so obtained to be the best:

Number of sets of data included	5	6	7	Forced slope
Yellow fluorescein				
Intercept on pH-axis	2.212	2.231	2.155	2.152
Slope	1.048	1.019	1.2416	1.000
R	0.9900	0.99049	0.975	
Red fluorescein				
Intercept on pH-axis	2.090	2.090	2.212	2.113
Slope	0.9961	0.9955	1.0429	1.000
R	0.9713	0.9853	0.9910	

The astonishing feature is that yellow fluorescein and red fluorescein yield practically the same value for the first dissociation constant. We believe that the various protonated species in water exist in only one structural form and accordingly average the values 2.152 and 2.113, and propose

$$K_{H_3Fl} = 7.41 \times 10^{-3};\ pK_{H_3Fl} = 2.13 \qquad (16)$$

To evaluate the second dissociation constant from the data on the high-pH side of the minimum, both equations (12) and (17) were used; for both equations a value must be selected for the intrinsic solubility (Table 2). When the S_i value was that obtained by equation (11), the values for K_{H_2Fl} [the intercept of equation (12)] varied with the number of data points included, for both fluoresceins. On the other hand, when the S_i value was that obtained by equation (15), second approximation, concordant values were obtained, with little variation with the number of sets of data included, and incorporated the high-pH data smoothly.

Thus application of equation (12) to yellow fluorescein, with use of $S_{i,yellow} = 3.48 \times 10^{-4}M$ and least-squares treatment forcing the slope to be 1.000 for all 8 sets of data in Fig. 5 curve B, gave $pK_{H_2Fl} = 4.43$. Similarly for red fluorescein, with $S_{i,red} = 1.30 \times 10^{-4}M$ and all 7 sets of data from Fig. 6 curve B, and a forced slope of 1.000, $pK_{H_2Fl} = 4.42$.

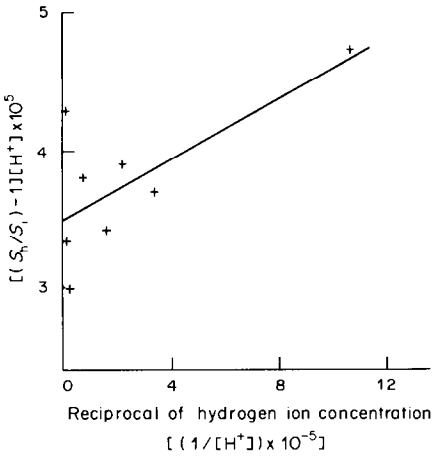

Fig. 7. Evaluation of the second dissociation constant, K_{H_2Fl}, of yellow fluorescein from solubility data on the high-pH side of the minimum solubility, with correction for the presence of the doubly-charged anion [equation (17)].

Equation (12) is based on the assumption that only the neutral species and the singly-charged anion are present, although a correction for the presence of the double-charged anion was made in arriving at the value of the intrinsic solubility used. A more rigorous treatment followed next, starting with the assumptions in equations (13)–(15). Equation (15), on rearrangement, yields

$$[(S_h/S_i) - 1][H^+] = K_{H_2Fl} + K_{H_2Fl}K_{HFl}/[H^+] \quad (17)$$

A plot of $[(S_h/S_i) - 1][H^+]$ *vs.* the reciprocal of the hydrogen-ion concentration for yellow fluorescein, again using $S_{i,yellow} = 3.48 \times 10^{-4}M$, is shown in Fig. 7; least-squares treatment gave $[(S_h/S_i) - 1][H^+] = 3.496 \times 10^{-5} + 1.103 \times 10^{-11}/[H^+]$, for all 8 sets of data ($R = 0.68511$), *i.e.*, $K_{H_2Fl} = 3.496 \times 10^{-5}$. The slope of almost zero makes equation (17) an interesting function, since the left-hand side is essentially independent of pH. A consequence of this is a low correlation coefficient of the least-squares line [for yellow fluorescein, $R = 0.01739$ for 4 sets of data, increasing to $R = 0.1492$ (6 sets), and to $R = 0.68511$ (8 sets, including the set at pH 6)]; thus, not surprisingly, the eight values for $[(S_h/S_i) - 1][H^+]$ yielded, on simple averaging, an intercept of 3.757×10^{-5}, and thus $pK_{H_2Fl} = 4.43$. Note that equations (12) and (17) yielded the same value for the second dissociation constant from the data for yellow fluorescein. Basically, then, the approach in equations (13)–(15) and (17) appears correct.

Application of equation (17) to red fluorescein, using $S_{i,red} = 1.30 \times 10^{-4}M$, yielded a linear plot (Fig. 8); least-squares treatment gave $[(S_h/S_i) - 1][H^+] = 3.690 \times 10^{-5} + 5.73 \times 10^{-12}/[H^+]$, so $pK_{H_2Fl} = 4.33$. As with yellow fluorescein, the slope was close to zero; a simple averaging of the seven values for $[(S_h/S_i) - 1][H^+]$ yielded 3.841×10^{-5}, *i.e.*, $pK_{H_2Fl} = 4.42$.

As reported above and in Table 3, equations (12) and (17) yielded the same values for the second dissociation constant for both the yellow and red fluoresceins. We therefore reiterate our belief that only one structure is present in the various prototropic forms of fluorescein existing in water solution and accordingly we average the results for both fluoresceins and propose $K_{H_2Fl} = 3.63 \times 10^{-5}$ ($pK_{H_2Fl} = 4.44$).

Comment on the pH of minimum solubility

Addition of equations (9) and (12) gives

$$\log[(S_h - S_i)/(S_j - S_i)] = 2pH - pK_{H_3Fl} - pK_{H_2Fl} \quad (18)$$

At the point of minimum solubility, the disproportionation of the undissociated species, the only species theoretically present, would produce equal amounts of the cation and the singly-charged anion:

$$2H_2Fl = H_3Fl^+ + HFl^- \quad (19)$$

and

$$S_j = S_h \quad (20)$$

At this pH, the left-hand side of equation (18) becomes zero, and

$$pH_{min.soly} = \tfrac{1}{2}(pK_{H_3Fl} + pK_{H_2Fl} \quad (21)$$

For the values presented in equations (16) and (18), $pH_{min.soly} = \frac{1}{2}(2.13 + 4.44) = 3.28$.

RESULTS AND DISCUSSION

The U-shaped curves of solubility as a function of pH, Fig. 1, for the yellow and red fluoresceins, are not expected to be symmetrical about the pH of min-

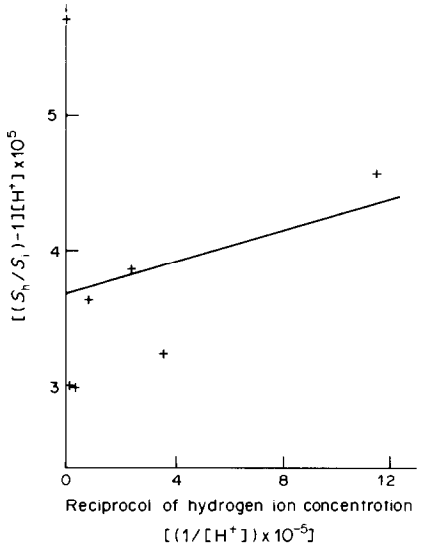

Fig. 8. Evaluation of the second dissociation constant, K_{H_2Fl}, of red fluorescein from solubility data on the high-pH side of the minimum solubility, with correction for the presence of the doubly-charged anion [equation (17)].

imum solubility, inasmuch as the branches are defined by different equations [(8) and (11)] and constants. The intrinsic solubility, however, is given the same definition, equation (4), in both equations and is assumed to be a constant independent of pH. Thus, the evaluation of the intrinsic solubility by equations (8) and (11), the first phase of the Krebs and Speakman treatment, would be expected to yield the same values, but failed to do so for the solubilities of the two fluoresceins. The treatment on the low-pH side of the minimum was straightforward, the linear least-squares treatment of the plots, Fig. 2, curves A and B, having high correlation coefficients, and the intercepts and slope showing essentially no variation with the number of sets of data used. The values found were: $S_{i,yellow} = 3.80 \times 10^{-4}M$; $S_{i,red} = 1.45 \times 10^{-4}M$ (Table 2). These values, when used in conjunction with the observed solubilities of the yellow and the red fluoresceins in the second phase of the Krebs and Speakman treatment [equation (9)] gave an identical value for the first dissociation constant $K_{H_3Fl} = 7.41 \times 10^{-3}$ ($pK_{H_3Fl} = 2.13$) (Table 3).

For both fluoresceins the data on the high-pH side of the minimum, however, gave by equation (11) significantly lower values for the intrinsic solubilities than those obtained from the data on the low-pH side, and moreover, gave values which shifted with the number of data points used. A similar effect was observed for the values of the second dissociation constants [equation (12), Krebs and Speakman second phase]. The supposition that the results were being distorted by the presence of appreciable amounts of the doubly-charged anion, Fl^{2-}, proved to be correct. The values for pK_{H_2Fl} and pK_{HFl} differ by only 1.5–1.8 and the dissociation of HFl^- is significant even at pH 4.5; at pH 5.5 it is completely dissociated and it is not surprising that the system does not conform to the assumption of the Krebs and Speakman approach.

The new theory, in which all three species (H_2Fl, HFl^- and Fl^{2-}) are assumed to be present [equations (13)–(17)], proved to be successful. Because of the nature of the equations involved, it was necessary to evaluate the intrinsic solubility by an approximation procedure. In practice, the second approximation was all that was necessary and the results from use of equation (15) conformed nicely to the theory and smoothly incorporated the data at high pH (pH > 6, data discarded in the simpler approach). The values found were $S_{i,yellow} = 3.48 \times 10^{-4}M$; $S_{i,red} = 1.30 \times 10^{-4}M$ (Table 2).

The second phase, the evaluation of the second dissociation constant, proved interesting. From the value for the intrinsic solubility obtained by use of equation (15) with the presence of Fl^{2-} taken into account, the same value for the second dissociation constant was obtained by both equation (12) (Krebs and Speakman) and equation (17) (new approach), for both yellow fluorescein and red fluorescein (Table 3); $pK_{H_2Fl} = 4.44$.

That sets of data on the solubility of two solid forms of the same chemical material should yield identical values for the pH of minimum solubility and for the two sets of dissociation constants is remarkable. The conclusion is that only one *structure* exists for fluorescein in water solution, for all three (and probably four) prototropic forms. Because the solutions at all pH values are yellow, the structure is probably the zwitterion structure **II**, with a positive charge located on the central oxygen-bearing ring and with protons and negative charges distributed about the periphery as determined by the prevailing pH.

REFERENCES

1. R. Markuszewski and H. Diehl, *Talanta*, 1980, **27**, 937.
2. H. A. Krebs and J. C. Speakman, *J. Chem. Soc.*, 1945, 593.

Talanta, Vol. 32, No. 2, pp.167-169, 1985
Pergamon Press Ltd. Printed in Great Britain

PRELIMINARY COMMUNICATION

A NEW FLUOROGENIC THIOL-SELECTIVE REAGENT: N-{p-[2-(6-DIMETHYLAMINO)BENZOFURANYL]PHENYL}MALEIMIDE[1)]

Kenichiro Nakashima, Hiroyuki Akimoto, Ken'ichi Nishida, Shin'ichi Nakatsuji and Shuzo Akiyama*

Faculty of Pharmaceutical Sciences, Nagasaki University, Bunkyo-machi, Nagasaki 852, Japan

(Received 3 October 1984. Accepted 4 December 1984)

Summary - N-{p-[2-(6-Dimethylamino)benzofuranyl]phenyl}maleimide (DBPM), has been synthesized and found to give fluorescent products when reacted with certain thiols. The reaction is very sensitive, and concentrations as low as 10^{-9}M can be detected.

Recently, several examples of thiol-selective reagents bearing the maleimide ring have been reported.[2-7] For the development of sensitive and useful fluorogenic thiol reagents, our attention has been directed to the synthesis of 2-phenylbenzofuran derivatives, which might be expected to be strongly fluorescent owing to the presence of a latent trans-stilbene skeleton.

In the work described here, a new fluorogenic reagent for thiols, DBPM (N-{p-[2-(6-dimethylamino)benzofuranyl]phenyl}maleimide), has been synthesized, and its application to the determination of glutathione (GSH), as a representative thiol, investigated.

The synthesis of DBPM (6) is shown. Treatment of the benzyl ether (2) obtained by the reaction of the aldehyde (1) with p-nitrobenzylbromide, with sodium methoxide, gave the nitro compound (3).

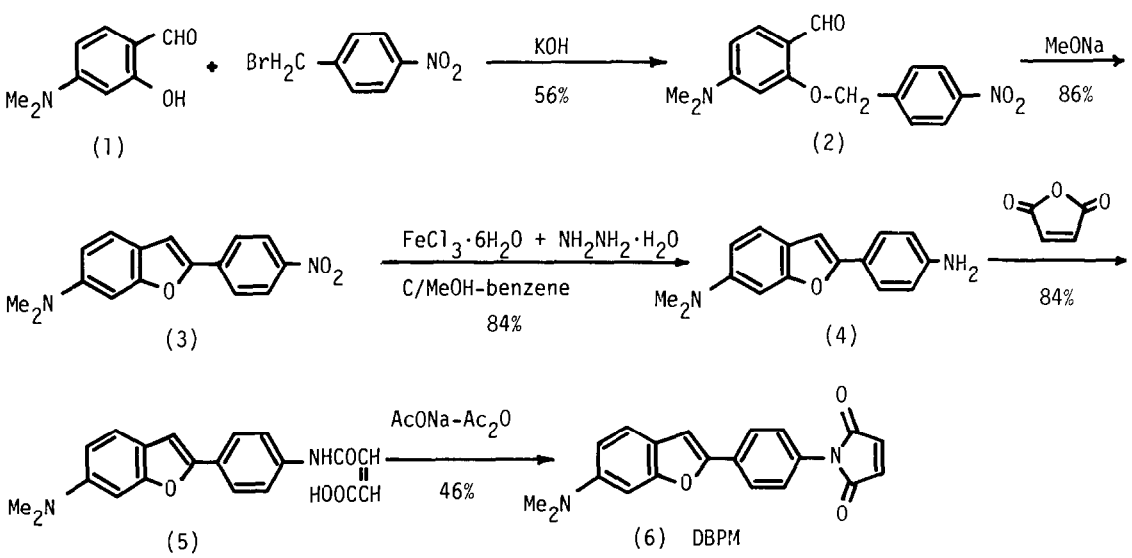

Reduction of (3) to (4), followed by treatment with maleic anhydride, and cyclization yielded DBPM. DBPM when combined with thiols shows strong fluorescence, with the emission maximum at 457 nm, and excitation at 355 nm, whereas the reagent itself is practically non-fluorescent. The large difference (ca. 100 nm) between the excitation and emission maxima makes the reagent advantageous for practical use. N-Acetyl-L-cysteine (taken as a representative thiol) reacts with DBPM to give a 1:1 adduct (m.p. 119 - 121°), the structure of which is under further investigation.

We have examined the application of DBPM to the determination of thiols, especially GSH, and have established the following procedure. To a standard solution (0.5 ml) of GSH ($\leq 2 \times 10^{-5}$M) in 0.02M EDTA, is added a buffer solution (pH 8.5, 0.1M borate-carbonate, 2.0 ml) and a solution of DBPM in CH_3CN (8×10^{-6}M, 2.5 ml). The well-mixed solution is heated for 30 min at 60°, cooled to room temperature, and then the relative fluorescence intensity (RFI) is measured at 457 nm with excitation at 355 nm. The RFI remains constant for 24 hr. The conditions given were chosen after examination of the effect of varying the DBPM and CH_3CN concentrations, pH, and reaction time. Maximal RFI is obtained with a final concentration of 4μM DBPM and 50 - 60% v/v CH_3CN over the pH range 8 - 10.5. The reaction of DBPM with thiols goes essentially to completion within 20 - 30 min at 60°.

The relationship between GSH concentration and RFI was linear over the range 2 - 2000nM (relative standard deviation 2.4% for 200nM GSH, 10 replicates). Oxidized glutathione (GSSG) can be quite easily reduced to GSH by means of KBH_4 within 5 min at 40° and determined by the proposed method. The excess of KBH_4 is easily removed with HPO_3. The calibration curve is linear over the GSSG concentration range 5 - 1000nM (r.s.d. 2.4% at the 200 nM level).

DBPM reacts with various thiol compounds, as shown in Table 1, which also gives the relative fluorescence yields. Cystine can be determined (after reduction to cysteine with KBH_4) 1 - 1000nM (r.s.d. 2.4% at the 200nM level).

Table 1. The reaction of thiol compounds with DBPM*

Compound	RFI
GSH	100
GSSG	13.2
Cysteine	109.4
Cystine	0
N-Acetyl-L-cysteine	83.8
Methionine	0
Coenzyme A	74.2

* The reaction and the measurement of the fluorescence intensity were performed according to the procedure described above. The final concentrations of the reaction products were 2 μM.

DBPM is easily prepared from commercially available materials and both its reactivity with thiols (reaction time 20 - 30 min at 60°) and the fluorescence stability of the reaction products (stable up to 24 hr) are rather superior to those of the known maleimide reagents.

Unfortunately, selective determination is not possible, because the fluorescence wavelengths of the reaction products from the thiols tested are almost identical. However, the proposed method has been successfully applied to the determination of total thiol group in rat tissue. The detailed results will be reported elsewhere. Use of DBPM after HPLC is being explored for determination of thiols in biological samples.

Acknowledgement

The authors wish to express their gratitude to the Ministry of Education of Japan for a Grant-in-Aid for Scientific Research.

REFERENCES

1. Development and Application of Organic Reagents for Analysis, Part 4. Part 3: K. Nakashima, T. Ando and S. Akiyama, Chem. Pharm. Bull., 1984, 32, 1654.
2. T. Kanaoka, T. Sekine, M. Machida, Y. Soma, K. Tanizawa and Y. Ban, ibid., 1964, 12, 127.
3. Y. Kanaoka, M. Machida, M.I. Machida and T. Sekine, Biochim. Biophys. Acta, 1973, 313, 563.
4. K. Yamamoto, T. Sekine and Y. Kanaoka, Anal. Biochem., 1977, 79, 83.
5. Y. Nara and K. Tuzimura, Agr. Biol. Chem., 1978, 42, 793.
6. H. Takahashi, Y. Nara and K. Tuzimura, ibid., 1979, 43, 1439.
7. Y. Kanaoka, Yakugaku Zasshi, 1980, 100, 973.

Talanta, Vol. 32, No. 3, pp. 171–175, 1985
Printed in Great Britain.

0039-9140/85 $3.00 + 0.00

MULTIPARAMETRIC CURVE FITTING—VII*

DETERMINATION OF THE NUMBER OF COMPLEX SPECIES BY FACTOR ANALYSIS OF POTENTIOMETRIC DATA

JOSEF HAVEL
Department of Analytical Chemistry, Purkyně University, Kotlářská 2, 611 37 Brno, Czechoslovakia

MILAN MELOUN†
Department of Analytical Chemistry, University of Chemical Technology, 532 10 Pardubice, Czechoslovakia

(*Received* 30 *May* 1984. *Accepted* 7 *November* 1984)

Summary—The number of complex species in solution may be determined by a computer-assisted factor analysis of a set of potentiometric titration curves, by finding the rank of the normalized data matrix. An application of the program SPECIES is demonstrated for some examples of titration data. The method is limited in that it can discriminate only between species with differing degrees of polymerization.

In the study of solution equilibria, it is not only necessary to determine the stoichiometry and stability constant of each complex species, but also to find out how many such species are present. This number can emerge from a careful least-squares treatment which seeks to find the best chemical model. One method is to use a species selector[1] in which the various complexes are tested and the best combination of them is determined. Such a treatment was first used for potentiometric data analysis by Sillén in the program LETAGROP,[1,2] and a new species selector was included recently in the program PSEQUAD.[3] The problem of species selection and determination is also discussed in a forthcoming publication.[4] With spectrophotometric data, the number of species in solution can be determined as the rank of the second moment of the absorbance matrix. This can be found by matrix-algebra operations[5] or by factor analysis.[6–8] Principal-component analysis[9,10] has been used to find the number of components from mass spectra,[11,12] fluorescence data,[13] *etc.* The use of the method in spectrophotometry is reviewed in a forthcoming monograph.[14]

This paper describes a factor-analysis method for finding the number of species present in a system studied by potentiometric titration. As with spectrophotometric data, the rank of the matrix constructed from normalized potentiometric data is shown to be less than or equal to the number of species in solution.

THEORY

Matrix analysis of normalized potentiometric data

Consider the complex-forming equilibria of components A, B and C; the general reaction equation and the corresponding overall stability constant are given by

$$pA + qB + rC \rightleftharpoons A_pB_qC_r \quad (1)$$

$$\beta_{pqr} = [A_pB_qC_r]/([A]^p[B]^q[C]^r) \quad (2)$$

The equation for the potentiometric titration curve must be transformed into the form of normalized variables $Z = f(\mathrm{pA})$ where the free equilibrium concentration of component A is usually measured potentiometrically as $\mathrm{pA} = -\log[A]$ (*e.g.*, pH) and Z represents the average number of one component (for example A) bound per B or C.

$$Z = (c_A - [A])/c_B = \left(\sum_{i=1}^{n_c} p_i[A_{p_i}B_{q_i}C_{r_i}]\right)\Big/ c_B = \left(\sum_{i=1}^{n_c} p_i c_i\right)\Big/ c_B \quad (3)$$

where c_A, c_B and c_C, are the total analytical concentrations of A, B and C, [A] is the free equilibrium concentration of A, and n_c is the number of complex species in solution.

Each curve $Z = F(\mathrm{pA})$ has n_s points, and curves may be measured for n_B total concentrations of either B or C (or both), to give finally an $n_s \times n_B$ matrix **Z** $[(Z_{k,j},\ k = 1,\ n_s),\ j = 1,\ n_B]$. Equation (3) may be written as

$$Z = \sum_{i=1}^{n_c} e_i\, c_i \quad (4)$$

where $e_i = p_i/c_B$, or in matrix notation

$$\mathbf{Z} = \mathbf{E}\,\mathbf{C} \quad (5)$$

where matrix **Z** is $(n_s \times n_B)$, **E** is $(n_B \times n_c)$ and the concentration matrix **C** is $(n_c \times n_s)$.

Equation (5) is analogous to the generalized form of the Beer–Lambert law for unit path-length, and element e_i of **E** is analogous to the molar absorptivity.

*Part VI: *Talanta* 1984, **31**, 1083.
†Author for correspondence.

The rank of matrix **Z** may be obtained from the equation

$$\text{rank}(\mathbf{Z}) = \min[\text{rank}(\mathbf{E}), \text{rank}(\mathbf{C})] \leqq \min(n_B, n_c, n_s) \quad (6)$$

If we now arrange experimentally that $n_B > n_c$ and $n_s > n_c$ we obtain

$$\text{rank}(\mathbf{E}) \leqq n_c \; [\text{rank}(\mathbf{E}) = \min(n_B, n_c)] \quad (7)$$

$$\text{rank}(\mathbf{C}) \leqq n_c \; [\text{rank}(\mathbf{C}) = \min(n_c, n_s)] \quad (8)$$

so

$$\text{rank}(\mathbf{Z}) \leqq n_c \quad (9)$$

Thus, the rank of **Z** gives directly the number of complex species in solution. The treatment is analogous to the factor analysis of absorbance matrices by Kankare[6] and Wernimont.[15] The "spectra" of the solutions in this case are replaced by the functions $Z = f(c_B)$ or $Z = f(c_c)$.

In continuance of the analogy with absorbance matrix analysis,[6] the matrix **Z** may be subjected to factor analysis. Thus, the second moment matrix **M** is defined by

$$\mathbf{M} = (1/n_s) \cdot \mathbf{Z}\,\mathbf{Z}^T \quad (10)$$

where $\mathbf{Z}^T$ denotes the transpose of **Z**. From equation (9),

$$\text{rank}(\mathbf{M}) \leqq n_c \quad (11)$$

This implies that matrix **M** has at most n_c non-zero eigenvalues. Because of experimental errors, the actual number of non-zero eigenvalues is $\min(n_B, n_s)$. Let the eigenvalues of **M** be r_i and suppose that there are k independent components in the equilibrium system. Then the residual standard deviation of Z is given by

$$s_k(Z) = \left[\left(\text{tr}(\mathbf{M}) - \sum_{i=1}^{k} r_i\right) \Big/ (n_B - k)\right]^{1/2} \quad (12)$$

where tr(**M**) is the trace of **M**. Let the precision of estimation of Z be $s_{inst}(Z)$; then it may be concluded that if $s_k(Z) < s_{inst}(Z)$ it is probable that $n_c < k$. Values for the eigenvalues r_i, and the standard deviation of Z, $s_k(Z)$, and also for the relative variance (expressed as a percentage), RV, the cumulative percentage relative variance, CRV, and the Malinowski factor indicator function,[16] IND, are calculated and printed by the program SPECIES.

$$\text{RV}\,(\%) = [r_i/\text{tr}(\mathbf{M})] \times 100 \quad (13)$$

$$\text{CRV}\,(\%) = \sum_{i=1}^{k} r_i \times 100/\text{tr}(\mathbf{M}) \quad (14)$$

$$\text{IND} = s_k(Z)/(n_B - k)^2 \quad (15)$$

The higher the value of the variance RV, the higher the contribution of the corresponding eigenvalue to the trace, and thus the more significant the eigenvalue. Eigenvalues with variance < 0.01% are regarded as negligible. Similarly, consideration of the CRV shows how 100% variance is approached as more eigenvalues are included. If inclusion of a certain eigenvalue brings the CRV to 99.99%, the remaining eigenvalues should be assumed to be of negligible significance. The Malinowski factor indicator function IND should reach a minimum when the correct number of factors (*i.e.*, species) has been chosen.[16]

PROPOSED PROCEDURE

For various possible integer values of the rank of **Z** the standard deviation, $s_k(Z)$, is calculated from equation (12). The graph of $s_k(Z) = f(k)$ where k is an actual value of the rank, consists of two nearly linear parts which intersect on extrapolation. The point of intersection should lie near to the experimental standard deviation value, $s_{inst}(Z)$. The coordinate k on the rank-axis for this intersection is the value sought for the rank of the matrix, and is equal to the number of complex species in solution (Fig. 1). At the same value of k, $s_k(Z)$ should be $\leqq s_{inst}(Z)$, the CRV should reach almost 99.99%, the variance of any remaining eigenvalues should be negligible (< 0.1%) and IND should reach a minimum. However, these criteria may *not* all be met at the same value of k.

Limitation of the method

The situation for potentiometric data is not strictly analogous to that for spectrophotometric data, in that the method is applicable *only* when a change in the total analytical concentration of component B or C, c_B or c_c, leads to a set of different curves for $Z_B = f(\text{pA})$ or $Z_C = f(\text{pA})$. That is, the complexes that can be detected must not be mononuclear (in B or C). For mononuclear complexes the curves of $Z_B = f(\text{pA})$ are identical; thus there is just one curve, and the rank of **Z** is one. The method cannot be used, therefore, to find the number of differently protonated species of a weak acid H_nL. [In such cases the number of species may be indicated by the number of inflection points on the $Z = f(\text{pH})$ curve.]

In the case of metal–ligand equilibria, curves for varied metal or varied ligand concentrations should be measured. The matrix **Z** is then obtained by taking vertical sections at constant pH values, or by taking horizontal sections at constant Z values. Only species with differing p_i indices can be distinguished.

Computation

Computations were done with use of a mainframe computer EC 1033. The program SPECIES is available, with specimen data, on request.

DISCUSSION

The program SPECIES was validated by use of literature titration data and simulated data sets.

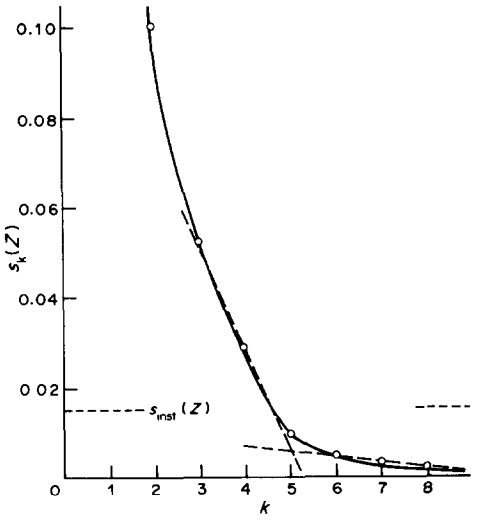

Fig. 1. Graphical determination of the number of complexes. The k-co-ordinate of the point of intersection of the two linear parts of $s_k(Z) = f(k)$ gives a good estimate of the matrix rank, and the $s_k(Z)$-co-ordinate should be close to the value of $s_{inst}(Z)$ (data from Table 2.).

Baldwin and Wiese[17] studied polymolybdate equilibria in $1M$ magnesium perchlorate solution and found three $H_p(MoO_4)_q$ species with (p, q) values (2, 1), (8, 6) and (9, 8). The normalized Z values for various pH values at different total concentrations of molybdate were taken from Fig. 1 in that paper and the matrix **Z** was constructed (Table 1). On the assumption that the precision of reading Z-values from this graph is $s_{inst}(Z) \approx 0.02$, the rank of the matrix should be three. It may be concluded that there are 3 polynuclear complexes in solution.

Sasaki and Sillén[18] studied the hydrolysis of molybdate in $3M$ sodium perchlorate and found eight $H_p(MoO_4)_q$ species with indices (1, 1), (2, 1), (8, 7), (9, 7), (10, 7) and (11,7). The Z values were read from Fig. 1 in that paper with precision $s_{inst}(Z) \approx 0.02$ for various pH values in the range 1.50–7.50. The resulting matrix **Z** was treated by program SPECIES (Table 2). The rank of the matrix is 5, in agreement with the five polynuclear species (with differing p_i indices) among those found in solution by the authors.

Biedermann and Ciavatta[19] found three complexes, $Y(OH)^{2+}$, $Y_2(OH)_2^{4+}$, and $Y_3(OH)_5^{4+}$ in hydrolysed solutions of Y(III) in $3M$ perchlorate. The matrix **Z** was constructed from the data of their Fig. 2 with precision $s_{inst}(Z) \approx 0.02$ (Table 3). The matrix rank is found to be 2, in accordance with the two polynuclear hydrolytic products formed in solution.

A data set was simulated for a metal-ion hydrolysis based on a study by Ahlberg[20] of Hg(II) in $3M$ perchlorate. Five species, $HgOH^+$, $Hg(OH)_2$, $Hg_2(OH)^{3+}$, $Hg_2(OH)_2^{2+}$ and $Hg_4(OH)_3^{5+}$ were found. The $Z = f(\text{pH})$ curves were simulated by the program POLET,[21] then the Z values were loaded with a random error so that $s_{inst}(Z) = 0.001$. Program SPECIES showed the rank of **Z** to be 2, which

Table 1. Determination of the number of complexes in a polymolybdate system from the potentiometric data of Baldwin and Wiese[17]

Part 1. Matrix **Z** (dimensions $n_s = 10$, $n_B = 8$); $s_{inst}(Z) = 0.02$

pH \ $c_{MoO_4^{2-}}$, $10^{-3}M$	13.25	11.07	9.86	8.603	7.299	5.947	4.545	3.088
5.25	0.25	0.14	0.11	0.06	0.04	0.03	0.02	0.02
5.00	0.55	0.46	0.38	0.32	0.26	0.20	0.10	0.05
4.75	0.82	0.77	0.74	0.70	0.65	0.58	0.40	0.25
4.50	1.02	0.99	0.97	0.90	0.88	0.86	0.79	0.65
4.25	1.15	1.14	1.13	1.11	1.10	1.09	1.04	0.98
4.00	1.24	1.23	1.23	1.23	1.23	1.23	1.22	1.21
3.75	1.35	1.35	1.35	1.33	1.32	1.31	1.30	1.30
3.50	1.46	1.45	1.41	1.40	1.38	1.36	1.35	1.35
3.25	1.60	1.50	1.46	1.44	1.42	1.41	1.39	1.38
3.00	1.70	1.60	1.55	1.50	1.48	1.48	1.42	1.41

Part 2. Values of eigenvalues, r, percentage relative variance, RV, percentage cumulative relative variance, CRV, residual standard deviation, $s_k(Z)$, and Malinowski indicator function, IND, for various postulated values of matrix rank, k; Trace = 9.722430

k	r	RV	CRV	$s_k(Z)$	IND
1	9.671622	99.477	99.477	0.085195	0.001739
2	0.046129	0.474	99.952	0.027924	0.000776
3	0.004098	0.042	99.994	0.010777	0.000431
4	0.000330	0.003	99.997	0.007922	0.000495
5	0.000187	0.002	99.999	0.004616	0.000513
6	0.000034	0.000	100.000	0.003865	0.000966
Estimated rank		4	3	3	3

Table 2. Determination of the number of complexes from a potentiometric study of molybdate hydrolysis by Sasaki and Sillén[18]

Part 1. Matrix **Z** (dimensions $n_s = 11$, $n_B = 10$); $s_{inst}(\mathbf{Z}) = 0.02$

pH \ $c_{MoO_4^{2-}}$, $10^{-3}M$	160	80	40	20	10	5	2.5	1.25	0.62	0.31
6.5	0.60	0.27	0.03	0.00	0.00	0.00	0.00	0.00	0.00	0.00
6.0	1.01	0.89	0.68	0.34	0.06	0.01	0.00	0.00	0.00	0.00
5.5	1.13	1.09	1.02	0.91	0.73	0.44	0.12	0.04	0.03	0.03
5.0	1.19	1.18	1.17	1.12	1.08	0.96	0.81	0.54	0.20	0.10
4.5	1.23	1.22	1.21	1.21	1.20	1.18	1.12	1.03	0.78	0.66
4.0	1.30	1.30	1.29	1.29	1.29	1.29	1.29	1.26	1.23	1.15
3.5	1.38	1.38	1.375	1.375	1.37	1.37	1.37	1.365	1.36	1.36
3.0	1.45	1.45	1.45	1.45	1.45	1.45	1.45	1.45	1.45	1.45
2.5	1.50	1.50	1.50	1.50	1.50	1.50	1.50	1.50	1.50	1.50
2.0	1.68	1.62	1.60	1.57	1.56	1.55	1.55	1.55	1.55	1.55
1.5	1.80	1.78	1.75	1.73	1.72	1.72	1.72	1.71	1.71	1.70

Part 2. Trace = 14.724625

k	r	RV	CRV	$s_k(Z)$	IND
1	14.255160	96.812	96.812	0.228392	0.002820
2	0.386226	2.623	99.435	0.102004	0.001594
3	0.063890	0.434	99.869	0.052574	0.001073
4	0.014082	0.096	99.964	0.029626	0.000823
5	0.004849	0.033	99.997	0.009131	0.000365
6	0.000321	0.002	99.999	0.004904	0.000306
7	0.000076	0.001	100.000	0.002582	0.000287
Estimated rank		6	5	5	(7)

Table 3. Determination of the number of complexes in the hydrolysis of Y(III), from normalized potentiometric data of Biedermann and Ciavatta[19]

Part 1. Matrix **pH** (dimensions $n_s = 8$, $n_y = 7$); $s_{inst}(\mathbf{Z}) = 0.002$

Z \ c_y, $10^{-3}M$	0.98	0.50	0.30	0.20	0.10	0.05	0.025
0.10	5.45	5.55	5.65	5.75	5.83	5.91	6.00
0.20	5.61	5.74	5.82	5.89	6.00	6.12	6.21
0.40	5.76	5.90	6.00	6.08	6.21	6.32	6.42
0.60	5.86	5.99	6.10	6.16	6.29	6.41	6.53
0.80	5.92	6.06	6.15	6.22	6.36	6.50	6.60
1.00	5.99	6.10	6.20	6.28	6.41	6.53	6.66
1.20	6.02	6.13	6.24	6.31	6.45	6.58	6.70
1.40	6.06	6.16	6.27	6.34	6.49	6.61	6.72

Part 2. Trace = 265.732100

k	r	RV	CRV	s_k(pH)	IND
1	265.731066	99.999	99.999	0.013126	0.000365
2	0.000710	0.000	100.000	0.008050	0.000322
3	0.000162	0.000	100.000	0.006362	0.000398
Estimated rank		1	1	2	2

corresponds to the two polynuclear species with different p_t indices (Table 4).

CONCLUSIONS

The graphical procedure for examination of $s_k(Z) = f(k)$ appears to yield results in agreement with the literature,[17–19] as shown in Tables 1–4. The commonly used methods for estimation of matrix rank in factor analysis, *viz.* IND, the Malinowski factor indicator function, and CRV, the cumulative relative variance, do not appear to be so reliable as criteria, at least for this particular application of factor analysis.

Table 4. Determination of the number of complexes from simulated potentiometric data for hydrolysis of Hg(II), based on the stability constants determined by Ahlberg[20]

Part 1. Matrix Z (dimensions $n_s = 9$, $n_B = 10$); imposed random error, $s_{inst}(Z) = 0.001$

pH \ c_{Hg}, 10^{-3}, M	2000	1300	1000	750	500	200	100	50	5	2.5
0.75	0.027	0.018	0.014	0.011	0.008	0.004	0.003	0.002	0.002	0.001
1.00	0.053	0.034	0.026	0.020	0.014	0.008	0.005	0.004	0.003	0.003
1.10	0.071	0.044	0.034	0.026	0.019	0.010	0.007	0.005	0.004	0.004
1.20	0.095	0.059	0.045	0.034	0.024	0.013	0.009	0.007	0.005	0.005
1.30	0.127	0.079	0.059	0.045	0.031	0.017	0.012	0.009	0.007	0.007
1.40	0.166	0.105	0.079	0.059	0.041	0.022	0.015	0.012	0.009	0.009
1.50	0.212	0.139	0.106	0.079	0.055	0.029	0.020	0.016	0.012	0.012
1.60	0.262	0.181	0.140	0.106	0.073	0.038	0.027	0.021	0.016	0.016
1.75	0.341	0.255	0.206	0.160	0.112	0.058	0.041	0.032	0.025	0.025

Part 2. Trace = 0.067746

k	r	RV	CRV	$s_k(Z)$	IND × 10^5
1	0.067600	99.783	99.783	0.004039	4.9864
2	0.000145	0.214	99.997	0.000473	0.7391
3	0.000002	0.002	100.000	0.000196	0.4000
4	0.000000	0.000	100.000	0.000164	0.4555
5	0.000000	0.000	100.000	0.000117	0.4680
Estimated rank		3	2	2	3

REFERENCES

1. L. G. Sillén and B. Warnqvist, *Ark. Kemi*, 1969, **31**, 341.
2. N. Ingri and L. G. Sillén, *ibid.*, 1969, **23**, 97.
3. I. Nagypál and L. Zékány, in D. J. Leggett (ed.), *Computational Methods for the Determination of Stability Constants*, Plenum Press, New York, 1984.
4. M. Meloun and J. Havel, *Computation of Solution Equilibria, Part 2, Potentiometry, Folia Fac. Sci. Nat. Univ. Purk. Brunensis*, Brno, 1985, in the press.
5. R. M. Wallace, *J. Phys. Chem.*, 1960, **64**, 899.
6. J. J. Kankare, *Anal. Chem.*, 1970, **42**, 1322.
7. M. Takatsuki and K. Yamaoka, *J. Sci. Hiroshima Univ., Ser. A.*, 1976, **40**, 387.
8. N. Ohta, *Anal. Chem.*, 1973, **45**, 553.
9. T. W. Anderson, *Ann. Math. Statist.*, 1963, **34**, 122.
10. D. Katakis, *Anal. Chem.*, 1965, **37**, 876.
11. G. L. Ritter, S. R. Lowry, T. L. Isenhour and C. L. Wilkins, *ibid.*, 1976, **48**, 591.
12. F. J. Knorr and J. H. Futrell, *ibid.*, 1979, **51**, 1236.
13. I. M. Warner, E. R. Davidson and G. D. Christian, *ibid.*, 1977, **49**, 2155.
14. M. Meloun and J. Havel, *Computation of Solution Equilibria, Part 1, Spectrophotometry, Folia Fac. Sci. Nat. Univ. Purk. Brunensis*, Brno, 1984, in the press.
15. G. Wernimont, *Anal. Chem.*, 1967, **39**, 554
16. E. R. Malinowski and D. G. Howery, *Factor Analysis in Chemistry*, Wiley, New York, 1980.
17. W. G. Baldwin and G. Wiese, *Ark. Kemi*, 1969, **31**, 419.
18. Y. Sasaki and L. G. Sillén, *ibid.*, 1968, **29**, 253.
19. G. Biedermann and L. Ciavatta, *ibid.*, 1964, **22**, 253.
20. I. Ahlberg, *Acta Chem. Scand.*, 1962, **16**, 887.
21. J. Havel and M. Meloun, *Talanta*, 1985, **32**, in the press.

Talanta, Vol. 32, No. 3, pp. 177–181, 1985
Printed in Great Britain.

0039-9140/85 $3.00 + 0.00

CHARACTERIZATION OF SEDIMENT REFERENCE MATERIALS BY X-RAY PHOTOELECTRON SPECTROSCOPY

M. SOMA, H. SEYAMA and K. OKAMOTO
National Institute for Environmental Studies, Tsukuba, Ibaraki 305, Japan

(*Received* 17 *September* 1984. *Accepted* 5 *November* 1984)

Summary—The chemical composition of surface layers of three sediment reference materials, Pond Sediment (Japan NIES CRM No. 2), River Sediment (US NBS SRM 1645) and Estuarine Sediment (US NBS SRM 1646), has been studied comparatively by X-ray photoelectron spectroscopy (XPS). The composition of River Sediment as determined by XPS is peculiar in that the concentration of Cr is much higher but that of Si is much lower than that expected from the bulk composition of the sample. This can be attributed to the structure of the sediment particles, which consist of silica-rich cores covered by surface layers rich in Cr(III). Organic substances are predominant in the surface layers of all three materials, as indicated by the C 1*s* and N 1*s* lines. The elemental composition of the surface layers can be reasonably related to the origin of the sediments. The bonding states of some elements in the sediment samples, deduced from the photoelectron binding energies, are briefly discussed.

It is well established that X-ray photoelectron spectroscopy (XPS), as a tool for analysing the elemental composition as well as the chemical state of surface layers of solids,[1] is applicable to a wide variety of solid materials, including those of geochemical and mineralogical interest.[2] However, in spite of its excellent capability for analysing solids of widely varied compositions, which may play important roles in environmental problems,[3] its application to environmental samples has been practically confined to the study of the surface chemical composition of aerosol[4] and fly-ash particles.[5]

In this report, an attempt has been made to characterize three reference sediment materials by XPS. It will be shown that, although there are difficulties in the quantification of XPS measurements made on such complex heterogeneous materials, the average elemental compositions of the surface layers of those materials, as determined by XPS, can deviate significantly from those given by total analysis (bulk composition), and reflect the origin and/or the history of the samples. Information obtained from the chemical shifts for certain elements will also be discussed. A brief account of the XPS of Pond Sediment has already been published.[6]

EXPERIMENTAL

Materials

The three reference materials studied are U.S. National Bureau of Standards (NBS) standard reference material (SRM) 1645 "River Sediment",[7,8] NBS SRM 1646 "Estuarine Sediment",[9] and Japan National Institute for Environmental Studies (NIES) certified reference material (CRM) No. 2 "Pond Sediment".[6,10,11] They were chosen because their properties and elemental compositions are well characterized, and they are in a form suitable for XPS measurements.

XPS measurement

The electron spectra were recorded on a Vacuum Generators ESCALAB 5 apparatus. The powdered sediment sample, as received, was fixed by double-sided adhesive tape on a stainless-steel sample holder 10 mm in diameter. The sample was irradiated by Al $K\alpha$ or Mg $K\alpha$ radiation from a twin anode. The typical measuring conditions were: X-ray power, 13 kV and 10 mA; electron pass-energy through the analyser, 50 eV; width of the analyser entrance slit, 4 mm. The instrumental resolution determined by the pass-energy and the slit-width was 1.25 eV. To determine the intensities of weak transitions, signals for narrow range scans were accumulated on a Nicolet 1070 signal averager until an acceptable signal-to-noise ratio was attained. For most elements measured, the electron emission intensity was stable enough for long exposure to the X-rays. However, the carbon and nitrogen lines of organic origin sometimes changed their intensities considerably during prolonged measurement (several hours) at room temperature. This instability was made negligible by cooling the sample with a continuous flow of liquid nitrogen through the specimen manipulator.

The electron binding energies were standardized against the Au $4f_{7/2}$ line (83.8 eV) of a gold film evaporated onto the sample. The uncertainty in the determination of binding energy for most of the emission lines was ± 0.2 eV.

The quantitative analysis was based on the relative atomic sensitivity factors for the photoelectron and Auger electron emissions tabulated in Table 1. These were determined either by integrating the experimental line intensities for the compounds of known stoichiometry or by theoretical estimation. The theoretical estimation was done by the procedure described by Seah,[12] with use of the theoretical ionization cross-section[13] and the asymmetry factor[14] given by Scofield and by Reilman *et al.*, respectively.

The reproducibilities in the determination of the relative area intensities for sediment samples, as examplified by Pond Sediment, have been shown to be within 10%.[6] The uncertainty in determining the elemental composition by XPS largely arises from the application of the atomic sensitivity factor to samples with different matrices, as has often been pointed out.[12] Our empirical estimation is that the error may be as large as 20%, but would rarely exceed this figure.

Table 1. Relative atomic sensitivity of the elements (Si $2s = 1$)

Element	Line	X-ray source: Al $K\alpha$	X-ray source: Mg $K\alpha$	Note
Al	$2p$	0.520	0.74	*a*
Fe	$2p$	10.2	11.0	*b*
Mg	$KL_{23}L_{23}$Auger	8.0	—	*c*
Ca	$2p$	4.64	5.75	*c*
Na	$KL_{23}L_{23}$Auger	5.08	6.69	*c*
K	$2p$	3.94	4.98	*c*
Ti	$2p$	4.81	5.95	*d*
Cr	$2p$	7.19	8.73	*c*
O	$1s$	1.83	2.19	*d*
C	$1s$	0.70	0.87	*d*
N	$1s$	1.24	1.51	*d*
P	$2p$	1.15	1.50	*d*

a Based on the measurement of halloysite, molecular sieve 4A and 13X. The given sensitivity was proved to reproduce the Al/Si ratio in NBS standard reference materials 97a (flint clay) and 98a (plastic clay) within 10%.
b Based on the measurement of $K_3[Fe(CN)_6]$ and $K_4[Fe(CN)_6]$.
c Based on the measurement of fluoride, sulphate and chloride.
d Theoretical estimation (see text), but also substantiated by the experimental measurement of reference materials.

RESULTS AND DISCUSSION

Elemental composition

Figure 1 shows the XPS spectra of the three sediment reference materials, excited by Al $K\alpha$ radiation. Since all the materials contain at least about 20% of silicon, the spectrum of River Sediment is evidently anomalous. Its silicon peaks ($2p$ and $2s$) are very weak, whereas the C $1s$ and Cr $2p$ lines are prominent. At first glance it would be presumed that the sample is a mixture of carbonaceous material and oxides of chromium and iron. Such survey spectra, obtained by scanning a wide energy range within a short time (~60 eV/min in the present case), give a rough idea of the relative abundance of the major elements (>1% w/w) and reveal the existence of the minor elements (~0.1% w/w). For environmental samples, in our experience, most of the useful information can be provided at this stage of the measurement if preliminary knowledge of the bulk composition is available. In addition to the inorganic components, the elements of organic origin, such as carbon and nitrogen (see below), can be easily seen, although care must be taken with the carbon lines, because carbon contamination layers accumulated on the surface of the samples during the experimental procedures (especially from pump oil) always contribute carbon lines.

From the integrated intensities of the relevant emission lines and the atomic sensitivity factors listed in Table 1, the relative atomic compositions for the sediment samples were determined. Table 2 gives the atomic abundances of selected elements relative to Si, and Fig. 2 depicts the compositions in weight per cent

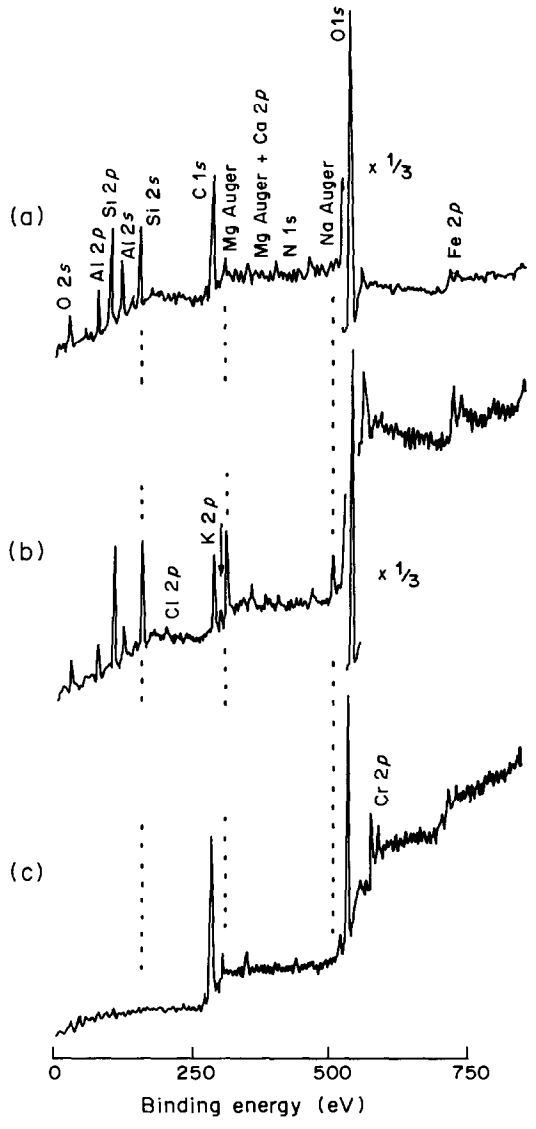

Fig. 1. X-Ray photoelectron spectra of (a) Pond Sediment, (b) Estuarine Sediment and (c) River Sediment.

and compares them with the corresponding analytical values for the bulk composition.[6-9] In representing the XPS results in weight per cent, the contribution of hydrogen is not considered, since it is not determined by XPS. The amount of carbon includes the contribution from contamination. However, for Pond Sediment as an example, the C/N ratio (16.4) determined by XPS is comparable to that (14.8) for the bulk composition, and therefore the contribution of the carbon contamination is not significant. Though various factors (*e.g.*, the probe depth in XPS, which depends both on the kinetic energy of the photoelectron and on the composition of the individual particles,[12,15] and the structure of the surface in an actual sample[16-19]) complicate evaluation of the relation of elemental composition determined by XPS to the true average surface composition, the result

Table 2. Atomic composition of the sediment reference materials, determined by XPS (Si = 1)*

Element	Line	Source target	NIES No. 2	NBS 1645	NBS 1646
Al	2*p*	Al	0.82 (1.5)	0.80 (8.8)	0.40 (1.9)
Fe	2*p*	Al	0.26 (1.6)	1.7 (7.0)	0.13 (2.5)
Mg	$KL_{23}L_{23}$Auger	Al	0.030 (0.59)	0.52 (4.5)	0.11 (2.8)
Ca	2*p*	Mg	0.026 (0.96)	0.89 (11)	0.0091 (0.48)
Na	$KL_{23}L_{23}$Auger	Al	0.010 (0.30)	0.25 (8.8)	0.090 (1.1)
K	2*p*	Al	—	—	0.048 (1.5)
Ti	2*p*	Mg	0.017 (0.94)	—	—
Cr	2*p*	Al	—	3.1 (46)	—
P	2*p*	Al	0.01 (1.7)	—	0.041 (2.6)

*Relative to Si. For Si, the 2*s* line was used. The numbers in parentheses are the ratios to the corresponding value for the bulk composition.[6-9]

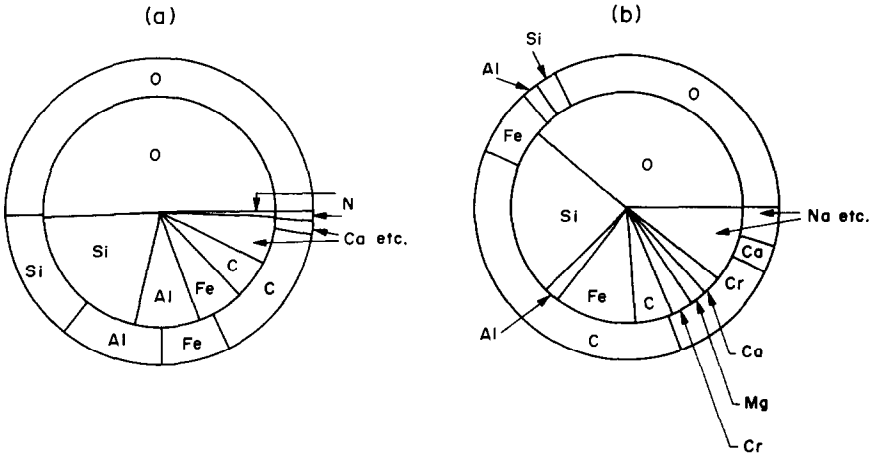

Fig. 2. Elemental composition of (a) Pond Sediment and (b) River Sediment in weight per cent. The inner circle represents bulk composition and the outer circle represents the composition determined by XPS.

may be regarded as representing the apparent surface composition "seen" by the X-ray flux. The peculiar features in the composition of River Sediment, as determined by XPS, are more clearly seen. As shown in Table 2, the atomic abundances of the major elements relative to Si, determined by XPS, are higher than those for the bulk composition, and the Cr/Si ratio is exceptionally large.

Since the finer particles are expected to contribute relatively more to the surface area seen by the X-ray flux (the contribution should be inversely proportional to the particle diameter if the particles are randomly arranged in the sample layer for the XPS measurement), we examined how the Cr/Si ratio determined by XPS depended on the particle size. Sieving of River Sediment powder revealed that it consisted of a 105–180 μm (particle diameter) fraction (80% in weight), a 44–105 μm fraction (20%) and a small amount of a finer portion. Table 3 shows the Cr/Si ratio of the coarser fraction is small but still more than an order of magnitude larger than the bulk ratio. Fine particles may be attached to coarse particles to form composite particles, and may not be separated by sieving. When the coarsest portion (105–180 μm) was subjected to ultrasonification in water, fine particles were dispersed. The coarse precipitate was separated and washed repeatedly (with ultrasonification) until no turbidity was visible in the supernatant liquid. The Cr/Si ratio (XPS) of the precipitate (Table 3) is significantly smaller than that for the sample before washing, but still far exceeds the bulk value. It can be concluded from these observations that in the River Sediment particles,

Table 3. Particle-size dependence of Cr/Si ratio for NBS 1645 River Sediment

	Cr/Si
(1) XPS	
44–105 μm	3.6
105–180 μm	2.1
105–180 μm washed with ultrasonification	0.86
(2) Bulk total	0.067*

*From refs. 7 and 8.

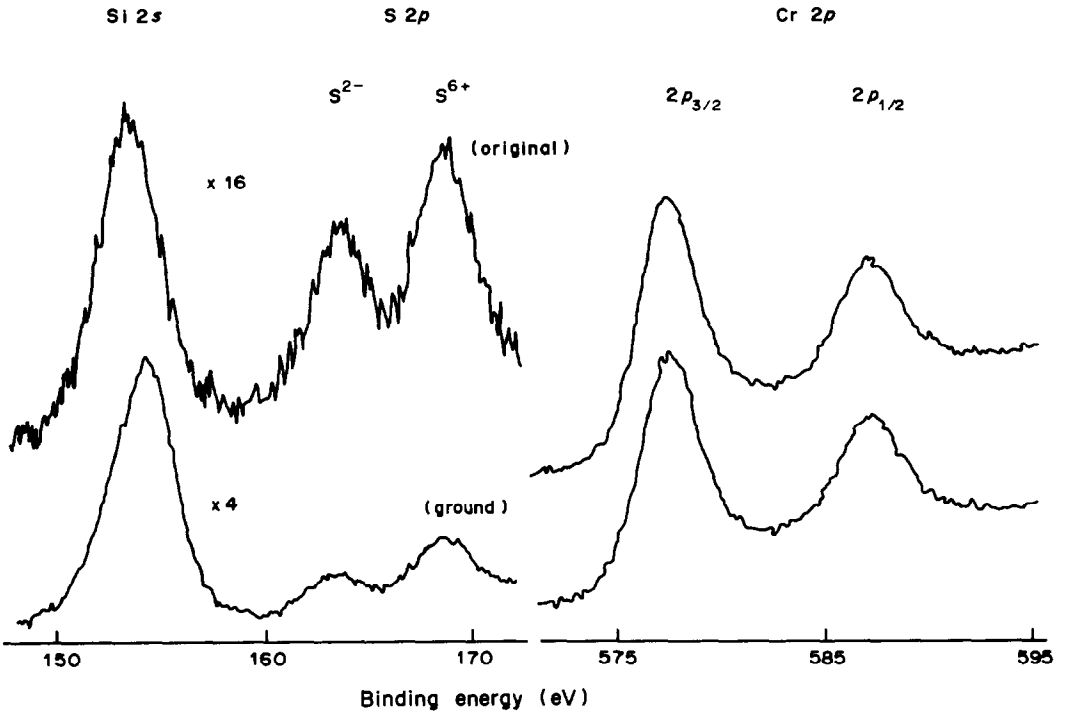

Fig. 3. Changes in the XPS spectra of River Sediment in the Si 2*s*, S 2*p* and Cr 2*p* regions after the powder has been ground in an agate mortar.

Si-rich particle cores are covered with Cr-rich surface layers, which include attached fine particles, and that Si is depleted in the surface layers. At least a part of the surface layers cannot be removed by physical methods such as ultrasonification.

Such a distribution of Cr and Si suggests that Cr was introduced into the river as a pollutant and deposited on the surface of the originally silica-rich sediment particles. The reported ease of acid extraction of Cr from River Sediment[20] is consistent with such a composition of the sediment particles. As Fig. 2b shows, carbon (and nitrogen) is most enriched in the surface layers, *i.e.*, the surface is rich in organic substances. Sulphur is also more abundant in the surface layers (1.8% w/w) compared to the bulk composition (*ca.* 0.5% as determined with a Carlo Erba 1108 Elemental Analyzer).

For other elements (Al, Fe, Mg, Ca, Na) in River Sediment, the amounts relative to Si are significantly larger in the surface than those in the bulk composition, because of the depletion of Si in the surface, but the amounts in terms of weight per cent are only slightly less than those in the bulk, owing to the diluting effect of organic substances in the surface. That is to say, unlike Si, they are mixed in the organic and chromium-rich surface layers.

Figure 3 shows the changes in the spectra when the sample of River Sediment was ground in a mortar (agate or alumina). The intensity of the Si 2*s* line relative to the lines of other elements increased remarkably after the grinding. This demonstrates that Si is exposed in the surface by grinding and that the Si-rich particles are covered by the surface overlayers in the original preparation.

In contrast to River Sediment, the deviation of the composition determined by XPS from that of the bulk for Pond Sediment (NIES No. 2) is much less pronounced (Fig. 2a). However, organic components (C, N) are again rich in the surface layers, as is also the case for Estuarine Sediment. Thus XPS offers direct evidence for the surface predominance of organic substances in soil or sediment particles.[21] The weight content of Si in the surface of Pond Sediment is about two-thirds of the bulk content, whereas the contents of Al and Fe in the surface are comparable to those in the bulk. As shown in Table 2, Na is depleted in the surface (one-fifth of the bulk content). K is also depleted in the surface, although the quantification is difficult because the energy-loss satellite of the C 1*s* line interferes with the weak K 2*p* lines. The depletion of alkali elements in the XPS analysis is also observed for a sample from the sedimentation pond of a water purification plant. Thus, it is probable that leaching causes the depletion of the alkali-metal elements from the surface. On the other hand, Al, Fe and P had the same concentration levels in the surface as in the bulk. There must be certain mechanisms, such as deposition from the aqueous phase, keeping the surface concentrations of those elements at a comparable level to the bulk

concentration, in spite of the diluting effect of organic substance.

The deviation of the surface elemental composition from the bulk composition for Estuarine Sediment is not as large as that for River Sediment but larger than that for Pond Sediment. The latter fact can be attributed to the mixing of river and sea-water causing more extensive reorganization of the surface composition for estuarine sediments.[21] The surface enrichment of Al and Fe relative to Si may thus be attributable to the deposition of these elements in the estuarine region.[21] The surface enrichment of Mg and depletion of Ca are also notable, but whether this is general behaviour for estuarine or coastal sediment is uncertain at the present stage.

Characterization of the bonding states of elements

We summarize here the information obtained from the photoelectron binding energies for the three reference materials. The peak positions of C 1*s* (284.7 ± 0.2 eV) and N 1*s* (399.8 ± 0.2 eV) indicate that the carbon and nitrogen are of organic origin, the latter being mainly due to the amino-group. The binding energies of Si 2*s* (153.6, 153.7 and 153.1 eV for Pond Sediment, Estuarine Sediment and River Sediment, respectively) are compatible with a range of silicate minerals.[22] They depend on the O/Si ratio and on the negative charge in the silicate skeleton. As can be seen in Fig. 3, the peak position of Si 2*s* for River Sediment shifted to 153.9 eV when the sample powder was ground. The binding energy after grinding was close to that for quartz (SiO_2, 154.2 eV).[22] This fact supports the preceding argument that the chemical composition of the surface layer of River Sediment is significantly different from that of the average (bulk) composition. Figure 3 also demonstrates that S^{6+} (168.5 eV; SO_4^{2-} should be the main species) and S^{2-} (163.5 eV) can be distinguished. As the latter energy is slightly higher than those observed for metal sulphides, we attribute it to organic sulphide(s). A comparison of the Cr $2p_{3/2}$ binding energy found in River Sediment (577.2 eV) with those of chromium compounds (Cr_2O_3, 576.6; $CrCl_3$, 577.0; $K_2Cr_2O_7$, 579.6 eV) shows that the chromium in the surface layers of River Sediment particles is tervalent. Since its binding energy is slightly higher than that for the oxide, the species is considered to be probably the hydrous oxide or Cr(III) adsorbed on minerals.[23] Similarly, the Fe $2p_{3/2}$ binding energies for Pond Sediment (711.2 eV) and River Sediment (711.4 eV) are slightly higher than that of ferric oxide (α-Fe_2O_3, 710.8 eV) and are consistent with hydrous oxides such as goethite[24] or Fe(III) adsorbed on minerals.[23] The Fe $2p_{3/2}$ binding energy for Estuarine Sediment (712.4 eV) is significantly higher and can be attributed to Fe(III) incorporated into clay minerals[23] or to amorphous ferric hydroxide.[23,24]

Acknowledgement—The authors are grateful to Mr. Masataka Nishikawa for the determination of sulphur in the River Sediment.

REFERENCES

1. For examples see: W. M. Briggs and M. J. Parker, in A. W. Czanderna, *Methods of Surface Analysis*, p. 103, Elsevier, Amsterdam, 1975; L. A. Casper and C. J. Powell (eds.), *Industrial Applications of Surface Analysis*, ACS Symposium Series, 1982, 199; H. Windawi and F. F.-L. Ho (eds), *Applied Electron Spectroscopy for Chemical Analysis*, Wiley, New York, 1982.
2. G. M. Bancroft, J. R. Brown and W. S. Fyfe, *Chem. Geol.*, 1979, **25**, 227.
3. I. J. Tinsley, *Chemical Concepts in Pollutant Behavior*, Wiley, New York, 1979.
4. For reviews see: D. Briggs, in C. R. Brundle and A. D. Baker, *Electron Spectroscopy*, Vol. 3, p. 305, Academic Press, New York, 1979; T. Novakov, S.-G. Chang, R. L. Dod and L. Gundel in D. S. Natusch and P. K. Hopke, *Analytical Aspects of Environmental Chemistry*, p. 191, Wiley, New York, 1983.
5. For a review see: R. W. Linton, D. T. Harvey and G. E. Cabaniss, in D. S. Natusch and P. K. Hopke, *Analytical Aspects of Environmental Chemistry*, p. 137, Wiley, New York, 1983.
6. K. Okamoto (ed.), *Preparation, Analysis and Certification of Pond Sediment Certified Reference Material, Research Report from the National Institute for Environmental Studies, Japan*, No. 38, 1982.
7. *Certificate of Analysis, River Sediment SRM 1645*, U.S. Department of Commerce, National Bureau of Standards, Washington D.C., 1978.
8. E. S. Gladney, *Anal. Chim. Acta*, 1980, **118**, 385.
9. *Certificate of Analysis, Estuarine Sediment SRM 1646*, U.S. Department of Commerce, National Bureau of Standards, Washington D.C., 1982.
10. Y. Iwata, K. Matsumoto, H. Haraguchi, K. Fuwa and K. Okamoto, *Anal. Chem.*, 1981, **53**, 1136.
11. Y. Iwata, H. Haraguchi, J. C. Van Loon and K. Fuwa, *Bull. Chem. Soc. Japan*, 1983, **56**, 434.
12. M. P. Seah, *Surf. Interface Anal.*, 1980, **2**, 222.
13. J. H. Scofield, *J. Electron Spectrosc.*, 1976, **8**, 129.
14. R. E. Reilman, A. Msezane and S. T. Manson, *ibid.*, 1976, **8**, 389.
15. D. M. Wyatt, J. C. Carver and D. M. Hercules, *Anal. Chem.*, 1975, **48**, 1297; K. T. Ng and D. M. Hercules, *J. Electron Spectrosc.*, 1975, **7**, 257.
16. C. S. Fadley, R. J. Baird, W. Siekhaus, T. Novakov and S. Å. L. Bergstrom, *ibid.*, 1974, **4**, 93.
17. H. Ebel, M. F. Ebel and E. Hillbrand, *ibid.*, 1973, **2**, 277.
18. K. Hirokawa and M. Oku, *Talanta*, 1980, **27**, 741.
19. H. Windawi and C. D. Wagner in *Applied Electron Spectroscopy in Chemical Analysis*, H. Windawi and F. F.-L. Ho (eds.), p. 191, Wiley, New York, 1982.
20. S. A. Sinex, A. Y. Cantillo and G. R. Helz, *Anal. Chem.*, 1980, **52**, 2342.
21. H. J. M. Bowen, *Environmental Chemistry of the Elements*, Academic Press, London, 1979.
22. H. Seyama and M. Soma, *J. Chem. Soc. Faraday I*, in the press.
23. M. H. Koppelman and J. G. Dillard, in *Marine Chemistry in the Coastal Environment*, T. M. Church (ed.), p. 186. American Chemical Society, Washington, D.C., 1975.
24. D. T. Harvey and R. W. Linton, *Anal. Chem.*, 1981, **53**, 1684.

Talanta, Vol. 32, No. 3, pp. 183–187, 1985
Printed in Great Britain.

0039-9140/85 $3.00 + 0.00

FLUORIMETRIC DETERMINATION OF DISSOCIATION CONSTANTS AND pH-CONTROLLED FLUORESCENCE ANALYSIS OF PURINES AND PYRIMIDINES

DIARIATOU GNINGUE and JEAN-JACQUES AARON*
Laboratoire de Chimie Physique Organique et d'Analyse Instrumentale, Département de Chimie, Faculté des Sciences, Université de Dakar, Dakar-Fann, Sénégal

(*Received* 11 *July* 1984. *Accepted* 28 *October* 1984)

Summary—Fluorimetrically determined pH-titration curves have been obtained for twelve purines and pyrimidines at room temperature, in aqueous solution. The pK_a values for these compounds have been determined fluorimetrically and potentiometrically. Except for 6-mercaptopurine and uric acid, there is close agreement between the two sets of pK_a values, but a large difference for the corresponding excited singlet-state values, $pK_a^{S_1}$, which were calculated previously. This indicates that the excited singlet-state proton-transfer rate is much slower than the fluorescence-decay rate of purines and pyrimidines in our experimental conditions. A direct, simple, pH-controlled fluorimetric method is proposed for the determination of purines and pyrimidines. The limits of detection vary between 60 ng/ml and 5.4 μg/ml.

In recent years, fluorimetry has been demonstrated to be a simple and relatively accurate method for the determination of dissociation constants of organic acids and bases.[1–5] For those cases in which excited-state proton-transfer takes place during the fluorescence lifetimes of acids and conjugate bases,[6–8] instrumental and chemical means have been proposed to overcome its interference with the fluorimetric measurement of the ground-state pK_a values.[1–9] However, for most nitrogen- and oxygen-containing heterocyclic compounds, with pK_a values in the range 3–10, the rate of deactivation of the excited singlet-state was found to be much larger than that of excited-state proton-exchange, resulting in fluorimetrically determined pK_a values that were in good agreement with absorptiometrically or potentiometrically measured ground-state pK_a values.[1,3–5,10,11] The effect of pH also has important consequences for the sensitivity and selectivity of the fluorimetric determination of acids and bases, owing to the large differences in fluorescence spectra and quantum yields between the various dissociated and undissociated species. For this reason, pH-dependent fluorimetry has recently aroused considerable interest.[4,7,8]

However, there have been relatively few reports concerning the pH effects on the fluorescence of purines and pyrimidines.[12–15] Börresen[12] found that the fluorimetrically determined dissociation constants of purine and guanine were significantly higher than the ground-state values obtained by potentiometric titration, whereas for adenine there was no difference between the pK_a values measured fluorimetrically and potentiometrically. The existence of a highly fluorescent tautomer was postulated by Börresen[13] to explain the broadening and red-shift in the fluorescence of protonated adenine derivatives relative to that of the corresponding neutral species, and confirmed recently by Knighton *et al.*[14] Finally, dissociation constants of purines and pyrimidines in the excited singlet-state were determined very recently by Parkanyi *et al.*,[15] using the Förster cycle method. These authors found that in the excited singlet-state the basicity of most of the purines and pyrimidines is increased for the equilibria between the cationic and neutral species, but for the equilibria between the neutral and anionic species, all purines and pyrimidines are more acidic.[15]

In the present work, we wish to report on the fluorimetric measurement of the dissociation constants of some purines and pyrimidines, and to evaluate the performance of a pH-controlled method of fluorescence analysis for the determination of these compounds.

EXPERIMENTAL

Reagents

Purine and guanine were purchased from CDC Chemicals, adenine, 6-chloropurine, 6-mercaptopurine, hypoxanthine, cytosine, and 5-fluorouracil from US Biochemical Co., theobromine and uric acid from Eastman Kodak, and thymine and uracil from Aldrich Chemical Co. Distilled water, hydrochloric acid and sodium hydroxide were used for preparing solutions in the pH range 1–10.

Instrumentation

A Turner model 111 fluorometer, an ultraviolet lamp model 110-855 (which gives an excitation band between 270 and 340 nm), 7-54 excitation and 2-A emission filters, and 10% and 1% neutral density filters. A Metrohm model E520 pH-meter.

Procedure

The pK_a values were determined from the inflection points of the fluorimetric-titration plots of relative fluorescence intensity (I_F) *vs.* acidity (pH or Hammett function H_0). The

*Author to whom all correspondence should be addressed.

excitation wavelength used was an isobestic wavelength of the pH-dependent absorption spectrum to ensure that the same amount of radiation was absorbed at all points of the titration curve. For some compounds, the pK_a values were also calculated from the equation:[1,3]

$$pK_a = pH - \log \frac{(I_F - I_F^{BH^+})}{I_F^B - I_F} \quad (1)$$

where I_F^B and $I_F^{BH^+}$ are the relative fluorescent intensities of the free base and the conjugate acid respectively.

The pK_a^{CN} values are those for the equilibria (2a) and (2b) between the cationic and neutral species of purines and pyrimidines:

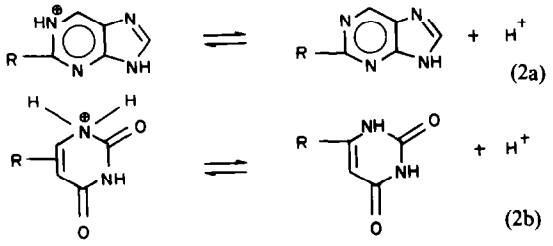

(2a)

(2b)

The pK_a^{NA} values refer to the equilibria (3a) and (3b) between the neutral and anionic species:

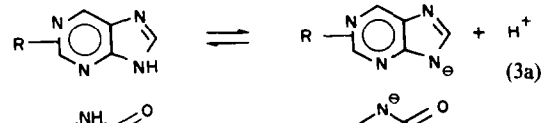

(3a)

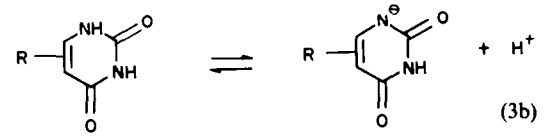

(3b)

Note that B is the neutral species in equilibria (2a) and (2b) but the anionic species in equilibria (3a) and (3b), and BH^+ is the cationic species in (2a) and (2b) but the neutral species in (3a) and (3b).

RESULTS AND DISCUSSION

Effect of pH on fluorescence intensity

The fluorescence intensity of purines and pyrimidines changes drastically with pH, as can be seen in Figs. 1–4, which give some examples of fluorimetric titration curves. In the case of purine (Fig. 1), 6-chloropurine, thymine (Fig. 3, curve b), and 5-fluorouracil (Fig. 4), the fluorescence intensity increases strongly between pH 6 and 11, because of the formation of the anionic species, which generally have a larger fluorescence quantum yield than neutral molecules.[15] At higher sodium hydroxide concentrations (pH > 12), the fluorescence of the anions of purine and thymine is partially quenched (Fig. 1 and Fig. 3, curve b).

In the case of adenine, cytosine (Fig. 3, curve a), and uric acid (Fig. 2, curve b), the fluorescence signal increases at around pH 4, which corresponds to the dissociation of the cationic species into the neutral molecule. Between pH 7 and pH 11, the titration curves level off, and the fluorescence is partially quenched in more alkaline solution (pH > 12). In the case of cytosine, there is a second inflection point at about pH 12, which corresponds to the neutral molecule–anion equilibrium (3b), (Fig. 3, curve a).

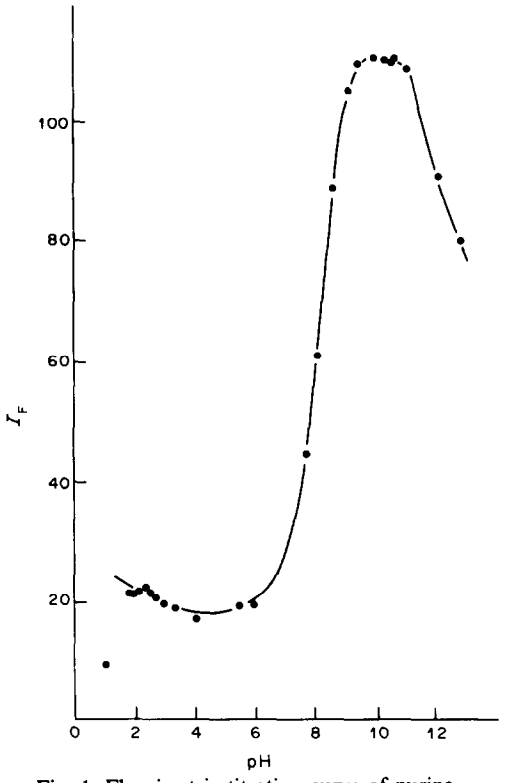

Fig. 1. Fluorimetric titration curve of purine.

A fluorimetric titration curve with two inflection points at around pH 3.9 and pH 8.9 is also found for guanine (Fig. 2, curve a). The first inflection point, characterized by a decrease in fluorescence intensity

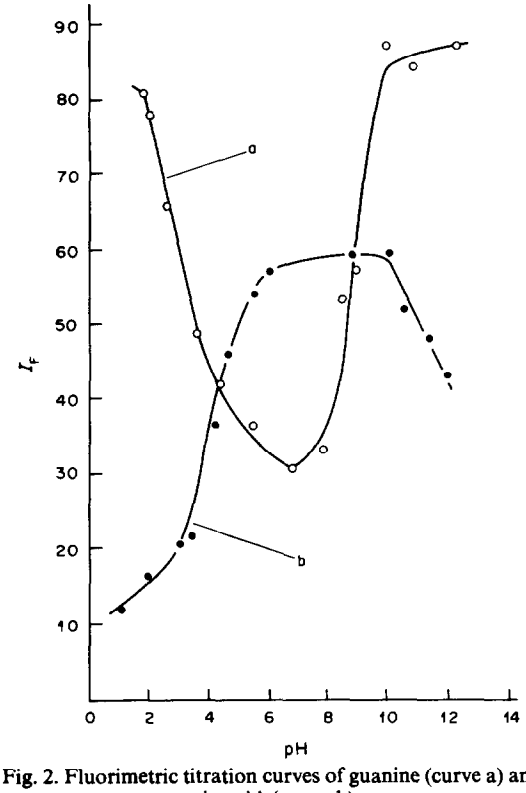

Fig. 2. Fluorimetric titration curves of guanine (curve a) and uric acid (curve b).

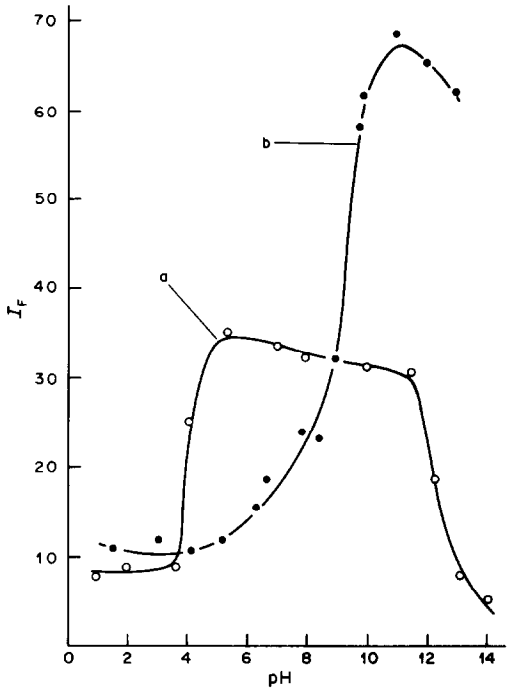

Fig. 3. Fluorimetric titration curves of cytosine (curve a) and thymine (curve b).

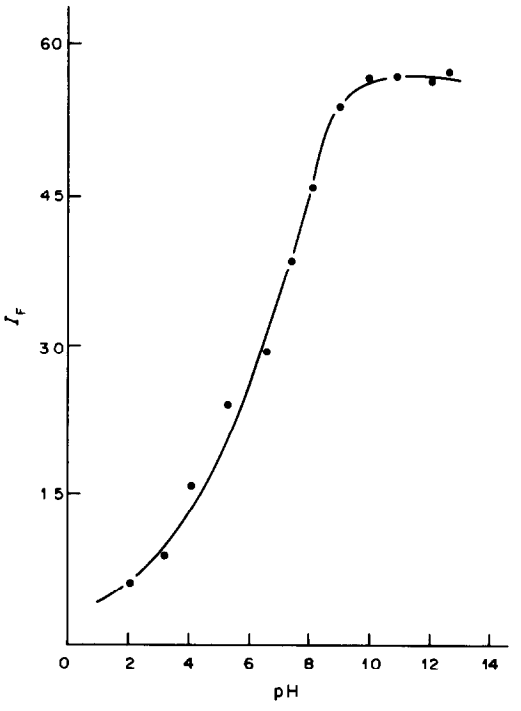

Fig. 4. Fluorimetric titration curve of 5-fluorouracil.

between pH 2 and pH 5, is due to the deprotonation of the cation, while the second, showing a strong increase in the fluorescence signal between pH 8 and pH 10.5, results from the formation of the more fluorescent anionic species of guanine.

Fluorimetric determination of pK_a

Table 1 summarizes the pK_a values of the purines and pyrimidines, calculated from the fluorescence titration curves, and also the ground-state dissociation constants determined potentiometrically and absorptiometrically. Our findings show that, for most of the compounds, the values of pK_a obtained fluorimetrically agree very well, within experimental error, with the ground-state pK_a value; the difference between the fluorimetric and the ground-state pK_a values is generally less than 0.2. There is also a good agreement between the pK_a values calculated from

Table 1. Dissociation constants (pK_a) of purine and pyrimidine cations and neutral molecules, calculated from fluorimetric, absorptiometric and potentiometric data

	Fluorimetry			Absorptiometry	Potentiometry	
Species[a]	Inflection point pK_a[b]	Equation (1) pK_a[c]	Literature values pK_a[d]	pK_a[e]	This work pK_a[f]	Literature values pK_a[g]
Purine	8.2 ± 0.2	8.5	9.2	8.95	9.0 ± 0.2	8.93
Adenine cation	4.1 ± 0.2	—	4.2	—	4.1 ± 0.2	4.25
6-Chloropurine	8.3 ± 0.2	7.5	—	7.85	7.7 ± 0.2	7.88
6-Mercaptopurine	7.0 ± 0.2	—	—	7.77	7.7 ± 0.2	7.77
Guanine cation	3.4 ± 0.1	3.2	3.4	—	3.5 ± 0.25	3.0
Guanine	8.9 ± 0.1	9.0	9.3	9.35	8.8 ± 0.3	9.35
Theobromine	—[h]	—	—	10.04	9.6 ± 0.2	10.00
Uric acid	4.2 ± 0.2	4.9	—	5.45	5.3 ± 0.1	5.40
Cytosine cation	4.6 ± 0.2	4.7	—	—	4.7 ± 0.3	4.65
Cytosine	12.15 ± 0.1	—	—	12.24	—	12.15
Thymine	9.5 ± 0.2	—	—	9.86	9.75 ± 0.2	9.94
5-Fluorouracil	7.4 ± 0.4	7.6	—	7.98	7.6 ± 0.3	8.04

[a] Neutral molecule, when not specified in the table.
[b] Mean values calculated from 3 or 4 fluorimetric curves.
[c] Mean values calculated from 3 or 4 points on each fluorimetric curve.
[d] Values taken from Börresen.[12]
[e] Values determined absorptiometrically at 293 K.[15]
[f] Mean values determined potentiometrically in triplicate at 298 K.
[g] Values taken from Albert.[16,17]
[h] No meaningful pK_a value could be determined from the unusually flat portion of the fluorimetric titration curve of theobromine in the pH region 7–12.

Table 2. Statistical treatment of the fluorimetric analytical curves and detection limits of purines and pyrimidines

Compound	pH	LDR,* M	Slope†	Intercept†	Correlation coefficient	LOD,§ $\mu g/ml$
Purine	10	5×10^{-6}–10^{-3}	0.68	4.19	0.993	0.9
Adenine	10	5×10^{-5}–10^{-3}	0.52	3.33	0.996	5.4
6-Chloropurine	10.3	10^{-6}–10^{-3}	0.35	2.43	0.984	0.07
Guanine	11	8×10^{-6}–4×10^{-5}	0.47	3.29	0.962	0.09
Hypoxanthine	9.5	10^{-5}–5×10^{-4}	0.70	3.90	0.987	0.2
Theobromine	10	10^{-5}–10^{-3}	0.26	2.13	0.950	0.1
Uric acid	10	10^{-5}–10^{-3}	0.27	1.83	0.978	1.1
Cytosine	6.5	10^{-6}–10^{-3}	0.21	2.03	0.989	0.06
Thymine	11	10^{-6}–10^{-4}	0.36	2.83	0.991	0.06
5-Fluorouracil	12	10^{-6}–10^{-4}	0.35	2.75	0.993	0.08

*LDR = linear dynamic range, defined by the concentrations between which the log–log analytical curve is linear.

†Values calculated by the statistical treatment of 9–12 measurements for each analytical curve.

§LOD = limit of detection, defined as the concentration (in μg/ml) of compound giving a fluorescence signal equal to three times the fluctuations of the background fluroescence signal.

the inflection point of the fluorescence titration curve and from equation (1).

In contrast, the pK_a values obtained fluorimetrically present large differences from the corresponding excited singlet-state dissociation constants ($pK_a^{S_1}$), calculated earlier[15] by the Förster cycle method. For example, for adenine a pK_a^{CN,S_1} value of 10.03 was found,[15] which is much higher than the fluorimetric pK_a^{CN} value of 4.10; for thymine the pK_a^{NA,S_1} value[15] was 3.85, whereas the pK_a^{NA} value determined fluorimetrically is 9.50. This results from the fact that the rate of excited singlet-state proton-transfer is much slower than the rate of fluorescence decay of the purine and pyrimidine cations, anions and neutral species; therefore, the prototropic equilibrium is not attained during the lifetime of the S_1 state, and the inflection points of the fluorimetric titration curves correspond to the ground-state pK_a values. Similar behaviour has been observed for other nitrogen- and oxygen-containing heterocycles, with $pK_a^{S_1}$ values in the range 3–10.[1,3,7,10,11]

Two exceptions are 6-mercaptopurine and uric acid, for which the fluorimetric pK_a^{NA} values (7.0 and 4.2 respectively) differ by more than 0.7 from the ground-state pK_a^{NA} values (Table 1). For 6-mercaptopurine, the fluorimetric value is closer to the excited-state pK_a^{NA,S_1} value[15] of 7.29, while for uric acid the fluorimetric value is between the excited-state pK_a^{NA,S_1} value[15] of 0.05 and the ground-state pK_a^{NA} value of 5.3. This may be due to partial establishment of the prototropic equilibrium in the lowest excited singlet-state of both compounds.

Quantitative analytical applications

The fluorimetric titration curves also have important consequences for the determination of purines and pyrimidines. They have allowed us to select, for each compound, the optimal pH region corresponding to the maximum sensitivity of fluorimetry. We found that, except for cytosine, the anionic species gave larger relative fluorescence intensities than the neutral molecules, the fluorescence signal generally being maximal at around pH 10, which corresponds to the predominant presence of the anionic species. This is in agreement with our previous results for the relative fluorescence quantum yields of neutral and anionic species of some purines.[15] Pyrimidines have also been found to be much more phosphorescent in basic than in neutral media.[18]

Although purines and pyrimidines are generally considered to be relatively weak fluorophores,[19] most of the compounds studied here were shown to have analytically useful fluorescence signals when our pH-controlled fluorimetric technique is used. Table 2 gives the pH values used, the statistical characteristics of the fluorimetric calibration curves, and the limits of detection (LOD). The linear dynamic ranges (LDR) are relatively large since they cover 2–3 orders of magnitude. However, the slopes of the log–log curves are much smaller than unity, indicating non-linearity for non-logarithmic calibration plots. This is thought to be due to concentration-independent secondary Rayleigh scattering intensity at wavelengths longer than 500 nm for most purines and pyrimidines,[15] which results in interference in the fluorescence measurements under the instrumental conditions used.

The limits of detection, defined here as the concentration giving a signal-to-noise ratio equal to 3, ranged between 60 ng/ml and 5.4 μg/ml, depending on the particular compound. Specially low LOD values (all lower than 90 ng/ml) were obtained for 6-chloropurine, guanine, cytosine, thymine, and 5-fluorouracil. It was only for adenine and uric acid that the LOD values were larger than 1 μg/ml (Table 2).

Purine and pyrimidine bases and nucleotides have been detected and separated, often in biological media, by chromatographic methods such as

TLC,[20,21] GC[22,23] and HPLC.[24–26] The use of low-temperature phosphorimetry (LTP)[18,27,28] and fluorimetry of derivatives[29–33] has also been reported for the determination of these compounds, with LOD values in the low ng/ml range. In spite of their high sensitivity, both techniques suffer from some limitations. LTP needs cryogenic equipment,[34,35] and preparation of highly fluorescent derivatives of purines and pyrimidines is time-consuming and often complicated.[31] Therefore, pH-controlled fluorimetry offers a convenient alternative method which, though sometimes less sensitive than the other technqiues, presents the great advantage of permitting direct, simple, and rapid determiantion of purines and pyrimidines.

REFERENCES

1. L. S. Rosenberg, J. Simons and S. G. Schulman, *Talanta*, 1979, **26**, 867.
2. S. G. Schulman and W. J. M. Underberg, *Anal. Chim. Acta*, 1979, **108**, 249.
3. R. Schipfer, O. S. Wolfbeis and A. Knierzinger, *J. Chem. Soc. Perkin Trans.*, 2, 1981, 1443.
4. O. S. Wolfbeis, *Z. Phys. Chem. (Frankfurt)*, 1981, **125**, 15.
5. O. S. Wolfbeis, A. Knierzinger and R. Schipfer, *J. Photochem.*, 1983, **21**, 67.
6. A. U. Acuna and J. M. Oton, *J. Luminescence*, 1979, **20**, 379.
7. O. S. Wolfbeis and E. Furlinger, *Z. Phys. Chem. (Frankfurt)*, 1982, **129**, 171.
8. S. G. Schulman, in *Modern Fluorescence Spectroscopy*, E. L. Wehry (ed.), Vol. 2, p. 239. Dekker, New York, 1976.
9. W. J. M. Underberg and S. G. Schulman, *Anal. Chim. Acta*, 1979, **105**, 311.
10. M. Swaminathan and S. K. Dogra, *J. Photochem.*, 1983, **21**, 245.
11. *Idem*, *J. Chem. Soc. Perkin Trans.* 2, 1983, 1641.
12. H. C. Börresen, *Acta Chem. Scand.*, 1963, **17**, 921.
13. *Idem*, *ibid.*, 1967, **21**, 11.
14. W. B. Knighton, G. Ogiskaas and P. R. Callis, *J. Phys. Chem.*, 1982, **86**, 49.
15. C. Parkanyi, D. Bouin, D.-C. Shieh, S. Tunbrant, J. J. Aaron and A. Tine, *J. Chim. Phys.*, 1984, **81**, 21.
16. A. Albert, in *Physical Methods in Heterocyclic Chemistry*, Vol. I, A. R. Katritzky (ed.), pp. 1–108. Academic Press, New York, 1963.
17. A. Albert, in *Physical Methods in Heterocyclic Chemistry*, Vol. III, A. R. Katritzky (ed.), pp. 1–26. Academic Press, New York, 1971.
18. J. J. Aaron, R. Fisher and J. D. Winefordner, *Talanta*, 1974, **21**, 1129.
19. M. Gueron, J. Eisinger and A. A. Lamola, in *Basic Principles in Nucleic Chemistry*, Vol. I, Chapter 4, Academic Press, New York, 1974.
20. R. Cardinaud, *J. Chromatog.*, 1978, **154**, 345.
21. J. F. Tomashevski, R. J. Barrios and O. Sudilovsky, *Anal. Biochem.*, 1974, **60**, 589.
22. C. W. Gehrke and C. D. Ruyle, *J. Chromatog.*, 1968, **38**, 473.
23. V. Miller, V. Pacáková and E. Smolková, *ibid.*, 1976, **119**, 355.
24. N. Christophidis, G. Mihaly, F. Vajda and W. Louis, *Clin. Chem.*, 1979, **25**, 83.
25. M. Zakaria and P. R. Brown, *J. Chromatog.*, 1981, **226**, 267.
26. K. Štulík and V. Pacáková, *ibid.*, 1983, **273**, 77.
27. J. J. Aaron and J. D. Winefordner, *Anal. Chem.*, 1972, **44**, 2127.
28. J. J. Aaron, W. J. Spann and J. D. Winefordner, *Talanta*, 1973, **20**, 855.
29. R. D. Hosmane and N. J. Leonard, *J. Org. Chem.*, 1981, **46**, 1457.
30. D. E. Bergstrom, H. Inoue and P. A. Reddy, *ibid.*, 1982, **47**, 2174.
31. J. A. Zoltewicz and E. Wyrzykiewicz, *ibid.*, 1983, **48**, 2481.
32. W. P. McCann, L. M. Hall and W. K. Nonidez, *Anal. Chem.*, 1983, **55**, 1454.
33. R. B. Triplett and L. D. Smith, *Anal. Biochem.*, 1977, **80**, 490.
34. J. J. Aaron and J. D. Winefordner, *Analusis*, 1982, **10**, 299.
35. R. J. Hurtubise, *Anal. Chem.*, 1983, **55**, 669A.

Talanta, Vol. 32, No. 3, pp. 189–193, 1985
Printed in Great Britain.

0039-9140/85 $3.00 + 0.00

ANALYTICAL APPLICATION OF THE COMPLEXATION OF Nb(V) WITH BROMOPYROGALLOL RED IN MICELLAR MEDIA

M. E. DIAZ GARCIA and A. SANZ-MEDEL
Department of Analytical Chemistry, Faculty of Chemistry, University of Oviedo, Oviedo, Spain

(*Received* 6 *February* 1984. *Revised* 10 *September* 1984. *Accepted* 29 *September* 1984)

Summary—A spectrophotometric method for the determination of trace amounts of Nb(V) based on the formation of a ternary complex with Bromopyrogallol Red (L) and cetylpyridinium bromide (CPB) in 1*M* hydrochloric acid/15% dimethylformamide medium has been developed. The ternary 1:2:2 Nb–L–CPB complex is formed. The absorbance maximum is at 645 nm, the molar absorptivity being $(4.00 \pm 0.04) \times 10^4$ l.mole^{-1}.cm^{-1}. The relative standard deviation is 1.9% and Beer's law is obeyed up to 1.4 μg of Nb(V) per ml. The application of the method to the determination of Nb in pyrochlore-bearing rocks is described. A possible mechanism of interaction of the surfactant with the Nb–L complex is discussed.

The characteristics of analytically useful anionic metal complexes are known to be modified by the addition of cationic surfactants. The charged micelles (through their large superficial electrostatic potential and hydrophobic forces) are able to promote formation of "new" complexes which exhibit markedly improved spectrophotometric properties, *viz.* higher molar absorptivities, stability over a wider pH range, larger bathochromic shifts in comparison with the binary complex, and so on.[1]

These unique properties of micellar systems have been extensively exploited,[1,2] mainly for improving the sensitivity of analytical methods ("surfactant-sensitized reactions"). Less attention has been paid, however, to the solution chemistry involved in this kind of reaction.

It is well known that surfactant molecules in aqueous solution associate upon reaching the so-called "critical micelle concentration" (c.m.c.) to form micelles capable of solubilizing a great variety of organic-like solutes (which otherwise would be insoluble in water). In this context, a binary chelate complex solubilized (or incorporated) in a micelle is exposed to a microenvironment quite different from that in bulk water. In fact, a micellar medium is best characterized as a mixed aqueous–organic solvent,[3] where reaction rates, spectral characteristics, redox processes, *etc.* of a given complex may change drastically.

The principles which are operative in the effects of micelles in analytical reactions are poorly known. No satisfactory theory exists so far to explain the possible mechanism(s) associated with sensitized reactions. Therefore, a better understanding of the nature of surfactant sensitization is a major goal of research in our laboratory.[4–6]

The ternary system Nb(V)–BPR–EDTA has been used to determine niobium in steels in a cetyltrimethylammonium medium of pH 4.5.[7] The object of the present paper is a detailed study of the niobium–Bromopyrogallol Red complex in micellar media. Some special features of using mixed solvents are discussed and attempts are made to extend some physico-chemical observations of micellar systems to surfactant-sensitized analytical reactions.

As a result, a mechanism for the reaction of Nb(V) with Bromopyrogallol Red and cetylpyridinium bromide is proposed, and the analytical characteristics of a new "sensitized" spectrophotometric method for Nb(V) determination are given. The method has been successfully applied to the determination of the metal in pyrochlore-bearing rocks.

EXPERIMENTAL

Reagents

Nb(V) stock solution (200 μg/ml). Prepared as described elsewhere.[4] Diluted further with 2% tartaric acid solution as required, immediately before use.

Cetylpyridinium bromide (CPB) solution, 0.2%. Prepared by dissolving the solid in water by warming, and standardized by titration.[8]

Bromopyrogallol Red solution, 0.1%. Prepared by dissolving 0.1 g of BPR in water containing 0.5 ml of 0.1*M* sodium hydroxide and diluting accurately to 100 ml with water.

All reagents were analytical-reagent grade and distilled demineralized water was used to prepare all solutions.

Spectrophotometric procedure

Pipette standard Nb(V) solution (up to 12 μg of the metal) into a series of 10-ml volumetric flasks already containing the following, added in the order shown and mixed after each addition: 0.5 ml of the reagent solution, 1.5 ml of dimethylformamide (DMF), 1.7 ml of 6*M* hydrochloric acid and 0.5 ml of CPB solution. Mix thoroughly and dilute to the mark with distilled demineralized water. After about 60 min measure the absorbance at 645 nm against a reagent blank.

Determination of Nb in pyrochlore-bearing rocks

Decompose the rock samples as described elsewhere,[9] and prepare a known volume of stock solution. Transfer a suitable aliquot (< 2 ml) containing 2–14 μg of Nb(V) into

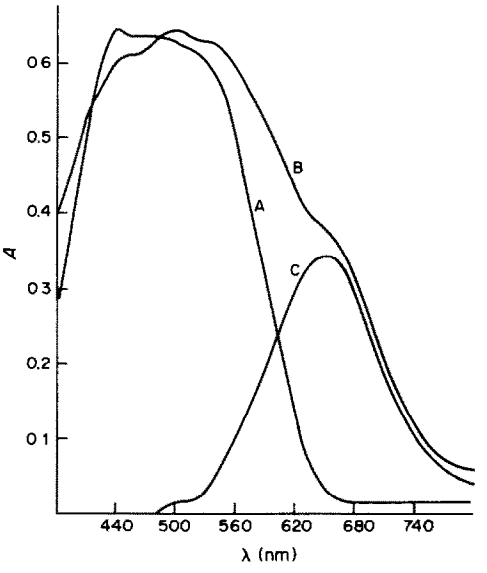

Fig. 1. Absorption spectra of: A, reagent blank against water as reference; B, Nb(V)–Bromopyrogallol Red–CPB complex measured against water as reference; C, Nb(V)–Bromopyrogallol Red–CPB complex against reagent blank. [Nb(V)] = $1.07 \times 10^{-5}M$; [BPR] = $5.37 \times 10^{-5}M$; [CPB] = $2.53 \times 10^{-4}M$. Medium, $1M$ HCl–15% DMF.

a 100-ml separatory funnel and dilute with 11 ml of concentrated hydrochloric acid. Add 10 ml of isopentyl acetate and shake the mixture vigorously for 10 min. Allow the layers to separate and discard the aqueous lower layer. Then add 3 ml of 2% tartaric acid solution, shaking the funnel for 10 min. Transfer the aqueous layer to a 10-ml standard flask which already contains the reagents (0.5 ml of 0.1% BPR solution, 1.5 ml of DMF, 0.2 ml of concentrated hydrochloric acid and 0.5 ml of 0.2% surfactant solution). Wash the remaining organic layer with 2 ml of $1M$ hydrochloric acid to collect any suspended water droplets; add this aqueous portion to the 10-ml standard flask. Dilute to the mark with distilled water and mix thoroughly. After 60 min measure the absorbance of the solution at 645 nm against a reagent blank prepared in the same way (2 ml of "blank ore" solution).

Prepare the calibration curve by treating independent portions of dilute standard niobium solution according to the method above.

RESULTS AND DISCUSSION

Spectral characteristics

The nature of the complex species formed in the presence of CPB depends on the acidity of the medium: in more acidic media (0.3–1.6M hydrochloric acid) a complex predominates which has its absorption maximum in the region 645–650 nm; as the pH increases a second complex with λ_{max} at 620–625 nm starts to appear and predominates between pH 2 and 6.

As $1M$ hydrochloric acid medium provides similar sensitivity to that observed at higher pH values, but higher selectivity, this medium was used in subsequent studies.

In Fig. 1, curves A and B show the absorption spectra of Bromopyrogallol Red and its Nb(V) complex in the presence of CPB in $1M$ hydrochloric acid. The maximum absorbance difference (curve C) for the Nb(V) complex is observed at 645 nm. Figure 2 shows that the spectrum of the ternary complex is very different from that of the binary Nb–Bromopyrogallol Red complex. The spectrum of the binary complex shows peaks corresponding to the 1:1 and 1:3 (Nb:BPR) complexes (see below).

Influence of experimental variables

Water-miscible solvent effect. Increasing turbidity and fading of the colour takes place on standing. A large surfactant concentration eliminates the precipitation, but also undesirably reduces the absorbance. Therefore, several water-soluble solvents were tested for stabilization: methanol, acetone, dimethylsulphoxide and *N,N'*-dimethylformamide (DMF). A final DMF concentration of 15% proved to be most suitable.

Mixing order and standing time. The absorbance was independent of the order in which the components of the reaction mixture were mixed, but in practice the order dye, DMF, acid, surfactant and Nb(V) solution was followed. Maximal constant absorbance was obtained in 60 min and remained unchanged for at least 12 hr.

Ionic strength effects. Callahan and Cook[10] have reported the effects of added electrolytes on the Be–Chrome Azurol S complex sensitized by cetyltrimethylammonium bromide: the molar absorptivity increases with addition of salt and the wavelength of maximum absorbance is shifted to a wavelength 12–14 nm longer.

The influence of the ionic strength (I) on the complex formation of Nb(V) and BPR in presence of CPB micelles was studied in the range 1.4–3M by adding increasing amounts of $4M$ sodium chloride. The results show that the shape of the spectrum remains practically unchanged but the turbidity (as

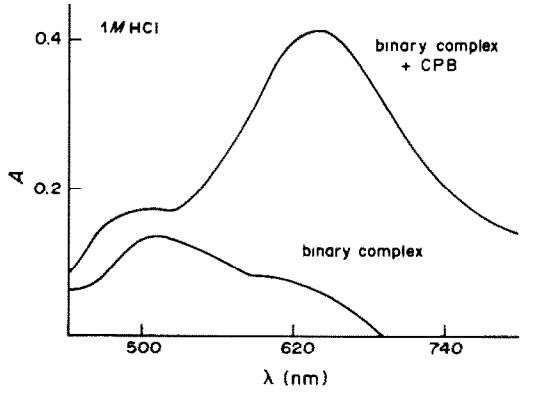

Fig. 2. Absorption spectra of the binary and ternary complexes measured against a reagent blank, in $1M$ HCl medium.

Table 1. Determination of niobium in natural and synthetic samples*

Sample	Nb expected, %	Nb found, %	
		Proposed method	Dichloro-oxine method
OKA-1 No 82†	0.36 ± 0.01	0.35 ± 0.04	0.35 ± 0.02
OKA-2 No 56†	0.36 ± 0.01	—	0.36 ± 0.02
A§	0.117 ± 0.01	—	0.12 ± 0.01
B§	0.705 ± 0.01	0.71 ± 0.03	0.70 ± 0.02
C§	1.010 ± 0.01	—	1.05 ± 0.02
D§	1.248 ± 0.01	1.28 ± 0.04	—

*Each value is the average of four separate determinations.
†Calcite-base pyrochlore ores from Oka (Canada).
§Synthetic samples.

absorbance measured at 800 nm) increases with I (Fig. 3). No turbidity was observed in the reagent blanks.

In the light of our observations it seems that a high electrolyte level may have a profound effect on the properties of the micellar medium. It is known that at high salt concentrations the shape of the micelles changes,[11] and that when the micelles change from spherical to rod-like, the viscosity increases markedly.[12]

Changes in viscosity, due not only to changes of the micellar structure but also to a higher salt content, could affect the solubility of the solutes. In this context, the turbidity observed in the Nb system could be attributed to the Nb–BPR–CPB complex becoming more insoluble as the salt concentration increases, but it is hard to draw any general conclusion, since it would be difficult to disentangle the effects due to changes in the medium viscosity from those due to influence of the micellar structure on the solubilizing capacity.

Surfactant concentration. The c.m.c. of CPB in a 1M hydrochloric acid medium was found to be $4.96 \times 10^{-4}M$, as determined by surface-tension measurement; the presence of 15% DMF lowered the c.m.c. to $2.39 \times 10^{-4}M$. This trend seems to be related to the solubility of the DMF in the micelles, which affects the hydrophobic forces in the micellar surface.[13]

During the study of the influence of surfactant concentration (in the presence of 15% DMF) we observed no precipitation of the ternary ion-association complex at surfactant concentrations below the c.m.c., whereas precipitation in such conditions is usually observed in many sensitized systems.[6] The formation of premicelles (mixed micelles) between DMF and surfactant monomers seems to play an important role; these mixed-micelles should be responsible for solubilization of the chelate–surfactant ion-association complex to give a clear and stable solution, even at low surfactant concentrations (DMF acts as a co-surfactant).

As shown in Fig. 4, the absorbance of the ternary system increases linearly with increasing CPB concentration up to a sharp break [at about 11-fold molar excess of surfactant relative to Nb(V)], after which,

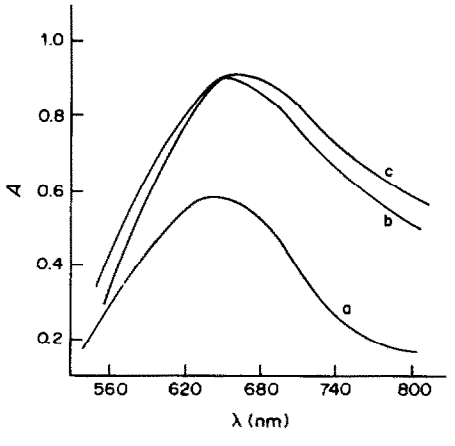

Fig. 3. Spectra of Nb(V)–BPR–CPB complex in 1M HCl–15% DMF medium with (a) no salt (b) 0.8M NaCl and (c) 2M NaCl. [Nb(V)] = $1.07 \times 10^{-5}M$; [BPR] = $8.95 \times 10^{-5}M$; [CPB] = $2.73 \times 10^{-4}M$.

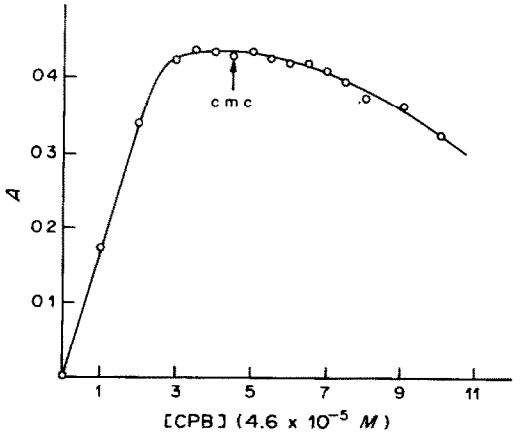

Fig. 4. Effect of cetylpyridinium bromide concentration on the Nb–BPR complex in 1M HCl–15% DMF medium. Wavelength, 645 nm. [Nb(V)] = $1.07 \times 10^{-5}M$; [BPR] = $8.95 \times 10^{-5}M$.

the absorbance remains virtually constant. For CPB concentrations above the c.m.c. a further increase in surfactant concentration produces a progressive decrease in absorbance.

Analytical characteristics

Beer's law, sensitivity and precision. The calibration graph was found to obey Beer's law in the Nb(V) range 0.1–1.4 μg/ml. At 645 nm the molar absorptivity was $(4.00 \pm 0.04) \times 10^4$ $l.mole^{-1}.cm^{-1}$. Absorbance measurements on ten independent 0.6 μg/ml solutions gave a relative standard deviation of 1.9%.

Interferences. The selectivity was investigated by determination of 0.8 μg/ml Nb(V) in the presence of a series of other ions. An ion was considered to interfere only if it produced a change of at least 2% in the absorbance obtained for niobium alone.

The following ions did not interfere: 400 μg/ml B; 80 μg/ml Si(IV), Ni, Co(II), Mn (II), Ca, Pb, Ce(III), U(VI); 40 μg/ml Cu(II), Al, Cr(III) and Sb(III); 0.8 μg/ml Fe(III), V(V) and Hg(II). The interference of 0.8 μg/ml Zr was eliminated by the addition of EDTA. The other interferences are dealt with by preliminary extraction of the Nb(V), see below.

Large amounts of common masking agents for Nb(V), *viz.* phosphate (up to 2.37*M*), EDTA (0.003*M*), citrate (0.085*M*), ascorbate (0.23*M*), fluoride (0.42*M*), oxalate (0.009*M*) and tartrate (0.053*M*) did not interfere.

Although the proposed method has lower sensitivity than that of the method reported by Jadhav and Venkateswarlu,[7] it is rather more selective; of 22 cations and 7 anions only Ta(V), Mo(VI), W(VI), Sn(IV) and Ti(IV) interfered. These interferences can be easily overcome by selectively separating Nb(V) before its determination, as in the surfactant-free method of Ramakrishna *et al.*[14] (see procedure for determination of Nb in pyrochlore-bearing rocks).

Nature of the sensitized reaction

Composition of the species formed. The continuous-variation method indicated that in the absence of surfactant two binary complexes were formed between Nb(V) and BPR in 1*M* hydrochloric acid medium, with Nb/L ratios of 1:1 ($\lambda_{max} = 524$ nm) and 1:3 ($\lambda_{max} = 645$ nm). In the presence of excess of CPB two complexes were again found, but of composition 1:1 and 1:2 (Nb/L).

Figure 4 shows that sensitization starts at well below the c.m.c. of CPB, indicating that a true ternary complex Nb:BPR:CPB of the type 1:1:*a* or 1:2:*b* might be responsible for the observed spectral changes on addition of surfactant. If this is so, a fixed stoichiometric ratio of chelate to surfactant is to be expected.[5]

To establish the values of *a* and *b*, equimolar solutions of surfactant and chelate (NbL or NbL_2) were prepared. Continuous-variation plots indicated a 1:1 chelate:surfactant ratio for the NbL system and a 1:2 ratio for NbL_2. In other words, at the relatively high dye concentrations used in the analytical procedure a 1:2:2 ternary complex seems to be formed. Complete formation of this complex, however, apparently necessitates an excess of surfactant (Fig. 3).

Reaction mechanism. The sensitization by the cationic surfactant appears to be the result of concurrently electrostatic and hydrophobic interactions.

Formation of the ion-association ternary complex NbL_2^{2-} $(CP^+)_2$ is attributable to *electrostatic interactions* through the sulphonate group of the dye. This kind of interaction alone, however, is not sufficient to explain the spectral changes observed on addition of CPB, because non-micelle-forming counter-ions, *viz.* diphenylguanidinium or tetraethylammonium, did not change the spectral characteristics of the binary complexes at all. In fact, simple ion-pairing between the sulphonate group of the dye and a quaternary ammonium counter-ion does not perturb the chromophore.[15] Therefore, surface-active agents do not simply act as counter-ions but clearly change the microenvironment of the chromophore (*hydrophobic interactions*), bringing about remarkable spectral changes.

Hydrophobic interactions, then, have to be considered: even at stoichiometric concentrations of the CPB, sensitization is observed and such hydrophobic interactions must then occur. As shown previously[5] the cationic surfactant electrostatically bound to the chelate would originate, probably by twisting of its long hydrocarbon chains towards the inner complex, a special microenvironment in which the physical properties (dielectric constant, viscosity, solubility, *etc.*) must be different from those of bulk water. This is more probable in our case where the ion-association complex is solubilized by surfactant–DMF premicelles. The more this microenvironment approaches that existing in the micelles of CPB the bigger is the sensitization observed (which would explain that maximum sensitization is observed around the c.m.c., see Fig. 3).

In any case, the overall effect of the cationic surfactant is quite involved and it cannot be attributed only to the addition of the electrostatic and hydrophobic contributions. Adding to the NbL_2 complex a mixture formed of a bulky non-micelle-forming cation (to provide the electrostatic contribution) and a non-ionic surfactant (Triton X-100, which would provide the hydrophobic effect) does not sensitize the binary complex.

Now, let us consider what happens if we secure maximum sensitization as in the analytical procedure (at CPB concentration around the c.m.c.): in this case the binary complex is incorporated into the Stern layer through the sulphonate groups.[12] This incorporation facilitates the reorientation of water molecules around the metal ion, and owing to the lower di-

electric constant near the micellar surface[16] the weakening of the hydration forces would make it possible for the central ion to co-ordinate more dye molecules (there would be an increase in the co-ordination number). This is a general trend observed in micellar systems.[17] In our systems, an $NbOL_3$ binary complex was detected: the presence of micelles should favour formation of this complex instead of the 1:1 or 1:2 complexes. Experiments showed, however, that the 1:2 complex was favoured by the presence of CPB micelles. This proves that exceptions to the rule above are quite common.[18] In our case, the CPB micelles seem to shift the equilibria towards the formation of the more stable complex, as it is known[19] that the $NbOL_3$ binary complex is very weak even at pH 6. The low stability of these binary complexes could be due to the effect of stereochemical factors.

Determination of niobium in pyrochlore-bearing rocks

The proposed method has been applied to the determination of Nb(V) in certified and synthetic rocks (synthetic samples were prepared from calcite-based Canadian pyrochlores by mixing them with pure Nb_2O_5 powder).

Table 1 summarizes the results obtained by the present method and by an independent solvent-extraction method using dichloro-oxine.[9]

REFERENCES

1. W. L. Hinze, *Solution Chemistry of Surfactants*, K. L. Mittall (ed.), Vol. 1, 1979.
2. V. N. Tikhonov, *Zh. Analit. Khim.*, 1977, **32**, 1435.
3. N. Muller and R. H. Birkhahn, *J. Phys. Chem.*, 1967, **71**, 957.
4. A. Sanz-Medel, C. Cámara Rica and J. A. Pérez-Bustamante, *Anal. Chem.*, 1980, **52**, 1035.
5. I. Alonso García, M. E. Díaz-García and A. Sanz-Medel, *Talanta*, 1984, **31**, 361.
6. E. Blanco González, M. E. Díaz-García and A. Sanz-Medel, *Microchem. J*, 1984, **30(2)**, 211.
7. S. G. Jadhav and Ch. Venkateswarlu, *Indian J. Chem.*, 1978, **16A**, 263.
8. J. T. Cross, *Analyst*, 1965, **90**, 315.
9. A. Sanz-Medel and M. E. Díaz-García, *ibid.*, 1981, **106**, 1268.
10. J. H. Callahan and K. D. Cook, *Anal. Chem.*, 1982, **54**, 59.
11. S. Ikeda, S. Hayashi and T. Inaae, *J. Phys. Chem.*, 1981, **85**, 106.
12. C. A. Bunton, M. J. Minch, J. Hidalgo and L. Sepúlveda, *J. Am. Chem. Soc.*, 1973, **95**, 3262.
13. M. F. Emerson and A. Holtzer, *J. Phys. Chem.*, 1967, **71**, 3320.
14. T. V. Ramakrishna, S. A. Rahim and T. S. West, *Talanta*, 1969, **16**, 347.
15. G. J. Yakatan and S. G. Schulman, *J. Phys. Chem.*, 1972, **76**, 508.
16. C. A. Bunton and M. J. Minch, *ibid.*, 1974, **78**, 1490.
17. T. M. Doscher, G. E. Myers and D. C. Atkins, *J. Colloid. Sci.*, 1951, **6**, 223.
18. S. B. Savvin, R. K. Chernova and I. V. Lobacheva, *Zh. Analit. Khim.*, 1981, **36**, 9.
19. R. Belcher, T. V. Ramakrishna and T. S. West, *Talanta*, 1965, **12**, 681.

Talanta, Vol. 32, No. 3, pp. 195–201, 1985
Printed in Great Britain.

0039-9140/85 $3.00 + 0.00

INVESTIGATIONS OF TRACE ANALYSIS OF $A^{III}B^{V}$ SEMICONDUCTOR MICROSAMPLES BY ATOMIC SPECTROSCOPY—VII*

INVESTIGATION OF TRACE AND THIN-LAYER ANALYSIS OF DOPING ELEMENTS (Ag, Au, Bi, Cd, Sn, Tl) IN InAs BY ATOMIC-ABSORPTION WITH ELECTROTHERMAL EVAPORATION

K. DITTRICH
Analytical Centre, Department of Chemistry, Karl-Marx University Leipzig, Liebigstr. 18, DDR 7010 Leipzig, G.D.R.

W. MOTHES
VEB Metallaufbereitung Halle, Betrieb Leipzig, Industriestr., DDR 7031 Leipzig, G.D.R.

I. G. YUDELEVICH and T. S. PAPINA
Institute of Inorganic Chemistry, Siberian Division of the Academy of Sciences of the U.S.S.R., 630090 Novosibirsk, U.S.S.R.

(*Received* 6 *April* 1984. *Revised* 6 *September* 1984. *Accepted* 29 *September* 1984)

Summary—Etching procedures for separation of thin layers of InAs (up to 1.4 μm thick) have been developed and optimized. A solid-state microtome has been used for cutting layers thicker than 1 μm. AAS/ETA methods for determination of traces of Ag, Au, Bi, Cd, Sn, and Tl have been developed. The matrix interferences of nitric acid, hydrobromic acid, and As^{3+} or In^{3+} in nitric or hydrobromic acid have been studied. The main causes of the matrix interference are the formation of diatomic molecules between the trace and matrix components, and the effect of the evaporation processes. By use of the platform technique with special platforms some matrix interferences could be minimized. For the determination of traces of Sn, matrix modification with $Ni(NO_3)_2$ as additive gave the best analytical values. For the trace determination of Au, separation of In from Au by evaporation of $InBr_3$ from 0.6*M* HBR medium in the AAS ashing phase was developed. The detection limits are in the 10^{16} atoms/cm^3 region for layers of 1 μm thickness and surface area 1 cm^2.

For thin-layer and layer-by-layer analysis of semiconductor materials reproducible methods of layer separation and very sensitive methods for trace analysis of microsamples are needed. So far we have investigated the possibility of determining doping elements in thin layers of GaAs,[1] and InSb,[2] separating the layers by anodic oxidation followed by chemical etching, by chemical etching alone, and by mechanical separation with a diamond knife in a solid-state microtome. The anodic oxidation procedure gave the best depth resolution. For the determinations we used atomic-absorption spectrometry with electrothermal atomization (AAS/ETA).

The purpose of the present work was to extend these researches to thin layers of InAs. We have proved that chemical etching and mechanical separation are both useful for the purpose and have developed sensitive determination methods for trace amounts of Ag, Au, Bi, Cd, Sn, and Tl by AAS/ETA. The influence of the matrix substances was investigated.

*Part VI, *Talanta*, 1982, **29**, 577.

EXPERIMENTAL

Materials

InAs monocrystals with 111B surface; "suprapur" In, As, hydrobromic acid and nitric acid; acetone (quartz-distilled), purified paraffin, and doubly quartz-distilled water. Stock 0.1-mg/ml solutions of Ag, Au, Cd, Bi, Sn, Tl in nitric acid or a mixture of nitric and hydrochloric acids were used, and for the analytical investigations were diluted with 0.1*M* nitric acid (Ag, Bi, Cd, Sn, Tl) or 0.6*M* hydrobromic acid (Au). Purified $Ni(NO_3)_2$ solution (1*M*) was used as matrix modifier.

Apparatus

A Jarrell–Ash 811 atomic-absorption spectrometer, and Beckmann 1268 graphite cuvette, with background compensation by the two-line method, and a Perkin-Elmer 303 atomic-absorption spectrometer and HGA 74 graphite tube atomizer, with background correction by continuous light-source, were used.

Chemical etching and mechanical separation

InAs with an appropriate plane-polished surface was washed with distilled acetone to remove traces of grease. The non-planar surface was coated with paraffin to avoid any etching effects. Then 0.15 ml of etching reagent was placed on 1 cm^2 of the InAs surface. After an etching time of about 3 min this solution was removed with a Teflon capillary and used for the analytical determinations.

Table 1. Experimental conditions for the determination of trace elements by AAS/ETA

Element	Wavelength, nm	Wavelength for background corr., nm	Temperatures, °C drying phase t = 30–60 sec	ashing phase t = 15–30 sec	atomization phase‡ t = 5–15 sec with gas stop	
Ag	328.1	326.2 (Sn)	150	500	2400*	3000†
Au	242.8	242.1 (Sn)	150	750	2550*	3000†
Bi	306.8	307.3 (Hf)	150	750	2100*	2600†
Cd	228.8	231.1 (Sb)	150	400	2000*	2600†
Sn§	224.8†	226.8 (Sn)	160	1200		3300†
	286.3		200	1150	2400*	
Tl	276.8	277.9 (Ga)	150	750	2150*	2600†

*Perkin-Elmer AA spectrometer 303/HGA 74.
†Jarrell-Ash AA spectrometer 811/Beckman GC 1268.
‡The temperature differences are due to the different electrical conditions.
§Sensitivity of AA with Sn EDL twice as good.

For separation of layers >2 μm thick chemical etching is very time-consuming, but such layers can be separated in 1-μm steps by use of a diamond knife in a solid-state microtome. The powder separated was collected, weighed, and dissolved in dilute nitric acid.

Determination of added traces

The etching solutions or nitric acid solutions were evaporated to dryness under infrared radiation at a temperature not exceeding 60°. For determination of Ag, Bi, Cd, Sn, and Tl, 0.1 ml of 1*M* nitric acid was added to the dry residue and evaporated to dryness to remove residues of hydrobromic acid. This step was repeated, then the residue was dissolved in 0.1*M* nitric acid (0.1–1.0 ml, accurately measured, depending on the amount of residue). For the determination of Au the dry residues were dissolved in 0.1–1.0 ml of 0.6*M* hydrobromic acid (accurately measured). Finally a 20-μl portion of the solution was placed in the graphite tube. The optimal working conditions for the AAS/ETA determination are shown in Table 1.

For the investigations using the L'vov platform technique we made special 10 × 6 mm platforms from normal graphite tubes. These platforms are chamfered to fit snugly on the inner surface of the graphite tube (*cf.* L'vov *et al.*[3]).

RESULTS AND DISCUSSION

Optimization of the separation method

First we tested some polishing reagents[4–6] for etching properties, but none was suitable for etching purposes. The polishing reagent proposed by Luft *et al.*[6] was based on sulphuric acid, which is a very bad reagent for use in AAS/ETA. We therefore tried other mixtures of acids and finally found the combination of hydrobromic and nitric acid to be the best. The etching properties of this reagent are due to the elemental bromine formed by oxidation. For etching of layers between 0.1 and 1.4 μm thick the reagents used were mixtures of concentrated hydrobromic acid, nitric acid and water in the ratios 20:1:40, 20:1:60 and 20:1:80 v/v. Before use the mixtures must stand for at least 2 hr, during which a brown colour due to bromine develops. The solutions are usable for 14 days.

The results of etching the 111B surface of InAs are shown in Fig. 1. The etching rate and depth depend on the water content of the etching solutions. In all cases a constant etch depth is achieved in 2–3 min, and increases with decreasing water content. Figure 1 shows that the etch depth can be varied by adjusting the acid concentration or the etching time. The first is recommended.

Ellipsometric measurement of the roughness of the etched surfaces showed a relative standard deviation of 10% for the depth. The mean depths of replicate etches had a relative standard deviation of 6%.

Effect matrix substances on the AAS/ETA results

Hydrobromic acid. Figure 2 shows the effect of hydrobromic acid concentration on the determination of Ag, Au, Bi, Cd, Sn, and Tl traces by AAS/ETA, at a fixed 0.1*M* nitric acid concentration. Use of the special platforms decreases this matrix effect (cf. Table 2), especially for Cd. The determination of Bi, Sn and Tl in 1.2*M* hydrobromic acid medium is practically impossible, even with use of the special platforms. There is no matrix effect on the signal for Ag when the platform is used, but the signal for Au is doubled at hydrobromic acid concentrations >0.6*M*.

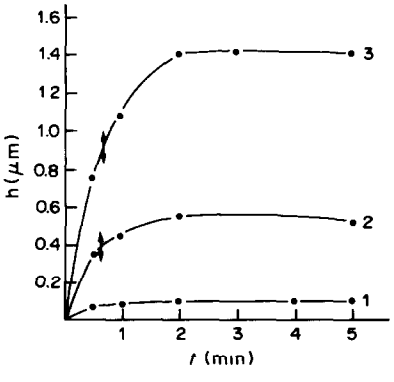

Fig. 1. Quantitative characteristics of the etching of InAs (111)B with 1, $HBr:HNO_3:H_2O = 20:1:80$; 2. $HBr:HNO_3:H_2O = 20:1:60$; 3. $Hbr:HNO_3:H_2O = 20:1:40$. The double arrow shows the uncertainty for $P = 95\%$.

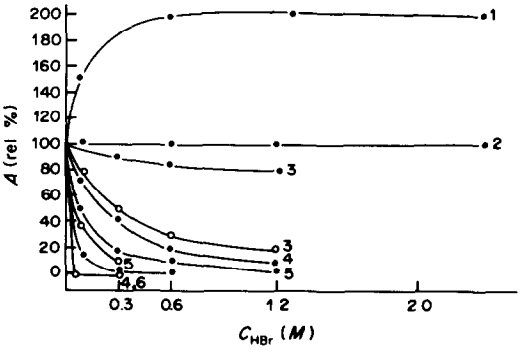

Fig. 2. Influence of the concentration of hydrobromic acid on trace element determinations by AAS/ETA, normalized to the signal for 0.1*M* HNO_3 medium: ● with platform; ○ without platform; 1-Au, 2—Ag, 3—Cd, 4—Sn, 5—Bi, 6—Tl.

Table 2 gives the improvement factors achieved by using the platform technique for both nitric and hydrobromic acid media. Except for the tin determination the improvement factors are small for nitric acid medium. With hydrobromic acid medium the signal improvement is significant for Ag and Cd trace determinations. The improvement in the determination of tin and thallium is very great, because there is zero signal if no platform is used (Fig. 2). The depression of the signals can be explained in terms of the thermal properties of the compounds which are probably formed in the hot tubes. Some of these are shown in Table 3.

The strong depression of the Bi and Sn signals by hydrobromic acid is due to the formation of the low-boiling bromides $BiBr_3$ (b.p. 461°) and $SnBr_4$ (b.p. 208°), which volatilize in the ashing phase. The signal for Tl is also strongly depressed, because of formation of sparingly soluble and easily volatilized TlBr. Katzkov[7] showed that in the AAS determination of Tl in nitric acid solution the Tl volatilizes as the metal in the temperature range 1200–1500°. The metal is formed from the salts by reaction with the hot graphite tube surface. This process is theoretically possible at high temperatures in presence of bromide but the TlBr will already have been lost by volatilization in the ashing phase and the beginning of the atomization phase. In earlier work on molecular absorption[8] we showed that in the vapour phase TlBr is a stable diatomic molecule (dissociation energy 3.4 eV) and exists at high temperatures in the gas phase inside the graphite tube. Its molecular absorption can be used for determination of traces of bromide, and the existence of TlBr molecules in the gas phase under the conditions used in this work was established by light-absorption measurements at 342.9 nm[9].

In principle, bromide should also influence the AAS determination of silver. In acid media the sparingly soluble AgBr is formed, which volatilizes at comparatively low temperature, with incomplete dissociation. We could detect the AgBr molecule by its light-absorption at 318.4 nm in hot graphite tubes.[9] The dissociation energy of this molecule is smaller than that of TlBr (3.2 eV). This fact and the incomplete dissociation on volatilization lead to the situation that all the silver species dissociate in the high-temperature gas phase before the AgBr has disappeared by diffusion.

The explanation for the depression of the Cd signal by hydrobromic acid is less well defined. Sturgeon *et al.*[10] showed that the atomization of Cd takes place by dissociation of gaseous CdO if nitric acid medium is used and by dissociation of gaseous CdCl if hydrochloric acid medium is used. The appearance temperature for Cd atoms in hydrochloric acid medium is 50° lower than that in nitric acid medium.

In presence of hydrobromic acid the appearance temperature is still lower than in hydrochloric acid medium because the b.p. of $CdBr_2$ is about 100° lower than that of $CdCl_2$. As we have shown,[11] hydrochloric acid has much less influence than nitric acid on the Cd AAS signals. From these facts we can conclude that the depressive effect of hydrobromic acid arises from the high volatility of $CdBr_2$ and diffusion of undissociated CdBr particles. This opinion is confirmed by the marked change when the platform technique is used, since the CdBr molecules are more extensively dissociated in a given atomization time by the higher temperature of the gas phase in the tube/platform system.

The improvement of the Au signals by hydrobromic acid can be explained as due to better and faster volatilization, with increased dissociation of AuBr particles.

Table 2. Influence of the platform technique on the AA determinations

Element and concentration,			Ratio of improvement*	
	μg/ml	*pg/20 μl*	0.1*M* HNO_3	0.2*M* HBr
Ag	0.004	80	1	1.6
Au	0.012	240	1.4	1.1
Bi	0.1	2000	1.2	1.3
Cd	0.001	20	1.1	1.8
Sn	0.2	4000	2.5	
Tl	0.1	2000	1.4	

*Ratio of improvement = $\frac{\text{AA signal with platform}}{\text{AA signal without platform}}$.

Table 3. Melting and boiling points of trace metals, In, and their compounds

Element or compound	m.p., °C	b.p., °C	Element or compound	m.p., °C	b.p., °C
Ag	960	2167	In	156.2	2020
AgBr	424	700 (d)	InBr	285	687
$AgNO_3$	209.7	300 (d)	$InBr_3$	420	371 (s)
AgO		100 (d)	$InBr_2$	197	633
Ag_2O		200 (d)	In_2O		~700 (s)
Au	1063	2677	In_2O_3	1910	
Bi	271	1552	Sn	232	2260
$BiBr_3$	218	461	$SnBr_4$	30	208
Bi_2O_3	825	1890	SnO	1080 (d)	
Cd	321	766	SnO_2	2000	2500
$CdBr_2$	568	865	Tl	303	1475
$CdCl_2$	568	960	TlBr	460	815
CdO	—	1560 (s)	Tl_2O	300	1800
			Tl_2O_3	717 ± 5	—

(d) = decomposition.
(s) = sublimation.

Effect of As(III) on AAS determination of Ag, Bi, Cd, Sn and Tl

The influence of the matrix As(III) formed from the InAs by oxidation with nitric acid and partly by the etching process, was investigated, for traces of Bi, Sn and Tl in only the nitric acid medium and for traces of Ag, Au and Cd in both nitric and hydrobromic acid media. It was found that As concentrations between 0.05 and 4 mg/ml have no influence on the AAS signals of these elements. Considering that up to 85–95% of the arsenic is lost during the evaporation of the etching solution (mixture of hydrobromic and nitric acids), this means that the residual arsenic does not influence the AAS determinations of Ag, Bi, Cd, Sn, Tl and Au. In the case of Au the evaporation of the arsenic is complete during drying of its solution in hydrobromic acid in the graphite tube.

Influence of In^{3+} on the AAS determination of Ag, Au, Bi, Cd, Sn and Tl

In nitric acid medium the presence of In^{3+} in concentrations up to 5 mg/ml does not affect the height of the signals for Ag, Bi, Cd, Sn and Tl, but the non-specific background for the determination of Bi, Cd and Tl is very high and cannot be compensated by use of a deuterium lamp. Use of the platform technique improves the background by fractional volatilization. The effect of the matrix substances is stronger in hydrobromic acid medium than nitric acid medium.

The AAS signals of Bi, Sn and Tl are completely depressed, and those of Ag and Cd are up to 50–90% depressed, even when the platform technique is used (Fig. 3). Comparison of Figs. 2 and 3 shows that the influence of the combination of In^{3+} and hydrobromic acid is much stronger than that of the acid alone.

The influence of the In^{3+}/HBr combination is due to $InBr_3$ being formed in the drying and ashing processes in the graphite tube, and only incompletely thermally decomposed at high temperatures. There are some losses of volatile InBr species in the ashing phase (Table 3), but the bulk of the indium bromide volatilizes only in the atomization phase. At the high temperatures of the atomization phase the indium bromide is partly dissociated (dissociation energy 4.2 eV)[8] into In and Br atoms. This leads to a high Br concentration in the graphite cuvette, which affects the complete (Bi, Sn, Tl) or incomplete but strong (Ag, Cd) formation of the diatomic metal bromides in the graphite tube, *cf.* Layson and Holcombe.[12] The strong influence of In^{3+} in hydrochloric acid medium is caused in the same way and was described by us earlier.[11]

The signal enhancement by the platform technique is caused first by the fractionated volatilizations and secondly by the increased dissociation at the higher temperatures achieved.

When the mixed matrix In^{3+}/As(III)/HBr is present in the determinations, there is a small improvement in the AAS determinations, caused by volatilization of part of the bromide as $AsBr_3$ and by the fact that the weak but volatile arsenious acid forms $InAsO_3$ at higher temperatures. The extent of

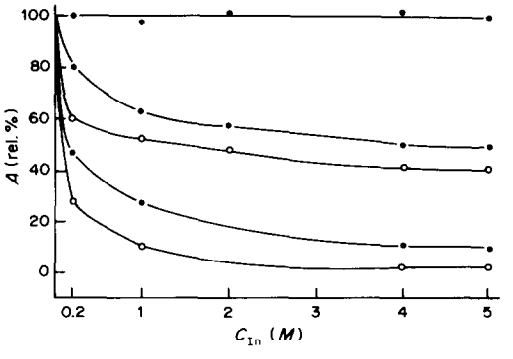

Fig. 3. Influence of the In^{3+} concentration in 0.2*M* hydrobromic acid on trace element determinations by AAS/ETA, normalized to the signal for 0.2*M* HBr medium: ● with platform; ○ without platform; 1—Au, 2—Ag, 3—Cd.

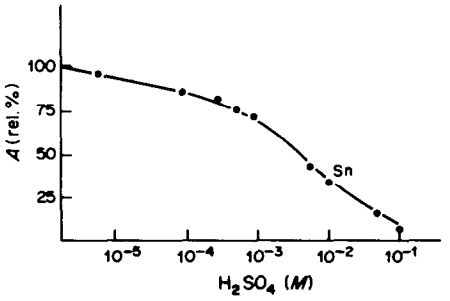

Fig. 4. Influence of sulphuric acid concentration on determination of Sn by AAS/ETA: signal for 0.1*M* HNO_3 medium = 100%.

these reactions also depends on the nitric acid concentration in the medium (cf. Dittrich *et al.*[11]).

Optimization of the Sn determination by matrix modification

The determination of Sn traces by AAS/ETA in hydrobromic acid medium is impossible, and in nitric acid medium is not very sensitive. The improvement of the sensitivity in both media by use of the platform technique shows the strong influence of the vaporization and dissociation processes on the determination.[12] To improve the sensitivity of the Sn determination we first tried sulphuric acid medium. The results are shown in Fig. 4. Low concentrations of sulphuric acid strongly depress the Sn signal by formation of the stable diatomic molecule SnS (dissociation energy 4.8 eV). We tried to detect this molecule in the gas phase in the graphite cuvette. The result is shown in Fig. 5, which shows characteristic differences in the molecular absorbance of Sn species in presence and absence of sodium sulphide, *cf.* Dittrich and Vorberg.[13] We therefore investigated some marix modifiers.[14] The results shown in Fig. 6 indicate that some metal nitrates improve the Sn signals significantly. It could also be shown that the parent acid and base, *e.g.*, nitric acid or barium hydroxide, also improve the analytical results when present at higher concentrations.

The salts are more effective however, stabilizing the easily volatilized and easily decomposed SnO by formation of the metal stannites and stannates, which

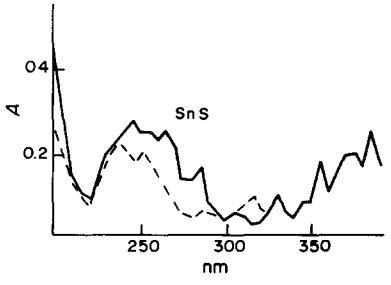

Fig. 5. Molecular absorption spectra of Sn species volatilized in the graphite tube in presence and absence of S: ——with S (as Na_2S); ---without S.

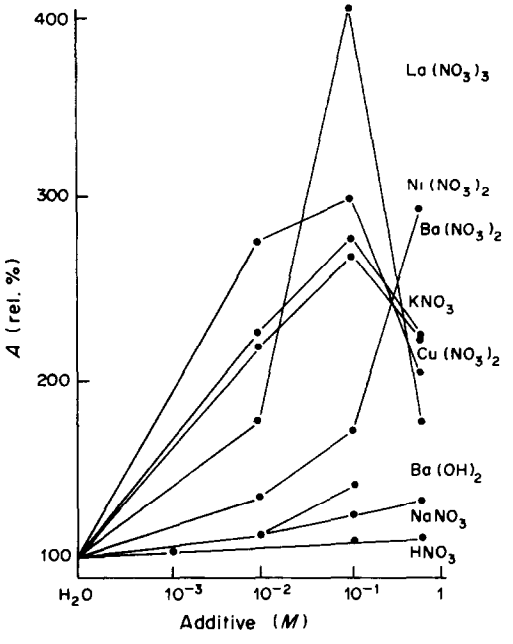

Fig. 6. Influence of various substances on AAS/ETA Sn signals.

are thermally stable and non-volatile. The metal stannites can also be formed in the presence of only the metal ion, but in presence of nitric acid only SnO_2 can be formed. The stannates are more stable than SnO_2 and the stannites, so the analytical results are best in the presence of metal nitrates. We also suppose that a high concentration of the metal nitrate influences the surface of the graphite. The direct contact of reducible substances with graphite at high temperatures leads to reduction processes. It is possible that active carbon centres on the surface are removed by oxidation by nitrates.

The truth of our hypothesis was demonstrated by the fact that the appearance temperatures for Sn are much higher in presence of metal nitrates: 800–1000° in the absence and 1500–1700° in the presence of metal nitrates such as $Ni(NO_3)_2$ or $Ba(NO_3)_2$, irrespective of whether nitric or hydrochloric acid me-

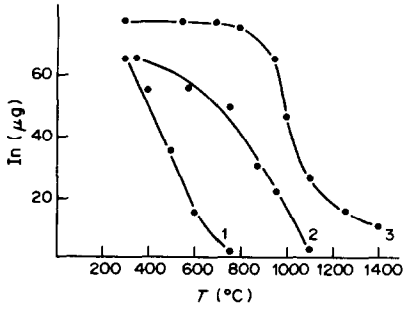

Fig. 7. Influence of the ashing temperature on the vaporization of indium in different media when platforms are used. 1—0.2*M* HBr, 2—0.2*M* HCl, 3—0.1*M* HNO_3; RSD ≤ 15%.

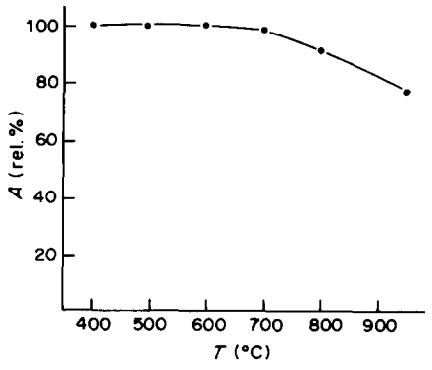

Fig. 8. Influence of the ashing temperature on the AA signals of Au in the AAS/ETA atomization phase: Au 40 μg/ml in 5% v/v HBr solution; RSD ≤ 4%.

Table 4. Detection limits of the trace element determinations in thin layers of InAs (area 1 cm^2) by AAS/ETA

Element	Thickness, μm	Detection limit, *atoms/cm³*
Ag	1.4	8×10^{15}
	5	2×10^{15}
Au	1.4	1×10^{16}
	5	3×10^{15}
Bi	1.4	2×10^{16}
	5	6×10^{15}
Cd	1.4	1×10^{15}
	5	3×10^{14}
Sn	1.4	6×10^{15}
	5	2×10^{15}
Tl	1.4	2×10^{16}
	5	6×10^{15}

dium is used. In the absence of metal nitrates the Sn signal is lower for hydrochloric acid medium than for nitric acid medium. In presence of metal nitrates the Sn signals are the same for both media. Hence the improvement of the signals by metal nitrates is relatively greater for hydrochloric acid medium.

Use of the platform technique as well, brings no further improvement. The best results were achieved by using $Ni(NO_3)_2$ as matrix modifier, but $Ba(NO_3)_2$ and $La(NO_3)_3$ also gave good results. For the Sn determination by AAS/ETA we used 0.2–0.5*M* $Ni(NO_3)_2$. The analytical signals were then greater by a factor of 4 than these in the absence of $Ni(NO_3)_2$.

Interference of In^{3+} in the Au determination, and optimization of the determination

As shown in Fig. 2 the AAS signal for Au in 0.6 *M* hydrobromic acid was twice that for Au in 0.1*M* nitric acid. We found that in presence of In^{3+}, irrespective of the medium (nitric, hydrochloric or hydrobromic acid), there was a high background at both 242.8 and 267.6 nm. The background absorption was directly proportional to the In^{3+} concentration. Background compensation by use of a continuous light-source, *e.g.*, a deuterium lamp, improves the situation, but accurate measurement of the Au atomic absorption is impossible. For example, at low concentrations of Au we found "negative" AA signals. Höhn and Jackwerth[15] investigated the reason for this interference in hydrochloric acid medium. In the vaporization phase most of the indium[13] volatilized as InCl (or InBr or InO, depending on the medium, cf. earlier results[8,9,16]. These molecular species absorb light in this 240–270 nm range very strongly. Because the absorption bands are strongly structured (pseudo line spectra), accurate compensation of the background is not possible. The Au absorption line at 267.6 nm lies between two rotational lines for the InCl molecule. The reason for the "negative" results is the inaccurate compensation.

Because it was necessary to determine traces of Au in InAs we tried to avoid the interference of In compounds. Table 3 shows that the b.p. of $InBr_3$ is very low, and we hoped to separate the matrix and the trace element by optimization of the chemical and thermal conditions. Therefore we studied the vaporization of 80 μg of In^{3+} from different acid media by use of the platform technique. After the appropriate thermal treatment the platforms were treated with nitric acid to dissolve any residual In^{3+}, and the In^{3+} content of these solutions was determined by flame AAS.

Figure 7 shows the results. It can be seen that indium volatilizes completely from hydrobromic acid medium at temperatures >750°, but in nitric acid medium the vaporization of indium is low and incomplete up to 1000°.

We also investigated whether the combined presence of hydrobromic acid and In^{3+} depresses the Au signal. Figure 8 shows that up to ashing temperatures

Table 5. Accuracy of trace determination in thin layers of InAs by AAS/ETA

Trace	Amount added in the etching step, *ng*	Amount found, *ng*	Absolute standard deviation, *ng* (P = 95%)
Ag	1.5	1.4	0.15
Au	5	4.9	0.5
Bi	5	5.2	0.4
Cd	0.2	0.2	0.02
Sn	20	22	3
Tl	10	10.5	0.5

of 750° there is no loss of Au. Therefore it is possible to separate In in hydrobromic acid medium (0.6*M*) from Au traces by using the optimal ashing temperature of 750°. The analytical results could be improved by this procedure.

Analytical results

The thin-layer or layer-by-layer analysis of InAs can be done in the following way. Etching with $HBr/HNO_3/H_2O$ mixtures is used for removal of layers up to a thickness of 1.4 μm, and for thicker layers a solid state microtome is used, in steps of 1 μm, to obtain the desired thickness. The residue from evaporation of the etching solution, or the product from the microtome sectioning, is dissolved in 0.1*M* nitric acid for the determination of Ag, Bi, Cd, Tl, in 0.1*M* HNO_3/0.2–0.5*M* $Ni(NO_3)_2$ medium for determination of Sn, and in 0.6*M* hydrobromic acid for Au determination by AAS/ETA, with 20-μl samples. Table 4 gives the analytical results. The accuracy of the results was established by the standard-addition method. Table 5 shows that the analytical results are accurate within the limits of the reproducibility.

REFERENCES

1. I. R. Schelpakowa, I. G. Judelewitsch, S. A. Soltan, O. I. Schtscherbakowa, K. Dittrich and R. Zschocke, *Talanta*, 1979, **25**, 243.
2. I. R. Schelpakowa, O. I. Schtscherbakowa, I. G. Judelewitsch, N. F. Beisel, K. Dittrich and W. Mothes, *ibid.*, 1982, **29**, 577.
3. B.V. L'vov, L. A. Pelieva and A. I. Sharnopolski, *Zh. Priklad. Spektrosk.*, 1977, **27**, 395.
4. J. Frost, *Etching of Semiconductor Materials*, p. 220, Mir, Moscow, 1965.
5. *Semiconductor Compounds of $A^{III}B^{V}$ Type*, R. Willardson and C. Hering (eds.), p. 637. Metallurgia, Moscow, 1967.
6. B. D. Luft, L. N. Pereboshtshikov and L. N. Vosmilova, in: *Physico-chemical methods of overworking the surfaces of semiconductor materials*, p. 127. Radio i zvyas, Moscow, 1982.
7. D. A. Katzkov, I. L. Grinshtein and L. P. Kruglikova, *Zh. Priklad. Spektrosk.*, 1980, **33**, 804.
8. K. Dittrich and S. Schneider, *Anal. Chim. Acta*, 1980, **115**, 189.
9. K. Dittrich, B. Vorberg, J. Funk and V. Beyer, *Spectrochim. Acta*, 1984, **39B**, 349.
10. R. E. Sturgeon, C. L. Chakrabarti and C. Langford, *Anal. Chem.*, 1976, **48**, 1792.
11. K. Dittrich, W. Mothes and P. Weber, *Spectrochim. Acta*, 1978, **33B**, 325.
12. G. D. Rayson and J. A. Holcombe, *Anal. Chim. Acta*, 1982, **136**, 249.
13. K. Dittrich and B. Vorberg, *ibid.*, 1983, **152**, 149.
14. K. Dittrich, in *Wissenschaftliche Beiträge der Karl-Marx-Universität Leipzig, D.D.R. zu Analytiktreffen 1982*, p. 76. Atomspektroskopie, Leipzig, 1982.
15. R. Höhn and E. Jackwerth, *Anal. Chim. Acta*, 1976, **85**, 407.
16. K. Dittrich, S. Schneider, B. Ya. Spivakov, L. N. Suchoveyeva and Yu. A. Zolotov, *Spectrochim. Acta*, 1979, **34B**, 257.

Talanta, Vol. 32, No 3, pp. 203–206, 1985
Printed in Great Britain.

0039-9140/85 $3.00 + 0.00

FLUORIMETRIC DETERMINATION OF SULPHATE BY TERNARY COMPLEX FORMATION WITH ZIRCONIUM AND BIACETYLMONOXIME NICOTINYLHYDRAZONE

S. RUBIO, A. GOMEZ-HENS and M. VALCARCEL
Department of Analytical Chemistry, Faculty of Sciences, University of Córdoba, Córdoba, Spain

(*Received* 30 *April* 1984. *Accepted* 14 *September* 1984)

Summary—A fluorimetric procedure for the determination of sulphate (0.5–6 μg/ml) based on the formation of a ternary complex with biacetylmonoxime nicotinylhydrazone and zirconium(IV) is described. The excitation and fluorescence maxima are at 415 and 505 nm, respectively. The method is rapid and the procedure reproducible. The precision is ±2% near to the middle range of the calibration curves. There is no interference from most common ions. Phosphate and fluoride are tolerated at 100-fold molar ratio to sulphate. The method has been applied to the determination of sulphate in a variety of water samples.

Fluorimetric methods for determining sulphate are mainly based on the ability of this anion to liberate an organic reagent (*e.g.*, salicylfluorone,[1] flavonol[2] or morin[3]) from its complex with thorium. The salicylfluorone method is the most sensitive. Only one fluorimetric method based on a complex *formation* reaction has been proposed.[4] Although it was necessary to use a considerable (100–1000 molar ratio) amount of the sulphate ion to obtain a linear calibration graph, the authors suggest the probable existence of a 1:1:1 ternary complex, but this cannot be proved.

Several applications of these fluorimetric methods have been described. Vlasov *et al.*[5,6] used the thorium–morin method to determine sulphate in weakly mineralized waters and Nasu[7] used it to analyse snow and river waters. Nasu *et al.*[2] have also used the thorium–flavonol system to determine sulphate in lake, river and mine waters and snow. The thorium–salicylfluorone system has been proposed for determining sulphate in germanium dioxide[1] and distilled water.[8] These methods are subject to serious interference from ions such as phosphate and fluoride and also several other ions, and it is generally impossible to determine sulphate in the presence of phosphate ions.[2,5–7]

In this paper, a direct fluorimetric determination of sulphate, based on the formation of a 1:2:1 ternary complex between zirconium(IV), biacetylmonoxime nicotinylhydrazone (BMNH) and sulphate, is described. BMNH has been used previously as a fluorimetric reagent for the determination of titanium, zirconium and hafnium.[9] It was found that the addition of sulphate to the zirconium–BMNH and hafnium–BMNH complexes resulted in an enhancement of the fluorescence intensity and the stoichiometry of the ternary complexes found to be formed was evaluated by the continuous-variation and molar-ratio methods. We now describe an investigation of this effect, and its use for the determination of sulphate. Although the methods based on substitution reactions[1–3] are more sensitive, they are also less selective. Interference by phosphate and fluoride is eliminated by addition of tartrate and aluminium respectively. Sulphate can be determined in the presence of 100-fold amounts of these ions. The method has been applied to water analysis.

EXPERIMENTAL

Reagents

All experiments were performed with reagent-grade chemicals and pure solvents.

Biacetylmonoxime nicotinylhydrazone (BMNH)[9], 5.5×10^{-4}M *solution in ethanol.*

Zirconium solution, 0.01M. Prepared by dissolving 3.22 g of $ZrOCl_2 \cdot 8H_2O$ in 1 litre of 3*M* hydrochloric acid. This solution should not polymerize on storage.[10] Lower concentrations were obtained by dilution with 3*M* hydrochloric acid.

Standard sulphate solution, ~0.01M. Anhydrous sodium sulphate (1.40 g) was dissolved in 1 litre of distilled water and the solution was standardized gravimetrically by precipitation with barium chloride.

Apparatus

A Perkin-Elmer fluorescence spectrophotometer, model MPF-43A, fitted with 1-cm quartz cells and a xenon arc source was used. Because of day-to-day variations in lamp intensity, it is necessary to run two or three standards with each batch of unknowns, as in all single-beam fluorimetric procedures, to establish the position and slope of the calibration curve. The slit-widths were adjusted to give a 6-nm band-width, both in the excitation and the emission monochromators.

Procedure

To a sample solution containing 12.5–150 μg of sulphate, in a 25-ml standard flask, add 0.25 ml of $2 \times 10^{-4}M$ zirconium, 6 ml of $5.5 \times 10^{-4}M$ BMNH and enough 1*M* hydrochloric acid to make the pH of the final solution between 1.75 and 2. Mix, dilute to volume, and measure the fluorescence intensity (λ_{ex} 415 nm, λ_{em} 505 nm) at 20 ± 0.1°.

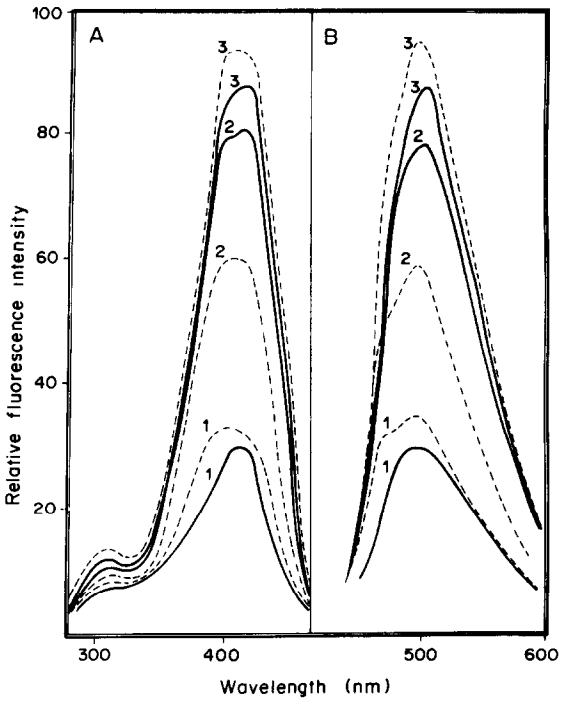

Fig. 1. Uncorrected excitation (A) and emission (B) spectra, showing the effect of the sulphate ion on the 1:2 Zr(IV)–BMNH and Hf(IV)–BMNH complexes. Broken lines: Hf(IV), complexes, bold lines: Zr(IV) complexes. Sulphate concentration: curves 1: 0, curves 2: 10 μg/ml, curves 3: 100 μg/ml. [Zr(IV)] = [Hf(IV)] = 50 ng/ml, [BMNH] = $10^{-4}M$.

Apply a correction for a reagent blank. Prepare a calibration graph in the same way.

RESULTS AND DISCUSSION

Spectral characteristics

BMNH reacts with zirconium(IV) and hafnium(IV) in mineral acid medium to produce fluorescent 2:1 BMNH–metal complexes. Sulphate enhances the fluorescence of these complexes but causes no changes in the wavelengths of the excitation or emission maxima and 2:1:1 BMNH–metal–sulphate ternary complexes have been formulated.[9] A comparative study has been made to decide which system is the more sensitive for sulphate determination. Figure 1 shows the uncorrected excitation and emission spectra of solutions containing BMNH, zirconium or hafnium, and sulphate at three levels (0, 10 and 100 μg/ml). The zirconium system gives a much greater sensitivity of response for sulphate levels < 10 μg/ml, and is therefore preferred. Maximum fluorescence intensity is reached in 10 min and remains constant for at least 3 hr.

Influence of variables

The effect of acidity was studied with use of sodium hydroxide and hydrochloric acid for adjustment. The fluorescence intensity was maximal and independent of pH in the range 1.7–2 (Fig. 2a). The effect of the type of buffer was examined. Phthalate and monochloroacetate buffers gave a fluorescence intensity for the ternary complex that was about half that obtained with hydrochloric acid (although there was no effect on the fluorescence intensity of the binary complex). Therefore, hydrochloric acid medium is preferred.

Increasing the zirconium concentration raised the fluorescence intensity of the ternary complex (Fig. 2b), the effect being maximal over the range 0.17–0.22 μg/ml. A level of 0.2 μg/ml was chosen.

As BMNH is insoluble in water, various solvents were tested. Ethanolic media gave the highest fluorescence intensity, which was independent of the ethanol content over a wide range. The fluorescence intensity was found to increase linearly with BMNH concentration in the range $1–5 \times 10^{-5}M$ and then remain constant from $5 \times 10^{-5}M$ up to at least $2.2 \times 10^{-4}M$ (Fig. 2c).

Variation in the ionic strength or in the order of mixing of the solutions had no influence on the fluorescence.

A temperature coefficient of about $-1\%/°C$ was found over the range of 15–35°, so the temperature should be controlled to within 1–2°. Under the recommended conditions, the system is stable for at least 2 hr.

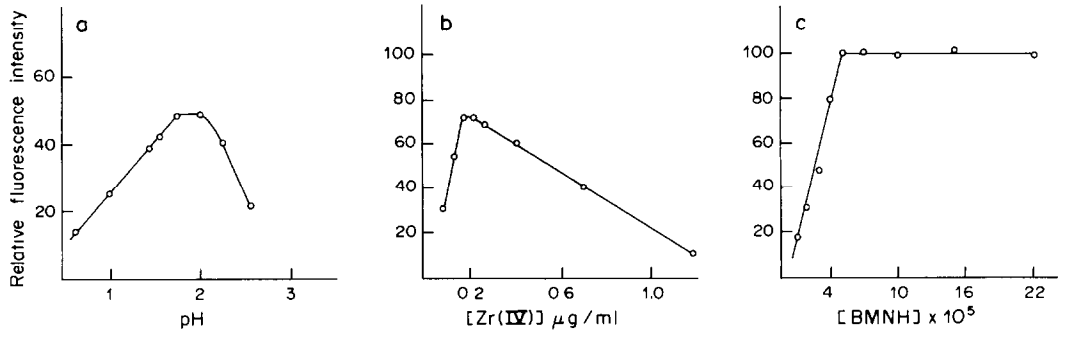

Fig. 2. Influence of (*a*) the acidity and the concentrations of (*b*) Zr(IV) and (*c*) BMNH on the effect caused by the sulphate ion on the Zr–BMNH complex.

Table 1. Effect of various ions on the determination of 3 μg/ml of sulphate

Ion added, (mole ratio of ion/sulphate)		Interference, %	Ion added, (mole ratio of ion/sulphate)		Interference, %
Cl^-	(100)	0	MoO_4^{2-}	(10)	−45
NO_3^-	(100)	0		(5)	−15
BrO_3^-	(100)	0		(1)	0
CO_3^{2-}	(100)	0	WO_4^{2-}	(25)	−100
ClO_3^-	(100)	0		(1)	0
$S_2O_3^{2-}$	(100)	0	VO_3^-	(10)	−37
Acetate	(100)	0		(1)	0
Tartrate	(100)	0	Cd^{2+}	(100)	0
Br^-	(100)	−12	Ni^{2+}	(100)	0
	(75)	0	Ca^{2+}	(100)	0
I^-	(100)	−25	Mg^{2+}	(100)	0
	(75)	0	Zn^{2+}	(100)	0
F^-	(75)*	0	Co^{2+}	(100)	0
	(50)	0	Sr^{2+}	(100)	0
$B_4O_7^{2-}$	(100)	−42	Be^{2+}	(100)	0
	(25)	0	Al^{3+}	(100)	0
SCN^-	(100)	−16	Ga^{3+}	(100)	0
	(75)	0	Cu^{2+}	(100)	−5
NO_2^-	(100)	−8		(75)	0
	(75)	0	Mn^{2+}	(100)	−22
SO_3^{2-}	(10)	+40		(50)	0
	(1)	+4	Pb^{2+}	(100)	−4
$C_2O_4^{2-}$	(1)	+100		(75)	0
PO_4^{3-}	(100)†	0	Fe^{2+}	(20)	−100
S^{2-}	(100)	−48		(5)	0
	(10)	0	Fe^{3+}	(1)	−28
AsO_2^-	(100)	−27			
	(25)	0			
AsO_4^{3-}	(100)	−100			
	(10)	−22			
	(1)	0			

*Plus aluminium nitrate (Al^{3+}/F^- molar ratio = 1).
†Plus tartrate (tartrate/PO_4^{3-} molar ratio = 2).

Characteristics of the method

The calibration graph was linear over the sulphate concentration range 0.5–6 μg/ml. The relative standard deviation for 3 μg/ml ($P = 0.05$, $n = 11$) was ±2%.

Interferences

The influence of various ions likely to interfere by forming complexes or precipitates with zirconium, BMNH or sulphate was examined. The results are summarized in Table 1. The most serious cationic interference found was that of iron(III), caused by strong absorption of both the excitation and the emission radiation by the Fe(III)–BMNH complex. Reduction to iron(II) permitted the direct determination of sulphate in the presence of a 5-fold molar ratio of iron. Oxalate interferes at the same level as sulphate, probably owing to the formation of a fluorescent ternary complex with zirconium and BMNH. The positive interference caused by sulphite can be attributed to its oxidation to sulphate in dilute solutions. It is not regarded as a reaction of the sulphite ion itself, since addition of sulphite to a deoxygenated sulphate-free medium did not cause any effect.

It is important to emphasize the effect of fluoride and phosphate, since they are serious interferences in all fluorimetric methods proposed for the determination of sulphate. Fluoride does not interfere at 50-fold molar ratio to sulphate. Higher ratios yield low recoveries but Al(III) can be used as a masking agent. Phosphate causes very serious negative error

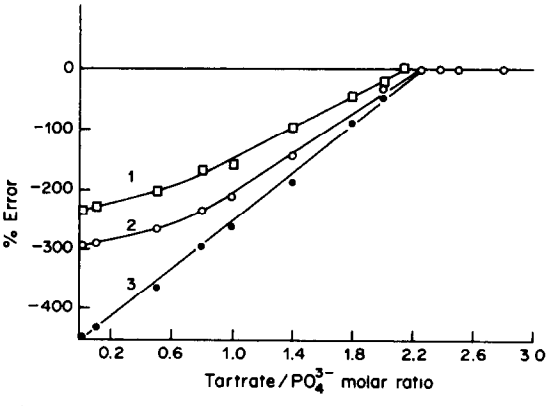

Fig. 3. Effect of the tartrate ion on the phosphate interference in the determination of sulphate. All the samples have $10^{-3}M$ phosphate, and the PO_4^{3-}/SO_4^{2-} molar ratios are: curve 1:20, curve 2:33, curve 3:100.

Table 2. Recovery of sulphate added to water samples

Sample	Sample volume, ml	Sulphate Added, μg	Found,* μg	Expected, μg	Recovery, %
River water	0.5	—	32	—	—
		25	62	57	109 ± 2
		50	80	82	98 ± 4
		75	106	107	99 ± 3
		100	137	132	104 ± 4
Mineral water	2.0	—	25	—	—
		25	48	50	96 ± 3
		50	71	75	95 ± 1
		75	105	100	105 ± 5
		100	111	125	89 ± 3
Tap water	1.0	—	27	—	—
		25	54	52	104 ± 4
		50	81	77	105 ± 6
		75	98	102	96 ± 1
		100	135	127	106 ± 2
Stream water	0.5	—	33	—	—
		25	54	58	93 ± 5
		50	86	83	104 ± 4
		75	108	108	100 ± 6
		100	131	133	98 ± 3
Well water	0.3	—	32	—	—
		25	53	57	93 ± 3
		50	84	82	102 ± 5
		75	109	107	102 ± 3
		100	128	132	97 ± 4
Pond water	0.3	—	30	—	—
		25	57	55	104 ± 6
		50	74	80	93 ± 3
		75	104	105	99 ± 4
		100	127	130	98 ± 4
Reservoir water	0.2	—	22	—	—
		25	43	47	91 ± 4
		50	70	72	97 ± 2
		75	101	97	104 ± 6
		100	123	122	101 ± 3

*Mean of six determinations.

by reducing the zirconium concentration. Common methods for the elimination of this error are precipitation of this ion with magnesium or lanthanum, its retention on a weak-base anion-exchange resin *etc.*, but these procedures are time-consuming. In our method, tartrate is used to eliminate the phosphate interference. The use of tartrate as masking agent for phosphate is mentioned in Table 3.3 of Perrin's monograph.[11] Initially a zirconium–phosphate complex is formed, but the tartrate ions destroy this complex. The fluorescence intensity is measured when it has reached a maximum. Figure 3 shows the error obtained for different PO_4^{3-}/SO_4^{2-} molar ratios, as the tartrate/PO_4^{3-} molar ratio changes. From this graph it can be inferred that: (*a*) the interference increases with PO_4^{3-}/SO_4^{2-} molar ratio for a fixed tartrate/PO_4^{3-} molar ratio; (*b*) as the tartrate/PO_4^{3-} ratio increases, the error is reduced, reaching zero when this ratio is about 2. In this way, sulphate can be determined in the presence of a 100-fold molar ratio of phosphate.

Applications

To test the applicability of the procedure to the determination of sulphate in water samples, various amounts of sulphate were added to each sample. The results obtained are shown in Table 2. The recoveries were calculated by comparing the results obtained before and after the addition of standard sulphate solutions. The data obtained show the precision of the method over a wide range.

REFERENCES

1. V. A. Nazarenko and M. B. Shustova, *Zavodsk. Lab.*, 1958, **24**, 1344.
2. T. Nasu, T. Kitagawa and T. Mori, *Bunseki Kagaku*, 1970, **19**, 673.
3. J. C. Guyon and E. J. Lorah, *Anal. Chem.*, 1966, **38**, 155.
4. L. H. Tan and T. S. West, *Analyst*, 1971, **96**, 281.
5. N. A. Vlasov, E. A. Morgen and V. A. Tyutin, *Izv. Nauch.-Issled. Inst. Nefte-Uglekhim. Sin. Irkutsk. Univ.*, 1969, **11**, (Pt. 1) 136; *Ref. Zh. Khim.*, 1969, 23G162.
6. *Idem, Gidrokhim. Mater.*, 1969, **50**, 92.
7. T. Nasu, *Hokkaido Kyoiku Daigaku Kiyo, Dai-2-Bu, A*, 1972, **23**, 35.
8. V. S. Yanysheva and Z. A. Sazonova, *Metody Anal. Khim. Reakt. Prep., Gos. Kom. Sov. Min. SSSR Khim.*, 1962, **4**, 133.
9. M. A. Cejas, A. Gómez-Hens and M. Valcárcel, *Anal. Chim. Acta*, 1984, **158**, 287.
10. B. C. Sinha and S. Das Gupta, *Analyst*, 1967, **92**, 558.
11. D. D. Perrin, *Masking and Demasking of Chemical Reactions*, p. 45. Wiley-Interscience, 1970.

Talanta, Vol. 32, No. 3, pp. 207–208, 1985
Printed in Great Britain

0039-9140/85 $3.00 + 0.00

SHORT COMMUNICATIONS

DETERMINATION OF BISMUTH BY FLAME ATOMIC-ABSORPTION SPECTROPHOTOMETRY AFTER SEPARATION BY ADSORPTION OF ITS 2-MERCAPTOBENZOTHIAZOLE COMPLEX ON MICROCRYSTALLINE NAPHTHALENE

KOICHI ISHIDA, BAL KRISHAN PURI and MASATADA SATAKE
Faculty of Engineering, Fukui University, Fukui 910, Japan

MOOL CHAND MEHRA
Chemistry Department, Université de Moncton, Moncton, Canada

(*Received* 2 *November* 1984. *Accepted* 8 *November* 1984)

Summary—Trace amounts of bismuth have been determined by atomic-absorption spectrophotometry after adsorption of the 2-mercaptobenzothiazole complex on naphthalene. The method has been applied to the determination of bismuth in aluminium alloys.

2-Mercaptobenzothiazole forms water-insoluble complexes with various metals. The bismuth complex is not extractable into the usual organic solvents such as chloroform, benzene, nitrobenzene and methyl isobutyl ketone. Several metals have been separated by adsorption of their complexes on microcrystalline naphthalene,[1–5] and this technique can be applied to the 2-mercaptobenzothiazole of bismuth.

EXPERIMENTAL

Reagents

Standard bismuth solution, 20 ppm.
2-Mercaptobenzothiazole solution in ethanol, 2%.
Acetic acid/ammonium acetate buffer, 1*M*, pH 4.5.
Naphthalene solution in acetone, 20%.

Procedure

Pipette a volume of sample containing 20–200 μg of bismuth into an 80-ml stoppered Erlenmeyer flask and dilute with water to about 35 ml. Add 4.0 ml of 2% 2-mercaptobenzothiazole solution and 2.0 ml of buffer. Mix and let stand for a few minutes. Add 2.0 ml of 20% naphthalene solution and shake the mixture vigorously for 30 sec. Filter through a paper (*e.g.*, No. 5C, Toyo Roshi Co., Japan) placed flat on a perforated Teflon disc (3 cm in diameter) in an ordinary filter funnel, or a sintered glass filter (porosity 2). Wash with water, then add dimethylformamide to the filter to dissolve the naphthalene and bismuth complex, and collect the solution in a 10-ml standard flask. Aspirate the solution into an air–acetylene flame and measure the absorbance at 223.1 nm, using a bismuth hollow-cathode lamp as light-source.

RESULTS AND DISCUSSION

The optimum pH range for the adsorption step is 2.2–6.4 (Fig. 1). Adsorption of the bismuth complex is quantitative when 1.0–6.0 ml of 2-mercaptobenzothiazole solution and 1–5 ml of buffer are used. Formation of the complex is complete in a few minutes. For complete adsorption of the complex 0.5–4.0 ml of the naphthalene solution is enough. The adsorption is very fast. Varying the aqueous phase volume from 30 to 100 ml has no effect on the bismuth absorbance measured but the absorbance decreases with larger volumes of aqueous phase. Beer's law is obeyed for bismuth concentrations up to 20 μg/ml in the final dimethylformamide solution. For ten replicate determinations of 100 μg of bismuth, the relative standard deviation found was 1.1%. The concentration giving 1% absorption was 0.34 μg/ml. The mixture of complex and naphthalene is soluble in dioxan, dimethylformamide, propylene carbonate and dimethyl sulphoxide, but dimethyl-

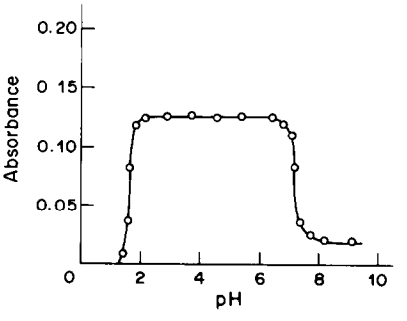

Fig. 1. Effect of pH, Bi, 100 μg; 2% 2-mercaptobenzothiazole solution, 2.0 ml; 20% naphthalene solution, 2.0 ml; shaking time, 30 sec; wavelength, 223 nm; reference, reagent blank.

Table 1. Effect of diverse ions

Salt	Tolerance limit	Ion	Tolerance limit
KI	70 mg	Mg^{2+}	2 mg
$NaClO_4$	1 g	Mo(VI)	10 mg
KNO_3	2 g*	Ca^{2+}	2 mg
$CH_3COONa \cdot 3H_2O$	1 g	W(VI)	50 μg
NaCl	9 mg	Mn^{2+}	2 mg*
NH_4Cl	80 mg	Pb^{2+}	2 mg*
Sodium tartrate	10 mg	Cr(VI)	1.5 mg
Na_2SO_4	80 mg	Hg^{2+}	2 mg
KSCN	1 g	V(V)	500 μg
NaF	50 mg	Pt(IV)	2 mg
Sodium citrate	1 mg	Ni^{2+}	500 μg
$Na_2C_2O_4$	2 mg	Cd^{2+}	300 μg
KH_2PO_4	8 mg	Al^{3+}	150 mg
KCN	1 mg	Cu^{2+}	1.8 mg
Disodium EDTA	8 μg	Zn^{2+}	1 mg
Na_2CO_3	0.1 g	Fe^{3+}	1.5 mg
Thiourea	1 g	Co^{2+}	200 μg
Na_2SO_3	500 mg	Ti(IV)	300 μg
		Sn^{2+}	200 μg
		Sb^{3+}	200 μg

*Maximum value tested.

Table 2. Analysis of alloys for bismuth

Sample	Composition %	Bismuth certified value, %	Bismuth*, %	
			Present method	Direct AAS
N.K.K. No. 916 aluminium alloy	Si:0.41,Fe:0.54,Cu:0.27 Mn:0.11,Mg:0.10,Cr:0.05 Ni:0.06,Zn:0.30,Ti:0.10 Sn:0.05,Pb:0.04,V:0.02 Zr:0.05,Ga:0.03,Co:0.03 Sb:0.01,B:0.0006,Ca:0.03	0.03	0.026 ± 0.001	—
N.K.K. No. 1021 aluminium alloy	Si:5.56,Fe:0.99,Cu:2.72 Mn:0.20,Mg:0.29,Cr:0.03 Ni:0.14,Zn:1.76,Ti:0.04 Sn:0.10,Pb:0.18,V:0.007 Zr:0.01,Sb:0.01,Ca:0.004	0.01	0.009 ± 0.001	—
Sumitomo Co. M-2-1 aluminium alloy	Si:0.29,Fe:0.071,Cu:0.0042 Ti:0.14,Mn:0.025,Mg:4.90 Cr:0.23,Zn:0.040,Be:0.0013 B:0.0002	0.022	0.022 ± 0.001	—
Sumitomo Co. 2011-4 aluminium alloy	Si:0.030,Fe:0.063,Cu:6.58 Ti:0.050,Mn:0.003,Ni:0.048 Pb:0.30,Zn:0.003	0.32	0.30 ± 0.01	—
Aluminium alloy	—	—	0.55 ± 0.03	0.56

*Mean of five determinations. Adsorption at pH 3.5. 500 mg of thiourea added.

formamide is the most suitable for the atomic-absorption measurements.

Effect of diverse ions

The procedure was applied to solutions containing 100 μg of bismuth and various amounts of other ions, adjusted to pH 1.5–1.8 to prevent precipitation of bismuth hydroxide. The results are shown in Table 1. EDTA interferes seriously. Bismuth can be determined in aluminium alloys without prior removal of other metal ions. Table 2 gives results obtained for analysis of some standards; they are in reasonable agreement with the certified values of those obtained by direct AAS determination.

REFERENCES

1. M. Satake, Y. Matsumura and M. C. Mehra, *Mikrochim. Acta*, 1980 **I**, 455.
2. M. Satake and M. C. Mehra, *Microchem. J.*, 1982, **27**, 182.
3. M. Satake, M. C. Mehra, H. B. Singh and T. Fujinaga, *Bunseki Kagaku*, 1983, **32**, E165.
4. L. F. Chang, M. Satake, B. K. Puri and S. P. Bag, *Bull. Chem. Soc. Japan*, 1983, **56**, 2000.
5. T. Nagahiro, M. Satake, J. L. Lin and B. K. Puri, *Analyst*, 1984, **109**, 163.

Talanta, Vol. 32, No. 3, pp. 209–211, 1985
Printed in Great Britain

0039-9140/85 $3.00 + 0.00
Pergamon Press Ltd

SOME SPECTROPHOTOMETRIC METHODS FOR DETERMINATION OF CERTAIN ANTIPYRETIC AND ANTIRHEUMATIC DRUGS

A. S. ISSA, Y. A. BELTAGY, M. GABR KASSEM and H. G. DAABEES
Pharmaceutical Chemistry Department, Faculty of Pharmacy, Alexandria University, Alexandria, Egypt

(*Received* 10 *February* 1984. *Revised* 10 *July* 1984. *Accepted* 5 *November* 1984)

Summary—Heating paracetamol in strongly alkaline medium with 4-nitrosoantipyrine gives a red colour with maximum absorption at 515 nm. Mefenamic and flufenamic acids can be determined colorimetrically after extraction as ion-pairs with Methylene Blue.

Paracetamol can be determined spectrophotometrically by reaction with sodium nitrite[1,2] or sodium cobaltinitrite,[3] or can be hydrolysed to *p*-aminophenol which is then either condensed with aldehydes[4–9] or diazotized and coupled with phenols.[10,11] Titration with sodium nitrite[12–14] or ceric sulphate[15–17] has also been reported. Fluorimetric and HPLC techniques are also used.[18–22] 4-Nitrosoantipyrine gives coloured products with α-naphthylamine, naphthalene-1,5-di-isocyanate and 8-amino-1-naphtholdisulphonic acid.[23] Mefenamic and flufenamic acids are determined alkalimetrically,[24,25] fluorimetrically[26] or by atomic-absorption,[27] and also with Fast Red Salt B.[28] Methylene Blue was first used by Jones[29] for determination of surfactants and has been used for the determination of probencid, saccharin, penicillins, some organic acids and sodium lauryl sulphate.[30–33]

Here we describe the use of 4-nitrosoantipyrine and Methylene Blue for the determination of some antipyretic and antirheumatic drugs.

EXPERIMENTAL

Reagents

4-Nitrosoantipyrine reagent.[23] Dissolve 1 g of antipyrine in 20 ml of acetic acid (1 + 1), add 0.6 g of sodium nitrite and let stand for 10 min. Then add 0.75 g of sulphamic acid and dilute to 150 ml with acetic acid (1 + 1).

Sodium hydroxide solution, 40%.

Methylene Blue solution, 0.5%.

Buffer, pH 6.8.[34] Mix 50.8 ml of 0.0667*M* potassium dihydrogen phosphate with 49.2 ml of 0.0667*M* disodium hydrogen phosphate.

Procedure for paracetamol

Dissolve 10–50 mg of paracetamol (accurately weighed) in 25 ml of 0.1*M* sodium hydroxide and dilute accurately to 1000 ml with water. Transfer 5 ml of this solution to a 25-ml standard flask, add 3 ml of 40% sodium hydroxide solution and 0.3 ml of 4-nitrosoantipyrine reagent, heat in a boiling water-bath for 15 min, cool, dilute to volume with ethanol, then allow to stand for 100 min. Measure the absorbance at 515 nm against a reagent blank treated in the same way.

Procedure for tablets. Weigh and powder 20 tablets. Weigh out a quantity of powder equivalent to 30–40 mg of the drug, into a 100-ml standard flask, and shake it for 15 min with 25 ml of 0.1*M* sodium hydroxide, then dilute to volume with water and filter. Dilute 10 ml of the filtrate to 100 ml with water, then analyse 5 ml of this solution as described above.

Procedure for liquid preparations. Dilute a known volume of syrup or drops with water to a volume large enough to give a final paracetamol concentration of 0.03–0.04 mg/ml. Transfer 5 ml of this solution to a 25-ml standard flask and analyse as above.

Procedure for mefenamic and flufenamic acids

Dissolve 1–3 mg of the drug in 5 ml of chloroform, and dilute accurately to 100 ml with methylene chloride. Transfer a known volume containing 0.05–0.15 mg of the drug to a 100-ml separatory funnel, add 20 ml of buffer (pH 6.8) and 1 ml of Methylene Blue solution, and extract with three 10-ml portions of methylene chloride, shaking for 5 min each time. Dry the combined extracts with anhydrous sodium sulphate and transfer to a 50-ml standard flask. Wash the sodium sulphate with 10 ml of methylene chloride, transferring the washings to the flask, and dilute to volume with the same solvent. Measure the absorbance at 658 nm against a blank prepared by the procedure.

Procedure for capsules. Empty 20 capsules, mix the contents and weigh. Transfer a weighed quantity equivalent to about 20 mg of mefenamic or flufenamic acid to a 50-ml standard flask, add 30 ml of chloroform, shake the flask for 15 min, then dilute to volume with chloroform. Transfer 5 ml of the clear solution to a 100-ml standard flask and dilute to volume with methylene chloride. Transfer 5 ml of the solution to a 100-ml separatory funnel and analyse as described above.

RESULTS AND DISCUSSION

The 4-nitrosoantipyrine procedure involves the use of a high alkali concentration to hydrolyse the drug to *p*-aminophenol, which is then condensed with 4-nitrosoantipyrine to give a red colour. Heating the reaction mixture and the addition of an alcohol are essential for colour formation. Methanol gives an unstable colour and isopropyl or n-butyl alcohol gives only a faint colour and is immiscible with the alkaline solution. Ethanol gives a stable colour and is completely miscible. Absolute ethanol gives the best colour development and stability. The common tablet fillers such as lactose, talc, starch and magnesium stearate do not interfere, nor do the other drugs present in paracetamol compound tablets (salicylamide, caffeine, aspirin, codeine phosphate and

Table 1. Results of determination of paracetamol by the 4-nitrosoantipyrine and B.P. 1980 methods

Drug form	4-Nitrosoanti-pyrine	B.P. 1980	
	Mean recovery, %	Sample wt., *mg*	Mean* recovery, %
Paracetamol	100.1 ± 0.9	300	100.0 ± 0.4
Paracetamol tab.[M] (500 mg/tab.)	95.9 ± 0.3	150	96.7 ± 0.2
Asco tablet[C] (200 mg/tab.)	98.7 ± 0.9	—	—
Vegaskin tab.[A] (200 mg/tab.)	100.6 ± 0.8	—	—
Pyral drops[K] (10 g/100 ml)	95.8 ± 0.6	—	—
Paracetamol syrup[M] (120 mg/5 ml)	100.9 ± 0.7	—	—
Pyral syrup[K] (120 mg/5 ml)	100.5 ± 1.0	—	—

*Mean and standard deviation (6 results) calculated with respect to nominal content in sample.

M = Misr company; C = Cid company; A = Alexandria company; K = Kahira company.

Asco contains 200 mg of paracetamol, 250 mg of salicylamide, 60 mg of caffeine, 7 mg of codeine phosphate and 15 mg of phenyltoloxamine dihydrogen citrate per tablet.

Vegaskin contains 200 mg of paracetamol, 300 mg of aspirin and 10 mg of codeine phosphate per tablet.

phenyltoloxamine dihydrogen citrate). Beer's law is valid over the concentration range 0.2–1.0 mg/100 ml. Results are shown in Table 1. The applicability of the method to some commercial preparations was compared with the B.P. 1980 method (Table 1). Efficient extraction of Methylene Blue ion-pairs into methylene chloride was achieved with Sørensen's pH-6.8 phosphate buffer. The use of methylene chloride gives higher sensitivity and better stability than use of chloroform does. The reacting ratio was found to be 1:1 by the mole-ratio method, indicating that the carboxylic group of the drug and not the imino group is involved in the reaction. Beer's law is valid over a concentration range of 0.12–0.28/100 ml; results are shown in Table 2. The method is applicable to some preparations (Table 2).

REFERENCES

1. M. C. Inamdar and N. N. Kagi, *Indian J. Pharm.*, 1969, **31**, 79.
2. A. Abou-Ouf, M. I. Walash, S. M. Hassan and S. M. Elsayed, *Arch. Pharm. Chem. Sci.*, 1978, **6**, 164.
3. M. Abdel Salam and M. A. Korany, *Egypt. J. Pharm. Sci.*, 1979, **18**, 29.
4. J. B. Vaughan, *J. Pharmac. Sci.*, 1969, **58**, 469.
5. F. M. Plakogiannis and A. M. Saad, *ibid.*, 1978, **67**, 581.
6. A. A. D'Souza and K. G. Shenoy, *Can. J. Pharm. Sci.*, 1968, **3**, 90.
7. D. R. Vishwasrao, *Indian J. Pharm.*, 1973, **35**, 172.
8. N. M. Sanghavi, *East. Pharm.*, 1974, **17**, 53.
9. T. Inoue, M. Tatsuzawa, S.C. Lee and T. Ishii, *Eisei Kagaku*, 1975, **21**, 313; *Chem. Abstr.*, 1976, **85**, 10491e.
10. J. Kos, *Farm. Glanisk*, 1966, **22**, 51.
11. C. T. H. Ellcock and A. G. Fogg, *Analyst*, 1975, **100**, 16.
12. M. C. Inamdar, J. C. Saboo, C. N. Kandar and N. M. Sanghavi, *Indian J. Pharm.*, 1973, **35**, 187.
13. U. Elste and H. Duda, *Deut. Apoth. Ztg.*, 1972, **112**, 711.
14. N. S. Soebito, *Acta. Pharm.*, 1974, **4**, 64.
15. Z. E. Kalinowska and H. Hasztar, *Farm. Pol.*, 1967, **23**, 447.
16. *Idem, ibid.*, 1965, **21**, 570.

Table 2. Results for determination of mefenamic and flufenamic acids by Methylene Blue and B.P. 1980 methods

Drug form	Methylene Blue method	B.P. 1980	
	Mean recovery, %	Sample wt., *mg*	Mean recovery,* %
Mefenamic acid	99.8 ± 0.7	600	100.3 ± 0.9
Ponstan capsules[P D] (250 mg/Cap.)	101.0 ± 0.8	500	101.3 ± 0.8
Flufenamic acid	99.6 ± 0.7	600	101.5 ± 0.8
Arlef Capsules[P D] (100 mg/Cap.)	100.1 ± 0.7	600	103.3 ± 0.7

P.D. = Park Davis.

*Mean and standard deviation (6 results) calculated with respect to nominal content in sample.

17. M. Rasburn and D. B. Dixon, *Pharm. J.*, 1974, **213**, 596.
18. T. Kaito, K. Sagara, T. Yoshida and Y. Ito, *Yakugaku Zasshi* 1974, **94**, 633.
19. *Idem*, *ibid.*, 1974, **94**, 639.
20. D. Blair and B. H. Rumock, *Clin. Chem.*, 1977, **23**, 743.
21. J. W. Munson and E. J. Kubiak, *Anal. Lett.*, 1980, **13**, 705.
22. G. Drehsen and P. Rohdewald, *J. Chromatog.*, 1981, **12**, 497.
23. F. Feigl, *Spot Tests in Organic Analysis*, 7th Ed., pp. 509, 579, 695. Elsevier, Amsterdam, 1966.
24. *British Pharmacopoeia*, 1980.
25. M. I. Walash and M. Rizk, *Indian J. Pharm.*, 1977, **39**, 82.
26. Y. Hattori, T. Arai, T. Mori and E. Fujihira, *Chem. Pharm. Bull.*, 1970, **18**, 1063.
27. I. Minamikawa, K. Sakai, N. Hashitani, E. Fukushima and N. Yamagishi, *ibid.*, 1973, **21**, 4632.
28. A. V. Vinnikova, *Farm. Zh.*, 1979, **3**, 74.
29. J. H. Jones, *J. Assoc. Off. Agr. Chem.*, 1945, **28**, 398.
30. I. K. Shin and F. W. Teare, *Can. J. Pharm. Sci.*, 1966, **1**, 35.
31. Y. A. Beltagy, S. M. Rida and A. S. Issa, *Pharmazie*, 1974, **29**, 64.
32. I. M. Korenman and I. A. Borisova, *Khim. Tekhnol.*, 1972, **1**, 104.
33. P. Mukerjee, *Anal. Chem.*, 1956, **28**, 870.
34. *Documenta Geigy*, 6th Ed., p. 314. Geigy, Basel, 1962.

Talanta, Vol. 32, No. 3, pp. 212–214, 1985
Printed in Great Britain.

0039-9140/85 $3 00 + 0.00

AN INEXPENSIVE AND ROBUST CONDUCTANCE ELECTRODE

J. P. LORIMER, K. JAGIT and TIMOTHY J. MASON
Department of Applied Chemistry, Coventry (Lanchester) Polytechnic, Priory Street, Coventry, England

(*Received* 18 *June* 1984. *Revised* 5 *October* 1984. *Accepted* 29 *October* 1984)

Summary—A conductance electrode consisting of carbon "pultrusion" rod embedded in PTFE has been shown to have similar characteristics to those of the traditional platinum-on-glass type. The new electrode has the advantages of being both robust and inexpensive and could prove particularly useful in Karl Fischer analyses of biological material where maceration of the sample is required.

In our recent conductometric studies[1] into the effect of ultrasonic irradiation on chemical reactivity, the traditional platinum-on-glass electrodes were found to suffer occasional irreversible mechanical breakdown (*i.e.*, foil chipping) owing to the hostile ultrasound environment. This difficulty was overcome by using an electrode system in which disks of carbon fibre composite (5 mm diameter "pultrusion" rod[2]) were embedded in Perspex.[3] The design proved a suitable replacement for the traditional electrode in a number of routine conductance measurements[4] with the exception of water determination by the Karl Fischer method. In this instance, although the electrode responded adequately, its repeated use led to physical breakdown due to attack by the Karl Fischer reagent on the adhesive used in fabrication.

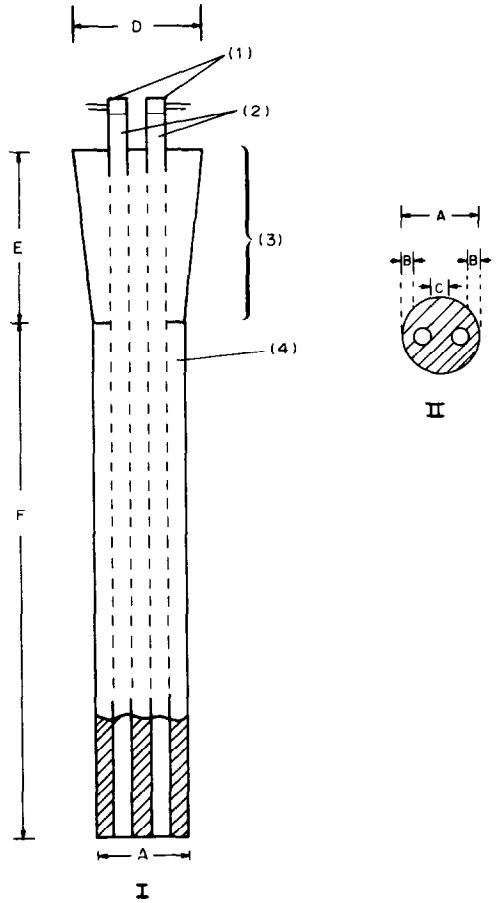

Fig. 1. Electrode assembly. I, longitudinal section; II, lower end view. (1) Electrical connections, (2) carbon "pultrusion" rod (3 mm section), (3) standard taper (1 in 10), (4) Teflon body. Dimensions (mm): A, 12; B, 1.5; C, 3; D, 14; E, 20; F, 75 (not critical).

We report here a new and simpler design (Fig. 1) which has proved to have both improved solvent resistance and better performance than the previous model.[5] In addition it has been found that neither the response nor the reproducibility of the system was affected by the application of ultrasound either during, or prior to, the Karl Fischer determination. This suggests a potential application to Karl Fischer analyses of biological material where the hostile environment of high-speed maceration or ultrasonic disruption may cause damage to traditional electrode systems.

The general performance of the electrode in a number of conductometric experiments has also been assessed and compared with that of platinum. Since the techniques used are all well known, experimental details have been kept to a minimum.

EXPERIMENTAL

Reagents

The following reagents were used as received: sodium lauryl sulphate and magnesium sulphate from BDH, barium chloride (analytical grade) from Fisons. Solutions of these salts (approximately 0.1*M*, 0.01*M* and 0.02*M* respectively) were prepared with demineralized water.

Stock solutions (0.5*M*) of all acids and bases were prepared by dilution of the appropriate concentrated solutions (BDH ampoules). Further dilution provided approximately 0.1*M* solutions for analysis.

Karl Fischer reagent (1 ml ≡ 5 mg of water) and standard methanol (1 ml ≡ 5 mg of water) were used as supplied by BDH.

Cells and measuring devices

The new assembly (Fig. 1) consists of two lengths of 3 mm diameter "pultrusion" rod (supplied by Carbon Fibres

Division, Courtaulds Ltd), push-fitted through a drilled PTFE plug machined from a 14 mm diameter rod.

The dimensions were such as to give a cell constant of approximately 2.5. A conventional (dip-type) platinum-on-glass conductance cell, of cell constant 1.0, was used for comparison.

A Portland conductance meter (P335) was used to monitor the conductance changes in the acid–base and precipitation titrations, and in the determination of critical micelle concentration (CMC). A Corning 109 mV/pH-meter was employed for the Karl Fischer determination.

General procedures

Conductometric titrations. In all cases 20 ml of the reagent under investigation, together with 50 ml of demineralized water to minimize dilution effects, were added to the titration vessel. Titrant was delivered in 0.2-ml aliquots from a 10-ml microburette. The solutions were stirred magnetically.

CMC. Sodium lauryl sulphate (0.1*M*) was added in 0.5-ml aliquots from a 25-ml burette to continually stirred demineralized water (100 ml) at 25 ± 0.1°.

Karl Fischer. The dead-stop method was employed. The stability of the assembly was assessed by subjecting the system to ultrasonic irradiation (4 min) prior to a determination, and also by continuous irradiation during the course of a determination. A Heat Systems Inc. W-225R Sonicator, operating at 60% power and 20 kHz, with a $\frac{1}{4}$-in. probe, was used as the ultrasonic source.

Speed of response and reproducibility of the electrode systems. Two methods were employed for comparing the response times of the systems to rapid changes in conductance. In the first, the electrodes, after drying, were rapidly dipped into an aqueous solution of hydrochloric acid. The conductance change was monitored on a chart recorder (Rikadenki, DBEI) and the response time taken to be the difference between the time of electrode insertion and the attainment of a constant conductance value. In the second, each electrode, after being washed and dried, was inserted into 50 ml of demineralized water, then 1 ml of 0.1*M* hydrochloric acid was rapidly injected with a syringe and the response recorded as previously.

Table 1. Comparison of platinum (Pt) and carbon rod (C) electrodes in conductometric titrations

System*	End-point, *ml*		Rel. std. devn., %	
	Pt	C	Pt	C
HCl/NaOH	4.54	4.48	0.8	0.5
HOAc/NaOH	3.98	3.96	1.0	1.1
NH_4OH/HCl	3.88	3.88	0.9	1.3
NH_4OH/HCl	3.80	3.80	1.0	1.0
$BaCl_2/MgSO_4$	3.92	3.92	1.0	0.5

*In all cases the first reagent is the titrand (0.1*M*), and the second is the titrant (0.5*M*).

Table 2. Comparison of platinum (Pt) and carbon rod (C) electrodes in other determinations

Determination	End-point, *ml*		Rel. std. devn., %	
	Pt	C	Pt	C
CMC	9.85	9.75	0.5	0.7
Karl Fischer*	11.5	11.8	1.3	1.1
Karl Fischer†	—	11.9	—	4.6

*Without ultrasound.
†With ultrasound.

RESULTS AND DISCUSSION

Titrations

The results in Tables 1 and 2 are the means of 6 determinations and demonstrate that the carbon rod assembly is a good inexpensive replacement for the traditional platinum model. The reproducibility of the results, even in the presence of ultrasonic irradiation, suggests that leakage around the joints (even after repeated usage) is not significant under the reaction conditions used.

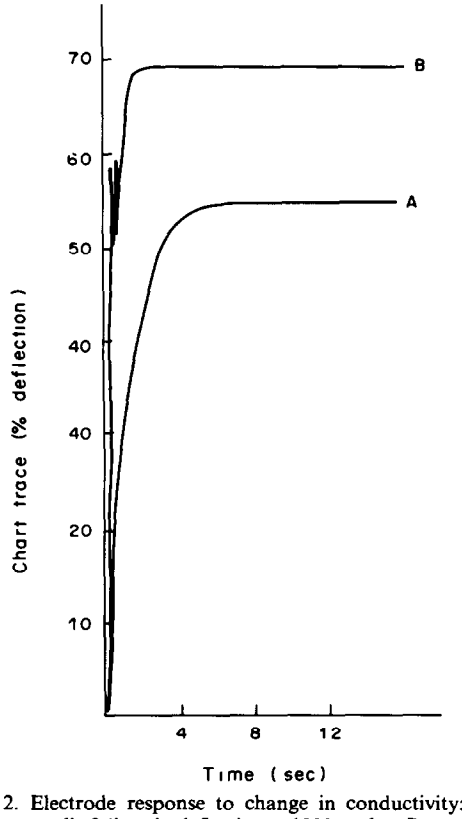

Fig. 2. Electrode response to change in conductivity: A, platinum cell, full-scale deflection = 1000 μmho; B, carbon rod cell, full-scale deflection = 300 μmho.

Table 3. Response and reproducibility of the electrode systems (8 replicates)

Method	Response time, *sec*		Rel. std. devn., %		Constant conductance value, *μmho*		Rel. std. devn., %	
	Pt	C	Pt	C	Pt	C	Pt	C
Electrode immersion	0.5	0.7	31	40	530	200	0.1	0.6
Solution addition	8.0	3.6	7	3	548	210	0.5	1.0

Response and reproducibility

Table 3 demonstrates that the speeds of response of both systems to changes in conductance are similar. The slightly longer response time of the traditional model to addition of a conducting solution is due mainly to its design, which is not conducive to efficient mixing. Typical response curves are given in Fig. 2.

Surface adsorption

At the reagent concentrations examined, no evidence was seen for the adsorption of species from solution. Both electrode systems gave constant conductance values ($\pm 0.5\%$) over periods of 2 hr.

REFERENCES

1. T. J. Mason, J. P. Lorimer and B. P. Mistry, *Tetrahedron Lett.* 1983, **24,** 4371.
2. "Pultrusion" rod consists of Grafil E/A-S fibre (10,000 filaments) sized with approximately 0.5% w/w of an epoxy resin. Process details were presented at the Symposium "Fabrication Techniques for Advanced Reinforced Plastics", University of Salford, April 1980.
3. *Brit. Pat. Appl.* 83-30073.
4. J. P. Lorimer and T. J. Mason, *Educ. in Chem.*, 1984, **21,** 46.
5. *Brit. Pat. Appl.* 84-08351.

Talanta, Vol. 32, No. 3, pp. 215–217, 1985
Printed in Great Britain

0039-9140/85 $3.00 + 0.00

INDIRECT DETERMINATION OF TRACE PHENOL IN WATER BY ATOMIC-ABSORPTION SPECTROPHOTOMETRY

XU BO-XING, XU TONG-MING, SHEN MING-NENG and FANG YU-ZHI
Department of Chemistry, East China Normal University, 3663 Chung Shan Road (N.), Shanghai, People's Republic of China

(*Received* 30 *March* 1984. *Revised* 11 *August* 1984. *Accepted* 24 *October* 1984)

Summary—An indirect method for determination of trace phenol in water by atomic-absorption spectrophotometry (AAS) is described. The phenol is brominated in acidic solution with $KBrO_3$–KBr solution at room temperature. The excess of bromine is reacted with KI and the I_2 produced is extracted into cyclohexane and then reduced back to I^- with ascorbic acid. The I^- is then complexed with Cd^{2+} in sulphuric acid medium and the complex extracted into MIBK. The extract is analysed by flame AAS for Cd (and hence indirectly for phenol). The linear concentration range for determination of phenol is 6×10^{-7}–$0.9 \times 10^{-5}M$ in aqueous solution. Several foreign ions and organic substances do not interfere.

The determination of trace phenol is difficult but important in monitoring water quality. The methods usually used include bromination,[1] colorimetry[2] and gas chromatography.[3] The recommended method is colorimetry, but it is time-consuming because of the distillation step needed to remove interferences. Bromination is the traditional titrimetric method, but it cannot be used for phenol concentration < 10 mg/l. We have made an attempt to determine trace phenol in water samples by AAS, as part of a programme of indirect determination of organic compounds by AAS.

Indirect determinations of phenol by AAS have already been reported. Yamamoto *et al.*[4] determined pentachlorophenol by AAS determination of iron after extraction of the iron(III)–pentachlorophenol ion-pair complex into nitrobenzene. Mitsui and Fujimura[5] reacted nitrosated phenol with sodium cobaltinitrite to form nitrosophenol which further reacts with cobalt (III) to form a cobalt–phenol complex, which can be extracted into methyl isobutyl ketone (MIBK) and determined by AAS.

The present method is based on the bromination of phenol to form tribromophenol. The excess of bromine is then reacted with iodide, and the iodine formed is extracted into cyclohexane and reduced back to iodide, which is then reacted with cadmium in sulphuric acid solution to form H_2CdI_4, which in turn is extracted into MIBK. This extract is aspirated into an air–acetylene flame to be analysed for Cd.

Bromine can react with several other classes of organic compounds, such as unsaturated organic acids, aniline, *etc.* Therefore, it is first necessary to remove these interferences by solvent extraction of the phenol with 1:1 v/v chloroform/ether mixture at pH 8–9, which can be done with nearly 100% efficiency.[6] At this pH the organic acids are not extracted. The extracted phenol is then stripped with $0.1M$ potassium hydroxide, and the aniline remains behind in the organic solvent. In this way the phenol can not only be preconcentrated but also freed from interferences. This paper shows that the method is highly sensitive and can be used to analyse for relatively low concentrations of trace phenol in water.

EXPERIMENTAL

Reagents

Use demineralized water and analytical grade reagents throughout.

Phenol stock solution (*1 g/l.*). Dissolve 0.1 g of freshly distilled phenol in 100 ml of water, and standardize the solution by iodometry. Prepare a working solution ($1 \times 10^{-5}M$), just before use, by diluting 1 ml of the phenol stock solution to 100 ml and then diluting 10 ml of this solution to 100 ml with water.

Bromate–bromide solution (5×10^{-4}M Br_2). Dissolve 2.78 g of dried potassium bromate and 10 g of potassium bromide in 1000 ml of water, then before use, dilute 1 ml of this solution to 100 ml with water.

Potassium iodide solution (1.0×10^{-3}M). Dissolve 1.66 g of potassium iodide in 100 ml of water and dilute 1 ml of this solution to 100 ml with water.

Cadmium working solution (1.37×10^{-3}M). Dissolve 38.5 mg of $CdSO_4 \cdot 4H_2O$ in 100 ml of water.

Ascorbic acid solution, *0.01*M.

Mixed solvent. Mix equal volumes of chloroform and diethyl ether.

Procedure

In a 60-ml separatory funnel place 10 ml (or more) of the water sample (depending on the phenol concentration), adjust the pH to 8–9 with $0.1M$ potassium hydroxide, and add 2 ml of mixed solvent (the amount of solvent should be increased in proportion to the volume of the sample. Shake the funnel for 2 min. Transfer the organic phase to a 25-ml separatory funnel, add 2 ml of $0.1M$ potassium hydroxide, shake the funnel for 1 min, separate the organic phase and add the following solutions to the aqueous phase in the order given: 0.3 ml of bromate–bromide solution, 0.5 ml of cyclohexane and 2 ml of $2M$ hydrochloric acid, mix well and leave to stand for 20 min, then add 0.5 ml of $10^{-3}M$

Table 1. Effect of foreign ions on determination of 1.13 μg of phenol in 10 ml of water

Foreign ion	Added, μg	Phenol found, μg	Error,%
Fe^{3+}	200	1.15	+2
Cr^{3+}	220*	0.99	−12
Zn^{2+}	100	1.11	−2
Al^{3+}	50*	1.21	+7
Ca^{2+}	100†	1.23	+9
Pb^{2+}	100†	1.10	−3
Mg^{2+}	100†	1.13	0
S^{2-}	500	1.11	−2
CO_3^{2-}	200	1.11	−2
Acetate	500	1.18	+4
EDTA	1000	1.09	−4
Oxalate	200	1.25	+11
Citrate	200	1.05	−7
Urea	200	1.22	+8
Nitrobenzene	200	1.23	+9
Aniline	50	1.17	+4
Methylbenzene	200	1.12	−1
Aminophenylsulphonic acid	300	1.13	0

*After addition of 200 μg of EDTA.
†After addition of 1000 μg of EDTA.

postassium iodide and shake the funnel for 1 min. Separate the aqueous phase and add to the cyclohexane layer 0.1 ml of 0.01*M* ascorbic acid and 0.2 ml of $1.37 \times 10^{-3}M$ cadmium solution, shake, then add 1 ml of 10*M* sulphuric acid and 1 ml of MIBK. Shake the funnel for 1 min, then run off the aqueous phase. Aspirate the mixed cyclohexane/MIBK phase directly into the air–acetylene flame for determination of cadmium under the following conditions:

Wavelength	228.8 nm
Cd lamp current	10 mA
Band-width	1.3 nm
Air flow	9.4 l./min
Acetylene flow	2.3 l./min

RESULTS AND DISCUSSION

Bromination

The initial reaction between bromine and phenol is rapid in acid solution, but the trisubstitution is slower and so a waiting period is needed to avoid negative errors; on the other hand, if this period is too long, side-reactions can take place and cause positive errors. From the data presented in Fig. 1 it can be seen that 10–20 min is a suitable period.

The hydrochloric acid concentration is fairly critical—it affects both the generation of bromine and the rate of bromination of phenol. The results shown in Fig. 2 indicate that the optimum acid concentration is 1*M*.

Extraction

Cadmium reacts with iodide in acid solution to form the iodide complex, which can be extracted into certain organic solvents, such as the MIBK/cyclohexane mixture used here, with high efficiency. The data plotted in Fig. 3 suggest that the 1:4 complex is extracted, presumably as H_2CdI_4; Fig. 4 shows that the sulphuric acid concentration must be at least 7*M* for extraction to be complete.

Interferences

The effect of various ionic species on the complete procedure was investigated. The results are summarized in Table 1. Some metal ions can cause problems by hydrolysing and precipitating when the pH is raised to 8–9 for the clean-up extraction of the phenol, and some phenol may then be lost by adsorption on the surface of the precipitate. The effect may be minimized by adding EDTA to keep the metal ions in solution.

Calibration and performance

The calibration graph is linear up to 2.3 μg of phenol in the original sample, and with a 100-ml

Table 2. Determination and recovery of phenol (5 determinations)

Sample	Sample volume, *ml*	Phenol added, μg	Phenol found, μg	R.S.D., %	Recovery, %
Huang Pu	10		1.09	8	
river water	10	0.23	1.32		100
Industrial area	5		1.47	6	
waste water	5	0.57	2.11		112
Laboratory	2		0.32	5	
waste water	2	0.57	0.88		98

Table 3. Bromination efficiency

Compound	Efficiency of bromination,* %
Distilled water	0
Phenol	100
o-Chlorophenol	46
p-Chlorophenol	35
2,4-Dinitrophenol	2
2,4,6-Trichlorophenol	6
Pentachlorophenol	−1
o-Methylphenol	87
m-Methylphenol	108

*Referred to phenol as 100%.

sample, the limit of detection is 1.2 μg/l. For 7 determinations of 1.13 μg of phenol the relative standard deviation was 3.3% and the recovery 98–112%. The result for the determination of phenol in three water samples are shown in Table 2. They indicate that method is sensitive and useful for low levels of phenol, though of course other phenolic compounds would interfere and to different extents, depending on the nature of their bromination reactions. Some apparent efficiencies of bromination of various phenols (at the $10^{-5}M$ level) under the conditions given in the procedure are listed in Table 3, and indicate which substituted phenols would interfere.

Acknowledgement—We are very grateful to Professor Hsu Chung-Gin for his enthusiastic help in finishing this work.

REFERENCES

1. A. I. Vogel, *Elementary Practical Organic Chemistry*, Part 3, p. 686. Longmans, London, 1958.
2. *Standard Methods for the Examination of Water and Waste Water*, 13th Ed., p. 507. American Public Health Association, New York, 1971.
3. *Ibid.*, p. 510.
4. Y. Yamamoto, T. Kumamaru and Y. Hayashi, *Talanta*, 1967, **14**, 611.
5. T. Mitsui and Y. Fujimura, *Bunseki Kagaku*, 1974, **23**, 1303.
6. Shi Ming-Shui, *Fenxi Huaxue*, 1980, **8**, 511.

Talanta, Vol. 32, No. 3, pp. 218–220, 1985
Printed in Great Britain.

0039-9140/85 $3.00 + 0.00

CATALYTIC TITRATION OF IODIDE, BROMIDE AND THIOCYANATE BY USE OF THE SILVER CATALYSED PHLOXIN–PERSULPHATE REACTION

C. SANCHEZ-PEDREÑO,* M. HERNANDEZ CORDOBA and P. VIÑAS
Department of Analytical Chemistry, University of Murcia, Murcia, Spain

(*Received* 12 *March* 1984. *Revised* 19 *September* 1984. *Accepted* 5 *October* 1984)

Summary—A method for the catalytic titrimetric determination of iodide, bromide and thiocyanate is described, based on the inhibitory effect of these anions on the silver-catalysed oxidation of phloxin by persulphate in the presence of 2,2′-bipyridyl. The end-point is determined photometrically by measuring the absorbance at 537 nm. Amounts of iodide, bromide and thiocyanate in the 0.01–7.94, 0.11–4.73 and 0.12–3.59 mg ranges, respectively, are titrated with a relative error of about 1%.

The oxidation of phloxin by persulphate, catalysed by silver in the presence of 2,2′-bipyridyl as an activator, has recently been described.[1] Iodide, bromide and thiocyanate have an inhibitory effect on the catalytic reaction and the phloxin–persulphate system can be used for indication of the end-point in their titration with silver nitrate. When the inhibitor has been titrated, the first excess of the titrant will immediately accelerate the indicator reaction, and this effect can be used to locate the end-point.

Catalytic reactions were first applied for end-point determination in titrimetric analysis by Weisz *et al.*[2–5] and later studied in depth by Mottola.[6] Titrimetric procedures with visual,[7] spectrophotometric,[2,3,7–15] potentiometric,[4,9–11] biamperometric[7,10,16] and thermometric[5,7,9,17–21] catalytic indication of the end-point have been used for the determination of several inorganic and organic compounds.

Although some titrations of iodide with silver, based on use of different catalytic indicator systems, have been described,[2,22–25] we have found only two references to similar determination of bromide and thiocyanate.[2,7]

This paper describes a semi-automatic method for the determination of iodide, bromide and thiocyanate, based on their inhibitory effect on the silver-catalysed phloxin–persulphate reaction.

EXPERIMENTAL

Reagents

All inorganic chemicals used were of analytical reagent grade and the solutions were prepared with doubly distilled water.

Phloxin solution. An aqueous $5 \times 10^{-4}M$ solution was prepared from the commercial product (Geigy) without further purification.

Bromide, iodide and thiocyanate solutions, 0.02M. These were prepared from the potassium salts and standardized with standard silver nitrate solution. Dilute solutions were prepared just before the measurements.

Other reagent stock solutions were $1M$ acetate buffer (pH 5) and $0.003M$ 2,2′-bipyridyl. A $0.15M$ potassium persulphate solution was prepared daily.

Apparatus

A Metrohm 616 photometric titrator was coupled to an Omniscribe recorder and an ABU 12 Radiometer automatic constant-rate burette.

Procedure

Fill the automatic burette with standard silver nitrate solution of concentration appropriate to that of the titrand in the sample. Set the wavelength of the photometric titrator at 537 nm, the rate of titrant addition at about 0.3 ml/min and the chart-speed at 0.5 in./min. To the titration vessel, add the reactants in the following order: 1 ml of $5 \times 10^{-4}M$ phloxin, 10 ml of $1M$ acetate buffer (pH 5), 10 ml of $0.003M$ 2,2′-bipyridyl, the sample containing the inhibitor ion, and 10 ml of $0.15M$ potassium persulphate. Dilute to 50 ml with doubly distilled water. Stir the solution with the magnetic stirrer. Switch on the recorder and the autoburette simultaneously and record the absorbance–volume curve.

Obtain the end-point by extrapolation of the linear segments of the curve and calculate the titrand concentration by simple proportion from the results for the sample and a standard titrand solution.

RESULTS AND DISCUSSION

The reaction is followed by monitoring the decrease in absorbance at 537 nm. During the precipitation process, the photometric signal decreases slowly. When the equivalence point is reached, the first excess of silver catalyses the indicator reaction and a sharp decrease in absorbance is recorded. There is always a blank because a small excess of silver is needed to start the indicator reaction. There is also a contribution to the absorbance from the scattering of incident radiation by the precipitate produced. The

*Author for correspondence.

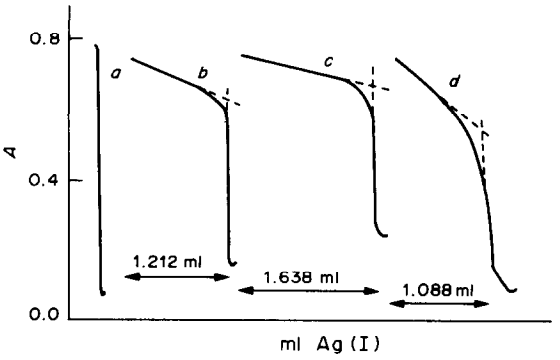

Fig. 1. Catalytic spectrophotometric titration of iodide, thiocyanate and bromide with 0.01*M* silver nitrate. Curve *a*, without inhibitory ion; *b*, 1.589 mg of I^-; *c*, 0.957 mg of SCN^-; *d*, 0.898 *mg of* Br^-.

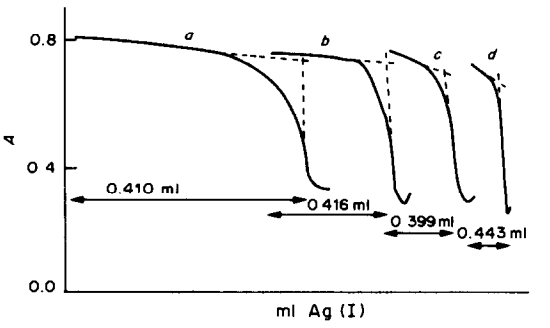

Fig. 2. Influence of the rate of addition of titrant for the determination of 2.641 mg of iodide with 0.05*M* silver nitrate. Chart-speed 1 in./min. Rate of addition, ml/min; *a*, 0.0712; *b* 0.1425; *c*, 0.285; *d* 0.570.

blank value and the sharpness of the end-point depend on the concentration of the reagents, and the concentration of the titrant and its rate of addition. When all these variables are kept constant, the blank is highly reproducible.

The effect of varying the reagent concentrations was studied, and the optimum values (indicated in the procedure) were found to be the same as those[1] for maximum rate of the catalysed reaction in the absence of inhibitor. The catalytic reaction starts before the equivalence point, but because of the dynamic nature of the titration system, does not become fast enough to give a large signal until the equivalence point is reached.

Titration curves obtained for iodide, thiocyanate and bromide are shown in Fig. 1.

The end-point indication is obviously sharper for iodide because the solubility of silver iodide is lower than that of silver thiocyanate or bromide, and the indicator reaction does not begin until nearer the end-point. Chloride cannot be titrated by this procedure because the indicator reaction is completed before the equivalence point is reached.

The influence of the rate of titrant addition on the determination of iodide is shown in Fig. 2. The addition rates ranged from 0.071 to 0.570 ml/min and the recorder was run at 1 in./min. To obtain optimal results, an addition rate of 0.285 ml/min was selected.

Since phloxin is a fluorescein derivative which has been used as an adsorption indicator,[26] several titrations were performed in the absence of persulphate to decide whether an adsorption mechanism is involved. The results indicate that the catalytic process is responsible for the sharp decrease in absorbance at 537 nm.

Results and performance characteristics for the catalytic titration of iodide, bromide and thiocyanate with silver nitrate are shown in Tables 1–3.

Table 1 shows that iodide can be titrated over a wide range of concentrations. The average error was 1%, with an average coefficient of variation of 0.7%. The best results were obtained with 10^{-3} and $10^{-2}M$

Table 1. Results for potassium iodide (5 determinations at each level)

$[AgNO_3]$, M	I^- taken, *mg*	I^- found, *mg*	Error, %	Standard deviation, *μg*	Coefficient of variation, %
1×10^{-3}	0.0106	0.0109	+2.8	0.4	3.6
	0.0265	0.0267	+0.8	0.6	2.1
	0.0530	0.0525	−0.9	0.1	0.2
	0.1060	0.1054	−0.6	0.2	0.2
	0.1590	0.1601	+0.7	0.5	0.3
	0.2120	0.2103	−0.8	0.6	0.3
	0.2650	0.2626	−0.9	1.4	0.6
1×10^{-2}	0.106	0.105	−0.9	1.0	1.0
	0.265	0.266	+0.4	1.6	0.6
	0.530	0.535	+0.9	1.9	0.4
	1.059	1.068	+0.9	3.1	0.3
	1.589	1.600	+0.7	3.5	0.2
	2.118	2.090	−1.3	7.4	0.4
	2.648	2.600	−1.8	14	0.6
5×10^{-2}	2.648	2.614	−1.3	63	2.4
	5.295	5.213	−1.6	41	0.8
	7.943	7.855	−1.1	81	1.0

Table 2. Results for potassium thiocyanate (5 determinations at each level)

$[AgNO_3]$, M	SCN^- taken, mg	SCN^- found, mg	Error, %	Standard deviation, μg	Coefficient of variation, %
1×10^{-2}	0.120	0.120	0	2.6	2.2
	0.239	0.236	−1.3	2.7	1.1
	0.479	0.474	−1.0	3.5	0.7
	0.718	0.712	−0.8	6.8	1.0
	0.957	0.950	−0.7	5.1	0.5
	1.196	1.178	−1.5	4.2	0.4
5×10^{-2}	1.196	1.209	+1.1	23	1.9
	2.392	2.386	−0.3	21	0.9
	3.589	3.562	−0.8	39	1.1

Table 3. Results for sodium bromide (5 determinations at each level)

$[AgNO_3]$, M	Br^- taken, mg	Br^- found, mg	Error, %	Standard deviation, μg	Coefficient of variation, %
1×10^{-2}	0.112	0.113	+0.9	4.9	4.4
	0.224	0.221	−1.3	3.7	1.7
	0.449	0.453	+0.9	3.7	0.8
	0.673	0.665	−1.2	6.2	0.9
	0.898	0.881	−1.9	9.3	1.1
	1.122	1.100	−2.0	13	1.2
5×10^{-2}	1.577	1.592	+1.0	21	1.4
	3.154	3.201	+1.5	52	1.6
	4.731	4.857	+2.7	98	2.1

silver nitrate as titrant. The concentration of iodide in the reaction vessel must be kept below $10^{-3}M$. More concentrated solutions produce abundant precipitates and location of the end-point becomes difficult.

For the thiocyanate determination the average error was 0.9% and the coefficient of variation 1.1%. Similar results were found in the catalytic titration of bromide. The titrand concentration must be in the range 3×10^{-5}–$10^{-3}M$ for the titration of thiocyanate or bromide. More dilute solutions cannot be titrated because the catalysis then takes place at a considerable rate before the equivalence point is reached.

As always in the use of chart-recorded titration curves, errors can arise from extrapolation, line thickness, variation in chart-speed *etc.*, and this is reflected in the higher coefficients of variation for the lower levels of analyte.

REFERENCES

1. M. Hernández Córdoba, C. Sánchez-Pedreño and P. Viñas, *Microchem. J.*, in the press.
2. H. Weisz and U. Muschelknautz, *Z. Anal. Chem.*, 1966, **215**, 17.
3. H. Weisz and T. Janjic, *ibid.*, 1967, **227**, 1.
4. H. Weisz and D. Klockow, *ibid.*, 1967, **232**, 321.
5. H. Weisz, T. Kiss and D. Klockow, *ibid.*, 1969, **247**, 248.
6. H. A. Mottola, *Talanta*, 1969, **16**, 1267.
7. H. Weisz and S. Pantel, *Anal. Chim. Acta*, 1972, **62**, 361.
8. H. A. Mottola, *Anal. Chem.*, 1970, **42**, 630.
9. H. Weisz, *Allg. Prakt. Chem.*, 1971, **22**, 98.
10. H. Weisz, S. Pantel and H. Ludwig, *Z. Anal. Chem.*, 1972, **262**, 269.
11. T. P. Hadjiioannou, E. A. Piperaki and D. S. Papastathopoulus, *Anal. Chim. Acta*, 1974, **68**, 447.
12. M. Ternero, F. Pino, D. Pérez-Bendito and M. Valcárcel, *ibid.*, 1979, **109**, 401
13. S. Pantel and H. Weisz, *ibid.*, 1980, **116**, 421.
14. M. Ternero, D. Pérez-Bendito and M. Valcárcel, *Microchem. J.*, 1981, **26**, 61.
15. T. Raya-Saro and D. Pérez-Bendito, *Analyst*, 1983, **108**, 857.
16. S. Pantel and H. Weisz, *Z. Anal. Chem.*, 1976, **281**, 211.
17. H. Weisz and T. Kiss, *ibid.*, 1970, **249**, 302.
18. T. Kiss, *ibid.*, 1970, **252**, 12.
19. K. C. Burton and H. M. N. H. Irving, *Anal. Chim. Acta*, 1970, **52**, 441.
20. T. Kiss, *Mikrochim. Acta*, 1973, 847.
21. N. Kiba and M. Furosawa, *Anal. Chim. Acta*, 1978, **98**, 343.
22. T. P. Hadjiioannou and E. A. Piperaki, *ibid.*, 1977, **90**, 329.
23. T. I. Fedorova, K. B. Yatsimirskii, E. V. Vasil'eva and V. G. Markichev, *Zh. Analit. Khim.*, 1977, **32**, 1951.
24. T. Braun, *Rev. Chim. Bucharest*, 1956, **7**, 309.
25. M. M. Timotheou-Potamia and T. P. Hadjiioannou, *Mikrochim. Acta*, 1983 **II**, 59.
26. E. Bishop, *Indicators*, p. 440. Pergamon Press, Oxford, 1972.

Talanta, Vol. 32, No 3, pp. 221–223, 1985
Printed in Great Britain

0039-9140/85 $3.00 + 0.00
Pergamon Press Ltd

KINETIC DETERMINATION OF TRACES OF CYSTEINE BY ITS INHIBITORY EFFECT ON THE SILVER-CATALYSED PHLOXIN–PERSULPHATE REACTION

M. HERNANDEZ CORDOBA, P. VIÑAS and C. SANCHEZ-PEDREÑO*
Department of Analytical Chemistry, University of Murcia, Murcia, Spain

(*Received* 13 *June* 1984. *Revised* 19 *September* 1984. *Accepted* 5 *October* 1984)

Summary—Cysteine has an inhibitory effect on the silver-catalysed phloxin–persulphate reaction at pH 5. When the cysteine/silver ratio is < 1, a decrease in the reaction rate is the only observed effect. However, when the ratio is > 1, an induction period appears. The length of the induction period is proportional to the cysteine concentration and allows the quantitative determination of cysteine and silver.

Many kinetic determinations of microquantities of inorganic ions have been reported, but few for organic compounds.[1] Recently, some kinetic methods for amino-acid determination based on inhibition of a given catalytic reaction have been proposed.[2–7]

We have reported earlier[8] the kinetic determination of silver by means of its catalytic action on the phloxin–persulphate system, with 2,2′-bipyridyl as activator. We have found that cysteine has an inhibitory effect on this reaction. A similar action of cysteine on a silver-catalysed reaction has already been reported by Alexiev and Angelova,[6] but in our work a different process is involved, since the nature of the inhibitory effect depends on the cysteine/silver ratio, resulting in either an induction period (with a length related to the cysteine/silver ratio) or reduction in the reaction rate. Based on this, a new method has been developed for the determination of cysteine in the presence of various amino-acids.

EXPERIMENTAL

Apparatus

A Pye Unicam SP8-100 double-beam spectrophotometer with 1-cm cells and constant-temperature cell-holder was used for recording absorbance–time curves.

Reagents

All chemicals used were analytical-reagent grade and the solutions were prepared with doubly distilled water. Aqueous $5 \times 10^{-4}M$ phloxin solution was prepared from the commercial product (Geigy), without further purification, by dissolving 0.2074 g in 500 ml of water. A $5 \times 10^{-3}M$ cysteine stock solution was prepared in $0.01M$ hydrochloric acid in order to stabilize it. The solution was prepared every week and stored in a dark bottle.

Other reagent stock solutions were: $1M$ acetate buffer, pH 5, $3 \times 10^{-3}M$ 2,2′-bipyridyl and $0.01M$ silver nitrate.

Working solutions of silver, cysteine and $0.15M$ potassium persulphate were prepared daily.

*Author to whom correspondence should be addressed.

Procedure

In a 25-ml standard flask place 1 ml of $5 \times 10^{-4}M$ phloxin, 5 ml of $1M$ acetate buffer, 5 ml of $3 \times 10^{-3}M$ 2,2′-bipyridyl and appropriate volumes of silver nitrate and cysteine solutions. Keep the flask in a thermostat at $25.0 \pm 0.1°$ for 30 min and then add 5 ml of $0.15M$ potassium persulphate solution and dilute to volume with water, but do not mix. Turn on the recorder, mix the solution by vigorous shaking, transfer it to the spectrophotometer cell (kept at $25.0 \pm 0.1°$) and record the absorbance–time curve. Evaluate the length of the induction period by extrapolation of the two segments of the reaction curve, and measurement of the elapsed time corresponding to the point of intersection. Prepare a calibration graph by the same procedure.

RESULTS AND DISCUSSION

The oxidation of phloxin by persulphate is catalysed by silver, in presence of 2,2′-bipyridyl as activator. The reaction can be followed spectrophotometrically by measuring the change in absorbance at 537 nm.[8]

When cysteine is present in this system, the catalytic effect of silver is decreased because the silver is bound by the thiol group of the cysteine, which thus acts as an inhibitor. The nature of the inhibitory effect depends on the cysteine/silver ratio in the sample.

Influence of the cysteine concentration

At cysteine/silver ratios < 1 the only effect is a decrease in the reaction rate. At cysteine/silver ratios > 1, however, an induction period appears (Fig. 1), which increases in length with increase in cysteine concentration.

Figure 2 shows the dependence of the induction period on the pH. A pH of 5 was selected for use because it maximizes the catalysed reaction rate and gives adequate length of the induction period for a given concentration of cysteine and silver.

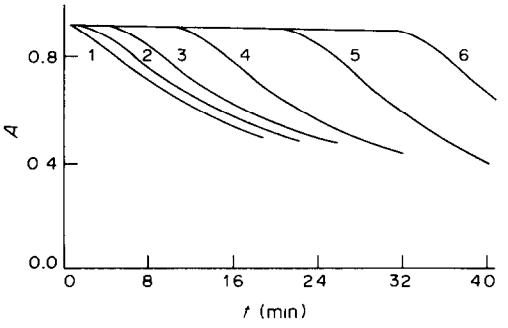

Fig. 1. Absorbance–time curves for [Cys]/[Ag] > 1: $2 \times 10^{-5}M$ phloxin, $0.2M$ acetate buffer (pH 5), $6 \times 10^{-4}M$ 2,2′-bipyridyl, $4.82 \times 10^{-7}M$ Ag^+, $0.03M$ potassium persulphate, 25°, λ 537 nm. [Cys]: (1) $0.6 \times 10^{-6}M$, (2) $1.0 \times 10^{-6}M$, (3) $1.4 \times 10^{-6}M$, (4) $2.0 \times 10^{-6}M$, (5) $3.0 \times 10^{-6}M$, (6) $4.0 \times 10^{-6}M$.

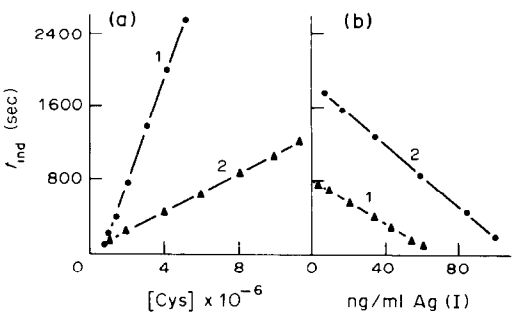

Fig. 3. Calibration graphs for cysteine and silver determination by the induction-period method. (*a*) Cysteine; (1) $4.82 \times 10^{-7}M$ Ag^+, (2) $9.64 \times 10^{-7}M$ Ag^+. (*b*) Silver; (1) $10^{-6}M$ cysteine, (2) $2 \times 10^{-6}M$ cysteine.

The other experimental variables were also chosen to give maximum rate of the catalysed reaction and hence sharper indication of the end of the induction period.[8] They were: $2 \times 10^{-5}M$ phloxin, $0.2M$ acetate buffer (pH 5), $6 \times 10^{-4}M$ 2,2′-bipyridyl, $0.03M$ potassium persulphate and temperature $25 \pm 0.1°$.

The following mechanism for the inhibitory effect is proposed. When the cysteine/silver ratio is below 1, some of the silver is bound by the thiol group of the amino-acid, so the concentration of the catalytically active Ag–bipyridyl complex is decreased, and consequently so is the rate of oxidation of phloxin.

The presence of excess of cysteine produces an induction period, however. Presumably all the silver is bound as the catalytically inactive Ag–cysteine complex and the persulphate acts on the excess of amino-acid. When all the free cysteine has been oxidized, the oxidant acts on the Ag–cysteine complex, releasing the metal ion, which can then combine with the activator so the induction period ends and the catalytic cycle starts.

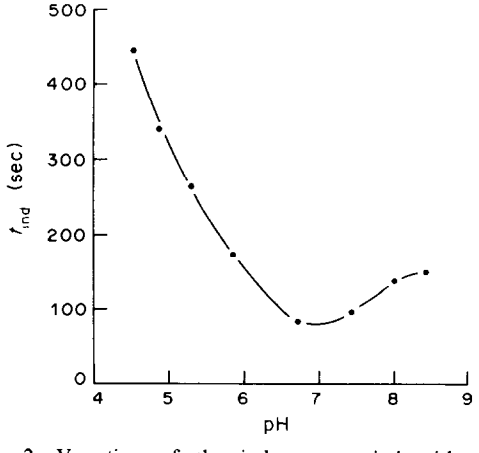

Fig. 2. Variation of the induction period with pH: $2 \times 10^{-5}M$ phloxin, $6 \times 10^{-4}M$ 2,2′-bipyridyl, $9.64 \times 10^{-7}M$ Ag^+, $2 \times 10^{-6}M$ cysteine, $0.03M$ potassium persulphate, 25°, λ 537 nm.

Thus, the cysteine can be determined by measurement of the induction period. Obviously, the measurable cysteine concentration range varies according to the silver concentration in the medium. Figure 3a shows two calibration graphs for the kinetic determination of cysteine by this procedure.

The relative error for ten measurements of $1.6 \times 10^{-6}M$ cysteine in the presence of $4.82 \times 10^{-7}M$ silver was $\pm 2.8\%$. A value of $t = 0.47$ was obtained in a Student's t-test, showing the absence of a systematic error in the method (the tabulated t-value for the 95% confidence level is 2.26).

If the cysteine concentration is kept constant, the length of the induction period decreases with increase in silver concentration, and calibration graphs for silver determination can be obtained (Fig. 3b).

Interference studies

The influence of the most important amino-acids on the determination of $1.5 \times 10^{-6}M$ cysteine was studied, and the results are summarized in Table 1. The tolerance limit was taken as the concentration which causes an error of not more than 5% in the cysteine determination.

The effect of adding greater amounts of interfering amino-acids is always to increase the length of the induction period.

Table 1. Interference of the most important amino-acids on the determination of $1.5 \times 10^{-6}M$ cysteine

Limiting molar ratio [Amino-acid]/[Cys]	Amino-acid
200*	Glycine, alanine, valine, leucine, isoleucine, threonine, serine, histidine, proline, lysine, asparagine, glutamine, aspartate, glutamate, arginine, phenylalanine
12	Methionine
4	Cystine
0.5	Tryptophan, tyrosine

*Maximum ratio tested.

REFERENCES

1. G. A. Milovanovic, *Microchem. J.*, 1983, **28,** 437.
2. T. J. Janjic and G. A. Milovanovic, *Anal. Chem.*, 1973, **45,** 390.
3. A. Vanni, P. Amico and E. Roletto, *Ann. Chim. (Rome)*, 1976, **66,** 213.
4. B. I. Nabivanets and L. V. Kalabina, *Zh. Analit. Khim.*, 1977, **32,** 2018.
5. H. Müller, H. Schurig and G. Werner, *Talanta*, 1979, **26,** 785.
6. A. A. Alexiev and M. G. Angelova, *Mikrochim. Acta*, 1983 **II,** 369.
7. M. Phull and P. C. Nigam, *Talanta*, 1983, **30,** 401.
8. M. Hernandez Cordoba, C. Sanchez-Pedreño and P. Viñas, *Microchem. J.*, in the press.

Talanta, Vol. 32, No 3, pp. 224–226, 1985
Printed in Great Britain.

0039-9140/85 $3 00 + 0 00

SPECTROPHOTOMETRIC DETERMINATION OF FLUORIDE IN FLUORIDE-BEARING MINERALS AFTER DECOMPOSITION BY FUSION WITH SODIUM HYDROXIDE

J. V. GIMENO ADELANTADO, V. PERIS MARTINEZ, A. CHECA MORENO and F. BOSCH REIG

Department of Analytical Chemistry, Faculty of Chemistry, University of Valencia, Burjasot (Valencia), Spain

(*Received* 9 *May* 1984. *Revised* 24 *August* 1984. *Accepted* 5 *October* 1984)

Summary—The decomposition of highly insoluble minerals (fluorspar and cryolite) by fusion with molten alkali-metal hydroxides is studied. The introduction of additives such as aluminium compounds or sodium peroxide to obtain total liberation of fluoride from calcium fluoride samples, is tested. The fusion is done in a silver crucible with a Bunsen burner. The cooled melt is easily soluble, giving solutions suitable for spectrophotometric fluoride determination by the Zr(IV)–fluoride–Erichrome Cyanine R method.

The difficulty of decomposing highly insoluble fluoride compounds such as fluorspar or cryolite for fluoride determination is well-known. Most methods employ fusion with silica and alkali-metal carbonates to bind the fluoride. Adolph uses an equimolar ratio of silica to fluoride, and a 6-fold molar ratio of sodium–potassium carbonate mixture,[1] whereas Hawley says that a 4-fold ratio of the carbonate is enough.[2] Treadwell recommends mixing the sample with twice its weight of silica and six times its weight of sodium–potassium carbonate, and Shehyn a weight ratio of 0.2:4:0.7 for CaF_2, $NaKCO_3$ and SiO_2.[3] Shell and Craig[4] and Grimaldi *et al.*[5] advise addition of zinc oxide to the mixture. Even so, the residue from the fusion must still be distilled by using the Willard and Winter method[6] or one of its modifications.[7–9] Distillation without previous carbonate fusion has been used but is slow and needs complicated apparatus.[10–12] Other methods use pyrohydrolysis,[13] fusion with vanadium pentoxide[14] or treatment with aluminium chloride solution.[15]

In the opening-out of cryolite samples, sodium–potassium carbonate and silica in various ratios,[3,6] or potassium carbonate and silica,[17] are used for the fusion.

Although molten alkali-metal hydroxides are powerful decomposition agents, according to Bogen, they are little used because platinum crucibles cannot be employed, and gold, silver or nickel crucibles become damaged;[18] this is a pity, because they completely retain even highly volatile elements such as arsenic.[19] Fusion with these hydroxides has been used to decompose compounds containing fluoride such as fluorinated minerals,[20–22] silicate materials,[23–25] zinc concentrates[26] and even organic compounds.[27]

The effectiveness of molten alkali-metal hydroxides in the decomposition of fluoride compounds and its improvement by introduction of some chemicals which have an influence on the solvent action are studied in this paper. A silver crucible is used, as recommended earlier by us[18,28] because the melt is less contaminated.[29] Fluoride can then be determined spectrophotometrically by the Zr(IV)–F^-–Eriochrome Cyanine R method.[30,31]

EXPERIMENTAL

Reagents

Eriochrome Cyanine R solution, 0.18%.

Zirconium solution. Dissolve 0.2650 g of $ZrO_2Cl_2 \cdot 8H_2O$ in 700 ml of concentrated hydrochloric acid and dilute to 1 litre.

Fluoride solution. Dissolve 0.2210 g of sodium fluoride in distilled water and dilute to 1 litre. Store in a polyethylene bottle.

Procedures

Alkaline fusion. In a silver crucible fuse 1 g of sodium hydroxide pellets. Allow to cool, shaking the crucible so that the melt solidifies on the bottom and walls. Add 0.1 g of cryolite or fluorspar sample (for the latter also add 0.1 g of sodium peroxide or an aluminium salt or alumina). Heat gently with a moderate flame until the alkali is molten, swirling the crucible to assist dissolution. Then heat more strongly, increasing the intensity of the flame, and continue heating for 2 min. Cool to room temperature. Leach the melt with small portions of hot water, transferring them to a 250-ml polyethylene beaker, dilute to 100 ml and cool. Add 0.2 g of boric acid or 0.1 g of an aluminium salt if a fluorspar sample has been decomposed in the presence of sodium peroxide. Add 3*M* hydrochloric acid dropwise with vigorous stirring to expel the carbon dioxide released, until a clear solution is obtained. Transfer to a 250-ml standard flask and dilute to the mark.

Fluoride determination. Transfer a 2-ml aliquot of the solution to a 100-ml standard flask and dilute to volume. Pipette a 10-ml aliquot into a 50-ml standard flask (if aluminium is present add one drop of 0.1% phenolphthalein solution and then 0.1 M sodium hydroxide dropwise until the colour changes). Add 5 ml each of the Eriochrome

Cyanine R and zirconium solutions. Dilute to the mark, mix, wait for 15–20 min, and read the absorbance at 527–528 nm against a reference prepared with 10 ml of Eriochrome Cyanine R solution and 7 ml of concentrated hydrochloric acid, diluted to 100 ml.[32]

Prepare a calibration curve with aliquots of standard fluoride solution to cover the fluoride range 0.2–1.2 ppm in the solution measured.

RESULTS AND DISCUSSION

Determination of fluoride

The suitability of the changes in the spectrophotometric method has been checked for samples that contain interfering elements arising either in the sample or in its treatment.

Boron. Boric acid is added to avoid loss of fluoride from fluorspar samples when the solution of the alkaline melt is acidified. Because of the ready complexation of boron with fluoride, its influence on the Zr(IV)–F^-–Eriochrome Cyanine system was studied. Solutions containing 0, 10, 20, 30 and 40 ppm of boric acid and 1 ppm of fluoride were found to give the same absorbance (which was stable) provided that the measurements were taken after 5–10 min.

Aluminium salts. Aluminium will be present in cryolite analyses as a component of the sample, and in fluorite analyses because it is added to ensure complete decomposition and/or to avoid loss of fluoride by volatilization when the solution of the cooled melt is acidified.

Aluminium interferes in the spectrophotometric determination of fluoride by retarding the formation of the zirconium–fluoride complex, so the modification proposed by Megregian is used.[30] The tolerance level for aluminium was tested with 1 ppm of fluoride and 0, 10, 20, 30 and 40 ppm of aluminium. For up to 20 ppm of aluminium the results were satisfactory if the absorbance was measured after a development time of 15 min; for 30 ppm a stable reading may be obtained after 45 min, but the delay time increases with aluminium concentration and for 40 ppm even an hour is not long enough for complete reaction.

Sulphate does not produce appreciable interference[30] when potassium alum is used as the additive, because its concentration is low.

Decomposition of the sample

The molten alkali appears to dissolve the whole sample, giving a clear fluid which may contain greyish-white suspended matter, principally calcium oxide.[33] The suspension does not affect the subsequent analytical treatment.

The trials performed are shown schematically in Table 1. The use of potassium hydroxide, recommended by some authors,[26] proved not to be advisable, because it causes greater attack on the crucible but does not give better decomposition than sodium hydroxide does.

The low recoveries obtained with potassium nitrate as additive seem to indicate that sodium peroxide does not produce only an oxidative effect.

The aluminium compounds tested as auxiliary agents were the nitrate, chloride, potassium alum and the oxide.

In all cases the effect of fusion time and amount of sodium peroxide or aluminium added was studied. The optimum working conditions found are included in the procedure.

Fluoride determination

Fluorspar and fluorite. Table 2 shows the results for calcium fluoride recoveries for the samples studied.

The accuracy of the proposed method when applied to a BCS standard fluorspar (certificate value 97.2% CaF_2) was studied for both decomposition procedures (*i.e.*, with sodium peroxide or aluminium compounds as auxiliary agents). If the fusion is done with added sodium peroxide, then boric acid or aluminium salts are added after the fusion, to retain fluoride. The mean values were statistically the same as the certificate values (t-test), with no systematic error (95% probability level). The relative standard deviation was 0.2%. Analysis of the standard by the reference method gave a mean CaF_2 content of 96.9%, relative standard deviation 0.2% (10 replicates). All r.s.d. values were calculated[34] as $ts/\bar{x}\sqrt{n}$.

Table 1. Effect of additives on completeness of decomposition

Alkaline fusion			CaF_2	
Hydroxide	Auxiliary agent	Cryolite	Precipitated	Natural
NaOH	—	q.d.†	q.d.†	i.d.†
KOH	—	q.d.	q.d.	i.d.
NaOH + KOH*	—	q.d.	q.d.	i.d.
NaOH	H_3BO_3	—	q.d.	i.d.
NaOH	SiO_2	—	q.d.	i.d.
NaOH	Na_2O_2	—	q.d.	q.d.
NaOH	KNO_3	—	q.d.	i.d.
NaOH	Al(III)	—	q.d.	q.d.

*Eutectic mixture.
†q.d., quantitative decomposition; i.d., incomplete decomposition.

Table 2. Determination of fluoride in minerals: precision of the methods used ($n = 10$)

Sample (No.)	Fusion with alkali-metal hydroxide: CaF_2 found, %	Na_3AlF_6 found, %	s, %	Relative std. devn., %	Reference fusion*: CaF_2 found, %	Na_3AlF_6 found, %	s, %	Relative std. devn., %
Fluorspar (1)	97.1[a1]		0.2	0.2				
(standard BCS,	97.2[a2]		0.2	0.2				
97.2% certif.)	97.3[b]		0.2	0.2				
Fluorspar (2)	98.9[a1]		0.3	0.2	98.3		0.3	0.2
(violet)	98.8[a2]		0.3	0.2				
	98.6[b]		0.2	0.2				
Fluorspar (3)	99.1[a1]		0.2	0.2	98.7		0.3	0.2
(colourless)	99.0[a2]		0.2	0.2				
	99.2[b]		0.2	0.2				
Fluorite (4)	24.6[a1]		0.2	0.6	24.3		0.3	0.9
(mineral)	24.8[a2]		0.2	0.6				
	24.5[b]		0.2	0.6				
Fluorite (5)	96.5[a1]		0.2	0.2	96.1		0.3	0.2
(precipitated)	96.4[a2]		0.2	0.2				
	96.9[b]		0.2	0.2				
	96.0[c1]		0.2	0.2				
	96.2[c2]		0.3	0.2				
Cryolite (6)		99.0[c]	0.2	0.2		98.5	0.3	0.2

a_1, auxiliary reactant sodium peroxide, boric acid added; a_2, *idem*, aluminium compounds added.
b, auxiliary reactant aluminium compounds.
c, without auxilary reactant; c_1, *idem*, boric acid added; c_2, *idem*, aluminium salts added.
*Samples (1–5): sodium carbonate (1.75 g) + potassium carbonate (2.25 g) + silica (0.7 g)/0.2 g of sample; (6): sodium carbonate (2.2 g) + potassium carbonate (2.8 g) + silica (1.0 g)/0.5 g of sample.

A statistical study[34] showed that both decomposition methods were equally effective. The relative standard deviations for calcium fluoride recovery ranged between 0.2 and 0.6 (95% probability level). The mean values obtained by the proposed method and a reference method gave t-values indicating no significant difference in performance. This was confirmed by the Snedecor F-test, but the proposed method always gave better precision.

Cryolite. The cryolite sample was decomposed by fusion with molten sodium hydroxide, auxiliary agents not being necessary. Additives for retention of fluoride during acidification are not required, because there is already aluminium in the solution, from the cryolite itself. The recoveries obtained by the proposed method and a reference method[3] are shown in Table 2. The proposed method gave a relative standard deviation of 0.2% (95% probability level).

The mean values obtained by both procedures were statistically comparable (t-test and F-test), but the proposed method gave better precision).

REFERENCES

1. W. J. Adolph, *J. Am. Chem. Soc.*, 1915, **37,** 2500.
2. F. G. Hawley, *Ind. Eng. Chem.*, 1926, **18,** 573.
3. H. Shehyn, *Anal. Chem.*, 1957. **29,** 1467.
4. H. R. Shell and R. Craig, *ibid.*, 1954, **26,** 996.
5. F. S. Grimaldi, B. Ingram and F. Cuttitta, *ibid.*, 1955, **27,** 918.
6. H. H. Willard and D. B. Winter, *Ind. Eng. Chem., Anal. Ed.*, 1933, **5,** 7.
7. J. Samachson, N. Slovick and A. E. Sobel, *Anal. Chem.*, 1957, **29,** 1888.
8. M. A. Wade and S. S. Yamamura, *ibid.*, 1950, **22,** 1190.
9. F. Seel, E. Steiner and I. Burger, *Angew. Chem.*, 1964, **76,** 532.
10. J. K. Wilkeyson, *Anal. Chem.*, 1975, **47,** 2053.
11. N. R. Sen Gupta and A. N. Chowdhury, *Indian J. Appl. Chem.*, 1972, **35,** 69.
12. S. Akos and L. Papp, *Zavodsk. Lab.*, 1978, **44,** 936.
13. K. Kawamura, S. Watanabe and H. Sasaki, *Nippon Kinzoku Gakkaishi*, 1970, **34,** 656.
14. L. Kai-Hsiang and Ch. Hui, *Fen Hsi Hua Hsueh*, 1978, **6,** 360.
15. Z. Sosin and L. Ciba, *Chem. Anal.*, 1976, **21,** 1383.
16. L. D. Zinov'eva and K. F. Gladysheva, *Zavodsk. Lab.*, 1973, **39,** 23.
17. H. Spielhaczek, *Z. Anal. Chem.*, 1939, **118,** 161.
18. D. C. Bogen, in *Treatise on Analytical Chemistry*, P. J. Elving, E. Grushka and I. M. Kolthoff (eds.), 2nd Ed., Part I, Vol. 5, p. 15. Interscience, New York, 1982.
19. F. Bosch Reig and J. V. Gimeno Adelantado, *Talanta*, 1983, **30,** 437.
20. J. C. Van Loon, *Anal. Lett.*, 1968, **1,** 393.
21. G. Jecko and D. Ravaine, *Rev. Metall. (Paris)*, 1977, **74,** 649.
22. Th.A. Palmer, *Talanta*, 1972, **19,** 1141.
23. B. Fabbri and F. Donati, *Analyst*, 1981, **106,** 1338.
24. *Idem*, *Ceramurgia*, 1981, **11,** 93.
25. S. J. Haynes, *Talanta*, 1978, **25,** 85.
26. D. S. Russell, H. B. MacPherson and V. P. Clancy, *ibid.*, 1980, **27,** 403.
27. R. L. Baker, *Anal. Chem.*, 1972, **44,** 1326.
28. J. V. Gimeno Adelantado, F. Bosch Reig, A. Pastor Garcia and V. Peris Martinez, *Talanta*, 1983, **30,** 974.
29. V. Peris Martinez, J. V. Gimeno Adelantado and F. Bosch Reig, *Z. Anal. Chem.*, 1983, **314,** 665.
30. S. Megregian, *Anal. Chem.*, 1954, **26,** 1161.
31. N. T. Crosby, A. L. Dennis and J. G. Stevens, *Analyst*, 1968, **93,** 643.
32. G. Charlot, *Dosages colorimétriques des eléments minéraux*, p. 232, Masson, Paris, 1961.
33. J. Goret and B. Trémillon, *Bull. Soc. Chim. France*, 1966, 2872.
34. Y. Lacroix, *Analyse Chimique: Interprétation des résultats par le calcul statistique*, Masson, Paris, 1973.

Talanta, Vol. 32, No. 3, pp. 227–229, 1985
Printed in Great Britain

0039-9140/85 $3.00 + 0.00
Pergamon Press Ltd

DETERMINATION OF *N*-ACETYLMURAMOYL-L-ALANYL-D-ISOGLUTAMINE IN LIPOSOMES BY HPLC

E. POSTAIRE*, M. HAMON*, E. SPONTON† and D. PRADEAU*

Laboratoires de contrôle de qualité* et de mise au point galéniquet, Pharmacie Centrale des Hôpitaux de Paris, 7, rue de Fer à Moulin, 75221 Paris Cedex 05, France

(*Received* 9 *August* 1984. *Accepted* 5 *October* 1984)

Summary—A method using reversed-phase high-pressure liquid chromatography (with spectrometric detection at 218 nm) is described for the determination in new pharmaceutical preparations (liposomes) of a new immunostimulating agent (*N*-acetylmuramoyl-L-alanyl-D-isoglutamine). Separation was achieved with a μ-bondapak column and phosphate buffer (pH 2.5)–methanol mixture (93:7 v/v) as eluent, at a flow-rate of 2 ml/min. Sodium acetate was used as an internal standard. The detector response at 218 nm was linear in the range 10–170 μg/ml. The method is simple and accurate.

N-Acetylmuramoyl-L-alanyl-D-isoglutamine (MDP) is a combination of a dipeptide and an *N*-acetylosamine. It is a new compound marketed as a lyophilisate (Institut Pasteur production). MDP is characterized by marked adjuvant activity, and thus can be a helpful substitute for Freund's complete adjuvant immunotherapy.[1-3]

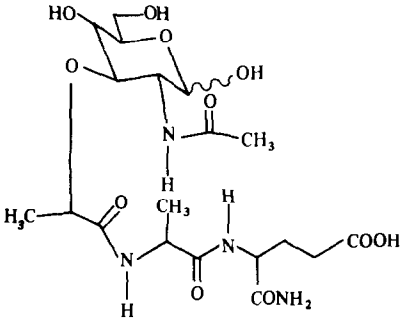

MDP

Administered in aqueous solution, MDP increases non-specific immunity of mice after *Klebsiella pneumoniae* injection.[4-6] Even oral administration is effective. In this study MDP encapsulated in liposomes has been tested. Many antitumoral drugs are currently proposed in this pharmaceutical form.[8]

Using such a vehicle for MDP seems to be of interest for various reasons: plasmatic wash-out decreases, but drug activity increases,[9] and liposomes have shown a specific tropism toward the tumoral cells.[10,11]

Direct analytical techniques (spectroscopy, polarimetry) cannot be applied because of the nature of the liposome constituents (phospholipids, sterols, ions) and the structure of MDP. Therefore a liquid chromatography technique has been chosen to separate the MDP from the vehicle. Liquid chromatography is widely used in peptide determination,[12-14] and is simple, specific and sensitive. This technique can also be applied to the control of pharmaceutical preparations containing MDP.

EXPERIMENTAL

Apparatus

The chromatographic system was equipped with a pump (Chromatem-Model 330), a universal injector (Rheodyne 7125, 20 μl), a stainless-steel column (15 cm long, 4.6 mm bore) packed with μ-bondapack (5 μm) (Touzart et Matignon) and a variable wavelength detector (Schoffel GM 70).

Standards

Internal standard solution. A 1-mg/ml aqueous sodium acetate solution (solution A).

Standard preparation. Made by weighing 170 mg of MDP into a 10-ml standard flask and dissolving and diluting to volume.

Sample preparation

Solution B. Liposome "suspension" containing 40 μg of MDP per ml.

Solution C. Lyophilisate containing 2 mg of MDP and 10 mg of lactose. This lyophilisate was dissolved and diluted to volume in a 50-ml standard flask with eluent.

Solutions D and E. Solutions B and C were diluted tenfold to give D and E respectively.

Chromatographic conditions

The eluent was a 93:7 v/v mixture of pH-2.5 phosphate buffer (0.1*M* phosphoric acid/0.1*M* disodium phosphate) and methanol.

The detector was set at 218 nm, and a 20-μl portion of solution D or E was injected into the column and eluted at a flow-rate of 2 ml/min. The chromatographic peaks were recorded and integrated. Quantitative analysis was accomplished by use of a peak area calibration graph obtained by use of standard preparations (170, 85, 42.5 and 21.25 μg/ml).

RESULTS AND DISCUSSION

As shown in Fig. 1 the two anomeric forms of MDP (pyranose or furanose form of the α or β

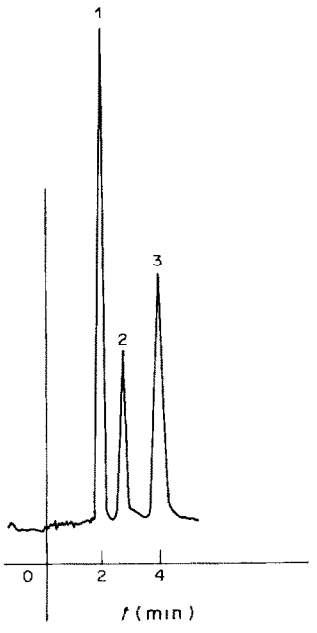

Fig. 1. HPLC analysis of MDP injection (42.5 μg/ml). 1, internal standard; 2, α-D anomer, 3, β-D anomer.

osamine) and sodium acetate as an internal standard were distinctly separated under the conditions used, having retention times of 4.11, 2.86 and 2.05 min, respectively. Blank samples tested by the same procedure showed no significant interfering peaks. It is of interest to separate these two anomeric forms; since the pharmacological activity of each form has yet not been studied.

The precision and accuracy of the method were demonstrated by replicate analyses of the lyophilisate and liposome suspension containing known concentrations of MDP. The overall relative standard deviations ranged from 2.1 to 4.0% (Table 1).

Table 1. Reproducibility of replicate standards at four concentrations

[MDP], μg/ml	RSD ($n = 10$), %
170	4.0
85	2.5
42.5	2.1
21.2	3.2

The limit of detection (10 μg/ml) could be improved by using a more concentrated internal standard solution. For example, with a 5-mg/ml sodium acetate solution, solutions B or C could be diluted only twofold with solution A.

During the development of the method, a number of variations were tested. Methanol and acetonitrile performed equally well as the mobile phase; methanol was chosen because it has lower absorptivity at 218 nm. The pH, buffer concentration and methanol concentration were chosen to give retention times < 6 min and good resolution. The absorption maximum of MDP is at wavelength shorter than 200 nm, but the absorbance at 218 nm is high enough to allow evaluation by liquid chromatography with ultraviolet detection. Sodium acetate was chosen as the internal standard, first because of its rapid elution under the conditions used and secondly because its absorbance is similar to that of MDP at 218 nm (Table 2).

Further investigations showed that the chromatographic system is not only suitable for the determination of the relative amounts of each component but also for determination of the lyophilisate stability. There are no reports in the literature which discuss the decomposition products of MDP. Knowledge of its liquid-chromatography behaviour might provide valuable insight into the decomposition of MDP.

Conclusion

Liquid chromatography allows the easy separation and determination of both anomeric forms of MDP, which would not be easily achieved by direct spectroscopic methods. It thus provides information complementary to that from direct spectroscopy. It appears to have considerable value as a rapid and sensitive method to be used as a routine procedure, and should help in the analysis of MDP pharmaceutical preparations.

Acknowledgements—The authors thank J. F. Petit (Université d'Orsay, Paris XI) and R. Larchee (Pharmacie Centrale des Hôpitaux de Paris) for their helpful collaboration.

REFERENCES

1. F. Ellouz, A. Adam, R. Ciorbaru and E. Lederer, *Biochem. Biophys. Res. Commun.*, 1974, **59**, 1317.

Table 2. Choice of eluent

	Capacity factor, k'			Resolution of peaks
	1	2	3	2 and 3
Buffer pH				
3.0	1.52	2.41	3.59	2.0
2.5	0.71	1.38	2.42	2.5
2.0	the columns do not operate at pH 2			
Methanol concentration, %				
10	0.25	0.92	1.58	0.8
7	0.71	1.38	2.48	2.5
5	1.82	2.65	3.73	1.9

1, Internal standard; 2 and 3, MDP.

2. C. Merser, P. Sinay and A. Adam, *ibid.*, 1975, **66,** 1316.
3. A. Adam, F. Ellouz, R. Ciorbaru, J. F. Petit and E. Lederer, *Z. Immun. Forsch.*, 1975, **149,** 341.
4. R. G. Webster, W. P. Glezen, C. Hannoun and W. G. Laver, *J. Immunol.*, 1977, **119,** 2073.
5. F. Audibert, L. Chedid and C. Hannoun, *Compt. Rend.*, 1977, **285D** 467.
6. V. Souvannavong, A. Adam and E. Lederer, *Infect. Immun.*, 1978, **19,** 966.
7. L. Chedid, F. Audibert, P. Lefrancier, J. Choay and E. Lederer, *Proc. Natl. Acad. Sci. USA*, 1976, **73,** 2472.
8. S. B. Kaye and V. J. Richardson, *Cancer Chemother. Pharmacol.*, 1979, **3,** 81.
9. R. L. Juliano, D. Stamp and N. McCullough, *Ann. New York Acad. Sci.*, 1978, **308,** 411.
10. P. Couvreur, P. Kante and M. Rolland, *J. Pharm. Belg.*, 1980, **35,** 51.
11. B. E. Ryman, R. F. Jewkes, K. Jeyasingh, M. P. Osborne, M. H. N. Patel and D. A. Tyrell, *Ann. New York Acad. Sci.*, 1978, **308,** 281.
12. K. Krummen and R. W. Frei, *J. Chromatog.*, 1976, **132,** 27.
13. R. W. Frei, L. Michel and W. Santi, *ibid.*, 1976, **126,** 665.
14. T. D J. Halls, S. Rasum, E. Wenkert, M. Zuber, F. Lefrancier and E. Lederer, *Carbohydrate Res.*, 1980, **81,** 173.

Talanta, Vol 32, No. 3, pp. 230–234, 1985
Printed in Great Britain

0039-9140/85 $3.00 + 0 00
Pergamon Press Ltd

A SOFTWARE PACKAGE FOR COMPUTER-CONTROLLED FLOW-INJECTION ANALYSIS

L. T. M. PROP and P. C. THIJSSEN*

Department of Analytical Chemistry, University of Nijmegen, Toernooiveld, 6525ED Nijmegen, The Netherlands

L. G. G. VAN DONGEN

Electronic Department, Faculty of Science, University of Nijmegen, The Netherlands

(*Received* 1 *August* 1984. *Accepted* 5 *October* 1984)

Summary—An automated flow-injection system is described, with a computer-controlled sample changer, injection device and photometer. The modular software package is understandable, flexible and easily adaptable to different computers.

Flow-injection analysis is a widely used, reliable and versatile routine method for the determination of various chemical constituents, such as nitrate, phosphate, chloride, glucose.[1] An automated version is attractive for processing large numbers of samples, because it offers the possibility of on-line calibration and evaluation of unknown samples.[2] Our aim was to develop a system which is able to function for some hours without supervision.

The system described below uses a computer for the execution of some basic tasks, such as control of the sample changer, control of the injection valve, and registration of the signal. The program can easily be extended to other tasks such as data-processing and report-generation.

Hardware

The entire system comprises:

(1) an HP9845B desk-top computer with a real-time clock;
(2) a 16-bit parallel I/O interface (HP98032A);
(3) a BIFOK FIA 05 flow-injection device equipped with L100-1 valve; after the injection the valve returns to its normal position within an adjustable time period;
(4) a BIFOK FIA 06 photometer with electronic equipment provided with a 3-digit BCD parallel output (0–1 V);
(5) a Gilson Minipuls II pump;
(6) a Skalar Sampler 1000 sample changer.

The following modifications have been made. The sample changer is connected to the I/O interface of the computer. In the "external mode" the switches for the wash, turntable disk, and two sampler arm motors (left and right) are controlled by the parallel output. The status of the microrelays indicating the positions of the disk and the sampler arm is read in by the parallel input. Thus the computer may take over all the functions of the sample changer. In the "internal mode" these connections are non-effective and the sample changer is manually operated. In a similar way the injection valve is rotated by the computer. The BCD-output of the photometric device is connected to the parallel input of the computer (12 bits for 3 digits).

An example of an automated flow-injection system is depicted in Fig. 1. The interface connections between the computer and the instrumental set-up are shown in Fig. 2.

Software

The software package comprises ten subroutines and functions written in BASIC. The program is written in a top/down structure, meaning that the more advanced routines are found at the highest level, and call lower-level routines, down to the most

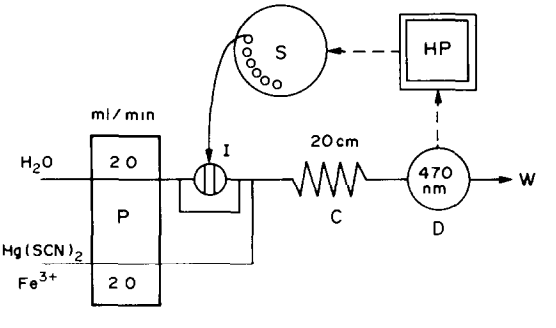

Fig. 1. Scheme of the flow-injection system for the determination of chloride with $Hg(SCN)_2$ and Fe^{3+}. The hardware consists of a peristaltic pump P, an automatic sample changer S, an injection valve I, the waste W, a reaction coil C, a photometric detector D (set at 470 nm) and an interfaced computer HP.

*Author for correspondence.

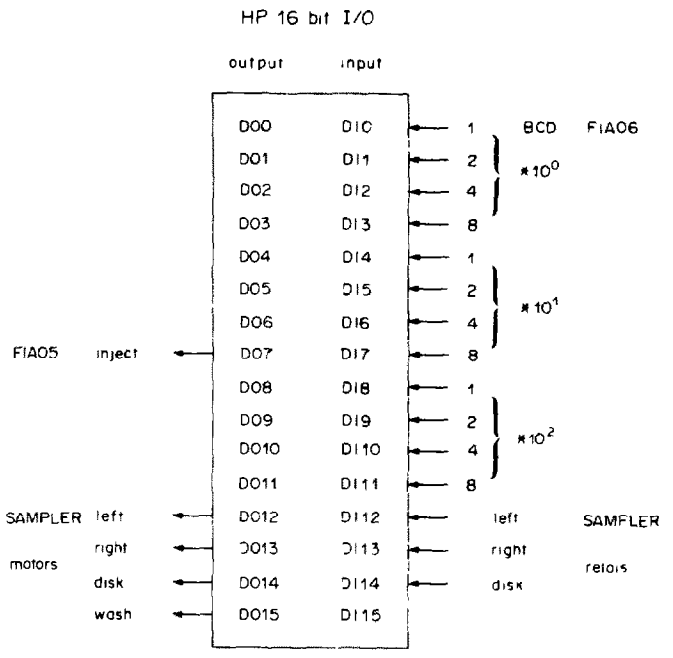

Fig. 2. Scheme of the most important connections of the computer, sample changer, injection device and photometer. The different functions are explained in the text.

primitive ones. The user has only to deal with the highest levels and to initialize some strings and variables.

The program structure is as follows:

level 2: main section;

level 1: subroutines Init, Check, Plot, Read_bcd, Inject, Wash, Disk and Sampler;

level 0: subroutine Output and function FNInput.

In the main section, after initialization the program checks the status of the system and asks for the number of samples. Thereafter, the samples are repeatedly taken, injected and measured and the results are plotted. The disk and sampler arm are manipulated in between other operations, to economise in time.

The lower level routines can be described briefly as follows.

Init: defines and initializes the connections of the 16-bit parallel I/O interface, *i.e.*, clock, input, output, inject, left motor, right motor, disk and wash.

Check: the status of the interface card and the position of the disk and sampler arm are checked for a proper start; if they are not correct, the routine will signal and ask for action.

Plot [Y(*),Names$,Number,Ymax]: performs the layout for the graphics and plotting on the screen.

Read_bcd [Y(*),Number,Delay]: reads a number of measurements, each with a given delay time, from the photometric device and converts the BCD code into a decimal value.

Inject: rotates the injection valve that introduces the sample into the flow system.

Wash: switches the wash motor either on or off.

Disk (Step): steps the disk a given number of places forward.

Sampler: the sampler arm is moved to the right-hand position when the arm is in the left-hand position, and *vice versa*.

Output (Bit): switches and masks the desired bit to the parallel output.

FNInput (Bit): returns the required bit from the parallel input.

The parameters involved are as follows,

Y(*): is an array in which the measurements are stored.

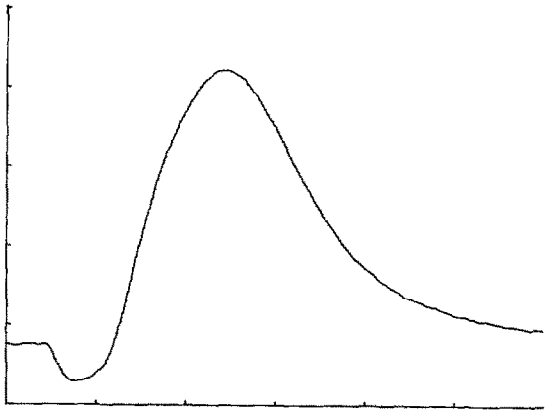

Fig. 3. An example of a digitized peak as displayed by the graphics part of the software package. Number = 600 and Delay = 40.

Number: denotes the number of data-points to be measured.

Delay: denotes the time between measurements (msec).

Name$: is the heading text used in the graphics plot.

Ymax: is a scaling variable to plot the measurements.

Step: is the number of steps the disk moves forward.

Bit: is the required I/O-line of the parallel interface.

Implementation

The computer-controlled flow-injection system has been employed for the determination of chloride in aqueous samples with mercuric thiocyanate in the presence of iron(III), with spectrophotometric measurement at 470 nm. The photometric signal is sampled 600 times during 24 sec and the time for plotting of the measurements, inclusive of taking the sample into the injection loop (100 μl), is about 16 sec, so for each sample a total of 40 sec is required. An example of the graphics plot of a flow-injection peak for a 10-ppm sample is shown in Fig. 3.

Although the package was developed for use with a professional computer, a similar set-up should be possible with a low-cost personal computer. The software package is flexible and may easily be extended to advanced data-processing techniques.

REFERENCES

1. J. Růžička and E. H. Hansen, *Flow Injection Analysis*, Wiley, New York, 1981.
2. P. C. Thijssen, S. M. Wolfrum, G. Kateman and H. C. Smit, *Anal. Chim Acta*, 1984, **156**, 87.

```
10
20
30          A SOFTWARE PACKAGE FOR A FLOW INJECTION SYSTEM
40
50          WRITTEN BY: Leon Prop & Pierre Thijssen
60                      Analytical Chemistry
70                      Faculty of Science
80                      Toernooiveld
90                      Nijmegen (Netherlands)
100
110
120
130       COM Input,Output,Clock,Inject,Left,Right,Disk,Wash
140       COM Io_mask, Disk_position
150       DIM Y(1:600),Name$[99]
160       READ Name$,Number,Delay,Ymax,Step
170   Data:DATA "FLOW INJECTION ANALYSIS",600,40,1,1
180       CALL Init
190   Again:INPUT "GIVE NUMBER OF SAMPLES?",Samples
200       CALL Check
210       FOR I = 1 TO Samples
220       CALL Inject
230       CALL Sampler
240       CALL Read_bcd(Y*),Number,Delay)
250       CALL Disk(Step)
260       CALL Sampler
270       CALL Plot(Y(*),Name$,Number,Ymax)
280       NEXT I
290       GOTO Again
300       END
310     !
320     ! INITIALIZATION OF I/O-VARIABLES
330     !
340       SUB Init
350       COM Input,Output,Clock,Inject,Left,Right,Disk,Wash
360       COM Io_mask,Disk_position
370       Input = 5
380       Output = 5
390       Clock = 3
400       Inject = 7
410       Left = 12
420       Right = 13
430       Disk = 14
440       Wash = 15
450       CALL Output(-1)
460       OVERLAP
470       Disk_position = 0
480       CALL Check
490       SUBEND
```

```
500       !
510       ! CHECK SYSTEM FOR START
520       !
530         SUB Check
540         COM Input,Output,Clock,Inject,Left,Right,Disk,Wash
550         COM Io_mask,Disk_position
560       Check_interface: STATUS Output;A
570         IF A = 292 THEN GOTO Check_disk
580         BEEP
590       DISP "STATUS 5 = ";A;" SWITCH INTERFACE TO 'S'";
600         INPUT A
610         GOTO Check_interface
620       Check_disk:IF NOT FNInput(Disk) THEN Check_sampler
630         BEEP
640         INPUT "PRESS CONTINUE TO START DISK",A
650         CALL Output(Disk)
660         IF FNInput(Disk) THEN 660
670         CALL Output(Disk)
680       Check_sampler:IF NOT FNInput(Left) THEN SUBEXIT
690         BEEP
700         INPUT "PRESS CONTINUE TO SUCK SAMPLE",A
710         CALL Output(Left)
720         IF FNInput(Left) THEN GOTO 720
730         CALL Output(Left)
740         WAIT 15000
750         SUBEND
760       !
770       ! FAST PLOT ROUTINE
780       !
790         SUB Plot(Y(*),Name$,Number,Ymax)
800         PLOTTER IS 13,"GRAPHICS"
810         SCALE 1,Number,0,Ymax
820         GRAPHICS
830         AXES 100,.2,1,0
840         LORG 5
850         MOVE Number/2,.9*Ymax
860         LABEL Name$
870         PENUP
880         FOR Count = 1 TO Number
890         PLOT Count,Y(Count)
900         NEXT Count
910         WAIT 6000
920         SUBEND
930       !
940       ! READ SIGNAL OF PHOTOMETER
950       !
960         SUB Read_bcd(Y(*),Number,Delay)
970         COM Input,Output,Clock,Inject,Left,Right,Disk,Wash
980         COM Io_mask,Disk_position
990         OUTPUT Delay$ USING "#,DDDDD";Delay
1000        OUTPUT Clock;"AU1 = O1U1P"&Delay$
1010        ON INT #Clock GOTO Read
1020        CONTROL MASK Clock;128
1030        Count = 1
1040        Bcd_mask = 2^12-1
1050        OUTPUT Clock;"U1G"
1060      Next:CARD ENABLE Clock
1070      Wait:GOTO Wait
1080      Read:WAIT READ Input,4;A
1090        B = BINEOR(BINAND(A,Bcd_mask),Bcd_mask)
1100        Y(Count = B DIV 256*100 + B MOD 256 DIV 16*10 + B MOD 256 MOD 16
1110        Count = Count + 1
1120        IF Count <= Number THEN Next
1130        MAT Y = Y(.001)
1140        SUBEND
1150      !
1160      ! INJECT THE SAMPLE
1170      !
1180        SUB Inject
1190        COM Input,Output,Clock,Inject,Left,Right,Disk,Wash
1200        COM Io_mask,Disk_position
1210        CALL Output(Inject)
1220        CALL Output(Inject)
1230        SUBEND
```

```
1240      !
1250      ! SWITCH WASH
1260      !
1270        SUB Wash
1280        COM Input,Output,Clock,Inject,Left,Right,Disk,Wash
1290        CALL Output(Wash)
1300        SUBEND
1310      !
1320      ! STEP WITH THE DISK
1330      !
1340        SUB Disk(Step)
1350        COM Input,Output,Clock,Inject,Left,Right,Disk,Wash
1360        COM Io_mask,Disk_position
1370        CALL Output(Disk)
1380        Count = MAX(1,Step)
1390        Disk_position = (Disk_position + Count) MOD 40
1400        IF NOT FNInput(Disk) THEN GOTO 1400
1410        IF FNInput(Disk) THEN GOTO 1410
1420        Count = Count-1
1430        IF Count THEN GOTO 1400
1440        CALL Output(Disk)
1450        SUBEND
1460      !
1470      ! SWITCH THE SAMPLER
1480      !
1490        SUB Sampler
1500        COM Input,Output,Clock,Inject,Left,Right,Disk,Wash
1510        Target = 0
1520        IF NOT FNInput(Left) THEN Target = Right
1530        IF NOT FNInput(Right) THEN Target = Left
1540        IF Target < =0 THEN Error
1550        CALL Output(Target)
1560        IF FNInput(Target) THEN 1560
1570        CALL Output(Target)
1580        SUBEXIT
1590    Error: BEEP
1600        DISP "SAMPLER POSITION ERROR!!!"
1610        PAUSE
1620        SUBEND
1630      !
1640      ! BIT MASK OUTPUT
1650      !
1660        SUB Output(Bit)
1670        COM Input,Output,Clock,Inject,Left,Right,Disk,Wash
1680        COM Io_mask,Disk_position
1690        IF Bit < 0 THEN GOTO Zero
1700        Power = 2^Bit
1710        IF Bit = 15 THEN Power = -Power
1720    Io_mask = BINEOR (Io_mask,Power)
1730        GOTO 1750
1740    Zero:Io_mask = 0
1750        RESET Output
1760        WRITE BIN Output;BINEOR(Io_mask,2^Inject)
1770        CONTROL MASK Output;2^5 + 2^4
1780        CARD ENABLE Output
1790        SUBEND
1800      !
1810      ! BIT MASK INPUT
1820      !
1830        DEF FNInput,(Bit)
1840        COM Input,Output,Clock,Inject,Left,Right,Disk,Wash
1850        COM Io_mask,Disk_position
1860        WAIT READ Input,4;A
1870        RETURN BIT(A,Bit)
1880        FNEND
```

Talanta, Vol. 32, No. 3, pp. 235–237, 1985
Printed in Great Britain

0039-9140/85 $3.00 + 0.00
Pergamon Press Ltd

EFFECT OF EDTA/NaF SOLUTIONS ON THE ORION Cu(II) ION-SELECTIVE ELECTRODE

HENRY F. STEGER
Canada Centre for Mineral and Energy Technology, 555, Booth St., Ottawa, Canada

(*Received* 9 *May* 1984. *Revised* 26 *June* 1984. *Accepted* 29 *September* 1984)

Summary—The titration of ethylenediaminetetra-acetic acid in fluoride medium with Cu(II) solution with the Orion Cu(II) ion-selective electrode as indicator, results (after several titrations) in a broad end-point which is unsatisfactory for exact analytical purposes. This effect has been found to arise from an enhanced rate of response to changes in EDTA concentration when the electrode has been exposed to an EDTA/NaF medium for prolonged periods.

In 1979, the Canadian Certified Reference Materials Project (CCRMP) initiated a programme to confirm the homogeneity of a suite of seven zinc–aluminium alloys (Al 7–30%). For aluminium, a method was developed in which an excess of ethylenediaminetetra-acetic acid (EDTA) was added to the sample and the mixture was boiled to form the Al–EDTA complex; the uncomplexed EDTA was titrated with standard Cu(II) solution. The Al–EDTA complex was then decomposed by the addition of fluoride and boiling; the EDTA released was also titrated with the Cu(II) solution. The end-points were detected with an Orion Cu(II)-selective electrode.[1]

The quality of the response of this electrode was found to deteriorate on continuous use, until a single sharp end-point was not obtained unless the electrode was permitted sufficient recovery time in water or Cu(II) solution between titrations. This paper reports the results of an investigation on the reduced response of the Orion Cu(II)-selective electrode (Ag_2S/CuS homogeneous membrane) under the conditions used in the determination of aluminium in these alloys.

EXPERIMENTAL

Apparatus and titration procedure

Titrations of EDTA with standard Cu(II) solution were performed with a Mettler Automatic Titrator equipped with an Orion 94–29 Cu(II) ion-selective electrode and a calomel reference electrode. All data were collected and mathematically treated by a home-made dedicated microprocessor. The titrations were of 6.00 ml of 0.1000*M* EDTA, 10.00 ml of pH 5.20 acetate buffer (75.0 g of sodium acetate and 8 ml of glacial acetic acid per litre) and 84.0 ml of water and were performed in a water-jacketed vessel maintained at 25°. Copper titrant (0.1000*M*) was added in 0.5 or 1 ml increments until the total volume added was 5.5 ml or greater than 6.5 ml. Within this range, however, titrant was added either at the minimum continuous rate possible, 0.003 ml/sec or in an "equilibrium" titration mode, wherein 0.1-ml increments were added at 3-min intervals. The end-points of the titration were calculated by the method of Wolf.[2]

General conditions

EDTA solutions, 10^{-2}, 10^{-3} and $10^{-4}M$, containing 10.0 ml of acetate buffer per 100 ml were prepared in order to establish electrode calibration graphs. To simulate the effect of continuous titration in a fluoride-medium,[1] the Cu(II)-selective electrode was stored for various periods in a mixture of 6 ml of 0.1*M* of acetate buffer, 54 ml of water and 25 ml of sodium fluoride solution (42 g/l.).

RESULTS AND DISCUSSION

Storing the Cu(II)-selective electrode in a solution similar to the titration samples containing fluoride hastened the degradation of the end-point response of the electrode. Indeed a 16-hr or longer storage period makes the electrode ineffective as an end-point indicator in EDTA/Cu(II) titrations. Figure 1 shows the titration curves and corresponding $\Delta E/\Delta V$ *vs.* V curves for the titration of EDTA with Cu(II), with end-point detection by use of the Cu(II)-selective electrode in (*a*) polished condition and (*b*) after treatment for 24 hr with EDTA/NaF solution. The earlier break in the titration curve when the treated electrode is used is typical whenever the $\Delta E/\Delta V$ *vs.* V curve displays multiple peaks or appreciable broadening.

When the titration data are presented as plots of electrode potential *vs.* either log [EDTA] or log [Cu(II)], linear plots are obtained for the region where the potential increases after the first few additions of Cu(II) titrant. Figure 2 illustrates this for the titration data in Fig. 1. Table 1 summarizes the slopes of such plots for different treatments of the Cu(II)-selective electrode. It must be pointed out that the electrode potentials, particularly those near the end-point in titrations, do not necessarily attain a steady value before the next addition of titrant. For most applications, this does not have a significant effect on the accuracy of the titration.

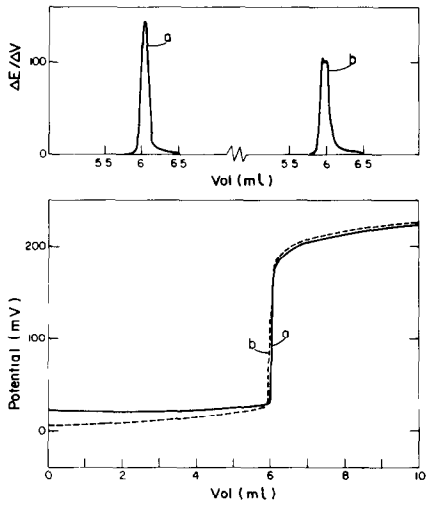

Fig. 1. Titration and $\Delta E/\Delta V$ *vs.* V curves obtained by continuous addition of titrant, with detection by use of (*a*) the polished electrode and (*b*) the electrode stored in EDTA/NaF solution.

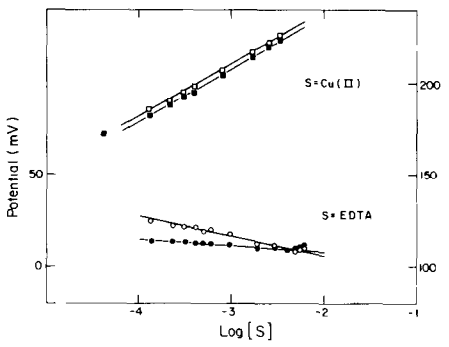

Fig. 2. Plot of electrode potential log [EDTA] and log [Cu(II)] for the curves of Fig. 1: ●—polished electrode, ○—electrode stored in EDTA/NaF solution.

The major point of interest in Table 1 is that storing the electrode in EDTA/NaF solution appears to increase its sensitivity to changes in [EDTA]. Since the rate of titrant addition was the same in these titrations, the electrode sensitivity is in effect the rate of electrode response to changes in [EDTA] before the end-point and to changes in [Cu(II)] after the end-point. To study the effect of response time, several "equilibrium" titrations of EDTA with Cu(II) solution were performed in which there were 3-min intervals between additions of titrant, to allow the potential of the electrode (in polished condition) to reach a steady value. Figure 3a shows a typical titration curve for these "equilibrium" titrations. It is evident that the break in the curve occurs earlier than when the continuous-addition procedure is used. The corresponding $\Delta E/\Delta V$ *vs.* V peak is broadened and can be resolved into two peaks. These observations are best explained as due to the rate of response of the polished electrode to changes in [EDTA] being appreciably slower than that to changes in [Cu(II)]. The rate of electrode response to relative changes in [EDTA] is not important until the end-point is closely approached because such changes are small for a given increment of Cu(II) titrant. Very near the end-point, however, the relative changes in [EDTA] become large for a given increment of titrant, but in a continuous-addition titration the electrode cannot give full response unless complete response is instantaneous. The result is a potential increase that is delayed and smaller than expected. Indeed, the end-point has been passed and the electrode is responding to free Cu(II) before it has been able to respond fully to EDTA. The steep potential increase associated with the single end-point suggests that in a continuous-addition titration the polished electrode responds only in a minor fashion to change in [EDTA] and essentially reflects changes in [Cu(II)]. In "equilibrium" titrations, however, the electrode has time to respond fully to changes in [EDTA] before the end-point and to changes in [Cu(II)] after it. That there appear to be two end-points where only one true end-point exists suggests that the electrode cannot respond instantaneously to free Cu(II) immediately after the end-point. This delay is analogous to the time required for the electrode to reach a stable potential on a change in sample composition. The existence of such a delay is also strongly implied in continuous-addition titrations of EDTA with Cu(II). In 29 titrations of $0.1000M$ EDTA with $0.1000M$ Cu(II), the concentration of EDTA in the reagent solution was calculated to be $0.1008M$ ($\sigma = 0.002M$) if [Cu(II)] = $0.1000M$. With the same reagents, the reverse titration, where the electrode responds initially to decreasing [Cu(II)] gave the EDTA concentration as $0.1000M$ ($\sigma = 0.0002M$) for 11 runs. The titration of EDTA with Cu(II) has a small bias that is consistent with a delay in the response of the Cu(II)-selective electrode to the initial free Cu(II) immediately after the end-point in titrations of EDTA.

Table 1. Slopes of plots of titration curves

Electrode condition	Slope, *mV/decade*	
	log [EDTA]	log [Cu(II)]
Polished	−7.8	29.1
Stored in EDTA/NaF for 24 hr	−10.0	29.8
Stored in EDTA/NaF for 48 hr	−12 6	30.0
Stored in EDTA/NaF for 96 hr	−15.4	30.4

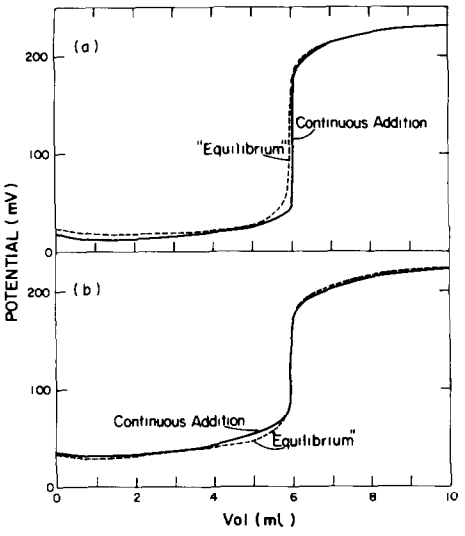

Fig. 3. Titration curves for continuous-addition and "equilibrium" procedures with (*a*) the polished electrode and (*b*) the electrode stored for 48 hr in EDTA/NaF solution.

The similarity in the curves for the "equilibrium" titrations with the polished electrode and for the continuous-addition titrations with the electrode treated with EDTA/NaF solution, strongly suggests the same cause. Storage or continuous use of the electrode in EDTA/NaF medium results in an enhanced rate of response to changes in [EDTA]. Figure 3b compares the titration curves of EDTA with Cu(II), using the electrode treated for 48 hr with EDTA/NaF solution, by the continuous-addition and "equilibrium" procedures. The strong similarity, especially in the end-point region, substantiates the contention that the EDTA/NaF treatment of the electrode leads to an enhanced rate of response to changes in [EDTA] before the end-point. Neither titration gave a satisfactory single end-point.

The treatment of the Cu(II)-selective electrode with EDTA/NaF solution has been postulated to form a sparingly-soluble fluoride compound, because the normal response of the electrode is readily restored by light polishing of the surface.[1] The physical presence of such a compound has not been unequivocally established. There is, however, a visually detectable dulling of the lustre and a corresponding slight decrease in the specular reflectance (in the region 5100–6000 Å) of the electrode surface on treatment with EDTA/NaF. The results of this investigation nevertheless do indicate that the surface of the electrode is affected by storage in EDTA/NaF solution.

This effect of storage in EDTA/NaF solution was investigated for two Orion 94–29 Cu(II) electrodes. The first, purchased in 1976 but used very infrequently until 1980,[1] displayed an immediate sensitivity to storage or continuous use in EDTA/NaF solutions. This electrode was accidentally broken during the initial stages of the present study. The second electrode, obtained in March 1983, remained unaffected by EDTA/NaF solutions for approximately two weeks but thereafter rapidly developed a sensitivity to EDTA-NaF comparable to that observed for the first electrode. This report summarizes the experimental results for the second electrode.

It should be emphasized that the findings of this study should not be taken to mean that all EDTA titrations with Cu(II) are unsatisfactory. Indeed, the opposite is true for all but very exact analysis. The phenomenon discussed here is observed primarily because of the resolving power of an up-to-date microcomputerized collection and reduction of data. Without it, the end-point in the titrations of EDTA with Cu(II) and of Cu(II) with EDTA could not have been determined with sufficient precision to show the slight differences observed. Indeed, the analyst must wonder if, in practical terms, there is any difference. The degeneration of the sharpness of the end-point in titrations of EDTA with Cu(II) after the electrode has been used or stored in EDTA/fluoride medium may not be noticed at all under less favourable conditions, and only be observed as a reduction in the reproducibility of the end-point.

REFERENCES

1. H. F. Steger, *Talanta*, 1983, **30**, 717.
2. S. Wolf, *Z. Anal. Chem.*, 1970, **250**, 13.

Talanta, Vol. 32, No. 3, pp. 238–240, 1985
Printed in Great Britain

0039-9140/85 $3.00 + 0.00
Pergamon Press Ltd

SPECTROPHOTOMETRIC DETERMINATION OF PARACETAMOL WITH IODYLBENZENE

KRISHNA K. VERMA and ARCHANA JAIN
Department of Chemistry, R.D. University of Jabalpur, Jabalpur 482001, India

(*Received* 29 *May* 1984. *Accepted* 29 *September* 1984)

Summary—Paracetamol (*N*-acetyl-4-aminophenol) has been determined spectrophotometrically by its oxidation with iodylbenzene in acetone to produce the yellow-orange *N*-acetyl-1,4-benzoquinoneimine, which attains maximum colour intensity within 1 min and absorbs maximally at 430 nm. The maximum molar absorptivity is 1.58×10^3 l.mole^{-1}.cm^{-1}. The method is simple and rapid and has been found to be unaffected by the presence of salicylamide, oxyphenbutazone, acetylsalicylic acid, dipyrone and a number of other excipients.

Paracetamol (acetaminophen, *N*-acetyl-4-aminophenol) is an extensively employed antipyretic analgesic drug. Dipyrone (analgin), oxyphenbutazone, acetylsalicylic acid and salicylamide are found along with it in various pharmaceutical preparations. These substances interfere severely in one or another of the currently available methods of determining paracetamol. The titrimetric methods involve the reaction of either the phenolic group with a base in dimethylformamide medium[1,2] or of the aromatic amino group (formed by hydrolysis) with nitrite,[3] but there is interference with the acid–base method by salicylamide, oxyphenbutazone and acetylsalicylic acid (which are also acidic), and any free 4-aminophenol present (which is a product of decomposition). In the other method, Vitamin C, dipyrone and 4-aminophenol will all consume nitrous acid. Hydrolysis of paracetamol to 4-aminophenol which is then reacted with a substituted benzaldehyde[4–6] or 4-dimethylaminocinnamaldehyde[7] to form coloured Schiff's bases is naturally affected by the presence of 4-aminophenol and phenetidine (formed by hydrolysis of phenacetin). The nitrosation and chelation reaction[8] of paracetamol is also given by salicylamide[8] and oxyphenbutazone.[9] Indophenol formation[10,11] constitutes a simple spectrophotometric determination, but it is based on the oxidative coupling of 4-aminophenol with alkaline phenol, so dipyrone (being a strong antioxidant) interferes and causes low results for paracetamol. Determinations based on ultraviolet absorption[12] and its change with pH[13] are too sensitive to be of general use for compound drug tablets.

A rapid and highly selective spectrophotometric method for the determination of paracetamol in drug formulations is now reported. Iodylbenzene (iodoxybenzene) is insoluble in common organic solvents but its suspension in acetone brings about specific oxidation of paracetamol to a yellow-orange substance that shows maximum absorption at 430 nm. The colour is stable for about an hour and obeys Beer's law over a wide range of paracetamol concentration.

EXPERIMENTAL

Reagent

Iodylbenzene was synthesized by the procedure described by Fieser and Fieser,[14] and by the bromate oxidation method of Banerjee *et al.*[15] modified as follows.

To a mixture of 20 g of iodobenzene, 200 ml of 40% v/v sulphuric acid and 50 ml of glacial acetic acid, heated on a boiling water-bath, slowly add a solution of 15 g of potassium bromate in 150 ml of warm water during a period of 30 min with vigorous stirring (in a fume-chamber). Continue the heating for 90 min, during which all the bromine evolved is removed. Cool to room temperature, decant the supernatant liquid, wash the product (oily owing to unreacted iodobenzene) with water, macerate it with 50 ml of chloroform, filter it off and wash it with chloroform to furnish a silky white solid, m.p. 222° (decomposition). The product obtained in this way (12 g, 50% yield) was found to be 98% pure, by iodometric analysis.[16]

Samples

A high-purity sample of paracetamol, found to be 98.8% pure by the indophenol method[10] and 98.6% pure by the nitrosation method,[8] was used. All drug samples tested were fresh.

Procedure

Preparation of calibration graph. Into a 50-ml calibrated flask accurately weigh 10 mg of paracetamol, dissolve it in acetone and make up to the mark with the same solvent; mix 1–5 ml portions of this solution with about 20 mg of finely powdered iodylbenzene in 10-ml beakers, dilute each to about 5 ml with acetone and stir for 1 min. Filter the coloured solution through a small fluted Whatman No. 41 filter paper into a 10-ml standard flask, washing the residue and making up to the mark with acetone. Measure the absorbance at 430 nm in a 1-cm cell against acetone.

Drug samples. Grind a known number of tablets, accurately weighed, into a fine powder, weigh out a portion containing about 10 mg of paracetamol and stir it with 20 ml of acetone. Filter off the residue on a fluted Whatman No. 41 filter paper, wash it with three successive 5-ml portions of acetone and make up filtrate and washings to volume with acetone in a 50-ml standard flask. Treat a 2-ml

portion of this solution by the procedure described for preparation of the calibration graph.

RESULTS AND DISCUSSION

Iodylbenzene is insoluble in the commonly used organic solvents, but a suspension of it in acetone oxidizes paracetamol to a yellow-orange product that has maximum absorption at 430 nm. The reaction is reversible, the product being decolorized on addition of ascorbic acid and reoxidized to the coloured product by iodylbenzene. The observation that iodosobenzene does not yield a colour reaction and that paracetamol acetylated at the phenolic group fails to give any colour with iodylbenzene, led us to believe that the colour reaction is:

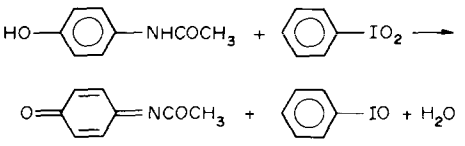

The colour develops almost instantaneously and remains stable for about 1 hr. There is a 10% decrease in colour intensity after 2 hr. Other common oxidizing agents, *e.g.*, iodosobenzene diacetate or dichloride, chloramine-T and *N*-bromosuccinimide, do not produce a colour, perhaps because the

Table 1. Determination of paracetamol in drugs

Drug*	Paracetamol, *mg/tablet*†			
	Maker's specification	Present method	CV, %	Comparison method
Laboratory-made tablet				
No. 1[i]	258	263	0.4	
No. 2[ii]	504	502	0.2	
No. 3[iii]	246	244	0.3	
Crocin	500	538	0.2	540§
Metacin	500	497	0.2	503‡
Panjon[iv]	150	142	0.3	139§
Arumin[v]	200	181	0.4	
Malidens[vi]	250	267	0.4	271§
Arthopar[vii]	500	512	0.5	
Actimol[viii]	500	475	0.3	480‡
Canapar[ix]	250	225	0.5	
Neogene[x]	250	236	0.5	243#
Flamar-P[xi]	250	210	0.3	
Parazolandin[xii]	500	506	0.4	510‡
Panbin[xiii]	150	138	0.3	135§
Reducin A[xiv]	650	596	0.4	
Paramide[xv]	250	284	0.3	278§
Vikoryl[xvi]	120	140	0.2	139§
Ultragin[xvii]	250	228	0.2	232§
Corbutyl[xviii]	650	600	0.4	612‡
Contac-CC[xix]	450	409	0.4	416‡
Prydonnal[xx]	400	415	0.5	405§
Spasmindon[xxi]	250	246	0.2	248§

Other substances present include the following: (*i*) 4-aminophenol (50 mg); (*ii*) dipyrone (250 mg) and salicylamide (100 mg); (*iii*) oxyphenbutazone (100 mg) and acetylsalicylic acid (150 mg); (*iv*) acetylsalicylic acid (300 mg) and caffeine (30 mg); (*v*) oxyphenbutazone (500 mg), dried aluminium hydroxide gel (750 mg) and magnesium trisilicate (500 mg); (*vi*) salicylamide (250 mg) and caffeine (25 mg); (*vii*) oxyphenbutazone (100 mg) and diazepam (2.5 mg); (*viii*) phenylbutazone (500 mg); (*ix*) dipyrone (250 mg) and caffeine (25 mg); (*x*) dipyrone (250 mg), caffeine (30 mg), codeine phosphate (7.5 mg) and chlorpromazine hydrate (7.5 mg); (*xi*) oxyphenbutazone (100 mg); (*xii*) salicylamide (200 mg), methaqualone hydrochloride (20 mg), caffeine (20 mg) and chlorpheniramine (2 mg); (*xiii*) phenylephrine hydrochloride (5 mg), salicylamide (200 mg) and chlorpheniramine maleate (2 mg); (*xiv*) dextropropoxyphene hydrochloride (65 mg); (*xv*) noscapine (15 mg) and phenylpropanolamine hydrochloride (25 mg); (*xvi*) hyoscyamine sulphate (0.22 mg), scopolamine hydrobromide (0.02 mg), atropine sulphate (0.02 mg) and phenobarbitone (30 mg); and (*xvii*) phenylisopropyl pyrazolone (150 mg), dicyclomine hydrochloride (10 mg) and ethylmorphine hydrochloride (11 mg).

†Mean of 6 replicates; CV = coefficient of variation.

§Method in reference 10.

‡Method in reference 8.

#Method in reference 1.

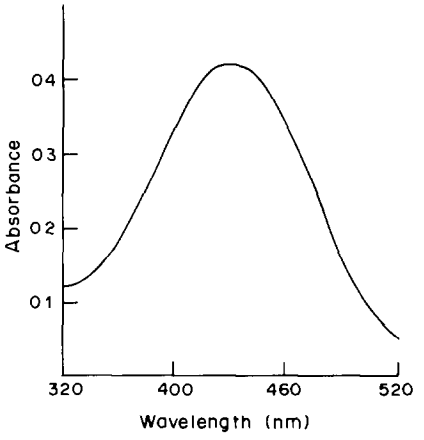

Fig. 1. Absorption spectrum of paracetamol–iodylbenzene reaction product (paracetamol 40 μg/ml).

oxidation continues beyond the *N*-acetyl-1,4-benzoquinoneimine. The visible spectrum of the chromogen is shown in Fig. 1. The molar absorptivity is 1.58×10^3 l.mole^{-1}.cm^{-1} at 430 nm. The method is more rapid and simple than the existing procedures, and Beer's law is obeyed over a wide range of paracetamol concentration, 0–100 μg/ml in the final solution. The absorption spectrum is unaffected by the use of as high as 100-fold molar excess of iodylbenzene.

A large number of pharmaceutical preparations containing paracetamol have been analysed by the method and the results are given in Table 1 together with comparative values obtained by using established methods. Dipyrone, oxyphenbutazone, acetylsalicylic acid, salicylamide, vitamin C, phenacetin and caffeine do not affect the results. Other substances which can be tolerated are listed in a footnote to Table 1. 4-Aminophenol is a product of decomposition of paracetamol and interferes in almost all available methods for determining paracetamol, but the present method is free from this interference.

Acknowledgement—Thanks are due to the University Grants Commission (New Delhi) for the award of a Junior Research Fellowship to A.J.

REFERENCES

1. M. I. Walash, S. P. Agarwal and M. I. Martin, *Can. J. Pharm. Sci.*, 1972, **7**, 123.
2. S. P. Agarwal and M. I. Walash, *Indian J. Pharm.*, 1974, **36**, 47.
3. M. C. Inamdar, M. A. Gore and R. V. Bhide, *ibid.*, 1974, **36**, 7.
4. N. M. Sanghavi and D. R. Vishwasrao, *ibid.*, 1973, **35**, 172.
5. F. M. Plakoviannis and A. M. Saad, *J. Pharm. Sci.*, 1975, **64**, 1547.
6. E. Kalatzis and I. Zarbi, *ibid.*, 1976, **65**, 71.
7. T. Inoue, M. Tatsuzawa, S. Lee and T. Ishii, *Eisei Kagaku*, 1975, **21**, 313.
8. S. F. Belal, M. A. H. Elsayed, A. Elwalily and H. Abdine, *Analyst*, 1979, **104**, 919.
9. A. A. Ouf, M. I. Walash, S. M. Hassan and S. M. Elsayed, *ibid.*, 1980, **105**, 169.
10. C. T. H. Ellcock and A. G. Fogg, *ibid.*, 1975, **100**, 16.
11. D. R. Davis, A. G. Fogg, D. T. Burns and J. S. Wragg, *ibid.*, 1974, **99**, 12.
12. *British Pharmacopoeia 1973*, p. 340. HMSO, London, 1973.
13. M. A. H. Elsayed, S. F. Belal, A. F. M. Elwalily and H. Abdine, *Analyst*, 1979, **104**, 620.
14. L. F. Fieser and M. Fieser, *Reagents for Organic Synthesis*, Vol. 1, p. 511. Wiley-Interscience, New York, 1967.
15. A. Banerjee, G. C. Banerjee, S. Bhattacharya, S. Banerjee and H. Samaddar, *J. Indian Chem. Soc.*, 1981, **58**, 605.
16. L. F. Fieser and M. Fieser, *op. cit.*, p. 507.

Talanta, Vol. 32, No. 3, pp. 241–243, 1985
Printed in Great Britain.

0039-9140/85 $3.00 + 0.00

PHOSPHATE DETERMINATION BY USE OF MOLYBDOANTIMONYLPHOSPHORIC ACID AND POLYURETHANE FOAM

A. S. KHAN and A. CHOW*
Department of Chemistry, University of Manitoba, Winnipeg, Manitoba, Canada

(*Received* 1 *August* 1984. *Accepted* 14 *September* 1984)

Summary—Preconcentration of phosphate as molybdoantimonylphosphoric acid on polyurethane foam has been combined with X-ray fluorescence measurement of antimony for the indirect determination of phosphate. The extraction is optimum between pH 1 and 3.6 and no interference is observed from silicate. The precision is 5% RSD at the 0.25-μg/ml level and the detection limit is 20 ng/ml for 100 ml of sample solution.

The most widely used spectrophotometric procedures for the determination of phosphate in aqueous solutions are based on the formation of 12-molybdophosphate in reduced or non-reduced forms. At the trace level, the reduced (heteropoly blue) form is preferred, owing to the higher absorptivity. The Murphy and Riley method,[1] using ascorbic acid and potassium antimony tartrate as the reducing agent, has become one of the standard procedures[2] for phosphate determination. Going and Eisenreich,[3] have established the stoichiometry of the reduced heteropoly product as $PSb_2Mo_{10}O_{40}$. Besides the traditional spectrophometric methods,[4] the determination of phosphate can be based on extraction of molybdoantimonylphosphoric acid ($PSb_2Mo_{10}O_{40}$) into isobutyl acetate and measurement of the antimony content in the extract by atomic-fluorescence spectrophotometry.[5]

X-Ray fluorescence (XRF) has also been employed for phosphate determination. Phosphate has been extracted[6] as 12-molybdophosphoric acid ($H_3PMo_{12}O_{40}$) into ethyl acetate, the organic layer then being coated onto a specially treated silica gel, pressed into pellets and analysed for molybdenum. Dube *et al.*[7] have estimated phosphate directly by XRF after precipitating it as quinine molybdophosphate.

Recently polyurethane foam has been used for the preconcentration and *in situ* XRF determination of trace elements.[8,9] In an earlier communication,[10] we reported the indirect XRF determination of phosphate after its extraction as molybdophosphoric acid into polyether foam. Further study has shown that molybdoantimonylphosphoric acid can be used similarly, and gives a selective and more sensitive method.

EXPERIMENTAL

Apparatus

The energy-dispersive XRF unit used to measure the intensity of the antimony K_α line included an annular 0.5-Ci ^{241}Am source (New England Nuclear) coupled with an Si(Li) detector, a Nuclear SemiConductor 512 amplifier and a Tracor Northern TN1705 pulse-height analyser. A thermostatically-controlled multiple automatic squeezer was used for squeezing the foam in the sample solutions.

Reagents

The stock solutions of molybdate, phosphate and antimony were prepared by dissolving the required amounts of sodium molybdate, potassium dihydrogen phosphate and potassium antimony tartrate. A 1% solution of ascorbic acid was prepared daily.

A mixed reagent was prepared as described by Going and Eisenreich,[3] except that half of the recommended amount of potassium antimony tartrate was used. Sodium molybdate dihydrate (2.12 g) was dissolved in 150 ml of water, and 20.8 ml of concentrated sulphuric acid were added slowly with continuous stirring. The solution was cooled to room temperature, 0.344 g of potassium antimony tartrate was added, and the volume was made up to 250 ml. This solution was usable for several weeks.

All chemicals were of reagent grade. and doubly distilled and demineralized water was used for dilutions. The phosphate, molybdate and mixed reagent solutions were stored in plastic bottles. Extran "300" (B.D.H.), a phosphate-free cleaning agent, was used to clean all glassware.

Foam discs, approximately 2 cm in diameter and 0.8 cm in thickness were cut from a sheet of polyether-based polyurethane foam obtained locally and washed according to a procedure described earlier.[11]

Procedure

An aliquot of phosphate solution, containing not more than 0.1 mg of phosphate, was transferred into a 100-ml standard flask, followed by 2.5 ml of the mixed reagent and 1 ml of ascorbic acid solution. This solution was diluted and mixed and after 10–15 min was equilibrated with a foam disc in an extraction cell for 30 min. The foam disc was then removed from the solution, washed with water and finally dried by squeezing between paper towels. The dried foam disc was placed on Mylar film, which was then stretched across the X-ray source and analysed for 200 sec. The area under the antimony K_α peak was obtained by integration with the TN1705 unit.

RESULTS AND DISCUSSION

Using the procedure recommended by Going *et al.*[4] for the extraction of molybdoantimonyl phosphate

*Author for correspondence.

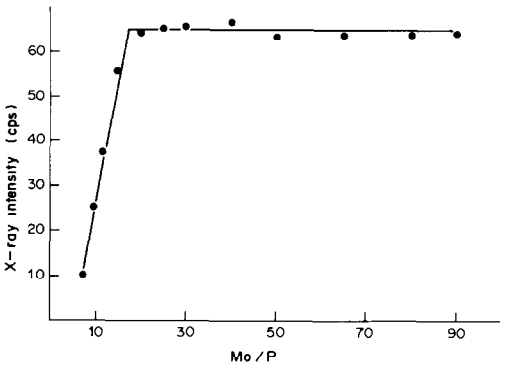

Fig. 1. Extraction of molybdoantimonylphosphoric acid as a function of initial molybdate concentration.

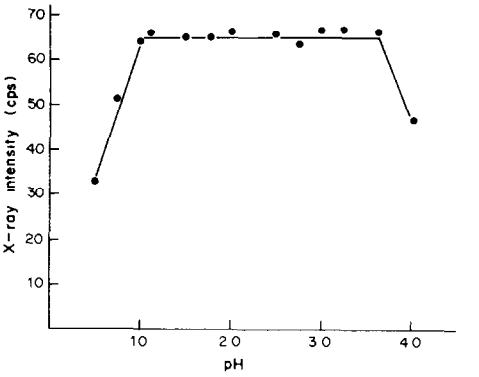

Fig. 2. Extraction of molybdoantimonylphosphoric acid as a function of solution acidity.

into organic solvents, it was found by absorption spectrophotometry that the extraction of molybdoantimonyl phosphate (MSbP) by polyurethane foam is quantitative. Initial experiments also showed that the extraction efficiency remains almost constant if the squeezing time is 15 min or more. In all later studies, the foam discs were squeezed in the sample solutions for half an hour or more to ensure equilibration.

The effect of molybdate concentration on the extraction was tested by squeezing foam discs in a series of solutions, 100 ml in volume, $1.5 \times 10^{-5} M$ in phosphate, $4 \times 10^{-5} M$ in antimony and containing varying amounts of molybdate and sufficient acid to maintain the H^+/Mo ratio at 75. It has been established that the formation of MSbP is maximal under these conditions.[3] From the results shown in Fig. 1, it is clear that a 20-fold excess of molybdate is sufficient for optimal extraction of MSbP. Similar results were obtained for the extraction of 12-molybdophosphoric acid by polyurethane foam,[12] but more molybdate is necessary for the quantitative extraction of molybdoarsenate.[13] It is most likely that the excess of molybdate is necessary to ensure complete formation of the particular heteropolymolybdate rather than to maximize the extraction efficiency.

The optimal pH range for the extraction was studied with a series of solutions (100 ml) with fixed concentrations of phosphate ($1.5 \times 10^{-5} M$), antimony ($4 \times 10^{-5} M$) and molybdate ($1 \times 10^{-3} M$). Figure 2 shows that pH 1–3.6 is optimal. Similar results have been reported by Going *et al.*[4] The optimum range for extraction of 12-molybdophosphate by polyurethane foam is pH 1–2,[12] owing to $PSb_2Mo_{10}O_{40}$ being stable over a wider pH range than the $PMo_{12}O_{40}$ complex is.

The effect of the Sb/P ratio was also studied. The results indicate that at least a 2:1 ratio is necessary for the efficient extraction of MSbP (since this concentration is required stoichiometrically), but a large excess of antimony results in precipitation.

It is evident that the extraction of MSbP by polyurethane foam is optimal under the conditions for maximum complex formation. For this Going and Eisenreich[3] recommended use of a mixed reagent containing sufficient molybdate, antimony and acid. Use of this mixed reagent was examined and it was found that 2 ml will suffice for the extraction of 100 μg of phosphate from 100 ml of sample solution.

The X-ray response was studied with 100-ml samples containing 0–100 μg of phosphate, 2.5 ml of mixed reagent and 1 ml of ascorbic acid solution. It was linear over this concentration range (correlation coefficient 0.998). The detection limit (X) defined as the mean blank value ($\bar{X}$) plus three standard deviations (σ) of the blank value, (*i.e.*, $X = \bar{X} + 3\sigma$), is 20 ng/ml for 100-ml sample solutions. The detection limit can be improved by using a more sensitive X-ray instrument or larger sample volumes.

The precision (relative standard deviation) was evaluated from replicate analyses for 25 μg of phosphate, and found to be 5%. As the extraction of MSbP by polyurethane foam is quantitative under the conditions used, it is most likely that the X-ray measurement is the major source of uncertainty.

The effect of As, Si and Ge was evaluated by analysing a series of 100-ml sample solutions containing 50 μg of phosphate and various amounts of the interfering elements. It was found that silicon did not interfere even when present in large excess (up to 10 mg) whereas only 250 μg of germanium and less than 50 μg arsenic can be tolerated. Although the solution chemistry of these systems has not been reported in the literature, it seems likely that germanium and arsenic also form mixed heteropoly complexes containing antimony. Since the heteropolymolybdate complexes of germanium and arsenic are extractable by polyurethane,[14] these mixed complexes are probably also extractable and thus give positive interference.

The X-ray fluorescence technique in conjunction with foam extraction can be used for the determination of phosphate, with a performance comparable to that of the existing solvent extraction methods, and should produce greater sensitivity when used with better X-ray equipment. The technique has several advantages over the previous method based

on molybdenum determination.[10] The antimony determination has a detection limit of 0.02 ppm compared with 0.10 ppm for molybdenum, and is more selective since phosphate can be determined even in the presence of large amounts of silicon, and also the optimal pH-range is wider.

Acknowledgement—This work was supported by the Natural Science and Engineering Research Council of Canada.

REFERENCES

1. J. Murphy and J. P. Riley, *Anal. Chim. Acta*, 1962, **27**, 31.
2. *Standard Methods for the Examination of Water and Wastewater*, 14th Ed., p. 479. American Public Health Assoc., Washington, 1975.
3. J. E. Going and S. J. Eisenreich, *Anal. Chim. Acta*, 1974, **70**, 95.
4. J. Going, S. Wenzel and J. Thompson, *Microchem. J.*, 1975, **20**, 126.
5. K. Tsujii, K. Kuga and E. Kitazume, *Anal. Chim. Acta*, 1980, **115**, 143.
6. D. E. Leyden, W. K. Nonidez and P. W. Carr, *Anal. Chem.*, 1975, **47**, 1449.
7. G. Dube, G. Boullay and F. M. Kimmerle, *ibid.*, 1976, **48**, 1950.
8. A. Chow, G. T. Yamashita and R. F. Hamon, *Talanta*, 1981, **28**, 437.
9. A. Chow and S. L. Ginsberg, *ibid.*, 1983, **30**, 620.
10. A. S. Khan and A. Chow, *Anal. Lett.*, 1983, **16**, 265.
11. R. F. Hamon, A. S. Khan and A. Chow, *Talanta*, 1982, **29**, 313.
12. A. S. Khan and A. Chow, *ibid.*, 1983, **30**, 173.
13. *Idem*, *ibid.*, 1984, **31**, 304.
14. A. S. Khan, *Ph.D. Thesis*, University of Manitoba, 1982.

Talanta, Vol. 32, No. 4, pp. 245–255, 1985
Printed in Great Britain.

0039-9140/85 $3.00 + 0.00

MICMAC—UN PROGRAMME GENERAL ET RIGOUREUX D'AFFINEMENT MULTIPARAMETRIQUE POUR LA DETERMINATION DE CONSTANTES D'EQUILIBRE A PARTIR DE METHODES PHYSIQUES VARIEES

ANDRÉ LAOUENAN* et ELISABETH SUET
Laboratoire de Chimie Analytique, LA CNRS 322, Université de Bretagne Occidentale, 6, Avenue le Gorgeu, 29283 Brest-Cédex, France

(*Reçu le* 9 *âout* 1984. *Accepté le* 12 *décembre* 1984)

Résumé—Le programme basic MICMAC a été développé pour l'ajustement sur micro-ordinateur de constantes d'équilibre à partir de méthodes physiques très variées. Le programme utilise la méthode particulièrement fiable de Gauss–Newton–Marquardt et permet l'ajustement multiparamétrique de fonctions non linéaires. Hautement interactif, d'utilisation aisée et de conception modulaire, il fait intervenir une pondération rigoureuse et peut prendre en compte des erreurs systématiques. Ce programme autorise la résolution de problèmes où interviennent plusieurs variables dépendantes, indépendantes et plusieurs séries de mesures. Quelques exemples traitant de polarographie, pH-métrie et RMN, illustrent la généralité du programme MICMAC et donnent lieu à une étude comparative avec des programmes récents.

Depuis les premiers travaux de Sillén,[1] de nombreux programmes permettant la détermination de constantes de stabilité ont vu le jour[2,3] et les résolutions graphiques tendent à être remplacées de plus en plus par des techniques numériques fondées sur la méthode des moindres carrés. Cependant, en dépit des avantages que présentent ces techniques (estimations objectives des incertitudes selon des critères statistiques, aptitude à traiter des problèmes complexes sans recourir à des approximations parfois discutables ou être conduit à linéariser à tout prix les équations descriptives du modèle), il est assez surprenant de constater que de nombreux travaux récents continuent à faire appel aux résolutions graphiques. Nous pensons que cet état de fait, à l'heure où tant de programmes ont été publiés, peut s'expliquer de la façon suivante:

—d'une part, la familiarisation avec des programmes généraux, tel LETAGROP-VRID,[4] exige un effort assez considérable et leur exécution nécessite de gros moyens informatiques;

—d'autre part, la plupart des programmes existants ne permettent de traiter qu'un seul type d'expérience: potentiométrie (SCOGS,[5] MINIQUAD,[6] BEST,[7] TITFIT,[8] MUCOMP[9]), spectrophotométrie (MINISPEF,[10] DCLET,[11] SQUAD[12]), résonance magnétique nucléaire (PHFIT[13]), polarographie (POLAG[14]).

Il nous semble que la demande du chimiste analyticien est de pouvoir disposer d'un programme d'utilisation aisée (*i.e.*, interactif, ne nécessitant pas de connaissances informatiques approfondies et éxécutable sur micro- ou mini-ordinateur) et d'une généralité telle qu'il puisse s'adapter à différents types d'expériences. En effet, devant un problème chimique, le choix primordial quant à la technique expérimentale doit être un *choix chimique* (il n'est pas souhaitable qu'un seul type de manipulation soit systématiquement utilisé quel que soit le problème envisagé). Ce choix ne pourra être fait librement que si l'on est assuré de disposer d'une méthode de calcul appropriée. Ainsi, la seule démarche valable est d'adapter un programme à l'expérience, et non de concevoir l'expérience en fonction du programme dont on dispose. En clair, le plus important est d'assurer le libre choix des manipulations. Qui plus est, il arrive que pour une expérience donnée des modèles différents conduisent à des ajustements comparables. La discrimination entre les modèles nécessite alors d'autres approches expérimentales; il est donc important de pouvoir traiter différents types de données.

Ces diverses constatations nous ont conduits à écrire un programme *d'utilisation générale* pouvant s'adapter à l'exploitation de résultats expérimentaux acquis par diverses techniques. L'investissement nécessaire à l'utilisation de ce programme sera donc largement rentabilisé par ses applications multiples. Le programme MICMAC, écrit en BASIC standard (Microsoft) est éxécutable sur micro-ordinateur.

Ce programme est conçu de façon à ce que tout paramètre expérimental puisse être rendu ajustable sans difficulté. Jusqu'ici, seuls des programmes comme LETAGROP,[4] DALSFEK,[15] TITFIT[8] et MUCOMP[9] permettent de rendre ajustables certains paramètres autres que les constantes d'équilibre.

*Auteur pour correspondance.

TRAITEMENT MATHEMATIQUE

Pour un modèle donné, la variable observée est fonction des paramètres $\alpha_j (j = 1, \ldots n)$ et des variables indépendantes $x_l (l = 1, \ldots k)$

$$y = f(\alpha_1, \ldots \alpha_n, x_1, \ldots, x_k) \tag{1}$$

(Pour la clarté de l'exposé, nous nous limitons à une variable dépendante. L'extension au cas de plusieurs variables se fait sans difficulté.)

Le but est d'obtenir les "meilleures" estimations des paramètres (au sens des moindres carrés), c'est-à-dire de minimiser la somme des carrés des résiduels:

$$U = \sum_{i=1}^{m} W_i [y_{i(\text{exp})} - f(\alpha_1, \ldots \alpha_n, x_{i1}, \ldots x_{ik})]^2 \tag{2}$$

où W_i représente le poids du point i ($i = 1$ à m, nombre de mesures).

Cette somme doit être rendue minimum par rapport à chacun des paramètres ajustables, ce qui conduit à un système de n équations

$$\frac{\partial U}{\partial \alpha_j} = 0; \; j = 1 \text{ à } n \tag{3}$$

La fonction f est développée en série de Taylor, en négligeant les termes d'ordre supérieur. Si y_i^0 représente la valeur calculée de y_i à partir d'un jeu de paramètres initiaux α_j^0, le développement en série de Taylor de f s'écrit:

$$f(\alpha_1, \ldots \alpha_n, x_{i1}, \ldots x_{ik}) = y_i^0 + \sum_j \frac{\partial f_i}{\partial \alpha_j} \Delta\alpha_j \qquad \begin{matrix} i = 1 \text{ à } m \\ j = 1 \text{ à } n \end{matrix}$$

soit

$$y_i - y_i^0 = \sum_j \frac{\partial f_i}{\partial \alpha_j} \Delta\alpha_j \tag{4}$$

Il est plus facile pour la programmation d'utiliser la notation matricielle selon laquelle l'équation (4) s'écrit

$$\Delta y = \mathbf{J} \cdot \Delta\alpha \tag{5}$$

Δy représente l'incrément sur la fonction f_i produit par l'incrément $\Delta\alpha$ sur les paramètres α_j. $\mathbf{J}$ est la matrice jacobienne dont les éléments sont définis par

$$\mathbf{J}_{ij} = \frac{\partial f_i}{\partial \alpha_j}; \quad i = 1 \text{ à } m, \quad j = 1 \text{ à } n.$$

Soit $\boldsymbol{\varepsilon}$ le vecteur des résiduels dont les éléments ε_i correspondent à la différence $(y_{i(\text{exp})} - y_i^0)$, y_i^0 étant calculé à partir du jeu de paramètres estimés. La fonction U à minimiser devient:

$$U = \widetilde{[\boldsymbol{\varepsilon} - \mathbf{J} \cdot \Delta\alpha]} \cdot \mathbf{W} \cdot [\boldsymbol{\varepsilon} - \mathbf{J} \cdot \Delta\alpha] \tag{6}$$

où $\mathbf{W}$ désigne la matrice de pondération (le symbole $\sim$ désigne la transposée de la matrice considérée). La condition de minimisation (3) s'écrit alors:

$$\frac{\partial U}{\partial \alpha_j} = -2\tilde{\boldsymbol{\varepsilon}} \cdot \mathbf{W} \cdot \mathbf{J} + 2\widetilde{\Delta\alpha} \cdot \tilde{\mathbf{J}} \cdot \mathbf{W} \cdot \mathbf{J} = 0$$

d'où l'on tire la relation, après transposition:

$$\mathbf{A} \cdot \Delta\alpha = \mathbf{S} \tag{7}$$

où

$\mathbf{A} = \tilde{\mathbf{J}} \cdot \mathbf{W} \cdot \mathbf{J}$ est le Hessien
$\mathbf{S} = \tilde{\mathbf{J}} \cdot \mathbf{W} \cdot \boldsymbol{\varepsilon}$ le vecteur des seconds membres.

L'expression des déplacements sur les paramètres $(\Delta\alpha_j)$ est donc:

$$\Delta\alpha = \mathbf{B} \cdot \mathbf{S} \tag{8}$$

où $\mathbf{B} = (\tilde{\mathbf{J}} \cdot \mathbf{W} \cdot \mathbf{J})^{-1}$ représente l'inverse du Hessien $\mathbf{A}$ et peut être calculé lorsque celui-ci n'est pas singulier. Le problème n'étant généralement pas linéaire, la nouvelle estimation des paramètres $\alpha_j = \alpha_j^0 + \Delta\alpha_j$ ne conduit pas directement au minimum de U; un ajustement itératif est nécessaire, et le calcul précédent est répété à partir des nouvelles estimations jusqu'à convergence. Chaque itération conduit idéalement à une valeur plus faible de la variance sur y:

$$\sigma^2 = \frac{1}{m - n} \sum_i W_i (y_{i(\text{exp})} - y_{i(\text{calc})})^2 \tag{9}$$

La variance sur chaque paramètre est obtenue à partir des éléments diagonaux de la matrice de variance-covariance $\mathbf{B}\sigma^2$ et la racine carrée de ses éléments conduit à la déviation standard sur le paramètre correspondant.

Enfin, la matrice de corrélation $\mathbf{C}$ s'obtient en normalisant la matrice $\mathbf{B}$ selon

$$\mathbf{C}_{ij} = \frac{b_{ij}}{\sqrt{b_{ii}}\sqrt{b_{jj}}} \tag{10}$$

LE PROGRAMME MICMAC

Caractéristiques du programme

Les équations mathématiques écrites ci-dessus permettent de constater que la méthode des moindres carrés n'est nullement restrictive. L'essentiel du traitement mathématique est indépendant de la forme de la fonction $f(\alpha_1, \ldots, \alpha_n, x_1, \ldots, x_k)$, qui le plus souvent ne sera pas connue de façon explicite. Nous avons cherché à exploiter cette qualité en écrivant un programme qui soit, lui aussi, le plus indépendant possible quant à la forme de f.

Un choix correct de la variable y sur laquelle est effectué l'ajustement est primordial. Il nous paraît naturel que la grandeur ajustée soit la *grandeur mesurée*. Il est ainsi possible d'interpréter en termes chimiques le déroulement du calcul. Les résidus ont une signification directe et peuvent être immédiatement comparés à une estimation de l'erreur expérimentale. L'étude des écarts observés pourra consti-

tuer pour l'expérimentateur un guide précieux dans sa recherche d'un modèle plus satisfaisant. Dans le cas où existent des erreurs systématiques, leur détection sera facilitée par l'examen critique des déviations sur telle ou telle fraction des valeurs calculées de y. De plus, lorsque l'ajustement se fait sur la grandeur mesurée, la pondération en $1/\sigma^2$ est aisément établie, et peut à l'occasion être prise égale à l'unité. Par contre, l'utilisation de fonctions indirectes impose une pondération plus complexe qui doit tenir compte de la propagation des erreurs, afin que l'analyse statistique demeure rigoureuse.[16] Ainsi, lorsque l'on utilise $\bar{n}$, les expressions mathématiques deviennent rapidement inextricables.[17]

Dans le cas d'analyse de dosages pH-métriques par exemple, la minimisation de $\Sigma(\mathrm{pH_{calc}} - \mathrm{pH_{exp}})^2$ constitue, comme l'affirment les auteurs de BEST,[7] le bon choix tant au sens chimique que mathématique. Dans ce cas, la pondération établie en tenant compte des erreurs sur la mesure du pH et le volume de titrant est nécessaire, afin de ne pas donner une importance dangereuse aux zones de plus grande pente.

Il faut remarquer que la distinction introduite précédemment entre variables indépendantes (x) et paramètres ajustables (α) est purement arbitraire. Il est d'un grand intérêt que cette distinction soit faite par l'utilisateur en fonction de ses besoins, et non imposée par la structure du programme. Une caractéristique majeure de notre programme est la *banalisation* de toutes les grandeurs utiles à la définition de f. Chacune de ces grandeurs, selon qu'elle sera déclarée fixe ou ajustable au moment de l'exécution, jouera le rôle d'un x ou d'un α. Ceci permet de prendre en compte d'éventuelles erreurs systématiques, comme le préconisent Sillén[18] et Wentworth *et al.*[19] De telles erreurs sont souvent compensées par l'introduction d'une espèce artificielle, qui devient inutile lorsque l'erreur est corrigée. La correction des erreurs systématiques permet donc une analyse plus fine du modèle et autorise une plus grande confiance dans la détection d'espèces mineures. Bien entendu, la valeur ainsi ajustée d'un paramètre ne pourra être retenue que si elle est raisonnable; l'examen des nouveaux coefficients de corrélation infirmera ou confirmera l'opportunité d'une telle démarche. En effet, si la corrélation de ce nouveau paramètre avec chacun des paramètres initiaux est grande, il est indispensable de procéder à d'autres mesures expérimentales selon un nouveau protocole.

Afin de maintenir au programme un haut degré de généralité, nous avons opté pour la *dérivation numérique*. L'obtention d'un code compact et plus lisible est une conséquence avantageuse de ce choix. L'écriture de programmes généraux utilisant la dérivation analytique est possible,[20] mais nécessite une capacité-mémoire supplémentaire.

Pour la recherche des coordonnées du minimum de U, la méthode de Gauss–Newton, facile à mettre en oeuvre, converge rapidement à partir d'estimations initiales satisfaisantes. Lorsque celles-ci sont trop éloignées de la solution, la fonction U n'est plus correctement approximée par le développement en série de Taylor limité au premier ordre, et il n'est pas rare que le calcul diverge. Nous avons donc introduit la modification proposée par Marquardt,[21] qui combine l'approche précédente avec la méthode du gradient (connue pour être plus sûre, mais extrêmement lente lorsque l'on approche de la solution). L'algorithme de Gauss–Newton–Marquardt permet d'assurer la convergence à partir d'estimations initiales mêmes médiocres, tout en conservant la rapidité de la méthode de Gauss–Newton. L'équation (7) est remplacée par

$$\mathbf{A}^* \cdot \Delta\alpha^* = \mathbf{S}^* \tag{11}$$

$\mathbf{A}^*$ est le Hessien normalisé selon:

$$\mathbf{A}^* = (a_{ij})^* = \frac{a_{ij}}{\sqrt{a_{ii}}\sqrt{a_{jj}}} \tag{12}$$

$\mathbf{S}^*$ est le nouveau vecteur des seconds membres

$$\mathbf{S}^* = (s_i)^* = \frac{s_i}{\sqrt{a_{ii}}} \tag{13}$$

L'expression des déplacements sur les paramètres devient

$$\Delta\alpha_j = (\Delta\alpha_j)^*/\sqrt{a_{jj}} \tag{14}$$

Le facteur de Marquardt c est alors introduit dans l'équation (11):

$$(\mathbf{A}^* + c\mathbf{I}) \cdot \Delta\alpha^* = \mathbf{S}^* \tag{15}$$

L'algorithme est construit de façon à ce que c augmente lors d'une itération divergente, et diminue jusqu'à tendre vers zéro lorsqu'il y a convergence. Cette méthode s'avère remarquablement efficace, et confère au programme une grande fiabilité.

L'hypothèse fondamentale de la méthode des moindres carrés repose sur le caractère aléatoire des erreurs et leur distribution gaussienne. L'emploi de cette méthode impose donc que chaque observation soit affectée d'un poids qui reflète exactement l'erreur commise. Le point a été largement discuté par Wentworth.[16,19,22] Il est toutefois surprenant de constater que beaucoup de programmes se limitent à la pondération unité.[3] D'autres n'introduisent que les variances sur les observables, ce qui est parfois insuffisant, les variances sur les variables indépendantes n'étant pas toujours négligeables. La théorie de la propagation des erreurs permet d'écrire, pour plusieurs observables et plusieurs variables indépendantes:

$$\frac{1}{W_{ij}} = \sigma^2_{y_{ij}} + \sum_k \sigma^2_{x_{ik}} \left(\frac{\partial y_{ij}}{\partial x_{ik}}\right)^2 \tag{16}$$

(i-ème mesure, j-ième observable).

La somme des carrés des résiduels s'écrit donc:

$$U = \sum_i \sum_j W_{ij}(y_{ij_{calc}} - y_{ij_{exp}})^2 \qquad (17)$$

La matrice de pondération obtenue est une matrice diagonale d'ordre $m \times n$ (m = nombre de mesures, n = nombre d'observables). Quand plusieurs observations sont faites sur une même solution (spectrophotométrie à plusieurs longueurs d'onde en particulier), il est théoriquement nécessaire de faire intervenir les termes de covariance. Cependant, Lingane et Hugus[23] ont démontré que, lorsque les mesures sont précises, la covariance peut être négligée sans inconvénient.

Toutes les caractéristiques que nous venons de mentionner sont inhérentes au programme principal. Il est bien sûr nécessaire d'introduire un module spécifique (MOSP) à chaque type d'expérience.

—Ce module, dont la longueur n'excède pas quelques dizaines de lignes, inclut la définition de la fonction f, ainsi que l'expression adéquate du facteur de pondération dans les cas où les poids calculés selon l'expression (16) ne sont pas adaptés. Notre schéma général de pondération suppose en effet que la variance sur les x et les y est constante. Dans le cas où cette hypothèse n'est pas vérifiée, il est nécessaire d'introduire une estimation de la variance en chaque point expérimental. Cette option d'une expression spécifique de la pondération pourra également être utilisée dans le cas d'un changement de variables (Fig. 1).

—Dans la plupart des cas, le calcul des concentrations des constituants sous forme libre, à partir de leur concentration analytique est une étape nécessaire. Les équations de conservation de la masse sont introduites dans le module MOSP selon

$$T_j = t_j + a_{j1}c_1 + \cdots + a_{jn}c_n \qquad (18)$$

où T_j représente la concentration analytique du constituant j, avec a_{ji} = nombre d'atomes de ce constituant dans l'espèce i, c_i = concentration de l'espèce i définie à partir des constantes β_i ou K_i.

—Ce module pourra également inclure une correction sur les y, utile notamment en potentiométrie (par exemple, correction de l'erreur alcaline de l'électrode de verre), ou permettre un changement de variables (Fig. 1).

Cette conception permet une économie appréciable de mémoire centrale et une plus grande rapidité d'exécution; elle autorise également une grande souplesse. Ainsi, l'écriture de l'expression des bilans (18), selon qu'elle fera intervenir β, $\log\beta$, K ou pK, entraînera l'ajustement sur ces mêmes grandeurs. Le problème est en effet communément posé.[3] L'ajustement sur $\log\beta$, fréquemment employé, conduit à des ordres de grandeur comparables des éléments du Hessien. Toutefois, il arrive que celui-ci soit alors mal conditionne.[18,24] L'étape de normalisation du Hessien (12) permet de s'affranchir de ces considérations et d'ajuster directement sur les constantes.

En ce qui concerne l'utilisation des constantes globales de formation β ou des constantes successives K, nous n'avons pas observé de différence significative sur les valeurs obtenues lors de l'emploi de l'une ou l'autre de ces constantes. Cependant, l'utilisation d'un micro-ordinateur peut orienter le choix en faveur des constantes K; il n'est pas rare, en effet, de rencontrer des valeurs de β supérieures à 10^{38}, dont la représentation en virgule flottante est impossible sur la plupart des micro-ordinateurs. Ce fut le cas lors de nos études sur les tétra-azamacrocycles.[25,26] Cependant, nous avons parfois observé un abaissement notable des coefficients de corrélation lors de l'emploi de constantes β. Ainsi, il n'y a pas de règle générale quant à l'utilisation de l'une ou l'autre des constantes, le choix qui conduit aux coefficients de corrélation les plus faibles dépend du degré de recouvrement des équilibres.

Tous les appels entraînant le calcul des diverses fonctions définies dans le module MOSP sont gérés exclusivement par le programme principal; aucune modification de celui-ci n'est nécessaire.

La résolution du système d'équations non linéaires (18) utilise la méthode de Newton–Raphson. Si cette méthode est généralement satisfaisante, on observe parfois une absence de convergence, notamment à l'équivalence et dans son voisinage où les concentrations calculées en un point ne constituent pas une bonne approximation pour le point suivant. Pour remédier à cet inconvénient majeur, nous limitons l'accroissement relatif de la concentration d'un constituant ce qui assure également que les concentrations restent positives. Cet accroissement relatif, correspondant dans le programme au "facteur pour Newton–Raphson", doit être compris entre 0 et 1; la valeur 0,8 est généralement satisfaisante. Cette technique peut s'avérer parfois insuffisante; une seconde modification, apparentée à la méthode de la cible mouvante,[27] est alors introduite automatiquement. Une cible intermédiaire est choisie suffisamment proche du point initial de telle sorte que l'itération soit convergente. En se déplaçant ainsi de proche en proche vers la cible finale, la convergence peut toujours être forcée. Lors des cycles d'itérations suivants, on dispose d'approximations satisfaisantes, et la méthode de Newton–Raphson s'avère alors très efficace. La modification de cette méthode proposée par Marquardt[21] ne semble pas intéressante pour le calcul des concentrations, probablement en raison d'une trop forte corrélation.

Utilisation de BASIC

L'utilisation d'un micro-ordinateur présente de nombreux avantages. Parmi ceux-ci, il faut noter le faible coût du matériel, sa disponibilité constante et la familiarisation rapide avec la machine en raison de sa simplicité d'utilisation. BASIC est le langage le plus largement répandu sur ce type de matériel. D'un

apprentissage aisé, il permet l'écriture de programmes lisibles et hautement interactifs. Ces avantages nous paraissent compenser largement les inconvénients inhérents à ce langage, au nombre desquels il faut compter la lenteur d'exécution.

L'introduction d'un module approprié au problème traité entraine bien entendu la nécessité de son écriture en BASIC, donc une connaissance minimale du langage. D'autre part, le module doit être partiellement réécrit quand le modèle est modifié. Afin de limiter ces contraintes, nous avons écrit un programme BASIC interactif GENPROG, qui permet de générer facilement le module nécessaire pour le problème le plus courant: l'analyse de courbes pH-métriques ou potentiométriques. A partir de la description du modéle (nomenclature des espèces,

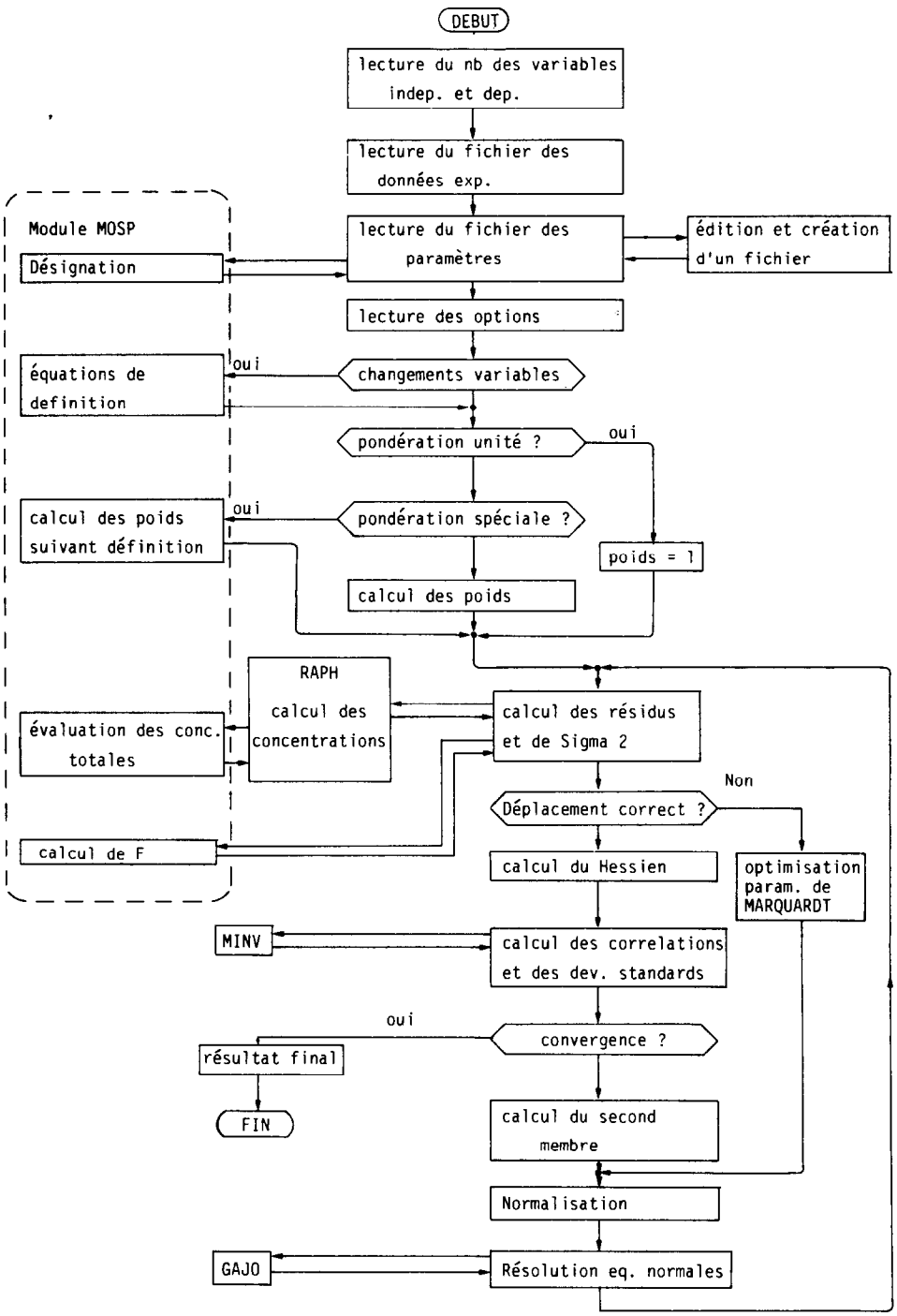

Fig. 1.

stoechiométrie, définition des constantes), le code engendré est très proche de l'écriture chimique et se résume à quelques expressions algébriques (bilans, équations). Aucun constituant ne joue de rôle particulier; leur nombre, ainsi que celui des espèces formées, n'est limité que par la capacité mémoire du système. Le BASIC étant interprété, le problème de la compilation du nouveau module ne se pose pas. Celui-ci vient simplement s'ajouter au programme principal.

Mise en oeuvre

L'éxécution débute par la lecture sur disquette du module MOSP et son chargement en mémoire centrale à la suite du programme principal. L'entrée des données et le choix des différentes options se font de manière interactive, les messages suivants sont affichés à l'écran.

1—Simulation (O/N)?
2—Nombre de variables indépendantes et de variables mesurées?
Nom du ficher des mesures?
Impression des couples (O/N)?
3—Nombre de points lus: *m*
Nombre de points à éliminer?
4—Nom du fichier des paramètres:
Corrections?
Nom du fichier des paramètres à créer:
5—Impressions intermédiares
Mise au point?
Edition du tableau valeurs calculées?
Edition des concentrations?
Edition de la courbe?
6—Valeurs initiales des concentrations:
7—Valeur initiale du facteur de Marquardt:
Facteur pour Newton–Raphson: 0.8
Facteur pour dérivation/paramètres: 1.001
Facteur pour dérivation/concentrations: 1.001
Précision: 10
OK?
8—Nombre maximum de cycles?
Calcul du Hessien tous les N cycles?
9—Correction sur les Y_i/Changement de variable?
10—Déviation standard sur les var. dépendantes?
Déviation standard sur les var. indépendantes?
Pondération (ENTER si poids égaux)?
Pondération spéciale? (ENTER = non).

Point 1—Si la réponse est oui, le calcul des observables conformément au modèle est fait à partir des valeurs fournies, l'étape de minimisation n'est pas effectuée; à l'issue de ce calcul, l'utilisateur est appelé à modifier tout ou partie des paramètres d'entrée, ce qui lui permet d'en évaluer l'incidence. Cette option pourra être utile notamment pour obtenir des approximations initiales satisfaisantes. Elle permet également d'évaluer l'intérêt potentiel d'une manipulation envisagée.

Point 2—Le fichier des mesures a été créé auparavant à l'aide d'un programme auxiliaire SAISIE V6. Ce programme est un éditeur de texte simplifié et adapté à la saisie des mesures, il évite le recours à un éditeur de texte standard.

Point 4—S'il existe déjà, le fichier des paramètres est lu. Sinon, la saisie se fait au clavier, elle est guidée par les informations présentes dans le module MOSP (la désignation de chaque paramétre s'affiche à l'écran). L'utilisateur répond en fournissant une valeur qu'il déclarera fixe ou ajustable. Une procédure de correction est prévue, et les données définitives sont éventuellement copiées dans un fichier.

Point 5—Ces diverses options assurent un contrôle des impressions des résultats intermédiaires.

Point 6—L'utilisateur fournit les valeurs des estimations initiales nécessaires au premier calcul des concentrations.

Point 7—Après avoir fourni une valeur initiale du facteur de Marquardt, (généralement 0.01), l'utilisateur peut, s'il le souhaite, modifier les valeurs par défaut des facteurs répertoriés. La constante introduite à la question "précision" est un terme multiplicatif qui contrôle la précision demandée sur les concentrations. Ainsi, la valeur typique 10 conduit à une précision $10^{-7}M$.

Point 8—Lorsque l'on est proche de la solution, un gain de temps appréciable peut fréquemment être obtenu en n'effectuant le calcul du Hessien que tous les deux ou trois cycles d'itération. Dans tous les cas, le Hessien sera calculé lors de l'itération finale.

Point 9—Une réponse positive entraîne le calcul de la correction ou du changement de variables définis dans le module MOSP.

Point 10—L'utilisateur est appelé à introduire les déviations standards sur les différentes variables dépendantes et indépendantes. Si l'option par défaut est retenue, un poids unité est affecté à chaque point. Sinon, l'évaluation des poids est faite selon l'expression générale (16) dans le programme principal, ou selon les modalités définies si l'option pondération spéciale a été retenue. Le calcul des dérivées partielles (16) au point i se fait en calculant les coefficients d'un polynôme du second degré approximant la courbe aux points de rang $(i-1)$, i, $(i+1)$; on en déduit la valeur de la dérivée au point i.

L'essentiel des données est rappelé sur l'imprimante au fur et à mesure de la saisie. A l'issue de celle-ci, on entre dans la boucle itérative principale (Fig. 1). En chaque point sont calculés les valeurs de Y et le résiduel correspondant en appelant RAPH, routine de calcul des concentrations selon Newton–Raphson. Cette routine incorpore les instructions d'appel du module MOSP qui fournit les expressions algébriques nécessaires au calcul des bilans. La somme pondérée des carrés des résiduels SIGMA est alors calculée.

Si le SIGMA ainsi obtenu est inférieur à la valeur de la précédente itération (à la première itération, la

comparaison se fait avec 10^{10}), les estimations des paramètres sont actualisées. On calcule le Jacobien, le Hessien, puis la matrice des coefficients de corrélation. Le Hessien est inversé dans la routine MINV utilisant la méthode du pivot maximal, et les variances sont calculées. La somme des carrés des résiduels SIGMA, la matrice de corrélation et les variances sont imprimées à chaque itération.

Dans le cas d'une itération divergente, le facteur de Marquardt est augmenté. Le système des équations normales modifiées (15) est à nouveau résolu et un nouveau SIGMA calculé. L'opération est répétée jusqu'à obtenir une itération convergente. Lorsque l'amélioration relative sur SIGMA devient inférieure à 0.001, le calcul se termine. Sinon, on procède à l'évaluation des seconds membres des équations normales, et de nouveaux déplacements sont calculés.

Les systèmes linéaires sont résolus par la méthode de Gauss–Jordan dans la routine GAJO.

Le développement de ce programme a été réalisé sur un TRS80 Model I Level II (48 K) équipé de deux unités de minidisquettes travaillant en double densité sous NEWDOS-80 V2 0. Le programme occupe 20 koctets (5 koctets sont dûs aux commentaires): 18 koctets sont donc utilisables pour les données. Tous les calculs sont exécutés en simple précision. Un listing du programme est disponible auprès des auteurs qui envisagent de réaliser une version utilisable sous CP/M 2.0.

RESULTATS

Afin d'illustrer quelques-unes des possibilités du programme MICMAC et d'en apprécier la validité, nous avons effectué une étude comparative avec des programmes récents traitant de problèmes divers.

Polarographie

Les travaux de Heath et Hefter[28] sur la détermination des constantes de stabilité des complexes cadmium–chlorure ont été exploités par Leggett[14] à l'aide du programme POLAG, puis plus récemment par Gomez-Nieto *et al.*[29] Il nous a donc semblé intéressant d'analyser à notre tour les mesures de Heath et Hefter.

L'ajustement sur la grandeur mesurée E_p conduit à minimiser l'expression:

$$U = \sum_i (E_{p_i}^{calc} - E_{p_i}^{exp})^2$$

avec

$$E_p^{calc} = E_p^0 - \frac{RT}{nF}\left(\log\frac{M_T}{M} - \log\frac{I_{p_0}}{I_p}\right)$$

où

M est solution des deux équations:

$M_T = M + M \cdot L \cdot \beta_1 + M \cdot L^2 \cdot \beta_2 + M \cdot L^3 \cdot \beta_3$ métal total

$L_T = L + M \cdot L \cdot \beta_1 + 2M \cdot L^2 \cdot \beta_2 + 3 \cdot M \cdot L^3 \cdot \beta_3$ ligand total

Il est également possible d'utiliser le traitement de DeFord et Hume[30] qui conduit à minimiser:

$$U = \sum_i (F0_i^{calc} - F0_i^{exp})^2$$

avec

$$F0^{calc} = \frac{M_T}{M}$$

$$F0^{exp} = \exp\left[\frac{nF}{RT}(E_p^0 - E_p) + \log\frac{I_{p_0}}{I_p}\right]$$

Nos résultats, ainsi que ceux de la littérature, sont rassemblés dans le tableau 1.

Nos valeurs de constantes sont identiques à celles obtenues par Gomez-Nieto *et al.* à l'aide des programmes F0W et GIP II.

Les différences observées avec Leggett ne peuvent s'expliquer par la simple lecture de son article. Par contre, l'examen de son listing permet de constater des erreurs dans les données ($10^{-3}M$ en cadmium au lieu de $4 \times 10^{-5}M$, ainsi que $I_p = 7.40$ au lieu de 7.37

Tableau 1. Système cadmium–chlorure ($I = 1{,}0M$; $T = 25°C$; $[Cd^{2+}]_T = 4{,}0 \times 10^{-5}M$; $\beta_1 = 22{,}5 \pm 0{,}5$; $\beta_2 = 56 \pm 1$; $\beta_3 = 35 \pm 3$)[28]

Grandeur ajustée	E_p		$F0$			
	ce travail*	Leggett[14]	ce travail $W \neq 1$	ce travail $W = 1$	Gómez *et al.*[29] $W \neq 1$§	Gómez *et al.*[29]‡
β_1	21,0	21,4	21,0	21,3	21,0	21,2
s.d.†	0,2		0,2	0,4	0,3	0,3
β_2	55,2	54,5	55,2	54,4	55,2	54,4
s.d.†	1,0		1,0	1,3	1,0	0,8
β_3	31,8	32,7	31,8	32,4	31,7	32,4
s.d.†	1,1		1,3	0,9	0,8	0,6

*Pente théorique 29,579 mV.
†Déviation standard.
§Programme F0W.
‡Programme GIP II.

Tableau 2. Valeurs calculées du pH pour le système PXBDE, en, Co^{2+} et O_2

Volume, *ml*	pH_{obs}	Résiduels calculés BEST	Résiduels calculés MICMAC ($W = 1$)
0,200	2,634	0,003	0,004
0,400	2,717	0,007	0,008
0,600	2,812	0,005	0,007
0,800	2,932	0,003	−0,004
1,000	3,092	−0,007	−0,024
1,200	3,346	−0,031	−0,018
1,400	4,233	−0,060	−0,027
1,800	6,162	−0,030	−0,009
2,000	6,265	−0,012	−0,002
2,200	6,322	−0,006	0,003
2,450	6,373	−0,001	0,005
2,700	6,413	0,002	0,007
2,950	6,448	0,004	0,010
3,200	6,482	0,006	0,006
3,400	6,502	0,002	0,009
3,600	6,529	0,005	0,009
3,800	6,553	0,004	0,007
4,000	6,576	0,003	0,005
4,200	6,600	0,001	0,006
4,400	6,627	0,002	0,006
4,600	6,654	0,002	0,004
4,800	6,681	−0,000	0,004
5,000	6,711	−0,001	0,003
5,200	6,748	0,002	0,007
5,400	6,785	0,003	0,007
5,600	6,824	0,002	0,004
5,800	6,862	−0,006	−0,001
6,000	6,917	−0,003	0,002
6,200	6,975	−0,007	−0,002
6,400	7,048	−0,011	−0,005
6,850	7,169	−0,024	−0,017
6,900	7,367	−0,066	−0,056
7,130	8,927	−0,082	−0,011
σ^2		$5,47 \times 10^{-4}$	$2,02 \times 10^{-4}$

pour $[Cl^-]_T = 0.4M$). Nous ne mettons pas en cause le programme POLAG puisque, en introduisant ces mêmes données, nous retrouvons des résultats identiques à ceux publiés par Leggett.

Il est assez remarquable de constater que les résultats obtenus en ajustant sur la grandeur mesurée E_p, sont identiques à ceux obtenus par ajustement pondéré, sur $F0$, mettant ainsi en évidence la nécessité de pondérer lorsque l'on n'ajuste pas sur la grandeur mesurée. Dans ce cas précis, nous avons estimé que l'erreur sur les concentrations était négligeable. L'expression du poids est donc:

$$\frac{1}{W_i} = \left(\frac{\partial F0}{\partial y}\sigma y\right)_i^2 = \left(\frac{nF}{RT}F0\,\sigma y\right)_i^2$$

pH-métrie: comparaison avec BEST

BEST[7] est l'un des rares programmes à ajuster sur la grandeur mesurée, ici le pH, se prêtant ainsi particulièrement bien à une étude comparative, d'autant plus que les auteurs fournissent un tableau des résiduels.

Complexes du cobalt. L'étude porte sur les complexes du cobalt en présence de deux ligands sous atmosphère d'oxygène; le système ne comporte pas moins de vingt-quatre espèces. Nous avons été satisfaits de constater l'excellent accord avec les auteurs de BEST, les résiduels obtenus à partir des mêmes paramètres étant strictement identiques. Les auteurs soulignant l'existence d'un léger déséquilibre des concentrations en acide et en base, nous avons entrepris d'ajuster conjointement le titre en acide et la constante β_{2210} de l'espèce 24. Les résultats sont rassemblés dans les tableaux 2 et 3.

L'ajustement simultané du titre en acide et de la constante améliore les résidus (σ^2 divisé par 2,5), les écarts autour des stoechiométries 1 et 5 sont moindres. La valeur $1.5009 \times 10^{-2}M$ obtenue pour l'acide est proche de la valeur initiale $1.5002 \times 10^{-2}M$, la variance est très faible et la corrélation entre les deux paramètres ajustés est de 0,2. L'ajustement du titre en acide nous paraît donc justifié et satisfaisant.

Nous avons d'autre part effectué les calculs avec et sans poids ($\sigma_x = 0.02$ ml; $\sigma_y = 0.002$ pH). Il apparaît que les deux valeurs sont compatibles entre elles, celle obtenue avec pondération se rapprochant davantage de celle de BEST; on peut cependant regretter que les auteurs ne donnent pas d'incertitude sur leur constante.

Dans le cadre de cette étude, nous avons pu vérifier l'efficacité de la méthode de la cible mouvante sans laquelle le calcul des concentrations diverge aux stoechiométries 1 et 5. Les auteurs de BEST, quant à eux, introduisent de nouvelles estimations initiales aux points critiques.

Base de Schiff. Le système étudié comporte treize espèces, l'ajustement porte sur les constantes de formation de la base de Schiff et de ses trois formes protonées. Comme précédemment, l'introduction des

Tableau 3. Résultat de l'ajustement

	BEST	MICMAC	
Titre en acide	$1,5002 \times 10^{-2}M$*	$1,5009 \times 10^{-2}M \pm 8,09 \times 10^{-7}M$†	
		$W = 1$	$W \neq 1$
pK_{2210}	6,71	6,739	6,717
		0,022§	0,010§
σ^2	$5,47 \times 10^{-4}$	$2,02 \times 10^{-4}$	$4,2 \times 10^{-5}$

*Valeur fixe.
†Valeur ajustée.
§Déviation standard.

Tableau 4. Formation de base de Schiff

	$W = 1$	$W \neq 1$	$W = 1$	$W \neq 1$	Ref. 7
log β_{110}	−6,0	−4,0	—	—	0,1
s.d.*	10	13			
log β_{111}	11,81	11,86	11,85	11,87	11,98
s.d.*	0,06	0,06	0,02	0,02	
log β_{112}	18,75	18,80	18,83	18,82	19,00
s.d.*	0,14	0,12	0,05	0,04	
log β_{113}	24,69	24,75	24,76	24,76	24,90
s.d.*	0,11	0,09	0,04	0,03	
σ^2	$1{,}253 \times 10^{-3}$	$3{,}23 \times 10^{-4}$	$9{,}17 \times 10^{-4}$	$3{,}00 \times 10^{-4}$	$1{,}356 \times 10^{-3}$
σ			0,0303		0,0368

*Déviation standard.

paramètres obtenus par BEST donne des résiduels identiques. Par contre, l'ajustement nous conduit à des conclusions différentes (Tableau 4).

Que ce soit avec ou sans pondération, la constante de formation de la base de Schiff β_{110} est rejetée par le programme (valeurs négatives, déviations standards démesurées, corrélation importante). Nous avons donc repris les calculs en éliminant cette espèce; l'ajustement est meilleur et les déviations standards diminuent de façon significative. L'influence du poids est plus particulièrement sensible lorsque cette espèce (110) est prise en compte: la colonne 1 se distingue des colonnes 2, 3 et 4 où les résultats obtenus sont très voisins.

Au vu de ces résultats, nous concluons que la base de Schiff totalement déprotonée n'existe pas et que le programme MICMAC semble à même de déterminer le minimum avec plus de précision. Cette différence est peut-être imputable au fait que BEST utilise un algorithme de type heuristique.

pH-métrie: comparaison avec TITFIT[8]

Le système Ni^{2+}–glycine a été très largement étudié ces dernières années. Il constitue donc une bonne base de comparaison. Nous avons repris les mesures des auteurs de TITFIT à partir des données figurant dans leur listing (ces données correspondent aux trois courbes de la figure 2 de leur article[8]). La comparaison nous paraît d'autant plus intéressante que TITFIT réalise l'ajustement sur les volumes de base titrante, alors que notre ajustement porte sur le pH.

Dans un premier temps, nous avons ajusté sur chacune des courbes les concentrations de l'acide fort ajouté et de la base titrante; cette démarche est analogue à l'ajustement des grandeurs Exac et EQ effectué par les auteurs.[8] L'ajustement des constantes a ensuite été réalisé en traitant simultanément les trois courbes et en utilisant les concentrations en acide et en base précédemment calculées (Tableau 5).

Nous sommes satisfaits de constater que deux programmes utilisant des démarches différentes conduisent à des valeurs de constantes identiques à partir des mêmes données. Dans ce cas précis, les résiduels sont très faibles, y compris au voisinage des points d'équivalence; la pondération faisant intervenir σ_{ml} et σ_{pH} n'a donc que peu d'influence. D'autre part, nous sommes en accord aves les auteurs de TITFIT lorsqu'ils rejettent l'hypothése d'un complexe hydroxylé Ni(gly)OH. En effet, l'introduction d'un tel complexe n'entraîne aucune amélioration de l'ajustement.

Résonance magnétique nucléaire du carbone-13

La résonance magnétique nucléaire, largement employée à des fins d'identification, a suscité relativement peu d'études quantitatives; cette méthode se prête pourtant bien à la détermination des constantes de stabilité, comme le montre l'étude menée par Surprenant *et al.*[13] sur la protonation de la lysine (programme PHFIT). Ne disposant pas de leurs données originales (couples déplacement chimique–pH), nous avons choisi de générer des courbes synthétiques à partir des résultats publiés par les auteurs (constantes d'acidité, déplacements chimiques des espèces libres et protonées). Nous avons ensuite ajouté aux déplacements chimiques ainsi calculés des erreurs aléatoires normalement distribuées afin d'obtenir des pseudo-valeurs expérimentales. L'ajustement porte sur les déplacements chimiques des deux carbones: C=O et C_δ, qui sont les plus influencés en présence de proton. La fonction à minimiser est:

$$U = \Sigma\Sigma\,(\delta_{calc} - \delta_{exp})^2$$

Tableau 5. Système Ni^{2+}–glycine (log $\beta_{011} = 9{,}57$; log $\beta_{012} = 11{,}99$)

	Ref. 8	Ref. 31	$W = 1$	$W \neq 1$†
log β_{110}	5,58	5,638	5,569	5,574
s.d.*		0,071	0,006	0,005
log β_{120}	10,30	10,391	10,298	10,296
s.d.*		0,089	0,010	0,008
log β_{130}	13,75	13,922	13,741	13,742
s.d.*		0,191	0,021	0,020
σ^2			$1{,}8 \times 10^{-4}$	$2{,}6 \times 10^{-5}$
Moyenne			$-1{,}5 \times 10^{-3}$	$1{,}3 \times 10^{-3}$

*Déviation standard.
†$\sigma_x = 10^{-3}$ ml; $\sigma_y = 2 \times 10^{-3}$ pH.[32]

Tableau 6. Protonation de la lysine

				C=O†				C_δ			
	pK_1^*	pK_2^*	pK_3^*	Z_0	Z_1	Z_2	Z_3	Z_0	Z_1	Z_2	Z_3
Reference 13	1,87	9,38	11,17	175,53	173,84	166,48	164,55	27,60	22,94	22,24	22,07
This work§	1,87	9,37	11,18	175,54	173,81	166,49	164,56	27,64	27,64	22,24	22,04
Standard déviation	$0,03_6$	$0,00_7$	$0,01_1$	$0,01_7$	$0,03_4$	$0,01_3$	$0,04_2$	$0,02_0$	$0,02_0$	$0,01_1$	$0,02_9$

*Valeurs des constantes de dissociation de la lysine triprotonée.

†Z_0, Z_1, Z_2, Z_3 = déplacements chimiques (en ppm) des formes libres, mono-, di- et tri- protonées de la lysine par rapport au TMS.

§$\sigma^2 = 7,87 \times 10^{-4}$; distribution des erreurs sur le pH: moyenne 0, déviation standard 0; sur Z: moyenne 0, déviation standard; 0,05 ppm.

avec

$$\delta_{calc} = \sum_{i=1}^{4} F_i \delta_i$$

où F_i = fraction molaire de l'espèce i et δ_i son déplacement chimique. Les paramètres ajustables sont les trois constantes d'acidité de la lysine et, pour chaque carbone, les déplacements chimiques des espèces libres et protonées, soient onze paramètres ajustables. Nos résultats sont rassemblés dans le Tableau 6.

Les estimations des paramètres sont très proches des valeurs exactes et la variance obtenue est inférieure à la valeur attendue, ce qui indique un excellent ajustement. De plus, les écarts entre valeurs exactes et valeurs calculées sont en plein accord avec les estimations des déviations standards.

Cet exemple illustre la capacité du programme à effectuer l'ajustement de nombreux paramètres (onze ici) sur deux grandeurs observées. Des mesures spectrophotométriques à deux longueurs d'ondes, qui conduisent à des équations de même forme, peuvent être traitées de manière similaire.

Cette étude comparative démontre la validité du programme MICMAC et illustre sa très grande généralité et son aptitude à traiter des problèmes très divers, puisque nous avons pu montrer la capacité de ce seul programme à traiter des sujets nécessitant cinq programmes spécifiques. De plus, MICMAC semble dans certains cas à même de cerner le minimum avec plus de précision.

DISCUSSION

Le programme MICMAC exploite les avantages liés à l'utilisation d'un micro-ordinateur sans sacrifier aucunement à la rigueur du traitement statistique. Son champ d'applications est potentiellement très vaste et nous avons fait en sorte qu'il n'y ait aucune limitation (autre que la capacité-mémoire) dans la complexité du problème envisagé. Ce programme réunit diverses caractéristiques qui nous semblent particulièrement importantes: ajustement sur la grandeur mesurée, prise en compte des erreurs systématiques, expression rigoureuse de la pondération, utilisation de la méthode de Marquardt, estimations des erreurs. A notre connaissance, aucun programme publié à ce jour, excepté DALSFEK,[15] n'offre simultanément ces possibilités.

Cette approche générale n'est vraisemblablement pas la plus efficace pour l'étude spectrophotométrique à plus de trois ou quatre longueurs d'onde. Le programme de Maeder et Gampp[32] est dans ce cas plus performant. Par contre, le programme MICMAC est bien adapté au traitement simultané de plusieurs variables dépendantes (absorbance et pH par exemple à quelques longueurs d'onde).

En conclusion, le programme MICMAC offre de nombreuses possibilités dans le domaine de la détermination des constantes de stabilité. Il est également applicable à la détermination de concentrations lors de l'analyse des solutions par différents moyens. De plus, son côté hautement interactif et le fait qu'il permette une approche heuristique le rendent utilisable à des fins d'enseignement.

Remerciements—Certains auteurs cités dans ce travail nous ont fait parvenir leur listing et nous tenons à les en remercier.

LITTERATURE

1. L. G. Sillén, *Acta Chem. Scand.*, 1962, **16,** 173.
2. P. Gans, *Coord. Chem. Rev.*, 1976, **19,** 99.
3. F. Gaizer, *ibid.*, 1979, **27,** 195.
4. L. G. Sillén, *Acta Chem. Scand.*, 1964, **18,** 1085.
5. I. G. Sayce, *Talanta*, 1968, **15,** 1397.
6. A. Sabatini, A. Vacca et P. Gans, *ibid.*, 1974, **21,** 53.
7. R. J. Motekaitis et A. E. Martell, *Can. J. Chem.*, 1982, **60,** 2403.
8. A. D. Zuberbühler et T. A. Kaden, *Talanta*, 1982, **29,** 201.
9. M. Wozniak et G. Nowogrocki, *ibid.*, 1978, **25,** 643.
10. F. Gaizer et A. Puskás, *ibid.*, 1981, **28,** 925.
11. M. Meloun et J. Čermák, *ibid.*, 1979, **26,** 569.
12. D. J. Leggett et W. A. E. McBryde, *Anal. Chem.*, 1975, **47,** 1065.
13. H. L. Surprenant, J. E. Sarnesi, R. R. Key, J. T. Byrd et C. N. Reillcy, *J. Magn. Res.*, 1980, **40,** 231.
14. D. J. Leggett, *Talanta*, 1980, **27,** 787.
15. R. M. Alcock, F. R. Hartley et D. E. Rogers, *J. Chem. Soc., Dalton Trans.*, 1978, 115.
16. W. E. Wentworth, *J. Chem. Ed.*, 1965, **42,** 96.
17. G. L. Cumming, J. S. Rollett, F. J. C. Rossotti et R. J. Whewell, *J. Chem Soc., Dalton Trans.*, 1972, 2652.
18. L. G. Sillén, *Acta Chem. Scand.*, 1962, **16,** 159.
19. W. E. Wentworth, W. Hirsch et E. Chen, *J. Phys. Chem.*, 1967, **71,** 218.

20. I. Nagypál, I. Páka et L. Zékány, *Talanta*, 1978, **25,** 549.
21. D. W. Marquardt, *J. Soc. Ind. Appl. Maths.*, 1963, **11,** 431.
22. W. E. Wentworth, *J. Chem. Ed.*, 1965, **42,** 163.
23. P. J. Lingane et Z. Z. Hugus Jr., *Inorg. Chem.*, 1970, **9,** 757.
24. P. Gans et A. Vacca, *Talanta*, 1974, **21,** 45.
25. E. Suet et H. Handel, *Tetrahedron Lett.*, 1984, **25,** 645.
26. E. Suet, H. Handel, A. Laouenan et R. Guglielmetti, *Helv. Chim. Acta*, 1984, **67,** 441.
27. F. V. Zeggeren et S. H. Storey, *The Computation of Chemical Equilibria*, p. 109. Cambridge University Press, Cambridge, 1970.
28. G. A. Heath et G. Hefter, *J. Electroanal. Chem.*, 1977, **84,** 295.
29. M. A. Gómez-Nieto, M. D. Luque de Castro, M. Valcárcel et J. L. Cruz-Soto, *Anal. Chim. Acta*, 1984, **156,** 77.
30. D. D. DeFord et D. N. Hume, *J. Am. Chem. Soc.*, 1951, **73,** 1634.
31. E. Bottari, A. Braibanti, L. Ciavatta, A. M. Corrie, P. G. Daniele, F. Delavalle, M. Grimaldi, A. Mastroiani, G. Mori, G. Ostacoli, P. Paoletti, E. Rizarelli, S. Sammartano, C. Severini, A. Vacca et D. R. Williams, *Ann. Chim. (Rome)*, 1978, **68,** 813.
32. M. Maeder et H. Gampp, *Anal. Chim. Acta*, 1980, **122,** 303.

Summary—The basic computer program MICMAC has been developed to fit equilibrium constants to various types of experimental data with a microcomputer. The program uses the very efficient Gauss–Newton–Marquardt algorithm for non-linear least-squares multiparametric refinement. Highly interactive, convenient to use and of modular design, it allows for a rigorous weighting scheme, and it takes account of possible systematic errors. This program is useful for solving problems with several sets of experimental data. Some examples dealing with polarography, pH-metric titration and ^{13}C-NMR are given, illustrating the versatility of MICMAC. Comparison is made with some recently published programs.

Talanta, Vol. 32, No. 4, pp. 257–264, 1985
Printed in Great Britain.

0039-9140/85 $3.00 + 0.00

CALCULATION OF EQUILIBRIUM CONSTANTS FROM MULTIWAVELENGTH SPECTROSCOPIC DATA—II*

SPECFIT: TWO USER-FRIENDLY PROGRAMS IN BASIC AND STANDARD FORTRAN 77

HARALD GAMPP, MARCEL MAEDER, CHARLES J. MEYER and ANDREAS D. ZUBERBÜHLER
Institute of Inorganic Chemistry, University of Basel, CH-4056 Basel, Switzerland

(*Received* 5 *October* 1984. *Accepted* 5 *December* 1984)

Summary—A new program (SPECFIT), written in HP BASIC or FORTRAN 77, for the calculation of stability constants from spectroscopic data, is presented. Stability constants have been successfully calculated from multiwavelength spectrophotometric and EPR data, but the program can be equally well applied to the numerical treatment of other spectroscopic measurements. The special features included in SPECFIT to improve convergence, increase numerical reliability, and minimize memory as well as computing time requirements, include (*i*) elimination of the linear parameters (*i.e.*, molar absorptivities), (*ii*) the use of analytical instead of numerical derivatives and (*iii*) factor analysis. Calculation of stability constants from spectroscopic data is then as straightforward as from potentiometric titration curves and gives results of analogous reproducibility. The spectroscopic method has proved, however, to be superior in discrimination between chemical models.

Spectrophotometry has long been used for analysis of chemical equilibria,[1–3] but generally only for relatively simple systems which can be described by linearized functions, as for example in the Benesi–Hildebrand method.[4] This may be partly due to the still widespread belief that spectrophotometric measurements are inherently less precise than potentiometric ones,[5] though this is definitely not the case with suitable instrumentation.[6] The paucity of reliable general computer programs that could deal successfully with spectrophotometric data for more complicated equilibrium systems[2,3,7,8] may be another reason.

As discussed in Part I of this work,[9] three main features have been combined in our program SPECFIT with the Marquardt algorithm[10,11] for the non-linear least-squares refinement of the unknown equilibrium constants. (*i*) The molar absorptivities (ε) are replaced by their least-squares estimates ($\hat{\varepsilon}$), making the matrix of the residuals (**R**) a function of only the species concentrations (**C**) and the measured absorbances (**Y**):[12–15]

$$\mathbf{R} = \mathbf{F} - \mathbf{Y} = \mathbf{C}\varepsilon - \mathbf{Y} = \mathbf{C}\hat{\varepsilon} - \mathbf{Y}$$
$$= \mathbf{C}(\mathbf{C}^t\mathbf{C})^{-1}\mathbf{C}^t\mathbf{Y} - \mathbf{Y} \qquad (1)$$

R, **F** and **Y** all are $M \times W$ matrices for M solutions measured at W wavelengths. (*ii*) The numerical derivatives generally used in previous programs for the treatment of spectrophotometric data[7,13–15] are replaced by the exact analytical expressions in the calculation of the Jacobian matrix **J** (the partial derivatives of the fitting function **F** with respect to the unknown equilibrium constants):

$$\mathbf{J} = \mathbf{DR} = \mathbf{DF} = \mathbf{D}(\mathbf{C}\hat{\varepsilon}) = \mathbf{DC}\hat{\varepsilon} + \mathbf{CD}\hat{\varepsilon} \qquad (2)$$

J and **DC** are tensors with dimensions $M \times W \times N$ and $M \times S \times N$, respectively (S = number of absorbing species, N = number of unknown stability constants).

Analytical derivatives have been used in the calculation of equilibrium constants from potentiometric data[16–19] and a general expression for functions containing both linear and non-linear parameters as in equation (1) has been discussed,[20] but the algorithm implemented in SPECFIT does not seem to have been previously applied to the determination of equilibrium constants from spectroscopic data. (*iii*) The original data matrix **Y** is subjected to factor analysis:

$$\mathbf{Y} = \mathbf{LV} \simeq \mathbf{L}_I\mathbf{V}_I \qquad (3)$$

where **V** contains the eigenvectors of the second moment matrix $\mathbf{Y}^t\mathbf{Y}$ and **L** is the matrix of the corresponding linear coefficients, and parameter refinement is then done with the $M \times I$ matrix $\mathbf{L}_I$ instead of **Y** in equations (1) and (2). Factor analysis has been used to find the number of linearly independent absorbing species in a chemical system[21–24] and applied to the determination of equilibrium constants from spectrophotometric data.[25,26] In the absence of experimental errors, the number of significant eigenvectors, I, would be identical with the mathematical rank of **Y**. Replacement of **Y** by $\mathbf{L}_I$ saves a lot of computer space without significant loss of information from multiwavelength data.

SPECFIT—HP 9835 VERSION

We have long advocated use of desk-top computers,[15,19,27,28] and as we collect all our data online,[6,28] our first (and preferred) version of SPECFIT, which is analogous to TITFIT,[19] was developed for

*Part I: *Talanta*, 1985, **32**, 95.

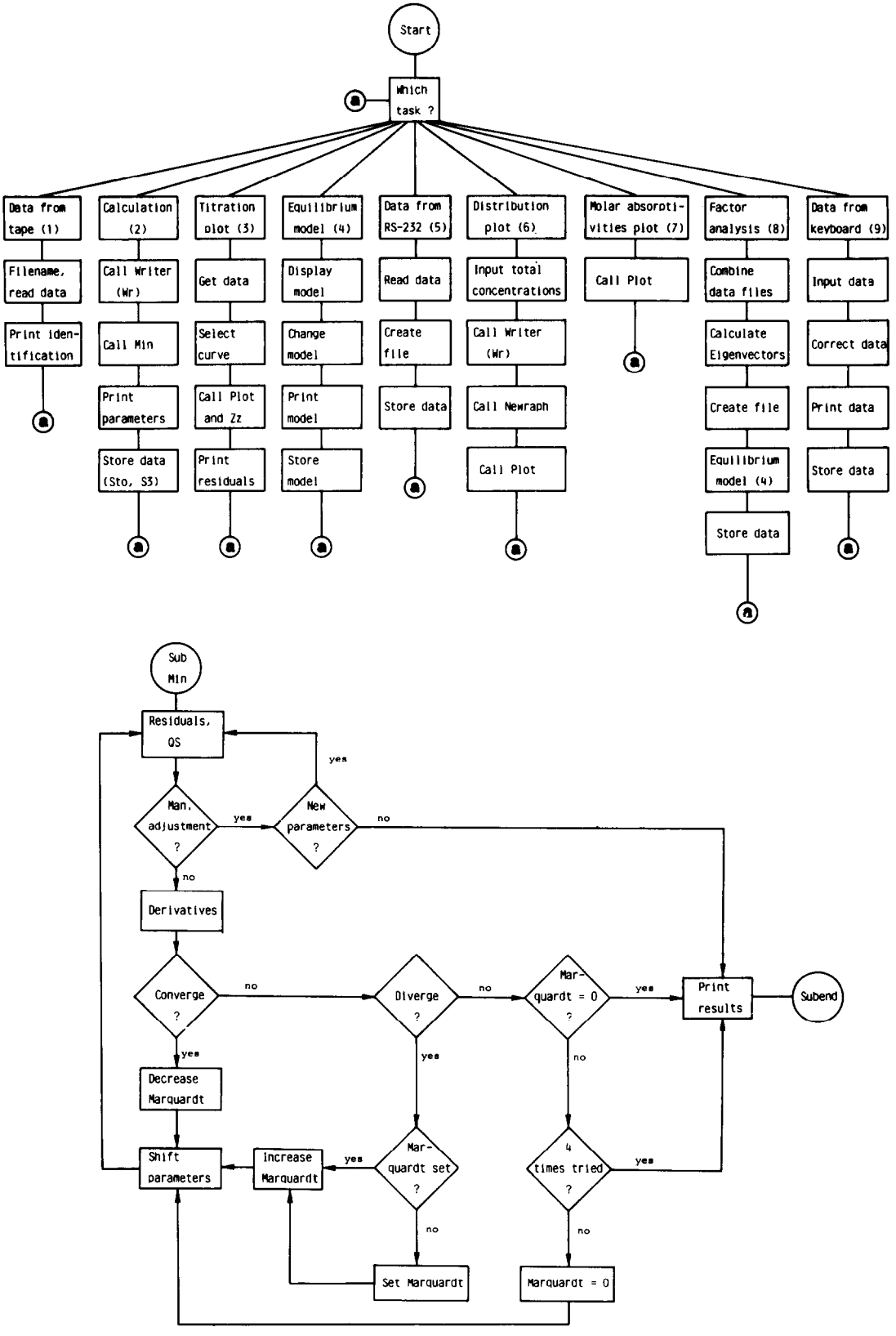

Fig. 1. Flow diagram for the program SPECFIT.

a 128-K Hewlett-Packard HP 9835 calculator. It performs nine different tasks, shown in Fig. 1.

Our experimental data are read through an RS-232 serial interface (task 5) from our data-acquisition system,[6,15] but data can also be input through the keyboard (task 9). In both cases, the number of wavelengths (W) and spectra (M), the maximum wavelength (Lm) and the interval between the wavelengths used for absorbance readings (Dl) are read first, followed by the arrays of absorbances, proton activities and analytical concentrations of metal and ligand. The data are then stored on tape and can be retrieved by task 1.

The least-squares fitting can be done on the original data, but the absorbances are usually first subjected to factor analysis (task 8). Data from up to 6 experiments are combined into a single array and the maximum number of eigenvectors Ne is entered. The program then tries to obtain the Ne most significant eigenvectors by vector iteration.[29] If the residual standard error falls below a prespecified limit or no convergence is obtained after 50 cycles for a given eigenvector, the calculation is terminated and the number of eigenvectors is set accordingly. The appropriate model is then defined (task 4) and the eigenvectors, their linear coefficients, and the chemical model are stored on tape. All the tasks are independent and can be accessed in any logical order by stopping execution of the program at any time, and executing CONTF from the keyboard.

When task 4 is called, the current model is displayed on the screen. Each species is defined by a number, the value of the stability constant $\beta_{mlh} = [M_m L_l H_h]/[M]^m[L]^l[H]^h$, the defining code (*e.g.*, $11-2$ for MLH_{-2}), an index (0 for fixed parameters, 1 for variable parameters, 2 to eliminate the species from the model), and whether the species is absorbing (Y) or not (N). An example is given in Table 1. Species may be added or deleted in any given order. After correction the model is stored on tape and a flag set to indicate whether the model or only the stability constant values had been changed.

The least-squares refinement is done in task 2, as already described in detail for TITFIT.[19] A simplified flow diagram of the minimization routine Min is also given in Fig. 1. In Newraph, the $M \times S$ concentration matrix **C** is established along with the tensor of partial derivatives **DC** with $M \times S \times N$ elements $\partial \mathbf{C}(m, s)/\partial \log\beta_n$. Back in the main minimization routine, the residuals and their dot product (sum of squares, SQ) are calculated.

If manual adjustment of parameters has been selected, the program now asks for their change and repeats the calculation. Normally, however, the refinement is done fully automatically, the Jacobian matrix $\mathbf{J} = \mathbf{DF}$ [equation (2)] being calculated in the subprogram Deriv and the Hessian[30] $\mathbf{J}^t\mathbf{J}$ as well as $\mathbf{J}^t\mathbf{R}$ built; calculation of the parameter shifts and the iterative refinement then proceed, essentially as in TITFIT.[19] Again it is advantageous to introduce the Marquardt correction only in the case of divergence, and to change the Marquardt parameter by less than a factor of 10. There is no unique optimal strategy, but increase by a factor of 5 for divergence and decrease by a factor of 3 for convergence perform satisfactorily. When the final set of parameters has been found or manual adjustment abandoned, the spectra of all absorbing species are calculated and all species concentrations, equilibrium constants and molar absorptivities are printed, with their standard errors. Finally, λ_{max} and ε_{max} are calculated by quadratic interpolation and all parameters and species concentrations are stored on tape.

Various plotting routines are available for graphical presentation of the results. Task 3 can plot experimental data and calculated titration curves for any selected wavelength(s) or can print out the complete matrix of residuals, **R**, and/or its graphical representation. For economy in memory Newraph is destroyed if this last option is selected, and is automatically reconstructed before further calculation of equilibrium constants.

Task 6 calculates the species distributions between pH 2 and 12 for a given chemical model and associated equilibrium constants, for any selected analytical (total) concentrations of the components. Again, Newraph is destroyed and then rewritten for further calculations.

Task 7 automatically plots the spectra of all the absorbing species from the latest calculation. In our HP 9835 version of SPECFIT, **C** and ε are kept on tape for only the latest calculation, for purely economic reasons; this can easily be changed by rewriting three or four lines of program code, or **C** and ε can be recalculated in a single iterative cycle with the final complexation model.

This version of SPECFIT provides for the handling of up to 125 spectra with 9 absorbing species and 16

Table 1. Display of defining model for Cu^{2+}/L-alaninamide

No.	Formula	Value	log K*	Parameters fixed/variable	log[(K + s)/K]*	Colour
1	011	1.510×10^8	8.18	0	0.0000	N
2	110	1.800×10^5	5.26	1	0.0000	Y
3	120	1.900×10^9	9.28	1	0.0000	Y
4	11 − 1	2.000×10^{-2}	−1.70	1	0.0000	Y
5	12 − 1	2.400×10^2	2.38	1	0.0000	Y
6	12 − 2	1.800×10^{-6}	−5.74	1	0.0000	Y

*Taken care of by the program.

equilibrium constants. Since the matrices can be redimensioned, more spectra can be handled with models made up of fewer species, and vice versa. SPECFIT is about 30 kbytes long and needs 2–4 additional kbytes for Newraph, but not all dimensions can be set simultaneously at their maximum values without producing memory overflow. The $M \times S \times N$ tensor DC [equation (2)] is the most problematic in this respect (the other tensor J is needed only column by column in SPECFIT). For 100 spectra, 9 species, 9 unknown equilibrium constants and normal precision (10 bytes per data variable) DC would occupy 81 kbytes of memory, which is not allowed, since no single array may occupy more than 64 kbytes of memory. The situation can be eased by using the SHORT notation (6 bytes per variable) but some restrictions remain. Because of the variability of the program code and the size of many matrices it is impossible to give exact limits. The complexation of Cu^{2+} with L-alaninamide (L), see below (62 spectra, 17 wavelengths, 7 eigenvectors) could be handled in the normal way for the model Cu^{2+}, L, LH^{+}, CuL^{2+}, CuL_2^{2+}, $CuLH_{-1}^{+}$, $CuL_2H_{-1}^{+}$ and CuL_2H_{-2} with 6 (5 unknown) equilibrium constants, but the SHORT notation was necessary with the additional species $CuLH_{-2}$.

Space may also be saved by loading only those parts of the program which are actually needed, or by continuous shuffling of data between memory and the data cartridge. A calculator of the HP 9835 type has its limits, however, and the algorithm developed for SPECFIT[9] can handle bigger problems.

SPECFIT—FORTRAN 77 VERSION

For the reasons just given, SPECFIT has been rewritten in standard FORTRAN 77 and implemented on a UNIVAC 1100/61 computer. Only standard instructions were used, and the program should run with almost any version of FORTRAN IV with a minimum of alterations. Our data are transferred directly from an APPLE II (which is used as an intelligent terminal; *cf.* task 5 in Fig. 1) and tasks 1, 2, 4, 8 and 9 are performed under remote control through a DIGITAL VT 132 terminal. Plotting routines are not implemented, but otherwise the interactive facilities of this program are practically identical with the HP 9835 version. However, the program is not easily transferable to other computers or usable without the necessary on-line facilities. We have therefore developed a third and easily transferable version designed to operate in batch mode. The FORTRAN programs differ from the HP 9835 version in several points. (*i*) The number of components (metal ions and ligands) is not restricted to two. (*ii*) A completely general subroutine is used for calculation of the concentration matrix C and its derivative DC. (*iii*) Known spectra may be included and kept constant as described earlier.[9] (*iv*) Dimensions have been set at 6 components, 10 absorbing species and eigenvectors, 20 equilibrium constants (10 adjustable), 15 fixed spectra, 150 measurements at 50 wavelengths, all changeable by simple modification of the PARAMETER statements, to allow for more involved models or less powerful computer systems. Data input differs from the interactive versions, because all the options must now be defined at the

Listings of both the HP 9835 and the FORTRAN 77 version are available from the authors upon request. The programs may also be provided on an HP 200 data Cartridge, in the form of punched cards, or on tape (FORTRAN version), together with the sample data for the complexation of Cu^{2+} by 3,6,9-triazaundecane. Detailed input instructions will be provided with the FORTRAN 77 version.

RESULTS AND DISCUSSION

SPECFIT has been successfully used both for spectrophotometric[31–35] and for EPR[36,37] titration data. Over 30 equilibrium systems have been studied. Complexation models containing between two[32] and ten[35] absorbing species (1–9 equilibrium constants) were successfully fitted to the experimental data. Additional results have been obtained with the precursor of SPECFIT, ELORMA.[15,38–40] In all cases which permitted direct comparison, the spectrophotometric method was equal to or better than potentiometric titration in discriminatory power between different models,[34,35,40] with comparable reproducibility and estimated standard errors. Spectrophotometric titrations have the additional advantage of providing valuable structural information through the spectra of the individual species, which is not possible by potentiometry.

Some aspects of practical interest will now be discussed, namely the ability of SPECFIT to find the correct parameters, starting from poor estimates; the usefulness of SPECFIT for discrimination between several chemical models of complexation; the application of SPECFIT to rather complicated equilibrium systems.

(*i*) In order to test the ability of the program to find the best set of parameters, starting from poor estimates, a spectrophotometric titration of Cu^{2+} and 3,6,9-triazaundecane (diethyldien, DED) was selected. In this system, which has been studied both potentiometrically and spectrophotometrically, the complexes $CuLH^{3+}$, CuL^{2+} and $CuLH_{-1}^{+}$ [$=CuL(OH)^{+}$] are formed.[34] Under the experimental conditions (*cf.* footnote to Table 2) $CuLH^{3+}$ is never more than 10% of the total, with a maximum at around pH 4, which makes the system reasonably critical. In Table 2 the results of systematically varying the estimates are given. The same parameters and sum of squares of residuals are calculated, even if the estimates are out by a factor of 1000 in either direction. A factor of 1000 is in fact close to a blind guess and substantially better estimates can normally be obtained even without inspection of the actual data. For instance, the deprotonation of CuL^{2+} to

Table 2. Results of varying the estimates of the non-linear parameters for the titration of Cu^{2+} and 3,6,9-triazaundecane (DED)*

Initial estimates†			Number of iterations required with			
β_{110}	β_{111}	β_{11-1}	$f=2$	$f=10$	$f=100$	$f=1000$
$\times f$	$\times f$	$\times f$	9	8	11	33
$\times f$	$/f$	$\times f$	4	16	12	36
$/f$	$\times f$	$/f$	4	18	29	30
$/f$	$/f$	$/f$	4	7	9	10
1.03×10^{15}	$\times f$	1.85×10^{5}‡	3	14	30	11
1.03×10^{15}	$/f$	1.85×10^{5}‡	3	3	3	3

*Experimental conditions: $[Cu^{2+}] = 4mM$, $[DED] = 5mM$, $[H^+] = 10mM$; 31 spectra between pH 2 and 12 were taken at 10-nm intervals between 800 and 550 nm.[34]

†As initial estimates, the least-squares estimates $\beta_{110} = 1.04 \times 10^{15}$, $\beta_{111} = 3.79 \times 10^{18}$, and $\beta_{11-1} = 2.21 \times 10^{5}$, were used and multiplied ($\times$) or divided ($/$) by the factor f. The overall standard deviation of the data is $\sigma_y = 0.0008$.

‡For β_{110} and β_{11-1} the results of the calculation without taking into account $CuLH^{3+}$ (1.03×10^{15} and 1.85×10^{5}, respectively) were used as estimates. The reduced model gave $\sigma_y = 0.004$.

form the hydroxo complex $CuLH_{-1}^{+}$ must occur around pH 9–10, while pK^{H}-values of 6 and 12 are equally absurd for this complex with an N_3O set of donor atoms. As one iteration takes 62.5 sec on the HP 9835, even with the poorest and quite unrealistic estimates the calculation does not take more than about 30 min.

A remarkable fact shown in Table 2 is that the number of iterations is not strongly correlated to the quality of the estimates unless all of them are chosen too small. However, starting from low estimates still seems to be the best approach since the number of iterations is always less than for any other combination.

Of course, more realistically the calculation would first be done with a reduced model, where only β_{110} and β_{11-1} (corresponding to the major and primarily expected species[34]) are refined. $CuLH^{3+}$ would only be introduced at a later stage, when it had become obvious that the simple model was unsatisfactory. The corresponding results are summarized in Table 2 (last two lines) and show that the best strategy is to start from estimates which are likely to be too small (*i.e.*, assuming a low stability of the complex), if an additional species has to be introduced. This consistently requires only three iterations, even if the estimate is out by three orders of magnitude, whereas with too large a starting value for β_{111} the use of good estimates for the other parameters is of no advantage.

(*ii*) The fact that spectrophotometric titrations are superior to potentiometric ones with respect to differentiation between several models of complexation has already been demonstrated for several systems.[34,35,40] Here we want to show that EPR titration data also allow an easy distinction between chemical models and are useful for the calculation of equilibrium constants. As an example we discuss the equilibria between Cu(II) and the ligand 4,7,10-triazatridecane-1,13-diamine (AMINE).[37] The experimental conditions are given in the caption to Fig. 2. The data set consisting of 31 spectra at 50 magnetic field strengths was first subjected to an eigenvector analysis. Representing the data by three eigenvectors resulted in a standard deviation of 1.7%. Including a fourth eigenvector reduced this value to 1.0% of the average measured signal (median of the first derivative of the intensity with respect to the magnetic field strength) as is to be expected for a representation of the data within the limits of the experimental error.[36] Therefore, it can be concluded that four paramagnetic species occur in the chemical system, in accordance with the results of a combined potentiometric and spectrophotometric study[34] which revealed the paramagnetic species Cu^{2+}, $CuLH_2^{4+}$, $CuLH^{3+}$ and CuL^{2+}. Nevertheless, we first tried to omit $CuLH_4^{2+}$ (a complex which is never more than 30% of the total, with a maximum at around pH 3.5 under the experimental conditions). The standard deviation thus obtained was 6.0% and the parameters $\log\beta_{110}$ and $\log\beta_{111}$ were calculated to be 20.91 (± 0.07) and 30.55 (± 0.02), respectively. Including the species $CuLH_2^{4+}$ reduced the overall standard deviation by a factor of five to 1.1% and gave $\log\beta$-values of 21.63, 30.58 and 33.78. The standard error in the calculated parameters was decreased to 0.01 in each case. The satisfactory description of the data by the complete model is nicely demonstrated by the respective plots of the residuals, Fig. 2. With the complete model a rather smooth error surface is obtained (Fig. 2a), but this is not at all the case if the complex $CuLH_2^{4+}$ is omitted (Fig. 2b), the errors then being much larger and also by no means randomly distributed, but obviously giving a spectrum-like distribution, corresponding to the missing species. This illustrates how clearly we can distinguish between different chemical models, even in cases where not all the complexes are formed to a major extent.

It is also satisfying to note the easy adaptation of the method to use of data other than spectrophotometric, especially EPR, which so far has hardly been used for the numerical analysis of complexation equilibria involving several species.[36,41]

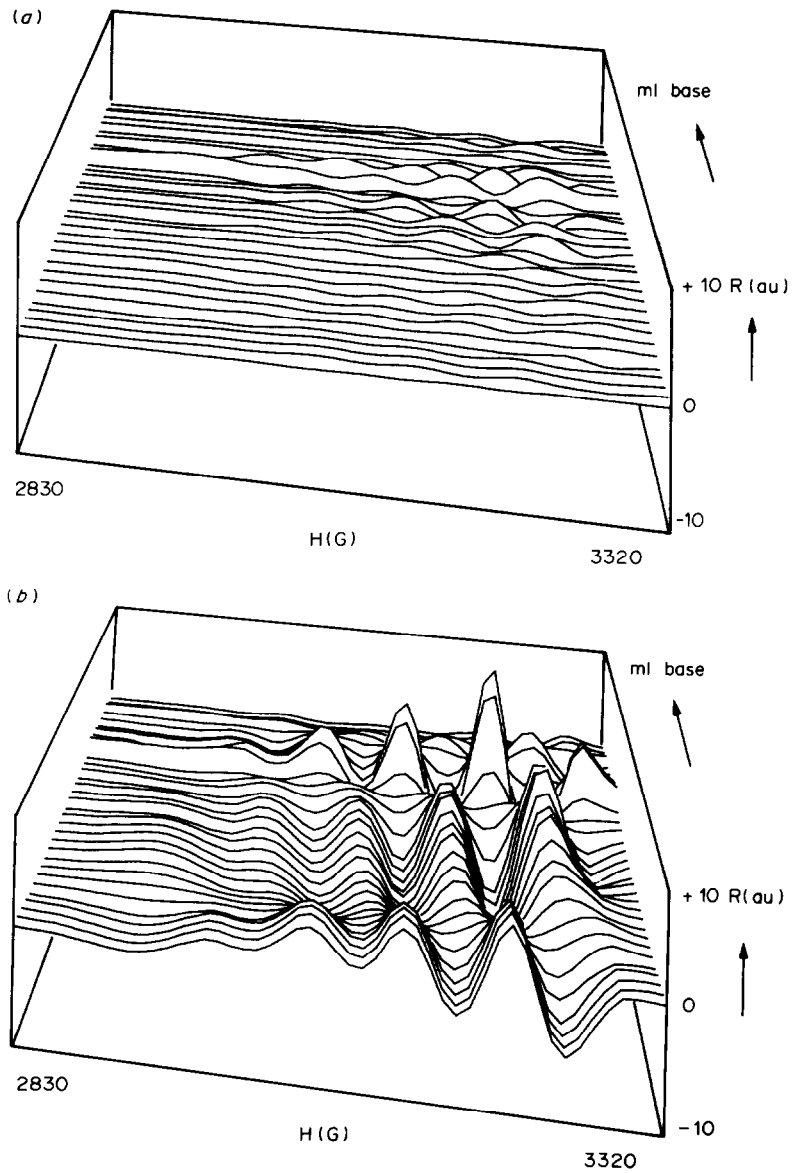

Fig. 2. Three-dimensional plot of the residuals from EPR titration of the Cu^{2+}/AMINE system. A mixture of Cu^{2+} (19.4m*M*), AMINE (20.0m*M*), and HCl (20.0m*M*) was titrated with NaOH (0.5*M*) at 25°, $I = 0.5M$; (*a*) complete model, including Cu^{2+}, $CuLH_2^{4+}$, $CuLH^{3+}$ and CuL^{2+}; overall standard error 1.1% (=0.4 arbitrary units) (*b*) same without $CuLH_2^{4+}$; overall standard error 6% (=2.0 arbitrary units).

(*iii*) Spectrophotometric data have been successfully used to deal with rather complicated systems described by six,[40] seven,[40] or even ten[35] absorbing species. We may cite the performance of SPECFIT in elucidating the equilibria between Cu^{2+} and L-alaninamide. A previous potentiometric study had shown the existence of Cu^{2+}, CuL^{2+}, $CuLH_{-1}^{+}$, CuL_2^{2+}, $CuL_2H_{-1}^{+}$ and CuL_2H_{-2}, *i.e.*, six cupric species.[31] Because the 1:1 and 1:2 complexes coexist the stability constants cannot be determined from a single experiment, and two titrations with metal:ligand ratios of 0.46 and 0.25 were combined for the calculation.

The data set consisted of 62 spectra recorded at 17 wavelengths, between 460 and 780 nm, *i.e.*, 1054 absorbance data. Representing the measured spectra as a linear combination of 7 eigenvectors reduced the number of data to be handled in the least-squares calculation to $7 \times 62 = 434$. Even if the data had been collected at many more wavelengths, the eigenvector representation would have reduced the data set to this same number.

With the model suggested by potentiometry, an overall standard deviation of 0.0009 for the absorbance was calculated. Although this value indicates a satisfactory fit of the data (corresponding to 0.35% of the maximum measured absorbance, or to 0.9% of the average of the data), the calculated logarithmic

Table 3. Stability constants for the Cu^{2+}/L-alaninamide system with standard errors

Stoichiometry MLH	$\log \beta^*_{mlh}$	$\log \beta^\dagger_{mlh}$	$\log \beta^\ddagger_{mlh}$
110	5.06 (0.009)	5.07 (0.004)	5.08 ($\leq$0.02)
120	8.85 (0.020)	8.93 (0.009)	8.99 ($\leq$0.02)
11 − 1	−2.13 (0.023)	−2.14 (0.010)	−2.14 (0.04)
12 − 1	1.84 (0.025)	1.95 (0.011)	2.01 ($\leq$0.02)
12 − 2	−6.31 (0.027)	−6.19 (0.012)	−6.14 ($\leq$0.02)
11 − 2		−10.87 (0.046)	

*From spectrophotometry, without $CuLH_{-2}$, $\sigma_y = 0.0009$.
†From spectrophotometry, complete model, $\sigma_y = 0.0003$.
‡From potentiometry.[31]

stability constants of the 1:2 complexes were on average smaller than the corresponding potentiometric values by 0.16, as shown in Table 3. Inclusion of the species $CuLH_{-2}$, a species which is to be expected from chemical reasoning (but could not be found potentiometrically), significantly improves the fit of the data. As shown in Table 3, the overall standard deviation of the absorbance is reduced to 0.0003 and the discrepancy between the logarithmic stability constants obtained by the two methods becomes 0.06. Surprisingly, although $CuLH_{-2}$ significantly improves the fit to the data, it forms no more than 2% of the total, as can be seen from the distribution curves in Fig. 3.

The standard error of the logarithmic stability constants (*cf.* Table 3) is 0.01; only for $\log \beta_{11-2}$ is a larger value (0.05) obtained. In contrast, potentiometry[34] did not suggest a species $CuLH_{-2}$ and even the error for β_{11-1} was relatively large. That spectrophotometry leads to a more complete description of this complicated system is indicated not only by statistical criteria. The calculated stability of $CuLH_{-2}$ corresponds to the formation of this species at pH 8.73, which is as expected for a Cu^{2+} complex containing the N_2O_2 donor set, with one amino and one deprotonated amide group.[42] The spectra of the individual species (Fig. 4) are typical for Cu(II), and their characteristics are readily understood in terms of the expected structures.[34] Even the spectrum of $CuLH_{-2}$ is reasonably well defined. Because of the small concentration of this species, it is not a perfectly smooth curve, however.

Thus, equilibrium constants calculated from potentiometric or from spectrophotometric data compare very well in the system Cu(II)–L-alaninamide. Again, spectrophotometry has proved superior in its discriminatory power between different chemical models of complexation. It should be noted that determination of $CuLH_{-2}$ with a maximum formation of 2% is close to the limits of the spectrophotometric method in our laboratory. In fact, overall standard deviations of 0.0003 for the absorbance cannot be obtained consistently for the combination of two or more titrations. As working criteria, errors of 0.0006–0.0009 in the absorbances and a minimum of 5% complex formation would be more realistic. This has, however, nothing to do with the performance of SPECFIT, but is simply a question of the quality of the experimental data.

In conclusion, we state that with use of SPECFIT the evaluation of spectroscopic titrations is completely straightforward. Both versions are easily handled because the programs can be used as black boxes and only estimates for the stability constants are

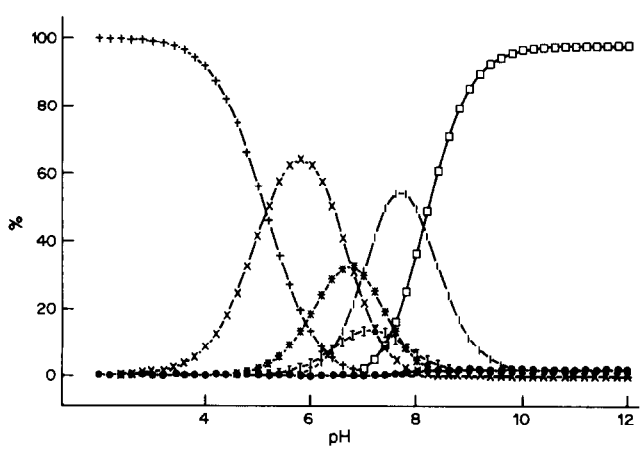

Fig. 3. Species distribution as a function of pH for the Cu^{2+}/L-alaninamide system. + Cu^{2+}_{aq}, × CuL^{2+}, ★ CuL_2^{2+}, I $CuLH^{+}_{-1}$, I $CuL_2H^{+}_{-1}$, □ CuL_2H_{-2}, ● $CuLH_{-2}$. The results are given as the percentage of the total metal present and are calculated for $[Cu^{2+}] = 5.5mM$ and $[L] = 12mM$) with the stability constants obtained spectrophotometrically (*cf.* Table 3).

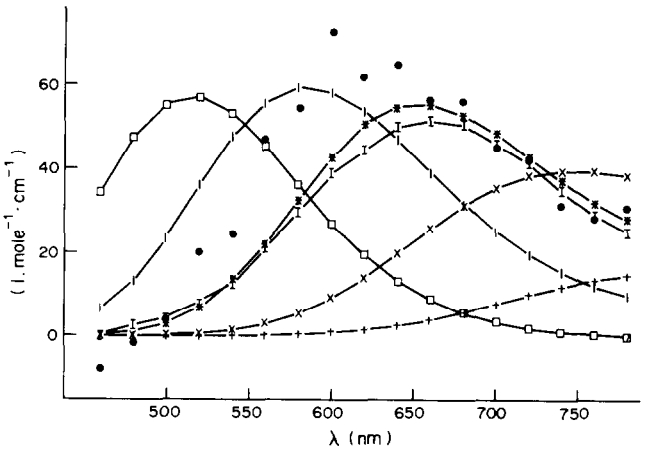

Fig. 4. Absorption spectra in the Cu^{2+}/L-alaninamide system (symbols as in Fig. 3).

required. Owing to the eigenvector representation, both computer memory and time requirements are minimized, and rather complicated systems can be treated even by a chemist who has no access to a mainframe computer.

Acknowledgements—We thank Dr. H. Christen (University Computer Centre, Basel) for useful discussions concerning transferability of FORTRAN code. Support by the Swiss National Science Foundation (Grant No. 2. 213-081) is gratefully acknowledged.

REFERENCES

1. W. A. E. McBryde, *Talanta*, 1974, **21**, 979.
2. F. Gaizer, *Coord. Chem. Rev.*, 1979, **27**, 195.
3. D. J. Leggett, *Am. Lab.*, 1982, **14**, No. 1, 29.
4. H. A. Benesi and J. H. Hildebrand, *J. Am. Chem. Soc.*, 1949, **71**, 2703; R. W. Ramette, *J. Chem. Educ.*, 1967, **44**, 647.
5. D. J. Leggett, S. L. Kelly, L. R. Shiue, Y. T. Wu, D. Chang and K. M. Kadish, *Talanta*, 1983, **30**, 579.
6. G. Hänisch, Th. A. Kaden and A. D. Zuberbühler, *ibid.*, 1979, **26**, 563.
7. R. M. Alcock, F. R. Hartley and D. E. Rogers, *J. Chem. Soc. Dalton Trans.*, **1978**, 115.
8. P. Gans, *Coord. Chem. Rev.*, 1976, **19**, 99.
9. H. Gampp, M. Maeder, C. J. Meyer and A. D. Zuberbühler, *Talanta*, 1985, **32**, 95.
10. D. W. Marquardt, *J. Soc. Ind. Appl. Math.*, 1963, **11**, 431.
11. P. R. Bevington, *Data Reduction and Error Analysis for the Physical Sciences*, McGraw-Hill, New York, 1969.
12. W. H. Lawton and E. A. Sylvestre, *Technometrics*, 1971, **13**, 461.
13. D. J. Leggett and W. A. E. McBryde, *Anal. Chem.*, 1975, **47**, 1065.
14. L. G. Sillén, *Acta Chem. Scand.*, 1964, **18**, 1085.
15. H. Gampp, M. Maeder and A. D. Zuberbühler, *Talanta*, 1980, **27**, 1037.
16. A. A. Bugaevsky and B. A. Dunai, *Zh. Analit. Khim.*, 1971, **26**, 205; A. A. Bugaevsky, L. E. Rudnaya and T. P. Mukhina, *ibid.*, 1972, **27**, 1675.
17. A. Sabatini, A. Vacca and P. Gans, *Talanta*, 1974, **21**, 53.
18. I. Nagypál, I. Páka and L. Zékány, *ibid.*, 1978, **25**, 549.
19. A. D. Zuberbühler and Th. A. Kaden, *ibid.*, 1982, **29**, 201.
20. G. H. Golub and V. Pereyra, *SIAM J. Numer. Anal.*, 1973, **10**, 413.
21. Z. Z. Hugus and A. A. El-Awady, *J. Phys. Chem.*, 1971, **75**, 2954.
22. R. N. Cochran and F. H. Horne, *Anal. Chem.*, 1977, **49**, 846.
23. E. R. Malinovsky, *ibid.*, 1977, **49**, 606.
24. S. Wold, *Technometrics*, 1978, **20**, 397.
25. J. J. Kankare, *Anal. Chem.*, 1970, **42**, 1322.
26. M. Maeder and H. Gampp, *Anal. Chim. Acta*, 1980, **122**, 303.
27. A. D. Zuberbühler and Th. A. Kaden, *Talanta*, 1979, **26**, 1111.
28. H. Gampp, M. Maeder, A. D. Zuberbühler and Th. A. Kaden, *ibid.*, 1980, **27**, 513.
29. H. R. Schwarz, H. Rutishauser and E. Stiefel, *Matrizen-Numerik*, Teubner, Stuttgart, 1972.
30. U. Hoffmann and H. Hofmann, *Einführung in die Optimierung*, Verlag Chemie, Weinheim, 1971.
31. H. Gampp, H. Sigel and A. D. Zuberbühler, *Inorg. Chem.*, 1982, **21**, 1190.
32. A. K. Basak and Th. A. Kaden, *Helv. Chim. Acta*, 1983, **66**, 2086.
33. K. P. Balakrishnan, Th. A. Kaden, L. Siegfried and A. D. Zuberbühler, *ibid.*, 1984, **67**, 1060.
34. H. Gampp, D. Haspra, M. Maeder and A. D. Zuberbühler, *Inorg. Chem.*, 1984, **23**, 3724.
35. D. Küry, P. Sandmeier and A. D. Zuberbühler, to be published.
36. H. Gampp, *Inorg. Chem.*, 1984, **23**, 1553.
37. *Idem*, submitted to *Helv. Chim. Acta.*
38. W. Schibler and Th. A. Kaden, *J. Chem. Soc. Chem. Commun.*, 1981, 603.
39. M. Micheloni, P. Paoletti, S. Bürki and Th. A. Kaden, *Helv. Chim. Acta*, 1982, **65**, 587.
40. M. Briellmann and A. D. Zuberbühler, *Helv. Chim. Acta*, 1982, **65**, 46.
41. W. S. Kittl and B. M. Rode, *J. Chem. Soc. Dalton*
42. Th. A. Kaden and A. D. Zuberbühler, *Helv. Chim. Acta*, 1968, **51**, 1797.

Talanta, Vol. 32, No. 4, pp. 265–272, 1985
Printed in Great Britain

0039-9140/85 $3.00 + 0.00
Pergamon Press Ltd

GRAPHICAL EVALUATION OF COMPLEXOMETRIC TITRATION CURVES

JOSE L. GUINON
Departamento de Química, E.T.S.I. Industriales, Universidad Politécnica de Valencia, Spain

(*Received* 4 *October* 1983. *Revised* 15 *May* 1984. *Accepted* 5 *December* 1984)

Summary—A graphical method, based on logarithmic concentration diagrams, for construction, without any calculations, of complexometric titration curves is examined. The titration curves obtained for different kinds of unidentate, bidentate and quadridentate ligands clearly show why only chelating ligands are usually used in titrimetric analysis. The method has also been applied to two practical cases where unidentate ligands are used: (*a*) the complexometric determination of mercury(II) with halides and (*b*) the determination of cyanide with silver, which involves both a complexation and a precipitation system; for this purpose construction of the diagrams for the $HgCl_2/HgCl^+/Hg^{2+}$ and $Ag(CN)_2^-/AgCN/CN^-$ systems is considered in detail.

In the teaching of titrimetric analysis, titration curves are effective illustrations of the sharp jump in certain parameters (pH, pM, pL, *etc.*) in the vicinity of the equivalence point, which allows detection of the end-point by means of chemical indicators or instrumental methods (*e.g.* potentiometry).

For complexometric titrations, however, the usual textbooks give calculations of points on the theoretical titration curve only for the chelating ligands which form ML complexes, whereas for unidentate and bidentate ligands forming compounds of type ML, only the graphs of the corresponding titration curves are shown, without details of the calculation. The reader may therefore miss the reason why the curves for titration with unidentate or bidentate ligands do not generally show sharp jumps in pM or pL in the region of the points corresponding to the individual complexes which are formed stepwise.

The logarithmic concentration diagrams developed and popularized by Scandinavian chemists have been used for solving graphically several problems related to equilibria in solution and/or titrimetric analysis, *e.g.*, in the determination of the sharpness index at the equivalence point of acid–base titrations,[1] evaluation of the solubility of hydrolysable salts,[2] estimation of titration errors in acid–base titration,[3] and the theoretical feasibility of complexometric back-titrations.[4] The graphical method has several times been applied to construction of complexometric titration curves,[5–8] but has either been used only for chelating ligands,[5,6] or has failed to prove of general application.[7,8]

The present paper reports the use of logarithmic concentration diagrams for obtaining complexometric titration curves for several types of ligand, and its application to some particular cases, such as the determination of mercury(II) with halides and the titration of cyanide with a standard solution of a silver salt.

TITRATION CURVES OF METAL IONS WITH LIGANDS

Let us consider a metal ion M with a co-ordination number of 4, and unidentate, bidentate and quadridentate ligands (L), which form different complexes with it, all of them having the same value of the overall formation constant, $\beta_1 = \beta_2 = \beta_4 = 10^{20}$. We will use the values employed in Skoog and West's textbook.[9] Charges are omitted, for both clarity and generality.

Quadridentate ligand

$$M + L \rightleftharpoons ML \qquad K_1 = [ML]/[M][L] = 10^{20} \qquad (1)$$

Bidentate ligand

$$M + L \rightleftharpoons ML \qquad K_1 = [ML/[M][L] = 10^{12} \qquad (2)$$

$$ML + L \rightleftharpoons ML_2 \qquad K_2 = [ML_2]/[ML][L] = 10^{8} \qquad (3)$$

Unidentate ligand

$$M + L \rightleftharpoons ML \qquad K_1 = [ML]/[M][L] = 10^{8} \qquad (4)$$

$$ML + L \rightleftharpoons ML_2 \qquad K_2 = [ML_2]/[ML][L] = 10^{6} \qquad (5)$$

$$ML_2 + L \rightleftharpoons ML_3 \qquad K_3 = [ML_3]/[ML_2][L] = 10^{4} \qquad (6)$$

$$ML_3 + L \rightleftharpoons ML_4 \qquad K_4 = [ML_4]/[ML_3][L] = 10^{2} \qquad (7)$$

To conform with practical use, these equilibrium constants, K_i, should be considered to be conditional stability constants, K_i'.

Example 1. *Quadridentate ligand*

The concentrations of the various species can be expressed for different concentrations of L by the following equations, obtained by combining the mass balance, $c_M = [M] + [ML]$, with equation (1):

$$\log [M] = \log c_M - \log (1 + K_1[L]) \qquad (8)$$

$$\log [ML] = \log c_M + \log K_1 - pL - \log (1 + K_1[L]) \qquad (9)$$

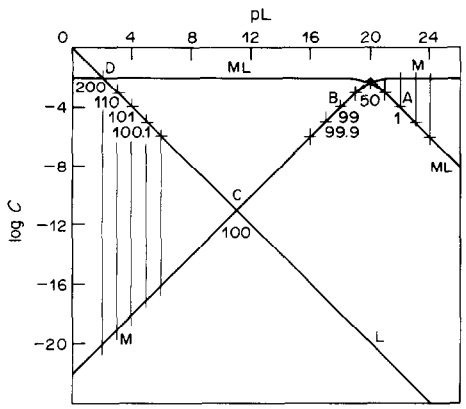

Fig. 1. Logarithmic concentration diagram of system ML/M, $c_M = 10^{-2}M$, $\log K_1 = 20$.

The master variable is the free ligand concentration [L], expressed as $pL = -\log [L]$. On the basis of these equations, graphs of $\log [M]$ and $\log [ML]$ *vs.* pL can be drawn by the usual procedure.[10-13] The logarithmic concentration diagram of system ML/M for $c_M = 10^{-2}M$ and $\log K_1 = 20$ is shown in Fig. 1.

The titration curve of pM *vs.* X, where $X = 100\, c_L/c_M$ is the degree of titration expressed as a percentage, is easily obtained from the logarithmic diagram in the way discussed by various authors.[5-8] In Fig. 1, several values of X (point A, $X = 1\%$, pM = 2; point S, $X = 50\%$, pM = 2.3; point B, $X = 99\%$, pM = 4; .... point C, $X = 100\%$, pM = 11; ... point D, $X = 200\%$, pM = 20) are shown on lines ML, M and L of the diagram, and from them the titration curve of pM *vs.* X is plotted, as shown in Fig. 2.

Example 2. Bidentate ligand

The concentration of the various species can be expressed in a similar way as for the case of the quadridentate ligand, for different concentrations of L, by the following equations, which are obtained by combining the mass balance, $c_M = [M] + [ML] + [ML_2]$, with equations (2) and (3).

$$\log [M] = \log c_M - \log (1 + K_1[L] + K_1K_2[L]^2) \quad (10)$$

$$\log [ML] = \log c_M + \log K_1[L] - \log (1 + K_1[L] + K_1K_2[L]^2) \quad (11)$$

$$\log [ML_2] = \log c_M + \log K_1K_2[L]^2 - \log (1 + K_1[L] + K_1K_2[L]_2) \quad (12)$$

Equations (10)–(12) yield a family of curves, the shapes of which depend on the ratio of the two formation constants. The logarithmic concentration diagram of system $ML_2/ML/M$ for $c_M = 10^{-2}M$ and $\log K_1 = 12$, $\log K_2 = 8$, is shown in Fig. 3.

The graphical method outlined above may be extended to obtain the titration curve of pM *vs.* X. The first part of the titration, corresponding to the formation of the complex ML, will be similar to that for the quadridentate ligand ($X = 1\%$, pM = 2; $X = 10\%$, pM = 2; $X = 50\%$, pM = 2.3; $X = 90\%$, pM = 3) (see Fig. 3). The crossing point A corresponds to the equality $[M] = [ML_2]$, so the equilibrium $2ML \rightleftharpoons M + ML_2$ gives

$$[ML] = c_M - [M] - [ML_2] = c_M - 2[ML_2],$$

and

$$[ML] = c_L - 2[ML_2] - [L] \sim c_L - 2[ML_2].$$

Thus, $c_M = c_L$ and therefore $X = 100\%$, so at the first equivalence point, $pM_{x=100} = 4$.

The formation of the complex ML_2 occurs mainly after the first equivalence point, according to the reaction $ML + L \rightleftharpoons ML_2$, and the corresponding values of X and pM are obtained in an analogous way ($X = 110\%$, pM = 5; $X = 150\%$, pM = 6.3; $X = 190\%$, pM = 8; $X = 199\%$, pM = 10) (see Fig. 3). The crossing point B corresponds to the equality $[ML] = [L] = 10^{-5}M$, and $[M] = 10^{-12}$, so

$$[ML_2] = c_M - [ML] - [M] \sim c_M,$$

and

$$c_L = [L] + [ML] + 2[ML_2] \sim 2[ML_2] \sim 2c_M,$$

so $X = 200\%$, and at the second equivalence point $pM_{X=200\%} = 12$.

After the second equivalence point, there is excess of free ligand and therefore the values of X and pM ($X = 20\%$, pM = 14; $X = 210\%$, pM = 16; $X = 300\%$, pM = 18) (see Fig. 3), are obtained analogously to those for the quadridentate ligand.

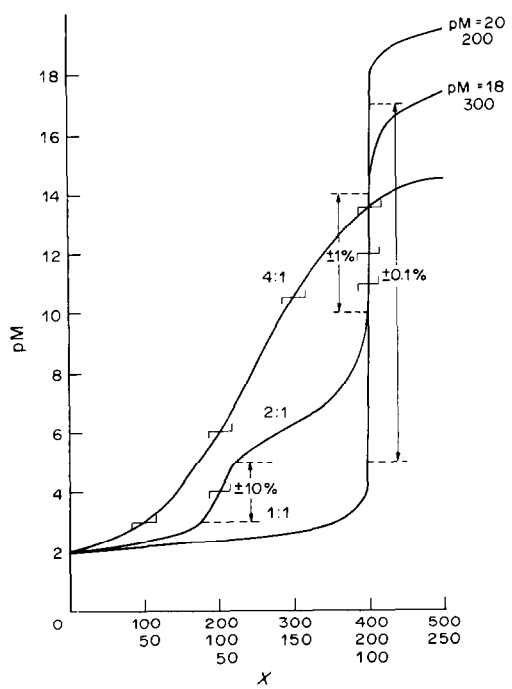

Fig. 2. Titration curves, pM *vs.* $X\%$, of $10^{-2}M$ metal ion M with monodentate (4:1), bidentate (2:1), tetradentate (1:1) ligands.

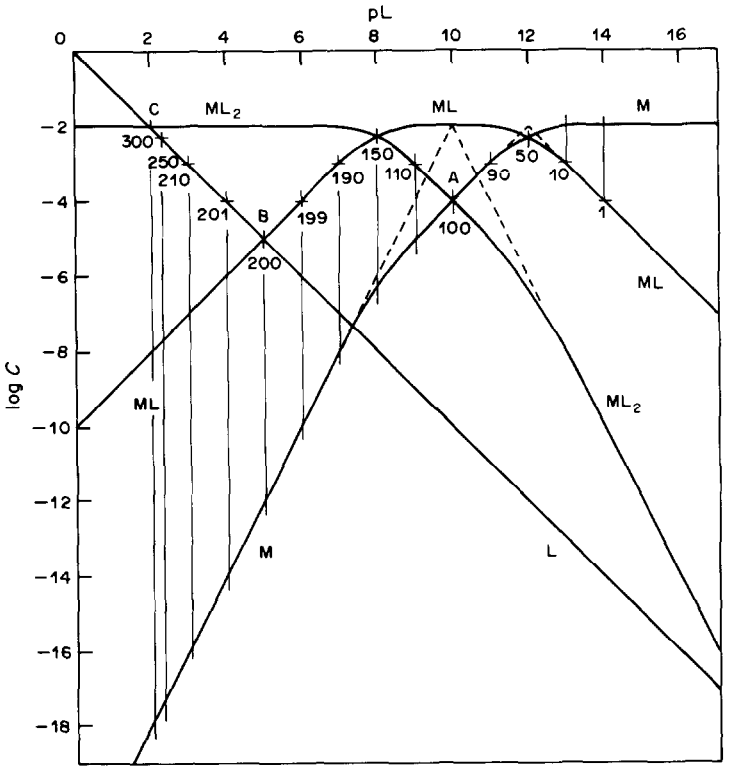

Fig. 3. Logarithmic concentration diagram of system $ML_2/ML/M$, $c_M = 10^{-2}M$, $\log K_1 = 12$, $\log K_2 = 8$.

With the set of values of X and pM shown in Fig. 3, the titration curve is easily plotted, as shown in Fig. 2.

Example 3. *Unidentate ligand*

The concentrations of the various ions can be expressed for different concentrations of L by the following equations, which are obtained by combining the mass balance

$$c_M = [M] + [ML] + [ML_2] + [ML_3] + [ML_4],$$

with equations (4)–(7).

$$\log [M] = \log c_M - \log A \quad (13)$$

$$\log [ML] = \log c_M + \log K_1[L] - \log A \quad (14)$$

$$\log [ML_2] = \log c_M + \log K_1K_2[L]^2 - \log A \quad (15)$$

$$\log [ML_3] = \log c_M + \log K_1K_2K_3[L]^3 - \log A \quad (16)$$

$$\log [ML_4] = \log c_M + \log K_1K_2K_3K_4[L]^4 - \log A \quad (17)$$

where

$$A = (1 + K_1[L] + K_1K_2[L]^2 + K_1K_2K_3[L]^3 + K_1K_2K_3K_4[L]^4)$$

Equations (13)–(17) yield a family of curves, the shapes of which depend on the ratios of the successive formation constants. The logarithmic concentration diagram for the system $ML_4/ML_3/ML_2/ML/M$ for $c_M = 10^{-2}M$ and $\log K_1 = 8$, $\log K_2 = 6$, $\log K_3 = 4$, $\log K_4 = 2$, is shown in Fig. 4. In this case, because of the closeness of the values of K_i and $K_{(i+1)}$, equations (13)–(17) cannot be simplified and hence

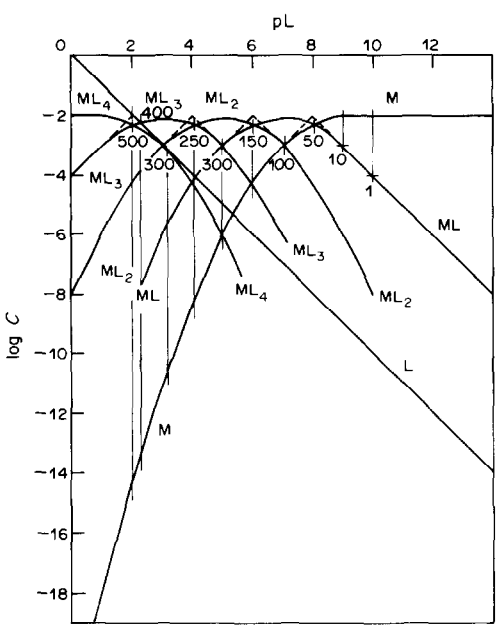

Fig. 4. Logarithmic concentration diagram of system $ML_4/ML_3/ML_2/ML/M$, $c_M = 10^{-2}M$, $\log K_1 = 8$, $\log K_2 = 6$, $\log K_3 = 4$, $\log K_4 = 2$.

log c_i would be given by curves for the whole range of values of pL. For convenience of plotting, and since we are mainly interested in knowing the variation of $-\log [M] = pM$ during the course of the titration, only the variation of log [M] with pL is plotted in Fig. 4.

The same procedure as for quadridentate and bidentate ligands can be used to obtain the titration curve of pM *vs.* X (for X up to 250%) from Fig. 4. Thus we have $X = 0\%$, pM = 2; $X = 50\%$, pM = 2.3; $X = 100\%$, pM = 3; $X = 150\%$, pM = 4.3; $X = 200\%$, pM = 6; $X = 250\%$, pM = 8.3. For values of $X = 300$, 400, 500%, however, the values of pM are obtained in a different way, since the concentration of L is of the same order as the concentrations of ML_3 or ML_4, as can be observed in Fig. 4. Thus, for $X = 300\%$, we have $c_L = 3c_M = 3 \times 10^{-2} M$, and substituting these values in the mass balance gives

$$c_L = [L] + [ML] + 2[ML_2] + 3[ML_3] + 4[ML_4] \quad (18)$$

$$c_M = [M] + [ML] + [ML_2] + [ML_3] + [ML_4] \quad (19)$$

From (18) and (19) we obtain

$$[L] + [ML_4] = 3[M] + 2[ML] + [ML_2] \sim [ML_2] \quad (20)$$

In this equation [M] and [ML] are neglected, owing to the predominance of $[ML_2]$ in the range $\log K_4 < pL < \log K_3$, as can be observed in Fig. 4. Let us suppose that for $X = 300\%$, the graphical procedure were followed as for $X = 100$ or 200%; then we would reach the condition $[ML_4] = [ML_2]$, and the value $pM_{x=300} = 11$ read from the diagram would be incorrect. The graphical solution of equation (20) can be achieved by putting $[L] \sim [ML_4]$, and thus obtaining the condition $\log [L] + 0.30 = \log [ML_2]$, which allows us to obtain graphically the value $pM_{x=300} = 10.5$

At the fourth equivalence point, $X = 400\%$, we have $c_L = 4c_M = 4 \times 10^{-2} M$, and substitution of these values in the mass balances gives, after some rearrangements,

$$[L] = 4[M] + 3[ML] + 2[ML_2] + [ML_3] \sim [ML_3] \quad (21)$$

Here [M], [ML] and $[ML_2]$ are neglected because of the predominance of ML_3 in the range $pL \sim \log K_4$, as can be observed in the diagram. The condition $[L] \sim [ML_3]$ yields graphically the value $pM_{X=400} = 13.5$.

For $X = 500\%$, we have $c_L = 5c_M = 5 \times 10^{-2} M$, and with a first approximation of $[L] \sim 10^{-2} M$, the diagram yields the value $pM_{X=500} = 14.6$.

If instead of using the graphical method just described, we consider the exact solution of the system of equations which results from combining the mass balances

$$c_L = [L] + [ML] + 2[ML_2] + 3[ML_3] + 4[ML_4],$$

and

$$c_M = 10^{-2} M = [M] + [ML_2] + [ML_3] + [ML_4],$$

with equations (4)–(7) we obtain the fifth degree polynomial equations

$$10^{20}[L]^5 + (5 - a)10^{18}L^4 + (3 - a - 10^{-2})10^{16}[L]^3 + (2 - a - 10^{-4})10^{12}[L]^2 + (1 - a - 10^{-6})10^6[L] - 10^{-2}a = 0 \quad (22)$$

where $a = c_L/c_M = 0, 1, 2, \ldots 5$.

This equation can be evaluated with a computer or a programmable calculator, *e.g.*, a Hewlett-Packard HP97. Once the value of [L] has been obtained we can evaluate [M] by using the equation:

$$[M] = c_M/(1 + 10^8[L] + 10^{14}[L]^2 + 10^{18}[L]^3 + 10^{20}[L]^4) \quad (23)$$

In this way, we obtain the table

a	$pM_{computed}$	$pM_{graphical}$
1	3.08	3
2	6.08	6
3	10.65	10.5
4	13.62	13.5
5	14.82	14.6

The agreement between the graphically evaluated pM values and those obtained by computer calculations is good.

DISCUSSION

The analysis shown in these examples gives us the fundamentals for a systematic and rapid approach for obtaining titration curves from the logarithmic concentration diagrams. The values of X are marked on the corresponding log c_i lines, and from them we can obtain directly the values of pM or pL. Note that the values of $X = 10, 90, 190, 210\%$ *etc.*, can be found on the respective log c_i lines, at $\log c_i = \log c_M - 1.0$. Analogously, the values of $X = 1, 99, 199, 210\%$, *etc.*, can be found on the log c_i lines, $\log c_i = \log c_M - 2.0$, and so on. The values of $X = 50, 150, 250\%$ *etc.*, are at the crossing points of log [M] and log [ML], log [ML] and log $[ML_2]$, log $[ML_2]$ and log $[ML_3]$, *etc.*, for values of $pL = \log K_1$, $\log K_2$, $\log K_3$, *etc.* Finally, the values of $X = 100, 200, 300\%$ *etc.*, can be found, in general, for the maximum concentration of species ML, ML_2, ML_3, *etc.*, respectively, and are easily obtained according to the stoichiometry at the successive equivalence points.

This graphical treatment does not take dilution into account, however. The effect of dilution on the pM and pL values at the end-point of the titration depends on the equilibrium constants and the stoichiometry of the complex ion. If we use equimolar metal and ligand solutions, we will have two-, three- and five-fold dilution by the end of the titration, for

quadridentate, bidentate and unidentate ligands respectively, which will correspondingly shift log c_M by $-\log 2$, $-\log 3$ and $-\log 5$. The new pM and pL values so obtained will be: pM = 11.15, 12 and 12.4, pL = 11.15, 5.25 and 2.8 respectively (compared with pM = 11, 12 and 13.5, pL = 11, 5 and 2.2 if the dilution is ignored). The dilution effect on the pM and pL value is only significant for a unidentate ligand.

The titration curves of pM *vs.* X for the different kinds of ligand are plotted in Fig. 2. Note that in the case of unidentate ligands, there is no sharp jump at any of the four equivalence points and therefore they cannot be commonly used in complexometric determination of metal ions. For the bidentate ligand two jumps are observed, the first of them moderate, but the second sharp enough to allow a potentiometric determination of metal ion. Finally, with the quadridentate ligand there is a big jump in pM in the vicinity of the equivalence point, which allows an accurate determination and explains why the chelating ligands which form stable 1:1 chelates with metal ions are the most often used in complexometric titration.

THE USE OF UNIDENTATE LIGANDS IN COMPLEXOMETRIC TITRATIONS

Metal ions form several complexes with most of the unidentate ligands, and even when exactly stoichiometric amounts of metal ion and ligand have been mixed, there is not a rapid enough change in the concentration of any of the species to indicate an end-point. Only when one species of a family of successive complexes is very much more stable than any of the others, is a successful titrimetric determination possible. Examples are the titration of mercury(II) with halides (and *vice versa*) and the titration of cyanide with a standard solution of silver or nickel (and *vice versa*), with either potentiometric or visual detection of the end-point. The calculation of the titration curves is not generally included in textbooks, so let us consider the application of logarithmic concentration diagrams for the purpose.

Example 1. *Titration of Hg(II) with* X^- (Cl^-, Br^-, I^-, CN^-, SCN^-)

Plotting the titration curve. To illustrate the approach, the curve for titration with chloride will be considered. In this case, the equilibrium constants are:

$$Hg^{2+} + Cl^- \rightleftharpoons HgCl^+$$

$$K_1 = [HgCl^+]/[Hg^{2+}][Cl^-] = 10^{6.74} \quad (24)$$

$$HgCl^+ + Cl^- \rightleftharpoons HgCl_2$$

$$K_2 = [HgCl_2]/[HgCl^+][Cl^-] = 10^{6.48} \quad (25)$$

$$HgCl_2 + Cl^- \rightleftharpoons HgCl_3^-$$

$$K_3 = [HgCl_3^-]/[HgCl_2][Cl^-] = 10^{0.85} \quad (26)$$

$$HgCl_3^- + Cl^- \rightleftharpoons HgCl_4^{2-}$$

$$K_4 = [HgCl_4^{2-}]/[HgCl_3^-][Cl^-] = 10^{1.00} \quad (27)$$

By substitution of these values of K_i into equations (13)–(17), the corresponding family of curves of log c_i *vs.* pCl can be obtained. Nevertheless, given the values of log $K_3 = 0.85$ and log $K_4 = 1.00$, it is clear that at low chloride concentrations meaningful amounts of the complexes $HgCl_3^-$ and $HgCl_4^{2-}$ will not be formed, so these will not be taken into account in the following discussion. Hence, by combining the mass balance $c_{Hg} \sim [Hg^{2+}] + [HgCl^+] + [HgCl_2]$ and equations (24) and (25), we obtain:

$$\log [Hg^{2+}] = \log c_{Hg} - \log A \quad (28)$$

$$\log [HgCl^+] = \log c_{Hg} + \log K_1[Cl^-] - \log A \quad (29)$$

$$\log [HgCl_2] = \log c_{Hg} + \log K_1K_2[Cl^-]^2 - \log A \quad (30)$$

where $A = 1 + K_1[Cl^-] + K_1K_2[Cl^-]^2$. Equations (28)–(30) are valid only when pCl is $> \log K_3$.

The construction of the logarithmic concentration diagram for the system $HgCl_2/HgCl^+/Hg^{2+}$ needs an additional explanation, because although equations (28)–(30) have the same mathematical form as equations (10)–(12) respectively, they cannot be simplified to give straight lines for the range pCl $\sim \log k_1 \sim \log K_2$, and so the curves must be plotted point by point. However, we can obtain approximate plots of these curves, if we take into account that two singular points exist; one point, S_1, corresponds to the maximum concentration of the complex ion $HgCl^+$. By expressing the mass-balance equation,

$$c_{Hg} = 10^{-2}M = [Hg^{2+}] + [HgCl^+] + [HgCl_2]$$

as a function of $[HgCl^+]$, and equating its first derivative to zero, we obtain $[HgCl^+]_{max}$ at pCl $= \frac{1}{2}$ log $K_1K_2 = 6.61$. The other singular point, S_2, corresponds to the equality $[HgCl_2] = [Hg^{2+}]$ and by introducing this value into the evaluation of $\beta_2 = K_1K_2 = 10^{13.22}$, we obtain pCl = 13.22/2 = 6.61. Considering now the expressions for the mass balance and the value of K_1, and operating with $[Cl^-] = 10^{-6.61}M$ and $[HgCl_2] = [Hg^{2+}]$, we obtain $[HgCl^+] = 10^{-2.40}M$ and $[HgCl_2] = [Hg^{2+}] = 10^{-2.53}M$. Therefore, the two singular points are S_1 (pCl = 6.61, log $[HgCl^+] = -2.40$) and S_2 (pCl = 6.61, log $[HgCl_2] =$ log $[Hg^{2+}] = -2.53$). The two singular points S_1 and S_2, and the simplified linear relationship of equations (28)–(30) for pCl $>$ log K_1 and log $K_3 <$ pCl $<$ log K_2, allow us to draw readily the logarithmic diagram of the system $HgCl_2/HgCl^+/Hg^{2+}$ for $c_{Hg} = 10^{-2}M$, as shown in Fig. 5.

Figure 5 also shows the values of X from which the corresponding values of pHg and pCl can be obtained. In Fig. 6 the titration curves pHg *vs.* X and pCl *vs.* X are plotted. Note that the first equivalence point, $X = 100\%$, cannot be distinguished on the

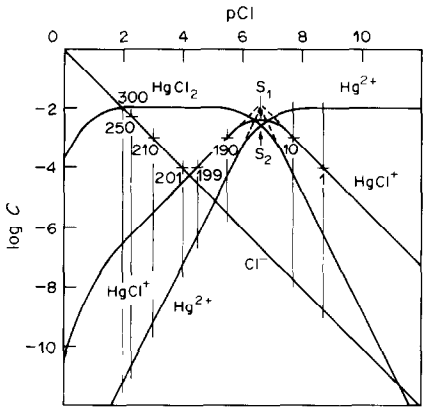

Fig. 5. Logarithmic concentration diagram of system $HgCl_2/HgCl^+/Hg^{2+}$, $c_{Hg} = 10^{-2}M$, log $K_1 = 6.74$, log $K_2 = 6.48$.

titration curve and that there is only one sharp jump in pHg or pCl, at the second equivalence point. The curves for titration of Hg(II) with Br^-, I^-, CN^- or SCN^- can be obtained analogously.

Practical examples. Practical examples of titration of Hg(II) with X^-, with use of the graphical method, can be presented as a laboratory exercise. For instance, 20 ml of $10^{-2}M$ mercuric nitrate, acidified with nitric acid, can be titrated potentiometrically with $10^{-2}M$ MX, where MX can be NaCl, KCl, KBr, KI, KCN or KSCN. The reference electrode can be an Hg/Hg_2SO_4 electrode, or a calomel electrode (used with an auxiliary salt-bridge for titration with Cl^- and Br^-). As indicator electrode an ion-selective electrode for Cl^-, Br^-, I^-, CN^- or SCN^-, as appropriate, or a silver electrode can be used. The experimental titration curves can then be compared with the curves for pHg *vs.* X or pX *vs.* X obtained from logarithmic diagrams of the system $HgX_2/HgX^+/Hg^{2+}$ for $c_{Hg} = 10^{-2}M$. It will be found that the first equivalence point can hardly be distinguished on the titration curve, but the sharp jump of potential is similar to the jump of pX and pHg in the vicinity of the second equivalence point.

It is interesting to note that because the equilibrium constant for $HgX_{2(s)} \rightleftharpoons HgX_{2(aq)}$ is $> 10^{-2}$ for $X = Cl^-$, Br^-, CN^- and SCN^-, the species HgX_2 formed during the titration of $10^{-2}M$ mercury(II) will not be precipitated. However, when $X = I^-$, this equilibrium constant is $10^{-3.88}$. This means that in the logarithmic diagram, the line corresponding to this equilibrium, log $[HgI_2] = -3.88$, is a straight line independent of pI, which intercepts the line log $[HgI_2]_{aq} = \log c_{Hg} + \log K_1K_2 - 2pI$, at pI = 12.85, a value very close to log K_1 (12.87). As outlined above, when pX = pI = log K_1, the degree of titration is $X = 50\%$, so we conclude that precipitation of HgI_2 theoretically begins close to the first half-titration point. In the experimental titration of 20 ml of $10^{-2}M$ mercury(II) with $10^{-2}M$ potassium iodide, the first turbidity due to precipitation of HgI_2 is observed at a somewhat larger degree of titration (about 70%).

Example 2. Titration of CN^- with Ag^+

Silver reacts with cyanide to form a series of species:

$$AgCN_{(s)} \rightleftharpoons Ag^+ + CN^-$$

$$K_{s0} = [Ag^+][CN^-] = 10^{-15.92} \quad (31)$$

$$AgCN_{(s)} + CN^- \rightleftharpoons Ag(CN)_2^-$$

$$K_2 = [Ag(CN)_2^-]/[CN^-] = 10^{4.62} \quad (32)$$

$$Ag(CN)_2^- + CN^- \rightleftharpoons Ag(CN)_3^{2-}$$

$$K_3 = [Ag(CN)_3^{2-}]/[Ag(CN)_2^-][CN^-] = 10^{1.00} \quad (33)$$

$$Ag(CN)_3^{2-} + CN^- \rightleftharpoons Ag(CN)_4^{3-}$$

$$K_4 = [Ag(CN)_4^{3-}]/[Ag(CN)_3^{2-}][CN^-] = 10^{0.50} \quad (34)$$

To obtain the curve for titration of CN^- with Ag^+, we must first plot the logarithmic concentration diagram of the system $Ag(CN)_2^-/AgCN_{(s)}/CN^-$ for $c_{CN} = 10^{-2}M$, with pAg as master variable. In this diagram, the higher complexes $Ag(CN)_3^{2-}$ and $Ag(CN)_4^{3-}$ need not be represented, since from the values of K_3 and K_4 it is clear that with sufficiently dilute cyanide solutions only the complex $Ag(CN)_2^-$ will be formed.

The log c_i lines can be obtained as follows. If we consider the mass balance $c_{CN} = 10^{-2}M = [CN^-] + 2[Ag(CN)_2^-]$ and the expression for the overall formation constant for $Ag(CN)_2^-$, $\beta_2 = K_2/K_{s0} = 10^{20.54}$, we obtain:

$$[CN^-] = \frac{-1 + (1 + 8c_{CN}\beta_2[Ag^+])^{1/2}}{4\beta_2[Ag^+]} \quad (35)$$

$$[Ag(CN)_2^-] = \frac{[-1 + (1 + 8c_{CN}\beta_2[Ag^+])^{1/2}]^2}{16\beta_2[Ag^+]} \quad (36)$$

Equations (35) and (36) can be simplified to linear relationships when (*a*) pAg > log β_2 + log c_{CN}, (*b*) pAg < log β_2 + log c_{CN}.

(*a*) For pAg > log β_2 + log c_{CN}, if $1 \gg 8c_{CN}\beta_2[Ag^+]$, the series expansion of the square-root term gives the approximation value $(1 + 4c_{CN}\beta_2[Ag^+])$, and substitution into (35) and (36) gives $[CN^-] = c_{CN}$ and

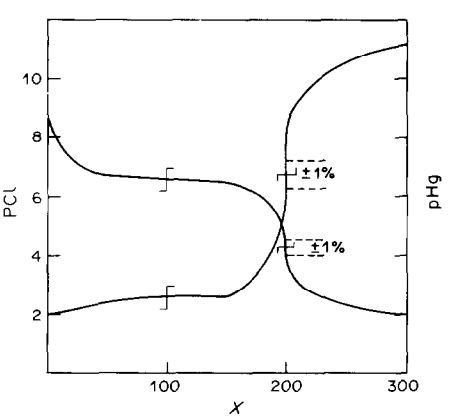

Fig. 6. Titration curves, pCl *vs.* $X\%$, pHg *vs.* $X\%$, of $10^{-2}M$ Hg^{2+} with chloride as titrant.

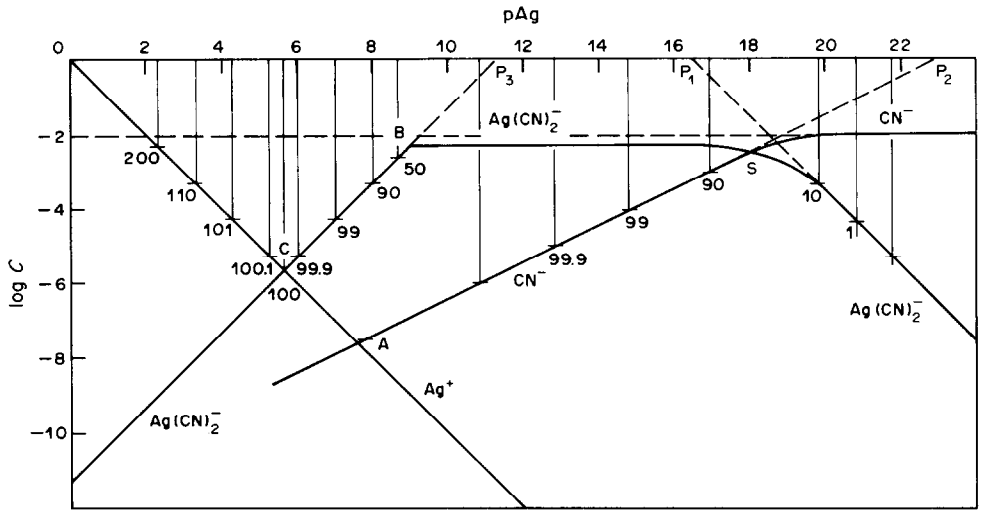

Fig. 7. Logarithmic concentration diagram of system $Ag(CN)_2^-/AgCN_2/CN^-$, $c_{CN} = 10^{-2}M$, log $K_{s0} = -15.92$, log $K_2 = 4.62$.

$[Ag(CN)_2^-] = c_{CN}^2\beta_2[Ag^+]$. Therefore, for a total concentration $c_{CN} = 10^{-2}M$, log $[CN^-] = \log c_{CN} = -2$, and log $[Ag(CN)_2^-] = 2 \log c_{CN} + \log \beta_2 - pAg = 16.54 - pAg$.

The plot of log $[Ag(CN)_2^-]$ *vs.* pAg is a straight line of slope -1 and when extrapolated reaches the point P_1 (pAg = 16.54; log $[Ag(CN)_2^-] = 0$) (see Fig. 7).

(*b*) For $pAg < \log \beta_2 + \log c_{CN}$, $1 \ll 8c_{CN}\beta_2[Ag^+]$. Substituting in (35) and (36), we obtain $[CN^-] = \{c_{CN}/2\beta_2[Ag^+]\}^{1/2}$ and $[Ag(CN)_2^-] = c_{CN}/2$. Hence for $c_{CN} = 10^{-2}M$, log $[CN^-] = \frac{1}{2}\log c_{CN} = \frac{1}{2}\log 2 - \frac{1}{2} \log \beta_2 + \frac{1}{2}pAg = 11.42 + \frac{1}{2}pAg$, and log $[Ag(CN)_2^-] = \log c_{CN} - \log 2 = -2.3$.

The plot of log $[CN^-]$*vs.* pAg is a straight line of slope $+0.5$ and when extrapolated reaches the point P_2 (pAg = 22.84; log $[CN^-] = 0$) (see Fig. 7).

When $pAg \sim (\log \beta_2 + \log c_{CN})$, however, equations (35) and (36) cannot be approximated by linear relationships and the points on the curves must be calculated pointwise. Nevertheless, an approximate diagram can be obtained if we know the crossing point, S, of the lines for log $[CN^-]$ and log $[Ag(CN)_2^-]$. For this purpose, we consider the cyanide mass balance and the overall formation constant β_2, and operating with $[CN^-] = [Ag(CN)_2^-]$, we obtain $[CN^-] = [Ag(CN)_2^-] = 10^{-2.48}M$ and $[Ag^+] = 10^{-18.06}M$. Therefore, the coordinates of point S are pAg = 18.06; log $[CN^-] = \log [Ag(CN)_2^-] = -2.48$ (see Fig. 7).

If, once $Ag(CN)_2^-$ is completely formed, we continue to add successive amounts of Ag^+, pAg decreases and the precipitation reaction $Ag(CN)_2^- + Ag^+ \rightleftharpoons Ag_2(CN)_{2(s)}$ (or $2AgCN_{(s)}$) takes place, for which the effective equilibrium constant is $K = K_{s0}K_2 = 10^{-11.3}$. Therefore, in the range of pAg where $AgCN_{(s)}$ precipitates, the line for log $[Ag(CN)_2^-]$ has the equation log $[Ag(CN)_2^-] = -11.3 + pAg$, slope $+1$, and when extrapolated reaches the point P_3 (pAg = 11.3; log $[Ag(CN)_2^- = 0]$) (Fig. 7).

The logarithmic diagram for the system $Ag(CN)_2^-/AgCN_{(s)}/CN^-$ for $c_{CN} = 10^{-2}M$ is shown in Fig. 7 and from this the titration curve pAg *vs.* X can be obtained, as for the preceding examples. Note that in the first titration, the one corresponding to the reaction $2CN^- + Ag^+ \rightleftharpoons Ag(CN)_2^-$, the degree of titration is $X = 200c_{Ag}/c_{CN}$, so the values of $X = \ldots 0.1, 1, 10\%$ shown on the log $Ag(CN)_2^-$ line will be situated at $\ldots 3.3, 2.3, 1.3$ logarithmic units below log c_{CN}. It is interesting that before the first equivalence point, given by the condition $[CN^-] = 2[Ag^+]$, *i.e.*, log $[CN^-] = \log [Ag^+] + 0.30$, point A (pAg = 7.8), is reached, precipitation begins according to the reaction $Ag(CN)_2^- + Ag^+ \rightleftharpoons 2AgCN_{(s)}$, since in the vicinity of the first equivalence point $[Ag(CN)_2^-] \sim 0.5 \times 10^{-2}M$ and the

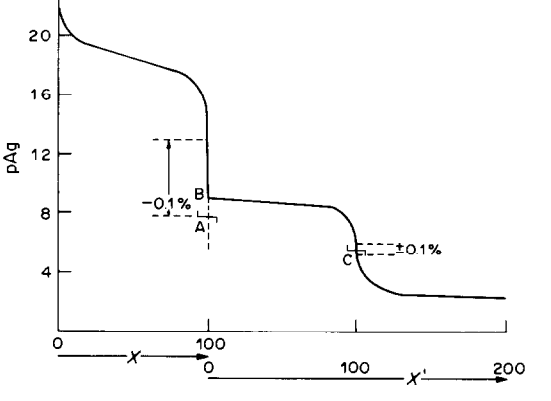

Fig. 8. Titration curve of pAg *vs.* X% for $10^{-2}M$ cyanide ion with silver as titrant.

$[Ag^+]$ necessary to begin the precipitation will be $10^{-11.3}/10^{-2.3} = 10^{-9}M$, point B (pAg = 9.0).

The second stage of the titration corresponds to the precipitation reaction of a solution of $Ag(CN)_2^-$ of initial concentration $\sim 0.5 \times 10^{-2}M$. The titration plot of pAg *vs.* X', where $X' = 100\ c_{Ag}/c_{Ag(CN)_2}$ can easily be obtained from the logarithmic diagram in an analogous way to that for the complexometric titration.[6,8]

In Fig. 7 the several values of X and X' and the corresponding values of pAg are shown, and the titration curve deduced from them is plotted in Fig. 8. Theoretically, the first end-point (at the break point at pAg = 9) could be detected by means of the turbidity due to precipitation of $AgCN_{(s)}$, but a slight excess of silver nitrate would have to be added to yield a perceptible turbidity. Both end-points can be detected potentiometrically, with a cyanide-selective or silver electrode as indicator electrode and an Hg/Hg_2SO_4 reference electrode.

REFERENCES

1. J. N. Butler, *Ionic Equilibrium*, p. 161. Addison-Wesley, Reading, Mass. 1964.
2. R. Palombari, *J. Chem. Educ.*, 1977, **54**, 222.
3. E. Wänninen, *Talanta*, 1980, **27**, 29.
4. C. Maccà, *Analyst*, 1983, **108**, 395.
5. A. Johansson, *Talanta*, 1973, **20**, 89.
6. O. Budevsky, *Foundations of Chemical Analysis*, pp. 208, 269. Horwood, Chichester, 1979.
7. S. Vicente Perez, *Química de las Disoluciones: diagramas y cálculos gráficos*, pp. 43, 149, 181. Alhambra, Madrid, 1979.
8. S. Johansson, *Talanta*, 1981, **28**, 241.
9. D. A. Skoog and D. N. West, *Fundamentals of Analytical Chemistry*, 1st Ed., p. 270. Holt, Rinehart and Winston, New York, 1963.
10. J. N. Butler, *Ionic Equilibrium*, Addison-Wesley, Reading, Massachusetts, 1964.
11. E. Högfeldt, in *Treatise on Analytical Chemistry*, I. M. Kolthoff and P. J. Elving (eds.), 2nd Ed., Part I, Vol. 2, p. 1. Interscience, New York, 1979.
12. Q. Fernando and H. Freiser, *Ionic Equilibria in Analytical Chemistry*, Wiley, New York, 1963.
13. L. Sůcha and S. Kotrlý, *Solution Equilibria in Analytical Chemistry*, Van Nostrand-Reinhold, London, 1972.

Talanta, Vol. 32, No. 4, pp. 273–278, 1985
Printed in Great Britain

0039-9140/85 $3.00 + 0.00
Pergamon Press Ltd

DIFFERENTIAL PULSE STRIPPING VOLTAMMETRY FOR THE DETERMINATION OF NICKEL AND COBALT IN SIMULATED PWR COOLANT

K. TORRANCE and C. GATFORD
Central Electricity Generating Board, Central Electricity Research Laboratories, Kelvin Avenue, Leatherhead, Surrey, England

(*Received* 24 *August* 1984. *Revised* 22 *November* 1984. *Accepted* 5 *December* 1984)

Summary—The determination of ionic nickel and cobalt in simulated PWR coolant at concentrations below 1 μg/l. by differential pulse stripping voltammetry at a hanging mercury-drop electrode has been investigated. The high sensitivity for these ions results from the adsorptive accumulation of their dimethylglyoximate complexes on the mercury drop. Boric acid does not interfere and if the samples are adjusted to pH 9 with an ammonia–ammonium chloride buffer, both nickel and cobalt can be determined in the same run. The relative standard deviations at concentrations below 2 μg/l. are of the order of 5–7% and the limits of detection for nickel and cobalt are about 8 and 2 ng/l. respectively. These performance statistics show that this method is the most sensitive method currently available for determination of soluble nickel and cobalt in PWR coolant and it should prove to be most valuable in any corrosion studies of the materials of construction of the primary circuit of a PWR.

The coolant used in the primary circuit of a pressurized water reactor (PWR) is a dilute solution of boric acid and lithium hydroxide to which hydrogen gas has been added. The concentrations of these additives are carefully controlled and operational experience has shown that only slight corrosion of the materials of construction occurs. It is necessary, however, to confirm the efficacy of the chemical treatment by periodic analysis of the coolant for corrosion products of the materials of construction, and nickel and cobalt derived from stainless steels are two of the principal elements of interest. Hitherto, the determination of these elements has involved either a lengthy accumulation on ion-exchange filters, or concentration, followed by γ-ray spectroscopy and/or electrothermal atomic-absorption spectrometry. This paper describes the determination of ionic nickel and cobalt in simulated PWR coolant by differential pulse stripping voltammetry after adsorptive accumulation of their dimethylglyoximate (DMG) complexes at a hanging mercury-drop electrode. Pihlar *et al.*[1] used this technique for the determination of nickel in natural waters, and Meyer and Neeb[2] used it for the determination of nickel and cobalt in ashed plant samples. The reported limits of detection of a few ng/l. were much lower than those obtained with the same reagents by differential pulse polarography at a dropping mercury electrode.[3–5] The increased sensitivity arises from the adsorptive accumulation of the metal DMG complexes on the mercury drop during a period in which the potential at the drop is held at a value more positive than that required for reduction of the complexes. This accumulation step is followed by a differential pulse voltammetric stripping scan during which the accumulated complexes are reduced.

EXPERIMENTAL

Reagents

All the reagents used were analytical reagent grade or better and, for accurate determinations below the 1-μg/l. level, all the reagents were purified.

Dimethylglyoxime. Analytical reagent grade dimethylglyoxime was recrystallized twice from methanol, and dried at 40°. A 1% solution was prepared in "Spectrosol" ethanol.

Boric acid. A standard solution containing 6000 mg of boron per litre was prepared from "Aristar" boric acid. It contained a small amount of nickel, but this could be substantially removed by adsorption on manganese dioxide powder.[6] Solutions containing lower concentrations of boric acid were prepared by dilution with demineralized water.

Ammonia–ammonium chloride buffer. Pure hydrochloric acid and ammonia solutions were prepared in polythene vessels by isothermal distillation, and mixed in 1:2 molar ratio (acid:base) to give a final concentration of 0.5*M* ammonium chloride at a pH of 9.2 ± 0.1.

Standard nickel and cobalt solutions. These were prepared by sequential dilution of 100-mg/l. Ni and Co solutions prepared from $Ni(NO_3)_2 \cdot 6H_2O$ and $CoSO_4 \cdot 7H_2O$ respectively. Solutions with metal-ion concentrations of 0.1–10 μg/l. were prepared by micropipette additions of 100-μg/l. solutions directly into the 10-ml portions of analysis solution taken in the polarographic cell.

Demineralized water. Prepared by circulating a bulk supply of water continuously through a mixed cation/anion-exchange column to give a final product with a conductivity of 0.06–0.07 μS/cm at 25°. The best quality water was obtained from a unit which had a microfilter and an activated-carbon column after the ion-exchange column.

Storage of reagents. Polythene containers were used exclusively, but cleaning by filling with 0.1*M* hydrochloric acid, leaving for a week, then washing thoroughly was shown to be inadequate. A cleaning procedure based on that described by Moody and Lindstrom[7] was therefore used, in which the bottles were filled with hydrochloric acid (1 + 1), let stand for a week, emptied, rinsed and refilled with nitric acid (1 + 1), let stand for a further week at room temperature, then subsequently rinsed and left filled with demineralized water, the water being changed every day for a week.

Polarograph and voltammetric conditions

An EG&G Princeton Applied Research model 264 polarographic analyser in conjunction with a model 303 mercury electrode assembly and a model RE0089 X-Y recorder was used. The polarograph incorporates a microprocessor which was programmed for differential pulse stripping analysis, involving deaeration of the sample solution, suspension of a mercury drop, a deposition period and a voltage sweep between preset values. The deaeration period necessary to reduce the background current over the voltage range from −0.9 to −1.0 V was 12 min for concentrations above 1 μg/l. and 16 min for lower concentrations. The purge gas used was 99.999% pure nitrogen, further purified by bubbling through pyrogallol solution. In the deposition period, the metal complexes are adsorbed onto the hanging mercury drop; for concentrations below 0.1 μg/l. a 200-sec adsorption time was used, and 100 sec for higher concentrations. The voltage was held at −0.75 V during this period, and then scanned to −1.25 V. Although some advantage in sensitivity can be gained by increasing the drop-size and the voltage scan-rate the best compromise between resolution and sensitivity was obtained by using either a medium (2.5 mg) or small (1.25 mg) drop and a scan-rate of 5 mV/sec. In all cases 50-mV pulses were applied at a rate of 2 per sec.

The standard reference half-cell supplied with the model 303 dropping mercury assembly has a "Vycor" frit liquid junction. Experiments indicated that the prolonged washing necessary to reduce the nickel response for blank solutions was largely associated with this junction. Washing for 2 hr was required after two days of disuse. Comments on nickel and cobalt contamination from Vycor frits have been made by Mart.[8] An experimental junction (Fig. 2) was constructed from a borosilicate glass tube and a crack-junction was formed by controlled local heating applied to a surface scratch. The resistance of this junction, when the reservoir was filled with 3*M* potassium chloride, was 5–6 kΩ. No prolonged washing was necessary with this junction.

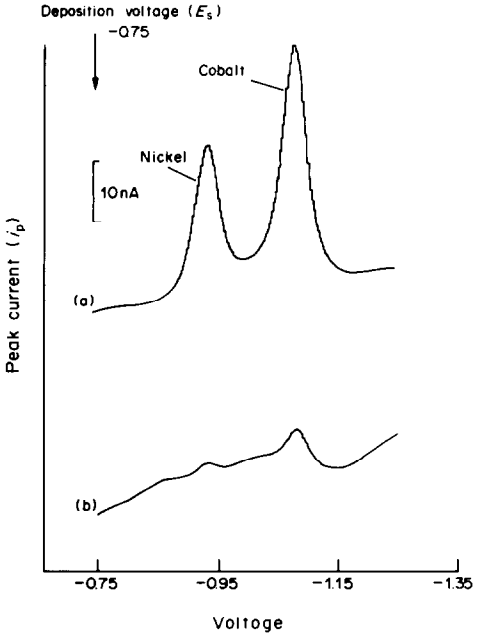

Fig. 1. Typical voltamperograms from precision experiments: (a) $Nc^{2+} = Co^{2+} = 0.4$ μg/l., (b) blank (plus 10 μg of Co^{2+} per litre). Scan-rate, 5 mV/sec; pulse amplitude, 50 mV; drop size, medium; deposition time (a) = 100 sec, (b) = 200 sec; applied voltage *vs.* Ag/AgCl (3*M* KCl).

Most experiments were done at room temperature (25 ± 2°) but for accurate temperature control a glass cell fitted with a water-jacket was used, with water circulated from a constant-temperature water-bath.

RESULTS

Preliminary experiments

In previously reported work on linear sweep voltammetric determination of nickel[1] and of nickel and cobalt[4] by adsorption of the dimethylglyoxime complexes on a mercury drop, an ammonia–ammonium chloride electrolyte was added to the sample. The pH of the test solution was found to affect the sensitivity, particularly for cobalt, which gave optimal response over only a narrow range of pH.[4]

Solutions containing 5 μg each of nickel and cobalt and 1000 mg of boron (as boric acid) per litre and buffered to pH 8.7, 9.0 and 9.4 with ammonia–ammonium chloride buffer were prepared. Voltamperograms of these solutions were recorded and the peak currents for the reduction of the metal ion complexes measured. The nickel peak was relatively unaffected (< 5% change) by the variation in pH. The cobalt peak was reduced by 13% when the pH was changed from 9.0 to 9.4 and it was therefore decided to control the pH at 9.0 ± 0.1. Under these conditions the peaks for reduction of the nickel and cobalt complexes were separated by about 130 mV (Fig. 1). The nickel peak was at −0.93 V and the cobalt peak at −1.06 V *vs.* the silver–silver chloride (3*M* potassium chloride) reference electrode.

The peak heights for reduction of the complexes increase with increasing concentration of dimethylglyoxime but above a certain excess no further advantage is gained.[3] In our experiments an approximately 1000-fold molar excess of DMG was added, and at this level essentially all the metal was complexed.

Adsorptive accumulation of nickel and cobalt

The adsorptive accumulation of the metal complexes on a hanging mercury drop is dependent on a number of factors and a closer examination was

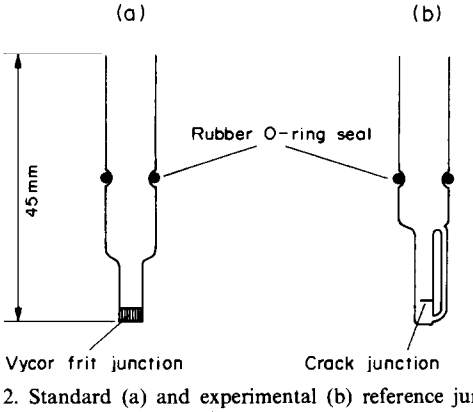

Fig. 2. Standard (a) and experimental (b) reference junctions.

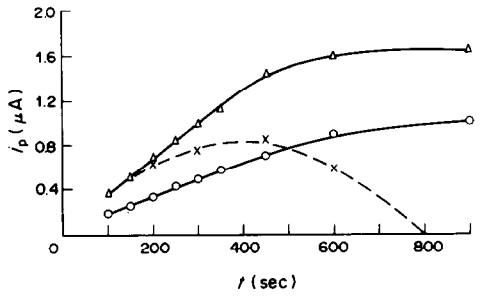

Fig. 3. Peak current *vs.* time curves for nickel at 25°: [Ni^{2+}], μg/l.—○ 2.5; △ 5; × 5 (in presence of Co^{2+}, 5 μg/l).

made of the effects of deposition time and temperature on the peak current, with metal:DMG mole ratio 1:10^3, pH 9.0, and 1100-mg/l. boron concentration (as boric acid).

The effect of deposition time was investigated at 25°. The results for solutions containing only nickel (2.5 and 5 μg/l.) are shown in Fig. 3. The peak currents initially increase linearly with time, then approach a constant value asymptotically and the general form is analogous to an adsorption isotherm. The corresponding plots for cobalt (Fig. 4) were similar in the initial stages, but a constant value was not reached in a reasonably short accumulation time.

When nickel and cobalt were both present there was a significant difference in behaviour. The values of i_p for nickel were suppressed (see Fig. 3) and passed through a maximum, whereas the values for cobalt in the same solution (Fig. 4) were significantly higher than in the absence of nickel, but there was no obvious stoichiometric relationship between the simultaneous changes in i_p for nickel and cobalt. The mutual effects of nickel and cobalt obviously change the slopes of the calibration graphs.

The effect of temperature was investigated at 15, 25 and 35°. In solutions containing only nickel or cobalt

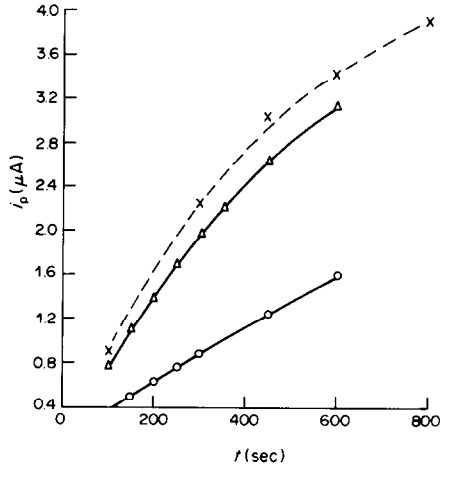

Fig. 4. Peak current *vs.* time curves for cobalt at 25°: [Co^{2+}] μg/l.—○ 2.5; △ 5; × 5 (in presence of Ni^{2+}, 5 μg/l.).

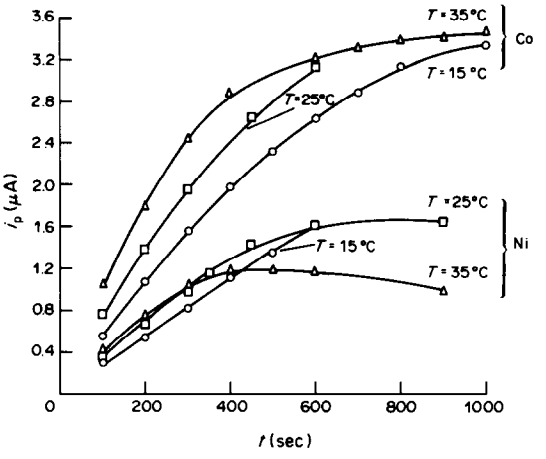

Fig. 5. Effect of temperature on i_p *vs.* time curves for 5-μg/l. nickel and 5-μg/l. cobalt solutions.

(Fig. 5), the slope of the initial linear portion increased with temperature. For nickel, the values at 35° passed through a maximum.

The major difference when nickel and cobalt were both present was shortening of the linear portion of the plots for nickel, and at 35° there was no useful linear range (Fig. 6).

For analytical purposes it is preferable to operate within the linear portion of the i_p *vs.* time plot. At the concentrations of interest in this paper, suitable adsorptive accumulation will be obtained at room temperature with deposition times of 100–400 sec.

Calibration graphs

Preliminary experiments indicated that calibration graphs for nickel in the presence of boric acid were linear over the range 0.1–10 μg/l. Detailed calibration data were obtained at concentrations < 3 μg/l., the

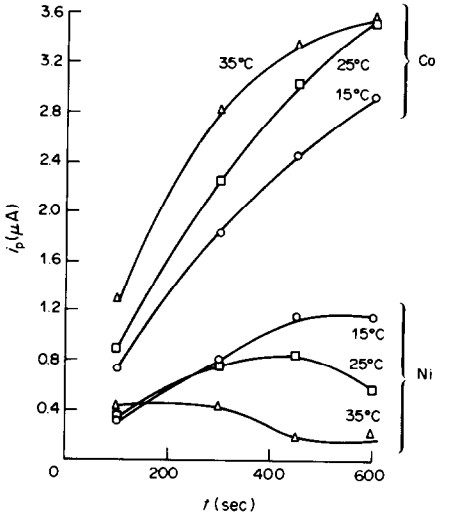

Fig. 6. Effect of temperature on i_p *vs.* time curves for a solution containing both nickel and cobalt at 5 μg/l.

most pertinent region for PWR coolant. Portions of nickel nitrate solution were added by micropipette to a mixture of 10 μl of 1% DMG solution, 2 ml of ammonium chloride buffer and 8 ml of simulated coolant containing boric acid at a concentration equivalent to 1100 mg of boron per litre. The voltamperograms were recorded and the peak currents corrected for that for a reagent blank. Peak current data for nickel in the concentration range 0.12–2.4 μg/l. were obtained at scan-rates of 5, 10 and 20 mV/sec. Linear regression analysis gave correlation coefficients, r^2, > 0.999 for all these sets of data. The sensitivity at 20 mV/sec was about twice that at 5 mV/sec but the gain in sensitivity was offset by a loss of resolution. This is a very important consideration when cobalt and nickel are both being determined since their peaks are separated by only 130 mV. For 5-mV/sec scan-rate, i_p (nA) was equal to $1.51 + 53.7c_{Ni}$, where c_{Ni} was the nickel concentration in μg/l.

Linear calibration graphs, $r^2 > 0.999$; $i_p = 0.09 + 96.9\ c_{Co}$, were similarly obtained for cobalt over the concentration range 0.13–1.11 μg/l. The sensitivity for cobalt was about 70% greater than that for nickel.

Blank-corrected calibration graphs prepared with solutions containing equal w/v concentrations of nickel and cobalt were linear ($r^2 > 0.999$, $i_p = 0.65 + 51.4\ c_{Ni}$ and $i_p = 0.01 + 105.7\ c_{Co}$), but significant day-to-day variation in slope was found, making the use of permanent calibration graphs impractical. In addition, the slope of the cobalt calibration graph (*cf.* 86.9 c_{Co} and 105.7 c_{Co}) is dependent on the nickel:cobalt ratio. For these reasons calibration by standard addition is recommended.

Interferences

The effect of other metal ions expected to be present in the primary coolant because of corrosion of the materials of construction was investigated. The principal ions expected are iron, chromium and manganese. The presence of Fe(III) (40 μg/l.), Mn(II) (10 μg/l.) and Cr(III) (10 μg/l.) had no significant effect (95% confidence level) on the peak heights for nickel (0.8 μg/l.) and cobalt (0.2 μg/l.).

The effect of oil was investigated by recording voltamperograms for nickel (0.2 μg/l.) and cobalt (0.1 μg/l.) in demineralized water saturated at 25° with a pump oil typical of those used in reactor feed-pumps, and for equivalent solutions prepared from uncontaminated demineralized water. A deposition time of 200 sec was used. There was no significant difference for nickel, but in the presence of oil the cobalt peak was largely obscured by a broad asymmetric peak and no determination was possible. Voltamperograms of the oil-saturated water containing no added metal ions did not have this broad peak and it was concluded that the oil interfered with the adsorption of the cobalt complex at the metal surface but not that of the nickel.

Precision

The standard deviations of the peak heights corresponding to the reduction of the nickel and cobalt complexes were determined for concentrations of 5 and 0.4 μg/l., and for blanks (six replicates). The results are given in Table 1, and typical traces are shown in Fig. 1. The relative standard deviations of nickel and cobalt were about the same at both levels and were in the range 5–7%. For the blanks, prepared with solutions purified as described, the voltamperograms always displayed a small peak for nickel but none for cobalt. A small amount (~10 ng/l.) of cobalt was added to the blank, which was estimated to contain about 10 ng/l. nickel, and it was assumed that the standard deviation at this level (Table 1) would be typical of that for a blank. The statistical limit of detection was calculated (95% confidence level) as 4.65 times the standard deviation of the blank. For nickel, the limit of detection was 8 ng/l. and for cobalt 2 ng/l.

Recovery tests on synthetic samples

Synthetic PWR coolant was prepared at two levels of boric acid and lithium hydroxide; B 2000 mg/l., Li 2.2 mg/l., and B 1100 mg/l., Li 2 mg/l., and known amounts of nickel and cobalt were added. The resulting solutions were analysed by the standard-addition technique. First the voltamperogram (peak current i_S) for V ml of a solution consisting of 8 ml of sample, 2 ml of buffer, and 10 μl of DMG solution was recorded. A small known volume, δ_A, of standard metal solution of concentration c_A was then added and a second voltamperogram recorded (peak current i_{S+A}). The concentration, c_S, of the determinand in the test solution was then calculated from:

$$c_S = \frac{i_S\,\delta_A c_A}{i_{S+A}\delta_A + (i_{S+A} - i_S)V}.$$

The original concentration of the metal in the sample before addition of the buffer was then 1.25 c_S. The results for solutions containing a number of different proportions of nickel and cobalt are given in Table 2. The recoveries were mainly in the range 100 ± 10% and the variations between duplicate values were 3–6%.

Table 1. Precision of nickel and cobalt determinations in the presence of boron (1100 mg/l.)

Metal concentration, $\mu g/l.$	Standard deviation		
	nA	$\mu g/l.$	%
Nickel			
5	16	0.24	4.8
0.4	2.4	0.024	6.1
Blank	0.33	0.0017	—
Cobalt			
5	36	0.34	6.7
0.4	3.2	0.023	5.8
Blank*	0.15	0.0004	—

*With added Co (10 ng/l.)

Table 2. Recovery of nickel and cobalt from simulated PWR coolant by standard addition

Coolant composition, mg/l.		Concentration added, μg/l.		Concentration found, μg/l.	
B	Li	Ni	Co	Ni	Co
2000	2.2	0.1	0.05	0.088	0.043
2000	2.2	0.4	0.2	0.38	0.17
1100	2.0	0.1	0.05	0.090	0.051
1100	2.0	0.4	0.2	0.39	0.20
1100	2.0	—	0.2	—	0.21
1100	2.0	0.4	0.4	0.41	0.37
1100	2.0	0	0.4	0.97	0.40

A water sample obtained from a rig operating under simulated PWR coolant conditions was analysed by the standard-addition technique and the nickel content was found to be 0.37 μg/l. and the cobalt content 0.014 μg/l. Analysis of the same sample by electrothermal atomic-absorption spectroscopy gave the nickel content as < 1 μg/l. and no cobalt was detectable. No alternative method of analysis was available for comparison with the voltammetric results at these very low levels.

DISCUSSION

Adsorption process

A characteristic of the differential pulse stripping voltammetry for nickel and cobalt is the higher sensitivity for the latter under identical analytical conditions. This is unexpected in view of the similarity of their complexes with dimethylglyoxime.[9] In addition, the i_p *vs.* time plots for nickel and cobalt present in the same solution are considerably different from those obtained for separate solutions of the two. In every case, for the mixed solution the cobalt signal is enhanced while the nickel signal is reduced (see the broken lines of Figs. 3 and 4). Figure 3 shows the value of i_p for nickel was reduced to zero if the collection time was long enough, suggesting that the complex had been completely displaced from the surface. These observations indicate a far from simple adsorption process at the electrode surface.

This interaction of cobalt and nickel was not observed when similar experimental conditions were used, but with a dropping mercury electrode,[10] and in DPP experiments only small differences in the slopes of the nickel and cobalt calibration graphs were detected. Figure 7 shows a polarogram and a voltamperogram of a solution containing nickel and cobalt (both at the 5-μg/l. level) and the ratios of the peak currents i_p(Ni):i_p(Co) were 0.8:1 in the former and 0.43:1 in the latter.

Purity of reagents

At the determination levels discussed here, the purity of the reagents is critical. The quality of the demineralized water has already been emphasized, and the water obtained after passage through an activated carbon bed after the ion-exchange did not have the broad peak (from -0.85 to -1.0 V) otherwise present. Similar broad peaks were associated with the presence of oxygen, and extensive deoxygenation (for 16 min) was necessary.

Appreciable blanks were found even for Aristar-grade reagents, and the boric acid, dimethylglyoxime, ammonia and hydrochloric acid all required purification. Purification of boric acid solutions by adsorption of trace metals on a manganese dioxide suspension was very successful and the cobalt content of a 1000-mg/l. boron solution was reduced from about 20 to <2 ng/l. Dimethylglyoxime was readily recrystallized from methanol, but tended to give an unidentifiable voltammetric peak after storage of the

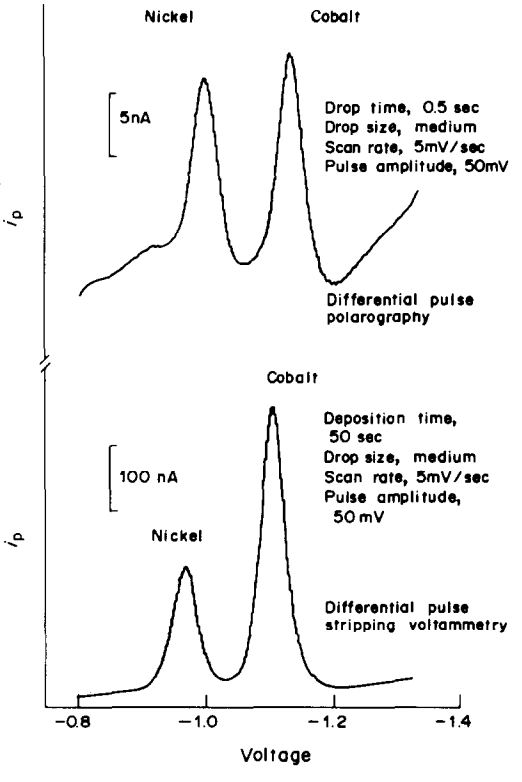

Fig. 7. Comparison of relative peak heights for solution containing 5 μg/l. each of nickel and cobalt.

1% ethanol solution in a polythene bottle for approximately two weeks. This was perhaps due to dissolution of the plasticizer from the bottle. The isothermal distillation of hydrochloric acid and ammonia was entirely successful. In blank solutions containing boric acid and prepared from these purified reagents no cobalt could be detected and the nickel levels were 10–15 ng/l. The nickel was considered to be present in the water used and reduction of its concentration was not attempted since the sensitivity was satisfactory for the immediate applications.

Analytical precision and limits of detection

It has been shown[10] that boric acid does not affect the determination of nickel and cobalt by differential pulse polarography provided consideration is given to the change in pH brought about by the weak acid. The same was found for the differential pulse stripping voltammetry. Of the substances normally expected in PWR coolant only the transition metal ions were considered as possible interferents and excesses of these were shown to have no significant effect.

Because of the interaction of nickel and cobalt in the adsorption step, a fixed calibration graph is impractical when the Ni:Co ratio varies from sample to sample. The standard-addition method gives recoveries of 88–103% for nickel and 86–105% for cobalt, which are considered satisfactory for the very low levels investigated. The relative standard deviations are in the range 5–7% for determination of nickel or cobalt (each in the absence of the other) in simulated PWR coolant. In any determination using a single standard-addition, the standard deviation will be greater, since the calculation involves a ratio as well as a sum and difference of measurements, and an overall relative standard deviation in the range 10–14% would be more appropriate. The limits of detection were calculated from the standard deviations for blank solutions which contained only traces of the two metals. At the 95% confidence level the limits of detection for nickel and cobalt were about 8 and 2 ng/l. respectively. These levels are very much lower than those obtainable by electrothermal atomic-absorption spectrometry, thus making this form of stripping voltammetry the most sensitive method for trace determinations of these metal ions in PWR coolant.

Acknowledgements—The authors wish to acknowledge the contribution of Mr. P. E. Madden to the design of the crack-junction reference electrode. The work was done at the Central Electricity Research Laboratories of the CEGB Technical Planning and Research Division and is published by permission of the Central Electricity Generating Board.

REFERENCES

1. B. Pihlar, P. Valenta and H. W. Nürnberg, *Anal. Chem.*, 1981, **307**, 337.
2. A. Meyer and R. Neeb, *Z. Anal. Chem.*, 1983, **315**, 118.
3. C. J. Flora and E. Nieboer, *Anal. Chem.*, 1980, **52**, 1013.
4. J. Weinzierl and F. Umland, *Z. Anal. Chem.*, 1982, **312**, 608.
5. H. Chen and R. Neeb, *ibid.*, 1983, **314**, 657.
6. C. M. G. Van den Berg and J. R. Kramer, *Anal. Chim. Acta*, 1979, **106**, 113.
7. J. R. Moody and R. M. Lindstrom, *Anal. Chem.*, 1977, **49**, 2264.
8. L. Mart, *Talanta*, 1982, **29**, 1035.
9. C. V. Banks and S. Anderson, *Inorg. Chem.*, 1963, **2**, 112.
10. K. Torrance, *Analyst*, 1984, **109**, 1035.

Talanta, Vol. 32, No. 4, pp. 279–283, 1985
Printed in Great Britain.

0039-9140/85 $3.00 + 0.00

MONITORING OF AROMATIC AMINES BY HPLC WITH ELECTROCHEMICAL DETECTION

COMPARISON OF METHODS FOR DESTRUCTION OF CARCINOGENIC AROMATIC AMINES IN LABORATORY WASTES

JIŘÍ BAREK, VĚRA PACÁKOVÁ, KAREL ŠTULÍK* and JIŘÍ ZIMA
Department of Analytical Chemistry, Charles University, Albertov 2030, 128 40 Prague 2, Czechoslovakia

(*Received* 21 *May* 1984. *Revised* 31 *October* 1984. *Accepted* 21 *November* 1984)

Summary—A new chemical method for destruction of carcinogenic aromatic amines in laboratory wastes has been developed. The method is based on enzymatic oxidation of the amines in solution (with hydrogen peroxide and horseradish peroxidase), followed by oxidation of the solid residues with permanganate in sulphuric acid medium. To monitor the efficiency of destruction, a reversed-phase HPLC system has been developed, with voltammetric detection with a carbon-fibre detector, which is substantially more sensitive (detection limits from a few ng down to a few pg of amine) than the commonly used ultraviolet photometric detection. It has been demonstrated that the proposed method of destruction is highly efficient (>99.8% destruction).

Many aromatic amines are known or suspected to be carcinogenic towards humans,[1] and therefore must be effectively destroyed in industrial and laboratory wastes before these are disposed of. Solution of this problem requires first a sufficiently effective, simple, cheap and rapid procedure for conversion of the carcinogens into harmless products, and secondly a reliable analytical method to check the completeness of destruction.

Several methods have been proposed[2] for the destruction. The most useful involves oxidation with permanganate in sulphuric acid medium,[3] but is unsuitable for wastes containing oxidizable solvents, such as methanol or ethanol, or large amounts of other oxidizable substances. Decontamination of large volumes of aqueous solution is also inconvenient, as large amounts of permanganate are required.

A very promising method has been proposed by Kalibanov and Morris,[4] based on oxidation of the aromatic amines by hydrogen peroxide, catalysed by horseradish peroxidase, to give the corresponding aromatic amine free radicals, which diffuse from the enzyme active site into the solution, where they polymerize. In contrast to the monomers the polymers are virtually insoluble in water, and can be separated by sedimentation, filtration or centrifugation. Unfortunately, the solid residues have been found to be mutagenic.[5]

The present work deals with the combination of these two methods, the enzymatic oxidation to preconcentrate the carcinogens from large volumes of wastes, and the permanganate treatment to destroy the solid residues. Representative aromatic amines were selected for the study (see Table 1).

Various methods can be used to determine trace concentrations of aromatic amines, and hence to monitor the effectiveness of their destruction.[6] Titration and spectrophotometric methods are insufficiently selective for analysis of complex samples, and better results are obtained by combining spectrofluorimetric determination with TLC separation.[7] Gas chromatography has been widely used[6] but mostly requires use of derivatives, which complicates the determination and increases the error. HPLC is therefore most suitable, as direct determination of the aromatic amines is then possible.[6,8–15] With ultraviolet photometric detection, a detection limit of $5 \times 10^{-6} M$ has been achieved.[3] The sensitivity can be considerably improved by use of electrochemical detection.[9–15] In view of the polar character of amines, non-polar stationary phases (*e.g.*, C_{18} bonded phases) are suitable in combination with aqueous solutions of methanol or acetonitrile; to increase the electrical conductivity of the mobile phase, aqueous buffers or salt solutions are used. Amines are readily oxidized at solid electrodes, monoamines at potentials close to +1.0 V (*vs.* SCE), diamines at around +0.5 V (*vs.* SCE).

In the present work, the conditions for HPLC determination of selected aromatic amines in a reversed-phase system with a C_{18} chemically bonded stationary phase and a methanol–aqueous buffer mobile phase, with combined ultraviolet photometric and voltammetric detection were studied. The method was then applied to monitor the effectiveness of degradation of some amines.

*Author for correspondence.

Table 1. Characteristics of the substances studied, and their detection limits

No.	Substance	pK_{a1}^{*}	pK_{a2}^{*}	λ_{max},[18] *nm*	$E_{1/2}$ (E_p), *V*	Detection limit, *ng*	
						Photometric	Electrochemical
1	Benzidine (4,4′-diaminobiphenyl)	4.7	3.7	268	+0.36	3	0.003
2	*o*-Dianisidine (3,3′-dimethoxybenzidine)	4.7	3.6	212; 303	+0.29 (+1.23)	4	0.05
3	3,3′-Dichlorobenzidine			285†	(+0.51)	16	0.45
4	3,3′-Diaminobenzidine			211; 224; 278	+0.17	3	0.05
5	*o*-Tolidine (3,3′-dimethylbenzidine)	4.7	3.7	282	+0.33	4	0.03
6	4-Aminobiphenyl	4.2		278	(+0.58)	10	1.1
7	4-Nitrobiphenyl			222; 305	−0.73 (DME)	12	—
8	1-Naphthylamine	4.0		243; 318; 328	(+0.51)	11.4	1.4
9	2-Naphthylamine	4.2		237; 259; 291; 337	(+0.58)	11.4	9.0
10	2,5-Diaminotoluene	5.1	3.3	294	+0.45	12.2	0.06
11	MOCA [4,4′-methylenebis-(*o*-chloroaniline)]	3.5	3.0	247; 298	+0.29 (+0.63)	5	4.6

*pK_a values for the conjugate acids of the bases; pK_{a1} refers to the singly protonated base, pK_{a2} to the doubly protonated base.

†The value recommended in Castegnaro.[2]

EXPERIMENTAL

Apparatus

The polarization curves of the substances were obtained with a PA-3 polarographic analyser (Laboratorní Přístroje, Czechoslovakia) with a glassy-carbon rotating disk electrode or a dropping mercury electrode. For determination of the conditional dissociation constants of the amines, an ABU13/TTT60/REC61 automatic titrator (Radiometer) was used. The pH values in mixed water–methanol media were not corrected.

The chromatographic system included a Pye Unicam LC-XP liquid chromatograph with a TZ4200 dual-line recorder (Laboratorní Přístroje), a stainless-steel column 25 cm long, 3 mm bore, packed with 10 μm Partisil ODS (Pye Unicam), an LC-UV variable-wavelength photometric detector (Pye Unicam), and a carbon-fibre voltammetric detector constructed by the authors and described elsewhere.[17] The two detectors were connected in series by a short (5 cm long, 0.2 mm bore) stainless-steel capillary. On the basis of published data,[2,18] the photometric detector was operated at 280 nm, and the voltammetric detector (see Table 1) at a potential of +0.6 V for a mobile-phase pH of *ca.* 7 and a potential of +0.9 V for a pH of *ca.* 3.5. The samples were injected through a 20-μl loop.

The mobile phase was deaerated by continuous passage of helium. The measurements were made at laboratory temperature and all the potentials were measured *vs.* the SCE.

Reagents

The aromatic amines were of analytical purity and obtained from Fluka (benzidine), Merck (3,3′-dimethoxybenzidine and 3,3′-dichlorobenzidine), Sigma (2-naphthylamine, 1-naphthylamine, 4-aminobiphenyl, 2,5-diaminotoluene and 4-nitrobiphenyl), Lachema, Czechoslovakia (3,3′-diaminobenzidine) and Serlabo, France [4,4′-methylenebis(*o*-chloroaniline)]. The substances were dissolved in 0.1*M* hydrochloric acid to give $5 \times 10^{-3}M$ concentration. If necessary, the dissolution was hastened by sonication.

Horseradish peroxidase (hydrogen peroxidase oxidoreductase), from Sigma, was used as a salt-free powder with a specific activity of 175 purpurogallin units per mg.

All other solvents and chemicals used were of analytical purity.

The mobile phase consisted of 0.1*M* ammonium acetate containing various amounts of methanol; the pH was adjusted with perchloric acid and sodium hydroxide.

Procedures

Determination of the conditional dissociation constants of the conjugate acids. A 20-ml portion of a $10^{-3}M$ solution of amine in a 1:1 mixture of methanol and 0.2*M* aqueous sodium perchlorate was potentiometrically titrated with 0.01*M* hydrochloric acid standardized with sodium tetraborate. The pK_a values were taken as the pH corresponding to half-neutralization. The values given in Table 1 are averages of two determinations.

Determination of the half-wave (peak) potentials. The polarization curves were obtained by using a three-electrode circuit with a 1:1 v/v mixture of methanol and aqueous 0.1*M* ammonium acetate, with an SCE (aqueous inner solution) as reference; no correction was made for liquid-junction potential. The solution was deaerated by passage of purified nitrogen.

Decontamination of laboratory wastes

Simple permanganate method. About 9 mg of test amine was dissolved in 10 ml of 0.1*M* hydrochloric acid (10 ml of glacial acetic acid for substances Nos. 6 and 11), then 5 ml of 0.2*M* potassium permanganate and 5 ml of 2*M* sulphuric acid were added and the mixture was allowed to react overnight. The solution was then subjected to HPLC analysis to check the completeness of degradation.

Combined enzymatic and permanganate oxidation. The pH of the waste solution (containing up to 100 mg of an aromatic amine per litre and up to 20% v/v methanol or ethanol) was adjusted to pH 5–7 with sodium hydroxide or sulphuric acid, and 3.5 ml of 3% hydrogen peroxide solution and 1000 units of horseradish peroxidase (*i.e.*, *ca.* 6 mg) were added per litre of waste solution. After 3 hr, the precipitate formed was filtered off with a porosity-4 frit. The frit and precipitate were then immersed in a mixture of 50 ml of 0.2*M* potassium permanganate and 50 ml of 2*M* sulphuric acid and stirred magnetically overnight. The precipitate was thus completely dissolved, and the solution was then subjected to HPLC analysis.

HPLC analysis

Solid ascorbic acid was gradually added to an aliquot of the solution from the permanganate oxidation until the solution became colourless, then the pH was adjusted to about 8 with 10*M* sodium hydroxide and the solution was centrifuged. One ml of the supernatant liquid was diluted with 3 ml of methanol and centrifuged, and 20 μl of the supernatant solution were injected into the column. The

separation was done with a mobile phase consisting of 40% methanol and 60% aqueous 0.1*M* ammonium acetate, pH 3.5–4.0, at a flow-rate of 1 ml/min. The detectors were operated at 280 nm and +0.9 V respectively and the amine concentration was determined from the voltammetric peak height by the standard-addition method (standard amine solution added to the sample immediately after the ascorbic acid).

RESULTS AND DISCUSSION

HPLC of aromatic amines

The substances studied are listed in Table 1, and the conjugate acids had very similar conditional dissociation constants in water–methanol mixtures. The pK_a values of substances Nos. 3 and 4 could not be measured by the technique used, because the substances were available only as the hydrochlorides.

The absorption maxima[2,18] given in Table 1 indicate that the optimal wavelength for detection of the studied substances is around 280 nm.

All the substances studied, except 4-nitrobiphenyl, are readily oxidized at a glassy-carbon electrode. The values given in Table 1 were obtained for a 1:1 mixture of methanol and aqueous 0.1*M* ammonium acetate, pH 7.1. With some substances (Nos. 3, 6, 8 and 9) there is strong adsorption of the oxidation products on the electrode surface, leading to pronounced drops in the limiting currents; the polarization curves then appear as peaks rather than normal waves and in these cases the peak potentials are given in Table 1 instead of the half-wave potentials. It follows from Table 1 that a potential of *ca.* +0.6 V is sufficient for the detection of all the substances (except No. 7) at pH 7.1. However, the anodic waves shift to more positive potentials with decreasing pH, by about 80 mV/pH. Therefore, the working electrode potential of the detector must be made more positive than +0.6 V when working at lower pH. To maximize the signal-to-noise ratio, the working electrode potential should be as low as possible (to suppress the background current); the best compromise is a potential of +0.9 V and a mobile-phase pH of 3.5.

As 4-nitrobiphenyl is not oxidized at carbon electrodes, it cannot be voltammetrically determined. However, as seen from Table 1, it can be reduced at a dropping mercury electrode and thus can be detected polarographically.

With the mobile phase used, methanol/aqueous ammonium acetate, the separation efficiency and resolution can in principle be modified by varying the methanol content and the pH. The dependence of the capacity factors on the methanol content of the mobile phase is given in Fig. 1. The dependences are similar for all the substances studied and thus it is impossible to attain a substantial improvement in the separation by changing the methanol content. To optimize the absolute values of the capacity factors (between *ca.* 1.0 and 10.0), a methanol content of 40% v/v is most suitable.

With a 40% v/v methanol mobile phase, the

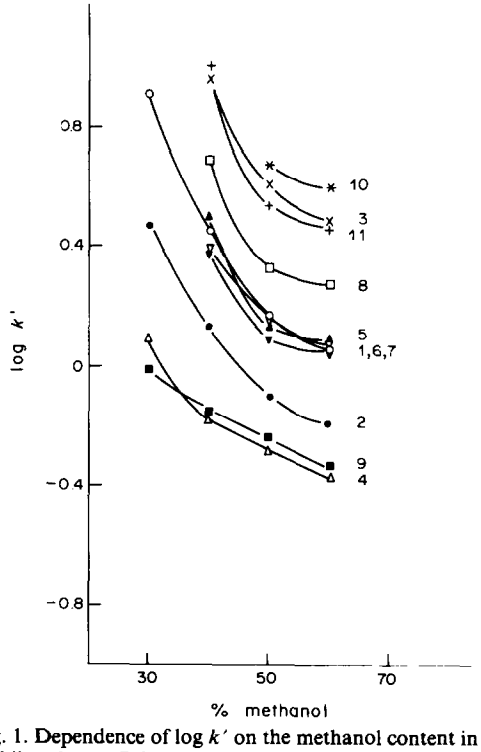

Fig. 1. Dependence of log k' on the methanol content in the mobile phase. Substance: 1—○, 2—●, 3—×, 4—△, 5—▲, 6—▽, 7—▼, 8—□, 9—■, 10—✳, 11—+. Conditions: 0.1*M* aqueous ammonium acetate +x% v/v methanol, pH 7.1; flow-rate, 1 ml/min. For list of substances see Table 1.

dependences of log k' on pH were then measured (Fig. 2). Although the pK_a values of the studied substances are similar, the pH-dependence of the capacity factors varies more significantly than the methanol-dependence. The greatest changes occur between pH 3 and 5, corresponding to the pK_a values of most of the substances. A decrease in the pH leads to a greater protonation of the amines, *i.e.*, to an increase in their polarity (and solubility), and thus to a decrease in their retention times. With some substances the elution order is also changed (Nos. 1, 5, 6 and 7). As follows from Fig. 2, the optimal mobile-phase pH for the separation is about 3.5–4.0. However, the detector electrode potential must be increased accordingly, see above.

The optimal conditions for the separation and determination are: a mobile phase consisting of 40% methanol +60% aqueous 0.1*M* ammonium acetate, pH 3.5–4.0; photometric detector wavelength 280 nm; detector electrode potential, +0.9 V *vs.* SCE.

The response of the two detectors to the studied substances was measured under these conditions for various amounts injected. The detection limits (for a signal equal to twice the absolute noise value) are given in Table 1. It can be seen that for most of the substances the voltammetric detector is substantially more sensitive than the photometric detector and the lowest detection limit is a few picograms. The greatest difference in sensitivity between the two detectors is

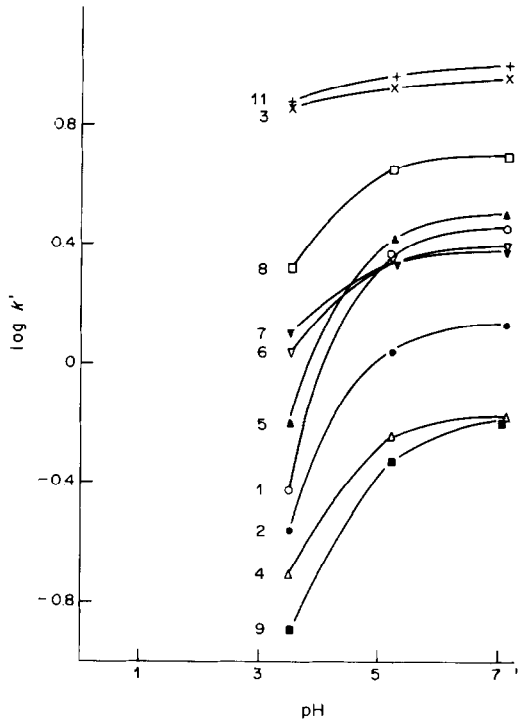

Fig. 2. Dependence of log k' on the mobile phase pH. For list of symbols see Fig. 1. Conditions: 0.1*M* aqueous ammonium acetate +40% v/v methanol; flow-rate, 1 ml/min. For list of substances see Table 1.

for substances Nos. 1, 2, 4, 5 and 10, for which the voltammetric detector is 2–3 orders of magnitude more sensitive than the photometric detector; the difference is *ca.* one order of magnitude for substances Nos. 3, 6 and 8, and the sensitivities are similar for substances Nos. 9 and 11.

It follows that the voltammetric detector is clearly preferable for use in trace analyses. The calibration data show that the linear dynamic range of the voltammetric detector extends from the detection limit to *ca.* 50 ng. The calibration graphs exhibit good linearity (correlation coefficients ranging from 0.9996 for 1-naphthylamine to 0.9978 for 2-naphthylamine) and satisfactory precision (the relative standard deviations of the peak height amount to only a few per cent and do not exceed 10–12% (5 replicates, 95% limits) even at the lowest measured concentrations. Therefore, the method can be used to monitor the effectiveness of the degradation treatment. A chromatogram of the solution after degradation of 3,3′-diaminobenzidine is shown in Fig. 3.

Chemical degradation of the amines

Typical results for the degradation procedures, as monitored by HPLC with electrochemical detection, are summarized in Table 2. The degradation methods are highly efficient and lead to destruction of more than 99.95% of most of the substances tested. The efficiencies found by electrochemical detection are higher than those found by photometric detection[3] because of the higher sensitivity. The apparently less

Table 2. The efficiency of the degradation of the substances studied, as determined by HPLC with electrochemical detection (four parallel determinations; $\alpha = 0.05$)

No.	Substance	Initial concentration taken, M	Final concentration found, M		Efficiency of degradation, %	
			Procedure (*a*)	Procedure (*b*)	Procedure (*a*)	Procedure (*b*)
1	Benzidine	4.07×10^{-3}	$1.2 \pm 0.1 \times 10^{-7}$	$< 4.4 \pm 0.7 \times 10^{-8}$	99.997	> 99.999
2	*o*-Dianisidine	3.07×10^{-3}	$< 4.1 \pm 0.8 \times 10^{-8}$	$< 4.1 \pm 0.8 \times 10^{-8}$	> 99.998	> 99.998
3	3,3′-Dichlorobenzidine	2.30×10^{-3}	$< 2.8 \pm 0.3 \times 10^{-7}$	$< 2.8 \pm 0.2 \times 10^{-7}$	> 99.988	> 99.988
4	3,3′-Diaminobenzidine	2.10×10^{-3}	$5.1 \pm 0.4 \times 10^{-7}$	$< 2.8 \pm 0.6 \times 10^{-8}$	99.976	> 99.989
5	*o*-Tolidine	3.54×10^{-3}	$7.1 \pm 0.4 \times 10^{-7}$	$< 8.0 \pm 0.7 \times 10^{-8}$	99.980	> 99.998
6	4-Aminobiphenyl	4.44×10^{-3}	$1.3 \pm 0.1 \times 10^{-6}$	$4.0 \pm 0.2 \times 10^{-6}$	99.971	99.910
8	1-Naphthylamine	5.24×10^{-3}	$2.1 \pm 0.2 \times 10^{-6}$	$2.0 \pm 0.1 \times 10^{-6}$	99.960	99.962
9	2-Naphthylamine	5.24×10^{-3}	$< 1.26 \pm 0.04 \times 10^{-5}$	$< 1.30 \pm 0.02 \times 10^{-5}$	> 99.718	> 99.752
10	2,5-Diaminotoluene	6.14×10^{-3}	$5.2 \pm 0.4 \times 10^{-8}$	(*c*)	99.999	(*c*)
11	MOCA	2.61×10^{-3}	$< 3.60 \pm 0.08 \times 10^{-6}$	$< 3.60 \pm 0.08 \times 10^{-6}$	> 99.862	> 99.862

(*a*) Simple permanganate method, (*b*) after oxidation of the residues formed by the enzymatic oxidation of the solution containing 10 mg of the test amine per 100 ml, (*c*) no precipitate formed during the enzymatic oxidation.
Note: The final concentration values are recalculated to refer to the original volume of the waste solution.

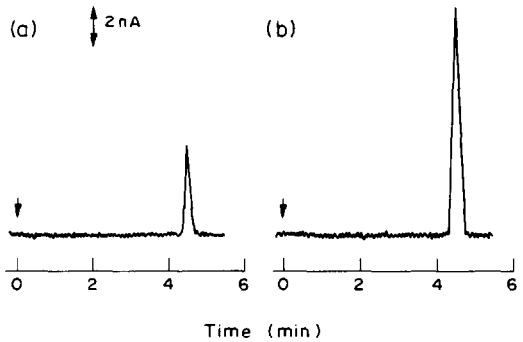

Fig. 3. Chromatogram of 3,3′-diaminobenzidine after the decomposition of the waste solution (a) and the same with a standard addition corresponding to $7.65 \times 10^{-7} M$ concentration (b). Conditions: 0.1*M* aqueous ammonium acetate + 40% v/v methanol; pH 3.7; flow-rate 1 ml/min, voltammetric detection at +0.9 V.

favourable values for substances Nos. 9 and 11 are probably due to the poorer detection sensitivity (for substances Nos. 2, 3, 9 and 11 the detection limit was higher than the residual amine concentration). The enzymatic method cannot be used for 2,5-diaminotoluene, as no precipitate is formed. For all the other amines tested, the permanganate oxidation is a highly efficient method for destruction of the solid mutagenic residues. It has been found[5] that the resulting solutions have no mutagenic effects and are thus environmentally harmless. It can be concluded that the method combining the enzymatic and chemical oxidation is suitable for large volumes of wastes containing small amounts of aromatic amines, and in the presence of oxidizable solvents and other oxidizable substances, where the simple permanganate method fails. The combined method is also somewhat more efficient than the simple permanganate method (see Table 2).

The HPLC method with electrochemical detection is suitable not only for monitoring the effectiveness of such degradation procedures, but also for trace analyses for these important substances in general.

REFERENCES

1. *IARC Monographs on the Evaluation of the Carcinogenic Risk of Chemicals to Humans. Supplement 1, Chemicals and Industrial Processes Associated with Cancer in Humans*, International Agency for Research on Cancer, Lyon, 1979.
2. M. Castegnaro (ed.), *Laboratory Decontamination and Destruction of Aromatic Amines in Laboratory Wastes*, International Agency for Research on Cancer, Lyon, in the press.
3. M. Castegnaro, Ch. Malaveille, I. Brouet and J. Barek, *Am. Ind. Hyg. Assoc. J.*, in the press.
4. A. M. Kalibanov and E. D. Morris, *Enzyme Microbiol. Technol.*, 1981, **3**, 119.
5. M. Casteganro, unpublished results.
6. H. Egan (ed.), *Environmental Carcinogens—Selected Methods of Analysis*, Vol. 4, *Some Aromatic Amines and Azo Dyes in the General and Industrial Environment.* International Agency for Research on Cancer, Lyon, 1981.
7. I. M. Jakovljevic, J. Zynger and R. H. Bishara, *Anal. Chem.*, 1975, **47**, 2045.
8. R. J. Passarelli and E. C. Jacobs, *J. Chromatog. Sci.*, 1975, **13**, 153.
9. I. Mefford, R. W. Keller, R. N. Adams, C. A. Sternson and M. S. Yelo, *Anal. Chem.*, 1977, **49**, 683.
10. J. R. Rice and P. T. Kissinger, *J. Anal. Toxicol.*, 1979, **3**, 64.
11. D. N. Armentrout and J. Cutie, *J. Chromatog. Sci.*, 1980, **18**, 370.
12. R. I. Riggin and C. C. Howard, *Anal. Chem.*, 1979, **51**, 210.
13. J. R. Rice and P. T. Kissinger, *Environ. Sci. Technol.*, 1980, **16**, 263.
14. C. J. Purnell and C. J. Warwick, *Analyst*, 1980, **105**, 861.
15. V. Concialini, G. Chiavari and P. Vitali, *J. Chromatog.*, 1983, **258**, 244.
16. K. Štulík and V. Pacáková, *CRC Crit. Rev. Anal. Chem.*, 1984, **14**, 297.
17. *Idem, J. Chromatog.*, 1984, **298**, 225.
18. *CRC Atlas of Spectral Data and Physical Constants for Organic Compounds*, 2nd Ed., CRC Press, Boca Raton, 1975.

Talanta, Vol. 32, No. 4, pp. 285–289, 1985
Printed in Great Britain.

0039-9140/85 $3.00 + 0.00

FLUORIMETRIC DETECTION OF TAUTOMERIC EQUILIBRIA IN 8-AMINOQUINOLINES

PEDRO J. ZAVALA, MARC D. RADCLIFFE* and STEPHEN G. SCHULMAN†
College of Pharmacy, University of Florida, Gainesville, Florida 32610, U.S.A.

(*Received* 28 *June* 1984. *Revised* 9 *November* 1984. *Accepted* 20 *November* 1984)

Summary—The 1-methylquinolinium cations derived from 8-aminoquinoline and 8-amino-6-methoxyquinoline were prepared by methylation of the corresponding nitroquinolines and reduction of the nitro-compounds. The dissociation constants of the protonated species of these compounds are almost identical to those of doubly-protonated 8-aminoquinoline and 8-amino-6-methoxyquinoline, respectively, suggesting that the parent quinolines are exclusively first protonated at the ring nitrogen atom. However, the molar absorptivities of the 1-methyl derivatives at their longest-wavelength absorption maxima are substantially greater than the corresponding absorptivities of the unmethylated aminoquinolines, a result which suggests tautomerism of the singly-protonated parent quinolines, with a proportion of the population protonated at the amino group. Fluorescence spectroscopy reveals a single emission from the 8-amino-6-methoxy-1-methylquinolinium ion and two excitation-wavelength-dependent fluorescences from the 8-amino-6-methoxyquinolinium ion, confirming the occurrence of tautomerism and supporting choice of the absorptiometric approach rather than the titrimetric approach as the preferred method for the detection of tautomerism and the calculation of tautomeric equilibrium constants.

The aminoquinolines have long been known to form singly-charged cations by protonation of their ring nitrogen atoms.[1-4] The assignments of the protonation sites were based on the red-shift of the ultraviolet and visible region spectra of the neutral aminoquinolines on protonation. However, the arylamino groups and the ring nitrogen atoms have inherently comparable basicity. If the amino groups in some of the molecules and the heterocyclic nitrogen atoms in the others were protonated, there would be a tautomeric equilibrium (Fig. 1). While protonation of a ring nitrogen atom should indeed cause a red-shift of the electronic absorption spectrum, protonation of an amino group would cause a blue-shift. If both phenomena occurred as a result of tautomerism, the red-shift would be the more obvious because the long-wavelength side of the spectrum would shift into regions which would be devoid of absorption bands for the neutral molecule. The blue-shift would be much less obvious, especially if the tautomeric equilibrium favoured protonation of the ring nitrogen atom.

To test the possibility of tautomerism in aminoquinolines the pH-dependence of the absorption spectra of 8-aminoquinoline and 8-amino-6-methoxyquinoline and their ring *N*-methylated cations was examined. Two methods commonly used to detect and measure tautomeric equilibria, one titrimetric and the other spectroscopic, were used to analyse the data. Since these approaches gave conflicting results, a third method, fluorescence spectroscopy, was used to establish the existence of the tautomeric equilibria.

*Department of Chemistry, University of Florida, Gainesville, Florida 32611, U.S.A.
†To whom correspondence should be addressed.

EXPERIMENTAL

8-Aminoquinoline was recrystallized from n-hexane and stored under nitrogen. The purified material gave a single spot ($R_f = 0.71$) on a silica gel TLC plate with methanol as the mobile phase and had m.p. (corrected) 64–65° (dec.) (literature value[5] 65°). 8-Amino-6-methoxyquinoline was purified by column chromatography on silica gel, with 1:24 v/v acetone–benzene solution as mobile phase. The compound was collected as a yellow oil which gave a single spot on a silica gel TLC plate with 15:85 v/v acetone/benzene as the mobile phase ($R_f = 0.6$). Crystals were obtainable from the oil only on standing for two months at −10°. The crystals were stored under nitrogen and had m.p. 49–50° (literature values of 38°,[6] and 53°,[7] have been reported). However, the red-shift (followed by a blue-shift) in the absorption spectrum with decreasing pH, together with the agreement of the proton NMR spectrum ($CDCl_3$), with the literature,[8] as well as the TLC check for purity seems convincing evidence that the compound isolated was 8-amino-6-methoxyquinoline.

8-Amino-1-methylquinolinium perchlorate was prepared by methylating 8-nitroquinoline with dimethyl sulphate and then reducing the 1-methyl derivative with iron and glacial acetic acid according to the method of Deady and Yusoff.[9] The product had m.p. 159–160°, in excellent agreement with the literature.[9] 8-Amino-6-methoxy-1-methylquinolinium perchlorate was similarly prepared from 6-methyl-8-nitroquinoline; the product was recrystallized twice from ethanol and obtained as orange crystals which decomposed at 165° to a brown material which melted sharply at 193°. The proton NMR spectrum (d_6-DMSO) corresponded to that predicted for the 8-amino-6-methoxy-1-methylquinolium ion.

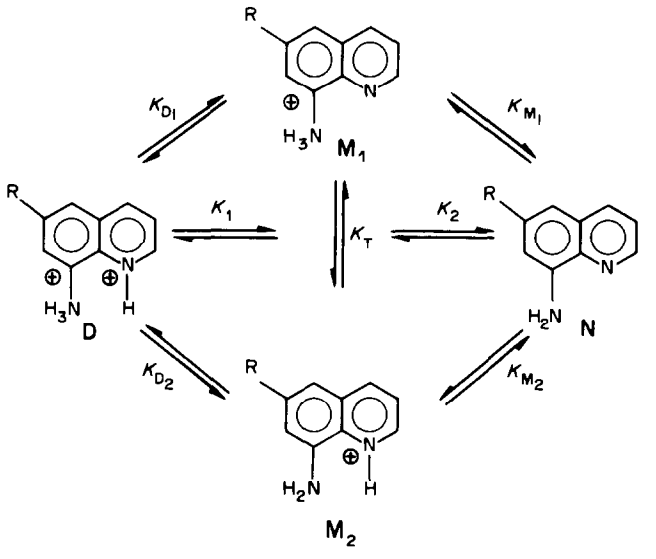

Fig. 1. Dissociation scheme for doubly-protonated (D) 8-aminoquinoline (R = −H) and 8-amino-6-methoxyquinoline (R = $-OCH_3$). K_{D_1} and K_{D_2} are the equilibrium constants for the dissociation pathways to M_1 and M_2, the amino-protonated and ring-protonated singly-charged cations, respectively. K_1 is the macro-equilibrium constant for dissociation of D to all singly-charged species. K_{M_1} and K_{M_2} are the respective dissociation constants for M_1 and M_2 dissociating to the neutral molecule (N). K_2 is the macro-equilibrium constant for dissociation of all single-charged cations to A and K_T is the tautomeric equilibrium constant for $M_2 \rightleftharpoons M_1$.

Absorption spectra were taken on a Beckman DB-GT spectrophotometer. Fluorescence spectra were taken on a Perkin-Elmer MPF-2A fluorescence spectrophotometer with monochromators calibrated against the xenon line-emission spectrum and its output corrected for instrumental response by means of a Rhodamine-B quantum-counter. All pH measurements were made with an Orion 801 pH-meter with a Sargent-Welch combination Ag/AgCl–glass electrode.

Sulphuric acid solutions were prepared by dilution with distilled, demineralized water and those with pH < 2 were calibrated by the H_+ acidity scale of Vetešnik *et al.*[10] Solutions used for absorption and fluorescence spectroscopy were *ca.* $2 \times 10^{-5} M$. All spectral measurements were made at $25.5 \pm 0.3°$.

RESULTS AND DISCUSSION

The dissociation constants of 8-aminoquinoline, 8-amino-6-methoxyquinoline and their protonated 1-methyl derivatives, determined absorptiometrically, are presented in Table 1. Representative titration curves for 6-methoxyguinoline and its 1-methyl derivative are shown in Figs. 2–4. The pK_2 of singly-protonated 8-aminoquinoline is in excellent agreement with the literature value.[5] The pK_1 of doubly-protonated 8-aminoquinoline reported previously[11] was based on calculations using an H_0 acidity scale for the moderately concentrated acid solutions employed in the determination. In the present study, the H_+ scale was used to determine pK_1, because the conjugate base is singly positively charged. The value obtained is in good agreement with that reported previously.[11] To the best of our knowledge the dissociation constants of protonated 8-amino-6-methoxyquinoline have not been reported previously.

The dissociation constants, pK_1, of the protonated 1-methylated aminoquinolines are for all intents and purposes identical to those of the doubly-protonated 8-aminoquinolines. According to Ebert's method,[12] which identifies the pK of the protonated *N*-methylated derivative (D in Fig. 5) with pK_{D_2} in Fig. 1, the 8-aminoquinolines do not measurably exist in tautomeric forms but rather are singly-protonated exclusively at the heterocyclic nitrogen atoms. If tautomerism of the protonated 8-aminoquinolines *did*

Table 1. Dissociation constants of the doubly (pK_1) and singly (pK_2) charged cations derived from 8-aminoquinoline, 8-amino-6-methoxyquinoline and their respective 1-methyl perchlorates, at 25.5°

Parent compound	pK_1	pK_2
8-aminoquinoline	-0.12 ± 0.02	3.91 ± 0.01
8-amino-1-methylquinolinium	-0.14 ± 0.02	—
8-amino-6-methoxyquinoline	-0.51 ± 0.02	3.90 ± 0.02
8-amino-6-methoxy-1-methylquinolinium	-0.56 ± 0.02	—

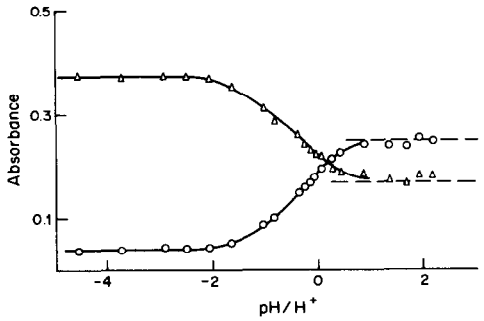

Fig. 2. Absorbance *vs.* pH/H_+ for $1 \times 10^{-5}M$ 8-amino-6-methoxyquinoline in dilute sulphuric acid at two analytical wavelengths (△ 249 nm, ⊙ 268 nm) at 25.5°C.

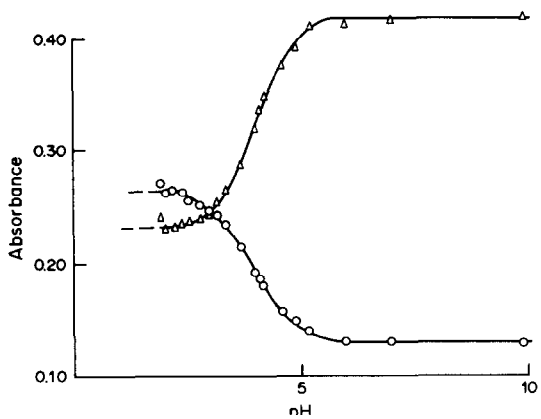

Fig. 3. Absorbance *vs.* pH for $1 \times 10^{-5}M$ 8-amino-6-methoxyquinoline in water at two analytical wavelengths (△ 250 nm, ⊙ 272 nm) at 25.5°C.

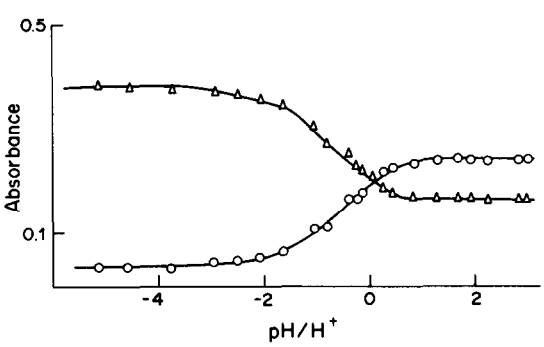

Fig. 4. Absorbance *vs.* pH/H_+ for $1 \times 10^{-5}M$ 8-amino-6-methoxy-1-methylquinolinium perchlorate, in dilute sulphuric acid at two analytical wavelengths (△ 250 nm, ⊙ 273 nm) at 25.5°C.

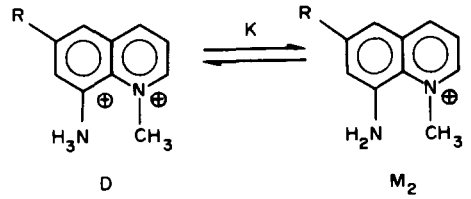

Fig. 5. Dissociation scheme for protonated (D) 8-amino-1-methylquinolinium cations (R = –H or –OCH_3) to the singly-charged cations (M_2).

occur, the pK values of the doubly-protonated 8-aminoquinolines and of the singly-protonated 1-methyl-8-aminoquinolines should differ by at least 0.3.

The molar absorptivities of the longest-wavelength absorption bands of the aminoquinolines and their 1-methyl derivatives are presented in Table 2 and give information about the tautomerism of the 8-aminoquinolines which is in conflict with that from the titrimetric approach (Ebert's method). At pH 1.9, where 8-aminoquinoline and 8-amino-6-methoxyquinoline are more than 99% in their singly-protonated forms, the absorbance, A_M, at some chosen analytical wavelength is given (if tautomerism occurs) by

$$A_M = A_{M_1} + A_{M_2} \quad (1)$$

where A_{M_1} and A_{M_2} are the absorbances due to the amino-protonated and ring-protonated singly-charged cations, respectively. Equation (1) may be rewritten

$$\epsilon_M[M]l = \epsilon_{M_1}[M_1]l + + \epsilon_{M_2}[M_2]l \quad (2)$$

where $[M_1]$ and $[M_2]$ are the equilibrium concentrations of the amino-protonated and ring-protonated species, respectively, ϵ_{M_1} and ϵ_{M_2} are the corresponding molar absorptivities and l is the optical path-length. Equation (2) can be rewritten as

$$\epsilon_M[M_1] + \epsilon_M[M_2] = \epsilon_{M_1}[M_1] + \epsilon_{M_2}[M_2] \quad (3)$$

so if the tautomeric ratio (equilibrium constant) is

$$K_t = [M_1]/[M_2] \quad (4)$$

then

$$K_t = (\epsilon_{M_2} - \epsilon_M)/(\epsilon_M - \epsilon_{M_1}) \quad (5)$$

According to equation (5) a non-zero numerator would imply the occurrence of tautomerism. In the

Table 2. Molar absorptivities and tautomeric ratios (K_t) of the singly charged cations at 25.5° and pH 1.8

Cation	λ_{max}, *nm*	ϵ_{max}, $10^3 l.mole^{-1}.cm^{-1}$	K_t*
8-aminoquinolinium	383	1.19 ± 0.01	0.62 ± 0.03
8-amino-1-methylquinolinium	393	1.93 ± 0.02	—
8-amino-6-methoxyquinolinium	382	1.49 ± 0.01	0.14 ± 0.02
8-amino-6-methoxy-1-methylquinolinium	392	1.70 ± 0.02	—

*K_t = [amino-protonated ion]/[ring-nitrogen protonated ion].

systems of interest here, ϵ_M would be the apparent molar absorptivity of 8-aminoquinoline or 8-amino-6-methoxyquinoline measured at pH 1.9, and ϵ_{M_2} could be estimated from the corresponding spectral features of the 1-methyl derivatives. A particularly useful analytical wavelength to use in each case would be that of the maximum of the longest-wavelength absorption band in each compound. Not only would these wavelengths correspond to the same spectral features in the aminoquinolines and in their ring-methylated derivatives, but the use of these spectral bands would also obviate the necessity to prepare the trimethylammonium derivatives of the aminoquinolines. It is assumed that the methylated and non-methylated cations have equal transition probabilities and that because the band-widths at half peak-height are almost identical, the molar absorptivities at λ_{max} will also be the same. Because of the shift of the absorption spectra of amino-aromatics to shorter wavelengths on protonation of the amino group, at the long-wavelength absorption maxima of the ring-protonated or methylated aminoquinolines $\epsilon_{M_1} = 0$. Equation (5) then becomes

$$K_t = (\epsilon_{M_2} - \epsilon_M)/\epsilon_M \qquad (6)$$

Also presented in Table 2 are the values of K_t for the 8-aminoquinolinium and 8-amino-6-methoxyquinolinium singly-charged cations. The spectroscopic method just described and the data of Table 2 indicate that there is substantial tautomerism between the two singly-charged cations for both 8-aminoquinoline and 8-amino-6-methoxyquinoline. These results are clearly in conflict with those obtained by Ebert's method.[12]

In order to resolve the apparent dilemma it was decided to find whether the various tautomeric species in question are fluorescent. For 8-aminoquinoline, no fluorescence could be found at any pH, in agreement with an earlier investigation of this compound.[13] Nor could fluorescence from the 8-amino-1-methylquinolinium ion be detected in aqueous solutions at any pH. The 8-amino-6-methoxy-1-methylquinolinium ion, however, did demonstrate a single moderately intense fluorescence band with a maximum at 440 nm at pH 1–10. The excitation spectrum or this species had maxima near the absorption maxima of the methylated derivative at 393, 338 and 272 nm. At pH < 1 the emission at 440 nm increased in intensity (Fig. 6) and shifted to 435 nm. Presumably, the latter emission originated from the doubly-charged cation. The fluorescences of the singly- and doubly-charged 8-amino-6-methoxy-1-methylquinolinium ions are both close to the fluorescence maximum of protonated 6-methoxquinoline, which lies at 438 nm.[14] This would certainly be expected for the doubly-charged cation, in which the protonated amino group can have almost no effect on the position of the bands in the electronic spectra. The similarity of the fluorescence of the singly-charged ring-nitrogen methylated cation to that of protonated 6-methoxyquinoline indicates that either the interaction of the lone-pair of the amino group with the aromatic ring does not appreciably affect the state from which the emission originates, or that the interaction leads to an emitting state which is accidentally essentially isoenergetic with the emitting state of protonated 6-methoxyquinoline.

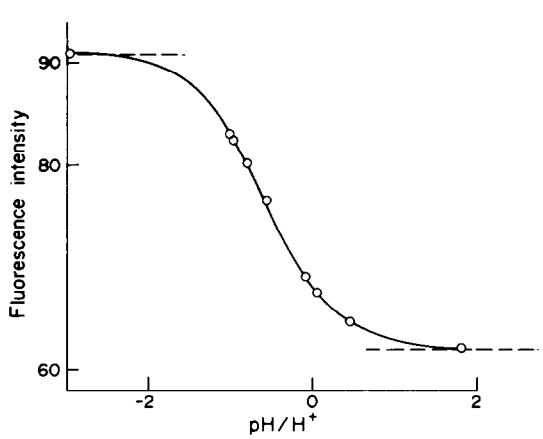

Fig. 6. Fluorescence intensity *vs.* pH/H_+ for $1 \times 10^{-5}M$ 8-amino-6-methoxy-1-methylquinolinium ion in dilute sulphuric acid ($\lambda_{ex} = 316$ nm., $\lambda_{em} = 435$ nm) at 25.5°C.

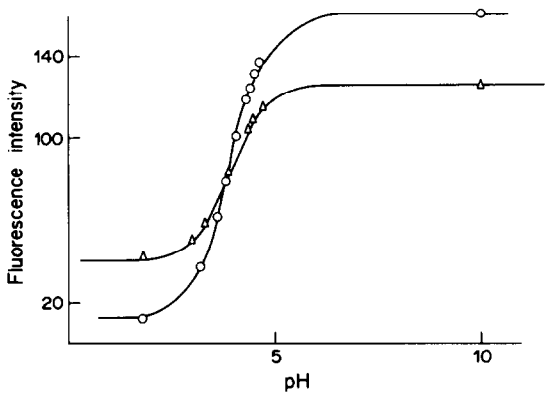

Fig. 7. Fluorescence intensity *vs.* pH for $1 \times 10^{-4}M$ 8-amino-6-methoxyquinoline in water (△, $\lambda_{ex} = 354$ nm, $\lambda_{em} = 460$ nm; ⊙, $\lambda_{ex} = 280$ nm, $\lambda_{em} = 365$ nm) at 25.5°C.

At pH 1.9, 8-amino-6-methoxyquinoline has two fluorescence bands, at 365 and 460 nm. As the pH is varied, both bands increase in intensity and coalesce to give a single fluorescence band which at high pH is centred at 380 nm. The inflection region of the fluorescence *vs.* pH graph is centred at pH 3.9 (Fig. 7), corresponding to pK for dissociation of the singly-charged species. This suggests that the emissions at both 365 and 460 nm arise from the singly-protonated species. Moreover, at pH < 1 the two emissions decrease and give way to a single fluorescence band at 435 nm, presumably that of the doubly-charged cation. The inflection for this change is centred at $H_+ = -0.5$, corresponding to the pK of the doubly-charged cation.

The fluorescence bands of 8-amino-6-methoxyquinoline at pH 1.9 have different excitation spectra. That at 460 nm has excitation peaks near 380, 333 and 269 nm, similar to the excitation spectrum of the 1-methyl derivative, and the emission at 365 nm has excitation peaks near 325 and 272 nm, not unlike the excitation spectrum of neutral 6-methoxyquinoline.[14] The fluorescence at 365 nm is, moreover, close to the emission maximum of neutral 6-methoxyquinoline,[14] which lies at 362 nm. The fact that the two fluorescence bands which seem to originate from singly-protonated 8-amino-6-methoxyquinoline have very different excitation spectra indicates that there are two ground-state species of substantially different electronic structure, rather than a single species giving two emissions. The most likely explanation for this would be that there are two tautomeric forms of the singly-charged cation. One, protonated at the ring nitrogen atom, would have emission and excitation spectra similar to those of the 8-amino-6-methoxy-1-methylquinolinium ion in which the 1-methyl group is similar to a "non-dissociating proton." The other, protonated at the 8-amino group, would have emission and excitation spectra similar to those of uncharged 6-methoxyquinoline (protonation of the amino group alone would effectively prevent it from having a substantial effect on the aromatic portion of 8-amino-6-methoxyquinoline, and give it essentially the electronic structure of 6-methoxyquinoline). Presumably, singly-protonated 8-aminoquinoline also exists as two tautomers. Unfortunately, the fluorescence approach, though qualitatively indicating the occurrence of tautomers, requires the specification of too many parameters for the acquisition of quantitative information about the tautomeric ratios. It may be concluded, however, that the use of the absorption spectra of alkylated model compounds to evaluate tautomeric equilibria is more accurate than the evaluation of the tautomeric equilibria by comparison of the dissociation constants of the model compounds with those of the substances in question.

REFERENCES

1. J. L. Irvin and E. M. Irvin, *J. Am. Chem. Soc.*, 1947, **69**, 1091.
2. D. P. Craig and L. N. Short, *J. Chem. Soc.*, 1945, 419.
3. E. A. Steck and G. W. Ewing, *J. Am. Chem. Soc.*, 1948, **70**, 3397.
4. J. C. Craig and D. E. Pearson, *J. Heterocyclic Chem.*, 1968, **5**, 3397.
5. A. Albert, R. Goldacre and J. N. Phillips, *J. Chem. Soc.*, 1948, 2240.
6. *Handbook of Chemistry and Physics*, p. C-486. C.R.C. Press, Cleveland, 1980.
7. *Beilstein's Handbuch der Organische Chemie*, 22 III-IV, p. 5747. Springer-Verlag, Berlin, 1980.
8. *Sadtler Standard Spectra*, NMR-2010, Sadtler Research Laboratories, Philadelphia, 1976.
9. L. W. Deady and N. I. Yusoff, *J. Heterocyclic Chem.*, 1976, **13**, 125.
10. P. Vetešník, J. Bielavský and M. Večeřa, *Collection Czech. Chem. Commun.*, 1968, **33**, 1687.
11. E. V. Brown and A. C. Plasz, *J. Heterocyclic Chem.*, 1971, **7**, 335.
12. L. Ebert, *Z. Phys. Chem.* (*Leipzig*), 1926, **121**, 385.
13. S. G. Schulman and L. B. Sanders, *Anal. Chim. Acta*, 1971, **56**, 83.
14. S. G. Schulman, R. M. Threatte, A. C. Capomacchia and W. L. Paul, *J. Pharm. Sci.*, 1974, **63**, 867.

Talanta, Vol. 32, No. 4, pp. 291–294, 1985
Printed in Great Britain.

0039-9140/85 $3.00 + 0.00

SENSITIVE FLOTATION-SPECTROPHOTOMETRIC DETERMINATION OF GOLD, BASED ON THE GOLD(I)–IODIDE–METHYLENE BLUE SYSTEM

Z. MARCZENKO and K. JANKOWSKI
Department of Analytical Chemistry, Technical University, Warsaw, Poland

(*Received* 25 *February* 1984. *Revised* 7 *October* 1984. *Accepted* 8 *November* 1984)

Summary—The gold(I)–iodide–Methylene Blue (MB) system is suitable for flotation separation and spectrophotometric determination of gold. Under the optimum conditions $[(MB^+)(AuI_2^-)]\cdot 3[(MB^+)(I_3^-)]$ is formed, and floated with cyclohexane. The product is dissolved in methanol and its absorbance measured. The molar absorptivity is 3.4×10^5 l.mole^{-1}.cm^{-1} at 655 nm. The proposed method is more than three times as sensitive as the Rhodamine B method. Pt, Pd, Ag and Hg interfere seriously, and Ir, Rh, Bi and Cd to a smaller extent. Preliminary separation of gold by precipitation with tellurium as a collector is recommended. The method has been applied to determination of gold traces (about 1×10^{-4}%) in a copper sample.

We have used the sparingly soluble ion-association compounds formed by some anionic complexes of platinum metals with appropriate basic dyes to develop very sensitive flotation–spectrophotometric methods for determination of all six platinum metals.[1–8] The molar absorptivities (ε) are in the range $1.7–4.0 \times 10^5$ l.mole^{-1}.cm^{-1}, because one atom of metal is associated with 2–5 dye molecules. The sparingly soluble compounds accumulate at the phase boundary or on the wall of the separatory funnel when the aqueous phase is shaken with a suitable solvent of low polarity. The washed precipitate is dissolved in a polar solvent and the absorbance of the solution is measured. In this modification of flotation separation, droplets of the low-polarity solvent, dispersed in the aqueous phase by shaking, act like inert gas bubbles and cause flotation of the precipitate.[9,10] The ion-association compounds formed with the basic dyes are hydrophobic, which makes it useless to add surfactants to the system.

This paper describes extension of the technique to spectrophotometric determination of gold. Some of the most sensitive spectrophotometric methods of gold determination yet reported are based on the extraction of ion-pairs of $AuCl_4^-$ or $AuBr_4^-$ with univalent basic dye cations,[11–17] the Rhodamine B method ($\varepsilon = 9.7 \times 10^4$) being the best known; the determination with thio-Michler's ketone[18,19] ($\varepsilon = 1.2 \times 10^5$) is slightly more sensitive.

EXPERIMENTAL

Reagents

Gold(III) standard solution (1 *mg/ml*). Dissolve 0.1000 g of pure gold in 4 ml of *aqua regia*. Evaporate the solution almost to dryness on a water-bath. Add 4 ml of concentrated hydrochloric acid, evaporate to half the volume, and dilute to the mark with water in a 100-ml standard flask. Dilute further with 0.1*M* hydrochloric acid as required.

Methylene Blue hydrochloride (*MB*) (*Merck*) *solution*, 1×10^{-3}M.

Potassium iodide, *0.01*M *solution.*

Potassium iodate, 5×10^{-5}M *solution.*

*Iodine-125, as sodium iodide, in 0.1*M *sodium hydroxide.*

Procedure

Place the sample solution (in about 0.5*M* hydrochloric acid, containing not more than 4 μg of gold) in a separatory funnel, and add 2 ml of iodide solution and 2 ml of iodate solution, with swirling, followed by enough hydrochloric acid to give 0.5*M* concentration. Then add 1.5 ml of Methylene Blue solution and shake with 10 ml of cyclohexane for 1 min. After separation of the phases, remove the aqueous phase and wash the precipitate and organic solvent by shaking (for 1 min) with 20 ml of water. After separation of the phases, remove them carefully, and dissolve the precipitate off the wall with methanol. Dilute the solution to volume with methanol in a 10-ml standard flask and measure its absorbance at 655 nm against a reagent blank prepared in the same way.

RESULTS AND DISCUSSION

Preliminary investigations

The extraction of the anionic complexes of gold with chloride, bromide, iodide, thiocyanate, thiosulphate and oxalate by means of Methylene Blue, Toluidine Blue, Methylene Green, Azure II (thiazine dyes), Capri Blue, Meldola Blue, Nile Blue A (oxazine dyes), Crystal Violet, Brilliant Green, Malachite Green (triphenylmethane dyes), Rhodamine 6G and Rhodamine B (xanthene dyes) from various media (ranging from pH 3 to 3*M* hydrochloric acid or sulphuric acid) into benzene, toluene, xylene, cylcohexane and di-isopropyl ether was examined.

Only the iodide, bromide and thiocyanate systems gave flotation, mainly with the azine dyes. Most of the systems (but not thiosulphate and oxalate systems) gave products extractable into the organic phase.

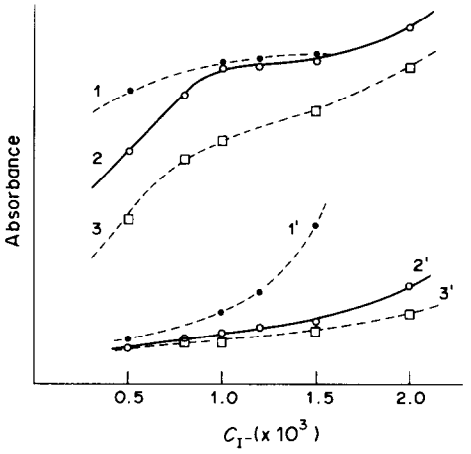

Fig. 1. Effect of the iodide and iodate concentrations on formation and flotation of the gold compound. Concentration of IO_3^-: curve 1, $6 \times 10^{-6}M$; 2, $5 \times 10^{-6}M$; 3, $3.5 \times 10^{-6}M$ (absorbance measurements against the blank). Blank values (curves 1′, 2′, 3′) measured against methanol.

The iodide/Methylene Blue system was the most promising and was investigated further.

Formation and flotation of the gold compound

When dilute hydrochloric or sulphuric acid containing gold (as $AuCl_4^-$), is mixed with iodide and Methylene Blue, and shaken with cyclohexane, a dark precipitate, containing all the gold, accumulates on the wall of the separatory funnel. The absorbance of a methanolic solution of the precipitate indicates that several dye molecules are associated with each gold atom, but this high absorbance is achieved only if iodine was also present in the aqueous phase.

It is known[12] that in acid medium gold(III) is reduced to gold(I):

$$AuCl_4^- + 4I^- \rightarrow AuI_2^- + I_2 + 4Cl^-$$

and it appears that the simple ion-pair $[(MB^+)(AuI_2^-)]$ may be associated with the tri-iodide/dyestuff ion-pair $[(MB^+)(I_3^-)]$.

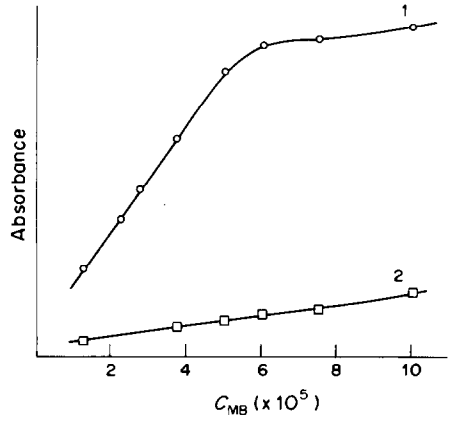

Fig. 2. Dependence of the absorbance of the methanol solution of the gold compound on the Methylene Blue concentration: curve 1, absorbance of the gold compound solution measured against the blank; 2, blank absorbance measured against methanol.

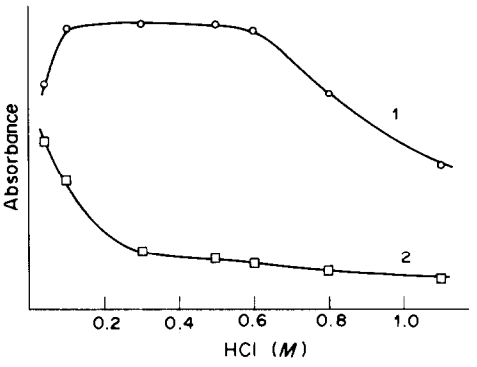

Fig. 3. Effect of the hydrochloric acid concentration on formation and flotation of the gold compound: curve 1, absorbance of the gold compound solution measured against the blank; 2, blank absorbance measured against methanol.

Reproducible and maximal absorbances are obtained if the aqueous phase, before the flotation, contains a fixed iodine concentration that is stoichiometrically smaller than the amount of dye added afterwards. The amount of iodine can be controlled by adding a known amount of potassium iodate and a suitable excess of potassium iodide. The solution should be protected from direct sunlight to avoid photochemical oxidation of the iodide. From Fig. 1, it is evident that at an iodate concentration of $5 \times 10^{-6}M$, the iodide concentration should be $1.0\text{–}1.3 \times 10^{-3}M$.

A Methylene Blue concentration of $6 \times 10^{-5}M$ (60–80-fold molar excess with respect to 2 μg of gold) gives maximal absorbance (Fig. 2). The optimum acidity range is rather narrow: 0.3–0.6M hydrochloric acid (Fig. 3). From a practical point of view, hydrochloric acid medium is more convenient than sulphuric acid medium, and gives lower blank values. Cyclohexane appears to be the best organic phase, its use resulting in maximum dye:metal molar ratio.

The precipitate accumulates on the wall of the separatory funnel above the liquid-phase level when the shaking has been completed, if the separatory funnel is opened, and presumably the precipitate clings to the wall as the thin film of organic solvent evaporates. Complete separation requires shaking of the phases for about 1 min. The volume of organic solvent is not critical and may be much smaller than that of the aqueous solution.

The precipitate, after removal of the liquid phase, must be washed free from excess of dye. A single washing with 20 ml of water (shaking for 60 sec) gives reproducible results, and the absorbance of the reagent blank is about 0.10.

The washed compound is readily dissolved in methanol or acetone but the methanolic solution is more stable. There is a small shift of about 5 nm in λ_{max} for the gold compound relative to the dye

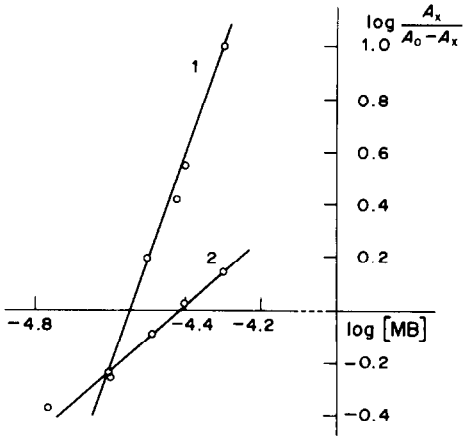

Fig. 4. Determination of the Au:MB molar ratio in the floated compound: curve 1, single washing; 2, double washing.

solution, which can be attributed to the influence of I_3^- and AuI_2^- on the dyestuff ions.

Composition of the gold compound

The molar ratio of metal to Methylene Blue in the complex was found to be 1:4 (on the basis of the ratio of the absorbance of the gold compound in the methanol to the absorbance of the solution of the free dye. This ratio was confirmed by the Bent and French method[20] (line 1 in Fig. 4).

Additional shaking (for 60 sec) of the precipitate with a second portion of water leads to a compound in which the gold:dye ratio is only 1:1 (line 2 in Fig. 4). Shaking for at least 45 sec is necessary to ensure complete conversion into the 1:1 complex.

Attempts were made to determine radiometrically, with ^{125}I, the ratio of gold to iodine in the precipitate separated by flotation. From 9 tests, it was found that on average one gold atom corresponds to 11 or 12 iodine atoms (the range of results was 9.7–13.2). Taking into consideration the limited precision of the method, this ratio may be postulated to be 1:11, which would correspond to the precipitate separated and washed with one portion of water being an adduct of two ion-association complexes:

$$[(MB^+)(AuI_2^-)]\cdot 3[(MB^+)(I_3^-)]$$

This adduct is rather unstable and decomposes during the second washing. The dye and iodide (I^-) pass to the aqueous phase and the iodine (I_2) to the residual cyclohexane present. The remaining compound is the simple ion-association complex $[(MB^+)(AuI_2^-)]$. From the analytical point of view, only the first compound is of interest, because it leads to a very sensitive spectrophotometric method for the determination of gold.

It must be emphasized that in contrast to the flotation–spectrophotometric methods for the determination of platinum metals[1-8] and other methods of this kind, based on ion-association complexes, the basis of the present method is a compound which does not contain a multivalent anionic complex of the element to be determined.

Determination of gold

The calibration graph obtained according to the procedure obeys Beer's law up to a gold concentration of 0.4 μg/ml. The molar absorptivity is 3.4×10^5 l.mole^{-1}.cm^{-1} at 655 nm. The method is therefore about 3.5 times as sensitive as the commonly used Rhodamine B method.

The method has been used for determination of gold at three concentration levels. The statistical evaluation of the results is presented in Table 1. The results for determination of trace amounts of gold in the presence of certain elements are listed in Table 2. Platinum, palladium, silver and mercury interfere considerably. Small quantities of iridium, rhodium, bismuth and cadmium can be tolerated. Copper does not interfere at 1000-fold weight ratio to gold, and tellurium practically does not interfere at all. It follows that before traces of gold are determined by the method, they can be separated by precipitation with tellurium as collector.[11-13]

The method was applied to determination of trace amounts of gold in copper. The sample was dissolved in 2–3*M* nitric acid, then diluted, some filter-paper pulp was added, and filtered off, washed with dilute nitric acid and water, then ignited. The residue from

Table 1. Statistical evaluation of the results (7 determinations) for gold

Gold added, μg	Gold found, μg	Standard deviation, μg	Relative standard deviation, %	Confidence limits (probability level 0.95)
0.80	0.84	0.06	7.2	0.84 ± 0.06
2.00	2.06	0.08	3.9	2.06 ± 0.08
3.50	3.48	0.09	2.6	3.48 ± 0.09

Table 2. Effect of some elements on the determination of gold (2 μg) with Methylene Blue

Metal	Mass ratio M:Au	Gold recovery, %		Metal	Mass ratio M:Au	Gold recovery, %	
Pt	0.1	115	113	Hg	0.2	104	106
	0.2	130	132		0.5	116	118
	0.5	177	170		1	147	147
Pd	0.1	109	107	Bi	10	99	100
	0.2	125	127		50	124	121
	0.5	144	142		200	135	137
Ir	5	102	103	Cd	50	103	105
	10	105	110		200	109	109
	50	152	152		1000	111	112
Rh	5	100	101	Cu	200	100	107
	10	107	105		1000	107	107
	50	130	128		5000	143	138
Ag	0.4	129	128	Te	50	97	100
	1	148	144		500	100	101
	5	220	215		2000	103	105

Table 3. Determination of Au in copper

Sample weight, g	Gold added, μg	Gold found, μg	Au content in copper*, $\times 10^{-5}$%
2.99		2.55	9.2
3.00		2.60	9.3
3.00		2.65	9.5
1.51		1.35	9.6
1.50		1.25	9.0
1.51		1.50	10.4
3.00	1.50	4.05	9.4
3.00	1.50	3.85	9.2
3.01	1.50	4.00	9.3
1.50	1.50	2.65	9.6
1.50	1.50	2.80	9.8
1.51	1.50	2.80	9.8

*Statistical data: $\bar{x} = 9.5 \times 10^{-5}$%; $s = 0.47 \times 10^{-5}$%; $s_r = 5.0$%; $\mu_{0.95} = (9.5 \pm 0.31) \times 10^{-5}$%.

the ignition was dissolved in *aqua regia* and the solution was evaporated to dryness. Hydrochloric acid was added to the residue and the solution again evaporated to dryness, and this step was repeated twice more. The residue was taken up in 1.5*M* hydrochloric acid and the gold was precipitated with tellurium as collector and hydrazine as reductant.[13] The precipitate was filtered off, washed with 1.5*M* hydrochloric acid and water and ignited. The product was dissolved in *aqua regia*, 20 mg of sodium chloride were added, and the solution was evaporated to dryness on a boiling water-bath. The evaporation was repeated after addition of hydrochloric acid. Gold was then determined according to the procedure given. Table 3 gives the results. The recovery of a known amount of gold added was 90–95%. The same result was obtained for the gold content of the copper by the Rhodamine B method.

Acknowledgement—This work was supported by Research Program MR-I-32.

REFERENCES

1. Z. Marczenko, *Crit. Rev. Anal. Chem.*, 1981, **11,** 195.
2. Z. Marczenko and J. Uścińska, *Microchem. J.*, 1981, **26,** 453.
3. Z. Marczenko and M. Jarosz, *Analyst*, 1981, **106,** 751.
4. *Idem, Talanta*, 1981, **28,** 561.
5. Z. Marczenko, M. Balcerzak and H. Pasek, *Mikrochim. Acta*, 1982**II,** 371.
6. Z. Marczenko and K. Kalinowski, *Anal. Chim. Acta*, 1982, **144,** 173.
7. *Idem, Mikrochim. Acta*, 1983**II,** 169.
8. *Idem, Anal. Chim. Acta*, 1983, **153,** 219.
9. E. B. Sandell and H. Onishi, *Photometric Determination of Traces of Metals; General Aspects*, Interscience, New York, 1978.
10. A. Mizuike and M. Hiraide, *Pure Appl. Chem.*, 1982, **54,** 1555.
11. F. E. Beamish and J. C. Van Loon, *Recent Advances in the Analytical Chemistry of the Noble Metals*, Pergamon Press, Oxford, 1972.
12. A. I. Busev and V. M. Ivanov, *Analiticheskaya khimiya zolota*, Izdat. Nauka, Moscow, 1973.
13. Z. Marczenko, *Spectrophotometric Determination of Elements*, Horwood, Chichester, 1976.
14. *Idem, Mikrochim. Acta*, 1977**II,** 651.
15. A. V. Radushev and G. Ackermann, *Zavodsk. Lab.*, 1978, **44,** 1431.
16. B. I. Nabivanets, E. M. Zadorozhnaya and N. N. Maslei, *Zh. Analit. Khim.*, 1973, **28,** 1901.
17. V. M. Ivanov, N. N. Yurzhenko and P. N. Nesterenko, *ibid.*, 1982, **37,** 1193.
18. I. Tsukahara, *Talanta*, 1977, **24,** 633.
19. A. T. Pilipenko, O. P. Riabushko and G. S. Matsibura, *Zh. Analit. Khim.* 1979, **34,** 1088.
20. M. Bent and C. French, *J. Am. Chem. Soc.*, 1941, **63,** 568.

Talanta, Vol. 32, No. 4, pp. 295–299, 1985
Printed in Great Britain

0039-9140/85 $3.00 + 0.00
Pergamon Press Ltd

DETERMINATION OF SULPHA-DRUGS WITH ION-SELECTIVE MEMBRANE ELECTRODES—II

G. E. BAIULESCU
Department of Analytical Chemistry, Institute of Chemistry, Polytechnic Institute of Bucharest, Spl. Independenţei 89, 77207 Bucharest, Romania

GÖNÜL KANDEMIR
Department of Analytical Chemistry, University of Istanbul, Beyazit, Faculty of Pharmacy, Istanbul, Turkey

M. S. IONESCU* and C. CRISTESCU
Institute of Chemical and Pharmaceutical Research, Bucharest, 74351, Sos. Vitan 112, Bucharest-3, Romania

(*Received* 10 *January* 1984. *Revised* 19 *September* 1984. *Accepted* 8 *November* 1984)

Summary—Two liquid-membrane electrodes, one sensitive to Cu^{2+} and the other to Ag^+, were used for the determination of various sulpha-drugs with $pK_a \geqslant 6$ (as the sodium salts) by potentiometric titration with $CuSO_4$ and $AgNO_3$. The construction and basic characteristics of these two electrodes are discussed.

For the determination of sulpha-drugs with the aid of ion-selective electrodes, the literature so far gives only two methods. The first uses electrodes sensitive to sulphamerazine and sulphisomidine.[1] These electrodes are based on a nitrobenzene solution of the ion-association complex of the iron(II)–bathophenanthroline chelate and the respective sulpha-drug. The second,[2] which is more rapid and accurate, is based on the well-known ability of these compounds to form highly insoluble mercury(II) compounds.[3,4] For the determination, an Hg^{2+}-selective electrode and a commercial silver sulphide crystal electrode were used. Recently, new results for the determination of some sulpha-drugs by using Ag^+- or Cu^{2+}-membrane electrodes have been reported.[5–7]

In this paper, we report our further researches in the field of sulpha-drug determination with ion-selective electrodes, dealing with their determination in alkaline medium, in which they are found as sodium salts. We have chosen this direction for research because the injectable solutions of these sulpha-drugs are prepared by dissolving the sulpha-drug in 20% sodium hydroxide solution. The determination method we are proposing is based on the metathetic reaction:

$$z(R\text{–}SO_2\text{–}\underset{\displaystyle R'}{\underset{|}{N}}\text{–}Na) + M^{z+} \rightarrow (R\text{–}SO_2\text{–}\underset{\displaystyle R'}{\underset{|}{N}}\text{–})M^{z+} + z\,Na^+$$

$$(M^{z+} = Cu^{2+}, Ag^+)$$

The copper and silver salts of the sulpha-drugs are insoluble, so the sulpha-drugs may be determined by direct titration with copper sulphate or silver nitrate.

We have used both commercially available Cu^{2+}- and Ag^+-selective electrodes, and two electrodes of our own construction. The literature mentions numerous Cu^{2+}- and Ag^+-selective electrodes, having membranes which consist of copper or silver complexes, dissolved in suitable organic solvents.[8–18]

The electrodes prepared by us have membranes

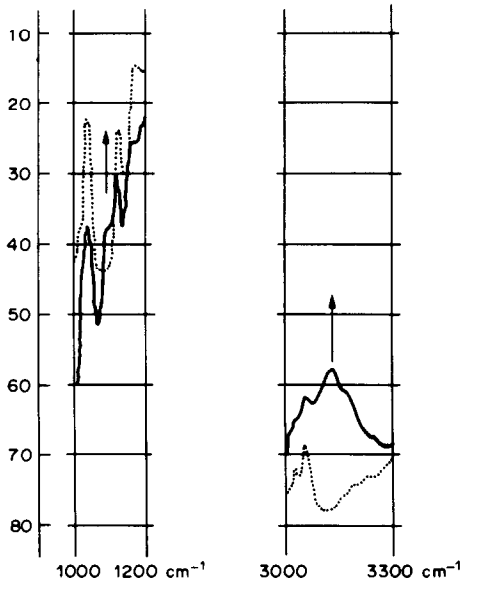

Fig. 1. Infrared spectra of the HRI ligand and $Cu(RI)_2$ complex —— HRI. ----- $Cu(RI)_2$.

*To whom correspondence may be sent.

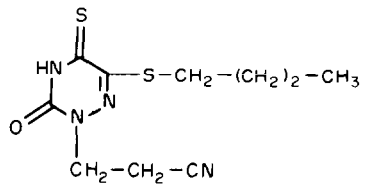

(HRI)

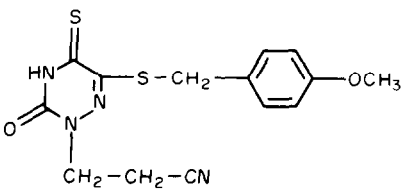

(HRII)

made with the copper and silver complexes of two derivatives (HRI and HRII) of aza-uracil.[19]

The functional groups of these compounds react in the thiol form, binding the metal to nitrogen and sulphur atoms; this is confirmed by the infrared spectra (Fig. 1). The characteristic band for thiocarbonyl ($C=S$) which appears in the ligand spectrum at 1113 cm^{-1} (as a shoulder), disappears in the spectra of the complexes. Further proof of coordination of the metal ion to the ligand in thiolic form is the disappearance of the ν_{NH} stretching band at 3100 cm^{-1}.

The proposed composition of the Cu^{2+} and Ag^{+} complexes was confirmed by elementary analysis of the compounds obtained in the solid state ($Cu_{theory} = 9.52\%$; $S_{theory} = 21.14\%$; $Cu_{found} = 9.86\%$; $S_{found} = 21.2\%$; $Ag_{theory} = 24.43\%$; $S_{theory} = 14.50\%$; $Ag_{found} = 24.0\%$; $S_{found} = 14.8\%$) and by determination of the combining ratios (1:2, 1:1) by the method of continuous variations.

EXPERIMENTAL

Apparatus and reagents

The e.m.f. values were measured at room temperature in stirred solutions, with an MV-87 digital pH/mV—meter (Prăcitronic, East Germany). The potentiometric titration curves were recorded with an automated outfit composed of a Radiometer TTT2 titrator, ABU 12 autoburette and SBR 2c recorder. A saturated calomel electrode (Radiometer K 401) was used as reference electrode. The pH measurements were made with a glass–calomel electrode pair (Radiometer types G 202 C and K 401).

All reagents used were of analytical grade, except HRI and HRII, which were obtained and purified by Cristescu.[19]

Preparation of the Cu^{2+}-selective membrane

Ten ml of $10^{-2}M$ $CuSO_4 \cdot 5H_2O$ were shaken in a separating funnel for 5 min with 15 ml of chloroform containing 0.0406 g of HRI, then the phases were separated and the organic layer was dried by passage through anhydrous sodium sulphate, transferred to a 100-ml standard flask and diluted to volume with chloroform. The concentration of the complex in this solution was $5 \times 10^{-4}M$.

Preparation of the Ag^{+}-selective membrane

Ten ml of $10^{-2}M$ $AgNO_3$ were mixed with 10 ml of chloroform containing 6.68 mg of HRII and shaken for 10 min. The phases were separated and the organic layer was dried and diluted to 100 ml as described above. The concentration of the complex in this solution was $10^{-3}M$.

Construction of electrodes

The construction of the electrodes has been described previously[20] and consists of impregnating the support material (a graphite rod 15 mm long, 6.5 mm in diameter, made water-repellent) with Cu–HRI or Ag–HRII solution in chloroform. The internal reference electrodes were eliminated by using a stainless-steel wire introduced into the graphite rod. The electrodes were stored in the appropriate organic phase and washed with distilled water between measurements.

Procedures

Potentiometric titration. The pair of electrodes (Cu^{2+}- or Ag^{+}-selective as indicator electrode and SCE as reference) were placed in the sample solution (20–30 ml, concentration *ca.* $10^{-2}M$). The sample was titrated with $0.1M$ $CuSO_4$ and/or $0.1M$ $AgNO_3$ solution. The end-point corresponds to the maximum slope on the E *vs.* volume titration curve.

Injectable aqueous solution of sulphamethoxidiazine. The contents of an ampoule were transferred with distilled water into a 25-ml standard flask and diluted to volume. A volume of 2.5 ml of this solution was transferred to a 50-ml beaker and 20 ml of distilled water were added. The solution was potentiometrically titrated with $0.1M$ $CuSO_4$ and/or $0.1M$ $AgNO_3$ solution, as above.

RESULTS AND DISCUSSIONS

The electrode function, E–pM^{z+}

The e.m.f. measurements were made with the electrochemical cell:

M^{z+}-selective membrane electrode	M^{z+} ($C_{Cu^{2+}}$, $C_{Ag^{+}}$) $I = 0.4M$ KNO_3 for Cu^{2+} $I = 0.1M$ KNO_3 for Ag^{+}	Satd. KNO_3 soln.	SCE	(I)

where $C_{Cu^{2+}}$ and $C_{Ag^{+}}$ represent the Cu^{2+} and Ag^{+} concentrations, respectively, varied in the range 10^{-6}–$10^{-1}M$. The measurements were made at constant ionic strength ($0.4M$ for Cu^{2+} and $0.1M$ for Ag^{+} adjusted with potassium nitrate) and the junction potential was kept constant. The variation of e.m.f. with pM^{z+} is presented in Fig. 2.

For the Cu^{2+}-selective electrode, the linear response range is 10^{-5}–$10^{-1}M$ with a slope of 30.6 mV/decade and for the Ag^{+}-selective electrode the linear response range is smaller (10^{-4}–$10^{-1}M$) but the slope is nearly Nernstian (59.7 mV/decade). The inability to obtain a better detection limit with this electrode is probably due to the adsorption of Ag^{+} ions at the end of the electrolyte bridge and on the surface of the glass vessel.

Extrapolation of both lines to $pM^{z+} = 0$ leads to values of $E_0' = 400$ mV for the Cu^{2+}-selective electrode and $E_0' = 548$ mV for the Ag^{+}-selective electrode.

Table 1. Effect of solvent on sensitivity of the Ag^+-selective membrane electrode

Solvent	Dielectric constant	Slope, *mV/decade*	Concentration range of linear response, M
Nitrobenzene	34.8	59.7	10^{-4}–10^{-1}
1,2-Dichloroethane	10.4	60	10^{-3}–10^{-1}
Chloroform	4.8	61	10^{-3}–10^{-1}

The linear response range of the Ag^+-selective electrode is reduced to 10^{-3}–$10^{-1}M$ when 1,2-dichloroethane or chloroform is used as solvent for the liquid membrane (Table 1).

Influence of pH. The pH range in which the potential remains constant is 3–7 for the Ag^+-selective electrode and 3–5.5 for the Cu^{2+}-selective electrode. The direct potential measurements for calibration of both electrodes were done at pH 5.

Response time. The response characteristics of the electrodes were evaluated by introducing them into copper sulphate and silver nitrate solutions, as appropriate, of different concentrations but identical acidity (pH 5) and recording the e.m.f. values as a function of time. The response time of the electrodes in dilute solutions ($pM^{z+} = 4$ and 5) is about 4 min, and in concentrated solutions only a few seconds.

Selectivity. The selectivity coefficients $K_{M^{z+},M^{z'+}}$ were calculated by the method of Srinivasan and Rechnitz[21] from the relation:

$$\log K_{M^{z+},M^{z'+}} = \frac{E_{II} - E_I}{S} + \log [M^{z+}] - \log [M^{z'+}]^{z/z'}$$

where S is the slope of the electrode function, E_I is the e.m.f. of cell (I) for $C_{M^{z+}} = 0.01M$ and E_{II} is the e.m.f. of an electrochemical cell of the type:

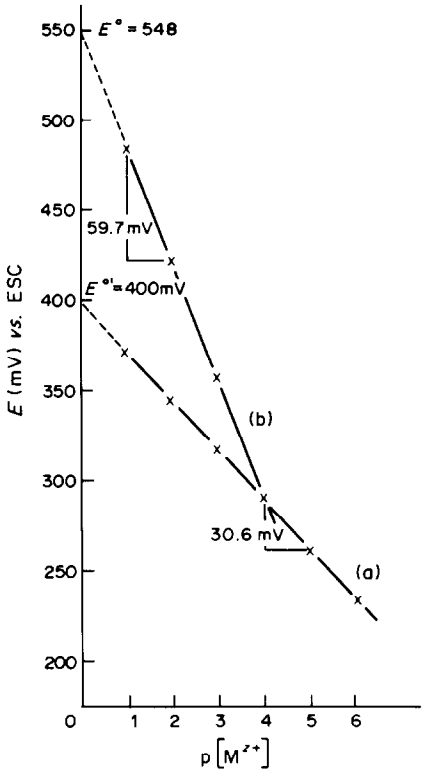

Fig. 2. The electrode functions of (*a*) the Cu^{2+}- and (*b*) Ag^+-selective electrodes.

M^{z+}-selective membrane electrode	$M^{z'+}$ ($C_{M^{z'+}} = 10^{-2}M$ $I = 0.4M$ for Cu^{2+} $I = 0.1M$ for Ag^+	Satd. KNO_3 soln.	SCE	(II)

where $M^{z'+}$ represents the main metal cations that form more or less stable compounds with HRI and HRII. With the exception of copper, all cations tested were in the form of the nitrates, at pH 3. The values of the selectivity coefficients may be seen in Table 2. The cations which interfere in the Cu^{2+}-selective electrode response are Ag^+ and Hg^{2+}, and Hg^{2+} also interferes in the response of the Ag^+-selective electrode.

Applications to sulpha-drug determination

All the sulpha-drugs listed in Table 3 could be directly titrated (as the sodium salts) with $CuSO_4$ and/or $AgNO_3$ solutions.

The potentiometric jumps at the equivalence point are big enough for the maximum error of determination to be 0.5% with the Ag^+-selective electrode and 1.9% with the Cu^{2+}-selective electrode. The amounts of sulpha-drug taken for determination varied from 25 to 87 mg.

Table 3 also lists the values of the acidity constants of the sulpha-drugs. The proposed method is applicable only to sulpha-drugs with $pK_a \geqslant 6$. Sulphafurazol

Table 2. Selectivity coefficients, $K_{M^{z+},M^{z'+}}$

Interferent cation ($M^{z'+}$)	log $K_{M^{z+},M^{z'+}}$	
	Cu^{2+} electrode	Ag^+-electrode
Ni^{2+}	−5.42	−2.76
Pb^{2+}	−5.13	−2.19
Zn^{2+}	−5.23	−2.47
Hg^{2+}	3.86	−0.15
Al^{3+}	−3.22	−2.25
Cu^{2+}	—	−4.99
Ag^+	3.93	—

Table 3. Sulpha-drugs determined with membrane-electrode

Sulpha-drug (name and formula)	pK_a	Cu^{2+} electrode taken, mg	found, mg	error, %	Ag^+ electrode taken, mg	found, mg	error %
Sulphadiazine 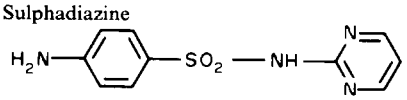	6.5	25.5	25.1	1.6	38.6	38.5	0.3
		32.0	31.4	1.0	42.7	42.6	0.2
		40.4	39.8	1.5	59.8	59.8	0.0
		87.1	86.9	0.2			
Sulphamerazine 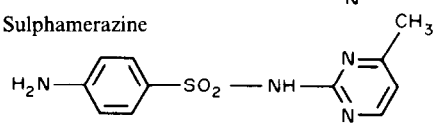		30.0	29.8	0.7	37.3	37.1	0.5
		34.0	34.7	0.9	50.9	50.7	0.4
		33.3	33.2	0.3	72.0	72.1	0.1
		41.2	41.2	0.0			
		119.5	119.2	0.3			
Sulphamethoxidiazine 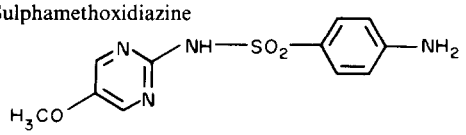	7.0	39.8	40.0	0.5	20.7	20.7	0.0
		45.7	45.5	0.4	26.8	26.9	0.4
		50.3	50.5	0.4	28.9	28.8	0.4
		54.4	54.6	0.4			
		74.7	74.6	0.1			
Sulphadimidine 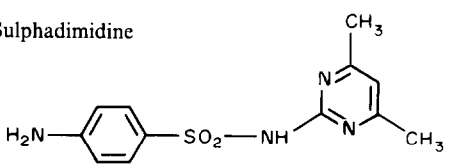	7.7	37.3	37.2	0.3	30.0	30.0	0.3
		43.0	42.8	0.5	36.4	26.5	0.3
		56.5	56.5	0.0	47.6	47.6	0.0
		57.2	57.3	0.2			
Sulphapyridine 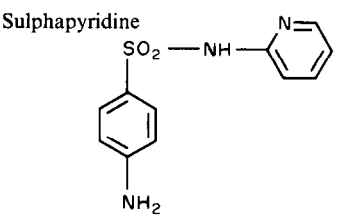	8.3	21.6	21.5	0.5	31.3	31.2	0.3
		39.6	39.5	0.3	41.5	41.4	0.2
		45.8	45.9	0.2	77.9	77.8	0.1
		55.0	54.9	0.2			

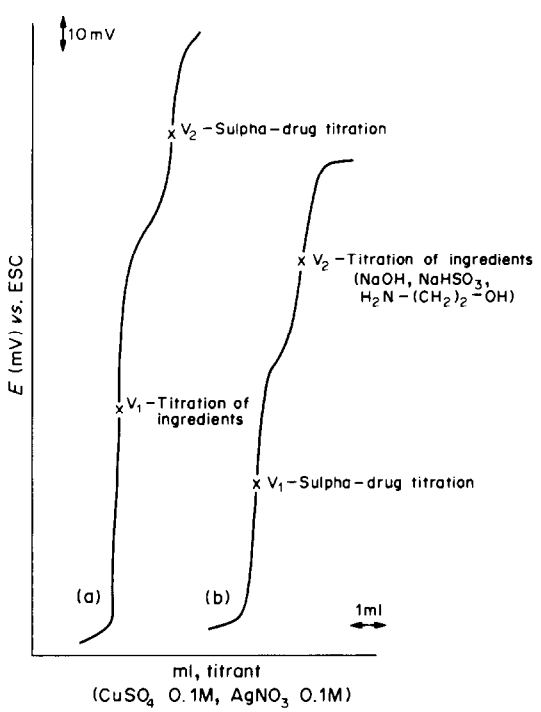

Fig. 3. Potentiometric titration of an injectable solution of sulphamethoxidiazine with the (a) Cu^{2+}-selective electrode; (b) Ag^+-selective electrode.

(pK_a = 5.5) does not form insoluble salts with $CuSO_4$ or $AgNO_3$.

Further, the determination of sulphamethoxidiazine (Sulphametin, Bayerena) in injectable solutions for veterinary use was examined. These solutions contain the sulpha-drug dissolved in 20% sodium hydroxide solution, together with $NaHSO_3$ and ethanolamine. All these ingredients can form salts or complexes with both $CuSO_4$ and $AgNO_3$. The potentiometric titration curves obtained are presented in Fig. 3; two significant potential jumps are obtained.

In the titration with $CuSO_4$, all the ingredients are titrated together in the first step of the titration curve, whereas in the titration with $AgNO_3$, the first potential jump corresponds to the sulpha-drug and the second to the other ingredients. For this reason we prefer the titration with $AgNO_3$ for determination of sulphamethoxidiazine in injectable solutions. The method is not applicable to formulations containing more than one titratable sulpha-drug.

REFERENCES

1. N. Hazemoto, N. Kamo and Y. Kobatake, *J. Pharm. Sci.*, 1976, **65**, 435.
2. M. S. Ionescu, S. Cilianu, A. A. Bunaciu and V. V. Coşofreţ, *Talanta*, 1981, **28**, 383.

3. Z. Blagojevic and P. Bradic, *Archiv. Farm.* (*Beograd*), 1960, **4,** 193.
4. I. Popa and A. Voicu, *Farmacia* (*Bucharest*), 1962, **7,** 399.
5. S. S. M. Hassan and M. M. Habib, *Microchem. J.*, 1981, **26,** 181.
6. F. Malecki and R. Starościk, *Anal. Chim. Acta*, 1982, **139,** 353.
7. S. S. M. Hassan and M. H. Eldesouki, *J. Assoc. Off. Anal. Chem.*, 1981, **64,** 1158.
8. W. Szczepaniak, M. Ren and K. Ren, *Chem. Anal.* (*Warsaw*), 1979, **24,** 51.
9. G. E. Baiulescu and V. V. Coşofreţ, *Rev. Chim.* (*Bucharest*), 1976, **27,** 158.
10. *Idem, ibid.*, 1975, **26,** 1051.
11. J. Růžička and J. C. Tjell, *Anal. Chim. Acta*, 1970, **51,** 1.
12. A. Burdin, J. Mesplede and M. Porthault, Compt. Rend., 1973, **276C,** 65.
13. J. Růžička and J. C. Tjell, *Anal. Chim. Acta*, 1970, **49,** 346.
14. V. V. Coşofreţ, *Rev. Chim* (*Bucharest*), 1976, **27,** 240.
15. S. Lal, *Z. Anal. Chem.*, 1971, **255,** 209.
16. V. V. Coşofreţ, *Rev. Roum. Chim.*, 1978, **23,** 1489.
17. V. V. Coşofreţ, C. Cristescu and P. G. Zugrăvescu, in *Ion-Selective Electrodes, Conference 1977*, E. Pungor and I. Buzás (eds.), p. 352. Elsevier, Amsterdam, 1978.
18. V. V. Coşofreţ, *Rev. Chim.* (*Bucharest*), 1974, **25,** 836.
19. C. Cristescu, unpublished data.
20. G. E. Baiulescu, V. V. Coşofreţ and C. Cristescu, *Rev. Chim.* (*Bucharest*) 1975, **26,** 429.
21. K. Srinivasan and G. A. Rechnitz, *Anal. Chem.*, 1969, **41,** 1203.

Talanta, Vol. 32, No. 4, pp. 301–305, 1985
Printed in Great Britain.

0039-9140/85 $3.00 + 0.00

SPECTROPHOTOMETRIC DETERMINATION OF ALIPHATIC PRIMARY AND SECONDARY AMINES BY REACTION WITH *p*-BENZOQUINONE

SAAD S. M. HASSAN*, M. L. ISKANDER and N. E. NASHED
Department of Chemistry, Faculty of Science, Ain Shams University, Cairo, Egypt

(*Received* 12 *March* 1984. *Revised* 3 *October* 1984. *Accepted* 5 *November* 1984)

Summary—A simple, sensitive and selective spectrophotometric method has been developed for determination of aliphatic primary and secondary amines. It is based on a reaction with excess of *p*-benzoquinone in ethanol whereby 1:1 (amine:quinone) coloured products are obtained, which have maximum absorption at 510 nm and $E^{1\%}_{1cm}$ in the range 400–650. The effect of solvent, temperature, concentration of quinone and the presence of water have been kinetically investigated by the initial rate method. The conditions for monitoring amine concentrations as low as 0.1 μg/ml are optimized in the light of the kinetic data. Results with an average recovery of 98.5% and mean standard deviation of 1.9% are obtained with 9 different amines without interference from tertiary amines, ammonia, amides, imides, anilides, hydrazines and α-amino-acids.

Existing methods for the spectrophotometric determination of aliphatic primary and secondary amines are based on reactions with nitro compounds substituted with active halogen or sulphonic groups, carbonyl compounds, organic dyes and inorganic reagents. In this connection, chromogenic reagents such as 2,4-dinitrofluorobenzene,[1] nitrophenylazobenzoyl chloride,[2] dinitrobenzyl chloride,[3] dinitrobenzenesulphonyl chloride,[4] and trinitrobenzenesulphonic acid[5] have been suggested. A method based on the reaction of aliphatic amines with picric acid and 18-crown-6-ether to yield a 1:1:1 complex, followed by extraction of the complex and absorbance measurement at 377 nm, has been proposed.[6] Reaction of *cis*-α,β-dinitrostilbene with aliphatic amines, and subsequent treatment with alkali, gives a coloured product with maximum absorption at 410 nm.[7] Many of these methods, however, entail a time-consuming extraction step, involve the use of water-sensitive reagents and suffer from lack of selectivity.

Aliphatic amines have also been spectrophotometrically determined by reaction with 1,2-naphthoquinone-4-sulphonic acid,[8] salicylaldehyde,[9,10] acetyl chloride and iron(III),[11] Methyl Orange,[12] Bromothymol Blue,[13] Chrome Azurol-S and aluminium,[14] alcoholic copper(II) chloride,[15] ascorbic acid and dimethylformamide,[16] and cobalt(II) thiocyanate.[17] The initial rate of colour development with chloranil,[18] and the depressive effect of amines on the absorbance of the copper–EDTA complex in aqueous and non-aqueous solvents[15,19,20] have been adapted for the determination of some aliphatic amines. Many of these methods suffer serious interference from metal ions, amines and α-amino-acids.

On the other hand, quinones have long been known to react with amines to give coloured products. Some of these reactions have been utilized for qualitative and quantitative determination of some quinones[21–24] and amines.[25–27] The present work demonstrates that the fairly simple reaction of aliphatic primary and secondary amines with *p*-benzoquinone under optimized conditions is suitable for determination of low levels of amines without interference from many compounds containing nitrogen and hydrogen.

EXPERIMENTAL

Reagents

All reagents used were of analytical grade unless otherwise stated. Doubly distilled water and solvents were used throughout. The aliphatic amines (purity ≮ 97%) were obtained commercially and used without purification. Ethanolic stock solutions ($10^{-3}M$) were prepared and standardized by potentiometric titration with copper.[28] *p*-Benzoquinone was purified by repeated sublimation and a $10^{-2}M$ stock solution in ethanol prepared.

Procedures

Kinetic measurements. Stock solutions ($1–25 \times 10^{-4}M$) of piperidine and of *p*-benzoquinone in ethanol, acetonitrile and dioxan, and the pure solvents were brought to the required temperature (25, 30 or 35 ± 0.1°) by standing them in a water-bath for 20 min. Then 1.00, 1.50, 2.00, 2.50, 3.00, 4.00 and 5.00 ml portions of *p*-benzoquinone solution were transferred to 25-ml standard flasks (brought to the same temperature) and containing 1.00–5.00 ml of piperidine solution and enough solvent to bring the mixture to the mark, and the solutions were mixed. The quinone:piperidine molar ratio covered the range from 1:5 to 5:1. A portion of the mixture was immediately transferred to a 1.00-cm silica cuvette placed in the constant-temperature cell-

*Author for correspondence. Current address: Department of Chemistry, Qatar University, Doha, Qatar.

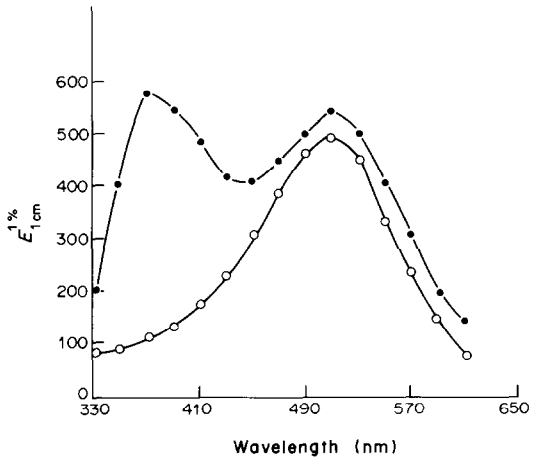

Fig. 1. Absorption spectra of the reaction product of *p*-benzoquinone with piperidine in: (○) pure ethanol; (●) 50% v/v water–ethanol mixture.

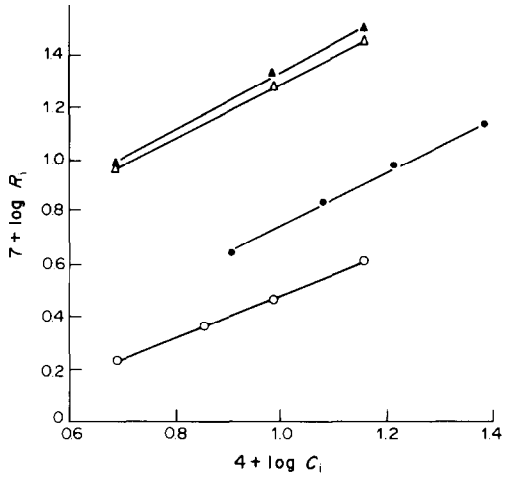

Fig. 2. Relationship between logarithmic initial rate of colour development (R_i) at 30° and logarithmic initial concentration (C_i) of: (●, ▲) *p*-benzoquinone and (○, △) piperidine in (○, ●) pure ethanol and (△, ▲) 50% v/v water–ethanol mixture.

compartment of the spectrometer. The absorbance at 510 nm was monitored as a function of time, against a blank similarly prepared without piperidine. From the absorbance–time curves, the initial slopes (dA/dt), initial rates, rate constants and thermodynamic parameters were calculated by standard methods.[29,30]

Determination of aliphatic amines. Portions (0.05, 0.10, 0.50, 1.00, 2.00, 3.00 and 5.00 ml) of $10^{-3}M$ standard amine solution in ethanol were transferred into 10-ml standard flasks, followed by 1.0-ml portions of $10^{-2}M$ ethanolic *p*-benzoquinone. Each test was run in triplicate. The flasks were left for 30 min in a water-bath kept at 50 ± 5°, then cooled, diluted to the mark with pure ethanol and mixed. The absorbance was measured at 510 nm in a matched set of 1.00-cm silica cuvettes against a blank prepared similarly but without the amine. A calibration graph was drawn for each amine and used for subsequent measurement of unknown concentrations.

RESULTS AND DISCUSSION

p-Benzoquinone has a maximum absorption at 430 nm with $E^{1\%}_{1\,cm} \sim 2$, and readily reacts with aliphatic primary and secondary amines in various water-miscible organic solvents to give an intense colour with maximum absorption at 510 nm and $E^{1\%}_{1\,cm}$ in the range 400–650. In the presence of >20% v/v water or low concentrations of the quinone reagent, two absorption maxima, at 370 and 510 nm, are obtained (Fig. 1). The nature, stability and rate of colour development are mainly dependent on the reactivity of the amines, nature of the solvent, concentration of quinone and presence of water.

Effect of solvent

The slopes of log–log plots of initial concentration of piperidine or *p*-benzoquinone *vs.* initial rate of colour development in pure ethanol are both unity, indicating first-order kinetics with respect to the amine and quinone, and that the overall reaction is second-order.[29,30] Similar results were obtained with 50% v/v water–ethanol mixture, and pure dioxan and acetonitrile as media. Thus the rate-determining step involves an equimolar ratio of the reactants.

The kinetic data (Table 1) show that the rate of reaction decreases in the order: ethanol > acetonitrile > dioxan. The reaction in dioxan requires an induction period of at least 22 min, and the rate constant is two orders of magnitude less than that for ethanol medium. This is probably due to the low dielectric constant and polarity of dioxan and also to solvent–solute interaction. Dioxan solvates piperidine and thus deactivates it in the reaction with *p*-benzoquinone. This was confirmed from the infrared spectra of piperidine, dioxan and a mixture of both. The N–H stretching absorption band at 3450 cm^{-1} in the spectrum of pure piperidine appears at 3400 cm^{-1} in the spectrum of piperidine–dioxan mixture but not in the spectra of piperidine in either ethanol or acetonitrile, where the band-shift did not exceed 10 cm^{-1}.

Table 1. Kinetics and thermodynamic parameters of the reaction of *p*-benzoquinone with piperidine in different pure solvents

Solvent	K_2, $l.mole^{-1}.sec^{-1}$ 25°C	30°C	35°C	$\Delta E^{\#}$, *kcal/mole*	$\Delta H^{\#}$, *kcal/mole*	$\Delta S^{\#}$, $cal.mole^{-1}.deg^{-1}$	$\Delta G^{\#}$, *kcal/mole*
Ethanol	0.46	0.70	1.22	16.0	15.4	−8.4	18.0
Acetonitrile	0.33	0.54	0.85	17.2	16.6	−5.1	18.1
Dioxan	0.017	0.026	0.045	19.1	18.5	−9.2	21.9

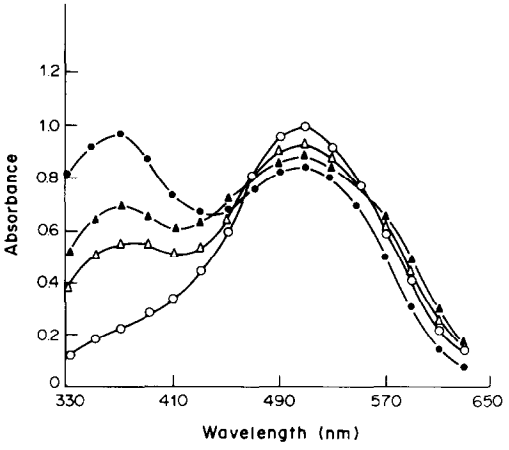

Fig. 3. Effect of *p*-benzoquinone concentration on the absorption spectrum of piperidine in pure ethanol at 30°. Piperidine:quinone molar ratios were: (●) 1:5; (▲) 1:10; (△) 1:30; (○) 1:40–1:60.

The activation parameters at 30° were calculated by the Arrhenius equation.[29,30] $\Delta G^{\#}$ in ethanol was very close to that in acetonitrile and both were less by about 4 kcal/mole than that in dioxan, indicating that dioxan is a less favourable medium. In ethanol, however, $\Delta H^{\#}$, $\Delta S^{\#}$ and $\Delta E^{\#}$ are all smaller.

Effect of water and quinone concentration

In ethanolic solutions containing 20–80% v/v water, the products from all the amines investigated display two maxima, at 510 and 370 nm. Although the order of the reaction is not affected by the presence of water, the rate of colour development substantially increases to a maximum and constant value ($k_2 = 4.51\ \text{l.mole}^{-1}.\text{sec}^{-1}$ at 30°) in 50–80% v/v water–ethanol mixtures. The stoichiometry of the reaction of piperidine with *p*-benzoquinone at a total molar concentration of $2.5 \times 10^{-4}M$ and temperature of 30° was examined in pure ethanol and 50% v/v aqueous ethanol by the continuous-variations method,[31] with measurement at 510 and 370 nm. Maximum absorbances were obtained at mole ratios of about 2:1 and 3:2 (quinone:piperidine) in the pure and aqueous ethanolic solutions, respectively. No evidence for formation of other species was noticed when the amine and quinone concentrations were varied in the range $0.6–5.0 \times 10^{-4}M$. Mole-ratio plots confirmed these conclusions.

The effect of quinone concentration on the nature of the spectra was also investigated by varying the piperidine:*p*-benzoquinone mole ratio (in pure ethanol) from 1:5 to 1:60. Figure 3 shows only one maximum (at 510 nm) when the quinone:piperidine mole ratio is greater than 30. As the mole-ratio of the quinone decreases, a band at 370 nm begins to appear and increases in intensity with decrease in quinone:piperidine mole ratio. The product when the reaction is done in ethanolic solutions containing >20% v/v water has an absorption spectrum with two maxima at 510 and 370 nm, irrespective of the quinone:piperidine mole ratio. These data indicate the possible formation of two different chromogens. Further studies showed that absorbance measurement at 370 nm, though sensitive for most amines, is not analytically useful, owing to irreproducible readings and poor precision.

Nature of the reaction and products

The chromogen produced by reaction of piperidine with excess of *p*-benzoquinone (quinone:piperidine mole ratio ~30) in pure ethanol was isolated as red crystals, m.p. 140°. The elemental analysis corresponded to formation of piperidyl-*p*-benzoquinone. The absorption spectrum of the compound displays maximum absorption at 510 nm. The infrared spectrum confirms the identity of the product, showing absorption bands at 2930, 1635, 1645, 880 and 810 cm^{-1}, due to the stretching vibrations of piperidyl C–H, quinonoid carbonyl, conjugated double bonds, and wagging vibrations of one isolated and two adjacent aromatic hydrogen atoms, respectively. Another chromogen was isolated as brown crystals (m.p. 177°) from an aqueous ethanolic reaction mixture containing an equimolar ratio of both reactants. This product has only one absorption maximum, at 370 nm, and both the elemental analysis and infrared data agree with the formation of 2,5-bis(dipiperidyl)-*p*-benzoquinone.

It is possible to suggest that the reaction of amines with *p*-benzoquinone in pure ethanol proceeds by 1,4 addition of one mole of amine to one mole of quinone to give piperidylhydroquinone, which on oxidation with a second mole of quinone gives piperidyl-*p*-benzoquinone (1:2 amine–quinone reaction). The latter product adds a second mole of amine in the presence of water or low concentrations of the quinone, to give 2,5-bis(dipiperidyl)-*p*-hydroquinone, which on further oxidation with a third mole of quinone yields 2,5-bis(dipiperidyl)-*p*-benzoquinone (2:3 amine–quinone reaction). Water probably en-

hances the reactivity and polarizability of the quinone carbonyl group by increasing the dielectric constant of the reaction medium. The reaction can thus be represented by the following scheme:

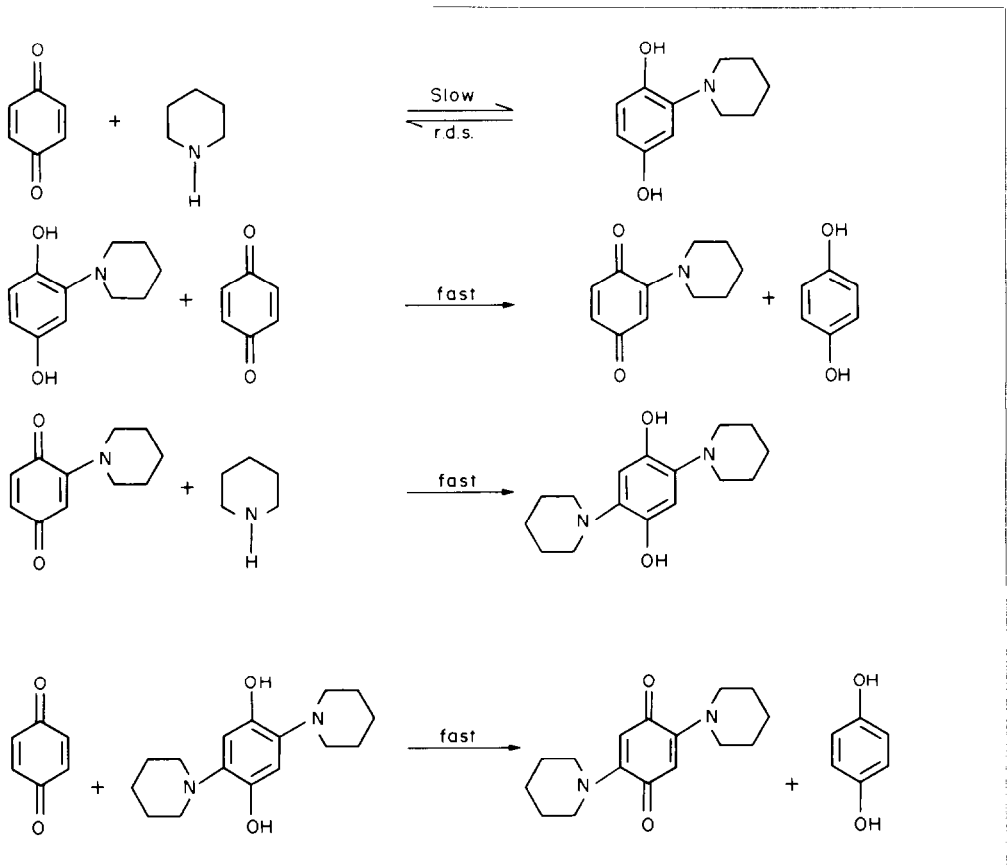

Optimum reaction conditions

The time required for maximum colour development at 510 nm by reaction of various aliphatic amines with >30-fold mole ratio of *p*-benzoquinone in pure ethanol at 30° is ~2 hr. At 50 ± 5°, the colour intensity reaches 95% of its maximum after ~30 min (Fig. 4). The presence of up to 15% v/v water has no significant effect on the absorbance and 1 ml of 10 ^{2}M ethanolic *p*-benzoquinone solution is adequate for the determination of various amines in the concentration range 0.1–20 μg/ml. These conditions give reproducible results and small variations in timing, quinone concentration, temperature and water content introduce no significant error. The intensity and nature of the colour are independent of pH in the range 7.5–10. At pH <5, no reaction takes place, probably because of the low nucleophilicity of the protonated amines.

Determination of amines

The colour developed at 510 nm with primary and secondary aliphatic amines under the optimized conditions is stable after 1 hr, and remains so for at least 24 hr. Beer's law holds over the amine concentration range 0.1–20 μg/ml. Linear regression analysis of the calibration data for some amines gave the values shown in Table 2 for the relation $A = a + bc$ where A is the absorbance at 510 nm in a 1.00-cm cell, a and b are respectively the intercept and slope of the calibration graph, and c is the concentration of the amine (μg/ml) in the final solution. The relative standard deviation (5 replicates) for 1–10 μg/ml concentration of the amines was 1.9%, and the average recovery 98.2%.

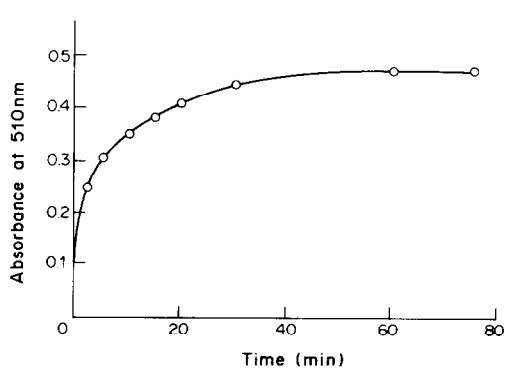

Fig. 4. Effect of time on the absorbance of the colour developed by reaction of 9.4 μg/ml piperidine with excess of *p*-benzoquinone in pure ethanol at 50°.

Table 2. Statistical analysis of the calibration graphs ($A = a + bc$) and results for the determination of some aliphatic amines by reaction with *p*-benzoquinone in pure ethanol at 50°C

Amine	Intercept, a*	Slope, b†	Correlation coefficient	[Amine] taken, c, $\mu g/ml$	Mean recovery,§ %	Standard deviation, %
Benzylamine	0.002	0.027	0.999	2.0–30.0	98.5	2.1
n-Butylamine	0.003	0.042	0.999	2.0–25.0	97.3	1.8
Dibutylamine	0.009	0.048	0.999	1.0–28.0	99.3	2.2
Diethanolamine	−0.006	0.035	0.999	1.0–30.0	98.3	2.0
Di-isopropylamine	0.007	0.065	0.998	1.0–20.0	98.0	1.6
Dipropylamine	0.013	0.046	0.999	1.0–30.0	99.0	2.0
Ethanolamine	−0.046	0.039	0.998	1.0–20.0	98.2	1.8
Morpholine	−0.044	0.059	0.999	1.0–22.0	96.9	2.0
Piperidine	0.009	0.047	0.996	1.0–20.0	98.5	1.8

*Absorbance.

†Absorbance.ml.μg^{-1}.

§The calibration graphs were prepared by use of amine solutions standardized by potentiometric titration with copper sulphate; the recovery values are based on nominal concentrations of amines assumed to be 100% pure.

Aromatic primary amines under the same conditions give a less intense colour, which depends on both the nature and position of the substituent group. Electron-attracting groups tend to give lower colour intensity than electron-repelling groups do. This effect decreases with substitutional position in the order *para* > *meta* > *ortho*. The $E^{1\%}_{1cm}$ values at 510 nm for aniline and its *p*-Cl, *m*-Cl, *o*-Cl, *p*-NO_2, *m*-NO_2, *p*-CH_3, *m*-CH_3 and *o*-CH_3 derivatives are 380, 280, 170, 90, 50, 130, 450, 360 and 340, respectively. No interference is caused by up to 1 mg/ml of ammonia, tertiary amines (*e.g.*, tripropylamine), amides (*e.g.*, benzamide, acetamide), imide (*e.g.*, succinimide), anilides (*e.g.*, acetanilide, benzanilide), α-amino-acids (*e.g.*, glycine, alanine) and hydrazines (*e.g.*, phenylhydrazine, methylhydrazine).

It can be seen that the present method offers the advantages of: (*a*) reagent availability and stability; (*b*) reasonable selectivity in the presence of many other NH-containing compounds; (*c*) less time consumption and fewer manipulation steps; (*d*) higher sensitivity than many of the most commonly used[5,8,9,11] or recently proposed[6,7,14] spectrophotometric procedures.

REFERENCES

1. F. C. McIntire, L. M. Clements and M. Sproull, *Anal. Chem.*, 1953, **25**, 1757.
2. J. Bartos, *Talanta*, 1961, **8**, 619.
3. S. J. Obtemperanskaya, *Zh. Analit. Khim.*, 1970, **25**, 2033.
4. S. I. Kaya and K. K. Ngiyen, *ibid.*, 1979, **34**, 2421.
5. K. Satake, T. Okuyame, M. Ohashi and T. Shinoda, *J. Biochem. (Tokyo)*, 1960, **47**, 654.
6. H. Naguchi, M. Yashia, K. Kawahara, H. Nakamura and M. Nagamatsu, *Anal. Lett.*, 1980, **13**, 271.
7. P. Dubois, P. Levillain and C. Viel, *Talanta*, 1981, **28**, 843.
8. D. H. Rosenblatt, P. Hlinka and J. Epstein, *Anal. Chem.*, 1979 **51**, 752.
9. A. J. Milun, *ibid.*, 1957, **29**, 1502.
10. F. E. Critchfield and J. B. Johnson, *ibid.*, 1956, **28**, 436.
11. J. P. Rawat and J. P. Singh, *ibid.*, 1975, **47**, 738.
12. R. Silverstein, *ibid.*, 1963, **35**, 154.
13. G. Schill and M. Svensk, *Farm. Tidskr.*, 1963, **67**, 385.
14. Y. Saito, J. Tanaka, J. Odo and Y. Tanaka, *Bunseki Kagaku*, 1980, **29**, 385.
15. H. M. Hershenson and D. N. Hume, *Anal. Chem.*, 1957, **29**, 16.
16. J. Bartos, *Ann. Pharm. Franc.*, 1964, **22**, 383.
17. M. Pesez and J. Bartos, *Colorimetric and Fluorimetric Analysis of Organic Compounds and Drugs*, pp. 125, 126. Dekker, New York, 1974.
18. S. U. Kreingol'd, V. N. Antonov and E. M. Yutal, *Zh. Analit. Khim.*, 1977, **32**, 1618.
19. I. M. Citron and A. Mills, *Anal. Chem.*, 1964, **36**, 208.
20. I. M. Citron and D. Dolan., *Anal. Chim. Acta*, 1965, **33**, 612.
21. H. Karius and G. E. Mapstone, *Chem. Ind. (London)*, 1956, 266.
22. D. P. Johnson and F. E. Critchfield, *Anal. Chem.*, 1961, **33**, 910.
23. S. S. M. Hassan, *J. Assoc. Off. Anal. Chem.*, 1981, **64**, 611.
24. K. Finley. *The Chemistry of Quinonoid Compounds*, p. 1049. Wiley, New York, 1974.
25. N. P. Yavorskii, V. S. Koval and M. M. Starushchenko, *Farmatsevt Zh. (Kiev)*, 1965, **20**, 31.
26. G. L. Ryzhova and R. G. L. Mishustina. *Tr. Tomsk Gas. Univ.*, 1968, **192**, 177.
27. S. Patai, *The Chemistry of the Amino Group*, p. 118. Interscience, London, 1968.
28. S. S. M. Hassan, F. Tadros and W. Selig, *Microchem. J.*, 1981, **26**, 426.
29. P. Atkins, *Physical Chemistry*, p. 855. Oxford Press, Oxford, 1979.
30. B. Stevens, *Chemical Kinetics for General Students of Chemistry*, 2nd Ed; pp. 9, 50. Chapman & Hall, London, 1970.
31. P. Job, *Ann. Chim. Phys. Paris*, 1936, **6**, 97.

Talanta, Vol. 32, No. 4, pp. 307–311, 1985
Printed in Great Britain.

0039-9140/85 $3.00 + 0.00

CORROSION MEASUREMENTS BY POTENTIAL-STEP CHRONOAMPEROMETRY

R. VON WANDRUSZKA, S. W. ORCHARD and A. GREEFF
Department of Chemistry, University of the Witwatersrand, Johannesburg, South Africa

(*Received* 20 *July* 1984. *Revised* 20 *September* 1984. *Accepted* 31 *October* 1984)

Summary—A solid-state computer-controlled system has been developed for the measurement of corrosion currents under potentiostatic anodic conditions. The system applies a potential step and measures the resulting current for a variable number of cycles. Data are stored and manipulated by the computer. Tests show that corrosion behaviour of metals in various environments can be evaluated.

Potentiostatic current–time curves have been used to study the attack on the passive surface of steel by chloride ions.[1,2] Similar studies on aluminium were reported subsequently,[3] and various aspects of the measurements involved have been discussed. In all cases the metal surfaces were passivated anodically in sulphuric acid medium and then disturbed by the addition of an aggressive anion[1-3] or by mechanical means.[4]

The similar technique of potential-step chronoamperometry with a clean surface is well-suited as an alternative procedure for the comparative evaluation of the corrosive behaviour of different environments on metals. The metal electrode is subjected to an anodic potential step and the resulting current is monitored for a period of about 30 sec. Depending on the nature of the metal and its environment, the current varies in a characteristic manner during this relatively short time. The potential preceding the anodic step must be sufficiently cathodic to prevent premature attack on the metal.

In principle, these measurements may be done with a potentiostat linked to a chart recorder. In such an arrangement, however, some readings within the first second of the potential step may be missed because of recorder lag. Furthermore, it may be difficult to eliminate the noise that invariably arises.[3]

The present paper describes a microcomputer-controlled system comprising a solid-state potentiostat and a synchronized current-measurement circuit. Current readings are taken at a rate of 4 per sec, and data manipulation, such as plotting, smoothing and storing, is done quickly and easily by the computer. Relevant calculations can be done conveniently on the stored data. The system was tested with representative chronoamperometric measurements involving mild steel and two stainless steels in a variety of electrolyte solutions. Comparative assessment of corrosion and passivation behaviour appears to be possible.

EXPERIMENTAL

Apparatus

A standard three-electrode cell, comprising a steel working electrode, a platinum counter-electrode and a calomel reference electrode, was used for the measurments. The cell contained 40 ml of solution and had a water jacket for temperature control. It was closed from the atmosphere by a standard titration-cell lid. A solid-state potentiostat and a current-measurement circuit were custom-built on a single board and interfaced to an Apple IIe microcomputer. The interface circuitry was included on the same board.

Circuit construction

The circuit is shown in Fig. 1. The computer interface is based on a Motorola 6821 peripheral interface adaptor (PIA), which has two peripheral registers, PA and PB, each comprising an 8-bit bus. The buses function independently and may be configured for either input or output. They are accessed through a bi-directional data bus, which is linked directly to the corresponding data lines in the computer input/output (I/O) slot. Register selection in the PIA is achieved by means of two "Register Select" lines, RS-0 and RS-1. These lines are controlled by the two least significant bits (lsb; A0 and A1) of the computer address bus. While all 16 bits of the address bus appear in the I/O slot, only the 12 most significant ones are involved in slot addressing, leaving the 4 lsb free for interfacing use. The circuit construction allows for PIA register selection in every address directed at the I/O slot.

The PIA is enabled by means of three "Chip Select" (CS) lines and the Read/Write selection is made through the R/$\overline{W}$ bit. These controls are manipulated with the "$\overline{\text{Dev Sel}}$" and "R/W" bits in the I/O slot. The $\overline{\text{Dev Sel}}$ line pulses low when the I/O slot is addressed and the R/$\overline{W}$ line assumes the state corresponding to either input or output. The signals are decoded as shown in Fig. 1, the PIA being enabled only when the I/O signals are true, during the 300-nsec period following an I/O address. This lay-out eliminates the possibility of accidental decoding of random I/O signals.

In the present application, the PA-bus is configured for input and the PB-bus for output. The PB-bus is linked to an 8-bit digital-to-analogue converter (DAC-08, PMI),[6] which generates the potential step. It is connected to an adder-type solid-state potentiostat[7] and controls the potential applied to the counter-electrode. The reference electrode is included in the feedback loop of the control amplifier, which also contains a voltage follower for impedance matching. The current at the working electrode is converted into a voltage by a current follower with adjustable feedback resistance. For the duration of the measurement the voltage is held constant by a sample-and-hold amplifier (SMP-11, PMI) with a gain of unity.

The analogue signal is digitized with a 12-bit analogue-to-digital converter (ADC 7109, Intersil). This is a dual-slope integrating converter, operating on a 5-MHz time base provided by an external crystal oscillator. Completion of a conversion is indicated by a "Status" line, which is used to interrupt the computer.

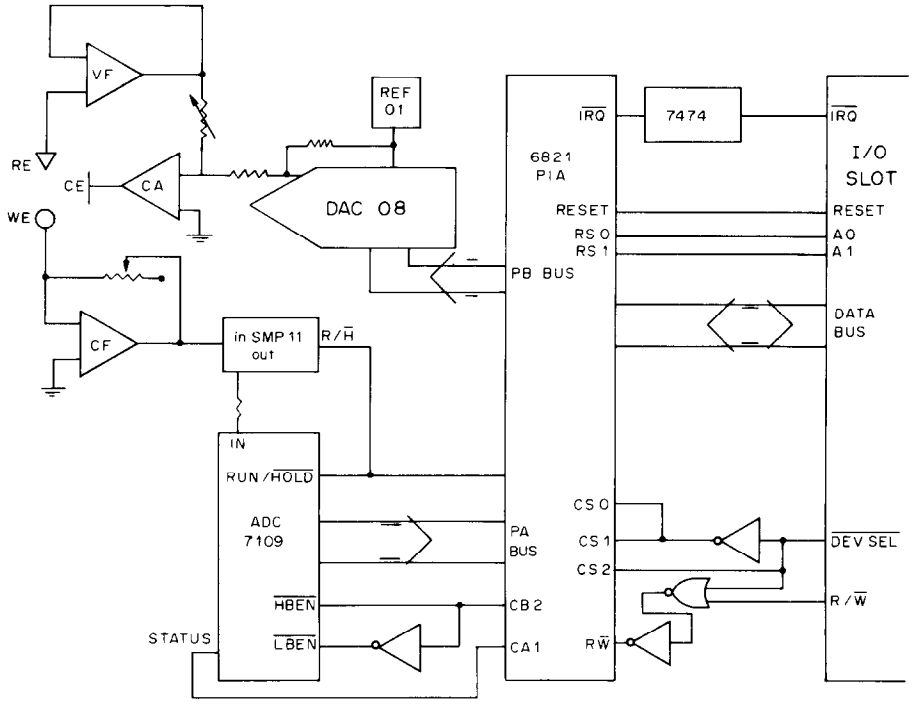

Fig. 1. Potentiostat and corrosion measurement circuit. WE = working electrode; CE = counter-electrode; RE = reference electrode; CA = control amplifier; CF = current follower; VF = voltage follower.

The interrupt signal is processed through the PIA (CA-2 line), giving a negative transition on the IRQ line on activation. It was found that direct application of this signal to the I/O interrupt line was not satisfactory: it invariably caused the program to crash after a few cycles. This problem was eliminated by the inclusion of a 7474 flip-flop as shown in Fig. 1. The flip-flop is clocked with the Apple Φ0 clock, allowing the interrupt to pass only after completion of a timing cycle.

The ADC output comprises 12 bits, as well as an over-range and a polarity bit. This necessitates a 2-part reading protocol for each conversion, the Apple data bus being only 8 bits long. This is facilitated by the provision of separate enabling lines on the ADC: LBEN for the 8 lower bits and HBEN for the 4 higher, and the over-range and polarity bits. All these are 3-state outputs, so enabled and disabled lines can simply be connected together to allow for 14-to-8 bit multiplexing.

Enabling control is achieved with a PIA control line (CB-2), which is in turn controlled through internal registers. The bits in these registers, and hence the CB-2 output, can be changed with a single computer command. As shown in Fig. 1, high-byte and low-byte enabling are mutually exclusive.

A further ADC input, the "Run/Hold" line, is controlled by the CA-2 output of the PIA. This output is similar to CB-2 and can be similarly accessed. The ADC is configured with external RC-components to give the maximum reading of 4095 for a working electrode current of 3 mA.

Circuit operation

The relatively slow reading speed required for the experiments allows for various circuit operations to be performed under software control. The first step consists of the application of a starting potential to the counter-electrode. This is achieved by placing the appropriate byte on the DAC. Next, by the same method, the potential is stepped anodically to a value at which current flows. The DAC has an output settling time of 85 nsec and the 741 operational amplifier has a rise time of less than 0.5 μsec, so the circuit responds virtually instantaneously relative to the experimental time scale of 4 readings per second.

During these manipulations the ADC is in the HOLD mode, switched by the software-controlled CA2 line of the PIA. Following the potential step, the ADC RUN mode is instituted by a high transition on CA2. The same line is used to put the SMP-11 in the HOLD mode, to prevent changes of signal during the measurement. Completion of a conversion is signalled by the status line and used to interrupt the computer. The program responds by switching the ADC to the HOLD mode and reading the output.

The high-byte and low-byte readings thus obtained are each temporarily stored as a variable. During each cycle, the contents of the two variables are combined to give a single decimal number. This number is stored in an array for later manipulation. The process is repeated for a software-controlled number of cycles. The conversion speed of the ADC depends to some degree on the magnitude of the signal. However, comparative tests revealed that in this circuit the differences involved are negligible.

A flow chart of the control program is shown in Fig. 2. The data obtained are filed on a floppy disk for future reference. A program for data manipulation and plotting current/time curves was written. This includes Savitsky–Golay smoothing,[8] curve-area determination by Simpson's rule integration, and passivation time and charge calculations. Hard copies of plots can be obtained on a dot matrix printer.

Sample preparation

The steels used in this study were mild steel, 409SS stainless steel and 316L stainless steel. The compositions of

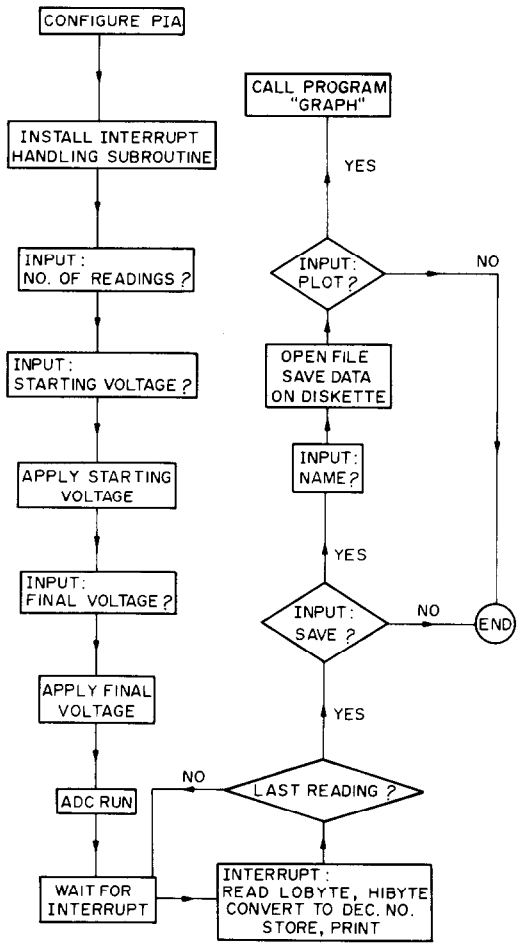

Fig. 2. Flow-chart of circuit control program.

the stainless steels are given in Table 1. The steels were formed into cylindrical electrodes and polished to optical smoothness. The electrode areas exposed to the solution were 79.8 mm^2 (mild steel), 153.15 mm^2 (409SS) and 157.87 mm^2 (316L). After each run the electrodes were thoroughly cleaned with ultrafine emery paper.

The deaerated solutions used in certain measurements were prepared by passage of high-purity nitrogen for 20 min.

RESULTS AND DISCUSSION

Mild steel

The results of measurements taken with mild steel are summarized in Table 2. The height of the potential step was limited by the maximum allowable corrosion current (3 mA). However, depending on the passivation characteristics of the system under investigation, the anodic voltages employed gave rise to significant currents. Figure 3 shows a number of current/time curves for non-passivating systems.

It can be seen that the aggressive sodium chloride solution gave a steadily rising current after an initial decrease. This decrease probably arose because the very first reading was high, owing to a brief capacitive surge accompanying the potential step. The sulphate solution gave a similar curve, but with a more gradual initial rise. Moreover, from measurements taken over a longer time, it was found that the current in the sulphate solution reached a steady value after about 50 sec, whereas the current in the chloride solution continued to rise after 90 sec. This is consistent with pitting corrosion and hence progressive surface-area enlargement in the chloride solution.

The fluoride solution gave a constant current after 20 sec, whereas in the thiocyanate solution the current first fell and then rose slowly. Interestingly, in the latter solution the current still continued to rise after 100 sec. This indicates that thiocyanate, too, has a surface-roughening effect.

After the initial surge, the current in the perchlorate solution first rose, resembling that in sulphate medium, but then gradually decreased. It reached a relatively high constant value after about 22 sec.

The curve for the passivating nitrate solutions is shown in Fig. 4. Clearly, the current decreased strongly in the passivation process. If, for the present purpose, "passivity" is defined as the situation in which the current has fallen to 3% of its initial maximum value, then the passivation time was 6 sec. The area under the curve was integrated and the charge involved in passivation was found to be 2.02 mC. This corresponds to 25 $\mu C/mm^2$. Nitrate concentrations of 0.1, 0.25 and 0.5*M* gave similar passivation times and charges.

Table 1. Compositions of stainless steels (%)

Element	409SS	316L
C	0.025	0.024
S	0.11	0.004
P	0.018	0.024
Mn	0.89	1.25
Si	0.63	0.55
Cu	0.08	0
Co	0.08	0.08
Ti	0.24	0
Mo	0.08	2.05
Cr	11.12	16.41
Ni	0.33	16.08

Table 2. Passivation behaviour of mild steel in various solutions

Solution (1*M*)	Observation	Potential step, *V vs.* SCE
NaCl	No passivation	−0.7 to −0.45
Na_2SO_4	No passivation	−0.7 to −0.3
$NaClO_4$	No passivation	−0.7 to −0.45
KF	No passivation	−0.3 to −0.11
LiCl	No passivation	−0.55 to −0.3
KSCN	No passivation	−0.55 to −0.4
KNO_3	Passivation	−0.3 to +0.63
$NaClO_3$	Passivation	−0.55 to −0.06
$Ca(NO_3)_2$	Passivation	−0.55 to +0.6

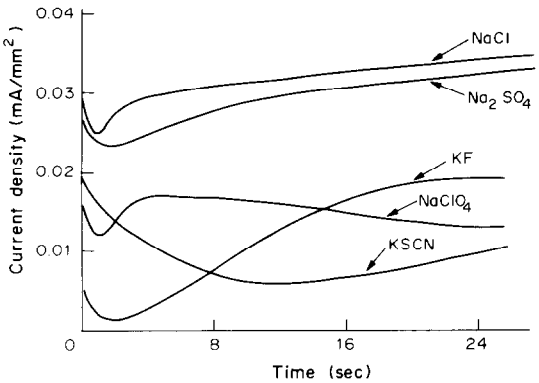

Fig. 3. Current/time curves for mild steel in non-passivating solutions (all 1*M*). Potential step from −0.55 to −0.2 V *vs.* SCE.

Passivation was also observed with chlorate solutions (Fig. 4). The initial currents involved were about a quarter of those found for nitrate solutions. At these low currents, passivation (3% criterion) was reached after 16 sec. However, in absolute terms, a current similar to that flowing at passivity in the nitrate solution (0.09 mA) was reached after only 4.7 sec. The anodic range of voltages which led to passivation was larger for nitrate solutions than chlorate solutions. With nitrate, passivity resulted even with potential steps from −0.55 to +0.67 V. In chlorate medium it was no longer reached at anodic potentials of 0.03 V and higher (all voltages *vs.* SCE).

Phosphate and benzoate are known corrosion inhibitors. It was found that 1*M* sodium chloride prepared in pH-7 phosphate and benzoate buffers gave current–time curves closely resembling those obtained in nitrate solutions. Initial current densities were generally below 13 μA/mm^2.

Dissolved oxygen

The role of oxygen in passivation was monitored chronoamperometrically. A 1*M* potassium nitrate solution was saturated with oxygen by passage of the gas for 20 min. Immediately after this, the determinations were done as described above. Further measurements were taken at approximately 15-min intervals and finally the solution was deoxygenated with nitrogen. The results are shown in Table 3.

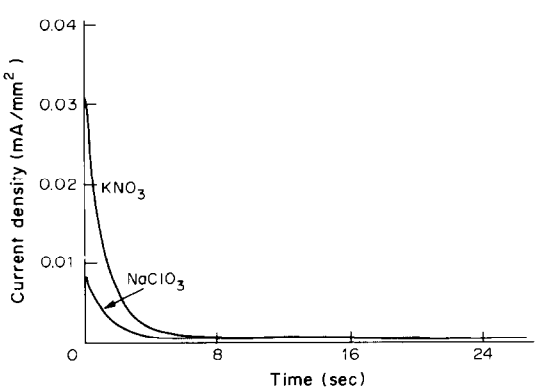

Fig. 4. Current/time curves for mild steel in passivating solutions (1*M*). Potential step from −0.55 to −0.2 V *vs.* SCE.

Table 3. The role of oxygen in passivation of mild steel in 1*M* KNO_3; potential step from −0.55 to +0.08 V *vs.* SCE

Time after oxygenation, *min*	Passivation time, *sec*	Passivation charge, *mC*
0	5	0.77
15	7	1.01
30	9	2.40
45	12	5.11
Deaerated	14	7.00

Table 4. The effect of temperature on passivation of mild steel in 1*M* KNO_3; potential step from −0.55 to +0.08 V *vs.* SCE

Temperature, °C	Passivation time, *sec*	Passivation charge, *mC*
6	2	0.16
15	6	1.65
20	8	3.31
31	14	6.22
41	No passivation	—
50	No passivation	—
60	No passivation	—

Clearly, passivation times and charges decreased with increasing oxygen content of the solution. As noted elsewhere,[4] however, passivation still occurred in deaerated nitrate solutions. Oxygenation of chloride solutions did not lead to passivating behaviour.

Temperature

The effects of temperature on mild steel passivation in 1*M* potassium nitrate are shown in Table 4. As expected, passivation time and charge increased with temperature. Above 41° no passivation was observed, although the current–time curves retained their original shape. At these higher temperatures the corrosion currents still initially decreased with time, but then settled to a relatively high constant value (*e.g.*, 8 μA/mm^2 at 50°).

Stainless steel

Table 5 shows that the stainless steels were passivated more rapidly than mild steel in 1*M* potassium nitrate and 1*M* sodium chlorate. Passivation charges

Table 5. Passivation times (sec) for stainless steels in various solutions

Solution (1*M*)	409SS	316L	Potential step, *V vs.* SCE
KNO_3	2	2	−0.55 to −0.06
$NaClO_3$	1	2	−0.55 to −0.06
$NaClO_3$	9	6	−0.55 to +0.08
NaCl	No passivation	5	−0.55 to −0.06
NaCl (60 C)	No passivation	10	−0.55 to −0.06

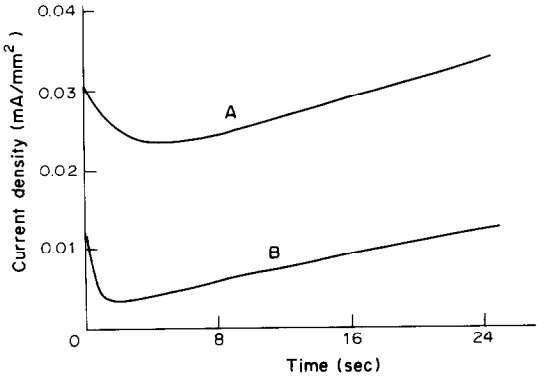

Fig. 5. Current/time curves for 409SS stainless steel in 1*M* NaCl. Potential steps: A, from −0.55 to +0.08 V; B, from −0.55 to −0.06 V *vs.* SCE.

were relatively low. In both cases passivation occurred at temperatures up to 60°. However, in 1*M* sodium chloride the 409SS steel did not become passivated, but gave a current–time curve similar to that for mild steel. Figure 5 shows the corrosion currents for two different potential steps. In contrast, the 316L steel was passivated in 1*M* sodium chloride at temperatures up to 60°.

The results show that the system and method described can be used for comparative evaluation of corrosion behaviour. Advantages include quickness and convenience of measurements, as well as the relatively low price of the system. Importantly, a potentiostat and an X–Y recorder are not needed.

REFERENCES

1. H. J. Engell and N. D. Stolica, *Z. Phys. Chem. Frankfurt*, 1959, **20**, 113.
2. T. P. Hoar and W. R. Jacob, *Nature*, 1967, **216**, 1299.
3. F. D. Bogar and R. T. Foley, *J. Electrochem. Soc.*, 1972, **119**, 462.
4. I. Epelboin and M. Keddam in *Passivity of Metals*, R. P. Frankenthal and J. Kruger (eds.). Electrochemical Society, Princeton, N.J., 1978.
5. R. von Wandruszka and M. Maraschin, *Anal. Lett.*, 1981, **14**, 463.
6. R. von Wandruszka, *S. African J. Chem.*, 1982, **35**, 121.
7. J. A. von Fraunhofer and C. H. Banks, *The Potentiostat and its Applications*, Chapter 1. Butterworths, London, 1972.
8. A. Savitzky and M. J. E. Golay, *Anal. Chem.*, 1964, **36**, 1627 (see also: J. Steiner, Y. Termonia and J. Deltour, *ibid.*, 1972, **44**, 1906.)

Talanta, Vol. 32, No. 4, pp. 313–317, 1985
Printed in Great Britain.

0039-9140/85 $3.00 + 0.00

SEPARATION OF IRON-52 FROM CHROMIUM CYCLOTRON TARGETS ON THE 2% CROSS-LINKED ANION-EXCHANGE RESIN AG1-X2 IN HYDROCHLORIC ACID

TJAART N. VAN DER WALT and FRANZ W. E. STRELOW
National Chemical Research Laboratory, P.O. Box 395, Pretoria 0001, Republic of South Africa

FLORIS J. HAASBROEK
National Accelerator Centre, P.O. Box 395, Pretoria 0001, Republic of South Africa

(*Received* 26 *June* 1984. *Revised* 26 *September* 1984. *Accepted* 29 *October* 1984)

Summary—Iron-52 can be separated from solutions of chromium cyclotron targets by eluting chromium, copper and radioactive impurities with 9.0*M* hydrochloric acid from a column containing 1.0 g of AG1-X2 anion-exchange resin. Iron-52 is retained and can then be eluted with 6.0*M* hydrochloric acid containing 0.05*M* hydrogen iodide or 0.05*M* sodium iodide. The separations are sharp and quantitative. Less than 2 μg of chromium will remain with the iron-52, from 2.0 g originally present.

Iron-52 is a radioisotope which is useful in nuclear medicine.[1–4] It has a short half-life ($t_{1/2} = 8.27$ hr), permitting studies to be repeated at short intervals. The decay is by positron emission (56%, 0.80 MeV) and electron capture.[5] Both decay modes involve de-excitation solely through a 169-keV level into manganese-52m ($t_{1/2} = 21$ min).

Many nuclear reactions can be utilized for the production of iron-52: $^{50}Cr(^{4}He, 2n)^{52}Fe$, $^{52}Cr(^{3}He, 3n)^{52}Fe$, $^{55}Mn(p, 4n)^{52}Fe$ and p-spallation. Some experimental methods and results have been discussed by Atcher *et al.*[6] The energy and type of accelerated particles available determine the method chosen for production. The reaction should be one that yields a maximum amount of iron-52 and a minimum amount of iron-55, because iron-55 ($t_{1/2} = 2.6$ yr) adds significantly to the radiation dose received by the patient.[7] In the Pretoria cyclotron natural chromium is bombarded with 32-MeV ^{3}He particles to obtain iron-52.

The preparation of chromium cyclotron targets[8,9] and the separation of iron-52 from chromium targets[6,7,9–14] have been described by several authors. Solvent extraction and ion-exchange methods or a combination of both have been applied. In this laboratory a solvent extraction method has been used, the iron-52 being extracted with di-isopropyl ether from 8*M* hydrochloric acid.

The most common impurities found in the final iron-52 fractions are residual amounts of copper and chromium (from the target), zinc-65 ($t_{1/2} = 244$ d), gallium-66 ($t_{1/2} = 9.4$ hr), gallium-67 ($t_{1/2} = 78.3$ hr), copper-64 ($t_{1/2} = 12.70$ hr), manganese-52 ($t_{1/2} = 5.6$ d), manganese-54 ($t_{1/2} = 312.2$ d), manganese-56 ($t_{1/2} = 2.58$ hr) and chromium-51 ($t_{1/2} = 27.70$ d), depending on the nuclear particles used for irradiation. In the Pretoria cyclotron some of these radioisotopes are formed by the reactions $^{65}Cu(^{3}He,n)^{67}Ga$, $^{65}Cu(^{3}He, 2n)^{66}Ga$ and $^{63}Cu(^{3}He,p)^{65}Zn$. In order to obtain a product of high purity the separation procedure should make provision for the removal of all these impurities. Our extraction method separated iron-52 from chromium, copper and zinc-65, but not from the radioactive gallium isotopes, and small amounts of the first two also remained with the iron.

Furthermore, copper, zinc-65 and the gallium radioisotopes are not completely separated from iron-52 when anion-exchange chromatography on AG1-X8 resin is applied at hydrochloric acid concentrations ranging from 4 to 12*M*. However it has been shown that the anion-exchange separation of iron(III) from copper at high concentrations of hydrochloric acid can be considerably improved by using the 4% cross-linked anion-exchanger AG1-X4 instead of the usual 8% cross-linked resin AG1-X8.[15] Additional studies conducted in this laboratory indicated that separation of iron(III) from copper is further improved by use of a 2% cross-linked resin, and quantitative separation of zinc also becomes possible.

Distribution coefficients were determined for copper, zinc, gallium, manganese, iron(III) and chromium(III) with the 2% cross-linked anion-exchanger AG1-X2 in 9.0*M* hydrochloric acid. From the results obtained a separation procedure was developed to purify iron-52 from large amounts of chromium and copper and from radioisotope impurities of manganese, zinc and gallium, by a single-column procedure.

EXPERIMENTAL

Reagents and apparatus

Analytical-reagent grade chemicals were used and purified from iron by anion-exchange chromatography. "Suprapur" hydrochloric acid was used. Water was distilled

Table 1. Analytical methods used

Element	Method
Cu	complexometric titration with DCTA at pH 5.5 in acetate medium; Methylthymol Blue plus, 1,10-phenanthroline as indicator
Zn	complexometric titration with EDTA at pH 5.5; Xylenol Orange as indicator
Mn	complexometric titration with DTPA at pH 10.0 in presence of ascorbic acid; Methylthymol Blue as indicator
Ga	complexometric titration, excess of DCTA and back-titration with thorium at pH 2.5–3.0; Xylenol Orange as indicator
Fe	oxidation to Fe(III) with bromine water; complexometric titration, excess of EDTA and back-titration with bismuth at pH 2.5–3.0; Methylthymol Blue as indicator
Cr	atomic-absorption spectrometry; air–acetylene flame at 357.9 nm

and then passed through an Elgastat demineralizer. Hydriodic acid was obtained by passing a solution of potassium iodide through a cation-exchanger (H^+ form) and eluting with water. The resin used was AG1-X2 polystyrene anion-exchanger with quaternary ammonium exchange groups, (Bio-Rad Laboratories, Richmond, California). A borosilicate glass tube (10 mm bore and 350 mm long) fitted with a fused-in porosity-1 glass sinter and a tap, was used as a column. It was filled with a slurry of resin until the settled resin reached a mark at 4.4 ml ($\equiv$ 1.0 g dry resin). The resin was then equilibrated with 10 ml of 9.0*M* hydrochloric acid.

Cyclotron-produced gallium-66, gallium-67 and zinc-65 were used to simulate the separation of gallium and zinc radioisotope impurities from iron-52 made by bombarding a chromium cyclotron target with ^{3}He particles.

Atomic-absorption measurements were made with a Varian-Techtron AA-5 instrument. An automatic fractionator was used to collect fractions for construction of the elution curve. A 4096-channel analyser, coupled to a Ge(Li) detector, was used to identify the radioisotopes and to measure their activities.

Distribution coefficients

The resin was dried at 60° over anhydrous silica gel in a vacuum pistol and stored over the same drying agent in a desiccator.

Distribution coefficients were determined by equilibrating 2.500 g of dry resin with 250 ml of 9.0*M* hydrochloric acid containing one of the following: 1.0 mmole of copper, zinc or manganese(II), or 0.67 mmole of gallium, chromium(III) or iron(III). The mixture was shaken for 24 hr at 20° in a mechanical shaker. After equilibration the resin was filtered off with a short borosilicate glass tube, and blown dry. The adsorbed fraction was then eluted with 150 ml of 0.50*M* hydrochloric acid (150 ml of 1.0*M* nitric acid for zinc) and determined by appropriate analytical methods (Table 1). The mass equilibrium distribution coefficients

$$K_d = \frac{\text{mass of element on resin}}{\text{mass of element in solution}} \times 100,$$

were calculated (Table 2).

Elution curves

Cu–Cr(III)–Fe(III). Hydrochloric acid (9.0*M*, 100 ml) containing 2.0 g of chromium(III), 100 mg of copper and 1.0 mg of iron(III) was passed through an equilibrated AG1-X2 resin column as described above, and the resin washed with small portions of 9.0*M* hydrochloric acid; chromium and copper were eluted with more 9.0*M* hydrochloric acid (300 ml in total). Iron was then eluted with 100 ml of 0.5*M* hydrochloric acid; 20-ml fractions were collected and a flow-rate of 5.5 $\pm$ 0.3 ml/min was maintained throughout. The 9.0*M* hydrochloric acid fractions were evaporated to dryness on a steam-bath and the residues dissolved, each in 20 ml of 0.5*M* hydrochloric acid. These solutions were analysed by atomic-absorption spectrometry, with an air–acetylene flame and the 357.9, 324.8 and 248.3 nm lines for chromium, copper and iron, respectively. The elution curve is presented in Fig. 1.

Mn–Zn–Fe(III)–Ga. Figure 2 shows an elution curve for a mixture containing 2.0 mg of manganese, 2.0 mg of zinc, 1.0 mg of iron(III) and 1.0 mg of gallium, dissolved in 50 ml of 9.0*M* hydrochloric acid. Zinc and manganese were eluted with 250 ml of 9.0*M* hydrochloric acid, and iron with 100 ml of 6.0*M* hydrochloric acid/0.05*M* hydriodic acid (freshly prepared), gallium being retained on the column. The mixed acid was then displaced with 20 ml of 6.0*M* hydrochloric acid and gallium was eluted with 100 ml of 0.5*M* hydrochloric acid/1% sodium sulphite, to reduce any iodine to iodide. The flow-rate was again 5.5 $\pm$ 0.3 ml/min and 20-ml fractions were collected throughout. Manganese, zinc and iron were determined in each fraction by atomic-absorption spectrometry (air–acetylene flame) at the 279.5, 213.9 and 248.3 nm lines for manganese, zinc and iron, respectively. For gallium the acetylene–nitrous oxide flame and the 294.4 nm line were used.

Separation of iron-52 from chromium and other impurities

A cyclotron target was prepared by electroplating a chromium layer onto a water-cooled copper base. It was bombarded in the cyclotron with 32-MeV α-particles for 8 hr at a beam current of 95 μA, and "cooled" for 2 hr to let the short-lived radioactive impurities decay. Chromium was etched from the surface of the target with 10-ml portions of

Table 2. Distribution coefficients on anion-exchange resin AG1-X2 in 9.0*M* hydrochloric acid

Element	K_d
Ga(III)	2570
Fe(III)	1660
Zn(II)	39.9
Mn(II)	4.5
Cu(II)	3.4
Cr(III)	2.7

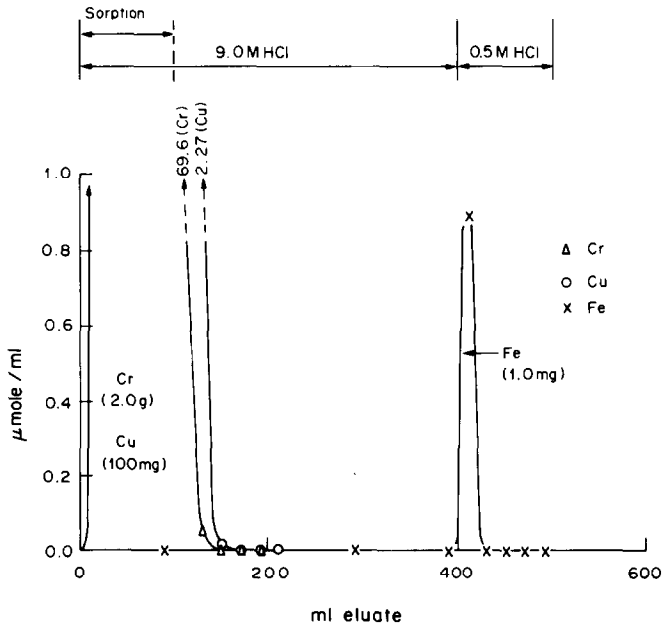

Fig. 1. Elution curve for Cu–Cr(III)–Fe(III).

hot concentrated hydrochloric acid to which 1 ml of concentrated nitric acid had been added. After all the chromium had dissolved, accurately measured gallium-66, gallium-67 and zinc-65 activities were added to the combined portions, which were then evaporated to 50 ml, and the activities of ^{52}Fe, ^{51}Cr, ^{54}Mn, ^{56}Mn, ^{65}Zn, ^{66}Ga and ^{67}Ga were measured. The solution was then evaporated to dryness and the nitrates were converted into chlorides. These were dissolved in 100 ml of 9.0*M* hydrochloric acid and the solution was passed through an equilibrated AG1-X2 resin column as described. Chromium and other impurities were eluted with 9.0*M* hydrochloric acid (200 ml in total) and the solution was evaporated to 50 ml. Finally, iron-52 was eluted with three 50-ml portions of 6.0*M* hydrochloric acid/0.05*M* sodium iodide. Gallium isotopes were retained by the resin. ^{52}Fe activities were measured in the "iron-52" eluates and the results are presented in Table 3. The combined iron-52 fractions were evaporated almost to dryness, then treated with nitric acid to expel iodide, and the nitrates were converted into chlorides. The salts were dissolved in 50 ml of 0.1*M* hydrochloric acid and the activities of the radioisotope impurities, ^{51}Cr, ^{54}Mn, ^{56}Mn, ^{65}Zn, ^{66}Ga and ^{67}Ga, were measured, the results are presented in Table 4.

RESULTS AND DISCUSSION

According to the distribution coefficients of the elements on AG1-X2 (Table 2) chromium, copper

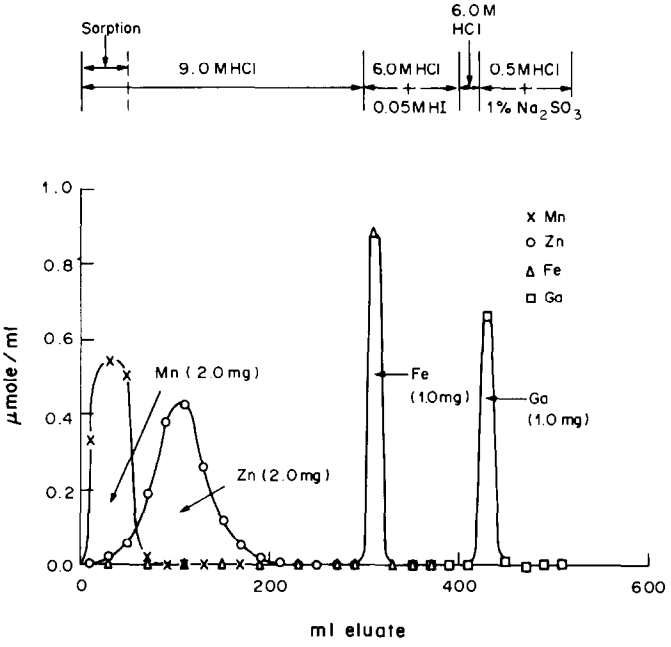

Fig. 2. Elution curve for Mn–Zn–Fe(III)–Ga.

Table 3. Separation of iron-52 from chromium cyclotron-target material on anion-exchange resin AG1-X2

Fraction	^{52}Fe activity*, *counts*/200 *sec*	Recovery, %
Solution (before separation)	7766 (± 5%)	—
"Other element" eluate (eluted with 9.0*M* HCl)	30 (± 5%)	0.4
First "^{52}Fe" fraction (eluted with 6.0*M* HCl + 0.05*M* NaI)	6887 (± 5%)	88.7
Second "^{52}Fe" fraction (eluted with 6.0*M* HCl + 0.05*M* NaI)	430 (± 5%)	5.5
Third "^{52}Fe" fraction (eluted with 6.0*M* HCl + 0.05*M* NaI)	244 (± 5%)	3.1

*All measurements on a volume of 50 ml in a 100-ml beaker, and corrected for decay.

and manganese should easily be eluted with 9.0*M* hydrochloric acid. This was confirmed by the elution curves (Figs. 1 and 2). Although zinc has a relatively large distribution coefficient ($K_d = 39.9$) on AG1-X2 resin in 9.0*M* hydrochloric acid, 2.0 mg of zinc were completely eluted with 9.0*M* hydrochloric acid. This is because the 2% cross-linked resin has exchange kinetics much superior to those of the 8% cross-linked resin. Zinc also has a distribution coefficient of *ca.* 40 on AG1-X8 resin in 12*M* hydrochloric acid, but cannot be eluted completely and shows serious tailing.

In ion-exchange procedures gallium behaves similarly to iron(III). For this reason iron(III) is usually reduced to iron(II) before separation from gallium. Hydriodic acid is especially effective as a reducing reagent[16] and does not introduce foreign solids, but has to be freshly prepared because free iodine forms very easily. For medical purposes iron-52 is usually prepared in an isotonic solution and hydriodic acid can be replaced by sodium iodide.

Less than 2 μg of chromium, copper, zinc, manganese or gallium was found in the "iron-52" fraction when 2.0 g of chromium, 100 mg of copper, 2.0 mg of manganese, 2.0 mg of zinc and 1.0 mg of gallium were present originally. In most cases the amounts of chromium in the iron fraction were below the detection limit of the atomic-absorption method (*ca.* 0.05 μg/ml). It can be expected that the amounts of chromium found in the iron fraction will further decrease with decreasing amounts of total chromium, though not linearly. Less than 50 μg of iron was found in the "iron-52" fraction after a separation done without iron-52 radiotracer. This iron was apparently present as a trace component in the reagents used.

Table 3 shows that the recovery of iron-52 is better than 90% in a typical separation. The product is of high purity, as indicated by Table 4. The amounts of gallium-66, gallium-67 and zinc-65 activities originally present, 3.6, 215 and 0.7 MBq, respectively, are much higher than would be encountered in practice, and were used merely to demonstrate the efficiency of the separation. The time for the total procedure including the target etching, is between 2 and 3 hr. An advantage is that the whole operation can easily be performed behind a lead shield in a fume cupboard. This considerably reduces the irradiation dose received by the operator, compared with that received when the di-isopropyl ether extraction of iron-52 is used. In addition the product contains considerably fewer impurities. The procedure is less tedious and more reliable, and has completely replaced the solvent extraction procedure for the production of iron-52 at the Pretoria Cyclotron. The purified iron-52 can also be used as a ^{52}Fe/^{52m}Mn generator, by selective elution of manganese-52m from an anion-exchange resin column with 8 or 9*M* hydrochloric acid.[18]

REFERENCES

1. P. E. Francois and L. Szur, *Nature*, 1958, **182**, 1665.
2. G. V. S. Rayudu, S. P. H. Shirazi, E. W. Fordham and A. M. Friedman, *Int. J. Appl. Radiat. Isot.*, 1973, **24**, 451.

Table 4. Radioisotope impurities separated from iron-52 on anion-exchange resin AG1-X2

Radioisotope present	Activity*, *counts*/*200 sec*	
	in solution before separation	in "iron-52" fraction
^{51}Cr	1774	⩽ 4 (mainly background)
^{54}Mn	5101	⩽ 2 (mainly background)
^{56}Mn	15975	⩽ 2 (mainly background)
^{65}Zn	1226	⩽ 25 (mainly background)
^{66}Ga	4338	⩽ 10 (mainly background)
^{67}Ga	360857	96

*All measurements on a volume of 50 ml in a 100-ml beaker. Coefficients of variations were 5% for all measurements.

3. H. O. Anger and D. C. van Dyke, *Science*, 1964, **144**, 1587.
4. W. H. Knospe, G. V. S. Rayudu, M. Cardello, A. M. Friedman and E. W. Fordham, *Cancer*, 1976, **37**, 1432.
5. C. M. Lederer and V. S. Shirley, *Table of Isotopes*, 7th Ed., p. 146. Wiley, New York, 1978.
6. R. W. Atcher, A. M. Friedman and R. J. Huizenga, *Int. J. Nucl. Med. Biol.*, 1980, **7**, 75.
7. D. M. Lyster, R. Thaller, J. S. Vincent, H. Dougan and R. T. Morrison, *Appl. Nucl. Radiochem.*, 1982, 45.
8. F. Akiha and Y. Murakami, *Nippon Genshiryoku Gakkaishi*, 1970, **12**, 382.
9. Y. Yano and H. O. Anger, *Int. J. Appl. Radiot. Isot.*, 1965, **16**, 153.
10. T. H. Ku, P. Richards, L. G. Stang and T. Prach, *Report* 1979, BNL–25802, CONF-790321-5.
11. M. L. Thakur, A. D. Nunn and S. L. Waters, *Int. J. Appl. Radiat. Isot.*, 1971, **22**, 481.
12. F. Akiha and Y. Murakami, *Bunseki Kagaku*, 1971, **20**, 1530.
13. J. R. Dahl and R. S. Tilbury, *Int. J. Appl. Radiat. Isot.*, 1972, **23**, 431.
14. F. Akiha, T. Aburai, T. Nozaki and Y. Murakami, *Radioisotopes*, 1972, **21**, 155.
15. F. W. E. Strelow, *Talanta*, 1980, **27**, 727.
16. T. N. van der Walt and F. W. E. Strelow, *Anal. Chem.*, 1983, **55**, 212.
17. R. W. Atcher, A. M. Friedman, J. R. Huizenga, G. V. S. Rayudu, E. A. Silverstein and D. A. Turner, *J. Nucl. Med.*, 1980, **21**, 565.
18. T. N. van der Walt, F. W. E. Strelow and F. J. Haasbroek, *Int. J. Appl. Radiat. Isot.*, 1985, **36**, 159.

Talanta, Vol. 32, No. 4, pp. 319–324, 1985
Printed in Great Britain.

0039-9140/85 $3.00 + 0.00

PREDICTION OF THE BEHAVIOUR OF A SINGLE FLOW-INJECTION MANIFOLD

MIGUEL ANGEL GOMEZ-NIETO*, MARIA DOLORES LUQUE DE CASTRO*
ANTONIO MARTIN† and MIGUEL VALCARCEL*
Department of Analytical Chemistry* and Department of Chemical Engineering,† Faculty of Sciences, University of Córdoba, Córdoba, Spain

(*Received* 19 *October* 1983. *Revised* 19 *July* 1984. *Accepted* 4 *October* 1984)

Summary—This paper suggests a handy method of obtaining equations to predict the fundamental parameters of an FIA peak—travel time, baseline-to-baseline time, peak height and appearance time of the maximum for a simple configuration—by performing a small number of preliminary experiments in the region in which FIA system usually operates.

The theory of FIA has not yet been definitively established, particularly that of the profile of the signal peak. Up till now, three different approaches have been taken. Růžička and Hansen use the traditional tanks-in-series model.[1,2] The theoretical expressions derived from this model are basically related to the height of the peak, expressed in terms of the dispersion coefficient.[3] Vanderslice *et al.*[4] examined the breadth of the peak, developing expressions to define the travel time and baseline-to-baseline time, deduced from numerical solutions of the general diffusion and convection equations for the conditions normally employed in FIA.[4] Painton and Mottola[5] considered the chemical contribution to the dispersion coefficient.

The theoretical approaches mentioned above must be judged not only in terms of the agreement given with experimental results but also in terms of the ability to predict the behaviour of any FIA manifold. The expression that relates the dispersion coefficient to various experimental parameters has the practical drawback of including the Levenspiel and Smith dispersion number,[6] which prevents its immediate application. One of the shortcomings of the expressions given by Vanderslice *et al.*[4] is the existence of the accommodation factor which, as shown in this paper, has to be experimentally calculated beforehand for each FIA manifold.

Our aim was to develop a simple alternative to the theoretical approaches taken by Vanderslice *et al.* and Růžička *et al.* It requires a simple experimental programme which allows development of expressions relating the characteristics of the manifold to the factors determining an FIA peak: travel time, appearance time of the maximum, and baseline peak-width. We have found that the equations of Vanderslice *et al.* do not always agree with the experimental results and that the accommodation factors are not constant. The expressions given here are applicable to simple FIA configurations without confluence points and in which no chemical reaction occurs during the transport process.

EXPERIMENTAL

Reagents

A Bromocresol Green stock solution was prepared by dissolving 0.400 g of the dye in 25 ml of 96% ethanol and diluting to 100 ml with 0.01*M* borax. The working solution was prepared by mixing 1 ml of the stock solution with 199 ml of 0.01*M* borax. The carrier stream was 0.01*M* borax.

The diffusion coefficient of the monitored substance was calculated by a traditional method.[7]

Apparatus

A Pye Unicam SP-500 spectrophotometer, equipped with a Hellma 178.12 QS flow-cell (inner volume 18 μl) was used. Gilson Minipuls 2 and Ismatec S.840 peristaltic pumps, a Tecator L 100-1 injection valve and a Tecator TM III "chemifold" were employed.

As can be seen from Fig. 1, the experiments were monitored with a Hewlett-Packard HP-85 microcomputer with built-in tape-cartridge drive, equipped with an HP-IB interface connected to the detector by an HP-3478A digital multimeter. A program for data-acquisition control was written in BASIC. The program was self-documented and easily operated. The input data necessary were L (the system length, cm), q (flow-rate, ml/min), d (tube internal diameter, mm), D (diffusion coefficient of the monitored substance, cm^2/sec), and A^* (the maximum absorbance obtained when the sample, without carrier, is passed through the flow-cell). The program allowed use of up to 1500 data points (absorbance, time) per sample. From these points the parameters such as peak area, residence time, statistical residence time, equivalent length, accommodation factors, co-ordinates of the maximum, travel time and baseline-to-baseline time

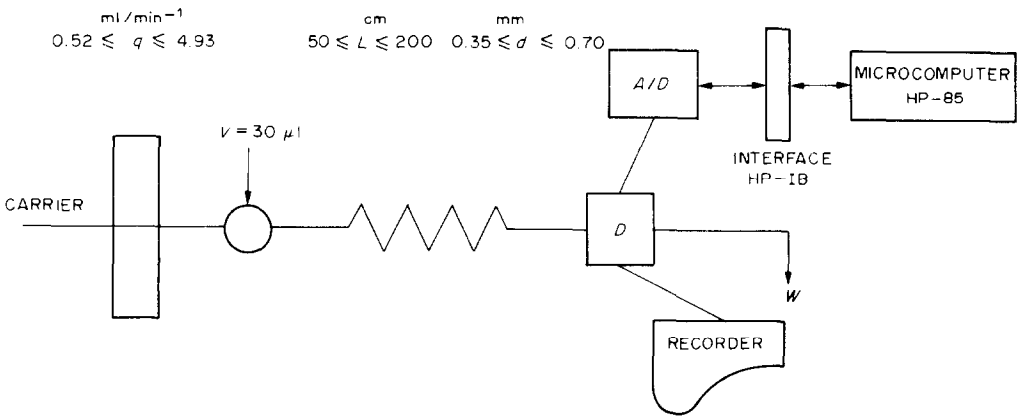

Fig. 1. Microcomputer system and interfacing to flow system (for details see text).

were calculated. The recorded signals were corrected for the background signal, taken as the average of three measurements. The system permitted plotting of the FIA peak by means of an $X-Y$ recorder connected in parallel to the microcomputer.

RESULTS AND DISCUSSION

Corroboration of the Vanderslice et al. *equations*

Vanderslice *et al.*[4] reported equations which, according to them, can predict two characteristic and very important parameters of an FIA peak: travel time, t_A, and dispersion or baseline-to-baseline time, Δt_B. These equations are:

$$t_A = \frac{109 a^2 D^{0.025}}{f} \left| \frac{L}{q} \right|^{1.025} \quad (1)$$

$$\Delta t_B = \frac{35.4 \alpha^2 f}{D^{0.36}} \left| \frac{L}{q} \right|^{0.64} \quad (2)$$

where D is the diffusion coefficient of the injected sample, L the length (cm) and a the inner radius (mm) of the tubing, q the flow-rate (ml/min) and f the accommodation factor, which according to these authors is characteristic for each system and depends on the bore of the tubing.

In order to test these expressions we have performed series of experiments in which both the flow-rate and the length and inner diameter of the tubing were changed. Some results are given in Table 1, in which the calculated data, such as theoretical travel time, baseline-to-baseline time, mean residence time and statistical residence time are also listed. The accommodation factors are denoted by f_{t_A} for expression (1) and $f_{\Delta t_B}$ for expression (2), since they are different. Thus,

$$f_{t_A} = \frac{(t_A)_{\text{calculated}}}{(t_A)_{\text{experimental}}}; \quad f_{\Delta t_B} = \frac{(\Delta t_B)_{\text{experimental}}}{(\Delta t_B)_{\text{calculated}}}$$

These factors were calculated for each run from the experimental values of t_A and Δt_B and from those calculated from expressions (1) and (2) with f taken as unity. As seen from Table 1, values for the two factors are not constant, but vary markedly as a function of the parameters of the system.

To test equations (1) and (2) we made a regression analysis of $\ln(t_A/a^2)$ and $\ln(\Delta t_B/a^2)$ *vs.* $\ln(L/q)$. Theoretically we should have obtained straight lines with slopes of 1.025 and 0.64, respectively, but in fact we did not. There are two fundamental reasons for this.

(*a*) The working conditions used by Vanderslice *et al.* are very extreme. These authors used very low flow-rates ($q < 0.1$ ml/min) and very small injection volumes (2 μl). Generally higher flow-rates (1–4 ml/min) and larger sample volumes (20–100 μl) are used in FIA. (*b*) The accommodation factors are not identical. The variation of the calculated accommodation factors with the length and bore of the tubing and flow-rate is plotted in Fig. 2. From the data in Table 1 and from these plots it is obvious that f_{t_A} and $f_{\Delta t_B}$ are different, and affected differently by the three variables.

The concept of "equivalent length", which takes into account connections, injection valves and irregularities in diameter throughout the whole manifold, besides the reactor length, allows us to eliminate the Vanderslice accommodation factor from expressions (1) and (2) by substitution of this parameter (L_{eq}) for the tube length.

For calculating the equivalent length in an FIA system, it is necessary to know the statistical residence time $(t_r)_{st}$, deduced from integration of the peak, by means of the Levenspiel–Smith equation:[8]

$$(t_r)_{st} = \frac{\int_0^\infty t C \, dt}{\int_0^\infty C \, dt} \quad (3)$$

where C is the molar concentration of the monitored substance at time t. Then L_{eq} can be obtained from

$$(t_r)_{st} = \frac{L_{eq}}{2\bar{u}} = \frac{\pi L_{eq} d^2}{8q} \quad (4)$$

Since $\bar{u} = 4q/\pi d^2$ is the mean linear velocity of the fluid.

In the regression analysis of $\ln(t_A/a^2)$ *vs.* $\ln(L_{eq}/q)$

Table 1. Experimental and calculated data obtained for the FIA system in Fig. 1.

Experimental							Calculated						
q,ml/min	*d,mm*	*L,cm*	t_A,*sec*	*T*	*A**	Δt_B,*sec*	$(t_A)_c$,*sec*	f_{t_A}	$(\Delta t_B)_c$,*sec*	$f_{\Delta t_B}$	t_r,*sec*	$(t_r)_{st}$,*sec*	*f'*
0.52	0.50	104.0	18.54	33.15	0.248	115.8	11.34	0.61	61.8	1.87	23.56	47.4	0.49
0.52	0.50	104.0	18.54	33.15	0.248	115.8	11.34	0.61	61.8	1.87	23.56	47.4	0.49
0.52	0.50	104.0	19.00	34.70	0.271	108.0	11.34	0.59	61.8	1.74	23.56	46.3	0.50
0.52	0.50	104.0	19.95	34.50	0.278	103.2	11.34	0.56	61.8	1.67	23.56	45.7	0.51
1.14	0.35	104.0	8.64	15.78	0.335	63.6	2.48	0.28	18.3	3.47	5.26	23.1	0.22
1.14	0.35	104.0	8.51	15.83	0.332	65.6	2.48	0.29	18.3	3.58	5.26	23.1	0.22
1.14	0.35	104.0	8.39	15.59	0.333	64.3	2.48	0.30	18.3	3.50	5.26	23.2	0.22
1.14	0.50	54.0	7.14	13.41	0.302	68.0	2.59	0.36	24.6	2.76	5.58	22.3	0.25
1.14	0.50	54.0	7.11	13.31	0.299	68.0	2.59	0.36	24.6	2.76	5.58	22.3	0.25
1.14	0.50	54.0	7.26	13.71	0.300	67.3	2.59	0.35	24.6	2.74	5.58	22.3	0.25
1.14	0.50	104.0	11.73	20.16	0.272	70.6	5.07	0.43	37.4	1.88	10.74	28.4	0.37
1.14	0.50	104.0	11.81	20.25	0.273	70.2	5.07	0.42	37.4	1.87	10.74	28.2	0.38
1.14	0.50	154.0	17.26	27.06	0.272	74.8	7.58	0.43	48.1	1.55	15.91	35.4	0.45
1.14	0.50	154.0	16.73	26.58	0.262	75.7	7.58	0.45	48.1	1.57	15.91	35.4	0.45
1.14	0.50	154.0	17.08	27.02	0.277	75.7	7.58	0.44	48.1	1.57	15.91	35.4	0.45
1.14	0.50	204.0	21.33	32.61	0.248	75.6	10.12	0.45	57.5	1.31	21.08	40.3	0.52
1.14	0.50	204.0	21.06	32.46	0.244	77.4	10.12	0.48	57.5	1.34	21.08	40.7	0.51
1.14	0.50	204.0	21.15	32.55	0.245	76.6	10.12	0.47	57.5	1.33	21.08	40.3	0.52
1.14	0.70	104.0	15.68	23.85	0.246	73.2	9.94	0.63	73.3	1.00	21.06	33.4	0.63
1.14	0.70	104.0	15.48	24.11	0.231	76.7	9.94	0.64	73.3	1.04	21.06	33.9	0.62
1.14	0.70	104.0	15.51	23.93	0.237	76.4	9.94	0.64	73.3	1.04	21.06	33.8	0.62
2.07	0.35	104.0	4.44	8.06	0.373	32.8	1.34	0.30	12.5	2.62	2.90	16.5	0.17
2.07	0.35	104.0	4.43	8.06	0.372	33.6	1.34	0.30	12.5	2.68	2.90	16.7	0.17
2.07	0.35	104.0	4.43	7.89	0.378	33.2	1.34	0.30	12.5	2.65	2.90	16.2	0.17
2.07	0.35	104.0	4.43	8.06	0.372	33.6	1.34	0.30	12.5	2.68	2.90	16.7	0.17
2.07	0.35	104.0	4.44	8.06	0.373	32.8	1.34	0.30	12.5	2.62	2.90	16.5	0.17
2.07	0.50	54.0	4.13	7.66	0.362	36.7	1.40	0.34	16.8	2.18	3.07	15.9	0.19
2.07	0.50	54.0	4.31	7.61	0.386	35.8	1.40	0.32	16.8	2.13	3.07	15.4	0.20
2.07	0.50	54.0	3.99	7.56	0.353	37.2	1.40	0.35	16.8	2.21	3.07	14.7	0.20
2.07	0.50	104.0	6.59	10.43	0.285	43.1	2.75	0.41	25.5	1.68	5.91	19.7	0.30
2.07	0.50	104.0	6.59	10.74	0.282	43.8	2.75	0.41	25.5	1.71	5.91	19.4	0.30
2.07	0.50	104.0	6.76	11.56	0.311	38.9	2.75	0.40	25.5	1.52	5.91	19.8	0.30
2.07	0.50	104.0	6.59	10.74	0.282	43.8	2.75	0.41	25.5	1.71	5.91	19.4	0.30
2.07	0.50	104.0	6.59	10.43	0.285	43.5	2.75	0.41	25.5	1.68	5.91	19.7	0.30
2.07	0.50	154.0	9.98	15.09	0.314	40.0	4.11	0.41	32.8	1.21	8.76	23.1	0.38
2.07	0.50	154.0	9.83	14.83	0.316	40.8	4.11	0.41	32.8	1.24	8.76	25.0	0.35
2.07	0.50	154.0	9.94	15.18	0.318	49.9	4.11	0.41	32.8	1.21	8.76	27.3	0.32
2.07	0.50	154.0	9.94	15.18	0.318	49.9	4.11	0.41	32.8	1.21	8.76	27.3	0.32
2.07	0.50	204.0	12.44	18.16	0.302	38.6	5.49	0.44	39.3	0.98	11.61	24.6	0.47
2.07	0.50	204.0	12.26	18.06	0.299	38.1	5.49	0.44	39.3	0.97	11.61	25.5	0.45
2.07	0.70	104.0	8.73	14.14	0.258	43.3	5.39	0.61	50.0	0.86	11.60	23.2	0.49
2.07	0.70	104.0	8.86	14.28	0.258	44.6	5.39	0.60	50.0	0.89	11.60	24.5	0.47
2.07	0.70	104.0	8.89	14.39	0.258	43.2	5.39	0.60	50.0	0.86	11.60	23.8	0.49
2.95	0.70	104.0	6.24	8.93	0.297	27.6	3.75	0.60	39.9	0.69	8.14	12.1	0.67
2.95	0.70	104.0	6.13	8.94	0.300	23.3	3.75	0.61	39.9	0.58	8.14	11.7	0.69
2.95	0.70	104.0	6.53	9.54	0.391	24.6	3.75	0.57	39.9	0.61	8.14	12.3	0.66
2.95	0.70	104.0	6.24	8.93	0.297	27.6	3.75	0.60	39.9	0.69	8.14	12.1	0.67
3.07	0.35	104.0	3.08	5.74	0.426	19.6	0.90	0.29	9.7	2.01	1.95	11.8	0.17
3.07	0.35	104.0	3.19	5.78	0.426	19.7	0.90	0.28	9.7	2.02	1.95	11.4	0.17
3.07	0.35	104.0	3.22	5.78	0.417	19.8	0.90	0.27	9.7	2.02	1.95	11.7	0.17
3.07	0.50	54.0	3.03	5.24	0.428	19.9	0.93	0.30	13.0	1.52	2.07	7.18	0.29
3.07	0.50	54.0	2.98	5.20	0.418	20.0	0.93	0.31	13.0	1.53	2.07	7.26	0.28
3.07	0.50	54.0	2.98	5.20	0.418	20.0	0.93	0.31	13.0	1.53	2.07	7.26	0.28
3.07	0.50	54.0	3.16	5.29	0.422	19.4	0.93	0.29	13.0	1.48	2.07	7.23	0.29
3.07	0.50	54.0	3.16	5.29	0.422	19.4	0.93	0.29	13.0	1.48	2.07	2.73	0.29
3.07	0.50	54.0	2.98	5.20	0.418	20.0	0.93	0.31	13.0	1.53	2.07	7.26	0.28
3.07	0.50	104.0	4.89	7.88	0.370	24.3	1.83	0.37	19.8	1.22	3.99	10.5	0.38
3.07	0.50	104.0	5.03	7.93	0.370	22.6	1.83	0.36	19.8	1.14	3.99	10.0	0.40
3.07	0.50	104.0	5.10	8.06	0.369	22.5	1.83	0.36	19.8	1.13	3.99	10.2	0.39
3.07	0.50	154.0	6.56	9.96	0.320	20.6	2.74	0.41	25.5	0.80	5.90	11.7	0.50
3.07	0.50	154.0	6.45	9.75	0.300	21.6	2.74	0.42	25.5	0.84	5.90	11.7	0.50
3.07	0.50	154.0	6.46	9.71	0.295	21.7	2.74	0.42	25.5	0.84	5.90	11.8	0.50
3.07	0.50	204.0	9.03	12.16	0.352	22.5	3.66	0.40	30.5	0.73	7.82	18.4	0.42
3.07	0.50	204.0	8.93	12.18	0.349	22.3	3.76	0.41	30.5	0.72	7.82	20.5	0.38
3.07	0.50	204.0	8.91	12.04	0.352	22.9	3.66	0.41	30.5	0.75	7.82	17.5	0.45
4.93	0.50	104.0	2.74	4.53	0.374	12.3	1.13	0.41	14.6	0.83	2.48	6.01	0.41
4.93	0.50	104.0	2.58	4.33	0.352	12.1	1.13	0.43	14.6	0.82	2.48	5.55	0.45
4.93	0.50	104.0	2.66	4.41	0.348	12.2	1.13	0.42	14.6	0.82	2.48	5.64	0.44

* $A_t = 0.845$.

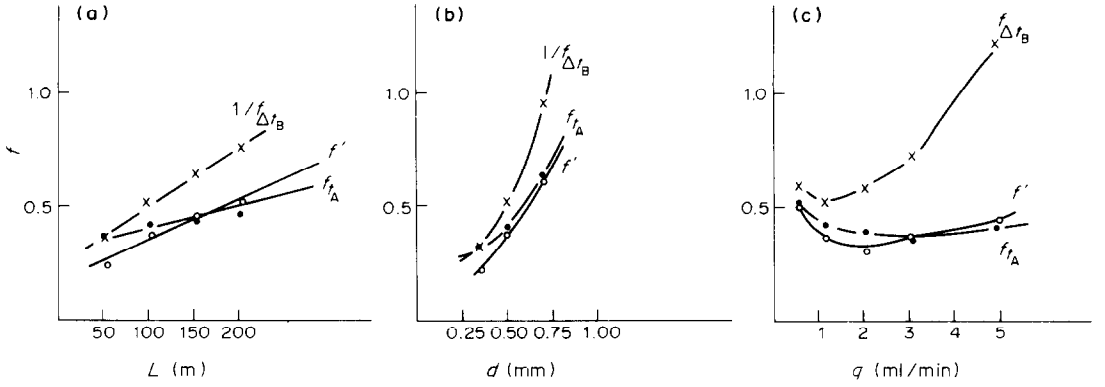

Fig. 2. Behaviour of accommodation factors *vs.* FIA variables. (a) $d = 0.50$ mm, $q = 1.14$ ml.min^{-1}; (b) $L = 104$ cm, $q = 1.14$ ml.min^{-1}; (c) $L = 104$ cm, $d = 0.50$ mm.

we found that the slope was very close to 1.025, the value suggested by Vanderslice *et al.*, confirming that our equation for L_{eq} gives results in agreement with $f_{t_A} = (L_{tube}L_{eq})^{1.025}$.

However, this alone does not advance or improve the theory and practice of FIA, since to be able to predict the travel time it is first necessary to calculate the equivalent length of the system (which depends on physical factors, such as q, d and the dimensions of the experimental manifold) and also to integrate the experimental FIA peaks, to calculate the statistical residence time $(t_r)_{st}$.

We must therefore examine $f_{\Delta t_B}$. Qualitatively, f_{t_A} and $f_{\Delta t_B}$ both depend on L and on d, but in different ways. The influence of these variables is roughly similar for f_{t_A} and $1/f_{\Delta t_B}$ but that of q on $1/f_{\Delta t_B}$ is considerably different from that on f_{t_A} (Fig. 2). The error in the measurement of $(t_r)_{st}$, and hence of f_{t_A} and $f_{\Delta t_B}$, is higher than that of the travel time, owing to the shape of the FIA peaks. Vanderslice *et al.* did not report the uncertainty in the exponents of the variables, and we predict that these exponents should be higher than those in equation (1). From regression analysis of the data obtained in our experiments, values very different from those reported by Vanderslice *et al.* were found, together with uncertainties in the values, which leads us to conclude the inapplicability of equation (2) under the general working conditions of FIA.

Accommodation factor f'.

A new factor, f', is therefore defined here as the ratio of the mean residence time, (t_r, calculated from geometric considerations) to the statistical residence time, $(t_r)_{st}$, deduced from equation (3).

The influence of L and d on f' is qualitatively similar to that on f_{t_A} and $1/f_{\Delta t_B}$, but is closest to that on $1/f_{\Delta t_B}$. On the other hand, the influence of the flow-rate on f_{t_A} and f' is similar, but very different from that on $1/f_{\Delta t_B}$.

The dependence of these accommodation factors on the diffusion coefficients has not been taken into account, since all the experiments were done with the same compound. Nevertheless, we can predict that its effect will be minimal, owing to the small value of its exponents. The varied influence of the dimensional parameters of an FIA system on the f values considerably restricts the application of the Vanderslice *et al.* equations. It is not possible to predict the features of an FIA peak from them since it is necessary to know the value of the f factors, which can only be found experimentally.

A NEW METHOD OF DEVELOPING EQUATIONS TO DESCRIBE A GIVEN FIA MANIFOLD

The experimental data obtained in the runs (Table 1) were statistically analysed as follows.

First the variables were grouped in various combinations, and by multiple regression analysis the exponents of these variables were calculated. In this and subsequent analysis the diffusion coefficient was not regarded as an independent variable, since a single compound was used. However, the equations tested, such as:

$$\frac{Dt}{L^2} = f\left|\frac{q}{DL}, \frac{L}{d}\right|; \frac{D\Delta t}{L^2} = f\left|\frac{q}{DL}, \frac{L}{d}\right|$$

did not give satisfactory results.

The problem was therefore approached in a different manner. The multiple regression analysis was performed directly with the original variables for two cases: (*a*) equations with two parameters, (*b*) equations with three parameters, *i.e.*, with (L/q) considered as one variable [case (*a*)] or as two independent ones [case (*b*)].

The same behaviour was found for the travel time in both cases, so for simplicity the two-parameter system was chosen, and gave the following equation:

$$t_A = 0.465\, d^{0.950}\left|\frac{L}{q}\right|^{0.850} \quad (5)$$

This equation correctly predicts the travel time for more than 85% of the experiments performed, with a relative error of less than 10%.

To predict the baseline-to-baseline time the three-parameter model is necessary, since there is rather a

large error when the two-parameter model is used. The following equation is proposed:

$$\Delta t_B = 56.7\, d^{0.293}\, L^{0.107}\, q^{1.057} \quad (6)$$

This equation predicts the results of more than 85% of the experiments, with a relative error of less than 15%.

Neither equation involves the diffusion coefficient, which is taken as constant as already explained, and its influence is included in the intercept of both equations, along with that of the type of FIA manifold.

It should be pointed out that in both equations only variables known beforehand are used; for this reason the equations are suitable for predicting the two time-parameters (travel time and dispersion time) for an FIA run, with an error similar to that of the measurement.

Equations (5) and (6) define characteristic parameters of an FIA peak that provide information about the time characteristics of this peak. In order to define the peak fully, two other parameters are necessary: the appearance time of the maximum and the peak height. A statistical procedure similar to the one already used was applied to find two equations that permit prediction of these parameters. The equations obtained are as follows:

$$\mathbf{D} = \frac{C_0}{C} = 2.342\, L^{0.167}\, q^{-0.206}\, d^{0.496} \quad (7)$$

$$t_{max} = 0.840\, L^{0.801}\, d^{0.683}\, q^{-0.977} \quad (8)$$

where **D** is the dispersion, C the concentration of the test substance monitored at time t, and C_0 the concentration of test substance monitored for zero dispersion.

Both equations predict the results of over 85% of the experiments with an error of less than 10%. As in equations (5) and (6), the diffusion coefficient and the injected volume have not been taken into account; both are kept constant throughout the experiments and their influence is included in the intercept of both equations.

These expressions are partially justified by the dispersion model deduced by Levenspiel,[8] but as he has demonstrated, the shape of the curve obtained is dramatically influenced by the methods of injection and the measurement of the tracer concentration.

These four expressions (5)–(8) provide sufficient information to characterize an FIA system, with the advantage that the features of a peak can be predicted. Obviously, from one FIA system to another, the injection valve, detector, coils and type volume of sample are likely to be changed, so the coefficients in the four equations will vary, but the variation will not be appreciable since it will mainly affect the intercepts of the expressions, since all the modified factors (L, d, q) are included in it. Therefore, the experimenter must adapt these equations to his own system, by a few simple operations, as follows.

(1) Running experiments in which the values of L, d and q are varied between the limits to be used in applications. At least 5 points in triplicate must be obtained for each variable, whilst the other two are kept constant.

(2) From the runs in (1), the data for travel time, baseline-to-baseline time, peak height and appearance time of the maximum are obtained.

(3) Multiple regressions for the logarithmic forms of equations (5)–(8) are performed. From the coefficients, the exponents of the variables and the intercept are obtained.

By this method and in a short time, with a few runs and the aid of multiple regression analysis [either manual or by computer (software packages are commercially available)] the experimenter can work out the equations for his own FIA system. From these equations the features of the FIA peaks obtained can be predicted for future experiments with an error of less than 10%.

CONCLUSIONS

The equations of Vanderslice *et al.* are not suitable for predicting the travel time and dispersion time of an FIA peak obtained under normal working conditions, because of the dependence of f_{t_A} and $f_{\Delta t_B}$ on L, d and q and the need to perform preliminary runs for the calculation of f_{t_A} or $f_{\Delta t_B}$ or equivalent length (since the equations are only fulfilled by this parameter, and not by the tube length).

Nor is the Ramsing *et al.* equation[3] related to the peak height practical for predicting the dispersion, since it is necessary to find experimentally the Levenspiel–Smith dispersion number, which is a function of the shape of the curve.

The dispersion volume, ΔV_B, can be predicted from equation (6). Since $\Delta V_B = q\Delta t_B$, the following expression is obtained:

$$\Delta V_B = 56.7\, d^{0.293}\, L^{0.107}\, q^{-0.057} \quad (9)$$

The equations reported in this paper permit the prediction of the fundamental parameters of an FIA peak with relative errors of under 10%, and a simple method is proposed for adapting them to the features of any given FIA system.

REFERENCES

1. J. Růžička and E. H. Hansen, *Flow Injection Analysis*, p. 40. Wiley, New York, 1981.
2. *Idem*, *Anal. Chim. Acta*, 1978, **99**, 37.
3. A. U. Ramsing, J. Růžička and E. H. Hansen, *ibid.*, 1981, **129**, 1.
4. J. T. Vanderslice, K. K. Stewart, A. G. Rosenfeld and D. J. Higgs, *Talanta*, 1981, **28**, 11.

5. C. C. Painton and H. A. Mottola, *Anal. Chem.*, 1981, **53,** 1713.
6. O. Levenspiel and W. H. Smith, *Chem. Eng. Sci.*, 1957, **6,** 227.
7. R. C. Reld and T. K. Sherwood, *The Properties of Gases and Liquids*, McGraw-Hill, New York, 1968.
8. O. Levenspiel, *Chemical Reaction Engineering*, Wiley, New York, 1973.

Talanta, Vol. 32, No. 4, pp. 325–327, 1985
Printed in Great Britain.

0039-9140/85 $3.00 + 0.00

SHORT COMMUNICATION

SPECTROPHOTOMETRIC DETERMINATION OF SACCHARIN IN DIFFERENT MATERIALS BY A SOLVENT EXTRACTION METHOD USING NILE BLUE AS REAGENT

M. HERNANDEZ CORDOBA, I. LOPEZ GARCIA and C. SANCHEZ-PEDREÑO*
Department of Analytical Chemistry, University of Murcia, Murcia, Spain

(*Received* 26 *June* 1984. *Revised* 3 *October* 1984. *Accepted* 6 *November* 1984)

Summary—In a slightly acidic medium (sodium acetate–acetic acid buffer, pH 4) saccharin and Nile Blue form an ion-association compound which is extractable into methyl isobutyl ketone and allows the spectrophotometric determination of saccharin. At 630 nm Beer's law is obeyed over the saccharin concentration range 0.1–3.5 μg/ml in the aqueous phase and the apparent molar absorptivity is 5.8×10^4 $l.mole^{-1}.cm^{-1}$. The method shows good selectivity and can be applied to the determination of saccharin in artificial sweeteners, soft drinks and toothpastes.

Saccharin and its salts are widely used as non-fattening sweetening agents. Several methods for their determination have been proposed.[1–6] Some are time-consuming and others need costly equipment. The formation and extraction of ion-association compounds of saccharin with basic dyes may offer a simple alternative for rapid spectrophotometric determination of saccharin, and thiazine dyes,[7–9] Basic Fuchsin[10] and phenazines[11] have been proposed for the purpose, but some of the methods have limitations in sensitivity and selectivity. We have therefore examined a large number of ion-association systems, looking for a compromise between minimum blank reading and maximum extraction of saccharin, with the aim of developing a rapid, highly sensitive and selective spectrophotometric method for the determination of saccharin. Nile Blue is the best of the reagents tested.

EXPERIMENTAL

Reagents

All inorganic chemicals used were of analytical reagent grade and doubly distilled water was used throughout.

Saccharin solution. A stock solution was prepared by dissolving 200 mg of the sodium salt in water and diluting to 200 ml. Working solutions were prepared daily by further dilution.

Sodium acetate–acetic acid buffer. A pH 4 buffer was prepared by mixing 90 ml of 1*M* sodium acetate and 410 ml of 1*M* acetic acid.

Nile Blue solution. An aqueous solution of the dye (Basic Blue 12, C.I. 51180) (Carlo Erba) was prepared and purified as follows before use. In a separating funnel, 375 ml of $2 \times 10^{-3}M$ dye solution, 50 ml of 1*M* acetate buffer (pH 4) and 75 ml of water were mixed and shaken for 10 min with 100 ml of methyl isobutyl ketone (MIBK). The organic layer was discarded and the aqueous phase, to be employed in the analysis, was filtered through filter-paper.

General procedure

Place the sample saccharin solution (no more than 9 ml, containing up to 35 μg of saccharin) in a separating funnel, add 1 ml of the purified and buffered dye solution and dilute to 10 ml with water. Add 5 ml of MIBK, shake the funnel vigorously for about 2 min and allow the phases to separate. Transfer the organic layer into a centrifuge tube and centrifuge it. Measure the absorbance of the organic layer at 630 nm against a reagent blank prepared in a similar way.

Prepare a calibration graph by applying the procedure to different volumes of standard saccharin solution. Beer's law is obeyed over the concentration range 1–35 μg of saccharin per 10 ml of aqueous phase.

Procedure for tablets and liquid sweeteners

Weigh accurately 10 saccharin tablets and grind them to a fine powder in an agate mortar. Transfer an accurately weighed amount of the powder, containing about 50 mg of saccharin, into a 100-ml standard flask. Dissolve with water and make up to the mark. Dilute 5 ml of this solution accurately to 100 ml with water. Take a 1-ml aliquot and apply the general procedure.

For the analysis of liquid sweeteners pipette 1 ml of the sample into a 100-ml standard flask and make up to the mark with water. Dilute 1 ml of this solution accurately to 100 ml with water. Apply the general procedure to a 1-ml aliquot of this solution.

Analysis of soft drinks

Remove carbon dioxide from the sample by repeated shaking. Take up to 10 ml of sample containing no more than 35 μg of saccharin, and transfer it into a separating funnel, add 1 ml of 1*N* sulphuric acid and 9 ml of 0.5*M* potassium sulphate, shake with 5 ml of MIBK for about 2 min, allow the phases to separate and discard the aqueous phase. Add 1 ml of the dye solution and 9 ml of water and shake for about 2 min. After separation of the phases measure the absorbance of the organic layer as described in the general procedure. Prepare a calibration graph with different amounts of saccharin treated in the same way.

Analysis of toothpastes

Extract a 1-g sample with water, filter, and dilute the filtrate to volume in a 100-ml standard flask. Transfer up to 5 ml of the solution into a separating funnel and add 10 ml of 0.5*M* potassium sulphate. Extract with 5 ml of MIBK and discard the organic layer. Add 1 ml of 1*N* sulphuric acid and extract with 5 ml of MIBK. Discard the aqueous phase, add 1 ml of the dye solution and 9 ml of water and shake for about 2 min. Measure the absorbance of the organic layer. Prepare a calibration graph, by treating different amounts of saccharin in the same way.

*Author to whom correspondence should be addressed.

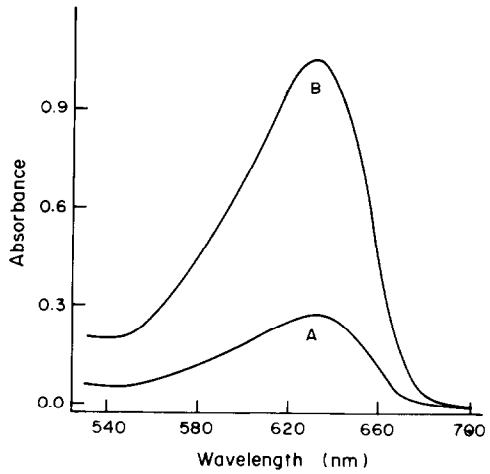

Fig. 1. Absorption spectra of extracts into MIBK: (A) reagent blank; (B) in the presence of 28 μg of saccharin.

RESULTS AND DISCUSSION

In the preliminary experiments several basic dyes (phenosafranine, Acridine Yellow, Acridine Orange, Rhodamine B, Pyronine G, Ethyl Violet, Malachite Green, gallocyanine, new Methylene Blue, Brilliant Cresyl Blue and Nile Blue) were tested at different pH values as ion-pairing reagents for the extraction of saccharin (Sac^-). Chloroform, carbon tetrachloride, benzene, toluene, isobutyl acetate, ethyl acetate, isoamyl acetate, cyclohexanone, isobutyl alcohol and methyl isobutyl ketone were tried as the solvents.

None of these systems showed better results than the Nile Blue (NB^+) and methyl isobutyl ketone (MIBK) system. The absorbance of the reagent blank is not high and this system gave the highest degree of extraction of saccharin.

Absorption spectra

Figure 1 shows the absorption spectra of the ion-pair [NB^+, Sac^-] extracted into MIBK and of the reagent blank, obtained as described in the procedure. The spectra are very similar in shape to the absorption spectrum of an aqueous solution of the dye, and all three spectra have maximum absorption at 630 nm.

Effect of pH and Nile Blue concentration

Figure 2 shows that the absorbance is maximal and constant over the pH range 3.2–4.8. The decrease in the absorbance at pH < 3.2 may be attributed to protonation of the saccharin anion, and at pH > 4.8 to conversion of Nile Blue into neutral form.

The extraction is also affected by the dye concentration. Figure 3 shows that maximal and constant absorbance is obtained by use of at least 1 ml of $10^{-3}M$ Nile Blue. It was found that better reproducibility and a lower reagent blank were achieved if the dye was purified by extraction with MIBK.

Characteristics of the ion-pair

The continuous-variations method with measurement at three different wavelengths showed that the ion-pair [NB^+, Sac^-] is the only compound extracted into MIBK under the recommended conditions.

The extraction efficiency was about 65%. However, a single extraction is recommended, because further extractions would complicate the procedure and the increased volume of organic phase would reduce the sensitivity. Hence accurate volume measurement is essential.

There were no measurable changes in the absorbance of the extract even after standing for 8 hr in a glass-stoppered tube at room temperature. Shaking times ranging from 1.5 to 5 min produced no change in absorbance, so a 2-min shaking time was selected.

Calibration graph

The calibration graph is linear in the range 1–35 μg

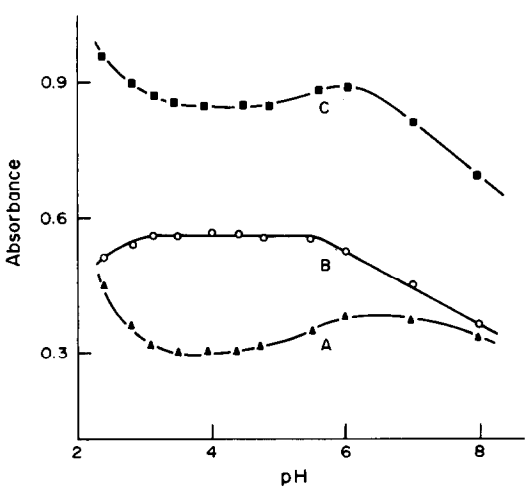

Fig. 2. Influence of pH: (A) reagent blank; (B) and (C) with 20 μg of saccharin (B, reference reagent blank; C, reference water).

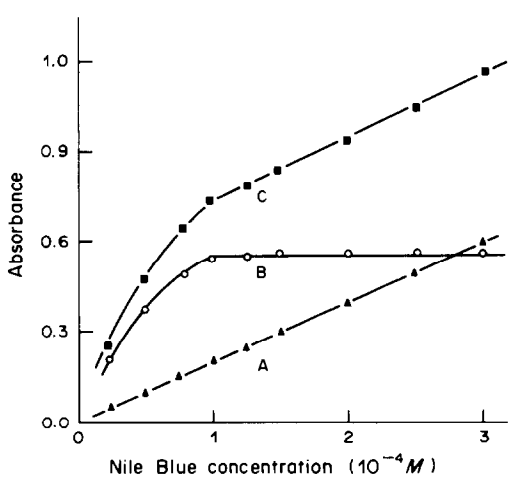

Fig. 3. Effect of Nile blue concentration: (A) reagent blank; (B) and (C) with 20 μg of saccharin (B, reference reagent blank; C, reference water).

Table 1. Effect of various species on the determination of 5 μg of saccharin

Species added	Tolerance limit*, μg
Ascorbic acid, gelatin, gum acacia, starch, talc, caffeine, maltose, fructose, sucrose, galactose, lactose, glucose, sodium citrate†, sodium tartrate†, sodium hydrogen carbonate†, sodium dodecyl sulphate§	10,000
Sorbic acid†, acetylsalicylic acid§, benzoic acid†	1000
Sodium cyclamate†	400

*Amount causing an error of no more than $\pm 3\%$.
†Using previous extraction with MIBK in acidic medium.
§Using previous extraction with MIBK from 0.5*M* potassium sulphate solution at pH 4.

of saccharin per 10 ml of aqueous phase. The apparent molar absorptivity at 630 nm is 5.8×10^4 l.mole^{-1}.cm^{-1}. The precision was estimated from 10 analyses for 9-ml aliquots of $7.2 \times 10^{-6}M$ saccharin. The standard deviation of the absorbance and the relative standard deviation were 0.006 and 1.3% respectively. The standard deviation of the absorbance of the reagent blank was less than 0.005.

Effect of foreign substances

The tolerance limit for permissible foreign substances was taken as the concentration which caused an error of not more than $\pm 3\%$ in the absorbance for 5 μg of saccharin in the sample. The selectivity can be enhanced by a previous separation of saccharin with MIBK from 0.1*N* sulphuric acid medium. In that way, 6 μg of dodecyl sulphate, 50 μg of acetylsalicylic acid, 400 μg of cyclamate, 1000 μg of sorbic acid and benzoic acid and 10 mg of tartrate, citrate and bicarbonate can be tolerated. Even with the use of this separation step, sodium dodecyl sulphate and acetylsalicylic acid are serious interferents, but their interference is easily overcome if the sample is treated with a large excess of potassium sulphate (0.5*M*) and extracted at pH 4 with MIBK. Potassium dodecyl sulphate and acetylsalicylate are transferred into the organic layer and the saccharin remains in the aqueous phase. Experimental results are given in Table 1.

Table 2. Determination of saccharin in artificial sweeteners

Sample	Saccharin content, *mg/tablet or g/l.* Label claim	Found*
Tablets A	5	4.92
B	15	15.0
C	25	24.4
D	30	30.1
Liquids A	12	11.8
B	226.8	227
C	125	123
D	15	15.9

*Average of four determinations.

Table 4. Determination of saccharin in toothpastes

Sample	Label claim, %	Saccharin found, %*
1	0.3	0.31
2	0.1	0.98
3	0.2	0.21
4	0.05	0.06

*Average of four determinations.

Determination of saccharin in samples

The method has been successfully applied to the determination of saccharin in tablets and liquid sweeteners, soft drinks and toothpastes, by the procedures given. The results are given in Tables 2–4.

Some of the soft drinks assayed did not contain saccharin and a known amount of saccharin was added to these to assess the recovery.

Conclusion

In comparison with the earlier spectrophotometric methods using ion-pairing reagents,[7–11] the extraction with Nile Blue reported here is highly sensitive and selective for the determination of saccharin, and is suitable for routine analysis.

Table 3. Recovery of saccharin from various soft drinks

Soft drink	Saccharin found without addition, μg/ml	Saccharin found with 2.0 μg/ml added	Recovery, %*
Tonic	—	2.06	103
Cola	—	1.98	99
Cola (non-caloric)	88	90.1	105
Bitter	1.9	3.95	102
Soda	—	1.96	99
Ginger ale	—	2.00	100

*Average of four determinations.

REFERENCES

1. J. W. Weyland, H. Roliuk and P. A. Doornbos, *J. Chromatog.*, 1982, **247,** 221.
2. E. R. Clark and A. K. Yacoub El-Sayed, *Analyst*, 1982, **107,** 414.
3. M. Geissler, B. Schiffel and C. Kuhnhardt, *Anal. Chim. Acta*, 1981, **124,** 237.
4. E. C. P. Gillyon, *Chromatog. Newsl.*, 1980, **8,** 50.
5. N. Hazemoto, N. Kamo and Y. Kobatake, *J. Assoc. Off. Anal. Chem.*, 1974, **57,** 1205.
6. R. Belcher, S. L. Bogdanski, R. A. Sheikh and A. Townshend, *Analyst*, 1976, **101,** 562.
7. Y. Beltagy, S. M. Rida and A. Issa, *Pharmazie*, 1974, **29,** 64.
8. K. C. Guven and F. Ozaydin, *Eczacilik Bul.*, 1980, **22,** 58.
9. P. G. Ramappa and N. N. Anant, *Analyst*, 1983, **108,** 966.
10. A. M. Wahbi, H. Abdine, M. A. Korany and M. H. Abdel-Hay, *ibid.*, 1978, **103,** 876.
11. Y. Beltagy, *Zentralbl. Pharm., Pharmakother. Laboratoriums Diagn.*, 1977, **116,** 925.

Talanta, Vol. 32, No. 4, pp. 329–333, 1985
Printed in Great Britain

0039-9140/85 $3.00 + 0.00
Pergamon Press Ltd

ANNOTATIONS

CADMIUM-113 AND CARBON-13 NUCLEAR MAGNETIC RESONANCE SPECTROMETRY OF CADMIUM PEPTIDE COMPLEXES

S. M. WANG* and R. K. GILPIN†
Kent State Universtiy, Kent, Ohio 44242, U.S.A.

(*Received* 14 *November* 1983. *Revised* 24 *October* 1984. *Accepted* 4 *December* 1984)

Summary—The cadmium complexes of glycylglycine, glycylglycylglycine, glycyl-γ-aminobutyric acid and β-alanylglycine (β-Ala-Gly) have been investigated by ^{113}Cd and ^{13}C nuclear magnetic resonance spectrometry. The minima observed in plots of the ^{113}Cd chemical shift *vs.* pH are consistent with cadmium binding first at the carboxylic site and then at the amino-group site. The chemical shift *vs.* pH profile for the β-Ala-Gly system is different from that for the other peptides, and is interpreted as suggesting formation of a five-membered chelate between Cd(II) and glycyl residues at the N-terminal groups and not at the C-terminal groups. The data further indicate that the NH groups of the peptide linkages are probably not involved in complexation with cadmium. Finally, a reported pH-dependent ^{113}Cd resonance for parvalbumin has been reassigned.

The role of several trace metals in living organisms has been designated as either structure-promotion or enzyme activation/deactivation. For elements such as zinc, cadmium and mercury, general complexation studies are important in obtaining a more fundamental understanding of the biochemical systems. However, because zinc, cadmium and mercury have completely filled *d*-orbitals, ultraviolet spectrometry is unsuitable for investigating their complexation, and hence other techniques such as nuclear magnetic resonance (NMR) spectometry have become popular, especially for acquiring information at the molecular level.

The ^{113}Cd nucleus, with its chemical shift range of over 800 ppm, gives an NMR sensitivity five times that of the ^{13}C nucleus[1] and thus is better suited for probing metal–ligand interactions. In addition to metallothionein,[2–7] a cadmium-induced metalloprotein, a variety of metalloproteins and metalloenzymes have been examined by ^{113}Cd NMR techniques.

NMR studies with cadmium as the probe ion have been used to elucidate the nature of metal binding in zinc-activated metalloenzymes,[8–18] and in metalloproteins modulated by calcium.[19–25] Also, Sudmeier *et al.*[25,26] have studied zinc and calcium binding sites in insulin.

Although considerable amounts of data on various cadmium systems have been collected, wide variations in results have been reported,[10,11] which may often be ascribed to the effect of changes in solution parameters, or to exchange of co-ordinated solvent molecules. As summarized in Table 1, the chemical shift of ^{113}Cd is especially sensitive to changes in pH and the counter-ions studied. As a result, systematic fundamental investigations of model compounds and systems are needed before the nature of more complex interactions such as metal binding in metalloproteins can be pictured clearly.

Combined ^{113}Cd and ^{13}C NMR studies of a homologous series of cadmium–amino-acid complexes have already been reported,[27] and interpreted as suggesting that five-membered chelate rings form between cadmium and molecules similar to glycine. In aqueous solutions, the highest complex formed with glycine was found to be $CdGly_3$. Similar results for supercooled aqueous solutions have been reported by Jakobsen and Ellis.[28]

To extend our earlier work, cadmium binding with selected peptides has been studied. Such studies are important in establishing general models for protein systems and as aids in elucidating specific properties such as the biological activity of carboxypepidase A, which breaks up polypeptide chains from the C-terminal end to give the consituent amino-acids[29] and also catalyses the hydrolysis of esters. The first of these properties is attributed to increase in the susceptibility of the peptide linkage to hydrolysis, owing to binding of the C-terminal group of the peptide to the zinc atom at the active site of the enzyme. Replacement of zinc by cadmium, lead or mercury results in partial loss of the catalytic activity for cleavage of the C-terminal amino-acid residue, but the modified enzymes still catalyse the hydrolysis of esters.[30] Indeed, with the cadmium-substituted car-

*Present address: GAF Corporation, Wayne, NJ 07470, U.S.A.
†To whom correspondence should be addressed.

Table 1. ^{113}Cd chemical shifts of various metalloproteins

Metalloproteins and metalloenzymes	Ligand binding sites*	pH-sensitive?	Counter-ion-sensitive?	Chemical shift, *ppm*	Reference
Alkaline phosphatase	3 N	yes	yes	55–170	9,10
	1 substrate				15,16
Calmodulin	6 O			−88.5, −115	24,25
Carbonic anhydrase	3 N	yes	yes	145–241	9–14
	1 substrate			410	
Carboxypeptidase A	2 N, 1 O	yes	yes	240,217	8,9
	1 substrate				
Concanavalin A	6 O	no	no	−125, −132	19,20
	5 O, 1 N				
Dehydrogenase	2 S, 1 N	yes	yes	483,519	17
	1 substrate			751	
Insulin	6 O	no		−36	25
	3 N, 3 O (H_2O)			201	26
Metallothionein	4 S			614–670	2–7
Parvalbumin	6 O	no	no	−90, −100	21,22
Superoxide dismutase	3 N, 1 O	no	no	310–330	18
Troponin C	4 O			−110, −107	23
	2 various				

*O = Oxygen binding; N = Nitrogen binding; S = Sulphur binding.

Table 2. ^{113}Cd chemical shifts and pH_{min} values for cadmium–peptide complexes

Peptide	pK_{a1}*	pK_{a2}*	*ppm*†	pH_{min}§	$pK_{a2} - pH_{min}$
Gly-Gly	3.16‡	8.23¶	−13.88	3.8	4.4
Gly-Gly-Gly	3.22‡	8.09¶	—	—	—
Gly-γ-ABA	4.17‡	8.25¶	−17.41	3.9	4.4
β-Ala-Gly	3.25¶	9.38¶	−16.97	5.4	3.8

*First and second acid dissociation constants of ligands.
†Chemical shift for curve minimum.
§pH value of curve minimum (pH_{min}).
‡Reference 37.
‖Reference 38.

boxypeptidase A, the hydrolysis is even faster than with the natural enzyme.

In the current investigation, binding of cadmium with glycylglycine (Gly-Gly), glycylglycylglycine (Gly-Gly-Gly), glycyl-γ-aminobutyric acid (Gly-γ-ABA) and β-alanylglycine (β-Ala-Gly) has been examined by use of ^{113}Cd and ^{13}C NMR.

EXPERIMENTAL

Reagents

Fisher buffers, pH 4.00, 7.00 and 10.00, were used as calibration standards. Gly-Gly, Gly-Gly-Gly, Gly-γ-ABA and β-Ala-Gly (Sigma) were used as received.

The deuterium oxide (Merck Isotope) was NMR spectroscopic grade. All additional chemicals, unless otherwise specified, were reagent grade.

Solid chemicals were weighed directly into standard flasks, and dissolved and diluted to volume with triply distilled water, which was degassed by boiling. These solutions were stored under nitrogen. The cadmium perchlorate solutions were standardized either titrimetrically with EDTA or by atomic-absorption spectrometry.

Measurements

All pH and NMR measurements were made at 25° as described earlier,[27] with the following exceptions. All the ^{13}C measurements except those for β-Ala-Gly were made with a Varian FT-80 NMR spectrometer using a 25° flip angle and a 1.20-sec acquisition time. The ^{13}C spectra of β-Al-Gly and its cadmium complex were measured at 50.3 MHz on a Varian model XL-200 NMR spectrometer at 25°.

For the ^{113}Cd measurements, an aqueous 1.0*M* solution of cadmium perchlorate was used as an external standard, but all reported chemical shifts are referred to 0.1*M* cadmium perchlorate, for which the signal is 1.87 ppm upfield from that of the 1.0*M* solution. Chemical shifts at higher and lower frequencies than the reference value are reported as positive and negative values respectively. No bulk susceptibility correction was applied, since it was negligible.

RESULTS AND DISCUSSION

Figure 1 shows the ^{113}Cd chemical shifts plotted *vs.* pH for the cadmium–peptide systems. Because of solubility problems, data could not be collected for solutions with pH values below 4.5 or above 7.6 for the Cd–Gly-Gly-Gly complex or for Cd–Gly-Gly,

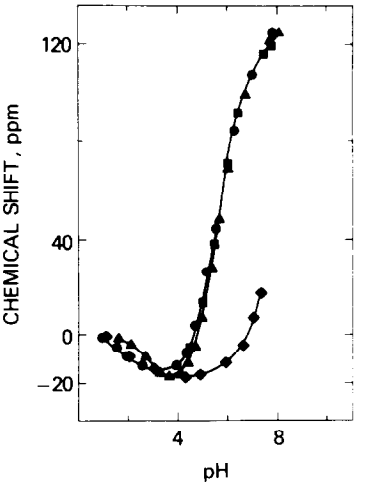

Fig. 1. ^{113}Cd chemical shift for mixtures of 0.3*M* $Cd(ClO_4)_2$ with 0.6*M* peptides, *vs.* pH. Gly-Gly (●), Gly-Gly-Gly (■), Gly-γ-ABA (▲), β-Ala-Gly (◆).

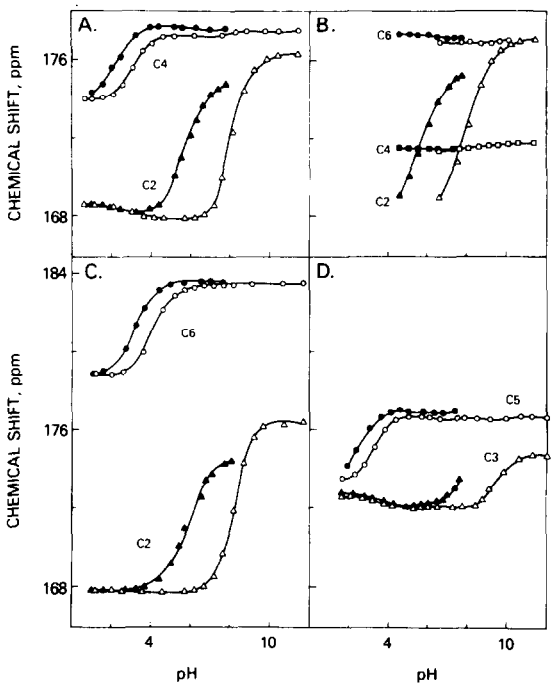

Fig. 2. ^{13}C chemical shift of carbonyl carbon atoms for 0.6*M* peptides alone (○, △, □) and with 0.3*M* $Cd(ClO_4)_2$ (●, ▲, ■), *vs.* pH. Symbols as for Fig. 1. A. C_2 and C_4 carbons of Gly-Gly. B. C_2, C_4 and C_6 carbons of Gly-Gly-Gly. C. C_2 and C_6 carbons of Gly-γ-ABA. D. C_3 and C_5 carbons of β-Ala-Gly.

Cd–Gly-γ-ABA and Cd–γ-Ala-Gly at pH above 8. As the pH is increased, there is first a negative shift, and then a positive shift, and this is consistent with cadmium binding initially at the carboxylate site, and then at the amino site analogously to the simpler amino-acid systems already reported,[27] but the minimum in the curve is sharper.

The difference between the profiles of the curves for Gly-Gly and Gly-γ-ABA at low pH is not unexpected, since the C-terminal group of the latter contains a longer alkyl chain, *cf.* the simple cadmium–amino-acid complexes.[27] The minima on the curves (pH_{min}) for Cd–Gly-Gly and Cd–Gly-γ-ABA were at pH 3.8 and 3.9 respectively, *cf.* Cd–glycine.[27] The difference between pK_{a2} and pH_{min} for these two peptides was 4.4, (Table 2) significantly smaller than that obtained for Cd–glycine (5.9) and suggests that the cadmium does not promote deprotonation of the amide groups in the peptides. Further, within experimental error, the chemical shift profiles for the three complexes were superimposable at pH > 5, which is reasonable since all three peptides contain an N-terminal glycyl group.

The curves for Cd–Gly-Gly and Cd–β-Ala-Gly were superimposable at lower pH. Both compounds contain the C-terminal glycyl group. Also of interest is the difference (Fig. 1) between the profile for the β-Ala-Gly system at pH > 4 and those for the other two systems. The chemical shift minimum was broader for the β-Ala-Gly system, in which there is a longer carbon chain at the N-terminal end. The pH for the chemical shift minimum was close to that reported for the β-alanine system,[27] and the smaller value of $pK_{a2} - pH_{min}$ (Table 2) suggests the absence of a chelate ring. The chemical shift profiles also demonstrate that chain-lengthening has a more significant effect when it occurs at the N-terminal position (*e.g.*, Cd–Gly-γ-Gly) than it does when at the C-terminal position (*e.g.*, Cd–Gly-γ-ABA). The results suggest that five-membered chelates of cadmium with glycyl residues may form only at the N-terminal groups of peptides.

Figure 2 shows the ^{13}C chemical shift *vs.* pH for the carbonyl carbon atoms of the free peptides and their complexes. Usually, for dipeptides which have large differences in consecutive pK_a values, assignments of NMR peaks to carbon atoms can be made directly from the pH-dependence of the ^{13}C resonances. However, for Gly-Gly-Gly the assignment is no longer straightforward. We have to make two assumptions in making assignments. First, that the chemical shifts for the carboxylate carbon atom of Gly-Gly-Gly before and after deprotonation are similar to those for Gly-Gly, 174 and 177 ppm. Secondly, that the changes in chemical shifts of the N-terminal carbonyl group, 8 ppm, due to the deprotonation of the protonated amino group, are similar for all glycyl groups in the N-terminal position, *e.g.*, in Gly-Gly, Gly-Gly-Gly, and Gly-γ-ABA. A method adapted from Feeney *et al.*[31] was also used to help make assignments. In solutions, exchange of solvent with the peptide-linkage proton is slower than that with quarternary amino-group protons or carboxylic-group protons. Therefore, in a 1:1 v/v mixture of H_2O and D_2O, the slow exchange of solvent with the peptide-linkage protons gives rise to doublet resonances for neighbouring carbonyl carbon atoms and α-carbon atoms, but singlets for carboxylic-group carbon atoms and other more remote groups. As shown in Fig. 3A, at pH 6.5, a doublet was observed at 171.8 ppm for Gly-Gly-Gly. Since the β-peptide proton is exchanged more quickly than the α-peptide proton,[32] the doublet was assigned to the C_4 carbon in the α-peptide linkage of Gly-Gly-Gly (numbering is shown in Fig. 4). A doublet was also observed for Cd–Gly-Gly-Gly at pH 5.5 under similar conditions. Figure 3B shows the full spectrum of Gly-Gly-Gly.

Another problem arises from ^{13}C resonance cross-over, which occurs as the solution pH is altered. This leads to serious ambiguities in using the chemical shift data to construct a titration curve. In the current studies cross-over ambiguities were minimized by collecting spectra at closely spaced pH values or by fitting the data to the Henderson–Hasselbalch equation,

$$pH = pK_a + \frac{\log [A^-]}{[HA]}$$

$$\delta_{obs} = \chi_{HA}\delta_{HA} + (1 - \chi_{HA})\delta_{\bar{A}}$$

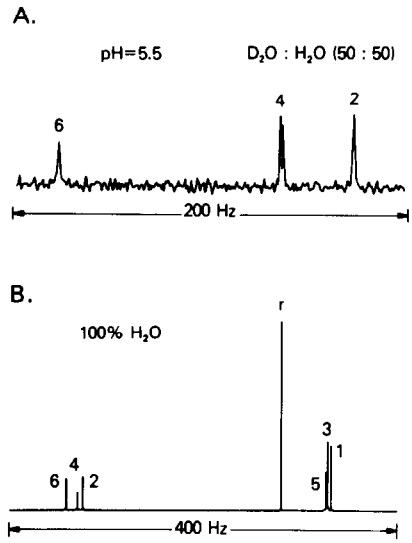

Fig. 3. A. ^{13}C spectrum of Gly-Gly-Gly in 50% D_2O, at pH 6.5, carbonyl region only. B. ^{13}C spectrum of Gly-Gly-Gly in 100% H_2O; r is dioxan (as reference, 67.39 ppm from TMS); C_1–C_6 correspond to the carbon atoms numbered in Fig. 4.

where HA and A^- are a peptide and its conjugate base, respectively, χ_{HA} is the mole fraction of the undissociated form of the peptide, δ_{HA} and δ_{A^-} are the chemical shift values before and after dissociation, respectively, and δ_{obs} is the observed chemical shift value.

The assignments made for the ^{13}C data by these methods are shown in Fig. 2. At low pH cadmium is bound weakly with the carboxylic groups of Gly-Gly (C_4), Gly-γ-ABA (C_6) and β-Ala-Gly (C_5). The pH shift caused by binding was approximately -0.9. Because of the solubility problem previously mentioned, the NMR behaviour of Gly-Gly-Gly could not be observed in this pH region.

In the pH range 4–10, the pH shift caused by the binding is -2.5 for Gly-Gly and Gly-γ-ABA, -2.1 for Gly-Gly-Gly, and -2.0 for β-Ala-Gly. Although all of these shifts are smaller than that for the Cd–glycine complex (-3.8) they are similar to that for Cd–β-Ala (-2.5).[27] This may be taken as indicating that the cadmium binding in these complexes does not involve deprotonation of the protonated amino group. Since a six-membered chelate ring is less stable than a five-membered ring, the pH shift on binding is smaller for β-Ala-Gly than for Gly-Gly and Gly-γ-ABA. Nearly the same chemical shifts were obtained from the C_4 atoms in free and complexed Gly-Gly-Gly, which implies that the α-peptide linkage does not serve as a binding site.

In the pH region 4–8 where cadmium binding occurs through the amino-group of the peptide, the small changes in chemical shifts observed for the C-terminal carboxylic group suggest simultaneous co-ordination with cadmium. However, from molecular models it seems unlikely that the amino nitrogen atom, the carbonyl oxygen atoms of the α- and β-peptide linkage and the carboxylate group for Gly-Gly-Gly can all be co-ordinated to the same metal ion. Although the amino nitrogen atom, the carbonyl oxygen atom of the β-peptide linkage and carboxylate group could be brought together, only the first two would form a thermodynamically stable structure, since the carboxylate group would be involved in a chelate ring with at least 10 members, which would be thermodynamically unstable. Therefore, it seems more likely that simultaneous co-ordination of the amino and the carboxylate ends would involve binding by metal ions to form polynuclear complexes. Likewise, competition for the metal co-ordination sites by the amino end potentially explains the reduced binding at the carboxylate end. As a result, smaller changes in the shifts of the C_6 carbonyl groups were observed at higher pH values.

Evidence for such polynuclear complexes has been reported, *e.g.*, by Kim and Martell,[34] who used ^1H-NMR to study copper and nickel complexes of

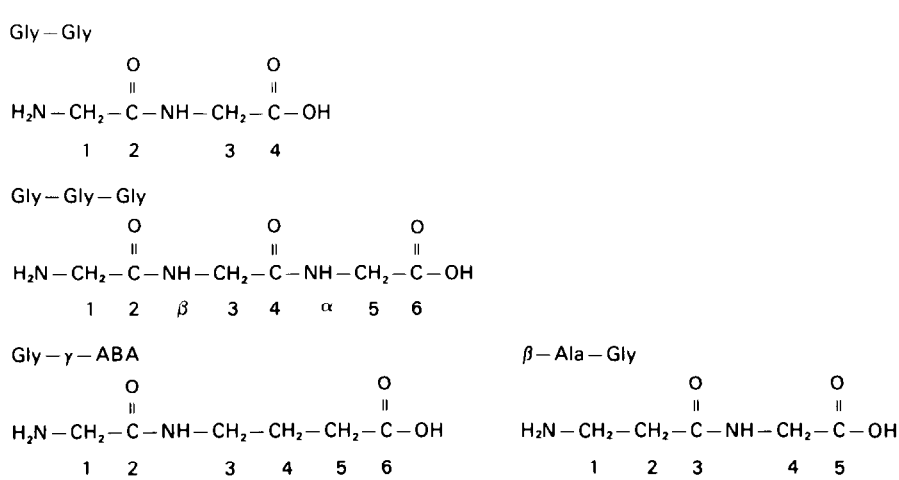

Fig. 4. Numbering of formulae of Gly-Gly, Gly-Gly-Gly, Gly-γ-ABA and β-Ala-Gly.

glycine peptides, and by Rabenstein and Libich[32] who reported on heavy metal complexes of the same peptides.

It has been suggested that Co(II), Ni(II) and Pb(II) can cause deprotonation of the peptide linkage,[35,36] but the present work gave no evidence for this. The plots of ^{13}C shift *vs.* pH were all simple S-shaped curves, not multi-stepped.

The α-peptide proton of Gly-Gly-Gly has been reported as being labilized by metal ions such as Zn(II) and Cd(II).[32] However, in the presence of cadmium the exchange between solvent and an α-peptide proton is slow on the NMR time scale, which is indicated by a doublet when 50% D_2O medium is used. In addition, the competition from a more stable five-membered chelate ring forming between cadmium ion and the N-terminal group, makes the C-terminal co-ordination become less likely at higher pH. The activity of carboxypeptidase A may thus be decreased in the presence of cadmium.

The results reported here provide at least partial explanation of the literature data for metalloproteins and metalloenzymes summarized in Table 1. For parvalbumin, in addition to the two signals (at -90 and -100 ppm) which correspond to the EF site and the CD site respectively, a pH-dependent signal was also observed. This resonance shifted from 0 to 67 ppm as the solution pH was changed from 4 to 8. This signal was assigned by Drakenberg[21] to the result of excess of cadmium complexing with the glycyl residues of parvalbumin. However, that chemical shift profile does not fit the curves obtained in the present study for either the C-terminal glycyl or the N-terminal glycyl group. Additionally, the current study shows that the binding between cadmium and the peptide linkage of the glycyl group is minimal. Therefore, the pH-dependent ^{113}Cd signal reported by Drakenberg[21] might be attributed to complexation of excess of cadmium with the Tris buffer used (pK_a for Tris is 8.5).

REFERENCES

1. R. K. Harris and B. E. Mann, *NMR and the Periodic Table*, Academic Press, New York, 1978.
2. P. J. Sadler, A. Bakka and P. J. Beynon, *FEBS Letters*, 1978, **94,** 315.
3. J. D. Otvos and I. M. Armitage, *Metallothionein, First International Meeting on Metallothionein and Other Low Molecular Weight Metal-Binding Proteins, 17 July 1978*, pp. 41–122. Birkhauser Verlag, Basel.
4. *Idem, J. Am. Chem. Soc.*, 1979, **101,** 7734.
5. I. M. Armitage, J. D. Otvos, R. W. Briggs and Y. Boulanger, *Fed. Proc.*, 1982, **41,** 2974.
6. Y. Boulanger and I. M. Armitage, *J. Inorg. Biochem.*, 1982, **17,** 147.
7. Y. Boulanger, I. M. Armitage, K. A. Miklossy and D. R. Winge, *J. Biol. Chem.*, 1982, **257,** 13717.
8. D. B. Bailey, *Dissertation*, Department of Chemistry, University of South Carolina, 1980.
9. I. M. Armitage, A. J. M. Schoot Uiterkamp, J. F. Chelbowski and J. E. Coleman, *J. Mag. Res.*, 1978, **29,** 375.
10. I. M. Armitage, R. T. Pages, A. J. M. Uiterkamp, J. F. Chelbowski and J. E. Coleman, *J. Am. Chem. Soc.*, 1976, **98,** 5710.
11. J. L. Sudmeier, *ibid.*, 1977, **99,** 4499.
12. N. B. H. Jonsson, L. A. E. Tibell, J. L. Evelhoch, S. J. Bell and J. L. Sudmeier, *Proc. Natl. Acad. Sci. USA*, 1980, **77,** 3269.
13. A. J. M. Uiterkamp, I. M. Armitage and J. E. Coleman, *J. Biol. Chem.*, 1980, **255,** 3911.
14. J. L. Evelhoch, D. F. Bocian and J. L. Sudmeier, *Biochemistry*, 1981, **20,** 4951.
15. J. D. Otvos and I. M. Armitage, *ibid.*, 1980, **19,** 4031.
16. P. Gettins, and J. E. Coleman, *J. Biol. Chem.*, 1983, **258,** 396.
17. B. R. Robsein and R. J. Myers, *J. Am. Chem. Soc.*, 1980, **102,** 2454.
18. D. B. Bailey, P. D. Ellis and J. A. Fee, *Biochemistry*, 1980, **19,** 591.
19. D. B. Bailey, P. D. Ellis, A. D. Cardin and W. D. Behnke, *J. Am. Chem. Soc.*, 1978, **100,** 5236.
20. A. R. Palmer, D. B. Bailey, W. D. Benhke, A. D. Cardin, P. D. Ellis and P. P. Yang, *Biochemistry*, 1980, **19,** 5063.
21. T. Drakenberg, B. Lindman, A. Cavé and B. Parello, *FEBS Letters*, 1978, **92,** 346.
22. A. Cavé, J. Parello, T. Drakenberg, E. Thulin and B. Lindman, *ibid.*, 1979, **100,** 148.
23. S. Forsen, E. Thulin and H. Lilja, *ibid.*, 1979, **104,** 123.
24. S. Forsen, E. Thulin, T. Drakenberg, J. Krebs and K. Seamon, *ibid.*, 1980, **117,** 189.
25. J. L. Sudmeier, J. L. Evelhoch, S. J. Bell, M. C. Storm and M. F. Dunn, *Dev. Biochem.*, 1980, **14,** 235.
26. J. L. Sudmeier, S. J. Bell, and M. D. Storm, *Science*, 1981, **212,** 560.
27. S. M. Wang and R. Gilpin, *Anal. Chem.*, 1983, **55,** 493.
28. H. J. Jakobsen and P. D. Ellis, *J. Phys. Chem.*, 1981, **85,** 3367.
29. W. N. Lipscomb, *Accounts Chem. Res.*, 1970, **3,** 81.
30. J. E. Coleman and B. L. Vallee, *J. Biol. Chem.*, 1960, **235,** 390.
31. J. Feeney, P. Partington and G. C. K. Roberts, *J. Mag. Res.* 1974, **13,** 268.
32. D. L. Rabenstein and S. Libich, *Inorg. Chem.*, 1972, **11,** 2960.
33. A. E. Martell, *Coordination Chemistry*, Vol. 1, p. 470, 1971.
34. M. K. Kim and A. E. Martell, *J. Am. Chem. Soc.*, 1969, **91,** 872.
35. P. J. Morris and R. B. Martin, *Inorg. Chem.* 1971, **10,** 964.
36. M. K. Kim and A. E. Martell, *J. Am. Chem. Soc.*, 1966, **88,** 914.
37. L. G. Sillén and A. E. Martell, *Stability Constants of Metal Ion Complexes*, The Chemical Society, Spec. Pubn. No. 17, London, 1964.
38. S. M. Wang and R. K. Gilpin, unpublished results.

Talanta, Vol. 32, No. 4, pp. 334–335, 1985
Printed in Great Britain

0039-9140/85 $3.00 + 0.00
Pergamon Press Ltd

COMMENTS ON THE PAPER BY GOMEZ-NIETO, LUQUE DE CASTRO, MARTIN AND VALCARCEL*

JOSEPH T. VANDERSLICE and GARY R. BEECHER
U.S. Department of Agriculture, Agricultural Research Service, Nutrient Composition Laboratory, Beltsville, Maryland 20705, U.S.A.

(*Received* 13 *November* 1984. *Accepted* 1 *February* 1985)

Gomez-Nieto *et al.* have correctly concluded that the equations derived by Vanderslice *et al.*[1] for flow in small capillary tubes do not apply to their system. They also infer, incorrectly, that the equations are inappropriate for any flow-injection analysis studies. However, these equations were derived under certain restrictive conditions,[2] and were obtained by numerical solution of the convection–diffusion equation for laminar flow in straight cylindrical tubing, on the assumption that the heights of peaks for components eluted at different times would all be $80 \pm 5\%$ of full-scale deflection on the recorder chart. The scaling factor, f, was introduced[2] to allow for the fact that experimenters would not necessarily adjust the recorder sensitivity to achieve this relative constancy of signal height. The initial purpose of the study was to elucidate what was happening at the molecular level in capillary tubing. In our laboratory, the equations do predict reasonably well not only the appearance times, t_a, and the baseline-to-baseline times, Δt_B, for simple systems, but also the peak shapes; they have also been used by others for accurate determination of diffusion coefficients for molecules of biochemical interest.[3]

To see why our equations would not apply to the system used by Gomez-Nieto *et al.* we have only to look at their experimental parameters for each of the twenty different configurations they studied and consider two imaginary situations: (1) where the bolus retains its original shape and moves down a straight tube at the average flow-rate, q; (2) where a true laminar situation exists with no diffusion, and the sample at the centre of the tube moves ahead of the bolus at a maximum flow-rate, q_{max}, which is twice the average velocity. For these two imaginary situations, the initial appearance times would be for case 1, $t_1\,(\text{sec}) = (60\pi a^2 L)/q$ and, for case 2, $t_2\,(\text{sec}) = (30\pi a^2 L)/q$. These times, together with the experimental appearance times given by Gomez-Nieto *et al.* are given in Table 1. Also shown are the appearance times, t_A, calculated from our original expression with $f = 1$. Note that t_2 is much smaller than t_{meas} and t_1 is also smaller than t_{meas} in three-quarters of the cases. Note also that t_A is very close to t_2, as it should be, since the effect of axial diffusion is small under these conditions.[4]

What are we to conclude from these results? First, as far as appearance times are concerned, the experimental conditions are such that they do not all resemble laminar flow systems. Secondly, the measured initial appearance times more nearly correspond to a non-distorted slug moving at the average flow-rate q; even here, in about three-quarters of the experiments, the slug seems to be moving at less than the average flow-rate. Such results are hardly compatible with laminar flow in a straight tube. It may be that the flow-injection system used contained one or more unsuspected mixing volumes which would tend to slow down the movement of sample. If so, this would also tend to increase Δt_B and indeed, the measured Δt_B values were larger than expected in three-quarters of the configurations studied. If the measured peak heights were not kept at similar values, this would introduce more uncertainty into the meaning of the measured t_A and Δt_B.

It is our experience that our proposed expressions for t_A and Δt_B, when used under the stated[2] re-

Table 1. Peak appearance times calculated on different assumptions

q, *ml/min*	d, *mm*	L, *cm*	t_{meas}, *sec*	t_1, *sec*	t_2, *sec*	t_A, *sec*
0.52	0.50	104.0	18.54	23.54	11.77	11.34
1.14	0.35	104.0	8.64	5.26	2.63	2.48
1.14	0.50	54.0	7.14	5.58	2.79	2.59
1.14	0.50	104.0	11.73	10.73	5.37	5.07
1.14	0.50	154.0	17.26	15.89	7.95	7.58
1.14	0.50	204.0	21.33	21.05	10.53	10.12
1.14	0.70	104.0	15.68	21.05	10.53	9.94
2.07	0.35	104.0	4.44	2.90	1.45	1.34
2.07	0.50	54.0	4.13	3.07	1.53	1.40
2.07	0.50	104.0	6.59	5.91	2.96	2.75
2.07	0.50	154.0	9.98	8.75	4.38	4.11
2.07	0.50	204.0	12.44	11.59	5.80	5.49
2.07	0.70	104.0	8.73	11.59	5.80	5.39
2.95	0.70	104.0	6.24	8.14	4.07	3.75
3.07	0.35	104.0	3.08	1.95	0.98	0.90
3.07	0.50	54.0	3.03	2.07	1.04	0.93
3.07	0.50	104.0	4.89	3.99	2.00	1.83
3.07	0.50	154.0	6.56	5.90	2.95	2.74
3.07	0.50	204.0	9.03	7.82	3.91	3.66
4.93	0.50	104.0	2.74	2.48	1.24	1.13

Talanta, 1985, **32**, 319.

strictions and applied to simple laminar flow systems, will give approximate values for these times over a wide range of experimental parameters. It it becomes necessary to determine a value for the scaling factor, f, then the instrument can be calibrated with a substance of known diffusion coefficient, as shown by Gerhardt and Adams.[3] We would prefer this method to the procedure proposed by Gomez-Nieto *et al.* It seems to us that these authors have taken laminar-flow expressions designed for simple systems and attempted to apply them to situations for which they were not designed. A sounder approach, it seems to us, would be to start with the simplest of systems and perturb it by adding connectors, mixing volumes, *etc.*, in a step-by-step sequence to see what effect each would have on the measured times. In this way, guidelines might be obtained developing practical working systems which, at present, are well-nigh impossible to design theoretically. One caveat is in order, however. With departure from simple laminar-flow systems, it becomes more difficult to determine, unambiguously, molecular parameters such as diffusion coefficients and rate constants.[2,5]

No apologies have to be made for the fact that our expressions are restricted to simple systems, for if we do not know what is happening at the molecular level in such systems, it is going to be impossible to understand what is occurring in more complicated ones.

REFERENCES

1. J. T. Vanderslice, K. K. Stewart, A. G. Rosenfeld and D. J. Higgs, *Talanta*, 1981, **28,** 11.
2. J. T. Vanderslice, G. R. Beecher and A. G. Rosenfeld, *Anal. Chem.*, 1984, **56,** 292.
3. G. Gerhardt and R. N. Adams, *ibid.*, 1982, **54,** 2618.
4. V. Ananthakrishnan, W. N. Gill and A. J. Barduhor, *A. I. Chem. Eng. J.* 1965, **11,** 1063.
5. J. T. Vanderslice, G. R. Beecher and A. G. Rosenfeld, *Anal. Chem.*, 1984, **56,** 268.

Talanta, Vol. 32, No. 4, pp.337-338, 1985
Pergamon Press Ltd. Printed in Great Britain

PRELIMINARY COMMUNICATION

FLUORESCENT REAGENT FOR VARIOUS REDUCING AGENTS

HARVEY W. YUROW

Chemical Research and Development Center, Aberdeen Proving Ground, Maryland 21010-5423, USA

(Received 7 January 1985. Accepted 6 February 1985)

The basis of many fluorescence-producing reactions of analytical importance is the displacement of a quenching and labile halogen moiety from an inherently fluorescent molecule. The quenching effect is assumed to involve an increase in the rate of internal conversion for the compound in question. Most of these reactions[1] involve the breaking of halogen-carbon or halogen-sulphur bonds. We wish to report fluorescence production from the cleavage of a halogen-nitrogen bond.

It was observed in our laboratory that though acridone sulphonamide in aqueous solution exhibited an intense blue fluorescence, chlorination of the nitrogen moiety in basic solution gave a non-fluorescent oxidizing agent. Reaction of the latter with a variety of reductants returned the fluorescence, presumably by reformation of the sulphonamide.

The sulphonamide was synthesized by heating acridone with an equimolar amount of pyrosulphuryl chloride (prepared[2] from sulphur trioxide and carbon tetrachloride) in a ten-fold excess of chlorosulphonic acid for 1 hr at 110°. The cooled mixture was poured onto ice to precipitate the sulphonyl chloride,[3] which was converted into the sulphonamide in 30% yield by dissolution in concentrated ammonia solution, removal of residual ammonia under reduced pressure, and precipitation with excess of dilute acid. Thin-layer chromatography (TLC) on silica gel[4] gave two spots having blue fluorescence, indicating the probable presence of the isomeric 2- and 4-sulphonamides.

The N,N-dichloroacridone sulphonamide was prepared by dissolving the acridone sulphonamide in dilute base, and passing chlorine through the solution. The precipitate was collected and dried, yielding a yellow powder which was found to be essentially insoluble in water. Stored in a freezer, the substance remained stable for extended periods.

Several media for application of the reagent to the determination of trace amounts of reducing agents were studied. Fluorescence rapidly developed when the compound was dissolved in acetone - water (9:1 v/v) or in acetonitrile ("Spectro" grade) or was formed directly on a silica-gel TLC plate. Greater sensitivity was obtained in a procedure in which the solid was shaken with aqueous test solution. Thus, when 0.1 mg of the solid was shaken for 1 min with 1 ml of aqueous 0.5 ppm sodium sulphide solution, a noticeable blue fluorescence was produced. Similar behaviour at this concentration was shown by sodium thiosulphate, sodium sulphide, ascorbic acid, hydrazine hydrochloride and pentamethylene sulphide, among others. Therefore, the reagent may have applicability to trace analysis for certain reducing agents in water samples or in the atmosphere. In this connection, further studies are being made on the purification and utilization of this novel reagent.

REFERENCES

1. A.T. Rhys Williams, Fluorescence Detection in Liquid Chromatography, Perkin-Elmer, Beaconsfield, England, 1980.
2. G.E. Brauer, Handbook of Preparative Inorganic Chemistry, Vol. 1, p. 386. Academic Press, New York, 1963.
3. R.B. Herbert and F.G. Holliman, Tetrahedron, 1965, 21, 663.
4. J.G. Kirshner, Thin Layer Chromatography, 2nd Ed., p. 760. Wiley, New York, 1978.
5. A.I. Vogel, Textbook of Practical Organic Chemistry, 4th Ed., p. 650. Longmans, London, 1978.

Talanta, Vol. 32, No. 3, pp.339-340, 1985
Pergamon Press Ltd. Printed in Great Britain

LETTER TO THE EDITOR

REPLY TO THE COMMENTS BY VANDERSLICE AND BEECHER*

SIR,

The aim of our work[1] was not to refute the expressions proposed by Vanderslice *et al.*[2] and by Ramsing *et al.*,[3] but rather to develop a simple and practical method for predicting the behaviour of an FIA system under the usual working conditions of this technique and hence to establish a relationship between the set of parameters (*L*, *q*, *d*) defining the flow system and those defining the FIA peak (t_A, Δt_B, t_{max} and D).

The experimental facts and therefore the contribution of the injection system, connectors, flow-cell geometry, *etc.* to the dispersion of the injected plug have been taken into account.

Vanderslice *et al.* state later[4] that their expressions were obtained (and are valid) for seven restrictive conditions, and in this respect their work differs from ours, because our method is subject to no restriction and should therefore be applicable to any FIA system.

The less restrictive (and so the more in accord with general practice) the working conditions, the more significant is the *f* factor. Vanderslice *et al.* do not enlarge on the importance of this factor, and do not indicate that it is different for the t_A and Δt_B expressions. Nor do they clearly indicate its critical dependence on the experimental variables of the FIA configurations. The conclusions obtained in our paper do not differ appreciably from those reported by Painton and Mottola.[5]

The fact that the Vanderslice expressions are adequate for the determination of molecular diffusion coefficients[6] does not imply that the *f* factor is insignificant, since those experiments were always performed with the same FIA system and under the same working conditions, *i.e.*, with a constant *f*.

The table in the comment by Vanderslice and Beecher is an excellent corroboration of how divergent the theoretical values are from the experimental data. This discrepancy was the main cause for development of our work. Furthermore, the correspondence between the t_2 values (second theoretical situation) and the t_a values (from the general expression in which $f = 1$) should not be at all surprising. Both are calculated from what are essentially almost identical theoretical expressions.

We agree with Vanderslice and Beecher that the usual working conditions in FIA distort the results in such a manner that a purely laminar flow cannot be considered. These systems themselves have distorting effects which contribute in a decisive way to the dispersion, thus increasing the appearance time values.

The method proposed by us, which is based on the experimental facts, can also be applied to more complex configurations (several channels with splitting and confluence points, *etc.*) which, like the simple ones considered in our work, will show a deviation from the theoretical behaviour at molecular level in a laminar flow, owing to the influence of these design factors, but the appropriate correction (or accommodation) factors can easily be assessed, as described in our paper.[1]

* Talanta, 1985, 32, 334.

REFERENCES

1. M.A. Gómez-Nieto, M.D. Luque de Castro, A. Martin and M. Valcárcel, Talanta, 1985, 32, 319.
2. J.T. Vanderslice, K.K. Stewart, A.G. Rosenfeld and D.J. Higgs, ibid., 1981, 28, 11.
3. A.U. Ramsing, J. Růžička and E.H. Hansen, Anal. Chim. Acta, 1981, 129, 1.
4. J.T. Vanderslice, G.R. Beecher and A.G. Rosenfeld, Anal. Chem., 1984, 56, 292.
5. C.C. Painton and H.A. Mottola, Anal. Chim. Acta, 1984, 158, 67.
6. J. Růžička and E.H. Hansen, ibid., 1983, 145, 1.

17 December 1984

MIGUEL VALCARCEL and M. DOLORES LUQUE DE CASTRO

Department of Analytical Chemistry,
Faculty of Sciences,
University of Córdoba,
Spain

Talanta, Vol. 32, No 5, pp 341–344, 1985
Printed in Great Britain

0039-9140/85 $3.00 + 0.00

DIFFERENTIAL DETERMINATION OF ANTIMONY(III) AND ANTIMONY(V) BY SOLVENT EXTRACTION–SPECTROPHOTOMETRY WITH MANDELIC ACID AND MALACHITE GREEN, BASED ON THE DIFFERENCE IN REACTION RATES

SHIGEYA SATO
Faculty of Education, Kumamoto University, 2-40-1, Kurokami, Kumamoto 860, Japan

(*Received* 6 *June* 1984. *Revised* 29 *December* 1984. *Accepted* 11 *January* 1985)

Summary—Highly sensitive and reproducible extraction–spectrophotometric methods for differential determination of antimony(III) and antimony(V) were investigated. It was found that antimony(III) reacts easily with mandelic acid to form a complex anion extractable into chlorobenzene with Malachite Green from weakly acidic media (pH 2.2–3.5) at room temperature, whereas antimony(V) reacts only slowly, and heating for 15 min at 45° is needed to obtain maximum sensitivity. The significant difference between the rates of reaction of mandelic acid with antimony(III) and antimony(V) was applied to the differential determination of these two species. The calibration graph was linear over the range 0.15–6.0 μg for antimony(III), and 0.20–10 μg for antimony(V).

A number of spectrophotometric determinations of antimony have been reported.[1-7] Most of them are based on the extraction of antimony as $SbCl_6^-$, prepared by the addition of an oxidizing agent such as cerium(IV) in acidic medium (6*M* hydrochloric acid), but often suffer from poor reproducibility.[8,9] Few studies have been made of the determination of antimony(III) or the differential determination of antimony(III) and antimony(V) by spectrophotometry, although several atomic-absorption studies have been made.[10-14]

We have recently reported that antimony(III) reacts with mandelic acid to form a complex anion extractable into chlorobenzene with Malachite Green from weakly acidic media at room temperature.[15] In further work, it was found that antimony(V) reacts similarly with mandelic acid on heating for 15 min at 45°, to give a complex extractable into chlorobenzene, but the rate of reaction of antimony(V) with mandelic acid at room temperature is very slow compared with that of antimony(III). This difference in reaction rate can be used for determination of both antimony(III) and antimony(V). In this differential method, no redox reagents are necessary and the reproducibility is very good because of the stability of the antimony complex at low acidity.

EXPERIMENTAL

Reagents

Standard antimony(III) solution, 1000 μg/ml. Prepared by dissolving potassium antimony tartrate in demineralized water; working solutions were prepared by suitable dilution.

Standard antimony(V) solution, 1000 μg/ml. Prepared by dissolving potassium pyroantimonate in water; working solutions were prepared by dilution.

Malachite Green (MG) solution, 1×10^{-3}M.

*Mandelic acid (MA) solution, 0.10*M. Adjusted to pH 3.0 with sodium hydroxide.

Standard procedure A

Transfer 1.0 ml of the sample solution containing up to 6.00 μg of antimony to a stoppered 10-ml test-tube, and add 0.2 ml of the mandelic acid solution, 1.0 ml of Malachite Green solution and dilute to 4.0 ml with water. Shake the solution with 4.0 ml of chlorobenzene for 5 min. After phase separation, measure the absorbance of the organic phase at 628 nm, in a 10-mm glass cell, against a reagent blank as a reference.

Standard procedure B

Transfer 1.0 ml of the sample solution containing up to 6.00 μg of antimony to a stoppered 10-ml test-tube, add 0.2 ml of mandelic acid solution, heat the solution for 15 min at 45°, then follow the extraction method given in procedure (A).

RESULTS AND DISCUSSION

Reaction conditions

Various complexing agents, dyes and solvents were tested for determination of antimony(III): glycollic acid, lactic acid, 2-hydroxyisobutyric acid, 2-hydroxy-2-methylbutyric acid, 2-hydroxyisocaproic acid and mandelic acid as complexing agents; Ethyl Violet, Methyl Violet, Crystal Violet, Brilliant Green, Malachite Green, Rhodamine B, Methylene Blue and fuchsin as dyes; 1,2-dichloroethane, dichloromethane, *o*-dichlorobenzene, chlorobenzene, benzene, toluene, chloroform, carbon tetrachloride, n-hexane and cyclohexane as solvents.

With each acid, different combinations of solvents and dyes were examined. From the apparent molar absorptivity (ε) of the extracted complexes and the

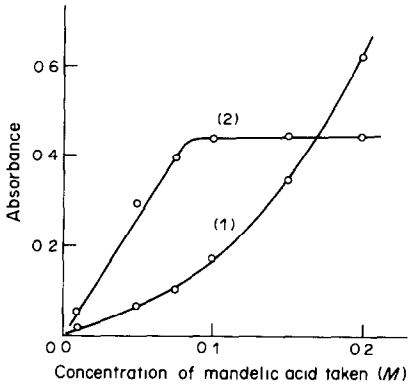

Fig. 1. Effect of mandelic acid concentration (0.2 ml of solution added). (1) Reagent blank. (2) Net absorbance [Sb(V) = 5.0 μg], Malachite Green $2.5 \times 10^{-4} M$; pH 3.0.

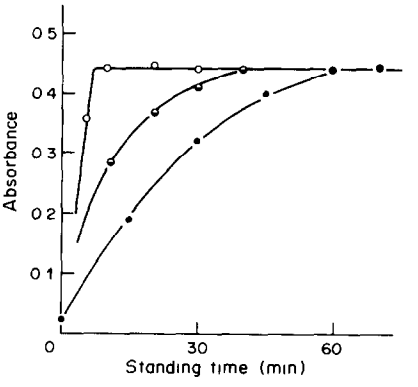

Fig. 2. Effect of standing time. Sb(V) = 5.0 μg; mandelic acid $5.0 \times 10^{-3} M$; Malachite Green $2.5 \times 10^{-4} M$; pH 3.0; reference chlorobenzene: ●——● at 20°, ◒——◒ at 30°, ○——○ at 45°.

absorbances of the reagent blanks, it was concluded that the mandelic acid–Malachite Green–chlorobenzene system was the most useful for determination of antimony(III) because it gave the highest sensitivity and lower reagent blank.

In the previous work[15] a phosphate buffer was used, but the mandelic acid solution (pH 3.0) has some buffering ability, and it was found that use of a phosphate buffer made no significant difference.

The experimental variables for the determination of antimony(V) with mandelic acid and malachite Green were similarly examined. The reaction rate was very slow at room temperature. The effect of the mandelic acid concentration in procedure B was examined and Fig. 1 shows that increasing it led to increased absorbance of both the reagent blank and sample extract, but maximum constant extraction was obtained with more than 0.2 ml of 0.1M mandelic acid, when the reagent blank was used as reference. Accordingly, 1.0 ml of sample solution and 0.2 ml of 0.1M mandelic acid were used, to keep the reagent blank as low as possible.

The effect of reaction temperature and time on the complex formation were also examined. Figure 2 shows that use of higher reaction temperatures considerably shortens the reaction time needed, from more than 60 min at room temperature (20°) to only 10 min at 45°. Once formed, the complex was stable for at least two weeks. Accordingly, heating the mixture of antimony(V) and mandelic acid at 45° for 15 min was chosen. The effect of pH was examined by heating the mixture at various pH values, then adjusting the pH to 3.0 for the extraction. The optimal range for complex formation was found to be 2.2–3.5. Mandelic acid solution adjusted to pH 3.0 was chosen for use.

Dichloromethane, chloroform, chlorobenzene, benzene and toluene were tested as solvents for the extraction, and Ethyl Violet, Crystal Violet, Methyl Violet, Brilliant Green, Malachite Green and Methylene Blue as the cationic dyestuffs. As shown in Table 1, the Malachite Green–chlorobenzene system gave the highest molar absorptivity. The net absorbance reached a constant plateau with Malachite Green concentrations exceeding $2.0 \times 10^{-4} M$, and a concentration of $2.5 \times 10^{-4} M$ was selected for use. The effect of pH on the extraction was examined and the range 2.2–3.5 found optimal. A pH of 3.0 is therefore convenient for both the complex formation and the extraction. An extraction time of about 3 min was found necessary for constant absorbance to be obtained. It was fixed at 5 min for safety.

Reaction mechanism

To confirm that antimony(V) is not reduced to antimony(III) by heating with mandelic acid, the Brilliant Green method[16] for antimony(V) was applied to a mixture of antimony(III) and antimony(V) heated with mandelic acid for various times. It was found that no antimony(III) or mandelic acid was extracted with Brilliant Green, and that the degree of

Table 1. The apparent molar absorptivity (ε) for antimony(V) and the reagent blank with selected cationic dyes and solvents

Cationic dye	Solvent	λ_{max}, *nm*	ε, $10^4 l.mole^{-1}.cm^{-1}$	Blank absorbance
Ethyl Violet	Toluene	610	2.74	0.13
Crystal Violet	Benzene	610	1.27	0.27
Methyl Violet	Benzene	605	2.50	0.34
Brilliant Green	Chlorobenzene	633	2.05	0.26
Malachite Green	Chlorobenzene	628	4.31	0.18
Methylene Blue	Chloroform	649	1.17	0.23

Table 2. Permissible amounts of interfering ions in the determination of antimony(V) and (III)*

Ion	Added as	Permissible amounts† Sb(V)	Sb(III)
Cl^-	NaCl	1440§	2900§
Br^-	NaBr	60	125
I^-	NaI	2.0	4.0
ClO_4^-	$NaClO_4$	0.1	0.2
SCN^-	KSCN	0.1	0.2
NO_3^-	$NaNO_3$	12	26
$H_2BO_3^-$	H_3BO_3	0.1	0.3
As(III)	As_2O_3	58	120
Fe^{3+}	Fe-alum	10‡	25‡
Sn^{2+}	$SnCl_2$	0.7	2.1
Sn^{4+}	$SnCl_4$	10	20

*Sb(V) 5.0 μg/4 ml; Sb(III) 2.5 μg/4 ml.
†Permissible amounts (ion/Sb weight ratio) corresponding to the concentration that gives <5% positive error.
§2% positive error.
‡5% negative error.

extraction of antimony(V) was not changed even when the heating time was as long as 60 min.

Further evidence was obtained by heating antimony(V) with mandelic acid and applying ammonium pyrrolidinedithiocarbamate/chloroform extraction at pH 5, followed by atomic-absorption spectrometry[10,14] to detect any antimony(III) formed; no antimony(III) was found. Antimony(V) at about the $10^{-5}M$ level exists mainly as $Sb(OH)_6^-$ in weakly acid media,[17] and the reaction of antimony(V) with mandelic acid is probably very slow because of the inert nature of the hydroxo-complex. The composition of the Sb(V)–MA–MG species extracted could not be determined by the continuous-variations and mole-ratio methods, because of the large excess of complexing agent and dyestuff required for its formation. It is suggested that a complex anion $[Sb(MA)_2(OH)_2]^-$ is formed and extracted as its ion-pair with Malachite Green. The antimony(III) species extracted is most likely the ion-pair $[Sb(MA)_2]^-[MG]^+$.

Calibration graph

At 628 nm Beer's law was obeyed over the range 0.20–10.0 μg of antimony(V). The apparent molar absorptivity [$\varepsilon_{V(45°)}$] calculated from the slope of the graph was 4.31×10^4 $l.mole^{-1}.cm^{-1}$. The absorbance of the reagent blank was 0.175 with chlorobenzene as reference, and the coefficient of variation was 2.8% for ten runs with 5.00 μg of antimony(V). The absorbance of the organic phase did not vary during at least 60 min. If the volume of extracting solvent was halved, the apparent molar absorptivity was increased by a factor of 1.8, but the absorbance of the reagent blank increased to only 0.318.

Table 4. Recovery of antimony(III) and antimony(V) in sample solutions

Taken, μg Sb(III)	Sb(V)	Found,* μg Sb(III)	Sb(V)
6.00	0.00	5.98	0.08
5.00	1.00	5.02	1.04
4.00	2.00	3.98	1.98
3.00	3.00	3.01†	3.02§
2.00	4.00	1.93	4.06
1.00	5.00	0.97	4.99
0.00	6.00	0.02	6.01

*Average of eight determinations.
†Standard deviation ± 0.07 μg.
§Standard deviation 0.05 μg.

Effect of other ions

The permissible amounts of foreign ions which strongly interfere with the determination of antimony(V) and antimony(III) are shown in Table 2. Borate gives a positive error because it reacts with mandelic acid to form an extractable complex anion. Iodide, perchlorate, thiocyanate and nitrate, which are bulky and of low surface charge-density, cause positive errors even when present at low levels. Arsenic(III) gives a positive error when present in 58-fold w/w ratio to antimony(V), and iron(III) gives a negative error when present in 10-fold ratio to antimony(V). These errors seem likely to be due to formation of an extractable anionic arsenic complex and the adsorption of antimony by iron(III) hydroxide, respectively. Tin(II) gives rise to a positive error for the determination of antimony(V) because of the reduction of antimony(V) to antimony(III), whereas the interference of tin(IV) is not as severe as that of tin(II).

Table 3. Effect of other ions on determination of Sb(V) and Sb(III)*

Ion	Added as	Amounts† added, μg	Recovery, % Sb(V)	Sb(III)	Ion	Added as	Amounts† added, μg	Recovery, % Sb(V)	Sb(III)
SO_4^{2-}	Na_2SO_4	19600	100	99	Cu^{2+}	$CuSO_4$	1400	100	99
$H_2PO_4^-$	KH_2PO_4	20000	98	100	Co^{2+}	$CoCl_2$	1200	102	100
Pb^{2+}	$PbCl_2$	600	99	100	Ni^{2+}	$NiCl_2$	1200	98	98
Zn^{2+}	$ZnSO_4$	600	101	98	Ca^{2+}	$CaCl_2$	800	100	102
Cd^{2+}	$CdCl_2$	2000	95	97	Mg^{2+}	$MgCl_2$	500	98	102
Mn^{2+}	$MnCl_2$	200	101	98	Ba^{2+}	$BaCl_2$	2800	103	102
		1000	108	110	Al^{3+}	K-alum	560	102	102
Te^{4+}	$TeCl_4$	600	102	100	Bi^{3+}	$BiCl_3$	500	100	99
							840	92	87

*Sb(V) 5.0 μg/4 ml; Sb(III) 2.5 μg/4 ml.
†Amounts added per 4 ml.

The effect of other ions is shown in Table 3, where recovery of antimony(V) or antimony(III) is described. Sulphate and phosphate do not interfere even at very high concentrations. Most cations do not interfere when present in 100-fold ratio to antimony(V) or antimony(III).

Differential determination of antimony(III) and antimony(V)

The most characteristic difference between the methods for antimony(III) and antimony(V) was the rate of reaction with mandelic acid. Antimony(III) reacts quickly irrespective of the temperature, but antimony(V) reacts very slowly at room temperature (20°), but rapidly on heating. Therefore, antimony(III) and (V) can be differentially determined by means of this difference in reaction rate. The method previously reported[15] for antimony(III) was modified to give standard procedure A, with which the calibration graph was linear over the range 0.15–6.00 μg of antimony(III), and the apparent molar absorptivity (ε_{III}) was 6.88×10^4 l.mole^{-1}.cm^{-1}, and the coefficient of variation 2.8% for ten runs with 2.50 μg of antimony(III). Under the same conditions the apparent molar absorptivity [$\varepsilon_{V(20)}$] for antimony(V) was $4.60 \pm 0.14 \times 10^3$ l.mole^{-1}.cm^{-1}.

Calibration graphs for antimony(V) were prepared by procedures A and B for antimony(V) in the range 0–10 μg, in the presence of fixed amounts of antimony(III) up to 5.00 μg. Linear graphs were obtained and the apparent molar absorptivities calculated from the slopes were the same irrespective of the antimony(III) concentration. Similarly, the apparent molar absorptivity of antimony(III) was found not to be affected by the concentration of antimony(V). Consequently, the concentrations of antimony(III) and (V) can be calculated from the total absorbances (Ab_A and Ab_B) obtained by procedures A and B respectively:

$$Ab_A = \varepsilon_{III}[Sb(III)] + \varepsilon_{V(20)}[Sb(V)]$$

$$Ab_B = \varepsilon_{III}[Sb(III)] + \varepsilon_{V(45)}[Sb(V)]$$

$$[Sb(V)] = (Ab_B - Ab_A)/[\varepsilon_{V(45)} - \varepsilon_{V(20)}]$$

$$[Sb(III)] = \{Ab_A - \varepsilon_{V(20)}[Sb(V)]\}/\varepsilon_{III}.$$

Recovery tests showed (Table 4) that the combination of the recommended procedures gave satisfactory results.

Acknowledgement—The author expresses his thanks to Professor Y. Yamamoto of Hiroshima University for his kind guidance and helpful discussions. the author is also indebted to Professor S. Uchikawa of Kumamoto University for his useful suggestions and warm encouragement.

REFERENCES

1. E. Eegriwe, *Z. Anal. Chem.*, 1927, **70,** 400.
2. R. W. Ramette, *Anal. Chem.*, 1958, **30,** 1185.
3. R. E. Stanton and A. J. Macdonald, *Analyst*, 1962, **87,** 299.
4. K. Študlar and I. Janoušek, *Collection Czech. Chem. Commun.*, 1960, **25,** 1965.
5. E. B. Sandell, *The Colorimetric Determination of Traces of Metals*, 3rd Ed., Interscience, New York, 1959.
6. R. W. Ramette and E. B. Sandell, *Anal. Chim. Acta*, 1955, **13,** 455.
7. H. M. Neumann, *J. Am. Chem. Soc.*, 1954, **76,** 2611.
8. M. Tanaka and M. Kawahara, *Bunseki Kagaku*, **1961, 10,** 185.
9. H. Imai, *ibid.*, 1962, **11,** 806.
10. T. Kamada and Y. Yamamoto, *Talanta*, 1977, **24,** 330.
11. M. Yamamoto, K. Urata and Y. Yamamoto, *Anal. Lett.*, 1981, **14,** 21.
12. M. Yamamoto, K. Urata, K. Murashige and Y. Yamamoto, *Spectrochim. Acta*, 1981, **36B,** 671.
13. S. Nakashima, *Analyst*, 1980, **105,** 732.
14. C. H. Chung, E. Iwamoto, M. Yamamoto and Y. Yamamoto, *Spectrochim. Acta*, 1984, **39B,** 459.
15. S. Sato, S. Uchikawa, E. Iwamoto and Y. Yamamoto, *Anal. Lett.*, 1983, **16,** 827.
16. R. W. Burke, *Anal. Chem.*, 1966, **38,** 1719.
17. C. F. Baes, Jr. and R. E. Mesmer, *The Hydrolysis of Cations*, Wiley, New York, 1976.
18. S. Sato, *Anal. Chim. Acta*, 1983, **151,** 465.

Talanta, Vol. 32, No 5, pp. 345–352, 1985
Printed in Great Britain.

0039-9140/85 $3.00 + 0.00

ION-EXCHANGER PHASE ABSORPTIOMETRY FOR TRACE ANALYSIS

KAZUHISA YOSHIMURA and HIROHIKO WAKI
Department of Chemistry, Faculty of Science, Kyushu University 33, Hakozaki, Higashiku, Fukuoka 812, Japan

(*Received* 17 *July* 1984. *Revised* 18 *December* 1984. *Accepted* 11 *January* 1985)

Summary—Ion-exchanger phase absorptiometry is based on the direct measurement of the degree of light-absorption by an ion-exchange resin phase which has sorbed a sample component. Direct application of the method makes it possible to determine trace elements in natural water samples without preconcentration. In this paper, all systems hitherto developed are reviewed and the theoretical background of solid-phase absorptiometry is described.

Although a number of chemical methods have been employed for the determination of chemical components present in solution at low levels, absorptiometry is most frequently used because of improvements in instrumental design and the development of more sensitive and selective chromogenic agents. Direct application of absorption spectrophotometry to the determination of trace elements in natural water samples is, however, difficult. Preliminary concentration procedures such as solvent extraction or ion-exchange have been used in some cases. With solvent extraction, a high phase-volume ratio to give an effective concentration of the traces cannot be adopted, because of difficulties in phase separation and mutual solubility. Ion-exchange concentration may often be more convenient, but the chemical components sorbed on the ion-exchanger usually have to be eluted for spectrophotometric measurement, leading to an undesirable dilution of the component. A higher sensitivity can be expected if the sorbed sample species is determined directly in the solid phase by absorption spectrophotometry.

A spot-test using ion-exchange resin beads and a visual observation of the coloured component on the ion-exchanger was proposed by Fujimoto[1] and by Kakihana and Murase.[2] Although this test has been proposed as a highly sensitive method of detection, it cannot be considered as a reliable colorimetric method for quantitative or even semi-quantitative analysis, because of interference by other coloured substances and difficulties in expression of colour intensity.

Measurement of the resin phase colour with a spectrophotometer was first suggested by us.[3] We found a linear relation between the resin-phase light-absorbance and the sample-component concentration in the initial solution. Ion-exchanger phase absorption spectra of metal complexes with inorganic ligands had been reported earlier[4] and have since been used for various investigative purposes.[5–7] The first analytical application was for the sensitive determination of chromium, iron, copper and cobalt in water. Even with a resin layer only 1 mm thick the sensitivity obtained was much higher than with the corresponding solution spectrophotometry. Several further systems have been developed for the analysis of natural water samples (see Table 1).

A technique for rapid collection of the resin beads and preparation of the sample resin layers for measurement has been proposed,[8] and the spectral range has been extended from the visible to the ultraviolet region by the use of aliphatic ion-exchangers.[9] Furthermore, the employment of thicker ion-exchanger layers (*e.g.*, 1 cm) is being investigated in order to enhance analytical sensitivity.[10] Another technical approach, based on analyses of differential spectra, has been tried to give more certain measurement in ion-exchanger phase absorptiometry.[11] Solid-phase spectrophotometry can also be applied with other types of sorbent[12] and other spectroscopic methods such as fluorimetry.[13]

All the systems developed are listed in Table 1 and described in the individual sections below.

Procedure for colour development in the ion-exchanger phase

There are three ways of developing the colour in the ion-exchanger phase, depending on the nature of the individual sample component and the chromogenic agent.

(1) The ion-exchanger is added to the sample solution together with the chromogenic agent. This procedure can be applied when the colour reaction is highly specific for the analyte and the complex formed can be sorbed on the ion-exchanger. Examples are the systems: chromium–diphenylcarbazide,[3,8,14,15] iron–1,10-phenanthroline,[3,16] iron–bathophenanthroline,[17] iron–Ferrozine,[18] cobalt–thiocyanate,[3,19] copper–tetrakis(4-*N*-methylpyridyl)-

Table 1. Summary of ion-exchanger absorptiometry

Element	Ion-exchanger (particle size)	Chromogenic agent	Wavelength, *nm*	Sensitivity* Ion-exchanger absorptiometry,† M	*V/m* ratio, *ml/g*	Conventional absorptiometry,§ M	*D*, *l./kg*	References
Si	Dowex 1-X8-MoO_4^{2-} (100–200 mesh)	molybdate**	700	8.4×10^{-7}	1000	4.5×10^{-6}		28
	Sephadex G-25 (medium)	molybdate	805–450	1.2×10^{-7}‡	500	4.5×10^{-6}	1.5×10^{3}	12
P	Dowex 1-X8-MoO_4^{2-} (100–200 mesh)	molybdate**	705	1.6×10^{-7}	2000	3.6×10^{-6}		29
	Amberlyst A-27-Cl^- (0.2–30 μm)	molybdate	700	2.1×10^{-8}	700#	3.6×10^{-6}		23,24¶
S	Amberlyst A-27-Cl^- (0.2–30 μm)	DPDA	675	7.6×10^{-8}	700#			25¶
Cr(VI)	Dowex 50W-X2-H^+ (100–200 mesh)	diphenylcarbazide	550–700	1.2×10^{-7}	400	3.6×10^{-6}	1.2×10^{4}	3
	Amberlyst 15-H^+ (0.2–30 μm)	diphenylcarbazide	550–700	1.9×10^{-8}	1400#	3.6×10^{-6}		8¶
	Shanghai 732-H^+ (200–300 mesh)	diphenylcarbazide	580–680	4.9×10^{-8}	1250	3.6×10^{-6}		14
Cr(III) Cr(VI)	Dowex 50W-X4-H^+ (200–400 mesh)	diphenylcarbazide	550–700	2.4×10^{-8}	2000	3.6×10^{-6}		15
Fe total	Dowex 50W-X2-H^+ (100–200 mesh)	1,10-phenanthroline	514–700	3.8×10^{-7}	400	4.4×10^{-6}		3
	Amberlyst 15-H^+ (0.2–30 μm)	bathophenanthroline	540	6.2×10^{-7}	700#			17¶
	Shanghai 717-Cl^- (20–40 mesh)	Ferrozine	575	3.8×10^{-7}‡	67	3.6×10^{-6}		18
Fe(II) Fe(III)	Dowex 50W-X4-H^+ (200–400 mesh)	1,10-phenanthroline	514–700	9.0×10^{-8}	2000	4.4×10^{-6}		16
$Fe(CN)_6$	Amberlyst A-27-Cl^- (0.2–30 μm)	iron(II)	630	7.5×10^{-7}	700#			32††

Co	Dowex 1-X2-Cl^- (100–200 mesh)	NH_4SCN	630–700	1.9×10^{-6}	2000	6.0×10^{-4}		3
	Amberlyst A-27-Cl^- (0.2–30 μm)	NK_4SCN	625		570			19††
Ni	Dowex 50W-X4-H^+ (200–400 mesh)	PAN**	566–700	1.7×10^{-8}	2000	2.0×10^{-6}	5.1×10^4	26
Cu	Dowex 1-X2-Cl^- (100–200 mesh)	Zincon**	630–700	5.0×10^{-7}	400	4.4×10^{-6}	1.0×10^4	3
	AV 17-X8 (0.1–0.25 mm)	TAN-3,6S**	582					27
	Dowex 50W-X2-H^+ (100–200 mesh)	T(4-MPy)P	424–510	5.0×10^{-9}	2000	2.8×10^{-7}		20
Zn	Dowex 1-X8-Cl^- (200–400 mesh)	Zincon‡‡	650–800	3.2×10^{-7}	2000	3.4×10^{-6}	5.6×10^2	30
Cd	Dowex 1-X2-SO_4^{2-} (200–400 mesh)	PAR‡‡	510–700	2.0×10^{-8}	2000	1.7×10^{-6}	5.2×10^4	31
Bi	Dowex 1-X2-SO_4^{2-} (200–400 mesh)	KI	492–700	9.2×10^{-8}	2000	1.2×10^{-5}	$>10^7$	21
	QAE-Sephadex A-25-Cl^-	HCl (50% isoPrOH)	328–360	2.9×10^{-8}§	2000		2.8×10^3	22
U	QAE-Sephadex A-25-Cl^-	NH_4SCN	300–600	3.9×10^{-7}	1000	1.1×10^{-5}	4×10^3	9

*Element concentration giving a final absorbance of 0.1.
†1-mm cell.
‡5-mm cell.
§1-cm cell.
Suspension of the resin pipetted; volume of resin about 0.07 ml.
¶Coagulated by addition of oppositely-charged resin particles; thickness of the resin layer for measurement about 0.3 mm.
††Reflectance of coloured complex in mixed-resin thin-layer measured.
**Chromogenic agent presorbed on resin.
‡‡Zinc and cadmium presorbed on the resin, as chloro- and iodo-complexes respectively.

porphine,[20] bismuth–iodide,[21] bismuth–chloride,[22] uranium–thiocyanate,[9] phosphate–molybdate,[23,24] and sulphide–*N*,*N*-dimethyl-*p*-phenylenediamine.[25]

(2) The chromogenic agent, presorbed on the ion-exchanger, is added to the sample solution. This procedure is applied when the coloured complex cannot be directly sorbed from the sample solution. The chromogenic agent should be sorbed irreversibly on the ion-exchanger under conditions such that it is retained on the exchanger during the equilibration with the sample solution. In this case the ion-exchanger behaves like a chelating resin. Examples are the systems: nickel–PAN,[26] copper–Zincon,[3] copper–TAN-3,6-disulphonic acid,[27] silicate–molybdate,[28] and phosphate–molybdate.[29]

(3) The analyte is first sorbed on the ion-exchanger from solution and then the chromogenic agent is added. This procedure is applied when the chromogenic agent has poor selectivity for the analyte, for example zinc[30] or cadmium[31] (as complex anions) or hexacyanoferrate[32] can be concentrated on an anion-exchanger and then reacted with Zincon, PAR and ammonium iron(II) sulphate, respectively, to give the coloured species.

Light-absorption measurement

Some of the ion-exchanger containing the coloured sample species is packed as a slurry into a quartz cell (with or without an appropriate transparent spacer), after most of the equilibrated solution has been decanted or filtered. The sedimentation and collection may be accelerated by adding finely powdered oppositely-charged ion-exchanger as coagulant. In this case the coagulated particles are collected on a filter paper under suction, to make a uniform thin layer. The cell containing the ion-exchanger is set in a spectrophotometer and the light transmitted through the cell is measured. When necessary, a reference ion-exchanger layer or a perforated metal plate may be inserted in the reference beam to cancel out the scattering background in the spectrum.

Here the term "attenuance" is conveniently introduced instead of "absorbance", because in the solid-particle layer both absorption and scattering of light contribute to the attenuation of the incident radiation intensity. The overall attenuance of the sample layer is given by

$$A = A_{RC} + A_{soln} + A_R + A_{RL} \qquad (1)$$

where A_{RC} represents the net absorbance by the complex species in the solid phase, A_{soln} the absorbance of the interstitial solution between the solid beads, A_{RL} the absorbance of the free chromogenic agent in the solid phase and A_R the background attenuance due to light scattering and absorption by the matrix material itself. Of course, A_{soln} may be neglected when the distribution ratios of the sample components are very high. A_R is a function of the packing in the cell and the values of A_{RC} and A_{RL} also depend on the packing. In an ideal case, A_{RC} could be obtained directly by measuring the absorbance at the wavelength characteristic of the sample species, with a reference layer containing no sample component and prepared under exactly the same conditions. In general, however, complete cancellation of the background attenuance cannot be expected, and it is more reliable to compare the difference (ΔA) between the values measured at the wavelength characteristic of the coloured species and at a wavelength at which the sample species does not absorb, with the difference (ΔA_{ref}) measured at the same two wavelengths for the reference layer, as shown in Fig. 1. Then, if $A_{RL} = 0$,

$$\Delta A^* = \Delta A - \Delta A_{ref} = A_{RC} + (A_R - A'_R) - (A_{R,ref} - A'_{R,ref}) \qquad (2)$$

where attenuance at the non-absorption wavelength is identified by a prime. In most cases, the ion-exchanger background spectra are parallel provided that the packing is not greatly different. Accordingly, $(A_R - A'_R) - (A_{R,ref} - A'_{R,ref}) = 0$ to a first approximation and $\Delta A^* = A_{RC}$. The use of a reference layer may be omitted if the spectral behaviour of the ion-exchanger layer is completely known, *i.e.*, $(A_R - A'_R)$ in equation (2) is a known constant. The sample attenuance may then be measured against air, which simplifies the procedure.

The sample concentration can be evaluated by means of a calibration graph or the standard-additions method.

If m g of ion-exchanger are equilibrated with V ml of sample solution, the concentration of sample species sorbed, C_{RC} (mole/kg), is

$$C_{RC} = \frac{C_0 V}{mv(1 + V/Dm)} \qquad (3)$$

where C_0 is the initial concentration in the sample solution (mole/l.), v the equilibrated ion-exchanger

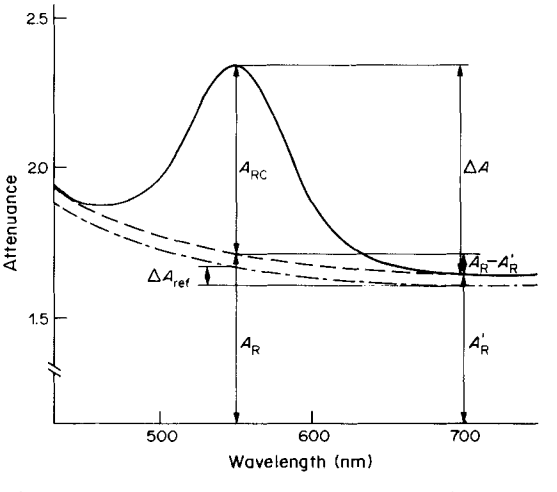

Fig. 1. Absorption spectra of Dowex 50W-X2 resin containing chromium diphenylcarbazide complex: --- assumed resin background of sample; —·— reference resin spectrum.

volume per unit weight (ml/g) and D the distribution ratio of the sample component (ml/g). The net absorbance due to the sample species sorbed, A_{RC}, is given by

$$A_{RC} = \varepsilon_{RC} l_R C_{RC} = \varepsilon_{RC} l_R C_0 V/[mv(1 + V/Dm)] \quad (4)$$

where ε_{RC} is the molar absorptivity of the sample species in the ion-exchanger phase and l_R the mean light-path length through the solid phase (which is different from the cell length). A good linear relationship is often found between A_{RC} and C_0.

Sensitivity

Equation (4) indicates that high sensitivity is attained by use of large ε_{RC}, V/mv, D and l_R values. In general, a sensitive reagent for conventional solution absorptiometry may also be satisfactory for the ion-exchanger method, provided that the resulting complex is strongly retained by the ion-exchanger. For example, porphyrin has been proposed[20] for the determination of copper at concentrations less than 1 ng/ml by ion-exchanger spectrophotometry.

In a heterogeneous method the sensitivity depends on the volume ratio of the phases. Using a high V/mv ratio leads to enhancement of sensitivity provided that a sufficiently high D value can be attained. Therefore it may be desirable to use just enough ion-exchanger to provide the sample layer in the cell. The use of a large sample volume increases the time required for equilibration and is inconvenient for handling, so the practical limit may be a few litres.

A further way of increasing the sensitivity is to use a thicker sample layer to increase l_R. However, measurements at very large values of l_R may be made difficult by the large light loss due to scattering and/or background absorption. So far, it has been customary to use a 1-mm cell for ion-exchanger spectrophotometry, but it has recently been found that increasing the cell length gives only a moderate increase in the background attenuance (in contradiction to Lambert's law).[33] On the other hand, increasing the cell length gives a proportional (or sometimes even greater) increase in the absorbance of the sample species. This suggests that it is advantageous to use the longest cell length compatible with accurate absorbance measurement. To minimize the light-loss by scattering, the cell can be set as close as possible to the light detector window to give the best

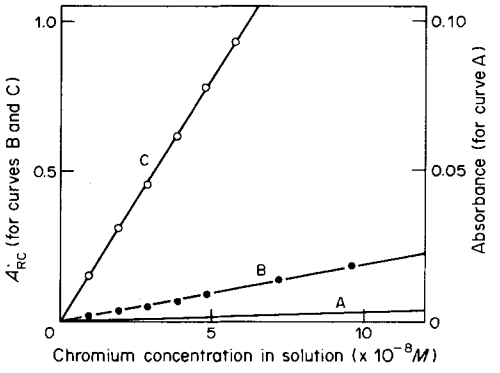

Fig. 2. Comparison of calibration graphs for the chromium–diphenylcarbazide system: A, conventional absorptiometry; B and C, ion-exchanger absorptiometry. Sample volume 1 litre; resin AG 50W-X2-H^+ (200–400 mesh), 0.50 g; stirring time 30 min; cell length, A 10 mm, B 1 mm, C 10 mm.

geometry for light-collection, or a slotted cylinder, with its inner surface a mirror, can be placed between the cell and the detector to collect to some extent the light scattered from the layer. With these modifications a cell length of 1–2 cm is the limit for reliable measurements with a commercial spectrophotometer. A longer cell requires use of more ion-exchanger, of course, and hence of a proportionately larger volume of sample solution to preserve high sensitivity. Use of spacers so that only the light-path is occupied by the resin, or use of a narrow black-sided cell has been tried to reduce the amount of ion-exchangers required.[10]

In these ways, ion-exchanger spectrophotometry is made 100–1000 times more sensitive than the corresponding solution methods, provided that the analysis is performed with a 1-cm cell and a 1-litre sample volume and that high distribution ratios are achieved. A typical comparison is given in Fig. 2, for the chromium–diphenylcarbazide system.

Precision

It might be thought that the precision of the ion-exchanger spectrophotometric method, involving as it does, an unorthodox solid-phase optical medium, would be inferior to that obtainable with conventional solution spectrophotometry. However, the analytical data given in Table 2 show that the errors are not serious for such low sample concen-

Table 2. Reproducibility of measurements

Sample species	Concentration, M	Volume, *ml*	Cell length, *mm*	A_{RC}	References
Cr(VI)	1.0×10^{-7}	1000	1	0.384 ± 0.013 ($n = 10$)	15
Cu(II)	7.9×10^{-9}	1000	1	0.162 ± 0.011 ($n = 5$)	20
Zn(II)	1.1×10^{-6}	1000	1	0.530 ± 0.023 ($n = 10$)	30
Bi(III)	8.9×10^{-8}	1000	1	0.083 ± 0.004 ($n = 5$)	21
U(VI)	1.7×10^{-6}	200	1	0.432 ± 0.02 ($n = 3$)	9
P(V)	3.2×10^{-8}	50	0.3	0.148 ± 0.005 ($n = 3$)	24

trations, for which the conventional solution method is inapplicable.

Determination of trace concentrations in solution

Silicate. Silicic acid in solutions at pH 3–9 was sorbed on an anion-exchange resin in the molybdate form. Molybdosilicate in the resin phase was reduced to "molybdenum blue" and the resin phase absorbance at 700 nm measured.[28] Sephadex gels strongly retain this blue species and this has been utilized as a new solid-phase colorimetric method for trace determination of silicate in industrial waters of high purity.[12]

Phosphate. Anion-exchange resins in the molybdate form can concentrate phosphate as molybdophosphate from 0.2–1*M* acid. The blue colour obtained on reduction has been measured for the determination of phosphate, although the sensitivity is not very high.[29] As an alternative, the reduced molybdophosphate was rapidly sorbed on a finely-divided macroreticular anion-exchanger, Amberlyst A-27 (0.2–30 μm), and the resin particles were coagulated by adding a finely-divided cation-exchanger, Amberlyst 15 (0.2–30 μm). After filtration, the coagulated resin was immersed in a solution containing sulphuric acid, ascorbic acid and potassium antimonyl tartrate. The orthophosphate or total phosphate (including organophosphates) at ng/ml levels in environmental water samples such as rain, snow, lake and sea waters was determined.[23,24]

Sulphide. Sulphide ions were converted into Methylene Blue by reaction with *N,N*-dimethyl-*p*-phenylenediamine (DPDA) in the presence of iron(II). The coagulation technique has been employed to concentrate the resulting coloured species.[25]

Chromium. Diphenylcarbazide selectively forms a soluble red-violet cationic complex with chromium(VI) and the complex can easily be concentrated with cation-exchangers.[3,8,14] Total chromium can also be determined by oxidizing chromium(III) to chromium(VI) with ceric sulphate.[15] Only copper(II) at ten times the chromium level interferes. Chromium(VI) in urine[14] and total chromium in natural waters[15] have been determined without preconcentration.

Iron. Ion-exchanger spectrophotometry for iron was developed with 1,10-phenanthroline[3,16] and 4,7-diphenyl-1,10-phenanthroline (bathophenanthroline).[17] Total iron could be determined after reduction of iron(III) to iron(II) with hydroxylamine. If citrate is used to mask iron(III), only iron(II) is determined.[16] Copper interferes considerably in the 1,10-phenanthroline method. The bathophenanthroline complex of iron(II) can also be strongly retained by finely divided cation/anion-exchange resin mixture. In this case copper does not interfere even in 40-fold amount relative to iron.[17]

Hexacyanoferrate(III). Hexacyanoferrate was concentrated on an anion-exchange resin and a coagulation technique was employed. The sorbed species was converted into Turnbull's Blue by treatment with ammonium iron(II) sulphate.[32]

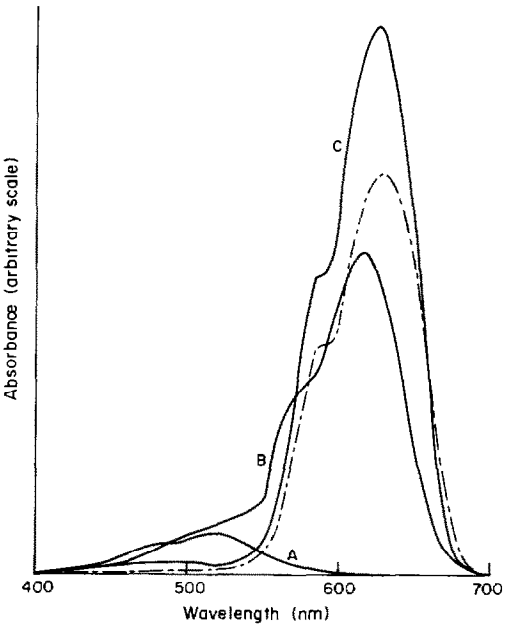

Fig. 3. Absorption spectra of isothiocyanato complexes of cobalt(II): —— solution spectra, A, 0.7*M* NH_4SCN + Co(II); B, 8*M* NH_4SCN + Co(II); C, 0.7*M* NH_4SCN + Co(II), in 1:1 acetone–water; –·–·– resin-phase spectrum (equilibrated with solution A), resin Dowex 1-X2-Cl^- (100–200 mesh).

Cobalt. Figure 3 shows the absorption spectrum of cobalt(II)–thiocyanate complexes sorbed on the anion-exchanger Dowex 1-X4.[3] The complexes formed in thiocyanate solution are also shown for comparison. It was found that the absorption spectra for the anion-exchanger correspond to the complexes formed at much higher ligand concentrations than those in the equilibrating solution. The sorbed complex is taken to be $Co(NCS)_4^{2-}$. This enhancing effect on ligand number when anion-exchangers are used has often been observed in inorganic complex systems and is advantageous in view of analytical sensitivity. The calibration graph is linear in the range 1–15 μg of cobalt in 40 ml of sample.[19] Interference by iron(III) or copper(II) can be removed by masking with fluoride or EGTA.

Nickel. 1-(2-Pyridylazo)-2-naphthol (PAN) shows high sorbability on a cation-exchange resin from an acidic alcohol solution. The PAN cannot be desorbed from the resin with aqueous solutions and therefore the resin behaves as a chelating resin. The resin phase develops a colour (λ_{max} 566 nm) with a very small amount of nickel. Copper and zinc, which form coloured complexes with PAN in the resin phase, can be completely stripped with a masking solution composed of EDTA and thioglycollic acid (pH 7.8). Cobalt can be determined in the presence of nickel by measurement at 628 nm.[26]

Copper. Both *o*-{2-[α-(2-hydroxy-5-sulphophenylazo)-benzylidene]hydrazino}benzoic acid (Zincon)[3]

and 1-(2-thiazolylazo)-2-naphthol-3,6-disulphonic acid (TAN-3,6S)[27] are irreversibly sorbed on anion-exchange resins. These reagent-loaded resins have been utilized for ion-exchanger colorimetry of copper. The mechanism of copper sorption from mixed solvents was deduced from the dependence of sorption rate on particle size and on the nature and content of the organic solvent.[27] The sorption of copper is controlled by the diffusion of copper ions through the film surrounding the ion-exchange resin particle.

The porphyrin $\alpha,\beta,\gamma,\delta$-tetrakis(4-*N*-methylpyridyl)porphine [T(4-MPy)P] has also been used as the chromogenic agent. After complexation at pH 4.5 and 40°, the surplus ligand was converted into the protonated species by addition of sulphuric acid. The complex and the ligand were easily sorbed on the cation-exchange resin because of their high positive charge. The resin-phase attenuance of the complex species at 424 nm and of the background at 510 nm were used for the measurements. There were no interferences by the foreign ions expected to be present in natural waters.[20] The copper contents of ground-waters in the Akiyoshi-dai karst area (Japan) were determined by this method.[34] The content in a ground-water dissolving only Akiyoshi limestone could be calculated to be 0.03 ng/ml from the average content of copper of the limestone, and this value was in good agreement with the lowest content of copper in the ground-waters.

Zinc. Zinc in water samples can be determined by its sorption onto an anion-exchange resin from 2*M* chloride solution, followed by transformation into a coloured complex with Zincon.[30] The Zincon complex of zinc has an absorption maximum at 650 nm in the resin phase, but at 620 nm in solution. This complex is stable in the pH range 8.5–9.5. The zinc:Zincon ratio of the complex in the resin phase was found to be 1:1 by the molar-ratio method, the same as that in solution. The difference between the absorption spectra in the two phases may be due to Zincon in the resin phase being deformed owing to spatial restriction and subject to non-electrostatic interaction with the resin skeleton.

Cadmium. 4-(2-Pyridylazo)resorcinol (PAR) forms soluble complexes of very high absorptivity with many metal ions, and is not selective for cadmium. Therefore cadmium in a water sample was first concentrated selectively as iodo-complexes on an anion-exchange resin, by sorption from 0.015*M* potassium iodide solution, and thereafter PAR was applied to the resin phase. Only copper and lead interfere (when present in concentrations greater than that of cadmium). By use of an anion-exchange resin column cadmium can be concentrated as chloro-complex anions and separated from the interfering ions. The combination of preliminary column operation and ion-exchanger colorimetry makes it possible to determine cadmium at ng/ml concentrations, or below, in natural water samples.[31]

Bismuth. The yellow bismuth–iodide complexes are specifically and strongly sorbed on an anion-exchange resin in the sulphate form, with $D > 10^7$. The spectrum of the resin phase indicates that the absorption maximum significantly shifts to longer wavelengths (492 nm), corresponding to the formation of higher ligand-number complexes than those formed in solution. This can be attributed to the effective ligand concentration being much higher in an anion-exchange resin than in solution. Bismuth in the ng/ml–μg/ml range can be determined without interference, except in the presence of a large amount of copper(II), silver and lead.[21] Very recently, ultraviolet spectrophotometry was applied to the ion-exchanger system of bismuth, chloride and QAE-Sephadex.[22] By use of a cell of long path-length (10 mm), ng/ml levels of bismuth could be determined.

Uranium. Ion-exchanger phase ultraviolet spectrophotometry was used for the determination of uranium.[9] Although aromatic ion-exchange resins show very high absorption background in the ultraviolet region, crosslinked dextran-type ion-exchangers, such as Sephadex ion-exchangers, have a much lower background. Isothiocyanato complexes of the uranyl ion are sorbed on Sephadex anion-exchanger and have an absorption maximum at about 300 nm. The difference between the attenuances at 300 or 330 and 600 nm is linear up to a uranium concentration of 0.5 ppm in the sample solution.

2,4,6-Trinitrotoluene (TNT). The fluorescence of the ion-exchanger phase was used for the microdetermination of TNT. The fluorescence of fluorescein sorbed on Dowex 2-X10 (cyanide form; 35–60 mesh) was quenched by traces of TNT. The resin, in a Pyrex U-tube, was subjected to ultraviolet radiation and the fluorescence measured with a photomultiplier. The detection limit was 70 ng/ml.[13]

REFERENCES

1. M. Fujimoto, *Bull. Chem. Soc. Japan*, 1954, **27**, 48.
2. H. Kakihana and T. Murase, *Nippon Kagaku Zasshi*, 1954, **75**, 907.
3. K. Yoshimura, H. Waki and S. Ohashi, *Talanta*, 1976, **23**, 449.
4. J. L. Ryan, *J. Phys. Chem.*, 1960, **64**, 1375.
5. P. Van Acker, F. De Corte and J. Hoste, *ibid.*, 1975, **37**, 2549.
6. K. Yoshimura, H. Waki and S. Ohashi, *ibid.*, 1977, **39**, 1697, and references therein.
7. P. J. Hoek and J. Reedijk, *ibid.*, 1979, **41**, 401.
8. K. Ohzeki, T. Sakuma and T. Kambara, *Bull. Chem. Soc. Japan*, 1980, **53**, 2878.
9. H. Waki and J. Korkisch, *Talanta*, 1983, **30**, 95.
10. K. Yoshimura and H. Waki, work in preparation.
11. H. Ishii, *Z. Anal. Chem.*, 1984, **319**, 23.
12. K. Yoshimura, M. Motomura, T. Tarutani and T. Shimono, *Anal. Chem.*, 1984, **56**, 2342.
13. C. A. Heller, R. R. McBride and M. A. Ronning, *ibid.*, 1977, **49**, 2251.

14. Ge Wueng-Xeng and Meng Li, *Anal. Chem. (China)*, 1978, **8,** 349.
15. K. Yoshimura and S. Ohashi, *Talanta*, 1978, **25,** 103.
16. S. Nigo, K. Yoshimura and T. Tarutani, *ibid.*, 1981, **28,** 669.
17. K. Ohzeki, Y. Satoh, Y. Kawamura and T. Kambara, *Bull. Chem. Soc. Japan*, 1983, **56,** 2618.
18. Li Shi-Yu and Gao Wei-Ping, *Talanta*, 1984, **31,** 844.
19. K. Suzuki, K. Ohzeki and T. Kambara, *Bull. Chem. Soc. Japan*, 1983, **56,** 2624.
20. K. Yoshimura, S. Nigo and T. Tarutani, *Talanta*, 1982, **29,** 173.
21. Y. Toshimitsu, K. Yoshimura and S. Ohashi, *ibid.*, 1979, **26,** 273.
22. H. Waki and S. Noda, unpublished data.
23. K. Matsuhisa, K. Ohzeki and T. Kambara, *Bull. Chem. Soc. Japan*, 1981, **54,** 2675.
24. *Idem, ibid.*, 1982, **55,** 3335.
25. *Idem, ibid.*, 1983, **56,** 3847.
26. K. Yoshimura, Y. Toshimitsu and S. Ohashi, *Talanta*, 1980, **27,** 693.
27. G. D. Brykina, T. V. Marchak, L. S. Krysina and T. A. Belyavskaya, *J. Anal. Chem. USSR*, 1980, **35,** 1480; *Zh. Analit. Khim.*, 1980, **35,** 2291.
28. T. Tanaka, K. Hiiro and A. Kawahara, *Bunseki Kagaku*, 1981, **30,** 131.
29. *Idem, ibid.*, 1979, **28,** 43.
30. K. Yoshimura, H. Waki and S. Ohashi, *Talanta*, 1978, **25,** 579.
31. K. Yoshimura and S. Ohashi, *Mem. Fac. Sci., Kyushu Univ., Ser. C.*, 1978, **11,** 181.
32. K. Suzuki, G. D. Park, K. Ohzeki and T. Kambara, *Bull. Chem. Soc. Japan*, 1982, **55,** 2851.
33. H. Waki, in D. Naden and M. Streat, *Ion Exchange Technology*, p. 595. Ellis Horwood, Chichester, 1984.
34. K. Yoshimura, M. Ota and T. Tarutani, *Bull. Akiyoshi-dai Mus. Nat. Hist.*, 1983, **18,** 21.

Talanta, Vol. 32, No. 5, pp. 353–357, 1985
Printed in Great Britain

0039-9140/85 $3.00 + 0.00

SPECTROPHOTOMETRIC DETERMINATION OF SILICON IN SILICATES BY FLOW-INJECTION ANALYSIS

ROKURO KURODA, IWAO IDA and HIDEKI KIMURA
Laboratory for Analytical Chemistry, Faculty of Engineering, University of Chiba, Yayoi-cho, Chiba, Japan

(*Received* 25 *July* 1984. *Revised* 13 *December* 1984. *Accepted* 11 *January* 1985)

Summary—A flow-injection spectrophotometric method has been developed for the accurate, continuous determination of silicon in silicate rocks. A rock sample solution is prepared by fusion with a 1:1 mixture of lithium carbonate and boric acid and subsequent dissolution of the cake in 1*M* hydrochloric acid. The preparation technique is the same as that used for the determination of total iron, aluminium, calcium, titanium, and phosphorus in silicate rocks by flow-injection spectrophotometry. Because of the marked polymerization of silicic acid in acid solution, silicic acid is depolymerized in alkaline medium after a simple cation-exchange column filtration of the rock sample solution and then determined by a static or an FIA spectrophotometric method. The FIA system consists of two channels which carry the carrier solution and molybdate reagent, and allows the colour reaction to proceed under controlled conditions. The FIA system permits high throughput of 70 samples per hour. The procedure has been applied to a variety of standard silicate rocks of the U.S. Geological Survey and the Geological Survey of Japan, and gave satisfactory agreement with the recommended values.

Flow-injection analysis (FIA) has been widely used for automatic continuous analysis in agricultural, clinical, pharmaceutical and environmental chemistry, *etc.*, owing to the high throughput and cost performance. We have been attempting to apply FIA to the determination of major and minor elements in silicate rocks, and have already reported on aluminium and iron,[1] titanium,[2] calcium[3] and phosphorus.[4] The work has now been extended to silicon. Little information is available about the determination of silicon by FIA. Spectrophotometric methods based on silicomolybdic acid have been reported[5,6] and recently the determination of reactive silicate in seawater has been automated by FIA, with use of the molybdenum blue method. A flow-injection voltammetric method has been worked out for the determination of soluble silicate and total phosphate in commercial washing powders.[8] Since FIA is concerned with liquid samples, we decided to use the same rock sample solution as in our earlier work.[1–4] A simple cation-exchange column filtration was used before the FIA, in order to isolate silicic acid, which was then depolymerized in alkaline medium to allow its photometric determination as yellow silicomolybdic acid. FIA is advantageous in that the critical conditions in silicomolybdic acid method, including reaction time, temperature, reagent concentrations, *etc.*, can be precisely controlled, so reproducible, continuous, rapid determination of silicon can be achieved.

EXPERIMENTAL

Reagents

Stock silicon solution, 1000 μg/ml in 0.1M sodium hydroxide. A piece of high-purity silicon was crushed between nickel plates, digested with 1*M* hydrochloric acid, and then washed with distilled water and ethanol; 0.05 g of the crushed silicon was fused with a mixture of 0.45 g sodium carbonate and 0.05 g of potassium nitrate for 15 min. The cooled melt was dissolved in 0.1*M* sodium hydroxide and diluted to exactly 50 ml with the same base.

Molybdate reagent. For the FIA work, 5.0 g of ammonium heptamolybdate, $(NH_4)_6Mo_7O_{24}\cdot 4H_2O$ was dissolved in 0.2*M* sulphuric acid and diluted to 500 ml with the same acid, and used after standing overnight. For the conventional spectrophotometry 5.0 g of the ammonium molybdate was dissolved in distilled water to yield 100 ml of solution.

Flux solution. Lithium carbonate and boric acid mixture (1:1, 600 mg) was fused for 15 min at *ca.* 1000°. The cooled cake was dissolved in 1*M* hydrochloric acid and the solution diluted to 100 ml with the same acid.

Apparatus

The FIA system is shown in Fig. 1. It consisted of a reciprocating pump (plunger type, KHU-W-104, Kyowa Seimitsu), six-way sample-injection valve (NV-508-6M, Nihon Seimitsu), spectrophotometer (UV-180, Shimazu) with a flow-through cell (volume 8 μl, 1 mm bore, 10 mm long), an analogue/digital converter data-processor (Chromatopac C-RIA, Shimazu) and a thermostatic water-bath. The flow line was made from 1.0-mm bore Teflon tubing, except for the back-pressure coil (0.5 mm bore).

Procedures

Decomposition. Weigh out about 100 mg of rock sample into a platinum crucible and mix it with 600 mg of 1:1 mixture of lithium carbonate and boric acid. Fuse the mixture for 15 min at 1000°. Dissolve the cooled melt in 1*M* hydrochloric acid (with magnetic stirring) and dilute to exactly 100 ml with the same acid. Store in an air-tight polyethylene bottle.

Pretreatment of sample solution. Take a 2.5-ml aliquot of sample solution, add 2.5 ml of distilled water and load the mixture into a cation-exchange column (Bio-Rad AG 50W-X8, hydrogen form, 100–200 mesh; bore 8 mm, bed 30 mm long). Wash the column with five 2-ml portions of 0.5*M* hydrochloric acid, collecting all the effluent in a 50-ml

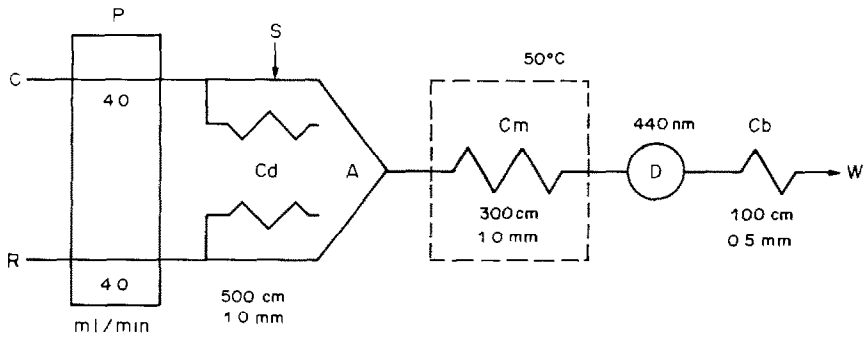

Fig. 1. Flow diagram. C, carrier (0.1*M* NaOH); R, reagent solution (1% ammonium molybdate in 0.2*M* sulphuric acid); S, sample (318 μl); Cd, damper coil; A, confluence point; Cm, mixing coil; D, spectrophotometer; Cb, back-pressure coil; P, pump; W, waste.

Teflon beaker. Add 4 ml of 2.5*M* sodium hydroxide to the combined effluent. Heat the mixture at 80° for 20 min to depolymerize the silicic acid. Cool and transfer to a 25-ml polypropylene standard flask. For FIA dilute this solution to the mark with distilled water, but for conventional spectrophotometry use a 50-ml polypropylene standard flask and proceed as described below.

Determination

Conventional spectrophotometry. Add 10 ml of a 1:1 v/v mixture of the 5% molybdate reagent and 1*M* sulphuric acid to the standard flask. Dilute to the mark with distilled water. Let stand for 20 min and measure the absorbance at 440 nm against distilled water as reference. For calibration place 2.5 ml of the flux solution, 10 ml of 0.5*M* hydrochloric acid, 4 ml of 2.5*M* sodium hydroxide and appropriate amounts of standard silicon solution into 50-ml standard flasks, and proceed as just described for samples.

Flow-injection analysis. Use the flow system illustrated in Fig. 1. Inject the pretreated sample solution (318 μl) into the carrier solution (0.1*M* sodium hydroxide) flowing at 4.0 ml/min and merging at A with the molybdate reagent stream (R) flowing at the same rate. Allow the sample slug to pass through a mixing coil Cm in a water-bath kept at 50°, to accelerate the colour-forming reaction. Read the absorbance in the flow-through cell at 440 nm against air as reference. Prepare a series of standard solutions by placing 2.5 ml of flux solution, 10 ml of 0.5*M* hydrochloric acid, 4 ml of 2.5*M* sodium hydroxide solution, and appropriate amounts of silicon stock solution in 25-ml polypropylene standard flasks and diluting to the mark with distilled water. Injected these into the carrier solution, as for sample solutions, before and after the sample run.

RESULTS AND DISCUSSION

Polymerization of silicic acid

There are many papers describing the spectrophotometric determination of silicon, but almost all are variations of two basic methods, *i.e.*, the yellow silicomolybdate and the molybdenum blue methods. The conditions for colour development in the yellow silicomolybdate method are rather critical and polysilicic acids react more slowly at higher degrees of polymerization, and at a certain degree of polymerization do not react at all with molybdate.[9] Formation of polysilicic acid is dependent on acidity and other conditions,[10–12] and proceeds rather rapidly even in 1*M* hydrochloric acid.[12] Since it is essential in this work to determine all species of silicic acid in the sample solutions (which are in 1*M* hydrochloric acid), the solution is made alkaline (0.13*M* in sodium hydroxide) and heated to depolymerize the polysilicic acid. Addition of EDTA to prevent precipitation of hydroxides was examined, and it was found that for iron-rich silicate rocks some brownish precipitate always appeared, and somewhat low results for silicon were obtained. We therefore decided to remove heavy metals and magnesium by cation-exchange before depolymerization of the silicic acid. This can simply be accomplished by passing the sample solution (diluted with distilled water to be 0.5*M* in hydrochloric acid) through a small cation-exchange column (hydrogen form). Results thus obtained for the recovery of silicon in the presence of iron and magnesium are quoted in Table 1. Though the data are somewhat scattered, the overall recovery of silicon is 99.5 ± 1.7% ($n = 16$), and there is no indication that silicate is adsorbed on the magnesium and iron forms of the resin that are formed during the ion-exchange.

Special attention should be drawn to possible error arising from use of commercially available standard

Table 1. Recovery of silicon after cation-exchange on AG 50W-X8

Forcign ion, μg		Si present, μg	Si found†, μg
Fe(III)	528	970	975
	264		991
	132		954
	528	495	482
	264		487
	132		478
	528	198	203
	132		193
Mg(II)	707	990	987
	353		996
	118		990
	707	495	485
	353		490
	118		502
	707	198	196
	118		199

†Average recovery of silicon = 99.5 ± 1.7%.

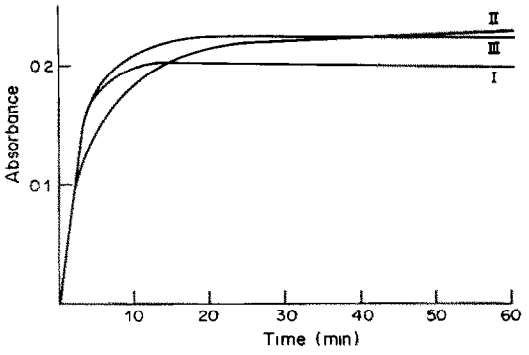

Fig. 2. Colour development of yellow silicomolybdate as a function of time. I: Rock sample (andesite AGV-1); rock solution treated as described in procedure. II: Silicic acid alone; standard solution of silicic acid treated as described in procedure without addition of flux solution. III: Silicic acid + flux solution; processed as described for the preparation of calibration standards in procedure.

silicon solutions for atomic-absorption. When used as received, silicon standards (nominal Si contents 1003, 990, 1000 ppm) obtained from three companies yielded apparent contents of 958, 927 and 756 ppm when used instead of our standard prepared as described above. This is partly because of polymerization of the silicic acid, which can occur even in weakly alkaline media[11,12] as well as in acid media.

Colour development

To obtain accurate results, matrix matching of samples and standards is of primary importance in the yellow silicomolybdate method. When an appropriate amount of silicon stock solution was diluted with 0.1*M* sodium hydroxide to yield a working standard, and aliquots of this solution and of a standard rock sample solution (prepared as described in the procedure) were taken, the colour was developed, and the absorbance of both solutions was plotted as a function of time (Fig. 2), the colour development for the silicon standard was much slower than that for the rock sample. This could obviously cause a systematic error for silicon determination since the absorbance is measured within an hour. If the working standard is prepared in the same way as the rock samples, however, colour development proceeds at the same rate for both standards and samples (Fig. 2). Therefore, the presence of the flux solution is of importance for obtaining accurate results in the silicomolybdate method.

Table 2. Effect of foreign ions on the determination of silicon (623 μg)

Ion	Amount present, μg	Si found, % Spectrophotometric	FIA
Fe(III)	528	$100._3$	$101._3$
Al(III)	436	$100._2$	$101._7$
Ca(II)	450	$101._1$	$100._8$
Mg(II)	1190	$99._2$	$101._5$
Ti(IV)	80	$101._1$	$99._6$
Mn(II)	11	$100._5$	$101._2$
P(V)	14	$100._5$	$99._0$
V(V)	2	$99._9$	$100._8$

Five ml of solution 0.5*M* in hydrochloric acid, which contained 2.5 ml of the flux solution, 623 μg of Si and a varied amount of foreign ion, was loaded on the column in accordance with the procedure, and the silicon in the effluent was determined.

Table 3. Effect of phosphorus on the determination of silicon (spectrophotometric method)

Si taken, μg	P taken, μg	Si found, %		
594	6.7	$101._6$	$101._3$	$99._6$
	13.5	$100._6$	$100._5$	$100._3$
	26.9	$101._4$	$100._3$	$100._3$
	40.4	$101._8$	$99._3$	$99._3$
891	6.7	$100._8$	$98._8$	$99._5$
	13.5	$100._4$	$99._6$	$99._3$
	26.9	$100._8$	$99._1$	$100._1$
	40.4	$100._7$	$100._3$	$99._9$

See Table 2, footnote, for the conditions. For a 2.5 mg sample in a 5-ml aliquot, 40.4 μg of P corresponds to 3.7% P_2O_5.

Interferences

The effect of foreign ions on the determination is summarized in Table 2. Five-ml portions of 0.5*M* hydrochloric acid, which contained silicic acid, flux, and either a major or a minor element were analysed for silicon in accordance with the full procedure. These elements do not interfere. A more detailed study of phosphorus was made (Table 3). For two levels of silicon (equivalent to 50.8 and 76.3% SiO_2 in rocks), 6.7–40.4 μg of phosphorus (equivalent to 0.6–3.7% P_2O_5 in rocks) do not interfere. The phosphorus content in igneous rocks ranges up to about 2% P_2O_5. The abundance in common sediments, sedimentary rocks and metamorphic rocks seldom exceeds 0.5% P_2O_5. Therefore the method can be applied to analysis of silicate rocks without interference from phosphorus. The reason seems to be that the molybdate method is not sensitive to phosphorus in the conditions used.

To assess the accuracy the spectrophotometric method was applied to 12 U.S. Geological Survey standard rocks and two standard rocks of the Geological Survey of Japan. Results are given in Table 4. The values refer to individual rock samples, each processed completely. Agreement of the results with the literature values is excellent, showing that the method is applicable to at least the rock types represented by these standard rocks. The rock sample solutions G2, GSP-1, AGV-1 and BCR-1 were prepared 10 months before the determination of silicon. The results indicate that the rock sample solutions are very stable, and able to serve as master solutions for the determination of other major and minor elements.

Table 4. Determination of silicon in standard rocks

Sample	SiO_2 found, %		1972 values,* Flanagan[13]	1980 usable values, Abbey[14]
	Spectrophotometric	FIA		
AGV-1 andesite	58.9, 58.8	59.1, 59.0	59.00 (r)	59.61
BCR-1 basalt	54.7, 53.8	54.4, 54.8	54.50 (r)	54.53
DTS-1 dunite	41.1, 40.9	40.6, 40.1	40.50 (r)	40.61
G-2 granite	69.2, 68.5	70.0, 68.9	69.11 (r)	69.22
GSP-1 granodiorite	67.2, 67.5	68.0, 67.2	67.38 (r)	67.32
PCC-1 peridotite	41.3, 41.4	42.3, 41.9	41.90 (m)	42.10
BHVO-1 basalt	50.0, 49.9	50.4, 50.3		49.9?
MAG-1 marine mud	49.6, 49.6	50.0, 50.5		50.9?
QLO-1 quartz latite	65.5, 65.9	64.4, 65.7		65.5?
RGM-1 rhyolite	72.6, 72.9	73.0, 73.0		73.4?
SDC-1 mica schist	66.5, 66.1	65.8, 65.3		66.0?
SGR-1 shale	28.3, 28.2	28.9, 28.2		28.3?
JB-1 basalt	52.2, 51.9	52.7, 51.9	52.09 (av)	52.60?
JG-1 granodiorite	72.1, 72.5	72.5, 71.8	72.24 (av.)	72.36

*r = recommended value; av. = average; m = magnitude.

Determination of silicon by FIA

The FIA colour development system was designed to reproduce the spectrophotometric method with respect to acidity, reagent concentration, *etc.* However, as shown in Fig. 2, the colour formation reaction is rather slow at room temperature. Hence, the reaction was accelerated by raising the temperature of the water-bath containing the mixing coil Cm (Fig. 1) to 50° (35° at the outlet of Cm). The stopped-flow signal for these conditions is given in Fig. 3. As can be seen, the colour formation reaction is complete at this temperature, below which the reaction proceeded more or less incompletely.

Secondly, the effect of mixing-coil length was tested as a function of the flow-rate of the carrier and the reagent solution (both these being the same). The result is illustrated in Fig. 4. The peak height is maximal with 200-cm coil length, over the flow-rate range tested. The variation of peak height is somewhat larger for shorter coil lengths (100, 200 cm), so a length of 300 cm was finally chosen, with a flow-rate of 4.0 ml/min, which gives a sufficiently high throughput, with good precision. The effect of concentration of molybdate reagent is also shown in Fig. 4, as a function of the flow-rate, with the mixing coil length fixed at 300 cm. As 1% and 2% molybdate solutions yield almost the same response, we decided to use 1.0% molybdate solution for economy.

The sample injection volume also has a significant effect on the peak height. Injection (214, 318, 406 μl) of standard silicon solutions of various concentration (5–40 μg/ml), gave results which showed that larger sample volumes led to higher peak heights, and for each injection volume a linear working curve passing through the origin was obtained over the silicon concentration range tested. We chose an injection volume of 318 μl, taking into account the throughput.

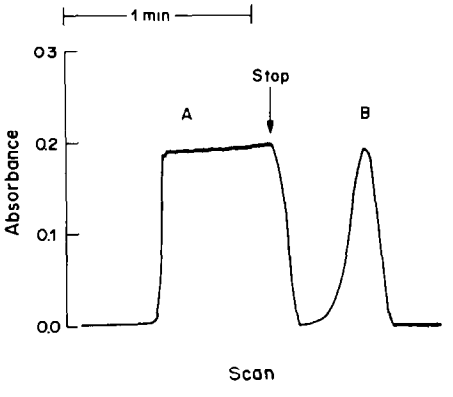

Fig. 3. Stopped-flow signal (A) and normal FIA peak (B) obtained with the flow system.

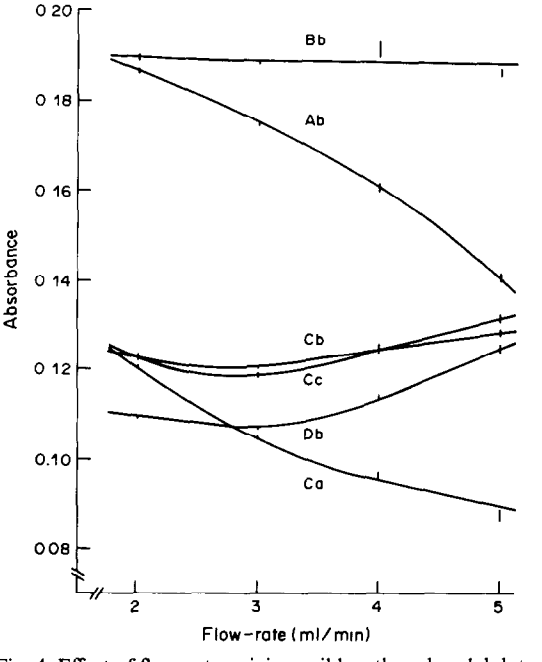

Fig. 4. Effect of flow-rate, mixing coil length and molybdate reagent concentration on peak height (absorbance). Coil length: A, 100 cm; B, 200 cm; C, 300 cm; D, 500 cm. Concentration: a, 0.5%; b, 1.0%; c, 2.0%.

Under the optimized conditions the colour development reached completion, and the dispersion D, defined by $D = H_0/H_{max}$, where H_0 is the peak height for the undiluted coloured species and H_{max} is that for the coloured slug in the flow system, was 2.2, *i.e.*, there was medium dispersion.

The FIA method described here gave good precision (0.5% relative standard deviation) and accuracy, and a throughput of 70 samples per hour, with no carry-over, and is applicable to a wide range of silicon content. It is particularly convenient to be able to use the method with a master sample solution prepared for determination of iron, aluminium, titanium, phosphorus and calcium in silicate rocks.

REFERENCES

1. T. Mochizuki, Y. Toda and R. Kuroda, *Talanta*, 1982, **29**, 659.
2. T. Mochizuki and R. Kuroda, *Analyst*, 1982, **107**, 1255.
3. H. Kimura, K. Oguma and R. Kuroda, *Bunseki Kagaku*, 1983, **32**, T79.
4. R. Kuroda, I. Ida and K. Oguma, *Mikrochim. Acta*, 1984, **I**, 337.
5. Y. Hirai, T. Yokoyama, N. Yoza, T. Tarutani and S. Ohashi, *Bunseki Kagaku*, 1981, **30**, 350.
6. T. Yokoyama, Y. Hirai, N. Yoza, T. Tarutani and S. Ohashi, *Bull. Chem. Soc. Japan*, 1982, **55**, 3477.
7. J. Thomsen, K. S. Johnson and R. L. Petty, *Anal. Chem.*, 1983, **55**, 2378.
8. A. G. Fogg and G. C. Cripps, *Analyst*, 1983, **108**, 1485.
9. L. V. Myshlyaeva and V. V. Krasnoshchekov, *Analytical Chemistry of Silicon*, p. 91. Wiley, New York, 1974.
10. T. Tarutani, *J. Chromatog.*, 1970, **50**, 523.
11. T. Shimono, T. Isobe and T. Tarutani, *ibid.*, 1983, **258**, 73.
12. K. Shimada and T. Tarutani, *ibid.*, 1979, **168**, 401.
13. F. J. Flanagan, *Geochim. Cosmochim. Acta*, 1973, **37**, 1189.
14. S. Abbey, *Geostds. Newslett.*, 1980, **4**, 190.

Talanta, Vol. 32, No. 5, pp. 359–362, 1985
Printed in Great Britain.

0039-9140/85 $3.00 + 0.00

INFLUENCE OF SOME METAL IONS ON OXIDATION OF NADH AND ON FORMATION OF THE SUPEROXIDE ANION RADICAL (O_2^-), DURING ENZYMATIC CATALYSIS BY E.C. 1.2.3.2 XANTHINE OXIDASE*

ANNA MARIA GHE†, CLAUDIO STEFANELLI, PAGONA TSINTIKI and GABRIELE VESCHI
Istituto Chimico "G. Ciamician" dell'Università, Scuola di Specializzazione in Chimica Analitica, Via Selmi 2, 40126 Bologna, Italy

(*Received* 3 *July* 1984. *Revised* 14 *November* 1984. *Accepted* 11 *January* 1985)

Summary—The inhibitory effect of selected metal ions [Ag(I), Hg(II), Cu(II), Cr(VI), V(V), Au(III), Tl(I) and Zn(II)], on the xanthine oxidase (XOD) catalysis of xanthine oxidation, has been investigated with reference to the XOD catalysis of oxidation of NADH. Hg(II), Ag(I), Zn(II) and Au(III) act as inhibitors, Tl(I) has no effect and Cu(II), Cr(VI) and V(V) act as activators. The formation of O_2^- during XOD catalysis of oxidation of either xanthine or NADH has also been studied. All the metal ions considered act as inhibitors with respect to O_2^- production when the reducing substrate is xanthine, but only a few of them when the substrate is NADH, the others showing no effect whatsoever whether or not they activate NADH oxidation in the course of the same reaction. Vanadium (V) has an anomalous effect: it inhibits xanthine oxidation but considerably increases NADH oxidation, and thus appears to modify the catalytic properties of the enzyme. This behaviour appears promising as the basis for a kinetic method for determination of V(V).

Xanthine oxidase (E.C. 1.2.3.2 XOD) is a complex enzyme containing four different prosthetic groups in each subunit: one molybdenum atom, a flavin adeninedinucleotide molecule (FAD), and two iron/sulphur centres.

The enzyme catalyses the oxidation of xanthine to uric acid, molecular oxygen acting as electron acceptor and being reduced to hydrogen peroxide and the superoxide radical anion O_2^-.

The overall reaction is very complex and can be subdivided into two half-reactions: the enzyme reductive step, that takes place at the molybdenum active site, leading to the formation of uric acid,[1] and the oxidative half-reaction, at the flavine site, leading to the formation of H_2O_2 and O_2^-.[2-4]

The fully reduced enzyme is reoxidized by a four-step six-electron mechanism. During the first and second steps electrons are transferred in pairs to oxygen molecules, producing two H_2O_2 molecules, and in the third and fourth steps only one electron at a time is transferred, with consequent reduction of O_2 to O_2^-, according to the scheme:

$$XOD_6 \xrightarrow[O_2]{H_2O_2} XOD_4 \xrightarrow[O_2]{H_2O_2} XOD_2 \xrightarrow[O_2]{O_2^-} XOD_1 \xrightarrow[O_2]{O_2^-} XOD_0 \qquad (I)$$

where the subscript to XOD stands for the number of electrons used in reduction of the original enzyme (XOD_0).

In a previous paper[5] we reported on the influence of metal ions on the XOD-catalysed oxidation of xanthine to uric acid and the inhibitory action of Ag(I), Hg(II), Cu(II), Cr(VI), V(V), Au(III), and Tl(I). In the present work we have concentrated our attention on the interactions of these inhibitors with the flavin site of the enzyme, studying their effects on the XOD-catalysed NADH → NAD^+ oxidation.

We have also examined the influence of the same species on the formation of O_2^- during the catalytic action of XOD, because of the importance of this radical in the biological context. The superoxide radical, reacting with the H_2O_2 formed in reaction scheme (I), may originate other highly reactive intermediates,[6] such as the hydroxyl radical ·OH, in the presence of metal chelates as catalysts,[7-9] and singlet oxygen O_2 ($^1\Delta g$).[10,11] All these species are extremely toxic and have profound effects on biological structures, and especially on macromolecular systems such as nucleic acids and biomembranes.[12] The oxygen free radicals are involved in several pathological processes,[13-16] but on the other hand they may also be involved in the defence mechanisms of the organisms;[17,18] hence the importance of the factors affecting the production of O_2^-.

EXPERIMENTAL

Reagents

Xanthine oxidase, Grade I, specific activity 0.76 U/mg of protein at 25°; NADH (β-nicotinamide adenine dinu-

*Work done with the financial support of the Ministero della Pubblica Istruzione (Italy), for research of national interest, no. 11835.
†Author to whom correspondence should be addressed.

cleotide, reduced form, disodium salt) Grade III; cytochrome C, type IV, from horse heart, Trizma base and Trizma-HCl, were obtained from Sigma Chemical Co. Xanthine was from U.S. Biochemical Corp., Cleveland, Ohio, and the salts of the metal ions were Merck analytical grade reagents. All solutions were prepared with doubly distilled demineralized water (conductance = 1×10^{-6} mho at 25°). The 0.05*M* Tris-HCl buffer (pH 7.4 at 37°), xanthine, and metal ion solutions were prepared as described earlier.[5]

The following solutions were prepared daily in Tris-buffer and stored at 4°.

NADH. The concentration ($1 \times 10^{-3}M$) was checked spectrophotometrically on the basis of a molar absorptivity of 6.21.mole^{-1}.cm^{-1} at 340 nm; this solution gave a ratio $\leqslant 2.3$ for the absorbances at 260 and 340 nm, as recommended.[19]

Cytochrome C. 1.5×10^{-4}M.

Xanthine oxidase. Concentration 0.37 mg/ml for the experiments with xanthine alone as reducing substrate, and 3.0 mg/ml when NADH was also present.

Analytical procedure

The reactions were monitored spectrophotometrically, with a Perkin-Elmer 554 double-beam spectrophotometer, a microcomputer-driven recorder, and constant-temperature 10-mm quartz cells.

All experiments were done with 0.05*M* Tris-HCl buffer (or Tris-HNO_3 if Ag^+ was present), pH 7.4 at 37 ± 0.1°, ionic strength 0.04*M*, final volume 3 ml, as reaction medium, containing all the reagents except the enzyme. The reaction mixture was brought to 37°, then the reaction was started by adding the enzyme.

The oxidation of NADH to NAD^+ was monitored by measuring the decrease in absorbance at 340 nm. The NADH concentration was $1 \times 10^{-4}M$; the reaction was started by addition of 50 μl of 3-mg/ml XOD solution (final enzyme concentration in cell = 50 μg/ml, corresponding to about $1.7 \times 10^{-7}M$).

The formation of the superoxide anion radical was examined by following at 550 nm the reduction of cytochrome $C_{Fe(III)}$ ($1 \times 10^{-5}M$ in the cell) by the reaction:

$$O_2^- + \text{cytochrome } C_{Fe(III)} \rightarrow O_2 + \text{cytochrome } C_{Fe(II)}.$$

When NADH was the reducing substrate the procedure was similar to that for NADH oxidation, except that cytochrome C was present in the reaction mixture.

When xanthine was the reducing substrate, its concentration was $6 \times 10^{-5}M$: the reaction was started by adding 20 μl of 0.37-mg/ml XOD solution to give a final enzyme concentration in the cell equal to 2.5 μg/ml (corresponding to about $8.9 \times 10^{-9}M$).

Absorbance readings were taken against a reagent blank containing no enzyme; the kinetic behaviour was studied by means of the initial-rate method.[20] Plots of absorbance *vs.* time were used to determine the initial reaction rate v_0 expressed as ΔA/min, in the presence or absence of metal ions.

In order to minimize errors due to possible loss of activity of the enzyme, the relative activity α was used:

$$\alpha = \frac{v_0 \text{ in presence of interfering metal ion}}{v_0 \text{ in absence of interfering metal ion}} = \frac{v_{0_i}}{v_0}.$$

RESULTS AND DISCUSSION

Influence of metals on NADH oxidation

The possibility of the flavin group being the active site for interaction with the metals which inhibit the XOD-catalysed xanthine oxidation, was explored by studying the XOD-catalysed oxidation of NADH to NAD^+. NADH, in fact, directly interacts with the flavin site of the enzyme,[21,22] instead of acting on the molybdenum site, as other reducing substrates such as xanthine do. In this way, the transfer of electrons is from NAD to FAD to molecular oxygen, and the remaining prosthetic groups of the enzyme are not involved.

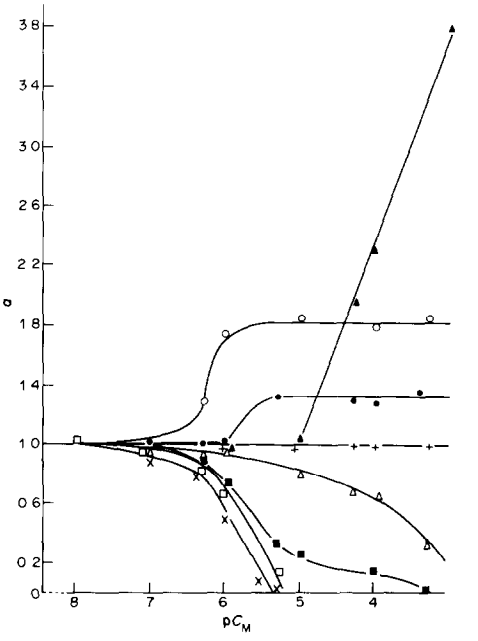

Fig. 1. Effect of various metal ions on the rate of the XOD-catalysed NADH → NAD^+ oxidation (α), *vs.* metal ion concentration (pC_M). $\alpha = v_{0_i}/v_0$; $pC_M = -\log[\text{metal}]$. [NADH] = $1 \times 10^{-4}M$; [XOD] = 50 μg/ml. × Hg(II); □ Ag(I); ■ Zn(II); △ Au(III); + Tl(I); ● Cu(II); ○ Cr(VI); ▲ V(V).

Some of the metal ions examined and found to be inhibitors of xanthine oxidation[5] exhibit a different effect on NADH oxidation (Fig. 1). Tl(I) has no effect on the reaction, whereas Cu(II), Cr(VI) and V(V), particularly the last,[23] are activators.

The effect of V(V) is proportional to its concentration when this is $> 1 \times 10^{-5}M$, but Cu(II) and Cr(VI), for which the threshold concentrations are 1×10^{-6} and $1 \times 10^{-7}M$ respectively, show a plateau region at $1 \times 10^{-5}M$.

Hg(II), Ag(I), Zn(II), and Au(III), in low concentration ($< 1 \times 10^{-6}M$), inhibit the XOD-catalysed NADH oxidation [Zn(II) behaves as an inhibitor of xanthine oxidation only at concentrations higher than $1 \times 10^{-2}M$].

The inhibiting effect of these metals in the XOD-catalysed NADH oxidation suggests the presence of an essential thiol group, presumably close to the flavin site, with which the metal can interact. The presence of such a group would be a prerequisite for oxidation of NADH to be catalysed by the enzyme.

Influence of metal ions on O_2^- formation

The effect of the metal ions which inhibit uric acid formation in the XOD-catalysed xanthine oxidation,[5]

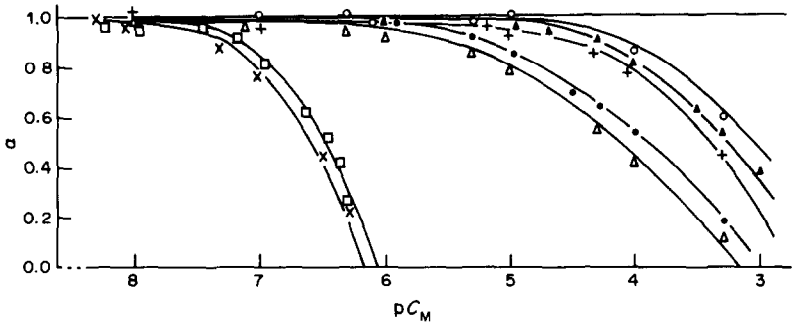

Fig. 2. Effect of various metal ions on the rate of formation of O_2^- during XOD-catalysed conversion of xanthine into uric acid (α), *vs.* metal ion concentration (pC_M). $\alpha = v_0/v_0$; $pC_M = -\log[\text{metal}]$. [Xanthine] = $6 \times 10^{-5}M$; [XOD] = 2.5 μg/ml; [cytochrome C] = $1 \times 10^{-5}M$. × Hg(II); □ Ag(I); △ Au(III); ● Cu(II); + Tl(I); ▲ V(V); ○ Cr(VI).

was studied—with the same reaction—with reference to O_2^- formation.

All those tested behave as inhibitors (see Fig. 2), although the inhibitory strength, related to O_2^- formation, shows values and sequences different from those observed for uric acid formation.

The sequence of inhibitory power was found to be

$$\text{Hg(II)} \geqslant \text{Ag(I)} >>> \text{Au(III)} > \text{Cu(II)} > \text{Tl(I)} > \text{V(V)} > \text{Cr(VI)}$$

with respect to the formation of O_2^-, whereas it was

$$\text{Ag(I)} > \text{Hg(II)} >>> \text{Cu(II)} > \text{Cr(VI)} > \text{V(V)} > \text{Au(III)} > \text{Tl(I)}$$

in the case of uric acid formation.[5]

The difference in sequence can be explained by assuming that the metal ion might act directly on the active site (flavin) at which the superoxide is produced; this action might influence the one- or two-electron reduction of O_2 (see introduction), consequently varying the ratio of H_2O_2 to O_2^- formed.

The influence of the same metal ions on the rate of O_2^- production during NADH oxidation is shown in Fig. 3. It can be seen that all the metal ions examined act as inhibitors, except Tl(I), which has no effect on the O_2^- formation.

The inhibition curves show a complex behaviour, which could be due to the effect of the metal ions on the successive reactions of newly formed O_2^-, such as its spontaneous dismutation;[12] however, the possibility of interference in the O_2^- detection system [O_2^- + cytochrome $C_{Fe(III)} \rightarrow O_2$ + cytochrome $C_{Fe(II)}$] cannot be ruled out.

It deserves mention that Cu(II), Cr(VI) and V(V), which are activators of NADH oxidation (see Fig. 1), either have no effect at all or inhibit O_2^- formation in this reaction (see Fig. 3); this is particularly evident in the case of V(V). A possible explanation of this behaviour would be that these ions are capable of oxidizing NADH directly, *e.g.*, in Tris-buffer (pH 7.4) there is slight oxidation of NADH by V(V) concentrations higher than 0.1M.

However, the enzyme-bound NADH (in an enzyme–substrate complex) might be more susceptible to oxidation occurring at lower metal concentrations by direct electron-transfer from nucleotide to the metal ion. The normal electron transfer sequence NADH → FAD → O_2 would thus be interrupted, which would explain the increased oxidation of NADH and the concomitant decrease of O_2^- formation.

Another explanation could be formation of an NADH–metal ion complex which would render the

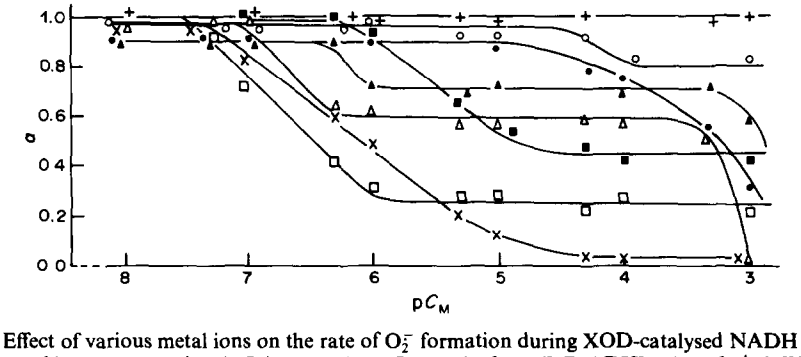

Fig. 3. Effect of various metal ions on the rate of O_2^- formation during XOD-catalysed NADH oxidation (α), *vs.* metal ion concentration (pC_M). $\alpha = v_0/v_0$; $pC_M = -\log[\text{metal}]$. [NADH] = $1 \times 10^{-4}M$; [XOD] = 50 μg/ml; [cytochrome C] = $1 \times 10^{-5}M$. □ Ag(I); × Hg(II); △ Au(III); ▲ V(V); ■ Zn(II); ● Cu(II); ○ Cr(VI); + Tl(I).

nucleotide easily oxidizable by O_2^-, with consequent decrease of the radical levels, and a simultaneous rise in NAD^+ formation.

In conclusion, all the metals tested are either inhibitors or have no effect on O_2^- formation during the enzymatic catalysis of XOD, with both xanthine and NADH as reducing substrates, but some are activators of NADH oxidation.

It should be pointed out that V(V) inhibits xanthine oxidation,[5] but at the same concentrations is a strong activator of NADH oxidation (see Fig. 2), substantially modifying the catalytic properties of the enzyme. This differential behaviour can be used for kinetic determination of V(V).[24]

REFERENCES

1. J. S. Olson, D. P. Ballou, G. Palmer and V. Massey, *J. Biol. Chem.*, 1974, **249,** 4363.
2. R. Hille and V. Massey, *ibid.*, 1981, **256,** 9090.
3. A. G. Porras, J. S. Olson and G. Palmer, *ibid.*, 1981, **256,** 9096.
4. A. G. Porras and G. Palmer, *ibid.*, 1982, **257,** 11617.
5. A. M. Ghe, C. Stefanelli and D. Carati, *Talanta*, 1984, **31,** 241.
6. G. Cohen, in *Superoxide and Superoxide Dismutases*, A. M. Michelson, J. M. McCord and J. Fridovic (eds.), p. 317. Academic Press, New York, 1977.
7. F. Haber and J. Weiss, *Proc. Roy. Soc.* 1934, **147A,** 332.
8. W. H. Koppenol, J. Butler and J. W. Van Leenwen, *Photochem. Photobiol.*, 1978, **28,** 655.
9. G. Czapski and Y. A. Ilan, *ibid.*, 1978, **28,** 651.
10. E. W. Kellog and I. Fridovich, *J. Biol. Chem.*, 1975, **250,** 8812.
11. A. U. Khan, *Science*, 1970, **168,** 476.
12. R. F. Del Maestro, *Acta Physiol. Scand.*, 1980, **492,** 153.
13. A. Petkan, *ibid.*, 1980, **492,** 81.
14. Y. R. Totter, *Proc. Natl. Acad. Sci. USA*, 1980, **77,** 1763.
15. C. F. Mills, T. T. El-Gallad, J. Bremmer and G. Wenbam, *J. Inorg. Biochem.*, 1981, **14,** 163.
16. P. C. H. Mitchell and D. A. Parker, *J. Chem. Soc. Dalton*, 1976, 1821.
17. B. M. Babior, J. T. Curnutte and R. S. Kipnes, *J. Lab. Clin. Med.*, 1975, **85,** 235.
18. H. Rosen and S. J. Klebanoff, *Arch. Biochem. Biophys.*, 1981, **208,** 512.
19. W. Gerhardt, B. Kofoed, L. Westlund and B. Pavlu, *Scand. J. Clin. Lab. Invest. Stockolm, Supplement*, 1974, 40.
20. H. B. Mark and G. A. Rechnitz, *Kinetics in Analytical Chemistry*, p. 27ff. Interscience, New York, 1968.
21. D. Edmonson, V. Massey, G. Palmer, L. M. Beacham and G. B. Elian, *J. Biol. Chem.*, 1972, **247,** 1597.
22. H. Komai, V. Massey and G. Palmer, *ibid.*, 1969, **244,** 1692.
23. C. S. Ramadoss, *Z. Naturforsch.*, 1980, **35C,** 702.
24. A. M. Ghe, C. Stefanelli, G. Chiavari and P. Tsintiki, *Talanta*, in press.

Talanta, Vol 32, No. 5, pp. 363–372, 1985
Printed in Great Britain

0039-9140/85 $3.00 + 0.00

ETUDE PAR SPECTROSCOPIE RAMAN DU CHLORHYDRATE DE COCAINE

A. P. GAMOT*, G. VERGOTEN† et G. FLEURY†
Laboratoires de *Chimie Analytique et de †Physique, Faculté de Pharmacie, Université de Lille II, rue du Professeur Laguesse, 59045 Lille, et
Centre de Technologie Biomédicale INSERM, 13-17, rue C. Guérin, 59000 Lille, France

(*Reçu le* 18 *juillet* 1983. *Revisé le* 30 *novembre* 1984. *Accepté le* 19 *décembre* 1984)

Résumé—Les spectres Raman complets du chlorhydrate de cocaïne à l'état polycristallin et en solution aqueuse saturée ont été enregistrés à température ambiante de 0 à 4000 cm^{-1} et à 9 K de 0 à 200 cm^{-1} (pour l'état polycristallin). Une attribution des raies observée est proposée. Elle montre que la cocaïne (méthyl benzoyl ecgonine) de structure bicyclique (noyau tropane) peut être caractérisée par les éléments suivants: la présence du noyau tropane peut être affirmée essentiellement par les raies intenses apparaissant à 851 et 786 cm^{-1} pour la partie pipéridinique et par les raies observées à 896 et 870 cm^{-1} pour la partie pyrrolidinique (ces raies sont attribuées aux vibrations ν_{C-C} des cycles); les fonctions esters qui se manifestent par les raies situées à 1713 cm^{-1} ($\nu_{C=O}$) et 1203 cm^{-1} (ν_{C-O-C}); la présence du noyau benzénique qui marque particulièrement le spectre du chlorhydrate de cocaïne et dont les raies les plus spécifiques se trouvent à 616, 990, 1000, 1026 et 1596 cm^{-1}. Une mention particulière a été faite en ce qui concerne les études réalisées dans le domaine des basses fréquences à température ambiante et à 9 K, et les études de polarisation en solution aqueuse saturée entre 700 et 1726 cm^{-1}. Ces résultats forment un ensemble de caractéristiques analytiques destinées à être utilisées à des fins d'identifications toxicologiques et montrent les multiples possibilités de la spectrométrie Raman dans ce domaine.

Ce travail s'inscrit dans le cadre d'une étude par spectrométrie Raman de composés polycycliques à propriétés thérapeutiques dont le but initial était la constitution d'un catalogue de spectres Raman destinés à des fins d'identifications toxicologiques utilisant des moyens informatisés. Cependant il nous est apparu indispensable de compléter ce travail en proposant d'une part une attribution des fréquences caractéristiques des produits concernés et d'autre part de mettre en évidence l'intérêt de la spectrométrie Raman dans l'étude de tels composés.

Nous présentons et discutons dans cet article les spectres Raman complets en phase solide et en phase liquide d'un composé bicyclique à propriété anesthésique locale dérivant du noyau tropane: le chlorhydrate de cocaïne. L'importance de ce noyau est considérable puisque cette structure est non seulement retrouvée chez les alcaloïdes du groupe de la cocaïne mais aussi chez les alcaloïdes du groupe de l'atropine à propriétés parasympatholytiques. Il est par ailleurs important de préciser que les indications thérapeutiques de l'atropine sont extrêmement nombreuses ce qui a induit la recherche de succédanés de synthèse d'où le développement extrêmement intense de cette série.

Avant d'entreprendre la description de la partie expérimentale et l'exposé des résultats obtenus il nous a semblé nécessaire de faire succintement le point des études diverses réalisées pour établir la structure de la cocaïne.

CONSIDERATIONS GENERALES SUR LA STRUCTURE DE LA COCAINE

La structure générale du noyau tropane est constituée par la fusion de deux hétérocycles, l'un pipéridinique et l'autre pyrrolidinique, avec une charnière commune de trois atomes, dont l'atome d'azote central est méthylé.

La cocaïne est un dérivé d'estérification de l'ecognine (acide tropanol carboxylique) par méthylation et benzoylation. Il existe quatre stéréoisomères de l'ecgonine différant par les orientations des deux substituants hydroxyle et carboxyle par rapport à l'azote. Dans les alcaloïdes naturels, ces deux fonctions sont en position *cis* par rapport à l'azote.

La configuration stéréochimique de la *l*-ecgonine et de la *l*-cocaïne fut élucidée avec certitude entre 1954 et 1956.[1] Enfin en 1963 les travaux de Gabe et Barnes[2] sur la structure cristalline du chlorhydrate de *l*-cocaïne, ont donné une preuve directe de la configuration stéréochimique de la molécule:

—le cycle pipéridinique a la forme chaise avec un groupement CH_3 sur l'atome d'azote;
—la chaîne latérale benzoxy en C_3 est en position équatoriale;
—la chaîne carbométhoxy en C_2 est en position axiale.

Par conséquent les substituants en C_2 et C_3 sont en position *cis* vis-à-vis d'eux-mêmes et de l'azote.

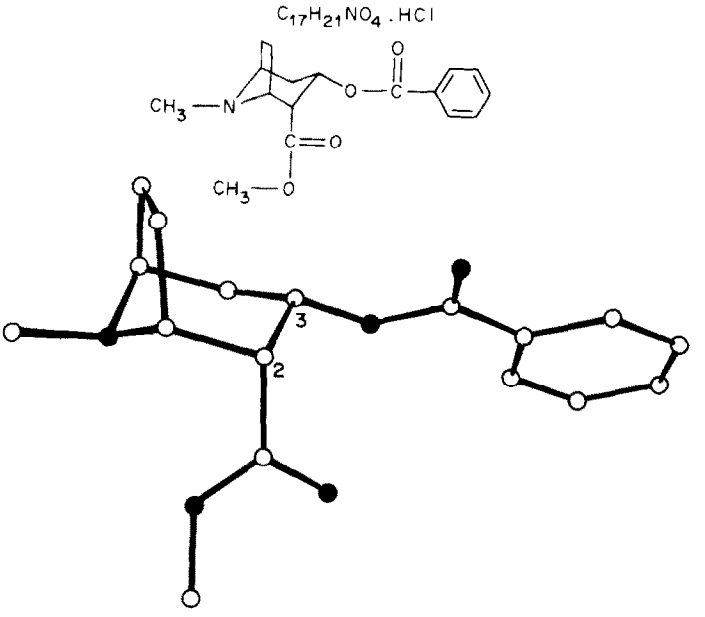

Fig. 1. Structure tridimensionelle de la cocaïne.

La figure 1 montre la structure tridimensionnelle de la cocaïne.

PARTIE EXPERIMENTALE

Appareillage

Les spectres Raman ont été enregistrés sur un spectromètre Coderg T800 comprenant un triple monochromateur de 800 mm de distance focale, équipé de trois réseaux plans gravés (1800 traits par mm) qui permet d'enregistrer toute la gamme spectrale (0–4000 cm^{-1}) en une seule fois sans changement de spectromètre.

Le principe actif est introduit, soit sous forme de poudre polycristalline dans un tube capillaire, soit sous forme de solution aqueuse saturée dans une cellule adéquate.

Un laser à argon ionisé (514,5 nm), Spectra-Physics modèle 165 03, délivre 500 mW sur l'échantillon solide et 1100 mW sur l'échantillon liquide.

L'utilisation d'un cryostat à hélium liquide a été nécessaire pour la prise des spectres de basses fréquences à 9 K.

Méthode

Le chlorhydrate de cocaïne utilisé a été purifié par recristallisation à partir de l'éthanol absolu.

Les spectres Raman de ce composé sous forme de poudre polycristalline ou en solution aqueuse saturée ont été enregistrés à la vitesse de 25 cm^{-1}/mn avec une résolution spectrale de 2 cm^{-1}. Cette vitesse a été choisie de façon à pointer les raies avec la meilleure précision. Elle peut être augmentée lors d'étude de routine pour devenir comparable à celle couramment employée en spectrométrie infra rouge. Les valeurs moyennes (Tableau 1) sont obtenues à partir de deux enregistrements par échantillon.

Bien que les deux types de spectroscopie IR et Raman soient complémentaires, la spectrométrie Raman présente un certain nombre d'avantages dont certains ont déjà été décrits dans un précédent article.[3] Cependant dans le cadre d'une étude adaptée aux problèmes biologiques et toxicologiques il en est un incontestable, découlant du principe même de la spectrométrie de diffusion Raman: les modes de vibrations actifs dans ce type de spectroscopie sont accompagnés d'une variation dans la polarisabilité de la molécule, il en résulte que l'eau est un faible diffuseur et par voie de conséquence un solvant idéal des échantillons.

Enfin dans le cas des solutions aqueuses, en utilisant une lame demi onde qui permet la rotation du champ électrique incident et en plaçant un polariseur ainsi qu'un "scrambler" ou bien une lame quart d'onde il a été possible d'analyser les composantes $I_\perp$ et $I_{/\!/}$ de la lumière diffusée. Si le mouvement de transition et le vecteur électrique de la radiation polarisée sont perpendiculaires l'un à l'autre, aucune raie de diffusion ne peut être observée. Par contre, s'ils sont parallèles, la diffusion est maximum. Entre ces deux extrêmes une transition graduelle a lieu ce qui permet en outre d'apprécier le taux de polarisation des raies.

Cette étude a été faite dans la région 700–1726 cm^{-1} en enregistrant successivement deux spectres Raman avec le plan de polarisation de la radiation excitatrice respectivement perpendiculaire et parallèle à la direction d'observation.

RESULTATS ET DISCUSSION

La substance étudiée présente une structure polycyclique sur laquelle se trouve deux chaînes latérales estérifiées en position *cis*. Nous étudierons donc dans un premier temps les vibrations de la partie bicyclique, et dans un deuxième temps les vibrations de la partie estérifiée.

Les résultats sont rassemblés dans le tableau 1 où figurent les fréquences observées dans les spectres Raman du composé sous forme polycristalline et en solution aqueuse saturée qui ont servi de base à l'attribution. Nous donnons également les fréquences infrarouge des divers composés. La discussion portera essentiellement sur les spectres Raman de la forme polycristalline du composé à température ambiante et à 9 K pour les basses fréquences. Cependant quelques commentaires seront faits à propos du spectre obtenu avec la solution saturée. Les taux de dépolarisation n'ont pas été donnés, car dans une

Tableau 1. Chlorhydrate de cocaïne: fréquences observées (cm^{-1})

Raman							
Température ambiante				9 K			
Solution aqueuse		Poudre polycristalline		Poudre polycristalline			
$\bar{\nu}$	I^*	$\bar{\nu}$	I^*	$\bar{\nu}$	I^*		
		19	FF	20	m	T†	
		29	mF	32,5	f	T + R†	
		34	mF	39	f	T + R	Vibrations du réseau cristallin + vibrations intramoléculaires de basse fréquence
				50	f		
		54	mF	59	F	R	
		73	ep	75	m		
		85	F	81	ep	R	
				93,5	FF	R	
		100	m				
				111	m	R	
		118	m	120	m	R + T	
				133	F		
		175	f				
		198	m				
		209	m				
		235	F				
		275	f				
		284	f				
		307	f				
310	f			I.R. Température ambiante			
		321	f				
325	f	334	m	$\bar{\nu}$	I		
368	f						
		374	m				
		394	f ←				Cycle benzénique 16a déformation hors du plan
396	f						
				410	f		
				425	f		
		427	f ←				δ (C_3N^+)
				450	f		
		456	ff ←				
				470	f		
				480	f		
486	f			490	f		
		492	f				
				500	f		
518	f			522	f		
				527	f		
		547	f	550	f		
555	ff						
				565	f		
		567	f	582	f		
		585	m				
589	m						
		616	F ←				Déformation du cycle dérivée de la vibration 6b du benzène
619	f						
				620	f		
		639	f ←				δ(O—C=O) déformation dans le plan (acétate)
				640	f		
680	f						
		683	m ←				cycle benzénique 4 déformation hors du plan
				685	f		
		730	m	730	FF		
				750	f		
		754	m				
780	m						
		786	FF ←				ν(C—C) cycle pipéridinique
				790	F		
813	f						
		817	m ←				ν(C—N^+)
				820	f		
		830	m ←	830	f		ν(C—CH_3) acétate élongation
832	f						
				850	m		

Tableau 1—*suite*

Tableau 1—*suite*

Raman Température ambiante				9 K		
Solution aqueuse		Poudre polycristalline		Poudre polycristalline		
$\bar{\nu}$	I^*	$\bar{\nu}$	I^*	$\bar{\nu}$	I^*	
		851	m			ν(C—C) cycle pipéridinique (élongation du cycle)
853	m					
		870	FF			ν(C—C) cycle pyrrolidinique (élongation du cycle)
887	FF					
		896	m			ν(C—C) respiration du cycle pyrrolidinique.
				898	f	
918	f					
		924	f			
				925	f	
		953	f			
				960	F	
966	f					
				980	m	
		981	m			
989	ep					
		990	ep			δ(C—H) 5 respiration trigonale du cycle benzénique ν(C—C)
1000	FF	1000	FF			
		1009	F			
				1010	m	
1012	FF					
1018	ep					
1024	FF	1021	FF			$\rho(CH_2)$
				1025	F	
		1026	FF			δ(C—H) (benzène) déformation dans le plan dérivée de la 18a
1055	f					
		1057	m			
				1060	m	
				1075	F	
		1077	m			
1080	f					
		1106	f			
				1110	FF	
1123	ff					
				1130	m	
		1139	m			
1144	ff					
				1150	m	
		1152	m			δ(CH) benzène 15
		1161	m			
1163	f	1168	m			δ(CH) (benzène) e_{2g} 9a $+\tau(CH_2)$
1181	f			1175	m	
		1185	f			
		1203	m			ν(C—O) ester $\nu(C_6H_5—C)$
				1210	m	
		1223	f			
1232	f			1230	F	
		1233	f			
				1250	ep	
1260	F					
		1266	FF			$\omega(CH_2)$
		1275	FF	1275	FF	
1276	F					
				1280	ep	
		1297	m			
				1300	ep	ν (cycle benzénique) b_{2u} 14 + vibration de torsion et balancement des méthylènes des substituants
		1314	m			
1316	f					
				1320	m	
				1325	m	
		1330	f			

Tableau 1—*suite*

Tableau 1—*suite*

Raman Température ambiante				9 K		
Solution aqueuse		Poudre polycristalline		Poudre polycristalline		
$\bar{\nu}$	I*	$\bar{\nu}$	I*	$\bar{\nu}$	I*	
		1353	f			$\omega(CH_2)$
				1360	m	
		1374	f			
				1375	m	
1385	f					
		1395	m			
				1400	m	
				1425	F	
		1428	m			
				1450	F	
1452	m					
		1456	m			$\delta(CH_3)$ déformation symétrique dans le plan (acétate) + δ_s (CH_2)
		1487	m			ν (cycle benzénique) e_{1u} 19a, 19b
1490	f			1490	F	
				1590	ff	
		1596	FF			ν(C—C) cycle benzénique e_{2g} (8a, 8b)
1598	FF					
				1600	m	
				1710	FF	
1712	FF					
		1713	FF			ν(C=O) élongation (acétate / benzoate)
				1730	FF	
				2550	m	
				2650	f	
				2700	m	
				2775	m	
		2840	f			
		2874	f			
2892	f					
		2897	F			ν(C—H) pipéridinique
				2900	m	
		2935	FF			ν(C—H) pipéridinique
2952	F					
				2955	m	
		2956	FF			ν(C—H) pyrrolidinique
				2965	m	
		2968	F			$\nu_s(CH_3)\ NH^+—CH_3$
2978	F					
		2986	FF			
		3021	F			
				3025	m	
		3034	m			$\nu_{as}(CH_3)\ NH^+—CH_3$
3067	F					
		3068	FF			ν(C—H) cycle benzénique
				3420	f	

*f = faible; ep = épaulement; FF = très forte; mF = moyennement forte; F = forte; m = moyenne; ff = très faible; I = intensité; †T = translation; R = rotation.

molécule de faible symétrie comme le chlorhydrate de cocaïne, ceux-ci ont une valeur limitée.

Il sera souvent fait référence au cours de l'exposé au spectre Raman du tropanol *trans* (alcool dérivant du noyau tropane), seul dérivé tropanique figurant à notre connaissance dans la littérature[4] en précisant toutefois:

—que la cocaïne dérive du pseudotropane ou tropanol *cis*,
—et que le spectromètre que nous avons utilisé est plus performant que celui cité dans la référence précédente.

Enfin la nomenclature adoptée pour les modes de vibration du noyau benzénique de la chaîne latérale estérifiée est celle de Wilson.[5]

Vibrations de la partie bicyclique

Cette partie dérive, comme cela a déjà été signalé, de la fusion de deux hétérocycles, l'un pipéridinique et l'autre pyrrolidinique (Fig. 1) avec une charnière

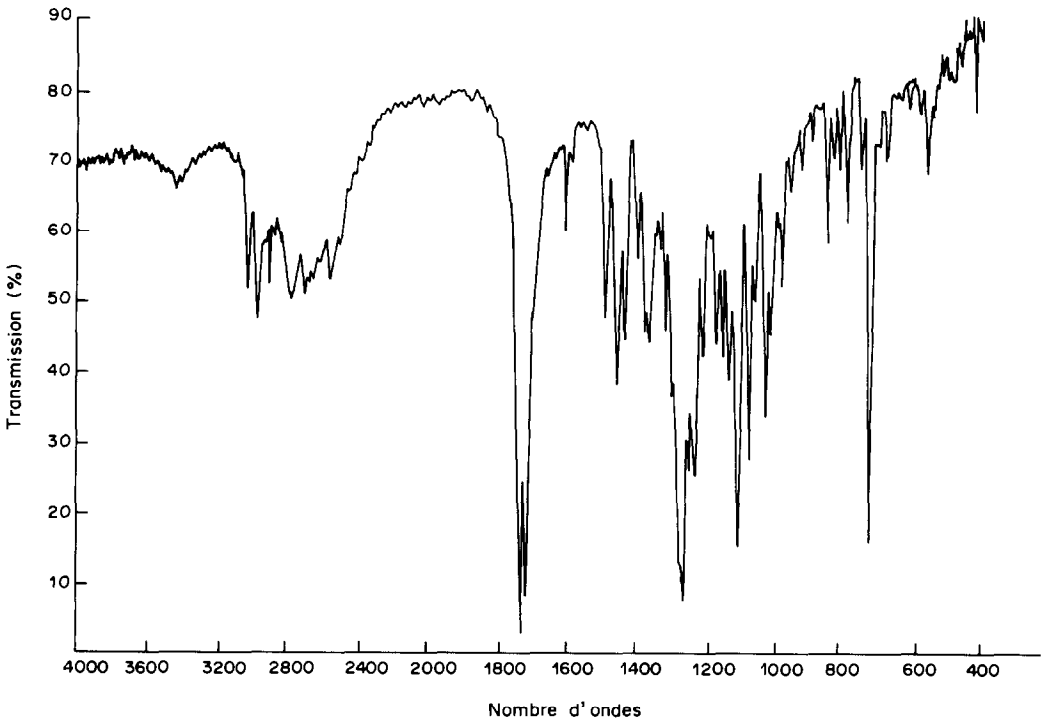

Fig. 2. Chlorhydrate de cocaïne dans KBr spectre d'absorption infrarouge.

commune de trois atomes dont l'atome d'azote central est méthylé.

L'attribution des fréquences fondamentales sera faite essentiellement par analogie avec la pyrrolidine, la N-méthyl pyrrolidine; la pipéridine, la N-méthyl pipéridine ainsi qu'avec d'autres hétérocycles et composés cycliques voisins. Enfin il sera proposé une attribution des fréquences caractéristiques de la partie bicyclique (noyau tropane).

Nous analyserons successivement:

—les vibrations du squelette carboné dans le domaine des moyennes et basses fréquences;
—les vibrations des atomes d'hydrogène;
—les vibrations du groupement alkyl ammonium.

Vibrations du squelette carboné. La cocaïne peut être considérée comme dérivant, soit de la N-méthyl pipéridine substituée en 2 et en 3, avec un pont —CH_2—CH_2— reliant les atomes de carbone 1 et 5, soit de la N-méthyl pyrrolidine avec un pont à trois chaînons CH_2 dont deux sont l'objet de substitutions. La fusion de deux hétérocycles qui permet d'obtenir un ensemble bicyclique introduit des tensions additionnelles qui modifieront, de façon plus ou moins grandes, les fréquences de base observées pour chaque hétérocycle pris séparément.

Les vibrations les plus affectées seront vraisemblablement celles qui sont communément appelées "respiration des cycles" constituées essentiellement par un mouvement de valence C—C symétrique d'espèce a_1g.

Ces vibrations d'intensité élevée qui apparaissent respectivement à 900 et 898 cm^{-1} dans le cas de la pyrrolidine et de la N-méthyl pyrrolidine[6] sont retrouvées avec une diminution importante de l'intensité des raies à 904 et 896 cm^{-1} pour le tropanol et le chlorhydrate de cocaïne.

Beaucoup plus perturbées sont les vibrations du cycle à 6 sommets traduisant la respiration: en effet dans le cas du cyclohexane elle apparaît avec une intensité forte à 802 cm^{-1}, à 815 cm^{-1} pour la pipéridine, passe à 774 cm^{-1} pour la N-méthyl pipéridine.[7] En ce qui concerne les dérivés bicycliques cette vibration est retrouvée respectivement à 744 cm^{-1} et 786 cm^{-1} pour le tropanol et le chlorhydrate de cocaïne.

Parmi les autres vibrations correspondant à l'élongation des cycles la raie située à 872 cm^{-1} de forte intensité pour la pyrrolidine et la N-méthyl pyrrolidine est retrouvée dans les spectres du tropanol et du chlorhydrate de cocaïne respectivement à 873 et 870 cm^{-1}. Enfin la vibration d'élongation du cycle située à 858–856 cm^{-1},[8] et 860 cm^{-1},[9] pour la pipéridine et son dérivé N-méthylé est retrouvée à 858 cm^{-1} pour le tropanol et à 851 cm^{-1} pour le chlorhydrate de cocaïne. Cette différence en fréquence est sans doute due à la présence de chaînes latérales sur le cycle à 6 sommets de la pipéridine.

Les spectres Raman de basses fréquences (<250 cm^{-1}) sont très caractéristiques de la structure d'un composé et sont très utiles pour leur identification. En effet les bandes observées sont très intenses, en particulier à basse température (9 K).

Dans cette région spectrale on observe généralement des raies dues aux vibrations de réseau cristallin (cas des échantillons sous forme de poudre cristalline) en plus des raies intenses dues à des mouvements de torsion (rotation interne) et à des mouvements du squelette de la molécule, donc d'un grand intérêt dans l'étude de composés polycycliques. Néanmoins l'attribution reste très difficile et nécessite l'emploi de techniques variées telles la spectroscopie d'absorption du rayonnement infra rouge lointain, l'étude de la polarisation des raies Raman observées sur un monocristal ainsi que le calcul à priori des fréquences de vibration du cristal. Un tel travail sur le chlorhydrate de cocaïne a été publié par notre équipe.[9,10]

Si le spectre de basses fréquences à température ambiante est déjà très caractéristique de la structure de la molécule de part la position et l'intensité des raies observées (notons au passage la raie intense à 19 cm^{-1}) le spectre obtenu à 9 K l'est encore plus. L'abaissement de température a pour effet de figer les molécules. Les raies observées sont beaucoup plus fines et mieux résolues d'une part et d'autre part il est possible de noter des glissements vers des fréquences plus élevées et des modifications d'intensité pour certaines d'entre elles.

Dans le tableau 1, il est proposé une attribution globale pour certaines fréquences observées. Le détail de cette attribution sort du cadre de cet article, nous nous bornerons à préciser que pour la réaliser un traitement en coordonnée normale utilisant le modèle de l'approximation du corps rigide a été utilisé.[10]

Vibration des groupements hydrocarbonés. Les vibrations de valence ν(CH) apparaissent en Raman dans l'intervalle 3000–2700 cm^{-1}. Ces vibrations sont intenses et plus ou moins faciles à attribuer spécifiquement. Cependant il a été observé un certain nombre de similitudes entre les dérivés du noyau tropane et les hétérocycles azotés qui composent ce noyau. Une attribution sera donc proposée sur ces bases.

Parmi les vibrations les plus caractéristiques citons:

—celle qui apparaît intensément à 2956 cm^{-1} dans le tropanol et le chlorhydrate de cocaïne et que l'on retrouve à 2957 cm^{-1} dans le spectre de la pyrrolidine;
—celle située à 2935 cm^{-1} pour les deux dérivés du noyau tropane et à 2936 cm^{-1} pour la pipéridine (2933 cm^{-1} pour le cyclohexane).

Ce groupe de vibrations pourrait donc être attribué dans le cas des groupements méthylènes à des vibrations antisymétriques.

Enfin citons la vibration ν(CH) à 2897 cm^{-1} que l'on peut comparer à celle de la pipéridine à 2890 cm^{-1} attribuée comme vibration d'élongation symétrique et que l'on retrouve d'ailleurs à 2897 cm^{-1} dans le cyclohexane, composé pour lequel la vibration à 2933 cm^{-1} ainsi que celle citée précédemment sont caractéristiques de la forme chaise.

Notons enfin que dans le cas du composé bicyclique étudié, la contribution des vibrations symétriques est apparemment discrète.

L'attribution spécifique des vibrations de déformation reste délicate du fait des possibilités de recouvrement de certaines raies. Dans l'intervalle étroit 1475–1450 cm^{-1} les spectres Raman peuvent présenter des bandes relativement larges dues à la contribution de plusieurs types de vibration des groupements CH_3 et CH_2. La plus caractéristique du chlorhydrate de cocaïne semble être celle qui apparaît à 1456 cm^{-1} déjà attribuée à la vibration de déformation symétrique de CH_3 du groupement acétate et qui peut aussi être attribuée à la vibration de cisaillement des groupements CH_2 du système bicyclique. Signalons que cette dernière est retrouvée[11] à 1450 cm^{-1} pour le cyclohexane [100% δ_s (CH_2)], à 1448 cm^{-1} pour la pyrrolidine et la N-méthyl pipéridine et à 1451 cm^{-1} pour la pipéridine. Notons enfin qu'elle apparaît à 1455 cm^{-1} dans le cas de cycles pentagonaux et hexagonaux (cyclopentane, cyclohexane). Ceci est donc en accord avec le fait que la cyclisation produit une légère diminution de fréquence par rapport à celle observée pour les alkanes non cycliques correspondant (vers 1468 cm^{-1}).

Parmi les vibrations de va et vient $\omega(CH_2)$ citons:

—les raies situées à 1350 et 1353 cm^{-1} pour les composés bicycliques (tropanol et chlorhydrate de cocaïne) que l'on retrouve[11] à 1349 et 1353–55 cm^{-1} dans le cyclohexane forme chaise;
—celles situées à 1260 et 1266 cm^{-1} (composés bicycliques) retrouvée à 1264 cm^{-1} dans le cas de la pipéridine.

Les vibrations de torsion $\tau(CH)_2$ sont attribuées aux raies apparaissant à 1168 cm^{-1} (chlorhydrate de cocaïne) par analogie avec la pipéridine 1166 cm^{-1} et 1268 cm^{-1} (cyclopentane).

Les vibrations de balancement $\rho(CH_2)$ sont caractérisées essentiellement par la raie à 1021 cm^{-1} (tropanol 1023 cm^{-1}) que l'on retrouve avec des intensités comparables dans la pipéridine et la pyrrolidine (1023 cm^{-1} et 1021 cm^{-1}).

Vibrations du groupement alkyl ammonium inclus dans un cycle ($>NH^+—CH_3$). L'attribution sera faite essentiellement d'après les spectres Raman du chlorure de polyméthylammonium rapportés par Edsall[12] et interprétés par Ebsworth et Sheppard.[13] Parmi les raies les plus caractéristiques dans le cas du chlorhydrate de cocaïne citons les vibrations $\nu_{as}(CH_3)$ à 3034 cm^{-1} et $\nu_s(CH_3)$ à 2968 cm^{-1} qui représentent la contribution du groupement méthyle. En ce qui concerne les vibrations de l'atome d'azote quaternaire inclus dans le cycle pyrrolidinique ou pipéridinique les vibrations ν(—C—N^+) à 817 cm^{-1} et $\nu(C_3N^+)$ à 427 et 456 cm^{-1} sont les plus importantes.

Vibrations de la partie estérifiée

Cette partie est obtenue par estérification de la fonction acide et de la fonction alcool de l'ecgonine

(Fig. 1), respectivement par méthylation et benzoylation.

Les deux chaînes latérales

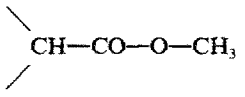

et

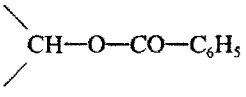

sont caractérisées par le groupement C=O qui se traduit pour le spectre Raman de la cocaïne par une seule bande très intense à 1713 cm^{-1} attribuée à la vibration d'élongation ν(C=O). Ceci peut s'expliquer pour les alkyl esters saturés dont le carbone adjacent au groupement C=O est inclus dans un cycle ce qui diminue les fréquences où cette vibration est le plus souvent observée (1734 cm^{-1}) de 15 à 20 cm^{-1}. En ce qui concerne les esters insaturés et en particulier les esters aromatiques, la fréquence correspondant à la vibration C=O est abaissée dans les mêmes proportions par effet de conjugaison. Signalons enfin la bande caractérisant l'élongation de la liaison C—O à 1203 cm^{-1}.

La vibration δ(O—C=O) de déformation dans le plan est caractérisée par une raie faible située à 639 cm^{-1}. Plus spécifique de l'ester méthylique sont les bandes d'intensité moyenne apparaissant à 830 cm^{-1} et 1456 cm^{-1} qui correspondent respectivement à la vibration d'élongation ν(C—CH_3) et à la vibration de déformation dans le plan $\delta(CH_3)$.

La présence d'un noyau aromatique dans la partie estérifiée confère à la molécule un moyen d'identification aisée en Raman de part le nombre et l'intensité des raies observées. En effet pour le cycle benzénique monosubstitué 24 vibrations sont essentiellement indépendantes du substituant attaché au noyau, les 6 autres sont sensibles aux substitutions puisque dans ces modes le substituant vibre avec une amplitude appréciable.[3]

Il y a 5 vibrations de valence des C—H dont les fréquences tombent dans l'intervalle 3100–3000 cm^{-1}. Pour le composé étudié la plus caractéristique est celle qui apparaît avec une intensité très forte à 3068 cm^{-1} ν(CH aromatique). Elle peut être accompagnée suivant les cas de 2 ou 3 épaulements.

La raie dégénérée e_{2g} (Tableau 1, 8a, 8b) correspondant à l'élongation du cycle n'est pas fortement perturbée par la substitution, de sorte que la fréquence résultante apparaît ici à la même fréquence que celle observée pour le benzène (1596 cm^{-1}). Cette vibration intense indique la présence d'un noyau aromatique mais ne permet pas de distinguer le type de substitution. Cependant, signalons que lors de l'étude en solution aqueuse entre 700 et 1726 cm^{-1} cette raie est la seule qui soit dépolarisée ce qui confirme l'attribution.

La vibration dégénérée e_{1u} du benzène à 1487 cm^{-1} peut aussi éclater en deux bandes (Tableau 1, 19a, 19b) qui sont très proches de la fréquence primitive. Dans le cas du chlorhydrate de cocaïne la vibration résultante est située à 1487 cm^{-1}.

La vibration b_{2u} (1310 cm^{-1}) d'élongation du cycle (Tableau 1, 14) est seulement légèrement décalée par la substitution et apparaît avec une intensité moyenne (1314 cm^{-1}) pour le composé étudié dans l'intervalle de fréquence couvert par les vibrations de torsion et de balancement des méthylènes des substituants alkyle. Elle peut donc difficilement être attribuée seule à la vibration b_{2u}.

La vibration d'élongation du cycle monosubstitué (992 cm^{-1}) correspondant à la vibration (Tableau 1, 1) a_{1g} du benzène est sensible aux substituants et selon Varsayni[14] doit se trouver dans l'intervalle 1100–1060 cm^{-1} pour les substituants lourds (masse > 25) et dans l'intervalle 830–620 cm^{-1} pour les substituants légers (masse < 25). Nous n'avons pas pu sur nos spectres caractériser avec précision cette vibration.

Plus intéressante est la vibration correspondant à la déformation du cycle dans le plan ou respiration trigonale du cycle. Elle dérive de la vibration b_{1u} du benzène (Tableau 1, 12) (1010 cm^{-1}) et donne lieu pour les benzènes monosubstitués à une intense bande Raman située dans l'intervalle 1010–990 cm^{-1}. Cette bande très caractéristique s'est manifestée sur les spectres du composé à 1000 cm^{-1}.

Pour les benzènes monosubstitués une autre vibration de déformation du cycle dérivée de la vibration du benzène (6b) (606 cm^{-1}) donne lieu à une bande d'intensité moyenne aux environs de 618 cm^{-1}. Elle s'est manifestée à 616 cm^{-1} d'une façon intense sur les spectres du chlorhydrate de cocaïne.

La fréquence de vibration 6a des benzènes monosubstitués est assez variable par conséquent il n'a pas été fait de tentative d'attribution.

Des vibrations de déformation des C—H dans le plan (3, 9a, 9b, 15, 18a, 18b) c'est celle qui dérive de la 18a qui est la plus utile pour l'identification; elle se traduit par une bande intense en Raman dans l'intervalle 1030–1018 cm^{-1}, de plus elle est caractéristique de la monosubstitution. Cette bande a aussi une intensité élevée en infrarouge. Elle a été repérée sur les spectres à 1026 cm^{-1} en Raman et à 1025 cm^{-1} en infrarouge.

La bande issue de la 18b devrait être comprise dans l'intervalle 1082–1065 cm^{-1} mais son intensité très faible aussi bien en Raman qu'en infrarouge n'a pas permis de la situer dans l'intervalle cité précédemment en raison de la présence d'autres bandes d'intensité moyenne.

La vibration e_{2g} dégénérée (9a, 9b) à 1178 cm^{-1} est perturbée et donnerait une bande spécifique en Raman à 1180–1170 cm^{-1} (9a) et une bande non spécifique à 410–160 cm^{-1} (9b). La première de ces bandes a été observée sur les spectres à 1168 cm^{-1}.

La vibration 15 (1160–1150 cm^{-1}) s'est manifestée

Tableau 2. Raies les plus caractéristiques du chlorhydrate de cocaïne ($\bar{\nu}$, cm^{-1})

	Noyau tropane	Fonction ester	Noyau benzénique
Moyennes fréquences	896	1713	616
	870	1203	990
	851		1000
	786		1026
			1596
Basses fréquences			
Vibration réseau cristallin + squellette de la molécule			
Température ambiante	19		
	29		
	34		
	54		
	73		
	85		
9 K	20		
	59		
	75		
	94		
	133		
	174		

par une bande faible située à 1152 cm^{-1}. La vibration 3 (1330–1250 cm^{-1}) est très faible et n'est pas apparue sur les enregistrements de manière significative d'autant plus que cet intervalle est couvert par des bandes d'intensité moyenne et deux bandes de très forte intensité à 1266 cm^{-1} et 1275 cm^{-1} dont l'attribution a été proposée das la première partie de cet article.

Les vibrations de déformation du cycle hors du plan d'intensité moyenne 4 (700–680 cm^{-1}) et d'intensité faible 16a (420–390 cm^{-1}) sont apparues respectivement à 683 et 394 cm^{-1}.

Pour les vibrations de déformation des C—H hors du plan du cycle seule la vibration 5 donne lieu en Raman à une bande très intense (1000–970 cm^{-1}) qui est caractérisée par un épaulement du côté des basses fréquences. Cette bande et son épaulement situés respectivement à 1000 et 990 cm^{-1} sont attribué à la respiration trigonale du cycle. Enfin signalons que la bande d'intensité moyenne observée à 1203 cm^{-1} pourrait être caractéristique du groupe C_6H_5—C.

Conclusion

Les principaux résultats permettant de caractériser le chlorhydrate de cocaïne sont consignés dans le tableau 2. La partie bicyclique de ce composé peut être mise en évidence grâce aux raies intenses apparaissant dans le domaine des moyennes fréquences. De plus le domaine des basses fréquences à température ambiante et à 9 K présente lui aussi un grand intérêt pour les molécules polycycliques puisque les raies observées sont spécifiques de la molécule et dues aux vibrations du réseau cristallin (cas des échantillons à l'état polycristallin), aux mouvements de torsion (rotation interne) et aux mouvements du squelette de la molécule; cet ensemble constitue une véritable fiche d'identité du composé.

Le reste de la molécule est surtout caractérisé par la présence du noyau benzénique qui se manifeste sur les spectres par de nombreuses raies intenses et par les deux fonctions esters.

Les spectres en solutions aqueuses saturées, outre certains glissements de fréquences, ont montré lors de l'étude de polarisation que seule la raie située à 1598 cm^{-1} correspondant à la vibration e_{2g} du benzène est dépolarisée.

Ce travail montre donc l'intérêt de la spectrométrie Raman dans l'étude réalisée d'une part grâce à la commodité d'obtention des spectres à l'état polycristallin et en solution aqueuse dans un intervalle spectral de 0 à 4000 cm^{-1} et d'autre part grâce à l'importance des caractéristiques analytiques fournies. Rappelons que cette étude préliminaire est destinée à être utilisée à des fins d'identification toxicologique utilisant des moyens informatisés et une microsonde Raman ce qui permet de descendre la limite de détection d'un composé aux environs du picogramme.

LITTERATURE

1. G. Fodor, *The Alkaloids*, Vol. VI, Chap. V. Academic Press, New York, 1960.
2. E. J. Gabe et W. H. Barnes, *Acta Cryst.*, 1963, **16**, 796.
3. A. P. Gamot, G. Vergoten et G. Fleury, *Talanta*, 1981,
4. B. Schrader et W. Meier, *Raman/I.R. Atlas of Organic Compounds*, I, 16-04. Verlag Chemie, Weinheim, 1974.
5. E. B. Wilson, Jr., *Phys. Rev.*, 1934, **45**, 706.
6. B. Schrader et W. Meier, *op. cit.*, I, 1-01; I, 1-06.
7. F. R. Dollish, W. G. Fateley et F. F. Bentley, *Characteristic Raman Frequencies of Organic Compounds*, p. 244, Wiley, New York, 1974.
8. *Idem, op. cit.*, p. 243.
9. A. P. Gamot, G. Vergoten et G. Fleury, *The Use of Raman Spectroscopy in Analytical Chemistry: Characterization of Cocaine Hydrochloride*, presented at

Hungarian Annual Conference on Spectral Analysis, Sopron, 14–18 June, 1982.
10. G. Vergoten, A. P. Gamot et G. Fleury, *J. Raman Spectrosc.*, 1983, **14,** 371.
11. J. P. Huvenne, G. Vergoten, G. Fleury, S. Odiot et S. Fliszar, *Can. J. Chem.*, 1982, **60,** 1347.
12. J. T. Edsall, *J. Chem. Phys.*, 1937, **5,** 225.
13. E. A. V. Ebsworth et N. Sheppard, *Spectrochim. Acta*, 1959, **13,** 261.
14. G. Varsanyi, *Acta. Chim. Acad. Sci. Hung.*, 1966, **50,** 225.

Summary—Raman spectra of cocaine hydrochloride in the polycrystalline state and in saturated aqueous solutions have been recorded at room temperature from 0 to 4000 cm^{-1} and at 9 K from 0 to 200 cm^{-1} (only for the polycrystalline state). They show that cocaine can be characterized by the following proposed assignments. For the tropane nucleus the frequencies 851 and 786 cm^{-1} (piperidine) and 896, 870 cm^{-1} (pyrrolidine); these frequencies are assigned to ring carbon stretching vibrations ν_{C-C}. Bands for the ester functional groups can be observed at 1713 cm^{-1} ($\nu_{C=O}$) and 1203 cm^{-1} (ν_{C-O-C}). The benzene nucleus is also important in characterization of cocaine hydrochloride because of its bands at 616, 990, 1000, 1026 and 1596 cm^{-1}. Special reference is made first to the work in the low-frequency range at room temperature and 9 K and secondly to the polarization studies of saturated aqueous solutions in the range 700–1726 cm^{-1}. The results constitute a pool of analytical characteristics which can be used for toxicological investigations, and also show all the possibilities of Raman spectroscopy in this field.

Talanta, Vol 32, No. 5, pp. 373–382, 1985
Printed in Great Britain

0039-9140/85 $3.00 + 0.00

ETUDE PAR SPECTROMETRIE RAMAN DE CORTICOSTEROIDES DERIVES DE LA FLUOCORTOLONE: TRIMETHYLACETATE ET CAPROATE

A. P. GAMOT,* G. VERGOTEN,† M. SAUDEMON et G. FLEURY†
Centre de Technologie Biomédicale INSERM 13–17, rue C. Guérin—59000 Lille, et
Laboratoire de *Chimie Analytique et de †Physique, Faculté de Pharmacie, Université de Lille II,
Rue du Professeur Laguesse, 59045 Lille Cedex, France

(*Reçu le* 18 *juillet* 1983. *Revisé le* 30 *novembre* 1984. *Accepté le* 19 *decembre* 1984)

Résumé—Les spectres Raman de trois corticostéroïdes: fluocortolone base, triméthylacétate et caproate de fluocortolone (TMAF et CAF) ont été enregistrés à l'état polycristallin entre 150 et 4000 cm^{-1}. Une attribution des raies observées est proposée. Elle a montré la complexité du problème posé à savoir la différenciation de trois composés de structure très voisine. Cependant quelques intervalles de fréquences contenant des raies spécifiques sont susceptibles d'être utilisés afin de permettre l'identification des composés étudiés. Il convient en premier lieu de distinguer tout particulièrement les raies situées entre 1500 et 1800 cm^{-1}. Dans l'intervalle 1580–1690 cm^{-1} celles-ci sont intenses et spécifiques de la structure conjuguée $\Delta^{1,4}$ 3-one des corticostéroïdes ce qui permet de distinguer la classe de médicament à laquelle appartiennent les substances étudiées. La zone de fréquence comprise entre 1690 et 1750 cm^{-1} témoigne non seulement de la présence d'une fonction cétonique sur la chaîne latérale mais aussi de l'existence d'une fonction ester suivant que l'on y trouve respectivement une ou deux raies (fluocortolone base 1701 cm^{-1}; TMAF 1728, 1745 cm^{-1}; CAF 1723, 1745 cm^{-1}). La fluocortolone base présente à 1635 cm^{-1} une raie qui n'est pas retrouvée chez les dérivés estérifiés. En second lieu, nous retiendrons les zones spectrales représentatives des chaînes latérales estérifiées fixées sur le carbone C_{21}: chaîne triméthylacétate 340–360, 570–610, 750–810 cm^{-1} (dans cette dernière région commune au caproate et au triméthylacétate la différenciation des deux composés se fait grâce à la raie à 796 cm^{-1} absente dans le spectre du caproate); chaîne caproate 1310–1350 cm^{-1} (dans cet intervalle, le caproate présente un profil très particulier avec trois raies d'intensité voisine). Cet ensemble de résultats doit être utilisé pour identifier ces substances par spectroscopie Raman sur des quantitiés de l'ordre du picogramme provenant d'éluat d'HPLC.

Ce travail s'inscrit dans le cadre de notre programme d'étude par spectrométrie Raman de composés à propriétés thérapeutiques. Son but initial était la constitution d'un catalogue de spectres Raman dont les données devaient permettre l'identification informatisée des substances étudiées. Cependant il nous est apparu indispensable de rendre ce travail plus complet en proposant une attribution des fréquences caractéristiques des composés polycycliques concernés.

Nous présentons et discutons les spectres Raman en phase solide de trois corticostéroïdes: la fluocortolone base et ses esters triméthylacétique et caproïque. Les résultats permettront de définir les caractéristiques de chaque ester afin de les identifier spécifiquement à l'état de trace (10^{-12} g) à partir d'une forme galénique, après une séparation préalable par chromatographie liquide haute pression. Ces travaux déjà réalisés seront publiés prochainement. Ils sont en quelque sorte la suite logique du travail préliminaire présenté ici.

PARTIE EXPERIMENTALE

Appareillage

Les spectres Raman ont été enregistrés sur un spectromètre Coderg T 800 comprenant un triple monochromateur de 800 mm de distance focale, équipé de trois réseaux plans gravés (1800 traits par mm). Ce monochromateur est caractérisé par un taux de lumière parasite très faible qui permet l'observation de raies Raman dans le domaine des très basses fréquences. Un laser à argon ionisé (514,5 nm), Spectra-Physics modèle 165.03, délivre 600 mW sur l'échantillon.

L'ensemble décrit est équipé d'un microordinateur Apple II permettant l'accumulation de données et la gestion du spectromètre.

Méthode

Les principes actifs étalons sont introduits sous forme de poudre polycristalline dans un tube capillaire sans purification supplémentaire. Leur pureté a été contrôlée à l'issue de leur synthèse par le fabricant. Les spectres Raman des composés corticostéroïdiques ont été enregistrés à la vitesse de 25 cm^{-1}/mn avec une résolution spectrale de 2 cm^{-1}. Les valeurs moyennes des fréquences du tableau 1 sont obtenues à partir de deux enregistrements par échantillon.

RESULTATS ET DISCUSSION

Les stéroïdes constituent une classe de composés abondamment répandus dans la nature (règne végétal et animal) dérivant du squelette du perhydrocyclopentanophénanthrène (Fig. 1) et portant en outre diverses fonctions ou insaturations, ainsi que des chaînes latérales sur le carbone 17.

Dans l'esprit d'une identification, l'attention doit être portée sur la chaîne latérale fixée sur le carbone 17 (Fig. 2). En effet, celle de la fluocortolone base

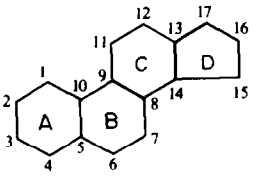

Fig. 1. Squelette du perhydrocyclopentanophénanthrène.

comprend une fonction cétone en C_{20} avec une fonction alcool primaire terminale en C_{21}. Cette chaîne est estérifiée par l'acide triméthylacétique pour le premier dérivé et par l'acide caproïque pour l'autre. C'est-à-dire une chaîne ramifiée dans le premier cas et une chaîne linéaire dans le second cas. Pour les deux esters, la différenciation ne portera que sur ce caractère et sur le nombre d'atomes de carbones et d'hydrogènes présents après la fonction ester.

Par conséquent un tel travail constitue un réel problème analytique, problème qui ne peut être solutionné que par la connaissance parfaite des spectres Raman dont une attribution est proposée sur les spectres établis à partir des substances étalons.

Il nous a semblé logique de concevoir cette attribution non pas par régions spectrales mais plutôt en présentant les éléments permettant d'identifier la classe de médicaments en se rapportant donc à la structure commune, puis par la suite en présentant ceux qui permettront d'identifier chaque substance.

ETUDE DES SPECTRES DES PRODUITS PURS SOUS FORME POLYCRISTALLINE

Les raies correspondant aux spectres des trois composes sont répertoriées dans le tableau 1.

Ces spectres ont été enregistrés en continu entre 150 et 3100 cm^{-1}. Leur interprétation a été rendue possible en partie grâce aux travaux de Schrader et Steigner[1-4] qui ont étudié les vibrations les plus caractéristiques du noyau stéroïdique ainsi que les variations possibles lors d'adjonction de substituants ou de deshydrogénation à l'intérieur du noyau perhydrocyclopentanophénanthrène.

Nous citerons également, dans le domaine des stéroïdes en spectrométrie Raman, un travail

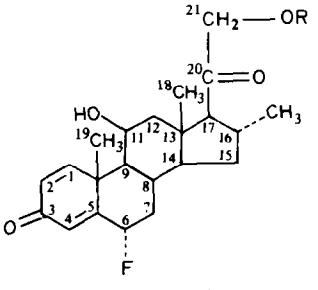

Fig. 2. Structure des corticostéroïdes etudiés: R=H, fluocortolone base; R = —(CO)C(CH$_3$)$_3$, fluocortolone triméthylacétate; R = —(CO)(CH$_2$)$_4$CH$_3$, fluocortolone caproate. Fluocortolone base = 6α fluoro-16α méthyl $\Delta^{1,4}$ pregnanedieñe 11β, 21 diol-3,20 dione.

d'interprétation du spectre de basses fréquences que nous avons effectué à basse température sur le caproate de fluocortolone.[5] Cet aspect que nous ne développerons pas dans ce travail mérite cependant d'être signalé puisque les raies observées sont très intenses d'une part, et d'autre part, celles-ci sont dûes essentiellement aux vibrations du réseau cristallin en plus des raies dûes à des mouvements de torsion et à des mouvements du squelette de la molécule. Elles constituent donc une "fiche d'identité" très spécifique de la molécule. Néanmoins, dans ce domaine de fréquence, l'attribution est difficile et nécessite l'emploi de techniques variées telles que la spectroscopie d'absorption du rayonnement infrarouge lointain, l'étude de la polarisation des raies Raman observées sur un monocristal ainsi que le calcul à priori des fréquences de vibration du cristal.

Vibrations des éléments de structure communs aux trois corticostéroïdes

Une forte modulation de la polarisabilité apparaît avec les vibrations localisées sur des liaisons riches en électrons; c'est pourquoi il est possible de prévoir que les raies Raman les plus intenses apparaîtront pour des vibrations dûes aux liaisons multiples. Les stéroïdes étudiés présentent en commun cette particularité de structure dite $\Delta^{1,4}$ 3-one.

Par ailleurs, les vibrations "en phase" du squelette carboné donneront aussi des vibrations intenses caractéristiques.

Enfin la fonction cétonique en 20 est aussi un élément d'identification important dans cet ordre d'idée.

Structure $\Delta^{1,4}$ 3-one. La vibration d'élongation d'une double liaison ν(C=C) isolée (1620–1672 cm^{-1}) présente une très forte intensité en spectroscopie Raman. Une liaison C=O isolée possède normalement une vibration d'élongation plus faible que celle de C=C. En Raman, deux doubles liaisons isolées C=O et C=C peuvent vibrer au même nombre d'onde, ainsi qu'en infrarouge où la vibration très importante du C=O peut masquer complètement la vibration du C=C. Par contre, pour des liaisons conjuguées C=O et C=C, on obtiendra un système très caractéristique avec autant de raies qu'il existe de doubles liaisons. La place de ces doubles liaisons peut être aisément déterminée en s'inspirant des travaux de Schrader. Des raies supplémentaires dans la région spectrale 900–1300 cm^{-1} peuvent aider à la confirmation des résultats.

Il apparait avec toutes les molécules de ce type, trois raies caractéristiques vers 1600–1620 et 1660 cm^{-1}. Si l'on considère des molécules plus simples comme:

—le cyclohexène qui présente une vibration d'élongation dûe à la liaison C=C à 1656 cm^{-1};[6]

—le 1,4 cyclohexadiène, molécule parfaitement symétrique à deux doubles liaisons qui ne donne qu'une seule raie très intense située aux alentours de 1675 cm^{-1};[7]

—la cyclohexanone pour laquelle en spectrométrie Raman n'est observée qu'une raie moyenne représentative de la vibration d'élongation ν(C=O) vers 1710 cm^{-1} pour les alkyls-cétones;[8] par des effets de conjugaison, cette raie peut se déplacer vers de plus faibles nombres d'onde comme par exemple avec la 1,2 cyclohexane dione qui présente une raie d'intensité moyenne à 1658 cm^{-1};[9]

—la parabenzoquinone qui montre trois raies d'intensités différentes: deux moyennes à 1610 et 1680 cm^{-1} et une raie intense à 1655 cm^{-1}.[10]

Il est donc possible de penser que la présence d'une fonction cétonique s'intercalant dans un système de deux doubles liaisons et établissant de ce fait un système conjugué, fera apparaître des raies d'un profil très particulier; l'ensemble constituant un moyen d'identification de la molécule en caractérisant la structure $\Delta^{1,4}$ 3-one. La position des raies, du fait des différentes interactions existantes, se trouve modifiée par rapport aux valeurs de fréquences décrites précédemment pour des molécules plus simples.

L'étude des profils de raies dans l'intervalle 1500–1700 cm^{-1} donné par Schrader[4] confirme les observations faites à propos des trois corticoïdes étudiés dans ce travail. La raie située vers 1600 cm^{-1} dans le cas des Δ^1 3-one et Δ^4 3-one stéroïdes se dédouble ce qui permet d'observer dans le cas des $\Delta^{1,4}$ 3-one stéroïdes trois raies caractéristiques dans cette zone de fréquences (voir tableau 1).

Signalons par ailleurs que le passage d'un Δ^1 3-one stéroïde à un Δ^4 3-one stéroïde fait apparaitre en spectrométrie Raman un dédoublement de la raie située à 1662 cm^{-1} (tableau 2).

Groupements CH, CH_2 du cycle et CH_3 substitués. Parmi les vibrations de valence ν(CH) les plus caractéristiques des stéroïdes, il faut citer celles du cycle A correspondant aux vibrations C–H des carbones doublement liés qui apparaissent dans l'intervalle 3030–3070 cm^{-1}. Les trois composés présentent ce type de raies à 3046 pour la fluocortolone base (F), 3045 pour le triméthylacétate (TMAF), 3048 pour le caproate (CAF) et 3066 (F), 3067 (TMAF), 3069 (CAF) et reflètent l'insaturation du cycle.[11] En dessous de 3000 cm^{-1} sont retrouvées les vibrations ν(CH) correspondant aux groupements CH_2 et CH_3. Les valeurs observées généralement attribuées dans l'ordre croissant des fréquences avec en premier lieu les vibrations symétriques ν_s puis les vibrations antisymétriques ν_a.

Des informations supplémentaires sur le squelette de la molécule stéroïdique peuvent être obtenues en considérant les intensités des bandes dans différentes régions du spectre.

Notamment la région 1440–1460 cm^{-1} montre une bande intense attribuée aux vibrations de déformation δ_s des groupements CH_2 et CH_3 et que l'on retrouve dans les spectres de tous les stéroïdes.[1] Cette bande a été observée pour les stéroïdes étudiés respectivement à 1454 (F), 1452 (TMAF) et 1450 cm^{-1} (CAF). L'intensité de cette bande comparée à celle des bandes situées de part et d'autre permet par ailleurs d'obtenir des informations concernant le type de stéroïde étudié. En effet:

—pour les stéroïdes saturés la vibration à 1450 cm^{-1} correspond à la bande la plus intense,

—pour ceux présentant des systèmes de doubles liaisons conjuguées, intracycliques ou branchées sur les cycles, les bandes situées au-dessus et en dessous sont plus intenses; ce fait a été noté pour les stéroïdes que nous avons étudiés,

—pour les systèmes non conjugués, des bandes de forte intensité sont observées à des fréquences plus élevées que 1450 cm^{-1},

—pour les stéroïdes comprenant des cycles aro-

Tableau 1. Fréquences observées pour les trois composés (cm^{-1})

Base		Triméthylacétate		Caproate		
Infrarouge	Raman	Infrarouge	Raman	Infrarouge	Raman	Essais d'attribution
				3742		
3421		3478		3464		
				3225		
	3075 f					
	3066 f		3067 f		3069 f	Vibrations de valence ν(C—H) des carbones doublement liés du cycle A
3058						
	3046 f		3045 m		3048 f	
3043						
3023						
	3014 f		3011 ep		3024 f	
					2996 f	
	2985 m	2988		2985	2988 f	$\nu_a(CH_3)$
			2974 ep		2972 ep	
	2967 m	2954	2960 ep	2960	2962 ep	$\nu_a(CH_2)$
	2945 F			2945	2940 ep	
		2929	2932 FF			$\nu_s(CH_3)$
2921				2925	2927 FF	
	2912 FF		2907 ep		2911 ep	$\nu_s(CH_2)$
					2899 ep	
	2874 F	2870	2876 ep		2871 F	

Tableau 1—*suite*

Tableau 1—*suite*

Base		Triméthylacétate		Caproate		Essais d'attribution
Infrarouge	Raman	Infrarouge	Raman	Infrarouge	Raman	
2869	2867 ep		2869 ep	2866		
			2857 ep		2859 ep	
			2786 ff			
			2731 ff			
			1782 ff			
			1745 m	1746	1745 f	—élongation ν(C=O) des fonctions esters
		1738				
1706			1728 m	1719	1723 f	—ν(C=O) en C_{20} des deux esters
1701	1701 f					—ν(C=O) en C_{20} de la fluocortolone base
			1668 ep			
1660	1666 FF	1660	1662 FF		1660 FF	raies caractéristiques rencontrées pour tous les stéroïdes présentant la structure $\Delta^{1,4}$ 3-one
	1661 ep			1656		
	1635 ff					
1622	1625 f	1625	1629 FF	1619	1623 m	
1602	1606 f	1604	1608 FF	1601	1604 m	
				1585		
1558		1560		1562		
1541		1542		1541		
1523		1524				
1505		1507				
		1478				
			1465 ep		1465 ep	—$\delta(CH_2)$ (scissoring) du CAF
		1457			1459 f	—$\delta_a(CH_3)$ du CAF
1450	1454 f		1452 F	1456	1450 f	—$\delta_s(CH_2)$ et $\delta_s(CH_3)$ des méthylènes
	1449		1448		1443 f	intracycliques et méthyles branchés directement sur le cycle.
1406	?	1409	1410 f	1411	1417 f	—déformation du CH_2 en α de la cétone.
		1394	1399 ff			
1389				1385		
1374	1374 ff	1378	1377 f	1378	1379 f	—déformation symétrique $\omega(CH_3)$ (wagging) du méthyl en α de la double liaison 1—2.
1364		1366	1370 f			
	1340 f		1336 F		1335 m	
	1319 f				1325 m	—$\delta_w(CH_2)$ (wagging) du CAF
1315		1315	1317 F	1315	1315 m	
	1304 ff		1302 f		1304 f	
1295		1284	1294 f	1297	1294 f	
1274	1276 f		1274 m	1276	1277 f	
				1268		
1253	1255 ff	1253	1254 ff		1252 ff	
				1247		
1229	1232 m	1229	1233 ff	1233	1235 m	—vibrations d'élongation du squelette et vibrations de déformation des C—H.
1203	1205 f		1204 m		1203 f	
1183			1191 m		1189 f	
1172	1169 f		1174 m	1172	1175 f	
1155		1154	1156 ep	1160		
1146	1149 f		1149 m		1150 m	élongation antisymétrique ν_a(C—CO—C) en C_{20}
	1117 m	1111	1115 FF	1113	1119 F	—vibrations d'élongation du squelette
1094		1100		1100	1094 ff	et vibrations de déformation des C—H.
1082		1085	1090 m	1085	1087 ff	
					1073 ep	
1065	1069 m		1067 m	1066	1067 f	
					1062 ep	
		1051	1054 ep	1053	1057 ep	
1043		1040	1038 f	1040	1043 ff	
			1028 f	1026	1029 ff	
			1010		1012 f	
	1006 f	1007	1001 f	1006	1007 f	
986		989		986	990 ff	—ν(C—C) du CAF
				969	971 ep	
964	966 m	966	972 m		965 m	—vibrations du squelette et déformation des C—H.
			959 m		948 f	ν(C—C) du TMAF et δ_r (rocking) des deux esters.

Tableau 1—*suite*

Tableau 1—*suite*

Base		Triméthylacétate		Caproate		
Infrarouge	Raman	Infrarouge	Raman	Infrarouge	Raman	Essais d'attribution
933	933 m	933	937 m	934	936 m	—vibrations du squelette et déformation
			928 m		930 m	des C—H.
	924 ep			919	921 ep	
912		915			910 f	
897	898 ff	897	893 ff	902	904 f	
	886 ff		882 ff	881	883 ff	
	873 ff	871				
	861 ff		861 f	866	868 ff	
857		856		857	859 ff	
				849		
837	839 f	839	842 m		839 ff	
				829		
821	820 ff	821	825 f		822 ff	
		794	796 ep			—ν(C—C) et ν_s du groupe en C_5 (TMAF)
			782 ep		782 ep	—déformation dans le plan du groupement
				778		(O—C=O) ester
		774	774 ep			
770	771 m		770 m	770	772 m	—élongation symétrique ν_s(C—CO—C) en C_{20}
	769 ep					
				751		
738		739	741 f		740 ff	
				729		
716	717 m	715	717 F	719	720 f	—Vibrations de déformation du squelette.
705	705 ff				712 f	
				699	699 ff	
672	674 f	670	674 f	670	674 ff	
		658		657		
	643	645	643 f	637		
629	630 f	633	628 f	629	629 f	—Déformation dans le plan δ(C—CO) en C_{20}
		625		619		
		607				
589		594	595 f	594		
		584				
		572				
		558		562		
547	550 m	550	551 F	549	551 m	—Vibrations de déformation du squelette.
	532 ff		531 f	531	535 ff	
517	518 ff	523		517	520 ff	
504	507 ff	514	506 f	506	508 ff	
488	489 ff	485	489 f	486	490 ff	Déformation hors du plan δ(C—CO) en C_{20}
		475		470	466 ff	
460	461 f	458	462 f	460		
		451		453		
				445		
423	437 ff	427	436 ff	429	431 ff	
418	419 ff	417	417 ff	419	420 ff	
		409		411		Déformation dans le plan δ(C—CO—C) en C_{20}
				403		
	401 m		398 F	403	402 f	
	384 f				380 f	
	363 f		370 m		368 f	
			350 f			—Déformation (C—C—C) du TMAF
			322 f		317 f	
	302 f		302 F		304 f	
	289 ff		285 ep			
	258 f		250 m		259 f	
	235 f		223 m		225 f	
			193 f		191 m	
			175 f		181 m	
			145 m		147 m	
			131 ff			

*f = faible.
m = moyen.
ep = épaulement.
F = fort
FF = très fort.
ff = très faible.

Tableau 2. Comparaison $\Delta^{1,4}$ 3-one, Δ^{1} 3-one, Δ^{4} 3-one dans l'intervalle 1550–1700 cm^{-1}

		Base	$\bar{\nu}$, cm^{-1} 1606	$\bar{\nu}$, cm^{-1} 1625	$\bar{\nu}$, cm^{-1} 1666
$\Delta^{1,4}$ 3-one	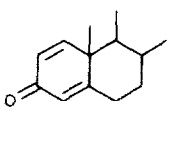 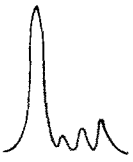				
	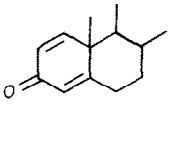 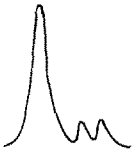	Triméthylacétate	1608	1629	1662
	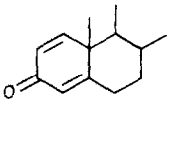 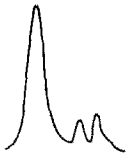	Caproate	1604	1623	1660
Δ^{1} 3-one	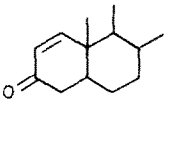 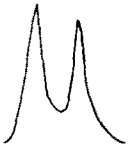	Selon Schrader[6]	1612		1662
Δ^{1} 3-one	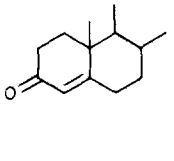 	Schrader[6]	1614		1650 et 1669

matiques, les bandes les plus intenses se trouvent en dessous de 1450 cm^{-1}.

En ce qui concerne les fréquences inférieures à 1450 cm^{-1}, l'intervalle 1360–1390 cm^{-1} montre pour les trois composés une bande située à 1374 (F), (TMAF), 1379 (CAF) qui peut correspondre à la déformation symétrique $\omega(CH_3)$ du groupement CH_3 porté par le carbone en α de la double liaison en 1–2,[12] bien que le phénomène d'exaltation escompté n'apparaisse pas de façon significative.

Parmi les autres bandes, citons les plus intenses qui se situent à 1232 (F), 1233 (TMAF), 1235 (CAF), 1117 (F), 1115 (TMAF), 1119 (CAF) et qui sont caractéristiques des composés étudiés. Il en est de même pour les raies observées à 966 (F), 972 (TMAF), 965 (CAF) et 933 (F), 937 (TMAF), 936 (CAF). Toutes ces raies sont difficilement attribuables, en effet dans la région 1350–800 cm^{-1} on trouve[1] les vibrations d'élongation du squelette de la molécule en même temps que les vibrations de déformation hors du plan, symétrique (wagging) et antisymétrique (twisting), ainsi que les vibrations asymétriques dans le plan (rocking) des liaisons C–H. Elles constituent cependant une bonne "empreinte digitale" de la molécule.

Enfin, parmi les bandes observées entre 800 et 200 cm^{-1}, les plus caractéristiques sont situées à 717 (F), 717 (TMAF), 720–712 (doublet, CAF) et 550 (F), 551 (TMAF), 551 (CAF). Elles correspondent aux déformations du squelette de la molécule et peu d'entre elles peuvent être attribuées directement.

Fonction cétonique en C_{20}. Des deux fonctions cétoniques fixées sur la molécule stéroïdique, nous avions envisagé la possibilité de distinguer celle provenant du système conjugué $\Delta^{1,4}$ 3-one donnant lieu à un ensemble très particulier de trois raies entre 1500 et 1690 cm^{-1}.

L'autre fonction cétonique, appartenant à la chaîne latérale fixée sur le carbone C_{17} va pouvoir être différenciée de la précédente de par son caractère aliphatique. En effet, la fréquence de la vibration d'élongation ν(C=O) d'une cétone de type R—CO—R a pour valeur moyenne 1715 cm^{-1}.[15] Cette valeur peut varier pour ce groupement dans l'intervalle 1705–1725 cm^{-1}.[14,15]

Le spectre de la fluocortolone base montre une raie à 1701 cm^{-1} pour la vibration ν(C=O). Celle-ci est d'ailleurs retrouvée à 1699 cm^{-1} dans le spectre Raman d'un Δ^{5} 20-one stéroïde,[2] comprenant une double liaison isolée et un groupement cétonique isolé sur une chaîne aliphatique. Par ailleurs d'autres $\Delta^{1,4}$ stéroïde[2] comme le $\Delta^{1,4}$ pregnadiène 3,20-dione, possédant une chaîne acétyle (CH_3—CO—) en C_{17}, présente cette raie à 1700 cm^{-1}.

Par contre pour les esters de la fluocortolone, la vibration ν(C=O) est déplacée vers de plus hautes

fréquences: 1728 cm^{-1} (TMAF) et 1723 cm^{-1} (CAF). Ce phénomène pourrait être induit par la présence dans les chaînes latérales d'une fonction carbonylée de type ester.

Parmi les autres vibrations caractéristiques de cette cétone, on peut citer:

—une vibration d'élongation antisymétrique ν_a (C—CO—C) d'intensité moyenne dans la zone allant de 1110 à 1170 cm^{-1} et que nous pourrions attribuer aux raies à 1149 cm^{-1} (F), 1149 cm^{-1} (TMAF) et 1150 cm^{-1} (CAF);[15]

—une vibration d'élongation symétrique ν_s (C—CO—C) vers 770 cm^{-1};[16]

—une vibration de déformation dans le plan de δ(C—CO) vers 630 cm^{-1};[17]

—une vibration de déformation hors du plan attribuable à l'une des deux raies situées dans la zone 460–490 cm^{-1};[17]

—une vibration de déformation dans le plan de l'ensemble C—CO—C dans la région allant de 390 à 430 cm^{-1},[17] et que nous n'avons pu discerner parmi les trois raies communes situées dans cette zone;

—enfin, une raie qui n'est pas spécifique d'une cètone mais qui en découle, a pu être mis en évidence.

Il s'agit de la déformation du CH_2 en α de la cétone qui varie peu quelque soit le type de cétone et qui se situe entre 1405 et 1420 cm^{-1}.[15,16]

Vibrations caractéristiques de la fonction ester

La raie la plus caractéristique est celle qui est dûe à la fréquence d'élongation ν(C=O) située entre 1730 et 1750 cm^{-1}.[18,19] Quant à la raie correspondant à l'élongation de la liaison —C—O—, inexistante en Raman, elle présente comme attendue une forte intensité vers 1150–1160 cm^{-1} en spectroscopie infrarouge. Une autre raie bien définie, située à 782 cm^{-1} peut être attribuée à une vibration de déformation dans le plan du groupement O—C=0.[18]

Habituellement, dans le cas des esters, on peut trouver de nombreuses bandes entre 1000 et 1300 cm^{-1} qui forment une "empreinte digitale" permettant d'identifier le type d'ester.[20] Nous n'avons pas pu mettre en évidence, dans nos spectres, de raies qui puissent être communes, dans cette région, aux deux seuls esters.

Vibrations caractéristiques de la chaîne latérale

Les chaînes latérales, constituées par des CH_2 et CH_3, présenteront de très nombreuses raies de vibration, que ce soit d'élongation ou de déformation. Elles vont se retrouver dans plusieurs régions du spectre, bien souvent en association avec les vibrations CH, CH_2 et CH_3 du noyau stèroïdique. Du fait de ces recouvrements possibles, il sera très difficile d'attribuer avec certitude les différentes bandes spectrales retrouvées.

Triméthylacétate. Le groupement *ter*-butyl—$C(CH_3)_3$ du triméthylacétate devrait théoriquement présenter des raies caractéristiques dans les zones spectrales hachurées sur la figure 3.

Sur les spectres, nous avons observé les raies suivantes, spécifiques du triméthylacétate:

—une raie à 959 cm^{-1} légèrement décalée vers les plus hautes fréquences par rapport à ce que l'on peut observer avec un 2,2,3,3-tétraméthylbutane ou un 2,2,3 triméthylpentane où cette raie se situe entre 930 et 940 cm^{-1};[21,22] cette raie correspond à un mode couplé: élongation ν(C—C) et $\delta_r(CH_3)$ (rocking);

—une raie à 796 cm^{-1} dûe à une élongation ν(C—C)[23] et à l'ensemble élongation symétrique du groupe en C_5;[23]

—une raie à 595 cm^{-1} qui est présente uniquement dans le triméthylacétate mais qui ne semble pas provenir du groupement *ter*butyl;

—de par les groupements méthyles, on retrouve des vibrations d'élongation antisymétriques vers 2960 cm^{-1} et symétriques vers 2870 cm^{-1}.

Caproate. En raison de sa chaîne latérale linéaire en CH_2 et CH_3, le spectre de ce produit présente de nombreuses raies spécifiques:

—un épaulement qui semble se situer vers 1465 cm^{-1} et qui est attribué à la vibration de cisaillement du groupement méthylène $\delta(CH_2)$;[24]

—à 1459 cm^{-1}, une vibration de déformation asymétrique du groupement méthyle $\delta_a(CH_3)$;[24]

—une raie très caractéristique à 1325 cm^{-1} provenant de la vibration de balancement $\delta_b(CH_2)$;[25]

—une autre également très spécifique à 990 cm^{-1} qui est une élongation C—C;[25]

—à 948 cm^{-1}, une raie attribuée à la vibration $\delta_r(CH_3)$ d'un groupement méthyle terminal;[25]

—comme pour le triméthylacétate, le spectre présente des vibrations d'élongation symétriques et antisymétriques dans les mêmes zones, avec en plus des raies à 2927 cm^{-1} d'intensité forte et 2859 cm^{-1} d'intensité moyenne, responsables respectivement des élongations antisymétriques et symétriques des groupements CH_2.[26]

Base: groupement alcoolique primaire en C_{21}. Dans le paragraphe qui suit, quelques informations d'ordre général seront indiquées pour la fluocortolone base. Rappelons tout d'abord que seuls les deux dérivés estérifiés entrent dans la composition de la prépara-

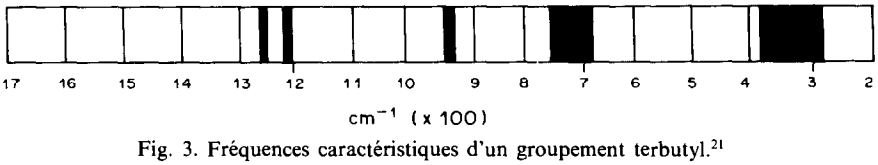

Fig. 3. Fréquences caractéristiques d'un groupement terbutyl.[21]

tion galénique pour laquelle l'étude préalable en spectrométrie Raman avait été envisagée.

Par rapport à ses dérivés d'estérification, la fluocortolone base ne présente que le groupement hydroxyle en C_{21} comme élément possible de différenciation. L'hydroxyle du cycle C en 11 présent sur les molécules des trois corticoïdes ajoutera sans aucun doute un élément de complexité au problème.

De plus, la vibration d'élongation ν(O–H) est très peu intense en spectrométrie Raman (environ vingt fois moins que le massif correspondant aux vibrations ν(C—H).[27] C'est pourquoi dans ce cas précis la spectrométrie d'absorption infrarouge se révèle plus démonstrative par l'intensité et la position des bandes observées.

Sans envisager de façon exhaustive le problème des différents types de liaisons hydrogène, qui nécessiterait une étude plus complète, il a été possible de noter pour la fluocortolone base une bande intense à 3421 cm^{-1} avec un épaulement à 3529 cm^{-1}. Les deux autres esters présentent une bande d'intensité moyenne à 3478 cm^{-1} avec un épaulement à 3357 cm^{-1} (TMAF) et une raie fine intense à 3464 cm^{-1} (CAF). Ces bandes et cette raie peuvent être attribuées à la vibration ν(O–H) des groupements hydroxyles en 11 pour les esters et dans le case de la fluocortolone base, la bande intense et large témoignerait de la contribution du groupement hydroxyle en 11 (groupement alcoolique secondaire cyclique) et du groupement alcoolique primaire en C_{21}.

La région spectrale 1000–1075 cm^{-1} qui signale l'existence des vibrations ν(C—O) des groupements alcooliques, primaire aliphatique et secondaire cyclique[28] reste difficile à interpréter pour ce type de composé.

Par contre, la vibration ν(C=O) des composés estérifiés apparait de façon très intense à 1154 cm^{-1} (TMAF) et 1160 cm^{-1} (CAF) alors que l'on ne la retrouve pas pour la fluocortolone base. Son absence, ainsi que la présence à 3421 cm^{-1} d'une bande d'élongation ν(O—H) peuvent confirmer une fonction alcoolique primaire non estérifiée.

ETUDE DES INTERVALLES DE FREQUENCES UTILISABLES POUR LA CARACTERISATION DE CHAQUE SUBSTANCE

Le paragraphe précédent concernant l'étude des spectres des produits purs sous forme polycristalline et les essais d'attribution, a montré la complexité du problème posé, à savoir la différenciation de trois composés polycycliques de structure très voisine. Cependant quelques intervalles de fréquences sont susceptibles d'être utilisés afin de permettre l'identification de la fluocortolone et de ses dérivés dans les éluats receuillis en sortie de colonne HPLC.

En premier lieu, il convient tout particulièrement de distinguer les raies situés entre 1500 et 1800 cm^{-1} (Fig. 4):

—dans l'intervalle 1580–1690 cm^{-1}, il a été démontré qu'elles sont intenses et spécifiques de la structure conjugée $\Delta^{1,4}$ 3-one des stéroïdes, ce qui permet de distinguer la classe à laquelle appartiennent les substances étudiées;

—la zone de fréquences comprise entre 1690 et 1750 cm^{-1} témoigne non seulement de la présence d'une fonction cétonique sur la chaîne latérale mais

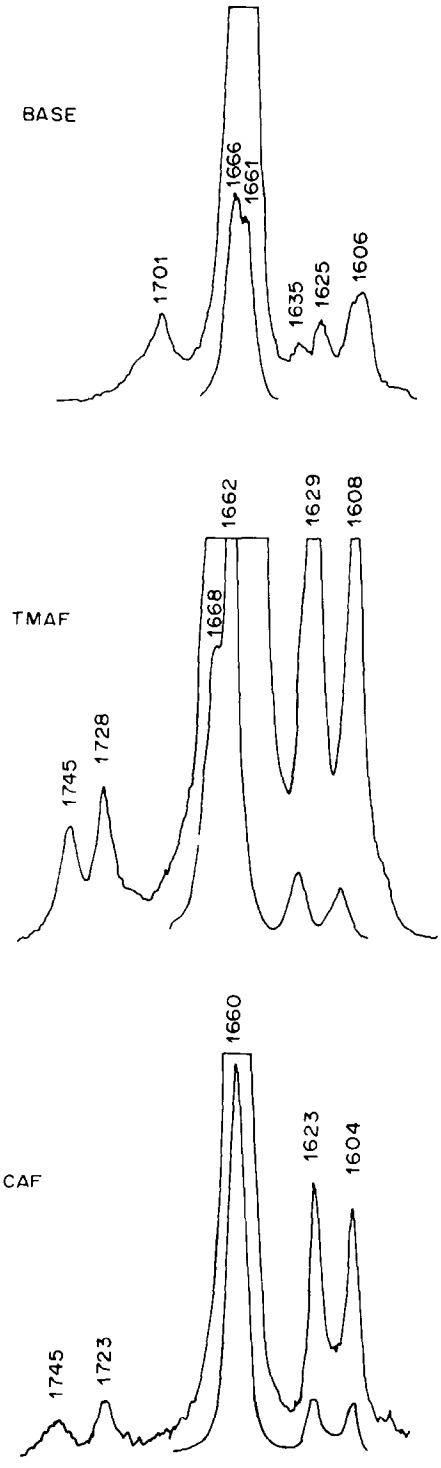

Fig. 4. Spectres Raman; région 1500–1800 cm^{-1}.

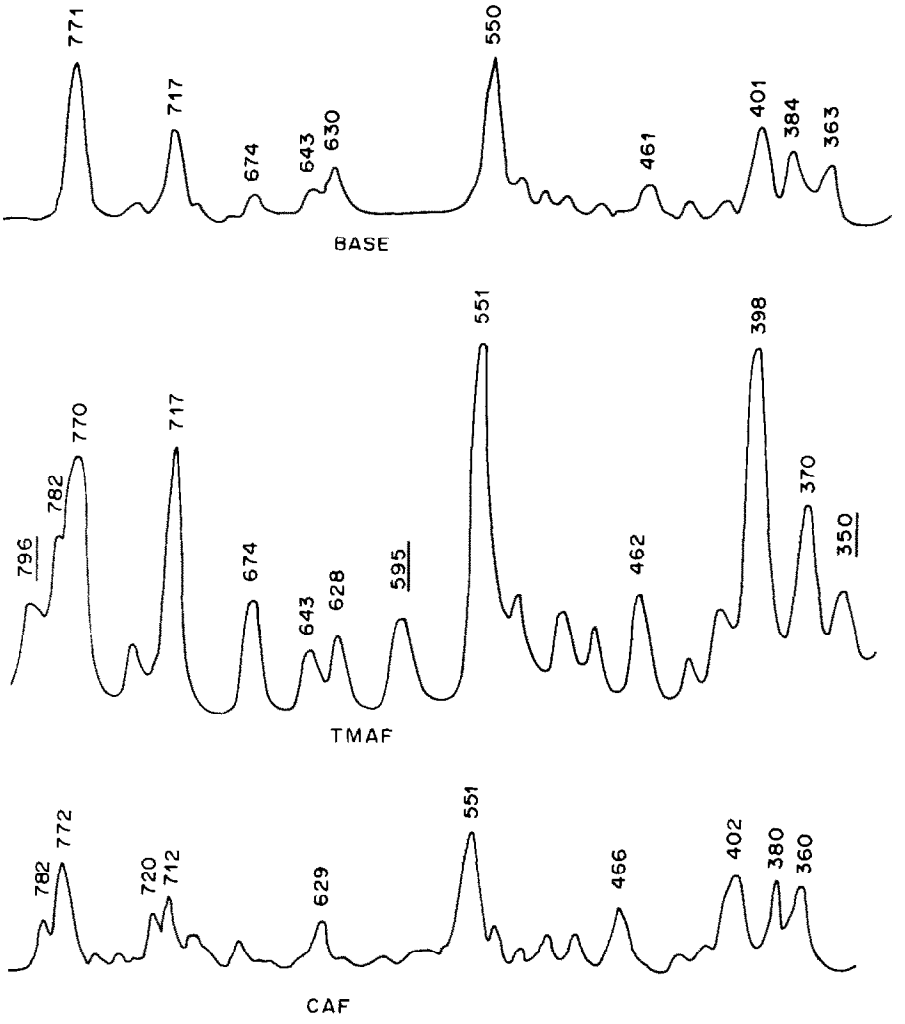

Fig. 5. Spectres Raman; région 340–810 cm^{-1} permettant de caractériser le triméthylacétate.

aussi de l'existence d'une fonction ester suivant que l'on y trouve respectivement une ou deux raies;

—rappelons que la fluocortolone base présente à 1635 cm^{-1} une raie qui n'est pas retrouvée chez les dérivés estérifiés.

En second lieu, nous retiendrons également les zones spectrales représentatives des chaînes latérales estérifiées fixées sur le carbone 21:

—chaîne triméthylacétate (Fig. 5): 340–360 cm^{-1}, 570–610 cm^{-1}, 750–810 cm^{-1}; dans cette dernière région, commune au caproate et au triméthylacétate, la differenciation des deux composés se fait grâce à la raie à 796 cm^{-1} absente dans le spectre du caproate;

—chaîne caproate (Fig. 6): 1310–1350 cm^{-1}; dans cet intervalle, le caproate présente un profil très particulier avec trois raies d'intensité voisine.

CONCLUSION

Ce travail portant sur l'étude par spectrométrie Raman d'esters de la fluocortolone (TMAF) (CAF) a montré qu'il était possible de caractériser aisément cette classe de médicaments corticostéroïdiques marqués par leur structure $\Delta^{1,4}$ 3-one. Nous avons par ailleurs apporté des éléments permettant de différencier d'une part la fluocortolone base de ses deux esters et d'autre part chacun des deux esters. Ces éléments essentiels ont été regroupés dans cette publication et sont destinés à être utilisés comme nous l'avons annoncé dans l'introduction, pour un travail d'identification fine par microspectrométrie Raman permettant d'atteindre la limite du picogramme.

LITTERATURE

1. B. Schrader et E. Steigner, *Modern Methods of Steroid Analysis*, pp. 231–243. Academic Press, New York, 1973.
2. *Idem, Z. Anal. Chem.*, 1971, **254**, 177.
3. E. Steigner et B. Schrader, *Liebigs Ann. Chem.*, 1970, 735, 15.
4. B. Schrader et E. Steigner, *ibid.*, 1979, **735**, 6.
5. A. P. Gamot, E. Cuingnet, G. Vergoten et G. Fleury, *Bulg. J. Phys.*, 1977, IV, 6, 679.
6. F. R. Dollish, W. G. Fateley et F. F. Bentley, *Charac-*

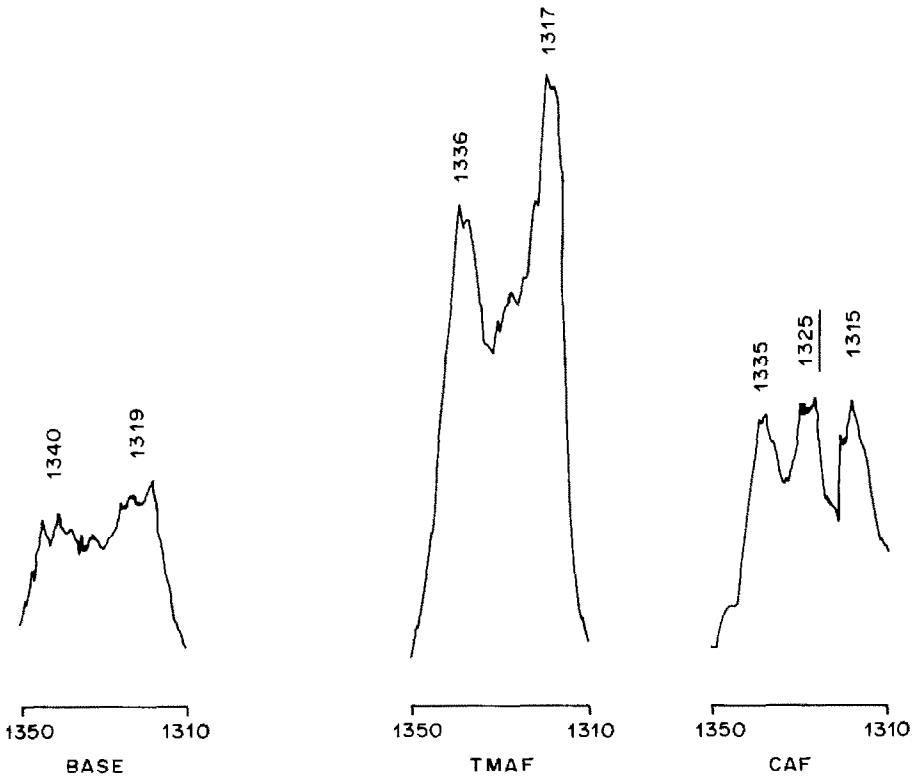

Fig. 6. Spectres Raman; région 1310–1350 cm^{-1} permettant la caractérisation du caproate.

teristic Raman Frequencies of Organic Compounds, p. 85, Wiley, New York, 1974.
7. B. Schrader et W. Meier, *Raman/I.R. Atlas*, E. 6–03.
8. *Idem, ibid.*, E. 1–02.
9. *Idem, ibid.*, E. 1–11.
10. *Idem, ibid.*, H. 1–01.
11. B. Wojtkowiak et M. Chabanel, *Spectrochimie moléculaire*, p. 152. Technique et Documentation, Paris, 1977.
12. F. R. Dollish, W. G. Fateley et F. F. Bentley, *op. cit.*, pp. 62–67.
13. B. Wojtkowiak et M. Chabanel, *op. cit.*, p. 219.
14. *Idem, op. cit.*, p. 222.
15. F. R. Dollish, W. G. Fateley et F. F. Bentley, *op. cit.*, p. 100.
16. *Idem, ibid.*, p. 102.
17. *Idem, ibid.*, p. 101.
18. *Idem, ibid.*, p. 111.
19. B. Wojtkowiak et M. Chabanel, *op. cit.*, p. 229.
20. *Idem, ibid.*, p. 228.
21. F. R. Dollish, W. G. Fateley et F. F. Bentley, *op. cit.*, p. 5.
22. B. Schrader et W. Meier, *op. cit.*, A. 1–14; A. 1–15.
23. F. R. Dollish, W. G. Fateley et F. F. Bentley, *op. cit.*, p. 4.
24. B. Wojtkowiak et M. Chabanel, *op. cit.*, p. 153.
25. F. R. Dollish, W. G. Fateley, F. F. Bentley, *op. cit.*, p. 3.
26. B. Wojtkowiak et M. Chabanel, *op. cit.*, p. 152.
27. *Idem, op. cit.*, p. 209.
28. N. B. Colthup, L. H. Daly et S. E. Wiberley, *Introduction to Infrared and Raman Spectroscopy*, p. 274. Academic Press, New York, 1964.

Summary—Raman spectra of a series of three corticosteroid drugs: fluocortolone and its trimethylacetate and caproate esters (TMAF and CAF) in the polycrystalline state have been recorded from 150 to 4000 cm^{-1}. Assignment of the observed frequencies is proposed. The problem is complex because the drugs have the same polycyclic structure, but frequency ranges with specific bands can be used to characterize the compounds. We first mention the frequencies observed between 1500 and 1800 cm^{-1}: in the range 1580–1690 cm^{-1} strong and specific bands assigned to the $\Delta^{1,4}$-3-one conjugated structure of corticosteroids characterize the class of drugs; the frequencies in the range 1690–1750 cm^{-1} characterize not only a ketone group on the side-chain but also an ester group, which gives one or two bands (fluocortolone base 1701 cm^{-1}; TMAF 1728, 1745 cm^{-1}; CAF 1723, 1745 cm^{-1}). Fluocortolone base shows a band at 1635 cm^{-1} which is not found in the spectra of the esters. Secondly we mention the specific spectral ranges of the esterified side chain on C_{21}: trimethylacetate chain 340–360, 570–610, 750–810 cm^{-1} (this last range is common to the two esters, and differentiation is made with the band found at 796 cm^{-1}, which is absent from the caproate spectrum); caproate chain 1310–1350 cm^{-1} (in this range, caproate shows a specific pattern with three bands of the same intensity). These results can be used to characterize these compounds by Raman spectroscopy of pg quantities in HPLC eluates

Talanta, Vol. 32, No. 5, pp. 383–386, 1985
Printed in Great Britain

0039-9140/85 $3.00 + 0.00
Pergamon Press Ltd

NON-DISPERSIVE ATOMIC-FLUORESCENCE SPECTROMETRIC DETERMINATION OF LEAD BY THE HYDRIDE-GENERATION TECHNIQUE

A. D'ULIVO and P. PAPOFF
Istituto di Chimica Analitica Strumentale del C.N.R., c/o Istituto di Chimica Analitica ed Elettrochimica dell'Università di Pisa, Via Risorgimento 35, 56100 Pisa, Italy

(*Received* 18 *October* 1984. *Accepted* 19 *December* 1984)

Summary—Non-dispersive atomic-fluorescence spectrometry combined with hydride-generation has been developed for lead determination. A radiofrequency-excited electrodeless discharge lamp was used as light-source and a small argon–hydrogen flame as atomizer. The detection limit was 0.06 ng/ml and the linear calibration graph was linear up to 300 ng/ml, with a precision of 5–6% over the dynamic range. Interference studies and optimization of the experimental parameters are reported. Severe suppression of the lead signal was observed in presence of Cu, Se or Te. An empirical equation was obtained for predicting the effect of copper on the lead signal at various concentration ratios. The strong effect of complexing agents such as EDTA was removed by addition of zinc salts.

Over the past ten years the spectroscopic determination of lead with use of sodium tetrahydroborate for generation of plumbane (PbH_4) has been attempted by several authors,[1–8] but because of the poor reaction efficiency the method was unsuitable until Fleming and Ide[2] and Vijan and Wood[3] discovered that the efficiency can be consistently enhanced by addition of an oxidant before injection of the tetrahydroborate. It was assumed that Pb(IV) is obtained in the oxidation step and is much more suitable than Pb(II) for formation of PbH_4.

Various oxidants and acids have been proposed as the reaction matrices,[2–8] but use of 10% hydrogen peroxide and 0.1–0.12*M* perchloric or nitric acid in the sample solution appears to be the best compromise in terms of sensitivity, reagent blank and interference effects.

Atomic-absorption spectrometry (AAS) was used in all the studies mentioned, except that by Ikeda *et al.*,[8] who used inductively-coupled plasma atomic-emission spectrometry (ICP–AES). Owing to the variation in the definitions of sensitivity and detection limit, the merits of the different procedures are difficult to compare. In the AAS methods, a typical sensitivity was an absorbance of 0.0044 for a lead concentration of 1 ng/ml. Taking the blank concentration as 1–2 ng/ml and the instability of the output of a commercial instrument as an absorbance of at least 0.003, a realistic estimate of the standard deviation, based on a small set of observation data, would be 0.004 absorbance at the blank concentration level. This corresponds to a detection limit (three times the standard deviation) of 3–4 ng/ml.

This value is comparable with those recently obtained by Sthapit[10] and Omenetto[11] by microwave-EDL or laser-excited atomic-fluorescence spectrometry with direct aspiration of the sample into the flame.

To achieve a lower detection limit and extend the linear dynamic range, we have tested the use of non-dispersive atomic-fluorescence spectrometry (NDAFS) with the instrument described previously.[9]

EXPERIMENTAL

Apparatus

A home-made non-dispersive atomic-fluorescence spectrometer with multielement capabilities was used, in the single-channel mode. The light-source was a Perkin-Elmer electrodeless discharge lamp (EDL) operating at 10 W mean power. The input power was square-wave modulated at 7500 Hz with 100% amplitude modulation and 0.5 duty cycle (duty cycle = pulse width/pulse period). Details of the non-dispersive apparatus and EDL behaviour are reported elsewhere.[9]

A hydride-reaction vessel (70 ml in volume) similar to those reported by other authors[1,12] was constructed from borosilicate glass. It had two ports, for the injection of the oxidizing and reducing solutions.

Disposable micropipettes (0.5 and 1 ml) were employed for manual injection of the reagents. The atomizer was a small argon–hydrogen/entrained-air flame[12] obtained with flow-rates of 0.3 l./min for the hydrogen and 1.0 l./min for the argon. Argon also acted as the carrier for volatile hydrides. The flame was supported on a simple glass tube (8.5 mm bore). A summary of the experimental conditions is reported in Table 1.

Reagents

A stock solution of lead (1000 μg/ml) was prepared from lead nitrate. More dilute solutions were prepared just before use. Demineralized doubly-distilled water was used in all operations.

All reagents were high purity products (Merck, "Suprapur" grade), unless otherwise specified.

Hydrogen peroxide solution (10% w/w) was used as oxidant. Sodium tetrahydroborate solution (10%) was used as reductant and prepared by dissolving the solid reagent

Table 1. Experimental conditions

Radiofrequency power for EDL	10 W (expressed as mean power)
Power modulation for EDL	Square-wave, 0–100% amplitude modulation, 0.5 duty cycle
Modulation frequency	7500 Hz
Photomultiplier voltage	750 V
Focusing height	8 mm above the burner top
Gas flow-rates	Hydrogen 0.3 l./min, argon 1.0 l./min
Sample size	5 ml
Acidity	0.12*M* HCl
Oxidant	0.5 ml of 10% H_2O_2 solution
Oxidation time	40–50 sec
Reductant	1 ml of 10% $NaBH_4$ solution
RC time-constant	10 sec

(BDH, reagent for AAS, pellets) in 0.1*M* sodium hydroxide and filtering with a 0.45-μm filter.

Lead-free sodium chloride solution (5*M*) was obtained by co-precipitating[13] lead with lanthanum hydroxide at pH 10–11 (by addition of sodium hydroxide), filtering, and neutralizing the filtrate with dilute hydrochloric acid.

Procedure

Five ml of sample or standard solution were transferred into the reaction vessel. Two micropipettes, one containing 0.5 ml of hydrogen peroxide solution and the other 1 ml of tetrahydroborate solution, were placed in the injection ports. Argon was then allowed to flow through the reaction vessel. Once the baseline was stabilized, the peroxide was injected and 40 sec later the tetrahydroborate; no stirring was used. The standard-additions method should be used (with correction for the blank), and if complexing agents such as EDTA are thought to be present, 0.05 ml of 10^{-3}*M* zinc solution should be added before injection of the peroxide. All the other experimental conditions are summarized in Table 1.

RESULTS AND DISCUSSION

Optimization of parameters

Burner. Observation at 8–10 mm above the burner top was found to give the best signal to noise ratio (SNR) and the highest signal. By increasing the burner bore, the path-length of the optical cell and the signal are enhanced, but the enhancement is not a linear function of the burner bore (Fig. 1). With a burner bore larger than 6 mm the hydrogen flow-rate can be reduced to 0.3 l./min without the flame being extinguished after the tetrahydroborate injection.

Argon. Changing the argon flow-rate in the range 0.9–1.2 l./min does not affect the signal. At an argon flow of 1.0 l./min the peak-width of the signal at half-height was about 12 sec, so using a 10-sec time-constant at the output of the lock-in amplifier gives a further increase in SNR.

Hydride generation. The effect of sample acidity, and peroxide and tetrahydroborate concentrations was studied in order to achieve higher sensitivity. Patterns similar to those observed by Vijan and Wood[3] were found (see Figs. 2–4). The maximal sensitivity was obtained with 0.1–0.12*M* hydrochloric acid, 8–10% hydrogen peroxide and 10–12% sodium tetrahydroborate solution.

The chemical parameters involved in the hydride generation were also optimized for 0.5*M* sodium chloride medium, in view of a possible application to sea-water analysis. The effect of sodium chloride is discussed below.

When magnetic stirring was used, a 70% suppression of the signal was always observed.

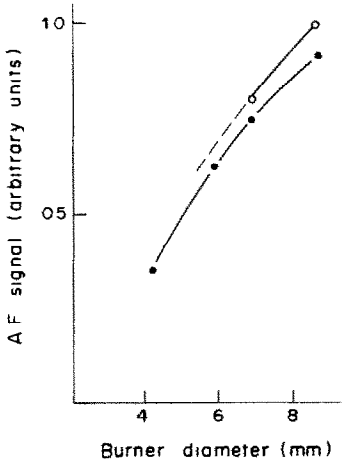

Fig. 1. Effect of glass burner internal diameter on lead signal. Conditions: see Table 1, hydrogen 0.4 (—●—) and 0.3 (—○—) l./min, lead 10 ng/ml. Flame extinguished (----).

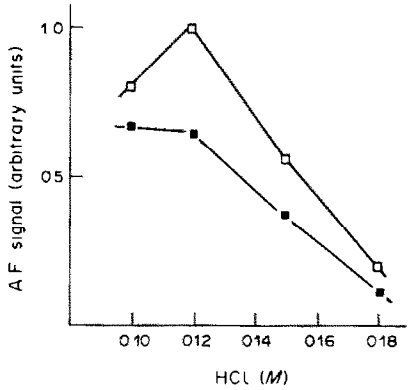

Fig. 2. Effect of sample acidity on lead signal. Conditions: see Table 1, lead 10 ng/ml; in absence (—■—) and in presence of 0.5*M* NaCl (—□—).

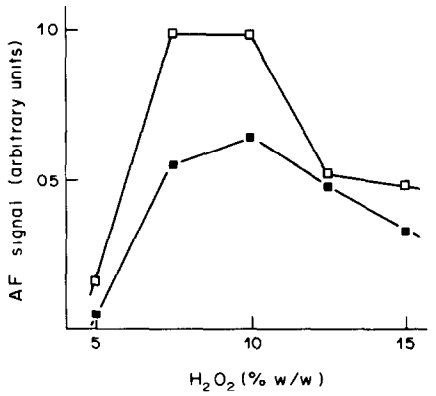

Fig. 3. Effect of concentration of added H_2O_2 solution. Added volume 0.5 ml. Conditions: see Table 1, lead 10 ng/ml; in absence (—■—) and in presence of 0.5*M* NaCl (—□—).

Detection limit, dynamic range and precision

Blank signal. To identify various contributions to the blank, the signal was recorded (*a*) before the addition of borohydride; (*b*) after its addition to a reagent blank solution; (*c*) as in (*b*) except for the presence of 2 μg/ml of copper and the absence of peroxide, to suppress the plumbane formation. It was found that the EDL light reflected by the surroundings onto the photomultiplier was responsible for the continuum component (14% of the peak amplitude for the blank), and that the flame contributes about 8%, the solution droplets dispersed in the flame 15%, and the lead present in the reagent about 63% of the blank. A silaned glass-wool filter placed before the atomizer retains the solution droplets and suppresses their effect.

With the present purity of available reagents, the reagent blank was found to be 0.35 ng/ml, with 6% RSD ($n = 10$). The calculated detection limit (three times the RSD of the blank) was 0.06 ng/ml.

Calibration graphs and precision. Calibration graphs were linear up to 300 ng/ml (4 decades). The

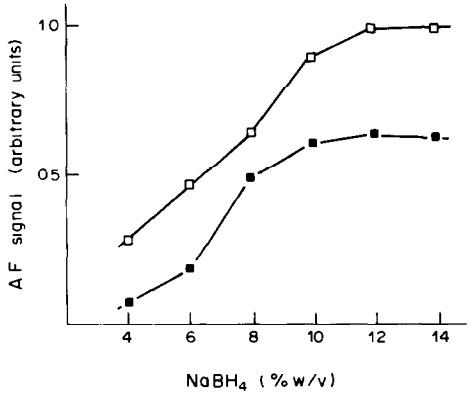

Fig. 4. Effect of concentration of added $NaBH_4$ solution. Added volume 1 ml. Conditions: see Table 1, lead 10 ng/ml; in absence (—■—) and in presence of 0.5*M* NaCl (—□—).

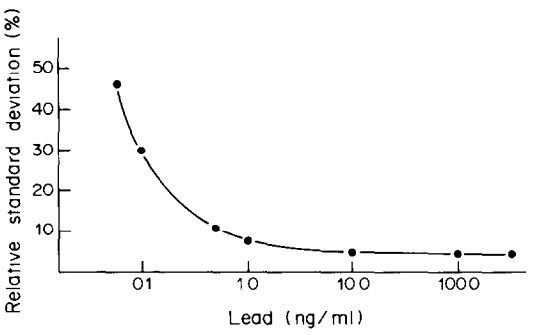

Fig. 5. Precision diagram for lead determination. Conditions: see Table 1.

relative standard deviation over the range 0.06–300 ng/ml was given by

$$\mathrm{RSD} = [(0.06S_B)^2 + (0.05S_i)^2]^{1/2}/S_i,$$

where S_B was the blank signal, S_i the signal relevant to concentration i and 0.06 and 0.05 were the relative standard deviations ($n = 10$) of S_B and S_i respectively. The precision is shown in Fig. 5. The intercept in the $(S_i + S_B)$ *vs.* C_i plot, obtained from the experimental points in the lead range 0–5 ng/ml was equivalent to 0.4 ng/ml. The fairly good agreement with the value calculated in the direct measurement of the blank shows that S_B is constant in the concentration range tested.

Effect of foreign compounds

Anions. Chloride (KCl, NaCl) and bromide (KBr) were found to enhance S_i by up to 50%. Figure 6 shows the effect of increasing concentration of chloride on the peak amplitude of lead. The effect was found to be independent of the lead concentration within the dynamic range. In the absence of hydrogen peroxide the small signal due to the quantity of PbH_4 produced by direct reduction of Pb(II) was further decreased by the presence of chloride. These effects can be explained by considering that Pb(IV) forms more stable complexes than Pb(II) with chloride, so the redox reaction:

$$PbCl_m^{(m-2)-} + 2H_2O_2 + 4H^+ + \overset{Cl^-}{\rightleftharpoons} PbCl_n^{(n-4)-} + 4H_2O$$

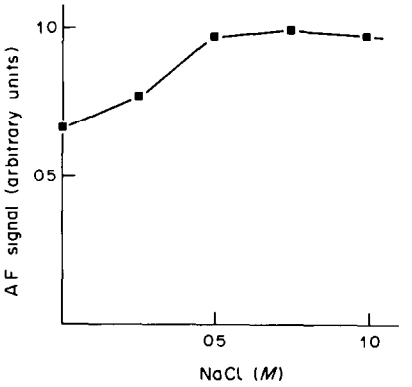

Fig. 6. Effect of sodium chloride present in the sample. Conditions: see Table 1, lead 10 ng/ml.

Table 2. Interference effect of foreign elements (200 ng/ml)*

Element	Interference, %	Element	Interference, %
As(III)	−50(−45)†	Cd(II)	0(0)
Sb(III)	−25(−25)	Co(II)	0(0)
Bi(III)	−13(0)	Ni(II)	0(0)
Sn(IV)	0(0)	Cu(II)	−85(−85)
Se(IV)	−78(−68)	Cr(III)	0(0)
Te(IV)	−77(−65)	Fe(III)	0(0)

*Expressed as percentage variation with respect to the signal of lead alone.
†Interference effect in presence of 0.5*M* NaCl.
Conditions: see Table 1, lead 5 ng/ml.

is shifted toward the right and the yield of PbH_4 in the subsequent reaction with borohydride is increased.

Sulphate ($5 \times 10^{-3}M$), perchlorate ($0.2M$), phosphate ($2 \times 10^{-3}M$) and EDTA ($5 \times 10^{-7}M$; 0.2 ppm) do not affect the signal for a 5-ng/ml level of lead. EDTA at 2 ppm level does not affect the signal for lead at 5-ng/ml level if the solution is made $10^{-5}M$ in zinc

Interferences. Several elements which are reported to have a strong effect on plumbane generation[2-8] were studied. The effect of these elements at the 200-ng/ml level on the signal for 5-ng/ml lead is reported in Table 2. More detailed information on copper, selenium and tellurium interference is given in Tables 3 and 4.

An empirical equation which allows prediction of the signal decrease as a function of lead and copper concentration was found to be: % decrease = $1.15C_{Cu}/C_{Pb}^{0.55}$ (C expressed in ng/ml). Thus for any matrix composition the problem is how much the detection limit and linearity of the calibration graphs are affected by interferents. Whenever a fairly linear calibration graph is obtained for a real sample, it is necessary to calculate the value of S'_B—the blank signal in the presence of interferences—in order to calculate S_l. S'_B is given by $S'_B = S_B\, m'/m$, where m' and m are the sensitivities in the presence and absence of the interferences, respectively. It was found that in presence of copper at the 50-ng/ml level, the standard-addition procedure gives a linear plot for lead from 0.2 to 7 ng/ml, which allows determination of an initial lead concentration in the range from about 0.2 to 2 ng/ml.

Table 3. Concentration interference effect of Se, Te and Cu*

Interferent concentration, ng/ml	Interference, %		
	Se(IV)	Te(IV)	Cu(II)
2.5	0	0	0
5	0	−12	0
10	−10	−20	0
50	−25	−25	−45
200	−78	−77	−82

*Expressed as percentage variation with respect to the signal of lead alone.
Conditions: See Table 1, lead 5 ng/ml.

Table 4. Copper interference effect: dependence on copper to lead ratio*

Pb, ng/ml	Interference, %					
	1†	2†	5†	10†	20†	40†
0.2	0	0	0	0	—	−28
1	0	0	0	0	−20	−42
5	0	0	−8	−45	—	−82
10	0	−10	−23	−65	—	—
100	−12	−35	—	−85	—	−100

*Expressed as percentage variation with respect to the signal for lead alone.
†Cu/Pb mass concentration ratio.
Conditions: see Table 1.

Experiments are in progress for comparison of the results obtained by this procedure with those obtained by anodic-stripping voltammetry in analysis of sea-water.

Conclusions

Non-dispersive atomic-fluorescence spectrometry combined with hydride-generation has proved to be superior to hydride generation and AAS or ICP–AES[1-8] in terms of detection limits and dynamic range, although the most sensitive fluorescence line of lead (at 405.1 nm) lies outside the spectral response of the solar-blind photomultiplier used in the present work.

Proper modulation of the EDL source,[9] adjustment of the burner parameters, and careful choice of the experimental conditions in the hydride generation step are essential for obtaining a low detection limit.

Chloride and bromide enhance the lead signal, but the enhancement is independent of the lead concentration. The depressant effects of other interferents are comparable with those observed in the continuous-flow automatic generation of the lead hydride.[7]

Acknowledgement—One of the authors (P.P.) acknowledges financial support by the Italian M.P.I.

REFERENCES

1. K. C. Thompson and D. R. Thomerson, *Analyst*, 1974, **99**, 595.
2. H. D. Fleming and R. G. Ide, *Anal. Chim. Acta*, 1976, **83**, 67.
3. P. N. Vijan and G. R. Wood, *Analyst*, 1976, **101**, 966.
4. P. N. Vijan and R. S. Sadana, *Talanta*, 1980, **27**, 321.
5. K. Jin, M. Taga, H. Yoshida and S. Hikime, *Bunseki Kagaku*, 1978, **27**, 759.
6. K. Jin and M. Taga, *ibid.*, 1980, **29**, 522
7. *Idem, Anal. Chim. Acta*, 1982, **143**, 229.
8. M. Ikeda, J. Nishibe, S Hamada and R. Tujino, *ibid.*, 1981, **125**, 109.
9. A. D'Ulivo, C. Festa and P. Papoff, *Talanta*, 1983, **30**, 907.
10. R. Sthapit, J. M. Ottaway and G. S. Fell, *Analyst*, 1984, **109**, 1061.
11. N. Omenetto, H. G. C. Human, P. Cavalli and G. Rossi, *ibid.*, 1984, **109**, 1067.
12. K. Tsuji and K. Kuga, *Anal. Chim. Acta*, 1978, **97**, 51.
13. W. Reichel and B. G. Bleakley, *Anal. Chem.*, 1974, **46**, 59.

Talanta, Vol. 32, No. 5, pp. 387–390, 1985
Printed in Great Britain

0039-9140/85 $3.00 + 0.00
Pergamon Press Ltd

SPECTROPHOTOMETRIC DETERMINATION OF IRON AND COPPER IN MILK, FOODSTUFFS AND BODY TISSUES WITH 1-(2-QUINOLYLAZO)-2,4,5-TRIHYDROXYBENZENE

ISHWAR SINGH, MRS. POONAM and P. S. KADYAN
Department of Chemistry, Maharshi Dayanand University, Rohtak-124001, India

(*Received* 26 *September* 1984. *Accepted* 19 *December* 1984)

Summary—1-(2-Quinolylazo)-2,4,5-trihydroxybenzene has been proposed as a sensitive chromogenic reagent for the simultaneous determination of iron and copper in presence of thiosemicarbazide. The molar absorptivities are 1.86×10^4 l.mole^{-1}.cm^{-1} at 510 nm for iron and 2.54×10^4 l.mole^{-1}.cm^{-1} at 550 nm for copper. Trace levels of these two metals have been determined in some foodstuffs, body tissues and milk samples.

Iron and copper are widely distributed in foods of plant and animal origin, but are present in very low concentrations in milk. In the northern areas of India, adults as well as infants are dependent on a milk diet. Excess of copper is objectionable in milk as it oxidizes the ascorbic acid content and causes an off-flavour.[1] These two metals are also distributed in blood and body tissues in the human system, and in some cases can be a pointer to various diseases (*e.g.*, copper, in Wilson's disease).

In an earlier publication,[2] we described use of a new reagent, 1-(2-quinolylazo)-2,4,5-trihydroxybenzene (QATB), for determination of manganese in foodstuffs, and now extend its use to determination of iron and copper.

EXPERIMENTAL

Reagents

QATB was synthesized[2] as described earlier, and used as a $2 \times 10^{-3}M$ solution prepared by dissolving 0.562 g in 1 litre of ethanol. Solutions more than a week old were discarded. Stock solutions ($0.01M$) of iron(II) and copper(II) were prepared by dissolving appropriate amounts of analytical grade ferrous ammonium sulphate hexahydrate and copper sulphate pentahydrate in doubly distilled water and were standardized with EDTA.[3] A 2% solution of thiosemicarbazide was prepared in water.

All other reagents were of analytical grade and doubly distilled water was used throughout.

Procedures

Calibration graphs. To each of a series of 1-ml aliquots (taken in dry 10-ml standard flasks) containing 4–28 μg of iron(II) or 3–30 μg of copper(II), add 2 ml of $2 \times 10^{-3}M$ QATB, 1 ml of $1M$ sodium acetate and dilute to volume with 1:1 v/v water–ethanol mixture. Record the absorbance at 510 nm for iron(II) and 550 nm for copper(II) against a reagent blank prepared under similar conditions. Draw the calibration graphs.

Determination of iron(II) in presence of copper(II). To 1 ml of sample solution (taken in dry 10-ml standard flask) containing not more than 28 μg of iron(II) and 100 μg of copper(II), add 1 ml of 2% thiosemicarbazide solution and after a minute, 2 ml of $2 \times 10^{-3}M$ QATB, 1 ml of $1M$ sodium acetate and 1 ml of ethanol. Dilute to volume with 1:1 water–ethanol mixture. Measure the absorbance at 510 nm against a reagent blank and deduce the amount of iron(II) from the calibration curve.

Determination of iron(II) and copper(II). Treat 1 ml of sample solution containing not more than 30 μg of iron(II) and/or copper(II) as just described, and measure the absorbance at 510 and 550 nm (readings 1 and 2, respectively) against a reagent blank. Repeat the procedure without adding the thiosemicarbazide, but measure only the absorbance at 550 nm (reading 3). Absorbance 1 gives the iron concentration from the calibration graph for iron(II). The difference between absorbances 2 and 3 gives the copper concentration from the calibration graph for copper(II).

RESULTS AND DISCUSSION

QATB immediately gives a very stable dark brown complex with iron(II) and a red complex with copper(II) in the neutral pH range, but corresponding precipitates when the ethanol concentration is below 40%. At ethanol concentrations >40% the precipitates dissolve. Higher ethanol levels do not affect the absorbance of the complex. Figure 1 shows the spectra of the complexes in 50% v/v aqueous ethanol solution buffered with sodium acetate (final concentration $0.1M$), the optimal conditions. Table 1 records the physicochemical characteristics of the complexes. Both complexes have 1:2 metal:ligand molar ratio.

In sodium acetate medium only iron(II) and copper(II) produce colour reactions with QATB; other transition metals only form coloured complexes in either concentrated sodium hydroxide medium or at above pH 10. Addition of 1–2 ml of 2% thiosemicarbazide solution completely prevents interaction of copper(II) with QATB but has no effect on formation of the iron(II) complex. The iron(II) complex has considerable absorbance at 550 nm, at which the copper complex has maximum absorbance, but

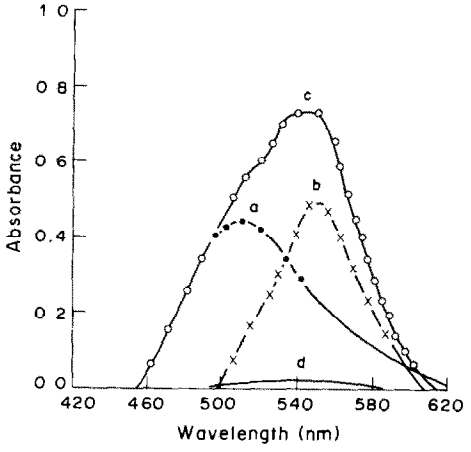

Fig. 1. Absorption spectra of (a) iron-QATB (b) copper-QATB complexes, (c) mixed in equal concentration (d) copper-QATB complex in presence of thiosemicarbazide, measured against reagent blank in sodium acetate medium; Fe 1.1 ppm, Cu 1.3 ppm, QATB $4 \times 10^{-4} M$.

this can be corrected for as described in the procedure, by measuring the absorbance at 550 nm in the presence and absence of thiosemicarbazide, for equal aliquots of sample.

Iron(II) also forms a coloured complex with QATB at neutral pH. When iron(II) is oxidized to iron(III) with nitric acid or persulphate and the pH is adjusted to 7.0–8.0, QATB produces a dark brown 1:2 complex with molar extinction coefficient of 1.8×10^4 $l.mole^{-1}.cm^{-1}$ at 510 nm, but hydrogen peroxide prevents the colour formation when it is used for oxidation purposes. Iron can, therefore, be determined in either of the oxidation states with the same accuracy at pH 8.0.

Effect of diverse ions

In the determination of iron(II) and copper(II) at the 1.12 μg/ml and 1.27 μg/ml level respectively, fluoride, chloride, bromide, iodide, thiocyanate, nitrate, nitrite, sulphite, sulphate, alkaline-earth metals, lanthanides, aluminium, indium, antimony(III), bismuth, chromium(III), platinum metals [except palladium(II)], thorium, cerium and tin(II) do not interfere. Cyanide, EDTA, nickel, cobalt(II) and vanadium(V) interfere seriously in both cases, even in 1:1 mole ratio to the analyte. Sulphide and phosphate also interfere in the iron(II) determination. Certain metal ions are precipitated at the pH used and the precipitates should be removed by centrifugation. For other ions, the tolerance limits, defined as the concentration (μg/ml in the final solution) causing a deviation of less than ±2% in the absorbance, are as follows. For iron(II): thiosulphate, 200; citrate, 50; molybdenum(VI), tungsten(VI), 40; oxalate, borate, uranium(VI), cadmium, mercury(II), palladium(II), 20; copper(II), silver (both masked by thiosemicarbazide), 10. For copper(II): sulphide, thiocyanate, citrate, tartrate, 100; phosphate, oxalate, molybdenum(VI), tungsten(VI), 40; borate, 25; cadmium, mercury(II), 20; palladium (II), silver (without masking), 10 (masking with thiocyanate and iodide respectively), 25; zinc, manganese(II), 5.

Table 1. Physicochemical and analytical characteristics of the complexes

Characteristic	Fe-QATB	Cu-QATB
λ_{max}, *nm*	510	550
pH range	8.0–10.0	7.0–9.0
Moles of reagent required per mole of metal ion for complete complexation	6	10
Beer's law validity range, *ppm*	0–3.0	0–3.0
Ringbom optimum concentration range, *ppm*	0.65–2.7	0.36–2.4
Molar absorptivity at λ_{max}, $l.mole^{-1}.cm^{-1}$	1.86×10^4	2.54×10^4

Table 2. Results for quadruplicate determination of iron in foodstuffs

Food sample	Sample ashed, *g*	Fe found, *μg*	Fe added, *μg*	Total Fe recovered, *μg*	Range of recovery, %
Wheatflour	5.0	3.75, 3.68, 3.70, 3.55	11.2	15.0, 14.5, 14.8, 14.9	97.5–101.2
Rice	5.0	9.57, 9.50, 9.48, 9.64	11.2	21.5, 21.0, 19.8, 21.2	95.7–103.7
Potato-chips	4.0	3.30, 3.40, 3.38, 3.25	11.2	15.0, 14.3, 15.0, 14.0	96.9–103.5
Apple	5.0	16.1, 16.2, 16.0, 15.2	10.2	26.9, 26.2 26.4, 25.0	98.2–102.2
Banana	5.0	8.09, 8.24 8.18, 8.12	11.2	19.5, 18.9, 19.4, 19.1	97.2–100.8
Tomato	5.0	13.7, 13.1, 13.8, 13.8	11.2	25.4, 25.2, 24.8, 25.2	99.2–103.5
Peas	3.0	5.26, 5.30, 5.18, 5.10	11.2	16.9, 16.5, 16.6, 16.0	99.7–102.6

Table 3. Results for quadruplicate determination of copper in foodstuffs (5-g samples)

Food sample	Cu found, μg	Cu added, μg	Total Cu recovered, μg	Range of recovery, %
Wheatflour	2.89, 2.82, 2.79, 2.94	12.7	15.8, 15.3, 16.0, 15.0	97.0–102.2
Rice	8.16, 8.26, 8.20, 8.09	12.7	21.4, 21.2, 20.5, 19.5	93.5–102.6
Tomato	5.00, 5.09, 5.05, 5.15	12.7	17.2, 17.6, 18.0, 18.2	97.3–102.5
Cabbage	6.85, 6.81, 6.93, 6.89	12.7	20.0, 19.1, 19.0, 18.7	95.5–102.3
Apple	5.58, 5.51, 5.49, 5.47	12.7	18.0, 18.7, 18.5, 17.7	97.1–102.7
Banana	3.38, 3.32, 3.43, 3.29	12.7	16.5, 16.2, 15.8, 16.0	98.9–102.7

APPLICATIONS

Some foodstuffs and fruits which contain negligible amounts of cobalt and nickel in comparison to iron or copper were selected for analysis. Body tissues are also found to contain negligible amounts of cobalt and nickel, but fair amounts of iron and copper. Milk contains very little iron, so only copper was determined in the milk samples.

Determination of iron and copper in foodstuffs

Wet-ash 5 g of food or fruit (dried for ~24 hr at ~70° in an oven) with nitric and perchloric acids.[4,5] Take up the ash with 5 ml of hydrochloric acid (1 + 9) and evaporate to dryness; repeat this step. Dissolve the dry residue in water, filter the solution into a 25-ml standard flask, add 1 or 2 drops of concentrated hydrochloric acid and make up to volume. Analyse 1-ml aliquots as already described, adjusting the pH to 7–8 with dilute sodium hydroxide solution.

Determination of iron in body tissues

Wet-ash 5-g sample with a 1:1 mixture of nitric acid and perchloric acids.[6,7] Evaporate the solution to dryness and ash the residue at 300°. Dissolve the ash in 2 ml of 1*M* sulphuric acid, make up to volume in a 25-ml standard flask and determine iron as already described, adjusting the pH to 7–8 with dilute sodium hydroxide solution.

Determination of copper in milk samples

The amount of natural copper present in fresh raw milk is rather low and the "oxidized" flavour of milk is correlated with the copper content.[1] Excess of copper is objectionable and is indicative of contamination. Hence its determination in milk is of importance during processing. Milk samples are usually dry-ashed for copper determination, and though time-consuming, this method is considered to be the most accurate.[8,9]

Add 100 ml of milk dropwise to a heated crucible to evaporate it without frothing. After the moisture has been removed, heat strongly to 450–500°. Cool and add 1 ml of concentrated nitric acid. Evaporate to dryness and ignite again at 450–500° for ~1 hr. Take utmost care to avoid loss by sputtering. Dissolve the white ash in the minimum of dilute nitric acid and make up to volume in a 10-ml standard flask. Pipette a 1-ml aliquot and determine the copper

Table 4. Contents of iron in body tissues (quadruplicate 5-g samples)

Sample	Aliquot taken, ml	Fe found, μg	Fe added, μg	Total Fe recovered, μg	Range of recovery, %
Prostate	1.0	6.77, 6.57, 6.48, 6.32	11.2	18.4, 18.0, 17.4, 17.0	98.4–102.4
Benign enlargement of prostate	0.5	12.9, 12.8, 12.8, 12.7	11.2	24.2, 23.5, 23.8, 23.6	97.8–100.6

Table 5. Recovery of copper from various milk samples by the dry-ashing procedure (quadruplicate analyses)

Sample	Cu found, μg	Cu added, μg	Cu recovered, μg	Range of recovery, %
Cow milk	4.06, 4.09, 4.08, 3.39	12.7	16.5, 17.1, 16.2, 16.2	96.8–101.9
Buffalo milk	3.86, 3.94, 3.58, 3.73	12.7	16.4, 16.9, 16.6, 16.1	98.9–101.7

contents as already described (in all cases adjust the pH to 7–8 with dilute sodium hydroxide).

Results for these analyses are given in Tables 2–5. Recovery experiments with spiked samples gave 95–104% recovery for iron and 93–103% for copper.

Acknowledgement—One of the authors (Mrs. P) is thankful to the Council of Scientific and Industrial Research, New Delhi, India for financial assistance.

REFERENCES

1. R. L. King and W. L. Dunkley, *J. Dairy Sci.*, 1959, **42**, 420.
2. I. Singh and Mrs. Poonam, *Talanta*, 1984, **31**, 109.
3. A. I. Vogel, *A Text Book of Quantitative Inorganic Analysis*, 4th Ed., Longmans, London, 1978.
4. M. M. Barling and C. V. Banks, *Anal. Chem.*, 1964, **36**, 2359.
5. J. F. Goodwin and B. Murphy, *Clin. Chem.*, 1966, **12**, 58; *Anal. Abstr.*, 1967, **14**, 3378.
6. V. Kauppinen, *Suomen Kem. B*, 1961, **34**, 27; *Anal. Abstr.* 1961, **8**, 3856.
7. G. Ceniotti and L. Spandrio, *Clin. Chim. Acta*, 1961, **6**, 233.
8. A. A. Schilt and P. J. Taylor, *Anal. Chem.*, 1970, **42**, 220.
9. G. L. Traister and A. A. Schilt, *ibid.*, 1976, **48**, 1216.

Talanta, Vol. 32, No. 5, pp. 391–394, 1985
Printed in Great Britain

0039-9140/85 $3.00 + 0.00

APPLICATION OF ORGANIC SOLVENT-SOLUBLE MEMBRANE FILTERS IN THE PRECONCENTRATION AND DETERMINATION OF TRACE ELEMENTS: SPECTROPHOTOMETRIC DETERMINATION OF PHOSPHORUS AS PHOSPHOMOLYBDENUM BLUE

SHIGERU TAGUCHI, EIYUKI ITO-OKA, KEIKO MASUYAMA,
ISSEI KASAHARA and KATSUMI GOTO
Faculty of Science, Toyama University, Toyama, 930 Japan

(*Received* 25 *July* 1984. *Accepted* 19 *December* 1984)

Summary—A simple and rapid preconcentration technique, based on collecting trace elements on a membrane filter and dissolving the membrane filter in an organic solvent, has been applied to the spectrophotometric determination of phosphorus in water. Phosphorus, 0.5–7 μg in 50–500 ml of water sample, is collected as phosphomolybdenum blue on a nitrocellulose or acetylcellulose membrane in the presence of n-dodecyltrimethylammonium bromide, the membrane is dissolved in 5 ml of dimethylsulphoxide (DMSO), and the absorbance of the DMSO solution is measured at 710 nm against a reagent blank. Moderate concentrations of silicate, anionic and non-ionic surfactants and high concentrations of sodium chloride do not interfere. Interference from arsenate can be eliminated by reducing the arsenate to arsenite. Condensed and organic phosphates can be determined if they are first converted into orthophosphoric acid by digestion with persulphate. The limit of determination is 0.002 μg of phosphorus in 100 ml of sample.

Adsorption on hydrophobic adsorbents is a simple and reliable means of preconcentrating trace elements from water.[1] We have proposed the use of C_{18}-bonded glass beads, C_{18}-bonded silica gel and polypropylene wool for this purpose. Traces of metals, phosphorus and arsenic can be adsorbed as coloured complexes on these adsorbents, eluted with a small volume of eluent, and determined either by spectrophotometry, inductively-coupled plasma atomic emission spectrometry or anodic stripping voltammetry.[2–9]

Recently we have proposed a simpler and faster preconcentration technique,[10] which is based on collecting trace elements as complexes on a membrane filter and dissolving the filter in a small volume of organic solvent. This technique was applied to the spectrophotometric determination of phosphorus. The phosphorus was collected as phosphomolybdenum blue on a nitrocellulose or acetylcellulose membrane in the presence of n-dodecyltrimethylammonium bromide, and the membrane was dissolved in a small volume of dimethylsulphoxide (DMSO). The absorbance of the DMSO solution was measured at 710 nm against a reagent blank. A 100-fold enrichment could easily be achieved and μg/l. levels of phosphorus determined with satisfactory precision. Because our earlier paper was only a preliminary report, we now present the method in more detail.

EXPERIMENTAL

Reagents

Ammonium molybdate solution.[11] Dissolve 6 g of ammonium heptamolybdate tetrahydrate and 0.24 g of potassium antimonyl tartrate in 500 ml of 3*M* sulphuric acid.

L-Ascorbic acid solution.[11] Dissolve 7.2 g of L-ascorbic acid in 100 ml of water. Prepare fresh daily.

Mixed reagent.[11] Mix 50 ml of the ammonium molybdate solution and 10 ml of the L-ascorbic acid solution. Prepare fresh daily.

Standard phosphorus solution. Prepare by dissolving an appropriate amount of potassium dihydrogen phosphate in water.

n-Dodecyltrimethylammonium bromide (C_{12}TMAB) solution. Dissolve 0.08 g of C_{12}TMAB in 100 ml of water. If necessary, remove any phosphate in this solution in the following manner:[12] add 0.5 ml of 10% aluminium sulphate solution to 100 ml of the C_{12}TMAB solution, adjust the pH to 8.5 with aqueous ammonia, stir for about 15 min, and filter off the aluminium hydroxide formed.

Reducing agent. Prepared as described by Schouwenburg and Walinga[13] and modified by Johnson.[14] Mix 20 ml of 1.75*M* sulphuric acid, 40 ml of 14% sodium metabisulphite solution and 40 ml of 1.4% sodium thiosulphate solution. Prepare fresh daily.

Membrane filters and holder

Most of the data presented in this paper were obtained with Toyo TM2 membranes (25 mm in diameter, 0.45-μm pore size, nitrocellulose membrane), but other membranes can be used equally satisfactorily as long as they are made of nitrocellulose or acetylcellulose. A Toyo KG-25 filter holder (effective filtration area 1.3 cm^2) was used.

Procedure

Take 100 ml of sample solution, containing less than 7 μg of phosphorus, add 8 ml of the mixed reagent, set aside for at least 15 min in a water-bath controlled at 20–40°, then add 1 ml of C_{12}TMAB solution (samples up to 500 ml in volume can be used if 8 ml of mixed reagent and 1 ml of C_{12}TMAB solution are added per 100 ml of sample). Filter off the phosphomolybdenum blue on the membrane filter, and wash the membrane with about 20 ml of water. Dissolve the filter in 5 ml of DMSO, and measure the absorbance of the DMSO solution at 710 nm against a reagent blank.

RESULTS AND DISCUSSION

Optimum conditions for colour development

The conditions for the formation of the phosphomolybdenum blue[11] and the masking of arsenic(V)[13,14] are similar to those reported by earlier workers. The volumes of reagents added are varied in proportion to the sample volume. A 15-min reaction time is sufficient for complete colour development.

Cationic surfactant

The collection of phosphorus as phosphomolybdenum blue on membrane filters was originally proposed by Hiiro *et al.*,[15] but was not quantitative, and the fraction retained on the filter varied widely, depending on the manufacturer and the pore size of the membranes used.

During the course of our study, our attention was drawn to a paper by Ohashi *et al.*,[16] stating that the addition of zephiramine, a cationic surfactant, greatly enhanced the extractability of phosphomolybdenum blue. This led us to examine the use of cationic surfactants to enhance the adsorption of phosphomolybdenum blue on membrane filters. Of those tested, dodecyltrimethylammonium bromide (C_{12}TMAB) was the most satisfactory.

Figure 1 shows that the absorbance of the DMSO solution increases with increasing amount of C_{12}TMAB added and reaches a constant value with at least 0.5 ml of 0.08% solution per 100 ml of sample.

Membrane filter for collection

Several filters of different sorts and pore-sizes were examined for their usefulness for collecting phosphomolybdenum blue. Nitrocellulose and acetylcellulose membrane filters are suitable because they readily dissolve in DMSO. Although any nitrocellulose membrane filter with pore sizes between 0.2 and 0.45 μm can be used, 0.45-μm filters are recommended because of their higher filtration rate.

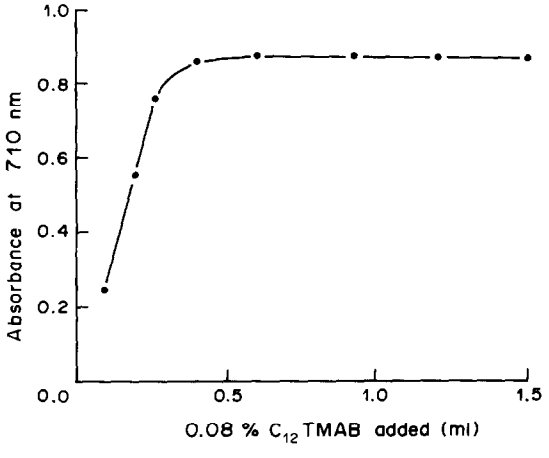

Fig. 1. Effect of C_{12}TMAB on the absorbance from 7.3 μg of P per 100 ml.

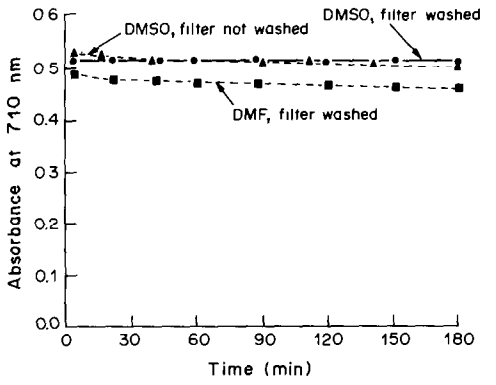

Fig. 2. Effect of different solvents on the absorbance and stability of phosphomolybdenum blue (P 4.17 μg).

Solvent

Several water-miscible organic solvents were tested as solvents for the wet membranes. DMSO, *N,N*-dimethylformamide (DMF) and acetone readily dissolve the nitrocellulose and acetylcellulose membranes, but acetone is not recommended, because of its high volatility.

Figure 2 shows the stability of the colour of phosphomolybdenum blue in DMSO and DMF. The colour intensity decreases slightly with time in DMF, but only very slowly in DMSO. If the membrane is washed with water before being dissolved in DMSO, the colour intensity is stable for at least 3 hr. Other water-miscible solvents, such as ethanol, methanol and acetonitrile, will not dissolve the membrane at room temperature.

Absorption spectrum

The visible-region absorption spectrum of phosphomolybdenum blue in DMSO is shown in Fig. 3. There are two absorption maxima: one at 710 nm and the other at 875 nm. The first was chosen for use, in view of the useful wavelength range of most spectrophotometers. Beer's law is obeyed for 0.5–7 μg of phosphorus in 5 ml of DMSO at both wavelengths.

Sensitivity and precision

Table 1 shows that microgram quantities of phosphorus in 50–500 ml of sample can be determined

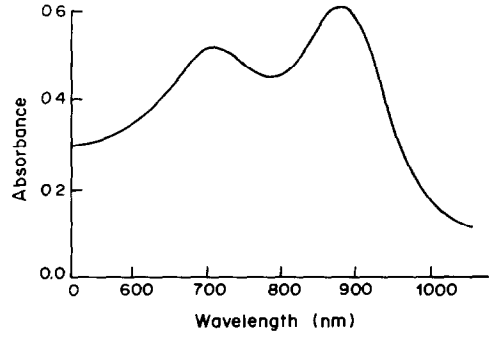

Fig. 3. Absorption spectrum of phosphomolybdenum blue in DMSO (P 0.834 μg/ml).

Table 1. Collection of phosphorus from different sample volumes

P taken, μg	Volume of aqueous sample, ml	P concn., μg/l.	Absorbance at 710 nm	C.V.,† %	No. of detns.
0.522	500	1.04	0.062	2.2	5
	200	2.61	0.062	1.8	5
	100	5.22	0.062	1.1	5
2.09	200	10.4	0.255	0.8	5
	50	41.7	0.251	0.9	5
3.13	100	31.3	0.386	0.7	10
4.17	100	41.7	0.517	0.8	5
	50	83.4	0.517	0.8	5
7.30	100	73.0	0.898	0.6	5
	50	146	0.889	0.7	5

*Filter dissolved in 5 ml of DMSO.
†Coefficient of variation.

with satisfactory precision. The lower limit of determination (taken as three times the standard deviation of the blank) is about 0.002 μg of phosphorus per 100 ml of sample.

Efficiency of collection

The collection efficiency was estimated by determining the phosphorus on the membrane after digestion of the membrane in a mixture of nitric and perchloric acids.[17] The results indicated that more than 99% of the phosphorus was retained on the filter from 100 ml of water containing 3 μg of phosphorus.

Table 2. Effect of foreign substances on the determination of 3.13 μg of phosphorus in 100 ml of sample

Substance	Concn., mg/l.	Absorbance at 710 nm	Error, %
None	—	0.386	—
Silicate	100 (as SiO_2)	0.389	+0.7
SSS*	0.5	0.384	−0.5
	1.0	0.378	−2.1
Triton X-100†	1.0	0.393	+1.8
As(V)	0.1	0.716	+85
	1.0	0.393§	+1.8§
	5.0	0.404§	+4.7§
NaCl	0.5*M*	0.389	+0.7

*Sodium di(2-ethylhexyl)sulphosuccinate; anionic surfactant.
†Non-ionic surfactant.
§In the presence of 10 ml of reducing agent

Effect of foreign substances

Silicate, arsenate and germanate also form molybdenum blues. Of these, germanate is not likely to be present in concentrations high enough to cause significant interference. Table 2 shows the effects of commonly occurring substances on the determination of phosphorus. It is clear that moderate concentrations of silicate and anionic and non-ionic surfactants, and high concentrations of sodium chloride, do not interfere.

Arsenate causes large positive errors even when present at very low concentrations, but this interference can be eliminated by reducing the arsenate to arsenite, as shown in Table 3.

Condensed phosphates and organic phosphorus compounds

Phosphorus in the forms of condensed phosphates and organic phosphorus compounds can be determined after conversion into orthophosphoric acid. A common procedure for this step is to heat the sample with potassium persulphate in an autoclave.[18] The Environmental Agency of Japan uses this as the official method. Table 3 shows results for the determination of pyrophosphate, tripolyphosphate and

Table 3. Determination of condensed and organic phosphates after treatment with potassium persulphate (sample volume 100 ml)

Phosphate	P taken, μg	P found, μg	Recovery, %
Sodium pyrophosphate	2.0	1.98	99
	4.01	4.08	102
	6.01	6.02	100
Sodium tripolyphosphate	2.00	1.96	98
	4.00	3.90	98
	6.00	5.86	98
Sodium phenylphosphate	2.00	2.03	101
	4.01	4.06	101
	6.01	5.98	100

Table 4. Analyses of river water and sea-water samples (50 ml) and recovery tests

P added, μg	P found, μg	Recovery of P added, μg	Recovery of P added, %
Sea-water			
none	1.67	—	—
1.04	2.71	1.04	100
2.09	3.69	2.02	97
3.13	4.73	3.06	98
River water			
none	2.82	—	—
1.04	3.83	1.01	97
2.09	4.90	2.08	100
3.13	6.01	3.19	102

phenylphosphate after persulphate digestion. It is clear that our proposed method can be applied successfully to samples digested with persulphate.

Application to river water and sea-water

The proposed method was applied for the analysis of river water and sea-water samples filtered through a 0.45-μm membrane filter. Table 4 shows the analyses of original samples and samples to which known quantities of phosphorus had been added. Recovery of the added phosphorus was nearly quantitative as shown in this table.

CONCLUSION

Solvent extraction is the commonest of the techniques used for the preconcentration of trace elements,[19-21] but can be tedious and time-consuming, and solubility of the organic solvents in the aqueous phase poses limitations on the enrichment factor which can be achieved.

The preconcentration technique proposed in the present paper is simple and very rapid. Once the phosphorus has been converted into phosphomolybdenum blue, collection on a membrane filter and the measurement of the absorbance can be completed in less than 5 min. An enrichment factor of 100 can easily be attained. The proposed technique may find many other applications for the determination of trace elements in water samples.

Acknowledgement—The authors wish to express their thanks to the Tamura Foundation for the Promotion of Science and Technology for supporting part of the investigation.

REFERENCES

1. D. E. Leyden and W. Wegscheider, *Anal. Chem.*, 1981, **53**, 1059A.
2. S. Taguchi and K. Goto, *Talanta*, 1980, **27**, 819.
3. S. Taguchi, K. Goto and H. Watanabe, *ibid.*, 1981, **28**, 613.
4. *Idem*, *Mizushori Gijutsu*, 1981, **22**, 769.
5. S. Taguchi, S. Amano and K. Goto, *Kankyo Gijutsu*, 1981, **10**, 628.
6. S. Taguchi, C. Yoshikura and K. Goto, *Bunseki Kagaku*, 1982, **31**, 32.
7. H. Watanabe, K. Goto, S. Taguchi, J. W. McLaren, S. S. Berman and D. S. Russell, *Anal. Chem.*, 1981, **53**, 738.
8. S. Taguchi, T. Yai, Y. Shimada, K. Goto and M. Hara, *Talanta*, 1983, **30**, 169.
9. S. Taguchi, H. Sugihara, I. Kasahara, K. Goto and M. Hara, *Mizushori Gijutsu*, 1984, **25**, 699.
10. S. Taguchi, E. Ito-oka and K. Goto, *Bunseki Kagaku*, 1984, **33**, 453.
11. J. Murphy and J P. Riley, *Anal. Chim. Acta*, 1962, **27**, 31.
12. M. Aoyama, T. Hobo and S. Suzuki, *Anal. Chim. Acta*, 1983, **153**, 291.
13. J. C. van Schouwenburg and I. Walinga, *ibid.*, 1967, **37**, 271.
14. D. L. Johnson, *Environ. Sci. Technol.*, 1971, **5**, 411.
15. K. Hiiro, T. Tanaka, A. Kawahara, M. Adachi and K. Fukushi, *Bunseki Kagaku*, 1982, **31**, E401.
16. K. Ohashi, T. Suzuki and K. Yamamoto, *ibid.*, 1979, **28**, 523.
17. H. S. Golterman, *Methods for Chemical Analysis of Fresh Waters*, p. 69, Blackwell Scientific Publications, Oxford, 1969.
18. D. W. Mentzel and N. Corwin, *Limnol. Oceanog.*, 1965, **10**, 280.
19. M. A. Chaube and V. K. Gupta, *Analyst*, 1983, **108**, 1141.
20. T. Matsuo, J. Shida and W. Kurihara, *Anal. Chim. Acta*, 1977, **91**, 385
21. S. Motomizu, T. Wakimoto and K. Toei, *Talanta*, 1984, **31**, 235.

Talanta, Vol. 32, No. 5, pp. 395–398, 1985
Printed in Great Britain

0039-9140/85 $3.00 + 0.00
Pergamon Press Ltd

A METHOD FOR THE DETERMINATION OF VANADIUM AND IRON OXIDATION STATES IN NATURALLY OCCURRING OXIDES AND SILICATES

RICHARD B. WANTY and MARTIN B. GOLDHABER
U.S. Geological Survey, MS 916, Box 25046 Denver Federal Center, Denver, CO 80225, U.S.A.

(*Received* 21 *September* 1984. *Accepted* 14 *December* 1984)

Summary—A valence-specific analytical method for determining V^{3+} in ore minerals has been developed that involves two steps: dissolution of a mineral sample without disturbing the V^{3+}/V^{tot} ratio, followed by determination of V^{3+} in the presence of V^{4+}. The samples are dissolved in a mixture of hydrofluoric and sulphuric acids at 100° in Teflon-lined reaction vessels. Tervalent vanadium is then determined colorimetrically by formation of a V^{3+}-thiocyanate complex in aqueous-acetone medium. Fe^{3+} is measured semi-quantitatively in the same solution. The method has been tested with two naturally occurring samples containing vanadium and iron. The results obtained were supported by those obtained by other methods, including electron spin resonance spectroscopy, thermogravimetric analysis, and Mössbauer spectroscopy.

In natural systems, vanadium is present in minerals and waters in the +3, +4 and +5 oxidation states. This fact may be advantageously applied in the determination of the redox state of an entire system. For instance, the presence of tervalent vanadium is an indication of an extremely reducing environment,[1–3] whereas the quadrivalent and quinquevalent states predominate in systems of intermediate and high oxidation potential, respectively. Many analytical techniques have been developed for the determination of total vanadium in rock samples,[4–7] but no techniques have been reported whereby one vanadium oxidation state in a mineral sample is measured in the presence of another. This paper presents an analytical procedure that has been developed to detect tervalent vanadium in minerals in the presence of quadrivalent vanadium. Tervalent iron in the minerals is also measured. The method has been tested with samples of the mineral roscoelite, a vanadiferous mica, and of a vanadium oxide phase from a sandstone-hosted vanadium–uranium orebody from the Colorado Plateaus. The results should aid in the interpretation of the processes of ore genesis and contribute to our understanding of the importance of redox processes in ore genesis.

EXPERIMENTAL

Sample collection and handling

Vanadium(III) is unstable in the presence of oxygen. Therefore, all sample handling must be done in an inert atmosphere. In this study, high-purity nitrogen containing <50 ppm of oxygen was used. Roscoelite samples were obtained from an inactive mine at Placerville, Colorado. Samples of vanadium oxide were collected from freshly exposed faces in the Tony M mine, near Hanksville, Utah. The samples were stored in Mason jars flushed with nitrogen immediately after sample collection.

Once the samples had been collected and brought back to the laboratory, all sample handling (grinding, size and density separation) was done under nitrogen in a glove-bag. All reagents which were to contact the samples were purged with nitrogen for at least 30 min. The efficiency of this purging process was verified by Winkler titration.[9] Heavy-mineral separations were performed with fresh bromoform which had been purged with nitrogen for >2 hr, and the samples were then rinsed with nitrogen-purged acetone. All size and density fractions were dried in a vacuum desiccator and stored in nitrogen-purged desiccators.

Although the roscoelite samples were not collected from freshly exposed mine faces, repeated analyses over the course of several months showed no change in the V^{3+}/V^{tot} ratio. Similar experiments on the vanadium oxide mineral showed that after several weeks significant oxidation had occurred. Typical results (vanadium oxide sample TM-5 from the Tony M mine) are shown in Fig. 1. The analysis at zero time corresponds to a fresh sample stored under nitrogen. After one week of exposure to air, the V^{3+}/V^{tot} ratio was virtually unchanged from the initial value of 0.82. After 6 weeks, the ratio had dropped to a value of 0.46. A split of the sample was stored in a cloth bag to allow complete exposure to air. Analysis of this split after 22 months exposure to air gave a V^{3+}/V^{tot} ratio of 0.10, assumed to be the lowest achievable value. It is interesting to note that two of the four analyses reported by Weeks *et al.*[8] on the vanadium oxide mineral montroseite yielded V^{3+}/V^{tot} ratios of approximately 0.15, and a third showed no V^{3+}. These values are close to our "infinite time" value of 0.10, suggesting that the earlier analyses[8] were performed on oxidized material.

Reagents

Ammonium thiocyanate solution (*2.50*M) *in acetone*. Dissolve 28.5 g of reagent-grade ammonium thiocyanate in 150 ml of acetone. Prepare fresh daily.

Stock vanadium solution (*0.050*M). Dissolve 0.585 g of reagent-grade ammonium metavanadate, NH_4VO_3, in 100 ml of 6*M* hydrochloric acid. On standing for about 2 months, this solution will turn bright blue as quinquevalent vanadium is reduced to the quadrivalent form, with liberation of chlorine.

Procedure

Introduce the samples (approximately 0.1 g) into the reaction vessels. Add to each 5.0 ml of 5*M* sulphuric acid and 5 ml of concentrated hydrofluoric acid, and seal the

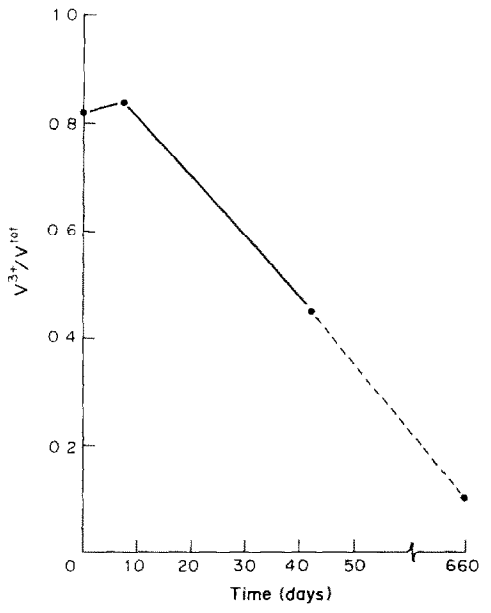

Fig. 1. Effect of time on the oxidation of the vanadium oxide sample TM-5 collected from the Tony M mine. The data point at 660 days represents the V^{3+}/V^{tot} ratio of the sample stored in air.

bombs. Heat the bombs at 100° for 3 hr in a vacuum oven. Prepare standard solutions of V^{3+} in 25-ml standard flasks by mixing portions of V^{4+} stock solution (2, 5, 10 and 25 μl) with 2 ml of concentrated hydrochloric acid and adding about 50 mg of crystalline stannous chloride dihydrate, and leave for an hour to reduce the V^{4+} quantitatively to V^{3+}. Prepare two reagent blanks, one with and one without stannous chloride. Set aside two standard flasks for each sample, one with and one without stannous chloride. On completion of the 3-hr digestion period, quench the bombs and put them in a glove-bag filled with nitrogen. Withdraw 5 ml of solution from each of the bombs and accurately dilute each to 50 ml with saturated boric acid solution. Using an automatic pipette, transfer pairs of 1.0-ml portions of these solutions to the pairs of sample flasks. Add 15 ml of thiocyanate solution to each flask, and dilute to volume with distilled water. Quickly measure the absorbance of the unreduced solutions at 475 and 395 nm. Calculate the V^{3+} content from the calibration graph for the standards measured at 395 nm. Determine the Fe^{3+} content from the differences in absorbance at 475 nm for the pairs of unreduced and reduced solutions. Use distilled water as reference, and correct the sample absorbances for the absorbance of appropriate reagent blanks. Determine the total V and Fe concentrations by atomic-absorption spectroscopy or some other method.

RESULTS AND DISCUSSION

Sample decomposition and analysis

The samples were decomposed in Teflon-lined reaction vessels similar to those described by Bernas.[10] The Teflon liners were found to be somewhat porous. To avoid oxidation by residual air in the pores during sample dissolution, all the Teflon liners were kept for at least 3 days in a vacuum oven at 100° prior to use. Experiments in which a V^{3+} solution was kept in the degassed bombs for the normal digestion period showed that no oxidation then occurred. Therefore, the three-day purging process is sufficient to remove all air.

Initial dissolution experiments involved heating with a 1:1 mixture of 5*M* hydrochloric acid and concentrated hydrofluoric acid at 100° for 3 hr. The results were widely scattered and did not vary systematically with any of the controlled variables (temperature, duration of decomposition, *etc.*). In subsequent experiments, this acid mixture was found to reduce V^{4+} to V^{3+} spontaneously under the conditions of the dissolution.[11] This reduction seems to be catalysed by iron, and the varied concentrations of iron in the samples (and subsequent solutions) may have been the cause for the wide scatter in the data. After this finding, the acid mixture was replaced by a 1:1 mixture of 5*M* sulphuric acid and concentrated hydrofluoric acid in all further experiments. "Blank" decompositions done with a V^{4+} or V^{3+} solution in the new acid mixture verified that no oxidation or reduction occurs as a result of redox reactions between vanadium and the acids used. Approximately 0.1–0.2 g of sample was used with 10 ml of the acid mixture. The mineral samples were completely dissolved by heating for 3 hr at 100°.

After formation of the strongly coloured vanadium thiocyanate complex, the solutions were analysed colorimetrically. This method was first proposed by Furman and Garner.[12] Crouthamel *et al.*[13] modified the method by using an acetone–water (3:2 v/v) medium. We have further modified the technique as described below, to remove the interference by ferric iron, which is present in the samples and also forms a strongly coloured thiocyanate complex. The absorbance maximum, λ_{max}, for the V^{3+}–thiocyanate complex is at 395 nm, and λ_{max} for the Fe^{3+}–thiocyanate complex is at 475 nm.

The Fe^{3+}–thiocyanate complex absorbs significantly at the λ_{max} of the V^{3+}–SCN complex. This interference may be easily removed by the addition of a small amount ($\sim$50 mg) of crystalline stannous chloride. The ferric iron is immediately reduced to the ferrous state, which has no coloured thiocyanate complex, but the V^{3+} is not affected. Any V^{4+} in solution is also unaffected during the time needed for the analysis (<1 hr after preparation of the solutions). To prove this point, V^{4+} solution was added to a test solution containing V^{3+} and stannous chloride. The absorbance was monitored for about 1 hr, and no change was detected. The absorbance of the V^{3+}–thiocyanate complex at λ_{max} for the Fe^{3+}–thiocyanate complex is minimal and automatically compensated in the procedure, since it should be identical for the reduced and unreduced solutions, and the difference between the absorbances gives the absorbance of the ferric iron complex.

The V^{3+} complex obeys Beer's law at 395 nm up to a V^{3+} concentration of $5 \times 10^{-5}M$. The ferric complex obeys Beer's law up to an Fe^{3+} concentration of $3.6 \times 10^{-5}M$. The concentration of thiocyanate is kept constant at 1.50*M*. The molar

absorptivities are 1.2×10^4 l.mole^{-1}.cm^{-1} for the V^{3+}-complex at 395 nm and 2.3×10^4 for the ferric complex at 475 nm. The limit of detection for V^{3+} is approximately $5.0 \times 10^{-7}M$, and that for Fe^{3+} is approximately $3.6 \times 10^{-7}M$. Repeated runs gave V^{3+}/V^{tot} ratios that agreed within ± 0.07. The technique was validated as described below.

Typical concentrations of V^{3+} in the sample solutions ranged from 0.2 to $4.0 \times 10^{-5}M$, and Fe^{3+} concentrations in the same solutions ranged from 0.72 to $7.2 \times 10^{-6}M$. The vanadium oxide minerals had V^{3+}/Fe^{3+} molar ratios between 2 and 7, and the vanadiferous clays had ratios close to unity.

The stoichiometry of the V^{3+}–thiocyanate complex is somewhat uncertain. Furman and Garner[12] applied Job's method and found the complex was probably 1:1, but the Job plot indicates that the complex is quite weak and does not preclude the existence of higher complexes. The ferric thiocyanate complex is 1:1, as determined by a variety of techniques.[14,15]

Validation of the procedure

Various simple experiments were run in order to show that the results are not affected by any redox reactions that occur during the decomposition or analysis. In addition, samples were analysed by the procedure developed and the results compared favourably with those of other techniques that do not require sample decomposition prior to analysis. The advantage of the technique reported here is that it does not require any exotic apparatus or expensive electronic equipment.

Three sets of experiments were performed to ascertain that no redox reactions occur during the decomposition procedure. In the first set, a solution of V^{3+} was added to the sulphuric/hydrofluoric acid mixture and heated for 3 hr at 100°; all the V^{3+} was recovered, *i.e.*, no oxidation of V^{3+} had occurred. A corresponding run with V^{4+} verified that no reduction of V^{4+} took place. Finally, in a run with V^{4+} and a known mixture of ferrous and ferric iron no V^{3+} was produced, and the initial and final ferrous/ferric ratios were identical. The samples that were to be analysed by this and other independent methods contained tervalent vanadium and iron, so there was the possibility of a redox reaction between them to produce V^{4+} and Fe^{2+}. Test runs were performed in which known amounts of Fe^{3+} or V^{3+} were added to the reaction vessel with a sample. In all cases, the additional V^{3+} or Fe^{3+} was recovered, verifying that no redox reactions occur. A possible reason for this is the formation of fluoride complexes of V^{3+} and Fe^{3+}, which would tend to inhibit any such reaction, though the fluoride present should be almost all in the protonated form at the acidity used.

The validity of the method when applied to minerals was established by analysing two standard samples and comparing the results with those of independent techniques.

The first standard was roscoelite, a vanadiferous mica, from Placerville, Colorado. Roscoelite from other localities has been reported to contain predominantly tervalent vanadium.[16–18] In the sample used in this study, 85% of the vanadium was found to be in the tervalent state. The presence of a small amount of quadrivalent vanadium was confirmed by electron spin resonance (ESR) spectroscopy, but the result was not quantitative. The V^{3+}/V^{tot} ratio (0.85) was also supported by thermogravimetric analysis (TGA). The TGA was run from 20° to 900° in two phases. The first phase was executed under an atmosphere of high-purity nitrogen. The sample was observed to lose weight as adsorbed water, structural water, and structural hydroxide ions were lost. The apparatus was then cooled, and the TGA was rerun under an oxygen atmosphere. The sample gained weight as V^{3+} was oxidized to V^{4+}, and then to V^{5+}, and as Fe^{2+} was oxidized to Fe^{3+}. After correction for the weight gain due to Fe^{2+} oxidation, the calculated V^{3+}/V^{tot} ratio was approximately 0.5. Assuming the oxygen content of the high-purity nitrogen to be 50 ppm (the maximum value specified) it was calculated that the amount of oxygen that would have flowed past the sample during the first heating period would have been sufficient to cause complete oxidation of V^{3+} to V^{5+}. Therefore, the calculated V^{3+}/V^{tot} ratio of 0.5 was taken as a minimum value, consistent with the result of the chemical determination, but somewhat inconclusive. The Fe^{3+}/Fe^{tot} ratio was found to be approximately 0.05 by our technique, near the detection limit for Fe^{3+}. This result compares favourably with the value of 0.10 found by Mössbauer spectroscopy.[19]

The second sample (TM-1) was a vanadium oxide mineral collected in the Tony M mine near Hanksville, Utah. The sample was collected as already described. The V^{3+}/V^{tot} ratio found by our method was 0.37 and the Fe^{3+}/Fe^{tot} ratio 0.75 ± 0.08. The Fe^{3+}/Fe^{tot} ratio determined by Mössbauer spectroscopy[19] was 0.75 ± 0.05. The V^{3+}/V^{tot} ratio was not checked by independent methods. The results of four replicate analyses of sample TM-1 (Table 1) are fairly close, and the Fe^{3+}/Fe^{tot} ratio agrees very well with the Mössbauer result, indicating that the analysis is reliable. Similar precision was obtained for replicate analyses of the roscoelite sample. The presence of V^{3+} and Fe^{3+} in the same sample indicates a narrow range of redox conditions that could have prevailed during formation of the Tony M orebody. Work is continuing to explore further the implications of this for the ore-forming processes.

Table 1. Replicate analyses of the vanadium oxide sample TM-1 collected in the Tony M mine

V^{3+}/V^{tot}	Fe^{3+}/Fe^{tot}	V^{tot}/Fe^{tot}
0.41	0.76	4.4
0.39	0.83	4.3
0.37	0.72	4.1
0.31	0.68	4.3

Acknowledgements—We wish to thank Dr. C. G. Whitney of the U.S. Geological Survey for help with the thermogravimetric analysis and Dr. D. L. Williamson of the Colorado School of Mines for performing the Mössbauer analysis. We also thank Mr. D. Underhill of Plateau Resources, Ltd. for permitting access to the Tony M mine. Drs. T. T. Chao and W. H. Ficklin of the U.S. Geological Survey provided excellent constructive reviews of the manuscript. Special thanks go to Dixie Termin for careful typing of the manuscript.

REFERENCES

1. P. B. Hostettler and R. M. Garrels, *Econ. Geol.*, 1962, **57,** 137.
2. J. O. Hill, I. G. Worsley and L. G. Hepler, *Chem. Rev.*, 1971, **71,** 127.
3. D. Langmuir, *Geochim. Cosmochim. Acta*, 1978, **42,** 547.
4. F. N. Ward, H. W. Lakin and F. C. Canney *et al.*, *U.S. Geol. Survey Bull.*, No. 1152, 1963, p. 89.
5. R. Goecke, *Talanta*, 1968, **15,** 871.
6. J. Warren and D. Carter, *Can. J. Spectrosc.*, 1975, **20,** 1.
7. G. Svehla and G. Tölg, *Talanta*, 1976, **23,** 755.
8. A. D. Weeks, E. A. Cisney and A. M. Sherwood, *Am. Mineral.*, 1953, **38,** 1235.
9. D. A. Skoog and D. M. West, *Fundamentals of Analytical Chemistry*, 3rd Ed., p. 750. Holt, Rinehart and Winston, New York, 1976.
10. B. Bernas, *Anal. Chem.*, 1968, **40,** 1682.
11. D. Palermo and S. R. Daniel, Colorado School of Mines, written communication, 1984.
12. S. C. Furman and C. S. Garner, *J. Am. Chem. Soc.*, 1951, **73,** 4528.
13. C. E. Crouthamel, B. E. Hjelte and C. E. Johnson, *Anal. Chem.*, 1955, **27,** 507.
14. H. E. Bent and C. L. French, *J. Am. Chem. Soc.*, 1941, **63,** 568.
15. S. M. Edmonds and N. Birnbaum, *ibid.*, 1941, **63,** 1471.
16. W. F. Hillebrand, H. W. Turner and F. W. Clarke, *Am. J. Sci.*, 1899, **7,** 451.
17. E. W. Heinrich and A. A. Levinson, *ibid.*, 1955, **253,** 39.
18. D. H. Maylotte, J. Wong, R. L. St. Peters, F. W. Lytle and R. B. Greegor, *Science*, 1981, **214,** 554.
19. D. Williamson, Colorado School of Mines, written communication, 1983.

Talanta, Vol. 32, No. 5, pp. 399–405, 1985
Printed in Great Britain

0039-9140/85 $3.00 + 0.00
Pergamon Press Ltd

SORPTION AND PERMEATION BEHAVIOUR OF METAL THIOCYANATE COMPLEXES ON CELLULOSE ACETATE POLYMERS

TAKASHI HAYASHITA and MAKOTO TAKAGI
Department of Organic Synthesis, Faculty of Engineering, Kyushu University, Higashi-ku, Fukuoka 812, Japan

(*Received* 28 *August* 1984. *Accepted* 14 *December* 1984)

Summary—Various metal thiocyanate complexes in aqueous solution were sorbed on solid cellulose acetate polymers. The sorption selectivity increased in the order $Zn^{2+} > Fe^{3+} > Cu^{2+} > Co^{2+} > Ni^{2+}$. The sorption behaviour followed a Langmuir-type adsorption isotherm, and the maximum adsorption capacity was 6.1×10^{-5} mole of complex per g of polymer under optimum conditions. The zinc species sorbed appear to be $NH_4Zn(H_2O)(SCN)_3$ or $(NH_4)_2Zn(SCN)_4$ according to analysis of the sorption equilibrium. The ion-association species formed by the complex zinc anion and the ammonium ion was supposed to be sorbed (or "extracted") onto the polymer matrix. As an application of sorption of metal complexes, a new hyperfiltration process was proposed for selective separation of metal ions. Thus, a mixture of metal thiocyanate complexes was hyperfiltered through cellulose acetate membranes. Permeation of certain metal complexes was preferred, and the selectivity was found to be similar to the sorption selectivity. These findings lead to a generalized idea that hyperfiltration separation of ionic species, particularly anionic metal complexes, can be attained by using polymer membranes which selectively adsorb or extract such ionic species as ion-association complexes onto the polymer matrix.

It is known that metal thiocyanate complexes are effectively extracted in the form of ion-association complexes into oxygen-containing organic solvents,[1,2] and this has been widely used for the separation of metals,[3] but the volatility and toxicity of organic solvents sometimes pose problems in the practical operation of the process. The sorption behaviour of solid polymers has recently been studied, and polymers such as polyurethane foam are found to be effective substitutes for organic solvents for the sorption or "extraction" of some ion-association complexes.[4,5] Several metal thiocyanate complexes are effectively extracted by solid polymers.[6–9]

Metal-selective separation by solid polymer membranes under hydraulic pressure is one of the future membrane technologies yet to be explored. To date, only a few studies have been made of this aspect,[10–13] and the sorption of ion-association complexes may be important in the development of solid membranes which selectively reject metal species or are permeated by them. The principle is that the active membrane phase acts as a "polymer solvent" for the extraction of ion-association complexes and the extracted metal species are transported through the membrane by some coupling processes with a solvent flow under hydraulic pressure. Metal species which lack affinity for the active membrane phase do not permeate it.

The aim of the present study was to examine and verify these ideas. The sorption of metal thiocyanate complexes by polymer membrane materials was studied, and the permeation selectivity of the complexes under hyperfiltration conditions is discussed in the light of the equilibrium sorption behaviour.

EXPERIMENTAL

Reagents

Cellulose acetate (acetyl content 39.8%, ASTM viscosity 3 sec), cellulose acetate butyrate (acetyl content 29.5%, butyryl content 17%, ASTM viscosity 15 sec) and cellulose acetate hydrogen phthalate were purchased from Eastman Kodak Co. Poly(ethylene glycol) succinate, poly(neopentyl glycol) succinate (for gas chromatography) and penta-acetyl-β-D-glucose were purchased from Tokyo Kasei Co. Cellulose (100–200 mesh) and poly(vinyl chloride) ($n = 1100$) were obtained from Toyo Roshi Co. and Wako Pure Chemical Co., respectively. Polyacrylonitrile was gifted by Mitsubishi Reiyon Co. All these polymers were used in powder form (finer than 50 mesh). Other reagents were reagent-grade commercial products and used without further purification.

Stock solutions of metal nitrates (in 0.1*M* nitric acid), ammonium thiocyanate and ammonium nitrate were stored in polyethylene bottles. Concentrations of metal complexes were determined by atomic-absorption spectrophotometry with a Japan Jarrel Ash Co. AA-1 instrument.

Sorption experiment

Metal thiocyanate solutions were prepared by mixing and diluting the stock solutions. An appropriate amount of polymer (2.0 g) was suspended in the solution and the mixture was shaken on a mechanical shaker for 90 min at 25°. The residual metal-ion concentration in the bulk solution was then measured by atomic-absorption spectrophotometry after centrifuging or filtering. A preliminary 3-hr study indicated that shaking for 90 min was sufficient for evaluation of the equilibrium sorption behaviour. The effect of polymer degradation (*e.g.*, by hydrolysis) was neglected. Prolonged shaking (10–15 hr) caused a small increase (~5%) in sorption, but a compromise was made between achieving complete equilibration and risking a possible structural change of the polymer matrix during an extended experiment. In addition, the 90-min equilibration data were better related to the hyperfiltration study, since

Table 1. Sorption of metal thiocyanate complexes on solid polymers*

No.	Polymer	Fe^{3+}	Co^{2+}	Ni^{2+}	Cu^{2+}§	Zn^{2+}
1	Cellulose acetate 398 (CA-398)	63.4	9.6	1.2	47.2	92 2
2	Polyacrylonitrile (PAN)	18.0	6.8	0.8	13.8	57.6
3	Cellulose (CE)	0.0	0.0	0.0	5.6	0.4
4	Poly(vinyl chloride) (PVC)	0.0	0.0	0.0	0.0	0.0
5	Penta-acetyl-β-D-glucose (PAG)	1.2	0.0	0 0	0.0	1.6

*Polymer (2.0 g, powder) was suspended in 20 ml of aqueous solution containing 0.5*M* NH_4SCN, 0.1*M* HNO_3, and 0.5m*M* $M^{II}(NO_3)_2$ or $M^{III}(NO_3)_3$.

§Prolonged contact of cupric ion with thiocyanate ion leads to the formation of cuprous species. The extent of this reaction was difficult to assess under the sorption conditions used. The solution, however, remained completely homogeneous.

the permeation data in the latter were collected in the period from 40 min to 4 hr after the membrane had been set up in the permeation cell (see below).

The sorption behaviour of the complexes were evaluated from the degree of sorption (E) and the distribution ratio (D):

$$E = \frac{[M]_i - [M]_f}{[M]_i} \times 100 \quad (1)$$

$$D = \frac{[M]_i - [M]_f}{[M]_f} \times \frac{V_w}{W_m} \quad (2)$$

where $[M]_i$ and $[M]_f$ are the initial and final metal concentrations, respectively, in the solution; V_w is the volume of solution (ml), and W_m the weight of polymer (g).

Membranes

Cellulose acetate (CA) membranes were prepared by either the casting or the coating method. The cast CA membrane was an asymmetric membrane for reverse osmosis, similar to that described earlier[11] (membrane annealing temperature 87°, membrane thickness, 36–40 μm). Coated CA membranes were prepared by dissolving 0.2 g of cellulose acetate in 40 ml of acetone, spraying the solution onto a "Fluoropore" membrane (pore-size 0.1 μm, Sumitomo Denki Co.) and drying at room temperature, the procedure being repeated until a polymer phase of appropriate thickness was formed (0.3–0.4 mg of CA per cm^2)[13]

Hyperfiltration

A batch type hyperfiltration cell of 16.6 cm^2 effective membrane area and 300 ml feed capacity (Atsuryoku Kiki Engineering Co., Tokyo) was used. The cell was specifically designed for the present purpose. It was protected from corrosion by using either Teflon or dense polyethylene as inner cell material. Permeation experiments were performed at 20 atm and 25°. Before and after each experiment, the membrane was tested for water flux with pressurized pure water, and the absence of any damage or deterioration during the experiment was confirmed.

The permeation experiments were done with 250 ml of feed solution. The first 5 ml of solution permeated were

Table 2. Sorption of zinc(II) thiocyanate complexes on solid polymers*

No.	Polymer	$E^\circ_{,0}$	Structure
1	Cellulose acetate 398 (CA-398)	89	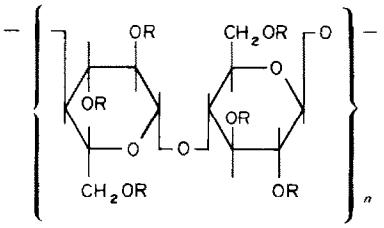
2	Cellulose acetate butyrate 171-15 (CAB-171-15)	22	
3	Cellulose acetate hydrogen phthalate (CAHP)	50	No. 1 R = —H, —$COCH_3$
4	Cellulose (CE)	1	2 —H, —$COCH_3$, —COC_2H_7
5	Penta-acetyl-β-D-glucose (PAG)	4	3 —H, —$COCH_3$, —COC_6H_4COOH
6	Polyacrylonitrile (PAN)	41	4 —H $-(CH_2CH-)_n-$ CN
7	Poly(vinyl chloride) (PVC)	0	$-(CH_2CH-)_n-$ Cl
8	Poly(neopentyl glycol succinate) (PNGS)	52	$-(OCH_2C(CH_3)_2CH_2OCCH_2CH_2C-)_n-$ O O
9	Poly(ethylene glycol succinate) (PEGS)	76	$-(OCH_2CH_2OCCH_2CH_2C-)_n-$ O O

*Polymer (2.0 g, powder) was suspended in 20 ml of aqueous solution (pH = 1) containing 0.5*M* NH_4SCN, 0.1*M* HNO_3, and 1m*M* $Zn(NO_3)_2$.

discarded, and the second 5 ml were collected for analysis. Further fractions were usually not collected, since they were similar to the analysed fraction in composition. The permeability (P) for metal ions was defined as follows:

$$P = \frac{\text{concentration of metal ion in the permeate}}{\text{concentration of metal ion in the feed}} \quad (3)$$

RESULTS AND DISCUSSION

Sorption of metal complexes

Sorption of metal thiocyanate complexes on some typical solid polymers is summarized in Table 1. Sorption of zinc thiocyanate complexes was studied in detail for other varieties of polymer or "monomer" sorbents, and the results are summarized in Table 2. It is seen that a hydrophilic polymer such as cellulose and a hydrophobic polymer such as poly(vinyl chloride) show no sorption capabilities. Metal thiocyanate complexes are sorbed only by polymers with intermediate polarity, such as cellulose acetate and polyacrylonitrile. Cellulose acetate has by far the highest sorption capability. As metal thiocyanates are not sorbed on the monomeric sorbent penta-acetyl glucose, a polymer environment or some microstructure of the solid polymer matrix seems to be of vital importance for sorption to take place.

The degree of sorption of metal thiocyanate complexes on cellulose acetate polymer increases in the order $Zn^{2+} > Fe^{3+} > Cu^{2+} > Co^{2+} > Ni^{2+}$. Under our conditions, cobalt was not effectively sorbed. It has also been reported that cobalt(II) and iron(III) thiocyante complexes are not sorbed on polyester type polyurethane foam.[7,14] On the other hand, it is reported that polyether-type polyurethane foam successfully sorbs these complexes.[6] It is interesting that the chemical structure of the polymer material has such a subtle effect on the sorptivity of metal complexes, analogous to that in metal extraction by organic solvents of various structure and polarity.

Sorption equilibrium

Figure 1 shows the effect of thiocyanate concentration on the sorption of zinc. The degree of sorption (E) increases with thiocyanate concentration. This suggests that complexes such as $(NH_4)_{2-n}Zn(SCN)_n$ are the main species involved in the sorption.

The effect of the medium on the sorption of zinc thiocyanate complexes was studied for cellulose polymers. Addition of ethanol to the bulk aqueous solution first tended to increase the sorption, but further addition caused a strong decrease in the sorption. Thus, plots of E *vs.* ethanol content in the bulk solution show maxima at an ethanol weight fraction of about 0.20–0.25 (Fig. 2). Addition of a small amount of ethanol is considered to promote the formation of sorption-active species (lipophilic ion-association complexes) in aqueous solution. It is also expected that ethanol brings about a sort of swelling effect and increases the effective surface area of the polymer for the sorption of such metal species.

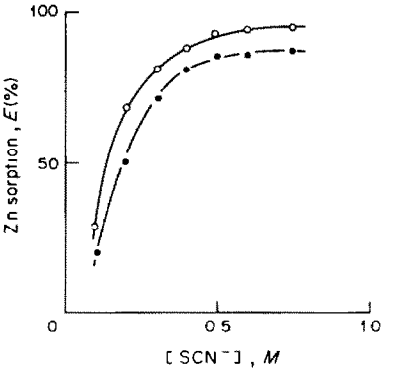

Fig. 1. Effect of thiocyanate concentration on the sorption of zinc on cellulose acetate: 20 ml of aqueous NH_4SCN–HNO_3 solution (pH 1.6) containing 0.5mM $Zn(NO_3)_2$ were used; total concentration of ammonium ion adjusted to 0.75M with NH_4NO_3. Cellulose acetate: 1.0 g (●), 2.0 g (○).

These effects seem to explain the increase in sorption (Fig. 2) when a small fraction of ethanol is added to the aqueous metal salt solution. However, excess of ethanol reduces the dielectric constant of the solution, bringing the polarities (or environments) of the bulk aqueous solution and the polymer matrix closer to each other. This in effect reduces the sorption of ion-association complexes onto the polymer matrix. This behaviour seems to be especially marked in the case of cellulose acetate butyrate.

The effect of pH on the sorption of zinc thiocyanate complexes is shown in Fig. 3. Since the solutions were not well buffered, the pH values were measured immediately after sorption equilibrium was attained. It is seen that sorption of zinc was constant in the pH range 1–6. It is known that cellulose acetate contains a small amount of carboxyl functional groups, and there is a possibility that sorption of zinc is partially due to cation-exchange at the carboxylate sites of the polymer matrix. However, the results in

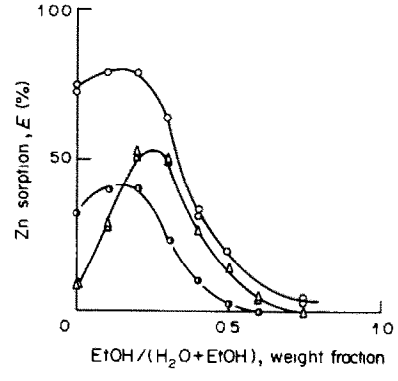

Fig. 2. Effect of ethanol content on the sorption of zinc thiocyanate complexes: 20 ml of solution containing 0.25M NH_4SCN, 25mM HCl, and 0.5mM $Zn(NO_3)_2$ were used. Polymers: cellulose acetate, 0.5 g (◑), 2.0 g (○); cellulose acetate butyrate, 2.0 g (△).

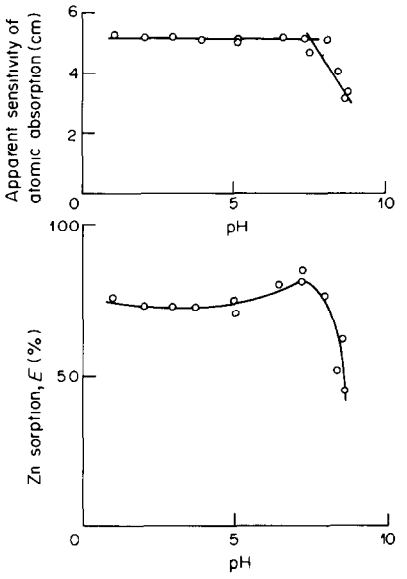

Fig. 3. Effect of pH on the sorption of zinc thiocyanate complexes; 20 ml of 0.25*M* NH_4SCN solution containing 0.5m*M* $Zn(NO_3)_2$ were used. The pH was altered by adding HCl or KOH. The amount of cellullose acetate was 2.0 g. The apparent sensitivity (peak height) of atomic absorption for 0.5m*M* $Zn(NO_3)_2$ in 0.25*M* NH_4SCN solution is shown in the upper figure as a function of pH.

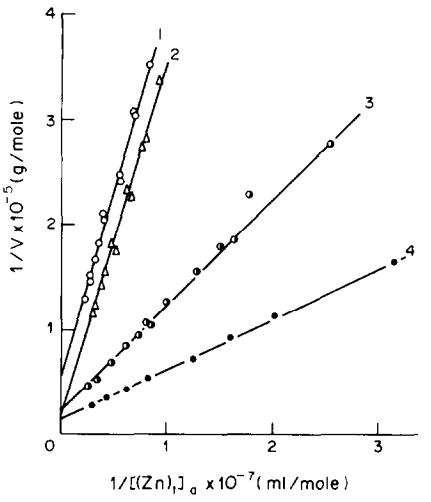

Fig. 4. Langmuir plots for the sorption of zinc thiocyanate complexes on cellulose acetate; 20 ml of solution containing $Zn(NO_3)_2$ in various concentrations were shaken with 0.5–2.0 g of cellulose acetate. The solution contained NH_4SCN in concentrations of 0.25*M* (1, ○), 0.25*M* (2, △; 25 wt% EtOH), 0.50*M* (3, ◑), and 0.75*M* (4, ●).

Fig. 3 indicate that the contribution from the ion-exchange mechanisms is negligible. The decrease in zinc sorption at pH > 7.5 was found to be due to hydrolysis of the metal ions in the bulk solution. This is also experimentally reflected in the decrease of sensitivity in the atomic-absorption measurements (Fig. 3).

Langmuir-type adsorption isotherm

When (*i*) there is no interaction between the sorbed species, (*ii*) the polymer "surface" is homogeneous and has the same sorption characteristics, and (*iii*) only monolayer sorption takes place, the sorption of metal thiocyanate complexes should follow a Langmuir-type adsorption isotherm:

$$\frac{1}{A} = \frac{1}{K_d A_M [(NH_4)_{n-2}M(SCN)_n]_a} + \frac{1}{A_M} \qquad (4)$$

where K_d is the equilibrium constant for adsorption of metal complexes from the bulk solution onto the polymer surface, A is the amount of metal species adsorbed (mole/g), and A_M the maximum adsorption capacity (mole/g). The sorbed species are assumed to have the compositions $(NH_4)_{n-2}M(SCN)_n$ (M is a bivalent metal; $n = 2$–4; co-ordinated or solvation water molecules are not shown).

When the concentration of ammonium thiocyanate in the bulk solution is kept constant, the concentration of complexed species is proportional to the total concentration of metal ion in solution. Thus,

$$[(NH_4)_{n-2}M(SCN)_n]_a = \alpha_n[(M)_t]_a \qquad (5)$$

where $[(M)_t]_a$ is the total concentration of metal and α_n is a conditional proportionality constant for the nth species. Substitution of equation (5) into equation (4) gives equation (6). Plots of $1/A$ *vs.* $1/[(M)_t]_a$ should be linear if a Langmuir-type isotherm is followed (*e.g.*, Fig. 4).

$$\frac{1}{A} = \frac{1}{\alpha_n K_d A_M [(M)_t]_a} + \frac{1}{A_M} \qquad (6)$$

Though the slopes and the intercepts varied with conditions, the plots were all linear within experimental error. The values of $\alpha_n K_d$ and A_M obtained from the plots are listed in Table 3. Increasing the ammonium thiocyanate concentration increases the A_M values (Nos. 1, 3, 4). The A_M value also increases when ethanol is added (Nos. 1, 2). This change is considered to be related to the change in aggregation of the polymer chains at the surface of cellulose

Table 3. Parameters of Langmuir plots for the sorption of zinc thiocyanate complexes on cellulose acetate

No.	$[NH_4SCN]$, M	[EtOH], *wt*%	$\alpha_n K_d \times 10^{-6}$	A_M 10^{-5} *mole/g*
1	0.25	0	1.6	1.9
2	0.25	25	0.5	5.7
3	0.50	0	2.3	4.4
4	0.75	0	3.5	6.1

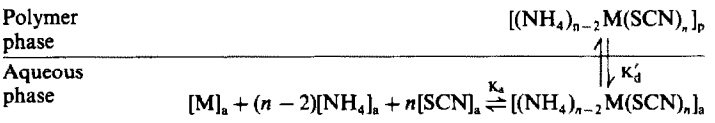

Scheme I. Sorption equilibrium of metal thiocyanate complexes

acetate. Increase in ammonium thiocyanate concentration also leads to increased $\alpha_n K_d$ values. This effect is most probably related to increase in α_n rather than in K_d since formation of the ion-association complexes is favoured by higher thiocyanate concentrations.

Mechanism of sorption

Scheme I shows a simplified expression of the sorption equilibrium, where the sorbent polymer is supposed to be present in sufficient excess for sorption to take place. The sorption and association constants, K'_d and K_a, respectively, are defined in the following equations, where the suffixes p and a refer to the polymer and aqueous phases, respectively:

$$K'_d = [(NH_4)_{n-2}M(SCN)_n]_p/[(NH_4)_{n-2}M(SCN)_n]_a \quad (7)$$

$$K_a = [(NH_4)_{n-2}M(SCN)_n]_a/[M]_a[NH_4]_a^{n-2}[SCN]_a^n \quad (8)$$

The metal distribution ratio (D') and the stepwise metal complex formation constants in aqueous solution are defined conventionally as follows:

$$D' = [(NH_4)_{n-2}M(SCN)_n]_p/[(M)_t]_a \quad (9)$$

$$M(SCN)_{n-1} + SCN \rightleftharpoons M(SCN)_n$$

$$K_n = [M(SCN)_n]/[M(SCN)_{n-1}][SCN] \quad (10)$$

(charges are omitted for simplicity). The concentration of free metal ion in aqueous solution is written as

$$[M]_a = [(M)_t]_a/\beta \quad (11)$$

where

$$\beta = 1 + K_1[SCN] + K_1K_2[SCN]^2 + \ldots + K_1K_2\ldots K_n[SCN]^n \quad (12)$$

Appropriate substitution and rearrangement leads to

$$\beta D' = K'_d K_a [NH_4]_a^{n-2}[SCN]_a^n \quad (13)$$

When ammonium and thiocyanate ions are present in large excess, *i.e.*, $[(NH_4)_t]_a$, $[(SCN)_t]_a \gg [(M)_t]_a$, equation (13) is more conveniently expressed as

$$\log\beta D' = (n-2)\log[(NH_4)_t]_a + n\log[(SCN)_t]_a + \log K'_d K_a \quad (14)$$

Equation (14) indicates that the co-ordination number n can be determined from log–log plots of $\beta D'$ *vs.* thiocyanate concentration. The plot for zinc thiocyanate sorption is linear with a slope of $n = 3.5$.[15] Thus, $NH_4Zn(SCN)_3$ or $(NH_4)_2Zn(SCN)_4$ (or a mixture of the two) seems to be the main sorption species. This result also verifies that the sorption of zinc thiocyanate complexes occurs by sorption of the ion-association complex on the polymer matrix.

The uptake of the ion-association complex by the solid polymer may be considered as due to stabilization of either the cationic or the anionic part of the complex through some specific interaction with the polymer matrix. Hamon *et al.* recently proposed the "cation chelation mechanism" in extraction with polyether-type polyurethane foam, where a counter-cation-selective extraction of metal thiocyanate complexes was observed.[16] This was a particular case in which a cation–matrix interaction (polyether oxygens atoms acting as electron-donors to cations) dominated. However, the sorption of a neutral complex such as $M(SCN)_2$ could occur, depending on experimental conditions, as reported elsewhere.[9,17]

In the present sorption study, specific interaction (in the sense above) between the ammonium ion and the cellulose acetate is yet to be investigated. However, such sophisticated considerations may not be needed here. According to the established principles of conventional ion-pair extraction,[3] a change in the ionic components or extraction solvents exercises a considerable effect on the extraction behaviour because of the difference in the lipophilicity of the ions or the difference in ion–solvent interaction. In this sense, the polymer surface may well be deemed a pseudo-solvent, and the sorption is a solvent extraction which uses the polymer as solvent. It would be pertinent to note in this connection that the Langmuir isotherm cannot be a critical basis for discriminating between sorption (or adsorption) phenomena and conventional solvent extraction equilibria, in the present type of study. An adsorption study is usually made under conditions where the loading of sorbed species on the surface is relatively high and the saturation effect has to be taken into account in terms of the Langmuir isotherm. If the adsorption conditions are such that only a small fraction of the surface is covered by the sorbed species (*i.e.*, the saturation effect is unimportant), the Langmuir isotherm can effectively be replaced by the Nernst distribution law, on the basis of which conventional extraction equilibria are formulated. Thus, under low-loading conditions, equilibria of sorption on polymer matrix may well be treated in the same manner as those of extraction by an organic solvent.

The actual nature of the "polymer solvent" depends not only on the chemical structure of the monomer unit of the polymer but also on the state of aggregation of the polymer chain, which may be

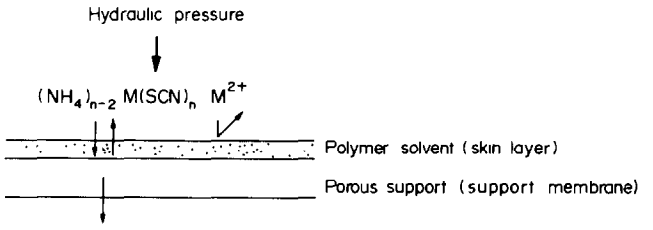

Scheme II. Selective permeation of metal species on the basis of ion-association extraction.

classified in a simplified manner into crystalline and amorphous. It would be reasonable to suppose that the amorphous region is the site responsible for extraction of the ion-association complex. Tables 1 and 2 show that cellulose acetate is an effective sorbent whereas the chemically related penta-acetyl-β-*D*-glucose is not. The latter forms a well-defined crystalline solid, and the lack of an amorphous polymeric region is certainly the cause of its poor extraction capability.

A change in the particle size of the sorbent material had little effect on the results in Table 1 and 2. This suggests that the sorption is related not to the apparent macrosurface obtained by simple physical grinding but to the microsurface or microstructure of the polymer material. The importance of the polymer microstructure for the sorption of lipophilic chemical species has also been exemplified by studying the sorption behaviour of organic dyes in aqueous solution on asymmetric polysulphone ultrafiltration membranes.[18] The sorption obeyed the Langmuir isotherm, and took place preferentially on the "active side" or "skin layer" of the membrane.

Hyperfiltration

As an application of the idea of ion-association extraction by solid polymers, selective hyperfiltration

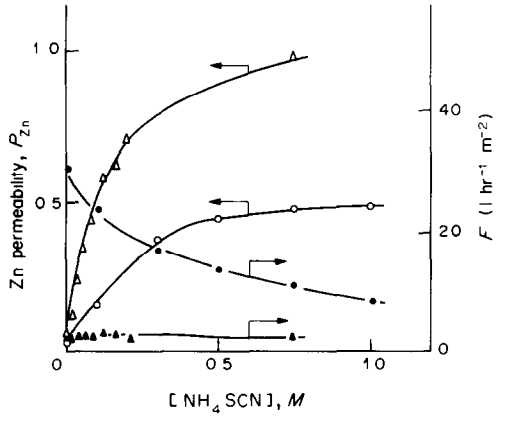

Fig. 5. Permeation of zinc thiocyanate complexes through cellulose acetate membranes; coated (△, ▲) and cast (○, ●); cellulose acetate membranes; feed solution, 250 ml of NH_4SCN–HCl solution (pH 2.0) containing 1 m*M* $Zn(NO_3)_2$; applied pressure, 20 atm at 25°C. P_{Zn}, permeability of zinc ion; *F*, flux of permeate solution.

separation of metal species in solution may be envisaged as taking place according to Scheme II. Therefore, cellulose acetate membranes were prepared by the casting or the coating method, and the permeation behaviour of the metal thiocyanate complexes under hydraulic pressure was investigated.

The effect of ammonium thiocyanate concentration on the permeation by zinc is shown in Fig. 5. The permeability increases with the increase in thiocyanate concentration. Such behaviour is particularly pronounced for coated membranes, which have effectively a much thicker polymer solvent phase than the cast membranes. This is also reflected in the lower permeation flux for coated membranes. A comparison experiment with the uncoated support material showed that there was no sorption on the support.

Permeability of metal thiocyanate complexes was also investigated in two-component systems by using zinc as the reference ion (Table 4). Selective permeation by metal thiocyanate complexes was observed, with permselectivity in the order $Zn^{2+} > Cu^{2+} > Fe^{3+} > Co^{2+} > Ni^{2+}$. It should be noted that the permselectivity is the same as that obtained for sorption experiments, except for copper (for which there is some ambiguity about the complex species in solution; see footnote to Table 1). This strongly indicates that selective separation of ionic solutes by hyperfiltration is made possible by use of the principle of ion-association extraction by solid polymers.

Finally, it is to be added that the mechanism of permeation of solutes is not fully elucidated by the present study. Not only the sorption on the mem-

Table 4. Permeation selectivity of metal thiocyanate complexes*

	Cast membrane			Coated membrane		
Metal	*P*	P/P_{Zn}	*F*, $l.hr^{-1}m^{-2}$	*P*	P/P_{Zn}	*F*, $l.hr^{-1}m^{-2}$
Zn^{2+}	0.44	1.00		0.90	1.00	
Cu^{2+}	0.42	0.96	15.8	0.78	0.84	2.4
Ni^{2+}	0.12	0.32	14.6	0.21	0.24	2.2
Co^{2+}	—	—	—	0.29	0.33	2.2
Fe^{3+}	0.22	0.50	14.3	0.51	0.55	2.4

*Feed solution, 250 ml of solution containing 0.5*M* NH_4SCN, 0.1*M* HCl, 1m*M* $Zn(NO_3)_2$, and $M(NO_3)_2$ (pH = 1); applied pressure, 20 atm at 25°C.

brane matrix but also the coupling with solvent flow through the membrane seem to be contributory factors. The nature of the permeation process is now under study.

Conclusion

Transition-metal thiocyanate complexes [Fe(III), Co(II), Ni(II), Cu(II), Zn(II)] in aqueous solution are sorbed on various solid polymers. Polymers with relatively high polarity, particularly cellulose acetate, are effective sorbents. The sorption involves ion-association complexes formed between cations (ammonium ion) and anionic metal thiocyanate complexes. The process is well described as ion-association extraction by "polymer solvents". Such a polymer solvent is useful not only as a substitute for conventional extraction solvents but also as basic material for preparing ion-selective separation membranes. Lamination of the polymer into hyperfiltration-type membranes is useful for such purposes. The metal permeation selectively follows essentially the metal sorption selectivity on the polymer material. These findings open a new prospect for developing metal-selective hyperfiltration membranes for separating metals in solution.

Acknowledgements—The present work was partially supported by a Grant-in-Aid for Scientific Research from the Ministry of Education, Science and Culture of Japan.

REFERENCES

1. R. Bock, *Z. Anal. Chem.*, 1951, **133,** 110.
2. C. Rozycki, *Chem. Anal.*, 1969, **14,** 755.
3. T. Sekine and Y. Hasegawa, *Solvent Extraction Chemistry*, Dekker, New York, 1977.
4. H. J. M. Bowen, *J. Chem. Soc.* (*A*), 1970, 1082.
5. P. Schiller and G. B. Cook, *Anal. Chim. Acta*, 1971, **54,** 364.
6. M. P. Maloney, G. J. Moody and J. D. R. Thomas, *Analyst*, 1980, **105,** 1087.
7. T. Braun and A. B. Farag, *Anal. Chim. Acta*, 1978, **98,** 133.
8. S. T. Al-Bazi and A. Chow, *Talanta*, 1982, **29,** 507.
9. *Idem, ibid.*, 1983, **30,** 487.
10. Q. T. Nguyen, P. Aptel and J. Neel, *J. Membr. Sci*, 1980, **6,** 71.
11. T. Hayashita, M. Takagi and K. Ueno, *Sepn. Sci. Techn.*, 1983, **18,** 461.
12. *Idem, ibid.*, 1984, **19,** 315.
13. M. Igawa, A. Saito, N. Sasamura, M. Tanaka, and M. Seno, *J. Membr. Sci.*, 1983, **14,** 59.
14. T. Braun and A. B. Farag, *Anal. Chim. Acta*, 1978, **99,** 1.
15. Complex formation constants of zinc thiocyanate complexes used in this calculation were obtained from L. G. Sillén and A. E. Martell, *Stability Constants of Metal-Ion Complexes*, Chemical Society, London, 1964.
16. R. F. Hamon, A. S. Khan and A. Chow, *Talanta*, 1982, **29,** 313.
17. J. J. Oren, K. M. Gough and H. D. Gesser, *Can. J. Chem.*, 1979, **57,** 2032.
18. S. Sakurai, T. Hayashita and M. Takagi, unpublished work.

Talanta, Vol 32, No 5, pp. 407–410, 1985
Printed in Great Britain

0039-9140/85 $3.00 + 0.00

POLAROGRAPHIC DETERMINATION OF ZIRCONIUM AT TRACE LEVEL

Y. CASTRILLEJO, R. PARDO, E. BARRADO and
P. SANCHEZ BATANERO
Departamento de Química Analítica, Facultad de Ciencias, Universidad de Valladolid, Valladolid, Spain

(*Received* 16 *August* 1984. *Revised* 13 *November* 1984. *Accepted* 12 *December* 1984)

Summary—An indirect polarographic method has been developed for the determination of zirconium by formation of molybdozirconophosphoric acid, its extraction with MIBK or a mixture of diethyl ether and 1-butanol, stripping with alkali and measurement of the Mo(VI) by its catalytic effect on the polarographic reduction of hydrogen peroxide. Depending on the extractant, a detection limit of 2.5 or 8.9 μg/l. can be achieved.

Zirconium is a non-electroactive element which gives refractory oxides, so a determination based on its direct reduction is not possible, and the AAS methods, when used at trace level, achieve poor results.[1] Until the advent of the spectroscopic methods with plasma source, which give lower zirconium detection limits,[2] the only possibility for determining zirconium at trace level was by spectrophotometric measurement of zirconium complexes with organic[3,4] or inorganic[5,6] reagents. The detection limits of these methods all are around 1 mg/ml.

Electrochemical determination of zirconium is only possible by means of an indirect procedure, as proposed by Harto and Sánchez Batanero,[7] who used stripping and coulometric techniques, or by Ye Hua-Li and He You-Hua, based on the adsorption polarographic wave of a Zr–oxalic acid–cupferron–diphenylguanidine complex.[8]

In this paper we describe an indirect method based on formation of molybdozirconophosphoric acid (MZrPA), its extraction with an organic solvent, stripping with alkali and determination of the resulting Mo(VI) by means of its catalytic effect on the polarographic reduction of hydrogen peroxide.[9] The method is thus a variant of that used earlier for the indirect determination of phosphorus.[10] The detection limit for the zirconium determination is significantly lowered because of the combination of release of 11 molybdenum atoms per zirconium atom in the MPZrA, and the sensitive Mo(VI) determination used. We have obtained a detection limit of 2.5 μg/l., very similar to that of the plasma techniques.

Because the Mo(VI) determination is non-specific with respect to parent molybdenum species, it is necessary to remove all these except the MZrPA before the stripping step. This is done by selective extraction of the molybdophosphoric acid (MPA) with ethyl acetate, followed by selective extraction of the MZrPA, the isopolymolybdic acid(s) being left in the aqueous phase. The molybdenum in the MZrPA can then be stripped with alkali and determined polarographically. Because of the number of conditions to be optimized a simplex technique[11–15] was preferred to the more tedious classical approach.

The optimized procedure has been applied to a certified zirconium-containing aluminium sample with good results.

EXPERIMENTAL

Apparatus

A Radiometer PO4d polarographic analyser was used with a dropping mercury electrode and a saturated calomel reference electrode. The sweep rate was 100 mV/min and deaeration of the test solution was not required. The temperature was controlled by using a double-wall polarographic cell and a Selecta thermoregulator.

Reagents

Molybdate solution, 0.1 M. Dissolve 24.20 g of sodium molybdate dihydrate in 1 litre of water.

Phosphate solution, 2.0×10^{-3} M. Dissolve 0.240 g of sodium dihydrogen phosphate in 1 litre of water.

Standard zirconium solution 1.00×10^{-2} M. Dissolve 2.86 g of zirconium oxychloride hexahydrate, dried at 110°, in 1 litre of 2*M* perchloric acid. Prepare less concentrated solutions by dilution.

All reagents were of analytical grade and demineralized water was used throughout.

Procedures

Standardization of zirconium solution. Adjust an aliquot to contain about 10% of sulphuric acid by volume. Add a 50-fold excess of 10% diammonium hydrogen phosphate solution and readjust the acidity to 10% acid content, adding 1 ml of concentrated sulphuric acid per ml of phosphate solution added. Digest the precipitate at 45° for 3 hr. Filter off the precipitate on an ashless paper and wash it with cold 5% ammonium nitrate solution until the washings are free from phosphate. Dry and ignite to ZrP_2O_7 in a platinum crucible at 1000°, cool and weigh.

Zirconium determination. Transfer 1 ml of 0.1*M* molybdate, 2 ml of 2×10^{-3}*M* phosphate and 1.3 ml of 60% perchloric acid into a separating funnel. Add a known volume of the zirconium sample and dilute with water to 25 ml. Add 25 ml of ethyl acetate, shake the mixture for 3 min and remove the organic phase 20 min later. If diethyl ether–1-butanol (2:1 v/v) mixture is used for the MZrPA extraction, shake the aqueous phase with 15 ml of it for 3 min, remove the aqueous layer 20 min later, wash the organic phase with three 10-ml portions of 0.5*M* perchloric

Table 1. Simplex optimization progress (centroid and reflected vertexes not shown; $[Zr] = 2.00 \times 10^{-6} M$ throughout)

Vertex	Simplex	Retained vertexes	Reagent amounts, *ml*			i_s, μA	Response
			$HClO_4$	Mo	P		
1	1		1.30	1.00	2.00	9.46	0.899
2	1		1.80	1.00	2.00	8.12	0.256
3	1		1.50	3.00	2.00	8.10	0.450
4	1		1.50	2.00	10.00	6.18	0.548
5	2	1,3,4	0.62	4.20	10.60	1.30	0.029
6*	3	1,2,4	1.43	1.98	8.00	7.30	0.342
7	4	1,6,4	1.40	2.06	4.57	9.65	0.960
8	5	1,7,4	1.40	1.70	5.45	9.30	0.522
9*	6	1,7,6	1.40	1.68	5.52	8.90	0.589
1†	6	1,7,6	1.30	1.00	2.00	9.56	0.930
10	7	1,7,9	1.34	1.48	2.57	9.72	0.377
11	8	1,7,9	1.37	1.58	4.01	10.90	0.908
12	9	1,7,11	1.37	1.42	4.28	6.70	0.504
7†	9	1,7,11	1.40	2.06	4.57	9.55	0.920
13	10	1,7,11	1.32	0.86	1.64	9.50	0.905

*"Next-to-worst" rule[13] used.
†"$n + 1$" rule[11] violated; point re-evaluated and mean value taken.

acid, shaking for 3 min each time, to remove any isopolymolybdic acid(s), then strip Mo(VI) from the organic phase by shaking it for 1 min with 25 ml of $1M$ sodium hydroxide. If methyl isobutyl ketone (MIBK) is used as the extractant for the MZrPA, add 5 ml of 60% perchloric acid to the aqueous phase from the ethyl acetate extraction, shake it with 15 ml of MIBK for 3 min, remove the aqueous phase 20 min later, wash the organic layer with two 10-ml portions of $2M$ perchloric acid, then strip the Mo(VI) as before.

Acidify the alkaline solution containing the stripped molybdenum to pH 2.5 with $4M$ sulphuric acid, then add 2.5 ml of $4M$ sulphuric acid and 5 ml of $0.2M$ hydrogen peroxide and dilute to volume in a 50-ml standard flask with water. Transfer an aliquot of this solution into the polarographic cell and run a d.c. polarogram between 0.40 and 0.00 V (*vs.* SCE). Deaeration is not required but the temperature must be kept constant ($25.0 \pm 0.1°$). Measure the current at 0.20 V and a run a blank solution through the whole procedure. Find the zirconium concentration of the sample from a calibration graph constructed by use of standard zirconium solutions under the same conditions.

Analysis of aluminium samples. Place a 0.5-g sample, accurately weighed, in a Teflon bomb with 3 ml of concentrated nitric acid, 2 ml of concentrated hydrofluoric acid and 1 ml of 30% hydrogen peroxide. Tightly seal the bomb and heat it at 100° for 15 min. After cooling, transfer the sample solution into a platinum crucible and evaporate it to dryness; add 2 ml of 60% perchloric acid and evaporate to fumes, repeating this step at least 5 times to ensure removal of all silicon and fluoride. Dissolve the residue in water adding the necessary perchloric acid amount to ensure its complete dissolution and make up to known volume. Adjust the pH of an aliquot with sodium hydroxide to pH 3 and analyse the solution by the procedure above, with MIBK as extractant for the MPZrA.

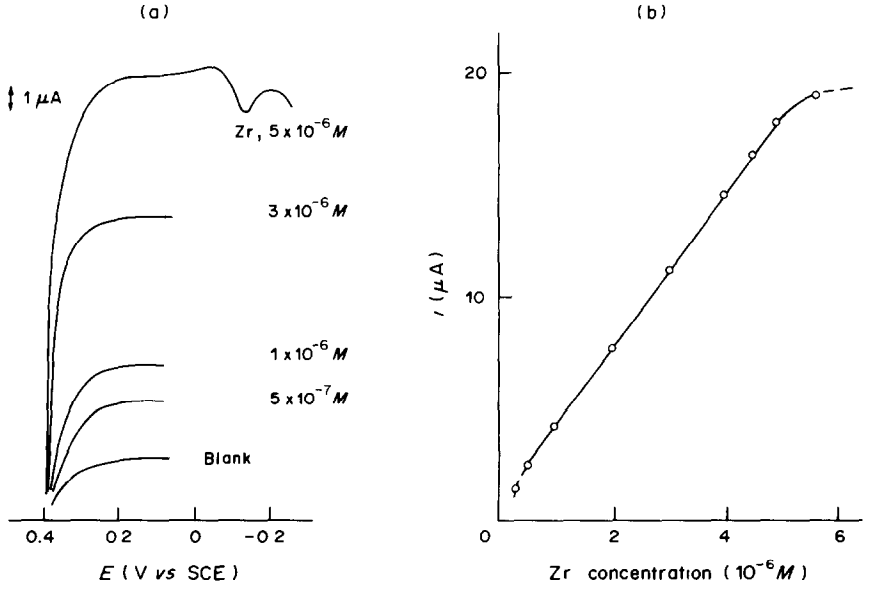

Fig. 1. Calibration graph for zirconium determined by using the 2:1 v/v diethyl ether–1-butanol mixture as extractant. (a) Polarograms; (b) calibration line.

Table 2. Interference of some elements in the zirconium determination

Species	Maximum allowed values: Concentration, M	Maximum allowed values: Molar ratio to zirconium*
Arsenic(V)	5.2×10^{-5}	104
Silicon	5.3×10^{-6}	11
Germanium	1.9×10^{-4}	380
Vanadium(V)	2.0×10^{-6}	4
Thorium	9.0×10^{-6}	18
Titanium	6.0×10^{-6}	12
Iron(III)	3.5×10^{-4}	700

*Assuming a mean zirconium concentration of $5.0 \times 10^{-7} M$.

RESULTS AND DISCUSSION

The experimental conditions to be optimized are (*a*) the pH, molybdate and phosphate concentrations, order of addition of the reagents and the reaction time for formation of MZrPA, (*b*) the solvent and pH for extracting the MPA, (*c*) the solvent and acidity for extracting the MZrPA, and the washing sequence for removal of isopolymolybdic acid(s), (*d*) stripping of Mo(VI) from the MZrPA and its polarographic determination.

The conditions for steps (*b*) and (*d*) have already been optimized and reported[10] so details need not be repeated here. The extractants for the MZrPA were chosen after a literature search and some preliminary spectrophotometric studies. Johnson *et al.*[16] concluded that ternary molybdophosphoric acids are best extracted with mixtures of oxygen-containing solvents, for example diethyl ether, mixed with aliphatic alcohols such as 1-butanol, 3-methylbutanol or 1-pentanol. Our previous work indicated that MIBK would also be suitable, so we selected 2:1 v:v diethyl ether–1-butanol mixture and MIBK for the purpose.

Although most of the conditions needed were already known, so many still needed to be optimized that a simplex method was used for economy of effort.

Simplex optimization was first proposed by Spendley *et al.*[11] and later modified by Nelder and Mead[12] and Routh *et al.*[13] These methods, usually referred to as Simplex, Modified Simplex (MS) and Super Modified Simplex (SMS) respectively, involve the movement of a simplex [an $(n + 1)$-point geometrical figure] through n-dimensional space, n being the number of experimental factors involved in the system studied. Each corner of the simplex (called a vertex) represents a different combination of the experimental factors and therefore gives a different response. The goal is to maximize (or minimize in some cases) the response, and some simple rules (depending on the variety of simplex) are used to move from regions of poor response towards regions of improved response and eventually to an optimum. We used the SMS variety.[13]

The response to be optimized was the ratio of net signal to blank signal for the currents obtained in the measurement step. The blank is due to any zirconium in the reagents and to any non-zirconium-containing molybdenum species that escape separation from the MZrPA, and must be corrected for. The order of addition of the reagents, and the reaction times were known from previous work so only the amounts of phosphate and molybdate (expressed as ml of reagent solution) and the acidity (expressed as ml of 60% perchloric acid) for formation of MZrPA needed optimization. To simplify the overall procedure, the two extractions were done at the acidity used for formation of the MZrPA, and the same acidity was used for washing the MZrPA extract.

The experimental procedure was similar to that given in the experimental section, with appropriate variations in the amounts of reagents added. Table 1 shows the progress of the optimization for the mixed solvent system. The optimization was stopped at simplex no. 10 because at this stage all the vertices retained had a similar amount of perchloric acid and a molar ratio of about 50:1 for Mo:P. An attempt to improve the response by varying the acidity for step (*c*) produced no advantage. For simplicity, the conditions chosen were the ones corresponding to vertex no. 1. Figure 1 shows a calibration graph obtained for zirconium under these conditions, together with the polarograms recorded. The linear range was from $5.0 \times 10^{-7} M$ (46 μg/l.) to $5.0 \times 10^{-6} M$ (466 μg/l.). The sensitivity was 3.28 A.l.mole^{-1} and the calculated detection limit 8.9 μg/l. The mean recovery of zirconium in the whole procedure was only $40 \pm 4\%$. Although this low value is compensated for by running the standards through the whole procedure, we also studied the use of MIBK as extractant, but not by simplex optimization. The conditions for the mixed extractant system were tried first but also gave very poor recovery. It was found that the recovery could be increased to $81 \pm 2\%$ by adding 5 ml more 60% perchloric acid before the extraction, as described in the procedure. The calibration graph obtained was linear from $1.0 \times 10^{-7} M$ (9 μg/l.) to $1.3 \times 10^{-6} M$ (120 μg/l.). The sensitivity was 9.6 A.l.mole^{-1} and the calculated detection limit 2.5 μg/l. MIBK was therefore used in all subsequent studies.

Interference may be expected from all those elements which give binary and/or ternary heteropolymolybdic acids and therefore, if they accompanied MZrPA throughout, could increase the final Mo(VI) concentration, giving a positive error. The determination of zirconium can only be made selective by choice of conditions and not by choice of organic solvent, since all those commonly used for these systems can extract all the isopoly and heteropolymolybdic acid species to some extent. The method (with MIBK as extractant) was therefore applied to solutions containing arsenic, silicon, germanium, vanadium, thorium and titanium. Table 2

shows the tolerance limits, expressed as maximum concentration and element/zirconium molar ratio allowed in "real samples".

As zirconium is often determined in metallic samples, the study was extended to metals likely to be present in such samples, and also to several anions to cover various methods of sample dissolution. Of the metals, only iron(III) gives interference, but this can be eliminated by initial reduction to iron(II) with hydroxylamine hydrochloride.[10] No interference by anions was found except for fluoride and sulphate, which produce negative errors by complexation of zirconium, and must be absent.

PRACTICAL APPLICATIONS

The recommended MIBK procedure was applied to determination of zirconium in a certified aluminium sample. The certified value of zirconium is 0.02% and all the interfering elements were at levels below their tolerance limits, except for silicon, which was removed as indicated in the experimental section. The result obtained was $0.0204 \pm 0.0002\%$ (mean of 5 determinations, 95% confidence level), which confirms the validity of the procedure. The sensitivity is greater than that of previous methods for determination of zirconium.

Acknowledgement—This work was supported by a grant from the CAICYT of the Ministerio de Educación y Ciencia.

REFERENCES

1. G. D. Christian and F. J. Feldman, *Appl. Spectrosc.*, 1971, **25**, 663.
2. S. Greenfield, H. McD. McGeachin and P. P. Smith, *Talanta*, 195, **22**, 1; 1975, **22**, 553; 1976, **23**, 1.
3. H. J. G. Challis, *Analyst*, 1969, **94**, 94.
4. M. Gallego, M. Valcárcel and M. García-Vargas, *Anal. Chim. Acta*, 1982, **138**, 311.
5. K. Mukaya, Y. Yokoyama and S. Ikeda, *ibid.*, 1969, **48**, 349.
6. Y. F. Shkaravskii, A. I. Bortun and T. A. Karaseva, *Ukr. Khim. Zh.*, 1982, **48**, 754.
7. A. Harto and P. Sánchez Batanero, *Analusis*, 1982, **10**, 229; 1983, **11**, 84.
8. Ye Hua-Li and He You-Hua, *Talanta*, 1984, **31**, 638.
9. I. M. Kolthoff and E. P. Parry, *J. Am. Chem. Soc.*, 1951, **73**, 5315.
10. R. Pardo, E. Barrado, Y. Castrillejo and P. Sánchez Batanero, *Talanta*, 1983, **30**, 655.
11. J. M. Spendley, G. R. Hext and F. R. Himsworth, *Technometrics*, 1962, **4**, 441.
12. J. A. Nelder and R. Mead, *Computer J.*, 1965, **7**, 308.
13. M. W. Routh, P. A. Swartz and M. B. Denton, *Anal. Chem.*, 1977, **49**, 1422.
14. M. L. H. Turoff and S. N. Deming, *Talanta*, 1977, **24**, 567.
15. R. J. McDevitt and B. J. Barker, *Anal. Chim. Acta*, 1980, **122**, 222.
16. B. H. N. Johnson, G. F. Kirkbright and T. S. West, *Analyst*, 1972, **97**, 696.

Talanta, Vol. 32, No. 5, pp. 411–417, 1985
Printed in Great Britain.

0039-9140/85 $3.00 + 0.00

AUTOMATED FLOW-INJECTION PSEUDOTITRATION OF STRONG AND WEAK ACIDS, ASCORBIC ACID AND CALCIUM, AND CATALYTIC PSEUDOTITRATIONS OF AMINOPOLYCARBOXYLIC ACIDS BY USE OF A MICROCOMPUTER-CONTROLLED ANALYSER

M. A. KOUPPARIS* and P. ANAGNOSTOPOULOU
Laboratory of Analytical Chemistry, University of Athens, 104 Solonos Street, Athens 106 80, Greece

H. V. MALMSTADT
Pacific and Asia Christian University, P.O. Box YWAM, Kailua-Kona, HI 96740, USA

(*Received* 5 *October* 1984. *Accepted* 12 *December* 1984)

Summary—A simple, inexpensive, fully automated spectrophotometric system for flow-injection pseudotitrations is used to perform acid–base, redox, complexometric and catalytic "titrations". Peak widths (in time units) in the range 10–100 sec can be measured with a precision of better than 0.3% in most cases. Strong and weak acids in the range 5.0×10^{-4}–$1.0 \times 10^{-2}M$ are measured by using sodium hydroxide–Bromothymol Blue "titrant". Ascorbic acid (1×10^{-4}–$1 \times 10^{-2}M$) is "titrated" with 2,6-dichlorophenolindophenol, and calcium (5.0×10^{-4}–$5.0 \times 10^{-2}M$) with EDTA, with calmagite as indicator in the presence of magnesium. Aminopolycarboxylic acids (5×10^{-6}–$1 \times 10^{-2}M$) are measured by use of catalytic indication based on the manganese-catalysed periodate–diethylaniline reaction. The ascorbic acid method has been applied to analysis of pharmaceutical preparations, and the calcium method to water analysis.

Since its introduction in 1975,[1,2] flow-injection analysis (FIA) has aroused considerable interest amongst analysts developing high-speed routine analytical methods in various fields.[3–7] During the rapid evolution of the new approach, in only a few years, many classical techniques used in the batch mode of analysis have been adapted to the continuous mode using FIA.

The FIA titration technique is attractive and has been studied and used in several applications.[8–20] One important difference between flow-injection pseudotitrations and other FIA procedures is the use of peak width rather than peak height as the analytical measurement. As shown by Růžička *et al.*,[8] the peak width measured in time units is linearly related to the logarithm of the analyte concentration:

$$\Delta t_{eq} = k_1 \ln \frac{C_a^0}{C_t^0} + k_2$$

where Δt_{eq} is the "equivalence" time for pseudotitration, C_a^0 the original concentration of analyte, C_t^0 the original concentration of titrant, and k_1 and k_2 are constants of the FIA system used. When peak width is used as the parameter to be measured, a large dispersion of the injected sample in the carrier-reagent stream is advantageous for increasing precision. This is achieved by placing a mixer between the sample injector and the detector. However, it has recently been suggested that the mixer is not necessary. The dispersion of the sample during its movement through the tubular reactor provides a mixing stage which is capable of serving the same function as the mixing chamber.

Pardue and Fields[21] have discussed in great detail various continuous-flow pseudotitrations and suggested that very dilute carrier solutions (or even a pure water stream) should be used in order to increase sensitivity. They also emphasized the variable-time kinetic view of this procedure and suggested that it is most accurately described as a "kinetic titration". The term FIA titration or pseudotitration[19] is widely used, however.

Stewart and Rosenfeld[18] pointed out that FIA titrations are part of a more general approach in unsegmented flow systems, where exponential dilution chambers are used for scale expansion in FIA.

Spectrophotometry is the most used detection technique in FIA titrations because of the large number of visual indicators available for neutralization, complexometric and redox titrations. Potentiometry with glass and ion-selective electrodes[21] has also been used.

The most serious drawback in FIA titration is the logarithmic relation between the time interval measured and the analyte concentration. Highly accurate and precise measurements of time are required, in conjunction with high precision of the flow-rate and the sampling.

*To whom correspondence should be addressed.

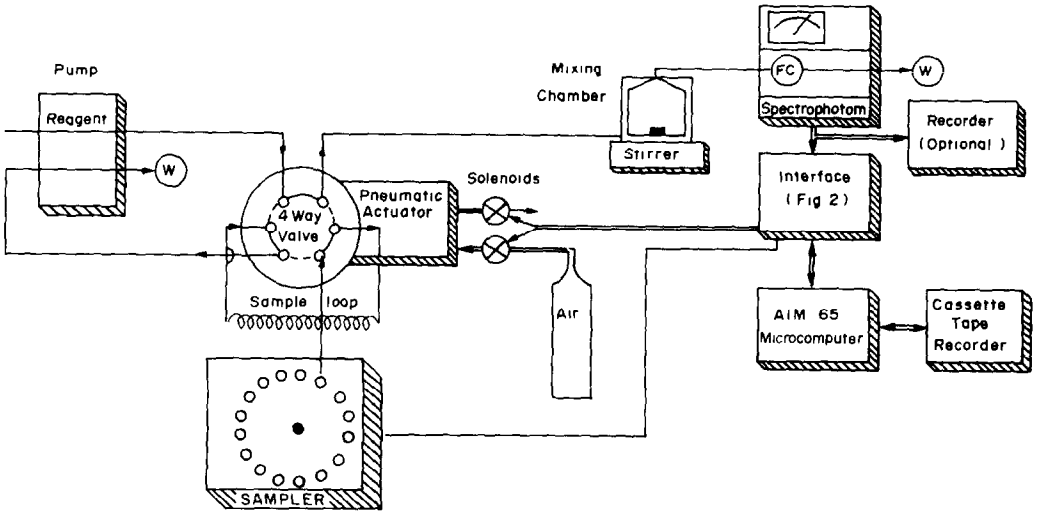

Fig. 1. Schematic diagram of the automated flow injection pseudotitration system.

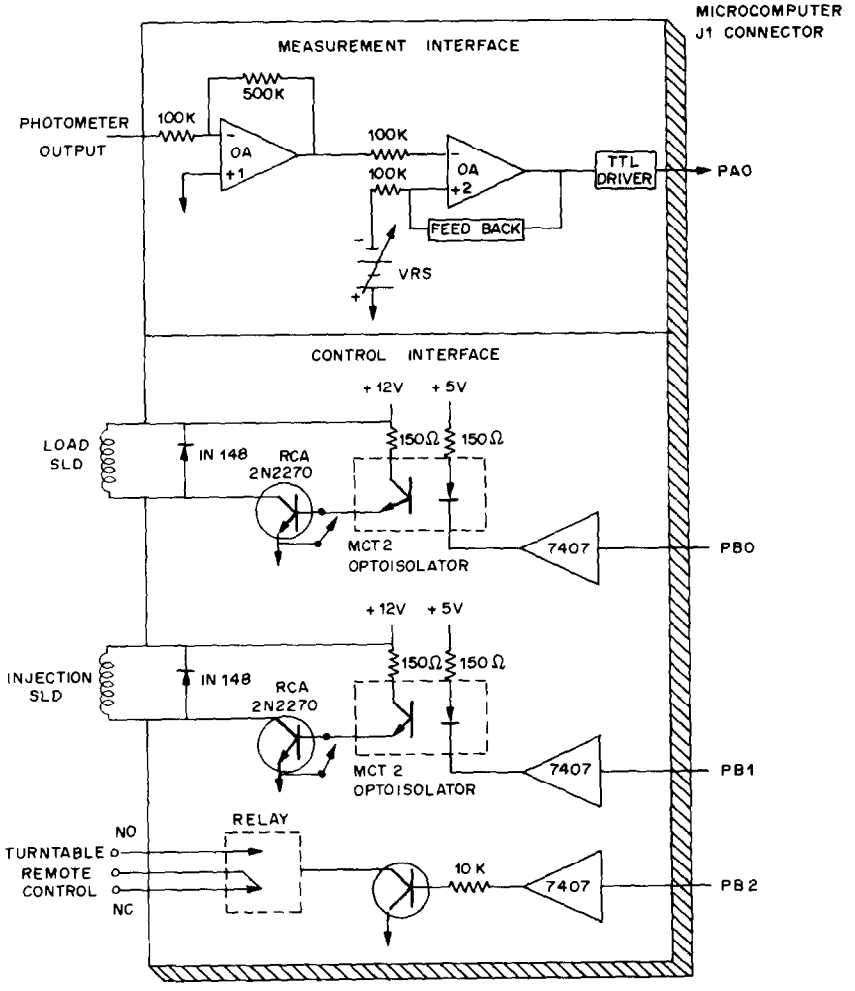

Fig. 2. Diagram of the measurement and control interface.

Microcomputers[17,18,23] and an electronic system[22] have been used to increase the precision of the measurement step. In this paper, we demonstrate the flexibility of the technique, and develop automated pseudotitrimetric acid–base, redox and complexometric determinations. The usefulness of the new concept is shown in "titrations" where secondary reactions are involved, such as the catalytic indicator reaction in aminopolycarboxylic acid determination. A simple, inexpensive, fully automated spectrophotometric system is used, based on an AIM 65 microcomputer to control all the steps—sampling, injection, time measurement and calculation.

EXPERIMENTAL

Apparatus

A block diagram of the automated system used (which is similar to previously reported systems[17,19]) is shown in Fig. 1.

The sample injection system consists of a 4-way Teflon rotary valve (Rheodyne Type 50) operated by a pneumatic two-position actuator (Rheodyne model 5001). An optional sampler (Hook and Tucker, England, model A40, modified for automatic control) is used for fully automated operation. A 1-ml capacity mixing chamber made from Plexiglas is used for sample dispersion, and the reaction and mixing coils are made from Teflon tubing, 0.8 mm bore.

The spectrophotometer used is the inexpensive Bausch and Lomb Spectronic 21 model, incorporating an 18-μl flow-cell with a 10-mm light-path. The spectrophotometer output signal [1.000 V for 100% transmittance (T)] is fed to the microcomputer interface and to an optional chart-recorder.

The microcomputer used is the Rockwell AIM 65, with visual display and a thermal printer. Input/output operations are performed through an on-board peripheral chip, the R6522 Versatile Interface Adapter (VIA) containing two 8-bit parallel I/O ports [port A (PA) and port B (PB)]. Programs are written in Basic, as a series of subroutines performing selected tasks and stored in a tape-recorder cassette.

The control and measurement interface is shown in Fig. 2. It was built with the Analog-Digital Designer[24] (E & L Instruments, model ADD 8000) provided with various useful and versatile circuit cards, power supplies and a voltage reference source (VRS). The control interface consists of two identical circuits which control the load and injection solenoids associated with the pneumatic actuator. The two control signals (low output), *load* and *injection*, are provided from outputs PB0 and PB1. The modified sampler is controlled by output PB2.

The measurement interface consists of two operational amplifiers. OA 1, acting as an inverter, amplifies the photometer output fivefold. The amplified signal (-5 V for 100% T) is then fed to OA 2 which acts as a comparator with positive feedback to avoid oscillation of the operational amplifier output, caused by transient signals in the transition region. By use of the feedback signal, the comparison voltage is divided at the amplifier input by a factor of two. In order to start the measurement at one preselected $\%T$ level, the VRS comparison voltage is set to the value calculated from the equation:

$$V_{ref} = \frac{-5 \times 2 \times \%T}{100}$$

The comparator output is fed to the PA0 input of the microcomputer. This input is high during the measurement time for pseudotitrations in which the transmittance increases, and low for those in which the transmittance decreases.

Software and system operation

The interactive routine program, written in Basic, is capable of running a series of standards and samples without attention by the operator. A selected number of standards are run, after which a complete least-squares analysis of the data is performed. This calibration curve is then used for determination of the analyte in any sample that is subsequently measured. Initially the operator provides the measurement parameters for the standards and samples that follow. The injection time (varied from 1 to 5 sec, depending on the sample volume and the flow-rate), the load time (required for the washing out of the previous sample), the number of standards and samples, the number of runs per standard and sample, and the standard concentrations are required. The direction of the titration peaks (increasing or decreasing transmittance) is also provided to the program so that it can select the appropriate statements in the measurement subroutine. After calibration of the spectrophotometer and stabilization of the base-line, a manual injection is used to select the appropriate transmittance level for triggering the time-measurement step. Half peak-height was found to be the optimum.

After each injection the program passes to the time-measurement subroutine, waiting for the transmittance to increase or decrease to the preselected trigger level, and making the PA0 input high or low respectively. The timing procedure is accurate to 0.01 sec, as tested by using a square-wave signal generator. After the "equivalence" time measurement and printing, the program waits for a preselected "load" time to ensure complete washing of the flow system before injection of the next sample. This time, 5–30 sec, depends on the sample size and the flow-rate.

EVALUATION OF THE SYSTEM

The automated system has been evaluated with typical neutralization, redox and complexometric determinations, along with determinations requiring secondary reactions such as catalytic titrations with end-point indication reactions.

Neutralization titrations

The model system chosen was the titration of hydrochloric acid with $1 \times 10^{-4}M$ sodium hydroxide, with Bromothymol Blue as indicator, added directly to the sodium hydroxide carrier stream (at a level of $8 \times 10^{-5}M$). As the carrier is blue, the detector, set at 600 nm, provides a steady base-line at 8% transmittance level. During each pseudotitration the indicator goes through two transitions (blue–yellow–blue), resulting in a peak, the width of which increases with the concentration of the acid injected. Once the indicator has turned either completely blue or yellow, the detector reaches a limiting level, and therefore all the recorded curves have a common base-line as well as a common top level, regardless of the concentration of the acid titrated. In the experiment described, a transmittance level of 50% was chosen as the triggering level, corresponding to about half the peak height.

The reagent was stored in a well-stoppered polyethylene flask provided with an Ascarite-filled guard-tube to prevent absorption of carbon dioxide from the air. A pumping rate of 5.0 ml/min was found to

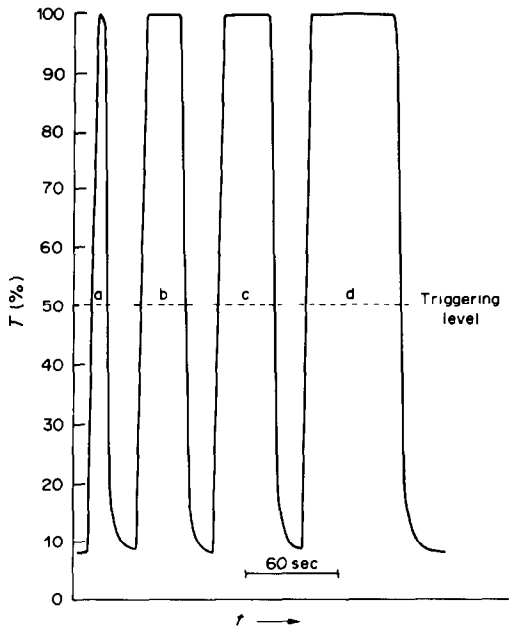

Fig. 3. Flow-injection pseudotitration curves for HCl. Carrier reagent: NaOH $1 \times 10^{-4}M$, Bromothymol Blue $8 \times 10^{-5}M$. Flow-rate 5 ml/min; sample volume 200 μl; λ 600 nm. HCl concentrations: (*a*) $1 \times 10^{-3}M$, (*b*) $5 \times 10^{-3}M$, (*c*) $1 \times 10^{-2}M$, (*d*) $1 \times 10^{-1}M$. Times measured: 10.68–59.72 sec, RSD 0.8–0.3% ($n = 5$). Calibration curve: Δt (sec) $= 84.32 + 24.56 \times \log C$, $r = 0.99994$.

be optimum, giving a compromise between good precision and high sample-throughput. Typical flow injection titrations of hydrochloric acid, along with the reproducibility and the calculated calibration curve, are shown in Fig. 3.

Three weak acids, benzoic, salicylic and citric, were also determined. The peaks were similar to those for the strong acid titration except that the falling edge was less abrupt because of the buffer-system generated during the reaction. The results obtained for calibration curves are similar in precision and linearity to those for hydrochloric acid in Fig. 3.

Redox titrations

The titration of ascorbic acid with 2,6-dichlorophenolindophenol (DCPI) was examined. The carrier stream consisted of $3 \times 10^{-5}M$ DCPI in 210-mg/l. sodium bicarbonate solution and was pumped at a rate of 5 ml/min through the mixing chamber; the spectrophotometer was set at 522 nm (the isosbestic point of DCPI). The coloured carrier solution had a transmittance level of 62%, which served as the base-line. The triggering level was set arbitrarily at 75% transmittance so that the pink–colourless–pink transitions were observed. Typical titration curves for 1×10^{-4}–$1 \times 10^{-2}M$ ascorbic acid standards (in $0.05M$ oxalic acid to prevent oxidation), along with the statistical treatment, are shown in Fig. 4. The automated method was applied to the determination of ascorbic acid in pharmaceutical preparations, and the results obtained were compared with those of the official titrimetric procedure (Table 1).

Complexometric titrations

The titration of calcium with EDTA–Mg^{2+} complex in ammonia buffer at pH 10, with calmagite as indicator, was studied as an example. The composition of the carrier stream was $5 \times 10^{-5}M$ EDTA, $5 \times 10^{-5}M$ Mg^{2+} (*i.e.*, equivalent to $5 \times 10^{-5}M$ EDTA–Mg^{2+}) and $1.3 \times 10^{-5}M$ calmagite indicator in $1M$ NH_3/NH_4Cl buffer. The carrier stream, pumped at 5 ml/min, was monitored at 520 nm. The base-line was set at 100% transmittance for the blue carrier stream (the colour of the free indicator). The triggering level was set at 92% transmittance (half the peak height), so monitoring of the indicator transition started when about 50% of the indicator was bound by the magnesium liberated from the EDTA–Mg^{2+} complex by the calcium, to give the pink calmagite–Mg^{2+} complex. Typical "titration" peaks for calcium in the range 5×10^{-4}–$5 \times 10^{-2}M$ are shown in Fig. 5 along with the statistical treatment of data used for the calibration curve. The method was also applied to determination of total hardness in synthetic and real water samples (Table 2).

Catalytic titrations

In catalytic titrations,[25] the catalyst is used as the titrant, and the solution titrated contains the reagents for the indicator reaction which is catalysed by the titrant, and also an inhibitor of this reaction. The inhibitor is the species that is to be determined, and it reacts stoichiometrically with the catalyst faster than the catalyst reacts with the indicator mixture. Catalytic titrations are especially useful for the determination of minute amounts of substances, for which conventional titrimetric methods are difficult to use, particularly in the case of complexometric titrations, where metallochromic indicators are ineffective for concentration ranges much below $10^{-4}M$.

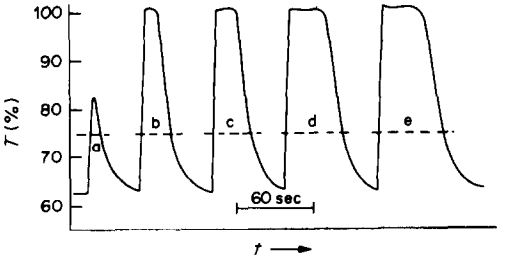

Fig. 4. Flow-injection pseudotitration curves for ascorbic acid. Carrier reagent: dichlorophenolindophenol $3 \times 10^{-5}M$. Flow-rate 5 ml/min; sample volume 200 μl; λ 522 nm. Ascorbic acid concentrations: (*a*) $1 \times 10^{-4}M$, (*b*) $5 \times 10^{-4}M$, (*c*) $1 \times 10^{-3}M$, (*d*) $5 \times 10^{-3}M$, (*e*) $1 \times 10^{-2}M$ Times measured: 9.25–49.29 sec, RSD 0.3–0.06% ($n = 5$). Calibration curve: Δt (sec) $= 89.96 + 20.10 \times \log C$, $r = 0.9997$.

Table 1. Determination of ascorbic acid in pharmaceutical preparations

Preparation	Found	
	FIA method*	Official method†
Ampoules (500 mg/5 ml)	A 101.8 ± 0.1 mg/ml	101.2 mg/ml
	B 100.8 ± 0.2 mg/ml	101.0 mg/ml
Effervescent tablets (1 g/tablet)	A 988 ± 1.6 mg/tablet	986 mg/tablet
	B 973 ± 6.4 mg/tablet	978 mg/tablet

*Average of three measurements.
†Average of two measurements.

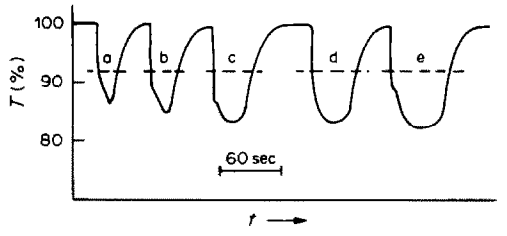

Fig. 5. Flow-injection pseudotitration curves for calcium. Carrier reagent: Mg^{2+}-EDTA $5 \times 10^{-5}M$, Calmagite $1.3 \times 10^{-5}M$, pH 10. Flow-rate 5 ml/min; sample volume 200 μl; λ 520 nm. Calcium concentrations: (*a*) $5 \times 10^{-4}M$, (*b*) $1 \times 10^{-3}M$, (*c*) $5 \times 10^{-3}M$, (*d*) $1 \times 10^{-2}M$ (*e*) $5 \times 10^{-2}M$. Times measured: 24.33–76.54 sec, RSD 0.2–0.08% ($n = 5$). Calibration curve: Δt (sec) = 109.96 + 25.82 × log *C*, $r = 0.9998$.

The catalytic titration of aminopolycarboxylic acids (EDTA, EGTA, DCTA, and DTPA) with Mn^{2+} as titrant and the manganese-catalysed periodate–diethylaniline reaction[26,27] as indicator reaction, has been developed to demonstrate the usefulness of FIA titration in catalytic titrimetry. The analytical manifold is shown in Fig. 6. The titrant and indicator reaction reagents are mixed in a 100-cm mixing coil and the mixing chamber and then allowed to react in a 3-m reaction coil. The product of the manganese-catalysed reaction is monitored at 470 nm, and gives a stable base-line at 32% transmittance for $1 \times 10^{-6}M$ Mn^{2+} and 3% for $1 \times 10^{-5}M$ Mn^{2+}. When an aminopolycarboxylic acid sample (200 μl) is injected into the reacting flow-stream, the catalysis is inhibited by formation of the manganese–aminopolycarboxylic acid complex, and the uncatalysed reaction is monitored, resulting in the transmittance being increased to 75%. The result is a peak with a width which depends on the aminopolycarboxylic acid concentration.

The experimental parameters were optimized to give the maximum difference in transmittance for the catalysed and uncatalysed reactions, high sample throughput, and high precision. Two manganese and periodate concentrations were chosen: $1 \times 10^{-6}M$ Mn^{2+} and $7 \times 10^{-3}M$ periodate for the aminopolycarboxylic acid range 5×10^{-6}–$5 \times 10^{-4}M$, and $1 \times 10^{-5}M$ Mn^{2+} and $3.5 \times 10^{-3}M$ periodate for the 1×10^{-4}–$1 \times 10^{-2}M$ range. The triggering levels were set at 60% and 20% transmittance respectively for the two ranges.

A series of typical peaks for EDTA titration are shown in Fig. 7 and results for the calibration in Table 3. Identical results were obtained with EGTA, DCTA and DTPA.

DISCUSSION

The system described is a simple, relatively inexpensive means of automating flow-injection pseudotitrations. A sample throughput of 60 samples per hour can be obtained in most cases, with small

Table 2. Total hardness determination in water samples

Sample	Total hardness calculated or determined by other methods, *mg $CaCO_3$/l.*	Total hardness found by FIA titration, *mg $CaCO_3$/l.* ($n = 3$)
1. Synthetic, Ca^{2+} $4 \times 10^{-3}M$	400	394 ± 0.6
2. Synthetic, Ca^{2+} $5 \times 10^{-3}M$	500	491 ± 2.7
3. Synthetic, Mg^{2+} $5 \times 10^{-3}M$	500	490 ± 2.0
4. Synthetic, Ca^{2+} $2 \times 10^{-3}M$ Mg^{2+} $3 \times 10^{-3}M$	500	507 ± 0.1
5. Commercial table water A	375*	392 ± 1.5
6. Commercial table water B	389*	394 ± 4.0
7. Water from well	595†	591 ± 0.2

*Ca and Mg determined by AAS.
†Total hardness determined by classical complexometric method.

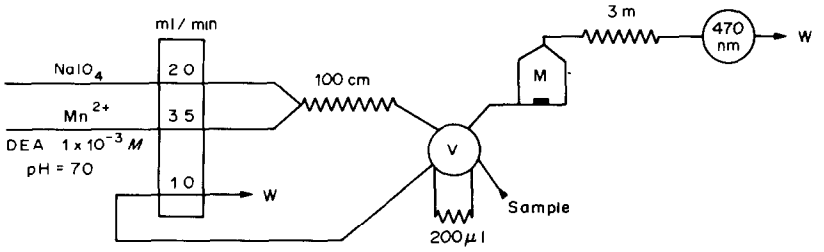

Fig. 6. Analytical manifold for catalytic pseudotitrations of aminopolycarboxylic acids. DEA = diethylaniline; W = waste, V = rotary valve, M = mixer; $[NaIO_4]$ $7 \times 10^{-3}M$ or $3.5 \times 10^{-3}M$, $[Mn^{2+}]$ $1 \times 10^{-6}M$ or $1 \times 10^{-5}M$. Buffer pH 7.0; citrate $0.007M$–phosphate $0.014M$.

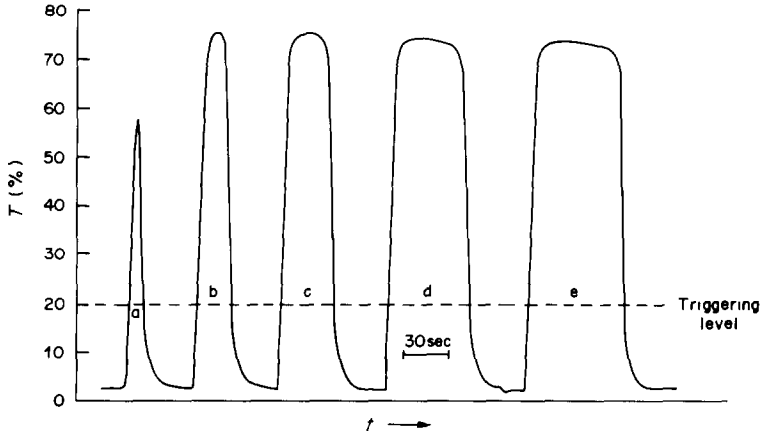

Fig. 7. Flow-injection pseudotitration curves of EDTA, obtained with the manifold shown in Fig. 6. $[Mn^{2+}]$ $1.0 \times 10^{-5}M$, $[IO_4^-]$ $3.5 \times 10^{-3}M$; [EDTA] (*a*) $1 \times 10^{-4}M$, (*b*) $3 \times 10^{-4}M$, (*c*) $1 \times 10^{-3}M$, (*d*) $5 \times 10^{-3}M$, (*e*) $1 \times 10^{-2}M$.

sample and reagent consumption. Any kind of conventional titration which can be monitored spectrophotometrically can be performed with excellent precision (less than 0.3% relative standard deviation in most cases) and accuracy. The logarithmic relation of the time measured to the concentration of the analyte can be an advantage when a wide range of sample concentrations is expected. A closed system is used for the titration, so unstable titrants can be prepared *in situ* and used in special analytical procedures.

The adaptation of catalytic titrations to the flow-injection technique provides a very fast and simple way to determine low concentrations of analytes without the tedious addition of the indicator reaction reagents and the time-consuming graphical estimation of the end-point. The automated measurement of the peak width in time units is simpler

Table 3. Results for the FIA titration determination of EDTA

[EDTA], M	Δt, *sec*	RSD, ($n = 5$), %
A		
5.0×10^{-6}	23.58	1.38
1.0×10^{-5}	31.00	0.72
5.0×10^{-5}	47.87	0.03
1.0×10^{-4}	55.07	0.28
5.0×10^{-4}	71.57	0.19
Calibration curve: Δt (sec) = 150.94 + 24.0 × log$C$; $r = 0.99997$		
Mn^{2+} "titrant" concentration: $1.0 \times 10^{-6}M$		
B		
1.0×10^{-4}	6.212	0.14
3.0×10^{-4}	21.41	0.32
1.0×10^{-3}	37.61	0.28
5.0×10^{-3}	59.24	0.04
1.0×10^{-2}	68.43	0.19
Calibration curve: Δt (sec) = 130.71 + 31.08 log$C$; $r = 0.99998$.		
Mn^{2+} "titrant" concentration: $1.0 \times 10^{-5}M$.		

and more precise than graphical end-point location and illustrates the kinetic view of flow-injection pseudotitrations.

REFERENCES

1. J. Růžička and E. H. Hansen, *Anal. Chim. Acta*, 1975, **78,** 145.
2. K. K. Stewart, G. R. Beecher and P. E. Hare, *Anal. Biochem.*, 1976, **70,** 167.
3. D. Betteridge, *Anal. Chem.*, 1978, **50,** 832A.
4. J. Růžička and E. H. Hansen, *Anal. Chim. Acta*, 1980, **114,** 19.
5. C. Ranger, *Anal. Chem.*, 1981, **53,** 20A.
6. J. Růžička and E. H. Hansen, *Flow Injection Analysis*, Wiley-Interscience, New York, 1981.
7. B. Rocks and C. Riley, *Clin. Chem.*, 1982, **28,** 409.
8. J. Růžička, E. H. Hansen and H. Mosbaek, *Anal. Chim. Acta*, 1977, **92,** 235.
9. G. Nagy, Zs. Fehér, K. Tóth and E. Pungor, *ibid.*, 1977, **91,** 87.
10. B. Griepink and H. B. Verbruggen, *Proc. Anal. Div. Chem. Soc.*, 1977, 141.
11. H. F. R. Reijnders, J. J. van Staden, G. H. B. Eelderink and B. Griepink, *Z. Anal. Chem.*, 1978, **292,** 290.
12. G. Nagy, Zs. Fehér, K. Tóth and E. Pungor, *Anal. Chim. Acta*, 1978, **100,** 181.
13. O. Astrom, *ibid.*, 1979, **105,** 67.
14. H. F. R. Reijnders, J. J. van Staden and B. Griepink, *Z. Anal. Chem.*, 1979, **295,** 409; 1979, **298,** 155.
15. K. K. Stewart, J. F. Brown and B. M. Golden, *Anal. Chim. Acta*, 1980, **114,** 119.
16. H. F. R. Reijnders, J. J. van Staden, G. H. B. Eelderink and B. Griepink, *ibid.*, 1980, **114,** 235.
17. K. K. Stewart and A. G. Rosenfeld, *J. Autom. Chem.*, 1981, **3,** 30.
18. *Idem, Anal. Chem.*, 1982, **54,** 2368.
19. K. K. Stewart, *ibid.*, 1983, **55,** 931A.
20. J. G. Williams, M. Holmes and D. G. Porter, *J. Autom. Chem.*, 1982, **4,** 176.
21. H. L. Pardue and B. Fields, *Anal. Chim. Acta*, 1981, **124,** 39, 65.
22. S. F. Simpson and F. J. Holler, *Anal. Chem.*, 1982, **54,** 43.
23. A. U. Ramsing, J. Růžička and E. H. Hansen, *Anal. Chim. Acta*, 1981, **129,** 1.
24. H. V. Malmstadt, C. G. Enke and S. R. Crouch, *Experiments in Digital and Analog Electronics*, E & L Instruments Inc., Derby, Conn., 1977.
25. T. P. Hadjiioannou, *Rev. Anal. Chem.*, 1976, **3,** 82.
26. E. A. Piperaki and T. P. Hadjiioannou, *Chim. Chronica*, 1977, **6,** 375.
27. T. P. Hadjiioannou, M. A. Koupparis and C. E. Efstathiou, *Anal. Chim. Acta*, 1977, **88,** 281.

Talanta, Vol. 32, No. 5, pp. 419–422, 1985
Printed in Great Britain.

0039-9140/85 $3.00 + 0.00

A CHEMICAL AMPLIFICATION METHOD FOR THE SEQUENTIAL ESTIMATION OF PHOSPHORUS, ARSENIC AND SILICON AT ng/ml LEVELS BY d.c. POLAROGRAPHY

R. KANNAN, T. V. RAMAKRISHNA* and S. R. RAJAGOPALAN
Materials Science Division, National Aeronautical Laboratory, Bangalore 560017, India and
*Department of Chemistry, Indian Institute of Technology, Madras 600036, India

(*Received* 22 *June* 1984. *Accepted* 12 *December* 1984)

Summary—A method is described for the sequential determination of phosphorus, arsenic and silicon at ng/ml levels by d.c. polarography. These elements are converted into their heteropolymolybdates and separated by selective solvent extraction. Determination of the molybdenum in the extract gives an enhancement factor of 12 for determination of the hetero-atom. A further enhancement by a factor of 40 is achieved by determining the molybdenum by catalytic polarography in nitrate medium. Charging-current compensation is employed to improve precision and the detection limit. The detection limits for phosphorus, arsenic and silicon are 0.5, 4.7 and 3.1 μg/l., respectively and the relative standard deviation is 2–2.5%.

Indirect methods for the estimation of phosphorus, arsenic and silicon may be based on the formation of the heteropoly molybdic acids (HPMA), extraction into an organic solvent and determination of the molybdenum in the extract either directly or after stripping into aqueous solution.[1–6]

This approach increases the sensitivity because 12 molybdenum atoms per hetero-atom become available for measurement. The sensitivity can be still further increased by choosing a highly sensitive method of measurement, such as the catalytic polarographic wave given by molybdenum under suitable conditions. The sensitivity of the catalytic polarographic wave is at least 40 times that of the corresponding diffusion wave. We have reported earlier the use of this approach for determining arsenic, phosphorus and silicon at ng/ml level by d.c. polarography.[7–9] Height *et al.* have similarly used differential pulse polarography for the determination of phosphorus.[10] Here we present a procedure for the sequential determination of phosphorus, arsenic and silicon in a mixture.

EXPERIMENTAL

Instrumentation

The polarograph used incorporates compensation for charging-current and was described earlier.[11,12] A Metrohm polarographic cell with a mercury pool as counter-electrode and an SCE as reference electrode was used with a 3-sec Sargent capillary, the drop-time being kept at 0.5 sec by an electromechanically controlled knocker. The water-jacketed polarographic cell was maintained at $34 \pm 0.1°$. Solutions were deaerated by passage of purified hydrogen for 20 min.

Reagents

Analytical grade chemicals were used throughout. Doubly distilled water was collected and stored in a polypropylene container and all reagent solutions were stored in polypropylene containers to avoid contamination with silicon.

Standard molybdenum solution (10^{-2}M). Dissolve 2.420 g of $Na_2MoO_4 \cdot 2H_2O$ in 2*M* sulphuric acid and make up to 1 litre with the same acid. Make further dilutions with 0.25*M* sulphuric acid.

Standard phosphorus solution (25 $\mu g/ml$). Dissolve 0.929 g of ammonium dihydrogen phosphate in 1 litre of distilled water.

Standard arsenic solution (100 $\mu g/ml$). Add 10 ml of concentrated nitric acid to 0.1320 g of As_2O_3 in a 100-ml beaker, heat to dissolve, and dilute to 1 litre with water.

Standard silicon solution (100 $\mu g/ml$). Fuse 0.1070 g of pure dry precipitated silica with 1 g of anhydrous sodium carbonate in a platinum crucible. Cool the melt, extract with water and dilute to 500 ml. Prepare working standard solutions by appropriate dilution of the stock solutions.

Wash solution for phosphorus. Equilibrate 2*M* hydrochloric acid with isobutyl acetate, then discard the organic phase.

Wash solution for arsenic. Equilibrate 2*M* hydrochloric acid with a 1:1 (v/v) mixture of 1-butanol and ethyl acetate, then discard the organic phase.

Wash solution for silicon. Equilibrate 2*M* hydrochloric acid with methyl isobutyl ketone (MIBK), then discard the organic phase.

Citrate solution. Dissolve 100 g of citric acid in about 80 ml of distilled water, adjust to pH 3.2 with sodium hydroxide, then dilute to 1 litre with water.

Supporting electrolyte. Dissolve 85 g of sodium nitrate in 0.25*M* sulphuric acid and dilute to 1 litre with the same acid.

Ammonium heptamolybdate tetrahydrate solution, 5%.

Procedure

Take 10 ml of sample or an aliquot containing up to 5 μg each of phosphorus, arsenic and silicon and diluted to 10 ml with distilled water. Add 2 ml of ammonium molybdate solution and adjust to pH 0.7 with dilute nitric acid. Transfer to a separatory funnel and let stand for 20 min.

Determination of phosphorus. Add 10 ml of isobutyl acetate and shake the funnel for 1 min. When the phases

have separated, carefully transfer the lower (aqueous) phase (*A*) into another separatory funnel and reserve it for determination of arsenic and silicon. Wash the organic layer three times with 15-ml portions of phosphorus wash solution (shaking time 30 sec), discarding the washings. Add 10 ml of 0.5*M* sodium hydroxide to the organic layer and shake for 1 min. When the layers have separated collect the lower layer in a 50-ml standard flask. Add 6.7 ml of 2.3*M* sulphuric acid and 4.25 g of sodium nitrate and make up to the mark. If there is less than 0.6 μg of phosphorus in the original aliquot, transfer the solution to the polarographic cell and record the polarogram. If there is more, dilute the solution suitably with supporting electrolyte and then record the polarogram. Run a blank determination simultaneously and subtract the blank value.

Determination of arsenic. To the aqueous phase (*A*) or, in the absence of phosphorus, the sample plus ammonium molybdate and adjusted to pH 0.7, add 5 ml of 1:1 v/v 1-butanol/ethyl acetate mixture and shake for 1 min. Add 5 ml of isoamyl acetate and shake again for 30 sec. Allow the phases to separate and drain the aqueous phase (*B*) into another funnel for the determination of silicon. Add exactly 5.00 ml of cylcohexane to the organic phase and wash, shaking vigorously for 30 sec each time, with three 15-ml portions of the arsenic wash solution. Discard the washings. Strip the molybdenum from the organic layer and complete the determination as for phosphorus. Further dilution is only necessary for >8 μg of arsenic.

Determination of silicon. Adjust the aqueous phase (*A* or *B*), or the sample if arsenic and phosphorus are absent, to pH 1.2–1.3 with silicon-free ammonia. Wait for 10 min, then add 2 ml of 7*M* nitric acid and wait for 10 min. Add 2 ml of citrate solution and wait for 10 min. Transfer quantitatively into a separatory funnel with the minimum of water. Add 10 ml of MIBK and shake for 1 min. Allow the phases to separate and discard the lower phase. Wash the organic phase by shaking it vigorously for 30 sec each time with three 10-ml portions of silicon wash solution, discarding the washings. Strip the molybdenum and complete the determination as for phosphorus, but adding a suitable aliquot of the 50 ml of final solution to 20 ml of supporting electrolyte, for the polarography.

Calibration graphs. Prepare these by applying the procedure to standard solutions containing 0–0.8 μg of phosphorus, 0.5–8 μg of arsenic and 0.5–5 μg of silicon.

RESULTS AND DISCUSSION

Polarographic determination of the molybdenum

Catalytic currents are given by molybdate in perchlorate,[13] nitrate[14] and chlorate[15] solutions and some arguments still remain about the character of the wave and the species involved in the catalysis.[16] Optimum conditions for the determination of molybdenum in this way have been reported.[17,18] Figure 1 shows the d.c. polarograms for 7.7-μg/l. molybdenum solution in nitrate and perchlorate media with and without charging-current compensation.

The wave is better and larger in the nitrate medium, which was therefore used for further work. Figure 1 also shows that charging-current compensation flattens the base-line and improves the precision of measurement.

The chosen concentrations of nitrate (1*M*) and sulphuric acid (0.25*M*) agree with those reported earlier.[7,17] The catalytic wave is highly temperature-dependent, and more sensitive at higher temperatures. Hence temperature control is imperative and our experiments were done at $34 \pm 0.1°$ unless otherwise stated.

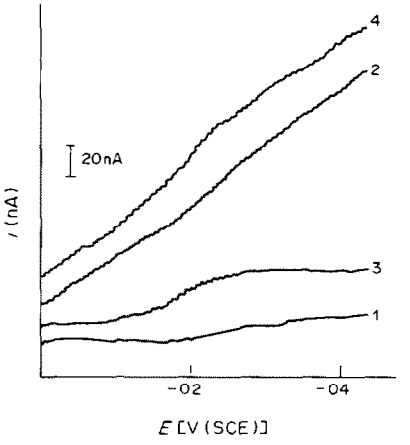

Fig. 1. Polarograms of 7.7-μg/l. molybdenum in (1) perchlorate medium with CCC (charging-current compensation), (2) perchlorate medium without CCC, (3) nitrate medium with CCC, and (4) nitrate medium without CCC.

Figure 2 shows typical polarograms used to construct the calibration graph for molybdenum. A sensitivity of 2 nA.ml.ng^{-1} was obtained at 34°; under the same conditions, the diffusion-controlled wave of molybdenum in 0.25*M* sulphuric acid gives a sensitivity of only 50 nA.ml.μg^{-1}.

The high blank problem. Whichever analytical technique is employed to determine the molybdenum stripped from the organic layer, a major problem is the high blank due to the simultaneous extraction of isopolymolybdic acid (IPMA), especially in the optical methods, where the large blank value may shift

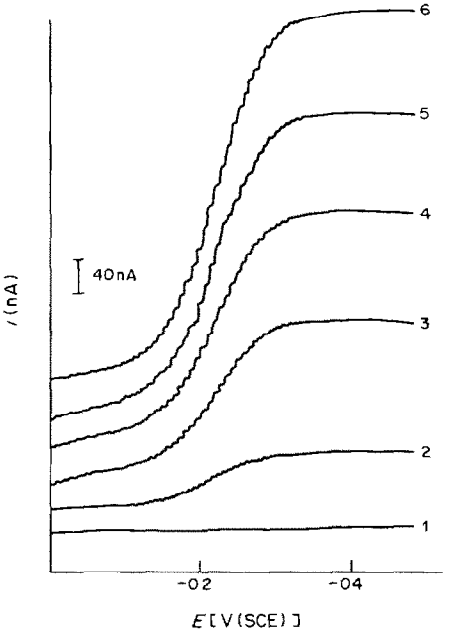

Fig. 2. Polarograms which were used for construction of the calibration graph for estimation of molybdenum in 0.25*M* sulphuric acid and 1*M* sodium nitrate. [Mo], ng/ml: (1) 0; (2) 47.5; (3) 94.1; (4) 140; (5) 184.6; (6) 230.7.

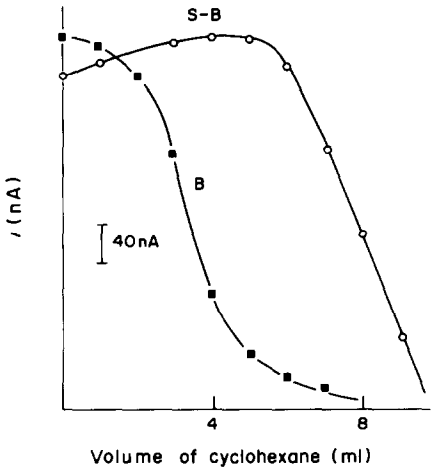

Fig. 3. Variation of blank and blank-corrected sample values with the addition of cyclohexane to the organic layer for 48 μg/l. arsenic. B = blank, S − B = blank-corrected sample values.

the sample absorbance to the non-linear region of the calibration graph. This shift does not arise in polarography because the calibration graph is linear up to a molybdenum concentration of $10^{-5}M$ (~ 1 μg/ml), but high blank values will necessitate operating the polarographic recorder at low current sensitivity, resulting in loss of overall sensitivity. Generally the organic layer is given an acidic wash to remove traces of IPMA, but the treatment varies considerably.[10,19,20] Chromatographic separation of IPMA has also been tried.[20]

A systematic study was undertaken to decrease this blank and it was found that the addition of small amounts of hydrocarbons (such as benzene or cyclohexane) to the organic layer, after extraction of the heteropoly acids, followed by a rigorous acidic wash, removed most of the IPMA from the organic layer. However, washing the isobutyl acetate extract of phosphomolybdic acid thrice with $2M$ hydrochloric acid was found to remove most of the IPMA and give maximum signal to blank ratio. Any effort to remove the residual IPMA was found to decrease the signal value as well.

In the case of arsenic, addition of hydrocarbons followed by an acid wash had a profound effect in decreasing the blank value. Figure 3 shows that addition of 5 ml of cyclohexane to the organic layer and then three washes each with 15 ml of $2M$ hydrochloric acid (30 sec shaking) was optimal.

In the case of silicomolybdic acid, addition of the citrate solution minimized the simultaneous extraction of IPMA, and acid washing still further decreased the blank value. The blank for silicon determination was quite high compared with that for arsenic and phosphorus, however, probably because of the presence of silicon as an impurity in the reagents used.

Extraction and stripping. The extraction conditions are based on earlier work[1,21] and give good sequential separation of the three heteropoly acids. For convenience, the same acidity can be used for extraction of phosphomolybdic acid and arsenomolybdic acid.

For silicon it is better to add the acid in two portions, first to form the HPMA and then to protonate it for extraction.[22,23] Although silicomolybdic acid is not formed at high acidity ($>0.7M$ H^+), once formed at lower acidity it remains quite stable on further acidification and is extractable even from $1M$ acid. Methyl isobutyl ketone (MIBK), 1-butanol, diethyl ether/1-pentanol (5:1), 1-pentanol and isoamyl alcohol were tested as solvents. The lowest blank values were obtained with the diethyl ether/pentanol mixture, but the best signal to blank ratio was obtained with MIBK, which was therefore chosen for the extraction. Shaking the organic phase for 1 min with 10 ml of $0.5M$ sodium hydroxide gave complete stripping for all three heteropoly acids.

Simultaneous determination of phosphorus, arsenic and silicon

The procedure was employed for the sequential determination of phosphorus, arsenic and silicon and the results are shown in Table 1.

Interference studies

Foreign ions may interfere at two stages: in the formation and extraction of the HPMA, and in the polarography. The first type of interference has already been studied[1] and confirmed by our observations. The second type of interference was investigated in this study and it was found that none of the reagents used in the procedure caused any interference. The shapes of the polarograms were also not distorted. This is clearly seen in Fig. 4, which shows typical polarograms for determination of arsenic, silicon and phosphorus.

Table 1. Determination of phosphorus, arsenic and silicon in the presence of each other

Phosphorus, μg		Arsenic, μg		Silicon, μg	
taken	found	taken	found	taken	found
0.020	0.017	0.50	0.52	0.50	0.55
0.050	0.058	2.00	2.17	3.00	3.15
0.50	0.51	3.00	2.94	2.00	2.03
0.20	0.25	5.00	5.04	1.00	0.94
1.00	0.98	1.00	1.10	5.00	4.90

Table 2. Sensitivity and detection limit for the estimation of phosphorus, arsenic and silicon

Element	Inherent sensitivity, $mA.l.\mu g^{-1}$	Inherent detection limit, $\mu g/l.$	Detection limit obtained by the present procedure, $\mu g/l.$
Phosphorus	80	0.1	0.5
Arsenic	8.5	0.94	4.7
Silicon	65	0.12	3.0

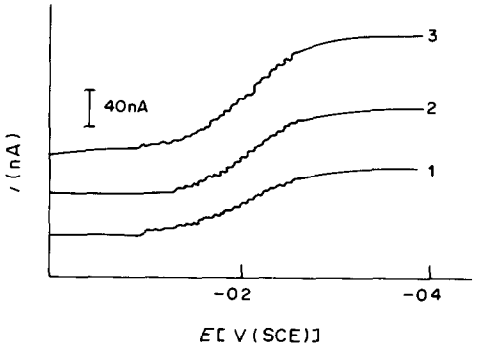

Fig. 4. Polarograms of stripped molybdenum equivalent to (1) 9.3 μg/l. arsenic; (2) 1.9 μg/l. silicon; (3) 0.8 μg/l. phosphorus.

Precision

The relative standard deviations were established (eight determinations) and were 2.3% for phosphorus (0.5 μg), 2.4% for arsenic (5.0 μg) and 2.3% for silicon (4.0 μg).

Sensitivity and detection limit

The sensitivities and detection limits are summarized in Table 2. Inherent sensitivity means the slope of the calibration graph. The values given were obtained from polarograms recorded at a recorder sensitivity of 40 nA/cm. The concentration which would give a wave-height of 8 nA (*i.e.*, twice the noise level of the instrument used) is called the inherent detection limit. The practical detection limits obtained by the present procedure were 5 times the inherent detection limit for phosphorus and arsenic, but 25 times that for silicon because of the high blank values and necessity to operate the recorder at lower sensitivity.

Conclusions

It is shown that the combination of two methods of increasing the sensitivity makes it possible to determine phosphorus, arsenic and silicon at ng/ml levels by d.c. polarography. The methods proposed give greater sensitivity than any of the other indirect methods reported earlier for determination of these elements.

REFERENCES

1. T. V. Ramakrishna, J. W. Robinson and P. W. West, *Anal. Chim. Acta*, 1969, **45,** 43.
2. G. F. Kirkbright, A. M. Smith and T. S. West, *Analyst*, 1967, **92,** 411.
3. T. R. Hurford and D. F. Boltz, *Anal. Chem.*, 1968, **40,** 379.
4. D. E. Leyden, W. K. Nonidex and P. W. Carr, *ibid.*, 1975, **47,** 1449.
5. A. Bazzi and D. F. Boltz, *Anal. Lett.*, 1976, **9,** 1111.
6. A. G. Fogg and K. S. Yoo, *ibid.*, 1976, **9,** 1035.
7. R. Kannan and S. R. Rajagopalan, *Proceedings of the Second International Symposium on Industrial and Oriented Basic Electrochemistry* at IIT, Madras, December 1980, p. 4.7.1.
8. R. Kannan and S. R. Rajagopalan, in M. Sankar Das (ed.), *Trace Analysis and Technological Development*, p. 86. Wiley Eastern Limited, 1983.
9. S. R. Rajagopalan, *Bull. Mater. Sci.*, 1983, **5,** 317.
10. S. C. Height, F. Bet-Pera and B. Jaselskis, *Talanta*, 1982, **29,** 721.
11. A. Poojari and S. R. Rajagopalan, *J. Electroanal. Chem.*, 1975, **62,** 51.
12. S. R. Rajagopalan, A. Poojari and S. K. Rangarajan, *ibid.*, 1977, **75,** 135.
13. R. Holtge and R. Geyer *Z. Anorg. Chem.*, 1941, **246,** 243.
14. M. G. Johnson and R. J. Robinson, *Anal. Chem.*, 1952, **24,** 366.
15. I. M. Kolthoff and I. Hodara, *J. Electroanal. Chem.*, 1963, **5,** 2.
16. K. Yokoi, T. Ozeki, I. Watanabe and S. Ikeda, *ibid.*, 1982, **132,** 191.
17. B. Stach and K. Schöne., *Mikrochim. Acta*, 1977 **II,** 565.
18. A. T. Violanda and W. D. Cooke, *Anal. Chem.*, 1964, **36,** 2287.
19. P. Tekula-Buxbaum, *Mikrochim. Acta*, 1981 **II,** 183.
20. J. F. Tyson and G. D. Stewart, *Anal. Proc.*, 1981, **18,** 184.
21. J. Paul, *Mikrochim. Acta*, 1965, 830, 836.
22. C. H. Leuck and D. F. Boltz, *Anal. Chem.*, 1958, **30,** 183.
23. A. Halász, K. Polyák and E. Pungor, *Talanta*, 1971, **18,** 691.

Talanta, Vol. 32, No. 5, pp. 423–429, 1985
Printed in Great Britain

0039-9140/85 $3.00 + 0.00

APPLICATIONS OF THE DICARBOLLYLCOBALTATE(III) ANION IN THE WATER/NITROBENZENE EXTRACTION SYSTEM

EMANUEL MAKRLÍK and PETR VAŇURA
Nuclear Research Institute, 250 68 Řež, Czechoslovakia

(*Received* 25 *July* 1984. *Accepted* 31 *October* 1984)

Summary—The fundamental properties of the polyhedral sandwich dicarbollylcobaltate(III) anion $\{[\pi\text{-}(3)\text{-}1,2\text{-}B_9C_2H_{11}]_2Co(III)\}^-$ are given, together with results for extraction of alkali-metal, alkaline-earth metal and some other cations (*e.g.*, H^+, Pb^{2+}, Pd^{2+} and Ce^{3+}) into nitrobenzene and corresponding analytical applications. Considerable attention is paid to charge-transfer through the water–nitrobenzene interface in the presence of this hydrophobic anion.

The complex dicarbollylcobaltate(III) anion $\{[\pi\text{-}(3)\text{-}1,2\text{-}B_9C_2H_{11}]_2Co(III)\}^-$ may be prepared by the original method[1,2] or more advantageously by its modification[3] according to the following scheme:

$$1,2\text{-}B_{10}C_2H_{12} \xrightarrow{KOH/CH_3OH} [(3)\text{-}1,2\text{-}B_9C_2H_{12}]^- \quad (1)$$

$$[(3)\text{-}1,2\text{-}B_9C_2H_{12}] \xrightarrow{Co^{2+},KOH/H_2O} \{[\pi\text{-}(3)\text{-}1,2\text{-}B_9C_2H_{11}]_2Co(III)\}^- \quad (2)$$

The surface of this voluminous anion, the symmetric sandwich structure[4] of which is presented in Fig. 1, is formed of hydrogen atoms, which increase the hydrophobic character of the anion, and therefore the solubility of salts of this anion in non-aqueous solvents, *e.g.*, nitrobenzene, nitromethane, 2,2′-dichlorodiethyl ether, is relatively high.

Dicarbollylcobaltate(III) is a member of the group of polyhedral heteroborane anions that do not possess a free electron pair for binding a proton, so the compound $H^+\{[\pi\text{-}(3)\text{-}1,2\text{-}B_9C_2H_{11}]_2Co(III)\}^-$ is totally dissociated in aqueous as well as in nitrobenzene solutions and is one of the strongest acids at present known.

The anion $\{[\pi\text{-}(3)\text{-}1,2\text{-}B_9C_2H_{11}]_2Co(III)\}^-$ is considered to have a sandwich-type spatial configuration in which the central cobalt atom is in the formal oxidation state +III, with two hexaelectron ligands $[(3)\text{-}1,2\text{-}B_9C_2H_{11}]^{2-}$ π-bonded to it. Six vacant orbitals of the central Co(III) atom are supposed to be filled with the 2×6 binding electrons of the two $[(3)\text{-}1,2\text{-}B_9C_2H_{11}]^{2-}$ ligands so that the d^6-configuration of Co(III) is completed to give stable 18-electron valence shell. At the same time, each of the two supposed twelve-vertex fragment units of $Co(III)B_9C_2H_{11}$ (see Fig. 1) exhibits a stable[5–7] closed structure with $2n + 2$ ($n = 12$) skeletal electrons and consequently with the maximum delocalized electron density.[8] In accord with that, the skeleton of this voluminous diamagnetic anion is highly resistant to radiation,[9–13] heat,[14] and strong acids and oxidation–reduction agents.[8]

These properties of the dicarbollylcobaltate(III) anion, together with its low specific charge, make this anion and some of its halogen derivatives excellent agents for the extraction of cations from aqueous solutions into some organic solvents, especially polar ones (*e.g.*, nitrobenzene), or their mixtures.

Extraction of cations from the aqueous phase into nitrobenzene

The dicarbollylcobaltate(III) anion (henceforth referred to as DCC^-), in the form of the acid (HDCC) was first utilized by Rais *et al.*[15] as an agent mainly suitable for the extraction of caesium* or other large cations from water into organic solvents containing

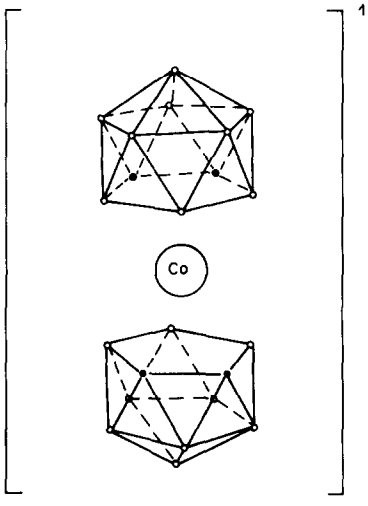

Fig. 1. Structure of dicarbollylcobaltate anion (symbols ● and ○ denote groups CH and BH, respectively).

*This has found application in a registered patent for caesium isolation[16] (*e.g.*, from irradiated nuclear fuel), that is shortly to be put into operation on at least a pilot-plant scale.

nitro-group (nitrobenzene, nitromethane, nitropropane). As the equilibrium distribution ratio of DCC^- between nitrobenzene and water in the HDCC extraction system did not depend (within experimental error) on the initial concentration of HDCC in the organic phase, the distribution of HDCC in this system may be expressed as a two-phase equilibrium

$$H^+(w) + DCC^-(w) \overset{K_{ex}(H^+,DCC^-)}{\rightleftharpoons} H^+(nb) + DCC^-(nb) \quad (3)$$

where $\log K_{ex}(H^+, DCC^-) \approx 3.1$; symbols w and nb refer to the aqueous and nitrobenzene phases, respectively. The exchange extraction constants K_M^{Cs} (M = Li, H, Na, NH_4, K, Rb) reported,[15] corresponding to the reaction

$$Cs^+(w) + M^+(nb) \overset{K_M^{Cs}}{\rightleftharpoons} Cs^+(nb) + M^+(w) \quad (4)$$

were in good agreement with those determined earlier.[17] The selectivity of the extraction separation of alkali-metal cation pairs Cs^+/M^+, estimated from the K_M^{Cs} value, did not depend on the particular DCC^- derivative used.

Macášek *et al.*[18] found that the exchange extraction constant K_H^{Cs} was practically the same whether the organic phase used was nitrobenzene–bromoform (4:1 v/v), nitrobenzene–tetrachloromethane (3:2 v/v) or nitrobenzene.

On the basis of the assumption that the ΔG values for transfer of tetraphenylarsonium cations (TPA^+) and tetraphenylborate anions (TPB^-) from water into nitrobenzene are equal, individual extraction constants of several derivatives of DCC^- have been determined radiometrically (see Table 1).[19] These constants (K'_{A^-}) express in principle the affinity of the anion for the nitrobenzene phase and are therefore a quantitative measure of the hydrophobicity of the anion. From comparison of the values for tetraphenylborate or dipicrylaminate (DPA^-) anions ($\log K'_{TPB^-} = 6.3$, $\log K'_{DPA^-} = 6.9$)[17] with the values in Table 1 it follows that the DCC^- anion and especially its derivatives are still more hydrophobic than the TPB^- and DPA^- anions.

Škarda *et al.*[20] proved by conductivity measurements that the salts of the type MDCC ($M^+ = Li^+$, H^+, Na^+, K^+, Rb^+, Cs^+, Tl^+ and Et_4N^+) were totally dissociated in nitrobenzene saturated with water, to the corresponding solvated ions M^+ and DCC^-, in contrast to the dipicrylaminates, tetraphenylborates and α-hexylates of alkali or alkaline-earth metals, which form ion-pairs in nitrobenzene.[21–23] The hydration numbers (h) of these univalent ions (mean number of water molecules co-extracted per cation in the equilibrium nitrobenzene phase) were determined:[20]

$$h_{Li^+} = 6.5,\ h_{H^+} = 5.5,\ h_{Na^+} = 3.9,\ h_{K^+} = 1.5,$$
$$h_{Rb^+} = 0.8,\ h_{Cs^+} = 0.5,\ h_{Et_4N^+} = h_{DCC^-} = 0.0.$$

It follows that the degree of hydration of these ions in the non-aqueous phase decreases with increasing affinity of the ions for the nitrobenzene phase. For the tetraethylammonium cation, no evidence of hydration was found experimentally.[20] It was also found that the degree of hydration of Li^+ and H^+ in 2,2′-dichlorodiethyl ether saturated with water was practically identical with that in water-saturated nitrobenzene, whereas in nitromethane saturated with water it was much higher.[20]

From a large number of experimental data it was found[24–26] that the extraction of both trace and weighable amounts of Ba^{2+} and Ce^{3+} from aqueous solutions of nitric or perchloric acids into nitrobenzene (in the presence of HDCC) could be satis-

Table 1. Individual extraction constants (K'_{A^-}) of some dicarbollylcobaltate(III) anions in the water-nitrobenzene system[19] at 298 ± 1 K

Anion	$\log K'_{A^-}$
$[(B_9C_2H_{11})_2Co]^-$; 3,3′-*commo*-bis(undecahydro-1,2-dicarba-3-3-cobalta-*closo*-dodecaborate)	8.8
$[(B_9C_2H_{10}Br)_2Co]^-$; 3,3′-*commo*-bis(8-bromoundecahydro-1,2-dicarba-3-cobalta-*closo*-dodecaborate)	10.0
$[(B_9C_2H_{10}I)_2Co]^-$; 3,3′-*commo*-bis(8-iodoundecahydro-1,2-dicarba-3-cobalta-*closo*-dodecaborate)	10.2
$[(B_9C_2H_8Br_3)_2Co]^-$; 3,3′-*commo*-bis(8,9,12-tribromoundecahydro-1,2-dicarba-3-cobalta-*closo*-dodecaborate)	10.7
$[C_6H_4(B_9C_2H_{10})_2Co]^-$; 8,8′[*o*-phenylene]-3,3′-*commo*-bis(undecahydro-1,2-dicarba-3-cobalta-*closo*-dodecaborate)	9.3
$[C_6H_2(CH_3)_2(B_9C_2H_{10})_2Co]^-$; 8,8′[*o*-xylylene]-3,3′-*commo*-bis(undecahydro-1,2-dicarba-3-cobalta-*closo*-dodecaborate)	9.8
$[C_6H_2(CH_3)_2(B_9C_2H_{10})_2Co]^-$; 8,8′[*p*-xylylene]-3,3′-*commo*-bis(undecahydro-1,2-dicarba-3-cobalta-*closo*-dodecaborate)	9.8
$[C_{10}H_{10}(B_9C_2H_{10})_2Co]^-$; 8,8′[tetrahydronaphthylene]-3,3′-*commo*-bis(undecahydro-1,2-dicarba-3-cobalta-*closo*-dodecaborate)	9.9
$[C_6H_5—C_6H_3(B_9C_2H_{10})_2Co]^-$; 8,8′[phenyl-*o*-phenylene]-3,3′-*commo*-bis(undecahydro-1,2-dicarba-3-cobalta-*closo*-dodecaborate)	10.2

factorily described by the equilibria:

$$Ba^{2+}(w) + 2H^+(nb) \overset{K_{2H}^{Ba}}{\rightleftharpoons} Ba^{2+}(nb) + 2H^+(w) \quad (5)$$

$$Ce^{3+}(w) + 3H^+(nb) \overset{K_{3H}^{Ce}}{\rightleftharpoons} Ce^{3+}(nb) + 3H^+(w) \quad (6)$$

It was proved experimentally that the hydration number h_{H^+} increases with increasing concentration of HDCC in the non-aqueous phase as well as with decreasing acidity of the aqueous phase; in the two-phase nitric acid/HDCC–nitrobenzene and perchloric acid/HDCC–nitrobenzene systems with identical initial mineral acid concentration and identical HDCC content in the initial organic phases, h_{H^+} was always higher in the nitric acid system. The mean hydration numbers of Ba^{2+} and Ce^{3+} in nitrobenzene saturated with water were also determined ($h_{Ba^{2+}} = 11.5 \pm 1.0$, $h_{Ce^{3+}} = 16.2 \pm 2.0$) together with the extraction constants ($\log K'_{Ba^{2+}} = -10.5 \pm 0.1$, $\log K'_{Ce^{3+}} = -15.8 \pm 0.2$). The logarithms of the extraction constants of the alkali-metal cations, the proton, and Ba^{2+} and Ce^{3+}, decrease linearly with the hydration number of the ions extracted into the nitrobenzene phase.[24–26]

Extraction of tervalent actinide and lanthanide ions from acidic aqueous solutions by means of HDCC or $H[B_{18}C_4H_{15}Cl_7Co]$ in nitrobenzene was studied by Benešová *et al.*[27] To increase the difference between the densities of the aqueous and organic phases, the nitrobenzene was diluted with tetrachloromethane or bromoform. The distribution ratios of the actinides and lanthanides are very similar, so these elements cannot be efficiently separated by extraction. The tervalent cations can be stripped from the organic phase with a sufficiently high concentration of nitric acid or sodium nitrate solution, or with some basic compounds (*e.g.*, 1-propanol, hydrazine, urea).[27]

Thiourea complexes of technetium (most likely cationic) have been extracted from nitric acid into nitrobenzene–bromoform (4:1 v/v) mixture with HDCC;[28] this has been employed for separation of ^{99m}Tc from ^{95}Zr–^{95}Nb nuclide decay products.

Equilibrium distribution ratios $>10^2$ have been found for palladium in the nitric acid/nitrobenzene–$H[(B_9C_2H_{10}Br)_2Co]$–1,10-phenanthroline (or α,α′-bipyridyl) systems.[29] These systems seem to be potentially useful for the isolation of palladium even from highly radioactive solutions, because 1,10-phenanthroline in particular is very stable towards radiation.

Rais *et al.*[30] observed a large synergic effect during the extraction of microamounts of Ca^{2+}, Sr^{2+}, Ba^{2+} or Pb^{2+} into nitrobenzene with hydrophobic anions (DCC^-, polyiodides, dipicrylaminate, tetraphenylborate) in the presence of polyethylene glycols with molecular weights of 200, 300, 400, 600 and 1000 (PEG 200, PEG 300, PEG 400, PEG 600, PEG 1000). This effect was ascribed to increase in the cation hydrophobicity caused by polyethylene glycol.

Šebesta *et al.*[31] studied the distribution of Ba^{2+} and Ra^{2+} between hydrochloric acid and nitrobenzene in the presence of HDCC and PEG 1000. The presence of 0.1% PEG 1000 in the aqueous phase gave the highest distribution ratios for both elements when the initial concentration of HCl in the aqueous phase (c_{HCl}) was $0.1M$ and the initial concentration of HDCC in nitrobenzene was $0.01M$. In the hydrochloric acid concentration range $0.1–1.0M$ (under otherwise unchanged conditions), the synergic effect of the PEG 1000 increased the distribution ratios by a factor of about 10^4, whereas at $c_{HCl} < 0.1M$ the distribution ratios decreased with decreasing acidity down to $c_{HCl} \approx 0.01M$, at which an antagonistic effect began. No explanation of this effect of PEG 1000 has been found. Experiments in our laboratory indicate that the original duration of shaking used was insufficient for equilibrium to be reached in the low acidity systems, and the apparent decrease in degree of extraction may have been due to a lower rate of equilibration.

Vaňura *et al.*[32] studied the extraction of microamounts of ^{85}Sr in the presence of PEG 400 with DCC^- from water into nitrobenzene. Maxima on plots of the distribution ratio of strontium as a function of the analytical concentration of polyethylene glycol in the aqueous phase was attributed to competitive action between the charged complex $SrPEG^{2+}$ and the protonated polyethylene glycol $HPEG^+$ as counter-ions of DCC^- in the organic phase. Theoretical relations were derived for the shape of these plots and also for the effect of the concentration of DCC^- in the organic phase on the shape of the plots and the positions of the maxima. The theoretically derived relationships were in accord with the experimental data.

The following equilibria characterize the distribution of microamounts of $^{85}Sr^{2+}$ or $^{133}Ba^{2+}$ in the perchloric (or nitric acid)/nitrobenzene–PEG–HDCC system[32,33]

$$M^{2+}(w) + 2H^+(nb) \overset{K_{ex}(M^{2+})}{\rightleftharpoons} M^{2+}(nb) + 2H^+(w) \quad (7)$$

$$L(w) \overset{K_D}{\rightleftharpoons} L(nb) \quad (8)$$

$$L(w) + H^+(nb) \overset{K_{ex}(HL^+)}{\rightleftharpoons} HL^+(nb) \quad (9)$$

$$M^{2+}(w) + L(w) + 2H^+(nb) \overset{K_{ex}(ML^{2+})}{\rightleftharpoons} ML^{2+}(nb) + 2H^+(w) \quad (10)$$

where $M^{2+} = Sr^{2+}$ or Ba^{2+}, L = PEG 200, PEG 300 or PEG 400, $\log K_{ex}(Sr^{2+}) = 0.70$ and $\log K_{ex}(Ba^{2+}) = 0.85$. The values of the other equilibrium constants are collected in Table 2. The hydration numbers decrease with increasing stability of the complexes.[33] Similar conclusions apply[34] to the hydration of complex cations of the ML^+ type, where $M^+ = Li^+$, Na^+, NH_4^+, K^+, Rb^+ and Cs^+.

These results[30–33] demonstrate that polyethylene glycols are effective synergic agents, especially in the extraction of alkaline-earth metals. This property of

Table 2. Values deduced from the data for the M^{2+}–mineral acid–L/nitrobenzene–HDCC systems[33]

	PEG 200	PEG 300	PEG 400
K_D	1.6×10^{-3}	1.5×10^{-3}	1.3×10^{-3}
log $K_{ex}(HL^+)$	1.72	2.51	2.87
log $K_{ex}(SrL^{2+})$	6.96	8.29	8.84
log $K_{ex}(BaL^{2+})$	8.98	10.19	10.76
log $\beta(HL^+)$	4.52	5.33	5.75
log $\beta(SrL^{2+})$	9.06	10.41	11.03
log $\beta(BaL^{2+})$	10.93	12.17	12.80
h_{HL^+}	3.7	2.9	2.3
$h_{SrL^{2+}}$	2.8	2.0	1.6
$h_{BaL^{2+}}$	1.7	1.3	1.0

polyethylene glycols and of some similar compounds has been utilized for extractive separation of strontium[35] and radium[36] from aqueous solutions.

Electrochemical study of the charge transfer across the water/nitrobenzene interface

The fundamental principles, concepts, and general relations that characterize the transfer of ions across the interface between two immiscible electrolyte solutions, studied by means of electroanalytical methods (polarography with the dropping electrolyte electrode, cyclic voltammetry, chronopotentiometry), together with applications and the demands made on the measuring technique and equipment, have been reviewed.[37,38]

As with classical electrochemical methods, it is necessary for both phases to be practically immiscible and to contain background electrolytes in sufficiently high concentrations. Very hydrophilic electrolytes suitable for the aqueous phase include the chlorides, bromides and sulphates of the alkali metals and magnesium. The background electrolyte of the organic phase must be very hydrophobic, and tetrabutylammonium (TBA^+), tetraphenylarsonium (TPA^+), tetraphenylborate (TPB^-) and dicarbollylcobaltate(III) compounds are suitable components. Tetrabutylammonium dicarbollylcobaltate (TBADCC) has been employed in several studies[39–42] but was probably contaminated with anionic impurities and these attempts to extend the "potential window"[38] were not successful. Only the use of sufficiently pure TBADCC or TPADCC led to this aim being achieved.

In contrast to the tetraphenylborate anion (until recently the anion most often used for the purpose, generally as TBATPB), which decomposes under the influence of light and mineral acids, DCC^- is completely inert towards strong acids (except fairly concentrated solutions of nitric acid) and light, and is also relatively thermally stable as well as not much affected by radiation. As HDCC and MDCC (M^+ is an alkali-metal cation or Tl^+) are completely dissociated in nitrobenzene saturated with water,[20] the use of TBADCC or TPADCC as background electrolyte in the nitrobenzene phase ensures that transfer of protons and M^+ across the water/nitrobenzene interface is not complicated by ion-association in the nitrobenzene phase and may be taken as a "simple" transfer.[43,44]

The transfer of caesium and tetramethylammonium (TMA^+) ions across the water–LiCl/nitrobenzene–TBADCC interface has been studied by cyclic voltammetry.[43] The temperature-dependence of the polarographic half-wave potentials for the transfer of Cs^+ and TMA^+ across the interface, together with some thermodynamic data published earlier,[17,45,46] made it possible to determine the enthalpy and entropy changes of transfer of certain ions from the aqueous into the nitrobenzene phase[43] (see Table 3). Transfer of the hydrophilic cations Li^+, Na^+ and H^+ is endothermic, the "endothermicity" increasing in the order $H^+ < Na^+ < Li^+$. Conversely, the transfer of K^+, Rb^+, Cs^+ and TMA^+, similarly to transfer of the hydrophobic dipicrylaminate anion (DPA^-) from the aqueous phase into nitrobenzene, is always exothermic. From the thermodynamic point of view it is significant that the transfer of the univalent ions listed in Table 3 is always accompanied by an entropy decrease ($\Delta S^{*,w\to nb}_{tr,i} < 0$), which means that each of these ions is in a more ordered environment in the nitrobenzene phase than in the aqueous phase. It is interesting[43] that the absolute values of the entropy changes $|\Delta S^{*,w\to nb}_{tr,i}|$ increase in the order $Li^+ < Na^+ < H^+ < K^+$ but decrease in the order $K^+ > Rb^+ > Cs^+ > TMA^+ > DPA^-$.

If TBATPB is the supporting electrolyte used in the nitrobenzene phase, then Cs^+ is transferred from the aqueous into the organic phase at a more negative Galvani potential difference, $\Delta^w_{nb}\phi = \phi(w) - \phi(nb)$, than when the electrolyte is TBADCC. This effect has been explained as due to formation of the ion-pair Cs^+TPB^- in the nitrobenzene phase:[44]

$$Cs^+(nb) + TPB^-(nb) \overset{K_a}{\rightleftharpoons} Cs^+TPB^-(nb) \qquad (11)$$

The following relation was derived for the polarographic half-wave potential $E^{(1)}_{1/2}$ for the reversible transfer of Cs^+ from the aqueous into the organic phase, in which the ion-pair Cs^+TPB^- is formed:[44]

$$E^{(1)}_{1/2} = \Delta^w_{nb}\phi^\circ_{Cs^+} + (RT/2F)\ln[D^w_{Cs^+}/(D^{nb}_{Cs^+} + D_{CsTPB}K_a c^{o,nb}_{TPB^-})(1 + K_a c^{o,nb}_{TPB^-})] \qquad (12)$$

where $\Delta^w_{nb}\phi^\circ_{Cs^+}$ is the standard Galvani potential difference for the Cs^+ cation between the aqueous

Table 3. Thermodynamic values[17,43] for transfer of some univalent ions in the mutually saturated water–nitrobenzene system at 298 K

Ion	$\Delta G^{*,w\to nb}_{tr,i}$, *kJ/mole*	$\Delta H^{*,w\to nb}_{tr,i}$, *kJ/mole*	$\Delta S^{*,w\to nb}_{tr,i}$, $J.mole^{-1}.K^{-1}$
Li^+	38.2	37.1	−3.6
Na^+	34.2	25.6	−28.9
H^+	32.5	16.8	−52.7
K^+	23.4	−8.1	−105.6
Rb^+	19.4	−7.8	−91.1
Cs^+	15.4	−10.3	−86.3
TMA^+	3.4	−9.3	−42.6
DPA^-	−39.4	−44.3	−16.6

and nitrobenzene phase,[37,47] D^{w}_{Cs+} and D^{nb}_{Cs+} are the diffusion coefficients of Cs^+ in the aqueous and nitrobenzene phases respectively, D^{nb}_{CsTPB} is the diffusion coefficient of the ion-pair Cs^+TPB^- in the nitrobenzene phase, $c^{o,nb}_{TPB-}$ is the initial analytical concentration of TPB^- in the nitrobenzene phase, and K_a is the association constant corresponding to equilibrium (11). For the polarographic half-wave potential $E^{(2)}_{1/2}$ of a "simple" reversible transfer of the Cs^+ ion from water into nitrobenzene, uncomplicated by the formation of an ion-pair or by chemical reactions in both phases:

$$E^{(2)}_{1/2} = \Delta^{w}_{nb}\phi^{o}_{Cs+} + (RT/2F)\ln(D^{w}_{Cs+}/D^{nb}_{Cs+}) \qquad (13)$$

Relation (13) follows from (12) when $K_a = 0$. The difference $\Delta E_{1/2}$ between $E^{(2)}_{1/2}$ and $E^{(1)}_{1/2}$ is

$$\Delta E_{1/2} = E^{(2)}_{1/2} - E^{(1)}_{1/2} = (RT/2F)\ln\{1 + (1+\delta)K_a c^{o,nb}_{TPB-} + \delta K_a^2[c^{o,nb}_{TPB-}]^2\} \qquad (14)$$

where $\delta = D^{nb}_{CsTPB}/D^{nb}_{Cs+} \approx D^{nb}_{TPB-}/D^{nb}_{Cs+}$. Relation (14) was employed when calculating the individual K_a values in the temperature interval between 278 and 338 K from experimentally determined $\Delta E_{1/2}$ values. From the linear dependence of log K_a on $1/T$, the value of ΔH for reaction (11) was found to be -17.2 kJ/mole (for the temperature range 293–338 K). The voltammetric measurements gave a value of 1×10^2 for K_a at 298 K (corresponding to $\Delta G = -11.4$ kJ/mole), which does not significantly differ from the value $K_a = 1.2 \times 10^{-2}$, obtained from extraction measurements at 298 ± 1 K. The corresponding entropy change is $\Delta S = -19.5$ J.mole^{-1}.K^{-1}.

It was also proved by cyclic voltammetry that proton transfer across the water/nitrobenzene interface, facilitated by an electroneutral ligand L (L = 18-crown-6) in the nitrobenzene phase (Fig. 2, System 1) or by DPA^- present as TPADPA in the non-aqueous phase (Fig. 2, System 2), is in any case a very fast process controlled by diffusion of L or DPA^- to the interface.[48–50] The results can be used to determine the values of $\beta(HL^+)$ and K for the equilibria (15) and (16) in the nitrobenzene phase of Systems 1 and 2.

$$H^+(nb) + L(nb) \overset{\beta(HL^+)}{\rightleftharpoons} HL^+(nb) \qquad (15)$$

$$H^+(nb) + DPA^-(nb) \overset{K}{\rightleftharpoons} HDPA(nb) \qquad (16)$$

For the polarographic half-wave potentials $E_{1/2}$ and $E'_{1/2}$ corresponding to reversible transfer of protons from the aqueous into the nitrobenzene phase, the following relations hold[48–50] (a general relation for cation transfer facilitated by an electroneutral ligand was first published by Koryta[37]):

$$E_{1/2} = \Delta^{w}_{nb}\phi^{o}_{H+} - (RT/F)\ln[\beta(HL^+)c^{o,w}_{H+}] \qquad (17)$$

$$E'_{1/2} = \Delta^{w}_{nb}\phi^{o}_{H+} - (RT/F)\ln(Kc^{o,w}_{H+}) \qquad (18)$$

where $\Delta^{w}_{nb}\phi^{o}_{H+} = 0.337$ V is the standard Galvani potential difference for protons between the aqueous and nitrobenzene phases,[37,47] found from extraction data.[17] Relations (17) and (18) are based on the simplifying assumption (evidently justified) that the diffusion coefficients of L and DPA^- in the nitrobenzene phase do not differ substantially from those of their protonated forms, *i.e.*, $D^{nb}_{L} \approx D^{nb}_{HL+}$ and $D^{nb}_{DPA-} \approx D^{nb}_{HDPA}$. From the experimentally determined half-wave potential $E_{1/2}$ and the known values of $\Delta^{w}_{nb}\phi^{o}_{H+}$ and $c^{o,w}_{H+}$, the value log $\beta(HL^+) = 5.9$ was determined by means of relation (17). The value log $K = 6.9$ was similarly calculated from equation (18).

aqueous phase	nitrobenzene phase	aqueous phase	nitrobenzene phase
HCl	TBADCC (TPADCC) L	HCl	TPADCC TPADPA
$c^{o,w}_{H+} \gg c^{o,nb}_{L}$		$c^{o,w}_{H+} \gg c^{o,nb}_{DPA-}$	
System 1		System 2	

Fig. 2. Two-phase systems for electrochemical study of proton transfer across the water/nitrobenzene interface; TBADCC (or TPADCC) is the supporting electrolyte in the nitrobenzene phase; $c^{o,w}_{H+}$, $c^{o,nb}_{L}$ and $c^{o,nb}_{DPA-}$ denote the initial concentrations of protons, L and DPA^- in the aqueous (w) or nitrobenzene (nb) phase.

Hung[51] found that synthetic DL-α-lecithine ($C_{40}H_{82}NO_9P$) dissolved in the nitrobenzene phase considerably slowed down both the simple transfer of the picrate anion and several cations (Cs^+, TMA^+, Li^+, TBA^+), and also the transfer of Na^+ (facilitated by dibenzo-18-crown-6) from the aqueous into the nitrobenzene phase (in the presence of TBADCC). This effect most likely resulted from the existence of a compact lecithine monolayer at the interface. The effect decreased with increasing temperature, which may be explained as a result of transition of the rigid crystalline structure of the monolayer to a liquid crystal structure or as a result of thermal increase of the disorder of the lecithine monolayer.[51] Lecithine has also been observed to slow down interfacial electron transfer between the $[Fe(CN)_6]^{3-}/[Fe(CN)_6]^{4-}$ couple in the aqueous phase and ferrocene dissolved in nitrobenzene.[51] Conversely, the transport of alkaline-earth metal cations (Ca^{2+}, Sr^{2+} and Ba^{2+}) across the water/nitrobenzene interface was facilitated by lecithine in the organic phase, probably by formation of lecithine complexes of the bivalent cations.[51]

Kolicine E_3 dissolved in the aqueous phase slows down transport of Cs^+ across the water–LiCl/nitrobenzene–TBADCC interface.[52]

Analytical application of extraction systems with the dicarbollylcobaltate(III) anion

Štefek *et al.*[53] found that the extraction system Sr^{2+}–PEG 400–$H^+\{[\pi\text{-}(3)\text{-}1,2\text{-}B_9C_2H_8Br_3]_2Co(III)\}^-$–water/nitrobenzene is not suitable for substoichiometric determination of strontium but can be

used for its determination by the concentration-dependent distribution method, which could be combined with isotopic dilution to allow the determination of strontium in the presence of barium and calcium.

A rapid method of separation of ^{90}Sr and ^{137}Cs from a solution of long-lived fission products has been developed for radioanalytical purposes.[54] The ^{137}Cs is extracted from a solution containing diethylenetriaminepenta-acetic acid (DTPA) and citrate (pH = 8) by HDCC solution in nitrobenzene, followed by extraction of the strontium at pH 4 by HDCC solution in nitrobenzene in the presence of PEG 400. The separation factors for the couples Cs/Sr and Sr/fission-products exceeded 10^4.

Selucký *et al.*[55] have developed a rapid extraction separation of radium from acidic solutions of thorium and its decay products. The radium is extracted with HDCC solution in nitrobenzene in the presence of *p*-nonylphenylnonaethylene glycol (Slovafol 909). The radium can easily be stripped into aqueous solution after dilution of the organic phase with di-isopropyl ether. This method may be used for the preparation of ^{224}Ra stock solutions.

HDCC or its chlorinated derivative $H[C_4B_{18}H_{15}Cl_7Co]$ can be used for the extraction of trace amounts of ^{137}Cs from nitric acid containing some radionuclides (^{144}Ce, ^{60}Co, ^{106}Ru–^{106}Rh, ^{95}Zr–^{95}Nb, ^{65}Zn) into nitrobenzene.[56] Microamounts of ^{137}Cs were found to be extracted nearly quantitatively, especially at low acidities of the aqueous phase; ^{106}Ru and ^{95}Zr passed into the organic phase only in small amounts, and ^{144}Ce, ^{60}Co and ^{65}Zn were practically not extracted at all. The equilibrium distribution ratios of these radionuclides decreased with increasing nitric acid concentration in the aqueous phase, but the separation factors for isolation of ^{137}Cs from the other radioisotopes increased with increasing nitric acid content in the initial aqueous phase, except for that from ^{106}Ru (which did not change much).

A study of the effect of macroamounts of some alkali-metal cations (Li^+, Na^+, K^+) on the distribution ratio of caesium in the nitric acid/nitrobenzene–HDCC system showed the possibility of direct separation of caesium from acid-digests of biological materials that did not contain large amounts of potassium (Li^+ and Na^+ did not interfere).[57]

Ščasnár and Koprda[58] also studied the chemical yield for ^{137}Cs as well as the selectivity of separation of ^{137}Cs from ^{144}Ce, ^{106}Ru, ^{60}Co, ^{65}Zn and ^{95}Zr, with a model mixture in nitric acid and also with acid-digests of spiked biological tissues, for a variety of analytical separation methods (adsorption on precipitates of $Co_2[Fe(CN)_6]$, $Cu_2[Fe(CN)_6]$ and ammonium phosphomolybdate; liquid–liquid extraction in the water–nitrobenzene system by means of HDCC or its chlorinated derivative $H[C_4B_{18}H_{15}Cl_7Co]$). It was found that only the extraction method could simultaneously ensure both high separation selectivity and sufficient yield of ^{137}Cs, and it was made the basis of the rapid routine isolation of ^{137}Cs from milk,[59] urine,[60] faeces[60] and biological materials[61] contaminated with a mixture of radionuclides.

Finally, a rapid and selective method for extractive isolation of radiostrontium from urea by using a nitrobenzene solution of HDCC in the presence of PEG has been developed.[62]

Conclusions

The dicarbollylcobaltate(III) anion and some of its halogen derivatives are very useful reagents for the extraction of alkali-metal cations (especially Cs^+), and also (in the presence of polyoxyethylene compounds) for the extraction of Sr^{2+} and Ba^{2+} from aqueous solution into an organic phase consisting of pure nitrobenzene or its mixtures with some less polar solvents (*e.g.*, CCl_4, $CHBr_3$), both under laboratory conditions for purely theoretical or analytical purposes, and on the technological scale for the separation of some high-activity isotopes in the reprocessing of irradiated nuclear fuel.

The dicarbollylcobaltate(III) anion, when employed as a component of the supporting electrolyte in the organic phase, has also found application in electrochemical studies on the processes taking place at the water/nitrobenzene interface. The results of these studies provide important information on the processes taking place in biological membranes and also in classical liquid–liquid extraction, especially in the water–nitrobenzene system.

REFERENCES

1. M. F. Hawthorne and T. D. Andrews, *J. Chem. Soc., Chem. Commun.*, 1965, **19,** 443.
2. M. F. Hawthorne, D. C. Young and P. A. Wegner, *J. Am. Chem. Soc.*, 1965, **87,** 1818.
3. M. F. Hawthorne, D. C. Young, T. D. Andrews, D. V. Hove, R. L. Pilling, A. D. Pitts, M. Reintjes, L. F. Warren and P. A. Wegner, *ibid.*, 1968, **90,** 879.
4. G. B. Dunks and M. F. Hawthorne, *Boron Hydride Chemistry*, E. L. Muetterties (ed.), p. 383. Academic Press, New York, 1975.
5. R. E. Williams, *Advan. Inorg. Chem. Radiochem.*, 1976, **18,** 67.
6. K. Wade, *ibid.*, 1976, **18,** 1.
7. R. Rudolph, *Acc. Chem. Res.*, 1976, **9,** 446.
8. J. Plešek, K. Baše, F. Mareš, F. Hanousek, B. Štíbr and S. Heřmánek, *Collection Czech. Chem. Commun.*, in preparation.
9. J. Rais and J. Teplý, *Radiochem. Radioanal. Lett.*, 1975, **22,** 119.
10. L'. Mátel and R. Čech, *ibid.*, 1977, **28,** 67.
11. L'. Mátel, R. Čech, F. Macášek, S. Heřmánek and J. Plešek, *ibid.*, 1977, **29,** 317.
12. *Idem, ibid.*, 1978, **35,** 241.
13. L'. Mátel, F. Macášek and H. Kamenistá, *ibid.*, 1981, **46,** 1.
14. V. Škarda, *Thesis*, Nuclear Research Institute, Řež, 1976.
15. J. Rais, P. Selucký and M. Kyrš, *J. Inorg. Nucl. Chem.*, 1976, **38,** 1376.

16. M. Kyrš, S. Heřmánek, J. Rais and J. Plešek, *Czech. Patent* 182 913.
17. J. Rais, *Collection Czech. Chem. Commun.*, 1971, **36,** 3253.
18. F. Macášek, L'. Mátel and M. Kyrš, *Radiochem. Radioanal. Lett.*, 1978, **35,** 247.
19. E. Makrlík, J. Rais, K. Baše, J. Plešek and M. Kyrš, *Collection Czech. Chem. Commun.*, in press.
20. V. Škarda, J. Rais and M. Kyrš, *J. Inorg. Nucl. Chem.*, 1979, **41,** 1443.
21. J. Rais, M. Kyrš and M. Pivoňková, *ibid.*, 1968, **30,** 611.
22. M. Pivoňková and M. Kyrš, *ibid.*, 1969, **31,** 175.
23. J. Rais and M. Kyrš, *ibid.*, 1969, **31,** 2903.
24. I. Podzimek, M. Kyrš and J. Rais, *ibid.*, 1980, **42,** 1481.
25. I. Podzimek, M. Kyrš, J. Rais and P. Vaňura, *Polyhedron*, 1983, **2,** 331.
26. I. Podzimek, *Thesis*, Nuclear Research Institute, Řež, 1978.
27. M. Benešová, L. Kuča, M. Kyrš, H. Petržílová and J. Rais, *Management of Alpha-Contamined Wastes*, p. 563. International Atomic Energy, Vienna (IAEA-SM-246/72), 1980.
28. P. Rajec, R. Kopunec and F. Macášek, *Radiochem. Radioanal. Lett.*, 1976, **26,** 51.
29. F. Macášek, R. Kopunec, V. Mikulaj, R. Čech, L'. Másel, J. Kadrabová, P. Rajec, A. Švec, H. Kamenistá, V. Širaňová, J. Kuruc, P. Tarapčík and M. Koreňovská, *Report, J. A. Komenský University of Bratislava, Department of Nuclear Chemistry*, 1980.
30. J. Rais, E. Šebestová, P. Selucký and M. Kyrš, *J. Inorg. Nucl. Chem.*, 1976, **38,** 1742.
31. F. Šebesta, E. Bílková and J. Sedláček, *Radiochem. Radional. Lett.*, 1979, **40,** 135.
32. P. Vaňura, J. Rais, P. Selucký and M. Kyrš, *Collection Czech. Chem. Commun.*, 1979, **44,** 157.
33. P. Vaňura, E. Makrlík, J. Rais and M. Kyrš, *ibid.*, 1982, **47,** 1444.
34. E. Makrlík and M. Kyrš, *ibid.*, in preparation.
35. J. Rais, M. Kyrš and S. Heřmánek, *Czech. Patent* 153 933.
36. F. Šebesta, V. Jirásek, J. Sedláček and J. Rais, *Czech. Patent* 180 850.
37. J. Koryta, *Electrochim. Acta*, 1979, **24,** 293.
38. Z. Samec, V. Mareček, P. Vanýsek, and J. Koryta, *Chem. Listy*, 1980, **74,** 715.
39. P. Vanýsek, *Thesis*, Charles University, Prague, 1976.
40. *Idem, Thesis*, Charles University, Prague, 1977.
41. J. Koryta, P. Vanýsek and M. Březina, *J. Electroanal. Chem.*, 1977, **75,** 211.
42. J. Koryta, P. Vanýsek, H. Jänchenová and M. Březina, *Elektrokhimiya*, 1977, **13,** 706.
43. E. Makrlík and L. Q. Hung, *J. Electroanal. Chem.*, 1983, **158,** 269.
44. *Idem, ibid.*, 1983, **158,** 285.
45. J. Rais, M. Benešová-Pacltová, P. Selucký and M. Kyrš, *J. Inorg. Nucl. Chem.*, 1973, **35,** 633.
46. M. Kyrš, M. Benešová-Pacltová, Z. B. Maksimovič and A. G. Maddock, *ibid.*, 1974, **36,** 1865.
47. L. Q. Hung, *J. Electroanal. Chem.*, 1980, **115,** 159.
48. A. Hofmanová, L. Q. Hung and E. Makrlík, *Proc. J. Heyrovský Memorial Congress on Polarography*, Prague, 25–29 August 1980, p. 66.
49. E. Makrlík, A. Hofmanová and L. Q. Hung, *J. Electroanal. Chem.*, in preparation.
50. Z. Samec, D. Homolka, V. Mareček and E. Makrlík, *ibid.*, in preparation.
51. L. Q. Hung, *Thesis*, J. Heyrovský Institute of Physical Chemistry and Electrochemistry, Prague, 1980.
52. M. Behrendt, *Thesis*, Charles University, Prague, 1981.
53. M. Štefek, M. Kyrš and J. Rais, *Zh. Analit. Khim.*, 1976, **31,** 1364.
54. P. Selucký, P. Vaňura, J. Rais and M. Kyrš, *Radiochem. Radioanal. Lett.*, 1979, **38,** 297.
55. P. Selucký, J. Rais and K. Jindřich, *ibid.*, 1980, **42,** 115.
56. V. Ščasnár and V. Koprda, *ibid.*, 1978, **34,** 23.
57. V. Koprda and V. Ščasnár, *J. Radioanal. Chem.*, 1979, **51,** 245.
58. V. Ščasnár and V. Koprda, *Radiochem. Radioanal. Lett.*, 1979, **39,** 75.
59. V. Koprda and V. Ščasnár, *ibid.*, 1980, **44,** 349.
60. V. Ščasnár and V. Koprda, *J. Radioanal. Chem.*, 1980, **59,** 389.
61. V. Koprda and V. Ščasnár, *Chem. Zvesti*, 1980, **34,** 480.
62. V. Ščasnár and V. Koprda, *ibid.*, 1982, **36,** 379.

Talanta, Vol. 32, No 5, pp. 431–433, 1985
Printed in Great Britain

0039-9140/85 $3.00 + 0.00

SHORT COMMUNICATION

A TIMED SOLENOID INJECTOR FOR FLOW ANALYSIS

S. D. ROTHWELL and A. A. WOOLF
School of Chemistry, Bath University, Bath, England

(*Received* 17 *July* 1984. *Revised* 18 *October* 1984. *Accepted* 12 *December* 1984)

Summary—Samples can be reproducibly injected into flow-streams by timed switching of a sample stream with a miniature solenoid valve and timer circuit. The device is simpler to assemble and use than the standard rotary valve and a direct comparison under the same operating conditions shows that the solenoid valve is an adequate replacement for the rotary valve.

Samples are generally introduced into flow-analysis systems by means of rotary valves with fixed-volume loops.[1] Such valves are expensive because they require careful construction to ensure alignment of the fine bores in the stators and rotors. Also a continuous variation in sample size is not possible. A change in sample size requires a change in the loop or rotor.

An economical timed solenoid valve is described which can provide samples in a continuous range of sizes at any time intervals desired. It can be readily assembled from "off the shelf" components and can be adapted for more complicated flow regimes. In essence it uses temporal, as opposed to spatial, control of injections. The performance of the timed solenoid valve has been compared with that of a standard rotary valve in a typical flow analysis, the determination of phosphate.

EXPERIMENTAL

Apparatus for phosphate determination

This was based on Růžička and Hansen's manifold[1] illustrated in Fig. 1, labelled according to their conventions. Different injectors were inserted at S. The rotary valve shown by Růžička and Hansen[2] was improved by inserting four O-rings (5 mm inner diameter, 8 mm outer diameter) around the bores on the inside faces of the stators, and clamping the assembly with four peripheral bolts rather than a central one. Rotary friction was reduced because the discs rotated on the small bearing surface of the compressed O-rings and not on the whole disc areas. This enabled us to dispense with the difficultly machinable polytetrafluoroethylene stator and to use only polystyrene discs. The quality of the surface finish of the polystyrene could also be lowered without causing leakage.

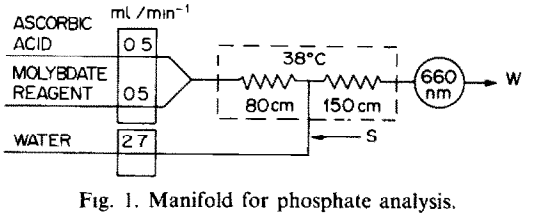

Fig. 1. Manifold for phosphate analysis.

The alternative injector was a three-way solenoid valve [Lee No. LFAA 1200118A][3] of overall size 33 × 12 mm. The actual working volume of fluid is only 100 μl and the valve-rubber travel about 1 mm on activation. At 12 V d.c. and 23 mA the solenoid will work against a pressure differential of 0.69 atm and at 19 V d.c. against a differential of up to 2 atm. The inlet and outlet had a bore of 0.8 mm and could be inserted into the 1-mm bore manifold tubing without use of special seals. This valve was attached at S as shown in Fig. 2. A simple timer circuit, which can turn the coil current on and off at fixed intervals, is shown in Fig. 3. The start switch initiates a sequence which leaves the solenoid inactive for 5–250 sec intervals, adjustable by means of R_1, followed by activation for 0.1–100 sec intervals, adjustable with R_2. The sequence carries on without resetting. The sample stream was run at a suitable flow-rate through a restricting coil to give a steady positive insertion pressure.

Reproducibility test on solenoid valve

The water emerging from the carrier-stream line during a time-period corresponding to 40 "valve open" cycles was collected and weighed. The difference between this weight and that of the water emerging from the carrier-stream line in the same period of time with the valve permanently closed gave the weight (and hence volume) of 40 samples. Times were not measured accurately, but set to approximately the required value by adjusting the timer resistances.

Dispersion measurements

Dispersions were measured with Bromothymol Blue indicator as described by Růžička and Hansen.[4] Residence times were obtained from the recorder traces and chart-speed.

RESULTS AND DISCUSSION

The mean relative deviations for injections of 380, 65.0 and 26.5 μl with the solenoid valve were 0.3, 0.3 and 1.2% respectively. The injection time for the last set of measurements was about 0.4 sec. The reproducibilities obtained with the solenoid valve were better than the range of timing error. The "555" timer has a specified maximum error of 0.5%, and for the larger volumes, averaged over 40 samples, the mean deviations were about half this value. For the smallest samples the deviations increased because the response time of the valve, quoted as 3 msec, became

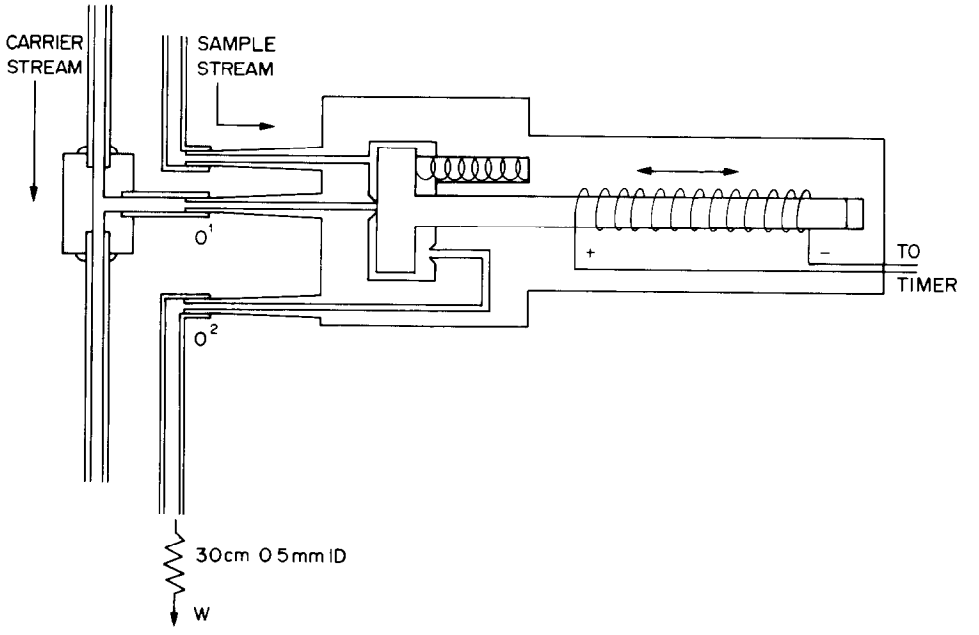

Fig. 2. Solenoid valve injector. Solenoid off, O^1 closed; solenoid on, O^2 closed.

an appreciable fraction (0.75%) of the time the valve was open. Smaller samples could be injected with the same accuracy as larger ones by reducing the sample flow-rate.

The sample residence time within the manifold was less when the solenoid valve was used, because of the higher flow-rate during injection (Table 1). A simple calculation shows that there is no appreciable change in resistance to flow on substituting the new valve. The equivalent-resistance length L of 1 mm tubing for the solenoid valve is given by:[5]

$$17.0 = \pi(0.05)^2 L \left(\frac{13}{17 Q_c} + \frac{4}{17 Q_o}\right)$$

where Q_c and Q_o are the carrier and sample stream flow-rates, with the valve closed and open respectively. This gives $L = 154$ cm for the solenoid valve, compared with $L = 151$ cm, calculated for the rotary valve at the Q_o rate, with the valve closed for

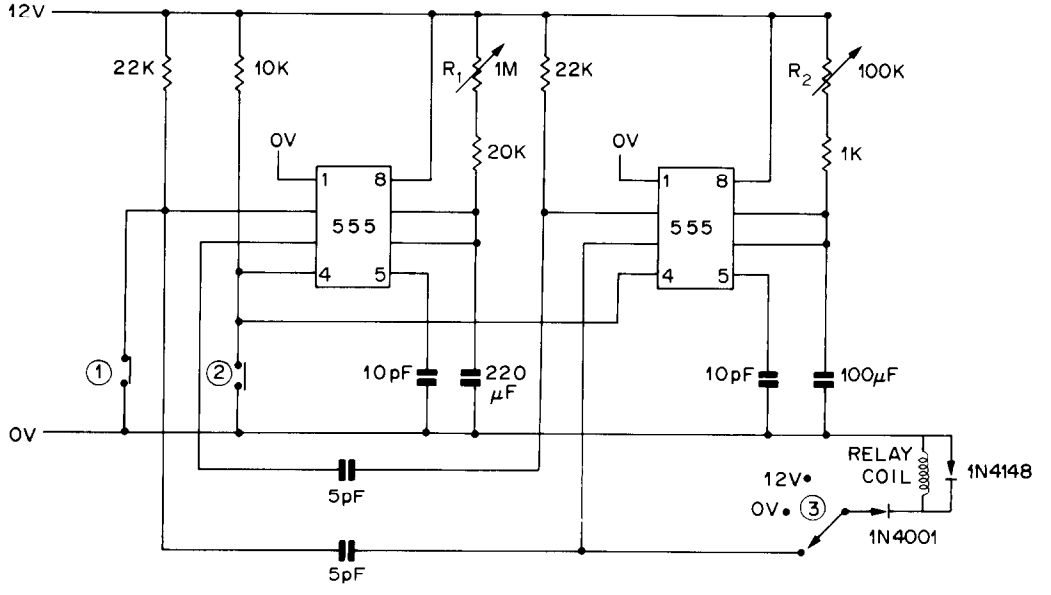

Fig. 3. Timer circuit. Start switch (1); reset switch (2); on, off and continuous cycle positions on switch (3).

Table 1. Comparison of dispersions and residence times with rotary valve (R) and solenoid valve(s)

Sample size, *µl*	Residence time, *sec*	Dispersion, *D**
340 (S)	16.3	2.33
289 (S)	17.0	2.47
285 (R)	19.2	2.69

* $D = C^{\circ}/C^{max}$ where C° is the undiluted dye concentration and C^{max} the concentration recorded at the peak maximum.

13 sec and open for 4 sec. The actual length of tubing used was 150 ± 1 cm.

The dispersion obtained was about 9% less with the solenoid valve, probably because the faster flow produces a shorter residence time. The absorption peaks recorded when the solenoid valve was used were still non-Gaussian (Fig. 4). If the peak width at half-height is taken as 2σ, the sampling rate can be between 110 and 170 samples/hr for peak separations of 6σ and 4σ respectively. The solenoid valve was operated at 105 samples/hr without any peak overlap resulting. This contrasted with only 77 samples/hr possible with the rotary valve. For both valves peristaltic pump pulsations were observed on the trace recorded at 50 mm/min, but were not detectable at the normal recording rate of 5 mm/min. Such fluctuations have been found not to be eliminated by using a pulse-damping device.[6]

The overall reproducibility of peak heights is marginally inferior when the solenoid valve is used (the average deviation is about 0.6% more than for rotary valve injection) (Table 2). It should be noted that almost half of the standard deviation results from errors in measuring peak heights. These readings were accurate to 0.3 mm which is 1.2, 0.6 and 0.4% of the heights of the 1, 2 and 4 ppm peaks respectively. Other inaccuracies arose from variations in sample volume (~0.3%) and colour development. The calibration graph obtained by use of the solenoid valve could be made less curved by adjusting parameters such as sample size or flow-rate.

Further miniaturization of solenoid-valve injection is an obvious development, since integrated-circuit timers accurate to 0.01% and smaller valves with fluid volumes as small as 10 µl are available, but for normal flow-injection analysis the unmodified device is a satisfactory replacement for the rotary valve. Timed-injection solenoid valves could also replace the multiple injection valves used in merging-zone flow analysis.[7]

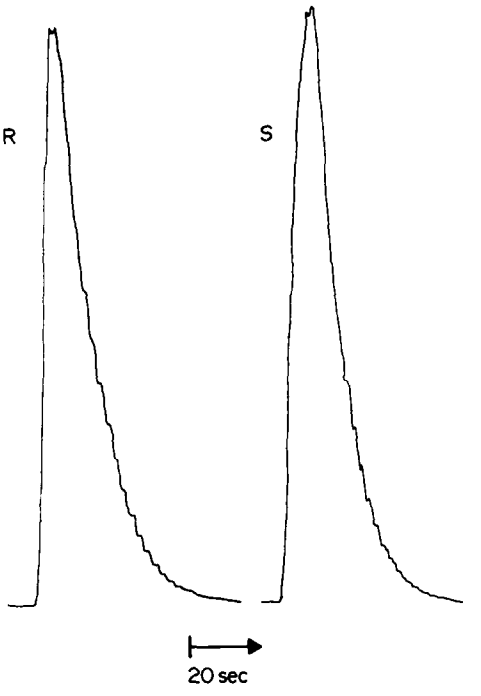

Fig. 4. Profile of absorption–time curves for rotary (R) and solenoid (S) valves.

REFERENCES

1. J. Růžiča and E. H. Hansen, *Flow Injection Analysis*, p. 135. Wiley, New York, 1981.
2. *Idem*, *op. cit.*, p. 105.
3. The Lee Company, 2 Pettipang Road, Westbrook CTO 6498.
4. J. Růžička and E. H. Hansen, *op. cit.*, p. 131.
5. *Idem*, *op. cit.*, p. 20.
6. H. Bergamin Filho, B. F. Ries and E. A. G. Zagatto, *Anal. Chim. Acta*, 1978, **97**, 427.
7. H. Bergamin Filho, E. A. G. Zagatto, F. J. Krug and B. F. Ries, *ibid.*, 1978, **101**, 17.

Table 2. Comparison of calibration data for phosphate determinations with rotary (R) and solenoid (S) valves

Valve	S			R		
Sample size, *µl*	380			285		
Conc., *ppm*	1	2	4	1	2	4
Mean peak height, *mm*	25.1	47.7	76.2	25.1	45.9	87.1
Number of readings	12	11	11	11	10	10
Sampling rate/*hr*$^{-1}$	105			77		
Standard deviation, *mm*	0.6	0.8	1.1	0.4	0.4	1.0
Relative std. devn., %	2.4	1.7	1.4	1.7	1.0	1.1

Talanta, Vol. 32, No. 5, pp. 435–438, 1985
Printed in Great Britain

0039-9140/85 $3.00 + 0.00
Pergamon Press Ltd

ANNOTATION

EFFECT OF CONTAINER MATERIAL, STORAGE TIME AND TEMPERATURE ON DETERMINATIONS OF CADMIUM LEVELS IN HUMAN URINE

KUNNATH S. SUBRAMANIAN, JEAN-CHARLES MERANGER and JOHN CONNOR
Environmental Health Directorate, Health and Welfare Canada, Tunney's Pasture, Ottawa, Ontario, Canada

(*Received* 6 *July* 1984. *Revised* 6 *December* 1984. *Accepted* 11 *January* 1985)

Summary—The effect of container material (polyethylene, polypropylene, polystyrene, borosilicate glass and flint glass), storage time (0–86 days), and temperature (22° and 4°) on the cadmium content found by graphite-furnace atomic-absorption spectrometry for spiked and unspiked urine samples has been studied. No loss of cadmium occurred for at least 10 and 28 days when unspiked and spiked samples respectively, were stored in polyethylene containers at 22°. For storage up to 3–4 days at 22°, polypropylene, polystyrene, borosilicate glass and flint glass containers were also found suitable. Storage at 4° was not effective in preventing loss of cadmium.

The detection of cadmium in human urine may be used for identifying groups at risk of cadmium toxicity.[1] Sensitive and selective methods capable of determining ng/ml levels of cadmium in human urine are now available,[2] but the data obtained by their use are meaningful only if the various factors affecting the accuracy and precision of the determination have been identified and controlled. Some of these factors are: (*i*) type of container material used for collecting and storing the urine samples; (*ii*) temperature of storage; (*iii*) duration of storage. In spite of the importance of these factors no studies seem to have been made of the stability of cadmium in urine on storage. In view of this, it was thought advisable to study the effect of container type, storage time and temperature on the levels of cadmium in unspiked and spiked human urine samples. The findings of this study are reported here.

EXPERIMENTAL

Apparatus

A Perkin–Elmer model 603 atomic-absorption spectrophotometer equipped with an HGA-500 graphite furnace, a deuterium-arc background-corrector and a Hamamatsu hollow-cathode lamp operated at 10 mA and a resonance wavelength of 228.8 nm (spectral band-pass 2.0 nm) was used for the determination of cadmium. Nitrogen was used as the purge gas and its flow was interrupted during the atomization step.

The containers used for storing the spiked and unspiked urine samples were: (*i*) polyethylene bottles, 250-ml capacity, with Teflon-lined plastic screw-caps (cat. no. F10610-0008, Canus Plastics, Ottawa, Ontario); (*ii*) sterile polystyrene urine specimen containers, 90-ml capacity, with white plastic screw-caps (cat. no. C8841-57, Starplex, Scientific, Mississauga, Ontario); (*iii*) sterile polypropylene urine specimen-containers, 115-ml capacity, with polyethylene screw-caps (cat. no. C8841-201, Canadian Laboratory Supplies); (*iv*) borosilicate glass serum bottles, 100-ml capacity (cat. no. B7761-100, Canadian Laboratory Supplies); (*v*) flint glass bottles, 125-ml capacity, with polypropylene screw-caps (cat. no. B7772-125, Canadian Laboratory Supplies). The red rubber stoppers recommended by the manufacturer for the glass serum bottles were found to be contaminated with cadmium, so they were replaced with parafilm closures.

All the containers were cylindrical in shape and were purchased from Canadian Laboratory Supplies Limited, Ottawa, Ontario. Before use, all the containers were freed from traces of cadmium as described earlier,[3] by a detergent wash, tap-water rinse, soaking in 2% ultrapure nitric acid for 24 hr, distilled water rinse (6 times) and ultrapure water rinse (6 times). After the cleaning operation, any containers found to give blanks when filled with ultrapure water acidified to pH 1.0 with ultrapure nitric acid having no detectable levels of cadmium, were rejected.

Reagents

High-purity water was obtained by passing tap water through a cellulose adsorbent and two mixed-bed ion-exchange columns, and finally distilling in a Corning AG-11 unit. The quality of the water conformed to ASTM Type 1 specification.[4] In addition, the cadmium level in the water was below the graphite-furnace atomic-absorption (GFAA) detection limit (3 times the standard deviation of the blank) of 0.1 ng/ml.

A certified atomic-absorption standard containing 1000 mg of cadmium per litre was obtained from Fisher Scientific. Fresh working standards of lower concentrations were prepared daily by serial dilution of the stock solution with high-purity water.

A 10% aqueous solution of diammonium hydrogen phosphate (Baker Analyzed Reagent) was prepared and purified as described elsewhere.[5]

All other reagents and solutions used were of the highest purity available.

Sample collection and storage

For studies with unspiked urine a 24-hr sample was collected from a laboratory volunteer, in a 2-litre Nalgene linear polyethylene bottle fitted with a polyethylene screw-cap, previously freed from traces of cadmium as described above. The pooled urine was homogenized by vortex mixing and its cadmium content immediately determined by graphite-furnace atomic-absorption spectrometry with addition of diammonium hydrogen phosphate and nitric acid as matrix-modifiers.[2] The measurement was done in quintuplicate.

From the homogenized pooled sample, 25-ml aliquots were pipetted into the polypropylene (PP), polystyrene (PS), borosilicate (BS), and flint glass (FG) containers, and 50-ml aliquots into polyethylene (PE) containers. The surface area of contact of the urine with the various containers was (cm^2): PP, 96; PS, 82; BS, 99; FG, 89; PE, 111. The containers were then stored at room temperature (22°) in a Class 100 clean hood and also at refrigerator temperature (4°). Each combination of container and temperature was run in triplicate. The samples from each container were then analysed on days 0, 1, 2, 4, 6, 10, 16, 20, 28, 58 and 86. Before analysis the refrigerated samples were allowed to attain room temperature, and all the samples in the various containers were thoroughly homogenized by vigorous vortex mixing.

For the studies with spiked urine, another 24-hr sample was collected from the same donor. The sample was vigorously vortex-mixed and spiked to give an added cadmium concentration of approximately 5 ng/ml. The same storage procedure was used and the sample were analysed on days 0, 1, 3, 7, 11, 14, 21, 28, 42, 59 and 66.

Analytical procedure

The concentration of cadmium in the unspiked urine sample was monitored by using the procedure developed earlier.[2] For each container, a 0.5-ml aliquot of sample was pipetted into a precleaned 1-ml Pyrex standard flask, followed by the addition of 20 μl each of 10% diammonium hydrogen phosphate solution and 10% v/v nitric acid. The solution was made up to the mark with high-purity water and vigorously vortex-mixed for 30 sec. A 10-μl aliquot of this solution was introduced into the graphite furnace with an Eppendorf pipette fitted with a disposable polypropylene tip which had been decontaminated as described elsewhere.[3] The cadmium in the sample was atomized by raising the temperature to 120° in 20 sec and holding at that temperature for 30 sec (drying), heating to 550° in 10 sec and holding there for 30 sec (ashing), heating to 2100° in 1 sec and holding for 5 sec (atomization) and finally heating to 2500° in 1 sec and holding for 2 sec (cleaning). The peak absorbance values for four replicate injections were averaged. A duplicate was run for each container at each temperature. The cumulative averages of the duplicates from each of the three containers at each temperature (*i.e.*, the average of 24 measurements) were then used to calculate the recovery of cadmium as a function of time.

The amount of cadmium in the urine sample immediately after pooling (time "zero", in fact approximately 60 min), and on the various days of storage, were calculated by use of a calibration graph prepared from a cadmium-free control urine (Product no. 2934-80. Level I, Fisher Scientific) spiked with various amounts of cadmium (0.5, 1.0 and 2.0 ng/ml) and the matrix modifiers as already described. A blank containing only the matrix modifiers, and a urine control spiked with 1.0 ng/ml cadmium and the matrix modifiers, were run once every 30 min during the analytical measurements to compensate for any small changes in the working graphs, resulting from conditions beyond the analyst's control. Also, a fresh matrix-matched calibration graph was prepared on each day the sample were tested. In addition, the blank and the 1-ng/ml spike prepared on day 0 (zero) were re-analysed on other days of sample measurement, to obtain the day-to-day precision.

The procedure for the spiked urine sample was basically the same as that above except that the sample and the control were diluted five-fold (*i.e.*, 0.2 ml of urine plus 20 μl of each matrix modifier, diluted to 1 ml with high-purity water).

RESULTS AND DISCUSSION

Analytical methodology

The atomic-absorption method has been fully described elsewhere, and gave within-run and between-day precision values, expressed as coefficient of variation (% CV), within 3–11% at cadmium concentrations of 0.5–2.4 ng/ml in human urine.[2] In the present study the within-run and day-to-day CV were found to be 3.5 and 5.0% respectively, for a cadmium concentration of 2.17 ng/ml in the pooled 24-hr urine sample, and 3.4 and 3.8% respectively, for the urine control containing a cadmium spike concentration of 1.0 ng/ml. In the earlier work, the overall mean analytical recovery of cadmium from five urine samples (native contents ranging from 0.5 to 2.7 ng/ml, supplemented with 0.4–1.0 ng of Cd per ml) was $103.24 \pm 4.3\%$. The method has a detection limit (concentration corresponding to 3 times the standard deviation of the blank) of 0.1 ng/ml and a linear range of 0–3 ng/ml. These analytical figures of merit demonstrate the suitability of the procedure[2] for the stability study conducted here.

Storage study

Preliminary studies showed little change in the cadmium concentration of a spot urine sample stored in PE, PP, PS BS or FG containers at 22° or 4° for at least a two-day period. Therefore it was decided to use a 24-hr collection from the same donor for the stability study.

The initial cadmium concentration (*i.e.*, value on day "zero") in the unspiked and spiked urine composite were 2.17 ± 0.08 and 7.06 ± 0.11 ng/ml respectively (the latter includes a spike of approximately 5.0 ng/ml). In the ensuing discussion these values are designated as 100%; the values on subsequent days are calculated as a percentage of the level on day 0 (zero).

Table 1 shows the recovery of cadmium from the unspiked urine as a function of time. No significant change occurred for at least 10 days of storage at 22° for any of the containers except the polystyrene ones. At refrigeration temperature significant loss of cadmium occurred even on the second day of storage from all the containers except those made of polypropylene, for which no loss was found for at least 4 days.

Table 2 shows the corresponding results for the spiked urine. At 22° no loss of cadmium occurred from any of the containers for at least 3 days, whereas at 4° there was no loss for 7 days except from the flint glass containers. At room temperature, by the 7th

Table 1. Effect of container material, time and temperature on cadmium levels in unspiked human urine

Container*	Recovery range of cadmium at various storage times (days), %							
	0† & 1	2	4	6 & 10	16 & 20	28	58	86
	Room temperature (22°)							
PE	90–110	90–100	90–110	90–110	75–81	68–80	16–20	13–15
PP	90–110	90–110	90–110	90–110	75–77	69–73	16–20	11–15
PS	90–110	90–110	90–110	81–85	79–81	69–75	15–19	12–16
BS	90–110	90–110	90–100	90–110	83–91	65–77	20–24	13–15
FG	90–110	90–110	90–110	90–110	82–86	74–76	15–17	14–16
	Refrigeration temperature (4°)							
PE	90–110	83–91	80–86	80–84	60–68	57–63	46–50	37–41
PP	90–110	90–110	90–110	75–83	64–72	63–65	49–51	39–43
PS	90–110	79–85	74–80	70–78	63–69	63–65	43–49	32–34
BS	90–110	85–91	81–87	68–76	60–72	53–63	53–55	33–41
FG	90–110	82–92	69–81	61–69	64–72	56–60	53–59	38–44

*PE = polyethylene; PP = polypropylene; PS = polystyrene; BS = borosilicate glass; FG = flint glass.
†"0" days corresponds to measurement within 60 min of sample pooling.

day of storage, losses had occurred from all the containers except those made of polyethylene or polystyrene. The urine stored in polyethylene showed no loss of cadmium for at least 28 days.

For the unspiked samples the losses at refrigeration temperature were higher than those at room temperature for at least 28 days. For the spiked samples the pattern was not so simple, but in general the loss at refrigeration temperature was lower than that at room temperature for at least 28 days, except for the samples stored in polyethylene containers.

From the results, storage of urine samples in PE at room temperature is seen to be best because no loss of cadmium occurred for at least 10 and 28 days respectively, when unspiked and spiked samples were stored in this material at 22°. For storage up to 3–4 days at 22° all five types of containers are suitable. Storage at refrigeration temperature did not improve the stability of the samples with respect to cadmium, the loss, especially from unspiked samples, being greater than at 22°. The reason for this is not clear. The loss of cadmium species from urine may occur by a number of mechanisms which could be chemical, physical or microbiological in nature. For example, urine is clear when voided but often precipitation (of uric acid and the oxalates, urates and phosphates of alkali and alkaline-earth metal ions) occurs on cooling.[6] Such crystalline substances are known to be surface-active and to remove metal ions by adsorption, occlusion and inclusion.[7] During refrigeration the extent of precipitation is generally greater, resulting in an increased loss of cadmium.

The loss of cadmium increases with storage time. On storage the urea in the urine samples is slowly converted into ammonium carbonate with release of ammonia and a consequent increase in pH.[6] It is generally known that the amount of trace metals adsorbed on surface increases with increasing pH.[8] Thus, one of the reasons for the increased loss of cadmium with increasing storage time could be the

Table 2. Effect of container material, time and temperature on cadmium levels in spiked urine*

Container†	Recovery range of cadmium at various storage times (days), %						
	0§ & 1 & 3	7	11 & 14	21 & 28	42	59	66
	Room temperature (22°)						
PE	90–110	90–110	90–110	90–110	78–82	69–77	62–78
PP	90–110	81–93	71–77	58–66	55–65	49–55	51–53
PS	90–110	90–110	69–77	65–69	51–65	49–53	45–51
BS	90–110	70–78	44–52	54–56	50–56	47–51	40–48
FG	90–110	77–83	49–59	52–56	42–52	43–45	32–40
	Refrigeration temperature (4°)						
PE	90–110	90–110	78–90	78–82	64–72	43–49	30–36
PP	90–110	90–110	78–86	72–74	55–59	23–31	14–16
PS	90–110	90–110	78–86	68–72	55–59	30–38	23–27
BS	90–110	90–110	81–87	58–62	44–48	26–28	13–17
FG	90–110	81–91	80–86	55–61	44–46	20–24	15–21

*The cadmium concentration of the spiked urine pool was 7.06 ± 011 ng/ml.
†PE = polyethylene; PP = polypropylene; PS = polystyrene; BS = borosilicate; FG = flint glass.
§"0" days corresponds to measurement within 60 min of sample preparation.

increased adsorption and co-precipitation of the metal, resulting from the increase in pH.

The cadmium concentration of urine is subject to temporal and diurnal variation but the average calculated for consecutive 24-hr collections shows little change.[9] Thus, 24-hr urine collection should be used for screening programmes and for identifying groups at risk of cadmium toxicity. The present study shows further that it is desirable to analyse the 24-hr sample either immediately or within ten days of collection. Storage in polyethylene containers at room temperature is found to be the most suitable. Finally, the observation that acidification and addition of bactericidal agents to urine samples are no longer a prerequisite, at least for ten days of storage in PE containers, may facilitate speciation studies undertaken to improve our knowledge of the nature of urinary cadmium compounds and cadmium metabolism.

REFERENCES

1. L. Friberg and M. Vahter, in *Analytical Techniques for Heavy Metals in Biological Fluids*, S. Facchetti (ed.), pp. 1–15. Elsevier, Amsterdam, 1983.
2. K. S. Subramanian, J. C. Méranger and J. E. Mackeen, *Anal. Chem.*, 1983, **55**, 1064.
3. K. S. Subramanian, C. L. Chakrabarti, J. E. Sueiras, and I. S. Maines, *ibid.*, 1978, **50**, 444.
4. *Annual Book of ASTM Standards*, Part 31, D1193-77, pp. 29–31. A.S.T.M., Philadelphia, 1981.
5. K. S. Subramanian and J. C. Méranger, *Int. J. Environ. Anal. Chem.*, 1979, **7**, 25.
6. H. Varley, A. H. Gowenlock and M. Bell, *Practical Clinical Biochemistry*, 5th Ed., Vol. 1, Chapters 12 and 33. Heinemann, London, 1980.
7. L. J. Stryker and E. Matijevic, in *Absorption from Aqueous Solution*, W. Weber, Jr, (ed.), p. 44. ACS, Washington, DC, 1968.
8. P. Beneš and I. Rajman, *Collection Czech. Chem. Commun.*, 1969, **34**, 1375.
9. K. S. Subramanian and J. C. Méranger, *Clin. Chem.*, 1984, **30**, 1110.

Talanta, Vol. 32, No. 6, pp. 439–445, 1985
Printed in Great Britain

0039-9140/85 $3.00 + 0.00
Pergamon Press Ltd

THE USE OF CERTIFIED REFERENCE MATERIALS IN THE VERIFICATION OF ANALYTICAL DATA AND METHODS*

R. SUTARNO and H. F. STEGER
Mineral Sciences Laboratories, CANMET, Energy, Mines and Resources Canada, Ottawa, Ontario, Canada

(*Received* 1 *June* 1984. *Revised* 24 *January* 1985. *Accepted* 7 *February* 1985)

Summary—An experimental design is proposed for the verification of the accuracy and precision of an analytical method by its application to certified reference materials.

The importance of certified reference materials, CRMs, in analytical chemistry is widely accepted. There are at least 130 producers of CRMs of all types in the Western World alone.[1] If only compositional CRMs such as ores, rocks and metal alloys are considered, there are at least 39 producers, who together offer approximately 250 reference ores, concentrates, rocks, soils and cements and over 2400 metal alloys.

CRMs are widely applied for quality control of analytical data by their use for the direct calibration of methods and instruments, verification of the precision, accuracy and sensitivity of methods used in control analyses, and the development and evaluation of new or reference methods. In spite of this, no general guidelines for the use of CRMs have been published. To remedy this, REMCO, the Council Committee on Reference Materials of the International Organization for Standardization, initiated the preparation of such a guide in September 1983.[2]

In the present paper we are not concerned with the appropriateness or the mechanics of the use of CRMs for these applications, but only the statistical transfer of the stated uncertainty in the certified value(s) and the application of this uncertainty by the analyst.

The use of CRMs in the direct calibration of methods and instruments has been studied by Oster *et al.* (France)[3] and by Mashiko *et al.* (Japan)[4] and is currently being expanded by Eberhardt (U.S.A.)[5] as contributions to the forthcoming REMCO guide. The use of CRMs in the determination of precision and accuracy and the sensitivity of methods, established or new, may have greater significance for the readers of analytical journals dedicated to the improvement of methodology. Most issues of such journals include one or more papers where CRMs are applied in this manner. A comparison of such papers readily shows that there is a variety of procedures for validating a modified or new method by applying it to CRMs. These vary from those based on statistical concepts to those based on subjective considerations. The latter approach has the potential danger that after the assessment with a CRM a user-analyst striving for high accuracy and precision may have doubts about his method that prove unfounded if the uncertainty in the certified values is taken into account.

To make analysts more aware of the concepts behind the use of CRMs, the Canadian Certified Reference Materials Project (CCRMP), on the basis of the experience of 13 years in the preparation of reference ores and related materials,[6,7] proposes the following experimental design for the use of CRMs in determination of the accuracy and precision of analytical methods†. The use of the proposed design should of course, do away with subjectivity.

Nature of CRMs

CRMs can be liquid, gaseous, or solid (as pure or mixed powders or individual artifacts). Regardless of their physical state, CRMs are packaged either in individually certified units or, more commonly, in units which are all assumed to be representative of a larger lot. In the latter case, the between-unit homogeneity is generally acceptable for all but the most exacting analytical purposes. Some CRMs however cannot be made truly homogeneous; the use of such materials will not be considered in this paper.

Certification

There are basically three types of analytical programmes for certification of a reference material. The first is by interlaboratory consensus,[8] a minimum of 10 laboratories analysing in replicate one or more units of the reference material for the elements of interest. A one-way analysis of variance is performed on the data. In one version of this programme the participating laboratories use the method of their

†This experimental design has also been submitted by CCRMP to REMCO.

choice. The following statistical parameters are then usually reported on the certification document.

A_c = the certified value for the content of an element. A_c is usually the overall mean of the results of the certification programme (or the mean of the laboratory means) but is sometimes some other central value such as the geometric mean or the median.

$V[A_c]$ = the variance of A_c, a measure of precision of the estimate of the consensus value. Alternatively, the precision may be expressed in terms of a confidence interval (usually 95%, which means that if the interlaboratory programme is repeated 100 times, it is expected that 95 of the resultant consensus means will fall within this confidence interval).

S_{Lc} = the between-laboratories standard deviation when each laboratory uses the method of its choice.

S_{rc} = the within-laboratory standard deviation when each laboratory uses the method of its choice.

In the second version of the programme, the participating laboratories use the same well-established widely-accepted analytical method. The statistical parameters usually reported are A_c, $V[A_c]$, defined as above, and σ_{Lc} and σ_{rc}.

σ_{Lc} = the between-laboratories standard deviation when all laboratories use the same method.

σ_{rc} = the within-laboratory standard deviation when all laboratories use the same method.

Certification by interlaboratory consensus is the most frequently encountered type of programme.

The second type of programme is met in certain specialized fields where it is impossible or impractical to arrive at a consensus value by a full interlaboratory programme. A small number of "expert" laboratories analyse the candidate reference material and the certified value A_c is arrived at by accepting the consensus value or taking into account "methodological" considerations.[9] There is no formal statistical evaluation of the analytical results. The uncertainty of the certified value of an element is based on chemical considerations.

In the third type of programme the certification is done by a single laboratory using a definitive method, *i.e.*, a method that is based on first principles, has high precision and for which the limits of uncertainty can be stated with a high degree of confidence.[10] In addition to accepting that the definitive method is the best available, the user assumes that the method is applied without bias. This assumption is usually made when the producer laboratory is a national or industrial reference laboratory where "superior" resources are available, or when the analysis involves a certain "art", and specialized skill is required. The statistical parameters reported are A_c and σ_{rc} of the definitive method as performed by the "expert" certifying laboratory. Some producers of reference materials also report an evaluation of any systematic error not included in σ_{rc}.

Validation of analytical methods

The concept presented here, of using CRMs to determine the precision and accuracy of an analytical method, rests on three basic premises. First, that the certified value of an element in a reference material is the best estimate of the true value. Second, when tested with a reference material certified by interlaboratory consensus, an analytical method is validated if the results are sufficiently precise and accurate to qualify for inclusion in the calculation of the statistical parameters for the interlaboratory programme for the CRM. That is, in statistical terms, they belong to the distribution used to characterize the CRM. Third, the relationship between the within-laboratory and between-laboratories standard deviation found to hold for reference materials certified by interlaboratory consensus, would also apply to a reference material certified by an "expert" certifying laboratory using a definitive method, if that material were certified by interlaboratory consensus. This last assumption is necessary because very few users can expect to achieve the same accuracy and precision as an "expert" certifying laboratory. In principle a between-laboratories variation must exist for every method.

Use of CRMs

All analytical methods have inherent errors. Random error is always present and may be accompanied by systematic error (bias). It is therefore highly unlikely that the result obtained by a method being tested will be exactly the same as the certified value of a CRM; an acceptable tolerance limit must therefore be defined for each CRM. This limit will depend partly on the mode of certification. The following criteria are proposed in assessing an analytical method by applying it to a CRM.

Precision. An analytical method is sufficiently precise if it produces results for a CRM that are statistically as precise as the within-laboratory precision stated in the certification document.

Accuracy. An analytical method is sufficiently accurate if it produces results for a CRM that do not differ from the certified value by more than can be accounted for by within- and between-laboratory statistical fluctuations.

GENERAL PROCEDURES FOR APPLYING AN ANALYTICAL METHOD TO A CRM

Validation of the CRM

Before a CRM is used, the following should be checked.

Certificate—certified value, precision, method of characterization, suggested sub-sample weight, and expiration date of certification (particularly for a relatively unstable CRM).

Visual check—segregation, discoloration and quantity.

Analysis of the CRM

Perform replicate determinations (on separate sub-samples) by the analytical method to be tested; n should be at least 10. For a periodic check of accuracy of an analytical method, duplicate analysis on each occasion is sufficient, but the total number of replicates should be at least 10.

Outliers

Use an outlier test such as the Dixon test to decide whether any of the results may be regarded as outliers. If an outlier is found, investigate possible physical causes for it. If an excessive number of results are found to be outliers and no physical cause can be identified, reinvestigate the analytical procedure.

Mean and standard deviation

Compute the following statistics for the results remaining after rejection of outliers.

$$\bar{X} = \sum_{i=1}^{n} X_i/n = \text{mean}$$

$$S_W = \sqrt{\sum_{i=1}^{n} \frac{(X_i - \bar{X})^2}{(n-1)}}$$

= estimated within-laboratory standard deviation, *i.e.*, precision of the method

Check of precision

This can only be performed if S_{rc} or σ_{rc}, the certified within-laboratory standard deviation, is given in the certificate, otherwise the precision should be judged by chemical considerations.

Compute

$$F = \frac{(S_W)^2}{(S_{rc})^2}$$

and compare F with the value of $F_c = F_{0\,95,n-1,DF_c}$ (obtainable from any statistics book). If the number of degrees of freedom DF_c for the CRM certification tests is not given in the certificate, use $DF_c = 60$. If $F \leqslant F_c$, the analytical method is sufficiently precise; if $F > F_c$, the analytical method is not as precise as those used for certification of the reference material.

Check of accuracy

If the between-laboratories standard deviation S_{Lc} or σ_{Lc} is reported for the CRM, *i.e.*, it was certified by interlaboratory consensus, then the following test should be used. If

$$|\bar{X} - A_c| \leqslant 2S_{Lc} \quad \text{or} \quad |\bar{X} - A_c| \leqslant 2\sigma_{Lc}$$

then the analytical method is sufficiently accurate. Otherwise it is not considered to be as accurate as those used by the laboratories participating in the certification programme.

For reference materials certified by interlaboratory consensus for which the between-laboratories standard deviation is not reported, or by a partial interlaboratory programme, or by interlaboratory consensus on the basis of one widely-accepted method that is not the same as the method being tested, or by

Table 1. Relation between the number of replicates (n) and the chance (β) that an analytical method will be accepted as valid, when the ratio of its standard deviation to the within-laboratories standard deviation of the CRM (at $\alpha = 0.05$) is greater than the tabulated value (calculated from data in *Handbook of Tables of Probability and Statistics*, 2nd Ed., p. 299, CRC, Cleveland, Ohio, 1968)

	$\alpha = 0.05$			
$n-1$	$\beta = 0.01$	$\beta = 0.05$	$\beta = 0.1$	$\beta = 0.5$
1	159.5	31.3	15.6	2.73
2	17.3	7.64	5.33	2.08
3	6.25	4.71	3.66	1.82
4	5.65	3.65	2.99	1.68
5	4.47	3.11	2.62	1.59
6	3.80	2.77	2.39	1.53
7	3.37	2.55	2.23	1.49
8	3.07	2.38	2.11	1.45
9	2.85	2.26	2.01	1.42
10	2.67	2.15	1.94	1.40
12	2.43	2.01	1.83	1.36
15	2.19	1.85	1.71	1.32
20	1.95	1.70	1.59	1.27
24	1.83	1.62	1.52	1.25
30	1.71	1.54	1.46	1.22
40	1.59	1.45	1.38	1.19
60	1.45	1.35	1.30	1.15
120	1.30	1.24	1.21	1.11

Table 2. Permissible tolerance ($2S_{Lc}$) values and S_{Lc}/S_{rc} ratios for CCRMP reference materials

RM	Certified species	A_c	S_{Lc}/S_{rc}	$2S_{Lc}$
CT-1	Tungsten, %	1.04	1.3	0.066
BH-1	Tungsten, %	0.422	1.6	0.0285
TLG-1	Tungsten, %	0.083	2.0	0.0140
BL-1	Uranium, %	0.022	1.2	0.0016
BL-2	Uranium, %	0.453	1.1	0.0137
BL-3	Uranium, %	1.02	0.9	0.024
BL-4	Uranium, %	0.173	1.2	0.0099
BL-5	Uranium, %	7.09	1.0	0.152
CCU-1	Silver, $\mu g/g$	139	3.6	15.3
CCU-1	Alumina, %	0.247	1.1	0.0217
CCU-1	Gold, $\mu g/g$	7.5	1.8	1.05
CCU-1	Copper, %	24.71	1.3	0.231
CCU-1	Mercury, $\mu g/g$	61	2.0	7.8
CCU-1	Lead, %	0.106	2.1	0.0236
CCU-1	Silica, %	2.61	2.5	0.260
CCU-1	Zinc, %	3.22	2.6	0.173
CD-1	Antimony, %	3.57	2.3	0.152
CD-1	Arsenic, %	0.66	2.3	0.66
CPB-1	Silver, $\mu g/g$	62.6	1.9	26.4
CPB-1	Alumina, %	0.28	1.8	0.039
CPB-1	Arsenic, %	0.056	1.5	0.0136
CPB-1	Bismuth, %	0.023	2.0	0.0040
CPB-1	Cadmium, %	0.0143	1.5	0.0016
CPB-1	Copper, %	0.254	1.8	0.0167
CPB-1	Iron, %	8.43	2.5	0.251
CPB-1	Mercury, $\mu g/g$	5.15	1.4	1.59
CPB-1	Lead, %	64.74	2.2	0.586
CPB-1	Sulphur, %	17.8	2.2	0.41
CPB-1	Antimony, %	0.36	2.4	0.045
CPB-1	Silica, %	0.74	1.7	0.109
CPB-1	Zinc, %	4.42	1.9	0.191
CZN-1	Silver, $\mu g/g$	93	2.4	10.2
CZN-1	Alumina, %	0.25	2.2	0.043
CZN-1	Arsenic, %	0.026	2.5	0.0089
CZN-1	Cadmium, %	0.132	1.7	0.0085
CZN-1	Copper, %	0.144	2.2	0.0138
CZN-1	Iron, %	10.93	2.7	0.284
CZN-1	Mercury, $\mu g/g$	43	2.3	11.9
CZN-1	Manganese, %	0.219	3.0	0.0258
CZN-1	Lead, %	7.43	1.6	0.246
CZN-1	Sulphur, %	30.2	2.8	0.78
CZN-1	Antimony, %	0.052	1.9	0.0081
CZN-1	Zinc, %	44.74	2.2	0.573
DH-1A	Thorium, %	0.091	2.7	0.0101
DL-1A	Uranium, %	0.0116	1.2	0.0013
DL-1A	Thorium, %	0.0076	2.0	0.0016
HV-1	Copper, %	0.522	1.1	0.0201
HV-1	Molybdenum, %	0.058	1.0	0.0047
KC-1	Lead, %	6.87	2.0	0.222
KC-1	Copper, %	0.112	2.1	0.0097
KC-1	Tin, %	0.67	3.2	0.700
KC-1	Silver, %	0.112	2.2	0.0064
KC-1	Zinc, %	20.07	1.3	0.209
MA-1	Gold, *oz/ton*	0.519	0.7	0.0224
MA-2	Gold, $\mu g/g$	1.86	1.6	0.244
MP-1	Tin, %	2.43	1.6	0.313
MP-1	Copper, %	2.09	2.3	0.113
MP-1	Lead, %	1.88	1.7	0.105
MP-1	Molybdenum, %	0.014	0.9	0.0028
MP-1	Indium, %	0.069	1.7	0.0067
MP-1	Bismuth, %	0.024	1.9	0.0069
MP-1	Arsenic, %	0.77	2.6	0.080
MP-1	Silver, $\mu g/g$	57.9	3.1	6.72
MP-1	Zinc, %	15.90	1.4	0.236
MP-1A	Zinc, %	19.02	1.7	0.417
MP-1A	Tin, %	1.28	2.6	0.137
MP-1A	Copper, %	1.44	1.5	0.037
MP-1A	Lead, %	4.33	2.8	0.140

RM	Certified species	A_c	S_{Lc}/S_{rc}	$2S_{Lc}$
MP-1A	Molybdenum, %	0.029	3.3	0.0044
MP-1A	Indium, %	0.033	2.2	0.0042
MP-1A	Bismuth, %	0.032	3.3	0.0062
MP-1A	Arsenic, %	0.84	2.1	0.070
MP-1A	Silver, $\mu g/g$	69.7	2.5	6.94
MP-2	Silver, $\mu g/g$	4.9	2.3	1.0
MP-2	Bismuth, %	0.246	3.8	0.0210
MP-2	Molybdenum, %	0.281	3.5	0.0386
MP-2	Tungsten, %	0.65	3.3	0.070
MW-1	Iron, %	66.08	1.4	0.210
MW-1	Iron(II), %	1.36	1.5	0.107
MW-1	Alumina, %	0.30	2.7	0.042
MW-1	Silica, %	4.60	2.5	0.216
MW-1	Lime, %	0.053	1.2	0.0095
MW-1	Magnesia, %	0.034	2.2	0.0079
MW-1	Phosphorus, %	0.011	2.4	0.0031
MW-1	Potassium, %	0.011	2.3	0.0024
OKA-1	Niobium, %	0.37	3.7	0.047
PD-1	Lead, %	2.75	3.0	0.287
PD-1	Arsenic, %	0.77	2.2	0.118
PD-1	Mercury, $\mu g/g$	389	2.0	66.6
PR-1	Molybdenum, %	0.594	3.1	0.0450
PR-1	Bismuth, %	0.111	1.4	0.0102
PR-1	Iron, %	1.244	1.9	0.0522
PR-1	Sulphur, %	0.793	2.6	0.0522
PTA-1	Platinum, *oz/ton*	0.089	0.2	0.0065
PTC-1	Palladium, *oz/ton*	0.37	0.8	0.073
PTC-1	Platinum, *oz/ton*	0.087	0.7	0.0194
PTC-1	Rhodium, *oz/ton*	0.018	1.2	0.0038
PTC-1	Gold, *oz/ton*	0.019	0.8	0.0083
PTM-1	Gold, *oz/ton*	0.052	1.0	0.0131
PTM-1	Palladium, *oz/ton*	0.24	1.1	0.051
PTM-1	Platinum, *oz/ton*	0.17	0.9	0.023
RU-1	Zinc, %	2.24	2.4	0.084
RU-1	Copper, %	0.85	1.8	0.035
RU-1	Iron, %	24.40	2.2	0.322
RU-1	Sulphur, %	21.71	2.5	0.454
SL-1	Silica, %	35.73	1.7	0.466
SL-1	Lime, %	37.48	2.5	0.773
SL-1	Magnesia, %	12.27	2.4	0.686
SL-1	Alumina, %	9.63	1.1	0.266
SL-1	Iron, %	0.72	1.5	0.106
SL-1	Sulphur, %	1.26	2.1	0.094
SU-1	Copper, %	0.87	1.7	0.035
SU-1	Nickel, %	1.51	1.1	0.053
SU-1A	Nickel, %	1.233	1.8	0.0327
SU-1A	Copper, %	0.967	1.3	0.0224
SU-1A	Cobalt, %	0.041	1.3	0.0039
SU-1A	Platinum, $\mu g/g$	0.41	1.9	0.148
SU-1A	Palladium, $\mu g/g$	0.371	1.7	0.062
SU-1A	Silver, $\mu g/g$	4.3	1.3	0.76
TAN-1	Tantalum	0.236	1.1	0.0217
UM-1	Copper, %	0.43	1.7	0.021
UM-1	Nickel, %	0.88	1.5	0.038
UM-1	Cobalt, %	0.035	1.9	0.0039
SCH-1	Iron, %	60.73	2.2	0.396
SCH-1	Silicon, %	3.78	2.0	0.173
SCH-1	Aluminium, %	0.509	1.6	0.0390
SCH-1	Calcium, %	0.029	2.9	0.0097
SCH-1	Magnesium, %	0.020	1.9	0.0053
SCH-1	Manganese, %	0.777	1.9	0.0377
SCH-1	Titanium, %	0.031	1.7	0.0072
SCH-1	Sulphur, %	0.007	2.0	0.0026
SCH-1	Phosphorus, %	0.054	1.2	0.0102
SCH-1	Sodium, %	0.019	2.6	0.0090
SCH-1	Potassium, %	0.026	2.6	0.0096

one "expert" laboratory using a definitive method, the following test is suggested. If

$$|\bar{X} - A_c| \leqslant 4S_W$$

then the analytical method being tested is sufficiently accurate.

STATISTICAL JUSTIFICATION

A significance level of $\alpha = 0.05$ is used for all statistical tests.

Number of replicate determinations, n

The number of replicate determinations to be performed directly affects the precision of the estimate of the within-laboratory precision, S_W. Table 1 shows the relation between n and the maximum ratio of the standard deviation of the analytical method and the within-laboratories standard deviation for the CRM, S_W/S_{rc}, at various values of β, and $\alpha = 0.05$, β being the probability that the method will be accepted if the standard deviation is greater than the ratio times the certified value of S_{rc}. For example, at $\beta = 0.05$ for $n = 10$, if the analytical method has passed the appropriate F-test, there is no more than a 5% chance that it has a standard deviation in excess of $2.26S_{rc}$.

CRMs for which S_{Lc} *is reported*

There are two factors to consider: the uncertainty of the certified value and the uncertainty of the analytical method. The following formula can be used as the criterion for acceptance.

$$|\bar{X} - A_c| \leqslant 2\sqrt{\sigma_C^2 + \sigma_D^2} \qquad (1)$$

where σ_C^2 is the uncertainty associated with the certified value and σ_D^2 is the uncertainty associated with the analytical method being examined. The factor 2 is an approximation for the fractile of *Student's* t-distribution for 95% probability. This assumption, although somewhat crude, has been widely accepted and used in various ISO standard methods. The value of σ_C^2 depends on the method of certification of the reference material.

For certification by interlaboratory consensus from use of several methods:

$$\sigma_C^2 = (S_{Lc}^2 + S_{rc}^2/n_c)/N_c \qquad (2)$$

For certification by interlaboratory consensus by use of one method:

$$\sigma_C^2 = (\sigma_{Lc}^2 + \sigma_{rc}^2/n_c)/N_c \qquad (3)$$

where N_c is the number of laboratories which produced results used in certification of the reference material, and n_c is the average number of replicate determinations performed by each participating laboratory for the certification programme. For most certifications by interlaboratory consensus, N_c is usually > 10, so σ_C^2 is small enough in relation to σ_D^2 to be neglected, and then

$$\sigma_D^2 = \sigma_{Lc}^2 + S_W^2/n \quad \text{or} \quad S_{Lc}^2 + S_W^2/n$$

depending on the type of CRM used. For $n = 10$, S_W^2/n becomes small and equation (1) can be simplified to

$$|\bar{X} - A_c| \leqslant 2S_{Lc} \quad \text{or} \quad |X - \bar{A}_c| \leqslant 2\sigma_{Lc} \qquad (4)$$

CRMs for which S_{Lc} *is not available*

Experience in interlaboratory consensus programmes based on use of one method, by ISO Technical Committee 102 on iron ores, shows that an analytical method is considered to be well standardized if $\sigma_{Lc}/\sigma_{rc} \leqslant 2$. On this basis, S_{Lc} can be replaced by $2\sigma_{rc}$ and the criterion for acceptance is:

$$|\bar{X} - A_c| \leqslant 4\sigma_{rc} \qquad (5)$$

Table 2 reports the value of S_{Lc}/S_{rc} for 135 elements and constituents that have been certified by CCRMP by interlaboratory consensus based on use of multiple methods. Of these, 77 show $S_{Lc}/S_{rc} \leqslant 2.0$ and all but 22 show S_{Lc}/S_{rc} or $\sigma_{Lc}/\sigma_{rc} \leqslant 2.5$. These data suggest that the criterion S_{Lc}/S_{rc} or $\sigma_{Lc}/\sigma_{rc} \leqslant 2.0$ is too harsh for most interlaboratory consensus programmes, but nevertheless is reasonable, particularly in view of the fact that some estimate of the between-laboratories standard deviation is required before the CRM can be used for validation of an analytical method. On this premise, S_{Lc} can be replaced by $2S_{rc}$ and the criterion for acceptance becomes:

$$|\bar{X} - A_c| \leqslant 4S_{rc} \qquad (6)$$

An analytical method can be verified for accuracy by use of equation (5) or (6) provided the value of σ_{rc} or S_{rc} for the CRM is reported. We propose, however, that the accuracy of the method can equally well be judged by:

$$|\bar{X} - A_c| \leqslant 4S_W \qquad (7)$$

if the precision of the method can be verified as stated above, *i.e.*,

$$F_0 > F = \frac{S_W^2}{S_{rc}^2} \quad \text{or} \quad \frac{S_W^2}{\sigma_{rc}^2}$$

in which case $4S_W$ is statistically equal to $4\sigma_{rc}$ or $4S_{rc}$, *i.e.*, the upper limit of $|\bar{X} - A_c|$ for acceptance of the method is not significantly raised. The advantage in the use of equation (7) is that, to be accepted, a method with higher precision must also have greater accuracy, *i.e.*, give a lower value of $|\bar{X} - A_c|$, than would be necessary if equation (5) or (6) were used as criterion.

In use of CRMs for which σ_{rc} or S_{rc} is not reported, we propose the use of equation (7) to test accuracy. The acceptability of the value of S_W must be decided by the analyst on chemical grounds.

EXAMPLES OF USE OF CRMs

Table 3 summarizes the results of the validation of some analytical methods by their application to some

Table 3. Validation of analytical methods

CRM	DL-1a	SU-1a	SCH-1	BL-2a
Element	Th	Co	Na	U
Certification	Interlaboratory, multiple methods	Interlaboratory, multiple methods	Interlaboratory, single method	Definitive method, volumetric umpire
A_c	0.0076%	0.041%	0.0186%	0.426%
S_{Lc}, σ_{Lc}	0.0008	0.0020	0.0045	—
S_{rc}, σ_{rc}	0.0004	0.0013	0.0017	0.0015
Method	Colorimetry	Atomic-absorption	Same as above	Neutron activation
$\bar{X}$	0.0080%	0.0474%	0.0201%	0.423%
n	10	10	10	45
S_W	0.0005	0.0005	0.0006	0.0033
Precision check	$F = 1.563$ $F_{0\,95,9,60} = 2.04$ —accepted	$F = 0.148$ $F_{0\,95,9,60} = 2.04$ —accepted	$F = 0.125$ $F_{0\,95,9,60} = 2.04$ —accepted	$F = 4.84$ $F_{0\,95,44,24} = 1.88$ —failed
Accuracy check				
$\lvert \bar{X} - A_c \rvert$	0.0004	0.0064	0.0015	0.003
$2S_{Lc}$ or $2\sigma_{Lc}$ or $4S_W$	$2S_{Lc} = 0.0016$ —accepted	$2S_{Lc} = 0.0040$ —failed	$2\sigma_{Lc} = 0.0090$ —accepted	$4S_W = 0.013$ —accepted

CRMs from the CCRMP. The examples are taken from CCRMP certification programmes. For DL-1a,[12] SU-1a[13] and SCH-1,[14] the method illustrated was used by one laboratory participating in the interlaboratory programme. In all three instances, the method is capable of acceptable precision in comparison with the overall results of the interlaboratory programme. The atomic-absorption method used to determine cobalt in SU-1a, as used by a particular laboratory, does not give acceptable accuracy. Indeed the results from this laboratory were designated as outliers and rejected for use in the interlaboratory programme.

BL-2a[15] was certified for uranium content solely on the basis of the results obtained by the volumetric umpire method performed at the Canada Centre for Mineral and Energy Technology. The neutron-activation method being validated was applied by a commercial laboratory to confirm the between-unit homogeneity of BL-2a. A precision check for this type of CRM is not recommended but has been performed for illustrative purposes. A definitive method is sufficiently precise for almost all other methods to fail the precision check. The acceptance of the accuracy is contingent on a value of $S_W = 0.0033$ being acceptable to the experimenter.

Caveat

For certain reference materials internationally available, no certified values are given, and only "best" or "usable" values are supplied, for which uncertainties are not reported. These values are often based on very few results or on results in relatively poor agreement. The reference rocks available from many sources are a typical example. The validation of the accuracy of an analytical method, by use of such reference materials and the experimental design proposed here, should be performed with caution, and only for elements and constituents for which the reported value, V, is well defined. The criterion of accuracy is then, of course, $\lvert \bar{X} - V \rvert \leqslant 4S_W$.

REFERENCES

1. *ISO Directory of Certified Reference Materials*, 1st Ed., 1982.
2. *Ninth Meeting of REMCO*, Geneva, 12–15 September 1983.
3. D. Oster, J. P. Caliste and A. Marschal, *ISO/REMCO* 72, 1981.
4. Y. Mashiko, K. Iizuki and S. Seaki, *ISO/REMCO* 86, 1982.
5. K. R. Eberhardt, personal communication.
6. H. F. Steger, *CANMET Report* 83-3E, Energy, Mines and Resources Canada, Ottawa, 1983.
7. R. Sutarno and G. M. Faye, *Talanta*, 1975, **22**, 675.
8. H. Marchandise and E. Colinet, *Z. Anal. Chem.*, 1983, **316**, 669.
9. J. P. Cali and W. P. Reed, in *Accuracy in Trace Analysis: Sampling, Sample Handling and Analysis*, P. D. Lafleur (ed.), Vol. I, p. 56. U.S. Department of Commerce, Washington D.C., 1976.
10. *Idem, op. cit.*, p. 47.
11. H. F. Steger and W. S. Bowman, *CANMET Report* 80-10E, Energy, Mines and Resources Canada, Ottawa, 1980.
12. *Idem, CANMET Report* 80-9E, Energy, Mines and Resources Canada, Ottawa, 1980.
13. R. Sutarno, D. J. Charette, W. S. Bowman and G. H. Faye, *CANMET Report* 78-5, Energy, Mines and Resources Canada, Ottawa, 1978.
14. H. F. Steger, W. S. Bowman, G. Zechanowitsch and R. Sutarno, *CANMET Report* 82-6E, Energy, Mines and Resources Canada, Ottawa, 1982.

Talanta, Vol. 32, No 6, pp. 447–450, 1985
Printed in Great Britain.

0039-9140/85 $3.00 + 0.00

EXTRACTION–SPECTROPHOTOMETRIC DETERMINATION OF BORON AND ANTIMONY IN CARBON AND LOW-ALLOY STEELS WITH MANDELIC ACID AND MALACHITE GREEN

SHIGEYA SATO
Faculty of Education, Kumamoto University, 2-40-1, Kurokami, Kumamoto 860, Japan

(*Received* 31 *August* 1984. *Revised* 9 *January* 1985. *Accepted* 23 *January* 1985)

Summary—A very simple and sensitive extraction method using mandelic acid and Malachite Green has been applied to the determination of boron and antimony in steels (carbon and low-alloy). When chlorobenzene is used as the solvent, boron and antimony are simultaneously extracted as ion-pairs of their mandelates with Malachite Green from weak acidic media, but only the boron compound is extracted in the presence of tartrate. Antimony is determined from the difference in absorbance of the extracts. In the case of benzene, boron alone was extracted and determined. Large amounts of iron(II) and other metal cations do not interfere, so the steel samples are dissolved in dilute sulphuric acid. Very low boron (0.0009–0.0091%) and antimony (0.002–0.02%) contents in steel are easily determined without any pretreatment.

Many spectrophotometric methods for determination of boron in steel have been reported. The methods using Methylene Blue[1–3] or curcumin[4–6] have been widely used routinely, but involve rather troublesome and time-consuming procedures.

Recently, methods based on extraction of ion-pairs formed by boron complex anions and large coloured cations have been developed and applied to steels.[7–8] These methods have advantages such as high sensitivity and selectivity, but again the procedures are complicated and analysis of steel samples requires pretreatment to avoid interference by iron. Most methods for the spectrophotometric determination of antimony are based on the extraction of antimony(V) as hexachloroantimonate with cationic dyes such as Rhodamine B[9] and Crystal Violet,[10] but often suffer from poor reproducibility;[11,12] they may be complicated[13] and problems may arise in the conversion of antimony(III) into $SbCl_6^-$,[14,15] and with the stability of the latter in strong acidic media.[16] Few studies have been made of the spectrophotometric determination of antimony(III), however, and for the determination of antimony in steel and various metals the Rhodamine B method[17] has been widely used, although the procedures are as troublesome as those for the boron determination.

It has recently been found that boron[18] and antimony(III)[19] both react with mandelic acid to form complex anions which are extractable as ion-pairs with Malachite Green into organic solvents from weakly acidic media at room temperature, and determined spectrophotometrically. These methods have now been combined and applied to analysis of low-alloy and carbon steels. The proposed method is very simple, rapid and reproducible; removal of the iron and the addition of redox reagents are not necessary, and the complex anion formed with mandelic acid is very stable in weakly acidic media.

EXPERIMENTAL

Reagents

Standard boron solution, *0.02*M. Prepared from boric acid; working solutions are prepared by suitable dilution.

Standard antimony(III) solution, *0.01*M. Prepared by dissolving antimony potassium tartrate in water; working solutions are prepared by dilution.

Malachite Green solution, 10^{-3}M.

Mandelic acid solution, *0.1*M. Adjusted to pH 3.0 with sodium hydroxide solution.

Tartrate solution (*pH 4.8*). Prepared from 0.1*M* tartaric acid and sodium hydroxide solution.

Sodium acetate solution, *0.1*M.

Use demineralized water throughout.

Preparation of the steel sample solution

Weigh the steel sample (up to 0.8 g) into a 100-ml silica flask, and dissolve it in 20 ml of sulphuric acid (1 + 6) by heating under reflux. Cool, rinse the condenser with 5 ml of water, and filter off any residue on a small filter paper (fine and ashless, Toyo Roshi, No. 5C) in a polyethylene funnel, and wash the paper with water. Transfer the filtrate and washings to a silica beaker, adjust to pH 1.8–2.0 with 8*M* sodium hydroxide, transfer the solution into a 100-ml standard flask and make up to volume with water.

Procedure A for boron

Transfer 1.0 ml of sample solution into a stoppered 10-ml test-tube. Add 1.0 ml of mandelic acid solution and 0.5 ml of Malachite Green solution; if necessary, adjust to pH 2.2–3.0 with sodium hydroxide solution. Dilute to 4.0 ml with water and shake the solution with 4.0 ml of benzene for 10 min. After phase separation, measure the absorbance of the organic phase at 633 nm, in a 10-mm glass cell, against benzene as reference.

Procedure B for the sum of boron and antimony

Transfer 1.5 ml of sample solution into a stoppered 10-ml test-tube. Add 0.2 ml of mandelic acid solution and 0.5 ml of Malachite Green solution, and adjust to pH 2.2–3.0 by

adding 1.0 ml of 0.1*M* sodium acetate. Dilute to 4.0 ml with water, and shake the solution with 4.0 ml of chlorobenzene for 10 min. After phase separation, measure the absorbance of the organic phase at 628 nm, in a 10-mm glass cell, against chlorobenzene as reference.

Procedure C for boron, in the presence of tartrate

Apply procedure B, but with 1.0 ml of 0.1*M* tartrate solution (pH 4.8) instead of the 0.1*M* sodium acetate.

RESULTS AND DISCUSSION

As described previously,[7,8] both borate and antimony(III) react with mandelic acid to form complex anions extractable with Malachite Green into an organic solvent from weakly acidic media (pH 2.2–3.5) at room temperature, and can be determined by measurement of the absorbance of the extract.

In further work on these systems, it has been found that iron(II) does not interfere at concentrations up to *ca.* 0.07*M* if the extraction is done at pH <3.0. When benzene is used as the solvent (procedure A), the sensitivity for boron is high (apparent molar absorptivity $\varepsilon = 6.52 \times 10^4$ l. mole^{-1}. cm^{-1}), whereas that for antimony is lower ($\varepsilon = 1.27 \pm 0.04 \times 10^4$). With chlorobenzene as solvent (procedure B), the opposite is the case, $\varepsilon_{Sb} = 6.08 \pm 0.19 \times 10^4$, $\varepsilon_B = 1.12 \pm 0.04 \times 10^4$. Antimony at concentrations $< 2.00 \times 10^{-4}M$ (25 mg/l.) cannot be extracted in the presence of tartrate ($2.5 \times 10^{-2}M$), procedure C, whereas boron can ($\varepsilon_B = 1.32 \pm 0.03 \times 10^4$). Accordingly, the three methods can cover determination of a range of boron and antimony contents in low-alloy and carbon steels.

Dissolution of steel sample

In spectrophotometric determination of boron in steels, sulphuric acid[20–23] and sulphuric–phosphoric acid mixtures have been widely used for dissolving the samples, and so have hydrochloric acid–hydrogen peroxide mixtures[6–8] and *aqua regia*.[24] However, when the last two mentioned are used, the excess of hydrogen peroxide or nitric acid must be removed by heating, or they interfere in the determination of boron. In the Japanese Industrial Standards method for determination of antimony,[25] it was concluded that sulphuric acid was a suitable solvent for low-alloy and carbon steels, so it was chosen for use in the present method, without any auxiliary oxidizing agents.

Most steels give some silicic acid and undissolved carbides when dissolved in dilute sulphuric acid. The residues from selected steels were therefore collected and analysed for boron and antimony. Each steel sample was treated as described in the procedure and the filter paper and residue were dried at 110°, then ignited in a platinum crucible at 600°. The ignition product was fused with 2.0 g of sodium carbonate, then the melt was cooled and dissolved in 8 ml of sulphuric acid (1 + 6). The solution (filtered if necessary) was transferred into a silica beaker, adjusted to pH 1.8–2.0 with 8*M* sodium hydroxide, transferred to a 50-ml standard flask and diluted to volume. This solution was analysed for boron and antimony by procedures A and B. No significant amounts were found to be present, so it is concluded that any residue from the dissolution step can safely be discarded.

It is known that boron is susceptible to volatilization during the dissolution of steel in acid, and antimony to reduction to a volatile hydride under reducing conditions. Possible loss of boron and antimony was therefore examined by dissolving the steel together with known amounts of boron, antimony and various metals and testing the recoveries. Table

Table 1. Recovery test of boron and antimony obtained by procedures B and C

Sample (Certified value, %)	Sample weight, g	Present in sample		Added			Found‡			
		Sb, μg	B, μg	Sb†, μg	B†, μg	Metal§	Sb, μg	Recovery, %	B, μg	Recovery, %
JSS 361-1	0.3801		3.4		6.5				9.8	99 #
(B 0.0009)	0.8018		7.2		6.5				13.9	101 #
JSS 175-3	0.1998*	39.2	18.2		43.2		38	98	60.0	98
(B 0.0091)	0.1999*	39.2	18.2	100			138	99	17.8	98
(Sb 0.0196)	0.2055	40.3	18.7	100			142	101	18.5	99
	0.3093	60.6	28.1	100			159	99	28.3	101
	0.4127	80.9	37.6	100			181	100	36.3	97
	0.2005	39.3	18.3	100		Al	142	102	18.5	101
	0.2007	39.3	18.3	100		Zn	138	99	17.9	98
	0.2007	39.3	18.3	100		Co	139	100	19.1	104
	0.2004	39.3	18.2	100		Cu	142	102	17.9	98
	0.2002	39.2	18.2	100		Mn	141	101	18.6	102
	0.1987	39.0	18.1	100		Pb	137	99	18.4	102

*Dissolved in 5 ml of sulphuric acid (1 + 6).
†Added as solution before dissolution of sample.
‡Mean of 8 determinations.
§Added as metal (~20 mg, Al, Zn, Co, Mn) or solution (equivalent to ~20 mg of Cu, Pb) before dissolution of sample.
Measured by procedure A.

Table 2. Determination of boron in steel

Sample (Certified value, %)	Sample solution,* *g per 100 ml*	Procedure A: Boron found,† *μg*	Procedure A: Boron content, %	Procedure C: Boron found,† *μg*	Procedure C: Boron content, %
JSS 175-3	0.2000	0.180	0.00900	0.265	0.00884
(B = 0.0091)	0.3002	0.274	0.00913	0.409	0.00909
(Sb = 0.0196)	0.4000	0.363	0.00908	0.537	0.00895
JSS 173-3	0.2012	0.064	0.00317	0.102	0.00336
(B = 0.0033)	0.4000	0.136	0.00341	0.192	0.00320
(Sb = 0.0048)	0.4009	0.130	0.00325	0.206	0.00343
	0.5992	0.200	0.00334	0.288	0.00321
JSS 172-3	0.4020	0.087§	0.00216	0.136‡	0.00226
(B = 0.0022)	0.4060	0.091	0.00224	0.128	0.00210
(Sb = 0.0020)	0.7995	0.173	0.00216	0.272	0.00227
	0.8000	0.166	0.00207	0.278	0.00232
JSS 361-1	0.4004	0.035	0.00087	#	#
(B = 0.0009)	0.7960	0.066	0.00083	0.102	0.00085
	0.8000	0.073	0.00091	0.112	0.00094
	0.8024	0.075	0.00093	0.105	0.00087
NBS 362	0.2018	0.050	0.00246	0.079	0.00260
(B = 0.0025)	0.2251	0.058	0.00256	0.085	0.00260
(Sb = 0.013)	0.3025	0.074	0.00246	0.108	0.00238
	0.3004	0.074	0.00247	0.118	0.00262
	0.4023	0.104	0.00259	0.147	0.00244

*1.0 ml of 1.5 ml of sample solution was analysed by procedure A or C, respectively.
†Mean of ten determinations.
‡Standard deviation 0.0028 μg.
§Standard deviation 0.0015 μg.
Not measurable.

Table 3. Determination of boron and antimony in steel by the combination of procedures B and C

Sample (Certified value, %)	Sample solution,* *g per 100 ml*	Boron found,† *μg*	Boron content, %	Antimony found,† *μg*	Antimony content, %
JSS 175-3	0.1005	0.131	0.00869	0.309	0.0205
(B = 0.0091)	0.2000	0.265	0.00884	0.597	0.0189
(Sb = 0.0196)	0.3002	0.409	0.00909	0.906	0.0201
	0.4000	0.537	0.00895	1.15	0.0192
JSS 173-3	0.2000	0.092	0.00306	0.134	0.00446
(B = 0.0033)	0.2012	0.102	0.00336	0.154	0.00512
(Sb = 0.0048)	0.4009	0.206	0.00343	0.299	0.00496
	0.4000	0.192	0.00320	0.288	0.00480
	0.5992	0.288	0.00321	0.422	0.00470
	0.5994	0.287	0.00319	0.432	0.00481
JSS 172-3	0.4020	0.136	0.00226	0.128	0.00213
(B = 0.0022)	0.4060	0.128	0.00210	0.144	0.00237
(Sb = 0.0020)	0.7995	0.288	0.00240	0.257	0.00215
	0.8000	0.278	0.00232	0.278	0.00232
NBS 362	0.2018	0.079	0.00260	0.385	0.0127
(B = 0.0025)	0.3025	0.108	0.00238	0.570	0.0126
(Sb = 0.013)	0.4023	0.147	0.00244	0.803	0.0133
	0.5006	0.190§	0.00253	0.955‡	0.0127
	0.6418	0.233	0.00242	1.28	0.0133
	0.8000	0.305	0.00254	1.53	0.0127

*1.5 ml of sample solution was analysed.
†Mean of ten determinations.
‡Standard deviation 0.017 μg.
§Standard deviation 0.0036 μg.

1 shows that no loss of boron or antimony was observed.

Analysis of steel samples

Table 2 shows that the values obtained for boron by procedures A and C are in good agreement with the certified values. Procedure A can be used for steels containing up to 0.01% of boron without interference by up to 0.02% antimony. In analysis for antimony and boron, their sum is determined by procedure B and the boron by procedure C, and the antimony is calculated by difference. Table 3 shows the results are in good agreement with the certified values.

Acknowledgements—The author expresses his thanks to Professor Y. Yamamoto of Hiroshima University for his kind guidance and helpful discussions. The author is also indebted to Professor S. Uchikawa of Kumamoto University for his useful suggestions and warm encouragement.

REFERENCES

1. L. Pasztor, J. D. Bode and Q. Fernando, *Anal. Chem.*, 1960, **32,** 277.
2. R. Rosotte, *Chim. Anal. Paris*, 1962, **44,** 204.
3. L. R. Uppstrom, *Anal. Chim. Acta*, 1968, **43,** 475.
4. J. Borrowdale, R. H. Jenkins and C. E. A. Shanahan, *Analyst*, 1959, **84,** 426.
5. M. R. Hayes and J. Metcalfe, *ibid.*, 1962, **87,** 956.
6. H. Goto, Y. Kakita and K. Takada, *Bunseki Kagaku*, 1969, **18,** 52.
7. K. Toei, S. Motomizu, M. Oshima and H. Watari, *Analyst*, 1981, **106,** 776.
8. M. Oshima, K. Fujimoto, S. Motomizu and K. Toei, *Anal. Chim. Acta*, 1982, **134,** 73.
9. E. Eegriwe, *Z. Anal. Chem.*, 1927, **70,** 400.
10. K. Študlar and I. Janoušek, *Collection Czech. Chem. Commun.*, 1960, **25,** 1965.
11. M. Tanaka and M. Kawahara, *Bunseki Kagaku*, 1961, **10,** 185.
12. M. Imai, *ibid.*, 1962, **11,** 806.
13. E. B. Sandell, *The Colorimetric Determination of Traces of Metals*, 3rd Ed., Interscience, New York, 1959.
14. R. W. Ramette and E. B. Sandell, *Anal. Chim. Acta*, 1955, **13,** 455.
15. R. W. Burke and O. Menis, *Anal. Chem.*, 1966, **38,** 1719.
16. H. M. Neumann, *J. Am. Chem. Soc.*, 1954, **76,** 2611.
17. L. Kidman and C. B. Waite, *Metallurgia*, 1962, **66,** 143.
18. S. Sato, *Anal. Chim. Acta*, 1983, **151,** 465.
19. S. Sato, S. Uchikawa, E. Iwamoto and Y. Yamamoto, *Anal. Lett.*, 1983, **16,** 827.
20. N. Fukushima and Y. Kakita, *Bunseki Kagaku*, 1966, **15,** 553.
21. O. P. Bhargava and W. G. Hines, *Talanta*, 1970, **17,** 61.
22. F. Vernon and J. M. Williams, *Anal. Chim. Acta*, 1970, **51,** 533.
23. *Japan Industrial Standards*, G 1227, 1980.
24. T. Kamada and Y. Yamamoto, *Talanta*, 1977, **24,** 330.
25. *Japan Industrial Standards*, G 1235, 1981.

Talanta, Vol. 32, No. 6, pp. 451–455, 1985
Printed in Great Britain.

0039-9140/85 $3.00 + 0.00

STABILITY CONSTANTS OF THE TERNARY COMPLEXES OF CuDTPA, NiDCTA, CrEDTA, CoHEEDTA, NiHEEDTA AND CuHEEDTA WITH OH^-

J. KORSSE, G. A. J. LEURS and P. W. F. LOUWRIER
National Institute for Nuclear and High-Energy Physics (NIKHEF, section K), P.O. Box 4395, 1009 AJ Amsterdam, The Netherlands

(*Received* 20 *September* 1984. *Accepted* 18 *January* 1985)

Summary—The acid dissociation constants of the metal chelates H_3CuDTPA, H_2NiDCTA, HCrEDTA, HCoHEEDTA, HNiHEEDTA and HCuHEEDTA were determined by potentiometric titration. The constants determined at an ionic strength of 0.1 were $pK_{a,1} = 2.1$; $pK_{a,2} = 2.8$ and $pK_{a,3} = 4.75$ for H_3CuDTPA (296 K), $pK_{a,1} = 2.16$ for HCrEDTA (298 K); $pK_{a,1} = 1.6$ and $pK_{a,2} = 2.0$ for H_2NiDCTA (298 K); $pK_{a,1} = 2.24$ for HCoHEEDTA, $pK_{a,1} = 2.47$ for HCuHEEDTA and $pK_{a,1} = 1.73$ for HNiHEEDTA. At high pH the formation of ternary hydroxo-complexes was observed for the chelates $CrEDTA^-$ ($pK_{a,2} = 7.35$; $pK_{a,3} = 12.35$), $CoHEEDTA^-$ ($pK_{a,2} = 11.74$), $NiHEEDTA^-$ ($pK_{a,2} = 12.44$) and $CuHEEDTA^-$ ($pK_{a,2} = 10.45$).

The ligands $EDTA^{4-}$, $HEEDTA^{3-}$, $DCTA^{4-}$ and $DTPA^{5-}$† form very stable chelates with transition metal ions.[1,2] The stability constant is defined by:

$$K^{L}_{ML} = \frac{[ML]}{[M][L]} \quad (1)$$

In strongly acid and strongly alkaline solutions these chelates dissociate and free metal ions or hydroxide complexes are formed.[3] In weakly alkaline regions there is the possibility of ternary complex formation according to:

$$ML^{n-} + H_2O \rightleftharpoons ML(OH)^{(n+1)-} + H^+ \quad (2)$$

$$ML(OH)^{(n+1)-} + H_2O \rightleftharpoons ML(OH)_2^{(n+2)-} + H^+ \quad (2a)$$

The stability constants are defined by:

$$K^{OH}_{MLOH} = \frac{[MLOH]}{[ML][OH]} = \frac{1}{K_b(MLOH)} \quad (3)$$

where k_b (MLOH) is the basic dissociation constant of MLOH. In order to determine the composition of aqueous solutions of these complexes at various pH values, in kinetic experiments,[4] the stability constants were determined by using a titration procedure.

EXPERIMENTAL

Preparation of the complexes

$H_3CuDTPA.3H_2O$ was prepared according to a modification of the method of Sievers and Bailar:[5] 7.65 mmoles of H_5DTPA and 9.65 mmoles of $CuSO_4 \cdot 5H_2O$ were dissolved in 60 ml of water. The pH was brought to 10 with sodium hydroxide solution and the copper hydroxide precipitate was filtered off. The pH of the filtrate was brought to 1.7 with dilute sulphuric acid. After reduction of the volume to 8 ml by use of a rotary evaporator, 4.5 ml of absolute ethanol were added slowly to the hot solution (348 K), with stirring. After cooling, the blue solid product was collected by filtration. It was washed with 2 ml of absolute ethanol. By further reduction of the volume a second crop was obtained after addition of 2 ml of absolute ethanol. The product was recrystallized from pure water and dried at 353 K.

$HCr(III)EDTA \cdot 2H_2O$ was prepared by dissolving 4.27 mmoles of $KCr(SO_4)_2 \cdot 12H_2O$ and 4.27 mmoles of H_4EDTA in 25 ml of water. After 1 hr of refluxing, the volume of deep purple solution was reduced to 10 ml by evaporation. To the hot solution (353 K), 15 ml of absolute ethanol were added. The mixture was cooled to room temperature, then the precipitate was collected and washed with 5 ml of absolute ethanol. This product was dissolved in 50 ml of water. The volume was reduced to 25 ml by evaporation and 20 ml of tert-butanol were added. After the solution had stood for several days at 268 K, purple-black crystals formed. These were collected, washed with absolute ethanol and dried over silica gel.

$H_2NiDCTA \cdot 4H_2O$. About 7 g of H_4DCTA was dissolved in 100 ml of water by stirring and addition of sodium hydroxide pellets. The pH was kept at about 11. Subsequently the stoichiometric amount of nickel perchlorate was added, and when this had dissolved the solution was deep blue and the pH was about 2. The solution was filtered. After a few days standing at room temperature light green-blue crystals formed. The crystals were recrystallized once from pure water and dried over phosphorus pentoxide.

$HCo(II)HEEDTA \cdot H_2O$; $HNiHEEDTA \cdot H_2O$; $HCu(II)HEEDTA \cdot H_2O$. These were all formed by the same method: 9 mmoles of cobalt perchlorate, 18 mmoles of nickel perchlorate or 18 mmoles of Cu(II) as $CuCO_3 \cdot Cu(OH)_2$ were dissolved in 100 ml of water together with the stoichiometric amount of H_3HEEDTA. After the reaction the volume was reduced by evaporation to 25 ml. After the solutions had stood for a few days at room temperature, pink, blue, or light-blue crystals formed. These were recrystallized once from pure water.

Analyses. The results of the elemental analysis are given in Table 1. These values were determined at the Organisch Chemisch Instituut TNO, Zeist, The Netherlands.

†EDTA = ethylenediaminetetra-acetate;
HEEDTA = hydroxyethylethylenediaminetriacetate;
DCTA = diaminocyclohexanetetra-acetate;
DTPA = diethylenetriaminepenta-acetate.

The data indicate that the water of crystallization is only loosely bound and that it can be released during the analysis. All the results are consistent with the stoichiometric formulae except those for $HNiHEEDTA \cdot H_2O$. However, the titration results (Table 2) indicate that the composition of this compound does not differ very much from the theoretical value. Thus, the results found for NiHEEDTA by elemental analysis should be treated with reservation.

Titration procedure

The pH was measured with a Philips CA-11 combined glass electrode fitted to a Philips PW9408 digital pH-meter, readable to ± 0.01 pH. The system was calibrated with freshly prepared reference buffers: $0.25M$ Na_2HPO_4/KH_2PO_4, pH = 6.86 at 298 K, and $0.01M$ $Na_2B_4O_7 \cdot 10H_2O$, pH = 9.18 at 298 K.[6]

The titrant was $0.1M$ sodium hydroxide, prepared with CO_2-free water. Titrations were done in a 100-ml closed vessel flushed with nitrogen, a Metrohm precision burette being used. The solutions were prepared by dissolving 0.2–0.5 mmole of the acid complex in $0.1M$ sodium chloride. During the dissolution and the titration, nitrogen was continuously bubbled through the solution. The temperature was not controlled but remained constant within 0.5 K during each experiment. The titrant was standardized against potassium hydrogen phthalate that had been dried at 393 K for 2 hr. The correlation between pH reading and $[H^+]$ and $[OH^-]$ was established by a titration of hydrochloric acid under the same conditions. These correlations gave an experimental value for pK_W which was used for the conversion of pK_a values into pK_b values.

RESULTS AND DISCUSSION

We report the equilibrium constants as acid or base dissociation constants defined by:

$$K_a(HA) = \frac{[H^+][A^-]}{[HA]} \qquad (4a)$$

$$K_b(BOH) = \frac{[B^+][OH^-]}{[BOH]} \qquad (4b)$$

Equations (4a) and (4b) refer to concentrations rather than activities and thus the reported pK values are valid only at the particular ionic strength used for the experiment. For a comparison of the results with literature values activity coefficients should be taken into account: these can be estimated by using the Debye–Hückel limiting law.[7] Unfortunately, it is not always clear whether the constants reported in the literature are activity constants or concentration constants. Moreover, at high ionic strengths (>0.1) activity coefficients cannot be calculated accurately.[7]

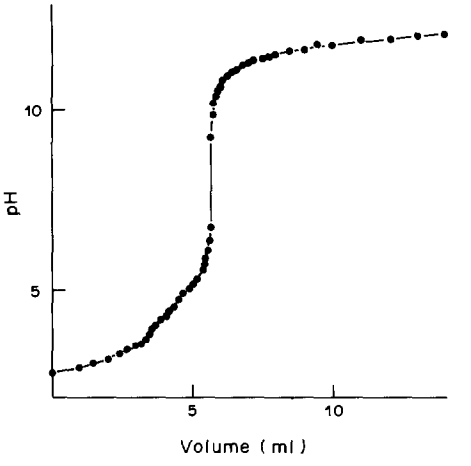

Fig. 1. Titration of 0.2129 mmole of $H_3CuDTPA$ with $0.1125M$ NaOH. Temperature 296 K, ionic strength 0.1 (NaCl). The curve was calculated by taking pK_a values of 2.1, 2.8 and 4.75. The points are the observed values

From the present experiments it appeared that equilibrium (2) is not important for pH < 12 in the case of $CuDTPA^{3-}$, $NiHEEDTA^-$ and $NiDCTA^{2-}$. Equilibrium (2a) was significant only for $CrEDTA^-$. A compilation of the results is given in Table 2. Some titration curves are shown in Figs. 1 and 2.

$H_3CuDTPA$

This complex is very stable, even at low pH. When the free ligand is in the form H_2DTPA^{3-} there are still six ligand atoms available for co-ordination to the copper ion. The stability constant $K^{H_2DTPA^{3-}}_{CuH_2DTPA^-}$ has been given as $10^{10.2}$. It was calculated that at pH 2 and a total complex concentration of $2mM$, the degree of dissociation α_D is less than 1%. Consequently, the only equilibria taken into account for our experiment are:

$$H_3CuDTPA \rightleftharpoons H^+ + H_2CuDTPA^- \qquad (5)$$

$$H_2CuDTPA^- \rightleftharpoons H^+ + HCuDTPA^{2-} \qquad (6)$$

$$HCuDTPA^{2-} \rightleftharpoons H^+ + CuDTPA^{3-} \qquad (7)$$

Table 1. Analyses of the compounds

Compound	Found, %				Calculated, %			
	C	H	N	O	C	H	N	O
$H_3CuDTPA \cdot 3H_2O$	34.3	4.8	8.5	38.0	33.04	5.35	8.25	40.87
$HCrEDTA \cdot 2H_2O$	32.3	4.3	7.5	40.9	31.84	4.54	7.42	42.41
$H_2NiDCTA \cdot 4H_2O$	38.0	4.9	6.3	34.6	35.39	5.94	5.89	40.42
$HCoHEEDTA \cdot H_2O$	33.9	5.1	7.8	36.2	34.01	5.14	7.93	36.25
$HNiHEEDTA \cdot H_2O$*	30.2	5.1	7.1	41.4	34.03	5.14	7.93	36.27
$HCuHEEDTA \cdot H_2O$	33.6	5.1	7.7	35.8	33.57	5.07	7.83	35.77

*The results for this compound are unsatisfactory; it is possible that combustion was incomplete, resulting in carbon monoxide being formed as well as carbon dioxide. From other evidence (Table 2) we believe the formula is correct.

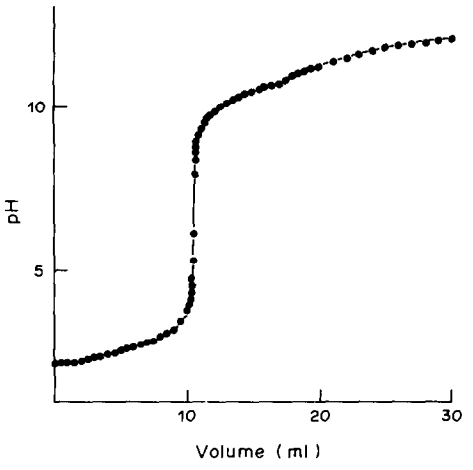

Fig. 2. Titration of 1.190 mmole of HCuHEEDTA with 0.1126*M* NaOH. Temperature 298 K, ionic strength 0.1 (NaCl). The curve is calculated by taking pK_a values of 2.44 and 10.44.

From literature data,[3] the pK_a values for equilibria (6) and (7) can be calculated:

$$\frac{[H^+][HCuDTPA^{2-}]}{[H_2CuDTPA^-]} = \frac{[H^+][HDTPA^{4-}]}{[H_2DTPA^{3-}]} \times \frac{[HCuDTPA^{2-}]}{[HDTPA^{4-}][Cu^{2+}]} \times \frac{[Cu^{2+}][H_2DTPA^{3-}]}{[H_2CuDTPA^-]} = K_a(H_2DTPA^{3-})\, K^{HDTPA^{4-}}_{CuHDTPA^{2-}} / K^{H_2DTPA^{3-}}_{CuHDTPA^-}$$

Thus

$$pK_a(H_2CuDTPA^-) = 8.59 - 15.7 + 10.2 = 3.09.$$

Similarly,[3]

$$pK_a(HCuDTPA^{2-}) = 4.75.$$

We tried to compute a curve to fit the experimental points by using these pK_a values, but the fit was not good around pH 3 for any value of pK_a (H_3CuDTPA). By using the graphical methods described by Schwarzenbach *et al.*,[8] the approximate values

$$pK_a(H_3CuDTPA) = 2.2 \pm 0.2$$

and

$$pK_a(H_2CuDTPA^-) = 2.7 \pm 0.2$$

were calculated. The values giving the best fit to the experimental points were then deduced to be

$$pK_a(H_3CuDTPA) = 2.1 \pm 0.2$$

and

$$pK_a(H_2CuDTPA^-) = 2.8 \pm 0.2$$

taking pK_a($HCuDTPA^{2-}$) as 4.75 (Fig. 1).

From the experimental points in the alkaline region it was estimated that pK_a for the complex $CuDTPA^{3-}$ is $\gtrsim 13$.

HCr(III)EDTA

Dissociation of the complex $CrEDTA^-$ into Cr^{3+} and the free ligand is of no importance even at pH 2 ($\alpha_D < 0.01\%$), because of the high stability of the complex. The stability constants are $K^{EDTA^{4-}}_{CrEDTA^-} = 10^{23.4}$ and $K^{HEDTA^{3-}}_{CrHEDTA} = 10^{15.1}$.[3]

The following equilibria were taken into account:

$$HCrEDTA \rightleftharpoons H^+ + CrEDTA^- \quad (8)$$

$$H_2O + CrEDTA^- \rightleftharpoons H^+ + CrEDTA(OH)^{2-} \quad (9)$$

$$H_2O + CrEDTA(OH)^{2-} \rightleftharpoons H^+ + CrEDTA(OH)_2^{3-} \quad (10)$$

The agreement between our experimental values and the literature data[3,9] is reasonable, especially since the lowest and the highest pK_a values lie outside the experimental pH range.

H_2NiDCTA

From the acid dissociation constants of H_4DCTA and the stability constants[3] $K^{DCTA^{4-}}_{NiDCTA^{2-}}$ and $K^{HDCTA^{3-}}_{NiHDCTA^-}$ it can be estimated that α_D of the $NiDCTA^{2-}$ chelate is about 6% at pH 2 and about 1% at pH 2.5. This dissociation was neglected in our calculations. As a consequence the calculated pK_a values will be slightly too high. However, this systematic error is smaller than the experimental error, which we estimate at about 0.2 pK unit. The pK_a values were calculated according to the graphical method,[8] leading to the approximate values 1.6 and 2.0 (at ionic strength 0.1). In the literature the values 1.8 and 2.74 are reported at ionic strength 1.25 and 25°.[10]

There seems to be a large discrepancy, as it is expected that concentration dissociation constants should increase with ionic strength; *i.e.*, the pK_a values decrease. The discrepancy, however, is not real, as the pK_a values reported by Margerum and Bydalek[10] are neither concentration constants nor activity constants. When the activity coefficient of H^+ is taken into account (according to the Debye–Hückel theory) smaller pK_a values are found.

HCo(HEEDTA), HNi(HEEDTA) and HCu(HEEDTA)

In the acid region the important equilibrium is:

$$HM(HEEDTA) \rightleftharpoons H^+ + M(HEEDTA)^- \quad (11)$$

For the calculation of the acid dissociation constants, it was assumed that no significant dissociation of $M(HEEDTA)^-$ occurred. The validity of this assumption was checked after the calculation of the pK_a values for equilibrium (11). It was found to be justified for nickel ($\alpha_D < 1\%$) and copper ($\alpha_D < 0.4\%$). In the case of cobalt, $\alpha_D < 15\%$ only at the lowest pH, so the calculated value for pK_a (HCoHEEDTA) may

Table 2. Hydrolysis reactions of some acid metal chelates studied by potentiometric titration; the pK_a and pK_b values refer to concentration constants; the medium is 0.1 *M* NaCl; $pK_w = 13.89 \pm 0.01$; the values for *n* in parentheses are the numbers of experimental points on which the calculations of the pK values are based; if no value is given, all the experimental points were used

Compound	Molecular weight: Theor.	Molecular weight: Expt.	C_o, *m*M	pK values	Literature values (reference)
$H_3CuDTPA \cdot 3H_2O$	508.9	505.4	2.129	$pK_{a,1} = 2.1 \pm 0.3$ (296 K)	—
				$pK_{a,2} = 2.8 \pm 0.2$	3.09 (3)
				$pK_{a,3} = 4.75 \pm 0.05$	4.75 (3)
				$pK_{b,1} \leqslant 1$	—
$HCrEDTA \cdot 2H_2O$	377.3	373.5	4.144	$pK_{a,1} = 2.2 \pm 0.2$ ($n = 12$) (298 K)	2.04[3a], 2.27[9b]
				$pK_{a,2} = 7.35 \pm 0.01$ ($n = 8$)	7.40[3], 7.41[9b]
				$pK_{a,3} = 12.35 \pm 0.05$ ($n = 15$)	12.2[9]
$H_2NiDCTA \cdot 4H_2O$	475.1	478.5	4.80	$pK_{a,1} = 1.6 \pm 0.2$ (298 K)	1.80[10c]
				$pK_{a,2} = 2.0 \pm 0.1$	2.74[10c]
				$pK_{b,1} \leqslant 1$	—
$HCoHEEDTA \cdot H_2O$	353.2	355.9	5.811	$pK_{a,1} = 2.2 \pm 0.2$ ($n = 10$) (297 K)	—
				$pK_{b,1} = 2.14 \pm 0.05$ ($n = 24$)	—
$HNiHEEDTA \cdot H_2O$	353.0	349.3	6.112	$pK_{a,1} = 1.73 \pm 0.03$ ($n = 22$) (298 K)	2.54[11]
				$pK_{b,1} = 1.46 \pm 0.1$ ($n = 16$)	—
$HCuHEEDTA \cdot H_2O$	357.8	358.6	2.998	$pK_{a,1} = 2.51 \pm 0.05$ ($n = 5$) (297 K)	2.32[11]
				$pK_{b,1} = 3.42 \pm 0.03$ ($n = 20$)	—
$HCuHEEDTA \cdot H_2O$		358.1	11.90	$pK_{a,1} = 2.44 \pm 0.02$ ($n = 19$) (298 K)	—
				$pK_{b,1} = 3.46 \pm 0.02$ ($n = 34$)	—

[a] Calculated from data given in Ref. 3.
[b] Values measured at 18°C and ionic strength 0.15 (spectrophotometry).
[c] Values measured at 25°C and ionic strength 1.25 (potentiometry).

be somewhat high, as the free ligand takes up two or three protons in this pH region. This systematic error should be less than 0.1 pK unit. Table 2 shows that HNiHEEDTA appears to be a stronger acid than HCuHEEDTA, contrary to the results of Bydalek and Margerum.[11] Their values do not refer to concentration constants, which can be obtained by taking the activity coefficient of H^+ into account.

However, this cannot explain the discrepancy mentioned. Thermodynamic data reported by Brunetti *et al.*[12] show that $HNiEDTA^-$ is a somewhat weaker acid than $HCoEDTA^-$ and $HCuEDTA^-$, the respective pK_a values being 3.23, 3.01 and 3.01. In view of these results and the elemental analysis results for HNiHEEDTA (Table 1), our pK_a and pK_b values for HNiHEEDTA appear to be doubtful (Table 2).

In alkaline solutions a ternary complex with OH^- is formed:

$$MHEEDTA^- + OH^- \rightleftharpoons MHEEDTA(OH)^{2-} \quad (12)$$

The pK_b values for these equilibria (Table 2) may be compared with those for the corresponding EDTA complexes. Bhat and Krishnamurthy[13] reported concentration pK_b values at 25° and ionic strength 1. They gave $pK_b = 0.83$ for $CoEDTA(OH)^{3-}$, $pK_b = 0.48$ for $NiEDTA(OH)^{3-}$ and $pK_b = 2.40$ for $CuEDTA(OH)^{3-}$.

The order of base strength is similar to that for the $MHEEDTA(OH)^{2-}$ chelates (Table 2). Recalculation of the pK_b values reported by Bhat and Krishnamurthy to ionic strength 0.1, according to the Debye–Hückel limiting laws[7] (although only an approximate procedure), leads to pK_b values for the $MEDTA(OH)^{3-}$ chelates that are smaller by about 0.5. Thus it is concluded that the $MHEEDTA(OH)^{2-}$ species are much weaker bases than the corresponding $MEDTA(OH)^{3-}$ species. This implies that Beck's rule[14] is valid: the more stable chelate forms the less stable ternary complex (Table 3):

$$K^{L_1}_{ML_1} > K^{L_2}_{ML_2} \rightarrow K^{X}_{ML_1X} < K^{X}_{ML_2X} \quad (13)$$

The validity of Beck's rule has also been demonstrated for other cases in recent publications.[16,17]

Table 3. Relative stabilities of the HEEDTA and EDTA chelates of cobalt, nickel and copper and their ternary hydroxo-complexes

Metal	$\log \{K^{EDTA}_{MEDTA}/K^{HEEDTA}_{MHEEDTA}\}$	$\log \{K^{OH}_{MEDTA(OH)}/K^{OH}_{MHEEDTA(OH)}\}$
Co	1.7[a]	≈ -1.8[b]
Ni	1.4[a]	≈ -1.5[b]
Cu	0.9[a]	≈ -1.5[b]

[a] Values taken from Ref. 15.
[b] Approximate values—see text.

Acknowledgement—This work is part of the research program of the National Institute for Nuclear Physics and High-Energy Physics (NIKHEF, section K), made possible by financial support from the Foundation for Fundamental Research on Matter (FOM) and the Netherlands Organization for the Advancement of Pure Research (ZWO).

REFERENCES

1. G. Schwarzenbach and H. Flaschka, *Die komplexometrische Titration*, Enke Verlag, Stuttgart, 1965.
2. D. D. Perrin, *Stability Constants of Metal–Ion Complexes, Part B, Organic Ligands*, Pergamon Press, Oxford, 1979.
3. J. Kragten, *Atlas of Metal–Ligand Equilibria in Aqueous Solution*, Horwood, Chichester, 1978.
4. J. Korsse, *Kinetics of the Reactions of Hydrated Electrons with Metal Complexes. Pulse Radiolysis Experiments and Theoretical Considerations*, Thesis, University of Amsterdam, 1983.
5. R. E. Sievers and J. C. Bailar, *Inorg. Chem.*, 1962, **1**, 174.
6. R. G. Bates, *Determination of pH. Theory and Practice*. Wiley, New York, 1973.
7. W. J. Moore, *Physical Chemistry*, 5th Ed., p. 454 ff. Longmans, London, 1972.
8. G. Schwarzenbach, A. Willi and R. O. Bach, *Helv. Chim. Acta*, 1947, **30**, 1303.
9. C. Furlani, G. Morpurgo and G. Sartori, *Z. Anorg. Allgem. Chem.*, 1960, **303**, 1.
10. D. W. Margerum and T. J. Bydalek, *Inorg. Chem.*, 1963, **2**, 683.
11. T. J. Bydalek and D. W. Margerum, *ibid.*, 1963, **2**, 678.
12. A. P. Brunetti, G. H. Nancollas and P. N. Smith, *J. Am. Chem. Soc.*, 1969, **91**, 4680.
13. T. R. Bhat and M. Krishnamurthy, *J. Inorg. Nucl.* Chem., 1963, **25**, 1147.
14. M. T. Beck, *Chemistry of Complex Equilibrium*, p. 196. Van Nostrand, London, 1970.
15. S. Chaberek, Jr. and A. E. Martell, *J. Am. Chem. Soc.*, 1955, **77**, 1477.
16. J. Korsse, L. A. Pronk, C. van Embden, G. A. J. Leurs and P. W. F. Louwrier, *Talanta*, 1983, **30**, 1.
17. E. A. Polyak, *Russ. J. Gen. Chem.*, 1975, **45**, 622.

Talanta, Vol. 32, No. 6, pp. 457–460, 1985
Printed in Great Britain.

0039-9140/85 $3.00 + 0.00

SEPARATION AND CONCENTRATION OF SOME PLATINUM METAL IONS WITH A NEW CHELATING RESIN CONTAINING THIOSEMICARBAZIDE AS FUNCTIONAL GROUP

S. SIDDHANTA and H. R. DAS
Department of Chemistry, Presidency College, Calcutta-700073, India

(*Received* 13 *September* 1982. *Revised* 10 *December* 1984. *Accepted* 12 *January* 1985)

Summary—A new chelating ion-exchange resin containing thiosemicarbazide as functional group and based on macroreticular polystyrene–divinylbenzene (8%) has been prepared. Its sorption characteristics for palladium(II), platinum(IV), rhodium(III), ruthenium(III) and iridium(III) have been studied. These platinum metal ions can be quantitatively separated by sorption on this chelating resin and selective elution. The resin is highly stable in acid and alkaline solution.

Thiosemicarbazide forms chelate compounds with a number of metal ions.[1,2] Its incorporation in a resin matrix was therefore deemed of interest in connection with concentration and separation of platinum metals. This paper deals with the synthesis and sorption characteristics of a macroreticular polystyrene-based resin containing thiosemicarbazide as a functional group, with special reference to separation and concentration of platinum metals.

EXPERIMENTAL

Synthesis of the resin

Air-dried styrene–divinylbenzene copolymer beads (5 g, 100–120 mesh) were first nitrated and reduced to the amino form.[3] This resin was then converted into the isothiocyanate derivative[4] by a two-step process. In the first step a 250-ml two-necked flask equipped with a powerful mechanical stirrer was cooled in a freezing mixture of ice and salt, and 30 ml of pure carbon disulphide and 50 ml of concentrated ammonia solution were introduced into it. The mixture was stirred and the amino-resin added. The stirring was continued for 6 hr, and the product was then filtered off. In the second step the product obtained was agitated with aqueous lead nitrate solution (20%) for 12 hr, to form the isothiocyanate derivative. The product was collected and the lead sulphide formed in the reaction was removed from it by repeated washing with hot hydrochloric acid (1 + 2) until the washings were free from lead ions. The product was finally washed with water.

The isothiocyanate derivative thus obtained was then refluxed with 25 ml of 99% hydrazine hydrate solution for 30 hr, a further 5 ml of the hydrazine hydrate solution being added every 5 hr. The final product, the chelating resin containing thiosemicarbazide as functional group, was filtered off and washed with demineralized water, then extracted in a Soxhlet extractor with a 1:1 v/v alcohol and benzene mixture for 3 days. Finally it was washed with dilute hydrochloric acid and then with demineralized water, air-dried, and sieved, the particles of 100–200 mesh size being retained for use.

Resin characterization

Stability. The resin is stable towards alkalis and non-oxidizing acids. A 0.5-g portion of the resin was shaken with 50 ml of acid or alkali for 1–7 days, filtered off, washed with water until the washings were neutral, dried, and analysed for nitrogen and sulphur.

Stability in the sorption–desorption cycle was examined by shaking 0.5 g of the resin with 50 ml of 0.1*M* palladium(II) in 1*M* hydrochloric acid for 24 hr, filtering off, and eluting palladium by shaking with 4*M* hydrochloric acid for 24 hr. The palladium content was determined spectrophotometrically. This loading and acid washing cycle was repeated 25 times, and the results were studied to assess the resin stability.

Water regain. The dry resin was allowed to stand in demineralized water for 48 hr, then filtered off, pressed between filter papers, weighed, dried at 100° for 48 hr and reweighed.

Chemical analysis of the resin. The sulphur content of the resin was determined as sulphate after fusion with potassium carbonate, and the nitrogen content was determined by the Dumas method.

Exchange capacity. Palladium(II), platinum(IV), rhodium(III), ruthenium(III) and iridium(III) solutions, 0.1*M*, were prepared by dissolving the chlorides (Johnson–Matthey) in dilute hydrochloric acid. Ten-ml portions were adjusted to various acidities ranging from 5*M* hydrogen-ion concentration to pH 6.0 with hydrochloric acid and sodium acetate solution (10%) and each was equilibrated with 0.1 g of air-dried resin for 24 hr. The resin was filtered off and washed with a solution of the same acidity as the test solution until the washings were free from metal ions. Palladium(II) and platinum(IV) were desorbed with 4*M* hydrochloric acid; rhodium(III) and ruthenium(III) were eluted with 9*M* hydrochloric acid. The metal ions were determined by the *N*,*N*-diphenylthiourea method.[5]

Equilibration rate. The time required for 50% uptake of palladium(II), platinum(IV), rhodium(III) and ruthenium(III) was determined at the acidity for maximal sorption.

Column operation. A glass tube (35 cm long, 9 mm bore) was filled with a 21-cm long bed of swollen resin (prepared by standing 5 g of air-dried resin in demineralized water for 24 hr); the bed volume was 13 ml. The resin bed was thoroughly washed with 1*M* hydrochloric acid and then with demineralized water until free from acid. The sorption and elution characteristics of palladium(II), platinum(IV), rhodium(III) and ruthenium(III) were then studied.

Separation procedures

To separate the five platinum metal ions examined, 1-ml portions of their 20-ppm solutions were mixed and diluted to 25 ml with 1.0*M* hydrochloric acid. The column was equilibrated with 1*M* hydrochloric acid and the mixture passed through the column at 1.0 ml/min. For larger quantities of the metal ions it was found necessary to recycle the solution to ensure complete sorption. Iridium(III) passed through the column unsorbed, but the other four metal species were completely sorbed. Palladium(II) was selectively eluted with 15 bed-volumes of 5% *N,N*-diphenylthiourea solution in ethanol at a flow-rate of 1 ml/min, and the column was freed from the reagent by repeated washing with ethanol. Next platinum(IV) was eluted with 20 bed-volumes of 4*M* hydrochloric acid and then rhodium(III) and ruthenium(III) with 9*M* hydrochloric acid. These last two were separated by adding 10 ml of 10% hydroxylamine hydrochloride solution to the eluate containing them, adjusting the acidity to 1*M*, and passing the solution through the column (conditioned by passage of 1*M* hydrochloric acid); the rhodium(III) was sorbed but not the ruthenium. The rhodium was then desorbed with 15 bed-volumes of 9*M* hydrochloric acid.

The metal ions in the effluents were determined spectrophotometrically with *N,N*-diphenylthiourea in ethanol.

RESULTS AND DISCUSSION

Synthesis and characterization of resin

The method of preparation of the thiosemicarbazide resin is shown schematically below.

The nitrogen content of compound **V** was 9.0% and that of **VI** 7.6%, the sulphur contents being 6.2% and 2.7% respectively. Calculation shows that there should be 0.84 mmole of sulphur per gram of dry chelating resin. The maximal exchange capacity for palladium(II) was found to be 0.78 mmole/g. The resin–metal complexes therefore probably have 1:1 stoichiometry; steric factors are probably responsible for the exchange capacities being lower than theoretical (Table 1). No decrease in nitrogen and sulphur content was observed after treatment of the resin with 1–6*M* acid or 0.1*M* sodium hydroxide, but sulphur was formed after treatment with 1*M* nitric acid for 2 hr or with 1*M* sodium hydroxide for 3 days. The resin was completely stable in the 25 metal uptake–elution cycles, in 1*M* hydrochloric acid medium.

Table 1. Exchange capacities and uptake times

Metal ion	Maximal capacity, *mmole/g*	Time required for 50% uptake, *min*
Pd(II)	0.78 (pH 0)	32
Pt(IV)	0.71 (pH 0)	35
Ru(III)	0.685 (1.5*M* HCl)	40
Rh(III)	0.615 (2*M* HCl)	45

The infrared spectrum of the chelating resin has a band at 1612 cm^{-1} which may be assigned[6,7] to the C—N stretching mode in the —N—C=S grouping, a band at 1500 cm^{-1} due to the C—N stretching mode, and a band at 1340 cm^{-1} due to C=S stretching vibrations corresponding to the "Amide I" band.

The time required for 50% uptake of the metal ions by the H^+ form of the resin is shown in Table 1. From the equilibrium rate study, the resin seems suitable for column operation if the flow-rate is low enough.

The water regain of the resin (0.48 g/g) is quite satisfactory.

Sorption and desorption of metal ions

The sorption behaviour of palladium(II), platinum(IV), rhodium(III) and ruthenium(III) in the batch method is shown in Fig. 1. The capacities are maximal in 1–2*M* hydrochloric acid medium, in which these platinum metal ions form stable complexes.[8–10] Sorption of silver(I) is zero at pH 0 but increases with increase in pH. Gold(III) and osmium(VI) are instantaneously reduced to the

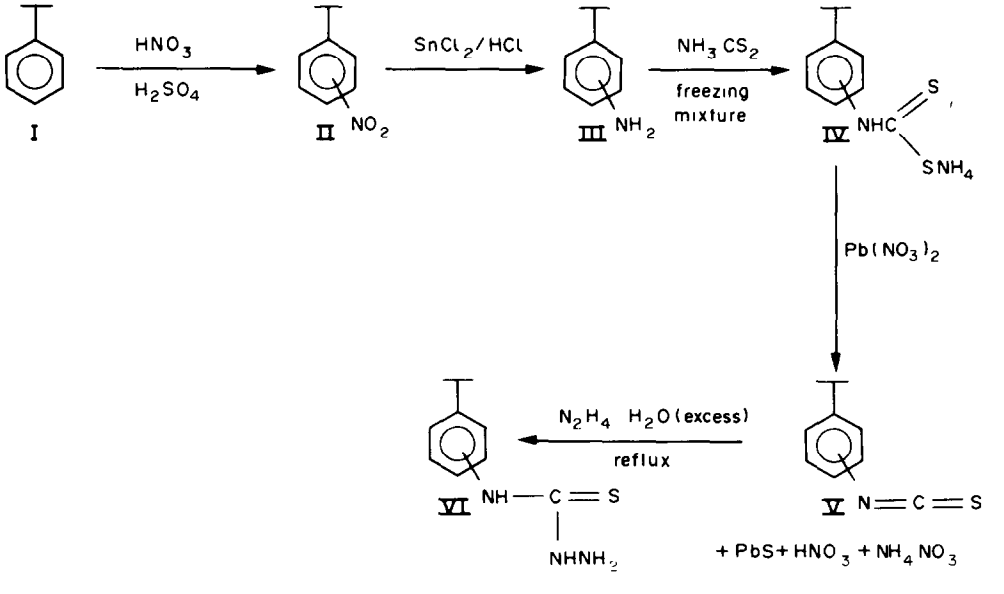

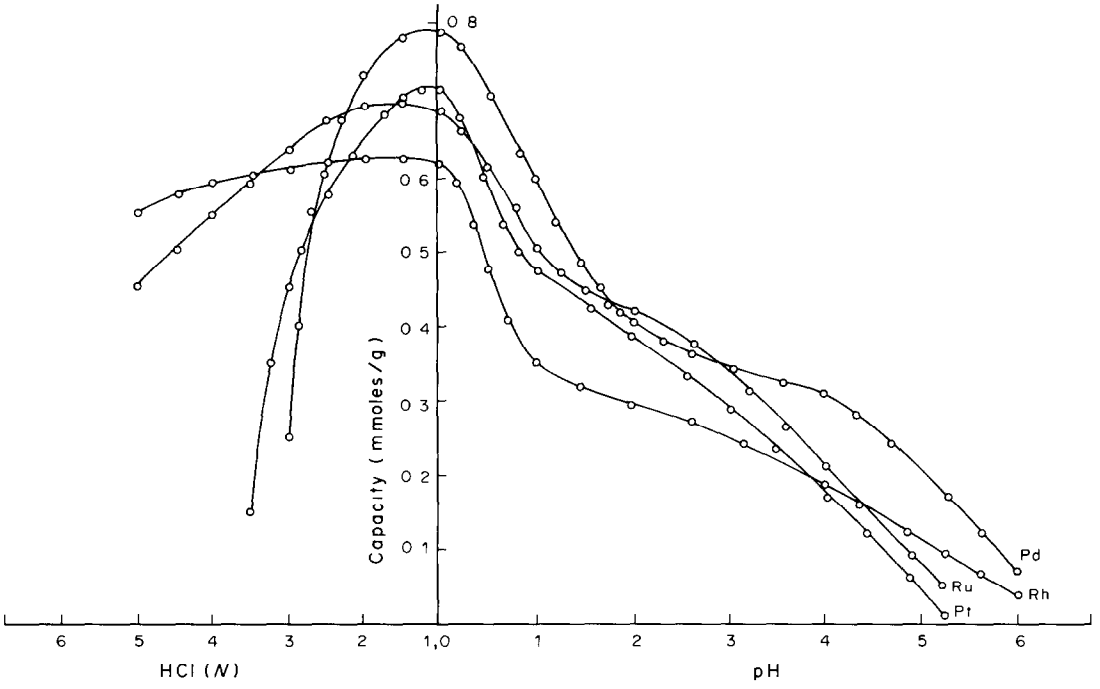

Fig. 1. Total exchange capacity of the thiosemicarbazide resin for different platinum metal ions.

metals by the resin. Base metal ions such as copper(II), bismuth, mercury(II), iron (III), vanadium(V), aluminium and uranium(VI) are not sorbed under the experimental conditions. The resin does not sorb iridium(III) at pH 0, which makes its separation from the other platinum metals easy. If the concentration ratio of palladium to the other platinum metals exceeds 10, the resin preferentially sorbs the palladium (Table 2), and a separate column is necessary for the separation of the others. In the normal case, after elution of palladium(II) and platinum(IV), the rhodium and ruthenium are eluted together with 9*M* hydrochloric acid, and the ruthenium is reduced with hydroxylamine hydrochloride to ruthenium(II),[5] which is not sorbed by the resin. The rhodium(III) can be separated from the ruthenium(II) by sorption on the resin from 1*M* hydrochloric acid and elution with 9*M* hydrochloric acid.

The recovery of platinum is 95.5% with 15 bed-volumes of eluent, and 99.5% with 20 or more bed-volumes; the recoveries of the other metals are between 99.5 and 100% (Table 2).

Results for separation from base metals are given in Table 3, which also shows the reproducibility.

Table 2. Separation of Pd(II), Pt(IV), Ru(III) and Rh(III) from mixtures

Sample	Metal ion	Taken, μg	Found, μg
1	Pd(II)	200	200
	Pt(IV)	20	0
	Ru(III)	20	0
	Rh(III)	20	0
2	Pd(II)	20	20.0
	Pt(IV)	200	199
	Ru(III)	20	19.9
	Rh(III)	20	19.8
3	Pd(II)	20	20.0
	Pt(IV)	20	19.9
	Ru(III)	200	199
	Rh(III)	20	19.8
4	Pd(II)	20	20.0
	Pt(IV)	20	19.9
	Ru(III)	20	19.9
	Rh(III)	200	198

Scheme for concentration and analysis of native Pt, Rh–Ir, Ir and most other alloys[11,12]

Mix the weighed sample with ten times its weight of sodium chloride in a porcelain boat. Place the boat in the centre of a clear fused-quartz tube and put the tube into an electric furnace for dry chlorination. Attach a receiver train, place 10 ml of water saturated with sulphur dioxide in the first receiver and 6*M* hydrochloric acid saturated with sulphur dioxide in

Table 3. Separation from a mixture of Au(III), Ag(I), Bi(III), Hg(II), Fe(III), V(V), Al(III), and Cu(II), (20 μg each)

Metal determined (20 μg)	Relative mean error, %	Standard deviation, μg
Pd(II)	0.1	0.09
Pt(IV)	0.2	0.09
Ru(III)	0.4	0.08
Rh(III)	0.6	0.08

the other three receivers. Heat the tube to 700° and pass dry chlorine through it for 7–8 hr. Cool, and displace the chlorine with nitrogen. Detach the receivers, wash the chlorinated product out of the tube with about 10 ml of hot 1*M* hydrochloric acid, into a beaker, taking care that no residue is left. Combine the contents of the receivers in a beaker and evaporate the solution to about 5–10 ml. Transfer it together with the main solution to a 500-ml distillation flask with water. Connect the flask to a distillation unit containing a trap for perchloric acid vapour, a condenser and three receiver in series. Distil the ruthenium and osmium by heating to fuming with 70% perchloric acid, collecting the tetroxides in concentrated hydrochloric acid.[13] Combine the solutions from the receivers in a beaker and evaporate the mixture slowly (Solution **I**). Solution **I** is then allowed to pass through the column at pH 0 (after conditioning at the same pH). Osmium will be reduced to the metallic state and ruthenium will be sorbed on the column and may be eluted with 9*M* hydrochloric acid (Solution **II**).

Transfer the residue from the distillation flask to a beaker, add concentrated nitric acid and evaporate to dryness. Repeat the addition of concentrated hydrochloric acid and the evaporation several times. Cool, add *aqua regia* and digest on a steam-bath. Convert into the chloride by repeated evaporation with concentrated hydrochloric acid. Take up the residue with 3*M* hydrochloric acid. Gold will be present as $AuCl_4^-$, platinum as $PtCl_6^{2-}$, iridium as $IrCl_6^{2-}$ (partly as $IrCl_6^{3-}$), rhodium as $RhCl_6^{3-}$, iron and copper as their corresponding chlorides.

Removal of gold[14]

Dilute the solution and adjust the pH to 1.5 with dilute sodium hydroxide solution. Heat and add 10 ml of 10% sodium nitrite solution. Gold is precipitated. Filter off the precipitate and wash it with water and then with hot dilute nitric acid.

Evaporate the filtrate and washings to dryness. Add concentrated hydrochloric acid and evaporate on a steam-bath; repeat this step three times. Dissolve the residue in 1*M* hydrochloric acid.

If gold is not completely separated then cycle the solution through the resin column (conditioned at pH 0) at the rate of 1 ml/min. The gold will be reduced and remain in the bed. Run 9*M* hydrochloric acid through the column. Collect the effluent and concentrate it (Solution **III**). Mix solution **II** and solution **III**, and dilute to 100 ml.

Analysis for Pd, Pt, Rh, Ru, Ir

Take an aliquot (the amount of platinum metal should not exceed 3 mg) and add 1 ml of ethanol. Adjust the acidity to 1*M* hydrochloric acid and cycle the solution through the resin column (conditioned with 1*M* hydrochloric acid) at a flow-rate of 1 ml/min. Palladium(II), platinum(IV), rhodium(III) and ruthenium(III) will be sorbed, and iridium(III) will pass through. First elute palladium(II) and then platinum(IV) as discussed above. Finally separate rhodium(III) and ruthenium(III) as discussed earlier.

Acknowledgement—One of the authors (S.S.) is grateful to The University Grants Commission, New Delhi, for the award of a Teacher Fellowship.

REFERENCES

1. J. Welcher, *Organic Analytical Reagents*, Vol. IV, p. 189. Van Nostrand, Princeton, 1948.
2. K. Kodama, *Methods of Quantitative Inorganic Analysis*, p. 63. Interscience, New York, 1963.
3. R. V. Davies, J. Kennedy, E. S. Lane and J. L. Will, *J. Appl. Chem.*, 1959, **9**, 368.
4. A. I. Vogel, *A Text Book of Practical Organic Chemistry*, 3rd Ed., p. 643. Longmans, London, 1968.
5. M. Chakraborty and S. C. Shome, *J. Indian Chem. Soc.*, 1977, **54**, 225.
6. L. J. Bellamy, *The Infrared Spectra of Complex Molecules*, 3rd Ed., Vol. I, pp. 400, 401. Chapman & Hall, London, 1975.
7. K. Nakanishi and H. Solomon, *Infrared Absorption Spectroscopy*, 2nd Ed., p. 50. Holden-Day, New York, 1977.
8. K. Kodama, *op. cit.*, p. 240.
9. S. Komatsu and K. Onishi, *J. Chem. Soc Japan*, 1955, **76**, 661.
10. S. Komatsu, *ibid.*, 1956, **77**, 1439.
11. J. G. Sen Gupta, *Anal. Chim. Acta*, 1972, **58**, 23.
12. K. Kodama, *op. cit.*, p. 231.
13. J. G. Sen Gupta and F. E. Beamish, *Anal. Chem.*, 1962, **34**, 1761.
14. K. Kodama, *op. cit.*, p 228.

Talanta, Vol. 32, No. 6, pp. 461–465, 1985
Printed in Great Britain

0039-9140/85 $3.00 + 0.00
Pergamon Press Ltd

MATHEMATICAL OPTIMIZATION IN THE DETERMINATION OF THE DISSOCIATION CONSTANTS OF A TRIBASIC ORGANIC ACID BY ^{13}C NMR SPECTROSCOPY

ANNE-MARIE SALONEN
Department of Chemistry and Biochemistry, University of Turku, SF-20500 Turku, Finland

(*Received* 6 *September* 1984. *Revised* 15 *December* 1984. *Accepted* 11 *January* 1985)

Summary—The calculation of dissociation constants from the chemical shifts of ^{13}C NMR spectra leads to a complicated non-linear equation. Two different mathematical methods for solution of this equation have been chosen—an iterative step method and a matrix pseudo-inversion method. When the iteration method is used the initial guesses for the parameters, the initial value of the step size and the escalation of the iteration must be optimized. For comparison the matrix pseudo-inversion method was used because it gives a unique result. With the optimized step method the results were as accurate or even better than those obtained with the matrix method. Although it takes time to optimize the system, the step method is the more suitable method of solving the problem. The matrix inversion can be done only with a computer with 13 significant digits and exponent capacity larger than ± 38.

In the case of strongly overlapping ionization processes, *i.e.*, $\Delta pK_a < 2.7$,[1] it has been difficult with classical methods to determine the dissociation constants of polyprotic acids.[2] Computers have proved their worth for resolving this problem. The purpose of this paper is to show that complicated non-linear least-squares minimization problems can be solved even with micro-computers.

An organic tribasic acid, 6-(4-carboxy-2-oxabutyl)-6-ethyl-4,8-dioxaundecanedioic acid, $C_{15}H_{26}O_9$, with both ΔpK_a values ~ 0.6, has been examined as an example.

FORMULATION OF THE PROBLEM

The chemical shifts in the NMR spectra of acids and bases are a function of pH.[3] For systems involving several ionized species the observed chemical shift is

$$\delta_{obs} = \sum x_i \delta_i \qquad (1)$$

where for the ith species x_i is the mole fraction and δ_i the chemical shift relative to the standard.[4] To calculate the mole fractions it is first necessary to derive the concentrations of the species. For an acid with n dissociable hydrogen ions the following equilibria exist:

$$\begin{aligned} H_nA &\rightleftharpoons H^+ + H_{n-1}A^- \\ H_nA &\rightleftharpoons 2H^+ + H_{n-2}A^{2-} \\ H_nA &\rightleftharpoons jH^+ + H_{n-j}A^{j-} \\ &\vdots \quad\quad \vdots \quad\quad \vdots \\ H_nA &\rightleftharpoons nH^+ + A^{n-} \end{aligned}$$

The corresponding cumulative dissociation constants are

$$\beta_i = \frac{[H_{n-i}A^{i-}][H^+]^i}{[H_nA]}; \quad i = 1, \ldots, n$$

$$\beta_n = K_1K_2 \ldots K_n = \prod_{i=1}^{n} K_i$$

The total concentration of the acid is

$$C_a = [H_nA] + [H_{n-1}A^-] + \ldots + [A^{n-}] = \sum_{i=0}^{n} [H_{n-i}A^{i-}] \qquad (2)$$

and from the expressions for the dissociation constants,

$$[H_{n-i}A^{i-}] = \frac{[H_nA]\beta_i}{[H^+]^i}$$

By substitution of these concentrations in equation (2) and rearrangement, the concentration of undissociated acid is found to be

$$[H_nA] = \frac{\sum_{i=0}^{n} [H_{n-i}A^{i-}]}{1 + \sum_{i=1}^{n} \beta_i/[H^+]^i}$$

Use of these expressions easily gives a general expression for the mole fractions:

$$x_j = \frac{[H^+]^{n-j} \prod_{i=0}^{j} K_i}{\sum_{i=0}^{n} \left([H^+]^{n-i} \prod_{i=0}^{n} K_i \right)}; \quad j = 0, 1, \ldots n$$

where K_0 is defined as unity for convenience in notation, and x_0 is the mole fraction of undissociated acid. Substitution of the mole-fraction expressions into equation (1) gives

$$\delta_{obs} = \sum_{j=0}^{n} \left\{ \frac{[H^+]^{n-j} \prod_{i=0}^{j} K_i}{\sum_{i=0}^{n} \left([H^+]^{n-i} \prod_{i=0}^{n} K_i \right)} \delta_j \right\} \quad (3)$$

After rearrangement, equation (3) can be written in the form

$$\sum_{i=1}^{n} \left(\frac{\delta_i - \delta_{obs}}{[H^+]^i (\delta_{obs} - \delta_0)} \right) \beta_i = 1 \quad (4)$$

MATHEMATICAL TREATMENT OF EQUATION (4)

Optimized iterative step method

To solve equation (4) two programs have been written in FORTRAN, program NDISS for the cumulative dissociation constants and program KDISS for the corresponding stepwise constants. Subprogram ST608[5] was chosen for iteration and subprogram QUENO[6] for error calculation. The optimization has been done by changing the initial guesses of the parameters, the initial step size and the escalation* of the iteration. The optimization criterion is minimization of the sum of the squares of the differences between the observed and calculated chemical shifts:

$$F = \sum (\delta_{obs} - \delta_{calc})^2$$

The calculations were run with an APPLE II+ (Apple Computer Inc., California) equipped with a CP/M-FORTRAN translator in addition to the standard Applesoft BASIC interpreter. The FORTRAN translator uses 6 or 7 significant digits and the exponent capacity is less than ± 38.

Error estimation

The standard deviations of the parameters were estimated by Quenouille's method,[6]

$$s(\beta) \sim \sqrt{\frac{n-1}{n} \sum_{i=1}^{n} (a - \bar{a}_i)^2}; \quad a = \frac{1}{n} \sum_{i=1}^{n} \bar{a}_i$$

where n denotes the number of data-points, and $\bar{a}_i$ is the value of a parameter when function F has been minimized with omission of the ith data-point. To find the errors of the pβ- and pK-values the variance[7] of an arbitrary function, $Z = \psi(a, b)$, must be used:

$$\text{var}(Z) = s_Z^2 = \left(\frac{\partial \psi}{\partial a}\right)^2 s_a^2 + \left(\frac{\partial \psi}{\partial b}\right)^2 s_b^2 + 2\left(\frac{\partial \psi}{\partial a}\right)\left(\frac{\partial \psi}{\partial b}\right) s_{ab}^2$$

to yield

$$\text{var}(p\beta) = s_{p\beta}^2 = \left(-\frac{\log e}{\beta} \right)^2 s_\beta^2$$

and

$$\text{var}(pK) = s_{pK}^2 = \left(-\frac{\log e}{K} \right)^2 s_K^2$$

Matrix pseudo-inversion method

For comparison with the iteration method the matrix method was used because it gives a unique result. The program was written in BASIC and the computer used was a WANG 2200 (Wang Laboratories, Massachusetts) with 13 significant digits and exponent capacity ± 99. Equation (4) must be changed into the matrix form

$$\mathbf{Nb} = \mathbf{h} \quad (5)$$

where $\mathbf{h}$ is a column vector of ones, $\mathbf{N}$ is a $k \times n$ matrix, k is the number of parameters, n the number of data-points and $\mathbf{b}$ is a column vector of the parameters.

Because $\mathbf{N}$ is not a square matrix, when $n > k$, $\mathbf{N}$ must be multiplied by its transpose, $\mathbf{N}^T$. The matrix $\mathbf{N}^T\mathbf{N}$ is then a square matrix and the solved form of equation (5) is

$$\mathbf{b} = (\mathbf{N}^T\mathbf{N})^{-1}\mathbf{N}^T\mathbf{h} \quad (6)$$

where $(\mathbf{N}^T\mathbf{N})^{-1}\mathbf{N}^T$ is the pseudo-inverse[8] of $\mathbf{N}$.

Error estimation[9]

For the matrix equation (5) it is possible to write the covariance matrix

$$\text{cov}(\mathbf{b}) = \text{cov}[(\mathbf{N}^T\mathbf{N})^{-1}\mathbf{N}^T\mathbf{h}]$$

According to the theorem

$$\text{cov}(\mathbf{AX}) = \mathbf{A}\,\text{cov}(\mathbf{X})\mathbf{A}^T$$

we can write

$$\text{cov}(\mathbf{b}) = (\mathbf{N}^T\mathbf{N})^{-1}\mathbf{N}^T\text{cov}(\mathbf{h})[(\mathbf{N}^T\mathbf{N})^{-1}\mathbf{N}^T]^T$$
$$= (\mathbf{N}^T\mathbf{N})^{-1}\mathbf{N}^T\text{cov}(\mathbf{h})\mathbf{N}(\mathbf{N}^T\mathbf{N})^{-1}.$$

It is assumed that the error is normally distributed, with mean zero and variance σ^2, and $\mathbf{h}_i$ elements are independent with equal errors, so

$$\text{cov}(\mathbf{h}) = f\mathbf{I}$$

where f = sum of squares/degrees of freedom and $\mathbf{I}$ is the identity matrix.

Thus

$$\text{cov}(\mathbf{b}) = (\mathbf{N}^T\mathbf{N})\mathbf{N}^T f\mathbf{I}\mathbf{N}(\mathbf{N}^T\mathbf{N})^{-1}$$

and

$$f = \frac{(\mathbf{h} - \mathbf{Nb})^T(\mathbf{h} - \mathbf{Nb})}{n - k}$$

The errors of the pβ- and pK-values have been calculated in the same way as in the iteration method.

EXPERIMENTAL

NMR system

The ^{13}C NMR-titrations were done at 298 ± 1 K on a Jeol FX-60 FT NMR spectrometer operating at 15.03 MHz,

*Escalation refers to the multiplication factor used in the iteration. It is sometimes called the magnification.

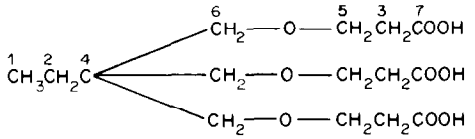

Fig. 1. The structural formula of the acid $C_{15}H_{26}O_9$.

using 8000 data-points with a precision of ± 0.06 ppm. Aqueous samples were placed in a 10-mm probe inside which was a 5-mm probe of D_2O + DSS as an external standard.

Potentiometric system

Values of pH were measured at 298 ± 0.5 K with a Radiometer ABL-3 potentiometer equipped with an Orion model 91-03-00 combined semimicro glass electrode assembly, standardized with NBS buffer solutions (pH 4.008 and 6.865 at 298 K).

Sample preparation

The concentration of the acid was $0.0501M$ ($\pm 4 \times 10^{-4}M$). The samples were delivered by micropipettes to give a total volume of 1.5 ml and the titrant used was a standard $0.9989M$ ($\pm 6 \times 10^{-4}M$) CO_2-free potassium hydroxide solution (Merck "Titrisol"). The volume change has no effect on the chemical shift.[10]

RESULTS AND DISCUSSION

The structural formula of the acid is shown in Fig. 1 and the ^{13}C NMR spectrum of the acid is shown in Fig. 2; numbering of the peaks refers to the scheme in Fig. 1 and the external standard peaks are marked with an x. The chemical shifts of the carboxyl groups—peak number 7—were the object of this study.

The chemical shifts of species H_3A and A^{3-} were measured in highly buffered solutions and $\delta(H_2A^-)$ and $\delta(HA^{2-})$ were calculated by the second method devised by Loewenstein and Roberts.[10] The ^{13}C NMR titration curve, δ *vs.* pH, is plotted in Fig. 3. In Tables 1–3 it is quite easy to find the optimal values for the calculations of the dissociation constants: they are

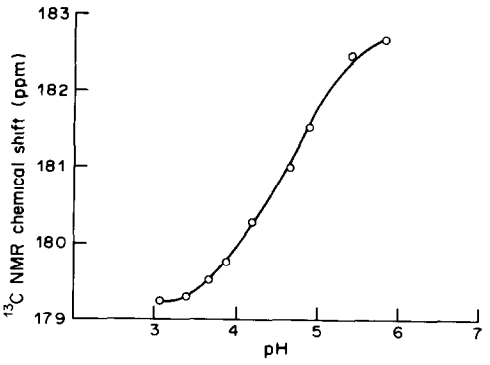

Fig. 3. ^{13}C NMR titration curve, chemical shift *vs.* pH.

denoted by asterisks. The optimum values of the initial guesses for the parameters were 10^{-4}, 10^{-9} and 10^{-14}, with initial step sizes of 10^{-10}, 10^{-15} and 10^{-20} respectively. For the optimum escalation of the iteration two values were found, 10^3 and 10^5, which both gave the minimum value 0.12154 for the function F; the lower value (10^3) was chosen for the final calculations.

The optimization of the system suggests that the error function is very complicated, so the observed data were treated by graphical analysis.[11] The error function used in the iteration process is drawn as contour plots and three-dimensional surfaces in Figs. 4 and 5. The function F splits into many minima, but the global minimum is clearly distinguishable from the local ones. The optimization of the iteration is necessary, otherwise the iteration may lead into a wrong pit and give erroneous results.

In Table 4 the results calculated by the three different methods are collected together. The calculated $p\beta$- and pK-values are very close to each other and stay within the error limits. In the matrix method the error of the first dissociation constant is smaller than in the other methods, but the errors of the second and third constants are one and a half times

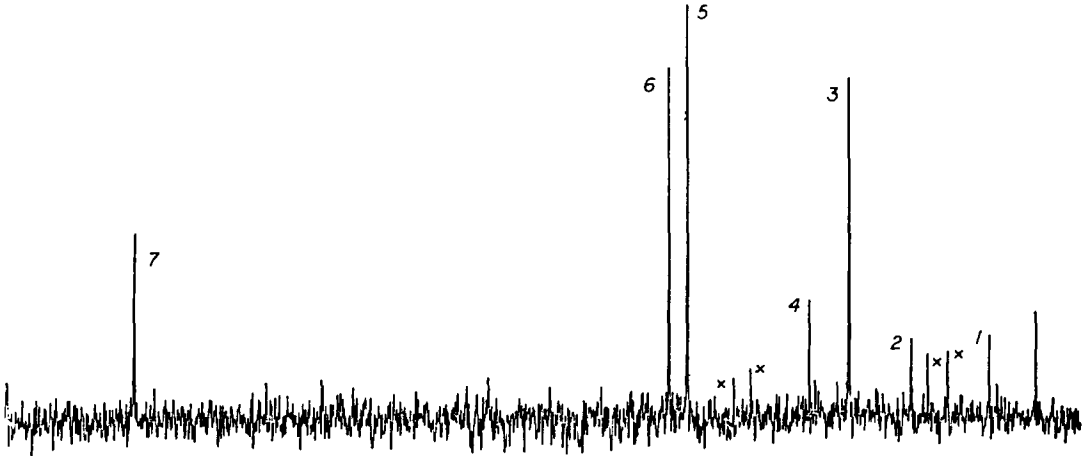

Fig. 2. ^{13}C NMR spectrum of the acid $C_{15}H_{26}O_9$.

Table 1. Effect of the initial guesses of the dissociation constants when the initial step size is 10^{-10}, 10^{-15} and 10^{-20} respectively for each parameter and the escalation of the iteration is 10^3

Initial guess			Computed parameters						
β_1	β_2	β_3	$10^4 \times \beta_1$	$10^9 \times \beta_2$	$10^{14} \times \beta_3$	pK_1	pK_2	pK_3	F
10^{-3}	10^{-8}	10^{-13}	1 652	4.940	3.069	3.782	4.525	5.207	0.47827
10^{-4}	10^{-9}	10^{-14}	1 255	3.812	2.360	3.901	4 517	5.208	0.12154*
10^{-5}	10^{-10}	10^{-15}	1 250	3.810	2.361	3.903	4 517	5.208	0.12247
10^{-6}	10^{-11}	10^{-16}	1.130	3.450	2.143	3.947	4.514	5.208	0.16241
10^{-4}	5×10^{-9}	10^{-14}	1.219	3.712	2.301	3.914	4.516	5.208	0.12586
10^{-4}	4×10^{-9}	3×10^{-14}	1.652	4.940	3.069	3.782	4.524	5.207	0.47827
10^{-4}	5×10^{-9}	3×10^{-14}	1.614	4.828	2.997	3.792	4.524	5.207	0.41325

Table 2. Effect of the initial step size when initial guesses are 10^{-4}, 10^{-9} and 10^{-14} respectively for each parameter and the escalation of the iteration is 10^3

Initial step size			Computed parameters						
β_1	β_2	β_3	$10^4 \times \beta_1$	$10^9 \times \beta_2$	$10^{14} \times \beta_3$	pK_1	pK_2	pK_3	F
10^{-5}	10^{-10}	10^{-15}	0.5072	1.693	1.041	4.295	4.476	5.211	1.46573
10^{-6}	10^{-11}	10^{-16}	0.5074	1.693	1.041	4.295	4.477	5.211	1.46567
10^{-7}	10^{-12}	10^{-17}	0.5074	1.693	1.041	4.295	4.477	5.211	1.46565
10^{-8}	10^{-13}	10^{-18}	0.5087	1.693	1.041	4.293	4.478	5.211	1.46544
10^{-9}	10^{-14}	10^{-19}	1.239	3.767	2.332	3.907	4.517	5.208	0.12254
10^{-10}	10^{-15}	10^{-20}	1.255	3.812	2.360	3.901	4.517	5.208	0.12154*
10^{-11}	10^{-16}	10^{-21}	1.227	3.731	2 310	3.911	4.517	5.208	0.12421
10^{-12}	10^{-17}	10^{-22}	1.249	3 795	2.349	3.903	4.517	5 208	0.12178
10^{-13}	10^{-18}	10^{-23}	1.178	3.593	2.224	3.929	4.515	5.208	0.13777
10^{-14}	10^{-19}	10^{-24}	1.000	1.452	1.000	4.000	4.838	5.162	44 22171

Table 3. Effect of the escalation of the iteration when initial guesses are 10^{-4}, 10^{-9} and 10^{-14} and initial step sizes are 10^{-10}, 10^{-15} and 10^{-20} respectively for each parameter

	Computed parameters						
Escalation	$10^4 \times \beta_1$	$10^9 \times \beta_2$	$10^{14} \times \beta_3$	pK_1	pK_2	pK_3	F
10	1.249	3.795	2.349	3.903	4.517	5.208	0.12178
10^2	1.227	3.731	2.310	3.911	4.516	5.208	0.12421
10^3	1.255	3.812	2.360	3.901	4.517	5.208	0.12154*
10^4	1.239	3.767	2.332	3.907	4.517	5.208	0.12254
10^5	1.255	3.810	2.359	3.901	4.517	5.208	0.12154*
10^6	1.087	3.335	2.063	3.964	4.513	5.209	0.19335
10^7	1.224	3 722	2.304	3.912	4.517	5.208	0.12477
10^8	1.075	3.299	2.041	3.969	4.513	5.209	0.20403
10^9	1.177	3.590	2.222	3.929	4.516	5.208	0.13827
10^{10}	1 149	3.510	2.172	3.940	4.515	5.208	0.15130

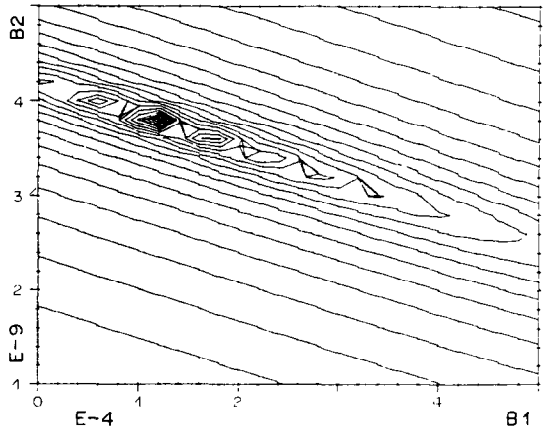

Fig. 4. Contour plot of the logarithm of the error function as a function of the cumulative dissociation constants β_1 and β_2: β_3 is fixed at the optimal value 2.36×10^{-14}.

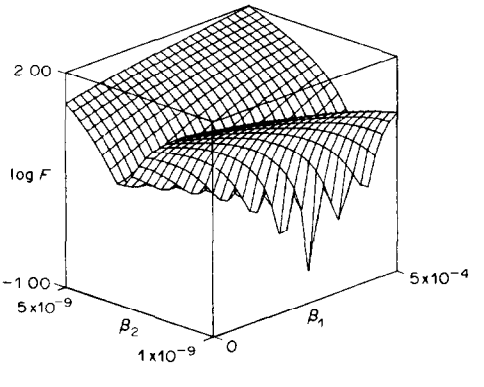

Fig. 5. Three-dimensional surface for the logarithm of the error function. The lowest contour line is -0.95 and the highest 5.35: the distance between the lines is 0.2.

Table 4. Cumulative and stepwise dissociation constants, with standard deviations computed with different programs

Parameters	Programs		
	NDISS	KDISS	Matrix method
$\beta_1 \pm s(\beta_1)$	$(1.25_5 \pm 0.12) \times 10^{-4}$	$1.25_8 \times 10^{-4}$	$(1.25_9 \pm 0.11) \times 10^{-4}$
$\beta_2 \pm s(\beta_2)$	$(3.81_2 \pm 0.18) \times 10^{-9}$	$3.82_1 \times 10^{-9}$	$(3.82_6 \pm 0.32) \times 10^{-9}$
$\beta_3 \pm s(\beta_3)$	$(2.36_0 \pm 0.13) \times 10^{-14}$	$2.36_5 \times 10^{-14}$	$(2.36_8 \pm 0.20) \times 10^{-14}$
$p\beta_1 \pm s(p\beta_1)$	3.901 ± 0.041	3.900	3.899 ± 0.039
$p\beta_2 \pm s(p\beta_2)$	8.418 ± 0.018	8.417	8.417 ± 0.036
$p\beta_3 \pm s(p\beta_3)$	13.627 ± 0.013	13.626	13.625 ± 0.037
$K_1 \pm s(K_1)$	$1.25_5 \times 10^{-4}$	$(1.25_8 \pm 0.17) \times 10^{-4}$	$1.25_9 \times 10^{-4}$
$K_2 \pm s(K_2)$	$3.03_7 \times 10^{-5}$	$(3.03_8 \pm 0.16) \times 10^{-5}$	$3.03_7 \times 10^{-5}$
$K_3 \pm s(K_3)$	$6.19_9 \times 10^{-6}$	$(6.19_0 \pm 0.05) \times 10^{-6}$	$6.19_0 \times 10^{-6}$
$pK_1 \pm s(pK_1)$	3.901	3.900 ± 0.059	3.899
$pK_2 \pm s(pK_2)$	4.517	$4\,517 \pm 0.022$	4.517
$pK_3 \pm s(pK_3)$	5.208	5.208 ± 0.035	5.208

as great as in the iteration method. It is thus obvious that the iteration method is quite useful after optimization. The matrix method is more rapid than the iteration method, but requires a computer capable of inverting a matrix with its elements distributed over a large number of orders of magnitude, and also requires great precision of calculation.

Acknowledgement—The author is grateful to Timo Nurmi and Mirja Samppala for recording the ^{13}C NMR spectra.

REFERENCES

1. A. Albert and E. P. Serjeant, *The Determination of Ionization Constants*, 3rd Ed., p. 61. Chapman and Hall, Cambridge, 1984.
2. R. F. Cookson, *Chem. Rev.*, 1974, **74**, 5.
3. E. Grundwald, A. Loewenstein and S. Meiboom, *J Chem. Phys.*, 1957, **27**, 641.
4. J. F Hinton and E. S. Amis, *Chem. Rev.*, 1967, **67**, 367.
5. J. P. Chandler, *Minimum of a Function of Several Variables*, Program 66.1, Quantum Chemistry Program Exchange, Indiana University, Bloomington, Ind., 1966.
6. M. H. Quenouille, *Biometrika*, 1956, **43**, 353.
7. A. A. Clifford, *Multivariate Error Analysis*, p. 30. Applied Science Publishers, London, 1973.
8. Y. Bard, *Nonlinear Parameter Estimation*, p. 290. Academic Press, New York, 1974.
9. N. Draper and H. Smith, *Applied Regression Analysis*, 2nd Ed., p. 70. Wiley, New York, 1981.
10. A. Loewenstein and J. D. Roberts, *J. Am. Chem. Soc.*, 1960, **82**, 2705
11. S. Pihlajamäki, University of Turku, Unpublished programs DACONT and THREE/2.

Talanta, Vol. 32, No 6, pp. 467–474, 1985
Printed in Great Britain

0039-9140/85 $3.00 + 0.00
Pergamon Press Ltd

ASYMMETRIC DERIVATIVES OF CARBOHYDRAZIDE AND THIOCARBOHYDRAZIDE AS ANALYTICAL REAGENTS

DANIEL ROSALES, GUSTAVO GONZALEZ and JOSE L. GOMEZ ARIZA
Department of Analytical Chemistry, Faculty of Chemistry, University of Seville, Seville-4, Spain

(*Received* 26 *June* 1984. *Revised* 10 *December* 1984. *Accepted* 11 *January* 1985)

Summary—The synthesis and analytical properties of two asymmetric derivatives of carbohydrazide and thiocarbohydrazide with pyridine and phenol have been studied. The compounds tested are 1-(2-pyridylmethylideneamino)-3-(salicylideneamino)urea and 1-(2-pyridylmethylideneamino)-3-(salicylideneamino)thiourea. The analytical utility of these reagents is outlined. A spectrophotometric method for determining the formation constants of the complexes is described.

Carbohydrazones and thiocarbohydrazones have been little used in analytical chemistry. Most of the work on their use has been done in our Department, and all of those studied were symmetric derivatives.[1–8]

The present paper deals with the synthesis and analytical study of two asymmetric derivatives with pyridine and phenol: 1-(2-pyridylmethylideneamino)-3-(salicylideneamino)urea (PSU) and 1-(2-pyridylmethylideneamino)-3-(salicylideneamino)thiourea (PST)

following results

PSU. HCl, $C_{14}H_{13}N_5O_2.HCl$	C	H	N	Cl
Theory, %	56.60	4.41	21.90	11.09
Found, %	52.9	4.5	22.1	10.7
PST. H_2O, $C_{14}H_{13}N_5OS.H_2O$	C	H	N	S
Theory, %	52.98	4.76	22.07	10.1
Found, %	52.7	4.5	22.2	10.3

Attempts to obtain the diaminoguanidine derivative were made but were unsuccessful.

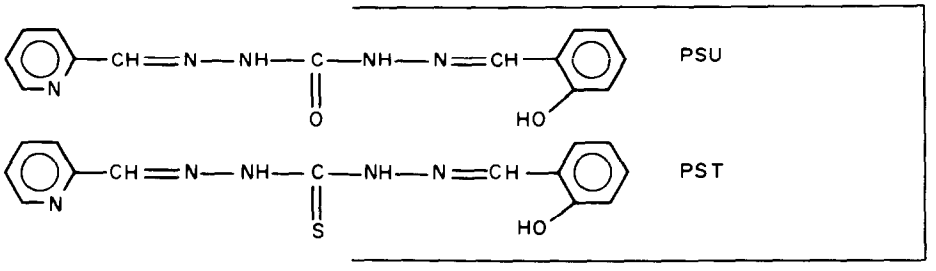

EXPERIMENTAL

Reagents

Synthesis. The reagents were obtained in two steps. First, the salicylaldehyde monoderivatives were obtained, by the method described by Brown *et al.*[9] The yields were higher than 80% and the microanalytical results in accordance with the empirical formulae. In the second step, these derivatives were condensed with 2-pyridinecarboxaldehyde in the usual way for Schiff's bases with some modifications. For PSU, to 1 g of mono(salicylidene)carbohydrazone, dissolved in 100 ml of boiling absolute ethanol, 2 ml of concentrated hydrochloric acid and 0.8 ml of 2-pyridinecarboxaldehyde were slowly added. The yellow product obtained was filtered off and washed with absolute ethanol and ether. The reagent was obtained as the monohydrochloride (m.p. 241–243°, decomp.). For PST, to 1 g of mono(salicylidene)thiocarbohydrazone, dissolved in 100 ml of boiling ethanol, 2 ml of glacial acetic acid and 0.7 ml of 2-pyridinecarboxaldehyde were added and the mixture was refluxed. After 1 hr, 200 ml of hot water were added and the mixture was cooled to room temperature. The yellow product was recrystallized from ethanol. This reagent was obtained as the monohydrate (m.p. 180–182°, decomp.).

The purity of both reagents was checked by thin-layer chromatography on silica gel. Microanalysis gave the

Other reagents. Salts and solvents were of analytical grade. All metal-ion solutions were standardized. Distilled water was used throughout.

Procedures

Evaluation of acid-dissociation constants. A 1-ml aliquot of a $10^{-3}M$ solution of PSU in 50% v/v aqueous ethanol, or a 0.75-ml aliquot of $10^{-3}M$ PST solution in ethanol, was placed in a 25-ml standard flask, and enough ethanol to make its final concentration 10% v/v was added. The ionic strength was fixed at 0.1 with potassium chloride and the pH adjusted with potassium hydroxide solution and hydrochloric acid. The solutions were then diluted to the mark with distilled water and mixed, and the absorbance, at five different wavelengths, and the pH were measured. The pH–absorbance curves were plotted for each reagent, and the pK_a values were evaluated by the two methods of Maroni and Calmon[10] (parallel straight lines and concurrent straight lines methods) and by Sommer's method.[11] The stability of the aqueous ethanol solutions at different pH values had been checked earlier.

Spectrophotometric study of reagent–metal ion reactions. The spectra of the chelates were recorded for samples with the reagent in excess (> 10-fold). The pH–absorbance curves were obtained, measurements being made at three wave-

lengths, and the buffers also serving to maintain the ionic strength at 0.01. The stoichiometry of the complexes was established by the continuous variation[12] and mole-ratio[13] methods, applied at a suitable pH, obtained with a buffer which also fixed the ionic strength at 0.01. The conditional overall formation constants were evaluated from the mole-ratio data by the method described below. For some complexes, the modification[14] of the Holme and Langmhyr method and the Asmus method[15] were also applied.

RESULTS AND DISCUSSION

Infrared spectra

The infrared spectra of the reagents (KBr discs) are complicated because the bands overlap. However, the assignments for the spectra of pyridine[16–18] and phenol[19–21] are well established, and so are those for carbohydrazide[22] and thiocarbohydrazide.[23] On the other hand, comparison of the spectra of the salicylaldehyde monoderivatives of carbohydrazide (**I**) and thiocarbohydrazide (**II**) shows that these have several absorption bands in similar regions. The principal bands and their assignments are listed in Table 1.

Ultraviolet spectra

The results obtained are given in Table 2. In general, as the dielectric constant of the solvent decreases, the wavelengths for maximum absorption become longer and the molar absorptivities decrease. The same effect was previously observed with symmetric derivatives of carbohydrazide and thiocarbohydrazide[5,24] and is characteristic of $n\rightarrow\pi^*$ transitions.

Acid–base equilibria

The spectra of aqueous solutions of both reagents are pH-dependent. The changes can be attributed to protonation of the pyridine nitrogen atom in acid medium, the dissociation of the imidol or thioimidol group in neutral or weakly alkaline medium, and the dissociation of the phenol group in alkaline medium, as shown in the scheme:

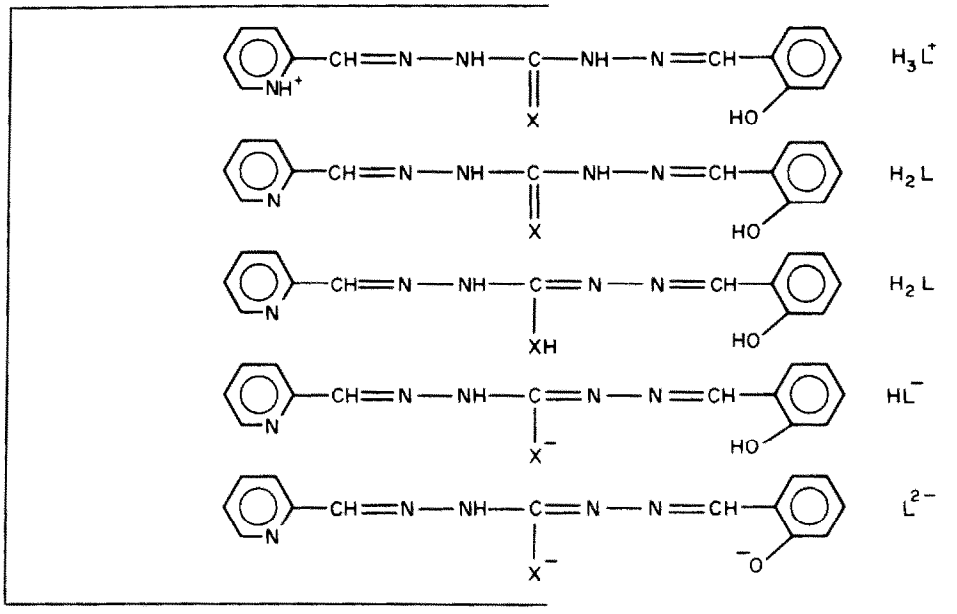

The molar absorptivity of the fully protonated species H_3R^+ of PSU could not be found experimentally because of the instability of this reagent in acid medium (pH <2), nor could the molar absorptivities of the HR^- species for both reagents, because K_{a_2} and K_{a_3} are too close together. The dissociation constants were therefore evaluated by using graphical methods in which the values of those molar absorptivities are not needed.[10,11] The pK_a values obtained are collected in Table 3.

Table 1. Infrared spectra

Frequency, cm^{-1}				
I	PSU	II	PST	Assignment
3350 m	3450 m	3280 s	3280 m	N—H and N=H_2 stretch
3050 w	3070 w	3140 w	3120 w	—OH intramolecular hydrogen bond
2920 w	2960 w	2960 w	2960 w	aromatic C—H stretch
1685 s	1700 s			C=O stretch
1640 s	1620 s	1640 s	1630 s	C=N stretch
1580–1490 s	1580–1460 s	1595–1460 s	1590–1470 s	aromatic C=C stretch
		1160 s	1150 s	C=S stretch
820–600 s	835–600 s	850–600 s	880–600 s	C—H in plane deformation

Table 2. Ultraviolet spectra of the reagents in common solvents

Solvent	Dielectric constant	PSU λ_{max}, nm	PSU ε, 10^4 l.mole^{-1}.cm^{-1}	PST λ_{max}, nm	PST ε, 10^4 l.mole^{-1}.cm^{-1}
Water	78.5	320	2.40	335	3.05
Dimethylsulphoxide	46.7	318	2.25	338	3.00
Dimethylformamide	37.6	318	2.45	338	3.60
Methanol	32.6	320	2.50	338	3.85
Ethanol	24.3	320	2.50	338	3.85
Acetone	20.7	326	2.00	350	1.50
Methyl isobutyl ketone	13.1	330	2.10	340	3.50
Chloroform	4.8	322	2.15	340	3.50
Ether	4.3	318	2.35	340	3.20
Benzene	2.4	324	1.95	344	3.65
Dioxan	2.2	318	2.35	356	2.70
Carbon tetrachloride	2.2	328	1.75	345	2.55

Table 3. pK_a values of the reagents*

Reagent	Method	pK_{a_1}	pK_{a_2}	pK_{a_3}
PSU	Parallel straight lines[10]	3.81 ± 0.05	9.58 ± 0.09	12.86 ± 0.08
	Concurrent straight lines[10]	3.77 ± 0.05	9.57 ± 0.09	12.89 ± 0.08
	Sommer[11]	3.81 ± 0.06	9.57 ± 0.08	12.87 ± 0.09
	Mean value	3.80 ± 0.05	9.57 ± 0.08	12.87 ± 0.08
PST	Parallel straight lines[10]	3.19 ± 0.04	7.80 ± 0.05	12.17 ± 0.08
	Concurrent straight lines[10]	3.20 ± 0.03	7.81 ± 0.08	12.23 ± 0.10
	Sommer[11]	3.20 ± 0.05	7.79 ± 0.05	12.23 ± 0.11
	Mean value	3.20 ± 0.04	7.80 ± 0.06	12.21 ± 0.09

*Mean of five determinations; medium containing 10% ethanol; $\mu = 0.1$.

Influence of oxidizing and reducing agents

Both reagents are readily oxidized or reduced (Table 4), but the products were not identified. No catalytic effect on the oxidation with hydrogen peroxide at pH 4.8 was exerted by Fe(III), V(V), Cu(II), Zn(II), Co(II), Ni(II), UO_2(II), Mn(II) or Ti(IV) at 1 ppm level. Hydroxylamine gives the well-known exchange reaction with the C=N group.

Fluorescence spectra

Both reagents showed weak fluorescence in ethanol and in aqueous media at pH >7; that for PSU is the more intense. The fluorescence spectra were not changed by addition of metal ions (at 1.0 ppm level), except for Fe(II) and Fe(III), which decreased the fluorescence intensity by about 20%.

COMPLEX FORMATION EQUILIBRIA

Reactions with metal ions

Comparison of the absorption spectra of the PSU–metal ion complexes with those of the corresponding complexes with the symmetric derivatives of carbohydrazide with salicylaldehyde (SAU) and 2-pyridinecarboxaldehyde (PMAU) and those of the PST–metal ion complexes with those of the corresponding complexes of the thiocarbohydrazide derivatives of salicylaldehyde (SAT) and 2-pyridinecarboxaldehyde (PMAT), indicates the effect of the asymmetric reagent structure on the reactivity with metal ions.

The results obtained with acetate-buffered medium are summarized in Table 5. The data for the Fe(III) complexes are not included because these complexes are very unstable and the spectra change to those of the Fe(II) complexes. Both reagents act as general chromogenic ligands and are only selective for iron(II), which gives a complex that absorbs at much longer wavelengths than the other complexes. The PSU complexes show similar spectrophotometric characteristics to the SAU and PMAU complexes, but PST is a better spectrophotometric reagent than SAT and PMAT because the complexes have higher molar absorptivities and generally absorb at longer wavelengths.

Table 4. Effect of oxidizing and reducing agents on the absorption spectra of the reagents (decrease in absorbance, %)

Agent*	pH	PSU at 1 hr	PSU at 24 hr	PST at 1 hr	PST at 24 hr
$(NH_4)_2S_2O_8$	4.7	7.1	40.0	31.1	95.1
	10.5	12.7	44.4	31.1	100
H_2O_2	4.7	4.0	21.6	14.1	81.2
	10.5	25.0	78.6	65.8	100
$NH_2OH.H_2SO_4$	4.7	21.7	47.8	16.9	58.5
	10.5	3.3	25.0	44.2	86.0
Ascorbic acid	4.7	5.0	21.1	3.1	16.9
	10.5	2.9	17.1	13.6	36.4

*Concentration of $(NH_4)_2S_2O_8$ 1.4%; concentration of the other agents 0.12%.

Table 5. Comparison of the spectrophotometric characteristics of the complexes in acetate-buffered medium

Cation	PSU λ_{max}, nm	PSU ε, 10^3 l.mole^{-1}.cm^{-1}	PMAU* λ_{max}, nm	PMAU* ε, 10^3 l.mole^{-1}.cm^{-1}	SAU† λ_{max}, nm	SAU† ε, 10^3 l.mole^{-1}.cm^{-1}	PST λ_{max}, nm	PST ε, 10^3 l.mole^{-1}.cm^{-1}	PMAT§ λ_{max}, nm	PMAT§ ε, 10^3 l.mole^{-1}.cm^{-1}	SAT‡ λ_{max}, nm	SAT‡ ε, 10^3 l.mole^{-1}.cm^{-1}
Co(II)	445	12.5	430	15.3	380	7.6	410	50.9	395	58.8	410	27.3
Cu(II)	370	7.3	366	16.0	380	8.2	410	18.0	400	16.5	400	22.2
Pd(II)	370	16.5	350	11.9	394	8.5	400	24.5	392	23.4	390	12.0
Zn(II)	385	21.6	363	20.4	386	13.0	410	67.5	394	11.2	390	12.0
Ni(II)	380	14.7	368	27.4	384	14.6	405	51.7	410	21.1	420	18.4
Fe(II)	380	12.5	384	10.0	382	19.5	400	65.0	384	34.4	390	22.8
	550	2.8	504	2.8	550	4.4	635	5.6	620	4.5	550	4.0
V(V)	380	9.6			388	14.2	400	15.9	430	7.3	396	19.3
Cd(II)	380	20.9	390	4.6			410	64.0	400	34.6		
Bi(III)							415	50.2	400	12.6		
In(III)							415	63.4	410	37.2	404	47.6
Hg(II)							400	64.2	396	57.7	382	37.1
Pb(II)							410	16.6	390	22.6		

*1,3-Bis(2-pyridylmethylideneamino)urea.[4,24]
†1,3-Bis(salicylideneamino)urea.[5]
§1,3-Bis(2-pyridylmethylideneamino)thiourea.[1]
‡1,3-Bis(salicylideneamino)thiourea.[5]

Influence of pH, and the stoichiometry

For both reagents, the pH–absorbance curves of the complexes were obtained at three different wavelengths (one of them always λ_{max}), buffers being used to ensure that the sample and the blank always had identical pH values. The stoichiometry was also evaluated at three wavelengths and at a pH in the optimum range. The medium used was 32% dimethylformamide (DMF) for the PSU complexes, and 40% DMF for the PST complexes.

The results are given in Tables 6 and 7. All the PSU complexes were destroyed at pH <3, and showed only one plateau at the three wavelengths tested. The graph for the Ni(II)–PSU complex was different from the others, because at pH 4 an additional band appeared in the spectrum (λ_{max} 440 nm), without affecting the band at 380 nm. The 2:1 (M:L) stoichiometry found for the Cu(II)–PSU complex appears to indicate the presence of a polynuclear complex.

The graphs for the PST complexes differed from those for the PSU species. The Co(II) and Pd(II) complexes showed two pH-independent zones, but there were no changes in the stoichiometry, so these zones probably reflected a change in the co-ordination. The Cu(II) complex showed 1:1 stoichiometry, but there was also evidence of a 2:1 (M:L) complex, analogous to the Cu(II)–PSU complex. The absorbances of the Co(II), Cu(II) and Bi(III) complexes remained unchanged at pH <2, whereas the absorbance of the other complexes decreased, but owing to the high absorbance of the reagent in acid medium, that pH-range is not useful for analytical purposes.

Evaluation of overall formation constants

The conventional methods of determining equilibrium constants from potentiometric or solvent-extraction experiments are time-consuming. Many spectrophotometric methods are based on Job's method, but they are extremely tedious and can result in erroneous values.[25] Sommer's method uses spectrophotometric data obtained from pH–absorbance curves,[11,26–31] but because it is based on linear extrapolation it requires careful experimental work to ensure that reliable results are obtained. We have developed a method based on the experimental data obtained by the mole-ratio method. The principles involved are summarized below.

The following symbols are used:

- A,B: total metal and ligand concentrations respectively
- a,b: free metal and ligand concentrations respectively
- α_B: side-reaction coefficient for the ligand
- ϕ_N: mole fraction of the AB_N complex
- β_i: overall formation constant of complex AB_i
- h: free hydrogen-ion concentration
- E: absorbance

Table 6. Spectrophotometric characteristics of the PSU complexes*

Cation	λ_{max}, nm	Optimum pH†	ε, 10^3 l.mole^{-1}.cm^{-1}	Stoichiometry (M:L)
Co(II)	445	4.5–7.0	11.0	1:1; 1:2
Cu(II)	370	3.8–4.7	8.0	2:1
Pd(II)	370	4.7–6.0	14.5	1:1
Zn(II)	385	6.7–7.5	21.0	1:2
Ni(II)	380	4.0–7.0	17.0	1:1
Fe(II)	550§	5.5–7.5	3.0	1:1; 1:2
V(V)	380	5.0–7.0	9.0	1:1

*Medium containing 32% dimethylformamide.
†All the pH values given are corrected.
§Shoulder; in the presence of asborbic acid.

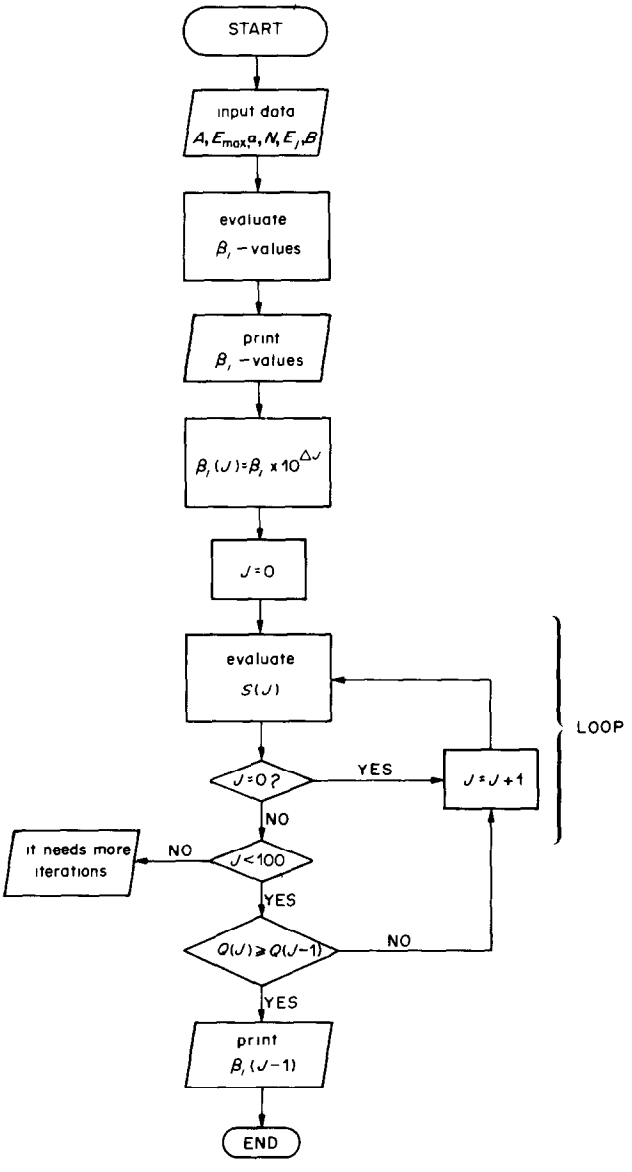

Fig. 1.

Table 7. Spectrophotometric characteristics of the PST complexes*

Cation	λ_{max}, nm	Optimum pH†	ε, 10^3 l.mole^{-1}.cm^{-1}	Stoichiometry (M:L)
Co(III)	410	2.0–4.5	53.0	1:1; 1:2
	460	6.5–8.0	59.0	1:1; 1:2
Cu(II)	410	2.0–6.0	20.0	2:1; 1:1
Pd(II)	400	4.2–5.5	28.0	1:1; 1:2
	500	7.5–10.0	16.0	1:1; 1:2
Zn(II)	410	4.5–6.7	65.0	1:1
Ni(II)	405	4.2–6.5	51.0	1:1; 1:2
Fe(II)	635§	4.0–10.5	5.6	1:1; 1:2
V(V)	400	3.5–6.5	16.0	1:1
Bi(III)	415	2.0–6.0	57.5	1:3
In(III)	415	4.0–5.5	63.0	1:1
Hg(II)	400	4.0–6.0	60.0	1:1; 1:2

*Medium containing 40% dimethylformamide.
†All the pH values given are corrected.
§Second maximum; in the presence of ascorbic acid.

The mole fraction expression for a complex AB_N can be written as a function of the overall formation constants $\beta_1, \beta_2 \ldots \beta_N$ and of the free ligand concentration b as follows:

$$\phi_N = \frac{[AB_N]}{A} = \frac{\beta_N b^N}{1 + \beta_1 b + \beta_2 b^2 + \ldots + \beta_N B^N}$$

or

$$\frac{1}{\phi_N} = \beta_N^{-1} b^{-N} + \beta_1 \beta_N^{-1} b^{1-N} + \beta_2 \beta_N^{-1} b^{2-N} + \ldots + \beta_{N-1} \beta_N^{-1} b + 1$$

and on rearranging:

$$\left(\frac{1}{\phi_N} - 1\right) b = \beta_N^{-1} b^{1-N} + \beta_1 \beta_N^{-1} b^{2-N} + \beta_2 \beta_N^{-1} b^{3-N} + \ldots + \beta_{N-1} \beta_N^{-1} \quad (1)$$

If the absorbance is measured against a reagent blank and it is assumed that the metal ion makes no contribution to the absorbance, the mole fraction ϕ_N can be experimentally obtained from the relation:

$$\phi_N = \frac{E_j}{E_{max}}$$

where E_{max} is the maximum absorbance obtained, which corresponds to the total complexation of A as AB_N, and E_j is the absorbance of the system in the range in which $B/A > (N-1)$ but $E_j < E_{max}$.

If it is further supposed that the ligand undergoes side-reactions only with the hydrogen ion, the free ligand concentration B is given approximately by:

$$b = (B - N[AB_N])/\alpha_B = (B - N\phi_N A)/\alpha_B$$

where the side-reaction coefficient α_B is:

$$\alpha_B = \frac{b'}{b} = 1 + \sum_1^q \beta_q h^q$$

in which

$$\beta_q = \frac{[H_q B]}{b\, h^q}$$

If the following substitutions are made in equation (1):

$$\left(\frac{1}{\phi_N} - 1\right) b = y;$$
$$\beta_i \beta_N^{-1} = p_i;$$
$$-1 + N = n;$$
$$b^{-1} = x,$$

we obtain:

$$y = p_0 x^n + p_1 x^{n-1} + p_2 x^{n-2} + \ldots + p_n$$

From the experimental data of the mole-ratio method a set of (x,y) values can be calculated, and by means of a least-squares procedure the p_i values can be obtained. From these, the overall formation constants can be directly evaluated. The β values obtained are "coarse", and can be refined by minimization of S in the equation:

$$S = \sum_j (\phi_{N(exp)} - \phi_{N(calc)})_j^2$$

Table 8. Conditional overall formation constants of the PSU complexes*

Cation	pH	$\log \beta_1'$	$\log \beta_2'$
Co(II)	5.1	4.22 ± 0.01	11.27 ± 0.10
Pd(II)	5.5	5.38 ± 0.03	
		5.46 ± 0.30†	
		4.67 ± 0.11§	
Zn(II)	6.5	4.50 ± 0.02	11.70 ± 0.19
			11.56 ± 0.33†
			9.48 ± 0.10§
Ni(II)	4.8	5.15 ± 0.07	
		5.04 ± 0.07†	
		4.41 ± 0.18§	
Fe(II)	5.5	4.39 ± 0.04	11.55 ± 0.04
V(V)	5.5	4.68 ± 0.03	
		4.86 ± 0.16†	
		4.01 ± 0.10§	

*Medium containing 32% (v/v) in dimethylformamide. Mean of three evaluations. $\mu = 0.01$.
†By the modified Holme and Langmhyr method.
§By the Asmus method.

The best β_i value, β_i^*, is given by:

$$\beta_i^* = \beta_i \, 10^{\Delta J}$$

where Δ is a positive or negative constant and J a counter.

Thus, if by successive iterations S is calculated for every J value, $J = J^*$ when S is a minimum, and the refined β_i values can evaluated from the expression:

$$\beta_i^* = \beta_i \, 10^{\Delta J^*}$$

We have written a BASIC program to evaluate the overall formation constants for 1:1, 1:2 and 1:3 complexes, by use of a TOSHIBA T-100 personal computer. Figure 1 shows the flow logic used in the program.

This program was used to evaluate the β_i' values for the PSU and PST complexes in water–dimethylformamide mixtures. For some complexes, the constants were also evaluated by the Asmus[15] and the modified Holme and Langmhyr[14] methods, which also use data from the mole-ratio method. The results obtained are summarized in Tables 8 and 9. There is good agreement with the results obtained by the modified Holme and Langmhyr method, but the Asmus method consistently gives low values because it takes the free ligand concentration as equal to the total ligand concentration, which is a good approximation only for very weak complexes (for which it was originally developed).

CONCLUSIONS

PST is clearly the more useful of the two reagents, as it forms highly coloured complexes at lower pH than PSU. It is also a better spectrophotometric reagent than the symmetric derivatives of thiocarbohydrazide with 2-pyridinecarboxaldehyde or salicylaldehyde, probably because it combines the best characteristics of both: the co-ordinative grouping of PMAT (pyridine) and the chromophore grouping of SAT (2-phenol). The reagent appear to be a terdentate ligand, through the pyridine nitrogen atom, the nitrogen atom at position 1 (see structure below) and the sulphur atom. In acetate-buffered medium, most PST complexes are uncharged.

The high molar absorptivity of the PST complexes can be explained by assuming that in the thio-enol form, the double bond is preferentially formed with the nitrogen atom at position 4 and not with the one at position 2. So the conjugated system of π-electrons is connected with the phenol ring, as shown in the structure:

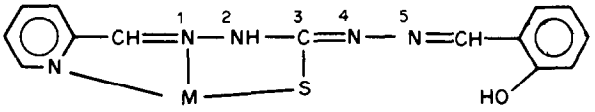

Hence half the molecule is involved in the co-ordination, and the other half is responsible for the colour. Further experiments in which the 2-phenol ring is replaced by other aromatic groups confirm this hypothesis.

Table 9. Conditional overall formation constants of the PST complexes*

Cation	pH	$\log \beta_1'$	$\log \beta_2'$	$\log \beta_3'$
Co(II)	4.5	5.23 ± 0.01	12.35 ± 0.17	
	7.1	5.28 ± 0.02†	11.56 ± 0.04†	
Pd(II)	4.5	5.57 ± 0.05	12.97 ± 0.36	
	9.0	10.69§	16.85§	
Zn(II)	4.7	4.69 ± 0.01		
		4.56 ± 0.03‡		
		4.29 ± 0.03 #		
Ni(II)	4.5	5.58 ± 0.24	12.21 ± 0.19	
Fe(II)	4.5	4.25 ± 0.22	10.23 ± 0.15	
V(V)	4.5	6.09 ± 0.08		
Bi(III)	4.5	6.54 ± 0.15	14.60 ± 0.26	21.70 ± 0.34
In(III)	4.1¶	5.05 ± 0.09		
		5.04 ± 0.12‡		
		4.60 ± 0.18 #		
	4.5**	5.25 ± 0.10		
		5.24 ± 0.17‡		
		4.72 ± 0.18 #		
Hg(II)	4.5	6.43 ± 0.09	12.31 ± 0.12	
			12.85 ± 0.32‡	

*Medium containing 40% dimethylformamide. Mean of three values unless otherwise stated; $\mu = 0.01$.
†Mean of two values.
§Single determination.
‡Modified Holme and Langmyhr method.
Asmus method.
¶Succinate buffer.
**Acetate buffer.

The sensitivity of PST is analogous to that of dithizone, a classical reagent for determination of metal ions, but PST exhibits some advantages because (*i*) the reagent solutions are stable for several weeks; (*ii*) it is not necessary to extract the complexes since they are soluble in water–dimethylformamide mixtures; (*iii*) the absorbance of the reagent blank is very low at λ_{max} of the complexes (about 0.050 at 400 nm *vs.* distilled water); (*iv*) it is more selective, since it does not react with Ag(I), Mn(II) or Sn(II); (*v*) its Pd(II) and Hg(II) complexes can be formed in EDTA medium.

On the basis of these characteristics, PST is an interesting analytical reagent.

The method developed for evaluating overall formation constants is less tiresome and time-consuming than the potentiometric or solvent-extraction methods, and far superior in accuracy to Job's method and related procedures. Furthermore, it is easy to use and does not need as many experimental results as Sommer's method does.[32] Also, the mole-ratio data on which this method is based are needed anyway, to establish the nature of the complexes.

REFERENCES

1. F. J. Barragán de la Rosa, J. L. Gómez Ariza and F. Pino, *Talanta*, 1983, **30,** 555.
2. *Idem, Mikrochim. Acta*, 1983 **II,** 455.
3. *Idem, ibid.*, 1983 **III,** 159.
4. *Idem, ibid.*, 1984 **I,** 171.
5. M. T. Montaña González and J. L. Gómez Ariza, *Anal. Quim.*, 1984, **80,** 129.
6. *Idem, Microchem. J.*, 1982, **27,** 290.
7. J. R. Bonilla Abascal, A. García de Torres and J. M. Cano-Pavón, *ibid.*, 1983, **28,** 132.
8. J. L. Gómez Ariza, F. J. Barragán de la Rosa and M. T. Montaña González, *Mikrochim. Acta*, in the press.
9. A. C. Brown, E. C. Pickering and F. J. Wilson, *J. Chem. Soc.*, 1927, 107.
10. P. Maroni and J. P. Calmon, *Bull. Soc. Chim. France*, 1964, 519.
11. L. Sommer, *Folia Fac. Sci. Nat. Univ. Purkynianae, Brno*, 1964, **5,** 1.
12. P. Job, *Ann. Chim.*, 1928, **9,** 113.
13. J. H. Yoe and A. L. Jones, *Ind. Eng. Chem., Anal. Ed*, 1964, **16,** 11.
14. J. C. Jiménez Sánchez, J. A. Mũnoz Leyva and M. Román Ceba, *Anal. Chim. Acta*, 1977, **90,** 223.
15. E. Asmus, *Z. Anal. Chem.*, 1960, **178,** 104.
16. L. Corssin, B. J. Fax and R. C. Lord, *J. Chem. Phys.*, 1953, **21,** 1170.
17. C. H. Kline and I. Turkevich, *ibid.*, 1944, **12,** 300.
18. J. K. Wilmshurst and H. J. Bernstein, *Can. J. Chem.*, 1957, **35,** 1183.
19. I. M. Hunsberger, *J. Am. Chem. Soc.*, 1950, **72,** 5626.
20. R. A. Friedel, *ibid.*, 1951, **73,** 2881.
21. R. B. Barnes, U. Liddel and V. Z. Williams, *Ind. Eng. Chem., Anal. Ed.*, 1943, **15,** 659.
22. Sadtler Research Laboratories Inc., *Sadtler's Standard Spectra Catalogue*, No. 570. Philadelphia.
23. F. Kurzer and M. Wilkinson, *Chem. Rev.*, 1970, **70,** 111.
24. F. J. Barragán de la Rosa, *Ph. D. Thesis*, Sevilla, 1982.
25. F. J. C. Rossotti and H. Rossotti, *The Determination of Stability Constants*, pp. 47–51. McGraw-Hill, New York, 1961.
26. M. Hniličková and L. Sommer, *Talanta*, 1966, **13,** 667.
27. V. Chromý and L. Sommer, *ibid.*, 1967, **14,** 393.
28. L. Sommer and M. Hniličková, *ibid.*, 1969, **16,** 83.
29. L Sommer and V. M. Ivanov, *ibid.*, 1967, **14,** 171.
30. L. Sommer, V. M. Ivanov and H. Novotná, *ibid.*, 1967, **14,** 329.
31. L. Sommer and H. Novotná, *ibid.*, 1967, **14,** 457.
32. D. Betteridge and D. John, *Analyst*, 1973, **98,** 390.

Talanta, Vol 32, No 6, pp. 475–478, 1985
Printed in Great Britain

0039-9140/85 $3.00 + 0.00
Pergamon Press Ltd

REMOVAL OF IRON INTERFERENCES BY SOLVENT EXTRACTION FOR GEOCHEMICAL ANALYSIS BY ATOMIC-ABSORPTION SPECTROPHOTOMETRY

LIYI ZHOU*, T. T. CHAO† and R. F. SANZOLONE
U.S. Geological Survey, Box 25046, Denver, Colorado 80225, U.S.A.

(*Received* 3 *December* 1984. *Accepted* 11 *January* 1985)

Summary—Iron is a common interferent in the determination of many elements in geochemical samples. Two approaches for its removal have been taken. The first involves removal of iron by extraction with methyl isobutyl ketone (MIBK) from hydrochloric acid medium, leaving the analytes in the aqueous phase. The second consists of reduction of iron(III) to iron(II) by ascorbic acid to minimize its extraction into MIBK, so that the analytes may be isolated by extraction. Elements of interest can then be determined using the aqueous solution or the organic extract, as appropriate. Operating factors such as the concentration of hydrochloric acid, amounts of iron present, number of extractions, the presence or absence of a salting-out agent, and the optimum ratio of ascorbic acid to iron have been determined. These factors have general applications in geochemical analysis by atomic-absorption spectrophotometry.

Iron has been recognized as one of the major interfering elements in geochemical analysis, owing to its abundance and widespread occurrence in geological materials. The complex spectrum and chemical properties of iron can cause spectral as well as other matrix interferences in the determination of elements by atomic-absorption spectrophotometry.[1,2]

There are two approaches to deal with the problem of iron interferences in geoanalysis. The first involves the long-known procedure for the solvent extraction of ferric iron from hydrochloric acid medium[3–5] before the analytes are determined. The chlorides of aluminium, magnesium, lithium, and ammonium have occasionally been added as salting-out agents in the extraction of iron into organic solvents.[7–9] The second approach consists of using ascorbic acid to reduce iron(III) to iron(II) so that only the analytes to be determined are extracted into the organic solvent. This technique has been successfully employed in the determination of a number of metals by both flame and furnace atomic-absorption spectrophotometry.[10–16]

Although both approaches have been applied satisfactorily to remove iron interferences in the analysis of geological materials, there has been a clear lack of systematic studies on the quantitative relationships among operating factors such as the concentration of hydrochloric acid, amounts of iron present, number of extractions, the presence or absence of a salting-out agent, and the optimum ratio of ascorbic acid to iron. Based on results obtained by using synthetic iron solutions, this report is aimed at contributing information for some general applications in geochemical analysis by atomic-absorption spectrophotometry.

EXPERIMENTAL

Reagents

Iron solution, 10%. Dissolve 10.00 g of "Specpure" iron powder in 53 ml of concentrated hydrochloric acid in a covered beaker, with heating on a hot-plate, and then slowly add 5 ml of 50% hydrogen peroxide to oxidize the iron(II). Heat the solution to remove the excess of peroxide, cool, and dilute it to volume with water in a 100-ml standard flask. This solution is approximately 1*M* in hydrochloric acid.

Ascorbic acid solution. Prepare fresh daily.

General procedure

A series of 20-ml portions of solutions containing different amounts of iron (10, 25, 50 and 100 mg) were shaken with 10 ml of methyl isobutyl ketone on a mechanical shaker for 1 min. After centrifugation, the organic phase was discarded and an aliquot of the aqueous phase was diluted at least 2000-fold for iron determination, so that the concentration of iron would fall within the range of the calibration graph.

Operating factors examined included the concentration of hydrochloric acid, number of MIBK extractions, the presence of lithium chloride as a salting-out agent, and the effect of reduction of Fe(III) to Fe(II) by ascorbic acid.

Determination of iron

Residual iron in the aqueous phase after the MIBK extraction was determined by atomic-absorption, with a Perkin-Elmer 272 spectrophotometer‡ with a lean air–acetylene flame. In the fuel-lean flame, iron(II) and iron(III) gave the same signal.[17] The instrument settings were: wavelength, 248.2 nm; lamp current, 10 mA; bandpass, 0.2 nm; air flowmeter reading, 40; fuel flowmeter reading, 10.

The iron calibration graph was prepared daily with 0, 1, 5 and 10 μg/ml iron solutions.

*Geochemist, The Institute of Geophysical and Geochemical Prospecting, Beijing, China.
†To whom correspondence should be addressed.
‡Use of brand names in this paper is for descriptive purposes only, and does not constitute endorsement by the U.S. Geological Survey.

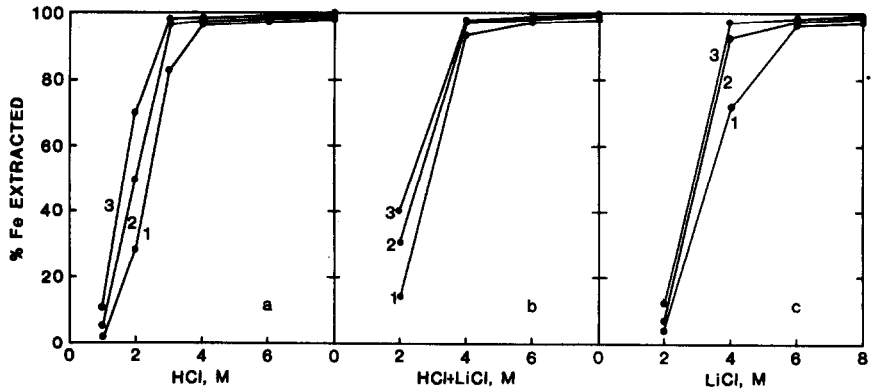

Fig. 1. Extraction of Fe (0.5 mg/ml) by MIBK as a function of the concentration of HCl, HCl + LiCl (equimolar concentrations), and LiCl in the aqueous phase. Number of extractions: 1, 2, and 3.

RESULTS AND DISCUSSION

Effect of acid concentration and the presence of lithium chloride

Because the extraction curves for different iron concentrations at various acidities and in the presence or absence of lithium chloride show similar trends, only those for 0.5 mg/ml and 5 mg/ml iron concentrations are presented, in Figs. 1 and 2. The degree of extraction of iron by MIBK is related to the concentration of hydrochloric acid in the aqueous phase (Figs. 1a and 2a). In order to remove more than 95% of the iron in the first extraction, an acidity equivalent to 6*M* hydrochloric acid in the aqueous phase is required. However, the degree of iron removal is also determined by the amount of iron present. While removal is 96.4% complete from 4*M* hydrochloric acid for the 0.5-mg/ml iron level, a second extraction is needed to reach a similar degree of removal for the 5-mg/ml iron level. Extraction from $>6M$ hydrochloric acid may cause miscibility of the phases, as observed by Menis and Rains.[4] Nearly complete removal of iron from solutions with an acidity $<6M$ hydrochloric acid can be accomplished if the extraction is repeated (Figs. 1 and 2).

Lithium chloride at concentrations equivalent to those of hydrochloric acid is not as efficient as a salting-out agent for iron removal by extraction with MIBK. The decreasing order of extraction of iron from the three systems is: HCl > HCl + LiCl > LiCl (Figs. 1 and 2). For example, for the 0.5-mg/ml iron level the degree of removal of iron in the first extraction from 4*M* background electrolyte medium is 96.4, 93.6, and 71.6% for the three systems respectively. The corresponding degree of removal at the 5 mg/ml iron level is 90.0, 82.4 and 48.0%. The comparative extraction efficiency of the three systems is readily seen by referring to Fig. 3 for the removal of iron at the 2.5 mg/ml level from the aqueous phase. Apparently a high hydrogen-ion concentration is essential for efficient extraction of iron. In the extraction of iron from various concentrations of hydrochloric acid by isopropyl ether, Dodson *et al.*[3] postulated that the chemical formula for the extracted iron chloro-complex might be $HFeCl_4$. If for some reason high acidity is not permissible, lithium chloride can be used as a salting-out agent to increase the efficiency of extraction of iron.

From the discussion above, it is evident that the extraction of iron by MIBK is influenced by the

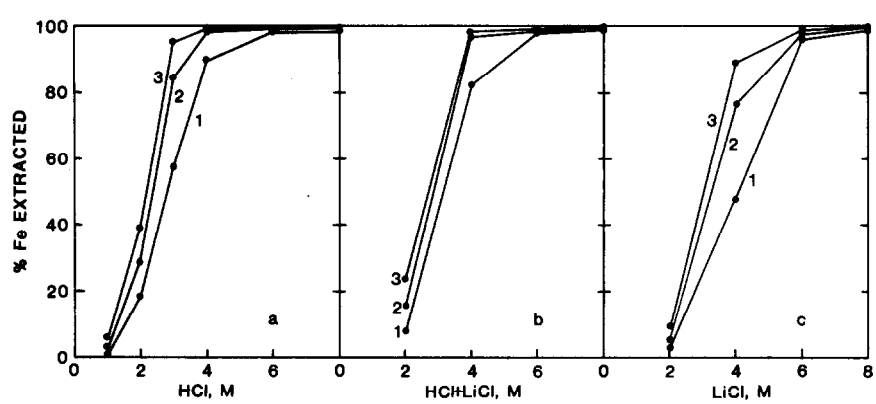

Fig. 2. Extraction of Fe (5 mg/ml) by MIBK as a function of the concentration of HCl, HCl + LiCl (equimolar concentrations), and LiCl in the aqueous phase. Number of extractions: 1, 2, and 3.

hydrochloric acid concentration in the aqueous solution, the number of extractions, the amount of iron to be extracted, and the presence of lithium chloride. Lithium chloride alone can be used if in sufficiently high concentrations and/or enough extraction steps are performed. Luke[5] has observed that iron(III) can be quantitatively extracted from 7*M* lithium chloride with MIBK.

Effect of ascorbic acid

Ascorbic acid can eliminate iron interference in the determination of various elements in geochemical analysis by virtue of its ability to reduce and complex iron so that the response of iron to solvent extraction and other chemical operations is altered. The amounts commonly used for this purpose range from an ascorbic acid/iron weight ratio from two[18] to ten.[19] Alternatively, ascorbic acid is added in increments until the iron colour fades to a light yellow or completely disappears. In this study, several iron levels (0.5, 1.25, 2.5 and 5 mg/ml) were treated with increasing amounts of ascorbic acid before MIBK extraction of iron from 1*M* and 2*M* hydrochloric acid. Only the results obtained for the highest iron level are presented in Fig. 4, as those for lower iron levels exhibit similar trends.

The degree of extraction of iron is inversely related to the amount of ascorbic acid added, but directly related to the acidity of the aqueous phase. While 200 mg of ascorbic acid is sufficient to prevent MIBK extraction of 100 mg of iron (weight ratio = 2) from 1*M* hydrochloric acid, 400 mg is necessary (weight ratio = 4) to do the same from 2*M* hydrochloric acid. In geochemical analysis, it is customary to digest the sample with mixed acids and evaporate to dryness. The residue may then be dissolved in dilute hydrochloric acid. It would be desirable to use less concentrated acid, such as 1*M*, for dissolution of the residue, so that a lower amount of ascorbic acid can be used to eliminate the iron interference. The highest iron level used in this work (5 mg/ml) is equivalent to 20.0% Fe or 28.6% Fe_2O_3 in the sample if a 0.5-g sample is taken for analysis.

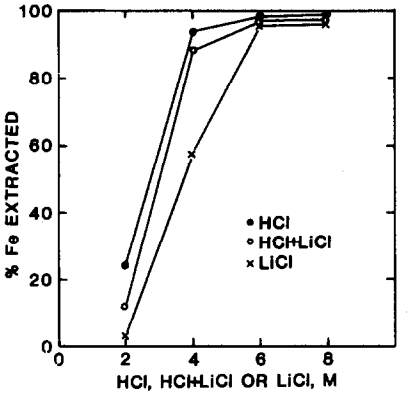

Fig. 3. Comparative efficiency of extraction for Fe (2.5 mg/ml) by MIBK as influenced by HCl, HCl + LiCl (equimolar concentrations), and LiCl in the aqueous solution.

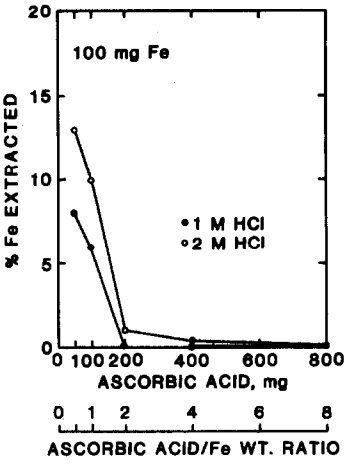

Fig. 4. Effect of different amounts of ascorbic acid on the extraction of Fe (5 mg/ml) by MIBK from 1*M* and 2*M* HCl.

From the reasoning above, geochemical samples can be analysed by atomic-absorption spectrophotometry for various elements in a hydrochloric acid medium, without iron interference, by use of the combination of reduction with ascorbic acid and solvent extraction.

Iron in hydrobromic acid medium behaves similarly toward extraction by MIBK.[20] Hubert and Chao[21] have taken advantage of this combination to circumvent iron interference in the determination of gold, indium, tellurium, and thallium in a singie sample solution of geological materials, by atomic-absorption spectrophotometry after a two-step solvent extraction. Gold and thallium are first quantitatively extracted into MIBK from 0.1*M* hydrobromic acid; the extraction of iron is minimal. The aqueous phase is then made 3*M* in hydrobromic acid and the indium and tellurium are extracted with MIBK, after reduction of iron by ascorbic acid. Before the development of this scheme, the four elements were individually determined in separate samples.[13,15,22,23]

Conclusions

Quantitative information has been provided in this paper for the removal of iron interference, by solvent extraction, in geochemical analysis. Based on the information given, adjustments can be made in procedures, either to extract the iron with MIBK from the aqueous solution adjusted to a certain concentration of hydrochloric acid, or to reduce Fe(III) to Fe(II) with ascorbic acid to prevent extraction of the iron into MIBK. The elements of interest can then be determined in the aqueous phase or the organic extract as appropriate by atomic-absorption spectrophotometry.

REFERENCES

1. G. J. S. Govett and R. E. Whitehead, *J. Geochem. Explor.*, 1973, **2**, 121.

2. P. Hannaker and T. C. Hughes, *ibid.*, 1978, **10,** 169.
3. R. W. Dodson, G. J. Forney and E. H. Swift, *J. Am. Chem. Soc.*, 1936, **58,** 2573.
4. O. Menis and T. C. Rains, *Anal. Chem.*, 1960, **32,** 1837.
5. C. L. Luke, *Anal. Chim. Acta*, 1966, **36,** 122.
6. E. Kiss, *ibid.*, 1967, **39,** 223.
7. S. K. Majumdar and A. K. De, *Talanta*, 1960, **7,** 1.
8. V. M. Shinde and S. M. Khopkar, *Sep. Sci.*, 1969, **4,** 161.
9. M. A. Qureshi, M. Farid, A. Aziz and M. Ejaz, *Talanta*, 1979, **36,** 166.
10. E. P. Welsch and T. T. Chao, *Anal. Chim. Acta*, 1975, **76,** 65.
11. *Idem*, *ibid.*, 1976, **82,** 337.
12. R. F. Sanzolone and T. T. Chao, *ibid.*, 1976, **86,** 163.
13. T. T. Chao, R. F. Sanzolone and A. E. Hubert, *ibid.*, 1978, **96,** 251.
14. Liyi Zhou, T. T. Chao and A. L. Meier, *Talanta*, 1984, **31,** 73.
15. *Idem*, *Anal. Chim. Acta*, in press.
16. J. G. Viets, J. R. Clark and W. L. Campbell, *J. Geochem. Explor.*, 1984, **20,** 355.
17. K. C. Thompson and K. Wagstaff, *Analyst*, 1980, **105,** 641.
18. C. H. Kim, C. M. Owens and L. E. Smythe, *Talanta*, **21,** 445.
19. T. C. Z. Jackman and S. Sivasubramaniam, *Analyst*, 1974, **99,** 296.
20. A. R. Denaro and V. J. Occleshaw, *Anal. Chim. Acta*, 1955, **13,** 239.
21. A. E. Hubert and T. T. Chao, *Talanta*, 1985, **32,** in press.
22. E. A. Hubert and H. W. Lakin, *Intern. Geochem. Explor. Symp. 4th, London* (1972), 1973, 383.
23. A. L. Meier, *J. Geochem. Explor.*, 1980, **13,** 77.

Talanta, Vol. 32, No 6, pp. 479–482, 1985
Printed in Great Britain.

0039-9140/85 $3.00 + 0.00

POLAROGRAPHY OF THE ALKALINE-EARTH METALS—II

THE ADSORPTION WAVE FOR THE MAGNESIUM–ERIOCHROME BLACK T COMPLEX

AN JINGRU, ZHOU JINKUI and WEN XIAODAN
Chemistry Department, Fuzhou University, Fuzhou, Fujian, China

(*Received* 11 *September* 1984. *Revised* 1 *December* 1984. *Accepted* 11 *January* 1985)

Summary—Magnesium–Eriochrome Black T in ethylenediamine medium gives a polarographic adsorptive wave at −0.7 V (*vs.* an Ag/Hg electrode). It gives a limit of detection for magnesium of $2 \times 10^{-8} M$. It is made the basis of a method for determination of magnesium in serum, water and various salts, without any pretreatment. The method is very rapid, sensitive and convenient for serum analysis.

Magnesium ions are very difficult to reduce at the dropping mercury electrode in aqueous solution, but give a polarographic wave at −2.2 V (*vs.* SCE) in tetramethylammonium chloride supporting electrolyte solution.[1] Richardson[2] determined magnesium in calcium carbonate by polarographically reducing the magnesium complex of Solochrome Violet R. S. at pH 11 in a piperidine buffer. In his method, calcium and iron were removed by precipitation and extraction. The detection limit for magnesium was $10^{-6} M$. Luo and Zhao[3] determined magnesium in hair by using the polarographic adsorption wave of the magnesium meso-tetra (4-trimethylammoniumphenyl)porphine complex in a methylamine buffer solution. In their method, the solution had to be heated at 100° for 50 min to form the complex. The detection limit was $10^{-7} M$.

In this report, we describe an adsorption wave for the magnesium–Eriochrome Black T complex in aqueous ethylenediamine medium. It can be used to determine magnesium in serum, water and chemical reagents, without any pretreatment.

Magnesium in serum is usually determined by flame photometry, atomic-absorption spectroscopy or spectrophotometry after appropriate sample pretreatment. Because of its sensitivity and good selectivity, our method can be used to determine magnesium in serum rapidly and conveniently.

EXPERIMENTAL

Apparatus

A single-sweep polarograph with three electrodes and a type 82-1 polarograph (made in Fuzhou University), with an Ag/Hg reference electrode. A PTFE polarographic cell was used.

Reagents

Standard magnesium solution. Magnesium oxide was ignited at 800° and 1.658 g of it was dissolved in 30 ml of 2*M* hydrochloric acid and the solution was diluted to 1000 ml. This 1000-μg/ml stock solution was further diluted as required.

Eriochrome Black T (EBT) solution, $5.0 \times 10^{-4} M$. Prepared in water as solvent. The solution was stable for two days.

Ethylenediamine, 10% aqueous solution. Demineralized water was used in all experiments.

All solutions were stored in polyethylene bottles, and contact between the solutions and glass vessels was avoided as much as possible.

Procedure

Transfer the magnesium solution into a 25-ml quartz standard flask, add 5 ml of 10% ethylenediamine solution and 3 ml of $5 \times 10^{-4} M$ EBT and dilute to the mark with water. Pour all the solution into the PTFE polarographic cell and record the derivative polarogram, starting the potential scan at −0.4 V. The temperature should be kept below 20°.

RESULTS

Oscillographic polarograms

In 2% ethylenediamine solution, EBT gave a reduction wave P_1, with a maximum at −0.53 V, and a derivative-peak potential of −0.50 V (see Fig. 1a,b). When magnesium ions were added, P_1 decreased and a new maximum P_2 appeared at a more negative potential, −0.72 V, and the derivative-peak potential was −0.70 V. The derivative mode is preferred because of its better resolution.

Dependence of peak current on the ethylenediamine concentration

The magnesium–EBT complex gives no wave in either acidic or ammoniacal medium, but does in the presence of ethylenediamine. The dependence of peak current on the concentration is shown in Fig. 2. The peak current reaches a maximum at 1% ethylenediamine and then remains constant, so 2% was chosen as the working concentration.

Dependence of peak current on the EBT concentraion

Magnesium does not give any reduction wave in ethylenediamine solution in the absence of EBT, but the Mg–EBT complex gives a polarographic wave at

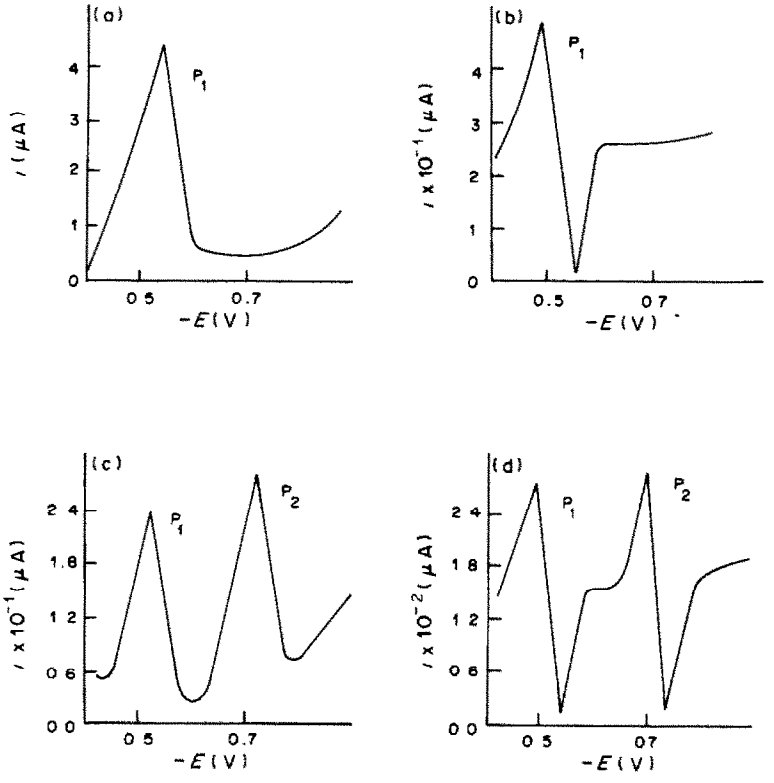

Fig. 1. Single-sweep polarograms: (a) 2% en + $6 \times 10^{-5}M$ EBT, normal wave; (b) derivative wave; (c) a + $8 \times 10^{-6}M$ Mg^{2+}, normal wave; (d) derivative wave.

-0.70 V. As shown in Fig. 3 the peak current remains maximal and constant for the EBT range 1.5×10^{-5}–$6 \times 10^{-5}M$: $6 \times 10^{-5}M$ EBT was chosen as the working concentration.

Effect of temperature

Figure 4 shows that the peak current was independent of temperature between 4° and 20°, so it is only necessary to keep the temperature below 20°.

Relation between peak current and magnesium concentration

Under the optimum conditions chosen, the peak current is proportional to the magnesium concen-

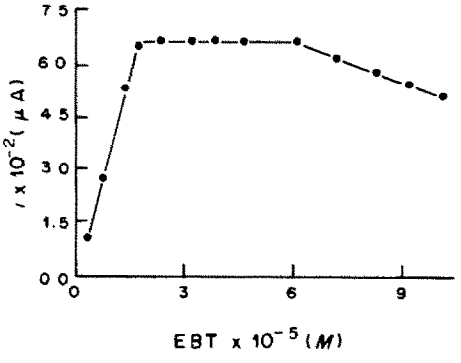

Fig. 3. Dependence of peak current on the concentration of EBT: 2% ethylenediamine + $5 \times 10^{-6}M$ Mg^{2+}.

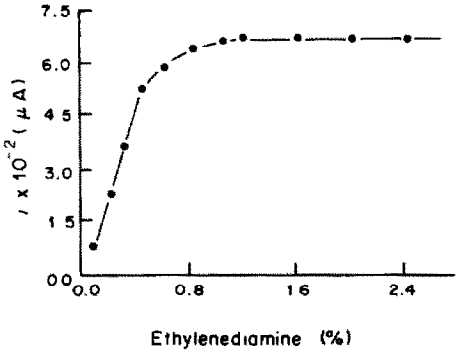

Fig. 2. Dependence of peak current on the concentration of ethylenediamine: $5 \times 10^{-6}M$ Mg^{2+} + $6 \times 10^{-5}M$ EBT.

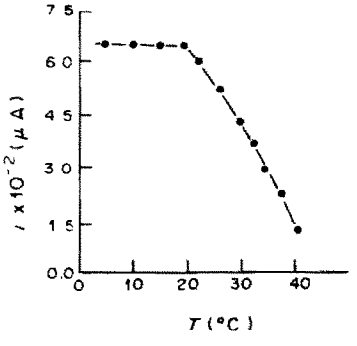

Fig 4. Effect of temperature on the peak current.

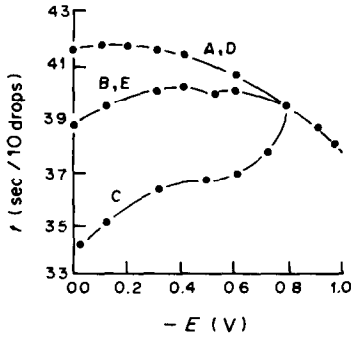

Fig. 5. Electrocapillary curves: (A) 2% ethylenediamine, (B) A + $6 \times 10^{-5}M$ EBT, (C) A + $1.8 \times 10^{-4}M$ EBT, (D) A + $1.5 \times 10^{-6}M$ Mg^{2+}, (E) B + $1.5 \times 10^{-6}M$ Mg^{2+}.

tration in the range 5×10^{-8}–$9 \times 10^{-6}M$, and the limit of detection is $2 \times 10^{-8}M$.

Effect of foreign substances

The effect of foreign substances was studied with 2 μg of magnesium in 25 ml of solution. The amounts of other ions which did not interfere (error < 10%) are as follows: large amounts of K, Na, 5 mg of Ca, Ba, Sr; 2 mg of Ge; 1 mg of Bi(III); 0.6 mg of W(VI), V(V); 0.4 mg of Mo(VI), Ag, Al; 0.3 mg of Zn; 0.2 mg of Be, Tl(III), As(III); 0.1 mg of Sn(II), Sc; 60 μg of In; 40 μg of Sb, Gd, Cr(VI); 30 μg of Pb, Cu(II); 20 μg of Ga, Ti(IV); 6 μg of Mn(II); 4 μg of Ni, Co(II); 1 μg of Fe(III). Fe(III) interfered by giving a peak at −0.67 V, but the interference of 200 μg could be eliminated by adding sodium sulphite (1 g per 25 ml). Sodium cyanide present at 0.2% concentration masked up to 80 μg of Fe(III), 100 μg of Co(II) or Ni, and 20 μg of Mn(II).

Small amounts of surfactants did not interfere, *e.g.*, 1.0 ml of 0.02% polyoxyethylene alkylphenol, 0.5 ml of 0.02% cetylpyridinium chloride, or 2.0 ml of 0.02% sodium dodecyl benzenesulphonate.

MECHANISM

Electrocapillary curves

Eriochrome Black T is a hydroxyazo dyestuff, and would be expected to be easily adsorbed at the mercury electrode. As shown in Fig. 5, the electrocapillary curves were considerably influenced by the presence of EBT, which was adsorbed very strongly at −0.50 V, resulting in the surface tension being reduced and the adsorption becoming stronger with increasing EBT concentration.

When magnesium ions were added they reacted with the EBT to form a red complex which was adsorbed at the electrode to give a reduction peak at −0.7 V. Curve A was the same as D, B the same as E, so we conclude that the adsorption depended mainly on the ligand EBT in the complex, and that the magnesium itself had little effect on the adsorption.

Relation between peak current and rest-time

The dependence of the maximum peak current on the rest-time was investigated with a hanging mercury drop electrode. For aqueous ethylenediamine solutions the peak currents for both reagents and complex increased with prolongation of the rest-time, which allowed much more reagent and complex to be adsorbed at the electrode. The conclusion from this experiment agreed with that from the electrocapillary curves.

Relationship between peak current and voltage scan-rate

The peak current i_p for the reagent and the complex varied with scan-rate V. The plot of i_p *vs.* $V^{1/2}$ is shown in Fig. 6 for scan-rates from 125 to 350 mV/sec: the plot is not linear, as it should be for a diffusion-controlled process, but is distinctly curved. Such deviations from the Randles-Ševčik equation have been explained by Anson.[4]

It is evident from the experiments described that both reagent and complex are strongly adsorbed on surface of the electrode. This has the effect of giving a significant increase in sensitivity.

Cyclic voltammetry

The cyclic voltammetry of the system was investigated with the Type 82-1 polarograph. Cyclic voltammetric curves for aqueous ethylenediamine solutions are shown in Fig. 7. EBT gives a cathodic peak at −0.5 V, owing to its reduction. If magnesium ions are present, a second peak appears at −0.7 V, due to reduction of the ligand in the complex.

No anodic peak was observed, from which we conclude that the reduction of EBT and of the Mg–EBT complex is irreversible.

Composition of the electroactive complex

The composition of the complex was examined by the linear[5] and continuous-variations methods and found to be 1:1, as expected. The conditional stability constant (2% ethylenediamine medium, pH = 11.8) was found to be 1.1×10^5.

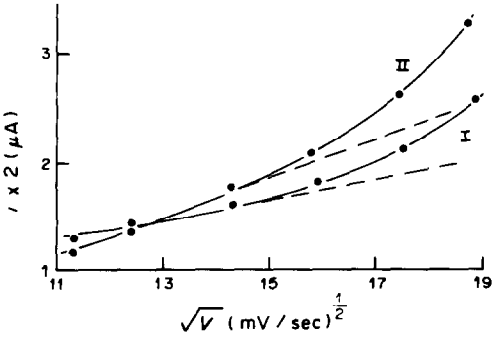

Fig. 6. Relationship between i_p and V: (I) 2% ethylenediamine + $6 \times 10^{-5}M$ EBT, (II) I + $7.5 \times 10^{-5}M$ Mg^{2+}.

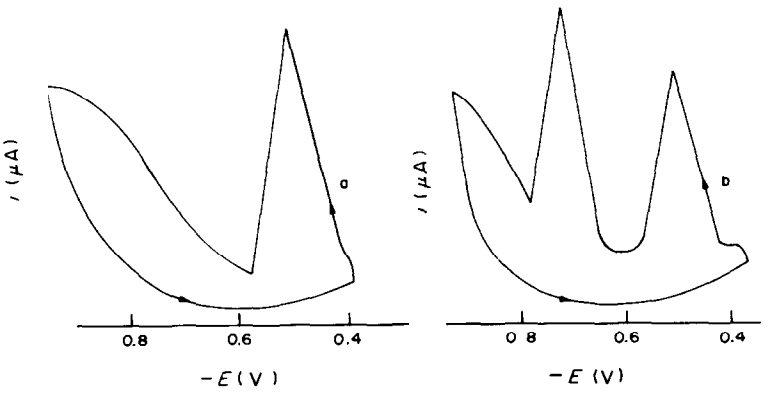

Fig. 7. Cyclic voltammetric curves.

APPLICATIONS

Determination of magnesium in water and serum

Transfer 2.5 ml of water into a 25-ml standard flask, then add 5 ml of 10% ethylenediamine and 3 ml of $5 \times 10^{-4}M$ EBT and dilute to the mark with water. Measure the peak current at −0.7 V.

Transfer 0.1 ml of serum, without any pretreatment, into a 25-ml standard flask, and continue as for a water sample. Determine the magnesium by the standard-additions method.

The results shown in Table 1 agreed satisfactorily with those obtained by atomic-absorption spectroscopy.

Table 1. Determination of Mg in water and serum

	Mg found by this method		Mg found by AAS	
Sample	μg	ppm	μg	ppm
Water	2.0	0.8	2.0	0.8
Serum A	2.26	22.6	2.21	22.1
Serum B	1.83	18.3	1.72	17.2
Serum C	2.24	22.4	2.18	21.8

Table 2. Analysis of various salts for Mg

Sample	Mg added, μg	Mg found, μg	Recovery, %	Content, %
Potassium nitrate, 200 mg	0	0.360		
	0.2	0.564	102	0.00018
Potassium chloride, 200 mg	0	0.408		
	0.2	0.600	96	0.000204
Barium nitrate, 0.8 mg	0	0.204		
	0.3	0.498	98	0.025
Strontium nitrate, 0.6 mg	0	0.276		
	0.2	0.474	99	0.046
*Calcium chloride, 0.3 mg	0	1.25		
	1.0	2.25	100	0.42

*For this sample, a chemically pure grade, the standard deviation (11 determinations) was 0.011 μg, coefficient of variation 0.9%. The other samples were analytical-reagent grade. All the results are the means of 3 determinations.

Determination of magnesium in salts

Transfer a weighed amount of salt to a 25-ml standard flask, dissolve it in water, then add the ethylenediamine and EBT solution as before and dilute to the mark with water. Record the derivative polarogram and measure as before.

REFERENCES

1. T. A. Kryukova, S. I. Sinyakova and T. B. Arefeva, *Polarographic Analysis* (in Russian), p. 685. National Chemical Publishers, Moscow, 1959.
2. M. L. Richardson, *Talanta*, 1965, **12**, 1009.
3. Luo Denbai and Zhao Zaofan, *J. Wuhan Univ. (Natural Sci. Ed.)*, 1982, 100.
4. F. Anson, *Electrochemistry and Electroanalytical Chemistry*, Huang Weiceng (ed.), (in Chinese), p. 6, Beijing Univ. Press, 1983.
5. E. Asmus, *Z. Anal. Chem.*, 1960, **178**, 104.

Talanta, Vol 32, No. 6, pp. 483–489, 1985
Printed in Great Britain.

0039-9140/85 $3.00 + 0.00

THE USE OF GLASS ELECTRODES FOR THE DETERMINATION OF FORMATION CONSTANTS—II

SIMULATION OF TITRATION DATA

PETER M. MAY*, KEVIN MURRAY and DAVID R. WILLIAMS
Department of Applied Chemistry, UWIST, Cardiff, Wales

(*Received* 16 *November* 1984. *Accepted* 11 *January* 1985)

Summary—Methods for simulating titration data, including various types of corrections for changes in activity, liquid-junction potential and ion-selectivity of electrodes are described. These form the basis of a new library of computer programs, called ESTA (Equilibrium Simulation for Titration Analysis). They permit the range of titration conditions employed in the determination of formation constants to be usefully extended. Simulations have been performed to illustrate the extent to which the effects mentioned above are manifest in many titrations of practical importance.

SYMBOLS

T_i^c = calculated total concentration of component i
T_i^r = real (analytical) concentration of component i
$[X_i]$ = free concentration of component i
$[C_j]$ = concentration of complex j
$[S_i]$ = concentration of species i (component or complex)
$\{S_i\}$ = activity of species i (component or complex)
$\{S_i^s\}$, $\{S_i^b\}$ = activity of species i in the test solution and bridge solution, respectively
γ_i = activity coefficient of species i
β_j = thermodynamic formation constant of complex j
r_{ji} = stoichiometric coefficient of component i in complex j
NC = number of components appearing in complexes
NI = total number of components (including inert ions, such as from background electrolyte, not appearing in complexes)
NJ = number of complexes
NB = number of burettes
C_i^v = initial concentration of component i in titration vessel
C_{im}^B = concentration of component i in solution in burette m
v_m = volume added from burette m
V° = initial volume in vessel
E_k = electrode potential k
E_k° = electrode response intercept
E^{LJ} = liquid-junction potential
E^{sel} = contribution of sodium ions to electrode potential
s_k = electrode response slope
C_H = empirical constant for H in liquid-junction term
C_{OH} = empirical constant for OH in liquid-junction term
K_{ki} = selectivity coefficient of component i
z_i = charge on species i
R = the gas constant
T = absolute temperature
F = Faraday constant
I = ionic strength
λ_i^S = ionic conductance of species i in the test solution
λ_i^b = ionic conductance of species i in the bridge solution
$\mathring{a}$ = ionic size parameter
A, B = parameters in the Debye–Hückel equation

The procedures developed by Sillén and his colleagues over twenty years ago[1] are still widely accepted as the most accurate way of determining formation constants potentiometrically. Experimental conditions were specifically chosen to minimize the adverse effects of various assumptions that had to be made in the analysis of their data. In particular, very high concentrations of supporting background electrolytes were employed to obviate such difficulties as the characterization of activity and liquid-junction potential changes.[2]

However, for many common applications, it is inappropriate to measure formation constants under such conditions. For instance, many biological solutions such as natural waters (*e.g.*, lakes, rivers and soil solutions) and physiological fluids (*e.g.*, plant xylem sap and blood plasma) have much lower ionic strengths, so that the relevant measurements ought to be performed in concentrations of background electrolyte less than, say, 0.2*M*. Under these conditions, the assumption of constant ionic strength throughout a titration is less valid and can lead to significant errors. Moreover, many systems have formation constants that require measurements to be made at pH values at which it is known that the effects of liquid-junction potentials and alkaline errors can be of a worrying magnitude.

*Author for correspondence.

Although a multitude of computer programs have been developed for the analysis of potentiometric titration data, only a few approach the problem in a generalized way. Of these, SCOGS[3] and, especially, MINIQUAD[4] have gained widespread popularity. However, neither of these accommodates variations in ionic strength, changes in liquid-junction potential or imperfect ion-selectivity of electrodes. Some programs, such as LETAGROP,[5] do permit simulation of changes in liquid-junction potential, albeit in a restricted way, but none allows corrections to be made for all three kinds of effect.

Each of these effects is well known and has been extensively studied in its own right. This paper describes how corrections for each may be applied in generalized computer programs for the analysis of potentiometric titration data. Although it is not possible to simulate electrode behaviour entirely satisfactorily for all practical circumstances, the proposed approach satisfies two paramount objectives, namely to improve the interpretation of certain observed data and to provide mathematical forms for the corrections that allow them to be simplified, or even neglected, if that is thought to be appropriate. In this way, the useful range of titration conditions can be extended, the necessity for corrections can be investigated and different forms of the equations used for correction can be readily compared.

THEORY

Mass-balance

The conditions of mass-balance are imposed in the standard way by equating calculated total concentrations with real (analytical) concentrations:

$$T_i^r = T_i^c, \quad i = 1, \ldots, NC \tag{1}$$

where

$$T_i^c = [X_i] + \sum_{j=1}^{NJ} r_{ji}\Gamma_j\beta_j \prod_{n=1}^{NC} [X_n]^{r_{jn}} \tag{2}$$

$$T_i^r = \frac{C_i^v V^\circ + \sum_{m=1}^{NB} C_{im}^B v_m}{V^\circ + \sum_{m=1}^{NB} v_m} \tag{3}$$

$$\Gamma_j = \left(\prod_{n=1}^{NC} \gamma_n^{r_{jn}}\right) \Big/ \gamma_j. \tag{4}$$

Electrode equation

In general, the equation relating the potential of an electrode to the activity of the electrode ion can be written in the form

$$E_k = E_k^\circ + E_k^{IS} + E_k^{LJ} \tag{5}$$

where E_k° is the electrode response intercept. For the purpose of formation-constant determination, E_k^{IS} is usually given by

$$E_k^{IS} = s_k \log\{X_k\} = s_k \log\gamma_k + s_k \log[X_k] \tag{6}$$

Some programs[4-6] assume that both the liquid-junction term, E_k^{LJ}, and the activity coefficient of the electrode ion, γ_k, are constant. The resulting electrode equation is

$$E_k = E_k^{const} + s_k \log[X_k] \tag{7}$$

where

$$E_k^{const} = E_k^\circ + s_k \log\gamma_k + E_k^{LJ}.$$

Others[7-10] assume that γ_k is constant and that E_k^{LJ} is a linear function of the free proton and hydroxide ion concentrations. The electrode equation is thus

$$E_k = E_k^{const} + s_k \log[X_H] + c_H[X_H] + K_w c_{OH}/[X_H] \tag{8}$$

where $E_k^{const} = E_k^\circ + s_k \log\gamma_k$.

Electrode selectivity

None of the above programs accommodates the well-known effects of interfering ions. It is possible to extend the useful range of detection by several orders of magnitude if these effects can be taken into account. However, the simple Nikolskii[11] equation (9),

$$E_k^{IS} = s_k \log(\{X_k\} + K_{ki}\{X_i\}) \tag{9}$$

often invoked to describe how the electrode response is ultimately dominated by the interfering ion, is unsatisfactory for this purpose. This is because it describes a very sharp transition in response whereas, in fact, the change is generally much more gradual.[12] As a result, even if equation (9) is used in an entirely empirical way, corrections in the region that is most important, *i.e.*, when the effect is first manifest, can never be more than a very small fraction of the effect itself.

At least in the case of glass electrodes, the behaviour observed in the presence of one univalent interfering ion is better described by the Eisenman equation:[13]

$$E_k^{IS} = s_k \log(\{X_k\}^{1/\alpha} + K_{ki}\{X_i\}^{1/\alpha})^\alpha \tag{10}$$

where α and K_{ki} are empirical parameters. Although a corresponding general multi-ion equation has not been formulated,[14] this has been done in the case of the Nikolskii equation, leading to

$$E_k^{IS} = s_k \log(\{X_k\} + \sum_i K_{ki}\{X_i\}^{z_k/z_i} \tag{11}$$

where the charges z_i have the same sign as z_k.[15] For the purpose of titration-data simulation, we therefore propose that an equation of the following form should be used:

$$E_k^{IS} = s_k \log[\{X_k\}^{1/\alpha} + \sum_i (K_{ki}\{X_i\}^{z_k/z_i})^{1/\alpha}]^\alpha \tag{12}$$

This has the advantage that equations (6), (10) and (11) can all be accommodated by making suitable choices for α and the K_{ki} values.

Liquid-junction potential

It is common for the liquid-junction coefficients of equation (8) to be obtained empirically. An extension which reduces to this linear form at low concentrations of acid is that derived from the Henderson equation[16] by Biedermann and Sillén.[2] It has the form

$$E_k^{LJ'} = -(RT/F)\ln(1 + d[X_H]/I) \qquad (13)$$

where I is the concentration of the background univalent electrolyte. This equation has been used to correct for liquid-junction potential changes in the calibration of glass electrodes.[17] The Henderson equation itself, equation (14), predicts potentials across junctions of different univalent electrolytes at constant ionic strength, with reasonable success.[18] It has also been shown to be useful in calculation of potentials across constant-ionic-medium junctions through potentiometric titrations.[19]

$$E_k^{LJ} = \frac{-RT}{F} \times \frac{\sum_i \gamma_i^s\{S_i^s\} - \lambda_i^b\{S_i^b\}}{\sum_i z_i(\lambda_i^s\{S_i^s\} - \lambda_i^b\{S_i^b\})} \times \ln \frac{\sum_i \lambda_i^s z_i\{S_i^s\}}{\sum_i \lambda_i^b z_i\{S_i^b\}} \qquad (14)$$

Much less is known about the applicability of the Henderson equation to salt bridges that have higher concentrations than that of the test solution, although Bates[20] has tabulated some typical values predicted for bridges containing saturated potassium chloride solution. Whilst such bridges clearly violate one of the principle tenets of the Henderson equation (namely that activity coefficients remain constant across the junction), they do serve to reduce the size of the junction potential, thus making relative errors in its characterization less significant. However, it remains to be seen whether the equation can be used effectively to simulate changes in the liquid-junction potential when high-concentration salt bridges are involved.

Although equation (14) predicts absolute liquid-junction potentials, these can be observed experimentally only as a difference in potentials. It is conventional to have this difference increasingly manifest towards the extremes of pH.

This property can be preserved by defining E_k^{LJ} as follows.

$$E_k^{LJ} = E_k^{LJ'} - E_k^{LJ_0} \qquad (15)$$

where $E_k^{LJ_0}$ is the liquid junction potential [calculated from equation (14)] between the bridge solution and a solution containing the bridge ions only (*i.e.*, at pH 7) at the reference ionic strength (*i.e.*, that at which the electrode constants E_k^{const} and s_k are applicable). This results in a calculated E_k^{LJ} that tends to a constant value (usually small or zero) as the pH tends to 7. Note that with a "constant ionic strength" bridge, *i.e.*, one containing electrolyte ions of the same type and concentration as the background medium, $E_k^{LJ_0} = 0$ and its size increases with the concentration of the bridge electrolyte. The advantage of equation (14) for the purpose of simulating titration data is that its general form permits further investigation of liquid-junction-potential phenomena, yet, by an appropriate choice of the ionic conductivities for each ion, it can be used to accommodate the simpler equation (13) when that is applicable. For example, with univalent electrolytes and a constant-ionic-strength junction of the type

$$I(AB) \,||\, [X_H](HB), I(AB)$$

equation (14) reduces to equation (13), with

$$d = (\lambda_H - \lambda_A)/(\lambda_A + \lambda_B).$$

There is evidence that liquid-junction potentials calculated from the Henderson equation are generally overestimated, especially for high ionic-strength bridges.[21,22] However, for any given background-electrolyte and salt-bridge concentrations, there is often only one ion that has an appreciable effect on changes in the liquid-junction potential.[23] Hence, for junctions involving H^+, λ_H can be empirically adjusted, either at the level of equation (13) or at that of equation (14).

Activity coefficients

For the calculation of activity coefficients the most common extension to the Debye–Hückel formula has the form

$$-\log\gamma = \frac{Az^2\sqrt{I}}{1 + B\mathring{a}\sqrt{I}} + cI \qquad (15)$$

where c is an empirical constant. Guggenheim[24] simplified this by choosing $\mathring{a} = 1/B$ and, under this condition, Davies[25] proposed that $c = 0.3Az^2$. The latter proposal is the IUPAC recommended equation for formation-constant work[26] and is widely used in geochemical equilibrium calculations.[27,28] Others have used Kielland's[29] values for $\mathring{a}$ and empirically determined values for c.[30,31]

Equation (16) seems a particularly sensible choice to incorporate in a computer program since the parameters $\mathring{a}$ and c for each ion can be chosen such that all of the approaches above can be accommodated. The constants A and B can be calculated within the program from

$$A = 1.8249 \times 10^6/D^3, \quad B = 50.293/D$$

where

$$D = (3686.2T^{1/2} - 135.15T)^{1/2}.$$

Although the coefficients depend on the particular values chosen for the dielectric constant of water, these formulae yield results which are more than adequate for the present purpose over the temperature range 0–100°.

At low concentrations of background electrolyte, variations in ionic strength occur during a titration, owing to changes in complexation. By using equation (16), corrections should be made to all the formation constants at each titration point so that they refer to the calculated ionic strength at the point. Corrections of this kind over a large range of ionic strength (say, from $I = 0.0$ to 0.2) may not be adequate in precise potentiometric work; however, in the majority of cases, variations in ionic strength, although significant, are sufficiently restricted to ensure that corrections with equation (16) are wholly satisfactory.

Conversion into thermodynamic constants

Equations (2), (12) and (14) require "thermodynamic" values of the parameters β_j, E_k°, K_{kl}, λ_i^s and λ_i^b, *i.e.*, those that are defined with respect to a standard state based on reactions occurring at infinite dilution in water at zero ionic strength. However, it is established practice to work with conditional constants (${}^I\beta_j$, ${}^IE_k^\circ$, ${}^IK_{kl}$, ${}^I\lambda_i^s$, ${}^I\lambda_i^b$) which refer to some other ionic strength (I). Such constants, therefore, need to be converted into the corresponding thermodynamic values in the following way:

$$\beta_j = {}^I\beta_j / {}^I\Gamma_j$$

${}^I\Gamma_j$ is defined as in equation (4).

Expressing equation (12) in terms of concentrations, and rearranging, yields

$$E_k^{IS} = s_k \log {}^I\gamma_k + s_k \log\left\{[X_k]^{1/\alpha} + \sum_i \left(\frac{K_{ki}({}^I\gamma_i[X_i]^{z_k/z_i})}{{}^I\gamma_k}\right)^{1/\alpha}\right\}^\alpha.$$

Hence, the supplied value of ${}^IE_k^\circ$ and the ion-selectivity coefficients are converted into thermodynamic values as follows.

$$E_k^\circ = {}^IE_k^\circ - s_k \log {}^I\gamma_k$$

$$K_{kl} = {}^IK_{kl}({}^I\gamma_k/({}^I\gamma_i)^{z_k/z_i})$$

The supplied ionic conductivities to be used in the calculation of E_k^{LJ} are treated similarly:

$$\lambda_i^s = {}^I\lambda_i^s / {}^I\gamma_i^s; \quad \lambda_i^b = {}^I\lambda_i^b / {}^I\gamma_i^b$$

Whether Debye-Hückel corrections are to be invoked or not, only conditional constants thus need to be supplied by the program user. In either case, the same values (say, for electrode potential) are calculated for any point in the titration which actually has the reference ionic strength.

Solution of mass-balance equations

The NC mass-balance equations (m.b.e.), equation (1), can, in principle, be solved for any NC unknowns as long as all remaining parameters are known. In particular, there are NC free concentrations that can be determined. On the other hand, if one of the free concentrations has been measured experimentally, the remaining free concentrations and one other parameter (such as v_m, β_j, C_i^v, C_{im}^B, or T_i^r) can be calculated. Consequently, the procedures for solution of the m.b.e. falls into two categories. In the first, these equations are solved for NC free concentrations without any reference to the electrode equation. The electrode potential can subsequently be obtained by substitution into equations (5), (12) and (15). In the second category, it is necessary to solve the electrode equation to obtain the free electrode-ion concentration, $[X_k]$, (given an observed potential, E_k), before solution of the m.b.e. Solving the electrode equation for $[X_k]$ requires a knowledge of all the free concentrations so it is necessary to implement an iterative solution of this equation and the m.b.e.

A Newton–Raphson procedure is generally the most efficient way to solve the m.b.e. The corresponding set of linear equations has the form

$$\mathbf{A}\bar{\mathbf{s}} = \bar{\mathbf{b}} \tag{17}$$

where

$$A_{im} = \left[\frac{\partial(T_i^c - T_i^r)}{\partial x_m}\right]_{\bar{x}^n}, \quad m = 1, \ldots, NC: \; i = 1, \ldots, NC.$$

$s_m = \Delta x_m^n =$ shift to m^{th} unknown $= x_m^{n+1} - x_m^n$.

$b_i = T_i^r(\bar{x}^n) - T_i^c(\bar{x}^n)$,

and

$\bar{x}^n = n^{th}$ iteration estimate of the unknowns.

The equations can be set up in terms of the absolute values of unknowns except for the free concentrations, $[X_k]$, and formation constants, β_j, for which natural logarithms are more convenient. The equations (17) can then rapidly be solved by forward and backward substitution using the Crout factors for **A** (obtained by using partial pivoting).[32] Scaling of the shift vector $\bar{\mathbf{s}}$ is only required when particularly large shifts are predicted or if $\bar{\mathbf{b}}^t.\bar{\mathbf{b}}$ increases. If a failure in the Newton–Raphson procedure occurs in those tasks for which the only unknowns are free concentrations, the slower but more robust secant method[33] can be used to solve the equations.

Initial estimates

It is well known that the efficiency of the Newton–Raphson method is considerably improved if good initial estimates can be obtained for the unknowns. Here, there are two classes of unknowns to consider. The first consists of the free concentrations of the components. Unless such concentrations can be obtained from electrode equations, they are very difficult to estimate. Secondly, there are those unknowns which are experimental parameters such as total titrand and titrant concentrations and titration volumes. Formation constants can also be included in this class. Generally it is possible to estimate reasonable initial values.

At the first and second points, initial estimates for the unknowns of the second kind can readily be

Table 1. Formation constants used in the simulations[36]

Species	log β
1. OH	−13.380
2. HCys	10.110
3. H_2Cys	18.078
4. H_3Cys	20.050
5 $ZnCys_2$	17.905
6. ZnHCys	14.604
7. $ZnHCys_2$	24.114
8. Zn_3Cys_4	42.278
9. Zn_3HCys_4	48.313
10. $Zn_3H_2Cys_4$	54.082

Table 2. Initial volumes (ml), concentrations (M), electrode parameters (mV) and selectivity parameters used

	Titration	
	H/Cys	Zn/Cys
V°	20.0	20.0
C^{V}_{H}	0.055	0.050
C^{V}_{Cys}	0.015	0.015
C^{V}_{Zn}	—	0.014
C^{V}_{Cl}	0.15	0.15
C^{V}_{Na}	0.125	0.102
C^{B}_{OH}	0.2	0.2
C^{B}_{Cl}	0.15	0.15
C^{B}_{Na}	0.35	0.35
E°_{H}	400.0	400.0
s_H	61.54	61.54
α	3.27	3.27
$K_{H,Na}$	4.17×10^{-16}	4.17×10^{-16}

provided from the experimental values. If measured electrode potentials are available, initial estimates of the corresponding free electrode-ion concentrations can readily be calculated from the simple electrode equation (7). At the first titration point, estimates of the other free concentrations can be obtained from a proportional formula of the kind used in COMICS[34] and ECCLES.[35] Initial estimates for these concentrations at the second point can then be taken as the values obtained for the solution of the equations at the first point.

Initial estimates of all parameters at the third and each subsequent point of a titration are best obtained by linear extrapolation of the solution from the previous two points. This can, in principle, be based on the change in either the observed electrode potentials or the titration volumes. Experience has shown that, when they are available, the potentials are the more effective. It is found that the number of Newton–Raphson iterations required to solve the m.b.e. at each point can be reduced by as much as 50% by this technique, compared with one which uses the solution of the previous point for the initial estimate. As storage and extrapolation of two previous solutions involves considerably less work than the application of a number of Newton–Raphson iterations, a correspondingly marked decrease in execution time is obtained. Quadratic extrapolation has also been investigated but proved to be less satisfactory, in part because the extra calculation over three points does not always lead to a decrease in the number of Newton–Raphson iterations required to solve the m.b.e.

RESULTS AND DISCUSSION

The ability to apply the more general electrode equation [see equations (5), (12) and (15)] and to correct for activity changes, forms the basis of a generalized computer library called ESTA (Equilibrium Simulation for Titration Analysis) which is currently being developed in this department.* The major objective of this project is to provide a flexible computing tool for investigating phenomena associated with chemical interactions in solution and for their quantitative characterization.

Although liquid-junction potential, sodium-ion interference and activity changes have long been individually characterized, they have been widely neglected in the context of potentiometric titrations. As no computer program for analysing titration data has hitherto incorporated all of these corrections, their importance has been difficult to assess and, as a result, has tended to be ignored. To illustrate the extent to which each effect is typically manifest in many titrations of practical importance, two simulations have been performed. These relate to the determination of proton and zinc formation constants of cysteine.[36] The titration conditions and parameters are shown in Tables 1–3. The Davies equation[25] was used to simulate activity-coefficient changes. Values for the formation constants, ionic conductivities and sodium-ion selectivity parameters were estimated from the literature, unless otherwise indicated.

The results of the simulations are shown in Tables 4 and 5. Distributions of the complexes during the titrations, as a percentage of total cysteine and total

Table 3. Ionic conductivities

		Constant-I bridge ($I = 0.15$)	Satd. KCl bridge ($I = 4.2$)
Bridge	Na	53	—
	K	—	36
	Cl	−83	−39
Test solution	Na	53	53
	K	—	81
	Cl	−83	−83
	Cys	−10	−10
	H	375	125*
	OH	−200	−100*

*Empirical values estimated experimentally.[37]

*Interested readers can obtain details of how to acquire copies of these programs by writing to PMM.

Table 4. Simulated liquid-junction potentials, sodium-ion interference and ionic-strength changes for a typical cysteinate protonation titration

Volume added, *ml*	$-\log\{H\}$	% of total Cys in species 2	3	4	$^1E^{LJ}$, *mV*	$^2E^{LJ}$, *mV*	E^{sel}, *mV*	*I*, *M*
0.0	1.92	0	40	60	−5.5	0.7	0.0	0.150
0.4	2.02	0	46	54	−4.4	0.8	0.0	0.150
0.8	2.14	0	53	47	−3.3	0.8	0.0	0.150
1.2	2.29	0	61	39	−2.4	0.8	0.0	0.150
1.6	2.49	0	71	29	−1 5	0.9	0.0	0.150
2.0	2.78	0	83	17	−0.8	0.9	0.0	0.150
2 4	3 52	0	96	4	−0.1	0.9	0.0	0.150
2.6	6.94	7	93	0	−0.1	0.9	0.1	0.151
2.8	7.49	20	80	0	−0.2	0.8	0.2	0 153
3.2	8 02	46	54	0	−0.4	0.8	0.3	0.156
3.6	8.49	71	28	0	−0.7	0.8	0.4	0.160
4.0	9.15	85	8	0	−0.9	0.7	0.6	0.163
4.4	9.79	72	1	0	−1.0	0.7	0.9	0.169
4.8	10.21	50	0	0	−1.1	0.7	1.2	0.175
5.2	10.58	30	0	0	−1.1	0.7	1.6	0.180
6.0	11.19	10	0	0	−0 5	0.7	2.4	0.187
6.8	11.51	5	0	0	0 5	0.8	3.0	0.193
7.4	11.65	4	0	0	1.1	0.9	3.4	0.196
7.8	11.72	3	0	0	1.6	0.9	3.6	0.199

zinc respectively, are also given. The magnitude of changes in ionic strength that commonly occur in titrations of this kind can be seen, emphasizing the need to correct formation constants to the appropriate ionic strength at each point. Secondly, the effect of sodium ion interference towards higher pH (E^{sel}), even at the concentrations which occur in these titrations, is significant. Moreover, as temperatures and sodium-ion concentrations increase, this effect will increase dramatically.[38] It is thus interesting to note that corrections of this kind are also important when higher concentrations of background electrolyte are employed to minimize ionic-strength and liquid-junction potential changes. For example, in 3.0*M* sodium perchlorate at 25°, errors of 1.0 mV may occur at pH values as low as 8.

The tables also show the liquid-junction potentials calculated from the Henderson equation for both constant ionic strength ($^1E^{LJ}$) and saturated potassium chloride ($^2E^{LJ}$) bridges. For titrations at these ionic strengths it is evident that constant-ionic-strength bridges may give rise to significant and somewhat irregular changes in liquid-junction potentials over the whole pH range. This is due to the opposing effects of hydrogen and hydroxide ions on the one hand and the steadily increasing concentration of sodium on the other. The saturated potassium chloride bridges are much less problematical in

Table 5. Simulated liquid-junction potentials, sodium-ion interference and ionic-strength changes for a typical zinc cysteinate titration

Volume added, *ml*	$-\log\{H\}$	% of total Zn in species 5	6	7	8	9	10	$^1E^{LJ}$, *mV*	$^2E^{LJ}$, *mV*	E^{sel}, *mV*	*I*, *M*
0.0	2.04	0	0	0	0	0	0	−2.7	1.1	0.0	0.164
0.4	2.17	0	0	0	0	0	0	−1.7	1.1	0.0	0.164
0.8	2.33	0	0	0	0	0	0	−0.7	1.1	0.0	0.164
1.2	2.54	0	0	0	0	0	0	0.2	1.1	0.0	0.163
1.6	2.88	0	0	0	0	0	0	0.9	1.1	0.0	0.163
2.0	3.93	0	3	0	0	0	0	1 5	1.1	0.0	0.162
2.4	4.87	0	15	1	0	0	4	1.3	1 1	0.0	0.160
2 8	5.07	0	15	3	0	2	14	1.1	1.1	0.0	0.159
3.2	5.25	0	14	4	1	5	23	0.8	1.0	0.0	0.157
3.6	5.44	1	11	5	2	10	29	0.6	1.1	0.0	0.157
4.0	5.68	1	8	5	6	18	28	0.4	0.9	0.1	0.156
4.4	6.00	2	5	5	17	25	19	0.2	0.9	0.1	0.157
4.8	6.55	4	2	3	46	18	4	−0.1	0.9	0.1	0.160
5.2	10.70	6	0	0	72	0	0	0.1	0.9	1.7	0.164
6.0	11.39	6	0	0	72	0	0	1.2	1.0	2.7	0.170
6.8	11 63	6	0	0	71	0	0	2.2	1.0	3.2	0.175
7.4	11.74	6	0	0	71	0	0	2.8	1.1	3.5	0.179

this respect. Thus, a choice must generally be made between the better characterized constant-ionic-strength bridge and the smaller, but not so well characterized, effects of saturated potassium chloride bridges. In either case, more experimental work is probably required to match the values of these parameters to the accuracy of modern research potentiometers. However, it is clear that with saturated potassium chloride bridges, under normal circumstances, errors from *changes* in the liquid-junction potential are likely to be much less than those arising from other sources.[39] They do not, therefore, justify the use of pH buffers[40] in preference to internal calibration of glass electrodes.

As is well known, the values of liquid-junction potentials and single-ion activity coefficients calculated as described here do not have any absolute significance. They cannot be measured experimentally and, as a corollary, they cannot, in themselves, be meaningfully interpreted in any data analysis. However, the effects of *differences* in these quantities can have an experimental reality and thus can validly be taken into account, either theoretically or empirically.

Although the approaches developed in this paper allow for large changes in liquid-junction potential, ionic strength and sodium-ion interference, it obviously remains desirable to design experiments which minimize these effects whenever possible. Nevertheless, it is envisaged that programs which apply such corrections will help to establish the extent to which titration conditions can be extended beneficially. This will permit a wider variety of equilibrium systems to be satisfactorily characterized. A major advantage in this respect will lie in the ability to integrate and quantify, simply and rapidly, expected effects *in the actual context of each application.* This will provide an insight, for the system under investigation, which has hitherto often proved elusive in practice.

REFERENCES

1. L. G. Sillén, *Laboratory Methods in Current Use at the Department of Inorganic Chemistry*, KTH, Stockholm, 1959.
2. G. Biedermann and L. G. Sillén, *Ark. Kemi*, 1953, **5**, 425.
3. I. G. Sayce, *Talanta*, 1968, **15**, 1397.
4. A. Sabatini, A. Vacca and P. Gans, *ibid.*, 1974, **21**, 53.
5. L. G. Sillén, *Acta Chem. Scand.*, 1964, **18**, 1085.
6. P. M. May, D. R. Williams, P. W. Linder and R. G. Torrington, *Talanta*, 1982, **29**, 249.
7. N. Ingri and L. G. Sillén, *Ark. Kemi*, 1964, **23**, 47.
8. G. Arena, E. Rizzarelli, S. Sammartano and C. Rigano, *Talanta*, 1979, **26**, 1.
9. M. Wozniak, J. Canonne and G. Nowogrocki, *J. Chem. Soc., Dalton*, 1981, 2419.
10. M. Molina, C. Melios, J. O. Tognolli, L. C. Luchiari and M. Jafelicci, Jr., *J. Electroanal. Chem.* 1979, **105**, 237.
11. B. P. Nikolskii, *Acta Physicochim. USSR*, 1937, **7**, 597.
12. B. P. Nicolsky (B. P. Nikolskii), M. M. Schultz, A. A. Belijustin (A. A. Belyustin) and A. A. Lev, in *Glass Electrodes for Hydrogen and Other Cations*, G. Eisenman (ed.), Chapter 6. Dekker, New York, 1961.
13. G. Eisenman, *Biophys. J.*, 1962, **2**, 259.
14. *Idem*, in *Glass Electrodes for Hydrogen and Other Cations*, G. Eisenman (ed.), Chapter 9. Dekker, New York, 1961.
15. G. G. Guilbault, *Pure Appl. Chem.*, 1976, **48**, 127.
16. P. Henderson, *Z. Phys. Chem.*, 1907, **59**, 118; 1908, **63**, 325.
17. H. S. Dunsmore and D. Midgley, *Anal. Chim. Acta*, 1972, **61**, 115.
18. D. A. MacInnes, *The Principles of Electrochemistry*, Dover, New York, 1961.
19. G. T. Hefter, *Anal. Chem.*, 1982, **54**, 2518.
20. R. G. Bates, *CRC Crit. Rev. Anal. Chem.*, 1981, **10**, 247.
21. R. G. Picknett, *Trans. Faraday Soc.*, 1968, **64**, 1059.
22. D. A. MacInnes and L. G. Langsworth, *Cold Spring Harbor Symposium Quant. Biol.*, 1936, **4**, 18.
23. C. F. Baes Jr. and R. E. Mesmer, *The Hydrolysis of Cations*, Wiley, New York, 1976.
24. E A. Guggenheim, *Phil. Mag.*, 1935, **19**, 588.
25. C. W. Davies, *Ion Association*, Butterworths, London, 1961.
26. G. H. Nancollas and M. B. Tomson, *Pure Appl. Chem.*, 1982, **54**, 2675.
27. G. Sposito and S. V. Mattigod, *GEOCHEM: A computer program for the calculation of chemical equilibria in soil solutions and other natural water systems*, University of California, 1980.
28. D. L. Parkhurst, D. C. Thorstenson and L. N. Plummer, *PHREEQE—A computer program for geochemical analysis*, U.S. Geological Survey, Water Research Division, Richmond V.A., PB 81-167801, 1980.
29. J. Kielland, *J. Am. Chem. Soc.*, 1937, **59**, 1675.
30. P. W. Linder and K. Murray, *Talanta*, 1982, **29**, 377.
31. Y. K. Kharaka and I. Barnes, *SOLMNEQ: Solution–mineral equilibrium computations*, U.S. Geological Survey, Water Research Division, Washington, D.C., PB-215-899, 1973.
32. J. H. Wilkinson and C. Reinsch, *Handbook for Automatic Computation*, Vol. II, *Linear Algebra*, p. 93. Springer-Verlag, Berlin, 1971.
33. N. Ingri, W. Kakolowicz, L. G. Sillén and B. Warnqvist, *Talanta*, 1969, **14**, 1261; corrections, 1970, **15**, No. 3, p. xi.
34. D. D. Perrin and I. G. Sayce, *ibid.*, 1967, **14**, 833.
35. P. M. May, P. W. Linder and D. R. Williams, *J. Chem Soc. Dalton*, 1977, 588.
36. G. Berthon, P. M. May and D. R. Williams, *ibid.*, 1978, 1433.
37. C F. Jones, P. M. May, K. Murray and D. R. Williams, unpublished work.
38. N. Linnet, *pH Measurements in Theory and Practice*, Radiometer, Copenhagen, 1970.
39. P. M. May, *Talanta*, 1983, **30**, 889.
40. H. K. J. Powell and M. C. Taylor, *Talanta*, 1983, **30**, 885

Talanta, Vol 32, No. 6, pp. 491–494, 1985
Printed in Great Britain.

0039-9140/85 $3.00 + 0.00

DETERMINATION OF POLYETHYLENE GLYCOLS BY PRECIPITATION WITH IODINE

M. FRANCOIS and R. DE NEVE*
Laboratorium Galenische en Magistrale Farmacie, Medische en Speciale Biochemie,
Vrije Universiteit Brussel, Laarbeeklaan, 103, 1090 Brussels, Belgium

(*Received* 5 *July* 1984. *Revised* 9 *November* 1984. *Accepted* 11 *January* 1985)

Summary—Two methods for the determination of polyethylene glycols (PEGs) in aqueous solution by precipitation with iodine have been developed. For PEGs with molecular weight 4×10^3–2×10^4 the excess of iodine is titrated with thiosulphate, and for PEGs with average m.w. $> 2 \times 10^4$ turbidimetric measurement is used. Both methods are relatively simple and give accurate and reproducible results.

Polyethylene glycols (PEGs) are non-toxic water-soluble polymers of ethylene oxide which have found wide application in the pharmaceutical,[1] biomedical[2] and many other sciences.[3] Most methods for their determination are based on precipitation of the Ba–PEG complex with sodium tetraphenylborate and determination of the precipitate by gravimetric,[4] potentiometric,[5] coulometric[6] or thermometric[7] analysis. The precipitates formed by the Ba–PEG complex with silicotungstic or phosphomolybdic acid can be determined gravimetrically[8] and the phosphomolybdic acid precipitate has also been determined colorimetrically.[9] Turbidimetry has been used for determination of the PEG–tannic acid precipitate[10] and of that of the Ba–PEG complex with trichloroacetic acid,[9] and nephelometry for the precipitate formed by reaction of PEG with Nessler's[11] or Mayer's[12] reagent. The oxidation of PEG with dichromate in acid solution[10,13] and splitting of the ether function with hydriodic acid[14] have also been used for the determination of PEGs.

We have developed two new and simple methods based on the reaction of PEG with iodine. In the first, the excess of iodine is titrated with thiosulphate after removal of the I_2–PEG precipitate, and in the second the turbidity of the I_2–PEG suspension is measured photometrically.

EXPERIMENTAL

Reagents

PEGs (Hoechst, Brussels), m.w. 200–20000, were "DAB 8" grade.[15] The other reagents were of analytical-reagent grade.

*Iodine (I_2) solution, 0.05*M. Made by dissolving 3.173 of iodine in a solution of 6.34 g of potassium iodide in about 50 ml of water and making up to 250 ml with water, and standardized with 0.1*M* sodium thiosulphate.

*Sodium thiosulphate solution, 0.1*M. Standardized by titration with potassium bromate. A 0.01*M* solution was made by appropriate dilution.

Apparatus

The turbidity of the I_2–PEG suspension was measured with a single-beam Coleman 55 spectrophotometer.

Procedures

Determination of iodine excess after filtration. Pipette 10 ml of PEG solution (100–200 mg/l.) into a 25-ml Erlenmeyer flask. Add 2 ml of 0.05*M* I_2 solution and mix carefully. Add 6 ml of 3M sulphuric acid and mix again. Filter off the precipitate on about 150 mg of glass wool placed on top of a sintered-glass filter (pore diameter 20–40 μm) and collect the filtrate in a 50-ml Erlenmeyer flask. Rinse the 25-ml flask and the glass wool with two 10-ml portions of 1*M* sulphuric acid and combine these with the filtrate. Titrate the iodine in the filtrate with 0.1*M* thiosulphate, adding 1 ml of 1% starch solution near the end of the titration.

Determination of iodine excess after centrifugation. Pipette 5 ml of the PEG solution into a dry 10-ml centrifuge tube. Add 1 ml of 0.05*M* I_2 solution and 3 ml of 3*M* sulphuric acid, mixing after each addition. Centrifuge for 5 min and pipette 3 ml of the clear supernatant liquid into a 50-ml Erlenmeyer flask. Add 20 ml of 1*M* sulphuric acid and titrate with 0.01*M* thiosulphate, adding 1 ml of 1% starch solution near the end of the titration.

Turbidity of the I_2-PEG suspension. Pipette 25 ml of 0.01*M* I_2 solution into a 50-ml beaker and add 5 ml of PEG solution (60–3000 mg/l.) dropwise, with vigorous magnetic stirring during addition of the PEG solution and for 3 min more. Then immediately transfer part of the suspension into a 1-cm glass cuvette and measure the absorbance at 750 nm after 5 min.

RESULTS

Titration method

On addition of iodine to a PEG solution a green ($300 \leqslant$ m.w. $\leqslant 2000$) or brown ($4000 \leqslant$ m.w. $\leqslant 20000$) precipitate is formed,[16] and becomes blue-black on acidification with sulphuric acid. The supernatant liquid is clear yellow and the iodine in it can be titrated with thiosulphate, with starch as indicator. If the titration is done in the presence of the precipitate an easily seen end-point is obtained, but within a few seconds iodine is released from the precipitate and the starch–iodine colour reappears. Very slow titration shows that all the iodine present can be released from the complex. It is therefore necessary to remove the

*To whom all correspondence should be addressed.

Table 1. Determination of PEGs by precipitation with I_2; parameters of the linear relation $y = a + bx$ (y = mole of I_2 and x = mg of PEG)

	Filtration method		Centrifugation method	
PEG	Slope ± S.D.	Intercept ± S.D.	Slope ± S.D.	Intercept ± S.D.
400	4.58 ± 0.14	$-4.0_5 \pm 0.5_3$		
4000	10.43 ± 0.23	$1.0_8 \pm 0.7_9$	10.25 ± 0.25	$0.3_2 \pm 0.4_3$
6000	10.39 ± 0.49	$0.1_7 \pm 1.6_3$	9.87 ± 0.26	$1.2_4 \pm 0.4_2$
10000	10.28 ± 0.18	$-0.1_0 \pm 0.6_1$	9.72 ± 0.25	$1.0_8 \pm 0.4_1$
20000	10.51 ± 0.30	$-1.0_3 \pm 0.9_9$	10.40 ± 0.33	$-0.5_8 \pm 0.5_6$

precipitate before the titration. The initial precipitate (before acidification) is so finely divided that it can only be separated by centrifugation at high centrifugal force, but the flocs formed by addition of sulphuric acid can be separated easily by filtration or centrifugation (at low centrifugal force).

The amount of iodine bound is linearly related to the amount of PEG. The regression equation data are summarized in Table 1. The reaction is much less sensitive for PEG 400 than for the PEGs of higher m.w. A t-test was applied to compare the regression-line slopes obtained for the filtration and centrifugation methods. The variance of the differences between the four pairs of slopes was 0.0398 and the best estimate of the population standard deviation was 0.23. The calculated t-value of 2.97 was smaller than the tabulated t-value of 3.182 (3 degrees of freedom, $P = 0.05$); the slopes were thus not significantly influenced by the separation method. The titration results were analysed statistically in more detail except for PEG 400 (excluded because it reacts very differently). Factorial analysis of variance[17] was applied to determine the influence of the following three factors on the amount of iodine bound to the PEG (μmole/mg):

M, the average molecular weight of the PEG (4000, 6000, 10000, 20000);
S, the method of separating the precipitate (filtration or centrifugation);
C, the concentration of the initial PEG solution (100, 200, 300, 400 or 500 mg/l.).

In all the determinations 0.2 ml of 0.05M I_2 solution was added per ml of PEG solution. There were 40 combinations ($2 \times 4 \times 5$) and each combination was executed twice, so 80 results were obtained.

The results of the analysis are summarized in Table 2. The variance estimates associated with the second-order (M–S–C) and first-order interactions (M–S, M–C and S–C), the separation method (S) and the PEG concentration (C) are not significantly greater than the residual variance estimate ($P = 0.05$). These results are in agreement with the conclusions drawn from the data in Table 1, where the linear relation indicated a constant I_2/PEG ratio and a t-test indicated that the slopes were not influenced by the separation method. However, the variance estimate associated with the molecular weight of the PEGs is significantly greater than the residual variance estimate (at $P = 0.01$). Since the separation method and the PEG concentration have no influence on the I_2/PEG ratio found, all results obtained for one specific PEG molecular weight were considered to belong to the same population. Thus 4 populations, each containing 20 results, were obtained (see Table 3). The "Studentized Range Procedure"[18] was used to see which means differed from the others. The pooled variance

$$S^2 = \sum(n_i - 1)\, S_i^2 \Big/ \sum_{i=l}^{i=k} (n_i - k)$$

was 0.421 and the "5% allowance" for n_i samples and n_j methods

$$\frac{Q}{\sqrt{2}} \sqrt{S^2\left(\frac{1}{n_i} + \frac{1}{n_j}\right)}$$

Table 2. Factorial analysis of variance to assess the influence of various parameters on the I_2/PEG ratio (μmole/mg)

Source of variance	Sum of squares	Degrees of freedom (df)	Variance estimate	F	Probability
M*	6.264	3	2.088	4.867‖	$P = 0.01$
S†	0.160	1	0.160	0.373‖	NS¶
C‡	1.367	4	0.342	0.797‖	NS¶
M–S	1.424	3	0.475	0.973§	NS¶
M–C	2.607	12	0.217	0.445§	NS¶
S–C	1.041	4	0.260	0.533§	NS¶
M–S–C	6.743	12	0.562	1.207	NS¶
Residual	18.628	40	$s^2 = 0.466$§		

*Molecular weight of PEG.
†Separation method
‡PEG concentration in solution.
§$s^2 = 0.488$ (df = 52), calculated successively according to Moroney.
‖$s^2 = 0.429$ (df = 71), calculated successively according to Moroney.
¶Not significant.

Table 3. I_2/PEG (*mole/mg*) and EOU/I_2 (*mole/mole*) ratios as a function of the PEG molecular weight

PEG m.w.	4000	6000	10000	20000
	I_2/PEG (*mole/mg*)			
mean*	10.7	10.7	10.4	10.0
SD	0.55	0.84	0.53	0.63
CV†	5.1	7.9	5.1	6.3
	EOU/I_2 (*mole/mole*)			
mean§	2.11	2.12	2.18	2.26
SD	0.11	0.17	0.11	0.14

*Any two means underscored by the same line do not differ statistically at $P = 0.01$ (1% allowance = 0.56).
†Coefficient of variation.
§Mean and standard deviation of 20 determinations.

was 0.54 ($Q = 3.74$ for 76 degrees of freedom and $P = 0.05$). In Table 3 any two means underscored by the same line do not differ statistically at $P = 0.05$ (difference smaller than 0.54). The I_2/PEG ratios for PEG 4000, 6000 and 10000 do not differ at $P = 0.05$. The I_2/PEG ratio for PEG 20000 is significantly smaller ($P = 0.05$) than the ratio for PEG 4000 and 6000 but does not differ from the ratio for PEG 10000. The EOU/I_2 molar ratios of the different PEGs are summarized. The EOU (ethylene oxide unit) concentration for a given quantity of PEG is calculated as weight of PEG per mole of EOU. The ratio is 2 for PEGs $4000 \leqslant$ m.w. $\leqslant 20000$, but 6 for PEG 400 (not included in Table 3) at PEG concentrations greater than 300 mg/l.

Turbidity method

As already mentioned, the I_2–PEG precipitate is very fine, so the particles settle slowly. Therefore turbidimetric measurement of the I_2–PEG suspension was investigated, but only for the PEG 20000 (which is frequently used in our laboratory). The absorbance was measured at 750 nm because iodine at the concentration in the assay mixture (about $8.3 \times 10^{-3} M$) does not absorb light at this wavelength. For reproducible absorbances to be obtained the suspension has to be formed by adding the PEG solution dropwise to the iodine solution and not *vice versa*. The absorbance was recorded as a function of time, after the initial standing time of 3 min, and Fig. 1 shows that the absorbance (measured for an optical path through the lower part of the cuvette) increases with time, on account of sedimentation. Hence the absorbance must be measured at a fixed time after transfer of the suspension into the cuvette. The reproducibility of the absorbance for five different PEG concentrations was studied; the absorbance was recorded immediately after transfer to the cuvette and after a time-lapse of 5 min. Each measurement was duplicated. An F-test ($F = 31.2$) indicated that the variance of the differences between duplicates is significantly smaller ($P = 0.01$) for the absorbances measured after 5 min.

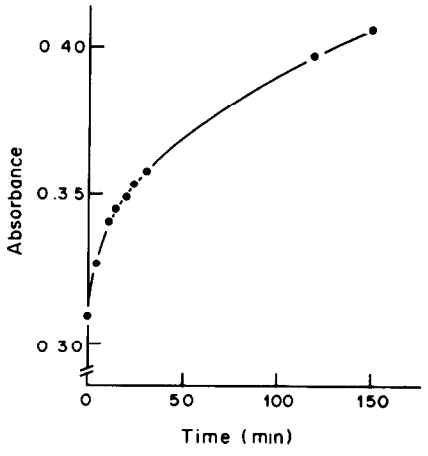

Fig. 1. Absorbance of an I_2–PEG suspension at 750 nm, as a function of time.

The calibration graph is linear over the range 60–2400 mg/l. in the final solution, which is much wider than that for the nephelometric determination of PEG 4000 with Nessler's reagent[11] (20–80 mg/l.) and the turbidimetric determination of the PEG–tannic acid precipitate (20–34 mg/l.). The results indicate that the turbidimetric method gives a simple and accurate determination of PEG 20000.

CONCLUSIONS

A novel, simple and rapid method for the accurate determination of PEG with iodine is presented. Only simple equipment is needed for the titrimetric method. In the turbidimetric method the order of addition of the reactants is important and so is the time-lapse between filling the cuvette and reading the light intensity. The concentration range for linear response is larger than for other methods.

In contrast to other methods in which the EOU/I_2 ratio found is 6, the ratio found here is 2; no explanation can be offered for the difference. An EOU/I_2 ratio of 6 was also found, but only for PEG 400 at concentrations > 300 ml/l.

REFERENCES

1. P. H. List and L. Hörhammer, *Hagers Handbuch der Pharmazeutischen Praxis*, 4th Ed., Band VII, Teil B, p. 405. Springer Verlag, Berlin, 1977.
2. W. Honig and M. R. Kulia, *Anal. Biochem.*, 1976, **72**, 502.
3. Polyglykole Hoechst, Hoechst Aktiengesellschaft, Frankfurt (Main), West-Germany, 1978.
4. R. Neu, *Arzneim. Forsch.*, 1959, **9**, 585.
5. R. J. Levins and R. M. Ikeda, *Anal. Chem.*, 1965, **37**, 671.
6. J. R. Moody, G. D. Christian and W. C. Purdy, *Anal. Chim. Acta*, 1968, **42**, 153.
7. K. Y. Khalaf and T. W. Gilbert, *Analyst*, 1978, **103**, 623.

8. C. B. Schaffer and F. H. Critchfield, *Anal. Chem.*, 1947, **19,** 32.
9. S. J. Malawer and D. W. Powell, *Gastroenterology*, 1967, **53,** 250.
10. J. Nuysink and L. K. Koopal, *Talanta*, 1982, **29,** 495.
11. K. C. Ingham and R. C. Ling, *Anal. Biochem.*, 1978, **85,** 139.
12. B. H. Lippold and G. F. Schneider, *Acta Pharm. Technol. APV-Informationsdienst*, 1977, **23,** 89.
13. A. V. Smirnova, E. K. Batischeva, G. I. Plotnikova, A. F. Koreckii and Yu. N. Ochonskaya, *Zavodsk. Lab.*, 1978, **44,** 25; *Z. Anal. Chem.*, 1979, **295,** 200.
14. P. W. Morgan, *Ind. Eng. Chem., Anal. Ed.*, 1946, **18,** 500.
15. *Deutches Arzneibuch*, 8th Ed., GOVI-Verlag, Frankfurt, FRG, 1978.
16. *Belgische Farmacopee V*, 5th Ed., Part II, pp. 253, 255, 1962.
17. M. J. Moroney, *Facts from Figures*, 2nd Ed., pp. 394–418. Penguin Books, London, reprint 1979.
18. L. K. Randolph and J. L. Ciminiera, in *Remington's Pharmaceutical Sciences*, 15th Ed., p. 133. Mack, Pennsylvania, 1975.

Talanta, Vol. 32, No. 6, pp 495–499, 1985
Printed in Great Britain.

0039-9140/85 $3.00 + 0.00

DETERMINATION OF THE RARE-EARTH ELEMENTS IN GEOLOGICAL MATERIALS BY THIN-FILM X-RAY FLUORESCENCE AND INDUCTIVELY-COUPLED PLASMA ATOMIC-EMISSION SPECTROMETRY

HOU QING-LIE*, T. C. HUGHES, MAUNU HAUKKA and PHILIP HANNAKER†
Department of Geology, School of Earth Sciences, University of Melbourne, Parkville, Victoria 3052, Australia

(*Received* 24 *March* 1984. *Revised* 24 *August* 1984. *Accepted* 12 *December* 1984)

Summary—Thin-film XRF and ICP–AES analytical procedures for the determination of the rare-earth elements (REE) in rocks, involving preconcentration by ion-exchange and co-precipitation with $Fe(OH)_3$ for thin-film preparation, and matrix modification, are described. The REE in five international reference rocks have been determined, with correction for spectral line overlap whenever necessary. The results obtained by using X-ray fluorescence spectrometry compare well with those of inductively-coupled plasma atomic-emission spectrometry, and with other values reported in the literature.

Several techniques have been used for determining the rare-earth elements (REE) in geological samples at the ppm level. Both inductively-coupled plasma atomic-emission spectrometry (ICP–AES)[1–6] and electrothermal atomic-absorption spectrometry (AAS)[7] have been used for REE determinations. REE values determined by other techniques, such as neutron-activation analysis (NAA)[8] and mass spectroscopy (MS)[9] have also been documented.

X-Ray fluorescence (XRF), available in many analytical laboratories, has also been used for REE determinations,[10,11] but matrix effects and line interferences are two of the major problems associated with REE determinations by this method. To cope with these problems, a thin-film technique was investigated in our laboratories, with $Lu(OH)_3$ as an internal standard and $Fe(OH)_3$ as the carrier for preconcentration. This, combined with a matrix modification, improved the sensitivity, accuracy and precision of the determinations.

The thin-film technique has long been used in XRF analysis. Gunn[12] demonstrated the linear relationship between fluorescence intensity and concentration of various elements in the thin film. Chung[13] examined the effect of the thickness of thin films on matrix effects. The great success of the technique is attributed to the reduction of matrix effects by use of the thin film and to the efficiency of preliminary separation and quantitative recovery of REE, using an internal standard and co-precipitation, similar to Miller's[14] procedure using fluoride precipitation.

The most important step in the procedure is the ion-exchange separation, in which the REE are separated from major elements in the rocks prior to XRF determination. According to the distribution coefficients for 50W-X8 resin,[15,16] most rock-forming cations [Fe(III), Ti, Al, Ca, Mg, Mn(II), Na, K] and some other heavy metal ions [Cu(II), Ni, Co, Cr(III), Zn, Cd, Ga, In, Tl, Bi, Au, Hg(II), Pb, U and V] are eluted quantitatively by 1*M* hydrochloric acid, 2*M* nitric acid and 1*M* sulphuric acid.

This paper presents a procedure suitable for determination of REE by ICP–AES or the XRF method. It involves sample decomposition by fusion with sodium peroxide and hydroxide, and separation of the REE by ion-exchange. For the XRF determination a further preconcentration by co-precipitation with $Fe(OH)_3$ and production of a thin film on a Millipore filter is necessary, but this is not required for the ICP–AES method. Results are given for five international reference samples and compared with other published values.

EXPERIMENTAL

Apparatus and operating parameters

For XRF determinations a Siemens sequential SRS-1 X-ray fluorescence spectrometer with ten-position sample changer was used. Between the primary and secondary beams home-made extra apertures were installed to mask all but the radiation from the 16-mm diameter sample surface.

For ICP–AES determinations a 34-channel direct-reading Applied Research Laboratories ICP spectrometer, which contained 6 REE channels for comparison with the XRF results, was used. The instrumental parameters are summarized in Tables 1 and 2.

Ion-exchange columns. All ion-exchange columns prepared in the laboratory were made of borosilicate glass tubes (18 mm bore, 170 mm long) with a reservoir at the top (57 mm diameter, 130 mm long, *ca.* 330 ml volume). Bio-Rad AG 50 W-X8 polystyrene cation-exchange resin (*ca.* 22 g), 200–400 mesh, was used in the hydrogen form. A flow-rate of 1–2 ml/min was obtained by constricting the plastic outlet tube (0.7 mm bore) with a screw-clamp.

*Current visiting Research Fellow from Baiyin Mining and Metallurgical Research Institute, Lanzhou, China.
†To whom correspondence should be addressed.

Table 1. XRF instrument parameters

X-Ray spectrometer	SIEMENS SRS-1
X-Ray generator:	CRYSTALLOFLEX 4 type H4
X-Ray tube target:	Au
Power:	40 kV; 60 mA
Collimator:	0.15° divergence
Analysing crystal	LiF (220)
Detector:	F.P.C. with P 10 gas
Counting time.	fixed time, 60 sec
Pulse height selection:	8.5/7 V
Sample changer.	10-position, under vacuum

Reagents

The eluents used (1*M* and 5.5*M* hydrochloric acid, 2*M* nitric acid and 1*M* sulphuric acid) were made by dilution of the analytical-grade concentrated acids with distilled demineralized water.

Stock solutions of the rare earths (1000 ppm) were prepared from the high-purity oxides (Johnson-Matthey) and 20% v/v nitric acid except for the cerium solution, which was made up with sulphuric acid (30% v/v). Mixed rare-earth standard solutions (containing 10 ppm of Lu and 4 ppm of each of the rest) were prepared from the 1000-ppm stock solutions and 10% v/v hydrochloric acid (note: *x*% v/v means *x* ml of concentrated acid diluted to 100 ml with water). The Millipore filters were either type GS with 0.22 μm pore size or GA-6 with 0.45 μm pore size (Millipore Co., Bedford, Mass., USA). All reagents were carefully checked for REE impurities, by applying the procedure to high-purity silica.

Procedures

Sample decomposition. The sample (1 g) was transferred into a nickel crucible and mixed with 3 g of sodium peroxide and 3 g of sodium hydroxide. The mixture was fused over a Méker burner at about 600° for 10 min and allowed to cool for 1–2 min. The crucible and lid were placed in a 150-ml beaker containing 20 ml of water to leach the fusion cake. After 10 min, the contents of the crucible were transferred to a 100-ml plastic centrifuge tube and centrifuged at 2000 rpm for 5 min. The supernatant liquid was decanted into another 100-ml centrifuge tube, and 1 ml of 1% ferric chloride solution was added to ensure that any REE in solution would be co-precipitated with hydrous ferric oxide, and the mixture was centrifuged. The supernatant liquid, containing most of the sodium silicate, was then discarded. The precipitates were dissolved in 10 ml of water and 5 ml of 6*M* hydrochloric acid, with heating on a steam-bath. The acid content of the solution was kept to a minimum (2*M*) to avoid precipitation of any residual silica The solution was then transferred to the ion-exchange column.

Ion-exchange separation. Once the sample solution had passed through, the column was washed successively with 150 ml of 1*M* hydrochloric acid, 170 ml of 2*M* nitric acid, 120 ml of 1*M* sulphuric acid, 120 ml of 1*M* hydrochloric acid and 300 ml of 5.5*M* hydrochloric acid. Between each acid wash, the column was washed with 15 ml of water. The final eluate (300 ml of 5.5*M* hydrochloric acid), containing the REE, was collected in a 400-ml beaker, and evaporated to dryness on a hot-plate. The residue was dissolved in a small quantitity of water and 0.5 ml of 10*M* nitric acid. This solution was then diluted to approximately 100 ml with water, for thin-film preparation. For ICP–AES measurement, dilution to 20 ml was found to be adequate.

Thin-film preparation for XRF. To each sample solution 300 μg of iron(III) (as carrier) and 50 μg of lutetium(III) (as internal standard) were added for co-precipitation of the rare-earth elements by addition of 10 ml of concentrated ammonia solution to raise the pH to >12. The thin film for XRF measurement was then made by filtering off the precipitate on a Millipore filter. A reference thin-film disk was made by running 5 ml of a working multi-element standard solution (containing 50 μg of Lu and 20 μg of each of the other REE) directly through the column as described above for ion-exchange separation, and processing the REE fraction as above. A blank disk, containing only the iron and lutetium, was prepared by applying the whole procedure to 1 g of pure silica. For identification of overlapping spectral lines, thin-film disks were prepared for the individual REE.

Constructing the calibration line. The REE peak and background intensities for a blank disk containing only Fe and Lu were measured and the corresponding peak/background ratios calculated. Multiplication of measured sample and standard backgrounds by these ratios produced the background intensity under the peaks.

Line overlap corrections were made by measuring the intensity of interfering lines at the appropriate analyte wavelengths, for a disk containing a known amount of an interfering element. This gave counts per unit quantity of interfering element, making it possible to subtract the interfering-element count from the analyte count for the multi-element standard disk. An alternative is to calculate and subtract the amount of analyte equivalent to the interfering-element concentration (see Table 3).

The final net counts obtained for the blank and the multi-element standard were expressed as ratios to the internal standard count and used to calculate calibration factors, on the assumption that the XRF count was a linear function of analyte concentration.

By these preparation, measurement and calculation procedures the calibration is fixed indefinitely, without any subsequent standard measurement. If a new batch of chemicals is used for sample preparation, it is only necessary to prepare and measure a new blank disk.

All XRF measurements were based on a fixed counting time of 60 sec, with sequential counting of line and background for each rare-earth element. The analytical lines, background measurement positions and lower limit of detection (L.L.D.) are summarized in Table 4.

ICP–AES analysis. The six rare-earth elements measured by ICP–AES were determined at the following wavelengths (nm): La 398.85, Ce 394.28, Sm 442.43, Eu 381.97, Gd 376.84, Yb 369.42, under the operating conditions outlined in Table 2.

ICP–AES calibration was done with a series of REE standards prepared in 5% v/v nitric acid.

Table 2. ICP instrument parameters

ICP spectrometer:	ARL 34000
RF generator:	air-cooled, 3 kW rating, 27.12 MHz
Incident power:	1600 W
Torch:	quartz, 18 mm outer diameter, two-turn coil surrounding the torch
Gas (Ar), coolant:	10.5 l./min
plasma:	1.5 l./min
carrier:	1.0 l./min
Grating:	1080 rulings/mm
Primary slit-width	20 μm
Pre-integration time:	25 sec
Integration time:	10 sec
Integration cycle:	3

Table 3. Line overlap interferences and required corrections

Analyte	Interferent (100 ppm)	Analyte apparent increase, *ppm*
Eu	Pr	12.4
Tb	Yb	44
Gd	Ce	5.8
Gd	Nd	0 19

Table 4. Measurement positions and detection limits by XRF

Analyte	Line	Background-peak 2θ,* *degrees*	L.L.D., *ppm*†
La	$L\alpha_1$	−2.590	0.06
Ce	$L\beta_1$	−1.378	0.14
Pr	$L\beta_1$	+1.008	0.16
Nd	$L\alpha_1$	−2.398	0.08
Sm	$L\beta_1$	+0.816	0.21
Eu	$L\alpha_1$	+1.784	0.15
Gd	$L\alpha_1$	−1.938	0.11
Tb	$L\beta_2$	+0.720	0.42
Dy	$L\beta_1$	−0.682	0.27
Ho	$L\beta_1$	−0.406	0.29
Er	$L\beta_1$	+0.821	0.31
Yb	$L\alpha_1$	+1.250	0.14
Lu	$L\alpha_1$	−0.730	—

*Background position relative to measured peak, negative if background 2θ lower than peak 2θ.

†Peak and background counting time is 1 min and the 95% confidence limit is 2σ. L.L.D. from counting statistics = standard concentration $\times 3 \times \sqrt{N_b/(N_p - N_b)}$ where N_p and N_b = total counts for peak position and background.

RESULTS AND DISCUSSION

The results for five international reference samples are given in Table 5. The recovery of REE by elution with 5.5*M* hydrochloric acid was found satisfactory, though Fe(III), Al, Si, Ca and Ni produced a small tail. This was not found to be serious, since Fe(III) was purposely added as a carrier to collect the REE. The interference of Ni with the Ho $L\beta_1$ line was expected, but the problem was overcome by co-precipitating the REE with $Fe(OH)_3$ by adding ammonia instead of sodium hydroxide, so that nickel remained in solution as the tetra-ammine complex. Silica particles, if present above trace level in the film, may present serious problems, as they do not adhere firmly to the filter. In that case, an additional column wash with 1*M* hydrochloric acid before the final elution with 5.5*M* hydrochloric acid is necessary to remove most of the silica in order to produce a perfect film. Blank level determinations made by a similar procedure were below the L.L.D. given in Table 4.

A series of ICP–AES determinations for six rare-earth elements in the range 50–10000 μg indicated 100% recovery after the ion-exchange. The quantity of REE co-precipitated with $Fe(OH)_3$ was found to be greater than 99.7% provided the pH of the solution was above 12.

All the REE were determined by XRF except Tm and Lu, which are usually present at sub-ppm levels and below the detection limits specified in this report. Lutetium was therefore used as an internal standard in this study. It has similar behaviour to the analyte elements, so it is more efficient than non-REE elements as an internal standard for correcting for chemical yield, mechanical losses and instrumental deviations. Substantial errors will only be encountered if the lutetium in the sample is present at more than sub-ppm level. When the lutetium content is high then generally so will be that of the other REE and they may be determined directly without preconcentration.

The lines for the determination of REE in this study were chosen on the basis of the spectrum resolution and sensitivity shown in Fig. 1, for 1 g of NIM-G standard rock (same disk as in Table 5). As can be seen, most of the rare-earth lines are well resolved, except Tb $L\beta_2$ which is overlapped by Yb $L\alpha_1$, Eu $L\alpha_1$ overlapped by Pr $L\beta_2$, and Gd $L\alpha_1$ overlapped by both Ce $L\gamma_1$ (not shown) and Nd $L\beta_2$.

The procedure allows the rare-earth elements to be separated from the bulk of other constituents in the

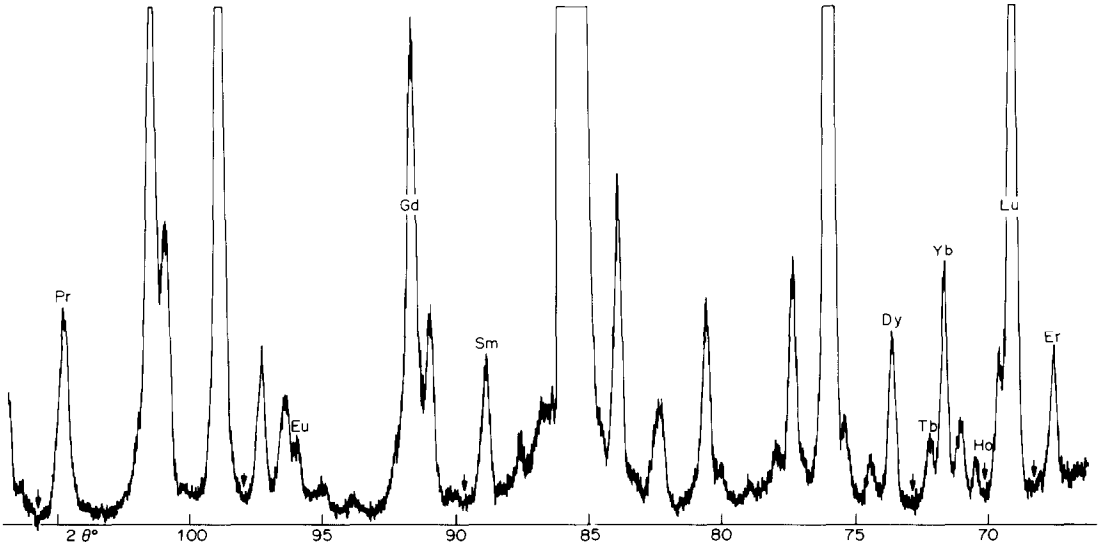

Fig. 1. XRF spectrum of REE, using NIM-G standard, scanning speed 0.5°/min, arrows show measured background positions, other parameters as in Table 1.

Table 5. Results for international reference samples (concentrations in *ppm*)

	NIM-G			BCR-1				BHVO-1				GSP-1			AGV-1			
	This work		Other	This work				This work				This work			This work			
Element	XRF	ICP	values	XRF	ICP	Other values		XRF	ICP	Other values		XRF	Other values		XRF	ICP	Other values	
La	114.4	118.4	105?†	28.5	26.8	26.6¶	27†	20.2	16.7	16.2¶	16.7 ± 0.8*	192.4	188¶	195†	43.5	41.0	39¶	36†
Ce	184.2	203.7	200†	51.6	54.6	53.8¶	53†	42.2	39.6	38.2¶	41 ± 4*	405.2	432¶	360†	66.2	68.4	69¶	71†
Pr	19.7		19.4‡	6.9		7.29¶	7?†	6.4		5.66¶	5.6*	51.7	56¶	50?§	8.4		8.5¶	7?§
Nd	78.3		68?†	32.8		29.7¶	26?†	31.9		25.4¶	24 ± 6*	229.0	206¶	190?†	36.3		32¶	37?†
Sm	13.0	16.8	16?†	6.9	7.3	6.7¶	6.5†	6.9	6.0	6.4¶	6.1 ± 0.7*	23.6	27.4¶	25?†	5.6	10.8	5.8¶	5.9†
Eu	—	0.49	0.4?†	1.8	1.9	1.98¶	2†	2.0	2.0	2.18¶	2.0 ± 0.4*	1.4	2.16¶	2.4?†	1.4	1.7	1.6¶	1.6?†
Gd	13.6	14 3	11?†	6.6	6.7	6.9¶	6.6§	6.6	5.7	7.0¶	7 ± 2*	11.5	12.4¶	15?§	4.5	7.4	4.6¶	5.5§
Tb	3.0		3?†	1.7		1.0¶	1.0†	1.6		0.86¶	1.0 ± 0.2*	1.6	0.4¶	1.47†	0.8		0.5¶	0.7?†
Dy	17.5		16§	6.5		6.72¶	7?†	5.4		5.59¶	4.8 ± 0.2*	5.1	5.8¶	5.7?†	3.3		3.7¶	3.5?†
Ho	3.5		3?§	1.3		1.4¶	1.2?†	1.1		1.06¶	0.94*	1.1	1.0¶		0.5		0.7¶	0.6§
Er	12.7		10?§	3.7		3 8¶	3.5?†	2.0		2.63¶	2.0 ± 0.3*	2.5	1.7¶	3?§	1.7		1.8¶	1.2?§
Yb	13.4	12.9	14†	3.3	3.0	3.7¶	3.4†	2.0	1.9	2.19¶	2.1 ± 0.5*	1.6	1.4¶	1.9†	1.6	1.6	1.72¶	1.9†

*Reported by Gladney and Goode.[20]
†"Usable value" of Abbey.[19]
‡Steele *et al.*[18]
§"Usable value" of Abbey.[17]
¶ICP–AES value of Crock and Lichte.[3]
?Uncertainty because it represents the median of only 5–9 available results.[19]

rock. The accuracy of measurement of the rare-earth elements is improved by reducing the spectral correction errors for both ICP–AES and XRF determination. Matrix errors in this procedure were found to be negligible in comparison with the possible errors associated with direct analysis of geological material.

The accuracy was shown to be satisfactory, by comparing two independent final analytical procedures (XRF, ICP–AES), as well as two independent types of standard (natural and synthetic).

The results presented in Table 5 show good agreement with those previously obtained by using either XRF or ICP–AES, or other analytical procedures such as neutron activation or mass spectrometry.

Acknowledgement—Work supported by the Department of Geology, University of Melbourne.

REFERENCES

1. J. N. Walsh, F. Buckley and J. Barker, *Chem. Geol.*, 1981, **33**, 141.
2. A. Balton, J. Hwang and A. V. Bolt, *Spectrochim. Acta*, 1983, **38B**, 165.
3. J. G. Crock and F. E. Lichte, *Anal. Chem.*, 1982, **54**, 1329.
4. J. A. C. Broekaert and P. K. Hormann, *Anal. Chim. Acta*, 1981, **124**, 421.
5. I. B. Brenner, A. E. Watson, T. W. Steele, E. A. Jones and M. Goncalves, *Spectrochim. Acta*, 1981, **36B**, 785.
6. S. E. Church, *Geostandards Newsl.*, 1981, **2**, 133.
7. J. G. Sen Gupta, *Talanta*, 1981, **28**, 31.
8. S. Meloni, M. Oddone, A. Cecchi and G. Poli, *J. Radioanal. Chem.*, 1982, **71**, 429.
9. F. W. E. Strelow and P. F. S. Jackson, *Anal. Chem.*, 1974, **46**, 1481.
10. G. N. Eby, *ibid.*, 1972, **44**, 2137.
11. B. J. Fryer, *Geochim. Cosmochim. Acta*, 1977, **41**, 361.
12. E. L. Gunn, *Anal. Chem.*, 1961, **33**, 921.
13. F. H. Chung, A. J. Lentz and R. W. Scott, *X-Ray Spectrom.*, 1974, **3**, 172.
14. A. G. Miller, *Anal. Chem.*, 1974, **46**, 1720.
15. F. W. E. Strelow, *ibid.*, 1960, **32**, 1185.
16. F. W. E. Strelow, R. Rethemeyer and C. J. C. Bothma, *ibid.*, 1965, **37**, 106.
17. S. Abbey, *Geol. Surv. Can. Paper*, 80–14.
18. T. W. Steele, A. Wilson, R. Goudvis, P. J. Ellis and A. J. Radford, *Geostandards Newsl.*, 1978, **2**, 71.
19. S. Abbey, *Geol. Surv. Can. Paper*, 83–15.
20. E. S. Gladney and W. E. Goode, *Geostandards Newsl.*, 1981, **5**, 31.

Talanta, Vol. 32, No. 6, pp. 501–503, 1985
Printed in Great Britain

0039-9140/85 $3.00 + 0.00
Pergamon Press Ltd

SHORT COMMUNICATIONS

INDIRECT DETERMINATION OF THALLIUM BY DIFFERENTIAL-PULSE POLAROGRAPHY*

ALI H. BAZZI and BRIAN R. KERSTEN
Department of Natural Sciences, University of Michigan-Dearborn, Dearborn, MI 48128, U.S.A.

(*Received* 6 *June* 1984. *Revised* 15 *November* 1984. *Accepted* 21 *January* 1985)

Summary—The method is based on the separation of Tl(I) as $Tl_2HPMo_{12}O_{40}$, stripping of the molybdate, and measurement of the peak current in differential-pulse polarography of the molybdenum. The calibration graph is linear over the range 2–12 ppm of thallium. The relative standard deviation is 1.2% (7 replicates each containing 500 μg of thallium). The current due to reduction of the molybdenum is three times that for reduction of the equivalent amount of Tl(I) in the thallous phosphomolybdate precipitate, making the indirect approach more sensitive than direct polarographic determination of the Tl(I).

The development of new methods for determination of thallium is of importance because of the toxicity of the element.[1] The polarographic behaviour of thallium in pyridine and in different buffer solutions and supporting electrolytes has long been investigated.[2–5] The determination of thallium by d.c. polarography in succinic acid medium has been reported.[6] Thallium has been determined in the presence of large amounts of copper and cadmium by means of the effect of the adsorption of camphor on the DME.[7] Other methods used include a.c. polarography, stripping analysis and differential pulse polarography.[8–11]

The present work deals with indirect determination of thallium by differential-pulse polarography. Tl(I) is separated as the phosphomolybdate and the molybdenum and Tl(I) in the precipitate are determined polarographically. The ratio of molybdenum to thallium in the precipitate has been shown to be 6:1.[12]

EXPERIMENTAL

Chemicals

Stock thallium solution (*1 mg/ml*). Dissolve 1.304 g of pure $TlNO_3$ in distilled water and dilute to the mark in a 1-litre standard flask. Transfer to a polyethylene bottle.

Standard thallium solution (*100 μg/ml*). Transfer 50 ml of the stock solution to a 500-ml standard flask and dilute to the mark with distilled water. Store in a polyethylene bottle.

Basic borate buffer. Transfer 15 ml of 50% sodium hydroxide solution to a 1-litre flask. Add about 300 ml of distilled water and 48.0 g of boric acid. Swirl to dissolve and dilute to the mark with distilled water. Store in a polyethylene bottle. The pH of this solution is 8.9.

*Perchloric acid, 0.5*M. Add 43 ml of concentrated (72%) perchloric acid to about 200 ml of distilled water, cool and dilute to 1 litre. Store in a polyethylene bottle.

*Perchloric acid, 4.0*M. Add 86 ml of concentrated (72%) perchloric acid to about 100 ml of distilled water, cool and dilute to 250 ml. Store in a polyethylene bottle.

Phosphomolybdic acid solution, 10%. Dissolve 10 g of phosphomolybdic acid in 100 ml of water. Filter the solution through a fine-porosity sintered-glass crucible and transfer into a polyethylene bottle.

Apparatus

Differential-pulse polarograms were obtained with an EG&G PAR 174 Polarographic Analyzer equipped with a model 303 static mercury-drop electrode and a Houston model RE0089 *X–Y* recorder.

Procedure

Transfer a sample containing between 100 and 600 μg of thallium(I) into a 30-ml centrifuge tube, acidify with 2.0 ml of 4.0*M* perchloric acid and dilute to 10 ml with distilled water. Add 5.0 ml of 10% phosphomolybdic acid solution and wait for 10 min for complete formation of the thallous phosphomolybdate precipitate.

Centrifuge for 10 min at about 16,000 rpm. Remove and discard the supernatant liquid. Wash the precipitate with 10.0 ml of 0.5*M* perchloric acid, being sure to start washing at the top of the tube and work down to ensure removal of any phosphomolybdic acid adhering to the sides of the tube. Centrifuge for 5 min, then remove and discard the wash solution. Add 25 ml of the borate buffer to the precipitate, directing the stream of the buffer at the precipitate, and wait for dissolution to become complete. Transfer the solution to a polyethylene beaker containing 0.62 g of citric acid monohydrate, and rinse the tube with distilled water into the beaker. Rinse the tube again, with 5 ml of borate buffer, and transfer the washings to the beaker. Transfer the contents of the beaker to a 50-ml standard flask, dilute to the mark with distilled water, and mix.

Transfer a portion of the solution into a polarographic cell and record the differential-pulse polarogram, scanning from −0.2 to −1.5 V *vs.* Ag/AgCl, at 5 mV/sec, using a modulation amplitude of 50 mV, with medium drop-size, a drop-time of 0.5 sec, and a purge time of 4 min.

RESULTS AND DISCUSSION

The effect of the acidity used in precipitation of $Tl_2HPMo_{12}O_{40}$ was studied with samples containing 400 μg of Tl(I). Table 1 shows that between 1.0 and

*Presented in part at the Pittsburgh Conference on Analytical Chemistry and Applied Spectroscopy, 7 March 1984, Atlantic City, N.J., U.S.A.

Table 1. Effect of acidity on the formation of $Tl_2HPMo_{12}O_{40}$ [400 μg of Tl(I), scan-rate 2 mV/sec, drop time 1.0 sec, modulation amplitude 50 mV]

4.0*M* $HClO_4$ added, *ml*	i_p(*), μA	
	Direct, Tl(I)	Indirect, molybdate
0.5	1.89	4.18
1.0	1.93	4.45
1.5	1.90	4.35
2.0	1.93	4.45

*Mean of three values.

2.0 ml of 4.0*M* perchloric acid can be used; 2.0 ml was chosen for the recommended procedure.

The voltage at which the peak of Tl(I) appears in the polarogram is rather insensitive to pH, and is about −0.4 V (*vs.* Ag/AgCl) at both pH 8.8 and 6.1. If the precipitate is decomposed in the pH-8.78 borate buffer without addition of citric acid, only Tl(I) is reduced, at −0.4 V (Fig. 1). If the acidity is adjusted with 0.62 g of citric acid monohydrate, both Tl(I) and the released molybdate are reduced, with good resolution between the two peaks. The pH of the resulting solution is 6.07, and this was chosen as the optimum pH. At a much lower pH the resolution is not adequate. The addition of the buffer serves two purposes: the first is to dissolve the precipitate, and the second to decompose the phosphomolybdate. The addition of citric acid also serves two purposes: the first is to adjust the pH, and the second to complex the molybdate to prevent re-formation of phosphomolybdate. For seven replicate determinations of 500 μg of thallium(I) by the procedure given, the thallium(I) peak gave E_p -0.413 ± 0.002 V, i_p 2.29–2.43 μA, and the molybdate peak gave E_p -1.245 ± 0.005 V, i_p 7.04–7.32 μA.

A typical differential-pulse polarogram at pH 6.1 is shown in Fig. 2. It exhibits two peaks, the first (at −0.4 V) due to reduction of Tl(I) and the second (at −1.2 V) due to reduction of the molybdate. Thus, the heights of the two peaks can be used for the simultaneous direct and indirect determination of thallium with the one polarogram.

The precision was estimated by analysing seven samples each containing 500 μg of thallium. The average current for the thallium peak was 2.33 μA and the relative standard deviation 2.6%, and the average current for the molybdate peak was 7.19 μA, relative standard deviation 1.2%. Hence mea-

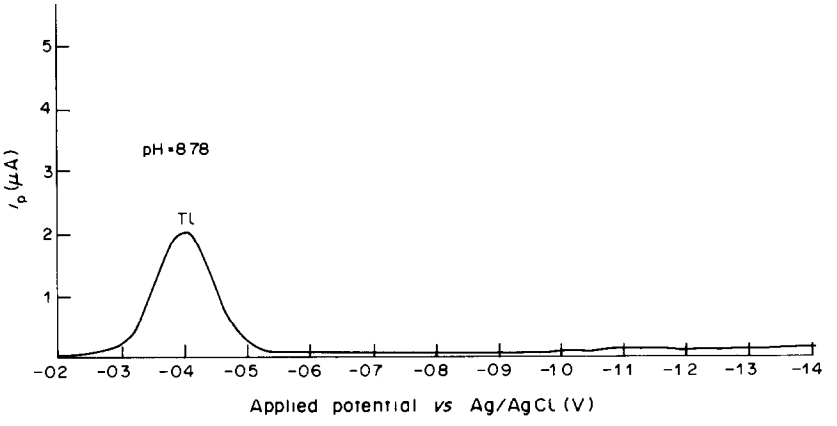

Fig. 1. A differential pulse polarogram of a sample containing 400 μg of Tl(I), pH = 8.78, without citric acid addition. Drop time = 1.0 sec. Scan-rate = 2 mV/sec.

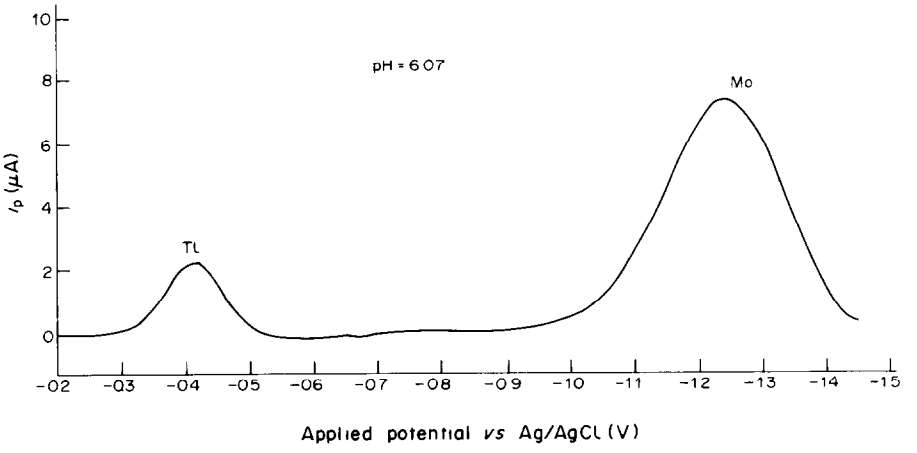

Fig. 2. A typical differential pulse polarogram of a sample containing 500 μg of Tl(I) at pH = 6.07, with citric acid addition.

Table 2. Effect of the presence of foreign ions on determination of 400 μg of Tl(I)

Ion	Added as*	Amount of ion added, μg	Tl peak Current†, μA	Tl peak RE,§ %	Mo peak Current†, μA	Mo peak RE,§ %
Ag^+	$AgNO_3$	100	1.90	+2.2	5.50	−1.3
Ag^+	$AgNO_3$	200	1.88	+1.1	5.52	−0.9
Ag^+	$AgNO_3$	400	1.88	+1.1	5.67	+1.8
Pb^{2+}	$PbNO_3$	400	1.83	−1.6	5.43	−2.5
Cd^{2+}	$CdCl_2$	100	1.85	−0.5	5.53	−0.7
Cd^{2+}	$CdCl_2$	200	1.88	+1.1	5.58	+0.2
Cd^{2+}	$CdCl_2$	400	1.87	−0.5	5.60	+0.5
Ba^{2+}	$Ba(NO_3)_2$	400	1.84	−1.1	5.48	−1.6
CrO_4^{2-}	K_2CrO_4	400	1.83	−1.6	5.52	−0.9
WO_4^{2-}	$Na_2WO_4 \cdot 2H_2O$	400	1.83	−1.6	5.45	−2.2
Cu^{2+}	$Cu(NO_3)_2 \cdot 2\frac{1}{2}H_2O$	400	1.79	−3.8	5.46	−2.0
Hg^{2+}	$Hg(NO_3)_2$	400	1.80	−3.2	5.52	−0.9
Ni^{2+}	$NiCl_2 \cdot 6H_2O$	400	1.87	+0.5	5.53	−0.7
Fe^{3+}	$Fe(NO_3)_3 \cdot 9H_2O$	400	1.85	−0.5	5.48	−1.6
NH_4^+	NH_4Cl	100	1.88	+1.1	5.67	+1.8
NH_4^+	NH_4Cl	200	1.85	−0.5	5.88	+5.6
NH_4^+	NH_4Cl	400	1.85	−0.5	6.13	+10.1

*Solutions were made in distilled water, except for $Hg(NO_3)_2$, which was dissolved in 0.032*M* HNO_3.

†Each value is the average from three separate samples.

§The relative error (RE) is calculated relative to 1.86 μA for the Tl current and 5.57 μA for the Mo current.

surement of thallium by means of the molybdate peak is more sensitive and precise.

Calibration graphs with good linearity are obtained for thallium in the range 2–12 μg/ml in the final 50 ml of solution, for both the thallium and molybdate measurements, the slope of the "molybdate" plot being about 3 times that of the "thallium" plot. Both plots give an intercept on the concentration axis at about 0.7 μg/ml thallium concentration, which implies a solubility of about $6 \times 10^{-6}M$ for $Tl_2HPMo_{12}O_{40}$ at the acidity used for the precipitation.

A study was made of the degree of interference by 100–400 μg amounts of various ions at the 400-μg Tl(I) level. Table 2 summarizes the results. The only significant interference is from the ammonium ion when present in amounts above about 100 μg, but even then only for the indirect determination, since it is due to precipitation of ammonium phosphomolybdate, which naturally results in a higher molybdate peak. The direct method is applicable in the presence of at least 400 μg of ammonium ion. Although thallous chromate is only sparingly soluble, its precipitation is prevented by the acidification of the sample with perchloric acid, because of conversion of the chromate into dichromate. Organic bases, rubidium and caesium were not tested, but would be expected to interfere in the indirect (but not the direct) determination because they form insoluble phosphomolybdate salts in acidic medium.[13–15]

The final test solution is fairly stable and there is a change of only +1.1% in peak current if the solution is kept for 24 or 48 hr before the direct measurement, and +1.3% (24-hr storage) and +2.2% (48-hr storage) in the peak current for the indirect measurement, for thallium at the 400-μg level (mean of three replicates).

REFERENCES

1. A Saddique and C. D. Peterson, *Vet. Hum. Toxicol.*, 1983, **25,** 16.
2. A Cisak and P. J. Elving, *J. Electrochem. Soc.*, 1963, **110,** 160.
3. I. C. Popescu and A. Craciun, *Rev. Chim. Bucharest*, 1961, **6,** 199.
4. A. I. Kamenev, E. N. Vinogradova and E. N. Sadinov, *Vestn. Mosk. Univ. Khim.*, 1968, **23,** No. 6, 91.
5. L. P. Petrova and V. P. Gladyshev, *Izv. Akad. Nauk Kaz. SSR, Ser. Khim.*, 1974, **24,** No. 15, 86.
6. G. S. Deshmukh and V. S. Naik, *Z. Anal. Chem.*, 1972, **259,** 123.
7. E. N. Shapovalova and G. V. Prokhorova, *Zavodsk. Lab.*, 1978, **44,** 536.
8. M. Kodama and T. Noda, *Bull. Chem. Soc. Japan*, 1968, 41.
9. A. V. Kon'kova, *Zh. Analit. Khim.*, 1968, **23,** 451.
10. J. P. Franke and R. A. De Zeeuw, *Pharm. Weekblad.*, 1976, **111,** 725.
11. W. Christmann, A. Lukaszewski and R. Neeb, *Z. Anal. Chem.*, 1980, **302,** 32.
12. L. G. Hargis and D. F. Boltz, *Anal. Chem.*, 1965, **37,** 240.
13. D. F. Boltz and S. J. Simon, *Microchem. J.*, 1975, **20,** 468.
14. E. A. Nikitina and O. N. Sokolova, *Zh. Obshchei Khim.*, 1954, **24,** 1123.
15. H. Buchwald and W. P. Thistlethwaite, *J. Inorg. Nucl. Chem.*, 1958, **7,** 292.

Talanta, Vol. 32, No 6, pp. 504–506, 1985
Printed in Great Britain

0039-9140/85 $3.00 + 0.00

FLUOROMETRIC DETERMINATION OF BIACETYL

A. J. MAROULIS*, A. N. VOULGAROPOULOS and C. P. HADJIANTONIOU-MAROULIS
Department of Chemistry, University of Thessaloniki, Thessaloniki, Greece

(*Received* 1 *August* 1984. *Revised* 12 *December* 1984. *Accepted* 11 *January* 1985)

Summary—The fluorometric determination of biacetyl is described. 3,4-Diaminoanisole reacts with biacetyl in alkaline ethanol–water solution to give strongly fluorescing 2,3-dimethyl-6-methoxyquinoxaline. Variables such as solvent composition, quenching by acetic and sulphuric acid, heating time and interference by other carbonyl compounds present are discussed. The method may be suitable for the determination of biacetyl in foodstuffs.

Biacetyl constitutes an important natural flavour component of a great variety of foodstuffs. Moreover it is a potential adulterant of frequently consumed products. As a consequence a great number of methods have been reported for its determination. The methods proposed during the past decade or so can be generally classified as those using chromatography (GLC and HPLC),[1–7] ultraviolet and visible absorption spectroscopy,[8–10] polarography[11,12] and miscellaneous techniques such as amperometric titration[13] and atomic-absorption spectrophotometry.[14]

However, none of these methods has the many advantages offered by fluorimetry and in particular its superior sensitivity and specificity.[15] Since biacetyl does not exhibit a significant native fluorescence[16] a method of developing fluorescence in the otherwise non-fluorescent biacetyl solutions had to be devised.

Here we describe a simple fluorimetric method for the estimation of biacetyl in water–ethanol solutions, which is based on formation of the strongly fluorescing 2,3-dimethyl-6-methoxyquinoxaline.

EXPERIMENTAL

Reagents

3,4-Diaminoanisole (DA) and its dichloride (DAD). These were synthesized in accord with established procedures from 4-aminoanisole, but the reagent can also be obtained commercially.

2,3-Dimethyl-6-methoxyquinoxaline (DMQ). This was obtained in crude form by refluxing equimolar amounts (0.013 mole) of 3,4-diaminoanisole and biacetyl in 80 ml of ethanol containing 1 ml of glacial acetic acid, for 1.5 hr, and then removing the solvent. Further purification by repeated recrystallization from ethanol yielded colourless crystals, m.p. 100.5–101.0° (literature value[17] 99–100°).

Biacetyl (Fluka puriss.). Distilled before use.

All other reagents were obtained from Merck and were *pro analysi* grade. The water was distilled twice and stored in polyethylene vessels.

Reagent solutions

3,4-Diaminoanisole solution. A $10^{-3}M$ solution was prepared by dissolving 0.0053 g of the dihydrochloride in 2 ml of $0.5M$ aqueous sodium hydroxide and diluting the solution to 25 ml with 10 ml of absolute ethanol and 13 ml of distilled water.

Biacetyl standard solutions. Prepared by weighing freshly distilled biacetyl, dissolving it in ethanol–water mixture, and diluting to known volume with the solvent mixture. Portions of these solutions were diluted with the solvent mixture to give the test samples. The ethanol–water mixture was prepared by diluting 400 ml of absolute ethanol to 1 litre with distilled water.

Procedure

In a 50-ml round-bottomed flask place 2.5 ml of sample, containing 0.3–1.9 μg of biacetyl, and add 1 ml of DA solution and 10 ml of absolute ethanol. Fit a condenser and reflux the mixture for 40 min, cool, then transfer the contents of the flask quantitatively to a 25-ml standard flask and dilute to the mark with ethanol–water mixture. Measure the fluorescence at 395 nm, using an excitation wavelength of 345 nm. Prepare a blank in the same way and measure its fluorescence.

Apply the procedure to three more 2.5-ml portions of the sample, to which have been added two, four and six times the amount of biacetyl in the initial sample (estimated by a calibration graph procedure). Use a plot of fluorescence intensity *vs.* added amount to compute the initial concentration.

RESULTS AND DISCUSSION

Characteristics of the fluorophore and the reagent

DMQ (**III**) is the product of the condensation reaction between DA (**I**) and biacetyl (**II**):

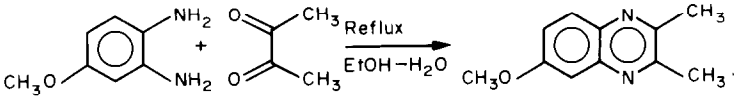

I II III

*Author for correspondence.

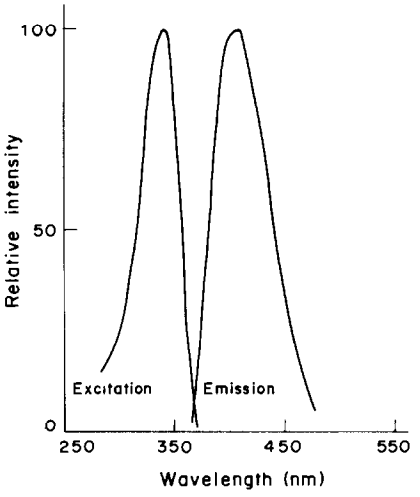

Fig. 1. Corrected excitation and emission spectra of 2,3-dimethyl-6-methoxyquinoxaline in ethanol–water solution. Excitation wavelength 345 nm. Emission wavelength 400 nm.

DMQ exhibits strong fluorescence not only in the ethanol–water solvent system used but also in pure ethanol, benzene and cyclohexane. Changing from the most to the least polar solvent shifts the λ_{max} of emission to longer wavelengths, with a concomitant decrease in fluorescence intensity.

The increased fluorescence observed in the hydroxylic solvents may be due to interchange of the lowest n, π^* and π, π^* excited singlet states in going from the hydrocarbon to the hydroxylic solvents.[18]

At this point it is worth mentioning that the presence of an electron-donating substituent such as the methoxy group in the 6-position of the quinoxaline ring is absolutely necessary, since the 2,3-dimethyl, 2,3,6-trimethyl and 2,3,6,7-tetramethyl quinoxalines (which we have also synthesized for this work) do not display significant fluorescence.

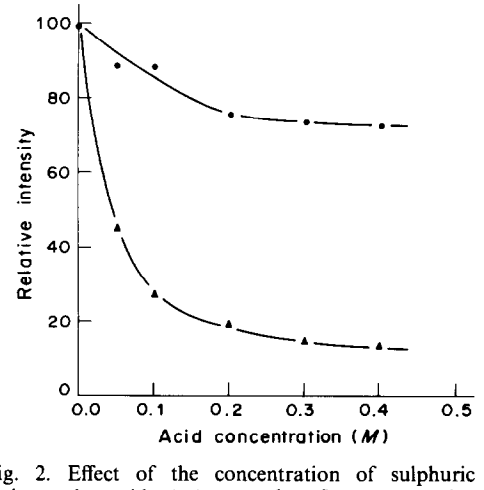

Fig. 2. Effect of the concentration of sulphuric (▲) and acetic acid (●) on the fluorescence intensity of 2,3-dimethyl 6-methoxyquinoxaline in ethanol–water solutions.

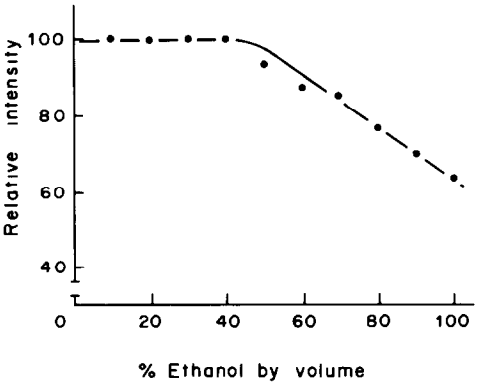

Fig. 3. Effect of solvent composition on the fluorescence intensity of 2,3-dimethyl-6-methoxyquinoxaline in ethanol–water solutions.

The corrected excitation and emission spectra of DMQ are shown in Fig. 1.

Our reagent (DA) does not fluoresce when excited at 395 nm in ethanol–water medium and therefore does not interfere. It does fluoresce, however, when excited at a shorter (*i.e.*, 304 nm) wavelength, displaying a maximum at *ca.* 360 nm.

Effect of added acid or base

Addition of various amounts of sulphuric or acetic acid to a solution of DMQ ($0.11 \times 10^{-5}\,M$) resulted in a decrease in fluorescence intensity (Fig. 2). Since addition of sodium hydroxide did not affect the fluorescence intensity we decided to use an alkaline medium to avoid the need for accurate pH control. There was no adverse effect on the rate or equilibrium of the condensation reaction.

Effect of solvent composition

As can be seen in Fig. 3, ethanol exerts a quenching effect which (fortunately) reaches a plateau when the ethanol concentration is larger than 40% v/v. We chose this particular solvent system so that determination of biacetyl in wine distillates would require minimum adjustment of the method.

Effect of reflux time

Prolonging the reflux time from 40 min to 5 hr did not affect the fluorescence development.

Stability of DMQ in solution

We submitted an analysis sample to extreme conditions (fully open excitation monochromator shutter

Table 1. Determination of biacetyl by standard-addition in ethanol–water solution

[Biacetyl], M		
Taken	Found	Std. devn., M
1.01×10^{-6}	1.10×10^{-6}	0.04×10^{-6}
1.0×10^{-7}	1.05×10^{-7}	0.04×10^{-7}

Table 2. Fluorescence excitation and emission maxima for carbonyl compounds subjected to the procedure

Compound	Excitation maximum*, nm	Emission maximum*, nm
Biacetyl	345	395
Glyoxal	345	422
Benzil	433	547
Acetone	432	544
Benzophenone	440	545

*Taken from the uncorrected spectra, for ethanol–water solution, ketone concentration *ca.* 1×10^{-5} *M*.

and longer exposure times than required for the actual measurement), but no photodecomposition occurred.

Precision of the determination

The precision was estimated by preparing two sets of solutions, each containing five identical samples and a blank.

The fluorescence intensity was measured twice in each determination. The results in Table 1 show that biacetyl was determined with fair precision.

A calibration graph can also be used. In preliminary experiments we found that the response was linear over the concentration range from 1×10^{-8} to 1×10^{-5} *M*.

Fluorescence from other carbonyl compounds

Other α-dicarbonyl compounds such as glyoxal and benzil also exhibit fluorescence under the conditions employed, presumably because the corresponding 6-methoxy- and 2,3-diphenyl-6-methoxyquinoxalines are formed. Fluorescence is also observed when monocarbonyl compounds such as benzophenone and acetone are treated with DA according to our procedure. However, with the exception of glyoxal, these compounds (Table 2) have different fluorescence characteristics and thus do not interfere in the determination of biacetyl when excitation at 345 nm is used.

Since glyoxal can easily be oxidized to oxalic acid, the proposed method can readily be adapted for determination of biacetyl and glyoxal in samples containing both substances. Moreover, it can be used for the determination of acetoin, since this yields biacetyl on oxidation.

Glucose, fructose and sucrose give no fluorescence in the procedure and do not quench that due to 2,3-dimethyl-6-methoxyquinoxaline.

REFERENCES

1. F. H. White and J. Wainwright, *J. Inst. Brew.*, 1975, **81**, 37.
2. E. M. Skibina, P. A. Artamonov and E. I. Gorshkova, *Zh. Analit. Khim.*, 1975, **30**, 1839.
3. P. C. Vocsavada and D. A. Lillard, *J. Chromatog. Sci.*, 1979, **17**, 215.
4. J. C. Buijten and B. Holm, *J. Autom. Chem.*, 1979, **1**, 91.
5. P. Moree-Testa and Y. Saint-Jalm, *J. Chromatog.*, 1981, **217**, 197.
6. W Postel and B. Meir, *Z. Lebensm. Unters. Forsch.*, 1981, **173**, 85.
7. D. Kasprick, R. Schaefer, H. P. Pietsch and B. Kunz, *Nahrung*, 1981, **25**, 943.
8. F. Kiermeir and H. J. Kyrein, *Z. Lebensm. Unters. Forsch.*, 1971, **147**, 128.
9. T. M. Cogan, *J. Dairy Sci.*, 1972, **55**, 382.
10. M. O. Serrano and R. G. Villanova, *Ars Pharm.*, 1978, **19**, 181.
11. E. Lechmer, I. Kunder and H. Klostermeyer, *Z. Lebensm. Unters. Forsch.*, 1981, **173**, 372.
12. E. Paspaleev, K. Kanchev, D. Dencheva and K. Batzalova, *Nahrung*, 1980, **24**, 303.
13. J. Vulterin and P. Straka, *Chemicky Prum.*, 1976, **26**, 242.
14. Y. Minami, T. Mitsui and Y. Fugimura, *Bunseki Kagaku*, 1979, **28**, 717.
15. A. J. MacLeod, *Instrumental Methods of Food Analysis*, p. 466. Elek Science, London, 1973.
16. F. Wilkinson, in *Organic Molecular Photophysics*, J. B. Birks (ed.), Vol. 2, p. 107. Wiley, London, 1975.
17. R. W. Bost and E. E. Towell, *J. Am. Chem. Soc.*, 1948, **70**, 903.
18. E. L. Wehry, in *Fluorescence*, G. G. Guilbault (ed.), p. 108 Dekker, New York, 1967.

Talanta, Vol 32, No. 6, pp. 507–509, 1985
Printed in Great Britain.

0039-9140/85 $3.00 + 0.00

STUDY OF THE TITANIUM–PHENYLFLUORONE COMPLEX FORMED IN THE PRESENCE OF TRITON X-305 AND EMULSIFIER OP

WU QUIANFENG
Shaanxi Research Institute of Environment Protection, 25 Chang An Road (N.), Xian, People's Republic of China

(*Received* 23 *May* 1984. *Revised* 19 *July* 1984. *Accepted* 11 *January* 1985)

Summary—A highly sensitive method for the spectrophotometric determination of titanium with phenylfluorone (PF) in the presence of Triton X-305 and emulsifier OP has been developed. In acid medium (pH 1.4–2.2) Ti(IV) forms red-violet complexes with PF, Triton X-305 and OP. The complex exhibits maximum absorption at 540 nm. The molar absorptivity is 1.63×10^5 l.mole^{-1}.cm^{-1}. The Ti:PF ratio in the complex is 1:2. Beer's law is obeyed in the titanium concentration range 0–0.2 μg/ml in the final solution. Fluoride and EDTA interfere. The method has been used for the rapid direct determination of microamounts of Ti(IV) in soils and cereals with satisfactory results.

Hydrogen peroxide[1] and diantipyrylmethane (DAM)[2] have long been used for spectrophotometric determination of microamounts of titanium. These methods have low sensitivity but high selectivity. Attempts have been made to enhance the sensitivity by addition of thiocyanate and use of solvent extraction,[3] but the methods are laborious and the sensitivity still not high.

Phenylfluorone (9-phenyl-2,3,7-trihydroxy-6-fluorone) (PF) yields intensely coloured complexes with a number of metals and has frequently been used for their spectrophotometric determination.[4–13] Many of these determinations also utilize cationic surfactants such as cetyltrimethylammonium bromide (CTAB),[4,7,8,12] cetylpyridinium bromide (CPB),[9,10,13] tetradecylbenzyldimethylammonium chloride (Zeph)[6] and so on. The molar absorptivity of the products obtained may exceed 10^5 l.mole^{-1}.cm^{-1}.

We have discovered that some non-ionic surfactants such as Triton X-305 or the emulsifier "OP"* may be used as solubilizing agents for the Ti–PF binary complex. It is of interest to note that a combination of Triton X-305 and OP has a very strong solubilizing effect. This paper reports an investigation of the conditions for formation of the Ti–PF–Triton X-305–OP complex in aqueous solution and the application of the system to direct determination of trace amounts of titanium in soils and cereals.

EXPERIMENTAL

Reagents

All chemicals were of analytical reagent grade.

Standard titanium solution. Prepared by dissolving 0.1668 g of high-purity titanium dioxide with 20 ml of concentrated sulphuric acid and 10 g of ammonium sulphate, heating till fuming, cooling and diluting accurately to 1 litre with demineralized water. Working solutions are prepared by accurate dilution of the stock solution.

PF solution, 0.03%. Prepared by dissolving 0.3 g of PF in absolute ethanol and 50 ml of sulphuric acid (1 + 1) and diluting to 1 litre with absolute ethanol. The working solution (0.01%) is prepared by mixing 150 ml of stock solution with 300 ml of absolute ethanol and adding 3 ml of concentrated sulphuric acid. It is stored in a brown bottle.

Mixed surfactant solution. Add 5 g of Triton X-305 to 2 ml of OP dissolved in 100 ml of water, and heat until it is completely dissolved.

Procedure

Transfer a portion of standard solution containing 5 μg of titanium into a 25-ml standard flask, add 5 ml of 0.025*M* hydrochloric acid, 4 ml of 0.01% PF solution and 3 ml of mixed surfactant solution. Dilute to volume with demineralized water. After 7 min measure the absorbance at 540 nm in a 1-cm cell against a reagent blank.

RESULTS AND DISCUSSION

Absorption spectra and effect of pH

Figure 1 shows that the Ti–PF complexes have maximum absorption at 540 nm, and the PF blanks at 470 nm, irrespective of the presence or absence of the surfactants. The absorbance is maximal and practically independent of pH in the range 1.4–2.2. A pH of 1.6 was selected for use.

Effect of PF concentration

The absorbance at 540 nm is constant when the volume of 0.01% PF used is varied between 3.8 and 4.2 ml, and decreases with higher or lower volumes. Hence 4 ml of 0.01% reagent solution was chosen for use.

Choice of non-ionic surfactants

Triton X-305, OP, Triton X-100, gelatin and poly-

*OP is $(CH_3)_3C.CH_2.C(CH_2)_2.C_6H_4(OCH_2.CH_2)_{10}OH$.

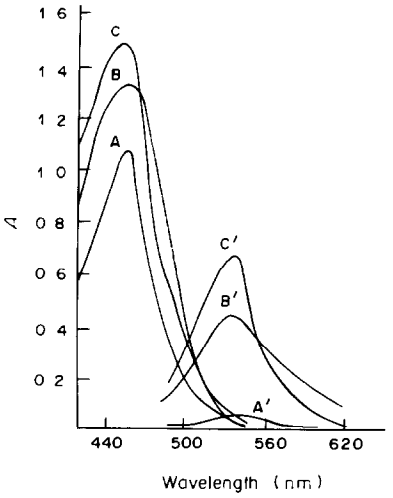

Fig 1. Absorption spectra (pH 1.6) of: A, PF reagent blank; B, PF–OP reagent blank; C, PF–Triton X-305–OP reagent blank, measured against water. A′, Ti–PF complex; B′, Ti–PF–OP complex; C′, Ti–PF–Triton X-305–OP complex, measured against a reagent blank [Ti(IV) 5 μg, pH 1.6, 1-cm cell].

Table 1. Influence of non-ionic surfactants on Ti–PF complex colour reaction (pH 1.6)

Reaction system	ε, 10^4 *l.mole*$^{-1}$.*cm*$^{-1}$
Ti–PF	3.4
Ti–PF–OP	10.8
Ti–PF–Triton X-305	12 9
Ti–PF–Triton X-305–OP	16.3

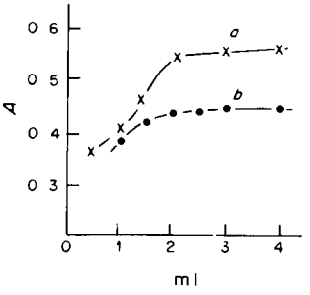

Fig. 2. Effect of non-ionic surfactant concentration: *a*, 5% Triton X-305; *b*, 2% OP.

(vinyl alcohol) were tested but only the first two showed any strong effect on the solubilization or sensitivity. Triton X-305 was better than OP, but a synergic effect was observed when both were used together (Table 1).

The effect of changing the concentration of Triton X-305 or OP is shown in Fig. 2. Maximum and constant intensity can be obtained with 2–4 ml of 5% Triton X-305 or 2% OP. Thus all further measurements were made with 3 ml of Triton X-305–OP mixture in the final solution.

Composition of the complex

The concentration of the Triton X-305–OP mixture was kept constant and a large excess was used, and the ratio of Ti(IV) to PF in the complex was determined by Job's method and found to be 1:2. Similar results were obtained from a molar ratio plot.

Calibration, sensitivity and precision

Beer's law is obeyed over the titanium concentration range 0–0.2 μg/ml in the final solution. The molar absorptivity is 1.63×10^5 l.mole^{-1}.cm^{-1}. The complex is formed quickly and its absorbance at 540 nm remains stable for at least 40 min for determination of 3 μg of Ti(IV). The standard deviation is 0.021 μg and the coefficient of variation 0.7%.

The method is much more sensitive than any of the methods using cationic surfactants, but similar in sensitivity to other methods based on fluorones (as shown in Table 2).

Effect of foreign ions

The effect of the most commonly encountered cations and anions was investigated. The tolerance limit was taken as the concentration of a foreign ion which caused an error of not more than 3% in the determination of 3 μg of Ti(IV). Up to at least 0.5 mg of the following did not interfere: zinc, nickel, copper, cadmium, cobalt(III), aluminium, lead. Manganese(VII), chromium(VI), vanadium(V), iron(III), zirconium(IV) and molybdenum(VI) interfere, but the interference of Fe(III), V(V), Cr(VI) and Mn(VII) can be eliminated by reduction with ascorbic acid, and their tolerance levels are then 10.0, 0.03, 0.5 and 0.5 mg respectively. Up to 0.3 mg of zirconium does not interfere if masked with EDTA. Up to 25 μg of Mo(VI) will not interfere if reduced with hydroxylammonium chloride and then masked with EDTA.

Table 2. Comparison of micellar solubilization spectrophotometric reagents for Ti(IV)

Colour system*	Acidity range	λ_{max}, nm	ε, 10^4 *l.mole*$^{-1}$.*cm*$^{-1}$	Ref.
Ti–PF–Triton X-305–OP	pH 1 4–2 2	540	16.3	This paper
Ti–SAF–CTAB	0.1–0 3*N* H_2SO_4	540	16.4	10
Ti–PF–CPB	0.08–0.2*M* HNO_3	535	14.6	11
Ti–PF–CTAB	pH 1 2–2 0	540	12.1	12
Ti–SPF–CPB	pH 1.0	610	12.0	13

*SAF = salicylfluorone; SPF = sulphenylfluorone.

Table 3. Results for determination of Ti(IV) by the proposed and DAM methods

Samples	Proposed method,* %	Relative standard, deviation, %	DAM method, %
Red soil	0.343	0.34	0.349
Black soil	0.316	0.55	0.324
Yellow soil	0.323	0.36	0.337
Alluvial soil 1	0.217	0	0.218
Alluvial soil 2	0.294	0.72	0.310
Violet soil	0.238	1.75	0.239
Rice	2.2×10^{-4}	2.62	2.4×10^{-4}
Wheat	2.4×10^{-4}	2.41	2.5×10^{-4}

*Average of three determinations.

Chloride, nitrate, sulphate, oxalate, phosphate, tartrate, ascorbic acid and hydroxylammonium chloride do not interfere, even in large amounts. Fluoride interferes but can easily be removed by fuming with concentrated sulphuric acid. Up to 2 mg of EDTA can be tolerated. The amount of chloride added in the procedure is enough to mask up to 20 μg bismuth.

Application of method

The method was applied to the determination of Ti(IV) in soil and cereal samples. The samples were freeze dried and ground (soil to 100 μm, cereal to 40 μm particle size) before analysis.

A 0.100-g soil sample was placed in a 100-ml conical beaker, 8 ml of concentrated sulphuric–phosphoric acid mixture (1 + 1) were added, and the beaker was heated on a hot-plate until the evolution of white fumes ceased. The beaker was cooled, 2 ml of concentrated nitric acid were added and heating was continued until the soil digest solution became colourless and dense fumes of sulphur trioxide appeared. After cooling, the residue was taken up with water and transferred into a 100-ml standard flask and the solution made up to volume. Some of the solution was filtered through a dry paper and 1 ml of filtrate was pipetted into a 25-ml standard flask. One drop of 0.1% *p*-nitrophenol solution and 2.2 ml of 4 g of sodium hydroxide and 4 g of sodium chloride in 100 ml of water were added, followed by 1*M* hydrochloric acid until the solution just became colourless. Five drops more of the acid were added, and 2 ml of 5% ascorbic acid solution, followed by 4 ml of 0.01% PF solution and 3 ml of mixed surfactant solution. The mixture was diluted to volume with water and after 7 min the absorbance was measured at 540 nm in a 1-cm cell against a reagent blank.

For analysis of cereals, a 2.0-g sample was placed in a 100-ml conical beaker, 10 ml of nitric–sulphuric–perchloric acid mixture (8:1:1 v/v) were added and the mixture was allowed to stand for at least 12 hr at room temperature (to avoid foaming on subsequent heating). The procedure for the soil digestion method was then applied.

Table 3 gives the results obtained for Ti(IV) in the samples tested. The results are in good agreement with those obtained by the DAM method. The results for the recovery tests were 82–94% for soil and 91–92% for cereal.

REFERENCES

1. I.U.P.A.C., *Spectrophotometric Data*, Butterworths, London, 1963.
2. L. Ya. Polyak, *Zh. Analit. Khim.*, 1962, **17**, 206.
3. M. M. Tananaiko, *Zavodsk. Lab.*, 1962, **28**, 263.
4. Zhan Caiqing, *Chemical World (China)*, 1982, **8**, 237.
5. I. Mori, *Bunseki Kagaku*, 1973, **22**, 1061.
6. S. Sakuraba and M. Kojima, *Nippon Kagaku Kaishi*, 1976, **2**, 345.
7. Hu Keren, *Physical Testing and Chemical Analysis (China)*, 1982, **6**, 7.
8. Y. Shijo and T. Takeuchi, *Bunseki Kagak*, 1967, **16**, 51.
9. M. Yamazaki, I. Mori and T. Enoki, *ibid.*, 1973, **22**, 112.
10. She Hanxi and Wang Zhenqing, *Fenxi Huaxue*, 1981, **6**, 665.
11. Wu Taibai, Chen Xianfu and Chen Xinzhen, *ibid.*, 1983, **7**, 529.
12. Liu Shaopu and Liu Zhongfang, *Chemical World (China)*, 1982, **4**, 107.
13. V. V. Belodsova and R. K. Chernova, *Zh. Analit. Khim.*, 1977, **32**, 1669.

Talanta, Vol 32, No. 6, pp 511–512, 1985
Printed in Great Britain.

0039-9140/85 $3.00 + 0.00

ANNOTATIONS

A NOTE ON THE APPLICATION OF SIGNIFICANCE TESTS BASED ON THE *R*-FACTOR RATIO TO THE SELECTION OF SPECIES IN COMPLEX-FORMATION EQUILIBRIA

MARIUSZ JASKÓLSKI and LECHOSŁAW ŁOMOZIK
Faculty of Chemistry, A. Mickiewicz University, ul. Grunwaldzka 6, 60-780 Poznań, Poland

(*Received* 15 *November* 1984. *Accepted* 24 *January* 1985)

Summary—The use of the significance test based on the *R*-factor ratio for the selection of species in complex formation equilibria studied by least-squares analysis of potentiometric titration data is discussed.

The significance test based on the *R*-factor ratio originally developed for crystallographic applications by Hamilton[1] was first applied to the selection of species in complex-formation equilibria by Vacca, Sabatini and Gristina[2] (hereafter VSG). However, in practical applications, VSG seem to have used the test incorrectly, and this weakened the power of the test and led in certain situations to wrong conclusions. Therefore, we decided to demonstrate the correct method of use of this test and to illustrate its application with a practical example.

The *R*-factor ratio test allows a decision to be made about whether the extension of a model to include additional parameters results in a *significant* improvement in the agreement between the observed and calculated quantities.

When complex-formation equilibria are investigated by least-squares analysis of potentiometric titration data, it is common practice to try various models and to compare the agreements between the experimental observations and the quantities calculated from the various models. A convenient measure of the agreement between the observed data and the values calculated by the least-squares fit is the generalized *R*-factor.[1] If there is no correlation between the data the *R*-factor has the form: $R = [\Sigma w_i(F_i^{obs} - F_i^{calc})^2/\Sigma w_i(F_i^{obs})^2]^{1/2}$, where F stands for the quantities to be compared and w_i is the weight associated with each observation (and equal to the inverse of the variance of the observation). Usually, the model that gives the best fit with the observations (lowest R value) is considered to be correct. However, as pointed out by Hamilton,[1] it is always possible to improve the agreement by including extra parameters in the model. Here, we describe the use of the *R*-factor ratio test to decide whether the inclusion of extra complex species in a model results in *significantly* better agreement between the values calculated from the model and the observations.

Suppose that a complex formation equilibrium can be described by two models: A and B. Let model A consist of m_A and model B of m_B complex species. Let the corresponding generalized *R*-factors be R_A and R_B and the number of observations (titration points) n. Let A be a subset of B, and $m_A < m_B$.

Model A can therefore be said to be *restrained* with respect to model B since some of its formation constants have been set to zero (non-existent species). We want to test the following hypothesis:

H_0: model A is correct.

The hypothesis is linear since it imposes linear relationships on the parameters of the model. The relationships are of the form

$$\beta_k = 0; \quad k = 1,\ldots b \tag{1}$$

with

$$b = m_B - m_A$$

Since the equations (1) are linearly independent, *the dimension of the hypothesis is b*. In practice, b will usually be a small integer. The approach adopted by VSG was incorrect in assuming that $b = m_B$. Moreover, their m_B included the free metal and free ligand concentrations at each titration point, which led to unrealistically large dimensions of the hypotheses.

We want to compare the R factors for the restrained model A, corresponding to the hypothesis, and the unrestrained model B, by calculating

$$\mathscr{R} = R_A/R_B$$

From the table of significance points for the *R*-factor ratio[3] we find a value $\mathscr{R}_{b,(n-m_B),p}$, where p is the level of significance and $(n - m_B)$ is the number of degrees of freedom calculated as (number of observations) – (number of parameters in the unrestrained model B). If

$$\mathscr{R} > \mathscr{R}_{b,(n-m_B),p} \tag{2}$$

we can reject the hypothesis at the p level. This is equivalent to saying that the probability of error if the hypothesis is rejected is less than p. Therefore, p should be as low as possible. In practice, one will *not* reject the H_0 hypothesis if the p level for which (2) is fulfilled is greater than 5%.

The practical example discussed is taken from VSG. For the system copper(II) + *N,N,N′,N′*-tetramethylethylenediamine, six different models were tried. The lowest R factor ($R_0 = 0.00141$) was obtained for a model comprising six complex species. The other models yielded: $R_1 = 0.00242$, $R_2 = 0.00184$, $R_3 = 00200$, $R_4 = 0.00194$, $R_5 = 0.00159$. The corresponding $\mathscr{R}$ values are: $\mathscr{R}_1 = 1.716$, $\mathscr{R}_2 = 1.305$, $\mathscr{R}_3 = 1.418$, $\mathscr{R}_4 = 1.376$, $\mathscr{R}_5 = 1.128$. VSG do not give the compositions of the systems 1–5 explicitly, but we can assume that they were obtained by excluding one or two species from model 0. The number of degrees of freedom given by VSG is 145. If we pessimistically assume that models 1–5 included only one species then the dimension of each of the five hypotheses (H_0: model i is correct; $i = 1,\ldots 5$) is 5. From the R-factor ratio tables we find $\mathscr{R}_{5,145,0\,005} = 1.059$. Therefore, by comparison of the models 1–5 with the unrestrained model 0 we can reject the hypotheses that any of the models 1–5 is correct, at the 0.5% level. Consequently, we are justified in accepting model 0 as correct.

In the example above, VSG used $b = 308$ which resulted in $\mathscr{R}_{308,145,0\,05} = 1.848$ for p as high as 5% and led to the wrong conclusion that there is no significant difference between the six models.

A word of caution may be appropriate. We strongly recommend that model selection should not be based on a single criterion only. In particular, it might be dangerous to try to reach conclusions about the chemical model from the R-factor alone. The R-factor ratio test can be, as illustrated in the example above, a very useful aid in making a decision in ambiguous situations. However, it should always be regarded as an auxiliary tool and used in connection with other tests. We shall discuss the problem of the various possible criteria for model selection in a forthcoming paper.

REFERENCES

1. W. C. Hamilton, *Acta Crystallog.*, 1965, **18,** 502.
2. A Vacca, A. Sabatini and M. A. Gristina, *Coord. Chem. Rev.*, 1972, **8,** 45.
3. *International Tables for X-ray Crystallography*, Vol. IV, pp. 289–292. The Kynoch Press, Birmingham, 1974.

Talanta, Vol. 32, No 6, pp. 513–516, 1985
Printed in Great Britain.

0039-9140/85 $3.00 + 0 00

EFFECT OF ACIDITY ON THE EXTRACTION AND KINETIC STABILITY OF THE COPPER(II)/APCD/IBMK SYSTEM IN STRONGLY ACIDIC MEDIA

MASAHIKO MURAKAMI and TAKEO TAKADA
Department of Chemistry, College of Science, Rikkyo (St. Paul's) University, Nishi-Ikebukuro, Toshima-ku, Tokyo 171, Japan

(*Received* 11 *September* 1984. *Accepted* 11 *January* 1985)

Summary—The extraction of copper(II) from strongly acidic solution (0.01–8*M* hydrochloric acid) with ammonium 1-pyrrolidinecarbodithioate in isobutyl methyl ketone has been investigated. The shaking time needed for quantitative extraction decreases as the acidity is increased. The effect of the mutual solubility of the organic solvent and the aqueous phase is significant when the acidity of the aqueous phase is increased. The acidity of the aqueous phase mainly affects the kinetic stability of the chelate during the shaking period, rather than the decomposition of the chelating agent. The kinetic stability of the chelate apparently depends on the mole ratio of reagent to copper, the half-lives for the chelate extracted from 4*M* hydrochloric acid being 29.0, 40.0 and 85.0 min for reagent: metal mole ratios of 10, 100 and 1000, respectively.

Generally, solvent extraction of metal chelates requires pH adjustment and does not work at very low pH (< 1), because the complexation is largely affected by the hydrogen-ion concentration of the aqueous phase. However, it has been reported[1,2] that Cd, Pb, Ni and Co(II) can be extracted at low pH (< 1) with ammonium 1-pyrrolidinecarbodithioate (APCD) into isobutyl methyl ketone (IBMK). Moreover, the hydrogen-ion concentration was said to affect the decomposition of the chelating agent rather than the formation of the metal chelate. It was also reported that the kinetic stability of the extracts in IBMK decreases as the pH is decreased.

In the preceding paper,[3] we reported on the extraction of Cu(II) from strongly acidic solution (0.01–6*M* hydrochloric acid) into IBMK with APCD. We found that the copper chelate can be extracted quantitatively even from the 6*M* acid if the extraction is done rapidly and the extract is stabilized by washing with water. Although several reports[4–9] have commented on the kinetic stability of metal–APCD chelates in IBMK, they have merely discussed, from a practical point of view, the effect of pH in the stability.

Therefore, we have systematically investigated the kinetic stability of the extracts and determined the optimum conditions for the extraction.

EXPERIMENTAL

Reagents

All chemicals used were of reagent grade. Water was redistilled from all-glass apparatus. Stock 1000-μg/ml copper solution was prepared from 99.99% pure copper metal, then adjusted in acidity to 0.01*M* hydrochloric acid, and diluted 100-fold with water to give the 10-μg/ml working solution.

APCD solution ($1.6 \times 10^{-2}M$) was prepared by dissolving 0.13 g of ammonium 1-pyrrolidinecarbodithioate in 50 ml of water containing 0.5 ml of 0.1*M* ammonia solution, and stored in a refrigerator; it was stable for at least 1 month. All solvents were used without further purification.

Procedure

Transfer 40 ml of hydrochloric acid of the desired concentration, and 5 ml of 10-μg/ml copper solution, to a 100-ml separatory funnel, add 25 ml of IBMK and 5 ml of APCD solution, and mechanically shake the mixture vigorously.

Measure the absorbance of the IBMK phase at 435 nm, in a 10-mm silica cell against IBMK as reference.

RESULTS AND DISCUSSION

Effect of shaking time

The effect of shaking time on the degree of extraction with a 100-fold reagent:copper molar ratio was studied at various acidities. After its separation, the organic phase was washed by shaking for 300 sec with 50 ml of water, then its absorbance was measured at 435 nm. The amount of copper left in the aqueous phase was checked by flame atomic-absorption spectrometry, but none was found.

Figure 1 shows that for each acidity there is an optimum shaking time (all curves have been normalized to make the maximum absorbance 1.0). The small variation between the maximum absorbances is attributed to the effect of increasing acidity on the mutual solubility of the two phases.

The minimum shaking time for quantitative extraction decreases as the acidity is increased: 300 sec for pH 7.5, 120 sec for 0.01*M* acid, 60 sec for 0.1*M* acid and 30 sec for 4*M* acid. These findings disagree with these reported by Irving and Williams,[10] who stated that the rate at which the metal chelates are formed and extracted decreases as the pH is reduced.

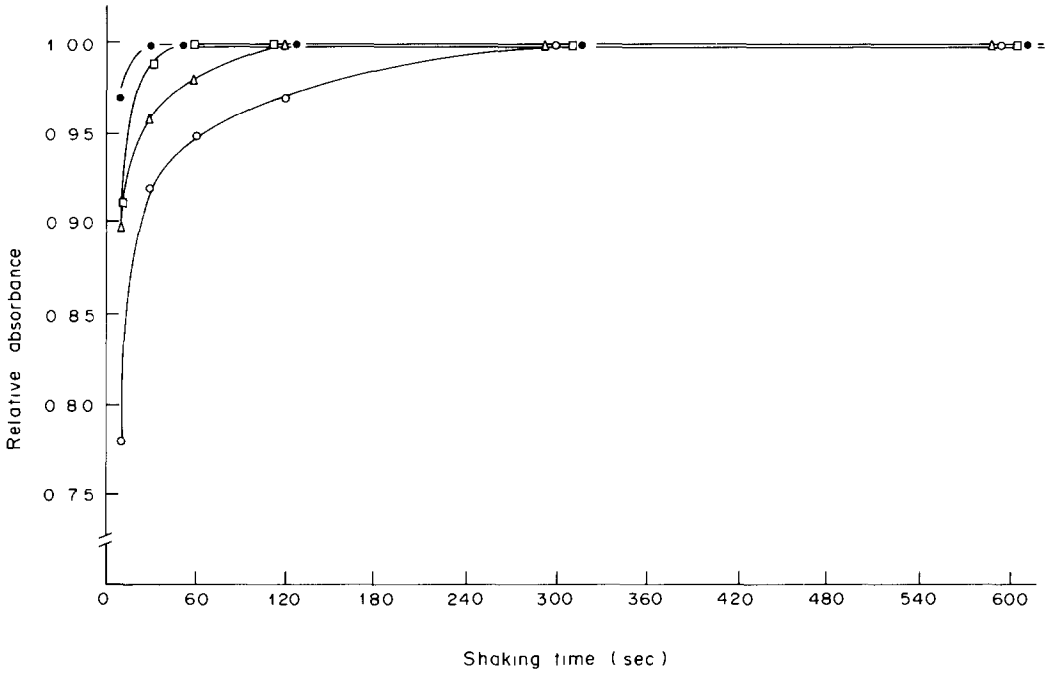

Fig. 1. Effect of shaking time on the extraction of Cu(II) with APCD: pH 7.5 (○), 0.01*M* HCl (△), 0.1 *M* HCl (□), 4*M* HCl (●); aqueous phase 50 ml; organic phase 25 ml; [Cu(II)] $1.5 \times 10^{-5}M$; [APCD] $1.5 \times 10^{-3}M$.

The absorbance was found not to decrease even with a 20-min shaking period under the proposed conditions. Hence a 300-sec shaking period is selected as optimum for extraction from 0.01–4*M* hydrochloric acid.

Effect of APCD concentration

The effect of acidity on the concentration of APCD needed for quantitative extraction was studied. First we studied the decomposition rate of free APCD in 0.01 and 4*M* hydrochloric acid, and found no difference in the half-life for decomposition (26.9 and 25.6 min for 0.01 and 4*M* acid respectively). This agrees with the report by Aspila *et al.*[11] that the decomposition rate of dithiocarbamic acid is not dependent on pH when this is less than 2.

The effect of APCD concentration on the degree of extraction under acidic conditions was then studied. Figure 2 shows the results. If the metal chelate is practically undissociated, the absorbance will increase linearly with APCD concentration until the ligand is just in excess, and then abruptly become constant. This is the case for 0.01*M* hydrochloric medium (Fig. 2a), even though free APCD slowly decomposes at this acidity. Extrapolation of the linear portions of the plot gives an intersection at [APCD]:[Cu] = 2:1, indicating that the predominant complex is $Cu(PCD)_2$.

For 4*M* hydrochloric acid medium, however, the curve is much more rounded in the region of the intersection (Fig. 2b) indicating that there is appre-

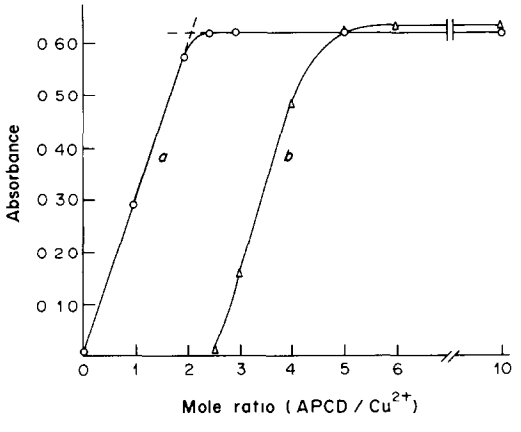

Fig. 2. Effect of APCD concentration on the extraction of Cu(II): (*a*) 0.01*M* HCl, (*b*) 4*M* HCl; aqueous phase 50 ml; organic phase 25 ml; [Cu(II)] $1.5 \times 10^{-5}M$; shaking time 300 sec.

Table 1. APCD/IBMK extraction of Cu(II) from 8*M* HCl

Shaking time, *sec*	A at 435 nm
300	0.142
120	0.179
60	0.264
30	0.721
10	1.124

$[Cu^{2+}]$ $1.5 \times 10^{-5}M$, [APCD] $1.5 \times 10^{-2}M$.

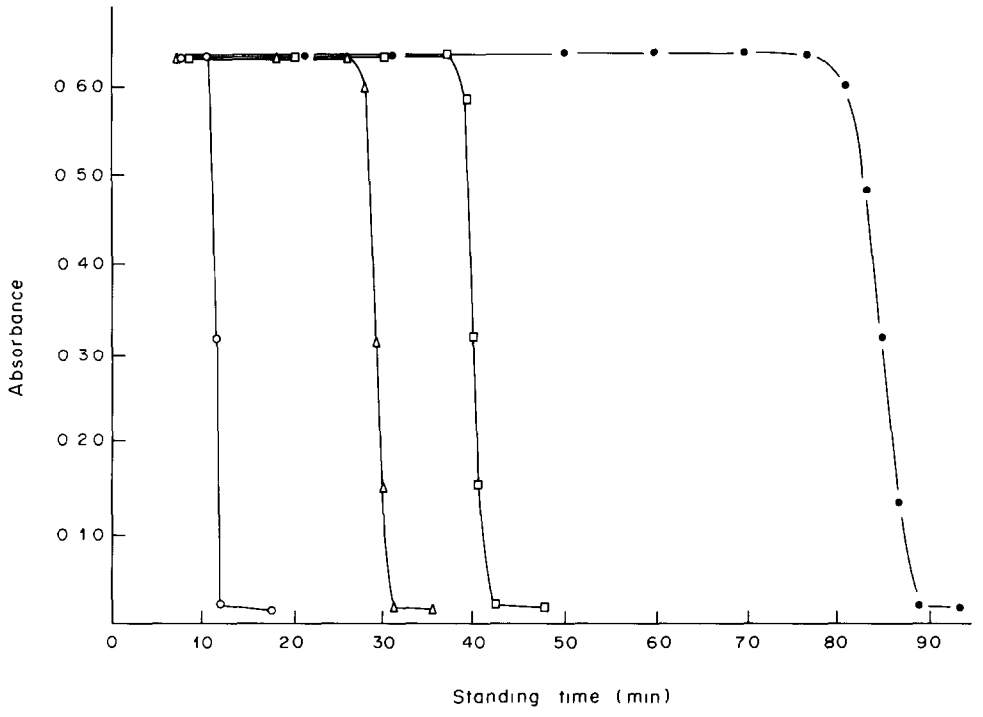

Fig. 3. Kinetic stability of Cu(II)–PCD chelate extracted from 4*M* HCl: [APCD] $7.5 \times 10^{-5}M$ (○), $1.5 \times 10^{-4}M$ (△), $1.5 \times 10^{-3}M$ (□), $1.5 \times 10^{-2}M$ (●); [Cu(II)] $1.5 \times 10^{-5}M$; shaking time 300 sec.

ciable decomposition of the complex during the shaking period. However, extraction is complete at mole ratios of ligand to metal 6:1, presumably because the excess of ligand is large enough to restore the complexation equilibrium in spite of the decomposition of APCD in the complex.

In the earlier work,[3] we observed that the copper chelate was not extracted from 8*M* hydrochloric acid even with 10 times as much APCD as copper, because of decomposition of the chelate during the 60-sec shaking period. We have therefore attempted to extract the copper chelate from 8*M* hydrochloric acid with a very large excess of reagent (1000-fold ratio to copper). The shaking time was varied from 10 to 300 sec, and the copper remaining in the aqueous phase was determined by flame atomic-absorption spectrophotometry. Table 1 shows that the absorbance decreases with increase in shaking time, which suggests that the decomposition of the chelate occurs during the shaking period. Moreover, although extraction of the chelate from 8*M* hydrochloric acid is incomplete (considerable amounts of copper are found in the aqueous phase), the absorbance of the organic phase is much higher (1.124) than that for extraction from 4*M* hydrochloric acid (0.635) for the same amount of copper. This is due to the remarkable decrease in volume of the organic phase. Irving and Rossotti[12] reported that the solubility of IBMK in hydrochloric acid increases considerably as the acidity is increased.

Hence IBMK is unsuitable for extraction from strongly acidic media, such as 8*M* hydrochloric acid.

Table 2. Half-life ($t_{1/2}$) for Cu(II)–PCD chelate extracted from 4*M* HCl

[APCD] *M*	$t_{1/2}$		
	Untreated	With wash	With filtration
7.5×10^{-5}	11.5 min	—	—
1.5×10^{-4}	29.0 min	88.0 min	44.0 min
1.5×10^{-3}	40.0 min	>24 hr	>24 hr
1.5×10^{-2}	85.0 min	—	—

[Cu^{2+}] $1.5 \times 10^{-5}M$, shaking time 300 sec.

Kinetic stability of extract

The kinetic stability of the chelate extracted from 4*M* hydrochloric acid into IBMK was studied as a function of reagent concentration, with various treatments of the extract, *viz.* with or without washing with water, and filtration of the organic phase through a dry filter paper after the extraction. The stability was determined by measuring the change of absorbance at 435 nm with time, the samples being kept in the spectrophotometer throughout. The timing was started when the reagent was added to the aqueous phase.

The variation of absorbance with time, when the extract is not washed with water, is shown in Fig. 3. Characteristically the absorbance is constant for a certain time, and then suddenly drops. Table 2 gives the time ($t_{1/2}$) needed for the absorbance of the extract

to decrease to half its original value, under various conditions; $t_{1/2}$ was found to depend on the concentration of the reagent added and on the treatment of the extract. Like washing,[3] filtration stabilizes the extract. When $1.5 \times 10^{-3}M$ APCD (100-fold ratio to copper) was used, the extract exhibited excellent stability (Table 2).

It is considered that decomposition of the extract is suppressed by removal of the free acid remaining in the separated IBMK, by means of washing or filtration (the separated IBMK phase tends to be turbid, containing fine droplets of the aqueous phase).

When the copper(II)–APCD chelate is extracted from strongly acidic solution, the kinetic stability of the chelate is a most important factor, and several of the conditions to be used should be selected according to their influence on the stability. The following conditions are recommended for extraction of the copper chelate from 0.01–4*M* hydrochloric acid: a large excess of reagent (>100-fold molar ratio to copper), 180–300 sec shaking time, rapid phase separation, and washing of the organic phase with water.

The kinetic stability of the copper chelate in IBMK after extraction from a strongly acidic aqueous phase is highly dependent on the concentration of APCD added, so a direct comparison of results reported by various authors is useless unless the concentrations of chelating agent and copper used are the same for the methods compared.

REFERENCES

1. R. J. Everson and H. E. Parker, *Anal. Chem.*, 1974, **46,** 1966.
2. I. Dellien and L. Persson, *Talanta*, 1979, **26,** 1101.
3. T. Takada, *ibid.*, 1982, **29,** 799.
4. R. E. Mansell, *At. Absorp. Newsl.*, 1965, **4,** 276
5. E. A. Jenne and J. W. Ball, *ibid.*, 1972, **11,** 90.
6. R. F. Roberts, *Anal. Chem.*, 1977, **49,** 186.
7. K. S. Tung and D. H. Karweik, *ibid.*, 1980, **52,** 1387.
8. K. S. Subramanian and J. C. Meranger, *Analyst*, 1980, **105,** 620.
9. D. M. Jonas and L. R. Parker, Jr., *Anal. Chim. Acta*, 1982, **134,** 389.
10. H. Irving and R. J. P. Williams, *J. Chem. Soc.*, 1949, 1841.
11. K. I. Aspila, V. S. Sastri and C. L. Chakrabarti, *Talanta* 1969, **16,** 1099.
12. H. Irving and F. J. C. Rossotti, *J. Chem. Soc.*, 1955, 1946.

Talanta, Vol 32, No 6, pp. 517–519, 1985
Printed in Great Britain.

0039-9140/85 $3.00 + 0.00

BORATE–POLYOL COMPLEXES IN AQUEOUS SOLUTION

DETERMINATION OF ENTHALPIES BY THERMOMETRIC TITRIMETRY

ROBERTO ARUGA
Institute of Analytical Chemistry, University of Turin, via Giuria 5, 10125 Turin, Italy

(*Received* 19 *December* 1984. *Accepted* 5 *February* 1985)

Summary—Enthalpies for the reaction of borate with 1,2-ethanediol, 1,2-propanediol, 1,2,3-propanetriol and D-mannitol have been determined by thermometric titrimetry. From these enthalpies and equilibrium constants taken from the literature, corresponding entropies have been calculated. The data refer to aqueous solutions at 25° and $I = 1.0M$ ($NaNO_3$). The results indicate reasons for the differences in the stabilities of the complexes.

The remarkable complex-forming ability of the borate ion with polyhydroxy compounds (polyols) in aqueous solution is well known. Biot,[1] as early as 1842, reported that a solution of boric acid became acid to litmus upon addition of sugars. Thomson[2] found that boric acid could be determined by titration in the presence of various polyhydroxy compounds, with phenolphthalein as indicator. More recently, these reactions have been shown to be not only of analytical but also of biological interest, as several compounds of biological importance, such as vitamins and coenzymes, can react with borate in the same manner.

The stoichiometry and stability of these complexes have been studied by various workers,[3–7] but values for the enthalpies and entropies of formation are both scarce and inconsistent. In fact only one calorimetric enthalpy value is available, which refers to the borate complex with mannitol.[7] It must be noted, in this connection, that there is serious disagreement between the -18.62 kJ/mole for the first step of reaction with mannitol, obtained by calorimetry, and the -33.68 kJ/mole obtained from values of the equilibrium constant at different temperatures.[5] The two methods give such inconsistent values for the entropy that these differ even in sign: $\Delta S_2^\circ = -27.2$ J . mole^{-1} . K^{-1} (ref. 7) and $+36.0$ J . mole^{-1} . K^{-1} (ref. 5).

Taking into account these observations, and also considering the value of thermodynamic quantities in elucidating the structures of the complexes formed, it was thought of interest in the present work to determine by thermometric titrimetry the enthalpies, and hence entropies, of the reaction of borate with 1,2-ethanediol (ethylene glycol), 1,2-propanediol (1,2-propylene glycol), 1,2,3-propanetriol (glycerol) and D-mannitol.

EXPERIMENTAL

Reagents

Analytical grade reagents were always used (Erba RPE), *viz.* boric acid (>99.8% pure); ethylene glycol and 1,2-propylene glycol (>99.5%); glycerol and D-mannitol (>99%). All solutions were prepared immediately before use. The background electrolyte was sodium nitrate.

Equipment

Calorimetric measurements were made at 25° with an LKB 8700-2 Precision Calorimetry System and an LKB 8726-1 100-ml titration vessel, provided with a standard resistor (50 Ω) and a thermistor (2000 Ω). The accuracy of the instrument was checked by measuring the molar enthalpy change of the reaction between tris(hydroxymethyl)methylamine and hydrochloric acid in aqueous solution. Fuller details of the instrument calibration have been reported.[8] The temperature of the titrant was kept at that of the calorimeter by immersing (for at least 12 hr before the measurement) the Teflon titrant reservoir in the thermostatic bath containing the calorimetric cell. The calorimeter was also equipped with a Radiometer ABU 12b autoburette for the addition of titrant. The calorimetric experiments were performed in a room kept at a temperature constant within ±0.3%.

Procedure

At least three series of measurements were made for each polyol–borate system, each series being performed in the following manner. Successive portions of 2.507 ± 0.002 ml of sodium borate solution were added to 88.00 ml of polyol solution in the calorimetric cell, and the heat liberated on each addition was measured (for the borate and polyol concentrations, see Table 1). The pH of all solutions was brought to 11.0 ± 0.2 by addition of sodium hydroxide before each measurement, and the ionic strength adjusted to $1.0M$ by addition of sodium nitrate. The corresponding heat of dilution was measured by adding the same amounts of the sodium borate solution to 88.00 ml of $1.0M$ sodium nitrate at pH 11.0, without any polyol. From these experiments the following conclusions can be drawn. (*a*) There is negligible association between the $B(OH)_4^-$ ion (which is the reacting species) and the proton, since the pK_a of boric acid is so high (8.69 at $I = 1.0M$).[9] (*b*) There is negligible dissociation of the polyols, since the pK_a values are all above 14.[10] (*c*) Complex species containing more than two molecules of polyol per borate ion are not present: their absence has been demonstrated[6] for polyol:borate ratios up to 200:1. (*d*) The contribution to the measured enthalpies from dissociation of polyborate species was negligible: since the borate concentration was lower than $0.025M$ at the end of the mixing process, it must have reacted[5] in the monomeric form and,

Table 1. Experimental data for the mixing of aqueous solutions of polyols (L) and sodium borate at 25°*

Ligand	C_L, M	ΣV_T, *ml*	$[BL^-]$, 10^{-3}M	$[BL_2^-]$, 10^{-3}M	[L], M	ΣQ_c, *J*
Ethylene glycol	2.000	2.507	4.73	0.755	1.938	11.25
		5.014	9.18	1.42	1.880	22.0
		7.521	13.4	2.01	1.825	32.2
		10.028	17.3	2.53	1.773	41.8
1,2-Propylene glycol	1.000	2.507	3.87	1.67	0.965	10.6
		5.014	7.54	3.15	0.932	20.6
		7.521	11.0	4.45	0.901	30.2
		10.028	14.3	5.60	0.872	39.5
Glycerol	0.205	2.507	4.47	1.29	0.192	8.76
		5.014	8.71	2.36	0.180	16.8
		7.521	12.7	3.23	0.170	24.5
		10.028	16.5	3.94	0.160	31.65
D-Mannitol	0.060	2.507	2.74	4.13	0.047	21.0
		5.014	6.18	7.14	0.036	39.9
		7.521	10.4	8.93	0.027	56.6
		10.028	15.3	9.51	0.019	69.8

Initial concentration of borate in the titrant solution: 0.250*M*.

moreover, the heat of dissociation of any polyborates which may be present in the initial solution is counterbalanced by an equal heat effect during the dilution experiment, so that it is eliminated in the calculation of the corrected heat (see below). (*e*) Thermal effects from the neutralization reaction between H^+ and OH^- and for changes in the optical rotatory properties of certain polyols in the presence of borate are negligible; in particular the latter process is extremely slow if compared with the time required for a calorimetric measurement.[7,11,12]

Treatment of the experimental data

Some experimental data are collected, as an example, in Table 1: the initial concentration of polyol in the calorimetric vessel (C_L); the cumulative volume of titrant added to the calorimetric vessel (ΣV_T); the concentrations of the complex species and of free polyol ($[BL^-]$, $[BL_2^-]$, [L]) after each addition of titrant; the mean cumulative heat, corrected for dilution (ΣQ_c).

Molar enthalpies of association were determined from the experimental heats (ΣQ_c) and the concentrations of the complex species: the latter were calculated from values of the corresponding stability constants determined potentiometrically by Paàl[6] (see Table 2) under the conditions of temperature and ionic strength used in the present work. No contraction in volume was found (in the limits of the instrumentation used) on mixing the reagents. The ΔH° values, with the corresponding standard deviations, were calculated by two different methods: (*a*) the numerical method of minimizing the sum of the squares of the deviations for each measurement;[13] (*b*) a graphical method derived from the equations of Leden and Fronaeus.[14] These two methods gave results in good accordance. In order to check the enthalpy values, the experimental heats were recalculated by using the ΔH° values obtained. Entropy values were calculated by means of the equation $\Delta G^\circ = \Delta H^\circ - T\Delta S^\circ$.

RESULTS AND DISCUSSION

The molar thermodynamic quantities for the first two steps of complex formation of borate with polyols are collected in Table 2. For ethylene glycol, values for only the first step are listed. In this case, in spite of the excess of polyol, the concentration of the BL_2^- species was too low to give reliable ΔH° values for the second step.

The present enthalpy and entropy values are in only partial agreement with those reported previously.[5] For mannitol, the entropies are in complete disagreement: -54 and $+36$ J.mole^{-1} K^{-1} in the cited paper,[5] and -7.9 and -50 from the present work, for the first and second steps, respectively. In any case, poor agreement between calorimetric values and those obtained from variation of an equilibrium constant with temperature[5] is fairly frequent. In general, calorimetric values are considered more reliable.[15] However, the present enthalpy data for mannitol are in fairly good accordance with those

Table 2. Thermodynamic parameters for complexation reactions of polyols (L) with the borate ion (B^-): $BL_{j-1}^- + L \rightarrow BL_j^-$, in aqueous solution at 25° and $I = 1.0M$*

L	*j*	log K_j†	ΔG_j°	ΔH_j°	ΔS_j°	$\Delta H_{j(\text{non})}$	$\Delta H_{j(\text{el})}$
Ethylene glycol	1	0.23 ± 0.01	-1.30 ± 0.08	-5.8 ± 0.5	-15 ± 2	-7.4	1.6
1,2-Propylene glycol	1	0.46 ± 0.01	-2.64 ± 0.08	-9.3 ± 0.6	-22 ± 2	-10.2	0.9
	2	-0.35 ± 0.04	2.0 ± 0.2	-38.9 ± 1.7	-138 ± 4	-30.1	-8.8
Glycerol	1	1.30 ± 0.02	-7.41 ± 0.12	-10.2 ± 0.5	-9.6 ± 1.6	-12.3	2.1
	2	0.18 ± 0.05	-1.0 ± 0.3	-28.9 ± 1.7	-92 ± 4	-23.9	-5.0
D-Mannitol	1	3.04 ± 0.08	-17.3 ± 0.5	-19.7 ± 0.2	-7.9 ± 1.6	$-21\,9$	2.2
	2	1.50 ± 0.09	-8.5 ± 0.5	-23.4 ± 0.5	-50 ± 2	-22.0	-1.4

*Gibbs function and enthalpies are expressed in kJ/mole, ΔS° in J.mole^{-1}.K^{-1}.
†See reference 6. The uncertainty given in each case is the estimated standard deviation.

obtained by Evans *et al.* calorimetrically:[7] -18.62 ± 0.25 and -19.9 ± 0.5 kJ/mole for ΔH_1° and ΔH_2° respectively, in comparison with -19.75 ± 0.25 and -23.4 ± 0.5 (Table 2). It is interesting to note that the standard deviations indicate that the data obtained by the two different calorimetric methods (*i.e.*, thermometric titrimetry in the present case, and continuous flow calorimetry[7]), have similar reproducibilities.

Examination of the results in Table 2 for the first step of reaction shows that the ΔG_1° values, in both sign and relative magnitude, are determined by ΔH_1°. The ΔS_1° values, on the other hand, are unfavourable to the complexation process, and are not very different from zero. These facts seem to indicate a greater influence of direct solute–solute interactions rather than external factors on the formation of the 1:1 complexes. In order to verify this conclusion, and for a better interpretation of the enthalpy values, the latter have been divided into electrostatic ($\Delta H_{(el)}$) and non-electrostatic ($\Delta H_{(non)}$) parts, following the calculation method proposed previously.[16,17] The electrostatic contribution to the enthalpy is a measure of long-range electrostatic interactions, depending on the dielectric constant of the medium; the non-electrostatic part is a measure of covalent, short-range interactions. The values obtained for $\Delta H_{(non)}$ and $\Delta H_{(el)}$ are listed in Table 2. They confirm that electrostatic contributions are almost non-existent, and that the direct covalent borate–polyol interactions are the controlling factors affecting ΔH°, and consequently ΔG°. Moreover, ΔH_1° and $\Delta H_{1(non)}$ become more favourable from ethylene glycol to mannitol; this seems to indicate the presence of progressively stronger solute–solute bonds. In fact, in propylene glycol, besides the two hydroxy-groups of ethylene glycol, a methyl group is present, which enhances the bond-forming properties with borate by inductive effects. In glycerol a third hydroxy-group is present, which can form hydrogen bonds with borate. Finally, the possible formation of a third C—O—B bond has been suggested for mannitol.[6]

The thermodynamic parameters for the second reaction step are remarkably different from those of the first step. ΔH_2° (again mainly due to $\Delta H_{(non)}$) is more favourable than ΔH_1°; ΔS_2°, on the other hand, is strongly negative. These values confirm, at least partially, the hypothesis of Paàl,[6] who suggested a much lower degree of hydration of borate in the 1:1 glycol–borate complex than in the uncomplexed form. Consequently, fewer borate–solvent bond ruptures would take place when the second molecule of polyol enters the complex. More particularly, the smallest difference between $\log K_1$ and $\log K_2$ is found for propylene glycol, together with the greatest difference between ΔH_1° and ΔH_2° and between ΔS_1° and ΔS_2°. This seems to confirm the hypothesis that the greatest desolvation of borate is caused by the methyl group of propylene glycol, as a consequence of its strong shielding properties.[6] In contrast, the greatest difference between $\log K_1$ and $\log K_2$ is found for mannitol, for which ΔH_2° is also the most unfavourable and very similar to ΔH_1°. This is in accordance with a possible formation, by the first polyol molecule, of a third C—O—B bond, which would hinder the binding with the second molecule of mannitol. It must be noted, in this connection, that in the previously mentioned calorimetric work on mannitol–borate complexation[7] the constancy of the corresponding ΔH_1° and ΔH_2° values was discussed. This constancy was justified by means of the general hypothesis of Poulsen and Bjerrum, according to which, for reactions with electrically neutral ligands, heats of successive steps will be approximately constant, variation in stability being mainly determined by the entropy changes. The data in Table 2, on the contrary, indicate that constancy of the ΔH° values for mannitol is peculiar to this compound and is not typical of the enthalpy data for the other polyols.

REFERENCES

1. M. Biot, *Compt. Rend.*, 1842, **14,** 49.
2. R. T. Thomson, *J. Soc. Chem. Ind.*, 1893, **12,** 432.
3. A. Deutsch and S. Osoling, *J. Am. Chem. Soc.*, 1949, **71,** 1637.
4. G. L. Roy, A. L. Laferriere and J. O. Edwards, *J. Inorg. Nucl. Chem.*, 1957, **4,** 106.
5. J. M. Conner and V. C. Bulgrın, *ibid.*, 1967, **29,** 1953.
6. T. Paàl, *Acta Chim. Acad. Sci. Hung.*, 1976, **91,** 393.
7. W. J. Evans, V. L. Frampton and A. D. French, *J. Phys. Chem.*, 1977, **81,** 1810.
8. R. Aruga, *Aust. J. Chem.*, 1981, **34,** 501.
9. M. Lourijsen-Teyssèdre, *Bull. Soc. Chim. France*, 1955, 1111.
10. E. Bottari, P. Ippoliti and R. Porto, *Ann. Chim. (Rome)*, 1983, **73,** 473.
11. L. Vignon, *Ann. Chim. Phys.*, 1874, **2,** 440.
12. *The Merck Index*, 10th Ed., p. 818. Merck, Rahway, N.J., 1983.
13. L. G. Sillén, *Acta Chem. Scand.*, 1962, **16,** 159.
14. R. Aruga, *J. Inorg. Nucl. Chem.*, 1977, **39,** 2159.
15. G. H. Nancollas, *Interactions in Electrolyte Solutions*, Elsevier, Amsterdam, 1966.
16. G. Degischer and G. H. Nancollas, *J. Chem. Soc.* A, 1970, 1125.
17. S. Murakami and T. Yoshıno, *J. Inorg. Nucl. Chem.*, 1981, **43,** 2065.

Talanta, Vol. 32, No. 7, pp. 521–524, 1985
Printed in Great Britain

0039-9140/85 $3.00 + 0.00
Pergamon Press Ltd

DETERMINATION OF BERYLLIUM IN Pt–Be ALLOY BY ATOMIC-ABSORPTION SPECTROMETRY AFTER ION-EXCHANGE SEPARATION

KRYSTYNA BRAJTER and KRZYSZTOF KLEJNY
Department of Chemistry, University of Warsaw, 02093 Warsaw, Poland

(*Received* 17 *January* 1984. *Revised* 21 *January* 1985. *Accepted* 9 *February* 1985)

Summary—Traces of beryllium in platinum have been determined by graphite-furnace atomic-absorption spectrometry, the graphite furnace being coated with lanthanum or titanium carbide. The coating improves the reproducibility, sensitivity and detection limit. Platinum interferes in the beryllium determination, and an ion-exchange separation is used in the determination of beryllium in Pt–Be alloy.

The determination of beryllium by atomic-absorption spectrometry (AAS) is difficult, whether flame or electrothermal atomization is used.[1–11] There are numerous interferences in the flame atomization methods, even when the high-temperature reducing nitrous oxide–acetylene flame is used,[4] and because of the formation of beryllium carbide the graphite furnace gives rather poor reproducibility and sensitivity.[7–11] According to the literature,[7,8,10,11] however, the reproducibility, sensitivity and determination limit may be considerably improved by coating the graphite furnace with a carbide or with pyrolytic graphite.

When we were asked to determine beryllium in Pt–Be alloy we decided to use AAS with electrothermal atomization (ETA) in graphite tubes coated with lanthanum or titanium carbide. We found there was spectral interference from platinum, and that the deuterium background corrector could not compensate for the high background absorption due to the platinum, so to avoid this matrix effect, we used ion-exchange to separate the beryllium.

EXPERIMENTAL

Instrumentation

Perkin-Elmer models 300 and 403 atomic-absorption spectrophotometers, equipped with the HGA model 72 and 74 graphite-furnace atomizers respectively, and a Beckman model 1272D atomic-absorption spectrophotometer equipped with a Unilam 1288 burner and a Pye-Unicam GRM 1268 graphite-furnace atomizer were used. The operating conditions are given in Tables 1 and 2. The Beckman instrument was also used for flame AAS determination of beryllium (wavelength 234 mm, band-pass 0.14 nm, lamp current 12 mA).

Carbide coating. A lanthanum chloride solution (La 1 mg/ml, 100 μl) or titanium sulphate solution (Ti 1 mg/ml, 200 μl) was injected into the tube and a heating programme was applied. The procedure was repeated two or three times, depending on the apparatus, for the lanthanum coating, and twice for titanium. For lanthanum the programme was heating at 100° for 100 sec, at 1100° for 30 sec and at maximum temperature for 10 sec. For titanium, the heating sequence was 100° for 120 sec, 1650° for 180 sec, 2850° for 20 sec.

Reagents

Standard beryllium solution. Beryllium (spectral grade, 0.5086 g) was dissolved in 2*M* hydrochloric acid and the solution was diluted to 250 ml. This solution was further diluted as required.

Standard platinum solution. Prepared by diluting a solution of H_2PtCl_6, standardized gravimetrically by precipitation of the ammonium salt.

Ion-exchange columns

The columns were made in tubes 25 cm long, 8 or 5 mm in bore, with a stopcock at the end. They were packed with Dowex 50W × 8, 20–50 mesh, sodium form.

Ion-exchange separation of platinum from beryllium

Static studies. Dowex 50W × 8 (sodium form, 400 mg) was mixed with 20 ml of beryllium solution containing 326 μg of Be(II) and the pH was adjusted with sodium hydroxide solution. The mixture was shaken for 8 hr, then the concentration of beryllium was measured by graphite-furnace AAS. The results are given in Table 3.

Column studies. To establish optimum conditions for the column separation of beryllium from platinum, an investigation was made of the effects of the amount of resin used. Recovery of 8 μg of Be was 99.2, 100.0, 99.9 and 93.5% complete, with use of 200, 400, 800 and 1200 mg of resin respectively. The efficiency of hydrochloric, nitric and citric acids as eluents was investigated, and 4–6*M* hydrochloric acid was chosen as the most efficient.

Procedure

A 5-ml portion of solution containing 2.5×10^{-4} mg of Be(II) and 7.14 mg of Pt(IV), adjusted to pH 3.5, was introduced into the Dowex column (bed height 3.5 cm, 400 mg of resin) and the platinum (as $PtCl_6^{2-}$) was washed through with 25 ml of water and collected in a 50-ml standard flask. The beryllium was eluted with 25 ml of 6*M* hydrochloric acid, into a 50-ml standard flask. Both eluates were diluted to the mark with water, and analysed by AAS according to the conditions given in Table 1. Blanks were run and appropriate corrections applied. The concentrations of Pt(IV) and Be(II) were obtained from calibration graphs.

Analysis of Pt–Be alloy. The alloy sample (0.741 g) was dissolved by heating with 20 ml of *aqua regia*. The solution was evaporated to dryness, a few ml of concentrated hydrochloric acid were added, and the evaporation was repeated, almost to dryness; this was repeated twice. The residue was dissolved in dilute hydrochloric acid and the solution was transferred into a 100-ml standard flask, and made up to volume. A 5-ml aliquot was adjusted to pH 3.5 and introduced into the Dowex column (sodium form).

Table 1. Operating conditions for determination of beryllium by flameless atomic-absorption spectrometry

	Perkin-Elmer 300/HGA 72	Perkin-Elmer 403/HGA 74	Beckman 1272/GRM 1268
Wavelength, *nm*	234.9	234.9	234.84
Band-pass, *nm*	0.7	0.7	0.6
Drying temperature, °C	100	100	120
Drying time, *sec*	25	25	30
Charring temperature, °C	1200	1200	1100
Charring time, *sec*	30	30	30
Atomization temperature, °C	maximum	maximum (2650)	2850
Atomization time, *sec*	12	12	20
Cleaning temperature, °C			2850
Cleaning time, *sec*			3
Injection volume, *µl*	20	20	20
Argon flow-rate, *l./min*	standard	50	standard

Platinum was removed from the column by washing with 25 ml of water. Beryllium was eluted with 25 ml of 6*M* hydrochloric acid, the eluate being collected in a 50-ml standard flask and diluted to volume. The flow-rate was 0.5 ml/min. Beryllium was determined by AAS according to the conditions given in Table 1, by use of the graphite furnace coated with titanium carbide; the results were corrected for the blank.

RESULTS AND DISCUSSION

As shown in Fig. 1 the calibration graphs are linear only over a certain concentration range, and above a certain beryllium concentration there appears to be a memory effect when the lanthanum coating is used, but not with the titanium coating. The memory effect is due to incomplete volatilization of Be in the firing, as shown by an absorption peak appearing during the cleaning step. The titanium carbide coating enhanced the absorbance from 0.1 to 0.25 for 0.2 ng of beryllium when the Pye-Unicam GRM 1268 furnace was used. Use of more than 400 µg of titanium for the coating gave slightly lower results.

A char temperature of 1200° applied for 30 sec was chosen for use with the Perkin-Elmer spectrometers and 1100° for 30 sec for the Beckman instrument (Fig. 2). Lower[8] and higher[12] temperatures have been recommended in the literature.

Table 2. Operating conditions for determination of platinum by flameless atomic-absorption spectrometry

Wavelength, *nm*	266; 273.4
Band-bass, *nm*	0.7; 0.2
Drying temperature, °C	103
Drying time, *sec*	30
Charring temperature, °C	1370
Charring time, *sec*	35
Atomization temperature, °C	2650
Atomization time, *sec*	30
Injection volume, *µl*	20
Argon flow-rate, *l./min*	standard

Table 3. Retention of beryllium on Dowex 50W × 8 as a function of pH

pH	Be retained on resin,* %	Be retained on column,† %
0.9	76.6	77.5
2.0	98.8	98.8
3.5	100.0	100.0
5.6§	99.7	99.9
11.9	77.9	85.0

*Batch method, 326 µg taken; after equilibration the solution was diluted, acidified to pH < 4 and analysed by AAS.

†Column method, 16.28 mg taken; the column was washed with 100 ml of water and the total effluent was diluted to 200 ml, acidified to pH < 4 and analysed by AAS.

§Precipitate observed.

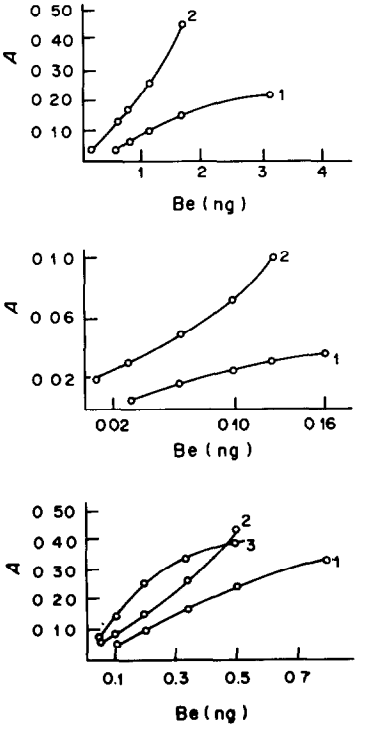

Fig. 1. Beryllium calibration graphs, with furnace (1) untreated, (2) coated with lanthanum carbide, (3) coated with titanium carbide; (a) HGA 72, 300 µg of La; (b) HGA 74, 200 µg of La; (c) Beckman spectrometer and GRM 1268, 300 µg of La or 400 µg of Ti.

With the Perkin-Elmer spectrometers the maximum attainable temperature was used as the atomization temperature, in agreement with the literature recommendations, but with the Beckman spectrometer an atomization temperature of 2750° (which is below the maximum) was chosen, since it gave a more linear calibration curve with the titanium coating (Fig. 3).

The conditions used for platinum determination were those established earlier.[12] Platinum was found to have a marked effect on the beryllium signal (Fig. 4), and this could not be eliminated by use of the deuterium-lamp background-compensator. It therefore seemed necessary to separate the traces of beryllium to avoid interference from the platinum matrix, and ion-exchange was chosen for the purpose.

The retention of beryllium on Dowex 50W × 8 was found to be maximal at pH ~ 3–4 (Table 3). The beryllium could be eluted from the column with 4–6*M* hydrochloric acid. Other eluents were also investigated; nitric acid interferes in the beryllium determination by AAS, and citric acid appears to be less efficient than hydrochloric.

To shorten the analysis time the conditions for column separation were investigated (as described above). As a result, a very short resin bed (3.5 cm long, 400 mg of resin) was used. The optimum flow-rate appears to be 0.5 ml/min. At higher flow-rates 25 ml of 4–6*M* hydrochloric acid will not be enough to elute the beryllium quantitatively. The optimum conditions for retention and elution of beryllium were adopted for the separation of platinum and beryllium and found to give good results (Table 4). The method was applied to the Be–Pt alloy which was the reason for the investigation and gave 0.0018 ± 0.00015% (mean and 95% confidence limits) for four AAS measurements in each of six separate determinations.

Our investigation confirmed that the sensitivity, reproducibility and detection limit of the beryllium

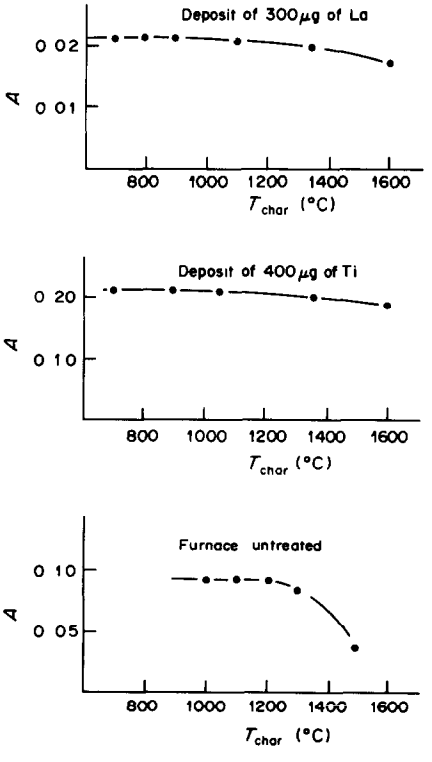

Fig. 2. Absorbance of Be as a function of charring temperature (Beckman spectrometer, $T_{atom} = 2850°C$, $c_{Be} = 0.01$ ppm).

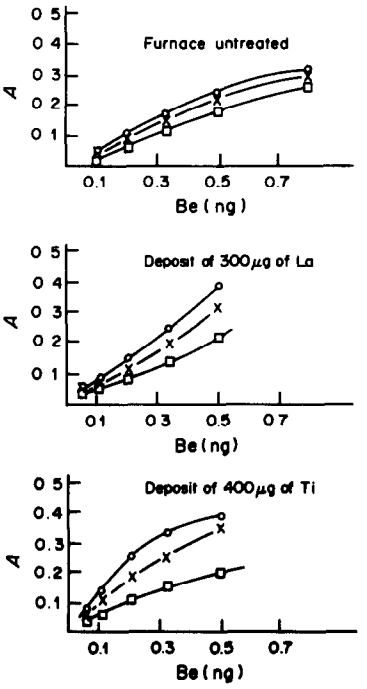

Fig. 3. Absorbance of Be as a function of atomization temperature with furnace (a) untreated, (b) treated with lanthanum, (c) treated with titanium; Beckman spectrometer. □–□–□– 2600°C; ×–×–×– 2750°C; ○–○–○– 2850°C.

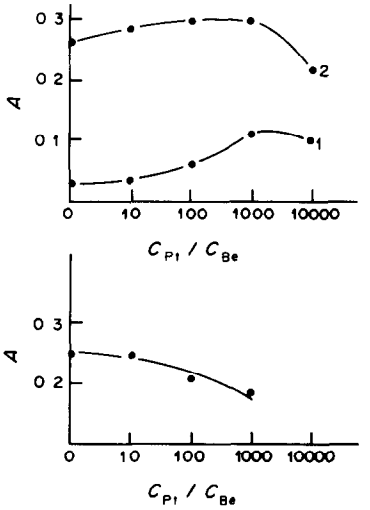

Fig. 4. Effect of Pt on Be determination. (a) with furnace untreated (curve 1) and treated with lanthanum (curve 2); (b) by flame AAS.

Table 4. Separation of beryllium from platinum on Dowex 50W × 8 (Na^+)

	Taken, *mg*		Found*, *mg*	
	Pt	Be	Pt	Be
1	3.57	0.025	$3.57 \pm 1.6 \times 10^{-2}$	$0.025 \pm 1.6 \times 10^{-3}$
2			$3.60 \pm 3.7 \times 10^{-2}$	$0.024 \pm 1.0 \times 10^{-3}$
3			$3.55 \pm 3.3 \times 10^{-2}$	$0.024 \pm 1.0 \times 10^{-3}$
4			$3.59 \pm 1.6 \times 10^{-2}$	$0.026 \pm 1.6 \times 10^{-3}$
1	7.14	0.25	$7.15 \pm 1.0 \times 10^{-2}$	$0.26 \pm 1.6 \times 10^{-2}$
2			$7.14 \pm 1.0 \times 10^{-2}$	$0.24 \pm 1.0 \times 10^{-2}$
3			$7.11 \pm 1.6 \times 10^{-2}$	$0.25 \pm 1.6 \times 10^{-2}$
4			$7.15 \pm 1.6 \times 10^{-2}$	$0.025 \pm 1.6 \times 10^{-2}$

*Each result is the mean and range (95% confidence limits) of four determinations.

For the first group of experiments 20 ml of test solution were passed through 2.0 g of resin and the column was washed with 50 ml of water to elute Pt. The Pt eluate was diluted to 250 ml for analysis. Be was eluted with 25 ml of 4*M* HCl and the eluate diluted to 50 ml for analysis. For the second group, 5 ml of test solution was passed through 400 mg of resin, and the Pt was eluted with water (total volume of eluate 50 ml; subsequently diluted for analysis). Be was eluted with 25 ml of 6*M* HCl and the eluate diluted to 50 ml for analysis.

Table 5. Detection limit and sensitivity (for 0.0044 absorbance) for determination of Be with different spectrometers and methods

		Perkin-Elmer 300* HGA-72		Perkin-Elmer 403* HGA-74		Beckman 1272D* Pye-Unicam GRM-1268				
		Without coating	With La deposit (300 μg)	Without coating	With La deposit (200 μg)	Without coating	With La deposit (300 μg)	With Ti deposit (400 μg)	Beckman 1272D Unilam 1288	
Detection limit,	*ng/ml*	9.8		0.72	0.56	0.053	0.24	0.016	0.013	3
	pg	196		14	11	1.0	4.8	0.33	0.25	
Sensitivity,	*ng/ml*	0.11		1.0	1.7	0.30	0.59	0.24	0.19	29
	pg	2200		4.4	34	6.0	12	4.9	3.8	
Reproducibility,†	*ng/ml*	±3		±0.22	±0.30	±0.016	±0.18	±0.29	±0.29	±12

*20 μl of test solution introduced into furnace.
†±20.

determination are improved if the graphite furnace is provided with a carbide coating, but also showed that these quantities depend on the apparatus used (Table 5). The improvement seems to be greater with the titanium coating.

For comparison, flame AAS with a reducing nitrous oxide–acetylene flame was used (conditions in Table 2), but as expected, it gave higher detection limits and poorer sensitivity than the flameless AAS (Table 5).

Our results were similar to[10] or better than[13] those in the literature.

It seems that the optimum amount of carbide coating depends on the size of the furnace. The HGA 74 is smaller than the others.

REFERENCES

1. T. V. Ramakrishna, P. W. West and J. W. Robinson, *Anal. Chim. Acta*, 1967, **39**, 81.
2. D. C. Manning, *At. Absorpt. Newsl.*, 1967, **6**, 35.
3. G. F. Kirkbright, M. Sargent and T. S. West, *Talanta*, 1969, **16**, 1467.
4. B. Fleet, K. V. Liberty and T. S. West, *ibid.*, 1970, **17**, 203.
5. S. L. Sachdev and P. W. West, *Environ. Sci. Technol.*, 1970, **4**, 745.
6. K. I. Aspila, C. L. Chakrabarti and M. P. Bratzel, Jr., *Anal. Chem.*, 1972, **44**, 1718.
7. K. C. Thomson, R. G. Godden and D. K. Thomerson, *Anal. Chim. Acta*, 1975, **74**, 289.
8. J. M. Runnels, R. Merryfield and H. B. Fisher, *Anal. Chem.*, 1975, **47**, 1258.
9. W. K. Robbins, J. H. Runnels and R. Merryfield, *ibid.*, 1975, **47**, 2095.
10. P. Lagas, *Anal. Chim. Acta*, 1978, **98**, 261.
11. Th. Stiefel, K. Schulze and G. Tölg, *ibid.*, 1976, **87**, 67.
12. K. Brajter, K. Słonawska and Z. Vorbrodt, *Chem. Anal., Warsaw*, 1982, **27**, 239.
13. E. Gladney, *At. Absorpt. Newsl.*, 1977, **16**, 42.

Talanta, Vol. 32, No. 7, pp. 525–530, 1985
Printed in Great Britain

0039-9140/85 $3.00 + 0.00
Pergamon Press Ltd

FURTHER DEVELOPMENTS IN THE HIGH-PRECISION COULOMETRIC TITRATION OF URANIUM

TATSUHIKO TANAKA,* GEORGE MARINENKO† and WILLIAM F. KOCH
Center for Analytical Chemistry, National Bureau of Standards, Washington, D.C. 20234, U.S.A.

(*Received* 2 *August* 1984. *Revised* 16 *January* 1985. *Accepted* 8 *February* 1985)

Summary—An experimental study of the current efficiency in the coulometric generation of Ti(III), as a function of electrolyte composition, current density and electrode material, has been performed. The cathodes investigated include platinum, mercury and graphite. The first two are suitable for high-precision determination of uranium. The graphite surface is readily poisoned, rendering it useless for high-accuracy work. The use of mercury requires thorough removal of chloride from the system. The precision and error obtained are comparable for both the mercury and platinum cathodes, and are of the order of 50 ppm.

In aqueous solutions titanium(III) is a powerful reductant, and was first introduced as a coulometric titrant by Arthur and Donahue.[1] $E°$ for the Ti(IV)–Ti(III) couple, +0.1 V, is very nearly equal to that of hydrogen. Hence, in any coulometric experiment there is a possibility of co-reduction of hydrogen ion along with Ti(IV), resulting in a significant loss of current efficiency. A high current efficiency for the electrogeneration of titanium(III) can easily be obtained if mercury, which has a high hydrogen overpotential, is used as the cathode, and the hydrogen-ion concentration in the supporting electrolyte is low.

For these reasons, Lingane and Iwamoto[2] coulometrically titrated uranium(VI) with titanium(III) electro-generated at a mercury-pool cathode in 0.2–1*M* citrate medium, containing 0.08*M* titanium tetrachloride, at pH 0.5–1.5 and 85°. The elevated temperature was required to increase the rate of reduction of U(V) with Ti(III), because at room temperature (25°) the rate is impracticably low. Later, Kennedy and Lingane successfully determined uranium(VI) by using a platinum cathode, which is more convenient to use than a mercury cathode. In their work, a medium of 6–9*M* sulphuric acid and 0.6*M* titanium(IV) was used as the supporting electrolyte. Under these conditions, titanium(III) can be generated with 100% efficiency for current densities as high as 3 mA/cm^2, but at elevated temperatures the efficiency decreases.[3] Kennedy and Lingane also found that iron(II) catalyses the reduction very effectively, eliminating the need for elevated temperatures.[3]

Takeuchi *et al.*[4] determined uranium(VI) in uranium(IV) oxide by use of Kennedy and Lingane's method. Marinenko *et al.*[5] improved the method and applied it to the analysis of Standard Reference Material (SRM) 960 Uranium Metal, issued by the National Bureau of Standards (NBS).

The generation of titanium(III) in a sulphuric acid medium, at a platinum cathode, is known to be less than 100% efficient.[5,6] Bishop and Hitchcock[7] investigated the electrode processes occurring at the platinum cathode during the reduction of titanium(IV) and found that trace impurities in the sulphuric acid can cause electrode poisoning, and emphasized the need not only to activate or condition the electrode, but also to purify the sulphuric acid. With 0.6*M* titanium(IV) sulphate/7*M* sulphuric acid purified by electrosorption, the loss of current efficiency is only 1 ppm at a current density of 59.2 mA/cm^2. However, according to Bishop and Hitchcock[7] it is difficult to purify sulphuric acid, and furthermore, after purification, the acid is soon recontaminated even when it is kept in an all-glass apparatus.

As mentioned above, the current efficiency for generation of titanium(III) has been extensively studied for the platinum cathode but not for other cathodes. Hence, systematic study of the efficiency of coulometric generation of titanium(III) at platinum, mercury and graphite electrodes was undertaken.

Coulometric generation efficiency for titanium(III)

The Ti(IV)–Ti(III) couple is reversible in 1–15*M* phosphoric acid,[8] but the Ti(IV) concentration cannot exceed 0.01*M* because of solution instability. Such a low concentration of Ti(IV) makes the system unusable for the coulometric generation of Ti(III) titrant. The titanium couple is also reversible in $\geq 4M$ sulphuric acid,[8] which is a preferred supporting electrolyte in cathodic titrations. Hydrochloric acid has also been employed as the medium for the generation of titanium(III), but the titanium couple is less reversible than in the same concentration of sulphuric acid.[8] Furthermore, both uranium(VI) and titanium(IV) are reduced by mercury in hydrochloric

*Guest worker at the National Bureau of Standards from Science University of Tokyo, Department of Industrial Chemistry, Kagurazaka, Shinjuka-Ku, Tokyo, 162 Japan.
†To whom correspondence should be addressed.

Table 1. Electrode potentials (*V vs. SCE*) on different cathodes, as a function of current density*

Current density	Hg			Graphite			Pt		
mA/cm^2	E'', V	E', V	ΔE, V	E'', V	E', V	ΔE, V	E'', V	E', V	ΔE, V
10^{-4}	+0.25	−0.35	0.60	+0.25	+0.05	0.20	+0.35	−0.10	0.45
10^{-1}	+0.23	−0.73	0.96	+0.20	−0.40	0.60	+0.25	−0.15	0.40
10	+0.15	−0.90	1.05	0.00	−0.65	0.65	0.00	−0.18	0.18

*E' determined in 9*M* H_2SO_4. E'' determined in 9*M* H_2SO_4/1*M* Ti(IV).

acid.[9] In perchloric acid the titanium couple is irreversible[8] because titanium(III) immediately reduces perchlorate to chloride. Consequently, of all the common acids considered, only sulphuric acid is suitable for the investigation.

The coulometric titration cell used throughout this work has already been described in detail.[5,10,11] Platinum gauze, high-purity mercury and spectrographic grade graphite rod were employed as the cathode materials. The areas of these electrodes were 80, 12 and 1.5 cm^2, respectively. The graphite rod was polished with fine carborundum paper and then rubbed with filter paper before each use. The anode was a piece of platinum gauze. The potential of the cathode was measured with respect to a saturated calomel electrode (SCE). All the work was done with 100 ml of electrolyte solution, containing 100 mg of ferrous ammonium sulphate hexahydrate as catalyst for the uranium(VI) titration, and stirred at constant rate with a Teflon-coated magnetic bar. The electrode potentials for the three types of cathode in different electrolytes, at three levels of current density (10^{-4}, 10^{-1} and 10 mA/cm^2), are listed in Table 1.

The current density *vs.* working electrode potential diagrams obtained are shown in Figs. 1–3, and the current efficiency for the generation of Ti(III) from Ti(IV) can be readily estimated from them.

The current due to the reduction of other species in the supporting electrolyte (*e.g.*, of protons) is subtracted from the total current to compute the current efficiency. For example, consider the curves a and b in Fig. 2. At a current density of 20 mA/cm^2 the potential of the graphite cathode in 9*M* sulphuric acid/1*M* titanium(IV) is −0.05 V *vs.* SCE (point × on curve b). At the same potential the corresponding current density in the absence of titanium(IV) is 3×10^{-3} mA/cm^2 (point x' on curve a). Then

$$\text{current efficiency} = \frac{(20\ \text{mA/cm}^2) - (3.0 \times 10^{-3}\ \text{mA/cm}^2)}{20\ \text{mA/cm}^2} \times 100$$

$$= 99.985\%$$

Current efficiencies calculated for different electrodes, different current densities and various electrolyte compositions are summarized in Table 2.

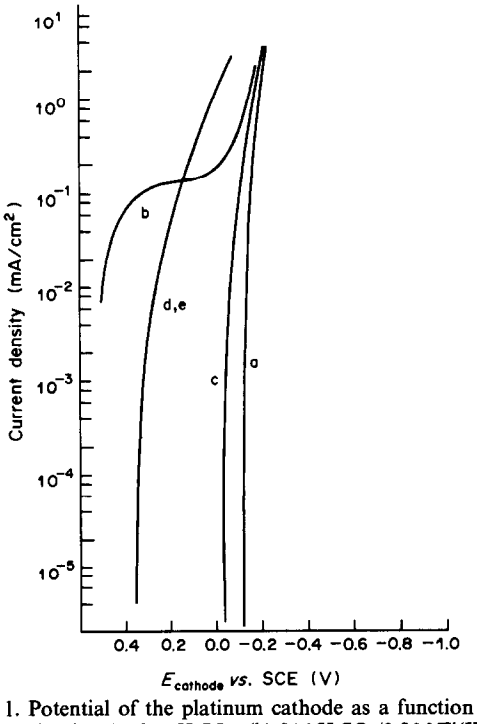

Fig. 1. Potential of the platinum cathode as a function of current density: (a) 2*M* H_2SO_4; (b) 2*M* H_2SO_4/0.2*M* Ti(IV); (c) 9*M* H_2SO_4; (d) 9*M* H_2SO_4/0.5*M* Ti(IV); (e) 9*M* H_2SO_4/1.0*M* Ti(IV).

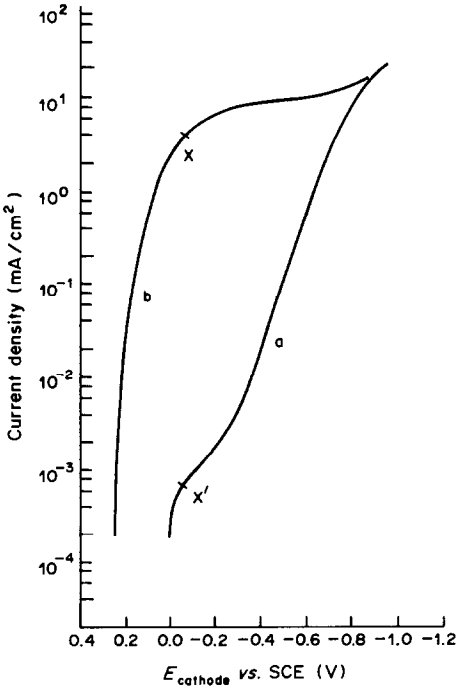

Fig. 2. Potential of the graphite cathode as a function of current density: (a) 9*M* H_2SO_4; (b) 9*M* H_2SO_4/1.0*M* Ti(IV).

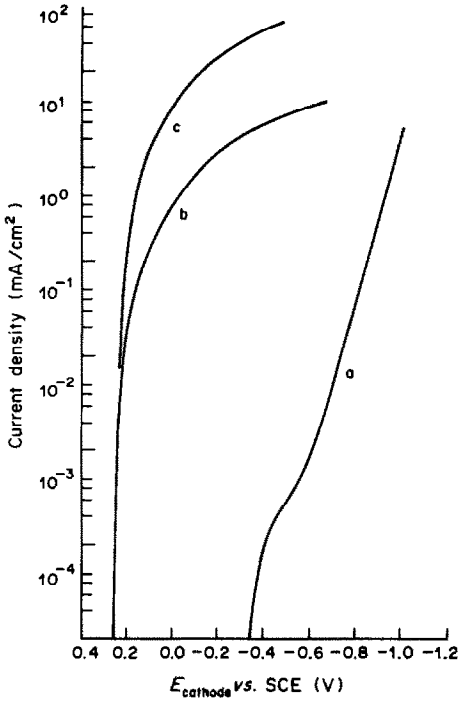

Fig. 3. Potential of the mercury cathode as a function of current density: (a) 2*M* or 9*M* H_2SO_4; (b) 2*M* H_2SO_4/0.2*M* Ti(IV); (c) 9*M* H_2SO_4/0.5*M* Ti(IV).

It is of interest to consider the potential of each of the cathodes investigated, at various current densities, for reactions in 9*M* sulphuric acid in the presence and absence of titanium(IV) (1*M*). In the latter case the primary potential-determining reaction is the reduction of protons to hydrogen gas (potential *E'*), and in the former it is the reduction of titanium(IV) (potential E''). A summary of the current-density/potential data is given in Table 1, and indicates that, between current densities of 10^{-4} and 10 mA/cm², $\Delta E = (E'' - E')$ increases dramatically for Hg and graphite cathodes (by 0.45 V). For platinum, under the same conditions, ΔE decreases by 0.27 V. The reason is evident from the values of *E'*. On both the mercury and graphite cathodes, the hydrogen overvoltage increases very markedly as a function of current density (0.55 V on mercury and 0.70 V on graphite), whereas on the platinum cathode the overvoltage increases by only 0.08 V over the same current-density range. The increase in overvoltage for the reduction of titanium(IV) on all three cathodes is comparable: 0.10 V for mercury, 0.25 V for graphite and 0.35 V for platinum over the 10^{-4}–10 mA/cm² current-density range. On the basis of only these data, mercury is the preferred cathode for 100% efficient generation of Ti(III) from titanium(IV) sulphate electrolyte, followed by graphite and platinum in order of decreasing efficiency. However, other considerations make platinum at least as attractive as the other two materials. As noted earlier, use of the mercury cathode results in significant titration errors when halides are present in the electrolyte. The addition of uranium(VI) chloride causes spontaneous oxidation of mercury to form mercurous chloride, in a reaction which is not reversible under these experimental conditions, so results for U(VI) are low. The graphite electrode used in our experiments became "poisoned" after a 30-min electrolysis and gave copious liberation of hydrogen with a concurrent loss of current efficiency. Thus, graphite was abandoned as cathode material for generation of Ti(III). For 1*M* titanium(IV) sulphate in 9*M* sulphuric acid the results obtained with the platinum cathode agree with those of Kennedy and Lingane.[3]

Kinetics of uranium reduction

It was found earlier by Kennedy and Lingane[3] that the slow reaction between U(VI) and Ti(III) at room temperature can be accelerated by the addition of small amounts of iron(II), but even then the reaction is quite slow as long as U(VI) is in excess. Only when excess of Ti(III) is present does the reaction proceed rapidly to completion.

This point is illustrated in Fig. 4 by three indicator-current curves measured in the equivalence-point region of the uranium titration. For each curve, 10 μeq of Ti(III) were coulometrically generated in the electrolyte [9*M* sulphuric acid/1*M* titanium(IV) sulphate containing 1 mg of ferrous ammonium sulphate hexahydrate per ml]. Curve 1 corresponds to

Table 2. Current efficiency of generation of Ti(III) on different electrode materials

Current density, mA/cm^2	[H_2SO_4] [Ti(IV)]	Platinum			Graphite			Mercury			
		2*M* 0.2*M*	9*M* 0.5*M*	9*M* 1*M*	9*M* 0.1*M*	9*M* 1*M*	2*M* 0.1*M*	2*M* 0.2*M*	9*M* 0.1*M*	9*M* 0.5*M*	9*M* 1*M*
0.01				100	100	100			100	100	100
0.05		100	100								
0.1											
0.5					100		100	100			
1		100			99.98		100	100	100		
3		99.33			99.98		99.91	99.999			
5		95	100	100			99.84	99.994			
8					36.25		99.77	99.96			
10					15		99.73	99.94			
20						99.997	99.49	99.87			
30						99.996	98.50	99.72	99.72	100	100

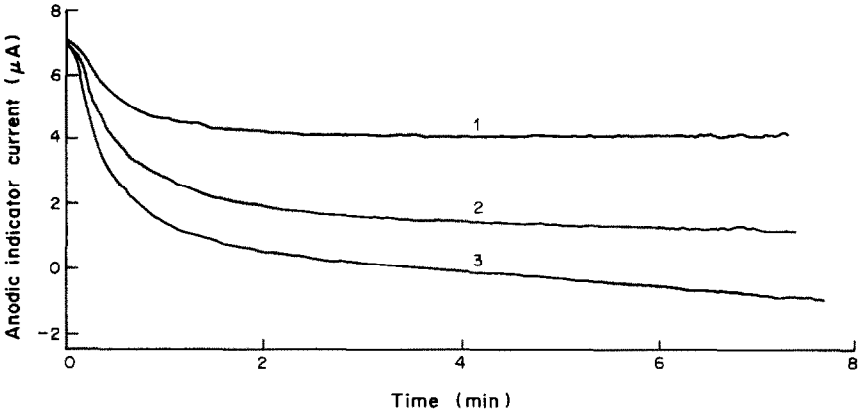

Fig. 4. Amperometric indicator current due to Ti(III), as a function of time. Electrolyte composition: 9*M* H_2SO_4/1*M* Ti(IV)/1-mg/ml $Fe(NH_4)_2(SO_4)_2 \cdot 6H_2O$, (1) 10 μeq Ti(III) + 5 μeq U(VI); (2) 10 μeq Ti(III) + 10 μeq U(VI); (3) 10 μeq Ti(III) + 15 μeq U(VI).

the region after the equivalence point. This curve was obtained by adding 5 μeq of U(VI) to the 10 μeq of Ti(III) generated. It can be seen that equilibrium is reached quite rapidly. The initial exponential decay of the indicator current reaches a constant value after $2\frac{1}{2}$ min. At the equivalence point (curve 2), the rate of reaction is significantly lower when 10 μeq of U(VI) are added to the generated 10 μeq of Ti(III), equilibrium being reached 7 min after addition of the U(VI) aliquot. Before the equivalence point (curve 3), the reaction rate when 15 μeq of U(VI) are added to the generated 10 μeq of Ti(III) is impracticably slow.

It is clear that, for stoichiometric reaction measurements, the system must be overtitrated to allow equilibration to take place at a reasonable rate and then the excess of titrant must be determined. On the basis of these studies the following experiments on the coulometric assay of uranium were performed.

EXPERIMENTAL

Coulometric assay of uranium metal

The instrumentation for coulometric generation of the titrant was similar to that described previously.[5,10,11] The electrolysis cell was also of the type described earlier,[5,10,11] with a few modifications. A silicic acid plug was cast in the bottom of the anode chamber to cover the glass frit. The remainder of the chamber was filled with 2*M* sulphuric acid and a glass tube with its bottom closed by a glass frit and a silicic acid plug, and filled with 2*M* sulphuric acid. The platinum anode and the SCE were immersed in the tube.

The end-point of the titration was determined amperometrically with a platinum foil indicator electrode (area approximately 1.2 cm^2) immersed in the cathode chamber. A polarograph was used to apply a constant potential between the indicator electrode and the SCE, and to record the indicator current. Argon, purified by passage through chromium(II) chloride and then 9*M* sulphuric acid, was used to purge oxygen from the cell and the electrolyte. The Faraday constant was taken as 96486.5 C/equivalent and the atomic weight of uranium as 238.0289.

Analytical-grade chemicals were used without further purification. Titanium(IV) sulphate solution was prepared by slowly adding 50% titanium tetrachloride solution to concentrated sulphuric acid, and removing all the hydrochloric acid by purging the solution overnight with argon. The final concentrations in the stock solution were 1*M* titanium(IV) and 9*M* sulphuric acid.

Uranium sample solution was prepared from uranium metal (NBS SRM 960) cut into approximately 1-g pieces. Immediately before the sample was weighed, the surface oxide was removed[12] by dipping the pieces in warm nitric acid (1 + 1) for 10 min, rinsing with distilled water, etching in hydrochloric acid (1 + 3) for 5 min, rinsing with distilled water again, immersing in acetone, air-drying for a few minutes, then placing them in a vacuum desiccator. The sample was weighed to the nearest microgram before any significant amount of surface oxide could form (*i.e.*, within 30 min), and the weight was corrected for air buoyancy. The sample was then dissolved in hydrochloric acid (1 + 1) in an inclined 125-ml Erlenmeyer flask (10 ml of acid per g of sample). After dissolution was complete, 0.5–1 ml of 30% hydrogen peroxide was added slowly to ensure that all uranium was in the hexavalent state and to dissolve any traces of black residue (ostensibly U_3O_8). The solution was then evaporated nearly to dryness under infrared lamps, the residue was taken up with water and the evaporation was repeated, to destroy the excess of hydrogen peroxide. Five ml of concentrated sulphuric acid were then pipetted slowly down the wall of the flask and the solution was evaporated till fuming. Finally the solution was diluted to about 15 ml with distilled water and then titrated. Reagent blank samples were prepared by the same procedure.

Titration procedure

The procedure was similar to that developed for the assay of NBS SRM 960 Uranium Metal by Marinenko *et al.*[5]

About 75 ml of titanium(IV) sulphate catholyte and 100 mg of ferrous ammonium sulphate hexahydrate were placed in the cathode chamber of the cell. Argon, purified from traces of oxygen by passage through chromous chloride solution, was passed through the contents of the cell for about 30 min, the solution being vigorously stirred with the magnetic stirrer. After purging, the catholyte was permitted to flow into the intermediate compartments of the coulometric cell until it just covered the bottom of each compartment. A current–voltage curve was run before each titration to determine the optimum potential for the indicator system.

For pretitration, *ca.* 10 μeq of uranium(VI) were added to the cathode chamber and titrated at 3.22 mA by passage of small increments of charge, each corresponding to 1 μeq. After a slight excess of titanium(III) had been generated, as evidenced by the indicator-current increase, the solution was allowed to equilibrate for 30 min. Additional amounts of titanium(III) were then generated and the indicator current

was measured after each charge increment. The linear portion of the indicator-current curve was extrapolated graphically, and its intersection with the zero-current line taken as the end-point.

After the pretitration, the intermediate cell compartments were rinsed by repeated emptying and filling with catholyte, by suction or argon pressure. The final reading of the indicator current was used to establish the amount of overtitration.

Next the intermediate compartments were filled with catholyte and the sample was transferred from the Erlenmeyer flask to the cathode chamber. The major part of the titration was then done at a constant current of about 102 mA for a precalculated time corresponding to a few μeq in excess of the theoretical amount. The intermediate compartment and the sample flask were then rinsed three times with the titrated solution, by suction or argon pressure. After equilibration of the solution for 30 min, the end-point was located by the procedure used for the pretitration.

ANALYTICAL RESULTS AND DISCUSSION

In view of the studies of the efficiency of generation of Ti(III) at different types of cathode it was of interest to verify independently the performance of the various cathodes in coulometric titrations. Hence, NBS SRM 960 Uranium Metal was analysed by the procedure of Marinenko *et al.*[5]

As mentioned earlier, work with the graphite cathode was abandoned because hydrogen was liberated and the current efficiency decreased. The results of analyses with the platinum cathode are shown in Table 3. The oxidimetric assay value is 99.981% ($s = 0.0048$). When this value is corrected for the iron and vanadium present, which are titrated along with uranium, the assay becomes 99.970% U, which is in excellent agreement with the certified value of 99.975%. It should be noted here that though the titration procedure was the same in this work as for the certification, the current densities were different (2.5 mA/cm^2 for certification, 1.27 mA/cm^2 in this work). The agreement of the results obtained at current densities differing by a factor of 2 is further evidence of the consistency of the titration process under selected conditions. Both current densities should provide 100% efficient generation of Ti(III) according to the data in Table 1.

Table 3. Coulometric assay of NBS SRM 960 Uranium Metal at a platinum cathode (supporting electrolyte 1*M* titanium(IV) sulphate/9*M* sulphuric acid; current density 1.27 mA/cm^2)

U metal, *mg*		
Taken	Found	Assay, % *w/w*
865.38_4	865.22_2	99.981
1033.58_0	1033.42_0	99.984
1028.65_6	1028.49_1	99.984
1075.75_7	1075.60_7	99.986
990.34_0	990.10_8	99.977
1033.71_4	1033.43_3	99.973
1287.81_4	1287.60_3	99.984
	Average	99.981
	Std. dev.	0.004_8

As a further test of the accuracy of the current efficiencies predicted from the current density/potential diagrams, uranium metal SRM 960 was coulometrically titrated with Ti(III) electrogenerated at the mercury cathode at a current density of 8.3 mA/cm^2. The electrolyte was 0.1*M* titanium(IV) sulphate/9*M* sulphuric acid. At a current density of 8.3 mA/cm^2, the predicted current efficiency is 99.96%. The assay of the uranium metal was 99.999%, which is 0.01% higher than the value obtained under 100% efficient generation conditions with a platinum cathode. The uranium assay expected from the current density data alone should be 100.029%. However, the titration "efficiency" should be higher than the current efficiency because uranium is directly reduced in the initial stages of the titration.

When the Ti(IV) concentration in the electrolyte was increased to 0.5*M*, the uranium assay was 99.987% ($n = 3$, $s = 0.0087\%$). The current-density studies indicate that this electrolyte should provide 100% efficient generation of Ti(III), which is borne out by the uranium assay.

A set of uranium metal samples, ranging in weight from 30 mg to 1.2 g, was analysed with the mercury cathode system with 0.2*M* titanium(IV) sulphate/9*M* sulphuric acid electrolyte. The results are presented in Table 4. The assay value for Uranium SRM 960 obtained with the platinum cathode system (99.981%) is in excellent agreement with the value obtained with the mercury cathode system (99.982%), under experimental conditions which are significantly different with respect to not only the nature of the cathode material but also the electrolyte composition and current density.

A word of caution is in order regarding the use of the mercury cathode for uranium determination. The use of the mercury cathode requires that great care be taken in preparing the supporting electrolyte. The absence of chloride is essential. When the 9*M* sulphuric acid supporting electrolyte contains chloride,

Table 4. Coulometric assay of NBS SRM 960 Uranium metal at a mercury cathode, (0.2*M* titanium(IV) sulphate/9*M* sulphuric acid; current density 8.3 mA/cm^2)

U metal, *mg*		
Taken	Found	Assay, % *w/w*
1078.13_9	1077.91_9	99.980
1176.48_8	1176.30_9	99.985
1169.49_3	1169.30_6	99.984
1180.50_1	1180.25_1	99.979
		Average 99.982
		Std. dev. 0.003_0
504.45_1	504.36_9	99.984
421.31_2	421.27_5	99.991
235.43_0	235.40_3	99.989
136.66_5	136.64_2	99.983
70.23_5	70.21_9	99.977
33.00_2	32.99_1	99.966
		Average 99.982
		Std. dev. 0.009_2

the introduction of uranium(VI) causes the spontaneous oxidation of mercury to form mercurous chloride on the surface of the cathode. In principle this is reversible, *i.e.*, Hg(I) is reduced back to metallic mercury, and should not cause any loss of generation efficiency as far as charge balance is concerned, but in practice complete electrochemical reduction of the calomel is not feasible. Thus, in the presence of chloride, the uranium assay is low.

The values of the reductometric assay of uranium metal reported in Tables 3 and 4 include all impurities which would oxidize Ti(III). In SRM 960 Uranium Metal two principal electroactive impurities are present: 42.1 ppm of iron and 4 ppm of vanadium, which are equivalent to 109 ppm of uranium. Therefore, to establish the uranium assay of SRM 960, a correction of 109 ppm must be applied to the reductometric assay. Thus, the corrected coulometric assay of SRM 960 is 99.970% ($s = 0.0048$) with the platinum cathode and 99.971% ($s = 0.0030$) with the mercury cathode. The two values, for all practical purposes, are identical. This uranium assay is in excellent agreement with the certified value of 99.975%.

REFERENCES

1. P. Arthur and J. F. Donahue, *Anal. Chem.*, 1952, **24,** 1612.
2. J. J. Lingane and R. T. Iwamoto, *Anal. Chim. Acta*, 1955, **13,** 465.
3. J. H. Kennedy and J. J. Lingane *ibid.*, 1958, **18,** 240.
4. T. Tekeuchi, T. Yoshimori and T. Kato, *Bunseki Kagaku*, 1963, **12,** 840.
5. G. Marinenko, W. F. Koch and E. S. Etz, *J. Res. Natl. Bur. Stds.*, 1983, **88,** 117.
6. T. Takahashi and H. Sakurai, *10th Annual Meeting Japan Society for Analytical Chemistry*, B107, Tokyo, 1961.
7. E. Bishop and P. H. Hitchcock, *Analyst*, 1973, **98,** 625.
8. J. J. Lingane and J. H. Kennedy, *Anal. Chim. Acta*, 1956, **15,** 294.
9. E. R. Caley and L. B. Rogers, *J. Am. Chem. Soc.*, 1946, **68,** 2202.
10. G. Marinenko and J. K. Taylor, *J. Res. Natl. Bur. Stds*, 1963, **67A,** 31.
11. *Idem, ibid.*, 1963, **67A** 453.
12. H. Hashitani, A. Hoshino and T. Adachi, *JAERI-M* 5343, 1973.

Talanta, Vol. 32, No. 7, pp. 531–537, 1985
Printed in Great Britain.

0039-9140/85 $3.00 + 0.00

ANIONIC INTERFERENCES WITH COPPER ION-SELECTIVE ELECTRODES

CHLORIDE AND BROMIDE INTERFERENCES

A. LEWENSTAM, T. SOKALSKI and A. HULANICKI
Department of Chemistry, University of Warsaw, Warsaw, Poland

(*Received* 14 *June* 1984. *Revised* 10 *January* 1985. *Accepted* 1 *February* 1985)

Summary—The effect of halide ions on copper ion-selective electrodes is connected with complexation and redox reactions, with the formation of amorphous sulphur, which by blocking the surface causes instability of potential response. It may be eliminated by addition of sodium thiosulphate solution. The electrode behaviour has been explained on the basis of the diffusion model. An equation is proposed for linearization of the calibration curve. The parameters of the semiempirical model which describes the electrode behaviour agree well with the physical meaning presented by the diffusion model. The treatment given enables analytical measurements of copper concentration to be made even in the presence of significant concentrations of chloride or bromide.

Copper-selective electrodes with membranes composed of copper(II) sulphide mixed with silver sulphide or of pure copper(I) sulphide show a rapid and Nernstian response (*i.e.*, 29.6 mV/decade at 25°) over a broad range of copper(II) concentration, but applications of these electrodes to real analytical samples often reveal non-Nernstian behaviour.[1] Such effects were observed when the Orion 94-29 electrode was used for measurements of copper concentrations in sea-water[2] or lake water.[3] Such facts have diminished the attraction of copper-selective electrodes as analytical tools, but at the same time have attracted the attention of scientists interested in electrode-response mechanisms, as the electrode behaviour could not be explained by existing theories.[4] Attempts to elucidate the super-Nernstian electrode slope, attributed to the presence of chloride ions, have been made in a number of papers. In some of them the source of anomalous electrode behaviour was considered to be exchange reactions occurring at the electrode surface:[4–8]

$$Ag_2S + 2Cu^{2+} + 2nCl^- \rightleftharpoons CuS + 2AgCl_n^{1-n} \quad (1)$$

$$Cu_2S + Cu^{2+} + 2nCl^- \rightleftharpoons CuS + 2CuCl_n^{1-n} \quad (2)$$

Others[9–11] have attributed the behaviour to redox reactions with participation of the membrane material:

$$Ag_2S + 2Cu^{2+} + 4nCl^- \rightleftharpoons 2CuCl_n^{1-n} + 2AgCl_n^{1-n} + S \quad (3)$$

$$Cu_2S + 2Cu^{2+} + 4nCl^- \rightleftharpoons 4CuCl_n^{1-n} + S \quad (4)$$

$$CuS + Cu^{2+} + 2nCl^- \rightleftharpoons 2CuCl_n^{1-n} + S \quad (5)$$

However, most papers do not offer a detailed explanation of the electrode response. Ross's interpretation[4] does not assume the occurrence of super-Nernstian slope, but indicates only that silver chloride is formed in the case of the CuS/Ag_2S membrane [reaction(1)]. The formation of electroactive AgCl has been experimentally confirmed by Moody and co-workers.[5,12] Lanza[7] suggests that the electrode interference is connected with the presence of Ag_2S and is due to reaction (1). His conclusions are not unequivocally confirmed by his own experimental data. There is also no explanation for super-Nernstian slope in the absence of chloride, and for electrodes which do not contain Ag_2S. Hepel,[8] extending the views of other authors, assumes reaction (2) to be the main reason for the interference. In his considerations, based only on potentiometric data, he neglects the role of redox processes in spite of some earlier remarks[9,13–15] about their importance. The influence of the redox reaction (5) has been discussed by Westall *et al.*[9] Their theoretical considerations were well supported by experiments, but these covered only a relatively narrow concentration range, namely pCu from 3.5 to 5.0, because according to the authors' statement this reaction is hindered by formation of AgCl at the membrane surface. They did not confirm the presence of sulphur at the membrane surface, but this has been reported independently.[10,11]

No complete explanation has so far been given, then, for the non-Nernstian electrode behaviour, especially the variation of slope between 0 and 120 mV/pCu in the pCu range from 2 to 5. In this paper we attempt to give a more general description of the interferences with copper electrodes in solutions containing copper-complexing anions, and propose a method for elimination of this interference and for practical utilization of the super-Nernstian slope.

EXPERIMENTAL

Measurements of the e.m.f. were made with Radiometer pHM 64 and Radelkis OP-206 instruments, with a Radio-

meter K-401 saturated calomel electrode as reference. All solutions were kept at $25 \pm 1°$. The indicator electrodes tested were an Orion 94-29A (CuS/Ag_2S), a CuS membrane electrode prepared as described earlier[10] and a Cu_2S single-crystal electrode prepared according to Hepel.[8]

All reagents were of analytical grade and doubly quartz-distilled water was used throughout.

RESULTS AND DISCUSSION

Electrode response in presence of chloride and bromide ions

Although the behaviour of several electrodes has been well documented, the response of the CuS/Ag_2S, CuS and Cu_2S electrodes was retested under comparable conditions. All measurements were performed in acetate buffers at pH 4.5. The solutions were not stirred during measurements, to ensure predominence of diffusion to and from the electrodes. The e.m.f. was recorded until its drift was less than 1 mV/hr. The results obtained (Figs. 1 and 2) indicated differences in the behaviour of various electrodes. A stable e.m.f. was reached first with the CuS/Ag_2S electrode (approx. 10 min), whereas for the two other electrodes stable e.m.f. values were obtained only after much longer times, even up to several tens of hours. The electrode potential drifted towards more positive values. Its reproducibility for the Orion electrode was better than 5 mV. The slope of the electrode response was found to be dependent on the concentrations of copper ion and interferent. The slope was constant only for the Orion electrode in the range pCu 3.5–5.0, which is in agreement with the findings of Westall *et al.*[9]

To obtain information on the state of the electrode surface, the dependence of the potential on pCl or pBr was investigated after each series of measurements. After treatment of the membrane with 1–3*M* potassium chloride or 1*M* potassium bromide,

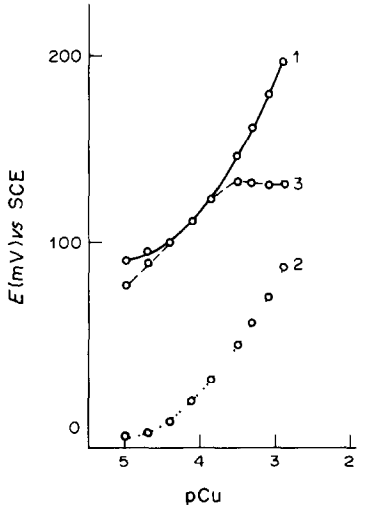

Fig. 1. Calibration graphs for copper electrodes in 1*M* potassium chloride. Curve 1—CuS membrane, curve 2—Cu_2S membrane, curve 3—Orion 94-29 electrode.

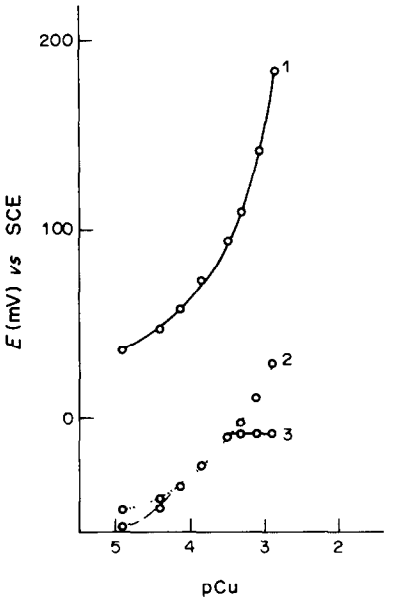

Fig. 2. Calibration graphs for copper electrodes in 1*M* potassium bromide. Curve 1—CuS membrane, curve 2—Cu_2S membrane, curve 3—Orion 94-29 electrode.

this function was linear only for the Orion electrode. For the other two electrodes (and also for the Orion electrode after previous exposure to 2 or 3*M* potassium bromide) such linearity was not observed. This indicates that in most cases no electroactive substances with composition different from that of the membrane are precipitated on the membrane surface. It may also suggest formation of soluble copper or silver complexes. The exceptional behaviour of the Orion electrode in the above-mentioned solutions indicates that in this case solid AgCl (or AgBr) has been formed. This process also seems to be responsible for the plateau of curve 3 in Figs. 1 and 2 for concentrations above pCu 3.5.

On the basis of previous data[5] and the results of this study the following interference mechanisms may be proposed for the various types of electrode:

$$Ag_2S + 2Cu^{2+} + 4nX^- \rightleftharpoons 2AgX_n^{1-n} + 2CuX_n^{1-n} + S \quad (6)$$

$$CuS + Cu^{2+} + 2nX^- \rightleftharpoons 2CuX_n^{1-n} + S \quad (7)$$

$$Cu_2S + 2Cu^{2+} + 4nX^- \rightleftharpoons 4CuX_n^{1-n} + S \quad (8)$$

These reactions explain the interference processes on the membrane surface, and the poor reproducibility and the instability of potential response are due to the formation of elemental sulphur. Considering the empirically established fact that electrochemical corrosion is stimulated by chloride and bromide ions[16] it seems reasonable to suppose that the rapidly formed amorphous sulphur mechanically blocks the electrode surface[10] and causes the irreversibility of reactions (6), (7) or (8). It becomes obvious that direct determination of copper in the presence of high

Table 1. Equilibrium constants used in calculations

Species	Constant	Values	Reference
CuS*	K_{s0CuS}	$10^{-36.2}$	18, 19
Cu_2S*	K_{s0Cu_2S}	$10^{-47.8}$	18, 19
Ag_2S	K_{s0Ag_2S}	$10^{-49.7}$	20
$CuCl_2^-$	β_2	$10^{5.30}$	21
$CuBr_2^-$	β_2	$10^{5.92}$	21
CuS_2O_3	β_1	$10^{10.35}$	21
$Cu(S_2O_3)_2^{2-}$	β_2	$10^{12.29}$	21
$Cu(S_2O_3)_2^{3-}$	β_2	$10^{12.86}$	21
$AgS_2O_3^-$	β_1	$10^{10.00}$	21
$Ag(S_2O_3)_2^{3-}$	β_2	$10^{13.36}$	21

*Calculated from thermodynamic data given in the literature.

concentrations of chloride or bromide ions is impossible.

Optimization of conditions for potentiometric determination of copper

It may be expected that addition of a reagent which binds copper(II), copper(I) and silver(I) more strongly than chloride or bromide does may act advantageously in the determination of copper(II). Thiosulphate was chosen as such a reagent, since it is known to diminish the strongly corrosive action of halide ions on copper and silver. The stability of the relevant thiosulphate complexes is greater than that of the halide complexes (Table 1). The reducing properties of thiosulphate ($E^0_{S_4O_6^{2-}/S_2O_3^{2-}} = 0.15$ V) are also advantageous. Those properties suggest that the halide ions will not participate in the redox reactions, and that these will proceed at lower rate. Therefore formation of crystalline sulphur instead of amorphous[17] is more probable, and the whole process becomes more reversible. In these experiments the Orion 94-29 electrode was used because its properties are well known and the response in halide solutions is the most reproducible.

The potential of the copper electrode in solutions containing thiosulphate depends significantly on the thiosulphate concentration (Fig. 3). Below a certain thiosulphate concentration the electrode potential is practically constant, but decreases linearly with higher thiosulphate concentrations. It also depends on the copper concentration. A thiosulphate concentration of 0.04M, in the middle of the linear decrease range, was used for further studies. Such a concentration is sufficient to mask the halide effect but is not large enough to cause rapid membrane dissolution.

For all the solutions containing both halide and thiosulphate ions the copper calibration curves are well reproducible, and so are the potential values. Measurement in 0.04M thiosulphate solution gave better results than that in 0.4M thiosulphate medium because with the latter the slope of the electrode response is lower for smaller copper concentrations (Fig. 4). The tangent to the calibration curve always has super-Nernstian slope, but the curves are not linear in any range. This behaviour can be explained by considering linearization of the standard curve.

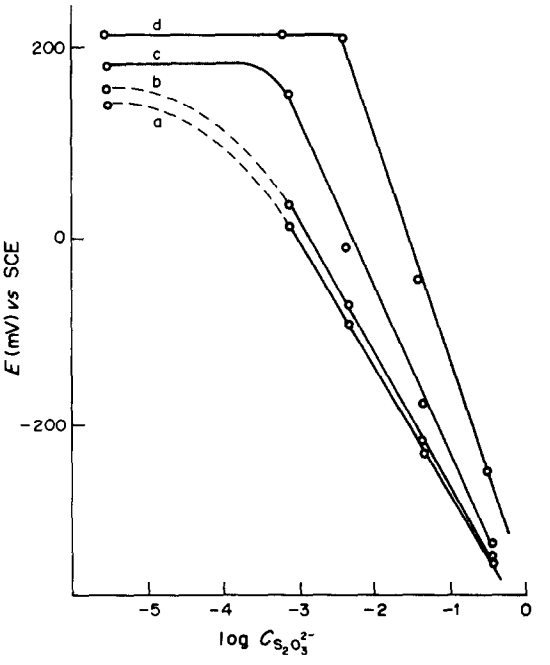

Fig. 3. Dependence of potential response of the Orion 94-29 electrode on thiosulphate concentration at various total copper concentrations in 2M KNO_3. Curve a—$10^{-4.7}M$ Cu^{2+}, curve b—$10^{-4.2}M$ Cu^{2+}, curve c—$10^{-3.3}M$ Cu^{2+}, curve d—$10^{-2.2}M$ Cu^{2+}.

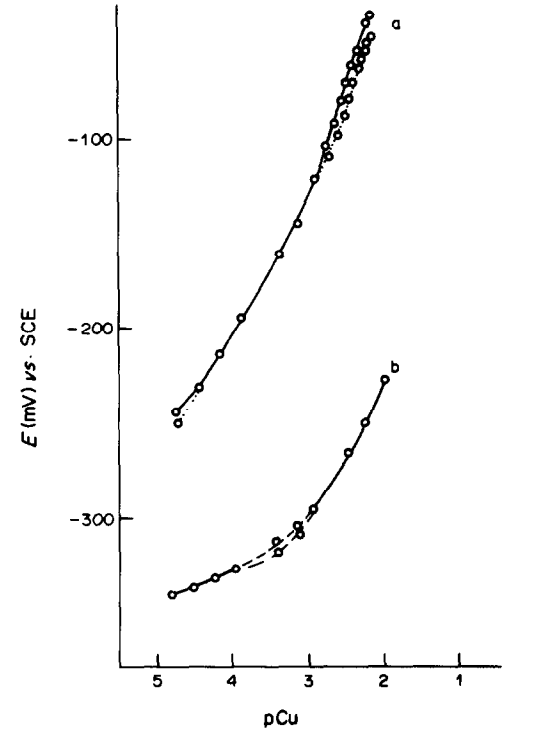

Fig. 4. Calibration graphs for Orion 94-29 electrode in solutions containing halide and thiosulphate ions. Curve a—0.04M sodium thiosulphate, curve b—0.4M sodium thiosulphate. Solid lines for 1M potassium chloride, dashed lines for 1M potassium bromide.

Linearization of the calibration graph

The linearization function is based on the diffusion model[6] with the following assumptions: (*a*) the electrode potential depends on the main-ion concentration at the membrane surface; (*b*) the concentrations of various species are different at the membrane surface and in the bulk solution; (*c*) concentrations at the membrane surface are controlled by rapid and reversible reactions at the membrane-solution interface; (*d*) these reactions do not change the bulk composition of the solution.

Because the electrode potential may be governed by the reactions of both components of the electrode the processes pertaining to each of them have been considered separately.

When CuS is the potential-defining species, then for the potential given by the equation

$$E = E^0_{ISE} + \frac{RT}{2F} \ln [Cu^{2+}]_0 \quad (9)$$

the concentration of copper ions at the membrane surface ($[Cu^{2+}]_0$) in the presence of thiosulphate is controlled by the redox reaction

$$Cu(S_2O_3)_2^{2-} + CuS + 2S_2O_3^{2-} = 2Cu(S_2O_3)_2^{3-} + S \quad (10)$$

Taking into account the stability constants of the thiosulphate complexes (Table 1) it is not a bad approximation to consider that at a total thiosulphate concentration of 0.04*M* the predominant species are the bis-complexes.

The equilibrium constant of reaction (10) is:

$$K_1 = \frac{[Cu(S_2O_3)_2^{3-}]_0^2}{[Cu(S_2O_3)_2^{2-}]_0 [S_2O_3^{2-}]_0^2} = \frac{\beta^2_{2,[Cu(S_2O_3)_2^{3-}]} K_{s0(Cu_2S)}}{\beta_{2,[Cu(S_2O_3)_2^{2-}]} K_{s0(CuS)}} = 10^{1.8} \quad (11)$$

where the subscript 0 refers to concentrations at the membrane surface.

In the bulk of the solution thiosulphate is present as free ions and as copper(II) complexes whereas at the membrane surface where copper(I) is formed, the copper(I) complexes must also be taken into account. For the bulk solution concentration the mass balance is given by the equation:

$$C_{S_2O_3^{2-}} = [S_2O_3^{2-}] + 2[Cu(S_2O_3)_2^{2-}] \quad (12)$$

whereas at the membrane surface

$$C_{S_2O_3^{2-}} = [S_2O_3^{2-}]_0 + 2[Cu(S_2O_3)_2^{3-}]_0 + 2[Cu(S_2O_3)_2^{2-}]_0 \quad (13)$$

but at equilibrium the last term is negligible compared to the others, so

$$C_{S_2O_3^{2-}} = [S_2O_3^{2-}]_0 + 2[Cu(S_2O_3)_2^{3-}]_0 \quad (14)$$

Assuming the fluxes of both thiosulphate complexes to be equal, than from equation (10):

$$2D''([Cu(S_2O_3)_2^{2-}] - [Cu(S_2O_3)_2^{2-}]_0) = D'([Cu(S_2O_3)_2^{3-}]_0 - [Cu(S_2O_3)_2^{3-}]) \quad (15)$$

where D' and D'' represent the diffusion coefficients of the copper(I) and copper(II) complexes, respectively, and if $[Cu(S_2O_3)_2^{3-}] = 0$, the concentration of copper(I) at the membrane surface is given by

$$[Cu(S_2O_3)_2^{3-}]_0 = \frac{D''}{D'}([Cu(S_2O_3)_2^{2-}] - [Cu(S_2O_3)_2^{2-}]_0) \quad (16)$$

It is also reasonable to accept that the surface concentration of $Cu(S_2O_3)_2^{2-}$ is negligible compared to the bulk concentration, so

$$[Cu(S_2O_3)_2^{3-}]_0 = 2\frac{D''}{D'}[Cu(S_2O_3)_2^{2-}] \quad (17)$$

By substitution of this expression into equation (14) and setting $D''/D' = B$, the surface concentration of the ligand can be evaluated:

$$[S_2O_3^{2-}]_0 = C_{S_2O_3^{2-}} - 4B[Cu(S_2O_3)_2^{2-}] \quad (18)$$

or, assuming that the predominant form of copper(II) in the solution is its complex:

$$[S_2O_3^{2-}]_0 = C_{S_2O_3^{2-}} - 4BC_{Cu^{2+}} \quad (19)$$

The surface concentration of the ligand (19) and the concentration of $Cu(S_2O_3)_2^{2-}$ expressed in terms of the stability constant β_2 and equation (11) can be used to calculate the potential-governing concentration of copper(II):

$$[Cu^{2+}]_0 = \frac{4B^2C^2_{Cu^{2+}}}{K_1\beta_2(C_{S_2O_3^{2-}} - 4BC_{Cu^{2+}})^2} \quad (20)$$

Thus the equation for the electrode potential (9) may be written in more extended form:

$$E = E^{0\prime} + \frac{RT}{F} \ln \frac{C_{Cu^{2+}}}{(C_{S_2O_3^{2-}} - 4BC_{Cu^{2+}})^2} \quad (21)$$

where

$$E^{0\prime} = E^0_{ISE} + \frac{RT}{F} \ln \frac{2B}{\sqrt{\beta_2 K_1}} \quad (22)$$

When Ag_2S is the potential-governing electrode component, the concentration of copper(II) ions is controlled by the reaction

$$2Cu(S_2O_3)_2^{2-} + Ag_2S + 4S_2O_3^{2-} \rightleftharpoons 2Cu(S_2O_3)_2^{3-} + 2Ag(S_2O_3)_2^{3-} + S \quad (23)$$

occurring at the membrane surface, for which the equilibrium constant is

$$K_2 = \frac{[Cu(S_2O_3)_2^{3-}]_0 [Ag(S_2O_3)_2^{3-}]_0}{[Cu(S_2O_3)_2^{2-}]_0 [S_2O_3^{2-}]_0^2} = 10^{2.8} \quad (24)$$

The mass balance for the ligand is expressed as

$$C_{S_2O_3^{2-}} = [S_2O_3^{2-}]_0 + 2[Cu(S_2O_3)_2^{2-}]_0 + 2[Cu(S_2O_3)_2^{3-}]_0 + 2[Ag(S_2O_3)_2^{3-}]_0 \quad (25)$$

and the stationary state is described by equality of the corresponding fluxes

$$D''([Cu(S_2O_3)_2^{2-}] - [Cu(S_2O_3)_2^{2-}]_0) = D'([Cu(S_2O_3)_2^{3-}]_0 - [Cu(S_2O_3)_2^{3-}]) \quad (26)$$

and

$$D''([Cu(S_2O_3)_2^{2-}] - [Cu(S_2O_3)_2^{2-}]_0) = D^{Ag}([Ag(S_2O_3)_2^{3-}]_0 - [Ag(S_2O_3)_2^{3-}]) \quad (27)$$

When $[Cu(S_2O_3)_2^{2-}]_0$, $[Cu(S_2O_3)_2^{3-}]$ and $[Ag(S_2O_3)_2^{3-}]$ are negligible in comparison with the respective concentrations in the equations above, then the concentrations in equation (24) may be expressed as

$$[Cu(S_2O_3)_2^{3-}]_0 = BC_{Cu^{2+}} \quad (28)$$

$$[Ag(S_2O_3)_2^{3-}]_0 = GC_{Cu^{2+}} \quad (29)$$

and

$$[S_2O_3^{2-}]_0 = C_{S_2O_3^{2-}} - 2(B+G)C_{Cu^{2+}} \quad (30)$$

where G represents D''/D^{Ag}.

Substitution into equation (24) gives the following expression for the potential of the copper ion-selective electrode:

$$E = E^0 + \frac{RT}{F} \ln \frac{C_{Cu^{2+}}}{(C_{S_2O_3^{2-}} - 2(B+G)C_{Cu^{2+}})^2} \quad (31)$$

where

$$E^0 = E^0_{ISE} + \frac{RT}{F} \ln \frac{\sqrt{BG}}{\sqrt{\beta_2 K_2}} \quad (32)$$

Some doubts may arise about the degree of reduction of copper in the bulk of the solution. The equilibrium constant of this reaction is probably not larger than 5×10^2, as can be evaluated on the basis of known redox potentials. This reaction has a large activation energy, however, and also the copper(I) complexes can be oxidized in the presence of oxygen.[22] To obtain experimental evidence on this, the copper(II) solutions were titrated with thiosulphate. When the reduction and complexation occur in the bulk, the consumption of titrant should be 3 moles of thiosulphate for 1 mole of copper(II);

$$2Cu^{2+} + 6S_2O_3^{2-} \rightleftharpoons 2Cu(S_2O_3)_2^{3-} + S_4O_6^{2-}; \quad (33)$$

otherwise only 2 moles of thiosulphate should be consumed in the complexation reaction:

$$Cu^{2+} + 2S_2O_3^{2-} \rightleftharpoons Cu(S_2O_3)_2^{2-} \quad (34)$$

In the experiment, about 2.2 moles were found to be consumed, which indicates that a small amount of reduction proceeds in the solution.

If the reduction is assumed to be complete, then $[Cu(S_2O_3)_2^{3-}]$ equals the total copper concentration and the potential should be interpreted only on the basis of the reaction stoichiometry. In such a case the final equation would have the form:

$$E = E^0 + \frac{RT}{F} \ln \frac{C_{Cu^{2+}}}{(C_{S_2O_3^{2-}} - ZC_{Cu^{2+}})^2} \quad (35)$$

where from the stoichiometry $Z = 3$, which is close to $2(B+G) = 3.5$, found experimentally as a best fit for the Orion-type electrode.

In order to check the agreement of the proposed model with the experimental data, equations (21) and (31) were written in the semi-empirical form with "constant", S and A_e as the equation parameters:

$$E = \text{constant} + S \log \frac{C_{Cu^{2+}}}{(C_{S_2O_3^{2-}} - A_e C_{Cu^{2+}})^2} \quad (36)$$

The "constant", S and A_e were calculated by the following numerical linearization procedure.

(*a*) For the set of $(pC_{Cu^{2+}})_i$ values corresponding to the set of E_i values for a fixed A_e value, the values n_i for

$$n_i = \log \frac{(C_{Cu^{2+}})_i}{[C_{S_2O_3^{2-}} - A_e(C_{Cu^{2+}})_i]^2} \quad (37)$$

were calculated.

(*b*) The E_i and n_i values were correlated by the least-squares method and the values of the "constant," S and r^2 were obtained (r is the correlation coefficient).

(*c*) The A_e value was changed by steps of $\Delta A_e = 0.1$, starting from $A_e = 0$, and the calculations were repeated until the best correlation coefficient was obtained (Table 2).

When the thiosulphate concentration was 0.4*M*, only potential values for total copper concentrations larger than $10^{-3}M$ were taken into account, whereas for 0.04*M* thiosulphate concentration only potential values for total copper concentrations less than $2 \times 10^{-3}M$ were used. This was done to avoid excessive membrane corrosion in the first case and incomplete conversion of Cu(II) into Cu(I) in the second. Neither of the linearized calibration curves for 0.04*M* and 0.4*M* thiosulphate media covers the whole analytical range (Fig. 5), but the linear parts are complementary and together cover the pCu range from 2 to 5. Two scales are shown on the abscissa, the linear scale n and the non-linear scale pCu. Their interrelation changes according to the thiosulphate concentration.

The experimentally found parameters of equation (36) should have a physical meaning which follows from the model presented for the interference mech-

Table 2. Numerical calculation of the parameters of equation (36)

Medium	const.	s	r^2	A
		0.04*M* $S_2O_3^{2-}$		
2*M* KNO_3	−136.3	59.2	0.999	3.5
1*M* KCl	−138.7	59.1	0.999	3.5
2*M* KCl	−144.8	59.3	0.999	3.5
3*M* KCl	−149.6	59.6	0.999	3.5
1*M* KBr	−143.4	57.5	1.000	3.5
2*M* KBr	−159.9	55.2	1.000	3.5
3*M* KBr	−182.9	51.5	0.999	3.5
		0.4*M* $S_2O_3^{2-}$		
2*M* KNO_3	−184.8	57.1	0.994	3.5
1*M* KCl	−185.2	57.4	0.995	3.5
2*M* KCl	−198.3	57.4	0.997	3.5
3*M* KCl	−196.0	56.5	0.999	3.5
1*M* KBr	−187.7	57.4	0.999	3.5
2*M* KBr	−195.7	56.9	0.999	3.5
3*M* KBr	−198.6	57.4	0.999	3.5

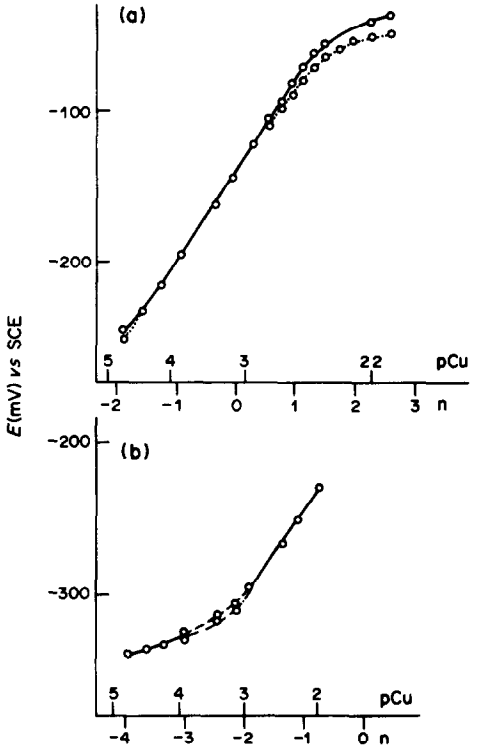

Fig. 5. Corrected calibration graphs for Orion 94-29 electrode in solutions containing halide and thiosulphate ions: a—0.04*M* sodium thiosulphate, b—0.4*M* sodium thiosulphate. Solid lines for 1*M* potassium chloride, dashed lines for 1*M* potassium bromide.

anism. The parameter $A_e = 4D''/D'$ cannot be exactly calculated, because of lack of precise values for the diffusion coefficients. However, they may be evaluated by taking into account that in the absence of complexing ligands the ratio of the diffusion coefficients for copper(II) and copper(I) species is 0.45.[23] It is known that complexation increases this value[24,25] and it may be assumed that it approaches unity.[26] Therefore the value of A_e should fit in the range 1.8–4 for linear diffusion transport, or even in the narrower range 2.5–4 when convection is taken into account.[27] The experimentally found value of 3.5 fits well in this range.

The constant corresponding to the standard potential E^0 can be calculated on the basis of equations (21) and (31), with the parameter B calculated from the experimentally found value of A_e. Assuming the activity of sulphur in the membrane to be unity (sulphur-rich electrode), the expected E^0 should be -57 mV *vs.* SCE. Assuming the activity of silver to be unity (silver-rich electrode), then $E^0 = -192$ mV *vs.* SCE. The values of the "constant," given in Table 2, are nearly bracketed by these two values, so they seem to be physically sound.

The slope of the linearized curve should be Nernstian, and the values in Table 2 are all, except for the 3*M* potassium bromide system, within the reasonable limits of 55.0–59.5 mV/pCu.

CONCLUSIONS

The interferences caused by the presence of chloride and bromide ions in the response of copper ion-selective electrodes are manifested by insufficient reproducibility, long response time, narrow range of linearity of electrode response and variable slope in the pCu range from 2 to 5. Such effects may be effectively counteracted by the addition of a proper concentration of thiosulphate, the strongly complexing and reducing properties of which can eliminate the membrane corrosion caused by halides and prevent precipitation of the slightly soluble silver halides. The exchange reactions at the membrane/solution interface are also stabilized, which permits the analytical utilization of the super-Nernstian electrode slope.

It may be suggested that a similar procedure may be applied for elimination of interferences with other solid-state ion-selective electrodes.

Acknowledgement—This study was financially supported through the project MR-I-32.

REFERENCES

1. J. Gulens, *Ion-Selective Electrode Rev.*, 1980, **2**, 117.
2. R. Jasiński, I. Trachtenberg and D. Andrychuk, *Anal. Chem.*, 1974, **46**, 364.
3. J. Barica, *J. Fish. Res. Board Can.*, 1978, **35**, 141.
4. J. W. Ross in *Ion-Selective Electrodes*, R. A. Durst (ed.), p. 82. National Bureau of Standards, Washington, 1969.
5. J. D. Crombie, G. J. Moody and J. D. R. Thomas, *Talanta*, 1974, **21**, 1094.
6. A. Hulanicki and A. Lewenstam, *ibid.*, 1976, **23**, 661.
7. P. Lanza, *Anal. Chim. Acta*, 1979, **105**, 53.
8. T. Hepel, *ibid.*, 1981, **123**, 151; 1981, **123**, 161; 1982, **142**, 217.
9. J. C. Westall, F. M. M. Morel and D. N. Hume, *Anal. Chem.*, 1979, **51**, 1792.
10. E. Ghali, B. Dandapani and A. Lewenstam, *J. Appl. Electrochem.*, 1982, **12**, 369.
11. A. Lewenstam, in *Theory and Application of Ion-Selective Electrodes in Medicine and Physiology*, M. Kessler (ed.), Springer Verlag, Berlin, in press.
12. G. J. Moody, N. S. Nassory, J. D. R. Thomas, D. Betteridge, P. Szepesvary and B. J. Wright, *Analyst*, 1979, **104**, 348.
13. G. Thomas and T. R. Ingraham, *Can. Met. Quart*, 1967, **6**, 153.
14. G. Thomas, T. R. Ingraham and R. J. C. MacDonald, *ibid.*, 1967, **6**, 281.
15. P. Brennet, S. Jafferali, J. M. Vansevaren, J. Vareecken and R. Winard, *Met. Trans.*, 1974, **5**, 127.
16. J. C. Scully, *Fundamentals of Corrosion*, Pergamon Press, Oxford, 1964.
17. T. Biegler and D. A. Swift, *J. Appl. Electrochem.*, 1979, **9**, 545.
18. H. J. Mathieu and H. Rickert, *Z. Phys. Chem. (Frankfurt)*, 1972, **79**, 315.
19. W. M. Latimer, *Oxidation Potentials*, 2nd Ed., Prentice-Hall, New York, 1952.
20. G. Schwarzenbach and M. Schellenberg, *Helv. Chim. Acta*, 1965, **48**, 28.
21. L. G. Sillén and A. E. Martell, *Stability Constants of Metal-Ion Complexes*, Spec. Publ. Nos. 17 and 25, The Chemical Society, London, 1964 and 1971.

22. H. A. Laitinen and W. E. Harris, *Chemical Analysis*, McGraw-Hill, New York, 1975.
23. G. W. Tindall and S. Bruckenstein, *Anal. Chem.*, 1968, **40**, 1402.
24. D. G. Peters and S. A. Cruser, *J. Electroanal. Chem.*, 1965, **9**, 27.
25. I. A. Semeonov, V. F. Lazarev and A. I. Levin, *Elektrokhimiya*, 1975, **11**, 1091.
26. J. Małyszko, *Thesis, Mechanism of copper(II) ion electro-reduction* (in Polish), School of Agriculture, Siedlce, 1978.
27. N.Ibl, *Advances in Electrochemistry and Electrochemical Engineering*, P. Delahay and C. W. Tobias (eds.), Vol. 2, p. 88, Wiley, New York, 1962.

Talanta, Vol. 32, No. 7, pp. 539–543, 1985
Printed in Great Britain

0039-9140/85 $3.00 + 0.00
Pergamon Press Ltd

DETERMINATION OF METALS BY SECOND-HARMONIC ALTERNATING-CURRENT VOLTAMMETRY WITH A SEMI-STATIONARY MERCURY ELECTRODE

CLINIO LOCATELLI, FRANCESCO FAGIOLI and CORRADO BIGHI
Department of Chemistry, University of Ferrara, Via L. Borsari 46, 44100 Ferrara, Italy

TIBOR GARAI
Research Laboratory for Inorganic Chemistry, Hungarian Academy of Sciences, Budaorsi Ut 45, H-1112 Budapest, Hungary

(*Received* 6 *December* 1984. *Accepted* 31 *January* 1985)

Summary—The simultaneous determination of tin(II) and lead(II) as well as of indium(III) and cadmium(II) by second-harmonic a.c. voltammetry using a semi-stationary mercury electrode with a drop-time of 240–300 sec (the long-lasting sessile-drop mercury electrode) has been investigated. Under the best experimental conditions, concentration ratios in the ranges $1:12 \leqslant c_{Sn}:c_{Pb} \leqslant 15:1$ and $1:15 \leqslant c_{In}:c_{Cd} \leqslant 15:1$ can be determined.

The half-wave potentials for the reduction of tin(II) and lead(II), and of indium(III) and cadmium(II), in the commonly used electrolytes, are very close and thus simultaneous polarographic determination of these pairs of elements is hindered. Various organic complexing agents or special solutions have been suggested as the supporting electrolytes for the determination of these elements. Kasagi and Banks[1] investigated the polarographic determination of small amounts of indium(III) in the presence of large amounts of cadmium(II), lead(II) and tin(II), using a solution of potassium iodide as the supporting electrolyte.

Metzger *et al.*[2–4] determined tin(II) and lead(II) by employing a mixture of hydrochloric acid and an alcohol (from C_1 to C_5) as solvent. In these supporting electrolytes the half-wave potentials of tin(II) and lead(II) are better separated and so the simultaneous determination of these ions is possible. Cinquantini *et al.*[5] determined tin(II) and lead(II) in 1*M* triammonium citrate medium at pH 4–7. Jacobsen and Tandberg[6] determined indium(III) and cadmium(II) in citrate buffer at pH 3.5 by d.c. and a.c. polarography. Perone and co-workers[7,8] and Bond and Grabaric[9] used microprocessor-controlled polarographs for the simultaneous determination of two species with overlapping polarographic waves. Fagioli *et al.*[10] employed second-harmonic a.c. polarography for the simultaneous determination of indium(III) and cadmium(II) in 1*M* hydrochloric acid with a conventional dropping mercury electrode. This work has now been extended to the simultaneous determination of tin(II) and lead(II) and of indium(III) and cadmium(II) by second-harmonic a.c. voltammetry by use of a semi-stationary mercury electrode with a drop-time of 240–300 sec.[11] This technique makes it possible to shorten the analysis time and gives lower detection limits than those attained by conventional a.c. polarography.

EXPERIMENTAL

Apparatus

Current *vs.* potential curves were recorded with an AMEL model 471 Multipolarograph equipped with a 291/LF stirrer and a 452/T timer. The three-electrode system consisted of a long-lasting sessile-drop mercury electrode as the working electrode, a saturated calomel reference electrode (SCE) and a platinum auxiliary electrode. The voltammetric cell was kept at 25.0 ± 0.5°. The solutions were deaerated by passage of pure nitrogen before analysis, and during the polarography a nitrogen atmosphere was maintained above the solution, and the solution was stirred with a magnetic stirrer.

Reagents and reference solutions

Hydrochloric acid and all other chemicals were Merck "Suprapur" grade. Intermediate reference solutions of various concentrations were prepared from BDH 1000-mg/l. stock solutions of Sn, Pb, In and Cd. The water used was demineralized and then twice distilled from potassium permanganate. The Teflon cell was periodically rinsed with concentrated nitric acid to eliminate contamination. Standard additions were made with Eppendorf micropipettes with disposable plastic tips.

RESULTS AND DISCUSSION

The voltammetric behaviour of the tin(II)–lead(II) and indium(III)–cadmium(II) pairs was studied by first and second harmonic a.c. polarography.

Calibration curves for tin(II) and lead(II)

Hydrochloric acid (1*M*) was chosen as supporting electrolyte. The measurement conditions used are

Table 1. Experimental conditions for the determination of tin(II) and lead(II) by a.c. voltammetry

Parameter*		Sn(II)	Pb(II)
E_i	*V vs. SCE*	−0.200	−0.200
t_d	*sec*	180	180
dE/dt	*mV/sec*	10	10
f	*Hz*	100	100
ΔE	*mV*	10	10
$\phi_{\text{first harmonic}}$	*degrees*	270 + 80	270 + 89
$\phi_{\text{second harmonic}}$	*degrees*	270 + 67	270 + 72

*E_i = initial potential; t_d = delay time for growth of drop before recording; dE/dt = potential scan-rate; f = frequency; ΔE = amplitude of a.c. voltage; ϕ = demodulation phase angle.

listed in Table 1. The demodulation phase angle ϕ was carefully set, since if properly chosen it can almost completely eliminate the capacitive current.

The polarographic wave parameters are reported in Table 2. The peak-width measured at half-height of the fundamental harmonic polarographic curve is $W_{1/2} = 90/n$ mV where n is the number of electrons involved in the electrode process. This relationship together with the equation $p\text{–}p = 68/n$ mV, where $p\text{–}p$ is the peak-to-peak separation of the potentials of the second harmonic a.c. polarographic curve,[12] are the simplest tests for the polarographic reversibility of an electrode reaction. The experimental half-peak widths and peak-to-peak separations of potential indicate that the polarographic reactions for both electroactive species are reversible. The half-wave potentials are also in excellent agreement with the literature values reported in the same Table.

The calibration curves for the determination of tin(II) and lead(II) were prepared for both first and second harmonic a.c. voltammetry. In all cases the standard addition method was used and each point was the mean of five readings. The second harmonic a.c. calibration curves were plotted on the basis of the cathodic peak current for tin(II) and the anodic peak current for lead(II).[13] The correlation coefficient is very satisfactory for all the regression functions reported in Table 3, while the relative standard deviation s_r is reasonably low. The corresponding detection limit is also reported for each calibration curve.

Simultaneous determination of tin(II) and lead(II)

The simultaneous determination of tin(II) and lead(II) was studied over the concentration ranges covered by the individual calibration curves. The voltamperograms were recorded under the experimental conditions reported in Table 1. The second (curve *a*) and the fundamental (curve *b*) harmonic a.c. voltamperograms of mixtures of tin(II) and lead(II) are shown in Fig. 1. The second harmonic a.c. voltamperogram indicates good resolution of the two electroactive species, whereas in the first harmonic a.c. voltamperogram the peaks for the two elements are not separated, and the combined peak has a half-width $>90/n$ mV.

Under the experimental conditions reported in Table 1, the simultaneous determination of tin(II) and lead(II) is possible in the range of concentration ratios $1{:}12 \leqslant c_{Sn}{:}c_{Pb} \leqslant 15{:}1$. The data were processed by univariate and bivariate analysis. The regression

Table 2. Polarographic wave parameters of tin(II) and lead(II)

Parameter*		Sn(II)	Pb(II)
$E_{p\ \text{first harmonic}}$	*V vs. SCE*	−0.480 ± 0.005	−0.440 ± 0.005
$E_{r\ \text{second harmonic}}$	*V vs. SCE*	−0.485 ± 0.005	−0.445 ± 0.005
$W_{1/2}$	*mV*	45 ± 5	50 ± 5
$p\text{–}p$	*mV*	35 ± 5	35 ± 5
$E_{1/2}$	*V vs. SCE* (1*M* HCl medium[14])	−0.470	−0.435

*E_p = peak potential; E_r = reversible potential; $W_{1/2}$ = peak-width at half height; $p\text{–}p$ = peak-to-peak separation of potentials; $E_{1/2}$ = reversible potential of electroactive species.

Table 3. Calibration curves for tin(II) and lead(II)*

Sn(II)	Pb(II)
First harmonic $i_p = 0.02 \pm 0.02 + (1.244 \pm 0.004) \times 10^5 c$ $r = 0.9999$; $s_r = 1.1\%$; D.L. $= 3.2 \times 10^{-7} M$	First harmonic $i_p = 0.03 \pm 0.03 + (1.846 \pm 0.094) \times 10^5 c$ $r = 0.9990$; $s_r = 3.1\%$; D.L. $= 2.2 \times 10^{-7} M$
Second harmonic $i_p = 0.001 \pm 0.001 + (1.378 \pm 0.012) \times 10^4 c$ $r = 0.9998$; $s_r = 2.8\%$; D.L. $= 2.9 \times 10^{-6} M$	Second harmonic $i_p = 0.01 \pm 0.01 + (1.950 \pm 0.026) \times 10^4 c$ $r = 0.9995$; $s_r = 2.4\%$; D.L. $= 2.1 \times 10^{-6} M$
Range of concentrations $0\text{–}5 \times 10^{-5} M$	Range of concentrations $0\text{–}3 \times 10^{-5} M$

*The limit of detection, D.L., is expressed according to the IUPAC recommendation[15] (99% probability). The units are μA for i_p and M for c.

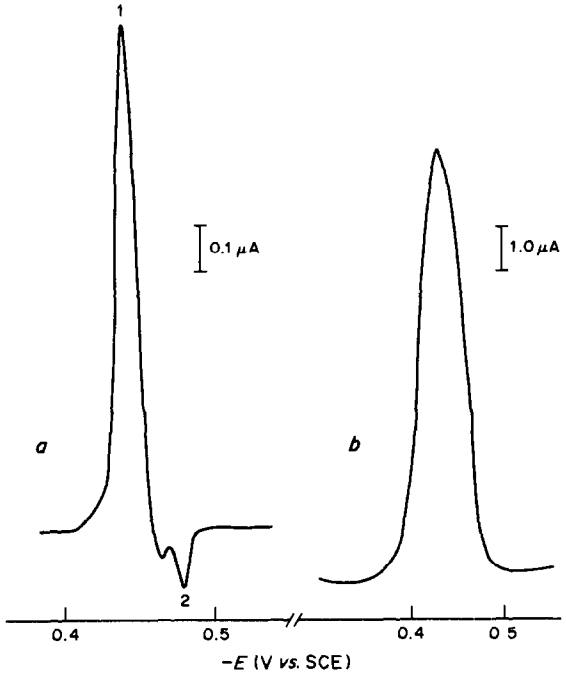

Fig. 1. Alternating current voltamperograms of tin(II) and lead(II): $c_{Pb} = 5.85 \times 10^{-5} M$; $c_{Sn} = 8.33 \times 10^{-6} M$. Curve *a*: second harmonic a.c. voltamperogram [Pb(II): peak 1, Sn(II): peak 2]. Curve *b*: first harmonic a.c. voltamperogram. Experimental conditions: Table 1.

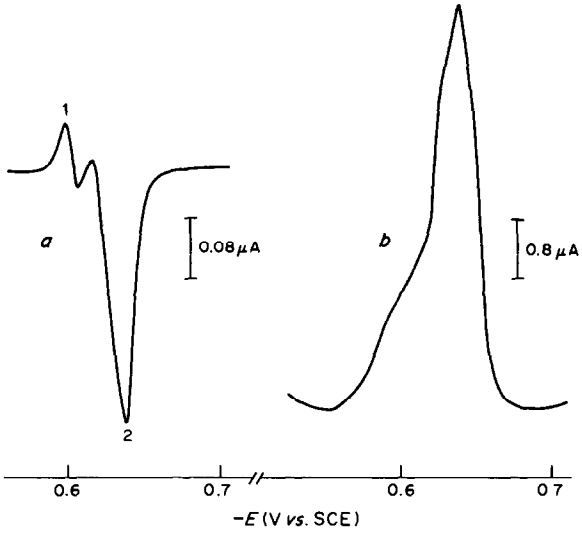

Fig. 2. Alternating current voltamperograms of indium(III) and cadmium(II): $c_{In} = 3.15 \times 10^{-6} M$; $c_{Cd} = 1.54 \times 10^{-5} M$. Curve *a*: second harmonic a.c. voltamperogram [In(III): peak 1, Cd(II): peak 2]. Curve *b*: first harmonic a.c. voltamperogram. Experimental conditions: Table 5.

functions calculated on the basis of the respective peak current values for tin(II) and lead(II) in mixtures are reported in Table 4. The univariate analysis neglects the presence of the interfering element, while the bivariate analysis takes into account the contribution of the interfering element as well. It is noteworthy that the slopes of the bivariate regression equations for both elements are practically equal to those of the individual calibration curves (*cf.* Table 3) and the univariate regression line. This proves that in the range of concentration ratios considered, the mutual interferences of tin(II) and lead(II) are negligible. The precision of the method, expressed as the relative standard deviation s_r, is 2–3% and the accuracy, expressed as relative error e, is 1–2%.

Calibration curves for indium(III) and cadmium(II)

The technique used for tin(II) and lead(II) determination was also employed for the a.c. voltammetric determination of indium(III) and cadmium(II). The

Table 4. Analysis of tin–lead mixtures*

Determination of tin(II) in the presence of lead(II)	Determination of lead(II) in the presence of tin(II)
Univariate analysis $i_p = 0.01 \pm 0.02 + (1.403 \pm 0.010) \times 10^4 c$ $r = 0.9997$; $s_r = 2.9\%$; $e = +1.8\%$ D.L. $= 2.9 \times 10^{-6} M$	Univariate analysis $i_p = -0.01 \pm 0.01 + (1.985 \pm 0.021) \times 10^4 c$ $r = 0.9991$; $s_r = 2.4\%$ $e = +1.8\%$ D.L. $= 2.0 \times 10^{-6} M$
Bivariate analysis $i_p = 0.0015 + (1.372 \pm 0.006) \times 10^4 c_{Sn} + (16 \pm 35) c_{Pb}$ $r = 0.9996$; $s_r = 2.0\%$; $e = -0.5\%$ D.L. $= 2.9 \times 10^{-6} M$	Bivariate analysis $i_p = 0.000085 + (1.982 \pm 0.008) \times 10^4 c_{Pb} + (35 \pm 127) c_{Sn}$ $r = 0.9996$; $s_r = 2.2\%$; $e = +1.6\%$ D.L. $= 2.0 \times 10^{-6} M$

*D.L. and units are defined in the footnote to Table 3.

Table 5. Experimental conditions for the determination of indium(III) and cadmium(II) by a.c. voltammetry

Parameter*		In(III)	Cd(II)
E_i	*V vs. SCE*	−0.400	−0.400
t_d	*sec*	180	180
dE/dt	*mV/sec*	10	10
f	*Hz*	100	100
ΔE	*mV*	10	10
$\phi_{\text{first harmonic}}$	*degrees*	0 + 0.5	0 + 0
$\phi_{\text{second harmonic}}$	*degrees*	270 + 65	270 + 64

*See footnote to Table 1.

experimental conditions are reported in Table 5 and the polarographic wave parameters in Table 6.

It is apparent that the literature and experimental data are in excellent agreement. The calibration curves and other statistical parameters for indium(III) and cadmium(II) are given in Table 7.

For the second harmonic a.c. calibration curves the cathodic peak current of cadmium(II) and the anodic current of indium(III)[13] were measured. The relative standard deviation (1–2%) is again low.

Simultaneous determination of indium(III) and cadmium(II)

Indium(III) and cadmium(II) were simultaneously determined in the concentration ranges covered by the individual calibration curves. One example of the second and first harmonic a.c. voltamperograms of indium(III) and cadmium(II) mixtures in 1*M* hydrochloric acid is shown in Fig. 2. In the second harmonic a.c. voltamperogram (curve *a*), the peaks for the species are separated, but in the first harmonic a.c. voltamperogram (curve *b*), they are not. Under the experimental conditions in Table 5, the determination of indium(III) and cadmium(II) is possible in the range of concentration ratios between 15:1 and 1:15. The regression functions relating to indium(III) and cadmium(II) mixtures are summarized in Table 8. The slopes of the bivariate functions for both elements are practically equal to the slopes of the individual calibration curves and of the univariate analysis, showing that the mutual interference is negligible. The relative standard deviation and the relative error are both 2–3%.

Table 6. Polarographic wave parameters of indium(III) and cadmium(II)

Parameter*		In(III)	Cd(II)
$E_{p\,\text{first harmonic}}$	*V vs. SCE*	−0.595 ± 0.005	−0.640 ± 0.005
$E_{r\,\text{second harmonic}}$	*V vs. SCE*	−0.595 ± 0.005	−0.645 ± 0.005
$W_{1/2}$	*mV*	35 ± 5	48 ± 5
p–p	*mV*	25 ± 5	35 ± 5
$E_{1/2}$	*V vs. SCE* (1*M* HCl medium[14])	−0.597	−0.642

*See footnote to Table 2.

Table 7. Calibration curves for indium(III) and cadmium(II)*

In(III)	Cd(II)
First harmonic $i_p = 0.001 \pm 0.002 + (1.040 \pm 0.030) \times 10^5 c$ $r = 0.9988$; $s_r = 2.3\%$; D.L. $= 1.9 \times 10^{-7} M$	First harmonic $i_p = -0.002 \pm 0.003 + (1.372 \pm 0.017) \times 10^5 c$ $r = 0.9995$; $s_r = 1.4\%$; D.L. $= 1.5 \times 10^{-7} M$
Second harmonic $i_p = 0.003 \pm 0.004 + (1.860 \pm 0.035) \times 10^4 c$ $r = 0.9990$; $s_r = 2.1\%$; D.L. $= 1.1 \times 10^{-6} M$	Second harmonic $i_p = 0.001 \pm 0.001 + (2.110 \pm 0.030) \times 10^4 c$ $r = 0.9994$; $s_r = 2.8\%$; D.L. $= 0.9 \times 10^{-6} M$
Range of concentrations 0–1 × $10^{-5} M$	Range of concentrations 0–1 × $10^{-5} M$

*D.L. and units are defined in the footnote to Table 3.

Table 8. Analysis of indium–cadmium mixtures*

Determination of indium(III) in the presence of cadmium(II)	Determination of cadmium(II) in the presence of indium(III)
Univariate analysis $i_p = 0.001 \pm 0.002 + (1.843 \pm 0.012) \times 10^4 c$ $r = 0.9994$; $s_r = 2.2\%$; $e = -1.9\%$ D.L. $= 1.1 \times 10^{-6} M$	Univariate analysis $i_p = 0.001 \pm 0.001 + (2.099 \pm 0.010) \times 10^4 c$ $r = 0.9997$; $s_r = 2.7\%$; $e = -1.0\%$ D.L. $= 1.0 \times 10^{-6} M$
Bivariate analysis $i_p = 0.0014 + (1.840 \pm 0.015) \times 10^4 c_{In} + (50 \pm 122) c_{Cd}$ $r = 0.9994$; $s_r = 1.1\%$; $e = -1.1\%$ D.L. $= 1.1 \times 10^{-6} M$	Bivariate analysis $i_p = 0.0015 + (2.104 \pm 0.012) \times 10^4 c_{Cd} + (109 \pm 90) c_{In}$ $r = 0.9997$; $s_r = 2.2\%$; $e = -0.3\%$ D.L. $= 1.0 \times 10^{-6} M$

*D.L. and units are defined in the footnote to Table 3.

Both the selectivity and the sensitivity of the measurements with the semi-stationary electrode showed a definite improvement over those obtained with the conventional dropping mercury electrode. This is due to the larger surface area of the semi-stationary electrode and to the elimination of the noise of the dropping mercury electrode capillary at low concentrations.

REFERENCES

1. M. Kasagi and C. V. Banks, *Anal. Chim. Acta*, 1964, **30**, 248.
2. L. Metzger, G. G. Willems and R. Neeb, *Z. Anal. Chem.*, 1977, **288**, 35.
3. *Idem, ibid.*, 1978, **292**, 20.
4. *Idem, ibid.*, 1978, **293**, 16.
5. A. Cinquantini, T. Garai and J. Dévay, *Hung. Sci. Instr.*, 1975, **34**, 7.
6. E. Jacobsen and G. Tandberg, *Anal. Chim. Acta*, 1969, **47**, 285.
7. S. P. Perone and W. F. Gutknecht, *Anal. Chem.*, 1970, **42**, 906.
8. S. P. Perone and L. B. Sybrandt, *ibid.*, 1971, **43**, 382.
9. A. M. Bond and B. S. Grabaric, *ibid.*, 1976, **48**, 1624.
10. F. Fagioli, F. Dondi and C. Bighi, *Ann. Chim. (Rome)*, 1978, **68**, 111.
11. R. Andruzzi and A. Trazza, *Talanta*, 1981, **28**, 839.
12. A. M. Bond, *Modern Polarographic Methods in Analytical Chemistry*, Dekker, New York, 1980.
13. F. Fagioli, T. Garai and J. Dévay, *Ann. Chim. (Rome)*, 1974, **64**, 633.
14. L. Meites, *Polarographic Techniques*, p. 629. Interscience Publishers, New York, 1965.
15. International Union of Pure and Applied Chemistry, Analytical Chemistry Division, *Spectrochim. Acta*, 1978, **33B**, 219.

Talanta, Vol. 32, No. 7, pp. 545–548, 1985
Printed in Great Britain

0039-9140/85 $3.00 + 0.00
Pergamon Press Ltd

DETERMINATION OF NEODYMIUM AND BORON IN IRON–NEODYMIUM–BORON ALLOYS BY DIRECT-CURRENT PLASMA ATOMIC-EMISSION SPECTROMETRY

NOEL M. POTTER and HARRY E. VERGOSEN, III
Analytical Chemistry Department, General Motors Research Laboratories, Warren, Michigan 48090, U.S.A.

(*Received* 20 *September* 1984. *Revised* 30 *November* 1984. *Accepted* 31 *January* 1985)

Summary—Rapid, accurate methods for the determination of neodymium and boron in iron–neodymium–boron alloys are presented. The procedure involves dissolution of the alloy with nitric acid and measurement of the elemental concentrations by direct-current plasma atomic-emission spectrometry. Lithium is added in the determination of neodymium, to control interferences. The relative standard deviations are approximately 1%, and the accuracies comparable to those obtained by classical chemical methods.

Current efforts in the development of improved permanent-magnet materials have been focused on various rare earth–transition metal alloys. Recently, an iron–neodymium–boron alloy which exhibits superior magnetic qualities was reported.[1] As part of the programme to characterize these alloys, analytical methods were required to determine the bulk concentrations of neodymium and boron.

Neodymium can be determined by classical gravimetric methods, such as precipitation with oxalate.[2] This method, however, suffers from the slight solubility of the oxalate, and iron contamination of the precipitate. The method is also not specific for neodymium and the precipitate will include any rare earths present as impurities. Instrumental methods have been used successfully to determine neodymium, *e.g.*, neutron-activation analysis[3,4] and inductively-coupled plasma atomic-emission spectrometry (ICP–AES).[5,6]

Boron can be determined in a wide variety of materials by classical chemical methods.[7] Titration of boric acid in the presence of mannitol is precise and accurate, but subject to interferences.[8] Spectrophotometric methods are commonly used to measure boron at low concentrations,[9] but are usually slow, and preliminary sample treatment, such as distillation of methyl borate, may be necessary before they can be applied.[10] Instrumental methods have included direct-current plasma atomic-emission spectrometry (DCP–AES).[11]

In view of the reported use of ICP–AES to determine neodymium and of DCP–AES to determine boron, we investigated DCP–AES methods for the determination of both elements in the iron–neodymium–boron alloys. With these methods, interferences are minimal, and no extractions or other chemical techniques are required.

EXPERIMENTAL

Apparatus

A SpectraSpan V plasma atomic-emission spectrometer (Spectrametrics, Inc., Andover, MA) equipped with a Model DBC-33 background corrector was used. Operating conditions are listed in Table 1.

Reagents

All chemicals were ACS reagent grade unless stated otherwise. A neodymium standard solution (3000 μg/ml) was prepared with neodymium oxide ignited at 750° for 16 hr to decompose any carbonate: 3.499 g was added to 100 ml of demineralized water, then 100 ml of concentrated nitric acid and 2 drops of 30% hydrogen peroxide solution were added and the mixture was swirled until the neodymium oxide had dissolved. The solution was diluted accurately to 1 litre and mixed.

A 25-ml aliquot was diluted to 250 ml and this solution was used to prepare calibration solutions. An iron stock solution (0.7 mg/ml) was prepared by dissolving 700 mg of pure iron in 50 ml of demineralized water plus 50 ml of concentrated nitric acid, and the solution was diluted to 1 litre and mixed. A lithium stock solution (10 mg/ml) was prepared by dissolving 53 g of lithium carbonate in 220 ml of nitric acid (1 + 1) and diluting to 1 litre.

Neodymium calibration solutions (15, 30 and 45 μg/ml) were prepared by adding 10.0 ml of iron stock solution, 20.0 ml (added by pipette) of the lithium stock solution and 10 ml of concentrated nitric acid to each of three standard 100-ml flasks, followed by 5.0, 10.0 and 15.0 ml of the diluted neodymium standard solution, diluting to volume and mixing.

A boron standard solution (100 μg/ml) was prepared by dissolving 0.5720 g of boric acid in 1 litre of demineralized water. This solution was stored in a plastic bottle. A 3-mg/ml neodymium stock solution was prepared by dissolving 1.5 g of neodymium metal (boron-free) in 50 ml of demineralized water and 20 ml of concentrated nitric acid, then adding 230 ml of concentrated nitric acid and diluting to 500 ml. An iron stock solution (7 mg/ml) was prepared from 3.5 g of iron metal by using the same procedure used to prepare the neodymium stock solution.

Calibration solutions containing 5, 10 and 15 μg of boron per ml were prepared by placing 10 ml each of the neo-

Table 1. DCP operating conditions

Wavelength–neodymium, *nm*	386.341, 489.693
Wavelength–boron, *nm*	208.893, 249.678
Entrance slit, *μm*	50 × 300
Exit slit, *μm*	50 × 300
Integration time, *sec*	30
Sleeve argon pressure, *atm*	3.4
Nebulizer argon pressure, *atm*	1.9
Sample flow-rate, *ml/min*	~2

dymium and iron stock solutions in 100-ml standard flasks, adding ~30 ml of water, cooling to room temperature, adding appropriate volumes of the 100-μg/ml standard boron solution and diluting to volume with water.

Procedure

All glassware and plastic ware was cleaned with nitric acid (1 + 1) and rinsed with demineralized water before use. Weighed portions of crushed sample material (250 mg) were put into 250-ml plastic standard flasks, 50 ml of demineralized water and 25 ml of concentrated nitric acid were added, and the flasks were lightly capped.

The samples dissolved completely within 1 hr at room temperature. The flasks were not heated, because of the potential volatilization of boron compounds. The solutions were then diluted to volume and mixed. Boron was determined in these solutions. For the determination of neodymium, 10-ml aliquots of these solutions were placed in 100-ml standard flasks; 10 ml of concentrated nitric acid and 20.0 ml (added by pipette) of lithium solution were added, and the solutions were diluted to volume with water. By use of this procedure the calibration and sample solutions all contain similar concentrations of iron, neodymium and boron, for alloys nominally containing 70% iron, 30% neodymium, and 0.5–1.5% boron.

Sample measurement

The neodymium emission lines at 386.341 and 489.693 nm and boron emission lines at 208.893 and 249.678 nm are satisfactory for use with this method. The boron line at 249.773 nm is not used, because there is a weak iron line at 249.772 nm. The instrument was calibrated with the 15- and 45-μg/ml neodymium calibration solutions and the 5- and 15-μg/ml boron calibration solutions, as the calibration graphs were found to be linear over these ranges. To compensate for instrumental drift, an integration time of 30 sec was used; frequent calibration checks were made. The calibration solution closest in concentration to the sample solutions was measured before and after each three sample solutions. The amount of drift in the response of the calibration solutions was calculated, and the sample solution responses were corrected accordingly. If the relative drift was >5%, the instrument was recalibrated before proceeding. Adequate precision (~1% relative) was obtained when each sample solution was measured three times, and the results were averaged.

RESULTS AND DISCUSSION

Selection of standards

Neodymium oxide was used to prepare the neodymium standard solutions. The metal was not used, because it is too easily oxidized. Neodymium oxide samples from three sources were examined by DCP and X-ray fluorescence, and the one considered to be of highest purity was used in this work.

Sample preparation

The dissolution at room temperature with dilute nitric acid (1 + 2) proceeds rapidly. Concentrated nitric acid is not used, because the heat generated during dissolution could cause volatilization of boron. No contamination with boron was observed when solutions were kept in borosilicate glass for up to 24 hr, but, to exclude all risk, plastic standard flasks were used.

Spectral interferences

Neodymium. Boron and iron at the concentrations normally encountered in the alloy solutions gave no spectral interferences with the neodymium lines at 386.341 and 489.693 nm. Cerium, lanthanum and praseodymium (which are potential impurities in the neodymium used to make the alloys), when present at the same concentration as the neodymium, gave only small signals in the vicinity of the neodymium lines (2%, or less, of the neodymium signal).

Boron. For the boron lines selected, interference from neodymium at 208.896 nm and iron at 249.653 nm could occur. However, no effect on the boron line at 208.893 nm appeared to be caused by iron and neodymium at the concentrations normally encountered in the alloy solutions. The iron line at 249.653 nm was adequately resolved from the boron line at 249.678 nm, so did not interfere.

Non-spectral interferences

Neodymium. Because chemical interferences can be troublesome in DCP techniques, calibration solutions are usually matrix-matched to the samples. A preliminary study was made of the possibility of direct measurement of neodymium in the solutions used for the boron determination, with matrix-loaded calibration solutions (0.7 mg/ml iron, 8 μg/ml boron, 10% v/v nitric acid). Although the first results appeared favourable, the apparent neodymium concentration was found to vary according to the iron concentrations. For example, a 50% change in the iron concentration caused a 5% change in the neodymium result. Hence, another approach was required to eliminate the need for exact matrix-matching of the calibration and sample solutions (which requires a preliminary approximate analysis).

To minimize chemical effects in DCP emission spectroscopy, lithium may be added to the sample and calibration solutions. Addition of lithium was found also to cause a considerable increase in neodymium response (Fig. 1).

Solutions containing more than 5000 μg of lithium per ml were not examined, because of considerable plasma disturbance. A lithium concentration of 2000 μg/ml was selected because it gave no disturbance of the plasma. In addition, at this concentration (2000 μg/ml) small errors in addition of the lithium (±1%) caused only about ±0.3% change in the neodymium response. The lithium solution was therefore added

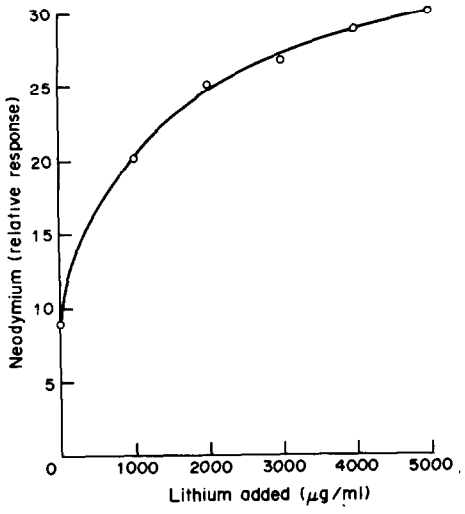

Fig. 1. Relative DCP response from solutions containing neodymium (30 μg/ml) and varying amounts of lithium.

by pipette. To facilitate the addition of lithium to the calibration and sample solutions and to allow use of the sample solutions used to determine boron, all the sample solutions were diluted tenfold. This dilution also minimized memory effects (caused by the DCP sample-delivery system) noted at higher neodymium concentrations.

With matrix-matched calibration and sample solutions, all containing 2000 μg of lithium per ml, changes of ±50% in the concentrations of iron and nitric acid caused no change in the neodymium responses. Boron had no effect on the neodymium response and was therefore not added to the calibration solutions.

Boron. Calibration solutions for the determination of boron were matrix-matched to the samples. All the solutions were adjusted to contain 10 ml of concentrated nitric acid per 100 ml, but no change in response was observed when the nitric acid concentration was varied by ±50%.

The iron–neodymium alloy used in this work nominally contains 70% iron and 30% neodymium, so the calibration solutions (0.7 mg/ml Fe, 0.3 mg/ml Nd) were made up to match this composition. When the iron and/or neodymium concentrations were varied by ±50%, no variations in response were noted except when the iron concentration was 1.05 mg/ml, which caused the boron response to increase by about 1%. Hence, addition of lithium to the solutions used for the determination of boron was not required.

Table 2. Precision data obtained with iron–neodymium–boron alloy

	Neodymium		Boron	
	386.341 nm	489.693 nm	208.893 nm	249.678 nm
Average concentration found*, %	30.8	30.8	0.88_2	0.88_5
Relative standard deviation, %	1.1	0.7	0.9	0.7

*Average from nine samples.

Table 3. Analyses of solutions containing known amounts of iron, neodymium and boron

Added, %*		Found, %			
		Neodymium		Boron	
Neodymium	Boron	DCP	Gravimetric†	DCP	Spectrophotometric§
29.8	0.599	30.0	30.0	0.603	0.595
29.8	0.596	29.7	29.8	0.600	0.594

*Balance is iron.
†Precipitation as oxalate.[2]
§Spectrophotometric quinalizarin method.[12]

Table 4. Comparison of results for iron–neodymium–boron alloys

	Neodymium found, %		Boron found, %	
Alloy	DCP	Gravimetric*	DCP	Spectrophotometric†
A	27.8	27.0	0.77	0.75
B	31.0	30.7	0.75	0.72
C	29.0	29.2	0.75	0.75
D	30.2	29.7	0.85	0.84
E	28.4	27.9	0.81	0.83
F	28.5	28.0	0.87	0.83
G	28.2	27.6	0.84	0.79

*Precipitation as oxalate[2].
†Spectrophotometric quinalizarin method.[12]

Precision and accuracy

Calibration solutions were analysed before and after each set of three sample solutions, and the responses were used to correct for instrumental drift. All sample solutions were measured three times to improve the precision.

A relative standard deviation of about 1% was obtained for both boron and neodymium in a sample containing 0.88% boron and 30.8% neodymium (Table 2). Nine replicates were run, each on a separate day, and fresh calibration solutions were prepared for each.

To evaluate accuracy, several iron–neodymium–boron alloys and two solutions containing known amounts of iron, neodymium and boron were analysed by the proposed method and also by classical chemical methods, neodymium being determined gravimetrically by oxalate precipitation,[2] and boron spectrophotometrically as the quinalizarin complex.[12] The results for the solutions (Table 3) show agreement within 1% relative, and those for the alloys (Table 4) show an average relative deviation (from the results for the reference method) of 1.7% for neodymium and 3.0% for boron.

A final advantage of the DCP methods is that ten samples, including sample preparation, can be analysed in 1 day, compared to the 2–3 days required for the chemical methods.

REFERENCES

1. J. J. Croat, J. F. Herbst, R. W. Lee and F. E. Pinkerton, *J. Appl. Phys.*, 1984, **55**, 2078.
2. M. M. Woyski and R. E. Harris, in *Treatise on Analytical Chemistry*, I. M. Kolthoff and P. J. Elving (eds.), Part II, Vol. 8, pp. 28–42. Wiley, New York, 1963.
3. C. C. Graham, M. D. Galscock, J. J. Carni, J. R. Vogt and T. G. Spalding, *Anal. Chem.*, 1982, **54**, 1623.
4. G. H. Morrison, J. T. Gerard, A. Travesi, R. L. Currie, S. F. Peterson and N. M. Potter, *ibid.*, 1969, **41**, 1633.
5. J. G. Crook and F. E. Lichte, *ibid.*, 1982, **54**, 1329.
6. H. Ishii and K. Satoh, *Talanta*, 1983, **30**, 111.
7. R. S. Braman, in *Treatise on Analytical Chemistry*, I. M. Kolthoff and P. J. Elving (eds.), Part II, Vol. 10, pp. 1–101. Wiley, New York, 1978.
8. *Idem*, *loc. cit.*, p. 87.
9. A. A. Nemodruk and Z. K. Karalava, *Analytical Chemistry of Boron*, Davey, New York, 1965.
10. *1983 Annual Book of ASTM Standards*, Vol. 03.05, p. 34. American Society for Testing and Materials, Philadelphia, 1983.
11. R. A. Burdo and M. L. Snyder, *Anal. Chem.*, 1979, **51**, 1502.
12. A. H. Jones, *ibid.*, 1957, **29**, 1101.

Talanta, Vol. 32, No. 7, pp. 549–558, 1985
Printed in Great Britain.

0039-9140/85 $3.00 + 0.00

CONTRIBUTIONS TO THE THEORY OF CATALYTIC TITRATIONS—II*

PRECIPITATION AND REDOX CATALYTIC TITRATIONS

BILJANA F. ABRAMOVIĆ and FERENC F. GAÁL
Institute of Chemistry, Faculty of Sciences, University of Novi Sad,
V.Vlahovića 2, YU-21000 Novi Sad, Yugoslavia

DJURA Ž. PAUNIĆ
Institute of Mathematics, Faculty of Sciences, University of Novi Sad,
V.Vlahovića 2, YU-21000 Novi Sad, Yugoslavia

(*Received* 3 *July* 1984. *Revised* 7 *December* 1984. *Accepted* 23 *January* 1985)

Summary—Precipitation and redox catalytic titration curves, obtained by both volumetric and coulometric addition of the titrant, have been simulated, taking into account the equilibrium concentration of the catalyst during the titration. The influence of several factors on the shape of the simulated catalytic titration curves has been investigated and is discussed in detail. Simulations of the blank titrations have also been made.

In previous papers we have described simulation of complexometric catalytic titration curves[1] and compared them with the experimental curves.[2] In continuation we now describe simulation of precipitation and redox catalytic titrations with both volumetric and coulometric addition of the titrant, taking into account, as before,[1,2] the equilibrium concentration of the catalyst during the entire course of the titration. The effect of a number of parameters (the solubility product and equilibrium constant, respectively, order of the indicator reaction, rate constants for both the spontaneous and the catalysed reaction, *etc.*) on the shape of the simulated titration curves has been investigated and is discussed. Blank titrations have also been simulated. Further, we have determined the conditions allowing usage of the approximative equations with satisfactory accuracy.[1]

Detailed information on catalytic titrations can be found in several reviews.[3–11]

The procedure for deriving the expressions for simulation of precipitation and redox catalytic titration curves consisted in setting up an equation for the equilibrium concentration of catalyst during the titration, introducing it into the corresponding equation for the rate of the indicator reaction, and integrating that for the limiting conditions. To simplify the mathematics we assumed the same approximations as in our previous work,[1] namely:

(1) titrant is added to an ideally stirred solution;
(2) temperature changes during titration do not affect the thermodynamics and kinetics of the reactions;
(3) the indicator reaction has an induction period short enough to be neglected;
(4) the rate constant of the titration reaction is high enough not to need to be taken into account;
(5) changes caused in the measured parameter by the titration reaction are negligible compared to the changes due to the indicator reaction.

SIMULATION OF PRECIPITATION CATALYTIC TITRATIONS

To obtain an expression for the equilibrium concentration of the catalyst during the titration, we started from the solubility product, K_{sp} (for an AK type of compound), characterizing the reaction product:

$$K_{sp} = c(\mathrm{K})c'(\mathrm{A}) \qquad (1)$$

where $c(\mathrm{K})$ is the molar concentration of catalyst K, and $c'(\mathrm{A})$ that of inhibitor A. Introduction of the appropriate expression for $c'(\mathrm{A})$ into (1) gives a relation for the equilibrium concentration of catalyst during the titration.

Volumetric addition of titrant

The inhibitor concentration, $c'(\mathrm{A})$, during volumetric addition of the titrant is given by the equation:

$$c'(\mathrm{A}) = \frac{V_r c(\mathrm{A}) - jtc(\mathrm{T})}{V_r + jt} + c(\mathrm{K}) \qquad (2)$$

where $c(\mathrm{A})$ is the initial molar concentration of the inhibitor, *i.e.*, of the titrand before the titration is started, $c(\mathrm{T})$ the concentration of the titrant, V_r the initial volume of the titrated solution (l.), j the rate of addition of titrant (l./sec), and t is time (sec).

*Part I—*Talanta*, 1984, **31**, 987.

Introducing expression (2) into (1) gives an equation for the catalyst concentration during titration:

$$c(\mathrm{K}) = \frac{c(\mathrm{T})jt - V_r c(\mathrm{A}) + (E_p + F_p t + G_p t^2)^{\frac{1}{2}}}{2(V_r + jt)} \quad (3)$$

where

$E_p = V_r^2[c^2(\mathrm{A}) + 4K_{sp}]$;

$F_p = 2V_r j[4K_{sp} - c(\mathrm{A})c(\mathrm{T})]$;

$G_p = j^2[c^2(\mathrm{T}) + 4K_{sp}]$.

First-order indicator reaction. After introduction of expression (3) into the equation for the rate of a first or pseudo-first order indicator reaction

$$-\frac{dc(\mathrm{X})}{dt} = [k'_o + k'_k c(\mathrm{K})]c(\mathrm{X}) + \frac{c(\mathrm{X})j}{V_r + jt} \quad (4)$$

where k'_o is the rate constant for the first-order spontaneous reaction (sec^{-1}), k'_k the rate constant for the first-order catalysed reaction ($l.mole^{-1}.sec^{-1}$), $c(\mathrm{X})$ the molar concentration of the indicator reaction component, and after integration for the limiting conditions $c(\mathrm{X}) = c_o(\mathrm{X})$ and $t = 0$, it follows that the concentration of component X at time t is given by

$$c(\mathrm{X}) = c_o(\mathrm{X})\frac{V_r}{V_r + jt}\exp(-M_p) \quad (5)$$

where $c_o(\mathrm{X})$ is the initial molar concentration of the indicator-reaction component, and

$$M_p = \left[k'_o + \frac{k'_k c(\mathrm{T})}{2}\right]t - \frac{k'_k V_r}{2j}[c(\mathrm{A}) + c(\mathrm{T})] \times \ln\frac{V_r + jt}{V_r} + \frac{k'_k}{2j}R_p \quad (6)$$

where

$$R_p = [A_k + B_p(V_r + jt) + C_p(V_r + jt)^2]^{\frac{1}{2}} - (A_k + B_p V_r + C_p V_r^2)^{\frac{1}{2}} + \frac{B_p}{2C_p^{\frac{1}{2}}} \times \ln\frac{2C_p(V_r + jt) + B_p + 2\{C_p[A_k + B_p(V_r + jt) + C_p(V_r + jt)^2]\}^{\frac{1}{2}}}{2C_p V_r + B_p + 2[C_p(A_k + B_p V_r + C_p V_r^2)]^{\frac{1}{2}}} - A_k^{\frac{1}{2}} \times \ln\frac{V_r\{2\{A_k[A_k + B_p(V_r + jt) + C_p(V_r + jt)^2]\}^{\frac{1}{2}} + B_p(V_r + jt) + 2A_k\}}{(V_r + jt)\{2[A_k(A_k + B_p V_r + C_p V_r^2)]^{\frac{1}{2}} + B_p V_r + 2A_k\}} \quad (7)$$

in which

$A_k = \{V_r[c(\mathrm{A}) + c(\mathrm{T})]\}^2$;

$B_p = -2V_r c(\mathrm{T})[c(\mathrm{A}) + c(\mathrm{T})]$;

$C_p = c^2(T) + 4K_{sp}$.

Analogously, for the concentration of product L,

$$c(\mathrm{L}) = c_o(\mathrm{X})\frac{V_r}{V_r + jt}[1 - \exp(-M_p)]. \quad (8)$$

Second-order indicator reaction. If expression (3) for the catalyst concentration is introduced into the expression for the rate of the second-order indicator reaction [when the initial concentrations of the indicator reaction components are equal, *i.e.*, $c(\mathrm{X}) = c(\mathrm{Y})$], then:

$$-\frac{dc(\mathrm{X})}{dt} = [k_o + k_k c(\mathrm{K})]c(\mathrm{X})^2 + \frac{c(\mathrm{X})j}{V_r + jt} \quad (9)$$

where k_o is the rate constant for the second-order spontaneous reaction ($l.mole^{-1}.sec^{-1}$), and k_k the rate constant for the second-order catalysed reaction ($l^2.mole^{-2}.sec^{-1}$); integration gives the following equation for the concentration of component X at time t:

$$c(\mathrm{X}) = \frac{c_o(\mathrm{X})V_r}{[1 + c_o(\mathrm{X})Q_p](V_r + jt)} \quad (10)$$

where

$$Q_p = \frac{k_o V_r}{j}\ln\frac{V_r + jt}{V_r} + \frac{k_k V_r c(\mathrm{T})}{2j}\left(\ln\frac{V_r + jt}{V_r} - \frac{jt}{V_r + jt}\right) - \frac{k_k V_r^2 c(\mathrm{A})}{2j}\left(\frac{1}{V_r} - \frac{1}{V_r + jt}\right) + \frac{k_k V_r}{2j}S_p \quad (11)$$

in which

$$S_p = \frac{-[A_k + B_p(V_r + jt) + C_p(V_r + jt)^2]^{\frac{1}{2}}}{V_r + jt} + \frac{(A_k + B_p V_r + C_p V_r^2)^{\frac{1}{2}}}{V_r} + C_p^{\frac{1}{2}} \times \ln\frac{2C_p(V_r + jt) + B_p + 2\{C_p[A_k + B_p(V_r + jt) + C_p(V_r + jt)^2]\}^{\frac{1}{2}}}{2C_p V_r + B_p + 2[C_p(A_k + B_p V_r + C_p V_r^2)]^{\frac{1}{2}}} - \frac{B_p}{2A_k^{\frac{1}{2}}} \times \ln\frac{V_r\{2\{A_k[A_k + B_p(V_r + jt) + C_p(V_r + jt)^2]\}^{\frac{1}{2}} + B_p(V_r + jt) + 2A_k\}}{(V_r + jt)\{2[A_k(A_k + B_p V_r + C_p V_r^2)]^{\frac{1}{2}} + B_p V_r + 2A_k\}}. \quad (12)$$

For the concentration of product L,

$$c(\mathrm{L}) = \frac{c_o^2(\mathrm{X})Q_p V_r}{[1 + c_o(\mathrm{X})Q_p](V_r + jt)}. \quad (13)$$

Coulometric addition of titrant

The inhibitor concentration, $c'(\mathrm{A})$, in coulometric addition of the titrant is given by

$$c'(\mathrm{A}) = c(\mathrm{A}) - \frac{It}{nFV_r} + c(\mathrm{K}) \quad (14)$$

where I is the generating current (A), F the Faraday constant (C/eq) and n the number of electrons in the half-reaction for electrochemical generation of the titrant. Introducing expression (14) into (1) gives a relation for the catalyst concentration during the

titration:

$$c(\mathrm{K}) = \frac{It - nFV_r c(\mathrm{A}) + (E'_p + F'_p t + G'_p t^2)^{\frac{1}{2}}}{2nFV_r} \quad (15)$$

where

$$E'_p = (nFV_r)^2[c^2(\mathrm{A}) + 4K_{sp}];$$
$$F'_p = -2nFV_r Ic(\mathrm{A});$$
$$G'_p = I^2.$$

First-order indicator reaction. If the indicator reaction is of first or pseudo-first order, then putting expression (15) into the expression for the rate of the indicator reaction gives

$$-\frac{dc(\mathrm{X})}{dt} = [k'_o + k'_k c(\mathrm{K})]c(\mathrm{X}) \quad (16)$$

and after integration for the limiting conditions $c(\mathrm{X}) = c_o(\mathrm{X})$ and $t = 0$, the following equation is obtained for the concentration of component X at time t:

$$c(\mathrm{X}) = c_o(\mathrm{X}) \exp(-M'_p) \quad (17)$$

where

$$M'_p = k'_o t + \frac{k'_k I t^2}{4nFV_r} - \frac{k'_k c(\mathrm{A}) t}{2} + \frac{k'_k}{2nFV_r} R'_p \quad (18)$$

in which

$$R'_p = \frac{(2G'_p t + F'_p)(E'_p + F'_p t + G'_p t^2)^{\frac{1}{2}} - F'_p (E'_p)^{\frac{1}{2}}}{4G'_p} + \frac{4E'_p G'_p - (F'_p)^2}{8(G'_p)^{\frac{3}{2}}} \times \ln \frac{2[G'_p(E'_p + F'_p t + G'_p t^2)]^{\frac{1}{2}} + 2G'_p t + F'_p}{2(G'_p E'_p)^{\frac{1}{2}} + F'_p}. \quad (19)$$

For the concentration of product L,

$$c(\mathrm{L}) = c_o(\mathrm{X})[1 - \exp(-M'_p)]. \quad (20)$$

Second-order indicator reaction. Taking into account the rate for the second-order indicator reaction in coulometric addition of the titrant $[c(\mathrm{X}) = c(\mathrm{Y})]$

$$-\frac{dc(\mathrm{X})}{dt} = [k_o + k_k c(\mathrm{K})]c(\mathrm{X})^2 \quad (21)$$

and expression (15) describing the catalyst concentration during the titration, gives, after integration of equation (21) for the limiting conditions $c(\mathrm{X}) = c_o(\mathrm{X})$ and $t = 0$, the following relation for the concentration of component X at time t:

$$c(\mathrm{X}) = \frac{c_o(\mathrm{X})}{1 + c_o(\mathrm{X})Q'_p}. \quad (22)$$

For the concentration of product L, it follows that

$$c(\mathrm{L}) = \frac{c_o^2(\mathrm{X})Q'_p}{1 + c_o(\mathrm{X})Q'_p} \quad (23)$$

where Q'_p is analogous to M'_p in equation (18) but with constants k_o and k_k instead of k'_o and k'_k.

SIMULATION OF REDOX CATALYTIC TITRATIONS

The starting point in deriving suitable expressions for simulation of redox catalytic titration curves was the equation for the equilibrium constant, K_e, for the redox couple $n_1\mathrm{A}_{\mathrm{Red}} + n_2\mathrm{K}_{\mathrm{Ox}} \rightleftharpoons n_1\mathrm{A}_{\mathrm{Ox}} + n_2\mathrm{K}_{\mathrm{Red}}$, where $n_1 = n_2$, viz.

$$K_e = \frac{c(\mathrm{K}_{\mathrm{Red}})c(\mathrm{A}_{\mathrm{Ox}})}{c(\mathrm{A}_{\mathrm{Red}})c(\mathrm{K}_{\mathrm{Ox}})} \quad (24)$$

where $c(\mathrm{A}_{\mathrm{Red}})$ is the molar inhibitor concentration, $c(\mathrm{K}_{\mathrm{Ox}})$ the catalyst concentration, and $c(\mathrm{K}_{\mathrm{Red}})$ and $c(\mathrm{A}_{\mathrm{Ox}})$ are the molar concentrations of the redox reaction products.

On the basis of expression (24) and the corresponding expressions for the rate of the indicator reaction, the suitable equations for simulation of redox catalytic titrations have been derived.

Volumetric addition of titrant

In volumetric addition of the titrant, the concentrations of the inhibitor, $c(\mathrm{A}_{\mathrm{Red}})$, and of the reaction products $c(\mathrm{A}_{\mathrm{Ox}})$ and $c(\mathrm{K}_{\mathrm{Red}})$, respectively, are given by

$$c(\mathrm{A}_{\mathrm{Ox}}) = c(\mathrm{K}_{\mathrm{Red}}) = \frac{jtc(\mathrm{T})}{V_r + jt} - c(\mathrm{K}_{\mathrm{Ox}}) \quad (25)$$

$$c(\mathrm{A}_{\mathrm{Red}}) = \frac{V_r c(\mathrm{A})}{V_r + jt} - \frac{jtc(\mathrm{T})}{V_r + jt} + c(\mathrm{K}_{\mathrm{Ox}}). \quad (26)$$

Introducing expressions (25) and (26) into (24) gives a relation describing the catalyst concentration during the titration:

$$c(\mathrm{K}_{\mathrm{Ox}}) = \frac{c(\mathrm{T})(K_e - 2)jt - E_r^{\frac{1}{2}} + (E_r + F_r t + G_r t^2)^{\frac{1}{2}}}{2(K_e - 1)(V_r + jt)} \quad (27)$$

where

$$E_r = [K_e V_r c(\mathrm{A})]^2;$$
$$F_r = 2K_e V_r c(\mathrm{A})jc(\mathrm{T})(2 - K_e);$$
$$G_r = [jK_e c(\mathrm{T})]^2.$$

First-order indicator reaction. Introducing expression (27) into equation (4) for the rate of an indicator reaction of first or pseudo-first order, and integrating for the limiting conditions $c(\mathrm{X}) = c_o(\mathrm{X})$ and $t = 0$, gives an expression for the concentration of component X at time t:

$$c(\mathrm{X}) = c_o(\mathrm{X}) \frac{V_r}{V_r + jt} \exp(-M_r) \quad (28)$$

where

$$M_r = k'_o t + \frac{k'_k c(\mathrm{T})(K_e - 2)t}{2(K_e - 1)} - \frac{k'_k V_r}{2(K_e - 1)j} \times [c(\mathrm{T})(K_e - 2) + c(\mathrm{A})K_e] \times \ln \frac{V_r + jt}{V_r} + \frac{k'_k}{2(K_e - 1)j} R_r \quad (29)$$

where R_r is analogous to R_p in equation (7) but with

constants A_r, B_r and C_r instead of A_k, B_p and C_p, in which

$$A_r = K_e V_r^2 \{K_e[c^2(A) + c^2(T)] - 2c(A)c(T)(2 - K_e)\}$$

$$B_r = 2V_r c(T)K_e[c(A)(2 - K_e) - c(T)K_e]$$

$$C_r = [c(T)K_e]^2.$$

For the concentration of product L,

$$c(L) = c_o(X)\frac{V_r}{V_r + jt}[1 - \exp(-M_r)]. \quad (30)$$

Second-order indicator reaction. Introduction of expression (27) for the catalyst concentration into relation (9) for the rate of a second-order indicator reaction [at $c(X) = c(Y)$] gives, after integration, the following expression for the concentration of component X at time t:

$$c(X) = \frac{c_o(X)V_r}{[1 + c_o(X)Q_r](V_r + jt)} \quad (31)$$

where

$$Q_r = \frac{k_o V_r}{j}\ln\frac{V_r + jt}{V_r} + \frac{k_k V_r c(T)(K_e - 2)}{2(K_e - 1)j} \times \left(\ln\frac{V_r + jt}{V_r} - \frac{jt}{V_r + jt}\right) - \frac{k_k V_r^2 c(A)K_e}{2(K_e - 1)j} \times \left(\frac{1}{V_r} - \frac{1}{V_r + jt}\right) + \frac{k_k V_r}{2(K_e - 1)j}S_r \quad (32)$$

in which S_r is analogous to S_p [equation (12)] but with constants A_r, B_r and C_r, instead of A_k, B_p and C_p.

For the concentration of product L, it follows that

$$c(L) = \frac{c_o^2(X)Q_r V_r}{[1 + c_o(X)Q_r](V_r + jt)}. \quad (33)$$

Coulometric addition of titrant

Taking the expressions for the concentrations of inhibitor $c(A_{Red})$ and of the products of the indicator reaction, $c(A_{Ox})$ and $c(K_{Red})$, in a coulometric addition of the titrant:

$$c(A_{Ox}) = c(K_{Red}) = \frac{It}{nFV_r} - c(K_{Ox}) \quad (34)$$

$$c(A_{Red}) = c(A) - \frac{It}{nFV_r} + c(K_{Ox}) \quad (35)$$

and introducing them into relation (24), gives the following expression for the catalyst concentration during the titration:

$$c(K_{Ox}) = \frac{(K_e - 2)It - (E_r')^{\frac{1}{2}} + (E_r' + F_r't + G_r't^2)^{\frac{1}{2}}}{2nFV_r(K_e - 1)} \quad (36)$$

where

$$E_r' = [nFV_r c(A)K_e]^2;$$
$$F_r' = 2nFV_r c(A)K_e I(2 - K_e);$$
$$G_r' = (K_e I)^2.$$

First-order indicator reaction. Introducing expression (36) into the corresponding relation for rate of the first-order indicator reaction [expression (16)] and integrating for the limiting conditions $c(X) = c_o(X)$ and $t = 0$, gives the following expression for the concentration of component X at time t:

$$c(X) = c_o(X)\exp(-M_r') \quad (37)$$

where

$$M_r' = k_o' t + \frac{k_k'(K_e - 2)It^2}{4nFV_r(K_e - 1)} - \frac{k_k' c(A)K_e t}{2(K_e - 1)} + \frac{k_k'}{2nFV_r(K_e - 1)}R_r' \quad (38)$$

in which R_r' is analogous to R_p' in equation (19) but with constants E_r', F_r' and G_r', instead of E_p', F_p' and G_p'.

For the concentration of product L, it follows that

$$c(L) = c_o(X)[1 - \exp(-M_r')]. \quad (39)$$

Second-order indicator reaction. If the indicator reaction is of second-order type, then introducing expression (36) into the corresponding expression for the rate of the indicator reaction [at $c(X) = c(Y)$], [expression (21)], and integrating gives the concentration of component X at time t as

$$c(X) = \frac{c_o(X)}{1 + c_o(X)Q_r'} \quad (40)$$

where Q_r' is analogous to M_r' in equation (38) but with constants k_o and k_k, instead of k_o' and k_k'.

For the concentration of product L,

$$c(L) = \frac{c_o^2(X)Q_r'}{1 + c_o(X)Q_r'}. \quad (41)$$

SIMULATION OF THE BLANK TITRATIONS

By employing the approach above it is also possible to write a mathematical expression describing the blank titrations. In this case, the catalyst concentration, $c(K)$, is a linear function of time, since there is no titrand in the reaction vessel. Here also, the two modes of titrant addition were considered.

Volumetric addition of titrant

The catalyst concentration is given by

$$c(K) = \frac{jtc(T)}{V_r + jt}. \quad (42)$$

First-order indicator reaction. Putting expression (42) into (4) and integrating gives, for the concentration of component X at time t:

$$c(X) = c_o(X)\frac{V_r}{V_r + jt}\exp\left\{-[k_o' + k_k' c(T)]t + \frac{k_k' V_r c(T)}{j}\ln\frac{V_r + jt}{V_r}\right\} \quad (43)$$

and for the concentration of product L:

$$c(\mathrm{L}) = c_o(\mathrm{X})\frac{V_r}{V_r+jt}\left(1-\exp\left\{-[k'_o+k'_k c(\mathrm{T})]t + \frac{k'_k V_r c(\mathrm{T})}{j}\ln\frac{V_r+jt}{V_r}\right\}\right). \quad (44)$$

Second-order indicator reaction. If the indicator reaction is second-order, then introducing expression (42) into the expression (9) for the rate of the indicator reaction gives a relation for simulation of the blank titration, expressed through the concentration changes of component X:

$$c(\mathrm{X}) = \frac{c_o(\mathrm{X})V_r}{[1+c_o(\mathrm{X})R^*](V_r+jt)} \quad (45)$$

where

$$R^* = \frac{V_r}{j}[k_o+k_k c(\mathrm{T})]\ln\frac{V_r+jt}{V_r} - \frac{k_k V_r c(\mathrm{T})t}{V_r+jt} \quad (46)$$

and expression (47) if it is the concentration changes of product L that are monitored:

$$c(\mathrm{L}) = \frac{c_o^2(\mathrm{X})R^*V_r}{[1+c_o(\mathrm{X})R^*](V_r+jt)}. \quad (47)$$

Coulometric addition of titrant

In coulometric addition of the titrant the catalyst concentration is given by

$$c(\mathrm{K}) = \frac{It}{nFV_r}. \quad (48)$$

First-order indicator reaction. Starting from expressions (48), and (16), integration gives a relation for the concentration of component X at time t:

$$c(\mathrm{X}) = c_o(\mathrm{X})\exp\left(-k'_o t - \frac{k'_k I t^2}{2nFV_r}\right) \quad (49)$$

and for the concentration of the indicator reaction product L:

$$c(\mathrm{L}) = c_o(\mathrm{X})\left[1-\exp\left(-k'_o t - \frac{k'_k I t^2}{2nFV_r}\right)\right]. \quad (50)$$

Second-order indicator reaction. On the basis of expression (21) for the rate of the second-order indicator reaction, expression (48) and integration for the limiting conditions given above, the following expression is obtained for the concentration of component X at time t:

$$c(\mathrm{X}) = \frac{2nFV_r c_o(\mathrm{X})}{2nFV_r[1+k_o c_o(\mathrm{X})t]+k_k c_o(\mathrm{X})It^2} \quad (51)$$

and for the concentration of product L:

$$c(\mathrm{L}) = \frac{c_o^2(\mathrm{X})(2k_o nFV_r t + k_k I t^2)}{2nFV_r[1+k_o c_o(\mathrm{X})t]+k_k c_o(\mathrm{X})It^2}. \quad (52)$$

Calculations

As can be seen, the equations obtained are rather complex. Therefore, for numerical treatment of data we used a Delta 340 computer (PDP 1134). The structure of the program, written in FORTRAN IV, was similar to that used in simulation of the complexometric catalytic titration curves.[1,2]

RESULTS AND DISCUSSION

After deriving the equations for simulation of precipitation and redox catalytic titration curves we investigated the effect of a number of parameters on the shapes of the curves, and present and discuss the results below.

Effect of the equilibrium constant of the titration reaction

Effect of the solubility product. From Fig. 1 it can be seen that the titration end-point may be determined (under the other working conditions mentioned) satisfactorily if the solubility product for the compound AK is $\leqslant 5\times10^{-11}$ (curves 3–6). However, for higher solubility product values, determination of the titration end-point is difficult (curve 2), or even impossible (curve 1). If the rate constant for the catalytic and spontaneous reactions were lower and the concentrations of the titrant and titrand higher, it would be possible to determine the titration end-point satisfactorily even with solubility products $>5\times10^{-11}$. Further, it can be seen that curves 5 and 6 practically do not differ, *i.e.*, for a solubility

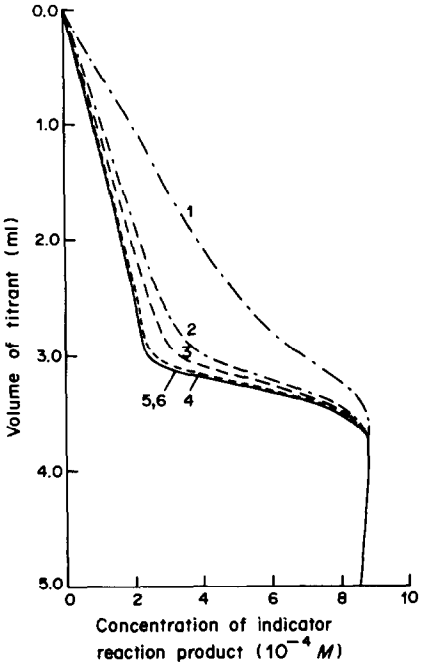

Fig. 1. Effect of solubility product, K_{sp}, on the shape of the simulated volumetric precipitation catalytic titration curves employing a first, or pseudo-first, order indicator reaction, and under the following conditions: $V_r = 3\times10^{-2}$ l.; $c_o(\mathrm{X}) = 10^{-3}M$; $k'_o = 10^{-3}$ sec^{-1}; $k'_k = 10^3$ l. mole^{-1}. sec^{-1}; $c(\mathrm{T}) = 5\times10^{-3}M$; $c(\mathrm{A}) = 5\times10^{-4}M$; $j = 10^{-5}$ l./sec. Values for K_{sp} are: (1) 5×10^{-10}; (2) 10^{-10}; (3) 5×10^{-11}; (4) 10^{-11}; (5) 10^{-12}; (6) 5×10^{-13}. Equivalence point: 3.00 ml.

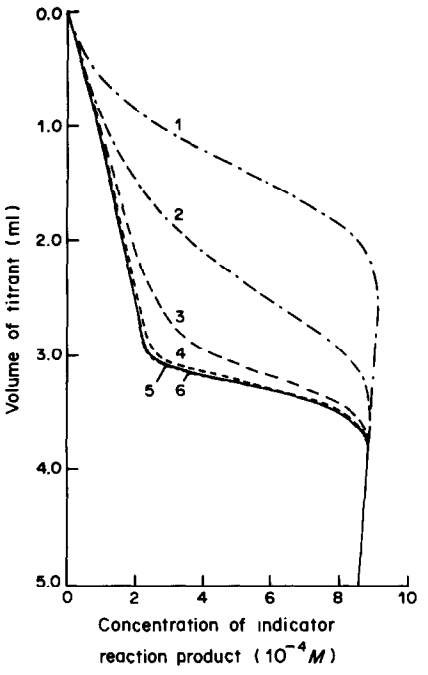

Fig. 2. Effect of equilibrium constant, K_e, on the shape of the simulated curves of volumetric redox catalytic titrations, obtained in case of the first, or pseudo-first, order indicator reaction under the following conditions: $V_t = 3 \times 10^{-2}$ l.; $c_o(X) = 10^{-3}M$; $k'_o = 10^{-3}$ sec^{-1}; $k'_k = 10^3$ l. mole^{-1}. sec^{-1}; $c(T) = 5 \times 10^{-3}M$; $c(A) = 5 \times 10^{-4}M$; $j = 10^{-5}$ l./sec. Values for K_e are: (1) 10; (2) 10^2; (3) 10^3; (4) 10^4; (5) 10^5; (6) 5×10^5. Equivalence point: 3.00 ml.

product below 10^{-12} (under the conditions mentioned) the equilibrium concentration of catalyst before the equivalence point can be neglected. That means it is possible to simulate the titration curves with the approximative expressions.[1]

Effect of the redox equilibrium constant. The equilibrium constant for the redox reaction on which the determination is based, has a significant effect on the shape of the catalytic titration curve (Fig. 2). As can be seen, the titration end-point can be determined satisfactorily if K_e is $\geqslant 10^4$ (under the given conditions, curves 4–6). For lower values of the equilibrium constant, determination of the titration end-point is difficult (curve 3), or even impossible (curves 1 and 2). Under the same conditions, as already mentioned, it is possible to determine the end-point satisfactorily in precipitation titrations provided the solubility product is $\leqslant 5 \times 10^{-11}$, and in complexometric catalytic titrations[1] if the instability constant of the complex is $\leqslant 10^{-7}$. These three conclusions are in good agreement, since for the stated values of the equilibrium constants of the titration reactions the equilibrium concentrations of catalyst in the solution are almost the same.

For somewhat lower values of the rate constant for both the spontaneous and catalysed reaction, and lower concentrations of the titrand and titrant, it could be possible to determine the titration end-point with K_e values slightly below 10^4. From the same figure, it can be seen that between curves 5 and 6 there is practically no difference, which means that for equilibrium constants above 10^5, it is possible to neglect the equilibrium concentration of the catalyst before the end-point, *i.e.*, it is possible to use the approximative expressions for simulation of the titration curves,[1] as in the case of precipitation titrations.

For this reason we have investigated the wide range of conditions under which it is possible to neglect the equilibrium concentration of the catalyst in simulation of precipitation and redox catalytic titrations. Figures 3 and 4 show these conditions for precipitation reactions, and Figs. 5 and 6 those for redox titrations (in both cases a first-order indicator reaction is assumed). The graphs in Figs. 3 and 5 give the conditions under which the approximation error does not exceed $0.03c_o(X)$ and Figs. 4 and 6 those for an error below $0.05c(L)$. For all conditions on the left-hand side of the figures it is more correct to use the complete expressions, while for those on the right-hand side it is possible to use the approximative expressions. Similar graphs are obtained irrespective of the mode of titrant addition, and also for a second-order indicator reaction except that the scale for the ordinate must be greatly expanded.

A comparison of Figs. 3 and 5 with Figs. 4 and 6 reveals certain differences. While the span of applicability safisfying the approximation error of $0.03c_o(X)$ (Figs. 3 and 5) depends only to a small extent on the rate constant of the spontaneous reaction, the same does not apply to Figs. 4 and 6, where the approximation error was preset not to exceed $0.05c(L)$. The difference can be easily explained if we assume that in the latter case the error is directly proportional to the concentration of the indicator reaction product, which is largely dependent on the value of the rate constant of the spontaneous reaction.

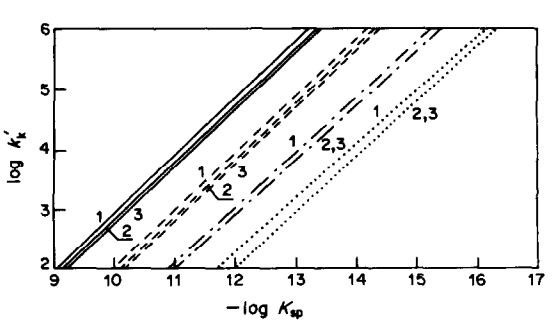

Fig. 3. Range of applicability of approximative equations for simulation of coulometric precipitation catalytic titrations with an approximation error not exceeding $0.03c_o(X)$ (first-order indicator reaction) under the following conditions: $V_t = 3 \times 10^{-2}$ l.; $c_o(X) = 10^{-3}M$; $n = 1$. —— $c(A) = 5 \times 10^{-3}M$; $I = 4.4 \times 10^{-2}$ A; --- $c(A) = 5 \times 10^{-4}M$; $I = 4.4 \times 10^{-3}$ A; -·-·- $c(A) = 5 \times 10^{-5}M$; $I = 4.4 \times 10^{-4}$ A; ····· $c(A) = 5 \times 10^{-6}M$; $I = 4.4 \times 10^{-5}$ A; (1) $k'_o = 10^{-3}$ sec^{-1}; (2) $k'_o = 10^{-4}$ sec^{-1}; (3) $k'_o = 10^{-5}$ sec^{-1}.

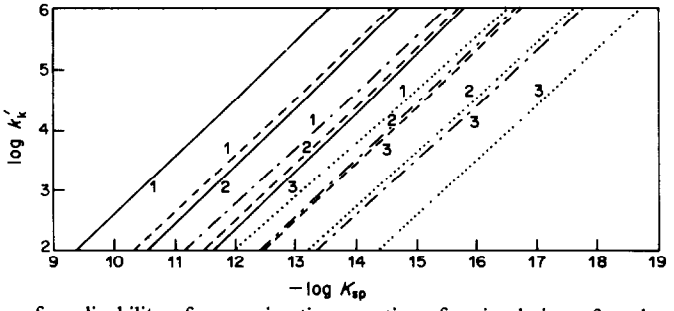

Fig. 4. Range of applicability of approximative equations for simulation of coulometric precipitation catalytic titrations with an approximation error not exceeding $0.05c$(L) (first-order indicator reaction) under the following conditions: $V_r = 3 \times 10^{-2}$ l.; $c_o(X) = 10^{-3}M$; $n = 1$. —— $c(A) = 5 \times 10^{-3}M$; $I = 4.4 \times 10^{-2}$ A; --- $c(A) = 5 \times 10^{-4}M$; $I = 4.4 \times 10^{-3}$ A; -·-·- $c(A) = 5 \times 10^{-5}M$; $I = 4.4 \times 10^{-4}$ A; ····· $c(A) = 5 \times 10^{-6}M$; $I = 4.4 \times 10^{-5}$ A; (1) $k'_k = 10^{-3}$ sec^{-1}; (2) $k'_o = 10^{-4}$ sec^{-1}; (3) $k'_o = 10^{-5}$ sec^{-1}.

If Figs. 3 and 4 are compared with Figs. 5 and 6, some substantial differences are discernible. These arise from the different dependence between the concentration of the titrant and the titrand, on the one hand, and the equilibrium concentration of the catalyst during titration, on the other, which will be discussed below.

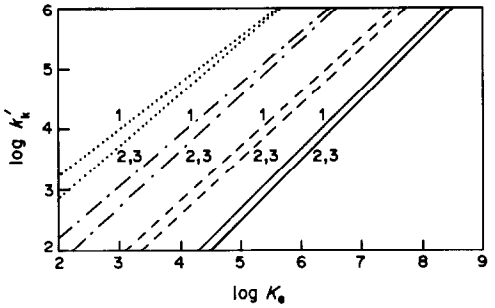

Fig. 5. Range of applicability of approximative equations for simulation of volumetric redox catalytic titrations with an approximation error not exceeding $0.03c_o(X)$ (first-order indicator reaction), under the following conditions: $V_r = 3 \times 10^{-2}$ l.; $c_o(X) = 10^{-3}M$; $j = 10^{-5}$ l./sec. —— $c(A) = 5 \times 10^{-3}M$; $c(T) = 5 \times 10^{-2}M$; --- $c(A) = 5 \times 10^{-4}M$; $c(T) = 5 \times 10^{-3}M$; -·-·- $c(A) = 5 \times 10^{-5}M$; $c(T) = 5 \times 10^{-4}M$; ····· $c(A) = 5 \times 10^{-6}M$; $c(T) \times 10^{-5}M$; (1) $k'_o = 10^{-3}$ sec^{-1}; (2) $k'_o = 10^{-4}$ sec^{-1}; (3) $k'_o = 10^{-5}$ sec^{-1}.

Effect of the rate constant for the catalysed reaction

From Fig. 7 it can be concluded that the end-point of the redox titration (with a second-order indicator reaction) can be determined satisfactorily provided k_k (under the given conditions) is $> 10^4$ l^2.mole^{-2}.sec^{-1} (curves 1–3). However, if the scale on the ordinate axis is expanded, it is possible to determine the end-point even for k_k as low as 10^3 l^2.mole^{-2}.sec^{-1}. With a first-order indicator reaction the titration end-point can be determined satisfactorily if $k_k > 10$ l.mole^{-1}.sec^{-1}. For precipitation titrations the corresponding condition is $K_{sp} \leqslant 10^{-11}$. However, the changes in the concentration of the indicator reaction product are not instantaneous in the vicinity of the equivalence point, which necessitates graphical extrapolation of the linear segments of the titration curve before and after the equivalence point, for determination of the end-point. The results thus obtained are somewhat higher than the true values, and it is necessary to correct them for the results of the blank titrations (Fig. 8). It is evident from Fig. 8 that the shape of the blank titration curve is not identical to that for titration of a sample, after the equivalence point. This is understandable if it is taken into account that in the titration of a sample the indicator reaction takes place from the beginning of the titration, so that the

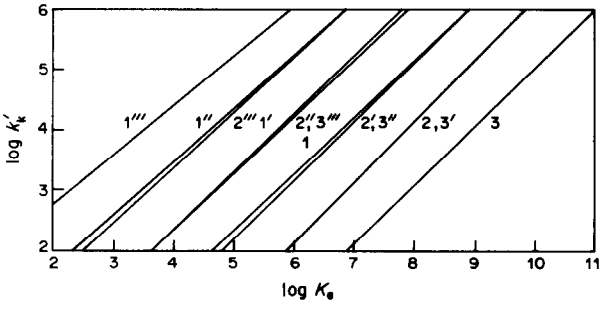

Fig. 6. Range of applicability of the approximative equations for simulation of volumetric redox catalytic titrations with an approximation error not exceeding $0.05c$(L) (first-order indicator reaction), under the following conditions: $V_r = 3 \times 10^{-2}$ l.; $c_o(X) = 10^{-3}M$; $j = 10^{-5}$ l./sec. 1–3 $c(A) = 5 \times 10^{-3}M$; $c(T) = 5 \times 10^{-2}M$; 1′–3′ $c(A) = 5 \times 10^{-4}M$; $c(T) = 5 \times 10^{-3}M$; 1″–3″ $c(A) = 5 \times 10^{-5}M$; $c(T) = 5 \times 10^{-4}M$; 1‴–3‴ $c(A) = 5 \times 10^{-6}M$; $c(T) = 5 \times 10^{-5}M$; 1, 1′, 1″, 1‴—$k'_o = 10^{-3}$ sec^{-1}; 2, 2′, 2″, 2‴—$k'_o = 10^{-4}$ sec^{-1}; 3, 3′, 3″, 3‴—$k'_o = 10^{-5}$ sec^{-1}.

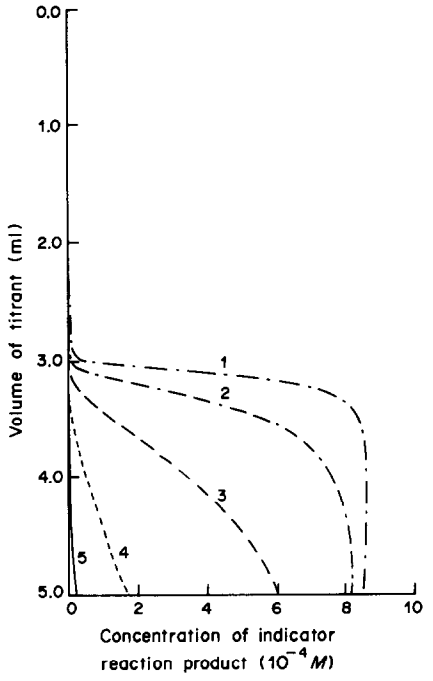

Fig. 7. Effect of rate constant for the second-order catalysed reaction, k_k, on the shape of the simulated curves in volumetric redox catalytic titrations obtained under the following conditions: $V_r = 3 \times 10^{-2}$ l.; $c_o(X) = 10^{-3}M$; $k_o = 10^{-3}$ l.mole^{-1}.sec^{-1}; $c(T) = 5 \times 10^{-3}M$; $c(A) = 5 \times 10^{-4}M$; $j = 10^{-5}$ l./sec; $K_e = 10^5$. Values for k_k (l^2.mole^{-2}.sec^{-1}) are: (1) 10^7; (2) 10^6; (3) 10^5; (4) 10^4; (5) 10^3. Equivalence point: 3.00 ml.

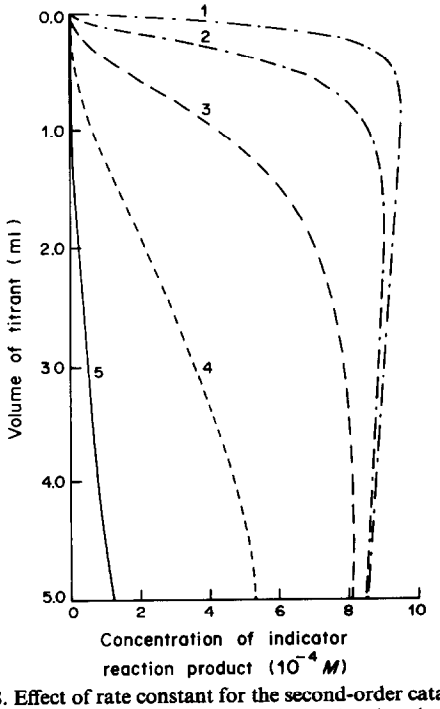

Fig. 8. Effect of rate constant for the second-order catalysed reaction, k_k, on the shape of the simulated volumetric blank titrations obtained under the following conditions: $V_r = 3 \times 10^{-2}$ l., $c_o(X) = 10^{-3}M$; $k_o = 10^{-3}$ l.mole^{-1}.sec^{-1}; $c(T) = 5 \times 10^{-3}M$; $j = 10^{-5}$ l./sec. Values for k_k (l^2.mole^{-2}.sec^{-1}) are: (1) 10^7; (2) 10^6; (3) 10^5; (4) 10^4; (5) 10^3.

concentration of the indicator reaction product at the equivalence point is generally higher than that at the start of the blank titration. The difference in shape of the curves is the greater: (*i*) the larger the rate constants for both the spontaneous and the catalysed reactions, (*ii*) the higher the equilibrium catalyst concentration before the equivalence point, and (*iii*) the longer the time interval between starting the titration and reaching its equivalence point. The last quantity depends on the concentrations of the titrand and of the titrant (or the value of the generating current, for coulometric titration) and the rate of titrant addition. However, in volumetric addition of the titrant, another effect comes into play, namely the volume change of the reaction mixture. This is more pronounced for a real titration (causing a significant decrease in the concentration of the reaction product) than for a blank, but the error due to this difference in shape of the titration curves is obviously less than that which occur if no blank titration correction were made.

It should be pointed out that the blank titration curves are the same for all types of catalytic titrations, which is understandable since there is no titrand present in the reaction mixture, and furthermore are the same irrespective of the value of K_e, K_{sp}, K_N, *etc.*

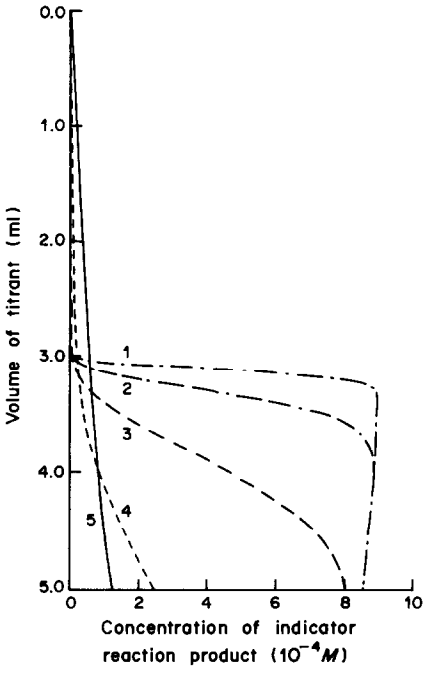

Fig. 9. Effect of concentration of titrant, c(T), and titrand, c(A), on the shape of simulated volumetric precipitation catalytic titration curves employing a first-order indicator reaction, under the following conditions: $V_r = 3 \times 10^{-2}$ l.; $c_o(X) = 10^{-3}M$; $k'_o = 10^{-5}$ sec^{-1}; $k'_k = 10^3$ l.mole^{-1}.sec^{-1}; $j = 10^{-5}$ l./sec; $K_{sp} = 10^{-13}$. Values for c(T) and c(A) (M) are: (1) 5×10^{-2} and 5×10^{-3}; (2) 5×10^{-3} and 5×10^{-4}; (3) 5×10^{-4} and 5×10^{-5}; (4) 5×10^{-5} and 5×10^{-6}; (5) 5×10^{-6} and 5×10^{-7}. Equivalence point: 3.00 ml.

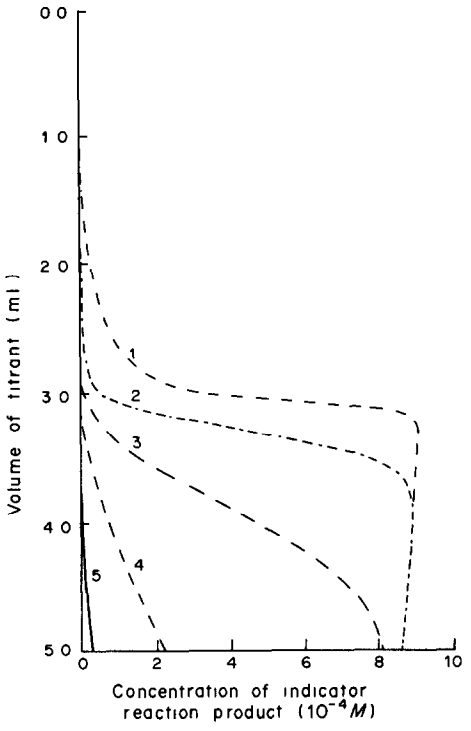

Fig. 10. Effect of concentration of titrant, c(T), and titrand, c(A), on the shape of simulated volumetric redox catalytic titration curves employing a first-order indicator reaction, under the following conditions: $V_r = 3 \times 10^{-2}$ l.; $c_o(X) = 10^{-3}M$; $k'_o = 10^{-5}$ sec^{-1}; $k'_k = 10^3$ l.mole^{-1}.sec^{-1}; $j = 10^{-5}$ l./sec; $k_e = 10^4$. Values for c(T) and c(A) (M) are: (1) 5×10^{-2} and 5×10^{-3}; (2) 5×10^{-3} and 5×10^{-4}; (3) 5×10^{-4} and 5×10^{-5}; (4) 5×10^{-5} and 5×10^{-6} (5) 5×10^{-6} and 5×10^{-7}. Equivalence point: 3.00 ml.

Effect of concentration of the titrant and titrand

The effect of the concentration of the titrant and titrand on the shape of the titration curves is markedly different in the precipitation (Fig. 9) and redox (Fig. 10) catalytic titrations. In precipitation catalytic titrations, a decrease in concentration of both titrant and titrand causes an increase in the equilibrium concentration of the catalyst before the equivalence point, and at the same time, in the rate of indicator reaction. On the other hand, in redox catalytic titrations, an increase in concentration of the titrant and titrand is accompanied by an increase in the equilibrium concentration of the catalyst, thus giving rise to an enhanced rate of the indicator reaction during the whole titration. These differences can be easily explained by considering expressions (1) and (24). It follows that if more concentrated solutions are to be titrated then precipitation titrations are best, whereas for more dilute solutions redox titrations would be more advantageous (under the given conditions). It is also implied by these two figures that the lowest concentrations allowing satisfactory location of the titration end-point are $5 \times 10^{-5}M$ and $5 \times 10^{-6}M$ for the titrant and titrand, respectively (Figs. 9 and 10, curve 4). By expansion of the ordinate axis it would be possible to employ even more dilute solutions in redox catalytic titrations. The titration end-point is determined by extrapolation of the linear parts of the titration curve before and after the equivalence point. The extrapolation is especially needed for lower titrant concentrations in precipitation titrations, and for higher concentration in redox catalytic titrations. Also, the results have to be corrected for the blank titration. Catalytic titration of more dilute solutions by precipitation reactions, or of more concentrated solutions by redox reactions could be achieved in several ways: (*i*) by employing a solvent in which the solubility of the titration reaction product is lower, or the redox equilibrium constant higher; (*ii*) by choosing a titration reaction giving a product with a lower solubility product, or a higher redox equilibrium constant, and (*iii*) by choosing an indicator reaction having a low rate constant for the spontaneous reaction and a high one for the catalysed reaction in precipitation titrations, and a low rate constant for the catalysed reaction in redox catalytic titrations. However, lower titrant concentrations necessarily correspond to a smaller change in the indicator-reaction product (*i.e.*, in the measured parameter intensity) in both kind of titrations, and necessitate the use of a more sensitive measuring instrument.

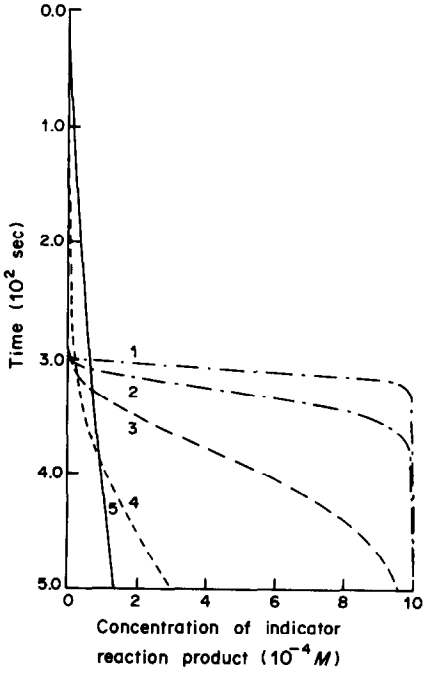

Fig. 11. Effect of generating current (I), and concentration of titrand, c(A), on the shape of simulated coulometric precipitation catalytic titration curves employing a first-order indicator reaction, under the following conditions: $V_r = 3 \times 10^{-2}$ l.; $c_o(X) = 10^{-3}M$; $k'_o = 10^{-5}$ sec^{-1}; $k'_k = 10^3$ l.mole^{-1}.sec^{-1}; $n = 1$; $K_{sp} = 10^{-13}$. Values for I and c(A) are: (1) 4.82×10^{-2} A and $5 \times 10^{-3}M$; (2) 4.82×10^{-3} A and $5 \times 10^{-4}M$; (3) 4.82×10^{-4} A and $5 \times 10^{-5}M$; (4) 4.82×10^{-5} A and $5 \times 10^{-6}M$; (5) 4.82×10^{-6} A and $5 \times 10^{-7}M$. Equivalence point: 300.3 sec.

Effect of the mode of titrant addition

If we compare the simulated curves obtained for precipitation catalytic titrations with volumetric (Fig. 9) and coulometric (Fig. 11) addition of the titrant, it can be seen that they are, contrary to the analogous redox titrations, almost identical up to the equivalence point. Afterwards, they differ significantly, as described in more detail in the previous paper.[1] This great similarity of the precipitation curves before the equivalence point is due to two effects. In volumetric precipitation titrations the volume changes of the reacting mixture cause an increase in the catalyst concentration during titration, which is the opposite to the case for redox catalytic titrations. On the other hand, the concentration of the indicator reaction product diminishes.Since the two effects act in opposite directions in the precipitation titration, the net effect is a titration curve that is almost independent of the mode of addition of the titrant in the period before the equivalence point. This effect will be more pronounced as K_{sp} and the rate constant k_k increase.

Other effects

The effect of the following parameters has also been studied: the rate constant of the spontaneous reaction, the initial concentration of the indicator reaction components, the rate of titrant addition, the magnitude of the generating current, and the number of electrons involved in the electrochemical generation of the titrant. The effect of all these parameters on the shape of simulated curves for precipitation and redox catalytic titrations is independent of the titration reaction employed, so conclusions similar to those for complexometric catalytic titrations can be drawn.[1]

Acknowledgements—The authors thank the SIZ for Research of SAP Vojvodina for partial financial support of the work.

REFERENCES

1. F. F. Gaál and B. F. Abramović, *Talanta*, 1984, **31**, 987.
2. B. F. Abramović and F. F. Gaál, *Microchem J.*, in press.
3. F. F. Gaál, *Ph.D. Thesis*, University of Belgrade, 1977.
4. B. F. Abramović, *Ph.D. Thesis*, University of Novi Sad, 1982.
5. H. A. Mottola, *Talanta*, 1969, **16**, 1267.
6. H. Weisz, *Allgem. Prakt. Chem.*, 1971, **22**, 98.
7. H. Weisz and S. Pantel, *Z. Anal. Chem.*, 1973, **264**, 389.
8. T. P. Hadjiioannou, *Rev. Anal. Chem.*, 1976, **3**, 82.
9. R. L. Parry-Jones, *Educ. in Chem.*, 1976, **13**, 76.
10. E. J. Greenhow, *Chem. Rev.*, 1977, **77**, 835.
11. Y. Rugu, *Chin. J. Pharm. Anal.*, 1981, **1**, 54.

Talanta, Vol. 32, No. 7, pp. 559–563, 1985
Printed in Great Britain.

0039-9140/85 $3.00 + 0.00

CONTRIBUTIONS TO THE THEORY OF CATALYTIC TITRATIONS—III*

NEUTRALIZATION CATALYTIC TITRATIONS

FERENC F. GAÁL and BILJANA F. ABRAMOVIĆ
Institute of Chemistry, Faculty of Sciences, University of Novi Sad, V. Vlahovića 2, YU-21000 Novi Sad, Yugoslavia

(*Received* 26 *September* 1984. *Accepted* 23 *January* 1985)

Summary—Neutralization catalytic titrations of weak monoprotic acids and bases with both volumetric and coulometric addition of the titrant (strong base/acid) have been simulated by taking into account the equilibrium concentration of the catalyst during the titration. The influence of several factors on the shape of the simulated catalytic titration curve has been investigated and is discussed.

In continuing our investigations on catalytic titrations[1-3] we now consider the simulation of neutralization catalytic titrations of weak monoprotic acids and bases. The mathematical modelling is done for both volumetric and coulometric addition of the titrant (strong base/acid), taking into account the equilibrium concentration of the catalyst during the titration. The necessary relations are derived and results calculated by a procedure similar to those employed in Parts I and II[1,3] of this series. The effect of various parameters on the shape of the simulated titration curve was investigated and is discussed. Also, the conditions under which it is possible to employ approximate equations (with the equilibrium concentration of the catalyst neglected) have been established. Catalytic titrations have been extensively reviewed.[4-12]

THEORY

Neutralization catalytic titrations have been employed mainly for determination of weak and very weak acids and bases.[4-12] Hence, we shall consider only simulation of these titrations. The mathematical procedure consists in setting up the equation for the equilibrium concentration of the catalyst during the titration and its introduction into the corresponding expression for the rate of the indicator reaction, followed by integration for the limiting conditions. The same assumptions on titrant addition, effect of temperature, and properties of the indicator reaction and titration reaction have been made as in our previous articles.[1,3]

SIMULATION OF CATALYTIC TITRATIONS OF WEAK MONOPROTIC ACIDS WITH STRONG BASE

When a weak acid HA (inhibitor) is titrated with strong base S^- (catalyst) in an amphiprotic solvent HS according to the reaction:

$$HA + S^- \rightleftharpoons A^- + HS$$

the concentration of catalyst (S^-) is one of the roots of the cubic equation:

$$c^3(S^-) + \left[c(a) - b + \frac{K_{HS}}{K_{HA}}\right]c^2(S^-) - K_{HS}\left[1 + \frac{b}{K_{HA}}\right]c(S^-) - \frac{K_{HS}^2}{K_{HA}} = 0 \quad (1)$$

where K_{HA} is the acidity constant of weak acid HA, given by:

$$K_{HA} = \frac{c(H_2S^+)c(A^-)}{c(HA)},$$

K_{HS} is the autoprotolysis constant, expressed as:

$$K_{HS} = c(H_2S^+)c(S^-),$$

$c(a)$ is the analytical (molar) concentration of weak acid HA, and b the concentration of strong base S^-.

The expressions describing $c(a)$ and b depend on the mode of titrant addition, as will be shown below.

Volumetric addition

The parameters $c(a)$ and b in volumetric addition of the titrant are:

$$c(a) = \frac{V_r c(A)}{V_r + jt} \quad (2)$$

$$b = \frac{jtc(T)}{V_r + jt} \quad (3)$$

where $c(A)$ is the initial molar concentration of the inhibitor (titrand), $c(T)$ the concentration of the titrant, V_r the initial volume of the titrated solution (l.), j the rate of addition of titrant (l./sec) and t is time (sec).

By introduction of expressions (2) and (3) into (1)

*Part II—*Talanta*, 1985, **32**, 549.

it is possible to derive the relation for the catalyst concentration, $c(S^-)$, during the titration. However, the expression thus obtained is rather complex, so its introduction into the relation for the rate of first or pseudo-first and second-order indicator reactions would result in a very complicated differential equation. For this reason the numerical tangent method[13] is employed for solving the third-order equation (1) (see Appendix).

First-order indicator reaction. If into the expression for an indicator reaction of first or pseudo-first order:

$$-\frac{dc(X)}{dt} = [k'_0 + k'_k c(K)]c(X) + \frac{c(X)j}{V_r + jt} \quad (4)$$

where k'_0 is the rate constant of the first-order spontaneous reaction (sec^{-1}), k'_k the rate constant of the first-order catalysed reaction ($l.mole^{-1}.sec^{-1}$), $c(K)$ the molar concentration of catalyst [in this case it is $c(S^-)$], $c(X)$ the concentration of the indicator reaction component, we introduce the corresponding root of equation (1) and then integrate (employing Romberg's numerical method[14]) for the limiting conditions $c(X) = c_0(X)$ at $t = 0$, the resulting expression describes catalytic titration of a weak acid for the case when concentration changes in the indicator reaction component X are monitored:

$$c(X) = c_0(X)\frac{V_r}{V_r + jt}\exp(-k'_0 t - k'_k Y_I) \quad (5)$$

where Y_I is the numerical solution of the integral $\int_0^t c(S^-)dt$, and $c_0(X)$ the initial molar concentration of the indicator reaction component.

If, however, the concentration changes of product L are monitored, the following expression holds:

$$c(L) = c_0(X)\frac{V_r}{V_r + jt}[1 - \exp(-k'_0 t - k'_k Y_I)] \quad (6)$$

Second-order indicator reaction. Similarly, starting from the corresponding root of equation (1) and the expression for the rate of the second-order indicator reaction [for $c(X) = c(Y)$]

$$-\frac{dc(X)}{dt} = [k_0 + k_k c(K)]c(X)^2 + \frac{c(X)j}{V_r + jt} \quad (7)$$

where k_0 is the rate constant for the second-order spontaneous reaction ($l.mole^{-1}.sec^{-1}$) and k_k the rate constant for the second-order catalysed reaction ($l^2.mole^{-2}.sec^{-1}$), and integrating, we can obtain an expression for simulation of catalytic titrations when the concentration changes of component X are to be monitored:

$$c(X) = \frac{c_0(X)V_r}{[1 + c_0(X)Q_n](V_r + jt)} \quad (8)$$

where

$$Q_n = \frac{k_0 V_r}{j}\ln\left(\frac{V_r + jt}{V_r}\right) + k_k V_r Y_{II} \quad (9)$$

and Y_{II} is the numerical solution of the integral

$$\int_0^t \frac{c(S^-)}{(V_r + jt)}dt.$$

The concentration of product L is:

$$c(L) = \frac{c_0^2(X)Q_n V_r}{[1 + c_0(X)Q_n](V_r + jt)} \quad (10)$$

Coulometric addition

In the coulometric mode of titrant addition, quantities $c(a)$ and b are given by:

$$c(a) = c(A) \quad (11)$$

$$b = \frac{It}{nFV_r} \quad (12)$$

where I is the generating current (A), F the Faraday constant (C/equivalent), and n the number of electrons in the half-reaction for the electrochemical generation of the titrant.

For the same reasons as in volumetric titrations, the Romberg's numerical method is employed for solving equation (1).

First-order indicator reaction. If the corresponding root of equation (1) is introduced into the expression for the rate of the indicator reaction of first or pseudo-first order:

$$-\frac{dc(X)}{dt} = [k'_0 + k'_k c(K)]c(X) \quad (13)$$

the numerical integration for the limiting conditions $c(X) = c_0(X)$ at $t = 0$ leads to an expression for the concentration of component X at time t:

$$c(X) = c_0(X)\exp(-k'_0 t - k'_k Y_{III}) \quad (14)$$

where Y_{III} is the numerical solution of the integral $\int_0^t c(S^-)dt$.

The concentration of product L is:

$$c(L) = c_0(X)[1 - \exp(-k'_0 t - k'_k Y_{III})] \quad (15)$$

Second-order indicator reaction. By introduction of the corresponding root of equation (1) into the expression for the rate of the second-order indicator reaction [at $c(X) = c(Y)$]:

$$-\frac{dc(X)}{dt} = [k_0 + k_k c(K)]c(X)^2 \quad (16)$$

and numerical integration for the limiting conditions $c(X) = c_0(X)$ at $t = 0$, an expression is obtained for the concentration of component X at time t:

$$c(X) = \frac{c_0(X)}{1 + c_0(X)Q'_n} \quad (17)$$

where $Q'_n = k_0 t + k_k Y_{III}$.

On the other hand, the concentration of product L is:

$$c(L) = \frac{c_0^2(X)Q'_n}{1 + c_0(X)Q'_n} \quad (18)$$

SIMULATION OF VOLUMETRIC AND COULOMETRIC CATALYTIC TITRATIONS OF WEAK MONOPROTIC BASES WITH STRONG ACID

In the titration of a weak base B (inhibitor) with strong acid H_2S^+ (catalyst) according to the reaction:

$$B + H_2S^+ \rightleftharpoons HB^+ + HS$$

the catalyst concentration is one of the roots of the third-order equation:

$$c^3(H_2S^+) + \left[c(b) - a + \frac{K_{HS}}{K_B}\right]c^2(H_2S^+) - K_{HS}\left[1 + \frac{a}{K_B}\right]c(H_2S^+) - \frac{K_{HS}^2}{K_B} = 0 \quad (19)$$

where K_B is the base constant of weak base B, defined as:

$$K_B = \frac{c(HB^+)c(S^-)}{c(B)}$$

$c(b)$ is the analytical (molar) concentration of weak base B and a the concentration of strong acid H_2S^+.

The expressions describing a and $c(b)$ again depend on the mode of titrant addition.

In volumetric titrations they are:

$$a = \frac{jtc(T)}{V_r + jt} \quad (20)$$

$$c(b) = \frac{V_r c(A)}{V_r + jt} \quad (21)$$

and in the coulometric titrations:

$$a = \frac{It}{nFV_r} \quad (22)$$

$$c(b) = c(A) \quad (23)$$

The mathematical procedure and expressions obtained for simulation of catalytic titrations of weak bases are analogous to those for the titrations of weak acids, both in volumetric and coulometric addition of the titrant. However, the concentration of H_2S^+ is involved instead of that of S^-, since the former ion is the catalyst in the reaction. For this reason the initial values (parameters) in the approximate solutions of equation (19) are of different form (see Appendix).

RESULTS AND DISCUSSION

By employing the expressions derived it is possible, in a relatively simple way, to choose the optimal conditions for catalytic titrations of weak monoprotic acids and bases. The effects of a number of parameters on the shape of the titration curve and the results of the determination will be discussed below.

Effect of the acid (base) constant

As can be expected, the shape of the catalytic titration curve for a weak acid (Fig. 1) is very

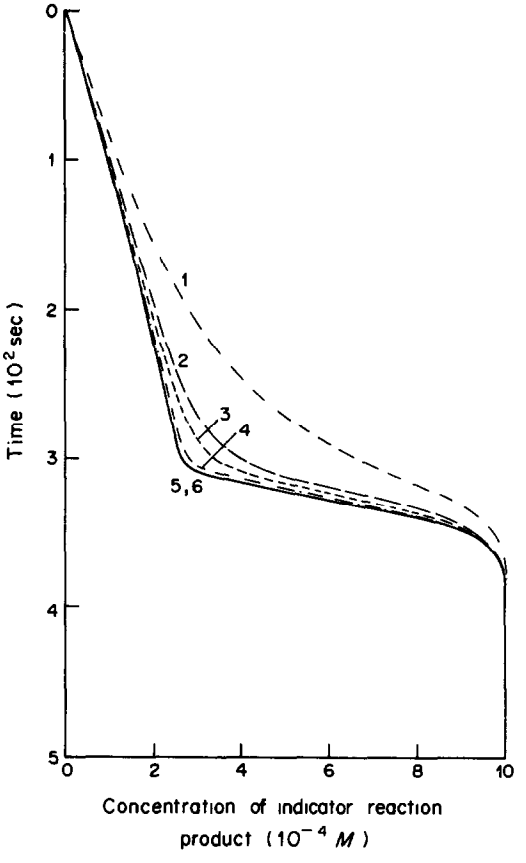

Fig. 1. Effect of acidity constant, K_{HA}, on the shape of the simulated curves for neutralization catalytic titrations of a weak monoprotic acid, with coulometric addition of titrant and a first or pseudo-first order indicator reaction, under the following conditions: $V_r = 3 \times 10^{-2}$ l.; $c_0(X) = 10^{-3}M$; $k_0' = 10^{-3}$ sec^{-1}; $k_k' = 10^3$ l.mole^{-1}.sec^{-1}; $I = 4.82 \times 10^{-3}M$; $c(A) = 5 \times 10^{-4}M$; $n = 1$; $K_{HS} = 10^{-14}$. Values for K_{HA} are: (1) 10^{-8}; (2) 5×10^{-8}; (3) 10^{-7}; (4) 5×10^{-7}; (5) 10^{-5}; (6) 10^{-4}. Equivalence point 300.3 sec.

dependent on the value of the acidity constant (the same also holds for the basicity constant of a weak base). It is clear that (other conditions being unchanged) the titration end-point can be satisfactorily determined provided K_{HA} (or K_B) is not lower than 10^{-7} (curves 3–6, for aqueous solutions). If another solvent, having a lower autoprotolysis constant, were used, it would be possible to titrate an even weaker acid, as described below. As in the other cases discussed previously,[1,3] by selecting an indicator reaction with lower values of the rate constants for both the spontaneous and catalysed reaction it would be possible to determine the titration end-point even for K_{HA} (K_B) below 10^{-7}. However, a proportional change in the concentration of the titrant and titrand (in the generating current in coulometric titrations) does not essentially affect (owing to the buffer effect) the titration curve in the period before the equivalence point. Therefore, unlike the situation for precipitation and redox titrations,[3] it is not possible to extend the limit in such a way toward lower values of K_{HA} (K_B). Further, it is evident that curves 5 and 6

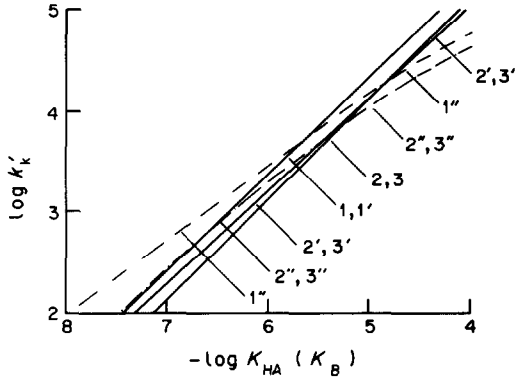

Fig. 2. Range of applicability of approximative equations for simulation of volumetric neutralization catalytic titrations with an approximation error not exceeding $0.03c_0(X)$ (first-order indicator reaction) under the following conditions: $V_r = 3 \times 10^{-2}$ l.; $c_0(X) = 10^{-3}M$; $j = 10^{-5}$ l./sec; $K_{HS} = 10^{-14}$. 1–3 $c(A) = 5 \times 10^{-3}M$; $c(T) = 5 \times 10^{-2}M$; 1'–3' $c(A) = 5 \times 10^{-4}M$; $c(T) = 5 \times 10^{-3}M$; 1''–3'' $c(A) = 5 \times 10^{-5}M$; $c(T) = 5 \times 10^{-4}M$; 1,1', 1''–$k'_0 = 10^{-3}$ sec^{-1}; 2,2', 2''–$k'_0 = 10^{-4}$ sec^{-1}; 3,3', 3''—$k'_0 = 10^{-5}$ sec^{-1}.

(Fig. 1) are identical, which means that under the given conditions and $K_{HA} > 10^{-5}$ it is possible for the equilibrium concentration of the catalyst to be reached before the equivalence point, *i.e.*, the approximate expressions[1] can be employed.

In Figs. 2 and 3 are shown the broad-range correlations of the characteristic parameters for a first-order indicator reaction with volumetric addition of the titrant. For all the conditions on the left-hand side of the graphs it is more correct to use the complete expression, and the approximate one can be employed with sufficient accuracy for those on the right-hand side. Similar graphs are obtained for coulometric addition of the titrant, as well as for the

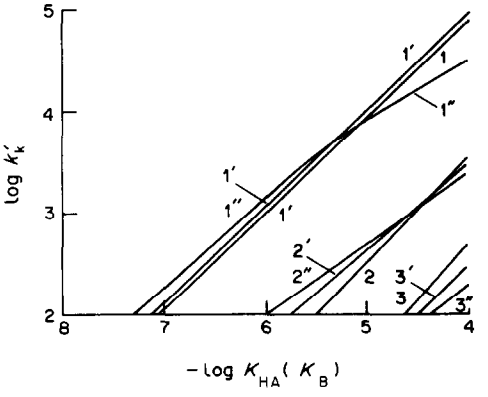

Fig. 3. Range of applicability of approximative equations for simulation of volumetric neutralization catalytic titrations with an approximation error not exceeding $0.05c(L)$ (first-order indicator reaction) under the following conditions: $V_r = 3 \times 10^{-2}$ l.; $c_0(X) = 10^{-3}M$; $j = 10^{-5}$ l./sec; $K_{HS} = 10^{-14}$. 1–3 $c(A) = 5 \times 10^{-3}M$; $c(T) = 5 \times 10^{-2}M$; 1'–3' $c(A) = 5 \times 10^{-4}M$; $c(T) = 5 \times 10^{-3}M$; 1''–3'' $c(A) = 5 \times 10^{-5}M$; $c(T) = 5 \times 10^{-4}M$; 1,1', 1''—$k'_0 = 10^{-3}$ sec^{-1}; 2,2', 2''—$k'_0 = 10^{-4}$ sec^{-1}; 3,3', 3''—$k'_0 = 10^{-5}$ sec^{-1}.

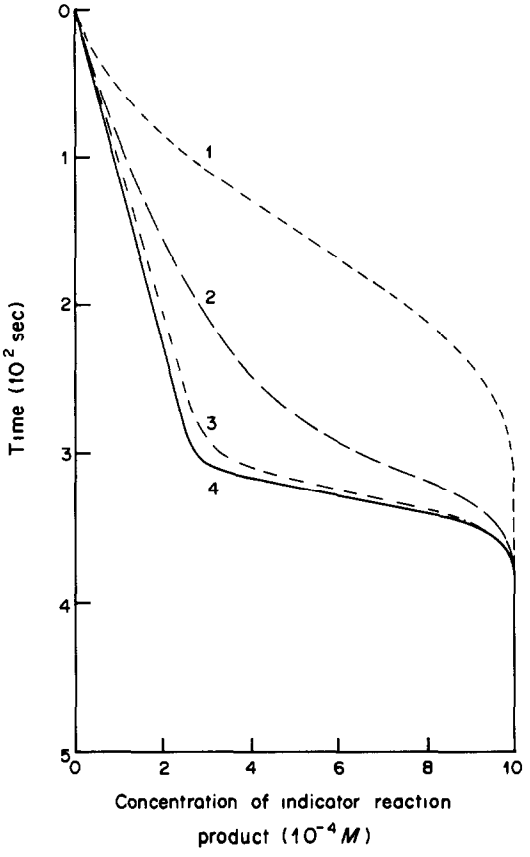

Fig. 4. Effect of autoprotolysis constant, K_{HS}, on the shape of the simulated coulometric neutralization catalytic titration curves for a weak monoprotic acid, with a first or pseudo-first order indicator reaction, under the following conditions: $V_r = 3 \times 10^{-2}$ l.; $c_0(X) = 10^{-3}M$; $k'_0 = 10^{-3}$ sec^{-1}; $k'_k = 10^{-3}$ l.mole^{-1}.sec^{-1}; $I = 4.82 \times 10^{-3}M$; $c(A) = 5 \times 10^{-4}M$; $n = 1$; $K_{HA} = 10^{-8}$. Values for K_{HS} are: (1) 10^{-13}; (2) 10^{-14}; (3) 10^{-15}; (4) 10^{-16}.

second-order indicator reaction. It should be noted that in the latter case the ordinate is about 1000 times longer if the same scale is used. A comparison of Figs. 2 and 3 shows that the position of the curves is only slightly dependent on the magnitude of the rate constant for spontaneous reaction when the approximation error is $0.03c_0(X)$. The same is not the case if the approximation error is $0.05c(L)$. This can be explained in the same way as before.[1,3] In addition, the effect of the concentration of both the titrant and titrand on the shape of titration curves is not significant, as mentioned above. Finally, the curves in Figs. 2 and 3 are similar to those for the complexometric titrations,[1] which indicates a similar dependence between the catalyst concentration and the parameters influencing the shape of the titration curves for these two groups of catalytic titrations.

Effect of the autoprotolysis constant

The effect of the solvent autoprotolysis constant on the shape of the titration curve of a weak acid is illustrated in Fig. 4. It is evident that for a fixed K_{HA},

the concentration changes of the indicator-reaction product at the titration end-point are more pronounced if K_{HS} is lower. It follows from Figs. 1 and 4 that the titration end-point can be determined satisfactorily provided the ratio K_{HS}/K_{HA} or K_{HS}/K_B is $\leqslant 10^{-7}$.

Other effects

We have also studied the effect of the following parameters: rate constants for both the spontaneous and catalysed reactions, initial concentration of the indicator reaction components, rate of titrant addition, magnitude of the generating current, and the number of electrons involved in the electrochemical generation of the titrant. The effect of all these parameters on the shape of simulated curves for catalytic titrations is independent of the titration reaction employed, so similar conclusions can be drawn as for complexometric,[1] precipitation[3] and redox[3] catalytic titrations. We have also studied the effect of concentration of both the titrant and titrand, as well as of the mode of addition of titrant. These effects are the same as for complexometric catalytic titrations,[1] *i.e.*, a proportional change in the concentration of the titrant and titrand has no significant effect on the shape of the titration curve before the equivalence point. On the other hand, the difference in effect of the mode of addition of the titrant lies only in the decrease of the concentration of the reaction product due to dilution in volumetric titration.

Acknowledgements—The authors thank the SIZ for Research, of SAP Vojvodina, for partial financial support of the work.

REFERENCES

1. F. F. Gaál and B. F. Abramović, *Talanta*, 1984, **31**, 987.
2. B. F. Abramović and F. F. Gaál, *Microchem J.*, in press.
3. B. F. Abramović, F. F. Gaál and Dj. Ž. Paunić, *Talanta*, 1985, **32**, 549.
4. F. F. Gaál, *Ph.D. Thesis*, University of Belgrade, 1977.
5. B. F. Abramović, *Ph.D. Thesis*, University of Novi Sad, 1982.
6. H. A. Mottola, *Talanta*, 1969, **16**, 1267.
7. H. Weisz, *Allgem. Prakt. Chem.*, 1971, **22**, 98.
8. H. Weisz and S. Pantel, *Z. Anal. Chem.*, 1973, **264**, 389.
9. T. P. Hadjiioannou, *Rev. Anal. Chem.*, 1976, **3**, 82.
10. R. L. Parry-Jones, *Educ. in Chem.*, 1976, **13**, 76.
11. E. J. Greenhow, *Chem. Rev.*, 1977, **77**, 835.
12. Y. Rugu, *Chin. J. Pharm. Anal.*, 1981, **1**, 54.
13. C. J. Brookes, I. G. Betteley and S. M. Loxston, *Mathematics and Statistics for Chemists*, Wiley, New York, 1966.
14. C. E. Fräberg, *Introduction to Numerical Analysis*, Addison-Wesley, Reading, Mass., 1969.

APPENDIX

Numerical determination of the root of the third-order equation by the tangent method (Newton's method)[13]

$$x_{n+1} = x_n - \frac{f(x_n)}{f'(x_n)} \qquad x = c(S^-) \text{ or } c(H_2S^+) \qquad n = 0, 1, 2 \ldots$$

The following values for x_0 are employed:
(*a*) in catalytic titrations of weak acids

$b = 0$ $\quad c(S^-) = K_{HS}[K_{HA}c(a)]^{-1/2}$
$c(a) > b$ $\quad c(S^-) = 2K_{HS}/(-(b + K_{HA}) + \{(b + K_{HA})^2 + 4K_{HA}[c(a) - b]\}^{1/2})$
$c(a) = b$ $\quad c(S^-) = [K_{HS}c(a)/K_{HA}]^{1/2}$
$c(a) < b$ $\quad c(S^-) = b - c(a)$

(*b*) in catalytic titrations of weak bases

$a = 0$ $\quad c(H_2S^+) = K_{HS}[K_Bc(b)]^{-1/2}$
$c(b) > a$ $\quad c(H_2S^+) = 2K_{HS}/(-(a + K_B) + \{(a + K_B)^2 + 4K_B[c(b) - a]\}^{1/2})$
$c(b) = a$ $\quad c(H_2S^+) = [K_{HS}c(b)/K_B]^{1/2}$
$c(b) < a$ $\quad c(H_2S^+) = a - c(b)$

Talanta, Vol. 32, No. 7, pp. 565–567, 1985
Printed in Great Britain.

0039-9140/85 $3.00 + 0.00

SHORT COMMUNICATIONS

SOLVENT EXTRACTION SEPARATION OF RUBIDIUM WITH DICYCLOHEXANO-18-CROWN-6

B. S. MOHITE and S. M. KHOPKAR
Department of Chemistry, Indian Institute of Technology, Bombay 400076, India

(*Received* 8 *May* 1984. *Revised* 8 *January* 1985. *Accepted* 28 *February* 1985)

Summary—Rubidium is extracted quantitatively at pH 3.0–7.0 by 0.01*M* dicyclohexano-18-crown-6 in methylene chloride from 0.01*M* picric acid, stripped with 2*M* nitric acid and determined by flame photometry or atomic-absorption spectrometry. It can be separated from the most alkali and alkaline-earth metals, but the tolerance levels for potassium, ammonium and barium are rather low. The common anions, including those of some organic acids, are tolerated in fairly high amounts. The method has been applied to analysis of chloride schist rock and lepidolite for rubidium. The analysis takes an hour.

The crown ethers have been extensively used for the extraction of alkali-metal ions, and these methods have been reviewed.[1] Dibenzo-18-crown-6 extracts alkali-metal ions from picrate media,[2] rubidium showing the highest degree of extraction. 12-Crown-4 in benzene[3] has also been used as the extractant. Several uni- and bivalent metal picrates have been extracted with dibenzo-24-crown-8, which has least selectivity for univalent metals; barium shows the highest extractibility.[4] Several bis-(crown ethers) form sandwich-type ion-pair complexes.[5] Dibenzo-18-crown-6 in nitrobenzene–toluene mixture extracts alkali-metal ions, potassium and rubidium being the most extractable.[6] In synergic extraction with 12-crown-4 or 15-crown-5 and tributyl phosphate[7], the formation constant of the complex increases with increase in the number of donor oxygen atoms. Other crown ethers have also been used to extract alkali and alkaline-earth metal ions.[8] The complexes of rubidium and caesium with crown ethers have also been characterized.[9–11] Crown dinitrophenylazophenol has been used for the photometric determination of rubidium and caesium.[11] 4′-Picrylaminobenzo-15-crown-5 has also been used for the extractive photometric determination of alkali metals, including rubidium.[12]

No systematic work has been done on the extractive separation of rubidium with macrocyclic polyethers. Such studies are reported in this paper and a method for determination of rubidium has been developed and applied to a rock sample and lepidolite.

EXPERIMENTAL

Apparatus and reagents

The apparatus used was similar to that described earlier.[1] A stock rubidium solution was prepared by dissolving 1.767 g of rubidium chloride in 250 ml of demineralized water and standardized gravimetrically.[13] A working standard solution (rubidium 250 μg/ml) was prepared by appropriate dilution. Methylene chloride solutions (0.01*M*) of dicyclohexano-18-crown-6, 18-crown-6, dibenzo-18-crown-6 and 15-crown-5 were prepared. A picric acid solution (0.05*M*) was prepared by dissolving 2.864 g of reagent in 250 ml of demineralized water and standardized by titration with standard alkali.

Procedure

To an aliquot of solution containing 250 μg of rubidium, 2 ml of 0.05*M* picric acid were added, the pH was adjusted to 2.0–8.0 with 0.01*M* lithium hydroxide or 0.01*M* picric acid, and the solution was diluted to 10 ml. It was then transferred to a separatory funnel, 10 ml of 0.01*M* crown ether solution were added, and the mixture was shaken on a wrist-action flask shaker for 10 min. The two layers were allowed to settle and the organic phase was separated and equilibrated with 10 ml of 2*M* nitric acid to strip the rubidium, which was then determined by the flame emission method (at 780 nm). The concentration of rubidium was computed from a calibration graph.

RESULTS AND DISCUSSION

Extraction as a function of pH

The pH range for the quantitative extraction of rubidium was found to be 3.0–7.0 for dicyclohexano-18-crown-6. The pH was adjusted with 0.01*M* lithium hydroxide or picric acid. The highest degree of extraction with the other reagents in the pH range tested was 90% with 15-crown-5, 48% with 18-crown-6 and 80% with dibenzo-18-crown-6 (Table 1). Thus only dicyclohexano-18-crown-6 was suitable for quantitative extraction of rubidium.

Effect of dicyclohexano-18-crown-6 concentration

Rubidium was extracted at pH 3.0 from $10^{-2}M$ picric acid medium with various concentrations of dicyclohexano-18-crown-6 in the range 2.00–$100 \times 10^{-4}M$, with methylene chloride as diluent. The extraction was 90% complete with $3 \times 10^{-4}M$ crown ether and quantitative with $\geq 70 \times 10^{-4}M$ crown ether. The concentration used for further work was $10^{-2}M$.

Table 1. Degree of extraction (%) of rubidium as a function of pH

pH	15-C-5	18-C-6	DB-18-C-6	DC-18-C-6
2	90	48	80	98
3	80	34	76	100
4	80	34	72	100
5	80	34	68	100
6	80	32	66	100
7	80	32	60	100
8	76	28	56	96
9	74	26	54	94

Effect of picric acid concentration

Extraction of rubidium at pH 3.0 with 0.01*M* dicyclohexano-18-crown-6 in methylene chloride was 70% complete with $8 \times 10^{-4}M$ picric acid, and quantitative with $4–10 \times 10^{-3}M$ picric acid. A 0.01*M* concentration of picric acid was used in further work.

Choice of diluents

Rubidium was extracted at pH 3.0 from 0.01*M* picric acid with 0.01*M* dicyclohexano-18-crown-6 in various solvents as diluents. The extraction was quantitative only with methylene chloride as diluent (Table 2).

Choice of stripping agent

The rubidium extracted under the conditions chosen as described above was stripped from the organic phase with various acids. The stripping was quantitative with 1.0–5.0*M* hydrochloric acid, 1.0–8.0*M* nitric acid or 3.0–6.0*M* perchloric acid but not with sulphuric or acetic acid. For practical application 2*M* nitric acid was chosen as it permits direct flame photometric determination of rubidium.

Equilibration period

Rubidium was found to be 92% extracted in 1 min, 98% in 3 min and 100% in 4 min. A shaking period of 10 min was therefore chosen for safety.

Nature of the extracted species

The probable composition of the extracted species was established from a plot of log *D vs.* log [crown ether] at fixed picric acid concentration (0.01*M*) and log *D vs.* log [picric acid] at fixed dicyclohexano-18-crown-6 concentration (0.01*M*). The slopes were 1.2 and 1.4 respectively, so the extracted species is probably 1:1:1 in composition in agreement with earlier work.[10]

Table 2. Effect of various diluents

Diluent	*E*, %
Benzene	80
Toluene	78
Xylene	76
Carbon tetrachloride	40
Chloroform	90
Methylene chloride	100
Ethylene chloride	94

Effect of other ions

About 250 μg of rubidium was extracted in the presence of several elements, including alkali and alkaline-earth metals. The tolerance limit was set as the amount of foreign ion showing not more than $\pm 2\%$ error in recovery of rubidium (Table 3).

It was noted that certain *s*-block elements such as lithium, beryllium and magnesium showed neither co-extraction nor spectral interference. Therefore they were tolerated in higher ratio.

Elements such as sodium, calcium, strontium and barium were co-extracted along with rubidium at pH 3.0–7.0 with dicyclohexano-18-crown-6 but none of them showed spectral interference.[14] The wavelength for their measurement was different from that for measurement of rubidium: sodium (589 nm), calcium (423 nm), strontium (461 nm), barium (554 nm), rubidium (780 nm).

Table 3. Tolerance limits for diverse ions in determination of 0.25 mg of Rb

Foreign ions	Added as	Tolerance limit, *mg*	Ratio to Rb
Li^+	LiCl	6.5	1:26
*Na^+	NaCl	2.5	1:10
*K^+	KCl	0.20	1:1
Cs^+	CsCl	2.5	1:10
Be^{2+}	$Be(NO_3)_2$	5.3	1:21
Mg^{2+}	$MgCl_2$	4.2	1:17
*Ca^{2+}	$CaCl_2$	3.5	1:14
*Sr^{2+}	$Sr(NO_3)_2$	2.1	1:8
*NH_4^+	NH_4Cl	0.15	1:0.6
*Ba^{2+}	$Ba(NO_3)_2$	1.9	1:8
UO_2^{2+}	$UO_2(NO_3)_2$	3.1	1:12
Pb^{2+}	$Pb(NO_3)_2$	4.5	1:18
Hg^{2+}	$HgCl_2$	5.0	1:20
Cl^-	HCl	5.1	1:20
Br^-	HBr	5.5	1:22
I^-	HI	6.5	1:26
NO_3^-	HNO_3	5.0	1:20
SO_4^{2-}	H_2SO_4	6.0	1:24
PO_4^{3-}	H_3PO_4	6.2	1:25
ClO_4^-	$HClO_4$	6.5	1:26
CH_3COO^-	CH_3COOH	6.0	1:24
$C_2O_4^{2-}$	$H_2C_2O_4$	5.8	1:23
Tartrate	Tartaric acid	2.5	1:10
Ascorbate	Ascorbic acid	3.0	1:12
EDTA	EDTA	2.5	1:10

*Co-extracted along with rubidium.

Potassium was co-extracted and also gave spectral interference (emission line at 767 nm). It could be tolerated only in 1:1 ratio. At a potassium:rubidium ratio of 2:1 the rubidium was only 96% extracted.

Although caesium was also co-extracted with rubidium it could be tolerated in 10:1 ratio, as no major spectral interference was encountered (emission line at 852 nm), and the rubidium was 100% extracted.

Ammonium ion interferes by competitive complex formation, as expected from its similarity to rubidium in ionic radius, but cannot cause spectral interference, of course.

Uranium, lead, mercury and various anions are tolerated at higher ratios to rubidium. Acids present can be neutralized with lithium hydroxide, and their ions are not extracted.

Determination of rubidium in geological samples

The proposed method was applied to determination of rubidium in a chloride schist rock and lepidolite. About 1 g of sample was dissolved in a mixture of 5 ml each of concentrated nitric acid and hydrofluoric acid in a platinum crucible. The solution was evaporated almost to dryness. Then 5 ml of concentrated nitric acid were added and the solution was evaporated again, and the residue was dissolved in demineralized water and the solution diluted to known volume. For the chloride schist sample the solution was used directly for the solvent extraction, but for the lepidolite the sample solution was first passed through a 20 × 1.4 cm Dowex 50W-X8 cation-exchange column (H^+-form) at a flow-rate of 2 ml/min. Potassium was eluted first with 1*M* hydrochloric acid in 40% ethanol, then rubidium with 2*M* hydrochloric acid.[15] The rubidium eluate was evaporated to dryness, the residue was taken up with water and the rubidium extracted as in the general procedure. The rubidium found was 0.029% for the chloride schist (certificate value 0.03%) and 1.31% in the lepidolite (certificate value 1.3%) from triplicate analysis.

Comparison with existing methods

The extraction methods involving use of tetraphenylborate,[16] dipicrylaminate,[17] 4-sec-butyl-2-(α-methylbenzyl)phenol (BAMBP)[18] and 2-thenoyltrifluoroacetone[19] suffer from several limitations. The extraction of rubidium with tetraphenylborate is quantitative only with freshly prepared reagent solution, and large amounts of the other alkali metals decrease the extraction of rubidium. The extraction with dipicrylaminate is not satisfactory as caesium is co-extracted and interferes, though this would not matter if AAS were used for the final determination. With BAMB in cyclohexane, lithium gives very strong interference, and the presence of other ions decreases the extraction of rubidium. In the extraction with 2-thenoyltrifluoroacetone a highly alkaline solution is required for extraction of rubidium, and the alkaline-earth and other alkali-metal ions show strong interference. The method proposed here permits extraction and flame photometric or atomic-absorption determination of rubidium in the presence of most of the alkaline-earth and alkali metals. The common sequestering agents such as tartrate, ascorbate, oxalate, EDTA and halides are tolerated in high ratio to rubidium.

The method is simple, rapid, reproducible and fairly selective. The total time required for extraction and flame photometric determination of rubidium is just one hour.

REFERENCES

1. B. S. Mohite and S. M. Khopkar, *Indian J. Chem.*, 1983, **22A**, 962.
2. A. Sadakane, T. Iwachido and K. Toei, *Bull. Chem. Soc. Japan*, 1975, **48**, 60.
3. Y. Takeda, *ibid.*, 1980, **53**, 2393.
4. *Idem, ibid.*, 1979, **52**, 2501.
5. K. H. Wong and H. L. Ng, *J. Coord. Chem.*, 1981, **11**, 49.
6. P. R. Danesi, H. Meider-Gorican, R. Chiarizia and G. Scibona, *J. Inorg. Nucl. Chem.*, 1975, **37**, 1479.
7. Y. Takeda, *Bull. Chem. Soc. Japan*, 1981, **54**, 526.
8. H. Holland, J. A. Ringseth and T. S. Brun, *J. Soln. Chem.*, 1979, **8**, 779.
9. T. Ikeda, A. Abe, K. Kikukawa and T. Matsuda, *Chem. Lett.*, 1983, 369.
10. U. Eliav and H. Levanon, *J. Phys. Chem.*, 1980, **84**, 842.
11. K. Nakashima, Y. Yamawaki, S. Nakatsuji, S. Akiyama, T. Kaneda and S. Misumi, *Chem. Lett.*, 1983, 1415.
12. H. Nakamura, M. Takagi and K. Ueno, *Talanta*, 1979, **26**, 921.
13. A. I. Vogel, *A Textbook of Quantitative Inorganic Analysis*, 4th Ed., p. 475. Longmans, London, 1978.
14. A. K. De, S. M. Khopkar and R. A. Chalmers, *Solvent Extraction of Metals*, p. 220. Van Nostrand Reinhold, London, 1970.
15. V. P. Mehta and S. M. Khopkar, *J. Indian Chem. Soc.*, 1981, **58**, 591.
16. K. Hayyama and T. Ashizawa, *Bunseki Kagaku*, 1965, **14**, 120.
17. M. Kyrš, *Collection Czech. Chem. Commun.*, 1962, **27**, 2380.
18. W. J. Ross and J. C. White, *Anal. Chem.*, 1964, **36**, 1998.
19. P. Crowther and F. L. Moore, *ibid.*, 1963, **35**, 2081.

Talanta, Vol. 32, No. 7, pp. 568–570, 1985
Printed in Great Britain.

0039-9140/85 $3.00 + 0.00

DETERMINATION OF GOLD, INDIUM, TELLURIUM AND THALLIUM IN THE SAME SAMPLE DIGEST OF GEOLOGICAL MATERIALS BY ATOMIC-ABSORPTION SPECTROSCOPY AND TWO-STEP SOLVENT EXTRACTION

A. E. HUBERT and T. T. CHAO
U.S. Geological Survey, Box 25046, MS 955, DFC, Denver, Colorado 80225, U.S.A.

(*Received* 27 *September* 1984. *Revised* 17 *January* 1985. *Accepted* 4 *February* 1985)

Summary—A rock, soil, or stream-sediment sample is decomposed with hydrofluoric acid, *aqua regia*, and hydrobromic acid–bromine solution. Gold, thallium, indium and tellurium are separated and concentrated from the sample digest by a two-step MIBK extraction at two concentrations of hydrobromic acid. Gold and thallium are first extracted from 0.1*M* hydrobromic acid medium, then indium and tellurium are extracted from 3*M* hydrobromic acid in the presence of ascorbic acid to eliminate iron interference. The elements are then determined by flame atomic-absorption spectrophotometry. The two-step solvent extraction can also be used in conjunction with electrothermal atomic-absorption methods to lower the detection limits for all four metals in geological materials.

Gold, indium, tellurium and thallium are present at very low concentrations in geological materials. The abundance in the earth's crust is estimated to be 0.001–0.0035 ppm for gold,[1,2] 0.11–0.14 ppm for indium,[3,4] 0.001 ppm for tellurium[5,6] and 0.3–1.3 ppm for thallium.[7] A method for determining the abundance of all four elements in the same sample digest of geological materials is particularly advantageous in geochemical prospecting, with respect to economy and speed of analysis, detection as ore elements in rocks or weathering products, use of the elements as a pathfinder for various types of mineral deposits[8–10] and the study of elemental associations.[9]

The flame atomic-absorption method described here provides a relatively fast and simple procedure for determining gold, indium and tellurium at concentrations much higher than the crustal abundance (anomalous concentrations) and thallium at both crustal and anomalous levels. The special feature of the procedure lies in a two-step solvent extraction whereby gold and thallium are first separated from sample solution adjusted to be 0.1*M* in hydrobromic acid, and then indium and tellurium are extracted from 3*M* hydrobromic acid medium, with ascorbic acid added to eliminate iron interference. If electrothermal atomic-absorption methods are used, the detection limits for all four analytes are considerably lowered.

EXPERIMENTAL

Apparatus

A Perkin-Elmer 603 atomic-absorption spectrophotometer was used. It was equipped with an automatic gas-control unit, a variable nebulizer, a 10-cm three-slot burner, a simultaneous background corrector, and an electrodeless-discharge lamp (EDL) power supply. Electrodeless-discharge lamps were used for tellurium and thallium, and hollow-cathode lamps for gold and indium. The instrumental and operating conditions were those recommended by the manufacturer, and an air–acetylene flame was used.

Reagents

All chemicals used were of reagent grade.

Aqua regia. A 1:3 v/v mixture of concentrated nitric acid and concentrated hydrochloric acid, prepared fresh when needed.

Hydrobromic acid, concentrated (48%).

Hydrobromic acid–10% bromine solution. Dilute 10 ml of bromine to 100 ml with concentrated hydrobromic acid.

Iron solution, 4%, in 3M hydrobromic acid. Dissolve 4 g of pure iron powder in concentrated hydrobromic acid, add 1 ml of bromine, and evaporate to dryness. Add 34 ml of concentrated hydrobromic acid, heat to dissolve the residue, and dilute to 100 ml.

Gold, indium, tellurium and thallium individual stock solutions, 1000-μg/ml. Dissolve 1.000 g of pure gold, indium or thallium, or 1.250 g of tellurium dioxide (TeO_2) in 20 ml of hydrobromic acid–10% bromine solution, heat gently to expel excess of bromine, and make up to volume in a 1000-ml standard flask with concentrated hydrobromic acid. The solution has a hydrobromic acid concentration of approximately 9*M*.

Gold and thallium working standards in MIBK. Prepare a series of 20-ml solutions containing 0.0, 0.5, 1.0, 2.5, 5.0 and 10.0 μg of Au or Tl by serial dilution of the stock solution with distilled water, and addition of hydrobromic acid so that the acidity of the final solution is equivalent to 0.1*M* hydrobromic acid. Shake the solution with 5 ml of methyl isobutyl ketone (MIBK) for 5 min. Centrifuge to separate the MIBK phase.

Indium and tellurium working standards in MIBK. Prepare standard solutions for indium and tellurium in the same concentration range as for gold and thallium, but in 3*M* hydrobromic acid containing 200-μg of iron as the bromide in 20 ml of the solution (0.1 ml of 4% iron solution per 20 ml of solution). Add 1 g of ascorbic acid to reduce the iron and make the the solution light yellow. Extract the solution with 5 ml of MIBK and centrifuge.

The concentrations of Au, Tl, In and Te in the MIBK working standards correspond to 0.00, 0.25, 0.50, 1.25, 2.50 and 5.00 ppm of the metal in a 2-g sample.

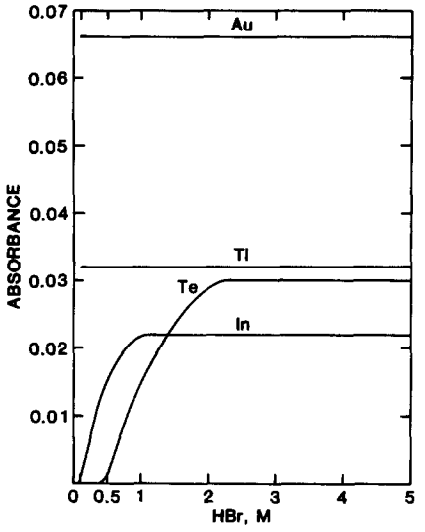

Fig. 1. Extraction of Au, In, Te and Tl (5 μg of each analyte in 20 ml of aqueous solution, extracted into 5 ml of MIBK) as a function of HBr concentration in the aqueous solution.

Procedure

Weigh a 2.00-g pulverized (< 100-mesh) rock, soil or stream-sediment sample into a 50-ml Teflon beaker. Wet the sample with 1 ml of distilled water and slowly add 10 ml of *aqua regia*. Add 10 ml of concentrated hydrofluoric acid and let stand on an oscillating hot-plate at room temperature for 2 hr to dissolve the sample. Then evaporate the solution to dryness at 100–110°. Cool and add 5 ml of concentrated hydrobromic acid. Again evaporate to dryness at 100–110°. Cool and add 0.22 ml of hydrobromic acid–10% bromine solution and 5 ml of distilled water. Warm, stir to dissolve the residue, wash the solution into a 25 × 200-mm screw-cap test-tube with distilled water, and make up to a volume of 20 ml. Add 5 ml of MIBK, cap the tube, and shake it for 5 min. Centrifuge to separate the layers and use the MIBK layer for the determination of gold and thallium.

Remove and discard the remaining MIBK layer. Add 10 ml of concentrated hydrobromic acid to the aqueous solution and mix. Add 1 g or more of ascorbic acid to reduce the iron and change the colour of the solution from brown to light yellow. Extract the solution with 5 ml of MIBK as above and use the organic solution for the determination of indium and tellurium.

Determine the absorbances for the four analytes in the organic extracts of the standards and samples, by measuring the peak heights.

RESULTS AND DISCUSSION

Sample decomposition

Aqua regia is a strongly oxidizing acidic reagent that is commonly used to dissolve elements from secondary weathering products such as soils and altered rocks. Hydrofluoric acid is added to the digestion mixture to decompose silicate minerals or other siliceous materials. Sighinolfi *et al.*[11] have used the combination of *aqua regia* and hydrofluoric acid for sample decomposition, in determining tellurium in geological materials by flameless atomic-absorption spectroscopy. Treatment with hydrobromic acid–bromine solution will further ensure complete dissolution of the four analytes, as shown by Thompson and Nakagawa[12] and Meier[13] for gold, Hubert and Lakin[14] for indium and thallium and Chao *et al.*[15] for tellurium. Therefore, analytical values obtained with this digestion step in the procedure should represent the total concentrations of the four elements in the samples.

Solvent extraction

In this procedure, the characteristics of MIBK extraction of the four analytes from hydrobromic acid were examined first. Figure 1 shows that gold and thallium can be extracted completely from 0.1–5*M* hydrobromic acid whereas the extraction of both indium and tellurium is complete only when the acidity is greater than 2.5*M*.

Iron is the major interfering element in the determination of the four analytes in geological materials. Prior removal of iron by solvent extraction, reduction of iron by ascorbic acid, stripping the co-extracted iron, and selective extraction of the analyte may be used to eliminate the iron interference. Because iron is practically unextracted into MIBK at low concentrations of hydrobromic acid,[16] gold and thallium can be separated from iron by MIBK extraction from a sample solution adjusted to 0.1*M* hydrobromic acid concentration. It is for this reason that the procedure uses the two-step extraction to isolate gold and thallium first for determination.

Both indium and tellurium can be extracted into MIBK from 3*M* hydrobromic acid, but an appreciable amount of iron is also extracted,[16] and interferes in both indium and tellurium determination.[15,17] Addition of ascorbic acid to reduce iron removes the interference completely, as shown in Fig. 2. Therefore, the extraction of indium and tellurium after addition of ascorbic acid constitutes the second phase of the two-step solvent-extraction procedure.

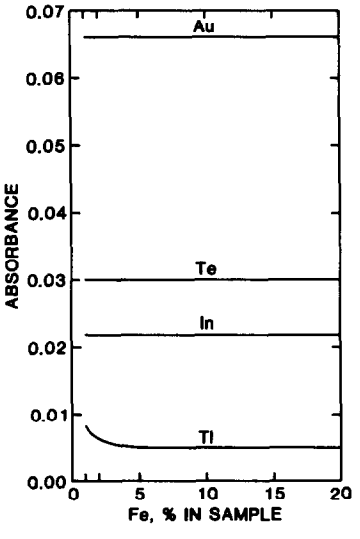

Fig. 2. Extraction of Au, In, Te, and Tl (5 μg of each analyte in 20 ml of aqueous solution) from 3*M* HBr in presence of various amounts of Fe, by 5 ml of MIBK after addition of ascorbic acid.

Table 1. Replicate analysis ($n = 6$) for Au, Tl, In and Te in six geochemical reference samples

Element		GXR-1	GXR-2	GXR-3	GXR-4	GXR-5	GXR-6
Au	Mean, *ppm*	3.1	*	*	0.43	*	*
	Lit. value,† *ppm*	3.0			0.35		
	RSD, %	4.3			11.9		
	Recovery,§ %					100, 98	96, 98
Tl	Mean, *ppm*	*	1.2	3.9	3.5	0.32	2.5
	Lit. value,‡ *ppm*		1.2	3.8	3.5	0.35	2.5
	R.S.D., %		4.2	1.6	2.4	12.5	2.0
	Recovery,§ %					96, 100	90, 102
In	Mean, *ppm*	0.53	*	*	*	0.32	*
	Lit. value,‖ *ppm*	0.39				0.11	
	R.S.D., %	9.7				12.9	
	Recovery,§ %					102, 98	96, 96
Te	Mean, *ppm*	9.3	0.83	*	0.92	*	*
	Lit. value,¶ *ppm*	8.7	0.88		1.0		
	R.S.D., %	7.3	6.2		4.5		
	Recovery,§ %					96, 90	96, 95

*Below detection limit, 0.1 ppm for Au and Te, 0.2 ppm for Tl and In.
†Meier.[13]
§For 0.5, 1.0 μg of the element, added to the sample.
‡Allcott and Lakin.[18]
‖Zhou *et al.*[17]
¶Chao *et al.*[15]

Though the extraction of gold is not affected by ascorbic acid, probably because of the formation of strong gold–bromide complexes in 3*M* hydrobromic acid, the extraction of thallium is drastically decreased (compare Figs. 1 and 2). For this reason, thallium is extracted along with gold from 0.1*M* hydrobromic acid in the first phase of the two-step extraction.

Sensitivity

For a 2.00-g sample, the practical lower range of concentration that can be accurately determined is 0.1 ppm Au, 0.2 ppm Tl, 0.2 ppm In, and 0.2 ppm Te (0.1 ppm if 2.5 ml of MIBK are used). Thus both anomalous and background levels of thallium can be determined, but only anomalous samples can be analysed for gold, indium and tellurium. However, the extraction procedure can also be used in conjunction with electrothermal atomic-absorption methods to enhance the sensitivity for gold, indium, and tellurium. The MIBK extract is analysed for gold by the method of Meier (with a lower limit of determination of 0.001 ppm),[13] for indium by the method of Zhou *et al.* (limit of determination 0.025 ppm)[17] and for tellurium by the method of Chao *et al.* (limit of determination 0.004 ppm).[15]

Results for geological samples

The method was applied to six U.S. Geological Survey geochemical exploration reference samples,[18] with the results presented in Table 1. The values for gold, thallium and tellurium are in good agreement with those reported in the literature. There is some difference of the two indium values from those reported by Zhou *et al.*,[17] but the two sets of values are still of the same order of magnitude. Overall recoveries for the four metals added to various samples ranged from 90 to 102% with an average of 97%.

Conclusion

The proposed two-step solvent extraction for isolation of the analytes from sample matrices can be used to determine a wide range of concentrations of Au, Tl, In, and Te in geochemical samples when coupled with flame or furnace atomic-absorption methods.

REFERENCES

1. V. M. Goldschmidt, *Geochemistry*, Clarendon Press, Oxford, 1954.
2. T. Lee and Chi-lung Yao, *Intern. Geology Rev.*, 1970, **12**, 778.
3. R. A. Weeks, *U.S. Geol. Surv. Prof. Paper*, 1973, **820**, 237.
4. D. M. Shaw, *Geochim. Cosmochim. Acta*, 1952, **2**, 185.
5. D. F. Davidson and H. W. Lakin, *U.S. Geol. Surv. Prof. Paper*, 1973, **820**, 627.
6. A. P. Vinogradov, *Geochemistry*, 1962, **7**, 641.
7. R. F. Parker, *U.S. Geol. Surv. Prof. Paper*, 1967, **440-D**, 17.
8. R. E. Learned and R. Boissen, *Intern. Geochem. Explor. Symp., 4th, London (1972)*, 1973, 93.
9. R. W. Boyle, *Geol. Surv. Can. Paper*, 1974, **74–75.**
10. M. Ikvamuddin, Y. Asmeron, P. M. Norstron, K. P. Kinart, W. M. Martin, S. J. M. Digby, D. D. Elder, W. F. Nijak and A. A. Afemari, *J. Geochem. Explor.*, 1983, **19**, 465.
11. G. P. Sighinolfi, A. M. Santos and G. Martinelli, *Talanta*, 1979, **26**, 143.
12. C. E. Thompson and H. M. Nakagawa, *U.S. Geol. Surv. Prof. Paper*, 1968, **600-B**, B130.
13. A. L. Meier, *J. Geochem. Explor.*, 1980, **13**, 77.
14. A. Hubert and H. W. Lakin, *Intern. Geochem. Explor. Symp., 4th, London (1972)*, 1973, 383.
15. T. T. Chao, R. F. Sanzolone and A. E. Hubert, *Anal. Chim. Acta*, 1978, **96**, 251.
16. A. R. Denaro and V. J. Occleshaw, *ibid.*, 1955, **13**, 239.
17. Liyi Zhou, T. T. Chao and A. L. Meier, *ibid.*, 1984, in press.
18. G. H. Allcott and H. W. Lakin, *Geochem. Explor.*, 1975, 659.

Talanta, Vol. 32, No. 7, pp. 571–573, 1985
Printed in Great Britain.

0039-9140/85 $3.00 + 0.00

USE OF THIOSEMICARBAZIDE AS MASKING AGENT FOR THE DIRECT DETERMINATION OF BISMUTH IN COPPER BY ATOMIC-ABSORPTION SPECTROMETRY WITH HYDRIDE GENERATION

TAKEO TAKADA and KATSUYUKI FUJITA
Department of Chemistry, College of Science, Rikkyo (St Paul's) University, Nishi-Ikebukuro, Toshima-ku, Tokyo 171, Japan

(*Received* 19 *November* 1984. *Accepted* 4 *February* 1985)

Summary—A simple atomic-absorption method for determining trace bismuth in copper metal is described. Interference from the matrix is eliminated by masking copper with thiosemicarbazide in acidic solution.

The hydride-generation atomic-absorption method provides one of the most widely used methods for the sensitive determination of bismuth, but suffers severe interference effects from various metal ions. Smith[1] studied the effects of 48 elements and reported that there was always some interference from copper. We also have found serious suppression of the bismuth signal by copper.

Bédard and Kerbyson[2] reported that bismuth in copper could be determined by co-precipitation of the bismuth with lanthanum hydroxide in ammoniacal medium, dissolution of the precipitate in nitric acid, and atomic-absorption determination of bismuth hydride generated in the usual way. Donaldson[3] used diethyldithiocarbamate extraction or co-precipitation with hydrous ferric oxide from ammoniacal medium, for determination of bismuth in ores, concentrates and non-ferrous alloys.

Various masking methods have been proposed for eliminating the interferences. For example, Drinkwater[4] suggested that addition of EDTA completely overcomes the matrix interference for the determination of low concentrations of bismuth in nickel-base alloys. One of the problems in application of masking to the hydride-generation technique is the limited choice of masking agent on account of the high acidity (generally, pH < 1) normally required for hydride generation.

In this paper thiosemicarbazide is proposed as masking agent for copper in the determination of bismuth at ppm levels in copper metal.

EXPERIMENTAL

Apparatus

A Nippon Jarrell-Ash Model AA8500 atomic-absorption spectrometer equipped with a 10-cm single-slot air–acetylene burner and a home-made hydride-generator (Fig. 1) was used. The apparatus for hydride generation and atomization consisted of the hydride generation and collection system with a "by-pass" and "sweep", and a quartz-tube atomizer. The reaction vessel was a 50-ml conical flask. A glass syringe and two tubes at the top of the flask served for introducing the reducing agent solution and flushing with carrier gas, respectively. The quartz tube atomizer (inner diameter 10 mm) was T-shaped, the horizontal arm being 160 mm long, aligned with the optical axis of the spectrometer system and heated by a wide-path air–acetylene burner.

Reagents and sample preparation

All reagents except the sodium tetrahydroborate were of analytical-reagent grade. Sodium tetrahydroborate powder (98% pure, Nisso-Ventron) was dissolved in 0.1% sodium hydroxide solution. This solution was filtered through a fine-pore filter paper (No. 131, Toyo Roshi) and was usable for a few days. A standard bismuth solution (1000 μg/ml) was prepared by dissolving 0.1000 g of the pure metal in 5 ml of 2*M* nitric acid, evaporating to dryness, dissolving the residue with a small amount of 1*M* hydrochloric acid, transferring the solution into a 100-ml standard flask and making up to the mark with 1*M* hydrochloric acid. This solution was diluted as required, with 1*M* hydrochloric acid. An aqueous 0.15*M* thiosemicarbazide solution was prepared.

Procedure

A 10-ml portion of test solution was placed in the reaction vessel, which was then connected to the hydride generation and collection system. The air in the reaction vessel was flushed out with nitrogen with the three-way stopcock in the "sweep" position. This cock was then turned to the "by-pass" position and the two-way stopcock was closed. The magnetic stirrer was switched on and 1 ml of reducing agent was injected into the reaction vessel from the glass syringe. The hydride generated was collected in the reaction vessel for 60 sec, and the three-way stopcock was then turned to the "sweep" position and the two-way stopcock immediately opened. In this way the flame and air backgrounds were virtually eliminated and better accuracy was achieved. All measurements were done under the following instrumental conditions: wavelength 223.1 nm; lamp current, 10 mA; air flow-rate, 6.5 l./min; acetylene flow-rate, 1.25 l./min; carrier gas flow-rate, 1.0 l./min.

RESULTS AND DISCUSSION

Optimizing the bismuth hydride generation

The effect of the sodium tetrahydroborate concentration on the hydride generation efficiency was stud-

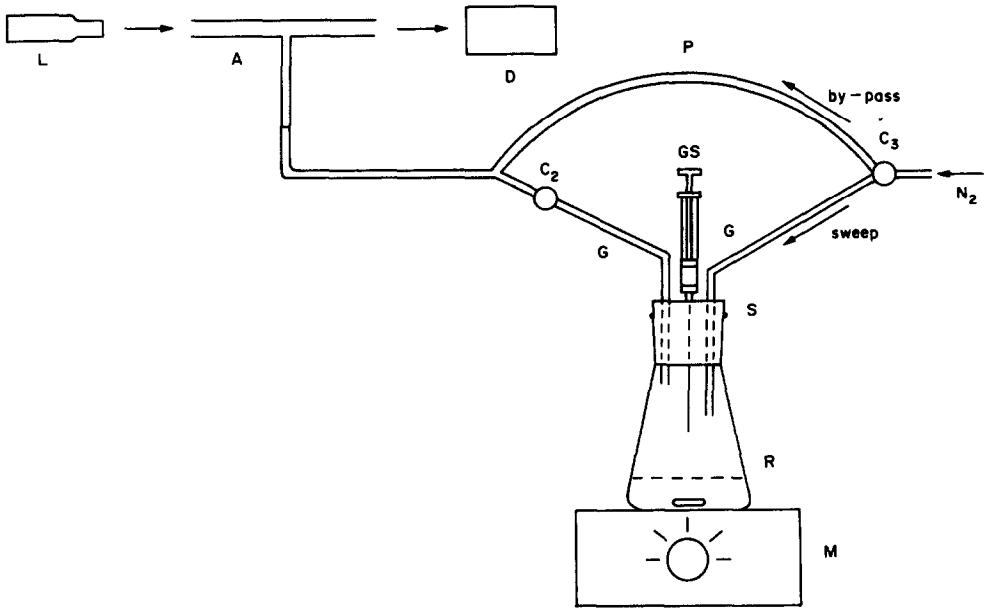

Fig. 1. Schematic diagram of apparatus: A, atomizing tube; C_2, two-way stopcock; C_3, three-way stopcock; D, detector; G, glass tube; GS, gas-tight syringe; L, light-source; M, magnetic stirrer; P, polyethylene tube; R, reaction vessel; S, silicone-rubber septum.

ied. One ml of reductant solution (of varied concentration) was added to 10 ml of 1*M* hydrochloric acid containing 40 ng of bismuth. The absorbance increased with reductant concentration up to 0.5%, became constant for the range 0.5–2.0% and then decreased again at higher reductant concentrations (2–3%) because of the high pressure developed in the hydride generation system by the larger volume of hydrogen evolved during the reaction period, which caused a faster flow of bismuth hydride through the atomizer tube. For this reason, 1 ml of 1% sodium tetrahydroborate solution was chosen for use.

The effect of hydrochloric acid concentration was investigated in the presence and absence of Cu(II). A 30-μl portion of standard bismuth solution (1 μg/ml) and 0.2 ml of Cu(II) solution (10 mg/ml) were added to the reaction vessel containing 5.0 ml of hydrochloric acid, and finally 5.0 ml of 0.15*M* thiosemicarbazide were added just before the reducing agent. The resulting test solutions contained 30 ng of bismuth, 2 mg of Cu(II), 0.75 mmole of thiosemicarbazide [*i.e.*, 25-fold mole ratio to copper(II)] and had a hydrochloric acid concentration between 0.1 and 4.0*M*. The results are shown in Fig. 2, and 0.1*M* hydrochloric acid medium was selected for use.

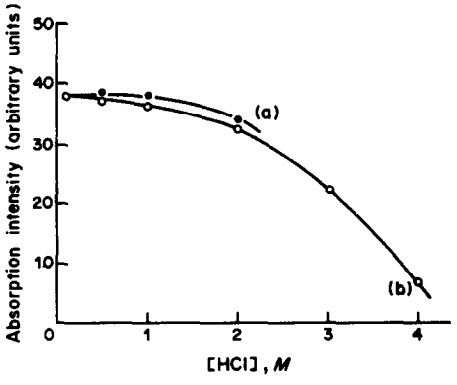

Fig. 2. Effect of acidity on the absorption intensity from 30 ng of Bi in the presence and absence of Cu(II); (a), without Cu(II); (b), with 2 mg of Cu(II). All other conditions are as in Table 1.

The collection time for the generated hydride (time period between adding the reducing agent and sweeping the generated gases into the atomizer) was found to be critical, and the optimum time at room temperature was found to lie in the range from 60 to 130 sec.[5] A collection time of 60 sec was chosen.

Effect of masking

The optimum thiosemicarbazide concentration was found by varying the volume of 0.15*M* masking agent added from 0 to 6.0 ml, with 1.0 ml of 1*M* hydrochloric acid, 50 μl of standard bismuth solution, and 0.2 ml of Cu(II) solution (10 mg/ml) present and the final total volume made 10 ml with distilled water. The resulting test solutions contained 50 ng of bismuth, 2 mg of Cu(II) and 0, 0.15, 0.30, 0.45, 0.60, 0.70 and 0.90 mmole of masking agent, in 0.1*M* hydrochloric acid medium.

The results are shown in Fig. 3. When no masking agent was present, practically no bismuth was found. A finely divided dark brown precipitate was produced by reaction of the reducing agent with the copper present. This precipitate was filtered off, dissolved in a small amount of 5*M* nitric acid and the solution

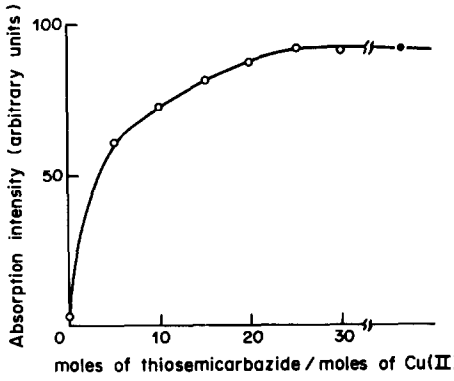

Fig. 3. Effect of thiosemicarbazide on the absorption intensity from 50 ng of Bi in the presence of and absence of Cu(II); ○, with 2 mg of Cu(II); ●, without Cu(II). All other instrumental conditions are as in Table 1.

was tested directly by atomic-absorption spectrometry, and copper was detected. It is thought that this precipitate results from reduction of cupric ions to the metal. Marked enhancement of the bismuth signal was observed on increasing the mole ratio of thiosemicarbazide to Cu(II), and a constant signal was obtained at mole ratios > 25. Thus, the interference of 2 mg of copper was removed by addition of 5 ml of 0.15*M* thiosemicarbazide.

Procedure for analysis of metal samples

Dissolve about 200 mg of sample, accurately weighed, in 5 ml of 5*M* nitric acid and heat the solution for about 7 min, then evaporate it to dryness on a boiling water-bath. Dissolve the residue in a small volume of 0.2*M* hydrochloric acid, transfer the solution into a 100-ml standard flask and dilute it to volume with 0.2*M* hydrochloric acid. Transfer a 1-ml aliquot of this solution to the reaction vessel, add 4 ml of 0.2*M* hydrochloric acid and 5 ml of 0.15*M* thiosemicarbazide and immediately attach the reaction vessel to the generation apparatus. Prepare a calibration graph with standard solutions containing bismuth (10, 30, 50 and 70 ng) in 0.1*M* hydrochloric acid without Cu(II) present. The optimum experimental conditions are given in Table 1.

Table 1. Experimental conditions

Sample solution in 0.2*M* HCl	1 ml
Hydrochloric acid, 0.2*M*	4 ml
Thiosemicarbazide, 0.15*M*	5 ml
Sodium tetrahydroborate solution 1%	1 ml
N_2 flow-rate	1.0 l./min
Collection time	60 sec
Air flow-rate	6.5 l./min
Acetylene flow-rate	1.25 l./min
Atomization temperature	*ca.* 830°

Table 2. Results of analysis of copper metals

Sample	Calibration curve method,* μg/g	Coefficient of variation, %	Standard addition method,† μg/g
S-1	4.1 ± 0.1	1.8	4.4
S-2	20.5 ± 0.3	1.9	20.0
S-3	10.4 ± 0.5	4.4	11.8

*Mean of 5 results.
†Mean of 2 results.

Table 3. Precision and accuracy of the method

Final conc. of Bi added to 2 mg of Cu(II), μg/g	Bismuth found, μg/ml	Coefficient of variation, %	Recovery, %
5	5.0	2.2	100
10	9.8	1.8	98
20	21.2	2.7	106

Applications

To test the reliability of the method, it was applied to the analysis of synthetic samples and of copper samples obtained from Nippon Mining. The standard-addition method was also tried. The results are given in Table 2, and agreed closely. The accuracy and precision were checked by analysis of synthetic standard solutions (6 replicates of each). The results are shown in Table 3. The linear calibration range was 0–70 ng of bismuth. The method is simple to use, no preseparation from the matrix is necessary and it is possible to analyse several samples within 90 min. Though the method is not recommended for samples with a very low bismuth content, it is suitable for samples containing 1 ppm or more of bismuth. It is also applicable to nickel and other non-ferrous metals.

Acknowledgements—The authors are grateful to The Nippon Mining Corporation for providing samples of copper metal.

REFERENCES

1. A. E. Smith, *Analyst*, 1975, **100**, 300.
2. M. Bédard and J. D. Kerbyson, *Anal. Chem.*, 1975, **47**, 1441.
3. E. M. Donaldson, *Talanta*, 1979, **26**, 1119.
4. J. E. Drinkwater, *Analyst*, 1976, **101**, 672.
5. K. Fujita and T. Takada, unpublished work.

Talanta, Vol. 32, No. 7, pp. 574–576, 1985
Printed in Great Britain.

0039-9140/85 $3.00 + 0.00

PREPARATION AND ANALYTICAL CHARACTERIZATION OF A CHELATING RESIN COATED WITH 1-(2-PYRIDYLAZO)-2-NAPHTHOL

J. CHWASTOWSKA and E. MOZER
Department of Analytical Chemistry, Faculty of Chemistry, Technical University of Warsaw, Warsaw, Poland

(*Received* 25 *April* 1984. *Revised* 6 *December* 1984. *Accepted* 1 *February* 1985)

Summary—A chelating sorbent was obtained by deposition of 1-(2-pyridylazo)-2-naphthol on Amberlite XAD-4. The analytical characteristics of the sorbent were established and optimum sorption conditions for Cu, Zn, Fe, Cd, Ni, and Pb under static and dynamic conditions were determined. The sorbent was applied to analysis of river water. After group separation of traces of metals on the sorbent and subsequent elution with hydrochloric acid, the metals were determined in the effluent by atomic-absorption spectrophotometry.

Styrene–divinylbenzene copolymers with a large surface area and macroporous structure, such as Amberlite XAD, are capable of adsorbing water-soluble organic substances. This property has been successfully utilized for separation of various organic compounds in analysis of water,[1–4] as well as for preparation of chelating sorbents by deposition of chelating reagents on Amberlite XAD as substrate. The method has been applied for preparation of a dithizone-coated resin (which was then used for isolation of mercury from sea-water)[5] and of a resin coated with ferroin-type compounds.[6]

In this work Amberlite XAD-4 was used as a substrate for deposition of 1-(2-pyridylazo)-2-naphthol (PAN), a heterocyclic azo compound capable of forming complexes with many metal ions. Polyurethane foams coated with PAN have already been reported as good sorbents for trace metals.[7–9]

EXPERIMENTAL

Reagents

Standard 1-mg/ml stock solutions of Fe, Pb, Ni, Cu, Zn and Cd were made by dissolving appropriate salts in distilled water suitably acidified to prevent hydrolysis, and were further diluted as required. PAN was used as a 0.45% solution in methanol.

Preparation of the sorbent

The copolymer was kept for one day in methanol, then filtered off and air-dried. PAN was deposited on the copolymer by two methods. In the first, a saturated solution of PAN in methanol (10 ml per g of resin) was passed at 1 ml/min through a column of Amberlite XAD-4, and the column was then washed with 5 bed-volumes of doubly distilled water. In the other, the resin was kept for 1 hr in a solution of PAN in methanol, with occasional stirring. The resin was then filtered off, washed with water, and air-dried.

The amount of PAN deposited on the resin was estimated by determining spectrophotometrically the amount of PAN left in the solution and washings. It was found that 78% of the PAN had been retained in the resin, which corresponds to 0.054 mmole per g of dry Amberlite XAD-4.

Procedures

The sorption of various metals was studied under static conditions by shaking a solution of the metal with a weighed quantity of the sorbent in a separating funnel, and under dynamic conditions by passing a solution of the metal through a column of the sorbent.

The static method was used in determination of the capacity and stability of the sorbent, the optimum sorption conditions (kinetics and pH), and the desorption conditions (stripping agent, its concentration, and shaking time).

The dynamic method was applied in determining the optimum pH, flow-rate, and sample volume.

The degree of sorption was found by atomic-absorption spectrophotometric determination of the test element in the effluent from the column and in the solution obtained by desorption. An air–acetylene flame was used under the conditions recommended by the instrument manufacturer, and the wavelengths (nm) used were: Cd—228.8, Cu—324.7, Fe—248.3, Ni—232.0, Pb—217.0, Zn—213.9.

Sorption kinetics (static conditions). A 10-ml portion of copper solution containing 75 μg of Cu at pH 8.5 was shaken for 30, 60, and 90 min with 1 g of the sorbent in a separating funnel.

Desorption conditions. One-g portions of resin were shaken for 60 min with 10-ml portions of copper solution (75 μg of Cu, pH 8.5), and then stripped by shaking for 15 min with 10 ml of 2, 3 and 4*M* hydrochloric acid.

Effect of pH on degree of sorption. Fixed amounts of the metals (Cu—75 μg, Fe—66 μg, Cd—130 μg, Ni—70 μg, Zn—75 μg, Pb—100 μg) in 10 ml of solution, at pH 2–10 for copper and pH 5–10 for the other metals, were shaken with 1-g portions of resin for 60 min.

Total sorption capacity. This was determined at pH 8.5 (assumed to be optimal for group separation of the test elements) with shaking for 60 min. The resin was separated, washed with water at pH 8.5, and stripped with 4*M* hydrochloric acid. The metals in the strippings were then determined by atomic-absorption spectrophotometry (AAS).

Sorption under dynamic conditions

Two columns, 9 and 6 mm in diameter respectively, were made with 2 g of the sorbent. A 200-ml portion of test solution at pH 8.5 and the concentration used in the static tests was passed through the resin, which was then washed with water at pH 8.5 and stripped with 10 ml of 4*M* hydrochloric acid. The metal stripped was determined by AAS.

Table 1. Total sorption capacity of the sorbent

Element	Sorption capacity per g of sorbent	
	μg	*mmole*
Cu	127	0.002
Fe	168	0.003
Ni	176	0.003
Zn	131	0.002
Cd	337	0.003

The effect of flow-rate on the sorption of copper was studied for the range 1.5–20 ml/min. The influence of the solution volume on copper sorption was studied by passing 200, 500, 1000 and 2000 ml volumes of copper solution through the column at a constant rate of 10 ml/min.

Analysis of water samples

Water samples (1 or 2 l.) were filtered, adjusted to pH 8.0, and passed at 5 ml/min through a column of 10 g of the chelating sorbent. The sorbed metals were eluted with 10 ml of 4*M* hydrochloric acid. The eluate was collected in a 25-ml standard flask, diluted to volume and analysed by AAS, after dilution if necessary (*e.g.*, for iron and zinc).

RESULTS AND DISCUSSION

Characteristics of the sorbent

Preparation of the sorbent is easy and quick; the batch method gives more uniform deposition of the reagent. The sorbent is highly stable. All attempts to remove the PAN from the Amberlite XAD-4 with organic solvents failed. The stability is confirmed by the fact that the sorbent can be repeatedly used: eight successive sorptions on the same sorbent gave almost identical results. The total sorption capacity is not very high (Table 1), which is typical for sorbents of this type.

Sorption under static conditions

The study of the sorption kinetics showed that shaking for 1 hr is necessary for equilibrium to be reached. Figure 1 shows that pH 8–9 is optimal for sorption of the elements studied. Under the batch conditions used, copper and iron are almost quantitatively sorbed, whereas lead, nickel, cadmium and zinc are only 80–85% sorbed.

All the elements retained by the sorbent are easily stripped by shaking it with 4*M* hydrochloric acid for 15 min.

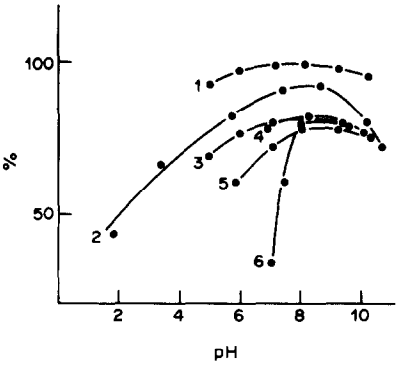

Fig. 1. Relationship between sorption and pH of solutions: 1—Fe, 2—Cu, 3—Zn, 4—Cd, 5—Pb, 6—Ni.

Column method

Table 2 shows that the column method gives more efficient overall sorption than the static method. Experiments with copper showed that varying the flow-rate in the range 1.5–20 ml/min did not affect the degree of sorption, which is advantageous for large volumes of sample, since a high flow-rate can be used to shorten the analysis time. The sample volume also does not affect performance with a fixed amount of resin and fixed *total* amount of metal. This is important for application to water analysis.

Application to analysis of water

Naturally occurring waters contain considerable amounts of sodium, potassium, magnesium and calcium salts, mainly the chlorides and sulphates. The influence of the major salts found in natural waters

Table 3. Group column sorption of metals in presence of other elements (synthetic drinking water, 200 ml, pH 8.5)

Element	Added, *μg*	Sorbed, *μg*	Sorption, %
Cu	30	21	70
Cd	52	36	69
Ni	42	30	71
Pb	50	40	80
Zn	30	22	73
Fe	66	48	73

Table 2. Column sorption of metals (as a group in 200 ml of solution, pH 8.5)

Element	Added, *μg*	Amount sorbed			
		Flow-rate 10 ml/min		Flow-rate 15 ml/min	
		μg	%	*μg*	%
Cu	30	29.0	97	28.0	93
Fe	25	24.5	98	23.0	92
Zn	30	28.0	93	27.0	90
Cd	52	45.0	87	47.0	90
Pb	100	90.0	90	90.0	90
Ni	28	25.0	90	25.0	90

Table 4. Group column sorption of metals in presence of other elements (synthetic drinking water) at different pH values (200 ml of solution, flow-rate 5 ml/min)

Element	Added, μg	pH 8.5 Sorbed, μg	pH 8.5 Sorption, %	pH 8.0 Sorbed, μg	pH 8.0 Sorption, %	pH 7.0 Sorbed, μg	pH 7.0 Sorption, %
Cu	30	21	70	26	87	23	77
Fe	66	48	73	62	94	64	97
Ni	42	30	71	31	74	12	30
Zn	30	22	73	25	83	21	70
Cd	52	36	69	44	84	16	31
Pb	50	40	80	40	80	32	64

Table 5. Analysis of river water

Element	Found,* μg/l. 1-l. sample	2-l. sample	1-l. sample after mineralization
Zn	56.3	56.0	56.5
Cu	2.1	2.0	2.0
Cd	<1	<1	<1
Fe	215	200	215
Ni	7.2	7.5	7.5
Pb	5.5	5.2	5.0

*Mean of 3 determinations.

on the sorption of metals on the PAN–XAD-4 sorbent was therefore examined, with a synthetic water (formulated on the basis of the acceptable limits for drinking water) having the composition: Na^+ 30, K^+ 8, Mg^{2+} 40, Ca^{2+} 110, Cl^- 248, and SO_4^{2-} 158 mg/l. A 100-ml portion of the synthetic water, to which a mixture of the elements under study had been added, was adjusted to pH 8.5 and passed at 5 ml/min through a column (9 mm diameter) of the sorbent.

It was found (Table 3) that the degree of sorption was lower than that in the absence of the salts present in the synthetic water. This was thought to be due to competitive sorption of calcium and magnesium. Further examination showed that at pH 8.5 the degree of sorption is 35% for magnesium, and 25% for calcium, and it decreases with decreasing pH. Since the concentration of these two elements in water can be very large compared with that of the trace elements, they can easily block the active centres of the sorbent. This effect can in principle be counteracted by using a lower pH for sorption of the trace elements, and/or by using more sorbent. The sorption experiment was therefore repeated with the synthetic water/trace element mixture at pH 7.0 and 8.0 with 4 g of sorbent. The results (Table 4) show that use of pH 7 is not profitable because of the considerably decreased sorption efficiency for all the trace metals, especially nickel and cadmium. Use of pH 8.0 and even more sorbent seemed a reasonable compromise. Under these conditions the sorption of the trace elements is sufficiently effective, and the sorption of calcium is reduced to 15% and of magnesium to 22%.

The procedure has been applied to analysis of river water (from the Jeziorka river). The water samples (1 and 2 l.) were passed through the column either directly after filtering or after preliminary mineralization by boiling with 15 ml of concentrated nitric acid for 30 min.

The results obtained are given in Table 5 show that preliminary mineralization is not necessary. This fact may be attributed to the elements being sorbed from organic as well as inorganic compounds. The similarity of the results obtained for the two sizes of sample proves that the sorption capacity of the amount of resin used (10 g) was sufficient for the purpose. The cadmium content was so low that even after concentration from 2 litres of water its amount was below the limit of determination. The iron and zinc contents were high enough for their determination after 2-fold and 5-fold dilution, respectively, of the final solutions.

REFERENCES

1. G. A. Junk, J. J. Richard, K. D. Greiser, D. Witiak, J. L. Witiak, M. D. Arguello, R. Vick, H. J. Svec, J. S. Fritz and G. V. Calder, *J. Chromatog.*, 1974, **99**, 745.
2. G. A. Junk, C. D. Chriswell, R. C. Chang, L. D. Kissinger, J. J. Richard, J. H. Fritz and H. J. Svec, *Z. Anal. Chem.*, 1976, **282**, 331.
3. J. P. Riley and D. Taylor, *Anal. Chim. Acta*, 1969, **46**, 307.
4. J. Zerbe, *Chem. Anal. Warsaw*, 1979, **24**, 85.
5. A. C. Howard and N. N. Arbab-Zawar, *Talanta*, 1979, **26**, 895.
6. J. L. Lundgren and A. A. Schilt, *Anal. Chem.*, 1977, **49**, 974.
7. T. Braun and M. N. Abbas, *Anal. Chim. Acta*, 1980, **119**, 113.
8. *Idem, ibid.*, 1982, **134**, 321.
9. M. P. Maloney, G. J. Moody and J. D. R. Thomas, *Analyst*, 1980, **105**, 1087.

Talanta, Vol. 32, No. 7, pp. 577–578, 1985
Printed in Great Britain

0039-9140/85 $3.00 + 0.00
Pergamon Press Ltd

MODIFICATION OF A PACKED COLUMN GAS CHROMATOGRAPH/MASS SPECTROMETER

YULIN L. TAN* and JOHN F. QUANCI
Environmental Measurements Laboratory, U.S. Department of Energy, New York, New York 10014, U.S.A.

(*Received* 23 *January* 1985. *Accepted* 28 *January* 1985)

Summary—A packed-column gas-chromatograph/mass-spectrometer (GC/MS), Hewlett-Packard 5982, was modified to accommodate fused silica capillary columns. The original GC/MS interface and chemical-ionization sample-line in the ion-source were changed to allow the end of a fused silica capillary column to enter the ion-chamber directly. For chemical-ionization operation, the reagent gas was brought into the MS through the direct-insertion probe port. The calibration compound was introduced through the electron-impact sample-inlet, which simplified the operation. The modified system yields higher sensitivity and more efficient separation, as well as simpler operation, without sacrificing any original instrument functions.

In the past decade, the demand for more efficient separations of analytical samples has accelerated developments in gas-chromatograph column technology, which has advanced from packed columns, to glass capillary columns, to flexible fused-silica capillary columns,[1,2] yielding higher sensitivity and efficiency.[3] While we have benefited from these advances, we are also faced with the rapid obsolescence of expensive instruments. The Hewlett-Packard 5982 gas-chromatograph/mass-spectrometer (GC/MS), which uses packed columns, is a case in point. We have modified this instrument to accommodate fused-silica capillary columns for trace organic analyses.

EXPERIMENTAL

Capillary column installed through the chemical-ionization sample-inlet

An SGE on-column injector and a fused-silica capillary column (J and W DB-5, 30 m long × 0.25 mm bore, 0.25-μm film) were installed on the gas chromatograph. The carrier gas used was helium, at a flow-rate of 0.6 ml/min.

In the ion-source assembly, the chemical-ionization sample-line was replaced with a stainless-steel guide tube (1.66 mm outside diameter, 0.51 mm bore, 15 cm long). Two stainless-steel sleeves (2.77 mm outside diameter, 1.66 mm bore, 3 mm long) were press-fitted on the two ends of the guide tube. The guide tube was placed in the ion-source assembly in such a way that the two sleeved ends were seated securely in the two chemical-ionization sample-holes, one in the sealing shoe and the other in the ion-chamber assembly. Gentle bends were made as needed so that the guide tube did not come into contact with any part of the source assembly, and the fused-silica capillary column could slide through the tube.

The two transfer lines, together with the jet separator and the two isolation valves between the GC and MS were removed. Instead, a simple stainless-steel tube, 3.18 mm outside diameter, 36 cm long ($\frac{1}{8}$ in. × 14 in.) was used as the support tube for the capillary column. One end of the support tube was reduced to 2.77 mm outer diameter over a length of 1 cm, to produce a shoulder that allowed a snug fit into the chemical-ionization sample-inlet hole on the ion-source flange.

To introduce the fused-silica capillary column into the ion-chamber, the following procedure was used. First, the end of the support tube without the shoulder was inserted into the GC oven. Before the end with the shoulder was fitted into the chemical-ionization sample-inlet hole, the column was slid through the support tube until it emerged from the shouldered end. This end of the column was then guided a distance of 18 cm through the chemical-ionization sample-inlet hole on the flange, through the guide tube in the ion-source and into the ion-chamber. The shoulder of the support tube was then fitted into the chemical-ionization sample-inlet hole on the flange, and the column was securely held in the support tube with a 3.18 mm × 1.59 mm ($\frac{1}{8}$ in. × $\frac{1}{16}$ in.) Swagelok reducing union in the GC oven.

Use of electron-impact sample-inlet for calibration compound

A $\frac{1}{16}$ in. (1.59 mm) outside diameter stainless-steel tube was used to bring the calibration compound into the MS through the electron-impact sample-inlet on the ion-source flange. The end of this sample line was assembled in a similar way to the batch-inlet probe, which introduces the calibration compound perfluorotributylamine (PFTBA). PFTBA was contained in the glass sample-bulb attached to a probe flow-valve. A shut-off valve for the supply of PFTBA was placed between the probe flow-valve and the electron-impact sample-inlet.

Chemical-ionization operation

Operation of the MS in the chemical-ionization mode for analysis of capillary GC effluents does not usually use reagent gas as the carrier gas. Hence the direct-insertion probe (DIP) port was used to provide the reagent gas.

The reagent-gas cylinder was connected to the GC carrier-gas inlet. After passing through one of the flow-rate controllers, the gas flowed through a $\frac{1}{16}$ in. (1.59 mm) stainless-steel tube connected to a $\frac{1}{4}$-in. (6.35 mm) stainless-steel tube which formed the insertion portion of the batch-inlet probe. The reagent gas was introduced into the MS by inserting the probe into the DIP port. A 5×10^{-4} mmHg ion-source manifold pressure was maintained by means of the flow-rate controller.

RESULTS AND DISCUSSION

The separation efficiency of the modified system is much higher than that of the original packed-column

*Author for correspondence.

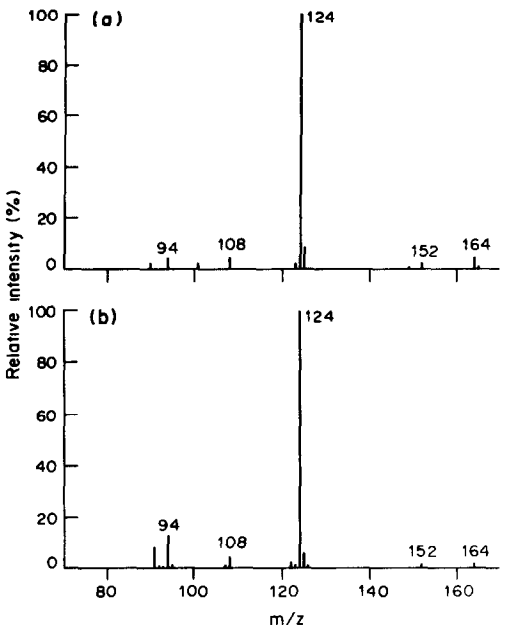

Fig. 1. Chemical-ionization mass spectra of nitrobenzene, with methane as reagent gas: (a) from modified capillary GC/MS; (b) from original packed-column GC/MS.

GC/MS. For example, for a GC run with the oven temperature starting at 60° and programmed to rise at 32°/min for the first 2.5 min, then at 4°/min to 280°, the total ion chromatogram shows complete separations for the isomeric pairs of phenanthrene/anthracene and benzo(*e*)pyrene/benzo(*a*)pyrene. At the same time, the sensitivity is also enhanced by an order of magnitude.

The constant flow of helium into the MS raises the ion-source manifold pressure to 6×10^{-6} mmHg, but does not have any adverse effect on the MS performance.

Introducing the calibration compound through the electron-impact sample-inlet simplifies calibration procedures. Once the probe flow-valve is adjusted to give a PFTBA pressure of $1\text{–}2 \times 10^{-6}$ mmHg, PFTBA can be injected into the MS by simply opening the shut-off valve. Therefore, the frequent insertion of the batch-inlet probe through the DIP port is avoided. Such insertions tend to degrade the vacuum and wear out the Teflon seals and *O*-rings in the DIP port. This arrangement is applicable to any other pure volatile-liquid samples.

The chemical-ionization mode for capillary GC effluents was operated by introducing reagent gas through the DIP port. The GC flow-rate controller successfully regulated the reagent-gas intake, giving rise to an ion-source manifold pressure in the mid-range of 10^{-4} mmHg. Similar chemical-ionization spectra for nitrobenzene were obtained from the present modified GC/MS and the original packed-column GC/MS,[4] as shown in Fig. 1. There is no degradation of spectral quality.

The modified Hewlett-Packard 5982 GC/MS is being used for complex trace organic pollutant analysis, which requires higher sensitivity and separation efficiency than those available with the original system.

REFERENCES

1. L. S. Ettre, *Open Tubular Columns in Gas Chromatography*, Plenum Press, New York, 1965.
2. W. G. Jennings, *Comparison of Fused Silica and Other Glass Columns in Gas Chromatography*, Hüthig, 1981.
3. M. Novotny, *Anal. Chem.*, 1978, **50**, 16A.
4. Y. L. Tan, *J. Chromatog.*, 1977, **140**, 41.

Talanta, Vol. 32, No. 7, pp. 579–580, 1985
Printed in Great Britain.

0039-9140/85 $3.00 + 0.00

EXTRACTION OF CHLORINATED HYDROCARBONS FROM FISH WITH SULPHURIC ACID

VITTORIO CONTARDI, BIANCA COSMA, GILDA ZANICCHI and VINCENZO MINGANTI
Istituto di Chimica Generale dell'Universita'/Gruppo Ricerca Oceanologica Genova (G.R.O.G.), viale Benedetto XV, 3, 16132 Genova, Italy

(*Received* 25 *October* 1983. *Revised* 20 *December* 1984. *Accepted* 17 *January* 1985)

Summary—A method is described for extraction of chlorinated hydrocarbons (DDTs and PCBs) from fish samples with sulphuric acid of various concentrations. The results are better than those obtained by an official method using Soxhlet extraction with n-hexane, especially with 9.5–13*M* sulphuric acid. The relative standard deviation is about 12% for analysis of portions of a homogenized single sample taken from the dorsal flesh of the same fish. Drawbacks and advantages in comparison with other methods are discussed.

The basic principles and practices of pesticide residue analysis have been summarized by various authors.[1–4] The analytical procedure consists of (1) extraction, (2) extract clean-up, (3) separation of the components, (4) identification and measurement. The first and third steps are the most critical, exhibiting higher uncertainty and inaccuracy in interlaboratory comparisons.

Components that have very similar gas chromatographic retention times are generally separated by column chromatography. We have already studied the effect of pore size (4, 6 and 10 nm) on the behaviour of silica gel in such separations, and have obtained very good separations and recoveries for fortified biological samples.[5]

For the initial extraction, organic solvents of various polarities can be used, either hot or cold. Stanley and Le Favoure[6] used a glacial acetic acid/perchloric acid mixture at temperatures above 90°, and back-extracted the chlorinated hydrocarbons with two portions of n-hexane. Smodlaka *et al.*[7] compared that method with Jensen's,[8] which extracts chlorinated hydrocarbons from macerated and homogenized samples with cold n-hexane, and found the results obtained from the two methods were comparable.

Norheim and Øckland[9] have described a rapid extraction method for some persistent chlorinated hydrocarbons (such as hexachlorobenzene and octachlorostyrene) in cod samples obtained from the Norwegian area. The samples (about 0.3% fat content) were treated with 95–97% sulphuric acid at 60° for 4 hr and, after cooling, extracted with heptane. The authors claim to have obtained very good recoveries for each component. The reproducibility was 5.5% for hexachlorobenzene and 9.5% for octachlorostyrene.

Veierov and Aharonson[10] have described a rapid procedure for extraction of various organochlorine pesticides in milk, utilizing sulphuric acid to precipitate the lipids. The organochlorine pesticides were subsequently extracted with petroleum ether. The method was applicable at the 5–10 μg/kg residue level and the recoveries were comparable with those obtained by widely used procedures such as the one by De Faubert Maunder *et al.*[11]

Because of the good results obtained with concentrated sulphuric acid and the simplicity of both the procedures described above, we thought it worth evaluating the behaviour of this acid at various concentrations and temperatures.

EXPERIMENTAL

Apparatus

Gas chromatographic analysis was performed with a Varian 2440 Aerograph Gas Chromatograph equipped with a tritium electron-capture detector and two glass columns, one containing 3% OV-101 on Chromosorb W-HP (80–100 mesh), and the other 5% QF-1 on the same support. Both columns were 1.8 m in length and 3 mm in internal diameter.

Glass 250-ml Erlenmeyer flasks were used for sample digestion and 250-ml glass separatory funnels with PTFE (polytetrafluoroethylene) stopcocks for extractions. The chromatographic columns were made of glass, 10 mm bore, 300 mm long, and fitted with coarse fritted discs and PTFE stopcocks at the bottom. The columns for clean-up had an internal diameter of 8 mm and length 150 mm.

Reagents

Sulphuric acid, anhydrous sodium sulphate, Florisil (60–100 mesh, ASTM), and Kieselgel 40 (70–100 mesh, ASTM), were all obtained from Merck. The n-hexane, benzene and diethyl ether (also from Merck) were distilled, and checked by gas chromatography. Analytical grade materials were used when ever possible.

The chlorinated hydrocarbons for standard solutions were *p,p'*-DDT, *p,p'*-DDD and *p,p'*-DDE (all from Riedel-de Haen, and > 99% pure). The polychlorinated biphenyls (PCBs) were Fenclor 54 (similar to Aroclor 1254) (containing 52–54% chlorine) and Fenclor 64 (similar to Aroclor 1260) (containing 61% chlorine) (both from Caffaro, Milan, Italy).

Procedure

Various samples from bonito caught in the Ligurian Sea were subjected to analytical investigation. They were taken from the dorsal muscle of the same fish, homogenized and freeze-dried (3% maximum water content, found by drying at 105°).

Chlorinated hydrocarbons were extracted by digesting 3 g (dry weight) of sample in an Erlenmeyer flask with 60 ml of sulphuric acid of 6, 8, 9.5, 11 or 13*M* concentration for

Table 1. Recovery of DDTs and PCBs (*ng/g*, dry weight) from bonito fish samples (mean and range of three results)

Chlorinated hydrocarbons	Soxhlet extraction with hot n-hexane	Cold extraction, [sulphuric acid]				
		6*M*	8*M*	9.5*M*	11*M*	13*M*
p,p'-DDT	38 ± 4	14 ± 8	30 ± 15	52 ± 9	91 ± 11	75 ± 7
p,p'-DDD	41 ± 6	19 ± 10	31 ± 12	55 ± 9	119 ± 14	86 ± 7
p,p'-DDE	63 ± 5	20 ± 8	49 ± 8	89 ± 14	130 ± 10	115 ± 9
PCBs	1410 ± 71	330 ± 97	870 ± 212	1551 ± 250	2430 ± 190	2086 ± 170

12 hr, and then equilibrating with three 30-ml portions of n-hexane in a 250-ml separatory funnel. The combined n-hexane fractions were evaporated to 3 ml, and cleaned-up and dehydrated on a glass microcolumn packed with 3 g of Florisil (activated by heating for 8 hr at 140°), topped with a 20-mm bed of anhydrous sodium sulphate. Chlorinated hydrocarbons were then eluted with 40 ml of 15% v/v solution of diethyl ether in n-hexane. The eluate was evaporated to 3 ml and chromatographed on a column of Kieselgel 40 (about 7 g dry weight, activated by heating for 12 hr at 200° and deactivated with 1.5% of water 5).

Identification and measurement were done by gas chromatography with columns packed with liquid phases of different polarity, such as OV-101 (methylsilicone) and QF-1 (fluorosilicone). The carrier-gas was high-purity research grade nitrogen further purified by magnesium perchlorate and molecular-sieve filters, and used at a flow-rate of 60 ml/min. The reference standards were n-hexane solutions of the determinants at the following concentrations: *p,p'*-DDT 0.4 ng/μl; *p,p'*-DDD 0.2 ng/μl; *p,p'*-DDE 0.1 ng/μl; a mixture of Fenclor 54 and Fenclor 64, each 1.0 ng/μl. The PBC mixture reproduced satisfactorily enough the gas chromatographic pattern obtained from fish sample extracts.

The purity of the reagents was checked and their contribution to the gas chromatographic peaks of the DDTs and PCBs was found to be insignificant.

RESULTS AND DISCUSSION

Table 1 compares the recoveries obtained by the sulphuric acid method with those obtained by the n-hexane Soxhlet extraction technique, which is one of the official methods of the FDA[1] and one of the most frequently employed for pesticide-residue analysis of marine organisms.

The recoveries, both for DDTs and PCBs, are strongly influenced by the sulphuric acid concentration. The best results are obtained with $\geqslant 9.5M$ acid. The low recoveries obtained with more dilute acid are probably due to incomplete digestion of the sample within the fixed time limit (12 hr).

The fat content can also influence the efficiency of the method. The extractable organic material of the fish samples used in this work was 8.2% (dry weight basis). No experiments were done on samples with higher fat contents, but the samples used have a notably higher fat content than the average for fish. The samples used by Norheim and Økland[9] contained only about 0.3% fat.

The influence of temperature on the extraction is shown in Fig. 1. With 11*M* sulphuric acid the best recoveries are obtained at room temperature (~20°).

It should be noted that when DDTs and PCBs were added as spikes to biological materials, both methods gave similar recoveries of the added material (92–98% by the hexane method, 89–100% by the 11*M* sulphuric acid method).

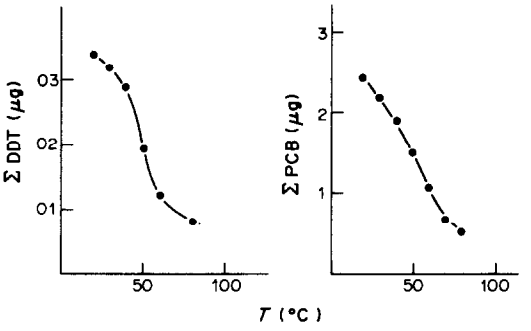

Fig. 1. PCBs and DDTs (μg/g dry weight) extracted from bonito fish with 11*M* sulphuric acid at various temperatures. temperatures.

Acknowledgements—The authors thank Professor R. Ferro, Director of the General Chemistry Institute, University of Genoa, and Professor C. Carpanelli of the Organic Chemistry Institute, University of Genoa, for useful suggestions during this work and Mr. P. Germano for his assistance in the chromatographic analysis. This work was supported by the Italian Consiglio Nazionale delle Ricerche (C.N.R.) under the Programme of Researches on Oceanography and Marine Shelves.

REFERENCES

1. F. D. A., *Pesticide Analytical Manual*, Vol. 1, Section 21114 a-19. U.S. Department of Health, Education and Welfare, Food and Drug Administration, Washington, D.C. 20201, 1971.
2. H. P. Burchfield, D. E. Johnson and E. E. Storrs, *Guide to the Analysis of Pesticide Residues*, Vols. 1 and 2, U.S. Department of Health, Education and Welfare, Office of Pesticides, Washington DC 20201, 1965.
3. O. Hutzinger, S. Safe and V. Zitko, *The Chemistry of PCBs*, p. 197. C.R.C. Press, Cleveland, Ohio, 1974.
4. L. W. Oller and M. F. Cranmer, *J. Chromatog. Sci.*, 1975, **13**, 269.
5. V. Contardi, R. Capelli, G. Zanicchi and M. Drago, *Analyst*, 1983, **108**, 510.
6. R. L. Stanley and H. T. Le Favoure, *J. Assoc. Off. Anal. Chem.*, 1965, **48**, 666.
7. N. Smodlaka, M. Devescovi and I. Ivancic, *Ves Journées Etud. Pollutions*, p. 43, C.I.E.S.M. Cagliari, 1980.
8. S. Jensen, *Manual of Methods in Aquatic Environment Research*, p. 77. *FAO Fisheries Tech. Paper*, 1975, No. 137.
9. G. Norheim and E. M. Økland, Analyst, 1980, **105**, 990.
10. D. Veierov and N. Aharonson, *J. Assoc. Off. Anal. Chem.*, 1980, **63**, 532.
11. M. J. De Faubert Maunder, H. Egan, E. W. Godly, E. W. Hammond, J. Roburn and J. Thomson, *Analyst*, 1964, **89**, 168.

Talanta, Vol. 32, No. 7, pp. 581–582, 1985
Printed in Great Britain.

0039-9140/85 $3.00 + 0.00

ANALYTICAL DATA

PHOSPHORUS-31 NUCLEAR MAGNETIC RESONANCE CHEMICAL SHIFTS OF PHOSPHORIC ACID DERIVATIVES

Zs. WITTMANN
Hungarian Oil and Gas Research Institute, H-8200 Veszprém, József Attila utca 34, Hungary

Zs. KOVÁCS
Research Institute for Heavy Chemical Industries, H-8200 Veszprém, Wartha Vince utca 1, Hungary

(*Received* 19 *July* 1984. *Revised* 5 *December* 1984. *Accepted* 25 *January* 1985)

Summary—^{31}P nuclear magnetic resonance chemical shifts of alkyl and alkylaryl phosphates, condensed phosphates, phosphoric acids and their salts, are reported. These are listed by classes of compounds so that relationships between chemical shifts and the substituent groups on phosphorus atoms can be recognized. These relationships are useful for qualitative identification of the specific compounds listed and of related compounds by extrapolation.

Correlation of the structure of the hydrocarbon moiety and the sulphur:oxygen atomic ratio of different alkyl or alkylaryl phosphates, condensed phosphates and phosphoric acids, with their chemical shifts in the ^{31}P NMR spectrum, have been investigated on the basis of literature data and measurements in our laboratories.

EXPERIMENTAL

The ^{31}P NMR spectra were obtained on a Varian CFT-20 high-resolution spectrometer. Chemical shifts are reported in parts per million (ppm) of the applied field, with 85% orthophosphoric acid as reference standard (zero shift). Upfield shifts are denoted by a plus sign, downfield shifts by a minus sign. Chemical shifts from the literature are given in the same way.

RESULTS AND DISCUSSION

The chemical shift depends most strongly on the nature of the atoms directly bonded to the phosphorus atom and on the type of bond involved.

The basic principle used to divide phosphoric acids and condensed phosphates into classes on the basis of their ^{31}P NMR chemical shifts[1–4] is the rule given by Stothers and Robinson.[5] The magnitudes of the chemical shifts change in the order $(RO)_2P(O)O^- < (RO)_2P(O)S^- < (RO)_2P(S)O^- < (RO)_2P(S)S^-$ and are similar for compounds containing the same groups. The chemical shifts of investigated compounds can be assigned according to this rule.

For a given member of the above-mentioned series the chemical shifts of salts of univalent cations are independent of the kind of cation, and those of salts of bivalent cations may also be independent of the kind of cation. The ^{31}P NMR chemical shifts of $>P(O)SM$ and $>P(S)OM$ isomers (M = univalent or bivalent cations) are equal, although in some cases only the $>P(O)SM$ form may exist. The latter statement seems to be in agreement with Kabachnic *et al.*[6,7] who reported that the tautomeric equilibrium in salts is shifted towards the $>P(O)SM$ isomer.

There is a difference of 10–15 ppm between the chemical shifts of the salts of univalent and bivalent cations, the chemical shifts of the bivalent cation salts being further downfield.

It is clear that changes in the environment of the second phosphorus nucleus in the condensed phosphates have a relatively small effect on the resonance of the phosphorus nucleus being considered. A condensed phosphate can be considered as a molecule consisting of two acids with a common sulphur or oxygen atom. The chemical shift (or shifts in the case of an asymmetric molecule) can be predicted from their structures.

On the basis of the Stothers and Robinson rule, the chemical shifts of the phosphates[1,2,4] can also be written in the order $(RO)_2P(O)OR < (RO)_2P(O)SR < (RO)_2P(S)OR < (RO)_2P(S)SR$. The chemical shifts of the other "mixed" compounds can be fitted to this rule as follows: $(RO)_2P(O)OR < (RO)_2P(O)SR < (RS)_2P(O)OR \lesssim (RS)_2P(O)SR \lesssim (RO)_2P(S)OR < (RO)_2P(S)SR \sim (RS)_2P(S)RS$.

Substitution at some distance from the phosphorus atom has a relatively small effect. The effect on the ^{31}P NMR chemical shifts when the alkyl groups are changed is small except when R = methyl (chemical shift downfield from the average chemical shift for the compounds with different hydrocarbon moieties, for a given member of the Stothers–Robinson series). In the case of an aryl group the chemical shifts of the different compounds generally change upfield from

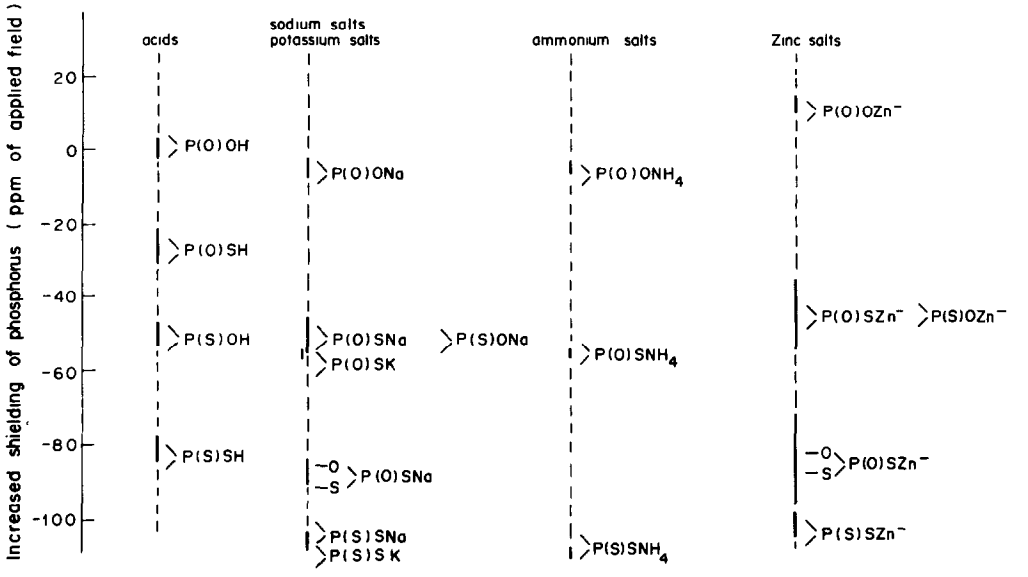

Fig. 1. ^{31}P NMR chemical shifts of phosphoric acids and their salts.

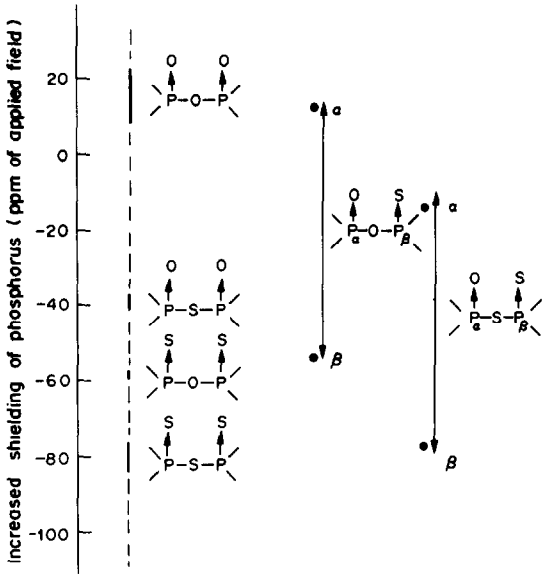

Fig. 2. ^{31}P NMR chemical shifts of condensed phosphates.

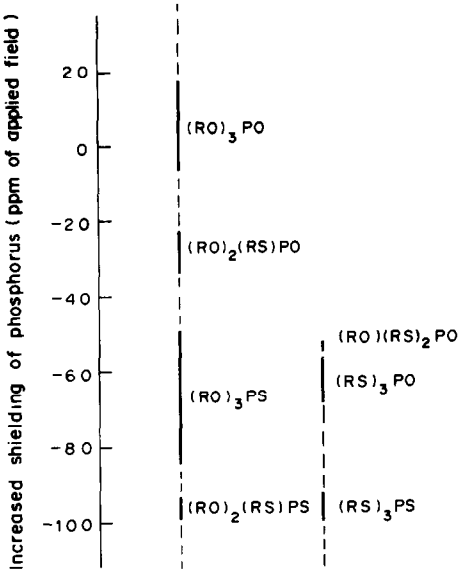

Fig. 3. ^{31}P NMR chemical shifts of phosphates.

the average value for similar compounds containing alkyl groups.

In Figs. 1–3 the ^{31}P NMR chemical shifts of the different phosphoric acids, condensed phosphates and phosphates are represented, independently of the hydrocarbon moiety, in a very simple way. These figures are useful for qualitative identification of these specific classes of compounds.

REFERENCES

1. V. Mark, C. H. Dungan, M. M. Crutchfield and J. R. Van Wazer, *Topics in Phosphorus Chemistry*, Vol. 5. ^{31}P *Nuclear Magnetic Resonance*. M. Grayson and E. I. Griffith (eds.), Interscience, London, 1967.
2. E. F. Mooney, *Annual Reports on NMR Spectroscopy*, Vol. 5B, Academic Press, London, 1973.
3. Zs. Wittmann and E. Pudmer, *ASLE Trans.*, in the press.
4. Zs. Wittmann, Z. Décsy and E. Pudmer, *Talanta*, 1985, **32**, 86.
5. J. B. Stothers and J. R. Robinson, *Can. J. Chem.*, 1964, **42**, 967.
6. M. J. Kabachnik and T. A. Mastryukova, *Zh. Obshch. Khim.*, 1955, **25**, 1924.
7. M. J. Kabachnik, T. A. Mastryukova and N. P. Radionova, E. M. Popov, *ibid.*, 1956, **26**, 120.

Talanta, Vol. 32, No. 8A, pp. 583–599, 1985
Printed in Great Britain

0039-9140/85 $3.00 + 0.00
Pergamon Press Ltd

BACKPLANE BUS STRUCTURES AND SYSTEMS

V. KARANASSIOS and G. HORLICK
Department of Chemistry, University of Alberta, Edmonton, Alberta, Canada

(*Received* 27 *August* 1984. *Revised* 15 *February* 1985. *Accepted* 1 *March* 1985)

Summary—A general survey is given of developments in the design of personal computers and implementation of their use in laboratory instrumentation and data handling *etc.* An extensive guide to commercial sources of hardware and software is given.

The advent of large-scale integration (LSI) devices, very large-scale integration (VLSI) devices, and the microprocessor in particular, has had a tremendous impact on the nature of scientific and electronic instrumentation that is just beginning to be felt. Microprocessors are replacing small- and medium-scale integration designs in the way that integrated circuits replaced discrete transistors more than a decade ago, and microcomputers have given instrumentation systems impressive intelligence capabilities quite inexpensively.

Most laboratory projects involving microcomputers, however, usually underestimate the computing power required, more from failure to realize the increased computing demand as a project develops than from a poor estimate of the computer's capabilities. Expandability is an important factor in the integration of a microcomputer system into the laboratory environment.

Most laboratory microcomputer systems are 8-bit designs, and because of limitations in speed, arithmetic and addressing power, often cannot accommodate the increasing needs that arise in development of applications. No matter how good today's 8-bit or 16-bit CPUs are, users are demanding more processing power, more powerful input/output (I/O) structure, a wealth of special function integrated circuits and megaword addressing capability.

The major obstacle to successful laboratory automation is frequently non-availability of interfaces between the computer and the experiment, or the inherent inability of a particular computer system to accommodate specific needs. Traditionally, computers were built with little or no regard for an intended application. The new generation of scientific instruments demands an "open-ended" computer architecture that can be tailored to fit specific needs. Modern laboratory applications require easily expandable computer systems with advanced data gathering and processing capabilities which provide both information management and information processing features. Bus-based systems are capable of satisfying these new demands.

BUS-BASED SYSTEMS

A bus can be defined as a set of conductors with a common function, providing communication between elements of a computer system (as shown in Fig. 1) and can be labelled according to its function, *e.g.*, as a data, address, or control bus. It can also be defined as an electrical connection between two or more digital system elements (Fig. 2).

The data bus transmits binary data between memory or I/O devices and the CPU, and is bidirectional. The address bus specifies the source or the destination of data and is unidirectional. The control bus synchronizes peripheral devices with the CPU and is bidirectional. (For more information and a glossary references 1 and 2 should be consulted.)

Buses can also be classified according to the hierarchical levels they occupy within the system.[3] At the lowest level is the component bus, which connects various integrated circuits (as in Fig. 1), and may be thought of as confined to a single printed-circuit board.

At the next level, the bus connects various modules (as in Fig. 2). The modules are usually printed-circuit boards that directly plug into the bus (as shown in Fig. 3). Physically, the bus is a baseboard (or "backplane") with connectors and a card-cage or motherboard carrying the slots for the modules to be plugged in. Table 1 lists selected mechanical and electrical specifications for selected bus structures. Modules are usually classified according to function, *e.g.*, memory, CPU, I/O or special function. A CPU board, for example, may contain a CPU, support logic (such as clock and/or transceivers), some local ROM, RAM and the appropriate bus interface. Such modules can be used to construct a modular bus-based computer system.

The backplane usually contains no active components. It merely provides the physical link between modules. Modules can be combined to meet the requirements of a specific application, giving a computer system that can be tailored to the user's needs. Motherboards containing active components such as CPU, memory and I/O, supervised by a single oper-

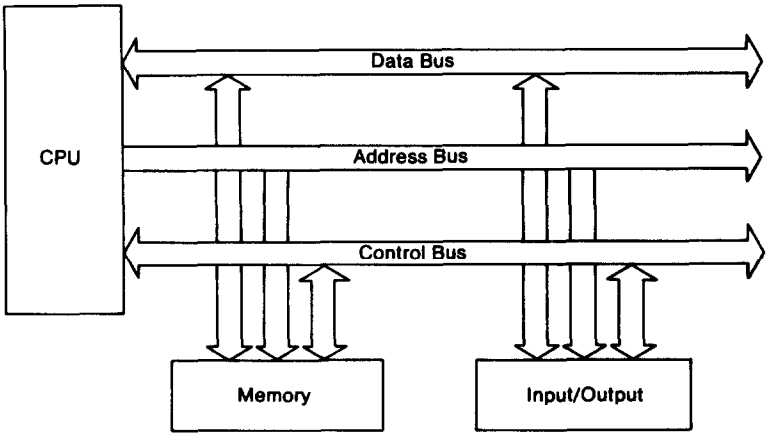

Fig. 1. Block diagram of a typical microcomputer system.

ating system, are often called "smart backplanes" and are used in microcomputer systems such as the Apple II and IBM PC. Smart backplanes are discussed in more detail elsewhere.[4,5]

At a higher level yet, system buses connect "racks" of computer systems together, and serial interface buses are usually used to link networks of computer systems. Further, parallel interface buses, such as the IEEE-488 GPIB (General Purpose Interface Bus), provide a communications path between instruments or peripheral units and a computer system. Buses can also be distinguished as local or global (Fig. 4).

Although all computer systems involve a bus structure at some level, the term "bus-based system" is usually applied to systems designed around backplanes.

Some of the most sophisticated desk-top computers are now designed to be so generally applicable that paradoxically they are unable to handle specific laboratory tasks. Furthermore, the general design[6] on which instruments are currently based must frequently include the microcomputer as a component in order to be successful.

For such a general plan to be effective, a microcomputer with different architectural features may have to be designed every time a unique application arises. Although for most laboratory applications the design of such a microcomputer system from discrete

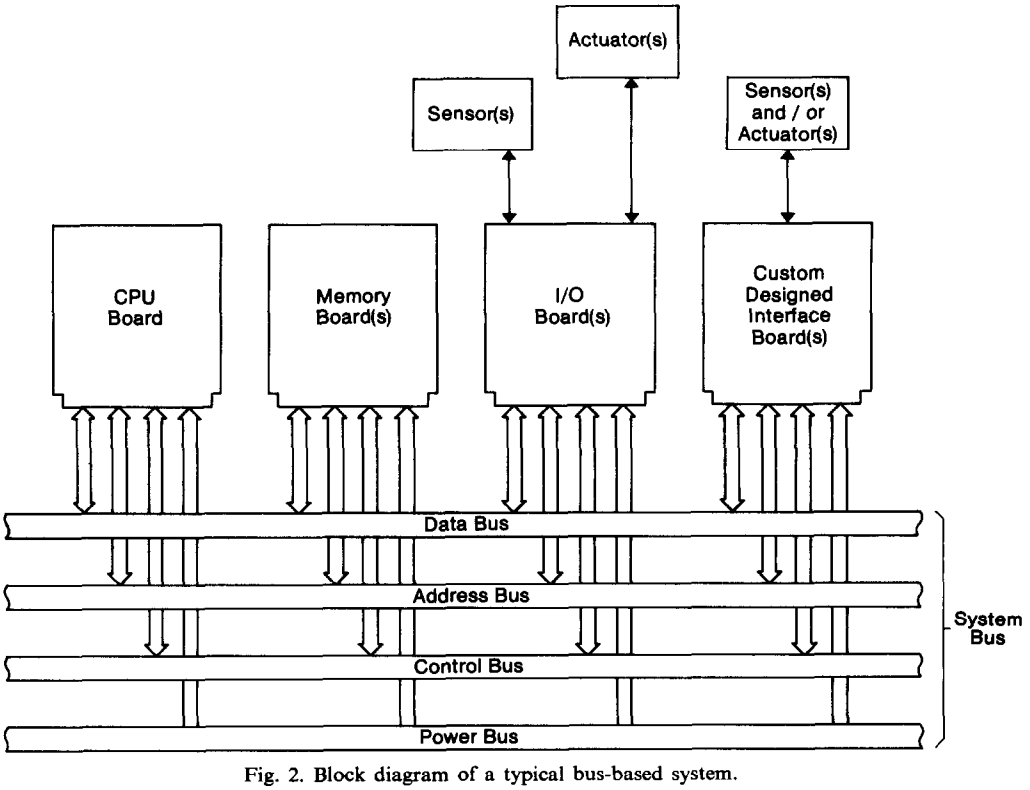

Fig. 2. Block diagram of a typical bus-based system.

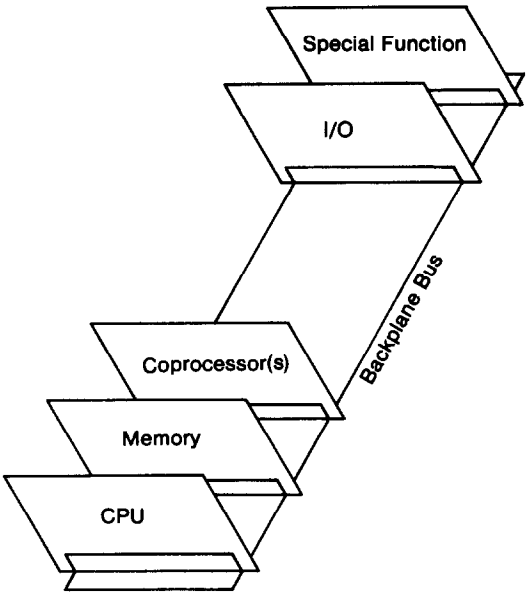

Fig. 3. Typical backplane bus.

components is prohibitive in terms of cost, time, and expertise, it can easily be realized as a bus-based system using commercially available modules. Such modules can be treated as single-function or multi-function components and selected in the same way as integrated circuits.

Advantages of modular bus-based systems

The major advantage is the modularity itself, since the modules can easily be interchanged (or replaced when they malfunction) or new ones added as required. In modular systems both hardware and software can be optimized for a specific task, and usually become less complicated.

Consider a system that controls several experimental parameters. If needs change, additional parameters can be controlled by simply adding more I/O boards. If one processor is not sufficient, more processors or intelligent I/O boards can be added to optimize response time. The modular design allows ready reorganization or expansion of a microcomputer system, making it more flexible and versatile. Such a system can be wheeled around the laboratory to provide intelligence and computing power whenever and wherever needed.[7]

As technology advances, more powerful ICs become available, for example, the new signal-processing ICs, arithmetic processors, high performance 16- and 32-bit CPUs and high-density memory chips. Each new crop of ICs usually creates new opportunities for design of higher performance systems. Ironically, these opportunities can lead to a system's obsolescence, often well before the end of its economic life. A modular system not only minimizes

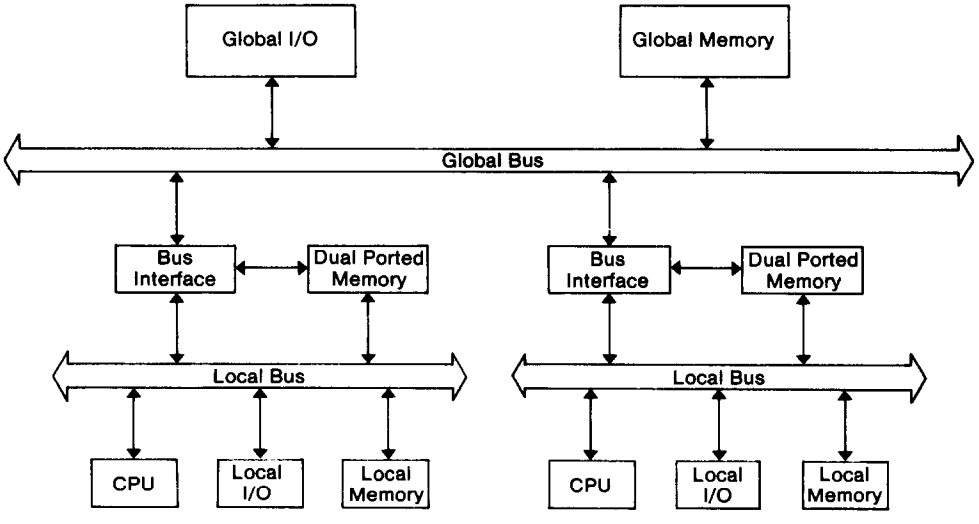

Fig. 4. Block diagram of a typical tightly coupled multiple processor system.

development cost, but also allows expansion with minimal disruption.

Invariably, some portion of a non-modular system eventually presents a bottleneck that forces replacement of the entire system. With modular designs, this portion of the system can be easily modified or upgraded (so the system can grow as technology progresses) and its lifespan is extended.

In many applications, the CPU limits the performance of a system. Bus-based systems can be designed to use several processors, making more computing power available at lower cost.

A good example of an analytical instrument with a high degree of modularity is Microsensor Technology's micromonitor,[8] a portable gas-analyser no bigger than a portable oscilloscope. It can carry up to five gas-chromatography modules, plugged into its backplane. Each module consists of a complete gas chromatograph, including valves, a capillary column and a thermal conductivity detector, integrated into a single 3-in. silicon wafer.[9] A library of such modules can be built, which can be combined to provide for analysis of various mixtures of gases. The instrument also gives direct concentration read-out.

Disadvantages

Assembling a system from off-the-shelf modules is a simple task requiring little or no experience in computer technology. A set of well-written manuals, although not common in the computer industry, is usually sufficient. However, writing software for such a system is not a casual undertaking, especially if the system supports several processors. To make software development easier, a bus that supports a well-known operating system is highly recommended.

The complexity of systems rises almost exponentially from the simple bus-based systems to more sophisticated backplanes, and so does the complexity of custom-designed interfaces.

Ideally, the design of a bus-based system should allow a free choice of technology, processors, and equipment-manufacturers. With the proliferation of vendors, compatibility between boards and buses becomes a major consideration.

Compatibility

As laboratory applications become more sophisticated, users have to buy components from more than one source and a possible mismatch of various boards and systems becomes a serious problem.

One solution is to use "standard" interfaces, which have specifications set out either by an authoritative standards-making organization (such as the IEEE microcomputer standards committee, ISO, EIA, CCIT or ANSI) or a manufacturer who imposes a *de facto* standard on the market, as is the case with the DEC's Q-bus. Interfaces are then designed according to such standards.

An obvious advantage of a single set of standards is that without it there is no assurance that two boards designed for the same backplane, but by two different manufacturers, will work together. It should be emphasized that several of the backplane bus standards appearing in Table 1 are still only proposals (hence the designation "P" in their title) and as such are subject to change.[10] It is the mechanical and electrical characteristics of backplane buses that are standardized. Several of the specifications appear in Table 1 and are discussed in detail below.

BACKPLANE BUS CHARACTERISTICS

Mechanical specifications

These refer to factors such as board size and connector type. Pin-type connectors are believed to be more reliable than edge-type connectors, especially in high-vibration environments.

Board size, often called form factor, is an important consideration in determining the capabilities and functions of a system. Small boards carry only a few functions per board, so board area and power are not wasted on unused functions. Consequently small boards are cheaper but give lower performance, and more are required for a complete system. The small size also means that usually no auxiliary functions are carried, so more traffic is carried on the backplane bus, resulting in lower system throughput. Boards designed with the newer, higher density ICs should give increased throughput, however.

Examples of buses supporting small boards are the STD and similar buses such as the RM-65. Because communication is simple with these buses, specialized interfaces can be built relatively easily.

For high-performance systems, buses supporting medium size or large boards must be used, such as the Multibus or VME-bus and VERSAbus. These larger boards carry more functions and also high-speed local buses, providing high throughput and performance, but there may be difficulty in finding boards providing only the functions required for a particular application, so they may not be cost-effective.

Because of the complexity of high-performance systems, interfaces are difficult to design. This problem can be alleviated by selecting boards that provide breadboarding area for the user, or are compatible with more than one bus, such as the Multibus and the IEEE-488 GPIB bus, in which case interfaces are built externally to the board and communications with the bus-based system are established through the GPIB bus. The latter approach, however, has limited applicability to sophisticated designs or high-performance systems.

Backplanes carrying small boards are well suited for simple data-acquisition and control applications, for portable instrumentation, and are in accord with the current trend towards miniaturization in analytical chemistry. Backplanes supporting medium to large boards are recommended for high-performance

Table 1. Selected backplane bus structures

Bus	STD	S-100	Multibus	VERSAbus	VMEbus	Futurebus
Controlling body	IEEE P961	IEEE 696	IEEE 796	IEEE P970	P1014	IEEE P896
Bus type	synchronous[a] non-multiplexed	asynchronous non-multiplexed	asynchronous non-multiplexed	asynchronous non-multiplexed	asynchronous non-multiplexed	asynchronous multiplexed
Address bus width (*bits*)	16	16/24[g]	24	16/24/32	16/24/32	16/24/32
Data bus width (*bits*)	8[b]	8/16	8/16	8/16/32	8/16/32	8/16/32
Max signal line length (*in.*)	c	25	15	18	19	NA
Popular processors supported	8080, 8085, 8088 6800, 6809 6502, 6512 Z80, NCS800 8088	8080, 8085, 8086 80186, 80286, 6800 6809, 68000, Z80[h] Z8000, NS16032	8080, 8085, 8086 8088, 80186, 80286 6800, 6802, 6808 68000, Z80, Z80000 NS16032	68000	68000, 8086 80186 NS16032	NA
Loads supported	d	22	16	15	20	32
Max multiple bus masters	NS	16	16	NS	NS	32
Bus arbitration	serial[e]	parallel	serial or parallel	parallel with daisy-chain	serial or parallel with daisy-chain	distributed
Interrupt levels	2	10	8	7	7	None
VLSI support	NA[f]	NA	Yes	Yes	Yes	NA
Power supply	± 5, ± 12	8, ± 16[i]	± 5, ± 12[j]	5, ± 12	5, ± 12	5[k]
Card dimensions (*in.*)	4.5×6.5	5.1×10	6.75×12	9.24×14.5	6.3×9.2	NA
Connector size	56	100	80/60	140/120	96/96	96
Connector type	Edge	Edge	Edge	Edge	DIN	DIN

[a]Can be configured to operate either in synchronous or asynchronous mode. Synchronous operation is the most common.
[b]A 16-bit bus version with 16-Mbyte addressing capability is under way.
[c]Confined within the backplane.
[d]Depends on the number of slots available on the backplane.
[e]Parallel bus arbitration requires extra lines for implementation.
[f]Owing to the simplicity of the bus, no VLSI support is needed.
[g]Standard/expanded.
[h]Several dual-CPU boards are also available.
[i]Voltage regulators are needed on each board.
[j]Has provisions for ± 15 V power supply.
[k]Other voltages can be either derived on board or provided through non-standard connectors.
NS: Not specified: NA: Not available.

systems and are best suited for applications demanding a multiple processor system.

Electrical specifications

These can be conveniently divided into power supply requirements and type of information exchange. The first is a major factor in the cost of a bus-based system, but does not affect the performance, and will not be discussed. The way information is exchanged between the various modules of a bus-based system is the important factor in the performance and complexity of the system.

Bus type (timing). The bus timing characteristics determine a system's throughput and complexity, and can be synchronous or asynchronous.

For synchronous operation, all processors and peripheral devices must be operated by the same clock. Synchronous operation provides high data-transfer rates because signals such as "bus request", "bus request acknowledge", and "bus grant" are not required. System throughput, however, is determined by the speed of the slowest module on the bus. Synchronous operation at bus level can impose limitations on the flexibility and expandability of the system by confining users to employing a specific family of CPUs and peripherals, but its simplicity makes software development easier.

A backplane bus operating asynchronously is more flexible and can easily adapt to the speed of different modules, although much tighter bus control is required for the successful operation of asynchronously operating modules within the system. There is usually advanced handshaking between several bus control signals. Such signals usually provide functions that could conceptually be termed "bus request", "bus request acknowledge" and "bus grant". Because of the handshake involved, asychronous systems can be slower than their synchronous counterparts. Also, asynchronous buses can "hang" if there is no response to a request. Consider, for example, an attempt to access a non-existent memory location or memory-mapped I/O device; the bus will hang for a short period of time, after which the bus and a "bus error" signal will be activated. Synchronous buses do not hang, but there is no indication that an error has occurred; this can be avoided by adding more software, but this imposes more load on the system.

Address-bus width. Memory requirements increase more rapidly than any other hardware requirement. Computer systems demand wide memory resources to accommodate large application programs and more sophisticated operating systems. Consider, for example, UNIX or the >2-Mbyte operating system for Apple Lisa. Manufacturers have been unable to integrate sophisticated operating systems on 8-bit microcomputers because of the limited addressing capability of such systems. Because the memory–processor bottleneck is becoming increasingly important, a backplane that supports a wide address bus is recommended, even if only a small portion of the bus may be utilized initially.

Data-bus width. Data-bus width is probably the most important single factor where system throughput is concerned. A 16-bit data-bus width can be considered the minimum for high-performance systems. For lower-performance systems, backplanes providing 8-bit data-bus widths can be used to support 16-bit CPUs. This can be achieved by utilizing two data transfers per 16-bit word. System throughput, however, is reduced and programming becomes more complicated and inefficient. Because of their inherent limitations, 8-bit buses are selected only for their simplicity, ease of interfacing and programming of low-level data-acquisition and control applications.

Bandwidth. Bandwidth can be defined as the maximum data-transfer rate of a bus or communications link. It is an important figure of merit, especially when system throughput is the prime consideration. With the possible exception of the STD-bus, maximum clock rate depends on memory-access time. For applications requiring fast response, a high-speed CPU supported by memory chips with short access time is recommended.

Number of loads supported. This determines the maximum number of boards that can be plugged in on a particular backplane. The backplanes listed in Table 1 are not likely to present any limitations, even for the most sophisticated applications. For applications demanding a larger number of boards than the backplane can support, a backplane that provides a bus-linking facility is recommended. This permits users to link two or more buses in such a way that one bus can address a device on the other as if they were on the same bus. The only bus that provides this facility is Eurobus.[11] For Multibus-based systems, two systems can be linked through a high-speed remote I/O bus.[12]

Supported processors

The type and number of processors supported by a backplane bus is a fundamental criterion of its success. There are several reasons for this, mainly concerned with independence of the processors, which is important in the following connections:

(*a*) For applications in which a particular CPU must be selected either for its architecture, speed, instruction set or the availability of a specific operating system. Consider, for example, applications requiring extensive assembly-language programming. A CPU supporting an extensive instruction set or providing specialized instructions is best suited for these applications. Operating speed is important for real-time applications or when the system has to respond rapidly to external events. In such a case a fast CPU may necessarily be selected instead of a slow one.

(*b*) In a laboratory environment where a bus-based

system must be frequently modified to accommodate the needs of various experimental configurations. This is particularly true for research laboratories, where the experimental set-up is dismantled after the data have been collected or when the use of a dedicated system cannot be justified.

(*c*) When the use of a specific CPU is dictated by peripheral controllers or specialized integrated circuits designed to mate with it (*e.g.*, signal-processing ICs, memory-management units, timer/counters).

(*d*) Because software has become more expensive than hardware, a particular CPU may be selected not because of its architectural characteristics or any other attributes but simply because a particular software package can run on it without modification.

Since use of independent CPUs enhances a system's modularity, versatility and flexibility, a backplane bus that supports a wide variety of CPU boards is highly recommended.

Multiple bus masters

For any given bus cycle, a bus master is a device that can take control of the bus;[13] that is, it can activate an information transfer by generating all the signals necessary for initiation and execution of bus cycles. Only one bus master can take control of the bus at any given time, according to its priority. Bus mastership is retained until either the bus master resigns or another potential bus master requests the bus by implementing a handshake.

Bus masters are often classified as permanent or temporary. A permanent master has highest priority in a system, while a temporary master may request the bus from a permanent master for an arbitrary number of bus cycles and then return control of the bus to the permanent master. The maximum number of masters supported by a bus-based system depends on the arbitration scheme used. Depending on the way control responsibility is distributed the modules can be organized in a master–master or a master–slave configuration.

Bus slaves monitor the bus status for all bus cycles but cannot activate a transfer. If addressed during a particular bus cycle, they accept or send the required message under control of the current bus master. The bus interface circuitry is much less complicated for a slave than it is for a master. Further, a system may or may not have a supervisor. A supervisory element monitors all bus transactions and can modify them. The IEEE P896/Futurebus, for example, has such a provision.[14]

Although this and the following sections attempt to utilize the most frequently used definitions, terminology often varies according to the literature used. To complicate matters, it is not unusual for a "vested interest" to create its own definitions to suit its own purpose. Because of such lack of clarity, good documentation becomes a very important issue in selecting commercially available bus-based systems.

The ability of a bus to support multiple bus masters becomes especially important when multiple processor configurations are being considered.

MULTIPLE PROCESSOR SYSTEMS

As the number of applications with more elaborate computational demands increases, high-performance CPUs become increasingly important. There are definite limits, however, to the extent and type of improvements possible with the existing CPUs. Even the newer stand-alone personal computers must incorporate more than one CPU or MCU to provide high performance. Consider, for example, the IBM PC and XT,[5] which incorporate an 8088 CPU and an 8048 single-chip microcomputer, the DEC Rainbow 100,[15,16] which uses a dual processor architecture (Z80A and 8088 CPUs), and the Apple Lisa with its five microprocessors. In fact, all but one of the I/O cards on the Lisa include a microprocessor.

Bus-based systems supporting multiple processors can provide appropriate solutions to the demands for higher program execution speed and for additional computing or control power. With the development of fabrication technology, it is peripherals and not processors which are the most expensive part of a computer system. Because multiple processor systems allow resource sharing, they provide better cost efficiency.

Fault tolerance can be defined as the ability of a computer system to recover automatically from failures and continue processing. According to Manuel,[17] the main characteristics of fault-tolerant computer systems are redundancy, failure detection, diagnosis and repair, and software recovery after failure. Although the implementation of these characteristics may vary from system to system, multiple processors are used to provide for processor redundancy and, consequently, fault tolerance. Taking this concept one step further, why not implement (on similar principles) fault-tolerant analytical instrumentation, especially for on-line real-time process control in an industrial environment?

Multiple processor systems also offer high processing power and throughput. Throughput, however, does not increase linearly with the number of processors used, because of problems of interprocessor synchronization and communication.[18] This can be dealt with by constructing parallel processing systems, which usually consist of identical processors. These processors are able to work synchronously and perform the same operation simultaneously, or are able to support a large number of parallel processes. Array processors and supercomputers are examples of systems providing parallel processing capabilities.[19]

It is often claimed that the need for high-performance computers with very high speed computational capabilities induces a shift towards paral-

lel processing. In such a system, the one processor-per-task approach is replaced by the several processors-per-task concept. Is there a fundamental limit imposed by the classical computer architecture that forces designers to use parallel-processor architectures? Basic computer architecture has not changed in the 35 or so years since its conception by von Neumann. The shortcomings of such highly serial architecture can be avoided by utilizing parallel processing in a multiple processor environment where many things are happening at once.[20]

To take full advantage of the computing power offered by multiple processor systems, a task might have to be partitioned between two, four, eight or more processors, but the algorithm required should be independent of the number of processors involved. The major difficulty is how to schedule a single task concurrently among several CPUs. Clearly, such systems require both sophisticated software and an advanced communications protocol. Moreover, because all existing software has been written for inherently sequential machines, new software will have to be developed for parallel systems. The shift from sequential to parallel processing appears to be a non-trivial task.

Until recently, only mainframes or supercomputers used parallel processing in order to provide high throughput. Cray, the designer of the fastest supercomputer, is utilizing this concept in his new designs. Cray-3, scheduled to be delivered in 1986, is expected to have up to 16 parallel processors designed with GaAs chips. Cray-2, due sometime in 1984, is expected to have a 4-nsec clock cycle and to house up to four processors. Parallel processing is neither unique to a mainframe environment nor foreign to "microcomputerland": it has already been incorporated into modern CPUs and implemented at the chip level.

In traditional microprocessors that do not facilitate "pipelining", a complete sequence of instruction fetching, decoding and execution must take place before the next instruction can be operated on. In modern CPUs such as Intel's iAPX 286 (often referred to as the 80286), these operations are performed in parallel. To put matters in perspective, an 80286 operating at 10 MHz offers three times the performance of an 8086 operating at the same speed, or ten times that of the same processor operating at 5 MHz.[21] Similar features have also been incorporated into Intel's 8086 and 80186 CPUs as well as National's 16000 and Motorola's 68000 CPUs.

Although the processors just mentioned offer improved performance, it should be emphasized that they do not provide a "true" parallel-processing environment. Their architecture can be considered as a hybrid between serial and parallel. Because these processors execute only one instruction at a time, their major bottleneck still lies in the serial nature of their architecture.

Another way to avoid the limitations imposed by classical architecture is to use an entirely different one. The TMS 320, a 32-bit signal-processor chip from Texas Instruments, may be the first VLSI device designed with other than von Neumann architecture. Based on a modified Harvard architecture, the TMS 320 provides separate locations for programs and data. Since it can fetch information from both memory areas in parallel, it is able to fetch and execute instructions at the same time. Because of such built-in capabilities, the TMS 320 can execute a single instruction in 200 nsec, which means an operating speed of 5 MIPS (million instructions per second), faster than that of many mainframes of the last decade.

Perhaps the most important current development is the vast amount of information pointing toward the design of multiple processor systems. Three basic trends can be distinguished. The first involves the incorporation of multiple CPUs in desk-top and bus-based systems. The second involves parallel processing, and its significance is stressed by the fact that parallel processing capabilities, though on a small scale, have already been included in commercially available CPUs, and "exotic" designs which attempt to incorporate several processors on the same IC are currently under development. The third deals with the realization of multiple processor architectures.

Although there seem to be innumerable ways of tying several processors together, multiple processor systems can be classified, based on the degree of physical coupling, as loosely, moderately and tightly coupled.[22] This classification is utilized in the following discussion. Several authors classify multiple processor systems only as tightly coupled and loosely coupled, because the distinctions between tightly and moderately coupled systems are not well defined.

Tightly coupled systems

Tightly coupled systems, also known as multiprocessor systems,[23] can be defined as those with two or more processing elements with similar capabilities, where all processors have access to common memory, I/O, control units and peripheral devices, and which are co-ordinated by a single operating system.

The most promising configuration for tightly coupled systems involves allocation of local resources, such as memory and I/O on each CPU board,[24] as shown in Fig. 4. Such boards are also known as "intelligent I/O" boards. Their ability to support a local bus and resources allows the CPUs to run concurrently and use the system bus only when specific information is required from global resources. A portion of the memory on such boards is "dual ported", *i.e.*, it can be accessed, asynchronously, by any of the processors on the backplane. This allows processors to pass "messages" to one another, a significant feature especially when advanced co-ordination for process control applications is needed. Because the global bus is utilized only

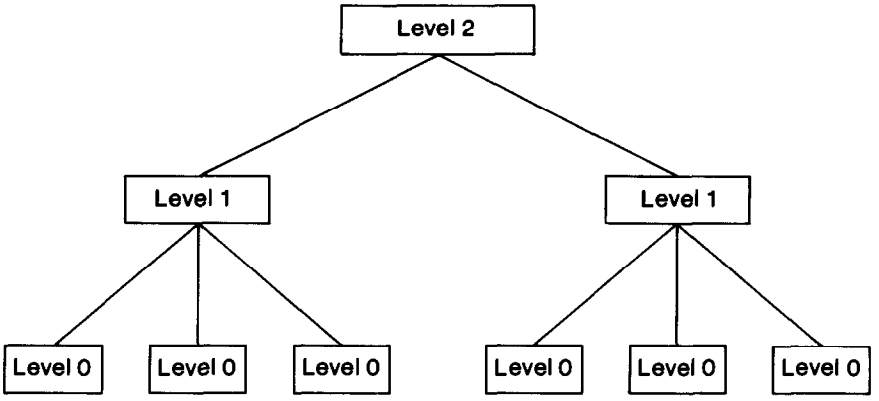

Fig. 5. A three-level hierarchical system.

when communication with global resources is required, bus throughput is increased.

To take care of special functions, "intelligent slaves" have also been developed. An intelligent slave is a board with local CPU, memory, I/O and dual-ported RAM. It cannot arbitrate for the system bus, however, and therefore has limited access to global resources.

For laboratory applications, tightly coupled systems may be utilized when sophisticated information and data-processing algorithms are implemented. Applications ranging from chemometrics to artificial intelligence and pattern recognition could also be included.

Moderately coupled systems

Moderately coupled systems are often referred to as distributed intelligence systems.[18] They involve computer systems close together and communicating via parallel or high-speed serial buses. Such systems do not usually give rise to general purpose microcomputer systems but are well suited for specialized applications. Applications are split up into relatively independent tasks, with local autonomy provided by assigning a processor or intelligent I/O for each task. The one processor-per-task concept utilized in such systems results in modular hardware and software and provides increased reliability through redundancy. Because distributed intelligence systems have resource-sharing capabilities, their cost–performance ratio decreases.

Although several topologies are possible, a hierarchical configuration seems to be the simplest and most promising for laboratory applications. Such a system, as its name implies, consists of a pyramidal structure of microcomputers assigned tasks of different complexity (Fig. 5). Its most important advantage is that routine or mundane tasks can be handled by subsidiary microcomputers or microprocessor-based designs at the bottom of the pyramid, and more complex tasks by processors at higher levels. As the number of levels increases, however, the response time becomes longer.

Loosely coupled systems

The current concept of distributed data-processing appears to be more closely related to loosely coupled than moderately coupled systems.

Loose coupling refers to widely separated multiple processor systems with resource-sharing capabilities. Each processor is an autonomous computer system utilizing local resources and providing on-site computation, control and storage capability. The interprocessor communications bandwidth is usually narrower than that provided by tightly coupled and moderately coupled systems. In addition, communications are message-oriented and operating systems are usually independent. Loose coupling characterizes computer networks, and because these have been extensively discussed in the literature[26,27] they will not be dealt with here.

SYNCHRONIZATION

Multiple processor systems sharing common resources, such as shared memory or peripherals, require some form of synchronization that co-ordinates the sequence of operations on common resources or on multiple tasks. A popular method of synchronization by software uses semaphores. A semaphore can be thought of as a "gate" to a restricted area or a critical section of software, thus protecting shared data or I/O. It is usually implemented by setting a memory bit which indicates that a resource is in use.

To avoid the shortcomings of this implementation, some form of mutual exclusion must be utilized. This enables a processor or a task to prevent access to a shared resource by other processors or tasks when it is in a critical section.[23] The way in which mutual exclusion is implemented depends on the particular bus-based system.

Interrupts

Microprocessor-based designs synchronize their operation with externally occurring events by means

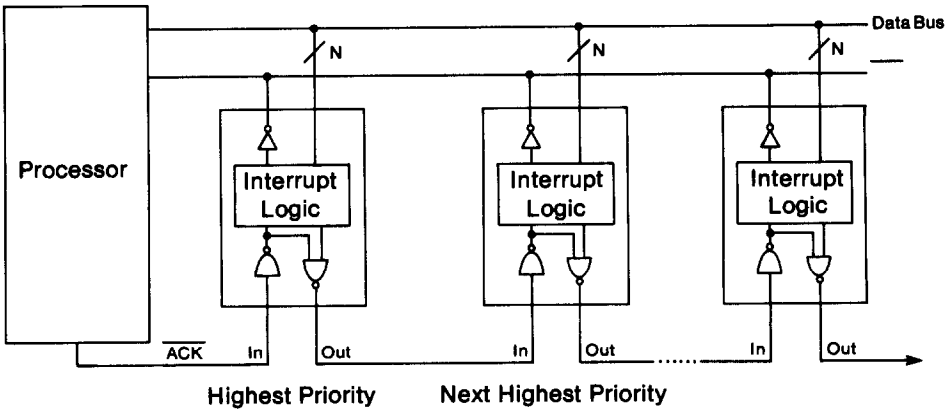

Fig. 6. Typical serial daisy-chained interrupt–acknowledge scheme.

of interrupts. For bus-based systems, the operations of various modules within the system must also be synchronized with each other. Ideally, each module has its own interrupt line, each line having different priority. The number of interrupting devices allowed is determined by the number of interrupt lines available. For bus-based systems supporting several modules and several interrupt levels, this approach is not practical, because it requires a large number of interrupt request lines. To avoid these shortcomings a serial scheme has been devised, which allows several modules to share a single interrupt-request line.

An interrupt–acknowledge signal passes through all modules on the shared interrupt line in a daisy-chain fashion, where each device connection is analogous to a link in a chain.[28] The interrupt–acknowledge output of the module with the highest priority is connected to the interrupt–acknowledge input of the module with the next highest priority and so on. Priority is then determined by the physical location of each module on the backplane, where the module closest to the processor has the highest priority. Although this implementation requires a small number of interrupt request lines, it spoils the positional independence of boards on the backplane.

A conceptual diagram of a daisy-chain interrupt–acknowledge scheme is shown in Fig. 6. Its exact implementation, however, depends on the backplane in question. Backplane bus structures utilizing daisy-chained interrupt–acknowledge schemes include the STDbus, VERSAbus and the VMEbus.

Bus arbitration

In a bus-based system providing DMA (direct memory access) facilities or one supporting a multiprocessing environment, the bus can be considered as time-shared among several bus masters. Only one bus master, however, is allowed to use the bus at any given time. If more than one processor attempts to use the bus at the same time, conflicts arise which can be resolved by implementing a communications protocol in the form of an arbitration scheme.[29]

Bus arbitration can be defined as "the procedure by means of which nodes may request and obtain exclusive usage of the bus".[23] More simply stated, a bus-arbitration unit "decides" which processor gets the bus and which has to wait. To avoid the possibility of a high-priority master monopolizing the bus, "fairness schemes" can be included in the priority mechanism.[14] Several bus-arbitration schemes are possible, although serial and parallel ones seem to be the most common.[30]

Parallel bus arbitration is the faster but requires more signal lines and external logic for its implementation. In this, all bus requests are usually routed into a bus-arbitration module which assigns priority and grants the bus to the chosen master. Serial daisy-chained bus arbitration is implemented in a similar fashion to a daisy-chained interrupt–acknowledge scheme and priority is assigned to the arbitrating module by virtue of its position on the backplane. The primary drawback is the logic delay experienced by the bus-grant signal as it travels down the chain. To avoid excessive delays, the number of modules on the backplane that can arbitrate for the bus must be limited. For Multibus-based systems to avoid excessive delays, there can be no more than 3 bus masters on the backplane when a serial scheme is utilized. With a parallel bus-arbitration scheme, up to 16 bus masters can be supported.[31]

Backplanes such as the VERSAbus and the VMEbus support parallel daisy-chain bus arbitration.[31,32] This implementation allows bus masters to share common bus-request lines, without the excessive delays imposed by true daisy-chain arbitration.

BUS-BASED STRUCTURES AND SYSTEMS

Bus selection

Several electrical and mechanical specifications that can influence bus selection have been discussed thus far. Non-technical issues, however, cannot be

ignored. Consider, for example, standardization in which the electrical and mechanical specifications of a proposed bus standard may be redefined before they become an adopted IEEE standard. This can give rise to incompatibility between the backplane and boards having a design based on the "new standard" specifications. Boards are often designed to fit both older and newer versions of the same backplane, as is the case with the S-100 bus and CompuPro's CPU Z board. This board is advertised as being "compatible with most S-100 mainframes", but there is no guarantee that it will be compatible with a particular user's system. Incompatibility can quickly lead to obsolescence and therefore to expensive replacements.

There is, however, a catch to the selection of adopted bus standards. Because standards take years to develop and mature, by the time they become widely accepted and endorsed by a standards-making organization they are no longer adequate for the newest applications. Consider, for example, Multibus. Although it is an adopted bus standard, it is unable to support CPUs with 32-bit data-bus widths. Moreover, proponents of the VMEbus, almost solely on the basis of Multibus's inability to support wide data paths advocate that Intel should use the VMEbus instead of the Multibus. Intel claims that a 16-bit data bus width is adequate for present needs, but is also working on Multibus II, a 32-bit Multibus-compatible version.[33] The ability to upgrade to 32 bits is becoming increasingly important for future laboratory applications.

Competitive supply is another important criterion because it gives lower prices and wider selection. Board availability is probably as important as software in selection of buses. What is available today is often more important than what will become available tomorrow, especially if a particular application requires immediate attention. Several backplanes do have the capability of supporting 32-bit CPUs, but currently there is neither a variety of 32-bit CPU boards nor applications software available for them, and 32-bit peripheral boards are non-existent. This current lack of hardware and software dictates the use of 16-bit boards in such backplanes and, as a consequence, users may have to pay "32-bit prices" to run, at least initially, 16-bit processors and software. However, because 32-bit backplanes are designed for the future, they are "here to stay". In the meantime, the user has been caught in the middle of a 16-bit *vs.* 32-bit controversy. The selection of a bus-based system is confusing at best, and essentially depends on the intended use.

Comments

Although no draft standards have been published for more than two years, the volume of information on activities leading to the present bus-based systems is overwhelming. Only a small fraction of it is presented in the short discussion that follows.

The STD-bus. A joint effort between Pro-Log Corp. and Mostek Corp. has resulted in the development of the STD-bus, a simple, compact, versatile, cost-effective but partially processor-independent bus for 8-bit microprocessors. Its specifications were announced at the 1978 Wescon, and the IEEE microcomputer standards committee allocated the project-authorization task P961 to the STD-bus in 1981. The STD-bus signals can be grouped into three sets of signal lines (the data bus, the address bus, and the control bus) and two sets of power lines (the logic power bus and the auxiliary power bus).

The electrical and mechanical specifications of the STD-bus are discussed by Elsmore[30] who also provides some insights into the bus's future. Cummings[34] concentrates on the bus's specifications and also includes a list of vendors of compatible boards, and Wilson[35] offers a guide to the STD-bus. Hanger[36] discusses tools available for software development for the STD-bus. Interfaces for the STD-bus are simpler and easier to build than those for high-performance 16- or 32-bit buses. Titus *et al.*[37] provide details of STD-bus interfacing.

At least one company[38] offers a complete, desk-top, STD-based microcomputer system, and a portable microcomputer designed around an 8-slot STD-backplane recently became available.[39] The Labtech 70,[40] described by Putnam *et al.*,[41] follows a different approach. This 14-slot STD-bus microcomputer is specifically designed for laboratory applications, offering real-time operation, networking capability, a 65-kHz data-acquisition rate, and process-control software.

The STD-bus can be used both as the main bus or in conjunction with other buses or personal computers. MassComp Inc.,[42] for instance, has developed a multiple CPU system designed around the Multibus, the STD-bus, and a proprietary bus. RMAC Corp.[43] is marketing an interface which links the IBM PC with the STD-bus and allows the PC to act either as a controller, *i.e.*, no intelligence is included on the bus, or as a development system for the same bus.

Communications Technology Corp.[44] offers a CMOS board with an interface to the Hewlett-Packard Interface-Loop (HP–IL). This board is built around National Semiconductor's NCS800 CMOS microprocessor and directly plugs into the CIMbus (CMOS Industrial Microcomputer bus), an STD-like bus developed by National. Both the CIMbus and the HP-IL are intended for small battery-operated systems which can withstand harsh environments, such as industrial plants.

The plethora of interface boards and data-acquisition subsystems available for the STD-bus, along with its inherent simplicity, compactness, small size and low cost, make it particularly attractive for certain laboratory or process-control applications, and for the design of distributed intelligence systems. However, the STD-bus imposes certain limitations. The processor- or timing-dependence prevents inter-

changeability of boards and therefore confines users to a specific family of CPUs and peripherals, and hence compatibility is referenced with respect to the CPU board utilized, for example, STD-Z80-I/O, STD-6800-I/O.

Although the STD-bus is 8-bit, 8/16-bit CPU boards designed around Intel's 8088 microprocessor are available for it. To accommodate the 20-bit address generated by the 8088, the higher-order address bits are multiplexed with the data bus, thus providing a 1-Mbyte addressing capability. The most important feature of this board, however, is that it provides compatibility with IBM PC software.

Even though the possibility of designing true 16-bit CPU boards for the STD-bus is under investigation, the bus is likely to remain "8-bits wide". An effort is being made to standardize a higher performance STD-bus, often referred to as the STE-bus. This bus is based on the Eurocard Format; it supports up to 21 slots and implements full bus arbitration.

Because of the renewed interest in 8-bit buses, the STD-bus and buses like it are expected to survive into the 1990s.

The S-100 bus. The S-100 bus has evolved, since its introduction in 1975, from an 8-bit "hobby bus" into a 16-bit high-performance bus for personal computers, and despite its initial difficulties, in December 1982 became the IEEE 696 bus standard. The backplane itself carries between 2 and 22 slots which now support both 8- and 16-bit processors and up to 16 Mbytes of memory, a considerable improvement over the original 8-bit, 64-kbyte version. The S-100 bus signals can be grouped into eight sets of signal lines (data, address, status, control output, control input, TMA access control, interrupt and utility) and a set of nine power lines. The eight TMA (temporary master access) signals allow a single bus-master and up to 16 temporary bus-masters to co-exist in a single system.

Perhaps the most important change from the original S-100 bus specifications was the addition of a mechanism for performing 16-bit data transfers. The data bus consists of two unidirectional 8-bit buses for byte transfers, in which different paths are followed for data input and output. These buses are combined to form a 16-bit bidirectional bus, which means that the bus can easily support both 8- and 16-bit processors. Almost every type of microprocessor, from the early 8085 to the latest NS16032, is available for the S-100 bus, which further contributes to its popularity. There are more than 100 active manufacturers marketing over 500 boards for this bus, according to one estimate.[45] This proliferation of vendors accounts for S-100 bus-based systems being cheaper than those designed with other high-performance buses. Only a limited number of such boards have been specifically designed for laboratory or industrial applications, but there is a trend towards the design of data-acquisition, signal-processing, and control boards. Probably the major advantage of these systems is in the large number of application programs, operating systems and languages available for use with them.

By virtue of its design, the S-100 bus cannot support multiprocessing, which appears to be the reason why a variety of dual CPU boards, ranging from an 8085/8088 pair to a 68000/Z80 combination have been introduced, a concept pioneered by Godbout's CompuPro.[46] Other vendors[47–50] are also marketing desk-top, S-100 based microcomputer systems, and Computershop Inc.[51] offers one of the first portable S-100 based systems.

Garetz,[45,52] the chairman of the IEEE committee, traces the history of the S-100 bus and discusses some of its specifications. He also discusses CompuPro's S-100 based multiuser systems. Wilson[54] discusses the electrical and mechanical specifications of this bus and describes several interface boards for it, and Cruce and Alexander[55–57] describe a hard-disk interface. Interface projects and reviews of S-100 systems appear in several microcomputer magazines, but Microsystems,[58] the CP/M user's journal, offers several such articles in every issue.

Bursky's book,[59] despite its title, provides a general but outdated view of microcomputer systems, and mentions the S-100 bus only in passing; it is included here because its appendices provide detailed schematic diagrams of commonly used S-100 boards and it incorporates a section on S-100 bus vendors. Poe and Goodwin's book[60] also has only minimal discussion of the S-100 bus. Libes and Garetz[61] give several interface projects for the bus. It should be emphasized, however, that some of the bus's specifications have been redefined since these books were published, and have become the IEEE-adopted 696 standard.[62,63]

The major advantages offered by S-100 bus systems are wide hardware support, a variety of software resources, and lower cost than other high-performance buses. However, the S-100 bus appears to have been completely defined and standardized a little too late. To accommodate 32-bit processors the bus may have to be redefined either by using RFU (reserved for future use) pins or by multiplexing data and/or address lines. In the meantime, the pressures exerted by Multibus and the emergence of the VMEbus may severely limit its growth.

Multibus. Just as the S-100 bus became a standard for personal computers, the Intel-developed and redesigned Multibus is becoming the dominant bus for scientific and engineering applications. The IEEE microcomputer standards committee officially approved Multibus as the IEEE 796 standard in December 1982. Long before this recognition, however, Multibus had established itself as a *de facto* industry standard.

The Multibus backplane supports 24 address lines, 16 data lines, 12 control lines, 9 interrupt lines and 6 bus-exchange lines, divided between two connectors. The primary connector (P1) contains all Multibus

signal lines except four of the address lines, which are routed onto the auxiliary connector (P2). The P2 connector supports the iLBX local bus extension which provides the ability for a processor to communicate with up to four memory boards without tying-up the Multibus. In other words, memory is considered to be logically on the board, but physically separate. This memory can be dual-ported; that is, it can be accessed either by the iLBX (P2 connector) or by the Multibus (P1 connector). The iLBX bus provides access for up to 16 Mbytes of local system RAM; it can handle 16-bit data-transfers and offers up to 19 Mbyte/sec data-rates.

The iSBX bus was the first major extension to Multibus's architecture. It meets the specifications of the IEEE-P959 draft standard and allows users to add a limited number of small-size "daughter" boards to a full-size board. The multichannel DMA (direct memory access) I/O bus was created to satisfy the need for high-speed I/O. It supports up to 16 I/O devices located up to 15 m away, provides 8- and 16-bit data-transfers, and provides a maximum throughput of 8 Mbyte/sec. The 16 I/O devices are classified as supervisors, controllers, talkers or listeners, in a manner similar to the IEEE-488 bus. The multiplicity of buses within the Multibus provides architectural flexibility unparalleled by any other high-performance bus.

The development of Multibus from its inception in 1974 until 1982 is traced by Boberg,[64] who also provides some details about its electrical and mechanical specifications. Wilson[33] provides a wealth of up-to-date information on Multibus, including specifications, and describes a limited number of boards available for it. Intel's Multibus data book[65] provides a survey and further details of the Multibus system architecture.

Several commercially available computer systems have been designed around Multibus. Mayers *et al.*[66] describe the Plexus P/40, a multiple-processor system based on Zilog's Z8000 CPUs. This system is assembled from off-the-shelf modules and operates under UNIX. Callan Data Systems[67] market a series of Multibus-based desk-top microcomputers, and Logical Microcomputer[68] offers the Megamicro, a virtual-memory microcomputer based on National Semiconductor's NS16032 microprocessor. One of the advantages offered by multiple-processor systems is increased reliability as a result of redundancy. August 300 is an example of a Multibus-based fault-tolerant computer system.[69] Portable Multibus-based computer systems are also available,[70] and ELAN,[71] an inductively-coupled plasma–mass spectrometry (ICP–MS) system, is one of the first analytical instruments with computing power derived from a Multibus-based system.

An adapter which makes an IBM PC or XT compatible with Multibus has recently become available.[72] This adapter allows the PC or XT to be used either as a bus-master or as a co-processor in a Multibus environment. Taking a different approach, SysteMathica[73] offer a board compatible with the IBM PC and the Multibus. This single-board computer offers a triple bus structure: a PC-compatible internal bus with on-board or off-board expansion capabilities; a Multibus interface; and a dual-ported memory bus which communicates with the internal-system bus and the Multibus. Such developments allow users to take advantage of popular software and provide access to applications that would normally require two sets of hardware.

Multibus is one of the most successful high-performance buses available to date. According to Intel Corp. there are more than 150 vendors marketing over 1000 boards for this bus. Ironoak Corp.[74] has compiled a complete up-to-date guide to Multibus manufacturers. The next step in the evolution of this bus standard is the introduction of Multibus II.

Multibus II is a multiplexed bus providing full 32-bit address and data paths and supporting the Eurocard format. The Multibus II specification defines five buses, three of which are new. The parallel system bus (iPSB) is the main bus supporting 8-, 16-, 24- and 32-bit data-transfers and a 32-bit address bus. In the burst mode the bus can sustain a 40 Mbyte/sec bandwidth. The local bus extension (iLBX) provides access for up to 64 Mbytes of local RAM and offers a 48-Mbyte/sec bandwidth. The serial system bus (iSSB) can be extended up to 10 m, is 1-bit wide, and runs at 2 MHz. Finally the iSBX I/O bus and the multichannel direct memory access (DMA) bus have been borrowed from the Multibus I architecture. Multibus II is described in some detail by Beaston.[75] Although Multibus II's bus structures have been designed to meet the needs of future high-performance bus-based systems, its effect on such systems and its compatibility with Multibus I still remain to be seen.

VERSAbus and VMEbus. The VERSAbus and the VMEbus, its Eurocard counterpart, are two different implementations of a very similar bus. They both support 16-bit and 32-bit processors, 32-bit data paths, multiple bus-masters and slaves, and incorporate a wide address bus which permits a direct addressing capability of over 4 Gbytes. Both backplanes consist of the data-transfer bus (DTB), a priority interrupt bus, the DTB arbitration bus and a utility bus.

The VMEbus (Versa Module Europa bus) specifications are a joint effort of Mostek, Motorola and Signetics/Philips Corp. The bus provides full 32-bit address and data lines in an asynchronous environment and supports the Eurocard format and DIN connectors. Although its functional characteristics have not changed since October 1981, the VMEbus specifications now define three separate and independent buses: the VMEbus, the VMXbus and the VMSbus. The VMEbus is used as the global bus. The VMXbus extends the local bus from the processor board to the adjacent boards so that the

Table 2. Attributes of multiple processor systems

Advantages	Disadvantages
High processing power	Increased software complexity
High throughput	Increased communications complexity
Increased reliability	Expensive
Fault-tolerance	
Increased versatility	
Improved cost/performance ratio	

processor can access additional memory without the need to arbitrate for the global bus. The VMSbus is a serial bus utilized to pass messages among boards on either the backplane or separate card racks.

Although the VMEbus has only recently been introduced, the IEEE committee P1014 began its standardization in March 1983, and several microcomputer systems have been designed around it. An example of a VMEbus-based system is the Consultant,[76] an early NS16032-based or NS32032-based desk-top computer which provides high-resolution graphics, multiprocessor capability, and a multi-user operating system. The computer's CPU board is equipped with an NS16082 memory-management chip, an NS16081 floating-point processor, a real-time clock/calendar, three 16-bit programmable interval timers and 7 levels of interrupt. Another example is Motorola's VME/10 desk-top computer.[77] The basic VME/10 system consists of three elements: the system-control unit, the keyboard, and a video display unit. The system-control unit contains an MC68010 and MC68451 MMU-based module, 5- or 15-Mbyte Winchester disk drive, and a 655-kbyte floppy disk. A choice of two card cages permitting different expansion capabilities is also provided. This system operates under VERSAdos, Motorola's real-time operating system. Willot[78] briefly describes the Victory Spirit, a system designed around the VMEbus and supporting CP/M-80 and CP/M-86 operating systems.

The VERSAbus is a proposed standard (P970) currently under review by the IEEE microcomputer standards committee. Perkin-Elmer's model 7500 is an example of a laboratory computer which has been designed around this bus.[79] Also, Varian's XL-NMR spectrometer is supported by two isolated VERSAbuses communicating with each other through serial ports.[80] UNI/VERS, an interface that links any VERSAbus-based system to a host PDP-11 or VAX is described by Russ.[81] The major advantage of this type of interface is that it merges features of two radically different families and offers expansion capabilities which broaden the user's range of options.

Additional information on the electrical and mechanical specifications of the VERSAbus and the VMEbus is given by DeBock,[82] and the VERSAbus is discussed in detail by Balph *et al.*[83] The VMEbus is described by Kaplinski[32] and Mackenna *et al.*[84] Lobelle[85] presents a case study of the interfacing of a 6809-based subsystem to the VMEbus.

The VERSAbus and VMEbus provide for the design of high-performance systems. Because of their ability to support 32-bit processors, they have the potential to become the dominant buses of the future. The VMEbus, because of its form factor, is a likely candidate for the design of high-performance desk-top computer systems or for the design of the "super-microcomputer" of the future.

Futurebus. Although no CPU or peripheral boards have been designed for the IEEE P896/Futurebus, it is included in Table 1 because it attempts to anticipate future needs in bus design and, *a priori*, influence the development of new bus standards. Despite the rejection of draft 5.2 by the IEEE microprocessor standards committee, the currently accepted 6.2 draft standard introduces several new concepts in bus design.

The Futurebus project is aimed at the development of a backplane bus architecture for use with the emerging 32-bit microprocessors and promotes multiprocessing and fault-tolerance. The bus is capable of performing 10 million 32-bit data-transfers over an asynchronous 32-bit data-bus. Both the address and data buses are multiplexed to make room for a redundant bus that can take over if the first one fails. The bus also provides fully distributed control without the need for a central master. Several papers that describe the Futurebus have appeared in the literature.[14,86,87]

National Semiconductor Corp. has committed itself to produce the new trapezoidal transceivers (the DS3896 and DS3897) required to drive this high-speed bus. Because of the interest shown in the P896 project, it is expected that several companies will soon start offering boards for the Futurebus.

Other backplane bus structures. A trend toward the introduction of both standard and proprietary bus structures is evident in the microcomputer industry. In the following discussion only the most prominent bus structures will be presented. The FASTBUS[88,89] is a development of the NIM Committee, National Bureau of Standards, as an upgraded version of the CAMAC (computer-automated measurement and control) bus standard.[90] There are several CAMAC-related standards adopted by the IEEE.[91–94] Although the FASTBUS was originally developed for nuclear physics apparatus requiring high data-rates, it is general enough to support a wide range of data-acquisition and control applications. The bus is based

on emitter-coupled logic, supports multiple bus-masters, and provides a flexible bus architecture. Larsen[95] provides background information on the FASTBUS and reports on developments of this bus standard. Laboratory applications of the CAMAC and the FASTBUS can be found in *J. Nucl. Instrum., Methods in Physics Research* and *IEEE Trans. Nucl. Sci.*, and a symposium report.[96]

The Eurobus[11,97] is a general-purpose backplane bus standard developed by the U.K. Ministry of Defence and Ferranti Computer Systems Ltd. Eurobus is one of the few general-purpose buses that can be operated as a data bus without the need for a processor to act as a bus-controller. The bus supports 8-, 16- and 32-bit data paths; the address bus is two bits wider in each case, and the data and address buses are multiplexed. To date, the major implementation of Eurobus is in Ferranti's military computer. Although the bus has its origins in the military sector, it is well suited for laboratory and industrial applications.

Perhaps one of the most important proprietary bus structures is Digital Equipment Corporation's Q-bus.[98] This is the slowest but most commonly used backplane bus structure. More than 300000 CPU boards compatible with the Q-bus have been sold since 1975, according to one estimate.[99] The bus has already undergone three stages of evolution. It began with a 16-bit address bus and one level of interrupt. It then moved to 18-bit addressing and 4 levels of interrupt and is currently supporting a 16-bit standard, 22-bit extended address bus and 4 levels of interrupt. In order to provide for higher throughput, DEC has recently announced several DMA enhancements for this bus. An M68000/UNIX combination is also available for this bus.

The Q-bus is currently defined as an asynchronous, multiplexed, single CPU bus. Its future, however, may be determined by the J-11 chip set which implements the complete PDP 11/70 instruction set, but requires a much faster bus than the Q-bus in order to provide for high throughput. Although the Q-bus appears to be on the verge of change, it still remains a widely used backplane because of the large number sold.

What does the future hold?

Undoubtedly, the microcomputer industry is undergoing a trend towards more powerful computer systems. The trend of functional architecture is towards computer systems made up of functional modules, resulting in a user-definable architecture. When such modules become popular enough, VLSI implementations will become available and ICs will replace boards as basic system-building blocks, as with Intel's iAPX 186 CPU "board on a chip". To the user there is another advantage besides higher performance at lower cost: these ICs can be chosen from "menu books" similar to a TTL (transistor transistor logic) data book, and advanced bus structures allow the desired functional modules to be plugged-in whenever and wherever needed. Such modules include not only hardware, but also software-oriented hardware devices such as electrically erasable PROMs and silicon-based software, such as ROM-based operating systems. The final outcome is vast computing power based on VLSI technology and bus-oriented solutions.

A step towards the implementation of unconventional bus structures has been taken by Philips Corp., which has developed two serial data buses, the Inter-Integrated-Circuit bus (I^2C-bus) and the Digital-Data-Bus (D^2B). By having the interface logic incorporated into the chip, single-chip microcomputers (derived from Intel's 80C48 and 80C51 series) act both as a network interface and as a processor or a controller, while support ICs or modules simply clip into the bus.[100]

The basic idea for both buses is quite simple. The bus provides the facilities of a small-area serial network within a single computer system or an instrument. Small-area networks are typical of local area networks. Their characteristics are somewhere between those of a simple serial-data link, such as the RS-232C or RS-422 and Ethernet. In the I^2C-bus implementation, each IC has a slave address and recognizes an ID code in order to respond. The D^2B implementation takes the I^2C-bus approach even further. It is designed to connect racks of equipment or computer systems together and thus is well suited for distributed intelligence applications. The D^2B concept can be thought of as the serial equivalent of the IEEE-488 bus.

Hewlett-Packard is taking a different approach by developing the HP-interface loop,[101–103] a two-wire link that turns the HP-41C handheld calculator into a powerful test, measurement, control, and data-analysis tool.[104,105] Texas Instruments is following a similar path in the development of HEXBUS, a 4-bit bus designed for communication between a calculator or a computer and intelligent peripherals. Such developments suggest that both the emerging and the next generation of proprietary bus structures will become "application driven" and, therefore, will no longer conform to traditional bus designs.

Undoubtedly, the future of high-performance computer systems supporting an open-ended user-definable architecture is bus-oriented, although the character of such systems is only vaguely defined. One thing is clear: those configured to operate in the laboratory environment will support multiple CPUs, sophisticated data-acquisition and control boards, special signal-processing boards, boards improving the quality of the man–machine interface, wide memory resources, vast mass storage, and multiprocessing and/or distributed processing.

Examples of specialized boards include the FFT-1, a single fast Fourier transform (FFT) processor board from DSP Systems. This Multibus-compatible board can perform a 1024-point complex FFT in 8.2

msec.[106] Multibus or Q-bus imaging boards, such as the Datacubes VG123 board providing 768 H × 512 V pixel resolution 8-bits deep, are available for medical imaging or robot vision.[107] Floating-point processors for the Multibus or Q-bus and array processors for the Q-bus, VERSAbus and Multibus are also available.[108] Such developments open new horizons for image-processing applications and are expected to affect many areas from spectroscopy to robot vision. This brief summary cannot mention all vendors marketing specialized signal-processing boards. For information concerning boards available for bus-based systems the Microcomputer Systems D.A.T.A. book[109] is recommended.

Clearly, the type of bus-based system just described out-performs many minicomputers. Are minicomputers dying? The evolution of the 32-bit superminicomputer is progressing from boxes to boards and will eventually progress to a few chips or even one. Data General's new microEAGLE chip set, for example, promises low-cost systems with performance nearly half that of the Eclipse MV8000, a 32-bit supermini. Developments of this type point in a single direction. Superminicomputers will eventually become small enough and cheap enough to be marketed as desk-top models, and today's minicomputers will have been sentenced to death by micros.

Although the next generation of personal computers will provide increased performance and 16-bit solutions, it cannot match the capabilities offered by "supermicrocomputers". The plethora of existing off-the-shelf modules that convert personal computers into programmable test and measurement equipment, however, suggests that their importance in the laboratory will not diminish. Because of the wide software resources, the variety of hardware modules available to them, and their low cost, personal computers have earned themselves a permanent place in the laboratory.

Currently, computer-system design is one of the fastest growing domains in the computer industry. To keep pace with the increasing power and performance of microcomputers, the design philosophy behind traditional measurement systems is changing, and the concept of an isolated stand-alone instrument appears to be fading. Emerging is an integrated "analytical work station" with capabilities never before thought possible.

In complementary developments, the new generation of silicon sensors which respond to more than one physical input, and the new domain-conversion ICs which provide an analogue or digital output in response to chemical stimuli (*i.e.*, chemical sensors), offer capabilities for new types of measurements. The new generation of ICs and microsensors is expected to play an increasing role in the laboratory, lead to a wider dissemination of electronic intelligence within analytical instrumentation, and help realize laboratory automation. Furthermore, semiconductor technology and silicon micromachining offer the basic framework for microminiaturization in analytical chemistry.

Finally, Kowalski's scenario,[110] in which a highly computerized instrument runs samples automatically, shortens execution times of algorithms and comments on the results, has not yet been completely implemented in a single instrument, but most of the modules exist for its implementation. It is believed that when sophisticated hardware, firmware and software modules are blended with novel microstructures and combined with innovative "*thinkware*", the nature of analytical instrumentation and laboratory computing will be altered, offering new and exciting possibilities.

REFERENCES

1. G. Horlick, *Talanta*, 1981, **28**, 487.
2. E. G. Codding, *ibid.*, 1981, **28**, 503.
3. P. L. Borrill, *IEEE Micro*, 1981, **1**, No. 7, 84.
4. V. Karanassios and G. Horlick, *Talanta*, 1985, **32**, 601.
5. *Idem, ibid.*, 1985, **32**, 615.
6. G. Horlick, *Phil. Trans. Roy. Soc., A*, 1982, **305**, 681.
7. G. Horlick, *Chem. in Canada*, May 1983, 21.
8. Microsensor Technology, Inc., 47747 Warm Springs Blvd., Fremont, CA 94539.
9. J. B. Angell, S. C. Terry and P. W. Barth, *Sci. Am.*, 1983, **248**, No. 4, 44.
10. P. Borrill, *Microprocessors and Microsystems*, 1982, **6**, No. 9, 450.
11. J. Hill, *ibid.*, 1982, **6**, No. 9, 484.
12. J. Dilbeck and J. Barthmaier, *Conf. Record Wescon*, Paper 27/2, San Francisco, 1981.
13. G. D. Kraft and W. N. Toy, *Mini/microcomputer Hardware Design*, Prentice Hall, New York, 1979.
14. A. A. Allison, *Conf. Record Wescon*, Paper 27/5, San Francisco, 1981.
15. D. B. Suits, *Byte*, 1984, **9**, No. 4, 170.
16. K. H. Olsen, B. J. Folson, R. H. Ham and J. D. Clarke, *Proc. IEEE* 1984, **72**, No. 3, 283.
17. T. Manuel, *Electronics*, 1983, **56**, No. 2, 93.
18. E. T. Fathi and M. Krieger, *Computer*, 1983, **16**, No. 3, 23.
19. P. G. Barker, *Computers in Analytical Chemistry*, Pergamon Press, Oxford, 1983.
20. T. Manuel, *Electronics*, 1983, **56**, No. 12, 105.
21. *Introduction to the iAPX 286*, Intel Corp., AP-note 210308-001.
22. C. Weitzman, *Distributed Micro/Minicomputer Systems. Structure, Implementation and Application*, Prentice-Hall, New York, 1980.
23. B. A. Bowen and R. J. A. Buhr, *The Logical Design of Multiple-Microprocessor Systems*, Prentice-Hall, New York, 1980.
24. T. Balph and J. Black, *Electronic Design*, 1982, **30**, No. 6, 219.
25. J. B. Peatman, *Digital Hardware Design*, McGraw-Hill, New York, 1980.
26. R. E. Dessy, *Anal. Chem.*, 1982, **54**, 1167A.
27. *Idem, ibid.*, 1982, **54**, 1295A.
28. G. D. Kraft and W. N. Toy, *Microprogrammed Control and Reliable Design of Small Computers*, Prentice-Hall, New York, 1981.
29. A. Osborne, *8089 I/O Processor Handbook*, Osborne/McGraw-Hill, Berkeley, 1980.
30. T. Elsmore, *Microprocessors and Microsystems*, 1982, **6**, No. 9, 455.

31. R. Allan, *Electronic Design*, 1982, **30**, No. 26, 107.
32. C. Kaplinski, *ibid.*, 1981, **29**, No. 23, 173.
33. D. Wilson, *Digital Design*, 1983, **13**, No. 2, 76.
34. W. C. Cummings, *Conf. Record Wescon*, Paper 27/1, San Francisco, 1981.
35. D. Wilson, *Digital Design*, 1983, **13**, No. 6, 55.
36. L. Hanger, *ibid.*, 1983, **13**, No. 4, 74.
37. C. A. Titus, J. A. Titus and D. G. Larsen, *STD Bus Interfacing*, Sams, Indianapolis, 1982.
38. Micro/sys, 1367 Foothill Blvd., La Canada, CA 91011.
39. Jonos Ltd., 920C Orangethorpe, Anaheim, CA 92801.
40. Laboratory Technologies Corp., 328 Broadway, Cambridge, MA 02139.
41. F. A. Putnam and C. Sawyer-Laucanno, *Am. Lab.*, 1983, **15**, No. 9, 38.
42. MassComp Inc., One Technology Park, Westford, MA 01886.
43. RMAC Corp., 716-G Capitola Ave., Capitola, CA 95010.
44. Communications Technology Corp., Electronics Division, 2237 Colby, Los Angeles, CA 90064.
45. M. Garetz, *Byte*, 1983, **8**, No. 2, 272.
46. CompuPro, 3506 Breakwater Court, Hayward, CA 94545.
47. Cromenco Inc., 280 Bernardo Ave., Mountain View, CA 94040.
48. Dynabyte Business Computers, 521 Cottonwood Drive, Milpitas, CA 95035.
49. Morrow Designs Inc., 5221 Central Ave., Richmond, CA 94804.
50. The Heath Co., Benton Harbor, MI 49022.
51. Computershop Inc., 139 First St., Cambridge, MA 02141.
52. M. Garetz, *Microprocessors and Microsystems*, 1982, **6**, No. 9, 466.
53. *Idem*, *Byte*, 1983, **8**, No. 1, 152.
54. D. Wilson, *Digital Design*, 1983, **13**, No. 9, 42.
55. A. C. Cruce and S. A. Alexander, *Byte*, 1983, **8**, No. 3, 130.
56. *Idem*, *ibid.*, 1983, **8**, No. 4, 304.
57. *Idem*, *ibid.*, 1983, **8**, No. 5, 368.
58. Microsystems, 270 St. Paul St., Denver, CO 80206.
59. D. Bursky, *The S-100 Bus Handbook*, Hayden, Rochelle Park NJ, 1980.
60. E. C. Poe and J. C. Goodwin, *The S-100 and Other Micro Buses*, Indianapolis, 1981.
61. S. Libes and M. Garetz, *Interfacing to S-100/IEEE 696 Microcomputers*, Osborne/McGraw-Hill, Berkeley, 1981.
62. M. Garetz, Chairman, IEEE-696 Committee, c/o CompuPro, P.O. Box 2355, Oakland Airport, CA 94614-0355.
63. IEEE Service Center, C.P. Dept., 445 Hoes Lane, Piscataway, NJ 08854.
64. R. Boberg, *Microprocessors and Microsystems*, 1982, **6**, No, 9, 471.
65. Intel Corp., Literature Dept., 3065 Bowers Ave., Santa Clara, CA 95051.
66. C. Myers and G. Munsey, *Comp. Design*, 1982, **21**, No. 2, 87.
67. Callan Data Systems, 2637 Townsgate Road, Westlake Village, CA 91361.
68. Logical Microcomputer Co., 140 South Dearborn St. Chicago, IL 60603.
69. August Systems Inc., 18277 S.W. Bonners Ferry Road, Tigard, OR 97223.
70. Cognex Corp., 72 River Park St., Needham, MA 02194.
71. SCIEX, 55 Glencameron Rd., Thonhill, Ontario L3T 1P2.
72. Bit3 Corp., 8120 Penn Ave. South, Minneapolis, MN 55431.
73. SysteMathica Microprocessor Development Group, 4732 Wallingford Street, Pittsburgh, PA 15213.
74. Ironoak Corp., 3239 Camito Ameca, La Jolla, CA 92037.
75. J. Beaston, *Electronics*, 1984, **57**, No. 6, 126.
76. Elite Corp., 906 N. Main, Wichita, KS 67203.
77. Motorola Semiconductor Products Inc., P.O. Box 20912, Phoenix, AZ 85036.
78. J. Willot, *Digital Design*, 1983, **13**, No. 7, 93.
79. Perkin–Elmer Corp., Main Ave. (MS-12), Norwalk, CT 06856.
80. S. H. Smallcombe and R. S. Codrington, *Am. Lab.*, 1983, **15**, No. 10, 105.
81. R. R. Russ, *Computer Design*, 1983, **22**, No. 11, 117.
82. R. DeBock, *Microprocessors and Microsystems*, 1982, **6**, No. 9, 475.
83. T. Balph and J. Kister, *Electronic Design*, 1980, **28**, No. 14, 97.
84. C. Mackenna, R. Main and J. Black, *Electronics*, 1984, **57**, No. 6, 132.
85. M. Lobelle, *Interfaces in Computing*, 1983, **1**, 193.
86. A. A. Allison, *IEEE Micro*, 1981, **1**, No. 7, 67.
87. P. Borrill, *Microprocessors and Microsystems*, 1982, **6**, No. 9, 489.
88. US NIM Committee, *FASTBUS Modular High Speed Data Acquisition System for High Energy Physics and Other Applications*, U.S. Dept. of Commerce, Natl. Bur. Stds., Washington, DC 20234.
89. US NIM Committee, *Future Data Bus Requirements for Laboratory High Speed Data Acquisition Systems*, *ERDA Tech. Doc.* TID-27621, June 1977, U.S. Energy and Research/Development Administration.
90. Modular Instrumentation and Digital Interface System (*CAMAC*), *IEEE-583*, 1975.
91. *IEEE-595*, 1976.
92. *IEEE-596*, 1976.
93. *IEEE-683*, 1976.
94. *IEEE-675*, 1979.
95. R. S. Larsen, *Interfaces in Computing*, 1982, **1**, 19.
96. A series of FASTBUS-related articles appears in the proceedings of the IEEE Nuclear Symposium, 1981, San Francisco.
97. C. Tyndale-Biscoe, G. R. Hobbs and R. J. Penny, *Interfaces in Computing*, 1982, **1**, 33.
98. Digital Equipment Corp., 146 Main St., Maynard, MA 01754.
99. *Electronics*, 1983, **56**, No. 19, 231.
100. T. Danbury and G. Allan, *Electronic Eng.*, 1984, **56**, No. 685, 41.
101. R. Katz, *Byte*, 1982, **7**, No. 4, 76.
102. S. Harper, C. Landsness and R. Quick, *Electronic Design*, 1981, **29**, No. 26, 78.
103. R. D. Quick and S. L. Harper, *HP Journal*, 1983, **34**, No. 1, 3.
104. J. P. Trautman and L. A. DesJardin, *ibid.*, 1983, **34**, No. 2, 3.
105. R. M. Miller and R. A. Coverstone, *ibid.*, 1982, **33**, No. 12, 16.
106. DSP Systems Corp., 1081 North Shepard St. M/S-E Anaheim, CA 92806.
107. Datacube Inc., 4 Dearborn Road, Peabody, MA 01960.
108. Sky Computers Inc., Foot of John Street, Lowell, MA 01852.
109. *Microcomputer Systems*, *D.A.T.A. Book*, D.A.T.A. Inc., 9889 Willow Creek Rd., P.O. Box 26875, San Diego, CA 92126.
110. S. A. Borman, *Anal. Chem.*, 1981, **53**, 703A.

Talanta, Vol. 32, No. 8A, pp. 601–614, 1985
Printed in Great Britain

0039-9140/85 $3.00 + 0.00
Pergamon Press Ltd

SMART BACKPLANES—I

THE APPLE II

V. KARANASSIOS and G. HORLICK
Department of Chemistry, University of Alberta, Edmonton, Alberta, Canada

(*Received* 27 *August* 1984. *Revised* 15 *February* 1985. *Accepted* 1 *March* 1985)

Summary—A comprehensive account is given of the characteristics of the Apple II family of personal computers, and the wide range of hardware and software available for it from various manufacturers. Pertinent books, magazines and journals are also listed.

From sources as diverse as hobby computers and minicomputer systems, a new generation of personal computers that can easily be adapted to the laboratory environment has emerged, ranging from professional versions of yesterday's "primitive" hobby machines to sophisticated bus-based systems that often outperform minicomputers.

Although laboratory automation has a lot to learn from office automation, it cannot follow exactly the same path. Some office computers are so specialized that they are not useful for anything but their assigned task, even some of the most sophisticated ones such as the Apple Lisa and the Xerox Star. For laboratory automation a different class of microcomputer system is required.

Although the descendants of hobby computers usually retain their ancestor's straightforward architecture, several trends can be distinguished, including wider data paths, more memory, "standard" operating systems, and use of a backplane bus on the motherboard. Motherboards containing active components such as CPU, memory and I/O in addition to a bus structure are often called "smart" or "intelligent" backplanes. Because they support a bus they give rise to microcomputer systems that can be adapted to some extent for specific needs. Though not offering the flexibility and performance of bus-based systems,[1] smart backplanes can be easily adapted to diverse applications.

The backplane bus structure in a personal computer motherboard is a key element for its successful use in the laboratory. For example, the Commodore PET has never had the success of the Apple II in the laboratory, a main reason being its lack of a backplane bus structure. Instead, the PET and its later versions relied primarily on the IEEE-488 interface for expansion and modification.[2] We purchased a PET long before an Apple II, but no longer use it. The backplane bus structure of the Apple II was undoubtedly very significant in its evolution as the most versatile computer of its type yet developed. This backplane constitutes a platform where devices ranging from co-processors to IEEE-488 interfaces can be added to the system. Because of this significance of the backplane bus in personal computer systems, this and the companion article[1] focus on the bus structure of such systems. The mechanical and electrical characteristics of each bus are presented after a brief survey of the system.

Boards and vendors have proliferated alongside the personal computer systems. The benefits include lower cost, a wide choice of boards and a better fit to specific requirements. There is only one problem. The information available about such boards is so massive that it would require volumes to present it completely. For this reason the section on boards compatible with the Apple II does not attempt to be all inclusive: the examples presented are indicative of the types of board commercially available, and are supplemented by a section on where to find additional information.

At the 1984 Pittsburgh Conference[3] it appeared that the two personal computers most widely used for laboratory applications were the Apple II+ and the IBM PC. The backplane bus structure of the latter is discussed in a companion article.[4]

THE APPLE II FAMILY OF PERSONAL COMPUTERS

From the original Apple I (a kit introduced in 1975) to the latest Apple Lisa, Apple[5] has come a long way. Apple II deserves its success for three main reasons: reliable design, complete documentation and a plethora of secondary source software and hardware.

Having avoided the mistakes that the mainframe and minicomputer giants made, namely unreadable documentation and "user-hostile" design, Steven Jobs and Steve Wozniac designed Apple II, probably under the influence of what was to become the IEEE 696/S-100 bus, as the first semi-reconfigurable, well documented personal computer system.

Both Apple II and its newer version, the Apple II+, have an 8-slot backplane bus on the main printed-circuit board, as shown in Fig. 1. The bus

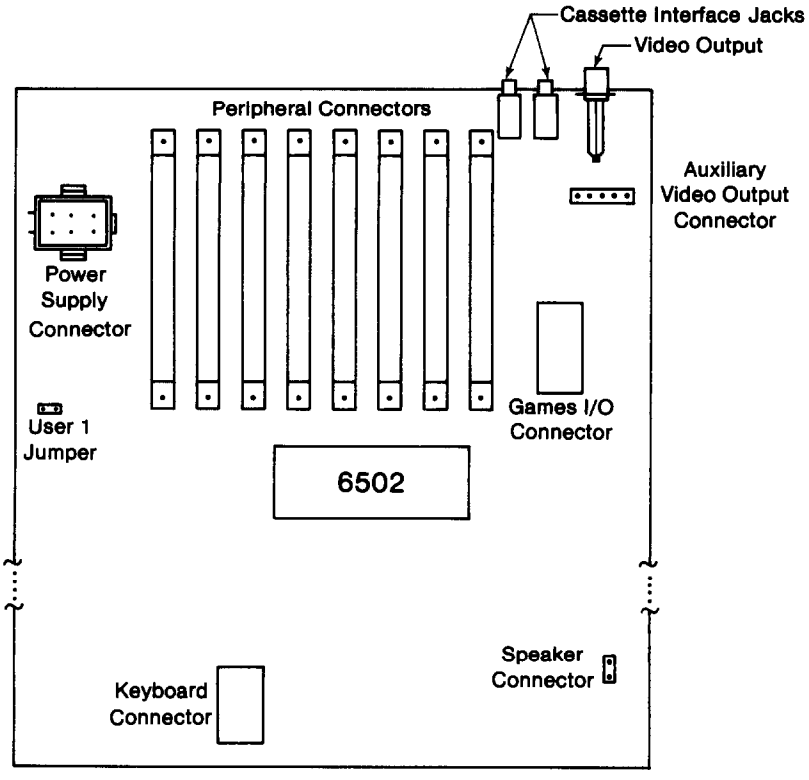

Fig. 1. Apple II+ printed-circuit board.

accepts any combination of peripheral boards with the exception of slot zero. Furthermore, Apple encouraged vendors to develop additional hardware and software for its systems, which has resulted in a variety of peripheral boards to choose from, a backplane bus to plug them into and software to support them. A system can be easily expanded or reconfigured as specific needs develop. This is of paramount importance for users with diverse needs, such as those found in a laboratory. No other system has had more software written for it than the Apple II+. It comes as no surprise that the Apple II+ is one of the most popular microcomputers for laboratory applications and among instrument manufacturers.

The standard Apple II+, though not the most modern design, is very reliable. Though its 6502 8-bit CPU with its 64-kbyte addressing capability imposes certain limitations, expansion to 128 kbytes can be achieved by bank-switching techniques, but this requires extensive software supervision and is not easily implemented for systems without memory-management capabilities. Integration of word processing with data-base management for automatic report writing is difficult because of the limited addressing capability. For such integration to be successful the Apple II+ must rely on disk I/O; one way to avoid the shortcomings of this is to utilize a "pseudodisk". The BUDDISK,[6,7] for instance, is a 128-kbyte memory board designed around Intel's 7110-4 bubble memory chips. This board allows the Apple II+ to access data at much higher speeds than by disk I/O.

Developments of this type could result in "diskless computer systems". "Soft disks" or "disk emulators" utilizing RAM chips offer an alternative to bubble memory-based mass-storage for high-speed data retrieval. Gilbert[8] describes four RAM disk emulators available for the Apple II.

The Apple II+ showed its age in 1982, when newer microcomputer designs appeared, and obviously buyers were choosing it not for its hardware but because of the software and add-on features available for it. Apple therefore introduced (early 1983) the Apple IIe,[9] an enhanced Apple II+ version. It has fewer parts, 64-kbyte memory easily upgradable to 128 kbytes, a 63-key keyboard with built in upper/lower case capability and special function keys. The main features of II+ and IIe are summarized in Table 1. The main differences are internal. The main printed circuit (pc) board of Apple IIe has been completely redisigned, and two custom-designed ICs, the IOU and the MMU, reside on the pc board. The Input Output Unit (IOU) and the Memory Management Unit (MMU) generate all memory addressing and I/O decoding signals. The IOU generates several other signals, including video (according to both American and European standards), video timing and keyboard control signals.

Table 1. Selected Apple II+ and Apple IIe features

	Apple II+	Apple IIe
Processor	6502	6502
Clock, *MHz*	1 MHz	same as II+
Selected add-on processors	Z80, 8088, 6809, 6502C, 68000, 8073	same as II+§
Arithmetic processors	9511, add-on module	same as II+§
Memory, min; max, *kbytes*	48, 128*,	64, 128*
Disk-drive, standard	140-kbyte, $5\frac{1}{4}$-in, floppy	same as II+
Keyboard	53-key, QWERTY	63-key, QWERTY
Upper/lower case	Optional plug-in module	Built-in
Function keys	No	Yes
Extras required†	Monitor (B/W)	same as II+
Screen format:		
Text	40 H × 24 V	same as II+
80-column display	Optional plug-in module	same as II+
Low-resolution graphics	48 H × 40 V, 16 colours	same as II+
High-resolution graphics	192 H × 200 V, 6 colours	same as II+
Peripheral slots	8	7§
Connectors	Games I/O connector	Games I/O connector, auxiliary connector
Operating systems	DOS, CP/M-80, Pro-DOS‡	same as II+

*Because it cannot address all memory at once, it cannot be considered as 128 kbytes.
†Minimum configuration.
‡For more details see R. Malloy, *Byte*, 1984, **9**, No. 2, 252.
§Most Apple II+ boards are claimed to be compatible with Apple IIe.

Apple IIe supports a 7-slot backplane bus. Pins, signals and backplane connector are identical with the ones found in Apple II+. The former slot zero is no longer present. The new auxiliary connector can be used in a variety of ways, including the interfacing of special test equipment. Most of the peripheral boards available for Apple II+ are claimed to be compatible with Apple IIe. The software situation is more complicated, however. Although high-level languages, such as BASIC or Pascal are compatible with both systems, the redesigned monitor can cause problems for programs containing assembly language subroutines or "strange" monitor calls. The new data-base management (Quickfile IIe) and the new word-processing software (Applewriter IIe) are compatible, meaning that word-processing software can access data-base management files, an important feature for automatic report-writing software.

Since all members of the Apple II family (II, II+ and IIe) have the same backplane bus structure, the term Apple II will be used hereafter to refer to the entire family.

THE APPLE II PERIPHERAL I/O BUS

This bus is an 8-slot (numbered from 0 to 7) backplane supporting a wide variety of I/O and memory boards. Peripheral I/O pins and signals are listed in Table 2, and a diagram of a peripheral slot is shown in Fig. 2. With BASIC, peripheral boards can be placed in any slot except slot zero (which is reserved for memory expansion). Apple II Pascal, however, is a slot-dependent language. For example, a super serial card supporting an RS-232C interface should be connected to slot 1 for communication with a printer or slot 3 for terminal emulation.

Bus characteristics

Since Apple II is a 6502-based design, its backplane bus supports all the signals delivered by that particular CPU. A line is also available for DMA operations. The bus accommodates non-maskable interrupts and provides daisy-chain maskable interrupt capability.

The bus is synchronous and non-multiplexed. The data-bus width is 8 bits, and the address-bus width 16 bits.

Sixteen memory locations are reserved for I/O for each of the peripheral slots, and are selected when the $\overline{\text{DEVICE SELECT}}$ signal becomes active. A 256-byte page is also reserved on every peripheral slot with the exception of slot zero. These memory locations are accessed by making the $\overline{\text{I/O SELECT}}$ line low.

Each peripheral slot can also support a 2-kbyte ROM, that usually holds the board's driving subroutines. This allows such routines to be placed on the peripheral card instead of being "patched" into the operating system later. This increases the reliability and ease of use of the peripheral board and the compatibility of Apple II with its interfaces. However, only one ROM can be active at a given time and each ROM must have an "enable" flip-flop, which is enabled (and disabled) by the $\overline{\text{DEVICE SELECT}}$ signal. ROM selection is achieved by combining the $\overline{\text{DEVICE SELECT}}$ and the $\overline{\text{I/O STROBE}}$ signals. In addition, there are 64 memory locations (8 bytes per slot) reserved in the system's RAM for use as scratch-pad memory.

Table 2. Peripheral I/O signals

Pin number	Signal name	Description	I/O function
1	$\overline{\text{I/O SELECT}}$	Derived from address decoders it can be used as a chip-select signal. This signal becomes active (low) on a particular slot when any of the 256 memory locations assigned to this slot are addressed. The signal is not present on slot 0. It can drive up to 10 LSTTL loads.*	O
2–17	A0–A15	Buffered address bus. Each line can drive up to 5 LSTTL loads.*	O
18	R/$\overline{\text{W}}$	Buffered Read/Write "Not" signal. This line can drive up to 2 LSTTL loads.*	O
19	SYNC	Available only on slot 7 and is connected to the video SYNC signal.	O
20	$\overline{\text{I/O STROBE}}$	This signal is common to all periperal slots. Becomes active during $\phi 0$ when a memory location between $C800 and $CFFF is addressed. This line can drive up to 4 LSTTL loads.*	O
21	RDY	Ready signal derived from 6502 CPU.†	I
22	$\overline{\text{DMA}}$	Direct Memory Access control line.† Any peripheral board can activate this line and thus gain access to the computer's buses. Data, address and R/$\overline{\text{W}}$ lines are floated and the $\phi 0$ clock is inhibited.	I
23	INT OUT	Daisy-chain interrupt output† to lower priority devices. Slot 0 has the highest priority, while slot 7 has the lowest. Any board not using interrupts must pass the INT IN to INT OUT to prevent a break in the chain.	O
24	DMA OUT	Daisy-chained Direct Memory Access output† to lower priority devices. If not used on a particular board, it should be connected to the DMA IN pin to avoid a break in the chain.	O
25	+5 V	+5 V d.c. regulated power supply providing up to 500 mA.‡	
26	GND	System ground.	
27	DMA IN	Daisy-chained DMA input from higher priority devices.	I
28	INT IN	Daisy-chained interrupt input from higher priority devices.	I
29	$\overline{\text{NMI}}$	Non-Maskable Interrupt. When this line becomes active (low), the processor begins an interrupt cycle and executes an interrupt handling routine. Memory locations $3FB, $3FC and $3FD hold the jump instruction to the NMI handling routine.	I
30	$\overline{\text{IRQ}}$	Interrupt Request. When this line becomes active (low), the processor begins an interrupt cycle only if the Interrupt Disable (I) status flag is reset. In such a case the processor executes the interrupt handling subroutine whose address is stored in locations $3FE and $3FF.	I
31	$\overline{\text{RES}}$	Microprocessor's RESET line.	I
32	$\overline{\text{INH}}$	When the inhibit line becomes active (low)†, it disables all on-board ROMs.	I
33	−12 V	−12 V d.c. regulated power supply providing up to 200 mA.‡	
34	−5 V	−5 V d.c. regulated power supply providing up to 200 mA.‡	
35	COLOUR REF	The 3.580-MHz Colour Reference line is available only in slot 7.	O
36	7 M	Provides a 7.159-MHz timing signal.	O
37	Q3	An asymmetrical, general-purpose timing signal operating at twice the frequency of the system clock. This line can drive up to 2 LSTTL loads.*	O
38	$\phi 1$	Phase 1 system clock, 1.023-MHz, complement of $\phi 0$.	O
39	USER 1	Used in conjunction with the USER 1 jumper. When the jumper is connected and pin 39 becomes active (low), all internal I/O decoding is disabled. The $\overline{\text{I/O SELECT}}$ and $\overline{\text{DEV SELECT}}$ lines remain high for as long as USER 1 is high, regardless of the status of the address bus.	I
40	$\phi 0$	Phase 0 (or microprocessor's $\phi 2$ clock), 1.023-MHz, complement to $\phi 1$. This line can drive 2 LSTTL loads.*	O
41	$\overline{\text{DEV SELECT}}$	The Device Select signal is derived from address decoders. It becomes active on a particular slot when any of the 16 bytes reserved for the same slot are addressed. This line can drive 10 LSTTL loads.*	O
42–49	D0–D7	Buffered bi-directional data bus. Each line can drive one LSTTL load.*	I/O
50	+12 V	+12 V d.c. regulated power supply providing up to 250 mA.‡	

*Loading limits refer to each peripheral board.
†This line is held high by a 3-kΩ resistor.
‡For all peripheral boards.

A comprehensive guide to Apple II hardware and firmware organization that provides specific information on more than 2000 memory locations or blocks of memory, including I/O memory allocation, has been written by Luebbert.[10] The programmers' gazette that accompanies this book provides listings for all named memory locations of the Apple II system, arranged in alphabetical order. The *Apple II monitors peeled manual*[5] provides descriptions of several routines that reside in the monitor and includes address tables that allow programmers to make use of routines in the monitor for their programs. Both the guide and the monitors peeled manual are recommended.

A daisy-chain interrupt ($\overline{\text{IRQ}}$) and a non-maskable interrupt ($\overline{\text{NMI}}$) are available on all slots. White[27] has

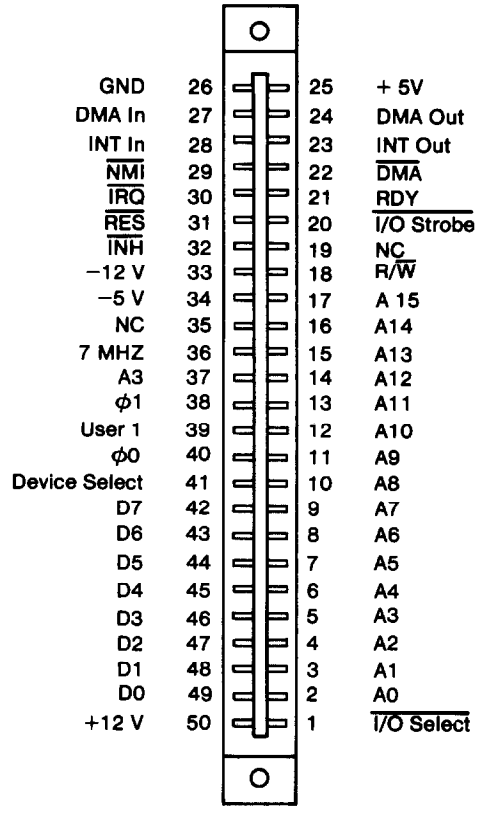

Fig. 2. Apple II peripheral connector.

discussed in detail how to use interrupts on the 6502-based Apple II.

The backplane connector has 25 contacts per side.

The number of loads supported is limited by the number of slots available on the backplane. If still more slots are needed, an expansion chassis[11] must be utilized.

The signal line length[13] is confined within the backplane or the backplane–expansion chassis combination.

Processors supported

Since the introduction of the original 16-kbyte 6502-based Apple II, new advanced CPUs have been introduced. To take advantage of these new chips and especially their vast software resources, various processor boards have been developed. Coffey[12] in an interesting, though slightly dated, article, compares several add-on processors available for the Apple II.

The "softcard".[13] The softcard was the first add-on processor card to be introduced for Apple II. Because it supports a Z80 CPU, it allows the Apple II to run a variety of programs written for CP/M. Although the softcard adds extra flexibility, it does not make the Apple II much faster. The computer's 6502 CPU must be utilized when access to I/O devices is required. The new softcard, specifically designed for Apple IIe, also provides 80-column upper–lower case video signals. The design of the softcard was innovative; it has been widely accepted and has initiated a trend. Since its introduction, add-on processor boards have been made available for almost every microcomputer on the market.

6502C Board.[14] This 6502C CPU supporting board is not intended for multiprocessing applications. Because it supports a much faster CPU, operating at 3.6 MHz as opposed to the standard 1-MHz 6502 CPU found on the Apple II, the 6502C board executes Apple software approximately 3.5 times faster. Although no software modification is necessary for successful operation of this board, extra boards populated with memory chips having shorter access times are required in order to take advantage of its speed. A 6502C board with its own 64-kbyte RAM on board is also available.[15]

8088 *Boards.*[16,17] Boards supporting an 8088 CPU permit the relatively new, though powerful and increasingly popular, CP/M-86 to be implemented on Apple II, thus allowing users to utilize the extensive CP/M-86 software library. The ALF 8088 board, for example, comes with software that makes Applesoft run 2–4 times faster. It requires, however, a 16-kbyte RAM card in slot zero.

6809 *Board.*[18] This 6809 CPU supporting board allows software developed for a 6809-based system (*i.e.* the TRS-80 colour computer) to run on Apple II. The board comes with its own operating system (OS-9) and a version of the BASIC language. The operating system includes Unix-like features such as multi-tasking and hierarchical file directories, while the language is a hybrid between BASIC and Pascal. It is claimed that the board increases Apple's throughput by approximately 25%.

68000 *Boards.* The "Dtack grounded board"[19] designed around Motorola's 68000 CPU, is aimed at sophisticated programmers who want the speed and power of a 16/32-bit CPU. The board does not fit inside the Apple case; it resides outside the computer and is connected to it by a ribbon cable. The package comes with a modified DOS version.

68000-based boards that fit inside the Apple II case are also available.[20–22] It is claimed[20] that such boards can increase Apple II's computational speed by a factor of 2–20. The PDQ II board,[20] for example, comes with 256-kbyte RAM, DOS 3.3 and UCSD p-system interpreter. The iBS board[21] supports a 7-MHz processor, a 14-bit timer and 128-kbyte RAM. Software for this board includes an Editor/Assembler and Forth for 68000, Pascal, BASIC and FORTRAN compilers for 68000 and CP/M-86K with C-compiler. Both boards have provisions for memory expansion up to 1 Mbyte.

A plug-in board that includes appropriate software allowing the Apple to act as a low-level development system for Assembly-language programming for the 68000 series of CPU's is also available.[22] The board employs a 68008 CPU, an 8-bit data-bus version of the 68000. It can be plugged into any slot and can

share all of the Apple II's I/O facilities, including the display. The processor may be started, stopped or interrupted from the keyboard. When executing, the 68008 runs simultaneously with the 6502, permitting 1-MHz operation. With its own 16-kbyte RAM (on-board expandable to 32 kbytes) the 68008 runs at 7 MHz. A 50-pin expansion connector attached to the board provides for peripheral or memory expansion.

Single board microcomputers. Microbasics[23] is marketing "Boothware", a set of hardware and software tools that facilitate program development for the National Semiconductor INS8073 processor. Boothware's hardware consists of a 4-MHz, 8073 CPU with Tiny BASIC included on chip, 8 kbytes of static RAM and a Universal asynchronous receiver–transmitter (UART). Although this board can be directly connected to a teletype for software development, the board must be connected to one of the Apple II's expansion slots in order to take full advantage of Boothware's software development tools. Apple-to-Boothware driver and development software is included on floppy disk. The software allows Apple II resources to be used for program development for the 8073.

All of the 8073's pins are available as wire-wrap pins, and the board provides a prototyping area for custom-designed interfaces. The board also supports vectored interrupts, external reset, and communication with the Apple through the UART. Up to six Boothware boards can be plugged into an Apple II. Such multiple boards can be used to monitor and control fully independent processes in the laboratory, thus forming an exciting low-level, low-cost multiple processor environment around the Apple II. The board can also function as a stand-alone single-board microcomputer system. Once the appropriate interfaces have been designed, the program(s) can be burned into an EPROM and the board can be removed from the Apple, connected to a +5 V power supply and used as a dedicated microcomputer.

Arithmetic processor—the 9511 board.[24] The MicroSPEED board houses a 9511, an Advanced Micro Devices floating-point processor chip. This board can be used to speed up the Apple II, especially for applications requiring extensive arithmetic. All data transfers, including commands and status information as well as operands and results, take place over an 8-bit bidirectional data bus. The board can fit in any slot, except slot zero, and comes with good documentation and extensive software, including BASIC, Pascal and Forth compatibility. The operator's manual that accompanies the board provides a detailed discussion of Forth. Although the 9511–Forth combination provides better performance than BASIC, programming and debugging in Forth is certainly more difficult than programming in BASIC. The 9511 can perform single (16-bit) and double (32-bit) precision arithmetic. However, it provides only seven decimal-digit precision as opposed to nine-digit precision provided by Applesoft BASIC.

For time-consuming functions such as sine, cosine or square roots, the 9511–6502 combination forms a winning team. It can be up to 100 times faster than plain Applesoft BASIC. For less complicated functions, such as multiplication and division, no real gain is realized. This is because format incompatibilities between the 9511 and the 6502 require a time-consuming conversion to be perfomed before any operation can take place. Finally, other 9511-based boards are also available.[25,26]

Power supply

Apple II's power supply provides ±5 V and ±12 V to the backplane. No more than 1.5 W should be drawn per board. An expansion chassis must provide its own power supply.

PERIPHERAL BOARDS

Prototyping boards

Boards for custom-designed interfaces and prototype development are commercially available. It is recommended that data, addresss and several control lines be buffered in order to avoid loading.

Data-acquisition and control boards and subsystems

The following is not intended to be an all-inclusive review of what is available for the Apple II and its backplane. Examples ranging from simple peripheral boards to specialized systems are chosen to represent the variety available.

For simple data-acquisition, interfaces such as the Interactive Structures.[28] 16-channel, 8-bit ADC board (the AI02), or the AI13, a 16-channel, 12-bit ADC front-ended with a programmable-gain amplifier can provide solutions to several laboratory problems. For more demanding applications, complete data-acquisition and control systems packaged on separate expansion chassis, such as Cyborg's ISAAC data-acquisition system,[29] can be utilized. This particular system has been described in the literature quite extensively. Hall and Winterlin,[30] for example, describe how the ISAAC system has been used in the acquisition of chromatographic data, and Kramer[31] describes the same system and discusses, in some detail, how it can be used to upgrade an X-ray diffractometer, a mass spectrometer, and a graphite-furnace atomic-absorption spectrometer.

A unique modular data-acquisition system has recently been introduced[32] by Acrotechnology.[33] The Acrosystem 800 is controlled by its own 8088 CPU and comes with Apple-compatible software. The system's modules interlock to form a single unit that supports up to eight I/O modules. Keithley's DAS 500 measurement and control system[34] is another recent introduction compatible with an Apple II (or IBM PC). This modular system is built around a card cage which supports up to 272 channels of analogue

input, 50 channels of analogue output, 160 channels of digital I/O, and AC/DC device-control. The maximum data-acquisition rate for the Apple II version is set at 27 kHz. Dynamic Solutions Corp.[35] is marketing yet another system which provides a 160-channel, 12-bit ADC and offers a 20-kHz data-acquisition rate. Software accompanying this system includes signal averaging, smoothing, peak detection, noise filtering and FFT (fast Fourier transform), among others. Further, a version of this software is available for Cyborg's ISAAC system. Interactive Microware[36] is marketing a data-acquisition and control system specifically designed for chromatography. This system can simultaneously control up to four GCs or HPLCs, support a gradient programmer which controls two pumps, and offer an event-controller for digital I/O.

Of course, other stand-alone data-acquisition and control systems, *i.e.*, systems providing their own intelligence and I/O and communicating with the host through serial or IEEE-488 interfaces, such as the Taurus systems,[37] can be easily coupled to an Apple II. Serial or IEEE-488 interface boards[38] are readily available and fairly inexpensive. Thomson[39] has briefly described automation of a laboratory temperature-control system with an Apple II and IEEE-488 interface. Sample software listings were provided.

Boards capable of turning an Apple II into a storage oscilloscope,[40] such as the aScope[41,42] have been available for quite some time. RC Electronics[43] have taken this idea one step further: their computer-scope can act as a user-programmable multifunction instrument. It can function as signal averager, digital-storage scope, spectrum analyser, programmable function-generator and strip-chart recorder. Software that provides high-resolution multiple trace display and histogram analysis is also included.

Boards accommodating specialized applications, such as pulse-height analysis,[45] or subsystems converting the Apple II into a real-time audiospectrum analyser,[44] have also been developed. Moreover, boards supporting digital I/O (serial or parallel), temperature sensors or even voice I/O, are just a part of the inventory of every "self-respecting" computer store.

Advanced interface boards

Since a personal computer usually functions both as the "main-processor" and as the "man–machine" interface processor, the way the computer presents data to the operator (*i.e.*, the graphics) or the way the operator presents control information to the computer (*i.e.*, task allocation in a menu-driven system) becomes increasingly important. Several boards that increase the quality of the man–machine interface have been developed for the Apple II. Computer Technology Associates,[46] for example, market a touch-sensitive display for Apple II, based on infrared emitter–sensor technology and offering a 96 × 64 point resolution. The interface card plugs into any of the peripheral slots. When an operator is busy doing several things at once, such as monitoring a process and a video display or a number of controls and indicators, voice data-entry and automatic speech-recognition become viable alternatives. Such systems are also commercially available.[47,48] It is worth noting that speech-recognition systems, although not based on Apple II, have already been incorporated into commercially available analytical instrumentation systems.[49]

The field of optical character- or object-recognition has been the subject of extensive research in the past several years. Optical recognition systems, however, have been quite expensive. The introduction of the IS32 optic RAM chip,[50] a 64-kbyte light-sensitive dynamic RAM assembled in a standard 16-pin caramic DIP package sealed with a glass window on top of the light-sensitive elements, is expected to affect the entire optical recognition field quite dramatically. The IS32 is organized into two rectangles of 128 × 256 pixels each and runs at 2–5 frames/sec in typical room lighting. A maximum operating speed of 15 frames/sec can be achieved with 64 × 128 resolution. Its spectral sensitivity covers the range from the visible to the near-infrared. A fairly inexpensive (< $300) board, including the optic RAM, a standard TV-camera lens and software that produces grey-scale high-resolution images, is available.[50,51]

Ciarcia[52,53] has provided a detailed description of the hardware and software needed to interface a camera based on the IS32 optic RAM to an Apple II. Wieland[54] describes the Microneye, a commercially available camera[50] based on the same optic RAM chip and suggests possible applications. However, he fails to mention some of the most exciting uses of the optic RAM chip, such as robotic vision systems, which could be utilized in an industrial environment to guide assembly-line robots or in the laboratory as an integral part of a sample-preparation station. Sample preparation and laboratory automation can benefit from inexpensive robots, such as Microbot's Alpha or Teachmover.[55] Taking a different approach, Rogers Labs[56] have recently introduced a robotics-development subsystem which can be utilized in diverse laboratory applications requiring two-axis motion control. This subsystem consists of an Apple II compatible plug-in board, a dual-axis driver board and a stepper motor. The board can also receive input pulses from rotary encoders or other position-measuring devices. For analytical applications, however, a board that provides an interface to a balance is at least as important as a robot or as a robot's "vision". Goegelman and Petrucelli[57] describe the "softweigh",[58] a two-channel balance-interface which is designed to mate Mettler[59] balances to an Apple II. This paper also provides several "how-to" examples. It should be noted that Mettler balances can also be interfaced to personal computers through an IEEE-488, RS-232C, or BCD interface.[60]

The notion that a picture is worth a thousand words has led to the design of modern data-presentation software and to hardware supporting high-resolution graphics. Number Nine Computer Engineering,[14] for example, market a high-resolution board that more than doubles the resolution provided by the standard Apple II. The board provides a 16-colour, 512 × 512 pixel resolution. Most of its functions, such as zoom, scroll and plane selection are software-controlled. Polaroid[61] market the Polaroid pallet, an interactive film recorder that produces quality 35-mm slides and instant photographs of computer graphic images, either from black and white or from a colour monitor. It connects to the computer through the video monitor and an RS-232C interface. The package also includes appropriate software.

Networks supported

One of the first "local area networks"[62] to be introduced was the Corvus Constellation network.[63] Its "star" topology supports up to 64 microcomputers. Corvus now offers Omninet,[64] a 1-Mbit/sec baseband carrier-sense multiple-access network, connecting many popular computers (*e.g.*, Apple, IBM PC, Corvus and DEC LSI-11) over a single twisted-pair cable meeting the RS-422 standard. As many as 64 microcomputers or peripheral devices, each with an intelligent interface installed, can be supported.

The Cluster/One network[65,66] uses a 16-wire cable to link up to 64 Apple II microcomputers. Because of its non-restrictive topology, it can support any configuration within a limit of 1000 ft of network cable. The network runs at 240 kbit/sec and utilizes carrier-sense multiple access with collision detection. The Plan 4000[65] is now replacing the older Cluster/One. It is a 2.5-Mbit/sec baseband token-passing LAN designed to connect up to 255 Apple IIs, Apple IIIs and IBM PCs.

A GLIMPSE OF APPLE II'S INFORMATION BASE

The information available for the Apple II is so massive that no one could hope to cover every single article or book ever written for it. What follows, however, is an attempt to direct users to where to find information related to Apple II.

Magazines

Traditionally, every successful personal computer system has had at least one magazine dedicated to it. The self-proclaimed reference magazine for Apple computing is *Nibble*.[67] This monthly publication contains a wealth of information concerning Apple II hardware and software. The *InCider*,[68] a monthly *80 Micro* sister publication, is also dedicated to Apple II hardware and software.

Although most personal computer magazines carry hardware and software reviews, *Peelings II*[69] is dedicated to Apple hardware and software evaluation. Some of its product reviews and comparisons are quite critical.

Call-A.P.P.L.E.[70] is a monthly publication dealing only with software. It contains easy-to-follow articles on programming techniques and Apple II firmware. It also publishes user-developed software. Programs appearing in Call-A.P.P.L.E. are available in *Source*.[71]

There are over 20 magazines and newsletters dedicated to Apple's microcomputers. Included are: *A+*,[72] the magazine for Apple microcomputing; *Apple Orchard*,[73] featuring articles on applications, peripherals and software; *Softalk for Apple Computers*,[74] a software-oriented publication. Other monthly publications carrying, in every issue, articles on Apple II or reviews of Apple II hardware and software, include: *Compute*,[75] a 6502 resource magazine publishing general interest articles; *Creative Computing*,[76] the magazine of personal computer applications and software; *Micro*,[77] the 6502/6809 resource magazine; and *Byte*,[78] a respected small-systems magazine.

Interfacing

Despite the variety of data-acquisition and control boards commercially available for the Apple II, certain laboratory applications require the construction of custom-designed interfaces. Selected books and articles dealing with Apple II interfacing are considered next.

The book by Gayler[79] is recommended for those who want to master Apple II's hardware. It provides a detailed circuit description of all Apple II motherboards, including the keyboard and power supply. An interesting book on Apple II interfacing, by Titus *et al.*,[80] includes several well-documented data-acquisition and control projects and provides listings of driving subroutines for all the interfaces described. This book, however, assumes that the user already has some experience with assembly language programming. Coffron's book[81] is one of the few written for the novice. Its primary focus is on software and hardware required to control external devices. The book by Hallgren[82] includes several well-thought-out interfacing projects. Unusual interfacing projects are included in a book by Hofacker *et al.*[83] Although it introduces several advanced interfacing concepts, most of the projects discussed are not suitable for implementation in laboratory applications.

An interface providing a 27 μsec analogue to digital conversion utilizing Analog Devices[84] integrated circuits (*e.g.*, the AD 582 sample-and-hold amplifier and AD 571 ADC) is described by Seeds,[85] while a simple interface of an x–y plotter with an Apple II is discussed by Hallgren.[86] Digital I/O is discussed by Ciszewski,[87] who also provides the interface schematics and driving subroutines for Motorola's 6821 chip. How to turn an Apple II into a storage oscilloscope is described by Korba.[88] Finally, five articles

dealing with real-world interfacing capabilities of microcomputers (including the Apple II) appeared in the April 1984 issue of *Byte*.

Several of the articles reviewed here provide detailed information, so the interfaces described can be fairly inexpensively built in the laboratory. Construction of such boards, however, is recommended only to those who want to gain experience with interfacing techniques.

Laboratory applications

Numerous examples can be found in the scientific literature of incorporation of an Apple II into a measurement system. A few examples are provided in this section. Chornik[89] provides a detailed hardware description of an interface between an Apple II and a Varian Auger spectrometer, including changes that had to be made in the original spectrometer to fit specific needs. The use of an Apple II in infrared work, for instrument control, data logging and data analysis has been presented by Adams *et al.*[90] The computer is interfaced with dispersive and Fourier-transform spectrometers and its performance is compared with that of commercially available instruments. Meiri *et al.*[91] provide the details of an Apple II controlled flash-photometry system with sub-microsecond resolution and of a Raman spectroscopy experiment. The interfacing of the two spectrophotometric systems is described in detail. Apple II's DMA (direct memory access) capability is also explained. A multichannel system for recording, viewing and plotting of multichannel analogue signals is described by Lee,[92] and Evans[93] describes the design and construction of a multiple photodiode-array direct-reading spectrometer controlled by an Apple II.

Bordes *et al.*[94] describe, in detail, a system based on a commercially available black-and-white TV camera and an Apple II microcomputer. Although the system is capable of real-time image analysis, the resolution offered (40 × 48 pixels) is poor. Russ *et al.*[95] describe an Apple II system capable of feature-discrimination and counting of images produced by techniques ranging from laboratory microscopy to aerial photography. This particular system is based on the ImagePlus + automatic image analyser.[96] It utilizes video and graphics tablet input, offers a 256 × 256 pixel resolution, and provides 64 levels of grey-scale.

Baadenhuijsen *et al.*[97] have designed a stand-alone read-out system for peak-recognition, data-processing and result-presentation, for a continuous-flow analyser. Deininger *et al.*[98] provide the details of an interface between an Apple II and a Technicon "AutoAnalyzer". Microcomputer software for data-acquisition and manipulation with an Apple II as the target system is discussed by Walling *et al.*,[99] who briefly discuss signal-conditioning electronics, and describe in some detail applications ranging from gas chromatography to Raman spectrometry. Dydula *et al.*[100] provide a set of guidelines for personal-computer selection for the clinical laboratory and discuss several practical examples based on an Apple II.

Gour-Salin *et al.*[101] have interfaced a spectrophotometer, an automatic titrator and a liquid chromatograph to an Apple II, using commercially available modules. The hardware and software used are described and a list of vendors is provided. Finally, Owens and Eckstein[102] describe the construction and performance of a robotic sample-preparation station, consisting of an Apple II microcomputer, a robot arm, a pipette/burette, a solvent dispenser, a pH-meter and a balance. Although their approach to sample manipulation is somewhat simplistic, it allows for total automation of a pH-titration, from standards preparation and calibration to final-report generation. Such an approach could be expanded to include sophisticated sample preparation, thus leading the way to a "complete" sample-preparation station.

Software

For most laboratory applications, there is a need for applications-specific software. The synopsis (by Poole *et al.*[103]) of Apple II manuals is highly recommended to both experienced and inexperienced programmers: it can be used as a guide complementing these manuals. DOS version 3.3 is the focus of a book by Worth *et al.*[104] This book is a valuable tool to those who wish to understand the structure and intracacies of Apple II's Disk Operating System (DOS). Other "bookware", such as "What's Where in the Apple"[10] and the Apple II monitors peeled manual,[5] as mentioned earlier, can help programmers take full advantage of the Apple II's power.

Several books specifically written for Apple II BASIC[105–110] address the need for custom-designed software. Books providing "ready-to-run" general purpose[111,112] or scientific and engineering programs,[113,114] may help programmers get started or may aid the novice in taking first steps in programming. For applications requiring faster execution than that provided by an interpreter BASIC, the use of a compiler BASIC is recommended. Taylor[115] sets the guidelines on how to choose a compiler and compares five compilers available for the Apple II. Callamaras[116] reviews the Einstein compiler,[117] which, in addition to speeding up Applesoft BASIC, provides statistical information on the programs compiled and can function as a debugging tool.

BASIC is not the only language that can be used with the Apple II. Pascal is gaining increasing popularity among users. Several reference texts are available for Apple II Pascal.[118–121] FORTRAN, however, has never had the success BASIC enjoys in use of personal computers. Blackwood *et al.*,[122] in a poorly written book, attempt to aid the beginning programmer wishing to learn Apple II's version of FORTRAN 77. A detailed discussion of the LOGO programming language, which has become famous

for its turtle graphics, is included in a book by Abelson.[123]

Assembly language programming, though not the favourite of many programmers, is essential when speed is the prime consideration. DeJong[124] has written an interesting book on Apple II assembly-language programming. It assumes that the reader has some working experience with the topic and places special emphasis on control applications. Both Scalcon's[125] assembly-language exercises, and Laventhal's[126] assembly-language subroutines include several well written and documented subroutines that can be incorporated in a variety of progams. However, both books are best suited for experienced assembly-language programmers. Unlike these volumes, Hyde's book[127] is recommended to beginners. It is intended for use with LISA, a disk-based assembler marketed by the book's publisher. The book by Inman *et al.*[128] can be consulted on Apple II machine-language programming, but it partially relies on the use of the mini-assembler which is available on the Apple II but not on the Apple II+. Finally, for those interested in a more specific presentation of 6502 assembly language topics, several books are available.[129–133]

The incorporation of graphics is an important feature for data display. Roybal[134] discusses Apple II's high-resolution features, and Lancaster[135] suggests various ways of mixing text with high- and low-resolution graphics, including three-dimensional representations. Pickholtz[136] discusses the theory of perspective as a means of understanding and reproducing three-dimensional graphics, and Sokol[137] provides special routines that link Apple's graphics tablet to UCSD Pascal for a computer-aided drafting project. Finally, books describing Apple II's graphic capabilities are also available.[138,139]

File manipulation and word processing are important for laboratory data-base management and report-generation software. Miller[140] discusses various ways of file manipulation, and Finkel *et al.*[141] provide a self-teaching guide to file manipulation in Apple BASIC. Eyes[142] describes how to use binary format for number storage on Apple II's disk, and Matthews[143] discusses how to exchange information between DOS and Pascal files. Poling[144] provides an in-depth, though not complete, survey of word processing with the Apple II. This book presents an examination of nine word-processing and two spelling-correction programs for the Apple II. However, "integrated software" packages are not included, because they did not appear until after the book was published. Carlson *et al.*[145] also critically review word processors (four) for the Apple II.

Although last year's software was claimed to be "user friendly", many programs proved difficult to master. The currently fashionable adjectives for the new generation of software are "integrated" and "supportive of multiple windows". Arktronics[146] market one of the first programs for Apple II that integrate list management, word processing and spreadsheet facilities within a single package. This program is accompanied by a "mouse" and an interface card.

Software that allows users to perform simulated experiments, such as VisiCalc[147,148] can be used in the laboratory as a data-analysis tool or for forecasting. Ouchi[149] has used VisiCalc and Apple II to simulate chromatography experiments. It should be noted that VisiCalc is the most popular software package ever developed. More than 700,000 copies have been sold since its introduction in 1979. Clearly, part of Apple II's success is due to software packages such as VisiCalc.

Product directories

Undoubtedly more hardware and software packages are available for the Apple II than for any other personal computer on the market. Ironically, the plethora of products compatible with Apple II makes it impossible for the individual to keep track of what is commercially available for this personal computer. Because of this information overload, or "information pollution" as it is often called, product directories become indispensable tools for the user. The new edition of the *Apple Blue Book*,[150] for example, is a well-documented where-to-find-it guide to products compatible with Apple II. The entries are categorized by function and by vendor. Approximately 10% of them are not software-oriented; these include boards, accessories, peripherals, and a limited number of books and magazines. *Vanloves Apple II/III Software Directory*,[151] includes over 2300 entries, classified under subject headings. It also features a cross-referenced list of vendors, listings of user groups and software publishers, and a glossary of computer terms. Although it proclaims itself the most comprehensive of Apple product directories, the lack of a comprehensive alphabetical index makes information retrieval difficult. Unlike the *Blue Book* or the *Addison-Wesley Directory*, the Vanloves directory omits both the hardware requirements and the price of each individual software package, thus providing an incomplete picture of the product in question.

Entries in the *Addison-Wesley Software Directory*,[152] are grouped into four major categories: business, education, utilities, and games. Listed for each software package are the vendor, the program language, the suggested retail price, and availability. Unlike Vanloves and the Blue Book, where the text accompanying an entry is often a direct copy of the vendor's promotional material, each item listed in the Addison-Wesley book appears to have been thoroughly tested, rated according to several criteria, and assigned a final score. This directory includes only five hundred entries. The number of non-software entries in both the Vanlove and Addison-Wesley directories is much smaller than that in the Blue Book.

The *Software Express*[153] lists over 800 software titles for personal computers, including the Apple II. This directory has a section for each computer, with each section divided into several categories. A short narrative describes each program, while another section lists the computer model, memory requirements, disk format and peripherals required for the program to run successfully. A directory of over 800 educational software packages for the Apple II is also available.[154] Finally, current issues of microcomputer magazines, especially those devoted exclusively to Apple II, constitute the best sources of information concerning interfaces and software compatible with Apple II.

COMMENTS

Undoubtedly, Apple II is one of the most popular personal computers ever built, with more than two million sold world-wide. The backplane-bus concept, an idea popularized on the Apple II, has become standard practice, while Apple II's backplane has itself long been an Apple-imposed standard. For number of boards and subsystems available, the Apple II has not yet been surpassed by any other personal computer, although the IBM PC has become a very strong competitor. As far as software is concerned, no other system has had more written for it. To take advantage of Apple II's resources, a program allowing the TRS-80 to run Apple II software has recently been published.[155] Also, Quadram Corp.[156] market Quadlink, a multifunction board which allows most Apple II software to run on an IBM PC and XT. Taking even further advantage of Apple II's popularity, several "me, too" companies have introduced low-priced, Apple II compatible or "look-alike" microcomputers.

Perhaps one of the most important Apple II features is its wide information base. Furthermore, several measurement and control systems based on Apple II are well documented in the scientific literature, and the Apple II is probably the most widely used microcomputer in the laboratory.

Despite all this success, Apple has remained, for the most part, a one-product company. An acceptable Apple III system, a business-oriented microcomputer, was marketed a little too late. It has never had the success of Apple II, and probably never will. After a long gestation period, in January 1983, Apple finally released Lisa (Local Integrated Software Architecture), an advanced desk-top computer system designed around the Motorola 68000, 16/32-bit CPU and supported by a total of five microprocessors or single-chip microcomputers.[157–159] In spite of its advanced software concepts, which are perhaps ahead of their time, Lisa is designed for a limited audience. Its limited success to date suggests that it has been introduced a little too early. Several companies, however, are beginning to market Lisa-like software for other personal computers, although such packages attempt to do solely with software what firmware accomplishes in Lisa. In practice, almost every new integrated software package attempts to incorporate Lisa-like features. Without a doubt, Lisa's innovative concepts will become an industry standard for the next generation of microcomputers. In spite of all this innovation, Lisa has so far been a great computer that not very many wanted to buy. To remedy the situation, Apple introduced, in January 1984, Lisa-2,[160] a cost-effective version of Lisa, which is expected to be more successful than its predecessor.

For the last year or so, there have been rumours and speculation about the introduction of yet another Apple-computer, code-named "Macintosh", which was finally released in January 1984.[161,162] This second-generation, easily transportable Lisa-like desk-top computer derives its power from a Motorola 68000, 16/32-bit CPU. It also supports a 128-kbyte RAM, 64 kbytes of ROM, an integral $3\frac{1}{2}$-in. Sony disk drive (the 400-kbyte storage capacity disk is encased in a rigid plastic housing), two high-speed serial ports, a "mouse", a detachable keyboard (with its own single-chip microcomputer), and an integral 9-in. monitor which offers 512 × 342 pixel resolution. Macintosh's main printed circuit board has only 50 ICs, including eight custom-designed PAL (programmable array logic) chips. Such a low number of ICs increases reliability and reduces size and cost. Although Macintosh behaves like Lisa-2, and in fact "Mac" software will run on Lisa-2, there are several differences from it, including higher clock-rate, lower memory capacity, inherent inability to allow more than one major application program to be active at any given time (with one exception), and no backplane bus structure.

Interestingly, the Macintosh is deviating from the backplane bus concept, which Apple itself has helped to establish. Instead of backplane slots and peripheral devices, the Macintosh has what Apple calls the "virtual slot" concept, which is implemented on high-speed (up to 1 Mbit/sec) serial ports. The reasoning behind this concept is that peripherals have become "smart enough" not to need to "tie-up" the processor. Indeed, the current trend is for local "intelligence" to be developed in all sorts of peripheral devices. This, however, requires an efficient communications link between the processor and the peripheral devices.

Communications and networking are emerging as areas crucial to the next generation of computer-related projects, not only in the laboratory, but in all segments of an information-driven society. Applications that utilize Macintosh's "virtual slot" concept, smart peripherals and multiple-processor systems that are moderately or loosely coupled, are not hard to envision within the realm of laboratory automation.

Undoubtedly, a related evolution is under way in software. The Macintosh can provide unique solu-

tions to several software-related laboratory needs. Of particular significance is the unique capability of current Macintosh software to integrate text and graphic information with exceptional ease of interfacing with the operator. In a way, this represents a small step towards the "Fifth Generation" concept of computer systems.

Clearly, the Macintosh has leap-frogged the current capabilities of personal computers with significant new hardware and software concepts and capabilities, and represents both an opportunity and a challenge for use in the laboratory. It has the potential not only to become a very powerful computer in the scientific world but also to trigger a major evolutionary change in the philosophy behind laboratory interfacing and computing.

Macintosh's information base is also expanding rapidly. *Macworld* magazine[163] and several Macintosh books are currently available. In summary, Macintosh has no backplane bus structure or colour graphics capability and so far only limited software is available, but its cost/performance ratio, the quality of its Human Processor Interface, its technological innovation, and the fact that it does not place heavy demands on the user's "computer literacy", offer it a promising future.

In April 1984, Apple introduced the IIc (c for compact), a 21-IC portable microcomputer.[164] The IIc merges features of two radically different personal computers: the IIe and the Macintosh. While it is claimed to be 90–95% software-compatible with the IIe, it supports Lisa-like features, such as "icons" and a mouse, much like those found on the Macintosh. Interestingly, the IIc uses the virtual slot concept instead of a backplane bus structure.

The IIc has 128 kbytes of RAM, 16 kbytes of ROM (including Applesoft BASIC and mouse-controlled icons) a $5\frac{1}{4}$-in. floppy-disk drive, a 63-key keyboard and the ProDOS[165] operating system. It also has built-in 80-column display capability, two RS-232 serial ports, two video ports (a 16-colour and a monochrome) providing 560 × 192 pixel resolution, an external disk-drive port and a combination mouse/joystick port. Thus, IIc users have access to functions that require as many as six of the Apple II's slots.

Perhaps the most interesting features of the IIc are its flat-panel display and mains or battery power supply, both of which contribute to its portability. However, the IIc is not CP/M-compatible, it does not have a built-in modem as most portables do and has limited built-in mass storage (140 kbyte). Although the IIe currently provides a much better alternative to laboratory automation than the IIc, the introduction of the IIc exemplifies Apple's commitment to the II family of personal computers and to the virtual slot concept.

There are now rumours about the introduction of yet another Lisa-like computer (an enhanced Macintosh), which is still being kept behind closed doors. In the meantime, the Apple II family is aging rapidly. Newer personal computer designs, such as the IBM PC, are taking away Apple II's lead in the market, while the Macintosh severely limits the II's audience. However, Apple II's hardware and software resources, along with its wide information base, guarantee its survival through the 80s.

NOTE ADDED IN PROOF

The following summarizes Apple-related developments which have occurred since the paper was first written. Although this is not a complete summary, it will aid the interested reader in keeping abreast of developments in Apple's family of personal computers. Apple[5] have released *AppleWorks for the Apple II*, an integrated software package incorporating word-processing, data-base management and electronic spreadsheet. They have also released *AppleMouse II* and *MousePaint*, allowing Apple II users to utilize Lisa-like features. Finally, they have introduced the previously rumoured enhanced version of the Macintosh (often referred to as the "Fat Mac") which supports 512 kbytes of random access memory, a high-speed laser printer, and *AppleTalk*, a Local Area Network (LAN) which supports up to 32 nodes. Both the LAN and the laser printer are briefly discussed by Markoff and Robinson.[166] Also available are several languages such as BASIC, Pascal, Modula-2, FORTH, C, and Assembler; software packages, such as Microsoft's[13] *Chart* and *Multiplan*, *Tk! Solver*,[167] *Thinktank*[168] and Lotus's *Jazz*;[169] and a limited number of hard disks.[170,171]

With respect to hardware interfaces,[10] tech Inc.[172] have introduced an IEEE-488 interface which is expected to help the Macintosh migrate into laboratory use. Finally, a 144-page section of the December 1984 issue of *Byte* magazine[78] was devoted to Apple's family of personal computers.

REFERENCES

1. V. Karanassios and G. Horlick, *Talanta*, 1985, **32**, 583.
2. E. Fisher and C. W. Jenson, *PET/CBM and the IEEE-488 (GPIB) Bus*, 2nd Ed., Osborne/McGraw-Hill, Berkeley, 1982.
3. Pittsburgh Conference on Analytical Chemistry and Applied Spectroscopy, Atlantic City, N.J., 5–9 March, 1984.
4. V. Karanassios and G. Horlick, *Talanta*, 1985, **32**, 615.
5. Apple Computer Inc., 20525 Mariani Avenue, Cupertino, CA 95014.
6. P. Callamaras, *Byte*, 1983, **8**, No. 7, 226.
7. MPC Peripherals Corp., 9424 Chesapeake Dr., San Diego, CA 92123.
8. M. G. Gilbert, *Byte*, 1984, **9**, No. 2, 318.
9. R. Moore, *ibid.*, 1983, **8**, No. 2, 68.
10. W. F. Luebbert, *What's Where in the Apple. A Complete Guide to Apple Computer*, Micro Inc., Amherst, 1982.
11. Mountain Computer Inc., 300 Harvey West Blvd., Santa Cruz CA 95060.
12. M. Coffey, *Creative Computing*, 1982, December, 30.

13. Microsoft Corp., 10700 Northup Way, Bellevue, WA 98004.
14. Number 9 Computer Engineering, P.O. Box 1802, Hatford, CT 06144.
15. Titan Technologies Inc., P.O. Box 8050, 3990 Varsity Dr., Ann Arbor, MI 48107.
16. ALF Products Inc., 1315F Nelson St., Denver, CO 80215.
17. Coprocessors Inc., 50 West Brokaw Rd., Suite 64, San Jose, CA 95110.
18. Stellation Two, P.O. Box 2342, Santa Barbara, CA 93120.
19. Digital Acoustics, 1451 E. McFadden, Suite F., Santa Anna, CA 92705.
20. Enhancement Technology Corp., P.O. Box 1267, Pittsfield, MA 01202.
21. iBS Computertechnik, 1011 Rose Marie Lane 16, Stockton, CA 95207.
22. QWERTY Corp., 9252 Chesapeake Dr., Suite 600, San Diego, CA 92123.
23. Microbasics Inc., Rte. 3, Box 136, Riber Falls, WI 54022.
24. Applied Analytics, 9810 Brookridge Dr., Upper Malboro, MD 20772.
25. California Computer Systems, 250 Caribbean, Sunnyvale, CA 94086.
26. Computer Station, 11610 Page Service Drive, St. Louis, MO 63141.
27. G. M. White, *Byte*, 1981, **6**, No. 5, 280.
28. Interactive Structures Inc., 112 Bala Ave., Box 444, Bala Cynwyd, PA 19004.
29. Cyborg Corp., 55 Chapel St., Newton, MA 02158.
30. G. Hall and W. Winterlin, *Am. Lab.*, 1983, **15**, No. 8, 84.
31. R. Kramer, *ibid.*, 1983, **15**, No. 9, 46.
32. *Electronics*, 1983, **56**, No. 22, 262.
33. Acrotechnology Corp., 66 Cherry Hill Dr., P.O. Box 487, Beverly, MA 01915.
34. Keithley DAS, 349 Congress St., Boston, MA 02210.
35. Dynamic Solutions Corp., 61 South Lake, Suite 309, Pasadena, CA 91101.
36. Interactive Microware Inc., P.O. Box 771, Dept. 10, Stage College, PA 16801.
37. Taurus Computer Products Inc., 4 Limbo Lane, Amhearst, NH 03031.
38. SSM Microcomputer Products Inc., 2190 Paragon Dr., San Jose, CA 95131.
39. T. Thomson, *Am. Lab.*, 1982, **14**, No. 12, 90.
40. L. Waller, *Electronics*, 1983, **56**, No. 4, 46.
41. Northwest Instruments Inc., P.O. Box 1309, Beaverton, OR 97075.
42. J. Birck and M. Maerz, *Electronics*, 1983, **56**, No. 7. 127.
43. RC Electronics Inc., 5368 Hollister Ave., Santa Barbara, CA 93111.
44. Eventide Clockworks Inc., 265 West 54th St., New York, NY 10019.
45. The Nucleus Inc., 461 Laboratory Rd., Box R, Oak Ridge, TN 37830.
46. Computer Technology Associates, 1704 Moon NE, Albuquerque, NM 87112.
47. Voice Recognition Systems, Suite 1716, 550 Battery St., San Francisco, CA 94111.
48. MCE Inc., Personal Computer Supply, 157 South Kalamazoo Mall, Kalamazoo, MI 49007.
49. J. E. Kahdeman, *Am. Lab.*, 1983, **15**, No. 9, 110.
50. Micron Technology Inc., Vision Systems Group, 2805 East Columbia Road, Boise, Idaho 83706.
51. The Micromint Inc., 561 Willow Ave., Cedarhurst, NY 11596.
52. S. Ciarcia, *Byte*, 1983, **8**, No. 9, 20.
53. *Idem, ibid.*, 1983, **8**, No. 10, 67.
54. C. Wieland, *ibid.*, 1983, **8**, No. 10, 316.
55. Microbot Inc., 435-H Ravendale Dr., Mountain View, CA 94043.
56. Rogers Labs, 2710 South Croddy Way, Santa Anna, CA 92704.
57. M. Goegelman and S. Petrucelli, *Am. Lab.*, 1983, **15**, No. 6, 58.
58. Microsystems Research Corporation, Box 1, Cranbury, NJ 08512.
59. Mettler Instrument Corp., Box 71, Highstown, NJ 08520.
60. K. M. Lang, *Am. Lab.*, 1983, **15**, No. 3, 72.
61. Polaroid Corp., 575 Technology Sq., Cambridge, MA 02139.
62. H. Saal, *Byte*, 1983, **8**, No. 5, 60.
63. Corvus Systems, 2029 O'Toole Ave., San Jose, CA 95131.
64. M. Hahn and P. Belanger, *Electronics*, 1981, **54**, No. 17, 125.
65. Nestar Systems Inc., 2585 East Bayshore Rd., Palo Alto, CA 94303.
66. E. P. Stirrer and L. J. Shustek, *Electronics*, 1981, **54**, No. 12, 171.
67. *Nibble*, Subscription Dept., P.O. Box 325, Lincoln, MA 01773.
68. *InCider*, Box 911, Farmingdale, NY 11737.
69. *Peelings II*, 2260 Oleander, Las Cruces, NM 88001.
70. *Call A.P.P.L.E.*, 21246 68th Ave. S., Kent, WA 98032.
71. Source Telecomputing Corp., 1616 Anderson Rd., McLean, VA 22102.
72. *A+*, P.O. Box 2964, Boulder, CO 80322.
73. Apple Orchard, International Apple Core Inc., 908 George St., Santa Clara, CA 95050.
74. Softalk Publications Inc., 11160 McCormick St., North Hollywood, CA 91603.
75. *Compute*, P.O. Box 5406, Greensboro, NC 27403.
76. *Creative Computing*, P.O. Box 789-M, Morristown, NJ 07960.
77. *Micro*, P.O. Box 6502, Chelmsford, MA 01824.
78. *Byte*, Subscription Dept., P.O. Box 590, Martinsville, NJ 08836.
79. W. D. Gayler, *Apple II Circuit Description*, Sams, Indianapolis, 1983.
80. J. A. Titus, D. G. Larsen and C. A. Titus, *Apple Interfacing*, Sams, Indianapolis, 1981.
81. J. W. Coffron, *The Apple Connection. Techniques and Principles of Apple II Interfacing*, Sybex, Berkeley, 1982.
82. R. C. Hallgren, *Interface Projects for the Apple II*, Prentice-Hall, Englewood Cliffs N.J., 1982.
83. W. Hofacker and E. Floegel, *The Custom Apple and Other Mysteries*, IJG, Upland Calif., 1982.
84. Analog Devices, Norwood, Mass., 02062.
85. M. A. Seeds, *Byte*, 1981, **6**, No. 10, 458.
86. R. C. Hallgren, *ibid.*, 1981, **6**, No. 5, 296.
87. K. J. Ciszewski, *ibid.*, 1982, **7**, No. 1, 324.
88. L. Korba, *ibid.*, 1982, **7**, No. 9, 520.
89. B. Chornik, *Rev. Sci. Instrum.*, 1983, **54**, 80.
90. M. J. Adams and I. Black, *J. Autom. Chem.*, 1983, **5**, 9.
91. Z. Meiri, Y. Berezin, A. Shemesh and B. Ehrenberg, *Appl. Spectrosc.*, 1983, **37**, 203.
92. Y. H. Lee and K. T. Park, *Rev. Sci. Instrum.*, 1982, **53**, 915.
93. R. G. E. Evans, *Ph.D. Dissertation*, University of Alberta, Edmonton, Alberta, 1983.
94. M. Bordes, J. C. Bernengo and J. F. Renaud, *Rev. Sci. Instrum.*, 1983, **54**, 1053.
95. J. C. Russ and W. D. Stewart, *Am. Lab.*, 1983, **15**, No. 12, 70.
96. Dapple Systems, P.O. Box 2160, Sunnyvale, CA 94087.
97. H. Baadenhuijsen and Th. Zelders, *J. Autom. Chem.*, 1983, **5**, 18.

98. R. A. Deininger, P. J. Capano, R. L. Miller and D. Tujaka, *Am. Lab.*, 1983, **15**, No. 2, 130.
99. P. L. Walling, T. E. Gentille and A. E. Gudat, *ibid.*, 1982, **14**, No. 2, 22.
100. J. I. Dydula, O. S. Lauritsen and R. Dybkaer, *J. Autom. Chem.*, 1982, **4**, 174.
101. B. J. Gour-Salin and E. Salin, *Am. Lab.*, 1982, **14**, No. 11, 110.
102. G. D. Owens and R. J. Eckstein, *Anal. Chem.*, 1982, **54**, 2347.
103. L. Poole, M. McNiff and S. Cook, *Apple II Users Guide*, Osborne/McGraw-Hill, Berkeley, 1981.
104. D. Worth and P. Lechner, *Beneath Apple DOS*, Quality Software, 1981.
105. A. B. Tucker, Jr., *BASIC/Apple IIe. A Programming Guide*. Holt, Reinhart & Winston, New York, 1983.
106. R. Haskel, *Apple BASIC*, Prentice-Hall, Englewood Cliffs N.J., 1982.
107. H. D. Peckham, *Hands on BASIC for the Apple II*, McGraw-Hill, New York, 1983.
108. B. Presley, *A Guide to Programming in Applesoft BASIC*, Van Nostrand/Reinhold, New York, 1982.
109. J. R. Brown, L. Finkel and B. Albrecht, *BASIC for the Apple II. A Self-teaching Guide*, Wiley, New York, 1982.
110. J. S. Coan, *Basic Apple BASIC*, Hayden, Rochell Park N.J., 1982.
111. T. Rugg and P. Feldman, 32 *BASIC Programs for the Apple Computer*, Dilithium Press, Forest Grove OR, 1981.
112. L. Poole, M. Borchers and D. M. Castlewitz, *Some Common Programs—Apple II Edition*, Osborne/McGraw-Hill, Berkeley, 1982.
113. H. M. Berlin, *Circuit Design Programs for the Apple II*, Sams, Indianapolis, 1982.
114. J. Heilborn, *Science and Engineering Programs, Apple II Edition*, Osborne/McGraw-Hill, Berkeley, 1981.
115. J. H. Taylor, *Byte*, 1982, **7**, No. 9, 440.
116. P. Callamaras, *ibid.*, 1984, **9**, No. 1, 349.
117. The Einstein Corp., 11340 W. Olympic Blvd., Los Angeles, CA 90064.
118. R. Zaks, *Introduction to Pascal Including USCD Pascal*, 2nd Ed., Sybex, Berkeley, 1981.
119. A. Leuherman and H. Peckham, *Apple Pascall: A Hands on Approach*, McGraw-Hill, New York, 1981.
120. T. G. Lewis, *Pascal Programming for the Apple*, Reston, Reston Virginia, 1980.
121. M. J. Borgerson, *A BASIC Programmer's Guide to Pascal*, Wiley, New York, 1982.
122. B. D. Blackwood and G. H. Blackwood, *Apple FORTRAN*, Sams, Indianapolis, 1982.
123. H. Abelson, *Apple LOGO*, Byte Publ., New York, 1982.
124. M. L. DeJong, *Apple II Assembly Language*, Sams Indianapolis, 1982.
125. L. J. Scalcon, *Apple II Assembly Language Exercises*, Wiley, New York, 1982.
126. L. A. Laventhal and W. Saville, 6502 *Assembly Language Subroutines*, Osborne/McGraw-Hill, Berkeley, 1982.
127. R. Hyde, *Using* 6502 *Assembly Language*, Reston, Reston Virginia, 1981.
128. D. Inman and K. Inman, *Apple Machine Language*, Reston, Reston Virginia, 1981.
129. L. A. Laventhal, 6502 *Assembly Language Programming*, Osborne/McGraw-Hill, Berkeley, 1979.
130. R. Zaks, *Programming the* 6502, 4th Ed., Sybex, Berkeley, 1983.
131. M. L. DeJong, *Programming and Interfacing the* 6502 *With Experiments*, Sams, Indianapolis, 1980.
132. L. J. Scalcon, 6502 *Software Design*, Sams, Indianapolis, 1980.
133. R. Findley, 6502 *Software Gourmet Guide and Cookbook*, Hayden, Rochelle Park N.J., 1979.
134. P. Roybal, *Byte*, 1981, **6**, No. 1, 226.
135. D. Lancaster, *Enhancing your Apple II*, Sams, Indianapolis, 1982.
136. A. Pickholtz, *Byte*, 1982, **7**, No. 11, 474.
137. D. Sokol, *ibid.*, 1981, **6**, No. 7, 381.
138. K. Williams and B. Kernaghan, *Apple II Computer Graphics*, Brady, Bowie Md, 1983.
139. K. Williams, *Apple Computer Graphics*, Brady, Bowie Md, 1983.
140. D. Miller, *Apple Files*, Reston, Reston Virginia, 1982.
141. L. Finkel and J. R. Brown, *Apple BASIC: Data File Programming. A Self-teaching Guide*, Wiley, New York, 1982.
142. D. Eyes, *Byte*, 1983, **8**, No. 3, 453.
143. J. B., Matthews, *Byte*, *ibid.*, 1982, **7**, No. 4, 447.
144. C. Poling, *Apple II Word Processing*, Que Corp., Indianapolis, 1981.
145. K. Carlson and S. Haber, *Byte*, 1981, **6**, No. 6, 176.
146. Arktronics Corp., 113 South Fourth Ave., Ann Arbor, MI 48104.
147. D. H. Beil, *The VisiCalc Book: Apple Edition*, Reston, Reston, Virginia, 1982.
148. V. Wolverton, *Visicalc, Advanced Version*, Visicorp., San Jose, 1983.
149. G. I. Ouchi, *Am. Lab.*, 1983, **15**, No. 2, 28.
150. *The Blue Book for the Apple Computer*, 1983/84 Ed., Wild Video, 5245 W. Diversy Ave., Chicago, IL 60639.
151. *Vanloves Apple II/III Software Directory*, Advanced Software Technology, Inc., 6720 W. 66th Terrace, Shawnee Mission, KS 66201.
152. *The Addison-Wesley Book of Apple Computer Software*, 1983 Ed., J. Stanton, R. P. Wells and S. Rochowansky (eds.), The Book Co., 1983, 11223 S. Hindry Ave., Los Angeles, CA 90045.
153. *The Software Express*, SKU Inc., 2600 Tenth St., Berkeley, CA 94710.
154. *Swift's 1982 Educational Software Directory, Apple II Edition*, Sterling Swift Publ. Co., 7901 South 1H-35, Austin, TX 78744.
155. G. Grout, 80 *Micro*, 1983, *June*, 78.
156. Quadram Corp., 4357 Park Dr., Norcross, GA 30093.
157. G. Williams, *Byte*, 1983, **8**, No. 2, 33.
158. B. Daniels, *Comp. Des.*, 1983, **22**, No. 9, 159.
159. *Idem, Proc. IEEE*, 1984, **72**, No. 3, 331.
160. G. Williams, *Byte*, 1984, **9**, No. 2, 84.
161. *Idem, ibid.*, 1984, **9**, No. 2, 30.
162. *Idem, ibid.*, 1984, **9**, No. 5, 339.
163. *Macworld*, P.O. Box 20300, Bergenfield, NJ 07621.
164. J. Markoff, *Byte*, 1984, **9**, No. 5, 276.
165. R. Malloy, *ibid.*, 1984, **9**, No. 2, 252.
166. J. Markoff and P. Robinson, *ibid.*, 1985, **10**, No. 2, 121.
167. Software Arts, 27 Mica Lane, MA 02181.
168. Living Videotext Inc., 2432 Charleston Rd., Mountain View, CA 94043.
169. Lotus Development Corp., 161 First St., Cambridge, MA 02142.
170. Tecmar Inc., Personal Computers Division, 6225 Cochran Rd., Solon, OH 44139-3377.
171. Davong Systems Inc., 217 Humboit Court, Sunnyvale, CA 94089.
172. IO tech Inc., P.O. Box 21204, Cleveland, OH 44121.

Talanta, Vol. 32, No. 8A, pp. 615–631, 1985
Printed in Great Britain

0039-9140/85 $3.00 + 0.00
Pergamon Press Ltd

SMART BACKPLANES—II

THE IBM PC

V. KARANASSIOS and G. HORLICK
Department of Chemistry, University of Alberta, Edmonton, Alberta, Canada

(*Received* 27 *August* 1984. *Revised* 15 *February* 1985. *Accepted* 1 *March* 1985)

Summary—A comprehensive account is given of the characteristics of the IBM PC personal computer and of the range of hardware and software available for it from various manufacturers, together with a list of books, magazines and journals of interest to the user.

With the possible exception of the operational amplifier (OA) no electronic device has affected analytical instrumentation as much as the microprocessor has. In fact, microprocessors are now replacing OAs as the basic building blocks in the laboratory, and microcomputers and microprocessor-based designs (along with semiconductor technology) figure largely on the chemist's work bench.

Until recently, design of personal computers was left to hobbyists, small firms and "garage-founded" companies. The introduction of the IBM PC marks the beginning of an era in which the significance of personal computers is recognized by traditional mainframe giants and mirocomputers are no longer considered as toys. Three and a half years after its introduction, the IBM PC has a broad range of scientific, engineering and industrial applications. Its success is attributed to its open architecture.

The idea of plugging a board into a personal computer's backplane bus to enhance or change its functionality is not new. Until recently, however, such boards had to be provided with tailored programs. Software which turns personal computers into multifunctional programmable test and measurement equipment is now becoming available. It is usually based on interactive menus and is often more thorough than that written by the user. Because the user can take advantage of data-processing, word-processing, data-base management, graphics, communications and control capabilities offered by personal computers, the marriage between traditional instrumental functions and personal computers does not result in just another piece of equipment but powerful, multifunctional instruments.

Without doubt, the trend to make instruments more "intelligent" will continue, and can only be paralleled by the shift from an industrial to an information-based society.[2] Future instruments will become information-driven: "the only way to handle information is by matching technology to the application".[2] A personal computer's backplane bus is a unique structure for the application-driven expansion of microcomputer based instrumentation.

THE IBM PC FAMILY

At present, the most widely used personal computer backplanes are those of the Apple II[3] and the IBM PC. Both have become industry-imposed standards and, because of the variety of data-acquisition and control boards available from other suppliers, the IBM PC is becoming increasingly popular for laboratory applications.

Owing to the PC's success, IBM has expanded its personal computer family to include both "senior" (such as the PC XT, the XT/370 and the 3270-PC) and "junior" members (such as the PCjr).

The IBM PC

This, introduced in August 1981, is typical of modern desk-top computers, offering basic arithmetic, word processing, high-resolution graphics and a backplane bus structure. The PC has become successful because of its modular design, good documentation, and the variety of hardware and software modules available for its backplane bus.

For users requiring extensive arithmetic capability, a socket on the main printed circuit (pc) board is available for Intel's 8087 arithmetic processor. The PC's five-slot backplane, which is also on the main pc board, allows several boards to be plugged in, making the PC particularly attractive to users with diverse applications. The scientific/engineering market appears to be as important as the business/home market for the PC, and currently the PC overshadows the CS 9000,[4,5] a 68000-based laboratory computer developed by IBM Laboratory Instruments division.

The PC consists of three major units: a detachable keyboard (with its own single-chip microcomputer), the main system unit (which has room for two $5\frac{1}{4}$-in. floppy-disk drives mounted horizontally in the front of the cabinet), and the monitor. The PC originally came with roughly the same memory as the now

defunct Radio Shack model I. IBM soon realized this drawback and corrected it in later versions. The current version provides 256-kbyte memory capacity on the motherboard itself, and can be expanded up to 640 kbytes with the aid of memory expansion boards. However, expanded memory is too large to accommodate on a single floppy disk, and a disk-drive supporting higher capacity floppy disks is needed.

Since there are only five slots on the PC's backplane, they may all be occupied by basic boards, and the user may have to introduce some multifunction boards. The keyboard is probably the most controversial of the PC's units. Its non-standard layout, the size of the ENTER key and the lack of indicator lamps for Caps Lock and Number Lock keys are but a few of the complaints. The remedy comes in the form of programs that redefine the keyboard. Although the PC supports a cassette interface (an obsolete feature), its motherboard is equipped with neither serial nor parallel ports. The lack of a serial port has been partially corrected on the PC XT version. The PC has had some further problems, most of which seem to have been corrected in the new PC XT version. Selected PC and PC XT features are summarized in Table 1.

The PC can be easily upgraded to a 3270-PC, as discussed in a later section, or to a PC XT. The requirements for the PC to be upgraded to an XT are: 128 kbytes of RAM, a floppy-disk drive, a communications card, a hard-disk interface and a hard disk. Although housing all this in the PC's cabinet is not impossible, an expansion chassis equipped with a hard disk provides a better alternative to upgrading the PC to a PC XT. Glinert-Cole[6] in an interesting article reviews three such expansion chassis. It should be noted that upgrading a PC to a PC XT is often cheaper than purchasing a PC XT.

The IBM PC XT

The IBM PC XT (XT for short), released in the spring of 1983, is an enhanced version of the IBM PC. It looks like the PC, except for its hard disk which replaces one of the two floppy disks available on the original PC, and its logo. Selected features are summarized in Table 1. The XT has the same three basic units as its predecessor. The basic unit, however, supports a 360-kbyte double-sided, double-density floppy-disk drive and a 10-Mbyte Winchester disk-drive. A cassette interface, an obsolete feature on the PC, is not present. Although the standard XT has 128-kbyte RAM, the redesigned motherboard supports up to 256-kbyte RAM based on 64-kbit DRAM chips instead of the 16-kbit DRAMs found on earlier PC versions. With expansion boards the

Table 1. Selected IBM PC and PC XT features

	IBM PC	IBM PC XT
Processor	Intel 8088	Same as PC
Clock, *MHz*	4.77	Same as PC
Selected add-on processors	Z80, 8086, 80286 68000, 16032	Same as PC
Arithmetic processors	Intel 8087, socket available on pc board 80287, 16081 add-on modules	Same as PC
Memory min, max, *kbytes*	64, 640	128, 640
Disk drives	Up to two 320-kbyte $5\frac{1}{4}$-in. floppies	One, 360-kbyte $5\frac{1}{4}$-in. floppy
Hard disk	Optional	10-Mbyte Winchester
Keyboard	83-key QWERTY, non-standard detachable, adjustable, includes numeric keypad	Same as PC
Function keys	10	Same as PC
Extras required*	Video adapter board, monitor	Same as PC
Screen format		Same as PC
Text	40 H × 24 V or 80 H × 24 V, 16 colours	
Medium-resolution graphics	320 H × 200 V	
High-resolution graphics†	640 H × 200 V	
Peripheral slots	5	8
I/O ports, standard	None	Serial port
Selected operating systems	PC-DOS, CP/M-86 USCD p-system MP/M-86, XENIX Oasis 16, RTOS Concurrent CP/M-86 Venix, QNX	Same as PC

*Minimum configuration.
†See text.

XT's memory capacity can be brought up to 640 kbytes.

The motherboard supports eight expansion slots (the PC has only five). Although PC and XT have the same backplane bus structure, not all slots are "equal" on the XT. Two of them are behind the floppy-disk drive and thus provide enough room for only half-length boards. One of these smaller slots, J8, which differs significantly from the other seven (more stringent timing requirements, and a "card select" signal must be generated when the board is selected), already carries an asynchronous communications board—a standard XT feature.

Because the XT's expansion slots are closer together than those on the PC, the six slots which can take full-length boards occupy the same space as the five slots on the PC and certain double-width boards or boards supporting "piggy-back" ICs are not likely to fit in. To provide the power required for the extra boards and the hard disk, the XT has a 130-W power supply.

At the time the XT was introduced, a new RGB (Red-Green-Blue) monitor, a new disk operating system (DOS) version 2.00, and a new version of BASIC were also introduced. However, not all programs written under PC–DOS version 1.10 will run under PC–DOS version 2.00. Some of the intricacies of PC–DOS 2.00 as it is used within the XT are discussed by Archer,[7] who also provides a short but interesting review of the XT. Several descriptive reviews of the XT can be found in microcomputer magazines (*e.g.*, those by Machrone[8,9]).

In summary, the standard XT comes with 128 kbytes of RAM, 40 kbytes of ROM where the BASIC interpreter and DOS I/O software are stored, a floppy-disk drive, a 10-Mbyte hard disk, a 50–9600 bites/sec asynchronous communications adapter, and disk adapters which take up three of the eight expansion slots.

The IBM XT/370

The once distinct boundaries between micro, mini and mainframe computer architectures are now blurred because of advances in very large scale integration technology. The recently introduced (late 1983) XT/370,[10,11] breaks down some of the barriers to concentrating "mainframe power" on a personal computer and thus officially marks the beginning of the "micro-mainframe" era.

The XT/370, as its name implies, has been designed to emulate the IBM System/370 mainframe. Externally it looks no different from an XT; internally, however, there are three additional boards. One provides 512 kbytes of RAM and, although this can be considered hardly adequate for System/370 emulation, the XT/370 also supports up to 4 Mbytes of virtual memory, which should provide ample resources for most users. The second board allows the XT/370 to act like an IBM 3277 terminal for communication with a host. The third contains two processors (a standard Motorola 68000 and an IBM-designed 68000) and an arithmetic processor (Intel 8087). This board emulates most of the mainframe's instruction set, but some of the System/370 specific instructions have not been included. IBM claims that the XT/370 executes most of the software written for the 370 at a speed nearly half that offered by a 4300 series mainframe. It also claims that versions of the FORTRAN, Pascal and COBOL compilers will run on the XT/370 without modification.

Further, a version of the System/370's VM/CMS (Virtual Memory/Conversational Monitor System), called the VM/PC (Virtual Memory/Personal Computer) has been developed for the XT/370. The VM/PC software runs under PC–DOS. When the VM/PC is invoked from within PC–DOS, the 8088 CPU remains idle until I/O is requested. The user can easily switch to "normal" XT mode and execute PC software. Although the XT/370 can still function as an ordinary PC, it is not a system for the novice and VM/CMS is not as friendly as PC–DOS. Clearly, the XT/370 places heavy demands on the user's "computer literacy". Moreover, IBM is keeping the System/370 hardware for the XT proprietary, which may signal IBM's final enhancement of the PC family and the end of the PC's open architecture. It may also mark the beginning of new rumour and speculation about the next generation of IBM's personal computers.

Finally, the XT/370 is expected to affect mainframe software radically, although software issues have been overshadowed by the announcement of the XT/370 hardware. Mainframe software is usually expensive; it often costs more than the XT/370 itself. How is such software going to become available to the end-user? Despite the number of software-related questions that have yet to be answered, less than $15000 can supply a miniature System/370 and thus provide the capability to run mainframe software at a fraction of mainframe cost.

The IBM PCjr

For several months in mid-1983 there was mounting conjecture about the introduction of yet another IBM personal computer, code-named "Peanut". In late 1983 IBM introduced the PCjr, which is thought to be the long-awaited "Peanut".

Two PCjr configurations are available. The basic one offers 64 kbytes of RAM (expandable to 128 kbytes), 64 kbytes of ROM, standard colour graphics, several connectors for peripheral devices, game connectors, and a cassette interface. The enhanced version has 128 kbytes of RAM, a $5\frac{1}{4}$-in. floppy-disk drive (mounted horizontally in the front of the main system cabinet), and advanced graphics capabilities. At the same time as the PCjr, PC–DOS 2.10 was introduced, which incorporates all the features of PC–DOS 2.00 and also allows the PCjr to access data stored in ROM cartridges and to access the disk drive. Cassette BASIC (a ROM-based version of the

PC's cassette BASIC) and Cartridge BASIC (a ROM-cartridge version of the PC's Advanced BASIC), are the major languages supported by the PCjr. Perhaps the most important feature of the PCjr is its compatibility with most, but not all, of the PC's software.

The *PCjr* magazine[12] offered in its first issue a table of PC-compatible software, and reviews of several programs (mainly for computer games) specifically written for the PCjr. Seger *et al.*[13] and Vose *et al.*[14] also provide relatively extensive tables of PC-compatible software.

Like the PC, the PCjr consists of three major units: the main system unit, the keyboard and the display. Its motherboard supports an 8088 CPU operating at the same clock-rate (4.77 MHz) as that of the PC, but this is where the similarities end. The PCjr's main system unit is about one-third the size of the PC's main system unit, and the Intel 8087 arithmetic processor is not present, nor are provisions made for it. There is no need for a video display adapter card: the colour graphics circuitry, designed around a proprietary gate-array chip, is built into the motherboard. An RF-modulator, four sources of sound, and an RS-232-compatible port are also built into the PCjr's motherboard. Finally, the keyboard can communicate with the main system unit by an infrared link.

The PCjr supports a variety of expansion connectors. Two cartridge slots in the front of the cabinet allow ROM cartridges to be added, and three expansion slots reside on the main pc board (one for a 64-kbyte RAM board, one for a disk-drive interface and the third for a modem). The main-board slots are neither PC-compatible nor interchangeable, however. Additional expansion can be made through the bus extension connector. Although both connector and pin assignments are different from those on the PC, their electrical specifications and functionality are claimed to be the same as for the PC. Such an arrangement, complicated even further by the junior's small power supply (33 W as opposed to 63.5 W for the PC), is not likely to allow the PCjr to take advantage of the variety of PC-compatible boards, unless an expansion chassis is utilized.

A few months after introduction of the PCjr, other vendors announced new products that enhance its capabilities, including a six-slot expansion chassis which accepts standard PC-compatible peripheral boards,[15] a 512-kbyte RAM board[16] and a board that turns the PCjr into an Apple II+.[17]

The detachable battery-operated QWERTY keyboard supports 62 small rectangular keys. The most interesting feature of this otherwise poor keyboard is that it can communicate with the processor by an infrared optical link. An optional keyboard cable is also available. Everything about this keyboard suggests that a vigorous market for keyboard replacements will develop. In fact, the May 1984 issue of *PCjr* magazine devoted several articles to the PCjr's keyboard, and described two replacements available for it.

PCjr literature appears to be expanding quickly. At least three magazines[12,18,19] are already available, and Microsoft[20] have published three books on PCjr.

From the information available to date,[14,17,21,22] the PCjr appears to be a hybrid between a personal computer and a home computer. However, because of its inadequate keyboard, its limited expansion capabilities—unless an expansion chassis is added—and its inability to run some of the more sophisticated PC software, it cannot be considered an up-to-date personal computer. As a home computer, it is currently more expensive than others with comparable capabilities. Finally, in the laboratory, the PCjr may be utilized either as a front-end processor that handles a variety of tasks for a PC or XT, or as a stand-alone microcomputer for low-level data-acquisition and control applications.

The IBM 3270-PC

To satisfy the growing demands for micro-to-mainframe communication, IBM introduced (Autumn 1983) the IBM 3270-PC, a microcomputer designed to serve both as a PC and a terminal.[23] It supports a variety of protocols and can emulate the IBM 3178, 3278 and 3279 terminals. Because the 3270-PC is not expected to contribute to laboratory automation, it will not be further considered here.

Comments

Despite the massive amount of information available on recently introduced microcomputers, most of it is vague, and more (even that concerning the older microcomputers) is in a state of flux. The information presented here represents the latest, but not the final, views of the authors.

Finally, since all members of the IBM PC family (PC, XT, XT/370) and the recently introduced portable PC[24,25] share the same backplane bus structure, the generic term "IBM PC" or just "PC" will be used hereafter to refer to the entire family.

BACKPLANE BUS STRUCTURE

The PC has a five-slot backplane bus, as shown in Fig. 1. The peripheral slots are identical and can house any combination of I/O and memory boards. The peripheral I/O pins and signals are listed in Table 2, and a diagram of a peripheral slot is shown in Fig. 2.

Bus characteristics

The backplate bus is a demultiplexed and enhanced version of the 8088 microprocessor bus. Enhancements are delivered to the bus by Intel's 8257 (DMA controller), 8259 (priority-interrupt controller) and 8253 (interval-timer/counter), and include six levels of interrupt, three channels of direct memory access (DMA), control lines for memory and I/O read or write, a dynamic memory-refresh signal, a channel-

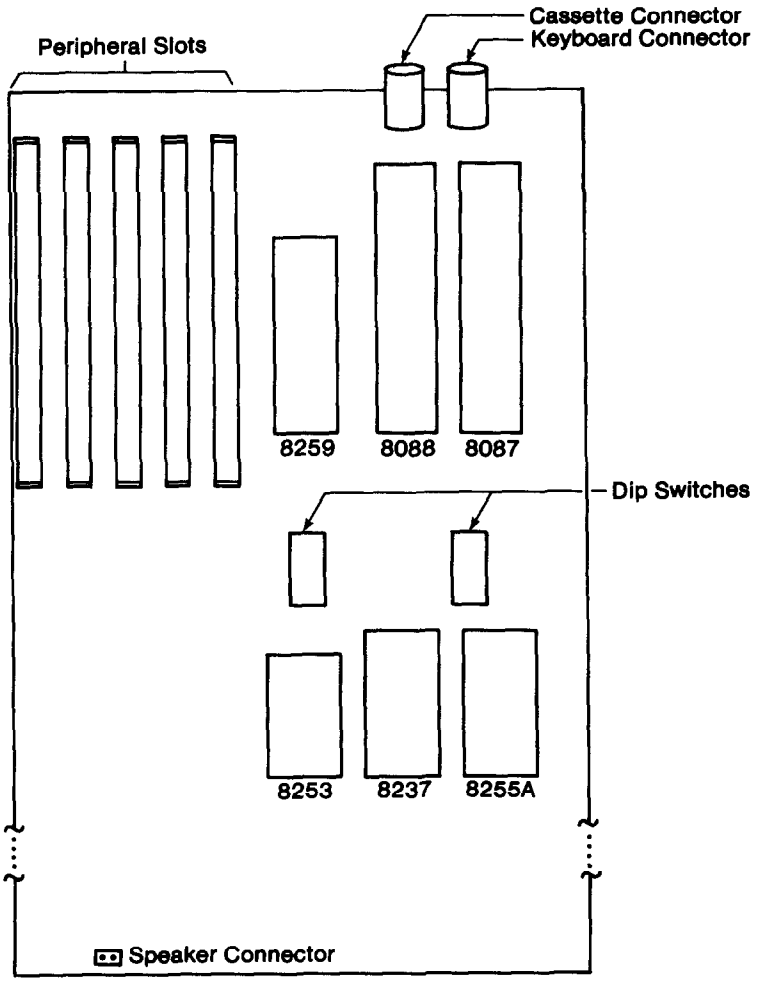

Fig. 1. IBM PC printed circuit board.

check line for parity error detection, and several clock and timing signals.

Although the PC's 8088 CPU represents current 8/16-bit microprocessor design, advanced interfacing schemes often require peripheral boards to take control of the bus. This is facilitated by Intel's 8257 DMA controller chip which resides on the main printed circuit (pc) board. The controller provides for three channels of bus-request arbitration and therefore allows up to three master modules to be present on the peripheral bus.

Bus type. Synchronous, non-multiplexed.

Bus timing. If stretching of the clock is not required, then all CPU-originated read or write operations require four clock cycles, while all I/O read or write operations require five clock cycles. Finally, all DMA-transfers require five clock cycles per transfer. A typical 4.77-MHz operation corresponds to 210 nsec per clock cycle.

Data bus width. Eight bits.

Address bus width. Twenty bits.

I/O memory allocation. Five hundred and twelve memory locations (512 bytes) are reserved on all peripheral slots. Each peripheral slot should provide its own address decoding.

Interrupt structure. Six levels of interrupt are available on the PC's backplane bus, which are managed by Intel's 8259 interrupt-controller chip. Dunford[26,27] describes how to use interrupts on the PC.

Backplane connector. The PC's backplane bus supports 62-contact connectors, as shown in Fig. 2.

Loads supported. The number of peripheral boards supported depends on the number of slots on the backplane. If there are not enough slots available at any given time, an expansion chassis should be utilized. Several expansion chassis are commercially available.[1,15,28-31] A hard disk[32] designed to mate with an expansion chassis,[28] or an expansion chassis incorporating a hard disk[1,15] can be used to upgrade a PC to an XT.

The PCI[33] takes a different approach to provide expandability and portability. It is a hybrid between a PC and an expansion chassis, and includes a power supply, a 12-in. monochrome display and two $5\frac{1}{4}$-in. double-sided double-density 320-kbyte half-height disk-drives, all housed in a cabinet no larger than a

Table 2. IBM PC peripheral I/O pins and signals

Pin number	Signal name	Description	I/O function
A1	$\overline{\text{I/O CH CK}}$	I/O channel check; when active, a parity error has occurred.	I
A2–A9	D7 to D0	Data lines.	I/O
A10	I/O CH RDY	I/O channel ready. Used for stretching clock cycles. It should not be active for more than 10 clock cycles.	I
A11	AEN	Address enable. When active, the DMA takes control of the bus.	O
A12–A31	A19–A0	Address lines, A19 (MSB) to A0 (LSB).	O
B1, B10, B31	GND	Ground	
B2	RESET DRV	Reset driver. Traditional CPU reset signal.	O
B3, B29	+5 V	+5 V d.c. power supply.	
B4	IRQ2	Highest priority interrupt request.	I
B5	−5 V	−5 V d.c. power supply.	
B6, B16, B18	DRQ	DRQ2, DRQ3, DRQ1. DMA request, channels 1–3.	I
B7	−12 V	−12 V d.c. power supply.	
B8		Reserved	
B9	+12 V	12 V d.c. power supply.	
B11	$\overline{\text{MEMW}}$	Memory write. Active (low) on a memory write cycle.	O
B12	$\overline{\text{MEMR}}$	Memory read. Active (low) on a memory read cycle.	O
B13	$\overline{\text{IOW}}$	I/O write. Active (low) when a peripheral device is written into.	O
B14	$\overline{\text{IOR}}$	I/O read. Active (low) when a peripheral device is being read.	O
B15, B26, B17, B19	$\overline{\text{DACK3}}$, $\overline{\text{DACK2}}$ $\overline{\text{DACK1}}$, $\overline{\text{DACK0}}$	DMA request acknowledge. $\overline{\text{DACK0}}$ is used for dynamic memory refresh.	O
B20	clock	System clock.	O
B21–B25	IRQ7–IRQ3	Interrupt request. IRQ7 has the lowest priority.	I
B28	ALE	Address latch enable.	O
B30	OSC	High-speed (14-MHz) clock.	O

portable oscilloscope. For true portability, a battery pack that provides $1\frac{1}{2}$ hr of operation is also available.

Signal line length. Confined within the constraints of the backplane bus or the backplane bus/expansion chassis combination.

Processors and systems supported

Co-processors. Applications that demand microprocessors do too much, too fast, increase at an accelerating pace. One way to enhance a microprocessor's computational power without increasing its chip size or its complexity is by off-loading computational tasks onto dedicated peripheral devices such as arithmetic processors, or co-processors, as they are often called.

Intel's 8087 NPX (numeric processor extension), for instance, has been designed to mate with the 8086 and 8088 CPUs. When an 8087 NPX is interfaced to a host, then it is called a numeric data processor (NDP). The 8087, whatever it is called, has an 80-bit internal architecture, performs 16-, 32- and 64-bit integer, 18-bit binary coded decimal (BCD) and 80-bit floating-point arithmetic and conforms to IEEE-standards. The 8087's architecture, instruction set and data format, along with its performance and interfacing to an 8086 or 8088 CPU, have been quite extensively discussed in the literature.[34–39]

The PC's motherboard includes a socket for an 8087. Once the 8087 has been plugged in, it can be immediately accessed, provided that the proper instructions have been issued, *i.e.*, appropriate software must be written to take advantage of the 8087's

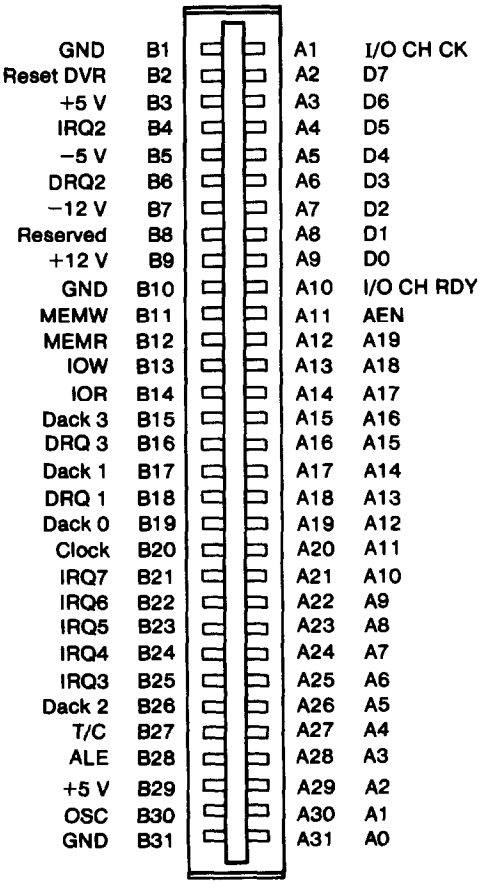

Fig. 2. IBM PC peripheral connector.

arithmetic capabilities. Field[40] offers several interesting comments about the 8087 NDP as it is used in the PC, and includes software utilities that make it easier to use with Assembly language. He also[41] provides software utilities that can speed up most Pascal programs by a factor of about three. Field's software utilities are also available on a floppy disk.[42] MicroWare[43] offer a set of software tools for the 8087, that run on the PC, including Maxpack, a set of subroutines designed for matrix manipulation (written in Assembly language) and several versions of assemblers and high-level language compilers that support the 8087. Hauppauge Computer Works[44] also offer Pascal, FORTRAN and Macro compilers that support the 8087. Admittedly, the performance of IBM's FORTRAN compiler is poor. However, the new FORTRAN compilers that take advantage of the 8087 are fast, and can even be recommended for use in laboratory applications,[45] but to take advantage of the PC's high-resolution graphics, some FORTRAN compilers must be accompanied by graphics software.[46]

Add-on processors. As the number of PC's installed increased, the PC found its way into many applications for which it was not initially designed. Moreover, the performance requirements for some of those applicatons revealed limitations of the PC that had to be overcome. To satisfy these new performance requirements and take advantage of the newer and more powerful CPUs available, several add-on processor modules have been developed. Included are modules containing CPUs (such as i8086, i80286, MC68000 and NS16032), accompanied by floating-point co-processors (such as i8087, i80287 and NS16081), and supported by memory-management units.[47,48] An MC68000-based board capable of running the Xenix 3.0 Operating System, which is Microsoft's version of Unix System III from Bell Laboratories, is currently available.[47] The same MC68000 board, under the RM/COS Operating System, turns the PC into a multi-user COBOL-oriented computer particularly suited for business applications.[49]

The Accelerator PC[50] is a board designed around a 10-MHz 8086 processor. It supports 128-kbyte RAM expandable to 640 kbytes, with a memory piggy-back option. This board is claimed to increase the PC's execution speed by a factor of about three. The Turbo-186 board[51] reportedly increases the PC's execution speed 3–10-fold depending on the program being run. The board contains an 8-MHz 80186 processor, 128 kbytes of RAM and comes with appropriate software. Ciarcia[52] describes the hardware and provides the diagrams required for the construction of a 10-MHz, Z8001-based add-on processor board that holds up to 512 kbytes of RAM. This board is also commercially available.[53] Quadlink[16,54] is a simulated Apple II computer that allows most of Apple II's software to be used with the PC. This multifunction board also provides 64-kbyte RAM and offers games, and parallel and serial I/O ports. A Z80-based add-on processor board allows PC users to run CP/M-80 software. Welch[55] lists nine such boards, some of which include, in addition to a standard 64-kbyte RAM, serial and parallel ports. The I/O processor,[56] for example, provides two serial ports, one parallel port and a real-time clock.

IBM has taken a different approach in designing add-on processors for the XT. Throughout the years, microprocessor architects have borrowed, modified, and incorporated mainframe concepts into their designs. Until recently, however, the ability to emulate mainframes had been a continuing challenge. The S/370 is a set of three add-on processor boards designed to emulate IBM System/370 mainframe's instruction set and thus provide the capability of running mainframe software on a microcomputer. Because the S/370 set has been discussed in conjunction with the XT/370 system, it will not be dealt with here.

Systems. There are several examples where the PC has been utilized as the "main processor" or a "front-end" processor. Advanced Digital Corp.,[57] for example, market a board that allows the PC to control up to five terminals. Analogic Corp.[58] offer a stand-alone general purpose computer with an array processor architecture. A typical configuration of this "APL-speaking machine" involves, among others, a 4-Mbyte array processor, a 124-Mbyte hard disk and an IBM PC serving as the programmer's work station. The system can execute as many as 10^7 floating-point operations per second and can display up to 10 concurrent tasks on overlapping windows. Even the minimum configuration of this system, however, is expensive (about $44000). At least one company[59] is marketing a less expensive (<$5000) array processor for the PC.

The PC can also be used in conjunction with bus-based systems.[60] Such combinations allow users to take advantage of the modularity, flexibility, versatility and computing power offered by bus-based systems, and also to exploit the PC's wide software resources. For example, an adaptor that links the PC with the IEEE 796 (Multibus) backplane bus recently became available.[61] The PC can be used either as a bus master or as a co-processor that stores, processes, and displays Multibus-acquired data. The PC's Macro-assembler and debugging facilities can be used to develop 8086 or 8088 software for use with the Multibus. The adaptor consists of two boards interconnected by a flat-ribbon cable: one board fits inside the PC and the other inside the Multibus card cage. The most important feature of this interface is that it allows users to take advantage of the high-performance boards available for Multibus.

In complementary developments, RMAC Corp.[62] market an adaptor that links the PC with the STD-bus (IEEE P961 backplane bus standard). This adaptor also consists of two boards interconnected with a flat-ribbon cable: one fits inside the PC and the

other fits inside the STD-bus card cage. The link allows the PC to act either as an STD-bus controller or as a development system. The STD-bus can also use DMA operations to access data directly from the PC's memory. An interface that links the IBM PC and the CAMAC backplane bus and allows the PC to take advantage of the high-speed data-acquisition and signal-processing plug-ins available for this backplane bus, has also been developed.[63]

Power supply

The PC's power supply provides ± 5 V and ± 12 V to the motherboard and to the backplane bus. An expansion chassis should provide its own power supply.

PERIPHERAL BOARDS AND SUBSYSTEMS

Undoubtedly, part of the PC's success is due to the availability of a large number of PC-compatible boards, subsystems, and software packages. It has been estimated that by mid-1983 there were over 3000 hardware and software products for the PC; this number was expected to grow to more than 6000 by the end of 1984.[64] Simple arithmetic suggests that an average of five new PC-compatible products have to be introduced daily to reach this projected number. Although such numbers seem quite high, it seems likely that users will have even more software and peripheral boards at their disposal in the future. The following examples have been chosen to illustrate the type of boards and subsystems currently available.

Multifunction boards

One of the most widespread criticisms of the PC's backplane is that it can easily be filled up with basic cards and therefore does not provide enough slots for application-driven expansion. For instance, a slot is needed for the disk-controller board, another for the display board and a third for a serial and/or parallel interface card. Adding memory to the fourth slot leaves only one to satisfy all of the expansion requirements, and more often than not that is simply not adequate. To remedy the situation, several vendors have developed either separate expansion chassis or multifunction boards. Although several combinations of functions are available on such boards, serial and parallel ports, RAM and a clock are the most common.

To provide a multiplicity of functions, some boards are designed to accept piggy-back modules. Although such boards are designed so that they will not interfere with other boards plugged in on the PC's backplane, they may not fit on the XT's backplane. Gleckler[65] provides helpful tips on how to choose a multifunction board, pinpoints some common problems (*e.g.*, software incompatibility, outdated documentation), and reviews sixteen such boards. Welch[55] has compiled a list of over 80 vendors marketing multifunction boards for the PC. He also provides the functionality included on each board and lists the board's retail price. It should be noted that the XT's backplane, since it offers eight expansion slots, no longer imposes expansion limitations for most applications.

Memory-expansion boards

Although the PC's 8088 CPU can address up to 1 Mbyte of memory, the basic PC is still equipped with only 64-kbyte RAM. Many application programs, however, require more than 64 kbyte of RAM to run on the PC. The solution comes in the form of memory-expansion boards. Welch[55] lists over 50 vendors marketing memory-expansion boards for the PC. Memory capacity, disk-emulation capability and the board's price are also included.

Although semiconductor memories offer short access times, they cannot retain their contents after the power is switched off. Therefore, they are only useful for temporary storage. There are two alternatives available: CMOS battery boards with battery back-up (a concept of limited applicability) or non-volatile mass-storage.

Magnetic-bubble memories have found their niche in portable computers, portable terminals and, because of their reliability and noise immunity, in military and industrial applications where semiconductor memories or disk drives cannot survive. In personal computers, bubble memories can be used to supplement non-volatile mass-storage, to replace conventional floppy-disk drives, or as disk emulators that allow fast access of disk data. A disk emulator is "a marvellous trick whereby you convince your computer that a lot of memory is really a disk drive".

Bubble-memory storage lies somewhere between RAM and disk storage. Like RAM, bubble memories offer solid-state storage. Unlike RAM, they provide non-volatile storage, but are slow [typically 40–50 msec access times, as opposed to 50–350 nsec for RAMs, and almost sub-nanosecond performance by use of ECL (emitter coupled logic)]. Like floppy disks, they offer non-volatile mass-storage, but are faster, require less power (about a third of that for a floppy-disk drive) and provide a much longer average time between failures.

Ecosea Technologies[66] market two bubble-memory boards (of 128- and 512-kbyte capacity) that directly plug into any of the PC's expansion slots. Other 512-kbyte bubble-memory boards are also available.[67,68] These boards are designed around Intel's 7110-4, 1-Mbit bubble memories and include all the appropriate interface circuitry. Hi Comp[68] has also developed a 512-kbyte and a 1-Mbyte bubble-memory subsystem controlled by its own microprocessor. This subsystem, designed for applications requiring high reliability or for hostile environments, allows personal computers to be used in harsh industrial environments. It can be interfaced to any microcomputer in two ways: it can be directly connected to the host disk controller and emulate an

industry standard $5\frac{1}{4}$-in. floppy disk, or it can communicate with the host through an RS-232C interface.

In summary, bubble memories are expected to find their way into applications in which reliability, non-volatility and speed are critical. Despite their speed and the expected increase in their capacity, however, both bubble and random access memories still require back-up.

Mass-storage subsystems

The XT utilizes the built-in floppy disk for hard-disk back-up, but about 30 floppy disks are required for the entire hard disk. A tape-based mass-storage device, though not always a cost-effective solution, is well suited for such back-up. For example, a cartridge tape system offering 13.4-Mbyte or 16-Mbyte storage capacity[69] and a 20-Mbyte cassette tape system[70] are commercially available. IBEX Corp.[71] market a $\frac{1}{2}$-in. 9-track magnetic storage device for the PC, which offers a 42-Mbyte storage capacity on a single reel.

Regardless of how much storage capacity modern mass-storage devices offer, the problem of waiting for the disk drive to respond still remains: even the speedier floppy-disk drives or Winchesters are not fast enough for some I/O-intensive applications. To boost the speed of disk-based mass-storage devices, semiconductor memories are again employed. A 100-fold improvement over a floppy disk's response time is not unusual,[72] but the improvement can vary considerably, depending on the type of semiconductor memory and the mass-storage device used.

Current laboratory applications requiring wide mass-storage resources include data-base management and data filing. In the future, mass-storage will become increasingly important for the implementation of pattern-recognition algorithms and for systems offering knowledge-management and information-processing capabilities. Although several hard disks are available for the PC,[73–78] applications such as those mentioned above may require mass-storage capacity greater than that provided by conventional Winchester disks.

Interface Corp's SMD PC-80 controller,[79] for example, enables the PC to take advantage of fast high-density disk drives using the storage–module–device (SMD) interface. This board packs the necessary circuitry (including a microprocessor and specially designed ICs) on a single board that handles up to two SMD units,[80] and allows data rates up to 20 Mbyte/sec. The PC-80 board allows the PC to control approximately 1 Gbyte of mass-storage (about 4×10^5 pages of text). Clearly, developments of this type pave the way for new laboratory applications that have thus far required a minicomputer or a mainframe for their implementation.

Data-acquisition boards and subsystems

Owing to the existence of a backplane bus and the variety of data-acquisition and control boards available, the PC can easily be configured as a programmable instrument that can perform tests, display and record measurements, and help analyse the results. The following section, which lists several examples of such boards, does not attempt to be all-inclusive; the examples chosen are considered to be representative of the types of interfaces available.

Data Translation[81] market two data-acquisition and control boards (the DT2801 and DT2805) which directly plug into any of the PC's expansion slots. These single boards perform digital and analogue I/O through the use of an on-board microprocessor. The DT2801 offers a 12-bit ADC front-ended with a programmable-gain amplifier (gain settings 1, 2, 4 or 8) and achieves a 13-kHz throughput. It also offers 2 analogue output channels, 16 digital I/O lines and a programmable clock. The DT2801-A offers the same features as the DT2801 but provides a 27.5-kHz throughput. The DT2801/5716 is a 16-bit, 2.5-kHz throughput version of the DT2801. Because of the on-board firmware and microprocessor, the board's functions can be controlled by three BASIC statements.[82] The DT2805 board offers 12- or 16-bit resolution and software-programmable gain.

Perhaps the broadest range of boards for laboratory and industrial applications is marketed by Tecmar.[15] A few examples of such boards are presented below. The digital to analogue and digital input/output (DADIO) board provides four independent channels of 12-bit DAC and 24 parallel I/O lines. The Lab Master provides up to 256 channels of analogue to digital conversion (ADC) with 12-, 14- and 16-bit resolution and offers a 30-, 40- or 100-kHz conversion rate. The Lab Master also includes 2 independent 12-bit DACs, 5 independent 16-bit timer/counters, 24 programmable I/O lines and an optional programmable-gain amplifier. Gates[83] describes how the Lab Master has been used in conjunction with a polarograph and in an undergraduate course. Listings of Assembly language subroutines required to drive the Lab Master, and of BASIC programs, are also provided. The Lab Tender is a data-acquisition and control card combining several functions on a single board, including 32 channels of 8-bit ADC with a 50-kHz conversion rate, 16 analogue output channels of 8-bit resolution, 24 I/O lines and 5 independently programmable timer/counters. The Labpack software-support package is a set of subroutines which eliminate the need for tailored machine-language programming for the Lab Tender and Lab Master boards. This software package also allows users to handle both "foreground" and "background" tasks.

The IEEE-488 interface board implements Intel's GPIB chip set and provides the facilities of talker, listener and controller. The board is capable of DMA-controlled data transfers, and offers programmable data-transfer rates and selectable software interrupts. The stepper-motor controller board allows simultaneous independent control of two stepper motors by utilizing two Cybernetic Micro

Systems CY512 Intelligent Positioning Stepper Motor Controller chips.

More sophisticated applications could require self-contained designs, such as Gould's DASA 9000 data acquisition and signal analysis system.[84] This modular system consists of a PC, an 8-channel front-end signal conditioner and digitizer (with 8 kbits of RAM allotted to each channel). The front-end analogue subsystem has a 50 mV–500 V input range, a frequency response from d.c. to 500 kHz, and a user-selectable sampling rate. The software that accompanies the system allows it to act as either an oscilloscope or a transient recorder.

In parallel developments, Keithley[85] have recently introduced the Series 500 work-station measurement and control system that can be interfaced with either the PC or the Apple II. The system offers a 31.4-kHz data-acquisition rate and is equipped with measurement and control software which extends BASIC by adding new data-acquisition and control statements. Finally, the Link 110[86] is intended for industrial data-acquisition and control applications. This subsystem can be expanded to support 64 analogue inputs, 32 analogue outputs and 256 digital I/O lines.

For the past few years, several newcomers have dominated the "plug-compatible" market for both the Apple II and the IBM PC, while traditional instrument manufacturers have been looking over their shoulders. The trend to increase the performance of an instrument through personal computers is reinforced by the introduction of personal computer-based test and measurement equipment by well-known instrument makers, such as Keithley and Gould. In complementary developments, personal computer-like instruments equipped with engineering software are also beginning to appear.

Advanced interface boards and subsystems

As PC-based test and measurement equipment moves into software-intensive areas, the benefits of using microprocessor-based intelligence become rather obvious. An example of integration of the PC's computational and graphic capabilities with data-acquisition modules comes from Ariel Corp.[87] Its real-time spectrum analyser, the RIA 311, consists of a PC-compatible board and a separate box that contains the analogue filter. The spectrum analyser divides the audio spectrum, from 20 Hz to 20 kHz, into 31 one-third octave bands, which are displayed in the PC's CRT as a bar-graph. The RTA 311 can also store more than 20 sec of 8-bit audio signal in 512-kbyte memory. The stored signal can be displayed on an oscilloscope through an on-board 8-bit DAC. The spectrum analyser also includes a pink-noise generator and appropriate software.

Data acquisition and control are not the only instrument functions which take advantage of the PC's intelligence. Northwest Instruments[88] model 2200 interactive timing analyser (ITA), for example, is a testing device that pinpoints faults as microprocessor or microcomputer systems are designed. When the ITA and the company's previously introduced model 2100 interactive state analyser (ISA) are housed on the μAnalyst model 2000 chassis, they create a powerful logic-analyser system. Other PC-based software or hardware debugging tools are also available.[89]

Using a 256×128 bit optical RAM chip and menu-driven software, Micro-D Cam,[3,90,91] a digital image sensor, can interpret, store or enhance images through a personal computer. Micro-D Cam interfaces are available for the PC, the Apple II and any RS-232C-supporting microcomputer. Imaging Technologies[92] and Datacopy Corp's[93] subsystems can also be used for image processing.

Tecmar's[15] Video Van Gogh board is a video digitizer interface that accepts TV camera signals. It provides 255×255 pixel resolution with an 8-bit intensity value and is capable of 256 levels of grey-scale. The main areas of application of this board are expected to be microscopy, signature recognition, pattern recognition and robotic vision. Von Stackelberg[94] discusses some problems encountered with robotic vision systems and comments on papers presented in the "Graphics Interface 83" conference. Feeley *et al.*[95] present a model for an elaborate robotic vision and display system based on the PC.

Human–processor interface

Because the interface between the operator and the computer has taken several steps forward in the past few years, "last year's" personal computers were invariably self-proclaimed as "user-friendly", although some of them were not so friendly after all. Undoubtedly, a successful human–processor interface (HPI) results in user-friendly systems.

Hardware. Perhaps the most important of all HPIs is the "user interface", which is that part of a program that bridges the gap between the computer and the operator. However, software alone cannot provide all the solutions. On the hardware side,[96] pointing devices such as a mouse, touch screens,[97] joysticks, trackballs, light pens and graphic input devices[98–100] in association with voice I/O boards[15] and high-resolution graphics can simplify the communication between the user and the PC. Also, the use of colour displays can simplify the differentiation and interpretation of complex information.

The introduction of low-cost voice I/O boards has already opened the door to speech-activated word processing and file searching. Clearly, speech recognition is an idea for which the time is ripe. SuperSoft,[101] for example, offer a voice-activated electronic spreadsheet. The mouse, so named because of its physical resemblance to the real thing, is a hand-held pointing device which controls cursor movement—a concept popularized on Apple's Lisa. Several "mice" are available for the PC,[45,102,103] and Peters[104] has described Microsoft's mouse in some detail. Mouse

technology is at an important stage, and it appears that it may provide a long-term solution for non-keyboard based input devices. Currently, an increasing number of system designers have jumped into Lisa-like technology, and designed systems which employ high-resolution graphics, icons, windows and a mouse. It is worth mentioning that windows and mice are both the result of research done at Xerox Corp's Palo Alto Research Center (PARC) during the early 70s.

Graphics. To date, high-resolution graphics are one of the most important of all HPIs in the laboratory.[105] Ironically, one of the major limitations of most personal computers used in the laboratory is their lack of high-resolution graphics. It appears that IBM did not, at least initially, place particular emphasis on the PC's graphics capabilities. While, for instance, the original PC was provided with a colour graphics board which offered a 640 × 200 pixel resolution, there was no colour monitor available for it. In fact, an RGB monitor was introduced only at the time the XT was announced. Several vendors seized this marketing opportunity and filled the gap. Welch,[55] for example, lists over 10 vendors marketing high-resolution boards for the PC. Thanks to the resolution offered by such boards, the PC can now be used as a work station for computer-aided design (CAD) projects.[106]

Field[107] briefly compares the features of a monochrome and a colour monitor and provides an easily modifiable program that takes advantage of both monitors' capabilities, and Waldow[108] describes the "Hercules" high-resolution board. In other graphics-related developments, Digital Research Corp.[109] recently released the graphics software extension (GSX) which extends PC-DOS to include graphics input/output functions. Vectrix Corp,[110] have developed a high-resolution colour graphics subsystem that can be interfaced with many personal computer systems. This subsystem consists of an 8088 processor, an NEC 7220 graphics processor and 348 kbytes of graphics RAM, and can simultaneously display 512 colours. Finally, several books which describe the PC's graphics features are currently available.[111-113]

Software. If last year's software was "user-friendly", this year's software is claimed to be "integrated". Although integrated software means different things to different people, such software usually includes data-base management, word processing, electronic spreadsheet, high-resolution graphics and communications facilities, all in a single software package. Integrated software packages range from a number of application programs designed to work together, exchange information with one another, and share the same data files, to complete operating system environments that can handle and display several tasks simultaneously (they do windows, too!), and share the same data base. Most of these software packages, however, require wide memory resources, ample mass-storage and high-resolution graphics.

Because the PC meets these key requirements, some of the most sophisticated integrated software packages were either developed or are available for it. Included are: *Lotus 1-2-3,*[114] which integrates data base, spreadsheet and graphics facilities; *T/Maker III,*[115] which combines word processing, list processing, spreadsheet and graphics facilities; and *MBA,*[116] which incorporates data-base, word processing, spreadsheet, graphics and communications facilities in a single package. Ouchi[117] describes how Lotus's software package has been used in the laboratory.

Some software developers feel, however, that integrated software should function as an integral part of the operating system, and Microsoft calls this "Operating Software". Software packages that follow this philosophy include Microsoft's *Windows,*[45] VisiCorp's *Visi-on*[118,119] and Quarterdeck's *DesQ* package.[120] Micropro's *StarBurst*[121,122] takes a different approach by allowing users to link applications-software (such as *WordStar, MailMerge, SpellStar, DataStar, ReportStar, VisiCalc, SuperCalc, dBASE II* or *1-2-3*) into a menu-driven system. *Savvy*[123,124] combines pattern-recognition software, a programming language, a program generator for data-base management and a set of business applications software. When integrated software is supplemented with relational data bases,[125-128] it can result in a PC with information-management capabilities or PC-based "expert systems".[129,130]

In conclusion, although a user-friendly system is currently easier to imagine than to describe, it is believed that when HPI hardware is combined with integrated software and blended with concepts such as "desk-top metaphors" (*i.e.*, symbolic representation of a desk top on a computer display), icons and windows, the result may be paperless offices or laboratories and truly user-friendly computer systems.

Communications and networking

Communications and networking are emerging as areas crucial to the next generation of computer projects, not only in the laboratory but in all sectors of an information-driven society. Although the significance of communications has not yet been recognized by many, it is not accidental that one of the characteristics of the entire PC family is its communication capability. Indeed IBM promotes schemes involving PCjrs, PCs and XTs or XT/370s linked together. A general treatment of the application of PC in data communications and a detailed discussion of local area networks (LANs) is offered by Jordan *et al.*[131] Jordan[132] also gives a short course on communications software and briefly compares 12 communications-supporting programs.

Modems. Until recently, microcomputers and mainframes served separate spheres. Currently, ad-

vanced communication schemes provide the necessary tools for micro-to-mainframe connection and allow personal computers to access information banks by telephone. Modems are the major tools for such implementations. Welch[55] lists over 13 vendors marketing PC-compatible modems, and Powers[133] reviews four such modems.

Currently, the so-called "dumb" modem is being replaced by "intelligent" ones that incorporate microprocessors, local memory and advanced communications ICs. Some of the new-generation modems also offer voice and data-handling capabilities, allow the PC to operate unattended, or users to run the PC by remote control. Durham[134] discusses some of the features of "high IQ modems". "Intelligent" modems accompanied by appropriate software are expected to find their way into applications ranging from central data-base access to remote diagnostics. Jordan[135] provides an introduction to remote and unattended software and briefly compares[136] six commercially available packages that facilitate its operation.

Following the same concept, but implementing a different design, Vynet Corp.[137] have developed a board that provides a unique solution to computer communications, by allowing multiple users to engage in two-way communication with the PC through a push-button telephone. It also allows users to call or be called by the PC and receive spoken information. Clearly, developments of this type open the way to unattended laboratory operations.

Networks. Although the tools for the creation of two-way links between personal computers have long been developed, there is neither a standard topology for a personal computer network nor standard network-accessing techniques. Despite all the standardization difficulties, however, current literature suggests that "personal computers that stand alone no longer stand a chance". Because of the significance of local area networks in the laboratory, a brief discussion of selected LANs available to PC users follows.

The PCnet,[51] one of the first LANs to be specifically designed for the PC, is a low-cost, medium-performance, carrier-sense multiple-access with collision-detection (CSMA/CD) network. Information is transmitted through a coaxial cable of a maximum length of 7000 ft. Unlike many LANs, the PCnet does not incorporate a hard disk, but provides users with a choice of disk drives.

3 Com's Etherseries[138–141] comprised of EtherLink, EtherShare, EtherPrint and EtherMail, allows as many as 100 PCs to communicate through coaxial cables not longer than 2100 ft. Repeaters can increase this distance and, in addition, allow up to 1000 PCs to be linked to the network. The peripheral boards required for this network have been designed around Seeq's Ethernet chips.[142] Members of this high-performance CSMA/CD network can exchange data at a rate of 10 Mbit/sec.

Although the debate to "Ethernet or Ethernot" rages on, Ethernet still remains one of the most widely used networks. Churchill[143] briefly discusses Ethernet and lists several vendors offering Ethernet-based networks for the PC. Recognizing Ethernet's significance, the editors of *Electronics* awarded the 1983 achievement award to Robert Metcalfe, co-designer of Ethernet, formerly at Xerox's PARC and currently chairman of 3 Com Corp.

Polynet[114] is a ring-topology token-passing network that utilizes a twisted-pair cable to support its 10 Mbit/sec ring. The network can support up to 254 nodes with a maximum internode distance of 150 ft. The Standard Microsystems[145] ARC–PC board provides a simplified interface between the PC and a modified, Datapoint-developed, token-passing ring. The board, which supports up to 255 nodes, includes the standard Microsystems single-chip COM 9026 LAN controller and COM 9026 ArcNet LAN transceiver chip. The Plan 4000[146–148] is a 2.5-Mbit/sec baseband token-passing LAN designed to connect up to 255 PCs, Apple IIs and Apple IIIs. PerCom Data Corp's interface card,[149] designed around Western Digital's WD2840 network-control processor, links 254 PCs to a 1-Mbit/sec LAN. Several other PC-compatible networks are also available.[150–152]

Along with the unveiling of the Portable PC (PPC), IBM announced a hardware and software scheme (the Personal Computer Cluster Program) aimed at connecting up to 64 PCjrs, PCs, PPCs and XTs to a bus-structured network. This CSMA/CD network transmits data at 375 kbits/sec over a coaxial cable of maximum length 3280 ft.

Finally, inexpensive schemes that facilitate Apple II–IBM PC communication (*i.e.*, file transfers) are either commercially available[153,154] or discussed in the literature.[155]

Terminal emulation. Because of the number of mainframes installed worldwide, a number of applications for the PC have involved its use as a terminal emulator. In fact, the release of the IBM 3270-PC attempts to satisfy these demands. In addition to IBM, AST Research[156] offers a variety of hardware/software products that allow the PC to emulate IBM 3274, 3278, 3270 terminals and IBM 2780/3780 RJE work stations. Further, software[157] or hardware[158] for IBM 3278 terminal emulation, or software for DEC VT52 or VT100[159,160] and Tektronix 4010[161] terminal emulation are also commercially available.

Prototyping boards

Because experiments frequently demand creativity and novelty, they often require functions which are not provided by any of the commercially available boards. Several prototyping boards,[55] which come in all shapes and sizes, are available for tailor-made interfaces. Backplane bus signals and supply voltages are provided to the board by means of a 2×31 pin edge-type connector. IBM recommmends that data,

address, and some control signals should be buffered in order to avoid loading. It also provides simple address-decoding schemes for use with the prototyping board.

A GLIMPSE OF THE PC INFORMATION BASE

The volume of IBM PC-related information is overwhelming. At least 150 books on the IBM PC were published in 1983 alone, and 1500 abstracts are indexed in the *PC Abstracts*.[162] Because of the massive amount of information, the *PC Magazine*,[163] which contains over 500 pages per issue, became a fortnightly in 1984. This means that a subscriber can expect to receive about 13000 pages of PC related information per year, approximately a twentieth of the number of pages in *Chemical Abstracts* in 1983, and this is only *one* publication! There are at least 15 others published monthly. Consequently, keeping up with PC developments can easily become a full-time job. Because the amount of material is so vast, it is possible to present only a small fraction of it in what follows.

The theme of the November 1983 issue of *Byte* [164] was the IBM PC. The issue contained over twenty PC-related articles. Lemmon's article[165] is a good starting point for beginners. Though slightly dated and highly descriptive, it raises several points of particular interest to new PC users. For more advanced users, Williams's[166] comprehensive review is recommended, and Field's article[167] is more technical but of limited scope. Howson[168] describes how to use PEEK and POKE commands on the PC and also develops subroutines[169] which transfer the parameters of a BASIC program into the BIOS (basic input/output system) and store BIOS results in memory.

There are over 20 books which describe the PC's hardware and operating system and provide "how-to" information. Also the well-written PC technical manual is a source of detailed hardware information. Ashton-Tate's IBM PC Reference Encyclopedia,[170] updated twice a year, is a two-volume work that does not quite seem to live up to expectation. DeVoney's[171] and Lewis's[172] books offer a survey of the PC and are well suited to beginners. Several books are useful to the experienced user.[173–176] Works explaining the intricacies of the PC's Assembly language[177–179] and of interfacing[180,181] have also been published.

Understanding the PC's operating system (PC–DOS) results in improved programming efficiency. King[182] explains in detail how to use PC–DOS. Field[183] briefly discusses PC–DOS 2.00 (IBM's version of MS–DOS 2.00) and explains why device drivers are important and how they work on the PC; Archer[7] presents PC–DOS 2.00 in conjunction with the IBM XT. Microsoft's MS–DOS is described in some detail by Peterson,[184] and Larson[185] discusses MS–DOS 2.00. Roscos[186] describes how to write device drivers for MS–DOS 2.00 and provides an example. Norton[187] provides an introduction to both MS–DOS and PC–DOS. Finally, Guzaitis[188] briefly explains Concurrent CP/M.

A personal computer's ability to support several languages means that users may not have to be retrained in another language. BASIC, Pascal, FORTRAN, FORTH, APL and COBOL are some of the compilers available for the PC. Currently, modula-2,[189–193] and C language compilers are being introduced at an accelerated rate. Whether modula-2 will replace Pascal still remains to be seen.[194]

The virtues of the C language have been discussed elsewhere.[195] Phraner,[196] in an interesting article, compares nine C compilers for the PC. Houston *et al.*[197] compare several C compilers for CP/M-86, Kern[198] compares five C compilers for CP/M-80, and Clark[199] compares two recent versions of C for CP/M-80. Despite such developments and the fact that it has become rather fashionable to denigrate BASIC, most of today's software for microcomputers is still written in BASIC.

Artificial intelligence (AI) is probably the most controversial area in computer science. Intelligent supercomputers and Japan's "Fifth Generation Computer Project", the "Japanese Computer Sputnik", are being widely publicized, from scientific journals to the popular press. An added reason for this popularity is the commercial availability of tools for the development of AI-based software on microcomputers: Prolog[200] and Lisp[201–203] compilers are currently available for the PC. Wong[204] reviews three Lisp implementations for the PC, and the *Tk!solver*,[205,206] an expert system in the area of numerical-problem solving, is implemented in a Lisp-like language. Without a doubt, AI software and AI-based expert systems will become increasingly important in the analytical laboratory.

Several attempts, besides the AI main-stream, have also been made in order to provide a framework for PC-assisted problem-solving in specific areas. *SPSS/PC*[207] is a menu-driven PC-version of the SPSS-X mainframe statistical analysis and data-management package. A PC or XT with 320 kbytes of RAM, a hard disk and an 8087 are necessary. *Thinktank*,[208,209] a self-proclaimed idea-processor, is nothing but a word processor with data-base management capabilities which can be used as an outlining and organizing tool. Finally, the *Lab Management System*[210] is specifically designed for use in the analytical laboratory. It offers data-base management, statistical analysis of results, and report-generation.

Magazines

PC Magazine,[163] an independent guide to IBMs personal computers, features low-level articles on hardware, software, communications, and applications. Regular columns include news, product announcements and the "PC Blue Book", a short guide to PC suppliers and services. *PC World*[211] also fea-

tures low-level articles, news and product announcements and the "PC World Directory", which contains listings of PC-related services and products. Beginning with the March 1984 issue, the *PC World* also includes the *PCjr World*, a detachable supplement devoted to the PCjr. The *PC Tech Journal*[212] is aimed at sophisticated programmers and users who want to develop special interfaces for the PC. Some of its articles are quite advanced.

Softalk for the IBM PC[213] provides information on hardware, software and applications. It also includes tutorials and software reviews. *Personal Computer Age*[214] features general interest articles on hardware, software and peripherals. *PC Disk Magazine*[215] offers ready-to-run general interest programs for the PC. Each issue is accompanied by a floppy disk and a user's manual. Two IBM-specific electronic magazines, the *IBM PC Gazette* and *Real Times Magazine* are available in *The Source*.[216] Finally, several other microcomputer magazines and trade journals feature PC-related articles; they include *Creative Computing*[217] and *Byte*.[164]

Product directories

The most important advantage offered by a multiplicity of vendors, besides lower cost, is that both the instrument manufacturer and the end-user do not have to waste their efforts "re-inventing the wheel". Such competition, however, appears to be a mixed blessing when it comes to finding out what is commercially available. The answer to this question comes in the form of product directories.

Infosource for the IBM PC,[218] for example, is a monthly publication providing information about new PC-compatible hardware, software and accessories. The *Buyers Guide for the IBM PC*[219] is a short-form catalogue published every six weeks. *PC: The Product Directory*[215] is a bi-annual publication describing PC-compatible hardware, software, and peripherals. *Vanloves CP/M and PC Software Directory*[220] is an annual publication which offers software information of interest to CP/M and PC users. The *Directory of Independent IBM PC Hardware and Software*[221] contains descriptions and evaluations of more than 400 PC-compatible products. *The Book of IBM Software 1984*[222] claims to be "the first consumers' guide to IBM PC/XT and compatible software". Programs included are graded on an A–F scale according to several criteria such as ease of use, visual appeal, reliability, and error handling. Several programs for IBM PC-compatible equipment are also reviewed and rated.

The *PC Buyers Guide*,[223] collated by the publishers of *PC Magazine*, offers over 500 pages of PC-compatible hardware, software and accessories. The *1983/1984 PC World Annual Software Review*, collated by the publishers of *PC World*,[211] provides short descriptions of more than 1200 software packages. Programs in this 480-page edition are listed under two general classifications (system software and applications software), which are further subdivided into several categories. The *Software Guide for the IBM PC/XT*,[224] which is updated four times a year, is a 1000-page publication describing PC-compatible software. *The Ratings Newsletter*,[225] published ten times a year, compares and rates PC-compatible software. The *Electronic Catalog for IBM PC Owners*,[226] is a $5\frac{1}{4}$-in. single-sided floppy disk that provides access to menu-driven information concerning a wide range of PC-compatible hardware, software and accessories.

Finally, current issues of microcomputer magazines, especially those exclusively devoted to the IBM PC, can serve as further sources of information concerning new IBM PC-compatible hardware or software.

COMMENTS

The IBM Personal Computer's backplane has become a *de facto* industry standard, as demonstrated by the number of other vendors marketing PC-compatible peripheral boards and software packages. Moreover, millions of PCs have been sold worldwide and the PC is currently outselling the Apple IIe.

The PC has helped establish Intel's 8086/8088 family as a standard personal-computer microprocessor. Although the 8088 is a fully modern 8/16-bit design, IBM did not go far enough in selecting a microprocessor for the PC family. Though it has been suggested that microprocessors will skip a generation or two and will directly move from 8- to 32-bits, IBM's choice along with Apple's MC68000 choice suggests that the evolution toward 32-bit data paths will be more gradual.

With the exception of the S/370 boards for the XT, there are no innovative concepts introduced by the PC family, and "technological elegance is an apparent irrelevance on the PC". Fastie[227] in the first issue of the *PC Tech Journal*, concludes that the PC is neither a sophisticated nor an advanced system. Could millions of PC users be wrong?[64] There is no doubt that the PC's name plate has played a vital role in its success. The growing list of PC imitators suggests that the PC will represent the standard personal-computer architecture for some time to come, but it also suggests that this influence in the personal computer community is "stifling innovation because so many companies are mimicking Big Blue".

Personal computers become successful not only because of their hardware features, but mostly because of the software available for them. There are approximately 2000 application programs running under PC–DOS,[64] which favourably compares with the more than 3000 software packages available for Apple II. Most of the new applications software is being written for the IBM PC. To widen further the PC's applications-software base, IBM has set up a

Personal Computer Software Department[228] which accepts user-written software and markets it on a royalty basis. IBM's software contracts, however, do not seem to be very appealing to many authors.[229]

Cashing in on the PC's success, several companies offer personal computers that are "a little better and a little cheaper" but essentially the same as the PC. Giant companies such as Sperry (Sperry PC: 7.16-MHz, 8088-based), ITT (ITT XTra: 7.16-MHz, 8088-based), Tandy (Tandy 2000: 8-MHz, 80186-based) and Texas Instruments (T.I. Professional: 5-MHz, 8088-based) also offer personal computers running under MS–DOS. Imitations of the IBM PC may provide a cheaper alternative for the same computing power, but that is not to say that they are recommended, only that they can be considered as an alternative.

NOTE ADDED IN PROOF

A brief update of developments since this paper was first written is presented in the following. Although this is by no means complete, it will aid the interested reader in keeping abreast of developments in the IBM PC family of personal computers. IBM[1] have released extensive colour-graphics hardware and software, a host of data-acquisition boards and a network for the PC. Haugdahl[230] offers an updated review of Local Area Networks for the PC. IBM[1] have also released the AT (Advanced Technology), a 6-MHz, 80286-based personal computer. The December 1984 issue of *PC Tech Journal*[212] includes several articles describing the AT. Also *Byte* magazine has devoted a special issue to the IBM PC family.[231]

In software-related developments, Macmillan Software Co.[232] have released the *ASYST*, a scientific software package which integrates data-acquisition, data-processing (*i.e.*, curve-fitting, least-squares, convolution, integration, differentiation, smoothing, fast Fourier transform) and data-display capabilities. Laboratory Technologies Corp's[233] *Notebook* takes a similar approach to software design for scientific applications. This general-purpose menu-driven program supports several commercially available data-acquisition boards and subsystems, and easily integrates with Lotus's *1-2-3* or *Symphony*.[114] It offers real-time data-acquisition, control and graphics data-display and can handle both foreground and background tasks. Some of its other functions include fast Fourier transform, curve-fitting, statistics, data-base management and report-generation. This type of software is expected to increase the performance of analytical instrumentation while reducing the tedium of software development.

REFERENCES

1. IBM, P.O. Box 1328, Boca Raton, FL 33432.
2. J. Naisbitt, *Megatrends*, Warner, New York, 1982.
3. V. Karanassios and G. Horlick, *Talanta*, 1985, **32**, 601.
4. C. Morgan, *Byte*, 1983, **8**, No. 1, 100.
5. T. R. Clune, *ibid.*, 1984, No. 2, 278.
6. S. Glinert-Cole, *PC Tech. J.*, 1984, No. 5, 75.
7. R. Archer, Jr., *Byte*, 1983, **8**, No. 11, 294.
8. B. Machrone, *PC Mag.*, 1983, **1**, No. 11, 51.
9. *Idem, ibid.*, 1983, **1**, No. 12, 105.
10. IBM National Marketing Division, 4111 Northside Parkway, Atlanta, GA 30327.
11. B. Machrone, *PC Mag.*, 1984, **3**, No. 1, 146.
12. *PCjr*, P.O. Box 2450, Boulder, CO 80321.
13. K. Seger and A. Mello, *PC World*, 1984, **2**, No. 2, 114.
14. G. M. Vose and R. S Shuford, *Byte*, 1984, **9**, No. 3, 320.
15. Tecmar Inc., Personal Computer Division, 23600 Merchantile Rd., Cleveland, OH 44122.
16. Quadram Corp., 4357 Park Dr., Norcross, GA 30093.
17. T. V. Hoffmann, *PC Tech. J.*, 1984, **1**, No. 8, 52.
18. *Jr*, Box 903, Farmingdale, NY 11737.
19. COMPUTE! *PC & PCjr Magazine*, P.O. Box 974, Farmingdale, NY 11737–9874.
20. Microsoft Press, 10700 Northup Way, Bellevue, WA 98004.
21. *PC World*, 1984, **2**, No. 2, 94.
22. P. D. Estridge, D. J. Bradley and D. A. Krummer, *Proc. IEEE*, 1984, **73**, No. 3, 322.
23. D. M. Tucker, *PC World*, 1984, **2**, No. 1, 48.
24. H. Miller and E. Brown, *ibid.*, 1984, **2**, No. 5, 84.
25. B. Machrone, *PC Mag.*, 1984, **3**, No. 10, 112.
26. C. Dunford, *PC Tech. J.*, 1983, **1**, No. 3, 173.
27. *Idem, ibid.*, 1984, **1**, No. 4, 144.
28. RCS Inc., 2116A Walsh Ave., Santa Clara, CA 95050.
29. P. C. Horizons Inc., 200 North Tustin Ave., Santa Ana, CA 92705.
30. Desert Technologies, P.O. Box 41628, Tucson, AZ 85717.
31. I-Bus Systems, 8863 Balboa Avenue, San Diego, CA 92123.
32. Appart Inc., 4401 S. Tamarac Parkway, Denver, CO 80237.
33. Colby Computer Inc., 2 Palo Alto Sq., Palo Alto, CA 94304.
34. J. Palmer, R. Nave, C. Wymore, R. Koebler and C. McMinn, *Electronics*, 1980, **53**, No. 11, 114.
35. C. McMinn, *Conf. Rec. Electro* 80, Paper 14/5, Boston, MA, 1980.
36. *T. Zingale, Conf. Rec. Electro* 82, Paper 18/1, Boston, MA, 1982.
37. R. Startz, *8087: Applications and Programming for the IBM PC and other PCs*, Brady, Bowie Md, 1983.
38. R. B. Simington, *Byte*, 1983, **8**, No. 4, 154.
39. W. Cooke, *PC World*, 1983, **1**, No 10, 256.
40. T. Field, *Byte*, 1983, **8**, No. 8, 331.
41. *Idem, ibid.*, 1983, **8**, No. 9, 331.
42. Field Computer Products, 909 North San Antonio Rd., Los Angeles, CA 94022.
43. MicroWare, P.O. Box 79, Kingston, MA 02364.
44. Hauppauge Computer Works Inc., 358 Veterans Memorial Highway, Suite MSI, Commack, NY 11725.
45. Microsoft Corp., 10700 Northup Way, Bellvue, WA 98004.
46. MICROCOMPATIBLES, 11443 Oak Leaf Drive, Silver Springs, MD 20901.
47. Sritek Inc., 6615 Snowville Rd., Cleveland, OH 44141.
48. S. Kavuru, *Byte*, 1983, **8**, No. 6, 194.
49. Ryan-McFarland Corp., 609 Deep Valley Dr., Cleveland, OH 44141.
50. Titan Technologies Inc., P.O. Box 8050, Ann Arbor, MI 48107.
51. Orchid Technology, 47790 Westinghouse Dr., Fermont, CA 94539.
52. S. Ciarcia, *Byte*, 1984, **9**, No. 5, 40.
53. Sweet Micro Systems Inc., 50 Freeway Dr., Cranston, RI 02910.

54. W. L. Rosch, *PC Mag.*, 1984, **3**, No. 3, 147.
55. M. J. Welch, *Byte*, 1983, **8**, No. 11, 168.
56. MA Systems, 2015 O'Toole Ave., San Jose, CA 95131.
57. Advanced Digital Corp., 5432 Production Dr., Huntington Beach, CA 92649.
58. Analogic Corp., Audubon Rd., Wakefield, MA 01880.
59. Marinco Computer Products, 3878 Ruffin Rd., San Diego, CA 92123.
60. V. Karanassios and G. Horlick, *Talanta*, 1985, **32**, 583.
61. Bit 3 Corp., 8120 Penn. Ave. South, Minneapolis, MN 55431.
62. RMAC Corp., 716-G Capitola Ave., Capitola, CA 95010.
63. Transiac Corp., 815 Maude Ave., Mountain View, CA 94043.
64. F. Gens and C. Christiansen, *Byte*, 1983, **8**, No. 11, 135.
65. A. A. Gleckler, *PC Tech. J.*, 1984, **1**, No. 4, 66.
66. Ecosea Technologies Corp., Unit 13, 465 King St., E. Toronto, Ontario M5A 1L5.
67. Xelix Systems and Development Corporation, 11952 Wilshire Blvd., Los Angeles, CA 90025.
68. Hicomp Computer Corp., 3860—148th Ave. N.E., Redmond, WA 98052.
69. Alloy Computer Products, 12 Mercer Rd., Natick, MA 01760.
70. Sysgen Inc., 47853 Warm Springs Rd., Fermont, CA 94539.
71. IBEX Computer Corp., 20741 Marilla St., Chatsworth, CA 91311.
72. Santa Clara Systems Inc., 1860 Hartog Dr., San Jose, CA 95131.
73. Computer Peripherals Inc., 220 West Higgins Rd., Suite 245, Hoffman Estates, IL 60195.
74. StarLogic, 20860 Plummer St., Chatsworth, CA 91311.
75. Chrislin Industries Inc., Computer Products Division, 31352 Via Colinas, #102 West Lake Village, CA 91361.
76. Microdisk Inc., 1422 Industrial Way, P.O. Box 1377, Gardnerville, NV 89410.
77. RanaSystems, 21300 Superior St., Chatsworth, CA 91311.
78. Falcon Technologies Inc., 6644 South 196th St., Suite T-101, Kent, WA 98032.
79. Interphase Corp., 2925 Merrell Rd., Dallas TX 75229.
80. Control Data Corp., 7725 Washington Ave. South, Edina, MN 55435.
81. Data Translation, 100 Locke Drive, Marlborough, MA 01752.
82. A. Davis and J. Fierke, *Computer Design*, 1983, **22**, No. 5, 101.
83. S. G. Gates, *Byte*, 1984, **9**, No. 5, 366.
84. Gould Inc., Recording Systems Division, 3631 Perkins Ave., Cleveland, OH 44114.
85. Keithley DAS, 349 Congress St., Boston, MA 02210.
86. Modular Integration Inc., P.O. Box 1079, 1145 12th Ave., NW, C-1, Issaquash, WA 98027.
87. Ariel Corp., Suite 84, 600 West 116th St., New York, NY 10027.
88. Northwest Instrument Systems Inc., P.O. Box 1309, Beaverton, OR 97075.
89. Atron Corp., 20665 Fourth St., Saratoga, CA 95070.
90. Micromint Inc., 561 Willow Ave., Cedarhurst, NY 11561.
91. Micron Technology Inc., 2805 East Columbia Rd., Boise, ID 83706.
92. Imaging Technologies Inc., 400 West Cummings Park, Suite 4350, Woburn, MA 01801.
93. Datacopy Corp., 1070 East Meadow Circle, Palo Alto, CA 94303.
94. P. Von Stackelberg, *PC Mag.*, 1983, **2**, No. 3, 445.
95. M. Feeley and N. F. Stewart, *Graphics Interface 83 Proceedings*, Canadian Information Processing Society, Edmonton, 9–13 May 1983.
96. R. E. Dessy, *Anal. Chem.*, 1984, **56**, 68A.
97. Microtouch Systems Inc., Suite 5050, 400 W. Cummings Park, Woburn, MA 1801.
98. Pencept Inc., 39 Green St., Waltham, MA 02154.
99. GTCO Corp., 1055 First St., Rockville, MD 20850.
100. Laboratory Computer Systems Inc., 139 Main St., Cambridge, MA 02142.
101. SuperSoft, P.O. Box 1628, Champaign, IL 61820.
102. Logitech Inc., 165 University Ave., Palo Alto, CA 94301.
103. Random Access Inc., 246 Highland Rd., Pittsburgh, PA 15253.
104. C. Peters, *Byte*, 1983, **8**, No. 7, 130.
105. R. E. Dessy, *Anal. Chem.*, 1984, **56**, 303A.
106. R. Jadrineck, *Byte*, 1984, **9**, No. 1, 172.
107. T. Field, *ibid.*, 1983, **8**, No. 11, 99.
108. T. Waldow, *ibid.*, 1983, **8**, No. 12, 343.
109. Digital Research, 160 Central Ave., Pacific Grove, CA 93950.
110. Vectrix Corp., 1416 Boston Rd., Greensboro, NC 27407.
111. D. Conklin, *Art and Animation on the IBM PC*, Wiley, New York, 1983.
112. N. Ford, *Business Graphics for the IBM PC*, Sybex, Berkeley, 1983.
113. M. Waite and C. Morgan, *Graphics Primer for the IBM PC*, Osborne/McGraw-Hill, Berkeley, 1983.
114. Lotus Development Corp., 161 First St., Cambridge, MA 02142.
115. T/Maker Co., 2115 Landings Dr., Mountain View, CA 94043.
116. Context Management Systems, Suite 101, 23864 Hawthorne Blvd., Torrace, CA 90505.
117. G. I. Ouchi, *PC World*, 1984, **2**, No. 2, 222.
118. VisiCorp., Inc., 2895 Zanker Rd., San Jose, CA 95134.
119. G. Woodmansee, *Byte*, 1983, **8**, No. 7, 166.
120. Quarterdeck Software, 1918 Main St., Suite 240, Santa Monica, CA 90405.
121. Micropro International Corp., 33 San Pablo Ave., San Rafael, CA 94903.
122. S. Vandor, *Byte*, 1983, **8**, No. 12, 189.
123. Excalibur Technologies Corp., 800 Rio Grande Blvd. NW, 21 Mercado Plaza, Albuquerque, NM 87104.
124. P. V. Callamaras, *Byte*, 1984, **9**, No. 2, 303.
125. Cypher, 121 Second St., San Francisco, CA 94105.
126. Rox Research Inc., 7005 Corporate Way, Dayton, OH 45459.
127. Mosaic Software Inc., 1972 Massachusetts Ave., Cambridge, MA 02140.
128. J. W. Walker, *Byte*, 1984, **9**, No. 2, 267.
129. Teknowledge Inc., 525 University Ave., Palo Alto, CA 94301.
130. Export Software International Ltd., 11 Olive St., Great Neck, N.Y. 11020.
131. L. E. Jordan and B. Churchill, *Communication and Networking for the IBM PC*, Brady, Bowie Md, 1983.
132. L. Jordan, *PC World*, 1983, **1**, No. 5, 74.
133. J. Powers, *PC Mag.*, 1983, **1**, No 9, 238.
134. S. Durham, *Byte*, 1983, **8**, No. 9, 51.
135. L. Jordan, *PC World*, 1984, **2**, No. 2, 66.
136. *Idem*, *ibid.*, 1984, **2**, No. 2, 132.
137. Vynet Corp., 160B Albright Way, Los Gatos, CA 95030.
138. 3 Com Corp., 1390 Shorebird Way, Mountain View, CA 94043.
139. K. Goldestein, *PC Mag.*, 1983, **1**, No. 9, 152.
140. L. Birenbaum, *Byte*, 1983, **8**, No. 11, 272.
141. S. Glinert-Cole, *PC Tech. J.*, 1984, **1**, No. 4, 54.
142. H. J. Hindin, *Electronics*, 1982, **55**, No. 20, 89.
143. B. W. Churchill, *PC Tech. J.*, 1983, **1**, No. 3, 87.
144. Logica Inc., 3 Embarcadero Center, San Francisco, CA 94939.

145. Standard Microsystems Corp., 35 Marcus Blvd., Hauppauge, NY 11788.
146. Nestar Systems Inc., 2585 E. Bayshore Rd., Palo Alto, CA 94303.
147. K. Goldestein, *PC Mag.*, 1983, **1**, No. 9, 162.
148. B. Churchill, *PC Tech. J.*, 1984, **1**, No. 5, 58.
149. PerCom Data Corp., 11220 Pagemill Rd., Dallas, TX 75234.
150. Novell Inc., 1170 N. Industrial Park Dr., Orem, Utah 84057.
151. Corvus Systems, 2029 O'Toole Ave., San Jose, CA 95131.
152. VLSI Networks Inc., 6214 W. Manchester Blvd., Suite 202, Los Angeles, CA 90045.
153. Alpha Software Corporation, 30 B Street, Burlington, MA 01803.
154. A. Holmes, *PC Mag.*, 1984, **3**, No. 3, 141.
155. R. Jones, *Byte*, 1984, **9**, No. 2, 331.
156. AST Research Inc., 2372 Morse Ave., Irvine, CA 92714.
157. Phone 1 Inc., 461 North Mulford Rd., Rockford, IL 61107.
158. Technical Analysis Corp., 120 West Wieuca Rd. NE, Atlanta, GA.
159. Coefficient Systems Corp., 611 Broadway, Suite 426B, New York, NY 10012.
160. Persoft Inc., 2740 Ski Lane, Madison, WI 53713.
161. MicroPlot Systems, 1897 Red Fern Dr., Columbus, OH 43229.
162. *PC Abstracts*, P.O. Box 1058, Jenks, OK 74037.
163. *PC Magazine*, P.O. Box 598, Morris Plains, NJ 07950.
164. *Byte*, P.O. Box 590, Martinsville, NJ 08836.
165. P. Lemmons, *Byte*, 1981, **6**, No. 10, 26.
166. G. Williams, *ibid.*, 1982, **7**, No. 1, 72.
167. T. Field, *ibid.*, 1983, **8**, No. 3, 331.
168. H. E. Howson, *ibid.*, 1983, **8**, No. 11, 121.
169. *Idem*, *ibid.*, 1983, **8**, No. 12, 417.
170. Ashton-Tate, 10150 West Jefferson Boulevard, Culver City, CA 90230.
171. C. DeVoney, *IBM's Personal Computer*, 2nd Ed., Que, Indianapolis, 1983.
172. T. G. Lewis, *Using the IBM Personal Computer*, Reston, Reston Virginia, 1983.
173. L. Poole, *Using Your IBM Personal Computer*, Sams, Indianapolis, 1983.
174. J. F. Kelley, Jr., *The IBM Personal Computer Guide*, Banbury Books, Dell Trade Plks, New York, 1983.
175. L. J. Graham, *Your IBM Personal Computer*, McGraw-Hill, New York, 1983.
176. P. Norton, *Inside the IBM PC: Access to Advanced Features and Programming*, Brady, Bowie Md, 1983.
177. L. J. Scalcon, *IBM PC/XT Assembly Language: A Guide for Programmers*, Brady, Bowie Md, 1983.
178. D. C. Willson and J. I. Kratnz, *8088 Assembler Language Programming*, Sams, Indianapolis, 1983.
179. R. Lafore, *Assembly Language Primer for the IBM PC*, Plume/Waite, New York, 1984.
180. M. Sargent and R. L. Shoemaker, *Interfacing the IBM PC to the Real World*, Addison-Wesley, Reading Mass., 1983.
181. J. W. Coffron, *IBM PC Connection*, Sybex, Berkeley, 1983.
182. R. A. King, *IBM PC–DOS Handbook*, Sybex, Berkeley, 1983.
183. T. Field, *Byte*, 1983, **8**, No. 11, 188.
184. T. Peterson, *ibid.*, 1983, **8**, No. 6, 230.
185. C. Larson, *ibid.*, 1983, **8**, No. 11, 285.
186. J. E. Roscos, *ibid.*, 1984, **9**, No. 2, 370.
187. P. Norton, *MS DOS and PC DOS: User's Guide*, Brady, Bowie MD, 1983.
188. J. Guzaitis, *Byte*, 1983, **8**, No. 11, 257.
189. J. McCormack and R. Gleaves, *ibid.*, 1983, **8**, No. 4, 385.
190. The Modula Research Institute, 950 North University, Provo, UT 84604.
191. Volition Systems, P.O. Box 1236, Del Mar, CA 92014.
192. JRT Systems Inc., 45 Camino Alto, Mill Valley, CA 94941.
193. Logitech, 165 University Ave., Solana Beach, CA 94301.
194. M. C. Johnson and A. Munro, *Byte*, 1984, **9**, No. 3, 371.
195. *Special Issue on the C Language*, *ibid.*, 1983, **8**, No. 8.
196. R. A. Phraner, *ibid.*, 1983, **8**, No. 8, 134.
197. J. Houston, J. Brodrick and L. Kent, *ibid.*, 1983, **8**, No. 8, 82.
198. C. O. Kern, *ibid.*, 1983, **8**, No. 8, 110.
199. D. D. Clark, *ibid.*, 1984, **9**, No. 5, 246.
200. Prolog Systems, 54 Edgemond Rd., Milford, CT 06460.
201. The LISP Company, 330 C Village Lane, Los Gatos, CA 95030.
202. The Soft Warehouse, P.O. Box 1328, Honolulu, Hawaii 96828.
203. Integral Quality, P.O. Box 31970, Seattle, WA 98103-0070.
204. W. G. Wong, *PC Tech. J.*, 1984, **1**, No. 7, 112.
205. Software Arts, 27 Mica Lane, Wellsley, MA 02181.
206. M. Konopasek and S. Jayaraman, *Byte*, 1984, **9**, No. 5, 137.
207. SPSS Inc., Marketing Dept., Suite 3000, 444 North Michigan Ave., Chicago, IL 60611.
208. Living Videotext Inc., 1000 Elwell Court, Palo Alto, CA 94303.
209. W. R. Hershey, *Byte*, 1984, **9**, No. 5, 189.
210. Scientific Software, 2 Sequoia Tree Lane, Irvine, CA 92715.
211. *PC World*, P.O. Box 6700, Bergenfield, NJ 07621.
212. *PC Tech. Journal*, P.O. Box 598, Morris Plains, NJ 07950.
213. Softalk Publishing Inc., 11160 McCormick St., North Hollywood, CA 91603.
214. *Personal Computer Age*, P.O. Box 70725, Pasadena, CA 91107.
215. Ziff-Davis Publishing Co., One Park Ave., New York, NY 10016.
216. Source Telecomputing Corp., 1616 Anderson Rd., McLean, VA 22012.
217. *Creative Computing*, P.O. Box 5214, Boulder, CO 80321.
218. QUERY, P.O. Box 417, Bogota, NJ 07603.
219. Starware, 1701 K St. NW, Washington, DC 20006.
220. R. Love (ed.), *Vanloves CP/M and PC Software Directory*, Software Technology Inc., 6720 W 66th Terrace, Shawnee Mission, KS 66201.
221. Infopro Inc., P.O. Box 22, Bensalem, PA 19020.
222. *The Book of IBM Software 1984*, The Book Co., Los Angeles, 1984.
223. *PC Buyers Guide*, CN 1914, Morristown, NJ 07960.
224. Micro-Information Publishing, 15420 Eagle Creek Ave., Prior Lake, MN 55374.
225. Software Digest, One Wynnewood Road, Wynnewood, PA 19096.
226. IBM Corp., P.O. Box 3148, Wallingfort, CT 06494.
227. W. Fastie, *PC Tech. J.*, 1983, **1**, No. 1, 50.
228. IBM External Submissions, Dept. 756 PC, Armonk, NY 10504.
229. J. Pournelle, *Byte*, 1983, **8**, No. 7, 340.
230. I. S. Haugdahl, *ibid.*, 1984, **9**, No. 12, 147.
231. *Ibid.*, 1984, **9**, No. 9.
232. Macmillan Software Co., 866 Third Av., New York, NY 10022.
233. Laboratory Technologies Corp., 255 Ballard St., Wilmington, MA 01887.

Talanta, Vol. 32, No. 8A, pp. 633–639, 1985
Printed in Great Britain

0039-9140/85 $3.00 + 0.00
Pergamon Press Ltd

GFAAS DETERMINATION OF ULTRATRACE QUANTITIES OF ORGANOTINS IN SEA-WATER BY USING ENHANCEMENT METHODS*

E. J. PARKS, W. R. BLAIR and F. E. BRINCKMAN
Chemical and Biodegradation Processes Group, National Bureau of Standards, Washington, D. C. 20234, U.S.A.

(*Received* 31 *December* 1984. *Revised* 18 *March* 1985. *Accepted* 30 *March* 1985)

Summary—Tributyltin in sea-water is preconcentrated by extraction into toluene and determined by enhanced graphite-furnace atomic-absorption (GFAAS) at ultratrace concentrations (as low as 1.0 μg/l.) equal to or lower than the toxic limits for aquatic organotins. Toluene is preferred to MIBK, chloroform or hexane as the solvent. Sea salts, in concentrations as low as 0.1%, critically interfere with GFAAS tin determinations, and must be removed by washing the extract with demineralized water. Signal enhancement effected by inserting L'vov platforms in the graphite furnace tubes or by adding ammonium dichromate to the analyte solution is nearly additive when both methods of enhancement are combined.

The determination of organotin species in sea-water at trace and ultratrace concentrations (from ng/ml to μg/ml) is becoming increasingly important as man-made sources of organotins increase in quantity relative to natural sources.[1]

Antifouling paints incorporating the toxic tributyltin moiety are finding widespread and increasing usage on ocean-going ships, buoys, and wooden pilings for long-term protection from marine microorganisms.[2–4]

Tributyltin compounds mixed with elastomers also serve as molluscicides, notably for the control of tropical parasites.[5] From an engineering standpoint, control of the kinetics and mechanisms by which organotins are released into saline waters is needed, in order to generate criteria for the performance and durability of such materials, as well as to evaluate the environmental impact of the species released. The solubility of the major organotin biocides, tributyltin chloride (TBTC) or tributyltin oxide (TBTO), in sea-water is about 10 μg/ml or less. This concentration far exceeds the toxic levels of the bioactive solvated tributyltin cation produced from either compound.[6] Consequently, reliable analytical data at ng/ml levels are necessary to characterize early-release rates from commercial "sustained-release" materials containing organotins. The concentration range of environmental importance extends below the ng/ml level, since certain non-target marine species are sensitive to tributyltin in concentrations of 0.6–1.5 ng/ml.[4]

All such studies have been hampered by the difficulty of determining heavy metals in saline waters at very low concentrations,[6] and these problems are exacerbated by the volatility and unusual decomposition behaviour of organometallics during analysis.[7] Graphite-furnace atomic-absorption spectroscopy (GFAAS) has the specificity and sensitivity needed to determine nanograms of tin in either organic solutions or in demineralized water,[7] but suffers sensitivity losses when the sample matrix contains salts. Moreover, special precautions may be required for reducing tin volatilization during the atomization procedure. Attempts to determine tin in sea-water by alternative methods gave highly erratic results, with apparent recoveries ranging from 50% to over 300% under the same experimental conditions, when applied to organic extracts from sea-water spiked with organotin at ng/ml level.[4]

Our results presented here spring from two novel developments. We have increased the sensitivity of GFAAS for organotins by chemical enhancement of the tin-specific GFAAS signal,[8] and have demonstrated the critical importance of removing salts, even at μg/ml levels, from the organic extract before measurement by GFAAS.

The extraction procedure described here is a sensitive method for determination of the levels of extractable tin compounds present in aqueous saline samples. As current analytical interest centres on the toxic tributyltin cation and its degradation products, di- and monobutyltin, efforts have been made to optimize the recovery of these species. However, to realize maximum information from samples showing the presence of tin, further analysis by a method designed for speciation of tin compounds is required.

*Portions of this work were presented at the 186th National Meeting of the American Chemical Society, Washington, D.C., 28 August–2 September 1983, paper ANYL 095. Contributions from the National Bureau of Standards are not subject to copyright.

EXPERIMENTAL*

Instrumentation

The graphite-furnace atomic-absorption spectrophotometer system used was a Perkin-Elmer Model 460 equipped with a tin EDL. A wavelength of 224.6 nm was used. Pyrolytically coated graphite-furnace tubes of two types were employed: regular tubes, and L'vov type tubes fitted with a graphite platform insert.[9] The GFAAS programme consisted of drying for 20 sec at 100°, charring with a temperature ramp from 100 to 1000° in 10 sec, and atomization for 6.5 sec at 2700°. The gas flow (argon, 400 ml/min) was interrupted during atomization.

The demineralized water (specific resistance greater than 10 megohm-cm) was prepared with a Culligan reverse-osmosis Reagent Water System. Extraction of aqueous organotin solutions with organic solvent was performed either manually or with a high-speed mechanical mixer (Vortex Genie, Scientific Industries, Bohemia, NY 11716).

Reagents

Artificial sea-water with a salinity of about 36 g/kg and dilutions thereof, were prepared from demineralized water and salts of reagent-grade purity in the molar concentrations: NaCl, 0.4106; $MgCl_2$, 0.0298; $MgSO_4$, 0.0284; KCl, 0.0093.[10] Natural estuarine water exhibits a considerable range of salinity. Measurements made in Chesapeake Bay showed that the salinity ranges from virtually open-ocean levels at the southern mouth of the Bay to only 1–2 g/kg at the northern end where the major fresh water influx occurs. Consequently, a sequence of diluted salt solutions, with the concentrations indicated in Fig. 1, was used to evaluate more realistically the estuarine salt concentration effects on the GFAAS background signal intensity.

All organic solvents were obtained commercially and were of reagent-grade purity, or better. Reagent grade ammonium dichromate dissolved in demineralized water was used for enhancement of GFAAS signals. Tributyltin chloride and dibutyltin dichloride (Alfa Products, Danvers, MA 01923) and monobutyltin trichloride (M & T Chemicals, Rahway, NJ 07065) were dissolved in "spectrograde" methanol at concentrations of approximately 1000 μg/ml and diluted with various solvents to provide organotin solutions of known concentration.

Samples

Samples of relatively uncontaminated Chesapeake Bay water were obtained at flood tide at a point near the centre of the Bay off the mouth of the Choptank River, from a depth of 6 m, by submerging acid-cleaned (10% nitric acid warmed overnight at 60°) Pyrex glass bottles from which the stoppers were removed at the measured depth.[11] Additional samples of estuarine water were obtained similarly at a depth of 1 m from the Inner Harbor area of Baltimore, Maryland, a water area of dense ship and motorboat traffic, also affected by urban-industrial waste-water.

To prepare samples spiked with organotin species at the desired concentrations, 50 μl of a methanolic organotin solution (1 g/l.) was diluted to a total volume of 50 ml to give a 1-μg/ml solution. Aliquots of the latter solution were added to specific volumes of solvents to provide the lower concentrations of organotin, *e.g.*, 400 μl added to 400 ml of sea-water provided reliable spiked solutions containing tin at 1 ng/ml concentration. Several measurements of organotin in demineralized water were made with and without extraction of the organotin species.

The saline solutions containing tin at 1 μg/ml concentration were prepared fresh each day. From such solutions, extraction of triorganotin into an aromatic solvent (benzene) is almost complete, and the aqueous solutions of Bu_3Sn^+ and Bu_2Sn^{2+} are stable over a period of several weeks.[12] Spiked samples of much lower tin concentration were usually extracted within a few minutes after addition of the organotin. For comparison of recovery from sea-water by toluene extraction, tri-, di-, and monobutyltin species (4 ng/ml) were extracted individually from 50-ml portions of artificial sea-water. Determinations were normally completed within 15 min of doing the extraction.

Extraction

The extraction procedure used depended on the concentration of the organotin. For the range 0–1 ng/ml, 400 ml of sea-water were vigorously shaken manually with 2 ml of toluene in a 500-ml separatory funnel for 5 min, and allowed to stand for at least 10 min before all but 10 ml of the aqueous phase was drained off. The organic phase and the small amount of aqueous solution retained were transferred to a smaller (30-ml) separatory funnel, for removal of the remaining sea-water by washing the organic phase three times with 6-ml portions of demineralized water. For organotin concentrations in the range 0–50 ng/ml, or higher, the high-speed mechanical mixer was used to extract smaller portions of solution with toluene, with 3 cycles of vigorous mixing (1 min) and standing (30 sec), before separation and washing of the organic phase.

Atomic-absorption (AA) measurements

For AA measurements, 20-μl aliquots were transferred automatically by a Perkin-Elmer AS-1 Autosampler from polyethylene cups into the graphite furnace. The optimized atomization programme was used. To each cup was added 0.1 ml of 0.1*M* ammonium dichromate in water, 0.6 ml of 2-propanol and 0.3 ml of toluene extract, resulting in a single-phase solution with a final dichromate concentration of 0.01*M*. For each concentration measured, 6 replicate AA measurements were made and the mean standard deviation is reported.

RESULTS AND DISCUSSION

Chemical enhancement

Figure 1 illustrates the effect of signal enhancement on detection of tributyltin in demineralized water by GFAAS. Ammonium dichromate is introduced into the furnace, together with analyte, in a single 20-μl aliquot. The GFAA signal intensity is a linear function of the tributyltin concentration for solutions containing between 0 and 5 ng of tin per aliquot in solutions 0.01*M* in ammonium dichromate. However, Beer's law is not obeyed at the higher organotin concentrations. The diminishing molar ratio of dichromate to tin may partially account for the deviation from linearity.[8] However, the range of organotin concentrations of interest in the present work requires measurement of less than 2 ng of tin, well within the linear range for tributyltin in demineralized water.

Background interference in the direct determination of heavy metals, including tin, in sea-water has necessitated inclusion of a variety of separation procedures in other methods: electrochemical deposi-

*Certain commercial equipment or material is identified in this paper in order to specify adequately the experimental procedure. In no case does such identification imply recommendation or endorsement by the National Bureau of Standards, nor does it imply that the material or equipment identified is necessarily the best available for the purpose.

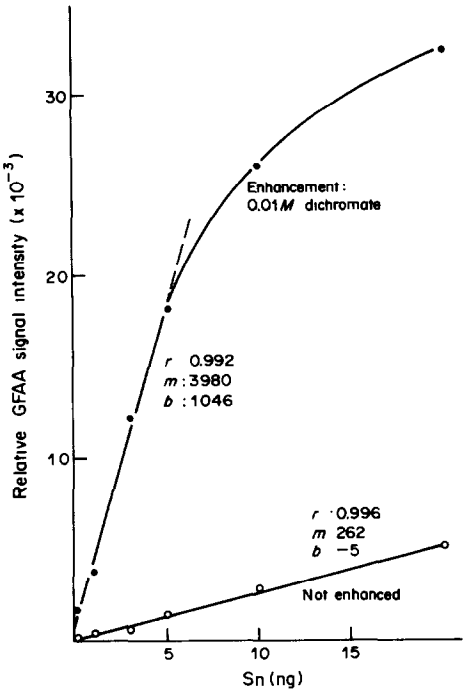

Fig. 1. GFAAS detection of tributyltin in demineralized water with and without chemical enhancement. Samples were prepared by diluting methanol stock solution (1 μg/ml) with water. Numbers along the abscissa represent quantities of atomized tin. Linear portion of the curve calculated between 0.0 and 5.0 ng (r = correlation coefficient; m = slope, μV . sec . ng^{-1}; b = intercept, μV . sec).

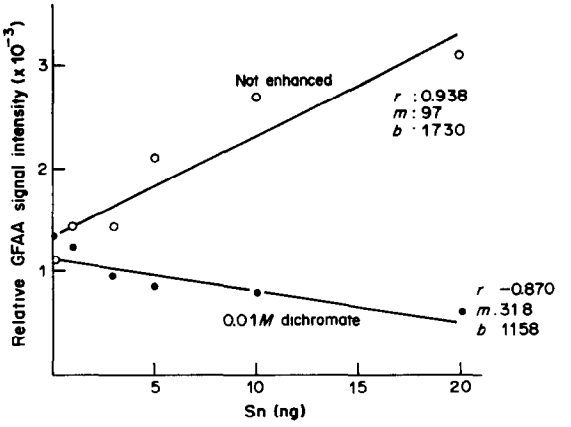

Fig. 2. Interference by sea salts in tin-specific GFAAS of varied concentrations of tin (r, m and b have same meanings as in Fig. 1).

tion of metals on refractory materials capable of withstanding high temperatures, followed by the volatilization of analytes for atomic-absorption spectroscopy;[13] solvent extraction processes aided[12,14,15] or not aided[15,16] by complexation; and volatilization of organotin compounds as their hydrides or alkyls.[17] Blair *et al.*[18] attempted to determine tin at μg/ml levels directly in samples of artificial sea-water during a kinetic, controlled-release experiment in which wooden piles impregnated with tributyltin and methacrylate polymer released the tributyltin moiety over a period of several days. However, they noted low precision for replicate determinations and poor correlations of tin concentration with time. Ward *et al.*[4] measured ^{14}C TBTO radiometrically over a period of 58 days in sea-water containing test fish, but there was unexplained scatter in their results, which ranged from 45 to 300% of the nominal concentrations.

In view of the successful GFAA enhancement methods discovered for lead and tin,[8] we decided to investigate whether sea salts would also interfere in the detection of tin in the presence of ammonium dichromate as enhancing agent.

In the absence of dichromate ions, the slope correlating GFAAS signal with tin content in demineralized water (Fig. 1) exceeds by a factor of three that for tin in sea-water (Fig. 2). With dichromate, no enhancement at all is obtained in the presence of sea salts. The apparently negative slope is probably an artifact of the high intercept and poor linear correlation.

Figure 3 illustrates the suppression of the GFAAS signal caused by increasing concentrations of sea salts when the organotin concentration is held constant at 20 ng per 20-μl aliquot, and the total salt concentration is increased from 0 to 36.7 mg/ml (0–734 μg per 20-μl aliquot). In the absence of added salts, the GFAAS signal intensity for tin is enhanced by dichromate by a factor of seven. The salts suppress the GFAAS signal intensity much more strongly in the absence of dichromate. As a net result, the enhancement factor increases to about 15 for a salt concentration of 0.03 mg/ml (0.6 mg per 20-μl aliquot). Thus, as little as 0.01% of the salt concentration typical of sea-water is sufficient to cause maximum

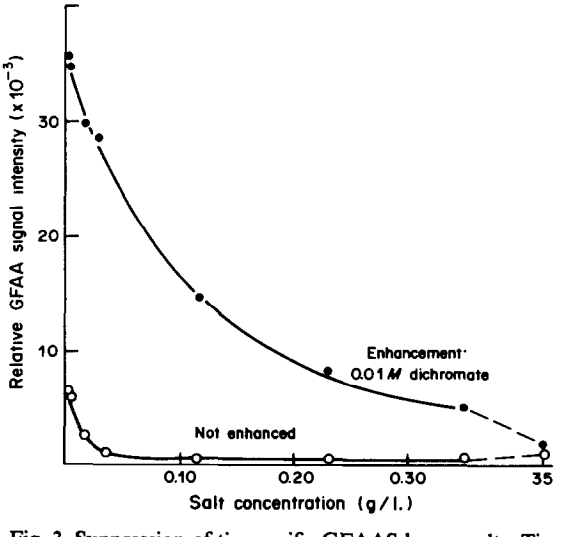

Fig. 3. Suppression of tin-specific GFAAS by sea salts. Tin concentration: 1 μg/ml (20 ng per specimen atomized). Salt concentration varied up to 36 g/kg (typical of sea-water).

Table 1. Determination of tin as Bu_3SnCl in demineralized water by GFAAS

Conditions	Slope,† $\mu V . sec . ng^{-1}$	Intercept, $\mu V . sec$	Detection limit, ng
Regular GFAA tube			
without dichromate	2030	650	0.41
with dichromate*	5550	1470	0.28
L'vov tube			
without dichromate	3790	810	0.25
with dichromate*	6800	1370	0.34

*0.01M $(NH_4)_2Cr_2O_7$.
†Range 0–20 ng of tin.

suppression of the tin signal in the absence of dichromate.

We may infer from these results that dichromate ions prevent the formation of volatile tin species at temperatures below that of atomization, but the molecular process is unclear. As the tin:chlorine ratio is about 1:25 at the point of maximum suppression, no simple chemical mechanism or direct stoichiometry between tin and chloride concentrations promoting formation of volatile species such as $SnCl_4$ can be deduced. The progressive suppression of the GFAAS signal with increasing salt concentrations in the presence of dichromate may indicate competition for tin between dichromate ions and, probably, chloride. Alternatively, chromyl chloride may be formed and volatilized, which would decrease the amount of dichromate available for enhancement purposes. In either case, it is critically important in organotin determinations to separate the covalent tin-bearing species from the chlorides in sea-water.

Physical enhancement

A recent development in GFAAS involves inserting graphite platforms, usually referred to as L'vov platforms,[9] into the conventional furnace tubes. Analyte volatilization is thus delayed because the elevated platform reaches maximum temperature somewhat more slowly than the furnace tube itself, and the probability that analyte will be volatilized before the absorption signal is measured is significantly diminished. The utility for determination of low-boiling covalent compounds, typified by organometallics is obvious. L'vov has reported an enhancement factor of two or three for lead, manganese and cadmium when platforms are used instead of ordinary pyrolytically coated furnace tubes.[9] Our results summarized in Table 1 demonstrate for tributyltin species in demineralized water a signal enhancement of 1.9 attributable to use of the L'vov platform. Dichromate provides even greater enhancement, with or without the platform, and the enhancement effects of *both* platform and dichromate when these are used together are approximately additive. Consequently, the minimum detectable concentration of tin in water is lowest for the combination of L'vov platform and enhancing agent. We cannot affirm whether or not relative enhancements for other specific organotin compounds, and other organometallics for that matter, will be as satisfactory, since preliminary results for a series of organotins indicate individual differences.[8]

Reduction of interference in the direct determination of metals in sea-water when L'vov tubes are employed has been reported.[19,20] However, our attempts to determine tin as tributyltin species in sea-water, by using L'vov tubes, with and without dichromate, gave highly erratic results, with frequent electrical shorting of the graphite furnace tubes owing to copious deposition of sea salts. The technique was therefore abandoned in favour of an improved extraction procedure.

Extraction coupled with enhancement

Table 2 summarizes a comparison of the effectiveness of several organic solvents for the extraction of tributyltin in quantities ranging from 0.0 to 0.8 ng per 20-μl GFAAS aliquot and concentrations of 0–40 μg/l. in sea-water. A relatively weak AA response is obtained for the organotin dissolved in chloroform, again suggesting that a volatile tin chloride is the product thermally favoured and lost during the atomization cycle. Although tin in n-hexane generates a much stronger GFAAS signal, n-hexane extracts only about 50% of the amount of organotin dissolved in the sea-water. Methyl isobutyl

Table 2. Comparison of solvents for extraction of tributyltin from sea-water

Solvent	Slope, $\mu V . sec . ng^{-1}$	Intercept, $\mu V . sec$	r*
Hexane			
Solution	11.12×10^3	43	0.997
Extract	5.20×10^3	570	0.885
$CHCl_3$			
Solution	6.19×10^3	76	0.986
MIBK			
Solution	11.10×10^3	715	0.993
Extract	13.90×10^3	500	0.965
Toluene			
Solution	13.50×10^3	980	0.994
Extract	11.10×10^3	560	0.973

*Correlation coefficient.

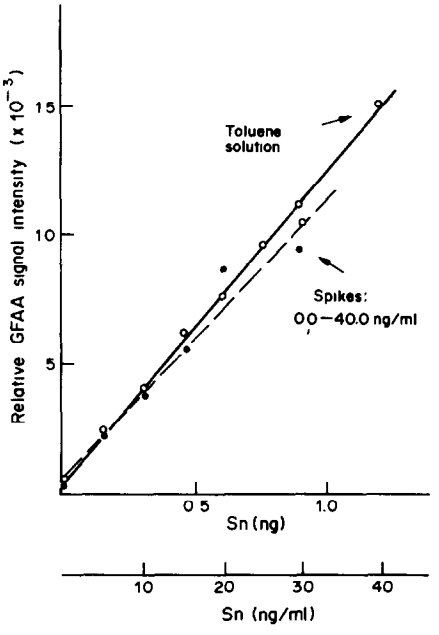

Fig. 4. Determination, by enhanced GFAAS, of tributyltin in spiked artificial sea-water in the range 0–40 ng/ml.

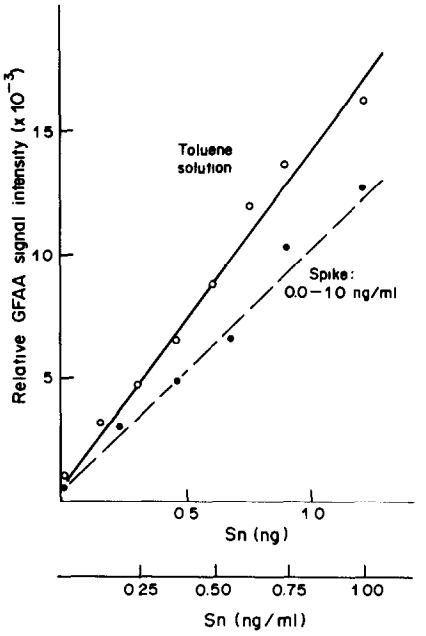

Fig. 5. Determination, by enhanced GFAAS, of tributyltin in spiked artificial sea-water in the range 0–1 ng/ml.

ketone (MIBK) is a much more effective extractant than hexane, but it forms a partial emulsion with sea-water, so phase separation is slow and incomplete. Toluene extracts 83% or more of tributyltin added to sea-water, with rapid separation and no apparent emulsification.

Figures 4 and 5 present results for the determination of tin in toluene and in toluene extracts from artificial sea-water, performed on successive days. To the artificial sea-water were added quantities of tributyltin sufficient to give the same concentrations of extracted tin as in the toluene control solutions, provided that extraction was 100% efficient. The volume of sea-water was varied to give concentrations of tin in the ranges 0–1 or 0–40 μg/l. The results show the effectiveness of the procedure for both extracting trace amounts of tributyltin and removing interference by sea salts. The recovery of 90% for tin in the range 0–40 μg/l. is slightly greater than that (77%) for tin in the range 0–1.0 μg/l. (Table 3). The detection limit in ng, conservatively estimated[21] at the 95% confidence level, is approximately the same for each range of tin concentrations in sea-water. For the lower range in sea-water, the lowest detectable tin concentration is 0.1 ng/ml. The extraction method coupled with the AA enhancements reported here appears suitable for environmental measurements of tributyltin as total tin.

Environmental application

Ward *et al.*[4] reported a 21-day median lethal concentration (LC 50) of tributyltin for sheepshead minnows, a tin-sensitive aquatic organism, of 0.64 ± 0.23 ng/ml. Results of toxicity experiments conducted with larvae of other marine organisms (Table 4) show similar sensitivities to TBTO,[22] based

Table 3. Detection of tin as tributyltin (0.0–1.5 ng) in control solution (toluene) and extracts of spiked artificial sea-water

Sample	Aqueous concentration range,* *ng/ml*	Organotin range,† *ng*	Slope, $\mu V . sec . ng^{-1}$	*r*	95% Confidence interval	Detection limit (95% confidence), *ng*§	*ng/ml*‡
Toluene	—	0.0–1.5	13.50×10^3	0.994	600	0.11	—
Sea-water	0.0–1.0	0.0–1.5	9.13×10^3	0.985	1340	0.15	0.13
Toluene	—	0.0–1.5	12.10×10^3	0.996	370	0.03	—
Sea-water	0.0–30.0	0.0–1.5	11.18×10^3	0.966	1300	0.13	4.33
Toluene	—	0.0–1.5	14.90×10^3	0.999	1020	0.07	—
Choptank water	0.0–1.0	0.0–1.5	9.59×10^3	0.969	2990	0.31	0.26
Choptank water	0.0–50.0	0.0–1.5	11.15×10^3	0.998	780	0.07	2.33

*Based on concentration and volume of spike solutions added to the water.
†Quantity of tin introduced into GFAAS furnace per 20-μl aliquot.
‡In water sample.
§In aliquot introduced into furnace.

Table 4. Toxicity of TBTO to larvae of five marine organisms

Species	Common Name	48-hr LC50, *ng/ml*	96-hr LC50, *ng/ml*
Crassostrea gigas	Japanese oyster	1.6	—
Mytilus edulis	Blue mussel	2 3	1
Crangon crangon	Grass shrimp	6.5	1.5
Carcinus maenas	Shore crab	110	10
Solea solea	Flat fish	8.5	2.1

on which a maximum allowable concentration of 0.64 ng/ml for tributyltin in water in shipyards has been proposed. In view of the analytical sensitivity of the method described here, we chose to examine, for a first trial, estuarine samples from both pristine and polluted locations in the Chesapeake Bay.

Similar sensitivities and detection levels were obtained for the determination of tributyltin dissolved in toluene and for the toluene extraction procedure applied to spiked samples of relatively clean bay water (Fig. 6, Table 3). With spikes in the lower concentration range of 0.0–1.0 ng/ml the detection limit (0.26 ng/ml) in clean bay water is only slightly higher than that for tin in artificial sea-water in the same range (Table 3) and is substantially lower than the toxic threshold of approximately 1 ng/ml suggested by the work of Ward *et al.*[4] and of Thain.[23] Thus, the method should be useful for monitoring tributyltin concentrations in environmental samples of non-polluted sea-water.

The results for the extraction of organotins from samples taken from Baltimore's Inner Harbor are very different. We found a tan, oily emulsion in the toluene layer, which dissolved on dilution with two parts of 2-propanol to one part of the toluene extract, indicating the presence of a polar, organic pollutant in these waters. The lower curve in Fig. 6 displays the GFAAS response to samples of this water spiked with tributyltin chloride in the range 0.0–1.0 ng/ml. The slope indicates an apparent recovery of only 18% of the added tin; the detection limit of 0.67 ng/ml suggests that, with these samples, ammonium dichromate does not give any pronounced enhancement of the GFAAS signal. The high intercept probably indicates environmental tin contamination, as previously noted for the area.[24] These results underscore the difficulty inherent in ultratrace measurements on environmental samples. Even though the present method is capable of determination within the concentration ranges significant for marine organisms, it may be limited by specific sampling-site conditions. Molecular speciation with complementary separatory strategies such as complexation with morin[15] and chromatographic techniques (size-exclusion chromatography or ion-exchange chromatography coupled with GFAAS) is critically important in order to resolve fully the true nature of the organotin species present. The degradation products of tributyltin chloride in natural environments presumably include the much less toxic di-, and mono-butyltin species.[25] As shown in Table 5, tin-specific GFAAS with dichromate enhancement gives signals of statistically equal intensity for these three organotin species in equal concentrations in toluene. Moreover, both dibutyltin and tributyltin are extracted from sea-water by toluene with nearly 100% recovery at concentrations of around 4 ng/ml, and monobutyltin is extracted by toluene containing tropolone.[25] The present results point the way to a unified HPLC technique for determination of all three species in saline waters.

Conclusions

Tributyltin in sea-water is detectable by GFAAS at concentrations as low as 0.1 ng/ml, following toluene extraction to separate the organotin species from interfering salts. The tin-specific GFAAS signal is strongly enhanced by dichromate ions in the absence of sea salts. In the absence of dichromate, the tin-specific GFAAS signal is totally suppressed by a 0.2 μg/ml concentration of sea salts. In the presence of 0.01*M* dichromate, signal suppression by sea salts

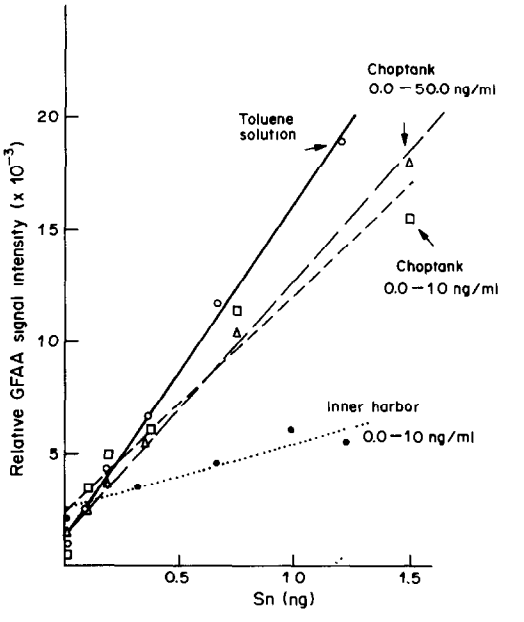

Fig. 6. Determination, by enhanced GFAAS, of tributyltin in spiked samples of relatively clean (Choptank) and relatively polluted (Inner Harbor) estuarine water. The tin recoveries are: Choptank (0.0–1.0 ng/ml) 64 + 20%; Choptank (0.0–50.0 ng/ml), 75 ± 5%; Inner Harbor (0.0–1.0 ng/ml), 18 ± 9%.

Table 5. Extraction of $Bu_{4-n}Sn^{n+}$ from sea-water as determined by tin-specific GFAAS enhanced by $Cr_2O_7^{2-}$

	GFAAS signals, *mV . sec*			
	Control		Extract†	
Organotin*	$\bar{x}$	s.d.	$\bar{x}$	s.d.
$BuSn^{3+}$	1.48×10^4	1.8×10^3	3.65×10^3	0.70×10^3
Bu_2Sn^{2+}	1.20×10^4	1.6×10^3	1.16×10^4	1.5×10^3
Bu_3Sn^{+}	1.67×10^4	3.5×10^3	1.70×10^4	1.4×10^3
Bu_4Sn	1.02×10^4	0.4×10^3	1.32×10^4	1.3×10^3

*0.6 ng per 20-μl aliquot for GFAAS.
†4 ng/ml, as tin.
§Mean ($\bar{x}$) and standard deviation (s.d.) for 5 determinations.

is much less pronounced but increases continuously with salt concentration up to the 35 mg/ml typically found in sea-water.

Toluene is preferred to MIBK, chloroform or n-hexane as the extractant. MIBK forms an emulsion with sea-water that only slowly separates into two phases. Hexane extracts only about 50% of the tributyltin present. Chloroform solutions of tributyltin give a relatively weak GFAAS signal, which indicates that volatile tin-containing species form and are lost before atomization of the tin.

Reportedly harmful concentration of tin (as tributyltin) in sea-water range from 0.6 ng/ml to the solubility limit of about 10 μg/ml. Thus, the present method is capable of determining tin within the significant concentration ranges, but may be limited by environmental factors. For example, heavy concentrations of unknown oily substances in harbour waters heavily traversed by ship and motorboat traffic and receiving polluted run-off reduced the sensitivity and increased the limit of detection substantially above the 0.1 ng/ml level, which indicated the need for additional separatory strategies (complexation and/or chromatography) for polluted waters.

Acknowledgements—For support of this work we are grateful to the United States Office of Naval Research and the Naval Civil Engineering Laboratory. We thank Drs. G. J. Olson, H. E. Guard, J. C. Means and J. S. Thayer for discussion and valuable suggestions.

REFERENCES

1. F. E. Brinckman, *Environmental Effects of Organotins*, presented at 4th International Conference on the Organometallic and Coordination Chemistry of Germanium, Tin and Lead, McGill University, Montreal, Canada, August 1983.
2. R. V. Subramanian, J. A. Mendoza and B. K. Garg, *Holzforschung*, 1981, **35**, 253.
3. W. L. Yeager and V. J. Castelli, in *Organometallic Polymers*, C. E. Carraher, Jr., J. E. Sheats and C. U. Pittman, Jr. (eds), p. 175. Academic Press, New York, 1978.
4. G. S. Ward, G. C. Cramm, P. R. Parrish, H. Trackman and A. Slesinger, *Aquatic Toxicology and Hazard Assessment: Fourth Conference ASTM STP 737*, D. R. Branson and K. L. Dickson (eds.), p. 183. American Society for Testing and Materials, 1981.
5. N. A. Ghanem, F. Youssef, E. M. Abdel-Barey, B. M. Badran and F. M. Hilaly, *7th International Symposium on Controlled Release of Bioactive Materials*, Ft. Lauderdale, FL, 1980, p. 141.
6. T. M. Florence and G. E. Bailey, *Talanta*, 1975, **23**, 179.
7. F. E. Brinckman, W. R. Blair, K. L. Jewett and W. P. Iverson, *J. Chromatog. Sci.*, 1977, **15**, 493.
8. K. L. Jewett, C. S. Weiss and F. E. Brinckman, *183rd National Meeting of the American Chemical Society, Division of Analytical Chemistry*, Abstract No. 40. 28 March–2 April 1982, Las Vegas, NV.
9. B. V. L'vov, *Spectrochim. Acta*, 1978, **33B**, 153.
10. Department of Microbiology, University of Maryland, College Park, MD, personal communication.
11. J. A. Jackson, W. R. Blair, F. E. Brinckman and W. P. Iverson, *Environ. Sci. Technol.*, 1982, **16**, 110.
12. H. A. Meinema, T. Burger-Wiersma, G. Versluis-de-Haan, and E. Ch. Geevers, *ibid.*, 1978, **12**, 288.
13. G. E. Baltey and J. P. Matousek, *Anal. Chem.*, 1977, **49**, 2031.
14. H. Imura and N. Suzuki, *ibid.*, 1983, **55**, 1107.
15. Y. Arakawa, O. Wada and M. Manabe, *ibid.*, 1983, **55**, 1901.
16. C. P. Monaghan, V. I. Kulkarni, M. Ozcan and M. L. Good, *Office of Naval Research, Project No. NR. 356–709, Technical Report*, No. 2, 1980.
17. V. F. Hodge, S. L. Seidel and E. D. Goldberg, *Anal. Chem.*, 1979, **51**, 1256.
18. W. R. Blair, E. J. Parks and F. E. Brinckman, *Characterization of Controlled Release Dynamics and Identification of Species Released from OMP Impregnated Wood Pilings*, U.S. Dept. of Commerce, National Bureau of Standards. NBSIR 83-2733 for the Naval Civil Engineering Laboratory, July 1983.
19. G. R. Carnick, W. Slavin and D. C. Manning, *Anal. Chem.*, 1981, **53**, 1866.
20. E. Pruskowska, G. R. Carnick and W. Slavin, *ibid.*, 1983, **55**, 182.
21. G. E. Parris, W. R. Blair and F. E. Brinckman, *ibid.*, 1977, **49**, 378.
22. W. A. Bailey and P. V. Mavraganis, *Environmental effects of organotin-contaminated drydock wastewater discharge*. Report No. NSRDC-SME CR 22-82 to David W. Taylor Naval Ship Research and Developmental Center, Annapolis, MD 21402, September 1982.
23. J. E. Thain, *Intern. Council for the Exploration of the Sea*, 1983, E. 13.
24. J. A. Jackson, W. R. Blair, F. E. Brinckman and W. P. Iverson, *Environ. Sci. Technol.*, 1982, **16**, 110.
25. F. E. Brinkman, J. A. Jackson, W. R. Blair, G. J. Olson and W. P. Iverson, In *Trace Metals in Sea Water*, C. S. Wong, E. Boyle, K. W. Bruland, J. D. Burton and E. D. Goldberg. (eds.), p. 39. Plenum Press, New York, 1982.
26. R. J. Maguire and H. Hineault, *J. Chromatog.*, 1981, **209**, 458.

Talanta, Vol. 32, No. 8A, pp. 641–644, 1985
Printed in Great Britain.

0039-9140/85 $3.00 + 0.00

ATOMIC-ABSORPTION SPECTROMETRIC DETERMINATION OF TRACE METALS IN ZIRCONIUM AND ZIRCALOY BY DISCRETE SAMPLE NEBULIZATION

DANIEL A. BATISTONI*, LIGIA H. ERLIJMAN and MARIA I. FUERTES
Departamento Química, Comisión Nacional de Energía Atómica, Avenida del Libertador 8250, 1429 Buenos Aires, Argentina

(*Received* 3 *January* 1985. *Accepted* 23 *March* 1985)

Summary—A discrete sample nebulization technique was employed to determine trace metals in nuclear grade zirconium and Zircaloy by flame atomic-absorption spectrometry. With 10% (w/v) sample solutions, detection limits for Cd, Cu, Mn, Ni, and Pb were 0.6, 2, 1, 3, and 10 μg/g. Micro standard-addition procedures and background correction were employed to minimize matrix interferences produced by the high salt content of the aspirated solutions.

Zirconium alloys (Zircaloy) employed as cladding materials in nuclear power reactors must fulfil strict purity specifications. Numerous analytical procedures have been developed to determine metallic contaminants present at the ppm and sub-ppm level.[1] Atomic-emission spectrographic and spectrometric methods[1–3] are commonly used for routine quality control in production plants. However, because of the relative nature of those techniques, based on calibration standards of known composition, independent determination procedures are necessary to maintain adequate levels of accuracy.

Methods for trace determination of calcium, copper, lithium, sodium and zinc in zirconium and its alloys by atomic-absorption spectrometry have been described by Elwell and Wood.[1] For copper and sodium, these authors recommended standard-addition calibration, with direct nebulization of 20% (w/v) sample solutions, and background correction.

Schlewitz and Shields[4] used atomic absorption to determine chromium, copper, iron, nickel and tin in Zircaloy-2 and Zircaloy-4. They investigated interferences arising from the dissolution medium (hydrofluoric acid) and interelement effects between the analytes and the zirconium matrix. Solutions containing 1% (w/v) metal were nebulized directly. Only nickel and copper, of those elements determined, were present at the ppm level.

The present paper deals with the direct determination of cadmium, copper, manganese, nickel and lead in zirconium and Zircaloy-4 by flame atomic-absorption spectrometry. Because of the high salt content of the aspirated solutions (necessary to attain low detection limits) and because of the corrosive nature of the acids employed to dissolve zirconium-containing materials, a discrete sample nebulization technique[5] was investigated. Microstandard-addition[6] and background correction were used to minimize matrix interferences.

*Author for correspondence.

EXPERIMENTAL

Reagents and apparatus

All chemicals and reagents were of analytical reagent grade. Demineralized water redistilled in quartz was used. Plastic or Teflon laboratory ware was used throughout.

Stock analyte solutions (1 mg/ml) were Merck "Titrisol". High-purity zirconium and various Zircaloy metals were used to prepare matrix solutions for background-absorption and interference studies.

A model 82-500 Jarrell-Ash atomic-absorption and emission spectrometer connected to a chart-recorder was employed. The spectrometer was operated at maximum sensitivity with an air–acetylene flame (premix burner) and single-element hollow-cathode lamps. Analytical wavelengths are listed in Table 1. Non-specific background absorption at or near the analyte wavelengths was measured by using non-absorbing lines from the hollow-cathode lamps or the continuum from a hydrogen discharge lamp.

A Teflon microsampling cone (2 cm diameter, 2 cm height, 1 cm deep), similar to that described by Fry *et al.*[6] was employed to nebulize small volumes of solutions (up to 250 μl, measured with Eppendorff micropipettes).

Procedures

Zirconium and Zircaloy-4 metal samples (5.0 g weighed to 1 mg) were dissolved in a mixture of 20 ml of hydrochloric acid (1 + 1), 10 ml of concentrated hydrofluoric acid and 2 ml of concentrated nitric acid, and finally diluted to 50 ml with water. Teflon beakers and plastic standard flasks were used. Blank solutions were prepared with similar amounts of the acids. Sample and blank solutions were stored in plastic (Nalgene) bottles.

Initial studies were made in order to optimize operating conditions, in particular the volume and flow-rate of the nebulized solutions and the response time of the spectrometer recording system. The absorbance of a 2-μg/ml copper solution at 324.7 nm was measured as a function of the volume injected into the microsampling cone (20–250 μl), for different rates of liquid aspiration (2.8, 3.7 and 5.1 ml/min) and for two settings of the instrument damping control, corresponding to recorder full-scale response times

Table 1. Analytical lines and background correction procedures

Element	Analytical line, *nm*	Element lamp and wavelength for background correction, *nm*
Cd	228.8	Cd 228.8*
Cu	324.7	Cu 323.1
Mn	279.5	H continuum 279.5
Ni	232.0	Ni 231.4
Pb	283.3	Pb 280.1 (or H continuum 283.3)

*Background absorbance measured with a high-purity Zr solution 10% (w/v).

of 2 and 4 sec respectively. The absorbance when the same solution was continuously nebulized under the same operating conditions was measured for comparison.

The wavelength distribution of the non-specific absorption was studied with the continuum from a hydrogen discharge lamp. The monochromator band-pass was set at 0.8 nm. Absorbances were measured at 10 nm intervals between 200 and 350 nm for nebulization of 100-μl volumes of 10% (w/v) zirconium or Zircaloy solutions.

To perform the analytical calibration, a trial run was required to give a preliminary estimate of the concentration of each element in the sample solution. The instrument was set to the optimized conditions and a 100-μl portion of sample was pipetted into the microsampling cone and aspirated by inserting the plastic nebulizer capillary into the cone. The peak absorbance was recorded and compared, after background correction, with that obtained similarly for an aqueous standard analyte solution of suitable concentration. An approximate concentration of analyte in the sample solution was then estimated.

Accurate calibration was subsequently performed for individual elements by a microstandard-addition procedure. A 10-μl volume of water was pipetted into the cone, followed by 100 μl of sample solution delivered rapidly to ensure complete mixing, and the mixture was aspirated. At least three replicates were recorded at the analytical wavelength. The procedure was repeated with the same volume of sample and 10-μl volumes of standard analyte solutions of increasing concentration. Usually, three calibration points were used. To correct the individual absorbances for non-specific absorption, a mean background absorbance was estimated at the appropriate wavelength (Table 1) by averaging the data from replicate injections of water–sample solution mixtures.

Background absorption for cadmium was estimated by measuring the absorbance of a 10% (w/v) solution of high-purity zirconium at the cadmium analytical line. A similar procedure was applied to the reagent blank solution in order to estimate any possible residual amount of analyte.

Calibration points were fitted to a straight line by a least-squares procedure and confidence limits for the extrapolated value were calculated by the method of Larsen *et al.*[7]

RESULTS AND DISCUSSION

Optimization of sample volume injected

When micro volumes of solutions are injected into premix burner systems, the atomic-absorption response signal increases until a plateau, which corresponds to the steady signal obtained by continuous nebulization, is eventually reached.

Several operating parameters which are known to influence the shape of the absorbance *vs.* injected-volume curves were investigated in order to decide the minimum volume suitable for the determinations. The results of a study performed with a 2-μg/ml copper solution can be summarized as follows.

(*i*) An increase of about 8% in the measured peak absorbance was observed when the length of the plastic capillary was reduced from 23 to 3 cm.

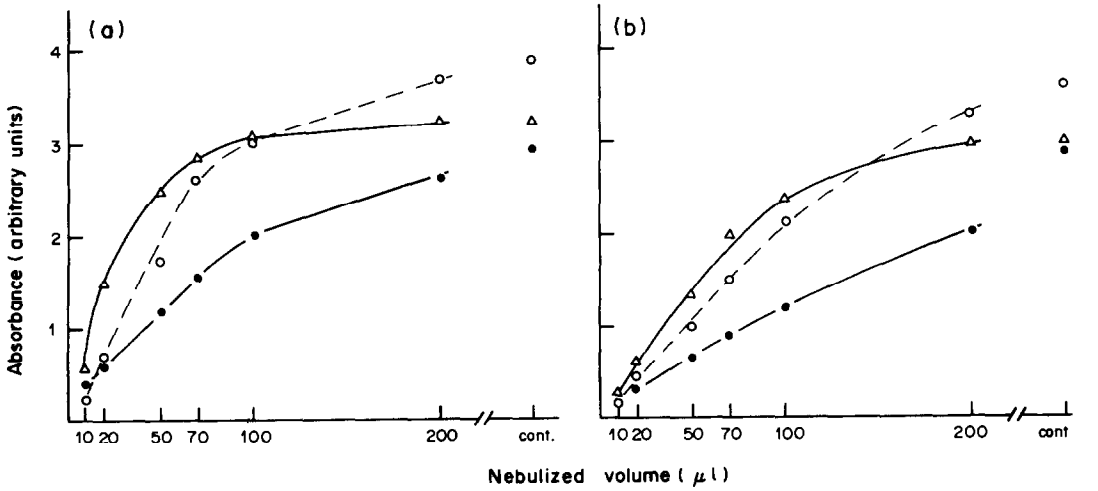

Fig. 1. Variation of absorbance with volume of sample nebulized, for recorder response times (*a*) 2 sec (*b*) 4 sec, and solution aspiration rates (△) 2.8 ml/min; (○) 3.7 ml/min; (●) 5.1 ml/min. Sample solution: Cu 2 μg/ml in water: cont. means continuous nebulization.

(*ii*) Plots of absorbance *vs.* volume of sample injected, for variable solution aspiration rates, and response times (t_r) of the signal recording system, are shown in Fig. 1. With the lower damping setting ($t_r = 2$ sec), a plateau (constant absorbance, 100% signal recovery) was reached for volumes larger than 100 μl only when the solution aspiration rate was maintained at 2.8 ml/min. For the other two rates tested, the absorbance increased steadily with volumes up to 200 μl, the signal recoveries for injected volumes of 200 μl being 95 and 89% for aspiration flow-rates of 3.7 and 5.1 ml/min respectively. The highest peak absorbance values were obtained for injections of 200 μl at a solution aspiration rate of 3.7 ml/min.

(*iii*) The relative standard deviation (rsd) of the peak absorbance measurements decreased as a function of volume nebulized. For volumes greater than 70 μl, a constant rsd of about 2% was observed.

On the basis of these experiments, we selected injection volumes of 100–200 μl, the minimum damping setting and a solution aspiration rate of 3.7 ml/min for routine work.

Matrix background interferences

It is well known that non-specific background absorption interferences are found when solutions containing a relatively large amount of dissolved salts, *i.e.*, more than 5% (w/v), are nebulized into an air–acetylene premixed flame.[8,9] Such interferences, which are critical when the standard-addition technique is to be used for calibration, are particularly severe for elements with analytical lines at short wavelengths.

The same phenomenon was observed for the system under study because of the high matrix (zirconium) concentration in the solutions to be analysed. Background absorption was measured for zirconium and Zircaloy solutions at different wavelengths, by use of a hydrogen continuum source. Results are shown in Fig. 2. For the wavelengths >220 nm the absorbance closely follows the inverse dependence on wavelength characteristic of Rayleigh scattering by solid particles in the light-beam. At shorter wavelengths the observed background absorbance is anomalously low; no explanation has been found for this. It can be seen from Fig. 2 that

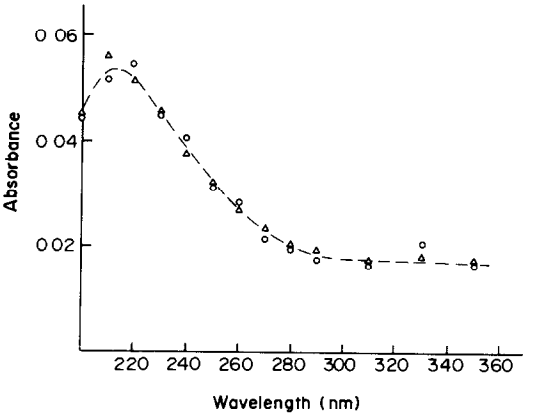

Fig. 2. Variation of background absorbance with wavelength for 10% (w/v) solutions of (○) zirconium, (△) Zircaloy. Volume nebulized 100 μl.

background correction is also necessary at rather longer wavelengths such as 327.4 nm for copper determination. However, checks on background absorbance at even longer wavelengths, made at 370.96 nm (Ne) and 495.14 nm (Pr) with a praseodymium hollow-cathode lamp, showed negligible absorption, even when continuous nebulization was used.

Signal to noise ratios were evaluated for background absorbance measurements made at the analytical wavelengths by using the hydrogen continuum source, and at nearby wavelengths by employing non-absorbing lines generated by the hollow-cathode lamps. Table 1 summarizes the analytical lines and background wavelengths which gave the best results. Average background absorbances agreeing within ±5% for the two measurement methods (continuum and line-source) were obtained for all the analytes studied, with the exception of cadmium.

A further investigation was made of the background near the Cd 228.8 line. Absorbances at 228.8 nm and 226.5 nm (non-absorbing line) were obtained for 10% (w/v) solutions of high-purity zirconium and Zircaloy-4 by means of the hollow-cathode lamp, and the values compared with those obtained at 228.8 nm by using the hydrogen continuum.

For both solutions the average absorbances measured in the first case were 0.040 and 0.041 for the analytical and non-absorbing lines, respectively, and the value of 0.046 obtained with the hydrogen con-

Table 2. Limits of detection

Element	Sample volume injected, μl	Detection limit		Specification limit,* $\mu g/g$
		ng	$\mu g/g$	
Cd	110	7	0.6	0.5
Cu	100	20	2	50
Mn	120	12	1	10
Ni	120	36	3	70
Pb	110	110	10	130

*For nuclear grade Zircaloy-4.

Table 3. Analysis of zirconium and Zircaloy-4 reference samples: levels of trace metals (*ppm*)

	Zirconium		Zircaloy-4§						
	NBS 1210		X-868			NBS 1239		X-869	
Element	NBS	This work	Wah-Chang	NBS‡	This work	NBS	This work	Wah-Chang	This work
Cd	n.r.*	—	<0.2	n.r.	<0.6	n.r.	<0.6	<0.2	<0.6
Cu	10†	9 ± 2	83	60	74 ± 13	30	35 ± 4	36	33 ± 3
Mn	5	4 ± 1	51	60	49 ± 9	50	38 ± 10	47	62 ± 11
Ni	8†	9 ± 3	146	100	109 ± 22	45	45 ± 13	88	46 ± 11
Pb	n.r.*	—	101	80	76 ± 28	30	32 ± 13	44	35 ± 15

*No reported values.
†Certified values.
§Samples NBS 1239 and Wah Chang X 869 are different cuts from the same original material.
‡Results reported under designation NBS 1238 for a different cut of the same original material.

tinuum indicated a small but measurable over-correction probably originating in extremely weak zirconium absorption lines falling within the monochromator spectral band-pass. These results showed the convenience of estimating the background by using a high-purity zirconium solution of the same concentration as the sample solutions, with measurement at the cadmium absorption line. It is worth mentioning that this procedure could only be applied successfully for cadmium determination because of the availability of zirconium materials containing very low concentrations of this element (less than 0.2 μg/g, estimated by emission spectrography).

Detection limits

A limit of detection (Table 2) was estimated for each element from the background-corrected standard-addition curves, as the concentration which produces a (corrected) absorbance signal equivalent to 3 times the standard deviation of the background signal. Absolute values (in ng) of the corresponding amount of the element in the sample volume nebulized are also included in Table 2, along with the nuclear specification limits. Only for cadmium is the minimum detectable concentration slightly higher than the limiting value for nuclear grade materials.

Application to zirconium and Zircaloy-4 samples

To test the procedure, zirconium metal standard NBS 1210, Zircaloy-4 metal standard NBS 1239 and two Zircaloy-4 reference samples obtained from Wah-Chang Corp., Albany, Oregon, U.S.A. were analysed. Results are shown in Table 3, together with available concentration values (non-certified) reported by NBS and Wah-Chang. Analytical calibration was done by the standard-addition method as described and the precision was estimated for each individual determination as the confidence limits (95% probability) for the concentration value calculated by extrapolation. Agreement between the "official" values and those found is reasonable for some of the trace elements, but for others the differences seem to be significant, and might suggest inhomogeneity of the sample from which the different subsamples were originally taken.

REFERENCES

1. W. T. Elwell and D. F. Wood, *Analysis of the New Metals*, pp. 134–223. Pergamon Press, Oxford, 1966.
2. ASTM Committee E-2, *Methods for Emission Spectrochemical Analysis*, 6th Ed., American Society for Testing and Materials, 1971.
3. C. P. Brown and C. R. Hillier, *Can. J. Spectrosc.*, 1975, **20,** 145.
4. J. H. Schlewitz and M. G. Shields, *At. Absorpt. Newsl.*, 1971, **10,** 39.
5. M. S. Cresser, *Prog. Anal. Atom. Spectrosc.*, 1981, **4,** 219.
6. R. C. Fry, S. J. Northway and M. B. Denton, *Anal. Chem.*, 1978, **50,** 1719.
7. I. L. Larsen, N. A. Hartmann and J. J. Wagner, *ibid.*, 1973, **45,** 1511.
8. W. T. Elwell and J. A. F. Gidley, *Atomic Absorption Spectrophotometry*, 2nd Ed., p. 47. Pergamon Press, Oxford, 1966.
9. S. R. Koirtyohann, in J. A. Dean and T. C. Rains (eds.), *Flame Emission and Atomic Absorption Spectrometry*, Vol. 1, p. 311. Dekker, New York, 1969.

Talanta, Vol. 32, No. 8A, pp. 645–649, 1985
Printed in Great Britain.

0039-9140/85 $3.00 + 0.00

DETERMINATION OF THE DEGREE OF SUBSTITUTION OF SODIUM CARBOXYMETHYLCELLULOSE BY POTENTIOMETRIC TITRATION AND USE OF THE EXTENDED HENDERSON–HASSELBALCH EQUATION AND THE SIMPLEX METHOD FOR THE EVALUATION

INGRID AGGERYD and ÅKE OLIN
Department of Analytical Chemistry, University of Uppsala, P.O.B. 531, S-751 21 Uppsala, Sweden

(*Received* 14 *November* 1984. *Accepted* 27 *February* 1985)

Summary—Determination of the degree of substitution, D.S., of purified sodium carboxymethylcellulose, CMC, by potentiometric titration has been studied. Different mathematical descriptions of the acid–base properties of polyelectrolytes were tested on the titration curve. It was found that the extended Henderson–Hasselbalch equation reproduced the measured data well. It was therefore used as a basis for evaluating D.S. by the simplex method. The influence of ionic strength, I, on the shape of the titration curve was investigated and the effect of I on the precision of the titrations was evaluated. The titrations showed a precision of ± 0.004 D.S.-units and the results were in agreement with those obtained from a dry-ashing method, within ± 0.02 D.S.-units. The whole method, including preparation of solutions and titration, showed a precision of ± 0.01 D.S.-units.

Sodium carboxymethylcellulose is a bulk chemical with wide applications in the cellulose and food industries, for instance. Its trade name is CMC or cellulose gum. By varying the length of the cellulose chain and the degree of substitution, D.S., CMC with different properties can be obtained. The D.S. is defined as the number of carboxymethyl groups per glucose unit. The highest theoretical value is 3, but for commercial products the D.S. is usually much lower, 0.6–0.8.

A number of methods for the determination of D.S. have been reported. In some of them CMC is quantitatively precipitated by multivalent metal ions: Cu^{2+},[1] UO_2^{2+},[2] or Pb^{2+}.[3] Two methods have been proposed by ASTM.[4] One is based on a non-aqueous acid–base titration. In the other, CMC is first converted into the insoluble acid form, separated, and dissolved in an excess of sodium hydroxide, and finally the excess of base is determined. The D.S. can also be determined by conductometric titration,[3,5] colorimetry[5] and by infrared spectrophotometry.[3] The methods are applicable only to purified samples of CMC or include a purification step in the analytical procedure.

CMC has been used as a model substance in studies of the acid–base properties of polyelectrolytes by the potentiometric titration technique, but the method has not been used for the determination of D.S. The slightly soluble acid form of CMC reacts slowly with added base and the shape of the titration curve is markedly affected by the speed of the titration.[6] Hence titration of the acid form cannot be used for any analytical purpose. The determination of D.S. must therefore be based on an acidimetric titration of CMC. Since polycarboxylic acids are fairly strong, evaluation of the equivalence volume directly from the titration curve can be expected to be imprecise. Numerical methods have been used to determine equivalence volumes from titrations of low molecular-weight acids and bases with unfavourable pK_a-values.[7] A numerical evaluation of the titration curve of a polyelectrolyte might also be possible, if a sufficiently accurate mathematical description of the shape of the titration curve could be found.

THEORY

Equations for description of the acid–base properties of polyelectrolytes have been proposed by Tanford.[8] For a macromolecule with identical binding sites and electrostatic interaction between the sites, the following expression was derived.

$$k = k_0 e^{\gamma \bar{z}} \tag{1}$$

or, in logarithmic form,

$$\ln k = \ln k_0 + \gamma \bar{z} \tag{2}$$

where k is the mean acidity constant of the sites at a particular ph, calculated in the usual way from ph (defined below) and the concentrations of dissociated and undissociated sites; $\bar{z}$ is the average charge of a site, and is proportional to the degree of dissociation, α; γ is a constant for a given fixed environment for the reaction, provided that the macromolecule does not change its conformation. In this equation $\ln k$ and $\bar{z}$ are both very sensitive to experimental errors; thus a linear evaluation of equation (2) requires that both $\ln k$ and $\bar{z}$ are weighted.

Another expression for description of the protolytic properties of polyelectrolytes is the extended Henderson–Hasselbalch equation, which was proposed by Katchalsky *et al.*[9]

$$ph = pK_a + n \log \frac{[A^-]}{[HA]} \quad (3)$$

where $[A^-]$ and [HA] are the concentrations of dissociated and undissociated substituent, respectively, and can be found from knowledge of the total concentration of the substituent and $[H^+]$; n is an empirical parameter which is equal to 1 for a low molecular-weight acid and larger than 1 for a polyelectrolyte.

The ph, which is defined by $ph = -\log[H^+]$, is measured by the glass electrode and calculated from

$$E = E_0 + g \log[H^+] + E_j \quad (4)$$

where E = measured potential (mV), $g = (RT/F) \ln 10 = 59.16$ mV (at 25°), and E_j = liquid-junction potential (mV). E_j is an empirical function of $[H^+]$: $E_j = K_h[H^+]$. Equation (3) can then be tested by plotting $y = \log([A^-]/[HA])$ against ph. The values of pK_a and n should be evaluated by a weighted linear regression since the variance of y is dependent on ph. The following estimate of $\sigma^2(y)$ may be used in the weighting scheme.

$$\sigma^2(y) = \left\{\frac{[A]^*}{[HA][A^-]}\right\}^2 \times \left\{\frac{(V_0 C_H)^2}{(V_0+V)^4}(\Delta V)^2 + \left(\frac{[H^+]}{RT/F}\right)^2 (\Delta E)^2\right\} \quad (5)$$

where [A]* is the total concentration of substituent, V_0 the initial volume, V the volume of added titrant of concentration C_H, and ΔV and ΔE are the estimated errors in the volume added and the potential, respectively. The influence of $[OH^-]$ was neglected in the derivation of equation (5).

Equation (3) appears to be applicable only when no changes in conformation occur. If this is not the case, models using more parameters must be resorted to.[10]

Equivalence volumes from inflection points of titration curves obeying equation (3)

If the titration curve has an inflection point, the condition $d^2(ph)/dV^2 = 0$ must be fulfilled somewhere along the curve. At the points where the second derivative is zero the following relationship can be shown to be valid for the titration of a polybasic acid obeying equation (3).

$$\frac{(1-\alpha)\alpha^{n+1}}{\alpha^{n+1} + Pn^2(1-\alpha)^{n-1}} = \frac{1}{2} \quad (6)$$

As before, α is the degree of dissociation, $P = K_a/C_A$ and C_A is the total concentration of acidic groups. The contributions from $[OH^-]$ and from dilution have been neglected in the derivation of equation (6). It can further be shown that for the equation to have a proper root, the value of P must not exceed a critical value given by

$$P = \frac{1}{108n^2}(n+3-\sqrt{n^2+3})^2(\sqrt{n^2+3}-n) \times \left\{\frac{n+1}{2+\sqrt{n^2+3}}\right\}^{n-1} \quad (7)$$

For a low molecular-weight acid this value is 1/27. For polymeric acids the limiting value of P is smaller because of the larger value of n. The difference between the inflection point and the equivalence point is shown in Table 1 for a few values of P and n. The data show that it is more difficult to evaluate a titration curve of a polymeric acid than of a monomeric one with the same acidity constant.

Calculation of the equivalence volume, V_e, from a titration curve obeying equation (3)

The following relationship between the experimental quantities V and $[H^+]$, and the parameters K_a, n and V_e, can be derived from equation (3) and the expressions for the total concentrations of substituents and protons.

$$V = V_e \frac{C_H}{(C_H - [H^+])\{1 + (K_a/[H^+])^{1/n}\}} + \frac{V_0[H^+]}{C_H - [H^+]} \quad (8)$$

It can be fitted to the measured data by the simplex method.[11] The sum of squared residuals, $U = \Sigma(V_{exp} - V_{calc})^2$, is minimized.

EXPERIMENTAL

Chemicals

The CMC used in the experiments was supplied by Billerud Uddeholm AB. Four types of CMC with different viscosities were titrated (see Table 2). The samples were

Table 1. The difference, Δ, between the equivalence point and the inflection point of a titration curve, for some values of n and $P = K_a/C_a$; $\Phi = V/V_e$ at the inflection point

P	Φ ($n = 1$)	Φ ($n = 1.3$)	Δ, % ($n = 1$)	Δ, % ($n = 1.3$)
10^{-2}	0.964	0.849	3.6	15.1
10^{-3}	0.997	0.966	0.3	3.4
10^{-4}	1.000	0.990	0.0	1.0

Table 2. Viscosity for 2% solutions of CMC in water, according to specifications from the manufacturer

Type of CMC	Viscosity, cP*
UV	20–50
LV	90–200
MV	400–800
HV	1200–2500

*SI equivalent of the centipoise is 10^{-3} N.sec.m^{-2}.

Fig. 1. Titration curve for a CMC sample of type UV. The curve is calculated from equation (8) with parameters from the simplex optimization. $V_e = 4.20$ ml and $I = 0.20M$.

purified according to the method described below. The D.S. was determined by dry-ashing the CMC and titrating the resulting sodium carbonate with hydrochloric acid.

All other chemicals were of p.a. grade. Potassium nitrate was recrystallized before use. Nitric acid solutions were prepared from the concentrated acid by dilution and standardized against tris(hydroxymethyl)aminomethane.

Purification of CMC

The CMC samples had a specified purity of 97–99%. The main impurities were sodium chloride, glycollate and carbonate. Carbonate was removed by treatment with acid. Then the sample was dissolved in sodium hydroxide solution and small amounts of undissolved material were removed by centrifugation. The CMC was reprecipitated with ethanol and washed with 70% v/v ethanol on a glass filter. CMC has very low solubility in this solvent, whereas sodium chloride and glycollate are quite soluble. Washing was continued until chloride could not be detected in the washings. Water was removed by washing with absolute ethanol and finally ether was passed through the CMC, which was then dried by sucking air through it. CMC is hygroscopic and the final product was equilibrated in a hygrostat to have a moisture content of about 10%. Glycollate and chloride ions could not be detected in the final product (*i.e.*, less than 0.05% of either was present).

Titrations

The titrations were done with a laboratory-built automatic titrator. An Ingold type 201 glass electrode was used as indicator electrode and a Metrohm Ag/AgCl electrode as reference electrode. The salt bridge contained $3M$ potassium nitrate. The emf was measured with a digital voltmeter to ± 0.01 mV.

The titrations were performed in a constant ionic medium to keep the activity coefficients constant. Before each titration the glass electrode was calibrated as follows. The ionic medium was titrated with 25.00mM nitric acid to pH 2. The parameters E_0 and K_h in equation (4) were evaluated from a plot of $E - g \log [H^+]$ as a function of $[H^+]$, with E_0 as the intercept and K_h as the slope of the straight line. It was found from these titrations that sodium chloride and nitrate, which are usually employed as ionic media, often contain acidic or alkaline impurities. Therefore potassium nitrate, which is easier to obtain pure, was used as the ionic medium in all experiments.

CMC solutions (1 g/l.) were titrated with 25.00mM nitric acid to pH 2. The experiments were done at 25.0°, with a protective atmosphere of nitrogen.

RESULTS AND DISCUSSION

The titration curve

A typical titration curve of CMC is shown in Fig. 1. No inflection point can be discerned visually and the equivalence volume must therefore be evaluated by a numerical method. To test the compatibility of our data with equations (2) and (3) the relevant quantities were calculated by using the values of D.S. obtained by the dry-ashing method (see experimental section).

Figure 2 gives a plot of $-\log k$ versus α. The plot is linear over most of the range of α values, but substantial deviations occur at low α. Since the calculated values of α and k are very sensitive to experimental errors, it is difficult to decide whether or not Tanford's equation fails to reproduce the acid–base properties of CMC. No explicit expression can be obtained from equation (1) for either $[H^+]$ or V. This makes the equation less suitable as the basis for numerical evaluation of the equivalence volume and hence no attempt was made to use it for determination of V_e.

The extended Henderson–Hasselbalch equation, equation (3), reproduces the data well in the range

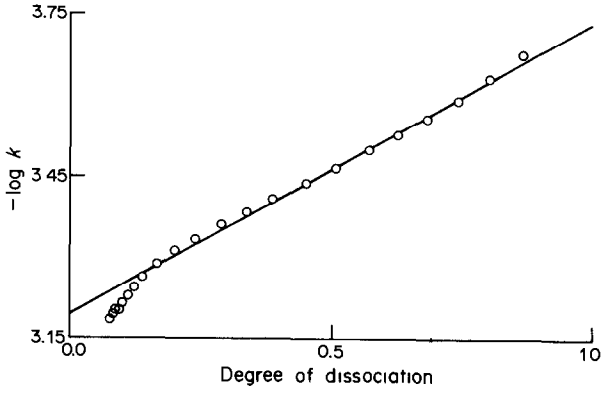

Fig. 2. Evaluation of a titration according to equation (2). [CMC] = 1 g/l., D.S. = 0.79, $I = 0.20M$.

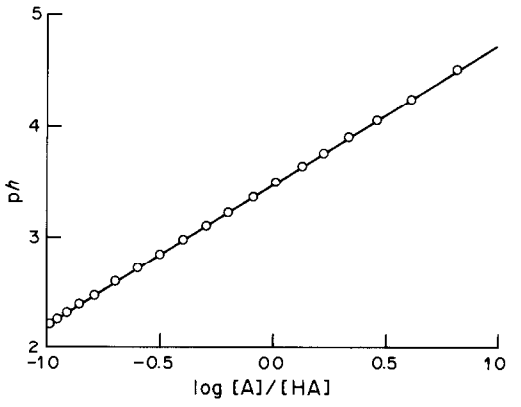

Fig. 3. Evaluation of a titration according to the extended Henderson–Hasselbalch equation. [CMC] = 1 g/l., D.S. = 0.79, $I = 0.20M$.

$-1 < \log([A^-]/[HA]) < 1$, as demonstrated by Fig. 3. Outside this interval the quotient $[A^-]/[HA]$, (where both concentrations are the experimental values) becomes increasingly sensitive to errors in E and V. The good fit of the data to a straight line led to the use of equation (8) for evaluation of V_e by the simplex method.

As will be detailed later the values of n and K_a in equation (3) are about 1.3 and $3 \times 10^{-4}M$, respectively. With a CMC concentration of 1 g/l. and a D.S. of 0.8, the value of P in equation (6) becomes 0.08. This P-value is larger than that given by equation (7) and shows that the titration curve has no inflection point, thus confirming the visual observation.

Influence of ionic strength on the titration curve

The ionic strength, I, affects the shape of the titration curve of a polyelectrolyte. The influence of I on pK_a and n has therefore been studied. The titrations were done with a CMC-sample of type UV with a D.S. of 0.79 and evaluated by weighted linear regression. The weights were calculated from equation (5) with $\Delta V = 0.01$ ml and $\Delta E = 0.1$ mV.

The results are presented in Table 3. An increase in I leads to a decrease in the values of n and pK_a, a result in agreement with other investigations.[12,13] An explanation of this behaviour has been given by Oosawa[14] in terms of the screening effect of the ions from the low molecular-weight salt on the charges on the polyelectrolyte chain. As a consequence n will approach unity when I rises, and pK_a will decrease when the attraction of protons to the macromolecule is weakened.

Table 3. The influence of the ionic strength, I, on pK_a and n for a CMC sample of type UV; D.S. = 0.79, [CMC] = 1 g/l.

I, mM	pK_a	n
500	3.37	1.17
200	3.46	1.26
100	3.55	1.34
50	3.68	1.40
25	3.82	1.43
12	3.96	1.57

An evaluation has also been made of the effect of the ionic strength on the precision in the titrations. It was found that the results obtained in 0.1–0.2M potassium nitrate media best agreed with equation (3), yielding R^2-values > 0.9998. For $I > 0.2M$ the solubility of CMC decreases, and at I below 0.1M the liquid-junction potentials are large and difficult to determine with high precision. Hence 0.2M potassium nitrate was chosen as medium for the determination of D.S. by titration.

Determination of D.S. by the simplex method

The D.S. was found by fitting equation (8) to the titration data by the simplex method with K_a, n and V_e as the adjustable parameters. The values of D.S. obtained for the four different CMC-samples investigated are presented in Table 4 and compared with the values obtained from the dry-ashing method. The difference between the two methods is less than ± 0.02 D.S. units.

As shown by the results in Table 5, the values of K_a and n obtained by the simplex method agree closely with those found by fitting the same titration data to equation (3) by weighted linear regression. In the latter calculations the D.S.-values from the dry-ashing method were used. The final result from the simplex optimization was independent of the starting values of the parameters. A bad initial guess merely results in many more iterations being required for the final values of K_a, n and V_e to be reached. The method was, however, found to be very vulnerable to systematic errors in the data, *e.g.*, arising from poor calibration of the electrodes.

Titrations of two different total concentrations of CMC, 1 g/l. and 2 g/l., indicated that the values of K_a, n, and D.S. are independent of the total concen-

Table 4. Determinations of D.S. for different types of CMC; $I = 0.2M$, [CMC] = 1 g/l.

Type of CMC	D.S. from dry-ashing	D.S. from simplex
UV	0.794	0.789
LV	0.716	0.734
MV	0.779	0.780
HV	0.772	0.783

Table 5. Comparison between values of pK_a and n obtained by simplex optimization and by weighted linear regression

Type of CMC	pK_a (simplex)	pK_a (lin. reg.)	n (simplex)	n (lin. reg.)
UV	3.47	3.46	1.26	1.27
LV	3.42	3.44	1.25	1.20
MV	3.45	3.44	1.27	1.26
HV	3.43	3.43	1.27	1.26

tration. The fit of the evaluation model to the measured data can be seen in Fig. 1. The curve is calculated from equation (8) with parameters from the simplex optimization.

The precision of the titrations was ± 0.004 D.S. units, and the precision for the whole method, including titration and preparation of solutions, was ± 0.01 D.S. units. The substantial increase in imprecision for the whole procedure is mainly due to the difficulties of handling and transferring CMC samples. The results show that potentiometric titration with simplex optimization to evaluate the titration curve is a feasible method for the determination of the D.S. of purified CMC samples with high precision.

REFERENCES

1. A. Z. Conner and R. W. Eyler, *Anal. Chem.*, 1950, **22**, 1129.
2. C. V. Francis, *ibid.*, 1953, **25**, 941.
3. A. Naterová and J. Polčin, *Faserforsch. Textiltech.*, 1975, **26**, 14.
4. American Society for Testing and Materials, *ASTM Standard* D1439-83.
5. R. W. Eyler, D. E. Klug and F. Diephuis, *Anal. Chem.*, 1947, **19**, 24.
6. B. Philipp and H. Dautzenberg, *Wiss. Z. Tech. Univ. Dresden*, 1975, **24**, 41.
7. L. Pehrsson, F. Ingman and S. Johansson, *Talanta*, 1976, **23**, 781.
8. C. Tanford, *Physical Chemistry of Macromolecules*, Chapter 8, Wiley, New York, 1961.
9. A. Katchalsky and P. Spitnik, *J. Polym. Sci.*, 1947, **2**, 432.
10. U. P. Strauss, *Macromolecules*, 1982, **15**, 1567.
11. M. C. Caceci and W. P. Cacheris, *Byte*, 1984, **5**, 340.
12. J. G. Zadow, *Cellulose Chem. Technol.*, 1975, **9**, 353.
13. Y. Muroga, K. Suzuki, Y. Kawaguchi and M. Nagasawa, *Biopolymers*, 1972, **11**, 137.
14. F. Oosawa, *Polyelectrolytes*, Dekker, New York, 1971.

Talanta, Vol. 32, No. 8A, pp. 651–653, 1985
Printed in Great Britain.

0039-9140/85 $3.00 + 0.00

SHORT COMMUNICATIONS

COLORIMETRIC DETERMINATION OF TWO FENAMATES IN CAPSULE DOSAGE FORM

MOHAMED S. MAHROUS, MAGDI M. ABDEL-KHALEK and MOHAMED E. ABDEL-HAMID
Faculty of Pharmacy, University of Alexandria, Alexandria, Egypt

(*Received* 20 *November* 1984. *Revised* 20 *February* 1985. *Accepted* 29 *March* 1985)

Summary—The colorimetric determination of mefenamic acid and flufenamic acid with potassium ferricyanide in sodium hydroxide medium is described. The orange product is measured at 464 nm. The molar absorptivities are 1.9×10^3 and 2.9×10^3 l.mole^{-1}.cm^{-1} for mefenamic acid and flufenamic acid, respectively. The method has been applied successfully to the determination of these drugs in capsules.

Mefenamic acid (2,3-xylyl-*N*-anthranilic acid) and flufenamic acid [(α,α,α-trifluoro-*m*-tolyl)-*N*-anthranilic acid] are potent non-steroidal analgesic and anti-inflammatory agents, extensively used in the management of rheumatoid arthritis. Titrimetric,[1,2] spectrophotometric,[3–5] colorimetric,[6] and fluorimetric[7–9] methods have been reported for the analysis of fenamate drugs. The official method[10] involves direct alkalimetric titration for the bulk drugs and capsule dosage forms.

The purpose of this work is to describe a simple and accurate colorimetric method for the determination of mefenamic acid and flufenamic acid by use of potassium ferricyanide in sodium hydroxide medium. The procedure has been applied to determination of these drugs in capsules.

EXPERIMENTAL

Reagents

Potassium ferricyanide solution, 1.5%.

Sodium hydroxide solution, 0.2N and 5M.

Test substances. Authentic samples of mefenamic acid and flufenamic acid were obtained from Nile Pharmaceuticals, Cairo, Egypt.

Standard solutions. A 20-mg portion of the drug (accurately weighed) was dissolved in 50 ml of ethanol and the solution made up to volume in a 100-ml standard flask with distilled water.

All chemicals and reagents used were of analytical-reagent grade.

General procedure

Transfer 1, 2, 3, 4, 5-ml portions of the standard solution into 10-ml standard flasks. Add to each flask 1 ml of potassium ferricyanide solution (by pipette), followed by 1 ml of 0.2*M* sodium hydroxide for mefenamic acid or 1 ml of 5*M* sodium hydroxide for flufenamic acid. Mix well, allow to stand for 3 min and dilute to volume with water. After 15 min, measure the absorbance at 464 nm, against a corresponding reagent blank.

For capsules. Weigh accurately a quantity of the mixed contents of 20 capsules, equivalent to about 20 mg of the drug, and transfer it into a 100-ml standard flask. Add 50 ml of ethanol, shake for 20 min and make up to volume with water. Filter, transfer 5 ml of the filtrate into a 10-ml standard flask and complete the assay by the general procedure.

RESULTS

Absorption spectra

Figure 1 shows the absorption spectra of the reaction products of potassium ferricyanide with mefenamic acid and flufenamic acid and of potassium ferricyanide in alkaline medium. The orange product from the fenamates exhibits an absorption maximum at 464 nm, and the alkaline solution of ferricyanide displays only slight absorption at this wavelength. Ferrocyanide shows no absorption in 464-nm region. Hence use of a carefully measured constant volume of ferricyanide solution and measurement against a reagent blank gives a linear calibration graph for the fenamates. The similarity of $\lambda_{max(s)}$ for both fenamate reaction products suggests indicates that the products formed have similar structures.

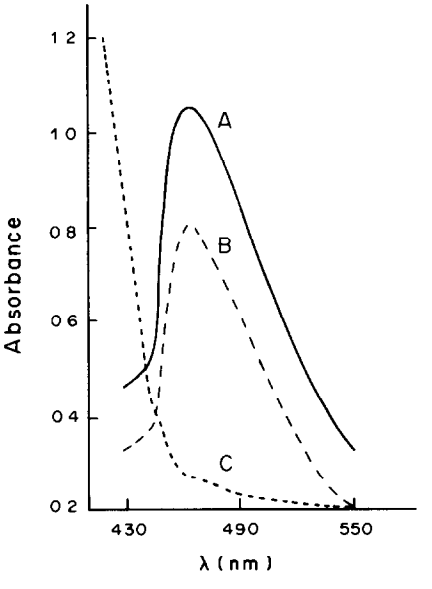

Fig. 1. Absorption spectra of the coloured products of: A, flufenamic acid; B, mefenamic acid; and C, reagent blank measured against distilled water. [Fenamate] = 100 μg/ml in each instance.

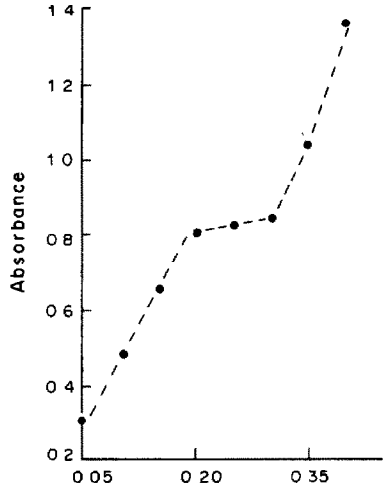

Fig. 2. Effect of alkalinity on the absorbance at λ_{max} of the coloured product of mefenamic acid. [Fenamate] = 100 μg/ml.

Effect of reagent concentrations

It was found that addition of 1 ml of 0.2*M* sodium hydroxide solution and 1 ml of 5*M* sodium hydroxide solution for mefenamic acid and flufenamic acid, respectively, gave a stable orange colour. Higher concentrations of sodium hydroxide resulted in increasing the intensity of the colour but slightly decreasing its stability (Figs. 2–4).

It was also found that 1 ml of 1.5% potassium ferricyanide solution in the total volume of 10 ml gave the most pronounced effect (Fig. 5).

Analytical data

Under the experimental conditions described, Beer's law is obeyed over the concentration range 20–100 μg/ml. The molar absorptivities at 464 nm were 1.9×10^3 and 2.9×10^3 l.mole^{-1}.cm^{-1} for

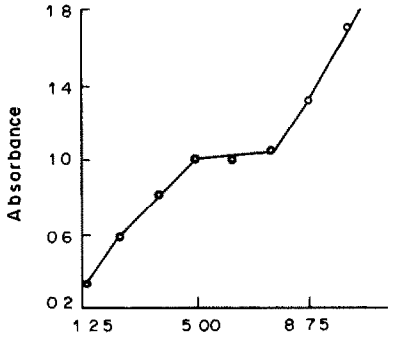

Fig. 3. Effect of alkalinity on the absorbance at λ_{max} of the coloured product of flufenamic acid. [Fenamate] = 100 μg/ml.

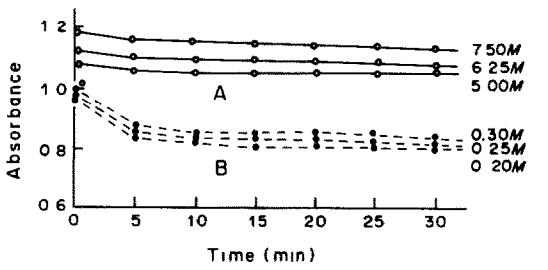

Fig. 4. Effect of alkalinity (addition of 1 ml of NaOH of concentration shown) on stability of the coloured products of: A, flufenamic acid; B, mefenamic acid. [Fenamate] = 100 μg/ml in each instance.

mefenamic acid and flufenamic acid respectively. The coefficients of variation (ten determinations) were less than 0.5%.

Results for determination of mefenamic acid and flufenamic acid in commercial capsules are given in Table 1, and are in good agreement with those obtained by using the BP method.[10] Application of the *Student* t-test and the F-test[13] indicated no significant difference in the accuracy and precision of the two methods.

Interferences

Frequently encountered excipients such as starch, lactose, talc and magnesium stearate did not interfere.

Mechanism

Mefenamic acid and flufenamic acid are *N*-phenylanthranilic acid derivatives. In acid medium, they are oxidized by many oxidants such as potassium dichromate, ceric ammonium sulphate, ammonium vanadate or potassium ferricyanide to unstable blue-green products. Mechanistic studies of the oxidation of *N*-phenylanthranilic acid in acid medium

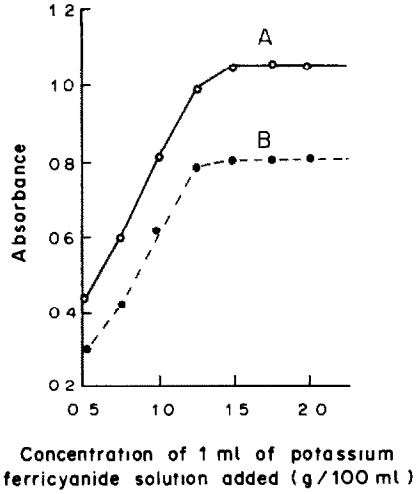

Fig. 5. Effect of reagent concentration on the reaction of fenamates with potassium ferricyanide. A, flufenamic acid; and B, mefenamic acid. [Fenamate] = 100 μg/ml in each instance.

have been reported.[14] The well-known but little understood use of potassium ferricyanide to assist in the nucleophilic displacement of hydrogen atoms in aromatic systems has been studied.[15] Accordingly, we postulate that in the present investigation the orange colour obtained by the interaction of fenamates with potassium ferricyanide in alkaline medium is a nucleophilic displacement of the *p*-hydrogen atom in the phenyl substituent of anthranilic acid, with subsequent oxidation of the intermediate enolate to the orange quinone-imine structure (see scheme below).

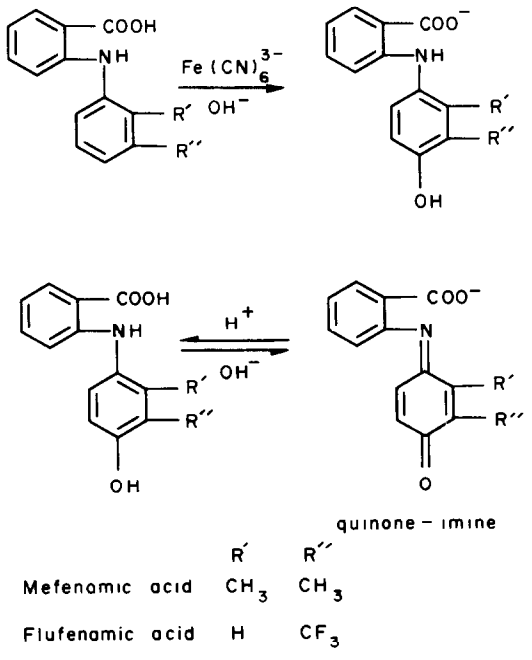

Scheme 1.

This postulate is substantiated by the fact that a similar orange product is obtained on oxidation of the two fenamates with potassium persulphate in alkaline solution. Electron-donating substituents (*e.g.*, CH_3) facilitate the nucleophilic displacement, whereas electron-attracting groups (*e.g.*, CF_3) have the opposite effect. The stabilization of the quinone-imine structure depends mainly on the pH of the medium. It was found that the colour is stable in alkaline solution and disappears in acid medium *i.e.*, the reaction is reversible, as shown in the scheme.

Table 1. Results for the determination of fenamates in pure form and in capsules

Drug	Found* ± S.D.% Proposed method	BP method	t_{calc} †	F_{calc} ‡
Mefenamic acid powder	99.4 ± 0.5	99.0 ± 0.8	0.67	2.56
Ponstan® capsules§	102.9 ± 0.7	102.0 ± 1.1	1.49	2.51
Flufenamic acid powder	100.4 ± 0.5	101.0 ± 0.8	1.58	2.56
Arlef® capsules #	101.8 ± 0.6	102.6 ± 1.0	1.54	2.78

*Average of 10 determinations.
†Theoretical value 2.1 ($p = 0.05$).
‡Theoretical value 3.2 ($p = 0.05$).
§Labelled to contain 250 mg of mefenamic acid per capsule (Parke Davis).
Labelled to contain 100 mg of flufenamic acid per capsule (Parke Davis).

REFERENCES

1. Y. K. Agrawal, *Sci. Cult.*, 1980, **46**, 309; *Anal. Abstr.*, 1981, **41**, 4E9.
2. M. I. Walash and M. Rizk, *Indian J. Pharm.*, 1977, **39**, 82.
3. A. V. Vinnikova, *Farm. Zh. (Kiev)*, 1978, No. 5, 56; *Anal. Abstr.*, 1980, **38**, 4E57.
4. *Idem, ibid.*, 1979, No. 3, 74; *Anal. Abstr.*, 1980, **39**, 4E46.
5. Y. A. Beltagy, *Zentralbl. Pharm., Pharmakother. Laboratoriumsdiagn.*, 1977, **116**, 925.
6. G. Devaux, P. Mesnard and A. M. Brisson, *Ann. Pharm. Franc.*, 1969, **27**, 239.
7. H. D. Dell and R. Kamp, *Arch. Pharm. (Weinheim)*, 1970, **303**, 785.
8. A. C. Mehta and S. G. Schulman, *Talanta*, 1973, **20**, 702.
9. W. Schmollack and U. Wenzel, *Pharmazie*, 1974, **29**, 583.
10. *British Pharmacopoeia 1980*, HM Stationery Office, London, 1980.
11. M. R. Spiegel, *Theory and Problems of Probability and Statistics*, pp. 215, 259. McGraw-Hill, New York, 1975.
12. E. B. Sandell, *Colorimetric Determination of Traces of Metals*, 2nd Ed., p. 50. Interscience, New York, 1953.
13. L. Saunders and R. Fleming, *Mathematics and Statistics*, 2nd Ed., pp. 192–197. The Pharmaceutical Press, London, 1971.
14. E. Bishop, *Indicators*, p. 597. Pergamon Press, Oxford, 1972.
15. R. A. Abramovitch and A. R. Vinutha, *J. Chem. Soc. B*, 1971, 131.

Talanta, Vol. 32, No. 8A, pp. 654–656, 1985
Printed in Great Britain.

0039-9140/85 $3.00 + 0.00

COPPER(I) ELECTRODE FUNCTION OF TWO TYPES OF COPPER(II) ION-SELECTIVE ELECTRODES

M. NESHKOVA and H. SHEYTANOV
Institute of General and Inorganic Chemistry, Bulgarian Academy of Sciences, 1040 Sofia, Bulgaria

(*Received* 13 *June* 1984. *Revised* 14 *December* 1984. *Accepted* 29 *March* 1984)

Summary—The response of two types of solid-state copper ion-selective electrodes with homogeneous membranes of CuAgSe and $Cu_{2-x}Se$ has been investigated in copper(I) solutions, prepared electrochemically by *in situ* generation from a copper anode in chloride medium. The selectivity coefficient $K^{pot.}_{Cu^+,Cu^{2+}}$ for both types of electrodes has been determined. It is $10^{-5\,7}$ for the copper selenide sensor, and $10^{-6\,2}$ for the copper silver selenide one. These values are very close to that calculated for an exchange reaction proceeding on the electrode surface. The similarity in $K^{pot}_{Cu^+,Cu^{2+}}$ values for different chalcogenide-based sensors suggests a common potential-generating mechanism. High chloride concentration does not interfere with the electrode response towards Cu(I), but distorts the electrode response to Cu(II).

Investigation of the behaviour of copper(II) ion-selective electrodes in copper(I) solutions over a sufficiently wide concentration range is important both for the elucidation of some theoretical problems, and from a purely analytical standpoint. The difficulties in such studies result from the instability of copper(I) in aqueous solutions—a problem which is aggravated as the copper(I) concentration decreases. These difficulties have been surmounted by some authors by using a non-aqueous medium[1,2] which stabilizes copper(I). A more convenient approach is to generate copper(I) electrochemically *in situ*, which offers the possibility of retaining the aqueous medium, and the experimental data can be used for the evaluation of important electrode characteristics.[3,4]

The present paper offers the results obtained during the investigation of the response of two types of solid copper(II) ion-selective electrodes in copper(I) solutions, prepared by coulometric generation.

EXPERIMENTAL

Radelkis OP-Cu-7113 electrodes with a pressed membrane of ternary CuAgSe,[5,6] and thin-film $Cu_{2-x}Se$ electrodes prepared electrochemically,[7] were used in the investigations. The emf was measured with a Radelkis OP-208 pH-meter *vs.* a saturated calomel reference electrode.

The copper(I) solutions were prepared *in situ*, within the concentration range 5×10^{-6}–$5 \times 10^{-2}M$ by potentiostatic anodic dissolution of a copper anode (purity 99.99%) in $2M$ potassium chloride–$0.005M$ acetate buffer supporting electrolyte (pH 4.7) at anodic potentials within the range from -150 to -100 mV *vs.* SCE. A Radelkis coulometric titrator type OP-404 was used, with which the quantity of electricity passed (mC) could be checked directly. The anodic dissolution yield of copper(I) under these conditions was tested by coulometric titration of a standard vanadium(V) solution, and the results confirmed a current efficiency above 99.8%.

RESULTS AND DISCUSSION

The corresponding couple of ion-selective and reference electrodes was immersed in the anodic compartment of the coulometric cell, containing an accurately measured volume of the supporting electrolyte, deaerated beforehand with argon. The potential of the supporting electrolyte was checked, and then the copper-anode was immersed in the solution. Copper(I) was generated in increments, the potential of the ion-selective electrode and the quantity of electricity passed being checked after each. The total copper(I) concentration was evaluated on the basis of the total quantity of electricity passed, and that of the free copper(I) (*i.e.*, not bonded into chloride complexes) by using the equation

$$[Cu^+] = [Cu^+]_{tot}/\{1 + \beta_1[L] + \beta_2[L]^2 + \beta_3[L]^3\} \quad (1)$$

where [L] = chloride, with $\log \beta_1 = 2.7$, $\log \beta_2 = 5.19$ and $\log \beta_3 = 5.7$.[8]

The experimental scheme of a single experimental run is given in Table 1. These experiments were repeated many times during a relatively long period of time, in order to confirm the reproducibility, which was within ± 3 mV for E°_{mean}, measured over a one-month period.

The coulometric generation allows calibration of the electrodes over the concentration range $10^{-5} - 5 \times 10^{-2}M$ total Cu(I). The lower limit is determined by the blank potential in presence of the copper anode, and the upper by the solubility of the cuprous chloride complexes. Under these conditions the Radelkis electrodes displayed a linear Nernstian response with a slope of 58.6 mV/decade, and the thin-layer $Cu_{2-x}Se$ electrodes a slope of 59 mV/decade.

An interesting experimental fact is that the high chloride concentration does not distort the electrode response towards copper(I), as it does for pure copper(II) solutions. The slope of the calibration graph for copper(II) changes from 29 to 60 mV/decade in presence of $2M$ potassium chloride, in the same manner as observed for other copper ion-selective electrodes.[9,10] This suggests that the chloride

Table 1. Experimental data from a single coulometric calibration run for each electrode, with Cu(I)

Quantity, of electricity, *mC*		*E vs.* SCE, *mV*		$pCu_{tot.}$		pCu_{free}	
CuAgSe	$Cu_{2-x}Se$	CuAgSe	$Cu_{2-x}Se$	CuAgSe	$Cu_{2-x}Se$	CuAgSe	$Cu_{2-x}Se$
—	—	−107.8	−139.2	—	—	—	—
50	99	−86.0	−78.8	5.24	4.94	11.9	11.6
137	303	−66.3	−53.9	4.80	4.46	11.5	11.1
445	786	−36.4	−33.2	4.29	4.04	10.9	10.7
758	2,030	−23.7	−9.1	4.06	3.63	10.7	10.3
1,364	7,825	−8.9	+25.5	3.80	3.04	10.5	9.7
5,500	10,580	+26.2	+33.0	3.20	2.91	9.9	9.6
10,457	30,061	+42.7	+59.9	2.92	2.46	9.6	9.1
22,026	61,089	+62.0	+76.5	2.60	2.15	9.3	8.8
50,002	77,960	+79.0	+81.4	2.24	2.04	8.9	8.7
78,563	119,397	+84.4	+86.4	2.04	1.86	8.7	8.5

interference follows an identical mechanism for both types of electrode, and does not depend on the chemical composition of the membrane material, *i.e.*, it is not due to blocking of the electrode surface as was assumed initially,[11] and is displayed only in the presence of copper(II) in the solution.

The two electrodes were separately calibrated with respect to copper(II) by using the multiple standard-addition method (potassium nitrate was used as ionic strength adjuster in this case). The data for copper(I) and copper(II) calibration for each type of electrode offer the possibility of determining experimentally the selectivity coefficient, $K^{pot}_{Cu^+,Cu^{2+}}$, by the separate solutions method. For the intersection point of the extrapolated linear parts of the calibration graphs, where the conditions $E_{Cu^+} = E_{Cu^{2+}}$ and $[Cu^+] = [Cu^{2+}]$ are simultaneously fulfilled (Fig. 1), it follows that

$$K^{pot}_{Cu^+,Cu^{2+}} = \frac{[Cu^+]}{[Cu^{2+}]^{1/2}}$$

The values of log $K^{pot}_{Cu^+,Cu^{2+}}$ found are −5.7 and −6.2 for the $Cu_{2-x}Se$ and CuAgSe sensors respectively. Since the Nernstian relationship is followed for both copper(I) and copper(II), these values are not affected by changes in the copper concentrations. It is impressive that the selectivity coefficients for the two types of selenide sensors are quite close to each other and to the value found for the Cu_2S-sensor[3] and the mixed sulphide Orion sensor,[2] thus suggesting that similar processes are responsible for the electrode responses.

As seen from the selectivity coefficients, both electrodes are far more sensitive towards copper(I) than copper(II), and consequently their behaviour is described more accurately by the extended Nikolskii equation:

$$E = E^\circ + \frac{RT}{nF} \ln \{a_{Cu^+} + K^{pot}_{Cu^+,Cu^{2+}} (a_{Cu^{2+}})^{1/2}\} \quad (2)$$

According to the concepts of Buck,[12] and of Pungor and Tóth,[13] the selectivity coefficients for solid ion-selective electrodes are related to the equilibrium constant of the exchange reaction which proceeds on the electrode surface. In the case of a $Cu_{2-x}Se$ sensor, using the notation proposed by Hepel *et al.*[4] for expressing the composition of a non-stoichiometric (n − s) phase, we may write

$$[Cu_{2-x}Se] = [(1-x)Cu_2Se_{(n-s)}\, x CuSe_{(n-s)}]$$

and hence for the exchange reaction:

$$Cu_2Se_{(n-s)} + Cu^{2+} \rightleftharpoons CuSe_{(n-s)} + 2Cu^+ \quad (3)$$

The equilibrium constant of this reaction is $K_{ex} = [Cu^+]^2/[Cu^{2+}] = K_{sp(Cu_2Se)}/K_{sp(CuSe)}$ and the general expression derived for the relation between K_{ex} and the selectivity coefficient is:

$$K^{pot.}_{Cu^+,Cu^{2+}} = K^{1/2}_{ex} = \left\{\frac{K_{sp(Cu_2Se)}}{K_{sp(CuSe)}}\right\}^{1/2} \quad (4)$$

where K_{sp} is the solubility product of the species indicated by subscript. From equation (4), the value −6.4 is obtained for log $K^{pot}_{Cu^+,Cu^{2+}}$.

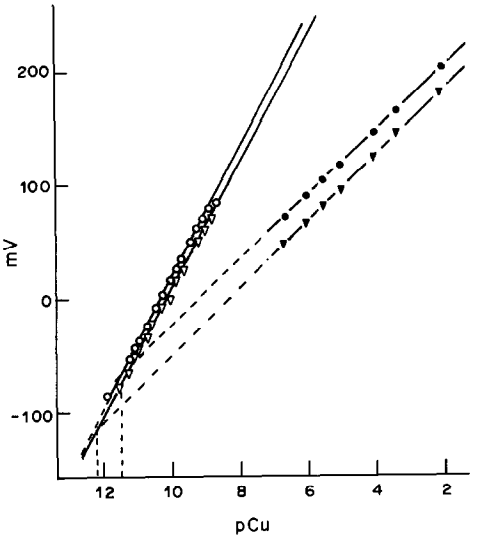

Fig. 1. Calibration curves for copper(I) (○, △) and copper(II) (●, ▲) with the CuAgSe electrode (△, ▲) and $Cu_{2-x}Se$ electrode (○, ●).

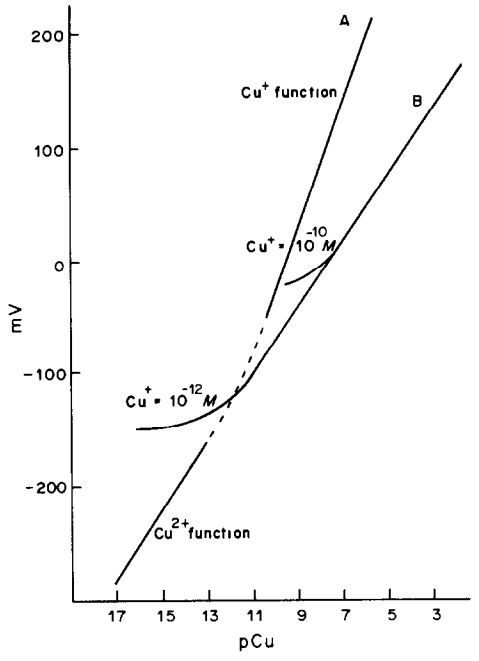

Fig. 2. Curve A, the theoretical emf calculated from equation (2) for the $Cu_{2-x}Se$ electrode for different equimolar concentrations of copper(I) and copper(II). Curve B, linearity limit of copper(II) dependence on the copper(I) surface activity.

By analogy, the composition of the ternary copper silver selenide membrane may be represented by

$$[2CuAgSe] = [(Cu_2Se)_{(n-s)}(Ag_2Se)_{(n-s)}]$$

and consequently equation (3) will be valid for the exchange reaction in this case too. Hence, the theoretical value for $K^{pot.}_{Cu^+,Cu^{2+}}$ will also be the same. The very good agreement between the experimentally determined and theoretically calculated values for the selectivity coefficients gives support to the Pungor model. Other models[4,14] also deserve attention and experimental check. Unfortunately, Hulanicki's diffusion model[15] leads to a very complicated expression for the selectivity coefficient for our membranes, difficult to interpret.

The experimental data also offer a possibility for determination of another very important electrode characteristic—E° in the extended Nikolskii equation (2). It was found that $E^\circ = 565 \pm 3$ mV for the CuAgSe membrane, and $E^\circ = 571 \pm 3$ mV for the $Cu_{2-x}Se$ membrane, both values *vs.* SCE. By use of the E° and $K^{pot.}_{Cu^+,Cu^{2+}}$ data for each type of electrode, the limit of sensitivity towards copper(II) could be determined as a function of the copper(I) activity (Fig. 2).

CONCLUSIONS

The present investigation shows that both types of ion-selective electrode offer a very sensitive and selective determination of copper(I) in the presence of a substantial excess of copper(II). This in turn provides the possibility of successful use of these electrodes for quantitative evaluation of equilibria involving copper(I).

The fact that both electrodes are much more selective towards copper(I) must always be taken into account if very low copper(II) activities are to be measured, since besides the extrinsic impurities, the electrode membrane itself is a generator of copper(I), at concentrations much higher than those expected on the basis of solubility data.

REFERENCES

1. L. F. Heerman and G. A. Rechnitz, *Anal. Chem.*, 1972, **44**, 1655.
2. H. Stünzi, *Talanta*, 1982, **29**, 75.
3. A. Hulanicki, M. Trojanowicz and M. Cichy, *ibid.*, 1976, **23**, 47.
4. T. Hepel, M. Hepel and M. Leszko, *Analyst*, 1977, **102**, 132.
5. M. Neshkova and J. Havas, *Hung. Patent*, 174, 627 (31 August 1976).
6. *Idem*, *Anal. Lett.*, 1983, **16**, 1567.
7. M. Neshkova and H. Sheytanov, *J. Electroanal. Chem.*, 1979, **102**, 189.
8. A. E. Martell and R. M. Smith, *Critical Stability Constants*, Vol. 4, Plenum Press, New York, 1976.
9. J. C. Westall, F. M. M. Morel and D. N. Hume, *Anal. Chem.*, 1979, **51**, 1792.
10. T. Hepel, *Anal. Chim. Acta*, 1981, **123**, 161.
11. G. J. Moody, N. S. Nassory, J. D. R. Thomas, D. Betteridge, P. Szepesvary and B. J. Wright, *Analyst*, 1979, **104**, 348.
12. R. P. Buck, *Anal. Chem.*, 1968, **40**, 1432.
13. E. Pungor and K. Tóth, *Analyst*, 1970, **95**, 625.
14. A. Hulanicki and A. Lewenstam, *Talanta*, 1976, **23**, 661.
15. *Idem*, *ibid.*, 1977, **24**, 171.
16. W. E. Morf, G. Kahr and W. Simon, *Anal. Chem.*, 1974, **46**, 1538.

Talanta, Vol. 32, No. 8A, pp. 657–658, 1985
Pergamon Press Ltd. Printed in Great Britain

0039-9140/85 $3.00 + 0.00
Pergamon Press Ltd

APPLICATION OF SOME COLORIMETRIC METHODS FOR THE SPECTROPHOTOMETRIC DETERMINATION OF PHENYLBUTAZONE AND OXYPHENBUTAZONE

A. S. Issa, Y. A. Beltagy, M. Gabr Kassem and H. S. Daabees
Pharmaceutical Chemistry Department, Faculty of Pharmacy, Alexandria University, Alexandria, Egypt

(*Received* 13 *November* 1984. *Accepted* 29 *March* 1985)

Summary—Two methods for determination of phenylbutazone and oxyphenbutazone are described. In the first, naphthoquinone reacts with the product of acid hydrolysis of phenylbutazone or oxyphenbutazone to give an orange colour, having maximum absorption at 480 and 465 nm respectively. In the second, lead tetra-acetate reacts with the hydrolysis product of phenylbutazone (benzidine) to develop a green colour which on heating or addition of excess of reagent changes to yellow, with maximum absorption at 340 nm. Oxyphenbutazone gives a yellow colour with the reagent in the cold, with maximum absorption at 359 nm.

Several methods have been reported for the colorimetric determination of phenylbutazone and oxyphenbutazone. Oxyphenbutazone has been determined through its reaction with sodium nitrite,[1] sodium cobaltinitrite,[2] diazotized sulphanilic acid, or diazotized *o*-nitroaniline.[3,4] The acid hydrolysis product of oxyphenbutazone has been condensed with an aromatic aldehyde and determined spectrophotometrically.[5] Phenylbutazone yields benzidine on acid hydrolysis, and this has been diazotized and coupled with different phenolic compounds.[6–8] Benzidine has also been oxidized with potassium ferricyanide and measured spectrophotometrically.[9] Phenylbutazone has been determined spectrophotometrically after reaction with a mixture of phosphomolybdic and phosphotungstic acids or with α,α′-bipyridyl and ferric chloride,[11] or with potassium permanganate in alkaline medium.[12,13] Other methods such as titrimetry[14–18] and gas or high-pressure liquid chromatography[19,20] have been reported for the determination of phenylbutazone and oxyphenbutazone.

EXPERIMENTAL

Reagents

Sodium 1,2-naphthoquinone-4-sulphonate. A 0.2% solution in 50% aqueous ethanol.

Potassium carbonate solution, 10%.

Borax solution, 1%.

Lead tetra-acetate reagent (LTA).[21,22] Heat 100 ml of glacial acetic acid to about 70° on a water-bath, then gradually add 3 g of lead dioxide. Stir the mixture for 30 min while keeping the temperature at 70°. Cool and filter the solution and store it in a dark bottle.

Procedure using naphthoquinone as reagent

For phenylbutazone and oxyphenbutazone powder. Weigh about 30 mg of phenylbutazone or oxyphenbutazone into a small round-bottomed flask, add 2 ml of concentrated hydrochloric acid and 1 ml of glacial acetic acid, heat under reflux, in a boiling water-bath, for 30 min, then cool. Transfer the contents of the flask with ethanol to a 100-ml standard flask and dilute to volume with ethanol. Transfer 25 ml of this solution to a 50-ml standard flask, add a small piece of litmus paper and neutralize by dropwise addition of 10% potassium carbonate solution, then dilute to volume with ethanol. Transfer an aliquot containing 0.075–0.75 mg of the drug to a 25-ml standard flask and add 4 ml of borax solution and 5 ml of naphthoquinone reagent. Let stand at room temperature for 30 min, then dilute to volume with ethanol. Measure the absorbance at 480 nm for phenylbutazone and 465 nm for oxyphenbutazone, against a reagent blank.

For tablets. Weigh and powder 20 tablets of phenylbutazone or oxyphenbutazone. Weigh out a quantity of the powder equivalent to about 150 mg of the drug and extract successively with 30, 10 and 10 ml of warm acetone, filtering each portion into a 100-ml standard flask. Cool and dilute to volume with acetone. Transfer 20 ml of this solution to a small round-bottomed flask and evaporate to dryness. Apply the procedure described above.

For phenylbutazone sodium ampoules. Mix the contents of 10 ampoules, transfer a volume containing about 600 mg of phenylbutazone to a 100-ml standard flask and add acetone up to the mark. Treat 5 ml of this solution, in a small round-bottomed flask, by the procedure for the powder.

Procedure using lead tetra-acetate (LTA) as reagent

For oxyphenbutazone powder. Prepare accurately a 0.03 mg/ml solution of oxyphenbutazone in glacial acetic acid. Transfer a suitable number of portions (1–5 ml) of the solution into 10-ml standard flasks, add 1 ml of LTA reagent to each and dilute to volume with glacial acetic acid. After 15 min measure the absorbance at 359 nm against a reagent blank, and construct a calibration graph. Analyse samples analogously.

For phenylbutazone powder. Weigh accurately about 100 mg into a small round-bottomed flask and add 10 ml of concentrated hydrochloric/acetic acid mixture (1:4 v/v). Heat under reflux in a boiling water-bath for 30 min, then cool. Transfer the contents of the flask to a 50-ml standard flask with glacial acetic acid, dissolve about 4 g of mercuric acetate in the solution and dilute to volume with glacial acetic acid. Accurately dilute 5 ml of this solution to 50 ml with glacial acetic acid, then transfer portions containing 0.2–0.8 mg of the drug into 10-ml standard flasks and add 3 ml of LTA reagent to each. Heat in a boiling water-bath for 15 min then cool and complete to volume with glacial acetic acid. Measure the absorbance at 340 nm against a

Table 1. Analysis of phenylbutazone and oxyphenbutazone products

Drug form	Napthoquinone method		Lead tetra-acetate method		B.P. 1980 method	
	Taken, *mg*	Mean* recovery,%	Taken, *mg*	Mean* recovery,%	Taken, *mg*	Mean* recovery,%
Phenylbutazone powder	0.3–2.4	99.7 ± 0.7	2.0–8.0	100.2 ± 0.6	500.0	100.1 ± 1.1
Phenylbutazone tablets[D] (200 mg/tablet)	0.3–2.4	85.1 ± 1.0	2.0–8.0	85.3 ± 0.4	500.0	86.7 ± 0.9
Adcobutazone ampoules[D] (1 g/5 ml)	0.3–2.4	103.7 ± 0.7	2.0–8.0	102.8 ± 0.9	—	—
Oxyphenbutazone powder	0.6–3.0	100.4 ± 1.0	0.3–1.5	100.5 ± 1.3	500.0	100.3 ± 1.0
Tanderil tablets[G] (100 mg/tablet)	0.6–3.0	95.7 ± 0.4	0.3–1.5	99.7 ± 1.4	500.0	94.3 ± 0.9
Rhumaxin tablets[A] (100 mg/tablet)	0.6–3.0	100.5 ± 0.9	0.3–1.5	100.6 ± 1.1	500.0	96.0 ± 1.3
Oxyzone tablets[N] (100 mg/tablet)	0.6–3.0	91.4 ± 0.5	0.3–1.5	98.5 ± 1.1	500.0	92.0 ± 1.3

D = Adco Company. G = Geigy Company. A = Alexandria Company. N = Nile Company.
*Mean and standard deviation (6 results) calculated with reference to nominal content in sample.

reagent blank and construct a calibration graph. Analyse samples analogously.

For tablets. Weigh and powder 20 tablets of phenylbutazone or oxyphenbutazone. Transfer a quantity of powder equivalent to about 40 mg of oxyphenbutazone or 500 mg of phenylbutazone to a 100-ml standard flask, shake it with 50 ml of glacial acetic acid for 10 min, then dilute to volume with glacial acetic acid and filter.

For oxyphenbutazone accurately dilute 10 ml of this sample solution to 100 ml with glacial acetic acid, and treat 3 ml of this solution with 1 ml of LTA reagent in a 10-ml standard flask, *etc.*, as described above.

For phenylbutazone add 2 ml of concentrated hydrochloric acid to 10 ml of the filtered sample solution in a small round-bottomed flask, then continue as described above, starting with heating for 30 min.

For phenylbutazone sodium ampoules. Mix the contents of 10 ampoules and transfer a known volume containing about 1 g of phenylbutazone to a 50-ml standard flask and dilute to volume with glacial acetic acid. Transfer 5 ml of this solution to a small round-bottomed flask and complete by the procedure for phenylbutazone powder.

RESULTS AND DISCUSSION

The naphthoquinone procedure involves hydrolysis of phenylbutazone or oxyphenbutazone to benzidine or a substituted benzidine, which was then condensed with naphthoquinone to give an orange product. The conditions given are those found to give maximal absorbance. The reacting ratio between the reagent and the hydrolysis product is 2:1, as found by the continuous-variations method.

In the LTA procedure oxyphenbutazone reacts in the cold to give a yellow colour that reaches maximum intensity in 15 min, but phenylbutazone must first be hydrolysed to benzidine, and heating is essential for complete colour development. Mercuric acetate is added before addition of the LTA reagent to prevent precipitation of lead chloride.

The two procedures were applied to the assay of tablets and ampoules (Table 1) and gave results in agreement with those obtained by using the B.P 1980 method.

REFERENCES

1. A. Abou-Ouf, M. I. Walash, S. M. Hassan and S. M. El-Sayed, *Analyst*, 1980, **105**, 1247.
2. A. M. Wahbi, H. Abdin, M. Korany and M. H. Abdel-Hady, *J. Assoc. Off. Anal. Chem.*, 1978, **61**, 1113.
3. S. M. Hassan, M. I. Walash, S. M. El-Sayed and A. Abou-Ouf, *ibid.*, 1981, **64**, 1442.
4. E. Svátek and A. Hrádková, *Cesk. Farm.*, 1966, **15**, 76.
5. N. M. Sanghavi, N. G. Jivani and P. D. Mulye, *Indian J. Pharm.*, 1977, **39**, 87.
6. H. Hasso, *Pharmazie*, 1966, **21**, 464.
7. E. Maggionelli, G. Gangeni and L. Conti, *Boll. Chim. Farm.*, 1966, **105**, 893.
8. J. F. Magalhacs and M. G. Piros, *Rev. Farm. Bioquim.* 1973, **11**, 41.
9. N. S. Simonova, *Farmatisya*, 1978, **27**, 29.
10. S. Bruno and G. Hupdi, *Farmaco, Ed. Sci.*, 1956, **11**, 462.
11. M. Deffner and A. Issidorides-Deffner, *Chim. Anal. (Paris)*, 1958, **40**, 460.
12. G. Stajer, E. Vinkler and A. E. Szabo, *Pharmazie*, 1970, **25**, 126.
13. J. E. Wallace, *J. Pharm. Sci.*, 1968, **57**, 2053.
14. A. Madraimov and A. I. Gregrinovich, *Farmatsiya*, 1968, **17**, 70.
15. F. Jančik, E. Kraus, B. Budějínský and O. Činková, *Cesk. Farm.*, 1957, **6**, 105.
16. F. Jančik, B. Kakáč and J. Körbl, *Czech. Patent* 134941, 1970.
17. Ž. Bezáková, M. Bachratá and L. Kŭažko, *Farm. Obz.*, 1979, **48**, 57.
18. M. I. Walash and M. Rizk, *Indian J. Pharm.*, 1977, **39**, 82.
19. H. Spahn and E. Mutschler, *Arzneim. Forsch.*, 1981, **31**, 495.
20. J. A. Bogan, *J. Pharm. Pharmacol.*, 1977, **29**, 125.
21. K. K. Verma and S. Bose, *Mikrochim. Acta*, 1976 **II**, 591.
22. M. H. Abdel-Hay, *Ph.D. Thesis*, University of Alexandria.

Talanta, Vol. 32, No. 8A, pp. 659–661, 1985
Printed in Great Britain.

0039-9140/85 $3.00 + 0.00

PROPERTIES AND ANALYTICAL APPLICATION OF A NEW MEMBRANE ELECTRODE SENSITIVE TO MOLYBDENUM(VI)

L. K. SHPIGUN
V.I. Vernadsky Institute of Geochemistry and Analytical Chemistry, USSR Academy of Sciences, Moscow, 117975, USSR

E. N. ABANINA, Z. A. GALLAI and N. M. SHEINA
Department of Chemistry, University of Moscow, 117234, USSR

(*Received* 4 *November* 1984. *Accepted* 15 *March* 1985)

Summary—A new liquid molybdenum(VI)-sensitive electrode with a membrane based on a solution of the molybdenum(VI)–*N*-benzoyl-*N*-phenylhydroxylamine chelate is proposed and its electrochemical behaviour and applicability have been critically investigated. The transfer of molybdenum(VI) across the water–organic solvent interface and across the membrane has been studied by use of sodium molybdate labelled with ^{99}Mo, and the response mechanism of the electrode is discussed.

The development and application of ion-selective electrodes continue to be exciting and expanding areas of analytical research. Only a few attempts have been made to find a membrane material suitable for a molybdenum-selective electrode.[1,2] Unfortunately, these electrodes have a narrow operational range, poor selectivity and limited lifetime, and therefore are not used in practical analysis.

In view of the correlation between the selective electrode response of liquid membranes (based on solvent extraction systems) and the corresponding extraction constants, metal chelates are an obvious choice as membrane components in liquid ISEs.[3] This report contains some results from the recent investigation of a new molybdenum(VI)-selective electrode which uses a solution of the molybdenum(VI)–*N*-benzoyl-*N*-phenylhydroxylamine (BPHA) complex as the liquid membrane.

EXPERIMENTAL

BPHA forms with molybdenum(VI) a highly stable complex $MoO_2(BPHA)_2$ ($\log \beta = 26.3$).[4] We have studied the extraction of molybdenum from aqueous solution with BPHA dissolved in various organic solvents and found that it can be rapidly and quantitatively extracted with high distribution coefficients ($\log D = 2.4$, 2.5, 2.8, for chloroform, 1,2-dichloroethane and nitrobenzene respectively, at $22 \pm 1°$ and pH 2). Therefore, we have chosen the chelate of molybdenum with BPHA as the membrane component for a molybdenum(VI)-sensitive electrode.

The liquid membranes were prepared in the usual way by solvent extraction: 1 ml of $4 \times 10^{-2}M$ BPHA in an organic solvent was shaken with a twofold molar excess of sodium molybdate solution at pH 2. These membranes were incorporated into an Orion liquid-liquid membrane electrode body and also into a home-made one of Růžička type. A potentiometric investigation showed that both types of electrode had similar characteristics. The internal solution of the electrode was $1 \times 10^{-3}M$ sodium molybdate/$1 \times 10^{-3}M$ potassium chloride saturated with silver chloride. The electrode potential was measured at $22 \pm 1°$ against a double-junction Ag/AgCl reference electrode (Orion model 90-02), with a salt-bridge filled with $0.1M$ sodium sulphate. All potential measurements were made with an Orion model 801A digital instrument.

RESULTS AND DISCUSSION

The electrodes were systematically checked for response slope and linear range, with pure solutions of sodium molybdate. Figure 1 shows the dependence of the electrode potential on the concentration of Mo(VI) for the electrodes in which $5 \times 10^{-3}M$ solutions of $MoO_2(BPHA)_2$ in various organic solvents were used as the membranes. The results clearly demonstrate that all three membranes are sensitive to Mo(VI), but the sensitivity is strongly dependent on the solvent used.

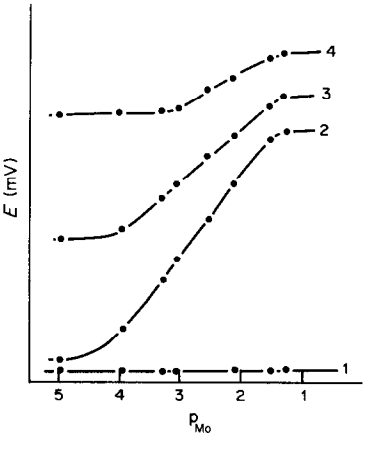

Fig. 1. *E vs.* P_{Mo} for the liquid membranes consisting of the $10^{-3}M$ solutions of chelate $MoO_2(BPHA)_2$ in nitrobenzene (2), 1,2-dichloroethane (3), chloroform (4), and for the pure solvents (1).

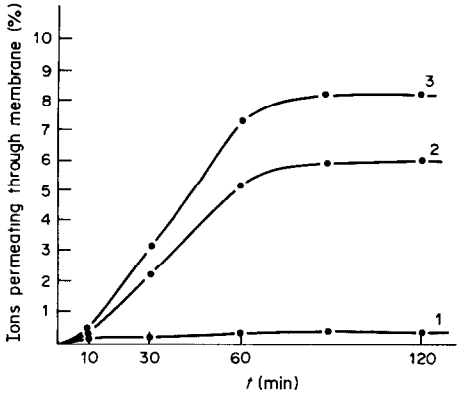

Fig. 2. Kinetics of the migration of ^{99}Mo across liquid membranes consisting of pure nibrobenzene (1), and the $MoO_2(BPHA)_2$ complex in 1,2-dichloroethane (2), or nitrobenzene (3). The concentration of Na_2MoO_4 in the aqueous phase was $1 \times 10^{-2}M$.

Increase in the dielectric constant of the solvent increases the linear range and slope of the electrode response. The distribution coefficients of the Mo–BPHA complex also increase with dielectric constant of the solvent. With nitrobenzene the electrode response is linear and practically Nernstian over the concentration range from $1 \times 10^{-5}M$ to $1 \times 10^{-1}M$, and this electrode has a more stable potential and better dynamic parameters than the others.

The electrode gives correct response in the pH-range 4–11. At lower pH the electrode response sharply increases, which may be mainly attributed to the effect of protons on the nature of the isopoly molybdate species and on the behaviour of the chelate in the membrane.

Since some other metals can also be quantitatively extracted as chelates with BPHA, their effect on the electrode response was tested. The values of the selectivity coefficients determined by the mixed-solution method are given in Table 1 and demonstrate that the electrode shows good selectivity towards molybdenum. Bivalent and multivalent anions do not affect the electrode potential. Anionic interference is caused only by lipophilic univalent anions.

Although several studies concerning the mechanism of the chelate-type membrane electrodes have been published[5] we thought it interesting to make a radiotracer investigation of the migration of ^{99}Mo at the water–membrane interface and through the membranes consisting of $MoO_2(BPHA)_2$ in organic solvents of different polarity (Figs. 2 and 3) and to discuss the correlation between the ion-transport data and the electrode function.

Table 1. Potentiometric selectivity coefficients of the liquid $MoO_2(BPHA)_2$ membranes; ion-exchanger concentration $1 \times 10^{-3}M$, C_{Me} $1 \times 10^{-2}M$

Interfering ion(Me)	$pK_{Mo/Me}$ nitrobenzene	$pK_{Mo/Me}$ 1,2-dichloroethane
Na	1.5×10^{-6}	—
Co(II)	3.9×10^{-4}	8.0×10^{-4}
W(VI)	1.7×10^{-4}	5.1×10^{-4}
Fe(III)	9.8×10^{-4}	7.5×10^{-3}
Cu(II)	1.2×10^{-3}	—
Mn(II)	2.0×10^{-3}	—
Ni(II)	3.9×10^{-3}	—
V(V)	1.7×10^{-2}	2.5×10^{-3}

Table 2. The conditional radiotracer-exchange rate-constants(r) of ^{99}Mo at the water/membrane interface; chelate concentration $1 \times 10^{-3}M$

pH	$r \times 10^2$, min^{-1} nitrobenzene	1,2-dichloroethane
2.8	5.7	6.0
7.0	4.8	5.2
11.0	4.8	5.2

The results obtained by both procedures clearly confirm the permeability of the $MoO_2(BPHA)_2$ liquid membrane to molybdenum(VI) species, in contrast to membranes consisting of the pure solvents, which give practically no diffusion of molybdenum. The extent of ion-exchange and the mobility of the molybdenum ions in the membrane decrease with decrease in the dielectric constant of the solvent. The data in Table 2 indicate the effects of the membrane solvents and pH of aqueous phase on the conditional radiotracer-exchange rate-constants for ^{99}Mo. The values of the trans-membrane diffusion coefficients were found to be of the order of 10^{-7} cm^2/sec.

A possible transport mode in such membranes is shown in Fig. 4. The electrode response mechanism is not fully understood, but it is evident that the electrochemical properties of these systems are determined by the rate of exchange of molybdenum ions with the chelate at the membrane–aqueous solution interface.

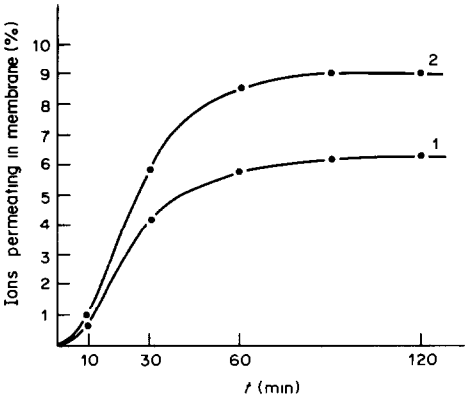

Fig. 3. Kinetics of the migration of ^{99}Mo at the aqueous solution/membrane interface for liquid membranes consisting of the chelate $MoO_2(BPHA)_2$ in 1,2-dichloroethane (1), and nitrobenzene (2).

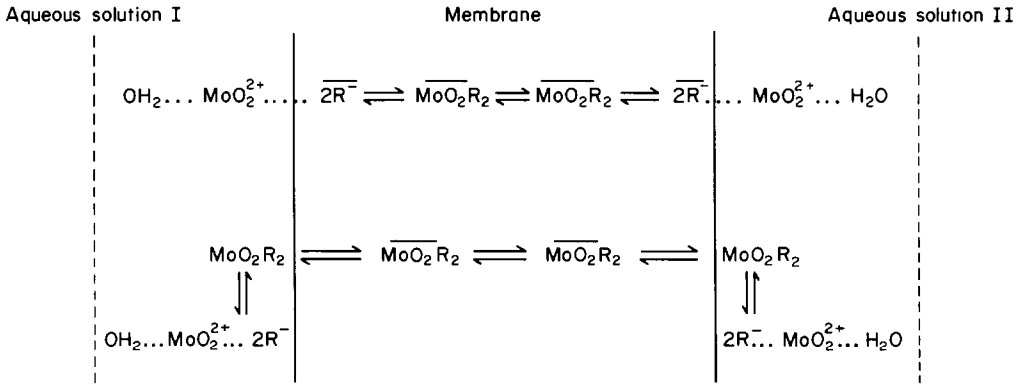

Fig. 4. The possible mode of transport for the liquid $MoO_2(BPHA)_2$ membrane.

REFERENCES

1. W. V. Malik, S. K. Srivastava and A. Bansal, *Anal. Chem.*, 1982, **54**, 1399.
2. S. K. Srivastava, A. K. Sharma and C. K. Jain, *Talanta*, 1983, **30**, 285.
3. W. Szczepaniak, M. Ren and K. Ren, *Chem. Anal., Warsaw*, 198, **24**, 51.
4. A. N. Bantysh, E. V. Dobizha and D. A. Knyazev, *Radiokhimiya*, 1968, **10**, 557.
5. J. Růžička and J. Ch. Tjell, *Anal. Chim. Acta*, 1970, **51**, 1.

Talanta, Vol. 32, No. 8A, pp. 662–664, 1985
Printed in Great Britain.

0039-9140/85 $3.00 + 0.00

DETERMINATION OF TRACE AMOUNTS OF COPPER, LEAD AND ZINC IN CEMENTS BY X-RAY FLUORESCENCE SPECTROMETRY AFTER PRECIPITATION SEPARATION WITH HEXAMETHYLENEAMMONIUM HEXAMETHYLENEDITHIOCARBAMATE

YOSHIKAZU YAMAMOTO, YASUHIRO NISHINO and KAZUMASA UEDA
Department of Industrial Chemistry, Faculty of Technology, Kanazawa University, Kanazawa, 920, Japan

(*Received* 22 *August* 1984. *Revised* 27 *December* 1984. *Accepted* 12 *March* 1985)

Summary—A rapid and precise X-ray fluorescence method is proposed for the simultaneous determination of trace amounts of copper, lead and zinc in cements. The method is based on prior removal of iron by extraction with methyl isobutyl ketone from 6*M* hydrochloric acid, followed by collection of copper, lead and zinc on a membrane filter as their hexamethyleneammonium hexamethylenedithiocarbamate complexes to give a thin layer suitable for X-ray fluorescence measurement. The use of an internal standard (nickel) improves the precision for the determination of copper, zinc and lead.

Various methods have been published for the determination of trace amounts of copper, lead or zinc in cements: spectrophotometric and atomic-absorption methods for copper,[1-4] an atomic-absorption method for lead,[5] and polarographic, fluorometric, spectrophotometric and atomic-absorption methods for zinc.[6-9] The spectrophotometric methods, however, have complicated procedures. Only atomic-absorption[10] has been applied to successive determination of the three elements in cements.

The present paper describes precipitation, followed by X-ray fluorescence spectrometry, for the simultaneous determination of trace amounts of copper, lead and zinc in cements. To separate and preconcentrate these trace elements from a cement solution, on a membrane filter, hexamethyleneammonium hexamethylenedithiocarbamate (HMA–HMDC) is used as precipitant, since it does not react with the major elements in cements (except iron) but forms stable insoluble complexes with the elements to be determined. Iron, which interferes, is extracted beforehand with MIBK from 6*M* hydrochloric acid medium. Nickel is used as an internal standard.

The HMA–HMDC complexes are collected on a membrane filter and the $K\alpha$ or $L\alpha_1$ fluorescence intensity of each element is measured. The calibration graphs are linear up to 100 μg for copper and lead, and 200 μg for zinc. The coefficients of variation found were 0.3, 0.6 and 1.1% respectively, for 50 μg of copper, lead and zinc. The results of analysis of cement samples by the proposed method agree with those obtained by atomic-absorption spectrophotometry.

EXPERIMENTAL

Apparatus

The X-ray fluorescence measurements were made with a Regaku-Denki KG-X type instrument equipped with a Philips tungsten target tube, a lithium fluoride ($2d = 4.028$ Å) analysing crystal, an NaI(Tl) scintillation counter and a pulse-height analyser. Toyo Roshi Co. TM-80 membrane filters (25 mm in diameter, 0.8 μm pore size) were used.

Reagents

Copper, lead and zinc standard solutions, 1000 ppm. Commercial standard solutions (Wako Junyaku Co.) were used.

Nickel standard solution, 1000 ppm. Prepared by dissolving nickel metal (99.9% pure) in hydrochloric acid (1 + 1) and diluting with water.

HMA–HMDC solution in ethanol, 0.5%. The HMA–HMDC was synthesized by Busev's method.[11]

All other chemicals used were of analytical-reagent grade; demineralized distilled water was used throughout. The stock standard solutions were diluted as required.

Procedure

Weigh a 1-g sample of the pulverized cement into a platinum crucible, add a mixture of 2 ml of 60% perchloric acid, 2 ml of water and 5 ml of concentrated hydrofluoric acid, and evaporate to dryness on a sand-bath. Heat the residue with 10 ml of hydrochloric acid and evaporate to dryness. Repeat this step, then take up the residue by heating with 10 ml of the acid. Filter off any residue (calcium fluoride) and wash it with hot water. Cool the filtrate and washings, and dilute to volume in a 50-ml standard flask with water. Transfer 20 ml of the solution and 20 ml of concentrated hydrochloric acid into a 100-ml separatory funnel, and shake the mixture for 3 min with 10 ml of methyl isobutyl ketone to extract iron. Separate the aqueous phase and transfer an aliquot of it (containing less than 100 μg each of copper and lead, and less than 200 μg of zinc) into a beaker, add 50 μg of nickel as internal standard and dilute the solution to about 50 ml with water. Adjust the pH to 4 with ammonia solution (1 + 3). Add 2 ml of 0.5% HMA–HMDC solution in ethanol, and let stand for 20 min at room temperature. Collect the precipitate on a 0.8-μm membrane filter, wash it with a small amount of water and dry it at room temperature. Fix the thin film of the complexes by covering it with a 6-μm Mylar film and a titanium mask, and place it in an aluminium holder. Measure the X-ray intensities of the $K\alpha$ lines for copper ($2\theta = 45.02°$) zinc ($2\theta = 45.81°$) and nickel ($2\theta = 45.64°$),

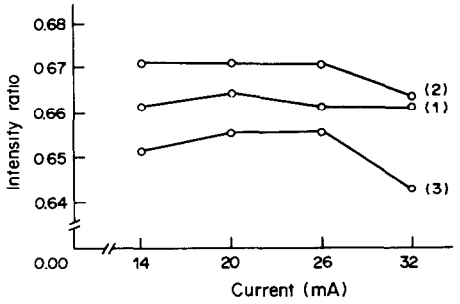

Fig. 1. Effect of voltage and current on X-ray intensity ratio; L_{Zn}/I_{Ni}. (1) 45 kV, (2) 40 kV, (3) 35 kV.

and the $L\alpha_1$ line for lead ($2\theta = 33.92°$) three times, for 20 sec each time, with vacuum-path X-rays, at 40 kV and 20 mA. Correct the background intensity of each element for the blank, measured in the same way as the sample. Calculate the amounts of copper, lead and zinc in the cement sample, from the calibration graphs.

RESULTS AND DISCUSSION

Choice of precipitant

Of the organic reagents commonly used for copper, lead and zinc, *viz.* cupferron,[12] 2-mercaptobenzothiazole (MBT),[13] sodium diethyldithiocarbamate (DDTC)[14] and HMA–HMDC,[15] cupferron also forms complexes with aluminium and iron, which are major elements in cement, MBT does not react with the major elements in cement and forms complexes with copper, lead and zinc in neutral or slightly alkaline media, but cannot be used because of its low reactivity with zinc, and DDTC forms stable complexes with iron, copper, lead and zinc in alkaline medium but is unstable in slightly acidic medium, which makes the complexes also less stable. However, HMA–HMDC forms stable complexes with these trace elements in acidic medium and does not react with the major elements (other than iron) in cement.

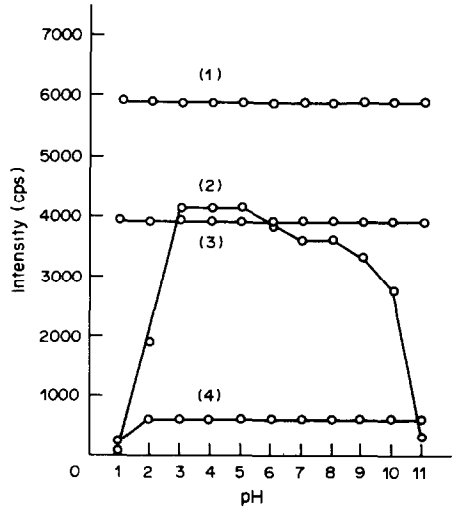

Fig. 2. Effect of pH on the formation of HMA–HMDC complexes. (1) Ni, (2) Zn, (3) Cu, (4) Pb.

The iron can be removed by prior extraction from 6*M* hydrochloric acid solution with MIBK. HMA–HMDC was therefore chosen as the complexing agent.

Effect of voltage and current on X-ray intensity ratios

The X-ray intensity ratios of copper, lead and zinc to nickel were examined with amounts of the HMA–HMDC complexes each containing 50 μg of the metal. The operating voltages and currents were varied in the ranges 35–45 kV and 14–32 mA respectively. The results shown in Fig. 1 indicate that a voltage of 40 kV and current of 20 mA would be optimal.

Precipitation conditions

Figure 2 shows that a pH range of 1–11 is suitable for precipitation of copper and nickel and 2–11 for that of lead, but only the narrow range 3–5 was found suitable for zinc. A pH of 4 was therefore selected as optimal for the group separation.

The optimum amount of HMA–HMDC for precipitation of 50 μg each of copper, lead, zinc and nickel was found by use of 50 μg each of the metals and varied amounts of reagent. The X-ray fluorescence intensity was constant and maximal with use of 3 ml or more of 0.1% HMA–HMDC solution, but too large an amount produced a very finely divided precipitate, which made the filtration more time-consuming. Use of 2 ml of 0.5% HMA–HMDC solution is therefore recommended.

Varying the aging time at room temperature in the range 5–60 min made no difference to the results, and an aging period of 20 min was selected, but 5 min could be used if speed is important.

Calibration graphs

The solutions for making the calibration graphs contained 10–100 μg each of copper and lead, 10–200 μg of zinc, and 50 μg of nickel as internal standard. Plots of the ratios of X-ray intensities for the three elements to those for nickel were all linear.

Precision, detection limit and recovery

The coefficients of variation for determination of 50 μg each of copper, lead and zinc, and the detection limits calculated as the amount of element giving three times the standard deviation of a 200-sec background count, are summarized in Table 1.

A solution containing 100 μg each of copper, lead and zinc, and 5000 μg of iron(III), was made 6*M* in

Table 1. Precision and detection limits

Metal	Metal added, μg	Metal found, μg	Coefficient of variation,* %	Detection limit, μg
Cu	50.0	50.0	0.3	0.09
Pb	50.0	49.8	0.6	0.7
Zn	50.0	50.1	1.1	0.07

*For five determinations.

Table 2. Copper, lead and zinc (*ppm*) in cements (200-mg sample)

	Cu		Pb		Zn	
Sample	XRF	AAS	XRF	AAS	XRF	AAS
Portland cement	151	151	55	57	657	659
Blast furnace cement A type	121	124	47	43	826	835
Blast furnace cement C type	85	90	49	47	621	628

Sample taken: 200 mg.

hydrochloric acid and the iron was extracted with MIBK.[16] The copper, lead and zinc in the aqueous phase were then determined by the proposed procedure, and recoveries of 99.2–100% were obtained.

Effect of other elements

Of the major elements in cement, only iron forms a complex with HMA–HMDC and it can be removed by extraction with MIBK. The other elements present were found not to cause interference by absorption or emission, and there was no need to correct the mass absorption coefficients of the three elements determined, since less than 200 μg of each was present and measurements were made on a membrane thin film.

Analysis of cements

The method was applied to determination of trace amounts of copper, lead and zinc in some cement samples. The results agreed with those obtained by atomic-absorption spectrometry, as shown in Table 2. The zinc content of the cements was 5–20 times that of copper and lead, so a 200-mg sample was adequate. The calcium fluoride residue was analysed by X-ray fluorescence, and found not to cause loss of copper, lead and zinc by adsorption or co-precipitation.

REFERENCES

1. H. Ishii, H. Einaga and E. Aoki, *Bunseki Kagaku*, 1966, **15**, 825.
2. H. Ishii, T. Mizoguchi and T. Odashima, *ibid.*, 1977, **26**, 540.
3. Cement Association of Japan, Committee on Chemical Analysis, *Determination of Trace Amounts of Elements in Cements and their Raw Materials*, pp. 42–44. Cement Association of Japan, Tokyo, 1981.
4. *Idem*, *op. cit.*, pp. 45–47.
5. *Idem*, *op. cit.*, pp. 82–84.
6. H. Ishii, H. Einaga and T. Suga, *Bunseki Kagaku*, 1965, **14**, 24.
7. K. Watanabe and K. Kawagaki, *Bull. Chem. Soc. Japan*, 1975, **48**, 1945.
8. Cement Association of Japan, Committee on Chemical Analysis, *op. cit.*, pp. 48–52.
9. *Idem*, *op. cit.*, pp. 52–55.
10. *Idem*, *op. cit.*, pp. 85–90.
11. A. I. Busev, V. M. Byr'ko, A. P. Tereshchenko, N. N. Novikova, V. P. Naidina and P. B. Terent'ev, *Zh. Analit. Khim.*, 1970, **25**, 665.
12. K. Hirokawa, *Z. Anal. Chem.*, 260, **4**, 1972.
13. O. N. Rushina, P. N. Kovalenko and Z. I. Ivanova, *Zh. Analit. Khim.*, 1965, **20**, 44.
14. Y. Yamamoto, H. Yamagishi and S. Ueda, *Nippon Kagaku Kaishi*, 1975, **9**, 1508.
15. Y. Yamamoto, M. Sugita and K. Ueda, *Bull. Chem. Soc. Japan*, 1982, **55**, 742.
16. H. Goto, Y. Kakita and T, Furukawa, *Nippon Kagaku Zasshi*, 1958, **79**, 1513.

Talanta, Vol. 32, No. 8A, pp. 665–667, 1985
Printed in Great Britain.

0039-9140/85 $3.00 + 0.00

EFFECT OF CYCLODEXTRIN CAVITY SIZE ON SENSITIZATION OF ROOM-TEMPERATURE PHOSPHORESCENCE OF BIACETYL

FRANK J. DELUCCIA and L. J. CLINE LOVE*
Seton Hall University, Department of Chemistry, South Orange, New Jersey 07079, U.S.A.

(*Received* 8 *January* 1985. *Accepted* 5 *March* 1985)

Summary—The triplet–triplet energy-transfer reactions of several polynuclear aromatic compounds are enhanced to different degrees in α-, β-, and γ-cyclodextrin (CD) media when biacetyl is used as the acceptor species. The phosphorescence intensity of biacetyl increases as the size of the CD cavity increases. The CD cavities have specific dimensions which place constraints on the number of donor and acceptor molecules that can be included in them. The larger the cavity, the better it is able to include the reactants and, apparently, position them to increase the rate of triplet–triplet energy transfer. Compounds such as chrysene and triphenylene, which are unresponsive as biacetyl sensitizers in α-CD and β-CD, are excellent sensitizers of biacetyl in the larger γ-CD. Typically, limits of detection of 1×10^{-6}, 5×10^{-7} and $1 \times 10^{-7} M$ were found with α-CD, β-CD and γ-CD, respectively.

In recent years, studies in our laboratory and by other workers have demonstrated that many excited phosphorescent compounds, when associated with micellar assemblies[1,2] or included in cyclodextrin (CD) cavities,[3,4] are deactivated in fluid solution at room temperature by triplet-state emission. An alternative method for studying molecular triplet-state processes is by energy-transfer interactions. Sensitized phosphorescence involves triplet–triplet energy transfer according to the equation[5]

$$D(T_1) + A(S_0) \rightleftharpoons D(S_0) + A(T_1) \qquad (1)$$

where D is the donor molecule (analyte of interest), A the acceptor molecule, and S_0 and T_1 are the ground state and excited triplet state, respectively.

Sensitization of the room-temperature phosphorescence of biacetyl has been observed to be enhanced through spatial organization of the reactants by various compounds.[6] Micelles of sodium dodecyl sulphate (SDS), and hosts such as β-CD were shown to enhance the energy-transfer reaction, presumably by organizing the donor–acceptor pair into a smaller reaction volume and thereby producing higher effective concentrations of both the acceptor and the donor. The sensitivities of the systems were dependent on the solubility of the donor in SDS, or on the ability of the donor to fit physically into the β-CD cavity, as well as on the nature of the hydrophobic and van der Waals interactions between the analyte and sensitizer and the host species. Indeed, large polynuclear aromatic compounds (PNAs) such as triphenylene and chrysene did not exhibit any measurable sensitization of the biacetyl phosphorescence in β-CD, although they do sensitize it in SDS micellar solution. A recent study by Cromwell *et al.* on the energetics of adamantanecarboxylate inclusion as a function of cyclodextrin cavity size found that the match in cavity size and ligand size was a very important factor in the strength of binding.[7] Inclusion by β-CD was the most energetically favoured ($\Delta G^\circ = -5.85$ kcal/mole) and exothermic ($\Delta H = -4.85$ kcal/mole), whereas the γ-CD interaction was endothermic. They also found that the neutral form of CD binds better than the anionic form.

This paper reports the photophysical and analytical characteristics of biacetyl room-temperature phosphorescence when sensitized by PNAs included in cyclodextrin hosts. The triplet–triplet energy-transfer reactions of several PNAs were evaluated in α-, β- and γ-CD, and found to be dependent on the size of the CD cavity. The larger the cavity, the greater the enhancement of the sensitized biacetyl phosphorescence intensity. In addition, compounds such as chrysene and triphenylene, unresponsive as sensitizers in α-CD and β-CD, were very responsive in the larger γ-CD. Analytical limits of detection for selected donor molecules in the three cyclodextrins are reported.

EXPERIMENTAL

Reagents

Chrysene, triphenylene (both from CHEM Services, Inc.), phenanthrene (Aldrich), and biacetyl (Merck) were used without further purification. Naphthalene and biphenyl (both from MCB Reagents) were recrystallized once from ethanol. α-CD and γ-CD (both from Aldrich) were used as received. β-CD (Aldrich) was recrystallized once from boiling water.

Apparatus

Phosphorescence spectra were obtained with a Fluorolog 2+2 spectrofluorometer (Spex Industries, Metuchen, NJ) with double excitation and emission monochromators. The

*Author for correspondence.

instrument was equipped with a 450-W xenon continuous light-source and a Peltier-cooled Hammamatsu R928 photomultiplier tube. The Spex Datamate computer was used to correct all spectra for lamp intensity and photomultiplier-tube response. Print-outs of the spectra were produced by a Houston Instruments x–y digital plotter.

Procedure

All glassware was rinsed with "spectrograde" methanol (Fisher) before use, and stock solutions ($0.01M$) of the donors and biacetyl acceptor were prepared in spectrograde methanol. The biacetyl solution was stored in an amber bottle away from direct light to minimize photodegradation. Inclusion complexes were prepared by adding aliquots of solutions of the donor of interest and biacetyl to a standard flask, followed by dilution to volume with $0.01M$ aqueous cyclodextrin solution. Blank samples were prepared in the same manner, but without the donor species present. The solutions were placed in a standard fluorescence cuvette equipped with a Teflon stopper, and deaerated by passage (for 20 min) of high-purity nitrogen that had first been passed through a self-indicating oxygen trap (Alltech Associates, Inc.).

Limits of detection

The analytical limits of detection were determined by extrapolating a plot of sensitized biacetyl phosphorescence intensity at 522 nm *vs.* donor concentration and finding the concentration at which the signal was equal to three times the noise, taken as the standard deviation of at least 5 measurements of the response of the biacetyl blank, measured at 522 nm.

RESULTS AND DISCUSSION

The cyclodextrins evaluated in this study were the α, β and γ forms, made up of six, seven and eight glucose units, respectively.[8] Coupling of the glucose monomers produces rigid, conical structures with inner cavity sizes of approximately 0.5 nm diameter for α-CD, 0.7 nm for β-CD, and 0.9 nm for γ-CD.[3] The interior of the cyclodextrin molecules is hydrophobic and contains water molecules (although this is thermodynamically unfavoured) and these can be displaced by more hydrophobic species which satisfy the size criterion of at least partially fitting into the cavity.[3] For the sensitized phosphorescence to be enhanced, both the donor and acceptor must fit at least partially into the CD at the same time. Favourable enthalpy changes give all three cyclodextrins the ability to form stable inclusion complexes with a wide variety of compounds.[9]

The five polynuclear aromatic molecules studied were selected to show the effect of systematic increase in donor size on the inclusion process, and the subsequent effects on the intensity of the sensitized biacetyl phosphorescence emission. For example, addition of an aromatic ring to naphthalene produces phenanthrene, and the addition of two aromatic rings produces chrysene. In this manner, the size is sequentially changed with little change in other molecular properties such as charge and polarity. Donor molecules larger than chrysene would not provide additional information since they would not fit in the α- and β-CD cavities. In addition, the choice of PNAs that can be studied is limited by the ability to sensitize biacetyl phosphorescence.

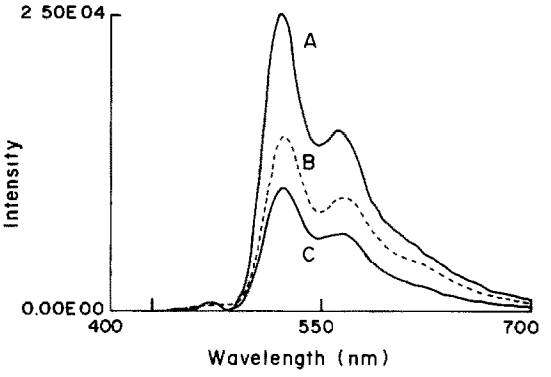

Fig. 1. Corrected phosphorescence emission of $1 \times 10^{-4}M$ biacetyl sensitized by $1.2 \times 10^{-5}M$ naphthalene in (A) γ-CD, (B) β-CD, and (C) α-CD; all CD concentrations are $0.01M$; excitation wavelength = 276 nm; slits, 14.4 nm for both excitation and emission; scan-rate = 1 nm/sec; 470 cut-off filter used.

Figure 1 shows the phosphorescence spectra of biacetyl sensitized by naphthalene in (A) γ-CD, (B) β-CD, and (C) α-CD solutions, showing an increase in intensity as the cavity size is increased. In order to separate the effects of cyclodextrin physical size from solvent-dependent effects on the biacetyl phosphorescence efficiency, θ_p^{Biac}, the ratio of the relative intensity at the phosphorescence wavelength maximum (522 nm) to that at the fluorescence wavelength maximum (490 nm) for a $0.01M$ solution of biacetyl was calculated for each of the three dextrins.[5] The values obtained are listed in Table 1. The similarity of the θ_p^{Biac} ratios found for the dextrins suggests that the increase in the sensitized signal, apparent in Fig. 1, is related to CD cavity-size, and not to any differences in the microenvironment provided by the three hosts. Thus, it may be generalized that for triplet–triplet energy transfer from a donor species to biacetyl, the larger the cavity, the greater the enhancement of the energy-transfer reaction.

Figure 2 shows the phosphorescence spectra of biacetyl sensitized by triphenylene in (A) γ-CD, (B) β-CD, and (C) α-CD media. No measurable signal was obtained for this species in the α- or β-cyclodextrins, but an intense signal was observed when the γ-CD medium was used. Most likely there was exclusion of this PNA and/or the biacetyl from the α-CD

Table 1. Ratio of phosphorescence intensities (I_p) at 522 nm to fluorescence intensities (I_f) at 490 nm for $0.01M$ biacetyl excited at 415 nm in $0.01M$ α-, β- and γ-CD

CD	I_p/I_f
γ	3.1
β	3.0
α	3.2

Table 2. Phosphorescence excitation and emission wavelengths and sensitized limits of detection (LODs) for selected polynuclear aromatic compounds in α-, β- and γ-CD solutions

Compound	$\lambda_{ex.}$* nm	$\lambda_{em.}$† nm	LOD,§ M		
			α-CD	β-CD	γ-CD
Biphenyl	272	476	2.3×10^{-6}	5.4×10^{-7}	4.1×10^{-7}
Naphthalene	276	513	5.6×10^{-6}	3.6×10^{-7}	2.9×10^{-7}
Chrysene	295	513	not detected	not detected	2.6×10^{-6}
Triphenylene	295	432	not detected	not detected	2.9×10^{-6}
Phenanthrene	295	501	3.2×10^{-6}	9.5×10^{-7}	5.0×10^{-7}

*Excitation wavelength of donors; precision ± 1 nm.
†Conventional phosphorescence wavelength of maximum intensity of donors in β-CD with 0.58*M* 1,2-dibromoethane added.[3,4]
§Measured at 522 nm with a typical precision of $\pm 0.2 \times 10^{-x}M$.

and β-CD cavities, owing to size limitations. However, the larger γ-CD cavity allowed inclusion of both molecules, enhancing the energy-transfer reaction. Table 2 lists the limits of detection (LODs) for several PNAs in the three different cyclodextrin media. The LODs increased with choice of cyclodextrin in the order γ-CD < β-CD < α-CD.

It is somewhat surprising that molecules which fit easily into α-CD or β-CD produce further enhancement in their spectroscopic effects when used with the larger γ-CD. This may result from inclusion of more than one biacetyl molecule into a single CD cavity. The concentration of biacetyl was always greater than that of the donor, so this could occur. Also, the CD might position the donor and acceptor in specific spatial configurations that would enhance the energy transfer; this may be easier in a larger cavity. These results can be rationalized on the basis of the data in reference 7, which showed that the better the match in size between the included species and the cavity, the stronger the binding constant. However, we have no estimate of the size of included species, not knowing how many biacetyl and donor molecules are included within the CD. Generally, it might be expected that many other types of photophysical reactions would be enhanced in cyclodextrin media, although any cavity-size effects might differ from those found here.

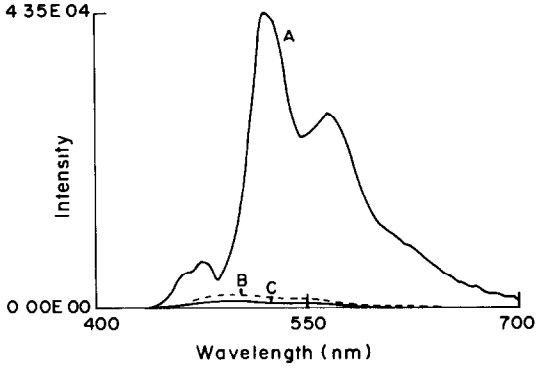

Fig. 2. Corrected phosphorescence emission of $1 \times 10^{-4}M$ biacetyl sensitized by $5.0 \times 10^{-5}M$ triphenylene in (A) γ-CD, (B) β-CD, and (C) α-CD; excitation wavelength = 495 nm. Other conditions as for Fig. 1.

Acknowledgement—This work was supported in part by a grant (CHE-8216878) to LJCL from the National Science Foundation.

REFERENCES

1. L. J. Cline Love, M. Skrilec and J. G. Habarta, *Anal. Chem.*, 1980, **52**, 754.
2. M. Skrilec and L. J. Cline Love, *ibid.*, 1980, **52**, 1559.
3. S. Scypinski and L. J. Cline Love, *ibid.*, 1984, **56**, 322.
4. *Idem, ibid.*, 1984, **56**, 331.
5. J. J. Donkerbroek, C. Gooijer, N. H. Velthorst and R. W. Frei, *ibid.*, 1982, **54**, 891.
6. F. J. DeLuccia and L. J. Cline Love, *ibid.*, 1984, **56**, 2811.
7. W. C. Cromwell, K. Bystrom and M. R. Eftink, *J. Phys. Chem.*, 1985, **89**, 326.
8. J. Szejtli, *Cyclodextrins and Their Inclusion Complexes*, Chapter 1, Akadémiai Kiadó, Budapest, 1982.
9. W. Saenger, *Angew. Chem., Int. Ed. Engl.* 1980, **19**, 344.

Talanta, Vol. 32, No. 8A, pp. 669–674, 1985
Printed in Great Britain

0039-9140/85 $3.00 + 0.00
Pergamon Press Ltd

ANALYTICAL DATA

DISSOCIATION CONSTANTS AND REACTIONS OF 3-PHENYL AND 3-CYCLOHEXYL-2-MERCAPTOPROPENOIC AND 3-PHENYL-2-MERCAPTOPROPANOIC ACIDS

A. IZQUIERDO and N. GARRIGA
Department of Analytical Chemistry, University of Barcelona, Barcelona, Spain

(*Received* 1 *March* 1985. *Accepted* 20 *March* 1985)

Summary—The dissociation constants of 3-phenyl- and 3-cyclohexyl-2-mercaptopropenoic acids have been determined spectrophotometrically ($I = 0.01M$) in aqueous medium, and potentiometrically for both reagents and for 3-phenyl-2-mercaptopropanoic acid in water–ethanol medium. The analytical properties of the three compounds have been studied and also the compositions of some of their insoluble metal chelates.

3-Aryl-2-mercaptopropenoic acids studied previously include the 2-furyl,[1] 2-pyrrolyl, 2-thienyl and 2-hydroxyphenyl,[2] and styryl and 1-naphthyl[3] compounds. These react with many ions and only small differences occur on changing the heteroatom of the aromatic ring or extending the unsaturated chain.

In the present work, 3-phenyl-2-mercaptopropenoic acid (3PH2MPE), 3-cyclohexyl-2-mercaptopropenoic acid (3CH2MPE) and 3-phenyl-2-mercaptopropanoic acid (3PH2MPA) were studied to examine the effects of a non-aromatic substituent in position 3 and of the absence of the conjugated double bond between the carboxyl and aryl groups.

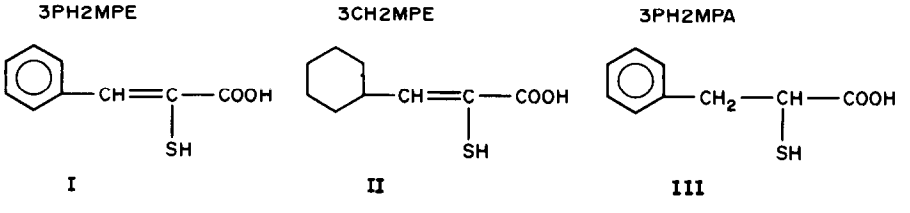

The dissociation constants were determined spectrophotometrically and potentiometrically, the reactions with metal ions were studied, and the compositions of some insoluble metal chelates were established.

EXPERIMENTAL

Instruments

A Beckman Acta M-VII spectrophotometer (1-cm cells) was used for spectrophotometric measurements. A Beckman IR-20A infrared spectrophotometer (KBr discs) and a Perkin-Elmer 12A NMR spectrophotometer were used. Crison Digilab 517 and Radiometer PHM 84 pH-meters were used with a Radiometer G202B glass electrode and a Radiometer K401 calomel reference electrode.

Solutions

Buffer solutions for spectrophotometry (ionic strength $0.01M$) were prepared as described by Perrin.[4] The ionic medium was prepared from potassium nitrate (Merck R. A.) recrystallized twice from water.

Carbonate-free potassium hydroxide solutions were standardized against potassium hydrogen phthalate, and nitric acid stock solution was standardized against borax and against potassium hydroxide by the Gran method.[5]

The mercapto acids were dissolved in deaerated ethanol (Merck).

Reagents

Compounds I and II were obtained by the method described by Campaigne and Cline[6] by condensation of benzaldehyde or cyclohexylaldehyde with rhodanine, then hydrolysis in alkaline medium and acidification with mineral acid. Recrystallization from benzene or petroleum ether (b.p. 50–70°) yielded products with m.p. 134–135° (I) and 139–140° (II). For 3PH2MPE, analysis gave: C 60.3%, H 4.5%, S 17.6%; $C_9H_8O_2S$ requires C 59.98%, H 4.47%, S 17.79%. For 3CH2MPE, analysis gave: C 57.9%, H 7.7%, S 17.1%; $C_9H_{14}O_2S$ requires C 58.03%, H 7.57%, S 17.21%.

3PH2MPA was prepared from I by reduction of the double bond with sodium amalgam,[7] acidification, and extraction with diethyl ether. Recrystallization from petroleum ether (b.p. 30–50°) yielded a product with m.p. 47–48°. For 3PH2MPA, analysis gave: C 59.3%, H 5.5%, S 17.5%; $C_9H_{10}O_2S$ requires C 59.32%, H 5.53%, S 17.59%.

The purity of all the reagents was examined by thin-layer chromatography and determined by potentiometric titration of the carboxyl group with sodium hydroxide and iodometric titration of the mercapto group (purity > 99.5%).

The solubilities (g/100 ml of solution at 25°) were deter-

mined by the Wittenberger technique[8] and were (**I, II, III**): water (0.02, 0.04, 0.5), ethanol (25.1, 25.0, 80.7), benzene (2.28, 5.58, 68.6), 3-methylbutan-1-ol (3.06, 16.6, v.s.), methyl isobutyl ketone (16.8, 14.5, v.s.), diethyl ether (28, 26.6, v.s.) (v.s. = very soluble).

The electronic spectrum of **I** was in accordance with the literature[6] and **II** shows a band at 263 nm. The infrared spectra (KBr discs) had characteristic bands (cm^{-1}) at 1265 (C—O), 1420 (O—H), 1665 (C=O) and 2585 (S—H) for **I**; 1260 (C—O), 1420 (O—H), 1675 (C=O) and 2590 (S—H) for **II**; 1250 (C—O), 1420 (O—H), 1710 (C=O) and 2590 (S—H) for **III**. The NMR spectra had the S—H peak for **I** ($\delta = 4.62$ ppm) and **II** ($\delta = 3.85$ ppm) further downfield than that for **III** ($\delta = 2.07$ ppm)

Procedures

Acidity constants. The pK_a values of **I** and **II** were determined spectrophotometrically[9] with use of a $10^{-4}M$

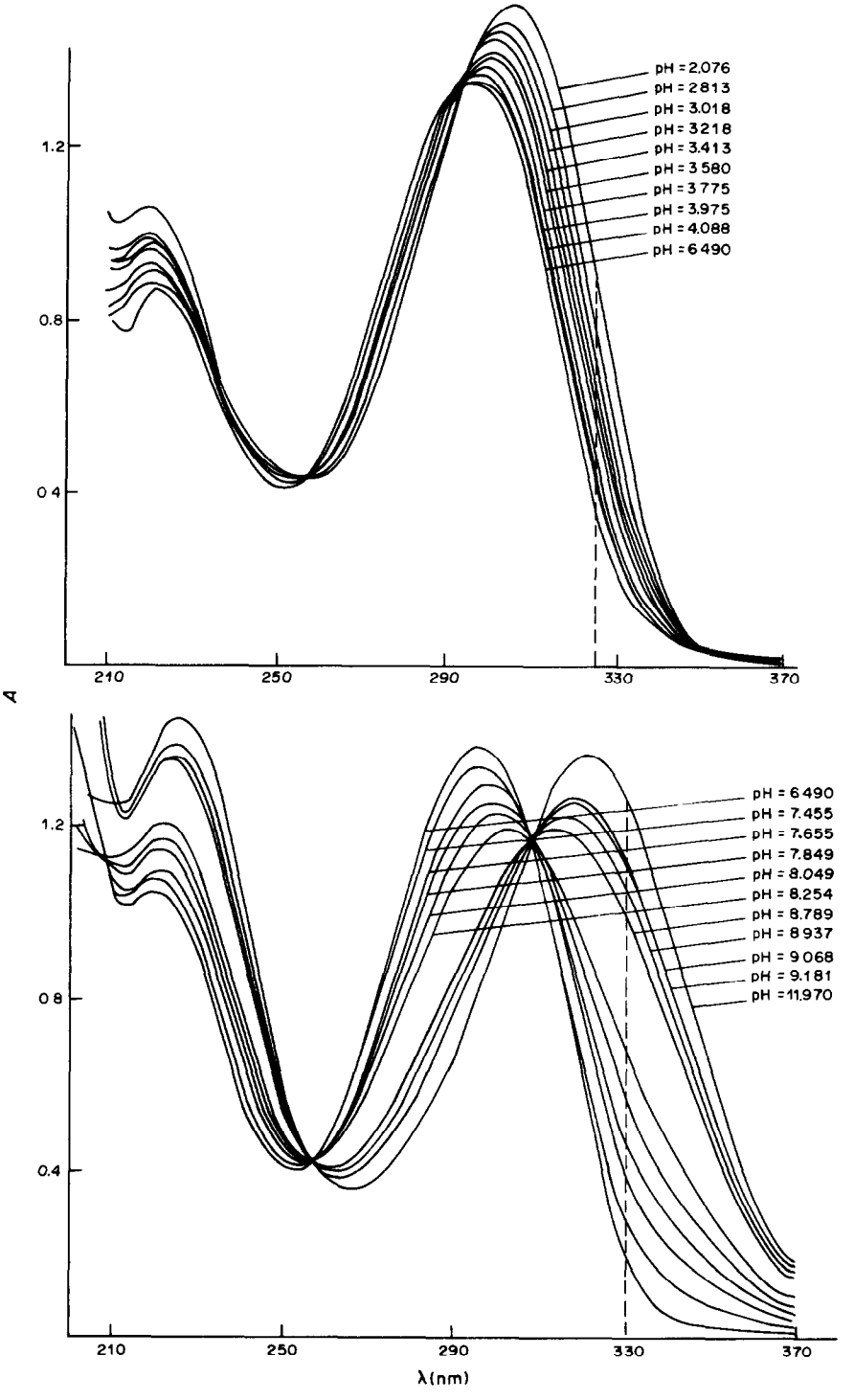

Fig. 1. Spectra for the determination of pK_{a_1} (above) and pK_{a_2} (below) of 3PH2MPE.

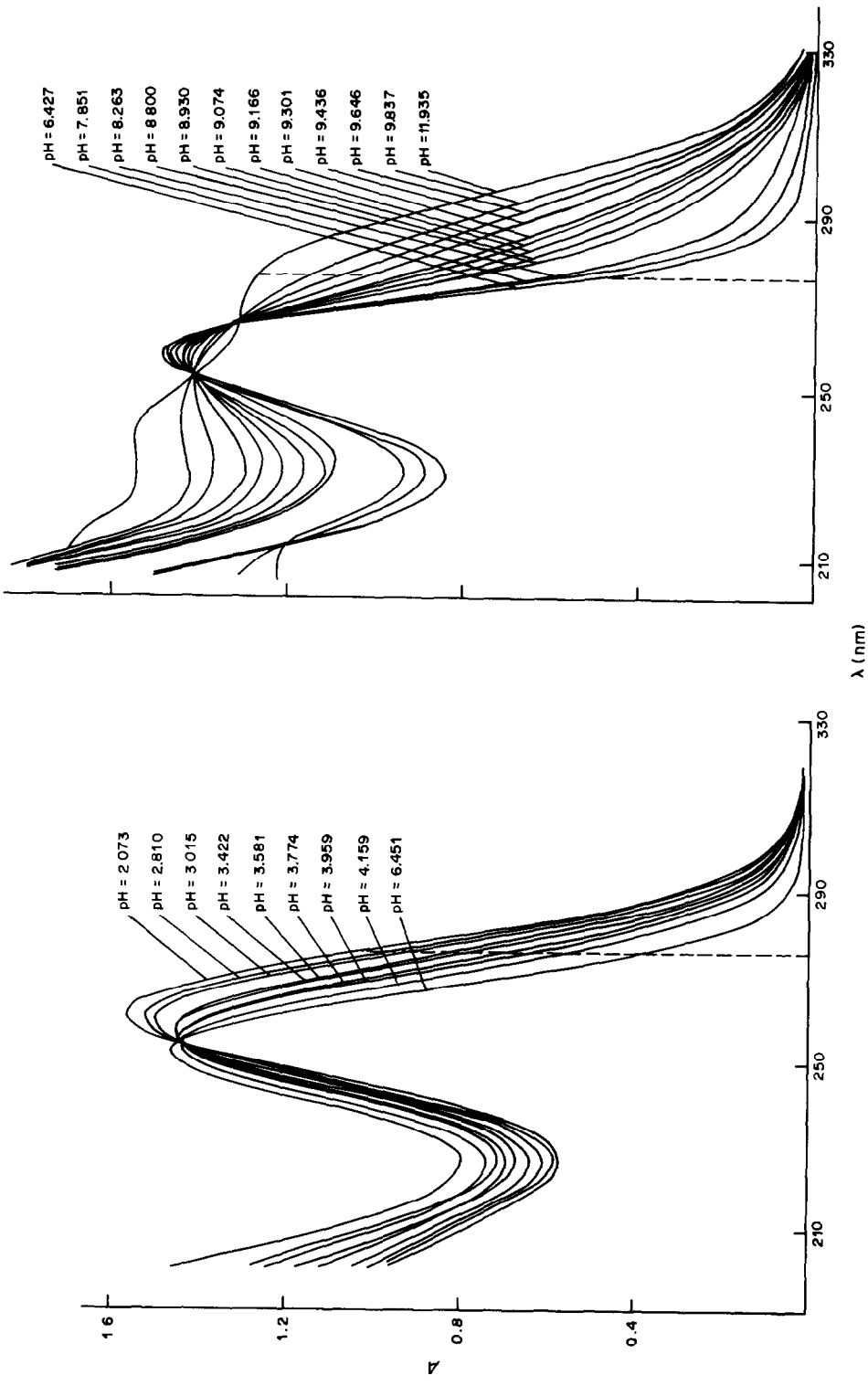

Fig. 2. Spectra for the determination of pK_{a1} and pK_{a2} of 3CH2MPE.

mercapto acid solution in aqueous medium containing 1% ethanol, at 0.01*M* ionic strength and 25°, and calculated from the pH and the relationship between the absorbances of the solution and of the molecular and ionized forms. The pK_a values for **III** could not be determined by this procedure because it did not have a suitable spectrum.

The dissociation equilibria of the three reagents were also studied by titration[10] at 25° with potassium hydroxide, in 30% v/v water–ethanol (because the compounds are poorly soluble in water) at ionic strength 0.1*M*, with potassium nitrate as ionic medium. Before and during the titration pure nitrogen was bubbled through the solution to remove dissolved oxygen.

Reactions with metal ions. These were investigated by the Benedetti-Pichler[11] technique for the whole pH-range, with a 1% ethanolic solution of the reagent and 1 g/l. solutions of the metal ions. The solubilities of the complexes in benzene, chloroform, diethyl ether, 3-methylbutan-1-ol and methyl isobutyl ketone were tested.

The insoluble metal chelates were prepared by reacting aqueous solutions of the metal ions with ethanolic solutions of the reagents, in various ratios. The precipitates were filtered off, washed with water, ethanol and acetone, and dried under reduced pressure over calcium chloride. Their elemental compositions and infrared spectra were determined.

RESULTS AND DISCUSSION

The dissociation constants for **I** and **II** were determined spectrophotometrically in aqueous medium (1% ethanol), at low ionic strength and low concentration, in order to obtain experimental pK_a values close to the thermodynamic ones and to compare them with those for other 3-aryl-2-mercaptopropenoic acids. Figures 1 and 2 show the spectra of 3PH2MPE and 3CH2MPE solutions at various pH values. Table 1 shows the analytical wavelengths used for the measurements, and the results obtained; these are comparable with those found for similar compounds.[1-3]

Dissociation constants for the three acids were also determined potentiometrically in water-ethanol medium. Gran's method[5] was used to determine $E^{\circ\prime}$ and E_j so that the hydrogen-ion concentration h could be found from E, the measured potential by means of

$$E\,(\text{mV}) = E^{\circ\prime} - 59.157 \log h + E_j$$

Also, the ionic product of the medium was determined, and found to be $pK_w = 14.20 \pm 0.01$. The protonation constants were then determined by use of the Bjerrum function $\bar{n}$:[12]

$$\bar{n} = \frac{H_T - h + K_w/h}{A_T} = \frac{\beta_1 h + 2\beta_2 h^2}{1 + \beta_1 h + \beta_2 h^2}$$

which is calculated from the experimental quantities h, the total concentration of titratable hydrogen-ion H_T and the total reagent concentration A_T. Figure 3 shows a typical example of the theoretical curve ($\bar{n}$ *vs.* log h) and the experimental points for titrations done at several reagent concentrations. The pK_a values were determined from the overall protonation constants β_1 and β_2 calculated by the linearization method of Irving and Rossotti[13] and the experimental data were treated by the least-squares program MINIPOT.[14] Table 2 shows the results obtained.

Table 1. pK_a values in aqueous medium at 25° and $I = 0.01M$

	3PH2MPE	3CH2MPE
pK_{a_1}	3.36 ± 0.03 (325 nm)	3.74 ± 0.02 (275 nm)
pK_{a_2}	8.34 ± 0.02 (330 nm)	9.14 ± 0.03 (280 nm)

Table 2. pK_a values in water–ethanol medium at 25° and $I = 0.1M$

	pK_{a_1}	pK_{a_2}
3PH2MPE	3.77 ± 0.01	8.98 ± 0.01
3CH2MPE	4.12 ± 0.01	9.71 ± 0.01
3PH2MPA	3.96 ± 0.01	10.53 ± 0.01

The differences between the mercapto group constants show the influence of the conjugated double bond; the greater acidity of **I** probably results from resonance of S^- with the aromatic ring; **II**, with no aromatic substituent, has lower acidity, and **III** cannot tautomerize, so has a high value of pK_{a_2}, similar to those obtained for saturated mercapto acids.[15]

The reactions of 3PH2MPE and 3CH2MPE are similar to those of other 3-aryl-2-mercaptopropenoic acids. They form insoluble compounds with many cations, and some coloured complexes with transition metals, which are readily extractable with polar organic solvents. Notable reactions of 3PH2MPE are the production of a red colour with titanium(IV) in acetic acid–acetate medium ($pD = 7$) and the reaction

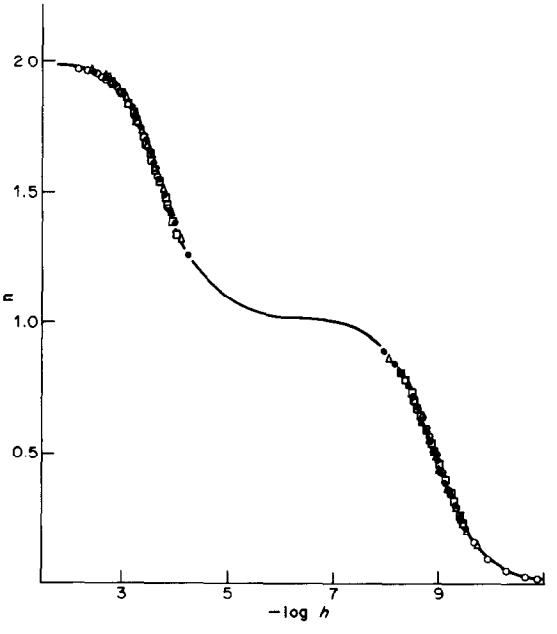

Fig. 3. Formation curve for 3PH2MPE (solid line = theoretical curve) △, [3PH2MPE] = 1.827 × $10^{-3}M$; □, [3PH2MPE] = 2.598 × $10^{-3}M$; ○, [3PH2MPE] = 4.086 × $10^{-3}M$; ●, [3PH2MPE] = 4.864 × $10^{-3}M$.

Table 3. Most sensitive reactions

Metal ion	3PH2MPE			3CH2MPE			3PH2MPA		
	Medium	Without extraction	With extraction	Medium	Without extraction	With extraction	Medium	Without extraction	With extraction
Cu(II)	all	g (5.4)		all	br (4.7)		HOAc, NaOAc	br (4.4)	br (4.4)B
	HCl, NaOAc		g (5.0) A, B, C						
	NH_3, NaOH		g (4.7) A, B						
Pd(II)	HCl, NaOAc	o (5.7)	o (6.0) B	all	r (5.0)		HCl, NaOAc	o (5.4)	
	NH_3, NaOH	o (5.0)	o (5.0) A, B	HCl, HOAc		r (6.0) A, B	HCl, HOAc		0 (5.7) B
Mo(VI)	HCl	o (5.7)	o (6.0) A, B	HCl, HOAc	o (5.4)	o (6.0) B	HCl	y (3.7)	y (4.0) B
	HOAc, NaOAc	o (6.0)		NaOAc	o (5.7)	0 (5.7) B	HOAc, NaOAc	y (4.0)	y (5.0) B
Fe(II)	HOAc	bl–g (5.7)	bl–g (6.0) A, B, C	NaOAc	bl (6.3)	bl (6.7) A, B	HOAc	bl (5.0)	
	NaOAc, NH_3	bl–g (6.0)	bl–g (6.3) A, B	NH_3	bl (6.3)	bl (6.4) A, B	NaOAc	vi (5.4)	
Co(II)	NaOAc	br–g (6.0)	br–g (6.0) A, B	HOAc	r (4.7)	r (4.7) B	NaOAc	br (5.4)	br (5.4) B
	NH_3, NaOH	br–g (5.7)		NaOAc	r (5.0)	r (5.0) B			
Ni(II)	NaOAc	y (6.0)	y (6.3) A, B	HOAc, NaOAc	r (4.4)	r (4.7) B	NaOAc	g (4.7)	g (4.7) B
	NH_3, NaOH	y (6.0)	y (6.0) A, B	NH_3, NaOH	r (4.0)	r (4.0) B			
Mn(II)	NaOAc, NH_3	bl (6.0)	bl (6.3) A, B	NaOAc, NH_3	bl (5.7)	bl (5.7) B			
Ti(IV)	HOAc, NaOAc	r (6.7)	r (7.0) A, B, C	HOAc, NaOAc	r (6.3)				
				HOAc		r (6.6) B			

Solvents
A = 3-methylbutan-1-ol
B = MIBK
C = ethyl ether

Colours
g = green
br = brown
y = yellow
vi = violet
o = orange
r = red
bl = blue

Table 4. Insoluble metal chelates of 3PH2MPE and 3PH2MPA

Stoichiometry	Complex	Asymmetric C=O band, cm^{-1}		Symmetric C=O band, cm^{-1}	
		Reagent	Complex	Reagent	Complex
MR	3PH2MPE–Ag	1665	1665	1265	1265
	3PH2MPA–Ag	1710	1710	1250	1250
M_2R	3PH2MPE–2Ag	1665	1550	1265	1345
MR	3PH2MPE–Pb	1665	1515	1265	1340
	3PH2MPE–Cd	1665	1520	1265	1380
	3PH2MPA–Pb	1710	1570	1250	1360
	3PH2MPA–Cd	1710	1550	1250	1395

with nickel in alkaline medium (pD = 6.3). Table 3 shows the most sensitive reactions of the three mercapto acids. The sensitivity of the reactions is expressed in terms of pD [*i.e.*, −log (dilution limit, M)].

The lower sensitivity of the reactions of 3CH2MPE suggests that the non-aromatic substituent in position 3 decreases the stability of the complexes, but has no influence on the reactivity of the functional group. Finally, 3PH2MPA gives similar insoluble compounds, but its soluble complexes are not strongly coloured and it does not react with titanium(IV). The differences in the reactivities of the three compounds can be related to the differences in the pK values of the mercapto groups.

The insoluble compounds of silver, lead and cadmium with 3PH2MPE and 3PH2MPA are 1:1 complexes, although for 3PH2MPE and silver the Ag_2R compound can also be obtained, if the appropriate conditions are used for precipitation. The infrared spectra of these compounds always show the disappearance of the mercapto group band and some show also a shift of the symmetric and asymmetric stretching bands of the carboxyl group. On this basis, the complexes can be divided into two groups, as shown in Table 4.

REFERENCES

1. A. Izquierdo and J. Calmet, *Quim. Anal.*, 1974, **28**, 148.
2. A. Izquierdo and M. Giné, *An. Quim.*, 1978, **74**, 53.
3. A. Izquierdo and J. L. Beltran, *Talanta*, 1984, **31**, 475.
4. D. D. Perrin and B. Dempsey, *Buffers for pH and Metal Ion Control*, Chapman & Hall, London, 1974.
5. G. Gran, *Analyst*, 1952, **77**, 661.
6. E. Campaigne and R. E. Cline, *J. Org. Chem.*, 1956, **21**, 32.
7. C. Ravazzoni and R. Valerio, *Ann. Chim. (Roma)*, 1962, **52**, 305.
8. W. Wittenberger, *Chemische Laboratoriumstechnik*, 6th Ed., Springer, Vienna, 1961.
9. A. Albert and E. P. Serjeant, *The Determination of Ionization Constants*, Chapman & Hall, London, 1971.
10. F. J. C. Rossotti and H. S. Rossotti, *The Determination of Stability Constants*, pp. 22, 53. McGraw-Hill, New York, 1961.
11. A. Benedetti-Pichler, *Microtechnique of Inorganic Analysis*, Wiley, New York, 1950.
12. N. Bjerrum, *Z. Anorg. Allgem. Chem.*, 1921, **119**, 197.
13. H. Irving and H. S. Rossotti, *J. Chem. Soc.*, 1953, 3397.
14. F. Gaizer and A. Puskás, *Talanta*, 1981, **28**, 565.
15. A. Izquierdo and J. Guasch, *An. Quim.*, 1984, **80**, 382.

Talanta, Vol. 32, No. 8A, pp. 675–677, 1985
Printed in Great Britain

0039-9140/85 $3.00 + 0.00
Pergamon Press Ltd

THERMODYNAMICS OF FORMATION OF MAGNESIUM, CALCIUM, STRONTIUM AND BARIUM COMPLEXES WITH 2,2′-BIPYRIDYL AND 1,10-PHENANTHROLINE, AT DIFFERENT IONIC STRENGTHS IN AQUEOUS SOLUTION

SANTI CAPONE, ALESSANDRO DE ROBERTIS, CONCETTA DE STEFANO and ROSARIO SCARCELLA
Istituto di Chimica Analitica dell'Università, via dei Verdi, 98100, Messina, Italy

(*Received* 26 *October* 1984. *Accepted* 15 *March* 1985)

Summary—The formation constants for the complexes of Mg^{2+}, Ca^{2+}, Sr^{2+} and Ba^{2+} with 2,2′-bipyridyl and 1,10-phenanthroline have been determined from pH measurements in aqueous solution, at 10, 25 and 40° and various ionic strengths in the range 0.05–0.95*M*. The species $[M(L)]^{2+}$ was found in all systems. The dependence on ionic strength was calculated for all the stability constants, and $\Delta H°$ values have been calculated from the temperature dependence of the stability constants. The formation constants are in the order $MgL^{2+} > CaL^{2+} > SrL^{2+} > BaL^{2+}$, and M–1,10-phenanthroline > M–2,2′-bipyridyl.

Recently some of us have been concerned with determination of the thermodynamic parameters for the formation of the complexes of alkali and alkaline-earth metal with low molecular-weight ligands,[1–4] and with the dependence of the formation constants on ionic strength.[5–9] We now describe a potentiometric study of the thermodynamic properties of the complexes of Mg^{2+}, Ca^{2+}, Sr^{2+} and Ba^{2+} with 2,2′-bipyridyl and 1,10-phenanthroline, in aqueous solution at various ionic strengths. The aims were (*a*) to elucidate the complexing capacities of alkaline-earth metal ions with respect to imines (few thermodynamic data are reported in the literature[10] and sometimes the alkaline-earth imine complexes are said not to exist, as in the case of 2,2′-bipyridyl[11]); (*b*) to confirm previous findings on the dependence of the stability constants for cationic species on ionic strength;[9] (*c*) to verify the reliability of a simple pH-measurement method in determining all the thermodynamic properties of systems in which weak complexes are formed.

EXPERIMENTAL

2,2′-Bipyridyl and 1,10-phenanthroline (Fluka *puriss.*) were used without further purification; the purity, by titration with acid, was ≥99.5%. Magnesium, calcium, strontium and barium chlorides (Fluka *purum* p.a.) were standardized by EDTA titration.[12] Hydrochloric acid and potassium hydroxide solutions were prepared by diluting concentrates (C. Erba or BDH). Potassium chloride (C. Erba R.P.) was used to adjust the ionic strength. Grade A glassware and doubly distilled water were used throughout. The apparatus and procedure were as previously reported.[1–4] Some experimental details of the potentiometric measurements are reported in Table 1.

The protonation formation constants were expressed as (c = free concentration):

$$K^{H} = c_{HL}/c_H c_L$$

$$K^{M} = c_{ML}/c_M c_L$$

The evaluation of $K^{H'}$ (by $K^{H'}$, we mean the conditional protonation constant, calculated without allowing for complex formation), K^{H}, the purity of the ligands and $E°$ was done by the non-linear least-squares computer programs ACBA[13] and ESAB.[14] The formation constants of weak $[M(L)]^{2+}$ complexes were calculated by the non-linear least-squares computer program WECO[3] (see also next section). In all the calculations, the pK_w values from reference 3 were used.

RESULTS AND DISCUSSION

Table 1 gives the log $K^{H'}$ values. It can be seen that increasing the values of the concentration of M^{2+} leads to lowering of the conditional protonation constants; since log $K^{H} = f(I)$ is a linear function with positive slope,[9] this behaviour indicates complex formation. The formation constants can be calculated from the equation:[3,5]

$$\log K^{H} = \log K^{H'} + \log (1 + K^{M} c_M) \qquad (1)$$

or

$$K^{M} = [10^{(\log K^{H} - \log K^{H'})} - 1]/c_M \qquad (2)$$

The calculations were done by the computer program WECO,[3] which allows the simultaneous determination of formation constants together with the parameters for the dependence on temperature and ionic strength.[3] Table 2 shows the log K values at 10, 25 and 40° and $I = 0.25M$, and $\Delta H°$ and $\Delta S°$ values at 25° and $I = 0.25M$. The ionic-strength dependence was found to be, as previously reported for protonation constants,[9] a simple linear relation:

$$\log K^{M}(I) = \log K^{M}(I') + c_0 (I - I') \qquad (3)$$

where I' is a reference ionic strength (within the range studied here, $I' = 0.25M$) and c_0 is a constant depending on temperature. The analysis of all the

Table 1. Conditional protonation constants and experimental details of potentiometric measurements*

M	I†	c_M‡	1,10-Phenanthroline§ 10°	1,10-Phenanthroline§ 25°	1,10-Phenanthroline§ 40°	2,2′-Bipyridyl§ 10°	2,2′-Bipyridyl§ 25°	2,2′-Bipyridyl§ 40°
Mg^{2+}	0.05	14	4.81 ± 0.02	4.71 ± 0.02	4.61 ± 0.01	4.45 ± 0.02	4.35 ± 0.01	4.24 ± 0.01
	0.15	47	4.60 ± 0.02	4.51 ± 0.01	4.39 ± 0.01	4.49 ± 0.02	4.35 ± 0.01	4.26 ± 0.01
	0.29	93	4.43 ± 0.03	4.33 ± 0.01	4.23 ± 0.01	4.48 ± 0.02	4.37 ± 0.01	4.25 ± 0.01
	0.29	47	4.65 ± 0.01	4.53 ± 0.01	4.42 ± 0.01	4.54 ± 0.01	4.42 ± 0.01	4.28 ± 0.01
	0.58	93	4.50 ± 0.01	4.39 ± 0.01	4.25 ± 0.01	4.57 ± 0.02	4.44 ± 0.01	4.33 ± 0.01
	0.85	280	4.12 ± 0.01	4.02 ± 0.01	3.91 ± 0.01	4.49 ± 0.01	4.36 ± 0.01	4.24 ± 0.01
	0.95	187	4.29 ± 0.01	4.17 ± 0.01	4.07 ± 0.01	4.62 ± 0.02	4.47 ± 0.01	4.31 ± 0.01
Ca^{2+}	0.05	13	4.85 ± 0.06	4.79 ± 0.02	4.69 ± 0.02	4.46 ± 0.06	4.36 ± 0.01	4.26 ± 0.01
	0.15	46	4.79 ± 0.03	4.70 ± 0.01	4.59 ± 0.01	4.49 ± 0.02	4.38 ± 0.01	4.26 ± 0.01
	0.29	93	4.68 ± 0.02	4.63 ± 0.02	4.55 ± 0.01	4.49 ± 0.04	4.42 ± 0.01	4.30 ± 0.01
	0.29	46	4.83 ± 0.04	4.73 ± 0.02	4.67 ± 0.02	4.57 ± 0.02	4.43 ± 0.01	4.32 ± 0.01
	0.58	93	4.77 ± 0.01	4.66 ± 0.01	4.59 ± 0.02	4.63 ± 0.02	4.51 ± 0.01	4.37 ± 0.01
	0.85	282	4.50 ± 0.01	4.42 ± 0.01	4.34 ± 0.02	4.62 ± 0.01	4.51 ± 0.01	4.37 ± 0.01
	0.95	187	4.65 ± 0.01	4.56 ± 0.01	4.49 ± 0.01	4.70 ± 0.01	4.56 ± 0.01	4.45 ± 0.01
Sr^{2+}	0.05	14	4.92 ± 0.06	4.81 ± 0.03	4.71 ± 0.01	4.48 ± 0.01	4.35 ± 0.01	4.25 ± 0.01
	0.15	47	4.86 ± 0.04	4.76 ± 0.02	4.68 ± 0.02	4.52 ± 0.01	4.40 ± 0.01	4.28 ± 0.01
	0.29	94	4.83 ± 0.02	4.74 ± 0.02	4.62 ± 0.01	4.55 ± 0.01	4.44 ± 0.01	4.29 ± 0.01
	0.29	47	4.94 ± 0.02	4.83 ± 0.03	4.72 ± 0.02	4.58 ± 0.01	4.45 ± 0.01	4.32 ± 0.01
	0.57	93	4.93 ± 0.02	4.79 ± 0.03	4.71 ± 0.02	4.66 ± 0.01	4.51 ± 0.01	4.40 ± 0.01
	0.86	282	4.71 ± 0.01	4.61 ± 0.02	4.54 ± 0.02	4.66 ± 0.01	4.52 ± 0.01	4.40 ± 0.01
	0.95	188	4.82 ± 0.02	4.75 ± 0.02	4.64 ± 0.01	4.73 ± 0.01	4.60 ± 0.01	4.47 ± 0.01
Ba^{2+}	0.05	14	4.90 ± 0.09	4.82 ± 0.02	4.72 ± 0.01	4.47 ± 0.02	4.37 ± 0.01	4.24 ± 0.01
	0.15	46	4.92 ± 0.04	4.81 ± 0.02	4.69 ± 0.01	4.51 ± 0.02	4.38 ± 0.01	4.24 ± 0.01
	0.29	93	4.86 ± 0.08	4.82 ± 0.02	4.71 ± 0.02	4.55 ± 0.02	4.44 ± 0.01	4.32 ± 0.01
	0.29	46	4.97 ± 0.03	4.87 ± 0.02	4.76 ± 0.02	4.57 ± 0.02	4.47 ± 0.01	4.33 ± 0.01
	0.57	93	5.02 ± 0.02	4.85 ± 0.02	4.75 ± 0.02	4.65 ± 0.01	4.51 ± 0.01	4.38 ± 0.01
	0.86	282	4.90 ± 0.02	4.77 ± 0.02	4.65 ± 0.01	4.67 ± 0.01	4.54 ± 0.01	4.40 ± 0.01
	0.95	187	5.00 ± 0.02	4.88 ± 0.02	4.77 ± 0.02	4.75 ± 0.01	4.61 ± 0.01	4.48 ± 0.01

*Initial volume: 30 ml; titrant 0.1M KOH; 30–40 data points for each titration.
†Ionic strength, M.
‡Free concentration of cations, mM.
§Value ± 3 standard deviations.

Table 2. Thermodynamic parameters at $I = 0.25M$ ($\Delta G°$ and $\Delta H°$ in *kcal/mole*, $\Delta S°$ in *cal. mole*$^{-1}$. K^{-1})

M	T,°C	log K	$-\Delta G°$	$-\Delta H°$	$\Delta S°$	Ref.	M	T,°C	log K	$-\Delta G°$	$-\Delta H°$	$\Delta S°$	Ref.
	1,10-Phenanthroline							2,2′-Bipyridyl					
H^+	10	5.15					H^+	10	4.60				
	25	4.99	6.81	4.3	8.5			25	4.46	6.08	3.8	8	
	40	4.83						40	4.32				
	25	5.00	6.82	4.3	9	[9]		25	4.47	6.10	3.8	8	[9]
	20	4.95	6.75	4.0	9	[15]†		20	4.52	6.17	3.7	8	[15]†
								25	4.46	6.08	3.5	9	[16]†
Mg^{2+}	10	1.61					Mg^{2+}	10	0.38				
	25	1.55	2.11	1.7	1			25	0.32	0.44	1.5	−4	
	40	1.49						40	0.26				
	20	1.2				[11]†							
Ca^{2+}	10	1.21					Ca^{2+}	10	0.09				
	25	1.09	1.49	3.3	−6			25	−0.05	−0.07	3.8	−13	
	40	0.97						40	−0.19				
	20	0.7				[11]†							
Sr^{2+}	10	0.93					Sr^{2+}	10	−0.02				
	25	0.82	1.12	3.0	−7			25	−0.16	−0.22	3.7	−13	
	40	0.71						40	−0.30				
Ba^{2+}	10	0.66					Ba^{2+}	10	−0.10				
	25	0.57	0.78	2.4	−5			25	−0.24	−0.33	3.9	−14	
	40	0.48						40	−0.38				

*Standard deviations:
Protonation: log K ± 0.015, $\Delta G°$ ± 0.02, $\Delta H°$ ± 0.3, $\Delta S°$ ± 1;
M^{2+} complex formation: log K ± 0.05, $\Delta G°$ ± 0.07, $\Delta H°$ ± 1.3, $\Delta S°$ ± 5.
†$I = 0.1M$.

formation constant data reported here allowed us to calculate:

$$c_0 = 0.26 - 2.0 \times 10^{-3}(T - 298) \quad (4)$$

where T is the absolute temperature.

From equations (3) and (4), bearing in mind the van't Hoff equation, we can write equations for the dependence of the thermodynamic parameters on ionic strength (at 25°):

$$\log K(I) = \log K(0.25) + 0.26(I - 0.25) \quad (5)$$

$$\Delta G(I) = \Delta G(0.25) + 0.35(I - 0.25)\ \text{kcal/mole} \quad (6)$$

$$\Delta H(I) = \Delta H(0.25) - 0.81(I - 0.25)\ \text{kcal/mole} \quad (7)$$

$$\Delta S(I) = \Delta S(0.25) - 1.2(I - 0.25)\ \text{cal.mole}^{-1}.\text{K}^{-1} \quad (8)$$

Note that equations (5)–(8) are valid for all reactions, including protonation: this is in agreement with the hypothesis[1-9] that the dependence of formation constants on ionic strength can be expressed (within experimental error) as a general equation valid for all reactions having the same stoichiometry. Moreover, the values of c_0 and $\partial c_0/\partial T$ agree quite well with previous findings.[9] A value of $c_0 = 0.3$ was also found for the first protonation constant (at 25°) of ethylenediamine.[17]

The formation constants show that the 1,10-phenanthroline complexes have greater stability than the 2,2′-bipyridyl complexes [the ratio between the formation constants K^M(phen)/K^M(bipy) is 17 for Ca^{2+} and 6 for Ba^{2+}]. For both ligands, the stabilities of the complexes follow the order $MgL^{2+} > CaL^{2+} > SrL^{2+} > BaL^{2+}$. The very low stability of the M^{2+}–2,2′-bipyridyl complexes explains the lack of published data. In fact, for 0.025M Ca^{2+}, the logarithm of the apparent protonation constant is lowered by <0.01. In practice, this means that the constant ionic-strength medium method cannot be used for low ionic strengths. However, our experimental method, which does not require a constant value of I, allows the determination of very low stability constants, down to $K^M \simeq 0.5$, for $I = 0$–1M. Our stability constant values for the Mg^{2+}– and Ca^{2+}–1,10-phenanthroline complexes are in fairly good agreement with those of Anderegg.[11] The ΔH° and ΔS° values show that the M^{2+} complexes are stabilized by the enthalpy term, for both ligands.

It should be noted that it was assumed in the calculations that the chloride ion does not form complexes with M^{2+}. There are several literature reports of studies of M^{2+}–chloride complexes[18-25] but the formation constants differ by as much as an order of magnitude. For example, for $MgCl^+$ at 25° and $I = 0$, the reported values range from 0.04 to 0.8. Calculation shows that if there were 10% association of M^{2+} with Cl^- the value of log $K^{H'}$ would be increased by 0.05. For 0.28M MCl_2 (the maximum concentration used) 10% association would require β_{MCl} to be $\leqslant 0.14$ for the change in log $K^{H'}$ to be $\leqslant 0.05$. We therefore feel that until the stability constants for the MCl^+ complexes have been definitively measured, the necessary correction can either be neglected or assigned an arbitrary value. In principle, if the conditional constants for the ML^{2+} complexes were accurately known, it should be possible to calculate the precise values from them and the experimental conditions.

Acknowledgements—We thank C.N.R. (Rome) and Ministero della Pubblica Istruzione for financial support, and Prof. S. Sammartano and Prof. C. Rigano for helpful discussions.

REFERENCES

1. P. G. Daniele, A. De Robertis, S. Sammartano and C. Rigano, *Thermochim. Acta*, 1984, **72**, 305.
2. P. G. Daniele, A. De Robertis, C. De Stefano, C. Rigano and S. Sammartano, *Ann. Chim. (Rome)*, 1983, **73**, 619.
3. A. De Robertis, C. Rigano and S. Sammartano, *Thermochim. Acta*, 1984, **74**, 343.
4. A. De Robertis, C. De Stefano, C. Rigano and R. Scarcella, *ibid.*, 1984, **80**, 197.
5. P. G. Daniele, C. Rigano and S. Sammartano. *Talanta*, 1983, **30**, 81.
6. *Idem, Transition Met. Chem.*, 1982, **7**, 109.
7. *Idem, Ann. Chim. (Rome)*, 1983, **73**, 741.
8. P. G. Daniele, G. Ostacoli, C. Rigano and S. Sammartano, *Transition Met. Chem.*, 1984, **9**, 385.
9. P. G. Daniele, C. Rigano and S. Sammartano, *Talanta*, 1985, **32**, 78.
10. L. G. Sillén and A. E. Martell, *Stability Constants*, Spec. Publ. No. 17, The Chemical Society, London, 1964; *Supplement*, Spec. Publ. No. 25, London, 1971; D. D. Perrin, *Stability Constants, Organic Ligands*, Pergamon Press, Oxford, 1979.
11. G. Anderegg, *Helv. Chim. Acta*, 1963, **46**, 2397.
12. H. A. Flaschka, *EDTA Titrations*, Pergamon Press, London, 1959.
13. G. Arena, E. Rizzarelli, S. Sammartano and C. Rigano, *Talanta*, 1979, **26**, 1.
14. C. Rigano, M. Grasso and S. Sammartano, *Ann. Chim. (Rome)*, 1984, **74**, 537.
15. G. Anderegg, *Helv. Chim. Acta*, 1963, **46**, 2813.
16. G. Arena, R. Calì, E. Rizzarelli and S. Sammartano, *Thermochim. Acta*, 1976, **17**, 155.
17. P. Paoletti, *Pure Appl. Chem.*, 1984, **56**, 491.
18. E. Högfeldt, *Stability Constants; Inorganic Ligands*, Pergamon Press, Oxford, 1982.
19. E. C. Righellato and C. W. Davies, *Trans. Faraday Soc.*, 1930, **26**, 592.
20. G. Macdougall and C. W. Davies, *J. Chem. Soc.*, 1935, 1416.
21. J. Kenttämaa, *Suomen Kem.*, 1959, **32B**, 68.
22. S. K. Patil and H. D. Sharma, *Can. J. Chem.*, 1969, **47**, 3851.
23. J. Havel and E. Högfeldt, *Acta Chem. Scand.*, 1973, **27**, 3323.
24. L. Šůcha, J. Čadek, K. Hrábek and J. Veselý, *Collection Czech. Chem. Commun.*, 1975, **40**, 2020.
25. V. Majer and K. Štulík, *Talanta*, 1982, **29**, 145.

Talanta, Vol. 32, No. 8B, pp. 679–696, 1985
Printed in Great Britain

0039-9140/85 $3.00 + 0.00
Pergamon Press Ltd

HENRY FREISER

HORACIO A. MOTTOLA
Department of Chemistry, Oklahoma State University, Stillwater, Oklahoma 74078, U.S.A.

A native of New York, Henry Freiser was born on August 27, 1920. He earned his Bachelor of Science degree in 1941 from the city College of New York where later he would be a lecturer (1945). His Master of Science and Doctor of Philosophy degrees are from Duke University; he earned them in 1942 and 1944, respectively. His academic career started as chairman of the Department of Physical and Analytical Chemistry at North Dakota State College (1944–1945). After a year as research fellow at the Mellon Institute of Industrial Research, Freiser joined the faculty of the University of Pittsburgh as associate professor (1946–1958). In 1958 his move to the west took him to the University of Arizona, Tucson, as professor and head of its Department of Chemistry. It was there that Freiser brought to realization his remarkable capabilities as a researcher, as a teacher, and as an administrator. He has been at Arizona since then, stepping down as head in 1968 to dedicate more time to his hobby of research in analytical chemistry, with short tenures as visiting professor at the University of California, Los Angeles (Fall, 1968) Kyoto University (Spring, 1972) and California Institute of Technology (Spring 1979). Freiser's professional activities are numerous; far too many to list here. Worth singling out, however, are his efforts in pioneering a meeting recognized globally as the single major gathering of analytical chemists: the Pittsburgh Conference. He has served in practically all capacities on its organizing committees, and he is still active today as a member of its programme committee. Also deserving mention are his services to different aspects of the activities and committees of the American Chemical Society, the National Research Council of the USA, and the International Union of Pure and Applied Chemistry. He has been on the Advisory Boards of *Analytical Chemistry* and *Talanta* and is a member of the *Separation Science and Technology* Editorial Board. His list of public appearances presenting lectures, short courses, and workshops all over the United States and in most of the world is too lengthy to include here. He loves to learn languages and it is no surprise that he has conducted courses in Spanish at the Universidad Autonoma de Guadalajara, Mexico. The large number of nationalities represented by those who have been associated with Henry Freiser as postdoctoral fellows can testify to his eagerness to learn about other people, other lands, other cultures, other languages. It is also an indication of his worldwide contributions to education and research in chemistry, particularly analytical chemistry.

His list of more than 260 publications is another mark of his enrichment of our subdiscipline with journal research articles, chapters, monographs, and books that are continuously cited and serve as inspiration in generating new research and in broadening the understanding of underlying principles for key analytical methodologies.

Professor Freiser started his graduate career in organic chemistry, receiving his M.S. degree for work on the direct fluorination of organic compounds. For his Ph.D. degree, which was in physical chemistry, he studied dielectric polarization of aromatic fluorine compounds (2),* thus displaying for the first time what became his lifelong interest in molecular structural influences on chemical behaviour. In the early part of his career he continued to use dipole moments for the elucidation of structural influences, in a series of papers (1, 3–5, 8, 10, 11, 28, 29, 39, 41, 73, 130) that clarified structural details of some heterocyclic nitrogen and sulphur compounds as well as of some organosilicon and organometallic compounds. The work provided early evidence for the free rotation of the cyclopentadienyl rings around the central iron atom in ferrocene (41) and made significant headway in the interpretation of dipole moments of metal chelates by providing a means of compensating for the unusually large contribution of atomic polarization encountered with chelates (10,130).

Freiser's interest in metal chelates and organic analytical reagents stems from his use of coordination compounds to purify and isolate heterocyclic nitrogen compounds (4,6). This work brought Professor Freiser closer and closer to the field of analytical chemistry. Around 1950 he began a wide ranging study of structure–behaviour correlations of organic chelating agents used in the determination of metal ions. He was perhaps the first analytical chemist to recognize the importance of the use of metal chelate formation equilibrium constants as a foundation for the evaluation of organic analytical reagents (12). Among the interesting findings by Freiser and his students are the following.

1. The recognition that the highly specific nickel reagent, dimethylglyoxime, does not owe its reputation to an anomalously high stability for the complex [for example, Cu(II) typically forms more stable

*Reference numbers from list of publications.

chelates than Ni(II) and this is also true for dimethylglyoxime (35)], but rather to the unusually low aqueous solubility of the nickel chelate (84).

2. The discovery that steric hindrance in 2-substituted-8-quinolinol chelates is significant for the bivalent-metal complexes (decreasing with increasing ionic radius) as well as in the case of Al(III) (36). Similar findings were reported for the sulphur-analogue, 8-mercaptoquinoline (129). Other important studies of steric factors in chelate formation included an examination of the role of chelate ring size (34,37) and the equivalence of one sulphur atom to two carbon atoms in such matters (52,64).

3. The systematic study of the effect of substituting sulphur [and selenium (99,110)] or oxygen as a bonding atom in producing reagents of greater selectivity as well as acid strength [as reflected by their ability to form chelates in more strongly acidic media (13,52,63,64,98,109,115,129,135,142,152].

4. The recognition that though crystal-field stabilization (CFS) plays a major role in the energetics of transforming gaseous transition metal ions into the hydrated metal ions (50–80 kcal/mole), the contribution of CFS to the stability of metal complexes in solution is small (2–3 kcal/mole) and fairly independent of ligand type (57). However, ligand type does exert a considerable influence on the extent of complex-stability increase from manganese to zinc; the less electronegative and more polarizable the bonding atoms, the greater the increase in stability (122).

5. The recognition that metal chelation can, by its effect on electron-density distribution, affect the chemical reactivity of the organic ligand. For example, metal chelation was found to increase the acidity of imidazole protons, to an extent that paralleled the stability of the metal chelate (42). Metal chelation was also found to affect profoundly the keto–enol tautomeric equilibria of various chelating agents, such as riboflavin (59), chelidamic acid (87), pyridine-2,6-dialdoxime (96) and various hydroxyquinaldinic acids (103). In a related area, metal ions were found capable of inducing molecular rearrangements in originally non-chelating compounds to form a chelating isomer (111,112). Work in these areas is of value in providing explanations of the role of trace metals in metabolism as well as in analytical chemistry.

6. The value of applying modern structural methods to problems of metal chelate chemistry. Freiser was among the first to use infrared spectroscopy with metal chelates and to observe a relation between the shift of a C—O stretching band in 8-hydroxyquinoline chelates and the fundamental chelating parameters (44). Electron spin resonance was ingeniously applied to resolve controversies in 8-mercaptoquinoline (102) and dithizone (161) chemistry. More recently, ESCA has been employed to assign unequivocal oxidation numbers to metal ions in chelates, where previous work had left some confusion (186). X-Ray crystallography was used to determine the structures of nickel (160) and zinc (168) dithizonates. This work not only served to define the atomic make-up of the chelate ring but the relation of the adjacent phenyl ring to it. From observations of the solution chemistry of these compounds, Freiser had suggested earlier (109) that in the case of nickel the phenyl ring would be perpendicular to the chelate ring while with zinc the two rings would be coplanar. This turned out to be the case. Explanations of electronic spectra, particularly in the case of low-spin nickel chelates, have been used to elucidate structure (154) as well as to provide a basis for new analytical methods (150).

7. Over the last thirty years, a great deal of effort has been devoted to the determination of metal chelate formation constants for a wide variety of metal ions and ligands and to the use of such data to obtain information about the role of various molecular structural parameters that affect chelate formation. Until recently, there has been no attempt to deal with any but a restricted series of compounds and metal ions rather than examine the rich data base available. Freiser and co-workers have applied pattern recognition techniques to three sets of metal chelate stability data, a sample population far larger than previously considered (201). For the stability constant data for the bivalent metal chelates of (*a*) β-diketones, (*b*) 8-quinolinols and (*c*) polyaminocarboxylic acids (such as EDTA), pattern-recognition computer programs were run which yielded linear equations with which stability constants could be predicted with (depending on the ligand family) a correlation coefficient of 0.95–0.98, by utilizing less than ten of the more than twenty structural parameters introduced at the beginning of the run. Further, it was found possible to maintain a correlation coefficient of $\geqslant 0.93$ even when the number of structural parameters used as independent variables was reduced to three, namely the pK_a values of the ligands, the second ionization potential of the gaseous metal ion, and a third which differed according to ligand family. The results of this application of pattern recognition to chelate chemistry are encouraging and strongly suggest the value of this approach to problems of reagent design.

Freiser's contributions to analytical chemistry extend over several interconnected areas. For instance, in the course of his study of metal chelate stabilities and their role in improving the evaluation of organic analytical reagents and the development of reagent design principles, several interesting and useful new reagents were developed, such as *o*-hydroxyphenylbenzoxazole (20) for the determination of cadmium in the presence of zinc, *o*-hydroxyphenylbenzimidazole as a selective reagent for mercury (23), quinoline-8-selenol (82,90,101) and others (25,32,50).

Professor Freiser has made significant contributions in the field of solvent extraction. He co-authored (with G. H. Morrison) the first book on the

principles and practices of solvent extraction in analytical chemistry (49), currently under revision, which even today is widely consulted and used throughout the world (translated into Russian, Chinese, Japanese, Czech, Polish). The Extraction Review appearing biennially since 1958 in the annual reviews issue of *Analytical Chemistry* (54,68,81,104,125,145), has served to update in almost encyclopaedic fashion the vast and still expanding literature in this field, at least part of which can be said to have derived inspiration from the work of Freiser and his students. Many other chapters and reviews on solvent extraction have appeared over the same period (65–67,79,80,82,89,90,126,163). In addition, Freiser and his students have conducted fundamental studies of various solvent extraction systems with a view to determining the contributory equilibrium constants, *e.g.*, for acetylacetone (33,46,60,74), 8-hydroxyquinolines (74,76), and pyridylazonaphthol (PAN) (95). Together with Starý, Freiser has compiled a volume of extraction equilibrium parameters of chelating extractants (195) as a supplement to the IUPAC *Stability Constants*.

Freiser developed a simple extraction method for study of the kinetics of fast reactions and its application to the mechanism of metal chelate chemistry. Structure–behaviour relations are often not fully explorable by equilibrium studies alone and attention is turned toward kinetics and mechanisms. Motivated by such considerations Freiser developed a unique and simple means of obtaining kinetic information about reactions having very high rate coefficients and applied his technique to the study of chelation reactions of analytical significance (83,114,136,139,155, 164). He and his students and associates found that under controlled conditions, the rate of the chelation extraction process was dependent on homogeneous chemical reactions in the aqueous phase and that extraction rates could therefore, be used to find reaction-rate coefficients of these rate-determining steps. The finding that, for most metal ions, the formation of the 1:1 chelate is rate-determining is interesting and corroborates testimony obtained with water-soluble chelate reaction-systems. They also found that the metal reaction-rate sequence (analogous to metal stability sequence) was essentially independent of the nature of the chelating agent, with $Cd > Zn > Co > Ni$ the rate order observed with about ten extractants in the dithizone family, as well as several 8-mercaptoquinolines. This sequence paralleled that found by Eigen for the rate of loss of water in the first co-ordination sphere of the metal ion. The importance of water was further emphasized by the finding that when metal ions such as zinc or nickel have had one co-ordinated water molecule replaced, even by an anionic ligand (which reduces the positive charge and presumably part of the driving force for combining with the anionic chelating ion), the rate of extraction usually increases. Thus it would appear, that for these metals, at least, the "first water to be replaced is the hardest".

The extraction technique developed by Freiser is the *only* way to study the kinetics of extremely water-insoluble chelate systems, and also represents a simple and convenient alternative to more sophisticated methods such as "stopped-flow," *etc.* By use of the extraction technique, the Ni(II)–phenanthroline (and bipyridyl) systems were investigated (194) and each of the stepwise formation and dissociation rate constants was experimentally determined, with results that were in good agreement with values obtained by the stopped-flow method. The solvent extraction technique is superior to the stopped-flow technique when secondary reactions of the ligand might be rate-determining under the experimental conditions required. Since its development in 1962, the solvent extraction kinetic technique has been used with increasing frequency in other laboratories.

Freiser has also tackled the question of the mechanism of back-extraction, or stripping. Using nickel dithizone in chloroform as a model system, he has shown that back-extraction can be catalysed better by such metal ions as Ag(I) and Hg(II) and by ligands such as cyanide and EDTA than by hydrogen ions (224). This work led naturally to the study of the kinetics of extraction of the commercially available chelating extractants of hydrometallurgical interest. Although some work by others (Flett, Spink, Atwood) had indicated that the extraction of Cu(II) by LIX65N (5-nonyl-2-hydroxybenzophenone) proceeded by mechanisms involving slow chemical reactions taking place at the interface, Freiser demonstrated that LIX65N, significantly less hydrophobic than dithizone, reacted, as did dithizone, through a slow aqueous homogeneous chemical reaction (216). In response to critics of this work, Freiser conclusively settled the argument by repeating the Cu(II)–LIX65N kinetic study in seven organic solvent–aqueous solvent pairs in which it was shown that, in quantitative agreement with the proposed mechanism, the observed reaction rates changed over three orders of magnitude as predicted from the change in the distribution constants of LIX65N (239). An analogous study of the Ni(II)-LIX65N system served to further emphasize the validity of the mechanism (241).

Freiser then turned his attention to the search for extraction systems in which the interface would play a part and, just as importantly, for experimental techniques that would be suitable for such studies. The latter problem was ingeniously solved by using a microporous Teflon membrane that permitted clean separation of very small ($\sim$100–200 μm diameter) organic solvent droplets from a highly agitated aqueous–organic solvent mixture (245). For the first time, therefore, extraction equilibria and kinetics could be studied under conditions in which there was a very large interfacial area. The search for inter-

facially active systems was also successful. Anions of dialkylated dithizones were shown to be selectively adsorbed into a water-like interface that resulted in changes of as much as five orders of magnitude [in the case of dihexyldithizone (246)] in heterogeneous acid–base equilibrium constants, induced by high-speed stirring. Understanding the selective adsorption of the extractant anion helps explain that the rate of metal-chelate formation in the interface is essentially the same as in bulk water (247). The Freiser group also demonstrated that the anion of Kelex 100 was adsorbed in the interface but that the neutral extractant was not (252). They are currently pursuing the opportunity afforded by their novel experimental approach, to study the unsupported liquid–liquid interface.

Most chelate-extraction equilibrium studies devoted to structural–behaviour considerations are directed toward elucidation of the effect of structural modification on metal chelate stability. Among the few workers who recognize the importance of understanding the influence of structural factors on the physical properties (distribution constants) of the extractants and their metal chelates, Freiser has undertaken a systematic study of the effect of substituents and the role of non-specific interactions on K_D values (123,134). In particular, he and his associates have brought recognition of the importance of the solubility parameter [of the organic solvent and of the distributing solute(s)] on K_D values. He was the first to observe that the solubility parameter, rather than dielectric constant or vaguely expressed "polarity" of the organic solvent was paramount in defining the extraction equilibrium constant of ion-association complexes as well as of neutral compounds (153).

Freiser and his group have conducted a broadly based study of extraction equilibria of ion-association complexes which resulted in the discovery of an extractability sequence for organic and inorganic anions (174). He has been able to correlate solvent extraction parameters with ion-selective electrode behaviour (174) and is on the way to employing novel electrochemical means of studying solvent extraction systems. He has also shown the broad analytical utility of highly coloured extractable ion-pair complexes in trace analysis (144, 179).

Initially through his interest in solvent extraction, Freiser and his group became involved with ion-selective electrodes of the liquid-membrane type. In the course of this work they developed the first organic anion-selective electrodes (148,151) including those involving amino-acid anions (162) and were able to clearly define the role of solvent extraction parameters in the selectivity of liquid-membrane ion-selective electrodes (174). He and his group discovered the novel coated-wire ion-selective electrode (197), which has great application potential in environmental and clinical as well as general analysis, because of its rugged simplicity and capability of miniaturization (181). Coated-wire electrodes (CWE) have been successfully applied to the determination of cations such as calcium (170), and potassium (188), as well as a wide series of organic and inorganic anions (175). Applications of coated-wire electrodes to atmospheric pollutant analysis for NO_x (178) and carbon disulphide (192) as well as in water analysis (189) have been developed. In more recent CWE work, the Freiser group has developed and studied a series of highly selective cation-responsive electrodes which permit the determination of drugs of abuse such as cocaine and phencyclidine (PCP or "angel dust") (217,219,235), as well as the new generation of pharmaceuticals for heart-disorder treatment (243). Freiser has also edited two volumes of a widely praised series dealing with ion-selective electrodes (221,222).

As further testimony to the vitality of Freiser's imaginative approach to research, mention can be made of his unique application of current-scan polarography in an organic–aqueous immiscible solvent-pair system to the study of transport of both ionic and neutral species across the liquid–liquid phase boundary. With the ascending water electrode (aqueous drops rising through the denser organic solvent, such as dichloroethane or nitrobenzene—so-named in analogy with the well-known dropping mercury electrode of classical polarography) Freiser has been able to demonstrate that, in the case of phenanthroline and similar extractants, the extractant diffuses into the aqueous phase, reacts with either a proton or a metal ion, and that the protonated or complexed extractant is transported back to the organic phase (258).

These experiments, as well as those currently under way, provide a powerful new approach to the study of both equilibrium and kinetic aspects of mass-transfer processes, that are capable of generating new insights into the role of the interface and other fundamental factors influencing such processes.

Although Freiser has not published extensively in the field of chromatography, he provided the first example of liquid adsorption-chromatography separation of metal chelates (14) and was the first to publish an application of gas–liquid chromatography to the separation of metal ions (61,72).

More recently, he has developed a novel reversed-phase liquid chromatography, termed dye-assisted chromatography, in which a dye such as Methylene Blue or Brilliant Green is incorporated in a polar eluent, and permits the separation and detection of a large number of individual compounds of various families of uncharged organic compounds: alcohols, aldehydes, ketones, esters, amides, *etc.* (228,244,249). Dye-assisted chromatography is particularly useful for compounds without chromophores, which now can be detected at much lower concentrations.

Freiser has also been active in the use of catalytic reactions for trace analysis. He and his group have applied metal-catalysed oxidation–reduction reactions to the determination of trace levels of various

complexing agents. By means of this approach methods for submicrogram quantities of EDTA (137), cysteine and other mercaptans, phenanthroline (146), cyanide (147), and arsenic (190) have been developed and applied to various environmental analytical problems.

In recognition of his leadership in the field, and confidence in the large contributions that he has yet to make, the University of Arizona in 1983 funded a research programme proposed by Professor Freiser, called the Strategic Metals Recovery Research Facility (SMRRF). SMRRF is designed to study new metal-recovery processes that are more economical, energy-efficient, and environmentally compatible. Professor Freiser, the chairman of SMRRF (or "Papa SMURF") has a research group of about 20 students, postdoctoral research associates, and visiting scholars and professors from all over the world.

In conclusion, Freiser's research record displays an interesting synthesis of the theoretical and the practical. The broad range of topics with which he has dealt mark him as one of the few "generalists" in analytical chemistry.

As for Freiser the man, he is always pictured to those with whom he has been associated, as a smiling face, a cunning intellect, a dynamic friend. This youngster of 65 years of age jogs every day, and put to shame and amazed younger colleagues during the First International Symposium on Kinetics in Analytical Chemistry (Córdoba, Spain, 27–30 September 1983) with his flamenco dancing and his request for more oil and garlic sauce for his chicken "a la Sevillana" when the rest of them were reaching for the bottle of anti-acid.

This informal reminiscence of Freiser's accomplishments should not be closed without mentioning a unique contribution to analytical chemistry, one for which his charming wife, Eddie, should claim major recognition. This unique contribution is Ben Freiser, their youngest son, who has recently received the ACS Award for outstanding contributions in basic chemistry. The ingenuity and charm of the Freisers can also be seen in their other two children: Debbie, a talented artist, and Manny, artist and entrepreneur. This special issue of *Talanta* is offered to him as a token of recognition from those whose life has been greatly benefited by their association with Henry Freiser, the scientist and the man.

PUBLICATIONS OF HENRY FREISER

1. H. Freiser and W. L. Glowacki, Some Physical Properties of 2-Picoline, *J. Am. Chem. Soc.*, 1948, **70,** 2575.
2. H. Freiser, M. E. Hobbs and P. M. Gross, The Electric Moments of Some Aromatic Fluorine Compounds, *ibid.*, 1949, **71,** 111.
3. R. Keswani and H. Freiser, Electric Moments and Structure of Substituted Thiophenes. I. Certain Halogenated Derivatives, *ibid.*, 1949, **71,** 218.
4. H. Freiser and W. L. Glowacki, Some Physical Properties of Isoquinoline, *ibid.*, 1949, **71,** 514.
5. R. Keswani and H. Freiser, Electric Moments and Structure of Substituted Thiophenes. II. Certain Thiotolene Derivatives, *ibid.*, 1949, **71,** 1789.
6. A. E. Spakowski and H. Freiser, Isoquinoline as a Reagent in Inorganic Analysis. *Anal. Chem.*, 1949, **21,** 986.
7.* H. Freiser, Analysis of Copper, in *Encyclopedia of Chemical Technology*, Vol. 4, Interscience, New York, 1949.
8. R. G. Charles and H. Freiser, Electric Moments and Structure of Substituted Thiophenes. III. Polysubstituted Thiophenes, *J. Am. Chem. Soc.*, 1950, **72,** 2233.
9. L. J. Uhlig and H. Freiser, Reaction of Nickel(II) and Beta-Isothioureidopropionic Acid, *Anal. Chem.*, 1951, **23,** 1014.
10. R. G. Charles and H. Freiser, Dielectric Polarization Studies of Metallic Chelates, *J. Am. Chem. Soc.*, 1951, **73,** 5223.
11. H. Freiser, R. G. Charles, J. Speier and M. Eagle, Electric Moments and Structures of Organosilicon Compounds. I. The Aliphatic Carbon–Silicon Bond, *ibid.*, 1951, **73,** 5229.
12. H. Freiser, R. G. Charles and W. D. Johnston, Structure and Behavior of Organic Analytical Reagents. I. The Calvin–Bjerrum Method for Determination of Chelate Stability, *ibid.*, 1952, **74,** 1383.
13. R. G. Charles and H. Freiser, Structure and Behavior or Organic Analytical Reagents. I. Stability of Chelates of *o*-Aminophenol and of *o*-Aminobenzenethiol, *ibid.*, 1952, **74,** 1385.
14. L. B. Hilliard and H. Freiser, Chromatographic Separation of Metallic Chelates, *Anal. Chem.*, 1952, **24,** 752.
15. M. Aven and H. Freiser, Use of Butyl Phosphate in Steel Analyses. I. Determination of Aluminum, *Anal. Chim. Acta*, 1952, **6,** 412.
16. J. L. Walter and H. Freiser, 2-(*o*-Hydroxyphenyl)-benzoxazole as a Reagent for Gravimetric Determination of Cadmium, *Anal. Chem.*, 1952, **24,** 984.
17. J. Steinbach and H. Freiser, Preparation of Standard Sodium Hydroxide Solutions by Use of a Strong Anion Exchange Resin, *ibid.*, 1952, **24,** 1027.
18. H. Freiser and R. Dessy, Neutralization Capacities of Buffer Solutions, *Anal. Chim. Acta*, 1952, **7,** 20.
19. W. D. Johnston and H. Freiser, Structure and Behavior of Organic Analytical Reagents. III. Stability of Chelates of 8-Hydroxyquinoline and Analogous Reagents, *J. Am. Chem. Soc.*, 1952, **74,** 5239.
20. J. L. Walter and H. Freiser, 2-(*o*-Hydroxy-

*Chapters.
†Books.

phenyl)benzoxazole as a Volumetric Reagent for Cadmium, *Anal. Chem.*, 1952, **24,** 1985.
21. H. Freiser, The Stability of Metal Chelates in Relation to Their Use in Analysis, *Analyst*, 1952, **77,** 830.
22. H. Freiser, Organic Analytical Reagents, *Baskerville Chem. J. City Coll. N.Y.*, 1952, **3,** No. 1, 20.
23. J. L. Walter and H. Freiser, 2-(*o*-Hydroxyphenyl)-benzimidazole as a Reagent for the Determination of Mercury, *Anal. Chem.*, 1953, **25,** 127.
24. H. Freiser and J. L. Walter, Preparation of Benzisoxazoles by Oxidative Ring Closure, *J. Org. Chem.*, 1953, **18,** 256.
25. R. G. Charles and H. Freiser, Synthesis of 2-(*o*-Hydroxyphenyl)benzothiazole and of 2-(*o*-Hydroxyphenyl)benzothiazoline, *ibid.*, 1953, **18,** 422.
26. L. Melnick, H. Freiser and H. F. Beeghly, Extraction of Metal Thiocyanate Complexes with Butyl Phosphate, *Anal. Chem.*, 1953, **25,** 856.
27. J. F. Steinbach and H. Freiser, Acetylacetone—In the Dual Role of Solvent and Reagent in Extraction of Metal Chelates, *ibid.*, 1953, **25,** 881.
28. H. Freiser, M. V. Eagle and J. Speier, Electric Moments and Structures of Organosilicon Compounds. II. The Aromatic Carbon–Silicon Bond, *J. Am. Chem. Soc.*, 1953, **75,** 2821.
29. H. Freiser, M. V. Eagle and J. Speier, Electron Moments and Structures of Organosilicon Compounds. III. The Oxygen–Silicon Bond, *ibid.*, 1953, **75,** 2824.
30. J. F. Hedenburg and H. Freiser, Anodic Voltammetry of Phenols, *Anal. Chem.*, 1953, **25,** 1355.
31. H. Freiser, Structure and Stability in Some Chelates of Analytical Significance, *Rec. Chem. Progr.*, 1953, **14,** 199.
32. J. L. Walter and H. Freiser, Analytical Aspects of Reactions of 2-(2-Pyridyl)-benzimidazole and 2-(2-Pyridyl)-imidazoline with Iron(II), *Anal. Chem.*, 1954, **26,** 217.
33. J. F. Steinbach and H. Freiser, Acetylacetone as an Analytical Extraction Agent—Extraction of Aluminum, Gallium, and Indium, *ibid.*, 1954, **26,** 375.
34. R. G. Charles and H. Freiser, Structure and Behavior of Organic Analytical Reagents. IV. Chelates of 2-(*o*-Hydroxyphenyl)-Benzoxazole, 2-(*o*-Hydroxyphenyl)-Benzothiazole and 2-(*o*-Hydroxyphenyl)-Benzothiazoline, *Anal. Chim. Acta*, 1954, **11,** 1.
35. R. G. Charles and H. Freiser, Structure and Behavior of Organic Analytical Reagents. V. Dimethylglyoxime and Its Oxygen Monomethyl Ether, *ibid.*, 1954, **11,** 101.
36. W. D. Johnston and H. Freiser, Structure and Behavior of Organic Analytical Reagents. VI. Heats and Entropies of Formation of Several Divalent Metal Chelates of 2- and 4-Methyl-8-Hydroxyquinoline, *ibid.*, 1954, **11,** 201.
37. W. D. Johnston and H. Freiser, Structure and Behavior of Organic Analytical Reagents. VII. Stability of Chelates of 2-(*o*-Hydroxyphenyl)-Benzimidazole and Analogous Reagents, *ibid.*, 1954, **11,** 301.
38. L. M. Melnick and H. Freiser, Extraction of Metal Thiocyanate Complexes with Tributyl Phosphate. Copper(II) Thiocyanate, *Anal. Chem.*, 1955, **27,** 462.
39. L. M. Shorr, H. Freiser and J. L. Speier, Methyl-Silicon Cleavage of Certain Substituted Carboxylic Acids in Sulfuric Acid. Kinetics and Mechanism, *J. Am. Chem. Soc.*, 1955, **77,** 547.
40. T. R. Harkins and H. Freiser, Thermodynamics of Ionization of 2,2′-Bipyridine and Analogs in Water and in 50% Aqueous Dioxane, *ibid.*, 1955, **77,** 1374.
41. H. H. Richmond and H. Freiser, The Electric Moments of Mono- and Diacetyl-ferrocene, *ibid.*, 1955, **77,** 2022.
42. T. R. Harkins, J. L. Walter, O. E. Harris and H. Freiser, An Infrared Study of the Metal Chelates of Some Imidazole Derivatives, *ibid.*, 1956, **78,** 260.
43. T. R. Harkins and H. Freiser, The Effect of Coordination on Some Imidazole Analogs, *ibid.*, 1956, **78,** 1143.
44. R. G. Charles, H. Freiser, R. A. Friedel, L. E. Hilliard and W. D. Johnston, Infrared Absorption Spectra of Metal Chelates Derived from 8-Hydroxyquinoline, 2-Methyl-8-Hydroxyquinoline, and 4-Methyl-8-Hydroxyquinoline, *Spectrochim. Acta*, 1956, **8,** 1.
45. H. Freiser, Quantitative Applications of pH Measurements in Analytical Chemistry, *Am. Soc. Testing Materials Symposium on pH Measurements*, 1956, Publication No. 190, 65.
46. A. Krishen and H. Freiser, Acetylacetone as Analytical Extraction Reagent. Increase in Selectivity with (Ethylenedinitrilo)tetraacetic Acid and Analytical Separation of Uranium from Bismuth, *Anal. Chem.*, 1957, **29,** 288.
47. J. P. McKavaney and H. Freiser, Analytical Solvent Extraction of Molybdenum Using Acetylacetone, *ibid.*, 1957, **29,** 290.
48. H. Freiser, Why Teach Qualitative Analysis? *J. Chem. Educ.* 1957, **34,** 387.
49.† G. H. Morrison and H. Freiser, *Solvent Extraction in Analytical Chemistry*, Wiley, New York, 1957. Translations into Japanese, Russian, Chinese, Polish and Czechoslovakian.
50. Q. Fernando and H. Freiser, Preparation and Metal-Complexing Properties of 2-Salicylideneimine-4:6 Diamino-1:3:5 Triazine, *Chem. Ind. London*, 1958, 1230.

51. T. R. Harkins and H. Freiser, Adenine-Metal Complexes, *J. Am. Chem. Soc.*, 1958, **80,** 1132.
52. Q. Fernando and H. Freiser, Chelating Properties of β-Mercaptopropionic Acid, *ibid.*, 1958, **80,** 4928.
53. J. P. McKavaney and H. Freiser, Analytical Solvent Extraction of Vanadium Using Acetylacetone, *Anal. Chem.*, 1958, **30,** 526.
54. G. H. Morrison and H. Freiser, Extraction, *ibid.*, 1958, **30,** 632.
55. H. Freiser and G. H. Morrison, Solvent Extraction in the Analysis of Metals, *Am. Soc. Test. Mater. Spec. Tech. Publ.* 1958, No. 238, 1.
56. J. P. McKavaney and H. Freiser, Solvent Extraction of Chromium with Acetylacetone, *Anal. Chem.*, 1958, **30,** 1965.
57. H. Freiser, Q. Fernando and G. E. Cheney, A New Approach to the Comparison of Metal Chelate Stability Constants, *J. Phys. Chem.*, 1959, **63,** 250.
58. D. Fleischer and H. Freiser, The Calorimetric Determination of the Heats of Coördination Reactions, *ibid.*, 1959, **63,** 260.
59. T. R. Harkins and H. Freiser, The Chelating Tendency of Riboflavin, *ibid.*, 1959, **63,** 309.
60. A. Krishen and H. Freiser, Acetylacetone as Analytical Extraction Reagent. Calculation of Successive Formation Constants from Extraction Data, *Anal. Chem.*, 1959, **31,** 923.
61. H. Freiser, Gas-Liquid Partition Chromatography for Metals Separations, *ibid.*, 1959, **31,** 1440.
62. Q. Fernando and H. Freiser, Polarography of 4-Benzothiazolol, *Anal. Chim. Acta*, 1959, **20,** 250.
63. G. E. Cheney, H. Freiser and Q. Fernando, Metal Complexes of Purine and Some of Its Derivatives, *J. Am. Chem. Soc.*, 1959, **81,** 2611.
64. G. E. Cheney, Q. Fernando and H. Freiser, Some Metal Chelates of Mercaptosuccinic Acid, *J. Phys. Chem.*, 1959, **63,** 2055.
65. H. Freiser and G. H. Morrison, Solvent Extraction in Radiochemical Separations, *Ann. Rev. Nucl. Sci.*, 1959, **9.**
66.* H. Freiser and G. H. Morrison, Solvent Extraction, in *Comprehensive Analytical Chemistry*, C. W. Wilson and D. L. Wilson (eds.), Vol. 1A, Elsevier, Amsterdam, 1959.
67.* G. H. Morrison and H. Freiser, Extraction, in *McGraw-Hill Encyclopedia of Science and Technology*, 1st Ed., McGraw-Hill, New York, 1960.
68. G. H. Morrison and H. Freiser, Extraction, *Anal. Chem.*, 1960, **32,** 37.
69. H.-S. Lee and H. Freiser, Solvolysis of *S*-Benzoyl-8-mercaptoquinoline and the Spectrum of 8-Mercaptoquinoline, *J. Org. Chem.*, 1960, **25,** 1277.
70. H. Freiser, Integrating Analytical Chemistry in the Undergraduate Curriculum, *J. Chem. Educ.*, 1960, **37,** 290.
71. M. Mendelsohn, E. M. Arnett and H. Freiser, Destructive Autoxidation of Metal Chelates. I. Effects of Variation of Ligand and Metal on Initial Rate, *J. Phys. Chem.*, 1960, **64,** 660.
72. R. A. Keller and H. Freiser, Gas–Liquid Partition Chromatography for Separation of Metal Halides, in *Gas Chromatography, 1960*, R. P. W. Scott (ed.), pp. 301–387. Butterworths, London, 1960.
73. A. M. Coleman and H. Freiser, Electric Moments and Structures of Organosilicon Compounds. IV. The Silicon–Hydrogen Bond. *J. Am. Chem. Soc.*, 1961, **83,** 4127.
74. S. J. Jankowski and H. Freiser, Extraction of Magnesium with 8-Quinolinol, *Anal. Chem.*, 1961, **33,** 776.
75. R. E. Kirby and H. Freiser, Polarography of Tantalum–Ethylenediaminetetraacetate Complex, *J. Phys. Chem.*, 1961, **65,** 191.
76. J. Fresco and H. Freiser, The Solubility of Bis-8-quinolinolo-zinc, *Talanta*, 1961, **8,** 693.
77. R. E. Kirby and H. Freiser, The Complexes of Niobium and Tantalum with Ethylenediaminetraacetic Acid, in *Advances in the Chemistry of the Coordination Compounds*, S. Kirschner, p. 444. Macmillan, New York, 1961.
78.* Q. Fernando and H. Freiser, The Analytical Chemistry of Cadmium, in Treatise on Analytical Chemistry, I. M. Kolthoff and P. J. Elving (eds.), Part II, Vol. 3, p. 171. Interscience, New York, 1961.
79. H. Freiser, Dithizone Extraction of the Elements, *Chemist-Analyst*, 1961, **50,** 62.
80. H. Freiser, 8-Quinolinol Extraction of the Elements, *ibid.*, 1961, **50,** 94.
81. G. H. Morrison and H. Freiser, Extraction, *Anal. Chem.*, 1962, **34,** 64R.
82. H. Freiser, Cupferron Extraction of the Elements, *Chemist-Analyst*, 1962, **51,** 62.
83. C. B. Honaker and H. Freiser, Kinetics of Extraction of Zinc Dithizonate, *J. Phys. Chem.*, 1962, **66,** 127.
84. D. Fleischer and H. Freiser, The Heats of Solution of Nickel and Copper Dimethylglyoximes, *ibid.*, 1962, **66,** 389.
85. A. Corsini, I. M. Yih, Q. Fernando and H. Freiser, Potentiometric Investigation of the Metal Complexes of 1-(2-Pyridylazo)-2-naphthol and 4-(2-Pyridylazo)-resorcinol, *Anal. Chem.*, 1962, **34,** 1090.
86. R. M. Arnett, H. Freiser and M. A. Mendelsohn, Destructive Autoxidation of Metal Chelates. II. Further Studies of the Effect of Ligand Structure on Initial Rate, *J. Am. Chem. Soc.*, 1962, **84,** 2482.
87. S. P. Bag, Q. Fernando and H. Freiser, The Influence of Metal Chelation on the Structure of Chelidamic Acid, *Inorg. Chem.*, 1962, **1,** 887.

88. C. R. Wasmuth and H. Freiser, Copper(II) Catalysis of 8-Acetoxyquinoline Hydrolysis, *Talanta*, 1962, **9**, 1059.
89. H. Freiser, Acetylacetone Extraction of the Elements, *Chemist-Analyst*, 1963, **52**, 55.
90.* G. H. Morrison, H. Freiser and J. Cosgrove, Solvent Extraction, in *Handbook of Analytical Chemistry*, L. Meites (ed.), McGraw-Hill, New York, 1963.
91. J. Fresco and H. Freiser, Stabilities of Chelates of Certain Substituted 8-Quinolinols, *Inorg. Chem.*, 1963, **2**, 82.
92. A. Corsini, Q. Fernando and H. Freiser, The Effect of Metal Ion Chelation on the Acid Dissociation of the Ligand 4-(2-Pyridylazo)-resorcinol, *ibid.*, 1963, **2**, 224.
93. C. Bostic, Q. Fernando and H. Freiser, Kinetics of Iodination of 8-Quinolinol-5-sulfonic Acid and Its Metal Chelates, *ibid.*, 1963, **2**, 232.
94. R. Kirby and H. Freiser, Polarography of Niobium-EDTA Complexes, *Anal. Chem.*, 1963, **35**, 122.
95. D. Betteridge, Q. Fernando and H. Freiser, Solvent Extraction of Certain Transition Metal Ions with 1-(2-Pyridylazo)-2-naphthol, *ibid.*, 1963, **35**, 294.
96. S. P. Bag, Q. Fernando and H. Freiser, A Spectrophotometric and Potentiometric Study of Certain Metal Chelates of Pyridine-2,6-Dialdoxime, *ibid.*, 1963, **35**, 719.
97. D. Betteridge, P. K. Todd, Q. Fernando and H. Freiser, An Investigation of the Metal Complexing Properties of 4-(2-Pyridylazo)-1-naphthol, *ibid.*, 1963, **35**, 729.
98. A. Corsini, Q. Fernando and H. Freiser, 8-Mercaptoquinoline as an Analytical Reagent. Dissociation and Metal Chelate Formation Constants, *ibid.*, 1963, **35**, 1424.
99. E. Sekido, Q. Fernando and H. Freiser, Quinoline-8-selenol, A New Chelating Agent, *ibid.*, 1963, **35**, 1550.
100. Q. Fernando, H. Freiser and E. N. Wise, Metal Chelates in Analytical Chemistry, *ibid.*, 1963, **35**, 1994.
101.† H. Freiser and Q. Fernando, *Ionic Equilibria in Analytical Chemistry*, Wiley, New York, 1963.
102. A. Corsini, Q. Fernando and H. Freiser, The Reaction of Copper (II) and Copper (I) with 8-Mercaptoquinoline, *Talanta*, 1964, **11**, 63.
103. S. P. Bag, Q. Fernando and H. Freiser, The Influence of Metal Chelation on the Structure of Certain Hydroxyquinaldinic Acids, *Inorg. Chem.*, 1964, **3**, 93.
104. G. H. Morrison and H. Freiser, Extraction, *Anal. Chem.*, 1964, **36**, 93R.
105. G. S. Kozak, Q. Fernando and H. Freiser, Kinetic Studies with Electrogenerated Halogens. Bromination of 8-Quinolinol and 2-Methyl-8-Quinolinol, *ibid.*, 1964, **36**, 296.
106. J. Fresco and H. Freiser, Solubilities of Certain Divalent Metal Complexes and 8-Quinolinol and Substituted 8-Quinolinols in Aqueous Media, *ibid.*, 1964, **36**, 372.
107. J. Fresco and H. Freiser, Distribution Coefficients of Certain 8-Quinolinols and Their Copper Chelates, *ibid.*, 1964, **36**, 631.
108. S. P. Bag, Q. Fernando and H. Freiser, Formation Constants of Certain Metal Complexes of Thioguanine, *Arch. Biochem. Biophys.*, 1964, **106**, 379.
109. K. S. Math, Q. Fernando and H. Freiser, Formation Constants of Nickel(II) and Zinc(II) Complexes of Dithizone and Related Compounds, *Anal. Chem.*, 1964, **36**, 1762.
110. E. Sekido, Q. Fernando and H. Freiser, An Investigation of the Dissociation Phenomena of Quinoline-8-Selenol in Water and Aqueous Dioxane. *ibid.*, 1964, **36**, 1768.
111. H. Jadamus, Q. Fernando and H. Freiser, Metal-Ion Induced Rearrangements of Bis-benzthiazolines to Schiff-Base Chelates, *J. Am. Chem. Soc.*, 1964, **86**, 3056.
112. H. Jadamus, Q. Fernando and H. Freiser, Metal-Ion Induced Rearrangements, *Inorg. Chem.*, 1964, **3**, 298.
113. G. Ehrlich and H. Freiser, The Study of Complexing Agents for Niobium and Tantalum, *Aerospace Research Labs., Report*, No. 64–190, 1964.
114. B. E. McClellan and H. Freiser, Kinetics and Mechanism of Extraction of Zinc, Nickel, Cobalt, and Cadmium with Diphenylthiocarbazone, Di-*o*-Tolylthiocarbazone, and Di-α-Naphthylthiocarbazone, *Anal. Chem.*, 1964, **36**, 2262.
115. P. Sun, Q. Fernando and H. Freiser, Structure and Behavior of Organic Analytical Reagents. Formation Constants of Transition Metal Complexes of 2-Hydroxypyridine-1-Oxide and 2-Mercaptopyridine-1-Oxide, *ibid.*, 1964, **36**, 2485.
116. H. Freiser and Q. Fernando, The Interpretation of Ionic Equilibria by Graphical Methods, *Proc. Soc. Anal. Chem.*, 1964, **1**, 124.
117. H. Freiser and Q. Fernando, Teaching Ionic Equilibrium, *J. Chem. Educ.*, 1965, **42**, 35.
118. F. Chou, Q. Fernando and H. Freiser, Solvent Extraction Equilibria of Certain 8-Quinolinols and Their Zinc(II) Chelates, *Anal. Chem.*, 1965, **37**, 361.
119. C. Bostic, Q. Fernando and H. Freiser, The Reactivity of Metal Chelates of 8-Quinolinol-5-sulfonic Acid, *Inorg. Chem.*, 1965, **4**, 602.
120. R. Prasad, H. L. D. Coffer, Q. Fernando and H. Freiser, The Monohalogenation of 8-Quinolinols, *J. Org. Chem.*, 1965, **30**, 1251.
121. S. Takamoto, Q. Fernando and H. Freiser, Structure and Behavior of Organic Analytical Reagents. Some Aryl Azo 8-Quinolinols, *Anal. Chem.*, 1965, **37**, 1249.

122. E. Sekido, Q. Fernando and H. Freiser, Absorption Spectra and Formation Constants of Some Metal Chelates of Quinoline-8-Selenol, *ibid.*, 1965, **37,** 1556.
123. H. A. Mottola and H. Freiser, Distribution of Certain 8-Quinolinols and Their Copper(II) Chelates in a Series of Organic Solvent–Aqueous Pairs, *Talanta*, 1966, **13,** 55.
124. H. Freiser, Comments on Analytical Chemistry in the Undergraduate Curriculum, *Anal. Chem.*, 1966, **38,** No. 2, 46A.
125. H. Freiser, Extraction, *ibid.*, 1966, **38,** 131R.
126. H. Freiser, Use of Solvent Extraction in Metals Purification, *Ann. N.Y. Acad. Sci.*, 1966, **137,** 1.
127. R. H. Barca and H. Freiser, Kinetics and Mechanism of the Metal Ion Catalyzed Hydrolysis of 8-Acetoxyquinoline, *J. Am. Chem. Soc.*, 1966, **88,** 3744.
128. D. Kealey and H. Freiser, Improved Synthesis of 8-Mercaptoquinoline and its Derivatives, *Talanta*, 1966, **13,** 1381.
129. D. Kealey and H. Freiser, Substituted 8-Mercaptoquinolines as Analytical Reagents. Dissociation and Metal Chelate Formation Constants of 2-Methyl-8-Mercaptoquinoline, *Anal. Chem.*, 1966, **38,** 1577.
130. R. H. Brook and H. Freiser, Electric Moments of Certain Substituted Tris(acetylacetonato)-chromium(III) Compounds, *Inorg. Chem.*, 1966, **5,** 2078.
131. F-Ch. Chou and H. Freiser, Formation of Mixed Ligand Complex in Extraction of Zinc in Presence of 8-Quinolinol and 1,10-Phenanthroline, *Anal. Chem.*, 1966, **38,** 1925.
132. H. Freiser, Modern pH Calculations, *Allgem. Prakt. Chem. (Wien)*, 1966, **17,** 697.
133. H. Freiser, Simplifying and Strengthening the Teaching of pH Concepts and Calculations Using Log-Chart Transparencies, *School Sci. Math.*, March, 1967.
134. H. A. Mottola and H. Freiser, Some Solvent Effects on the Solvent Extraction of 8-Quinolinol, *Talanta*, 1967, **14,** 864.
135. A. Kawase and H. Freiser, Acid Dissociation Phenomena of Certain Methyl- and Phenyl-Substituted 8-Mercaptoquinolines, *Anal. Chem.*, 1967, **39,** 22.
136. J. S. Oh and H. Freiser, Kinetics and Mechanism of Extraction of Zinc and Nickel with Substituted Diphenylthiocarbazones, *ibid.*, 1967, **39,** 295.
137. H. A. Mottola and H. Freiser, Use of Metal Ion Catalysis in the Detection and Determination of Microamounts of Complexing Agents. The Determination of Ethylenediamine-*NNN'N'*-Tetraacetic Acid, *Anal. Chem.*, 1967, **39,** 1294.
138. R. L. Stevenson and H. Freiser, Tridentate Ligands Derived from Substitution in the Methyl Group of 8-Hydroxyquinaldine, *ibid.*, 1967, **39,** 1354.
139. J. S. Oh and H. Freiser, Kinetics and Mechanism of Extraction of Cobalt(II) with Substituted Diphenylthiocarbazones, *ibid.*, 1967, **39,** 1671.
140. H. Freiser, Application of Solvent Extraction Techniques to the Study of Fast Reaction Techniques, in *Solvent Extraction Chemistry*, D. Dyrssen, J.-O. Liljeuzin and J. Rydberg (eds.), p. 85. North-Holland, Amsterdam, 1967.
141. F-Ch. Chou and H. Freiser, The Role of Adduct Formation in the Extraction of Zinc with Substituted 8-Quinolinols, *Anal. Chem.*, 1968, **40,** 34.
142. G. Gutnikov and H. Freiser, Heats and Entropies of Formation of Metal Chelates of Certain 8-Quinolinols, Quinolinol-8-thiols, and 2,4-Pentanedione, *ibid.*, 1968, **40,** 39.
143. C. Woodward and H. Freiser, Mixed Ligand Complex Formation in the Extraction of Zinc in the Presence of 8-Quinolinol and 1,10-Phenanthroline, *ibid.*, 1968, **40,** 345.
144. C. Woodward and H. Freiser, Calmagite as a Spectrophotometric Reagent for Aluminium, *Talanta*, 1968, **15,** 321.
145. H. Freiser, Extraction, *Anal. Chem.*, 1968, **40,** 522R.
146. H. A. Mottola, M. S. Haro and H. Freiser, Use of Metal Ion Catalysis in the Detection and Determination of Microamounts of Complexing Agents. The Autoxidation of L-Ascorbic Acid as an "Indicator" Reaction, *ibid.*, 1968, **40,** 1263.
147. H. A. Mottola and H. Freiser, Use of Metal Ion Catalysis in the Detection and Determination of Microamounts of Complexing Agents. Catalimetric Titration of Cyanide Ion, *ibid.*, 1968, **40,** 1266.
148. C. J. Coetzee and H. Freiser, Anion-Responsive Electrodes Based on Ion Association Extraction Systems, *ibid.*, 1968, **40,** 2071.
149. D. Kingston and H. Freiser, Influence of Structural Factor on the Thermal Stability of Metal Chelates of 8-Quinolinols, *U.S. Govt. Res. Develop. Rept.*, 1967, No. 67, 64.
150. K. S. Math, K. S. Bhatki and H. Freiser, A Highly Sensitive Extraction–Photometric Method for Nickel with Dithizone and Phenanthroline, *Talanta*, 1969, **16,** 412.
151. C. J. Coetzee and H. Freiser, Liquid–Liquid Membrane Electrodes Based on Ion Association Extraction Systems, *Anal. Chem.*, 1969, **41,** 1128.
152. H. G. Hamilton and H. Freiser, Extraction Equilibria for the System Toluene-3,4-Dithiol and Zinc, *ibid.*, 1969, **41,** 1310.
153. H. Freiser, Relevance of Solubility Parameter in Ion Association Extraction Systems, *ibid.*, 1969, **41,** 1354.
154. K. S. Math and H. Freiser, Reactions of Some Low-Spin Nickel Chelates with Heterocyclic Nitrogen Bases, *ibid.*, 1969, **41,** 1682.

155. P. R. Subbaraman, Sr. M. Cordes and H. Freiser, Effect of Auxiliary Complexing Agents on the Rate of Extraction of Zinc(II) and Nickel(II) with Diphenylthiocarbazone, *ibid.*, 1969, **41,** 1878.
156. H. Freiser, On the Occurrence of Adduct Formation in Metal Chelate Exchange in the Organic Phase, *Talanta*, 1969, **16,** 1501.
157. H. Freiser, Some Interesting Aspects of the Extraction of Zinc, *Pure Appl. Chem.*, 1969, **20,** 77.
158. A. R. Al-Salihy and H. Freiser, Acid Dissociation and Metal Chelate Formation Equilibria of Some Halogenated Diphenylthiocarbazones, *Talanta*, 1969, **17,** 182.
159. G. Colovos and H. Freiser, Determination of 2,3-Dimercaptopropanol-I (BAL) by Titration with Zinc, with Eriochrome Black T as Indicator, *Talanta*, 1969, **16,** 1605.
160. K. S. Math and H. Freiser, The Crystal and Molecular Structure of the Mixed-ligand Chelate Formed From Nickel Dithizonate and Bipyridyl, *Chem. Comm.*, 1970, **2,** 110.
161. B. S. Freiser and H. Freiser, On the Nature of the "Enol" or "Secondary" Series of Diphenylthiocarbazone Chelates, *Anal. Chem.*, 1970, **42,** 305.
162. M. Matsui and H. Freiser, Amino Acid-Responsive Liquid Membrane Electrodes, *Anal. Lett.*, 1970, **3,** 161.
163. H. Freiser, Some Recent Developments in Solvent Extraction, *CRC Crit. Rev. Anal. Chem.*, 1970, **1,** 47.
164. G. Colovos, M. Haro and H. Freiser, Reactions of 2′,7′-Bis(Acetoxymercuri)-Fluorescein with Certain Complexing Anions, *Talanta*, 1970, **17,** 173.
165. B. S. Freiser and H. Freiser, Analytical Applications of Mixed Ligand Extraction Equilibria. Nickel–Dithizone–Phenanthroline Complex, *ibid.*, 1970, **17,** 540.
166. H. Freiser, Acid-Base Reaction Parameters, *J. Chem. Educ.*, 1970, **47,** 809.
167. H. Freiser, Calculation of Hydrogen Ionic Concentrations, *ibid.*, 1971, **47,** 844.
168. K. S. Math and H. Freiser, The Crystal and Molecular Structure of Zinc Dithizonate, *Talanta*, 1971, **18,** 435.
169. W. J. Brinkman and H. Freiser, A Novel Method of Determining Certain Group VIII Metal Ions by Electron Paramagnetic Resonance Measurements, *Anal. Lett.* 1971, **4,** 513.
170. R. W. Cattrall and H. Freiser, Coated Wire Ion Selective Electrodes. *Anal. Chem.*, 1971, **43,** 1905.
171. H. Freiser, Application of Solvent Extraction Principles to the Development of Ion-Selective Electrodes, in *Solvent Extraction Proc. Int. Solvent Ext. Conf. 1971*, J. G. Gregory, B. Evans and P. C. Weston (eds.), Vol. 2, p. 1199. Society of Chemistry & Industry, London, 1971.
172. H. Freiser, Estrazione dentro Chimica Analitica, in *USES Encyclopedia Della Chimica*, 1971.
173. H. Freiser, Polywater and Analytical Chemistry: A Lesson for the Future, *J. Chem. Educ.*, 1972, **49,** 445.
174. H. J. James, G. D. Carmack and H. Freiser, Role of Solvent Extraction Parameters in Liquid Membrane Ion-Selective Electrodes, *Anal. Chem.*, 1972, **44,** 853.
175. H. J. James, G. D. Carmack and H. Freiser, Coated Wire Ion Selective Electrodes, *ibid.*, 1972, **44,** 856.
176. H. Freiser, The Two-Place Logarithm Table: An Aid to Understanding and Use of Logarithms, *J. Chem. Ed.*, 1972 **49,** 325.
177. R. L. Stevenson and H. Freiser, Standardization of Metal Ion Solutions Using a Batch Ion Exchange Technique, *Chem. Analit., Warsaw*, 1972, **17,** 675.
178. B. M. Kneebone and H. Freiser, Determination of NO_x in Ambient Air Using a Coated-Wire Nitrate Ion Selective Electrode, *Anal. Chem.*, 1973, **45,** 449.
179. C. Woodward and H. Freiser, Sulphonated Azo-Dyes as Extractive Metallochromic Reagents, *Talanta*, 1973, **20,** 417.
180. H. Freiser, Recent Research with some Sulfur-Containing Chelating Agents, *Bunseki Kagaku*, 1972, **21,** 1330.
181. H. Freiser, H. J. James, G. Carmack, B. M. Kneebone and R. W. Cattrall, Coated Wire Ion-Selective Electrodes, *United States Pat. App.* 519, 191 (30 Oct. 74); *Great Brit. Pat. App.* 15128/72 (30 March 72); *Japan Pat. App.* 28856/72 (22 March 72); *West Germ. Pat. App.* p. 22 15 378.2 (29 March 72); *Can. Pat. App.* 950536-issue (2 July 74), *Great Brit. Pat.* Pat.1375785 (24 March 75 issue).
182. H. Freiser, Ion Pair Partition, *Acta Pharm. Suecica*, 1972, **9,** 609.
183. G. D. Carmack and H. Freiser, Conductance of Quaternary Ammonium Salt Dispersions in Polymeric Films, *Anal. Chem.*, 1973, **45,** 1975.
184.* H. Freiser, Solvent Extraction, in *An Introduction to Separation Science*, B. L. Karger, S. C. Su, S. Marchese and B. A. Persson, Wiley, New York, 1973.
185.* H. Freiser, Separations Processes in Analytical Chemistry, in *The Industrial Environment—Its Evaluation and Control*, U.S. Govt. Printing Office, 1973.
186. H. Freiser and P. Brant, A Photoelectron Spectrometric Confirmation of the Oxidation State of Copper in So-Called Secondary Cu(II) Dithizonate, *Anal. Chem.*, 1974, **48,** 1147.
187. K. Math and H. Freiser, Formation Constants

of Cd(II) Complexes with Dithizone and Related Compounds, *Talanta*, 1974, **21**, 1215.
188. R. W. Cattrall, S. Tribuzio and H. Freiser, A Potassium Ion Responsive Coated Wire Electrode Based on Valinomycin, *Anal. Chem.*, 1974, **46**, 2223.
189. T. Fujinaga, S. Okazaki and H. Freiser, Ion Selective Electrodes Responsive to Anionic Detergents, *ibid.*, 1974, **46**, 1842.
190. T. Tarumoto and H. Freiser, Determination of Trace Level Quantities of Arsenic via a Novel Kinetic Method, *ibid.*, 1975, **47**, 180.
191. B. M. Kneebone and H. Freiser, Determination of Cr(VI) in Industrial Atmospheres by a Catalytic Method, *ibid.*, 1975, **47**, 595.
192. B. M. Kneebone and H. Freiser, Determination of Carbon Disulfide in Industrial Atmospheres by an Extraction–Atomic Absorption Method, *ibid.*, 1975, **47**, 942.
193. G. D. Carmack and H. Freiser, Electrical Charge Conduction Mechanism in Polymer Membrane Ion Selective Electrodes, *ibid.*, 1975, **47**, 2249.
194. G. Colovos, A. Yokoyama and H. Freiser, Application of the Solvent Extraction Technique to the Investigation of the Kinetics of the Reaction of Nickel(II) and Certain Bidentate Heterocyclic Nitrogen Ligands, *ibid.*, 1975, **47**, 2441.
195.† J. Starý and H. Freiser, *Liquid–Liquid Distribution in Equilibrium Constants*, Part IV, *Chelate Extractants*, IUPAC Special Publication, Oxford, 1978.
196. K. Uesugi and H. Freiser, Di(*p*-butylphenyl)-thiocarbazone, A New Metal Chelating Extractant, in *Essays on Analytical Chemistry*, E. Wänninen (ed.), p. 397. Pergamon Press, Oxford, 1976.
197. H. Freiser, Coated Wire Ion Selective Electrodes, *Research Devel.*, 1976, **27**, 28.
198. G. Carmack and H. Freiser, Effect of Pressure on Electrical Conduction in Ion Exchange Resins, *Anal. Chem.*, 1977, **49**, 767.
199. G. D. Carmack and H. Freiser, Assay of Phenobarbital Using an Ion Selective Electrode, *ibid.*, 1977, **49**, 1577.
200.* H. Freiser, Chapter 5 in *Platinum-Group Metals*, National Academy of Sciences, Washington, D.C., 1977.
201. D. L. Duewer and H. Freiser, Relating Molecular Structure to Metal Chelate Stability and Reagent Selectivity: Abstract Factor Analysis of the Chelate Formation Equilibria for some Diaminetetracarboxylic Acids, *Anal. Chem.*, 1977, **49**, 1960.
202. P. Baca and H. Freiser, Determination of Trace Levels of Nitrates by an Extraction-Photometric Method, *ibid.*, 1977, **49**, 2249.
203. K. S. Bhatki, A. T. Rane and H. Freiser, Reactions of Some Nickel Chelates of 8-Quinolinols with Heterocyclic Nitrogen Bases, *Inorg. Chim. Acta*, 1978, **26**, 183.
204.* H. Freiser, in *Theory, Design and Biomedical Applications of Solid State Chemical Sensors*, P. Cheung (ed.), CRC Press, Cleveland, 1978.
205.* H. Freiser, Instrumental Analysis: Solvent Extraction, in *Instrumental Analysis*, H. Bauer, G. Christian and J. O'Reilly (eds.), Allyn and Bacon, Boston, 1978.
206. K. S. Bhatki, A. T. Rane and H. Freiser, Self-adduct Formation in the Extraction of Nickel(II) Chelates of Certain 8-Quinolinols, *Indian J. Chem.*, 1977, **15A**, 983.
207. H. Freiser, Vegyes Ligandumu Kelat Extrakcios Rendszerek, *Kem. Kozlemen.*, 1977, **48**, 89.
208. P. K. Davis, H. S. Leaver and H. Freiser, Regeneration of Organic Extractants Containing *s*-Hydroxyoximes, *United States Patent*, No. 4,104,359, 1 August, 1978.
209. J. R. Jezorek and H. Freiser, 4-(Pyridylazo)-resorcinol-Based Continuous Detection System for Trace Levels of Metal Ions, *Anal. Chem.*, 1979, **51**, 373.
210. J. R. Jezorek and H. Freiser, Metal-Ion Chelation Chromatography on Silica-Immobilized 8-Hydroxyquinoline, *ibid.*, 1979, **51**, 366.
211.* H. Freiser (ed.), Chemical Analysis and Monitoring, in *Cleaning Our Environment A Chemical Perspective*; American Chemical Society, Washington, D.C., 1978.
212. C. R. Martin and H. Freiser, Microcomputer-Controlled Potentiometric Analysis System, *Anal. Chem.*, 1979, **51**, 803.
213. S. P. Carter and H. Freiser, Apparatus for Following Extraction Kinetics, *ibid.*, 1979, **51**, 1100.
214. J. DeNunzio and H. Freiser, The Use of Brilliant Green in Ion-Pair Chromatography, *Talanta*, 1979, **26**, 587.
215. C. R. Martin and H. Freiser, Coated-Wire Ion Selective Electrodes and Their Application to the Teaching Laboratory, *J. Chem. Educ.*, 1980, **57**, 512.
216. S. P. Carter and H. Freiser, Kinetics and Mechanism of the Extraction of Copper with 2-Hydroxy-5-Nonylbenzophenone Oxime (LIX65N), *Anal. Chem.*, 1980, **52**, 511.
217. C. R. Martin and H. Freiser, Response Characteristics of Ion Selective Electrodes Based on Dinonylnaphthalenesulfonic Acid (DNNS), *ibid.*, 1980, **52**, 562.
218. K. Ohashi and H. Freiser, Kinetics and Mechanism of Formation of Nickel(II)–Diarylthiocarbazone Complexes, *ibid.*, 1980, **52**, 767.
219. T. Hori, M. Kawashima and H. Freiser, Mixed Ligand Chelate Extraction of Lanthanides: 8-Quinolinol Systems, *Sep. Sci. Tech.*, 1980, **15**, 861.
220. C. Martin and H. Freiser, Ion Selective Elec-

trode for the Determination of Phencyclidine, *Anal. Chem*, 1980, **52,** 1772.
221.† H. Freiser, *Ion Selective Electrodes in Analytical Chemistry*, Vol. I, Plenum Press, New York, 1978.
222.† H. Freiser, *Ion Selective Electrodes in Analytical Chemistry*, Vol. II, Plenum Press, New York, 1980.
223. T. Yamada and H. Freiser, Propranolol Coated Wire Ion-Selective Electrode, *Anal. Chim. Acta*, 1981, **125,** 179.
224. K. Ohashi and H. Freiser, Kinetics of Back-Extraction of Nickel Dithizonate, *Anal. Chem.*, 1980, **52,** 2214.
225. M. Kawashima and H. Freiser, Mixed Ligand Chelate Extraction of Lanthanides in 8-Quinolinol Tetra-n-heptylammonium Chloride Systems, *ibid.*, 1981, **53,** 284.
226. C. Martin and H. Freiser, Ion-Selective Electrodes Based on an Ionic Polymer, *ibid.*, 1981, **53,** 902.
227. O. Tochiyama and H. Freiser, Mixed Ligand Chelate Extraction of Lanthanides With 5,7-Dibromo-8-Quinolinol Systems, *ibid.*, 1981, **53,** 874.
228. T. Gnanasambandan and H. Freiser, Paired Ion Chromatographic Separation of Neutral Species, *ibid.*, 1981, **53,** 909.
229. K. Ohashi, M. Ozaki and H. Freiser, Study on the Exchange of Nickel(II)-dithizone with Mercury(II) by Atomic Absorption Spectrophotometry, *Bunseki Kagaku*, 1981, **30,** 139.
230. H. Freiser, Kinetics of Solvent Extraction of Metal Chelates, *Proc. Intl. Solvent Extr. Conf. Liège, Belgium*, 1980, Paper 80–II.
231. T. Honjo and H. Freiser, Extraction of Nickel(II), Copper(II), and Zinc(II) in Carbon Tetrachloride with Monothiodibenzoylmethane and Derivatives, *Anal. Chem.*, 1981, **53,** 1258.
232. E. Yamada and H. Freiser, Mixed Ligand Chelate Extraction of Lanthanide Ions in Systems Involving 7-(1-Vinyl-3,3,6,6-tetramethyl)-8-quinolinol, 8-Quinolinol, and 1,10-Phenanthroline, *ibid.*, 1981, **53,** 2115.
233. H. Freiser, Solvent Extraction in Analytical Chemistry and Separation Science, *Bunseki Kagaku*, 1981, **30,** S47.
234. O. Tochiyama and H. Freiser, Mixed Ligand Chelate Extraction of Lanthanides with 1-Phenyl-3-Methyl-4-Octanoyl-5-Pyrazolone Systems, *Anal. Chim. Acta*, 1981, **131,** 233.
235. L. Cunningham and H. Freiser, Response and Selectivity Characteristics of Alkylammonium Ion-Selective Electrodes, *ibid.*, 1981, **132,** 43.
236. S. P. Bag and H. Freiser, Kinetics and Mechanism of Solvent Extraction of Copper with Kelex 100 in Presence of Nitrilotriacetic Acid, *ibid.*, 1982, **134,** 333.
237. S. Okazaki and H. Freiser, A Proposal to Account for the Selectivity Coefficient of ISE, *Denki Kagaku Oyobi Kogyo Butsuri Kagaku*, 1982, **50,** 117.
238. S. P. Bag and H. Freiser, Liquid Distribution Equilibria in the Copper(II)–7-(1-Vinyl-3,3,6,6-Tetramethylhexyl)-8-Quinolinol System, *Anal. Chim. Acta*, 1982, **135,** 319.
239. K. Akiba and H. Freiser, The Role of the Solvent in Equilibrium and Kinetic Aspects of Metal Extractions, *ibid.*, 1982, **136,** 329.
240. S. P. Bag and H. Freiser, Preferential Solvation of Dithizone in Chloroform in Cyclohexane, *ibid.*, 1982, **136,** 439.
241. K. Akiba and H. Freiser, Equilibrium and Kinetics of Nickel Extraction with 2-Hydroxy-5-nonylbenzophenone Oxime, *Sep. Sci. Tech.*, 1982 **17,** 745.
242. V. Bagreev and H. Freiser, Mechanistic Studies on the Extraction of Copper by 5,8-Diethyl-7-hydroxy-dodecane-6-One Oxime (LIX 63), *ibid.*, 1982, **17,** 751.
243. L. Cunningham and H. Freiser, Ion Selective Electrodes for Basic Drugs, *Anal. Chim. Acta*, 1982, **139,** 97.
244. T. Gnanasambandan and H. Freiser, Separation of Aliphatic Alcohols by Paired Ion Liquid Chromatography, *Anal. Chem.*, 1982, **54,** 1282.
245. H. Watarai, L. Cunningham and H. Freiser, Automated System for Solvent Extraction Kinetic Studies, *ibid.*, 1982, **54,** 2390.
246. H. Watarai and H. Freiser, Effect of Stirring on the Distribution Equilibria of N-Alkyl Substituted Dithizones, *J. Am. Chem. Soc.*, 1983, **105,** 191.
247. H. Watarai and H. Freiser, The Role of the Interface in the Extraction Kinetics of Zinc and Nickel Ions with Alkyl Substituted Dithizones, *ibid.*, 1983, **105,** 189.
248. L. Zhu and H. Freiser, Solvent Extraction Equilibria of Uranium with 7-Dodecenyl-8-Quinolinol, *Anal. Chim. Acta*, 1983, **146,** 237.
249. T. Gnanasambandan and H. Freiser, Paired Ion Chromatography of Certain Monosaccharides, *Anal. Chem.*, 1982, **54,** 2379.
250. K. Haraguchi and H. Freiser, Kinetics and Mechanism of Metal Exchange Reaction of Bis-8-Mercaptoquinolatonickel(II) Chelate with Copper(II) Ion by an Exchange Extraction Method, *Inorg. Chem.*, 1982, **22,** 653.
251. H. Freiser, Reagents Used in Inorganic Analysis Reagents, in *Treatise on Analytical Chemistry*, 2nd Ed., Part I, Vol. 3, I. M. Kolthoff and P. J. Elving (eds.), Wiley, New York, 1983.
252. K. Haraguchi and H. Freiser, Equilibrium and Kinetics of Extraction of Nickel with 7-Dodecenyl-8-Quinolinol (Kelex 100), *Inorg. Chem.*, 1983, **22,** 1187.
253. K. Haraguchi and H. Freiser, Kinetics of Extraction of Nickel with 8-Mercaptoquinoline. *Anal. Chem.*, 1983, **55,** 656.

254. Y. Sasaki and H. Freiser, Mixed Ligand Chelate Extraction of Lanthanides with 1-Phenyl-3-Methyl-4-Acyl-5-Pyrazolones, *Inorg. Chem.*, 1983, **22,** 2289.
255. C. Martin and H. Freiser, Large Organic Cation-Selective Electrodes, *United States Pat. App.* 239,081 (2-27-81), issued 4,399,002 (8-16-83).
256. E. Ma and H. Freiser, Mechanistic Studies on the Extraction of Palladium (II) with 2-Hydroxy-5-Nonylbenzophenone Oxime (LIX 65N), *Solvent Extr. Ion Exch.*, 1983, **1,** 485.
257. H. Freiser, Kinetics and Mechanism of Metal Chelation Processes Via Solvent Extraction Techniques, *Acc. Chem. Res.*, 1984, **17,** 126.
258. Z. Yoshida and H. Freiser, Ascending Water Electrode Studies of Metal Extractants. Faradaic Ion Transfer of Protonated 1,10-Phenanthroline and Its Derivatives Across An Aqueous 1,2-Dichloroethane Interface, *J. Electroanal. Chem.*, 1984, **162,** 307.
259. E. Ma and H. Freiser, Solvent Extraction Equilibria and Kinetics in the Palladium (II)–Hydrochloric Acid–7-(1-Vinyl-3,3,5,5-tetramethylhexyl)-8-Quinolinol System, *Inorg. Chem.*, 1984, **23,** 3334.
260. E. Ma and H. Freiser, Reactivity of Palladium Dithizonate with Lewis Acids and Bases, *ibid.*, 1984, **23,** 3342.
261. L. Cunningham and H. Freiser, Ion-Selective Electrodes For Some β-Adrenergic and Calcium Blockers, *Anal. Chim. Acta*, 1984, **157,** 157.
262. Z. Yoshida and H. Freiser, Ascending Water Electrode Studies of Metal Extractants. Role of Kinetic Factors In the Faradaic Ion Transfer of Metal-Phenanthroline Complex Ions Across an Aqueous-Organic Solvent Interface, *Inorg. Chem.*, 1984 **23,** 3931.
263. Z. Yoshida and H. Freiser, Mechanism of the Carrier-Mediated Transport of Potassium Ion Across the Water–Nitrobenzene Interface by Valinomycin, *J. Electroanal. Chem.*, 1984, **179,** 31.
264. A. Trujillo, T. Gnanasambandan and H. Freiser, Determination of Organophosphorus Compounds by Dye Assisted Chromatography, *Anal. Chim. Acta*, 1984, **162,** 333.
265. E. Aprahamian, Jr., F. F. Cantwell and H. Freiser, Measurement of Interfacial Adsorption and Interfacial Area in Vigorously Stirred Solvent Extraction Systems, *Langmuir*, 1985, **1,** 79.

POSTDOCTORAL ASSOCIATES OF PROFESSOR HENRY FREISER

Prof. Carl B. Honaker
Department of Chemistry
Tennessee Wesleyan College
Athens, Tenn. 37303

Prof. Alfio Corsini
Department of Chemistry
McMaster University
Hamilton, Ontario, Canada

Prof. Saswati P. Bag
Department of Chemistry
Jadavpur University
Calcutta-32, India

Prof. Carl R. Wasmuth
Department of Chemistry
University of Tennessee at
Martin, Tenn. 38237

Prof. D. (Jack) Betteridge
Department of Chemistry
University College of Swansea
Singleton Park, Swansea, UK

Prof. Eiichi Sekido
Department of Chemistry
Faculty of Science
Kobe University
Rokkodai, Nada
Kobe, Japan

Prof. Kumar Math
Reader in Chemistry
Karnatak University
Dharwar-58003, India

Dr. Hans Jadamus
Wientapper Wg 24
Hamburg 5555, Germany

Dr. G. Ehrlich
US Geological Survey
345 Middlefield Road
Menlo Park, CA

Prof. Susumu Takamoto
Faculty of Science
Gakushuin University
Mejiro, Tokyo, Japan

Prof. Horacio A. Mottola
Department of Chemistry
Oklahoma State University
Stillwater, Oklahoma 74078

Dr. David Kealey
Chemistry Department
Kingston Polytechnic Institute
London, UK

Dr. Akira Kawase
National Research Institute for Metals
300, 2-Chome, Nakameguro
Tokyo, Japan

Dr. Colin Woodward
17 Hardwich Road
Sedgefield, Cleveland,
England

Dr. Kumar S. Bhatki
Hot Laboratory
Tata Institute of Fundamental Research
Homi Bhabha Road
Bombay, India 400 005

Dr. Hobart G. Hamilton
Office of the Chancellor
Stanislaus State College
Turlock, CA 95380

Dr. P. R. Subbaraman
National Chemical Laboratory
Poona-8, India

Dr. Toshitaka Hori
Department of Chemistry
College of Liberal Arts
& Sciences
Kyoto University
Kyoto 606, Japan

Dr. Huang Chun-Hui
Department of Chemistry
Peking University
Beijing, China

Professor John Jezorek
Department of Chemistry
University of North Carolina
Greensboro, NC 27412

Dr. Munetsuga Kawashima
Shiga University
Faculty of Liberal Arts
& Education
2-5-1 Hiratsu-cho
Otsu-City, 520, Japan

Dr. Thomas McGrath
Department of Chemistry
Susquehanna University
Selinsgrove, PA 17870

Dr. Hoshimi Sasaki
Department of Industrial
Chemistry
Fukui Technical College
Geshi, Sabae City, 915
Japan

Dr. Osamu Tochiyama
Department of Nuclear
Engineering
Faculty of Engineering
Tohoku University
Aramaki-aza-aoba
Sendai, 980, Japan

Professor Robert Cattrall
Department of Chemistry
La Trobe University
Bundoora, Victoria
Australia 3083

Professor Rong Qing-Xin
Chemistry Department
Zhongshan (Sun Yatsen) University
Guangzhou, People's Republic of China

Dr. Hitoshi Watarai
Department of Chemistry
Faculty of Education
Akita University
Tegata-gakuencho
Akita 010, Japan

Dr. Takeshi Yamada
Faculty of Textile Science
Kyoto Technical University
Matsugasaki Goshokaido-cho
Sakyo-ku, Kyoto, 606, Japan

Dr. Zenko Yoshida
Analytical Chemistry Division
Japan Atomic Energy Research
Institute
Tokai-mura, Naka-gun
Ibaraki, 319-11, Japan

Professor Lin Zhu
Department of Chemistry
Sichuan University
Chengdu, Sichuan
People's Republic of China

Professor P. J. Sun
3 Fl., No. 244
Hsin I Road Sec. 4
Taipei, Taiwan 106
People's Republic of China

Dr. C. J. Coetzee
Department of Chemistry
University of the Western Cape
Bellville, South Africa

Professor Masakazu Matsui
27-5, Goshu-no-Uchi
Matsugasaki, Sakyo
Kyoto, Japan

Prof. Bob E. McClellan
Department of Chemistry
Murray State University
Murray, Kentucky 42071

Prof. Abdul R. Al-Salihy
Department of Chemistry
University of Baghdad
Adamiya, Baghdad, Iraq

Prof. Helen James
Weber State College
Department of Chemistry
Ogden, Utah 84403

Prof. Benjamin Kirson
The Hebrew University of Jerusalem
Department of Inorganic and Analytical Chemistry
Jerusalem, Israel

Dr. Takeshi Ashizawa
Atomic Fuel Corp.
Tokai, Ibaragi, Japan

Prof. Ted Haupert
Department of Chemistry
California State College
Sacramento, CA 95819

Dr. Kenichi Akiba
Res. Institute of Mineral Dressing & Metallurgy
Tohoku University
Katahira-2, Sendai, Japan

Dr. James DiNunzio
Department of Chemistry
Wright State University
Dayton, OH 45435

Dr. David L. Duewer
Monsanto Industrial Chemicals
St. Louis, Missouri 63167

Prof. Marcia Cordes
Department of Chemistry
Creighton University
Omaha, Nebraska 68131

Dr. George Colovos
Science Center
Rockwell International
P.O. Box 1085
Thousand Oaks, CA 91360

Prof. Takaharu Honjo
Department of Chemistry
Kanazawa University
Kanazawa, Ishikawa 920
Japan

Prof. Genkichi Nakagawa
Department of Chemistry
Nagoya Institute of Technology
Gokiso-Cho Show A-Ku
Nagoya, Japan

Prof. William Van Willis
Department of Chemistry
California State College
Fullerton, CA 92631

Dr. V. V. Bagreev
Institute of Geochemistry & Analytical Chemistry
Academy of Science of U.S.S.R.
Kosygin St. 19
Moscow V-334 U.S.S.R.

Dr. Enxin Ma
Shanghai Institute of Organic Chemistry
Academia Sinica
345 Linglin Lu
Shanghai, China

Dr. Kensaku Haraguchi
619-24 Kotoni-jutaku
95 Hachiken, Nishi-ku
Sapporo 063, Japan

Professor Akira Yokoyama
Faculty of Pharmaceutical Sciences
Kyoto University
Skayo-ku, Kyoto
Japan

Dr. Tsunehiko Tarumoto
c/o Imai
549 W. 123rd St.
New York, NY 10027

Professor Katsuya Uesugi
Laboratory of Chemistry
Himeji Institute of Technology
Shosya 2167
Himeji Hyogo 671-22, Japan

Dr. Satoshi Okazaki
Department of Chemistry
Kyoto University
Kyoto, Japan

Dr. Kousaburo Ohashi
Department of Chemistry
Ibaraki University 2-1-1 Bunkyo, Mito
310, Japan

Professor Quintus Fernando
Department of Chemistry
University of Arizona
Tucson, AZ 85721

Prof. Rong Qing-Xin
Zhongshan University
Guangzhou, People's Republic
of China

Prof. Zhao Zaofan
Department of Chemistry
Wuhan University
Wuhan, People's Republic
of China

Professor Fred Cantwell
Department of Chemistry
University of Alberta
Edmonton, Alberta
Canada

Dr. Lin Sinru
Shanghai Institute of Metallurgy
Academy of Sciences of China
Shanghai, China 200050

Dr. Shoji Motomizu
Department of Chemistry
Faculty of Science
Okayama University
Tsushima, Okayama 700
Japan

Dr. Kazuo Kondo
Department of Organic Synthesis
Kyushu University
Hakozaki, Higashi-ku
Fukuoka 812, Japan

Dr. Sargon J. Al-Bazi
Department of Chemistry
University of Manitoba
Winnipeg, Manitoba
Canada R3T 2N2

Dr. Shigeo Umetani
Institute for Chemical Research
Kyoto University
Kyoto, Japan

Dr. Maciej Kostanski
Institute of General Chemistry
Poznan Technical University
Poznan, Poland

Dr. Shigeru Taguchi
Department of Chemistry
Toyama University
Toyama, Japan

Dr. Li Ke-an
Department of Chemistry
Peking University
Beijing, People's Republic
of China

Dr. B. Buděšínský
Chemical Laboratory
Phelps Dodge
Morenci, AZ 85540

Dr. E. Yamada

Dr. N. Egan

Dr. R. Prasad

Dr. J. S. Oh
Dean of Academic Affairs
Ajou University
Suweon, Korea

Dr. Lawrence Cunningham
Department of Chemistry
University of Arizona
Tucson, AZ 85721

Ph.D. STUDENTS OF PROFESSOR HENRY FREISER

Dr. R. G. Charles
Westinghouse Research
Pittsburgh

Dr. W. D. Johnston
Pittsburgh Plate Glass Research
Pittsburgh

Prof. J. L. Walter
Department of Chemistry
Notre Dame University
Notre Dame, Ind. 46556

Prof. J. Steinbach
(U. of Kentucky, retired)

Dr. L. M. Melnick
Section Supervisor
Analytical Chemistry
US Steel Corp.
Applied Research Laboratory
Monroeville, PA 15146

Dr. John Hedenburg
Gulf Research

Dr. Leonard M. Shorr
Israel Mining Institute
Haifa, Israel

Dr. Thomas R. Harkins

Dr. Anoop Krishen
Goodrich Research
Akron, Ohio

Dr. J. P. McKaveney, Manager
Occidental Research Corp.
1855 Carrion Road
La Verne, CA 91750

Dr. D. Fleischer

Prof. G. E. Cheney
Department of Chemistry
Acadia University
deceased

Dr. Morris Mendelsohn
Westinghouse Research
Pittsburgh

Dr. Anna M. Coleman
Dow-Corning Research
Midland, Michigan

Dr. Stanley J. Jankowski
ICI United States Inc.
Wilmington, Del.

Prof. Robert E. Kirby
Queens College, CUNY
Department of Chemistry
65-30 Kissena Blvd.
Flushing, NY 11361

Dr. Gary Carmack
Pathology Lab
VA Hospital
Phoenix, Arizona

Dr. S. P. Carter
FMC Corporation
Princeton, NJ

Prof. James Fresco
Department of Chemistry
McGill University
P.O. Box 6070, Station A
Montreal, Quebeck H3C 3G1
Canada

Dr. Robert L. Stevenson, Manager
Research & Development
Varian, Aerograph Division
2700 Walnut Creek, CA 94598

Prof. George Gutnikov
Dept. of Physical Sciences
Cal. State Polytechnic College
Pomona, CA 91766

Dr. David Kingston

Dr. William J. Brinkman
Magma Copper Co.
San Manuel, AZ

Dr. Larry Cunningham
Department of Chemistry
University of Arizona
Tucson, AZ 85721

Dr. C. R. Martin
Department of Chemistry
Texas A&M University
College Station, Texas

Dr. O. E. Harris
Dr. F. Chou
Dr. T. Gnanasambandan

CURRENT Ph.D. STUDENTS OF PROFESSOR HENRY FREISER

Andres Trujillo-Rebollo
Ed Aprahamian, Jr.
V. G. Chamupathi
Anthony Stevens
Daro Ferrara
Ted Cecconie
Mark Dietz

MASTER OF SCIENCE STUDENTS OF PROFESSOR HENRY FREISER

Ram Keswani

Adolph E. Spakowski
NASA
Cleveland

R. G. Charles
Lydia J. Uhlig

Mary Eagle
W. D. Johnston
T. Christos
S. J. Jankowski
P. Baca
C. Sikabwe
H. S. Lee

Carl Bostic
Robert Barca

Prof. James Katekaru
Chemistry Department
Cal. State Polytechnic College
San Luis Obispo, CA 93420

Willow Frazier

Barbara Kneebone
Magma Copper Co.
San Manuel, AZ

Mark Fu-Pao Tsao
Department of Chemical Engineering
National Central University
College of Science
Chug-li, Taiwan 320
Republic of China

Carlos Fabara
Instituto Nacional de Investigaciones
Agropecuarias (INIAP)
P.O. Box 2600
Quito, Ecuador

Talanta, Vol. 32, No. 8B, pp. 697–708, 1985
Printed in Great Britain.

0039-9140/85 $3.00 + 0.00

INVESTIGATION OF REACTIONS OF METAL IONS AND THEIR CLUSTERS IN THE GAS PHASE BY LASER-IONIZATION FOURIER-TRANSFORM MASS SPECTROMETRY

BEN S. FREISER
Department of Chemistry, Purdue University, West Lafayette, Indiana 47907, U.S.A.

(*Received* 3 *December* 1984. *Accepted* 24 *January* 1985)

Summary—Recent developments in our laboratory involving both software and hardware modifications of the Nicolet FTMS-1000 Fourier-transform mass spectrometer now enable us to conduct research in what can be termed a "complete gas-phase chemical laboratory." Selected ions of interest can be mixed with various reagents and their detailed chemistries monitored through a series of as many as eight reaction sequences. At any point in these sequences, ion structures can be elucidated and fundamental kinetic and thermodynamic parameters of the reactions can be determined. In particular we have been applying these powerful new techniques to the examination of the gas-phase chemistry and photochemistry of metal ions, metal clusters and metal complexes, which have a bearing on the fundamentals of organometallic chemistry and catalysis. This paper presents some highlights of this work.

Over the last few years our laboratory has been working extensively in two main areas: (1) development of Fourier-transform mass spectrometry (FTMS) as a means of performing both analytical mass spectrometry and fundamental ion-molecule reaction chemistry and (2) study of bare metal ions, metal-ion complexes and metal-ion clusters. These two areas have been intimately related, in that new instrumental developments in FTMS have permitted increasingly sophisticated experiments to be performed. The desire to extend our knowledge of the chemistry of metal ions in the gas phase has often required the development of such new methodology. In this paper some highlights of this work are presented in the hope of providing the reader with a basic understanding and appreciation of both the methodology and the chemistry.

LASER GENERATION OF METAL IONS

The application of a pulsed laser source in our laboratory has proved to be a convenient and powerful method of generating metal ions for subsequent gas phase studies.[1] As shown schematically in Fig. 1, focusing the beam of a high-powered pulsed laser onto a metal target causes ejection of a plume of material from the surface. This phenomenon, known as "laser ionization" when ions are produced or "laser ablation" in general, gives what is seen visually as a "spark" and is attributed to the rapid heating of the surface.[2] The process is dependent on the laser power, with a threshold of the order of 10^7–10^8 W/cm^2, but is apparently independent of wavelength and is readily produced, for example, by the fundamental, doubled, tripled and quadrupled energy beams of an Nd:YAG laser, at 1066, 533, 355 and 267 nm, respectively. Although the plume consists predominantly of neutral metal atoms, these species rapidly condense on the first surface they strike and are not observed during the time taken by our experiments, as discussed below. By far the most abundant positive ion produced is the monatomic singly-charged metal ion, and the electron is the predominant negatively-charged species generated. Atomic metal anions, M^-, as well as metal cluster ions, M_n^+ and M_n^-, have also been produced by using laser ionization[3,4] but, unfortunately, are not produced in sufficient abundance to be studied by FTMS.

Laser ionization thus provides a convenient method for generating virtually any positive metal ion from the pure metal for subsequent gas-phase chemical studies, and has a number of clear advantages over other commonly used techniques. Electron impact on a volatile metal carbonyl such as $Fe(CO)_5$,

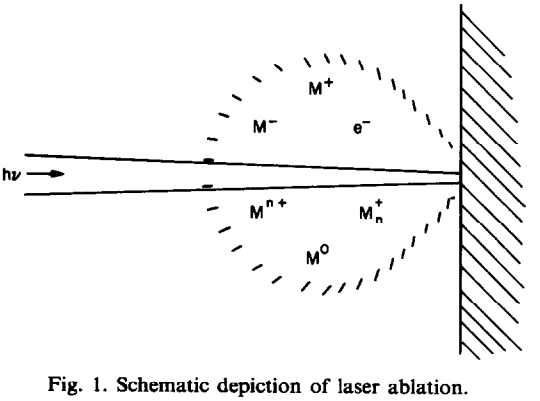

Fig. 1. Schematic depiction of laser ablation.

produces not only Fe^+ but also high abundances of $Fe(CO)_n^+$ $(n = 1 - 5)$.[5,6] In addition, in a study of the chemistry of Fe^+ with an organic substrate, the neutral carbonyl, which is highly reactive with the ions present, can obscure the chemistry. Finally, a convenient volatile complex of a more exotic metal may not be available. Surface ionization of metal atoms, produced by heating metal salts, has also been used quite successfully in ion-beam studies[7-9] but requires a somewhat cumbersome changing of the metal salts if different metals are to be studied. In addition, some of the more exotic metal ions are again difficult to produce by this method. In summary, while these other techniques continue to be quite useful, laser ionization offers a "clean" and convenient source of metal ions, the selection of which is rapidly accomplished by simply focusing the laser on a different target.

Our interest in studying metal ions is twofold. First, fundamental studies of metal ions in the gas phase provide kinetic, mechanistic and thermodynamic information of relevance to a broad range of areas, such as organometallic chemistry, atmospheric chemistry, corrosion chemistry and catalysis. Second, metal ions hold promise as selective chemical ionization reagents, as described below.

METAL IONS AS SELECTIVE CHEMICAL IONIZATION REAGENTS

In addition to the spectacular instrumental developments in mass spectrometry over the past two decades, there has also been a growing interest in the "chemistry taking place within the ionization chamber". In particular the ion source can be thought of as a reaction chamber in which chemical reactions can provide selectivity greater than that given by the instrumentation itself. The beginnings of this more chemical approach can be traced to the landmark paper by Munson and Field in 1966, introducing chemical ionization.[10] The most commonly recognized ionization method in mass spectrometry is electron impact, in which a sample is bombarded with electrons (usually at 70 eV). Electron impact on compound AB, for example, produces the fragments A^+ and B^+, and in fortunate cases, the molecular

$$AB \xrightarrow{e^-} A^+, B^+, AB^+ \qquad (1)$$

ion AB^+(reaction 1). It is both an advantage and a disadvantage of electron impact that it is a universal, non-selective ionization method whereby any sample that can be volatilized can be ionized. While under many circumstances this may be desirable, clearly a complex mixture will produce a complex spectrum. Furthermore, it is often the case that electron impact, especially at 70 eV, imparts too much energy to the parent molecular ions, causing decomposition and hence their absence from the spectrum. Chemical ionization on the other hand is a two-step process in which the first step involves the generation of a reagent ion, R^+, generally by electron impact on a reagent gas, R (reaction 2).

$$R \xrightarrow{e^-} R^+ \qquad (2)$$

The second step is that the reagent ion then undergoes an ion–molecule reaction with the sample, AB, to produce product ions (reaction 3).

$$R^+ + AB \longrightarrow \text{product ions} \qquad (3)$$

The sample is not ionized by electron impact, but by chemical reaction. Careful choice of the reagent ion can, in theory, permit this reaction to be as selective or universal as desired. A number of reagent gases have been used for chemical ionization, but most of them come into the categories of either proton- or charge-transfer reagents.[11,12] In contrast, we felt that the array of metal ions available would exhibit a far wider variety of reactivities, which would be particularly useful for selective chemical ionization. Thus, we set about a systematic study of reactions of metal ions with various classes of organic molecules. The goal of this research was to identify trends in reactivity, i.e., to find reaction mechanisms useful in interpreting the chemical ioniation spectra of unknown compounds and to test for the functional-group selectivity of the various metal ions. We have demonstrated the feasibility of these goals, thus far, in extensive studies of Cu^+ with esters and ketones,[13] Fe^+ with ethers, ketones and hydrocarbons,[14] Ti^+,[15] Rh^+,[16] V^+,[17] and Y^+,[18] with hydrocarbons, and of Fe^+ and Co^+ with sulphur-containing compounds.[19] Results have also been reported from a number of other laboratories.[6-9] Chemical ionization with Co^+, for example, has been applied to bifunctional compounds,[20] and in an elegant recent experiment Fe^+ was found to be useful for locating double bonds in a variety of long-chain compounds.[21] Finally, in view of the large data sets generated from the variety of metal ions and organic species studied, we have begun to apply pattern-recognition techniques as a powerful means for data analysis.[22]

FOURIER-TRANSFORM MASS SPECTROMETRY

Our work on metal-ion chemistry was greatly facilitated when we obtained the prototype Nicolet FTMS-1000 Fourier-transform mass spectrometer in 1981. Before this, all our studies had been performed on a conventional ion cyclotron resonance (ICR) spectrometer. FTMS is based on the principles of ICR and, in fact, is also referred to as FTICR as originally named by its inventors, Marshall and Comisarow. As first pointed out by these authors,[23] all the advantages of the Fourier-transform method achieved in NMR and infrared spectroscopy are also realized for ICR, with a few additional advantages as discussed below.

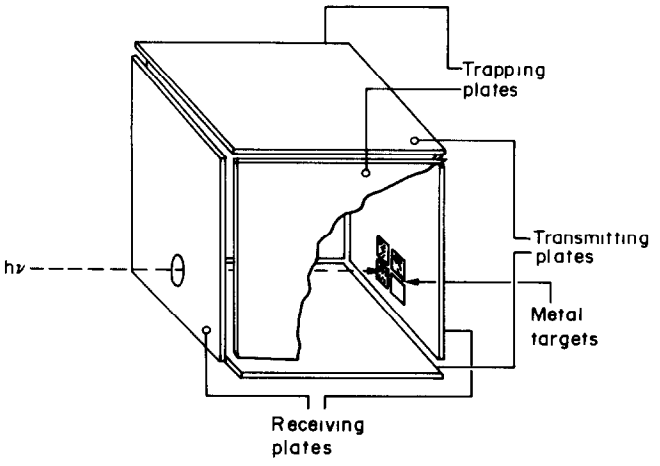

Fig. 2. Modified cubic trapping cell.

The heart of the FTMS instrument is the cubic trapping cell shown schematically in Fig. 2. Because of the applied electric and magnetic fields, the cell acts as an "electromagnetic bottle" in which ions may be stored for up to several seconds—much longer than the microsecond residence times available with conventional mass spectrometers. It is this feature which makes FTMS ideally suited for studying the chemistry and photochemistry of ions in the gas phase. The cell shown in Fig. 2 was constructed in our laboratory and is a 5.2-cm cube. The tolerances for the cell are not critical and the $\frac{1}{4}$-in. hole drilled in one of the plates to permit laser irradiation does not affect its performance. Several metal targets are spot-welded onto the back receiving plate, and are easily accessible for laser ionization. The entire cell is in a vacuum enclosure which is operated at between 10^{-8} and 10^{-5} mmHg pressure and placed between the pole faces of a 9-kG electromagnet.

The basis of FTMS can be described in relatively simple terms.[24-30] An ion in a magnetic field is constrained to move in a circular orbit perpendicular to the field, at a characteristic frequency proportional to the magnetic field and inversely proportional to its mass-to-charge ratio (m/z). If the ion is then placed between two plates and a radiofrequency field (*i.e.*, an oscillating electric field) having the same frequency as the cyclotron frequency of the ion is applied to the plates, there is a resonance effect and the ion absorbs energy, causing its orbital radius and velocity to increase. Ions of the same mass all orbit at the same frequency prior to excitation but are in different spatial positions in the orbits, and thus are out of phase with each other. After an excitation (RF) pulse, not only have the orbital radii and velocities increased, but the ions are all moving together coherently. It is this coherent motion that gives rise to a signal. The "packet" of ions attracts electrons to whichever plate it is approaching, and an "image" current is established between the two plates. As shown in Fig. 3, this image current provides the time-domain information which is then digitized and subjected to fast Fourier-transformation to yield the frequency-domain spectrum. A complete mass spectrum is obtained by applying a 0–1 MHz RF pulse, referred to as an RF "chirp", for about 0.1 msec. This excites all the ions in a coherent fashion, producing an image current consisting of all the superimposed frequencies. The Fourier transform yields the frequency spectrum and thus the mass spectrum. The intensities of the peaks are directly related to the concentrations of the ions present. A particularly interesting feature is that the width of a peak, and hence the resolution, is limited by the uncertainty principle, in that the longer the image-current transient is sampled, the higher the resolution. The decay of the image-current signal arises mainly because of ion collisions with the neutral gas molecules present. A collision of one of the ions in the packet results in that ion no longer moving coherently with the remainder of the ions in the packet. Thus with a high pressure in the cell, the signal decays rapidly (in times of the order of msec), producing a low-resolution spectrum, while at low pressures (especially, for example, on the space-shuttle) the transient may last for tens of seconds, producing an ultra high-resolution spectrum. It is interesting to note that the intramolecular relaxation mechanism for NMR, as opposed to the intermolecular process in ICR, is the reason that, unlike FTICR, there is no gain in resolution on going from

Fig. 3. Schematic depiction of the basic principles of FTMS. Coherent motion of ions in the cell produces an image-current signal which is digitized and then Fourier-transformed, resulting in a frequency or mass spectrum.

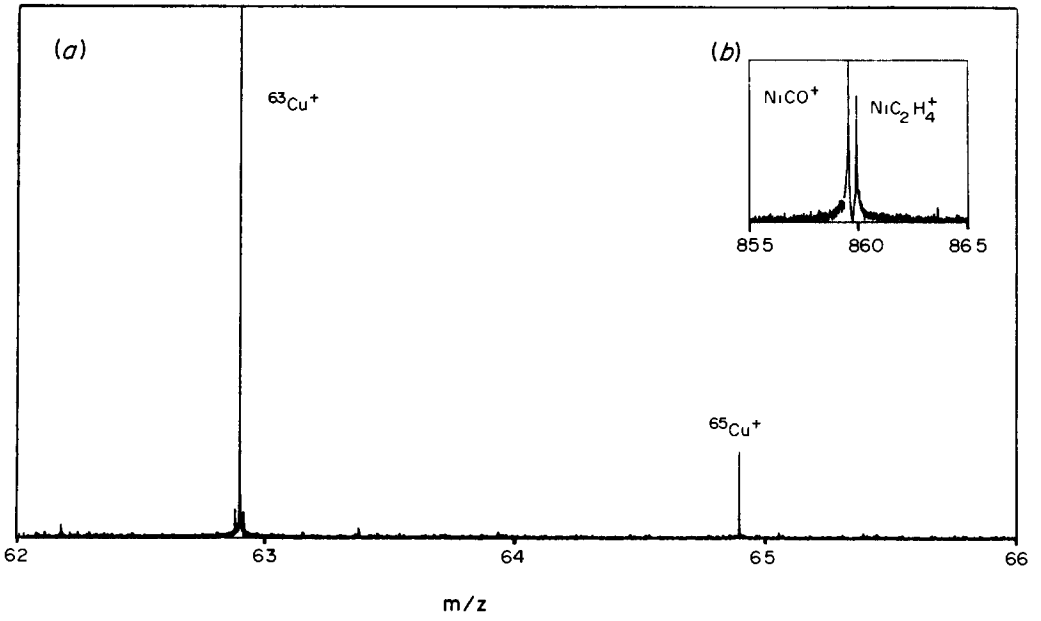

Fig. 4. (*a*) High-resolution spectrum (FWHH = 6×10^4) of Cu^+. (*b*) Mass spectrum (FWHH = 1.7×10^4) indicates the presence of two isobars at integral mass 86 [reactions (4) and (5) in text].

NMR to FTNMR. A resolution of 10^8 has been reported[31] at mass 18, which in theory could resolve He^+ in its ground state from He^+ in its first excited state, *i.e.*, the resolution is equivalent to the mass of a 21-eV photon! Conceivably, the gain of another order of magnitude in resolution could allow bond energies to be obtained directly from mass-defect measurements. A mass resolution of 10^8 at the present time, however, is still by no means routine, although resolutions of the order of 10^4–10^6 are easily achievable. Figure 4*a* shows a spectrum of Cu^+ at a resolution of 6×10^4 obtained in the presence of only background gas at 10^{-8} mmHg. Addition of a sample gas does degrade performance but, as shown in Fig. 4*b*, a resolution of 1.7×10^4 is sufficient to determine that both reactions (4) and (5) occur for Ni^+ and butanone at $\sim 5 \times 10^{-7}$ mmHg.

$$Ni^+ + CH_3COC_2H_5 \longrightarrow \begin{cases} NiCO^+ + C_3H_8 & (4) \\ NiC_2H_4^+ + C_2H_4O & (5) \end{cases}$$

MS/MS BY FTMS

One of the techniques currently in the forefront of mass spectrometry research is MS/MS (mass spectrometry/mass spectrometry) by analogy with GC/MS.[32–34] Figure 5 illustrates one of the basic differences between performing the MS/MS experiment with the more conventional tandem instrument, and doing it by using FTMS. In a tandem MS/MS experiment the ions are manipulated in space. An ion generated in the source is selected by using the first mass spectrometer (sector or quadrupole), MS_1, and undergoes a collision in the reaction chamber. The product ions from that collision are analysed by using a second mass spectrometer, MS_2. This is also the basis of the popular triple quadrupole instrument as well as those instruments employing magnetic and electrostatic analysers. Clearly, additional sectors or quadrupoles would be required for MS/MS/MS or further combinations. In contrast, in FTMS the ions are constrained in space and the experiments are carried out in time. A typical pulse-timing sequence is shown in Fig. 5. In our experiment the ion-formation pulse triggers the laser to generate metal ions. Following ion formation, a series of radio-frequency pulses (often referred to as double resonance pulses) of varied amplitude, frequency and

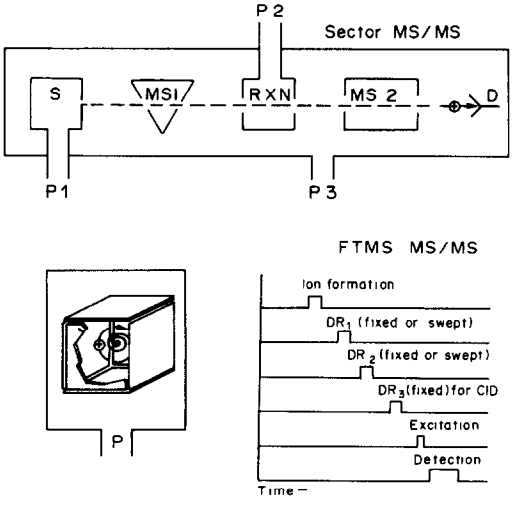

Fig. 5. Comparison of a generalized tandem mass spectrometer and a Fourier-transform mass spectrometer. Also shown is a typical FTMS pulse timing sequence.

duration occur to manipulate the ions (as discussed below), and finally a detection pulse permits a "snapshot" of the products generated. This pulse sequence is readily modified by teletype commands and, therefore, different experiments require changes only in software as opposed to hardware.

All the radiofrequency pulses are generated from a frequency synthesizer which is under computer control. This device literally calculates voltage as a function of time to achieve the desired frequency, and sends the signal to the cell. The radiofrequency from the synthesizer is used for three functions: (1) for detection as described above, (2) for ejection and (3) for collision-induced dissociation (CID). Ejection is achieved when a high-amplitude radiofrequency signal is applied at the cyclotron resonance frequency of an ion, causing its orbit to expand rapidly and resulting in the annihilation of the ion against one of the cell plates.[35,36] A single frequency can be applied to eject one ion selectively or a swept frequency can be applied to eject several ions. The spectrum shown in Fig. 6 illustrates the power of this technique to determine reactant-ion/product-ion relationships. Laser ionization of a titanium target in the presence of water vapour generates Ti^+ and TiO^+. Because titanium is such a reactive metal, it is not clear whether the TiO^+ arises from a gas phase reaction of Ti^+ with H_2O, or is being generated directly from the surface as a result of a surface reaction. Titanium has several isotopes and while the ions at m/z 46 and m/z 50 are observed, during this experiment the isotopes at m/z 47–49 are continuously ejected. Not only are these species absent from the spectrum in Fig. 6, but the corresponding oxide ions are also missing. This provides unambiguous evidence that the TiO^+ is a result of the gas phase reaction (6), and is not due to direct formation from the surface, since in the latter case ejection of Ti^+ would have had no effect on TiO^+.

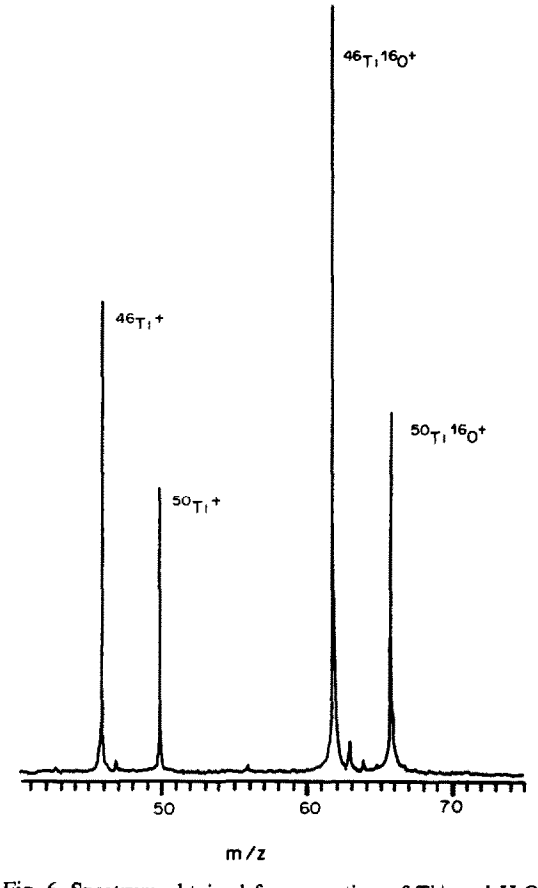

Fig. 6. Spectrum obtained from reaction of Ti^+ and H_2O.

$$Ti^+ + H_2O \rightarrow TiO^+ + H_2 \quad (6)$$

In collision-induced dissociation (CID), an ion is accelerated into a target gas, causing the ion to fragment and thus yield its mass spectrum. Collision-induced dissociation is readily accomplished in a Fourier-transform mass spectrometer by once again applying a radiofrequency pulse at the frequency appropriate for an ion of a particular mass.[37,38] With a pulse of moderate amplitude, the kinetic energy of the ion and the radius of its orbit increase at such a rate as to favour collisions with a target gas (usually argon at $\sim 5 \times 10^{-6}$ mmHg) rather than ejection. CID is one of the most powerful and certainly most widely used tools in mass spectrometry for ion-structure determination.[32–34] This technique has been particularly useful in our work, where a knowledge of the product-ion structure yields an insight into the reaction mechanism. CID, for example, was used to distinguish the four isomeric $NiC_4H_8^+$ ions generated in reactions (7)–(10).[39]

$$Ni^+ + n\text{-}C_4H_{10} \rightarrow Ni(C_2H_4)_2^+ + H_2 \quad (7)$$

$$Ni^+ + n\text{-}C_6H_{14} \rightarrow NiC_2H_5CH{=}CH_2^+ + C_2H_6 \quad (8)$$

$$Ni^+ + \begin{matrix} CH_2CH_2 \\ | \\ CH_2CH_2 \end{matrix} > CO \rightarrow \begin{matrix} CH_2CH_2 \\ | \\ CH_2CH_2 \end{matrix} > Ni^+ + CO \quad (9)$$

$$Ni^+ + (CH_3)_4C \rightarrow Ni(CH_3)_2C{=}CH_2^+ + CH_4 \quad (10)$$

As shown in Table 1, the bis-ethene product in reaction (7) loses one and two ethenes upon CID, while the butene complex in reaction (8) loses H_2 to form a stable butadiene complex, and so on. The particular significance of these results is that they provide direct evidence for initial C–C insertion as opposed to C–H insertion, in direct contrast to the behaviour observed for bare metal atoms and transition metal complexes in solution.

In addition to structure elucidation, we have found CID to be a powerful and convenient tool for synthesizing unusual ions *in situ*. We have employed this technique extensively to generate and study transition-metal atomic anions which could not be formed reproducibly or in sufficient yields by direct

Table 1. Neutral losses from CID of $NiC_4H_8^+$ complexes*†

Structure	H_2	C_2H_4	C_4H_8
$Ni(C_2H_4)_2^+$		×	×
$NiC_2H_5CH{=}CH_2^+$	×		×
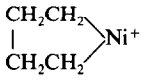	×	×	×
$Ni(CH_3)_2C{=}CH_2^+$			×

*CID fragments observed at 15 eV kinetic energy.
†Argon added to give total pressure of 1×10^{-5} mmHg.

laser ionization.[40] Figure 7 demonstrates this capability for generating Cr^-. This example shows the results of a study of $Cr(CO)_6$ which, like most metal carbonyls, has a large cross-section for dissociative electron-capture and produces a large signal for $Cr(CO)_5^-$. Next, CID results in the sequential loss of CO ligands, producing a variety of products, including Cr^-. The Cr^- is isolated by ejecting all the other species present. It is evident from Fig. 7 that there is a strong signal for Cr^- for subsequent study.

PULSED VALVE CHEMISTRY: STUDY OF MX^+ (X = LIGAND)

Thus far, the study of atomic metal-cations and anions has been discussed. A logical extension was to investigate the influence of various ligands on the chemistry observed. To perform this experiment properly, however, we needed to develop a method for manipulating the concentrations of neutral species with as much ease as we were able to manipulate the ion concentrations. Because the cell was in a single vacuum chamber, the use of differential pumping was not feasible. It become apparent, however, that since the entire experiment was pulsed, neutral gases could be pulsed in as well.[41] Figure 8 illustrates this idea. We have tried to draw an analogy between this concept and a conventional experiment in an organic or inorganic laboratory. The experiment begins with a synthesis step to generate the desired metal–ligand complex, followed by a separation step in which that ion is isolated from all others, a reaction step, and finally a product-analysis step. Thus, with this flexibility we have dubbed the FT mass spec-

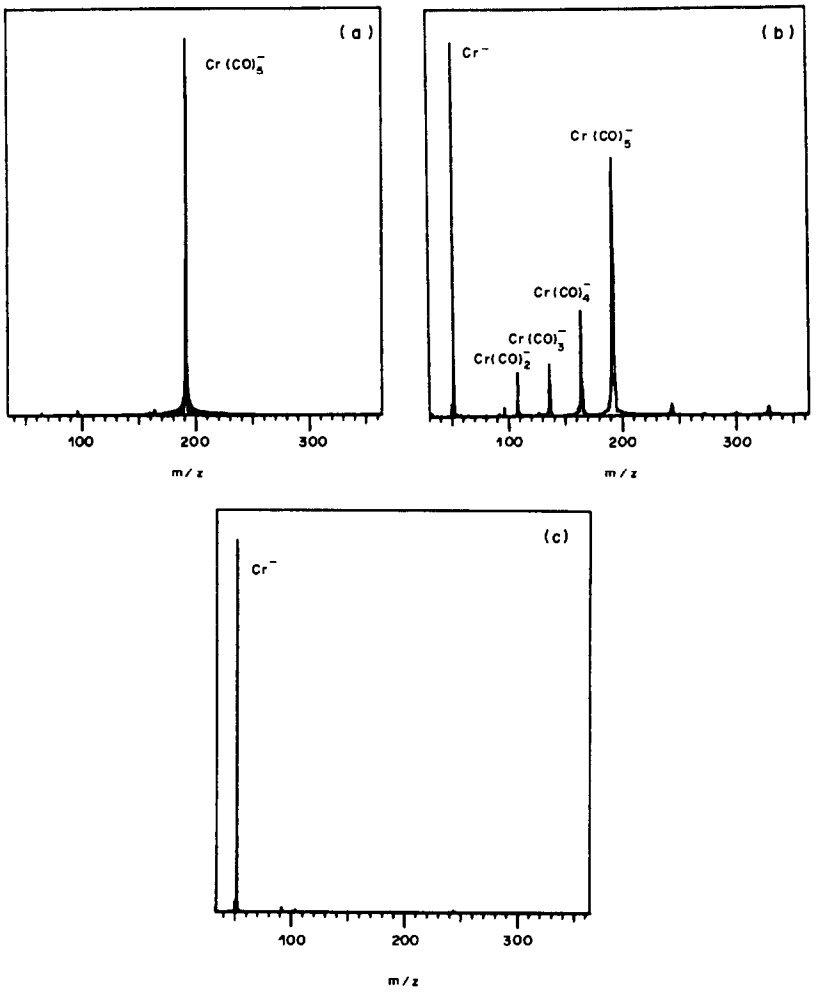

Fig. 7. Multi-step synthesis of Cr^-.[40]

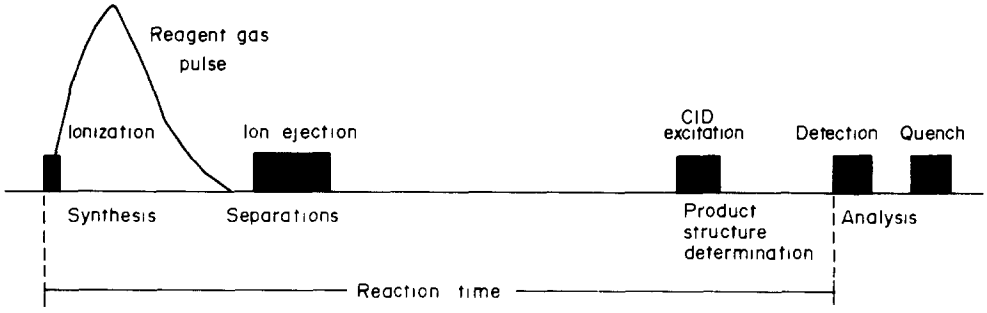

Fig. 8. Sequence of events for pulsed-valve addition of reagent gas for the FTMS experiment.

trometer "the complete gas-phase chemical laboratory".

The effect of sulphur on metal-ion reactivity is of particular interest, since sulphur has been found both to enhance and reduce the reactivity of selected catalysts. Figure 9 shows a sequence of reactions in which CoS^+ is generated and its reactions with butane are studied.[19] In the first step, ethylene sulphide is pulsed into the instrument concurrently with the laser generation of Co^+. Co^+ undergoes a series of reactions of the type shown in equation (11) to produce CoS^+, CoS_2^+, CoS_3^+ and CoS_4^+:

$$CoS_n^+ + C_2H_4S \rightarrow CoS_{n+1}^+ + C_2H_4 \; (n = 0\text{–}4) \quad (11)$$

The CoS^+ is then isolated by ejecting all the other ions present. The CoS^+ is then permitted to react with butane, reactions (12) and (13):

$$CoS^+ + \text{n-}C_4H_{10} \rightarrow CoC_4H_8^+ + H_2S \quad (12)$$

$$CoS^+ + \text{n-}C_4H_{10} \rightarrow CoC_4H_6^+ + H_2S + H_2 \quad (13)$$

By this time, all of the ethylene sulphide has been pumped out of the system, as evidenced by the absence of any polysulphide ions. Finally, the $CoC_4H_8^+$ product is isolated and collisionally activated. The products, shown in the bottom spectrum of Fig. 9, arise from the loss of H_2 and C_4H_8 and are indicative of a butene–metal ion structure. The results of this study are summarized by reactions (14)–(19).

Thus 98% of the reaction products from bare Co^+ are due to initial C–C insertion, whereas 100% of the reaction products from CoS^+ can be attributed to C–H insertion.

Figure 10 provides another striking example of multi-step chemistry using FTMS, in which NiD^+ is generated and its reactions with 2-methylpropane are studied.[42] In spectrum (*a*), CD_3ONO is pulsed into the instrument concurrently with laser generation of Ni^+. The $^{58}Ni^+$ isotope has been selected and a variety of primary and secondary reaction products are observed. Next, in spectrum (*b*), all but a selected group of ions have been ejected from the cell. In particular, one of these ions corresponds to $NiOCD_3^+$, generated by reaction (20).

$$Ni^+ + CD_3ONO \rightarrow NiOCD_3^+ + NO \quad (20)$$

Selective CID of $NiOCD_3^+$ is evidenced by its absence in spectrum (*c*) as well as the appearance of two product ions from reactions (21) and (22).

$$NiOCD_3^+ \xrightarrow[Ar]{CID} NiD^+ + CD_2O \quad (21)$$

$$NiOCD_3^+ \xrightarrow[Ar]{CID} Ni^+ + CD_2O + D \quad (22)$$

The NiD^+ is isolated, spectrum (*d*), and permitted to react with a background of 2-methylpropane, spectrum (*e*). Interestingly, the metal-containing products from reactions (23) and (24) show a complete loss of label.

$$NiD^+ + (CH_3)_2CHCH_3 \rightarrow NiC_3H_5^+ + CH_3D + H_2 \quad (23)$$

$$NiD^+ + (CH_3)_2CHCH_3 \rightarrow NiC_4H_7^+ + HD + H_2 \quad (24)$$

$$CoS^+ + \text{n-}C_4H_{10} \rightarrow Co^+C_2H_4 + C_2H_6 \quad 74\% \quad (14)$$

$$CoS^+ + \text{n-}C_4H_{10} \rightarrow Co^+C_3H_6 + CH_4 \quad 8\% \quad (15)$$

$$CoS^+ + \text{n-}C_4H_{10} \rightarrow Co^+(C_2H_4)_2 + H_2 \quad 16\% \quad (16)$$

(14)–(16): C–C process

$$CoS^+ + \text{n-}C_4H_{10} \rightarrow Co^+C_4H_8 + H_2 \quad 2\% \quad (17)$$

(17): C–H process

$$CoS^+ + \text{n-}C_4H_{10} \rightarrow Co^+C_4H_8 + H_2S \quad (18)$$

$$CoS^+ + \text{n-}C_4H_{10} \rightarrow Co^+C_4H_6 + H_2S + H_2 \quad (19)$$

(18)–(19): C–H process

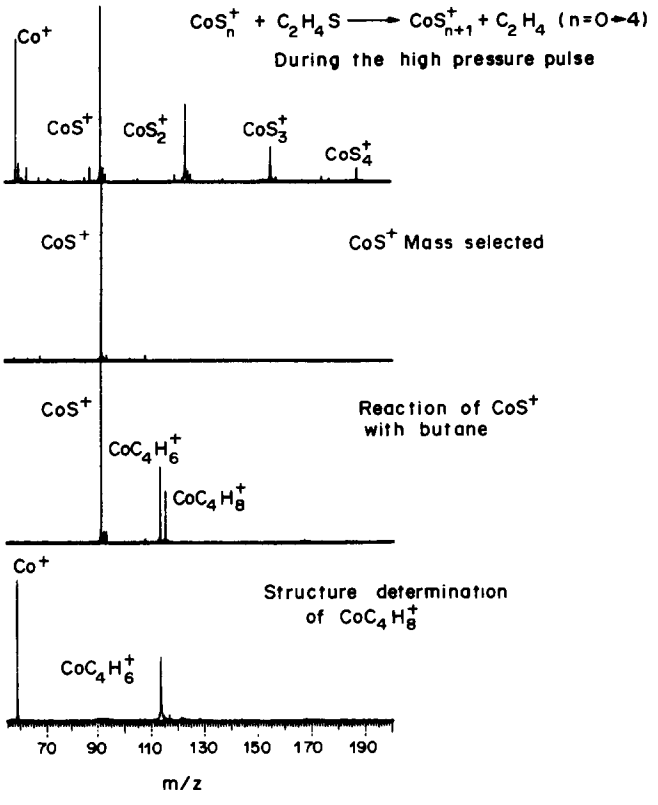

Fig. 9. Multi-step synthesis and reaction of CoS^+.[19]

It is probably fair to say that at this stage virtually any small ligand can be prepared from suitable precursors. A representative sample of some of the metal complexes of special interest that have been generated and reagent gases used, is listed in Table 2.

PHOTODISSOCIATION OF MX^+

An alternative method for obtaining structural information about ions is by examining their absorption spectra. Unfortunately, since the concentration of the ions in the trapping cell is only of the order of $10^{-20}M$, a direct absorption spectrum obviously cannot be obtained. By monitoring the disappearance of AB^+ or the appearance of A^+ in reaction (25) as a function of wavelength, however, the photodissociation spectrum of AB^+ can be derived, and this mimics the direct absorption spectrum.[43–46]

$$AB^+ + h\nu \rightarrow A^+ + B \qquad (25)$$

Table 2. Recommended reagent gases for pulsed-valve synthesis of metal-ion complexes

Metal ion complex	Reagent gas	Applicable metal ion*					
		Ti^+	V^+	Fe^+	Co^+	Ni^+	Rh^+
MO^+	oxygen	+	+				
	nitrous oxide			+			
	ozone				+	+	
MS^+	ethylene sulphide	+	+	+	+		+
	methyl mercaptan					+	
MOH^+	nitromethane			+	+		
$HMOCH_2^+$	methyl nitrite			+	+	+	
MCO^+	acetone			+	+	+	
MC^+	norbornadiene						+
MCH_2^+	1,3,5-cycloheptatriene			+	+	+	
	ethylene oxide						+
MCH_3^+	methyl iodide			+	+		
$MC_6H_6^+$	cyclohexene	+	+	+	+	+	+
$MC_4H_6^+$	butane	+	+				+
	1- and 2-butenes			+	+	+	
$MC_2H_4^+$	ethane	+					+

* + in the table indicates the simplest route known to occur with good yield; blanks indicate less efficient routes or reactions which have not been studied or do not occur.

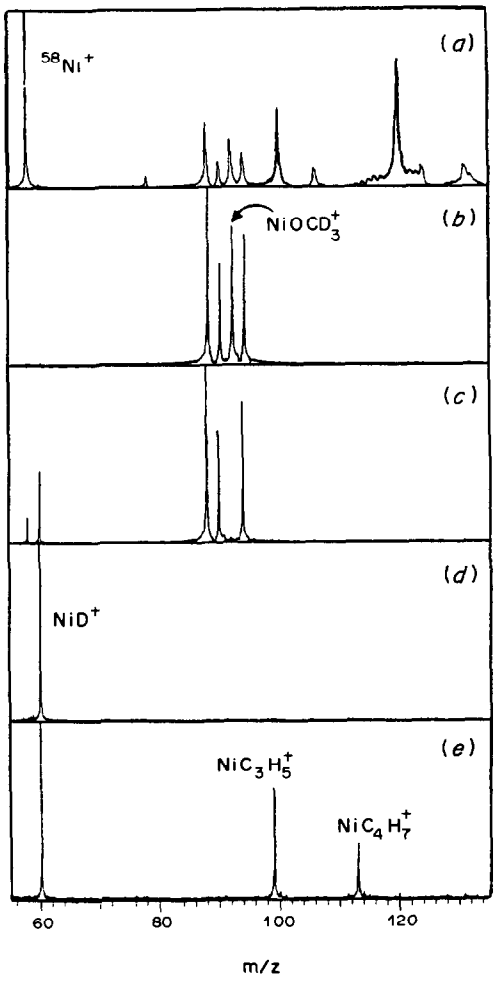

Fig. 10. Multi-step synthesis and reaction of NiD^+.

Preliminary results from our laboratory suggest that a wide variety of metal complexes will in fact photodissociate in the visible and near ultraviolet regions. Three representative examples which undergo reaction (26) are shown in Fig. 11.[47]

$$FeX^+ + h\nu \rightarrow Fe^+ + X \quad (26)$$

$$X = CO,\ C_2H_4 \text{ or } OH$$

Surprisingly, each of the spectra shows two maxima at about 290 and 340 nm, suggesting that the transitions are localized mainly on the metal. Of particular interest is the threshold observed for $FeOH^+$ at about 390 nm, not observed for the other two ions. This threshold can be attributed directly to the bond energy of Fe^+–OH. The threshold at 390 nm corresponds well to an estimated bond dissociation energy of about 76 kcal/mole. Therefore, even though the ion may absorb at longer wavelengths, the photons do not have enough energy to cause dissociation. Photodissociation of $FeCO^+$ and $FeC_2H_4^+$ at wavelengths longer than 600 nm is in accord with the fact that the bond energies are less than 40 kcal/mole.

SYNTHESIS OF MIXED-METAL CLUSTER IONS BY MS/MS/MS/MS

One of the most exciting areas in metal chemistry today is the study of small metal clusters, because of their relevance to catalysis. Despite this intense interest, relatively few studies on small metal cluster ions have appeared because of difficulties in generating and studying these species. Perhaps no other example, therefore, better illustrates the potential of FTMS than its application to the *in situ* synthesis and study of mixed-metal clusters, recently reported.[48,49] Metal ions undergo the clustering reaction (27) with $Fe(CO)_5$ in the gas phase, eliminating one or more carbonyl groups.

$$M^+ + Fe(CO)_5 \rightarrow MFe(CO)_{5-x}^+ + xCO \quad (27)$$

Subsequent CID of the product ions strips off the remaining CO groups to produce MFe^+, reaction (28).

$$MFe(CO)_{5-x}^+ \xrightarrow[-CO]{CID} MFe(CO)_{4-x}^+ \xrightarrow[-CO]{CID} \cdots \xrightarrow[-CO]{CID} MFe^+ \quad (28)$$

A similar reaction with $Co_2(CO)_8$ yields the bare trimer ion.[49] Figure 12 provides an interesting example. Spectrum (*a*) shows the reaction of Co^+ with a mixture of 1-pentene and $Fe(CO)_5$. The $CoFe(CO)_5^+$ [generated by reaction (27)] is isolated, spectrum (*b*). Subsequent application of CID [reaction (28)] and isolation of the product $CoFe^+$ results in spectrum (*c*). The $CoFe^+$ then reacts with the neutral gas mixture, but it is evident from spectrum (*d*) that it reacts more readily with 1-pentene [reactions (29) and (30)] than with $Fe(CO)_5$. One of the products, $CoFeC_{10}H_{14}^+$, is isolated, spectrum (*e*), and then collisionally activated, spectrum (*f*).

$$CoFe^+ + C_3H_7CH{=}CH_2 \rightarrow CoFeC_5H_8^+ + H_2 \quad (29)$$

$$CoFeC_5H_8^+ + C_3H_7CH{=}CH_2 \rightarrow CoFeC_{10}H_{14}^+ + 2H_2 \quad (30)$$

The products observed in reactions (31)–(33) correspond to metallocenes.

$$CoFe(C_{10}H_{14})^+ \xrightarrow[Ar]{CID} \begin{cases} CoFeC_{10}H_{10}^+ + 2H_2 & (31) \\ CoC_{10}H_{10}^+ + 2H_2 + Fe & (32) \\ FeC_{10}H_{10}^+ + 2H_2 + Co & (33) \end{cases}$$

Interestingly, the process of converting linear pentenes into cyclic products, termed dehydrocyclization, is analogous to that observed on surfaces. Finally, it is instructive to compare the simplicity of this FTMS experiment with the complications involved in performing an equivalent experiment with a generalized tandem instrument. It is clear from Fig. 13 that the final metallocene products are the result of $(MS)^4$ or MS/MS/MS/MS.

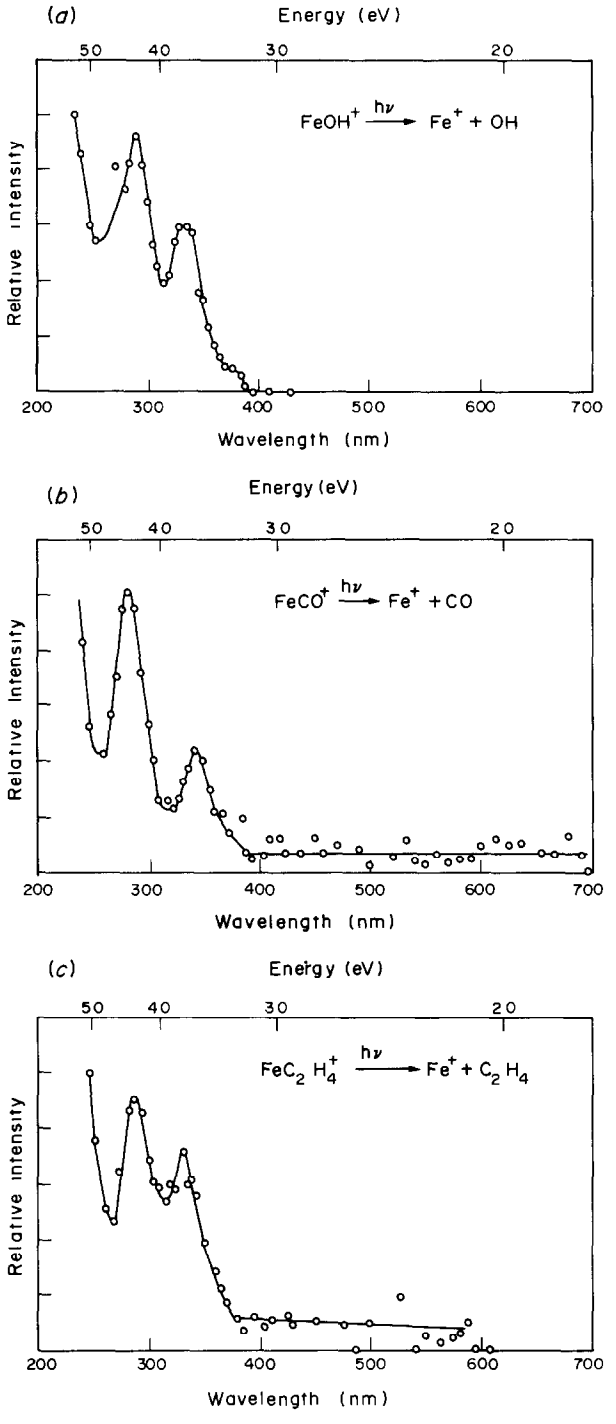

Fig. 11. Photodissociation spectra of (*a*) $FeOH^+$, (*b*) $FeCO^+$ and (*c*) $FeC_2H_4^+$.[47]

CONCLUSION

Fourier transform mass spectrometry is an emerging technology which holds tremendous potential for the future. Its unusual ability to store gaseous ions for periods of seconds, together with the ease with which both ion and neutral populations may be manipulated under computer control, makes a Fourier transform mass spectrometer a highly versatile instrument and FTMS a method of choice for studying fundamental ion-molecule reaction chemistry. In addition, the advantages of speed, signal averaging and high resolution, all bode well for the development of the instrument as a state-of-the-art analytical mass spectrometer.

The combined laser ionization–FTMS provides a convenient and powerful method of generating and studying metal ions in the gas phase. By using this

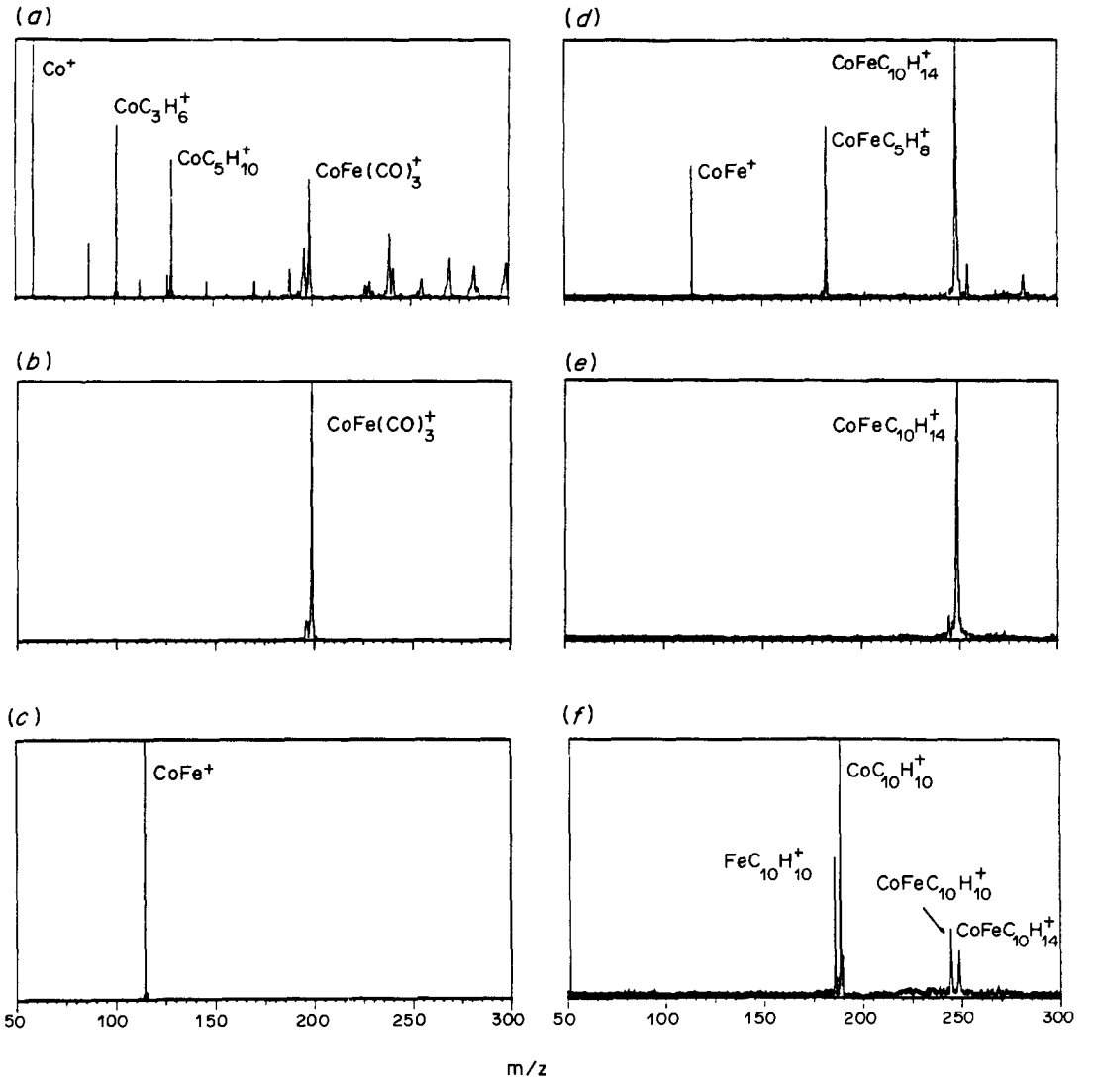

Fig. 12. Multi-step synthesis and reaction of $CoFe^+$.[48]

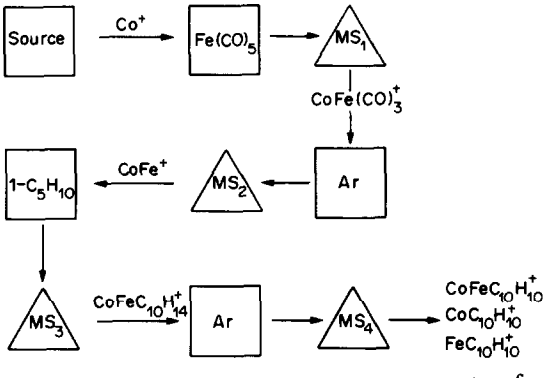

Fig. 13. Generalized tandem mass spectrometer for MS/MS/MS/MS required to perform an experiment equivalent to that shown in Fig. 12. The squares indicate collision regions and the triangles indicate sector or quadrupole mass-selectors.

technique, thermodynamic, kinetic and mechanistic information on atomic metal cations and anions, metal-ion complexes and metal-ion clusters can now be obtained. It is hoped that ultimately these studies will provide a better understanding of the fundamental controlling factors in organo–transition metal chemistry and catalysis.

Dedication—It is a personal honour and pleasure to be a part of this tribute to my father on his sixty-fifth birthday. His guidance and love, as well as his tremendous enthusiasm for chemistry, continue to be a real source of inspiration. In view of his current vigorous research programme, I look forward to writing another paper for "Papa SMRRF*" on his ninetieth birthday!

Acknowledgements—The author is indebted to the Division of Chemical Sciences in the Office of Basic Energy Sciences

*Strategic Metals Recovery Research Facility.

in the United States Department of Energy (DE-AC02-80ER10689) and to the National Science Foundation (CHE-8310039) for supporting this research.

REFERENCES

1. R. B. Cody, R. C. Burnier, W. D. Reents, Jr., T. J. Carlin, D. A. McCrery, R. K. Lengal and B. S. Freiser, *Int. J. Mass Spectrom. Ion Phys.*, 1980, **33,** 37.
2. J. R. Ready, *Effects of High-Power Laser Radiation*, Academic Press, New York, 1971.
3. K. R. Thomas, *Anal. Chem.*, 1976, **48,** 696.
4. M. A. Posthumus, P. G. Kistemaker, H. L. C. Meuzelaar and M. C. Ten Noever de Braun, *ibid.*, 1978, **50,** 985.
5. M. S. Foster and J. L. Beauchamp, *J. Am. Chem. Soc.*, 1971, **93,** 4924.
6. J. Allison and D. P. Ridge, *ibid.*, 1979, **101,** 4998.
7. P. B. Armentrout, L. F. Halle and J. L. Beauchamp, *ibid.*, 1981, **103,** 6624.
8. P. B. Armentrout and J. L. Beauchamp., *ibid.*, 1982, **103,** 6628.
9. N. Aristov and P. B. Armentrout, *ibid.*, 1984, **106,** 4065.
10. M. S. B. Munson and F. H. Field, *ibid.*, 1966, **88,** 2621.
11. A. Harrison, *Chemical Ionization*, Wiley–Interscience, New York, 1984.
12. S. Ghaderi, M. L. Gross, P. S. Kulkarni, E. B. Ledford and C. L. Wilkins, *Anal. Chem.*, 1981, **58,** 428.
13. R. C. Burnier, G. D. Byrd and B. S. Freiser, *ibid.*, 1980, **52,** 1641.
14. *Idem, J. Am. Chem. Soc.*, 1981, **103,** 4360.
15. *Idem, ibid.*, 1982, **104,** 3565.
16. G. D. Byrd and B. S. Freiser, *ibid.*, 1982, **104,** 5944.
17. T. C. Jackson, T. J. Carlin and B. S. Freiser, *ibid.*, submitted for publication.
18. M. B. Wise, *Ph.D. Thesis*, Purdue University, 1984.
19. T. J. Carlin, *Ph.D. Thesis*, Purdue University, 1983.
20. M. Lombarski and J. Allison, *Int. J. Mass Spectrom. Ion Phys.*, 1983, **49,** 281.
21. D. A. Peake and M. L. Gross, *J. Am. Chem. Soc.*, submitted for publication.
22. R. A. Forbes, M. B. Wise, S. P. Perone and B. S. Freiser, unpublished results.
23. A. Marshall and M. B. Comisarow, *Chem. Phys. Lett.*, 1974, **25,** 282.
24. T. A. Lehman and M. M. Bursey, *ICR Spectrometry*, Wiley–Interscience, New York, 1976.
25. J. L. Beauchamp, *Ann. Rev. Phys. Chem.*, 1971, **22,** 527.
26. M. B. Comisarow, *Adv. Mass Spectrom.*, 1978, **7,** 1042.
27. R. T. McIver, Jr., *Sci. Am.*, 1980, **243,** No. 5, 148.
28. C. L. Johlman, R. L. White and C. L. Wilkins, *Mass Spectrom. Rev.*, 1983, **2,** 389.
29. M. L. Gross and D. L. Rempel, *Science*, 1984, **226,** 261.
30. K. P. Wanczek, *Int. J. Mass Spectrom. Ion Phys.*, 1984, **60,** 11.
31. M. Allemann, H.-P. Kellerhals and K. P. Wanczek, *ibid.*, 1983, **46,** 193.
32. R. G. Cooks (ed.), *Collision Spectroscopy*, Plenum Press, New York, 1978.
33. F. W. McLafferty and F. M. Bockhoff, *Anal. Chem.*, 1978, **50,** 69.
34. R. A. Yost and C. G. Enke, *J. Am. Chem. Soc.*, 1978, **100,** 2274.
35. L. R. Anders, J. L. Beauchamp, R. C. Dunbar and J. D. Baldeschwieler, *J. Chem. Phys.*, 1966, **45,** 1062.
36. M. B. Comisarow, V. Grassi and G. Parisod, *Chem. Phys. Lett.*, 1978, **57,** 413.
37. R. B. Cody and B. S. Freiser, *Int. J. Mass Spectrom. Ion Phys.*, 1982, **41,** 199.
38. R. B. Cody, R. C. Burnier and B. S. Freiser, *Anal. Chem.*, 1982, **54,** 96.
39. D. B. Jacobson and B. S. Freiser, *J. Am. Chem. Soc.*, 1983, **105,** 736.
40. L. Sallans, K. Lane, R. R. Squires and B. S. Freiser, *ibid.*, 1983, **105,** 6352.
41. T. J. Carlin and B. S. Freiser, *Anal. Chem.*, 1983, **55,** 571.
42. T. J. Carlin, L. Sallans, C. J. Cassady, D. B. Jacobson and B. S. Freiser, *J. Am. Chem. Soc.*, 1983, **105,** 6320.
43. B. S. Freiser and J. L. Beauchamp, *ibid.*, 1976, **98,** 3136.
44. *Ions and Light; Gas Phase Ion Chemistry*, Vol. 3, Bowers, (ed), Academic Press, New York, 1984.
45. R. C. Dunbar, *Anal. Chem.*, 1976, **48,** 723.
46. E. W. Fu and R. C. Dunbar, *J. Am. Chem. Soc.*, 1978, **100,** 2283.
47. C. J. Cassady and B. S. Freiser, *ibid.*, 1984. **106,** 6176.
48. D. B. Jacobson and B. S. Freiser, *ibid.*, 1984, **106,** 4623.
49. *Idem, ibid.*, 1984, **106,** 5351.

Talanta, Vol. 32, No. 8B, pp. 709–722, 1985
Printed in Great Britain

0039-9140/85 $3.00 + 0.00
Pergamon Press Ltd

REFLECTIONS ON THE MODIFIED SIMPLEX—I

D. BETTERIDGE* and A. P. WADE
BP Research Centre, Chertsey Road, Sunbury-on-Thames, Middlesex, England, and
Department of Chemistry, University College, Singleton Park, Swansea, Wales

and

A. G. HOWARD
Department of Chemistry, University of Southampton, Highfield, Southampton, England

(*Received* 17 *December* 1984. *Accepted* (5 *March* 1985)

Summary—The modified simplex method is a well-known method of optimization. In this study several changes have been made to it. These include an adaptive weighted centroid and a Lagrange interpolation procedure. The latter is used to get a better value of the reflected point when a contraction succeeds or an expansion fails. The new method, called the composite modified simplex method (CMS) has been rigorously evaluated by means of mathematical functions, maps and chemical experimentation. The effect of the starting point and the size of the simplex have been investigated in detail. For flow-injection analysis it has proved possible to optimize 2–12 variables. The method has proved most suitable for rapid and effective optimization of polarography, flow-injection analysis and chemical synthesis. This paper describes the evaluation procedures and reviews the results obtained.

The simplex method of optimization, devised by Spendley *et al.*[1] and later modified by Nelder and Mead,[2] has proved of great value to analytical chemists, as shown by the many studies[3] which have followed the early work of Long[4] and Morgan and Deming.[5] The basic method is not completely satisfactory, however, as is evidenced by the number of proposals for further modification.[6–20] We have developed and evaluated a simplex algorithm which combines many of the modifications previously proposed, and described it here. Because it is difficult to arrive at acceptable criteria for evaluation of a method of optimization as general as the modified simplex, three different methods of evaluation have been employed.

The first uses mathematical formulae. This procedure is commonly used as the basis of evaluation. It has the advantage that it is exact and rapid, but the disadvantage that it has no experimental basis, is usually free from noise, and is difficult to visualise.

The second makes use of contour maps and thus has a high visual content, but is limited to two variables.

The third is an experimental evaluation based on chemical systems such as polarography, synthesis, and especially flow-injection analysis (FIA). This last is a very versatile form of continuous-flow analysis which can simulate many process systems and in which the number of variables studied can be altered with ease. In this study 2–12 variables have been used.

A common problem in this area is drawing general conclusions from too few systems. It is hoped that by use of such a large variety of response surfaces this difficulty will be minimized.

The paper is presented in two parts. The first gives an account of the chemical experiments and mathematical tests which have been used to evaluate the algorithm, and the second critically discusses the various modifications of the simplex method which have been proposed and compares the simplex method with other optimization procedures.

EXPERIMENTAL

Composite modified simplex method

The method used in this work is based on that of Nelder and Mead,[2] but includes some of the better modifications suggested recently and also a few that we have found advantageous. It is called the composite modified simplex (CMS), or referred to by the program name "OPTIMA". It has been implemented on a number of microcomputers, in particular the Commodore PET, APPLE and CP/M machines.

The algorithm employed is shown in Fig. 1. A detailed consideration of it is deferred to Part II.†

METHODS OF EVALUATION OF CMS

Use of mathematical functions. The performance of the CMS was investigated by applying it to the maximization of a number of functions, some of which had been used by other workers.[7,8] The functions are of a type that can be solved by iteration. The role of the simplex procedure is to reduce the number of iterative steps required. It follows that the final result depends critically on the initial estimates of the terms of the function. However, since the optimization procedure for a function is purely computational, it is possible to perform numerous optimizations from different starting points without taking up much time. In all, 500 optimizations were performed for each function. Simplex sizes of 50, 20, 10, 5 and 2.5% of the specified search domains, and variable ranges were used, 100 optimizations from different starting points being done for each size. The

*Author for correspondence.
†*Talanta*, 1985, **32**, 723.

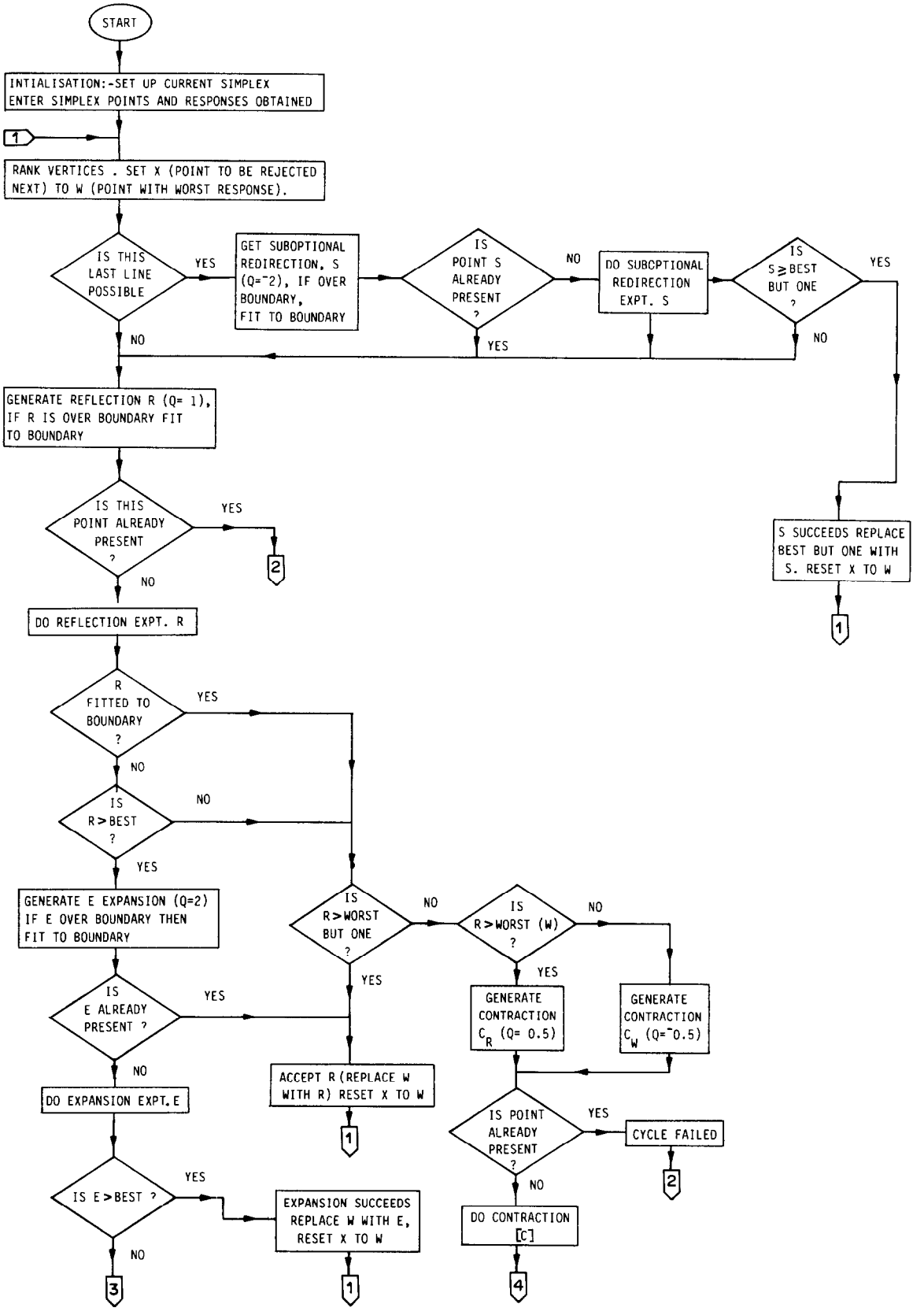
START
INTIALISATION:-SET UP CURRENT SIMPLEX ENTER SIMPLEX POINTS AND RESPONSES OBTAINED
1
RANK VERTICES . SET X (POINT TO BE REJECTED NEXT) TO W (POINT WITH WORST RESPONSE).
IS THIS LAST LINE POSSIBLE
YES
GET SUBOPTIONAL REDIRECTION, S (Q=⁻2), IF OVER BOUNDARY, FIT TO BOUNDARY
IS POINT S ALREADY PRESENT ?
NO
YES
DO SUBOPTIONAL REDIRECTION EXPT. S
IS S ≥ BEST BUT ONE ?
YES
NO
NO
GENERATE REFLECTION R (Q= 1), IF R IS OVER BOUNDARY FIT TO BOUNDARY
IS THIS POINT ALREADY PRESENT ?
YES
2
NO
S SUCCEEDS REPLACE BEST BUT ONE WITH S. RESET X TO W
1
DO REFLECTION EXPT. R
R FITTED TO BOUNDARY ?
YES
NO
IS R > BEST ?
NO
YES
GENERATE E EXPANSION (Q=2) IF E OVER BOUNDARY THEN FIT TO BOUNDARY
IS R > WORST BUT ONE ?
NO
IS R > WORST (W) ?
NO
YES
YES
GENERATE CONTRACTION C_R (Q= 0.5)
GENERATE CONTRACTION C_W (Q=⁻0.5)
IS E ALREADY PRESENT ?
YES
NO
ACCEPT R (REPLACE W WITH R) RESET X TO W
1
DO EXPANSION EXPT. E
IS POINT ALREADY PRESENT ?
YES
CYCLE FAILED
2
NO
IS E > BEST ?
YES
NO
EXPANSION SUCCEEDS REPLACE W WITH E, RESET X TO W
1
DO CONTRACTION [C]
4
3

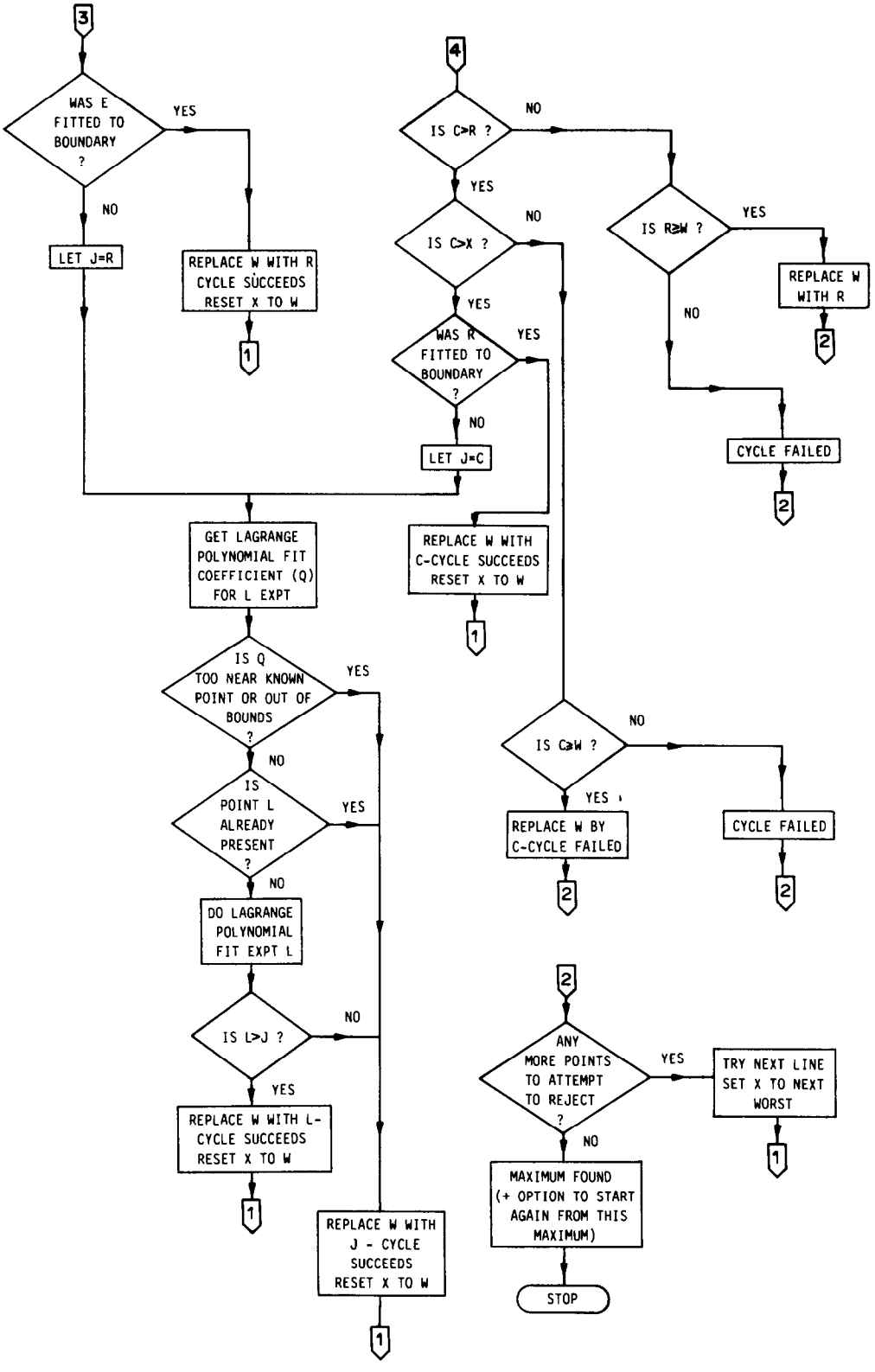

Fig. 1. Flow diagram of the CMS method—the OPTIMA program.

best response obtained after 20 and 40 experiments was noted for each function optimization. Other workers have rejected or omitted the results of some optimizations from their findings, to simplify the mathematical analysis of their methods.[7,8] In this paper, all results obtained are included.

Since the current CMS version maximizes the response of systems, and other workers[7,8] used minimizing algorithms, we used the negative of some of the functions (marked "min"). All functions were scaled so as to give a percentage response, R, which was 0% for the worst case and 100% for the best case (optimum). This allowed easy comparison of the performance of the algorithm for the various surfaces and can be related more directly to the requirements of chemical optimizations, namely reliability and rapid approach to the optimum. The transform used was:—

$$R(\%) = 100[F(\text{worst}) - F(i)]/[F(\text{worst}) - F(\text{best})]$$

where F(worst) is the worst value of the function within the allowed ranges of the variables, F(best) the optimum value, and $F(i)$ the value for the ith simplex point.

In the rare event that the simplex became trapped in an unfavourable orientation and a direction for further improvement could not be found, the optimization was terminated. If this occurred before the preset number of experiments had been completed, the simplex was restarted from the best point obtained up till then by using the initial simplex size, and run for the remaining number of experiments. If more than one termination occurred, then the simplex size used was halved so as to prevent reinvestigation of the same series of points.

The functions used were as follows.

(1) *A 2-variable paraboloid*[7,8]

$$Y = X_1^2 + X_2^2$$

$$-1000 \leqslant X_1, X_2 \leqslant 1000$$

(2) *A least-squares function*[7,8,21]

A_i and t_i are a set of experimental data given in Morgan and Deming's paper[17]

$$(\text{min})\ Y = \sum_{i=1}^{18} (A_i - X_1(1 - \exp[-X_2 t_i])^2$$

$$0 \leqslant X_1, X_2 \leqq 2$$

(3) *Rosenbrock's valley*[7,8,21]

$$(\text{min})\ Y = 100(X_2 - X_1^2)^2 + (1 - X_1)^2$$

$$-25 \leqslant X_1, X_2 \leqslant 25$$

(4) *A modification of Fletcher and Powell's helical valley*[8,22]

$$(\text{min})\ Y = 100(X_1 - 10\theta)^2 + (\sqrt{X_1^2 + X_2^2} - 1)^2 + X_2^2$$

$$-100 \leqslant X_1, X_2 \leqslant 100$$

$$X > 0\text{: } \theta = (1/2\pi)\tan^{-1}(X_2/X_1)$$

$$X < 0\text{: } \theta = (1/2\pi)[\pi + \tan^{-1}(X_2/X_1)]$$

(5) *A 5-variable paraboloid*[7,8]

$$(\text{min})\ Y = \sum_{i=1}^{5} X_i^2$$

$$-5 \leqslant X_i \leqslant 5$$

(6) *A sharp straight rising ridge*

This function is similar to the flame-ionization detector response surface obtained experimentally by Routh *et al.*[6] Other workers have applied an interpolation procedure to the experimental data.[7,8]

$$X \leqslant 6\text{: (max) } Y = \sqrt{7(6 - X_1)^2 + X_2^2}$$

$$X > 6\text{: (max) } Y = X_1 + X_2 - 6$$

$$0 \leqslant X_1, X_2 \leqslant 25$$

(7) *A complex surface with three equal maxima, as given by Himmelblau.*[14]

$$(\text{min})\ Y = (X_1^2 + X_2 - 11) + (X_1 + X_2^2 - 7)$$

$$-5 \leqslant X_1, X_2 \leqslant 5$$

(8) *A 10-variable constant-gradient system*

$$(\text{max})\ Y = \sum_{i=1}^{10} X_i$$

$$0 \leqslant X_i \leqslant 10$$

Use of contour maps. Mount Egmont, New Zealand (Fig. 2) was chosen as a test surface. Its volcanic origin has given it properties which are ideally suited to this application, namely (*i*) it is well defined and fairly smooth, (*ii*) it has one main maximum (8260 ft) with a suboptimal maximum (subsidiary top, 4590 ft) to the north-west of this, and (*iii*) there are several features (knolls, cliffs, river beds *etc.*) which would have a similar effect on the algorithm as that of "noise" or operator error in a chemical optimization. Maps and photographs were readily available.

The search was restricted to the area bounded by grid references 400400, 400700, 900400, 900700, and the precision of measurement in each variable (latitude and longitude) was taken as 1 unit in east or north co-ordinates (*i.e.* 1/10 of the side of a grid square). The optimum was therefore one point in 150000. Optimizations were started from a randomly chosen point (490423) situated on the lowland to the south-west of the main peak. Both the starting point and the suboptimal maximum therefore lay to the west of the main peak. Simplex sizes of between 50% and 2.5% of the specified ranges were used. The "response" optimized was height.

Where a point fell between two contour lines the height was estimated by interpolation, taking appropriate account of any local features.

For comparison, several univariate optimizations were performed, as were optimizations by earlier versions of the CMS algorithm, and by the CMS algorithm with some modifications removed.

Use of chemical systems. Four analytical systems of widely different types were selected and optimized.

(1) *Optimization of the sensitivity of the catalytic wave of the uranium(VI)/nitrate system*[23,24]

Polarograms for uranium(VI) in the presence of various concentrations of nitric and hydrochloric acids were obtained with a Radiometer PO-4 polarograph. Table 1 shows the initial data entered into the microcomputer to start the simplex operation.

For each experiment the potential was varied from −0.6 to −1.8 V, the working solution being $10^{-6}M$ uranium(VI) solution with hydrochloric and nitric acid concentrations as requested by the modified simplex program.

Improvement in sensitivity alone was not sufficient as an optimization criterion since, under the more acidic of the conditions tried, the definition of the uranyl catalytic wave became unacceptable: the uranyl wave became partially merged with the hydrogen discharge wave. Figure 3 shows some waves typical of those obtained. Waves 2 (flat limiting current) and 3 (peak formation) are well defined, and would be suitable for an analytical method. Wave 17, on the other hand, while more sensitive, is poorly defined and unacceptable. Clearly a wave-definition weighting factor had to be included in the optimization criteria.

The response function chosen was $R = h\cos(s)$ where h is the height of the catalytic wave and s the angle between the horizontal and the tangent to the top of the wave. For waves 2 and 3, $s = 0$ and $\cos(s) = 1$, giving $R = h$. For wave 17, $s > 0$ and $\cos(s) < 1$, therefore $R < h$, and the function discriminates against this poorly defined wave.

(2) *Optimization of the reaction between PAR and permanganate (4 variables)*[24]

Fig. 2. Mount Egmont, New Zealand (8260 ft).

In an earlier study[25] it had been noted that there is a colour-forming reaction between PAR and permanganate. The mechanism of the reaction was unclear and the conditions under which it took place were ill-defined. It was decided to investigate the optimum conditions for the reaction.

The four variables studied were reaction time, PAR concentration, pH and temperature. Various sets of these experimental conditions were tried, generated by the modified simplex optimization program. The optimization was for maximum sensitivity (absorbance) and was started from the best set of conditions found previously.

A phosphate buffer solution (0.667*M*) of the required pH was prepared by using an appropriate combination of phosphate and phosphoric acid solutions. A PAR working solution ($0–10^{-3}M$) was prepared by appropriate dilution of a $10^{-3}M$ stock solution. The test solution used was composed of 10 ml of $10^{-4}M$ permanganate, 10 ml of phosphate buffer and 10 ml of PAR working solution. The blank solution was the same as the test solution, but with 10 ml of distilled water instead of the permanganate solution.

When the solutions were at the required temperature the PAR solution was added to the permanganate plus buffer and the timing started. As closely as possible to the time requested by the modified simplex program the absorbance was measured at 500 nm, and the time elapsed from the PAR addition was noted. Finally the pH was checked again. These values, and the absorbance obtained, were entered into the microcomputer, and the conditions for the next experiment were generated by the program.

(3) *Optimization of the FIA determination of isoprenaline (4 and 5 variables)*[26]

The oxidation of isoprenaline by ferricyanide, which forms the basis of a manual spectrophotometric determination of isoprenaline, was adapted to a flow-injection analysis system and optimized. The experimental work for this system has been reported in detail elsewhere.[26]

Table 1. Initial data required by the OPTIMA program for optimization of the catalytic wave of the uranium(VI)/nitrate system

Variable	From	To	Precision	%	Origin
$[HNO_3]$	0	100m*M*	0.1m*M*	5	2.0m*M*
[HCl]	0	100m*M*	0.1m*M*	5	10.4m*M*

(4) *Optimization of the solvent extraction/FIA determination of uranium(VI) (12 variables)*

The system investigated was the flow-injection analysis of solutions of uranium ore, in which uranium(VI) is extracted from the ore solution with tributyl phosphate, and then reacted with PAN after suitable changes in the pH have been made. The procedure is based on the one described by Baban[27] and is similar to that reported by Lynch *et al.*[28] An important practical difference was the use of a displacement method for pumping the organic solvent.

The apparatus was set up as in Fig. 4. A carrier stream of concentrated aluminium nitrate solution, propelled by a peristaltic pump, was divided at a T-piece. One stream then passed through the sample valve, where the sample was injected into it. The other stream by-passed the valve, and passed through a coil before rejoining the sample-containing line at a second T-piece. This arrangement ensured uniform mixing of nitrate and injected sample, and minimized the pulsation effect of switching the valve.

A stream of tributyl phosphate (TBP) in chloroform then joined the sample stream at another T-junction. The TBP stream was propelled by the same peristaltic pump as the nitrate, but through a displacement tank. (This allowed the organic stream to be pumped with standard tubes, which would otherwise be attacked by the organic solvents.)

The aqueous and organic solutions are immiscible, so a segmented aqueous/organic stream resulted. This passed through a second coil, where the selective solvent extraction of uranium(VI) into the organic phase took place.

The segmented stream then passed on to the separator, which was as designed by Cockshott *et al.*[29] and used by Baban.[27] The aqueous component was bled off to waste, a needle valve being used to control the aqueous flow, as suggested by Rowles.[30] In analytical practice, interfering metals also pass to waste in the aqueous stream.

The organic phase, containing the uranium(VI)–TBP complex, then continued on and mixed with the colour-forming reagent solution, of PAN in pyridine and chloroform, which was directly pumped by a second peristaltic pump using "Acidflex" tubing resistant to organic solvent.

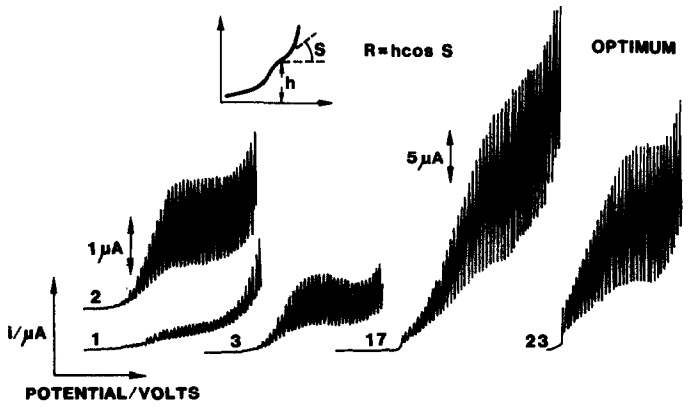

Fig. 3. Catalytic polarographic waves from the optimization of the uranium(VI)/nitrate system. Points 1–3 show the initial simplex, point 17 a loss of definition, and point 23 the final optimum.

The stream then entered a third coil, in which the colour-forming reaction took place.

The coloured PAN–uranium(VI) complex was detected photometrically at 565 nm, downstream of the coil, with an inexpensive light-emitting diode/phototransistor type of flow-through detector.[31]

The system was optimized for 12 variables. It is important in modified simplex methods to specify the limits of experimental precision accurately, and to maintain them during the experimentation. Consideration of 12 variables and the concomitant large number of experiments indicated the need for extra special experimental care.

RESULTS

Mathematical functions

Table 2 summarizes the performance of the CMS for each initial simplex size and for each mathematical function. It shows the values for the best points obtained by individual optimizations after 20 and 40 "experiments" (evaluations). Each row in the table shows the complete spread and distribution of "best" responses found for that simplex size of the function. As stated earlier, the responses shown are scaled percentage optimum values.

It can be seen that for all 8 functions (a total of 4000 optimizations), and in virtually all cases, the CMS procedure reached nearly 100% response within the allowed number of experiments.

Contour maps

The results of the five optimizations by the CMS are given in Table 3. In each case the optimum was found. The 20% simplex size optimization became attached to the suboptimal maximum. The algorithm terminated, restarted and brought the simplex back to the main peak.

The results of several univariate optimizations are given in Table 4. If, as is common practice in laboratory optimizations, each variable is considered once only, then the maximum heights found are 900–1100 ft. Moreover, analysis of the full set of results would leave the user none the wiser as to the existence of either major peak. If an iterative uni-

Table 2. Results of mathematical function optimizations; values shown are % of optimum for respective surfaces and limits; columns marked with an asterisk show that, *e.g.*, 50 of the 100 optimizations gave best values ≥ the % optimum shown.

2.1 *Optimization of a 2-variable paraboloid*

After 20 experiments

Initial simplex size, %	Distribution of best values obtained for 100 optimizations					
	Best	50 ≥ *	90 ≥ *	95 ≥ *	99 ≥ *	Worst
50	99.999 997	99.99	99.95	99.9	99.8	99.8
20	100	99.99	99.92	99.8	99.5	99.4
10	99.999 99	99.99	99.5	98.5	97.5	97.2
5	99.999 999	99.97	99.1	98.5	94.8	92.6
2.5	99.999 999	99.5	95.4	92.9	88.1	85.9

After 40 experiments

Initial simplex size, %	Distribution of best values obtained for 100 optimizations					
	Best	50 ≥ *	90 ≥ *	95 ≥ *	99 ≥ *	Worst
50	100	99.999 996	99.999 8	99.999	99.99	99.98
20	100	99.999 996	99.999 7	99.999	99.7	99.7
10	100	99.999 99	99.998	99.99	99.96	99.8
5	100	99.999 98	99.996	99.99	99.97	99.9
2.5	100	99.999 6	99.95	99.9	98.5	94.0

Table 2. (cont.)

2.2 *Optimization of a least-squares function*

After 20 experiments

Initial simple size, %	Distribution of best values obtained for 100 optimizations					
	Best	50 ≥ *	90 ≥ *	95 ≥ *	99 ≥ *	Worst
50	99.999 7	99.9	99.8	99.7	99.7	96.9
20	99.999 8	99.8	99.7	99.7	96.9	96.9
10	99.999 98	99.8	99.7	96.9	96.9	96.9
5	99.999 99	99.8	99.7	99.7	96.9	96.9
2.5	99.999 95	99.8	99.7	99.7	99.6	96.9

After 40 experiments

Initial simple size, %	Distribution of best values obtained for 100 optimizations					
	Best	50 ≥ *	90 ≥ *	95 ≥ *	99 ≥ *	Worst
50	99.999 99	99.99	99.9	99.7	99.7	96.9
20	99.999 993	99.98	99.8	99.7	96.9	96.9
10	99.999 995	99.98	99.8	96.9	96.9	96.9
5	99.999 995	99.94	99.8	99.7	96.9	96.9
2.5	99.999 995	99.9	99.7	99.7	99.7	96.9

2.3 *Optimization of Rosenbrock's valley*

After 20 experiments

Initial simple size, %	Distribution of best values obtained for 100 optimizations					
	Best	50 ≥ *	90 ≥ *	95 ≥ *	99 ≥ *	Worst
50	99.999 998	99.999 95	99.999	99.998	99.995	99.992
20	100	99.999 92	99.998	99.994	99.95	99.95
10	100	99.999 9	99.99	99.94	99.93	99.93
5	100	99.999 8	99.97	99.94	99.93	99.91
2.5	99.999 999 2	99.999	99.96	99.92	99.9	99.9

After 40 experiments

Initial simple size, %	Distribution of best values obtained for 100 optimizations					
	Best	50 ≥ *	90 ≥ *	95 ≥ *	99 ≥ *	Worst
50	100	99.999 98	99.999 7	99.999 3	99.996	99.996
20	100	99.999 98	99.999 7	99.999 3	99.997	99.997
10	100	99.999 99	99.999 8	99.997	99.94	99.94
5	100	99.999 99	99.999 95	99.999 3	99.998	99.98
2.5	100	99.999 99	99.999 9	99.999	99.97	99.94

2.4 *Optimization of modified Fletcher and Powell's helical valley*

After 20 experiments

Initial simple size, %	Distribution of best values obtained for 100 optimizations					
	Best	50 ≥ *	90 ≥ *	95 ≥ *	99 ≥ *	Worst
50	99.999 9	99.97	99.8	99.7	99.6	99.6
20	99.999 1	99.96	99.6	99.4	99.3	99.2
10	99.999	99.9	99.3	99.2	99.0	99.0
5	99.997	99.8	99.1	99.0	98.7	98.7
2.5	99.999 95	99.7	98.9	98.8	98.7	98.4

After 40 experiments

Initial simple size, %	Distribution of best values obtained for 100 optimizations					
	Best	50 ≥ *	90 ≥ *	95 ≥ *	99 ≥ *	Worst
50	99.999 94	99.999	99.97	99.92	99.8	99.8
20	99.999 996	99.997	99.97	99.95	99.6	99.4
10	99.999 98	99.996	99.9	99.7	99.1	99.0
5	99.999 96	99.995	99.8	99.7	99.5	99.1
2.5	99.999 95	99.99	99.4	99.1	98.8	98.8

Table 2. (cont.)

2.5 *Optimization of 5-variable paraboloid*

After 20 experiments

Initial simple size, %	Distribution of best values obtained for 100 optimizations					
	Best	50 ≥ *	90 ≥ *	95 ≥ *	99 ≥ *	Worst
50	99.8	98.8	97.2	96.9	96.1	95.9
20	99.8	97.4	94.5	92.6	88.6	88.0
10	99.8	97.2	94.2	91.4	86.8	85.4
5	99.8	97.4	92.1	90.8	86.8	86.6
2.5	99.8	96.8	91.1	89.4	85.0	83.9

After 40 experiments

Initial simple size, %	Distribution of best values obtained for 100 optimizations					
	Best	50 ≥ *	90 ≥ *	95 ≥ *	99 ≥ *	Worst
50	99.99	99.9	99.7	99.5	99.4	98.7
20	99.99	99.4	98.5	97.5	94.4	94.2
10	99.93	98.5	95.8	93.8	90.8	88.7
5	99.9	97.8	93.1	92.2	87.7	87.2
2.5	99.8	97.1	91.4	90.5	86.5	85.3

2.6 *Optimization of a sharp rising ridge*

After 20 experiments

Initial simple size, %	Distribution of best values obtained for 100 optimizations					
	Best	50 ≥ *	90 ≥ *	95 ≥ *	99 ≥ *	Worst
50	99.99	99.3	95.4	93.9	87.0	86.4
20	99.999	99.5	98.1	97.4	94.5	94.1
10	99.997	99.3	96.6	95.7	87.3	84.8
5	99.98	98.8	95.0	93.6	78.3	74.0
2.5	99.994	98.3	87.3	80.3	75.3	64.6

After 40 experiments

Initial simple size, %	Distribution of best values obtained for 100 optimizations					
	Best	50 ≥ *	90 ≥ *	95 ≥ *	99 ≥ *	Worst
50	99.999 97	99.992	98.8	97.2	95.8	92.9
20	99.999 9	99.98	99.3	99.1	96.3	94.1
10	99.999 7	99.99	99.5	98.3	94.5	88.1
5	99.999 998	99.98	99.1	98.1	96.2	95.9
2.5	99.999 8	99.97	98.1	96.1	88.9	88.4

2.7 *Optimization of a complex surface with three equal maxima*

After 20 experiments

Initial simple size, %	Distribution of best values obtained for 100 optimizations					
	Best	50 ≥ *	90 ≥ *	95 ≥ *	99 ≥ *	Worst
50	99.994	99.3	95.4	93.3	92.5	90.4
20	99.999 4	99.92	98.9	96.5	93.8	93.8
10	99.999 92	99.98	99.2	98.7	96.3	94.9
5	99.999 93	99.95	97.0	96.2	92.3	90.3
2.5	99.999 9	99.9	98.2	94.6	89.1	88.7

After 40 experiments

Initial simple size, %	Distribution of best values obtained for 100 optimizations					
	Best	50 ≥ *	90 ≥ *	95 ≥ *	99 ≥ *	Worst
50	99.999 997	99.97	99.1	98.0	97.7	97.0
20	100	99.999 6	99.9	99.7	99.1	98.7
10	100	99.999 96	99.96	99.92	99.4	96.1
5	100	99.999 9	99.99	99.93	98.9	96.6
2.5	100	99.999 8	99.8	99.1	89.8	88.8

Table 2. (cont.)
2.8 *Optimization of a 10-variable constant gradient system*

After 20 experiments

Initial simple size, %	Distribution of best values obtained for 100 optimizations					
	Best	50 ≥ *	90 ≥ *	95 ≥ *	99 ≥ *	Worst
50	100	100	100	99.8	96.3	96.0
20	100	97.4	92.7	91.4	89.7	86.8
10	88.5	79.2	71.0	68.3	65.6	65.2
5	82.0	63.8	54.5	52.6	45.9	42.5
2.5	75.4	57.8	46.1	43.0	35.6	31.2

After 40 experiments

Initial simple size, %	Distribution of best values obtained for 100 optimizations					
	Best	50 ≥ *	90 ≥ *	95 ≥ *	99 ≥ *	Worst
50	100	100	100	100	99.7	99.7
20	100	100	100	100	100	99.993
10	100	100	100	100	100	100
5	100	100	100	100	99.999 8	99.999 6
2.5	100	100	100	100	100	99.999

variate approach is taken, then matters improve somewhat, giving best values of 2850, 7250 and 7250 ft. These are still substantially lower than the true maximum (8260 ft).

This very limited study indicates that the univariate approach is ill-suited to this surface and inferior to multivariate methods. This is in agreement with the findings of a comparison of 4- and 5-variable FIA systems.[26]

In a limited study with Mt. Egmont as a test surface, previous versions of the CMS, and those with modifications removed, all proved to be less reliable in obtaining the optimum and did not exhibit any substantially faster rate of climb. Removal of the Lagrange fit led to a definite loss in performance. For brevity, these results and the versions used are not discussed here.

Chemical systems

(1) *The polarographic analysis*

Figure 3 showed the points of the initial simplex (points 1–3), a large but poorly defined wave (point 17) and the best wave found (point 23). The full set of results is given in Table 5 and plotted as a three-dimensional graph in Fig. 5. This shows the response surface to have its maximum on a very sharp diagonal ridge.

The response obtained rose from 12 mm (point 1) to 610 mm (point 23). In all, 26 experiments were performed.

(2) *The PAR/permanganate reaction*

Table 6 shows the 15 experiments done. Points 1–5 are the initial simplex. The response (product absorbance) rose from 0.065 (point 1) to 0.435 (point 11).

Table 3. Climbing Mt. Egmont (8260 ft) by CMS: heights (*ft*) obtained after various numbers of experiments for several initial simplex sizes

Initial simplex size, %	No. of experiments								
	10	20	30	40	50	60	70	to reach summit	to terminate algorithm
50	5500	7000	7900	8260	—	—	—	35	44
20	1850	4100	4500*	6500	7700	8100	8260	66	71
10	1030	3250	6000	6000	8000	8260	—	56	64
5	1900	1900	3400	7100	8000	8260	—	57	62
2.5	680	1250	4500	7800	8000	8260	—	57	66

*Simplex found sub-optimal maximum first.

Table 4. Climbing Mt. Egmont (8260 ft) by the iterative univariate method: heights (*ft*) obtained after various numbers of experiments for several step sizes

Step size %	No. of experiments						Best height obtained	(no. of experiments)
	10	20	30	40	50	60		
20	900*	2850	—	—	—	—	2850	(13)
10	700	900*	4500	7250	7250	—	7250	(38)
5	600	700	920	1100*	3800	6100	7250	(100)

*Maximum peak heights that would have been obtained in a standard univariate optimization with each variable considered once only.

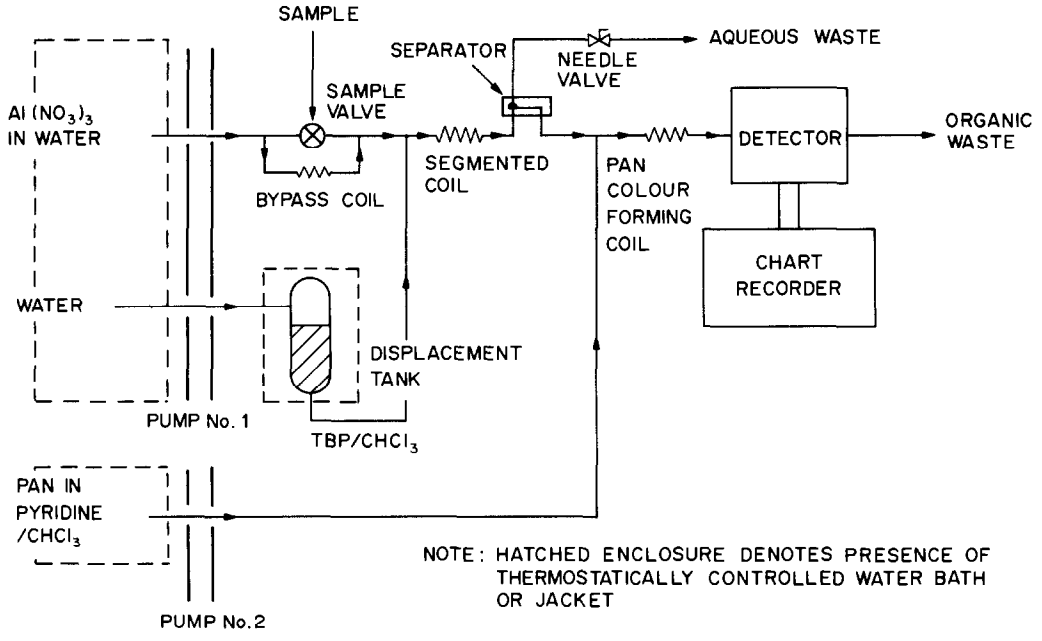

Fig. 4. Apparatus used for the optimization of uranium(VI) determination by FIA, including a solvent extraction stage.

(3) *The isoprenaline FIA system*

When four variables (reaction-coil length, flow-rate, pH and reagent concentration) were taken into account, the response rose from 35 mm to 168 mm in 34 experiments. When a fifth variable (sample size) was included, and the optimization restarted from the original conditions, the response rose from 35 mm to 192 mm in 37 experiments. Studies using the iterative univariate method of optimization, starting from the same conditions, took 88 and 168 experiments respectively to achieve the same improvement.

The full data sets for the four optimizations are given elsewhere.[26] The rate of approach to the optimum and the sequential decrease in the standard deviation of the peak heights of the current simplex are illustrated in Fig. 6.

Table 5

Expt. no.	Cycle	Operation	$[HNO_3]$, *m*M	[HCl], *m*M	Response, *mm*	Best, *mm*
1	1	Origin	2.0	10.4	12	12
2			7.0	10.4	75	
3			4.5	14.7	24	75
4	2	Reflection	10.8	12.5	125	
4		Expansion	15.2	13.5	216	216
6	3	Reflection	21.7	10.7	108	
7	4	Reflection	27.7	14.7	90	
8		Contraction	22.6	13.7	71	
9	5	Reflection	4.5	14.7	24	
10		Contraction	17.4	11.7	360	360
11	6	Reflection	11.4	14.1	150	
12		Contraction	14.0	13.2	260	
13	7	Reflection	16.7	11.2	248	
14		Contraction	16.4	11.7	320	
15	8	Reflection	19.9	10.2	362	
16		Expansion	22.8	8.7	530	530
17	9	Reflection	24.8	8.1	110	
18		Contraction	18.5	10.8	396	
19		Fit	19.3	10.5	415	
20	10	Reflection	25.1	7.3	126	
21		Contraction	19.3	10.5	415	
22		Fit	19.8	10.3	399	
23	11	Reflection	23.2	8.5	610	
24		Expansion	25.2	7.5	595	
25		Fit	23.8	8.2	161	610
26	12	Reflection	26.7	6.7	132	

Table 6. Optimization of the PAR/permanganate system by CMS (4 variables)

Expt. no.	Time, *min*	PAR, *ml*	pH	Temperature, °C	Absorbance	Best absorbance
1	11.0	20.0	6.9	20	0.065	0.065
2	20.0	20.0	6.9	21	0.030	
3	15.0	28.65	7.1	21	0.125	
4	16.6	22.9	7.6	21	0.110	
5	15.5	22.9	7.3	28	0.076	0.125
6 R	10.0	32.1	7.6	24	0.166	
7 E	6.0	38.15	7.8	24	0.175	0.175
8 R	8.5	46.7	8.4	26	0.224	
9 E	7.6	60.0	9.15	30	0.223	
10 L	8.2	53.1	8.7	28	0.165	0.224
11 R	4.1	58.45	8.8	22	0.435	
12 E	1.0	76.25	9.4	18	0.170	
13 L	6.3	51.5	8.4	21	0.195	0.435
14 R	0.6	83.0	9.4	23	0.170	
15 R	0.9	86.3	10.3	24	0.275	

R = reflection; E = expansion; L = Lagrange fit.

(4) *The solvent extraction/FIA system*

Table 7 shows the experiments done and the responses obtained. Each set of conditions was investigated with between 7 and 10 consecutive replicate injections to check that stable repeatable analytical results could be obtained.

The experimental conditions initially used were the best found by Baban.[27] Before the modified simplex optimization a 30% improvement in sensitivity was obtained by using an injection-valve by-pass coil to obtain mixing of sample with nitrate, instead of the 1.5-m mixing coil used previously.[17] The resultant peak height was 107 mm. Peak heights of up to 171 mm were obtained during the optimization, but under these conditions the repeatability was unacceptable.

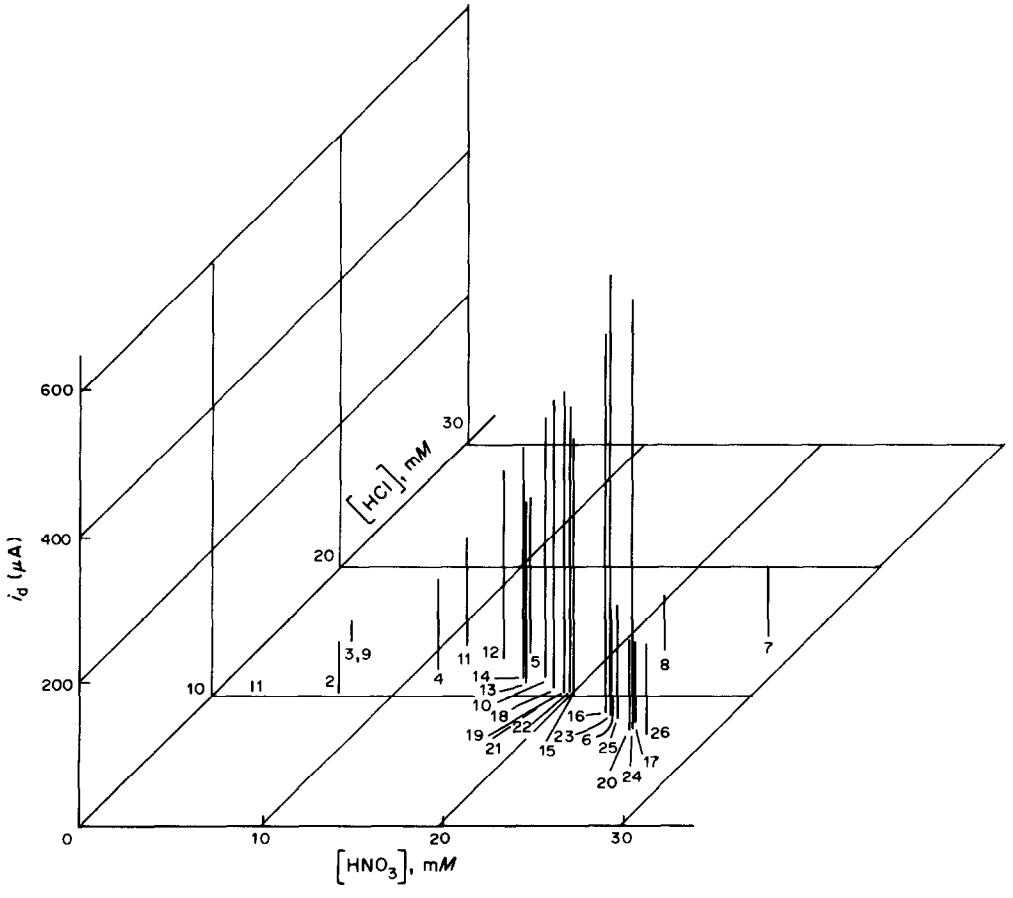

Fig 5. Three-dimensional graph of modified simplex experiments for the uranium(VI) polarographic analysis.

Table 7. Results for the optimization of the solvent extraction/FIA determination of uranyl ion (12 variables)

Expt. no.	Cycle/ Type	Master flow	PAN flow	Sample size, *μl*	PAN coil, *cm*	SEG coil, *cm*	MIX coil, *cm*	TBP tube	[PAN], *ml/50*	[Pyridine], *% v/v*	[TBP], *% v/v*	[Nitrate], *g/100ml*	Temp., *°C*	Peak height, *mm*		s.d., *mm*	*R*
1	0I	250	2	250	300	150	70	1.2	5	6	40	36	24.6	107		3.00	26.7
2		150	2	250	300	150	70	1.2	5	6	40	36	24.6	98.5		1.41	40.8
3		200	3.2	250	300	150	70	1.2	5	6	40	36	26.0	74		0.82	40.7
4		200	2.4	170	300	150	70	1.2	5	6	40	36	26.0	86		1.07	41.5
5		200	2.4	220	205	150	70	1.2	5	6	40	36	26.4	101.5		1.04	49.9
6		200	2.4	220	280	55	70	1.2	5	6	40	36	25.8	91.5		1.03	44.9
7		200	2.4	220	280	135	160	1.2	5	6	40	26	25.3	63.5		0.48	43.1
8		200	2.4	220	280	135	90	0.8	5	6	40	36	25.3	69.5		0.66	41.8
9		200	2.4	220	280	135	90	1.0	9.5	6	40	36	24.8	47		1.48	18.9
10		200	2.4	220	280	135	90	1.0	5.5	3.8	40	36	24.9	48.5		0.45	33.5
11		200	2.4	220	280	135	90	1.0	5.5	5.8	28.9	36	25.3	29		0.84	15.6
12		200	2.4	220	280	135	90	1.0	5.5	5.8	39	26.69	25.8	38		0.49	25.7
13		200	2.4	220	280	135	90	1.0	5.5	5.8	39	32.4	35.3	44		0.69	25.9
14	1R	257	1.9	260	300	150	60	1.4	4.85	6.1	51	35.29	25.3	113.5		0.76	64.8
15	E	286	1.7	280	315	160	50	1.4	4.5	6.2	62	35.29	25	0	a	+	0
16	2R	270	1.8	270	300	155	50	1.6	4.6	6.2	54.3	44.26	25.6	0	a	+	0
17	C	217	2.2	230	280	140	80	1.2	5.3	5.9	42.8	31.08	25.8	75.5		2.19	23.7
18	3R	270	1.8	270	305	155	50	1.6	4.6	6.2	54.4	38.39	20	0	b	+	0
19	C	217	2.2	230	280	140	80	1.2	5.3	5.9	42.8	33.9	30.4	56.5		1.42	23.4
20	4R	270	1.8	270	305	155	50	1.6	0.4	6.0	53.4	34.67	26.2	0	b	+	0
21	C	218	2.2	230	280	140	80	1.2	7.2	6.0	43.4	35.67	25.4	102.5		2.18	32.2
22	5R	240d	1.8	270	305	155	50	1.4d	4.55	8.3	53.4	36.03	25.0	84		2.08	27.3
23	6R	254	1.9	260	305	150	60	1.4	4.7	6.4	51.3	40.0	19.6	125		9.08	12.4
24	E	273	1.8	280	315	155	50	1.4	4.4	6.6	55.5	42.5	20.6	0	a	+	0
25	7R	273	1.7	280	315	155	0	1.4	4.8	6.6	55.5	40.22	20.0	0	b	+	0
26	C	218	2.2	450	290	140	110	1.2	5.0	6.2	44	50	25.6	171		13.93	11.5

R = reflection, E = expansion, C = contraction.
Master flow: speed setting on Gilson minipuls pump.
PAN flow: speed setting on Desaga pump.
Sample size: loop size used; for total sample volume including connecting tubing, add 80 μl.
TBP tube: flow-rating of tube used (ml/min),—N.B. actual flow-rate is dependent on master flow setting; $Al(NO_3)_3$ flow used 1.2 ml/min tubing.
[PAN]: volume of $5 \times 10^{-3} M$ PAN diluted to 50 ml.
For meaning of a, b, d, see text.

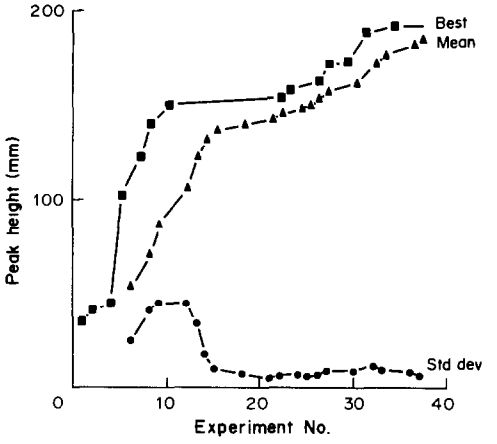

Fig 6. Rate of approach to the optimum and sequential decrease in the standard deviation of the peak heights of the current simplex for the isoprenaline determination.

The conditions of experiment 14 (peak height 113.5 mm) proved not only to give better sensitivity than the starting conditions, but very much better stability as well, giving a 19-fold improvement in signal to noise ratio relative to the previous system.[27]

It was found that some sets of experimental conditions requested by the simplex procedure were unstable and not suitable as the basis for an analytical method. In particular, it was found that the separator ceased to function acceptably when the flow-rate of the incoming segmented stream exceeded 2 ml/min. The unstable experiments, marked "a", were therefore assigned a response of 0 mm. Other experiments, marked "b", were then known to be unstable too, and therefore were not performed but were assigned a response of 0 mm. Polynomial-fit experiments were not done for cycles which included experiments marked "a" or "b". In experiment 18, the temperature used was fitted to the lower working boundary by the simplex. In experiment 22, the master flow and TBP tube-size suggested by the program were known to lead to instability. These were therefore decreased by the operator to the values (marked "d") shown. In experiment 26, the operator increased the sample size and nitrate concentration values. A further improvement in sensitivity was obtained, but repeatability was unacceptably poor.

It therefore became apparent that, for this system, sensitivity was the wrong parameter to optimize. Table 7 also shows the standard deviations (s.d.) of the heights of the consecutive replicate peaks (typically 7), and the values for an alternative response function:

$$R = (\text{mean peak height})/[\text{s.d.} + 1]$$

This function correctly reflects the merit of each set of results, since it places appropriate emphasis on both sensitivity and repeatability, and should have been used instead of peak height alone.

DISCUSSION

The results above show that the CSM works well on all the test systems. It has been found versatile and easy to apply to a wide range of mathematical, geographical and analytical systems. It is superior to univariate methods, and compares favourably with previous versions, and those we have tried with modifications removed.

The one system which gave difficulty was the solvent extraction of uranium. Study of the system has emphasized the importance of correct choice of response or response function. Box considered the consequences of propagation of errors in multivariate systems and concluded that, if the systems were linear, the errors tended to cancel. However, if the systems were non-linear, uneven behaviour resulted. Sometimes the errors cancelled, but at others they compounded so as to give instability.[32] This was encountered experimentally in the extraction system, and had the effect of slowing down the simplex. One practical solution to the problem is to change the starting point of the simplex if instability occurs and try a different route, in the hope that it is a stable one. Another solution, which has been used elsewhere,[23] is to optimize a response function which heavily penalizes instability.

Further discussion of the details of the algorithm and of specific points raised by these results is deferred to Part II* of this paper.

Acknowledgements—The authors would like to thank British petroleum for a research studentship award to A.P.W., the High Commissioner for New Zealand for photographs of Mt. Egmont, Prof. E. Neves and Dr. I. Gutz (University of São Paulo, Brazil) for their efforts and expertise in polarography, Dr. A. F. Taylor (BP Sunbury) for valued guidance and discussion, and D. J. Evans (University College, Swansea) for experimental work in the PAR/permanganate optimization. D.B. thanks Henry Freiser for demonstrating, in the laboratory and whilst jogging, the way in which a mathematical viewpoint can sharpen appreciation of this quantitative science of ours.

REFERENCES

1. W. Spendley, G. R. Hext and F. R. Himsworth, *Technometrics*, 1962, **4**, 441.
2. J. A. Nelder and R. Mead, *Computer J.*, 1965, **7**, 308.
3. S. N. Deming and S. L. Morgan, *Anal. Chim. Acta*, 1983, **150**, 183.
4. D. E. Long, *ibid.*, 1969, **46**, 193.
5. S. L. Morgan and S. N. Deming, *Anal. Chem.*, 1974, **46**, 1170.
6. M. W. Routh, P. A. Swartz and M. B. Denton, *ibid.*, 1977, **49**, 1422.
7. P. B. Ryan, R. L. Barr and H. D. Todd, *ibid.*, 1980, **52**, 1460.
8. E. R. Åberg and A. G. T. Gustavsson, *Anal. Chim. Acta*, 1982, **144**, 39.
9. S. N. Deming and L. R. Parker, *CRC Crit. Rev. Anal. Chem.*, 1978, **7**, 187.
10. J. W. Gorman and J. E. Hinman, *Technometrics*, 1962, **4**, 463.
11. M. J. Box, *Computer J.*, 1965, **8**, 42.
12. R. R. Ernst, *Rev. Sci. Instrum.*, 1968, **39**, 998.

Talanta, 1985, **32**, 723.

13. T. Umeda and A. Ichikawa, *Ind. Eng. Chem. Process Des. Develop.*, 1971, **10**, 229.
14. D. M. Himmelblau, *Applied Non-linear Programming*, McGraw-Hill, New York, 1972.
15. D. L. Keefer, *Ind. Eng. Chem. Process Des. Develop.*, 1973, **12**, 92.
16. L. A. Yarbro and S. N. Deming, *Anal. Chim. Acta*, 1974, **73**, 391.
17. S. L. Morgan and S. N. Deming, *J. Chromatog.*, 1975, **112**, 267.
18. P. F. A. van der Wiel, *Anal. Chim. Acta*, 1980, **122**, 421.
19. P. F. A. van der Wiel, R. Maassen and G. Kateman, *ibid.*, 1983, **153**, 83.
20. L. G. Sabaté and X. Tomás, *J. High Resn. Chromatog. Chromatog. Commun.*, 1984, **7**, 104.
21. H. H. Rosenbrock, *Computer J.*, 1960, **3**, 175.
22. R. Fletcher and M. J. D. Powell, *ibid.*, 1963, **6**, 163.
23. D. Betteridge, A. P. Wade, E. A. Neves and I. Gutz, *An. Simp. Bras. Electroquim. Electroanal., 3rd*, 1982, **2**, 411.
24. A. P. Wade, *Anal. Proc.*, 1983, **20**, 108.
25. T. B. Goad, *Ph.D. Thesis*, University of Wales, 1981.
26. D. Betteridge, T. J. Sly, A. P. Wade and J. E. W. Tillman, *Anal. Chem.*, 1983, **55**, 1292.
27. S. Baban, *Ph.D. Thesis*, University of Wales, 1981.
28. T. P. Lynch, A. F. Taylor and J. N. Wilson, *Analyst*, 1983, **108**, 470.
29. I. D. Cockshott, R. Payne and P. B. Copsey, *Research Disclosure*, 18721, November, 1979.
30. R. S. Rowles, private communication.
31. T. J. Sly, D. Betteridge, D. Wibberley and D. G. Porter, *J. Autom. Chem.*, 1982, **4**, 186.
32. G.E.P. Box, *Technometrics*, 1963, **5**, 247.

Talanta, Vol. 32, No. 8B, pp. 723–734, 1985
Printed in Great Britain

0039-9140/85 $3.00 + 0.00
Pergamon Press Ltd

REFLECTIONS ON THE MODIFIED SIMPLEX—II*

D. BETTERIDGE† and A. P. WADE
BP Research Centre, Chertsey Road, Sunbury-on-Thames, Middlesex, England, and
Department of Chemistry, University College, Singleton Park, Swansea, Wales

A. G. HOWARD
Department of Chemistry, University of Southampton, Highfield, Southampton, England

(*Received* 17 *December* 1984. *Revised* 16 *March* 1985. *Accepted* 23 *March* 1985)

Summary—This paper discusses the details of the composite modified simplex, critically compares it with other simplex methods, and reviews the value of this type of optimization procedure.

Simplex optimization has proved to be a simple and effective means of optimizing chemical systems which have several variables. In recent years, much effort has gone into obtaining improvements in both the speed and reliability of the method. Figure 1 shows the history of the many modifications which have been suggested.[1–21] We have embodied several of these published modifications, and some of our own devising, into an algorithm called the composite modified simplex (CMS). This attempts to overcome the shortcomings that Nelder and Mead recognized in their "modified simplex" method (MSM),[3] whilst maintaining its many advantages. Its primary use has been in the optimization of chemical systems.[17–19,22–31]

Part I of this work[19] described the use of the CMS for the optimization of a number of known surfaces, both mathematical and geographical, and of a wide variety of chemical and analytical systems. The results presented show that the CMS works well, and is capable of reliably giving acceptable levels of optimization with relatively few experiments. The results are in accordance with those of other workers for modified simplex methods in general, yielding their best performance when large initial simplex sizes are used.[10,14,16] In this part of the work, the rationale of the method is described in detail and comparisons are made with other simplex methods and alternative methods of optimization.

COMPARISON OF CMS FEATURES WITH THOSE OF OTHER SIMPLEX PROCEDURES

Figure 2 shows the initial simplex (*BNW*) for a two-variable system. It also defines Q, which indicates the positional co-ordinates for points on the current line of search. This facilitates easier description of the various operations. A reflection, *R*, has Q = 1. Expansion points, *E*, normally have Q = 2, and contractions, C_W and C_R, normally have Q = −0.5 and Q = 0.5 respectively.

Initial simplex

All simplex methods first involve performance of the experiments corresponding to the $n + 1$ vertices of the initial simplex in n-dimensional space. They then rank the vertices in order of the responses obtained. For our two-dimensional example we refer to these as *B* (best), *N* (next best) and *W* (worst).

Reflection

All the simplex methods considered in detail[1,3,12–17,20,21] initially generate a "reflection", *R*, of the point with worst response, *W*, through some point, *P*, on the side opposite it. The value of Q = 1 for reflection is common to all the simplex methods considered. It was retained for the CMS on the basis of the findings of Nelder and Mead.[3]

Most of the methods, including the CMS, evaluate the response at the reflection point. Some make an approximation to it, without performing the experiment. This practice is discussed later.

Weighted centroid

Most of the methods considered take *P* as the centre of the line *BN*. In the general n-variable case, this is the centroid of all the current simplex points, excluding *W*. It was Umeda and Ichikawa[7] who first suggested using a centroid weighted towards the better point(s) (*e.g.*, *P′* in Fig. 2). This has the advantage of giving a faster climb to the region of the optimum and decreases the problems that simplex methods usually have with sharply rising ridges. Its disadvantage is that the simplex becomes more distorted and loss of a dimension through narrowing of the angle of search may result if adequate protection features are not incorporated.[14] Ryan *et al.*[14] found the weighted centroid approach to be beneficial in exploring response surfaces to find the region of the optimum, but that Nelder and Mead's unweighted approach[3] was better in the region of the optimum,

*Part I—*Talanta*, 1985, **32**, 709.
†Author for correspondence.

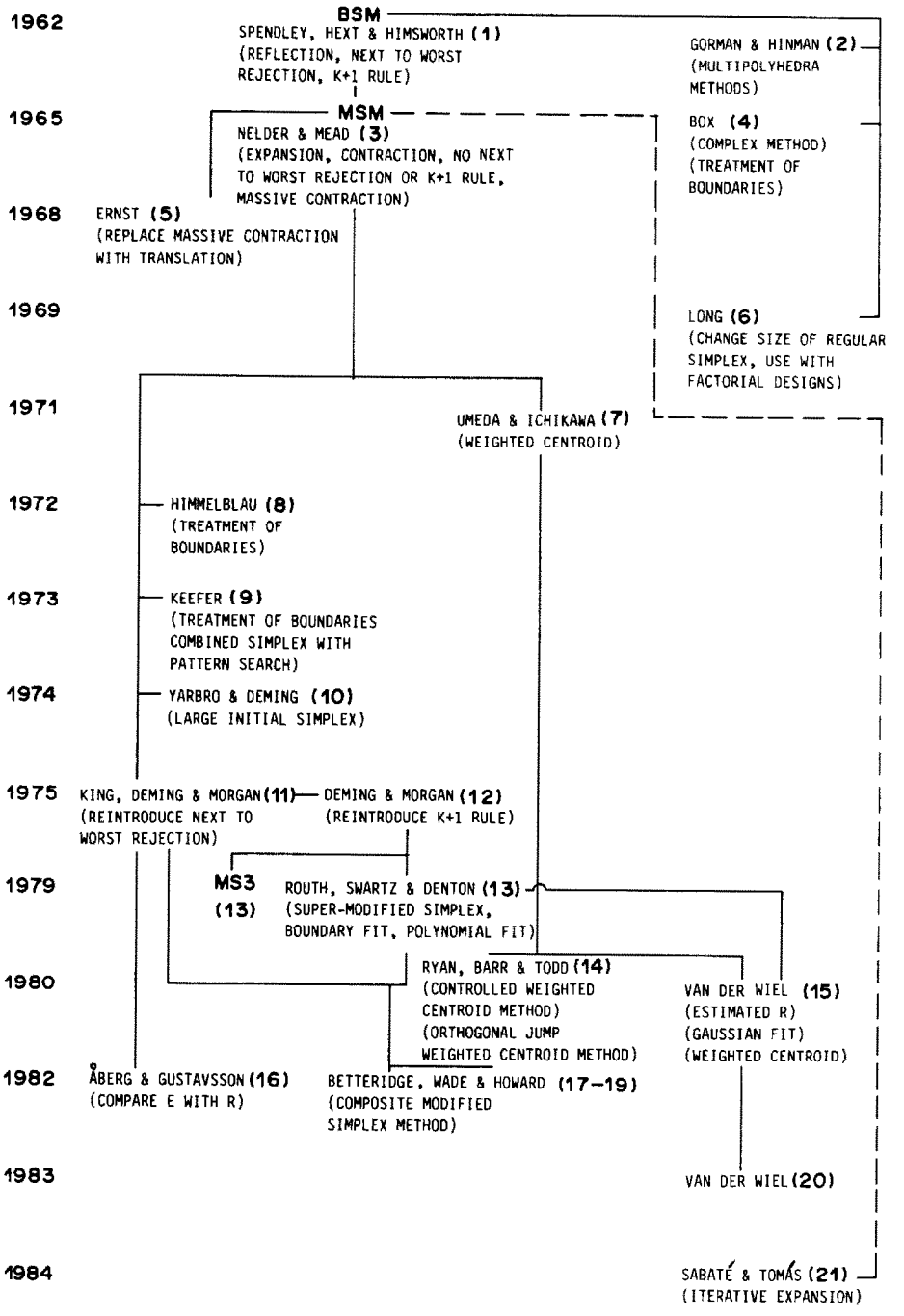

Fig. 1. A history of simplex optimization, 1962–1984.

where (with the exception of some cases where the obtainable optimum lies on an experimental boundary) the gradient is usually smaller. They also found that weighted centroid methods performed better than the MSM for optimizations which used the hundreds of experiments needed to satisfy high-precision convergence criteria.

Ryan *et al.*[14] used the difference between point responses and the current worst response in calculating the weighting factor to be used. The CMS also uses a controlled weighted centroid but, by using a weighting calculated from actual response values (rather than differences), it attempts to combine the advantages of both methods so that the amount of weighting decreases as the point responses become closer together. In this way it is also made less prone to error (caused by experimental noise) in choice of the direction of search. The weighting function used is

$$\mathrm{WF}(i) = 1 - [\mathrm{R}_{P(1)}/(\mathrm{R}_{P(1)} + \mathrm{R}_{P(i)})] \qquad (1)$$

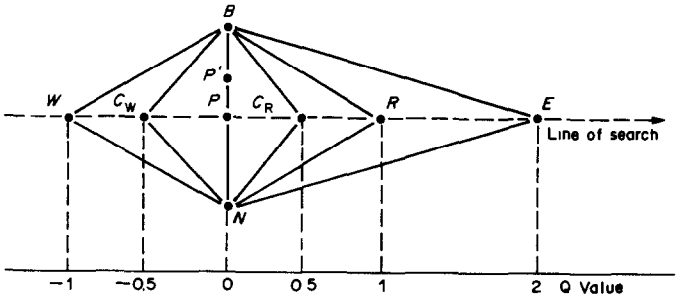

B	Best response point
N	Next best response point
W	Worst response point
C_W,C_R	Contractions
R	Reflection
E	Expansion
P	"Centroid of opposite face"
P'	Example weighted centroid

Fig. 2. Possible vertex positions for a modified simplex in two dimensions.

where WF(i) is the weighting factor and $R_{P(i)}$ the response for the ith point, and $R_{P(1)}$ is usually the response at B, the best point in the current simplex. A weighting limit, WL, is defined to guard against degeneracy (*i.e.*, loss of the ability to search in all directions in the parameter space) when $R_{P(i)} \ll R_{P(1)}$. WF(i) is not allowed to be less than WL. In our work WL was set equal to 0.1, although in other circumstances this might be too low a value.

P', the weighted centroid to be used, is then given by:

$$P' = P(1) + \frac{1}{n-1} \times \sum_{i=2}^{n} \mathrm{WF}(i) \times [P(i) - P(1)] \quad (2)$$

Here $P(n+1)$ is the point being reflected, usually W.

Expansion

All the modified simplex algorithms in common use allow expansion of the simplex and have an expansion coefficient of Q = 2, as originally tested and used by Nelder and Mead.[3] The work of Sabaté and Tomás allows several expansion steps to be made (Q = 2, 3, 4 *etc.*).[21]

Nelder and Mead[3] showed that as the expansion coefficient for their test function was increased (to 3 or 4) the efficiency of their method became progressively worse. An expansion coefficient of Q = 2 was therefore retained in the CMS.

Contractions

Nelder and Mead's values of Q = −0.5 and Q = 0.5 for contractions have proved to be effective. Use of these values is similar to the commonly used "binary search" procedure in which the area of search is halved with each successive approximation. This is known to be very efficient.[32] In view of this, and since there have been no studies using other values, these values were retained in the CMS. The other modified methods also use these values, with the exception of that of Sabaté and Tomás[21] which makes no mention of any contraction at all. Nelder and Mead's algorithm also featured a "massive contraction", which decreased the simplex size by a factor of ten when highly unfavourable circumstances were encountered.[3] This was first removed by King *et al.*[11] and does not feature in other modified simplex algorithms. It was not included in the CMS because in typical analytical systems there would be a danger of degeneracy for some variables, and all experimental studies agree that large simplexes are the most efficient.[10,14,16,19]

Comparison of expansion and reflection responses

Like the method of Åberg and Gustavsson,[16] the CMS compares the response at an expansion point, E, with that at its reflection point, R, rather than with that at B. This guarantees retention of the highest response found.

"Next-to-worst" rule

The CMS adopts the approach suggested by King,[11] which was present in Spendley's original method,[1] but neglected by others. If a line of search (called a "cycle") fails to give an improvement over the point with next-to-worst response, then a new cycle is started, with the next worst point treated as though it were the worst. In this way oscillation between two points is prevented.

In evaluation of the weighted centroid for such cases the point being rejected is exchanged for $P(n+1)$. If the point being rejected is B, the current best, then N, the point of next best response, is used in place of B in equations (1) and (2).

In the CMS, once a cycle giving an improvement has been obtained, the best point from that cycle is retained and the worst point discarded.

The algorithm terminates if no line of search gives an improvement.

Polynomial fit

Nelder and Mead observed that their method (the MSM) was better than quadratic methods for obtaining a fast rise to the region of the optimum, but that in that region, quadratic methods had the advantage.[3]

The super-modified simplex method (SMS) was the first to incorporate a quadratic fitting facility into the modified simplex approach.[13] This is of obvious utility when the simplex straddles a ridge or maximum. The SMS requires three experiments per cycle, these being at the centroid, P, the reflection, R, and a fit point, F. This last is a point on the line passing through W, P and R which corresponds to the maximum of the curve given by a quadratic fit to the responses at W, P and R. Routh *et al.* extrapolated the fit to Q-values outside the normal limits of $-1 \leqslant Q \leqslant 2$, but did not state the boundaries of the extended range they used.[13] If the maximum lies within the allowed range, but is not within a given safety interval of P (degeneracy can occur if F is too close to P), then the response for these conditions is evaluated, and retained as the new vertex if an improvement is found. If there is no maximum within the extended range, then the new vertex is taken as whichever boundary of the extended range is predicted will give the higher response. The method has been shown to work well, and has formed the basis of more recent further modified methods.[15,20]

Despite Nelder and Mead's findings that large expansions were not beneficial, the SMS has been shown to be more efficient than the MSM in a chemical optimization.[13]

In this work we have assumed that extrapolations outside the range of the current simplex are less likely to give an improved response than interpolation within it. The CMS algorithm incorporates a Lagrange polynomial fit, which is used only when the local response topography indicates that a maximum lies within the interval of the current simplex, *i.e.*, when a failed expansion or successful contraction has occurred. In this event, a quadratic equation is fitted to the responses at W, R and the point corresponding to the expansion or contraction. The maximum is found and an experiment at this point, L, is only performed if the Q value of L differs by at least 0.1 from that of the points already evaluated. If L were too close to P, and were accepted, then degeneracy would occur. Therefore a safety interval $(-0.25 < Q < 0.25)$ is set and if L lies within it, the boundary of the interval that is nearer to L is used as the new vertex. The response is evaluated and the vertex retained if an improvement is found, otherwise the reflection or contraction already evaluated is retained.

Variable number of points per cycle

The MSM is more flexible than the SMS in one respect: the number of experiments per cycle is allowed to vary with local response surface topography. If a "good" direction of search has been chosen, the MSM cycle will consist of two experiments, a reflection and an expansion. If it is a "bad" direction, then again two experiments will be done, these being a reflection and a contraction (either C_R or C_W). If the direction chosen yields a response which is neither "good" nor "bad" then the cycle is restricted to one experiment only, *viz.* the reflection, since neither expansion nor contraction is likely to give further improvement.

The SMS algorithm always uses three experiments per cycle. Although the response at P is always evaluated, this point can never be retained in the resultant simplex because degeneracy would be caused.

We have assumed that the flexible approach of the Nelder and Mead algorithm is likely to minimize the number of experiments which are unlikely to (or cannot) give a direct improvement, and have retained the principle given by these authors. The typical cycle for the CMS algorithm is therefore of one, two or three experiments. We have found the average number of experiments required per cycle to be about two, and that it depends on the nature of the surface and the initial simplex size.

Fitting to boundaries

In many systems there are experimental boundaries beyond which the user does not wish the simplex to venture. These may be physical constraints imposed by the apparatus or chemistry involved.

The SMS was the first widely used method to advocate fitting to a boundary, and was demonstrably more efficient than other methods which do not allow this.[13]

The CMS algorithm again follows the SMS example and allows fitting to boundaries, but it also retains the full moves in the variables which remain within their allowed ranges, shortening only the moves of those variables which would otherwise violate their boundaries. This leads to a distortion of the simplex, but guards against premature contraction in the more significant variables.

Squashing to boundary

Nelder and Mead noted that if all the points in the current simplex are set at the same value for one variable, the simplex is constrained to search in one dimension less.[3] Parker *et al.* showed that this had no adverse affect on the search in the remaining dimensions.[33] The loss of one dimension can sometimes be a desirable feature of the system.[29] The CMS allows the simplex not only to explore points along a boundary, but where the system dictates it to be desirable, to flatten itself out along it.

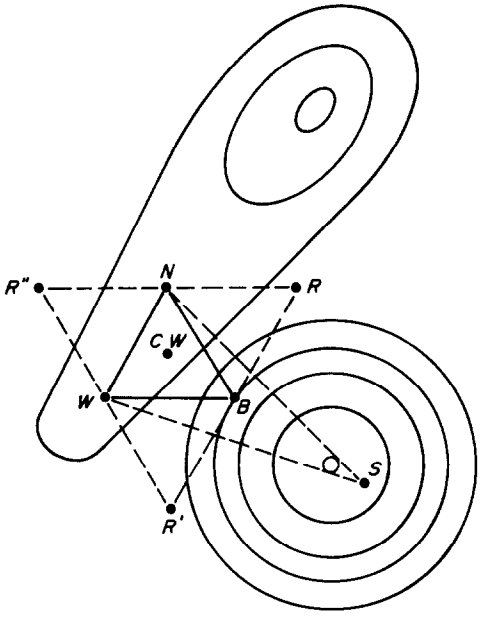

Fig. 3. Suboptimal redirection succeeds in relocating the simplex onto one of the maxima.

Suboptimal redirection

It is known that simplex methods can have problems with surfaces containing more than one maximum. In the development of the CMS by use of contour maps, a circumstance similar to that in Fig. 3 arose. The algorithm, as it stood, would have become stranded between the two peaks. A procedure, known as "suboptimal redirection" was therefore suggested by which the algorithm could escape onto one or the other, choosing the one more likely to be higher. This is shown in Fig. 3, which is explained as follows.

Reflecting away from W gave R, which was worse than W. C_W was still no better, so the next line of search was tried. Reflecting N gave R' (no better) and the subsequent contraction again gave no improvement. On most surfaces reflection of B (the next and final line of attack) is very unlikely to give an improvement, so before attempting R'', the suboptimal redirection, S, was tried. This corresponds to a Q value of -2 on the final line of search, and the approach is similar to the extended range argument used by the SMS in every cycle. If S is successful, then N is rejected, rather than W or B, since N is the point most likely to be situated on the second maximum. This leaves the new simplex, WBS, correctly oriented to climb the maximum on which B was lying. This approach is also of obvious value when a surface contains a sharply rising ridge, a feature on which simplexes can fail.[34] If S fails, then R'' is tried. If R'' fails, and the subsequent contraction also fails, then the optimization terminates, and B is taken as the best value obtainable.

Precision limiting

It was thought advantageous to limit the precisions of the variables manipulated by the CMS to the levels actually measurable in the experimental system being optimized. The measurement precisions are entered into the microcomputer as part of the initial data. This limiting not only makes the output clearer and more intelligent but also enables a "projected point check" to be made.

Projected point check

When the simplex size approaches the precisions to which the variables are measured, it is possible that the next experiment to be done (R, E, C_W, C_R, L or S) has effectively the same co-ordinates as a point already in the current simplex. If this were accepted, then degeneracy would result. In the CMS this is detected and the experiment is not (re)tried, but the cycle is terminated prematurely.

Premature cycle termination

When R results in a point on one or more of the experimental boundaries it is necessary to terminate the cycle prematurely. If the reflection is successful, it is accepted and the cycle terminated, since an expansion point, E, would lie even further over the boundary and result in an even greater distortion of the simplex. If the reflection fails, then C_W is automatically chosen, rather than C_R. If C_W is successful then no boundary fit is made.

The cycle is also terminated prematurely when an expansion which has been fitted to one or more of the experimental boundaries has failed. The fit experiment is not done since W, R and E are usually no longer collinear.

Retesting of old points

One feature of Spendley's method[1] which was retained in the SMS,[13] but neglected by the other algorithms, is the periodic re-evaluation of the response at points which have been resident in the simplex for a number of cycles. This is of great utility in locating responses that are falsely high owing to equipment instability or experimental error and helps the simplex to avoid getting stuck on a "false maximum". This should really have been included in the CMS, and was an omission on our part. In experimental optimizations we have tended to restart the simplex from the best point found so far once the rate of improvement suggests a maximum (false or otherwise) has been located.[18] Also, when replicate experiments have been rapid and easy to do, the average response of several replicates has been used.[18,19]

Setting up the initial simplex

The CMS software allows users either to define their own initial simplex in terms of individual experiments or to use the geometric method of Spendley *et al.*[1] A design for an initial simplex based on either approach is given in Table 1.

Table 1. Design of the initial simplex

Variable No.	Experiment 1	2	3	4	5	6	7
1	—	+	0	0	0	0	0
2	—	—	+	0	0	0	0
3	—	—	—	+	0	0	0
4	—	—	—	—	+	0	0
5	—	—	—	—	—	+	0
6	—	—	—	—	—	—	+

Key: — 1st level; 0 intermediate level; + 2nd level.

Termination of the algorithm

Various criteria for termination of multivariate optimizations have been suggested.[3,35] The ones used here are generally of rather more empirical nature than mathematical convergence, and are probably more applicable to analytical chemistry.[18] They include terminating the algorithm once the observed rate of improvement is considered not to be worth the experimental effort or cost involved, and terminating after a prespecified number of experiments or cycles.

Aids to performance

Even the best modified simplex algorithms can sometimes fail on noisy or very complex response surfaces. Various approaches, such as filtering,[36] averaging,[18] use of definition-weighted[17] or noise-weighted[19] response functions, retesting old points[13] and restarting optimizations from the current best point with a larger than current simplex[18] have been suggested as means of countering this. Although not the complete answer, these methods can greatly minimize the problem.

Experimental noise in response and variable values is the major cause of failure of modified simplex methods. Studies in the literature have investigated the effect of "white" ("shot") noise on the modified simplex.[14,16] In systems where this is the main type of noise (*e.g.*, ultraviolet/visible spectrophotometers), response-value precision can be improved by averaging a number of readings.[18,37] In many measurement systems, "flicker" ("$1/f$") noise and "interference" noise are also likely to be present.[38] If $1/f$ noise (or worse) predominates, as is the case with some inductively-coupled plasma optical-emission spectrometers, averaging will not improve precision, and may even decrease it.[37,39] Precautions should therefore be taken to limit noise and improve experimental precision as much as possible.

COMPARISON OF MODIFIED SIMPLEX PROCEDURES

The main features of the main modified simplex algorithms are listed in Table 2.

Since no complete study exists of the performance of all the modified simplex methods for a larger number of systems, and indeed could not practicably be undertaken, no completely accurate comparison is

Table 2. A profile of various modified simplex algorithms (Y = yes)

Method	BSM	MSM	KDM	SMS	MS3	CWC	OJWC	AGM	CMS
Reflection ($Q = 1$)	Y	Y	Y	Y	Y	Y	Y	Y	Y
Weighted centroid	—	—	—	—	—	Y	Y	—	Y
Expansion ($Q = 2$)	—	Y	Y	Y	Y	Y	Y	Y	Y
Contraction ($Q = \pm 0.05$)	—	Y	Y	Y	Y	Y	Y	Y	Y
$E > R$ Comparison	—	—	—	—	—	—	—	Y	Y
Reject next worst	Y	—	Y	Y	—	?	?	Y	Y
Polynomial fit	—	—	—	Y	—	—	—	—	Y
Variable points/cycle	—	Y	Y	—	Y	Y	Y	Y	Y
Fit to boundary	—	—	—	Y	—	?	?	?	Y
Squash to boundary	—	—	—	Y	—	?	—	?	Y
Suboptimal redirection	—	—	—	—	—	—	—	—	Y
Precision limiting	—	—	—	—	—	—	—	—	Y
Point present check	—	—	—	—	—	—	—	—	Y
Own initial simplex	—	—	—	—	—	—	—	—	Y
Retest old points	Y	—	—	Y	—	—	—	—	—
Tested on:									
Chemical systems	Y	Y	Y	Y	Y	?	?	?	Y
Mathematical functions	Y	Y	?	Y	?	Y	Y	Y	Y
Map surfaces	—	—	—	—	—	—	—	—	Y

BSM: basic simplex method of Spendley, Hext and Himsworth.[1]
MSM: modified simplex method of Nelder and Mead.[3]
KDM: method used by King, Deming and Morgan.[11]
SMS: super modified simplex method of Routh, Swartz and Denton.[13]
MS3: MS3 modified method tested by Routh, Swartz and Denton.[13]
CWC: controlled weighted centroid method of Ryan, Barr and Todd.[14]
OJWC: orthogonal jump weighted centroid method of Ryan, Barr and Todd.[14]
AGM: method of Åberg and Gustavsson.[16]
CMS: composite modified simplex method of Betteridge, Howard and Wade.[17-19]

possible. The efficiency and reliability of each method will vary from surface to surface and so comparisons based on just a few systems are prone to error. However, a number of tentative conclusions can be reached from the literature.

1. All modified simplex methods have proved to be of utility in experimental optimization.[1-31,33,34]
2. The MSM is a robust multivariate optimization procedure.[3,13-15]
3. The method of King *et al.*[11] is an improvement on the MSM.
4. The SMS exhibits a faster initial rate of climb than the MSM, King's method and MS3 algorithms.[13]
5. Weighted centroid methods give a faster rise to the region of the optimum, and are usually more efficient when evaluating the position of a maximum with high precision (using a large number of experiments).[14]
6. Åberg and Gustavsson's method[16] may be a small improvement on the controlled weighted centroid algorithm of Ryan *et al.*[14]

Comparisons are made more difficult by the wide range of possible measures for the merit of each method.

Comparisons of several modified simplex methods by use of mathematical function optimizations have appeared in the literature.[14,16] These define "efficiency" in terms of the number of experiments required to get within a given tolerance of optimum, and show "reliability" by the numbers of "critical" and "non-critical" failures to reach this target. The initial size and orientation of the simplex has an effect on the speed of convergence to the optimum[3] and these studies[14,16] take this into account. They consider several surfaces, and several initial simplex sizes, using 100 randomly chosen starting points for each. The results are summarized in Tables 3 and 4. The functions referred to are those used in Part I of this paper,[19] with the exception of function 6, the flame-ionization detector response surface. For this, Routh *et al.*, used experimental data and an interpolation program.[13] We have used a mathematical function having a similar response surface. There has been no study of comparable size which makes use of chemical systems.

Table 3. Comparison of efficiency of the MSM, SMS, CWC and OJWC modified simplex procedures by use of 5 functions*

	Average number of evaluations			
Function	MSM	SMS	CWC	OJWC
1	89	147	99	82
2	52	161	46	54
3	371	435	385	484
5	174	231	139	130
5†	162	222	110	108
6	111	171	114	106
Average	160	228	149	161

For each function the number of evaluations shown is the average over eight simplex sizes and 100 optimizations per size.[14]
*For meaning of acronyms see footnotes to Table 2.
†Convergence criteria relaxed.

Table 4. Comparison of the efficiencies of Åberg and Gustavsson's method[16] (AGM) and the controlled weighted centroid method[14] (CWC)

	Average number of evaluations	
Function	AGM	CWC
1	85	92
2	65	57
3	180	189
4	142	156
Average	118	124

For each function the number of evaluations shown is the average over eight simplex sizes and 100 optimizations per size.[16]

Routh *et al.* made experimental comparisons of several modified simplex methods for the optimization of the performance of a computer-controlled flame spectrophotometer.[13] They found no failures (critical or otherwise) for any of the methods they tried, although differences in the rate of approach to optimum were demonstrated. They evaluated method efficiency in terms of numbers of experiments and of cycles (a cycle is the number of experiments required to obtain a translation from one simplex to the next), needed to reach the optimum. They found SMS to be the most efficient method, the ratios of average number of evaluations needed by the test method to average number by the SMS method being 1.11 for MSM, 1.08 for KDM and 1.17 for MS3 (for identification of the methods see footnotes to Table 2). The values may be compared with those in Table 3. In comparing methods, the number of cycles needed to get within a given tolerance of optimum is not the most helpful measure, since in most modified simplex methods the number of experiments performed per cycle is variable, and experimentalists would prefer to know how many experiments they have to perform.

All the simplex methods considered are of use in rapidly improving an experimental response. For the CMS in the examples considered here, it can generally be noted that acceptable levels of improvement are obtained within relatively few experiments, and that the additional effort required to reach the absolute optimum would often not be justifiable.

Comparisons of efficiency in reaching a target and of failure rate are certainly useful. However, from an experimentalist's point view a more complete measure of merit would also include the initial rate of improvement and the capability for dealing with noise. For this, one number might well be insufficient, and therefore the full range of results ought to be shown. These would then give grounds for confidence

that acceptable improvements can be obtained within a limited predefined number of experiments on the vast majority of (unknown) experimental surfaces.

Relative efficiencies

The results in Tables 3 and 4, and those quoted by Routh *et al.*,[13] show that each group of workers has grounds for claiming its own algorithm to be "the best". The results of Routh *et al.*,[13] and Ryan *et al.*,[14] appear to differ regarding the relative merit of the SMS and MSM algorithms. Routh *et al.* were dealing with a real experimental system and so based their conclusions on optimizations of only 40 experiments. In contrast, the function optimizations by Ryan *et al.*,[14] and Åberg and Gustavsson[16] (Table 4) were run for up to 500 evaluations, with an average of well over 100 evaluations. Since no information is given as to the performance of the methods for the functions after 20 and 40 evaluations (or indeed on the chemical system after more than 100 experiments per method!), it is difficult to draw any real conclusions as to how the methods would compare in laboratory optimizations. We think it likely, however, that the SMS is indeed capable of a more rapid initial climb than the MSM type approaches. We have been unable to investigate this experimentally, but would suggest that this may be due to the quadratic fitting procedure it employs, this enabling a better approximation to the position of a maximum or a ridge on the current line of search.

EVALUATION OF THE CMS

Since the CMS was designed specifically for experimental use, the number of evaluations used per optimization and the mode of evaluation procedure differ markedly from those used by other workers.[14,16] The evaluation procedures were reported in Part I of this paper.[19] We believe our approach to be more applicable to the development of analytical methods for laboratory use, whereas the approach reported elsewhere is more suited to theoretical branches of chemistry where optimization can be done solely by computer calculation, without the need for time-consuming sequential chemical experimentation. We give the following justifications for this statement. (*i*) Following the experimental example of Routh *et al.*,[13] we used a maximum of 40 evaluations (experiments) per optimization rather than up to 500 evaluations per optimization as used elsewhere.[14,16] For routine laboratory use, optimizations requiring more than about 40 experiments are usually impractical. (*ii*) The other workers reported their results in terms of the average number of evaluations required to obtain the optimum within a given tolerance. In optimization of chemical systems the true optimum value is often not known, and it cannot be known when a value reached is within the tolerance range of the optimum necessary to terminate the optimization. We therefore report the full range and distribution of best values obtained after a prespecified number of experiments. (*iii*) The tolerances specified in the other papers correspond to a small fraction of 1% of the response range lying within the chosen boundaries. In the laboratory, a system reaching 99% of optimum would be warmly received, and figures as low as 90%, if economically achieved, are often perfectly acceptable. (*iv*) In real situations it is usually not worth the extra experimentation to slowly obtain the last fractional improvement, and in any case such experiments are less likely to succeed because of the increasing size of the experimental noise relative to the improvement left to be achieved. (*v*) In real systems, fractions of 1% may correspond to very small changes in the values of critical variables, and these changes may be smaller than can practically and reproducibly be achieved. (*vi*) Our results show the full range and distribution of best values found; the other papers quote numbers of "critical failures", without saying just how critical the failures were! For these reasons then, we feel that a modified approach to the evaluation of optimization methods for experimental optimization is required, and the method suggested in these papers is one possibility.

COMPARISON OF THE CMS WITH OTHER METHODS OF OPTIMIZATION

Although many methods of optimization exist,[40,41] Murray[40] felt that there was still a long way to go before any one computer program could claim to be able to provide effective and efficient solution for even the majority of current optimization problems. This was thought likely to remain the situation for some time. He felt it necessary to first acquire background knowledge of the problem if an appropriate choice of optimization algorithm was to be made.[36]

Optimization methods are used primarily to find the best set of conditions, rather than investigate and model the complete response surface. There is therefore a trade-off inherent in any optimization, *i.e.*, that of speed of improvement *vs.* detailed knowledge of the system. It has been shown that a reasonable understanding of system behaviour can be obtained from the results of a CMS modified simplex optimization.[18]

Optimization by trial and error

Even today, many laboratory "optimizations" are done by the "finger in the wind" method. Variables are altered in either a random fashion or in accordance with assumed relationships between individual variables and system response, and the best set of conditions found is taken as "optimum". It has been recognized for some time that this approach is worse than use of univariate methods.[6] The efficiency and reliability of such an approach is heavily dependent on the expertise of the operator. Interaction between variables may be complex[18] and can easily be missed or misinterpreted, even by experts. For systems which

are not totally understood (the vast majority), a more systematic method of search, such as the CMS or other modified simplex algorithm, should be used.

Grid search

By investigation of a large number of points distributed regularly over the response surface, an idea of its contours can be obtained. For a two-variable system, with a $k \times k$ grid pattern for the search, a typical value of k is 8, requiring 64 experiments. Even then the optimum would only be known to within 12% of the range of each variable. The major disadvantage of this method is the number of experiments required. An n-variable system would need k^n experiments. This clearly is impracticable for many systems. Also, some systems have very sharp maxima which could lie between known points and so be missed altogether.

Univariate optimization

The results given in Part I of this paper[19] and elsewhere[18] indicate that this commonly used method has difficulty in coping with interaction of variables and may lead to erroneous conclusions being made (see Table 5). This is in agreement with the observations of Morgan and Deming.[12]

Iterative univariate optimization

Considering each variable several times does improve reliability, but dramatically increases the number of experiments required.[18]

Table 5 compares the univariate, iterative univariate and CMS methods for the systems we studied. It is clear that the CMS is greatly superior to univariate and iterative univariate optimization, both in terms of efficiency and reliability.

Univariate or iterative univariate optimization with polynomial approximation

The number of experiments required may be reduced somewhat by interpolating between known points to locate a maximum more accurately. This still, however, does not alter the strictly univariate nature of the data, and so the method will still be prone to error due to interactions. The quintic equations obtained for peak height, P, for the first round of a four-variable univariate optimization[18] are given in Table 6. It is evident that no physical understanding of the system can be gained from these.

Multivariate techniques

From the discussion above we conclude that univariate optimization procedures are unreliable and often lengthy, and that grid searches can be ruled out whenever more than 3 variables are involved, or the optimum needs to be known to high precision. This leaves multivariate methods.

Of the many multivariate methods,[40,41] the modified simplex approach is by far the most widely applied to experimental optimization.[42] This is largely due to the simple principles on which it is based, and the energy with which Deming and Morgan (in particular) have investigated it since the early seventies.[10–12,33,34] We have found the modified simplex to be good with experimental systems, although there is general agreement that it is worthwhile to apply an

Table 5. Comparison of performance of univariate, iterative univariate and CMS modified simplex optimization methods

System: Mount Egmont contour map optimization (2 variables)			
Size*	Method	Experiments	Response
20%	Univariate	10	900
10%	Univariate	20	900
5%	Univariate	40	1100
20%	Iterative univariate	20	2850
10%	Iterative univariate	50	7250
5%	Iterative univariate	100	7250
50%	CMS modified simplex	35	8260
20%	CMS modified simplex	66	8260
10%	CMS modified simplex	56	8260
5%	CMS modified simplex	57	8260
2.5%	CMS modified simplex	57	8260
System: Optimization of FIA determination for isoprenaline			
	Method	Experiments	Response
With 4 variables:			
	Univariate	28	85
	Iterative univariate	80	162
	CMS modified simplex	31	162
With 5 variables:			
	Univariate	43	127
	Iterative univariate	150	192
	CMS modified simplex	34	192

*Initial size as fraction of range.

Table 6. Equations modelling first univariate optimization of the FIA determination for isoprenaline

Variable	a_0	a_1	a_2	a_3	a_4	a_5
1	22.12	0.23	-1.74×10^{-3}	8.08×10^{-6}	-1.79×10^{-8}	1.49×10^{-11}
2	22.39	43.13	−22.88	4.97	−0.50	0.02
3	52.89	170.03	−135.75	35.29	−3.79	0.15
4	37.07	76.66	−45.95	12.86	−1.69	0.08

Peak height (mm) $= \sum_{i=0}^{5} a_i X^i$.

Variables and ranges were: 1, reaction coil length (50–450 mm); 2, flow-rate (1.51–5.21 ml/min); 3, pH of carrier stream (3.91–8.21); 4, concentration of potassium ferricyanide in carrier stream (0.24–6.08 mM).

experimental design in the vicinity of the "optimum".[6,42]

Other multivariate methods may well be applicable to experimental optimization, but have not been widely accepted by the analytical community. The "Quasi-Newton" is one such method.[40,43] This is more difficult to understand than the modified simplex since it is mathematically complex. It still relies on differences between response values (which will be noisy, of course).

Van Terheyden[44] has pointed out that where algebraic solutions are possible, these should be considered first. Simplex comes into its own where these techniques "cannot" be used, such as for experimental systems for which no algebraic approximation exists.

Optimization by modelling

Simulation and modelling of chemical analysis systems is an area currently receiving greater attention[45–47] and is an alternative strategy for optimization. In this a mathematical model of the system is constructed and then optimized by either nonlinear programming or a guided search procedure.

The main pitfall is that while a model may accurately fit the experimental data obtained, it may not be representative of the whole surface. For example, by combination of the univariate equations given in Table 6, a "system" model of 21 terms can be constructed which closely fits the experimental data (all values within an uncertainty range from +1.5 mm to −1 mm). It gives a maximum of 85.3 mm, and fails to predict the true optimum (192 mm) since it takes no account of interactions of variables. A better approach would be to use data from a truly multivariate search procedure and allow cross-terms (X1·X2, X2·X3 etc) in the system model equation.

Alternatively, the example of Erni and Muller[48] could be followed. They combined relevant flow-rates, concentration changes, mass- and flow-balance equations, *etc.*, to model a continuous-flow analysis system. A few experiments were undertaken to obtain values for model constants. Nonlinear programming was then used to optimize the model. A 15-fold improvement in response was forecast. The actual improvement obtained was 10-fold.

In flow-injection analysis (FIA), modelling is complicated by the dispersion process. It is insufficient to modify Erni and Muller's equations to include physical dispersion, since the degree of mixing and sample dispersion interact with the chemical kinetics in a complex manner.[49]

Painton and Mottola[50] have suggested a model for FIA, based on a set of differential equations. Optimization of FIA systems with such a model is not a trivial problem, but may yield useful information.

Betteridge *et al.*[49] have proposed a stochastic model for simple FIA systems, using a random walk approach. This has recently been extended to include merging-zones FIA systems.[51] This is a simple approach which has been most useful in obtaining insight into the effect of the mixing process and gives a highly visual output. The major disadvantage is that, since it deals individually with the movements of large numbers of molecules, the calculations take a long while to run on a microcomputer.

FURTHER WORK

Through the CMS has been proved a reliable and efficient means of experimental optimization, there still exists room for improvement. The potentially hazardous effects of one noisy result could be minimized by a method of direct-search optimization making use of all available data when calculating the next point to try, rather than just the points of the most recent simplex. Since experimental systems are prone to drift and need frequent recalibration, the validity of individual results will decrease with age.[52] Weighting should therefore be given to the age and uncertainty of each value. Analytical science would benefit greatly from having an optimization procedure able to produce some mathematical model or set of local models for the system as the optimization progresses. Some form of pattern recognition approach would probably be used to highlight the effects of each variable and identify major interactions.[53] Such information would allow intelligent judgements to be made on possible trade-offs to obtain, for example, improved economy in reagents without substantially decreasing sensitivity. From a system model it should be possible to estimate values

for other untried sets of conditions, and give confidence levels for these, based on the regularity of the surface fitted to the measured data and the distance from known values.

CONCLUSIONS

Nelder and Mead's modified simplex method is of great utility in achieving rapid and reliable optimization of multivariate systems. Modifications to their method have been shown to improve the efficiency in some instances. The test procedures used in these papers (maps, mathematical functions and chemical systems) should be *de rigeur*.

In investigation of the performance of an optimization procedure, the mode of evaluation should be decided upon as a consequence of, and in relation to, the intended use of the method. This should determine the number of experiments to be used per optimization.

For comparisons using function optimizations done by computer, a large number of test surfaces should be used. Each surface should be representative of those likely to be optimized by the final method. Several initial simplex sizes should be used with at least 100 optimizations for each, on each surface. Those wishing to follow this path would do well to heed the words of Hocking[54] when he states that the value of a particular method can only be established by its performance in practice, and cautions potential investigators to examine the magnitude of the required computation before proceeding.

Acknowledgement—The authors would like to thank The British Petroleum Company for a research studentship to APW, which made this work possible.

REFERENCES

1. W. Spendley, G. R. Hext and F. R. Himsworth, *Technometrics*, 1962, **4**, 441.
2. J. W. Gorman and J. E. Hinman, *ibid.*, 1962, **4**, 463.
3. J. A. Nelder and R. Mead, *Computer J.*, 1965, **7**, 308.
4. M. J. Box, *ibid.*, 1965, **8**, 42.
5. R. R. Ernst, *Rev. Sci. Instrum.* 1968, **39**, 998.
6. D. E. Long, *Anal. Chim. Acta*, 1969, **46**, 193.
7. T. Umeda and A. Ichikawa, *Ind. Eng. Chem. Process Des. Develop.*, 1971, **10**, 229.
8. D. M. Himmelblau, *Applied Non-linear Programming*, McGraw-Hill, New York, 1972.
9. D. L. Keefer, *Ind. Eng. Chem. Process Des. Develop.*, 1973, **12**, 92.
10. L. A Yarbro and S. N. Deming, *Anal. Chim. Acta*, 1974, **73**, 391.
11. P. G. King, S. N. Deming and S. L. Morgan, *Anal. Lett.*, 1975, **8**, 369.
12. S. L. Morgan and S. N. Deming, *Anal. Chem.*, 1974, **46**, 1170.
13. M. W. Routh, P. A. Swartz and M. B. Denton, *ibid.*, 1977, **49**, 1422.
14. P. B. Ryan, R. L. Barr and H. D. Todd, *ibid.*, 1980, **52**, 1460.
15. P. F. A. van der Wiel, *Anal. Chim. Acta*, 1980, **122**, 421.
16. E. R. Åberg and A. G. T. Gustavsson, *ibid.*, 1982, **144**, 39.
17. D. Betteridge, A. P. Wade, E. A. Neves and I. Gutz, *An. Simp. Bras. Electroquim. Electroanal., 3rd*, 1982, **2**, 411.
18. D. Betteridge, T. J. Sly, A. P. Wade and J. E. W. Tillman, *Anal. Chem.*, 1983, **55**, 1292.
19. D. Betteridge, A. G. Howard and A. P. Wade, *Talanta*, 1985, **32**, 709.
20. P. F. A. van der Wiel, R. Maassen and G. Kateman, *Anal. Chim. Acta*, 1983, **153**, 83.
21. L. G. Sabaté and X. Tomás, *J. High Res. Chromatog. Chromatog. Commun.*, 1984, **7**, 104.
22. A. P. Wade, *Anal. Proc.*, 1983, **20**, 108.
23. G. C. M. Bourke, G. Stedman and A. P. Wade, *Anal. Chim. Acta*, 1983, **153**, 277.
24. R. M. Belchamber, D. Betteridge, P. Y. T. Chow, T. J. Sly and A. P. Wade, *ibid.*, 1983, **150**, 115.
25. A. P. Wade, *Anal. Proc.*, 1983, **20**, 523.
26. D. Betteridge, A. F. Taylor and A. P. Wade, *ibid.*, 1984, **21**, 373.
27. R. M. Belchamber, D. Betteridge, J. Cruikshank, P. Davison and A. P. Wade, *Spectrochim. Acta*, in the press.
28. T. P. Lynch, N. J. Kernoghan and J. N. Wilson, *Analyst*, 1984, **109**, 843.
29. S. Al-Najafi, A. P. Wade, C. A. Wellington, T. J. Sly and D. Betteridge, *ibid.*, in the press.
30. D. Betteridge, T. J. Sly and A. P. Wade, *Anal. Chem.*, in the press.
31. J. J. Kosman, J. E. Thompson and A. W. Varnes, Internal Report, Warrensville Laboratory, The Standard Oil Company, Cleveland, USA, 1983.
32. E. S. Page and L. B. Wilson, *Information Representation and Manipulation in a Computer*, 2nd Ed., Cambridge University Press, London, 1979.
33. L. R. Parker, S. L. Morgan and S. N. Deming, *Appl. Spectrosc.*, 1975, **29**, 429.
34. S. N. Deming and S. L. Morgan, *Anal. Chem.*, 1973, **45**, 278A.
35. M. J. D. Powell, *Computer J.*, 1964, **7**, 155.
36. T. Lilley, *Anal. Proc.*, 1984, **21**, 147.
37. R. M. Belchamber and G. Horlick, *Spectrochim. Acta*, 1982, **37B**, 71.
38. H. V. Malmstadt, C. G. Enke, S. R. Crouch and G. Horlick, *Optimization of Electronic Measurements*, Benjamin, California, 1974.
39. R. M. Belchamber and G. Horlick, *Spectrochim. Acta*, 1982, **37B**, 17.
40. W. Murray (ed.), *Numerical Methods for Unconstrained Optimization*, Academic Press, London, 1972.
41. G. R. Walsh, *Methods of Optimization*, Wiley, New York, 1979.
42. S. N. Deming and S. L. Morgan, *Anal. Chim. Acta*, 1983, **150**, 183.
43. J. Creighton, *Ph.D. Thesis*, Dundee University, 1980.
44. G. Van Terheyden, private communication, September 1984.
45. H. H. Willard, L. L. Merritt, Jr., J. A. Dean and F. A. Settle, Jr., *Instrumental Methods of Analysis*, 6th Ed., pp. 431–564. Van Nostrand, New York, 1981.
46. C. J. Suckling, K. E. Suckling and C. W. Suckling, *Chemistry Through Models*, pp. 260–266. Cambridge University Press, Cambridge, 1978.
47. D. N. Burghes and M. S. Borrie, *Modelling with Differential Equations*, pp. 70–71, 130–133. Horwood, Chichester, 1982.
48. P. K. Erni and H. Muller, *Anal. Chim. Acta*, 1978, **103**, 189.
49. D. Betteridge, A. P. Wade and C. Z. Marczewski, *ibid.*, 1984, **165**, 227.
50. C. C. Painton and H. A. Mottola, *ibid.*, 1984, **158**, 67.
51. C. D. Crowe, H. Levin, D. Betteridge and A. P. Wade,

Proc. FACCS 11 Conf., Paper 291, Federation of Analytical Chemistry and Spectroscopy Societies, Philadelphia, USA, 16–21 September 1984.
52. B. G. M. Vandeginste, unpublished results, 1984.
53. R. M. Belchamber, D. Betteridge, P. Y. T. Chow, T. Lilley, M. E. A. Cudby and D. G. M. Wood, *J. Acoustic Emission*, in the press.
54. R. R. Hocking, *Biometrics*, 1976, **32**, 1.

Talanta, Vol. 32, No. 8B, pp. 735–743, 1985
Printed in Great Britain.

0039-9140/85 $3.00 + 0.00

ANALYTICAL USE OF SOLVENT EXTRACTION WITH ACETONITRILE/WATER/CHLOROFORM AND 1-PROPANOL/WATER/CYCLOHEXANE MIXTURES

T. HORI*
Department of Chemistry, College of Liberal Arts and Sciences, Kyoto University, Kyoto 606, Japan

T. FUJINAGA
Professor Emeritus of Kyoto University, Kyoto University, Kyoto 606, Japan

(*Received* 12 *October* 1984. *Accepted* 12 *February* 1985)

Summary—To obtain an organic phase containing acetonitrile or 1-propanol from aqueous acetonitrile or aqueous 1-propanol solution, the effect of chloroform and cyclohexane as auxiliary solvents has been investigated. Use of such ternary systems offers an alternative to the so-called salting-out method, in which inorganic salts or hydrophilic organic materials are used to separate organic phases from otherwise miscible solvent mixtures. It also seems preferable for solvent-extraction procedures, since only a small amount of auxiliary solvent is needed instead of the usually large amount of a salt (impurities in which may cause undue contamination); also, the volume and composition of the organic phase can be predicted from phase diagrams and the overall composition of the solvent mixture. Volume-fraction diagrams are especially easy to use. Furthermore, equilibrium is attained in solvent mixtures more rapidly than in salting-out systems. The utility of the ternary solvent systems has been demonstrated for extraction of intermediate molybdophosphate complexes which are specifically formed in aqueous acetonitrile solutions.

When aqueous solutions are extracted with organic solvents, certain solvents such as acetonitrile and acetone cannot be used as extracting solvents because they are miscible with water in all proportions. For the same reason, methanol, ethanol, dimethylsulphoxide, hexamethylphosphoramide, *etc.* are omitted from use as extractants from aqueous solution, although their high dielectric constants, donor numbers, and solubility parameters would make them especially useful if they *could* be employed. If some means could be found to separate these solvents as organic phases from aqueous solutions, the versatility of solvent extraction would be greatly increased.

An attempt to separate acetone as an organic phase was made by Matkovich and Christian,[1,2] by using the salting-out effect, and the acetone phase thus obtained served not only to extract certain metal chelates but also to increase the sensitivity in the subsequent determination of the metals by flame-emission or atomic-absorption spectrophotometry. Of 79 salts tested, these authors recommended calcium chloride and sucrose as suitable agents for salting-out of acetone, but the metal impurities in the calcium salt and the high viscosity in the aqueous phase given by the sucrose caused problems in practical analysis.

Nagaosa[3–6] and Fujinaga and Nagaosa[7] separated an acetonitrile phase by salting-out, and extracted various ion-pairs and metal chelates, which were then measured directly in the extract by polarography, after addition of suitable supporting electrolytes. More recently,[8] they extended salting-out to the separation of such solvents as dioxan, tetrahydrofuran, ethanol and 1-propanol.

Kofanov and Nevinnaya[9] employed such methods for the extractive concentration of traces of hydrophilic materials present in natural waters.

In work on the partition behaviour for a given compound between a pair of solvents, *e.g.*, 1-butanol and water or 4-methyl-2-pentanone and water, we had earlier sought suitable means of minimizing the mutual solubilities of the solvents and found[10,11] it very effective to add an auxiliary solvent such as cyclohexane to the binary solvent system. It was noted in particular that even a completely miscible solvent pair such as acetonitrile and water could be separated into two phases by addition of chloroform as an auxiliary solvent.[12]

Although such auxiliary solvents need to be found empirically, once a suitable one has been found and the phase diagrams for the ternary system have been constructed, the phases obtainable by use of various ternary solvent compositions can be used for solvent extraction as easily as the solvent pairs in conventional solvent extraction systems.

We describe in this paper the acetonitrile/water/chloroform and 1-propanol/water/cyclohexane systems and report on their possible uses for extraction analysis of aqueous samples. A way to search for other ternary systems which would separate otherwise miscible solvents will also be discussed by introducing simulated phase diagrams.

EXPERIMENTAL

Reagents

Acetonitrile, cyclohexane and 1-propanol were G.R. grade reagents from Wako Pure Chemicals Co. and purified by distillation[13–15] for use in establishing the phase diagrams.

*Author for correspondence.

Chloroform, G.R. grade, was washed three times with water, just before use, to remove ethanol present as stabilizer, and dried over anhydrous sodium sulphate.

Tris(trifluoroacetylacetonato)iron(III), $Fe(TFA)_3$, was synthesized[16] by adding an aqueous solution of ferric chloride dropwise to a methanol solution of TFA and extracting with chloroform. The crude chelate was purified by recrystallization from methanol–hexane mixture.

β-Molybdophosphate, $PMo_{12}O_{40}^{3-}$, was prepared in a medium consisting of 0.05*M* Mo(VI)/1.2*M* hydrochloric acid/40% v/v acetonitrile as described previously, and the yellow complex anion was electrolytically reduced to phosphomolybdenum blue.[17,18]

Apparatus

A Shimadzu model GC-4C gas chromatograph equipped with thermal conductivity detectors was used. The column was a 1.0 m × 3 mm bore stainless-steel coil packed with Polapak Q (80–100 mesh). The ovens for the column, injection port and detectors were maintained at 170°, 170° and 200°, respectively. Helium was used as carrier gas at a flow-rate of 50 ml/min.

Volume-fraction phase diagram for the acetonitrile/water/chloroform system

Into 10-ml (or 20-ml, if necessary) graduated centrifuge tubes (with standard-taper glass stoppers and previously calibrated), were placed V_A ml of acetonitrile, V_B ml of water, and V_C ml of chloroform, all at 25°, the sum of the volumes being kept constant at 10 (or 20) ml, *i.e.*, $V_0 = V_A + V_B + V_C = 10$ (or 20) ml, and the composition varied from sample to sample. The tubes were tightly stoppered and shaken well. The samples were left for approximately 1 hr in a bath kept at 25 ± 0.1°, and shaken occasionally. When equilibrium had been attained, the total volume and the volumes of the lower and the upper layers of the sample (V_T, V_L, and V_U respectively) were read. The organic and aqueous phases in this solvent system change their relative positions according to the chloroform content of the phases, so the layer which was the organic phase was identified, and hence the volume of the organic phase, V_{org}. Then $R_{org} = V_{org}/V_0$ was calculated for each sample and the values were plotted in equilateral triangle co-ordinates, expressed in terms of volume-fractions of the component solvents. Finally, a smooth line was drawn through the points which had equal values of R_{org} (when necessary, approximating by interpolation).

Such a diagram is shown in Fig. 1, for R_{org} (thin lines) from 0.1 to 0.9. The solubility curve is shown by the thicker line in Fig. 1, and indicates the boundary between the single-phase and two-phase regions of the ternary system. The broken line indicates the critical compositions at which the two phases change position: for the region above the broken line the organic phase is the lower layer and for the region below the line the organic phase is the upper layer. The organic phase can be identified either by means of its interface being convex towards the aqueous phase, or by adding certain organophilic coloured materials (as shown in Plates 1 and 2). At the critical composition, the two phases (being of equal density) will not separate into two layers, the organic phase remaining suspended in the other phase, and extractions at these solvent compositions are thus impracticable.

Points P, Q, and R on line AB of the triangle are introduced to facilitate description of the characteristics of this ternary system, as described later. Three series of points (a–f, g–l, m–r) are shown on lines PC, QC, and RC, respectively, and series of solvent extractions were performed with the solvent compositions indicated by these points, as described later.

Weight-fraction phase diagram

Besides measurement of the volumes of the separated phases, their phase compositions were obtained by gas chromatography. The results are shown in Fig. 2 in terms of weight-fractions of the components. The solubility curve and the tie-lines are shown with a thick line and thinner lines, respectively. As usual, the points at the ends of the tie-lines show the composition of the two phases in equilibrium, the full circles indicating that the phase formed is

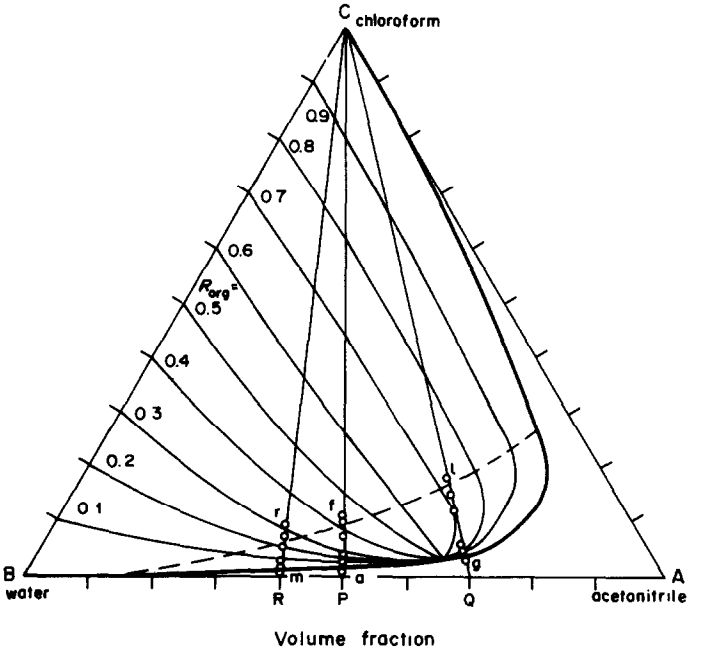

Fig. 1. A phase-separation diagram for the ternary system of acetonitrile (A)/water(B)/chloroform (C) at 25°C. The values for R_{org}, *i.e.*, volume-ratios of V_{org}/V_0, where $V_0 = V_A + V_B + V_C$, are presented as a function of the total compositions of the component solvents. Lines PC, QC, and RC, and points a–f, g–l, and m–r are introduced to explain the phase-separations shown in Plates 1–3.

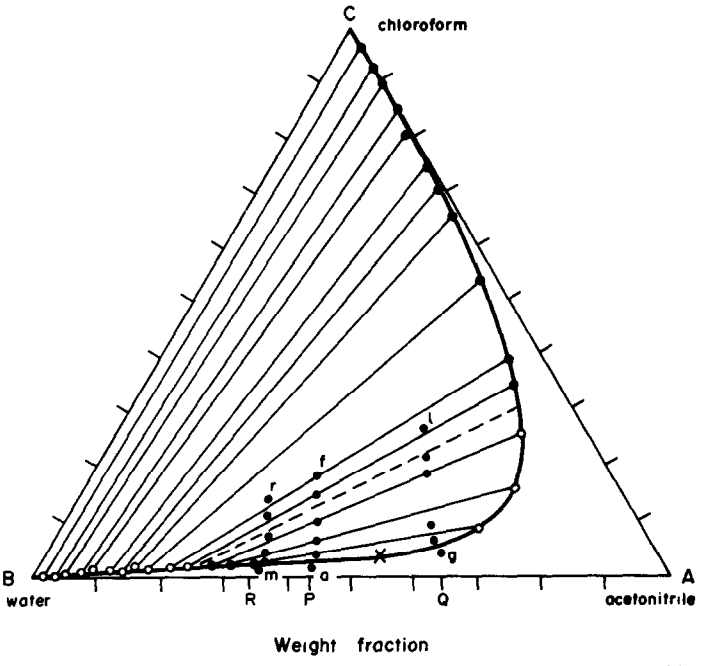

Fig. 2. A weight-fraction phase diagram for the ternary system of acetonitrile/water/chloroform at 25°C. Points P, Q, and R on line AB, and points a–f, g–l, and m–r in the triangle are transferred from Fig. 1. Details for other lines and points are described in the text.

the lower layer and the open circles that the phase is the upper layer. The broken line shows the critical tie-line at which the specific gravities of the equilibrated phases are identical. The plait point in the system, which was approximated by extrapolation, is marked with a cross on the lower branch of the solubility curve. Points P, Q and R on line AB and the series of points a–f; g–l; m–r inside the triangle, are transferred from Fig. 1 by converting the volume-fractions into weight-fractions by using specific gravities[19] of 0.777, 0.997 and 1.480 (at 25°) for pure acetonitrile, water and chloroform, respectively.

RESULTS AND DISCUSSION

Formation of organic phases from aqueous acetonitrile solutions by addition of chloroform

Plate 1 shows the effect of adding increasing amounts of chloroform to a mixture of 10 ml of water and 10 ml of acetonitrile containing about 10 mg of $Fe(TFA)_3$ to indicate the organic phase formed, and equilibrating at 25°. Addition of only 0.2 ml of chloroform causes no phase separation, but 0.4 ml results in approximately 5 ml of organic phase being separated, into which the chelate is extracted almost quantitatively. Obviously the organic phase in tube b is almost entirely acetonitrile, and does not increase much in volume on further addition of chloroform (tubes c–f), but the phases change position when the chloroform content is changed from 1.6 to 2.2 ml.

Similar experiments with 6 ml of water and 14 ml of acetonitrile are illustrated in Plate 2. Sample h shows that more than 14 ml of organic phase is obtained by addition of as little as 0.8 ml of chloroform, and it might be said that the aqueous phase is squeezed from the aqueous acetonitrile solution by the chloroform. It is interesting that addition of 1.2 ml of chloroform (sample i) results in a slight decrease of the organic phase volume.

The addition of chloroform is thus very effective for separating an organic phase from aqueous acetonitrile, although the volume of the organic phase changes in a rather complicated manner, depending not only on the volume of chloroform added but also on the initial composition of the aqueous acetonitrile solution. In general, it is difficult to predict, by non-empirical means, the volumes as a function of the composition of the ternary mixtures. It is for this reason that ternary (or even more complicated) solvent systems have not been extensively investigated for solvent extraction, and only a few applications have been reported so far (*e.g.*, by Mitra and Mitra,[20] Natusch and Tomkins[21]).

On the other hand, it is fairly easy to measure such phase volumes empirically and represent them quantitatively on phase diagrams, according to thermodynamic procedures, as shown in Fig. 1. In Fig. 1 point P corresponds to a 1:1 v/v mixture of acetonitrile and water. As chloroform is added, the total (volume) composition of the ternary mixture moves from point P towards C along line PC. The phase separations in Plate 1 are, therefore, interpreted according to the line PC, the samples a–f corresponding to the points a–f in Fig. 1.

Conversely, when such a diagram as Fig. 1 is provided and the volumes of chloroform to be added, V_C, are properly chosen, the volume of organic phase obtained can be calculated. For each value of V_C, we can calculate the volume fraction of chloroform in the ternary mixture (since $V_A = V_B = 10$ ml) and read R_{org} from line PC. As $V_0 = V_A + V_B + V_C$ and

Table 1. Volumes and compositions of organic phases attained from mixtures of acetonitrile (A) and water (B) by addition of chloroform (C) at 25°C

Sample	V_C, ml*	Total composition† A	B	C	V_{org}, ml§	Composition of equilibrium org. phase, wt. fraction‡ A	B	C
		[V_A = 10.0 ml, V_B = 10.0 ml]¶						
a	0.20	0.495	0.495	0.010	—	—	—	—
		0.431	0.553	0.016				
b	0.40	0.490	0.490	0.020	5.06	0.657	0.258	0.085
		0.424	0.544	0.032				
c	0.80	0.481	0.481	0.039	6.72	0.670	0.167	0.163
		0.410	0.527	0.063				
d	1.60	0.643	0.643	0.074	8.32	0.629	0.104	0.267
		0.386	0.496	0.118				
e	2.20	0.450	0.450	0.099	10.2	0.569	0.075	0.356
		0.370	0.475	0.155				
f	2.60	0.444	0.444	0.111	10.6	0.538	0.060	0.402
		0.360	0.462	0.178				
		[V_A = 14.0 ml, V_B = 6.0 ml]¶						
g	0.60	0.680	0.291	0.029	—	—	—	—
		0.613	0.337	0.050				
h	0.80	0.673	0.288	0.034	14.2	0.627	0.300	0.073
		0.603	0.332	0.066				
i	1.20	0.660	0.283	0.056	13.9	0.666	0.213	0.121
		0.584	0.321	0.095				
j	2.80	0.614	0.263	0.123	15.5	0.629	0.104	0.267
		0.518	0.285	0.197				
k	3.60	0.593	0.254	0.153	16.3	0.604	0.088	0.308
		0.430	0.270	0.240				
l	4.40	0.574	0.246	0.180	17.5	0.558	0.071	0.371
		0.465	0.256	0.279				
		[V_A = 8.0 ml, V_B = 12.0 ml]¶						
m	0.10	0.398	0.597	0.005	—	—	—	—
		0.339	0.653	0.008				
n	0.20	0.396	0.594	0.010	0.75 (0.95)#	0.657	0.258	0.085
		0.336	0.648	0.016				
o	0.40	0.392	0.588	0.020	2.07 (2.64)#	0.657	0.146	0.197
		0.332	0.637	0.032				
p	1.00	0.381	0.571	0.048	4.08 (6.36)#	0.604	0.088	0.308
		0.316	0.609	0.075				
q	1.50	0.372	0.558	0.070	4.93 (7.14)#	0.558	0.067	0.375
		0.305	0.587	0.109				
r	2.00	0.364	0.545	0.091	6.45 (8.06)#	0.521	0.050	0.429
		0.294	0.566	0.140				

*Volumes of chloroform added.
†Upper value is the volume–fraction, lower value is the weight-fraction.
§Volumes of organic phases calculated by reading R_{org} values from the phase-separation diagram (Fig. 1) and using the relation $V_{org} = R_{org} \times V_0$, where $V_0 = V_A + V_B + V_C$.
‡Values read off from the phase-diagram (Fig. 2).
¶Binary mixtures subjected to phase separation by addition of chloroform.
#Values in parentheses are those attained in the aqueous acetonitrile medium composed of 0.05*M* Mo(VI)/1.2*M* HCl/40% v/v acetonitrile.

$R_{org} = V_{org}/V_0$ for any composition on the triangle, V_{org} can be found by solving these equations with the given value of V_C. Representative results calculated for V_{org} are listed in Table 1, and explain the volumes observed in the experiments shown in Plate 1, since the chelate concentration was low enough not to disturb the phase equilibrium in the ternary system.

The composition of the organic phase can be read from the phase diagram in Fig. 2 by using the tie-line and the solubility curve, and these results are also

Plate 1. Phase-separations from 50% v/v aqueous acetonitrile medium by addition of chloroform. From left to right, the volume of chloroform increases: 0.2, 0.4, 0.8, 1.6, 2.2 and 2.6 ml. The organic phases separated are indicated by the partition of $Fe(TFA)_3$.

Plate 2. Phase-separations from 70% v/v aqueous acetonitrile by chloroform. From left to right, the chloroform volume increases: 0.6, 0.8, 1.2, 2.8, 3.6 and 4.4 ml.

Plate 3. Extraction of an intermediate molybdophosphate (β-molybdophosphate) in the yellow (oxidized) state. The complexes were formed in 0.05*M* Mo(VI)/1.2*M* HCl/40% v/v acetonitrile medium, and extracted by adding increasing amounts of chloroform (0.1, 0.2, 0.4, 1.0, 1.5 and 2.0 ml).

Plate 4. Extraction of the blue reduced β-molybdophosphate. Conditions as for Plate 3.

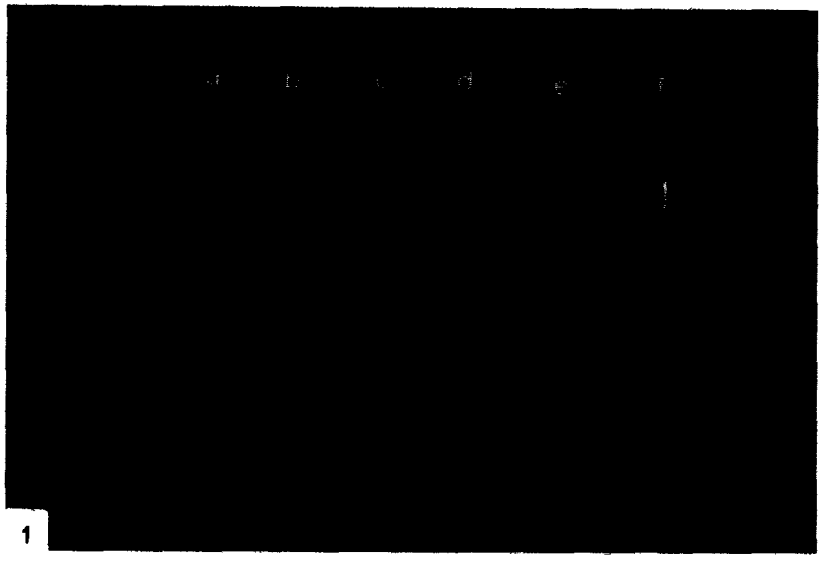

1

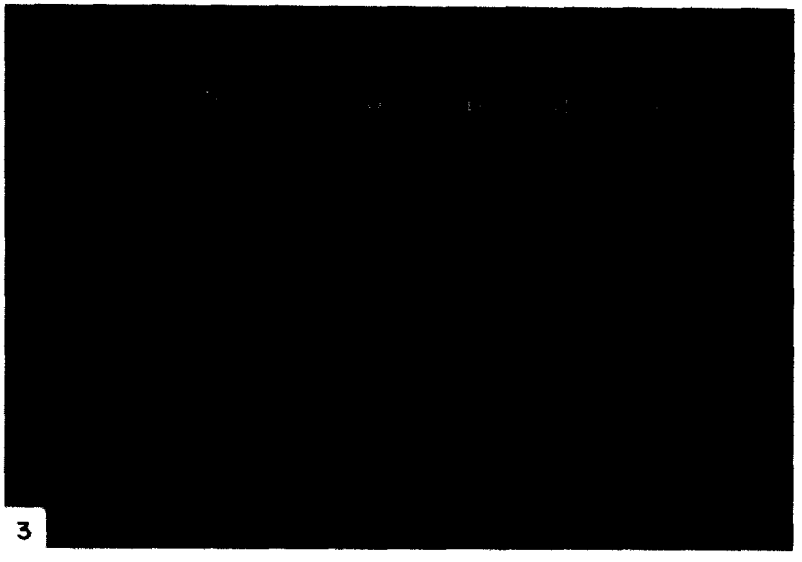

3

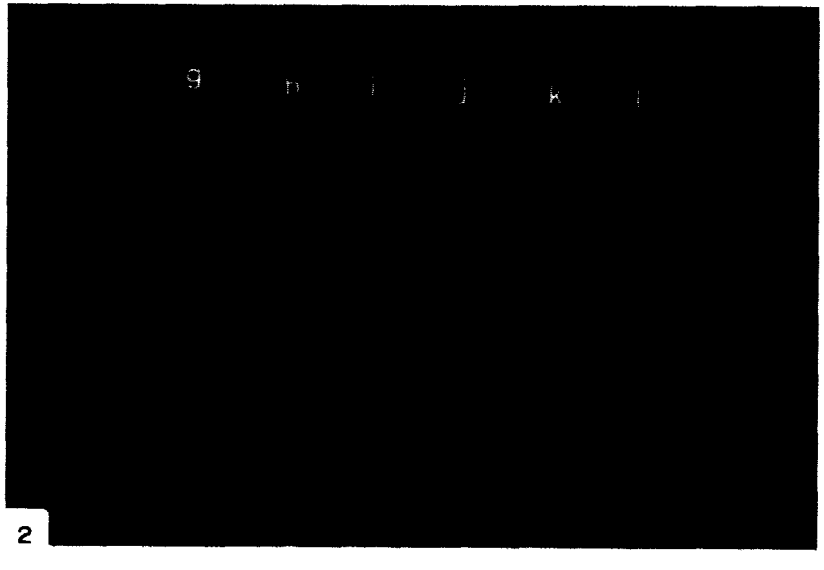

2

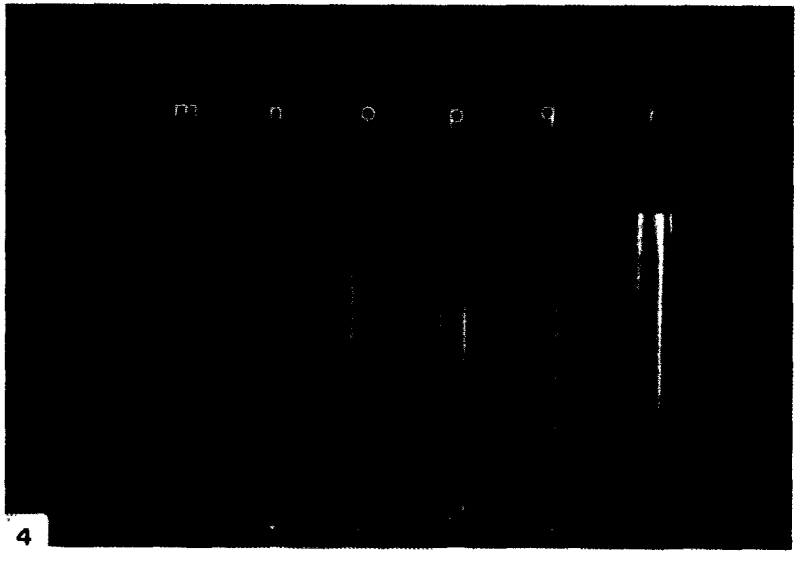

4

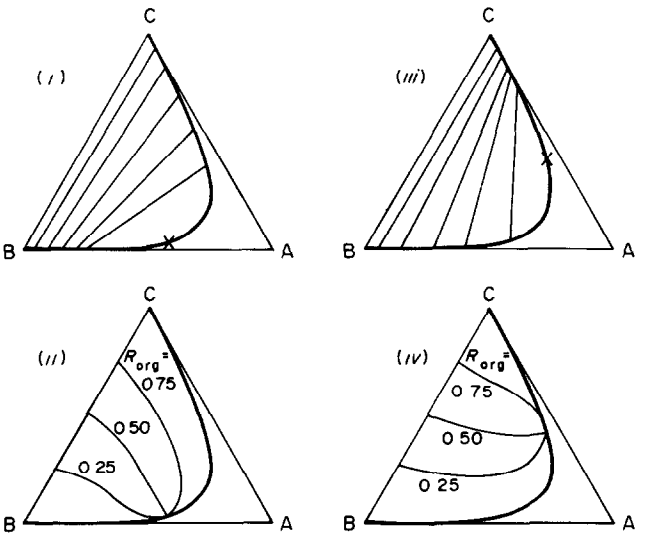

Fig. 3. Ternary solvent systems available for the phase-separation of otherwise miscible solvents. For generalized ternary systems consisting of solvents A, B and C, weight-fraction phase diagrams, (*i*) and (*iii*), and volume fraction, (*ii*) *and* (*iv*), phase-separation diagrams were simulated by supposing that each component solvent has a specific gravity of unity and that their specific volumes are unchanged on mixing. The positions of the plait points and the slopes of the tie-lines in (*i*) and (*iii*) are well characterized by the R_{org} curves in diagrams (*ii*) and (*iv*).

listed in Table 1. As can be seen in the last three columns of the table, the organic phase produced by relatively small amounts of chloroform contains acetonitrile as the main component. Such systems could be said to correspond to virtual extraction into acetonitrile.

The extractions shown in Plate 2 can be similarly interpreted, by using line QC in Fig. 1, where AQ:QB is 3:7, which corresponds to the aqueous acetonitrile solution used. The volumes and compositions of the organic phases are again summarized, in Table 1, as a function of the added volume of chloroform, V_C.

It is obvious that the compositions of the organic phases for both the 50 and 70% aqueous acetonitrile solutions simply change according to the same solubility curve and the increase in volume of chloroform added. Thus it is made possible to use acetonitrile as an extracting solvent even from aqueous solutions.

Application of the ternary system to extraction of an intermediate molybdophosphate complex.

The ternary solvent system described above was used for extraction of an intermediate molybdophosphate complex which is known to form neither in purely aqueous nor in purely acetonitrile medium, but in aqueous acetonitrile medium.[17]

The volumes of organic phase to be separated from the 40% aqueous acetonitrile medium used were first calculated, as before, for various amounts of chloroform (points m–r on line RC in Fig. 1) and are given in Table 1 along with the compositions of the organic phase (read from Fig. 2). As can be seen, organic phases containing acetonitrile would be expected to form.

The extractions of the molybdophosphate complex are demonstrated in Plate 3 (for the complex in the yellow oxidized state) and Plate 4 (for the blue reduced state). The complex in either state can be quantitatively extracted into the organic phase, in which acetonitrile is the operative solvent, as chloroform is known not to extract the complex at all.

Other ternary systems for phase separation of otherwise miscible solvents

The ternary system of acetonitrile/water/chloroform can be symbolized as in Fig. 3(*i*). As can be deduced from (*i*), for good phase separation the solubility curve has to be close to sides AB and AC of the triangle. The closer the two branches of the solubility curve approach to AB and AC, the smaller the addition of component C needed to give effective phase separation. The position of the plait point of the system is also important. Two extreme cases can be considered, as shown in Fig. 3(*i*) and (*iii*); in (*i*) the plait point appears on the lower branch of the solubility curve and very close to line AB, whereas in (*iii*) it is on the opposite branch close to line AC. Obviously (*i*) represents a ternary system such as acetonitrile/water/chloroform and (*iii*) would represent such a system as ethanol (A)/water (B)/2,2,4-trimethylpentane (C), which was reported by Huber[22] in his studies on solvent mixtures for liquid–liquid chromatography. These two phase diagrams are the same with respect to efficiency of phase separation by addition of the same small volume of the third component C, but differ considerably in terms of the composition of the equilibrated phases. In such a system as that shown by (*i*), the slopes of the tie-lines show that the organic phase should contain fair amounts of component A, whereas in the

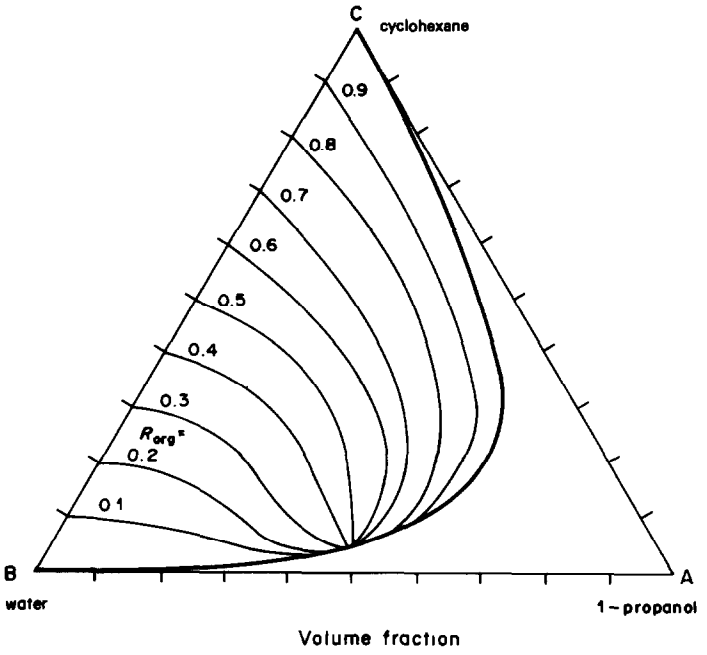

Fig. 4. Phase-separation diagram for the ternary system of 1-propanol (A)/water (B)/cyclohexane (C) at 25°C.

other system, (*iii*), the organic phase mainly contains component C and is rather poor in component A. Hence if the organic phase is desired to be rich in component A, the third component should be one that gives a diagram of type (*i*).

The volume-fraction diagrams (*ii*) and (*iv*) in Fig. 3 were obtained by simulating types (*i*) and (*iii*), on the assumptions that every component solvent has a specific gravity of unity and their specific volumes are unchanged on mixing, but that the two phases will separate into layers. As shown in (*ii*) and (*iv*), the simulated R_{org} curves merge towards the plait point of the system and approximate well to the weight-fraction phase diagrams (*i*) and (*iii*). For detailed discussion of the thermodynamic properties of the system, of course, it is necessary to establish the weight- or molar-fraction phase diagrams, but the volume-fraction diagrams are sufficient to reveal the characteristics for phase separations in solvent mixtures.

Numerous solvent systems investigated in liquid–liquid phase-equilibria studies have been comprehensively reported.[23,24] In addition to such experimental data, theoretical calculations based on the NRTL, UNIFAC and UNIQUAC equations[25] have been successfully used for predicting the phase equilibria in various ternary solvent systems, even though the systems include highly non-ideal components such as water and alcohols. Reference to these empirical and/or theoretical results will suggest suitable media for exploration in selective extraction. As indicated above, the acetonitrile/water/chloroform system has considerable potential in this field.

Similarly, the ternary system of 1-propanol/water/cyclohexane[26,27] would be another choice, since it readily provides a propanol-rich phase from aqueous 1-propanol solutions on addition of cyclohexane. That is to say, solvent extractions with 1-propanol could be conducted practically, even with aqueous samples.

Recently, we measured the volume-fraction phase diagram for 1-propanol(A)/water(B)/cyclohexane(C). As shown in Fig. 4, the pattern of R_{org} curves resembles that in diagram (*ii*) in Fig. 3, confirming that this solvent system promises formation of a useful propanol-rich organic phase from 1-propanol/water mixture by addition of cyclohexane, but we have not yet worked out any practical applications.

Acknowledgement—The authors' thanks are due to Mr. A. Shuhara for measuring phase-separation diagrams for the ternary solvent systems cited in this report.

REFERENCES

1. C. E. Matkovich and G. D. Christian, *Anal. Chem.*, 1973, **45**, 1915.
2. *Idem, ibid.*, 1974, **46**, 102.
3. Y. Nagaosa, *Mikrochim. Acta*, 1979 **I**, 495.
4. *Idem, Z. Anal. Chem.*, 1979, **296**, 259.
5. *Idem, Talanta*, 1979, **26**, 987.
6. *Idem, Anal. Chim. Acta*, 1980, **115**, 81; 1980, **120**, 279.
7. T. Fujinaga and Y. Nagaosa, *Bull. Chem. Soc. Japan*, 1980, **53**, 416.
8. *Idem, Chem. Lett.*, 1978, 587.
9. V. I. Kofanov and L. V. Nevinnaya, Paper presented at IInd USSR–Japan Symposium Anal. Chem., Moscow, 1984.
10. T. Fujinaga, T. Hori and Y. Kanada, *Bunseki Kagaku*, 1977, **26**, 829.
11. *Idem, ibid.*, 1978, **27**, 395.

12. T. Fujinaga, A. Shuhara and T. Hori, *ibid.*, 1984, **33**, 159.
13. E. O. Sherman and V. C. Olson, *Anal. Chem.*, 1968, **40**, 1174.
14. T. L. Brown, *J. Am. Chem. Soc.*, 1959, **81**, 3232.
15. J. F. Mathews and J. J. McKetta, *J. Phys. Chem.*, 1961, **65**, 758.
16. T. Fujinaga, T. Kuwamoto, K. Sugiura, S. Ichiki and N. Matsubara, *Bunseki Kagaku*, 1980, **29**, 796.
17. T. Hori and T. Fujinaga, *Chem. Lett.*, 1983, 687.
18. *Idem*, *Bull. Chem. Soc. Japan*, 1985, **58**, 1380.
19. J. A. Riddick and W. B. Bunger, *Techniques of Chemistry, Vol. II, Organic Solvents*, 3rd Ed., Wiley–Interscience, New York.
20. M. Mitra and B. K. Mitra, *Talanta*, 1977, **24**, 698
21. D. F. S. Natusch and B. A. Tomkins, *Anal. Chem.*, 1978, **50**, 1429.
22. J. F. K. Huber, *J. Chromatog. Sci.*, 1971, **9**, 72.
23. J. Wisniak and A. Tamir, *Physical Sciences Data 7A, Liquid-Liquid Equilibrium and Extraction*, Elsevier, Amsterdam, 1980.
24. J. M. Sørensen and W. Arlt, *DECHEMA Chemistry Data Series, Volume V, Liquid–Liquid Equilibrium Data Collection*, DECHEMA, Frankfurt, 1980.
25. S. A. Newman (ed.), *Chemical Engineering Thermodynamics*, Ann Arbor Science, Ann Arbor, Michigan, 1982.
26. A. S. Smith, *Ind. Eng. Chem.*, 1950, **42**, 1206.
27. I. Hanssens, J. Mullens, C. Deneuter and P. Huyskens, *Bull. Soc. Chim. France*, 1968, 3942.

Talanta, Vol. 32, No. 8B, pp. 745–749, 1985
Printed in Great Britain.

0039-9140/85 $3.00 + 0.00

LUMINESCENCE PROBE STUDIES OF IONOMERS—II

STEADY-STATE MEASUREMENTS FROM SULPHONATED POLYETHYLENE AND TEFLON MEMBRANES

MARILYN N. SZENTIRMAY, NELSON E. PRIETO and CHARLES R. MARTIN*
Department of Chemistry, Texas A&M University, College Station, Texas 77843, U.S.A.

(*Received* 5 *December* 1984. *Accepted* 18 *January* 1985)

Summary—Luminescence probe studies of sulphonated Teflon and sulphonated polyethylene ionomer membranes are described. These studies have shown that the micropolarities of the ionic clusters within these ionomers are quite dynamic, varying with the nature of the chain material and the membrane water content. These studies also suggest that polymer chain material intrudes into the ionic cluster phase.

Ion-containing polymers, or "ionomers",[1,2] are used in a variety of chemical and electrochemical processes and devices, including fuel cells,[3] solar-energy conversion systems,[4] batteries,[5] chemically modified electrodes[6] and industrial electrolytic processes.[7] Because of their technological importance, a broad range of chemical methods is currently being used to study the chemical and morphological properties of these polymers.[8–12] This research effort has shown that the charged groups in ionomers can aggregate to form micelle-like domains called ionic clusters. The structural and chemical details of these microdomains have not yet been elucidated.

Because luminescence probe methods have proved useful in studies of micelles[13] and other chemical microdomains, we and others have been using luminescence methods to study ionomers.[14–16] We have recently examined the micropolarity of the ionic clusters in Nafion, a perfluorosulphonate ionomer, by following changes in the luminescence properties of incorporated probes.[16] The micropolarity varied significantly, depending on the water content and the type of counter-ion.[16] These results are valuable in that the polarity of Nafion, as indicated by the luminescent probe, can be used to predict the chemical properties of the microenvironment around other molecules or ions (*e.g.*, electroactive species, catalysts, diffusants) incorporated into the membrane. These data can in turn aid in the prediction or interpretation of the rates and courses of chemical and electrochemical processes occurring within the membrane.[16] For example, by using the results of luminescence probe experiments, we have recently succeeded in changing the redox potential of ferrocene in a Nafion film at an electrode surface, by adjusting the film polarity through incorporation of a hydrophobic counter-ion.[16]

Ionomers prepared by grafting styrenesulphonate side-chains onto sheets of hydrocarbon or fluorocarbon polymers are proving to be important membrane materials.[17] For this reason, we have used luminescence probe experiments to study the chemical and morphological properties of styrenesulphonate-grafted Teflon and polyethylene membranes. The results of these studies are reported here.

EXPERIMENTAL

Materials

Sulphonated polyethylene (PE-SS, 700 g per mole of $-SO_3H$) and sulphonated polytetrafluoroethylene (PFE-SS 850 g per mole of $-SO_3H$) were donated by RAI Research Corporation (Hauppage, NY). These polymers are prepared by radiation-grafting styrene side-chains onto preformed Teflon or polyethylene sheets; the side-chains are then sulphonated by use of sulphuric acid.[17] 5-Dimethylaminonaphthalene-1-sulphonamidoethyltrimethylammonium perchlorate ($DAClO_4$) was obtained from Sigma. $Ru(bpy)_3Cl_2 \cdot 6H_2O$ (bpy = 2,2′-bipyridine) was obtained from G.F. Smith. Pyrene (Py) (99 + % pure) and caesium hydroxide were obtained from Aldrich. All other chemicals were of reagent grade. Water was either triply distilled or circulated through a Milli-Q water-purification system (Millipore Corp.).

Procedures

PFE-SS was cleaned ultrasonically in ethanol for 4 hr. PE-SS was cleaned ultrasonically in 1:1 ethanol–water mixture for 1 hr. After cleaning, all membranes were boiled in water for 4 hr. Membranes in various counter-ionic forms were prepared by soaking the H^+-form membranes in concentrated solutions of the appropriate metal hydroxide. Excess of base was then removed by stirring the membranes in several portions of pure water. The luminescent probes [Py, DA^+, $Ru(bpy)_3^{2+}$] were incorporated (loaded) by stirring the membranes in aqueous solutions of the probes. The quantity of probe incorporated was determined spectrophotometrically;[16] loading levels were kept low [DA^+ and $Ru(bpy)_3^{2+}$ less than 3 probe ions per 100 $-SO_3^-$ sites, Py *ca.* 3 probe molecules per 1000 $-SO_3^-$ sites] so as to minimize the effect of the probe on the membrane microenvironment.

The effects of membrane water content on the emission characteristics of the probes were investigated by gradually drying the membranes, first by exposure to air, then in a

*Author for correspondence.

desiccator, and finally in a vacuum oven (temperature <70°). The water content of each membrane was determined from the average of weights recorded immediately before and after each spectrum was acquired. The water content is reported as per cent by weight (100 × wt. of H_2O/wt. of dry polymer) and as the number of water molecules per $-SO_3^-$ site. Membranes dried in a vacuum oven at 100° for 1–3 days served as "zero" water-content references.[16]

Spectroscopy

Emission spectra were obtained with a Spex Fluorolog 2 spectrofluorometer. The Spex solid-sample holder with front-surface viewing geometry was used. Excitation wavelengths for Py, $Ru(bpy)_3^{2+}$ and DA^+ were 310, 445 and 340 nm respectively, unless otherwise noted. Emission monochromator band-widths of 0.8 nm (Py spectra) and 4.1 nm [$Ru(bpy)_3^{2+}$ and DA^+ spectra] were used. Absorption spectra were recorded on a Beckman 26 spectrophotometer. The PFE-SS did not absorb light of wavelengths longer than 350 nm and no PFE-SS emission was detected when the excitation wavelengths stated above were used. In contrast, the PE-SS absorbed light of wavelengths shorter than 400 nm and showed an absorbance maximum at 374 nm. PE-SS also gave a weak emission when excited at any of the wavelengths used in these studies.

The spectroscopic characteristics of the PE-SS were both enigmatic and undesirable. A polyethylene film containing styrenesulphonate groups would not be expected to absorb light at wavelengths longer than *ca.* 300 nm, so it seems likely that some impurity was present. This impurity could not, however, be cleaned from the membrane by using conventional membrane pretreatment procedures.[14,16,18] This suggests that the impurities might be covalently attached and result from damage incurred during the grafting or sulphonation steps. The spurious absorbance/emission of the PE-SS was undesirable because it caused interference in the analysis of the probe's luminescence data. This interference precluded the use of Py as a probe in PE-SS and make it difficult to interpret the effect of drying on emission by DA^+ in PE-SS.

RESULTS AND DISCUSSION

Luminescent probes

Three luminescent molecules, Py, DA^+ and $Ru(bpy)_3^{2+}$, were chosen as probes of the microenvironments within the radiation-grafted membranes. As discussed in detail in our previous paper,[16] these probes were chosen because the effects of environment polarity on their emission characteristics have been extensively studied. Briefly, emission spectra of pyrene contain partly resolved vibronic bands, which have relative intensities that vary with solvent polarity.[19] In general, an increase in solvent polarity results in a decrease of the ratio of the third and first vibronic band intensities (I_3/I_1).[19] Derivatives of dimethylaminonaphthalenesulphonate (DNS) such as DA^+ have been used as polarity probes for a number of chemical systems.[20] The wavelengths of maximum emission intensity (λ_{max}) for 1,5-DNS derivatives are sensitive to solvent polarity, giving a blue shift with decreasing polarity.[20] The fluorescence quantum yields for 1,5-DNS derivatives are also solvent-sensitive, with water producing one of the lowest quantum yields.[20]

The emission characteristics of the excited species $Ru(bpy)_3^{2+*}$ have been studied extensively.[21] $Ru(bpy)_3^{2+*}$ emission energies do not correlate well with solvent polarity.[16] However, our luminescence probe studies of aqueous solutions of Nafion polyelectrolytes have show that increasing emission energies and quantum yields result when $Ru(bpy)_3^{2+}$ is taken from a purely aqueous environment into an environment where interaction with fluorocarbon chain material is possible.[15] A similar effect is observed when $Ru(bpy)_3^{2+}$ is placed in fluorocarbon micelles[22] or in Nafion membranes.[14,16] In contrast, the emission energies of $Ru(bpy)_3^{2+*}$ in long-chain alcohols or hydrocarbon micelles are less than that for $Ru(bpy)_3^{2+*}$ in water. These results suggest that $Ru(bpy)_3^{2+}$ is sensitive to the nature of its chemical environment and, of particular interest to this study, can discriminate between hydrocarbon- and fluorocarbon-containing environments. The effects of various solvents on the emission characteristics of the probes used here are shown in Table 1.

Emission from fully hydrated membranes

Luminescence probe studies of Nafion membranes have shown that the polarity of the microenvironment around a probe molecule or ion is an average of contributions from the components which constitute the microenvironment.[14,16] Hence, if the environment around a probe is essentially aqueous, the probe should give a λ_{max} or I_3/I_1 ratio equivalent to that for the probe in water. Conversely, if the immediate environment contains both water and chain material, an environment polarity significantly lower than that of a bulk aqueous phase will be experienced and reported by the probe. This was the case when the probes used here were incorporated into Nafion.[16]

Table 2 shows that the water contents of the fully hydrated (boiled for 4 hr) PE-SS membranes are extremely high, much higher than those for both Nafion (40% H_2O[16]) and PFE-SS. In spite of these very high water contents, λ_{max} for DA^+ in PE-SS is smaller than λ_{max} for DA^+ in water; however, the extent of the blue shift is much less than that observed for DA^+ in Nafion, PFE-SS or a relatively

Table 1. Wavelengths of maximum emission intensity (λ_{max}) for DA^+ and $Ru(bpy)_3^{2+}$ and I_3/I_1 for Py in various solvents

Solvent	λ_{max}, nm		Py, I_3/I_1
	DA^+	$Ru(bpy)_3^{2+}$	
Water	571	613	0.58
Ethylene glycol	544	—	0.79
Methanol	534	610	0.72
Ethanol	526	606	0.80
Butanol	522	608	0.94
Pentanol	519	616	0.98
Decanol	513	622	1.24
Hexane	—	—	1.50
p-Xylene	—	—	0.95

Table 2. Emission characteristics of probes in fully hydrated PFE-SS and PE-SS

Membrane	H_2O, %	H_2O/SO_3^-	λ_{max}, nm		Py, I_3/I_1
			DA^+	$Ru(bpy)_3^{2+}$	
PFE-SS-H^+	27	13	510	608	0.90
PFE-SS-Na^+	19	9	509	—	0.91§
PFE-SS-K^+	19	9	510	—	0.86§
PFE-SS-Cs^+	19	10	510	—	0.90§
PE-SS-H^+	118	46	—	628	—
PE-SS-Na^+	116	46	559*	—	—
PE-SS-K^+	107	44	543*	—	—
PE-SS-Cs^+	102	42	544†	—	—

*Excitation $\lambda = 360$ nm.
†Excitation $\lambda = 380$ nm.
§Excitation $\lambda = 335$ nm.

non-polar hydrocarbon solvent (see Table 1). These data suggest that, as was the case in Nafion, DA^+ is experiencing an effective microenvironment polarity which is made up of contributions from water and chain material, and because of the relatively high water contents, the polarity is much higher than that for DA^+ in either Nafion or PFE-SS.

The PFE-SS studied here contains significantly more $-SO_3H$ sites per gram than Nafion does. It is, therefore, somewhat surprising that PFE-SS contains much less water than Nafion. This lower water content may result from the higher crystallinity of the Teflon-based PFE-SS membrane.[23] In perfect agreement with the arguments presented above, both DA^+ and Py indicate PFE-SS microenvironment polarities which are much lower than those for these probes in either PE-SS or Nafion.[16] In the case of Py this agreement may be fortuitous, because drying experiments have shown that the microenvironment of Py in PFE-SS is insensitive to changes in water content (*vide infra*).

As noted above, $Ru(bpy)_3^{2+}$ can apparently differentiate between a hydrocarbon and a fluorocarbon environment. This is evident in the data shown in Table 2 in that the emission from $Ru(bpy)_3^{2+}$ is red-shifted (relative to water) in PE-SS and blue-shifted in PFE-SS. These data again indicate that the probe has access to the chain material. More importantly, the PFE-SS data indicate that $Ru(bpy)_3^{2+}$ interacts with the fluorocarbon main chain more extensively than with the aromatic hydrocarbon side-chain.

Experimental evidence suggests that, by analogy with Nafion and other ionomers,[24] the $-SO_3^-$ sites, their counter-ions and the water of hydration for each are aggregated into ionic clusters in PFE-SS.[25,26] Most recent models of ionomer clustering predict clusters which are devoid of chain material and which are lined with the ionic sites.[27,28] The hydrocarbon side-chains in PFE-SS, which contain the $-SO_3^-$ groups, are of sufficient length (3–10 repeat units[29]) for a cluster having a structure of this type to have hydrocarbon walls. This would preclude or at least greatly hinder $Ru(bpy)_3^{2+}$–fluorocarbon interactions. The $Ru(bpy)_3^{2+}$ emission data from PFE-SS strongly suggest, then, that chain material intrudes into the ionic cluster. It is of interest to note that Eisenberg has proposed a model which allows for main-chain penetration into the cluster[30] and that both infrared[12] and transport[6] studies of Nafion provide evidence which supports this model.

Effect of water content on microenvironment polarity

If the properties of a probe's microenvironment are determined by the relative concentrations of water and chain material, then the polarity of this environment should decrease as water is removed from the membrane. All the probes used here indicated decreasing microenvironment polarities when water was removed from Nafion membrane.[16] In contrast, the polarity changes observed on removal of water from PFE-SS and PE-SS depended on the probe used. DA^+ in PFE-SS and $Ru(bpy)_3^{2+}$ in both PFE-SS and PE-SS behaved in the expected manner. As water was removed from PFE-SS, the λ_{max} values for both DA^+ and $Ru(bpy)_3^{2+}$ were blue-shifted (Fig. 1, A and B) and the $Ru(bpy)_3^{2+}$ emission intensity increased (Fig. 1, C). All these effects indicate a less polar microenvironment for these probes.[16] The λ_{max} values for DA^+ in the driest PFE-SS membranes studied here (*ca.* 498 nm) are very similar to the λ_{max} values obtained for very dry Nafion membranes (*ca.* 503 nm).[16] Reference to Table 1 suggests that it would be difficult to dissolve DA^+ in homogeneous solvents of low enough polarity to produce a λ_{max} value of 498 nm. This is an interesting point, because it suggests that a microenvironment which would be impossible to create in homogeneous solution can be created in the PFE-SS membrane.

As water is removed from PE-SS, λ_{max} for $Ru(bpy)_3^{2+}$ is red-shifted and the emission intensity increased (Fig. 2, A and B). As noted above, the red-shift indicates that, as water is removed, $Ru(bpy)_3^{2+}$ is interacting more strongly with the hydrocarbon chain material.

In contrast to the spectral changes observed for the other probes, the I_3/I_1 ratio for Py was essentially unchanged when water was removed from PFE-SS (Fig. 3). This suggests that the Py is located in some region of the membrane which is inaccessible to

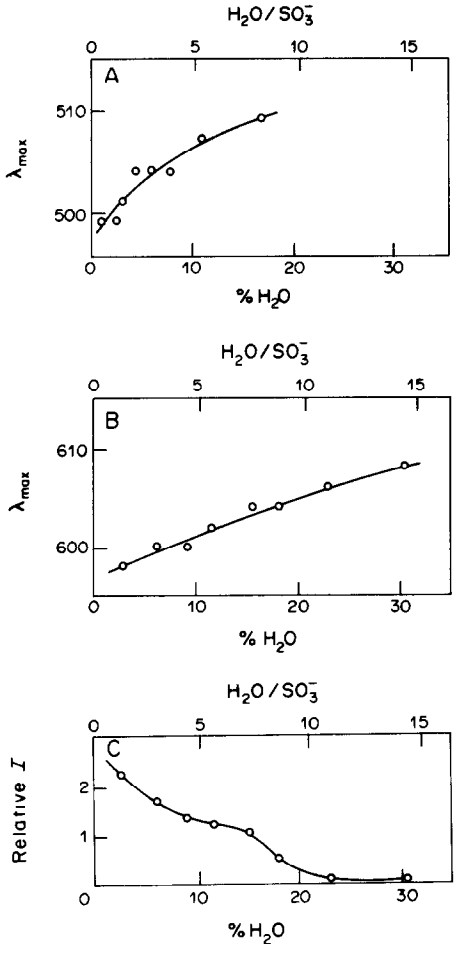

Fig. 1. Emission characteristics of probes *vs.* PFE-SS water content. A, DA^+ λ_{max} in Na^+-form PFE-SS. B, $Ru(bpy)_3^{2+}$ λ_{max} in H^+-form PFE-SS. C, $Ru(bpy)_3^{2+}$ relative intensity in H^+-form PFE-SS.

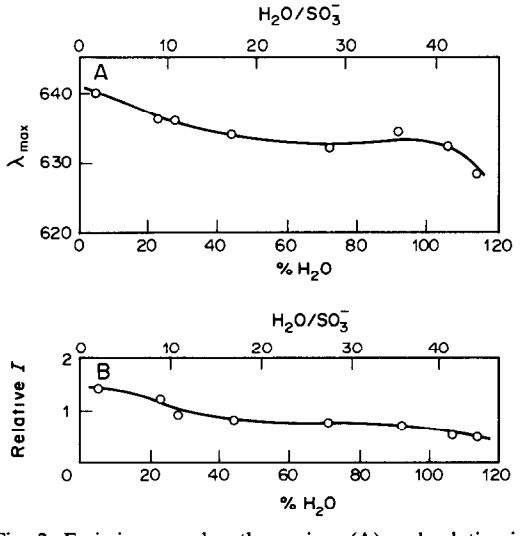

Fig. 2. Emission wavelength maxima (A) and relative intensities (B) of $Ru(bpy)_3^{2+}$ *vs.* water content of PE-SS, H^+-form.

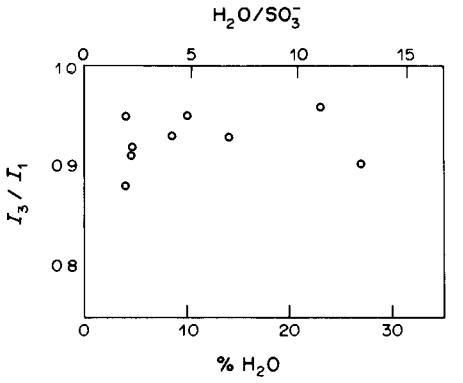

Fig. 3. Py I_3/I_1 *vs.* water content of PFE-SS, H^+-form.

water. One possible explanation is that Py is partitioned into the polymer chain-material phase which separates the ionic clusters. This seems unlikely, however, in that if Py were dissolved in a fluorocarbon phase, I_3/I_1 would be expected to be close to 2.0.[19] Another possibility is that Py is partitioned into an interfacial region as described by Yeager and Steck.[31] Further study of the effects of water and of counter-ion[16] on the emission from Py in PFE-SS will be required.

Conclusions

These studies have shown that the microenvironment experienced by a probe within sulphonated ionomer membranes is determined by the nature of the polymer chain material and by the membrane water content. The microenvironment can be quite dynamic, in general, becoming much less polar as water is removed from the membrane. Furthermore, these studies have shown that microenvironments can be created in the ionomer membrane which, because of solubility limitations, would be difficult to create in homogeneous solutions. These results corroborate the conclusions of analogous studies conducted on the perfluorosulphonate ionomer Nafion.[16]

Luminescence data from $Ru(bpy)_3^{2+}$ in PFE-SS suggest that chain material intrudes into the ionic cluster. This conclusion is supported by both transport[6] and spectroscopic[12] data. This is an important issue because intrusion of chain material into the cluster phase undoubtedly has the deleterious effect of retarding the rate of transport through the membrane. We are therefore conducting further studies of the extent of chain-material penetration.

Finally, it is important to note that all the probes studied here are relatively hydrophobic, so they undoubtedly seek out the more hydrophobic parts of the ionic cluster. It is not surprising, then, that these probes indicate that the microenvironments are rather non-polar. To complement these data from hydrophobic probes, we are currently studying the emission characteristics of hydrophilic probes (*e.g.*, lanthanide ions) in ionomer membranes.

Acknowledgement—This work was supported in part by the Office of Naval Research.

REFERENCES

1. A. Eisenberg and H. L. Yeager (eds.), *Perfluorinated Ionomer Membranes*, ACS, Washington, D.C., 1982.
2. A. Eisenberg (ed.), *Ions in Polymers*, ACS, Washington, D.C., 1980.
3. E. Gileadi, S. Srinivasan, F. J. Salzano, C. Braun, A. Beaufrere, S. Gottesfleld, L. J. Nuttall and A. B. Laconti, *J. Power Sources*, 1977, **2**, 191.
4. T. H. Teherani, S. N. Frank and K. Carson, Presented at the Spring ACS National Meeting, 10 April 1984, St. Louis, MO.
5. F. G. Will and H. S. Spacil, *J. Power Sources*, 1980, **5**, 173.
6. C. R. Martin and K. A. Dollard, *J. Electroanal. Chem.*, 1983, **159**, 127 and references therein.
7. S. G. Cutler, in *Ions in Polymers*, A. Eisenberg (ed.), Chap. 9. ACS, Washington, D.C., 1980.
8. E. J. Roche, M. Pineri and R. Duplessix, *J. Polym. Sci. Polym. Phys. Ed.*, 1982, **20**, 107.
9. E. J. Roche, R. S. Stein and W. J. MacKnight, *ibid.*, 1980, **18**, 1035.
10. H. K. Pan, D. J. Yarusso, G. S. Knapp and S. L. Cooper, *ibid.*, 1983, **21**, 1389.
11. B. A. Brozoski, M. M. Coleman and P. C. Painter, *Macromolecules*, 1984, **17**, 230.
12. M. Falk, *Can. J. Chem.*, 1980, **58**, 1495.
13. N. J. Turro, M. W. Geiger, R. R. Hautala and N. E. Schore, in *Micellization, Solubilization and Microemulsions*, K. L. Mittal (ed.), p. 75. Plenum Press, New York, 1977.
14. P. C. Lee and D. Meisel, *J. Am. Chem. Soc.*, 1982, **104**, 4824.
15. N. E. Prieto and C. R. Martin, *J. Electrochem. Soc.*, 1984, **131**, 751.
16. M. N. Szentirmay, N. E. Prieto and C. R. Martin, *J. Phys. Chem.*, to be published.
17. V. D'Agostino, J. Lee and E. Lu, in *Ion Exchange*, R. S. Yeo and R. P. Buck (eds.), p. 148. Electrochemical Society, Pennington, NJ, 1981.
18. C. R. Martin and H. Freiser, *Anal. Chem.*, 1981, **53**, 902.
19. K. Kalyanasundaram and J. K. Thomas, *J. Am. Chem. Soc.*, 1977, **99**, 2039.
20. Y.-H. Li, L.-M. Chan, L. Tyler, R. T. Moody, C. M. Himel and D. M. Hercules, *ibid.*, 1975, **97**, 3118.
21. K. Kalyanasundaram, *Coord. Chem. Rev.*, 1982, **46**, 159.
22. N. J. Turro and P. C. Lee, *J. Phys. Chem.*, 1982, **86**, 3367.
23. M. N. Szentirmay and C. R. Martin, *J. Electrochem. Soc.*, 1984, **131**, 1652.
24. C. G. Bazuin and A. Eisenberg, *J. Chem. Ed.*, 1981, **58**, 938.
25. L. Y. Levy, A. Jenard and H. D. Hurwitz, *J. Chem. Soc., Faraday I*, 1980, **76**, 2558.
26. R. Vasquez, J. Avalos, F. Volino, M. Pineri and D. Galland, *Appl. J. Polym. Sci.*, 1983, **28**, 1093.
27. W. Y. Hsu and T. D. Gierke, *Macromolecules*, 1982, **15**, 101.
28. K. A. Mauritz, C. J. Hora and A. J. Hopfinger, in *Ions in Polymers*, A. Elsemberg (ed.), p. 123. ACS, Washington, D.C., 1980.
29. J. Y. C. Lee, Private communication.
30. A. Eisenberg, *Macromolecules*, 1960, **33**, 147.
31. H. L. Yeager and A. Steck, *J. Electrochem. Soc.*, 1981, **128**, 1880.

Talanta, Vol. 32, No. 8B, pp. 751–756, 1985
Printed in Great Britain.

0039-9140/85 $3.00 + 0.00

PREPARATION AND GAS CHROMATOGRAPHIC CHARACTERIZATION OF SOME CROWN-ETHER STATIONARY PHASES

DENNIS D. FINE,* HARRY L. GEARHART, II,† and HORACIO A. MOTTOLA‡
Department of Chemistry, Oklahoma State University, Stillwater, Oklahoma 74078, U.S.A.

(*Received* 6 *December* 1984. *Accepted* 9 *February* 1985)

Summary—Three open tubular glass capillary chromatographic columns containing poly(vinylbenzo-15-crown-5), vinylmethylsila-17-crown-6, and vinylmethylsila-14-crown-5 have been prepared and characterized. The silacrown-ether stationary phases were polymerized inside the capillary and copolymerized with a methacryloxysilane bound to the inner surface. The poly(vinylbenzo-15-crown-5) was prepared and used as a coating in a capillary which had been roughened and deactivated. Characterization was performed by use of gas chromatography and included determination of column bleed character, phase transition changes, polarity and selectivity. Differential scanning calorimetry confirmed the phase transition temperature of the poly(vinylbenzo-15-crown-5) phase. The polarity and selectivity of these phases are comparable to those of Carbowax 20M.

Crown ethers have found several applications in analytical chemistry: (1) as solvent extraction reagents for separation and isolation of alkali and alkaline-earth metal ions, (2) in membranes for ion-selective electrodes, and (3) as stationary phases or mobile phases in liquid chromatography.[1-3] Crown ethers constitute unique components of stationary phases, with a highly polar site localized within the centre of the ring formed by the crown-ether oxygen atoms.

Polar compounds, including alcohols, amines, carboxylic acids, and compounds which have methyl groups attached to electron-withdrawing groups, such as acetonitrile or nitromethane, and alkali and alkaline-earth metal ions are capable of interaction with the localized polarity provided by a crown ether.[4]

The preparation and characterization of three glass capillary columns containing the crown ethers shown in Fig. 1 are discussed in this paper. Columns containing vinylmethylsila-17-crown-6 (VMSi17C6) and vinylmethylsila-14-crown-5 (VMSi14C5) were prepared by polymerization of the crown ether inside the capillary. Before this *in situ* polymerization, the capillary was treated with γ-methacryloxypropyltrimethoxysilane (MAPTMS). This silane provides methacryloxy groups which copolymerize with the vinylsilacrown ether. Hydrolysis of the methoxy groups provides silanols which bond to the glass surface. Another column containing poly(vinylbenzo-15-crown-5) (PVB15C5) was prepared by statically coating the inside of a roughened, deactivated capillary with the polymer. Roughening was achieved by etching with ammonium hydrogen flouride.[5] This was followed by deactivation of the capillary with a thin non-extractable film of Carbowax 20M.[6] Gas chromatographic characterization was accomplished by comparing the retention behaviour of a mixture of alcohols on each column. Phase transitions obtained by "inverse phase gas chromatography"[7] were studied and provided explanations for anomalies in the chromatographic behaviour occurring when the column temperature was decreased. "Inverse phase gas chromatography" implies determining the prop-

*Present address: Lorillard, Research Center, P.O. Box 21688, Greensboro, NC 27420, U.S.A.
†Permanent address: CONOCO, Inc., Ponca City, OK 74601, U.S.A.
‡Author to whom correspondence and reprint requests should be addressed.

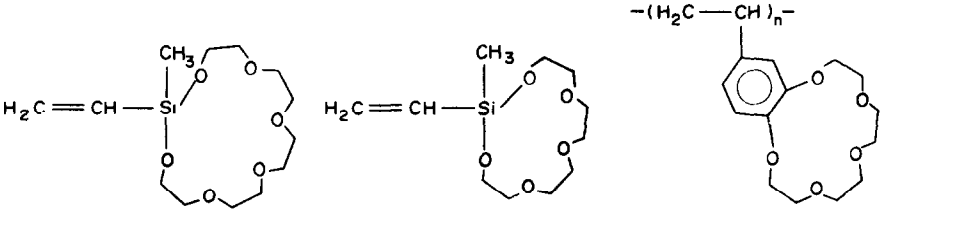

Vinylmethylsila-17-crown-6 Vinylmethylsila-14-crown-5 Polyvinylbenzo-15-crown-5

Fig. 1. Structures of crown ethers used in this work.

erties of the stationary phase by using known molecular probes, whereas conventional chromatography utilizes a well-characterized stationary phase to determine the properties of unknown solutes. Minimum and maximum operating temperatures were determined for each column. In addition, the differences in retention of homologous series of alkanes, alcohols, and diols on the PVB15C5 column provided selectivity information for this type of crown-ether stationary phase.

EXPERIMENTAL

Instrumentation

A Hewlett–Packard 5880A gas chromatograph equipped with level 4 integrator and computing system, capillary split injection, and a flame-ionization detector was used for the chromatographic evaluation. Pyrex glass capillaries were drawn on a Hewlett–Packard 1045A capillary-drawing machine. A Shimadzu MCT-1A micro-column treating stand was used to apply stationary phases to the glass capillary columns. Characterization of some species used or prepared was by NMR spectrometry [Varian XL-100 and Varian XL-300 spectrometers] and infrared spectrophotometry [Perkin-Elmer 681 IR spectrophotometer]. A Du Pont differential scanning calorimeter with a single-crucible cell and scanning rate of 10°/min was used to determine phase transitions of poly(vinylbenzo-15-crown-5).

Reagents.

Vinylmethylsila-17-crown-6 (VMSi17C6) and vinylmethylsila-14-crown-5-(VMSi14C5) were obtained from Petrach Systems, Inc. (Bristo, PA, U.S.A.) and were used without further purification. Benzo-15-crown-5 was obtained from Parish Chemical Co. (Orem, Utah, U.S.A.) and Chemalog (Chemical Dynamics Corporation, South Plainfield, NJ, U.S.A.). The γ-methacryloxypropyltrimethoxysilane (MAPTMS) was obtained from Dow Corning (Midland, MI, U.S.A.). All other chemicals used for preparation or characterization purposes were analytical reagent grade.

Synthesis

Poly(vinylbenzo-15-crown-5) was prepared by a synthetic route described by Kopolow[8], with the first step replaced by a higher yielding reaction which used benzo-15-crown-5 as starting material.[9]

VMSi17C6 and VMSi14C5 column preparation

Capillaries containing the silacrown ethers were prepared in the same manner. Pyrex capillaries were first leached by filling 92% of the capillary with hydrochloric acid (1 + 4), sealing, and heating at 180° for 16 hr.[10] After flushing with one column volume of distilled water, the capillary was dehydrated at 300° for 1 hr with a helium flow of 5 ml/min. The capillary was then dynamically coated with a 0.50% v/v MAPTMS solution. Before introduction into the column, the silane was hydrolysed by adding it to distilled water acidified to pH 3.7 with acetic acid.[11] This solution was left in the capillary for 1 hr before being pushed out at a linear velocity of 3 cm/min. A long buffer column at the end of the treated column and a crimped metal restrictor at the front of the column were used to maintain this linear velocity. After removal of the solution, the column was dried at 115° for 15 min while being flushed with helium flowing at 1 ml/min. A solution of 20% v/v VMSi17C6 or VMSi14C5, 0.50% v/v divinylbenzene, and 0.10% w/v 2,2-azo-bis-(isobutyronitrile) in benzene was deaerated by reducing the pressure with a water aspirator and agitating with an ultrasonic bath. After all but 8% of the capillary had been filled with this solution, the capillary was sealed and heated at 60° for 72 hr. It was then attached to a buffer column and the liquid was pushed out at a linear velocity of 5 cm/min. Conditioning was accomplished by heating at 2°/min up to 200° and then holding at that temperature for 3 hr, with a helium flow maintained at 5 ml/min. In addition to these silacrown-ether columns, two further capillaries were prepared, with the treatment stopped at different stages, the first after the acid leach and dehydration, the second after the MAPTMS coating and drying.

PVB15C5 column preparation

The capillary containing the PVB15C5 polymer was prepared in a different manner. Following a hydrochloric acid leach and dehydration, an ammonium hydrogen fluoride etch was performed as described by Peters.[5] After another hydrochloric acid leach and dehydration, the column was deactivated with Carbowax 20M.[6] The capillary was then statically coated with a 1-μm thick film of PVB15C5 by the procedure described by Grob.[12] Column conditioning consisted of heating at 2°/min from 60° up to 220° and holding at that temperature for 2 hr. The helium flow was maintained at 3 ml/min.

RESULTS AND DISCUSSION

Separation of alcohols

Initial column characterization was performed by injecting a mixture of fourteen alcohols into each column. Comparison of chromatograms obtained from the HCl-leached and MAPTMS-silaned columns [Fig. 2, (a) and (b)] with the chromatograms from the two silacrown-ether columns (Figs. 3 and 4) shows that it is the silacrown ether that allows separation of the alcohols. The severe adsorption which results after the acid leach and MAPTMS silanation is reduced after the silacrown-ether treatment. The silacrown ethers increase the efficiency and capacity of the stationary phase and may also deactivate the surface silanols left on the capillary wall after the MAPTMS treatment. Interaction of the polar ends of the silanol chain with the oxygen atoms in the crown-ether ring can prevent polar solutes from interacting with the surface silanol and thereby reduce tailing.

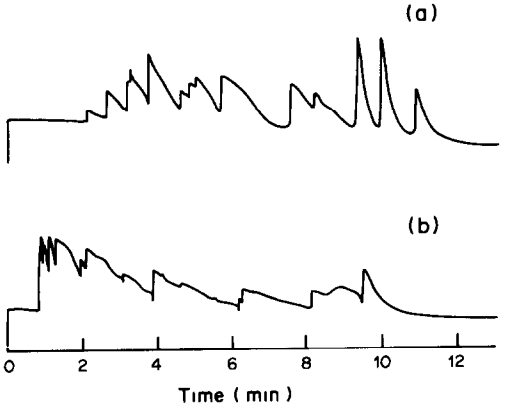

Fig. 2. Chromatograms of an alcohol mixture on (a) an HCl-leached capillary column; (b) an MAPTMS and HCl-leached capillary column. (For temperature programme and components of alcohol mixture see Fig. 3.)

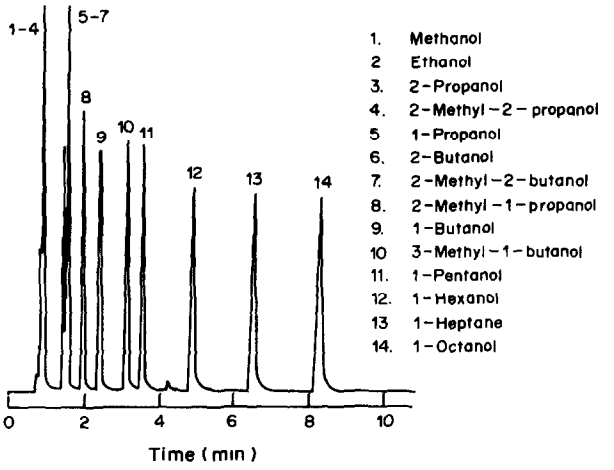

Fig. 3. Chromatogram of an alcohol mixture on VMSi17C6 capillary column. Linear carrier velocity (He at 60°) 38.4 cm/sec. Volume injected: 0.10 μl of a mixture of alcohols (equal volumes of each). Split ratio 1/31. Attenuation 2^6. Temperature programme: hold at −10° for 3 min then heat at 10°/min to 30°, 5°/min to 65°, 30°/min to 100°, and hold at 100° for 10 min.

A temperature programme over the range used in the silacrown-ether columns could not be used for separation of the alcohol mixture on the PVB15C5 because of severe band broadening and tailing at low temperatures. Isothermal chromatograms obtained at 130° and 180° (Fig. 5) show that column temperatures above 130° are required for well-resolved peaks to be obtained. Possible reasons for this temperature effect can be found in the phase transitions occuring in the column.

Phase transition studies

To determine the phase transition temperatures for each phase (see Table 1), the partition ratio, k', of each probe was calculated at 10° intervals. Figure 6 shows the log k' *vs.* $1/T$ plot for 1-pentanol on the VMSi17C6 and VMSi14C5 columns. Changes in the slope at 70° for VMSi17C6 and at 58° for VMSi14C5 correspond to phase changes in the columns. These phase changes may be liquid–liquid transitions rather than melting transitions. The rationale for this is seen in Figs. 3 and 4 where reasonably good chromatographic peaks are obtained throughout the temperature programme. If solid–liquid transitions were occurring, adsorption of solutes, as evidenced by peak tailing and broadening, would dominate at temperatures below the transition temperatures. Figure 7 shows the log k' *vs.* $1/T$ plot for acetonitrile, when chromatographed on the PVB15C5 phase. Acetonitrile was chosen as a phase-transition probe because of its solubility in polystyrene and in poly-

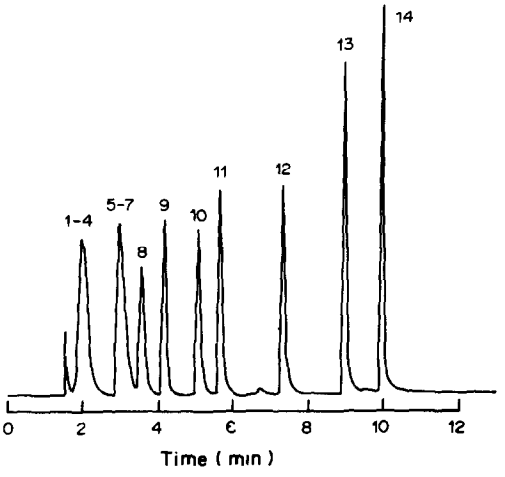

Fig. 4. Chromatogram of alcohol mixture on VMSi14C5 capillary column. Linear carrier velocity (He at 60°) 26.1 cm/sec. Volume injected 0.10 μl. Split ratio 1/57. Attenuation 2^6. (For temperature programme and alcohol mixture see Fig. 3.)

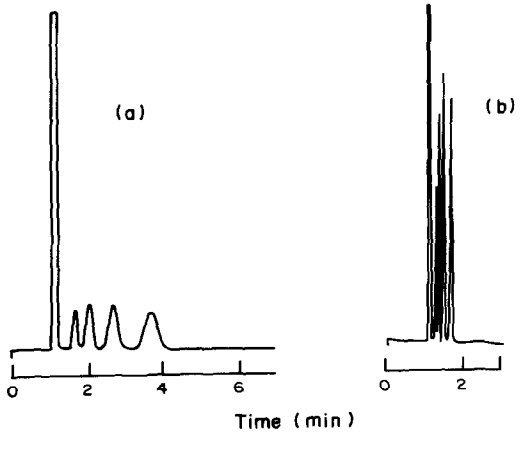

Fig. 5. Chromatograms of alcohol mixture on PVB15C5 capillary column at (a) 130° and (b) 180°. Film thickness 1 μm. Linear Carrier velocity 29.0 cm/sec. Volume injected 0.20 μl of mixture of 0.10% v/v mixture of 1-pentanol, 1-hexanol, 1-heptanol and 1-octanol in hexane. Split ratio 1/140 at 180°.

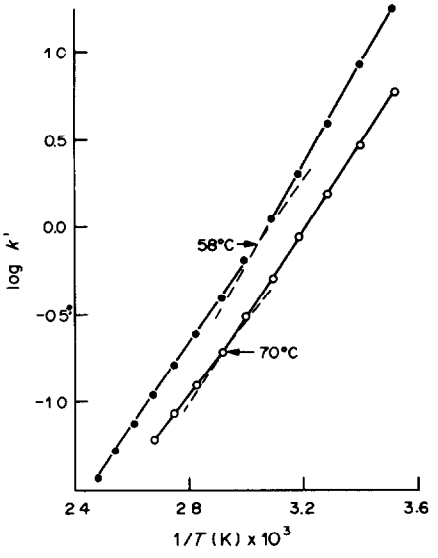

Fig. 6. Plots of log(partition ratio) against inverse of absolute temperature for 1-pentanol on VMSi17C6 (○) and VMSi14C5 (●) capillary columns.

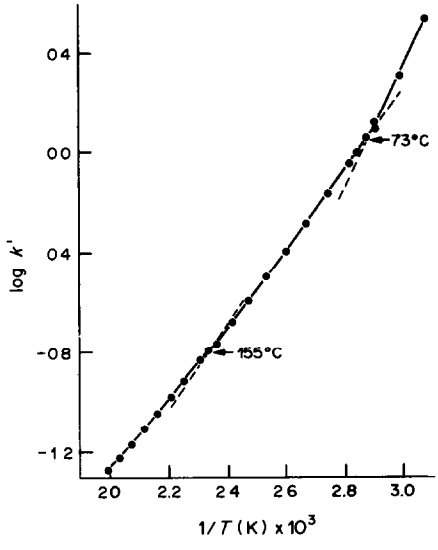

Fig. 7. Plots of log(partition ratio) against inverse of absolute temperature for acetonitrile on PVB15C5 capillary column.

ethylene glycol. It also provides acidic methyl group protons which can interact with several of the crown-ether oxygen atoms at the same time.[4] Changes in the retention behaviour of acetonitrile on PVB15C5 occur at 73° and 155°. These transitions occur at temperatures which may correspond to a softening or glass-phase transition and a liquid–liquid transition. Chromatography at temperatures below the glass-phase transition at 73° is characterized by severe tailing. Above this transition temperature the tailing diminishes, although broadening such as that seen in Fig. 5a is present. The transition at 155°, which is evidenced by the increase in efficiency (in Fig. 5b) may correspond to a liquid–liquid phase transition.[13,14] Such transitions, which have been observed in atactic polymers, including polystyrene, by Fourier-transform infrared spectroscopy and differential scanning calorimetry, may be related to temperatures where a liquid of fixed structure becomes a true liquid.

Differential scanning calorimetry (DSC) of the PVB15C5 polymer shows that a second-order phase transition in the polymer occurs at an extrapolated onset temperature of 60°. The mid-point of the phase transition occurs at 81°, which correlates well with the phase-transition temperature of 73° determined by gas chromatography. The DSC did not reveal, however, a transition at 155°. A possible explanation for this could be that the attendant change in the heat capacity of the polymer was too small to be detected by DSC. Transitions in the polymer that results in small changes in heat capacity could cause larger changes in the polarity of the polymer, which would easily be detectable through the change in retention behaviour.

Further comparisons of the crown-ether stationary phases

Tables 1 and 2 show some parameters of interest in the comparison of the crown-ether stationary phases reported here. The minimum operating temperature for each of the three phases was taken as the highest phase-transition temperature. Though this temperature provides a good lower working limit for the PVB15C5 phase (Fig. 5), the silicrown-ether phases exhibit reasonable gas chromatographic behaviour even at temperatures below the observed

Table 1. Comparison of column dimensions, phase-transition temperatures, minimum and maximum operating temperatures

Stationary phase	Bore (*mm*)/ length (*m*)	Phase-transition temperatures, °C	Min./max. operating temperatures, °C
Vinylmethylsila-17-crown-6	0.42/18	70	> 70/100
Vinylmethylsila-14-crown-5	0.40/16	58	> 58/154
Poly(vinylbenzo-15-crown-5)	0.32/20	73(66, 81)* 155	55/220

*Onset and mid-point transition temperatures determined by differential scanning calorimetry.

Table 2. Partition ratios (k'), retention indices (I), McReynolds' constants (ΔI) and average polarity for the McReynolds' probes on each of the crown ether capillary columns, along with the retention indices and McReynolds' constants for Carbowax 20M[16]

		McReynolds' probes					Average
		Benzene	n-Butanol	2-Pentanone	Nitropropane	Pyridine	polarity
VMSi17C6	ΔI	347	553	373	491	477	448
	I	1000	1143	1000	1143	1176	
	k'	0.008	0.030	0.008	0.030	0.038	
VMSi14C5	ΔI	243	398	280	378	359	327
	I	896	988	907	1030	1058	
	k'	0.019	0.036	0.020	0.048	0.056	
PVB15C5	ΔI	382	564	439	648	595	526
	I	1035	1154	1066	1300	1294	
	k'	0.225	0.426	0.264	0.959	0.923	
Carbowax 20M	ΔI	322	536	368	572	510	462
	I	975	1126	995	1224	1209	

transition temperatures. This is evident from the chromatogram for alcohols in Figs. 3 and 4. For each of these phases the practical lower working limit is, therefore, below the observed transition temperature.

The maximum allowable operating temperature (MAOT) of each column was determined by identifying the temperature at which a shift in baseline of 1.2×10^{-11} A occurred during application of a temperature programme. For the flame-ionization detector of the Hewlett–Packard 5880A GC this corresponds to a 10% baseline shift at an attenuation of 2^3, at which the sensitivity is 1.2×10^{-10} A full scale. A carrier-gas linear velocity of 25 cm/sec and temperature programme starting at 60° with a 5°/min temperature ramp were used in each case. This method is based on setting an arbitrary baseline shift as the criterion for acceptable bleed of stationary phase. The MAOT values for the silacrown-ether phases (100° and 154°) are lower than expected, probably because of incomplete polymerization of the vinyl groups in the silacrown ether. The low MAOT results from bleed of unpolymerized ether. Although NMR spectroscopy of the monomer solution emptied from the column containing VMSi17C6 after the heat treatment showed no evidence of a polyethylene backbone, this does not preclude the possibility that copolymerization occurred with MAPTMS on the column wall. The PVB15C5 phase showed much higher MAOT, owing to the stability of the polystyrene backbone, which was confirmed by NMR spectroscopy.

Measures of selectivity and polarity of the crown ether phases are given by the McReynolds' constants (ΔI), retention indices (I), partition ratios (k'), and average polarity, in Table 2. The column temperature for these retention parameters was 120° for the VMSi14C5 and PVB15C5 columns and 100° for the VMSi17C6 column. The lower column temperature was necessary in order to obtain a measurable partition ratio for the McReynolds' probes. Calculation of the McReynolds' constants for this column, by using the absolute retention indices of squalene at 120° instead of 100°, should introduce errors of only 1–3% in each ΔI value.[15] Though the temperatures used for determining the retention indices of the VMSi17C6 and VMSi14C5 were above the transition temperatures, the temperature for determination of the indices on the PVB15C5 phase was below the phase transition temperature (155°). Consequently, the McReynolds' constants for PVB15C5 were determined at a temperature at which the stationary phase was present as a fixed liquid.

Comparison of the values of the McReynolds' constants and the average polarity for the three crown-ether phases with other stationary phases in the McReynolds' table[16] shows that the crown-ether phases have an average polarity similar to that of Carbowax 20M. The McReynolds' constants, retention indices, and average polarity of Carbowax 20M are given in Table 2 for comparison. Of the three crown-ether phases, PVB15C5 has the highest polarity, owing to the induced dipole interactions contributed to the overall polarity by the aromatic rings. The lower polarity of the silacrown-ether phases is due to the weaker induction interactions of non-polymerized vinyl groups which may be present and to weak dispersion interactions of the methyl groups. The increased number of ethyleneoxy linkages in the crown ring results in the VMSi17C6 phase having higher polarity than the VMSi14C5 phase.

The retention indices also indicate that the PVB15C5 phase elutes the McReynolds' probes in the same sequence as Carbowax 20M does. The silacrown-ether phases differ from this sequence in that l-nitropropane and pyridine switch elution order. The polarity and selectivity of the PVB15C5 phase is also evident in Fig. 8 where log k' *vs.* boiling point is plotted for homologous series of diols, alcohols, and alkanes. In addition to the expected linearity within each homologous series, the plot shows selective retention of compounds which have the same boiling point but differ in polarity. This behaviour is typical of polar columns where retention of compounds is determined more by their polarity than their boiling point.

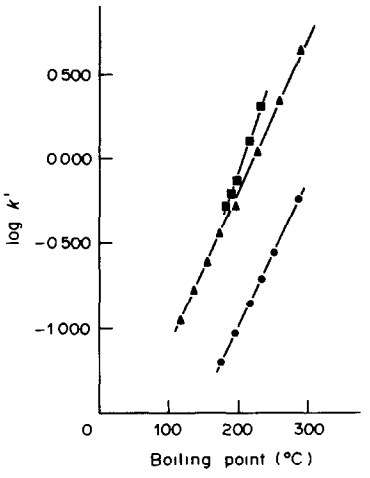

Fig. 8. Plot of log(partition ratio) against boiling point for alkanes (●), alcohols (▲), and diols (◆) on PVB15C5 capillary column. Alkanes: nC_{10}–nC_{16}. Alcohols: nC_4OH–$nC_{14}OH$. Diols: $HO(CH_2)_nOH$ ($n = 2,3,4$), 1,2-propanediol and 1,3-butanediol. Column temperature 180°.

CONCLUSIONS

In summary, the three crown-ether stationary phases reported here exhibit average polarity similar to that of Carbowax 20M and appear more suited for liquid than for gas chromatographic separations. The gas chromatographic separations of alcohols and alkanes which were obtained on capillary columns containing the phases reported here show, however, that there is some potential for use of crown ether phases in GC. These separations and the phase-transition studies point to the incorporation of crown ethers into polymers with low melting points (*e.g.*, polysiloxanes or polyethylene glycols) as providing more promising systems for phases to be used in gas chromatography.

It is of interest to note the usefulness of gas chromatographic characterization of stationary phases in its ability to detect phase changes not observable by differential scanning calorimetry. Gas chromatography revealed three transitions for the PVB15C5 phase whereas differential scanning calorimetry revealed only one of them.

Acknowledgements—This work was partially supported by the Water Research Institute, Oklahoma State University. One of the authors (DDF) acknowledges summer support from Conoco, Inc., Dowell, Inc., and the Phillips Petroleum Co. The authors thank Albert Buckholtz (Conoco Inc.) for work involving DSC studies.

REFERENCES

1. I. M. Kolthoff, *Anal. Chem.*, 1979, **51**, 1R.
2. M. Yoshio and H. Noguchi, *Anal. Lett.*, 1982, **15**, 1197.
3. K. Kimura and T. Shono, *J. Liq. Chromatog.*, **1982**, 5, 223.
4. E. Elbasyouny, H. J. Brugge, K. von Deuten, M. Dickel, A. Knochel, K. U. Koch, J. Kopf, D. Melzer and G. Rudolph, *J. Am. Chem. Soc.*, 1983, **105**, 6568.
5. T. L. Peters, T. J. Nestrick and L. L. Lamparski, *Anal. Chem.*, 1982, **54**, 2397.
6. L. Blomberg, *J. Chromatog.*, 1975, **115**, 365.
7. J. E. Guillet, in *Advances in Analytical Chemistry and Instrumentation*, H. Purnell (ed.), Vol. 11, Wiley, New York, 1973. p. 188.
8. S. Kopolow, T. E. Hogen Esch and J. Smid, *Macromolecules*, 1973, **6**, 133.
9. W. W. Parish, P. E. Scott, C. W. McCausland and J. S. Bradshaw, *J. Org. Chem.*, 1978, **43**, 4577.
10. K. Grob, G. Grob and K. Grob, Jr. *J. High Resn. Chromatog. Chromatog. Commun.*, 1979, **2**, 677.
11. Dow Corning. *Information on Organofunctional Chemicals, Z-6030 Silane*, Form No. 23-230-76.
12. K. Grob and G. Grob, *J. High Resn. Chromatog., Chromatog. Commun.*, 1982, **5**, 119.
13. R. F. Boyer, *J. Macromol. Sci. Phys.*, 1980, **B18**, 461.
14. J. B. Enns, R. F. Boyer, H. Ishida and J. L. Koenig, *Polymer Eng. Sci.*, 1979, **19**, 756.
15. L. S. Ettre, *Chromatographia*, 1973, **6**, 489; 1974, **7**, 39; 1974, **7**, 261.
16. W. O. McReynolds, *J. Chromatog. Sci.*, 1970, **8**, 685.

Talanta, Vol. 32, No. 8B, pp. 757–762, 1985
Printed in Great Britain.

0039-9140/85 $3.00 + 0.00

TOPOLOGICAL METHOD FOR THE DESIGN OF NEW LIGANDS

SUSUMU TAKAMOTO
Department of Chemistry, Faculty of Science, Gakushuin University, Mejiro, Tokyo 171, Japan

(*Received* 15 *October* 1984. *Accepted* 25 *January* 1985)

Summary—A purely geometrical investigation of ligand patterns systematically derived and documented by use of graph theory is described, as a means for designing future ligands. Various kinds of graphs represent the ligand patterns. The simple ligand graphs are most practical and useful for ligand design, and all of them are systematically derived from simpler patterns, although there remains difficulty for expressing certain ligands. Whereas the complex ligand graphs can exactly express the structures of all the ligands, they are so complicated that their derivation is much more difficult than that of the other types of graph. Several methods of deriving such ligand graphs are developed, and the merits and demerits of these representations are discussed.

A ligand can be regarded as a dress for a metal. The chemistry of complexes has had several fashion periods, analogous to the fashions in ladies' dresses. When complexometric titration was being developed, many complexone-type ligands were prepared; just after the remarkable discovery of ferrocene, various sandwich-bonded complexes were synthesized; since the applications of crown-ethers were exploited, a great many such compounds have been proposed; now studies of macrocyclic ligands are in fashion.

The conventional and easy way to design new ligands is to consider some analogues or derivatives of an already well established ligand. However, this way of developing new ligands is so short-sighted that it seems to have little connection with the creative discovery of ligands. As the properties and reactions of metal complexes are closely related to their geometrical structure, for designing the most suitable chelating reagent for a certain purpose it seems an obviously useful approach would be to look at all the geometrical patterns of ligand structure.

There are some reviews[1,2] on ligand design, and that by Black and Hartshorn[2] beautifully collects and systematically classifies the various ligands prepared up to the present, but these reviews give little guidance to planning future ligands and their topological diagrams are mathematically incomplete. Graph theory and the computer have been successfully applied to the enumeration and documentation of the chemical isomers and homologues of some organic compounds. This paper extends this approach and introduces a few purely geometrical studies on the representation and derivation of ligand patterns in order to design future ligands, and also provides some comments on topological treatments and graph-theory methods because many readers may be unfamiliar with them. Further details of graph theory may be obtained from monographs.[3,4]

THEORY AND METHODS

Simple ligand graph

A graph in graph theory is defined as a set of m points together with n lines joining certain pairs of these points. A ligand can be considered as a set of donor atoms joined by carbon chains capable of forming medium-sized chelate rings. Then a "simple ligand graph" L(m,n) can be defined for a ligand, its points and lines corresponding to m donor atoms and n carbon chains respectively.[5] Each of these carbon chains is called a "chelate path", which starts from one donor atom and ends at another after passing through two (or three) carbon atoms, if the chelate ring consists of five (or six) members, including a metal ion (or atom). Then it is obvious from the denticity of the donor atoms that the degree of each point is one, two or three (the degree of a point is the number of lines incident on it).

Some examples of simple ligand graphs for various ligands are shown in Fig. 1. Since any carbon atoms which do not participate in chelate rings are neglected, almost all bidentate ligands such as glycine, oxalate, dimethylglyoxime, 1,10-phenanthroline, acetylacetone, 8-quinolinol, are represented by the same simple ligand graph L(2,1). A graph in the narrow sense of the word does not include multiple lines; that is, two points may be joined by only one line. Piperazine (Fig. 1), however, is represented by a graph with double lines L(2,2), because it has two chelate paths between two nitrogen atoms. Triple lines are not needed, however, for such a donor atom would have lone-pair electrons oriented in opposite directions and could not form a chelate ring. To avoid complicating the design no multiple line is included in this simple ligand graph. If necessary such double line derivations can be easily produced by

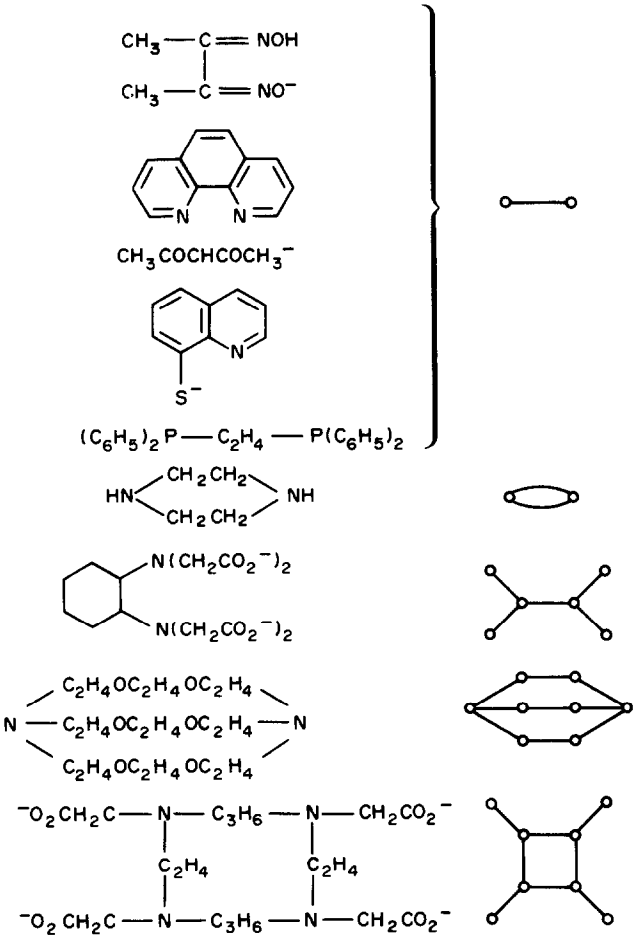

Fig. 1. Graph representation of ligands.

joining a pair of adjacent points, of degree one or two, in a simple ligand graph.

However complicated the ligand graph may be, it is a planar graph; that is, all its lines can be drawn on a plane so that no two lines cross each other. According to graph theory such a graph is identical with a spherical graph. To be spherical the criterion is that the chelate paths do not cross each other on a co-ordination sphere, because chelate paths are too short to be able to make detours.

All the simple ligand graphs with $m \leqslant 8$ can be systematically derived from fifteen basic patterns by adding points and/or side-chains, and the basic patterns are also obtainable, one by one, by starting from a circle and a segment. Each structure can then be documented by a code of eight figures.[5] The numbers of simple ligand graphs thus designed, and of their double-line derivatives, are summarized in Table 1.

Extension of ligand graph

There remains consideration of the graphical representation of ligands which have chelate paths branched at their carbon atoms. Such ligands form some fused chelate rings with a metal, because several of the chelate paths have parts in common. There are various ways to represent such ligands, and examples are shown in Fig. 2.

Extended ligand graph. An "extended ligand graph" is a set of several points corresponding to the donor atoms, which are joined by several single, double or triple lines, according to the number of chelate paths.[6] This is just an extension of the simple ligand graph, but the degree of a point may exceed the valence of the donor atom.

Donor-atom graph. A "donor-atom graph" is a set of several points corresponding to the donor atoms and several single lines corresponding to the chelate paths without regard to their numbers.[6] This is also quite similar to the simple ligand graph, and the degree of a point may again sometimes exceed the valence of the donor atom. Donor-atom graphs can

Table 1. Number of ligand graphs

Donor atoms	2	3	4	5	6	7	8
Simple ligand graphs	1	2	6	10	28	63	187
Double-line derivatives	1	2	6	12	37	102	318

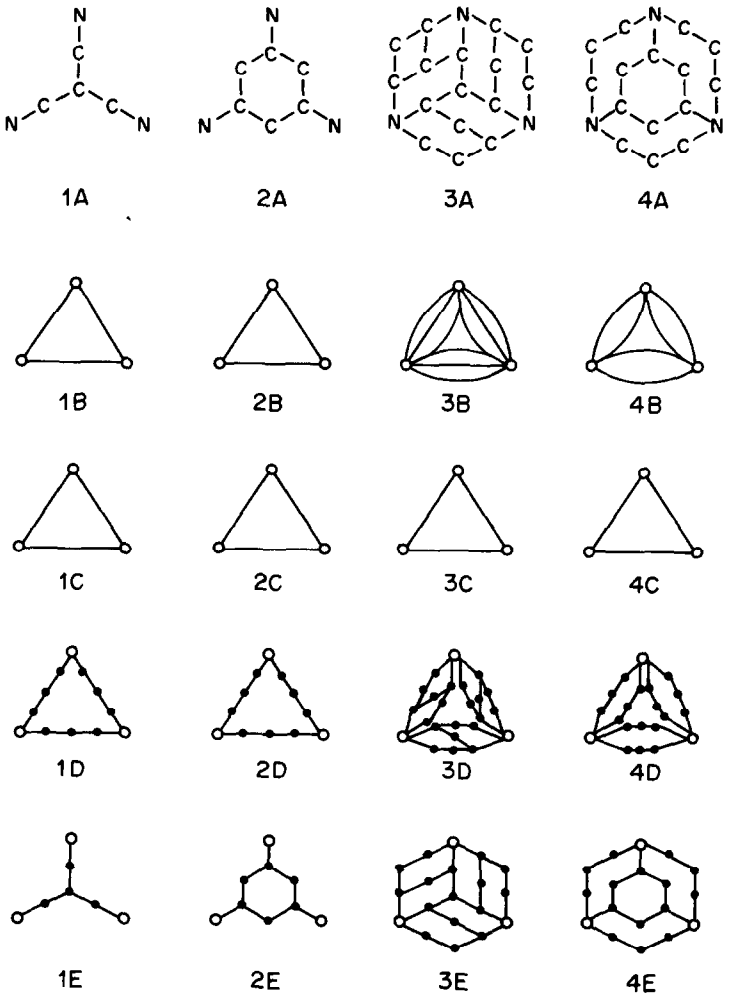

Fig. 2. Representations with diverse ligand graphs. 1A–4A: Ligands. 1B–4B: Extended ligand graphs. 1C–4C: Donor-atom graphs. 1D–4D: Composite graphs. 1E–4E: Complex ligand graphs.

be systematically derived from some basic patterns similarly to the simple ligand graphs. The extended ligand graphs are also derivable from the donor-atom graphs by substitution of a multiple line for a single line. Neither type of graph, however, expresses the geometrical structure of complicated ligands well enough for them to be discriminated. For example the ligands 1A and 2A in Fig. 2 are expressed by the same extended ligand graph 1B and 2B, and donor-atom graph 1C and 2C. In order to correct this defect, a complex graph, a new concept in graph theory, should be introduced. It is a set of main points and main lines, where each main line is also a graph composed of sub-points and sub-lines.

Complex ligand graph. A "complex ligand graph" is a set of several main points joined by sub-lines, where the main point, subpoints, and sub-lines correspond to donor atoms, carbon atoms becoming chelate members, and chemical bonds among these atcms, respectively.[6] Examples of complex ligand graphs are given as (1E)–(4E) in Fig. 2. The degree of the main points is 1–3, whereas that of the subpoints is 2 or 3, since no carbon atom can be an end-point. The complex ligand graph contains no multiple sub-line. Naturally, each chelate path has two or three sub-points between two main points. The complex ligand graphs can faithfully express the original ligand structure, but are so complicated that their systematic derivation is much more difficult than that of previous ligand graphs.

A method of deriving complex ligand graphs is to start from the donor-atom graph. Let us neglect three- and four-membered carbon-rings, for simplicity. When each line of a donor-atom graph is replaced by one of the six unit graphs in Fig. 3, the complex graph thus obtained is called a "composite graph", as shown in Fig. 2, 1D–4D. By various combinations of the six kinds of unit graphs, many composite graphs are obtained from a particular donor-atom graph.

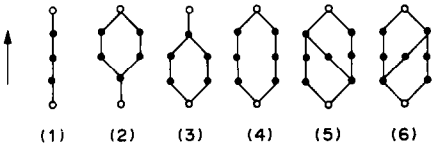

Fig. 3. Unit graphs.

Next, a new concept of "fusion" should be introduced.[6] It means a partial fusing of two patterns or graphs, as when the fusion of two benzene rings produces the naphthalene structure. Several adjacent unit graphs may be partially fused, then some sub-points and sub-lines are united. The fusion results in relieving the congestion of carbon chains, and in reducing the degree of the main points. Then a complex ligand graph is derived from a composite graph by fusing its adjacent unit graphs, as seen in Fig. 2. Sometimes one sub-point of degree two on each chelate path in the complex ligand graph thus obtained may be omitted, because every chelate path of a unit graph has three sub-points. Because of steric restrictions fusion is not always possible. All the combinations of adjacent unit graphs which are impossible to fuse have been checked in detail. That study will be published separately.

Ligand design for a given co-ordination structure

The derivation method given above for complex ligand graphs is sufficiently systematic, but these graphs do not necessarily fit a particular co-ordination structure. First, it should be confirmed that the original donor-atom graph can fit the desired co-ordination. A donor-atom graph for any planar co-ordination is always a linear or a circular graph, and the unit graphs in its composite graph cannot be fused. In other words, such a composite graph is identical with the corresponding complex ligand graph.

Parent graph. For a given co-ordination structure, a complex ligand graph to which no more sub-points or sub-lines can be added, *i.e.*, a complex graph of the highest density, is called a "parent graph". If all of these are found, the other complex ligand graphs for such a co-ordination can be derived as their "daughter graphs" by neglecting some sub-points and/or removing some sub-lines.

Both unit graphs (5) and (6) in Fig. 3 are identical and give only one parent graph for the bidentate ligand, whereas both 3E and 4E in Fig. 2 are parent graphs for the terdentate ligand. There are four kinds of parent graphs for square planar co-ordination, and nine kinds for tetrahedral co-ordination.[6]

It is much more difficult, however, to find all the parent graphs for octahedral co-ordination, which is the most popular one, and such a task can be executed only by use of the electronic computer. The donor-atom graph of the complete cage for octahedral co-ordination is naturally an octahedron (a complete cage means a spherical graph in which every adjacent pair of points is joined). There are 6^{12} ($=2,176,782,336$) permutations of six kinds of unit graphs placed on twelve edges of an octahedron, including symmetrical duplications. The computer examines each of these permutations, (*a*) to see whether they meet the conditions for becoming the parent graph, (*b*) to find whether the unit graphs can be fused and (*c*) to exclude duplication of structures. A "canonical name", which is a numerical code expressing the characteristic pattern of a graph, should be defined for the computer process. A composite graph, from which a complex ligand graph is derived, can be expressed by a code consisting of twelve figures, each of which represents the number of unit graphs on a particular edge and is placed in a definite order in the code. Twenty-four codes are possible for the same structure, because a definite order of edges may be started from any of the six vertices and in any of four directions. The canonical name of a structure is therefore defined as the code which gives the greatest sum of the component figures. Thus it is found that as many as 1055 kinds of parent graphs for octahedral co-ordination can exist, even if chiral isomers are excluded. The detailed computer process will be described elsewhere.

Simple cage graph. As the parent graphs are too complicated, simpler complex ligand graphs for octahedral co-ordination are sought. A "single cage graph" is a complex ligand graph where every pair of adjacent main points is jointed by one chelate path; consequently, both its donor-atom graph and its composite graph are octahedra. Since the degree of every vertex on an octahedron is four, at least one adjacent pair of unit graphs (1) in Fig. 3 at every vertex must be fused so that the degree of every main point becomes three. As there are four adjacent pairs of four edges at each of six vertices, the permutations come to 4^6 ($=4096$), including symmetrical duplications. Then a canonical name is defined as the minimum total of the six figures, each of which is 1–4. The computer has been used to check each structure of all the permutations above, and 90 chiral isomers and 12 achiral graphs are found for the simple cage graphs.

DISCUSSION

The representation of ligand patterns by a set of points and lines is a useful method for documenting and classifying a number of ligands, so that we can look over and compare all of them even though such ligands have never been synthesized. Since any atoms which cannot become members of medium-sized chelate rings are entirely neglected, the topological expression might abstract the chelating functions from a complicated ligand and explicitly illustrate them. As any donor atoms from the nitrogen- and oxygen-group elements may be located at any main points of these ligand graphs, ligands with mixed

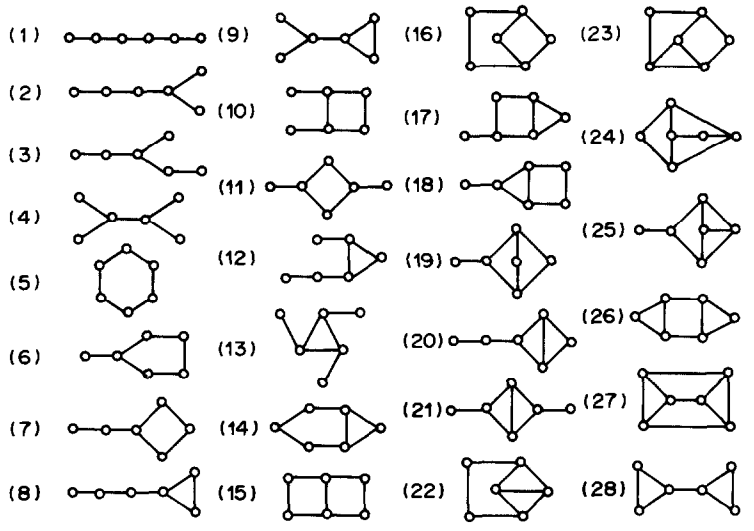

Fig. 4. Simple ligand graphs for $m = 6$.

donor atoms can also be expressed, and the lines may represent not only hydrocarbon chains but also boron, silicon and any other mixed or unmixed chains.

Since the simple ligand graphs are plainly defined and all of them can be systematically derived one by one, their representation is sufficiently practical and useful for general design purposes, although some considerations remain on some special ligands containing branched chelate paths.

All the simple ligand graphs with $m = 6$ are illustrated in Fig. 4. Looking over these various patterns of sexidentate ligands, we see that complexation chemistry has always pursued the use of only a quarter of these twenty-eight patterns. Accordingly it might be forecast that further and possibly more interesting ligands, having quite diverse structures, will be developed in the future.

At least one face on most regular polygons is an equilateral triangle. Hence the trigonal ligand 1,4,7-triazacyclononane should fit well in octahedral co-ordination, in terms of the length of its chelate paths and the three directions of its lone-pair electrons. As expected, it has been proved that of all the triamine ligands this forms the most stable metal chelates.[7] Furthermore, its complexone-type derivative, 1,4,7-triazacyclononane-*N*,*N*′,*N*″-triacetic acid[8] of type (13), and its bivalve-like derivative, 1,2-di(1,4,7-triazacyclononane-1-yl)ethane[9] of type (28), are extremely strong chelating agents, although their complexation rates are very slow because of their rigid structures.

Ligands 1A and 2A in Fig. 2 are also very suitable for facial co-ordination and able to form three fused six-membered chelate-rings with a metal ion.[10–13] Hence, their three-limbed sexidentate derivatives can form quite stable metal chelates.[14–17]

Since type (27) in Fig. 4 has a cage structure and all the lone-pair electrons of its donor atoms are directed towards the centre of an octahedron, no metal ion would enter inside or co-ordinate it. However, if such ligands could be synthesized around a metal ion by a template reaction, the metal ion should be encapsulated within the network and a highly hydrophobic spherical cation would be produced. Sargeson and co-workers[18–23] synthesized very interesting complexes similar to these. As the ligands have branched chelate paths, they belong to type (27) not as a simple ligand graph but as a donor-atom graph. Type (27) is not yet a complete-cage depth graph, as above mentioned. If a genuine complete-cage ligand could be synthesized round a metal ion the cation should be entirely confined within the network, no matter how weak the chelate bonds.

The complex ligand graphs can exactly express the ligand structures, but they are too complicated for all of them to be derived or enumerated. Especially when the number of donor atoms exceeds four, the systematic derivation of the daughter graphs from the parent graphs is practically impossible because there are so many complicated parent graphs. However, the ligands which will be synthesized in the near future will not have such complicated networks as those parent graphs. Hence it would be better for the ligand design to start from simpler graphs, *e.g.*, the simple cage graphs, the number of which is only a tenth of that of the parent graphs for octahedral co-ordination. The setting of proper restrictions on the complex ligand graphs would be the key to the solution of design problems. Thus, the topological conception, applied practically to ligand design, should lead to the finding of new and useful ligands.

REFERENCES

1. H. A. Goodwin, in *Chelating Agents and Metal Chelates*, F. P. Dwyer and D. P. Mellor (eds.), pp. 143–181. Academic Press, New York, 1964.

2. D. St. C. Black and A. J. Hartshorn, *Coord. Chem. Rev.*, 1973, **9**, 219.
3. A. T. Balaban (ed.), *Chemical Applications of Graph Theory*, Academic Press, London, 1976.
4. F. Harary and E. M. Palmer (eds.), *Graphical Enumeration*, Academic Press, New York, 1973.
5. S. Takamoto, *Bull. Chem. Soc. Japan*, 1979, **52**, 2477.
6. *Idem, ibid.*, 1980, **53**, 595.
7. T. Arishima, K. Hamada and S. Takamoto, *Nippon Kagaku Kaishi*, 1973, 1119.
8. H. Hama and S. Takamoto, *ibid.*, 1975, 1182.
9. N. Tanaka, Y. Kobayashi and S. Takamoto, *Chem. Lett.*, 1977, 107.
10. T. G. Spiro and C. G. Ballhausen, *Acta Chem. Scand.*, 1961, **15**, 1707.
11. G. Anderegg, *Helv. Chim. Acta*, 1962, **45**, 1303.
12. N. Kitajiri, T. Arishima and S. Takamoto, *Nippon Kagaku Zasshi*, 1970, **91**, 240.
13. P. A. Brauner and G. Schwarzenbach, *Helv. Chim. Acta*, 1962, **45**, 2030.
14. R. A. D. Wentworth and J. J. Felten, *J. Am. Chem. Soc.*, 1968, **90**, 621.
15. L. J. Zompa, *Inorg. Chem.*, 1971, **10**, 2647.
16. D. M. Higgins and L. J. Zompa, *J. Coord. Chem.*, 1977, **7**, 105.
17. M. Takahashi and S. Takamoto, *Bull. Chem. Soc. Japan*, 1977, **50**, 3413.
18. A. M. Sargeson, *Chem. Britain*, 1977, **15**, 23.
19. I. I. Creaser, J. MacB. Harrowfield, A. J. Herlt, A. M. Sargeson and J. Springborg, *J. Am. Chem. Soc.*, 1977, **99**, 3181.
20. *Idem, ibid.*, 1982, **104**, 6016.
21. J. MacB. Harrowfield, A. J. Herlt, P. A. Lay and A. M. Sargeson, *ibid.*, 1983, **105**, 5503.
22. A. M. Bond, G. A. Lawrance, P. A. Lay and A. M. Sargeson, *Inorg. Chem.*, 1983, **22**, 2010.
23. A. Hammershøi and A. M. Sargeson, *ibid.*, 1983, **22**, 3554.

Talanta, Vol. 32, No. 8B, pp. 763–770, 1985
Printed in Great Britain.

0039-9140/85 $3.00 + 0.00

SILICA-BOUND COMPLEXING AGENTS: SOME ASPECTS OF SYNTHESIS, STABILITY AND PORE SIZE

JOHN R. JEZOREK,* KATHLEEN H. FALTYNSKI, LARRY G. BLACKBURN, PEGGY J. HENDERSON and H. DARLENE MEDINA
Department of Chemistry, University of North Carolina at Greensboro, Greensboro, North Carolina 27412, U.S.A.

(*Received* 21 *November* 1984. *Revised* 4 *January* 1985. *Accepted* 8 *February* 1985)

Summary—A number of factors related to the metal-ion reactivity of silica-bound complexing agents are discussed. The metal-uptake capacity of alkylamines immobilized on silica is shown to be reduced by hydrolysis of bound ligand from the surface, by protonation in aqueous buffers, and by an apparent air oxidation of the amine group or other deactivation process. A one-step silylation reaction using triethoxysilylpropyl-*p*-nitrobenzamide is shown to produce nitrobenzamide silica gel (NBSG) and azo-coupled material equivalent to that obtained by the former two-step process. Significant time saving is realized. Organic solvent washing of the NBSG, and the azo-coupled chelating agents derived from it, removes organic matter from the surface. Adsorbed or weakly bound polymers or oligomers present in the original silane or formed during the silylation are apparently dissolved slowly by these washing solvents. Finally, metal uptake (and presumably surface coverage), expressed as μmole/m^2, of a series of 8-quinolinol controlled-pore glasses was found to decrease with decrease in pore size.

Chemically-modified silica materials have become important in several areas of science in recent years, for example as catalyst supports and as stationary phases in both gas and liquid chromatography. Silica modifications are typically effected by some type of silylation reaction, perhaps followed by one or more other reactions to produce the desired chemical character. Though there is a large body of data on silica modifications and the subsequent reactivity of these materials,[1] new applications are continually demanding further information.

Our primary interest in this field is in the use of chelating agents immobilized on silica, as stationary phases for the liquid-chromatographic separations of trace metal[2] and organic species,[3] but aspects of the preparation and characterization of these packings are also of concern, especially as they may have significant effects on chromatographic behaviour. For example, the chemical resistance of the covalently-bound moieties to hydrolysis is important in maintaining constant column characteristics. Should the bound group be an alkylamine, significant hydrolytic instability may exist, as has been suggested for some systems.[4,5] We report here further evidence of this instability for several amine phases.

When the intention is to produce a chemically complex material, several reactions may be needed to arrive at the final modified silica, and increased efficiencies of preparation are desirable. A significant reduction in the time necessary to prepare silica-bound, azo-coupled chelating agents has recently been reported by Marshall and Mottola[6] and we describe here an alternative, equally short, method of making these materials.

The physical character of the silica support material may also play a part in determining the qualities of the modified stationary phase. For example, the pore size of the base silica can have an effect, for good or ill, on the liquid chromatography of various organic species.[7] Further, it has recently been suggested that pore-size has an effect on the ligand-loading of 8-quinolinol silica-gel.[8,9] As chromatographic retention is normally directly proportional to surface coverage by the stationary phase, metal-ion retention on a bonded chelating-agent as stationary phase will then be affected by the pore-size of the native silica used to prepare the column packing. We report here corroborative evidence of the relationship of pore-size to coverage with azo-coupled ligand.

EXPERIMENTAL

Apparatus

A Hitachi 100-80 spectrophotometer and a Beckman 1301 or Perkin–Elmer 272 atomic-absorption spectrophotometer were used.

Reagents

Adsorbosil-LC, 10-μm silica gel (70 Å pore-size, specific surface area 480 m^2/g) was obtained from the Applied Science Division of the Milton Roy Company. The 37–75-μm controlled-pore glasses (CPG) were purchased from Pierce Chemical Company, Rockford, IL. Polygosil 60–20, 20-μm silica gel (60 Å pore-size, 500 m^2/g) manufactured by Machery-Nagel, was obtained from Rainin Instrument Company, Woburn, MA.

*Author for correspondence

The 3-(2-aminoethyl)aminopropyltrimethoxysilane (Corning Z-6020) and the trimethylchlorosilane (TMCS) were purchased from PCR Research Chemicals, Gainesville, FL, the 3-aminopropyltriethoxysilane was from Pierce Chemical and the trimethylsilylimidazole (TMSI) and triethoxysilylpropyl-*p*-nitrobenzamide were from Petrarch Systems Inc., Bristol, PA. The silanes were stored in a refrigerator and used as received. The *N*-(1-naphthyl)ethylenediamine dihydrochloride was obtained from Aldrich Chemical Co. All other chemicals were of reagent grade and used without further purification. Toluene and dimethylformamide (DMF) were dried over a 4 Å molecular sieve before use.

Syntheses

All silica materials were dried in an oven or under vacuum at 110° or higher temperature before silylation. The silica was cooled and subjected to vacuum to remove air from the pores before the silane solution was added.[8]

The silylated silica gels were prepared by refluxing with 5% toluene solution of the silane, unless otherwise noted. Aminopropyl silica gel (APSG) was prepared by using 20 g of Adsorbosil, 150 ml of the aminopropyltriethoxysilane solution, and 4 hr reaction time. The aminoethylaminopropyl silica gels (AEAPSG) were obtained by using 5 g of Polygosil, 70 ml of a toluene solution of aminoethylaminopropyltrimethoxysilane, and 2.5 hr reaction time, one batch being made at room temperature and the other at 73°. Non-refluxing conditions were used to make the AEAPSGs in order to reduce the surface coverages by this very reactive silane and so make them comparable to that of the APSG.

Nitrobenzamide-modified silica gel (NBSG) was obtained with 15 g of Adsorbosil, 100 ml of a toluene solution of the triethoxysilylpropyl-*p*-nitrobenzamide (a waxy solid) and refluxing for 7 hr. The nitrobenzamide-modified controlled-pore glass (NBCPG) preparation used 4 g of CPG which had been rinsed with 78 ml of 0.1*M* hydrochloric acid and 70 ml of water, and was refluxed for 3 hr with a 2% toluene solution of the nitrobenzamide silane.

After silylation the modified material was filtered off by suction, washed with 50–100 ml of toluene then 50–100 ml or more of methanol, and cured overnight in a vacuum oven at 70–80°.

End-capping of the APSG was performed by using trimethylsilylimidazole (TMSI) for selective deactivation of residual silanol groups, but not of the amine function. About 4 g of APSG was reacted overnight with 50 ml of a slightly warm 2% TMSI solution in DMF. The solid was filtered off and washed with 50 ml of dimethylformamide (DMF) and 50–100 ml of methanol.

The nitrobenzamide-modified Adsorbosil was end-capped by refluxing about 16 g of it with 100 ml of a toluene solution of trimethylchlorosilane for 5 hr, followed by filtration and washing with toluene and methanol.

All silylation reactions were protected from atmospheric moisture either by performing them in a sealed system, or, if refluxing conditions were used, by a "Drierite" trap on the reflux column.

The nitrobenzamide-modified materials were reduced to the aminobenzamide form by boiling about 4 g of the NBSG or NBCPG in 50 ml of 5% aqueous sodium dithionite solution for about 30 min. As the end-capped NBSG was extremely hydrophobic, it was necessary to wet the material with methanol before adding the dithionite solution. The water used to dissolve the dithionite was first deaerated with nitrogen to minimize oxidative decomposition of the dithionite. The aminobenzamide modified material was filtered off, washed with water, and added to 50 ml of 2% sodium nitrite solution in 2*M* hydrochloric acid and the mixture was left for 30 min in an ice-bath. The light yellow diazonium salt-modified material was filtered off and washed with 50 ml of cold water. The damp product could be immediately coupled or frozen for later use.[8]

The 8-quinolinol-modified controlled-pore glass was obtained by coupling the material bonded with the diazonium salt, in 60 ml of 1% 8-quinolinol solution in 95% ethanol, stirring for 30 min, filtering off and washing with ethanol, methanol and finally water.

N-(1-Naphthyl)ethylenediamine-modified silica gel was prepared by coupling 3 g of the Adsorbosil-based diazonium salt in 75 ml of 2% aqueous solution of the diamine dihydrochloride for 30 min. As discussed below, extensive water rinsing was required before the filtrate was free from the red colour produced.

Batch copper-uptake

About 100–200 mg of the modified silica was placed in a vial, 10 ml of 0.1*M* copper(II) solution were added and the mixture was shaken for at least 30 min. The solid was filtered off, washed with 50–100 ml of water to remove excess of metal ion, and the extracted copper(II) was stripped with hydrochloric acid. At first 0.1*M* hydrochloric acid was used, but to ensure complete copper removal[6] 1*M* acid was employed in later stages. A 25-ml water rinse followed. The stripped copper(II) and rinsings were made up accurately to 50 or 100 ml and copper was determined by atomic-absorption spectroscopy.

Column copper-uptake

A 15 cm × 4.6 mm stainless-steel column was slurry-packed with about 1.4 g of the appropriate silica gel at about 4000 psig pressure by using a Haskel pneumatically-amplified pump with methanol as the slurrying and packing solvent.

A typical copper-uptake cycle involved successive passage of 15 ml of water, 70–90 ml of 0.01*M* acetate buffer (pH 5), 25 ml of 0.02*M* copper(II) nitrate (an excess), 10–30 ml of water, 20–30 ml of nitric acid (pH 1.8) to elute the extracted copper, 15 ml of water and 15 ml of methanol. The first two of the five cycles employed 10 ml of 0.05*M* copper solution instead of 25 ml of the 0.02*M* solution, and 30–40 ml of nitric acid (pH 2.1) before the stripping step using nitric acid at pH 1.8. The more concentrated acid was employed to ensure complete removal of copper from the APSG. All solutions were pumped through the column at 1.0 ml/min. The appropriate solution was chosen by using a six-port selection valve on the low-pressure side of the Beckman 110A pump. The amount of copper stripped was determined by atomic-absorption spectroscopy.

RESULTS AND DISCUSSION

Stability of alkylamine silicas

Silica-bound complexing agents are being increasingly used for trace-metal preconcentration and both metal-ion and organic liquid-chromatographic separations. A class of ligands that seems promising for these uses is the alkylamine group, as much is known about their homogeneous solution chemistry. In a chromatographic study using aminopropyl silica gel (APSG) and aminoethylaminopropyl silica gel (AEAPSG) in our laboratory, it was found that retention times for the transition metals were unreasonably short when sulphate and acetate mobile phases were used. This finding suggested deactivation or a loss of complexing ligand from the stationary phase.

The occurrence of hydrolytic cleavage of bound alkylamines from the surface of silica gel has been

Table 1. Metal-uptake and surface coverage of aminoethylaminopropyl silica gel*

Material	Copper(II) uptake, μmole/g		Ligand coverage, from N determination, μmole/g	
	Freshly prepared	After extensive column use	Unused, 4-month old	After extensive column use
AEAPSG-batch 1	231	22	264	89†
AEAPSG-batch 2	310	7	—	—

*$\equiv SiCH_2CH_2CH_2NHCH_2CH_2NH_2$.
†Based on 0.2% nitrogen by weight (±0.1% absolute).

suggested by recent studies by Gimpel and Unger[4] and Waddell *et al.*[5] To investigate this possibility, two different columns packed with AEAPSG and used extensively for metal-ion separation studies were emptied and the copper(II)-uptake of the packings was measured by the batch method (Table 1). One batch, which had an original capacity of about 230 μmole/g yielded a capacity of only about 16–30 μmole/g for the used stationary phase, the lower value being for material taken from near the column inlet, the higher value for that near the outlet. The second batch of AEAPSG, originally displaying a metal-uptake capacity of 310 μmole/g, yielded a value of 7 μmole/g after use in the column. Silica-bound ligand freshly synthesized in non-aqueous solvent is unprotonated and reacts readily with copper(II), whereas column material which has been subjected to aqueous buffers in the pH range 2–5 is probably protonated and therefore less reactive toward metal complexation, which may result in low copper uptake values.[10] Another possibility is chemical deactivation (*e.g.*, oxidation) of the bound amine, which would also preclude reaction with metal-ions.

These results may also indicate, however, that ligand was hydrolysed from the silica surface by the aqueous mobile phases used in the chromatographic studies. That this indeed occurred was confirmed by the elemental analysis of AEAPSG taken from the first column, which gave a nitrogen content of 0.2%, corresponding to a ligand coverage of about 90 μmoles of diamine per gram (Table 1). This is to be compared with the diamine coverage of 264 μmole/g based on the nitrogen content of unused four-month old material. As the stoichiometry of the copper(II)–AEAPSG complex(es) is not known for these low coverages, the 89 μmole/g value cannot be converted into a metal-uptake capacity with any certainty. Furthermore, as the absolute precision of nitrogen determinations is itself ±0.1%,[11] strict comparison with the metal-uptake value is not warranted. Any bound but unreactive nitrogen would also lead to poor comparison. In any case, the important point is that the ligand coverage and metal uptake have been reduced to about 30% and 10% respectively, of their original values.

A more detailed study of the fate of APSG during column use was made, modelled on that by Waddell *et al.*[5] The on-column uptake of copper(II) was monitored during repeated cycling of acetate buffer and several other mobile phases. The usual cycle consisted of successive passage of portions of water, 0.01*M* acetate buffer (pH 5), 0.02*M* copper(II) solution, water, nitric acid (pH 1.8) to strip the copper, then water, and finally methanol. Five cycles were performed. The results are given in Table 2. As can be seen, the uptake capacity decreased from the 240 μmole/g batch-mode value for the unused material to between 50 and 60 μmole/g after only one cycle, with a levelling-off at around 10–15 μmole/g after the third cycle. The results were similar for both APSG and APSG which had been TMSI-end-capped to deactivate residual silanol groups and are also qualitatively similar to those of Waddell *et al.*,[5] although the reduction in uptake capacity was greater in the present study.

The experiment on column uptake of copper(II) was repeated with a fresh APSG column, the only difference being that 10 ml of water preceded the first copper loading, and 40 ml of buffer the second. The uptake values were 262 and 72 μmole/g respectively for these two cycles (Table 2). The initial uptake was greater than that in the five-cycle study in which the first copper-loading was preceded by passage of pH-5 acetate buffer.

The APSG and capped APSG, which had been used in the five-cycle column study, were also subjected to a batch copper(II)-uptake study after removal from the column, yielding values of 10 μmole/g in

Table 2. Effect of mobile-phase cycling on APSG metal-uptake

Material	Copper(II) uptake, μmole/g					
	Original value	After cycle number† 1	2	3	4	5
APSG*	240§	61	34	5	17	13 (10)‡
		262	72	—	—	—
APSG end-capped	147	53	32	11	12	15 (10)‡

*$\equiv SiCH_2CH_2CH_2NH_2$.
†The first two cycles employed 11 ml of 0.05*M* copper(II), 30–40 ml of pH 2.1 HNO_3, followed by pH 1.8 HNO_3.
§Batch copper-uptake value for unused material.
‡Batch copper-uptake values on material removed from column after fifth cycle are shown in parentheses.

Table 3. APSG elemental nitrogen determination

Material	N, %		Ligand coverage, μmole/g		Metal uptake, μmole/g		
	Unused	After cycles	Unused	After cycles	Unused	After cycles	% Decrease
APSG	1.66	1.26	1186	900	593	450	24
APSG end-capped	1.35	1.01	964	721	482	360	25

*Based on a stoichiometry of metal:ligand = 1:2, calculated from ligand coverage values.

both cases, in good agreement with the last three column values (Table 2). Another portion of the cycled APSG was treated with 0.1*M* ammonia buffer (pH 10) for 30 min, thoroughly washed with water, dried and then used for a batch study, in which a copper(II) uptake of 117 μmole/g was obtained. Evidently, the very low column uptake values were primarily the result of protonation of the amine functional group in the stripping step of the cycle, rather than of massive hydrolysis of ligand from the surface. The pH-5 acetate buffer simply maintained the APSG in the protonated state. This protonation effect was also observed qualitatively for the cycled APSG. The material from the column remained white (no copper uptake) when subjected to 0.1*M* copper(II) solution, but after brief contact (30 sec) with pH-10 ammonia buffer, and a thorough water rinse, the material was turned light blue by copper(II) solution, and the colour remained even after extensive water rinsing.

The unused and cycled APSG and capped APSG were also analysed for nitrogen, and the results are given in Table 3. Whereas the cycling study showed nearly total loss of copper-uptake capacity after several cycles, mostly due to protonation of active amine sites as mentioned above, the nitrogen determination revealed the disappearance of about a quarter of the original ligand coverage after only five cycles. This loss must be due to leaching of the ligand from the surface of the silica. The more extensive loss of ligand from the AEAPSG, discussed above, resulted from the longer use of that column for chromatographic studies. An observation that implies that substantial hydrolysis of ligand from the silica surface does indeed occur, is that the column effluent collected early in the cycling runs contained some sticky, polymer-like material after standing for a day or so. Although this material was not characterized further, we surmise that the aminopropylsilane hydrolysate polymerized in the aqueous acetate buffer.

However, on comparing the values in Tables 2 and 3, it is seen that metal-uptake values calculated from the nitrogen content, on the assumption of saturation with metal in 2:1 ligand–metal complexes,[10] are much higher than the experimental copper-uptake results, even for the unused materials. Protonation of the amine groups could account for some of this discrepancy for the used material, but not for the unused. There are apparently metal-inactive nitrogen groups bound to this material even when it is in the unused state, perhaps as a result of using a silane which was over a year old. Presumably oxidation or some other reaction of the amine groups occurred which deactivated the amine with respect to metal complexation. Similar (but smaller) disagreement between results based on copper-uptake and on calculation from carbon or nitrogen contents has previously been reported[10,12] (relatively fresh or distilled silane solutions were used in the earlier work). Interestingly, there is also some indication that the copper-uptake capacity of APSG decreases on standing, as the uptake values of stored material continuously decreased with time (Table 4). Again, this could be due to oxidation of the amine functional group, but more investigation is required before this can be firmly established. The 21-month value for APSG (168 μmole/g) was obtained after treating the material with pH-10 ammonia buffer for 30 min, and indicates that protonation is not the cause of this gradual loss of copper(II)-uptake capacity for unused material.

Table 4. Copper(II)-uptake capacities of alkylamine silica gels as a function of storage time

APSG		End-capped APSG		AEAPSG	
Capacity, μmole/g	Months after preparation	Capacity, μmole/g	Months after preparation	Capacity, μmole/g	Months after preparation
356	0	333	0	310	0
240	17	147	17	249	4
199	19	145	19		
173	20	110	20		
168	21				

It is clear that much of the metal-uptake capacity of the freshly prepared alkylamine silica gels is quickly lost when these materials are subjected to treatment with low-pH aqueous media. The bulk of this loss early in the column use is due to protonation of the amine group, rendering it unreactive toward metal ions at low pH. Treatment with basic buffers is necessary to deprotonate the amines and restore reactivity. This may be a slow process in dilute media[10] and cause further hydrolysis of ligand from the surface.

The nitrogen determination results suggest that true removal of ligand groups from the surface also occurs, significant loss (25%) occurring after only five of the cycles used in this study, and loss of as much as two-thirds of the original coverage after extended column use. Whether this results from true hydrolysis at the more accessible sites, leaching of adsorbed or hydrogen-bonded oligomers, or a combination of both is not known. It seems clear, however, that the alkylamine silicas are not suitable for long-term use with aqueous solutions because of protonation or other deactivation of amine groups and loss of ligand from the surface. Even commercial amine columns should be used with these findings in mind.

Stability of naphthylethylenediamine silica gel

In an attempt to prepare a stable alkylamine silica, a more rigid system was sought. Phenylazo-coupled *N*-(1-naphthyl)ethylenediamine was bound to the silica gel, by use of the shortened preparation of nitrobenzamide silica gel described below, followed by the usual nitro-group reduction, diazonium salt preparation and coupling procedure. However, even this bulky aromatic-substituted amine exhibited bleeding. As the final silica-bound material is highly coloured (red), like most azo-coupled chelating agents, any leaching of ligand can be observed visually, as well as spectrophotometrically. Aqueous acetate buffers, especially in the pH range 3–5, caused extensive bleeding of pink solution from a column packed with this material. Sulphate solution at pH 3 seemed to halt the bleeding, as did lowering the pH to 1.5, at which both nitrogen atoms of the ethylenediamine moiety are protonated. Non-aqueous solvents such as dimethylsulphoxide and 1-propanol also caused bleeding. Methanol–water solutions (1 : 1 v/v) caused the most extensive bleeding, however, as observed earlier for 8-quinolinol silica gel.[3]

The fact that non-aqueous solvents washed coloured material out of this column implies that some leaching process other than normal surface hydrolysis is taking place (see below). However, the pH-dependence of the bleeding (the leaching is less at low pH) implies conventional hydrolysis. In spite of all the washing done, however, the material retained its deep red colour, implying that only a small portion of the overall coverage was lost. It appears that two types of bleeding occur, normal hydrolysis with aqueous buffers, and dissolution of possible oligomeric material from the surface by non-aqueous solvents. More extensive studies are required to determine whether this aromatic amine is indeed more stable than the alkylamines described above. Initial results are promising, however, as extensive washing seemed to remove all leachable material, no further colour appearing in subsequent washings.

Improved synthesis of azo-coupled materials

While a number of alkylamine silanes are commercially available and make possible the one-step attachment of a complexing group to the surface of silica gel, the incorporation of other ligands may require further modification of the bound alkylamine. One productive route has been the preparation of azo-coupled ligands.[8,13,14] In the past this has required a multi-step process beginning with alkylamine silylation, amide formation by use of *p*-nitrobenzoyl chloride, reduction of the aromatic nitro group to the amine, formation of a diazonium salt and finally coupling to the ligand of interest. Marshall and Mottola[6] recently reported the use of *p*-aminophenyltrimethoxysilane which, in effect, combined the first three steps of the synthesis into one, thus eliminating the 48-hr acid–chloride reaction needed to produce the amide. This makes preparation of the azo-coupled ligand materials much more convenient. The modified silica obtained differs from those prepared in ealier studies in that it lacks the propylamide grouping between the silica surface and the aromatic function, which is present if aminopropylsilane is used to begin the synthesis. This presumably provides a smaller and more rigid silica-bound moiety, allowing somewhat higher surface coverages than those achieved in the past.[6] However, there are a number of reasons why azo-coupled ligands containing the propylamide grouping may be desired. First, all of the earlier work with these materials included this group and, for purposes of comparison with new work, the same surface-bound moiety should be present. Secondly, there may be some instances in which a more flexible attached group is needed, or a higher organic content desired for HPLC purposes. A third reason arises from the desirability of trimethylsilyl end-capping of these materials at the nitrobenzamide stage of the synthesis. When the initial silylation step produces the aminophenyl species,[6] there is a danger that end-capping will deactivate the amino group as well as the undesirable residual silanol groups.

Accordingly we have developed a more efficient route to the azo-coupled materials, which uses triethoxysilylpropyl-*p*-nitrobenzamide as the silylating agent. Use of this silane results in nitrobenzamide silica gel (NBSG) containing the propylamide spacer group between the surface and the benzene ring, as did the earlier syntheses. As with the Mottola procedure,[6] the lengthy acid–chloride reaction step is eliminated. Unlike the Mottola approach,

an additional step to convert the aromatic nitro group into the amine is required, but this involves only a 30-min reduction with sodium dithionite, and causes no difficulty.

Elemental nitrogen determinations on several batches of NBSG have revealed surface coverages ranging from 230 to 250 μmoles of the benzamide moiety per gram of modified silica gel. This is considerably less than the coverage which results from an initial silylation with an alkylamine reactant such as aminopropylsilane.[8,14,15] The smaller coverage is probably due to the steric effect of the bulky nitrobenzamide group, which hinders further surface reaction once a certain coverage is achieved. Of course, a larger number of residual silanol groups will remain than in the case of alkylamine silica gels, and the necessity to end-cap these silanol groups, if HPLC stationary phases are being prepared, is obvious. This underscores the advantage of being able to perform the end-capping reaction at the NBSG stage of the procedure.

After the NBSG has been end-capped it is clear that there are indeed more residual silanol groups present in it than in the same type of material prepared by the earlier procedure. Whereas the NBSG itself can be easily wetted with water after preparation, this is not the case after the end-capping reaction. The trimethylsilylation of residual silanol groups creates a moderately hydrophobic surface which is wetted only with difficulty. This hydrophobicity was not observed for capped NBSG prepared by the old procedure, as fewer silanol groups were present in it, owing to the greater initial alkylamine coverage.

Though the initial silylation reactions yield a greater coverage with alkylamine than nitrobenzamide groups, the final amount of ligand which is coupled through the azo linkage is at least as great as that obtained by the earlier approach. The 8-quinolinol silica gel (QSG) derived from NBSG prepared by our new procedure exhibits copper-uptake capacities of up to 175 μmole/g. Steric effects apparently limit the amount of 8-quinolinol (and presumably other bulky ligands) which can be azo-coupled to the surface of silica gel,[8,9] so greater coverage of the surface at earlier stages of the reaction sequence serves no useful purpose. In fact, greater coverage may result in unsubstituted bonded moieties being left, which can lead to unwanted interactions in chromatography, as well as causing steric effects which can limit reactions later in the sequence.

Other than the increased hydrophobicity, the NBSG prepared by the new procedure did not differ in reactivity from material prepared by the longer method. Infrared spectra of pellets of NBSG prepared by both methods were essentially identical.[8] All reactions were qualitatively similar to those reported earlier,[8] and the colours of the reaction intermediates and final products all agreed.

Leaching studies

An earlier study of NBSG and QSG prepared from APSG base material revealed that organic species continued to bleed from these materials long after the normal washing.[3] The effluent from QSG columns was red when methanol, acetonitrile, and especially 50% aqueous solutions of these solvents were used as eluents, and after the column had been stored with these solvents for extended periods. Ultraviolet spectra of these washings revealed absorption in the aromatic region, around 260 nm. Washings of NBSG exhibited a broad band around 265 nm and a sharp one around 195 nm. These bands matched those of a methanol solution of *p*-nitrobenzoyl chloride, the reagent used to obtain NBSG from APSG. Water washings had no colour or ultraviolet absorption. It was argued that adsorbed acid chloride, or alkylamine polymers or oligomers adsorbed or weakly bound to the surface and subsequently converted into the nitrobenzamide derivative, were slowly removed by the organic eluents. Likewise, Unger reported the presence of slightly soluble oligomeric sulphonated benzyl siloxanes in an extraction solution of a silica-based cation-exchanger.[16]

Because the NBSG used in the present study was prepared by the new method described above, with triethoxysilylpropyl-*p*-nitrobenzamide, and because of the existing information on leaching of organic species from modified silica gels,[3,16] the new materials were subjected to various washing procedures. The ultraviolet spectra of the washings were recorded for comparison.

A methanol solution of the silylating reagent itself exhibited an envelope of absorption bands in the aromatic region, around 265 nm, and also a sharp but much smaller peak near 210 nm, as expected. The first methanol wash of NBSG (after a 50–100-ml toluene rinse) yielded a spectrum qualitatively similar to that of the silylating reagent itself. On further washing, however, the longer wavelength band decreased substantially, while the shorter wavelength band did not. The spectrum of a methanol solution of a different batch of the nitrobenzamidesilane exhibited peaks at 265 and 207 nm which were of the same height. These facts seem to imply that these two bands are due to different species and that differences in the commercial silanes may exist from batch to batch. However, methanol washings of NBSG prepared from this second batch of silane yielded solutions having spectra which were similar to those of washings of NBSG prepared from the first batch of silane, implying that the NBSG produced was the same in both cases. Again, the longer wavelength band decreased more rapidly on washing than the shorter wavelength band.

One batch of NBSG was washed intermittently with methanol over a 3-month period. Organic material was always removed. For example, after standing overnight in methanol, the NBSG was filtered off and washed immediately with 25 ml of warm methanol;

the ultraviolet spectrum of this wash exhibited a peak at 210 nm, with an absorbance greater than 1.0. Repetitive methanol washing caused the absorbance of this peak to decrease to less than 0.4. The NBSG was allowed to dry, and one week later this experiment was repeated, and gave the same results. These findings parallel those obtained earlier,[3] and also in the present study, with azo-coupled ligands, such as 8-quinolinol silica gel (QSG). Columns packed with the QSG stationary phase were washed until the eluent was colourless. They were then filled with methanol, and after standing for several days were washed with methanol; the first few ml of the effluent were again slightly coloured.

Another batch of NBSG was washed with cyclohexane after the original toluene rinse, because of the suggestion[17] that methanol may cause some hydrolysis of silane from the silica surface. The ultraviolet spectrum of the cyclohexane washes was almost qualitatively identical with that of the nitrobenzamidesilane itself in methanol. Both the peak in the aromatic region (255 nm) and that at the shorter wavelength (215 nm) had absorbance values above 2.

These findings and earlier results[3] suggest that hydrolysis is not involved here. Washing with water does not remove organic material from the surface; the column effluents are colourless and their ultraviolet spectra exhibit little or no absorption. Methanol, acetonitrile, 50% aqueous solutions of these solvents, cyclohexane and hexane all remove substantial amounts of organic matter. The fact that consecutive washings with methanol remove less and less organic material, but subsequent overnight standing of the modified silica in methanol removes more material than the previous washes did, suggests slow "softening" or dissolving of weakly bound or adsorbed small polymers or oligomers, or a diffusion-controlled removal of material from deep within the pores of the silica gel. Eventually, columns packed with, for example, QSG, yield no more coloured effluent on flushing with methanol. It seems then, that some polymeric material forms during the silylation reaction despite our best efforts at drying the solvents and silica, and preventing introduction of moisture during the reaction, or that the silanes themselves contain polymerized material which is adsorbed on the silica surface.[12] However, the type of hydrolysis seen for the alkylamine-modified silicas does not occur with these aromatic-substituted materials. Once the polymeric material has been finally removed, very stable materials result.

In an effort to compare further methanol washing with cyclohexane washing, three batches of NBSG, one prepared from 60 Å pore-size Polygosil, the second from 240 Å controlled-pore glass (CPG) and the third from 500 Å CPG, were each divided into two equal parts. One portion of each batch was washed thoroughly with methanol, the other with cyclohexane. All portions were then used to prepare QSG or QCPG, and the copper-uptake of each product was measured. The results are given in Table 5.

It would appear that the polar methanol was a more effective washing solvent than the non-polar cyclohexane, except in the case of the smallest pore-size material, although the 7% lower capacities of the methanol-washed CPGs may not be significant. Much more extensive controlled studies will be necessary to determine whether any real difference exists between the effect of polar and non-polar washing solvents. The importance of these washing studies is the finding that organic material bleeds from the modified silica gels even when these are made with the usual preparative precautions to prevent polymer formation. However, the azo-coupled ligand columns eventually stabilized, leaving moderately high and constant capacity values, unlike other products in which there is total hydrolysis of the alkylamines from the surface.

Pore-size effects

An aspect of silica materials which can have an effect on the reactivity and metal-uptake capacity of bound chelating agents is the pore-size of the base silica gel. Roumeliotis and Unger found that the pore diameter and pore volume were reduced by up to 50% and 40% respectively, after reaction with hexadecyldimethylchlorosilane.[18] Roumeliotis also found that coverage of the surface decreased as the surface area of bound groups increased in a series of silanes.[19] Jezorek *et al.*[8] postulated that steric blockage of

Table 5. Effect of washing-solvent polarity on metal-uptake of QSG*

Washing solvent	Copper(II) uptake, $\mu mole/m^2$		
	60 Å Polygosil	240 Å CPG	500 Å CPG
methanol	0.16	0.41	0.62
cyclohexane	0.16	0.44	0.66

*8-Quinolinol silica gel,

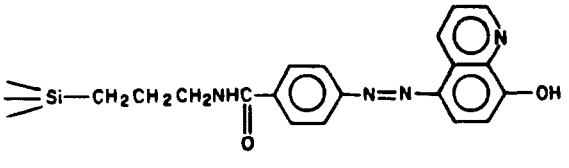

Table 6. Physical characteristics and copper(II)-uptake of 8-quinolinol-modified controlled-pore glass

Pore size, Å	Specific surface area, m^2/g	Copper(II) uptake capacity	
		$\mu mole/m^2$	$\mu mole/g$
40	190	0.26	48.6
240	130	0.40	52.5
500	70	0.62	43.1

reacting 8-quinolinol, by groups already present on the surface, was the reason why the amount of this ligand coupled through the azo-bond was only 25–50% of the original coverage of the silica by the aminopropyl moiety.[8,13] These investigators also speculated that the actual pore-size of the silica gel itself, for a given bound group such as 8-quinolinol, would affect the maximum amount of that group which could be bonded to the silica.

Recently, Marshall and Mottola provided evidence that this is indeed the case.[9] A series of base materials of various pore-sizes resulted in the production of phenylazo-8-quinolinol silica gels of varying capacity. Because the specific surface area of the silica gels decreases as the pore-size increases, an optimum metal-uptake capacity, expressed as μmoles of 8-quinolinol per gram of modified silica, was observed for 60 Å pore-size material. For materials with pore diameters smaller than 60 Å, the coverage was found to drop dramatically, owing to steric blockage of the pores. A similar result was previously found by Jezorek *et al.* for 22 Å pore-size material.[8]

In this paper we provide further evidence of this pore-size effect. To silylate the silica the nitrobenzamidesilane was used instead of the aminophenylsilane used by Marshall and Mottola,[9] so the steric bulk of the attached group was even greater. The base material used was controlled-pore glass. Table 6 shows the pore-size, specific surface area and copper-uptake capacity of three 8-quinolinol-modified controlled-pore glasses. The metal uptake by this bound propylamide-substituted phenylazo-8-quinolinol (expressed in $\mu mole/m^2$), increases with pore size. In fact, for the limited study of three pore-sizes reported here, the capacity, and by implication the surface density of the bound chelating group, seems to increase linearly with pore-size with a slope of 7.8×10^{-4} $\mu mole.m^{-2}.Å^{-1}$, an intercept of 0.22 $\mu mole/m^2$ and a correlation coefficient of 0.9996. However, only three pore-sizes were employed and this apparent linearity might not be found if a greater number of pore-sizes were used. The intercept of 0.22 $\mu mole/m^2$ may correspond to a limiting coverage, sterically controlled by the bulk of the bound moiety, which would be obtained for a non-porous material or one with very small pores.

Acknowledgements—The authors would like to thank the Research Corporation, the North Carolina Board of Science and Technology, and the University of North Carolina at Greensboro Research Council, for financial assistance with this work.

REFERENCES

1. K. K. Unger, *Porous Silica*, Elsevier, Amsterdam, 1979.
2. J. R. Jezorek and H. Freiser, *Anal. Chem.*, 1979, **51**, 366.
3. G. J. Shahwan and J. R. Jezorek, *J. Chromatog.*, 1983, **256**, 39.
4. M. Gimpel and K. Unger, *Chromatographia*, 1982, **16**, 117.
5. T. G. Waddell, D. E. Leyden and M. T. Debello, *J. Am. Chem. Soc.*, 1981, **103**, 5303.
6. M. A. Marshall and H. A. Mottola, *Anal. Chem.*, 1983, **55**, 2089.
7. S. A. Wise and W. E. May, *ibid.*, 1983, **55**, 1479.
8. C. Fulcher, M. A. Crowell, R. Bayliss, K. B. Holland and J. R. Jezorek, *Anal. Chim. Acta*, 1981, **129**, 29.
9. M. A. Marshall and H. A. Mottola, *ibid.*, 1984, **158**, 369.
10. J. R. Jezorek, C. Fulcher, M. A. Crowell, R. Bayliss, B. Greenwood and J. Lyon, *ibid.*, 1981, **131**, 223.
11. R. C. Johnson, Personal communication.
12. P. R. Moses, L. M. Wier, J. C. Lennox, H. O. Finklea, J. O. Lenhard and R. W. Murray, *Anal. Chem.*, 1978, **50**, 576.
13. J. M. Hill, *J. Chromatog.*, 1973, **76**, 455.
14. K. F. Sugawara, H. H. Weetall and G. D. Schucker, *Anal. Chem.*, 1974, **46**, 489.
15. D. E. Leyden and G. H. Luttrell, *ibid.*, 1975, **47**, 1612.
16. K. Unger and D. Nyamah, *Chromatographia*, 1974, **7**, 63.
17. Petrarch Systems, Inc., Personal communication.
18. P. Roumeliotis and K. K. Unger, *J. Chromatog.*, 1978, **149**, 211.
19. P. Roumeliotis, *Thesis*, Technische Hochschule, Darmstadt, FRG, 1977.

Talanta, Vol. 32, No. 8B, pp. 771–777, 1985
Printed in Great Britain

0039-9140/85 $3.00 + 0.00
Pergamon Press Ltd

EXTRACTION OF MANGANESE(II), IRON(II), COBALT(II), NICKEL(II), COPPER(II), ZINC(II), AND CADMIUM(II) INTO 1,2-DICHLOROETHANE WITH 4,7-DIPHENYL-1,10-PHENANTHROLINE AND PERCHLORATE

TAKAHARU HONJO, AKIKO OKAZAKI, KIKUO TERADA
Department of Chemistry, Faculty of Science, Kanazawa University, Kanazawa, Ishikawa 920, Japan

and TOSHIYASU KIBA
Kanazawa Institute of Technology (President, Professor Emeritus of Kanazawa University), Kanazawa, Ishikawa 921, Japan

(*Received* 6 *June* 1984. *Revised* 4 *March* 1985. *Accepted* 12 *March* 1985)

Summary—The extraction of the ion-association complexes formed by Mn(II), Fe(II), Co(II), Ni(II), Cu(II), Zn(II) and Cd(II)–4,7-diphenyl-1,10-phenanthroline (BP) chelates and perchlorate ions into 1,2-dichloroethane has been investigated. Extraction equilibrium for Mn(II), Cu(II), Zn(II) and Cd(II) is reached within 1 hr, but equilibration for Fe(II), Co(II) and Ni(II) is very slow; the equilibration rate depends on the structure of the chelating agent, the nature of the organic solvent, and pH. In the extraction equilibrium of Co(II) the rate-determining step seems to be the complexation of hydrated Co(II) by BP in the aqueous phase.

In general, the extraction equilibria of ion-pair complexes are attained within a few minutes.[1–3] However, an ion-pair extraction system involving pinacyanole and tetraphenylborate has been reported which takes over an hour to reach equilibrium.[4] During an investigation into the extraction of Mn(II), Fe(II), Co(II), Ni(II), Cu(II), Zn(II) and Cd(II) with 4,7-diphenyl-1,10-phenanthroline into 1,2-dichloroethane in the presence of perchlorate, we have found that the rate of extraction of Fe(II), Co(II) and Ni(II) is quite slow.

In this paper, the role of the central metal ion, the chelating agent, the extracting solvent, and the pH on the rate of extraction is reported. Furthermore, to identify the rate-determining step, the kinetics and mechanism of the Co(II)–4,7-diphenyl-1,10-phenanthroline–1,2-dichloroethane extraction system in the presence of perchlorate have been investigated and are discussed in detail.

EXPERIMENTAL

Apparatus

A Hitachi 170-50 atomic-absorption spectrophotometer, and Hirama 6 and Union Giken SM-401 spectrophotometers were used. Other apparatus was the same as previously described.[1–3]

Materials

All the reagents used were guaranteed-grade materials. The organic solvents, such as 1,2-dichloroethane, carbon tetrachloride and nitrobenzene, were used without further purification. Distilled water was further purified by passage through an ion-exchange column. The chelating agents, 4,7-diphenyl-1,10-phenanthroline (bathophenanthroline, BP), 4,7-dimethyl-1,10-phenanthroline (DMP), and 1,10-phenanthroline (OP), were obtained commercially. Manganese(II), iron(II), cobalt(II), nickel(II), zinc(II) and cadmium(II) sulphates were dissolved in $5 \times 10^{-3}M$ sulphuric acid to give $2 \times 10^{-2}M$ aqueous solutions. Sodium perchlorate was dissolved in purified water to make a $1M$ solution. A series of 0.01–0.1M anion solutions was prepared by dissolving sodium or potassium chloride, nitrate, acetate, sulphate and phosphate in purified water. A series of buffer solutions (pH 1.5–4.5) was prepared by mixing 0.1M phosphoric acid and 0.1M sodium dihydrogen phosphate solution. These buffer solutions had no specific influence on the extractability of the metals.

Extraction and stripping

The extraction procedure was as follows: 4.5 ml of 0–0.01M perchlorate adjusted to the desired pH (1.67–4.37), 0.5 ml of $10^{-3}M$ metal-ion solution, and 5 ml of $10^{-3}M$ phenanthroline derivative in organic solvent were placed in a 30-ml glass-stoppered centrifuge tube and agitated on a shaking machine for 0–4 hr. After separation of the phases, the amount of metal ion in the aqueous phase was determined by atomic-absorption spectrophotometry (AAS), and the pH of the aqueous phase was measured again. To determine the amount of metal ion in the organic phase, a 4-ml portion was pipetted into a test-tube and the solvent evaporated under reduced pressure. The residue was decomposed by evaporation to dryness with a 1:1 mixture of nitric and perchloric acids, and the residue was taken up in 0.5M hydrochloric acid for determination of the metal-ion by AAS. The stripping procedure was as follows. A 4-ml portion of organic extract containing known amounts of

metal ion, phenanthroline derivative and perchlorate was prepared by the extraction procedure. This organic phase was shaken for 1 hr with 4 ml of an aqueous solution adjusted to the desired pH and containing a known amount of perchlorate and phenanthroline derivative. The amount of metal ion in both phases was determined by AAS as just described. The pH and the amount of perchlorate in the aqueous phase were measured again after the stripping. All experiments were performed at 18–20°.

Determination of perchlorate[5]

One ml of 0.01*M* 1,10-phenanthroline, 1 ml of $2.5 \times 10^{-3}M$ ferrous ammonium sulphate, 2 ml of 1*M* sodium acetate (adjusted to pH 4.8–8.0), 2 ml of perchlorate solution of appropriate concentration and 4 ml of distilled water were placed in a stoppered glass tube (30- or 50-ml), and 5 ml of nitrobenzene were added. The mixture was shaken for 5 min, then left to stand for about 30 min. The organic phase was then transferred into a test-tube containing 1 g of anhydrous sodium sulphate, and shaken vigorously to remove entrained water. The absorbance of the nitrobenzene phase was measured at 510 nm.

Determination of the 1,10-phenanthroline derivative

The 1,10-phenanthroline derivatives in the organic phases after equilibration were determined as follows. A 1-ml portion of organic phase was pipetted into a test-tube, and the excess of solvent evaporated under reduced pressure. The residue was dissolved in a mixture of ethanol and $5 \times 10^{-4}M$ ferrous ammonium sulphate in 20:1 volume ratio, and left to stand for about 30 min. The absorbance of the solution was then measured at 510 nm for OP, 512 nm for DMP, and 533 nm for BP. A check was run by obtaining the residue from another 1-ml portion, dissolving it in absolute ethanol and measuring the absorbance at 265 nm for OP and DMP, and 273 nm for BP. The phenanthroline derivatives in the aqueous phases were determined by mixing an appropriate volume with 1*M* sodium acetate and $5 \times 10^{-4}M$ ferrous ammonium sulphate, leaving to stand for about 30 min, then measuring the absorbance at 510 nm (OP), 512 nm (DMP) and 533 nm (BP). If the amount of the phenanthroline derivative in the aqueous phase was very small, a 25-ml portion was shaken with 5 ml of 1,2-dichloroethane for 2 hr. After separation of the phases, a 4-ml portion of the organic phase was analysed for phenanthroline derivative as above.

Kinetics of extraction

In 30-ml glass-stoppered centrifuge tubes 4.5-ml portions of $0–10^{-3}M$ perchlorate adjusted to pH 1.67–4.37 were mixed with 5 ml of $10^{-3}M$ BP in 1,2-dichloroethane and 0.5 ml of $10^{-3}M$ Co(II) solution. The tubes were shaken at 300 strokes/min for various times at 18–20°. After separation of the phases, the amount of Co(II) in each was determined by AAS as already described, and the pH of the aqueous phase was measured again.

THEORY

Extraction equilibrium

The extraction equilibria for a bivalent metal ion with BP in the presence of perchlorate can be summarized in the following scheme:

$$\begin{array}{ccc} BP\,(BP\cdot H)^+ + A^- & \overset{\alpha_o}{\rightleftharpoons} & (BP\cdot H)^+A^- \\ \Big\| K_d & & \Big\| K_r \\ (BP\cdot H)^+ + A^- & \overset{\alpha}{\rightleftharpoons} & (BP\cdot H)^+A^- \\ BP + H^+ & \overset{K_a}{\rightleftharpoons} & (BP\cdot H)^+ \end{array} \qquad \begin{array}{ccc} (M\cdot BP_3)^{2+} + 2A^- & \overset{\gamma_o}{\rightleftharpoons} & (M\cdot BP_3)^{2+}\,(A^-)_2 \\ \Big\| K_r & & \Big\| K_c \quad \begin{matrix}\text{Org.}\\ \text{Aq.}\end{matrix} \\ (M\cdot BP_3)^{2+} + 2A^- & \overset{\gamma}{\rightleftharpoons} & (M\cdot BP_3)^{2+}\,(A^-)_2 \\ M^{2+} + 3BP & \overset{\beta}{\rightleftharpoons} & (M\cdot BP_3)^{2+} \end{array}$$

$$K_d = \frac{[BP]_o}{[BP]}; \quad K_r = \frac{[(BP\cdot H)^+A^-]_o}{[(BP\cdot H)^+A^-]}; \quad K_c = \frac{[(M\cdot BP_3)^{2+}(A^-)_2]_o}{[(M\cdot BP_3)^{2+}(A^-)_2]}; \quad k_a = \frac{[BP]\,[H^+]}{[(BP\cdot H)^+]};$$

$$\alpha = \frac{[(BP\cdot H)^+A^-]}{[(BP\cdot H)^+]\,[A^-]}; \quad \alpha_o = \frac{[(BP\cdot H)^+A^-]_o}{[(BP\cdot H)^+]_o\,[A^-]_o}; \quad \beta = \frac{[(M\cdot BP_3)^{2+}]}{[M^{2+}]\,[BP]^3}; \quad \gamma = \frac{[(M\cdot BP_3)^{2+}(A^-)_2]}{[(M\cdot BP_3)^{2+}]\,[A^-]^2};$$

$$\gamma_o = \frac{[(M\cdot BP_3)^{2+}(A^-)_2]_o}{[(M\cdot BP_3)^{2+}]\,[A^-]_o^2}; \quad D_M = \frac{[M^{2+}]_{o,\text{total}}}{[M^{2+}]_{\text{total}}}; \quad D_A = \frac{[A^-]_{o,\text{total}}}{[A^-]_{\text{total}}}; \quad D_{BP} = \frac{[BP]_{o,\text{total}}}{[BP]_{\text{total}}}$$

where A^- and M^{2+} stand for perchlorate and the metal-ion, respectively, and [ ] and [ ]$_o$ designate the concentrations of the chemical species in the aqueous and organic phase, respectively.

The extraction equilibrium for BP and perchlorate in the absence of M^{2+} can be treated as follows:

$$A^- + BP_{(o)} + H^+ \overset{K_{ex_1}}{\rightleftharpoons} (BP\cdot H)^+A^-_{(o)} \qquad (1)$$

$$K_{ex_1} = \frac{[(BP\cdot H)^+\,A^-]_o}{[A^-][BP]_o[H^+]} \qquad (2)$$

Equation (2) can be rewritten as

$$\log D_A = -\mathrm{pH} + \log [BP]_o + \log K_{ex_1} \qquad (3)$$

The extraction equilibrium of M^{2+} with BP in the presence of perchlorate can be represented by the equations:

$$M^{2+} + 3BP_{(o)} + 2A^- \overset{K_{ex_2}}{\rightleftharpoons} (M\cdot BP_3)^{2+}(A^-)_{2(o)} \qquad (4)$$

$$K_{ex_2} = \frac{[(M\cdot BP_3)^{2+}(A^-)_2]_o}{[M^{2+}]\,[BP]_o^3\,[A^-]^2} \qquad (5)$$

Equation (5) yields the equation

$$\log D_M = 3 \log [BP]_o + 2 \log [A^-] + \log K_{ex_2} \qquad (6)$$

Rate of extraction

The rate of extraction of M^{2+} with BP in the presence of perchlorate at a fixed pH may in general be represented by the following equation:

$$-\mathrm{d}\,[M^{2+}]/\mathrm{d}t = k\,[M^{2+}]^a\,[BP]_o^b\,[ClO_4^-]^c \qquad (7)$$

When BP and perchlorate are in large excess relative to M^{2+}, the rate equation can be written as

$$-d[M^{2+}]/dt = q\,[M^{2+}]^a \qquad (8)$$

where q is equal to $k\,[BP]_o^b\,[ClO_4^-]^c$, and the concentrations of BP in the organic phase and of perchlorate in the aqueous phase are kept constant in any given series of experiments. When the reaction order of the extraction system is unity with respect to the concentration of M^{2+}, the following equation will apply:

$$-\log[M^{2+}] = 2.3\,qt + \text{const.} \qquad (9)$$

In order to obtain the reaction order, b, a q_{BP} value can be defined by

$$\log q_{BP} = \log k\,[ClO_4^-]^c + b \log[BP]_o \qquad (10)$$

where the concentration of the perchlorate ion in the aqueous phase is kept at a constant known value. Likewise, a q_A value can also be defined in order to obtain the reaction order, c:

$$\log q_A = \log k\,[BP]_o^b + c \log[ClO_4^-] \qquad (11)$$

where the concentration of BP in the organic phase is kept at a constant known value. Then the reaction order of this extraction system, b, may be obtained from the slope of the log q_{BP} *vs.* log $[BP]_o$ plot. The value of c can be determined in the same way as b. By use of these values, the rate constant in the extraction system at a fixed pH, k, can be calculated from equation (7).

RESULTS AND DISCUSSION

Effect of metal ion

Mn(II), Fe(II), Co(II), Ni(II), Cu(II), Zn(II) and Cd(II) form 1:3 complexes with 1,10-phenanthroline.[6-9] As a preliminary test we checked the recovery of the metals in the extraction and stripping procedures as follows. The extraction was done by shaking 5 ml of $10^{-4}M$ metal solution and 5 ml of $0.01M$ perchlorate with 5 ml of $10^{-3}M$ BP in 1,2-dichloroethane for 1 hr. The stripping was done as already described. At pH 1.67 the degrees of extraction of Cu(II), Ni(II), Co(II) and Fe(II) were 100, 0, 45 and 80%, respectively, and no metal was stripped in the back-extraction. This suggests that only the nickel system reaches equilibrium in 1 hr (or that it reacts at an imperceptible rate). The extraction and stripping curves (as a function of pH) for Mn(II), Zn(II) and Cd(II) were mirror images, indicating that for these metals equilibrium was reached within 1 hr. At pH 4.37 the degree of extraction of Ni(II) was 45%, but it still was not stripped at this pH.

Effect of perchlorate concentration

The extraction and back-extraction behaviour of Co(II), Ni(II) and Zn(II) was examined by varying the perchlorate concentration. The extraction and stripping curves are given in Fig. 1. The symbols A→O and O→A denote the extraction and stripping of chemical species, respectively and [ ] and [ ]$_o$ designate the concentrations in the aqueous and organic phases, respectively. The extraction and stripping curves for Zn(II) are mirror images, and we again conclude that extraction equilibrium is reached within 1 hr. On the other hand, the extraction and stripping behaviour of Co(II) and Ni(II) is quite different; the degree of extraction of Ni(II) increases with increase in $[ClO_4^-]$, but that of Co(II) remains constant. Neither is stripped under the conditions used. The rate of extraction varies considerably and generally seems to increase in the order Ni(II) < Co(II) < Fe(II) < Zn(II) < Cd(II) < Cu(II) as shown in Fig. 2.

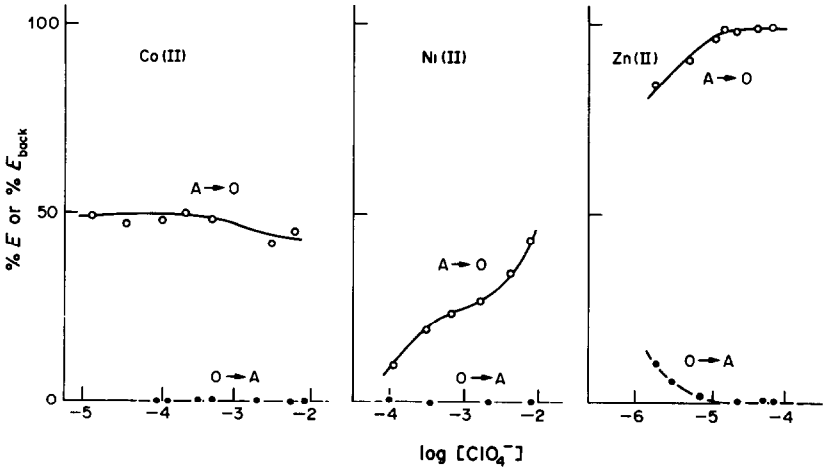

Fig. 1. Effect of concentration of perchlorate on the extraction and back-extraction of Co(II), Ni(II) and Zn(II) with BP in 1,2-dichloroethane. $[ClO_4^-]$ = concentration of perchlorate ion in aqueous phase after extraction; $[BP]_{o,initial} = 10^{-3}M$; $[M(II)]_{initial} = 10^{-4}M$; pH 1.67 for Co(II) and Zn(II), 4.39 for Ni(II); ○—extraction; ●—back-extraction.

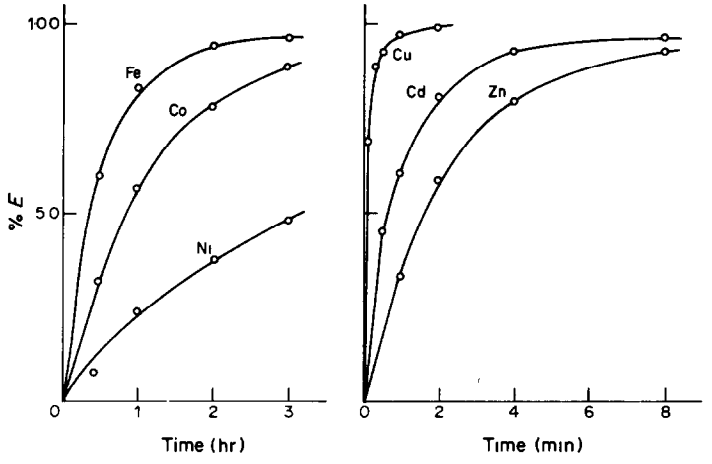

Fig. 2. Effect of shaking time on the extraction of Fe(II), Co(II) Ni(II), Cu(II), Zn(II) and Cd(II) with BP in 1,2-dichloroethane in the presence of perchlorate, $[M(II)]_{initial} = 10^{-4}M$; $[BP]_o$, initial $= 10^{-3}M$; $[ClO_4^-]_{initial} = 9 \times 10^{-4}M$; pH 1.67 for Fe(II), Co(II), Cu(II), Cd(II) and Zn(II), 4.37 for Ni(II).

Effect of 1,10-phenanthroline derivatives

Since the rates of extraction of Fe(II), Co(II) and Ni(II) in the BP–perchlorate–1,2-dichloroethane system were found to be low, it was decided to investigate the effect of substituted 1,10-phenanthrolines on the rate of extraction of Co(II) as a representative metal species under the conditions shown in Fig. 3. The extraction and stripping curves for Co(II) with OP and DMP are mirror images and the results show that extraction equilibrium was reached within 1 hr.

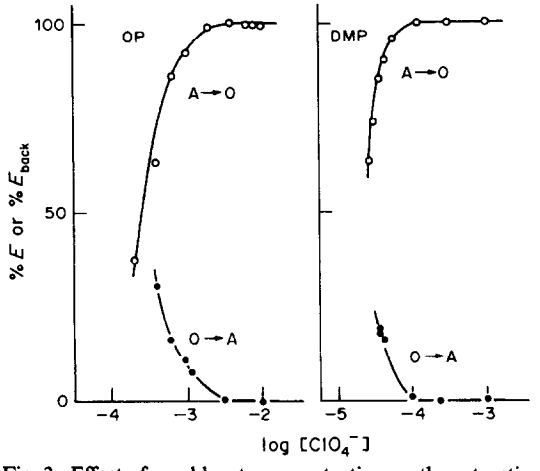

Fig. 3. Effect of perchlorate concentration on the extraction and back-extraction of Co(II) with OP or DMP in 1,2-dichloroethane. $[Co(II)]_{initial} = 10^{-4}M$; $[OP]_{o,initial}$ and $[DMP]_{o,initial} = 10^{-3}M$; shaking time 1 hr; pH 1.67 for DMP and 3.18 for OP; ○—extraction, ●—back-extraction.

Effect of extracting solvent

A binary mixture of carbon tetrachloride and 1,2-dichloroethane was used with the Co(II)–BP–perchlorate system. The extraction curves shown in Fig. 4 show that the rate of extraction increases remarkably as the volume ratio of carbon tetrachloride to 1,2-dichloroethane increases. This

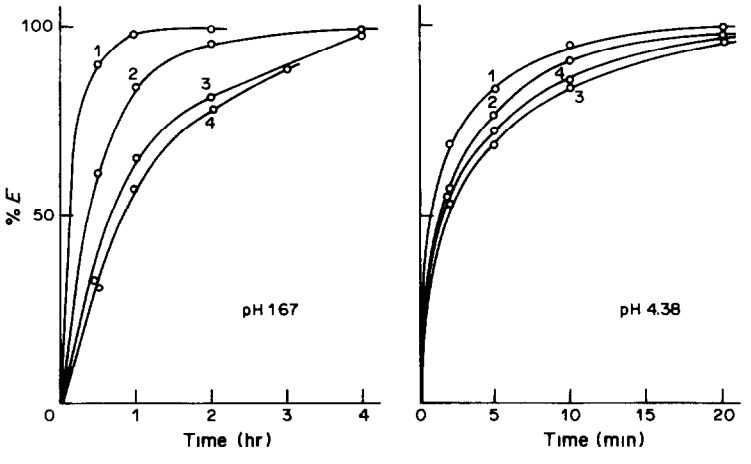

Fig. 4. Effect of shaking time on the extraction of Co(II) with BP in a mixture of carbon tetrachloride and 1,2-dichloroethane. Composition of extracting solvent (CCl_4/1,2-$C_2H_4Cl_2$, v/v); (1) 4/1, (2) 2.5/2.5, (3) 1/4, (4) 0/5; $[Co(II)]_{initial} = 10^{-4}M$; $[BP]_{o,initial} = 10^{-3}M$; $[ClO_4^-]_{initial} = 9 \times 10^{-4}M$.

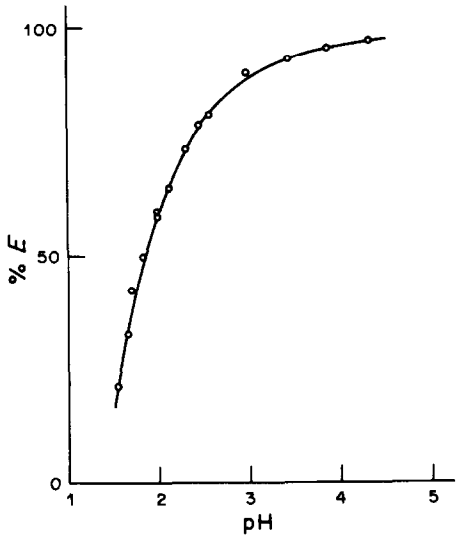

Fig. 5. Effect of pH on the extraction of Co(II) with 4,7-diphenyl-1,10-phenanthroline in 1,2-dichloroethane in the presence of perchlorate. $[Co(II)]_{initial} = 10^{-4}M$; $[BP]_{o,initial} = 10^{-3}M$; $[ClO_4^-]_{initial} = 9 \times 10^{-4}M$; shaking time 20 min.

may be due to the decreasing polarity favouring ion-association complex extraction.

Effect of pH on extraction equilibrium of the reagent

Experiments involving extraction of cobalt at different pH values with different shaking times have shown that pH affects both the extent of extraction (once equilibrium has been attained), and the rate at which the system reaches equilibrium, as shown in Fig. 2 and Fig. 5. A rigorous analysis of the data is very complex. The protonated phenanthrolines themselves are extracted as ion-pairs with perchlorate very rapidly and the distribution is pH-dependent. Plots of log $D_{reagent}$ *vs.* pH for the three reagents are shown in Fig. 6 and the apparent K_d values calculated from these results and the pK_a values from the literature[10] are listed in Table 1. The extraction and stripping curves for perchlorate in the absence of the transition metal ions, as a function of pH, were mirror images (with equilibration for 30 min). The dependence of the distribution on the perchlorate concentration [equation (3)] is demonstrated by the linearity of a plot of log D_A *vs.* pH, which has a slope of -1 and log $D_A = 0$ at pH 2.0.

Stoichiometry

Cobalt was extracted from an aqueous solution at pH 4.37 (so as to avoid extraction of $BP^+ClO_4^-$) and containing a known concentration of perchlorate into 1,2-dichloroethane containing a known concentration of BP. Then the organic phase contained BP (excess, free) with negligible $HBP^+ClO_4^- + CoBP_x(ClO_4)_y$, and the aqueous phase contained ClO_4^- (excess), negligible Co and BP. The excess of BP in the organic phase was determined as the $Fe(II)(BP)_3(ClO_4)_2$ ion-association complex, since

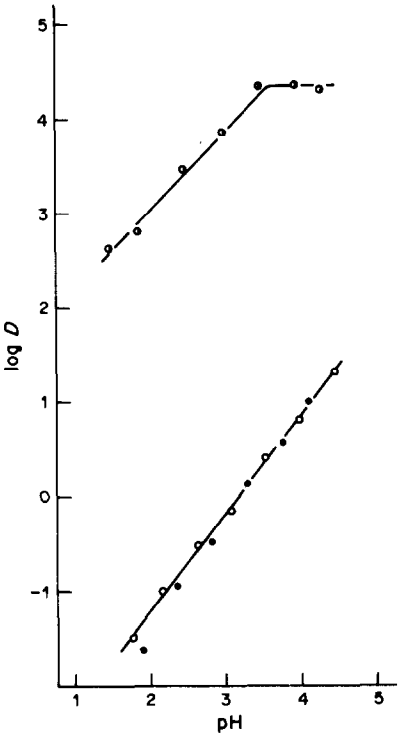

Fig. 6. Effect of pH on the distribution of BP, OP and DMP between 1,2-dichloroethane and aqueous solution. ○—1,10-phenanthroline, ●—4,7-dimethyl-1,10-phenanthroline, ◑—4,7,diphenyl-1,10-phenanthroline.

Fe(II) will not displace Co(II) from its BP complex. The excess of perchlorate remaining in the aqueous phase was determined by extraction as the red $Fe(OP)_3(ClO_4)_2$ ion-association complex. These analyses showed how much BP (from the organic phase) and perchlorate (from the aqueous phase) had combined with the cobalt, and proved the chelate ion-association complex to be $(Co \cdot BP_3)^{2+}(ClO_4^-)_2$, and justified the use of equations (2) and (5). We next tried to find which was the rate-determining step in the extraction process. The transfer of BP between the phases is rapid, and in our experiments, its initial concentration in the organic phase was kept constant. However, when cobalt was extracted into the mixed solvent, the rate of extraction increased as the proportion of carbon tetrachloride added to the dichlo-

Table 1. Acid dissociation constants of BP, OP, and DMP, and their apparent distribution constants between 1,2-dichloroethane and aqueous solution in the absence of perchlorate

Reagent	pK_a (ref.)	K_d^*
1,10-Phenanthroline	5.05(9)	2.0
4,7-Dimethyl-1,10-phenanthroline	6.04(9)	3.0
4,7-Diphenyl-1,10-phenanthroline	3.4*	4.3

*Apparent values from distribution curves without regard to protonation of species in aqueous solution.

Table 2. Apparent distribution ratio of BP between a carbon tetrachloride/1,2-dichloroethane mixture and aqueous solution at fixed pH in absence of perchlorate

	D_{BP}*	
$CCl_4/1,2\text{-}C_2H_4Cl_2$, *v/v*	pH 1.67	pH 4.37
5/0	21.7	3.5×10^3
4/1	123	8.5×10^3
2.5/2.5	287	1.57×10^4
1/4	429	1.58×10^4
0/5	435	1.57×10^4

*Without regard to protonation of species in aqueous solution.

roethane was increased. The data in Table 2 show that D_{BP} is lower for higher proportions of carbon tetrachloride, so the level of BP in the aqueous phase, although small, is greater than when pure dichloroethane is used. This suggests that an initial bimolecular complex formation reaction, $Co^{2+} + BP \rightleftharpoons (CoBP)^{2+}$, could be the rate-determining step, in agreement with the kinetic data fitting equation (13). Presumably, once the symmetry of the aquo-ion $Co(H_2O)_6^{2+}$ has been lost, it is then easy (and fast) to add the second and third BP molecules, to give the stoichiometry arrived at by chemical analysis.

Rate of extraction and its rate-controlling step

Co(II) was again extracted with BP and perchlorate into 1,2-dichloroethane at pH 4.37. The plots of log [Co(II)] *vs.* *t* were initially linear, indicating that the extraction is first-order with respect to [Co(II)]. The slope of the log q_{BP} *vs.* log $[BP]_o$ plot [equation (9)] was about unity, whereas that of log q_A *vs.* log $[ClO_4^-]$, equation (10), was zero. Thus the reaction order with respect to BP in the organic phase, *b*, is unity, while that with respect to perchlorate in the aqueous phase, *c*, is zero. Therefore, equation (7) may be rewritten as

$$-d[Co^{2+}]/dt = k[Co^{2+}][BP]_o[ClO_4^-]^0$$
$$= k[Co^{2+}][BP]_o \qquad (12)$$

The rate constant at pH 4.37 in the present extraction system was computed as $k = 6.39 \times 10^{-2}$ l. mole^{-1} min^{-1}. The distribution constant for BP, $K_d = [BP]_o/[BP]$ can now be combined with the kinetic expression in equation (12), to give

$$-d[Co^{2+}]/dt = k K_d [Co^{2+}][BP] \qquad (13)$$

The slow rate of extraction of Co^{2+} is due to the low concentration of free BP in the aqueous phase.

The extraction of Mn(II), Ni(II), Fe(II), Cu(II), Zn(II) and Cd(II) with BP in 1,2-dichloroethane is also dependent on the shaking time, as described in the previous section. All the plots of log $[M^{2+}]$ *vs.* *t* were linear, and the results suggest that the extraction rates are all first order with respect to $[M^{2+}]$. The relative rates of extraction are shown in Table 3, along with the rate of dissociation of water of hydration from the aquo-ions, k_{H_2O}, reported by Eigen and Tamm.[11] From these values, it is deduced that the higher the k_{H_2O} value, the higher the rate of extraction, confirming the choice of formation of $M \cdot BP^{2+}$ as the rate-determining step. The addition of perchlorate to form the ion-association complex would be expected to be very fast, and therefore not rate-determining, which is in keeping with the observed zero rate-order with respect to perchlorate concentration. The mixed-solvent effect on the rate was then examined in more detail. The plot of log q_{BP} or log q_A *vs.* log $[BP]_{total}$ gave a straight line with a slope of about unity. At low pH (≤ 1.4, since $pK_a = 3.4$ for BP), we can approximate $[BP]_{total} \approx [BP \cdot H^+]$. Then (13) becomes

$$-\frac{d[Co^{2+}]}{dt} = kK_d K_a \frac{[BP]_{total}}{[H^+]}[Co^{2+}] \qquad (14)$$

Thus we would expect a plot of apparent rate constant q_{H+} given by

$$-\frac{d[Co^{2+}]}{dt} = q_{H+}[Co^{2+}] \qquad (15)$$

A plot of log q_{H+} *vs.* pH would be expected to give a straight line of slope 1. However, the result shows a somewhat smaller slope of about 0.7. This suggests that the formation of protonated species[12-14] such as $(phen)H^+$, $(phen)_2H^+$ and $(phen)_3H^+$, which would decrease the free reactant concentration, may not be negligible in the present extraction. The earlier observation that cobalt was extracted very much more rapidly with phenanthroline (OP) and its dimethyl derivative (DMP), than with the diphenyl compound (BP) is now explainable in terms of the K_d values, which are concerned with the concentration of the free reactants in the aqueous phase and their salting-in effects.[15] However, a rigorous analysis of the data is very complex, as shown in Table 4. At any rate, it is evident that the formation of the aqueous complex $Co(BP)^{2+}$ is the rate-determining step in this extraction system, although more detailed information must be obtained before a definite conclusion can be reached.

Table 3. Relative rate of extraction of bivalent ions with BP into 1,2-dichloroethane in the presence of perchlorate

Ion	Relative rate†	k_{H_2O}§, *sec*$^{-1}$
Ni(II)*	0.30	1.4×10^4
Co(II)	1.0	2.2×10^5
Fe(II)	2.3	1.4×10^6
Mn(II)	—	5.0×10^6
Zn(II)	34	2.8×10^7
Cd(II)	54	1.8×10^8
Cu(II)	540	4.5×10^8

$[M(II)] = 10^{-4}M$, $[BP]_{o,initial} = 10^{-3}M$, $[ClO_4^-]_{initial} = 9 \times 10^{-4}M$, pH 1.67 ($0.1M$ H_3PO_4), 4.37 ($0.1M$ NaH_2PO_4).
*pH 4.37 ($0.1M$ NaH_2PO_4).
†Slope of log [M(II)] *vs.* time plot, relative to that for Co(II).
§From Eigen and Tamm.[11]

Table 4. Effect of pH on the apparent distribution coefficient of BP between 1,2-dichloroethane and aqueous solution in absence of perchlorate

pH	$[BP]_{total}$, M	[BP],* M	log K_d†
1.48	2.22×10^{-6}	2.7×10^{-8}	4.56
1.90	1.79×10^{-6}	5.6×10^{-8}	4.25
2.47	3.0×10^{-7}	3.5×10^{-8}	4.46
2.97	1.5×10^{-8}	5.6×10^{-8}	4.25
3.42	4.5×10^{-8}	4.5×10^{-8}	4.35
3.98	4.5×10^{-8}	4.5×10^{-8}	4.35
4.32	5.0×10^{-8}	5.0×10^{-8}	4.30

$[BP]_{o,\ initial} = 10^{-3}M$; $pK_a = 3.4$.
*Without regard to protonation of species in aqueous solution.
†Apparent distribution coefficient.

Acknowledgement—The authors wish to express their thanks to Prof. H. Freiser of the University of Arizona for his kind suggestions for this investigation when one of the authors, T. Honjo, was a research associate, sponsored by the University of Arizona, in solvent extraction research on both equilibrium and kinetic aspects.[16] Thanks are also due to Dr. E. Iwamoto of Hiroshima University for his valuable advice.

REFERENCES

1. T. Honjo, S. Ushijima and T. Kiba, *Bull. Chem. Soc. Japan*, 1973, **46**, 3764.
2. T. Kiba, H. Imura and T. Honjo, *Chem. Lett.*, 1977, 805.
3. H. Imura, T. Kiba and T. Honjo, *Bull. Chem. Soc. Japan*, 1979, **52**, 2563.
4. M. Tsubouchi and T. Sakai, *Bunseki Kagaku*, 1975, **24**, 754.
5. Y. Yamamoto, K. Kotsuji, S. Kinuwaki and H. Sawamura, *Nippon Kagaku Zasshi*, 1964, **85**, 870.
6. G. H. Walden, L. P. Hammett and R. P. Chapman, *J. Am. Chem. Soc.*, 1931, **53**, 3908.
7. J. M. Dole and C. V. Banks, *Inorg. Chem.*, 1963, **2**, 591.
8. G. Anderegg, *Helv. Chim. Acta*, 1963, **46**, 2397.
9. T. S. Lee, I. M. Kolthoff and D. L. Leussing, *J. Am. Chem. Soc.*, 1948, **70**, 2348.
10. H. G. Hamilton and H. Freiser, *Anal. Chem.*, 1969, **41**, 1310.
11. M. Eigen and K. Tamm, *Z. Electrochem.*, 1962, **66**, 107.
12. M. J. Fahsel and C. V. Banks, *J. Am. Chem. Soc.*, **88**, 878 (1966).
13. J. V. Rund and P. C. Keller, *J. Chem. Soc. A*, 1970, 2827.
14. P. Paoletti, A. Dei and A. Vacca, *ibid.*, 1971, 2656.
15. E. Iwamoto, Y. Hiyama and Y. Yamamoto, *J. Soln. Chem.*, 1977, **6**, 371.
16. T. Honjo and H. Freiser, *Anal. Chem.*, 1983, **53**, 1258.

Talanta, Vol. 32, No. 8B, pp. 779–784, 1985
Printed in Great Britain.

0039-9140/85 $3.00 + 0.00

DETERMINATION OF TRACE ORGANIC DICARBOXYLIC ACIDS AND AMINES BY ION-CHROMATOGRAPHY

SASWATI P. BAG
Department of Chemistry, Jadavpur University, Calcutta 700032, India

(*Received* 20 *November* 1984. *Accepted* 1 *February* 1985)

Summary—Retention times for various species in separator columns packed with Zipax SAX, Vydac SC, and MicroPak AX-10 anion-exchange resins were compared with those obtained with Dionex separator column for anions. The MicroPak column was found to separate organic dicarboxylic acids, and the logarithm of the retention time of the acids of a homologous series was found to bear a simple relationship to the number of methylene groups between the carboxylic groups. A modified column system, consisting of a post-separator column packed with Vydac CX cation-exchange resin placed between a Dionex separator column for cations and a suppressor column, was able to separate a nine-component mixture of Na^+, K^+, NH_4^+, methylamine, ethylamine, propylamine, butylamine, dimethylamine and trimethylamine, a separation that is not possible with any other current column system.

In recent years ion-chromatography has provided a reliable method for the rapid identification and simultaneous quantitative analysis of mixtures of inorganic and organic anions or cations in dilute aqueous solutions. It is a form of ion-exchange chromatography which utilizes (1) a separator column, (2) a background-ion suppression column, (3) various eluents, and (4) a conductivity detector. Immediately after its introduction in 1975,[1] a commercial instrument, the Dionex "Ion Chromatograph", was marketed. A multitude of applications, focusing almost entirely on inorganic ions, was quickly developed.[2–4] As the technique began to mature, many workers considered it in more detail in an effort to improve it. Fritz and co-workers[5–7] have worked on the retention behaviour of separator column resins and also on the effect of eluents. Stevens and Davis[8] have developed alternative suppressor columns. Slanina *et al.*[9] have developed methods for fast determination of ions by computerized ion-chromatography with multiple detectors.

The Dionex separator columns permit good resolution of many anion mixtures with high sensitivity and have, therefore, found wide application, especially in the analysis of environmental pollutants. Organic dicarboxylic acids, which are found in airborne particulate matter as products of photochemical smog, have thus far not been identified by ion-chromatography though they have been detected by electron-impact and chemical-ionization mass spectrometry.[10]

Qualitative and quantitative analysis for ammonia and lower alkylamines in ambient air is difficult at the levels at which they can be detected by smell.[11] Ion chromatography has been used to detect trace amounts of ammonia, methylamine (MA), dimethylamine (DMA) and trimethylamine (TMA) in dimethylformamide[12,13] and automobile exhaust fumes,[14] but the separator columns currently in use have poor resolution. From a Dionex separator column, potassium, MA, DMA and n-propylamine (PA) are eluted together. Therefore, to achieve better resolution and separation, the column systems have been modified as described here.

This paper describes several separator columns packed with different types of anion-exchange resins for simultaneous determination of organic dicarboxylic acids, and compares them with a Dionex separator column. When a MicroPak column is used, the logarithm of the retention time of dicarboxylic acids bears a simple relationship to the number of methylene groups between the carboxylic groups. This is perhaps the first ion-chromatographic identification of the anions of a homologous series of organic dicarboxylic acids.

The paper also records the modification of a column system to separate a number of protonated lower alkylamines and of Na^+, K^+ and NH_4^+ ions. A short post-separator column packed with Vydac CX resin is placed between a Dionex separator column and a suppressor column. Results are presented showing the separation of a nine-component mixture of Na^+, K^+, NH_4^+, MA, EA, PA, n-butylamine (BA), DMA and TMA on the modified column system.

EXPERIMENTAL

Apparatus

A Dionex model 10 Ion Chromatograph connected with a 7101 BM strip-chart recorder (Hewlett-Packard) was used to collect retention data. The chart-speed was 30 cm/hr throughout.

Separator columns. Glass columns (250 mm × 3 mm bore) were used as separator columns in most cases. A 250

mm × 6 mm bore column packed with Vydac CX resin was used for alkyl- or arylamine analysis. Columns (50 mm × 3 mm bore) packed with Zypax resins were used as pre-columns. The Dionex separator column and precolumn were used as supplied. No precolumn was used with Vydac or MicroPak separator columns.

Suppressor column. A 250 mm × 9 mm bore glass column was used as suppressor column.

Post-separator column. A 40 mm × 4 mm bore glass post-separator column was packed with Vydac CX resin and introduced between the Dionex separator column and the suppressor column.

Ion-exchange resins

Four kinds of ion-exchanger served as the stationary phase of the separator column used for obtaining retention data for organic dicarboxylic acids. Zipax SAX (Du Pont, Wilmington, DE, U.S.A.) anion-exchange resin (bead size 25–37 μm, capacity 0.01 meq/g), Vydac SC (U.S. Universal Scientific Inc., Atlanta, GA, U.S.A.) anion-exchange resin (bead size 30–44 μm, capacity 0.1 meq/g) and MicroPak AX-10 (Varian Associates, Palo Alto, CA, U.S.A.) anion-exchange resin (bead size 10 μm, capacity 2 meq/g) were used to pack separator columns in the laboratory. The columns were used when a steady-state pressure had been established at the desired flow-rate. The fourth resin, the standard Dionex-packed column material (Dionex Corp., Sunnyvale, CA, U.S.A.), was an anion-exchange resin (bead size 20–30 μm, capacity 0.02 meq/g).

Bio-Rad AG 50 W × 12 (200–400 mesh, hydrogen-form) strong cation-exchange resin (Bio-Rad Laboratories, Richmond, CA, U.S.A.) was used for preparation of the suppressor column for dicarboxylic acid analysis.

Zipax SCX (bead size 15–37 μm, capacity 0.005 meq/g) and Vydac CX (bead size 30–44 μm, capacity 0.1 meq/g) cation-exchange resins were used to prepare separator columns in the laboratory for determination of amines. A standard Dionex cation-exchanger (bead size 20–30 μm, capacity 0.02 meq/g) packed column was also used for the same purpose.

Bio-Rad AG 1 × 10, a strong anion-exchange resin (200–400 mesh, hydroxide form) was used in the suppressor column for cation analysis.

Eluents

Sodium carbonate and sodium bicarbonate of analytical reagent grade were used to prepare the 0.003*M* $NaHCO_3$/0.0024*M* Na_2CO_3 eluent for dicarboxylic acid analysis.

Dilute nitric or hydrochloric acid is usually used as the eluent to separate univalent inorganic and organic cations. However, acidifying samples with nitric acid increases the peak height, shortens the elution time, and prevents volatilization of amines more effectively than acidification with hydrochloric acid does. Therefore 0.01*M* nitric acid was used as the eluent for alkylamines. Because this acid depletes the suppressor column fairly rapidly, this column was regenerated every 4 hr.

Sample solutions

All solutions were made up with demineralized water. Standard solutions of oxalic, malonic, succinic, glutaric, adipic and pimelic acids and of various amines were prepared from the reagent grade chemicals. Standard cation solutions were prepared from reagent grade chlorides. All glassware and plastic ware was thoroughly rinsed and soaked in demineralized water before use.

RESULTS

Organic anions

Solutions containing 5.0 ppm oxalic acid, 10.0 ppm each of succinic, glutaric and adipic acids, and 50.0 ppm of pimelic acid were prepared in order to collect retention data on all columns, with a sensitivity of 10 μmho, under identical flow-rate (30% of maximum). In the case of the MicroPak column, the flow-rate was "10%", because of the high pressure developed due to the 10-μm particle size. Table 1 records the retention behaviour of the ions.

Table 1. Retention times of organic anions on different separator columns

Acid	Retention time, *min*			
	Dionex	Vydac	Zipax	MicroPak
Oxalic	20.86	3.15	9.64	10.20
Malonic	14.40	4.40	7.00	9.10
Succinic	12.20	4.50	6.84	10.30
Glutaric	11.50	4.40	6.44	12.50
Adipic	12.20	4.20	6.36	14.20
Pimelic	15.10	7.60	6.64	16.40

The type and capacity of the anion-exchange resin are important variables in anion-chromatography, as reflected in Table 1. The retention time was shortest on the Vydac column and longest on the Dionex column, the order being Vydac < Zipax < MicroPak < Dionex.

On the Vydac column, the peak heights were low and the peaks broad. A mixture of all the acids gave two bands; all but the pimelic acid were grouped together. The p*K* values of this series of dicarboxylic acids were rather close, except for oxalic and malonic acid, owing to their molecular structure, and this made separation difficult. However, the retention data cannot be explained on the basis of the p*K* values (see Table 2).

The chromatogram of a mixture of the acids on a Dionex column had three bands: succinic, glutaric and adipic acid were eluted first; malonic and pimelic acid formed another overlapping band; oxalic acid was eluted last. The retention time was very long. Here also, neither the acidity nor the molecular structure of the acids can explain the retention behavior. The peaks were broad, preventing clear-cut separation of all the acids.

The chromatogram of a mixture of the acids on a Zipax column was a single peak, broad at the base, with no separation. However, the peaks obtained for the acids chromatographed individually were much

Table 2. Retention data for organic anions on a MicroPak column

Acid	pK_1	pK_2	R_{t_a}, *min*	R_{t_b}, *min*
Oxalic	1.27	4.30	5.10	8.97
Malonic	2.80	5.70	4.55	8.45
Succinic	4.21	5.64	5.15	9.01
Glutaric	4.30	5.22	6.25	9.39
Adipic	4.41	5.28	7.10	9.90
Pimelic	4.49	5.43	8.20	11.58

Eluent 0.003*M* $NaHCO_3$/0.0024*M* Na_2CO_3. For R_{t_a} the flow-rate was 10% and the pressure 680 psig. For R_{t_b} the flow-rate was 6% and the pressure 480 psig.

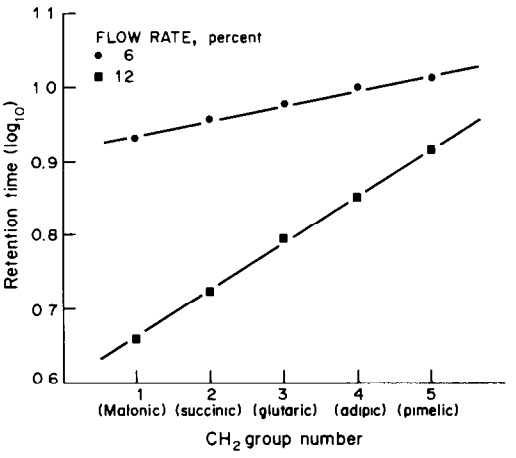

Fig. 1. Retention characteristics of organic dicarboxylic acids: $n = 1$, malonic; $n = 2$, succinic; $n = 3$, glutaric; $n = 4$, adipic; $n = 5$, pimelic acid. Flow-rate 10 or 6%; pressure 680 or 480 psig, respectively; sensitivity 10 μmho.

sharper and higher than any of those obtained on the other columns. A 10-ppm pimelic acid solution gave a higher and sharper peak on this column than a 50-ppm solution gave on the other columns. The retention data revealed that as ΔpK ($\Delta pK = pK_2 - pK_1$) increases, the retention time increases.

Examination of the retention data for the Micro-Pak column revealed several characteristics. Retention time gradually increased with molecular weight, except for oxalic acid. This exception may be due to the structure of oxalic acid, which can assume a hydrogen-bonded form after loss of the first proton, thereby increasing the retention time. The peaks were broader at the base. Because of the small particle size (10 μm) and irregular shape of the resin beads, the column pressure was high for the ion-chromatograph, even at low flow-rate. The retention data for a 250-mm column with 10% and 6% flow rates are given in Table 2. A plot of log R_t (R_t = retention time) *vs.* the number of methylene groups between the carboxylic groups was linear (Fig. 1). As the flow-rate increased, the retention time decreased and the slope of the straight line increased. This result means that for the first time a homologous series of compounds has been identified by ion-chromatography.

Separation of amines

The separation described represents a notable application of ion-chromatography in the determination of trace ammonia and organic lower alkylamines at ppm concentrations. The retention behaviour of these amines is indicative of the speed and resolution attainable with Zipax, Vydac and Dionex separator columns. The multicomponent cation mixtures were chromatographed to establish the feasibility of the separation rather than to optimize the analysis. These chromatograms helped to achieve the desired modification of the separator column system, leading to clear separation of the components of the mixtures.

The retention characteristics of a six-component mixture of four primary lower alkylamines, methylamine (MA), ethylamine (EA), n-propylamine (PA), n-butylamine (BA), a secondary amine, dimethylamine (DMA) and a tertiary amine, trimethylamine (TMA), were studied on Zipax, Vydac and Dionex separator columns. The retention data are recorded in Table 3. Except for TMA and BA, which are eluted together, the amines are eluted separately on both Zipax and Vydac columns in the elution order: MA < EA < DMA < PA < TMA ≈ BA. The retention behaviour is rather different on the Dionex column. The retention times of amines with the same empirical formula are approximately the same, and the retention times gradually increase with increasing carbon number of the compounds. Thus EA and DMA are eluted together, as are PA and TMA. The retention times are in the order MA < EA ≈ DMA < PA ≈ TMA < BA. On the Zipax column the peaks are broader and retention times longer (except for MA and EA) than on the Vydac column. Figures 2–4 show the chromatograms of the six-amine mixture on Zipax, Vydac and Dionex columns respectively.

The elution behaviour of Na^+, K^+ and NH_4^+ on

Table 3. Retention data for six-amine mixture on different column systems

Amines	Zipax*		Vydac†		Dionex§		Modified column‡	
	Conc., *ppm*	R_t, *min*	Conc., *ppm*	R_t, *min*	Conc., *ppm*	R_t, *min*	Conc., *ppm*	R_t, *min*
Methyl	1.5	6.44	1.5	9.50	0.17	6.04	0.75	7.60
Ethyl	3.0	12.50	3.0	13.04	0.33	6.90	1.50	9.46
n-Propyl	10.0	25.54	10.0	21.14	1.11	8.30	5.00	13.16
n-Butyl	20.0	42.86	20.0	32.76	2.22	12.30	10.00	19.94
Dimethyl	3.0	19.00	3.0	16.16	0.33	6.90	1.50	10.86
Trimethyl	10.0	42.86	10.0	32.76	1.11	8.30	5.00	16.80

*Flow-rate = 184 ml/hr, pressure = 650 psig.
†Flow-rate = 230 ml/hr, pressure = 400 psig.
§Flow-rate = 184 ml/hr, pressure = 430 psig; 4 × 50 mm precolumn.
‡Flow-rate = 184 ml/hr, pressure = 460 psig.

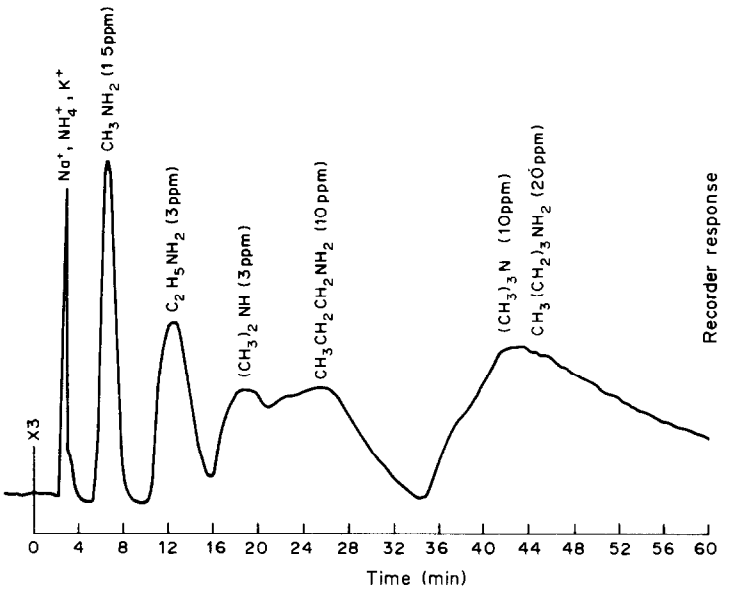

Fig. 2. Chromatogram of six amines on a Zipax column (250 mm × 3 mm): flow-rate 40%; 680 psig; eluent 0.01*M* HNO_3; ×3 attenuation.

Zipax, Vydac and Dionex columns is given in Fig. 5. NH_4^+ and K^+ are eluted together from the Vydac column. Though NH_4^+ and K^+ are eluted separately with 0.005*M* eluent from Zipax, they are eluted together with 0.01*M* eluent. NH_4^+ and K^+ do not interfere with elution of MA from either of these columns. From the Dionex column, however, NH_4^+ and K^+ are eluted separately, but K^+ is eluted together with MA. The Dionex column offers sensitive detection, with sharper peaks and lower retention

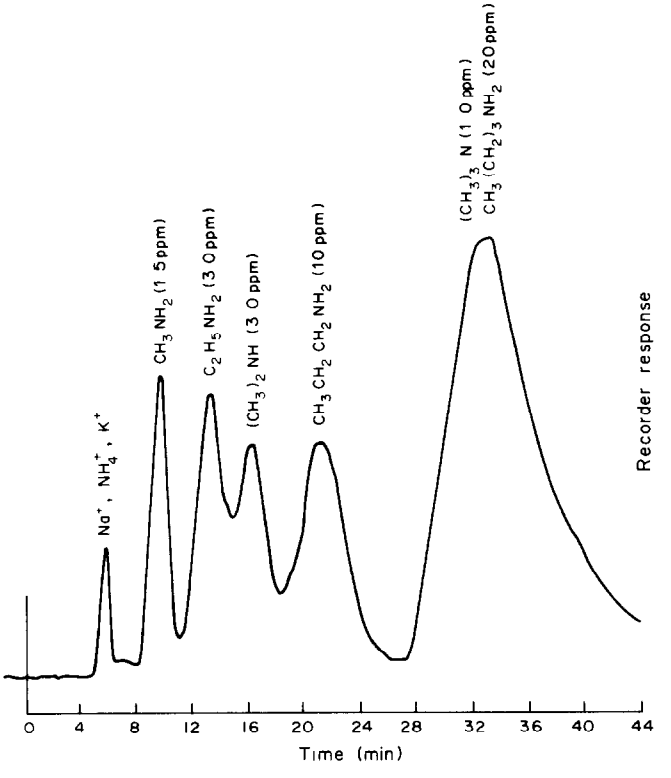

Fig. 3. Chromatogram of six amines on a Vydac column (250 mm × 6 mm): flow-rate 50%; 380 psig; eluent 0.01*M* HNO_3; ×3 attenuation.

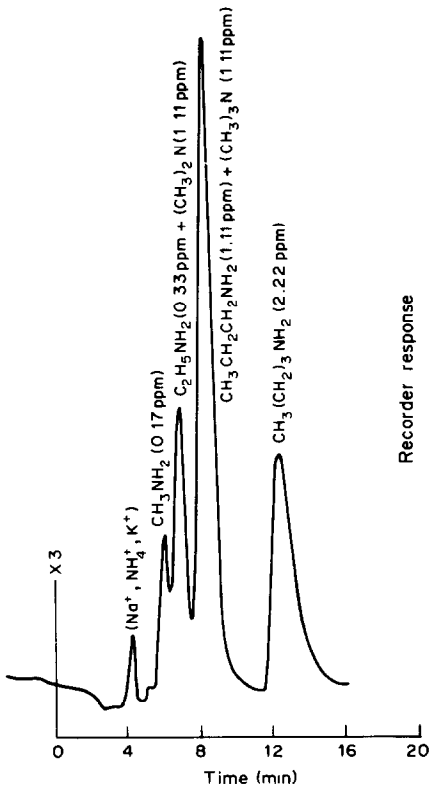

Fig. 4. Chromatogram of six amines on a Dionex column (250 mm × 4 mm): flow-rate 40%; 430 psig; eluent = 0.01*M* HNO_3; ×3 attenuation.

times than those for Vydac, but resolution of K^+ and MA, of EA and DMA, or of PA and TMA is not possible on this column.

Development of post-separator column

Though the elution pattern is similar with both the Zipax and Vydac columns, the latter gives much better sensitivity and resolution as well as faster elution. Only trimethylamine and n-butylamine are eluted together from the Vydac column, but they are eluted separately from the Dionex column. A combination of these columns was therefore tried. Since the peaks are sharper and the elution time shorter with the Dionex system, the Dionex column should be used as the separator column. The use of a short Vydac column as either a pre- or post-column should achieve the desired separation. Use as a precolumn did give the separation pattern of the Vydac system but the sensitivity and sharpness of the Dionex system was lost. Use of a 4 × 40 mm Vydac column as a post-column, however, gave good separation of the six-component amine mixture. Retention times are given in Table 3.

Potassium ions interfere in methylamine determination on Dionex, and NH_4^+ and K^+ are always eluted together from the Vydac column, but the coupled column system gave separation of all six amines, Na^+, K^+ and NH_4^+, as shown in Fig. 6.

DISCUSSION

The retention time data (Table 1) for the dicarboxylic acids show that the MicroPak column allows identification of organic dicarboxylic acids (malonic to pimelic) in a homologous series by ion-chromatography. The resolution increases with increasing flow-rate (Fig. 1). The retention time increases with increasing ΔpK_a as well as increasing

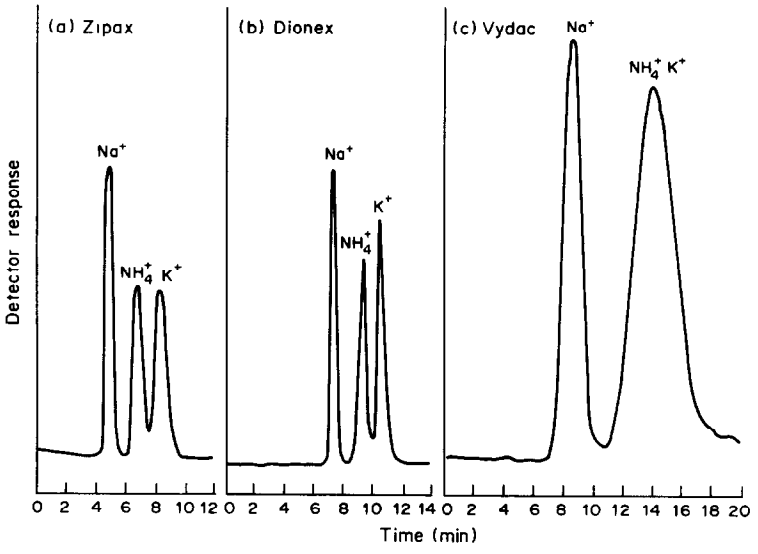

Fig. 5. Separation of Na^+, NH_4^+ and K^+. (a) Zipax 250 mm × 3 mm separator (SC), 50 mm × 3 mm precolumn (PC); (b) Dionex 250 mm × 4 mm SC, 50 mm × 4 mm PC; (c) Vydac 250 mm × 6 mm SC, 150 mm × 3 mm PC. Concentrations: (a) and (b) Na^+, 0.5 ppm; NH_4^+, 0.5 ppm; K^+, 1.0 ppm; (c) Na^+, 5.0 ppm; NH_4^+, 5.0 ppm; K^+, 10.0 ppm. Eluent 5.0m*M* HNO_3. Detector sensitivity 10 μmho. Flow-rates (a) and (b) 138 ml/hr; (c) 230 ml/hr.

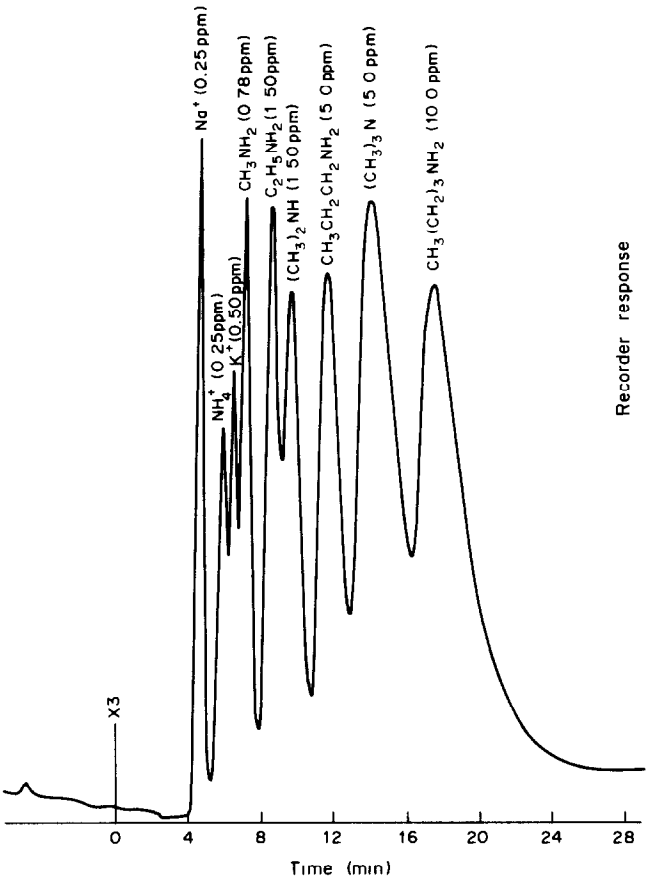

Fig. 6. Separation of Na^+, NH_4^+, K^+ and six amines on the modified column. Flow-rate 40%; 460 psig; eluent 0.01*M* HNO_3; ×3 attenuation.

molecular weight. It is also evident that the particle-size, capacity and type of resin are important in preparation of a column that will achieve separation. Incorporation of suitable functional groups in the resin may induce appropriate hydrophilic ion-pair formation which will result in separation of the ions.

When a sample is injected into the column, the sample cations replace the eluent cations from the cation-exchange resin at the top of the column. The displaced eluent cations, together with the sample anions, move with the solvent front to the conductivity detector. If these cations and anions give a greater conductance than that of the eluent, there will be a positive peak. If the conductance is less than that of the eluent background a negative peak will result. In the examples cited in this paper, positive peaks were obtained. Negative peaks were obtained for purines and pyrimidines (DNA-bases) with potassium hydrogen phthalate or ammonium hydrogen *o*-sulphobenzoic acid as eluents (unpublished results).

Acknowledgements—The author gratefully acknowledges the award of a research associateship by the National Research Council, U.S.A. and the laboratory facilities provided by the U.S. Environmental Protection Agency, Research Triangle Park, N.C., U.S.A.

REFERENCES

1. H. Small, T. S. Stevens and W. C. Bauman, *Anal. Chem.*, 1975, **47**, 1801.
2. E. Sawicki, J. D. Mulik and E. Wittgenstein (eds.), *Ion Chromatographic Analysis of Environmental Pollutants*, Vol. 1, Ann Arbor Sci. Publ., Ann Arbor, Mich., 1978.
3. J. D. Mulik and E. Sawicki (eds.), *Ion Chromatographic Analysis of Environmental Pollutants*, Vol. 2, Ann Arbor Sci. Publ., Ann Arbor, Mich., 1979.
4. C. A. Pohl and E. L. Johnson, *J. Chromatog. Sci.*, 1980, **18**, 442.
5. D. T. Gjerde, J. S. Fritz and G. Schmuckler, *J. Chromatog.*, 1979, **186**, 509.
6. D. T. Gjerde, G. Schmuckler and J. S. Fritz, *ibid.*, 1980, **187**, 35.
7. K. M. Roberts, D. T. Gjerde and J. S. Fritz, *Anal. Chem.*, 1981, **53**, 1691.
8. T. S. Stevens and J. C. Davis, *ibid.*, 1981, **53**, 1488.
9. J. Slanina, F. P. Bakker, P. A. C. Jongejan, L. Van Lamoen and J. J. Mols, *Anal. Chim. Acta*, 1981, **130**, 1.
10. D. Grosjean, K. Van Cauwenberghe, J. P. Schmid, P. E. Kelley and J. N. Pilts, Jr., *Environ. Sci. Technol.*, 1978, **12**, 313.
11. Y. Hoshika, *Anal. Chem.*, 1976, **48**, 1716.
12. S. A. Bouyoucos, *ibid.*, 1977, **49**, 401.
13. *Analysis of Ammonia and Amines in Dimethylformamide*, Application Note 6, 3/78, Dionex Corporation, Ion Chromatography Systems, Sunnyvale, CA.
14. R. B. Zweidinger, S. B. Tajeda, J. E. Sigsby, Jr., and R. L. Bradow, Chapter 11 in *Ion Chromatographic Analysis of Environmental Pollutants*, E. Sawicki, J. D. Mulik, and E. Wittgenstein (eds.), Vol. 1, p. 125. Ann Arbor Sci. Publ., Ann Arbor, Mich., 1978.

Talanta, Vol. 32, No. 8B, pp. 785–790, 1985
Printed in Great Britain

0039-9140/85 $3.00 + 0.00
Pergamon Press Ltd

SOLVENT EFFECT ON THE LIQUID–LIQUID PARTITION COEFFICIENTS OF COPPER(II) CHELATES WITH SOME β-DIKETONES

HISANORI IMURA and NOBUO SUZUKI
Department of Chemistry, Faculty of Science, Tohoku University, Sendai 980, Japan

(*Received* 7 *December* 1984. *Accepted* 15 *March* 1985)

Summary—Partition coefficients for the copper(II) chelates of trifluoroacetylacetone and thenoyltrifluoroacetone in eleven organic solvent–0.10*M* aqueous perchlorate solution systems have been determined at 25°. The effect of the organic solvents can be readily explained in term of the concept of regular solutions. The effect of water is discussed in terms of a modified equation based on the regular solution theory and also evaluated by the scaled particle theory. It is suggested that the partition coefficient of the copper(II) chelates is lowered by specific solvent effects of water, such as direct co-ordination to the central metal ion, and hydrogen-bonding to the ligands in the chelate.

The extractability and separability of metal chelates are governed by both the magnitude of the chelate formation constant in aqueous medium and the partition coefficient of the chelate formed. In most of the systematic and theoretical studies on chelate extraction, most attention has been focused on the former and little on the latter. Only a few data on the partition coefficients of metal chelates are listed in a monograph on extraction equilibrium constants.[1] In our laboratory, work on liquid–liquid partition of β-diketones and their metal chelates has been continued since the pioneering work in which the effect of organic solvents was successfully elucidated by means of the regular solution theory.[2–4] As the partition coefficient is essentially governed by the difference between the dissolution energy of a solute in an organic phase and that in an aqueous phase, the role of water in the partition should be considered in addition to the organic solvent effect. In our preceding paper,[5] the partition coefficient of bis(acetylacetonato)copper(II) was evaluated by a modified equation based on the regular solution theory, and the significance of specific interaction between the solute and solvents was pointed out.

In the present study, the partition coefficients of the copper(II) chelates of trifluoroacetylacetone (Htfa) and thenoyltrifluoroacetone (Htta) are determined in various organic solvent–0.10*M* aqueous perchlorate solution systems. These β-diketones have similar acid dissociation constants and metal-chelate formation constants:[6] The results are discussed with the aid of the modified regular solution theory and the scaled particle theory. The present approach is demonstrated to be a powerful one for evaluating the partition coefficient of uncharged solutes.[7–10]

EXPERIMENTAL

Reagents and apparatus

Trifluoroacetylacetone (1,1,1-trifluoro-2,4-pentanedione) and thenoyltrifluoroacetone [1-(2′-thienyl)-4,4,4-trifluoro-1,3-butanedione) were obtained from Dojindo Laboratories, and further purified by distillation and vacuum sublimation respectively. The copper(II) chelates were synthesized in the usual way and recrystallized from methanol, and their identity established by elemental analysis.

Carrier-free ^{67}Cu was produced by photonuclear reaction as described in the preceding paper.[5] An appropriate portion of ^{67}Cu was added to an aliquot of a standard solution of copper(II) perchlorate; the mixture was evaporated to dryness, and the residue dissolved in 0.01*M* perchloric acid. Other reagents and the apparatus were the same as those described previously.[5]

Procedures

Partition. An aqueous copper(II) solution (10^{-7}–10^{-4}*M*, labelled with ^{67}Cu) in 0.10*M* sodium perchlorate at pH 1–8 was shaken for 0.5–1 hr with an equal volume of an organic solution of 0.05–0.1*M* β-diketone at 25 ± 0.5°, then centrifuged. A 0.1–3 ml fraction was very carefully pipetted from each phase and the γ-activity of each was measured with an NaI(Tl) well-type scintillation counter, and the distribution ratio (D) of copper(II) was calculated. The equilibrium pH value was measured with a glass electrode. Attainment of partition equilibrium was checked by extraction and stripping experiments.

To determine the partition coefficient of the β-diketones (K_{DR}) a portion of 10^{-4}–10^{-3}*M* β-diketone solution in organic solvent was shaken with 0.10*M* sodium perchlorate at pH 2–3 and the equilibrium concentration of β-diketone in the organic phase was measured from the absorbance at 282 and 300 nm for Htfa and at 318 nm for Htta.

Solubility. The solubilities of the copper(II)–β-diketone chelates in an organic solvent saturated with water and in an aqueous solution saturated with the organic solvent were measured simultaneously as follows. To 10–100 mg of the copper(II) chelate labelled with ^{67}Cu were added a 0.05*M* organic solution of the β-diketone and 0.10*M* aqueous sodium perchlorate solution at pH 6–8. The mixture was shaken for 24–48 hr at 25 ± 0.5° and then centrifuged. A

portion of each saturated solution was pipetted after passage through a filter paper, and its γ-activity was measured. Comparison of this activity with that of the total amount of labelled chelate taken gave the solubility. It was ascertained that the solubility found was independent of the quantity of labelled chelate used.

RESULTS

Typical extraction curves for copper(II) with Htfa in benzene and Htta in heptane and toluene are shown in Fig. 1; the concentration of β-diketone anion in the aqueous phase was calculated by using the acid dissociation constant and partition coefficient for the β-diketone. The partition coefficient of the copper(II) chelate(K_{DM}) was determined as the limiting value of the distribution ratio in the plateau region and ascertained to be independent of the copper(II) concentration in the range 10^{-6}–$10^{-5}M$. However, the partition coefficient of $Cu(tta)_2$ in solvents other than alkanes was too high to be accurately measured by this technique. The partition coefficient K_{DM} is simply connected with the distribution ratio by $K_{DM} = D/(\beta_2[A^-]^2)$. This means that if we know β_2 accurately, K_{DM} for any organic solvent can be determined by plotting log D *vs.* log[A^-] and using the linear section which has a slope of two. As K_{DM} in alkane solvent systems can be determined directly as described above, the chelate formation constant, β_2, can be determined from the distribution ratios in these systems; the values of β_2 for $Cu(tfa)_2$ and $Cu(tta)_2$ were thus found to be $10^{9.14}$ and $10^{9.30}$ respectively. These values are close to each other as expected from the small difference between the acid dissociation constants of Htfa ($10^{-6.09}$) and Htta ($10^{-6.23}$).[6] The average values and standard deviations of the partition coefficients, obtained from more than four separate measurements, are listed in Table 1 together with some literature values for the β-diketones.[3,9,11] The reliability of the partition coefficients determined here was further checked by comparing them with those obtained from the solubilities of the chelates in both phases. The partition coefficient can be considered to be equal to the ratio

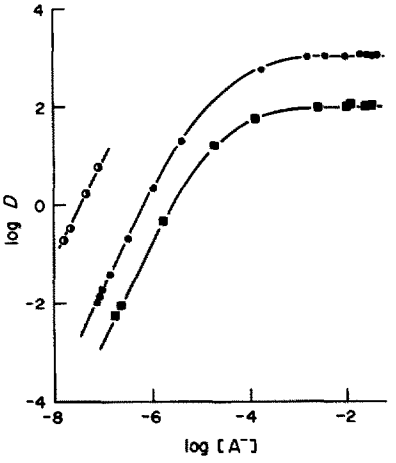

Fig. 1. Distribution ratio of copper(II) *vs.* concentration of β-diketone anion in the aqueous phase. Initial concentration of β-diketone, 0.05–0.1M; pH 1 – 8. ●Htta–heptane, ◑Htta–toluene, ■Htfa–benzene.

of the solubility in the organic phase to that in the aqueous phase provided the solubility is low enough for the solutions to be regarded as dilute. The solubilities of the copper(II) chelates in some organic phases and an aqueous phase are given in Table 2 along with the solubility ratios. Most of the solubility ratios are in agreement with the corresponding partition coefficients in Table 1, within experimental error. The partition coefficient of $Cu(tta)_2$ is remarkably higher than that of $Cu(tfa)_2$ for all the organic solvents tested. This may be due to the remarkably low solubility of $Cu(tta)_2$ in aqueous solution.

Since β-diketones exist in the keto and enol forms in solution, the partition coefficients for the β-diketones listed in Table 1 are the apparent values (*i.e.*, a weighted mean of those for the two tautomeric forms). The partition coefficient of the enol (K_{DE}) form (which is known to have a ring structure through intramolecular hydrogen-bonding) is calculated from the equation $K_{DE} = (f_{org}/f_{aq})K_{DR}$, where f_{org} and f_{aq} are the enol fractions in the organic and

Table 1. Partition coefficients of β-diketones and their copper(II) chelates at 25°C

No.	Solvent	Htfa	$Cu(tfa)_2$	Htta	$Cu(tta)_2$
1	Hexane	3.17×10^{-1}*	2.23 ± 0.05	4.79†	$(1.24 \pm 0.11) \times 10^3$
2	Heptane	$(2.67 \pm 0.00_1) \times 10^{-1}$	2.01 ± 0.02	3.72‡	$(1.11 \pm 0.05) \times 10^3$
3	Octane	$(2.39 \pm 0.00_2) \times 10^{-1}$	1.58 ± 0.09	4.05 ± 0.28	$(1.18 \pm 0.07) \times 10^3$
4	Dodecane	1.72×10^{-1}§	1.11 ± 0.12	3.19 ± 0.11	$(8.03 \pm 0.56) \times 10^2$
5	Carbon tetrachloride	7.18×10^{-1}*	$(1.77 \pm 0.02) \times 10$	2.00×10†	$(3.71 \pm 0.20) \times 10^4$‡
6	Isopropylbenzene	$(6.68 \pm 0.01) \times 10^{-1}$	$(2.40 \pm 0.08) \times 10$	2.34×10†	$(9.10 \pm 0.56) \times 10^4$‡
7	Toluene	1.02 ± 0.02	$(9.26 \pm 0.09) \times 10$	4.02×10†	$(4.44 \pm 0.07) \times 10^5$‡
8	Benzene	1.28*	$(1.05 \pm 0.03) \times 10^2$	4.20×10†	$(3.08 \pm 0.75) \times 10^5$‡
9	Chloroform	1.95*	$(1.46 \pm 0.02) \times 10^2$	5.33×10†	$(1.73 \pm 0.16) \times 10^5$‡
10	Dichloromethane	2.51*	$(3.97 \pm 0.19) \times 10^2$	6.84×10†	$(5.98 \pm 0.14) \times 10^5$‡
11	Dibutyl ether		$(5.25 \pm 0.10) \times 10$		$(1.67 \pm 0.03) \times 10^5$‡

*Reference 3.
†Reference 11.
§Reference 9.
‡Calculated from $K_{DM} = D/(\beta_2[A^-]^2)$.

Table 2. Solubility of the copper(II)–β-diketone chelates at 25°C

Solvent	S* or R†	$Cu(acac)_2$	$Cu(tfa)_2$	$Cu(tta)_2$
Heptane§	S	$(6.9 \pm 0.4) \times 10^{-5}$	$(1.2 \pm 0.1) \times 10^{-3}$	$(4.0 \pm 0.2) \times 10^{-5}$
	R	$(1.6 \pm 0.1) \times 10^{-1}$	1.1 ± 0.1	$(1.0 \pm 0.2) \times 10^{3}$
Toluene§	S	$(1.9 \pm 0.1) \times 10^{-3}$	$(7.2 \pm 0.1) \times 10^{-2}$	$(2.4 \pm 0.2) \times 10^{-2}$
	R	4.4 ± 0.4	$(6.5 \pm 0.6) \times 10$	$(5.9 \pm 1.4) \times 10^{5}$
Water‡	S	$(4.3 \pm 0.3) \times 10^{-4}$	$(1.1 \pm 0.1) \times 10^{-3}$	$(4.1 \pm 0.9) \times 10^{-8}$

*Solubility (M).
†Ratio of the solubility in the organic phase to that in the aqueous phase.
§Saturated with water; β-diketone concentration 0.01–0.03M.
‡Saturated with heptane; sodium perchlorate concentration, 0.10M. The following conditions were used for each chelate; $Cu(acac)_2$, 0.03M Hacac, pH 8.4; $Cu(tfa)_2$, 0.04M Htfa, pH 6.0; $Cu(tta)_2$, 0.03M Htta, pH 6.5.

aqueous phases respectively. The numerical values for the enol fraction were taken from the literature;[12] f_{aq} is 0.011 and 0.016 for Htfa and Htta, and f_{org} in benzene is 0.97 and 0.94 for Htfa and Htta respectively. In the four alkanes and carbon tetrachloride, f_{org} was assumed to be unity, and in the other solvents to be equal to that for benzene solution.

Figure 2 shows the plots of K_{DM} and K_{DE} *vs.* the molar volume of each solute, together with those for the acetylacetone system.[5] The molar volumes of the copper(II) chelates were estimated from an empirical relation between those of β-diketones[2] and their zirconium(IV) chelates,[3,13] *viz.* 223 cm³/mole for $Cu(tfa)_2$ and 304 cm³/mole for $Cu(tta)_2$. The value for $Cu(tta)_2$ agreed within 5% with that of the partial molar volume for bis(thenoyltrifluoroacetonato)beryllium(II), reported recently.[14] The partition

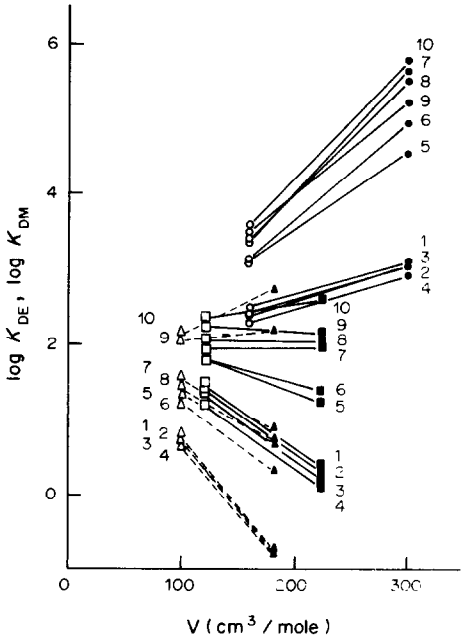

Fig. 2. Partition coefficients of enols and the copper(II) chelates *vs.* molar volume. The numbers correspond to those in Table 1. ○Htta, □Htfa, △Hacac,[5] ●$Cu(tta)_2$, ■$Cu(tfa)_2$, ▲$Cu(acac)_2$.[5]

coefficient of a series of β-diketone enols increases with increase in the molar volume of these solutes, *viz.* acac < tfa < tta. The same is true for the copper(II) chelates of these β-diketones.

DISCUSSION

The partition coefficient, expressed as a molar fraction, can be written by using the modified equation based on the regular solution theory:[5]

$$\ln K^{\circ}_{D2} = \frac{V_2}{RT}[C_{ww} - C_{oo} + 2(C_{o2} - C'_{w2})] \quad (1)$$

where V and C are the molar volume and cohesive energy density respectively, and the subscripts 2, w and o denote the solute, water and organic solvent respectively. The parameter C'_{w2} involves the correction terms for specific interactions between the solute and water molecules. If the interaction between the solute and the organic solvent molecules is mainly due to their dispersion forces, the geometric mean approximation for the solubility parameters, δ, is valid, *i.e.*, $C_{o2} \sim \delta_o \delta_2$. Equation (1) can be rewritten as

$$\frac{RT}{V_2} \ln K^{\circ}_{D2} + C_{oo} = 2\delta_2\delta_o + C_{ww} - 2C'_{w2} \quad (2)$$

Plots of the left-hand side of equation (2) *vs.* the solubility parameter $\delta_o (= \sqrt{C_{oo}})$, which is calculated from the heat of vaporization of the solvent, are expected to be linear. The apparent solubility parameter of the solute (δ_2) and the interaction term with water ($C_{ww} - 2C'_{w2}$) can be obtained from the slope and the intercept respectively. Figure 3 shows the plots for the enols and the copper(II) chelates. For the enol and chelate of the trifluoroacetylacetone and thenoyltrifluoroacetone systems, good linear relationships hold for almost all non-polar organic solvents. It seems that the organic solutions of these solutes can be taken as apparently regular solutions and the solvent effects can be quantitatively evaluated by means of equation (2). However, quite large deviations from straight lines are found for the chloroform and dichloromethane/acetylacetone systems, and these are ascribed to specific interaction between the solutes and the solvents, such as hydrogen-bonding.[5] Such deviations for the

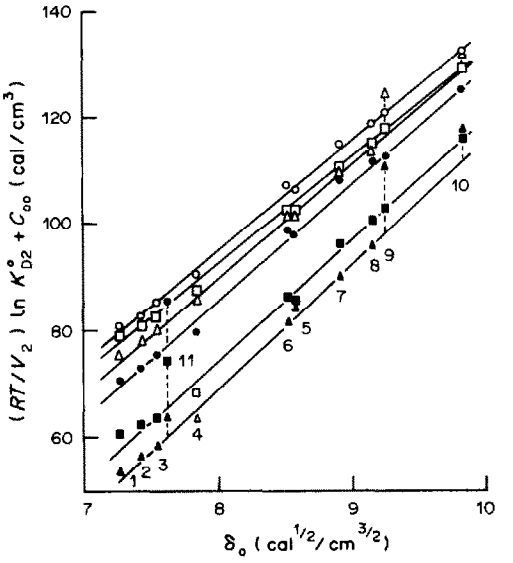

Fig. 3. Evaluation of partition coefficients with equation (2), based on the regular solution theory. The numbers correspond to those in Table 1. ○Htta, □Htfa, △Hacac,[5] ●Cu(tta)$_2$, ■Cu(tfa)$_2$, ▲Cu(acac)$_2$.[5]

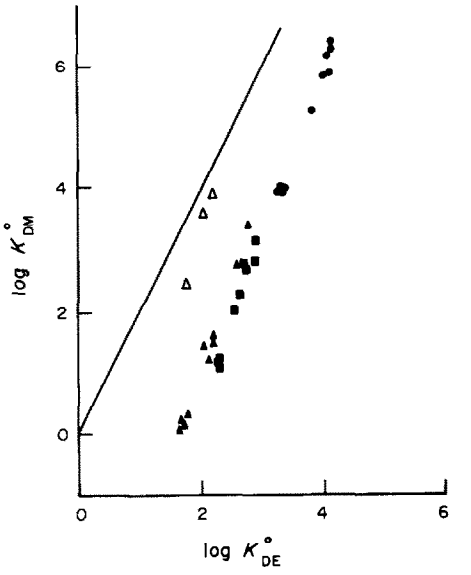

Fig. 4. Relationship between the partition coefficients of the copper(II) chelates and the enols. ●Cu(tta)$_2$, ■Cu(tfa)$_2$, ▲Cu(acac)$_2$,[5] △Pd(acac)$_2$.[9]

β-diketones may be interpreted by considering the electron density on the oxygen atoms in these β-diketones; a strong negative inductive effect of the trifluoromethyl group in the tfa and tta ligands remarkably decreases the electron density and consequently the strength of hydrogen-bonding to the ligand oxygen atom. The large deviation found for dibutyl ether in the copper(II) chelate systems is ascribable to another type of specific interaction, such as direct co-ordination of the basic solvent to the central metal ion. The magnitudes of the deviations, Cu(tfa)$_2$ ~ Cu(tta)$_2$ > Cu(acac)$_2$ are in reverse order of the trend in the formation constants of these chelates and in accord with the normal tendency toward additional co-ordination of Lewis bases.

The parameters of equation (2) were determined by the least-squares method from the plots, except for some solvent systems having the specific interactions described above and shown in the second and third columns in Table 3. The enols of trifluoroacetylacetone and thenoyltrifluoroacetone have similar values for δ_2 and $C_{ww} - 2C'_{w2}$, and this suggests that they have similar solute–solvent interactions with organic solvents and with water. On the other hand, the values of these parameters for the copper(II) chelates differ appreciably and are also larger than those of the enols. In particular the $C_{ww} - 2C'_{w2}$ parameters of the acetylacetonate and trifluoroacetylacetonate chelates have very negative values, which suggests a strong interaction between the solutes and water, as discussed later.

Since equation (2) holds for the partition of neutral solutes (and hence for both the chelate and the enol) the following relation is derived:

$$\ln K^{\circ}_{DM} = \frac{V_M}{V_E}\ln K^{\circ}_{DE} + \frac{2V_M}{RT}(\delta_M - \delta_E)\delta_o + \frac{2V_M}{RT}(C'_{wE} - C'_{wM}) \quad (3)$$

Figure 4 shows the logarithmic plots of K°_{DM} *vs.* K°_{DE}, for the copper(II) chelates, together with those for the palladium(II) acetylacetone chelate.[9] The plot of Pd(acac)$_2$ is close to the solid line (with slope two)

Table 3. Parameters from the regular solution theory and the scaled particle theory*

Solute	δ_2, $(cal/cm^3)^{1/2}$	$C_{ww} - 2C'_{w2}$, cal/cm^3	$\bar{G}_{c,w} - \bar{G}_{c,o}$, kcal/mole	$\bar{G}_{i,w} - \bar{G}_{i,o}$, kcal/mole
Hacac(enol)	10.4	−77	3.69	−2.63
Htfa(enol)	10.0	−68	4.22	−2.33
Htta(enol)	10.2	−68	5.21	−1.98
Cu(acac)$_2$	11.6	−116	5.76	−6.78
Cu(tfa)$_2$	11.2	−104	6.64	−6.23
Cu(tta)$_2$	11.0	−91	8.37	−4.21

*Heptane–water system.

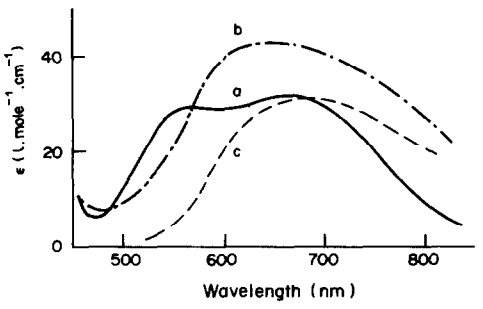

Fig. 5. Absorption spectra of $Cu(tfa)_2$ in various solvents. a, benzene; b, dibutyl ether; c, water containing 0.013*M* tfa^-.

passing through the origin, whereas the plots for the copper(II) chelates are in a much lower region. This difference can be understood by comparing the values of the third term in the right-hand side of equation (3). Here, we can use $(C_{ww} - 2C'_{w2})$ from Table 3 instead of $(C'_{WE} - C'_{WM})$ in equation (3). The parameter C'_{w2}, which expresses the solute–water interaction, is much larger for the copper(II) chelates than the respective enols. One of the possible interactions between copper(II) chelate and water may be direct co-ordination of water to the central metal ion. Figure 5 shows the electronic spectra of $Cu(tfa)_2$ in different media. The spectrum for the benzene solution is not influenced by the water content in that solvent and is almost the same as that for solutions in other inert solvents such as heptane and carbon tetrachloride, but the spectra for the dibutyl ether and water solutions are significantly different from those for solutions in inert solvents. The same was also observed for $Cu(acac)_2$.[5] This phenomenon suggests the direct co-ordination of the central metal ion with such polar solvent molecules containing a donor oxygen atom. However, in view of the lower tendency for direct co-ordination of a polar solvent to the central metal ion in $Cu(acac)_2$, the more negative value of the interaction parameter for $Cu(acac)_2$ cannot be due only to the direct co-ordination of water. In addition to direct hydration another type of specific interaction with water must be considered, such as the hydrogen-bonding of water to the acetylacetonate ligand in the chelate. This type of interaction was throughly discussed in connection with a chloroform anomaly in the acetylacetone system.[5] $Pd(acac)_2$ has a stable planar structure, and no adduct formation with bases has been reported, so it has practically no specific interaction with water or polar solvents, as shown in Fig. 5.

The solute–water interaction parameter included in equation (2) is useful as a comparative parameter, but it is difficult to discuss the strict physical significance of its absolute value, partly because this equation is based on the simple regular solution concept. Hence the partition coefficient of the copper(II) chelates is further discussed below with the aid of the scaled particle theory (SPT), which is applicable to aqueous solutions and was recently used in the evaluation of the liquid–liquid partition of halobenzenes, haloalkanes and metal chelates in our laboratory.[7–10]

The free energy for the liquid–liquid partition or the transfer free-energy from an aqueous to an organic phase is represented by the difference in the free energy for the dissolution of the solute in both phases,

$$RT \ln K_{D2} = -(\Delta\bar{G}_{s,o} - \Delta\bar{G}_{s,w}). \quad (4)$$

The dissolution process can be divided into two steps; the creation of a cavity of a suitable size to accommodate the solute molecule in the solvent, followed by the interaction of the surrounding solvent molecules with the solute introduced into the cavity. Equation (4) can be rewritten by using the free energies corresponding to these two steps in each phase:

$$RT \ln K_{D2} = (\bar{G}_{c,w} - \bar{G}_{c,o}) + (\bar{G}_{i,w} - \bar{G}_{i,o}) \quad (5)$$

where $\bar{G}_c$ and $\bar{G}_i$ denote the cavity-formation energy and interaction energy respectively. The cavity-formation energy can be calculated by using the scaled particle theory:[15]

$$\bar{G}_c = -RT\ln(1-y) + RT\frac{3y}{(1-y)}\left(\frac{\sigma_2}{\sigma_1}\right) + RT\left[\frac{3y}{1-y} + \frac{9}{2}\left(\frac{y}{1-y}\right)^2\right]\left(\frac{\sigma_2}{\sigma_1}\right)^2 + \frac{N_A y P}{\rho}\left(\frac{\sigma_2}{\sigma_1}\right)^3 \quad (6)$$

where σ_1 and σ_2 are the molecular diameters of the solvent and solute respectively, N_A is Avogadro's number, P is the pressure, ρ is the number density of the solvent and y is the packing fraction, $(y = \pi\rho\sigma_1^3/6)$. The molecular diameter of the solutes was estimated from the molar volume by using an empirical correlation, $\sigma(\text{Å}) = 1.356\,V^{1/3} - 0.8268$, which was found to hold for 36 kinds of solvents, such as alkanes, benzenes, alcohols and water, in the data from the literature.[15,16]

Figure 6 shows the transfer free energies of the solutes ($RT \ln K_{D2}$) and the difference in the cavity-formation energies $(\bar{G}_{c,w} - \bar{G}_{c,o})$ in both phases as a function of the cavity diameter. The transfer free energies of the enols of Hacac, Htfa and Htta increase with increase in σ_2 and lie close to the solid line calculated from the SPT. This means that the difference in the interaction energies for solute–heptane and solute–water is not so large for the three β-diketones. This result is similar to that obtained for halobenzenes.[7] On the other hand, the transfer free energies of the copper(II) chelates, especially the acetylacetonate and trifluoroacetylacetonate chelates, are remarkably lower than the values expected from the SPT. This means that the interactions of these solutes with water molecules are much stronger than those with heptane solvent

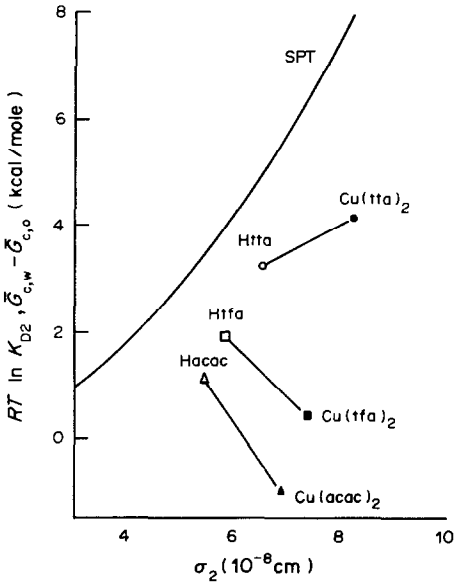

Fig. 6. Comparison of transfer free energy of enols and the copper(II) chelates with the cavity formation energy in heptane-water system.

molecules. If the cavity-formation energy calculated in the present way is valid, the interaction term, $\bar{G}_{i,w} - \bar{G}_{i,o}$, for each solute can be estimated from equation (5). The value is shown in Table 3 together with the cavity-formation energy. Good correlation is seen between the interaction term obtained from the SPT and the parameter $C_{ww} - 2C'_{w2}$ from the modified regular-solution theory. The peculiar effect of water on the partition coefficient can thus be elucidated in terms of both theories without inconsistency.

REFERENCES

1. J. Starý and H. Freiser, *Equilibrium Constants of Liquid–Liquid Distribution Reactions*, Part IV: *Chelating Extractants*, Pergamon Press, Oxford, 1975.
2. T. Wakahayashi, S. Oki, T. Omori and N. Suzuki, *J. Inorg. Nucl. Chem.*, 1964, **26**, 2255.
3. T. Omori, T. Wakahayashi, S. Oki and N. Suzuki, *ibid.*, 1964, **26**, 2265.
4. H. M. N. H. Irving, in *Ion Exchange and Solvent Extraction*, Vol. 6, J. A. Marinsky and Y. Marcus (eds.), pp. 139–187. Dekker, New York, 1974.
5. H. Imura and N. Suzuki, *J. Radioanal. Nucl. Chem.*, 1984, **88**, 65.
6. D. D. Perrin, *Stability Constants of Metal-Ion Complexes*, Part B, *Organic Ligands*, Pergamon Press, Oxford, 1979.
7. H. Watarai, M. Tanaka and N. Suzuki, *Anal. Chem.*, 1982, **54**, 702.
8. N. Suzuki, M. Itoh and H. Watarai, *Polyhedron*, 1982, **1**, 383.
9. H. Watarai, H. Oshima and N. Suzuki, *Quant. Struct.-Act. Relat.*, 1984, **3**, 17.
10. M. Takahashi, *M.Sc. Thesis*, Tohoku University, 1983.
11. K. Akiba, N. Suzuki and T. Kanno, *Bull. Chem. Soc. Japan*, 1969, **42**, 2537.
12. J. C. Reid and M. Calvin, *J. Am. Chem. Soc.*, 1950, **72**, 2948.
13. E. M. Larsen, G. Terry and J. Leddy, *ibid.*, 1953, **75**, 5107.
14. M. Saito, R. Kuroda and M. Shibukawa, *Anal. Chem.*, 1983, **55**, 1025.
15. R. A. Pierotti, *Chem. Rev.*, 1976, **76**, 717.
16. E. Wilhelm and R. Battino, *J. Chem. Phys.*, 1971, **55**, 4012.

Talanta, Vol. 32, No. 8B, pp. 791–795, 1985
Printed in Great Britain.

0039-9140/85 $3.00 + 0.00

MULTIELEMENT PRECONCENTRATION OF TRACE METALS WITH *meso*-TETRA(*p*-SULPHONATOPHENYL) PORPHINE

A. CORSINI, R. DIFRUSCIA* and O. HERRMANN†
Department of Chemistry, McMaster University, Hamilton, Ontario, Canada

(*Received* 27 *November* 1984. *Revised* 22 *January* 1985. *Accepted* 14 *March* 1985)

Summary—*Meso*-tetra(*p*-sulphonatophenyl)porphine reacts with several metal ions in ammoniacal aqueous solution. The resulting complexes are extractable into methyl isobutyl ketone with tricaprylmethylammonium chloride. The distribution ratios for the metal ions range from 8 for Mn(II) to about 1400 for Cd(II), corresponding, respectively, to single-stage extractions of 33–99% with a phase-volume ratio $V_w/V_o = 18$. A procedure has been developed for the multielement preconcentration of several trace metals (Mn, Co, Ni, Cu, Cd, Pb) from sea-water and their subsequent determination by graphite-furnace AAS.

Recently, synthetic porphines have been increasingly used as analytical reagents, primarily because the very intense absorption of the Soret band in the free or complexed porphine permits the measurement of trace amounts of analyte species. The spectrophotometric determination of low levels of carbon monoxide is an example.[1] Most of the applications, however, have involved the determination of metal ions at ng/ml concentrations.[2–12] The range of bivalent metal ions determined includes Mg, Mn, Co, Cu, Zn, Pd, Cd, Hg and Pb, usually measured individually but occasionally in groups of two or three.[3,4] Both cationic and anionic water-soluble porphines have been employed, mainly as spectrophotometric reagents, although the fluorescence of some porphines and complexes has also been used to advantage.[2] The reaction of the porphines with metal ions is generally slow and heating is normally required for quantitative complexation. The insertion of Mn(II) into the central cavity of the porphine is catalysed by Hg(II) and Cd(II) and this effect has been exploited in kinetic methods for the latter two ions.[8,9]

In the present study, the anionic porphine, *meso*-tetra(*p*-sulphonatophenyl)porphine ($TPPS_4$), is shown to react simultaneously with several ions in hot ammoniacal aqueous solution. The resulting anionic chelates are extracted into methyl isobutyl ketone (MIBK) as ion-association complexes with tricaprylmethylammonium chloride (Aliquat 336) to effect a multielement preconcentration. Distribution ratios for the extraction of metal ions from aqueous saline solution are reported and the preconcentration method is applied to synthetic test solutions and a sea-water sample.

*Present address: Dow Chemical Limited, Sarnia, Canada.
†Present address: Ontario Hydro Research, Toronto, Canada.

EXPERIMENTAL

Reagents

Distilled demineralized water (DDW) was used throughout. Buffer and sodium chloride solutions were purified before use by passage through a Chelex-100 (Bio-Rad, 200–400 mesh) column to remove any trace metals. All other common reagents were of analytical reagent grade or better (*e.g.*, Baker Instra-analyzed nitric acid and aqueous ammonia solution). Metal-ion solutions were prepared by dilution of Fisher 1000-ppm standard solutions.

Radioisotopes for the determination of distribution ratios were prepared from the metal nitrates by (n, γ) reactions performed in the McMaster Nuclear Reactor.

Tetraphenylporphine (TPP) was synthesized from benzaldehyde and freshly distilled pyrrole by the method of Adler *et al.*[13] It was purified on a column (2.5 × 45 cm) of Brockmann Activity I neutral alumina with chloroform as the mobile phase. The purple band of purified TPP was collected.

The ammonium salt of $TPPS_4$, $(NH_4)_4TPPS_4$, was prepared by the procedure of Fleischer *et al.*,[14] with some modification. After removal of unreacted TPP, the mixture was cooled in an ice-bath and a 6:1 v/v mixture of methanol and concentrated aqueous ammonia solution was added carefully until the colour of the mixture changed from green to purple. The ammonium sulphate produced was removed by filtration, the filtrate was reduced to about 100 ml, about 550 ml of absolute methanol was added and the mixture was then filtered to remove a further portion of ammonium sulphate. The volume was again reduced to about 100 ml and the $(NH_4)_4TPPS_4$ was precipitated by addition of 200 ml of acetone, filtered off, and further purified by chromatography.[15] Additional purification involved three precipitations from methanol by addition of acetone. It was then dissolved in DDW and passed through a 2.5 × 30 cm column of Dowex 1, 100–200 mesh, hydroxide form. This procedure converted residual ammonium sulphate into aqueous ammonia solution; the $(NH_4)_4TPPS_4$ was recovered by evaporation. Because the ammonium salt slowly loses ammonia on prolonged storage, it was converted into Na_4TPPS_4 by passage through a 2.5 × 30 cm column of Amberlite CG120, 100–200 mesh, sodium form. Drying overnight at 120° *in vacuo* produced the anhydrous salt but final traces of acetone could be removed only by drying for about a month. The structure was confirmed by proton

NMR[14] and elemental analysis showed that the product was of high purity.

Apparatus

Solutions were prepared and stored in polypropylene containers and standard flasks. As much as possible, laboratory operations were conducted at a laminar-flow clean-air work station. Spectrophotometric measurements were made with a GCA/McPherson Super 700 ratio-recording instrument interfaced with a Monroe 1860 programmable calculator for spectrophotometer control and data acquisition. Hellma Spectrosil Quartz cells (1- and 5-cm) were used.

Atomic-absorption measurements were made with a Perkin-Elmer Model 373 instrument equipped with an HGA-2200 graphite furnace and a Hitachi Perkin-Elmer 056 recorder. The wavelengths, slit-widths and lamp currents used were those recommended in the applications manual. The temperature programme was drying at 150° for 30 sec (75 sec for Co and Ni); charring at 600° (50 sec) for Mn and Cu, 600° (75 sec) for Co and Ni, 500° (50 sec) for Pb, 300° (50 sec) for Cd; atomization at 2700° for 7 sec for Mn, Co, Ni and Cu, 2100° for 7 sec for Cd, 2000° for 7 sec for Pb. During atomization, the argon gas "interrupt mode" was used because of the very low metal concentrations involved. Sample volumes of 10 or 25 μl were injected, except for Co and Ni, which required 75 μl.

Measurements of γ-radiation were made with a Ge/Li APTEC detector equipped with a Canberra Series 30 multichannel analyser and Teletype Model 43. All counts were corrected for background radiation and half-life.

Procedures

Reactivity. The general reactivity of $TPPS_4$ towards metal ions was tested in approximately neutral solution (pH 5–8) and at pH 10 (ammonia/ammonium acetate buffer). Final test solutions were $5 \times 10^{-5}M$ in $TPPS_4$ and $5 \times 10^{-4}M$ in metal ion. The solutions were heated on a steam-bath for up to 20 hr. Evidence for complexation was obtained by comparing spectra of the test solutions and of $TPPS_4$ in the intense Soret region, 400–450 nm (molar absorptivities, ε, $\sim 10^5$ l.mole^{-1}.cm^{-1}), and in the 500–700 nm region ($\varepsilon \sim 10^3$). In the presence of a tenfold excess of metal ion, the concentration of unreacted $TPPS_4$ was low when complexation occurred, and its spectral interference was minimized.

The stability of those metalloporphyrins which formed was tested over the pH range 2–14 by removing aliquots of the pH-10 test solutions, readjusting the pH and monitoring the absorbance of the complex at the appropriate wavelength.

The times required for maximum complex formation at *low* concentrations of the metal ions (50–200 ng/ml) was determined at pH 10. The concentration of $TPPS_4$ was $1.0 \times 10^{-5}M$. The test solutions were heated in polypropylene flasks to 90–98° for periods of time ranging from 10 to 100 min. Spectrophotometric measurements were made in 5-cm cells. In most cases, the Soret band of the individual metalloporphyrins could be used to monitor complex formation. The Soret band (412 nm) of $TPPS_4$ did not seriously interfere. The solutions contained sodium chloride ($0.75M$) to approximate the saline nature of seawater.

Extraction. Aqueous saline solutions (50 ml) of selected $TPPS_4$ complexes, containing 20–100 ng of metal per ml, were batch-extracted by shaking for 2 min with 5 ml of a 10% solution of tricaprylmethylammonium chloride (Aliquat 336, General Mills) in MIBK; (before use the Aliquat 336 was washed successively with $2M$ hydrochloric acid and $2M$ aqueous ammonia to remove any trace metals present). The phases were separated and the aqueous phase was extracted a second time. The degree of extraction (E, %) was measured as $E = 100A_1/(A_1 + A_2)$, where A_1 and A_2 are the Soret absorbances of the complex in the two organic extracts. After the second extraction the aqueous phase appeared colourless to the eye.

The composition of the extracted copper complex was determined by extracting 50-ml aliquots of saline solutions containing 30 ng of Cu (as the $CuTPPS_4$ complex) per ml with 5-ml volumes of MIBK solutions of Aliquat 336 ranging in concentration from 5.4×10^{-4} to $1.4 \times 10^{-3}M$. The concentration of $CuTPPS_4$ remaining in the aqueous phase was obtained by measurement of the Soret absorbance and reference to a calibration graph for standard saline solutions of $CuTPPS_4$. The concentration in the organic phase was determined similarly. Values of the distribution ratio D_R were calculated for each concentration of Aliquat 336.

The E and D_R values were measured for the *overall* chemical procedure, which involves reaction of the metal ion with $TPPS_4$ in the aqueous phase and subsequent extraction of the $TPPS_4$ complex. The aqueous phase (90 ml) was $0.75M$ in sodium chloride, $2 \times 10^{-6}M$ in $TPPS_4$ and contained 5–20 ng/ml of a radioisotope of the metal ion ($TPPS_4$:metal-ion molar ratio $\sim$ 6–25, depending on atomic weight and concentration of metal ion). The solution was heated to 90–98° for 1 hr in a water-bath and then extracted once with 5 ml of Aliquat 336 solution. The activity of the aqueous phase was measured before and after extraction. The activity of the organic phase was also measured, and good mass balance was obtained.

Application to sea-water. The use of $TPPS_4$ as a group-reagent for metal ions was tested on a synthetic saline solution containing 1 ng/ml each of Co, Ni, Cu, Zn and Pb and 0.1 ng/ml of Mn(II) and Cd. The procedure was then applied to sea-water samples obtained from Sandy Cove Bay, Nova Scotia. These samples were filtered through 0.45-μm filters, acidified with ultrapure nitric acid to pH 1.7 and stored in clean 10-l. polypropylene bottles. The standard-addition method was used for trace-metal determination.

To four 90-ml aliquots of acidified sea-water in 100-ml standard flasks were added a combined metal-ion spike, 200 μl of 95% hydrazine, a few drops of concentrated ammonia solution (to give pH $\sim$8), and a small volume of ammonia/ammonium acetate buffer ($4M$ ammonia, $0.4M$ acetate) to bring the solution to about pH 10. $TPPS_4$ ($\sim$200 μg) was then added (final concentration, $\sim 2 \times 10^{-6}M$) and the stoppered flasks were sealed with Teflon tape, wrapped in aluminium foil, and heated for 1.5 hr in a water-bath at 90–98°. The solutions were cooled, presaturated with 1 ml of MIBK, extracted with 5 ml of the Aliquat 336/MIBK solution ($\sim$2 min of vigorous shaking, one batch-extraction), and the phases were left for 1 hr to separate and clarify completely. The organic phases were withdrawn from the necks of the flasks and stored in capped polypropylene centrifuge tubes until ready for GFAAS measurement.

Blanks, prepared with $0.75M$ sodium chloride, were run in the same manner, always in duplicate. Good reproducibility of the blank was achieved.

RESULTS AND DISCUSSION

Reactivity

Of 33 ions tested at pH 10, evidence for reaction was obtained for only 11 bivalent ions and for silver (Table 1). The alkaline-earth metal ions and all tervalent and quadrivalent cations tested did not react under the conditions used. In neutral solution, evidence for reaction of Pb and Cd was uncertain. Below pH 6–7, the Pb and Cd complexes decompose completely. The Hg complex is stable only in the pH range 11–13. Below pH 10, decomposition is essen-

Table 1. Reactivity of $TPPS_4$ with metal ions, pH 10

Reaction observed		No reaction observed			
Mn^{2+}	Pd^{2+}	Be^{2+}	Cr^{3+}	Gd^{3+}	Th^{4+}
Fe^{2+}	Ag^{+}	Mg^{2+}	Fe^{3+}	Ho^{3+}	UO_2^{2+}
Co^{2+}	Cd^{2+}	Ca^{2+}	La^{3+}	Er^{3+}	VO^{2+}
Ni^{2+}	Hg^{2+}	Sr^{2+}	Ce^{3+}	In^{3+}	
Cu^{2+}	Sn^{2+}	Ba^{2+}	Nd^{3+}	Sc^{3+}	
Zn^{2+}	Pb^{2+}	Al^{3+}	Eu^{3+}	Y^{3+}	

tially quantitative. Ni appears to react very slowly, especially in neutral solution. The remaining complexes are more stable; in particular, the Zn complex persists to pH 3 before decomposing and the Sn(II), Co(II) and Cu(II) complexes remain stable at pH 2. All the complexes are stable up to at least pH 12.

The non-reactivity of $TPPS_4$ with the more highly charged ions appears to be due to kinetic rather than thermodynamic effects. Fe(III), for example, was not observed to react and has been reported elsewhere to react only extremely slowly.[16] Once formed, however, the Fe(III) complex is very stable. By comparison, Fe(II) reacts quickly but its electronic spectrum is the same as that for the Fe(III) complex, which is consistent with the observation that the higher oxidation state is stabilized in metalloporphyrins.[17] The same behaviour obtains with Sn(II) and Sn(IV).[17,18] The low reactivity of the more highly charged ions is probably a combined result of hydrolysis and the requirement for simultaneous removal of several water molecules from the ion before its insertion into the porphine cavity can occur.

The reactions of $TPPS_4$ with metal ions are much slower than those involving familiar organic analytical reagents and require application of heat if they are to proceed at practical rates. It was therefore necessary to determine the time required for attainment of equilibrium, particularly at low metal-ion concentrations. This study was done at pH 10 since the complexes (except for that of Hg) are stable at this pH. The acetate present served to reduce hydrolysis and prevent precipitation of lead chloride. A highly saline matrix was used with a view to later application to sea-water analysis. Equilibrium was *assumed* to have been established when the absorbance had reached a constant maximum. The group of ions (bivalent) tested included Cd, Co, Cu, Mn, Ni, Pb and Zn. Except for Ni, maximum constant absorbance was attained within 60 min. The addition of a few drops of fresh hydrazine effected much more rapid insertion of Ni, and constant absorbance was attained within 60 min. The use of auxiliary ligands to increase the rate of metal-ion insertion has been known for some time,[19] but the same ligand may affect different metals in different ways, which makes it difficult to choose optimum conditions for a group separation, such as that done here. In the present study, ammonia and acetate were present in the reaction solution, together with hydrazine, as auxiliary ligands. The Cd complex was found to be sensitive to light; accordingly, in subsequent work, the reaction flasks were wrapped in aluminium foil.

Table 2. Extraction of preformed $MTPPS_4$ complexes from saline solution (pH 10) with Aliquat 336

Metal	$\%E$*	D_R
Mn	96.7	3×10^2
Co	98.5	1.1×10^3
Ni	99.7	3.5×10^3
Cu	99.4	1.7×10^3
Zn	99.6	2.7×10^3

*$V_w/V_o = 10$, ionic strength = 0.75.

Extraction

Because of the presence of the four sulphonate groups in $TPPS_4$, its metal complexes are anionic and therefore it was expected that they could be extracted as ion-association complexes with large cations. The extraction data for standard solutions of several *preformed* $TPPS_4$ complexes extracted with a 10% w/v solution of Aliquat 336 in MIBK are summarized in Table 2. The extractions are extremely facile. In preliminary experiments, E was found to be independent of the Aliquat concentration if this was >5%, and 10% concentration was selected for practical use. The number of tricaprylmethylammonium (TCMA) cations associated with the extracted $CuTPPS_4$ complex was determined from the slope of the linear portion of a plot of log D_R *vs.* log[TCMA]. Two determinations yielded a value of 3.98 ± 0.01 for the slope. It is reasonable to assume that four TCMA cations are also associated with the other $TPPS_4$ complexes extracted.

The high values of E and D_R for the preformed complexes show only that the complexes, once formed, are readily extracted. More significant are the E and D_R values that represent the *overall* process involving the reaction between metal ion and $TPPS_4$ in the aqueous phase, and the extraction, *i.e.*,

$$M^{2+} + H_2TPPS_4^{4-} \rightleftharpoons MTPPS_4^{4-} + 2H^+ \text{ (aqueous)}$$

$$4R_3MeN^+ + MTPPS_4^{4-} \rightleftharpoons (R_3MeN^+)_4(MTPPS_4^{4-}) \text{ (organic)}.$$

The E values for the overall process are best determined by use of radioisotopes. In Table 3, some experimental details and extraction results are given for several metal ions. The E values are lower, significantly in some cases, than those in Table 2. The D_R values are also lower than the corresponding values in Table 2, although still highly favourable (for most ions) for analytical purposes. The reduction in E resulted from incomplete reaction in the aqueous phase, partly on account of the slow rate of metalloporphyrin formation but also because of some adsorption of metal ions on the vessel walls. Low levels of activity due to residual adsorbed metal were detected in acid washings of the vessels, after the

Table 3. Reaction/extraction of metal ions as $TPPS_4$ complexes in saline solution (pH 10)

Isotope	γ-Ray energy, *keV*	Conc. used, *ng/ml*	*E*,%	$D_R^{\dagger}$	V_w/V_o for 90% *E*
^{56}Mn	847 1811	4	33	8	—
^{60}Co	1332.5	4	60	27	—
Ni*	—	20	94	2.8×10^2	30
^{64}Cu	511	10	96.9	5.6×10^2	60
^{65}Zn	1115	20	93.6	2.65×10^2	30
^{115m}Cd	934.1	5	98.7	1.4×10^3	150
^{110m}Ag	657.7 884.7	10	98.5	1.3×10^3	150
Pb*	—	20	97	5.8×10^2	65

*Radioisotopes of Pb and Ni could not be produced in the reactor. *E* was obtained by GFAAS measurement, from $E = 100A_1/(A_1 + A_2)$ %.
†Based on the experimental V_w/V_o ratio, 18.

experimentation. The low *E* values for Mn and Co are mainly due to incomplete reaction with $TPPS_4$; the amount of adsorption on the vessel walls was too small to be significant. Once formed, the Mn and Co complexes are very extractable.

The values of D_R were calculated from $E = 100D_R/(D_R + V_w/V_o)$. With these experimental values, the attainable preconcentration factors, calculated on the assumption that 90% extraction is acceptable, are given in the last column of Table 3. Difficulties in working with large phase volume ratios (*e.g.*, $V_w/V_o = 150$) would limit their attainment in practice, however.

Application to sea-water

Application of the procedure to the synthetic sea-water sample gave excellent values (not reported here) for the trace metals present; the method was therefore applied to the sea-water sample. Results for the determination of total (soluble) trace metals in Sandy Cove sea-water are reported in Table 4. The values in the last column were obtained independently in another laboratory, by extraction with ammonium pyrrolidinedithiocarbamate (APDC) and measurement by GFAAS. Agreement between the $TPPS_4$ and APDC procedures is good. The advantage of the APDC procedure is the faster reaction between the reagent and metal ions; the disadvantage is the instability of the reagent in the aqueous phase and of the extracted metal chelates in the MIBK phase.[20,21] Fe(III) is not extracted in the $TPPS_4$ system, which could prove advantageous for plasma atomic-emission multielement measurements. The long phase-separation time in the $TPPS_4$ extraction system is a drawback, the 1-hr period was allowed for safety, separation usually being complete in 30 min. The use of hexane or xylene instead of MIBK with Aliquat 336 did not lead to any improvement.

Table 4. Analysis of sea-water sample by $TPPS_4$ procedure

Trace metal	$TPPS_4$ method,* *ng/ml*	APDC method,† *ng/ml*
Mn	0.83 ± 0.07	0.68 ± 0.05
Co	0.018 ± 0.007	0.015 ± 0.007
Ni	0.42 ± 0.02	0.31 ± 0.04
Cu	0.82 ± 0.02	0.96 ± 0.04
Cd	0.025 ± 0.002	0.027 ± 0.003
Pb	0.22 ± 0.02	0.22 ± 0.06

*Results represent the mean of 3–5 determinations and the standard deviation.
†Results reported by independent laboratory.

In preliminary work with a sea-water sample that was not acidified, the trace element concentrations were found to be unreasonably low, and ultraviolet irradiation was required to release additional amounts of trace metals. The results were not reproducible, however. The most consistent results for metal-ion concentrations were always obtained when the sea-water samples had been acidified to pH 1.6. On adustment of the pH to 10, any recomplexation of metal ions with naturally occurring ligands will affect the standard metal-ion spikes in the same way as the analytes, providing automatic compensation (provided the spike concentration does not exceed the natural ligand concentration).

Results for Zn (not reported) were not reproducible even when samples were prepared and processed in a clean-air station. The concentration of Hg was not measured because of the effect of pH on the stability of the complex and the low sensitivity of GFAAS for this element when it is directly injected into the furnace. The extraction of Mn and Co is not quantitative (Table 3) but the standard-additions method provides the necessary compensation, though the sensitivity is reduced.

Conclusions

$TPPS_4$ is an effective reagent for multielement preconcentration of Mn, Co, Ni, Cu, Cd and Pb from sea-water. $TPPS_4$ reacts slowly with metal ions and prolonged heating is required for metalloporphyrin formation. The reagent and the complexes of the metals above are stable, except for $CdTPPS_4$ (which

is light-sensitive). The complexes are very readily extracted by tricaprylmethylammonium chloride into MIBK.

Acknowledgements—The authors gratefully acknowledge financial support for this work from the National Research Council of Canada and the Natural Sciences and Engineering Council of Canada.

REFERENCES

1. A. Corsini, A. Chan and H. Mehdi, *Talanta*, 1984, **31**, 33.
2. S. Igarishi, T. Yotsuyanagi and K. Aomura, *Nippon Kagaku Kaishi*, 1981, 60.
3. S. Igarishi, M. Nakano and T. Yotsuyanagi, *Bunseki Kagaku*, 1983, **32**, 67.
4. H. Ishii, H. Koh and K. Satoh, *Nippon Kagaku Kaishi*, 1980, 1919.
5. *Idem*, *Analyst*, 1982, **107**, 647.
6. *Idem*, *Anal. Chim. Acta*, 1982, **136**, 347.
7. H. Ishii, K. Satoh, Y. Satoh and H. Koh, *Talanta*, 1982, **29**, 545.
8. M. Tabata and M. Tanaka, *Mikrochim. Acta*, 1982 **II**, 149.
9. *Idem*, *Anal. Lett.*, 1980, **13**, 427.
10. H. Ishii and H. Koh, *Nippon Kagaku Kaishi*, 1978, 390.
11. J. Itoh, M. Yamashira, T. Yotsuyanagi and K. Aomura, *Bunseki Kagaku*, 1976, **25**, 781.
12. H. Ishii and H. Koh, *Talanta*, 1977, **24**, 417.
13. A. D. Adler, F. R. Long, J. D. Finarelli, J. Goldmacher, J. Assour and L. Korsakoff, *J. Org. Chem.*, 1967, **32**, 476.
14. E. B. Fleischer, J. M. Palmer, T. S. Srivastava and A. Chatterjee, *J. Am. Chem. Soc.*, 1971, **93**, 3162.
15. W. DeW. Horrocks, Jr. and E. G. Hove, *ibid.*, 1978, **100**, 4386.
16. W. Schneider, *Structure and Bonding*, Vol. 23, p. 123. Springer-Verlag, New York, 1975.
17. J. H. Fuhrop, *Angew. Chem.*, 1974, **13**, 321.
18. N. W. G. Debye and A. D. Adler, *Inorg. Chem.*, 1974, **13**, 3037.
19. W. Schneider, in *The Nature of Seawater*, E. D. Goldberg (ed.), Dahlem Workshop Report, Dahlem Conference Berlin, 1975, p. 375.
20. K. S. Subramanian and J. C. Méranger, *Analyst*, 1980, **105**, 620.
21. I. Dellien and L. Persson, *Talanta*, 1979, **26**, 1101.

Talanta, Vol. 32, No. 8B, pp. 797–802, 1985
Printed in Great Britain

0039-9140/85 $3.00 + 0.00
Pergamon Press Ltd

LIQUID–LIQUID EXTRACTION OF UNIVALENT CLASS *b* METAL IONS BY THE THIACROWN COMPOUND 4′-PICRYLAMINOBENZO-1,4,8,11-TETRATHIACYCLOPENTADEC-13-ENE

EIICHI SEKIDO, KENJI CHAYAMA and MOTOHO MUROI*
Department of Chemistry, Faculty of Science, Kobe University, Rokkodai, Nada, Kobe 657, Japan

(*Received* 7 *December* 1984. *Accepted* 19 *February* 1985)

Summary—A new thiacrown compound in which the picrylamino group is introduced as the chromogenic group, 4′-picrylaminobenzo-1,4,8,11-tetrathiacyclopentadec-13-ene (4′-PicNHBz-TTCP), has been successfully synthesized and its characteristics as an extracting and spectrophotometric reagent have been examined. This compound (HL) forms ion-pair complexes (M^+L^-) with univalent class *b* metal ions (M^+) such as silver and copper(I). The M^+L^- species can be extracted into 1,2-dichloroethane and spectrophotometrically determined. Not only class *a* and *ab* metals but also bivalent class *b* metals such as mercury(II) and palladium(II) are not extracted at all. As silver and copper(I) ions are effectively extracted at pH above 8.0, a suitable masking agent such as tartrate is used in order to prevent the formation of hydroxides of foreign metals, if necessary.

The chemistry of thiacrown ethers, in which sulphur atoms replace the oxygen atoms in crown ethers, has been mainly advanced in the fields of co-ordination chemistry and analytical chemistry during the past fifteen years, since Rosen and Bush synthesized and studied the properties of some typical thiacrown ethers and their transition metal complexes.[1] Thiacrown ethers have the characteristics of polythioethers, and hence formation of their complexes with metal cations may be primarily attributed to the affinity of the metal ion for sulphur atoms. In general, organic reagents in which the sulphur atom is present as the mercapto group (R—SH) act as soft Lewis bases, and hence react with soft Lewis acids such as class *ab* and *b* metals. Thiacrown ethers, however, contain sulphur atoms in the thioether group (R—S—R′) so will act as softer Lewis bases than the reagents containing a mercapto group, and consequently will react with softer Lewis acids, mainly class *b* metals. The difference in the affinities of the thioether group for various groups of metals is particularly interesting in connection with the selective separation of class *b* metals from class *a* and *ab* metals, especially from the first-row transition metals. In addition, the separation of class *b* metals from each other by solvent extraction might be made more selective by the relative sizes of the metal ion and the cavity of the macrocyclic compound, the choice of anion for formation of the ion-pair, and the type of extraction solvent.

Recently, it was shown that the perchlorates and picrates of class *b* metals such as silver, copper(I), palladium(II) and mercury(II) are selectively extracted with a 1,2-dichloroethane solution of the thiacrown ether 1,4,8,11-tetrathiacyclotetradecane (TTCT).[2] Furthermore, the extraction and spectrophotometric determination of copper and silver with TTCT by the use of an appropriate coloured anion, such as Bromocresol Green or picrate, was reported.[3]

If a group which can act both as a counter-anion to form ion-pairs and as a chromophore is introduced into a thiacrown compound, the product should be able to extract class *b* metals selectively without the need for an auxiliary counter-anion, and to give a compound suitable for determining the metal by spectrophotometry after extraction. Moreover, if the group functions as a univalent counter-anion, the reagent should serve as a selective extracting and spectrophotometric reagent for univalent class *b* metals, and even be specific for a certain metal. Recently, new chromogenic crown ethers into which picrylamine or one of its derivatives is introduced have been synthesized, and their use for extraction and spectrophotometric determination of alkali metals has been reported.[4–7]

In the present study a new chromogenic thiacrown ether, 4′-picrylaminobenzo-1,4,8,11-tetrathiacyclopentadec-13-ene (4′-PicNHBz-TTCP), which has one dissociable proton in the picrylamino group, was synthesized and its properties as an extracting and spectrophotometric reagent were examined.

EXPERIMENTAL

Synthesis of 4′-PicNHBz-TTCP (Scheme 1)

4′-Nitrobenzo-1,4,8,11-tetrathiacyclopentadec-13-ene (4′-NO_2Bz-TTCP) (**III**). In 700 ml of absolute ethanol, under nitrogen, 1.02 g (44 mmoles) of sodium metal was dissolved. To this solution 5.02 g (22 mmoles) of

*Present address: Public Health Research Institute of Kobe City, Minatojima, Chuo, Kobe 650, Japan.

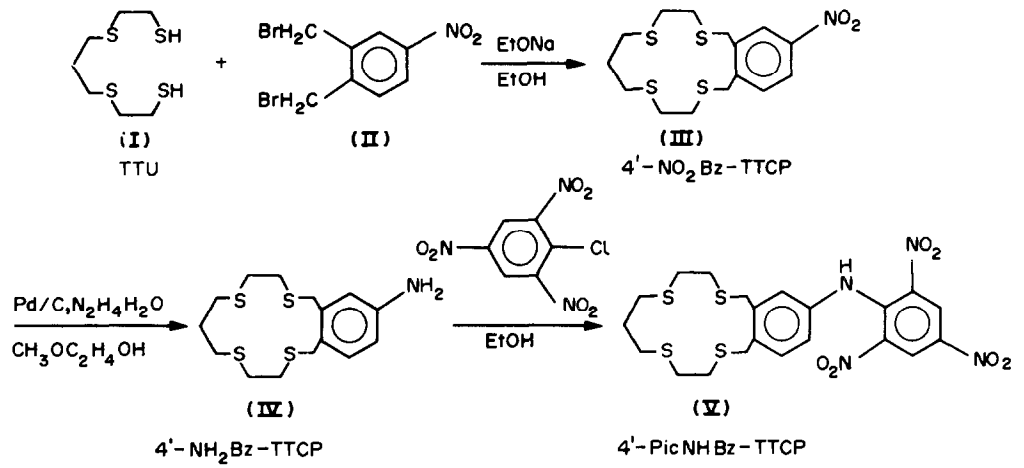

Scheme 1.

1,4,8,11-tetrathiaundecane (TTU) (I) dissolved in 200 ml of benzene and 6.80 g (22 mmoles) of α,α′-dibromo-4-nitro-*o*-xylene (II) dissolved in 200 ml of benzene were simultaneously added dropwise during 5 hr, at room temperature. After stirring overnight, the precipitate was filtered off and washed with benzene. The filtrate and washings were combined and evaporated under reduced pressure. The residue was dissolved in chloroform and water, then the organic layer was separated, washed with water and dried. The solvent was removed again under reduced pressure and the residual oil was chromatographed on a silica-gel column with benzene–dichloroethane (1:1 v/v) mixture. The first of two major bands was collected and on recrystallization from chloroform–ethanol gave colourless curdy crystals, m.p. 102–3°, yield 4.97 g (61%). Found: C 47.9%, H 5.7%, N 3.7%; $C_{15}H_{21}NO_2S_4$ requires C 47.97%, H 5.64%, N 3.73%. The infrared spectrum (KBr) had bands at 1510, 1350 cm^{-1}(NO_2), but no absorption by SH at 2550 cm^{-1}. ^1H NMR ($CDCl_3$) gave δ 1.80 (2H, m, $CH_2CH_2CH_2$), 2.50–3.00 (12H, overlapping t and s, $CH_2CH_2CH_2$, CH_2CH_2), 4.05 (4H, s, CH_2Ph), 7.30–8.40 (3H, m, aromatic H).

4′-Aminobenzo-1,4,8,11-tetrathiacyclopentadec-13-ene (4′-NH_2Bz-TTCP) (IV). Into 90 ml of 2-methoxyethanol 1.5 g (4 mmoles) of 4′-NO_2Bz-TTCP (III) was mixed and the reaction was started by addition of 0.2 g of 10% Pd/C catalyst and 10 ml of hydrazine monohydrate. After refluxing for 1 hr the hot reaction mixture was filtered and evaporated under reduced pressure. Recrystallization from ethanol gave colourless needles, m.p. 122–3°, yield 1.24 g (90%). Found: C 51.9% H 6.7%, N 4.2%; $C_{15}H_{23}NS_4$ requires C 52.13%, H 6.71%, N 4.05%. The infrared spectrum (KBr) had bands at 3430, 3350 cm^{-1} (NH_2). Mass spectrometry (MS) (70 eV) gave *m/z* (relative intensity) 345 (M^+, 9), 150 (100). ^1H NMR ($CDCl_3$) gave δ 1.90 (2H, m, $CH_2CH_2CH_2$), 2.60–3.00 (12H, overlapping t and s, $CH_2CH_2CH_2$, CH_2CH_2), 3.65 (2H, br. s, NH_2), 3.90 (4H, CH_2Ph), 6.40–7.25 (3H, m, aromatic H).

4′-Picrylaminobenzo-1,4,8,11-tetrathiacyclopentadec-13-ene (4′-PicNHBz-TTCP) (V). 4′-NH_2Bz-TTCP (IV) (1.04 g, 3 mmoles) was mixed with 400 ml of absolute ethanol and a solution of 0.74 g (3 mmoles) of picryl chloride in 100 ml of absolute ethanol was added dropwise at 40°. To the solution 0.41 g of sodium carbonate was added. After 15 min the reaction mixture was poured into chloroform, and the organic layer was separated and washed with water. The organic solvent was then evaporated under reduced pressure and the residual yellow crystals were recrystallized from benzene–ethanol mixture. The product had m.p. 161–2°, yield 1.3 g (80%). Found: C 45.4%, H 4.3%, N 10.0% $C_{21}H_{24}N_4O_6S_4$ requires C 45.31%, H 4.35%, N 10.06%. The infrared spectrum (KBr) had bands at 1530, 1510, 1350 cm^{-1}(NO_2). MS (70 eV) gave *m/z* (relative intensity) 556 (M^+, 3), 361 (89), 167 (59), 106 (100). ^1H NMR (DMSO-d_6) gave δ 1.80 (2H, m, $CH_2CH_2CH_2$), 2.80 (4H, s, $CH_2CH_2CH_2$), 3.30 (8H, s, CH_2CH_2), 3.95 (4H, s, CH_2Ph), 6.90–7.45 (3H, m, aromatic H), 9.00 (2H, s, aromatic H).

Reagents

Reagent solution. A $5 \times 10^{-5}M$ 4′-PicNHBz-TTCP solution in 1,2-dichloroethane was prepared.

Metal solutions. Metal sulphates of guaranteed-reagent grade were used to prepare $1 \times 10^{-2}M$ stock solutions, which were standardized by EDTA titration.

Dichloroethane. 1,2-Dichloroethane was shaken three times with 2*M* potassium chloride and three times with water, dried over anhydrous magnesium sulphate and distilled.

Dioxan. Commercial dioxan was treated with hydrochloric acid and metallic sodium and then distilled, the fraction boiling at 102.5–105.5° being collected.

Other reagents. The other reagents used were reagent grade where possible.

Apparatus

A Taiyo M incubator was used for shaking the stoppered 50-ml glass cylindrical tubes. A Seiko SAS-725 atomic-absorption spectrophotometer was used for the determination of silver and copper. Absorption spectra were measured with a Shimazu UV-240 recording spectrophotometer, and the pH of aqueous phases was measured with a Hitachi-Horiba H-5 pH-meter.

Determination of acid dissociation constant

In an 800-ml water-jacketed vessel controlled at 25°, 600 ml of $5 \times 10^{-5}M$ 4′-PicNHBz-TTCP (V) solution in 50% dioxan–water mixture were adjusted to pH 4.0 with sulphuric acid. The absorption spectrum was measured in the range 210–600 nm, with a small portion of the solution in a 1-cm quartz cell. The solution was returned to the 800-ml vessel and the pH was raised a little by addition of sodium hydroxide solution of suitable concentration (1–10*M*, according to the pH required). The spectrum was again recorded. By repetition of this procedure, the absorption spectra of the reagent over a wide range of pH values were measured. The volume change on addition of the hydroxide solution could be neglected. The acid dissociation constant of the reagent, K_a, was calculated from $pK_a = pH - \log[L^-]/[HL] = pH - \log(\varepsilon - \varepsilon_{L^-})/(\varepsilon_{HL} - \varepsilon)$ where ε_{HL} and ε_{L^-} are the molar absorptivities of pure HL and L^- solution at a selected wavelength and ε is the apparent molar absorptivity calculated from the absorbance of the mixed solution at various pH values. When ε is equal to

Table 1. Degree of extraction of various metals with 4′-PicNHBz-TTCP in 1,2-dichloroethane

Metal ion	Classification of metal by Ahrland *et al.**	α Value†	4′-PicNHBz-TTCP pH	4′-PicNHBz-TTCP *E*, %	TTCT§ pH	TTCT§ *E*, %
Na^+	*a*	0	10.3	0	5.4	0
Mg^{2+}	*a*	0	10.3	0	5.4	0
Mn^{2+}	*ab*	0	10.3	0	5.4	0.8
Co^{2+}	*ab*	1.39	10.3	0	5.8	0.8
Ni^{2+}	*ab*	1.41	10.3	0	5.4	0.7
Zn^{2+}	*ab*	1.25	10.3	0	5.4	0.5
Cu^{2+}	*ab*	1.64	10.3	0	5.4	5.9
Cd^{2+}	*b*	1.66	10.3	0	5.4	0.8
Cu^+	*b*	3.92	7.4	99.5	5.4	99.4
			3.6	15.4		
Ag^+	*b*	3.60	8.3	99.8	5.4	99.9
			3.5	8.0		
Pd^{2+}	*b*	5.33	10.3	0	5.4	14.3
Hg^{2+}	*b*	5.83	10.3	0	5.1	89.5

*S. Ahrland, J. Chatt and N. R. Davies, *Quant. Rev. Chem. Soc.*, 1958, **12**, 265.
†Ref. 7
§Ref. 2.

$(\varepsilon_{HL} + \varepsilon_{L^-})/2$, the pH value is equal to pK_a. The values of ε at 450 nm were plotted against pH and the values of pK_a deduced.

Liquid–liquid extraction of metals

An aliquot (10 ml) of aqueous solution containing the metal ion ($5 \times 10^{-5}M$) and sodium hydroxide–borax buffer solution ($1 \times 10^{-2}M$) was taken in a stoppered 50-ml glass cylindrical tube. The ionic strength was kept at 0.1 with sodium sulphate. To obtain a copper(I) solution, enough hydroxylammonium sulphate was added to copper(II) sulphate solution to give a $0.1M$ solution. After the addition of 10 ml of $2.5 \times 10^{-3}M$ 4′-PicNHBz-TTCP solution, the mixture was shaken for 30 min at 200 strokes/min and $25.0 \pm 0.1°$. The mixture was then centrifuged for 5 min, the pH of the aqueous phase was measured and the absorbance of the organic phase was measured at 510 nm against a reagent blank. When the degree of extraction was very high, as in the case of silver and copper(I), the metal concentration in the aqueous phase was measured by atomic-absorption spectrometry.

RESULTS AND DISCUSSION

Synthesis of reagent

The reagent, 4′-PicNHBz-TTCP, was synthesized in three steps as shown in Scheme 1. Benzo-1,4,8,11-tetrathiacyclopentadec-13-ene (Bz-TTCP) could not be used as the starting material, because the nitration of Bz-TTCP with nitric acid to obtain 4′-NO_2Bz-TTCP (III) oxidizes the thioether group in the Bz-TTCP, although Bz-15-crown-5 is easily nitrated.[4] Therefore, TTU (I), which was synthesized by Bush and co-workers,[1,8] and α,α′-dibromo-4-nitro-*o*-xylene (II) synthesized by Kleinschmidt and Braeuniger,[9] were used as starting materials. The cyclization reaction of the dithiol (I) and the dibromide (II) was performed by the high-dilution method, with sodium ethoxide in absolute ethanol. The cyclic polythioether, 4′-NO_2Bz-TTCP (III) was separated by silica-gel column chromatography, with benzene–dichloroethane. The reduction of the nitro group of (III) to the amino group of 4′-NH_2Bz-TTCP (IV) was successfully performed by use of Pd/C as a catalyst and hydrazine monohydrate as reducing agent, without inhibition of the catalysis by sulphur atoms. The final product, 4′-PicNHBz-TTCP (V), was obtained by the reaction of (IV) and picryl chloride. The compounds obtained at each step of the synthesis were identified by elemental analysis, infrared spectroscopy, mass spectrometry and ^1H NMR.

4′-PicNHBz-TTCP, when recrystallized from benzene–ethanol, gives orange needles. It is soluble in benzene, chloroform, 1,2-dichloroethane, MIBK, acetone and dioxan, sparingly soluble in ethanol and methanol and insoluble in water. 4′-PicNHBz-TTCP is stable in air for at least a month when dissolved in organic solvents, or in acidic or neutral (but not alkaline) aqueous solutions of solvents miscible with water.

Liquid–liquid extraction of various metals with 4′-PicNHBz-TTCP

The following ions were examined: Na^+ and Mg^{2+} (class *a*), Mn^{2+}, Ni^{2+}, Co^{2+}, Cu^{2+} and Zn^{2+} (class *ab*), and Cu^+, Ag^+, Hg^{2+} and Pd^{2+} (class *b*). The results are shown in Table 1 along with those for extraction with TTCT.[2] Na^+ and Mg^{2+} were not extracted at all, with either reagent. Mn^{2+}, Ni^{2+}, Co^{2+}, Cu^{2+} and Zn^{2+} were not extracted with 4′-PicNHBz-TTCP but slightly extracted with TTCT. Only Ag^+ and Cu^+ (of the species tested) were well extracted with 4′-PicNHBz-TTCP ($E > 99\%$). Bivalent class *b* ions such as Hg^{2+}, Cd^{2+} and Pd^{2+} were not extracted at all, although they are well extracted with TTCT. 4′-PicNHBz-TTCP, which has only one dissociable proton, will form intramolecular ion-pair metal complexes only with univalent class *b* metals.

Absorption spectra of 4′-PicNHBz-TTCP

The ultraviolet and visible absorption spectra of $5 \times 10^{-5}M$ 4′-PicNHBz-TTCP in 50% v/v

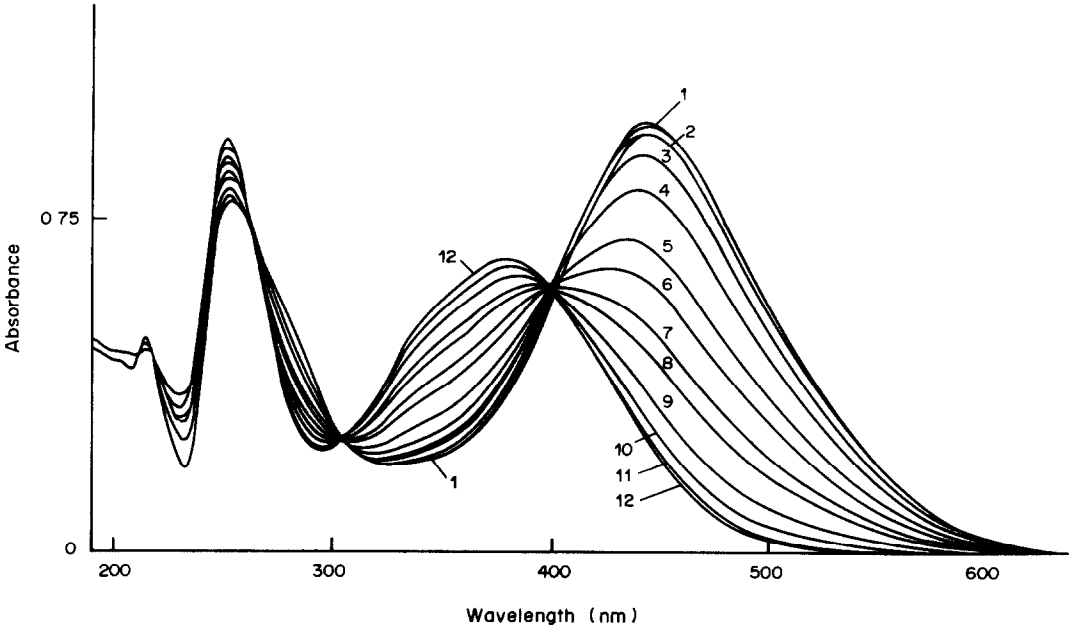

Fig. 1. Absorption spectra of 4′-PicNHBz-TTCP in 50% v/v dioxan–water mixture. Concentration of 4′-PicNHBz-TTCP: $5 \times 10^{-5}M$, pH: 1—11.10, 10.72; 2—10.33, 10.10, 9.86; 3—9.64; 4—9.46; 5—9.20; 6—8.96; 7—8.72; 8—8.50; 9—8.27; 10—8.01; 11—7.42; 12—5.50; 4.75—4.35, 4.30.

dioxan–water mixture in the pH range 4.0–11.0 are shown in Fig. 1. In acidic media (pH 4.3), absorption maxima appear at 253 and 380 nm. The absorption maximum at 380 nm decreases with increase in pH and a new absorption maximum appears at 445 nm. In alkaline media (pH > 11.0), absorption maxima exist at 253 and 445 nm. The absorption maximum at 253 nm exists in both acidic and alkaline media, although it becomes less intense in alkaline media. Three isobestic points are found, at 264, 308 and 400 nm. These changes in the electronic absorption spectra on change of pH indicate the existence of the acidic form, HL and basic form, L^-, due to the acid dissociation equilibrium of the amino group in 4′-PicNHBz-TTCP.

Acid dissociation constant of 4′-PicNHBz-TTCP

It was necessary to evaluate the dissociation constant of 4′-PicNHBz-TTCP in order to select the optimum pH for extraction of univalent class *b* metals, and to determine the effect of complexation on the apparent (conditional) dissociation constant.

The acid dissociation constant was determined spectrophotometrically, in 50% v/v dioxan–water mixture, and the effect of Ag^+ on pK_a was also examined. The results are shown in Table 2. In general, the proton of a secondary amine is difficult to dissociate. The inductive effect of the nitro groups on the picrylamino group results in a pK_a value of 9.74. This value is decreased in the presence of silver, reaching a practically constant value of 8.8 when the $[Ag^+]/[HL]$ ratio is $\geqslant 1.0$.

Table 2. Acid dissociation constants of 4′-PicNHBz-TTCP (HL) in 50% v/v dioxan–water mixture

[HL], M	[Silver], M	Mole ratio, HL:Ag	pK_a
5×10^{-5}	0	1:0	9.70
5×10^{-5}	1.66×10^{-5}	3:1	9.20
5×10^{-5}	3.33×10^{-5}	3:2	8.76
5×10^{-5}	5.00×10^{-5}	1:1	8.57
5×10^{-5}	1.00×10^{-4}	1:2	8.55
5×10^{-5}	2.00×10^{-4}	1:4	8.5

Liquid–liquid extraction behaviour of silver and copper(I)

The absorption spectra of the reagent and its silver and copper(I) complexes in 1,2-dichloroethane medium are shown in Fig. 2. The absorption band of HL has its maximum at 380 nm ($\varepsilon_{HL} = 1.40 \times 10^4$ l.mole^{-1}.cm^{-1}) and is almost the same as that in 50% dioxan–water medium. The absorption maxima of the extracted silver and copper(I) species are at 450 nm ($\varepsilon_{M+L^-} = 2.30 \times 10^4$ l.mole^{-1}.cm^{-1}).

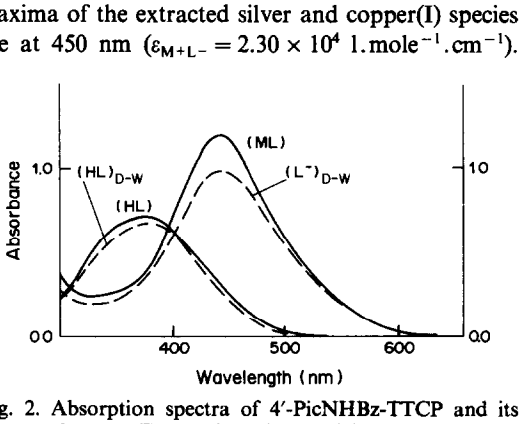

Fig. 2. Absorption spectra of 4′-PicNHBz-TTCP and its silver and copper(I) complexes in 1,2-dichloroethane. Concentration of 4′-PicNHBz-TTCP: $5 \times 10^{-5}M$. Dashed lines: HL and L^- species in 50% v/v dioxan–water mixture.

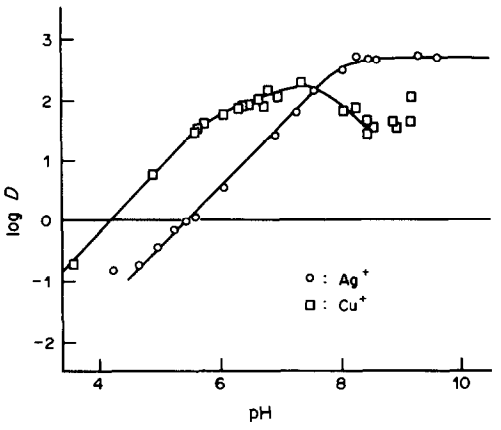

Fig. 3. Plots of log D *vs.* pH. Initial concentration of silver and copper(I): $5 \times 10^{-5}M$. Concentration of 4′-PicNHBz-TTCP in 1,2-dichloroethane: $2.5 \times 10^{-3}M$.

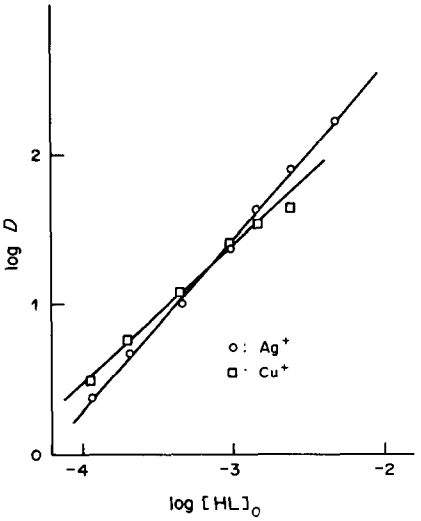

Fig. 4. Plots of log D *vs.* log $[HL]_o$ at pH 7.5 for silver and pH 6.2 for copper(I). Concentration of silver and copper(I): $5 \times 10^{-5}M$.

The absorption spectra of the two complexes are identical and very similar to the spectrum of the anion of the reagent, L^-, in 50% dioxan–water mixture. These facts seem to indicate that the deprotonated amino group in the reagent does not bond with silver or copper(I) but provides internal charge-compensation to form an intramolecular ion-pair in which the silver or copper(I) is co-ordinated with sulphur atoms of the macrocyclic polythioether.

If a univalent class *b* metal ion M^+ reacts with HL, the extraction equilibrium is generally represented by the equation

$$M^+ + nHL_0 \rightleftharpoons M^+L^-(HL)_{(n-1)_o} + H^+ \qquad (1)$$

The extraction constant is given by

$$K_{ex} = \frac{[M^+L^-(HL)_{(n-1)}]_o[H^+]}{[M^+][HL]_o^n} \qquad (2)$$

The distribution constants for the complex and reagent are $K_{Dc} = [M^+L^-]_o/[M^+L^-]$ and $K_{DR} = [HL]_o/[HL]$ respectively, and the formation constant for the complex and the adduct are $K_f = [M^+L^-]/[M^+][L^-]$ and $K_{add} = [M^+L^-(ML)_{n-1}]/[M^+L^-]_o[HL]_o^{n-1}$ respectively. The extraction constant can be written as

$$K_{ex} = K_a K_f K_{add} K_{Dc}/K_{DR} \qquad (3)$$

The distribution ratio of the metal ion is given by

$$D = \frac{[M^+L^-(HL)_{(n-1)}]_o}{[M^+] + [M^+L^-] + [MHL^+]} \qquad (4)$$

As the aqueous phase is completely colourless, the concentrations of the metal complexes M^+L^- and MHL^+ in the aqueous phase must be negligibly small, and the relationship between the distribution ratio, D, and the extraction constant, K_{ex}, therefore gives the logarithmic expression

$$\log D = \log K_{ex} + n \log[HL]_o + \mathrm{pH} \qquad (5)$$

Plots of the logarithmic distribution ratio for silver and copper(I) *vs.* the pH of the aqueous phase are shown in Fig. 3. A linear section with a slope of +1 was obtained for both silver and copper(I), as expected from equation (5).

For extraction of silver, log D becomes constant at pH > 8, but log D for copper(I) becomes maximal at pH ~ 7.5 then decreases at higher pH. Such decreases in log D on the alkaline side may be attributed to the formation of hydroxo-complexes of copper(I). As seen in Fig. 3, copper(I) is extracted at lower pH than silver. The values of $pH_{1/2}$ (pH at log $D = 0$) are 5.5 for silver and 4.2 for copper(I). The values of the parameter α,[10] representing the softness of the metals, are 3.9 for copper(I) and 3.6 for silver, as shown in Table 1. It would be expected that the affinity for a polythioether (*i.e.*, the bonding to the sulphur atoms of the polythioether), would be stronger for copper(I) than for silver. Consequently, formation of the copper(I) complex cation with the polythioether will facilitate dissociation of the proton on the amino group more readily than formation of the silver complex does.

Plots of the logarithmic distribution ratio of copper(I) and silver *vs.* the logarithm of the ligand concentration in the organic phase at constant pH [7.5 for silver and 6.2 for copper(I)] are shown in Fig. 4. Straight lines with slopes of 1.1 and 0.97 were obtained for silver and copper(I) respectively. Putting $n = 1$ in equation (5) yields

$$M^+ + HL_{(o)} \rightleftharpoons M^+L^-_{(o)} + H^+ \qquad (6)$$

and shows that silver and copper(I) form the (1:1 complex M^+L^- without formation of an adduct.

Effect of masking agents on extraction of silver

The univalent class *b* metal ions, silver and copper(I), were completely extracted with 4′-PicNHBz-TTCP into 1,2-dichloroethane from aqueous solution at pH > 8.0. At such a pH, many

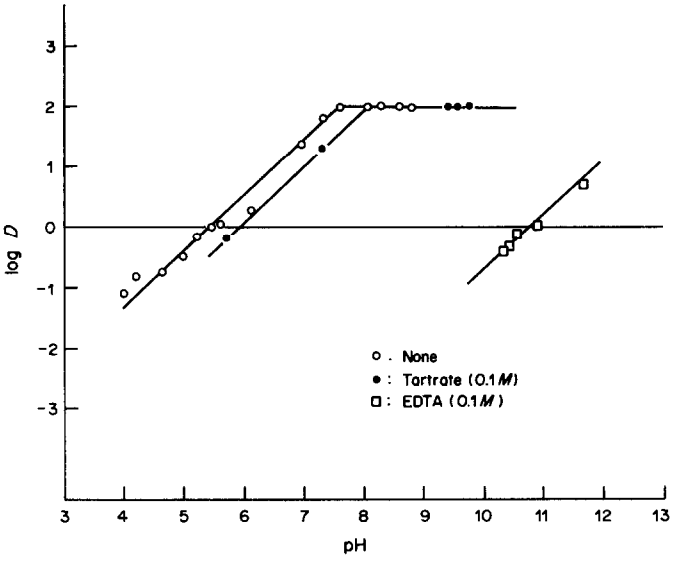

Fig. 5. Plots of log D *vs.* pH. Initial concentration of silver $5 \times 10^{-5}M$; —○—: no masking agent, —□—: $0.1M$ EDTA, —●— $0.1M$ tartrate.

Table 3. Effects of diverse ions

Ion	Concentration, M	pH	Absorbance at 500 nm	E, %
None	—	9.60	0.588	100.0
Mn^{2+}	1.0×10^{-2}	9.63	0.570	96.7
Co^{2+}	1.0×10^{-2}	8.80	0.592	100.7
Ni^{2+}	1.0×10^{-2}	8.83	0.590	100.3
Cu^{2+}	1.0×10^{-2}	8.56	0.590	100.3
Zn^{2+}	1.0×10^{-2}	9.32	0.595	101.2
Cd^{2+}	1.0×10^{-2}	9.30	0.584	99.3
Fe^{3+}	1.0×10^{-2}	9.63	0.586	99.7

Concentration of silver: $5 \times 10^{-5}M$.

foreign transition metal ions will precipitate as their hydroxides, and interfere in the extraction of silver and copper(I). Consequently, if large amounts of foreign transion metals are present, they must be masked by a suitable complexing agent. Hence, the effects of EDTA and tartrate on the extraction of silver were examined. The results are shown in Fig. 5. The presence of 0.1M EDTA shifts the extraction curve by about 5 pH units ($pH_{1/2} = 10.8$). This pH effect may be due to formation of the silver–EDTA complex, with an accompanying decrease in the free silver ion concentration, though it is difficult to see why, since the silver–EDTA complex has maximum stability at about this pH, but lower stability as the pH is decreased. On the other hand, $0.1M$ tartrate does not produce so large an effect on the extraction curve for silver ($pH_{1/2} = 5.8$), so $0.1M$ tartrate will serve as a suitable masking agent.

Effect of foreign ions on extraction of silver

The interference from Mn(II), Co(II), Ni(II), Cu(II), Zn(II), Cd(II) and Fe(III) in presence of $0.1M$ tartrate as masking agent was examined, with a shaking time of 5 min for extraction of silver. The results are shown in Table 3. Co^{2+}, Ni^{2+}, Cu^{2+}, Zn^{2+}, Cd^{2+} and Fe^{3+} in a 200-fold amount relative to silver do not interfere, and Mn^{2+} decreases the absorbance by only 3.1%. A $5 \times 10^{-5}M$ silver solution containing Mn^{2+}, Co^{2+}, Ni^{2+}, Cu^{2+}, Zn^{2+}, Cd^{2+} and Fe^{3+}, each at $1 \times 10^{-2}M$ concentration, was successfully analysed, with $0.1M$ tartrate as masking agent, the silver recovery being 98.6%.

REFERENCES

1. W. Rosen and D. H. Bush, *J. Am. Chem. Soc.*, 1969, **91**, 4694.
2. K. Saito, Y. Masuda and E. Sekido, *Anal. Chim. Acta*, 1983, **151**, 447.
3. *Idem, Bull. Chem. Soc. Japan*, 1984, **57**, 189.
4. H. Nakamura, M. Takagi and K. Ueno, *Talanta*, 1979, **26**, 921.
5. *Idem, Anal. Chem.*, 1980, **52**, 1668.
6. G. E. Pacey and B. P. Bubnis, *Anal. Lett.*, 1980, **13**, 1085.
7. *Idem, Analyst*, 1981, **106**, 636.
8. K. Travis and D. H. Bush, *Inorg. Chem.*, 1974, **11**, 2591.
9. E. G. Kleinschmidt and H. Braeuniger, *Pharmazie*, 1969, **24**, 31.
10. S. Yamada and M. Tanaka, *J. Inorg. Nucl. Chem.*, 1975, **37**, 587.

Talanta, Vol. 32, No. 8B, pp. 803–806, 1985
Printed in Great Britain.

0039-9140/85 $3.00 + 0.00

LIQUID CHROMATOGRAPHIC SEPARATION OF METALS BY ON-COLUMN CHELATION WITH 4-(2-PYRIDYLAZO) RESORCINOL

JAMES E. DINUNZIO, ROBERT W. YOST and EMORY K. HUTCHISON
Department of Chemistry, Wright State University, Dayton, Ohio 45435, U.S.A.

(*Received* 21 *November* 1984. *Accepted* 28 *February* 1985)

Summary—A method for the separation of trace levels of Zn(II), Fe(II), Ni(II) and Co(II) by on-column formation of their complexes with 4-(2-pyridylazo)resorcinol and subsequent separation of the complexes by reversed-phase liquid chromatography is described. Either acidic or buffered mobile phases can be used. For the separation using acidic mobile phases the role of the mobile-phase pH, concentration of PAR, and type of stationary phase is described. For buffered (slightly acidic) mobile phases it is shown that the complexing ability of the buffer can be used to influence the separation. Data on the use of this system for quantitative analysis are included.

In recent years ion-chromatography[1–3] has proven to be a convenient means of separating metals at trace levels. However, the separation of metals as metal chelates is a technique which offers some potential advantages. Reversed-phase systems generally perform with higher efficiency than ion-exchange systems. Because of the improved efficiency offered by the reversed-phase separation of metal chelates it may be possible to achieve otherwise difficult separations. Furthermore, the use of chelating agents that give high sensitivity for the determination of metals should result in good sensitivity for the separation of metal chelates. For these reasons the separation of metals as chelates has received modest but steady attention.

An extensive review on the high-pressure liquid chromatography of metal chelates has recently been published,[4] covering the separation of metal chelates with β-diketones, β-ketoamines, thiosemicarbazones, thiobenzohydrazones, hydrazones, dithizone, dithiocarbamates, 8-hydroxyquinolines, bipyridyl, 1,10-phenanthroline, crown ethers, macrocyclic amines, porphyrins and organophosphorus complexes, and both normal phase and reversed-phase separations.

One reagent which possess characteristics which make it attractive as a chelating agent in metal analysis is 4-(2-pyridylazo)resorcinol (PAR). PAR is water-soluble and forms soluble chelates with a large number of metals.[5] PAR chelates have high molar absorptivity, which makes it possible to determine them at very low concentrations. The chelation of metals by PAR is rapid and the stability constants are large,[6] but very little work has been reported[7,8] on the use of PAR as a chelating agent for the separation of metals. This paper reports on the use of PAR as an on-column chelating agent for the separation of metals by reversed-phase high-pressure liquid chromatography (HPLC).

EXPERIMENTAL

Apparatus

An Altex Model 420 liquid chromatograph (Altex Scientific Inc., Berkeley, CA) with a Schoeffel Instruments Spectroflow Monitor SF770 variable-wavelength detector (Schoeffel Instruments Corp., Westwood, NJ) and a Waters Model M-6000 pump with a Model UK-6 injector (Waters Associates, Milford, MA) were used to obtain chromatograms of the metal complexes. A Hewlett-Packard Model 7101B strip-chart recorder (Hewlett-Packard, Avondale, PA) was used to record the chromatograms. A 25-cm, 5-μm Alltech C-18 and C-8 column (Alltech Inc., Deerfield, IL) and a 15-cm, 5 μm Chromega C-2 column (ES Industries, Marlton, NJ) were used to separate the metals. A Whatman 37-μm ODS guard column (Whatman Inc., Clifton, NJ) was used with the C-18 column.

Reagents

HPLC grade methanol (Fisher Scientific) was used to prepare the mobile phase. Phosphate, acetate and tartrate buffers were passed through a glass column packed with Chelex 100 (100–200 mesh) to remove traces of metals. All other reagents were analytical-reagent grade and used as received. All solutions were prepared from doubly-distilled demineralized water and filtered through 0.5-μm membranes before use.

Procedure

Chromatograms were obtained at ambient temperature in the usual manner. The column was conditioned by pumping the mobile phase containing PAR until a stable base line was recorded. Samples were directly injected into the mobile phase. Sample volumes were 20 μl in all cases. In general, mobile phases were buffered with a single buffer system (bisulphate, acetate, tartrate or phosphate). For some experiments bisulphate–acetate mixed buffers were used. These were prepared by mixing the appropriate amount of 1*M* pH-5 acetate buffer with a known volume of 1*M* pH-2.4 bisulphate buffer to obtain the desired pH. The samples consisted of trace levels of metals in demineralized water. The metal–PAR complexes were monitored at 525 nm unless otherwise stated. The chromatographic system was rinsed with methanol at the end of each experiment and stored filled with methanol when not in use.

RESULTS AND DISCUSSION

This study investigated the reversed-phase separation of metals chelates on silica-based bonded-phase columns. Use of these phases is limited to the pH range between 2 and 8.[9] Over this range metals form either 1:1 or 1:2 metal:PAR complexes. Many more metals form PAR complexes at pH > 4 than at pH < 4. The separation of metals as PAR complexes was investigated for both pH regions.

Separations performed in the pH range 2–4 are characterized by good analytical selectivity, because few metals form PAR complexes under acidic conditions. Also, these metal complexes have shorter retention times. Figure 1 shows the effect of pH (<4) on the retention of the Zn(II), Fe(II), Ni(II) and Co(II) complexes. Two different types of behaviour are evident. For Fe(II) and Ni(II) the capacity factor is independent of mobile-phase pH. For Co(II) and Zn(II) the capacity factor increases as the pH increases.

These data seem related to the type of complex formed. All four metals form 1:2 complexes with PAR, but the cobalt complex is positively charged owing to the formation of Co(III).[8,10,11] This makes it much more polar than the uncharged cobalt complex, so it should be less easily retained than the uncharged complex by the non-polar stationary phase. When the pH of the mobile phase is increased, the $Co(III)(PAR)^+$ complex can be converted into uncharged Co(III)(PAR), which will be retained more strongly. This would explain the observed increases in retention for cobalt with increase in pH.

The behaviour of the zinc complex is due to the comparatively low stability constant ($\log \beta_2 = 19$). Although zinc chelates are usually more stable than the corresponding iron(II) chelates (Irving–Williams order[12]), this is not always the case, because iron(II) complexes can be stabilized by formation of a low-spin complex.[13] This effect has been observed indirectly in studies involving PAR[14] and other similar ligands.[15] The increased retention of zinc with increase in pH (Fig. 1) is due to an increase in the degree of formation of the neutral PAR complex, since the conditional stability constant[16] will increase as the pH of the mobile phase increases.

A second factor which was found to be important for the separation of metals as PAR complexes was the concentration of PAR in the mobile phase. Figure 2 shows the effect of PAR concentration on the retention of the metals studied. For Zn(II), Fe(II) and Ni(II) the capacity factor increases as the concentration of PAR in the mobile phase increases. This is consistent with an increased degree of formation of the 1:2 complexes in accordance with the law of mass action. When there is an excess of metal ion the charged 1:1 complexes will be formed,[5] which will be relatively poorly retained. Since the only difference

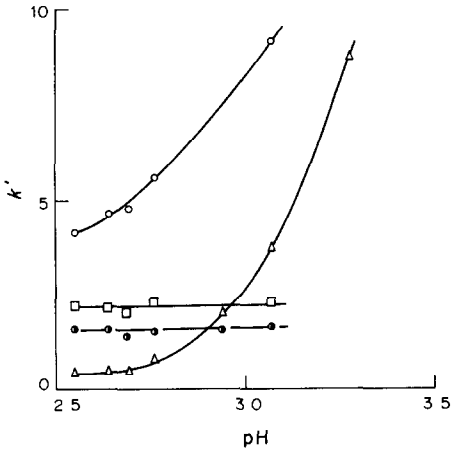

Fig. 1. Effect of pH on retention of metal–PAR complexes. Mobile phase methanol–0.01*M* bisulphate–acetate buffer mixture (55:45 v/v), PAR concentration $1.0 \times 10^{-4}M$ Co(II), ○; Zn (II) △; Ni(II) □; Fe(II) ◑.

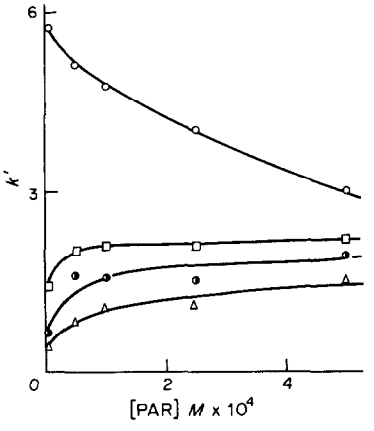

Fig. 2. Influence of the concentration of PAR on the retention of metal–PAR complexes. Mobile phase methanol–pH-2.54 0.01*M* bisulphate buffer (55:45 v/v). Symbols same as for Fig. 1.

Table 1. Chromatographic data from use of different non-polar stationary phases (mobile phase as for Fig. 3)

	Stationary phase					
	C-18		C-8		C-2	
Metal	k'	HEPT, *mm*	k'	HETP, *mm*	k'	HETP, *mm*
Zn	0.88	2.14	0.59	2.87	0.29	1.80
Fe	3.56	0.10	5.96	0.07	3.23	0.11
Ni	5.98	0.10	9.01	0.19	4.33	0.22
Co	11.56	0.76	2.13	0.12	1.75	0.40

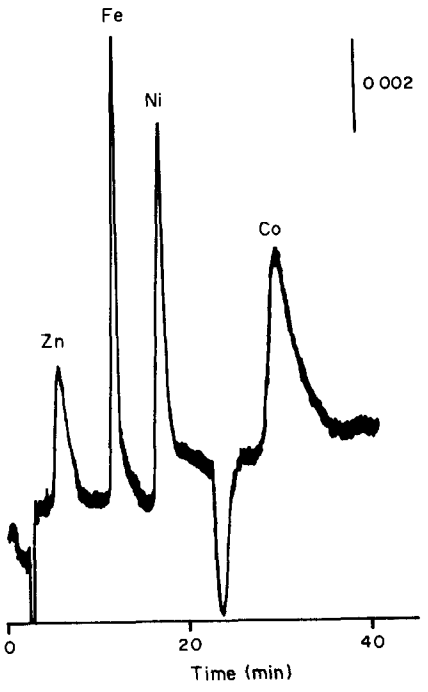

Fig. 3. Separation of metals with an acidic mobile phase on a C-18 column. Mobile phase methanol–pH-2.54 0.01*M* bisulphate buffer (52:48 v/v). PAR concentration $5 \times 10^{-4}M$. Flow-rate 1.0 ml/min. Detector setting 525 nm. Zn(II) 80 ng; Fe(II) 10 ng; Ni(II) 20 ng; Co(II) 40 ng.

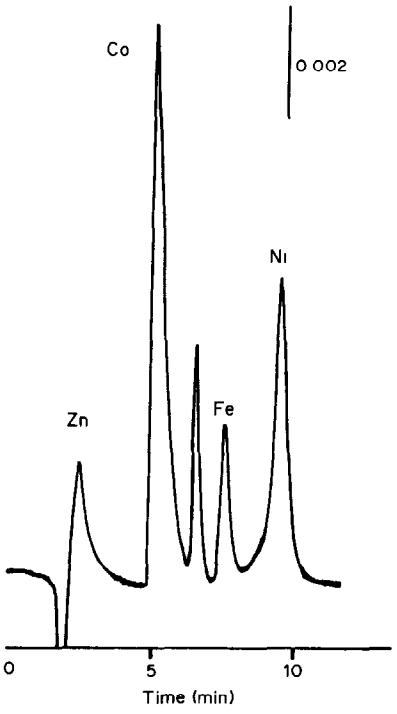

Fig. 4. Separation of metals with an acidic mobile phase on a C-2 column. Detector setting 546 nm. Zn(II) 24 ng; Co(II) 12 ng; Fe(II) 21 ng; Ni(II) 7 ng. Other conditions as for Fig. 3.

between these three complexes is in their stability, they should behave in a similar manner, as observed.

For Co(II) the retention decreases as the PAR concentration increases. This cannot be explained at present, but could be due to increase in degree of complexation and hence of degree of oxidation to the less strongly retained charged Co(III) complex.

Table 1 shows the data obtained for the separation of test metals under identical conditions but on different stationary phases. The most interesting aspect of this is the change in elution order with different stationary phases. Cobalt is eluted last from the C-18 column and second from the C-8 and C-2 columns. There is also a marked improvement in the theoretical plate height for cobalt when it comes earlier in the elution order.

The change in elution order and efficiency with different stationary phases may indicate differences in the separation mechanism of the metals on the different phases. It is important to note that the elution order of the metals on the C-8 and C-2 columns parallels the order of stability of the metal complexes.[6,10,14,15] This would support the idea that the separation is controlled mainly by the degree of formation of the metal complex. The unexpectedly long retention time for cobalt on the C-18 column indicates that some other factor also contributes to the retention process. Two possibilities are increased retention due to poor mass transfer of the Co–PAR complex in the C-18 bonded phase, and adsorption on the residual silanol sites on the column.

Figures 3 and 4 show chromatograms obtained for the separation of trace levels of Zn(II), Fe(II), Ni(II)

Table 2. Effect of buffer on the capacity factor

Metal	Acetate	Tartrate
Fe	5.10	2.45
Ni	6.25	3.40

Separation performed on a C-18 column, mobile phase as for Fig. 5.

Table 3. Calibration data for trace analysis (mobile phase and column as for Fig. 3)

Metal	Slope	Intercept	*r*	RSD, %	Abs. det. limit, ng*
Zn	0.37	0.23	0.996	7	20
Fe	1.91	12.3	0.997	7	1
Ni	3.01	5.4	0.993	5	2
Co	2.38	42.6	0.995	9	8

*Estimated for a signal/noise ratio of 2.

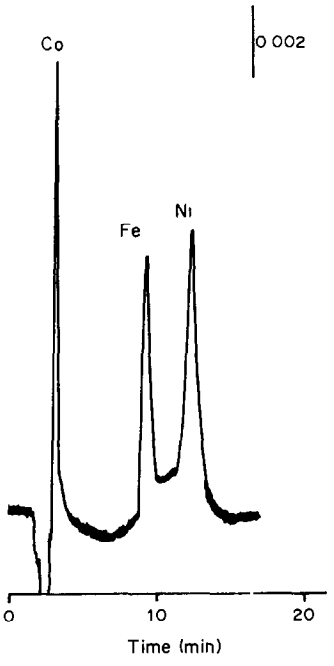

Fig. 5. Separation of metals with a slightly acidic mobile phase on a C-18 column. Mobile phase methanol–pH-5 0.01*M* acetate buffer. (50:50 v/v). PAR concentration $1.0 \times 10^{-4}M$. Flow-rate 1.0 ml/min. Detector setting 525 nm. Co(II) 1.2 ng; Fe(II) 4 ng; Ni(II) 8 ng.

and Co(II), on the C-18 and C-2 columns respectively, with an acidic mobile phase. The short-chain stationary phases, which can produce similar chromatograms, give good separations with short analysis times and good sensitivity.

Separations of metal–PAR complexes by use of a slightly acidic mobile phase (pH > 4) are characterized by low analytical selectivity since many metals form complexes, but high chromatographic selectivity since many of the complexes are strongly retained in this pH range. Figure 5 shows the separation of Co(II), Fe(II) and Ni(II) by use of a pH-5 acetate buffer.

In the slightly acidic pH range it is possible to use complexing buffers not only to control pH, but also to influence the separation through competition with PAR for the metal. This is not possible with acidic mobile phases because the acidity will prevent complex formation between the metal and the buffering anion unless the stability is very high. This is not usually the case for the most common buffer systems.

Table 2 shows a comparison of the influence of acetate and tartrate buffers on the capacity factors for Fe(II) and Ni(II) at pH 5. The tartrate buffer system, which is capable of forming complexes with transition metals, reduces the retention of both metals. Unfortunately, tartrate also lowers the efficiency of the system. The number of theoretical plates for the separation of Fe(II) and Ni(II) decreases by about 30% on changing from the acetate to the tartrate buffer.

On-column chelation of metals with PAR is suitable for trace analysis. Table 3 shows the linear regression data, relative precision and estimated detection limits for the test metals. Linear calibration curves over at least one order of magnitude were obtained.

Separation of trace levels of Zn(II), Fe(II), Ni(II) and Co(II) is possible by using on-column chelation with 4-(2-pyridylazo)resorcinol and reversed-phase chromatography. The most important factors to consider are the mobile-phase pH and the type of stationary phase. The ability to control the elution order of the metals by proper selection of either could be advantageous in some situations.

REFERENCES

1. H. Small, T. Stevens and W. Bauman, *Anal. Chem.*, 1975, **47**, 1801.
2. J. S. Fritz, *Ion Chromatography*, Hüthig, Heidelberg, 1982.
3. J. E. DiNunzio and M. Jubara, *Anal. Chem.*, 1983, **55**, 1013.
4. J. W. O'Laughlin, *J. Liq. Chromatog.*, 1984, **7**, 127.
5. E. B. Sandell and H. Onishi, *Photometric Determination of Traces of Metals*, Wiley, New York, 1978.
6. E. Bishop, *Indicators*, p. 293. Pergamon Press, Oxford, 1972.
7. D. Roston, *Anal. Chem.*, 1984, **56**, 241.
8. H. Hoshino, T. Yotsuyanagi and K. Aomura, *Bunseki Kagaku*, 1978, **27**, 315.
9. B. A. Bidlingmeyer, *J. Chromatog. Sci.*, 1980, **18**, 525.
10. A. Corsini, I. Yih, Q. Fernando and H. Freiser, *Anal. Chem.*, 1962, **34**, 1090.
11. A. Corsini, Q. Fernando and H. Freiser, *Inorg. Chem.*, 1963, **2**, 224.
12. H. Irving and R. J. P. Williams, *J. Chem. Soc.*, 1953, 3192.
13. C. S. G. Phillips and R. J. P. Williams, *Inorganic Chemistry*, Vol. 2. pp. 312–315. Clarendon Press, Oxford, 1966.
14. T. Yotsuyanagi, R. Yamashita and K. Aomura, *Anal. Chem.*, 1972, **44**, 1091.
15. R. G. Anderson and G. Nickless, *Anal. Chim. Acta.*, 1967, **39**, 469.
16. A. Ringbom, *Complexation in Analytical Chemistry*, Wiley-Interscience, New York, 1963.

Talanta, Vol. 32, No. 8B, pp. 807–810, 1985
Printed in Great Britain.

0039-9140/85 $3.00 + 0.00

DECONVOLUTION TECHNIQUES FOR RAPID FLOW-INJECTION ANALYSIS

JAMES T. DYKE and QUINTUS FERNANDO*
Department of Chemistry, University of Arizona, Tucson, Arizona 85721, U.S.A.

(*Received* 28 *May* 1984. *Accepted* 11 *January* 1985)

Summary—In the optimum configuration of any flow-injection analysis system there is a maximum experimentally attainable sampling rate. Any attempt to increase this sampling rate will result in overlapping output peaks. Use of deconvolution techniques to separate the overlapping peaks allows the sampling rate to be increased. Fourier-transform deconvolution and an iterative curve-fitting deconvolution technique have been compared with simulated as well as experimental data. It has been shown that the iterative curve-fitting technique is less sensitive than the Fourier-transform deconvolution to random noise.

Unsegmented continuous-flow analysis or flow-injection analysis, FIA,[1] is an established analytical technique in many clinical and environmental laboratories in which large numbers of samples have to be analysed daily. The major advantage of FIA is that small sample volumes (μl) can be analysed with a minimum expenditure of time and reagents. The procedure involves the injection or "intercalation"[2] of a small sample volume into a flowing carrier stream. The sample and carrier streams mix and a chemical reaction occurs between the components of the sample and carrier streams. Usually, one of the products formed in this chemical reaction is monitored with a detector located downstream. The mixing that occurs results in an increase in the sample volume[3] and consequently a broadening of the output peak. In conventional applications of FIA the sampling rate is limited by the requirement that successive output peaks should not overlap. If this maximum sampling rate is exceeded, the peak broadening will give rise to overlapping output peaks. The information contained in the overlapping peaks can be retrieved by using deconvolution techniques that mathematically remove the effect of peak broadening. The objective of this work was to develop a methodology for deconvolution of overlapping peaks obtained in FIA systems with rapid sampling, and to examine the factors that affect the accuracy and reproducibility of the results obtained by deconvolution. The FIA system was assembled from components available in our laboratory and the system is therefore not optimized for this investigation. As a consequence, the reproducibilities reported are probably poorer than the optimum values.

THEORY

The successive injection of a series of sample volumes into a flowing carrier stream results in the introduction of a corresponding series of narrow sample plugs into the carrier stream. A combination of the injection rate and the sample concentrations constitutes the input function of the FIA system. The narrow sample plugs become broadened, for a variety of reasons, while they are being carried towards a detector and this broadening is the response function of the FIA system. The detector response, therefore, is the convolution of the input function with the response function (Fig. 1). The requirement that successive sample volumes do not mix with each other during their journey to the detector sets an upper limit on the rate at which the samples can be injected into the carrier stream. This upper limit can be calculated from the width of the response function.

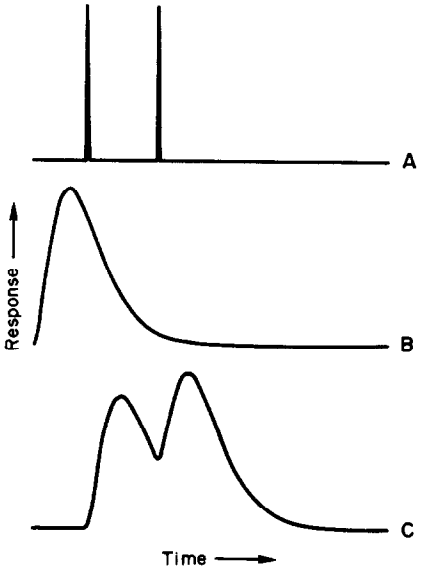

Fig. 1. Convolution of the input function with the response function in an FIA system. A, input function; B, response function; C, convolution of A and B to give the FIA output function.

*Author for correspondence.

If the peak broadening (the response function) can be deconvoluted from the output (the detector response), the rate of injection can be increased considerably and be limited only by the mechanical methods available for injection or intercalation of sample volumes in rapid succession into a carrier stream. Useful analytical data can be obtained, however, only if the output can be successfully analysed mathematically.

The feasibility of deconvoluting the response function from the output was examined first with a set of simulated data generated for this purpose. Several investigators have proposed various models and mathematical functions to explain the effect of dispersion on peak profiles in FIA systems.[4,5] In this work an empirical mathematical function that describes the peak profile obtained in an FIA system[1] was used to represent the response function of the system. The concentration at the detector, $C(t)$, when time t has elapsed after the initial injection, is represented by:

$$C(t) = \frac{1}{T}\left(\frac{t}{T}\right)^{N-1} \frac{1}{(N-1)!} e^{-t/T}$$

where T and N are constants.

The simulated data were generated for $N = 3$ and $T = 10$ and values of $C(t)$ were calculated for 1-sec time intervals. Simulated output data sets were generated by convoluting this response function with input functions representing two discrete injections of equal analyte concentration. The input function is $Y(t) = C_0$, where C_0 is the initial sample concentration for every value of t at which an injection is made; for all other values of t, $Y(t) = 0$. A 50-sec separation between the two injections was chosen to give convolution results that showed a significant overlap of the adjacent output peaks. The convolution can be expressed as con(τ), the time-averaged or integrated product of the input function, $Y(t)$, and the response function $C(t)$, where τ is the relative displacement.[6]

$$\text{con}(\tau) = \lim_{T\to\infty} \frac{1}{2T} \int_{-T}^{T} Y(t)C(-t \pm \tau)dt$$

A Fourier-transform deconvolution and an iterative convolution curve-fitting technique[4] were the two methods investigated for deconvoluting the response function from the output. The Fourier-transform deconvolution was performed by first taking the Fourier transforms of the response function and the output function and dividing the second by the first. The inverse transform of the resulting function then represented the original input function.[7] In the iterative convolution curve-fitting method, a trial input function was convoluted with the response function. The results of the convolution were compared with the original data and the goodness of fit was evaluated by a chi-squared test. The parameters of the trial input function (time of injection and sample concentration), were then iteratively adjusted until a minimum value for χ^2 was obtained.[8] The application of these deconvolution techniques should yield, in principle, an input function that represents two discrete injections of equal concentrations (or the corresponding peak heights). The variables investigated in this work were the effect of random noise and variation of the signal:noise ratio (from 20 to 2000) on the applicability of the two deconvolution techniques. The effect of the signal:noise ratio was determined by comparing the relative difference between the peak height, [peak height (1) − peak height (2)]/(average peak height), for the two injections, obtained after deconvolution by the Fourier transform and by the iterative convolution curve-fitting technique (Fig. 2). The results suggest that although the Fourier-transform deconvolution may provide better results at high signal:noise ratios, the iterative method is much less sensitive to noise when the time intervals between sample injections are relatively long.

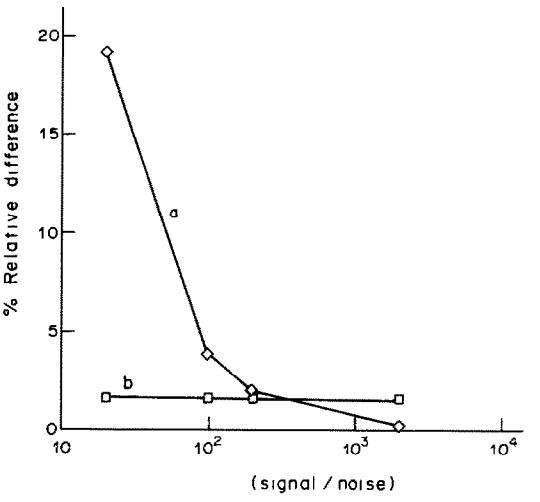

Fig. 2. Effect of signal:noise ratio on deconvolutions: a, Fourier-transform deconvolution; b, convolution curve-fitting.

These initial calculations with simulated data have shown that it is feasible, within certain limitations, to deconvolute an FIA output consisting of overlapping peaks. The next phase of this work was designed to identify the experimental variables in the FIA system that cause random noise and decreased signal:noise in the output, and therefore tend to invalidate the deconvolution technique selected.

EXPERIMENTAL

Instrumentation

The FIA system shown in Fig. 3 consisted of a Cole-Palmer "Masterflex" peristaltic pump (#7014), an Altex pneumatic injection valve with a sample loop (80 μl volume) and a mixing coil, 3 m in length and 0.8 mm in diameter, to

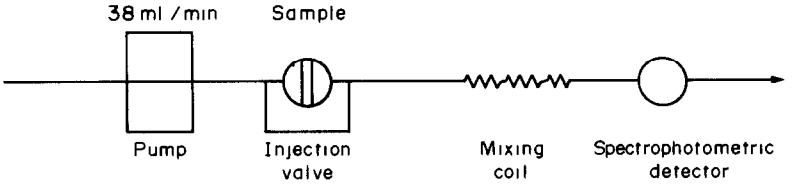

Fig. 3. Schematic representation of the FIA system used for the generation of overlapping peaks.

provide the dispersion normally encountered in FIA experiments. A Gilford 240 spectrophotometer fitted with a cylindrical flow-through cuvette with a capacity of 0.08 ml and 1-cm path length (NSG Precision Cells #513) was used as the detector. A flow-rate of 3.8 ml/min was used and the absorbance of the permanganate ion was monitored at 525 mm.

The data were collected and processed with the aid of a Digital Equipment Corporation LSI 11/02 microcomputer. The analogue output voltage from the Gilford spectrophotometer was digitized by a Data Translations 2781 analogue I/O system set at ± 1.0 V full scale. The DT2781 utilizes a 12-bit A/D converter with the 12th bit a sign bit. The D/A converter of the DT2781 was used to control the Altex injection valve.

RESULTS

Deconvolution of overlapping peaks

Several sets of experiments were performed in order to determine the practical limitations within which the overlapping peaks in the output could be deconvoluted. The simplest possible experimental conditions were selected for this initial study; the FIA system consisted of a single carrier stream into which was injected a species such as permanganate which absorbs in the visible region of the spectrum. This obviates the requirement for a chemical reaction between the injected sample and a component of the carrier stream, and thereby simplifies the system considerably.

In the first set of experiments, constant volume samples of a potassium permanganate solution ($\sim 4 \times 10^{-3} M$) were injected in rapid sequence into a flowing carrier stream of distilled water. The rate of sample injection was such that the absorbance of the carrier stream monitored by the detector at 525 nm as a function of time, *i.e.*, the output, consisted of a series of overlapping peaks. When a sample volume of 80 μl, a flow-rate of 3.8 ml/mm and a mixing coil 3 m long and 0.8 mm in diameter were used, the time between the first appearance of a peak and the return to within 1% of peak height from baseline was found to be 25 sec. A sample injection rate of one every 10 sec was used to provide a series of overlapping peaks as shown in Fig. 4A, in which the maximum peak height of each peak was influenced to a significant extent by the presence of adjacent peaks. A single injection of the permanganate solution into the carrier stream under these conditions gave an output (Fig. 4B) which was the response function of the system. This response function was used in the convolution curve-fitting method for a deconvolution of the overlapping peaks.

The composition of the carrier stream had a pronounced effect on the results obtained from the deconvolution. The height of the initial peak was always the lowest value in the set of peak heights. Some improvement in the overall precision of the results was achieved by the addition of an inert 1:1 electrolyte, such as potassium chloride, to the carrier stream. It was observed that the concentration of the electrolyte in the carrier stream could either increase or decrease the overall precision of the results. The best results, in which the peak height of the initial peak was not significantly lowered, were obtained when the concentration of the 1:1 electrolyte was slightly greater than that of the permanganate solution.

A second set of experiments was conducted to determine the effect of varying sample concentration

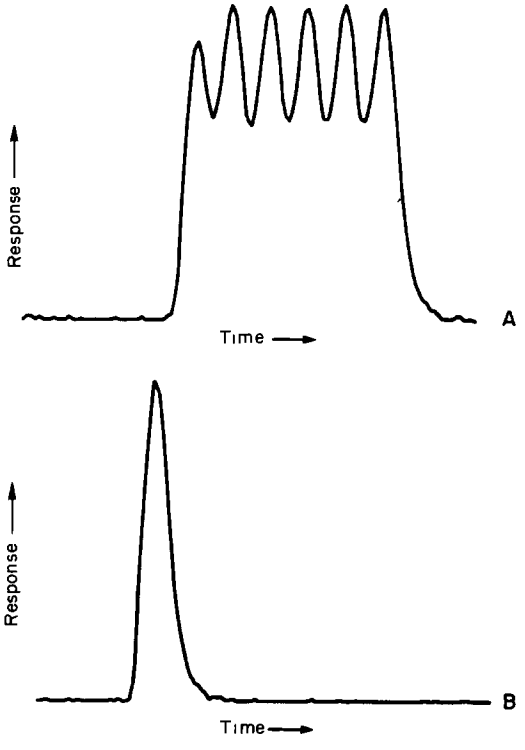

Fig. 4. Multiple overlapping peaks in the FIA output. A, output from six consecutive injections of the same concentration; B, response function obtained from a single injection.

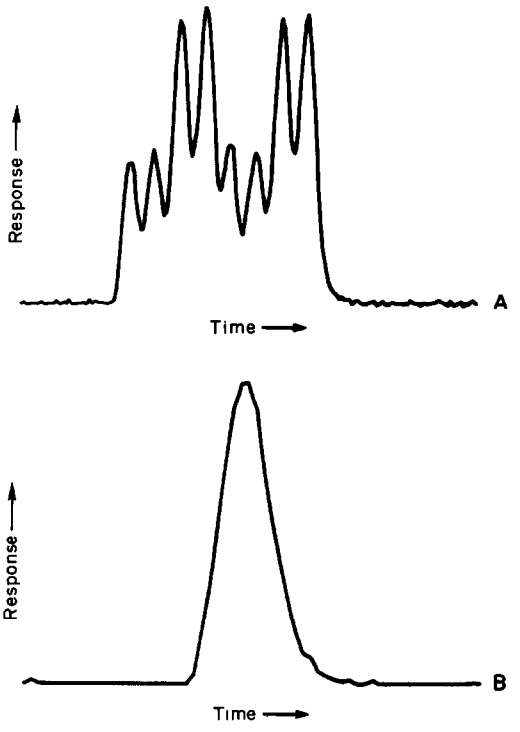

Fig. 5. Multiple overlapping FIA peaks obtained with different concentrations. A, output from consecutive injections of varying concentration; B, response function of the FIA system.

on the precision of the results obtained by the deconvolution technique. Pairs of alternately low ($2 \times 10^{-3}M$) and high ($4 \times 10^{-3}M$) concentrations of permanganate were injected into the carrier stream ($2.3 \times 10^{-3}M$ potassium chloride), and the resulting output is shown in Fig. 5A. The response function was obtained by injecting a single sample volume of the $4 \times 10^{-3}M$ permanganate solution into the carrier stream (Fig. 4B). The deconvolution of the output gave an average peak height ratio of 1.98 for the two concentrations of permanganate used in this experiment.

The effect of varying the sample injection rate on the precision of the peak heights obtained by the deconvolution technique was evaluated. When the interval between sample injections was 30 sec the output consisted of well-separated peaks under the experimental conditions described above. The relative standard deviation of the peak heights obtained by deconvolution increased perceptibly when the time interval between sample injections was decreased from 30 to 10 sec. When this time interval was decreased from 10 to 7 sec the standard deviation was quadrupled. Although the output consisted of multiple peaks that were readily apparent with sample injection every 7 sec, the number of experimental points was insufficient for acceptable results to be obtained by the deconvolution technique. This situation could be remedied, if necessary, by increasing the A/D sampling rate.

These results have demonstrated that rapid sampling with an FIA system in conjunction with an appropriate deconvolution technique is a useful addition to the methodology available for the study of the kinetics of moderately fast reactions. The method is especially useful for the automated sampling of the liquid phase in heterogeneous reaction systems in which the determination of initial rates is important.

REFERENCES

1. J. Růžička and E. H. Hansen, *Flow Injection Analysis*, Wiley, New York, 1981.
2. H. A. Mottola, *Anal. Chem.*, 1981, **53**, 1312A.
3. J. M. Reijn, W. E. Van Der Linden and H. Poppe, *Anal. Chim. Acta*, 1980, **114**, 105.
4. J. T. Vanderslice, K. K. Stewart, G. A. Rosenfeld and D. J. Higgs, *Talanta*, 1981, **28**, 11.
5. D. Betteridge, W. C. Cheng, E. L. Dagless, P. David, T. B. Goad, D. R. Deans, D. A. Newton and T. B. Pierce, *Analyst*, 1983, **108**, 17.
6. G. Horlick and G. M. Hieftje, *Contemporary Topics in Analytical and Clinical Chemistry*, Vol. 3, D. M. Hercules, G. M. Heiftje, L. R. Snyder and M. A. Evenson (eds.), Plenum Press, New York, 1978.
7. S. N. Chesler and S. P. Cram, *Anal. Chem.*, 1978, **45**, 1354.
8. P. R. Berington, *Data Reduction and Error Analysis for the Physical Sciences*, McGraw-Hill, New York, 1969.

Talanta, Vol. 32, No. 8B, pp. 811–815, 1985
Printed in Great Britain.

0039-9140/85 $3.00 + 0.00

REACTIONS OF NITROGEN BASES WITH NICKEL CHELATES OF DI-*o*-TOLYLCARBAZONE AND DI-*o*-TOLYLTHIOCARBAZONE

KUMAR S. MATH and T. SURESH
Department of Chemistry, Karnatak University, Dharwad-580 003, India

(*Received* 29 *October* 1984. *Revised* 16 *April* 1985. *Accepted* 7 *May* 1985)

Summary—The behaviour of nickel di-*o*-tolylcarbazonate and nickel di-*o*-tolylthiocarbazonate with organic nitrogen bases has been examined with a view to better understanding of the effect of different donor atoms in adduct formation. The adducts formed vary remarkably in composition and stability, and there are some interesting steric effects.

Nickel di-*o*-tolylcarbazonate, $Ni(OTC)_2$, is diamagnetic, in contrast to the nickel chelates of diphenylcarbazone, di-*m*-tolylcarbazone, and di-*p*-tolylcarbazone, which are paramagnetic.[1] The spectrum of $Ni(OTC)_2$ is remarkably different from the spectra of most other metal di-*o*-tolylcarbazonates, which closely resemble those of the nickel di-*o*-tolylcarbazonate adducts of phenanthroline or other nitrogen bases. This resembles the behaviour of nickel dithizonates towards nitrogen bases.[2] Much work has been done on the evaluation of factors such as ligand basicity, solvent, steric effects and metal chelate acidity in the study of adduct formation from metal chelates.[3–8] In this report, we give some results of a study of the adducts of nickel chelates of di-*o*-tolylcarbazone, $Ni(OTC)_2$ (**I**), and its sulphur analogue, di-*o*-tolylthiocarbazone, $Ni(OTTC)_2$ (**II**), with different nitrogen bases. The comparative study of adducts of $Ni(OTC)_2$ and $Ni(OTTC)_2$, both of which have square planar structures, may lead to a better understanding of the behaviour of different donor atoms in the formation of adducts.

EXPERIMENTAL

Apparatus

Absorption spectra were measured with a Bausch and Lomb Spectronic 2000 recording spectrophotometer.

Reagents

Di-*o*-tolylthiocarbazone was prepared by the method described by Hubbard and Scott,[9] involving persulphate oxidation of di-*o*-tolylcarbazide, and purified by the method suggested by Ghosh and Ray.[10] Di-*o*-tolylcarbazide was synthesized by heating *o*-tolylhydrazine and guaiacol carbonate for 3 hr at 160° as suggested by Noller.[11] The melting point of the di-*o*-tolylcarbazone was 137°. Pyridine (Fisher), picolines (Eastman), lutidines (B.D.H.), collidine (Fluka) and ethylenediamine (B.D.H.) were dried over solid potassium hydroxide and distilled. Constant-boiling fractions were collected and used. 2,2′-Bipyridyl (Eastman), 1,10-phenanthroline (G. Frederick Smith Co.), neocuproine (B.D.H.), nickel perchlorate (Fisher Reagent Grade), chloroform (Merck) and carbon tetrachloride (Merck) were used as received.

Preparation of nickel di-o-tolylcarbazonate

A slight excess of 0.01*M* nickel perchlorate buffered with 1*M* ammonia and 1*M* ammonium chloride was added to an alcoholic 0.01*M* solution of di-*o*-tolylcarbazone at room temperature. The mixture was stirred and the precipitate formed was collected under suction and washed several times with water and finally with ethanol. The complex was dried at room temperature over phosphorus pentoxide under vacuum. The nickel content of the complex was found to be 9.87% by the phenanthroline–dithizone method developed by Math *et al.*[12] (theory requires 9.91%).

Preparation of nickel di-o-tolylthiocarbazonate

A slight excess of 0.01*M* nickel perchlorate was added to 0.01*M* di-*o*-tolylthiocarbazone solution in 1,4-dioxan. The mixture was diluted with water and the precipitate obtained was filtered off, washed several times with water and finally with carbon tetrachloride. The product was dried over phosphorus pentoxide under vacuum at room temperature for 12 hr. Its nickel content was found to be 9.10% by the phenanthroline–dithizone method[12] (theory requires 9.39%).

Determination of equilibrium constants

Known volumes of chloroform solutions of the given nickel complex were pipetted into standard flasks containing various amounts of the nitrogen base (dissolved in chloroform) and the mixtures were diluted to the mark with the solvent. The absorption spectra of the solutions were obtained in the range 400–700 nm, with an optical path-length of 10 mm. The absorbance values at 630 and 665 nm were found to be suitable for study of formation of the $Ni(OTC)_2$ and $Ni(OTTC)_2$ adducts, respectively, the difference in absorbance between chelate and adduct being largest at these wavelengths. The absorbances were found to be constant for at least 1 hr unless otherwise stated. Typical plots are shown in Figs. 1 and 2. The absorbance values were also used to obtain mole-ratio plots (*e.g.*, Fig. 3).

RESULTS AND DISCUSSION

Chloroform solutions of $Ni(OTC)_2$ are slate-blue, with two absorption bands in the visible region at 630 nm ($\varepsilon_{630} \sim 2.1 \times 10^4$ $l.mole^{-1}.cm^{-1}$) and 465 nm ($\varepsilon_{465} \sim 1.4 \times 10^4$ $l.mole^{-1}.cm^{-1}$), in contrast to most of the other metal–OTC complexes, *e.g.*, those of Zn, Co, Cu, which each have a single absorption band at about 550 nm. The absorption spectrum of $Ni(OTC)_2$

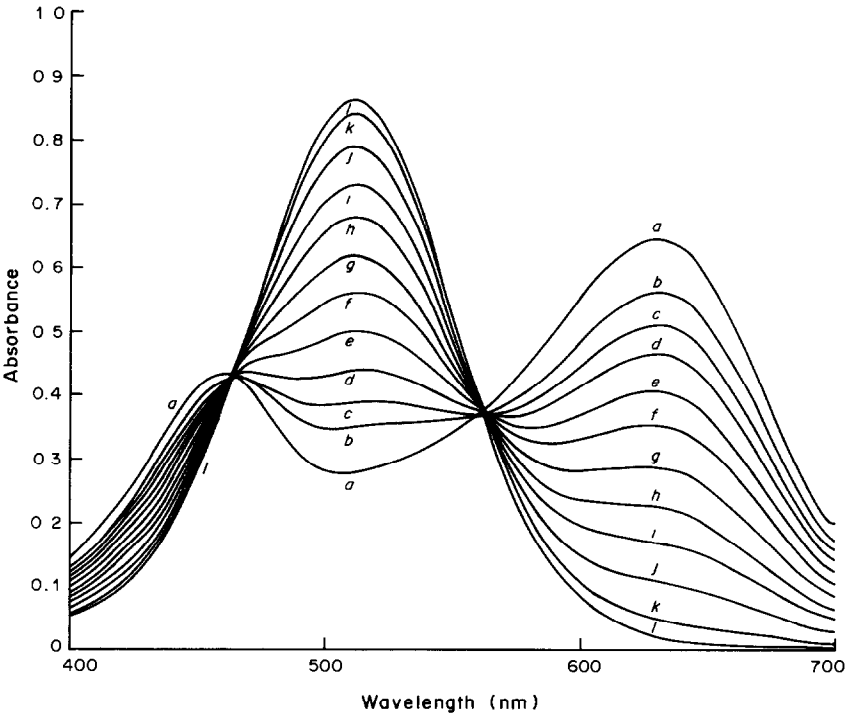

Fig. 1. Absorption spectra of $Ni(OTC)_2$ + 2,2′-bipyridyl mixtures in chloroform. $[Ni(OTC)_2]$: $3 \times 10^{-5}M$. [2,2′-bipy] μM: (*a*) 0.0, (*b*) 1.34, (*c*) 2.69, (*d*) 4.03, (*e*) 5.38, (*f*) 6.72, (*g*) 8.07, (*h*) 9.41, (*i*) 10.76, (*j*) 12.10, (*k*) 13.45, (*l*) 14.79.

also differs from that of the nickel complexes of diphenylcarbazone and di-*p*-tolylcarbazone, which have a single absorption band at around 500 nm. The spectrum of $Ni(OTC)_2$ undergoes a profound change on addition of certain nitrogen bases, giving a single absorption band at around 520 nm with $\varepsilon \sim 2.5 \times 10^4$ $l.mole^{-1}.cm^{-1}$. This closely resembles the behaviour of the nickel dithizonate adducts with nitrogen bases.[2] There are two isosbestic points in the visible region for the $Ni(OTC)_2$ adduct systems, at around 570 and 465 nm. In some cases the isosbestic points are not sharp, however, as the $Ni(OTC)_2$ itself is not stable in solution, and its colour slowly fades.

The absorption spectrum of the brown chloroform solution of $Ni(OTTC)_2$ also has multiple absorption bands ($\lambda_{max} = 665$, 550 and 420 nm with $\varepsilon \sim 2.2 \times 10^4$, 2.5×10^4 and 2.0×10^4 $l.mole^{-1}.cm^{-1}$ respectively), unlike those of other metal *o*-tolylthiocarbazonates (Hg, Co, Cd, Zn *etc.*) which have a single absorption band[13] at around 500 nm. On addition of nitrogen bases the multiple peaks of $Ni(OTTC)_2$ also coalesce to give a single band at around 500 nm, as might be expected from the behaviour of nickel dithizonate and $Ni(OTC)_2$.

The change in the spectra of nickel complexes on the addition of heterocyclic nitrogen bases could be used to determine the equilibrium constants of the adducts. The overall formation constants β_n^{ad} of the adduct for the reaction of the nickel chelate, NiL_2, with n molecules of base, B, to form the adduct, NiL_2B_n is given by:

$$\beta_n^{ad} = \frac{[NiL_2B_n]}{[NiL_2][B]^n} \tag{1}$$

when n is $\geqslant 1$.

If the initial concentrations of the chelate and base are C_{ch}^0 and C_B^0 respectively, then

$$C_{ch}^0 = [NiL_2] + [NiL_2B_n] \tag{2}$$

and

$$C_B^0 = [B] + n[NiL_2B_n] \tag{3}$$

The absorbance A at a wavelength at which both the adduct and the nickel chelate absorb radiation is given by:

$$A = \varepsilon_{ch}[NiL_2] + \varepsilon_{ad}[NiL_2B_n] \tag{4}$$

for 1-cm path-length, ε_{ch} and ε_{ad} being the molar absorptivities of the chelate and adduct respectively. Substitution and rearrangement gives

$$\beta_n^{ad} = \frac{\varepsilon_{ch}C_{ch}^0 - A}{(A - \varepsilon_{ad}C_{ch}^0)[B]^n} \tag{5}$$

Since the absorbance (A_{ch}) in the absence of base and the absorbance (A_{ad}) in the presence of a large excess of base (*i.e.*, when all the complex is in the adduct form) are given by $A_{ch} = \varepsilon_{ch}C_{ch}^0$ and $A_{ad} = \varepsilon_{ad}C_{ch}^0$,

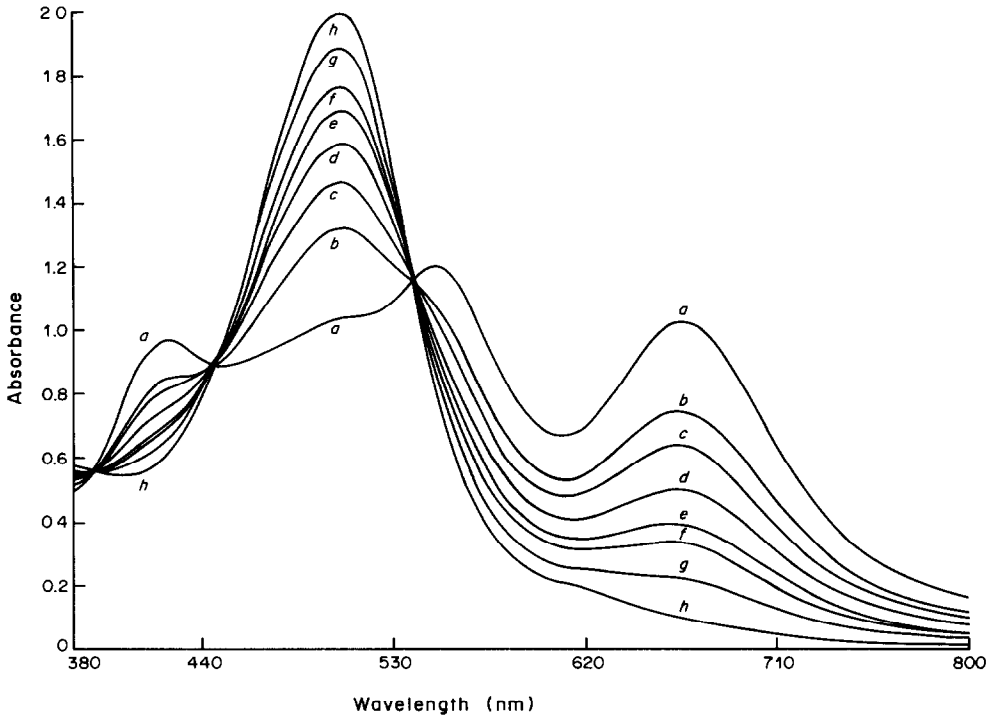

Fig. 2. Absorption spectra of $Ni(OTTC)_2$ + 1,10-phenanthroline mixtures in chloroform. [$Ni(OTTC)_2$]: $3 \times 10^{-5}M$. [1,10-phen], $10^{-5}M$: (*a*) 0.0, (*b*) 1.67, (*c*) 3.35, (*d*) 5.02, (*e*) 6.70, (*f*) 8.37, (*g*) 13.40, (*h*) 26.80.

equation (5) can be rewritten in logarithmic form as

$$\log \beta_n^{ad} = -n \log[B] + \log \frac{(A_{ch} - A)}{(A - A_{ad})} \quad (6)$$

The concentration of free base at equilibrium, [B], is calculated by using the relation:

$$[B] = C_B^0 - n \frac{(A - \varepsilon_{ch} C_{ch}^0)}{(\varepsilon_{ad} - \varepsilon_{ch})} \quad (7)$$

The second term on the right-hand side of equation (7) corresponds to the base bound to the chelate to form the adduct. When the adduct is weak, a large excess of base must be added to form the adduct, but only a small fraction is actually bound, so [B] can conveniently be taken as equal to C_B^0, and $\log \beta_n^{ad}$ can be taken as equal to $-n \log C_B^0$ when $(A_{ch} - A)/(A - A_{ad})$ is equal to unity. The stoichiometry of such adducts was eatablished by Job's and/or mole-ratio methods (Table 1). Because of the instability of the $Ni(OTC)_2$ solutions (mentioned above), accurate values for β_n^{ad} can be obtained only by making accurately timed absorbance measurements, and corrections to allow for the fading of the $Ni(OTC)_2$ colour, and this has not yet been achieved.

For the adducts of $Ni(OTC)_2$ with unidentate bases, the approximate $\log \beta_2^{ad}$ values increase linearly with pK_a for the conjugate acid of the base. These adducts contain two moles of base as shown by the slope of 2 for the plots of $\log (A_{ch} - A)/(A - A_{ad})$ *vs.* $-\log[B]$. This accounts for six co-ordination sites around nickel. It is interesting that the pink adducts of $Ni(OTC)_2$ with unidentate bases such as pyridine, or 3- and 4-picolines are unstable and rapidly decompose, whereas the adducts with 2-picoline, 2,6-lutidine, 2,4-lutidine and 2,4,6-collidine, which have sterically hindering groups, are stable for at least 1 hr. We have been unable to establish the reasons for this behaviour.

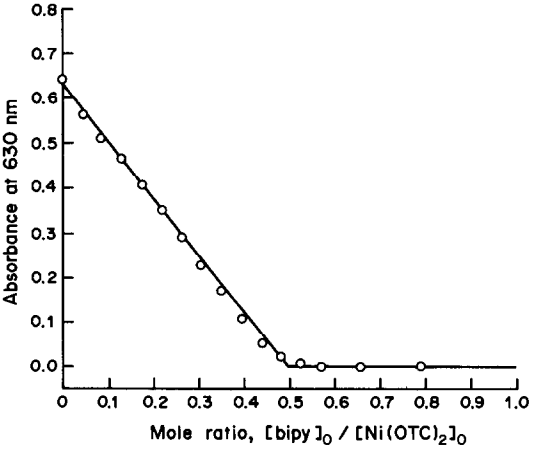

Fig. 3. Mole-ratio plot showing adduct formation between $Ni(OTC)_2$ and 2,2′-bipyridyl.

Table 1. Adduct formation from Ni(II) chelates

Base	Ni-di-*o*-tolylcarbazonate adducts			Ni-di-*o*-tolylthiocarbazonate adducts					
	n*	$\log \beta_n^{ad}$† (in $CHCl_3$)	λ_{max}, nm	n*	$\log \beta_n^{ad}$† (in CCl_4)	λ_{max} nm	n*	$\log \beta_n^{ad}$† (in $CHCl_3$)	λ_{max}, nm
Pyridine	—	—	—	—	—		2	−1.8	615
2-Picoline	2	2.2	520	2	2.4		No adduct formation		
4-Picoline	—	—	—	—	—		2	−1.2	615
2,6-Lutidine	2	1.4	520	2	1.8	520	No adduct formation		
2,4-Lutidine	2	2.7	520	2	3.3		No adduct formation		
2,4,6-Collidine	2	3.6	520	2	4.1	520	No adduct formation		
Aniline	2	1.2	530	2	2.1	530	No adduct formation		
2,2′-Bipyridyl	0.5	—	510	0.5	—	510	1	3.2	505
1,10-Phenanthroline	0.5	—	510	0.5	—	510	1	4.4	505
2,9-Neocuproine	0.5	—	515	—	—		No adduct formation		
Ethylenediamine	0.5	—	520	0.5	—	520	1	2.3	615
Dimethylformamide	—	—	—	2	1.8	520	—	—	—
Dimethylsulphoxide	—	—	—	2	3.2	520	—	—	—

*n = number of molecules of base per chelate molecule; $n = 0.5$ means 2:1 ratio of nickel chelate to base.

It is interesting that when carbon tetrachloride [a poorer solvent than chloroform for $Ni(OTC)_2$] is used as the solvent, the values of $\log \beta_n^{ad}$ are uniformly greater, which may reflect interaction between the nickel chelate and chloroform. DMF and DMSO form adducts with the chelate in carbon tetrachloride but not in chloroform, again suggesting interaction between the nickel chelate and chloroform.

Nickel di-*o*-tolylcarbazonate forms more stable adducts with bidentate bases, namely 2,2′-bipyridyl, 1,10-phenanthroline, neocuproine and ethylenediamine, and the mole-ratio and Job's methods have clearly shown the ratio of chelate to base to be 2:1 (Fig. 3). Therefore, equation (6) cannot be used for calculation of the adduct formation constants. In principle the stability constants could be calculated from the absorbance data:

$$\beta = [(NiL_2)_2B]/[NiL_2]^2[B] \quad (8)$$

$$C^0_{ch} = [NiL_2]_2 + 2[(NiL_2)_2B] \quad (9)$$

$$A = \varepsilon_{ch}[NiL_2] + \varepsilon_{ad}[(NiL_2)_2B] \quad (10)$$

$$= \varepsilon_{ch}[NiL_2] + \tfrac{1}{2}\varepsilon_{ad}(C^0_{ch} - [NiL_2]) \quad (11)$$

Again, however, the instability of the $Ni(OTC)_2$ solution causes difficulty and no values for the adduct formation constants can be deduced from the data so far available. The behaviour of $Ni(OTC)_2$ towards bidentate heterocyclic bases cannot be explained by assuming that the base acts as a bridging ligand between two chelate molecules, because the geometry of reagents such as 1,10-phenanthroline does not permit such a possibility. We therefore suggest that two molecules of chelate react with one molecule of phenanthroline to form an ion-pair which is soluble in chloroform:

$$2Ni(OTC)_2 + phen \rightleftharpoons Ni(OTC)phen^+ + Ni(OTC)_3^- \rightleftharpoons Ni(OTC)phen^+ \cdot Ni(OTC)_3^-$$

The formation constants of $Ni(OTTC)_2$ adducts, calculable by using equation (6), are also given in Table 1. It seems that most of the unidentate bases do not readily form adducts. $Ni(OTTC)_2$ in highly concentrated solutions of pyridine and 4-picoline given isosbestic points at around 515 and 650 nm respectively. The use of relation (6) gave a slope of 2 and the $\log \beta_2^{ad}$ values were obtained as twice the value of $-\log [B]$ at $\log(A_{ch} - A)/(A - A_{ad}) = 0$. Extremely low β_n^{ad} values for these bases are expected because of the *o*-methyl group in the benzene ring (which itself is perpendicular to the chelate plane[14]) of the ligand. This results in crowding around the central nickel atom, which will interfere with the interaction of the base with the chelate. This is clearly seen when $Ni(OTTC)_2$ fails to exhibit any kind of reaction towards bases having sterically hindering substituents, *e.g.*, 2-picoline.

The behaviour of $Ni(OTTC)_2$ towards bidentate nitrogen-bases differs from that of $Ni(OTC)_2$. It forms 1:1 adducts, which is clearly demonstrated by the slope of the plot of $\log(A_{ch} - A)/(A - A_{ad})$ *vs.* $-\log [B]$ and by the mole-ratio experiments, and this is in accordance with the hexaco-ordination of the nickel complex. The possibility of adduct formation arises as a result of the reorientation of di-*o*-tolylthiocarbazone molecules, which were in a plane, so as to provide a *cis*-position for bidentate bases such as 1,10-phenanthroline and 2,2′-bipyridyl. The β_1^{ad} values for these bases with $Ni(OTTC)_2$ are lower than those for the corresponding adducts of nickel–dithizone complexes,[2] probably because of the steric influence of the *o*-methyl group of the reagent. Furthermore, neocuproine does not form an adduct with $Ni(OTTC)_2$, demonstrating the adverse steric effect of the methyl groups *ortho* to the donor nitrogen-atoms, which introduce steric strain.

The adduct formation constants for $Ni(OTTC)_2$ are significantly lower than those for its oxygen analogue $Ni(OTC)_2$. In general, it seems that the adducts of nickel chelates with sulphur and nitrogen as donor atoms, *e.g.*, Ni–dithizone,[2] Ni–8-mercaptoquinoline,[2] nickel chelates of hydrazine-

S-methyldithiocarboxylate type Schiff's bases,[7] are considerably weaker than the adducts of chelates with oxygen and nitrogen donor atoms, *e.g.*, Ni–8-hydroxyquinoline,[8] probably reflecting the strong preference of sulphur donor atoms for a square planar structure.

We plan to investigate further why with bidentate bases $Ni(OTC)_2$ behaves differently from all other nickel chelate adducts studied hitherto, and to obtain better values for the adduct formation constants.

Acknowledgement—The authors gratefully acknowledge helpful discussions on this work with Prof. Henry Freiser, University of Arizona, Tucson, U.S.A.

REFERENCES

1. S. T. Hiremath, *Ph.D. Thesis*, Karnatak University, Dharwad, India, 1982.
2. K. S. Math and H. Freiser, *Anal. Chem.*, 1969, **41**, 1682.
3. F. C. Chou and H. Freiser, *ibid.*, 1968, **40**, 34.
4. M. Nanjo and T. Yamasaki, *J. Inorg. Nucl. Chem.*, 1970, **32**, 2411.
5. T. Marshall and Q. Fernando, *Anal. Chem.*, 1972, **44**, 1346.
6. M. Chikuma, A. Yokoyama and H. Tanaka, *J. Inorg. Nucl. Chem.*, 1974, **36**, 1243.
7. M. F. Iskander, M. A. E. Dessouky and S. A. Sallam, *ibid.*, 1976, **38**, 2201.
8. K. S. Bhatki, A. T. Rane and H. Freiser, *Inorg. Chim. Acta*, 1978, **26**, 183.
9. D. M. Hubbard and E. W. Scott, *J. Am. Chem. Soc.*, 1943, **65**, 2390.
10. N. N. Ghosh and J. N. Ray, *J. Indian Chem. Soc.*, 1960, **37**, 650.
11. C. R. Noller, *J. Am. Chem. Soc.*, 1930, **52**, 1132.
12. K. S. Math, K. S. Bhatki and H. Freiser, *Talanta*, 1969, **16**, 412.
13. K. S. Math, Q. Fernando and H. Freiser, *Anal. Chem.*, 1964, **36**, 1762.
14. K. S. Math and H. Freiser, *Chem. Commun.*, 1969, **41**, 1682.

Talanta, Vol. 32, No. 8B, pp. 817–820, 1985
Printed in Great Britain.

0039-9140/85 $3.00 + 0.00

EFFECT OF STIRRING ON THE ION-ASSOCIATION EXTRACTION OF COPPER AND ZINC 4,7-DIPHENYL-1,10-PHENANTHROLINE COMPLEXES

HITOSHI WATARAI
Department of Chemistry, Faculty of Education, Akita University, Akita 010, Japan

(*Received* 3 *December* 1984. *Revised* 22 *March* 1985. *Accepted* 29 *March* 1985)

Summary—The effect of high-speed stirring on the extraction of 4,7-diphenyl-1,10-phenanthroline (L) complexes into chloroform was examined for the copper(II)/perchlorate, copper(II)/chloride and zinc(II)/perchlorate systems. A significant reversible decrease in the organic phase concentration in all the systems was caused by stirring, but most evidently in the copper/perchlorate system, where the effect depended on the stirring rate, concentration of L, and metal-ion concentration. The phenomena are primarily explained in terms of an interfacial adsorption of the extracted complex, according to the Langmuir adsorption isotherm.

The role of the interface in solvent extraction has become one of the most stimulating subjects in the field of solvent extraction chemistry.[1] Although the interface has often been suggested to have an influence on the extraction mechanism, experimental evidence to confirm this has rarely been obtained, because of experimental difficulties. Thus a new technique is required as an alternative to the common methods such as measurement of interfacial tension and interfacial potential.[2] In this context, the recently reported two-phase stirring method for the measurement of interfacial adsorption[3] seems promising as a novel technique for examination of interfacial phenomena in solvent extraction systems. The stirring method, combined with spectrophotometry, has the advantages of permitting identification and determination of the species adsorbed by the interface, and allowing the estimation of the interfacial area of the stirred system. This method can be successfully used for kinetic studies of solvent extraction.[4] In the present study, the effect of two-phase stirring on the chloroform extraction of ion-association species formed by copper(II) and zinc 4,7-diphenyl-1,10-phenanthroline complexes with chloride and perchlorate was examined; the aqueous phase contained excess of the metal ion. The effect of stirring on the distribution of 1,10-phenanthrolines between chloroform and an acidic aqueous phase was determined earlier, and it was suggested that there is interfacial adsorption of the reagents owing to protonation at the interface.[5] The present study demonstrates the interfacial adsorption of the ion-association complexes in the dispersed-solvent extraction systems.

EXPERIMENTAL

Reagents

4,7-Diphenyl-1,10-phenanthroline (L) (general reagent grade) was used as purchased. Stock solutions of copper were prepared by dissolving general reagent grade cupric oxide or cupric chloride dihydrate in the appropriate acid. Zinc metal (general reagent grade) was dissolved to make the zinc stock solution. The general reagent grade chloroform was washed three times with water before use. Demineralized and distilled water was used throughout. Hydrochloric acid, perchloric acid, sodium hydroxide and other reagents were all analytical grade. The 1*M* stock solutions of sodium chloride and sodium perchlorate were washed with concentrated L solution in chloroform and then with fresh chloroform to remove trace impurities in the salts.

Extraction studies

Preliminary experiments showed that the metal ions were fairly completely extracted from the copper/0.1*M* perchlorate, copper/0.1*M* chloride and zinc/0.1*M* perchlorate systems with a tenfold excess of L in chloroform, but from the zinc/0.1*M* chloride system only 10% of the zinc was extracted. When an anion concentration lower than 0.1*M* was employed, the extractability was decreased, suggesting that the extracted species was an ion-association complex, as expected from charge considerations. Hence, only the first three systems were examined further. A dilute chloroform solution of L was shaken for 30 min at 25 ± 1° with an aqueous solution containing excess of copper or zinc, in order to produce the ion-association complex in the organic phase. The spectral changes in the chloroform phases, due to the complex formation, were measured with a Hitachi 200-20 or Uvidec 430 spectrophotometer. The metal-species concentrations in the organic phase were determined by spectrophotometry after addition of $2.3 \times 10^{-3}M$ 1-(2-pyridylazo)-2-naphthol (PAN) in ethanol and 0.1*M* ethanolic ammonia instead of the ethylenediamine recommended by Bhat *et al.*[6] The molar absorptivities of the Cu–PAN and Zn–PAN complexes in the 1:2 v/v mixed solvent of chloroform and ethanol were estimated to be 4.2×10^4 and 5.4×10^4 l.mole^{-1}.cm^{-1} respectively, at 550 nm.

Stirring experiments

The effect of stirring on the ion-association complex concentration in the chloroform phase was examined by means of the two-phase stirring apparatus described elsewhere in detail.[4,5] Fifty ml of 1.5×10^{-6}–$3.4 \times 10^{-5}M$ L solution in chloroform and an equal volume of 2.0×10^{-6}–$4.9 \times 10^{-3}M$ copper or 2.0×10^{-5}–$1.9 \times 10^{-2}M$ zinc solution at pH 3.9–4.7 were stirred in the dispersion

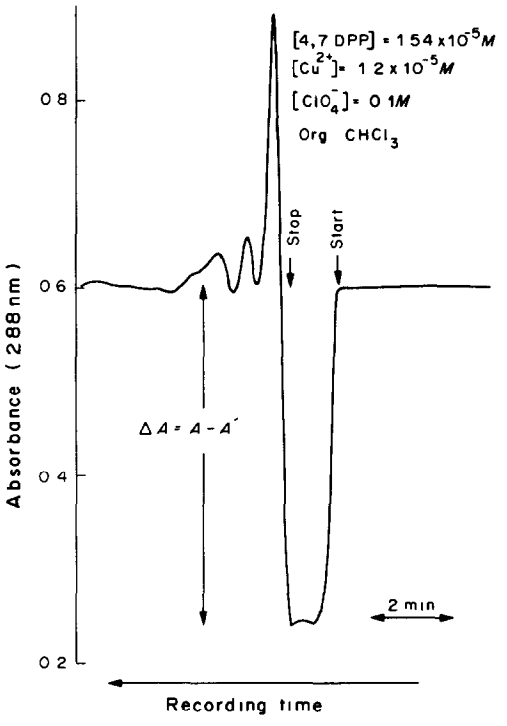

Fig. 1. A typical example of the stirring effect. The definition of ΔA is also illustrated in this figure.

cell, which was kept at $25 \pm 0.1°$. The organic phase was pumped out through a Teflon phase separator and circulated through a 100-μl flow-cell (10-mm light-pass) at a flow-rate of 7.5 ml/min. Change in the absorbance or spectrum of the complex was recorded. A typical example of the stirring effect is shown in Fig. 1, in which the absorbance of the Cu^{2+}–L complex decreases soon after the start of stirring and is restored to the original after the stirring has been stopped. The decrease in absorbance, ΔA, defined as $\Delta A = A - A'$ where A and A' are the absorbances before stirring and during stirring respectively, depends on the stirring rate, as shown in Fig. 2. A stirring rate of 4700 rpm was therefore adopted for the further studies.

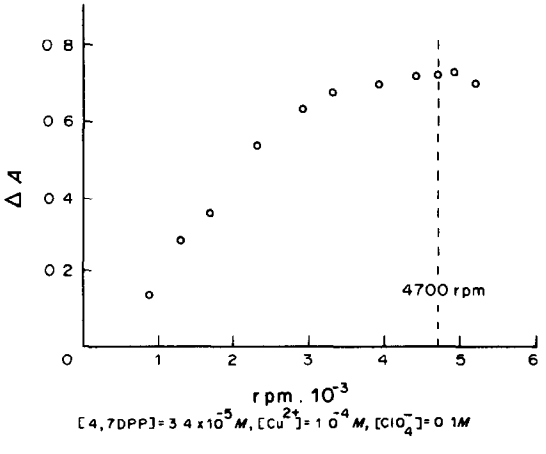

Fig. 2. Dependence of ΔA observed at 288 nm on the stirring rate; $[4,7DPP] = 3.4 \times 10^{-5}M$, $[Cu^{2+}] = 1.0 \times 10^{-4}M$, $[ClO_4^-] = 0.1M$.

RESULTS AND DISCUSSION

Ultraviolet spectra of the extracted species

When $2.87 \times 10^{-5}M$ L in chloroform was shaken with aqueous metal ion solutions of various concentrations, the ultraviolet spectrum of L ($\lambda_{max} = 275$ nm) shifted toward longer wavelengths, depending on the metal concentration and the counter-ion. The spectra of both anion systems were independent of copper concentration $> 10^{-4}M$, but showed characteristic absorption maxima depending on the counter-anion: 292 nm for the chloride system and 288 nm for the perchlorate system (Fig. 3). The extracted zinc complex showed a constant spectrum at zinc concentrations $> 10^{-2}M$, with the absorption maximum at 285 nm. The greater wavelength shift observed for the copper/chloride system may be due to co-ordination of chloride to copper rather than ion-association. In the aqueous phase, no absorbance due to complex formation was observed. The distribution of L into the aqueous phase is negligible since the distribution constant is about $10^{7.5}$ Therefore, all the L in the organic phase was assumed to react with metal ion. Determination of the metal in the chloroform phases by the PAN method allowed calculation of the mean numbers of molecules of L co-ordinating to the metal ion; 3.05, 2.58 and 2.17 for the $10^{-4}M$, $10^{-3}M$ and $10^{-2}M$ copper/perchlorate systems, 1.49 and 1.16 for $10^{-4}M$ and $10^{-3}M$ copper/chloride systems, and 3.14 for the $10^{-2}M$ zinc/perchlorate system. Hence, the compositions of the complexes extracted under the conditions described in Fig. 3 were assumed to be $CuLCl_2$, $CuL_2(ClO_4)_2$ which may co-exist with $CuL_3(ClO_4)_2$, and $ZnL_3(ClO_4)_2$.

Stirring effect

The decrease in the organic phase absorbance caused by stirring depended on the metal concen-

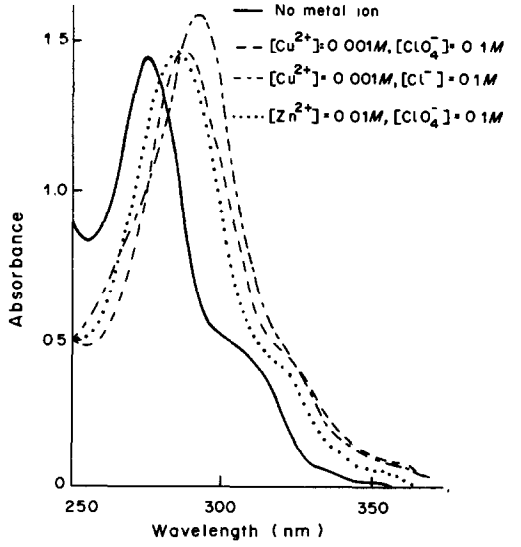

Fig. 3. Changes in the ultraviolet spectra of $2.87 \times 10^{-5}M$, 4,7DPP in chloroform, resulting from ion-pair formation in the organic phase.

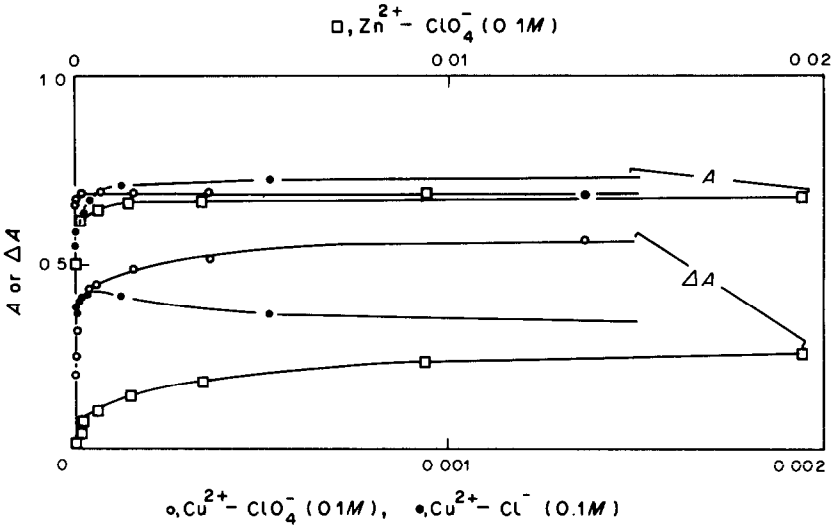

Fig. 4. Variation in A and ΔA observed at maximum absorption wavelengths, with metal ion concentration. [4,7DPP] = $1.54 \times 10^{-5}M$.

tration differently for the two anion systems, as shown in Fig. 4. In the copper/chloride system, a maximum in ΔA appeared for around $10^{-4}M$ copper, whereas in the perchlorate system ΔA continued to increase with metal-ion concentration up to $10^{-3}M$ copper or $10^{-2}M$ zinc. ΔA values were also measured for fixed $10^{-3}M$ copper and $10^{-2}M$ zinc concentrations and [L] varied over the range 0–$3 \times 10^{-5}M$. Figure 5 illustrates the results, as plots of ΔA and 100 $\Delta A/A$ *vs.* [L]. The percentage decrease in absorbance is highest in the copper/perchlorate system and goes up to 95% for $3.9 \times 10^{-6}M$ L, implying 95% of the copper complex is removed from the bulk organic phase by stirring. The shape of the spectrum of the organic phase during stirring was essentially the same as that before stirring. Hence, it is unlikely that the decrease in absorbance is caused by decomposition or conversion of the complexes in the organic phase.

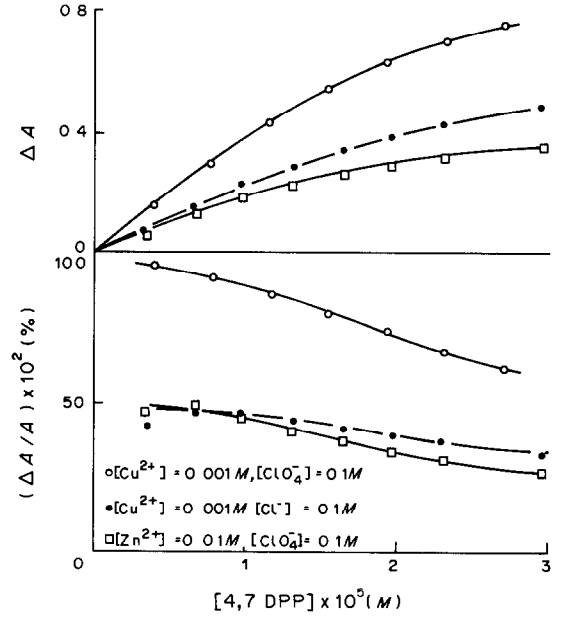

Fig. 5. Variations in ΔA and $(\Delta A/A) \times 10^2$ (%) with 4,7DPP concentration.

The dependence of ΔA on the stirring rate and the concentration of L seems to suggest participation of the interface. Assuming that the decrease in absorbance of a complex ML_n is due to interfacial adsorption, the mass-balance equation for L can be written as

$$[L]_t = n[ML_n]_o + n[ML_n]_i \frac{10^3 A_i}{V} \qquad (1)$$

where subscripts t, o and i indicate total (added initially to organic phase), organic and interfacial concentrations (the last in units of mole/cm^2), n the mean ligand numbers co-ordinated to the metal ion M, A_i (cm^2) is the total interfacial area during stirring and V (ml) is the volume of the bulk organic phase. In this equation and the following equations, the charges and counter-ions of the extracted ion-association complexes are omitted. As we are dealing with kinetic effects, the adsorption equilibrium of ML_n may be assumed to conform to the Langmuir adsorption isotherm,

$$[ML_n]_i = \frac{ab[ML_n]_o}{1 + b[ML_n]_o} \qquad (2)$$

where a and b are constants, a corresponding to the saturated interfacial concentration and ab to the adsorption equilibrium constant K' defined by,

$$ab \equiv K' = \lim_{[ML_n] \to 0} \frac{[ML_n]_i}{[ML_n]_o}. \qquad (3)$$

From these equations, and $A' = \varepsilon[ML_n]_o$ and $\Delta A = \varepsilon\{([L]_t/n) - [ML_n]_o\}$, where ε is the molar

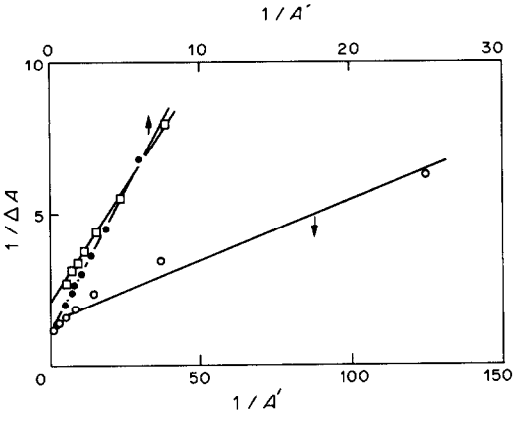

Fig. 6. Analyses of the 4,7DPP concentration dependences shown in Fig. 5. The keys in this figure are the same as those in Fig. 5.

absorptivity, the equation

$$\frac{1}{\Delta A} = \left(\frac{1}{a} + \frac{\varepsilon}{K'A'}\right)\frac{V}{\varepsilon 10^3 A_i} \qquad (4)$$

can be derived.

The observed dependences on [L] shown in Fig. 5 were analysed according to equation (4). The plots of $1/\Delta A$ against $1/A'$ for the copper/chloride and zinc/perchlorate systems gave straight lines, as shown in Fig. 6, with correlation coefficients $r = 0.998$ and $r = 1.000$, respectively, but the plot for the copper/perchlorate system was decidedly non-linear. The slopes of the straight lines allow the estimation of $K'A_i$, which is thought to be a measure of the interfacial activity of ML_n; they are 0.053 for the copper/chloride system and 0.065 for the zinc/perchlorate system. For the copper/perchlorate system the value for a least-squares linear fit is 1.2_5, but is not very reliable. The interfacial activity of $CuLCl_2$ may be small if this species is a mixed-ligand complex which behaves as a non-electrolyte, and that of $ZnL_3(ClO_4)_2$ may be small since the hydrophilic central ion is symmetrically surrounded by the large hydrophobic ligands. The large apparent value for the copper/perchlorate system may correspond to the higher interfacial activity of $CuL_2(ClO_4)_2$. The poor linearity in this system may be caused by variability in the area of the interface as a result of the effect of amount of adsorbed copper complex on the rate of coalescence of the dispersed drops.

The dependence of ΔA on the metal concentration (Fig. 4) may also be explained by the interfacial adsorption mechanism. The maximum in the $10^{-4}M$ copper/chloride system may be due to a higher fraction of $CuL_2Cl^+.Cl^-$ which is expected to be more interfacially active than $CuLCl_2$.

The surge after the stirring is stopped, shown in Fig. 1, may be due to localized adsorption of droplets at the interface. If the stirrer speed is slowly decreased instead of the stirrer being switched off, the oscillation in absorbance is not observed.

The significant effect of the interface demonstrated in the present study seems to require an alternative mechanism for extraction of ion-association complexes, taking account of adsorption equilibria at the interface.

Acknowledgements—The author thanks Professor N. Suzuki of Tohoku University for his continuing encouragement. This work was financially supported by a Grant-in-Aid for Scientific Research from the Ministry of Education, Japan (No. 59,540,353—1984).

REFERENCES

1. M. Cox and D. S. Flett, in *Handbook of Solvent Extraction*, T. C. Lo, M. H. I. Baird and C. Hanson (eds.), p. 53. Wiley, New York, 1983.
2. J. T. Davies and E. K. Rideal, *Interfacial Phenomena*, 2nd Ed., Academic Press, New York, 1963.
3. H. Watarai and H. Freiser, *J. Am. Chem. Soc.*, 1983, **105**, 191.
4. H. Watarai, L. Cunningham and H. Freiser, *Anal. Chem.*, 1982, **54**, 2390.
5. H. Watarai, *J. Phys. Chem.*, 1985, **89**, 384.
6. S. R. Bhat, P. T. Crisp, J. M. Eckert and N. A. Gibson, *Anal. Chim. Acta*, 1980, **116**, 191.

Talanta, Vol. 32, No. 8B, pp. 821–823, 1985
Printed in Great Britain.

0039-9140/85 $3.00 + 0.00

SHORT COMMUNICATIONS

PROPERTIES AND ANALYTICAL APPLICATION OF A THALLIUM(I) ION-SELECTIVE ELECTRODE

C. J. COETZEE
Department of Chemistry, University of the Western Cape, Bellville 7530, South Africa

(*Received* 16 *October* 1984. *Accepted* 23 *January* 1985)

Summary—A liquid-membrane electrode for the potentiometric determination of thallium(I) ions is described. Use as an indicator electrode in potentiometric titration of thallium(I) is outlined.

The use of commercial ion-selective electrode barrels for the preparation of various liquid membrane ion-selective electrodes has been described by Coetzee and Freiser.[1] Several types of ion-selective electrode for thallium(I) have been described. These include thallium(I) salts of heteropoly acids, supported in an epoxy resin membrane,[2–5] PVC-membrane electrodes based on bis(crown ethers),[6] polycrystalline membrane electrodes,[7] and a liquid ion-exchanger containing thallium *O,O'*-didecyldithiophosphate.[8] Fogg *et al.*[9] have reported the use of water-insoluble basic dye salts for the preparation of thallium ion-selective electrodes.

In contrast to a previously reported liquid membrane[10] in which thallium(I) tetrakis(*m*-trifluoromethylphenyl)borate was used as the active material, the procedure for the preparation of the active material (and hence the electrode) described here is much simpler.

EXPERIMENTAL

Reagents

The solvent 4-ethylnitrobenzene was distilled under reduced pressure. Thallium(I) cyanotriphenylborate was prepared by precipitation from an aqueous 1% thallium(I) nitrate solution with 1% sodium cyanotriphenylborate solution. The precipitate was washed with cold water, separated by centrifugation and dried at 120° for 3 hr.

All other chemicals used were of analytical reagent grade.

Electrode construction

Orion electrode barrels (Model 92-20, kindly supplied by J. W. Ross of Orion) were used, with Orion 92-20 membranes as separators for the organic and aqueous phases. The organic phase consisted of a saturated solution of thallium(I) cyanotriphenylborate in 4-ethylnitrobenzene. The aqueous phase was a 0.10*M* solution of thallium(I) nitrate saturated with thallium(I) chloride. After preparation the electrode was conditioned by immersion in 0.10*M* thallium(I) nitrate for at least 1 hr, and stored in this solution when not in use.

Apparatus

A Radiometer PHM 64 pH-meter fitted with the necessary adaptors and a Beckman 39170 saturated calomel electrode was used for all e.m.f. measurements. Because of the possibility of thallium(I) chloride precipitation caused by leakage of chloride from the calomel electrode, agar salt bridges (1% ammonium nitrate) were used. An Orion model 607 pH-meter equipped with an Orion 91-05-00 gel-filled pH electrode was used for pH measurements.

RESULTS AND DISCUSSION

Characteristics of the electrode

Linear response range. The electrode gave linear calibration graphs for thallium(I) in pure nitrate solutions in the concentration range $10^{-4.5}$–$10^{-1}M$. The graphs could be used to determine thallium concentrations as low as $10^{-5}M$. Activity coefficients were calculated from the extended Debye–Hückel equation $\log f = -0.51\, z^2\mu^{1/2}/(1 + \mu^{1/2})$. The slope of the calibration graphs for three different electrodes were 58.3, 58.0 and 58.0 mV/pTl at 25°. The useful lifespan of the electrodes was found to be 4–6 weeks, after which the organic phase turned dark yellow, probably because of oxidation of the organic solvent.

Response time. The response times for e.m.f. measurements were not studied in detail. With 10^{-3}–$10^{-1}M$ solutions stable readings were obtained within 30 sec; with more dilute solutions a 1–3 min period was required to obtain stable readings. Measurements were more stable with slow than with fast stirring.

Effect of pH. The pH-dependence of the electrode was studied for the pH range 1–12, adjusted by addition of nitric acid and sodium hydroxide solutions having the same thallium(I) concentration as the test solution. The results indicate the working range of the electrode to be between pH 2 and 11. The e.m.f. readings were the same over that range for 10^{-1}, 10^{-2} and $10^{-3}M$ thallium(I) solutions.

Selectivity. A systematic examination was made of interference by sodium, potassium, rubidium, caesium, ammonium and silver ions. Calibration graphs for the primary ion in the presence of a fixed concentration ($10^{-2}M$) of the interfering ions were

Table 1. Selectivity coefficient (k^{pot}_{TlM}) values for the thallium(I) electrode

Cation	k^{pot}_{TlM}
Na^+	4.1×10^{-2}
K^+	4.0×10^{-1}
Rb^+	9.2×10^{-1}
Cs^+	5.3
NH_4^+	2.2×10^{-1}
Ag^+	3.5×10^{-1}
Mg^{2+}, Ca^{2+}, Sr^{2+}	$< 10^{-2}$

prepared. Selectivity coefficients k^{pot}_{TlM} were calculated from these curves by means of the equation

$$k^{pot}_{TlM} = (10^{\Delta E/S} - 1)a_{Tl}/(a_m)^{1/z}$$

where ΔE is the change in e.m.f. in the presence of the interfering ion M^{z+}, S is the slope of the calibration graph for the primary ion, and a_{Tl} and a_M are the activities of the primary and the interfering ions respectively. The values obtained are shown in Table 1.

Bivalent ions do not have any appreciable influence on the electrode behaviour. The general response order is

$$Cs^+ > Tl^+ > Rb^+ > K^+ > Ag^+ > NH_4^+ > Na^+.$$

The values quoted in Table 1 also suggest the possibility of using the electrode as an indicator in potentiometric titrations of caesium and rubidium, as well as of thallium.

ANALYTICAL APPLICATIONS

Standard addition potentiometry

If the sample and standard solutions are prepared so that the ionic strength is kept high and almost constant, the liquid-junction potential and the activity coefficient of the analyte ion will not change appreciably. As the slope of the calibration graph for the primary ion is used in calculations, this technique can only be applied for the determination of thallium(I) ion at concentrations on the linear part of the graph, *i.e.*, above $5 \times 10^{-5}M$. This method was used successfully to determine thallium(I) concentrations varying between 0.2 and 2.0 mg/ml [at constant ionic strength $0.1M$ magnesium nitrate].

Precipitation titrations

A series of potentiometric precipitation titrations was performed in which the electrode was used as the indicator electrode. Standard solutions of the following salts were used as titrants: sodium tetraphenylborate, sodium cyanotriphenylborate, sodium chromate, sodium iodide, sodium bromide, sodium chloride, potassium chromate and potassium iodide, standardized where necessary by potentiometric titration with standard silver nitrate solution, an Orion 94-16A silver ion-selective electrode being used as indicator electrode. During these titrations no pH or ionic strength adjustments were made. All titrations were done with sample solutions varying between 40 and 60 ml in volume. A typical titration curve is shown in Fig. 1. The other titrants gave similar titration curves the steepness of the "potential jump" being inversely dependent on the solubility product as usual.

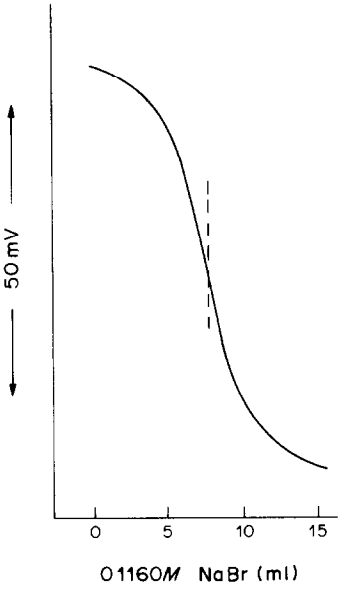

Fig. 1. Titration curve for the titration of 179 mg of thallium(I) with $0.1160M$ sodium bromide.

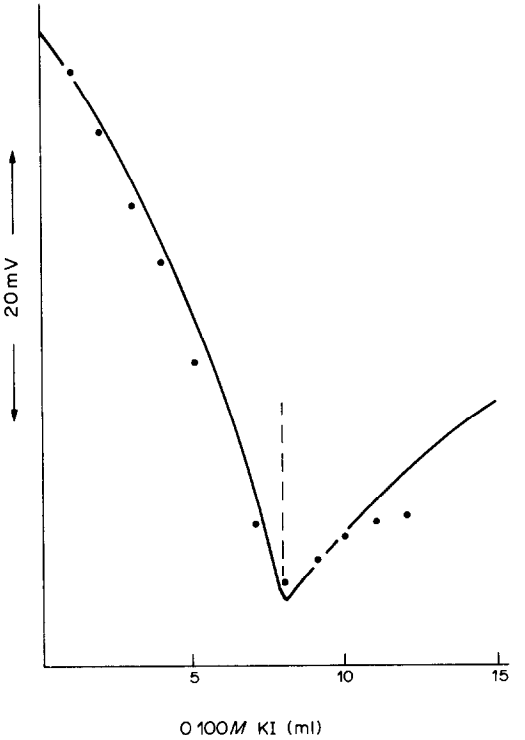

Fig. 2. Theoretical curve for the titration of 163.5 mg of thallium(I) with $0.100M$ potassium iodide (——); (●) experimental points.

Table 2. Solubility products for some insoluble thallium(I) salts at 25°C (reference in brackets)

Salt	pK_{sp}			
TlI	7.24*	7.24 (11)†	7.27 (12)†	7.19 (13)
TlBr	5.40*	5.47 (14)	5.42 (15)	5.41 (13)
TlCl	3.59*	3.75 (16)	3.66 (17)	3.74 (13, 18)
Tl_2CrO_4	12.17*	12.01 (19)	11.70 (20)	12.07 (13)
$TlB(CN)(C_6H_5)_3$	10.5 *			
$TlB(C_6H_5)_4$	9.54*			

*This work.
†20°C.

Most of the titration curves have the classical shape, the exception being those for potassium salts as titrants. In the latter titrations the potential increases again after the equivalence point has been reached, as a result of the electrode response to the potassium ions introduced by the titrant solution. Figure 2 shows a theoretical titration curve (full line) for titration with a potassium salt, together with the experimental points observed.

Solubility products at 25° were calculated from single titration curves and are listed, together with some literature values, in Table 2.

Acknowledgements—The author thanks the South African C.S.I.R. for financial support, and Dr. Gunnar Gran, Stockholm, for helpful discussion of calculation of theoretical titration curves.

REFERENCES

1. C. J. Coetzee and H. Freiser, *Anal. Chem.*, 1968, **40**, 2071.
2. C. J. Coetzee and A. J. Basson, *Anal. Chim. Acta*, 1973, **64**, 300,
3. W. K. Malik, S. K. Srivastava, P. Razdam and S. Kumar, *J. Electroanal. Chem.*, 1976, **72**, 111.
4. A. K. Jain, S. Agrawal and R. P. Singh, *Anal. Lett.*, 1979, **12**, 995.
5. A. K. Jain, R. P. Singh and S. Agrawal, *Z. Anal. Chem.*, 1980, **302**, 407.
6. H. Tamura, K. Kimura and T. Shona, *J. Electroanal. Chem.*, 1980, **115**, 115.
7. J. J. Fombon, Y. Oddon, J. Tacussel and A. Tranquard, *Analusis*, 1979, **7**, 494.
8. W. Szczepaniak and K. Ren, *Anal. Chim. Acta*, 1976, **82**, 37.
9. A. G. Fogg, A. A. Al-Sibaai and C. Burgess, *Anal. Lett.*, 1975, **8**, 129.
10. C. J. Coetzee and A. J. Basson, *Anal. Chim. Acta*, 1977, **92**, 399.
11. F. Ya. Kul'ba and V. E. Mironov, *Zh. Neorgan. Khim.*, 1957, **2**, 2741.
12. G. Jones and W. Schumb, *Proc. Am. Acad. Arts Sci.*, 1921, **56**, 199.
13. H. Freiser and Q. Fernando, *Ionic Equilibria in Analytical Chemistry*, 2nd Ed., Wiley, New York, 1966.
14. A. L. Anderson, *Thesis*, State College, Washington, 1955.
15. A. G. Scott, R. G. Dartan and S. Sapsoonthorn, *Inorg. Chem.*, 1962, **1**, 313.
16. A. A. Noyes, *Z. Phys. Chem.*, 1892, **9**, 603.
17. A. E. Hill and J. P. Simmons, *ibid.*, 1909, **67**, 594.
18. J. B. Macaskill and M. H. Panckhurst, *Austral. J. Chem.*, 1966, **19**, 915.
19. S. Suzuki, *J. Chem. Soc. Japan*, 1953, **74**, 219.
20. I. M. Korenman, V. G. Ganin and N. P. Lebedeva, *Zh. Neorgan. Khim.*, 1958, **3**, 219.

Talanta, Vol. 32, No. 8B, pp. 824–826, 1985
Printed in Great Britain

0039-9140/85 $3.00 + 0.00
Pergamon Press Ltd

EXTRACTION OF URANIUM BY A SUPPORTED LIQUID MEMBRANE CONTAINING MOBILE CARRIER

KENICHI AKIBA and HIROYUKI HASHIMOTO
Research Institute of Mineral Dressing and Metallurgy, Tohoku University, Katahira-2, Sendai, Japan

(*Received* 3 *December* 1984. *Accepted* 13 *March* 1985)

Summary—A study has been made of carrier-mediated transport of uranium(VI) by a liquid membrane of 7-dodecenyl-8-quinolinol (Kelex 100). Uranium is transported across the membrane and concentrated in a stripping acid. The apparent rate constant of uranium transport increases slightly with increase in carrier concentration and in the pH of the feed solution. Uranium can be effectively recovered from spiked sea-water through the liquid membrane without any preliminary treatment.

The use of liquid membranes has become of interest in recent years as a new technique for concentration and recovery of metal ions in analytical and process separation.[1,2] A membrane consisting of a carrier liquid supported on a hydrophobic polymer seems attractive, because the metal species can be transported through it against a concentration gradient, in a single step. Its utility for separation of metal ions will be governed by the choice of carrier. Several extracting reagents have been tried as carriers for the uranyl ion.[3–6] Recently, 7-dodecenyl-8-quinolinol (Kelex 100) has been employed for uranium extraction by Zhu and Freiser.[7] From its high distribution constant and low acid dissociation constant,[8] this reagent could be expected to act as a carrier up to around pH 10 without carrier losses due to dissolution in the aqueous phase.

This paper describes several variables affecting the transport of uranium from dilute solution by a liquid membrane containing Kelex 100 as the carrier.

EXPERIMENTAL

Materials

7-Dodecenyl-8-quinolinol, Kelex 100 (Sherex Chemical Co.) was purified as reported elsewhere.[9]

Uranium-237 ($t_{1/2} = 6.75$ d) was produced by the $^{238}U(\gamma,n)^{237}U$ reaction, and purified as previously described.[10]

A porous polytetrafluoroethylene film, Fluoropore FP-045 (Sumitomo Electric Ind.), was employed as the solid support. It was 80 μm thick and 74% porous and had an average pore size of 0.45 μm.

Procedure

Transport experiments were performed as already described.[6] The liquid membrane was prepared by impregnating the support with a kerosene solution of Kelex 100, and was attached to the bottom of the inner vessel. The uranium solution, containing ^{237}U as a tracer, was poured into the outer vessel, and its pH was adjusted to an appropriate value with $10^{-2}M$ acetate buffer solution.

The vessels were shaken at 150 strokes/min in a water-bath controlled at 25°. At various time intervals, the concentration of uranium was determined by measuring the activity of the ^{237}U with an NaI(Tl) scintillation detector.

RESULTS AND DISCUSSION

Transport of uranium

The transport of uranium through the supported liquid membrane (SLM) of Kelex 100 is shown in Fig. 1. The pH of the feed solution was adjusted to 4.7 with acetate buffer solution to enhance the extraction, and $0.1M$ nitric acid was chosen as the stripping solution, on the basis of the equilibrium data for the corresponding liquid–liquid extraction.[7] The fraction of uranium in the feed solution decreased with shaking time, while that in the product solution gradually increased. When $0.1M$ Kelex 100 was used, more than 99% of the uranium was moved across the SLM against its concentration gradient, and was concentrated into the small volume of product solution by continuous permeation. When a high carrier concentration ($1M$) was used, the fraction of uranium in the feed side smoothly decreased to nearly zero with shaking time, but that in the product side remained slightly less than 1.0, a small portion of uranium being retained in the SLM.

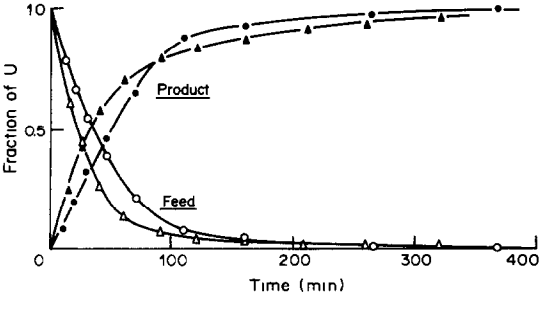

Fig. 1. Transport of uranium, through an SLM of Kelex 100. Feed 100 ml of $10^{-5}M$ uranium/$10^{-2}M$ acetate buffer solution, pH 4.7; product solution 10 ml of $0.1M$ HNO_3; (○, ●) $0.1M$ Kelex 100, (△, ▲) $1M$ Kelex 100. The open and closed symbols indicate the feed and product, respectively.

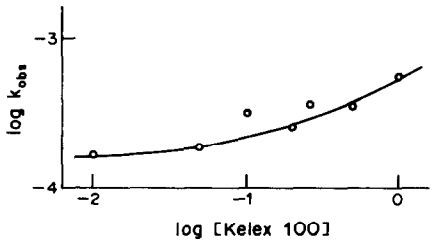

Fig. 2. Effect of the carrier concentrations on k_{obs}. Experimental conditions as for Fig. 1.

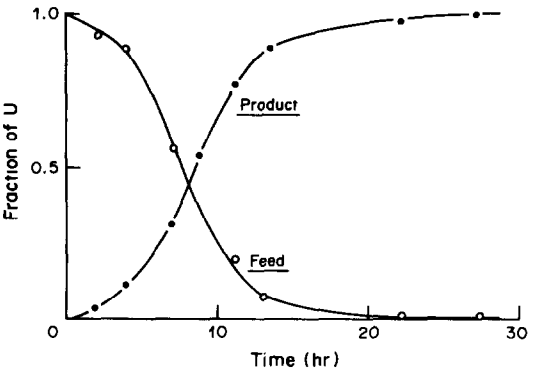

Fig. 3. Extraction of uranium from sea-water by an SLM of 0.1M Kelex 100. Feed—sea-water (Pacific Ocean at the shore at Miyagi, Japan) spiked with $10^{-6}M$ U, 100 ml; product solution—0.1M HNO_3, 10 ml.

Effect of carrier concentrations

The apparent rate constant of uranium transport, k_{obs} (sec^{-1}), was obtained from the slope of the linear plot of $\ln([U]_{f,t}/[U]_{f,0})$ against shaking time t ($[U]_f$ is the concentration in the feed solution). The k_{obs} value slightly increased with an increase in the carrier concentration, as shown in Fig. 2. Though from the kinetic point of view it is desirable to work with high carrier concentration, increasing the carrier concentration beyond a certain value might cause insufficient stripping. Thus, the optimum value was an intermediate concentration around 0.1M.

Effect of hydrogen-ion concentration

In order to move uranium across the membrane, it is necessary to maintain the hydrogen-ion concentration gradient between both sides of the membrane.

The k_{obs} value was found to increase with increasing pH of the feed solution, *e.g.*, from 1.9×10^{-4} at pH 4 to 5.5×10^{-4} at pH 6.

The effects of change in stripping solution are summarized in Table 1 for the transport of uranium from a feed solution initially $10^{-5}M$ in uranium. Changes in the kinds of acid and their concentrations over a wide range from 0.01M to 1M had little effect on the k_{obs} values.

After 5 hr shaking, the uranium concentration in the feed was only 2% of its initial value, and the uranium recovery in the product solution was over 95%, with a few exceptions. The concentration ratio of the product to the feed ($[U]_p/[U]_f$) reached 400 in 5 hr. Further shaking for a long time would result in almost quantitative recovery of uranium. The residual uranium in the SLM after 20 hr shaking was found to be less than 0.5% of the total amount present.

Effect of the feed volume

To concentrate uranium from dilute solutions, a high volume ratio, V_f/V_p, of feed to product solution is desirable, because it yields the limiting concentration factor $[U]_{p,t}/[U]_{f,0}$. The k_{obs} value is found to be inversely proportional to the feed volume. Thus we should make the volume of the product solution as small as possible in order to obtain a high concentration factor, and use a large membrane area to enhance the transport rate. This can be achieved by means of a tubular or hollow fibre type support for the carrier liquid.

Extraction of uranium from sea-water

Extraction of uranium from sea-water has recently become of interest both in analysis and in recovery of energy resources. In the extraction of uranium from

Table 1. Effect of stripping acid on uranium transport (5 hr shaking time)

Acid	Concn., M	$10^4 k_{obs}$, sec^{-1}	$10^7[U]_{f,5h}$, M	$10^5[U]_{p,5h}$, M	$\frac{[U]_{p,5h}}{[U]_{f,5h}}$
HNO_3	0.01	3.68	2.4	9.3	4×10^2
	0.1	3.47	1.6	9.6	6×10^2
	1.0	2.00	2.0	9.8	5×10^2
H_2SO_4	0.01	3.00	1.9	9.7	5×10^2
	0.1	3.52	1.9	9.8	5×10^2
	1.0	3.39	0.7	9.9	1.4×10^3
HCl	0.01	3.60	0.9	8.5	9×10^2
	0.1	3.30	2.4	9.6	4×10^2
	1.0	3.36	1.7	9.0	5×10^2

$V_f = 100$ ml; $V_p = 10$ ml; $[U]_{f,0} = 10^{-5}M$; $10^{-2}M$ acetate buffer solution (pH 4.7).

sea-water, the carrier-containing membrane must have high stability in sea-water at pH around 8.2. An SLM of Kelex 100 is well suited for this purpose, and was therefore tested with a 0.1M Kelex 100 membrane and natural sea-water. The results are illustrated in Fig. 3. The sea-water was initially spiked with $10^{-6}M$ uranium containing ^{237}U. The transport rate was rather low, but an essentially complete ($\sim 99\%$) extraction was achieved by shaking for 20 hr. Extraction of elements other than uranium was not examined in this work. No interferences from matrix species such as alkali-metal ions and halides were observed, and uranium could be effectively concentrated into the acid solution from sea-water without any supplementary treatment such as pH control. Thus, the supported liquid membrane method is rather simple and efficient for the purpose.

Acknowledgement—This study was partially supported by the Special Project Research on Energy under a Grant-in-Aid of Scientific Research of the Ministry of Education, Science and Culture.

REFERENCES

1. N. N. Li, *Recent Developments in Separation Science*, Vol. VI, CRC Press, Boca Raton, Florida, 1981.
2. K. H. Lee, D. F. Evance and E. L. Cussler, *AICh J.*, 1978, **24**, 860.
3. H. Matsuoka, M. Aizawa and S. Suzuki, *J. Membrane Sci.*, 1980, **7**, 11.
4. W. C. Babcock, R. W. Baker, E. D. LaChapelle and K. L. Smith, *ibid.*, 1980, **7**, 71.
5. S. Sifniades, T. Largman, A. A. Tunick and F. W. Koff, *Hydrometallurgy*, 1981, **7**, 201.
6. K. Akiba and T. Kanno, *Sep. Sci. Technol.*, 1983, **18**, 831.
7. L. Zhu and H. Freiser, *Anal. Chim. Acta*, 1983, **146**, 237.
8. S. P. Bag and H. Freiser, *ibid.*, 1982, **135**, 319.
9. V. I. Lakshmanan and G. J. Lawson, *J. Inorg. Nucl. Chem.*, 1973, **35**, 4285.
10. K. Akiba, N. Suzuki, H. Asano and T. Kanno, *J. Radioanal. Chem.*, 1971, **7**, 203.

Talanta, Vol. 32, No. 8B, pp. 827–829, 1985
Printed in Great Britain.

0039-9140/85 $3.00 + 0.00

POTENTIOMETRIC DETERMINATION OF SODIUM CONCENTRATIONS IN AQUEOUS-ETHANOLIC SOLUTIONS

C. J. COETZEE
Department of Chemistry, University of the Western Cape, Bellville 7530, South Africa

(*Received* 16 *October* 1984. *Revised* 5 *March* 1985. *Accepted* 18 *March* 1985)

Summary—The potentiometric behaviour of a sodium ion-selective glass electrode in aqueous ethanolic media was studied. The electrode was then used to determine sodium ion concentrations in aqueous ethanolic samples by standard-addition potentiometry.

The application of ion-selective electrodes in media other than water is still somewhat limited, although there were some applications in the early days of these sensors.[1–4] Reasons for this slow progress are many, and some are listed by Kakabadse.[5]

Little difficulty is encountered in the use of the glass pH-electrode in ethanol–water mixtures containing less than 90% w/w ethanol. At higher concentrations of alcohol and in water containing 50–90% acetone some contraction of the linear portion of the emf–pH curve has been found, as well as variation of the potential with time.[6]

Since a change in solvent may cause changes in the thermodynamic as well as the kinetic properties of the ions present and of exchange sites in ion-selective membranes, it is to be expected that the sensitivity, selectivity and response time of ion-selective electrodes might be dependent on the nature of the solvent.

The reproducibility of potentiometric measurements made in wholly or partially aqueous solvents is generally better than that for those made in pure non-aqueous solvents, because traces of water present in the non-aqueous solvent itself do not pose a problem in the mixed solvent systems, since they will seldom (if ever) be large enough to affect the overall water concentration significantly.

The behaviour of the reference electrode in the solvent used must also be known. The reference electrode most commonly used in non-aqueous systems is the aqueous calomel electrode, the use of which is very convenient. Its liquid-junction potential is evidently generally sufficiently constant for electrode potentials in non-aqueous or partly non-aqueous solutions to be measured with high precision.[7]

If a glass electrode is to be used in non-aqueous or partly non-aqueous media it must be soaked in the appropriate solvent so that the electrode surface layer obtained has a constant vacancy-concentration characteristic of the solvent.[8]

The use of the standard-addition technique in application of ion-selective electrodes is well known.[9,10] In this work a sodium ion-selective glass electrode was employed for determination of the sodium ion concentration in aqueous ethanol samples, by the standard-addition method.

Because of variations in the non-aqueous contents of the samples the technique was not simple to apply and various precautions had to be taken to standardize the conditions under which determinations could successfully be done.

One of the more important prerequisites is that the ionic strength of the solution to be analysed should be the same as that of the added standard. Also, the concentration range covered by the standard additions must fall within the linear part of the calibration graph for the electrode. In addition, if a partially aqueous solvent is used the added standard should have the same solvent composition as the sample in order to cut out any effects from heat of mixing.

EXPERIMENTAL

Reagents

All reagents used were of analytical-reagent grade. Sodium chloride was dried at 120° overnight.

Apparatus

A Radiometer PHM-64 pH-meter was used for all potentiometric measurements. The sodium ion-selective glass electrode used was a Beckman 39278. The manufacturers recommend that the pH of test solutions should be $\geqslant pNa + 4$ if sodium measurements are to be made.[11] The reference electrode was a Beckman 39170 fibre-junction saturated calomel electrode.

Preliminary experiments

The following experiments were planned and done in order to establish the effect of all the variables, before the standard-addition method for the determination of sodium concentration in ethanolic solutions was attempted.

1. Calibration of the electrode at 25° in sodium solutions containing from 0 to 50% v/v ethanol.
2. Repetition of the calibrations with the ionic strength adjusted to 0.1*M* with 0.1*M* magnesium sulphate. This was

necessary as the standard-additions technique calls for working with a constant ionic strength medium to minimize junction-potential effects.

3. Repetition of the calibration with sodium solutions in 50% v/v aqueous dimethylformamide, dioxan, acetone, ethanol, dimethylsulphoxide, methanol and 1-propanol media to obtain an overall picture of the response of the electrode in various aqueous/non-aqueous solvent mixtures. The glass electrode used was preconditioned in the appropriate solvent mixture for 24 hr before use.

On the basis of the preliminary experiments, 15% v/v ethanol solution was chosen as the medium for the standard-addition determinations with the glass electrode preconditioned in 15% v/v ethanol solution.

Standard-addition procedure

The alcohol content of the sample was first determined by density determination[12] at 20° and the solution was adjusted to 15% v/v ethanol content and 0.1*M* ionic strength with magnesium sulphate. The sample size was normally 25 ml. The ionic strength of the standard solutions was also adjusted to 0.1*M* with magnesium sulphate when necessary, and the solutions were prepared in 15% v/v ethanol medium. Their sodium concentration ranged between $5.00 \times 10^{-3}M$ and 0.1000*M*. Fixed volumes of sample were mixed with various volumes of standard and diluted to a fixed volume with 15% v/v aqueous ethanol at ionic strength 0.1*M* ($MgSO_4$), the sodium activities were measured with the sodium electrode, and the usual graph was drawn and interpreted. When necessary the pH was adjusted to pNa + 4 by addition of a drop or two of 3*M* ammonia solution.

RESULTS AND DISCUSSION

The calibration graphs for various sodium solutions in aqueous ethanol were linear between pNa 1 and 4.5. Stable potential readings were obtained within a minute. Figure 1 shows a selection of these graphs. The slopes of the linear sections were all in the range 58.3–58.7 mV/pNa. The general trend of increase in potential with increasing ratio of organic solvent was also found by Chaudhari and Cheng[13] for the response of a lead ion-selective electrode.

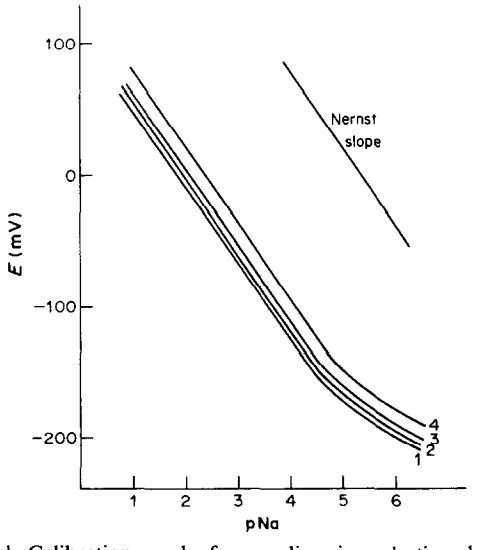

Fig. 1. Calibration graphs for a sodium ion-selective glass electrode in (1) water, (2) 10% ethanol, (3) 25% ethanol, (4) 50% ethanol.

Table 1. Slopes of calibration graphs for sodium in 50% v/v water–organic solvent media

Solvent	Slope, *mV/pNa*
Water	58.6
1-Propanol	56.5
Methanol	56.8
Dimethylsulphoxide	58.7
Ethanol	58.7
Acetone	52.4
Dioxan	56.5
Dimethylformamide	57.2

Table 2. Determination of the sodium content of aqueous ethanol solutions

Original ethanol content, % *v/v*	$[Na^+]$ found, M	
	Potentiometry	Flame photometry
12.0	0.0196_5	0.0196
12.0	0.0196_5	0.0196
15.0	0.0123_8	0.0124
15.0	0.0085_7	0.0086
15.0	0.0082_8	0.0083
15.0	0.0159_1	0.0159
15.0	0.0168_2	0.0168
21.0	0.0193_7	0.0194
18.0	0.0057_6	0.0058
16.0	0.0125_6	0.0126
14.0	0.0252_2	0.0252

At the ionic concentrations and solvent compositions used there does not seem to be any problem due to ion-pair formation.

The results show, however, that knowledge of the ethanol content of the sample is necessary before a potentiometric determination can be done either by direct measurement or by the standard-additions method.

It is also necessary that the ethanol content of both the sample and the standards be the same.

The slopes of the calibration graphs for the 0.1*M* ionic strength ($MgSO_4$) solutions also agreed within 0.5 mV, but there is a small parallel shift of the graphs with change in ionic strength, so close matching of the ionic strength of the unknown and standard solution is necessary.

Table 1 gives the slopes of the calibration graphs for the sodium electrode in the various 50% v/v aqueous/non-aqueous solvent mixtures tested. The graphs were linear over the sodium concentration range 10^{-1}–$3 \times 10^{-5}M$.

All the slopes except that for the acetone medium are within 3 mV of the value for purely aqueous medium. The cell emf depends on the solvent, and becomes more positive with change of solvent in the descending order given in the table. The shift does not have a direct correlation with the dielectric constant of the organic component of the solvent medium. It may probably be attributed to a combination of increase in activity of the cation, change in junction potentials, and dielectric constant effects.

Table 2 gives the results of a number of sodium determinations, in which the ethanol content of the sample was adjusted to 15% v/v. The sodium contents of the samples were also determined by flame-emission spectrometry and these results are listed for comparison. A set of 20 determinations of sodium covering the range 0.10–2.0 mg/ml gave an average recovery of 99.9$_5$% with a standard deviation of 0.3%.

These results show that with necessary precautions it is possible to use a sodium-selective glass electrode to determine the sodium content of aqueous ethanolic solutions successfully. The selectivity coefficients listed by the manufacturer indicate that only lithium, silver and hydrogen ions could interfere, and in most samples likely to be tested (*e.g.*, wines), the first two species are unlikely to be present in more than traces, and the pH adjustment will take care of the third.

Acknowledgements—The author wishes to thank the South African C.S.I.R. for financial assistance, and Dr. R. A. Chalmers for critical comments during preparation of the manuscript.

REFERENCES

1. J. J. Lingane, *Anal. Chem.*, 1967, **39**, 881; 1968, **40**, 935.
2. E. Pungor and K. Tóth, *Anal. Chim. Acta*, 1969, **47**, 291.
3. J. W. Ross and M. S. Frant, *Anal. Chem.*, 1969, **41**, 967.
4. G. A. Rechnitz and N. C. Kenny, *Anal. Lett.*, 1969, **2**, 395.
5. G. Kakabadse, *Ion-Selective Rev.*, 1982, **3**, 127.
6. R. G. Bates, *Determination of pH, Theory and Practice*, 2nd Ed., Wiley, New York, 1984, and references cited therein.
7. G. J. Hills, in *Reference Electrodes, Theory and Practice*, D. J. G. Ives and G. J. Janz (eds.), Academic Press, New York, 1961.
8. Z. Boksay and B. Csakvari, *Acta Chim. Acad. Sci. Hung.*, 1971, **67**, 157.
9. A. Liberti and M. Mascini, *Anal. Chem.*, 1969, **41**, 676.
10. C. J. Coetzee, A. J. Basson and S. R. Grobler, *Tydskr. Natuurwetenskappe*, 1975, **15**, 24.
11. *Beckman Instructions 1155B*, Beckman Instruments, Fullerton, Cal., August 1964.
12. R. C. Weast (ed.), *Handbook of Chemistry and Physics*, 47th Ed., The Chemical Rubber Co., Cleveland, Ohio, 1966.
13. S. N. K. Chaudhari and K. L. Cheng, *Mikrochim. Acta*, 1979 **II**, 411.

Talanta, Vol. 32, No. 8B, pp. 830–831, 1985
Printed in Great Britain.

0039-9140/85 $3.00 + 0.00

IRIDIUM IN SEA-WATER

JAMES FRESCO
Department of Chemistry, McGill University, Montreal, Quebec, Canada

HERBERT V. WEISS, RICHARD B. PHILLIPS and RONALD A. ASKELAND
Radiation Physics, Naval Ocean System Center, San Diego, California 92152, U.S.A.

(*Received* 26 *November* 1984. *Revised* 27 *February* 1985. *Accepted* 5 *March* 1985)

Summary—Iridium in sea-water has been measured (after isolation from the saline matrix by reduction with magnesium) by neutron bombardment, radiochemical purification and high-resolution γ-ray spectroscopy. The concentration obtained in a Pacific coastal water was $1.02 \pm 0.26 \times 10^{-14}$ g per g of sea-water. At such extremely low concentrations, seawater is an extremely unlikely source for anomalously high iridium concentrations measured in the Cretaceous-Tertiary boundary layer of deep-sea sediments.

Among the platinum-group elements only palladium has been detected in sea-water.[1,2] Interest in oceanic iridium has been aroused by recent investigations of the distribution of iridium in the earth's crust. For one location where the amount of iridium was anomalously large, an upper concentration limit for iridium in sea-water, 4×10^{-13} g/g, was used to reject the possibility of dissolved iridium as the source.[3]

It appeared the time was appropriate to measure iridium in sea-water. In the study to be presented here, iridium was removed from sea-water by reduction with magnesium and then bombarded with neutrons. A series of post-irradiation separations was performed to remove long-lived interferences, and then the γ-radiation of iridium-192 ($t_{1/2} = 74.2$ d) was measured to establish the mass of the precursor element.

EXPERIMENTAL

Isolation of iridium from sea-water

Since iridium has been reported to be quantitatively precipitated by reduction with magnesium[4] or by heating under pressure with magnesium or zinc,[5] conditions for recovery of iridium-192 tracer [dissolved as $(NH_4)_2IrCl_6$] from sea-water were investigated. Although the speciation of iridium in sea-water is unknown, the presence of iridium(III) in sea-water samples is unlikely since it is aerially oxidized in basic 0.50*M* sodium chloride solutions.[6]

Quantitative separation of the tracer from 1.5-litre volumes of sea-water was achieved by initial pH adjustment to 4, followed by continuous stirring with 75 mg of magnesium powder at 80° for a period of 2 hr. The stirring time was extended to 4 hr for the analyses.

Samples and sample treatment

Sea-water samples were collected close to the southern tip of Pt. Loma, CA, at a point 250 m from the shore line, 2 m above the sediment and, at mean-tide, 3 m from the water surface. Both 1- and 1.5-litre volumes of sea-water were passed through 0.4-μm Nuclepore filters immediately after collection. The filters were discarded and the iridium collection procedure immediately started.

The sea-water was discarded after collection of the reduction products and undissolved magnesium on a Nuclepore filter. The filter was washed with demineralized water, the magnesium was dissolved in the minimal amount of 8*M* nitric acid, and the solution was passed through the filter. The filter was then rinsed with additional small volumes of 8*M* nitric acid, the volume of combined filtrate and washings being 40 ml. This solution was evaporated to about 0.1 ml, then diluted to 2 ml with demineralized water, and evaporated again to about 0.1 ml. This final solution was transferred to a quartz vial and diluted to 2 ml, and the vial was sealed.

Irradiation and post-irradiation procedure

Samples, reagent blanks and standards (0.1 and 1.0 ng of Ir) were irradiated in the University of Missouri nuclear reactor for 166 hr at a flux of 1.8×10^{13} neutrons . cm^{-2} . sec^{-1}.

After a one-month cooling period, the vials were unsealed. The irradiated solutions were washed into beakers with nitric acid, and 10 mg of iridium carrier [as hexachloroiridate (IV)], 10 mg of cobalt (II) carrier and 3 ml of concentrated sulphuric acid were added. Studies of the recovery of magnesium-reduced iridium-192 tracer by the procedure to be described below, but without the separation steps to remove other γ-emitting nuclides, showed quantitative recovery of the tracer and carrier and thus indicated that carrier–tracer exchange was essentially complete.

The diluted irradiated solutions were heated to boiling and evaporated to fumes of sulphuric acid. This step was repeated after cooling and addition of nitric and hydrochloric acids. The intensely blue solutions were diluted to 20–25 ml and concentrated hydrochloric acid was added dropwise to the boiling solutions until a colour change to amber was noted. After further dilution to 150 ml, three successive precipitations with α-nitroso-β-naphthol were performed, with additional cobalt carrier introduced after the first and second precipitations. The γ-ray spectra of the cobalt precipitates were examined to confirm that decontamination from cobalt-60 was complete.

The excess of α-nitroso-β-naphthol in the final filtrate from the cobalt separation was destroyed by heating with nitric acid. This was followed by addition of 2 mg of silver carrier, dilution to 30 ml and precipitation of silver chloride by addition of sodium chloride.

The silver chloride filtrates were treated with 1 mg of iron(III) carrier, heated, and adjusted to pH 7.2–7.6 with ammonia to precipitate hydrous ferric oxide. The iron precipitates were filtered off and washed, and the filtrates were acidified, and the precipitations repeated after addition of a further 1 mg of iron(III) carrier to each. At least three such precipitations were necessary. The γ-ray spectra of the successive hydrous ferric oxide precipitates were recorded

and compared, first to document the removal of high-energy γ-emitters which would contribute to the Compton background of the sample, and secondly to minimize the number of iron(III) scavenges, since these could entail loss of iridium. Iridium losses of 50% or more were incurred at pH 7.6.

Ammonia, ammonium ions and chloride, which reduce the recovery of iridium oxide, were then expelled from the final filtrates from the iron-scavenges by heating first with sodium hydroxide and then with excess of concentrated nitric acid, and finally to fumes of sulphuric acid. Before volatilization of the nitric acid, 5 mg of chromium(III) carrier and 5 mg of zinc carrier were added to each of the samples. After the heating till fuming the solutions were diluted to 50 ml and heated, then sufficient potassium bromate was added to convert the chromium(III) into chromium(VI). The pH was raised to 5 with sodium bicarbonate and additional potassium bromate was introduced to precipitate the iridium.[7]

The iridium dioxide produced was collected on a Nuclepore filter, and washed first with 0.05*M* acetate–acetic acid buffer (pH 5) and then with demineralized water.

Measurements

The 296, 308, 316 and 468 keV photopeaks of iridium-192 were counted with a 75-cm^3 Ge(Li) detector coupled to a 1024-channel pulse-height analyser. After it had been verified that the relative intensities of the four peaks were of the correct order, the counting data for the 468 keV peak were corrected for Compton background and radioactive decay.

Iridium carrier recoveries

Sample and blank iridium dioxide precipitates and 0.1-mg iridium comparison samples were transferred to 1.4-ml polyethylene vials. The vials were irradiated for 30 min in the "lazy susan" compartment of the TRIGA nuclear reactor at the University of California, Irvine, operated at 40 kW. The original ^{192}Ir activities were corrected for chemical yield by comparison of the counting rates of samples and standards.

RESULTS AND DISCUSSION

Among the principal long-lived induced nuclides that appeared with the iridium recovered from sea-water were ^{60}Co, ^{65}Zn, ^{51}Cr, ^{46}Sc and ^{59}Fe. Small amounts of other nuclides such as ^{110}Ag were identified. Since iridium-carrier losses could be > 50% in the iron(III) separation steps and lesser losses were incurred in other radiochemical steps, the iridium-carrier chemical yields ranged between 10 and 30%. Counting periods were 72 hr or more and for samples of low activity the counting error was 15%.

The concentrations of iridium found in reagent blanks and replicate sea-water samples are presented in Table 1. The iridium concentration in six of the sea-water samples, after subtraction of the reagent blanks, averaged $1.02 \pm 0.26 \times 10^{-14}$ g/g. The other sample, no. 3, was omitted from calculation of the mean; the high value was presumed to be the result of contamination.

The mean value found for iridium is only a twentieth of the value reported earlier for palladium, 2.2×10^{-13} g/g, in the same waters.[1] This Ir/Pd ratio falls between the ratios calculable for the upper continental crust and deep-sea sediments. The crustal abundances (Ir 0.025 ng/g and Pd 1.05 ng/g), give a value of 1/42, while for deep-sea sediments the corresponding abundances, 0.31 and 3.5 ng/g, give an Ir/Pd value of 1/11.[8]

Table 1. The concentration of iridium in reagent blanks and sea-water samples corrected for blanks

	Iridium	
	pg	*fg/g*
Blanks		
40 ml of con. HNO_3	1.0	
75 mg of Mg	2.0	
*Samples**		
1		12.4
2		11.0
3		29.7†
4		07.8
5		08.4
6		13.7
7		07.6

*Samples 1–4 were 1-litre volumes; samples 5–7 were 1.5-litre volumes.
†Omitted from calculation of the mean.

The iridium anomaly for the deep-sea sediments has been ascribed by some[9] to a change in oceanic chemistry that resulted in precipitation of the dissolved species and prompt transport to the ocean bottom. If the concentration of iridium in sea-water reported here is correct, and the entire quantity of dissolved iridium in a water column of average ocean depth (4000 m) were suddenly transported to the sediment, it would result in a value of 4×10^{-9} g/cm^2. The average concentration of iridium in nine pelagic sediments is 64×10^{-9} g/cm^2.[10] Thus, even if some remarkable oceanic chemical condition occurred 65 million years ago, the consequence of such an event would not account for the quantities of iridium found in the sediments that were laid down at that period of time.

Acknowledgement—One of us, J. F., is grateful to the National Science and Engineering Research Council of Canada for financial support.

REFERENCES

1. H. V. Weiss and J. Fresco, *Can. J. Chem.*, 1983, **61**, 734.
2. D. S. Lee, *Nature*, 1983, **305**, 47.
3. L. W. Alvarez, W. Alvarez, F. Asaro and H. V. Michel, *Science*, 1980, **208**, 1095.
4. W. R. Schoeller and A. R. Powell, *Analysis of Minerals and Ores of the Rarer Elements*, 3rd Ed., p. 337. Hafner, New York, 1955.
5. S. I. Ginzburg *et al.*, *Analytical Chemistry of Platinum Metals*, p. 182. Wiley, New York, 1975.
6. G. van Loon and J. A. Page, *Can. J. Chem.*, 1966, **44**, 515.
7. R. Gilchrist and E. Wichers, *J. Am. Chem. Soc.*, 1935, **57**, 2565.
8. J. H. Crocket and H. Y. Kuo, *Geochim. Cosmochim. Acta*, 1979, **43**, 831.
9. Statement cited in L. W. Alvarez, *Proc. Natl. Acad. Sci. U.S.A.*, 1983, **80**, 627.
10. L. T. Silver and P. A. Schultz, *Eds. Geol. Sci. Am. Spec. Paper*, 1982, 190.

Talanta, Vol. 32, No. 8B, pp. 833–837, 1985
Printed in Great Britain.

0039-9140/85 $3.00 + 0.00

ANNOTATION

ADDUCT FORMATION BY THE OXINATES OF CERTAIN METALS

KASHINATH S. BHATKI
Chemistry Division, Bhabha Atomic Research Centre, Trombay, Bombay 400085, India

(*Received* 10 *October* 1984. *Accepted* 22 *March* 1985)

Summary—Various metal oxinates readily form adducts either with the reagent or other organic bases, and the adduct formation results in a synergic effect on the extraction of these oxinates into organic solvents. The nature of the adducts has been extensively explored but is still not completely understood. This paper surveys current knowledge of this field.

An adduct may be defined as a co-ordination compound in which there is addition of one or more molecules of a Lewis base (the donor) to one molecule of a Lewis acid (the acceptor), without any proton displacement. Formation of an adduct of a metal complex often supplies information about the co-ordination number of the metal ion and the structure of the complex. Formation of such adducts has been exploited for increasing the extractability of the metal complexes into organic solvents.

The metal complexes which form adducts are usually complexes of bidentate ligands and are co-ordinatively unsaturated, *i.e.*, the number of ligand anions required to neutralize the charge on the central metal ion is insufficient for all the co-ordination sites on the metal ion to be occupied by the donor atoms of the ligand, and the remaining sites are occupied by water molecules in the parent complex, or by other neutral ligands in the adduct.

Neutral co-ordinatively saturated complexes, which are in effect metal ions encased in an organic sheath, with no net charge, are readily soluble in solvents of low polarity but not in water, whereas neutral co-ordinatively unsaturated complexes are insoluble in both water and organic solvents, because there is no ion-dipole interaction with water to confer solubility, but equally there is sufficient intermolecular interaction between the water molecules of hydration of the complex to prevent dissolution in non-polar solvents. To extract these "insoluble" complexes, it is necessary to displace the water molecules with a co-ordinating solvent such as butylcellosolve,[1] or by neutral organic donor molecules, such as butylamine[2] or the neutral ligand species itself.

For example, the strontium complex of 8-quinolinol (oxine,8-hydroxyquinoline, HQ), $SrQ_2 \cdot 2H_2O$, is insoluble in chloroform, whereas the adduct $SrQ_2 \cdot HQ$ is extractable into chloroform containing a sufficiently high concentration of 8-quinolinol.[3] Starý has studied the 8-quinolinol complexes of 32 metal ions, and their formation of adducts with the reagent.[4] Substituted 8-quinolinols give similar behaviour in general, but modifications can be caused by steric effects or inductive effects, and the extensive work on this topic by Professor Freiser and his school is the main theme of this paper.

Adduct formation is usually inferred from equilibrium extraction data, and there are few instances[5,6] of the extracted species being isolated and characterized,[7] and their absorption spectra measured.[8,9] The formation constants of many adducts have been determined, mainly by spectrophotometry[10,11] and solvent extraction,[12,13] and the methods of calculation have been described.[14–18]

In their work, Freiser and his school have used a series of metals and substituted 8-quinolinols to examine inductive and steric hindrance effects on the formation of adducts with the reagent itself (self-adducts) and with various pyridines. Pyridine and various of its methyl derivatives were used to investigate more closely the effect of steric hindrance by the donor and of donor basicity. The value of this approach was evident from the earlier reports that 4-methylpyridine forms more stable adducts than pyridine does with copper(II) β-diketonate complexes, because of its higher basicity,[19,20] and that copper(II) ethylacetoacetate can be crystallized as a di-adduct with the solvent from pyridine or 4-methylpyridine but not (presumably because of steric hindrance) from 2-methylpyridine or 2,6-dimethylpyridine.[19]

The self-adduct $NiQ_2 \cdot HQ$ (where HQ represents 8-quinolinol or one of its derivatives) is extracted in all the systems so far investigated, except the 2-methyl-8-quinolinol system, where only the simple 1:2 chelate is extracted, which can be attributed to steric hindrance.[18] This steric effect must presumably also extend to hydration of the chelate itself. Steric

Table 1. Equilibrium constants* for nickel chelates of 8-quinolinols[18] at 28° ± 1°C (reproduced from K. S. Bhatki, A. T. Rane and H. Freiser, *Indian J. Chem.*, 1977, **15A**, 983, by permission, Copyright 1979, Indian Chemical Society)

Ligand	Species extracted	log K_{ex}	log K_{AD}	log K_{DC}	$pK_{a_1} + pK_{a_2}$†	log K_{DR}§	log K_f
8-Quinolinol	$NiQ_2 \cdot HQ$	−5.50	2.95	0.58	14.90	2.64	18.24
2-Methyl-	NiQ_2	−9.55	No adduct	1.25	15.90	3.22	18.10
4-Methyl-	$NiQ_2 \cdot HQ$	−5.10	3.10	1.14	15.66	3.27	23.80
5-Chloro-	$NiQ_2 \cdot HQ$	−5.65	2.85	1.40	13.00	3.32	19.40
5-Nitro-	$NiQ_2 \cdot HQ$	−3.20	3.40	0.55	8.79	2.64	20.20

*K_{ex} = extraction constant; $K_{ex} = [NiQ_2 \cdot nHQ]_0[H^+]^2/[Ni^{2+}][HQ]_0^{n+2}$.
K_{AD} = adduct formation constant in organic phase; $K_{AD} = [NiQ_2 \cdot nHQ]_0/[NiQ_2]_0[HQ]_0^n$.
K_{DC} = distribution constant for NiQ_2; $K_{DC} = [NiQ_2]_0/[NiQ_2]$.
K_{DR} = distribution constant for reagent; $K_{DR} = [HQ]_0/[HQ]$.
K_f = formation constant of chelate in aqueous phase; $K_f = [NiQ_2]/[Ni^{2+}][Q^-]^2$.
†Reference 17.
§Reference 27.

hindrance in complex formation is usually caused when a bulky group is attached either to the donor atom or is near enough to it to cause mutual repulsion between the ligands, weakening the metal–ligand bonds and making the sterically crowded complex unstable. Thus substitution in the chelating molecule may not only alter its basic strength (and hence the stability of the complex) but also introduce steric effects which can further weaken the complex. This is well shown by the difference in the extraction behaviour of nickel with 2-methyl- and 4-methyl-8-quinolinol.[18]

Healy[21] has suggested that during adduct formation some of the bidentate chelating ligands may break one bond to the metal ion and become unidentate ligands, thus freeing co-ordination sites for addition of adduct-forming donors. The simplest and most direct ways to form adducts are by direct addition of the donor to the central metal ion, increasing its co-ordination number, or by substitution for water ligands.[21,22] The first is exemplified[23] by addition of a ligand S to $UO_2(HX)_2$ to form a highly extractable adduct $UO_2(HX)_2 \cdot S$, with an increase in co-ordination number from 6 to 7, and the second by formation of an extractable adduct of zinc trifluorothenoylacetonate, $Zn(TTA)_2$, with tri-n-octyl phosphate (TOP),[24] as shown by NMR studies:

$$Zn(TTA)_2 \cdot 2H_2O + \overline{TOP} \rightleftharpoons \overline{Zn(TTA)_2 \cdot TOP} + 2H_2O$$

where the bars indicate the organic phase.

SELF-ADDUCT FORMATION IN VARIOUS 8-QUINOLINOL SYSTEMS

In aqueous solution, nickel forms the dihydrate $NiQ_2 \cdot 2H_2O$ with 8-quinolinols (except the 2-methyl derivative). X-Ray diffraction studies on the zinc[25,26] and copper[27] complexes have shown that the two water molecules are *trans* to each other in a hexa-co-ordinated octahedral structure. The zinc, cadmium, cobalt, nickel and lead complexes are isomorphous.

When the logarithms of the formation constants of the nickel[18] or zinc[17,28] chelates of various 8-quinolinols are plotted against the overall pK_a values (pK_a being the sum of pK_{a1} and pK_{a2} for dissociation of protons from the protonated 8-quinolinol), a linear relationship is found (since pK_a represents the basicity of the ligand). The logarithms of the adduct formation constants are also a linear function of the pK_a values but are almost the same as each other. This is because the chelating agent plays two roles, in which its basicity has opposing effects. Increased basicity increases the donor power of the reagent in adduct formation, but this is offset by a reduction in the acceptor power of the chelate complex, since the greater stability of the complex (because of the higher basicity of the ligand) results in a lower "residual Lewis acidity" of the chelate. Similar results are found for the cobalt(II) complexes[29] but manganese(II) does not form a self-adduct with 8-quinolinols, only the simple 1:2 chelate being extracted.[30]

Table 1 summarizes the equilibrium data for the nickel complexes. These values were all obtained by solvent extraction studies, and it was thought interesting to see what happens when the anhydrous solid chelates are treated with the adduct-forming species in an organic solvent, and to apply spectrophotometric methods to the investigation. In formation of chelates with 8-quinolinols there are bathochromic shifts of the absorption bands of the ligands.[31] Further change might be expected on adduct formation. The spectrum of the anhydrous nickel 8-quinolinol complex in chloroform medium[32] has absorption bands at 455 and 340 nm. The band at 455 nm decreases gradually on addition of 8-quinolinol, and the band at 340 nm shifts to 323 nm, with a large increase in absorbance. The 5-nitro-8-quinolinol complex in chloroform in the absence of free ligand has bands at 480, 430 and 345 nm. The weak band at 480 nm decreases on addition of the ligand; the other two show a large increase in absorbance and the 345-nm band shifts to 355 nm. These changes have been used to determine the adduct formation constants (by plotting

Table 2. Adduct-formation constants for various pyridine adducts of nickel-8-quinolinolates[34] at 28° ± 1°C (reproduced from K. S. Bhatki, A. T. Rane and H. Freiser, *Inorg. Chem.*, 1978, **17**, 2215; Copyright 1978 American Chemical Society)

		log K_{AD}				
Base	pK*	8-Quinolinol	2-Methyl-8-quinolinol	4-Methyl-8-quinolinol	5-Chloro-8-quinolinol	5-Nitro-8-quinolinol
Pyridine	5.20	3.12	2.70	2.76	4.50	5.14
2-Picoline	5.90	2.25	1.90	2.04	3.10	4.34
2,4-Lutidine	6.72	2.50	2.24	2.36	3.56	4.84
2,4,6-Collidine	7.50	2.92	2.55	2.80	4.25	4.60

*Dissociation constant for the protonated base.

$\log[A_0 - A]/A$ *vs.* log[HQ], A_0 and A being the maximum and variable absorbances respectively)[32] and the results obtained were in agreement with those obtained by solvent extraction.[18] It had been shown earlier[33] that the chelate does not exist as a polymer, so only formation of a monomeric adduct was considered.

There was no change, however, in the visible-region spectrum of the 2-methyl-8-quinolinol chleate on addition of free ligand, and this was attributed to steric hindrance by the 2-methyl group. Similar work with the 4-methyl-8-quinolinol and 5-chloro-8-quinolinol complexes[33] showed that di-adducts $NiQ_2 \cdot 2HQ$ are formed in the chloroform solution, in contrast to the mono-adducts found in the solvent extraction study.[18] Thus nickel can form two types of self-adducts with 8-quinolinols, depending on the conditions.

ADDUCTS WITH OTHER NITROGEN BASES

Because 2-methyl-8-quinolinol does not form an adduct with its nickel complex,[18] it was of interest to examine the effect of steric hindrance caused by the adduct-forming donor. For this purpose the effect of pyridine and a series of methyl-substituted pyridines on the extraction of the 2-methyl-8-quinolinol complex was examined.[34] Similar experiments were done with the 8-quinolinol and 4-methyl-8-quinolinol complexes for comparison. In all the systems studied, except the 2-methyl-8-quinolinol system, adducts of the type $NiQ_2 \cdot 2B$ were found (where B is the nitrogen base). Since the chelates formed in aqueous medium were the dihydrates, the nitrogen base obviously increases the extractability by replacing the water molecules with ligands that are more compatible with an organic solvent medium of low polarity.

Substitution of a methyl group in pyridine increases the basicity of the nitrogen atom,[35] but substitution in the 2- or 6-position can adversely affect the co-ordination to a metal ion, by steric hindrance. Thus pyridine is expected to form more stable adducts than 2-picoline does. The addition of a second methyl group in the 4-position results (as expected) in a further increase in basicity and hence in the adduct formation constant K_{AD}, but not enough to offset entirely the adverse steric influence of the 2-methyl group, as shown in Table 2. The effect of the basicity of the adduct-forming base and of that of the chelating ligand is seen to be in agreement with that predictable from the adduct-formation constants of the self-adducts (Table 1), *viz.* that for a series of chelates the smaller the residual Lewis acidity of the acceptor (*i.e.*, the higher the basicity of the ligand and hence stability of the chelate), the lower the adduct formation constant for a particular base, and the higher the basicity of the donor, the higher the adduct-formation constant for a particular chelate, except, of course, for the 2-methyl-8-quinolinol series, where the steric effect is dominant. This study confirmed the earlier findings by Willis and Mellor[36] and Patel *et al.*[37] that these adducts are octahedral with the two nitrogen-base ligands in *trans*-positions (except for the 2-methyl-8-quinolinol systems).

When the spectrophotometric approach[32] was applied to examination of these adducts,[38-40] the results listed in Table 3 were obtained, which show that the behaviour is as expected from the observation above, lower adduct stability being observed whenever steric hindrance is encountered. Thus the constants for the 2-methylpyridine (2-picoline) adducts are lower than those for the corresponding pyridine adducts, and those for the 2-methyl-8-quinolinol adducts lower than those for the corresponding 4-methyl-8-quinolinol products. If more methyl groups are introduced in positions where they can exert steric hindrance, as in 2,6-lutidine or 2,4,6-collidine, the resultant crowding that would occur on adduct formation can also have an adverse effect. That is seen when the methyl-8-quinolinol complexes (either 2- or 4-) are treated with 2,6-lutidine; no spectral shifts are seen in either case, indicating the absence of adduct formation.

An interesting situation arises when a second substituted quinolinol is used as the adduct-forming base. Since 5-nitro-8-quinolinol is considerably the least basic and 4-methyl-8-quinolinol the most basic of the 8-quinolinols tested, an adduct with the 5-nitro chelate as the acceptor and 4-methyl reagent as the donor should be the strongest, and that with the 4-methyl chelate as acceptor and the 5-nitro compound as donor the weakest. This prediction was examined spectrophotometrically by adding 4-methyl-8-quinolinol to a solution of the anhydrous 5-nitro chelate in chloroform and measuring the decrease in absorbance at 480 nm.[41] The value of log

Table 3. Adduct-formation constants of nickel(II) chelates of 8-quinolinols with various bases by direct addition in chloroform medium

Base	pK*	log K_{AD} 8-Quinolinoate[40]	2-Methyl-8-quinolinolate[38]	4-Methyl 8-quinolinolate[38]	5-Chloro-8-quinolinolate[40]	5-Nitro-8-quinolinolate[39]
Pyridine	5.20	4.33	0.65	3.40	3.90	3.42
2-Picoline	5.90	1.35	−0.48	0.05	1.43	2.63
4-Picoline	6.08	5.16	0.94	3.73	4.50	4.05
2,4-Lutidine	6.72	0.43	−0.33	0.28	0.87	2.00
2,6-Lutidine	4.95	No adduct	No adduct	No adduct	No adduct	No adduct
2,4,6-Collidine	7.48	1.67	−0.18	1.65	2.05	2.97
Ethylenediamine	6.84	9.00	2.87	8.47	7.47	9.90
2,2-Bipyridyl	4.37	9.35	3.13	8.65	6.83	10.20
1,10-Phenanthroline	4.95	9.20	3.23	8.47	7.07	9.77
2,9-Neocuproine	5.85	6.88	2.75	—	5.86	4.50

*Dissociation constant for protonated base.

K_{AD} for the mixed adduct was 4.60, which may be compared with log $K_{AD} = 3.35$ for the self-adduct, and shows that the behaviour is as predicted. This observation should also apply to the solvent extraction system, and Freiser has suggested that addition of a small amount of 4-methyl-8-quinolinol should give a synergic increase in the extraction of the nickel 5-nitro-8-quinolinol chelate.

Similar effects have been found for the zinc[28] and cobalt[42] quinolinol complexes, with pyridines as donors. With manganese, however, pyridine forms a mono-adduct of the 8-quinolinol complex.[30] 2-Picoline and 2,6-lutidine produce the expected steric hindrance. The stability of the adducts is also a function of the atomic number of the central metal ion, and increases in the order Mn < Co < Ni.

The indium system has also been examined.[43] It is not surprising that the simple anhydrous 1:3 chelate is extracted in the absence of pyridines. Addition of a pyridine, however, results in a synergic increase in extraction, with formation of a di-adduct $InQ_3 \cdot 2B$.

STRUCTURE OF THE ADDUCTS

Though the structure of the di-adducts is known, there being octahedral co-ordination with the two donor groups *trans* to each other, that of the mono-adducts has not been conclusively established and is open to conjecture. The possibilities seem to be either an octahedral structure with the two chelating ligands rearranged so that they are no longer planar as in the dihydrates, with the donor group also forming a chelate ring with the central metal ion, or a penta-co-ordinated system with the two chelating ligands forming the square base of a pyramid, with a unidentate donor group occupying the apex of the pyramid, the second water molecule in the original dihydrate being forced out of the co-ordination sphere. All the thermogravimetric evidence obtained points to the absence of a water molecule in the adduct, but of course gives no information about the structure. The only direct structural evidence seems to be from the X-ray study by Rane and Ravi,[44] but unfortunately they do not seem to have worked out the structure yet. Their report says that the anhydrous, dihydrate and self-adduct forms of the nickel 8-quinolinol complex are all monoclinic, and that the X-ray pattern for the adduct is different from that of the dihydrate. They propose a penta-co-ordinated square pyramidal structure for the adduct, on the basis of a reference to a review[45] that does not appear to mention this particular adduct. The general opinion of those who have worked on these adducts is that the structure is the postulated square-based pyramid, but confirmation must await a definitive structural analysis.

Acknowledgements—The author is grateful to Professor Henry Freiser for introducing him to the world of adducts, especially those of 8-quinolinol chelates, and for his advice and encouragement during the progress of this work at Tucson, Arizona. The author also gratefully acknowledges the financial support he received from the U.S.A.E.C. during his stay at the University of Arizona where part of this work was carried out. The author is obliged to Dr K. N. Rao, Director, Chemical Group and Dr R. M. Iyer, Head, Chemistry Division and Associate Director Chemical Group, BARC, for their support and constant encouragement. He is also grateful to his former student and now colleague, Dr A. T. Rane, who collaborated in the experimental part of T.I.F.R. during the work for his Ph.D from Bombay University. The author has benefited much during the writing of this review from discussions with Dr D. G. Vartak, Head, Reactor Chemistry Section, CIRUS, Bhabha Atomic Research Centre, Bombay.

REFERENCES

1. C. L. Luke *Anal. Chem.*, 1956, **28**, 1443.
2. F. Umland, W. Hoffmann and K.-U. Meckenstock, *Z. Anal. Chem.*, 1960, **173**, 211.
3. D. Dyrssen, *Svensk Kem. Tidskr.*, 1953, **65**, 43; 1955, **67**, 311.
4. J. Starý, *Anal. Chim. Acta*, 1963, **28**, 132.
5. J. R. Ferraro and T. V. Healy, *J. Inorg. Nucl. Chem.*, 1962, **24**, 1463.
6. T. V. Healy and J. R. Ferraro, *ibid.*, 1962, **24**, 1449.
7. H. M. Irving and N. S. Al-Niaimi, *ibid.*, 1965, **27**, 1671.
8. S. Oki, *Talanta*, 1969, **16**, 1153.
9. S. Oki and I. Terada, *Anal. Chim. Acta*, 1972, **61**, 49; 1973, **66**, 201.

10. D. Dyrssen and D. Petković, *Acta Chem. Scand.*, 1965, **19,** 653.
11. W. R. Walker and N. C. Li, *J. Inorg. Nucl. Chem.*, 1965, **27,** 2255.
12. T. V. Healy, *Nucl. Sci. Eng.*, 1963, **16,** 413.
13. H. Irving and D. N. Edgington, *J. Inorg. Nucl. Chem.*, 1965, **27,** 1359.
14. T. Sekine and Y. Hasegawa, *Solvent Extraction Chemistry*, p. 200 ff. Dekker, New York, 1977.
15. T. Sekine and D. Dyrssen, *J. Inorg. Nucl. Chem.*, 1964, **26,** 1727.
16. F. C. Chou, Q. Fernando and H. Freiser, *Anal. Chem.*, 1965, **37,** 361.
17. F. Chou and H. Freiser, *ibid.*, 1968, **40,** 34.
18. K. S. Bhatki, A. T. Rane and H. Freiser, *Indian J. Chem.*, 1977, **15A,** 983.
19. D. P. Graddon and E. C. Walton, *J. Inorg. Nucl. Chem.*, 1961, **21,** 49.
20. W. R. May and M. M. Jones, *ibid.*, 1963, **25,** 507.
21. T. V. Healy, in *Solvent Extraction Research*, A. S. Kertes and Y. Marcus (eds.), pp. 257–279. Wiley, New York, 1969.
22. Q. Fernando, in *Separation Techniques in Chemistry and Biochemistry*, R. A. Keller (ed.), pp. 357–376. Dekker, New York, 1967.
23. C. A. Blake, D. E. Horner and J. M. Schmitt. *U.S. At. Energy Comm. Rept.*, ORNL-2259, 1959.
24. W. R. Walker and W. C. Li, *J. Inorg. Nucl. Chem.*, 1965, **27,** 411.
25. L. L. Merritt, *Anal. Chem.*, 1963, **25,** 718.
26. L. L. Merritt, R. T. Cady and B. W. Mundy, *Acta Cryst.*, 1954, **7,** 473.
27. J. Fresco and H. Freiser, *Anal. Chem.*, 1964, **36,** 631.
28. F. Chou, *Ph.D. Thesis*, University of Arizona, 1967, and references therein.
29. A. T. Rane and K. S. Bhatki, *Can. J. Chem.*, 1979, **57,** 580.
30. A. T. Rane, *J. Inorg. Nucl. Chem.*, 1980, **42,** 1520.
31. O. Popovych and L. Rogers, *Spectrochim. Acta*, 1965, **21,** 1229.
32. A. T. Rane and K. S. Bhatki, *Indian J. Chem.*, 1979, **18A,** 92.
33. K. S. Bhatki and A. T. Rane, *Proc. Indian Acad. Sci.*, 1979, **88A,** (J-4), 313.
34. K. S. Bhatki, A. T. Rane and H. Freiser, *Inorg. Chem.*, 1978, **17,** 2215.
35. K. Schofield, *Hetero Aromatic Nitrogen Compounds: Pyrroles and Pyridines*, Butterworths, London, 1967.
36. J. B. Willis and D. P. Mellor, *J. Am. Chem. Soc.*, 1947, **69,** 1237.
37. D. C. Patel, R. C. Sharma and P. K. Bhattacharya, *J. Indian Chem. Soc.*, 1971, **48,** 233.
38. K. S. Bhatki, A. T. Rane and H. Freiser, *Inorg. Chim. Acta*, 1978, **26,** 183.
39. K. S. Bhatki and A. T. Rane, *Spectrochim. Acta*, 1979, **35A,** 573.
40. *Idem, J. Inorg. Nucl. Chem.*, 1980, **42,** 453.
41. *Idem, Indian J. Chem.*, 1981, **20A,** 424.
42. *Idem, Trans. Metal Chem.*, 1978, **3,** 181.
43. A. T. Rane, *Indian J. Chem.*, 1981, **20A,** 900.
44. A. T. Rane and V. V. Ravi, *ibid.*, 1982, **21A,** 311.
45. J. S. Wood, *Prog. Inorg. Chem.*, 1972, **16,** 227.

Talanta, Vol 32, No. 9, pp. 839–844, 1985
Printed in Great Britain.

0039-9140/85 $3.00 + 0.00

A THEORETICAL AND EXPERIMENTAL STUDY OF THE WAVEFORM IN POTENTIOMETRIC STRIPPING ANALYSIS WITH A ROTATING MERCURY-FILM ELECTRODE—THE REVERSIBLE CASE

BOY HØYER and LARS KRYGER

Department of Chemistry, Aarhus University, Langelandsgade 140, 8000 Aarhus C, Denmark

(*Received* 7 *February* 1985. *Accepted* 23 *April* 1985)

Summary—The potential–time transient in potentiometric stripping analysis with a rotating mercury-film electrode is simulated digitally by means of the finite-difference Cranck–Nicolson method. Good agreement with experimental results is obtained. The relations between peak shape and signal duration for reversible analyte systems are discussed, and it is shown that severe peak overlap gives rise to distortions of the composite signal.

In potentiometric stripping analysis (PSA)[1,2] or chemical stripping analysis,[3] trace analytes are preconcentrated by potentiostatic deposition on a working electrode and subsequently re-oxidized chemically by oxidizing agents present in the solution, with the potential–time behaviour of the working electrode being monitored in open circuit. With amalgamation of the analytes on thin-film mercury electrodes, PSA has proved useful for the accurate determination of several trace metals in a wide variety of media and materials, *e.g.*, sea-water,[4] beverages,[5] body fluids,[6,7] digested biological substances[8] and fly-ash.[9,10]

In PSA, if two analytes are redissolved at similar potentials, there is a risk of interanalyte interference due to overlap of the signals. The degree of overlap is partly determined by the separation of the peak potentials and by the amplitudes of the individual peaks. Generally, for reversible systems, the peak amplitudes and potentials are governed by factors which are well understood, and much can be done to minimize interference problems, for example by careful selection of the medium and the conditions for analyte deposition. The degree of overlap is, however, influenced even by the widths and general shapes of the individual stripping signals. Thus the chances of eliminating peak overlaps are better if the factors which govern the peak shape are equally well understood. Nevertheless, this aspect has so far received very little attention.[11,12] The present paper demonstrates how digital simulation can be used to provide a theoretical description of the waveform obtained with PSA under convective stripping conditions. More specifically, the reversible case is chosen for study. The proposed model is validated by comparison of theoretical and experimental data, and the results of the simulation are evaluated with respect to the applications of PSA.

To comply with the experimental conditions most frequently used in computerized batch PSA, the theoretical investigation assumes that analyte stripping as well as analyte deposition takes place under forced convective conditions at a mercury-coated rotating disk electrode (RDE), and, accordingly, the experimental study was done with this type of electrode. This forced-convection stripping scheme has one disadvantage: in PSA the sensitivity depends strongly on the hydrodynamic conditions, and a decrease of sensitivity results if the electrode rotation is not interrupted towards the end of the deposition period.[13] Consequently, if forced convection is maintained throughout the experiment, longer deposition periods will frequently be required, but this drawback is usually fully compensated by the improved precision and accuracy.

The rotating electrode creates a well-defined hydrodynamic pattern in the vicinity of its surface, which is stable towards mechanical disturbances in the cell. Therefore, electroactive species are transported to and from the surface in a highly reproducible manner, which eventually is reflected in improved precision of the analytical results. Under convective conditions, the flux of oxidant towards the electrode will respond rapidly to changes of electrode potential and will almost instantaneously reach a steady-state value which is proportional to the bulk concentration of the oxidant. Consequently, the flux of oxidant will be independent of the time spent at any particular potential. This facilitates application of the background subtraction method,[8] and with the RDE, an accurate correction for the capacitance contribution to the primary stripping signal can usually be achieved: a reliable estimate of the capacitance contribution can be obtained from a separate plating/stripping cycle using a deposition period of negligible duration. Once the flux of oxidant is constant in time, the electrode discharge proceeds at

equal rates in the two plating/stripping cycles. Hence a mutual scaling of the two signals[12] is no longer necessary, and the capacitance correction amounts to a simple subtraction of the capacitance signal from the primary stripping signal. Apart from this simplification, stripping at an RDE is particularly advantageous when samples contain electroactive substances which can be reduced to water-soluble species. Under convective conditions, such substances are much less likely to interfere in the determination of species which can be plated.[14]

THEORY

Principle of digital simulation

The basic equation describing the convective diffusional mass-transport of a species to or from the RDE in the absence of homogeneous reactions in the solution is given by:[15]

$$\frac{\partial c}{\partial t} = D\frac{\partial^2 c}{\partial x^2} - V_x\frac{\partial c}{\partial x} \tag{1}$$

where D is the diffusion coefficient of the species, V_x is the convective velocity of the solution normal to the electrode surface, and x is the distance from the electrode. V_x can be expanded into a power series in terms of x; however, when phenomena close to the electrode surface are studied, the first term suffices:

$$V_x = -0.510\,\omega^{3/2}\nu^{-1/2}x^2 \tag{2}$$

where ω is the angular velocity of the electrode in radians/sec, and ν is the kinematic viscosity of the medium. To bring equation (1) into dimensionless form, the following variable transformation is defined:[16]

$$X = x/\delta,\ T = Dt/\delta^2,\ C = c/c_{\text{bulk}} \tag{3}$$

where δ is the diffusion layer thickness:

$$\delta = 1.612D^{1/3}\nu^{1/6}\omega^{-1/2} \tag{4}$$

and equation (1) becomes:

$$\frac{\partial C}{\partial T} = \frac{\partial^2 C}{\partial X^2} + 2.139X^2\frac{\partial C}{\partial X} \tag{5}$$

In the finite-difference approach to solution of partial differential equations, the time and space variables are divided into discrete intervals of ΔT and ΔX, respectively. In this study, the derivatives in equation (5) have been thus divided by use of the implicit Cranck–Nicolson scheme, which is distinguished by great numerical stability. In particular, the simulation parameter $\lambda = (\Delta T)/(\Delta X)^2$ need not be less than 0.5, which is the stability limit by the explicit finite-difference method, and large savings in computation time can be achieved.

Boundary conditions and initial values

During the plating step in PSA, the electrolysis potential is normally chosen so that the rate of analyte deposition is limited by mass transport. In such cases, the surface concentration of analyte is essentially zero. With these boundary values and initial conditions (*i.e.*, $C(X,0) = 1$ for all X, $C(0,T) = 0$ for $T > 0$ and $C(X,T) = 1$ for $X \to \infty$, $T > 0$), the solution of equation (5) is trivial,[17] and a steady-state concentration profile is rapidly reached. This concentration profile can be calculated once and for all and serves as the initial value when the simulation of the stripping step is performed. Furthermore, it is assumed that the redox potentials of the analyte and the oxidant are sufficiently well separated to ensure that mass transport limits the flux of oxidant at the redissolution potential of the amalgamated analyte. With the analytes investigated in the present study [lead(II), cadmium(II) and indium(III)] and the oxidant applied (dissolved oxygen), this requirement is fulfilled, and the boundary condition at the electrode surface becomes:

$$\left(\frac{\partial C}{\partial X}\right)_{X=0} = K \tag{6}$$

Here, C refers to the analyte concentration, and K is a negative constant supplied as input to the simulation routine. As regards the digital simulation, PSA is therefore identical to constant-current chronopotentiometry.

The description of the mercury film during the stripping step is uncomplicated since it has been shown theoretically[18] that concentration gradients of amalgamated species within the film are important only at the very beginning of the stripping phase. Even for a relatively thick film (5 μm), this transition period lasts less than 1 msec, and is negligible on the time scale of a typical stripping signal. Hence the mercury film remains virtually uniform, and the concentration of dissolved metal decreases linearly with time during the redissolution process. In the case of reversible oxidation of an amalgamated metal M, which is the subject of this study, the electrode potential is governed by the Nernst equation:

$$E = E^0 + \frac{RT}{nF}\ln\frac{[M^{n+}]_{X=0}}{[M(Hg)]} \tag{7}$$

The thickness of the mercury film can be fixed arbitrarily, since a different choice merely shifts the stripping signal on the potential axis. This simplification, however, only applies to reversible behaviour.

When two analytes are re-oxidized at similar potentials, the boundary condition at the electrode surface is somewhat modified. The flux of newly oxidized material from the electrode surface must balance the constant supply of oxidant, which can be expressed in dimensionless form as:

$$\left(\frac{\partial C_1}{\partial X}\right)_{X=0} + \left(\frac{\partial C_2}{\partial X}\right)_{X=0} = K \tag{8}$$

where $C_2 = c_2/c_{2(\text{bulk})}$ and $C_1 = c_1 n_1 D_1/c_{2(\text{bulk})} n_2 D_2$. An additional boundary condition arises from the fact that the Nernst equation must be fulfilled for both

analytes *i.e.*, $E = E_1 = E_2$. At the beginning of the simulation, it is assumed that only the species with the most cathodic redox potential is re-oxidized, and the simulation proceeds as a single-component simulation until the concentration gradient of the second species becomes negative at the electrode surface, indicating the onset of oxidation of the second component.

Chronopotentiometric responses of amalgamated metals simultaneously undergoing re-oxidation from thin-film mercury electrodes have been calculated previously.[19] However, only stripping in stationary solutions was considered, and the semi-analytical approach employed in the calculation of the diffusive mass transport is not readily extendable to systems involving convection.

EXPERIMENTAL

Instrumentation

For data-acquisition and experimental control, a computerized instrument was employed.[20] During the stripping phase in the PSA, the potential of the working electrode was sampled at constant frequency and recorded as a potential distribution, the stripping of an amalgamated metal appearing as a peak. The background signal obtained with zero plating time was subtracted from the primary potentiograms. During all experiments, the data-acquisition rate was 6.7 kHz.

The electrochemical cell comprised a Metrohm 628–50 rotating disk electrode unit mounted with a 16-mm^2 glassy-carbon electrode (GCE) and equipped with a 50-ml beaker. The reference electrode was a Radiometer K801 Ag/AgCl electrode, and the counter-electrode was a glass-fitted platinum rod (1 cm long, 0.5 mm thick). The RDE was operated at a speed of 1500 rpm. Prior to measurements, the GCE was polished with 0.25-μm diamond paste and rinsed with ethanol. The GCE was preplated in $8 \times 10^{-5}M$ mercury (II) solution in $1M$ sodium acetate/hydrochloric acid buffer by electrolysis for 120 sec at -400 mV *vs.* Ag/AgCl.

Reagents

Triply distilled water and analytical grade chemicals were used in all experiments. Stock solutions of the analytes were $10^{-2}M$, made with triply distilled water and lead and cadmium nitrates and indium sulphate.

Experimental procedure

The medium used in all experiments was an acetate buffer prepared by adjusting $1M$ sodium acetate to pH 4.7 with concentrated hydrochloric acid. The solutions were not deaerated prior to PSA, and dissolved oxygen served as the oxidizing agent. Analytes were added as small aliquots of standard solutions from microlitre pipettes.

The lead signals reported were recorded after pre-electrolysis at -750 mV *vs.* Ag/AgCl. To obtain signals of widely differing magnitudes, the pre-electrolysis time was varied between 7.5 and 360 sec, and the lead concentration between 2.0×10^{-7} and $1.6 \times 10^{-6}M$.

In the investigation of additivity of overlapping PSA signals, the cadmium/indium system was chosen for study. Pre-electrolysis was done for 60 sec at -1300 mV *vs.* Ag/AgCl. First, 50 ml of blank buffer was divided equally between two identical beakers; cadmium solution was added to the first beaker, to give a level of $8.0 \times 10^{-7}M$ and indium solution to the second to give a level of $1.6 \times 10^{-6}M$. The cadmium signal was recorded, then the beakers were exchanged and the indium signal was recorded. During the exchange, the GCE was disconnected, and the electrodes were rinsed thoroughly. Finally, cadmium was added to the second beaker, again to give $8.0 \times 10^{-7}M$ concentration and the overlapping cadmium/indium signals were recorded. Each potentiogram was recorded three times.

Computation

All programs were written in FORTRAN-77 and run on the departmental VAX 11/780 computer. Simulated potentiograms were displayed in the multichannel mode to facilitate comparison with the experimental results. Copies of the programs are available on request.

RESULTS AND DISCUSSION

Single peak shapes

In quantitative PSA, the oxidant must always be present in large excess relative to the analyte, in order to control the oxidation rate and to eliminate inter-analyte interferences [*e.g.*, $2Tl^+ + Cd(Hg) \rightarrow 2Tl(Hg) + Cd^{2+}$]. Hence the flux of oxidized analyte from the working electrode in the stripping phase is much larger than the opposite flux during preconcentration. The simulations showed that for $C_{oxidant}/C_{analyte} > 30$ (assuming equal diffusion coefficients of oxidant and analyte), the concentration profile of analyte during stripping is entirely dominated by the flux from the electrode, and the steady-state concentration profile present at the commencement of stripping can be neglected. When equation (5) is solved with these boundary conditions, *i.e.*, $C(X,T) = 0$ for $T = 0$ and $(\partial C(X,T)/\partial X)_{X=0} = K$ for $0 < T \leq T_{strip}$, the solution for the concentration profile will be proportional to K in any time step. Owing to the logarithmic form of the Nernst equation, it can thus be concluded that the shape of the potential–time transient is governed by the duration of the stripping phase, T_{strip}, whereas the absolute values of the oxidant concentration and the pre-electrolysis time are unimportant. For instance, if both of the latter quantities are doubled in an experiment, no change in the shape or size of the PSA signal should be observed.

If the stripping phase lasts longer than $T = 2.5$ (called T_{ss} in the following), a steady-state concentration profile of re-oxidized analyte is established at the working electrode. At this point, the Cranck–Nicolson calculation of the concentration profile in the next time-step can be omitted, and a considerable saving in computational time is achieved. Inspection of the steady-state concentration profile showed that the effect of the electrode process is negligible at a distance of $X = 3$ from the electrode surface; hence consideration of the space axis beyond that point is redundant.

If simulated and experimental PSA signals are to be compared, the conversion factor between the physical and the dimensionless variable must be known. The transformation formulae can be written explicitly as:

$$X = 0.6211 D^{-1/3} \nu^{-1/6} \omega^{1/2} x$$

$$T = 0.3858 D^{1/3} \nu^{-1/3} \omega t \qquad (9)$$

Since D and ν enter these expressions with low powers, the accuracy with which they are known is not critical. Typical values are $\nu = 0.01$ cm^2/sec for aqueous media and $D = 10^{-5}$ cm^2/sec for non-complexed metal ions in such media.[17] With the applied rotation rate of $\omega/2\pi = 1500$ rpm, the conversions become: $x = 1.3 \times 10^{-2}X$ mm and $t = 0.17T$ sec.

In Fig. 1, simulated PSA curves corresponding to a reversible two-electron stripping process are displayed. For short stripping times, in which the steady-state concentration profile of analyte is not reached [curves (A) and (B)], the peak shape is relatively symmetrical and independent of the stripping time. With longer stripping times [curve (C)], a steady state is reached during the stripping phase, and the peak is sharper. Finally, when T_{strip} is so long that steady-state conditions prevail during most of the stripping phase [curve(D)], a very sharp and asymmetrical peak with a steeper cathodic branch is obtained. In quantitative PSA, the analytical signal usually evaluated is the stripping time, *i.e.*, the area of the peak when this is recorded in multichannel mode; however, it has also been reported[8] that the peak height is proportional to the analyte concentration when stripping is performed in a stationary solution. To examine whether this relation is valid for the RDE system as well, the peak height relative to T_{strip} is plotted against T_{strip} in Fig. 2. Proportionality should result in a horizontal line; however, it is seen that when $T_{strip} > 1$, the peak height grows disproportionately fast in accordance with the observed sharpening of the peak (Fig. 3). Under the experimental conditions of this study, $T_{strip} = 1$ corresponds to 170 msec in real time, and transition times in trace analysis by computerized PSA are usually well below this limit. Thus, for most practical applications, the peak height can be taken as the analytical response. This method of signal evaluation is particularly useful when neighbouring peaks overlap to some extent, and complete base-line resolution of the signals is then not required.

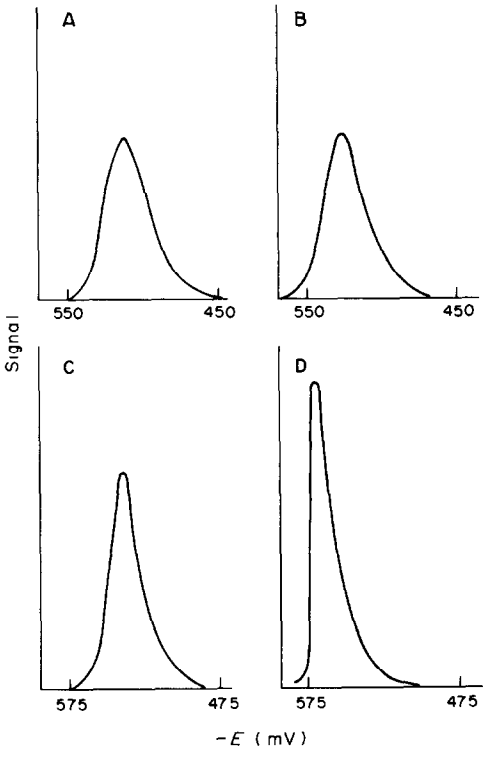

Fig. 1. Simulated PSA signals of an amalgamated analyte undergoing reversible oxidation at the mercury film RDE. The curves have been normalized to equal areas. T_{strip} is (A) 0.09; (B) 0.72; (C) 2.88; (D) 23.00. Simulation parameters: $n = 2$, $E^0 = -500$ mV, $[M(Hg)]_{T=0} = 10000$, $\Delta T = 2 \times 10^{-4}$, $\Delta X = 2 \times 10^{-2}$.

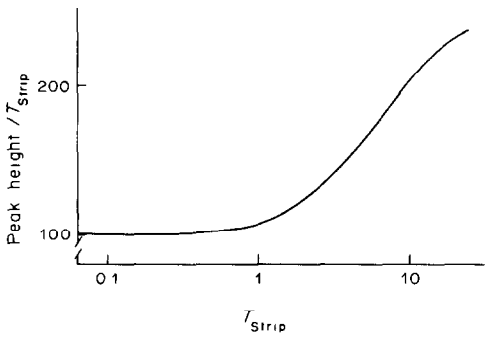

Fig. 2. Relative peak height of simulated PSA signals at the mercury film RDE as a function of T_{strip}. The ordinate has been normalized to 100 for $T_{strip} = 0.09$. Same conditions and simulation parameters as in Fig. 1. Note the logarithmic abscissa.

In Fig. 4, calculated and experimental PSA curves for lead are compared. Since the mercury film thickness and the exact value of the conditional redox potential are not known, the position of the simulated signal on the potential axis is indeterminate, *cf.* equation (7), so the theoretical curves were shifted along the potential axis until the best fit to the experimental data was obtained. Within the wide range of signal magnitudes covered, the agreement is

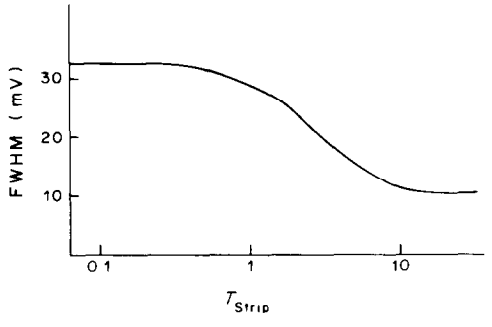

Fig. 3. Full width at half maximum height of simulated PSA signals at the mercury film RDE. Same conditions and simulation parameters as in Fig. 1. Note the logarithmic abscissa.

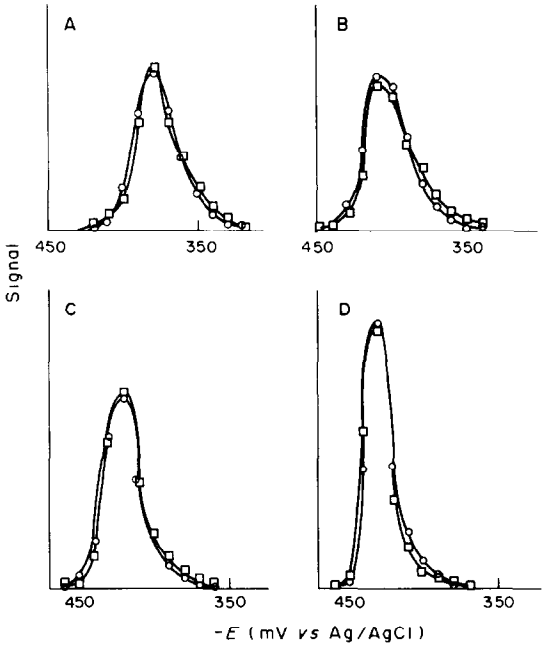

Fig. 4. Comparison of experimental (□) and simulated (○) PSA signals of lead. The curves are scaled to equal areas. The stripping time (sec) is: (A) 0.044; (B) 0.092; (C) 0.412; (D) 2.95. Simulation parameters: $n = 2$, $\Delta T = 4 \times 10^{-4}$, $\Delta X = 2 \times 10^{-2}$. For experimental details, see text.

good, and it can thus be concluded that the model proposed for the simulation of a PSA experiment is essentially correct.

Shapes of overlapping peaks

When the oxidation potentials of two amalgamated analytes are too close, oxidation of the second component will commence before oxidation of the first component is complete. If the extent of the resulting overlap is considerable, the potential distribution calculated as the sum of component signals will differ from that of the composite signal, and the waveform in PSA is no longer additive. As shown in Fig. 5, the peak height of the component stripped most cathodically is increased at the expense of the signal from the other component. The explanation of this finding is simply that during the time spent at the dissolution potential of the first component, a significant fraction of the second component is also oxidized. In Fig. 6, the fraction of the total oxidant flux consumed in the stripping of each component is plotted against the electrode potential, and it is seen that both oxidation processes take place in the potential range between the dissolution potentials of the analytes. The distortion of overlapping PSA signals was verified experimentally for the cadmium/indium system (Fig. 7). Whereas the sum of the cadmium and indium peak areas agreed with the area of the composite peak within experimental error, the potential distribution of the latter is clearly changed in the way predicted by the digital simulation.

Although severely overlapping PSA signals have been resolved numerically with satisfactory accuracy by the use of the generalized standard-addition method,[21] the applicability of this approach will eventually be limited by the lack of additivity of overlapping PSA signals. Therefore, it is recom-

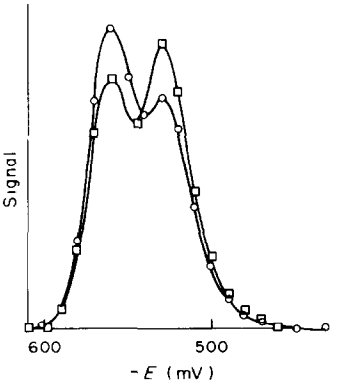

Fig. 5. Simulation of the peak overlap interference in PSA. (□) = sum of single-component signals, (○) = signal obtained when both species are present simultaneously. Simulation parameters: $n_1 = n_2 = 2$, $T_{strip(1)} = T_{strip(2)} = 1.4$, $E_1^0 = -500$ mV, $E_2^0 = -535$ mV, $[M_1(Hg)]_{T=0} = [M_2(Hg)]_{T=0} = 10000$.

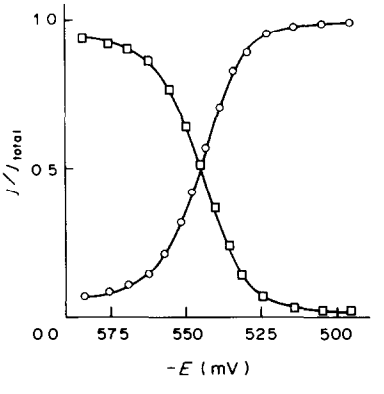

Fig. 6. Fraction of the total oxidant flux consumed by the oxidation of each analyte during the stripping of an overlapping two-component system in PSA: (□) $= j_1/j_{total}$, (○) $= j_2/j_{total}$. Simulation parameters as in Fig. 5.

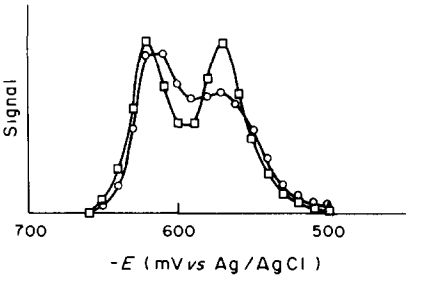

Fig. 7. Distortion of the waveform in PSA caused by severe peak overlap: (□) sum of Cd- and In-signals when measured separately, (○) signal obtained with both analytes present. For experimental details, see text.

mended that the interfering peaks should be resolved by instrumental or chemical means (*e.g.*, by matrix modification) whenever possible.

CONCLUSIONS

With the theoretical model proposed, an accurate description of the waveform in PSA in the case of a reversible electrode process can be obtained by digital simulation. In practical analysis, the theoretical signals are useful as diagnostic tools, since complications in the electrode process (*e.g.*, saturation of the amalgam electrode, accompanying homogeneous solution reactions or irreversible electrode kinetics) will lead to distortions of the peak shape. Conversely, if a species is known to behave reversibly under given experimental conditions, deviations from the theoretical values (particularly peak broadening) are indicative of poor instrumental performance.

A major advantage of the finite-difference approach in digital simulation is the ease by which kinetic effects are incorporated into the model, and it is our intention to expand the simulation of PSA signals to cover more complicated cases in the future.

Acknowledgements—A research fellowship (B.H.) from the Danish Technical Science Research Council (16-3499.K-810) and a grant (511-8032) from the Danish Natural Science Research Council for the computerized instrument are gratefully acknowledged.

REFERENCES

1. D. Jagner and A. Graneli, *Anal. Chim. Acta*, 1976, **83,** 19.
2. D. Jagner, *Anal. Chem.*, 1978, **50,** 1924.
3. S. Bruckenstein and J. W. Bixler, *ibid.*, 1965, **37,** 786.
4. D. Jagner, M. Josefson and S. Westerlund, *Anal. Chim. Acta*, 1981, **129,** 153.
5. D. Jagner and S. Westerlund, *ibid.*, 1980, **117,** 159.
6. D. Jagner, M. Josefson and S. Westerlund, *ibid.*, 1981, **128,** 155.
7. D. Jagner, M. Josefson, S. Westerlund and K. Åren, *Anal. Chem.*, 1981, **53,** 1406.
8. J. Mortensen, E. Ouziel, H. J. Skov and L. Kryger, *Anal. Chim. Acta*, 1979, **112,** 297.
9. J. K. Christensen, L. Kryger and N. Pind, *ibid.*, 1982, **141,** 131.
10. N. Pind, *Talanta*, 1984, **31,** 1118.
11. J. Mortensen, *Ph.D. Thesis*, University of Aarhus, Denmark, 1982.
12. J. Mortensen and D. Britz, *Anal. Chim. Acta*, 1981, **131,** 159.
13. C. Labar and L. Lamberts, *ibid.*, 1981, **132,** 23.
14. J. K. Christensen, L. Kryger and N. Pind, *ibid.*, 1982, **136,** 39.
15. V. G. Levich, *Physicochemical Hydrodynamics*, Prentice-Hall, Englewood Cliffs, 1962.
16. D. Britz, *Digital Simulation in Electrochemistry*, Springer Verlag, Berlin, 1981.
17. A. J. Bard and L. R. Faulkner, *Electrochemical Methods*, Wiley, New York, 1980.
18. S. P. Perone and A. Brumfield, *J. Electroanal. Chem.*, 1967, **13,** 124.
19. P. Bos, *ibid.*, 1972, **34,** 475.
20. H. J. Skov and L. Kryger, *Anal. Chim. Acta*, 1980, **122,** 179.
21. B. Høyer and L. Kryger, *ibid.*, 1985, **167,** 11.

Talanta, Vol. 32, No 9, pp. 845–850, 1985
Printed in Great Britain.

0039-9140/85 $3.00 + 0.00

INJECTION ANALYSIS WITH FLOW-GRADIENT SYSTEMS: A NEW APPROACH TO UNSEGMENTED FLOW TECHNIQUES

ANGEL RIOS, MARIA DOLORES LUQUE DE CASTRO
and MIGUEL VALCARCEL
Department of Analytical Chemistry, Faculty of Science, University of Córdoba, Córdoba, Spain

(*Received* 4 *September* 1984. *Accepted* 23 *April* 1985)

Summary—Flow gradients controlled by a variable hydrostatic head have been employed in FIA for the first time. The influence of these gradients on the most characteristic parameters of an FIA recording have been studied in systems with and without a chemical reaction. The potential of this technique for enhancing the applications of FIA is shown.

Gradient techniques in flow-injection analysis (FIA), defined as those that make use of peak measurement before or after the residence time, date from 1977, when Růžička *et al.* described their FIA titrations.[1] A year later Betteridge and Fields[2] suggested the first simultaneous determinations by use of a pH-gradient, and then new techniques followed, such as use of concentration-gradients established in the double carrier–sample–carrier interface, gradient dilution,[3] electronic calibration,[3] stopped-flow methods,[4,6] three-dimensional FIA scanning[7] and FIA systems with a gradient chamber.[8,9] All these are techniques based on concentration gradients, and up till now no gradient techniques based on hydrodynamics have been developed for FIA, although programmed-flow systems have been used in HPLC[10] which, modifying the retention times through successive changes of the flow-rate, afford better resolution in elution of the solutes.

In the work described here we studied the effect of a flow-rate gradient (flow-gradient) in FIA. The change in flow-rate from sample injection to exit through the detector results in substantial alterations in the parameters of the peaks obtained, which may be taken advantage of for several purposes. Moreover, when the FIA involves a chemical reaction, there will be a considerable effect of the reaction kinetics on the dispersion[11] as well as on the parameters which define the peak, and a flow-gradient allows manipulation of these parameters thanks to the possibility of controlling the degree of reaction that has occurred by the time the peak reaches the detector. The simplest way of creating a flow-gradient (used by us) is by controlled variation of a hydrostatic head. In earlier works[12–14] flow-rate control was obtained by use of a fixed hydrostatic head, with a reservoir of carrier solution at a given height. In our work the reservoir is raised or lowered to change the flow-velocity, thus creating a flow-gradient. We have studied the effect of the gradient in a system in which no chemical reaction takes place (injection of Bromocresol Green) and systems in which chemical reaction occurs at a moderate rate (ascorbic acid–potassium dichromate and cobalt–pyridoxal thiosemicarbazone) and for which the disappearance or appearance of a species is monitored.

A flow-rate gradient, Q, may be defined as the variation of the flow-rate, q, over a given period of time:

$$Q = \frac{\Delta q}{\Delta t} = \frac{q - q_0}{t - t_0} \quad (1)$$

where q_0, q and t_0, t are the initial and final flow-rates and times, respectively.

EXPERIMENTAL

Apparatus

The device used, Fig. 1, has a vertical column (2 m high) with a tray which can be moved up and down by a mechanical drive mechanism, at a controllable rate, the rate being set by means of a rheostat. The reservoir is connected by tubing to the injection valve of the FIA system, and the outlet from the flow-through cell of the detector is lengthened by tubing to end 50 cm below the base of the column, so that there is no return flow when the reservoir is at the base of the column. The flow-rates are adjustable in the normal range for FIA (0.76 and 2.42 ml/min) with our apparatus.

FIA manifold

This was very simple, consisting of a single channel for the carrier solution, into which the samples are injected in the usual way. A microcomputer (Hewlett-Packard HP-85) was used to collect the absorbance values from the spectrophotometer through an interface (HP-IB) every 0.2 sec.

Reagents

Bromocresol Green. A stock solution was prepared by dissolving 0.400 g of the dye in 25 ml of 96% ethanol and diluting to 100 ml with 0.01*M* borax. The working solution was prepared by mixing 0.5 ml of the stock solution with 99.5 ml of 0.01*M* borax. The carrier stream was 0.01*M* borax.

Potassium dichromate solution, 1×10^{-3}M (*pH varied*).
Ascorbic acid solution, 5×10^{-3}M, *pH* 5.45.
Pyridoxal thiosemicarbazone[15] (*PT*) *solution.* In 1:4 v/v ethanol–water mixture, pH 5.74.

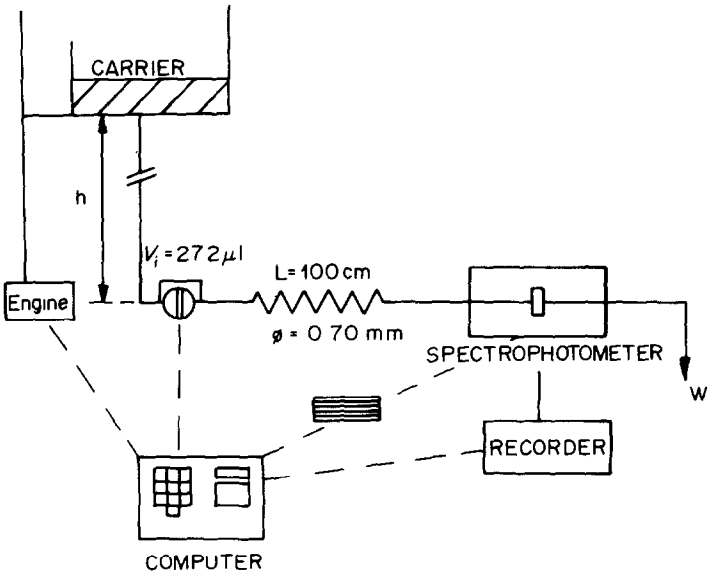

Fig. 1. Scheme used to establish a gravity-flow and FIA manifold.

Co(II) solutions (10 µg/ml). In 1:4 v/v ethanol–water mixture (pH varied).

Procedure for data collection

Injection and start-up of the microcomputer and recorder were simultaneous. A program was written in Basic to provide the following information for each peak: flow-rate gradient (Q); flow-rates at the start (q_0), end (q_f), signal appearance (q_a), peak maximum (q_T) and half peak-height for the rise (q_{w1}) and fall (q_{w2}) of the peak; the appearance time (t_a), residence time (*i.e.*, time from injection to appearance of the peak maximum) (t_r), baseline-to-baseline (Δt), and peak-width at half-height ($\Delta t_{1/2}$); the absorbance at the maximum (A_m); the peak area (A). The flow-chart of the program is shown in Fig. 2.

RESULTS AND DISCUSSION

The study was started by determining the most characteristic FIA parameters when the reservoir was kept at different heights. For our apparatus the equation relating the flow-rate to the height was found to be:

$$q_{(ml/min)} = 0.00832h_{(cm)} + 0.764$$

SYSTEM INVOLVING NO CHEMICAL REACTION

First, the signal provided by the injection of a dye (Bromocresol Green) into an aqueous carrier (with

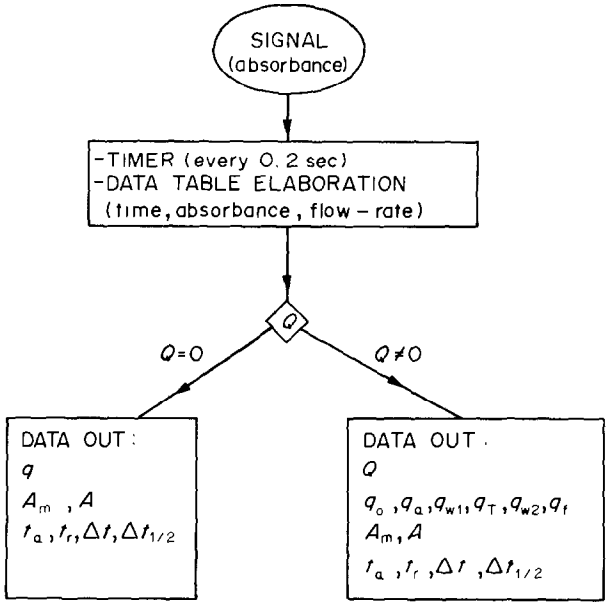

Fig. 2. Flow-chart of program.

both solutions at the same pH so that no chemical reaction occurred) was monitored and the FIA parameters were obtained. The flow-gradient was varied by changing the rheostat setting (Pr), to which Q was linearly related by the equations:

$$Q > 0: Q = 0.0278\text{Pr} - 0.5812 \text{ for } 35 \leqq \text{Pr} \leqq 80$$

$$Q < 0: Q = -0.0286\text{Pr} + 0.0256 \text{ for } 20 \geqq \text{Pr} \geqq 60$$

Figure 3 shows the peaks obtained with four of the Q values, together with the gradients. The changes in t_a, t_r and Δt with Q are more remarkable for positive than for negative gradients.

Washing effect

An immediate application of the flow-gradient in FIA is the washing effect,[16,17] by which a higher sampling frequency is obtained. If a positive flow-gradient is established at t_r (*i.e.*, at the maximum of the signal), the peak-tail can be dramatically diminished; the time to return to the baseline is shorter and the time lapse between consecutive injections if cross-contamination is to be avoided is minimized (Fig. 4).

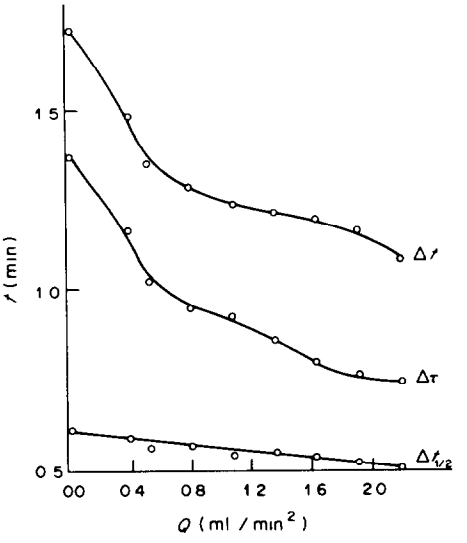

Fig. 4. Influence of Q on various peak parameters. The flow-rate gradient (positive) is established at time t_r to take advantage of the washing effect. The effect is shown for Bromocresol Green. The effect of Q on $\Delta t_{1/2}$ is small, whereas on Δt and $\Delta\tau$ it is very pronounced $[\Delta\tau = \Delta t - (t_r - t_a)]$.

SYSTEMS INVOLVING A CHEMICAL REACTION

Monitoring the disappearance of a reactant

The ascorbic acid–potassium dichromate system, employed by Painton and Mottola[11] to study the contribution of the chemical kinetics to the dispersion, was used in these experiments. This redox reaction is very suitable because its rate is dramatically affected by pH:

$$Cr_2O_7^{2-} + 3C_6H_8O_6 + 8H^+ \rightleftharpoons 2Cr^{3+} + 3C_6H_6O_6 + 7H_2O$$

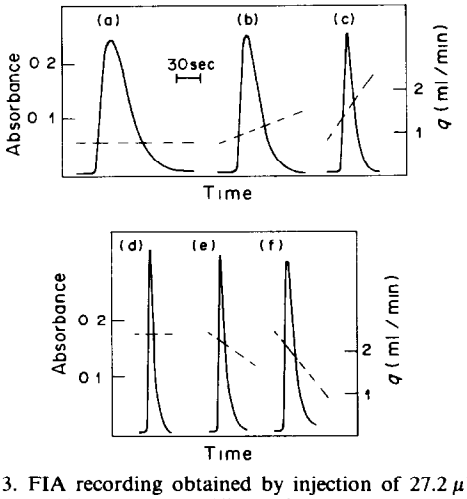

Fig. 3. FIA recording obtained by injection of 27.2 μl of Bromocresol Green under different flow conditions (dashed lines): (a) and (d) without a flow-gradient ($q = 0.764$ and 2.420 ml/min, respectively); (b) and (c) with a positive gradient ($Q = 0.392$ and 1.639 ml/min^2, respectively); (e) and (f) with a negative gradient ($Q = -0.831$ and -1.582 ml/min^2, respectively).

The rate of disappearance of the dichromate ion at different pH values was monitored photometrically (at 352 nm) by injecting samples sequentially into an ascorbic acid stream at pH 5.45.

When no flow-gradient is present the variation of the chemical dispersion, D_c, ($D_c = D_{\text{total}} - D_{\text{physical}}$) with q is described by curves similar to those found by Painton and Mottola[11] for this system. When a flow-gradient is established the dispersion is dramatically affected by Q, especially if Q is >0 (Fig. 5).

The effect of the pH of this system on parameters such as D_c, t_r and Δt when different flow-gradients are established is interesting. Figure 6 shows plots of D_c and Δt *vs.* pH, which are the most significant. In general, as might be expected, the introduction of a flow-gradient between two extreme q-values produces values of the characteristic parameters between those corresponding to the minimal and maximal flow-rate.

We have attempted to use the apparatus to measure the reaction-rate of the disappearance of dichromate (k) as a function of pH, on the basis of the differences (ΔD and ΔA) in the total dispersion and area, respectively, for the peak obtained in the presence (R) and absence (NR) of a chemical reaction ($\Delta D = D_R - D_{NR}$; $\Delta A = A_{NR} - A_R$). Obviously, ΔD, ΔA and k must be directly related. We have plotted ΔD *vs.* ΔA for different q and pH values in the absence of a flow-gradient, obtaining straight lines with slopes which increase as the pH decreases (*i.e.*, as the degree of reaction increases). These slopes, representing proportionality constants between ΔD and ΔA, must equal k, the intrinsic rate-constant of the FIA system as a function of pH: $\Delta D = k\Delta A + C$, where C is the intercept of the straight line at $\Delta A = 0$.

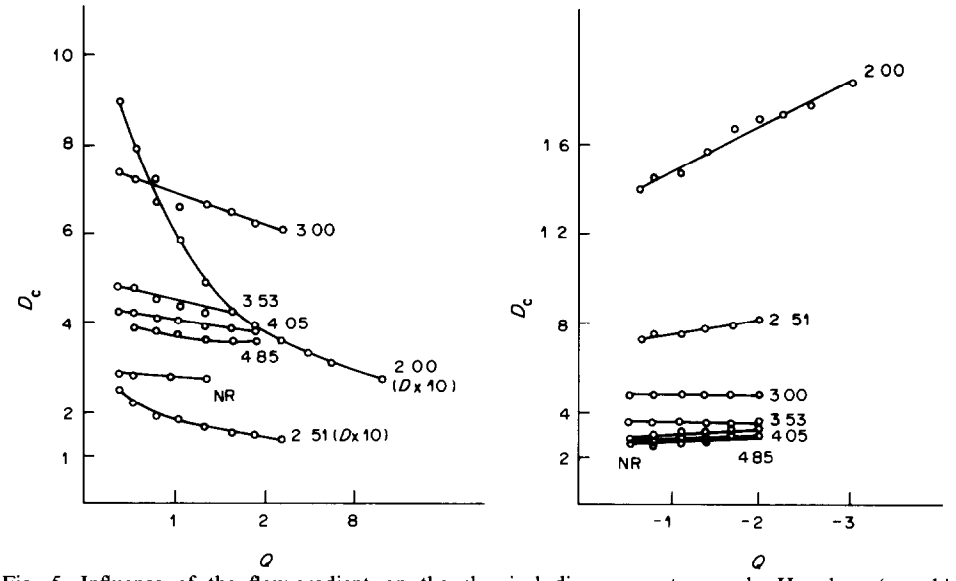

Fig. 5. Influence of the flow-gradient on the chemical dispersion at several pH values (ascorbic acid–potassium dichromate reaction); NR = no chemical reaction.

When a flow-gradient is established and the plots are recorded for different Q values, the straight lines obtained show slopes slightly smaller than those found in the absence of a gradient, except when the reaction rate increases sharply with decrease in pH, *i.e.*, at pH < 2.4, in which case $k_{(Q>0)} > k_{(Q=0)} > k_{(Q<0)}$, Fig. 7. This means that when the reaction-rate is maximal the differences in dispersion and peak area corresponding to the occurrence and absence of a reaction are maximized by a positive flow-gradient and minimized by a negative gradient.

Monitoring of formation of a product

The complex-formation reaction between cobalt and pyridoxal thiosemicarbazone (PT)[18] was chosen for studying the influence of a flow-gradient on the profile of the peak obtained:

$$Co^{2+} \xrightarrow{O_2} Co^{3+} \overset{3PT}{\rightleftharpoons} Co(PT)_3^{2+} + H^+$$

Because we start with Co(II) in solution the overall reaction is slow owing to the oxidation step, which is highly influenced by pH. The reaction can be photometrically monitored at 435 nm, the carrier being a solution of the ligand (see experimental section) at pH 5.75, into which 10-μg/ml Co(II) samples at different pH values are injected.

As the concentration of the complex is unknown, the dispersion cannot be calculated, but can be indirectly assessed from the maximal absorbance of the peaks.

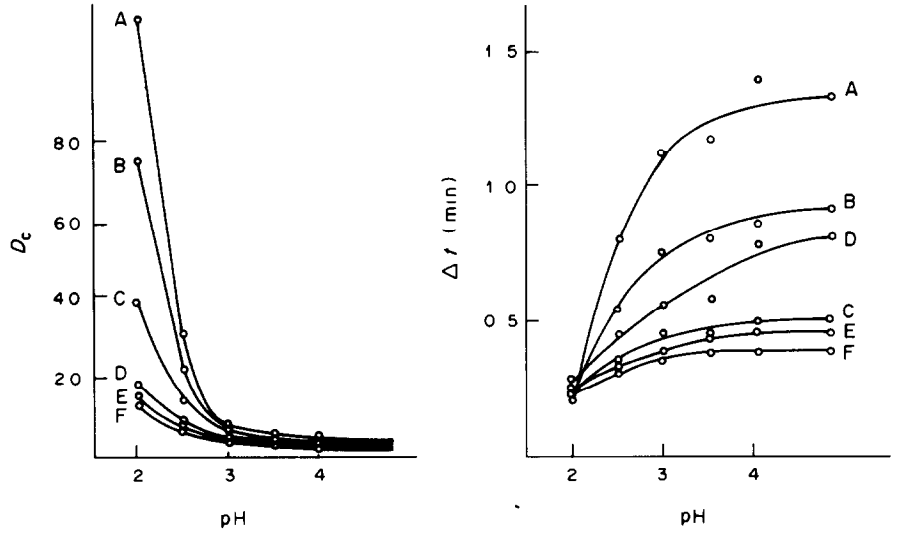

Fig. 6. Variation of the chemical dispersion and baseline-to-baseline time as a function of pH for the ascorbic acid–potassium dichromate system. A and F without a flow-gradient (q = 0.764 and 2.420 ml/min, respectively); B and C with a positive gradient (Q = 0.529 and 1.917 ml/min^2, respectively); D and E with a negative gradient (Q = −1.973 and −0.831 ml/min^2, respectively).

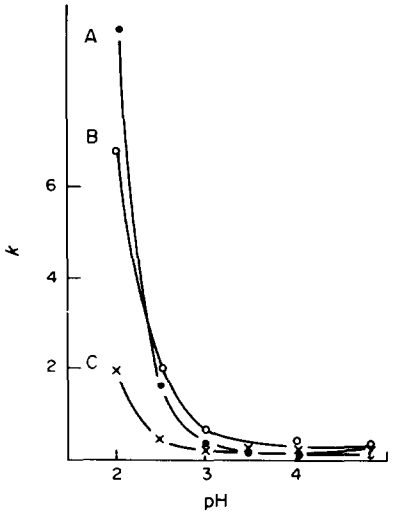

Fig. 7. Variation of k with the pH of the potassium dichromate sample in the ascorbic acid system with and without flow-gradients: A, positive gradient; B, without gradient; C, negative gradient.

When the reaction product is monitored, the reaction rate and dispersion have opposing effects on the peak profile: increase in reaction rate increases the transient signal, whereas increase in the dispersion decreases it. Therefore, the maximal absorbance of the peaks is less affected by the change in q than it is in the ascorbic acid–dichromate system.

When a flow-gradient is established the maximal absorbance for a fixed pH is only slightly affected by Q; A and Δt are the most significantly affected parameters. In this case, negative gradients have a greater influence on A (Fig. 8, A, B) and Δt (Fig. 9). For positive gradients the increase in Q diminishes A and Δt, whereas for negative gradients increase in Q increases A and Δt.

The variation in A and Δt with sample pH for different Q-values (Fig. 8, C and D, Fig. 9) gives curves similar to the plots of reaction-rate *vs.* pH obtained by a manual photometric method, but slightly shifted towards higher pH-values, possibly owing to the fact that the slower the reaction-rate, the more pronounced the effect of the dispersion on the signal.

CONCLUSIONS

The study performed allows the following conclusions to be drawn.

(1) The establishment of a flow-gradient in an FIA system modifies the peak profiles to give shapes between those obtained by use (at $Q = 0$) of the initial and final flow-rates of the gradient tested.

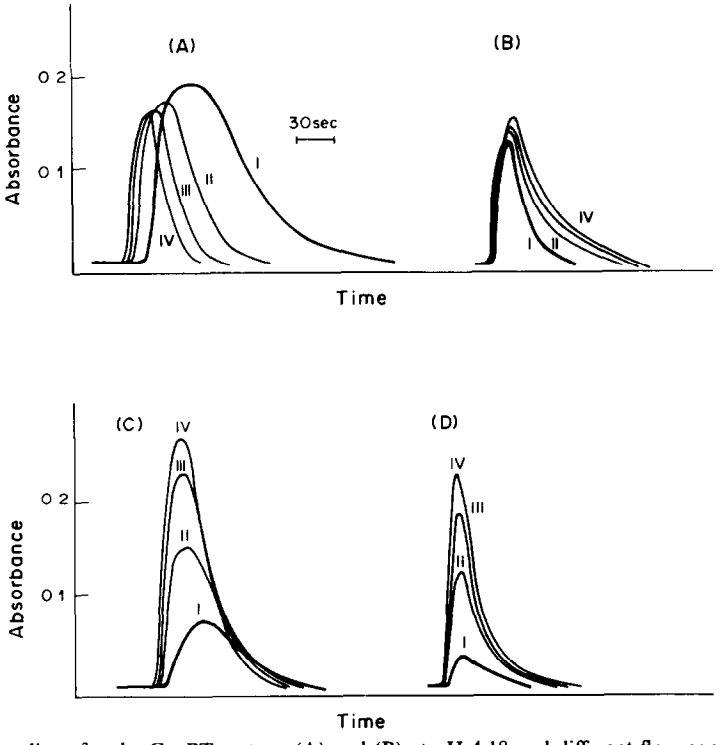

Fig. 8. FIA recordings for the Co–PT system: (A) and (B) at pH 4.18 and different flow-conditions; (C) with a positive gradient and (D) a negative gradient at different pH values. (A): I, without a gradient ($q = 0.764$ ml/min); II, III and IV with a positive gradient ($Q = 0.529$, 1.084 and 1.361 ml/min^2, respectively). (B): I, without a gradient ($q = 2.420$ ml/min); II, III and IV with a negative gradient ($Q = -0.831$, -1.117 and -1.402 ml/min^2, respectively). (C): I, with a positive gradient ($Q = 0.529$ ml/min^2) at different pH values: 3.25 (I); 3.63 (II); 4.85 (III) and 6.77 (IV). (D): With a negative gradient ($Q = -0.688$ ml/min^2) at the same pH values as (C).

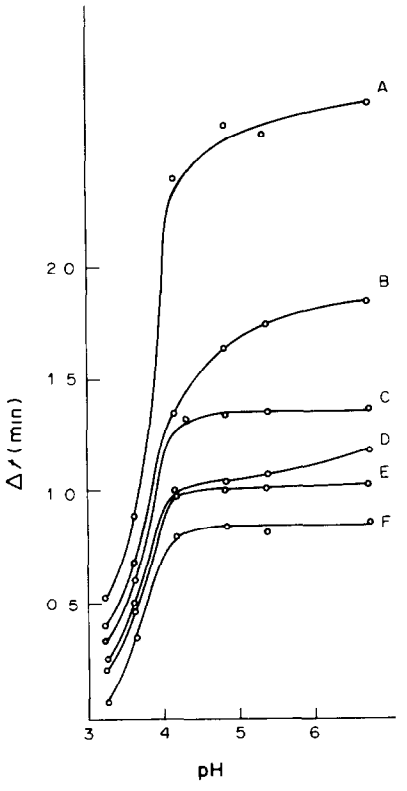

Fig. 9. Δt *vs.* pH of the injected Co(II) sample, for different flow-rates (Co-PT system). A and F without a flow-gradient ($q = 0.764$ and 2.420 ml/min, respectively); C and E with a positive gradient ($Q = 0.529$ and 1.084 ml/min^2, respectively); B and D with a negative gradient ($Q = -1.117$ and -0.688 ml/min^2, respectively).

(2) Positive or negative flow-gradients affect the parameters of an FIA peak differently according to whether a chemical reaction occurs or not, and in the first case the effect also depends on whether the species monitored is a reactant or a product.

When no chemical reaction takes place, the most significant influence of the gradient is on parameters such as Δt and A, and is stronger for positive gradients.

When the system involves a chemical reaction, use of a flow-gradient allows the degree of reaction at the instant of detection to be increased or decreased at will. When the disappearance of a reactant is monitored, the total dispersion is the parameter most significantly affected by Q, especially for positive flow-gradients. Both the reaction-rate and the dispersion decrease the transient signal when they increase. If formation of a product is monitored an increase in the dispersion decreases the signal, whereas an increase in the reaction-rate increases it. Thus, the effect of Q is more important for A and Δt, and negative flow-gradients exert the strongest influence. It is interesting that a positive flow-gradient significantly reduces the analysis time (Fig. 8) without an appreciable loss of sensitivity.

The practical advantages derived from the use of a flow-gradient in FIA are of two types: (*a*) increase in the sampling rate, based on the washing effect; (*b*) resolution of mixtures by differential kinetics, based on use of flow-gradients which initially favour the faster reaction and then enhance the slower one.

The most important limitation of the hydrodynamically controlled system is its limited versatility, since only a narrow range of flow-variation can be established and it may be used only in single-channel FIA systems, the length and inner diameter of which are also limited. The chief aim of this paper is to show the potential of this new technique in FIA; the limitations could be overcome by using electronically-controlled impulsion systems to achieve a wide range of flow-variation during the time in which the sample is within the system.

Acknowledgements—We are grateful to A. Valcárcel Cases for construction of the flow-gradient device.

REFERENCES

1. J. Růžička, E. H. Hansen and H. Mosbaek, *Anal. Chim. Acta*, 1977, **92,** 235.
2. D. Betteridge and B. Fields, *Anal. Chem.*, 1978, **50,** 654.
3. S. Olsen, J. Růžička and E. H. Hansen, *Anal. Chim. Acta*, 1982, **136,** 101.
4. J. Růžička and E. H. Hansen, *ibid.*, 1980, **114,** 19.
5. P. J. Worsfold, J. Růžička and E. H. Hansen, *Analyst*, 1981, **106,** 1309.
6. J. Růžička and E. H. Hansen, *Anal. Chim. Acta*, 1979, **106,** 207.
7. J. Janata and J. Růžička, *ibid.*, 1982, **139,** 105.
8. H. L. Pardue and B. Fields, *ibid.*, 1981, **124,** 39.
9. *Idem, ibid.*, 1981, **124,** 65.
10. R. P. W. Scott, *Contemporary Liquid Chromatography*, Wiley, New York, 1976.
11. C. C. Painton and H. A. Mottola, *Anal. Chem.*, 1981, **53,** 1713.
12. H. Müller, *Proc. 3rd Symposium on Ion-Selective Electrodes, Matrafüred*, pp. 279–286. Akadémiai Kiadó, Budapest, 1980.
13. J. Wang and B. A. Freiha, *Anal. Chem.*, 1983, **55,** 1285.
14. R. W. Pratt, Jr. and D. C. Johnson, *Anal. Chim. Acta*, 1983, **148,** 87.
15. D. Pérez-Bendito and M. Valcárcel, *Afinidad*, 1980, **18,** 336.
16. J. Růžička and E. H. Hansen, *Flow Injection Analysis*, p. 72. Wiley, New York, 1981.
17. E. A. G. Zagatto, A. O. Jacintho, J. Mortatti and H. Bergamin F°, *Anal. Chim. Acta*, 1980, **120,** 399.
18. L. Ballesteros and D. Pérez-Bendito, *Analyst*, 1983, **108,** 443.

Talanta, Vol. 32, No 9, pp. 851–858, 1985
Printed in Great Britain.

0039-9140/85 $3.00 + 0.00

SIMULTANEOUS KINETIC DETERMINATION OF COPPER, COBALT AND NICKEL BY MEANS OF >C=N— GROUP INTERCHANGE REACTIONS

ANGEL RIOS and MIGUEL VALCARCEL
Department of Analytical Chemistry, Faculty of Science, University of Córdoba, Córdoba, Spain

(*Received* 16 *January* 1984. *Revised* 14 *September* 1984. *Accepted* 10 *April* 1985)

Summary—The kinetic determination of copper, cobalt and nickel in binary and ternary mixtures without prior separation is described. The methods are based on the difference in the reaction rate of interchange of >C=N— groups between thiosemicarbazide and 6-methylpicolinaldehyde azine in the presence of these ions at pH 4.5. Through these reactions the corresponding metal thiosemicarbazone complexes are formed. Various ratios of these ions at the $10^{-5}M$ level can be determined photometrically by either the logarithmic extrapolation method or a combined initial-rate and fixed-time method proposed here for the first time.

Several analytical applications of the interchange reactions of >C=N— groups have recently been described by us.[1–3] These reactions have been used previously in organic[4–6] and inorganic[7–9] chemistry, but were first used in analytical chemistry by Pino and Valcárcel.[10]

The interchange reaction:[11]

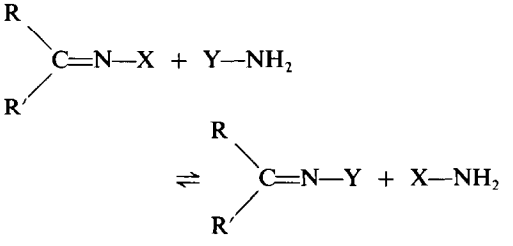

consists of exchange of X for Y by means of the action of excess of the amine on an azomethine compound. These reactions occur at reasonable speed in aqueous medium at an appropriate pH and are a cause of the instability of the ligands in solution.[12]

In this work we have made use of the reaction between 6-methylpicolinaldehyde azine (6-Me-PAA) and thiosemicarbazide.

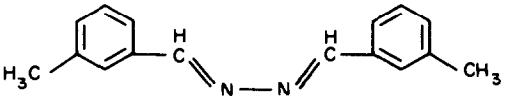

6 — Me — PAA

This reaction occurs at different rates in the presence of copper(I), cobalt(II) or nickel(II), and the corresponding metal thiosemicarbazone complexes are formed *in situ* in the reaction medium. This permits the application of differential kinetic methods for the simultaneous determination of these cations. However, a synergic effect with these mixtures limits use of the methods of differential kinetic analysis, only one of which can be employed: the traditional logarithmic extrapolation method. However, we have developed a new technique that consists of a combination of the initial-rate and fixed-time methods for the kinetic determination of a single species ("combined initial-rate and fixed-time" method).

Several differential rate methods for the analysis of mixtures of metals by use of redox reactions,[13–17] catalysed reactions,[18–21] ligand-exchange reactions[22–31] and complex-formation reactions[32,33] have been reported.[34] The >C=N— interchange reactions are here used for the first time in differential kinetic methods of analysis, and a method is presented for analysis of mixtures when a synergic effect is present.

EXPERIMENTAL

Reagents

All solvents and reagents were of analytical grade. The 6-methylpicolinaldehyde azine was easily synthesized by the condensation of 6-methylpicolinaldehyde with hydrazine.[35] The standard copper(II), cobalt(II) and nickel(II) solutions were prepared from the nitrates, standardized by atomic-absorption spectroscopy, and diluted as required before use. A sodium acetate–acetic acid buffer (total concentration $1.4M$, pH 4.5) was prepared.

Apparatus

A Perkin–Elmer 575 spectrophotometer with 1.0-cm glass cells and equipped with an electrothermal thermostat (Peltier effect) was used for the kinetic measurements.

Procedure

To a solution (in a calibrated 10-ml standard flask) containing up to 56 μg of copper and/or 20 μg of cobalt and/or 47 μg of nickel, add 1.5 ml of 0.1% 6-Me-PAA solution in ethanol (0.5 ml for copper–nickel mixtures), 4 ml of buffer solution and an appropriate volume of distilled water so that when 0.4 ml of $0.05M$ thiosemicarbazide solution is finally added (0.5 ml for copper–nickel mixtures), the total volume will be 10.0 ml. Add the thiosemicarbazide, mix, transfer a portion to a 1.0-cm cell and record the absorbance–time curve at $20 \pm 0.1°$ and 410 nm (396 nm for copper–nickel mixtures). Let the mixture stand until the reaction is complete and measure the final absorbance (A_∞). Treat the data as indicated below.

RESULTS AND DISCUSSION

Kinetic and photometric characteristics of metal-ion/6-Me-PAA/thiosemicarbazide systems

Photometric study. Spectrophotometric monitoring of solutions containing the metal ion, 6-Me-PAA and thiosemicarbazide shows that an excess of thiosemicarbazide relative to 6-Me-PAA at pH 3–7 in the presence of copper, cobalt or nickel leads to the >C=N— interchange reaction and formation of the metal thiosemicarbazone complex. The spectrophotometric characteristics of these complexes, at pH 4.5, are listed in Table 1. Copper will be complexed as Cu(I), owing to reduction by 6-Me-PAA, which also forms a chelate with it (λ_{max} 480 nm). Complex-formation reactions between cobalt or nickel with 6-Me-PAA are not observed photometrically under these conditions.

In the absence of the metal ions, the exchange reaction occurs at acidic pH values, but not at pH > 7. At pH 4.5 the reaction takes place easily (maximum rate). The reaction in the presence of copper is very interesting, since whereas 6-Me-PAA reacts with copper(I) selectively because it is a ligand of "cuproine" type,[36] the exchange product 6-Me-PAT, even though it still contains the "cuproine" group, is not selective for copper(I), probably because of preferential reaction of the copper with the thiosemicarbazide group in the 6-Me-PAT molecule[37] [copper(I) is classified by Ringbom in the B group,[38] as co-ordinating more favourably with sulphur than nitrogen]. However, we have proved that a copper(I)–thiosemicarbazide complex is also formed at pH 4.5 (λ_{max} 315 nm). This means that two reaction mechanisms are possible, depending on the relative concentrations of thiosemicarbazide and azine (Scheme 1 and Scheme 2).

Thus, for thiosemicarbazide/azine ratios <3 there is direct transformation of the copper(I)–azine complex into the copper(I)–thiosemicarbazone complex (mechanism 1), whereas for ratios >4 we propose mechanism 2, since the free-copper(I)/complexed-copper(I) concentration ratio in the equilibrium for the complexes involved is in agreement with the ligand-exchange reactions indicated. At ratios between 3 and 4 there is presumably participation of both mechanisms.

Table 1. Spectrophotometric characteristics of the metal ion/6-Me-PAT* complexes

Complex	Wavelength, *nm*	Molar absorptivity†, $\times 10^3$ *l.mole*$^{-1}$*.cm*$^{-1}$
Cu(I)/6-Me-PAT	395	8.65
Co(II)/6-Me-PAT	410	11.20
Ni(II)/6-Me-PAT	396	7.68

*6-Me-PAT = 6-methylpicolinaldehyde thiosemicarbazone.
†Obtained by "*in situ*" technique.

Kinetic study. The absorbance–time curves for the 6-Me-PAT complexes were recorded at the wavelengths indicated in Table 1. The reaction in the absence of metal ions was also studied at 323 nm (*in situ* formation of 6-Me-PAT). The partial orders of the reaction were calculated for each system by plotting log (initial rate) *vs.* log concentration, and the proposed rate equations at pH 4.5 are those in Table 2, where the rate constants [calculated by plotting log $(A_\infty - A_t)$ against time, where A_∞ = final absorbance and A_t = absorbance at time t], and the activation energies (obtained from the Arrhenius plot) are also given.

According to the rate equations, the reactions are pseudo first-order with respect to copper(I), cobalt(II) and nickel(II). These ions can be determined kinetically under these conditions, but the determinations are not of great interest, whereas the simultaneous determinations are more important.

The difference in rate for the 6-Me-PAA/6-Me-PAT transformation reaction in the presence and in the absence of cations was increased by the metal ions in the order Co(II) > Ni(II) > Cu(I). The reaction in the presence of copper(I) is less favoured owing to the complex-formation reactions with both 6-Me-PAA and thiosemicarbazide at pH 4.5. In the reactions with cobalt(II) or nickel(II) neither the 6-Me-PAA nor the thiosemicarbazide complex is observed photometrically under these experimental conditions. The interchange reaction in the presence of cobalt(II) is the most favoured because the pH-value for maximum rate is the same as the optimum pH for the complex formation with 6-Me-PAT.

Differential kinetic analysis of binary mixtures

Effect of experimental variables. The pH affects the three systems similarly (Fig. 1). The initial rate of the reactions is maximal at pH 4–5; at pH > 7 there is no interchange reaction. The ionic strength has little

Table 2. Kinetic parameters for the metal ion/6-Me-PAA/thiosemicarbazide systems (pH = 4.5)

System	Rate equation	Rate constant, 10^{-3} *sec*$^{-1}$	Activation energies*, *kcal/mole*
6-Me-PAA/TSC†	$V' = k'[\text{6-Me-PAA}][\text{TSC}]^{1/2}$	4.18	5.27
Cu(I)/6-Me-PAA/TSC	$V = k[\text{Cu}^+][\text{6-Me-PAA}]^{1/2}[\text{TSC}]^{1/2} - V'$	1.86	10.86
Co(II)/6-Me-PAA/TSC	$V = k[\text{Co}^{2+}][\text{6-Me-PAA}]^{1/2}[\text{TSC}]^{1/2} - V'$	8.27	3.07
Ni(II)/6-Me-PAA/TSC	$V = k[\text{Ni}^{2+}][\text{6-Me-PAA}]^{1/2}[\text{TSC}] - V'$	3.44	8.80

*Values obtained by plotting log k against $1/T$, (T in Kelvin; Arrhenius equation).
†TSC = thiosemicarbazide.

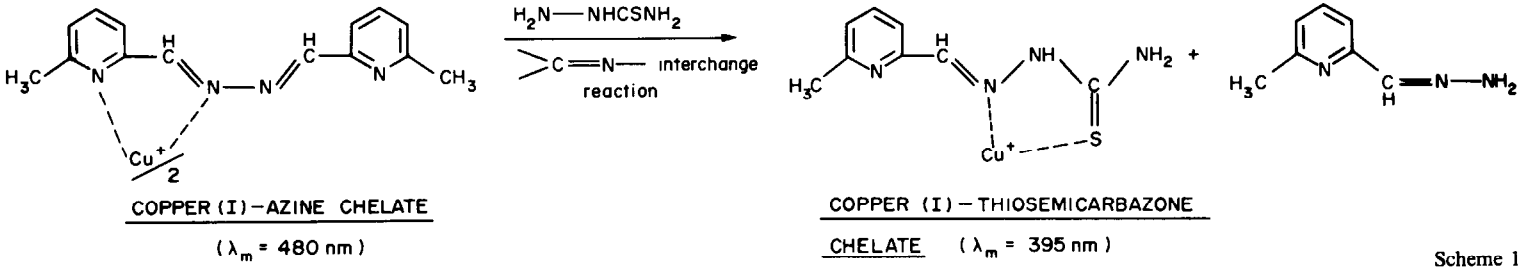

COPPER (I)–AZINE CHELATE (λ_m = 480 nm)

COPPER (I)–THIOSEMICARBAZONE CHELATE (λ_m = 395 nm)

Scheme 1

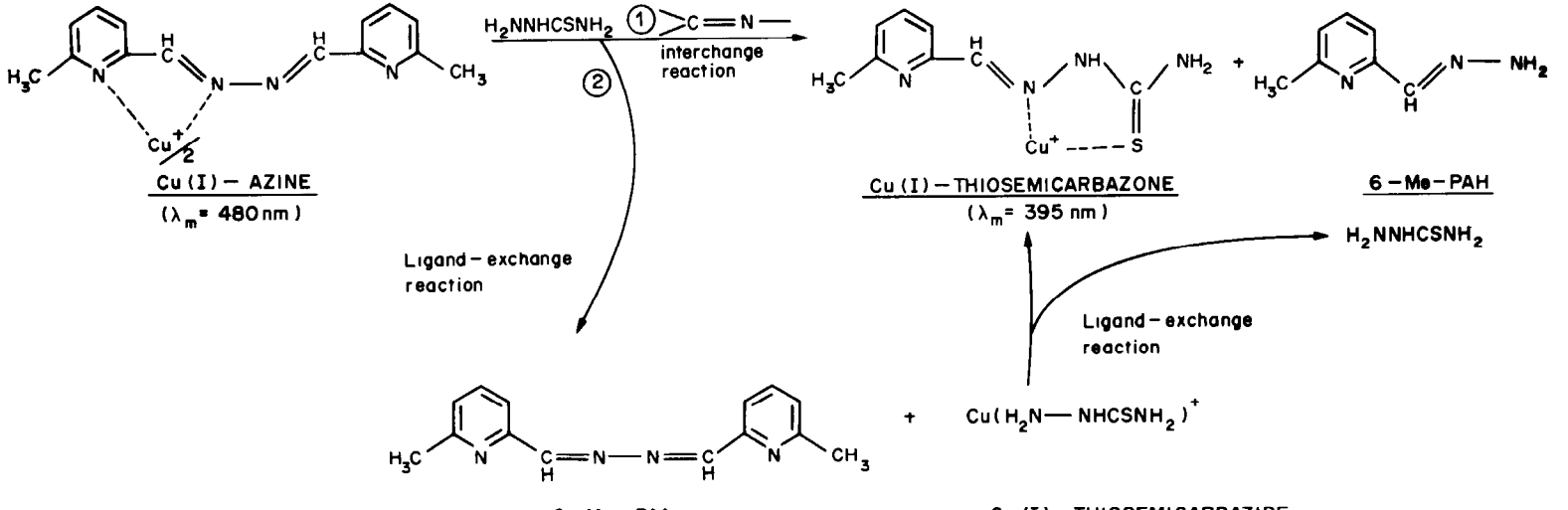

Cu (I)–AZINE (λ_m = 480 nm)

Cu (I)–THIOSEMICARBAZONE (λ_m = 395 nm)

6–Me–PAH

6–Me–PAA

Cu (I)–THIOSEMICARBAZIDE (λ_m = 315 nm)

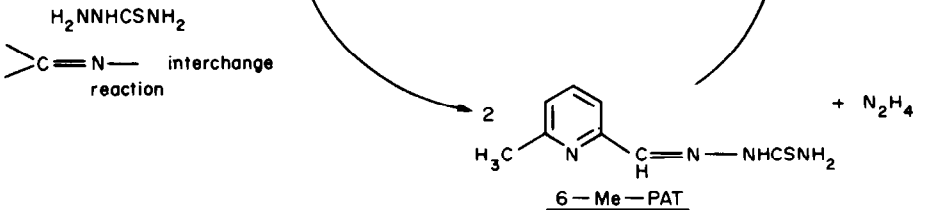

6–Me–PAT

Scheme 2

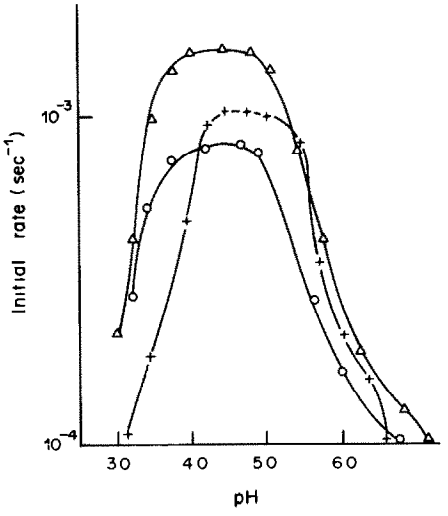

Fig. 1. Influence of pH on initial rate of interchange reactions in the presence of 4.9 μg/ml copper(I) (○), 2.9 μg/ml cobalt(II) (△), and 3.8 μg/ml nickel(II) (+).

influence on the rates (Fig. 2a), but increase in the ethanol concentration decreases them (Fig. 2b).

The effect of temperature was studied in the range 15–45°, and for each pair of the three cations the ratio of the rate constants was maximal at 20° (Fig. 3).

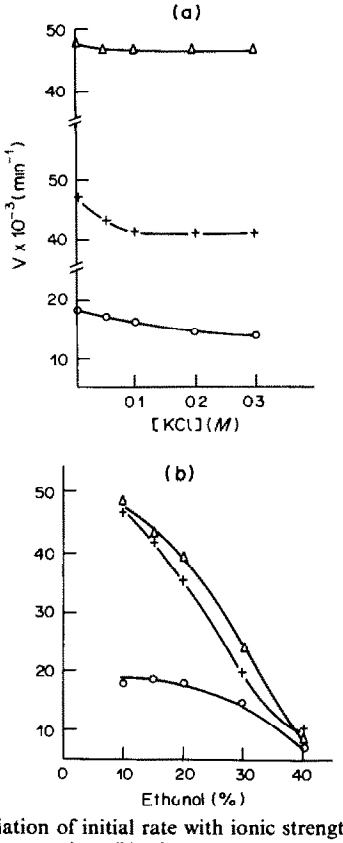

Fig. 2. Variation of initial rate with ionic strength (a), and ethanol concentration (b); for 3.5 μg/ml copper(I), 1.0 μg/ml cobalt(II) and 2.0 μg/ml nickel(II).

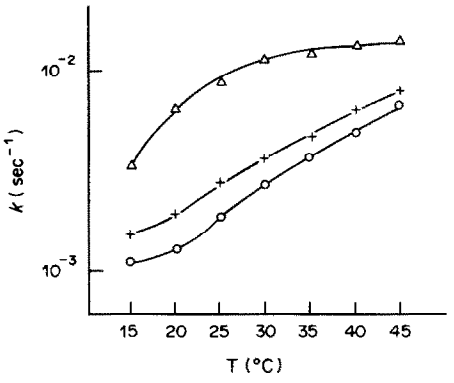

Fig. 3. Variation of the rate constants with temperature for interchange reactions in presence of copper(I) (○), cobalt(II) (△) and nickel(II) (+); concentrations as for Fig. 1.

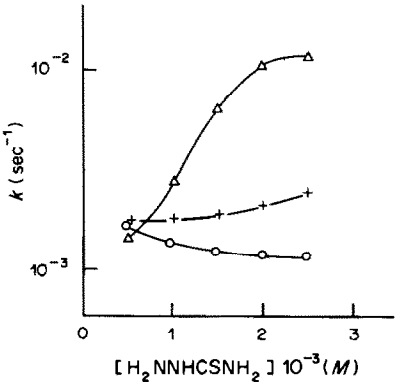

Fig. 4. Variation of the rate constants with concentration of thiosemicarbazide for interchange reactions in presence of copper(I) (○), cobalt(II) (△), and nickel(II) (+); concentrations as for Fig. 1.

The optimum 6-Me-PAA concentration for the copper–cobalt and copper–nickel mixtures was $6 \times 10^{-4} M$, and $2 \times 10^{-4} M$ for the copper–nickel mixture.

The thiosemicarbazide concentration is the most significant variable for the simultaneous determinations (Fig. 4). Increasing it results in increased k (rate constant) for the cobalt(II) and nickel(II) systems, but decreased k for the copper(I) system. This is in accordance with the rate constants and activation energies (Table 2). Cobalt and nickel form complexes only with 6-Me-PAT, whereas the copper(I)–thiosemicarbazide complex [together with the copper(I)–azine complex] is also formed. The increase is greater for cobalt than nickel because of the lower activation energy for the interchange reaction.

The effect of the relative concentrations of the metal ions on the rate-constant ratios is shown in Fig. 5.

Proposed methods. Only the logarithmic extrapolation and the "combined initial-rate and fixed-time" methods are satisfactory for the analysis of binary mixtures of the three metals, on account of the

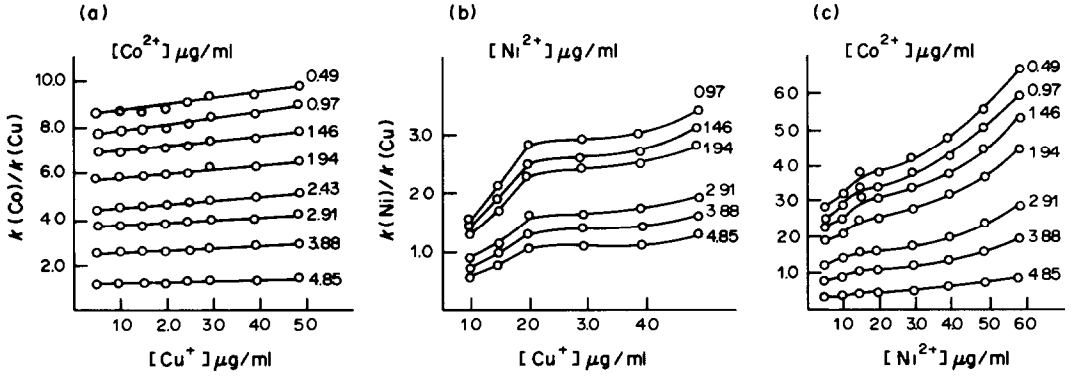

Fig. 5. Variation of the rate-constant ratios with the relative concentrations of the metal ions: (a) copper(I)–cobalt(II) (b) copper(I)–nickel(II), and (c) cobalt(II)–nickel(II).

synergism exhibited (as evidenced by the non-additivity of the absorbances and reaction rates).

The *logarithmic extrapolation method*[39] plots log $(A_\infty - A_t)$ against time (Fig. 6) and gives two straight-line segments. Extrapolation of the second segment to $t = 0$ yields the concentration of the slower reacting component, and the concentration of the other is calculated by difference from the final absorbance, A_∞. Thus, for

$$A + R \xrightarrow{k_A} P$$

$$B + R \xrightarrow{k_B} P$$

where $k_A \gg k_B$, the concentrations of A and B are calculated from $[B] = 10^n/\varepsilon_B$ and $[A] = (A_\infty - 10^n)/\varepsilon_A$, where ε_A and ε_B are the respective molar absorptivities of the complexes and n is the intercept at $t = 0$. This method is applied to the copper–cobalt and cobalt–nickel mixtures, since according to Mottola[40] it can be applied even when there is synergism.

The "*combined initial-rate and fixed-time*" *method*, proposed by us for the first time, is based on the fact that small amounts of copper(I) do not affect the initial rate of the Co(II)/6-Me-PAA/H_2NNHCSNH_2 or Ni(II)/6-Me-PAA/H_2NNHCSNH_2 systems.

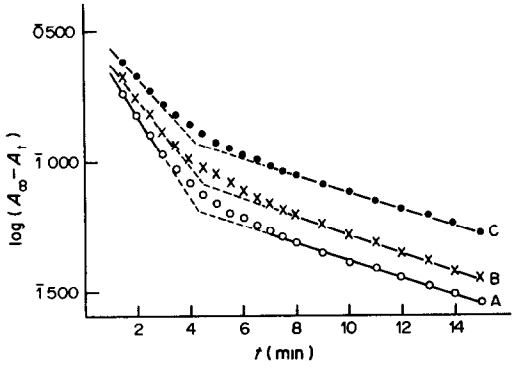

Fig. 6. Logarithmic extrapolation method for the simultaneous determination of copper(I) and cobalt(II). Concentrations 0.97 μg/ml cobalt(II) and (A) 0.93 (B) 1.40, and (C) 1.86 μg/ml copper(I).

Therefore, this method is applied only to copper–cobalt and copper–nickel mixtures.

The concentration of cobalt(II) or nickel(II) in the mixture can be obtained by the initial-rate method (Fig. 7a) and the copper(I) concentration by the fixed-time method at 5 min (copper–cobalt) or 7 min (copper–nickel). However, since the absorbance is not additive, owing to the synergism, it is necessary to draw calibration graphs for copper(I) in the presence of different amounts of cobalt or nickel (Fig. 7b). Extrapolation of the calibration lines to [Cu(I)] = 0 gives a set of values which are a linear function of the cobalt or nickel concentration *over a certain range* (*e.g.*, Fig. 7c). Once a straight-line equation of absorbance *vs.* copper concentration is defined, it is possible to calculate the concentration of copper(I) in the mixture. Thus, the experimental magnitudes for each mixture are the initial rate (V) and the absorbance (A) measured at 5 min (copper–cobalt) or 7 min (copper–nickel), and the equations obtained by us for the analysis of copper–cobalt and copper–nickel mixtures by this method, according to the arguments indicated above, were as follows (concentrations in μg/ml, velocity in $\mu g.ml^{-1}.sec^{-1}$).

Copper(I)–cobalt(II) mixtures:

$$V = 45.2[Co^{2+}] + 15$$

$$A = -0.0113[Cu^+][Co^{2+}] + 0.045\,[Cu^+] + 0.182[Co^{2+}] - 0.005$$

Copper(I)–nickel(II) mixtures:

$$V = 15.6[Ni^{2+}] + 6.2$$

$$A = 0.0035[Cu^+][Ni^{2+}] + 0.031[Cu^+] + 0.064[Ni^{2+}] + 0.031$$

The equations for the absorbance, containing the concentrations of both metal ions involved, show the similarity of the proposed method to the proportional-equations method suggested by Worthington and Pardue,[41] but the factors containing

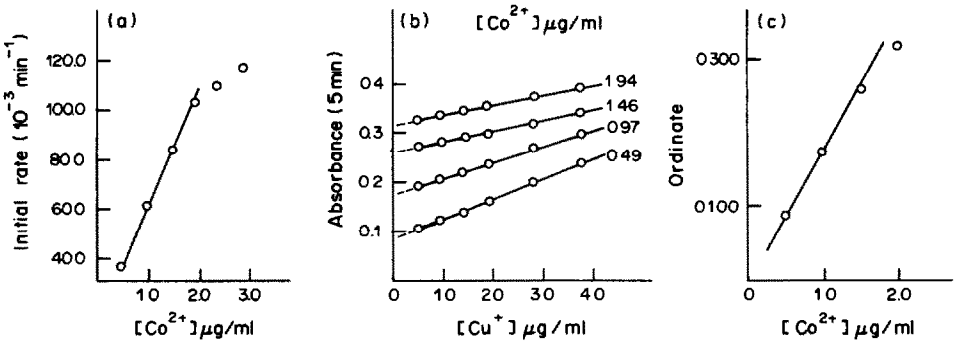

Fig. 7. Combined initial rate and fixed-time method for simultaneous determination of copper(I) and cobalt(II). (a) Calibration graph for cobalt(II) determination by the initial rate method (b) calibration graphs for copper(I) determination in the presence of different amounts of cobalt(II) (c) plot of intercept (at [Cu] = 0) *vs.* cobalt(II) concentration.

the product of both concentrations show mathematically the synergic effect in these systems. Furthermore, by this method, only one experiment is needed for the simultaneous determination of both components of the mixture.

Copper–cobalt mixtures

The logarithmic extrapolation and "combined initial rate and fixed time" methods can be employed for the determination of copper(I) and cobalt(II) in mixtures. Some examples are given in Table 3. The logarithmic extrapolation method is more favourable for copper/cobalt concentration ratios >1, whereas for ratios <1, the "combined initial rate fixed time" method gives the lowest errors.

Copper–nickel mixtures

Copper(I)–nickel(II) mixtures cannot be analysed by the logarithmic extrapolation method because $k_{Ni} \geqslant k_{Cu}$ (Fig. 5), but the "combined initial rate and fixed time" method gives acceptable results provided the [Cu]/[Ni] ratio is greater than ~ 1 (Table 4). If [Cu]/[Ni] is substantially less than 1, an accurately known amount of copper can be added to make the ratio >1 and an appropriate correction made to the results.

Cobalt–nickel mixtures

Only the logarithmic extrapolation method can be used for the analysis of mixtures of cobalt and nickel. Table 5 shows that the error is lowest for [Co]/[Ni] < 1.

Interferences

Tests were made with concentrations of 300 μg/ml for anions and 100 μg/ml for cations. The most important interferences can be classified as follows.

(*a*) Species which react with the azine (generally oxidizing it):
IO_4^-, $S_2O_8^{2-}$, $Cr_2O_7^{2-}$ and MnO_4^-.

(*b*) Species which complex the metal ions:
EDTA, citrate, tartrate.

(*c*) Species which give coloured solutions:
Fe(II), Pd(II), Pt(IV) and VO_3^-.

(*d*) Other interfering species:
Ag(I), Hg(II), Cd(II), Cr(III) and MoO_4^{2-}.

Comparison of results

Table 6 summarizes the range of application of the methods and the relative standard deviations (R.S.D.) calculated from 22 determinations. The logarithmic extrapolation method is more precise

Table 3. Analysis of some synthetic mixtures of copper(I) and cobalt(II)*

Added, μg/ml		Logarithmic extrapolation method				Combined initial rate and fixed-time method			
		Found, μg/ml		Relative error, %		Found, μg/ml		Relative error, %	
Copper	Cobalt	Copper	Cobalt	Copper	Cobalt	Copper	Cobalt	Copper	Cobalt
0.93	0.49	0.92	0.48	−1.1	−2.0	1.10	0.45	18.0	−8.2
1.86	0.97	1.80	1.02	−3.2	5.2	1.73	1.01	−6.9	4.1
0.93	0.97	1.00	0.94	7.5	−3.1	0.88	1.04	−5.4	7.2
0.47	1.46	0.59	1.40	25.0	−4.1	0.43	1.45	−8.5	−0.7
0.47	0.97	0.54	0.92	14.0	−5.2	0.44	1.05	−6.3	8.2

*Each result is the average value of three separate determinations.

Table 4. Analysis of mixtures of copper(I) and nickel(II) by the combined initial rate and fixed-time method*

Added, μg/ml		Found, μg/ml		Relative error, %	
Copper	Nickel	Copper	Nickel	Copper	Nickel
0.93	0.48	0.86	0.50	−7.5	4.1
3.73	1.92	3.75	1.91	0.5	−0.5
1.86	1.92	1.93	1.93	3.7	0.5
0.93	1.44	1.30	1.45	32	0.7
0.93	1.92	1.60	1.91	64	−0.5

*Each result is the average value of three separate determinations.

Table 5. Analysis of synthetic mixtures of cobalt(II) and nickel(II) by the logarithmic extrapolation method*

Added, μg/ml		Found, μg/ml		Relative error, %	
Cobalt	Nickel	Cobalt	Nickel	Cobalt	Nickel
0.97	0.48	0.88	0.46	−9.2	−4.1
1.46	0.48	1.43	0.44	−2.1	−8.3
0.49	0.48	0.45	0.48	−8.2	0.0
1.46	1.44	1.49	1.53	2.1	6.2
0.49	0.96	0.47	0.97	−4.1	1.0
0.97	4.70	0.98	4.72	1.0	0.4

*Each result is the average of three separate determinations.

Table 6. Summary of analytical characteristics of the analysis of binary mixtures of copper(I), cobalt(II) and nickel(II)

Mixture	Method employed		R.S.D.,* %	Application range, μg/ml
Cu(I) + Co(II)	Logarithmic extrapolation	Copper	1.4	0.5–5.0
		Cobalt	0.8	0.5–1.0
	Combined initial rate and fixed-time	Copper	2.3	0.5–≳5.0
		Cobalt	0.9	0.5–1.5
Cu(I) + Ni(II)	Combined initial rate and fixed-time	Copper	0.5	0.9–5.6
		Nickel	0.4	0.5–1.9
Co(II) + Ni(II)	Logarithmic extrapolation	Cobalt	1.0	0.5–1.9
		Nickel	0.6	0.5–4.7

*For 1.40 μg/ml copper(I), 0.97 μg/ml cobalt(II) and 1.44 μg/ml nickel(II).

than the "combined" method for copper–cobalt mixtures, but the "combined" method has the following advantages: (*a*) it is faster; (*b*) it does not require such high k/k' ratios as the logarithmic extrapolation method does; (*c*) the application range is slightly wider; (*d*) it takes synergism explicitly into account.

Analysis of ternary mixtures of copper(I), cobalt(II) and nickel(II)

First the copper concentration is determined photometrically by the complex-formation reaction with 6-Me-PAA,[42] then the cobalt and nickel concentrations are determined by logarithmic extrapolation method. The method is therefore a combination of both photometric and kinetic determinations. 6-Me-PAA is a selective photometric reagent for copper(I); cobalt(II) and nickel(II) in concentrations similar to that of the copper do not interfere. Small concentrations of copper(I) do not interfere in the simultaneous determination of cobalt and nickel by the logarithmic extrapolation method.

We have analysed several Cu/Co/Ni ternary mixtures by this technique and the accuracy and precision for a mixture containing 1.40 μg/ml copper(I), 0.97 μg/ml cobalt(II) and 2.88 μg/ml nickel(II) are given in Table 7. As expected, the precision is best for the copper(I) determination, but all the values are within acceptable limits.

Table 7. Accuracy and precision in the analysis of ternary mixtures of copper(I), cobalt(II) and nickel(II)

Ion	Relative error, %	R.S.D., %
Copper(I)	−2.1	0.5
Cobalt(II)	−3.2	1.3
Nickel(II)	1.4	1.0

CONCLUSION

A new analytical application of >C=N— interchange reactions has been developed, providing a further use for it in analytical chemistry. As the reactions are not instantaneous, they are mainly of kinetic interest, and their use in differential rate methods for the simultaneous determination of metal ions without prior separation holds clear advantages. We have also shown how to exploit the synergic effect in the reaction of some cation mixtures.

Acknowledgement—The authors would like to thank Prof. M. D. Pérez-Bendito, of their Department, for helpful comments and suggestions.

REFERENCES

1. M. D. Luque and M. Calcárcel, *Anal. Lett.*, 1978, **11**, 1.
2. A. Ríos and M. Valcárcel, *Analyst*, 1982, **107**, 737.
3. *Idem*, *Quím. Anal.*, 1983, **4**, 227.
4. T. Curtius and A. Lubin, *Ber.*, 1900, **33**, 2460.
5. R. L. Hinman, *J. Org. Chem.*, 1960, **25**, 1775.
6. H. H. Szmant and C. McGinnis, *J. Am. Chem. Soc.*, 1950, **72**, 2890.
7. Y. Muto, *Nippon Kagaku Zasshi*, 1955, **76**, 252.
8. H. S. Verter and A. E. Frost, *J. Am. Chem. Soc.*, 1960, **82**, 85.
9. D. F. Martin, *Advan. Chem. Ser.*, 1963, **37**, 192.
10. M. Valcárcel and F. Pino, *Talanta*, 1973, **20**, 224.
11. S. Patai, *The Chemistry of the Carbon–Nitrogen Double Bond*, p. 81. Interscience, New York, 1970.
12. A. Ríos, *Thesis*, University of Córdoba, 1983.
13. J. D. Ingle and S. R. Crouch, *Anal. Chem.*, 1971, **43**, 7.
14. K. Ohashi, H. Kawaguchi and K. Yamamoto, *Anal. Chim. Acta*, 1979, **111**, 301.
15. T. Yonekubo, Y. Nagaosa and Y. Nakahigashi, *Nippon Kagaku Kaishi*, 1974, 269.
16. Y. Nagasoa, T. Yonekubo, N. Satake and R. Seto, *Bunseki Kagaku*, 1972, **21**, 215.
17. Y. Nagasoa and T. Yonekubo, *Bull. Chem. Soc. Japan*, 1973, **46**, 1677.
18. J. B. Worthington and H. L. Pardue, *Anal. Chem.*, 1970, **42**, 1157.
19. S. N. Deming, *ibid.*, 1971, **43**, 1726.
20. I. I. Alekseeva, L. P. Ruzinov, L. M. Chernysheva and E. G. Khachaturyan, *Izv. Vyssh. Ucheb. Zaved., Khim. Khim. Tekhnol.*, 1974, **16**, 1445.
21. C. M. Wolff and J.-P. Schwing, *Bull. Soc. Chim. France*, 1976, **1**, 679.
22. M. Tanaka, S. Funahashi and D. Shirai, *Anal. Chim. Acta*, 1967, **39**, 437.
23. E. Mentasti, *ibid.*, 1979, **111**, 177.
24. G. M. Ridder and D. W. Margerum, in *Essays on Analytical Chemistry* (in Memory of Professor Anders Ringbom), E. Wänninen (ed.), p. 529. Pergamon Press, Oxford, 1977.
25. S. Ito, K. Haraguchi and K. Nakagawa, *Bunseki Kagaku*, 1978, **27**, 334.
26. S. Ito, K. Haraguchi, K. Nakagawa and K. Yamada, *ibid.*, 1977, **26**, 554.
27. J. B. Pausch and D. W. Margerum, *Anal. Chem.*, 1969, **41**, 226.
28. A. M. Albrecht-Gary, J. P. Collin, P. Jost, P. Lagrange and J. P. Schwing, *Analyst*, 1978, **103**, 227.
29. S. Funahashi, S. Yamada and M. Tanaka, *Anal. Chim. Acta*, 1971, **56**, 371.
30. M. Kopanica and V. Stará, *Collection Czech. Chem. Commun.*, 1976, **41**, 3275.
31. K. B. Yatsimirskii, A. G. Khachatryan and L. I. Budarin, *Dokl. Akad. Nauk SSSR*, 1973, **211**, 1139.
32. T. Kitagawa and K. Fujikawa, *Nippon Kagaku Kaishi*, 1977, **7**, 998.
33. L. Ballesteros and M. D. Pérez-Bendito, *Analyst*, 1983, **108**, 443.
34. M. D. Pérez-Bendito, *Analyst*, 1984, **109**, 891.
35. M. Valcárcel, *Thesis*, Anales Univ. Hispalense, Serie Ciencias, 1972.
36. H. Diehl and G. F. Smith, *The Copper Reagents: Cuproine, Neocuproine and Bathocuproine*, G. F. Smith Chemical Co., Colombus, Ohio, 1958.
37. C. Genestar, F. García, M. D. Pérez-Bendito and M. Valcárcel, *An. Quím.*, 1978, **74**, 1522.
38. A. Ringbom, *Complexation in Analytical Chemistry*, p. 7. Interscience, New York, 1963.
39. M. Kopanica and V. Stará, in *Comprehensive Analytical Chemistry*, Gy. Svehla (ed.), Vol. XVIII, p. 131. Elsevier, Amsterdam, 1983.
40. H. A. Mottola, *CRC Crit. Rev. Anal. Chem.*, 1975, **4**, 229.
41. J. B. Worthington and H. L. Pardue, *Anal. Chem.*, 1970, **42**, 1157.
42. M. Valcárcel, M. D. Pérez-Bendito and F. Pino, *Inform. Quím. Anal. (Madrid)*, 1971, **25**, 39.

Talanta, Vol 32, No 9, pp. 859–863, 1985
Printed in Great Britain.

0039-9140/85 $3.00 + 0.00

COMPARISON OF CHELATING AGENTS IMMOBILIZED ON GLASS WITH CHELEX 100 FOR REMOVAL AND PRECONCENTRATION OF TRACE COPPER(II)

DAVID K. RYAN* and JAMES H. WEBER
Chemistry Department, University of New Hampshire, Durham, New Hampshire 03824, U.S.A.

(*Received* 27 *August* 1984. *Accepted* 19 *April* 1985)

Summary—Three types of chelating agents immobilized on glass were compared with Chelex 100 for removing and preconcentrating trace Cu^{2+} from laboratory-prepared solutions. Columns of immobilized *N*-propylethylenediamine (diamine), its bis(dithiocarbamate) (DTC) and immobilized 8-hydroxyquinoline (8-HQ) quantitatively remove Cu^{2+} (10–200 μg/l.) from buffered solutions at pH 6.00. Addition of isolated natural organic matter at concentrations typical of organic-rich fresh waters (25–100 mg/l.) complexed Cu^{2+} and hindered the performance of Chelex and the immobilized chelating agents. In the presence of organic matter the DTC performed very well, removing about 98% of the Cu^{2+}. However, the Cu^{2+} removed could not be readily recovered from the column. Chelex gave the poorest results, removing only 62 and 75% of Cu^{2+} at the two levels tested. The other immobilized reagents gave results that were strongly dependent on their contact time with the solution. Longer columns and slower flow-rates tended to improve results. Overall, the immobilized 8-HQ is probably the most suitable of the materials tested for preconcentration work. A batch titration of 8-HQ with Cu^{2+} monitored by ion-selective electrode indicated a conditional stability constant of 6.2×10^7, which is larger than the corresponding value for the complex with non-immobilized 8-hydroxyquinoline, measured under the same conditions.

Determination of trace or ultratrace levels of metal ions in natural waters is often preceded by a preconcentration step to increase the analyte concentrations to levels that are easily and reliably measured. One commonly used method is to pass a large volume of sample through a column of a cation-exchange or chelating ion-exchange resin which will retain the trace metal ions. The metal ions can then be recovered in a much smaller volume by elution with acid, which gives a preconcentration factor equal to the ratio of the volume of sample to the volume of eluent. This is typically done before determination by flame atomic-absorption spectrometry (a.a.s.), which does not have low enough detection limits to be suitable for direct determination of environmental levels of many important trace metals. Other atomic spectrometric techniques (electrothermal a.a.s. and plasma atomic emission) can also benefit from preconcentration and isolation of trace metals from difficult matrices.

Chelex 100, a chelating resin with iminodiacetic acid functional groups anchored to a styrene–divinylbenzene copolymer support,[1] is used for trace metal preconcentration because it has been reported to be capable of quantitative sequestering of trace metals.[2,3] More recent work by different groups has shown that Chelex is ineffective for quantitative separation of many metal ions from water samples containing appreciable amounts of naturally occurring fulvic and humic acids.[4,5] This natural organic matter binds metals and competes with the Chelex, making it necessary to use additional sample treatments such as irradiation with ultraviolet light.[6]

This research investigated use of certain immobilized chelating agents for recovery and preconcentration of trace Cu^{2+} from media containing natural complexing agents. The chelating agents used are covalently anchored to a rigid glass support and offer a high degree of specificity for transition metal ions relative to alkali-metal and alkaline-earth metal ions, and increased mechanical strength for work at high pressures and flow-rates.

The immobilized chelating agents used included *N*-propylethylenediamine (diamine) and its bis(dithiocarbamate) (DTC), which have been studied extensively by Leyden and co-workers[6–11] and others.[12,13] In addition immobilized 8-hydroxyquinoline (8-HQ) was tested.[13–19]

EXPERIMENTAL

Materials

For most of the experiments described here Porasil B spherical porous silica beads (Waters Associates) were used as a support for immobilizing the chelating agents. This support is 80–100 mesh (125–177 μm diameter), has a surface area of 125–250 m^2/g and an average pore diameter of 100–200 Å. Initial experiments employed controlled-pore glass (CPG) (Pierce Chemical Co.) of 200–400 mesh with 40-Å pores and about the same surface areas as Porasil B.

The support was prepared for synthesis by cleaning with each of the following liquids in succession: distilled water, 1 *M* hydrochloric acid, distilled water, 1 *M* ammonia solution and finally distilled water. Each washing step consisted of stirring the slurry of support for 15 min with a motor-driven

*Author for correspondence: present address, Edgerton Research Laboratory, New England Aquarium, Central Wharf, Boston, MA 02110, U.S.A.

paddle-type stirrer, allowing the beads to settle and decanting the solution. Each distilled-water washing step was followed by drying the silica beads on a watch-glass at 180°. Care was taken in every step to avoid undue agitation or mechanical force that would cause breakage of beads.

Natural organic matter was modelled with a soil-derived fulvic acid (SFA) that had been well characterized with respect to chemical[20,21] and metal-ion binding properties.[22-25] These studies demonstrated that the concentrations of Cu^{2+} (10–200 μg/l.) and SFA (25 or 100 mg/l.) used here at pH 6.00 produce nearly complete complexation of the Cu^{2+}.

Immobilization of diamine

Two procedures were used for the silylation reaction. The aqueous preparation which was normally used employed a mixture of 9.0 ml of glacial acetic acid and 36 ml of distilled water. Exactly 5.0 ml of 3-(2-aminoethylamino)-propyltrimethoxysilane (Corning Z-6020, Petrarch Systems) was added slowly with stirring.[7,9] As much as 35 ml of cleaned and dried silica was added to this mixture, stirred for 10 min and filtered off on a medium glass frit. Some reactions were done under a reduced pressure of 40 mmHg to remove air trapped in the pores of the glass beads.

Dithiocarbamates

The bis(dithiocarbamate) derivative (DTC) of the immobilized ethylenediamine was synthesized according to the procedure of Leyden and Luttrell.[7] A monodithiocarbamate of the diamine was prepared according to Hercules *et al.*[12] under conditions which suffice only for reaction of a primary amine group and result in attachment of a single terminal dithiocarbamate group.

8-Hydroxyquinoline

An immobilized 8-hydroxyquinoline material was prepared by the method of Hill[14] with certain modifications. The immobilized diamine was used as the starting material and was reacted with *p*-nitrobenzoyl chloride in freshly distilled chloroform. Distilled triethylamine was added to neutralize the hydrogen chloride produced in the reaction and to help solubilize the acid chloride. In addition a few drops of 2,4,6-trimethylpyridine were usually added as a catalyst.[26] Typical concentrations of the reagents were 0.27*M* *p*-nitrobenzoyl chloride and 0.36*M* triethylamine with 10–15 g of the diamine. The reaction was conducted at 50° for about 48 hr. The product, nitrobenzoylated silica, was filtered off, washed with chloroform and allowed to dry in air. The immobilized nitro group was reduced to the amine by reacting with 100 ml of a 5% solution of sodium dithionite in distilled water. This aminophenyl derivative was diazotized with 100 ml of 2% sodium nitrite solution in 1% v/v acetic acid at 5° for 35 min. The silica was then filtered off, washed with cold distilled water and added to 50 ml of a 2% solution of 8-hydroxyquinoline in absolute ethanol. The final product, 8-hydroxyquinoline immobilized on silica, was filtered off from the reaction mixture and washed consecutively with ethanol, distilled water, 1*M* nitric acid and distilled water.

Copper(II) titrations of 8-HQ

An accurately weighed portion of the 8-HQ chelate (0.3–0.4 g) was titrated in duplicate with Cu^{2+} at pH 5. The titration was conducted under a nitrogen atmosphere in 0.1*M* potassium nitrate and was monitored with a copper ion-selective electrode and a pH electrode. The results were analysed by a Scatchard plot[27] to determine the end-point and stability constant.

Column methods

Chelating agents immobilized on Porasil B and the chelating ion-exchange resin Chelex 100 (Bio-Rad Laboratories, 100–200 mesh) were used in 7-mm bore borosilicate glass columns with polypropylene end-caps and a 35-μm pore-size polypropylene frit (Bio-Rad Econo Columns). Solution reservoirs were 1-litre polyethylene wash-bottles, and the 3-way valves were made of polypropylene, with Teflon stopcocks. Tygon tubing was used for all connections. Column flow-rates were maintained with a peristaltic pump (Sigmamotor, model TGS). All reagents were analytical-reagent grade except the nitric acid, which was Alfa "ultrapure HNO_3".

The immobilized chelating agents and Chelex 100 were slurry-packed into columns and washed with distilled water. Chelex 100 was cleaned of trace metals and converted into the calcium form by the method of Figura and McDuffie.[5] The 8-HQ and diamine columns were also washed with 1*M* ultrapure nitric acid prior to use. All columns, including the DTC, were then buffered to a pH of 6.00 ± 0.05 with 100–200 ml of dilute citrate buffer of 0.01*M* ionic strength.[28] The DTC-copper chelate has been shown to be stable at pH 6.00[7] and all the chelating ligands used, including Chelex 100, sequester metal ions at this pH[1,7,8,14,15] which makes it appropriate for this comparison study. Buffered sample solutions (pH 6.00 ± 0.05 and $I = 0.01$) containing Cu^{2+} (10–200 μg/l.) or Cu^{2+} and SFA (25 or 100 mg/l.) were then passed through the columns at known flow-rates and the effluents were collected in standard flasks. All solutions containing both metal ion and SFA were allowed to equilibrate overnight before use. The columns were then eluted with 1*M* ultrapure nitric acid, the eluates being collected in 25- or 50-ml standard flasks.

Buffer, acid and sample solutions as well as column effluents were analysed for Cu^{2+} by differential-pulse anodic-stripping voltammetry (a.s.v.) with Princeton Applied Research models 174A, 315 and 303. Solutions containing SFA were acidified to 0.1*M* with ultrapure nitric acid and subjected to ultraviolet irradiation in quartz cells overnight before analysis, to destroy organic matter.[29] Acid eluents were analysed by a.a.s.

Adsorption of organic matter on the immobilized chelating agents

In preliminary studies it was observed that a significant amount of organic matter was adsorbed on the immobilized chelating agents. To study this phenomenon further, as a function of chelating functional group and support medium, a series of columns was prepared with 1 ml each of untreated CPG, untreated silica gel, diamine on silica gel, DTC on silica gel and the monodithiocarbamate on CPG. Through each of these columns were passed 50 ml of 20-mg/l. SFA solution at pH 6.0. The absorbance of these solutions before and after passage through a column was measured at 260 nm with a Cary 14 spectrometer.

RESULTS AND DISCUSSION

Column results

Table 1 shows the results of the Chelex 100 experiments with Cu^{2+} solutions and 25-mg/l. SFA. Removal of Cu^{2+} was incomplete even when a fairly long column of Chelex (30 cm) was used. These results agree with those of Figura and McDuffie[30] and Pakalns *et al.*[31] Chelex did not give quantitative results for waters containing natural ligands. Others have also reported that in column operation Chelex only removes a certain labile fraction of metal ion in equilibrium with natural organic matter.[32,33] The fact that Chelex removed a lower percentage of Cu^{2+} when a longer column and slower flow-rate were employed (Table 1) is probably a function of the lability of the Cu^{2+} present. Since less total Cu^{2+} was used, a higher fraction was complexed by stronger binding and potentially less labile sites. This has the

Table 1. Chelex separations of Cu^{2+} from 25-mg/l. soil-derived fulvic acid solutions at pH 6.00

Column height, *cm*	Flow-rate, *ml/min*	Cu^{2+} taken, *μg/l.*	Cu^{2+} in effluent, *μg/l*	Cu^{2+} removed, %
10	3	100	25.0	75.0
30	2	27.8	10.6	61.9

overall effect of reducing the effectiveness of the Chelex separations.

The results obtained for the immobilized diamine are shown in Table 2 and are similar to those for Chelex 100. With no SFA present essentially all the Cu^{2+} was removed from solution. However, in the presence of SFA incomplete recovery was observed. The diamine is not an extremely strong ligand, so these results are not surprising. In addition a large amount of SFA was adsorbed on the chelate (see below).

The DTC gave better results in some respects and these are summarized in Table 3. Quantitative removal of Cu^{2+} was achieved from solutions with SFA levels as high as 100 mg/l. A problem encountered with the DTC was that the Cu^{2+} could not be eluted from the column by 1–4*M* nitric acid, presumably because of the high stability of the complex even under highly acidic conditions.[34]

Results were more promising for the 8-HQ chelate and are shown in Table 4. Cu^{2+} removal was complete from solutions containing only metal ion, but 25-mg/l. SFA solutions posed a more difficult problem and only 37% of the Cu^{2+} was removed under the same conditions but in the absence of SFA. However, use of longer columns and lower flow-rates gave much better results: 91–94% removal.

SFA loss to columns

Preliminary experiments with some of the immobilized chelating agents and the untreated supports demonstrated that the amine functional groups caused loss of SFA. Table 5 shows that untreated supports had little or no effect on SFA passing through the column, as shown by the absorbance. The DTC also retained no SFA. However, the diamine removed practically all the SFA and the monodithiocarbamate removed more than half of it. This was probably due to simple charge attraction between protonated amine groups and the anionic

Table 2. Column separations of Cu^{2+} at pH 6.00 with immobilized ethylenediamine

Bead weight, *g*	Flow-rate, *ml/min*	Sample		Cu^{2+} in effluent, *μg/l.*	Cu^{2+} removed, %
		Cu^{2+}, *μg/l.*	SFA, *mg/l.*		
0.5	10	223	0	1.51	99.3
1.0	10	90.3	0	1.77	98.0
0.4	10	100	25	23.0	77.0
1.0	4.3	100	100	15.4	84.6

Table 3. Column separations of Cu^{2+} with the immobilized bis(dithiocarbamate) at pH 6.00

Bead weight, *g*	Flow-rate, *ml/min*	Sample		Cu^{2+} in effluent, *μg/l.*	Cu^{2+} removed, %
		Cu^{2+}, *μg/l.*	SFA, *mg/l.*		
0.5	3.6	100	0	1.6	98.4
1.0	4	100	100	1.3	98.7
4.0	10	11.0	25	0.3	97.6

SFA. The monodithiocarbamate has a secondary amine group that removes some SFA, but not as much as the diamine does. The DTC does not contain nitrogen atoms that can be protonated at pH 6, so it does not remove SFA.

When solutions containing both SFA and Cu^{2+} were passed through columns of the immobilized chelating agents, a loss of colour occurred even for the DTC column. Table 6 shows the degree of loss of colour for different experiments with 8-HQ and DTC. Also included are the data for Cu^{2+} removal. As can be seen, the loss of colour increases as the degree of Cu^{2+} removal by a given chelating agent increases. We therefore believe that adsorption of SFA on the column occurs owing to the formation of a mixed ligand complex of the Cu^{2+} with the immobilized chelating agent and SFA.

Potentiometric titration of 8-HQ

The titration of the immobilized 8-HQ with Cu^{2+} was conducted exactly as if the ligand were in solution. A titration curve obtained by monitoring free Cu^{2+} potentiometrically with an ion-selective electrode is shown in Fig. 1 and is very similar to one for a solution phase complexometric titration. The endpoint for 1:1 complexation calculated by the second derivative method is $1.3 \times 10^{-3}M$ Cu^{2+}, corresponding to a capacity of 9.5×10^{-5} moles of Cu^{2+} per g of immobilized reagent. This is significantly higher than the early results reported for this system.[14–17] The reason for this higher value is that the diamine was used as the starting material for immobilizing the 8-HQ. Previous reports mentioned above used a monofunctional amine starting material. The diamine could potentially have twice the capacity for 8-HQ,

Table 4. Column separations of Cu^{2+} with the immobilized 8-hydroxyquinoline at pH 6.00

Bead weight, *g*	Flow-rate, *ml/min*	Sample		Cu^{2+} in effluent, *μg/l.*	Cu^{2+} removed, %
		Cu^{2+}, *μg/l.*	SFA, *mg/l.*		
0.5	10	197.8	0	5.3	97.4
0.5	10	198.4	0	0.6	99.7
0.5	10	10.5	0	*	100.0
0.5	30	10.5	0	*	93.9
0.5	30	11.2	25	*	30.4
0.5	10	11.2	25	*	37.1
1.7	5	24.8	25	1.5	93.9
2.7	5	26.8	25	2.4	91.0

*Not determined. Results based on a.a.s. of acid eluent.

Table 5. Adsorption of soil fulvic acid (SFA) on chelates and untreated supports at pH 6.00

Species immobilized	Support	SFA passing through column, %
—	Untreated CPG*	97.7
Monodithiocarbamate	CPG	46.9
—	Untreated silica gel	101.1
Diamine†	Silica gel	2.7
DTC§	Silica gel	103.4

*CPG is Controlled Pore Glass (Corning).
†Diamine is immobilized ethylenediamine.
§DTC is immobilized bis(dithiocarbamate).

but this is not fully achieved, because certain steps in the reaction sequences may not go to completion. An effort to optimize each step in the synthesis of the diamine[13] has resulted in rather high capacity values. Alternative synthetic routes[35] and supports with larger surface area[36] have also given high capacity values for immobilized 8-hydroxyquinoline.

The titration results were also analysed by the Scatchard method,[27] yielding a conditional stability constant of 6.2×10^7 at pH 5 for the 1:1 complex (this stoichiometry was assumed in calculating the end-point). This conditional stability constant is significantly higher than that calculated (2.8×10^7 at pH 5) from the thermodynamic stability constant and the acid dissociation constant.[37] One reason for this is that the 8-HQ is immobilized by reaction at its 5-position with a substituted diazobenzene, and thus is chemically different from 8-hydroxyquinoline. The substituted phenylazo-8-hydroxyquinoline is considerably more acidic[16] and this will increase the stability of the Cu^{2+} complex. The change in electron configuration, caused by the substitution, is evidenced by the red colour of the immobilized species.

One problem encountered in titrating the immobilized chelating agent was that very long equilibration times were needed in order to get constant potential readings from the Cu^{2+} electrode. This behaviour is in contrast to the fairly rapid uptake kinetics reported by Kvitek *et al.*,[38] and may be due to slow uptake of the metal ion by binding sites that are not readily accessible. Even with vigorous stirring of the system, there will be an unstirred layer around and in the pores and polymeric coating of each bead, through which the Cu^{2+} ions must diffuse. This diffusion was so slow and the equilibration time so long that completion of a titration took a period of days. No difficulty was encountered with electrode stability over this time period. The pH electrode was removed from the titration cell and recalibrated regularly and the Cu^{2+} electrode was calibrated before and after the titration. Both calibrations showed very good Nernstian response.

Table 6. Loss of soil fulvic acid (SFA) to immobilized reagent

Species immobilized	Loss of SFA, %	Cu^{2+} removed, %
8-HQ	5.1	37.1
8-HQ	59.2	85.1
8-HQ	70.9	93.9
DTC	74.9	90.0
DTC	93.3	97.6

CONCLUSIONS

Practically any ion-exchange or immobilized chelating group can remove Cu^{2+} from simple aqueous solutions at an appropriate pH. The real test of these materials, however, is in their performance for solutions containing competing ligands or high total ion concentrations, such as are encountered in many analytical problems. The results reported here show that immobilized chelating agents such as 8-HQ and DTC can give better results than Chelex 100 when a competing ligand is present in solution. The immobilized diamine was not very effective against the competing ligand SFA. All the immobilized reagents tested adsorbed a substantial quantity of this natural ligand. However, the adsorption phenomenon does not cause a problem for most applications, as it does not seem to seriously degrade performance.

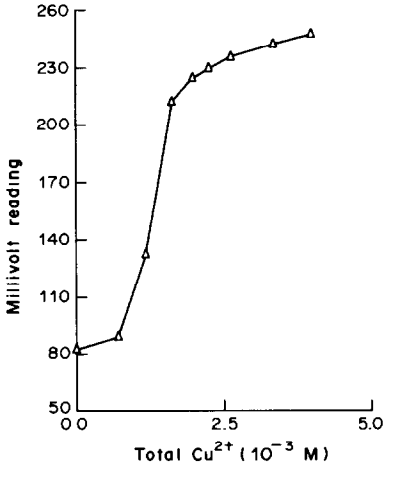

Fig. 1. Potentiometric titration curve for titration of immobilized 8-hydroxyquinoline with copper at pH 5.00.

Of the chelating agents used in this study 8-HQ seems best suited for analytical preconcentration. By choice of the proper conditions quantitative removal and recovery of Cu^{2+} can be obtained. DTC gives the best removal from solutions but does not readily release the bound Cu^{2+}. However, it is possible to recover the sequestered Cu^{2+} by complete destruction of the support, as done by Barnes and co-workers[39-41] for DTC immobilized on an organic resin.

Acknowledgements—D.K.R. acknowledges the helpful comments of T.R. Gilbert in the preparation of this manuscript. This research was supported in part by grant OCE 79-10571 from the National Science Foundation.

REFERENCES

1. Bio-Rad Laboratories, *Product Information* 2020, 1978.
2. J. P. Riley and D. Taylor, *Anal. Chim. Acta*, 1968, **40**, 479.
3. M. J. Abdullah and L. G. Royle, *ibid.*, 1972, **58**, 283.
4. T. M. Florence and G. E. Batley, *Talanta*, 1976, **23**, 179.
5. P. Figura and B. McDuffie, *Anal. Chem.*, 1977, **49**, 1950.
6. D. E. Leyden, J. T. Cronin and A. T. Ellis, *Intern. J. Environ. Anal. Chem.*, 1982, **11**, 105.
7. D. E. Leyden and G. H. Luttrell, *Anal. Chem.*, **1975**, 47, 1612.
8. D. E. Leyden, G. H. Luttrell and T. A. Patterson, *Anal. Lett.*, 1975, **8**, 51.
9. D. E. Leyden, G. H. Luttrell, A. E. Sloan and N. J. DeAngelis, *Anal. Chim. Acta*, 1976, **84**, 97.
10. D. E. Leyden, G. H. Luttrell, W. K. Nonidez and D. B. Werho, *Anal. Chem.*, 1976, **48**, 67.
11. D. E. Leyden, W. K. Nonidez and P. W. Carr, *ibid.*, 1975, **47**, 1449.
12. D. M. Hercules, L. E. Cox, S. Onisick, G. D. Nichols and J. C. Carver, *ibid.*, 1973, **45**, 1973.
13. C. Fulcher, M. A. Crowell, R. Bayliss, K. B. Holland and J. R. Jezorek, *Anal. Chim. Acta*, 1981, **129**, 29.
14. J. M. Hill, *J. Chromatog.*, 1973, **76**, 455.
15. K. F. Sugawara, H. H. Weetall and G. D. Schucker, *Anal. Chem.*, 1974, **46**, 489.
16. J. R. Jezorek and H. Freiser, *ibid.*, 1979, **51**, 366.
17. E. D. Moorhead and P. H. Davis, *ibid.*, 1974, **46**, 1879.
18. M. M. Guedes da Mota, F. G. Romer and B. Griepink, *Z. Anal. Chem.*, 1977, **287**, 19.
19. R. E. Sturgeon, S. S. Berman, S. N. Willie and J. A. H. Desaulniers, *Anal. Chem.*, 1981, **53**, 2337.
20. J. H. Weber and S. A. Wilson, *Water Res.*, 1975, **9**, 1079.
21. S. A. Wilson and J. H. Weber, *Chem. Geol.*, 1977, **19**, 285.
22. G. A. Bhat, R. A. Saar, R. B. Smart and J. H. Weber, *Anal. Chem.*, 1981, **53**, 2275.
23. R. E. Truitt and J. H. Weber, *ibid.*, 1981, **53**, 337.
24. R. A. Saar and J. H. Weber, *ibid.*, 1980, **52**, 2095.
25. D. K. Ryan and J. H. Weber, *ibid.*, 1982, **54**, 986.
26. P. R. Moses, L. M. Wier, J. C. Lennox, H. O. Finklea, J. R. Lenhard and R. W. Murray, *ibid.*, 1978, **50**, 576.
27. G. Scatchard, *Ann. N.Y. Acad. Sci.*, 1949, **51**, 660.
28. D. D. Perrin, *Aust. J. Chem.*, 1963, **16**, 572.
29. G. E. Batley and Y. J. Farrar, *Anal. Chim. Acta*, 1978, **99**, 283.
30. P. Figura and B. McDuffie, *Anal. Chem.*, 1979, **51**, 120.
31. P. Pakalns, G. E. Batley and A. J. Cameron, *Anal. Chim. Acta*, 1978, **99**, 333.
32. R. J. Stolzberg and D. Rosin, *Anal. Chem.*, 1977, **49**, 226.
33. D. D. Nygaard and S. R. Hill, *Anal. Lett.*, 1979, **12**, 491.
34. N. Strafford, P. Wyatt and F. Kershaw, *Analyst*, 1945, **70**, 232.
35. M. A. Marshall and H. A. Mottola, *Anal. Chem.*, 1983, **55**, 2089.
36. G. J. Shahwan and J. R. Jezorek, *J. Chromatog.*, 1983, **256**, 39.
37. A. E. Martell and R. M. Smith, *Critical Stability Constants*, Vol. 3, p. 186. Plenum Press, New York, 1977.
38. R. J. Kvitek, P. W. Carr and J. F. Evans, *Anal. Chim. Acta*, 1981, **124**, 229.
39. R. M. Barnes and J. S. Genna, *Anal. Chem.*, 1979, **51**, 1065.
40. A. Miyazaki and R. M. Barnes, *ibid.*, 1981, **53**, 299,364.
41. H. S. Mahanti and R. M. Barnes, *Anal. Chim. Acta*, 1983, **149**, 395.

Talanta, Vol. 32, No. 9, pp. 865–873, 1985
Printed in Great Britain.

0039-9140/85 $3.00 + 0.00

REVERSED-PHASE LIQUID CHROMATOGRAPHIC RETENTION BEHAVIOUR OF CATECHOL AMINO-ACIDS

T. ISHIMITSU and S. HIROSE
Kyoto Pharmaceutical University, 5 Nakauchi-cho, Misasagi, Yamashina-ku, Kyoto 607, Japan

H. SAKURAI
Faculty of Pharmaceutical Sciences, University of Tokushima, Scho-machi 1, Tokushima 770, Japan

(*Received* 3 *October* 1984. *Accepted* 18 *April* 1985)

Summary—For a group of catechol amino-acids varying widely in acid strength and hydrophobicity, the effects of mobile phase composition, pH and ionic strength on their reversed-phase chromatographic separation have been determined, with phosphate buffer as mobile phase. Retention data were measured for 18 catecholamine derivatives. The retardation factors and retention behaviour of all the compounds tested could be explained in terms of the acid dissociation and tautomeric constants.

Catecholamines and their derivatives are widely distributed in living systems, and their separation and determination are essential for understanding of their physiological importance.[1,2] High-pressure liquid chromatography (HPLC) has been successfully employed for this purpose.[3,4] We have reported the determination of methoxy derivatives of 3,4-dihydroxyphenylalanine (DOPA), including 3-hydroxy-4-methoxyphenylalanine (4-*O*-methyl-DOPA), in plasma by HPLC.[5,6] Recent chromatographic work has suggested a close relationship between the retardation factor and the acid dissociation constant of these compounds,[7,8] but the chromatographic retention mechanism has not been established. For this reason we have studied the relationship between the retention values and structures of 18 such compounds. The results allow prediction of the elution order in reversed-phase chromatography as well as identification of these compounds.

EXPERIMENTAL

Reagents

Noradrenaline (NA), adrenaline (A), normetanephrine (NMN), metanephrine (MN), 3,4-dihydroxymandelic acid (DOMA) and 3-methoxy-4-hydroxymandelic acid (VMA) were purchased from Nakarai Chemical Co., Kyoto. The following materials were synthesized: 4-*O*-methylnoradrenaline (4-*O*-methyl-NA) and 4-*O*-methyladrenaline (4-*O*-methyl-A);[9] 3,4-dimethoxynoradrenaline and 3,4-dimethoxyadrenaline.[10,11] Other reagents were obtained as described previously.[5] Potassium phosphate buffers (0.05*M*, pH 2.6–8.5) with and without 15% of methanol present were prepared. The ionic strength was adjusted in the range 0.01–1.0 with potassium chloride.

Chromatographic conditions

A Yanagimoto L-2000 high-speed liquid chromatograph equipped with a Yanagimoto VMD 101 detector was used for determination of the catecholamines. Yanapak ODS (10 μm) was packed in a 250 mm × 4.0 mm bore stainless-steel column; the flow-rate used was 0.58 ml/min. The working electrode was set at 0.9 V *vs.* an Ag/AgCl reference electrode. The chromatographic system was programmed for 6 min elution with the purely aqueous phosphate buffer, then for 30 min with a linearly increasing methanol concentration up to 15% in the buffer, and finally with the 15% methanol buffer. Organic solvents were HPLC grade. The chromatographic peaks were characterized by the retardation factor, k', calculated from $k' = (t_R - t_0)/t_0$, where t_0 and t_R are the retention times of a completely unretained solute and the test solute, respectively. Equation (1) shows that k' depends on the dissociation constant of the compound and the pH of the mobile phase.[12] K_1 and K_2 are the dissociation constants of the amino and/or phenol groups. For zwitterions

$$k' = \frac{k_0 + k_1\left(\frac{[H^+]}{K_1}\right) + k_{-1}\left(\frac{K_2}{[H^+]}\right)}{1 + \frac{[H^+]}{K_1} + \frac{K_2}{[H^+]}} \quad (1)$$

where k_0, k_1 and k_{-1} are the retardation factors for the zwitterion, cationic and anionic forms, respectively.

Procedure

The electrochemical detection method was tested for 18 catecholamine derivatives. The operating potential was increased stepwise from 0.3 to 0.9 V for each compound, and the signal produced by the electrochemical oxidation at each potential was displayed on the recorder and the peak current was noted. For each compound the peak current was plotted against the applied potential.

pH-titration

The titration procedure described in a previous paper[13] was employed. Catechol amino-acids are relatively stable in acidic solution but oxidized slowly at high pH. Therefore, the titrations were done with the solution in an atmosphere of nitrogen to prevent oxidation.

Determination of the macroscopic proton dissociation constants (macro-constants)

The macro-constants of the compounds were calculated according to the method of Schwarzenbach.[14]

Determination of the microscopic proton dissociation constants (micro-constants)

The micro-constants were determined as described in the calculation of the micro-constants of tyrosine.[13] The acid-

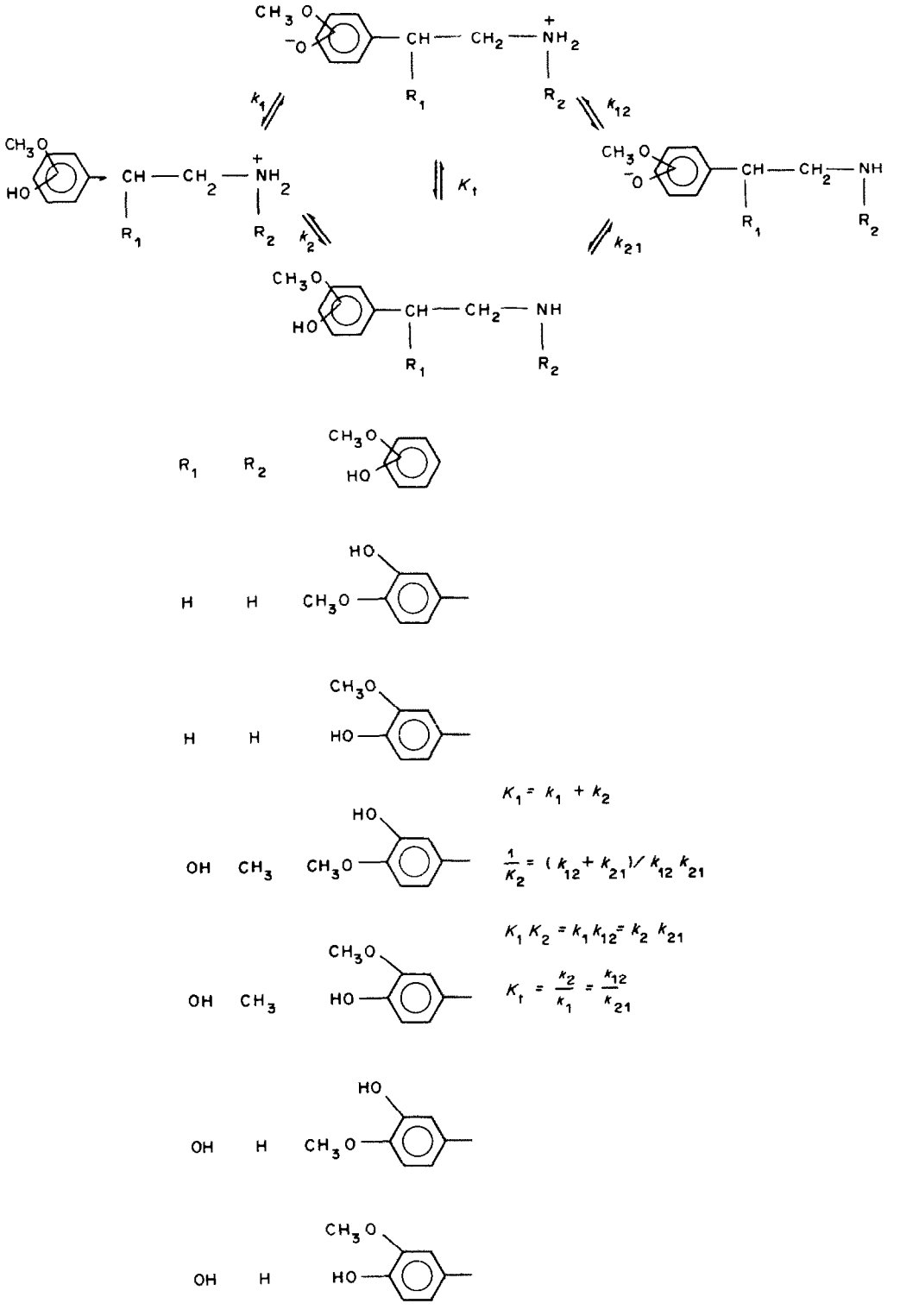

Fig. 1. Scheme of ionization equilibrium of catecholamine derivatives.

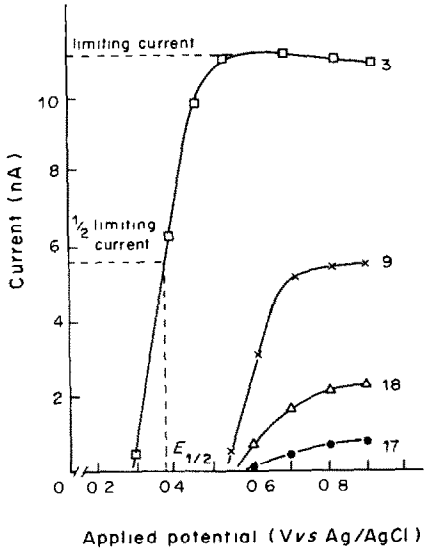

Fig. 2. Current–potential curves for catecholamine derivatives. The half-wave potential ($E_{1/2}$) is determined as the voltage at which the current produced by the oxidation is half of the limiting current. 3, DOMA; 9, VMA; 17, VPA; 18, VLA.

dissociation scheme is shown in Fig. 1. To determine the micro-constants of a catecholamine, the macro-constant of the methoxyphenyl derivative was conveniently used for k_2, which corresponds to proton dissociation from $-NH_3^+$.

RESULTS AND DISCUSSION

Electrochemical detection of the compounds and effect of ionic strength on their retention

The current–potential curves obtained from the chromatographic peak currents at each potential are shown in Fig. 2. It has been reported that the limiting current of a catecholamine reaches a plateau at about 0.5 V *vs.* Ag/AgCl,[15] but for DOMA, VMA, 3-methoxy-4-hydroxyphenyl-lactic acid (VLA) and 3-methoxy-4-hydroxyphenylpyruvic acid (VPA) the plateau is reached at 0.5, 0.7, 0.8 and 0.8 V *vs.* Ag/AgCl, respectively. The half-wave potentials ($E_{1/2}$) were determined as the potentials at which the peak current reached half its limiting value, as shown for DOMA (0.37 V) in Fig. 2, and are listed in Table 1. The correlation between chemical structure and half-wave potential is clearly seen: NA, A and DA, and the three catechol derivatives (DOPA, *N*-methyl-DOPA and DOMA) have lower $E_{1/2}$ values (about 0.35 V *vs.* Ag/AgCl) and the monohydroxy compounds have higher $E_{1/2}$ values (0.58–0.6 V *vs.* Ag/AgCl). This result can be used to identify the type of compound.

The electrochemical-detector signal showed a dependence on the ionic strength of the buffer (Fig. 3). The maximal response was obtained at $\mu = 0.05M$ for the phosphate buffer, for all compounds tested, and this was therefore used throughout.

k'–pH relationships

A mobile phase consisting of 0.05*M* phosphate buffer at various pH values was used for the separation of catecholamine derivatives. A chromatogram for pH 3.1 is shown in Fig. 4 as an example of the separation achievable, and the effects of pH on *k'* are shown in Figs. 5 and 6. Figure 5 suggests that the retardation behaviour depends largely on the type of functional group and the pK_a values of the compound as well as on the pH of the eluent. The pK_a values are listed in Table 2, where pK_1 and pK_2 correspond to the dissociation of the amino and/or phenol groups, and the dissociation constants of the carboxylic group are represented by pK_{COOH}. From Fig. 5, three general conclusions can be drawn. (*a*) The retardation factors of the catecholamines (NA, A, DA, NMN, MN, 3-*O*-methyl-DA, 4-*O*-methyl-DA, 4-*O*-methyl-NA and 4-*O*-methyl-A) that have no carboxylic group, are independent of the pH of the eluent up to 5.5. This is as expected, since their pK_a values are higher than 6.0, and these compounds therefore carry the same charge from pH 2.6 to 5.5. The elution order (retardation factor) of these compounds in the pH range 2.6–5.5 is NA < A < NMN < 4-*O*-methyl-NA < DA < MN < 4-*O*-methyl-A < 3-*O*-methyl-DA < 4-*O*-methyl-DA. This order may be understood on the basis of the hydrophobicity of the compounds, as suggested previously.[18] NA is the most polar catecholamine in the present study and hence has the lowest retardation factor. DA is more hydrophobic than NA and retained longer than NA. (*b*) The α-hydroxycarboxylic acid derivatives, especially VLA, VMA and DOMA, are strongly retarded compared with the corresponding amino-acids. This can be explained by the finding that ion-pair formation increases with increase in

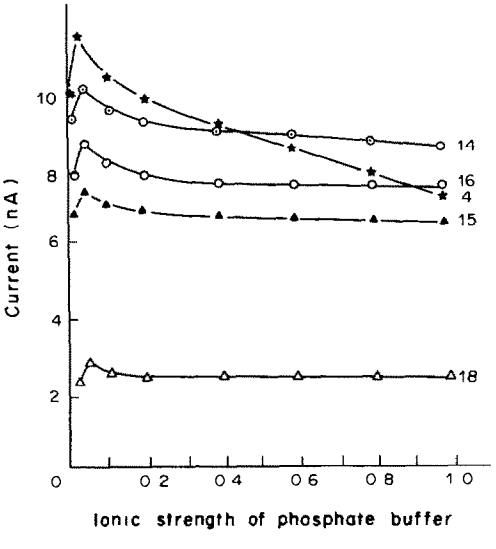

Fig. 3. Relationship between current–potential curve and ionic strength. 4, NMN; 14, 3-*O*-methyl-DA; 15, 4-*O*-methyl-DOPA; 16, 4-*O*-methyl-DA; 18, VLA.

Table 1. Half-wave potentials for catecholamines and amino-acids

Compound	Abbreviation	$E_{1/2}$, *V vs.* Ag/AgCl
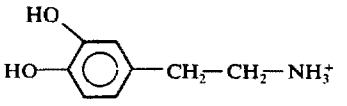	DA	0.34
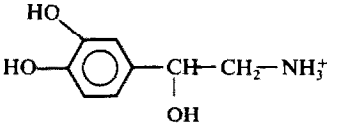	NA	0.35
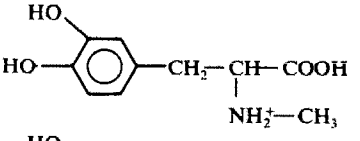	*N*-methyl-DOPA	0.35
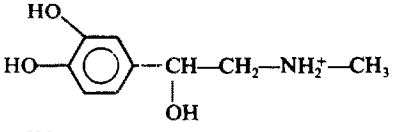	A	0.36
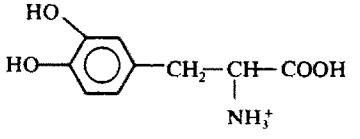	DOPA	0.36
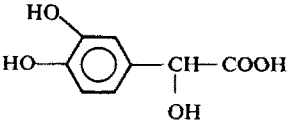	DOMA	0.37
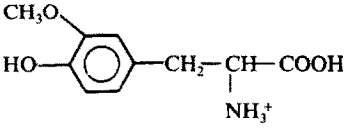	3-*O*-methyl-DOPA	0.58
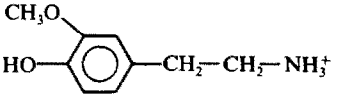	3-*O*-methyl-DA	0.59
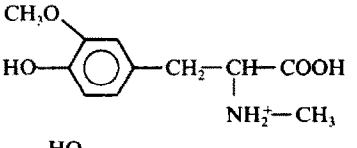	*N*-methyl-3-*O*-methyl-DOPA	0.59
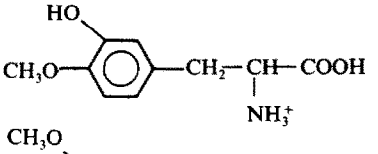	4-*O*-methyl-DOPA	0.61
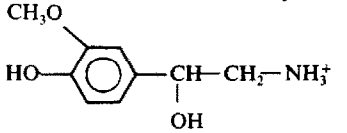	NMN	0.61
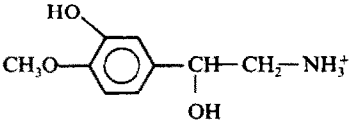	4-*O*-methyl-NA	0.63
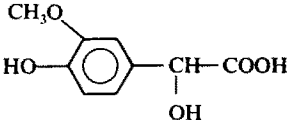	VMA	0.63

Table 1 (*cont.*)

Compound	Abbreviation	$E_{1/2}$, *V vs.* Ag/AgCl
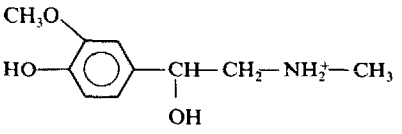	MN	0.64
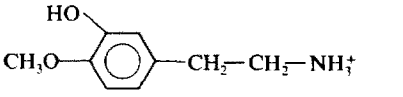	4-*O*-methyl-DA	0.65
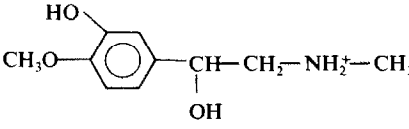	4-*O*-methyl-A	0.65
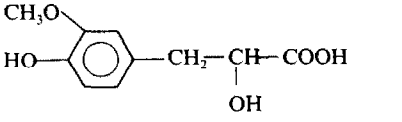	VLA	0.65
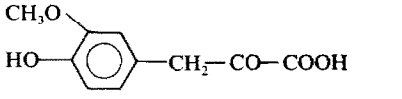	VPA	0.66

protonation of the carboxylic group (*i.e.*, as the pH decreases).[19,20] (*c*) For DOPA, *N*-methyl-DOPA, 3-*O*-methyl-DOPA, *N*-methyl-3-*O*-methyl-DOPA, 4-*O*-methyl-DOPA and VPA, the retardation factor changes slightly with pH up to 3.5 and at pH 3.5–5.5 is almost constant. For these compounds, which have pK_{COOH} values <2.62, the carboxylic groups are at least 90% in the carboxylate COO^- form at pH >3.6. The compounds having pK_{COOH} values >3.3 should show a pronounced increase in retardation factor as the pH falls below $pK_{COOH} + 1$, and the carboxylate group becomes progressively protonated. This is clearly shown for the three groups of compounds consisting of α-hydroxy (VLA, VMA,

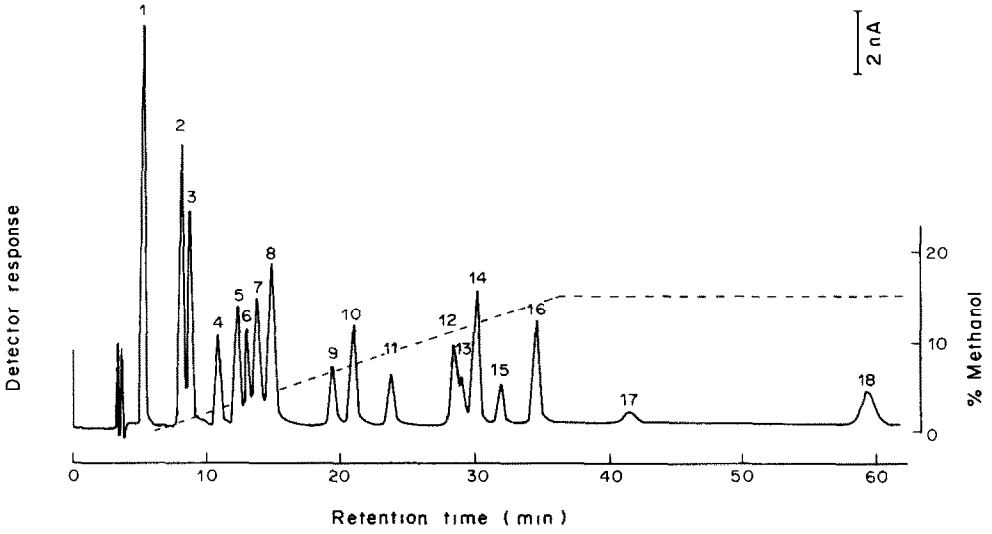

Fig. 4. Chromatograms of standard mixture containing catecholamine derivatives. Injection sample: 10 μl of solution containing 1 ng each of compounds. Column, Yanapak ODS; flow-rate, 0.58 ml/min; temperature 25°C; eluent, 0.05*M* phosphate buffer (pH 3.1) for the first 6 min, then a linear gradient of increasing methanol concentration in the buffer from 6 to 36 min. Peaks: 1, NA; 2, A; 3, DOMA; 4, NMN; 5, *N*-methyl-DOPA; 6, 4-*O*-methyl-NA; 7, DOPA; 8, DA; 9, VMA; 10, MN; 11, 4-*O*-methyl-A; 12, 3-*O*-methyl-DOPA; 13, *N*-methyl-3-*O*-methyl-DOPA; 14, 3-*O*-methyl-DA; 15, 4-*O*-methyl-DOPA; 16, 4-*O*-methyl-DA; 17, VPA; 18, VLA.

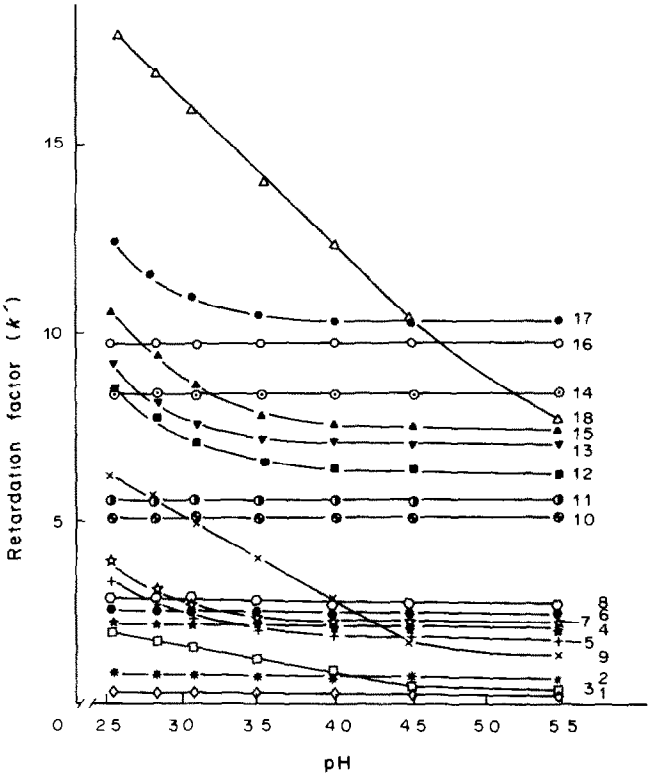

Fig. 5. pH-dependence of the retardation factor of the compounds. Chromatographic conditions as in Fig. 4. 1, NA; 2, A; 3, DOMA; 4, NMN; 5, *N*-methyl-DOPA; 6, 4-*O*-methyl-NA; 7, DOPA; 8, DA; 9, VMA; 10, MN; 11, 4-*O*-methyl-A; 12, 3-*O*-methyl-DOPA; 13, *N*-methyl-3-*O*methyl-DOPA; 14, 3-*O*-methyl-DA; 15, 4-*O*-methyl-DOPA; 16, 4-*O*-methyl-DA; 17, VPA; 18, VLA.

DOMA), monohydroxy (VPA, 4-*O*-methyl-DOPA, *N*-methyl-3-*O*-methyl-DOPA, 3-*O*-methyl-DOPA) and dihydroxy compounds (*N*-methyl-DOPA, DOPA) in the pH region 2.6–5.5. For all the groups a clear relationship between elution order and the pK_{COOH} values is shown in Table 3, and from Fig. 5 it can be seen that MN, 4-*O*-methyl-A, 3-*O*-methyl-DA, 4-*O*-methyl-DA, 3-*O*-methyl-DOPA and 4-*O*-methyl-DOPA were always retarded more strongly than the corresponding catecholamine and DOPA compounds.

A marked increase in the retardation factor was

Table 2. Dissociation constants of catecholamine derivatives

Compound	pK_{COOH}	pK_1	pK_2	pK_3	Ref.
VLA	3.80 ± 0.02	10.09 ± 0.06	—	—	
VMA	3.45 ± 0.03	9.96 ± 0.05	—	—	
DOMA	3.40 ± 0.03	9.53 ± 0.04	11.97 ± 0.04	—	
VPA	2.62 ± 0.03	10.11 ± 0.08	—	—	
4-*O*-methyl-DOPA	2.34 ± 0.03	8.95 ± 0.01	10.23 ± 0.01	—	16
N-methyl-3-*O*-methyl-DOPA	2.28 ± 0.04	8.91 ± 0.04	10.29 ± 0.06	—	
3-*O*-methyl-DOPA	2.24 ± 0.03	8.89 ± 0.01	10.25 ± 0.01	—	16
N-methyl-DOPA	2.32 ± 0.02	8.70 ± 0.03	10.08 ± 0.05	12.21 ± 0.06	
DOPA	2.29 ± 0.05	8.76 ± 0.06	9.96 ± 0.02	12.14 ± 0.08	16
4-*O*-methyl-NA	—	8.80 ± 0.02	9.90 ± 0.01	—	
NMN	—	8.82 ± 0.01	9.93 ± 0.02	—	
4-*O*-methyl-A	—	8.95 ± 0.02	10.11 ± 0.03	—	
MN	—	8.98 ± 0.03	10.03 ± 0.02	—	
4-*O*-methyl-DA	—	9.34 ± 0.01	10.49 ± 0.02	—	17
3-*O*-methyl-DA	—	9.45 ± 0.01	10.58 ± 0.02	—	17
A	—	8.63 ± 0.03	9.96 ± 0.05	12.07 ± 0.09	
NA	—	8.56 ± 0.01	9.64 ± 0.05	12.03 ± 0.07	
DA	—	9.05 ± 0.04	10.52 ± 0.02	11.98 ± 0.06	17

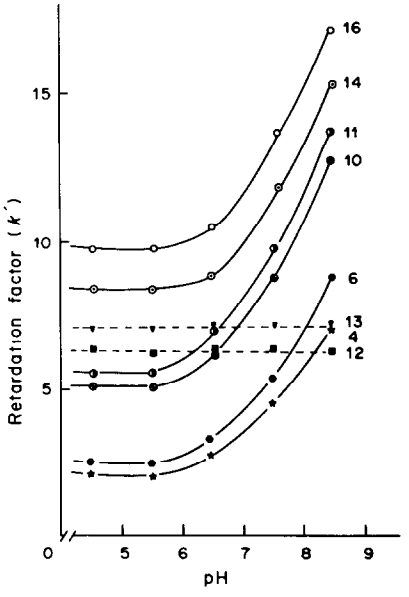

Fig. 6. pH-dependence of the retardation factor of the compounds. Chromatographic conditions as in Fig. 4. 4, NMN; 6, 4-*O*-methyl-NA; 10, MN; 11, 4-*O*-methyl-A; 12, 3-*O*-methyl-DOPA; 13, *N*-methyl-3-*O*-methyl-DOPA; 14, 3-*O*-methyl-DA; 16, 4-*O*-methyl-DA.

found for certain compounds when the pH of the mobile phase was raised from 4.5 to 8.5 (Fig. 6). This behaviour is probably due to the increase in availability of phosphate anionic species that can form ion-pairs with NMN, MN, 3-*O*-methyl-DA,

Table 3. Relationship between proton dissociation constants and retention behaviour of mandelic acid derivatives

	DOMA	VMA	VLA
pK_{COOH}	3.40	3.45	3.80
k'*	1.4	4.9	15.9
Retention time,[18] *min*	7.4	11.5	—
Retention time,[21] *min*	3.2	5.5	—
Retention time,[22] *min*	—	6.0	20.0
Retention time,[22] *min*	—	5.2	18.8
Retention time,[23] *min*	0.9	1.3	6.4
Retention time,[24] *min*	4.5	10.0	—

*This work, separation chromatogram at pH 3.1.

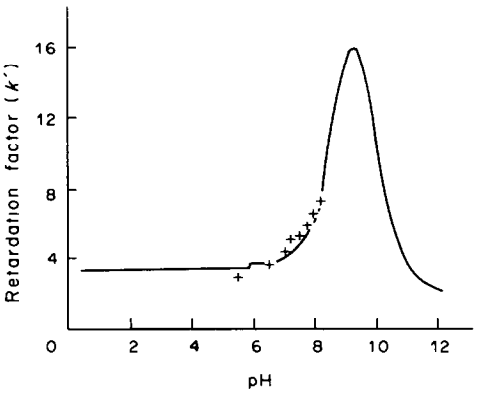

Fig. 7. Retardation factors for normetanephrine as a function of pH, with k_1, k_0 and k_{-1} calculated by equation (1) and a non-linear least-squares fit. For normetanephrine $k_0 = 23.71$, $k_1 = 3.63$ and $k_{-1} = 2.00$.

4-*O*-methyl-DA, 4-*O*-methyl-NA and 4-*O*-methyl-A, which have no carboxylic group. On the other hand, the retardation factors of 3-*O*-methyl-DOPA and *N*-methyl-3-*O*-methyl-DOPA, which have a carboxylic group, are independent of eluent pH in this region. The correlation between elution order and pK_a values for NMN, MN, 3-*O*-methyl-DA, 4-*O*-methyl-DA, 4-*O*-methyl-NA and 4-*O*-methyl-A was estimated as before, but no clear relationship was found. It is assumed that the reason for this is that these derivatives can dissociate the first proton from either the ammonium or the hydroxy group in the same pH range, as has been shown for tyramine and octopamine.[13] To obtain further information on the deprotonation of the six derivatives (NMN, 4-*O*-methyl-NA, MN, 4-*O*-methyl-A, 3-*O*-methyl-DA and 4-*O*-methyl-DA), the microconstants and $1/K_t$ values were calculated (Table 4). The concentration ratios of the two intermediates, represented by the $1/K_t$ values, show a definite trend, the $1/K_t$ values being 0.66, 0.74, 0.81, 0.95, 1.75 and 2.57 for NMN, 4-*O*-methyl-NA, MN, 4-*O*-methyl-A, 3-*O*-methyl-DA and 4-*O*-methyl-DA, respectively. The $1/K_t$ values and retention times for these compounds, listed in Table 5, suggest a relationship between the $1/K_t$ values and elution order: as the $1/K_t$

Table 4. Microscopic acid dissociation constants and tautomeric constants of catecholamine derivatives

Compound	k_1	k_2	k_{12}	k_{21}	$1/K_t$ (k_1/k_2)
NMN	9.22	9.04*	9.71	9.89	0.66
4-*O*-methyl-NA	9.17	9.04*	9.53	9.66	0.74
MN	9.33	9.24†	9.68	9.77	0.81
4-*O*-methyl-A	9.26	9.24†	9.80	9.82	0.95
3-*O*-methyl-DA[17]	9.65	9.89§	10.38	10.14	1.75
4-*O*-methyl-DA[17]	9.48	9.89§	10.35	9.94	2.57

*Dissociation constant of 3,4-dimethoxynoradrenaline (9.04 ± 0.05).
†Dissociation constant of 3,4-dimethoxyadrenaline (9.24 ± 0.03).
§Dissociation constant of 3,4-dimethoxyphenethylamine (9.89 ± 0.01).

Table 5. Relationship between tautomeric constants and retention behaviour of catecholamine derivatives

Compound	$1/K_t$ (k_1/k_2)	k'*	Retention time,[18] *min*	Retention time,[21] *min*	Retention time,[25] *min*	Retention time,[26] *min*	Retardation factor,[27] k'	Retention time,[28] *min*	Retardation factor,[29] k'	Retention time,[30] *min*
Octopamine	0.32[13]	4.3	—	—	—	—	0.26	—	2.05	—
NMN	0.66	7.2	4.0	—	—	5.9	0.48	3.8	2.09	11.2
4-*O*-methyl-NA	0.74	8.3	—	—	—	—	—	—	—	16.2
MN	0.81	12.7	5.7	12.2	—	8.6	0.93	6.0	3.14	15.4
4-*O*-methyl-A	0.95	13.8	—	—	—	—	—	—	—	22.7
Tyramine	1.15[13]	14.5	—	8.6	15.0	10.0	0.96	—	2.86	—
3-*O*-methyl-DA	1.75[17]	15.4	7.0	15.0	34.0	17.0	1.86	9.5	3.09	31.2
4-*O*-methyl-DA	2.57[17]	17.2	—	—	48.0	—	—	—	3.77	43.1

*This work; separation chromatogram at pH 8.5.

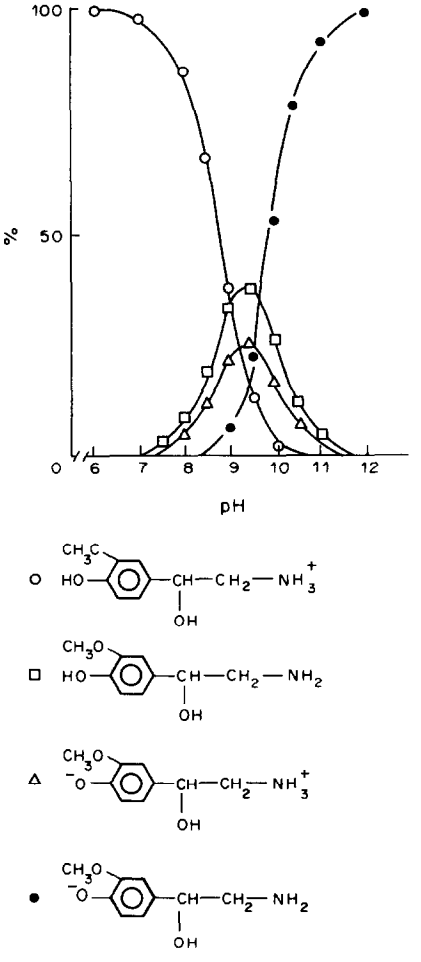

Fig. 8. Relative concentration of various ionic forms of normetanephrine.

value increases so does the retention time, except for MN.[21,29,30]

The relationship between the retardation factor and the pH-dependent distribution of the chemical species of the compound was examined. Figure 7 shows a plot of the experimentally determined k' values for the reversed-phase HPLC of NMN as a function of pH (5.5–8.5) at controlled ionic strength. High pH values could not be tested because of the effect on the ODS stationary phase used. The values of k_0, k_1 and k_{-1} for NMN were calculated from the experimental points by equation (1)[12] and a non-linear least-squares fit, and the back-calculated $k' = f(\text{pH})$ function for pH 0.5–12 is shown as the continuous line and shows that the retardation factor should reach a maximum at pH 9.5. The distribution of the various ionic forms of NMN as a function of pH is shown in Fig. 8. The fractions in tautomeric zwitterion or phenol forms, and their sum, are maximal at pH 9.5, which corresponds well with the maximum of the retardation factor (Fig. 7). The same trends were also seen for MN, 3-*O*-methyl-DA, 4-*O*-methyl-DA, 4-*O*-methyl-NA and 4-*O*-methyl-A.

Figures 7 and 8 suggest that the relative concentrations of the tautomeric forms as a function of pH are closely related to the retardation behaviour. Knowledge of the distribution of the tautomeric forms as a function of pH could prove valuable as an aid to prediction of chromatographic retardation behaviour.

REFERENCES

1. J. Axelson, *Ann. Rev. Physiol.*, 1971, **33**, 1.
2. L. P. Cooper, F. E. Bloom and R. H. Roth, *The Biochemical Basis of Neuropharmacology*, 2nd Ed., pp. 90–174. Oxford Univ. Press, New York, 1972.
3. J. H. Knox and J. Jurand, *J. Chromatog.*, 1976, **125**, 89.
4. C. Hansson, G. Agrup, H. Rorsman, A. M. Rosengren, E. Rosengren and L. E. Edholm, *ibid.*, 1979, **162**, 7.
5. T. Ishimitsu and S. Hirose, *Chem. Pharm. Bull.*, 1981, **29**, 3400.
6. T. Ishimitsu, S. Hirose, K. Asahara and M. Imaizumi, *ibid.*, 1984, **32**, 3320.
7. Cs. Horváth, W. Melander and I. Molnár, *Anal. Chem.*, 1977, **49**, 142.
8. Gy. Vigh, Z. Varga-Puchony, A. Bartha and S. Balogh, *J. Chromatog.*, 1982, **241**, 169.
9. E. A. Nodiff, J. M. Hulsizer and K. Tanabe, *Chem. Ind. (London)*, 1974, 962.
10. H. D. Moed, M. Asscher, P. J. A. van Praanen and H. Niewind, *Rec. Trav. Chim. Pays-Bas*, 1952, **71**, 933.
11. H. Biltz and K. Slotta, *J. Prakt. Chem.*, 1926, **113**, 252.
12. D. J. Pietrzyk, E. P. Kroeff and T. D. Rotsch, *Anal. Chem.*, 1978, **50**, 497.
13. T. Ishimitsu, S. Hirose and H. Sakurai, *Chem. Pharm. Bull.*, 1976, **24**, 3195.
14. G. Schwarzenbach, *Helv. Chim. Acta*, 1950, **33**, 252.
15. G. Wenk and R. Greenland, *J. Chromatog.*, 1980, **183**, 261.
16. T. Ishimitsu, S. Hirose and H. Sakurai, *Talanta*, 1977, **24**, 555.
17. *Idem, Chem. Pharm. Bull.*, 1978, **26**, 74.
18. I. Molnár and Cs. Horváth, *Clin. Chem.*, 1976, **22**, 1497.
19. Cs. Horváth and W. Melander, *J. Chromatog. Sci.*, 1977, **15**, 393.
20. J. Wagner, M. Palfreyman and M. Zraika, *J. Chromatog.*, 1979, **164**, 41.
21. Cs. Horváth, W. Melander and I. Molnár, *ibid.*, 1976, **125**, 129.
22. J. Mitchell and C. J. Coscia, *ibid.*, 1978, **145**, 295.
23. J. P. Crombeen, J. C. Kraak and H. Poppe, *ibid.*, 1978, **167**, 219.
24. A. M. Krstulovic, M. Zakaria, K. Lohse and L. Bertani-Dziedzic, *ibid.*, 1979, **186**, 733.
25. K. D. Mcmurtrey, L. R. Meyerson, J. L. Cashaw and V. E. Davis, *Anal. Biochem.*, 1976, **72**, 566.
26. R. E. Shoup and P. T. Kissinger, *Clin. Chem.*, 1977, **23**, 1268.
27. I. Molnár and Cs. Horváth, *J. Chromatog.*, 1978, **145**, 371.
28. S. Harapat and P. Rubin, *ibid.*, 1979, **163**, 77.
29. J.-N. Bidard and L. Cronenberger, *ibid.*, 1979, **164**, 139.
30. K. Uchikura, R. Horikawa, T. Tanimura and Y. Kabasawa, *ibid.*, 1981, **233**, 41.

Talanta, Vol. 32, No 9, pp 875–882, 1985
Printed in Great Britain

0039-9140/85 $3.00 + 0.00
Pergamon Press Ltd

DETERMINATION OF AROMATIC AMINES IN FD&C YELLOW NO. 5 BY DIAZOTIZATION AND COUPLING FOLLOWED BY REVERSED-PHASE HPLC

JOHN E. BAILEY, JR.* and CATHERINE J. BAILEY
Division of Color Technology, Food and Drug Administration, Washington, DC 20204, U.S.A.

(*Received* 1 *February* 1985. *Accepted* 14 *April* 1985)

Summary—Benzidine, aniline, 4-aminobiphenyl (4-ABP) and 4-aminoazobenzene are determined at trace levels in the colour additive FD&C Yellow No. 5 by diazotization and coupling with disodium 3-hydroxy-2,7-naphthalenedisulphonate (R-salt). The products are separated and determined by reversed-phase HPLC. All four amines were found in a survey of commercial colours. 4-ABP is determined with 4,5-dihydro-5-oxo-1-(4-sulphophenyl)-1*H*-pyrazole-3-carboxylic acid as the coupling agent. Calibration is done by spiking a reference commercial colour at several levels.

FD&C Yellow No. 5 (Tartrazine, Colour Index No. 19140) is a synthetic colour that is permitted in the United States for colouring foods, drugs and cosmetics.[1] It is synthesized by diazotization of 4-aminobenzenesulphonic acid (sulphanilic acid), followed by coupling with pyrazolone-T (Fig. 1). Commercially prepared FD&C Yellow No. 5 is rarely pure, because of impurities in the reactants and the occurrence of side-reactions during manufacture. The impurities include unsulphonated aromatic amines at trace levels. The method presented determines the aromatic amines in the dyestuff by diazotization and coupling followed by high-pressure liquid chromatography (HPLC) of the products.

EXPERIMENTAL

The method used for determination of the aromatic amines was the one already described for D&C Red No. 33,[2] modified as follows.

(*a*) The 254-nm signal from the detector was recorded only on the integrator.
(*b*) A 5-g sample was used.
(*c*) For calibration it was not necessary to use a specially purified reference sample, since a sufficiently pure commercial batch was available.
(*d*) Pyrazolone-T was used as the coupling agent to confirm the presence of 4-aminobiphenyl (4-ABP) in some samples.

The pyrazolone-T coupling solution was prepared by dissolving 0.5 g of purified pyrazolone-T hydrochloride and 0.9 g of anhydrous sodium carbonate in 100 ml of water. A 1-ml portion was used in the same way as the R-salt solution in the procedure for D&C Red No. 33.[2]

RESULTS AND DISCUSSION

An aqueous alkaline solution of the FD&C Yellow No. 5 is extracted into chloroform, the solvent is evaporated and the extract is dissolved in dilute acid, diazotized and coupled with R-salt. The coloured products are separated by reversed-phase HPLC with detection at 510 and 254 nm.

Extraction

FD&C Yellow No. 5 dissolves completely in the aqueous phase used, so there should be no loss of aromatic amines by occlusion in undissolved solids. Some samples may form agglomerations, but these are easily broken up by stirring. The chloroform extracts of most samples tested were essentially colourless, but a few were more or less strongly coloured. In nearly all the analyses, the extract residue was completely soluble in acid; only one or two left a visible residue on the walls of the flask.

Diazotization

The amount of sodium nitrite added is sufficient to diazotize the equivalent of 1.33 mg of aniline (266 ppm in the 5-g sample) and is adequate to ensure that an excess of nitrite is always present.

HPLC

It was discovered that some newly received HPLC columns used in the investigation did not separate the coupling products sufficiently to permit determination of aniline and benzidine. A slight change in column characteristics may have caused this change in resolution from that reported in the earlier work.[2] Although the work reported here was completed with the same column, future work may require the use of a different column or a change in the gradient programme. Investigation suggests that a Nova-Pak C-18 steel column (Waters Associates) provides adequate separation of the benzidine and aniline coupling products.

Calibration

The calibation was done by applying the method to separate 5-g samples of a specially selected (low

*Author to whom requests for reprints should be addressed.

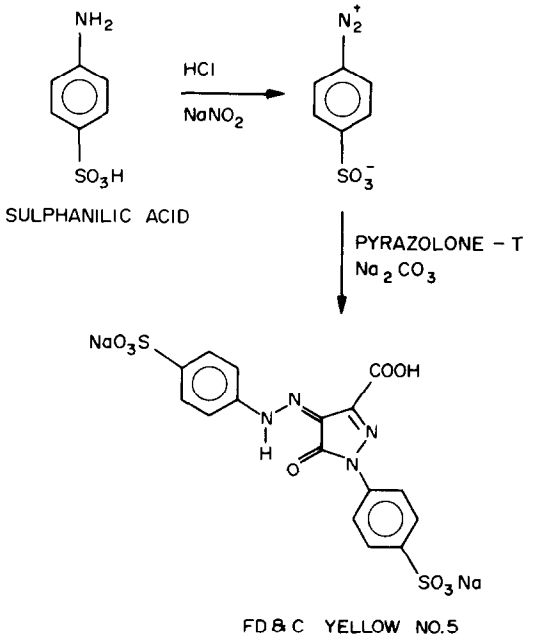

Fig. 1. Manufacturing procedure for synthesis of FD&C Yellow No. 5.

amine content) FD&C Yellow No. 5, with the four aromatic amines added at six or seven concentration levels.

The responses obtained for the amines (corrected for the contribution from the matrix reference material itself) were treated statistically to calculate the regression equation and evaluate the performance of the method.[3] The results of the regression analysis are shown in Table 1. The calibration data show good linearity ($r \geq 0.98$) and reasonably low intercepts. We consider the results to be excellent for trace analysis. The lower correlation coefficient for benzidine perhaps reflects the incomplete resolution of the benzidine and aniline products. The statistical data indicate reliable determination of benzidine and the other amines at the ng/g level in FD&C Yellow No. 5.

Analysis of dyes

A total of 25 commercial FD&C Yellow No. 5 samples were analysed for aromatic amines. The results are shown in Table 2. The samples were selected so that the major domestic manufacturers of the dyestuff were represented by two or more lots and the remaining manufacturers by at least one lot. Included in the survey was a sample from a pharmacology batch (sample G) used in animal feeding studies. Most of the samples were analysed once. The sample used as matrix reference in the calibration, sample E, was analysed three times. The reproducibility of the method was checked by analysing sample V five times.

Benzidine was found in five of the samples, but only one sample was found to contain more than 1 ng/g. The response for the benzidine coupling product in this analysis was confirmed by performing the HPLC with the detector wavelength set at 610 nm.[2] Under these conditions, only the benzidine product produces a response (Fig. 2).

All the samples contained measurable levels of aniline (mean 67 ng/g). The highest amount found was 487 ng/g in sample O (mean of results at 254 and 510 nm).

4-AAB was found in 10 of the samples, up to a level of 439 ng/g (in sample H; mean of results at 254 and 510 nm). Most of the high levels of 4-AAB were found in the batches manufactured by the same company. The pharmacology sample (sample G) contained 62 ng 4-AAB per g.

Most of the samples analysed in the survey produced an HPLC response corresponding to the 4-ABP/R-salt coupling product, but the absorption spectra of the products, obtained by use of a rapid-scan diode-array spectrophotometer, did not match the spectrum obtained for the authentic material. This suggested the presence of an interferent response that could augment the response from the 4-ABP actually present in the sample. This problem was dealt with by using pyrazolone-T as the coupling agent, as discussed below in detail.

The HPLC of the coupling products also produced a number of responses due to components other than the four aromatic amines of interest. The variation in the composition of the samples is illustrated in Fig. 3, which shows some of the chromatograms. Examination of the chromatograms obtained suggested

Table 1. Regression analysis[3] of calibration data for aromatic amines in FD&C Yellow No. 5

Amine	No. of data points	Range, *ng/g*	Wavelength, *nm*	Regression equation*	*r*†	X_{LD},‡ *ng/g*
Benzidine	6	2.9–14.5	254	$Y = 48.6X - 13.0$	0.9825	5
			510	—	—	—
Aniline	7	11–535	254	$Y = 57.2X + 7.2$	1.0000	6.5
			510	$Y = 464X - 651$	0.9999	13.5
4-Aminobiphenyl	7	2.0–20.2	254	$Y = 37.2X - 27.6$	0.9973	3.0
			510	$Y = 338X - 206$	0.9972	3.0
4-Aminoazobenzene	7	2.1–20.8	254	$Y = 20.2X - 4.5$	0.9953	4.0
			510	$Y = 284X + 60$	0.9971	3.0

Y = integrator counts, X = concentration in standard (*ng/g*).
†Correlation coefficient.
‡LD = limit of detection with 95% confidence.

Table 2. Results at 254 and 510 nm for analysis of FD&C Yellow No. 5 for aromatic amines

Sample	Maker	Benzidine,* ng/g	Aniline, ng/g		4-ABP,† ng/g		4-AAB, ng/g		Remaining responses calculated as 4-ABP, ng/g
			254	510	254	510	254	510	
A	1	1	43	44	≤2	≤2	ND‡	ND	29
B	1	ND	67	65	≤3	≤3	ND	ND	12
C	2	ND	10	11	≤6	≤6	2	1	116
D	2	ND	34	35	≤5	≤5	ND	ND	20
E	3	ND	12	13	≤2	≤3	ND	ND	14
F	3	ND	17	18	≤2	—	ND	ND	18
G§	4	1	60	59	≤1†	—	62	62	708
H	4	1	57	57	≤1	—	448	431	633
I	4	ND	179	169	≤3	≤4	111	111	990
J	4	ND	19	—¶	≤3	—	ND	ND	—
K	5	ND	9	10	ND	ND	ND	ND	7
L	5	ND	54	54	≤1	ND	ND	ND	23
M	6	ND	24	24	ND	ND	ND	ND	35
N	6	ND	31	32	≤2	≤2	ND	ND	45
O	7	13	491	483	≤5	≤5	2	2	241
P	8	ND	51	50	≤4	—	3	—	104
Q	9	1	10	12	ND	ND	ND	ND	76
R	10	ND	43	42	≤4	≤4	ND	ND	204
S	11	ND	85	82	≤1	—	ND	ND	107
T	12	ND	54	53	≤1	—	2	1	311
U	13	ND	5	7	ND	ND	ND	ND	32
V	14	ND	105	103	≤6	≤6	13	13	28
W	15	ND	93	93	≤4	≤5	6	6	17
X	16	ND	20	22	≤3	—	1	—	—
Y	17	ND	76	77	≤4	ND	ND	ND	617

*Determined at 254 nm.
†See discussion of 4-ABP in text.
‡ND = none detected, *i.e.*, no response was present.
§Pharmacology sample.
¶Response was present but was not detected by integrator.

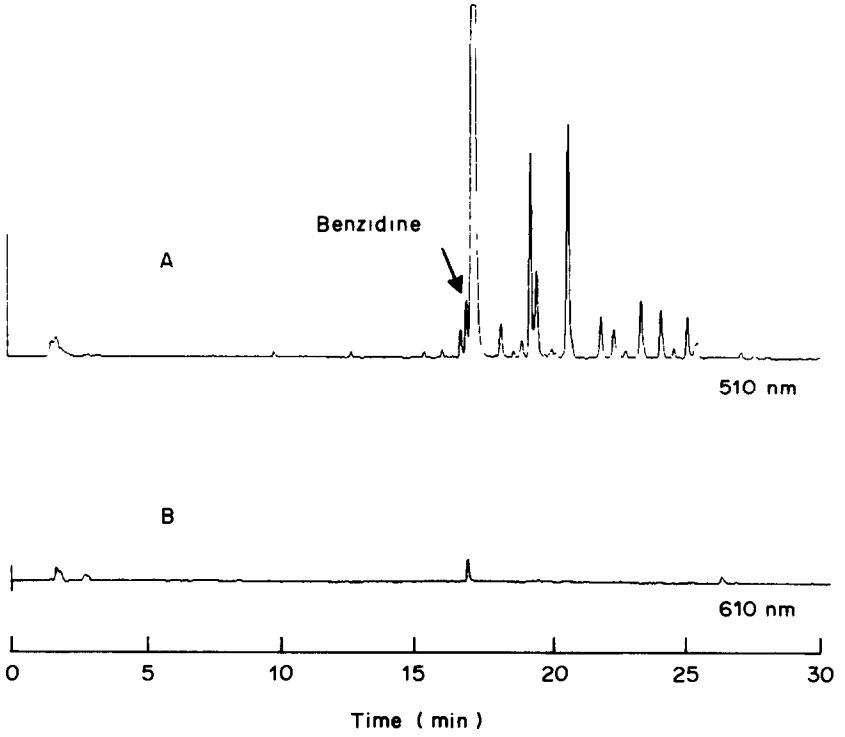

Fig. 2. HPLC chromatograms from analysis of FD&C Yellow No. 5 sample O (Table 2), illustrating the detection of the benzidine/R-salt coupling product at 610 nm.

that the colour additive manufacturers produce fairly consistent products with characteristic qualitative HPLC profiles. For example, for both samples from Manufacturer 1 some of the FD&C Yellow No. 5 migrated into the chloroform phase during the extraction. This can occur if surfactants are used during production of the colour additive; the presence of a cationic surfactant during the extraction would lead to extraction of the colour additive as an ion-pair into the chloroform. The chromatogram of the colour additive produced by Manufacturer 4 contained a large number of HPLC responses in addition to those corresponding to the four aromatic amines. These responses were observed at both 254 and 510 nm, and probably indicate the presence of aromatic amines other than benzidine, aniline, 4-ABP and 4-AAB. The amounts of these additional components can be estimated if we calculate "molar absorptivities" for the coupling products from aniline, 4-ABP and 4-AAB at 510 nm by multiplying the slopes of the

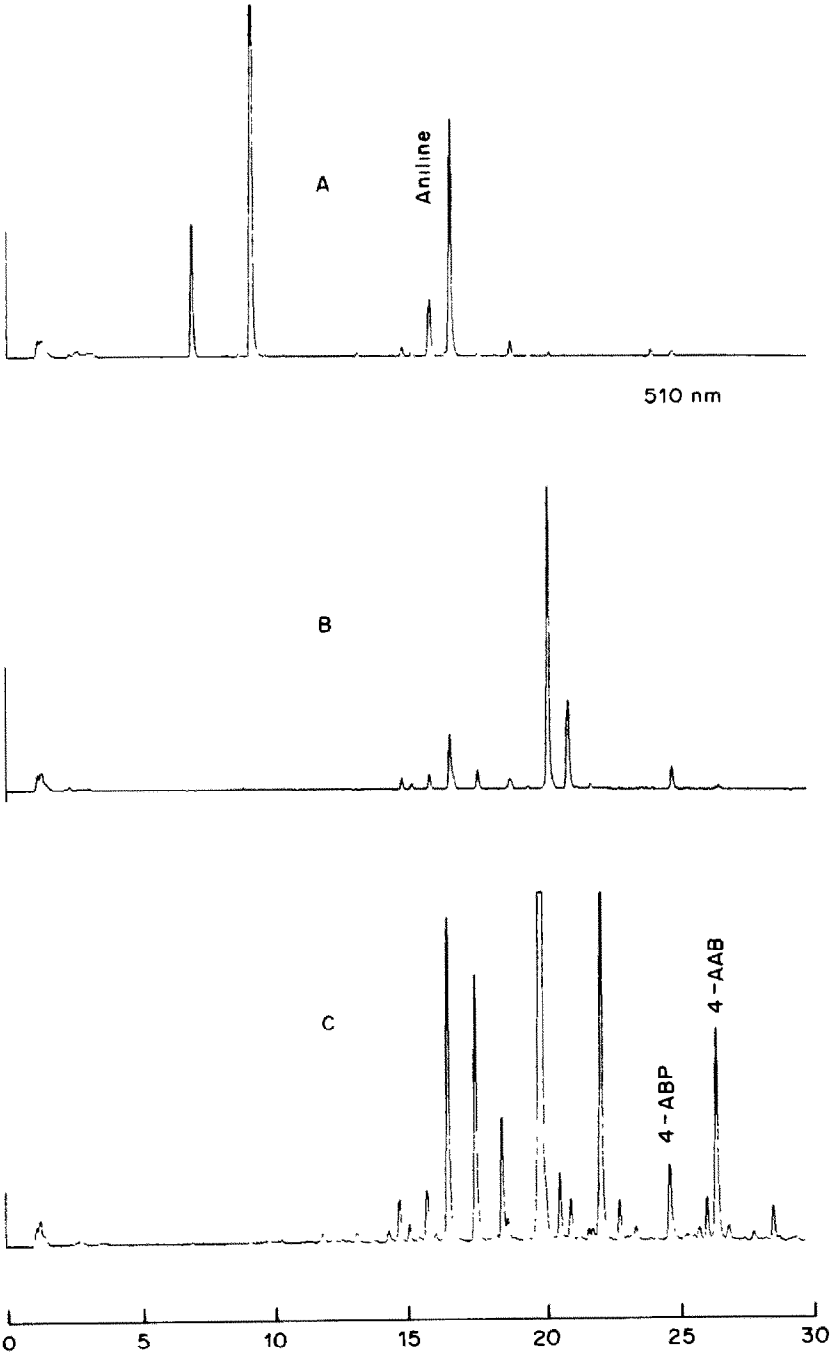

Fig. 3.

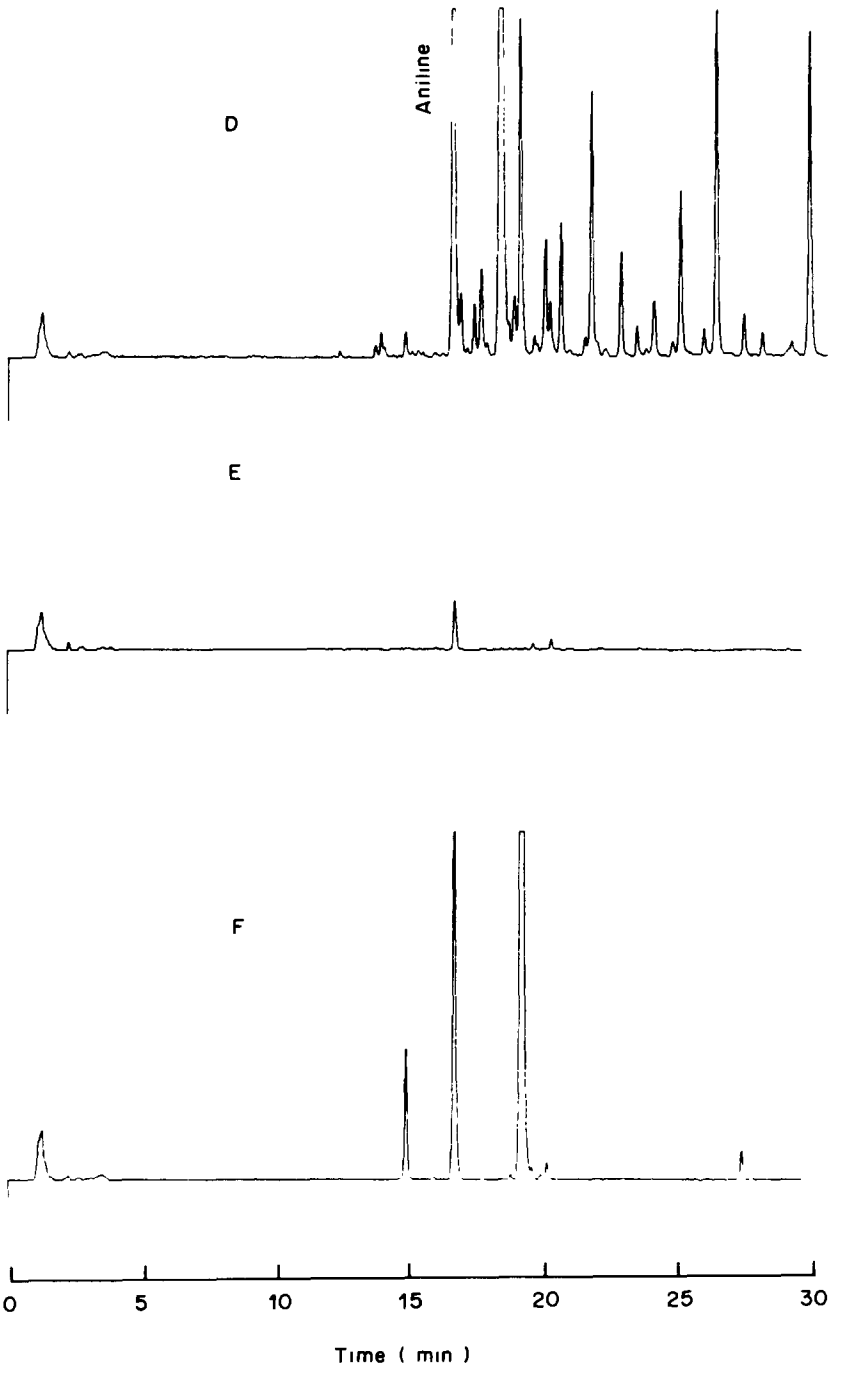

Fig. 3. HPLC chromatograms obtained at 510 nm from analysis of commercial samples of FD&C Yellow No. 5, using R-salt as the coupling agent: (A) sample A, (B) sample C, (C) sample G, (D) sample I, (E) sample K and (F) sample Y.

regression lines by the molecular weights of the products. The values for the other two are within about 20% of the value for the 4-ABP product, and similar behaviour would be expected for other amine coupling products if all the absorption spectra have similar maxima. In fact, scanning with the diode-array spectrophotometer showed that the spectra of the other coupling products were indeed similar to those for the aniline, 4-ABP and 4-AAB products. The levels of the other coupling products can then be estimated by summing the peak-height measurements reported by the 510-nm channel of the integrator, subtracting the contribution from known amine products, and calculating the remainder as 4-ABP. It should be noted that the integrator is programmed to report only data collected after 15 min, to eliminate

Table 3. Reproducibility results

	Aniline		4-ABP		4-AAB	
Analysis	254*	510*	254*	510*	254*	510*
Sample V†						
$\bar{X}$, *ng/g*	100	101	5.4	5.9	12.6	12.6
S, *ng/g*	3.0	2.0	0.2	0.3	0.3	0.3
CV, %	3.0	2.0	3.7	4.4	2.4	2.1
Sample E‡						
$\bar{X}$, *ng/g*	11.5	12.9	2.3	2.8	—	—
S, *ng/g*	0.7	0.35	0.06	0.15	—	—
CV, %	6.2	2.7	2.5	5.4	—	—

*Wavelength of measurement (*nm*).
†Five replicates.
‡Reference sample, three replicates.

the responses from the reagents used in the method and from any FD&C Yellow No. 5 carried over (see above). The values thus calculated are reported in the last column of Table 2, and indicate the degree to which the colour additive is contaminated with extractable (presumably unsulphonated) amine constituents other than the four aromatic amines identified. There is, however, no indication of the number of components that make up the additional contamination. Examination of Table 2 shows that some samples are almost completely free from such contaminants, whereas in others there is a total of more than 1 μg/g.

The precision of the method was measured by replicate analysis of a sample selected so that it contained significant levels of aniline, 4-ABP and 4-AAB (although it did not contain benzidine). Multiple analyses were also performed on the sample used as matrix for the calibration. The results, presented in Table 3, shows good reproducibility for trace analysis.

Spectra of coupling products

The coupling products were characterized for the purpose of confirming peak identity by obtaining the electronic absorption spectra as the compounds were eluted from the HPLC column, as described earlier.[2] The benzidine coupling product obtained during the analysis of sample O produced an absorption spectrum identical to that obtained from authentic material, thus confirming the presence of benzidine in this sample. Aniline was similarly confirmed in samples G, H and O, and 4-AAB in samples G and H.

As previously mentioned, attempts to confirm the identity of the product giving the "4-ABP" response failed because the absorption spectrum obtained did

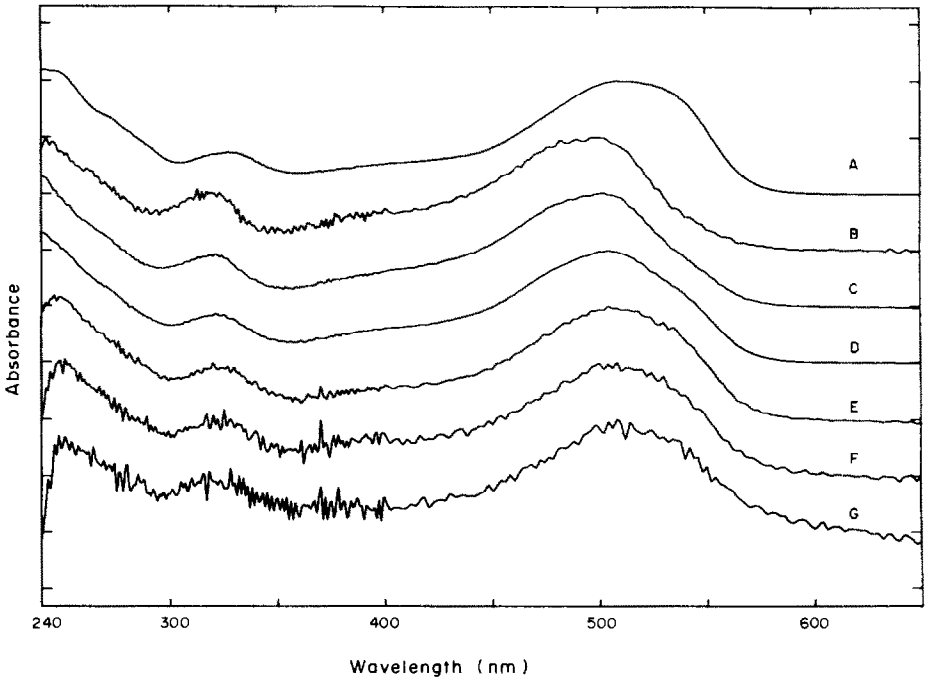

Fig. 4. Ultraviolet/visible spectral scan of the 4-ABP/R-salt coupling product in sample G: (A) authentic product, (B, C, D) leading edge of peak and (E, F, G) trailing edge of peak.

not match that of authentic material. Careful scanning of the entire 4-ABP peak obtained during the analysis of sample G, including the leading and trailing edges as shown in Fig. 4, suggested that some 4-ABP was present, but its level could not be measured. In an attempt to remove the interference and determine the levels of 4-ABP present in FD&C Yellow No. 5, the procedure was modified by substituting pyrazolone-T as the coupling agent. Otherwise the procedure was exactly the same as when R-salt was used. The eluate from the HPLC column was monitored only at 254 nm, since the spectrophotometer was connected to the system. Chromatogram A in Fig. 5 illustrates the HPLC separation obtained for the four aromatic amines when they are coupled with pyrazolone-T instead of R-salt. It is noteworthy that the elution order for the aniline and benzidine products is reversed and that these two components are well resolved. Chromatograms B–E are for some of the samples that were found to contain relatively high levels of 4-ABP when R-salt was used as the coupling agent (samples G, H, S and

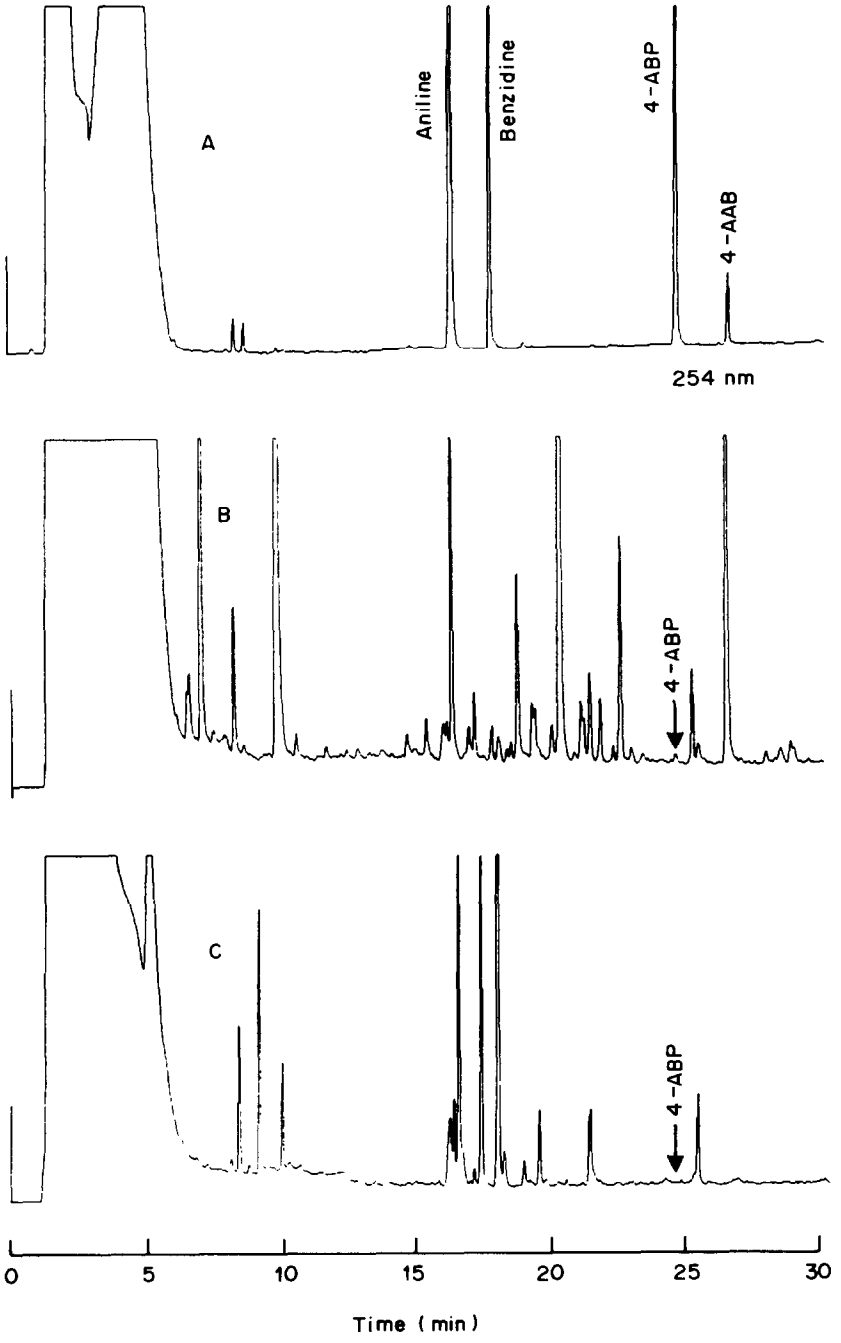

Fig. 5.

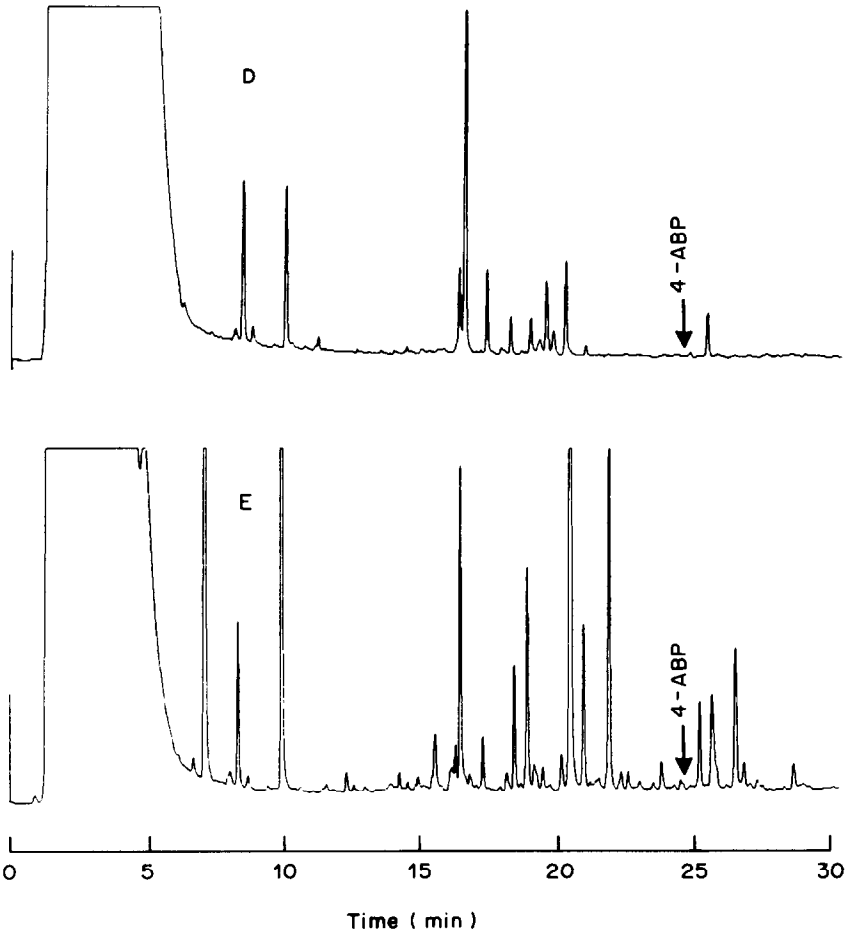

Fig. 5. HPLC chromatograms obtained at 254 nm from analysis of commercial samples of FD&C Yellow No. 5, using pyrazolone-T as the coupling agent: (A) qualitative mixture of aniline, benzidine, 4-ABP and 4-AAB, (B) sample G, (C) sample H, (D) sample S and (E) sample T.

T). These chromatograms show no significant response for the 4-ABP/pyrazolone-T coupling product. The sensitivity of the analysis was increased by concentrating the solutions containing the coupling products and analysing the concentrates by HPLC in an attempt to obtain the absorption spectra. The spectra obtained closely resembled the spectrum of the authentic coupling product, but the intensity was very weak and, therefore, identification was not definitive. On the basis of these results, the level of 4-ABP in these four samples are actually quite low, probably less than 1 ng/g. The other samples in the survey were not examined to confirm the identity of the 4-ABP coupling products. The values shown in Table 2 are those obtained with R-salt as the coupling agent and are reported as upper limits because of the likelihood of a co-eluted interference.

REFERENCES

1. *Code of Federal Regulations*, Title 21, Part 74. U.S. Government Printing Office, Washington, DC, 1984.
2. J. E. Bailey, *Anal. Chem.*, 1985, **57**, 189.
3. C. J. Bailey, E. A. Cox and J. A. Springer, *J. Assoc. Off. Anal. Chem.*, 1978, **61**, 1404.

Talanta, Vol. 32, No. 9, pp. 883–886, 1985
Printed in Great Britain

0039-9140/85 $3.00 + 0.00

AN ENZYME-CATALYSED METHOD FOR THE DETERMINATION OF MERCURY TRACES IN CARBONATED SOFT DRINKS, BY THE Hg^{2+} INHIBITION OF β-FRUCTOFURANOSIDASE

J. MASŁOWSKA and J. LESZCZYŃSKA
Bioinorganic and Analytical Chemistry Division, Institute of General Food Chemistry, Technical University of Łódź, Stefanowskiego st. 4/10, 90 924 Łódź, Poland

(*Received* 20 *June* 1983. *Revised* 28 *March* 1985. *Accepted* 12 *April* 1985)

Summary—This paper describes the utilization of the inhibition of β-fructofuranosidase by Hg(II) during the hydrolysis of saccharose, for the determination of Hg(II) in waters and drinks. The mercury levels in the samples tested ranged from 100 to 270 ng/l.

Enzyme-catalysed methods based on the effect of additives such as metal ions, anions and organic compounds on enzyme activities are amongst the most sensitive in trace analysis, allowing determination at concentrations below 10^{-8} *M*.

Inhibition effects on enzymes have been used for the determination of many compounds and ions, such as pesticides, antibiotics, organic acids, metal ions (*e.g.*, Mn^{2+}, Zn^{2+}, Mg^{2+}, Co^{2+}, Ca^{2+}) and anions (*e.g.*, $S_2O_3^{2-}$, CN^-, S^{2-}, F^-).[1-3]

Enzyme-catalysed methods have also been used for the determination of Hg(II) by its inhibition of enzymes such as xanthine oxidase,[4] urease,[5] glucosidase,[6] glucose oxidase,[7] alcohol dehydrogenase[8] and β-fructofuranosidase.[9] β-Fructofuranosidase has also been used for the determination of I^-, S^{2-}, CN^-,[10] and Ag(I) and thiocarbamide.[11]

In this work we have used semipurified β-fructofuranosidase (invertase–EC 3.2.1.26) to determine traces of mercury in samples of soft drinks. This enzyme catalyses the hydrolysis of β-fructofuranosides, including saccharose, as shown below, where R is 1-α-glucopyranosyl.

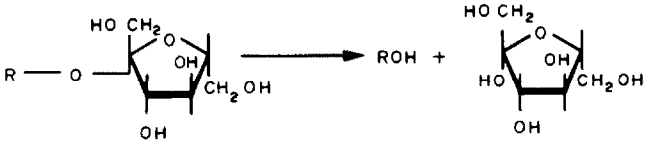

In solution the highest activity is exhibited by invertase between pH 4 and 5 (the optimum value lies near pH 4.8). The enzyme is stable to heat. Heavy metal ions such as mercury(II), mercury(I) and silver(I) are strong inhibitors of invertase, and copper(II), cadmium(II), zinc(II) and uranium(VI) are weaker ones. The inhibition is competitive and reversible—the activity recovers after dialysis or the addition of complexing agents. Acetone, glycerol, ethanol (in high concentrations), aromatic amines and some dyes[12] are organic inhibitors of this enzyme.

EXPERIMENTAL

Reagents

Water triply distilled in a glass unit, an acetone preparation of invertase extracted from yeast, 0.1*M* acetate buffer (pH 4.8), an aqueous solution of saccharose (as substrate), Folin–Ciocalteu reagent,[13] cupric reagent for protein determination,[13] cupric reagent for sugar determination,[14] Nelson's phosphomolybdic acid reagent,[14] soluble casein (BDH), and anhydrous glucose (Polfa, Cracow). The stock solutions of salts were 0.01*M* solutions of the chlorides or nitrates; more dilute solutions were obtained by appropriate dilution. Analytical grade chemicals were used for preparing 2.0*M* and 0.001*M* hydrochloric acid, 6% potassium permanganate solution and a 10% solution of anhydrous sodium sulphite.

Cupric reagent for protein determination.[13] A 50-ml portion of 2% anhydrous sodium carbonate solution in 0.1*M* sodium hydroxide is mixed with 1 ml of 0.5% solution of copper sulphate pentahydrate in 1% sodium citrate solution, half an hour before use.

Cupric reagent for sugar determination.[14] Four g of copper sulphate pentahydrate and 16 g of sodium bicarbonate are added to a solution of 24 g of anhydrous sodium carbonate and 12 g of sodium potassium tartrate in 250 ml of water. A separate solution of 180 g of anhydrous sodium sulphate in 500 ml of water is boiled to remove dissolved air. The two solutions are mixed, and the mixture is diluted to 1 litre with water, and filtered after standing for two days.

Preparation of vessels

The glass vessels used were washed with chromic acid cleaning mixture, rinsed with water, washed with a 0.001% solution of dithizone in carbon tetrachloride, then with acetone and again with water, to eliminate all traces of metals from the surface.

Preparation of invertase in acetone[15]

Five g of baker's yeast were finely ground in a mortar, mixed with water and centrifuged. The supernatant liquid

was fivefold diluted with purified[16] and cooled acetone, and centrifuged. The precipitate obtained was dissolved in 20 ml of water and filtered. The preparation thus obtained was stored at 4° and was stable for several weeks.

Determination of protein content

The protein in the enzyme preparation was determined by the method of Lowry *et al.*[13] The invertase solution was diluted tenfold with water and 0.4 ml of the diluted solution was pipetted into a test-tube and 2 ml of the cupric reagent[13] (prepared 30 min before use) were added. After 10 min, 0.2 ml of Folin–Ciocalteu reagent twofold diluted with water was added and the whole was quickly mixed. The absorbance was then measured at 650 nm against a reagent blank. The protein content was read from the calibration graph prepared in the same way with soluble casein standards, covering the range 5–100 μg/ml.

Determination of the invertase activity

Somogy's and Nelson's method[14] was used. In this, 0.5 ml of 0.2M saccharose was incubated at 37° for 50 min with 0.5 ml of 2000-fold buffer-dilution of the enzyme preparation plus 2 ml of acetate buffer. The reaction was then stopped by addition of 1 ml of the cupric reagent for sugar determination and the sample was heated for 10 min on a boiling water-bath, then cooled, and 1 ml of the phosphomolybdic acid reagent was added and all was stirred. The mixture was diluted to volume in a 10-ml standard flask with water and the absorbance was measured at 520 nm against a reagent blank (3 ml of acetate buffer) after 20 min. A calibration graph was prepared with glucose, covering the range 5–80 μg/ml.

The activity was calculated from the equation:

$$\text{activity} = nx/tp$$

when n is the sugar content read from the calibration graph, x is the dilution factor, t is the reaction time (min) and p the protein content of the preparation. The results are in activity units, *viz.* the amount of enzyme catalysing, under defined conditions, the conversion of 1 μmole of substrate in a 1 min period by 1 mg of protein.[17]

Investigation of invertase inhibition by metal cations

The decrease in the activity of invertase caused by incubation for 30 min with a salt solution was examined. The composition of the mixture incubated was 1 ml of buffer solution, 1 ml of the buffered salt solution, 0.5 ml of the enzyme preparation; after the 30-min incubation 0.5 ml of saccharose solution was added and the determination completed as for the activity measurements. The reference blank was run with 0.5 ml of the buffer instead of the 0.5 ml of enzyme preparation.

Calibration graph for Hg(II)

This graph (log enzyme activity *vs.* pHg) covered the mercury concentration range from 5×10^{-11} to $5 \times 10^{-7}M$, with mercuric chloride as the standard, the activity being measured as described above.

Sample preparation

In order to decompose organic mercury compounds 1 litre of the sample of water or carbonated drink was acidified with 200 ml of concentrated hydrochloric acid, and 50 ml of 6% potassium permanganate were added. The mixture was kept in a stoppered round-bottomed flask in a water-bath at 70° for 2 hr, then cooled. The excess of permanganate was reduced with 10% sodium sulphite solution, then the sample was filtered and passed through a column (26 cm × 1 cm^2) of Dowex 1 × 8 (50–100 mesh in the chloride form) at 2 ml/min. Under these conditions the mercury is present as the tetrachloro-complex and bound by the anion-exchanger. The mercury is eluted with 100 ml of 0.001M hydrochloric acid at 2 ml/min and is accompanied only by any Au, Te, Sb and platinum metals present.[18] The mercury recovery is only 87% but is reproducible and is automatically compensated for if all standards are treated in the same way as samples. For analysis, 1 ml of eluate, 1 ml of water, 1 ml of acetate buffer and 0.5 ml of the enzyme preparation solution were mixed. After 30 min 0.5 ml of the solution of saccharose was added and the procedure continued as for the activity determination. The absorbance was measured against that of a reference sample containing 1 ml of hydrochloric acid instead of the test sample. Finally 500 ml of 0.001M hydrochloric acid were passed through the anion-exchange column to remove residual mercury(II).

RESULTS

Because a different β-fructofuranosidase preparation and a different method for determining the enzyme activity were used, it was impossible to utilize the results obtained by Mealor and Townshend.[9] The effects of reaction time, temperature, and protein concentration in the enzyme preparation on the inhibition of invertase by mercury(II) were investigated to find the optimum conditions.

A pH of 4.8 was chosen as optimum.[12] Figure 1 shows that the amount of glucose released is a linear function of time in the reaction period from 10 to 40 min, and maximum release is obtained at between 50 and 60 min reaction time. A 50-min period was chosen for use. The effect of temperature is shown in Fig. 2. The effect of Hg(II) on the enzyme activity increases with the temperature, and the assays performed at 37° are more precise and reproducible than those done at lower temperatures. Figure 3 shows that if the protein content in the preparation is decreased and the specific activity is simultaneously increased, the sensitivity of the inhibition is increased. This is probably due to the fact that in preparations of lower specific activity mercury(II) also couples with other proteins besides β-fructofuranosidase, so the concentration ratio of mercury to the enzyme is lower. Therefore, preparations of high specific activity are the most suitable for Hg(II) determination at very low levels. A log–log plot of activity *vs.* mercury concentration, obtained with the preparation (*a*) referred to in Fig. 3, applied at 37°, is linear from

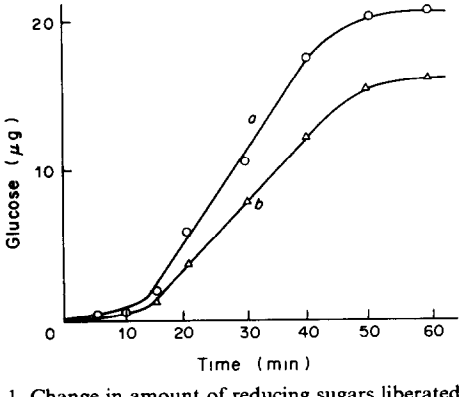

Fig. 1. Change in amount of reducing sugars liberated with duration of reaction: *a*, free enzyme; *b*, enzyme $+2.5 \times 10^{-8}M$ Hg^{2+}. Preparation with 0.588 mg/ml protein content, temperature 20°.

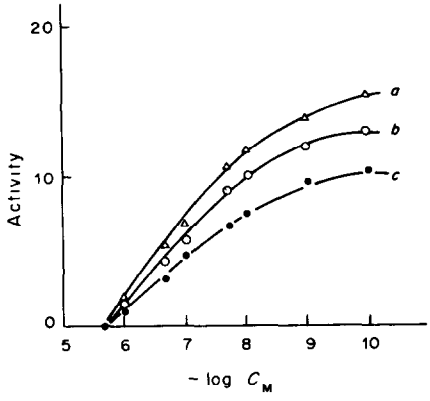

Fig. 2. β-Fructofuranosidase activity as a function of Hg^{2+} concentration (preparation with 0.588 mg/ml protein): incubation at *a*, 37°; *b*, 30°; *c*, 20°.

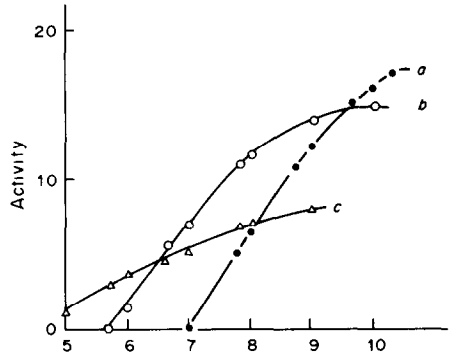

Fig. 3. β-Fructofuranosidase activity as a function of Hg^{2+} concentration for preparations with different protein content (and activity): *a*, 0.225 mg/ml (17.9); *b*, 0.588 mg/ml (15.4); *c*, 1.025 mg/ml (7.9).

Table 1. Statistical evaluation of the method (6 determinations, preparation with 0.588 mg/ml protein content)

$[HgCl_2]$	Mean specific activity, $\bar{X}$, *a.u.*	Standard deviation, $S_{\bar{X}}$, *a.u.*	Confidence interval, *a.u.* ($m = \bar{X} \pm tS_{\bar{X}}$)
2.5×10^{-8}	11.2	0.3	11.2 ± 0.9
5.0×10^{-8}	10.6	0.3	10.6 ± 0.9
2.5×10^{-7}	2.9	0.3	2.9 ± 0.8
5.0×10^{-7}	2.3	0.3	2.3 ± 0.8
2.5×10^{-6}	1.8	0.3	1.8 ± 0.8
5.0×10^{-6}	0.2	0.3	0.2 ± 0.7

*$t = 2.57$

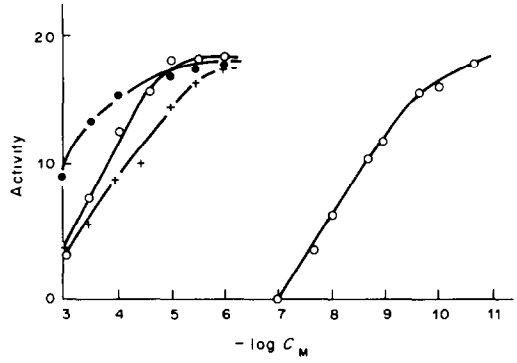

Fig. 4. β-Fructofuranosidase activity as a function of Zn^{2+}, Co^{2+}, Fe^{3+}, Cd^{2+} and Hg^{2+} concentration (0.255 mg/ml protein) ●—Zn^{2+}, ×—Co^{2+}, ⊙—Fe^{3+}, +—Cd^{2+}, ○—Hg^{2+}.

$10^{-7}M$ to $10^{-11}M$ mercury(II). The use of different mercuric salts (chloride, sulphate and nitrate) as standards did not affect the graph. The influence of Co^{2+}, Zn^{2+}, Fe^{3+}, Cd^{2+} and Hg^{2+} ions on the activity of invertase was investigated and the results plotted in Fig. 4 show that Fe^{3+} and Co^{2+} give the same degree of inhibition but do not interfere at concentrations lower than $10^{-5}M$. Contrary to the findings of Mealor and Townshend,[9] our results indicate that Cd^{2+} is a stronger inhibitor than Zn^{2+}, but neither interferes at $< 10^{-5}M$ concentration.

Table 1 presents a statistical evaluation of the results for the mercuric chloride standard. The standard deviation is practically constant, so the coefficient of variation increases with decreasing mercury concentration.

The results for mercury(II) in water and drinks are shown in Table 2. The samples were all mineralized and the mercury(II) separated on a column, to liberate mercury from its organic compounds and to eliminate ions which could interfere in the spectrophotometric determination of the reducing sugars. Mineralization of the orangeade and tangerine drink was necessary, because the flavourings and dyes interfere in the determination.

The mercury content in the samples tested was very low, ranging from 100 to 270 ng/l. The results agreed with those obtained for the same samples by cold-vapour atomic-absorption spectrometry.[19] The low detection limit in the enzyme method allows direct analysis of the samples without preconcentration step. The main disadvantage of the method is the need to use such a large volume of eluent (500 ml) in

Table 2. The results of mercury determinations in water and drinks ($\mu g/l. \pm$ standard deviation)

Drink	Origin			
	Łódź	Pabianice	Łask	Aleksandrów
Water	0.10 ± 0.01	—	—	—
Soda-water	0.10 ± 0.01	0.15 ± 0.01	0.20 ± 0.01	0.15 ± 0.01
Orangeade	0.16 ± 0.01	0.20 ± 0.02	0.20 ± 0.02	0.20 ± 0.02
Tangerine	0.20 ± 0.02	0.25 ± 0.02	0.27 ± 0.02	0.25 ± 0.02

the final clean-up of the column. Many eluents have been tried, but so far only 0.001*M* hydrochloric acid has proved not to interfere with the subsequent enzymatic determination. The search for a more efficient system continues, and any successful solution will be reported.

REFERENCES

1. G. G. Guilbault, *Anal. Chem.*, 1966, **38**, 527R.
2. *Idem*, *ibid.*, 1968, **40**, 459R.
3. *Idem*, *ibid.*, 1970, **42**, 334R.
4. G. G. Guilbault, D. N. Kramer and R. L. Cannon, *ibid.*, 1964, **36**, 606.
5. R. Hughes, S. Katz and S. Stubbins, *Enzymologia*, 1969, **36**, 332.
6. G. G. Guilbault and D. N. Kramer, *Anal. Biochem.*, 1967, **18**, 313.
7. G. Toren and F. Burger, *Mikrochim. Acta*, 1968, 538.
8. A. Townshend and A. Vaughan, *Talanta*, 1970, **17**, 299.
9. D. Mealor and A. Townshend, *ibid.*, 1968, **15**, 1747.
10. *Idem*, *ibid.*, 1968, **15**, 1477.
11. *Idem*, *ibid.*, 1968, **15**, 1371.
12. J. B. Sumner and K. Myrbäck, *The Enzymes*, Academic Press, New York, 1950.
13. O. H. Lowry, N. J. Rosebrough, A. L. Farr and R. J. Randall, *J. Biol. Chem.*, 1951, **193**, 265.
14. N. Nelson, *ibid.*, 1944, **153**, 375.
15. L. Kłyszejko-Stefanowicz, *Exercises in Biochemistry*, PWN, Warsaw, 1972, (in Polish).
16. *Handbook of Physico-Chemical Data*, WNT, Warsaw, 1972 (in Polish).
17. *Enzymes, Nomenclature and Classification, Recommendation of the International Union of Biochemistry*, (Polish translation of the English version), T. Korzybski (ed.), PWN, Warsaw, 1967.
18. R. E. Jervis and K. Y. Wong, *Nuclear Activation Techniques in the Life Sciences*, p. 137. IAEA, Vienna, 1967.
19. J. Masłowska and J. Leszczyńska, *Roczn. PZH*, 1983, **34**, 377.

Talanta, Vol. 32, No. 9, pp. 887–891, 1985
Printed in Great Britain

0039-9140/85 $3.00 + 0.00

DI-2-PYRIDYL KETONE 2-FUROYLHYDRAZONE AS A REAGENT FOR THE FLUORIMETRIC DETERMINATION OF LOW CONCENTRATIONS OF ALUMINIUM

M. SALGADO ORDOÑEZ, A. GARCIA DE TORRES and J. M. CANO PAVON
Department of Analytical Chemistry, Faculty of Sciences, The University, 29004 Málaga, Spain

(*Received* 17 *July* 1984. *Revised* 19 *December* 1984. *Accepted* 4 *April* 1985)

Summary—The synthesis and properties of di-2-pyridyl ketone 2-furoylhydrazone as an analytical reagent are described. A rapid procedure for the fluorimetric determination of aluminium at the 10–100 ng/ml level, at pH 6.1–6.5 (λ_{exc} 395 nm, λ_{em} 465 nm) has been established. Interferences have been evaluated, and the procedure has been applied satisfactorily to determination of aluminium in sea-water.

Hydrazones have been widely used as analytical reagents, especially in the spectrophotometric determinations of metals,[1,2] but there have been few applications of hydrazones in fluorimetric analysis. Some *N*-heterocyclic hydrazones have been studied in attempts to correlate the ligand structure with the fluorescence intensity of the zinc chelates.[3] In recent years, aroylhydrazones, which contain the atomic grouping —CO—NH—N=CH— have been tested as spectrophotometric and fluorimetric reagents.[4–8] The formation of complexes with a coplanar structure is conducive to production of fluorescence; reaction of a metal ion with a chelating agent induces rigidity in the resultant molecule and tends to produce fluorescence.[9]

The object of the present work was to find a simple method for the determination of aluminium that would be sufficiently sensitive for analysis of sea-water. Spectrophotometric methods are not sufficiently sensitive for use at these levels.[10] Atomic-absorption spectrometry with electrothermal atomization is sensitive enough, but cannot be applied directly to sea-water because of the interference caused by the high salt content. Lumogallion[11] has been used for fluorimetric determination of aluminium, but the procedure is slow, and heating is required for complete development of the fluorescence. 3-Hydroxypyridine-2-aldehyde 2-pyridylhydrazone has also been proposed[12] for the fluorimetric determination of aluminium but synthesis of the reagent is difficult and expensive.

The present paper describes a fluorimetric method for determination of aluminium, based on complex formation with di-2-pyridyl ketone 2-furoylhydrazone (DPFH), and its application to analysis sea-water.

EXPERIMENTAL

Reagents

DPFH was synthesized by refluxing equimolecular amounts of di-2-pyridyl ketone and 2-furoylhydrazine in ethanol for 3 hr. The reaction mixture was then cooled in the refrigerator and the yellow crystals formed were filtered off and recrystallized from ethanol (yield 60%, m.p. 132–134°). Elemental analysis gave C 65.5%, H 4.1%, N 19.2%: $C_{16}H_{12}N_4O_2$ requires C 65.75%; H 4.10%; N 19.18%. Solutions (0.025*M*) of the reagent in ethanol were prepared weekly.

A 0.001*M* stock solution of aluminium was prepared by dissolving $Al(NO_3)_3 \cdot 9H_2O$ in 100 ml of 0.5*M* nitric acid and diluting to 1 litre with demineralized water. This solution was standardized gravimetrically with oxine; working standards were prepared by suitable dilution.

Buffer solution (pH 6.3) was prepared by mixing 50.0 ml of 0.2*M* sodium hydrogen maleate with 38.0 ml of 0.2*M* sodium hydroxide and diluting to 200 ml with demineralized water.

Apparatus

The absorption measurements were made with a Shimadzu UV-240 Graphicord and a Unicam SP 6-550 spectrophotometer; all fluorescence measurements were made with a Perkin-Elmer model MPF-43 A spectrofluorimeter, equipped with an Osram XBO 150-W xenon lamp, grating excitation and emission monochromators, 1 × 1-cm quartz cells, an R-508 photomultiplier and an 023 recorder. A set of fluorescent polymer samples was used to adjust the spectrofluorimeter and compensate for changes in source intensity.

An ultrathermostatic water-bath circulator, Frigiterm model S-382, was used for temperature control.

The infrared spectrum was recorded on a Beckman Acculab-4 spectrophotometer (KBr disc). Proton NMR spectra were obtained ($CDCl_3$ medium, 200 MHz) with a Bruker WP-200 Y spectrometer; tetramethylsilane was used as internal reference.

Procedure

To a known volume of sample (containing 0.25–2.50 μg of aluminium) in a 25-ml standard flask add 5 ml of buffer solution (pH 6.3), 1 ml of 0.025*M* DPFH solution in

ethanol, and dilute to volume with distilled water. After not less than 15 min, measure the fluorescence at 465 nm, using excitation at 395 nm. Determine the amount of aluminium in the sample from a calibration graph prepared under the same conditions. Alternatively use a standard-addition procedure if ions are present which affect the slope of the graph.

Determination of aluminium in sea-water

Collect the samples in 100-ml polypropylene bottles previously cleaned by soaking in 0.1 *M* hydrochloric acid. Filter the sample and use 5 ml for analysis by the standard-addition method as described above. Analyse the samples as soon as possible after collection, to prevent loss of aluminium.

RESULTS AND DISCUSSION

Infrared and NMR spectra of DPFH

The infrared spectrum of the reagent is complicated because the aromatic portion of the molecule produces numerous bands, the overlap of which makes detailed assignments difficult. The band at 3440 cm^{-1} is attributed to N—H stretching, and the well-defined band at 3070 cm^{-1} is characteristic if aromatic C—H stretching frequencies. The spectrum in the "double-bond" region (1750–1450 cm^{-1}) shows strong bands at 1675 cm^{-1} (C=O stretching); the peak at 1575 cm^{-1} is attributed to a CNH overtone.

The NMR spectrum shows a peak at 15.3 ppm due to the OH group in the hydroxyimine tautomer; integration indicates that 71% of the reagent is in the imine form. Other peaks appear at 7.75, 6.52 and 7.30 ppm (multiplet), and are assigned respectively to the H*a*, H*b* and H*c* protons of the furan ring.

Proton equilibra

The spectrum of aqueous DPFH solution is pH-dependent. The spectrum in the pH interval 3.6–10.0 is attributed to the uncharged molecule (HL), with $\lambda_{max} = 325$ nm, that at pH 3.6 ($\lambda_{max} = 337$ nm) to the protonated species (H_2L^+), and that at pH 10.6 to the anion L^-.

The values of p*K* were calculated from the variation of absorbance with pH, by the Stenström and Goldsmith method[13] (Fig. 1a). Two dissociation constants were found: $pK_1 = 3.23$, $pK_2 = 10.23$, which can be attributed respectively to deprotonation of the protonated nitrogen atom in the pyridine ring and to loss of the proton of the OH group in the hydroxyimine tautomer.

For a more complete study of the protonation reactions, Buděšínský's graphical method,[14] as modified by Barragan de la Rosa *et al.*,[15] was used. This method requires the presence of two forms only of the reagent in the acidity range concerned. It is necessary to analyse the absorbance *vs.* pH graph to find whether only one proton participates in the acid–base equilibrium. The method involves the transformation of the absorbance–pH plot into the form $(A - A_{n-a})$ *vs.* pH and substitution of the slope of this graph into the equation

$$\Delta A / \Delta pH = -0.575a(A_n - A_{n-a})$$

where the value of *a* indicates the number of protons interchanged, and A_n and A_{n-a} are the absorbances of the two main species in solution in the pH range studied. The curves for DPFH at different wavelengths are plotted in Fig. 1b, and the values obtained for *a* in both dissociation steps are all close to 1. For

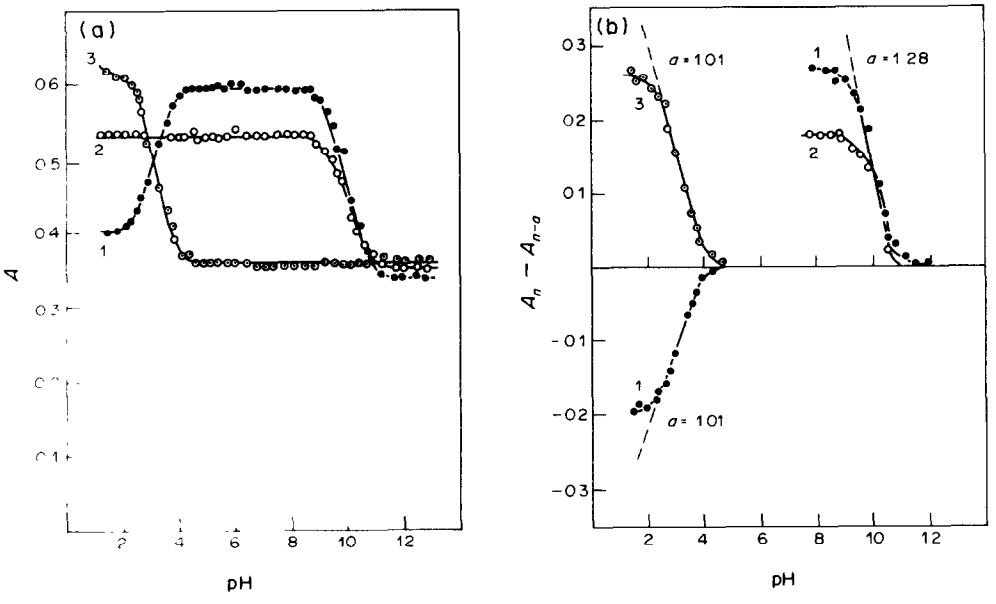

Fig. 1. Effect of pH on the absorbance of DPFH ($7.5 \times 10^{-5} M$): (a) absorbance–pH plots; (b) A_n–A_{n-a} *vs.* pH graphs; λ: 1–320 nm, 2–330 nm, 3–340 nm.

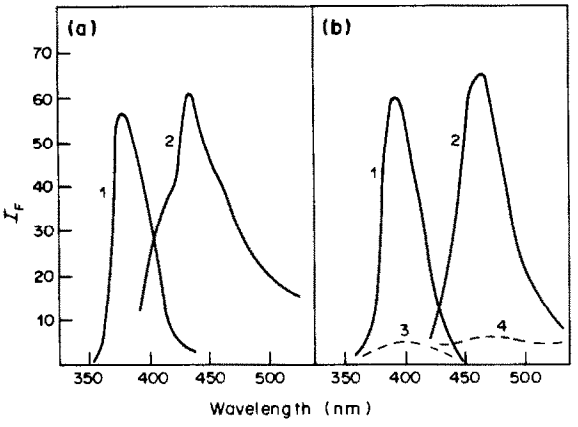

Fig. 2. (a) Fluorescence of DPFH ($1.25 \times 10^{-3}M$) in ethanol; 1—excitation spectrum, 2—emission spectrum. (b) Fluorescence of the Al–DPFH complex (pH 6.28). Curves 1 and 2, excitation and emission spectra, respectively for the complex. Curves 3 and 4, excitation and emission spectra for the reagent alone, in the same conditions.

this reason, it can be concluded that only one of the two pyridine rings is protonated in acid medium.

Fluorescence studies

The reagent shows fluorescence both in aqueous and ethanolic solution, and the intensity is much influenced by pH. The excitation wavelength is 380 nm and the emission wavelength 437 nm (Fig. 2a). It forms fluorescent complexes with aluminium, gallium, scandium, indium and lanthanum. The aluminium complex shows an intense blue fluorescence, which can be used for its determination. The excitation and emission spectra of the Al–DPFH complex at pH 6.0 in 4% ethanol solution are shown in Fig. 2b. The maxima are at 395 and 465 nm, respectively.

A detailed pH study (Fig. 3a) showed that the aluminium complex has maximum fluorescence intensity at pH 6.0. A sodium maleate–sodium hydroxide buffer (pH 6.2) was used in all subsequent work; in the recommended procedure the final apparent pH is 6.0. The use of a phosphate or acetate buffer is not recommended, owing to resultant appreciable decrease in the fluorescence. The fluorescence intensity decreases continuously as the ethanol concentration increases from 4 to 50% (Fig. 3b). Use of an ethanol concentration of 4% in the final solution measured is considered satisfactory.

The fluorescence intensity is temperature-dependent (Fig. 3c) and the optimum temperature is 20°. For convenience a temperature of $25 \pm 0.5°$ was used, but the lower temperature gives higher sensitivity.

The effect of DPFH concentration on the fluorescence intensity for a 50-ng/ml aluminium solution ($1.85\ \mu M$) was studied under the conditions of

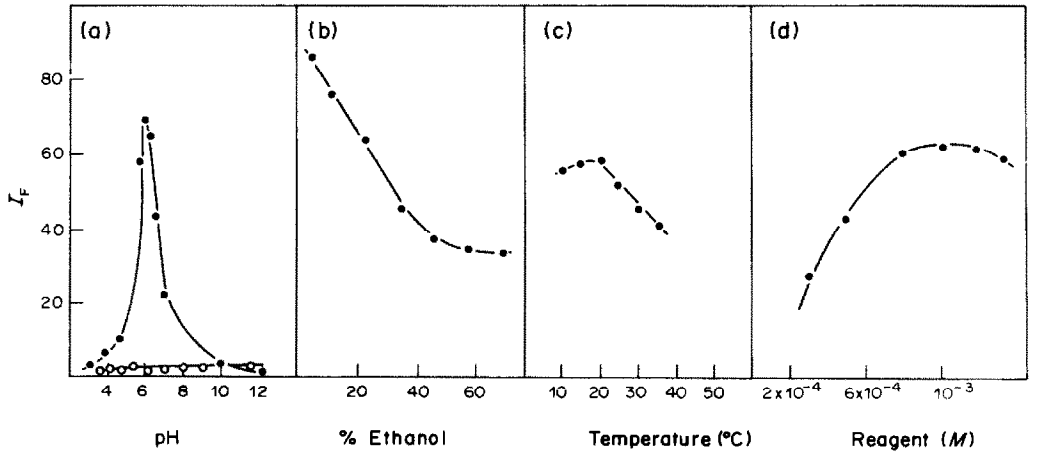

Fig. 3. Influence of experimental variables on the fluorescence of the Al–DPFH complex. Aluminium concentration 50 ng/ml. (a) Influence of pH. (b) Influence of percentage of ethanol. (c) Influence of temperature. (d) Influence of the reagent concentration.

Table 1. Effect of foreign ions on the determination of aluminium at the 50-ng/ml level

Foreign ions	Amount tolerated without masking agent, *ng/ml*
$S_2O_3^{2-}$, thioglycollic acid, Na^+, K^+	2.5×10^4
CN^-, Rb^+, H_2O_2	1.5×10^4
Thiourea, acetate	1.0×10^4
Mo(VI), Pb(II), Tl(I), As(V), Ba^{2+}, NO_2^-, IO_3^-, I^-, IO_4^-, $S_2O_8^{2-}$, ClO_3^-, NO_3^-, CO_3^{2-}, SO_3^{2-}, SCN^-, SO_4^{2-}, Br^-	5.0×10^3
Li^+, Mn(II), Hg(II), Ca^{2+}, S^{2-}	2.5×10^3
Y^{3+}	1.0×10^3
Be(II), Cr(III)	500
Co(II), Ag^+, Cd^{2+}, Sr^{2+}, EDTA	250
V(V), La^{3+}, Tl(III), Bi(III), Zr(IV), Ce(IV), Sc^{3+}, Hg(I), Zn^{2+}, U(VI), Fe(III), As(III), Ni^{2+}, Sb(III), $C_2O_4^{2-}$, $H_2PO_4^-$	50
Fe(II)	5

the recommended method (Fig. 3d). The fluorescence intensity increases with reagent concentration up to 0.0025*M*. A DPFH concentration of 0.001*M* was chosen because it ensures a sufficient reagent excess, and at higher reagent concentrations the fluorescence intensity decreases.

The stoichiometry of the complex was found to be 1:1 by the Bent and French method[16] (which is suitable for weak complexes), with fluorimetric measurement.

Determination of aluminium

There is a linear relationship between the fluorescence intensity and aluminium concentration over the range 10–100 ng/ml (3.7×10^{-7}–$3.1 \times 10^{-6}M$). The limit of detection[17] is 4 ng/ml. Negative deviation from linearity is observed at higher aluminium concentrations. Application of the recommended method to a series of 11 samples (Al 50 ng/ml) gave a relative standard deviation of 1.1%.

Effect of foreign ions

Cationic and anionic interferences were studied in detail. Some cations interfere because they form non-fluorescent complexes with DPFH; this reduces the length of the linear section of the calibration graph by decreasing the effective reagent concentration. Some other cations (gallium, scandium, indium and lanthanum) increase the fluorescence intensity appreciably, and give positive errors. The tolerance levels for foreign ions are given in Table 1. The amounts tolerated in presence of masking agents are shown in Table 2.

Aluminium in sea-water

The method has been applied to the determination of traces of aluminium in sea-water. The standard-addition procedure can be used, but similar results are obtained by using a calibration graph obtained by using standards for which the final ionic strength has been made the same as that for the sea-water samples ($\mu \sim 0.7$).

The procedure has been applied to spiked samples prepared by using an artificial sea-water (Table 3) and to three samples collected in the Andalusian sector of the Mediterranean (Table 4).

Table 2. Interferences in the presence of masking agents

Foreign ions	Amount tolerated with masking agent, *μg/ml*	Masking agent, *μg/ml*
Sr^{2+}	2.5	SO_4^{2-}, 1.0
Ag^+	1.0	SCN^-, 5.0
Ag^+	1.0	thiourea, 10.0
Ag^+	1.0	I^-, 5.0
Co^{2+}	0.50	H_2O_2, 15.0
Au(III)	0.50	Br^-, 5.0
Cd^{2+}	0.50	SCN^-, 5.0
Cd^{2+}	0.50	I^-, 5.0
Tl(III)	0.50	CN^-, 10.0
Sb(III)	0.25	I^-, 5.0
La^{3+}	0.25	EDTA, 0.25
Ni^{2+}	0.25	CN^-, 15.0
Cu^{2+}	0.25	CN^-, 15.0
Bi(III)	0.10	I^-, 1.0
Zr(IV)	0.10	SO_4^{2-}, 1.0
Fe(II)	0.25	CN^-, 10.0

Table 3. Results obtained with spiked samples

Aluminium added, *ng/ml*	Aluminium found, *ng/ml*	Recovery, %
50	47	94
100	97	97
150	154	103
200	200	100
250	260	104

Table 4. Determination of aluminium in sea-water

Sample	Found, *ng/ml*
Málaga bay (Huelin beach)	202
Málaga bay (Misericordia beach)	193
Marbella (Puerto Oais beach)	137

REFERENCES

1. M. Katyal and Y. Dutt, *Talanta*, 1975, **32,** 151.
2. R. B. Singh and P. Jain, *ibid.*, 1982, **29,** 77.
3. T. Uno and H. Taniguchi, *Bunseki Kagaku*, 1971, **20,** 997.
4. S. S. Katyar and S. N. Tandon, *Talanta*, 1964, **11,** 892.
5. G. S. Vasilikiotis and J. A. Tossidis, *Microchem. J.*, 1969, **14,** 380.
6. M. Gallego, M. García Vargas and M. Valcárcel, *Analyst*, 1980, **105,** 193.
7. M. Silva and M. Valcárcel, *ibid.*, 1980, **105,** 93.
8. E. Requena, J. J. Laserna, A. Navas and F. García Sanchez, *ibid.*, 1983, **108,** 933.
9. D. E. Ryan, F. Snape and M. Winpe, *Anal. Chim. Acta*, 1972, **58,** 101.
10. W. K. Dougan and A. J. Wilson, *Analyst*, 1974, **99,** 413.
11. D. J. Hydes and P. S. Liss, *ibid.*, 1976, **101,** 922.
12. J. M. Cano Pavón, M. G. Trujillo and A. García de Torres, *Anal. Chim. Acta*, 1980, **117,** 319.
13. W. Stenström and N. Goldsmith, *J. Phys. Chem.*, 1926, **30,** 1683.
14. B. Buděšínský, *Talanta*, 1969, **16,** 1277.
15. F. J. Barragán de la Rosa, J. L. Gómez Ariza and F. Pino, *ibid.*, 1983, **30,** 555.
16. H. E. Bent and C. L. French, *J. Am. Chem. Soc.*, 1941, **63,** 1568.
17. *Anal. Chem.*, 1980, **52,** 2242.

Talanta, Vol 32, No. 9, pp. 893–899, 1985
Printed in Great Britain

0039-9140/85 $3.00 + 0.00

VOLTAMMETRIC DETERMINATION OF THE STABILIZING ADDITIVES ACARDITE II, CENTRALITE I AND DIPHENYLAMINE IN PROPELLANTS

ARNE BERGENS,* KENT LUNDSTRÖM† and JAN ASPLUND§
Department of Analytical Chemistry, University of Uppsala, P.O. Box 531, S-751 21 Uppsala, Sweden

(*Received* 15 *January* 1985. *Accepted* 3 *April* 1985)

Summary—A method for the determination of the stabilizing additives Acardite II, Centralite I and diphenylamine in single- and double-base propellants has been developed, based on oxidative differential pulse voltammetry with a glassy-carbon electrode in a 1:1 v/v acetonitrile–methanol medium. The voltammetric behaviour of Acardite II and Centralite I was briefly studied to find the proper experimental conditions. For analysis, aliquots of a crude sample extract in dichloromethane are added directly, with no prior treatment, to the measurement cell. The analysis is performed by the standard-addition method. The relative standard deviation is typically 1.0–1.5%. The concentration range accessible with the differential pulse technique, 0.5–100 μM, is quite sufficient for the levels of stabilizers used in powders and propellants. The utility of the method is exemplified by the monitoring of stabilizer consumption in three different propellants subjected to accelerated degradation at 90°.

Diphenylamine (DPA) and certain derivatives of urea are commonly used as stabilizing additives in various propellants. The chemical structure of the two most commonly used urea derivatives, *N'*-methyl-*N,N*-diphenylurea (known as Acardite II, AII) and *N,N'*-diethyl-*N,N'*-diphenylurea (known as centralite I, CI), are shown below.

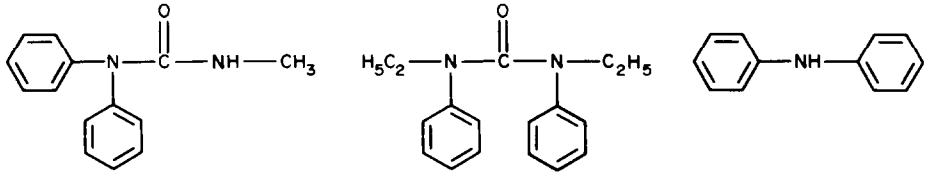

Acardite II Centralite I Diphenylamine

These compounds impart a significantly improved shelf-life to a propellant product, by capturing the reactive HNO_3 and different NO_x species liberated in the degradation of nitrocellulose.[1] Thus, nitroglycerine and nitrocellulose are protected from the accelerated degradation caused by exposure to HNO_3 and NO_x. The stabilizing action accordingly involves a transformation of the additives AII, CI and DPA into various nitro-derivatives. The safe storage period of a particular propellant batch can be conveniently established by monitoring the gradual consumption of the stabilizing additive. A reliable routine method for the determination of unreacted stabilizer in propellants is thus of great practical value.

Titrimetric assays based on bromination have traditionally been widely employed,[2] but the poor selectivity renders such methods suitable only for newly manufactured batches. In order to improve the selectivity, primarily towards the different nitro-derivatives formed during storage, various gas- and liquid-chromatography methods have been employed.[3–6]

The aromatic amine moiety can be oxidized electrochemically at carbon electrodes, for example, at a sufficient rate to make an analytical exploitation worthwhile.[7–9] The present work was undertaken with the object of evaluating a voltammetric method for routine use.

A brief voltammetric characterization of the two urea derivatives will be reported since there is an apparent lack of such data. Diphenylamine, on the other hand, has been well characterized voltammetrically.[7] A voltammetric method for the determination of these three compounds in propellants will be outlined. Finally, the feasibility of applying

*Author for correspondence.
†Present address: KabiVitrum AB, S-11287 Stockholm, Sweden.
§AB Bofors Nobel Kemi, P.O. Box 800, S-691 80 Bofors, Sweden.

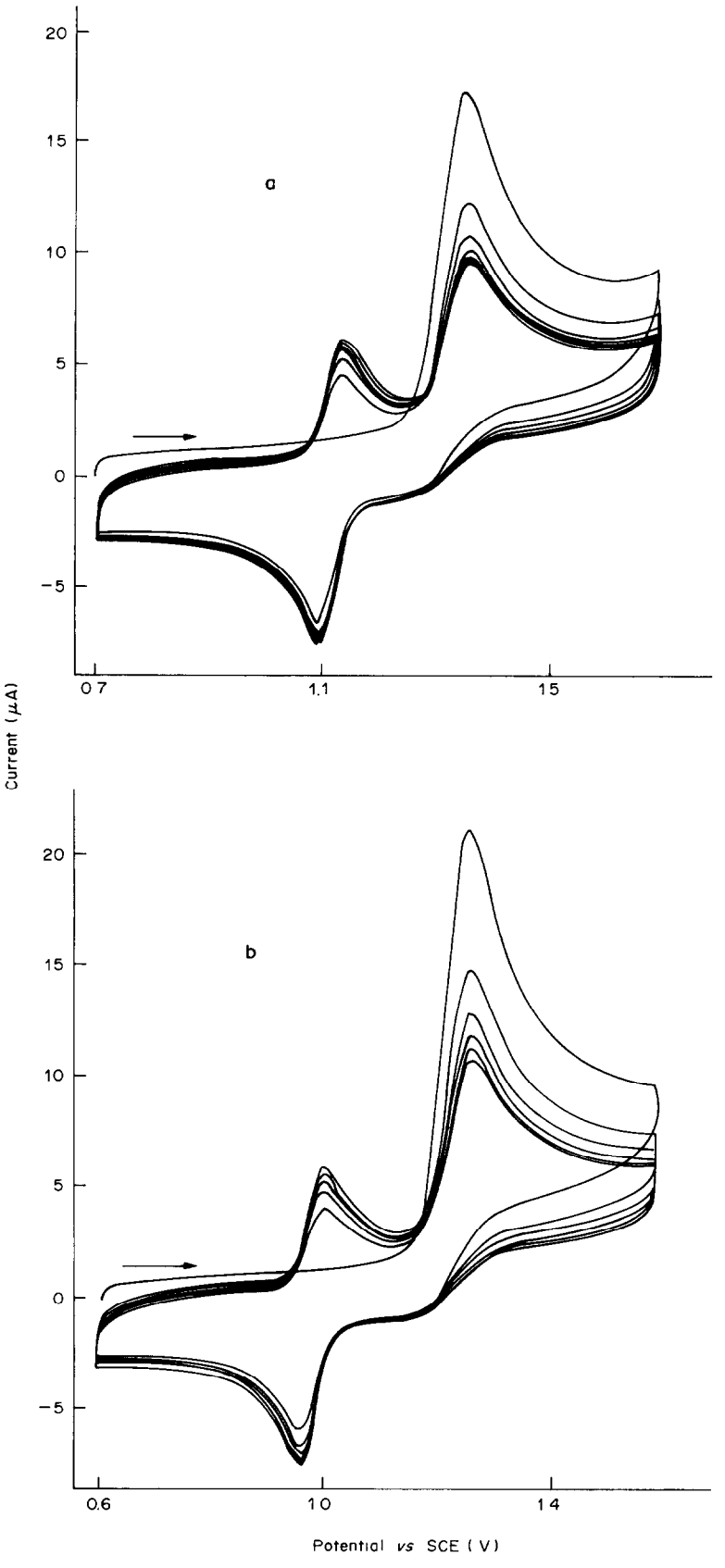
20
15
10
5
0
−5
a
0 7
1.1
15
Current (μA)
20
15
10
5
0
−5
b
0.6
1 0
1 4
Potential *vs* SCE (V)

Fig. 1.

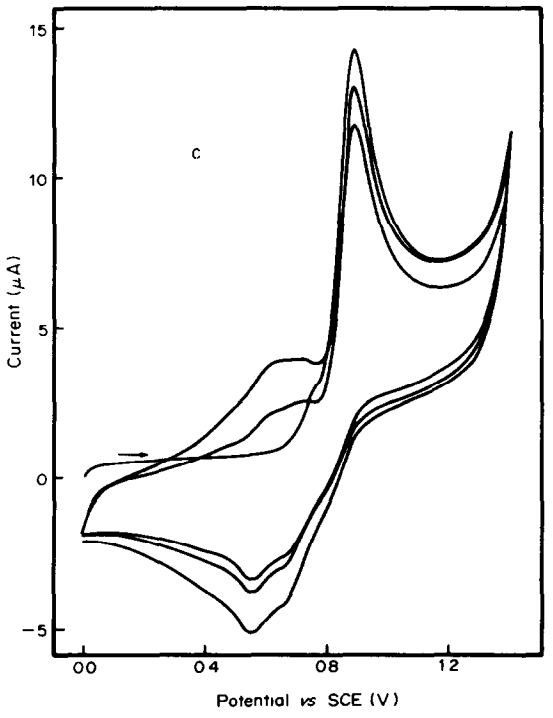

Fig. 1. Cyclic voltamperograms of (a) Acardite II, (b) Centralite I, (c) diphenylamine in acetonitrile. Sweep rate 100 mV/sec, concentration 0.2m*M*. In (a) and (b) the gradual development of steady-state behaviour is shown.

the voltammetric method directly to a crude sample extract for monitoring the entire course of consumption of a stabilizing additive will be demonstrated.

EXPERIMENTAL

Apparatus

Conventional polarographic instrumentation was employed for the cyclic voltammetric characterization experiments (PAR 170 Electrochemistry System) and for analytical determinations by differential pulse voltammetry (PAR 174 A). A conventional three-electrode potentiostat equipped with an integrator unit (made in our laboratory) was used for controlled potential coulometry.

The electrochemical cell was a 20-ml glass vessel with a water jacket (Metrohm, 6.1418.220), with a saturated calomel reference electrode (Radiometer, K 401), a separate salt-bridge, a platinum-wire auxiliary electrode and a glassy-carbon working electrode (GCE, area 7.07 mm^2) embedded in a Teflon housing (Metrohm, 6.1204.040), which fitted a rotating electrode assembly (Metrohm, 2.628.0020). The measurement cell was kept at constant temperature by a conventional thermostat. All potential values reported refer to the reference electrode system described above, whether this is explicitly stated or not.

Propellant samples were performed in a Soxhlet apparatus (Soxtec System 1040 Extraction Unit, Tecator).

Reagents

Acetonitrile, dichloromethane and methanol were of *p.a.* grade (Merck) and used as received. The supporting electrolyte was 0.05*M* lithium perchlorate (*p.a.*, G. F. Smith) in acetonitrile, methanol or a 1:1 v/v mixture of the two. For the salt-bridge 0.1*M* lithium perchlorate in acetonitrile was used throughout.

The compounds CI, AII and DPA were used as received (supplied by AB Bofors Nobel Kemi, Sweden). Stock solutions were prepared weekly in appropriate solvents.

Procedure

A 10-ml portion of supporting electrolyte was transferred to a thoroughly rinsed and dried measuring cell, kept at 25.0 ± 0.5°. Solutions were not deaerated.

Before each series of voltammetric experiments the GCE was polished with an aqueous slurry of 0.3-μm alumina powder (BDH) on a damp silk cloth (LAMPLAN 410) and thoroughly rinsed with water, an ultrasonic bath being used in the final stages. The GCE was then conditioned in the supporting electrolyte by cycling the applied potential between 0.0 and + 1.8 V at 50 mV/sec for about 20 min. This conditioning step also serves as a check on performance of the system with regard to magnitude of the residual current, the presence of impurities, and the positive potential limit. Typically, for the voltammetric parameters given above, a positive potential limit of 1.6–1.7 V was found for acetonitrile medium, the limit being taken as the potential at which the residual current density was 25 μA/cm^2. The apparent capacitance evaluated from the residual current[10] was *ca.* 140–160 μF/cm^2 at 1.0 V. Two different GCEs were used, but they showed very similar behaviour.

After conditioning, the GCE was left in the supporting electrolyte and appropriate quantities of test solutes were added from a 100-μl syringe. The parameters for the cyclic voltammetry are given in the text as appropriate, but for the differential pulse voltammetry (DPV) the following parameters were used throughout: scan-rate 10 mV/sec, modulation amplitude 50 mV, clock period 0.5 sec, and low-pass filter in the "off" position. Potential intervals for the differential pulse voltamperograms were from 0.2 to 1.2 V for DPA and from 0.8 to 1.7 V for AII and CI. Unless otherwise stated, all voltammetric measurements were made under quiescent conditions.

Table 1. Oxidation potentials for Acardite II, Centralite I and diphenylamine in acetonitrile

Compound	E_p, V	$E_p - E_{p/2}$, V	$i_p/Cv^{1/2}$
Acardite II	1.32	0.055	0.187
Centralite I	1.24	0.060	0.193
Diphenylamine	0.82	0.060	0.205

Units used for $i_p/Cv^{1/2}$: i_p in A, $C = 0.2mM$ for all three compounds, $v = 0.100V/sec$. Potentials are *vs.* SCE.

Propellants were subjected to the conventional stability test[1] of storage at elevated temperature. At regular intervals, samples of approximately 2 g were accurately weighed and the stabilizer was extracted with 75 ml of dichloromethane in the Soxhlet apparatus. The final volume of each extract was made 50 ml by evaporation of some solvent, transfer to a standard flask and dilution to volume. Portions of these extracts, typically 50–200 μl, were added to the 1:1 acetonitrile–methanol solution of supporting electrolyte in the cell. The stabilizer content was evaluated by the standard-addition method, with at least three additions (of 50 μl of 0.4mM stock solution) to each sample and two measurements for each concentration level.

RESULTS AND DISCUSSION

Cyclic voltammetry

The three compounds examined can all be oxidized at a glassy-carbon electrode, giving voltammetric waves well suited for analytical purposes (Fig. 1). The voltammetric characteristics of DPA have been extensively investigated in both aqueous and non-aqueous media, *e.g.*, by Adams,[7] and Chey and Adams,[11] and our experimental data are in full agreement with the reported behaviour. AII and CI have not hitherto been voltammetrically characterized.

From Fig. 1, it can be seen that the potential required for the oxidation of AII and CI falls outside the range accessible in an aqueous medium, at least for analytical purposes. A suitable non-aqueous solvent is hence required, and acetonitrile was used to obtain Fig. 1. Precautions were found to be necessary in order to avoid contamination by water, which would give rise to excessive background currents in the potential range in question. Use of a salt-bridge containing acetonitrile, to connect the reference electrode (which contained aqueous solution) and the cell compartment, was found essential for the same reason.

The following observations on the reactivity of AII and CI can be made from the cyclic voltammetric experiments. A single well-defined oxidation wave, suitable for analytical applications, is revealed in the initial positive potential sweep, Fig. 1. As summarized in Table 1, the peak potentials are at 1.32 and 1.24 V vs. SCE for AII and CI respectively. The primary electrode process generates a redox couple, the reduction wave for which appears on the reversed sweep in the voltamperograms shown in Fig. 1. The corresponding oxidation of this secondary redox couple can be seen on subsequent positive potential sweeps.

To study the appearance of this secondary redox couple, a solution of CI was electrolysed at a potential of 1.40 V to exhaustion (2 hr); application of differential pulse voltammetry then revealed that the yield of this secondary couple was less than 20%, as judged from the peak heights. Apparently, under these conditions, there are either further transformations of the secondary redox couple or additional reaction paths not involving it. The solutions became strongly coloured on oxidative electrolysis, red for CI and dark blue for AII, but the colour slowly faded on standing, and finally disappeared. The concentration of the secondary redox couple found immediately after exhaustive electrolysis (which gave the strongly coloured product) by cyclic voltammetry and in the same solution 24 hr later when it had been decolorized, was the same, indicating that the interpretation of the low yield of secondary couple was probably correct. Only a minor primary oxidation wave, representing roughly 1% of the original content of CI, could be discerned after such a bulk electrolysis experiment.

Cyclic voltammetry with a working electrode rotating at 1500 rpm did not reveal these follow-up reactions, and it is concluded that there is no adsorptive accumulation, on the electrode surface, of electroactive species generated in the oxidation process.

With a methanolic medium, which provides almost the same positive potential range as acetonitrile, only the primary oxidation wave can be distinguished. Apparently, the follow-up reactions take a different route in this medium from that in pure acetonitrile. The peak potentials are similar in the two media, and neither medium gives a sufficient resolution for determination of both compounds. However, mixtures of DPA and AII or of DPA and CI can be readily analysed (Table 1 and Fig. 2).

For all three compounds, in both media, the peak current was found to increase linearly with the square root of the sweep rate, showing that mass transport controls the primary oxidation process. Calibration graphs over the range 1–200μM were linear; typical regression equations are presented in Table 2. No intermittent polishing of the electrode surface was necessary. The repeatability of the peak current in repeated sweeps for a 100μM solution, with only a brief stirring between sweeps was typically in the range 1.0–1.5%. After about 20 measurements, however, there was a gradual deactivation of the electrode surface, resulting in a slow decrease in sensitivity. At higher concentrations. $> 100\mu M$, this deactivation was more pronounced and peak currents were no longer so reproducible. A fouled electrode surface could be completely cleaned by polishing as detailed above.

Differential pulse voltammetry

For analysis at lower concentrations, differential pulse voltammetry (DPV) was used. A further asset

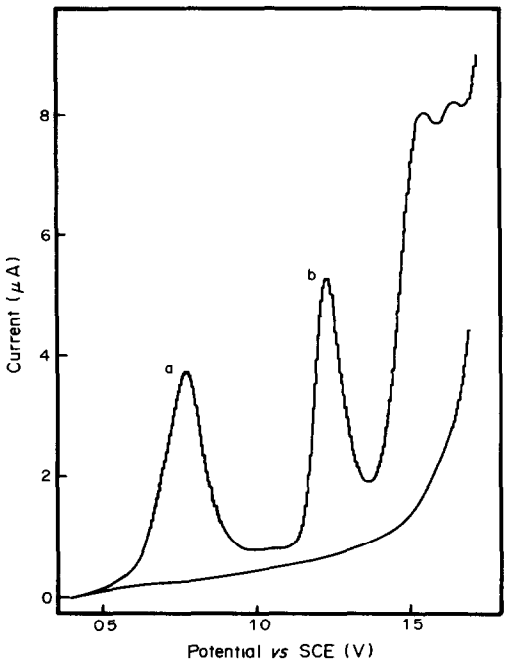

Fig. 2. DPV of sample from propellant C containing both DPA (a) and CI (b). The background current from pure supporting electrolyte, 0.05*M* $LiClO_4$ in 1:1 v/v acetonitrile–methanol mixture, is represented by the lower curve.

of this technique is that peak currents are easier to evaluate, especially when there is more than one voltammetric wave. Though the performance of GCEs is known to be far from ideal in DPV,[12] it proved possible to make measurements at the 1μM level with a reasonable signal to background ratio. When submicromolar levels were measured, which required high sensitivity settings, the base-line of background current was sloping and never quite reproducible, but interpolating the base-line under the DPV peak caused only minor problems (Fig. 2).

DPV calibration graphs were linear over the range 0.5–100μM, but deactivation became evident after only about 10 measurements. This is not surprising since increased susceptibility to the effect of altered electrode surface conditions is an inherent feature of DPV.[10,12]

Assay of stabilizing additives in propellants

The voltammetric assay developed was used to monitor the rate of breakdown of stabilizing additives in three different propellants, A, B and C, stored at 90° to accelerate the degradation.[1] The stabilizing agents used in these propellant formulations are AII, CI and DPA, respectively. In the case of C, a single-base propellant, there is a coating of CI, besides the presence of DPA.

Since the toxic properties of acetonitrile necessitate certain handling precautions, a purely methanolic medium would be preferable for routine purposes, but unfortunately gives a steeply sloping residual current when DPV is used, probably because of the presence of traces of water, and this restricts the positive potential range. Neither simple drying (with molecular sieves or dried alumina nor acidification with glacial acetic acid improved the residual current in the methanolic medium. However, a 1:1 v/v mixture of acetonitrile and methanol was found to provide essentially the same detection limits as acetonitrile alone, and this mixed medium was chosen for routine work.

A typical standard-additions analysis for AII is shown in Fig. 3. The AII concentration was 5.8μM corresponding to 0.67% in the propellant. Satisfactory repeatability is shown by the duplicate voltamperograms. Eleven separate analyses (each with four standard additions) of a single extract of CI from propellant B gave a mean content of 1.51% in the propellant and a relative standard deviation of 1.0%. In general, provided the standard additions were within the linear concentration region of the calibration graphs, the correlation coefficients for regression analysis of the standard addition data were always 0.998 or better.

Figure 2 shows a differential pulse voltamperogram for an unstored sample of propellant C. Both DPA and CI are seen to be present, and their voltammetric peaks are well enough resolved to allow determination of both components. It also appears that only the DPA and CI are electroactive in the range of potential covered. However, interference from intermediate or final decomposition products formed from the stabilizers during propellant storage must be considered. The final products have been identified by chromatography[3,5,13] as nitro-derivatives. The fact that the voltammetric reponse disappears completely on prolonged storage (see below) shows that there are no contributions from the final decomposition products. Interference from intermediate decomposition products cannot be ruled out, however. In general, the incorporation of one or more nitro groups close to the electro-oxidizable amine moiety renders it more difficult to oxidize.[14] We have verified this experimentally for several nitro-derivatives known to be formed, and voltammetric measurement of the intact stabilizer will hence be highly selective with respect to the decomposition products. This will be examined in more detail in subsequent work.

Two small peaks in the range 1.50–1.65 V can be seen in Fig. 2. Propellant C also contains *N*-nitroso-DPA (its amount being about a tenth of that of the

Table 2. Typical regression data [i_p (μA) = $ac - b$] for calibration curves

Compound	a, $\mu A.l.mole^{-1}$	b, μA	r
Acardite II	2.88×10^4	0.002	0.9994
Centralite I	2.89×10^5	0.064	0.9999
Diphenylamine	3.87×10^5	0.244	0.9977

r = correlation coefficient and c = concentration (M).

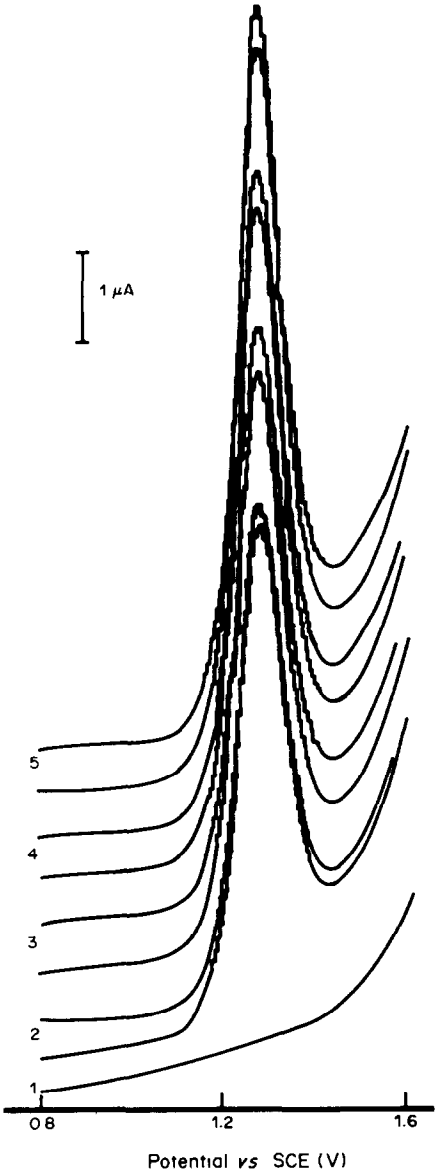

Fig. 3. Sequential standard additions of Acardite II to a sample from propellant A. Voltamperogram 1 is the background current, 2 is from 50μl of the extract of A, and voltamperograms 3–5 are for successive 0.02-μmole standard additions. Base-lines have been shifted for clarity.

DPA present) and separate experiments showed that the peak at the most positive potential was due to *N*-nitroso-DPA. The separate experiments gave no information about the peak at 1.50 V and the reason for this peak is at present not fully understood. The peak is not evident in voltamperograms of other unstored samples.

The selectivity is further illustrated in Fig. 4, by the differential pulse voltamperograms obtained for CI in a particular sample of propellant B before and after its storage for 6 days at 90°. The voltamperograms obtained after one standard addition are also shown. An additional peak at 1.40 V is seen for the stored

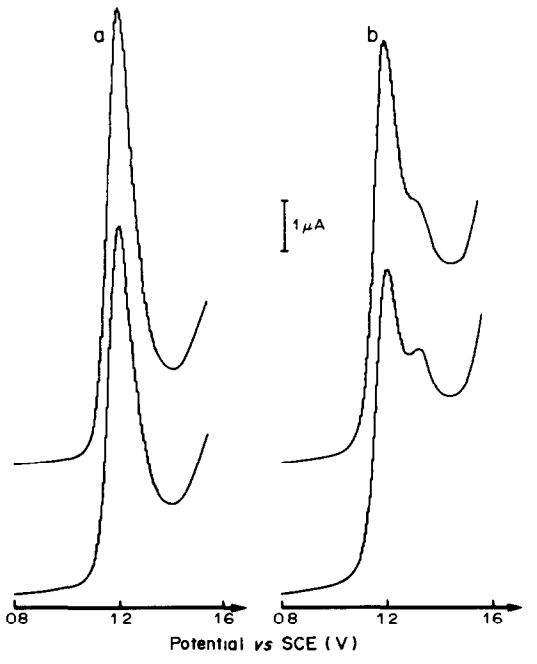

Fig. 4. DPV of two samples from propellant B, with and without standard additions; (a) unstored sample, (b) sample stored for 6 days. Base-lines have been shifted for clarity.

propellant and, as expected, it is not affected by the standard addition. Its development as a function of storage time is gradual, and its height eventually becomes larger than that of the peak for CI (which decreases with increasing time). Finally, this species, which is more difficult to oxidize, also completely disappears. Hence, this new peak is apparently due to a degradation product of CI. No attempt was made to identify this product unambiguously, but 4-nitro-CI has been identified by others[3,13] in stored propellants stabilized with CI, and the peak potential for 4-nitro-CI has been found to be the same as that of the unknown peak in Fig. 4, 1.40 V. We conclude that this peak does correspond to 4-nitro-CI.

Figure 5 shows the feasibility of using the method to monitor decomposition of the stabilizer. The concentration found in the fresh sample was taken as reference and taken as 100%. The rate of degradation follows first-order kinetics only in the early stages. The time found for the onset of autocatalytic decomposition of the propellant, defined as the appearance of visible amounts of NO_2, was about twice the time needed for the stabilizers to be no longer detectable by the voltammetric method. For these particular samples and storage conditions, autocatalytic decomposition began after 23, 24 and 9 days for propellants A, B, and C respectively.

CONCLUSIONS

Differential pulse voltammetry with a glassy-carbon electrode in acetonitrile or mixed

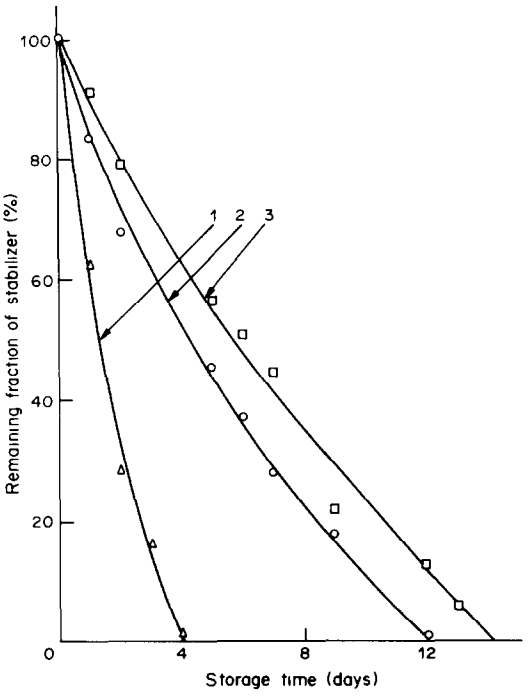

Fig. 5. Rate of stabilizer degradation during propellant storage at 90°C: (1) propellant C (0.82% initial DPA); (2) propellant B (2.25% initial CI); (3) propellant A (0.72% initial AII).

acetonitrile–methanol medium has been demonstrated to provide a convenient approach for determination of the stabilizing additives Acardite II, Centralite I and diphenylamine used in propellant formulations. The voltammetric characterization of Acardite II and Centralite I, for which voltammetric data had not previously been published, has shown that they behave with a chemically irreversible primary oxidation process and generation of a secondary redox couple. With the electrochemical techniques used, this secondary couple exhibits reversible behaviour and a less positive redox potential than that of the parent couple.

The proposed method does not require extensive sample pretreatment since the voltammetric measurement is directly applicable to aliquots of crude sample extracts. The optimum working range for the voltammetric technique is 1–100μM, which gives adequate sensitivity. When 2-g portions of sample are extracted, portions of 50–200 μl from 50 ml of extract are sufficient for monitoring the stabilizer content. However, the definite susceptibility to interference from other oxidizable species, owing to the positive potential required for the electrochemical oxidation of Acardite II and Centralite I, should be kept in mind, and in further applications of the method only simple sample types, such as most propellants, should be considered. Another general limitation of the method is the necessity to use non-aqueous voltammetric conditions.

Acknowledgement—We thank the AB Bofors Company for financial support of this research and for placing propellant samples at our disposal.

REFERENCES

1. *Analytical Methods for Powder and Explosives*, pp. 41–49. AB Bofors Nobelkrut, Bofors, Sweden, 1960.
2. *Ibid.*, pp. 181–183.
3. W. A. Schroeder, K. Wilson, C. Green, P. E. Wilcox, R. S. Mills and K. N. Trueblood, *Ind. Eng. Chem.*, 1950, **42**, 539.
4. W. A. Schroeder, E. W. Malmberg, L. L. Fong, K. N. Trueblood, J. D. Landerl and E. Hoerger, *ibid.*, 1949, **41**, 2818.
5. G. Wunsch, *Int. Jahrestag-Fraunhofer-Inst. Treib-Explosivst.*, 1977, 79.
6. J. Knobloch, *ibid.*, 1980, 103.
7. R. N. Adams, *Electrochemistry at Solid Electrodes*, p. 345. Dekker, New York, 1969.
8. M. M. Baizer, *Organic Electrochemistry*, p. 515. Dekker, New York, 1973.
9. R. N. Adams, *Accts. Chem. Res.*, 1969, **2**, 175.
10. C. Urbaniczky and K. Lundström, *J. Electroanal. Chem.*, 1983, **157**, 221.
11. W. M. Chey and R. N. Adams, *ibid.*, 1977, **75**, 731.
12. J. Wang and B. Freiha, *Talanta*, 1983, **30**, 317.
13. F. Volk, *Propellants and Explosives*, 1976, **1**, 90.
14. R. N. Adams, *Electrochemistry at Solid Electrodes*, p. 334. Dekker, New York, 1969.

Talanta, Vol 32, No. 9, pp. 901–906, 1985
Printed in Great Britain.

0039-9140/85 $3 00 + 0.00

PROPERTIES OF LOW-CAPACITY MACROPOROUS ANION-EXCHANGERS AND THEIR USE WITH HIGH-pH ELUENTS FOR THE DETERMINATION OF WEAK ACIDS IN URINE

ANJUM S. KHAN and FREDERICK F. CANTWELL*
Department of Chemistry, University of Alberta, Edmonton, Alberta, Canada

(*Received* 22 *February* 1985. *Accepted* 2 *April* 1985)

Summary—Low-capacity anion-exchangers have been synthesized from the macroporous styrene–divinylbenzene co-polymer Hamilton PRP-1. These anion-exchangers have non-polar adsorbent properties for neutral sample molecules. The dependence of the capacity factor for a polar weak-acid metabolite of the drug polythiazide on the type and concentration of electrolyte, the organic solvent concentration, and pH of aqueous eluents has been studied to characterize the exchangers. As an application, a method has been developed to determine the metabolite in urine at levels as low as 10 ng/ml. The method employs the exchangers in both a precolumn, which is used to preconcentrate and clean-up the metabolite from urine, and an analytical column. Eluents containing 0.001–0.01*M* sodium hydroxide are used to ionize the weak-acid metabolite.

Determination of trace concentrations of drugs in body fluids by liquid chromatography has been facilitated by the inclusion of adsorbent pre-columns in the chromatograph.[1,2] The pre-column achieves both a preconcentration and a preliminary separation of the drug from the majority of the components of the body fluid, because the drug is usually strongly sorbed on the pre-column packing under conditions in which the polar body-fluid components are weakly sorbed and readily washed off. However, when the analyte is fairly polar, *e.g.*, a drug metabolite, it becomes difficult to find conditions under which an adsorbent will selectively retain it in preference to the polar components of the body fluid. When the analyte is a weak acid an improvement in selectivity may be achieved if the pre-column packing is an anion-exchanger and the sample is loaded onto it under conditions in which the analyte is in its anionic conjugate base form.

If the analyte is a very weak acid it is necessary to use a high-pH solvent in the pre-column loading and washing steps in order to convert it into its conjugate base. This requirement generally precludes the use of silica-based bonded ion-exchangers and demands exchangers that are less susceptible to hydrolysis. In the present study, low-capacity anion-exchangers were synthesized from the styrene–divinylbenzene macroporous liquid-chromatography packing Hamilton PRP-1.

Earlier, a model was proposed to account for the sorption of organic anions from water by a low-capacity anion-exchanger and was verified experimentally with an exchanger prepared from another macroporous styrene–divinylbenzene co-polymer, Amberlite XAD-2.[3] A similar model was shown to be valid for cation-exchangers.[4] On the basis of the similarity between PRP-1 and XAD-2 it might be expected that a low-capacity anion-exchanger prepared from PRP-1 would resemble in its properties a similar exchanger prepared from XAD-2.[5–7] In the present study it has been demonstrated that retention of organic anions on the exchanger derived from PRP-1 exhibits the same kind of dependence on salt concentration as that found for the exchanger made from XAD-2 and the study has been extended to an aqueous–organic medium. Additionally, the anion retention has been studied as a function of other factors which affect retention and selectivity, including the type of electrolyte, the concentration of organic solvent, and the pH.

These studies were performed with the weakly acidic polar metabolite of the diuretic drug polythiazide as a model compound (Fig. 1). This compound was chosen for study mainly on account of its polar nature and high pK_a value. The former causes it to be very weakly retained on non-polar adsorbents and on reversed-phase bonded packings such as octadecylsilyl silica, and the latter necessitates the use of a high-pH mobile phase if the compound is to be retained as its anionic conjugate base. On the basis of previous studies of thiazide diuretics it is expected that polythiazide will be excreted unmetabolized by humans.[8–12] Although several liquid-chromatography methods have been reported for the determination of the relatively non-polar parent drug polythiazide, none has been reported for its metabolite.[13–15] Thus it was also of interest to attempt to develop a liquid-chromatography determination with a low detection

*Author to whom reprint requests should be directed.

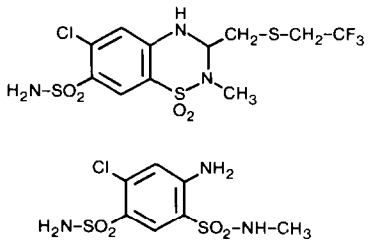

Fig. 1. Structures of polythiazide, 6-chloro-3,4-dihydro-2-methyl-3-{[(2,2-trifluoroethyl)thio]methyl}2H-1,2,4-benzothiadiazine-7-sulphonamide-1,1-dioxide, and its major hydrolytic metabolite, 4-amino-6-chloro-3-(methylsulphamyl)benzenesulphonamide.

limit for the metabolite in urine, in order to verify its virtual absence as an excreted component after ingestion of polythiazide.

EXPERIMENTAL

Reagents

All solvents and chemicals were reagent grade. Acetonitrile was distilled before use; chloroform and ethyl acetate were used as received. Water was demineralized, distilled and finally distilled from alkaline permanganate. The polythiazide and Renese Tablets were manufactured by Pfizer Co. of Canada. The metabolite was synthesized by hydrolysis of polythiazide by Richard Moskalyk of the Pharmacy Department of the University of Alberta, according to a published procedure.[16]

Stock solutions of polythiazide were prepared by dissolving known amounts of the drug in 20 ml of acetonitrile and diluting accurately to 100 ml with water. Stock metabolite solutions were prepared in water.

All mobile-phases were prepared by transferring the required volumes of aqueous reagent solutions and water into standard flasks and diluting to volume with acetonitrile.

Instruments

A schematic diagram of the chromatograph used for studying the pre-column characteristics and for performing the determinations on urine is shown in Fig. 2. Pump P_1 (Model 6000A, Waters Assoc.) pumped a weak eluent S_1 through a Teflon sample-injection valve (Model R6301, Laboratory Data Control) fitted with a 0.5-ml Teflon sample-loop L and then through the precolumn C_1 mounted in place of a sample loop in a high-pressure injection valve V_2 (Model 7010, Rheodyne Corp.) and finally to waste. At the same time, pump P_2 (Model 6000A, Waters Assoc.) pumped the strong eluent S_2 through V_2, through the analytical column C_2 and to the ultraviolet-absorbance detector (Model 770 Spectroflow Monitor, Schoeffel Instrument Corp.) set at 268 nm for monitoring metabolite or at 265 nm for monitoring polythiazide. The detector signal was displayed on a Recordall strip-chart recorder (Series 5000, Fisher Scientific Co.).

Another chromatograph, used for studying retention behaviour of the analytical column, consisted of one Model 6000A pump, a Model 7010 injection valve with a 20-μl loop, a Model 8200 (Spectra-Physics Corp.) ultraviolet-absorbance detector and a Recordall strip-chart recorder.

Measurements of pH were made with a low sodium-error glass and calomel reference electrode pair, calibrated with aqueous buffers, and a Model 520 pH-meter (Accumet, Fisher Scientific Co.). Values of pH reported for acetonitrile–water mixed solvents are "apparent" pH values (pH*) since they are made with respect to an aqueous reference state.[17]

Anion-exchangers

The non-ionic macroporous liquid-chromatography packing PRP-1 (Hamilton Co., Reno, Nev.) which consists of nominally 10-μm diameter spherical particles was converted into a low-capacity, surface-quaternized, strong-base type anion-exchanger by a slight modification of the chloromethylation/amination procedure described by Fritz and previously used in this laboratory.[3,13] Two batches of exchanger were prepared. The first, designated as QPRP (0.11 meq), was chloromethylated for 10 min and the second, designated as QPRP (0.20 meq), was chloromethylated for 30 min. The final product in each case was liberally washed with 1*M* hydrochloric acid, 2-propanol and water and dried overnight at 40° in vacuum before storage. The ion-exchange capacities of the two exchangers were found to be 0.11 meq/g and 0.20 meq/g, respectively, by the following procedure. A small glass column (5 cm × 2.8 mm bore) was dry-packed with exchanger and the weight of packing accurately measured. Then 1*M* sodium hydroxide (10 ml) was slowly pumped through the column under nitrogen pressure in order to convert the exchanger into the OH^- form. The column was washed with water until the effluent was neutral, after which 20 ml of 1*M* sodium chloride were pumped through it, collected and titrated with standard hydrochloric acid.

The C_1 precolumns (Fig. 2) were 2 cm × 2 mm bore modified stainless-steel "guard columns" (Part No. 84550, Waters Assoc.) dry-packed with QPRP (0.20 meq).

The analytical column C_2 was 15 cm × 4.1 mm bore stainless steel packed at a flow-rate of 6 ml/min by a stirred-slurry technique with a slurry of 3 g of QPRP (0.11 meq) in 80 ml of a solvent composed of 10% glycerol and 2.5% sodium chloride in water, as recommended by the Hamilton Corp. for packing PRP-1.[19] After packing, the column was flushed for several cycles with water and methanol alternately.

Extraction of urine

Before its chromatographic determination the metabolite was removed from urine and simultaneously separated from polythiazide by solvent extraction. The urine was adjusted

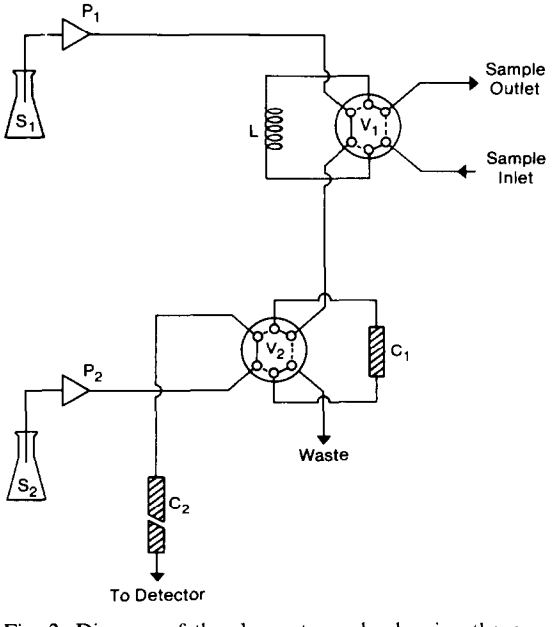

Fig. 2. Diagram of the chromatograph, showing the pre-column (C_1) and analytical column (C_2). See text for details.

to pH 8 by addition of solid sodium bicarbonate and a 50.0-ml portion was transferred to a separatory funnel and extracted with five 50-ml volumes of chloroform, which were then discarded (they contained the polythiazide). The aqueous phase was filtered through Whatman No. 1 filter paper and then extracted with two 50-ml portions of ethyl acetate. The combined ethyl acetate extracts, containing the metabolite, were washed with two 5-ml portions of water and the ethyl acetate phase was filtered through Whatman Phase Separating Paper to remove entrained water, and then evaporated to dryness at 40° on a rotary vacuum evaporator and the resulting residue was dissolved in 5.00 ml of 20% acetonitrile in water. Before this solution was loaded into the injection loop of the chromatograph it was filtered through a 0.45-μm Metricel membrane filter (Gelman Instruments Co.).

When the parent drug polythiazide was to be determined, the urine was adjusted to pH 8.0 with sodium bicarbonate and a 50.0-ml portion was extracted with an equal volume of ethyl acetate. The ethyl acetate phase was washed with two 10-ml portions of water, filtered through phase separating paper and evaporated to dryness on a rotary vacuum evaporator. The residue was dissolved in 5.00 ml of 20% acetonitrile solution and passed through a membrane filter before loading into the injection loop of the chromatograph.

Chromatographic determinations

Precolumn C_1 was packed with QPRP (0.20 meq). The weak eluent S_1 was 0.01*M* sodium acetate/0.01*M* sodium hydroxide in 20% acetonitrile; strong eluent S_2 was 0.01*M* sodium perchlorate/0.0001*M* sodium hydroxide in 10% acetonitrile. With valves V_1 and V_2 in the positions shown by solid lines in Fig. 2, C_1 was equilibrated with S_1 and C_2 was equilibrated with S_2. The 0.5-ml sample loop L was filled with the residue solution from the urine extraction step, and V_1 was switched to the injection position (dashed lines). A total of 20 ml of S_1 was allowed to flow through C_1 at a flow-rate of 1 ml/min, and during this the metabolite was retained and most urine components were washed off to waste. Valve V_2 was then rotated (dashed lines), allowing strong solvent S_2 to elute the metabolite and sorbed urine components out of C_1 and into C_2. After 1 min, during which metabolite was completely eluted from C_1, valves V_2 and V_1 were switched back.

The same chromatograph was used to determine the parent drug, polythiazide, in urine. There were only three changes in conditions from the metabolite determination: (*i*) the urine extract was obtained under different conditions (see above); (*ii*) water was used as eluent S_1, with only 10 ml allowed to flush C_1; (*iii*) S_2 was 0.10*M* sodium formate in 40% acetonitrile solution.

Calibration graphs of peak height *vs.* concentration of metabolite were obtained for both aqueous metabolite standard solutions and for metabolite-spiked urine standards. To obtain the former, aqueous metabolite solutions (250–1000 ng/ml concentration) were loaded into the injection loop without prior solvent extraction. To obtain the calibration graph for spiked urine, urine spiked to contain 25–50 ng/ml levels of metabolite were subjected to solvent extraction prior to chromatography, as described above for urine samples.

RESULTS AND DISCUSSION

Retention behaviour

The dependence of the capacity factor (k') on the concentration of sodium perchlorate in an aqueous eluent is shown in Fig. 3, curves A and B, for two anionic compounds. The first, *p*-nitrobenzenesulphonate, is an anion at all pH values and the second,

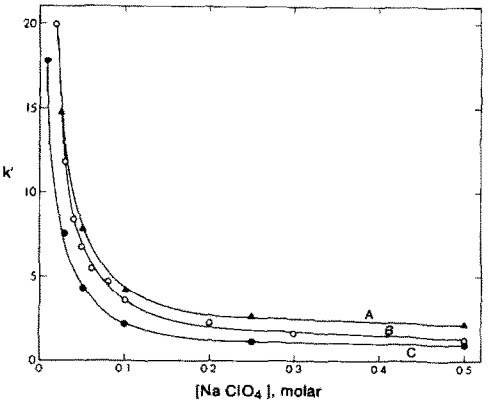

Fig. 3. Capacity factor of *m*-nitrobenzenesulphonate (NBS) anion and of metabolite anion on QPRP (0.11 meq) as a function of $NaClO_4$ concentration. A, NBS eluted with $NaClO_4/H_2O$; B, metabolite eluted with $NaClO_4$/0.01*M* NaOH; C, NBS eluted with $NaClO_4$/10% CH_3CN.

the metabolite of polythiazide, is an anion in 0.01*M* sodium hydroxide medium. As expected, the strength of the eluent is increased by increasing the concentration of sodium perchlorate. Comparison of curve A for the sulphonate ion with curve C for the same ion eluted with 10% acetonitrile medium shows that eluent strength is also increased by addition of organic solvent to the aqueous phase.

The relative strengths of the anions as eluents is in the order acetate < formate < chloride < perchlorate, as can be seen in Fig. 4 by comparing k' for the metabolite anion at any fixed percentage of aceto-

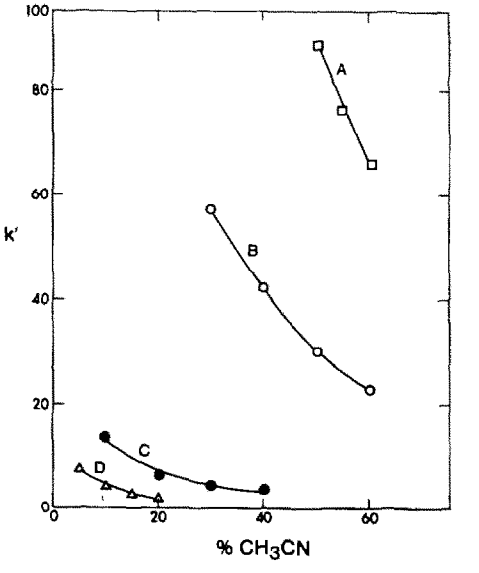

Fig. 4. Dependence of k' for metabolite on QPRP (0.11 meq) on the type of electrolyte and acetonitrile content. Eluents are: A, 0.1*M* CH_3COONa/0.01*M* NaOH; B, 0.1*M* HCOONa/0.01*M* NaOH; C, 0.1*M* NaCl/0.01*M* NaOH; D, 0.01*M* $NaClO_4$/0.01*M* NaOH.

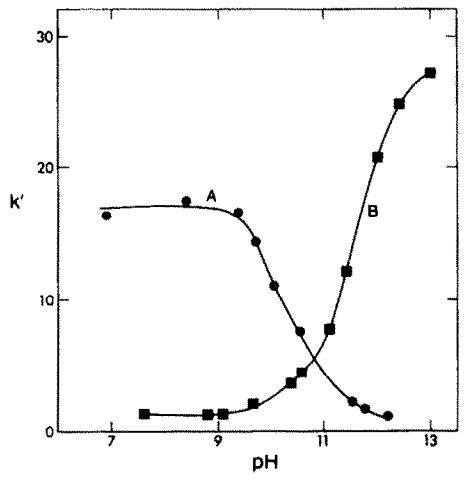

Fig. 5. Dependence of k' for metabolite on QPRP (0.11 meq) on pH* of the eluent. Eluents are: A, 0.025M $NaClO_4$/10% CH_3CN; B, 0.1M HCOONa/30% CH_3CN.

nitrile. This order of increasing eluent strength on the low-capacity exchanger is the same as the well known "selectivity sequence" for high-capacity anion-exchangers. Figure 4 also shows that eluent strength increases with increasing acetonitrile concentration.

Since the metabolite is a weak acid, with $pK_a = 9.8$, its chromatographic capacity factor depends on the pH of the mobile phase.[20] This is shown in Fig. 5 for two eluents. At pH* values well below its pK_a value, the metabolite is present as the undissociated conjugate species in both the mobile phase and the stationary phase. Since the acetonitrile concentration in the eluent is greater for curve B than for curve A, k at low pH* is lower for curve B than for curve A; at low pH* the type and concentration of anion in the eluent is much less important than the acetonitrile concentration as a factor influencing the eluent strength for neutral species. This is consistent with the expected behavior of QPRP (0.11 meq) as a non-polar (reversed-phase) adsorbent for neutral compounds.[3] As pH* is increased the curves become sigmoidal and cross each other as the metabolite begins to dissociate and the eluent anion effect begins to predominate over the acetonitrile effect. Since perchlorate is a very much stronger eluent anion than formate, at high pH* the eluent used for curve A is stronger than that used for curve B in spite of the fact that the latter contains a higher concentration of acetonitrile. Hence the relative strengths of these two eluents undergo a reversal as pH* is increased.

The fact that the inflection points ($pH^*_{1/2}$) in the sigmoidal regions of the two curves occur at different pH* values (10_4 and 11_5) and that neither occurs at the pK_a value (9.8) for the metabolite in aqueous medium is a consequence of both the neglect of transfer activity coefficients in measuring the pH, and the shift of pK_a to higher values in a less polar medium, which stabilizes the neutral conjugate species relative to the anionic species.[17]

The studies described above reveal the dependence of k' of a weak organic acid on type and concentration of electrolyte, concentration of organic solvent and pH used for the eluent. This information provides a rational basis for varying eluent composition in order to obtain the desired k' and selectivity in a chromatographic determination.

Metabolite in urine

In designing a chromatographic method for determining trace concentrations of the polar metabolite of polythiazide in urine it is necessary to include both a preconcentration of the metabolite and a clean-up of the sample to remove the majority of the large number of polar urine components which are, of course, present in much higher concentrations than is the metabolite. In addition, since the chromatographic operations involve high-pH* eluents it is desirable to remove polythiazide from the sample solution before the chromatography, even though polythiazide and its metabolite have very different retention times on the analytical column. This is because slow alkaline hydrolysis of polythiazide in the high-pH* eluent would produce the metabolite.

The first preconcentration and clean-up step consists of two solvent extractions. Polythiazide is extracted from the urine sample with chloroform, and then the metabolite is extracted from the urine into ethyl acetate. The distribution coefficients of the metabolite and polythiazide between chloroform and aqueous buffer at pH $\leqslant 8$ were found to be 0.013 and 3.0, respectively, and between ethyl acetate and aqueous buffer to be 1 and $\geqslant 10$, respectively. Thus, the five preliminary extractions of urine with chloroform remove $\sim 99.9\%$ of the polythiazide but leave $>93\%$ of the metabolite unextracted. Overall recovery of the metabolite from spiked urine standards by extraction and chromatography, compared with that from aqueous standards subjected only to chromatography, was $80 \pm 5\%$. The principal reason for the low recovery is the calculable loss in the ethyl acetate extraction and washing step, due to the low distribution coefficient of the metabolite.

The second preconcentration and clean-up step is performed on the QPRP (0.20 meq) precolumn in the chromatograph. Experiments were performed, with the chromatograph shown schematically in Fig. 2, on aqueous metabolite solutions and on dissolved residues of metabolite-free urine extracts in order to find compositions for the weak eluent S_1 and the strong eluent S_2 that would yield a metabolite peak in the final chromatogram at a retention time at which no urine-component peak appeared. These experiments demonstrated that the use of up to at least 50 ml of an S_1 with the composition 0.01M sodium acetate, 0.01M sodium hydroxide 20% acetonitrile did not remove any metabolite from the precolumn C_1. At

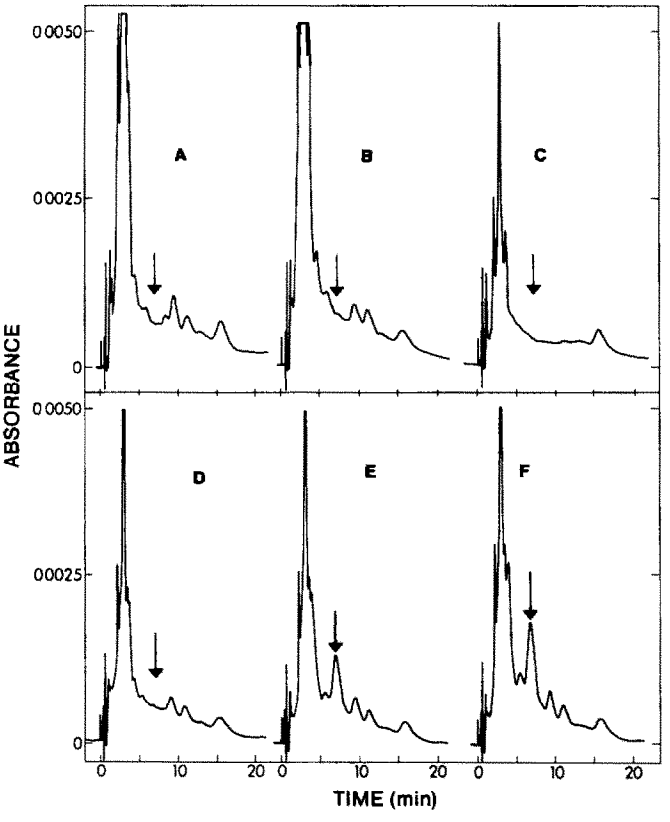

Fig. 6. Chromatograms of urine blanks from four subjects (A–D) and of urine (from subject D) spiked with (E) 50 ng/ml and (F) 75 ng/ml of metabolite. See experimental section for procedure. Eluent flow-rate 3 ml/min. The retention time corresponding to the metabolite peak is marked by the arrows.

the same time, for most urines studied washing the precolumn with 10 ml of this eluent provided adequate removal of normal urine components. The urine from some individuals, however, required 20 ml. Thus, a 20-ml wash of the precolumn C_1 with eluent S_1 was used routinely.

The final step in determination of the metabolite is its elution from the precolumn into the analytical column C_2 with the strong eluent S_2. The chromatographic capacity factors for urine components not removed in the extraction and precolumn clean-up steps, and for the metabolite, were varied empirically by employing various combinations of electrolyte type and concentration, organic solvent content and pH* of S_2. Urine samples from four subjects, each from a different ethnic and dietary background, served as the urine blanks in these studies. In general, it was observed that high-pH* eluents were more successful in eluting the metabolite from C_2 in a "clean" region of the chromatograms for the urine blanks. Substantial differences were observed in the chromatograms for urines of the four subjects, but for all four samples the eluent S_2 finally selected yields a relatively clean background at the metabolite retention time, as seen in Fig. 6. Chromatograms of metabolite-spiked urine are also shown. The detection limit of the technique is 10 ng/ml, defined as the concentration corresponding to a net signal that is three times the standard deviation of the background signal.

The polythiazide metabolite was determined in the urine of a subject who had ingested one commercial tablet containing a 1-mg dose of polythiazide. All urine excreted over a 40-hr period was collected in eight consecutive batches, each containing the pooled urine obtained over a 5-hr period. The results are summarized in Table 1, in which it can be seen from

Table 1. Urinary excretion of polythiazide and metabolite after administration of a 1-mg dose

Time, *hr*	Total urine volume, *ml*	Polythiazide found		Metabolite found, *μg/ml*
		μg/ml	*μg*	
0–5	690	0.029	20	<0.01
5–10	800	0.044	35	<0.01
10–15	580	0.019	11	<0.01
15–20	960	0.042	40	<0.01
20–25	600	0.054	32	<0.01
25–30	320	0.039	12.5	<0.01
30–35	440	0.057	25	<0.01
35–40	210	0.012	2.5	<0.01
Total	4590		178	

the last column that there was no detectable concentration of free metabolite excreted. This result is consistent with the expected stability of thiazide drugs in humans.[12]

Polythiazide in urine

Because of its non-polar character polythiazide is relatively easily determined in urine by the procedure described in the experimental section. The preliminary ethyl acetate extraction serves to exclude most urine components and to preconcentrate the drug. The metabolite extracted along with it is eluted well before polythiazide in the final chromatogram, causing no interference. The strong eluent S_2 used in this determination has a lower pH* than that used in the metabolite determination, and polythiazide has the same pK_a as its metabolite.[20] Thus, though polythiazide is retained in its anionic conjugate-base form on the precolumn, it migrates as the neutral conjugate species through the analytical column and is sorbed there not by ion-exchange, but rather by adsorption.

Polythiazide was determined in the same urine samples as was the metabolite. These results are also summarized in Table 1. The extraction–time profile of polythiazide given in the third column of Table 1 as well as the cumulative 40-hr excretion (178 μg or 18% of the 1 mg ingested) are both in agreement with the polythiazide excretion data reported by Hobbs and Twomey who used a derivative-formation gas chromatography method for the determination.[11]

CONCLUSIONS

In addition to extending the characterization of low-capacity anion-exchanger/adsorbents prepared from macroporous styrene–divinylbenzene copolymers, this study has shown the utility of such materials both in precolumns for on-stream preconcentration and clean-up of weakly acidic polar compounds, and in analytical columns for elution chromatography of these compounds. Compatibility with high-pH eluents is an important property of the ion-exchangers, which makes possible these applications.

Acknowledgements—This work was supported by an Alberta Heritage Foundation for Medical Research Postdoctoral Fellowship to A.S.K., by the Natural Sciences and Engineering Research Council of Canada and by the University of Alberta. Hamilton PRP-1 resin was kindly supplied by the Hamilton Co., Reno, Nevada. Polythiazide and its metabolite were supplied by Richard Moskalyk, Department of Pharmacy, University of Alberta, as was useful information on polythiazide.

REFERENCES

1. R. W. Frei, *Anal. Proc.*, 1980, **17**, 519.
2. R. A. Hux, H. Y. Mohammed and F. F. Cantwell, *Anal. Chem.*, 1982, **54**, 113.
3. S. Afrashtehfar and F. F. Cantwell, *ibid.*, 1982, **54**, 2422.
4. R. A. Hux and F. F. Cantwell, *ibid.*, 1984, **56**, 1258.
5. Z. Iskandarani and D. J. Pietrzyk, *ibid.*, 1981, **53**, 489.
6. T. D. Rotsch, W. R. Cahill, D. J. Pietrzyk and F. F. Cantwell, *Can. J. Chem.*, 1981, **59**, 2179.
7. D. P. Lee and J. H. Kindsvater, *Anal. Chem.*, 1980, **52**, 2425.
8. H. R. Brettell, J. K. Aikawa and G. S. Gordon, *A.M.A. Arch. Internal Med.*, 1960, **106**, 57.
9. J. E. Baer, H. L. Leidy, A. V. Brooks and K. H. Beyer, *J. Pharmacol. Expt. Therap.*, 1959, **125**, 295.
10. R. Pinson, E. C. Schreiber, E. H. Wiseman, J. Chiaini and D. Baumgartner, *J. Med. Pharm. Chem.*, 1962, **5**, 491.
11. D. C. Hobbs and T. M. Twomey, *Clin. Pharm. Ther.*, 1978, **23**, 241.
12. L. S. Goodman and A. Gilman (eds.), *The Pharmacological Basis of Therapeutics*, 5th Ed., Macmillan, New York, 1975.
13. R. E. Moskalyk, R. A. Locock, L. G. Chatten, A. M. Veltman and M. F. Bielech, *J. Pharm. Sci.*, 1975, **64**, 1406.
14. C. K. Wong, D. Y. J. Tsau, D. M. Cohen and K. P. Munnely, *ibid.*, 1977, **66**, 736.
15. V. P. Shah, J. Lee and V. K. Prasad, *Anal. Lett.*, 1982, **15**, 529.
16. U. G. Hennig, R. E. Moskalyk, L. G. Chatten and S. F. Chan, *J. Pharm. Sci.*, 1981, **70**, 317.
17. R. G. Bates, *Determination of pH*, 2nd Ed., Chapter 8. Wiley, New York, 1973.
18. D. T. Gjerde, J. S. Fritz and G. Schmuckler, *J. Chromatog.*, 1979, **186**, 599; 1980, **187**, 35.
19. R. G. Baum, R. Saetre and F. F. Cantwell, *Anal. Chem.*, 1980, **52**, 15.
20. A. S. Khan and F. F. Cantwell, to be published.

Talanta, Vol. 32, No. 9, pp. 907–913, 1985
Printed in Great Britain.

0039-9140/85 $3.00 + 0.00

SIZE FRACTIONATION TECHNIQUES IN THE DETERMINATION OF ELEMENTS ASSOCIATED WITH PARTICULATE OR COLLOIDAL MATERIAL IN NATURAL FRESH WATERS

B. SALBU, H. E. BJØRNSTAD, N. S. LINDSTRØM and E. LYDERSEN
Department of Chemistry, University of Oslo, Blindern, Oslo 3, Norway

E. M. BREVIK and J. P. RAMBAEK
Institute of Energy Technology, 2007 Kjeller, Norway

and

P. E. PAUS
Central Institute for Industrial Research, Blindern, Oslo 3, Norway

(*Received* 3 *December* 1984. *Accepted* 2 *April* 1985)

Summary—Among fractionation techniques which have been applied to trace-element speciation studies in natural water samples, methods based on size separations are by far most commonly applied. In the present work, methodological effects occurring in use of filtration, centrifugation, dialysis *in situ* and hollow-fibre ultrafiltration are discussed. By use of a combination of these techniques and different methods of analysis, information on the association of 20 elements with particulate or colloidal material in ground water and lake water has been obtained.

Most trace elements present in natural waters, especially multivalent metals, are to some degree associated with particulate or colloidal material.[1-3] This association strongly influences their transport and bioavailability. Valuable information can be obtained if species are fractionated according to particle size. However, when fractionation of samples is performed, the results obtained may depend on the technique applied. In the present work filtration, centrifugation, dialysis *in situ* and hollow fibre ultrafiltration were performed on aliquots of the "same" sample.

As the degree of association of elements with particulate or colloidal material depends not only on the element in question but also on other components present, waters that vary in composition have been investigated. Ground water is characterized by a relatively high content of salts and inorganic particulate/colloidal matter, whereas a relatively high content of organic matter is present in lake waters (Table 1). The present samples are part of a broad analytical programme[3] and a comparison of the values obtained, by different analytical methods, for the total concentrations and residual concentrations after filtration through 0.45-μm pore-size filters, has already been presented for eight elements.[4]

EXPERIMENTAL

Sampling

Ground-water samples (bore-hole) from Kise, Hedmark, Norway, were collected on 24 March 1981, during the winter stagnation period. The sampling depth was 6.7 m below the ground-water level (8.3 m below ground). Water samples from Lake Tyrifjorden, Norway, were collected on 1 June 1981, during the algal growth period. The sampling depth was 5 m. Samples from Lake Kjellingtjenn, Norway, were collected on 3 March 1982, 1 m under the ice surface (dialysis *in situ* and hollow-fibre ultrafiltration).

A Ruttner polyethylene sampler was used, from which portions were poured into individual prewashed containers for elemental analysis. Furthermore, samples were fractionated *in situ* (dialysis), in the field immediately after sampling (filtration), or in laboratory clean bench facilities a few hours later.

Filtration

Suction filtration was performed with 47-mm diameter filter membranes (Millipore: 0.45-μm HAWP, 0.1-μm VCWP, AP-20 borosilicate microfibre glass depth filter; Nuclepore: 0.4-μm polycarbonate) and Millipore polypropylene/polycarbonate filtration equipment. The membranes were first conditioned by passage of 250 ml of distilled demineralized water and then 50 ml of the sample. Then the filtrates (250 ml) were distributed between individual containers. Before use all filters were soaked in 0.1*M* nitric acid for one day, and then in distilled demineralized water for 3 days. The blank values demonstrated this to be a proper washing procedure.

Centrifugation

With a high-speed angle rotor (DIMON/IEC), 25-ml portions of the samples were centrifuged in 8 different polystyrene tubes, according to the specifications given in Table 2. The tubes were soaked in 0.1*M* nitric acid for three days before use. The supernatant phases (5 ml) were pipetted into individual containers. In timing the 83-sec centrifugation the acceleration and retardation of the centrifuge were taken into account.

Dialysis in situ

Dialysis *in situ* of ground water and lake waters

Table 1. Physical/chemical parameters for the ground water and lake waters

Parameters	Ground water	Lake waters	
	Kise	Tyrifjorden	Kjellingtjenn
pH	7.6	6.8	5.3
Temperature, °C	5.5	5.5	1.1
Conductivity, $\mu S/cm$	326	38	26.5
Turbidity, *FTU*	12	1	0.64(NTU)
MnO_4^- number, $mg(O)/l.$	1.8	2.9	4.0
Chlorophyll, $\mu g/l.$	0.11*	0.70*	0.28
O_2, $mg/l.$	3.2	9.9	3.3
HCO_3^-, $meq/l.$	2.4	0.04	< 0.04
Total N $mg/l.$	1.4	0.4	0.6
NO_3^-, $mg(N)/l.$	0.3	0.3	0.07
Total P, $\mu g/l.$	20	8	4
PO_4^{3-}, $\mu g(P)/l.$	12	3.5	1
SO_4^{2-}, $mg/l.$	9	2.7	6.7
B, $mg/l.$	0.3	0.04	n.d.
F^-, $mg/l.$	0.15	0.04	n.d.
Si, $mg/l.$	4.6	1.1	0.3
Rn, $nCi/l.$	0.12	0.11	n.d.

*K. Ormerod, personal communication.
n.d. = not determined.

(Kjellingtjenn) was performed by using dialysis bags similar to those applied by Beneš and Steinnes.[1] According to the specification (Scientific Instruments Centre Ltd., London) the nominal cut-off of the Visking membrane is about 5 nm diameter or close to 10^4 molecular weight.[1] Before use the bags were soaked in 0.1*M* nitric acid for one day and then in distilled demineralized water for three days. Four bags were each filled with 100 ml of distilled demineralized water, fastened with a nylon string and then submerged in the water at the chosen depth. The bags were kept in this position for 3 weeks. After withdrawal the dialysates were distributed between individual containers (in the field).

Ultrafiltration

Ultrafiltration was performed with an Amicon CH3 concentrator equipped with H1P10-8 hollow-fibre cartridges. According to the specification (Amicon Corporation, Mass., U.S.A.) the cartridge, consisting of cylindrical non-ionic polymer tubes with internal diameter 0.2 mm, has a total surface area of about 830 cm^2 and a nominal molecular-weight cut-off of 10^4. Before use the hollow fibres were soaked in dilute nitric acid (pH ~ 2) and then rinsed with several litres of distilled demineralized water. The blank values demonstrated this to be a proper washing procedure. The membrane was first conditioned by passage of 1 litre of distilled demineralized water and then 250 ml of the sample. Portions of the filtrate (250 ml) were transferred to individual containers.

Table 2. Particle sizes estimated from experimental conditions

Centrifugation time, *sec*	Rotation speed, *rad/min*	Particle density, g/cm^3	Particle diameter, μm	RCF*, g
83†	1.00×10^4	1.2	0.6	1.10×10^4
		1.5	0.4	
		2.5	0.2	
2387	1.40×10^4	1.2	0.1	2.50×10^4
		1.5	0.07	
		2.5	0.04	

*Relative centrifugation force. According to DIMON/IEC specification.
†Corrected for acceleration and retardation of the centrifuge.

Methods of elemental analysis

To obtain information on a large number of elements, the original and fractionated samples were analysed by 3 different laboratories, using instrumental neutron-activation analysis (INAA), atomic-absorption spectrometry (AAS), and inductively-coupled plasma atomic-emission spectrometry (ICP).

When INAA was used, the samples were stored in heat-sealed ampoules (prewashed: quartz in 1:1 v/v mixture of concentrated nitric and hydrochloric acids; polyethylene in 1:1 v/v mixture of concentrated nitric acid and demineralized water) to be irradiated. No conservation was needed as species sorbed on the walls were washed out with nitric acid after irradiation. When the other methods were employed the samples were acidified to pH 1 with concentrated nitric acid and kept in polyethylene or glass bottles prewashed with a 1:1 v/v mixture of concentrated nitric acid and demineralized water, according to the Norwegian Standard.[5]

The INAA method described by Salbu *et al.*[6] was applied, with short (10 min) and long (3 day) irradiation times. An Ortec Ge(Li) detector (efficiency 10%, resolution 2.0 keV, defined by means of the 1332.5-keV gamma radiation from ^{60}Co) and a Canberra Ge(Li) detector (efficiency 20.7% and resolution 1.9 keV, defined as above) were used for measurements of the short and long irradiation samples respectively.

Flame AAS (for Ca, K, Mg, Mn and Na) was done with a Perkin-Elmer 403 instrument and Cd and Zn were determined by graphite furnace AAS with the Perkin-Elmer 460/HGA 400.[7] ICP measurements were performed with a Jarrel Ash 975 ICAP instrument.[8]

The methods used were described earlier.[4]

RESULTS AND DISCUSSION

The concentrations of selected elements in total samples, filtrates, centrifuged fractions and ultrafiltrates are given in Table 3. The elements were selected to illustrate problems that may arise when the different fractionation techniques are applied.

Filtration

When filtration is performed, clogging, sorption

Table 3. Concentration of elements in different lake water fractions

Element	Total	Filtrate (0.4 μm)	Filtrate (AP − 20 + 0.4 μm)	Filtrate (0.45 μm)	Filtrate [0.45 (11) μm]	Centrif. (0.4 μm)	Filtrate (0.1 μm)	Centrif. (0.07 μm)	Ultrafilt. (M ≤ 10) (~0.005 μm)
(a) Mn, μg/l.	8 ± 1	1	3	4	3	4	4	< 1	4
(b) Al, μg/l.	61 ± 8	30	49	50	30	20	40	20	20
(c) Zn, μg/l.	≤ 5	25	30	37	10	3	30	3	5
(d) Cu, μg/l.	6 ± 1	4	5	5	28	13	5	17	1
(e) Sc, ng/l. (30 m)	18 ± 2	14	n.d.	14	n.d.	14	14	13	6
(f) Sc, ng/l. (5 m)	46 ± 5	18	n.d.	20	n.d.	30	20	20	9

n.d. = not determined.

and systematic or random contamination may seriously affect the results.

Depending on the sample volume, the amount of suspended material and the type of filter membrane, clogging may occur during filtration and reduce the pore size of the membrane, so the flow-rate and the inverse of the linear flow velocity ($1/v$, Fig. 1) will decrease during the filtration. As seen from Fig. 1 the first 50 ml of sample will serve to condition the membrane and should be discarded. For the polycarbonate (Nuclepore) membrane only a small fraction of the filtrate (100–200 ml) can be considered to be well defined and reproducible. With higher loads the filtration rate decreases drastically for the polycarbonate membrane, whereas only a slight lowering is seen for the cellulose acetate (Millipore) membrane. When 500 ml of ground water had been filtered through the Nuclepore membrane, the flow-rate corresponded to that for a 0.1-μm membrane. The Millipore membrane is not so seriously affected as the Nuclepore membrane by clogging and acts more as a depth filter, so a larger volume of filtrate can be considered representative and reproducible.

Clogging reduces the elemental concentrations in the filtrates. This is demonstrated for manganese (Table 3) in lake water (turbidity = 1 FTU), where the low value found for the Nuclepore filtrate may indicate a clogging/sorption effect. When a depth filter was used as a prefilter to the Nuclepore membrane clogging was reduced and the manganese value in the filtrate increased significantly, approaching

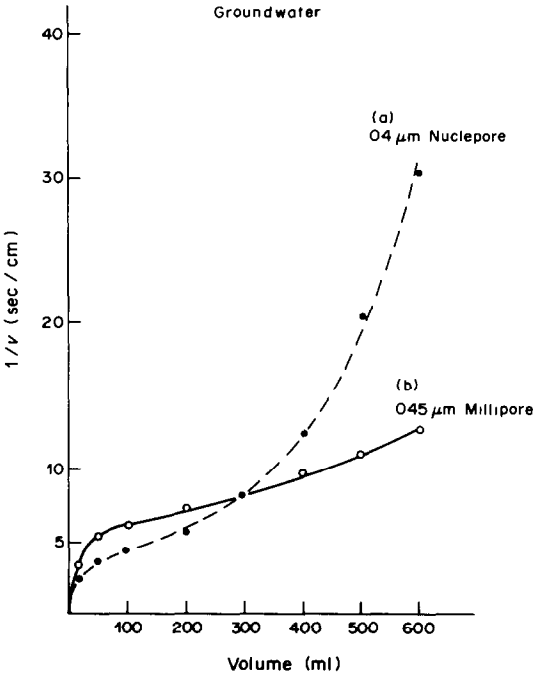

Fig. 1. Changes in filtration speed because of clogging effects when ground water is filtered through (a) a 0.4-μm Nuclepore polycarbonate membrane; (b) a 0.45-μm Millipore cellulose acetate membrane.

that obtained by using the Millipore membrane. When the volume filtered was increased to 1 litre the clogging effect became evident also for 0.45-μm Millipore filters as demonstrated for aluminium (Table 3). This effect was especially significant for multivalent metals.

Surface sorption effects are minimized when part of the sample is used to condition the filter. This has also been indicated by double filtration experiments, with radioactive tracers added to samples of the waters investigated (contact time 28 days). However, when particles are retained on the membranes the sorption of species by the particles and membrane is significantly increased. This is illustrated for instance, for manganese and aluminium (Table 3) where sorption of low molecular-weight forms seems to take place on the Nuclepore and the Millipore membranes, respectively.

During filtration, especially if this is done in the field, contamination is easily introduced even if a proper washing and handling procedure is followed. This is demonstrated for zinc in lake water (Table 3), where the contamination apparent for the filtrates is not observed in the centrifuged fractions or the ultrafiltrate.

Furthermore, random contamination is easily introduced; for example copper (Table 3) was higher in the Millipore filtrates than in the total sample or the Nuclepore filtrate. These results underline the importance of including the determination of the total concentrations in the analytical scheme. If only the filtrates are analysed, contamination (unless fairly severe) may not be detected.

Centrifugation

When centrifugation is performed the results may be affected by the density, aggregation/sorption effects and any contamination introduced. The centrifugation times and rotation speeds were chosen in order to obtain different fractions of the elements. However, during centrifugation small dense particles are sedimented together with larger particles of lower density. Therefore, particles of different densities must be considered when particle sizes are estimated according to Shaw[9] and Marshall[10] from the experimental conditions (Table 2).

The centrifuged fractions in Table 3 are based on an average particle density of 1.5 g/cm^3, as most organic material has lower, and inorganic material higher, particle density.[11] For scandium in lake water, at a depth of 30 m (Table 3), the results obtained for centrifuged fractions and filtrates are in good agreement, whereas for the samples from 5 m depth the amount retained on the membranes is significantly higher than that removed during centrifugation. Thus, an association of scandium with large particles (> 0.45 μm) of low density (< 1.5 g/cm^3) is indicated. Assuming a density of 1.2 g/cm^3, a particle diameter of 0.6 μm is estimated (Table 2). Thus, there should be retention on 0.45-μm membranes. For aluminium in lake water (Table 3) the low value in the centrifuged fraction (0.4 μm) may indicate that the aluminium is associated with inorganic, high-density (> 1.5 g/cm^3) small-sized (< 0.1 μm) particles which are not retained on the filters. However, the calculations imply particles of unrealistic densities even though shape corrections are made. As species such as clay minerals can cohere to one another and/or adhere to the tube wall during centrifugation, a loss of small-sized species in the centrifuged fraction can occur.[11] Sorption experiments where lake- and ground-water samples containing radioactive tracers were stored in the centrifuge tubes illustrated that pure adsorption was insignificant and could not account for the losses observed during centrifugation. For aluminium and manganese (Table 3) the removal of low molecular-weight species during centrifugation is most likely due to this aggregation effect. This effect was especially significant for multivalent metals. During centrifugation contamination was introduced for copper (Table 3) and also for lead, but was not observed for the other elements investigated.

Dialysis

When dialysis *in situ* is used, the results may be

Table 4. Relative standard deviation (r.s.d.%) for dialysis *in situ*

Element	Lake water (Kjellingtjenn) (replicate sampling) (4 × 1 l.)	Lake water (Kjellingtjenn) (dialysis bags) (4 × 100 ml)	Ground water (dialysis bags) (3 × 100 ml)
Na	3	3	6
Mg	3	3	10
Ca	2	3	3
Br	5	7	10
Cr	8	7	12
Fe	10	25	50*
Co	8	7	30
Zn	8	6	8
Sc		5	25
La	9	10	25
Ce	9	7	30

*Contaminated.

affected by clogging effects and contamination introduced during the sampling.

After dialysis *in situ* for 3 weeks in the slow-moving ground water, a coating of inorganic—probably iron—compounds on the external surface of the dialysis membrane was observed by microscopy (K. G. Ormerod, personal communication). This coating reduces the effective pore-size of the membrane, and for one of the four dialysis bags the very low values for several elements indicate that dialysis had been hindered. The results are therefore based on those for only three of the dialysis bags. As illustrated in Table 4, scattered results or high relative standard deviations (r.s.d.) were obtained for dialysable elements in the ground water, whereas the r.s.d. was within 5–10% for most elements in the lake water (Lake Kjellingtjenn). Therefore the coating formed also reduced the precision of this sampling technique. The coating also seemed to introduce contamination with several elements, especially iron, into the dialysate. The concentration of iron in the dialysis bags was about 5 times that found in the ultrafiltered water. Dialysis *in situ* therefore seems less suitable for slow moving ground waters than for lake waters or river waters.[1,2]

Ultrafiltration

When hollow-fibre cartridges are used, as described here, the results may be affected by sorption effects and contamination. Because of the high surface area of the fibre cartridges clogging of the membrane does not significantly affect ultrafiltration even when a 500-ml volume of the ground water is used (Fig. 2). However, the sorption of species by the membrane may be substantial owing to the large surface area available, even though the membrane is made of inert, non-ionic polymers. The sorption of radioactive tracers (added to already ultrafiltered ground water 10 days before the test ultrafiltration) as a function of volume filtered, is illustrated in Fig. 2. The first 250-ml fraction of ultrafiltrate serves for conditioning; afterwards less than 1% of $^{65}Zn(II)$, about 5% of $^{51}Cr(III)$, and about 15% of $^{51}Cr(VI)$ are retained by the membrane. Thus, anions seem to be more prone than cations to sorption effects when these cartridges are used. When the results obtained from hollow-fibre ultrafiltration are compared with those from dialysis *in situ* (Lake Kjellingtjenn) the concentration ratios for ultrafiltrate relative to dialysate for the elements investigated was about 1 for alkali-metal, alkaline-earth metal and halide ions and somewhat higher for trace metals which to a certain extent are associated with colloidal material. Thus, deformable species may penetrate the hollow-fibre membrane owing to the applied pressure (5 psi).

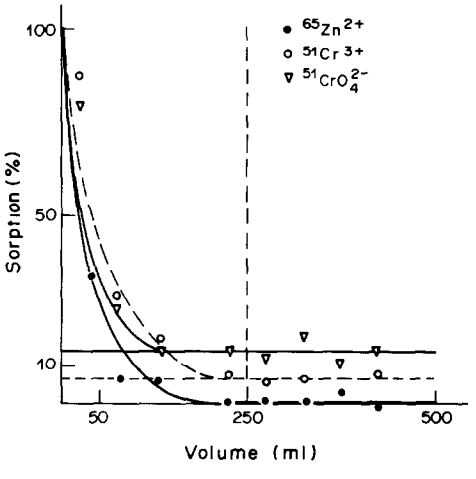

Fig. 2. Sorption of Zn(II), Cr(III) and Cr(VI) on an Amicon Hl P10-8 hollow fibre cartridge.

Neither contamination with the elements investigated nor leaching of organic constituents from the membrane could be detected after conditioning.

Distribution of elements as a function of particle size

The fractions (%) of 20 elements associated with the particulate material (> 0.45 μm), colloidal material in the ranges 0.1–0.45 μm and 0.005–0.1 μm, and low molecular-weight material (M < 10^4 ~ 0.005 μm) in ground water and lake water (Tyrifjorden), as found by the techniques described, are given in Fig. 3. For alkali-metal, alkaline-earth metal and halide ions there is good agreement between the results obtained by the different techniques.

Scattered results, especially for the multivalent trace metals, could be attributed to clogging of the polycarbonate (Nuclepore) membrane during filtration or to aggregation of small-sized species during centrifugation. In these cases, the results obtained by using the Millipore filters seem less affected by methodological effects, but contamination seems to be somewhat more easily introduced.

The fraction of elements present in low molecular-weight forms was determined from hollow fibre ultrafiltration, as a coating was formed during dialysis *in situ* sampling in ground water. Figure 3 shows that the fraction of elements associated with particulate material is high for the high-turbidity ground water, and the low molecular-weight fraction is high in the lake water containing organic material. Furthermore, the results show that colloids may contribute substantially to the transport of trace metals in natural aquatic systems. The low molecular-weight fractions (M < 10^4) in Lake Kjellingtjenn are similar to those of Lake Tyrifjorden except for Al (70% and 40%, in Lakes Kjellingtjenn and Tyrifjorden respectively), Ce (60% and 40%), Co (90% and 70%), Fe (30% and < 1%) and Zn (80% and 10%). Thus a higher fraction of mobile species seems to be present during winter stagnation than in an algal growth period.

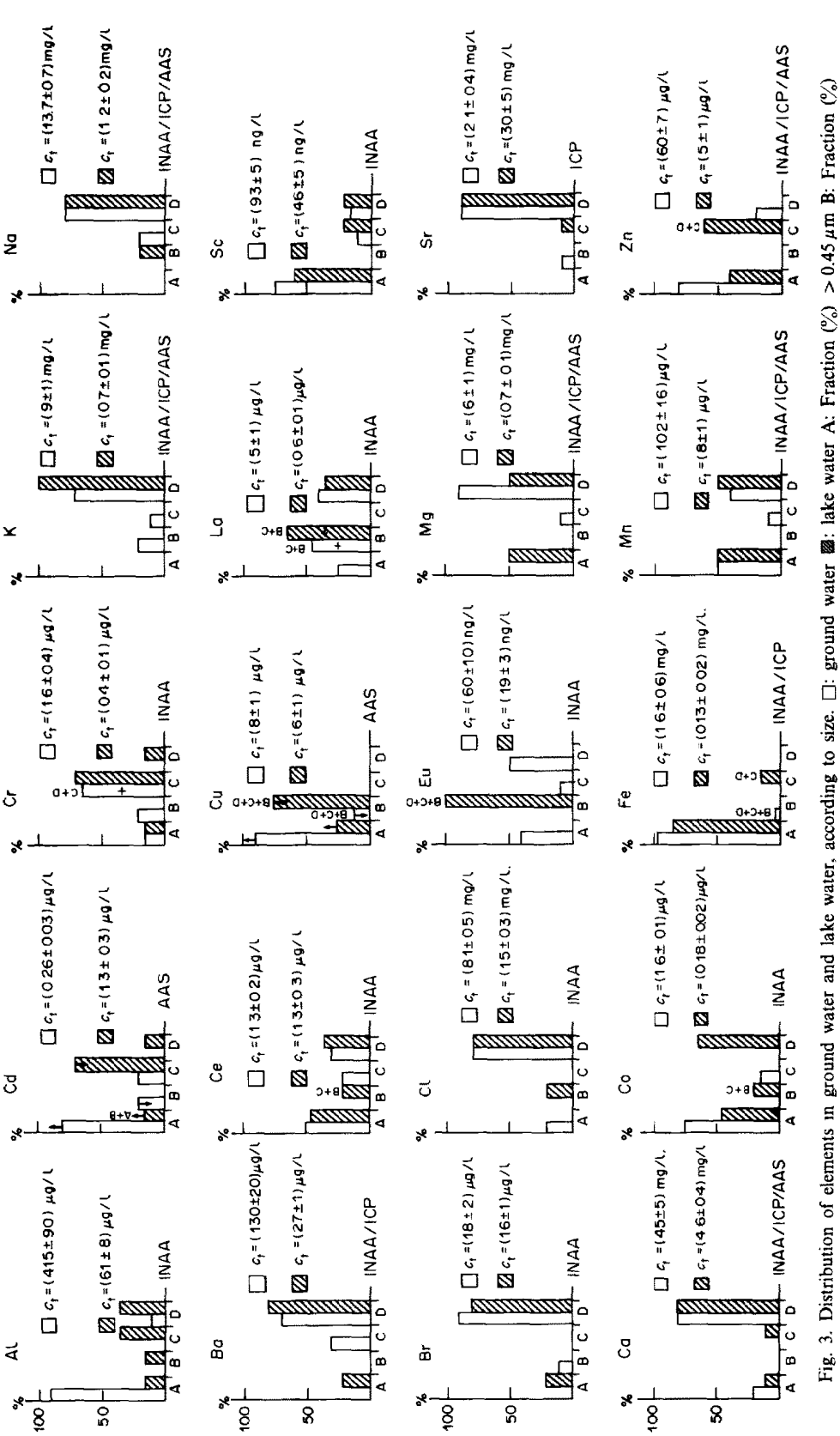

Fig. 3. Distribution of elements in ground water and lake water, according to size. □: ground water ▨: lake water A: Fraction (%) > 0.45 μm B: Fraction (%) 0.1–0.45 μm C: Fraction (%) 0.005–0.1 μm D: Fraction (%) < 0.005 μm.

CONCLUSION

The present work demonstrates that in studies of the distribution of elements according to size, a combination of different fractionation techniques and methods of analysis allows valuable information on several elements to be obtained, as methodological effects can then be accounted for. It also shows that the colloidal fraction can contribute significantly to the transport of trace metals in natural waters.

Acknowledgement—The authors wish to thank K. F. Meyer, Agricultural University of Norway, for assistance during sampling, and Professor A. C. Pappas, University of Oslo, for valuable discussions. B. Salbu expresses her appreciation to the Norwegian Research Council for Science and the Humanities for grants provided. The authors are also indebted to the Royal Norwegian Research Council for Scientific Technology for financial support to this project.

REFERENCES

1. P. Beneš and E. Steinnes, *Wat. Res.*, 1974, **8**, 947.
2. P. Beneš, E. Gjessing and E. Steinnes, *ibid.*, 1976, **10**, 711.
3. B. Salbu, *Michrochim. Acta*, 1981 **II**, 351.
4. B. Salbu, H. E. Bjørnstad, N. S. Lindstrøm, E. M. Brevik, J. P. Rambaek, J. O. Englund, K. F. Meyer, H. Hovind, P. E. Paus, B. Enger and E. Bjerkelund, *Anal. Chim. Acta*, 1985, **167**, 161.
5. Norwegian Standard Association, *Selected Norwegian Standards, Water Analysis*, 1980.
6. B. Salbu, E. Steinnes and A. C. Pappas, *Anal. Chem.*, 1975, **47**, 1011.
7. W. J. Price (ed.), *Spectrochemical Analysis by Atomic Absorption*, Heyden, London, 1979.
8. R. M. Barnes (ed.) *Application of Plasma Emission Spectrochemistry*, Heyden, Philadelphia, 1979.
9. D. J. Shaw (ed.), *Introduction to Colloid and Surface Chemistry*, Butterworths, Liverpool, 1966.
10. C. E. Marshall, *Proc. Roy. Soc.*, 1930, **126A**, 427.
11. W. T. Lammers, *Report* K-1749, Union Carbide Corp., Oak Ridge, 1968.

Talanta, Vol. 32, No. 9, pp. 915–920, 1985
Printed in Great Britain.

0039-9140/85 $3.00 + 0.00

EXTRACTIVE FLUORIMETRIC DETERMINATION OF ULTRATRACES OF LEAD WITH CRYPTAND 2.2.2 AND EOSIN

D. BLANCO GOMIS, E. FUENTE ALONSO and A. SANZ-MEDEL
Departamento de Química Analítica, Facultad de Química, Universidad de Oviedo, Oviedo, Spain

(*Received* 11 *February* 1985. *Accepted* 28 *March* 1985)

Summary—A new spectrofluorimetric method for determination of ultratraces of lead is based on solvent extraction into chloroform of the ion-pair formed between the positively-charged cryptate of lead with cryptand 2.2.2 and the eosinate anion. The detection limit for lead is 1 ng/ml, and the linear working range is from the detection limit to 250 ng/ml. The relative standard deviation is 3.7% at the 100 ng/ml level. The method is highly selective for the extraction and determination of lead in the presence of other cations, and has been tested for direct determination of lead contamination in soft drinks. Aggregation of the extracted ion-pair in the organic phase has been demonstrated in fundamental extraction studies.

Macrocyclic ligands have been of considerable analytical interest in recent years because of their ability to form remarkably stable and selective complexes with a number of metal cations, particularly with alkali-metal, alkaline-earth metal and toxic heavy metal cations. These macrocyclic ligands, which are neutral compounds, form cationic complexes with metal cations. One of the most fruitful analytical approaches for the determination of metals with macrocyclic ligands is extraction of the cationic complexes into a suitable organic phase as ion-pairs with bulky hydrophobic anions. Anionic dyes of the fluorescein series have proved to be excellent counter-ions; ion-association ternary complexes[1] are formed.

We recently reported a new sensitive and selective fluorimetric determination of lead with 18-crown-6 and eosin.[2] The lead complex of the crown ether was extracted at pH 8.5 into dichloromethane by forming an extractable ion-association species with the fluorescent eosinate anion.

It is well known that bicyclic ligands usually form complexes of higher stability, and have higher metal-ion selectivity, than monocyclic ligands. Thus, a bicyclic ligand such as 2.2.2 should be superior to 18-crown-6 for lead complexation because the cryptate complex is much more stable (log $\beta_{2\,2\,2\text{-Pb}} = 12.72$)[3] than that with the monocyclic ligand (log $\beta_{18\text{-C-6-Pb}} = 4.27$).[4] Also, better selectivity (as expressed by the logarithm of the ratio of the corresponding stability constants, $\Delta \log \beta_{ML^{n+}}$) relative to the alkali-metal, alkaline-earth metal and other cations frequently associated with lead, should be expected (except for the mercury cation, as shown by the values of the stability constants of the binary complexes).[3,4]

Extraction can sometimes further improve this selectivity: for instance we have established in preliminary investigations that the mercury cryptate is not extracted under the same experimental conditions as lead. In other words, although the stability constant of the Hg binary complex is very high, the extent of its interference depends also on the nature of the solvent and the type of counter-ion used.

If an appropriate extraction of such cryptate complexes were found, a new more selective and convenient method for the determination of ultratraces of lead could be developed. Szczepaniac *et al.*[5] have already reported a spectrophotometric determination of lead with cryptand 2.2.2, but to our knowledge, no fluorimetric determination of lead with use of macrobicyclic compounds has yet been reported.

Therefore, a detailed investigation of the extraction of the cryptand 2.2.2–Pb^{2+} complex with different fluorescent counter-ions and organic solvents was undertaken. As a result, a new and very useful fluorimetric determination of lead is reported here. Some fundamental extraction studies on the nature of the species extracted into chloroform were made, and the analytical method was tested for the determination of lead in soft drinks.

EXPERIMENTAL

Apparatus

Fluorescence intensity measurements were made with a Perkin–Elmer MPF-44A spectrofluorimeter; 2 nm bandwidths were used in both the excitation and emission systems. The pH of the aqueous phases was measured with a Weilheim WTW-D812 pH-meter.

Reagents

All reagents were of analytical grade, and doubly distilled demineralized water was used throughout.

Cryptand 2.2.2. The commercial product (Merck) was used as received. An aqueous stock solution ($1.7 \times 10^{-4} M$) of the cryptand was stored in a PVC container and was diluted as required before use.

Pb(II) stock solution (1000 ppm). Prepared by dissolving 1.598 g of lead nitrate in water, and diluting to 1 litre. Standardized gravimetrically by precipitation of lead sulphate. Dilute standard lead solutions were freshly prepared by dilution of this stock solution.

Eosin solution 3.4×10^{-4}M. An aqueous solution of the disodium salt (as received from Merck) was prepared daily to avoid possible dimerization of the dye.

Buffer solution (pH 8.3). Prepared by dissolving 121 g of tris(hydroxymethyl)aminomethane in about 800 ml of doubly distilled demineralized water. The pH of the solution was brought to the required value with hydrochloric acid, and use of a pH-meter. This solution was finally diluted to 1 litre with water.

Chloroform. Merck "Uvasol" grade for fluorimetry.

General procedure

Transfer into 50-ml separating funnels or centrifuge tubes known volumes of standard lead solution (containing up to 1.25 μg of Pb). To each funnel or tube add 0.3 ml of the cryptand 2.2.2 stock solution, 1 ml of buffer solution, 0.2 ml of eosin solution, and dilute to 5 ml with doubly distilled demineralized water (final pH 8.3 ± 0.1). After mixing, add 5 ml of chloroform (previously equilibrated with lead-free buffered aqueous phase) and extract the complex by shaking for 5 min. Measure the fluorescence intensity, I_F, of the organic phase at 552 nm (excitation wavelength 536 nm) against a reagent blank. Keep the temperature constant throughout.

Soak all glassware in nitric acid after conventional cleaning, and finally wash it with doubly distilled demineralized water. This cleaning procedure is essential for obtaining reproducible results when solutions of low lead concentration are handled.

Recommended procedure for the determination of lead in soft drinks

Pipette 2.5 ml of the sample into a 50-ml separating funnel or centrifuge tube, add the cryptand 2.2.2 solution and the other reagents as described for the general procedure. For carbonated drinks decarbonate the sample before analysis, by shaking.

RESULTS AND DISCUSSION

Preliminary investigations

Various acidic fluorescent dyes of the fluorescein group, including fluorescein, dichlorofluorescein, tetrabromofluorescein (eosin), tetraiodofluorescein (erythrosin) and tetrachlorotetraiodofluorescein (Rose Bengal) were studied as counter-ions for extraction of the cryptand 2.2.2–Pb^{2+} complex over a wide range of pH values. The results showed that eosin gave the best fluorescence signal. This behaviour agrees with the general rule of extraction of ion-association ternary complexes with fluorescein dyes; the degree of extraction increases with increase in halogenation, and with increase in the atomic number of the halogen substituent, but the quantum efficiency of fluorescence decreases at the same time, due to a "heavy atom" effect.[6] Probably because it represents a compromise between these two opposite effects, eosin proved to be the best counter-ion for the extraction of the lead–2.2.2 cryptate and the best reagent for the fluorimetric determination of the metal.

Benzene, chlorobenzene, dichloromethane, 1,2-dichloroethane, carbon tetrachloride and chloroform were tested as solvents for the extraction of the eosin complex. The corrected fluorescence intensities for 1 μg of lead in these solvents decreased in the order chloroform > 1,2-dichloroethane > dichloromethane. No fluorescence was observed when benzene, chlorobenzene or carbon tetrachloride was used. Therefore, eosin was selected as counter-ion, and chloroform as the organic solvent.

Excitation and fluorescence spectra

The excitation and emission spectra of the blank and the lead complex extracted into chloroform from an aqueous medium at pH 8.3 are shown in Fig. 1. The excitation spectrum has a maximum at 536 nm and the emission maximum is at 552 nm. A spectral band-pass of 2 nm was used for both excitation and emission. The spectra were not corrected for variations in the emission characteristics of the lamp nor for the response characteristics of the photomultiplier.

Effect of pH

The ion-pair extraction of the lead–cryptand complex has a complicated pH-dependence, because of

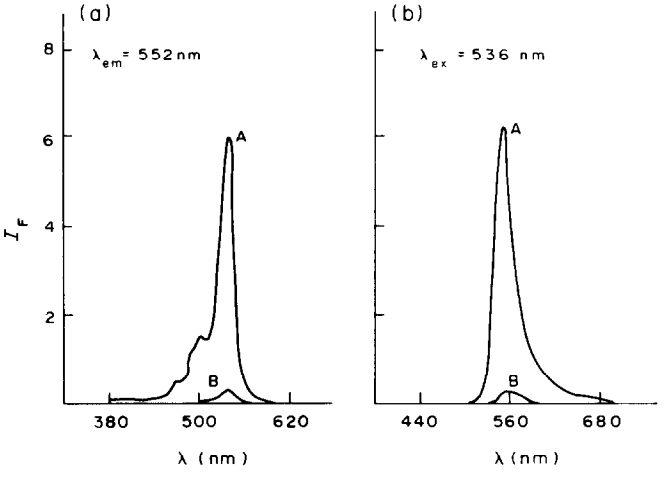

Fig. 1. Excitation (a) and emission (b) spectra of blank (B) and ion–association lead complex (A); I_F in arbitrary units.

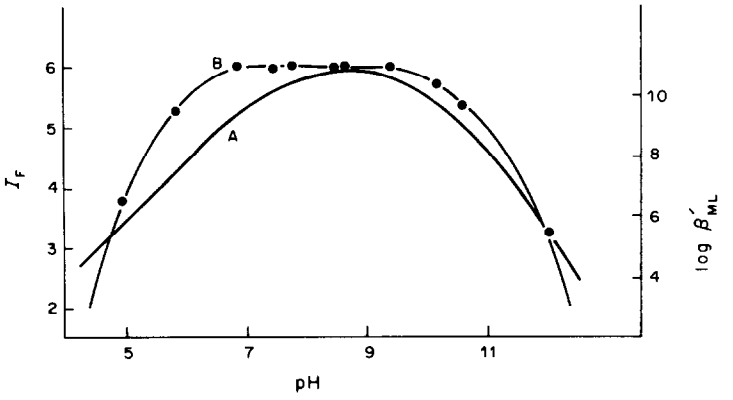

Fig. 2. (A) Variation of the conditional stability constant of the lead–cryptate complex with pH. (B) Variation of the fluorescence intensity of the lead ion-association complex (0.35 μg/ml Pb) with pH; I_F in arbitrary units.

the basic nature of the cryptands, the dissociation of eosin and the hydrolysis of the lead cation.

Figure 2, curve A, shows the pH-dependence of the conditional stability constant of the lead–cryptate complex in aqueous solution, as computed from the stability constant of the complex cryptand 2.2.2–Pb^{2+},[3] the pK_a values[7] of the mono- and biprotonated cryptand 2.2.2 and the stability constants of lead with hydroxide ions.[8] From the values of the conditional constant, and the actual reagent concentrations used, it can be calculated that the formation of the binary complex in the aqueous phase is quantitative between pH 6.5 and 11. The actual influence of pH on the extraction process was studied by measuring the fluorescence intensity due to 0.35 μg/ml of lead in test solutions corrected for the corresponding blanks, for the pH range 5–12 (adjusted by addition of acetic acid or tetramethylammonium hydroxide).

Figure 2, curve B, shows that maximum fluorescence was obtained for extractions between pH 6.8 and 9.5. This is in accordance with formation of the doubly charged eosinate anion at pH 5–6.[9] For subsequent studies, the pH was fixed at 8.3 by addition of tris(hydroxymethyl)aminomethane buffer.

Reagent concentrations

The influence of the concentrations of cryptand 2.2.2 and eosin on the fluorescence signal of the extracted ion-pair into chloroform was studied for two fixed amounts of lead (0.5 μg and 1.75 μg) and a single extraction step. The results (Fig. 3) show that the fluorescence signal becomes constant at a cryp-

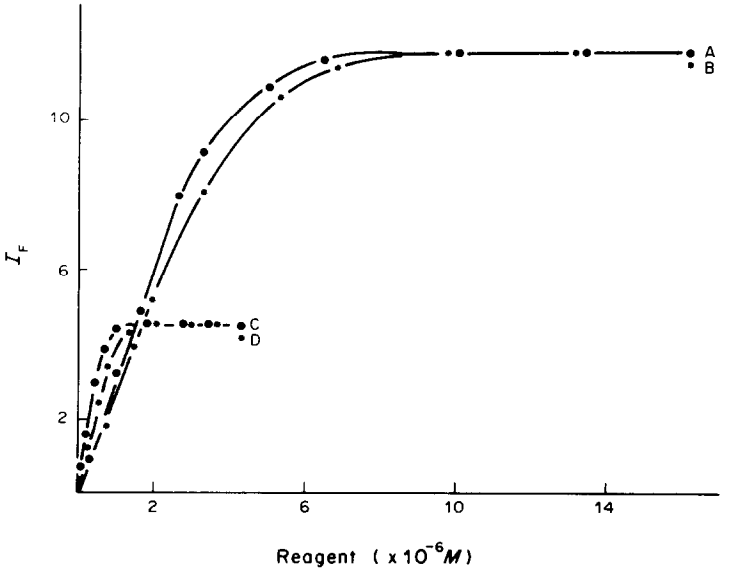

Fig. 3. Influence of the concentrations of cryptand 2.2.2 (A and C) and eosin (B and D) on fluorescence intensity. (A) $c_{Pb} = 1.69 \times 10^{-6}M$, $c_{eosin} = 2.03 \times 10^{-5}M$, c_L varied. (B) $c_{Pb} = 1.69 \times 10^{-6}M$, $c_L = 1.35 \times 10^{-5}M$, c_{eosin} varied. (C) $c_{Pb} = 4.76 \times 10^{-7}M$, $c_{eosin} = 2.03 \times 10^{-5}M$, c_L varied. (D) $c_{Pb} = 4.76 \times 10^{-7}M$, $c_L = 1.35 \times 10^{-5}M$, c_{eosin} varied. I_F in arbitrary units.

tand 2.2.2:lead molar ratio of about 3:1 (for a fixed eosin concentration of $2.03 \times 10^{-5}M$). With eosin, a maximum constant signal was observed for an eosin: lead molar ratio of about 4:1 (for a fixed cryptand 2.2.2 concentration of $1.35 \times 10^{-5}M$). Thus, with use of cryptand 2.2.2, the reagent excesses required are much smaller than those necessary for use of 18-crown-6.[2]

Rate of extraction and stability of the extract

Maximum constant extraction (fluorescence) was obtained after a shaking time of 1 min, and the green fluorescence produced in the chloroform layer remained constant for at least 18 hr. As observed with the 18-crown-6 method,[2] the order of addition of the reagents is unimportant, provided that the cryptand is added before pH adjustment. Increase of the ionic strength from 0.004 to $1.0M$ with the buffer solution and sodium chloride had no noticeable effect.

The temperature of the solutions was $20 \pm 5°$; no significant variation of I_F with temperature in this range was noted.

Calibration, limit of detection, recovery and precision

A linear relationship was observed between I_F and concentration of lead from the detection limit up to 250 ng/ml of lead. The limit of detection (evaluated as twice the standard deviation of the blank value) was 1 ng/ml.

ICP emission measurements were used to determine the amount of lead extracted, with five independent samples and blanks. The recovery of lead in a single extraction was found to be $97.8 \pm 2.4\%$. When 0.5 μg of lead was determined, the relative standard deviation for eleven replicate determinations was 3.7%.

Selectivity

Potential interferences by metals which form stable complexes with cryptand 2.2.2 (*e.g.*, alkali and alkaline-earth metals) and by some metals commonly associated with lead are shown in Table 1. The alkali-metal and alkaline-earth metal ions were tested at up to 1000-fold molar ratio to lead; for sodium and potassium, much higher concentrations were tested. For other potential interferents, a 500-fold molar ratio was first tested.

When ions were found to interfere at these levels (change in I_F for 0.4 μg of lead greater than $\pm 8\%$[2]) they were tested with lower concentrations.

As shown in Table 1, the alkali metals do not interfere. Indeed, sodium and potassium do not interfere at 2×10^6 molar ratio to lead.

Among the cations tested, only strontium interfered seriously in the determination of lead. Calcium and iron could be tolerated at the 100- and 200-fold levels respectively. The interference of strontium and of high levels of calcium could be eliminated by increasing the ionic strength of the aqueous phase.

The dramatic effect of the ionic strength of the aqueous phase in the extraction of alkaline-earth metals with 2.2.2 and eosin was studied in detail for the extraction of strontium. Figure 4 shows that the fluorescence intensity of the strontium ion-association complex (and correspondingly of the extraction[10]) decreases with ionic strength, and becomes virtually negligible at ionic strengths above $0.5M$. Measurements of the stability constant ($\beta_{LPb^{2+}}$) and of the ion-association extraction constant of the binary complex with eosin ($P_{cT} = [LM^{2+}E^{2-}]_0/[LM^{2+}][E^{2-}]$) tend to indicate that it is the ion-pairing that is influenced by ionic strength, rather than secondary

Table 1. Effects of metal ions on the determination of 0.4 μg of lead

Cation	M:Pb (molar ratio)	Apparent recovery, %
Li^+	1000	103.0
Na^+	1000	100.0
K^+	1000	100.0
Cs^+	1000	95.1
NH_4^+	1000	108.0
Tl^+	1000	95.1
Ag^+	1000	98.7
Mg^{2+}	1000	102.5
Ca^{2+}	200	128.0
	100	105.0
Sr^{2+}	5	152.0
	1	119.4
	0.5	95.7
Ba^{2+}	1000	104.0
Cu^{2+}	500	105.4
Cd^{2+}	500	105.4
Hg^{2+}	500	104.8
Ni^{2+}	500	105.5
Zn^{2+}	500	101.0
Co^{2+}	500	100.0
Al^{3+}	500	102.7
Cr^{3+}	500	104.1
La^{3+}	500	100.0
Fe^{3+}	500	84.4
	200	92.7

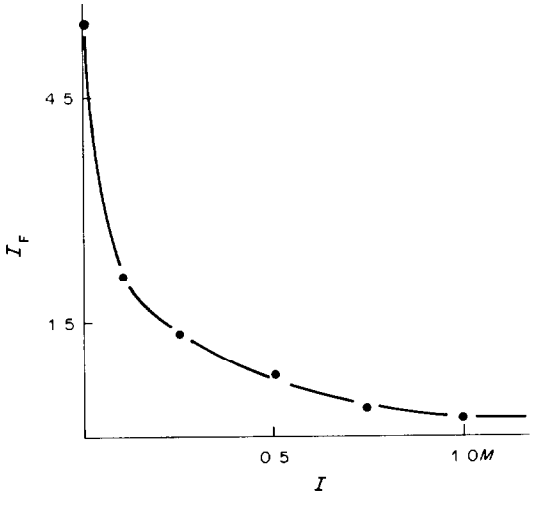

Fig. 4. Influence of ionic strength ($NaClO_4$) on the fluorescence intensity; pH = 11.5, $c_{Sr} = 1.1 \times 10^{-6}M$, $c_L = 1.01 \times 10^{-5}M$, $c_{eosin} = 2.03 \times 10^{-5}M$. I_F in arbitrary units.

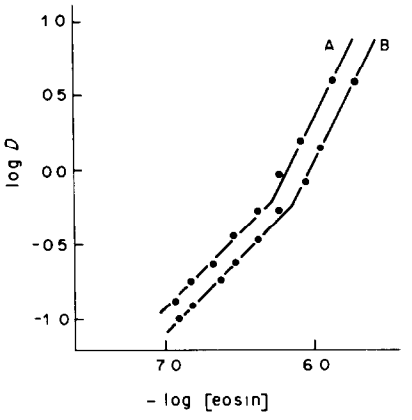

Fig. 5. Dependence of the distribution ratio for lead on the eosin concentration in the aqueous phase. (A) $c_{Pb} = 7.25 \times 10^{-5}M$, $c_L = 9.66 \times 10^{-5}M$, $c_{eosin} = (4.06–72.5) \times 10^{-6}M$; (B) $c_{Pb} = 9.66 \times 10^{-5}M$, $c_L = 9.66 \times 10^{-5}M$, $c_{eosin} = (9.66–172) \times 10^{-6}M$.

complex-formation reactions with the salt or the stability constant of the LPb^{2+} complex. This behaviour is different from that reported by Szczepaniak[5] in the spectrophotometric determination of lead with 2.2.2 and eosin by extraction into chlorobenzene. There, strontium interfered seriously in a manner which appeared to be independent of the ionic strength (see Fig. 3 in reference 5). In 1.0*M* sodium chloride, calcium (at molar ratio to lead of up to 10^4) and strontium (up to 25) can be tolerated. The slight depressive effect of Fe^{3+} observed here is probably due to the relatively high working pH, favouring the precipitation of hydrous ferric oxide, which would hinder the formation and extraction of the lead complex.[2] The iron interference is much reduced when 2.2.2 is used rather than 18-crown-6.[2] In fact there is improved selectivity for most metals.

The common anions fluoride, chloride, nitrate, sulphate and phosphate had negligible effect, even for amounts above 10^5 times that of the lead. Thus, the method proposed here is not only more sensitive for lead determination than previous methods based on macrocyclic[2] or macrobicylic[5] compounds, but also it is clearly superior to both in terms of selectivity.

Stoichiometry of the extracted complex

The crystal and molecular structures of the lead cryptate complex were determined by X-ray crystallography. The lead–cryptand ratio was 1:1, with lead occupying a central position in the cavity of the macrobicyclic ligand.[11] The dissociation constants of eosin[9] and the pH value of 8.3 used suggest that only a neutral complex (1:1:1, lead:cryptand:eosin) should be extracted.

Figure 5 shows the dependence of the distribution ratio of lead on eosin concentration. The lead concentrations for the two sets of experiments (total lead 15 and 20 μg/ml) were determined in the organic and aqueous layers by ICP emission photometry. Eosin equilibrium concentrations were measured in the aqueous layer spectrophotometrically at 516 nm and/or fluorimetrically at 535 nm (excitation wavelength 509 nm). The results obtained showed the same trends as observed previously for the system Pb^{2+}–18-crown-6–eosin,[2] in spite of the different ligands and concentration levels used. The displacement of the extraction curves for different lead concentrations indicates that polynuclear complexes are formed. The change in the slope at higher eosin concentrations is attributed (as with 18-crown-6) to aggregation processes in the organic phase.[12,13]

The distribution coefficient (D) for the extraction system

$$p\mathrm{Pb}^{2+} + q\mathrm{L} + r\mathrm{E}^{2-} \rightleftharpoons (\mathrm{Pb}_p\mathrm{L}_q\mathrm{E}_r)_o$$

is given by

$$D = \frac{\Sigma\,[\mathrm{Pb}^{2+}]_o}{\Sigma\,[\mathrm{Pb}^{2+}]} = \frac{\sum_1^{p,q,r} pK_{ex}[\mathrm{Pb}^{2+}]^p[\mathrm{L}]^q[\mathrm{E}^{2-}]^r}{[\mathrm{Pb}^{2+}] + [\mathrm{PbL}^{2+}] + \sum_1^{i,j}[\mathrm{Pb}_j(\mathrm{OH})_i^{2j-i}]}$$

$$= \frac{\sum_1^{p,q,r} pK_{ex}[\mathrm{Pb}^{2+}]^p[\mathrm{L}]^q[\mathrm{E}^{2-}]^r}{[\mathrm{Pb}^{2+}](1 + \beta_{ML}[\mathrm{L}] + \sum_1^{i,q} j\beta_{j,i}^{OH}[\mathrm{Pb}^{2+}]^{j-1}[\mathrm{OH}^-]^i)} \quad (1)$$

where Pb^{2+}, L and E^{2-} are the free lead ion, cryptand 2.2.2 and eosinate anion, respectively. The subscript o and the absence of a subscript denote the organic and aqueous phase respectively.

If the conditional distribution coefficient is $D' = D\alpha$, where $\alpha = (\Sigma[\mathrm{Pb}^{2+}])/[\mathrm{Pb}^{2+}]$, then

$$D' = (\Sigma[\mathrm{Pb}^{2+}]_o)/[\mathrm{Pb}^{2+}] \quad (2)$$

where $[Pb^{2+}]$ is the concentration of free lead in the aqueous phase. Then, from equations (1) and (2)

$$D' = \sum_1^{p,q,r} pK_{ex}[\mathrm{Pb}^{2+}]^{p-1}[\mathrm{L}]^q[\mathrm{E}^{2-}]^r.$$

Experimental plots of log D' *vs.* log$[E^{2-}]$ again show a clear displacement of the extraction curves for different lead concentrations (Fig. 6), indicating formation of polynuclear complexes. The slopes of the graphs (equal to 1) for free eosin indicate that the lead ion forms $(1:1:1)_n$ (lead:cryptand 2.2.2:eosin)$_n$ complexes. (Determination of total concentration of Pb^{2+} and eosin actually present in the organic phase confirmed that in all cases the molar ratio of lead to eosin was 1:1.)

Thus, here

$$D' = \sum_1^n n\,K_{ex,n}[\mathrm{Pb}^{2+}]^{n-1}[\mathrm{L}]^n[\mathrm{E}^{2-}]^n$$

If only a single species is present then

$$D' = n\,K_{ex,n}[\mathrm{Pb}^{2+}]^{n-1}[\mathrm{L}]^n[\mathrm{E}^{2-}]^n$$

or

$$\log\frac{D'}{[\mathrm{Pb}^{2+}]^{n-1}[L]^n} - n\log[\mathrm{E}^{2-}] = \log n\,K_{ex,n}$$

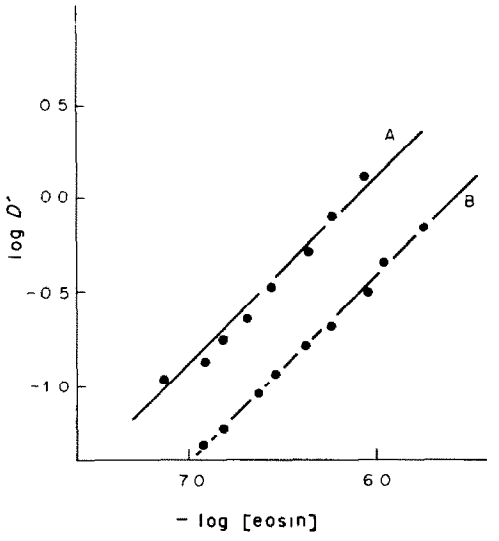

Fig. 6. Dependence of the conditional distribution ratio for lead on the concentration of eosin in the aqueous phase. (A) $c_{Pb} = 7.25 \times 10^{-5}M$, $c_L = 9.66 \times 10^{-5}M$, $c_{eosin} = (4.06–72.5) \times 10^{-6}M$; (B) $c_{Pb} = 9.66 \times 10^{-5}M$, $c_L = 9.66 \times 10^{-5}M$, $c_{eosin} = (9.66–172) \times 10^{-6}M$.

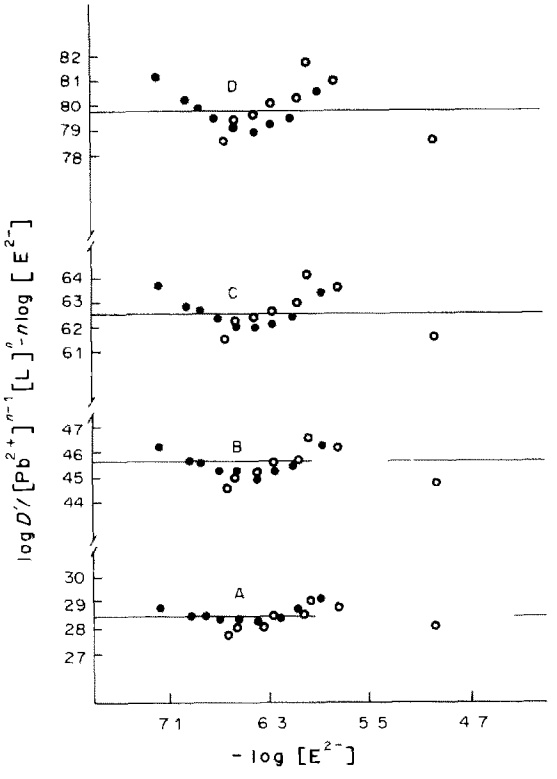

Fig. 7. Dependence of $(\log D'/[Pb^{2+}]^{n-1}[L]^n - n \log [E^{2-}])$ on $\log [E^{2-}]$. (A) $n = 2$; (B) $n = 3$; (C) $n = 4$; (D) $n = 5$. ● $c_{Pb} = 7.25 \times 10^{-5}M$, $c_L = 9.66 \times 10^{-5}M$, $c_{eosin} = (4.06–72.5) \times 10^{-6}M$; ○ $c_{Pb} = 9.66 \times 10^{-5}M$, $c_L = 9.66 \times 10^{-5}M$, $c_{eosin} = (9.66–172) \times 10^{-6}M$.

Table 2. Determination of lead in soft drinks

Sample	Extraction—flame method, μg/l.	Proposed method, μg/l.
Cola drink	43.3 ± 0.7	42.0 ± 1.0
Sweet lime drink	46.7 ± 1.7	43.7 ± 0.7
Apple juice	51.3 ± 1.3	50.3 ± 1.2
Lemon juice	54.7 ± 1.3	47.7 ± 0.3
Orange juice	49.3 ± 1.3	48.3 ± 0.9
Pineapple juice	74.7 ± 1.3	72.3 ± 1.4

Plots of $\log D'/[Pb^{2+}]^{n-1}[L]^n - n \log [E^{2-}]$ *vs.* $\log [E^{2-}]$ for different n values (Fig. 7) showed that the best fit is obtained for $n = 2$. Therefore, it seems that the predominant species in the organic layer is a dimer, although the fitting could be improved if several polymeric species are considered simultaneously.

Determination of lead in soft drinks

The proposed method was used, with no preconcentration step, for determination of lead in various soft drinks, juices and extracts. Table 2 shows that the results are in good agreement with those obtained by the extractive atomic-absorption method (which requires a ten-fold preconcentration with ammonium tetramethylenedithiocarbamate and isobutyl methyl ketone).[14] Therefore, the fluorimetric methods based on macrocyclic compounds seem to be extremely valuable for lead contamination control in water[2] and soft drinks. The method with cryptand 2.2.2 recommended here should be especially useful for ultratrace determinations of lead in a variety of samples (*e.g.*, water, foods, chemicals, alloys, metals) with minimum sample handling.

REFERENCES

1. A. Sanz-Medel, D. Blanco Gomis and J. R. García Alvarez, *Talanta*, 1981, **28**, 425.
2. A. Sanz-Medel, D. Blanco Gomis, E. Fuente and S. Arribas Jimeno, *ibid.*, 1984, **31**, 515.
3. F. Arnaud-Neu, B. Spiess and M. J. Schwing-Weill, *Helv. Chim. Acta*, 1977, **60**, 2633.
4. R. M. Izatt, R. E. Terry, B. L. Haymore, L. D Hansen, N. K. Dalley, A. G. Avondet and J. J. Christensen, *J. Am. Chem. Soc.*, 1976, **98**, 7620.
5. V. Szczepaniac and B. Juskowick, *Anal. Chim. Acta*, 1982, **140**, 261.
6. T. S. West, *Lab. Pract.*, 1965, 927.
7. J. M. Lehn and J. P. Sauvage, *J. Am. Chem. Soc.*, 1975, **97**, 6700.
8. A. Ringbom, *Complexation in Analytical Chemistry*, p. 348 (Spanish translation). Alhambra, Madrid, 1979.
9. N. O. Mchedlov-Petrosyan, L. B. Adanovich and L. E. Nikishima, *Zh. Analit. Khim.*, 1980, **35**, 1495.
10. J. L. Arias Alvarez, *Ph.D. Thesis*, University of Oviedo.
11. B. Metz and R. Weiss, *Inorg. Chem.*, 1974, **13**, 2094.
12. T. Sekine and Y. Hasegawa, *Solvent Extraction Chemistry*, p. 222. Dekker, New York, 1977.
13. W. Müller and R. M. Diamond, *J. Phys. Chem.*, 1966, **70**, 3469.
14. R. K.Roschnik, *Analyst*, 1973, **98**, 596.

Talanta, Vol. 32, No 9, pp 921–925, 1985
Printed in Great Britain.

0039-9140/85 $3.00 + 0.00

ENHANCEMENT OF SENSITIVITY IN ATOMIC-ABSORPTION SPECTROMETRY BY ADDITION OF A GRAPHITE LID TO A CUP FURNACE

KUNIO TAKADA
The Research Institute for Iron, Steel and Other Metals, Tohoku University, Sendai, 980, Japan

(*Received* 18 *February* 1985. *Accepted* 20 *March* 1985)

Summary—By using a cup furnace covered with a graphite lid, it is possible to enhance the atomic-absorption signal for Cd, Zn, Sb, Pb, In, Cu and Fe in solution and for Pb in tin metal (directly atomized). When the analyte is atomized in the cup furnace, part of it condenses on the lid, from which it can be re-evaporated and atomized to give a second absorption signal and hence greater sensitivity. When the lid is small, so that the temperature lag is short, the initial atomic-absorption intensity is also enhanced. The enhancement is due to an increased residence time of the atomized analyte in the cup.

In atomic-absorption spectrometry with an electrothermal graphite furnace, the sensitivity and precision vary with the shape (tube,[1–3] cup,[4] rod,[5] filament,[6] disc[7]) of the furnace. A tube furnace is most commonly used and experiments have been conducted to enhance the sensitivity obtained with this type of furnace. Some increase is obtained by the insertion of a graphite platform,[8] a graphite cup[9] or a graphite fibre ribbon[10] into the tube, or by closing both ends of a tube furnace with graphite lids.[5] The sensitivity obtained with a cup furnace is lower than that with a tube furnace, but the cup has certain advantages, *e.g.*, ease of liquid-sample injection and direct atomization[11–15] of a solid sample without cutting off the excitation beam. Modifications of the cup furnace include the addition of a miniature cup in the bottom of the furnace, as reported by Atsuya,[16,17] and closing the furnace with a lid as described by Siemer *et al.*[5] It was reported recently that when a cup furnace (Hitachi 170-5104) was covered with a graphite lid the scattering intensity from ground-state atoms increased and the influence of the matrix decreased,[18] in coherent forward-scattering spectrometry.

In the present work, the effect of putting a graphite lid on the cup furnace (which was different from Siemer's cup-type carbon furnace) was studied and the experimental results are discussed here.

EXPERIMENTAL

Apparatus

Experiments were performed with a Hitachi 180-80 Zeeman-polarized atomic-absorption spectrometer. The graphite cup furnace (Hitachi 180-7402) and home-made graphite lid (constructed from a Hitachi spectroscopic graphite electrode, diameter 6.15 mm, length 150 mm) are shown in Fig. 1. The thickness (T) of the lid rim was varied and the lid had a central hole. The temperatures of the cup furnace and graphite lid were measured with W5%Re–W26%Re thermocouples (diameter 0.254 mm, length 1 m, Furuya Kinzoku K.K.) at point A on the cup furnace and B on the lid (Fig. 1). The absorption signal was recorded with a Hitachi 056 recorder, and peak areas were measured with a Tokyo Kagaku RD-202 digital integrator. The hollow-cathode lamps used were Hitachi HLA-4s for cadmium (Cd 228.8 nm line, lamp current 7.5 mA), HLA-4 for zinc (Zn 213.8 nm, 7.5 mA), HLA-4s for antimony (Sb 217.6 nm, 10 mA), HLA-4s for lead (Pb 283.3 nm, 7.5 mA), HLA-4s for indium (In 304.0 nm, 10 mA), HLA-4 for copper (Cu 324.8 nm, 7.5 mA) and HLA-3 for iron (Fe 248.3 nm, 10 mA). The sample solutions were injected into the cup furnace with an Eppendorff micropipette (10 μl). The metal samples used for direct atomization were weighed on a Shimadzu LM-20 microbalance.

Standard solutions

An accurately weighed 100-mg portion of the pure metal (Cd, Zn, Pb, In, Cu and Fe, 99.9–99.999%) was dissolved in 8 ml of 3.5M nitric acid and diluted to volume with distilled water in a 100-ml standard flask. A stock solution (Sb 1.00 mg/ml) of antimony was prepared by dissolving 0.2743 g of antimonyl potassium tartrate hemihydrate in 100 ml of distilled water. Standard solutions were prepared by dilution of the stock solutions with distilled water.

Standard metal sample

To determine lead in tin by atomic-absorption spectrometry with direct atomization of the solid sample, a BCS 192f standard tin sample (certified lead value, 3.5 ppm) was used, a 0.1–0.6 mg sample being cut off with a pair of nippers.

Procedure

The cup furnace was set up in a chamber with argon flowing at 3 l./min as the sheath gas. A 10-μl portion of standard solution was placed in the cup furnace, and the carrier gas flow-rate through the furnace was set at 250 ml/min. The sample was dried and ashed, then the heating was interrupted, the cup furnace was closed with the graphite lid, the carrier gas was turned off, and the atomization programme was initiated. When solid samples were atomized directly, the sample was placed in the cup furnace with the carrier gas flowing at 250 ml/min, then the carrier gas was turned off after the lid had been placed on the cup furnace. The heating programme was then initiated. When no lid was used, the heating programme was initiated, with the carrier gas flowing during drying and ashing, but turned off at atomization. All absorbances were calculated from peak area measurements of the absorption signal.

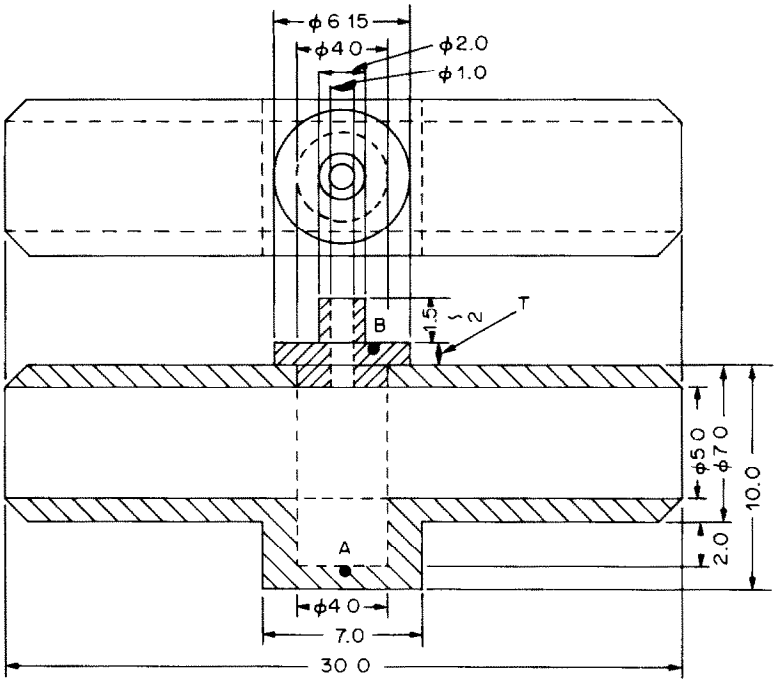

Fig. 1. Graphite cup furnace with graphite lid (dimensions in mm). T, rim thickness; A and B are locations of thermocouples.

Atomization conditions

The relationship between atomization temperature and the peak area obtained for cadmium by use of a cup furnace with and without a graphite lid (rim 1.0 mm thick, hole diameter 1.0 mm) is illustrated in Fig. 2. Drying was done by heating from 60° to 120° in 10 sec and ashing by heating at 200° for 10 sec. The atomization time was varied between 5 and 40 sec, depending on the temperature. As shown in Fig. 2, the peak area observed for cadmium with the lid on the cup was 20–60% larger than that obtained without it. The effect of the lid on enhancement of peak area for cadmium was studied with atomization for 15 sec at 1280°, at which the peak area was large and constant. Optimal atomization temperatures and times for other elements were chosen in a similar manner.

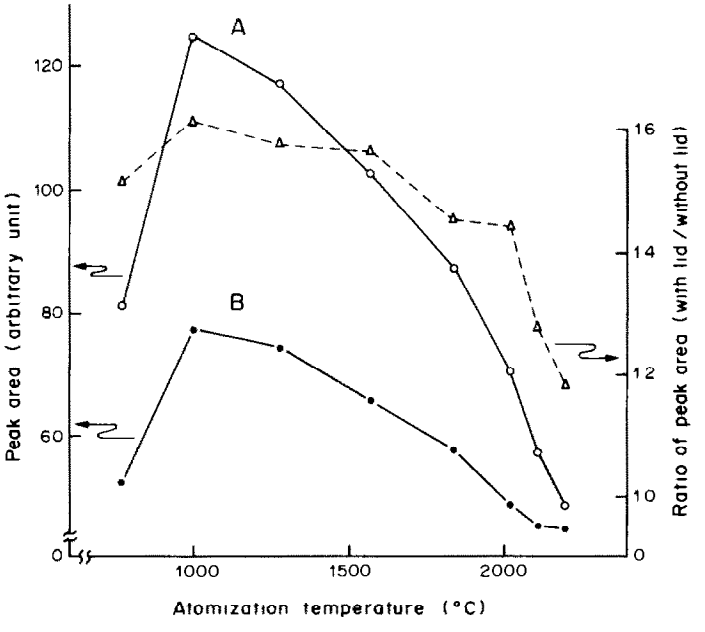

Fig. 2. Effect of atomization temperature on peak area for cadmium (2.51 ng/ml) in cup furnace with and without graphite lid (1.0 mm rim thickness, 1.0 mm hole diameter). A, with lid; B, without lid.

RESULTS AND DISCUSSION

Comparison with atomization in a tube furnace

The peak area observed for cadmium atomized in a cup furnace fitted with a graphite lid (rim 1.0 mm thick, hole diameter 1.0 mm) was 30% greater than that obtained by using a tube furnace. This suggests that the slower temperature rise of the lid, which was heated by radiation from the furnace, contributed to the increase in signal.

Effect of lid rim thickness

Figure 3 shows that as the thickness of the lid increases, the absorption peak becomes divided into two. The appearance times of the absorption maximum for these two peaks as a function of lid rim thickness are given in Fig. 4. The time for the first peak is independent of the rim thickness, indicating that this peak is the signal for cadmium deposited in the cup furnace. This is confirmed by the fact that the appearance time for the first peak maximum is the same as that for the single peak observed when the lid is left off the cup. The appearance of the maximum of the second peak was delayed by a time dependent on the thickness of the lid rim. This phenomenon was interpreted as follows. The temperature of the lid rises more slowly than that of the cup because it is heated by radiation from the furnace. When the first peak appears, the temperature of the lid is low enough to permit condensation of some of the cadmium on its surface. When the temperature of the lid has been raised sufficiently by radiation from the furnace, the condensate is re-evaporated and atomized to give the second peak. As the time taken for this temperature rise becomes longer with increasing thickness of the lid rim, the arrival time of the maximum of the second peak is correspondingly delayed. This interpretation was proved by the following experiment. The atomization was interrupted at the end of the first peak and the lid was then removed from the furnace. Any residual cadmium in the furnace was removed by atomization and a barely perceptible absorption signal was observed. The cup furnace was cleaned and the lid was replaced on the furnace and atomization continued. A single absorption peak was then observed, its appearance time being identical to that of the second peak, as shown by D, E and F in Fig. 3.

Time–temperature curves for the cup furnace and graphite lid are shown in Fig. 5. The temperature of the cup furnace at which the maximum of the first peak appeared and the temperature of the lid at

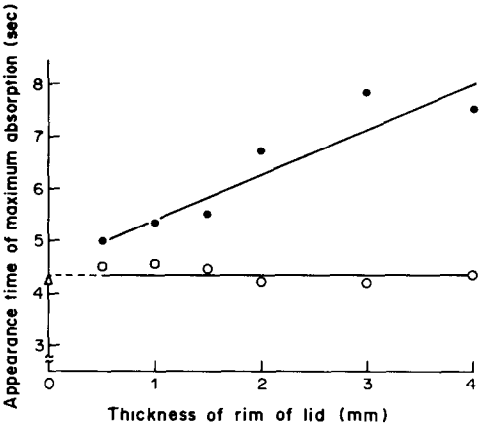

Fig. 4. Effect of lid rim thickness on appearance time of absorption maximum: ○ 1st peak, ● 2nd peak, △ without lid. Hole diameter 1.0 mm. Cd solution 2.51 ng/ml. Atomization temperature 1280°.

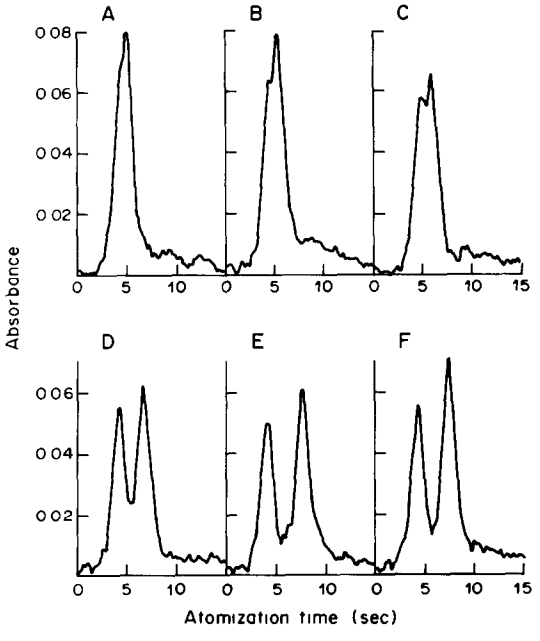

Fig. 3. Profiles of atomic-absorption signals for cadmium (2.51 ng/ml), by use of cup furnace with lids having various rim thicknesses (mm). A, 0.5; B, 1.0; C, 1.5; D, 2.0; E, 3.0; F, 4.0. Hole diameter 1.0 mm. Atomization temperature 1280°.

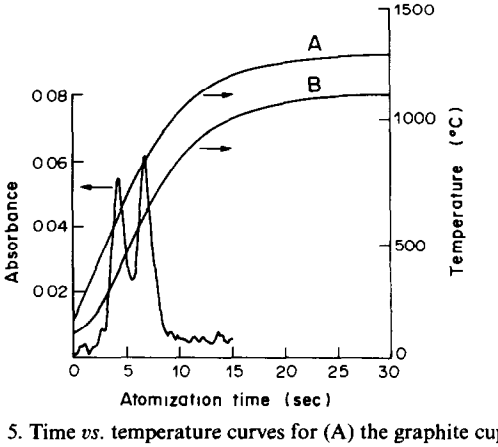

Fig. 5. Time *vs.* temperature curves for (A) the graphite cup furnace and (B) the lid. (Rim thickness 2.0 mm, hole diameter 1.0 mm). Cd solution 2.51 ng/ml.

which the maximum of the second peak appeared were both about 630°. In spite of the increased delay in the appearance of the second peak maximum (as shown in Fig. 4) with increasing thickness of the lid rim, the lid temperature at which the maximum of the second peak appeared was always about 600–630°. Although the shape of the atomic-absorption peaks changed with variation of lid rim thickness (Fig. 3), the peak area remained constant (relative standard deviation 2%) and the total peak areas were 60% greater than those obtained by using a cup furnace without a lid. The peak areas obtained by using a cup furnace with a lid were constant in spite of variation in rim thickness provided that the diameter of the central hole was kept the same. When its rim is thin enough the lid is heated so quickly that the two peaks merge (A in Fig. 3), and any enhancement of sensitivity is then due only to retention of the cadmium vapour within the furnace.

Effect of diameter of the hole

Figure 6 shows the profiles of the absorption peaks obtained by use of lids with different hole sizes. The appearance time of the first peak maximum is practically independent of the size of hole in the lid, but that of the second peak maximum decreases with increase in hole diameter. This is because the rate of temperature rise of the lid increases as the weight of the lid decreases. The area of the second peak decreases as the diameter of the hole is increased because the amount of cadmium condensing on the lid decreases and the retention time of cadmium vapour within the cup furnace is shortened. Therefore, the peak area for cadmium decreased with increasing diameter of the hole (Fig. 7). However, the peak area obtained by using a lid having a hole 3 mm in diameter was still 50% larger than that obtained without the lid.

Enhancement of sensitivity for other elements

The atomic-absorption signals for zinc, antimony, lead, indium, copper and iron were determined for use of a cup furnace with and without a lid (rim 1.0 mm thick, hole diameter 1.0 mm). The increase in peak area obtained when using a lid is shown in Table 1. The absorption signal for lead exhibited a double peak similar to that observed for cadmium, showing that the increase in total peak area was again due to condensation on the lid. The absorption signals for zinc, antimony, indium, copper and iron were in the form of single peaks even when a lid was used, but in each case the appearance time of the maximum was delayed and the peak was wider than that obtained without use of a lid. The increase in sensitivity for these elements was therefore due to prolongation of the retention of atomic vapour in the furnace.

Direct atomization of solid samples

In the examination of tin samples containing lead

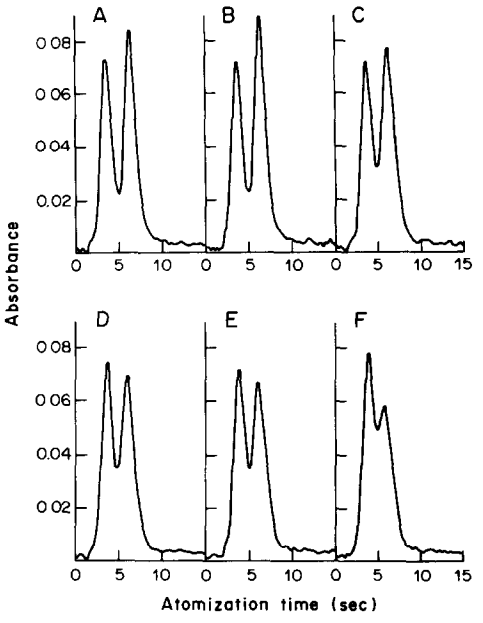

Fig. 6. Profiles of atomic-absorption signals for cadmium, by use of a cup furnace with lids having holes of various diameters (mm). A, 0.5; B, 1.0; C, 1.5; D, 2.0; E, 2.5; F, 3.0. Lid rim thickness 2.0 mm. Cd solution 4.02 ng/ml. Atomization temperature 1280°.

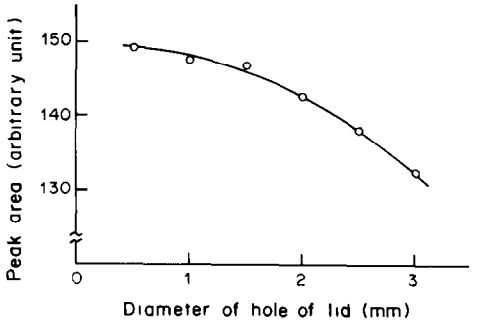

Fig. 7. Relationship between hole diameter (mm) and peak area for cadmium (4.02 ng/ml). Lid rim thickness 2.0 mm. Atomization temperature 1280°.

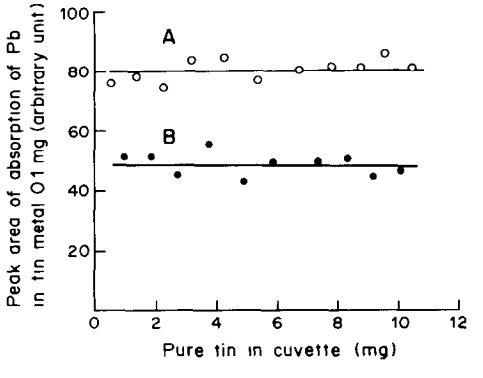

Fig. 8. Peak area for AAS of lead in tin (BCS 192f, Pb 3.5 ppm) by direct atomization of a solid sample in a cup furnace (A) with and (B) without a lid. Lid rim thickness 1.0 mm, hole diameter 1.0 mm. Atomization temperature 1840°.

Table 1. Enhancement of peak area for various elements by use of a cup furnace with graphite lid

Element	Boiling point, °C	Atomization conditions			Linear range of calibration curve, ng	Enhancement factor,§ %
		Drying*	Ashing*	Atomization		
Cd	766	60–120°	200°	1280° 15 sec	0.0025–0.05	50–70
Zn	930	60–120°	200°	1570° 10 sec	0.005–0.1	40–60
Sb	1640	60–120°	200°	2020° 15 sec	2†	50–80
Pb	1750	60–120°	260°	1840° 15 sec	0.05–1.5	40–60
In	2100	60–120°	260°	2110° 10 sec	5†	80–100
Cu	2630	60–120°	400°	2200° 15 sec	0.5–5	10–20
Fe	2730	60–120°	400°	2110° 20 sec	0.25–2	50–60

*For 10 sec.
†Calibration range not tested.
§100 × [(area with lid) − (area without lid)]/(area without lid)

(BCS 192f) by direct atomization, the absorption signal for lead was always in the form of a single peak (with and without use of a lid), but the appearance time of the peak maximum was influenced by the amount of pure tin which remained after atomization of the lead. The appearance time of the absorption signal for lead was increased by use of a lid. The specific area of the peak for lead, *i.e.*, the peak area per unit mass of sample, is shown in Fig. 8 to be practically independent of the amount of pure tin left in the cup, whether a lid is used or not, but there is about 60% enhancement when the lid is used. The reproducibility of the peak area was better (r.s.d. 4.7% for 11 replicates) when a lid was used than when it was not (r.s.d. 8.7% for 10 replicates). This is because there is less fluctuation in the atomic vapour concentration in the furnace (generated by the flow of sheath gas) when a lid is used.

CONCLUSION

In the atomic-absorption determination of many elements by electrothermal atomization in a cup furnace, an increase in sensitivity is obtained by fitting the cup furnace with a graphite lid having a central hole. The shape of the recorded atomic absorption signal is modified, the peak becoming wider or dividing into two. This alteration varies with the lid rim thickness and the diameter of the central hole and is due to retention of the metal vapour within the furnace, or condensation of metal on the lid and subsequent re-evaporation. The latter phenomenon, which causes the appearance of two peaks in the output signal, is due to a temperature lag between the cup furnace and the lid (which is heated only by radiation from the furnace). In the atomization of solid samples there is also an increase in the precision of determination.

Acknowledgements—The author would like to acknowledge the continuing guidance of Prof. Kichinosuke Hirokawa. This research was supported in part by a Grant-in-Aid for Scientific Research from the Ministry of Education.

REFERENCES

1. B. V. L'vov, *Spectrochim. Acta*, 1961, **17**, 761.
2. *Idem, ibid.*, 1969, **24B**, 53.
3. H. Massmann, *ibid.*, 1968, **23B**, 215.
4. H. Koizumi, K. Yasuda and M. Katayama, *Anal. Chem.*, 1977, **49**, 1106.
5. D. Siemer and W. Frech, *Spectrochim. Acta*, 1984, **39B**, 261.
6. T. S. West and X. K. Williams, *Anal. Chim. Acta*, 1969, **45**, 27.
7. V. Z. Krasil'shchik and M. G. Lifshits, *Zavodsk. Lab.*, 1977, **43**, 692; *Chem. Abstr.*, 1978, **88**, 68500k.
8. B. V. L'vov, *Spectrochim. Acta*, 1978, **33B**, 153.
9. W. J. Price, T. C. Dymott and P. J. Whiteside, *ibid.*, 1980, **35B**, 3.
10. C. H. Chung, E. Iwamoto, M. Yamamoto, Y. Yamamoto and M. Ikeda, *Anal. Chem.*, 1984, **56**, 829.
11. K. Hirokawa and K. Takada, *Bunseki Kagaku*, 1980, **29**, 675.
12. *Idem, Z. Anal. Chem.*, 1982, **312**, 109.
13. K. Takada, *Bunseki Kagaku*, 1983, **32**, 197.
14. K. Takada and K. Hirokawa, *Talanta*, 1983, **30**, 329.
15. K. Takada and T. Shoji, *Z. Anal. Chem.*, 1983, **315**, 34.
16. I. Atsuya and K. Itoh, *Bunseki Kagaku*, 1982, **31**, 708.
17. *Idem, Spectrochim. Acta*, 1983, **38B**, 1259.
18. K. Takada and K. Hirokawa, *ibid.*, 1984, **39B**, 1113.

Talanta, Vol. 32, No. 9, pp 927–929, 1985
Printed in Great Britain.

0039-9140/85 $3.00 + 0.00

SHORT COMMUNICATION

A RAPID EXTRACTIVE SPECTROPHOTOMETRIC METHOD FOR THE DETERMINATION OF TIN IN CANNED FOODS WITH 5,7-DICHLORO-8-QUINOLINOL

A. M. GUTIERREZ, C. PEREZ-CONDE, M. P. REBOLLAR and L. M. POLO DIEZ
Departamento de Química Analítica, Facultad de Ciencias Químicas, Universidad Complutense, 28040 Madrid, Spain

(*Received* 1 *February* 1985. *Revised* 20 *March* 1985. *Accepted* 3 *May* 1985)

Summary—A rapid method for the spectrophotometric determination of tin in canned foods, based on formation of the binary Sn(IV)–5,7-dichloro-8-quinolinol complex and extraction into chloroform has been developed. The absorption maximum at 390 nm ($\epsilon = 1.26 \times 10^4$ l.mole^{-1}.cm^{-1}) is used for the determination. Beer's law is obeyed up to 6 μg of tin per ml. Organic matter is destroyed by digestion with acid. Potential interferences have been studied. The detection limit for tin is 2.5 mg/kg.

Rapid determination of tin in canned foods is very important for several reasons: (*i*) it serves for assessing the degree of corrosion of the internal surface of the can, (*ii*) the amount of tin present in the food increases as a function of the temperature and duration of storage, (*iii*) there are maximum levels laid down by legislation.

The spectrophotometric reagents most often used for this purpose are Catechol Violet,[1,2] especially recommended by the IUPAC commission on food chemistry,[3] and quercetin.[4] Both lack selectivity and require prior extraction of tin as SnI_4 into toluene or cyclohexane.[5,6] We present here a new method, based on extraction of the complex formed by tin(IV) and 5,7-dichloro-8-quinolinol (HCQ).[7] Very sensitive analytical methods are not necessary for the determination of tin in canned foods, and our method has the advantage that interfering ions are unlikely to be present in foods at above their tolerance levels, so prior separation of the tin is unnecessary.

EXPERIMENTAL

Reagents

Tin(IV) stock solution (1000 μg/ml). Obtained by dissolving tin metal in concentrated sulphuric acid and diluting with water to give a final acid concentration of 3.6*M*. Fresh standard tin(IV) solutions were prepared daily by suitable dilution of this stock solution with 1.7*M* sulphuric acid.

HCQ solution in chloroform, 1%.

Citric acid/citrate buffer, 1M, *pH 4.5.*

Ammonia solution, 3M.

Hydroxylamine hydrochloride solution, 0.5%.

All chemicals were of analytical reagent grade. Demineralized distilled water was used throughout.

Sample solution

Digestion with $HClO_4$–H_2SO_4–HNO_3 mixture. Weigh accurately about 2 g of the canned foodstuff, previously homogenized and dried at 110°, into a 100-ml beaker, add 3 ml of concentrated sulphuric acid, 3 ml of 72% perchloric acid and 10 ml of concentrated nitric acid, cover with a watch-glass, and heat carefully to suppress foam formation. Continue heating until fumes of sulphur trioxide appear, cool, add 10 ml of concentrated nitric acid and repeat this treatment until the solution remains colourless (the attack takes about half an hour). Then dilute to volume in a 50-ml standard flask with demineralized distilled water.

Digestion with HCl–HNO_3 mixture. Weigh accurately about 2 g of the canned foodstuff, dried at 110°, into a 100-ml beaker, add 30 ml of concentrated nitric acid and 25 ml of concentrated hydrochloric acid, cover with a watch-glass, and heat the vessel on a sand-bath until a volume of about 25–30 ml remains. Add 10 ml of concentrated hydrochloric acid and reduce the volume again, and repeat the process until the solution remains colourless. Finally dilute to volume in a 50-ml standard flask with demineralized distilled water.

Tin determination by the proposed method

Transfer an aliquot of sample solution containing up to 60 μg of tin into a short-stemmed 100-ml separating funnel. Add, in the order given, 1 ml of hydroxylamine solution, 10 ml of HCQ solution, several drops* of 3*M* ammonia solution to neutralize the excess acidity, and 2 ml of the citric acid/citrate buffer to bring the solution to pH 4.5. Adjust the aqueous volume to approximately 10 ml with demineralized distilled water, shake the funnel for 3–4 min and allow the phases to separate. Transfer the chloroform phase into the spectrophotometric cell, through a rolled-up piece of dry Whatman No. 1 filter paper placed inside the funnel stem. Measure the absorbance at 390 nm against a blank, using 1-cm cells fitted with Teflon lids. Prepare a calibration graph by applying the procedure to standard solutions containing tin in the 12–60 μg range.

Tin determination by standard-addition atomic-absorption spectrometry (AAS)

Transfer aliquots of sample solution into a series of 5-ml standard flasks, add known amounts of standard tin solution (containing up to 500 μg of tin, in a graded series),

*A preliminary test on another aliquot, with use of a pH-meter, is useful for finding the amount of ammonia needed.

Table 1. Recovery of tin from canned foods*

Acid mixture	Sample	Tin, *mg* Added	Total	Found	Recovery %
HNO_3–H_2SO_4–$HClO_4$	Tomato I	2.00	2.00	2.00	100
		5.00	5.00	5.06	101
HCl–HNO_3	Sardines	0.95	1.32	1.31	99
		1.90	2.26	2.37	105
		4.75	5.13	5.00	97
	Peas	0.95	1.71	1.87	109
		1.90	2.67	2.50	94
		4.75	5.49	5.62	93
	Tomato II	0.95	2.93	2.93	100
		1.90	3.90	3.87	99
		4.75	6.85	6.87	100

*Determined by the AAS method.

dilute them to volume, and measure the absorbances at 235.5 nm, using a nitrous oxide–acetylene flame.

RESULTS AND DISCUSSION

Selection of sample decomposition method

Because of the known volatility of some tin compounds, including the chlorides, ashing methods were not considered. A comparative study was made of the three acid mixtures most often recommended for destruction for organic matter.[8] In general, sulphuric–nitric acid mixtures take quite a long time to give complete mineralization of food samples. In the presence of perchloric acid less nitric acid is necessary, and the oxidation of organic matter is faster and more complete. Although the hydrochloric–nitric acid mixture does not destroy the organic matter completely, its action is very rapid and in general it gives good results for the determination of tin by AAS.[9] The last two acid mixtures were used for mineralization purposes, and the recoveries were determined by AAS. Results obtained for several samples are shown in Table 1, and are mostly satisfactory. In our experience canned vegetables may be mineralized with good results by use of either acid mixture. However, for canned fish, the sulphuric–nitric–perchloric acid mixture is less suitable because a considerable precipitate appears, mainly composed of potassium perchlorate.

Analytical characteristics of the spectrophotometric method

The calibration graph shows that Beer's law is obeyed up to 6 μg of tin(IV) per ml. The apparent molar absorptivity is 1.26×10^4 $l.mole^{-1}.cm^{-1}$ at 390 nm. The relative standard deviation, evaluated from ten independent determinations at the 5-μg/ml tin level, is 1.0%.

Interferences from the species most often associated with tin(IV) in canned foods and some masking agents were studied. The ions under investigation were added to sulphuric acid solutions containing 50 μg of tin. Each test solution was treated by the determination procedure and the results are shown in Table 2. Of the species studied, only chloride and iron(III) may be found in these types of foodstuffs at above the tolerance ratios (see Table 2), but in any case some (such as fluoride and certain organic species) would be eliminated in the acid decomposition step. The interference of iron(III) can be eliminated by prior reduction to iron(II) with hydroxylamine hydrochloride in acidic medium. Chloride interference is due to formation of the $SnCl_2(HCQ)_2$ ternary complex and can be eliminated by working at a pH equal to or above 4.5. This is taken as the working pH because of the presence of large amounts of chloride in these kinds of sample; otherwise lower pH values, down to 2, could be used.[7]

Tin determination in several canned foods

The procedure described was applied to three different kinds of foodstuff, and the results, referred to dry weight of sample, are shown in Table 3. It can be seen that the relative standard deviation for each sample is reasonably low.

The accuracy was determined first by recovery studies on dissolved samples to which different amounts of standard tin solution had been added. Results are shown in Table 4. The recoveries of total

Table 2. Tolerance limits for diverse ions in the determination of tin (5 ppm)

Ions	Tolerance, foreign ion/Sn(IV), *w/w*
$C_4O_6H_4^{2-}$	3×10^{4}*
$C_2O_4^{2-}$	2×10^{3}*
H_2Cit^-, Cl^-, NO_3^-, Na^+	400*
Cr(III)	100*
PO_4^{3-}	80*
As(III), As(V)	80*
Mn^{2+}, Al^{3+}, U(VI), Pb^{2+}, Co^{2+}	10*
V(V)	2.5
Fe^{2+}	2
Cd^{2+}, Ni^{2+}	1
Hg(II), Zn^{2+}	0.5
Fe^{3+}	0.2
Cu^{2+}	0.1
Ti(IV), F^-, EDTA	<0.1

*Maximum ratio tested.

Table 3. Tin content in canned food samples

Sample*	Weight, g	Proposed method				AAS method		
		Sn†, μg/g	R.S.D., %	Mean, μg/g	R.S.D., %	Sn, μg/g	Mean, μg/g	R.S.D., %
Tomato (I) (*a*)	2.0000	512	3.6	513	3.2	581	570	3.3
	2.0002	500	4.1			581		
	2.0435	526	1.8			548		
Tomato (II) (*b*)	2.0279	838	3.5	837	3.6		—	
	2.0329	836	3.6					
Peas I (*a*)	1.9914	389	2.4	392	3.3	392	389	1.3
	1.9935	389	4.3			392		
	2.0360	405	2.2			384		
Peas II (*b*)	2.0087	386	4.4	393	3.3	—	377	1.8
	1.9745	390	2.5			370		
	1.9605	396	3.2			376		
	2.0328	393	4.1			384		
Sardines (*b*)	1.9621	200	3.4	205	3.8	188	188	2.4
	2.0171	210	4.2			184		
	2.0072	—	—			193		

*(*a*) and (*b*) refer to the use of H_2SO_4–$HClO_4$–HNO_3 and HCl–HNO_3 acid mixtures respectively.
†Each value is the mean of six replicates; R.S.D. = relative standard deviation.

Table 4. Recovery of tin, determined by the proposed method

Sample*	Weight, g	Tin, mg			Recovery of tin, %	
		Added	Total	Found	Total	Added
Tomato I (*a*)	2.0008	0.600	1.62	1.57	97	92
	1.9952	0.800	1.82	1.70	93	85
Tomato II (*b*)	1.9513	0.950	2.58	2.65	102	105
	1.9704	1.90	3.55	3.85	108	105
	2.0724	4.75	6.48	5.15	81	72
Peas I (*a*)	1.9923	0.600	1.38	1.20	87	70
	2.0554	0.800	1.61	1.47	92	83
	2.0563	1.00	1.81	1.72	95	91
Peas I (*b*)	2.0043	0.950	1.74	1.70	98	97
	2.0185	1.90	2.69	2.62	97	96
	1.9211	4.75	5.50	5.25	95	95
Sardines (*b*)	1.9400	1.90	2.30	2.30	100	100
	2.0620	4.75	5.17	5.15	99	100

*(*a*) Acid mixture H_2SO_4–$HClO_4$–HNO_3; (*b*) acid mixture HCl–HNO_3.

tin were generally >90%, with a mean of about 97%, but those for added tin were more variable, since they were based on the difference of two quantities, each with a relative standard deviation of 3–4%, so a range from 90–110% recovery might have been expected: The few recoveries outside this range could have been due to a variety of causes, and in general the method is of potential use. The results were also compared with those obtained by the AAS method,[9] with a nitrous oxide–acetylene flame (Table 3), each value being the mean of three AAS determinations by the standard-additions method. The results indicate that there are no significant differences between the two methods at the 95–99% confidence level.

Conclusions

The proposed spectrophotometric method is sensitive enough for the determination of tin in canned food, the accuracy is adequate, and the method is more rapid than other methods usually employed for this purpose.

REFERENCES

1. W. J. Ross and J. C. White, *Anal. Chem.*, 1961, **33**, 421.
2. Analytical Methods Committee, *Analyst*, 1967, **92**, 320.
3. L. E. Coles, *Pure Appl. Chem.*, 1982, **54**, 1737.
4. A. Engberg, *Analyst*, 1973, **98**, 137.
5. E. J. Newman and P. D. Jones, *ibid.*, 1966, **91**, 406.
6. K. Tanaka and N. Takagi, *Anal. Chim. Acta*, 1969, **48**, 357.
7. A. M. Gutiérrez, R. Gallego and A. Sanz-Medel, *ibid.*, 1983, **149**, 259.
8. Analytical Methods Committee, *Analyst*, 1960, **85**, 643.
9. R. W. Dabeka and A. D. McKenzie, *J. Assoc. Off. Anal. Chem.*, 1981, **64**, 1297.

Talanta, Vol. 32, No. 10, pp. 931–935, 1985
Printed in Great Britain.

0039-9140/85 $3.00 + 0.00

CONSEL, A LEAST-SQUARES PROGRAM FOR ESTIMATING STABILITY CONSTANTS FROM POLAROGRAPHIC DATA

J. A. SANTABALLA, C. BLANCO*, F. ARCE and J. CASADO
Departamento de Química Física, Facultad de Química, Universidad, E-Santiago de Compostela, Spain

(*Received* 6 *February* 1985. *Accepted* 24 *May* 1985)

Summary—This article describes CONSEL, a least-squares linear-regression program which, when applied to polarographic data, provides estimates of stability constants suitable for priming non-linear optimization programs. The use of CONSEL avoids the need for recourse to traditional graphical methods. The results of its application to three systems are presented.

The most widely used methods for the determination of the stability constants of complexes from polarographic data (that of DeFord and Hume[1] for a single ligand and that of Schaap and McMasters[2] for two) are both based on graphical extrapolation, which has made them the object of criticism.[3] Existing non-linear optimization programs for the calculation of stability constants nevertheless require to be primed initially with both an informed guess about the stoichiometry of the complexes formed, and approximate estimates of the constants. This article describes a computer program CONSEL, which can find such initial estimates non-graphically.

METHOD

The calculation of stability constants from half-wave potential shifts is based on the equations[2]

$$F = \exp\left[\frac{n\mathscr{F}}{RT}(E_{1/2s} - E_{1/2c}) + \ln\left(\frac{I_{ds}}{I_{dc}}\right)\right] \quad (1)$$

and

$$F = 1 + \sum_i \sum_j \beta_{ij}[L_1]^i[L_2]^j; \quad 1 \leqslant (i+j) \leqslant m \quad (2)$$

where $E_{1/2c}$ and $E_{1/2s}$ are the half-wave potentials of the complexed and uncomplexed metal ions respectively and I_{dc} and I_{ds} the diffusion currents for the complexed and uncomplexed ions, $[L_1]$ and $[L_2]$ are the equilibrium concentrations of ligands L_1 and L_2, m is the maximum number of ligands that can co-ordinate to the metal ion, and β_{ij} is the stability constant of the complex $M(L_1)_i(L_2)_j$, given by

$$\beta_{ij} = \frac{[M(L_1)_i(L_2)_j]}{[M][L_1]^i[L_2]^j} \quad (3)$$

The problem is to determine which complexes $M(L_1)_i(L_2)_j$ are actually formed, and the values of the stability constants. Once equation (1) has been used to calculate F from experimental data for several pairs of values ($[L_1]$, $[L_2]$), this amounts to finding the best regression equation of the form of equation (2),[4] *i.e.*, which terms of (2) contribute significantly to the function that gives the best fit to the experimental data, and the β_{ij} values in these terms.

The problem formulated above is at first sight a typical linear-regression problem. Therefore, a suitable least-squares algorithm for its solution, according to the criteria of Draper and Smith,[5] is that known as STEPWISE. Once the maximum set of terms possibly involved in the regression has been fixed, by fixing m in equation (2), this algorithm proceeds as follows.

1. The partial coefficients of correlation between the dependent variable (in this case F) and each of the independent variables ($[L_1]^i[L_2]^j$) are calculated.
2. The least-squares linear regression of the dependent variable on the independent variable with the largest of the partial correlation coefficients calculated in step 1 is obtained.
3. The partial coefficients of correlation between the dependent variable and the independent variables not included in the regression are calculated.
4. An appropriate statistical test is applied to determine whether the addition of the term with the greatest of the partial correlation coefficients calculated in step 3 significantly improves the fit. If not, the best regression equation is deemed to have been found and the algorithm halts.
5. If significant improvement has been detected in step 4, the corresponding variable is included in the regression, and the regression of the dependent variable on this enlarged set of terms is calculated.
6. An appropriate statistical test is applied to detect whether the introduction of the new term into the regression has caused any other term to cease to be significant.
7. After eliminating any insignificant term detected in step 6, the algorithm returns to step 3.

*Author for correspondence.

When algorithms such as STEPWISE are applied to polarographic data, it is necessary to make sure that the β_{ij} values found are physically meaningful.[6] If negative stability-constant values are obtained, the corresponding terms may be eliminated from the model and the whole algorithm rerun without them.[7] However, the main failing of such procedures for finding a best linear-regression model is that changing the set of terms initially proposed for inclusion in the model is very likely to affect the final results, even though none of the extra terms included in the larger set may appear in the model finally predicted by applying the algorithm to that set (see Table 5 for an example). For polarographic purposes, STEPWISE by itself is thus deficient—even as a method of priming non-linear optimization algorithms—in that it is necessary to make a good initial guess at the best choice of m, even if not at the actual complexes formed.

The solution we have adopted for this difficulty is to pre-select all the significant terms predicted by STEPWISE for all likely values of m, and subject them to non-linear optimization by the program POLAG[3] (though any other non-linear optimization program could also be used, of course). Thus if the greatest possible value of m is six, STEPWISE is applied to all the initial models listed in Table 1, where T_{ij} represents $\beta_{ij}[L_1]^i[L_2]^j$ and each initial model contains among its terms all those of the initial models corresponding to smaller values of m. Then, instead of trying to decide which of the six optimal regression equations calculated is really the best, which is not easy,[8] we simply pool the terms of all those with correlation coefficients greater than say, 0.9, and pass them to POLAG for further refinement. CONSEL thus consists essentially in the SELection of initial CONstants for POLAG by repeated application of STEPWISE to increasingly larger sets of terms up to some reasonable maximum (see Fig. 1). For CONSEL, only the maximum value of m must be fixed at the start, not each single value as in STEPWISE.

Once all the terms selected by CONSEL have been passed to POLAG, the decision process is as follows.

1. Non-linear optimization of the β_{ij} values is attempted.

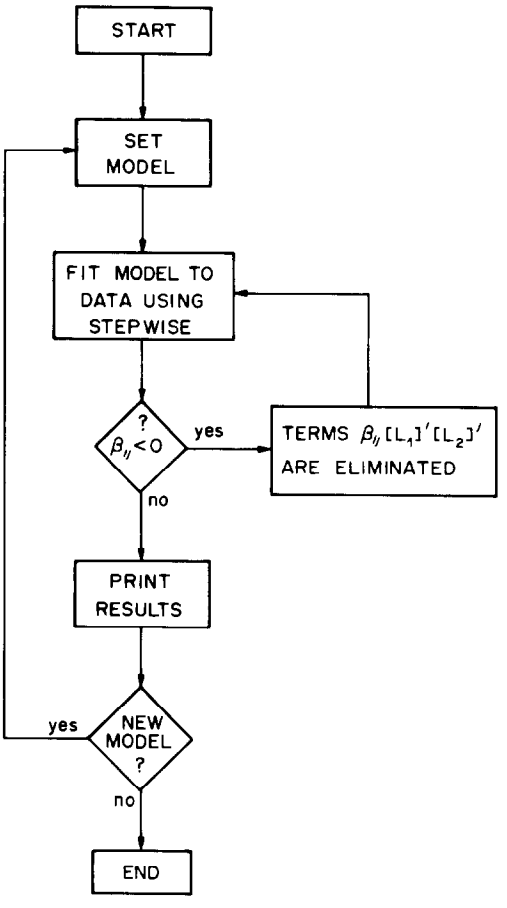

Fig. 1.

2. If no β_{ij} with a relative error greater than 15% has been calculated, this result is deemed good and the procedure is halted.

3. Otherwise, the complex for which the stability constant has the greatest relative error is dropped, and the algorithm returns to step 1.

The same procedure may of course be followed with use of any other non-linear optimization program.

A FORTRAN V version of CONSEL has been used in our laboratory with POLAG for the last year. A documented listing, together with sample data, is available from the authors on request.

Table 1. Initial models for fitting of polarographic data by CONSEL

Model	m	Terms*
I	1	T_{10}, T_{01}
II	2	I, T_{20}, T_{02}, T_{11}
III	3	II, T_{03}, T_{30}, T_{21}, T_{12}
IV	4	III, T_{40}, T_{04}, T_{31}, T_{13}, T_{22}
V	5	IV, T_{50}, T_{05}, T_{14}, T_{41}, T_{32}, T_{23}
VI	6	V, T_{60}, T_{06}, T_{15}, T_{51}, T_{42}, T_{24}, T_{33}

*The roman numerals here stand for the terms in the preceding set; thus I means T_{10}, T_{01}, II means T_{10}, T_{01}, T_{20}, T_{02}, T_{11}, and so on.

RESULTS AND DISCUSSION

We shall illustrate the use of CONSEL by analysing polarographic data for three systems. The data for two of these have been taken from the literature and the results obtained by using CONSEL–POLAG are compared with the results published previously. The third system is one of the hydroxide–metal–aminoalcohol complexes being studied in our own laboratory. The charges of the complexes have been omitted for convenience.

Cadmium–thiocyanate–nitrate system

Polarographic data for this system were published by Momoki.[9] Leggett[3] demonstrated the application of POLAG by using it to refine Momoki's data. For this article we have taken Momoki's experimental data and employed them to obtain initial values for POLAG by using CONSEL rather than a graphical method. The results are shown in Tables 2 and 3.

All the models fitted by STEPWISE have correlation coefficients greater than 0.9 except that obtained from model I. The stability constants of all the complexes predicted from models II–VI were therefore fed into POLAG. The final results are shown in Table 4 together with those obtained by Legget.[3] The two sets of results agree quite well except that that among the complexes predicted by Leggett, the complex for which the standard deviation of the stability constant is greatest—$Cd(NO_3)$—is no longer predicted when CONSEL is used.

Cadmium–thiocyanate–chloride system

This system was studied polarographically by Arevalo *et al.*[10] who, since they analysed their data by using the conventional method of Schaap and McMasters, also had to determine the complexes formed by cadmium with each of the ligands individually[11,12]. The results of applying CONSEL to their data for the mixed complexes are shown in Tables 5 and 6. The stability constants of all the complexes predicted by CONSEL were fed into POLAG, which produced the final results shown in Table 7. There is good agreement between the figures obtained by CONSEL–POLAG from mixed-complex data alone and those found by Arevalo *et al.* with the aid of additional experimental data for the complexes formed with the individual ligands.[10,11]

Lead–monoethanolamine (MEA)–OH system

The existence of mixed hydroxo-complexes of Pb^{2+} with aminoalcohols in basic media has been reported by Subrahmanya[13] together with the composition and stability constants of some of them. However, subsequent research by Migal *et al.*[14,15] failed to consider the possibility of the presence of hydroxide ions within the co-ordination sphere of the metal ion. In order to settle the question, we have made a polarographic study, the results of which have been analysed by both CONSEL–POLAG and the graphical method of Schaap and McMasters.

Table 2. Stability constants estimated by CONSEL for the cadmium–thiocyanate–nitrate system, $I = 2.0M$, $T = 25°$

Stoichiometry of the complex			Values of m for which the complex is predicted by STEPWISE	$\log \beta \pm$S.D.*
Cd	SCN	NO_3		
1	1	0	1	3.02 ± 0.98
1	2	0	2, 4, 5, 6	2.31 ± 0.01
1	3	0	3, 5, 6	2.30 ± 0.01
1	4	0	4	2.27 ± 0.01
1	5	0	5, 6	1.71 ± 0.04
1	1	1	5, 6	1.44 ± 0.12
1	2	1	4	1.72 ± 0.04
1	4	1	6	1.30 ± 0.14

*Standard deviation.

Table 3. Values of the correlation coefficients (r) for the six models predicted by CONSEL for the system Cd–SCN–NO_3

Model	I	II	III	IV	V	VI
r	0.877	0.997	0.998	0.999	0.999	0.999

Table 4. Complexes present in the Cd–SCN–NO_3 system, and their stability constants, $I = 2.0M$, $T = 25°$

Complex	$\log \beta \pm$ S.D.	
	Our results	Leggett's results[3]
$Cd(NO_3)$	—	1.247 ± 0.055
$Cd(SCN)_2$	2.327 ± 0.025	2.262 ± 0.019
$Cd(SCN)_4$	2.292 ± 0.028	2.328 ± 0.016
$Cd(SCN)(NO_3)$	1.527 ± 0.039	1.317 ± 0.046

Table 5. Stability constants estimated by CONSEL for the cadmium–thiocyanate-chloride system, $I = 1.0M$, $T = 25°$

Stoichiometry of the complex			Values of m for which the complex is predicted by STEPWISE	$\log \beta \pm$S.D.
Cd	SCN	Cl		
1	0	1	1	2.25 ± 0.01
1	1	0	1, 2	2.09 ± 0.04
1	2	0	3, 4	2.24 ± 0.03
1	3	0	5, 6	2.65 ± 0.03
1	0	2	2	1.95 ± 0.04
1	1	1	2, 3, 4, 5, 6	2.63 ± 0.03
1	1	2	3, 6	2.76 ± 0.02
1	1	3	4	2.71 ± 0.02
1	2	3	6	3.26 ± 0.04

Table 6. Values of the correlation coefficients (r) for the six models predicted by CONSEL for the system Cd–SCN–Cl

Model	I	II	III	IV	V	VI
r	0.976	0.995	0.997	0.997	0.994	0.997

Table 7. Complexes present in the cadmium–thiocyanate–chloride system, and their stability constants, $I = 1.0M$, $T = 25°$

$Cd(SCN)Cl$	$Cd(SCN)Cl_2$	$Cd(SCN)_2Cl$	$Cd(SCN)$	$Cd(SCN)_3$	Ref.
—	—	—	1.279 ± 0.023	2.262 ± 0.016	11
2.025 ± 0.041	2.193 ± 0.028	2.685 ± 0.072	—	—	10
2.453 ± 0.019	2.728 ± 0.019	—	1.483 ± 0.025	2.528 ± 0.021	This work

EXPERIMENTAL

All experiments were done at 25° in potassium nitrate medium ($I = 1.0\ M$). Polarographic data were obtained by using a Beckman Electroscan 30, and the pH (adjusted by adding nitric acid or sodium hydroxide solution) was measured with a Radiometer 26 pH meter. The total lead concentration was kept constant at $10^{-4}\ M$.

RESULTS

Well-defined polarograms were obtained and in all cases single-stage reversible two-electron reduction reactions were shown to occur. The data are given in Table 8. The contribution of the term I_{ds}/I_{dc} in equation (1) was in all cases negligible.

To obtain a graphical estimate of the complexes formed, $\Delta E_{1/2}$ was plotted against the logarithm of the concentration of one of the ligands, the concentration of the other being kept constant. Plotting $\Delta E_{1/2}$ against log[MEA] at constant pH resulted in all cases in straight lines with slopes of about 0.028, indicating the co-ordination of a single molecule of the aminoalcohol to the metal ion. Plotting $\Delta E_{1/2}$ against log[OH] for constant concentrations of MEA produced straight lines with slopes of between 0.058 and 0.063, suggesting that a single complex containing two hydroxide ions was present. Accordingly, the appropriate form of equation (2) is predicted by this method as

$$F = \beta_{12}[\mathrm{OH}]^2[\mathrm{MEA}]$$

Plotting F against [MEA] for each value of [OH] produced straight lines with slopes A given by

$$A = \beta_{12}[\mathrm{OH}]^2$$

Table 8. Polagraphic data for the lead–monoethanolamine–OH system*

MEA,M	pH	$-E_{1/2}$, V	MEA, M	pH	$-E_{1/2}$, V
—	—	0.4050	0.050	11.50	0.5685
0.100	10.50	0.5177	0.100	11.50	0.5776
0.150	10.50	0.5231	0.150	11.50	0.5814
0.200	10.50	0.5257	0.200	11.50	0.5789
0.250	10.50	0.5272	0.250	11.50	0.5839
0.300	10.50	0.5307	0.300	11.50	0.5865
0.400	10.50	0.5338	0.400	11.50	0.5932
0.500	10.50	0.5387	0.500	11.50	0.5938
0.600	10.50	0.5406	0.600	11.50	0.5964
0.700	10.50	0.5415	0.800	11.50	0.6012
0.800	11.00	0.5425	1.000	12.00	0.6017
0.050	11.00	0.5424	0.050	12.00	0.6055
0.100	11.00	0.5391	0.100	12.00	0.6109
0.150	11.00	0.5498	0.150	12.00	0.6147
0.200	11.00	0.5560	0.200	12.00	0.6173
0.250	11.00	0.5561	0.250	12.00	0.6198
0.300	11.00	0.5593	0.300	12.00	0.6209
0.400	11.00	0.5625	0.400	12.00	0.6239
0.500	11.00	0.5660	0.500	12.00	0.6272
0.600	11.00	0.5708	0.600	12.00	0.6276
0.700	11.00	0.5713	0.800	12.00	0.6319
1.000	11.00	0.5780			

*Each wave was measured at 15 points. The ionic strength of the solutions was kept at $1.0M$. The temperature was $25.0 \pm 0.1°$.

Table 9. Stability constants estimated by CONSEL for the lead–monoethanolamine–OH system, $I = 1.0M$, $T = 25°$

Stoichiometry of the complex			Values of m for which the complex is predicted by STEPWISE	$\log\beta \pm$S.D.
Pb	MEA	OH		
1	1	0	1	7.05 ± 1.13
1	0	1	1	9.38 ± 0.04
1	0	2	2, 5, 6	10.63 ± 0.03
1	0	3	3	12.63 ± 0.03
1	1	1	5, 6	8.98 ± 0.07
1	1	2	3	11.72 ± 0.01
1	2	3	5, 6	13.64 ± 0.02

Finally, plotting log A against log[OH] resulted in a straight line of slope 1.98 ± 0.01 with an intercept of 11.70 ± 0.03. In other words, according to the Schaap and McMasters graphical method the system contains the single complex Pb(MEA) $(OH)_2$, with a logarithmic stability constant $\log \beta_{12} = 11.70 \pm 0.03$.

The results of applying CONSEL to the polarographic data are given in Tables 9 and 10. The stability constants of the complexes predicted by all the stages except I and IV (for which STEPWISE was unable to fit an equation) were passed to POLAG, which yielded the final result shown in Table 11. The value of $\log \beta_{12}$ calculated by CONSEL–POLAG (11.701 ± 0.021) coincides with that found graphically (11.70 ± 0.03) and agrees well with Subramanya's value of 11.73. The value of $\log \beta_{03}$, 12.640 ± 0.73, may be compared with the published[16] values of 13.29 and 13.66 obtained in sodium perchlorate medium.

CONCLUSIONS

In this article we have demonstrated the utility of CONSEL for extracting from reversible polarographic data an initial set of stability constants for input to non-linear optimization programs such as POLAG. CONSEL is remarkably simple to use, since the only input required, apart from the polarographic data, is the maximum number of ligands with which the metal ion is capable of co-ordinating.

Table 10. Values of the correlation coefficients (r) for the six models predicted by CONSEL for the system Pb–MEA–OH

Model	I	II	III	IV	V	VI
r	0.862	0.976	0.999	—	0.999	0.999

Table 11. Complexes present in the lead–monoethanolamine–OH system, and their stability constants, $I = 1.0M$, $T = 25°$

Complex	$\log\beta \pm$S.D.
Pb(MEA)(OH)	8.377 ± 0.023
Pb(MEA)$(OH)_2$	11.701 ± 0.021
$Pb(OH)_3$	12.640 ± 0.073

When applied to the experimental data obtained in our laboratory for the lead–monoethanolamine–OH system, CONSEL and POLAG together found the complexes Pb(MEA)(OH), $Pb(MEA)(OH)_2$ and $Pb(OH)_3$. The logarithms of the stability constants of the last two (11.701 ± 0.021 and 12.640 ± 0.073 respectively) are comparable with values available in the literature.

REFERENCES

1. D. D. DeFord and D. N. Hume, *J. Am. Chem. Soc.*, 1951, **73**, 5321.
2. W. B. Schaap and D. L. McMasters, *ibid.*, 1961, **83**, 4699.
3. D. J. Leggett, *Talanta*, 1980, **27**, 787.
4. R. Hocking, *Technometrics*, 1983, **25**, 219.
5. N. R. Draper and H. Smith, *Applied Regression Analysis*, Wiley, New York, 1966.
6. L. G. Sillén, *Acta Chem. Scand.*, 1964, **18**, 1085.
7. J. Watters and J. Mason, *J. Am. Chem. Soc.*, 1956, **78**, 285.
8. C. Daniel and F. S. Wood, *Fitting Equations to Data*, Wiley, New York, 1980.
9. K. Momoki, H. Ogawa and H. Sato, *Anal. Chem.*, 1969, **41**, 1826.
10. A. Arevalo, J. C. Rodríguez-Placeres, T. Moreno and J. Segura, *J. Electroanal. Chem.*, 1978, **92**, 56.
11. *Idem*, *An. Real Soc. Espan. Fis. Quim.*, 1977, **73**, 784.
12. A. Arevalo, personal communication.
13. R. S. Subrahmanya, *Advances in Polarography*, Vol. 2, Pergamon Press, London, 1960.
14. P. K. Migal and G. F. Serova, *Russ. J. Inorg. Chem.*, 1962, **7**, 827.
15. *Idem*, *ibid.*, 1965, **10**, 1366.
16. B. Carell and A. Olin, *Acta Chem. Scand.*, 1960, **14**, 1999.

Talanta, Vol. 32, No. 10, pp 937–947, 1985
Printed in Great Britain.

0039-9140/85 $3.00 + 0.00

THE BEHAVIOUR OF TWO TYPES OF COPPER ION-SELECTIVE ELECTRODES IN DIFFERENT COPPER(II)–LIGAND SYSTEMS

M. NESHKOVA and H. SHEYTANOV
Institute of General and Inorganic Chemistry, Bulgarian Academy of Sciences, 1040 Sofia, Bulgaria

(*Received* 13 *June* 1984. *Revised* 3 *May* 1985. *Accepted* 10 *May* 1985)

Summary—The behaviour of two types of solid-state homogeneous sensors for copper(II), one based on pressed pellets of ternary CuAgSe and the other on thin-layer electroplated $Cu_{2-x}Se$, in 12 different copper(II)–ligand systems, has been thoroughly investigated. Both electrodes exhibit anomalous behaviour when the ligands are of complexone type, the effect of the complexones on the deviations increasing in the order IDA < NTA < EDTA ~ DTPA, and being practically the same for the two types of sensors, thus disproving a previous suggestion that the anomaly is due to the silver in the silver-containing sensors. The experimental data do not support the specific ligand-adsorption hypothesis either. The observed deviations are tentatively explained on the basis that, as suggested by the selectivity coefficients, both sensors act as primary copper(I) ion-selective electrodes rather than copper(II)–electrodes. Thus, at very low copper(II) concentrations, according to the extended Nikolskii equation, the [Cu(I)]/[Cu(II)] ratio at the electrode surface determines the electrode sensitivity towards Cu(II). The lower detection limit could be improved by pH-control and selective complexation of Cu(I). This hypothesis has been proved experimentally. If the copper(I) activity on the electrode surface is decreased, the anomaly observed for the Cu(II)–NTA system disappears and decreases considerably for the Cu(II)–EDTA and Cu(II)–DTPA systems.

Soon after the first ion-selective electrodes for heavy metal ions were developed, it was realized that they offer excellent possibilities for direct determination of stability constants, as well as for objective end-point location in complexometric titrations.[1] It is now generally known that the measurement of activities lower than $10^{-6}M$ is possible only by use of buffers to attain these low values reliably, and this requires knowledge of the behaviour of these electrodes in different metal–ligand systems. Hansen *et al.*[2] were the first to consider the fact that several commercially available copper(II) ion-selective electrodes of the mixed chalcogenide type display anomalous behaviour in the presence of EDTA. Later, other authors[3–7] also commented on this fact. Different reasons have been proposed for the observed deviations but no consensus has yet been reached. A definitive answer can only be obtained after comprehensive studies of the behaviour of membrane materials of different composition in a broad range of copper(II)–ligand systems which have been studied by independent methods.

The present paper offers a systematic investigation of two solid homogeneous copper(II) ion-selective electrodes of different chemical composition, one based on pressed ternary CuAgSe and the other on a thin membrane of electro-deposited $Cu_{2-x}Se$, in different Cu(II)–ligand systems, the ligands being carboxylic acids, amino-acids and polyaminopolycarboxic acids (complexones). The complexing agents were carefully chosen to enhance the chances of finding specific ligand effects.

EXPERIMENTAL

Radelkis OP-Cu-7113 ion-selective electrodes, with homogeneous CuAgSe membranes,[8] the performances of which have been reported,[9] and plated thin-layer $Cu_{2-x}Se$ membranes prepared as described earlier,[10] were selected for the studies. The following complexing agents were examined: tartaric, salicylic and sulphosalicylic acids, alanine, methionine, lysine, aspartic and glutamic acids, iminodiacetic acid (IDA), nitrilotriacetic acid (NTA), EDTA and DTPA, all of analytical grade and not further purified.

The emf was measured with a digital Radelkis OP-208 pH-meter at 20 or 25° (±0.2°), depending on the temperature at which the corresponding stability constants had been determined, *vs.* a Radelkis OP-830 double-junction Ag/AgCl reference electrode (1*M* potassium nitrate in the bridge). The measurements were made on solutions with a total Cu(II) concentration of $1 \times 10^{-3}M$ and at least a 10-fold excess of ligand.

A thermostatically controlled potentiometric cell was filled with approximately 100 ml of the copper(II)–ligand solution at a constant ionic strength of 0.1 (KNO_3). The electrode-pair was immersed in the solution, together with a combined glass electrode. The pH was changed gradually by adding dilute sodium hydroxide solution or nitric acid, the corresponding steady-state potential of the ion-selective electrode being measured at each pH value. A value which did not alter by more than 0.4 mV within 10 min was accepted as the steady-state potential. The stirring rate was kept constant. Three independent sets of measurements were made for each system with each type of electrode, in an effort to determine the reproducibility. For all systems except those containing complexones, the reproducibility was ±1.5 mV or better and the steady-state potential was reached very rapidly as the pH was changed. In the Cu(II)–complexone solutions the steady-state potential was reached after different periods, depending on the pH, and more quickly with copper selenide electrodes than with CuAgSe electrodes, but with a rather poor reproducibility

of ±5 mV. Before and immediately after each measurement, the copper ion-selective electrode was calibrated with standard copper solutions of the same ionic strength as the test solution. The relationship pCu/mV was extrapolated to the lowest measured potential, by using the slope of the calibration graph. The concentration of free copper(II) was calculated from the equation:

$$[Cu^{2+}] = [Cu^{2+}]_{tot} \Big/ \left(1 + \beta_1 \frac{[L]}{\alpha_{L(H)}} + \beta_2 \frac{[L]^2}{\alpha^2_{L(H)}} + \cdots \beta_n \frac{[L]^n}{\alpha^n_{L(H)}}\right) \quad (1)$$

where β_1–β_n are the stability constants for the CuL–CuL_n complexes, [L] is the total ligand concentration, and $\alpha_{L(H)}$ is the side-reaction coefficient for protonation of the ligand, calculated from

$$\alpha_{L(H)} = 1 + [H^+]K^H_{HL} + [H^+]^2 K^H_{HL} K^H_{H_2L} + \cdots [H^+]^n K^H_{HL} K^H_{H_2L} \cdots K^H_{H_nL} \quad (2)$$

Table 1 summarizes the values used for $K^H_{H_iL}$ and β_i. The use of the total ligand concentration in equation (1) is an approximation justified by $[L] \gg [Cu^{2+}]_{tot}$.

Corresponding single measurements were made for copper-free solutions of the ligand at the same pH values and ionic strength as for the copper solutions.

RESULTS AND DISCUSSION

The pCu(II)-values experimentally determined with the two types of sensor, and those calculated according to equation (1) for each system, are presented in Figs. 1–12. Use of only a twofold excess of ligand does not change the character of the experimental curves.

The following experimentally established facts should be noted.

(1) A serious discrepancy between the experimentally determined and theoretically calculated pCu(II) values is observed with both types of membrane only when the ligands are complexones, and it increases with change of ligand in the order IDA < NTA < EDTA ~ DTPA. The theoretical relationship is followed up to pH = 8 for IDA (Fig. 9).

(2) Regardless of the chemical composition of the membranes used (*i.e.*, with or without silver), the deviations follow approximately the same pattern. All the experimental values are several orders of magnitude higher than those theoretically predicted.

(3) The pCu/mV relationships for the other ligands can be divided into two regions: up to pH 8–9 there is good agreement between the theoretical and experimental values, but at higher pH some of the systems show slight discrepancies, again with experimental values higher than those calculated.

(4) An experimental straight line with a slope of 30 mV/pH was found for the Cu(II)–tartaric acid system at pH > 5, instead of the plateau expected from the stability constants. This suggests a mixed hydroxide–tartrate complex, which does not seem to have been reported. Investigation of this equilibrium is in progress.[11]

(5) The mV/pH relationship for the pure ligands follows closely, or even coincides with, that for the copper(II)–ligand system, when NTA, EDTA and DTPA are used as ligands.

All these experimental facts can hardly be explained as due to dissolution of the membrane—the thin membranes would tend to dissolve immediately, whereas we were able to use them for several months, exposing them daily to EDTA or DTPA solutions. The presumed role played by the silver in the membrane,[3,4,6] should obviously be rejected. The distribution of the ligand species as a function of pH (note the distribution diagrams in the upper right-hand corner of each figure) is not in accord with the nature of the anomalous behaviour, and gives no support to the hypothesis advanced that there is ligand adsorption, increasing with the charge of the ligand species.[4,5] For example, it is rather difficult to explain on this basis the fact that for salicylic, sulphosalicylic and tartaric acids (Figs. 6–8) excellent agreement between experimental and calculated data was observed even when a large excess of negatively charged ligand species was present in the solution, whereas in the case of NTA, EDTA and DTPA (Figs. 10–12) the

Table 1.

Complexing agent	β^H_{HL}	$\beta^{2H}_{H_2L}$	$\beta^{3H}_{H_3L}$	$\beta^{4H}_{H_4L}$	$\beta^{5H}_{H_5L}$	β^L_{CuL}	$\beta^{2L}_{CuL_2}$	$\beta^{3L}_{CuL_3}$	$\beta^{4L}_{CuL_4}$	Ref.
Alanine	9.69	11.99				8.13	14.92			22
Glutamic acid	9.2	13.15	15.35			7.87	14.16			22
Aspartic acid	9.62	13.32	15.26			8.4	15.20			24
Methionine	9.20	11.37				8.1	14.80			24
Lysine	10.69	19.77	21.81			7.56*	14.02*			22
Glycine	9.57	11.93				8.15	15.03			23
Tartaric acid	4.10	7.0				3.2	5.1	5.7	6.5	23
Salicylic acid	13.4	16.21				10.62	18.45			22
Sulphosalicylic acid	11.80	14.29				9.43	16.30			22
IDA	9.38	12.03				10.5	16.2			23
EDTA	10.34	16.58	19.33	21.40		18.8				23
NTA	9.81	12.38	14.35			12.7	16.3			23
DTPA	10.56	19.25	23.62	26.49	28.4	20.5				23

*The corresponding values for β^{HL}_{MHL} and $\beta^{2HL}_{M(HL)_2}$ are given.

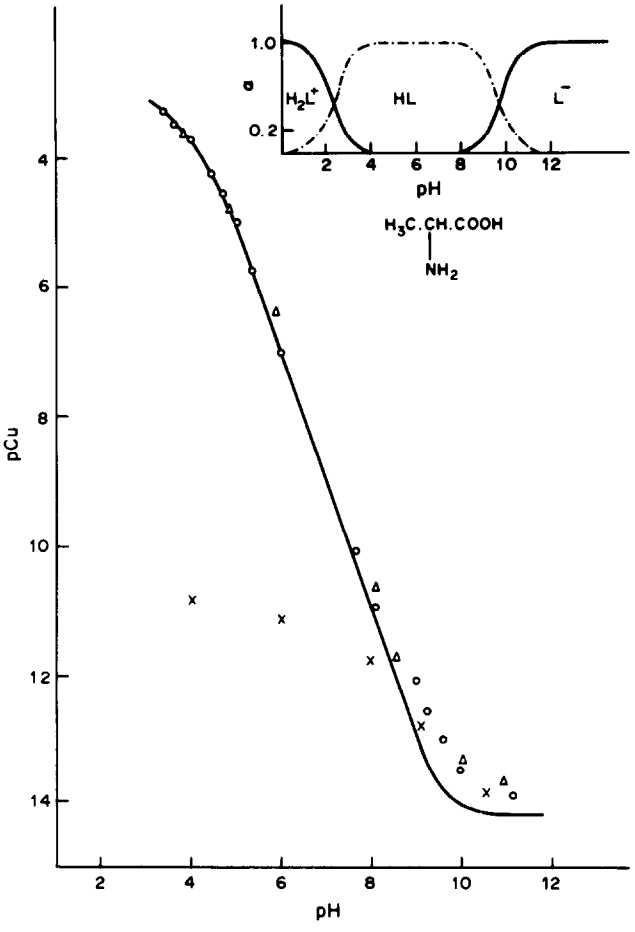

Fig. 1. pCu–pH relationship for $1 \times 10^{-3}M$ copper nitrate $+ 2 \times 10^{-2}M$ alanine with the CuAgSe membrane (○) and $Cu_{2-x}Se$ membrane (△). The curve drawn is calculated after equation (1). (×) values for the pure ligand.

observed deviations started at low pH, at which ions of high negative charge were not present. Nor does ligand adsorption explain why both electrodes measure pCu(II) values of 10 or 12 accurately in the alkaline and neutral pH region, but cannot measure the same values in the acidic region. Ligand species of higher negative charge are predominant in the far alkaline region for almost all the systems investigated, a region where in fact certain deviations were observed, but these cannot be related unambiguously to specific ligand adsorption by the membrane. Both electrodes displayed ideal reproducibility of the potential for copper standards immediately after measurements in the corresponding Cu(II)–ligand system, without application of special treatment. Any conclusions based on the observations in this pH region appear to be premature and ambiguous, as other equilibria may also exist in such alkaline solutions.

Hansen *et al.*[2] and later Hulanicki[7] have called attention to the fact that the effect of any Cu(I) in the composition of the membrane should also be considered as a factor which may cause the observed anomalous behaviour, and therefore deserves a comprehensive investigation.

We have assumed that a general cause for the anomalies we have observed is related to the fact that the two types of electrode are sensitive both to copper(I) and copper(II) and that their selectivity towards copper(I) is substantially the higher.[12] Consequently, their behaviour is better described by the extended Nikolskii equation:

$$E = E^\circ + \frac{RT}{nF} \ln \{a_{Cu^+} + K^{pot}_{Cu^+,Cu^{2+}} (a_{Cu^{2+}})^{1/2}\} \quad (3)$$

where $\log K^{pot}_{Cu^+,Cu^{2+}}$ is equal to -5.7 and -6.2 for the copper selenide and CuAgSe sensors respectively. It should be remembered that in equation (3), a_{Cu^+} and $a_{Cu^{2+}}$ are the activities at the membrane surface. Consequently, when we measure the activity of Cu(II), the activity of Cu(I) generated by the membrane material may be neglected (as a factor which affects the potential) only in the case of relatively higher copper(II) activities (above $10^{-7}M$).

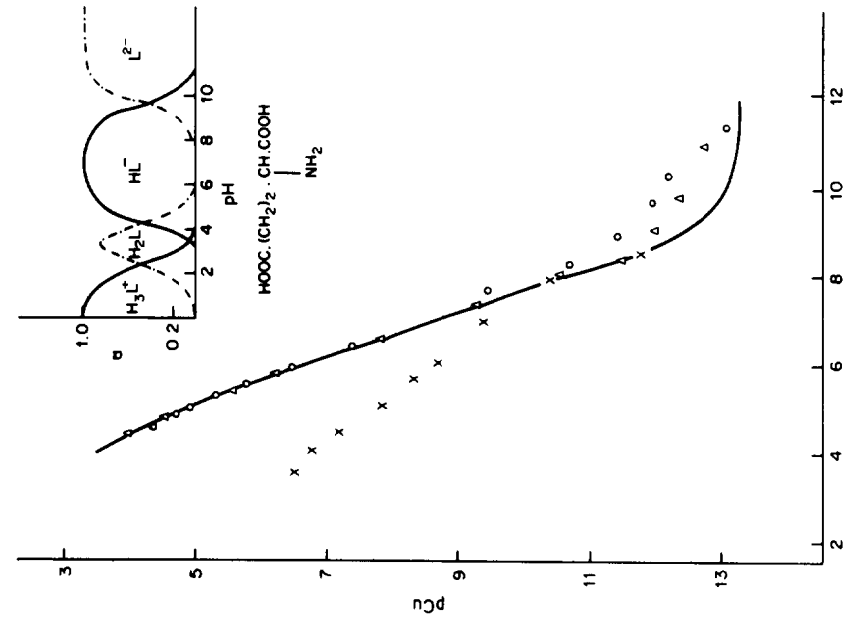

Fig. 3. pCu–pH relationship for $1 \times 10^{-3}M$ copper nitrate + $1 \times 10^{-2}M$ aspartic acid. Symbols as for Fig. 1.

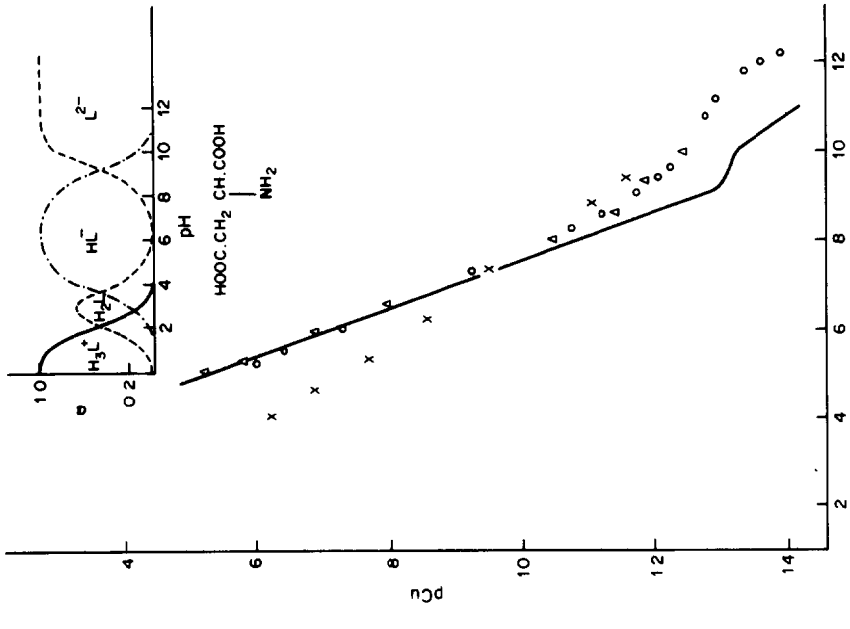

Fig. 2. pCu–pH relationship for $1 \times 10^{-3}M$ copper nitrate + $1 \times 10^{-2}M$ glutamic acid. Symbols as for Fig. 1.

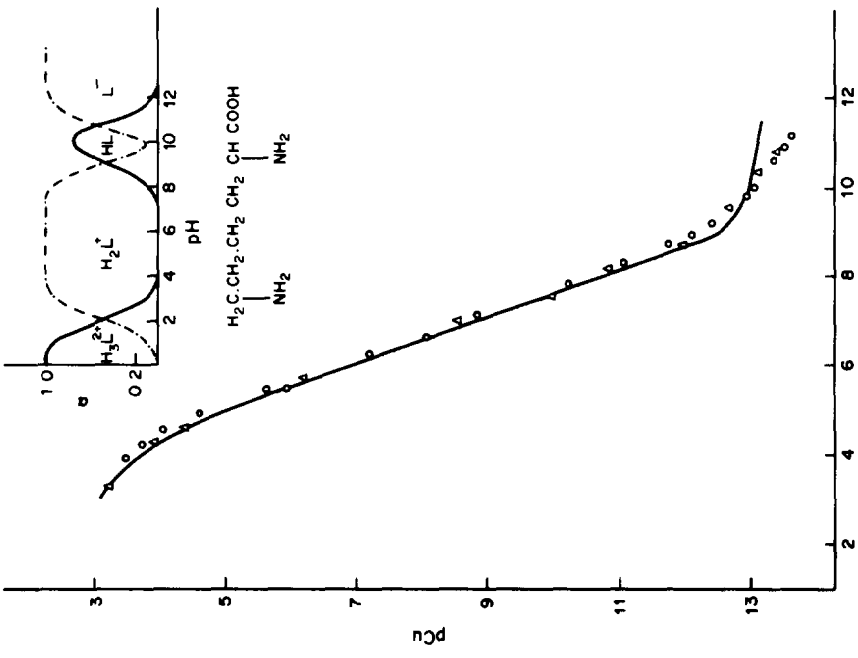

Fig. 5. pCu–pH relationship for $1 \times 10^{-3}M$ copper nitrate + $1 \times 10^{-2}M$ lysine, with the CuAgSe membrane (○) and $Cu_{2-x}Se$ membrane (△).

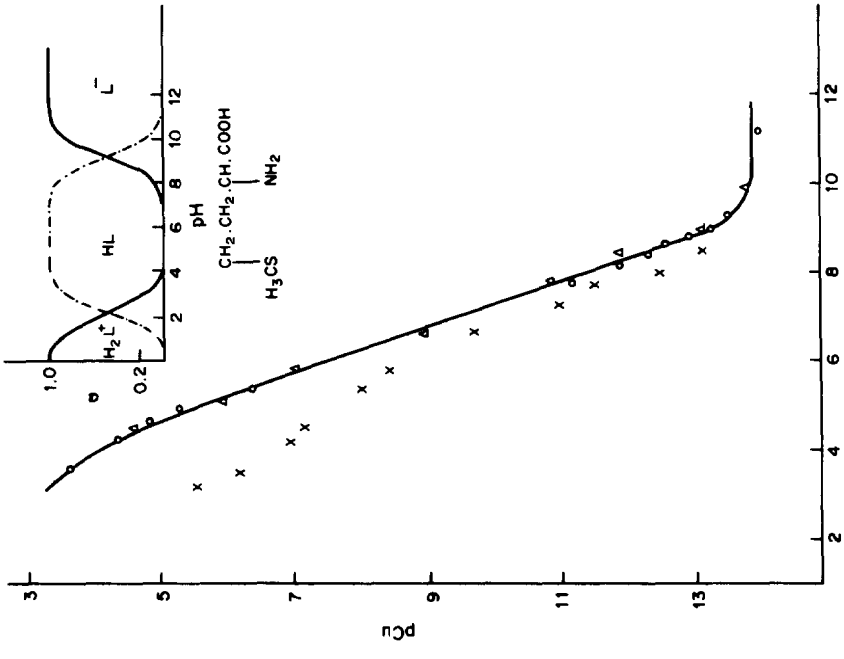

Fig. 4. pCu–pH relationship for $1 \times 10^{-3}M$ copper nitrate + $1 \times 10^{-2}M$ methionine. Symbols as for Fig. 1.

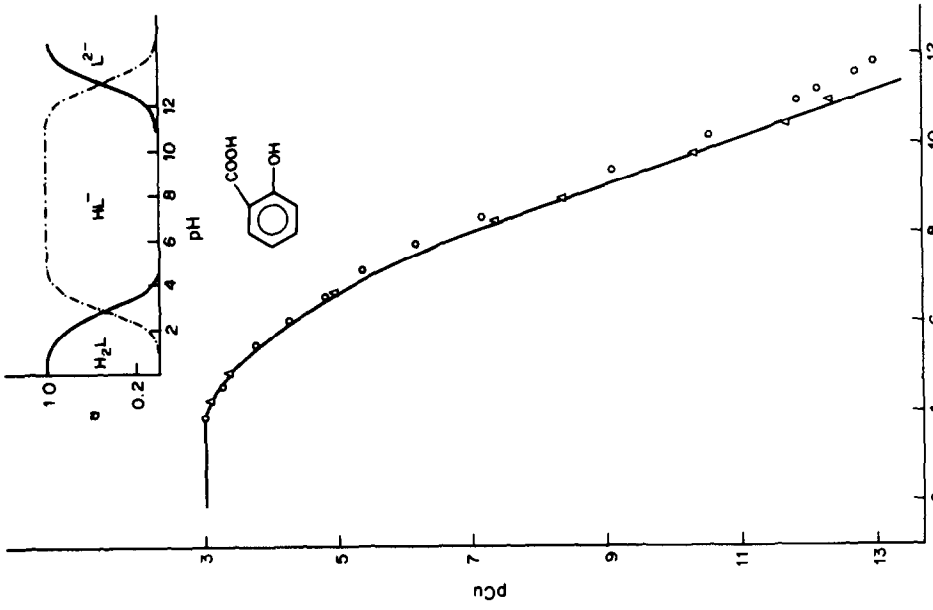

Fig. 6. pCu–pH relationship for $1 \times 10^{-3}M$ copper nitrate + $1 \times 10^{-2}M$ salicylic acid. Symbols as for Fig. 5.

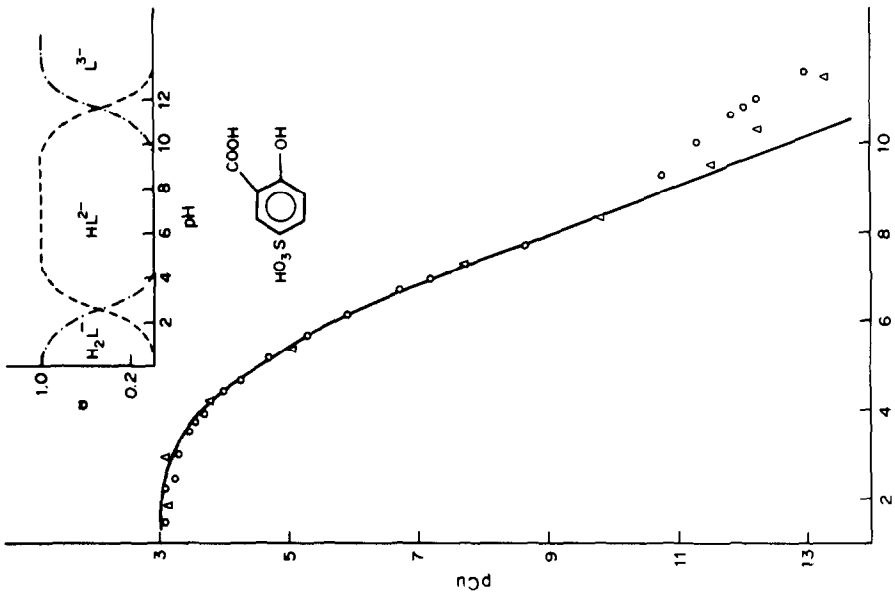

Fig. 7. pCu–pH relationship for $1 \times 10^{-3}M$ copper nitrate + $5 \times 10^{-2}M$ sulphosalicylic acid. Symbols as for Fig. 5.

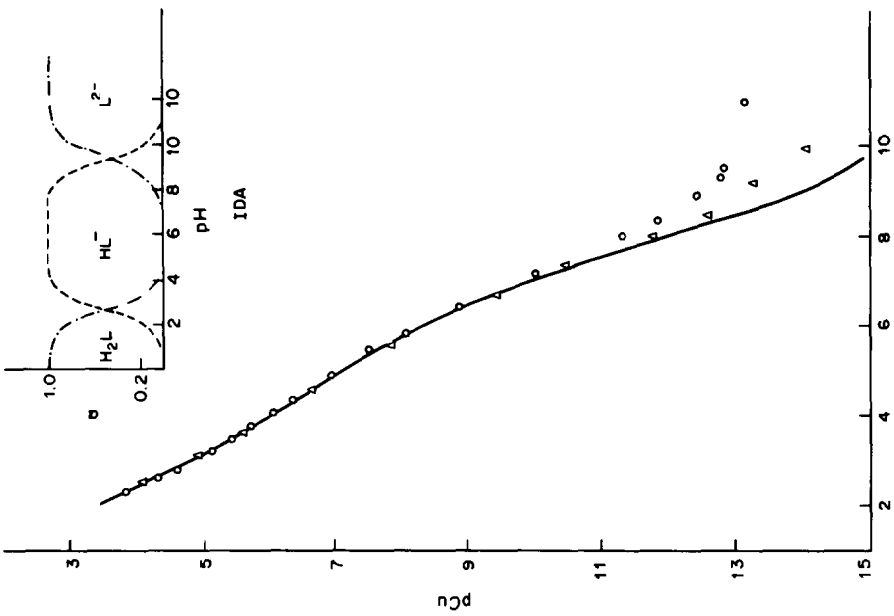

Fig. 9. pCu–pH relationship in $1 \times 10^{-3}M$ copper nitrate + $1 \times 10^{-2}M$ IDA. Symbols as for Fig. 5.

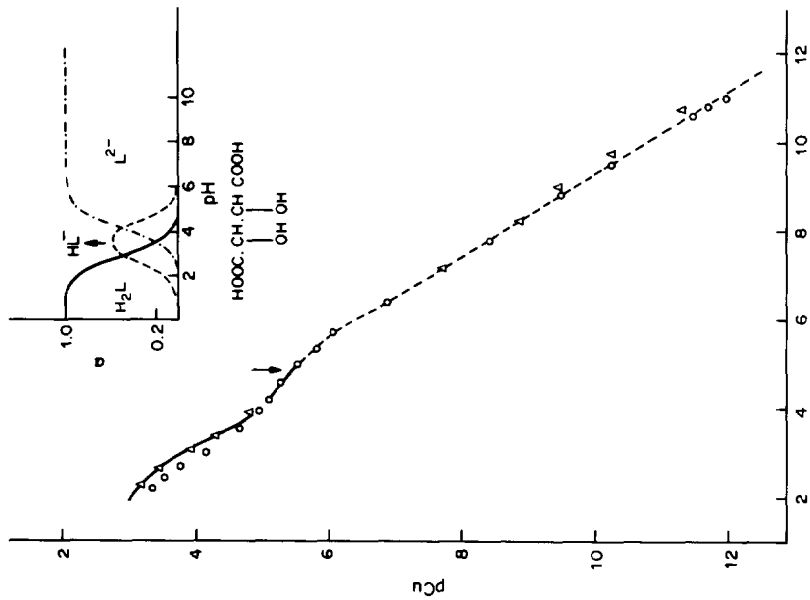

Fig. 8. pCu–pH relationship for $1 \times 10^{-3}M$ copper nitrate + $5 \times 10^{-2}M$ tartaric acid. Symbols as for Fig. 5.

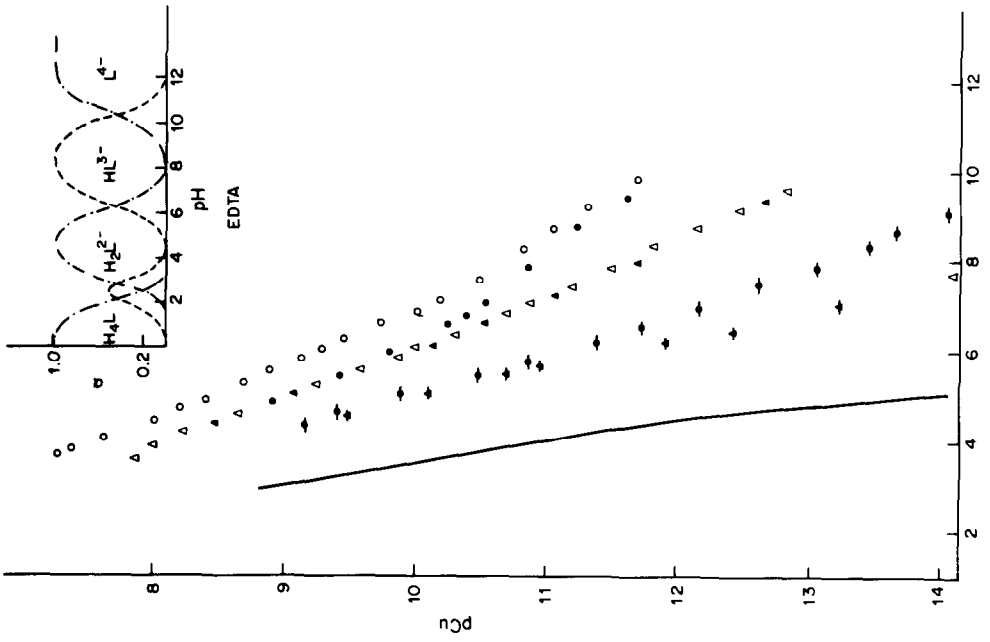

Fig. 11. pCu–pH relationship for $1 \times 10^{-3}M$ copper nitrate + $1 \times 10^{-2}M$ EDTA with the CuAgSe membrane (○, ●, -●-) and $Cu_{2-x}Se$ membrane (△, ▲, -▲-); (●, ▲) for the pure ligand solution; (-●-, -▲-) in presence of $0.1M$ glycine.

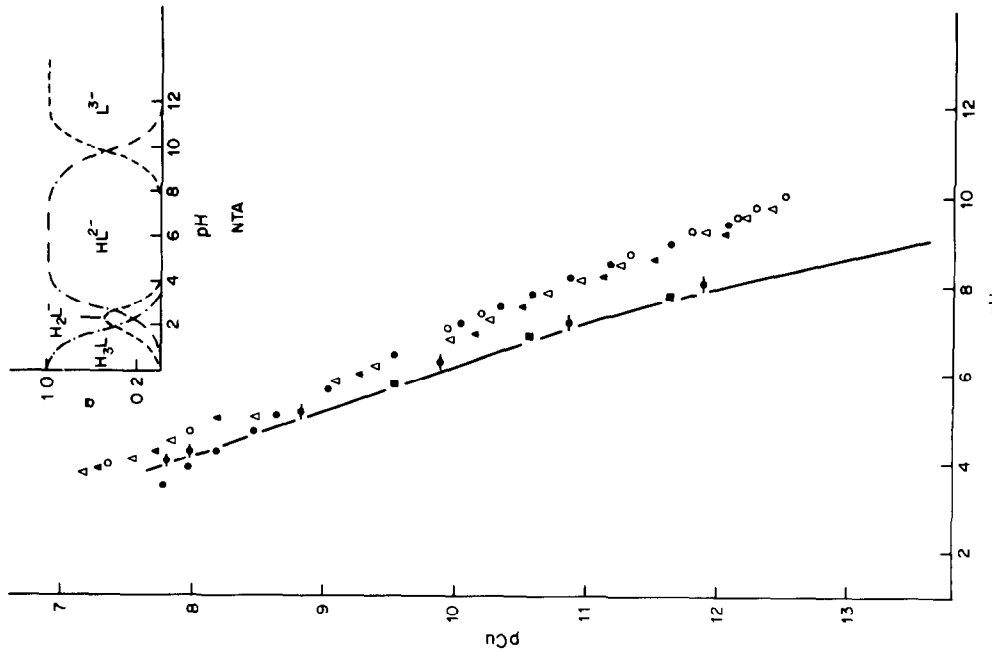

Fig. 10. pCu–pH relationship for $1 \times 10^{-3}M$ copper nitrate + $1 \times 10^{-2}M$ NTA with the CuAgSe membrane (○, ●, -●-) and $Cu_{2-x}Se$ membrane (△, ▲, ■); (●, ▲) for the pure ligand solution; (-●-, ■), in presence of $10^{-2}M$ glycine.

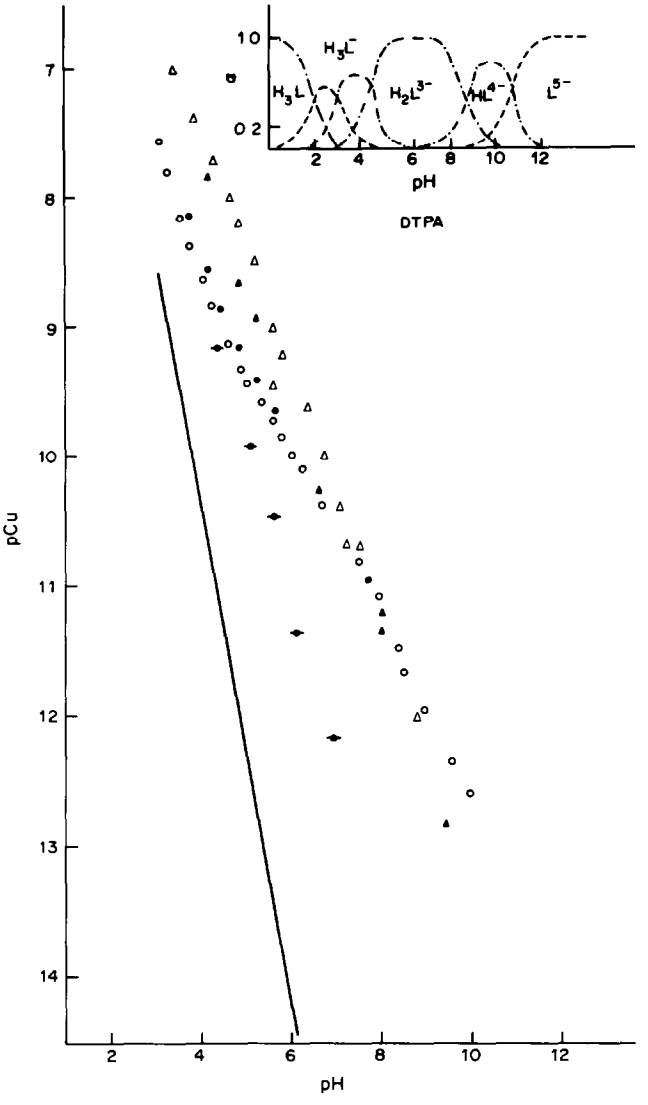

Fig. 12. pCu–pH relationship for $1 \times 10^{-3}M$ copper nitrate $+ 1 \times 10^{-2}M$ DTPA with the CuAgSe membrane (○, ●, -●-) and $Cu_{2-x}Se$ membrane (△, ▲); (●, ▲) for the pure ligand solution, (-●-) in presence of $0.1M$ glycine.

It is quite reasonable to presume[13] that the real activity of copper(I) at the electrode surface should be much higher than that calculated from the solubility data for the membrane material, and hence that the following equation for the surface copper(I) concentration will be valid:

$$[Cu^+]_0 = [Cu^+]_{0(K_{sp})} + [Cu^+]_{0(extran)} \qquad (4)$$

where the term $[Cu^+]_{0(extran)}$ depends on other factors than those related to the thermodynamic solubility $[Cu^+]_{0(K_{sp})}$ of the membrane. We think that these factors are intimately related to the defect structure and semiconductor character of the membrane materials.[14] The thermodynamic solubility contribution, $[Cu^+]_{0(K_{sp})}$, for the copper selenide sensor will be negligible, as calculated from $K_{sp(Cu_2Se)}$.[15] It varies from $2 \times 10^{-17}M$ at pH = 2 to $5.7 \times 10^{-20}M$ at pH = 8. Data for the solubility of CuAgSe are lacking, but it can be expected to be of the same order or lower. If we consider that the calibration limit for copper(I) buffer with both electrodes is[12] pCu(I) = 12, we have to accept a rather high concentration for $[Cu^+]_{0(extran)}$ in equation (4), *i.e.*, $[Cu^+]_{0(extran)} \gg [Cu^+]_{0(K_{sp})}$.

The experimental data strongly suggest that the Cu(I) activity at the electrode surface is pH-dependent. It decreases as the pH increases.

If all the above-mentioned circumstances are taken into consideration, equation (3) can be rewritten as

$$E = E^\circ + \frac{RT}{nF} \ln \left\{ \frac{[Cu^+]_{0(extran)}}{\alpha_{Cu^+(L)}} + K^{pot}_{Cu^+,Cu^{2+}} \left(\frac{[Cu^{2+}]}{\alpha_{Cu^{2+}(L)}} \right)^{1/2} \right\} \qquad (5)$$

for the general case. It follows that the electrodes should display anomalous behaviour when $[Cu^+]_{0(extran)}/\alpha_{Cu^+(L)}$ becomes commensurable with, or greater than, the second term in the bracket in equation (5). Thus equation (5) defines the "apparent" electrode sensitivity towards copper(II). Obviously all factors leading to decrease in the copper(I) activity at the electrode will increase the relative apparent sensitivity of the electrode with respect to copper(II).

On the basis of these assumptions, the observed experimental results can be interpreted as follows.

(1) Fairly good agreement between the measured and calculated pCu(II) values is observed for all systems over the pH range for which the equilibrium copper(II) concentration at any pH meets the condition

$$\left(\frac{[Cu^{2+}]}{\alpha_{Cu^{2+}(L)}}\right)^{1/2} K_{Cu^+,Cu^{2+}} \geqslant \frac{[Cu^+]_{0(extran)}}{\alpha_{Cu^+(L)}}$$

This requirement is easily met by complexes which exhibit only moderate stability in acidic medium.

(2) The deviations observed for the copper–complexone systems are due mainly to the high stability of the copper complexes even in acidic medium. It becomes more and more difficult to meet the above-stated requirement for a proper Nernstian response to Cu(II) as the stability of the Cu(II) complexes increases. That is why the extent of the observed deviations is in the same order as the stability of the complexes in acidic medium: Cu–IDA < Cu–NTA < Cu–EDTA ~ Cu–DTPA.

(3) It appears that the "apparent" electrode sensitivity towards Cu(II) will be different for each system since it will depend not only on the pH but also on the ability of the ligand to bind copper(I) in a complex too. Indeed, when the ligand also binds copper(I), the deviations are absent or start at higher pCu(II) in the alkaline region, *e.g.*, in the case of glycine, alanine, methionine and lysine.

(4) The electrode response in pure ligand solutions is a practical measure of the change in surface copper(I) concentration as a function of pH and complexation processes. The experimental curves in pure complexone solutions outline in fact the pCu(II)/pH region which can be used successfully in a particular Cu(II)–L system. Thus for the Cu–EDTA and Cu–DTPA systems the lowest copper(II) activity which can actually be measured varies from 8 to 12 as the pH is changed from 4 to 8.

It follows, on this hypothesis, that if an appropriate complexing agent for copper(I) which does not disturb the bulk equilibrium is introduced into the copper(II)–complexone solution, we should be able to decrease the discrepancy observed between the experimental and theoretical results, to an extent governed by the alteration in Cu(I)/Cu(II) ratio at the electrode surface. We used glycine, which forms complexes with copper(I) ($\log \beta_2 = 10.1$) and does not affect the Cu(II)–EDTA, Cu(II)–NTA and Cu(II)–DTPA equilibria when present in concentrations up to 0.1*M* at pH 8. The effect of addition of glycine to these systems was investigated over the concentration range 10^{-3}–$10^{-1}M$. Figures 10–12 present some of the results obtained.

As seen from the figures, the observed changes are in the predicted direction and also depend on the concentration of glycine. The expected decrease in the copper(I) activity at the electrode surface is adequate to eliminate the anomaly in the Cu(II)–NTA system, but is not sufficient to eliminate it in the other systems.

A logical question which arises is what is the limit of the relative sensitivity of the electrodes towards copper(II) which can be practically achieved. An attempt was made to reach this limit, by studying the effect of other ligands for copper(I) when introduced into the Cu(II)–EDTA system. The choice was restricted because of the requirement that the added ligand must not affect the Cu(II)–EDTA equilibrium. Thus, the effect of potassium chloride and potassium thiocyanate was investigated. An interesting phenomenon was observed in presence of 2*M* KCl and 0.1*M* KCNS. At all pH values >3, the membranes get "blocked", *i.e.*, they can no longer respond to change in the Cu(II) concentration and show an approximately constant and stable potential, corresponding to about pCu(II) = 12. When rinsed with water and introduced into copper(II) standards, the electrodes instantly regain their normal response. Lower concentrations of these ligands do not cause "blocking", but the response is heavily distorted, probably because the anomalous response to Cu(II) in presence of halides (or pseudohalides) is superimposed on it. The model for reduction of Cu(II) in the presence of chloride[16,17] seems very likely to be applicable in these cases too. No clear-cut explanation for the "blocking" can yet be presented, but the phenomenon does suggest that copper(I) plays a role in the potential-generating processes.

The assumption that the higher selectivity of the two electrodes towards copper(I) is the major reason for the observed anomalous behaviour can be further extended to other membranes of chalcogenide type. Moreover, it was recently established that even when the initial material is a CuS/Ag_2S mixture, a new phase containing copper(I) appears after pressing.[19] This offers an explanation of the fact that membranes differing in composition show similar anomalous behaviour in presence of EDTA, the differences being only in the extent of the deviations, which can be explained by a different copper(I) activity at the electrode surface, characteristic for each electrode material. The differences in the electrode materials in this respect can be simply established by comparative titration of copper(II) with EDTA and comparison of the experimental titration curves with the theoretical ones.

CONCLUSIONS

These investigations by no means provide grounds for pessimistic conclusions about the applicability of the different ion-selective electrodes for new equilibrium studies, but rather confirm that comprehensive understanding of the variable relative sensitivity limit towards Cu(II) and of the factors which affect it, can prevent erroneous interpretation of the experimental data, an example of which is a value proposed for the stability of the Cu(II)–NTA complex.[20] The results offer a possibility to formulate a practical criterion for the pCu(II)–pH region within which investigations must be confined. We recommend that before an investigation is attempted, the mV *vs.* pH relationship for the pure ligand and the Cu(II) + L systems be traced. The region where the two experimental curves are separated defines the values of pCu(II) which can be correctly measured. The success achieved by Baumann[21] in confirming the stability constants for Cu–EDTA and Cu–DTPA complexes by using the Orion copper ion-selective electrode, is due to the Cu–ligand ratio and pH being chosen so that the electrode measures pCu(II) values above its apparent limit of sensitivity.

This study strongly suggests that the potential-generation mechanism is identical for all chalcogenide copper electrodes, the role of copper(I) and the defect structure of the membranes being factors which undoubtedly deserve attention and deeper investigation.

A further theoretical exploration of these systems was presented at Euroanalysis V in Krakow, August 1984, and will be submitted to *Mikrochimica Acta* for publication.

REFERENCES

1. R. P. Buck, J. C. Thompsen and O. R. Melroy, in *ISEs in Analytical Chemistry*, Vol. 2, H. Freiser (ed.), p. 208. Plenum Press, New York, 1980.
2. E. Hansen, C. G. Lamm and J. Růžička, *Anal. Chim. Acta*, 1972, **59**, 403.
3. G. Nakagawa, H. Wada and T. Hayakawa, *Bull. Chem. Soc. Japan*, 1975, **48**, 424.
4. Y. Umezawa, Y. Imanishi, K. Sawatari and S. Fujiwara, *ibid.*, 1979, **52**, 945.
5. W. E. van der Linden and G. J. M. Heijne, *Anal. Chim. Acta*, 1978, **96**, 13.
6. G. Nakagawa, H. Wada and T. Sako, *Bull. Chem. Soc. Japan*, 1980, **53**, 1303.
7. A. Hulanicki, M. Trojanowicz and M. Cichy, *Talanta*, 1976, **23**, 47.
8. M. Neshkova and J. Havas, *Hung. Patent*, 174627, 31 August 1976.
9. *Idem*, *Anal. Lett.*, 1983, **16**, 1567.
10. M. Neshkova and H. Sheytanov, *J. Electroanal. Chem.*, 1979, **102**, 189.
11. *Idem*, investigation in progress.
12. *Idem*, *Talanta*, 1985, **32**, 654.
13. W. E. Morf, *The Principles of Ion-Selective Electrodes and of Membrane Transport*, Akadémiai Kiadó, Budapest, 1981.
14. W. E. Morf, G. Kahr and W. Simon, *Anal. Chem.*, 1974, **46**, 1538.
15. R. M. Smith and A. E. Martell *Critical Stability Constants*, Vol. 4, Plenum Press, New York, 1976.
16. J. C. Westall, F. M. M. Morel and D. N. Hume, *Anal. Chem.*, 1979, **51**, 1792.
17. T. Hepel, *Anal. Chim. Acta*, 1981, **123**, 151.
18. G. J. M. Heijne and W. E. van der Linden, *ibid.*, 1977, **93**, 99.
19. H. Stünzi, *Talanta*, 1982, **29**, 75.
20. S. Ramamoorthy, C. Guarnaschelli and D. Fecchio, *J. Inorg. Nucl. Chem.*, 1972, **34**, 1651.
21. E. W. Baumann, *ibid.*, 1974, **36**, 1827.
22. A. E. Martell and R. M. Smith, *Critical Stability Constants*, Vol. 1, Plenum Press, New York, 1974.
23. A. Ringbom, *Complexation in Analytical Chemistry*, Interscience, New York, 1963.
24. L. G. Sillén and A. E. Martell, *Stability Constants*, Special Publ. No. 25, The Chemical Society, London, 1971.

Talanta, Vol. 32, No. 10, pp. 949–952, 1985
Printed in Great Britain.

0039-9140/85 $3.00 + 0.00

DETERMINATION OF NICKEL IN THE SERUM OF OCCUPATIONALLY EXPOSED WORKERS, BY MEANS OF FLAME ATOMIC-ABSORPTION SPECTROSCOPY*

ANNA MARIA GHE†, MARIA TERESA LIPPOLIS and LUCIANA PASTORELLI
Istituto Chimico "G. Ciamician" dell'Università, Scuola di Specializzazione in Chimica Analitica, Via Selmi 2, 40126 Bologna, Italy

(*Received* 19 *October* 1983. *Revised* 2 *May* 1985. *Accepted* 8 *May* 1985)

Summary—A flame atomic-absorption spectroscopy method for determination of nickel in the serum of occupationally exposed subjects has been developed. Trichloroacetic acid is utilized for precipitating proteins and freeing bound nickel; sodium diethyldithiocarbamate is used as complexing agent and isopropyl acetate as the solvent for extraction. The method is characterized by good accuracy, precision and sensitivity, over a concentration range up to about 20 ng/ml. Calcium, which is present in serum in great excess with respect to typical nickel concentrations, does not interfere in the determination of the latter.

The determination of nickel has been the subject of numerous investigations in view of the industrial and environmental importance of this element on the one hand, and of its biological relevance on the other, since nickel is one of the essential trace elements in the human body.

Either lack of nickel or an excess of it with respect to the regular levels, such as can be induced by consumption in food or by industry-related exposure, can have toxic effects on humans.

The clinical consequences of such irregular levels range from common dermatitis, through skin intoxication, to chronic rhinitis and sinusitis,[1–3] and several types of cancer.[4–6] Its concentration in the serum of "normal" subjects ranges between 2.0 ± 0.9 ng/ml (in areas of low environmental nickel concentration) and 4.6 ± 1.4 ng/ml (levels recorded in North America industrial areas), but can rise to over 20 ng/ml in workers in the nickel industry who are "over-exposed".[7–9]

Recently, some AAS methods for the determination of nickel in the serum and urine of "normal subjects", based on use of electrothermal atomization, have been developed.[10,11]

In the work described here a simple and reliable method for the flame AAS determination of Ni in the serum of occupationally exposed workers has been developed.

EXPERIMENTAL

Apparatus

A double-beam Perkin-Elmer AAS spectrometer (model 372), equipped with an 057–0706 burner–nebulizer for an air–acetylene flame, a nickel hollow-cathode lamp (Intensitron 303–6047; lamp current 25 mA) and a Leeds-Northrup chart-recorder, was utilized. An Orion 701 A pH-meter, with a glass microelectrode, was used for pH measurement, which was done on a duplicate test solution to avoid possible contamination with nickel from the electrode.

Standard instrumental parameters

Spectrophotometric measurements were made at the 232-nm resonance line of nickel, which (with a 0.2-nm band-pass) gives the best reciprocal sensitivity for this element.[12]

The flow ratio of air to acetylene was 55:32 (for our spectrometer); the air and acetylene pressures were 3 and 1 kg/cm^2, respectively; the aspiration rate was 8 ml/min; the signal was integrated for 5 sec.

For the work with organic solvents the same experimental conditions were used, except for a different flow ratio of air to acetylene, namely 35/17.

Reagents, solvents and containers

Great care was taken to prevent contamination of the sample with nickel from the environment and from the operators, and to follow the recommendations outlined in a IUPAC reference work.[10]

All the reagents and solvents utilized (of ultrapure grade) were, whenever necessary, further recrystallized or distilled, and tested, by the method described here, for freedom from nickel.

Hydrochloric acid and nitric acid were J. T. Baker "Ultrex" products. Trichloroacetic acid (TAA), ammonia, potassium hydroxide, absolute ethanol and acetone were all Baker "ACS analyzed reagents", and the sodium diethyldithiocarbamate (NaDDC) and dithizone (DZ) were Eastman Kodak "ultra pure" reagents.

Isopropyl acetate (IPA) (b.p. 87–89°) and carbon tetrachloride, were Fluka "ultra pure" products. Before use, the IPA was distilled at atmospheric pressure in a protective stream of argon and the fraction boiling at $86 \pm 0.1°$ was utilized. The solvent thus produced gave a level base-line. Care was taken to saturate the solvent with water, so as to prevent volume changes during extraction; for the same reason, the aqueous solutions utilized in the extraction procedure were presaturated with IPA.

The standard nickel and calcium solutions for calibration purposes were obtained by diluting Carlo Erba standard 1000 ppm solutions for AAS.

*Work done with the financial support of the National Research Council (C.N.R.), Rome, Italy (No. 820781).
†Author for correspondence.

The aqueous 1% solution of the complexing agent (NaDDC) was freshly prepared before use. The ultrapure water used was demineralized and then distilled twice in quartz apparatus and stored in polyethylene containers. Its conductivity was 1×10^{-6} mho at 25°.

The more acidic solutions were stored either in polypropylene bottles or borosilicate glass bottles, depending on the pH, and were kept in the dark to prevent exchange of metal ions in solution.[13]

The necessary glassware and analytical utensils were kept immersed in 6% v/v nitric acid,[14] and washed in conductivity water (see above) immediately before use. Possible contamination of the glass was eliminated by soaking in $10^{-3}M$ dithizone solution[15] for 3 hr, rinsing with acetone and finally with the ultrapure water.

Optimum pH for complexation and extraction

The NaDDC–IPA combination was chosen as the most promising of those in the literature,[16] and from results obtained in this laboratory, because of its good sensitivity, extraction efficiency and enhancement for the element investigated.[17,18] Indeed NaDDC appears to be the most efficient extraction agent for nickel and IPA is superior to most of the other possible solvents in terms of the physical properties which have most influence on the atomization process.

The optimum pH for the complex-formation and the IPA extraction was found by adjusting the pH of 5 ml of standard nickel solutions (0.5 and 0.05 ppm) to various values in the range 0–6, adding 1 ml of 1% NaDDC solution, extracting with 5 ml of IPA, separating the organic phase and measuring the atomic absorption, under the conditions already described. Figure 1 shows the pH range 2.5–3.0 is optimal.

AAS calibration curves

Aqueous nickel solutions (concentration 0.1–1 ppm) were prepared by diluting a C. Erba standard solution for AAS and their absorbances were measured under the conditions described above. The calibration graph was linear and the characteristic concentration was 0.15 μg/ml for 1% absorption.

A corresponding calibration was done for the NaDDC–IPA system, by addition of 0.065 ml of hydrochloric acid (1 + 9) to 5 ml of nickel solution (0.1–0.9 ng/ml) to give pH 2.2, followed by addition of 1 ml of 1% NaDDC solution (pH shift to 2.5), stirring for 1 min, extraction with 5 ml of IPA and measurement of the organic phase by AAS. A blank was prepared analogously with 5 ml of ultrapure water. A calibration graph covering the nickel range 0.01–0.1 ng/ml was similarly obtained. Both graphs were linear.

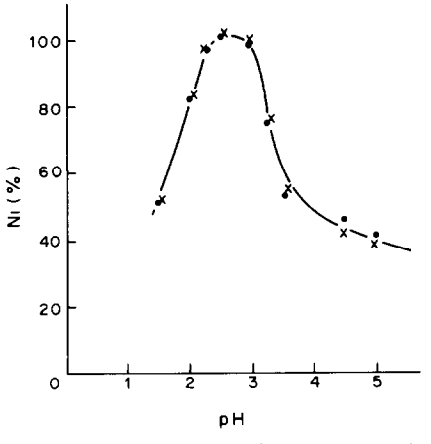

Fig. 1. Effect of pH on extraction of Ni–DDC complex with IPA. Ni: 0.5 μg/ml —●—●—; 0.05 μg/ml — × — × —.

Because the proteins present in serum, some of which are bound to nickel, interfere with the flame AAS, precipitation with 10% trichloroacetic acid (TAA) solution, which also liberates the bound nickel, was tested as the means for their elimination. The nickel standards (5 ml) were treated with 10 ml of 10% TAA solution (to obtain the optimum conditions for the deproteination), 1.8 ml of $1M$ potassium hydroxide and 1 ml of 1% NaDDC solution, and extracted with 5 ml of IPA as before. The trichloroacetic acid and the changed aqueous/organic phase-volume ratio did not appreciably alter the calibration graphs for the nickel ranges 0.02–0.10 and 0.2–1.0 μg/ml.

Although the calibration graphs were all satisfactory, the standard-additions method was used for the determination of nickel in serum, to eliminate any other possible interferences from the matrix.

Procedure for nickel in serum

A 20-ml serum sample from blood withdrawn with special care taken to avoid contamination with nickel,[10] was quantitatively transferred to a 100-ml polyethylene centrifuge tube and 40 ml of 10% TAA solution presaturated with IPA were slowly added. The mixture was stored for 18–24 hr at 4°, then centrifuged at 5000 rpm for 30 min.

The clear supernatant liquid was filtered into a separating funnel through a double Schleicher & Schull 587/E filter, two 2-ml portions of water being used to transfer and wash the precipitate. To the solution were added 4 ml of C. Erba pH-3 "Normex" buffer and then concentrated ammonia solution dropwise to give a final pH of 1.5–2.0. Then 4 ml of 1% NaDDC solution were added, the solution was shaken for 2 min, 20 ml of IPA saturated with water were added and the mixture was shaken for 2 min. After separation of the phases, the organic phase was collected and centrifuged. Each of a series of 2.5-ml aliquots of this extract was then shaken with a mixture of 2.5 ml of standard aqueous nickel soltuion and 0.5 ml of 1% NaDDC solution, buffered at pH 2.5. The nickel standards all differed in concentration over a range suitable for the sample analysed. After separation of the phases, the organic phase was centrifuged at 5000 rpm for 10 min and the AAS value for nickel was measured under the standard conditions prescribed. The same procedure was used with 2.5 ml of ultrapure water instead of a nickel standard, to obtain the "zero" for the standard-additions graph, from which the nickel concentration was determined in the usual way from the intercept of the straight line on the abscissa.

RESULTS AND DISCUSSION

The method was applied to the pooled serum from a group of "exposed workers" and linear regression analysis of the standard-additions graph gave a value of 18 ng/ml (90% confidence limits 14–22 ng/ml).

Statistical analysis gave the following equation for the straight line (90% confidence limits in parentheses):

$$A = 1.83(\pm 0.39) \times 10^{-3} + 1.04(\pm 0.05) \times 0.1[\text{Ni}](\mu\text{g/ml})$$

with correlation coefficient $r = 0.998$.

The technique was also applied to determine the recovery of nickel added at the 20-ng/ml level to a pooled serum which had previously been found to contain 19.1 ng/ml (mean of 20 determinations; standard deviation 0.5 ng/ml). The total nickel concentration found (mean of 20 determinations) was

Table 1. Determination of nickel (*ng/ml*) in pooled serum of "occupationally exposed" subjects*

Sample	AAS flame method		DMG-sensitized differential pulse polarography[19]‡	
	Mean†	*s*§	Mean‖	*s*§
A	18.5 ± 3.9	1.3	17.2	1.2
B	10.2 ± 3.8	1.2	11.8	1.3
C	28.2 ± 4.2	1.4	26.2	1.3
D	33.8 ± 4.3	1.5	34.0	1.9
E	22.0 ± 3.6	1.2	23.7	1.4

*Workers in industrial areas of Northern Italy.
†Mean and confidence limits for six determinations per sample.
‡Buffer 0.1*M* ammonium tartrate/0.1*M* ammonia, pH 9.2; [DMG] = $4.3 \times 10^{-5}M$.
§Estimated standard deviation.
‖Mean of six determinations per sample.

38.8 ng/ml (standard deviation 0.6 ng/ml), showing a recovery better than 98%.

Further analysis of pooled serum from occupationally "exposed" subjects gave the results in Table 1. The samples were also analysed, for comparison, by differential-pulse polarography.[19] The AAS and polarographic results agreed within 2 ng/ml.

Interferences

Determination of nickel by flame AAS has always appeared relatively free from interference.[20–25]

Nomoto and Sunderman,[7] in an examination of the Sprague and Slavin method,[26] studied the interference of most of the elements possibly present in serum and other matrices and found that only cadmium and gold caused deviations greater than ±1% from the absorbance values of nickel standards.

In the present investigation, possible interference by calcium was examined, because of its very high concentration relative to that of nickel[27] (Ca 100 μg/ml; Ni 20–30 ng/ml) in the serum of occupationally overexposed subjects.

Calibration graphs were prepared for nickel in the range 0.1–0.8 μg/ml in the presence of 0, 100 and 500 μg/ml calcium, and compared. The difference in absorbance caused by the presence of calcium was expressed as a fraction of the absorbance for the corresponding calcium-free nickel standard, to yield a percentage interference (*I*, %). The values obtained at the two fixed calcium concentrations are plotted against nickel concentration in Fig. 2A and the values for a fixed nickel concentration of 0.7 μg/ml and varied calcium concentration are plotted in Fig. 2B. Each point represents the average of ten determinations. Very similar results were obtained for calcium interference in determination of nickel in human serum.

As can be observed, a fixed level of calcium causes increasing enhancement of the signal up to a certain nickel concentration, above which the enhancement is constant. The degree of enhancement increases

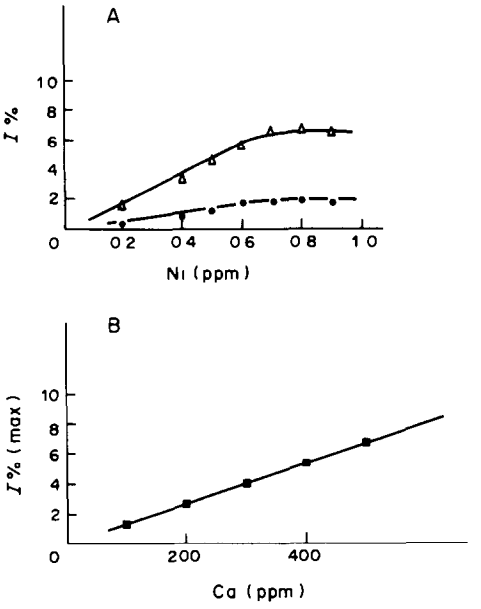

Fig. 2. Calcium interference. (A) Interference (*I*%) of calcium at constant concentration (● 100 μg/ml; △ 500 μg/ml) as a function of nickel concentration; (B) interference (*I*%) of increasing calcium concentrations at constant nickel concentration (0.7 μg/ml).

linearly with calcium concentration up to the limit examined. The enhancement could possibly be due to the ionization and boiling point of calcium being lower than those for nickel,[28] resulting in suppression of any ionization of nickel atoms, and lowering of the boiling point of nickel, thus increasing the number of free nickel atoms in the flame and hence the absorbance values. This hypothesis is in agreement with the results shown in Fig. 2B, where the interference effect is seen to increase linearly with calcium concentration. However, there is less than 2% enhancement when the nickel concentration is lower than 200 ng/ml, so this source of interference does not affect the determination of nickel in the concentration range of interest here (namely 20–30 ng/ml), where the uncertainty of the determination is itself higher than 2%. The proposed method is therefore applicable to determination of nickel in serum of occupationally exposed workers; it is simple and gives good accuracy and precision.

Acknowledgements—This work was done with the financial assistance of the National Research Council (C.N.R.), Rome, which is gratefully acknowledged.

REFERENCES

1. A. A. Tatarskaya, *Gig. Trud. Prof. Zabol.*, 1960, **6**, 35.
2. G. M. Kucharin, *Brit. J. Dermatol.*, 1975, **93** (Suppl.), 41.
3. A. V. Suschenko and K. E. Rafikova, *Gig. Trud. Prof. Zabol.*, 1972, **16**, 42.
4. J. G. Morgan, *Brit. J. Indust. Med.*, 1958, **15**, 224.
5. A. V. Sakiyn and N. K. Shabymine, *Gig Trud. Prof. Zabol.*, 1973, **17**, 25.

6. *IARC Monographs*, Vol. II, IARC Publishing Office, Lyon, 1976.
7. S. Nomoto and F. W. Sunderman, Jr., *Clin. Chem.*, 1970, **16,** 477.
8. M. D. McNeely, M. W. Nechay and F. W. Sunderman, Jr., *ibid.*, 1972, **18,** 992.
9. D. Mikac-Devic, F. W. Sunderman, Jr. and S. Nomoto, *ibid.*, 1977, **23,** 948.
10. S. S. Brown, S. Nomoto, M. Stoeppler and F. W. Sunderman, Jr., *Clin. Biochem.*, 1981, **14,** 295.
11. F. W. Sunderman, Jr., M. C. Crisostomo, M. Reid, S. M. Hoffer and S. Nomoto, *Ann. Clin. Lab. Sci.*, 1984, **14,** 232.
12. B. Weltz, *Spettroscopia di assorbimento atomico*, 1st Ed., p. 205. ETAS, Milan, 1976.
13. A. W. Struempler, *Anal. Chem.*, 1976, **45,** 2251.
14. K. M. Bone and W. D. Hibbert, *Anal. Chim. Acta*, 1979, **107,** 219.
15. A. Vanni and P. Amico, *Ann. Chim. (Roma)*, 1976, **66,** 719.
16. V. B. Stein and B. E. McClellan, *Environ. Sci. Technol.*, 1980, **14,** 872.
17. A. J. Lemonds and B. E. McClellan, *Anal. Chem.*, 1973, **45,** 1455.
18. C. L. Chakrabarti and S. P. Singhal, *Spectrochim. Acta*, 1969, **24B,** 663.
19. C. J. Flora and E. Nieboer, *Anal. Chem.*, 1980, **52,** 1013.
20. K. Kinson and C. B. Belcher, *Anal. Chim. Acta*, 1964, **30,** 64.
21. F. W. Sunderman, Jr., *Ann. J. Clin. Pathol.*, 1965, **44,** 182.
22. Y. A. Platte and V. W. Marcy, *Atom. Abs. Newslett.*, 1965, **4,** 289.
23. L. L. Sundberg, *Anal. Chem.*, 1973, **45,** 1460.
24. Y. A. Helsen and P. F. Hermans, *Atom. Abs. Newslett.*, 1977, **16,** 119.
25. C. T. Bishop and R. N. Harris, *ibid.*, 1969, **8,** 110.
26. S. Sprague and W. Slavin, *ibid.*, 1964, **3,** 160.
27. P. L. Altman and D. S. Dittmer, *Biology Data Book*, 2nd Ed., Vol. III, pp. 1751–1752. Fed. Am. Soc. Exper. Biol., Bethesda, Maryland, 1974.
28. *CRC Handbook of Chemistry and Physics*, R. C. Weast and M. Y. Astle (eds.), 60th Ed., pp. e68, b101, b64. Chemical Rubber Company, Boca Raton, Florida, 1979–1980.

Talanta, Vol. 32, No. 10, pp. 953–956, 1985
Printed in Great Britain.

0039-9140/85 $3.00 + 0.00

SEPARATION OF SILVER FROM ZINC, CADMIUM, COPPER, NICKEL AND OTHER ELEMENTS IN NITRIC ACID WITH A MACROPOROUS RESIN

F. W. E. STRELOW
National Chemical Research Laboratory, P.O. Box 395, Pretoria, Republic of South Africa

(*Received* 23 *November* 1984. *Revised* 9 *January* 1985. *Accepted* 7 *May* 1985)

Summary—Traces of silver and amounts up to 50 mg can be separated from up to gram amounts of Zn, Cu(II), Ni, Co(II), Mg, Be, Ti(IV), V(IV), Li and Na by eluting these with 2.0*M* nitric acid from a column containing 54 ml (20 g) of macroporous AG MP-50 cation-exchange resin of 100–200 mesh particle size, in the H^+-form. Silver is retained and can be eluted with 0.5*M* hydrobromic acid in 9:1 v/v acetone–water. Separations are sharp and quantitative and only a few μg of the other elements are found in the silver fraction. Cadmium and manganese (II) can also be separated quantitatively but show tailing and require larger elution volumes. Some typical elution curves and results of analyses of synthetic mixtures are presented.

Because silver can be determined accurately in the presence of many other metals its separation by ion-exchange chromatography has not received much attention. It has been suggested that at trace concentrations silver can be sorbed by strongly basic anion-exchange resins in the chloride form from dilute hydrochloric acid (0.1*M*) and eluted at high concentrations of the same acid.[1] This approach has been applied to the separation of silver from iron meteorites.[2] However, elution with hydrochloric acid is incomplete and nitric acid–acetone mixtures are more effective eluting agents.[3] Sorption of silver from seawater, on an anion-exchange resin, is considerably enhanced if the sample is made 0.05*M* in ammonium thiocyanate, and 0.4*M* thiourea is used as eluent.[4] Trace amounts of silver in rain water have been sorbed on a cation-exchange resin and selectively eluted with 0.1*M* ammonium thiocyanate.[5] Most of these methods are only applicable to trace amounts of silver and run into difficulties with amounts >100 μg because of formation of insoluble silver salts.

Probably the most selective method for the separation of larger amounts of silver from other elements is sorption by cation-exchange resins from solutions containing EDTA. Though this approach has been described in detail only for separation from nickel,[6] cobalt,[7] and mercury,[8] it should be applicable to separation from a large number of other elements. Its disadvantage is that the presence of EDTA and high salt concentrations in the eluates may be detrimental when highly accurate results are required. Lead and mercury(II) have been separated from silver by cation-exchange in ammonium acetate media,[9] but the separation factor for the Ag–Pb pair is only about 3.5 and the accuracy of quantitative results obtained is poor. The behaviour of other elements is also uncertain. Selective elution of silver from a cation-exchange column by elution with 2% sodium nitrite solution has been proposed for its separation from cobalt and nickel.[10] Elution with diethanolamine–nitric acid buffers has been suggested for separation of silver from lead.[11] In both methods the separation factors are not very large, and silver is eluted first. This is less attractive for separating small amounts of silver from large amounts of the other elements because gram amounts of these would seriously overload the columns in view of the small separation factors.

A systematic study of the macroporous cation-exchange resin AG MP-50[12] has shown that the distribution coefficient of silver is about 5 times that obtained with a gel-type resin of 8% cross-linkage such as AG 50W-X8, whereas the coefficients for the bivalent transition metals are much less increased. An exploitation of this fact is described in this paper.

EXPERIMENTAL

Reagents and apparatus

All chemicals used were of analytical reagent grade. Water was distilled and then passed through an Elgastat demineralization unit. Standard stock solutions were made up in 0.5*M* nitric acid. Those of titanium(IV) also contained 0.3% hydrogen peroxide. The resin used was the AG MP-50 macroporous cation-exchanger, a sulphonated polystyrene, 100–200 mesh, in the H^+-form. Borosilicate glass tubes, 400 mm long, 21 mm bore, fitted with a B19 joint at the top and a No. 2 porosity sintered-glass plate and a burette tap at the bottom were used for making the columns.

The glass columns were loaded with a slurry of the resin until the settled resin reached a 54-ml volume mark ($\equiv$20 g of dry resin in the H^+-form). The resin was purified by passage of about 500 ml of 5*M* nitric acid followed by 100 ml of demineralized water, shaking with water, and allowing the resin to resettle. The eluent for silver, "HBr/acetone", was prepared by mixing 1 part of 5.0*M* hydrobromic acid and 9 parts of acetone in a standard flask. After mixing, the solution was degassed by leaving the flask open for a few hours or overnight with the stopper inverted on the top and

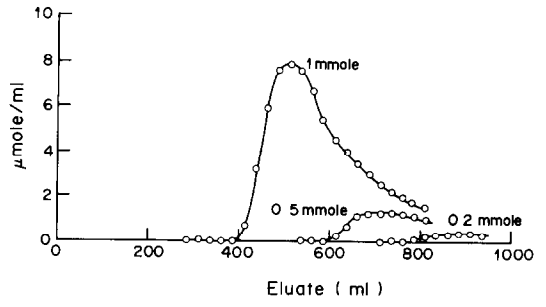

Fig. 1. Elution curves for various amounts of Ag with 2.0*M* HNO_3; 54 ml (20 g) of AG MP-50 resin, 100–200 mesh (155 mm length, 21 mm diam.). Flow rate 2.0 ± 0.3 ml/min.

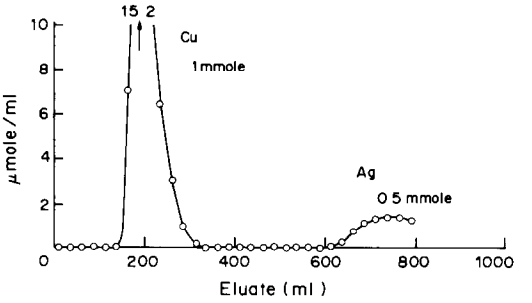

Fig. 2. Elution of Cu(II)–Ag with 2.0*M* HNO_3. Experimental conditions as for Fig. 1.

shaking the flask from time to time. Degassing is important to avoid or minimize bubble formation in the resin column. The silver eluent should not be too old (< 3 days), because the acetone tends to polymerize, and if too much polymer forms, recovery of traces of silver becomes incomplete.

Atomic-absorption measurements were made with a Varian–Techtron AA-5 instrument with either the air–acetylene or the nitrous oxide–acetylene flame, the latter for traces of beryllium.

Elution curves

Behaviour of various amounts of silver. A solution containing about 1 mmole of silver in about 50 ml of 0.5*M* nitric acid was passed through a column of clean resin as described above. The silver was washed into the column with several small portions of 2.0*M* nitric acid, and then eluted with 2.0*M* nitric acid at a flow-rate of 2.0 ± 0.3 ml/min. Fractions (25 ml) were taken with an automatic fraction collector from the beginning of the washing step, and the amounts of silver in the fractions determined by atomic-absorption spectrometry with appropriate dilutions when required. The experiment was repeated with 0.5 and 0.2 mmole amounts of silver and the same column. The experimental elution curves are shown in Fig. 1.

Separation of element pairs. A solution containing about 1 mmole of copper(II) and 0.5 mmole of silver in about 50 ml of 0.5*M* nitric acid was passed through a column as described above, and the elements (copper first) were eluted with 2.0*M* nitric acid at a flow-rate of 2.0 ± 0.3 ml/min. Fractions of 25 ml were collected as before and analysed for silver and copper. The copper concentration in the 350–375 ml fraction was less than 0.01 ppm. No silver (< 0.001 ppm) appeared in the first 550 ml. The experimental elution curve is shown in Fig. 2.

Figure 3 shows the curve for the zinc–silver pair. The elution of zinc with 2.0*M* nitric acid was terminated at 450 ml in this case, the nitric acid was washed from the column with 50 ml of 60:40 v/v acetone–water mixture ("60% acetone"), and the silver finally eluted with "HBr/acetone", a very effective eluent for silver.

This experiment was repeated with 10 mmoles of zinc and 1 mg of silver sorbed from 100 ml of 0.5*M* nitric acid but 900 ml of 2.0*M* nitric acid were used for the first elution step, followed by 250 ml of "HBr/acetone" eluent, with no wash step in between. After passage of 350 ml of nitric acid the concentration of zinc in the subsequent eluate was below the background level (~0.02 ppm). No silver could be detected in the 900 ml of nitric acid eluate, and all silver was eluted with 100 ml of the "HBr/acetone" eluent.

Ni, Co(II), Mg, Be, V(IV), Ti(IV) and Li were either eluted similarly to copper and zinc or even faster. Manganese(II) and cadmium are retained more strongly however, and show considerable tailing on elution with 2.0*M* nitric acid, 1 mmole of manganese requiring 600 ml of the acid for complete elution. Nevertheless, up to 0.2 mmole of silver can be separated from 1 mmole of manganese, since elution of silver begins only after passage of about 700 ml of the eluent. As shown in Fig. 1, however, large amounts of silver would not be adequately separated. Cadmium behaves similarly to manganese.

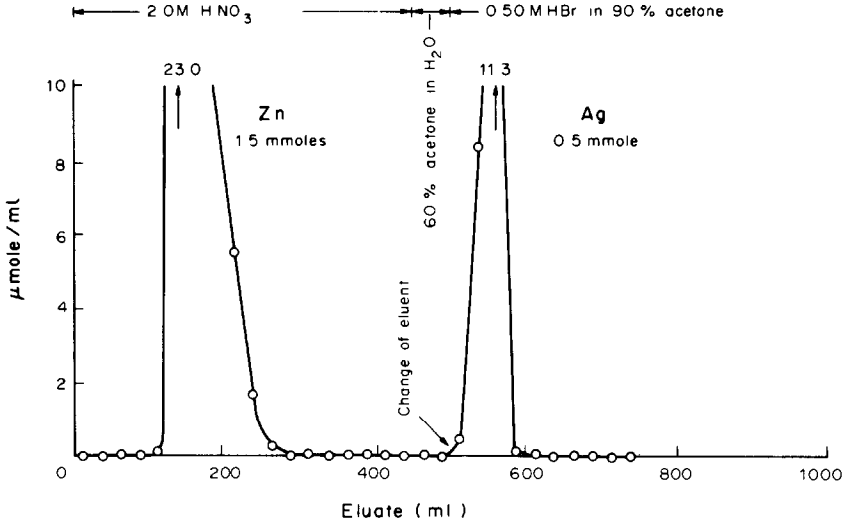

Fig. 3. Elution of Zn–Ag with 2.0*M* HNO_3, followed by 0.50*M* HBr in 90% acetone. Experimental conditions as for Fig. 1.

Table 1. Recovery of silver from binary synthetic solutions

Other ions				Silver	
Taken, *mg*		Found in 2*M* HNO_3 eluate, *mg*	Found in HBr/acetone eluate, *μg*	Taken, *μg*	Found in HBr/acetone eluate,§ *μg*
Zn^{2+}	65.84	65.85 ± 0.03	N.D.*	53.9×10^3	$(53.9 \pm 0.1) \times 10^3$
Zn^{2+}	658.4	658.3 ± 0.3	N.D.	1000	999 ± 2
Zn^{2+}	658.4	N.D.	3.8–9.6	100	100.2 ± 0.5
Zn^{2+}	1317	N.D.	4.9–10.8	20	19.9 ± 0.3
Cu^{2+}	667.1	667.0 ± 0.3	1.4–2.3	100	100.0 ± 0.3
Cu^{2+}	1334	N.D.	1.7–2.8	100	99.8 ± 0.3
Cd^{2+}	1117	1117 ± 1	13.6–15.9	100	99.8 ± 0.5
Ni^{2+}	591.7	591.7 ± 0.3	0.9–1.8	100	100.0 ± 0.3
Co^{2+}	590.9	590.8 ± 0.3	1.3–2.1	100	100.2 ± 0.5
Mn^{2+}	548.1	548.2 ± 0.3	1.8–8.2	100	99.8 ± 0.3
Mg^{2+}	244.6	244.7 ± 0.2	5.6–9.8	100	100.0 ± 0.3
Be^{2+}	91.4	91.4 ± 0.1	0.2–0.6	100	99.8 ± 0.5
Ti(IV)†	481.2	481.3 ± 0.2	N.D.	100	100.2 ± 0.5
V(IV)	510.1	510.0 ± 0.3	N.D.	100	100.0 ± 0.3
Li^+	69.5	69.6 ± 0.2	0.9–1.6	100	99.8 ± 0.3
Na^+	230.2	230.3 ± 0.4	12.8–17.4	100	100.0 ± 0.5

*N.D. = not determined.
†0.1% H_2O_2 present.
§Mean and standard deviation of 20 readings.

Quantitative separations

A series of columns each containing 54 ml of resin was prepared as described above. Appropriate volumes of standard solutions of silver and one other element (as the nitrates) were accurately measured out in triplicate, mixed and adjusted to yield about 100 ml of solution in about 0.5*M* nitric acid. Another set of standard solutions was also measured out in triplicate, but kept separate for comparative measurements. The mixed solutions were passed through the resin columns and the cations washed into the resin with several portions of 2.0*M* nitric acid. The elements were then eluted with a total of 425 ml of 2.0*M* nitric acid, including the washing step, at a flow-rate of 2.0 ± 0.3 ml/min. When about 1 g of copper was present 475 ml of eluent were used. For manganese(II) and cadmium 750 ml of the eluent were used because of the delayed elution and tailing. For Be, Li, Na, Ti(IV) and V(IV) the eluates were collected right from the beginning of the sorption step, but for the other elements they were collected from the beginning of the washing step. For titanium 0.10% hydrogen peroxide was present in the test solution and eluent. The nitric acid was then washed from the column with 60% acetone and the silver was eluted with "HBr/acetone" at a flow-rate of 3.0 ± 0.5 ml/min. For 50 mg of silver, 200 ml of the eluent were used, and 125 ml in all other cases. The eluates were evaporated to dryness on a water-bath and the elements determined by the analytical methods in Table 2 after dissolution and suitable dilution. Appropriate amounts of thiourea were added to the silver fractions to dissolve the bromide for AAS determination by atomic-absorption. For traces of silver the amount of the other element remaining in the silver fraction was determined, by AAS when possible.

RESULTS AND DISCUSSION

Results for the analysis of binary synthetic mixtures are presented in Table 1. Silver was determined by AAS at 328.1 nm, with the air–acetylene flame. Samples and standards were all 0.5*M* in nitric acid and 0.1*M* in thiourea. Small amounts of the other elements, except beryllium, titanium and vanadium, were determined by AAS, by use of the most sensitive resonance line and an air–acetylene flame. For beryllium a nitrous oxide–acetylene flame was used. Larger amounts of the elements were determined titrimetrically or gravimetrically by the methods listed in Table 2.

The method can separate traces or larger amounts of silver from large amounts of most bivalent transition metals. It gives a superior separation of traces of silver from large amounts of copper than that given

Table 2. Analytical methods used

Element	Method
Zn	EDTA titration, acetate medium, pH 5.5, Xylenol Orange indicator.
Cu	DCTA titration, acetate medium, pH 5.5, Methylthymol Blue indicator in the presence of 1,10-phenanthroline.
Cd	EDTA titration in slight excess of ammonia, Methylthymol Blue indicator.
Ni	DCTA titration, ammonia solution (pH 10), Murexide as indicator.
Co	EDTA titration, pH 6 (pyridine buffer), Naphthyl Azoxine S indicator
Mn	DCTA titration (after reduction with ascorbic acid), pH 10 (triethanolamine present), Methylthymol Blue indicator.
Mg	EDTA titration, pH 10, Eriochrome Blue Black B indicator.
V(IV)	Addition of excess of EDTA and back-titration with $ZnSO_4$, acetate medium at pH 5.5, Xylenol Orange indicator.
Be, Ti	Gravimetrically as the oxides after precipitation with ammonia.
Li, Na	Gravimetrically as the sulphates

by the classical solvent extraction of silver dithizonate. Furthermore, a few mg of silver can also easily be separated from copper. Table 1 shows that traces of silver can be separated from about 1 g of zinc, copper and even the strongly sorbed cadmium. In 2.0*M* nitric acid, Ni, Co(II), Mg, Be, Ti(IV), V(IV), Li and Na have distribution coefficients either similar to or smaller than those of zinc and copper and can also be separated from silver. Furthermore, only a slightly larger amount of 2.0*M* hydrochloric acid is needed to elute 10 mmoles of zinc than is required for 1.5 mmoles. In addition, silver appears very late in the elution with 2.0*M* nitric acid when only 1 mg or less is present, and it is probable that several grams of zinc could be separated from small amounts of silver ($\leqslant 1$ mg). This should also apply to separation from the other ions listed above. Only a few μg of these remain in the silver fraction. All these elements show little tailing, and the flow-rates can be increased to 3.0–3.5 ml/min without detrimental effects. An elution volume of 425 ml provides a considerable safety margin to ensure quantitative elution and adequate separation from silver.

The situation is different for manganese(II) and cadmium, which require considerably larger elution volumes (750 ml) for quantitative recovery, because of the serious tailing, which increases with increasing flow-rate. The large eluent volumes and slow flow-rate of 2.0 ml/min needed for elution of these two elements make the separation from silver less attractive, through qualitative recovery can be achieved. Using 200–400 mesh resin does not lead to much improvement. Generally, lowering the flow-rate seems to be more effective than reducing the particle size for improving separations with the macroporous resin.

Sorption should be done from about 0.5*M* nitric acid to ensure that silver is sorbed as a band at the top of the column. As the nitric acid concentration is lowered competition from the multivalent ions becomes progressively stronger. The appearance of silver in the nitric acid eluate is strongly dependent on the total amount present (Fig. 1). No silver could be detected in the first 900 ml of 2.0*M* nitric acid eluate when only 1 mg of silver was present. Attempts to elute silver quantitatively with 5.0*M* nitric acid were not successful (though the distribution coefficient[12] of 13 is not excessively large) because of very strong and prolonged tailing.

The "HBr/acetone" eluent proved very effective for eluting and dissolving silver. Apparently the acetone promotes the formation of anionic silver bromide complexes sufficiently to dissolve considerable amounts of precipitated silver bromide. When large amounts of silver, 50 or 100 mg, were separated, a precipitate initially formed on the column in the region where the silver had been sorbed, but dissolved rapidly in the eluent. A 0.5*M* ammonium thiocyanate solution in 90% acetone was found to be even more effective, but destruction of the thiocyanate presented problems, because oxidation with nitric acid gave very fast autocatalysed reactions which could not be controlled, and led to sample losses.

Evaporation of the hydrobromic acid eluate led to a precipitate of silver bromide, which was dissolved in nitric acid containing thiourea and made up to an appropriate volume in 0.5*M* nitric acid/0.1*M* thiourea for AAS determination. Standards containing the same concentrations of nitric acid and thiourea were used for calibration. Solutions containing thiourea gave no memory effects when the Varian–Techtron AA-5 instrument was used, but there were quite appreciable memory effects when the thiourea was omitted from bromide-free solutions. In fact, when a number of samples containing silver in nitric acid (0.5*M*) had been measured and silver-free 0.5*M* nitric acid containing thiourea was aspirated, an appreciable transient silver peak was observed. Though large amounts of silver can generally be determined without prior separation, the method described can be useful for the separation of traces of silver from large amounts of other elements before its final determination by AAS or other methods in which the presence of large amounts of salts can limit the sensitivity and accuracy. Up to 30 columns can be operated in parallel.

REFERENCES

1. K. A. Kraus and F. Nelson, *Proc. First Int. Conf. Peaceful Uses Atomic Energy, Geneva*, 1955, **7**, 113.
2. V. R. Murthy, *Geochim. Cosmochim. Acta*, 1962, **26**, 481.
3. T. T. Chao, M. J. Fishman and J. W. Ball, *Anal. Chim. Acta*, 1969, **47**, 189.
4. K. Kawabuchi and J. P. Ridley, *ibid.*, 1973, **65**, 271.
5. J. A. Warburton and L. G. Young, *Anal. Chem.*, 1972, **44**, 2043.
6. F. Burriel-Marti and C. A. Herrero, *Inf. Quim. Anal.*, 1964, **18**, 61.
7. *Idem, Rev. Univ. Santander*, 1965, **7**, 17.
8. R. L. Shrimal, *Talanta*, 1971, **18**, 1235.
9. A. K. De and S. K. Majumdar, *ibid.*, 1963, **10**, 201.
10. R. P. Bhatnager and R. P. Shukla, *Anal. Chem.*, 1960, **32**, 777.
11. H. Grays and H. F. Walton, *Sepn. Sci.* 1970, **5**, 653.
12. F. W. E. Strelow, *Anal. Chem.*, 1984, **56**, 1053.

Talanta, Vol. 32, No. 10, pp. 957–960, 1985
Printed in Great Britain

0039-9140/85 $3.00 + 0.00
Pergamon Press Ltd

RAPID AUTOMATIC POTENTIOMETRIC METHOD FOR ANALYTICAL CONTROL IN THE MANUFACTURE OF EXTRACTION PHOSPHORIC ACID

GEORGI VELINOV
Faculty of Pharmacy, Medical Academy, 15 Ekz. Josif Street, Sofia, Bulgaria

(*Received* 25 *July* 1984. *Revised* 25 *April* 1985. *Accepted* 3 *May* 1985)

Summary—A rapid automatic method for determination of free sulphuric acid in the manufacture of extraction phosphoric acid from apatite has been developed. It is based on potentiometric titration combined with the Gran approach for linearization of the titration curve. The analysis is done with an automatic potentiometric titrator controlled by an HP-85 microcomputer. BASIC software activates the system to perform the data acquisition and calculations, and the whole operation takes only 7–8 min.

The concentration of free sulphuric acid in the course of manufacture of extraction phosphoric acid is considered to be a main technological index for both the degree of extraction of P_2O_5 from the raw material, and the consumption of sulphuric acid. A pure mixture of phosphoric and sulphuric acid can be analysed by two consecutive titrations with a standard solution of sodium hydroxide, with Methyl Orange and phenolphthalein as indicators,[1] or by pH-titration, but as the ratio H_2SO_4:H_3PO_4 in the process product is 1:10, these methods tend to give wrong results for the sulphuric acid content. Recently it was shown[2] that the accuracy of this analysis can be significantly improved if the potentiometric data are treated by the methods giving linear plots for the titration curves.[3–5] Unfortunately, the extraction process solutions provide another difficulty—the presence of some impurities, mainly F^- (H_2SiF_6), Fe(III), Fe(II), Al(III) and Ca(II), extracted from the raw materials, so the above-mentioned methods are inapplicable. The elimination of these impurities is very difficult, and virtually impossible in process-control, where very fast analysis is required for maximizing efficiency. We have tried to solve the problem by using the Gran strategy, which provides the advantages of improving the accuracy of determination of the equivalence-point and giving an idea of the chemical behaviour of the system in the course of the titration.

The present work proposes a rapid method for determination of free sulphuric acid in the manufacture of extraction phosphoric acid from apatite. It is based on a potentiometric Gran titration, with an automatic system controlled by microcomputer.

EXPERIMENTAL

Reagents

Merck reagent-grade sulphuric acid, phosphoric acid, hydrofluoric acid, iron(III) nitrate, iron(II) sulphate, aluminium sulphate and calcium nitrate were used without additional purification. Fluorosilicic acid was prepared by addition of hydrofluoric acid to an excess of "Aerosil-300" and storage of the mixture for one month in a polyethylene vessel. The solution was analysed as described by Kolthoff and Stenger[6] and it was found that it contained 98.8% fluorosilicic acid and 1.2% hydrofluoric acid.

Procedure

A 100-μl portion of sample solution (containing 26–32% phosphoric acid, calculated as P_2O_5, and 1–4% sulphuric acid, calculated as SO_3) was diluted with 200 ml of 0.1*M* sodium chloride and titrated with *ca.* 0.75*M* carbonate-free sodium hydroxide.[7] The titration was stopped just before neutralization of the second proton of the phosphoric acid (pH 7.5–7.7), as precipitation begins at higher pH. A digital pH-meter accurate to 0.1 mV and a Radiometer type ABU-12 automatic burette with maximal volume 2.5 ml (accurate to 0.001 ml) were used. The automatic titration was performed by means of an HP-85 microcomputer with HP-IB interface and I/O ROM memory extension. The transfer of data and control commands between the computer and the measuring instruments was done by the interface unit developed earlier,[8] based on a MOTOROLA microprocessor.

RESULTS AND DISCUSSION

Chemical composition of the system

The most important point in the development of the method was the determination of the chemical composition of the impurities in the extract obtained after decomposition of the apatite by sulphuric acid. For this purpose a series of extraction solutions taken over a period of a month was investigated, which ensured the evaluation of possible variations of the chemical composition under the conditions of manufacture.

Fluoride was determined by direct potentiometry with a Radiometer "Selectrode" fluoride, type F1052F, by the TISAB procedure,[9] and found to be in the range 18–25 g/l. in the extraction solution.

Iron(II) was determined by redox titration with ceric sulphate.[10] The total amount of iron was determined after reduction of Fe(III) with a silver reduc-

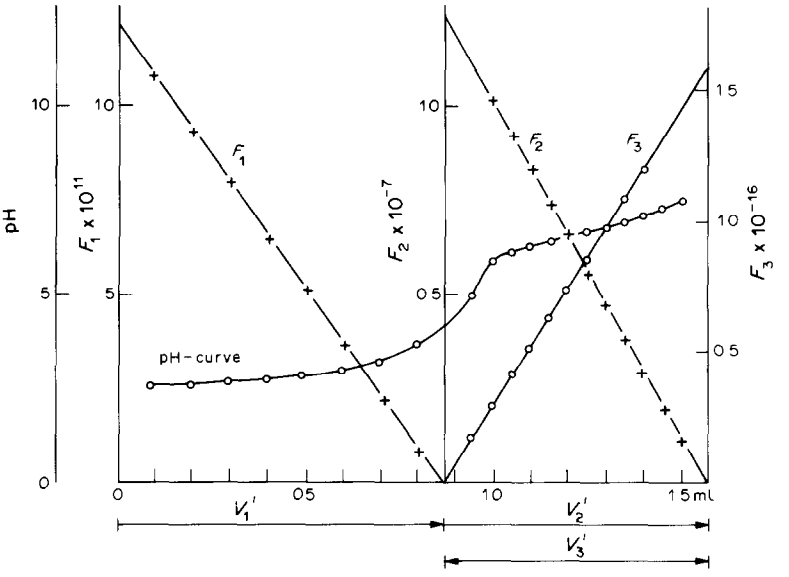

Fig. 1. Titration curve and its linearized plot for the titration of solution A, containing sulphuric and phosphoric acid.

tor, followed by titration of the total Fe(II) obtained.[10] The iron(III) was then calculated by difference. The iron(III) and iron(II) contents were found to be in the range 2.5–3.2 and 1.5–2.0 g/l. respectively.

The determination of aluminium in the system is difficult because of the presence of phosphate. The latter was therefore eliminated by ion-exchange with an anion-exchange resin in chloride form, and then Al(III) was determined complexometrically by a back-titration procedure.[11] Its content was found to be in the range 2.0–3.0 g/l.

Calcium was not determined experimentally since it has been reported[12] that the solubility of calcium sulphate in the solutions investigated is 9–10 g/l.

Effect of impurities

Three standard solutions were analysed; their compositions were as follows.

Solution A—phosphoric acid 378.8 g/l. (as P_2O_5) and sulphuric acid 42.35 g/l. (as SO_3), established gravimetrically.

Solution B—composition as for solution A plus F^- (H_2SiF_6) 26.0 g/l.

Solution C—composition as for solution A plus F^- (H_2SiF_6) 26.0 g/l., Ca(II) 2.94 g/l., Fe(III) 3.5 g/l., Fe(II) 2.0 g/l., and Al(III) 3.0 g/l.

Solution C contained the highest impurity concentrations found in "real" samples. All titrations were done as described above and the data-treatment was done with a program constructed for the Hewlett-Packard HP-85 desk computer working "off-line".

Figure 1 presents the titration curve and its linearized plot for the titration of solution A. F_1^* is the Gran function for the strongly acidic region, which determines the equivalence volume V_1' for the neutralization of the strong acids (the first proton of H_3PO_4 and the two protons of H_2SO_4). F_2^* is a linear function based on the extended Gran equation,[5] which determines the equivalence volume V_2' (for the neutralization of the second proton of H_3PO_4) and simultaneously the pK_2-value for H_3PO_4. Since the extended equation uses pH-values (not mV) a special block in the program deals with calibration of the galvanic cell according to Thencheva *et al.*[13] F_3^* is also a Gran function,[14] which determines the equivalence volume V_3' (also for neutralization of the second proton of H_3PO_4). When impurities are absent the values of V_2' and V_3' must agree. Solution A was titrated ten times and the following results were obtained: $P_2O_5 = 378.2 \pm 0.7$ g/l. and $SO_3 = 42.37 \pm 0.01$ g/l. In all the titrations good coincidence between V_2' and V_3' was observed.

Figure 2 presents the titration curve and its linearized plot for the titration of solution B. It is seen that the experimental points for some sections of F_1, F_2 and F_3 are not linear. Moreover $V_2 > V_3$, which

---

$$*F_1 = (V_0 + V_{ad})10^{-E/k},$$

$$F_2 = (V_{ad} - V_1')[H^+] + \frac{V_0 + (V_{ad} - V_1')}{C}[H^+]^2 - \frac{V_0 + (V_{ad} - V_1')}{C}K_w,$$

$$F_3 = (V_1' + V_2' - V_{ad})10^{E/k},$$

where V_0 is the original volume, V_{ad} the volume of titrant added, E the measured potential, C the concentration of the titrant, K_w the ion-product of water and k the Nernst coefficient (2.303RT/F).

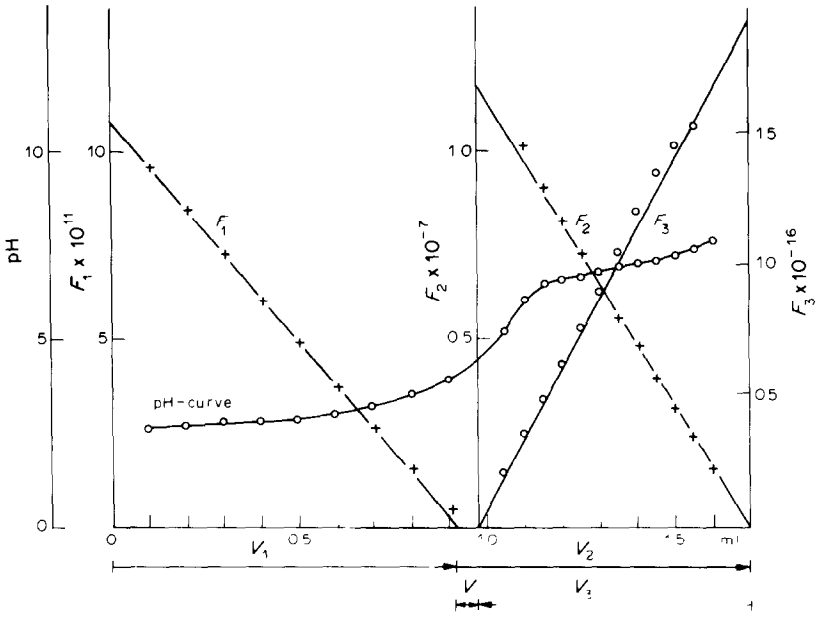

Fig. 2. Titration curve and its linearized plot for the titration of solution B, containing H_2SiF_6 as an impurity.

requires some corrections and iterative calculations with F_2 and F_3. After the second iteration the values of V_2 and V_3 agree and do not change by more than the corresponding standard deviations. The results significantly improve if the points of the non-linear sections of F_1, F_2 and F_3 are eliminated (*i.e.*, the full lines in Fig. 2 are used). Comparison of these results with those for solution A shows that $V_1 = V_1' + V$ and the values of V_2, V_3, V_2' and V_3' coincide after the iterations. The most important result is that the volume V is equivalent to neutralization of the two protons of fluorosilicic acid. It is known[6] that fluorosilicic acid is a strong electrolyte and can be titrated (though with poor accuracy) as a dibasic acid to a p_T (transition pH) of 3.5 with Methyl Yellow as indicator. Consequently, volume V_1 in Fig. 2 corresponds to the titration of first proton of H_3PO_4, the two protons of H_2SO_4 and the two protons of H_2SiF_6. At pH > 4 SiF_6^{2-} reacts according to the equation:

$$SiF_6^{2-} + 4OH^- = SiO_2 + 6F^- + 2H_2O$$

Completion of this reaction requires titration at boiling temperature to the rose colour of phenolphthalein or, as recommended, addition of excess of alkali, boiling for 5 min, and back-titration with hydrochloric acid.

Obviously, under the conditions of the proposed method (titration at room temperature to pH 7.5–7.7) the reaction with SiF_6^{2-} is not complete. The statement above, that volume V is equivalent to neutralization of the two protons of H_2SiF_6, was found experimentally and is statistical in character. As can be seen below, this determination has a comparatively high error, which increases in the presence of impurities.

Consequently, after proper choice of the points (from only the linear regions of F_1, F_2 and F_3) good results for the three acids can be obtained, though the accuracy of this determination is poorer: the error is $\pm 0.5\%$ for P_2O_5, $\pm 2\%$ for SO_3 (compared to the gravimetric determinations) and $\pm 5\%$ for fluoride (compared to potentiometric determination).

In the same way several titrations were done with solution C. The linearized plots were similar to those for solution B but the linear sections of F_2 and F_3 were shorter. Comparison of all the titration curves for solutions A, B and C leads to the following conclusions for the titration curve of solution C: (1) F_1 has a linear section up to $(0.6–0.7)V_1$; (2) F_2 has a linear part after $0.5V_2$; (3) F_3 has a linear section up to $0.5V_2$; (4) the linear regression of the functions from these sections determines the main components with an error of $\pm 0.5\%$ (P_2O_5), $\pm 5\%$ (SO_3) and $\pm 10\%$ (F^-).

The results obtained show that this complicated mixture can be analysed by a simple potentiometric titration procedure, combined with suitable selection of the experimental data, and use of Gran data-treatment.

BASIC program for automatic analysis

On the basis of the results obtained, a program was written for automatic titration of the extraction solutions obtained during manufacture. The block-diagram of the program is shown in Fig. 3. BEGIN takes data for the first two points at 0.000 and 0.100 ml and calculates a "rough" value for V_1;

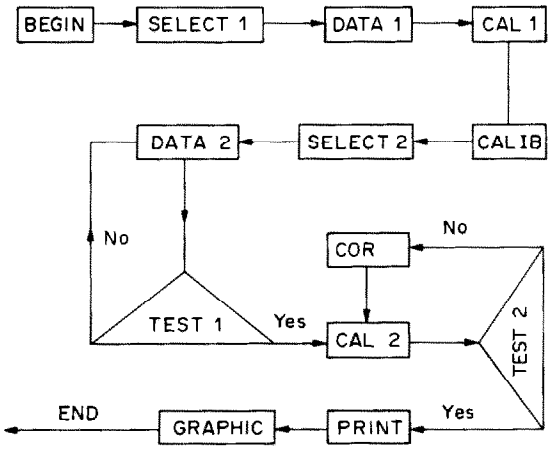

Fig. 3. The block-diagram of the BASIC program.

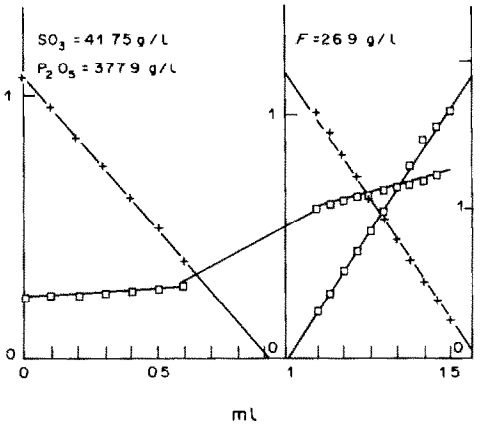

Fig. 4. The final results for the titration of extraction solution under the conditions of manufacture shown as the the CRT display of the HP-85, copied on the thermal printer.

SELECT 1 estimates how many 0.100-ml portions are necessary to collect the information from the linear region of F_1; DATA 1 makes the data acquisition as planned in SELECT 1; CAL 1 calculates V_1 from the data of DATA 1; CALIB calibrates the galvanic cell;[13] SELECT 2 estimates the titrant portion which must be added in order to reach the beginning of the linear part of F_3; DATA 2 performs data acquisition in the region of F_3 and F_2; TEST 1 checks whether the pH-value of every new point is greater than 7.6 (if so, the titration is stopped); CAL 2 calculates F_2 and F_3, obtains V_2, V_3 and the pK_2-value for the H_3PO_4; TEST 2 checks the agreement between V_2 and V_3; COR makes corrections before the iteration; PRINT prints the final results for P_2O_5, SO_3 and F^- in g/l.; GRAPHIC produces the titration curve and its linearized plot (see Fig. 4).

The program uses the procedures for data acquisition described earlier,[8] a procedure for least-squares linear regression and some procedures for graphical presentation of the curves. The values of the characteristic constant of the cell ($E^{0\prime}$) and pK_2 for the phosphoric acid as well as all standard deviations are printed, and if something is wrong with these values an alarm appears on the CRT display of the computer.

The method and the automatic titrator were tested under process-control conditions. A single determination takes 7–8 min and does not require any special training of the operator. The determination is simple to perform and satisfies the requirements of technology with respect to accuracy and speed.

Acknowledgement—The author is indebted to Professor Omortag Budevsky for his constructive comments in the course of this investigation.

REFERENCES

1. K. I. Godovskaya, L. V. Rebina, G. Y. Novic and M. M. Gerner, *Technicheski Analyz*, Izd. "Visshaya Shkola", Moscow, 1979.
2. I. R. Pavlova, I. K. Pajeva, G. Velinov and O. Budevsky, *Zh. Prikl. Khim.*, 1981, No. 9, 1946.
3. G. Gran, *Analyst*, 1952, **77**, 661.
4. A. Johansson, *ibid.*, 1970, **95**, 535.
5. L. Pehrsson, F. Ingman and A. Johansson, *Talanta*, 1976, **23**, 769.
6. I. M. Kolthoff and V. A. Stenger, *Volumetric Analysis*, Vol. II, pp. 120–122. Interscience, New York, 1974.
7. J. E. Powell and M. A. Hiller, *J. Chem. Educ.*, 1957, **34**, 330.
8. G. Velinov, N. Todorov and S. Karamphilov, *Talanta*, 1983, **30**, 687.
9. M. S. Frant and J. W. Ross Jr., *Anal. Chem.*, 1968, **40**, 1169.
10. G. H. Walden, L. P. Hammett and H. P. Chapman, *J. Am. Chem. Soc.*, 1931, **53**, 3908; 1933, **55**, 2649.
11. I. Sajó, *Acta Chim. Acad. Sci. Hung.*, 1955, **6**, 251.
12. B. D. Melnik, *Inzhenerni Spravochnik po Tekhnologii Neorganicheskikh Veshtestv*, Izd. "Khimia", Moscow, 1975.
13. J. Thencheva, G. Velinov and O. Budevsky, *J. Electroanal. Chem.*, 1976, **68**, 65.
14. G. Gran, *Acta Chem. Scand.*, 1950, **4**, 559.

Talanta, Vol. 32, No. 10, pp. 961–966, 1985
Printed in Great Britain.

0039-9140/85 $3.00 + 0.00

USE OF METHYLIMINODIACETIC ACID BOUND TO CELLULOSE FOR PRECONCENTRATION AND DETERMINATION OF TRACE-METAL CATIONS

M. C. GENNARO, C. SARZANINI, E. MENTASTI and C. BAIOCCHI
Dipartimento di Chimica Analitica, Università di Torino, Via P. Giuria 5, 10125 Torino, Italy

(*Received* 4 *December* 1984. *Revised* 16 *April* 1985. *Accepted* 3 *May* 1985)

Summary—Methyliminodiacetic acid immobilized on a cellulose support can be conveniently utilized for trace-metal uptake. Capacities and uptake yields as a function of pH have been evaluated for Pb(II), Cu(II), Mg(II), Ca(II), Cd(II), Zn(II), Co(II), Ni(II) and Hg(II) and the results compared with those predicted from the stability constants for the same systems in homogeneous solution. The immobilization of the ligand increases its co-ordinating ability. The applicability to speciation studies is considered.

In trace-metal analysis, efforts have to be devoted to working out suitable preconcentration techniques to raise the metal concentration to reliably measurable levels and also to improve the accuracy and precision; in many cases separation from the matrix can be achieved at the same time.

For these purposes, techniques which employ chelating materials to abstract metal ions from dilute solutions have found extensive development and application. Inert substrates have been used to absorb, adsorb, chemically bind, or be impregnated by, suitable chelating agents.[1-7]

In previous work[8] we made a study of preconcentration of a large series of metal ions by means of a chelating material in which iminodiacetic groups were chemically bound to cellulose filter discs. Good uptake efficiency, leading to high preconcentration factors, was obtained. The ease of preparation of the material, free from contamination, and its wide applicability, suggested the study of a similar material made with methyliminodiacetic acid (MIDA) as the functional group.

Since both ligands (IDA and MIDA) have the same bonding structure and MIDA generally forms more stable metal complexes in aqueous solution than IDA does, if this stability difference is maintained in the heterogeneous phase, the chelating properties of this new material should be superior to those of the IDA cellulose.

EXPERIMENTAL

Reagents

Stock standard metal solutions (1000 mg/l., Erba "for atomic absorption", Merck "Titrisol") were diluted as required. All other chemicals were analytical-grade reagents, checked by plasma emission spectroscopy for the absence of contaminating metals at detectable levels. Water (DDW) was doubly distilled from quartz.

Apparatus

All laboratory glassware and polyethylene and polypropylene equipment was always thoroughly cleaned by soaking in 6.0*M* nitric acid and repeated rinsing with DDW.

Adjustable Eppendorf pipettes and "Micrometric Instrument" precision syringes were used for solution preparation. A Millipore filtration system was used to ensure reproducible placement of the prepared cellulose discs.

All pH measurements were made with an Orion pH-meter model 811, equipped with a combined glass–calomel electrode.

For emission measurements, a Spectraspan IV d.c. plasma emission spectrometer (SMI, Andover, MA, U.S.A.) was used. Two-point calibration (high and low standard) was used, the standard solutions containing the same amount of hydrochloric acid as the samples. For each sample, at least three independent measurements were made. To check the reliability of the measurements of metal concentrations in mixtures and to choose the most suitable wavelengths, multicomponent mixtures were prepared in 1.0*M* hydrochloric acid and analysed with use of single-component as well as multi-component standards; no appreciable differences were observed between the results obtained with the two types of standard. Table 1 shows the wavelength, accuracy and reproducibility of measurement for each cation.

Preparation of the modified filters

The MIDA was bound to the paper discs by the methods already described.[3,7,8] First, the cellulose filters were checked for absence of contaminating metal impurities by passing

Table 1. Plasma emission spectroscopy data

Cation	λ, nm	Accuracy*
Pb(II)	405.8	97.2 ± 2.0
Cu(II)	324.7	99.5 ± 0.3
Cd(II)	214.4	98.5 ± 1.4
Co(II)	345.3	100.5 ± 1.2
Hg(II)	253.6	98.5 ± 1.8
Ni(II)	352.5	99.5 ± 0.8
Zn(II)	213.8	100.3 ± 1.5
Ca(II)	393.3	99.8 ± 0.2
Mg(II)	279.5	99.9 ± 0.1
Fe(III)	259.9	98.5 ± 1.1

*Statistical data calculated for solutions containing 0.5–1.5 ppm of each metal, and five replicate runs.

1.0*M* hydrochloric acid through them and testing it by plasma emission spectroscopy. About 20 Whatman No. 41 cellulose filter discs (47 mm diameter) were soaked for 60 min in about 400 ml of dry dimethylformamide (DMF) which had been freshly distilled in presence of 10% benzene; the anhydrous solvent thus obtained ensures maximum yield in the chlorination reaction. To another 400 ml of dry DMF, 12 ml of phosphorus oxychloride were added, the brown-red mixture was heated to 90° on a water-bath, and the cellulose filters were added. The brownish filters obtained after the chlorination reaction were washed with DMF, DDW, 5% sodium hydroxide solution, DDW, 5% acetic acid solution, DDW and DMF, in that order. The filters, now white again, were put to react at 105–110° for about 150 min with a saturated solution of disodium methyliminodiacetate in a mixture of DMF (about 600 ml) and DDW (250 ml); water was replaced as it evaporated. In this reaction the MIDA group replaces the chlorine atom previously attached to the cellulose.

The two steps in the preparation can be indicated schematically as follows:

$$\text{cellulose-OH} \xrightarrow[\text{DMF}]{POCl_3} \text{cellulose-Cl}$$

$$\text{cellulose-Cl} \xrightarrow[\text{DMF, DDW}]{Na_2\text{MIDA}} \text{cellulose-}\overset{\displaystyle CH_3}{\underset{|}{N}}{}^{+}\,(CH_2COO)_2^{2-}$$

It may be noted that the mechanism of attack by the ligand, proceeding through a nucleophilic substitution reaction, provides the nitrogen atom with a positive charge.

The prepared filters were repeatedly washed with DDW and left to dry on a glass plate. They were then ready for use: they appeared similar to untreated filters, apart from a certain surface roughness; their average weight was 160 mg.

Data treatment

The experimental values for retention of the metals by the bound ligand were compared with those calculated for complexation with the ligand in a homogeneous solution. The program BASECO[9] was used, which can process equilibrium calculations for up to 50 possible complexes formed by up to 20 possible components. The original program was partially modified so that it also gave the plot of the distribution of the complex species as a function of pH.

RESULTS AND DISCUSSION

The preconcentration yield, as a function of pH, was systematically studied for Pb(II), Cu(II), Mg(II), Ca(II), Cd(II), Zn(II), Co(II), Ni(II) and Hg(II), with 100.0 ml of solution containing 1.00 ppm of metal ion, adjusted with hydrochloric acid or potassium hydroxide solution to various pH values. Potassium hydroxide was preferred to sodium hydroxide, because potassium interfered less than sodium in the measurement of the other metals, but in any case the amount added was well below the interference level.

The test solution was passed through the Millipore system containing the modified filter, preconditioned at the pH of the test solution, and the metal retained was eluted with 10.00 ml of 1.0*M* hydrochloric acid. The filtrate (containing the unretained metal) and the eluate (containing the metal retained and then released) were both analysed by plasma emission spectrometry, with calibration by means of standards at the same pH as the samples. The percentage of metal uptake as a function of pH is shown in Table 2 and also as broken lines in Figs. 1–9.

Table 2. Uptake (%) on MIDA-filter, as a function of pH, from solutions (100.00 ml) containing 1.00 ppm of the metal indicated

pH	Pb(II)	pH	Cu(II)	pH	Mg(II)
2.00	86.5 ± 2.0	2.01	60.0 ± 0.5	1.99	32.6 ± 0.2
3.03	99.8 ± 1.0	3.02	100.0 ± 1.0	3.01	91.0 ± 0.1
4.01	100.0 ± 1.0	3.99	99.5 ± 0.6	4.00	92.7 ± 0.3
4.98	97.1 ± 1.5	5.01	97.1 ± 0.7	5.04	97.7 ± 0.3
7.03	83.5 ± 1.8	7.03	90.2 ± 0.5	7.01	90.5 ± 0.3
pH	Ca(II)	pH	Cd(II)	pH	Zn(II)
2.04	46.5 ± 0.3	2.01	89.1 ± 0.9	2.02	92.0 ± 1.5
3.00	92.0 ± 0.2	3.00	98.2 ± 0.8	3.02	100.0 ± 2.0
4.00	100.0 ± 0.4	3.98	85.3 ± 1.1	4.00	100.0 ± 2.0
5.02	93.7 ± 0.4	5.03	99.9 ± 1.1	5.06	100.0 ± 3.0
6.99	94.0 ± 0.5	7.00	95.2 ± 0.8	6.99	99.0 ± 3.0
pH	Co(II)	pH	Ni(II)	pH	Hg(II)
2.09	33.5 ± 1.1	1.98	99.5 ± 0.7	2.01	0.0
3.04	88.8 ± 1.2	3.00	96.3 ± 0.6	3.00	50.0 ± 2.0
4.02	91.2 ± 0.9	4.00	99.6 ± 0.5	3.97	23.0 ± 1.9
5.00	92.3 ± 0.8	5.02	98.0 ± 0.5	5.03	22.2 ± 2.0
7.05	94.2 ± 1.1	7.00	82.0 ± 0.8	7.00	28.0 ± 3.0

The elution with acid also regenerates the modified filter, making it ready for the next determination. No reduction of filter efficiency was observed, but as a precaution, the filter was changed after each ten or so passages.

The metal uptake as a function of pH shows different types of behaviour (Figs. 1–9): in particular, Hg(II) is poorly retained, its maximum uptake being only about 50%. However, in all cases, the uptake is maximal at about pH 3. The capacity of the filter for the various metals at this pH was therefore determined, by repeating the uptake experiment with 100.0 ml of solution containing 100.0 ppm of metal. The results are given in Table 3.

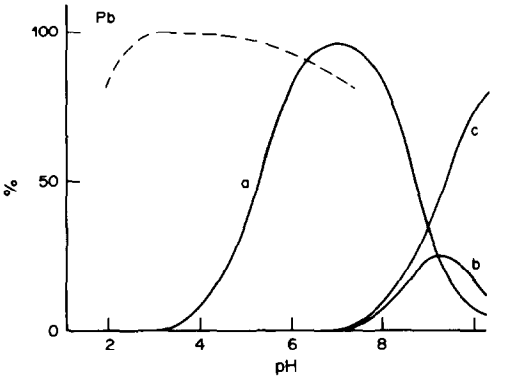

Fig. 1. Lead(II). Experimental uptake on MIDA-filter (dotted line) and relative species distribution computed for solutions with $C_{Me} = 1.00$ mg/l., $C_{MIDA} = 2.03 \times 10^{-4}M$. The distribution curves in Figs. 1–9 refer to: a, MeMIDA; b, $Me(MIDA)_2$; c, Me(MIDA)OH; d, MeOH; e, $Me(OH)_2$.

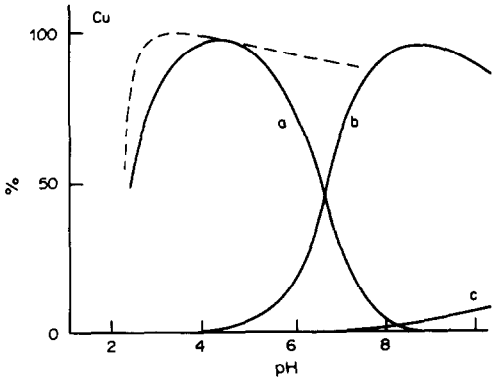

Fig. 2. Copper(II). See caption to Fig. 1.

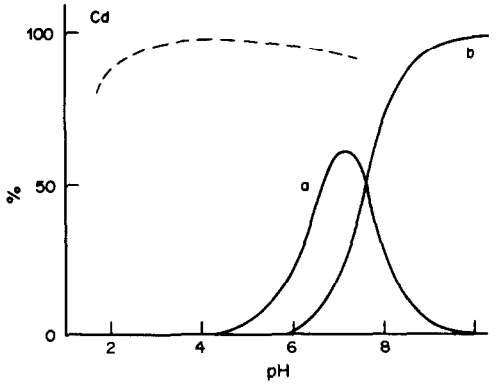

Fig. 5. Cadmium(II). See caption to Fig. 1.

In the pH range 3–5 the uptake from 1.00-ppm solutions was >90% for all the cations investigated, except Hg(II), and quantitative for Pb(II), Cu(II), Zn(II) and Ni(II). Similar results were obtained for these metals in mixtures at 0.100 ppm level (preconcentration factor equal to 100).

The results suggest that the proposed procedure can usefully be employed when non-selective metal preconcentration is required. It is, in fact, impossible to separate them, even Hg(II) which, though the least strongly retained, is still 50% sorbed. The method might also be very useful when removal or reduction of the total metal content is required. For this reason, it was of interest to evaluate the uptake behaviour of the modified material when the metal content of a sample was close to or greater than the average filter capacity. In particular, for practical application, it must be known whether the relative order of affinity

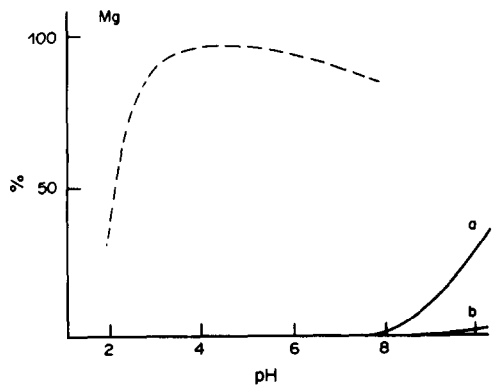

Fig. 3. Magnesium(II). See caption to Fig. 1.

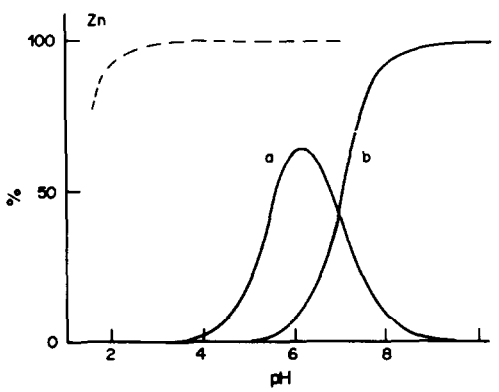

Fig. 6. Zinc(II). See caption to Fig. 1.

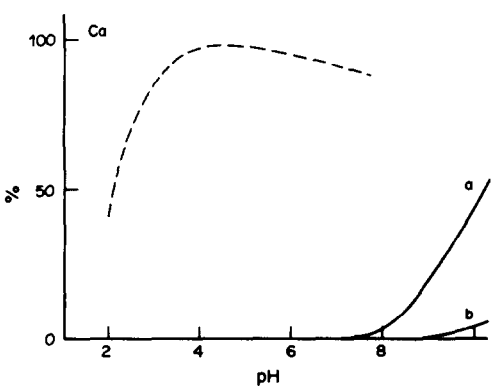

Fig. 4. Calcium(II). See caption to Fig. 1.

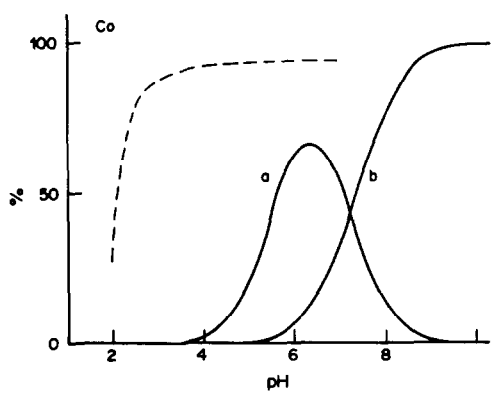

Fig. 7. Cobalt(II). See caption to Fig. 1.

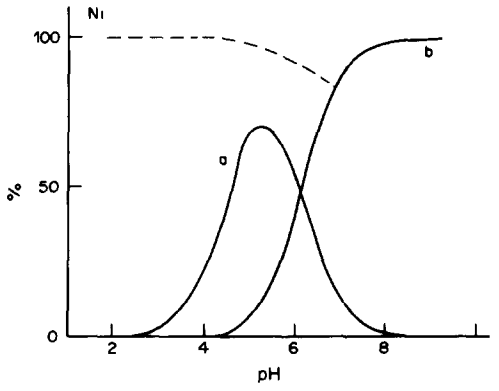

Fig. 8. Nickel(II). See caption to Fig. 1.

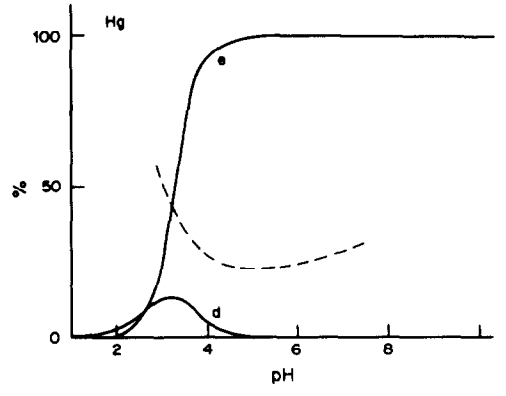

Fig. 9. Mercury(II). See caption to Fig. 1.

of the filter for different cations (as evidenced by the different capacity values) remains the same when the metals are present at different concentrations in a mixture, especially when a less easily retained metal is present at higher concentration than the others. Some binary mixtures (100.00 ml) were therefore prepared, containing Pb(II), Cu(II), Ca(II) and Mg(II) in different concentration ratios: the choice of

Table 4. Uptake from binary mixtures in saturation conditions for the chelating filters

Cation	Total amount, μg	Uptake, μg
Pb(II)	2000	1300 ± 4
Cu(II)	2000	660 ± 2
Pb(II)	4000	1250 ± 3
Mg(II)	8000	390 ± 1
Pb(II)	4000	1370 ± 5
Ca(II)	4000	110 ± 1
Cu(II)	4000	630 ± 2
Ca(II)	4000	330 ± 2
Cu(II)	2000	660 ± 2
Mg(II)	1000	200 ± 1
Ca(II)	4000	310 ± 2
Mg(II)	4000	240 ± 1

Ca(II) and Mg(II) as interferents was based on their frequent presence in appreciable concentration in real samples. Each mixture, brought to pH 3.00, was passed through the MIDA filter and the retention determined. The overall error was always within $\pm 2\%$. The results are given in Table 4. Obviously the behaviour of the filter when its capacity is close to or less than the total metal concentration cannot be readily predicted. There is evidently competition between the two metals for uptake by the filter, which readily becomes completely saturated, but the relative proportions of the metals sorbed depend on their concentrations as well as their affinity for the chelating material. To express this quantitatively, the equilibrium in the system of the two metals in solution (M_1^{2+}, M_2^{2+}) and bound to the filter (M_1-filter, M_2-filter) must be taken into account:

$$M_1^{2+} + M_2\text{-filter} \rightleftharpoons M_2^{2+} + M_1\text{-filter} \qquad (1)$$

The concentrations in solution may correctly be expressed as molar concentrations, whereas the amounts bound to the filter can only be expressed in absolute terms, *e.g.*, as the number of μmoles fixed (which is equivalent to assuming a fixed volume for the filter and the solution sorbed by it). The equi-

Table 3. Maximum capacity of the uptake of the investigated metals on a MIDA-filter (for comparison purposes, the last column reports the data for IDA-filters)

Cation	Fixed for each filter, *mg*	Error, %	Fixed for each filter, *μmole*	Specific uptake on MIDA-filter, *μmole/g*	Specific uptake on IDA-filter, *μmole/g*
Pb(II)	4.21	+3.0	20.3	127	218
Cu(II)	1.07	—	16.9	106	202
Mg(II)	0.51	+0.5	20.9	131	182
Ca(II)	0.70	+4.3	17.5	109	105
Fe(III)	0.97	+4.5	17.4	109	109
Co(II)	0.50	−8.3	8.4	53	171
Ni(II)	1.12	−1.4	19.0	119	184
Hg(II)	2.74	+2.5	13.6	85	88
Zn(II)	0.72	−0.1	11.0	69	157
Cd(II)	1.99	−1.1	17.7	111	172

librium is therefore characterized by a constant K' given by:

$$K' = \frac{[M_2^{2+}]}{[M_1^{2+}]} \times \frac{\mu\text{moles } M_1\text{-filter}}{\mu\text{moles } M_2\text{-filter}}$$

The K' values for the mixtures investigated are listed in Table 5; they show the affinity sequence of the metal ions for the filter to be: Pb(II) > Cu(II) > Mg(II) ≃ Ca(II), which agrees with the results previously collected. No relationship was found between the K' values found and those calculated from the reported formation constants[10–12] for the metal–MIDA complexes in aqueous solution and the metal concentrations in the experimental solution and the ligand concentration evaluated for the filter. The only conclusion which may be drawn from comparison of the calculated and experimental data is the general evidence of enhanced co-ordinating ability of MIDA, when bound to the filter, and information on the uptake behaviour of the filter for mixtures of metals in amounts close to the filter capacity can only be obtained experimentally, under the conditions to be used for application of the information.

A difference in the co-ordination behaviour of MIDA when in solution and when bound is also evidenced in Figs. 1–9, in which per cent metal uptake from dilute solution is plotted *vs.* pH. It is immediately obvious that the uptake on the filter is very similar, irrespective of the stability of the metal–MIDA complexes in solution.

To investigate this further, the complete composition of the solution system was calculated by computer. An assumption had to be made in order to assign a molar concentration to the ligand bound on the cellulose. The amount of MIDA fixed on the filter cannot be evaluated by direct measurement and was assumed to be the number of μmoles of the metal ion for which the filter had the highest capacity, *viz.* Pb(II). This assumption disregards the possible formation on the filter of complex species of different stoichiometry from that in solution. Anyway, in order to compare directly the experimental and the calculated behaviour, the predominant formation of the 1:1 complex was presumed, in view of the pH range investigated. This number of μmoles was then regarded as present in the total volume of solution passed through the filter. In Figs. 1–9 the continuous

Table 5. K' values evaluated for the equilibrium: $M_1^{2+} + M_2$-filter $\rightleftharpoons$ $M_2^{2+} + M_1$-filter

M_1	M_2	K'
Pb(II)	Ca(II)	18.90
Pb(II)	Mg(II)	8.87
Pb(II)	Cu(II)	3.82
Cu(II)	Ca(II)	2.09
Cu(II)	Mg(II)	1.95
Mg(II)	Ca(II)	0.78

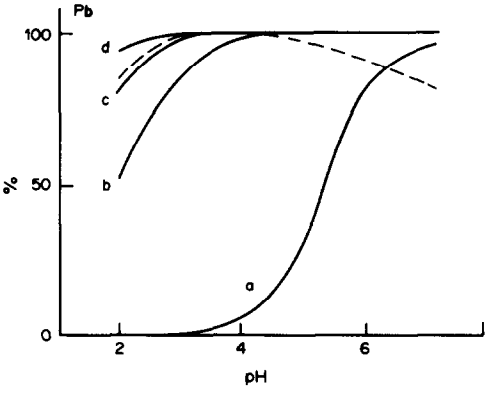

Fig. 10. Lead(II). Experimental uptake on MIDA-filter (dotted line) and computed uptake for various log β values: a, 8; b, 12; c, 13; d, 14.

lines represent the calculated behaviour. The differences between the experimental and calculated behaviour do not show a clear-cut trend for all the metal ions investigated, either for the pH of maximum uptake and/or the degree of uptake. The enhanced co-ordinating ability of MIDA groups when bound to cellulose is particularly important for those metal ions, *e.g.*, Ca(II), which form less stable complexes in aqueous solution but are quantitatively fixed on the MIDA filter (at pH > 3.0). This result perhaps suggests that the retention mechanism involves ion-exchange as well as chelation equilibria.

It seems reasonable, however, to assume that complex formation predominates and that the ligand has a much greater chelating ability when immobilized than when in solution. This could be regarded as simply the consequence of the much higher "concentration" of the ligand in the filter (*cf.* post-precipitation of zinc sulphide on mercuric sulphide in acid medium, because of the high surface concentration of adsorbed hydrosulphide ions). Alternatively, in an attempt to express this increased chelating strength by an equilibrium constant, we used the same metal and ligand concentrations, stoichiometries and formation constants of all the hydrolysed and complex species as before, except for the stability constant of the 1:1 metal–MIDA complex, which was progressively increased until the distribution curve calculated from it fitted the experimental curve. Figure 10 shows that in the Pb(II)–MIDA system at the concentrations indicated, a formation constant of about 10^{12} gave the best fit. Table 6 lists the values for the "observed" constants β_{obs} found in this way: they are around 10^{13} for all the metals showing a quantitative uptake at pH ≃ 3, and progressively decrease with decrease in uptake, down to the value for Hg(II), which is the least retained metal.

The data in Table 6 suggest a kind of "levelling" of the chelating strength of the filter towards the different cations. The weaker the complex in aqueous medium, the greater is the levelling effect.

Table 6. Observed log β_{obs} values for the uptake of cations on the MIDA-filter

Cation	log β_{obs}
Pb(II)	13.0
Cu(II)	12.0
Mg(II)	11.5
Ca(II)	11.5
Cd(II)	12.5
Zn(II)	13.0
Co(II)	11.5
Ni(II)	13.0
Hg(II)	10.5

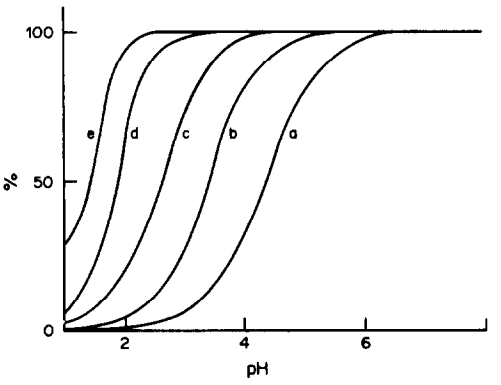

Fig. 11. Computed uptake on MIDA-filter for the following conditions: $C_{Me} = 1.00 \times 10^{-5} M$; $C_{MIDA} = 2.03 \times 10^{-4} M$; log β = a, 9; b, 10; c, 11; d, 12; e, 13.

It may also be noticed that the values of the "observed" constants are generally intermediate between those in aqueous solution for the MIDA and EDTA (ethylenediaminetetra-acetate) complexes. This might suggest that immobilization of the MIDA groups on cellulose could result in a molecular structure resembling that of EDTA, with two MIDA molecules bound to cellulose in such a way as to resemble an EDTA molecule. This should favour chelation, but would correspond to predominant formation of a 1:2 complex. The hypothesis should also hold when the bound ligand is IDA. In fact the IDA filter previously studied[8] also showed higher co-ordination power than IDA in solution.

Furthermore, in aqueous solution MIDA generally forms stronger metal complexes than IDA does, but the metal capacities of an IDA-filter[8] are higher than those reported here for a MIDA-filter (Table 3). If the suggested mechanism is indeed operative, with two IDA or MIDA molecules assuming a geometry and co-ordination behaviour similar to those of an EDTA molecule, the methyl group present in MIDA might induce a steric hindrance which would lower the chelating ability of the MIDA grouping relative to that of IDA, when attached to cellulose. Another possible reason for the lower chelating capacity of the MIDA filter could be the residual positive charge left on the nitrogen atom by the nucleophilic substitution reaction. Such a positive charge might, through electrostatic repulsion, hinder the fixing of metal cations.

The variation in metal uptake as a function of pH may also be described, for a series of cations, with the aid of the β_{obs} values. Because of the levelling effect, the behaviour can be plotted for a known concentration of any metal (for a given MIDA concentration on the filter) by using log $\beta_{obs} = 13$.

If we now consider the competitive effect of a ligand present in the sample, we can expect a reduced uptake which may be described by use of a log β'_{obs} value computed to match the experimental behaviour. Figure 11 shows, as an example, the behaviour computed for various log β'_{obs} values.

The presence of a ligand in a metal solution may therefore be detected and characterized by a simple flow-through uptake experiment on the MIDA filter; the difference in uptake in the presence (log β'_{obs}) or absence of the ligand (log $\beta_{obs} = 13$) gives an index of the overall complexing ability of the ligand in the matrix solution, which arises from the combined effect of type and concentration of the ligand. Such information may be very helpful in order to characterize the different forms in which a metal is present, when used in conjunction with other techniques (*e.g.*, ASV lability, uptake with chelating resins, ultrafiltration, *etc.*).

REFERENCES

1. D. E. Leyden and W. Wegscheider, *Anal. Chem.*, 1981, **53**, 1059A.
2. A. Mizuike, *Z. Anal. Chem.*, 1984, **319**, 415.
3. J. A. Smits and R. E. Van Grieken, *Anal. Chem.*, 1980, **50**, 1479.
4. K. H. Lieser and B. Gletsmann, *Z. Anal. Chem.*, 1982, **313**, 203.
5. K. Goldbach and K. H. Lieser, *ibid.*, 1982, **311**, 183.
6. P. Burba and P. G. Willmer, *Talanta*, 1983, **30**, 381.
7. G. Reggers and R. Van Grieken, *Z. Anal. Chem.*, 1984, **317**, 520.
8. M. C. Gennaro, C. Baiocchi, E. Campi, E. Mentasti and R. Aruga, *Anal. Chim. Acta*, 1983, **151**, 339.
9. C. Rigano and S. Sammartano, personal communication.
10. L. G. Sillén and A. E. Martell, *Stability Constants of Metal Ion Complexes*, Spec. Publs. 17 and 25, The Chemical Society, London, 1964 and 1971.
11. D. D. Perrin, *Stability Constants of Metal Ion Complexes*, Part B, Pergamon Press, Oxford, 1979.
12. A. E. Martell and R. M. Smith, *Critical Stability Constants*, Vol. 1, Plenum Press, New York, 1971.

Talanta, Vol. 32, No. 10, pp. 967–972, 1985
Printed in Great Britain.

0039-9140/85 $3.00 + 0.00

PHOTOMETRIC DETERMINATION OF COBALT BY MEANS OF PHOTOCHEMICALLY GENERATED *anti*-2-FURALDEHYDE 2-PYRIDYLHYDRAZONE

F. GARCIA SANCHEZ and M. HERNANDEZ LOPEZ
Department of Analytical Chemistry, Faculty of Sciences, The University, 29004-Malaga, Spain

(*Received* 20 *November* 1984. *Revised* 30 *January* 1985. *Accepted* 3 *May* 1985)

Summary—The photochemical *syn–anti* isomerization of 2-furaldehyde 2-pyridylhydrazone (FAPH) in ethanolic solutions has been investigated. A study of the infrared, visible and ultraviolet, and n.m.r. spectra of the two isomers was made. The *syn–anti* ratio at the photostationary state was determined. *syn*-FAPH scarcely reacts with metal ions but the *anti*-FAPH formed by irradiation gives sensitive reactions with several metal ions to form stable chelates. A photometric method for the determination of cobalt (0.025–1.0 μg/ml) in aqueous ethanolic medium (50% v/v) at pH 9.7 is described. A detection limit of 0.007 μg/ml and relative standard deviation of 0.5% were found. By consideration of the *syn–anti* ratio at the photostationary state, the stoichiometry of the chelate was determined. An application of this technique to determination of cobalt in environmental fume samples is also described.

Hydrazones and azomethines, characterized by the grouping >C=N—N<, are extensively used for detection and determination of several metal ions[1,2] and many hydrazones are now commercially available. This type of ligand often suffers photochemical transformation,[3–14] resulting in instability and poor precision of the analytical measurements.[15–19] Although this effect can be alleviated by employing reduced slit-widths in the apparatus, operating with a great excess of ligand, or keeping the samples in the dark, study of the mechanism and the variables affecting the photo-lability of the ligand is advisable as an aid to improvement of the analytical characteristics of photometric and fluorimetric methods.

However, this photochemical behaviour of the ligand could also prove to be a valuable advantage if it produces a favourable change in the chelate formed, and consequently improves the analytical characteristics of any quantitative application, such as the sensitivity, reproducibility or selectivity.

Although the light-induced reactions of the carbon–nitrogen double bond have been the subject of investigations since the nineteenth century, this area of photochemistry has only recently been exposed to the wealth of techniques available to the modern investigator.[20,21] Irradiation may lead to isomerization, phototropy, rearrangement, cycloaddition, oxidation, hydrolysis, cyclization, photoreduction or photo-alkylation.[22] However, although other radiationless paths which maintain geometric integrity are also important, *syn–anti* isomerization has been found to provide the major route for deactivation of the excited imine state.[23]

Because of the low thermal barrier between the two isomers,[24] the photochemically induced shift in the isomeric equilibrium is frequently followed by rapid thermal relaxation which re-establishes the initial configurational equilibrium.[22,25] This feature impedes the isolation of the isomers and complicates the photoisomerization studies. However, in the hydrazone derivatives of aromatic aldehydes and ketones this barrier is high enough to prevent thermal interconversion.

Photochemical isomerization of several hydrazones has been reported in the literature.[3–12] Recently, Costanzo *et al.* have studied the *syn–anti* photoisomerization of two pyridylhydrazones, and established the mechanism of direct[13] and sensitized[14] photoisomerization.

This paper deals with the light-induced transformation of 2-furaldehyde 2-pyridylhydrazone (FAPH) into the *anti*-isomer, which can be used as a complexing agent in the photometric determination of cobalt at trace levels.

EXPERIMENTAL

Apparatus

A Shimadzu UV-240 Graphicord spectrophotometer was used to record spectra and a Beckman DU-2 instrument for measurements at fixed wavelength, with matched 1.00-cm silica cells. Infrared spectra (KBr disks) were recorded with a Beckman IR-4240 spectrophotometer. Nuclear magnetic resonance spectra were recorded for solutions in DMSO, with a Hitachi–Perkin Elmer R-24b spectrometer; tetramethylsilane was used as internal reference.

The light-source used for the irradiation was an Atom-70 mercury vapour lamp (strongest line 365 nm). The irradiation equipment consisted of a black box equipped with the mercury lamp, and the reaction cells were Pyrex standard flasks (lowest limit of transparency 300 nm). The distance between radiation source and sample was 10 cm, and constant agitation was maintained during irradiation.

Reagents

syn-2-Furaldehyde 2-pyridylhydrazone was prepared as described previously.[26] The *anti*-isomer was prepared, starting from the *syn*-isomer ($1 \times 10^{-3} M$ in ethanolic solution)

Table 1. Ultraviolet data for the *syn–anti* conversion

Solvent	*syn*-band maximum		t^*_{ps},	*anti*-band maximum	
	λ, *nm*	ε†	*min*	λ, *nm*	ε†
Dioxan	330	3.05	15	325	2.80
Diethyl ether	328	3.25	15	324	3.02
Chloroform	328	2.97	20	324	2.77
Propanol	328	2.95	15	322	2.70
Ethanol	328	3.25	15	322	2.85
Methanol	326	3.10	15	321	2.85

*Time to reach the photostationary state.
†10^4 l.mole^{-1}.cm^{-1}.

by direct irradiation for 6 hr at 365 nm. It was isolated by HPTLC on silica gel (Merck 5719) with chloroform–ethyl acetate mixture (3:1 v/v) as eluent. The melting point of the *syn*-isomer is 133–134° and that of the *anti*-isomer 60–61°. The R_f values are 0.35 and 0.50 for the *syn*- and *anti*-isomers, respectively. The isomers were characterized by their ultraviolet infrared, and n.m.r. spectra.

syn-FAPH solution ($1 \times 10^{-3}M$, in absolute ethanol) was prepared daily and stored in the dark. A $0.1M$ cobalt stock solution was prepared from cobalt chloride hexahydrate and standardized complexometrically. Working solutions were prepared by dilution with demineralized, distilled water. A buffer solution, pH 8.05, was prepared from $0.1M$ boric acid and $0.1M$ sodium hydroxide.

Unless otherwise stated, the reagents were of analytical-reagent grade and used as supplied. Distilled, demineralized water was used throughout.

Procedures

Direct photoisomerization. For direct photoisomerization the pure *syn*-isomer ($2 \times 10^{-5}M$ and $1 \times 10^{-3}M$ ethanolic solutions) was irradiated in standard flasks. The course of the reaction was followed by measuring the spectral changes at regular intervals of time at 450–250 nm. The photostationary state was considered to be reached when subsequent irradiation did not alter the spectra. The constant isosbestic point and a chromatographic analysis indicated that only one product was formed by irradiation, and no side-reactions could be detected.

Spectrophotometric determination of cobalt. A volume of solution containing 0.625–2.225 μg of cobalt, 2 ml of $1 \times 10^{-3}M$ irradiated ethanolic FAPH solution, 5 ml of pH-8.05 buffer solution and 10.5 ml of ethanol were transferred to a 25-ml standard flask, and diluted to volume with demineralized water. The absorbance at 425 nm was measured against a reagent blank. A graph or an empirical equation was used to convert absorbance into concentration.

Procedure for environmental fume samples. Fume samples were collected in workshop environments according to the NIOSH Manual[27] as described previously.[28] An aliquot of the resulting solution was then treated according to the photometric procedure.

RESULTS AND DISCUSSION

Spectrometric studies

The ultraviolet spectra of the *syn*- and *anti*-isomers of FAPH in six different solvents are reported in Table 1. *syn*-FAPH absorbs strongly at long wavelengths, as expected for a substituted hydrazone[29] in which the planes of the two nitrogen-atom lone-pair orbitals are close to and interact with the extremities of the C=N bond π-orbital, so that their common axis is parallel to the C=N bond axis.

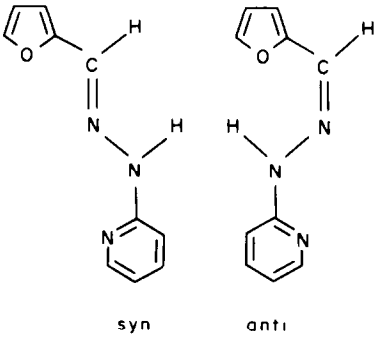

Under direct irradiation *syn*-FAPH undergoes *syn–anti* isomerization. In the ultraviolet spectrum of the *anti*-isomer, the long wavelength band is shifted towards the blue and decreased in intensity. This shift is related to repulsion between the aryl groups. Table 1 shows that the irradiation time needed to reach the photostationary state does not depend on the nature of the solvent.

The spectral changes during the photoisomerization of FAPH are shown in Fig. 1. *syn*-FAPH has its absorption maximum at 328 nm, ($\varepsilon = 3.25 \times 10^4$ l.mole^{-1}.cm^{-1}) and *anti*-FAPH at 322 nm, in the photostationary state ($t_{irr} = 15$ min, $\varepsilon = 2.85 \times 10^4$ l.mole^{-1}.cm^{-1}). The single isosbestic point (at 315 nm) indicates the presence of two related absorbing species.

At pH > 6, the *anti*-isomer shows a blue shift of 6 nm and $\Delta\varepsilon = -4.0 \times 10^3$ l.mole^{-1}.cm^{-1} with respect to *syn*-FAPH. At lower pH values, the spectral shapes are identical for both isomers, perhaps because of the formation of an intramolecular hydrogen bond between the lone-pair of the exocyclic nitrogen atom and the protonated ring-nitrogen atom.

The n.m.r. spectra of the *anti*- and *syn*-isomers were measured at 60 MHz, and the various proton peaks have been assigned according to reported data for *syn*- and *anti*-isomers of several pyridylhydrazones and related compounds.[30,31] Proton n.m.r. has been used to elucidate structural isomerism involving restricted rotation, as in the present case. In previous studies, both the aldehyde and the α-hydrogen atoms *syn*- to the anisotropic group were deshielded (shifted downfield relative to the corresponding hydrogen atoms *anti*- to the anisotropic

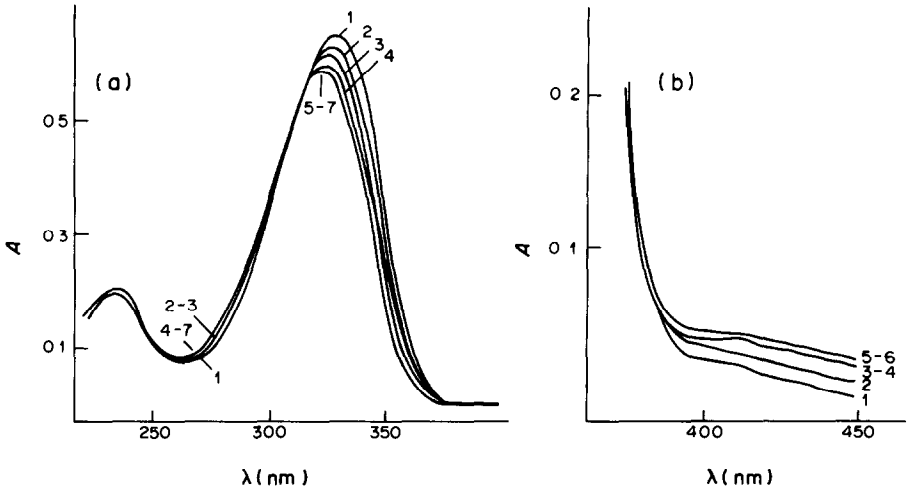

Fig. 1. Spectral changes of FAPH upon irradiation: (a) [FAPH] = $2 \times 10^{-5}M$; t_{irr} curves 1–7; 0, 2, 5, 10, 15, 25, 45 min. (b) [FAPH] = $1 \times 10^{-3}M$; t_{irr} curves 1–6; 0, 1, 3, 5, 6, 7 hr.

group). The most significant differences between the spectra of *syn*-FAPH and *anti*-FAPH are the analogous chemical shift differences of the aldehyde hydrogen atom (7.7 to 7.2 ppm) and the amine hydrogen atom (10.9 to 9.9 ppm). The other hydrogens atoms appear to be unaffected (Fig. 2).

The infrared spectra provide information about the relative configurations of two isomers, in that the N—H stretching vibration, at 3180 cm^{-1} in the *syn*-isomer, shifts to 3250 cm^{-1} in the *anti*-isomer. The higher frequency is due to steric compression of the *cis* NH and aryl groups, which approach each other in the *anti* configuration.[14,32] The observed increases in the pyridine ring vibration frequencies also provided evidence for the *syn* and *anti* configurations (stretching, from 1460 to 1470 cm^{-1}, 1340 to 1360 cm^{-1}).

The reversibility of the photo-equilibrium implies that no hydrogen bond is formed between the NH group and the furan oxygen atom, since the blue shift observed in the conversion into the *anti*-isomer indicates the transformation of an almost coplanar

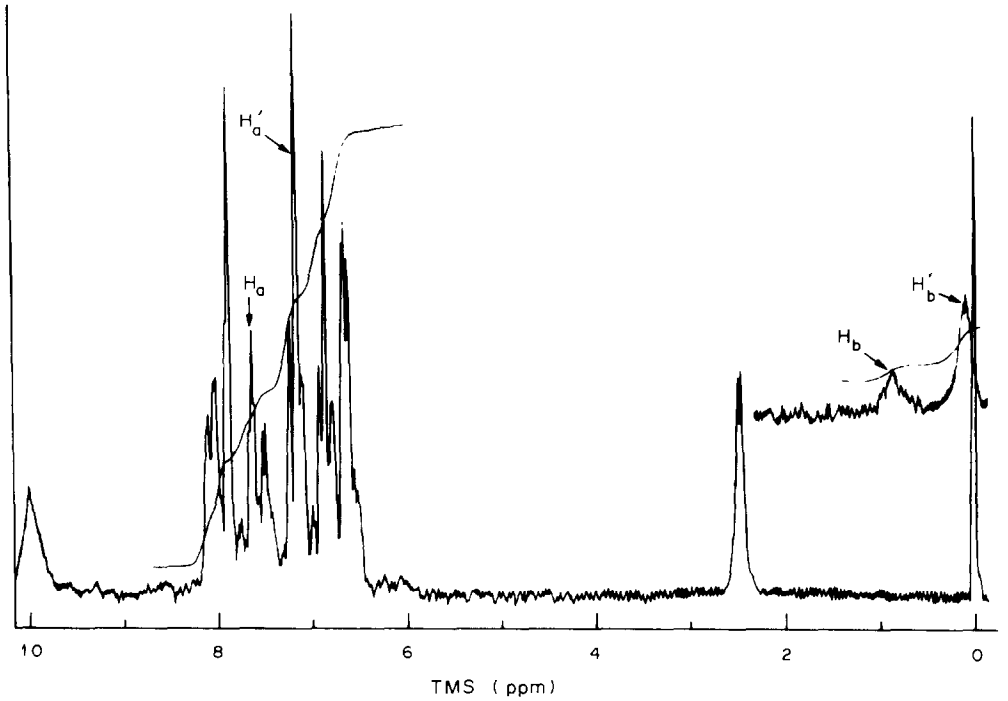

Fig. 2. 60 MHz proton NMR spectrum of *syn*- and *anti*-FAPH at the photostationary state. Solvent: DMSO. H_a and H_b refer to the *syn*-isomer and H'_a and H'_b to the *anti*-isomer.

Table 2. Spectrophotometric data for the determination of the *syn–anti* ratio

	$\lambda = 327$ nm		$\lambda = 337$ nm	
	ε^*	A_{mix}	ε^*	A_{mix}
syn-FAPH	3.22	0.560	3.00	0.440
anti-FAPH	1.87	0.560	1.25	0.440

*10^4 l.mole^{-1}.cm^{-1}.

molecule into a non-planar one, with restricted conjugation, whereas a hydrogen bond would confer rigidity and stabilize the structure.

Determination of the syn/anti *ratio in the photostationary state*

After irradiation, the *syn*- and *anti*-FAPH were separated from the mixture by silica-gel column chromatography with chloroform–ethyl acetate (57:25 v/v). The *syn–anti* concentration ratio was determined by n.m.r. and ultraviolet spectroscopy.

The ratio of concentrations of *syn–anti* isomers in the mixture is equal to the ratio of peak areas for the relevant amine peaks in the n.m.r. spectrum. For the stationary state the composition was found to be: *syn*-FAPH = 29.4%, and *anti*-FAPH = 70.6%.

The ultraviolet data from the isomers isolated by column chromatography showed the composition in the photostationary state to be: *syn*-FAPH = 32.2%; *anti*-FAPH = 67.8%. Table 2 summarizes the pertinent data for ethanol solutions.

Metal complexes

FAPH appears to be a bidentate or terdentate ligand with a convenient steric arrangement of its donor groups, and contains a system of π-electrons conjugated with the donor system.

The reactions of the two isomers of FAPH with 45 cations at various pH values were investigated qualitively. The absorption spectra of the potentially useful complexes are shown in Fig. 3, and their analytical characteristics are summarized in Table 3. Only one fluorogenic reaction was detected; that of the *syn*-isomer with zinc in alkaline medium.

Table 3. Spectral data for the chelates formed by *syn*- and *anti*-FAPH

	syn-FAPH		*anti*-FAPH	
Ion	λ_{max}, nm	ε_{max}, 10^3 l.mole^{-1}.cm^{-1}	λ_{max}, nm	ε_{max}, 10^3 l.mole^{-1}.cm^{-1}
Pd(II)	430	11.2	425	16.0
Ag(I)	400	7.5	400	8.0
Cu(II)	425	5.5	420	14.7
Zn(II)	425	1.7	410	1.2
Au(III)	400	6.2	400	6.7
Ni(II)	—	—	410	9.0
Co(II)	—	—	420	13.2

The most interesting observation is that the *anti*-isomer gives two new stable chelates with nickel and cobalt. With a large molar excess of *syn*-FAPH (sixtyfold or more) in alkaline media, cobalt forms an unstable yellow complex and nickel an orange complex which fades rapidly. Figure 4 shows the spectra of *syn*- and *anti*-FAPH cobalt complexes obtained in two distinct photochemical situations. Curves 7–10 were obtained by mixing *syn*-FAPH with cobalt and then exposing the mixture to sunlight. The increasing absorbance values at $\lambda_{max} = 418$ nm are consistent with the hypothesis that the *syn*-isomer is converted into the *anti*-isomer on irradiation. The λ_{max} values for the complexes range from 425 nm (*syn*-complex) to 418 nm (*anti*-complex). Curves 1–6 were obtained by keeping the *syn*-FAPH–cobalt complex in darkness until the absorbance measurements were made. The absorbance was constant at $\lambda_{max} = 425$ nm and no transformation occurred.

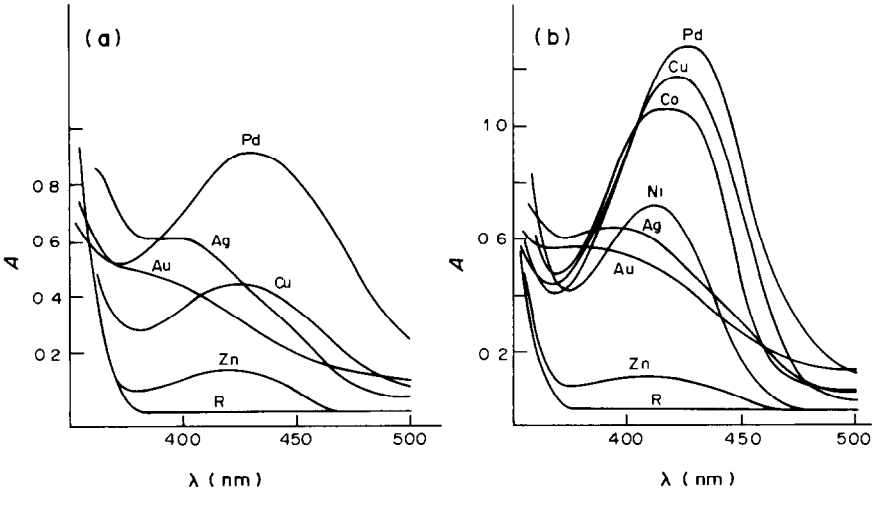

Fig. 3. Absorption spectra of FAPH chelates in 50% aqueous alcohol solutions at an apparent pH of 10.7; (a) *syn*-FAPH, (b) *anti*-FAPH. $C_R = C_M = 8 \times 10^{-5} M$.

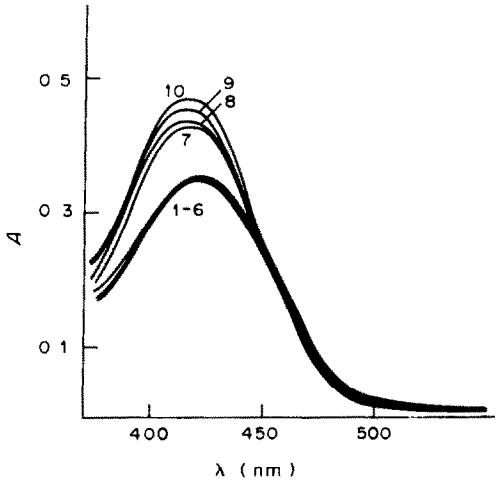

Fig. 4. Absorption spectra of the *syn*- and *anti*-FAPH–Co complexes. $C_R = 1.1 \times 10^{-3}M$; $C_M = 1.7 \times 10^{-5}M$; pH = 10.7.

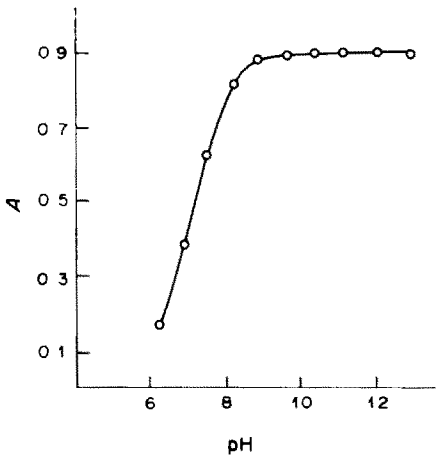

Fig. 5. Absorbance–pH graph for the *anti*-FAPH–cobalt complex. $C_M = 2 \times 10^{-5}M$; $C_R = 8 \times 10^{-5}M$.

syn-FAPH might act as a terdentate ligand because the linear arrangement of the furan oxygen, pyridine nitrogen and azomethene nitrogen atoms could give rise to two five-membered chelate rings. In the *anti* form, because of steric limitations, the torsion around the C=N bond would preclude electron donation by the oxygen atom and thus dictate the formation of only a single five-membered chelate ring involving the azomethene and pyridine nitrogen atoms.

With *syn*-FAPH the oxygen atom distorts the terdentate chelate because of the delocalization of the unshared heterocyclic lone-pair, to create a very unstable chelate.

In *anti*-FAPH, the oxygen atom does not participate as a donor atom so the chelates are not distorted. As a consequence, and surprisingly, the chelates with two five-membered rings are less stable than the chelate with one five-membered ring.

It was principally the stability of the coloured complexes produced by the photogeneration of the anti-isomer that made them useful as analytical ligands and, in turn, suggested this photometric method, in which the molar absorptivities are higher than with the analogous *syn*-isomer chelates.

STUDY OF THE *anti*-FAPH–Co(II) COMPLEX

Spectra of the complex

Study of the pH-dependence of the complexation of *anti*-FAPH with cobalt(II) showed that the yellow complex ($\lambda_{max} = 418$ nm) gave a constant absorbance at pH values above 9.0 (Fig. 5). For complete complexation, a 10-fold molar ratio of FAPH to Co(II) was sufficient. The complex formed quickly and the colour remained stable for at least 4 hr. Slight variations in absorbance were found when the concentration of ethanol in the medium was changed. Optimum results were obtained with 50% v/v ethanol–water. The pH was adjusted to (an apparent) pH 9.7 by the addition of 5 ml of borate buffer solution, pH 8.05.

Stoichiometry

The metal-to-ligand ratio in the complex was studied under the recommended working conditions by the molar-ratio method. The method was applied to a series of cobalt solutions with a fixed concentration of $4 \times 10^{-5}M$; and varied concentration of irradiated FAPH. A plot of absorbance *vs.* the molar ratio of FAPH:cobalt showed a break at 4:1. If it is assumed that the absorbing species are formed by *anti*-FAPH, then the true metal-to-ligand ratio may be obtained by multiplying the total FAPH concentration by a conversion factor to give the real concentration of *anti*-FAPH. In the photostationary state, the fraction in *anti*-form was 69%, and the modified stoichiometry gives a metal-to-ligand ratio of 1:2.76 (almost 1:3), which is to be expected because of the bidentate character of the *anti*-FAPH mentioned above, and the octahedral hexaco-ordinate nature of the cobalt ion.

Spectrophotometric determination of cobalt with anti-*FAPH*

Beer's law was obeyed for 0–1.0 μg/ml cobalt, and there was negligible blank absorbance. The molar absorptivity at $\lambda_{max} = 418$ nm is $\varepsilon = 4.70 \times 10^4$ l.mole^{-1}.cm^{-1}. The Ringbom plot shows the optimum cobalt range for accurate determination to be 0.2–1.0 μg/ml.

The precision of the method was checked by measuring the absorbance of ten separate samples each containing 0.7 μg/ml cobalt. The relative error ($P = 0.05$) was 0.4%, and the relative standard deviation 0.5%. The contribution of between-batch variation to the precision of the results was negligible. For between-day variation, triplicate measurements

Table 4. Characteristics of the analytical method

s_b	s_s	S_C, ml/μg	$1/S_A$, ng/ml	C_L ($k = 3$), ng/ml	C_Q ($k = 10$), ng/ml	Linear dynamic range, ng/ml
0.002	0.0031	0.79	4	7	25	25–1000

Table 5. Tolerance of foreign ions

Species added (x)	Tolerance ratio, [x]/[Co], w/w
Urea, acetate, thiocyanate	2.5×10^4
I^-	1.5×10^4
Thiourea	6×10^3
F^-	3×10^3
Tartrate	5×10^2
H_2O_2, ethylene glycol	3×10^2
$S_2O_3^{2-}$	1.5×10^2
NH_3	1×10^2
Ascorbic acid, triethanolamine	50
Oxalate, Fe(III)*	30
PO_4^{3-}, Cd(II), Zn(II), Cu(II)†	15
Pb(II)	10
Al(III)	3
Ag(I), Mn(II), Hg(II), Ni(II)§	1
EDTA, CN^-	0.2

*In presence of 2000 ppm fluoride.
†In presence of 4000 ppm thiourea.
§In presence of 60 ppm ammonia.

Table 6. Determination of cobalt in environmental fume samples

Sample	Cobalt present, μg/ml AAS	Present method
1	0.30	0.29_8
2	0.25	0.25_2
3	0.37	0.37_1

were made on each of ten days. All absorbances were within the range 0.555–0.565 (0.7 μg/ml Co).

Sensitivity and limit of detection

The sensitivity of the method is reported as the calibration sensitivity S_C (the slope of the calibration curve), and the analytical sensitivity $S_A = S_C/s_s$, where s_s is the standard deviation of the signal. Thus S_A is inversely related to the ability to distinguish a concentration difference. The limit of detection, C_L, is that defined by IUPAC.[33] The limit of quantification,[34] C_Q, was used to establish the lower limit of the linear dynamic range. The values are given in Table 4.

Interference study

The effects of several potentially interfering ions on the determination of 0.7 μg/ml cobalt were examined over a wide range of concentrations. The interference criterion was a relative absorbance error of ±2%. The main interferences could be reduced by using common masking agents (Table 5).

Application to real samples

This proposed procedure for cobalt determination was applied to environmental fume samples to evaluate its effectiveness. Table 6 summarizes the results.

REFERENCES

1. M. Katyal and Y. Dutt, *Talanta*, 1975, **22,** 151.
2. V. Zathka, J. Abraham, J. Holzbecher and D. E. Ryan, *Anal. Chim. Acta*, 1971, **54,** 65.
3. D. Schulte-Frohlinde, *Annalen*, 1959, **622,** 47.
4. I. D. Hausser, *Naturwissenschaften*, 1949, **36,** 313.
5. I. D. Hausser, D. Jerchel and R. Khun, *Chem. Ber.*, 1949, **82,** 515.
6. R. Khun and H. M. Weitz, *ibid.*, 1953, **86,** 1199.
7. J. L. Wong and M. F. Zady, *J. Org. Chem.*, 1975, **40,** 2512.
8. G. Condorelli and L. L. Costanzo, *Boll. Acad. Gioenia Sci. Nat.*, 1966, **8,** 753.
9. *Idem, ibid.*, 1967, **9,** 126.
10. G. Condorelli, L. L. Costanzo, S. Pistara and S. Giuffrida, *Z. Physik. Chem. Frankfurt*, 1974, **90,** 58.
11. *Idem, ibid.*, 1975, **96,** 97.
12. E. Fischer and M. Kaganowich, *Bull. Res. Counc. Isr., Sect. A*, 1961, **10,** 138.
13. L. L. Costanzo, U. Chiacchio, S. Guiffrida and G. Condorelli, *J. Photochem.*, 1980, **13,** 83.
14. *Idem, ibid.*, 1980, **14,** 125.
15. E. Requena, J. J. Laserna, A. Navas and F. Garcia Sanchez, *Analyst*, 1983, **108,** 933.
16. J. J. Laserna, A. Navas and F. Garcia Sanchez, *Anal. Lett.* 1981, **14,** 833.
17. H. Ishii, T. Odashima and T. Imamura, *Analyst*, 1982, **107,** 885.
18. S. P. Singhal and D. E. Ryan, *Anal. Chim. Acta*, 1967, **37,** 91.
19. M. Santiago, A. Navas, J. J. Laserna and F. Garcia Sanchez, *Mikrochim. Acta*, 1983 **II,** 197.
20. F. Ramirez and A. F. Kirby, *J. Chem. Soc.*, 1954, **76,** 1037.
21. G. J. Karabatsos and C. E. Osborne, *Tetrahedron*, 1968, **24,** 3361.
22. A. Padwa, *Chem. Rev.*, 1977, **77,** 37.
23. W. G. Herkstroeter, *J. Am. Chem. Soc.*, 1976, **98,** 330.
24. H. Izawa, P. de Mayo and T. Tabata, *Can. J. Chem.*, 1969, **47,** 51.
25. L. L. Costanzo, S. Giufffrida, U. Chiacchio and G. Condorelli, *J. Photochem.*, 1979, **11,** 39.
26. M. Hernández and F. Garcia Sanchez, *An. Quim.*, 1981, **77B,** 112.
27. National Institute of Safety and Hygiene, *Manual of Sampling Data Sheets*, Cincinnati, Ohio, 1976.
28. A. Navas and F. Sanchez Rojas, *Talanta*, 1984, **31,** 437.
29. D. C. Iffland, M. D. McAneny and D. J. Weber, *J. Chem. Soc.*, 1969, 1703.
30. G. J. Karabatsos, J. D. Graham and F. M. Vane, *J. Am. Chem. Soc.*, 1962, **84,** 753.
31. G. J. Karabatsos, B. L. Shapiro, F. M. Vane, J. S. Fleming and J. S. Ratka, *ibid.*, 1963, **85,** 2784.
32. H. Hadzi and J. Jan, *Rev. Roum. Chim.*, 1965, **10,** 1183.
33. G. L. Long and J. D. Winefordner, *Anal. Chem.*, 1983, **55,** 712A.
34. *Ibid.*, 1980, **52,** 2242.

Talanta, Vol. 32, No. 10, pp. 973–986, 1985
Printed in Great Britain

0039-9140/85 $3.00 + 0.00
Pergamon Press Ltd

MULTIPARAMETRIC CURVE FITTING—VIII

THE RELIABILITY OF DISSOCIATION CONSTANTS ESTIMATED BY ANALYSIS OF ABSORBANCE–pH CURVES

MILAN MELOUN
Department of Analytical Chemistry, College of Chemical Technology, CS-532 10 Pardubice, Czechoslovakia

and

MILAN JAVŮREK
Computer Centre, College of Chemical Technology, CS-532 10 Pardubice, Czechoslovakia

(*Received* 20 *November* 1984. *Revised* 29 *March* 1985. *Accepted* 19 *April* 1985)

Summary—The program SPOPT estimates stability constants β_{pqr} and molar absorptivities ε_{pqr} of all light-absorbing species $M_pL_qH_r$ by analysis of the absorbance–concentration (or absorbance–pH) curve. The program DCMINUIT estimates dissociation constants and molar absorptivities of protonated species. Both programs have been tested and compared with DCLET and LETAGROP–SPEFO for analysis of the overlapping equilibria of a triprotic acid. Computer plots of the residual-square-sum function are used to test the conditioning of parameters. Two approaches are made to formulation of the mathematical model, and several optimization algorithms are tested to find a reliable minimization procedure. The accuracy of ill-conditioned parameters is shown to be dependent on the precision of the absorbance measurements. General rules for investigation of A–pH curves are recommended.

The analysis of the absorbance–pH curve for a polyprotic acid to determine dissociation constants and molar absorptivities is not a straightforward procedure. In the application of regression analysis attention must be paid to formulation of a suitable mathematical model for the system and to the choice of an efficient minimization subroutine and minimization strategy. The precision of the spectrophotometric data should be as high as possible, especially for evaluation of ill-conditioned parameters. It must be discovered which parameters are well-conditioned and which ill-conditioned, and finally, criteria must be chosen to characterize the reliability of parameter estimates, and to terminate the minimization process.

This paper considers all these problems, warns against unthinking application of regression analysis, and suggests general rules for use of regression procedures to obtain reliable estimates of dissociation constants and molar absorptivities. Four regression programs are discussed, *viz.* DCLET,[1] LETAGROP–SPEFO[2] and two new programs, SPOPT and DCMINUIT in which several minimization subroutines and two formulations of the residual-square-sum function are available. The A–pH curve for a triprotic acid involving one overlapping protonation equilibrium is analysed and the reliability of the computer treatment is assessed.

THEORY

Structure of the regression programs used

Our "old" regression program DCLET,[1] Sillén's LETAGROP–SPEFO,[2] and our new programs SPOPT and DCMINUIT, were modified to have nearly the same structure (Fig. 1), as previously described for the ABLET regression system.

SPOPT AND DCMINUIT

The RESIDUAL-SQUARE-SUM block

The regression analysis of spectrophotometric data to provide molar absorptivities and stability constants for the individual absorbing species requires the minimization of the residual-square-sum function

$$U = \sum_{i=1}^{n} w_i(A_{\mathrm{exp},i} - A_{\mathrm{calc},i})^2 \qquad (1)$$

where $A_{\mathrm{exp},i}$ is the measured absorbance at a given wavelength for given concentration of the three main components M, L and H, for the equilibria

$$p\mathrm{M} + q\mathrm{L} + r\mathrm{H} \rightleftharpoons \mathrm{M}_p\mathrm{L}_q\mathrm{H}_r \qquad (2)$$

Part VII—*Talanta*, 1985, **32**, 171.

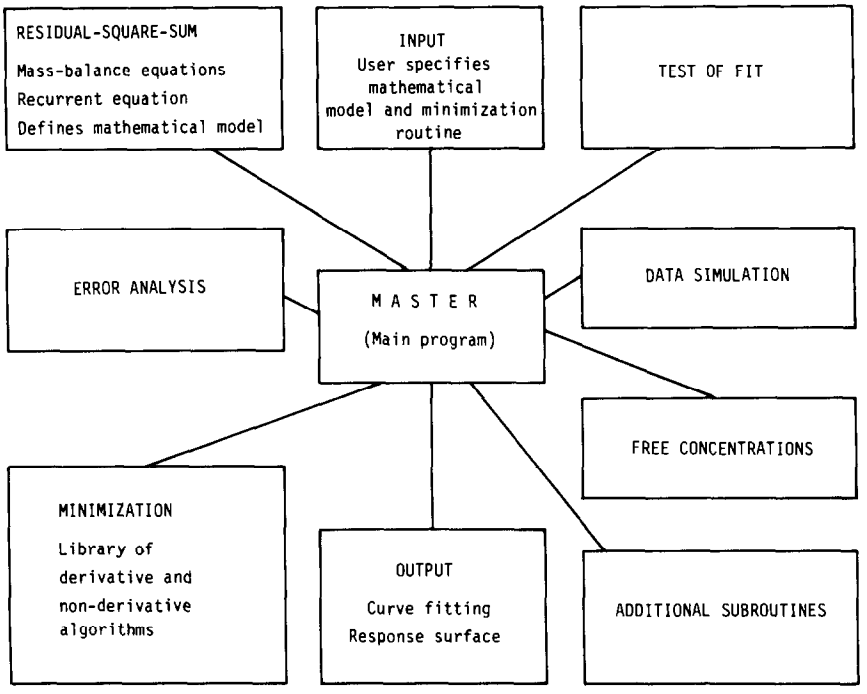

Fig. 1. Functional blocks of the program SPOPT.

with stability constants

$$\beta_{pqr} = [M_pL_qH_r]/([M]^p[L]^q[H]^r) \quad (3)$$

If J species absorb at the given wavelength, the absorbance A of the solution (in a cell of path-length d cm) is given by

$$A = d \sum_{j=1}^{J} \varepsilon_{pqr,j} [M_pL_qH_r]_j$$

$$= d \sum_{j=1}^{J} \varepsilon_{pqr,j} (\beta_{pqr}[M]^p[L]^q[H]^r)_j \quad (4)$$

where $\varepsilon_{pqr,j}$ is the molar absorptivity of the jth species and $[M_pL_qH_r]_j$ the free concentration of this species[4,5] and the mass-balance equations for the three basic components are given by

$$S = \sum_{j=1}^{J} (\beta_{pqr}[M]^p[L]^q[H]^r)_j \quad (5)$$

$$c_M = [M] + pS \quad (6)$$

$$c_L = [L] + qS \quad (7)$$

$$c_H = [H] + rS \quad (8)$$

U is assumed to be a second-degree function of m unknown parameters in $(m + 1)$ dimensional (and hence parametric) space, m being sufficient for calculation of a position for the minimum. Parameters are estimated by optimization in the multiparametric space in which values are given for absorbance and concentrations, and stability constants and molar absorptivities are adjusted by the computer.

There are two approaches to the formulation of U in the SPOPT program, corresponding to two different ways of determining A_{calc}. The first is a general method based on equation (4), in which an adjusted set of stability constants and molar absorptivities, and free concentrations of the components [M] and [L] are calculated ([H^+] is known from pH measurement), and hence A_{calc}. This version of SPOPT is referred to as SPOPT(MB) ($m$ass-$b$alance equation approach). In the second, the A–pH curve for a mononuclear acid is written with the assumption that base L is protonated to form the various forms LH_1, LH_2, ..., LH_r, *etc.* of the mononuclear acid LH_R. As discussed previously, the equation for the absorbance–pH curve may be written as

$$A = dc_L \left\{ \frac{\varepsilon_L + \sum_{r=1}^{R} \varepsilon_{LH_r} 10^{(r \log a_{H+} + \log \beta_{01r})}}{1 + \sum_{r=1}^{R} 10^{(r \log a_{H+} + \log \beta_{01r})}} \right\} \quad (9)$$

In the expression $(r \log a_{H+} + \log \beta_{01r})$, the conventional activity pH scale may be used and the protonation constants β_{01r} may be expressed as a function of the mixed stepwise dissociation constant $K_{a,i} = a_{H+}[LH_{i-1}]/[LH_i]$ and so

$$r \log a_{H+} + \log \beta_{01r} = \sum_{i=1}^{r} pK_{a,i} - r\,pH \quad (10)$$

This version of SPOPT is referred to as SPOPT(DC) (recurrent equation of the A–pH curve for $d$issociation $c$onstants determination).

DCMINUIT also contains a residual-square-sum function formulated by use of equations (9) and (10). Both SPOPT(DC) and DCMINUIT determine dissociation constants $pK_{a,i}$ and SPOPT(MB) determines stability constants or protonation constants $\log \beta_{0qr}$.

The MINIMIZATION block

Regression analysis finds estimates for the unknown parameters $\vec{\beta}_{pqr}$ and $\vec{\varepsilon}_{pqr}$ by minimizing the difference between the experimental and calculated data. The general problem is to find the best values of parameters $\beta_{pqr,j}$ and $\varepsilon_{pqr,j}$, $j = 1, J$, for which U is minimal. Here, $A_{exp,i}$ is a measured absorbance for the ith point and $A_{calc,i}$ is calculated from $A_{calc,i} = f(pH_i, \vec{\beta}_{pqr}, \vec{\varepsilon}_{pqr})$, where pH is known as an experimental quantity. The non-linear estimation problem is really simply a problem of optimization in the parameter space in which the A and pH values are known and the β and ε values are the variables. The function U must have its minimum at a point where either (*i*) all derivatives $\partial U/\partial \beta_j$ are zero ($j = 1, J$), (a stationary point), or (*ii*) some derivatives $\partial U/\partial \beta_j$ do not exist (a cusp), or (*iii*) the point β_j is on the boundary of the allowed region (an edge point). When it is realized that there may be any number of stationary points, cusps and edge points, all of which may be arbitrarily hard to find by simple sampling of the function value, the whole problem begins to appear hopeless unless some simplifying assumptions are made. The usual simplification consists of abandoning the attempt to find the global minimum and being satisfied with a local minimum for which the parameters have a physical meaning.

There are 30 minimization algorithms in the SPONA routines library,[6] and these may be divided into derivative and non-derivative routines. All may be called by SPOPT. If in the search for a minimum of U, the partial derivatives of U with respect to the parameters must be calculated, then the method is classified as derivative; otherwise, it is termed non-derivative.

Derivative methods used and selected for mention here are the Steepest Descent Method,[7] Gradient Method[8] and the Conjugate Gradients Method;[9] the Grid Method,[10] the Simplex Method[11] and Rosenbrock's Method[12] represent the non-derivative methods. However, the user is free to use any other minimization routine in the SPONA library.[6]

DCMINUIT incorporates three different minimization methods from the MINUIT regression system,[13] each of which may be used alone or in combination with the others, depending on the behaviour of U and on the requirements of the user. First, a Monte Carlo searching non-derivative subroutine[14] may be used at the beginning of a minimization when no reasonable initial value for the parameters can be guessed, or when it is suspected that there are several minima. Second, the Nelder and Mead non-derivative simplex method[11] is "safe" and fast when far from a minimum, and may also be used to converge to the exact minimum. Third, a derivative method developed by Fletcher[15] is extremely fast near a minimum or in any "nearly-quadratic" region, but slower if U is badly behaved. It uses the partial first derivatives of U, calculated either analytically or numerically. The program employs some "global" logic; if one method fails, the other is automatically caused to make another attempt. In addition, the minimization can be guided or separated into steps by the input data, which may cause a variable parameter to be fixed at a constant value or restored to variable status between minimization steps.

The ERROR ANALYSIS block

This block finds estimated confidence intervals for the parameters. The partial first derivatives of U for the estimates of the parameters may be calculated analytically or numerically for all the A–pH points. The square roots of the diagonal elements of the covariance matrix are the estimated errors, or standard deviations, of the parameters.

DCMINUIT also prints the correlation coefficients between the parameters (represented by the off-diagonal elements), and the global correlation coefficient for a given parameter, which is the correlation between it and that linear combination of the other parameters most highly correlated with it.[13]

The FITNESS TEST block

This test-of-fit block contains the STATS subroutine;[16] its function has been already described.[1,3]

The DATA SIMULATION block

This block contains the random error generator in the RANDOM subroutine, and also the additional subroutines SIMUL and NORAND.[3,18] It calculates a simulated A–pH curve by addition of generated random errors to the calculated precise values of absorbance for given pH values.

The user may select values for the errors in the parameters and for the instrumental error of the spectrophotometer. Then, for given values of the independent variable pH, the precise values of the independent variable A are calculated. Each precisely calculated point is then transformed into a simulated "experimental" one by addition of a random error having Gaussian distribution. The actual distribution of errors generated is then tested, and four statistical moments, Pearson's Chi-Square test[16] and the Hamilton R-factor test[19] are applied.

The FREE CONCENTRATIONS block

This block calculates for each experimental point the free concentrations [M] and [L] from the current set of stability constants β_{pqr}, the chemical composition of the solution and the stoichiometric coefficients pqr of each species, and given value of $[H^+]$. Subroutines COGSNR and CCSCC are used. CCSCC is a "book-keeping" routine of COGSNR,

which is used in SCOGS[20] to evaluate free concentrations of species by the Newton–Raphson method.

The ADDITIONAL SUBROUTINES block

This block contains subroutines for format-free reading of integers (READI) and reals (READR).[3]

The INPUT block

This contains subroutine DATA which reads the experimental data, the independent variable, pH, the dependent variable, A_{exp}, and does some preliminary calculations.[22] The measured values of pH_{read} are corrected for any deviation of the glass electrode from Nernstian slope (WK), for any difference in temperature from 298.16 K (WT), and for the liquid-junction potential correction in pH units (WW). WZ is pa_{H+} for the standard buffer solution used for calibration.

$$pH_{corr} = [(pH_{read} - WZ) \times 59.16 \times WT/(WK \times 298.16)] + WZ + WW \quad (11)$$

The OUTPUT block

This prints the parameter estimates and their standard deviations, and a printer-plotting subroutine PLOTT[21] makes a graph of experimental and calculated A–pH curves. A graph of U as a function of parameter values in the region of the pit may be plotted by DIGIGRAPH equipment to allow investigation of the conditioning of the parameters in the U function.[23] Computer-drawn plots of the hyperparaboloid response surface $(1 - U)$ as a function of any two chosen parameters are of great assistance in deciding whether parameters are ill-conditioned.

Computation

The computations were done with an EC 1033 (500 K) computer and the DCLET,[1] LETAGROP–SPEFO,[2] DCMINUIT, SPOPT, SQUAD(84),[26,27] and FA608 + EY608[25] programs in the Computing Centre of the College of Chemical Technology, Pardubice, Czechoslovakia.

DISCUSSION

Identification of ill-conditioned parameters

The reliability of any estimates of ill-conditioned parameters depends on the choice of minimization method. The refinement of parameters should lead to a minimum, preferably local rather than global, for which the parameter values have physical meaning. In the analysis of the absorbance–pH curve of a triprotic acid, for example, the seven parameters ε_L, ε_{LH}, pK_{a1}, ε_{LH_2}, pK_{a2}, ε_{LH_3}, pK_{a3} have to be estimated. If $|pK_{ai} - pK_{ai-1}| > 3$ the protonation equilibria do not overlap, but when $|pK_{ai} - pK_{ai-1}| < 3$, overlap does occur.

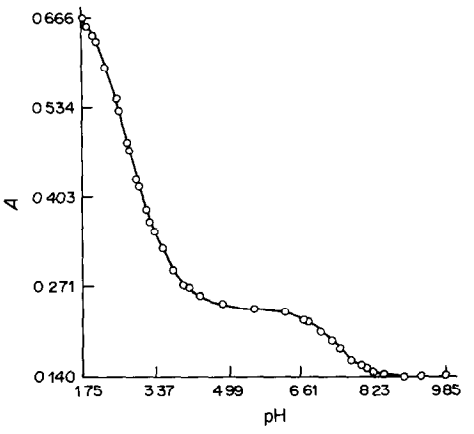

Fig. 2. Experimental A–pH curve for 7-(carboxyphenylazo)-8-hydroxy-quinoline-5-sulphonic acid measured by external titration, with spectrophotometer VSU2-G (Zeiss, Jena, GDR). Experimental conditions: $c_L = 4.18 \times 10^{-5} M$, $\lambda = 540$ nm, path-length 0.998 cm, $I = 0.1$ ($NaClO_4$ + Na_3PO_4 + $HClO_4$ + EDTA), 25°.

As an example, the absorbance–pH curve of 7-(3-carboxyphenylazo)-8-hydroxyquinoline-5-sulphonic acid[24] (I) illustrated in Fig. 2, was analysed by the regression program SPOPT(MB). A shortened output appears in Table 1. Since ε_L, pK_{a1}, ε_{LH} and ε_{LH_3} are well-conditioned in mathematical model (4), a graphical representation of the hyperparaboloid, simplified for two parametric co-ordinates ($m = 2$) in $(m + 1)$-dimensional space shows a well-developed minimum U_{min}. In Fig. 3 this appears as a maximum of $(1 - U_{min})$. The shape of the hyperparaboloid for the ill-conditioned parameters is a rather flat-bottomed saucer; this pit cannot be improved and also cannot be reached by any minimization method (Figs. 4–6).

The search for true estimates of the parameters, then, cannot give a certain answer, and no method is able safely to find a pit in U. Careful choice of a minimization subroutine and strategy is necessary, because some algorithms will fail, some will lead quickly to the global minimum, and others will terminate at local minima in dependence on the initial guesses for the parameters.

Choice of minimization algorithm

From the 30 minimization algorithms included in SPOPT (265 K) three derivative and three non-derivative methods were selected. The non-derivative method LETAG from DCLET[1] (82 K), LETAGROP–SPEFO[2] (240 K) and three minimization methods of DCMINUIT (150 K), were compared with selected algorithms of SPOPT.

The derivative Gradient[8] method and the non-derivative Grid,[10] Rosenbrock[12] and Simplex[11] methods of SPOPT and the derivative Fletcher method[15] of DCMINUIT, are algorithmic in nature and readily find the global minimum, $U_{min} = 3.60 \times 10^{-4}$ (Table 2). The derivative Steepest

Table 1. Non-linear regression of the experimental A–pH curve of (I) by algorithmic minimization by the Gradient method[8] of the SPOPT(MB) program; the free concentrations of the protonated species are expressed as percentages of the total concentration c_L

Minimization terminated at $U_{min} = 3.60 \times 10^{-4}$ with $s(A) = 0.00352$

Estimated values of parameters:
EPS(L) = 3290 ± 52
EPS(LH) = 5731 ± 81
PKA1 = 7.34 ± 0.06
EPS(LH2) = 7028 ± 181
PKA2 = 3.96 ± 0.08
EPS(LH3) = 16706 ± 18
PKA3 = 2.73 ± 0.08

i	pa_H	A_{exp}	A_{calc}	Residual	[L], %	[LH], %	[LH_2], %	[LH_3], %
1	1.565	0.6600	0.6721	−0.0121	0.00	0.03	7.18	92.80
2	1.750	0.6660	0.6594	0.0066	0.00	0.07	10.58	89.36
3	1.817	0.6530	0.6536	−0.0006	0.00	0.09	12.13	87.79
4	2.000	0.6400	0.6336	0.0064	0.00	0.19	17.36	82.45
5	2.058	0.6310	0.6259	0.0051	0.00	0.24	19.35	80.41
6	2.244	0.5930	0.5963	−0.0033	0.00	0.52	26.83	72.66
7	2.500	0.5470	0.5436	0.0034	0.00	1.37	39.42	59.21
8	2.550	0.5300	0.5319	−0.0019	0.00	1.64	42.06	56.31
9	2.750	0.4830	0.4828	0.0002	0.00	3.24	52.45	44.31
10	2.788	0.4710	0.4732	−0.0022	0.00	3.66	54.31	42.03
11	2.956	0.4280	0.4318	−0.0038	0.00	6.10	61.54	32.35
12	3.000	0.4200	0.4214	−0.0014	0.00	6.92	63.10	29.98
13	3.185	0.3820	0.3807	0.0013	0.00	11.36	67.65	20.99
14	3.250	0.3660	0.3678	−0.0018	0.00	13.34	68.39	18.27
15	3.364	0.3500	0.3474	0.0026	0.00	17.38	68.53	14.08
16	3.518	0.3270	0.3239	0.0031	0.00	24.01	66.41	9.57
17	3.772	0.2950	0.2945	0.0005	0.01	37.52	57.82	4.64
18	4.000	0.2730	0.2761	−0.0031	0.02	51.14	46.62	2.21
19	4.082	0.2720	0.2709	0.0011	0.03	56.02	42.29	1.66
20	4.369	0.2570	0.2574	−0.0004	0.08	71.49	27.87	0.57
21	4.872	0.2450	0.2455	−0.0005	0.30	88.76	10.87	0.07
22	5.569	0.2380	0.2393	−0.0013	1.63	96.00	2.36	0.00
23	6.266	0.2320	0.2320	0.0000	7.77	91.78	0.45	0.00
24	6.691	0.2220	0.2210	0.0010	18.36	81.49	0.15	0.00
25	6.750	0.2200	0.2188	0.0012	20.49	79.38	0.13	0.00
26	7.056	0.2050	0.2047	0.0003	34.28	65.67	0.05	0.00
27	7.295	0.1920	0.1912	0.0008	47.50	52.48	0.02	0.00
28	7.500	0.1800	0.1792	0.0008	59.20	40.79	0.01	0.00
29	7.740	0.1640	0.1665	−0.0025	71.60	28.39	0.00	0.00
30	8.000	0.1550	0.1558	−0.0008	82.11	17.89	0.00	0.00
31	8.072	0.1530	0.1534	−0.0004	84.41	15.59	0.00	0.00
32	8.250	0.1470	0.1486	−0.0016	89.08	10.92	0.00	0.00
33	8.464	0.1440	0.1446	−0.0006	93.03	6.97	0.00	0.00
34	8.915	0.1400	0.1401	−0.0001	97.42	2.58	0.00	0.00
35	9.316	0.1400	0.1385	0.0015	98.96	1.04	0.00	0.00
36	9.855	0.1400	0.1378	0.0022	99.70	0.30	0.00	0.00

Statistical analysis of residuals:
Residual mean = 7.65E-10
Mean residual = 0.00214
Standard deviation = 0.00316
Skewness = −1.023
Curtosis = 7.336
Pearson's $Chi^2 = 4.00$
Hamilton R-factor = 0.008302

CPU time (sec) = 1505.9

Descent[7] and Conjugate Gradients[9] methods are algorithmic in nature, but did not reach the global minimum and terminated at the local minima $U_{min} = 4.76 \times 10^{-4}$ and $U_{min} = 4.013 \times 10^{-4}$. LETAG[3] and LETAGROP,[2] and the algorithm MINUIT[13] allow use of both heuristic (trial-and-error) and algorithmic minimization processes. Generally, since algorithmic procedures lead mostly to the global minimum, heuristic minimization is used to allow the computer "to keep processing" near a local minimum which has a physical meaning and is supported by a preliminary graphical analysis. The local minimum may correspond to a higher value of U than the global value. The test for degree of fit

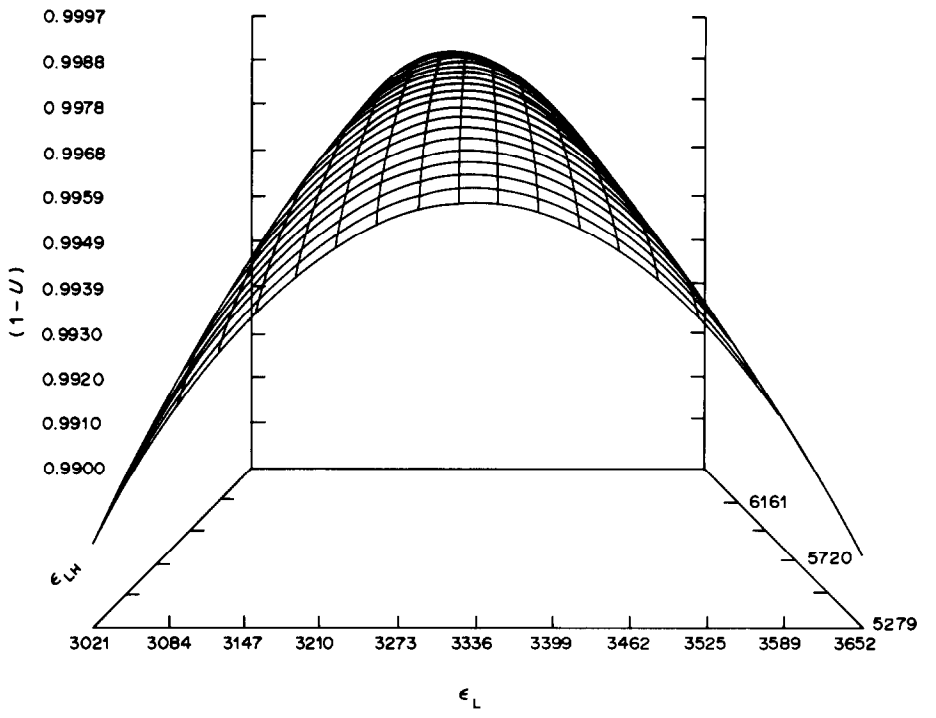

Fig. 3. The minimum of U for m parameters (for LH_3 $m = 7$) may be represented by a pit in the hyperparaboloid surface in $(m + 1)$-dimensional space. A three-dimensional representation of the surface is often helpful. Here, the response surface $(1 - U)$ is drawn for two well-conditioned parameters, ε_{LH} and ε_L.

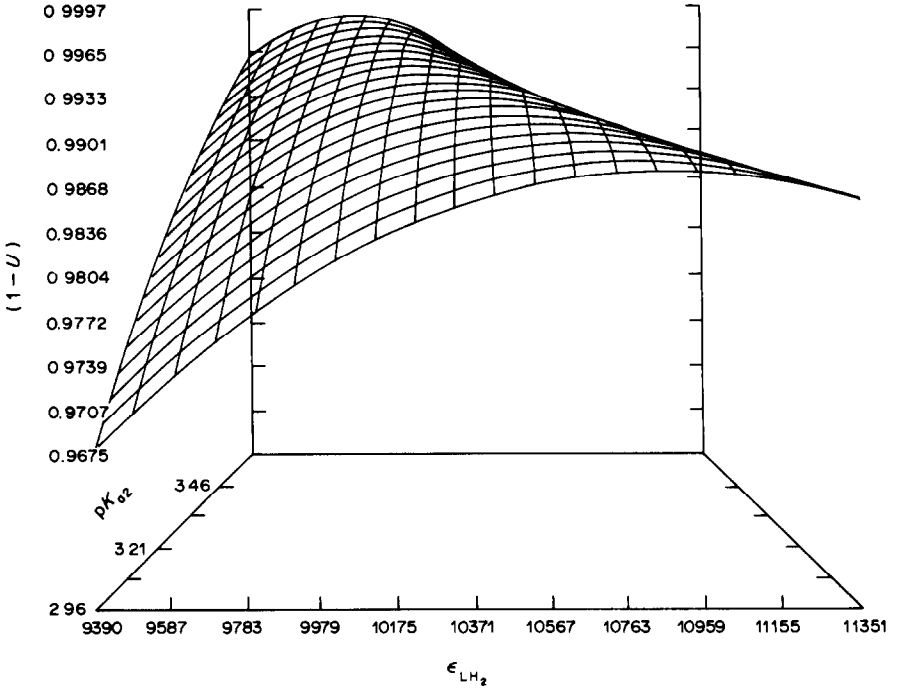

Fig. 4. Response surface $(1 - U)$ for the ill-conditioned parameters pK_{a2} and ε_{LH_2}.

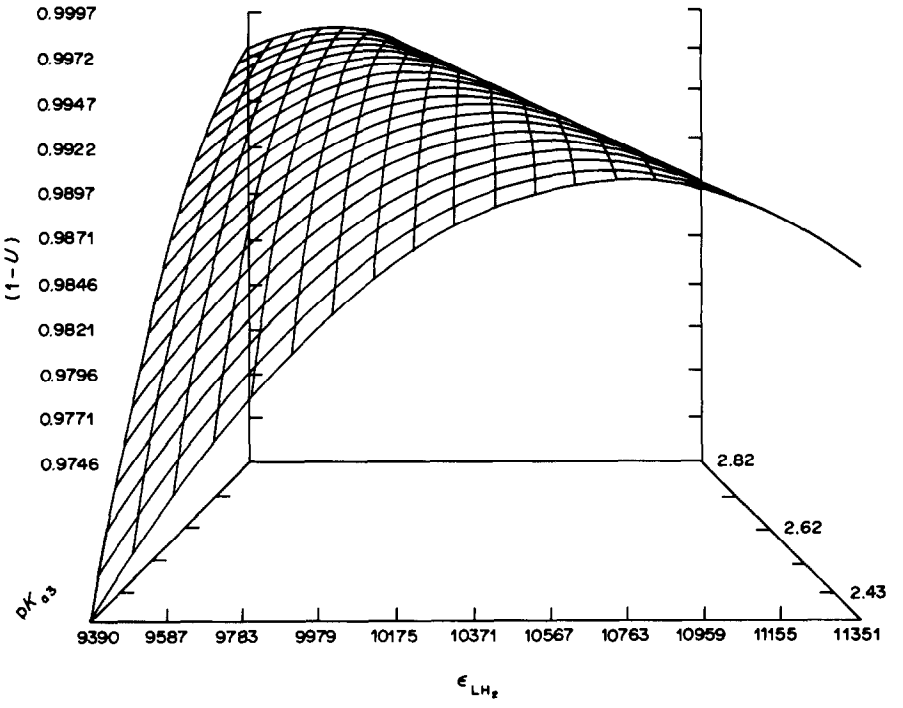

Fig. 5. Response surface $(1 - U)$ for the ill-conditioned parameters pK_{a3} and ε_{LH_2}.

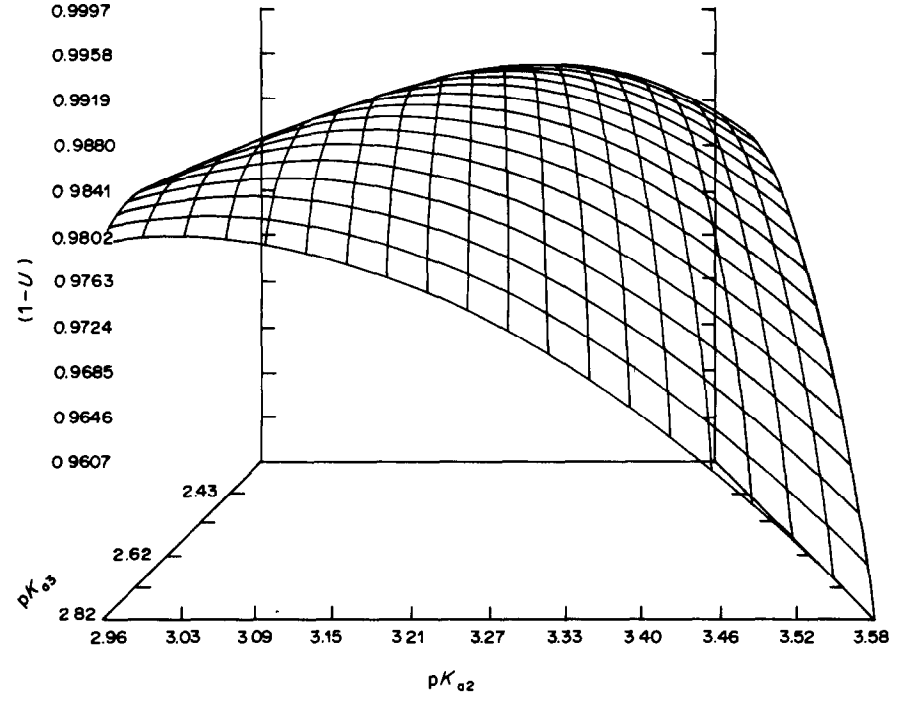

Fig. 6. Response surface $(1 - U)$ for the ill-conditioned parameters pK_{a2} and pK_{a3}.

Table 2. Non-linear regression of the experimental A–pH curve, with algorithmic (ALGOR), heuristic (HEURIST) or combination minimization methods in SPOPT(DC), DCMINUIT, DCLET[1] and LETAGROP-SPEFO[2] (data are from Table 1)

Program	SPOPT(DC)						DCMINUIT			DCLET		SPEFO
Algorithm	St. Desc.	Grad.	Con. G.	Grid	Simplex	Rosenb.	Combin.	Combin.	Combin.	LETAG	LETAG	LETAGROP
Minimization	ALGOR	ALGOR	ALGOR	ALGOR	ALGOR	ALGOR	ALGOR	HEURIST	HEURIST	HEURIST	COMBIN	HEURIST
EPS(L)	3294.9	3290.2	3295.5	3290.2	3290.2	3290.2	3288.4	3299.7	3292.9	3300.8	3288.4	3295.6
	± 61.0	± 53.3	± 64.9	± 53.3	± 53.3	± 53.3	± 4.1	± 35.6	± 0.0	± 43.5	± 2.7	± 31.6
EPS(LH)	5763.6	5731.1	5781.2	5731.1	5731.1	5731.1	5724.2	5799.3	5765.8	5799.3	5744.4	5770.3
	± 67.8	± 106.5	± 53.4	± 106.5	± 106.5	± 106.5	± 7.5	± 32.6	± 0.0	± 46.4	± 2.6	± 33.8
PKA1	7.3215	7.3383	7.3134	7.3383	7.3383	7.3383	7.3428	7.3035	7.3235	7.3017	7.3331	7.3184
	± 0.0626	± 0.0669	± 0.0636	± 0.0669	± 0.0669	± 0.0669	± 0.0668	± 0.0004	± 0.0000	± 0.0440	± 0.0030	± 0.1182
EPS(LH2)	8166.2	7028.4	8779.7	7029.0	7028.4	7028.5	6938.6	9736.4	8167.1	10020.5	7552.1	8149.0
	± 1124.2	± 664.4	± 1283.6	± 664.6	± 664.4	± 664.4	± 11.1	± 3.3	± 0.3	± 201.6	± 8.7	± 59.0
PKA2	3.5953	3.9600	3.4714	3.9597	3.9599	3.9599	4.0087	3.2339	3.5932	3.2913	3.7619	3.5925
	± 0.2608	± 0.3379	± 0.2274	± 0.3378	± 0.3376	± 0.3379	± 0.0115	± 0.0003	± 0.0000	± 0.0287	± 0.0064	± 0.1278
EPS(LH3)	16737.4	16706.4	16752.0	16706.5	16706.4	16706.4	16703.7	16762.0	16737.8	16812.8	16731.3	16731.0
	± 24.2	± 20.1	± 26.6	± 20.1	± 20.1	± 20.1	± 10.6	± 50.6	± 0.2	± 51.2	± 0.00	± 42.9
PKA3	2.6578	2.7263	2.6218	2.7263	2.7263	2.7263	2.7313	2.5601	2.6596	2.5250	2.6938	2.6625
	± 0.0654	± 0.0358	± 0.0800	± 0.0358	± 0.0358	± 0.0358	± 0.0016	± 0.0070	± 0.0000	± 0.0287	± 0.0000	± 0.1466
$U_{min} \times 10^4$	4.76	3.60	4.013	3.60	3.60	3.60	3.60	4.31	3.83	4.58	3.67	3.82
s(A)	0.00365	0.00352	0.00372	0.00352	0.00352	0.00352	0.00352	0.00385	0.00361	0.00390	0.00355	0.00365
Residual mean	1.1E-6	−1.3E-8	−3.7E-5	−5.9E-7	−5.8E-10	−4.4E-10	−1.4E-5	−2.9E-5	−1.6E-5	3.0E-4	2.4E-5	2.5E-9
Mean residual	0.00221	0.0021	0.0023	0.0021	0.0021	0.0021	0.0021	0.0024	0.0022	0.0024	0.0021	0.0022
Standard dev.	0.0033	0.0032	0.0033	0.0032	0.0032	0.0032	0.0032	0.0035	0.0033	0.0036	0.0032	0.0033
Skewness	−0.96	−1.02	−1.14	−1.08	−1.02	−1.02	−1.00	−1.05	−1.11	−1.02	−1.21	1.05
Curtosis	7.481	7.335	7.437	7.337	7.336	7.336	7.222	6.842	7.602	7.671	8.067	7.335
Pearson's Chi^2	4.89	4.00	4.44	4.00	4.00	4.00	6.22	7.17	4.44	9.33	6.67	4.00
R-factor	0.00856	0.00830	0.00876	0.00830	0.00830	0.00830	0.00831	0.00908	0.00856	0.00936	0.00838	0.00856
CPU time (*sec*)	564.4	563.1	220.0	554.3	299.9	572.9	134.1	380.1	850.0	23.7	35.7	64.16

usually cannot help much, because that achieved for the local minimum seems to be nearly the same as that for the global one.

To test the algorithms selected, the initial guesses of parameters from graphical analysis were $\varepsilon_L = 3300$, $\varepsilon_{LH} = 5800$, $pK_{a1} = 7.3$, $\varepsilon_{LH_2} = 9800$, $pK_{a2} = 3.3$, $\varepsilon_{LH_3} = 16800$, $pK_{a3} = 2.55$. The routines of SPOPT(DC) were applied several times with different sets of initial guesses and most led to the same global minimum, $U_{min} = 3.60 \times 10^{-4}$. This global minimum was also reached when mass-balance equations were used in the residual-square-sum function of SPOPT(MB) (Table 1).

In DCMINUIT, global logic was used (Table 2, Combination, ALGOR.); when one of the three minimization methods fails, another automatically makes another attempt. Minimization was guided by user's commands from data and three minimization routines of MINUIT[13] were used (Table 2, Combination, HEURIST.). The algorithmic strategy leads to the global minimum obtained with SPOPT, but the heuristic strategy terminates at another local minimum, $U_{min} = 4.31 \times 10^{-4}$.

DCLET[1] uses the heuristic strategy of LETAG,[3] and gave a local minimum of $U_{min} = 4.58 \times 10^{-4}$. A combined strategy (*i.e.*, heuristic followed by algorithmic) gave better refinement of the parametric values and a slightly better fit was achieved, $U_{min} = 3.67 \times 10^{-4}$.

LETAGROP–SPEFO[2] has a heuristic trial-and-error strategy totally under control of the user. Values for the minimization steps of all the parameters to be refined must be supplied, and good initial guesses are required to avoid divergence of the iterative process. Here, a local minimum of $U_{min} = 3.82 \times 10^{-4}$ was achieved, with a good fit to the curve, and the parameter estimates had a physical meaning.

Because the four programs terminate with refined estimates that differ in value, the user must decide which program to choose as the best for getting reliable parameter estimates. It would be useful to classify the various regression algorithms in application. Two approaches were used: (1) comparison with results of analysis of A–pH curves, (2) study of simulated data.

For comparison, 23 absorbance–pH curves for 19 wavelengths were analysed by the FA608 + EY608 program;[25] the results were $pK_{a1} = 7.32 \pm 0.03$, $pK_{a2} = 3.28 \pm 0.03$, $pK_{a3} = 2.60 \pm 0.02$ with $s(A) = 0.0030$.[24] SQUAD(84)[27] gave $pK_{a1} = 7.332 \pm 0.066$, $pK_{a2} = 3.206 \pm 0.173$, $pK_{a3} = 2.503 \pm 0.294$ with $s(A) = 0.0022$. The absorbance matrix for 19 wavelengths gives more information about the protonation equilibria studied, so the estimates of the constants should be more accurate than those found by an analysis at one wavelength only. The results found from the absorbance matrix appear to be in agreement with the parameters corresponding to the local minimum.

To select reliable algorithms for analysis of A–pH curves, simulated data were investigated.

Modelling absorbance–pH curves by use of simulated data

The use of simulated A–pH data allows the analysis of real experimental data to be tested in a situation where the parameters are known. Such modelling serves (*i*) to test whether each parameter is ill-conditioned or well-conditioned in the mathematical model in question, (*ii*) to examine the influence of the instrumental error of the spectrophotometer on the precision and accuracy of the parameter estimates, and (*iii*) to find a reliable minimization routine which, for a similar shape of experimental A–pH curve, will give the best parameter estimates in the shortest time.

"True" values of seven parameters were chosen to correspond roughly to the experimental parameters for (**I**): $\varepsilon_L = 3300$, $\varepsilon_{LH} = 5800$, $\varepsilon_{LH_2} = 9800$, $\varepsilon_{LH_3} = 16800$, $pK_{a1} = 7.3$, $p_{Ka2} = 3.3$ and $pK_{a3} = 2.6$. The instrumental error, $s_{inst}(A)$ was taken as 0.003. For set pH values, 35 absorbance values were calculated precisely, then loaded with random errors. The random errors had a normal distribution with the mean approximately zero, the standard deviation of the mean 0.003, the mean error 0.003, skewness 0, curtosis 3 and a Pearson Chi-Square value of 12.60 for 6 degrees of freedom and 0.95 significance level. These errors appear to be Gaussian in nature (Table 3).

In the analysis of the simulated A–pH curve, the minimization was started either with a bad initial guess ($\varepsilon_L = 6000$, $\varepsilon_{LH} = 8000$, $pK_{a1} = 8.2$, $\varepsilon_{LH_2} = 12000$, $pK_{a2} = 3.7$, $\varepsilon_{LH_3} = 20000$, $pK_{a3} = 3.0$) or a good initial guess (the corresponding values being 3300, 5800, 7.3, 9800, 3.3, 16800, 2.6).

The Conjugate Gradients algorithm[9] of SPOPT(MB) found the best estimates of all seven parameters either by the recurrent equation method or by formulation on the basis of the mass-balance equations (Tables 3 and 4).

The hyperparaboloid response surface shows that three parameters, ε_{LH_2}, pK_{a2} and pK_{a3}, are ill-conditioned, because the minima are broad and indefinite (Figs. 3–6). They cannot be determined accurately or precisely. The last U-contour (the "D boundary") may be expressed as the supercurve $U = U_{min} + s^2(A)$, so the standard deviation in each parameter b_i is defined by the expression $s(b_i) = \max(b_D - b_{min})_i$ which is the maximum difference between the value for b_i at any point on the "D boundary", and the value for b_i at the minimum. The standard deviations for the ill-conditioned parameters $s(\varepsilon_{LH_2})$, $s(pK_{a2})$ and $s(pK_{a3})$ have significantly greater values than those for the well-conditioned parameters. Because the response surface resembles a flat-bottomed saucer, there is a large amount of uncertainty in the location of the pit.

Table 3. Non-linear regression of a simulated A–pH curve by the Conjugate Gradients algorithm[9] of SPOPT(DC), with $s_{inst}(A) = 0.003$

True values of parameters	Estimated values of parameters
EPS(L) = 3300	3275 ± 30
EPS(LH) = 5800	5811 ± 13
PKA1 = 7.3	7.3 ± 0.03
EPS(LH2) = 9800	9851 ± 2716
PKA2 = 3.3	3.3 ± 0.31
EPS(LH3) = 16800	16776 ± 52
PKA3 = 2.6	2.60 ± 0.19

i	pH	$A_{accurate}$	Error	A_{exp}	A_{calc}	Residual
1	1.450	0.68248	−0.00222	0.6803	0.6817	−0.0014
2	1.610	0.67426	−0.00100	0.6733	0.6735	−0.0002
3	1.770	0.66294	0.00350	0.6664	0.6622	0.0042
4	1.930	0.64766	−0.00286	0.6448	0.6471	−0.0023
5	2.090	0.62756	0.00030	0.6279	0.6272	0.0007
6	2.250	0.60200	−0.00244	0.5996	0.6018	−0.0022
7	2.410	0.57084	0.00188	0.5727	0.5708	0.0019
8	2.570	0.53472	0.00111	0.5358	0.5349	0.0009
9	2.730	0.49514	0.00138	0.4965	0.4955	0.0010
10	2.890	0.45434	−0.00242	0.4519	0.4549	−0.0030
11	3.050	0.41474	−0.00043	0.4143	0.4155	−0.0012
12	3.210	0.37850	0.00287	0.3814	0.3794	0.0020
13	3.370	0.34704	−0.00251	0.3445	0.3479	−0.0034
14	3.530	0.32099	0.00657	0.3276	0.3219	0.0057
15	3.690	0.30027	−0.00226	0.2980	0.3010	−0.0030
16	3.850	0.28433	0.00165	0.2860	0.2851	0.0009
17	4.010	0.27239	0.00288	0.2753	0.2731	0.0022
18	4.170	0.26363	0.00119	0.2648	0.2642	0.0006
19	4.330	0.25730	0.00057	0.2579	0.2579	0.0000
20	4.490	0.25276	0.00018	0.2529	0.2533	−0.0004
21	4.580	0.25081	−0.00352	0.2473	0.2514	−0.0041
22	4.670	0.24919	−0.00365	0.2455	0.2497	−0.0042
23	4.760	0.24784	0.00005	0.2479	0.2484	−0.0005
24	4.850	0.24672	−0.00416	0.2426	0.2473	−0.0047
25	5.235	0.24347	0.00169	0.2452	0.2440	0.0012
26	5.620	0.24109	0.00356	0.2447	0.2417	0.0030
27	6.005	0.23772	0.00380	0.2415	0.2384	0.0031
28	6.390	0.23112	0.00215	0.2333	0.2321	0.0012
29	6.775	0.21846	0.00297	0.2214	0.2198	0.0016
30	7.160	0.19856	0.00250	0.2011	0.2002	0.0009
31	7.545	0.17584	−0.00138	0.1745	0.1770	−0.0025
32	7.930	0.15779	−0.00138	0.1564	0.1582	−0.0018
33	8.315	0.14715	−0.00116	0.1460	0.1468	−0.0008
34	8.700	0.14194	−0.00258	0.1394	0.1412	−0.0018
35	9.085	0.13963	0.00161	0.1412	0.1387	0.0025

Statistical analysis of random errors:	Statistical analysis of residuals:
Error mean = 2.41E-04	Residual mean = −1.14E-04
Mean error = 0.00218	Mean residual = 0.00203
Standard deviation = 0.00255	Standard deviation = 0.00246
Skewness = 0.471	Skewness = −0.041
Curtosis = 2.437	Curtosis = 2.482
Chi^2 (6, 0.95) = 5.46	Chi^2 (6, 0.95) = 4.09
Hamilton R-factor = 0.00660	Hamilton R-factor = 0.00633

To test whether a model represents the data adequately, the residuals are analysed. These should be randomly distributed about the predicted regression curve, and systematic departures from randomness indicate that either the model or the parametric estimates are not satisfactory. To analyse the residuals, their statistics are compared with the statistics of the imposed random errors; it is checked whether both distributions are Gaussian in nature, and whether the errors agree in magnitude and/or sign. The degree of fit of the curves in Table 4 is good enough, so the minimization process is assumed to have terminated successfully. Table 4 also shows how the instrumental error of absorbance affects the precision and accuracy of the parameter estimates, other things being equal.

Errors in absorbance cause systematic errors in the parametric estimates: the relative systematic error of the parametric estimates $e_{rel}(b_i)$ depends on the instrumental error $s_{inst}(A)$ approximately according to $e_{rel}(b_i) = q + k s_{inst}(A)$. The intercept q and slope k were calculated for seven parameters from the data of

Table 4, and found to be

Parameter b_i	ε_L	ε_{LH}	pK_{a1}	ε_{LH_2}	pK_{a2}	ε_{LH_3}	pK_{a3}
Intercept q	0.0091	−0.0164	0.0093	−4.9550	1.1236	−0.0998	2.1967
Slope k	195.79	29.45	92.18	6464.50	−1513.8	34.88	−2367.34

The higher values of the slope for the three ill-conditioned parameters ε_{LH_2}, pK_{a2} and pK_{a3} illustrate the greater importance of absorbance precision for accuracy of these estimates. Thus, for elucidation of overlapping equilibria, only high-precision data are suitable. Application of non-linear regression to imprecise data is very likely to lead to false values for the parameter estimates.

Tables 5 and 6 list the methods that did not fail, and which terminated reasonably quickly, selected from 15 derivative and 15 non-derivative algorithms of SPOPT, two of DCMINUIT, one of DCLET[1] and one of LETAGROP–SPEFO.[2] Derivative algorithms were tested with the use of good and bad initial guesses, but the non-derivative ones with just bad guesses. Good initial guesses were used in order to find a true minimum for comparison with any minimum found from a bad initial guess.

Starting from a good initial guess, the lowest value of U_{min} (2.086×10^{-4}, perhaps representing a global minimum) was found by the Gradient and Rosenbrock methods. Close to this was $U_{min} = 2.093 \times 10^{-4}$, found by the Steepest Descent, Conjugate gradients and Grid methods.

With good guesses, the relative systematic errors of the estimates found for the well-conditioned and ill-conditioned parameters had nearly the same magnitude: $e_{rel}(\varepsilon_{LH_2}) = 0.4\%$, $r_{rel}(pK_{a2}) = 0.2\%$, $e_{rel}(pK_{a3}) = 0.1\%$ for the ill-conditioned and $e_{rel}(\varepsilon_L) = 0.8\%$, $e_{rel}(\varepsilon_{LH}) = 0.1\%$, and $e_{rel}(\varepsilon_{LH_3}) = 0.4\%$ for the well-conditioned parameters. Starting from a bad initial guess the algorithms found the same estimates as before only for the well-conditioned parameters. The relative systematic errors of the ill-conditioned parameters were about 10 times greater than those for the well-conditioned ones: $e_{rel}(\varepsilon_{LH_2}) = 10\%$, $e_{rel}(pK_a2_2) = 3.4\%$ and $e_{rel}(pK_{a3}) = 2.7\%$.

Figure 7 demonstrates that well-conditioned parameters are not loaded by significant systematic errors, but the broader confidence interval for estimation of the ill-conditioned parameters indicates some uncertainty in the estimates.

The statistical analysis of the residues in Tables 5 and 6 shows that a good fit was achieved by most of the algorithms. The mean residual and its standard deviation are less than $s_{inst}(A) = 0.003$. The Hamilton R-factor is 0.6–0.7%. From a mathematical point of view, a satisfactory fit indicates that the parameter estimates have been refined sufficiently.

Table 4. Non-linear regression of the simulated A–pH curve by the derivative Conjugate Gradients algorithm[9] of SPOPT(DC); data are simulated for various instrumental errors of the absorbance, $s_{inst}(A)$; bad initial guesses of the parameters were used

$s_{inst}(A)$	0.000001	0.0005	0.001	0.002	0.004	0.006
Error mean	1.40E-7	6.98E-5	1.40E-4	2.79E-4	5.58E-4	8.37E-4
Mean error	8.69E-7	0.00043	0.0009	0.0017	0.0035	0.0052
Standard deviation	9.71E-7	0.00049	0.0010	0.0019	0.0039	0.0058
Skewness	0.561	0.561	0.561	0.561	0.561	0.561
Curtosis	1.689	1.689	1.689	1.689	1.689	1.689
Pearson's Chi²	9.57	9.57	9.57	9.57	9.57	9.57
R-factor	3.0E-6	0.00125	0.00251	0.00501	0.01002	0.01502
EPS(L) = 3300	3300	3303	3307	3314	3325	3339
EPS(LH) = 5800	5800	5801	5801	5802	5806	5809
PKA1 = 7.3	7.30	7.30	7.31	7.31	7.32	7.34
EPS(LH2) = 9800	9800.5	10191	9859	10453	12326	12854
PKA2 = 3.3	3.30	3.26	3.20	3.24	3.09	3.06
EPS(LH3) = 16800	16800	16800	16791	16790	16812	16816
PKA3 = 2.6	2.60	2.57	2.60	2.55	2.38	2.31
U_{min}	2.93E-11	7.30E-6	3.00E-5	1.81E-4	4.67E-4	1.05E-3
$s(A)$	1.00E-6	0.00051	0.00103	0.00205	0.00408	0.00613
Residual mean	−8.29E-11	−3.06E-7	1.28E-6	−5.91E-6	6.85E-6	−6.27E-6
Mean residual	8.44E-7	0.00042	0.0008	0.0017	0.0033	0.0050
Standard deviation	9.15E-7	0.00046	0.0009	0.0018	0.0037	0.0055
Skewness	0.158	0.141	0.185	0.154	0.154	0.147
Curtosis	1.574	1.578	1.598	1.588	1.599	1.599
Pearson's Chi²	11.86	8.66	14.14	11.86	10.03	8.66
R-factor	0.00000	0.00118	0.00237	0.00473	0.00942	0.01413
CPU time (sec)	150.02	411.44	173.98	305.42	159.46	279.52

Table 5. Non-linear regression of the simulated A–pH curve by various derivatives algorithms of SPOPT(DC) and DCMINUIT

Program	SPOPT(DC)						DCMINUIT			
Algorithm	Steepest Descent		Gradient		Conjugate Gradient		Fletcher		Combination	
Initial Guess	Bad	Good	Bad	Good	Bad	Good	Bad	Good	Bad	Good
EPS(L) = 3300	3260.4 ± 28.2	3259.6 ± 27.8	3258.9 ± 27.6	3258.9 ± 27.6	3260.0 ± 28.0	3275.4 ± 30.0	3316.8 ± 2.2	3318.5 ± 2.6	3323.9 ± 6.9	3313.9 ± 1.9
EPS(LH) = 5800	5810.9 ± 12.6	5806.9 ± 13.0	5803.5 ± 13.8	5803.5 ± 13.8	5809.2 ± 12.7	5811.3 ± 13.0	5794.8 ± 1.5	5800.0 ± 1.3	5805.4 ± 2.6	5797.8 ± 0.7
PKA1 = 7.30	7.3323 ± 0.0265	7.3345 ± 0.0260	7.3364 ± 0.0258	7.3364 ± 0.0258	7.3332 ± 0.0262	7.3297 ± 0.0263	7.3270 ± 0.0014	7.3234 ± 0.0000	7.3150 ± 0.0022	7.3300 ± 0.0000
EPS(LH2) = 9800	10842.8 ± 2688.8	9774.3 ± 2557.6	8949.5 ± 2335.3	8949.4 ± 2335.3	10333.8 ± 2643.3	9851.5 ± 2716.3	8707.6 ± 4.2	9826.4 ± 4.0	11242.6 ± 8.3	9854.6 ± 7.5
PKA2 = 3.3000	3.1978 ± 0.2428	3.3087 ± 0.2957	3.4174 ± 0.3446	3.4174 ± 0.3446	3.2473 ± 0.2665	3.2988 ± 0.3075	3.4618 ± 0.0001	3.3096 ± 0.0000	3.1693 ± 0.0009	3.3070 ± 0.0002
EPS(LH3) = 16800	16792.1 ± 56.5	16781.9 ± 49.5	16773.3 ± 45.0	16773.3 ± 45.0	16787.4 ± 52.9	16776.3 ± 51.7	16755.4 ± 2.5	16769.3 ± 2.3	16791.3 ± 6.5	16771.7 ± 5.3
PKA3 = 2.60	2.5245 ± 0.2197	2.6025 ± 0.1769	2.6554 ± 0.1447	2.6554 ± 0.1447	2.5632 ± 0.1988	2.5985 ± 0.1898	2.6698 ± 0.0003	2.5974 ± 0.0001	2.4869 ± 0.0016	2.5949 ± 0.0000
$U^{(0)}$	7.7E-1	7.67E-4	7.74E-1	7.67E-4	7.74E-1	7.67E-4	7.72E-1	2.97E-4	7.72E-1	2.97E-4
U_{min} terminated	2.11E-4	2.09E-4	2.08E-4	2.08E-4	2.10E-4	2.10E-4	2.71E-4	2.67E-4	2.64E-4	2.67E-4
s(Å)	0.00275	0.00273	0.00273	0.00273	0.00274	0.00274	0.00310	0.00308	0.00307	0.00308
Residual mean	7.64E-7	−1.21E-6	−1.91E-9	4.23E-10	−4.45E-6	−1.14E-4	4.49E-6	1.58E-6	−2.52E-7	1.64E-5
Mean residual	0.0020	0.0020	0.0020	0.0020	0.0020	0.0020	0.0025	0.0025	0.0025	0.0025
Standard deviation	0.0024	0.0024	0.0024	0.0024	0.0025	0.0025	0.0028	0.0027	0.0027	0.0027
Skewness	0.099	0.008	0.008	0.082	0.082	−0.041	0.215	0.182	0.141	0.213
Curtosis	2.531	2.446	2.416	2.416	2.486	2.482	1.629	1.595	1.584	1.607
Pearson's Chi^2	8.66	2.26	1.34	1.34	3.63	4.09	14.60	13.23	11.86	14.14
R-factor	0.00633	0.00630	0.00629	0.00629	0.00632	0.00633	0.00717	0.00712	0.00707	0.00712
CPU time (sec)	560.9	550.0	545.2	510.3	80.6	75.5	70.1	53.9	110.9	57.5

Table 6. Non-linear regression of the simulated A–pH curve by various non-derivative minimization algorithms of SPOPT(DC), DCMINUIT, DCLET and LETAGROP-SPEFO; the process was started with bad initial guesses of the parameters

Program	SPOPT(DC)			DCMINUIT	DCLET		SPEFO
Algorithm	Grid	Simplex	Rosenbr.	Simplex	LETAG-alg.	LETAG-comb.	LETAGROP
EPS(L) = 3300	3259	3413	3259	3331	2573	3322	3324
	± 28	± 141	± 28	± 5	± 34	± 15	± 41
EPS(LH) = 5800	5807	3276	5803	5805	5128	5787	5755
	± 13	± 832	± 14	± 12	± 43	± 3	± 59
PKA1 = 7.30	7.33	7.93	7.336	7.315	8.35	7.325	7.32
	± 0.026	± 0.97	± 0.026	± 0.0146	± 0.02	± 0.003	± 0.22
EPS(LH2) = 9800	9840	5826	8945	11243	8733	7823	5842
	± 2543	± 13	± 2334	± 20	± 31	± 1	± 23
PKA2 = 3.30	3.30	7.41	3.41	3.109	3.56	3.63	5.84
	± 0.29	± 0.14	± 0.34	± 0.008	± 0.00	± 0.00	± 0.22
	16784	16694	16773	16791	15818	16741	16668
	± 50	± 25	± 45	± 29	± 0	± 0	± 31
PKA3 = 2.60	2.60	2.83	2.66	2.486	2.98	2.72	2.83
	± 0.18	± 0.004	± 0.14	± 0.008	± 0.00	± 0.0000	± 0.22
$U^{(0)}$	0.774	0.774	0.773	0.771	0.773	0.773	0.773
U_{min} (terminated) × 10^4	2.093	2.608	2.086	2.638	195.7	2.647	3.191
Residual mean	−1.63E-6	−2.58E-5	4.064E-9	−2.01E-5	−6.92E-5	2.04E-5	−3.99E-11
Mean residual	0.0020	0.0020	0.0020	0.0025	0.0021	0.0025	0.0026
Standard deviation	0.0024	0.0027	0.0024	0.0027	0.0023	0.0027	0.0030
Skewness	0.076	0.566	0.789	0.121	−0.498	0.316	0.188
Curtosis	2.438	3.836	2.416	1.595	1.773	1.855	1.630
Pearson's Chi^2	2.26	9.11	1.34	8.20	25.11	10.49	9.11
R-factor	0.00630	0.00704	0.00629	0.00708	0.06099	0.00709	0.00779
CPU time (sec)	545.2	330.5	530.2	97.0	83.3	90.9	446.8

CONCLUSIONS

To determine ill-conditioned parameters in an overlapping equilibrium system, an efficient minimization routine is needed, which is safe, fast, and able to find true estimates of the parameters. Study of the effects of instrumental error shows that data of the highest precision should be used; otherwise, estimates of the ill-conditioned parameters are not accurate enough. A criterion for determination of the minimization process should be decided with the use of a simulated data set.

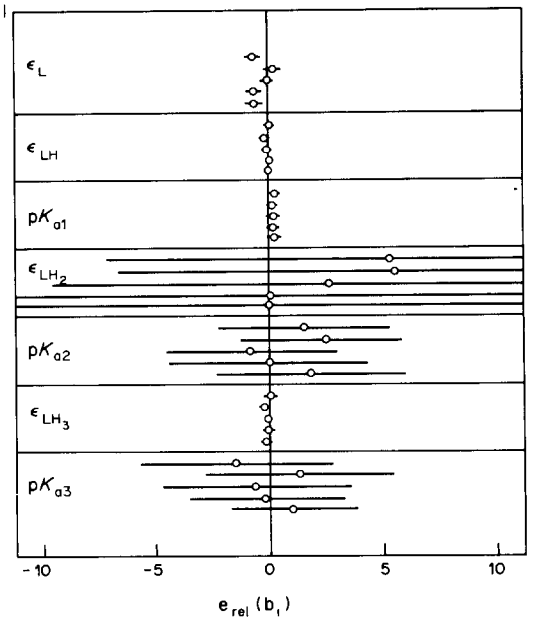

Fig. 7. Relative systematic errors of seven parameter estimates refined by the five minimization algorithms (Tables 5 and 6, from top to bottom) Steepest Descent, Fletcher, Conjugate Gradients, Grid and Rosenbrock methods. The positions of the parameter estimates and corresponding standard deviations are plotted on a relative percentage scale.

Diagnostic tools such as (*i*) graphical interpretation of the hyperparaboloid response surface, in parametric co-ordinates, (*ii*) examination of the degree of fit by statistical analysis of the residuals, (*iii*) comparison of the calculated parametric estimates with the preselected true values, (*iv*) comparison of the statistics of the imposed errors with those of the residuals, (*v*) the size of the standard deviations calculated from the last U contour (D boundary), help in the examination of the conditioning of parameters in a particular model, and to determine the best minimization strategy, the termination criterion, *etc.*

The following procedure is recommended for regression analysis.

(1) Formulate a suitable mathematical model.

(2) Choose and test (by use of simulated data) a minimization algorithm suitable for safe determination of ill-conditioned parameters.

(3) Set up computational conditions such as parameter limits, minimization steps, residuals statistics for best parametric estimates, an efficient minimization strategy and a termination criterion for the algorithm selected.

(4) Analyse the experimental A–pH curve.

REFERENCES

1. M. Meloun and J. Čermák, *Talanta*, 1979, **26**, 569.
2. L. G. Sillén and B. Warnqvist, *Ark. Kemi*, 1969, **31**, 377.
3. M. Meloun and J. Čermák, *Talanta*, 1984, **31**, 947.
4. M. Meloun and J. Havel, *Computation of Solution Equilibria, Part I, Spectrophotometry, Folia Fac. Sci. Nat. Univ. Purk. Brunensis*, Brno, 1985.
5. J. Havel and M. Meloun, in *Computational Methods for the Determination of Stability Constants*, D. J. Leggett (ed.), Plenum Press, New York, 1985.
6. L. Lukšan, *Research Report N. V-4*, Czechoslovak Academy of Sciences, Prague, 1976.
7. W. Murray, *Numerical Methods for Unconstrained Optimization*, Academic Press, London, 1972.
8. B. V. Shah, R. J. Buehler and O. Kempthorne, *SIAM J. Appl. Math.*, 1964, **12**, 74.
9. M. R. Hestenes and E. Stiefel, *J. Res. Natl. Bur. Stds.*, 1952, **49**, 409.
10. R. Hooke and T. A. Jeeves, *J. Assoc. Comp. Mach.*, 1961, **8**, 212.
11. J. A. Nelder and R. Mead, *Comput. J.*, 1965, **7**, 308.
12. H. H. Rosenbrock, *ibid.*, 1960, **3**, 175.
13. F. James, *Comp. Phys. Commun.*, 1975, **10**, 343.
14. *Idem, Proc. 1972 CERN Computing and Data Processing School*, CERN 72-21.
15. R. Fletcher, *Comput. J.*, 1970, **13**, 317.
16. A. Sabatini, A. Vacca and P. Gans, *Talanta*, 1974, **21**, 53.
17. M. Meloun and M. Javůrek, *ibid.*, 1984, **31**, 1083.
18. J. R. Bell, *Commun. Assoc. Comp. Mach.*, 1968, **11**, 498, Algorithm 334.
19. W. C. Hamilton, *Statistics in Physical Science*, Ronald Press, New York, 1964.
20. I. G. Sayce, *Talanta*, 1968, **15**, 1397.
21. C. F. Moore, *Comp. Phys. Commun.*, 1971, **2**, 53.
22. M. Meloun and J. Pancl, *Collection Czech. Chem. Commun.*, 1976, **41**, 2365.
23. M. Javůrek, *Thesis*, College of Chemical Technology, Pardubice, 1985.
24. M. Meloun and J. Chýlková, *Collection Czech. Chem. Commun.*, 1979, **44**, 2815.
25. J. J. Kankare, *Anal. Chem.*, 1970, **42**, 1322.
26. D. J. Leggett and W. A. E. McBryde, *ibid.*, 1975, **47**, 1065.
27. M. Meloun, J. Havel and M. Javůrek, *Talanta*, 1985, in the press.

Talanta, Vol. 32, No. 10, pp. 987–991, 1985
Printed in Great Britain.

0039-9140/85 $3.00 + 0.00

SPECTROPHOTOMETRIC, DIFFERENTIAL PULSE POLAROGRAPHIC AND DIFFERENTIAL PULSE VOLTAMMETRIC MONITORING OF THE CHEMICAL DESTRUCTION OF THE ANTI-TUMOUR PHARMACEUTICALS 6-MERCAPTOPURINE, 6-THIOGUANINE AND MELPHALANE

JIŘÍ BAREK, ANTONÍN BERKA and JIŘÍ ZIMA
Department of Analytical Chemistry, Charles University, Albertov 2030, 128 40, Prague 2, Czechoslovakia

(*Received* 29 *March* 1985. *Accepted* 17 *April* 1985)

Summary—A new method has been developed for the destruction of 6-mercaptopurine, 6-thioguanine and melphalane in laboratory waste, based on oxidation of these substances by potassium permanganate in sulphuric acid medium. To study the effectiveness of the decontamination, spectrophotometric and differential-pulse polarographic methods have been developed for the determination of 6-mercaptopurine and 6-thioguanine and spectrophotometric and differential-pulse voltammetric methods for melphalane. These techniques have been employed to demonstrate that the effectiveness of the proposed method is around 99.8%. Its usefulness for the destruction of various types of expired pharmaceuticals has been demonstrated.

Pharmaceuticals that have been successfully used in the treatment of various types of tumours include 6-mercaptopurine (I), 6-thioguanine (II) and melphalane (III).

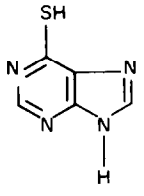

I

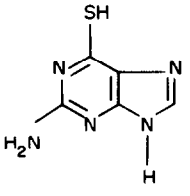

II

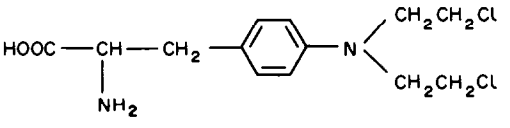

III

It is well known[1] that thiopurines inhibit the synthesis of DNA and RNA and have been used successfully in the treatment of acute leukaemia.[2] Melphalane is an alkylation agent used in the treatment of various types of tumours.[3] Because of their ability to interact with genetic material in the cell, all these substances have mutagenic or carcinogenic properties. Thus work with these substances yields biologically harmful waste materials, and glassware and instruments become contaminated. As part of a systematic study of methods for the destruction of chemical carcinogens on a laboratory scale, this work considers the oxidation of these substances with permanganate in sulphuric acid medium, which has been found to be useful for carcinogenic aromatic amines.[4] Simultaneously, a sufficiently sensitive method was sought for monitoring the effectiveness of the destruction. Reversed-phase high-pressure liquid chromatography has been used for the determination of 6-thioguanine[5–7] and melphalane[8,9] in biological materials. This method is sufficiently sensitive and selective but is demanding on time and requires complex instrumentation. Thus the simpler and faster spectrophotometric and differential-pulse polarographic or voltammetric determinations of these substances were developed, to monitor the effectiveness of the destruction.

EXPERIMENTAL

Apparatus

Potentiometric titrations were done with a Radiometer ABU1/TTT1 automatic titrator, a platinum indicator electrode and saturated calomel reference electrode. Polarization curves were measured with a PA2 polarographic analyser (Laboratorní přístroje, Czechoslovakia). Polarographic measurements were made with a dropping mercury electrode ($m = 5.77$ mg/sec and $t = 2.05$ sec at $h = 36$ cm in 0.1*M* KCl medium at an applied potential of 0 V). Voltammetric measurements were made by use of an RDE 1 rotating-disc electrode with a glassy-carbon active surface, 3 mm in diameter (Laboratorní přístroje). Both types of measurements were made with a three-electrode system involving a platinum auxiliary electrode and saturated calomel reference electrode. Spectrophotometric

measurements were made with a Pye-Unicam PU8 800 instrument and 1-cm cuvettes.

Reagents

Solutions of 6-mercaptopurine and 6-thioguanine (both $10^{-3}M$) and melphalane ($10^{-2}M$) in $0.1M$ sulphuric acid were prepared by dissolving precisely weighed amounts of the pure substances provided by the International Agency for Research on Cancer, Lyon, France. All other chemicals used ($KMnO_4$, H_2SO_4, $FeSO_4$, $Na_4P_2O_7$, Na_2SO_3 and zinc powder) were of *p.a.* purity (Lachema, Brno). Water was distilled twice in quartz apparatus.

Procedures

Time-dependence of the oxidation of the studied substances with permanganate. A 1.00-ml portion of the sample solution was transferred into the titration vessel, together with 1.00 ml of $0.025M$ potassium permanganate and 1 ml of $2M$ sulphuric acid. After time t, 5 ml of $0.1M$ manganese(II) sulphate and 3 g of solid sodium pyrophosphate decahydrate dissolved in 10 ml of $2M$ sulphuric acid were added. After 5 min, the pyrophosphate complex of manganese(III) was determined potentiometrically by titration with $0.01M$ iron(II) sulphate. A blank was run simultaneously and the consumption of the oxidizing agent in equivalents per mole of studied substance was found from the difference between the sample and blank titrations.

Spectrophotometric determination of unreacted 6-mercaptopurine and 6-thioguanine. A 10.0-ml portion of $10^{-3}M$ solution of the studied substance was mixed with 5.0 ml of $0.025M$ potassium permanganate and 5.0 ml of $2M$ sulphuric acid. After 12 hr, 200 mg of zinc powder were added and the solution stirred for 1 hr. Unreacted zinc was filtered off with a porosity-4 sintered-glass filter funnel and 10.0 ml of the filtrate were spiked by five successive additions of 50 μl of $10^{-4}M$ solution of the studied substance, the spectrum in the region 200–400 nm being recorded for the unspiked filtrate and again after each addition.

Spectrophotometric determination of unreacted melphalane. A procedure analogous to that described above was followed but because of the lower molar absorptivity of melphalane in $0.5M$ sulphuric acid, $10^{-3}M$ solution was used for the standard additions. Higher sensitivity was attained with a medium of pH 3. The pH of 10 ml of the filtrate was adjusted to 3.0 ± 0.1 with $2M$ sodium hydroxide; $10^{-3}M$ melphalane was used for the standard additions and the dilution of the filtrate with the sodium hydroxide solution was allowed for in the calculations.

If a yellow colour is formed as a result of localized oxidation of manganese(II) by atmospheric oxygen during the neutralization, it must be removed by addition of a small amount of zinc powder.

Determination of unreacted 6-mercaptopurine and 6-thioguanine by differential-pulse polarography (DPP). Ten ml of $10^{-3}M$ solution of the studied substance were mixed with 5 ml of $0.025M$ potassium permanganate and 5 ml of $2M$ sulphuric acid. After 12 hr, the unreacted permanganate was reduced by addition of 5 ml of $0.1M$ sodium sulphite, and 7.0 ml of the solution were transferred to the polarographic vessel and deaerated by passage for nitrogen for 15 min, then the DPP curve was recorded, for a drop time of 1 sec, a polarization rate of 5 mV/sec, a modulation amplitude of 50 mV, mercury reservoir height of 36 cm and sensitivity of 100 nA/cm. Then five successive additions of 35 μl of $10^{-3}M$ solution of the studied substance were made, the DPP curve being recorded after each.

Determination of unreacted melphalane by differential pulse voltammetry. Twenty ml of $10^{-3}M$ melphalane were mixed with 10 ml of $0.025M$ potassium permanganate and 10 ml of $2M$ sulphuric acid. After 12 hr, 200 mg of zinc powder were added and the solution was stirred for 1 hr. Undissolved zinc was filtered off with a porosity-4 sintered-glass funnel. The filtrate was transferred to the voltammetric vessel and its anodic DPV curve was measured by the use of a glassy-carbon disc electrode rotating at 2000 rpm, polarization rate of 5 mV/sec, modulation amplitude 12.5 mV, 1-sec interval between pulses and sensitivity 50 nA/cm.

Destruction of expired pharmaceuticals. 6-Thioguanine was studied by using a product containing 1.5 mg of the active substance and 10 ml of 5% dextrose solution. The 6-mercaptopurine product contained 10 mg of the substance and 10 ml of 5% dextrose solution. Ten ml of $6M$ sulphuric acid were added to the test solution, followed by 2 g of solid potassium permanganate in small amounts (the solution has a tendency of foam after addition of permanganate). The solution was left to stand overnight with stirring.

For spectrophotometric determination of the degree of destruction, 1 g of zinc powder was added to the solution, the mixture was stirred for 1 hr, then the solution was filtered through a porosity-4 frit. The spectrum of the filtrate was recorded, then six successive 50-μl additions were made of a solution containing 1.5 mg of 6-thioguanine or 10 mg of 6-mercaptopurine in 20 ml of $3M$ sulphuric acid, the spectrum being recorded after each. The efficiency of destruction was calculated from the absorbance values at 323 nm for 6-mercaptopurine and 343 nm for 6-thioguanine.

RESULTS AND DISCUSSION

It follows from the dependence of the consumption of oxidant on time (Table 1) that extensive oxidation of the studied substances occurs, involving destruction of the aromatic system. It might be expected that the substances would be oxidized to form carbon dioxide, sulphur dioxide and ammonia, requiring 18 equivalents of oxidant per mole of 6-mercaptopurine and 16 equivalents per mole of 6-thioguanine. The somewhat higher values obtained can be explained by assuming decomposition of the reagent, catalysed by the manganese dioxide formed, and this cannot be completely compensated for by the blank. The efficiency of the decomposition was also studied by determining the unreacted substance.

The substances could be directly determined spectrophotometrically because of their intense absorbance in the ultraviolet region of the spectrum (Figs. 1 and 2). In $0.5M$ sulphuric acid, for 6-mercaptopurine $\lambda_{max} = 323$ nm and $\varepsilon_{323} = 1.93 \times 10^4$ $l.mole^{-1}.cm^{-1}$, for 6-thioguanine $\lambda_{max} = 343$ nm and $\varepsilon_{343} = 2.09 \times 10^4$ $l.mole^{-1}.cm^{-1}$ and for melphalane

Table 1. Time-dependence of the oxidation of the studied substances with permanganate

Substance	Consumption of reagent at time t, *eq/mole*				
	0.25 hr	0.50 hr	1 hr	2 hr	6 hr
6-Mercaptopurine	13.9	14.0	14.1	16.5	17.5
6-Thioguanine	17.8	17.9	18.4	18.8	21.2
Melphalane	23.6	25.5	26.9	28.2	32.7

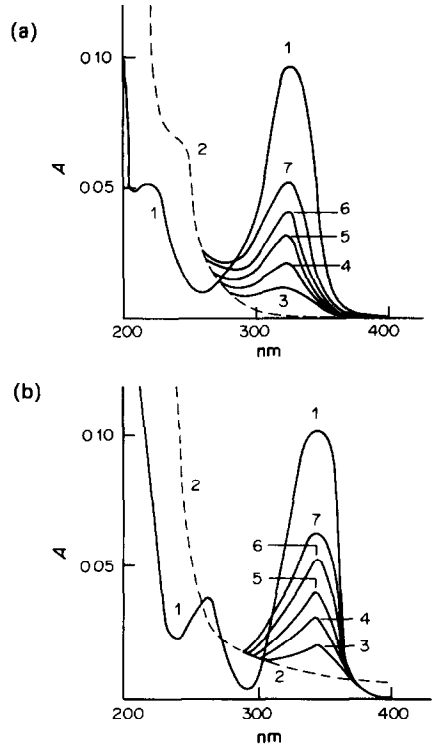

Fig. 1. The spectrophotometric determination of unreacted 6-mercaptopurine (a) and 6-thioguanine (b). (1)—5 × $10^{-6}M$ solution of the studied substance in 0.5M H_2SO_4, (2)—solution after decomposition, to 10 ml of which were added: 50 (3), 100 (4), 150 (5), 200 (6), 250 (7) μl of a $10^{-4}M$ solution of the substance studied.

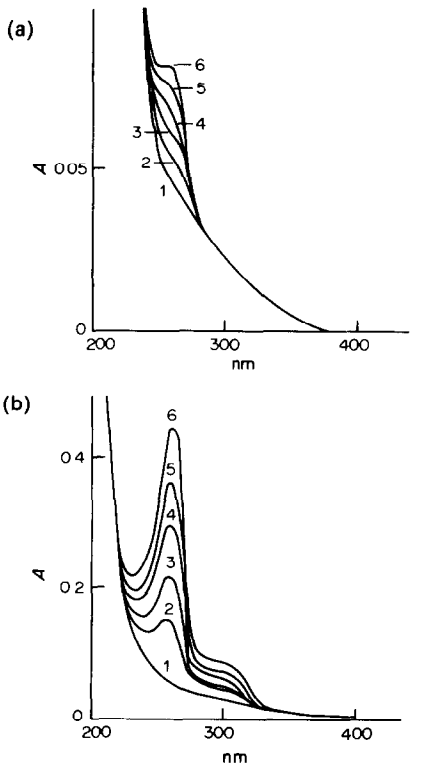

Fig. 2. Spectrophotometric determination of the unreacted melphalane in 0.5M H_2SO_4 (a) and in a medium at pH 3 (b). (1)—solution after decomposition, to 10 ml of which were added: 50 (2), 100 (3), 150 (4), 200 (5), 250 (6) μl of a $10^{-3}M$ solution of the substance studied.

$\lambda_{max} = 260$ nm and $\varepsilon_{260} = 1.20 \times 10^3$ l.mole^{-1}.cm^{-1}. It follows from Fig. 1 that the concentrations of 6-mercaptopurine or 6-thioguanine after destruction are lower than that corresponding to the first standard addition, *viz.* 5 × $10^{-7}M$ (50 μl of $10^{-4}M$ solution added to 10 ml). As the initial concentration of the test substance was 5 × $10^{-4}M$, at least 99.9% was destroyed by this method. It appears from the absorbance value at 260 nm for melphalane in 0.5M sulphuric acid (Fig. 2a) that the concentration after the destruction reaction is comparable with that resulting from the fifth standard addition, *viz.* 2.5 × $10^{-5}M$, corresponding to 95% destruction of the initial concentration of 5 × $10^{-4}M$. However, the molar absorptivity of melphalane strongly depends on acidity (Table 2), so the determination was modified as described above. It follows from Fig. 2b that the concentration of melphalane after the decomposition reaction is lower than that corresponding to the first standard addition, 5 × $10^{-6}M$ (50 μl of $10^{-3}M$ solution added to 10 ml). Hence at least 99% of the melphalane was destroyed.

It is apparent from these results that spectrophotometry is sufficiently sensitive for monitoring the efficiency of the destruction process. The method is not very selective, but a large number of those substances that would interfere under the given conditions would also be oxidized by permanganate.

As it is useful to have more than one independent method available for monitoring the destruction of chemical carcinogens, the use of differential-pulse polarography (DPP) and voltammetry (DPV) was also studied. The very sensitive DPP determinations of 6-mercaptopurine and 6-thioguanine[10] and the DPV determination of melphalane[11] were therefore modified so that they could be used to monitor the efficiency of the decomposition of these substances (see experimental section). In 0.5M sulphuric acid, 6-mercaptopurine yields a DPP recording with 1 peak at −0.96 V *vs.* –SCE (Fig. 3a) and 6-thioguanine yields 2 peaks at −0.96 V and −1.11 V *vs.* SCE (Fig. 3b). It is also apparent from Fig. 3 that the concentrations of both substances after the decom-

Table 2. Dependence of the molar absorptivity of melphalane at 260 nm on acidity

$[H_2SO_4]$, M	ε, 10^3 l.mole^{-1}.cm^{-1}
0.001	15.0
0.01	11.6
0.1	2.92
0.2	1.56
0.3	1.06
0.4	0.80
0.5	0.63

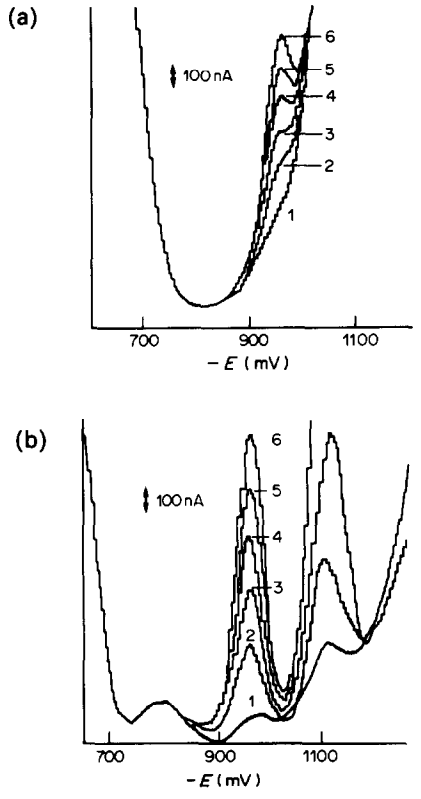

Fig. 3. Differential pulse polarographic determination of unreacted 6-mercaptopurine (a) and 6-thioguanine (b). The individual curves correspond to the solution after decomposition (1), to 7 ml of which were added: 35 (2), 70 (3), 105 (4), 140 (5), 175 (6) μl of a $10^{-3}M$ solution of the substance studied.

position are much lower than that corresponding to the first standard addition, ($5 \times 10^{-6}M$; 35 μl of $10^{-3}M$ solution added to 7 ml), and can be estimated as $\sim 10^{-6}M$. For an initial concentration of $5 \times 10^{-4}M$, this corresponds to 99.8% destruction, in good agreement with the result of the spectrophotometric measurements.

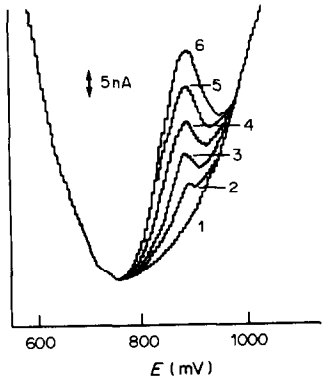

Fig. 4. The differential pulse voltammetric determination of melphalane. The individual curves correspond to the solution after decomposition (1), to 40 ml of which were added: 80 (2), 160 (3), 240 (4), 320 (5), 400 (6) μl of $10^{-3}M$ melphalane.

It is apparent from Fig. 4 that, under the given conditions, DPV of melphalane at a glassy-carbon rotating-disc electrode yields a well developed peak at a potential of about +0.88 V *vs.* SCE. It can also be seen that the concentration after degradation is lower than that corresponding to the first standard addition, $2 \times 10^{-6}M$ (80 μl of $10^{-3}M$ solution added to 40 ml). For an initial concentration of $5 \times 10^{-4}M$, this corresponds to 99.6% destruction. This procedure was repeated with $10^{-2}M$ melphalane, $0.2M$ potassium permanganate and 1 g of zinc powder, with additions of 20, 40, 60, 80 and 100 μl of $10^{-2}M$ melphalane. At least 99.8% of the substance was destroyed under these conditions.

It was found that this method can also be used to decompose a solution of the test substance in dimethylformamide or dimethylsulphoxide. In this case 50 mg of the substance were dissolved in 5 ml of dimethylformamide or dimethylsulphoxide and mixed with 40 ml of $3M$ sulphuric acid and 0.3 g of solid potassium permanganate. The solution was left to stand overnight, 0.5 g of zinc powder was added and the mixture stirred for 1 hr. The bleached solution was filtered through a porosity-4 sintered-glass funnel and the unreacted substance determined by DPP for 6-mercaptopurine or 6-thioguanine and DPV for melphalane. (The spectrophotometric method cannot be used in the presence of dimethylformamide or dimethylsulphoxide because of their absorbance in the ultraviolet region.) At least 99.5% destruction was attained under these conditions.

Finally the usefulness of this method for the destruction of expired pharmaceutical products consisting of 6-mercaptopurine or 6-thioguanine in 5% dextrose solution was studied. The dextrose is also oxidized, so a larger excess of permanganate must be used. The procedure described gave 99.9% destruction for both 6-mercaptopurine and 6-thioguanine.

The method can therefore be used to destroy the solid substances, solutions of these substances in water or mineral acids as well as in solvents miscible with water and not reacting with permanganate, and in expired pharmaceutical products. The solution in solvents immiscible with water or reacting with permanganate should first be evaporated in a vacuum evaporator and the solid residue oxidized with permanganate. It is useful that the effectiveness of the method can readily be monitored by the spectrophotometric or electrochemical techniques described. The instrumentally more demanding HPLC technique has to be used only when the sample contains interferents that are not oxidized by permanganate.

The residues of degradation of 6-mercaptopurine and 6-thioguanine have been tested for mutagenicity with *Salmonella typhimurium* strains TA 1535, TA 98 and TA 100. No mutagenic activity could be detected.[12] With melphalane, mutagenic activity of the residues has been found with the TA 100 and TA 1535 strains.[12] Therefore, a search for a more suitable method for destruction of melphalane will continue.

REFERENCES

1. J. A. Nelson, J. W. Carpenter, L. M. Rose and D. Y. Adamson, *Cancer Res.*, 1975, **35**, 2872.
2. C. B. Elion, S. Bieber and G. H. Hitchings, *Ann. N.Y. Acad. Sci.*, 1954, **60**, 297.
3. T. H. Wasserman, R. L. Comis, M. Goldsmith, H. Handelsman, J. S. Penta, M. Slavik, W. R. Soper and S. K. Carter, *Cancer Chemother. Rep., Part* 3, 1975, **6**, 399.
4. J. Barek, V. Pacáková, K. Štulík and J. Zima, *Talanta*, 1985, **32**, 279.
5. A. F. Fell, S. M. Plag and J. M. Neil, *J. Chromatog.*, 1979, **186**, 691.
6. P. K. Narang, R. L. Yeager and D. C. Chaterji, *ibid.*, 1982, **230**, 373.
7. R. E. Jonkers, B. Oosterhuis, R. I. M. Ten Berge and C. J. Van Boxtel, *ibid.*, 1982, **233**, 249.
8. A. G. Bosanquet and E. D. Gilby, *ibid.*, 1982, **232**, 345.
9. K. P. Flora, S. L. Smith and J. C. Cradock, *ibid.*, 1979, **177**, 91.
10. J. Barek, A. Berka and J. Zima, *Collection Czech. Chem. Commun.*, submitted for publication.
11. *Idem*, unpublished results.
12. M. Castegnaro, unpublished results.

Talanta, Vol. 32, No. 10, pp 993–995, 1985
Printed in Great Britain.

0039-9140/85 $3.00 + 0.00

SHORT COMMUNICATIONS

INDIRECT SPECTROPHOTOMETRIC DETERMINATION OF SILICATE

I-WEN SUN and FREDRICK BET-PERA*
Department of Chemistry, California State Polytechnic University, Pomona, California 91768, U.S.A.

(*Received* 4 *April* 1984. *Revised* 11 *April* 1985. *Accepted* 24 *May* 1985)

Summary—An indirect spectrophotometric method has been developed for trace determination of silicate in aqueous samples. The silicate is converted into silicomolybdic acid and extracted into a mixture of 1-butanol and butyl acetate. The silicomolybdic acid is then decomposed with sodium hydroxide and the molybdenum(VI) reduced to molybdenum(III) with a Jones reductor, followed by reoxidation to molybdenum(VI) with iron(III). The resulting iron(II) is complexed with ferrozine, and the absorbance of the complex measured at 562 nm. In this manner, submicroamounts of silicate can be determined.

Most methods for determination of microamounts of silicate are based on conversion into silicomolybdic acid and separation of this from isopolymolybdates by extraction with organic solvents. The silicon content is then determined by measurement of the absorbance of the yellow silicomolybdic acid[1–4] or its blue reduction product. Several reducing agents have been used, such as 1-amino-2-naphthol-4-sulphonic acid,[2,5] stannous chloride,[6] hydroquinone,[7] and sodium sulphite.[8]

Various methods have been used to overcome interference by phosphate. One approach is to add citric,[9] tartaric,[10] or oxalic acid[11] following formation of the heteropoly acids, to destroy the phosphomolybdic acid (silicomolybdic acid is thermodynamically slightly less stable than phosphomolybdic acid, but is kinetically protected by its very slow rate of reaction with these acids). Other approaches include sequential extraction,[12] control of the acidity,[13] use of differences in the rate of formation of heteropoly acids,[14] and precipitating the phosphate as ferric phosphate.[15]

Small amounts of silicate have also been determined indirectly by polarography[16,17] and by atomic-absorption.[18,19]

In the method described in this paper, silicate is first converted into silicomolybdic acid, which is then selectively extracted into a mixture of 1-butanol and butyl acetate. After evaporation of the organic solvent, the complex is dissolved in alkali, and molybdenum(VI) is reduced to molybdenum(III) by Jones reductor. The molybdenum(III) is reoxidized with iron(III) to molybdenum(VI) and the resulting iron(II) is determined as the iron(II)–ferrozine complex by measuring the absorbance at 562 nm. In this manner, submicroamounts of silicate have been determined.

*Author for correspondence.

EXPERIMENTAL

Apparatus

All spectrophotometric measurements were made with a Cary 118 spectrophotometer. The pH of solutions was determined with an Orion Model 12 pH-meter. Small amounts of reagents were weighed with a semimicrobalance. All glassware was washed with 6*M* hydrochloric acid and rinsed with distilled water.

Reagents

All chemicals were either of analytical or primary standard grade and used without further purification. All solutions were made with distilled or demineralized water.

Stock standard silicate solution. Prepared by dissolving 0.2131 g of sodium silicate, $Na_2SiO_3 \cdot 9H_2O$, in 100 ml of distilled water, standardized titrimetrically,[20] and stored in a polyethylene container. Working solutions were prepared daily by diluting the stock solution.

Molybdate solution. Prepared by dissolving 1.000 g of sodium molybdate, $Na_2MoO_4 \cdot 2H_2O$, in 100 ml of distilled water, and stored in a polyethylene container.

Iron(III) solution, 0.003M. Prepared by dissolving 0.1446 g of ferric ammonium sulphate 12-hydrate in about 50 ml of demineralized water plus 0.5 ml of concentrated perchloric acid and 0.2 ml of concentrated nitric acid, heating until perchloric acid fumes appear, cooling, and diluting to 100 ml with demineralized water.

Ferrozine solution, 0.012M. Prepared by dissolving 0.6125 g of ferrozine, 3-(2-pyridyl)-5,6-bis(4-phenylsulphonic acid)-1,2,4,-triazine monosodium salt monohydrate (Hach Chemical Co., Ames, IA), in 100 ml of demineralized water.

Jones reductor. Made by taking enough 20–30-mesh zinc to occupy 7–8 cm of a 50-ml burette, amalgamating it by stirring for about 10 min with a mixture of 15 ml of 3% mercuric chloride solution and 15 ml of ~1*M* sulphuric acid, washing the amalgamated zinc and packing the reductor as described in most quantitative analysis texts. The reductor is activated by running 10–20 ml of 1.44*M* hydrochloric acid through it before use. The reductor is kept filled with demineralized water when not in use.

Calibration graph and analysis

Transfer various volumes (0–5 ml) of the stock sodium silicate solution to 100-ml standard flasks and dilute to the mark with distilled water. For each of these diluted standards place 1 ml in a 25-ml separatory funnel, add 1 ml of 1% sodium molybdate solution, and 1 ml of 0.25*M* hydrochloric acid to bring the hydrogen-ion concentration to

0.08*M*. Shake the solution and let it stand for 20 min to ensure complete formation of the silicomolybdic acid. Then add 0.20 ml of 14% tartaric acid solution, and after 5 min 0.6 ml of 2*M* hydrochloric acid, shake the solution vigorously for 1 min with 6 ml of a 2:5 v/v 1-butanol and butyl acetate mixture, let it stand for 3 min for the phases to separate, then discard the lower aqueous phase. Pipette 1 ml of the organic phase into a 25-ml beaker and leave it in a fume-hood until the organic solvent has completely evaporated. Then add 2.0 ml of 0.125*M* sodium hydroxide to decompose the heteropoly acid, followed by 5.6 ml of 2*M* hydrochloric acid, added rapidly to bring the hydrogen-ion concentration to 1.44*M*. Pass this solution through the Jones reductor at a rate of 12 drops/min, collecting the effluent in a 25-ml beaker containing 5.0 ml of 0.003*M* iron(III), and keeping the collection beaker covered with "Para" film (with appropriate holes for inlets and outlets) and flushed with nitrogen throughout the operation. Wash the reductor column with three 4-ml portions of 1.44*M* hydrochloric acid. Immediately add 4 ml of 0.012*M* ferrozine to the collected effluent. Slowly add small amounts of solid sodium bicarbonate to adjust the pH of the solution to 4.0–4.5. Transfer the solution into a 100-ml standard flask and dilute it to the mark. Measure the absorbance of the complex at 562 nm against a reagent blank (to which the procedure has been applied), using 1-cm cells. Use an analogous procedure for analysis of samples.

Calculation

Because there is about 6% increase in the volume of the organic phase, owing to the mutual solubility of the phases, it is best to use a calibration curve constructed by plotting absorbance against the concentration of silicon in the 1 ml of standard solution used in the extraction. The absorbance for the test sample will then correspond to the silicon concentration of that sample if a 1-ml portion was used in the extraction procedure. This procedure automatically compensates for uncertainty in the solubility data, provided the reactant volumes are accurately measured.

Alternatively, it can be calculated from the molar absorptivity and the conditions used, that the weight of silicon in 1 ml of the aqueous solution taken for extraction is $18.9A$ μg, where A is the absorbance finally measured. Thus if an absorbance of 0.01 is taken as a working minimum, the limit of detection is ~ 0.2 μg/ml in the original sample.

RESULTS AND DISCUSSION

The effect of hydrogen-ion concentration and molybdate concentration on the formation of silicomolybdic acid has been examined by various investigators[21,22] and generally a pH range of 0.8–3.6 and a molybdate concentration of at least 50 times the silicate concentration have been recommended. In our method, the optimum conditions found by systematically varying the concentration of molybdate and hydrogen-ions were 0.013*M* molybdate and 0.083*M* hydrogen-ion concentration in the aqueous phase.

The efficiency of various organic solvents in extraction of heteropoly acids was investigated by Wadelin and Mellon.[23] They found that 1-butanol is a good extractant for silicomolybdic acid. Butyl acetate is also used in our method as a diluent for minimizing the co-extraction of molybdate. A small amount of molybdenum is still extracted, however, so it is necessary to run a blank determination along with the standard silicate solutions and unknown samples.

If the silicomolybdic acid is decomposed with alkali and the solution is made sufficiently acid, the heteropoly acid will not be reformed, and the molybdenum(VI) can then be reduced to molybdenum(III) by the Jones reductor. For quantitative reduction, not only must the hydrogen-ion concentration of the aqueous solution be adjusted to 1.4–1.5*M* with hydrochloric acid but the solution must be passed through the reductor at a rate of 12–15 drops/min: otherwise, the reduction will be incomplete. The molybdenum(III) is reoxidized with iron(III) to molybdenum(VI), and this step must be done in a completely oxygen-free medium to avoid oxidation of either the molybdenum(III) or the iron(II) that is produced from the iron(III).

Table 1. Absorbance as a function of silicate concentration

Si taken, *μmole*	Silicon, *ng/ml* Taken*	Found†	Absorbance§	Apparent molar absorptivity‡ $l.mole^{-1}.cm^{-1}$
0.0375	1.65	1.63	0.055	9.33×10^5
0.075	3.30	3.45	0.115	9.33×10^5
0.150	6.60	6.67	0.225	9.54×10^5
0.300	13.20	13.30	0.448	9.50×10^5
0.375	16.50	16.68	0.563	9.55×10^5
				Mean = 9.45×10^5

*The concentration of silicate was varied by taking suitable fractions of the standard solution, diluting to 100 ml, and taking 1.00 ml for extraction. The following were kept constant: sample volume, 1.00 ml; solvent volume, 6.00 ml; volume of organic phase taken for analysis, 1.00 ml; final volume, 100.0 ml. The concentration stated is that in the final 100 ml of solution measured.

†Calculated from the average absorbance value.

§Average of three independent determinations corrected for the blank.

‡Obtained by using Beer's law and allowing for a 6% increase in the volume of organic phase owing to the mutual solubility of water and the butanol/butyl acetate mixture.

Table 2. Analysis of synthetic samples

	Si taken, μmole	P taken, μmole	Silicon, ng/ml Taken	Found*	Absorbance†
A	0.0260	—	1.15	1.04	0.031
B	0.203	—	8.92	8.75	0.295
C	0.315	—	13.87	13.50	0.460
D	0.045	0.038	1.98	1.75	0.065
E	0.278	0.075	12.22	12.00	0.410
F	0.037	0.150	1.65	1.58	0.052

*Amount of silicon calculated by using calibration graph.
†Average absorbance for duplicate samples.

The iron(II) is then determined by forming its 1:3 complex with ferrozine at pH >4.0,[24] in the presence of ammonium bifluoride to prevent precipitation of hydrous iron(III) oxide from the surplus iron(III) present. The absorbance of the iron(II)–ferrozine complex is measured at 562 nm. Typical results used for making the calibration graph are reported in Table 1. The apparent molar absorptivity is 9.45×10^5 $l.mole^{-1}.cm^{-1}$, indicating that the overall efficiency of the system is 94%, since the theoretical value is 10.04×10^5 $l.mole^{-1}.cm^{-1}$ (the molar absorptivity of the ferrozine complex is 2.79×10^4 $l.mole^{-1}.cm^{-1}$,[24] and 36 moles of complex are produced per mole of silicon originally present). The relative standard deviation of the absorbance is 1–3%. For samples with absorbance values less than 0.1, the standard-addition method is recommended. Results for determination of silicate in synthetic mixtures with phosphate are summarized in Table 2.

REFERENCES

1. H. W. Knudson, C. Juday and V. W. Meloche, *Ind. Eng. Chem., Anal. Ed.*, 1940, **12**, 270.
2. D. F. Boltz, A. Trudell and G. Potter, *Colorimetric Determination of Nonmetals*, D. F. Boltz and J. A. Howell (eds.), Chapter 11. Wiley, New York, 1978.
3. F. E. Snell and C. T. Snell, *Colorimetric Methods of Analysis*, Vol. IIA, Van Nostrand, Princeton, NJ, 1959.
4. G. Charlot, *Colorimetric Determination of Elements*, p. 370. Elsevier, New York, 1964.
5. I. R. Morrison and A. L. Wilson, *Analyst*, 1963, **88**, 88.
6. F. Schaffer, J. Fong and P. Kirk, *Anal. Chem.*, 1953, **25**, 343.
7. G. S. Nelson, *ibid.*, 1956, **28**, 1330.
8. F. Dienert and F. Waldenbulk, *Compt. Rend.*, 1923, **176**, 1478.
9. F. K. Lindsay and R. G. Bielemberg, *Ind. Eng. Chem., Anal. Ed.*, 1953, **12**, 460.
10. A. J. Boyle and V. Hughey, *ibid.*, 1942, **15**, 618.
11. M. C. Schwartz, *ibid.*, 1942, **14**, 893.
12. G. F. Kirkbright, A. M. Smith and T. S. West, *Analyst*, 1967, **92**, 411.
13. H. C. Baghurst and V. J. Norman, *Anal. Chem.*, 1957, **29**, 778.
14. C. C. Kircher and S. R. Crouch, *ibid.*, 1983, **55**, 248.
15. E. J. King, B. D. Stacy, D. F. Holt, D. M. Yates and D. Dickles, *Analyst*, 1955, **80**, 441.
16. D. F. Boltz, T. DeVries and M. G. Mellon, *Anal. Chem.*, 1949, **21**, 563.
17. A. G. Fogg and A. A. Osakwe, *Talanta*, 1978, **25**, 226.
18. T. V. Ramakrishna, J. W. Robinson and P. W. West, *Anal. Chim. Acta*, 1969, **45**, 43.
19. T. R. Hurford and D. F. Boltz, *Anal. Chem.*, 1968, **40**, 379.
20. R. J. W. McLaughlin and V. S. Biskupsi, *Anal. Chim. Acta*, 1965, **32**, 165.
21. J. D. H. Strickland, *J. Am. Chem. Soc.*, 1952, **74**, 862.
22. C. C. Kircher and S. R. Crouch, *Anal. Chem.*, 1982, **54**, 1219.
23. C. Wadelin and M. G. Mellon, *ibid.*, 1953, **25**, 1668.
24. L. L. Stookey, *ibid.*, 1970, **42**, 779.

Talanta, Vol. 32, No. 10, pp. 996–998, 1985
Printed in Great Britain

0039-9140/85 $3.00 + 0.00
Pergamon Press Ltd

A RAPID METHOD FOR DETERMINING TIN AND MOLYBDENUM IN GEOLOGICAL SAMPLES BY FLAME ATOMIC-ABSORPTION SPECTROSCOPY

ERIC P. WELSCH
U.S. Geological Survey, Box 25046, Denver Federal Center, MS 973 Denver, Colorado 80225, U.S.A.

(*Received* 7 *March* 1985. *Accepted* 24 *May* 1985)

Summary—The proposed method uses a lithium metaborate fusion, dissolution of the fusion bead in 15% v/v hydrochloric acid, extraction into a 4% solution of trioctylphosphine oxide in methyl isobutyl ketone, and aspiration into a nitrous oxide–acetylene flame. The limits of detection for tin and molybdenum are 1.0 and 0.5 ppm, respectively. Approximately 50 samples can be analysed per day.

The combination of trioctylphosphine oxide and methyl isobutyl ketone (TOPO–MIBK) was first incorporated into a routine method of analysis for tin in alloys by Burke.[1] His method was adapted for use with geological samples by combining it with an iodide fusion.[2] Zhou *et al.*[3] used a lithium metaborate ($LiBO_2$) fusion and graphite-furnace atomic-absorption spectrophotometry (GFAAS) to achieve a more complete digestion[4] and better sensitivity, but GFAAS is slow compared to flame AAS even with the highly automated systems available today. It would seem advantageous to combine the $LiBO_2$ fusion and TOPO–MIBK extraction with a flame atomic-absorption method if the sensitivity were adequate to allow detection of tin at the crustal abundance level. The more advance background-correction and noise-suppression devices on the newer AA spectrometers make it possible to attain the necessary sensitivity.

An investigation of the extraction capabilities of the TOPO–MIBK system led to the discovery that molybdenum is also extracted. Hence both elements can be determined in the same solution by sequential measurement with a single-channel AA spectrometer or simultaneous measurement with a dual-channel instrument, since a nitrous oxide–acetylene flame can be used for both. Silver and tellurium are 90% and bismuth and gold nearly 100% extracted by this system. In the presence of 10% potassium iodide and ascorbic acid, as Burke[1] indicated in his work, antimony and lead can also be quantitatively extracted, but it has been found that zinc and cadmium as well under these conditions.

EXPERIMENTAL

Apparatus

A Perkin-Elmer 5000 atomic-absorption spectrophotometer* was the instrument primarily used for this study but models 603 and 2380 were also used occasionally. A Varian nitrous oxide burner-head was used at all times, in conjunction with the conventional flow-spoiler. An electrodeless discharge lamp (EDL) was used for tin and a hollow-cathode lamp for molybdenum.

The spectral lines employed were 235.5 nm for tin and 313.3 nm for molybdenum. A 1-sec integration time was used, along with deuterium-arc background correction. The gas flow-rates were adjusted to yield a $1\frac{1}{2}$-in. tall red feather and prevent clogging of the burner slot. For the Perkin-Elmer 5000 instrument, the appropriate fuel and oxidant settings were 20 and 35 respectively. The burner was positioned so that the light-beam was about 1 cm above the slot.

Reagents

TOPO–MIBK. Dissolve 4.0 g of TOPO in 100 ml of MIBK.

Stock and standard solutions. Prepare 1000-μg/ml stock in solution by dissolving 1.000 g of tin metal in 150 ml of concentrated hydrochloric acid and diluting to 1 litre with water. Prepare 1000-μg/ml molybdenum stock solution by dissolving 1.500 g of molybdenum trioxide in 40 ml of 1*M* sodium hydroxide and diluting to 1 litre with water. Make working standards by adding 100, 200 and 500 μl of the stock solutions to 1000-ml portions of 15% v/v hydrochloric acid, shaking these solutions for 1 min with 60 ml of TOPO–MIBK and discarding the aqueous phase. This provides a convenient quantity of standards which are stable for at least four weeks and correspond to 10, 20 and 50 μg of tin or molybdenum in a 1-g sample analysed as described below.

Procedure

Mix a 1-g sample of 80-mesh rock, soil or stream sediment with 3 g of $LiBO_2$ flux in a graphite crucible of 8 ml or more capacity. Fuse the samples in a furnace at 1100° for 20 min with a row of empty crucibles at the front as a heat barrier, and the door slightly ajar to allow free circulation of air. Pour the molten bead directly into a 150-ml beaker containing 100 ml of 15% v/v hydrochloric acid. (Caution: the underside of the glass beaker must be dry or the resulting stress when the bead is poured in will probably rupture the vessel.) Add a Teflon-coated magnetic stirring bar and place the beaker on a magnetic stirrer for about 15 min. Transfer the clear solution into a 125-ml separatory funnel and shake it with 6 ml of TOPO–MIBK solution for 1 min. Once the layers have separated, drain off most of the aqueous layer and collect the remaining liquid in a 16 × 150 mm test-tube, from which the extract can be conveniently aspirated into the AA instrument. Run a reagent blank and apply appropriate corrections.

*Any use of trade and company names is for descriptive purposes only and does not imply endorsement by the U.S. Geological Survey.

Table 1. Comparison of flux mixtures by analysis of GSD glass standard* (average of 5 replicates)

Flux	Sn, $\mu g/g$	Mo, $\mu g/g$
4:1 tetraborate–metaborate	37.6	34.4
1:1 $LiCO_3$–H_3BO_3	35.0	30.8
$LiBO_2$	36.2	31.2

*Emission spectroscopy values: Sn, median 43 $\mu g/g$, range 30–50 $\mu g/g$; Pb, median 46 $\mu g/g$, range 20–70 $\mu g/g$.

Table 2. Analysis of geochemical reference samples (six replicates)

		Sn,* $\mu g/g$		Mo,* $\mu g/g$	
Sample	Material	This work	Zhou *et al.*[3]	This work	Gladney *et al.*[10]
GXR 1	Jasperoid	57.7 ± 2.20	52.4 ± 1.9	14.5 ± 2.3	10 ± 2
2	Soil	1.7 ± 0.5	1.98 ± 0.06	1.4 ± 0.2	1.5 ± 0.5
3	Spring deposit	2.0 ± 0.9	0.94 ± 0.07	5.4 ± 0.5	6
4	Coppermill head	7.7 ± 0.8	4.79 ± 0.25	367 ± 16	310 ± 25
5	Soil	2.0 ± 0	2.84 ± 0.09	30.5 ± 1.4	30 ± 4
6	Soil	2.2 ± 0.4	0.86 ± 0.06	1.7 ± 0.3	1.7 ± 0.4

*Mean and standard deviation.

RESULTS AND DISCUSSION

Sample decomposition

Lithium metaborate, 1:1 lithium carbonate–boric acid mixture,[5] and 1:4 lithium tetraborate–metaborate mixture are all equally effective fluxes for the GXR reference samples. As expected,[6] the lithium tetraborate–metaborate mixture yielded better results for the GSC, GSD, and GSE[7] glass reference samples. No significant difference could be detected between the performance of the other two fluxes with regard to these samples (Table 1), and lithium metaborate was chosen simply because it was most readily available in quantity.

Pouring the molten bead directly into acid[8] has the advantage of disrupting the melt and facilitating rapid dissolution in a relatively small amount of acid. If the sample contains more than 10% of iron the melt adheres to the graphite crucible and cannot be quantitatively transferred to the beaker: however, the portion remaining in the crucible is small enough to be insignificant and is not detrimental to the results.

The amount and concentration of the acid used suffice to overcome the alkalinity of the $LiBO_2$ flux.

Sensitivity

A 20-μg molybdenum standard typically gave an absorbance of about 0.22 when the 313.3 nm line was used. The 235.5 nm line was chosen for tin as a compromise between the more sensitive but noisier 224.6 nm line and the quieter but less sensitive 286.3 nm line. The 20-μg tin standard normally gave 0.035 absorbance at 235.5 nm.

Extraction

Because the phases are not mutually saturated before use, there will be a volume change in the organic phase, but this is automatically allowed for in the calibration procedure.

Interferences

The method was tested for interference from 1000 μg of Cu, Pb, Zn, Hg, Mn, V, W, Ni, Co, Cr and Bi, 5.00 mg of Al and Mg, 10.0 mg of Ca, and 20.0 mg of Fe, added to 100 ml of standard solution in 15% v/v hydrochloric acid containing 3 g of lithium metaborate. Only iron gave appreciable interference, suppressing the Mo readings by 50%; however, no interference by iron was observed in analysis of the geochemical samples. Formation of an iron–molybdenum complex is thought to be responsible for the effect, but seems to be prevented by the other ions present in actual samples. Various masking agents failed to eliminate the interference and the effect was not further investigated.

Results for geological reference samples

The six GXR reference samples[9] were analysed six times each and the results for Sn and Mo are listed in Table 2. As expected, the worst results were obtained for samples low in tin, except for a "lucky" analysis of GXR 5. Relative standard deviations of up to 50% are not uncommon for geochemical analysis at or near the limit of detection of the method and such data are considered useful for geochemical exploration. The tin values agree reasonably well with those obtained by Zhou *et al.*[3] and the Mo values agree remarkably well with those of Gladney *et al.*[10]

REFERENCES

1. K. E. Burke, *Analyst*, 1972, **97**, 19.
2. E. P. Welsch and T. T. Chao, *Anal. Chim. Acta*, 1976, 82, 337.

3. Liyi Zhou, T. T. Chao and A. L. Meier, *Talanta*, 1984, **31**, 73.
4. A. Hall, *Chem. Geol.*, 1980, **30**, 135.
5. F. Bea Barredo and L. Polo Diez. *Talanta*, 1976, **23**, 859.
6. W. M. Johnson and J. A. Maxwell, *Rock and Mineral Analysis*, 2nd Ed. p.109, Wiley, New York, 1981.
7. T. Myers, R. G. Havens, J. J. Connor, N. M. Conklin and H. F. Rose, Jr., *U.S. Geol. Survey Paper*, 1976, No. 1013, 29.
8. L. Storms, A. Bonne and W. Viaene, *J. Geochem. Exploration*, 1980, **13**, 51.
9. G. H. Allcott and H. W. Lakin, *U.S. Geol. Survey Open-File Rep.*, 78–163, 1978.
10. E. S. Gladney , W. E. Goode, D. R. Porrin and C. E. Burne, *Los Alamos Natl. Lab. Rep.*, LA-8966-MS, 1980.

Talanta, Vol. 32, No. 10, pp. 999–1001, 1985
Printed in Great Britain

0039-9140/85 $3.00 + 0.00
Pergamon Press Ltd

DETERMINATION OF CERTAIN PHENOTHIAZINE DRUGS WITH DIAZOTIZED *p*-NITROANILINE

S. R. EL-SHABOURI
Department of Pharmaceutical Chemistry, Faculty of Pharmacy, University of Assiut, Assiut, Egypt

(*Received* 30 *January* 1985. *Accepted* 20 *May* 1985)

Summary—A colorimetric method for the determination of 7 phenothiazine drugs by interaction with diazotized *p*-nitroaniline has been developed. Neither the degradation products of the drugs nor the common excipients in pharmaceutical preparations interfere.

Phenothiazine drugs have been determined by titrimetric,[1,2] spectrophotometric,[3,4] polarographic,[5,6] gas chromatographic[7,8] and high-pressure liquid chromatographic methods.[9,10] The official methods are generally non-aqueous titration for the bulk drugs and ultraviolet spectrophotometry for dosage forms.

Diazotized *p*-nitroaniline can be used for the identification of phenothiazine drugs in TLC,[11] and this reagent is now shown to be suitable for the determination of promazine hydrochloride, alimemazine tartrate, perciazine, levomepromazine maleate, thioridazine hydrochloride, thiethylperazine maleate and sulphoridazine.

EXPERIMENTAL

Reagents

Diazotized p-*nitroaniline solution.* Weigh accurately about 25 mg of *p*-nitroaniline into a 25-ml standard flask and dissolve it in 1 ml of concentrated sulphuric acid. Cool in an ice-bath, add 0.5 ml of 2% sodium nitrite solution, and 5 min later add 0.2 ml of 10% sulphamic acid solution and dilute to volume with distilled water. Mix well and keep in an ice-bath. This reagent solution should be used within 5 hr.

Test solution. Freshly prepared 1 mg/ml solution of each phenothiazine drug in water. In case of bases, drops of concentrated hydrochloric acid were added to their solutions.

General procedure

Transfer 1 ml of an aqueous solution containing 100 μg of phenothiazine drug into a 10-ml standard flask. Add 0.5 ml of diazotized *p*-nitroaniline solution and mix well. Dilute to volume with concentrated hydrochloric acid. Measure the absorbance at the appropriate wavelength for the drug, against a blank treated similarly. Use tightly stoppered cuvettes.

For injections. Transfer into a 25-ml standard flask an accurately measured volume of the injection equivalent to about 25 mg of the drug (promazine hydrochloride), dilute to volume with water and mix well. Dilute further with water accurately to obtain an approximately 100 μg/ml solution, and assay as above.

For tablets. Weigh and powder 20 tablets. Transfer an accurately weighed amount of the powder equivalent to 10 mg of the drug (thioridazine hydrochloride or thiethylperazine maleate) to a 25-ml standard flask. Dissolve and make up to volume with distilled water. Filter, and dilute the filtrate accurately with water to give a concentration of about 100 μg/ml. Complete the determination as described above.

RESULTS AND DISCUSSION

The absorption spectra for the products obtained from all the phenothiazine drugs studied are presented in Fig. 1. Beer's law is valid for all the drugs over the ranges in Table 1. The colour is stable for at least 2 hr.

Owing to the lower solubility of *p*-nitroaniline in hydrochloric acid, sulphuric acid[12] is used for preparation of the diazotized *p*-nitroaniline. The influence of the amount of sulphuric acid used in this preparation was studied over the range 0.25-4 ml (at 0.25-ml intervals). All the solutions performed equally well in the general procedure, so 1 ml of concentrated sulphuric acid was selected for use, to avoid any possible effect of high acid concentration on the phenothiazine drugs.

The choice of diluent for the reaction mixture was also studied. Dilution with water, methanol, ethanol, 2-propanol or 1,4-dioxan gave an unstable colour, and dilution with dilute sodium hydroxide, potassium hydroxide or ammonia solution resulted in immediate disappearance of the colour.

Dilution with phosphoric, sulphuric, perchloric, nitric, glacial acetic, trichloroacetic or hydrochloric acid in different concentrations gave non-reproducible and/or lower colour intensity, except for hydrochloric acid, which gave a more intense and stable colour, the optimum final hydrochloric acid concentration being about 10*M*.

The method was tested in the presence of the oxidation products of the test drugs. The concentration of alimemazine tartrate was determined in several standard solutions containing alimemazine tartrate and oxomemazine (alimemazine-5,5-dioxide), and the other phenothiazine drugs were determined in the presence of their respective sulphoxides, prepared as described by Davidson.[3] Ex-

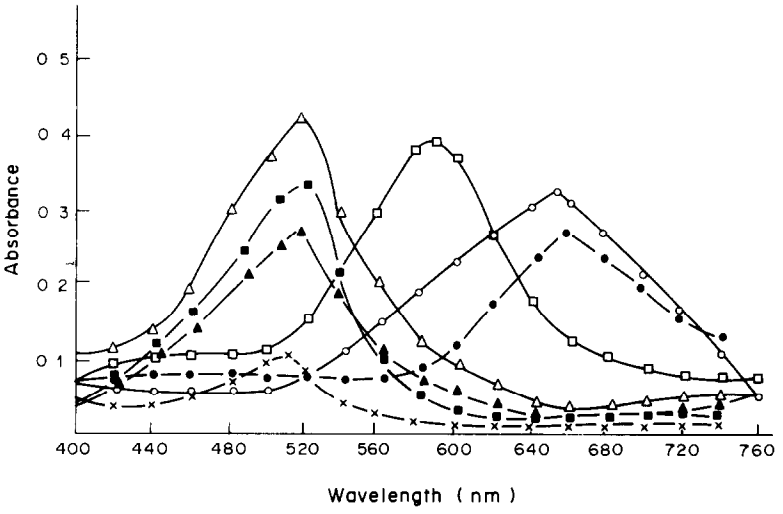

Fig. 1. Absorption spectra for colour produced on reaction of phenothiazine drugs with diazotized *p*-nitroaniline: promazine hydrochloride (△——△), alimemazine tartrate (■——■), perciazine (▲——▲), levomepromazine maleate (□——□), thioridazine hydrochloride (○——○), thiethylperazine maleate (●——●), sulphoridazine (×——×).

Table 1. Spectral characteristics

Drug	λ_{max}, *nm*	Beer's law range, *μg/ml*	Intercept*	Apparent molar absorptivity, 10^3 *l.mole*$^{-1}$*.cm*$^{-1}$
Promazine hydrochloride	520	2–20	−0.005	6.6
Alimemazine tartrate	520	2–30	0.012	7.5
Perciazine	520	2–30	0.027	4.9
Levomepromazine maleate	590	2–30	0.049	8.7
Thioridazine hydrochloride	655	2–20	−0.020	6.3
Thiethylperazine maleate	660	2–30	0.011	6.1
Sulphoridazine	510	5–30	0.031	2.0

*Of regression line.

Table 2. Determination of some phenothiazine drugs by the proposed procedure and an official method

Formulation	Found*, %	
	Proposed method	Official method
Promazine hydrochloride vial (Wyeth)	98.9 ± 0.6	99.7 ± 1.0
Thioridazine hydrochloride tablets (Swiss-Pharma)	100.9 ± 0.6	101.2 ± 0.7
Thiethylperazine maleate tablets (Swiss-Pharma)	98.9 ± 0.6	99.3 ± 0.5

*Mean and standard deviation of 5 determinations, expressed as fraction of nominal amount present.

cellent recovery (99.8–100.2%) for the intact phenothiazine drugs in these mixtures confirms that the assay is specific for the unchanged drugs in presence of their degradation products.

It was also found that there is no interference from the commonly encountered excipients or additives, such as glucose, lactose, starch, talc and magnesium stearate.

The method is applicable to analysis for some phenothiazine drugs in commercial pharmaceutical preparations. The results (Table 2) are comparable to those obtained by the official methods.[13,14]

The nature of the interaction coloured product has not been elucidated and will be the subject of further work.

REFERENCES

1. H. S. Gouda and S. A. Ahmed, *J. Indian Chem. Soc.*, 1978, **55**, 352.
2. K. Nowakowski and B. Dembinski, *Acta Pol. Pharm.*, 1975, **32**, 595.
3. A. G. Davidson, *J. Pharm. Pharmacol.*, 1976, **28**, 795.
4. A. S. Issa, Y. A. Beltagy and M. S. Mahrous, *Talanta*, 1978, **25**, 710.
5. F. W. Teare and R. N. Yadar, *Can. J. Pharm. Sci.*, 1978, **13**, 69.
6. A. D. Cowan, *Methodol. Dev. Biochem.*, 1976, **5**, 193.

7. L. Laithem, I. Bello and P. Gaspar, *J. Chromatog.*, 1978, **156,** 327.
8. N. E. Larsen and J. Naestoft, *ibid.*, 1975, **109,** 259.
9. C. Gonnet and J. L. Rocca, *ibid.*, 1976, **120,** 419.
10. A. C. Mehta, *Analyst*, 1981, **106,** 119.
11. S. R. El-Shabouri, A. M. Taha and S. A. Hussin, *Pharmazie*, 1982, **37,** 71.
12. I. Vogel, *Practical Organic Chemistry*, 1st Ed., p. 566. Longmans, London, 1954.
13. *British Pharmacopoeia*, pp. 813, 865. Pharmaceutical Press, London, 1980.
14. *United States Pharmacopeia XX*, p. 791. US Pharmacopeial Convention, Rockville, MD, 1980.

Talanta, Vol. 32, No. 10, pp. 1002–1004, 1985
Printed in Great Britain.

0039-9140/85 $3.00 + 0.00

UTILITY OF 2,3-DICHLORO-5,6-DICYANO-*p*-BENZOQUINONE IN ASSAY OF CODEINE, EMETINE AND PILOCARPINE

MOHAMED E. ABDEL-HAMID, MOHAMED ABDEL-SALAM,
MOHAMED S. MAHROUS and MAGDI M. ABDEL-KHALEK
Faculty of Pharmacy, University of Alexandria, Alexandria, Egypt

(*Received* 11 *January* 1985. *Revised* 24 *April* 1985. *Accepted* 15 *May* 1985)

Summary—A simple and sensitive spectrophotometric method for the assay of codeine, emetine and pilocarpine is described, based on the interaction of these drugs (as *n*-electron donors) with 2,3-dichloro-5,6-dicyano-*p*-benzoquinone (as π-acceptor) to give a highly coloured radical anion which exhibits maximum absorption at 460 nm. Formation of the radical anion has been established by electron spin resonance measurements. Beer's law is obeyed for the alkaloids investigated. The assay results are in accord with pharmacopoeial assay results. The procedure is sufficiently sensitive to permit unit dose assay of the individual alkaloids in pharmaceutical formulations.

Codeine phosphate (cough-sedative), emetine hydrochloride (anti-amoebic) and pilocarpine nitrate (anti-mydriatic) are widely used in pharmaceutical practice. The BP compendium[1] describes an acid–base titration for the analysis of codeine phosphate tablets and emetine hydrochloride injections, and the USP[2] reports a colorimetric method for the assay of pilocarpine eye drops. Several methods have been described for the assay of these alkaloids in the formulations, and include colorimetric[3–9] and chromatographic[10–12] methods.

Substituted quinones such as 2,5-dichloro-*p*-benzoquinone,[13] 7,7,8,8-tetracyanoquinodimethane[14,15] and *p*-chloranil[16] have been used as π-acceptors with various donors to form charge-transfer complexes and radicals. Application of 2,3-dichloro-5,6-dicyano-*p*-benzoquinone (DDQ) for the detection and determination of some medicinal drugs containing the imidazoline ring has recently been described.[17]

The present work describes the utility of DDQ reagent for the spectrophotometric determination of codeine, emetine and pilocarpine in dosage forms. In addition, the nature of the orange-red coloured chromogen was established by electron spin resonance spectroscopy.

EXPERIMENTAL

Instruments

A Perkin-Elmer Model 550 S spectrophotometer with matched 1-cm quartz cells and a Varian Model E 12 electron spin resonance spectrometer were used.

Reagents

Pharmaceutical grade codeine phosphate, pilocarpine nitrate (Merck) and emetine hydrochloride (B.D.H.) were used as working standards. DDQ solution, 0.2% was freshly prepared in methanol. All reagents used were of analytical grade.

Standard solutions

An accurately weighed amount of the drug salt (codeine phosphate, emetine hydrochloride and pilocarpine nitrate) equivalent to 0.1 g of the base was dissolved in about 20 ml of water. The solution was quantitatively transferred to a separatory funnel, made alkaline with ammonia solution and shaken with five 20-ml portions of chloroform. The extracts were pooled in a 100-ml standard flask and diluted to volume with chloroform, to provide a standard 1-mg/ml solution of the base.

Determination of codeine

For calibration serial volumes of standard base solution in the range 0.2–0.9 ml were transferred into a series of 10-ml standard flasks. The solvent was removed by immersing the flasks in a water-bath at 70°. The residue was dissolved in 5 ml of methanol and 1 ml of DDQ solution was added. The volume was made up to 10 ml with methanol and the absorbance at 460 nm was measured against a reagent blank similarly prepared.

For determination of codeine phosphate in tablets, 10 tablets were powdered and thoroughly mixed. An accurately weighed quantity equivalent to ~0.13 g of codeine phosphate (0.1 g of codeine base) was transferred into a separatory funnel containing 20 ml of water. The base was extracted as described above and the extracts were transferred into a 100-ml standard flask and diluted to volume with chloroform. Exactly 0.6 ml of the diluted solution was then treated by the calibration procedure.

Determination of emetine

Ten ml of standard emetine base solution were transferred into a 50-ml standard flask and diluted to volume with chloroform. For calibration serial volumes of 0.3–1.1 ml of this solution were treated as described above for codeine.

For the determination of emetine in injections, 5 injections were mixed and an accurately measured volume containing ~0.115 g of emetine hydrochloride (0.1 g of emetine base) was transferred into a separatory funnel containing 20 ml of water. The base was extracted and diluted as above, and 1 ml of this solution was analysed by the procedure for calibration.

Determination of pilocarpine

The calibration procedure was the same as that for codeine.

For the assay of pilocarpine in eye drops, the free base from an accurately measured volume containing ~0.13 g of pilocarpine nitrate (0.1 g of pilocarpine base) was extracted and diluted as described for codeine phosphate tablets, and

0.6 ml of the resulting solution was assayed by the calibration procedure.

Electron spin resonance

The DDQ radical anion was prepared by mixing $10^{-4}M$ solution of the drug base (codeine, emetine, pilocarpine) in methanol with $10^{-4}M$ DDQ solution in the same solvent. The electron spin resonance spectra were run with the solution protected by a nitrogen atmosphere.

RESULTS AND DISCUSSION

In spite of their structural differences, codeine, emetine and pilocarpine react with DDQ in methanol to give an intensely orange-red product which exhibits absorption maxima at 460, 520 and 560 nm (Fig. 1). The absorption bands are similar to those of the DDQ radical anion obtained by reduction with iodide.[14] Further support of this assignment was provided by the detection of the DDQ radical by electron spin resonance measurements. The ESR spectrum for the DDQ radical anion is shown in Fig. 2. The spectrum displays 5 bands with relative intensities 1:2:3:2:1. The observed lines are due to the hyperfine interactions caused by two equivalent nitrogen nuclei. Analysis of the spectrum gave a value of 0.55 ± 0.01 gauss for the coupling constant (a_N^2). The g-factor value, as calculated from the spectrum, was 2.0050. The band-width ($\Delta H = 0.39$ gauss) was greater than that for the TCNQ radical anion.[18] This is because the coupling in TCNQ occurs between the free electron and the hydrogen and nitrogen nuclei, whereas in DDQ it takes place between the free electron and the nitrogen and chlorine nuclei. The chlorine-interaction accounts for the relatively large band width for the DDQ radical anion.

On the basis of the ESR investigations, it is assumed that a charge-transfer complex is formed by the interaction of the alkaloids as n-donors and DDQ as π-acceptor. In polar solvents (*e.g.*, methanol, acetonitrile), complete electron transfer from the donor- to the acceptor moiety takes place (see below) with the formation of the DDQ radical anion as predominent chromogen.

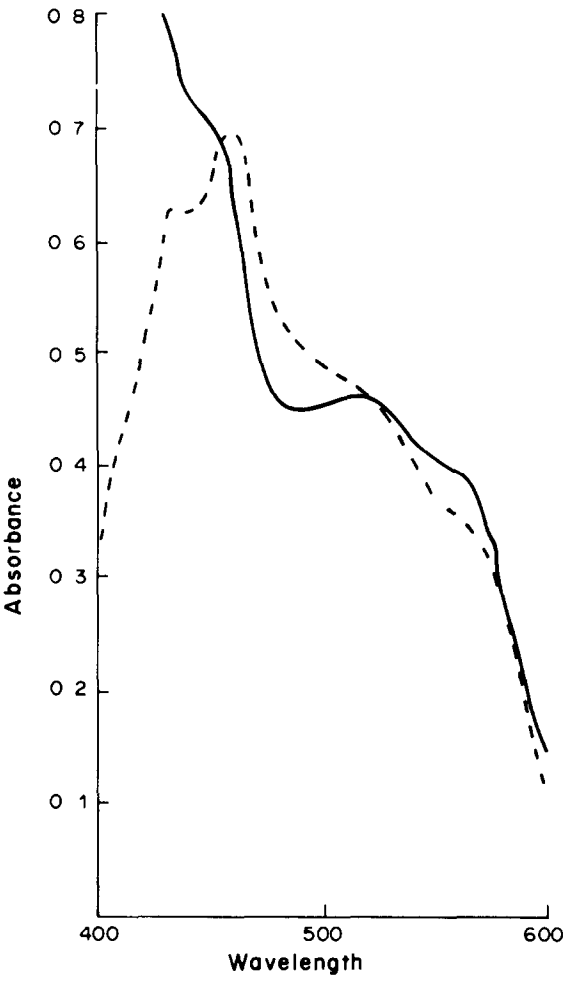

Fig. 1. Absorption spectra of (----) codeine–DDQ reaction product, measured against reagent blank, (——) DDQ radical anion obtained by iodide reduction method, measured against methanol. Codeine concentration = 9 mg/100 ml; DDQ concentration = 0.2 mg/ml.

$$\ddot{D} + A \longrightarrow \underset{\text{charge-transfer complex}}{[D \cdots A]} \longrightarrow \underset{\text{radical ions}}{D^{+}\cdot + A^{-}\cdot}$$

The spectral properties of the coloured radical and also the influence of various factors on the colour

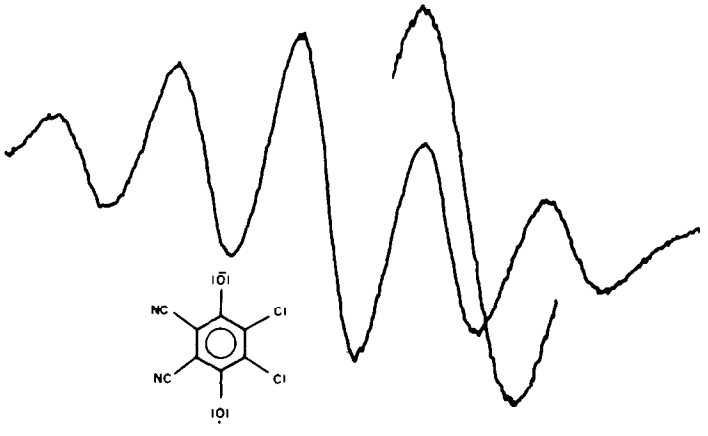

Fig. 2. ESR spectrum of DDQ radical anion in methanol.

Table 1. Assay results (6 replicates) for dosage forms of codeine phosphate, emetine hydrochloride and pilocarpine nitrate

Preparation	Nominal concentration*, *mg*/100 *ml*	Found,† %		
		Proposed method	Official methods[1,2]	*t*
Codeine phosphate® tablets‡	7.68	98.6 ± 1.1	98.0 ± 1.2	0.95
Emetine hydrochloride® injections#	2.30	99.0 ± 0.6	98.6 ± 0.7	1.09
Pilocarpine® eye drops¶	7.81	96.1 ± 0.8	96.6 ± 0.8	0.98

*The stated amounts of codeine phosphate, emetine hydrochloride and pilocarpine nitrate are equivalent to 6, 2, and 6 mg of the corresponding base per 100 ml, respectively.
†Mean and standard deviation.
§For $p = 0.05$ the critical t-value is 2.23.
‡Labelled to contain 30 mg of codeine phosphate per tablet (Adco Co., Egypt).
#Labelled to contain 30 mg of emetine hydrochloride per injection (Misr Co., Egypt).
¶Labelled to contain 3% of pilocarpine nitrate (Alexandria Co., Egypt).

development, were studied to determine the optimal conditions for the assay. Maximum absorption was obtained when 1 ml of 0.2% DDQ solution was used in the total volume of 10 ml. Non-polar solvents (benzene, carbon tetrachloride, chloroform) were found to be unsuitable, whereas polar solvents (methanol, acetonitrile) were considered as ideal solvents as high yields of the DDQ radical were obtained in these media. The reaction was found to be fast, the colour attaining maximum intensity in 5 min and then remaining stable for at least 30 min.

Under the conditions described, the calibration graphs for measurement at 460 nm are linear over the concentration ranges (for the solution measured) 2–9 mg/100 ml (codeine), 0.6–2.2 mg/100 ml (emetine) and 2–8 mg/100 ml (pilocarpine). The regression equations derived for our calibration systems by the least-squares method[19] were

$$A = -0.01 + 0.08C \quad \text{(codeine)}$$

$$A = 0.00 + 0.31C \quad \text{(emetine)}$$

$$A = -0.01 + 0.11C \quad \text{(pilocarpine)}$$

with regression coefficients of 0.9991, 0.9979 and 0.9970, respectively; C is the concentration of the drug in mg/100 ml. The slopes of the calibration curves reflect the degree of formation of the DDQ radical anion. The much higher slope for emetine is probably due to the presence of two basic centres in its molecule. The molar absorptivities for codeine, emetine and pilocarpine were 2.5×10^3, 1.54×10^4 and 2.2×10^3 $1.\text{mole}^{-1}.\text{cm}^{-1}$, respectively. The relative standard deviations (7 replicates) for the determination of the alkaloids investigated were all 0.2%. The method was applied to determination of codeine phosphate in tablets, emetine hydrochloride in injections and pilocarpine nitrate in eye drops, the official methods being used for comparative assays. The results are presented in Table 1. The performance of the method was assessed by a t-test. At the 95% confidence level, the calculated t-value did not exceed the tabulated value, indicating that the proposed and official methods are equally accurate. The proposed method is simpler, faster and more sensitive than the official procedures. These advantages favour its application in the analysis and quality-control of pharmaceutical formulations containing these alkaloids. However, other drugs with basic centres are expected to give similar reactions with DDQ, so the method is limited to the assay of single-drug formulations.

Acknowledgement—The authors wish to thank the Institute of Chemistry, University of Tübingen, West Germany, for measuring trhe ESR spectra; they are also grateful to Prof. K. A. Kovar, Institute of Pharmaceutical Sciences, University of Tübingen for his valuable suggestions and discussion.

REFERENCES

1. *British Pharmacopoeia*, pp. 605, 570. HM Stationary Office, London, 1980.
2. *U.S. Pharmacopeia*, 20th Revision, p. 628. Mack Publishing Company, Easton, Pa. 1980.
3. A. O. Gettler and I. Sunshine, *Anal. Chem.*, 1951, **23**, 779.
4. Y. A. Mohamed and M. Abdel-Hady, *Pharmazie*, 1975, **30**, 60.
5. A. M. Taha, A. K. S. Ahmed, C. S. Gomaa and H. El-Fattatry, *J. Pharm. Sci.*, 1974, **63**, 1853.
6. C. Gomaa and A. Taha, *ibid.*, 1975, **64**, 1398.
7. A. Taha and C. S. Gomaa, *ibid.*, 1976, **65**, 986.
8. M. E. Abdel-Hady, M. A. Abdel-Salam, N. A. Abdel-Salam and Y. A. Mohamed, *Planta Med.*, 1978, **34**, 430.
9. P. S. Agarwal and M. A. Elsayed, *Analyst*, 1981, **106**, 1157.
10. W. F. Bayne, L. C. Chu and F. T. Tao, *J. Pharm. Sci.*, 1976, **65**, 1724.
11. R. W. Frei, W. Santi and M. Thomas, *J. Chromatog.*, 1976, **116**, 365.
12. B. Aaroe, J. Remme and B. Salvesen, *Meddr. Horsk Farm. Selsk*, 1975, **37**, 274; *Anal. Abstr.*, 1976, **30**, 6E4.
13. H. Abdine, M. A. Elsayed, I. Chaaban and M. E. Abdel-Hamid, *Analyst*, 1978, **103**, 1227.
14. A. Taha and G. Rücker, *Arch. Pharm.*, 1977, **310**, 485.
15. K.-A. Kovar, W. Mayer and H. Auterhoff, *ibid.*, 1981, **314**, 447.
16. S. Belal, M. A. Elsayed, M. E. Abdel-Hamid and H. Abdine, *J. Pharm. Sci.*, 1981, **70**, 127.
17. K.-A. Kovar and M. Abdel-Hamid, *Arch. Pharm.*, 1984, **317**, 246.
18. M. E. Abdel-Hamid, *Dissertation*, Tübingen, 1983.
19. M. R. Spiegel, *Theory and Problems of Probability and Statistics*, pp. 215, 259. McGraw-Hill, New York, 1975.

Talanta, Vol. 32, No. 10, pp. 1005–1007, 1985
Printed in Great Britain.

0039-9140/85 $3.00 + 0.00

USE OF ENZYMATIC CATALYSIS WITH E.C. 1.2.3.2 XANTHINE OXIDASE FOR THE KINETIC DETERMINATION OF V(V) AT LOW CONCENTRATIONS*

ANNA MARIA GHE†, CLAUDIO STEFANELLI, GIUSEPPE CHIAVARI and PAGONA TSINTIKI
Istituto Chimico "G. Ciamician" dell'Università, Scuola di Specializzazione in Chimica Analitica, Via Selmi 2, 40126 Bologna, Italy

(*Received* 3 *July* 1984. *Revised* 5 *May* 1985. *Accepted* 14 *May* 1985)

Summary—An enzymatic kinetic method for the determination of V(V) is described, based on the activation of xanthine oxidase-catalysed NADH oxidation, in the presence of xanthine, dithiothreitol and Ag^+ ions. Under these conditions the activating power of V(V) was found to be enhanced. The linear relationship between relative enzyme activity and V(V) concentration allows the enzymatic determination of vanadium in the concentration range 20–500 ng/ml, the maximum relative error being ±3%, and relative standard deviation less than ±2.2%. Possible interferences have been studied.

In previous papers,[1–3] it was shown that V(V) changes the catalytic properties of xanthine oxidase E.C. 1.2.3.2 (XOD); it inhibits the XOD-catalysis of conversion of xanthine into uric acid but—at the same concentration—strongly activates the XOD-catalysed NADH oxidation, a reaction otherwise rather slow.[4] This latter property of V(V) has been investigated with a view to its use for kinetic determination of vanadium.

EXPERIMENTAL

Reagents

Xanthine oxidase, Grade I, with a specific activity of 0.76 U/mg of protein at 25°; NADH, Grade III (β-nicotinamide adenine dinucleotide, reduced form, disodium salt); dithiothreitol (1,4-dimercapto-2,3-butanediol) and Trizma base were obtained from Sigma Chemical Co.; xanthine was from U.S. Biochemical Corp., Cleveland, Ohio; sodium vanadate and the salts of other metal ions were Merck analytical-grade reagents.

All solutions were prepared with doubly distilled demineralized water (conductance 1×10^{-6} mho at 25°). The 0.05*M* Tris–HCl and Tris–HNO_3 buffers (pH 7.4 at 37 ± 0.1°), and xanthine and metal ion solutions, were prepared as described earlier.[1] A $1 \times 10^{-3}M$ NADH solution in Tris–buffer was prepared daily and kept refrigerated at 4° and protected from light. Its concentration was determined on the basis of a molar absorptivity of 6.2 $l.mole^{-1}.cm^{-1}$ at 340 nm.[5] A xanthine oxidase stock solution (3 mg/ml) in Tris-buffer was also prepared daily and stored at 4°.

The XOD-catalysed NADH oxidation was monitored spectrophotometrically at 340 nm and 37 ± 0.1°, by means of a Perkin–Elmer double-beam spectrophotometer (Model 554) with a microcomputer-driven recorder and a constant-temperature cell-holder.

*Work done with the financial support of the Ministero della Pubblica Istruzione (Italy), for research of national interest, no. 11835.
†Author to whom correspondence should be addressed.

Analytical procedure

Into a quartz cell (optical path 10 mm), place the following solutions in the order given: 0.18 ml of $1 \times 10^{-3}M$ xanthine; 0.3 ml of $1 \times 10^{-3}M$ NADH; 1.0 ml of $1.5 \times 10^{-2}M$ dithiothreitol in 0.05*M* Tris-HNO_3 buffer; 20 μl of $1.5 \times 10^{-3}M$ silver nitrate and 1.5 ml of sodium vanadate solution in Tris-HNO_3 buffer. Bring the mixture to 37°, and add 25 μl of 3-mg/ml XOD solution to give a final enzyme concentration of 25 μg/ml. Measure the absorbance against a reagent blank containing no enzyme.

Plot absorbance *vs.* time to determine the initial reaction rate v_0, expressed as ΔA_{340}/min, and to minimize errors due to possible loss of activity of the enzyme during successive determinations use the relative activity α:

$$\alpha = \frac{v_0 \text{ in presence of V(V)}}{v_0 \text{ in absence of V(V)}}$$

RESULTS AND DISCUSSION

In earlier work[2] the strong activating effect of V(V) on the XOD-catalysed NADH oxidation was observed and it was pointed out that the metal could modify the catalytic properties of the enzyme. This effect has now been examined with two reducing substrates present simultaneously, namely xanthine and NADH, which interact with different active sites of the enzyme, xanthine with the molybdenum site and NADH with the flavin site. Figure 1 clearly illustrates the difference in effect when NADH is present alone (curve 1), and together with xanthine (curve 2). When both reducing substrates are simultaneously present, the activating effect of V(V) on NADH oxidation begins at lower concentrations ($1 \times 10^{-6}M$ instead of $1 \times 10^{-5}M$).

In a previous paper[2] it was reported that in the presence of NADH alone as substrate, Hg(II), Ag(I), Zn(II) and Au(III) inhibited the XOD-catalysed NADH oxidation, and Cu(II) and Cr(VI) proved

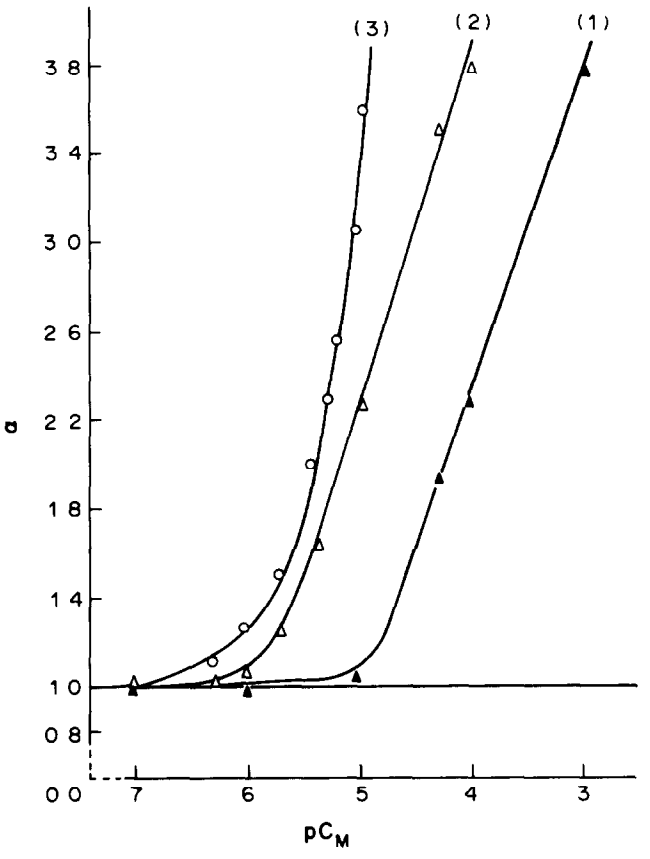

Fig. 1. Influence of V(V) concentration on XOD-catalysed NADH oxidation. Curve (1) substrate $1 \times 10^{-4}M$ NADH; curve (2) substrate $1 \times 10^{-4}M$ NADH plus $6 \times 10^{-5}M$ xanthine; curve (3) substrate $1 \times 10^{-4}M$ NADH plus $6 \times 10^{-5}M$ xanthine, in the presence of $5 \times 10^{-3}M$ dithiothreitol and $1 \times 10^{-5}M$ Ag^{+}; XOD concentration = 25 μg/ml; $pc_M = -\log[V(V)]$.

mild activators. We have therefore studied the possible effects of these species on the activation of XOD-catalysed NADH oxidation by V(V) when both xanthine and NADH are present.

The results obtained from equimolar ($1 \times 10^{-5}M$) concentrations of V(V) and of the other ions, in the presence of $1 \times 10^{-4}M$ NADH, $6 \times 10^{-5}M$ xanthine and 25 μg/ml XOD, are reported in Table 1.

There is strong inhibition of the reaction by Hg(II) and Ag(I), weaker inhibition by Au(III) and Zn(II), activation by Cu(II) and no effect from Cr(VI). These effects suggest the presence of an essential thiol group in the enzyme, with which the cations may interact. The experiment was therefore repeated with addition of dithiothreitol ($5 \times 10^{-3}M$) to protect the thiol group[5] of the enzyme. Table 1 shows that the inhibitory effect of Hg(II), Zn(II) and Au(III) is masked, Cu(II) now behaves as an inhibitor and Ag(I), which in the absence of dithiothreitol was a strong inhibitor, increases the activating effect of V(V) on NADH oxidation. Indeed the enhancement of the V(V) activating effect is sufficient (Fig. 1, curve 3) for detection of V(V) at concentrations lower than $5 \times 10^{-7}M$. This effect of dithiothreitol (enhancement of the reaction of interest and masking of some interferences) permitted development of the kinetic method for the determination of V(V) in low concentrations that is described here. The relative enzyme activity (α) is a linear function of vanadate concentration from 0.5 to 10 μM, corresponding to 25–500 ng of vanadium per ml.

Table 1. Influence of possibly interfering metal ions ($1 \times 10^{-5}M$) on the activation by $1 \times 10^{-5}M$ V(V) of XOD-catalysed NADH oxidation* in the presence or absence of dithiothreitol (DTT)

Interfering element	$\alpha^{\dagger}_{V(V)}$	
	[DTT] = 0	[DTT] = $5 \times 10^{-3}M$
Hg(II)	0	0.94
Ag(I)	0.14	1.60
Zn(II)	0.61	1.05
Au(III)	0.80	1.00
Cr(VI)	1	0.95
Cu(II)	3	0.14

*Experimental conditions: [NADH] = $1 \times 10^{-4}M$; [xanthine] = $6 \times 10^{-5}M$; [XOD] = 25 μg/ml.

$\dagger\alpha_{V(V)} = \dfrac{v_0 \text{ in the presence of V(V) plus interferent}}{v_0 \text{ in the presence of V(V) alone}}$.

Table 2. Effect of various species ($1 \times 10^{-5}M$) on the activation by $5 \times 10^{-6}M$ V(V) of XOD-catalysed NADH oxidation*

Species added	$\alpha_{V(V)}$
Ag(I)	1
Cd(II)	1
Mg(II)	1
Mo(VI)	1
Ca(II)	1
Cr(VI)	0.99
Zn(II)	0.91
Au(III)	0.90
Hg(II)	0.90
Al(III)	0.75
Cu(II)	0.17
Mn(II)	0.1
Ni(II)	0.07

*Experimental conditions: [NADH] = $1 \times 10^{-4}M$; [xanthine] = $6 \times 10^{-5}M$; [DTT] = $5 \times 10^{-3}M$; [Ag^+] = $1 \times 10^{-5}M$; [XOD] = 25 μg/ml. $\alpha_{V(V)}$ is defined in a footnote to Table 1.

The possible interferences of some elements present at concentrations twice that of the vanadium were studied (Table 2). Ag(I) concentrations ten times as large as that ($1 \times 10^{-5}M$) used in the standard assay do not affect the results. Of the species examined, Cd(II), Mg(II), Mo(VI), Ca(II) and Cr(VI) are tolerated at fairly high ratios to V(V), but Zn(II), Au(III), Hg(II) and Al(III) begin to interfere when present in equimolar ratio to V(V), and strong inhibition of the reaction is brought about by Cu(II), Mn(II) and Ni(II).

Table 3. Enzymatic determination of V(V), based on XOD-catalysed NADH oxidation in the presence of xanthine, dithiothreitol and Ag(I)

Sample	V(V), M		Relative error, %
	Taken	Found*	
1	5.0×10^{-7}	$5.15 \pm 0.10 \times 10^{-7}$	+3.0
2	8.4×10^{-7}	$8.52 \pm 0.08 \times 10^{-7}$	+1.4
3	3.3×10^{-6}	$3.20 \pm 0.05 \times 10^{-6}$	−3.0
4	5.2×10^{-6}	$5.31 \pm 0.11 \times 10^{-6}$	+2.1
5	6.5×10^{-6}	$6.40 \pm 0.14 \times 10^{-6}$	−1.5
6	8.2×10^{-6}	$8.15 \pm 0.06 \times 10^{-6}$	−0.6

*Average and standard deviation of 5 determinations.

For determination of known concentrations of V(V) in the absence of interfering elements (see Table 3) the relative error (average of five determinations) did not exceed $\pm 3\%$ and the relative standard deviation was not more than 2.2%. The method may therefore be recommended for determination of 0.5–10 μM V(V), provided the concentrations of the inhibitory species do not exceed the tolerance limits.

REFERENCES

1. A. M. Ghe, C. Stefanelli and D. Carati, *Talanta*, 1984, **31**, 241.
2. A. M. Ghe, C. Stefanelli, P. Tsintiki and G. Veschi, *ibid.*, 1985, **32**, 359.
3. C. S. Ramadoss, *Z. Naturforsch.*, 1980, **35C**, 702.
4. R. C. Bray, in *The Enzymes*, P. D. Boyer (ed.), Vol. 12, pp. 299–419. Academic Press, New York, 1975.
5. W. Gerhardt-Hansen, B. Kofaed, L. Westlund and B. Pavlu, *Scand. J. Clin. Lab. Invest., Suppl.* 1974, **33**, 40.

Talanta, Vol. 32, No. 10, pp. 1008–1010, 1985
Printed in Great Britain.

0039-9140/85 $3.00 + 0.00

EXTRACTIVE PHOTOMETRIC DETERMINATION OF GOLD(III) WITH 1-(2′,4′,6′-TRICHLOROPHENYL)-4,4,6-TRIMETHYL-(1H,4H)-2-PYRIMIDINETHIOL IN PRESENCE OF TRI-ISO-OCTYLAMINE

M. A. ANUSE, S. R. KUCHEKAR, N. A. MOTE and M. B. CHAVAN*
Analytical Chemistry Laboratory, Shivaji University, Kolhapur 416004, India

(*Received* 9 *January* 1984. *Revised* 25 *April* 1985. *Accepted* 9 *May* 1985)

Summary—Tervalent gold was determined spectrophotometrically as its anionic 1:4 gold–thiol complex extracted into chloroform from aqueous acidic medium (1.5*M* sulphuric acid) in the presence of tri-iso-octylamine. The complex exhibits maximum absorption at 480 nm (molar absorptivity 4.60×10^3 $l.mole^{-1}.cm^{-1}$) and Beer's law is obeyed in the concentration range 5–50 μg of gold(III) per ml. The relative standard deviation and relative error, calculated from ten determinations of solutions containing 15 μg of gold(III) per ml were 1.0% and 0.8%. The method is simple, selective and reproducible. It permits separation of gold(III) from associated elements and its determination in synthetic mixtures.

In earlier work we reported the use of 1-(2′-nitro-4′-tolyl)-4,4,6-trimethyl-(1H,4H)-2-pyrimidinethiol and 1-(4′-chlorophenyl)-4,4,6-trimethyl-(1H,4H)-2-pyrimidinethiol as extractants for platinum metals and gold(III).[1,2] In continuation of our studies, three new derivatives of mercaptopyrimidine with the structures shown below were synthesized with a view to investigating their reactions with gold(III). These reagents all extract gold(III) quantitatively from acidic media, but only 1-(2′,4′,6′-trichlorophenyl)-4,4,6-trimethyl-(1H,4H)-2-pyrimidinethiol (2′,4′,6′-trichloro-PTPT) forms a coloured product with gold(III) (in sulphuric acid medium, in presence of tri-iso-octylamine) which is suitable for use in spectrophotometric analysis.

Critical reviews on solvent extraction of gold(III) have been published by various authors.[3–5] Extractive photometric determination of gold is subject to many limitations, which have been critically discussed in the literature. β-Diketones[6,7] and 2,2′-dipyridylketoxime[8] require longer extraction times or multiple extractions, and the furil-α-dioxime[9] and 4-heptanone oxime[10] methods demand the separation of interfering ions before determination of gold(III). In the diphenylcarbazide method[11] it is necessary for the chloroform extract of the gold–trioctylamine complex to be evaporated to dryness, the residue mineralized and the gold determined with diphenylcarbazide; chromium(VI), molybdenum(VI), uranium(VI) and platinum metals interfere. Gold can be determined with Michler's thioketone[12] after extraction with tri-iso-octylamine (TIOA) in toluene, but although the method is highly sensitive, it is necessary for the organic phase to be scrubbed with wash solutions in order to get rid of interfering ions. Dyes such as Rhodamine B,[13–15] Methyl Violet,[16] Brilliant Green,[17] Acridine Orange,[18] PAR,[19] Acridine Yellow[20] and Chrompyrazol I[21] have also been used for extractive photometric determination of gold. Many of these are of practical importance but either the extraction periods are unusually long or the aqueous phase needs pre-equilibration, and reagent blanks are required. The reagent proposed here is colourless and extracts gold(III) readily and quantitatively from acidic medium in a single extraction. The method is simple, selective and reproducible, and permits separation of gold(III) from associated elements and its determination in mixtures.

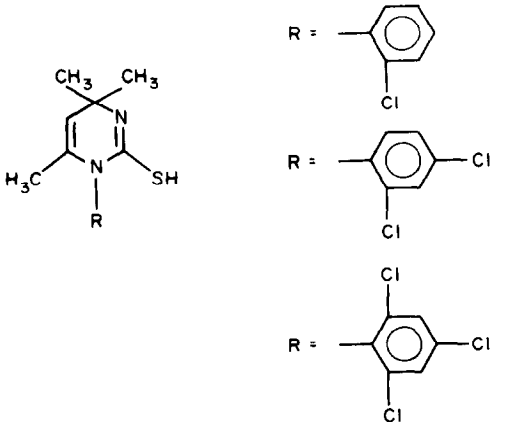

EXPERIMENTAL

Reagents

Standard solution of gold(III). Prepared by dissolving chloroauric acid in dilute hydrochloric acid, standardized[4] and diluted as required.

Reagent solution. 2′,4′,6′-Trichloro-PTPT was prepared by the method of Mathes[22] from 2,4,6-trichloroaniline. The compound is a colourless crystalline solid with a sharp m.p.

*To whom correspondence should be addressed.

(243°), and is used as a 0.01*M* solution in chloroform. This solution is colourless and stable.

*Tri-iso-octylamine (TIOA) solution in chloroform, 0.2*M. The chloroform and all other materials used were of guaranteed grade. Distilled water was used throughout.

Recommended procedures

Photometric determination of gold(III). Adjust the acidity of the gold(III) solution to 1.5*M* in sulphuric acid. Shake it for 10 sec with 5 ml each of the 0.01*M* reagent and 0.2*M* TIOA solutions. Collect the organic phase and make it up to a known volume with chloroform and measure the absorbance at 480 nm against chloroform. Compute the metal content from a calibration graph.

Extraction of gold(III). Adjust the acidity of the gold(III) solution to 8*M* in hydrochloric acid. Shake the solution for 10 sec with 5 ml of the 0.01*M* reagent solution. Collect the organic phase and evaporate it to dryness on a steam-bath. Destroy the complex by adding 1–2 ml of concentrated perchloric and hydrochloric acids and evaporating the solution until fumes appear, repeating this treatment at least twice. Dissolve the residue in a little concentrated hydrochloric acid and a few drops of nitric acid. Add a few milligrams of sodium chloride and evaporate to dryness on a steam-bath. Add a few drops of concentrated hydrochloric acid and evaporate again. Repeat this thrice. Dissolve the residue in dilute hydrochloric acid and determine gold photometrically as described above.

RESULTS AND DISCUSSION

The reagent reacts with gold(III) in sulphuric acid medium to form the yellow complex, which is readily extractable into chloroform (10 sec shaking), but is unstable in the organic medium. However, if the TIOA is also present in the organic phase, an orange ion-association complex of gold(III) is extracted from sulphuric acid medium, and is suitable for spectrophotometric determination of gold(III) at 480 nm (Fig. 1). The absorbance measured against the chloroform blank is independent of shaking time from 5 sec to 10 min and also of the acidity of the solution in the range 0.5–2*M* sulphuric acid. A 10-sec shake

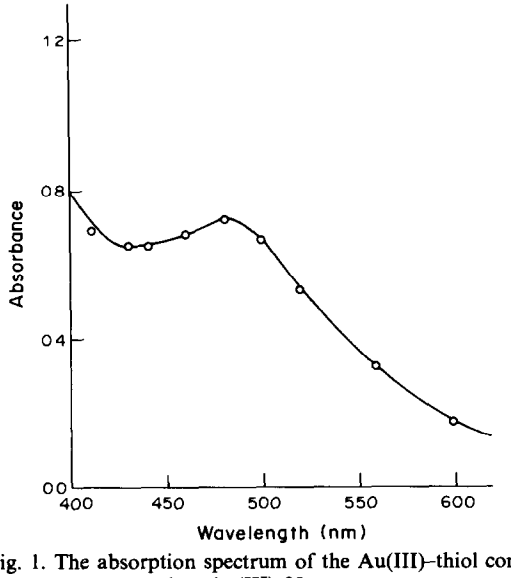

Fig. 1. The absorption spectrum of the Au(III)–thiol complex: Au(III) 30 ppm.

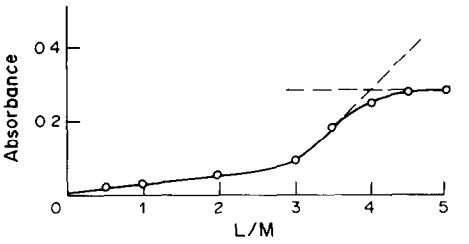

Fig. 2. Mole-ratio plot, [Au] = [Thiol] = $1.01 \times 10^{-3}M$, TIOA = 0.2*M*.

and 1.5*M* acidity were selected. Maximum absorbance was attained by using a reagent concentration at least 20 times that of the gold(III) and at least 3 ml of 0.2*M* TIOA in chloroform. The extraction was found to be quantitative from hydrochloric acid up to 8*M*, nitric acid up to 7*M*, sulphuric acid up to 2.5*M* and perchloric acid up to 8*M*, but to be more selective from 0.5–2.0*M* sulphuric acid. Variation in the volume of aqueous phase from 25 to 250 ml caused no marked effect on the absorbance. The mole-ratio method showed that the complex had a 1:4 metal-to-ligand ratio (Fig. 2). The molar absorptivity is 4.60×10^3 l.mole^{-1}.cm^{-1}, and Beer's law is obeyed over the gold concentration range 5–50 μg/ml in the final solution measured. The complex is stable for at least 5 hr.

Effect of diverse ions

For interference studies, different amounts of ionic species were added to the sample solution containing 150 μg of gold and the solution was adjusted to 1.5*M* in sulphuric acid or 8.0*M* in hydrochloric acid. Gold was determined as described by the recommended procedures. An error of $\pm 2\%$ in the absorbance readings was considered tolerable. Up to about 150 μg of gold(III) can be quantitatively extracted without interference from 20 mg of cobalt(II), nickel, copper(II) and uranium(VI); 15 mg of iron(III), zinc, platinum(IV) and barium; 10 mg of gallium, sodium, tungsten(VI) and selenium(IV); 7 mg of manganese(II), cadmium, iridium(III), mercury(II), lead and magnesium, 5 mg of chromium(VI), rhodium(III), tellurium(IV), cerium(IV) and bismuth; 3 mg of vanadium(V), molybdenum(VI), ruthenium(III), zirconium and silver. In photometric determination of gold(III) (150 μg) there is no interference from 10 mg of iron(III), sodium, cobalt(II), nickel, copper(II), zinc, barium, titanium(IV) and thorium; 5 mg of gallium, cadmium, uranium(VI) and selenium(IV); 3 mg of manganese(II), magnesium, tungsten(VI), lead, zirconium, aluminium and cerium(IV); 2 mg of molybdenum(VI), rhodium(III), iridium(III), silver and tellurium(IV); 1 mg of vanadium(V), ruthenium(III) and mercury(II). The only species showing interference in both procedures are iron(II), tin(II), thiourea and thiosulphate. In the photometric procedure chromium(VI), platinum(IV), bismuth, EDTA and

Table 1. Determination of gold in Cu–Ag–Au alloys (means of 6 analyses)

Composition of alloy %	Gold found, %	Relative mean deviation, %
Cu 49.35 Ag 7.25 Au 43.0	43.7	0.2
Cu 35.0 Ag 5.0 Au 60.0	60.0	0.1

bromide interfere. There is co-extraction of palladium(II) and osmium(VIII), but these can be separated by the scheme reported earlier.[1,2] The interference due to chromium(VI) and platinum(IV) in the photometric determination is eliminated by using the extraction procedure.

Determination of gold in alloys

Dissolution of gold–copper–silver alloy. About 0.1 g of the sample was transferred into a 250-ml conical flask with a short-stemmed funnel in its neck and heated gently with 10 ml of *aqua regia* to dissolve the alloy. The solution was treated with 10 ml of concentrated hydrochloric acid added in 2-ml portions, the solution being evaporated almost to dryness on the steam-bath after each addition. The residue was dissolved in dilute hydrochloric acid and the precipitated silver chloride was filtered off and washed with dilute hydrochloric acid. The filtrate and washings were collected in a 250-ml standard flask and made up to volume with distilled water.

Determination of gold. An appropriate aliquot of the solution was taken and the gold was separated from copper by the extraction procedure and determined by the photometric procedure. Results are reported in Table 1. The amount of gold found in the alloys is in agreement with the certified values. The relative standard deviation and relative error calculated from ten determinations on solutions containing 150 μg of gold(III) per 10 ml were 1.0% and 0.8%.

Acknowledgement—Thanks are due to the U.G.C., New Delhi, for providing a fellowship for SRK.

REFERENCES

1. M. A. Anuse, N. A. Mote and M. B. Chavan, *Talanta*, 1983, **30**, 323.
2. M. A. Anuse and M. B. Chavan, *Chem. Anal. (Warsaw)*, 1984, **29**, 409.
3. N. R. Das and S. N. Bhattacharyya, *Talanta*, 1976, **23**, 535.
4. F. E. Beamish and J. C. Van Loon, *Analysis of Noble Metals, Overview and Selected Methods*, pp. 129, 272. Academic Press, New York, 1977.
5. J. P. Richard, *The Chemistry of Gold*, Elsevier, Amsterdam, 1978.
6. A. V. Rangnekar and S. M. Khopkar, *Z. Anal. Chem.*, 1967, **230**, 425.
7. S. B. Akki and S. M. Khopkar, *Indian J. Chem.*, 1972, **10**, 125.
8. W. H. Holland and J. Bozic, *Anal. Chem.*, 1967, **39**, 109.
9. P. S. Patil and V. M. Shinde, *Mikrochim. Acta*, 1977 **II**, 331.
10. R. J. Walker and W. J. Holland, *ibid.*, 1974, 105.
11. J. Adam and R. Přibil, *Talanta*, 1971, **18**, 405.
12. I. Tsukahara, *ibid.*, 1977, **24**, 633.
13. B. J. MacNulty and L. D. Woollard, *Anal. Chim. Acta*, 1955, **13**, 154.
14. H. Onishi, *Mikrochim. Acta*, 1959, 9.
15. R. Dancheva and S. Beleva, *Khim.-Ind. Sofia*, 1964, **36**, 109; *Chem. Abstr.*, 1965, **62**, 19*a*.
16. L. Ducret and H. Maurel, *Anal. Chim. Acta*, 1959, **21**, 74.
17. R. E. Stanton and A. J. McDonald, *Analyst*, 1964, **89**, 767.
18. D. A. Mikaelyan and L. A. Mekhakyan, *Molodi Nauch. Rab. Estetr. Nauki*, 1972, No. 2, 79; *Chem. Abstr.*, 1974, **80**, 90751z.
19. S. G. Nagarkar and M. C. Eshwar, *Anal. Chim. Acta*, 1974, **71**, 461.
20. V. M. Tarayan and D. A. Mikaelyan, *Arm. Khim. Zh.*, 1981, **34**, 545.
21. P. N. Nesterenko and V. M. Ivanov, *Zh. Analit. Khim.*, 1982, **37**, 1977.
22. R. A. Mathes, *J. Am. Chem. Soc.*, 1953, **75**, 1747.

Talanta, Vol. 32, No. 10, pp. 1011–1012, 1985
Printed in Great Britain.

0039-9140/85 $3.00 + 0.00

SELECTIVE COMPLEXOMETRIC DETERMINATION OF BISMUTH WITH MERCAPTANS AS MASKING AGENTS, AND ITS ESTIMATION IN ALLOYS

SARALA RAOOT and K. N. RAOOT
Defence Metallurgical Research Laboratory Kanchanbagh, Hyderabad-500 258, India

(*Received* 22 *February* 1985. *Accepted* 9 *May* 1985)

Summary—A method is proposed for selective complexometric determination of bismuth. To a solution containing bismuth and other cations, excess of EDTA is added and the surplus is back-titrated at pH 5–6 with lead nitrate (Xylenol Orange as indicator). Thioglycollic or mercaptopropionic acid is then added to decompose the bismuth–EDTA complex and the liberated EDTA is titrated with lead nitrate. The interference of various cations has been studied and the method employed to determine bismuth in a variety of alloys.

Bismuth can be titrated with EDTA at pH as low as 1,[1] but cations forming comparably strong EDTA complexes, such as iron(III), thorium, zirconium, tin(IV) and titanium(IV), will interfere. This interference can be dealt with by titrating the total metal content, then treating the titrated solution with a releasing agent which will form a more stable complex with bismuth than EDTA does. The EDTA released from its bismuth complex can then be titrated with a suitable metal solution. Mercaptopropionic acid,[2] 2,3-mercaptopropane-1-sulphonic acid,[3,4] 2,3-dimercaptopropan-1-ol,[5] mercaptoacetic acid[6] and thioglycollic acid[7] have all been recommended for masking bismuth in acid medium, so should be useful as releasing agents. In our recent work on use of thioglycollic acid and mercaptopropionic acid as selective releasing agents for copper[8] and tin,[9] we found that bismuth caused serious interference, which might be expected from the earlier work quoted above. We therefore examined these two acids as agents for releasing bismuth from its EDTA complex.

EXPERIMENTAL

Reagents

Bismuth nitrate solution. Prepared by dissolving 1.0 g of high-purity bismuth in 20 ml of concentrated nitric acid, making up to 1 litre and standardizing.

*EDTA solution, 0.01*M.

*Lead nitrate solution, 0.01*M.

Xylenol Orange, 0.1% aqueous solution.

Thioglycollic acid and mercaptopropionic acid, 20% solutions.

Hexamine, 30% solution.

Solutions of various metal ions (1 mg/ml) were prepared from suitable salts. All chemicals used were of analytical reagent grade.

Determination of bismuth in presence of other cations

To a solution containing 5–50 mg of bismuth and various amounts of other metal ions, add excess of 0.01*M* EDTA, dilute to about 100 ml with water, adjust the pH to 5–6 with hexamine solution, add a few drops of Xylenol Orange indicator and back-titrate the excess of EDTA with 0.01*M* lead nitrate. Add 2–15 ml of thioglycollic or mercaptopropionic acid solution, heat to boiling and boil for 4–5 min, cool, adjust the pH to 5–6 with hexamine and titrate and liberated EDTA with 0.01*M* lead nitrate.

Application to alloys

Dissolve 0.2–0.5 g of alloy in the minimum amount of *aqua regia* necessary and make up to volume in a 100 ml standard flask containing sufficient potassium chloride solution to give an overall KCl concentration of 2%. Analyse a suitable aliquot as described above.

RESULTS AND DISCUSSION

The formation constant for the bismuth–EDTA complex[1] is variously reported as 10^{23}–10^{26}. The stability constants for the complexes of bismuth with thioglycollic and mercaptopropionic acid are not known, but because these acids release EDTA from its bismuth complex, their stability constants must be higher than that for the EDTA complex.

We have found that 5 ml of 20% thioglycollic or mercaptopropionic acid solution quantitatively releases EDTA from its complex with 20 mg of bismuth, on boiling for 4–5 min. The treatment with these acids lowers the pH from that at the end of the first titration, and to ensure a correct end-point in the second titration with lead, it is necessary to adjust the pH back to 5–6.

Table 1 shows that the method is selective for bismuth in the presence of nickel, zinc, cadmium, cobalt, lead, manganese, aluminium, iron(III), indium, yttrium, lanthanum, samarium, cerium(III), titanium(IV) and zirconium, but manganese gives some trouble in the end-point detection in both titrations when more than 5 mg of it is present. Copper(II) and tin(IV) are also quantitatively released from their EDTA complexes by means of mercaptans[8,9] and cause interference, but this can be prevented by masking copper with ascorbic acid and thiourea[10,11] and tin with tartaric acid[12] before the

Table 1. Determination of bismuth in presence of foreign metal ions

Foreign ion, *mg*		Bi^{3+}, *mg* Taken	Found MPA	Found TGA
Cu^{2+}	40.4[a]	12.00	12.07	12.07
	10.1[a]	50.0	49.9	50.2
Ni^{2+}	40.3	8.00	7.94	8.05
	10.1	45.0	44.7	45.1
Zn^{2+}	50.6	10.00	10.03	10.03
	10.1	40.0	39.8	40.1
Cd^{2+}	40.5	35.00	34.9	34.9
	20.3	45.0	45.1	45.2
Co^{2+}	20.4	5.00	5.02	4.96
	10.2	45.0	44.9	45.1
Pd^{2+}	18.0[b]	15.00	14.94	15.05
	6.0[b]	8.00	8.05	7.94
Hg^{2+}	40.4[b]	40.0	40.1	40.2
	10.1[b]	12.00	11.97	11.97
Pb^{2+}	30.8	18.00	17.97	18.13
	15.4	50.0	49.9	50.1
Mn^{2+}	5.0	10.00	10.08	9.93
	3.0	18.00	17.87	18.13
Al^{3+}	25.0[c]	5.00	4.96	4.96
	5.0[c]	30.0	30.1	29.9
Fe^{3+}	25.8	15.00	15.05	15.10
	12.9	25.0	24.9	25.1
In^{3+}	25.8	12.00	11.91	11.97
	12.9	30.0	30.1	29.9
Y^{3+}	28.4	8.00	8.05	7.94
	7.1	40.0	39.9	40.2
La^{3+}	30.5	12.00	12.07	12.02
	5.1	45.0	45.2	44.9
Sm^{3+}	28.4	20.00	20.06	19.91
	14.2	35.0	34.9	35.1
Ce^{3+}	40.2	10.00	9.93	10.03
	10.1	50.0	50.2	49.9
Ti^{4+}	20.4	15.00	15.05	15.05
	10.2	25.0	24.9	25.1
Zr^{4+}	40.1	10.00	10.03	9.98
	10.3	45.0	44.9	45.2
Sn^{4+}	50.5[d]	8.00	8.05	7.94
	25.3[d]	40.0	39.7	39.9

MPA = Mercaptopropionic acid.
TGA = Thioglycollic acid.
[a]Ascorbic acid and thiourea added to mask copper.
[b]Thiourea added to mask palladium and mercury.
[c]Excess of EDTA added, pH adjusted to 3, solution boiled for 3 min.
[d]Tartaric acid added to mask Sn(IV).

titration. Thiourea will likewise mask palladium[13] and mercury[14] which would also otherwise interfere. A notable feature of the method is its capability to determine bismuth in presence of metals such as iron, tin, titanium and zirconium, which seriously interfere in the direct titration at low pH.

Table 2. Determination of bismuth in solid and synthetic alloy samples

Alloy	Bi found, % a	b	c
Sn–Bi	59.9	59.7[b]	60.0
Pb–Bi	56.1	55.9[b]	56.4
Cd–Bi	40.0	40.2[b]	40.0
Wood's metal* Pb (25.0); Sn (12.5); Cd (12.5); Bi (50.0)	50.0	50.2[b]	49.7
Bismuth solder Pb (40.0); Sn (15.1); Bi (44.9)	44.9	44.7[b]	45.2
Eutectic fusible alloy Pb (32.0); Sn (14.8); Bi (53.2)	53.2	53.0[b]	53.5

[a]Gravimetric values by bismuth oxychloride precipitation.[15]
[b]Values by mercaptopropionic acid release.
[c]Values by thioglycollic acid release.
*Synthetic mixture.

Table 2 gives results obtained for bismuth in alloys and these are in good agreement with those obtained by a standard procedure,[15] the relative error in no case exceeding 1%. Besides being selective and accurate, the method is simple and rapid. A suite of three alloy samples can be analysed in 1 hr.

Acknowledgement—Grateful thanks are due to Dr P. Rama Rao, Director, Defence Metallurgical Research Laboratory, Hyderabad, for permission to communicate this paper.

REFERENCES

1. R. Přibil, *Applied Complexometry*, Pergamon Press, Oxford, 1982.
2. K. Yamaguchi and K. Ueno, *Talanta*, 1963, **10**, 1195.
3. L. A. Volf, *Zavodsk. Lab.*, 1960, **26**, 1353.
4. Yu. V. Morachevskii and L. A. Volf, *Zh. Analit. Khim.*, 1960, **15**, 656.
5. R. Přibil and Z. Roubal, *Collection Czech. Chem. Commun.*, 1954, **19**, 1162.
6. R. Přibil and Veselý, *Chemist-Analyst*, 1965, **54**, 12.
7. *Idem*, *Talanta*, 1961, **8**, 880.
8. S. Raoot, K. N. Raoot and N. R. Desikan, *Indian J. Technol.*, 1983, **21**, 39.
9. K. N. Raoot and S. Raoot, *Talanta*, 1984, **31**, 469.
10. O. B. Budevsky and L. Simova, *ibid.*, 1962, **9**, 769.
11. K. N. Raoot, S. Raoot, B. V. Rao and D. P. Lahiri, *Indian J. Technol.*, 1976, **14**, 254.
12. S. Raoot and K. N. Raoot, *ibid.*, 1983, **21**, 442.
13. K. N. Raoot, S. Raoot and V. L. Kumari, *Talanta*, 1983, **30**, 611.
14. R. P. Singh, *ibid.*, 1969, **16**, 1447.
15. N. H. Furman, *Standard Methods of Chemical Analysis*, 6th Ed., Vol. I, p. 195. Van Nostrand, New York, 1962.

Talanta, Vol. 32, No. 10, pp. 1013–1015, 1985
Printed in Great Britain.

0039-9140/85 $3.00 + 0.00

SPECTROPHOTOMETRIC DETERMINATION OF TRACE AMOUNTS OF CADMIUM AND ZINC IN WASTE WATER WITH 4-(2-PYRIDYLAZO)-RESORCINOL AND MIXED IONIC AND NON-IONIC SURFACTANTS

WEN-BIN QI and LI-ZHONG ZHU
Chemistry Department, Hangzhou University, Zhejiang, People's Republic of China

(*Received* 25 *October* 1984. *Revised* 1 *April* 1985. *Accepted* 7 *May* 1985)

Summary—A spectrophotometric method for determination of trace amounts of cadmium and zinc in waste water with PAR and mixed ionic and non-ionic surfactants is described. The interferences of foreign ions can be eliminated by masking with a mixture of triethanolamine, potassium fluoride, ethylenediamine and sodium hexametaphosphate. By virtue of the difference between the absorbances before and after addition of a little sodium diethyldithiocarbamate, cadmium and zinc can be determined directly in aqueous solution without separation. Beer's law is obeyed for 0–20 μg of Cd or 0–12 μg of Zn in 25 ml of solution. The apparent molar absorptivities at 505 nm are 8.65×10^4 l.mole^{-1}.cm^{-1} for Cd and 8.21×10^4 l.mole^{-1}.cm^{-1} for Zn. Results obtained by applying the proposed method to waste-water samples agree well with those obtained by atomic-absorption spectrophotometry.

The determination of trace amounts of cadmium and zinc has recently received considerable attention owing to concern with the problems of environmental pollution. At present, the most commonly used colour reagent for spectrophotometric determination of cadmium and zinc is dithizone, but the method is complicated and toxic solvents are used.

The analytical applications of 4-(2-pyridyl-azo)-resorcinol (PAR) have been extensively investigated. Determination of cadmium and zinc with PAR is highly sensitive, but poorly selective. However, it has been shown that the colour system of cadmium or zinc with PAR, cetyltrimethylammonium bromide (CTMAB) and a non-ionic surfactant possesses many advantages, such as high sensitivity, good stability and wide tolerance in the experimental conditions, over the simple Cd–PAR system, because of the synergic sensitizing effect of a mixture of ionic non-ionic surfactants on the colour reaction.[1] In this paper, continuous spectrophotometric determination of cadmium and zinc in waste water by use of PAR, CTMAB and "Peregal O" is described.

EXPERIMENTAL

Reagents

PAR solution, 5×10^{-4}M. Dissolve 0.1076 g of PAR in 1000 ml of water containing 1 ml of 1*M* sodium hydroxide.

Standard solutions of cadmium. Stock solution 1 mg/ml; working solution 10 μg/ml.

Standard solutions of zinc. Stock solution 1 mg/ml; working solution 10 μg/ml.

Cetyltrimethylammonium bromide (CTMAB) solution, 2×10^{-3}M.

"Peregal O" [$C_{18}H_{37}O(CH_2CH_2O)_{20}H$] *solution*, 4×10^{-3}M.

CTMAB–Peregal O solution, prepared by mixing 200 ml of CTMAB solution and 100 ml of Peregal O solution to give an equimolar mixture.

Buffer solutions. Buffers covering the pH-range 6.0–11.7 were prepared by mixing 0.05*M* sodium borate and 0.05*M* sodium carbonate in appropriate ratios.

Mixed masking-reagent solution. A mixture of 200 ml of 5.0% triethanolamine (TEA) solution, 150 ml of 10% potassium fluoride solution, 50 ml of 1.0% ethylenediamine (En) solution and 50 ml of 0.2% sodium hexametaphosphate solution, diluted to 500 ml.

All chemicals used were of analytical-reagent grade and demineralized water was used.

General procedure

Pipette into a 25-ml standard flask 1.0 ml of test or standard solution containing up to 20 μg of cadmium or 12 μg of zinc. Add 5.0 ml of mixed masking-reagent solution, 2.0 ml of PAR solution, 5 ml of borate buffer (pH 10), 7.5 ml of CTMAB–Peregal O solution, dilute to the mark with water, mix, and after 20 min measure the absorbance at 505 nm in a 1-cm cell against a reagent blank. Prepare a calibration graph with appropriate standards.

RESULTS AND DISCUSSION

The absorption spectra of the Cd–PAR–CTMAB–Peregal O complex and reagent blank were measured against water in the range 360–600 nm (1-cm cells). The absorption maximum of the complex is at 505 nm and that of the reagent blank is at 404 nm (Fig. 1).

Effect of amounts of reagents

The general procedure was followed with 10 μg of cadmium and various amounts of $5 \times 10^{-4}M$ PAR. Maximum and constant absorbance was obtained when 1.5–3.5 ml of the PAR solution were used, so 2.0 ml of the PAR solution was selected as optimal.

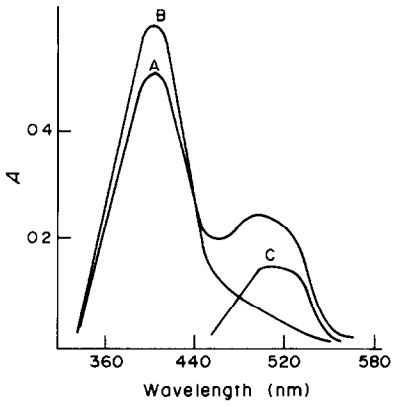

Fig. 1. Absorption spectra of Cd–PAR–CTMAB–Peregal O system. A, Cd–PAR–CTMAB–Peregal O *vs.* water; B, reagent blank *vs.* water; C, Cd–PAR–CTMAB–Peregal O *vs.* reagent blank; 0.5-cm path-length; Cd = 10 μg.

The effects of CTMAB and Peregal O were similarly tested in the range 4.0–8.0 ml of $2.0 \times 10^{-3}M$ CTMAB and 2.25–5.0 ml of $4.0 \times 10^{-3}M$ Peregal O. The absorbance was maximal and constant when the molar ratio of CTMAB to Peregal O ranged from 0.5 to 1.1; for convenience, we recommend use of a 1:1 molar ratio. It is important, however, to add the surfactants as a composite solution, otherwise the reproducibility of the determination is much poorer.

The allowable amounts of masking reagent in 25 ml of solution were likewise found to be 2.5 ml of 10% potassium fluoride solution, 1.5 ml of 5.0% TEA solution, 0.5 ml of 1.0% En solution and 0.5 ml of 0.2% sodium hexametaphosphate solution.

Characteristics of the complex

The molar ratio of cadmium to PAR in the complex was determined by the continuous-variations and molar-ratio methods and found to be 1:2. The molar ratio of cadmium to CTMAB and to Peregal O in the complex was found to be 1:1 in both cases by the Asmus and molar-ratio methods. Therefore, the complex is $Cd(PAR)_2(CTMAB)$ (Peregal O).

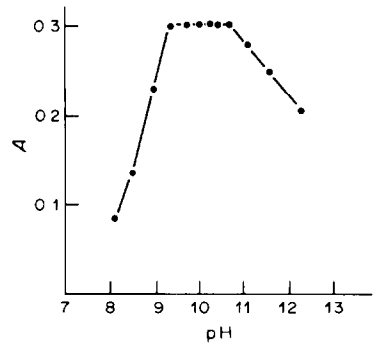

Fig. 2. Dependence of absorbance on pH $\lambda = 505$ nm; reference, reagent blank.

Beer's law is obeyed at 505 nm for 0–20 μg of cadmium or 0–12 μg of zinc in 25 ml of solution. The apparent molar absorptivities at 505 nm were found to be 8.65×10^4 and 8.21×10^4 $l.mole^{-1}.cm^{-1}$ for cadmium and zinc respectively. Complete colour development takes 20 min and the colour is then stable for at least 18 hr.

Interferences

The selectivity was investigated by determination of 10 μg of cadmium or zinc in the presence of various amounts of other ions. The results indicated that Ni^{2+}, Co^{2+}, Cu^{2+} and Mn^{2+} interfere severely and that there is mutual interference by cadmium and zinc. The interference of cobalt, copper, nickel and manganese may be reduced somewhat by adding the masking-reagent mixture. The tolerance limits for diverse ions when the mixed masking-reagent solution is used are given in Tables 1 and 2.

To eliminate the mutual interference of zinc and cadmium, we devised the following procedure, based on the difference in stability of the complexes concerned.[2-4] The total absorbance of the Zn–PAR–CTMAB–Peregal O and Cd–PAR–CTMAB–Peregal O complexes is measured, then 0.2 ml of 2% sodium diethyldithiocarbamate solution is added to the test solution. The Cd–PAR–CTMAB–Peregal O complex is destroyed but not the Zn–PAR–CTMAB–Peregal O complex. The change in absorbance corresponds to the amount of cadmium present in the sample. Thus, the method can be used for the spectrophotometric determination of trace amounts of both cadmium and zinc in the same sample. Provided less than 20 mg

Table 1. Effect of foreign ions on determination of 10 μg of Cd in presence of mixed masking reagents

Added		Ion/Cd ratio, *w/w*	Cd found, μg
Ion	μg		
PO_4^{3-}	6000	600	10.10
Al(III)	400	40	9.97
Bi(III)	50	5	10.00
Ca(II)	500	50	9.98
Co(II)	10	1	10.08
	0.5*	0.05	11.83
Cr(VI)	2000	200	9.77
Cu(II)	5	0.5	10.07
	0.5*	0.05	10.86
Fe(II)	10	1	10.16
Fe(III)	20	2	10.30
Hg(II)	40	4	10.12
Mg(II)	3000	300	9.80
Mn(II)	10	1	10.30
	0.5*	0.05	10.43
Mo(VI)	2000	200	9.80
Ni(II)	2	0.2	11.30
	1	0.1	10.00
	1*	0.1	10.57
Pb(II)	40	4	9.90
Sn(II)	20	2	10.13
Zn(II)	1	0.1	10.40

*In the absence of masking agents.

Table 2. Effect of foreign ions on determination of 10 μg of Zn in presence of mixed masking reagents

Added			
Ion	μg	Ion/Cd ratio, *w/w*	Cd found, μg
PO_4^{3-}	8000	800	10.04
Al(III)	700	70	9.86
Bi(III)	30	3	9.84
Ca(II)	1000	100	9.90
Co(II)	10	1	10.20
	0.5*	0.05	10.40
Cr(VI)	4000	400	9.90
Cu(II)	8	0.8	10.20
	0.5*	0.05	10.86
Fe(II)	20	2	10.18
Fe(III)	20	2	10.24
Hg(II)	200	20	10.12
Mg(II)	3000	300	9.96
Mn(II)	5	0.5	10.20
	0.5*	0.05	10.44
Mo(VI)	4000	400	9.82
Ni(II)	2	0.2	10.28
	1.0*	0.1	10.60
Pb(II)	100	10	10.16
Sn(II)	30	3	10.18
Cd(II)	30	3	10.04

*In the absence of masking agents.

of the diethyldithiocarbamate is added, up to 20 μg of copper, 10 μg of nickel, 10 μg of cobalt and 5 μg of manganese will not interfere.

Table 3. Results for determination of cadmium and zinc in waste water

	Atomic-absorption spectrophotometry		Present method	
Sample	Cd, *ppm*	Zn, *ppm*	Cd, *ppm*	Zn, *ppm*
1	0.008	4.05	0.0	4.08
2	0.0	1.70	0.0	1.75
3	0.0	11.70	0.0	11.67
4	0.0	55.00	0.0	54.6
5	0.54	2.34	0.53	2.22
6	1.23	10.19	1.25	10.24

The results for determination of cadmium and zinc in some waste-water samples by the proposed method are shown in Table 3, and are in reasonable agreement with those obtained by atomic-absorption spectrophotometry. The method could be adapted for on-line monitoring.

REFERENCES

1. Wen-bin Qi and Li-zhong Zhu, *Fenxi Huaxue*, in the press.
2. H. A. Flaschka and A. J. Barnard, *Chelates in Analytical Chemistry*, Vol. 4, p. 127. Dekker, New York, 1972.
3. H. Bode and K. J. Tusche, *Z. Anal. Chem.*, 1957, **157**, 414.
4. G. Eckert, *ibid.*, 1955/56, **148**, 14.

Talanta, Vol. 32, No. 10, pp. 1016–1018, 1985
Printed in Great Britain.

0039-9140/85 $3.00 + 0.00

DETERMINATION OF SUB-ng/ml LEVELS OF MERCURY IN WATER BY ELECTROLYTIC DEPOSITION AND ELECTROTHERMAL ATOMIC-ABSORPTION SPECTROPHOTOMETRY

XU BO-XING, XU TONG-MING, SHEN MING-NENG and FANG YU-ZHI
Department of Chemistry, East China Normal University, 3663 Chung Shan Road (N), Shanghai, People's Republic of China

(*Received* 31 *January* 1985. *Accepted* 3 *May* 1985)

Summary—The determination of trace mercury in water samples by electrolytic deposition and electrothermal atomic-absorption spectrophotometry is described. Traces of mercury in water are preconcentrated by electrolytic reduction and deposition on a platinum wire cathode, which is then put into a graphite cup for direct atomization and measurement. The method is sensitive and simple, with a detection limit of 0.04 ng/ml. Almost all the metal ions commonly found in water samples can be tolerated, because of the selective deposition at controlled potential.

Traces of mercury in water can be determined by colorimetry[1] or cold-vapour atomic-absorption spectrophotometry,[2,3] The latter approach is to be preferred on account of its sensitivity, but its precision is not always satisfactory, and large amounts of easily reducible elements must be absent from the sample solution. The aim of this work was to develop a new method which would overcome these disadvantages, minimize interferences and background absorption, and give maximum sensitivity. The use of controlled-potential electrolytic deposition as a separation and preconcentration technique for the determination of mercury in samples with complex matrices, by electrothermal atomic-absorption spectrometry (AAS), was developed several years ago,[4–8] but the equipment was not particularly simple and easy to operate and the method did not attract much attention for routine analysis. In this paper a simple electrolytic deposition is combined with electrothermal AAS for the determination of trace mercury in water.

EXPERIMENTAL

Reagents

Doubly distilled demineralized water was used throughout. Acetic acid (analytical grade) was redistilled in a quartz still before use. A stock solution ($1.3 \times 10^{-3}M$) of mercury(II) chloride was stored in a polyethylene bottle and a working solution ($1.3 \times 10^{-5}M$) was made by dilution with water just before use.

Apparatus

A Hitachi 180-80 polarized Zeeman atomic-absorption spectrophotometer was used with a Hitachi model 056 recorder and control unit (including temperature programmer). A model 75-4B polarograph was used as a potentiostat. A Hitachi mercury hollow-cathode lamp was out. Acetic acid (analytical grade) was redistilled in a quartz still before use. A stock solution ($1.3 \times 10^{-3}M$) of mercury (II) chloride was stored in a polyethylene bottle and a working solution ($1.3 \times 10^{-5}M$) was made by dilution with water just before use.

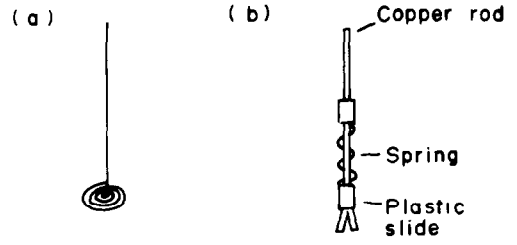

Fig. 1. Platinum cathode (a) and holder (b). The cathode is released by moving the sleeve on the holder.

General procedure

Transfer 60 ml of water sample and 0.5 ml of 12*M* acetic acid to a plastic electrolysis cell, submerge the three electrodes (platinum coil electrode, Ag/AgCl reference electrode and platinum foil anode) in the sample solution, start the magnetic stirrer and timer, and electrolyse at 0.0 V *vs.* the Ag/AgCl electrode. After 300 sec, transfer the platinum coil electrode from the cell into the graphite cup, then start the atomization procedure and measure the absorbance under the following conditions:

Wavelength	2537 Å
Bandpass	13 Å
Hg lamp current	6 mA
Sheathing gas (Ar) flow-rate	200 ml/min
Drying temperature and time	40–80°; 5 sec
Atomization temperature and time	700°; 7 sec (stopped Ar flow)
Cleaning temperature and time	1000°; 3 sec

RESULTS AND DISCUSSION

Effect of cathode potential

The potential of the platinum coil electrode strongly affects the electrolytic deposition of mercury and other metals. Figure 2 shows that the amount of mercury deposited in a given time is constant and

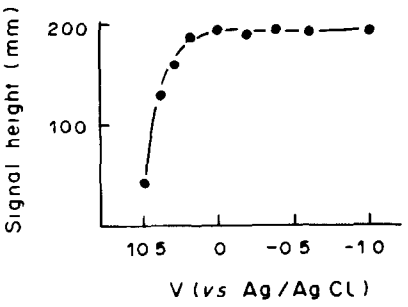

Fig. 2. Selection of cathode potential.

maximal over the range from +0.1 to −1.0 V (*vs.* Ag/AgCl electrode). To avoid interferences from other metal ions a potential of 0.0 V (*vs.* Ag/AgCl) is used.

Electrolysis time

Results for the determination of mercury at 4 ng/ml concentration indicate (Fig. 3) that there is initially a linear relationship between amount of mercury deposited and deposition time. Deposition times up to 6 min are best, but if the concentration of mercury is lower than 4 ng/ml the time may be extended. In this work a 5-min deposition time was used as standard.

Position of platinum wire in the graphite cup

The position of the coiled wire cathode in the graphite cup (Fig. 4) was found not to affect the repeatability of the results, because even if part of the wire is in the light-beam and scatters a little of it, there is almost the same degree of scattering of the measured beam (π) and the reference beam (σ) in the polarized Zeeman AAS.

Calibration graph, detection limit and precision

The calibration graph was linear from 0.08 to 5.2 ng/ml mercury concentration and the detection limit was 0.04 ng/ml. The relative standard deviation for 10 determinations at the 0.4-ng/ml level was 7.0%.

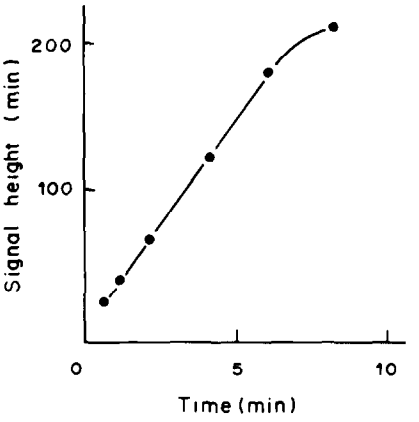

Fig. 3. Effect of electrolysis time on signal for a 4-ng/ml sample.

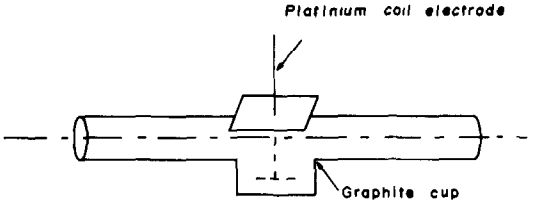

Fig. 4. Position of cathode in graphite cup.

Interferences

The determination of mercury at the 0.4-ng/ml level was not affected by the presence of 200-ng/ml levels of Fe^{2+}, Cd^{2+}, Mn^{2+}, Cr^{3+}, Pb^{2+}, Cu^{2+}, Ni^{2+} and Al^{3+} under the recommended conditions.

Determination of mercury in water samples

Four water samples (60 ml) were analysed by the standard-addition method. The results are shown in Table 1; apparent recoveries of 91–104% were obtained in the analysis of four 60-ml water samples spiked with 52.1 ng of mercury.

Conclusions

A major advantage of this method is that the whole atomization procedure is conducted in an ordinary

Table 1. Determination of mercury in 60-ml water samples

Water sample	Hg added, *ng*	Hg found*, *ng*	Recovery,† %
No. 1 mineral water	—	10.4	
	52.1	64.7	104
No. 2 mineral water	—	13.3	
	52.1	60.8	91
Dian Shan lake water	—	13.0	
	52.1	65.4	101
Campus river water	—	85.8	
	52.1	135.0	94

*Means of 3 determinations.
†Of added mercury.

graphite cup atomizer, without modification, so the method can conveniently be used for the routine determination of traces of mercury with any electrothermal AAS equipment, and requires in addition only a simple three-electrode system for controlling the potential of the platinum coil electrode, such as a common polarograph or other controlled-potential electrochemical instrument.

Acknowledgement—We are very grateful to Professor Xu Chung-Ging for his help in doing this work.

REFERENCES

1. G. Charlot, *Colorimetric Determination of Elements*, Elsevier, Amsterdam, 1964.
2. N. S. Poluektov, R. A. Vitkum and Y. V. Zelyukova, *Zh. Analit. Khim.*, 1964, **19,** 873.
3. W. R. Hatch and W. L. Ott, *Anal. Chem.*, 1968, **40,** 2085.
4. H. Brandenberger and H. Bader, *At. Abs. Newsl.*, 1967, **6,** 101.
5. *Idem*, *ibid.*, 1968, **7,** 53.
6. K. H. Schaller, P. Strasser, P. Woitowitz and D. Szadkowski, *Z. Anal. Chem.*, 1971, **256,** 123.
7. P. Deldime and Van Tran Trieu, *Anal. Lett.*, 1976, **9,** 169.
8. D. A. Frich and D. E. Tallman, *Anal. Chem.*, 1982, **54,** 1217.

Talanta, Vol. 32, No. 11, pp. 1019–1022, 1985
Printed in Great Britain.

0039-9140/85 $3.00 + 0.00

MOLECULAR ABSORPTION SPECTROMETRY (MAS) BY ELECTROTHERMAL EVAPORATION IN A GRAPHITE FURNACE—XIII*

DETERMINATION OF TRACES OF FLUORIDE BY MAS OF AlF AFTER LIQUID–LIQUID EXTRACTION OF FLUORIDE WITH TRIPHENYLANTIMONY(V) DIHYDROXIDE

K. DITTRICH†
Department of Chemistry, Karl-Marx-University Leipzig, 7010 Leipzig, G.D.R.

and

V. M. SHKINEV and B. V. SPIVAKOV
Vernadsky Institute of Geochemistry and Analytical Chemistry, Academy of Sciences, Moscow V334, U.S.S.R.

(*Received* 29 *October* 1984. *Revised* 5 *July* 1985. *Accepted* 9 *August* 1985)

Summary—The determination of traces of fluoride by means of the molecular absorption of AlF volatilized in graphite cuvettes is described. An extraction method for separation and preconcentration of the fluoride has been developed, to avoid matrix effects. The fluoride is extracted with $10^{-3}M$ triphenylantimony(V) dihydroxide in MIBK, and stripped with $0.025M$ barium hydroxide. The method is sensitive and specific for fluoride. The detection limit is about 0.3 ng of fluoride, and the fluoride content of 6 ml of $10^{-7}M$ solution can be determined. The determination is possible in presence of various ions, but it is estimated that usage of trace matrix separation leads to a considerable improvement in the relative detection limits (by 2–3 orders of magnitude), levels as low as 0.01 ppm being detectable in some matrices.

As indicated in our previous papers on chloride and bromide,[1,2] determination of fluoride is an important and difficult practical problem. Sensitive determination of fluoride is possible with ion-selective electrodes,[3–5] but the accuracy is not always adequate in the presence of various other ions. As shown by us[6–10] and others[3,11,12] sensitive and selective determination of fluoride is possible by means of molecular absorption spectrometry of diatomic metal–fluoride molecules (*e.g.*, AlF, GaF, InF, MgF).

An important problem in MAS with electrothermal atomization is the significant interference from the matrix. We showed earlier[1,2] that liquid–liquid extraction with triphenyltin hydroxide (TPTH) followed by stripping with sodium or barium hydroxide solution improves the sensitivity and accuracy of MAS determination of Br^- and Cl^- as AlBr and AlCl respectively. This extractant is not successful for fluoride, however, because the stripping is difficult.

Schweitzer and McCarthy[13] have shown the usefulness of triphenylantimony dihydroxide (TPSbDH) for extraction of anions, and Chermette *et al.* have used it for extraction of halides.[4,5,14,15]

In the present work we have studied the extraction of fluoride by TPSbDH from acidic solutions, for its preconcentration and separation from large amounts of other anions and cations. The data obtained were used to develop a method for determination of fluoride in aqueous solution by molecular absorption spectrometry (MAS) in hot graphite tubes.

*Part XII, *Anal. Chim. Acta*, 1984, **160**, 323
†Author for correspondence.

EXPERIMENTAL

Apparatus

The molecular absorption was measured with a Jarrell-Ash double-channel double-beam AA-spectrometer, type 811, fitted with a Beckman graphite-furnace, type 1268. The light-source was a hydrogen hollow-cathode lamp run at 35 mA. The molecular absorption of AlF was measured at 227.6 nm.

For background correction the two-line method was used, the non-specific wavelength being 226.4 nm. The distribution of fluoride between the organic and aqueous phase was estimated by MA measurements.

Reagents

TPSbDH solutions were prepared by equilibration (shaking time 3 min) of $10^{-3}M$ triphenylantimony(V) dibromide (12.5 mg in 25 ml) in *o*-xylene, MIBK, pentyl acetate, or mixed solvents, with successive portions of $0.2M$ sodium hydroxide in doubly distilled water (phase-volume ratio 1:1) until no further bromide was found in the aqueous phase. The organic phase was washed free from the hydroxide with water and then filtered. The last washing had pH < 7. The concentration in the diluent was $10^{-3}M$ ($10^{-2}M$ can be achieved if desired) and the concentration of fluoride in the initial aqueous solution was 10^{-7}–$10^{-4}M$ for the extraction studies.

The following aqueous stock solutions were used: Al^{3+} 10 mg/ml (prepared from the nitrate); NaOH 0.2*M*; $Ba(OH)_2$ 0.05*M*; F^- 0.1*M*; X 10 mg/ml (X = Cl^-, SO_4^{2-}, sodium salts), M 10 mg/ml (M = Al^{3+}, Li^+, Cu^+, Zn^{2+}, Mg^{2+}, Ca^{2+}, La^{3+}, Fe^{3+}, prepared from the nitrates).

Procedures

Analytical investigations without extraction. Volumes of 10 μl of solutions containing F^-, Al^{3+}, and Ba^{2+} were placed in the graphite furnace. After drying and ashing the substances were evaporated in the so-called atomization step (better termed the volatilization step) and the MA signal for AlF was measured.

Analytical determinations with extraction. Stoppered plastic test-tubes or separatory funnels were used for distribution of fluoride between the two phases. The extraction was done with different V_o/V_{aq} ratios. For $V_o = V_{aq}$ the volume of each phase was 1.5 ml. The extraction studies were done at room temperature and the phases were shaken for 3 min. It was established that equilibrium was attained in less than 3 min in all the systems studied. Back-extraction was done with 0.05*M* barium hydroxide containing 0.1 mg of Al^{3+} per ml. An aliquot of the resulting aqueous phase was placed directly in the graphite furnace.

To determine the degree of extraction, appropriate amounts of Al^{3+} and $Ba(OH)_2$ for direct determination of fluoride by MA were added to the aqueous phase left after the initial extraction.

RESULTS AND DISCUSSION

Investigation of the extraction

The data in Table 1 on the extraction of fluoride from water (pH = 6) with $V_o/V_{aq} = 1$, as a function of fluoride concentration in the initial aqueous solution (C_{F^-}) show that high recovery values are obtained for $C_{F^-} \leqslant 2 \times 10^{-4}M$ with $10^{-3}M$ triphenylantimony(V) dibromide (TPSbDBr) in *o*-xylene. This reagent was used at first because during preparation of TPSbDH solution in *o*-xylene a white precipitate was formed and after separation of this precipitate fluoride could not be extracted with the reagent. For back-extraction with barium hydroxide, however, TPSbDBr is not convenient, because a lot of bromide is also back-extracted and interferes with the AlF measurement.

We therefore tried other organic solvents, which could be used to prepare TPSbDH solutions as described above. The results are shown in Table 2. When mixed solvents were used a precipitate formed during the fluoride extraction and the recovery values showed that this precipitate contained fluoride. MIBK and PA gave good recovery and fast phase separation. For further investigation we used MIBK but PA could equally well be used. We found that shaking with $10^{-3}M$ TPSbDH in MIBK for 3 min at a phase-volume ratio $V_{aq}:V_o = 5:1$ would give a fivefold preconcentration and complete recovery of fluoride at concentrations from 2.5×10^{-6} up to $10^{-4}M$. For higher fluoride concentrations a more concentrated DPSbDH solution (*e.g.*, $10^{-2}M$) must be used. This is a useful technique for separation of fluoride from metals which form complexes with it (cf. Fig. 1).

Table 1. Influence of the fluoride concentration on the extraction into $10^{-3}M$ TPSbDBr ($V_o = V_{aq}$; 3 min extraction)

C_{F^-}, M	Extraction (recovery), %
1×10^{-4}	100
2×10^{-4}	100
4×10^{-4}	74

We also investigated the influence of the pH of the initial aqueous solution and found that the extraction of $10^{-4}M$ F^- ($V_o:V_{aq} = 1:1$ or 1:5) is quantitative between pH 6 and 0.

The back-extraction with barium hydroxide solution was also investigated, with phase-volume ratios $V_o:V_{aq} = 1:1$ or 2:1. The results in Table 3 show it is necessary to use a barium hydroxide concentration $>0.025M$. There is no interference caused in the back-extraction when aluminium ions are present in the aqueous phase, and this allows the stripping to be done with a reagent mixture that provides the correct medium for the MA measurements. It is also possible to use sodium hydroxide for back-extraction but this interferes in the MA determination.

Fluoride determination by MA

Optimization of conditions. In our previous papers[6,7] we showed that it is possible to determine traces of fluoride with a reciprocal sensitivity for AlF-measurement of 0.04 ng of fluoride per μl for an absorbance of 0.01. If barium hydroxide is used instead of sodium hydroxide this value can be improved to 0.03 ng/μl. This means it is possible to determine fluoride directly in the aqueous phase at initial concentrations down to $3.2 \times 10^{-6}M$ (the original sample is mixed with an equal volume of barium hydroxide/aluminium solution, so there is a dilution factor of 2).

From the investigation described above we found the following optimal conditions for extraction. In a stoppered 10-ml plastic (polyethylene) tube place 6 ml of aqueous sample and if necessary adjust the pH to 1–3 by addition of a small volume of concentrated nitric acid. Add 1.2 ml of 10^{-2}–$10^{-3}M$ TPSbDH in MIBK and shake the mixture for 3 min. Separate the phases and remove 0.8 ml of the organic phase in four 200-μl portions by micropipette, placing it in a 1.5-ml plastic tube. Add 0.4 ml of 0.05*M* barium hydroxide (containing 40 μg of Al^{3+}) and shake the mixture for 3 min. Place 10 μl of the separated aqueous phase in the furnace for analysis.

Table 2. Influence of organic solvents on the extraction of $2 \times 10^{-4}M$ fluoride by $10^{-3}M$ TPSbDH ($V_o = V_{aq}$; pH = 6; 3 min extraction)

Solvent	Extraction (recovery), %
Methyl isobutyl ketone (MIBK)	100
Pentyl acetate (PA)	100
o-Xylene/butan-1-ol (70/30)	87.5
o-Xylene/decan-1-ol (70/30)	90

Table 3. Fluoride determination by AlF MA in presence of various ions with and without extraction*

Matrix ion	Concentrations in the initial solution, M	Detection limit for F^-, without extraction, ppm†	Concentrations in the initial solution, M	Detection limit for F^-, with extraction, ppm†	Improvement factor
Li^+	$F^-:5\times10^{-6}/Li^+:1.4$	10	$F^-:1.5\times10^{-7}/Li^+:14$	0.03	3.3×10^2
Mg^{2+}	$F^-:6\times10^{-6}/Mg^{2+}:0.16$	30	$F^-:1.5\times10^{-7}/Mg^{2+}:4.1$	0.03	1×10^3
Ca^{2+}	$F^-:6\times10^{-6}/Ca^{2+}:5\times10^{-2}$	60	$F^-:3\times10^{-7}/Ca^{2+}:2.5$	0.06	1×10^3
Cu^{2+}	$F^-:4\times10^{-6}/Cu^{2+}:0.15$	8	$F^-:2\times10^{-7}/Cu^{2+}:0.8$	0.075	1.1×10^2
Zn^{2+}	$F^-:3.5\times10^{-6}/Zn^{2+}:0.15$	7	$F^-:2\times10^{-7}/Zn^{2+}:0.8$	0.07	1×10^2
La^{3+}	$F^-:6\times10^{-6}/La^{3+}:0.007$	120	$F^-:1.9\times10^{-7}/La^{3+}:0.7$	0.04	3×10^3
Fe^{3+}	$F^-:6\times10^{-6}/Fe^{3+}:0.09$	24	$F^-:3\times10^{-7}/Fe^{3+}:0.02$	5	48
Al^{3+}	$F^-:6\times10^{-6}/Al^{3+}:0.18$	24	$F^-:3\times10^{-7}/Al^{3+}:0.02$	12	2
Cl^-	$F^-:6\times10^{-6}/Cl^-:0.3$	12	$F^-:3\times10^{-7}/Cl^-:2.8$	0.06	2×10^2
SO_4^{2-}	$F^-:8\times10^{-6}/SO_4^{2-}:0.1$	15	$F^-:3\times10^{-7}/SO_4^{2-}:1.0$	0.03	5×10^2

*Conditions without extraction: 50-μl sample, 1:1 dilution with 0.1 *M* $Ba(OH)_2$ (containing 2 μg of Al^{3+} per 10 μl); injection volume 10 μl.
Conditions with extraction: 6000-μl sample for extraction with 1.2 ml of extractant and back-extraction of 0.8 ml of organic phase with 0.4 ml of aqueous phase, as described; injection volume 10 μl.
†Ratio of weight of fluoride to weight of matrix species. The detection limit refers to the ratio at which the MAS signal is 50% of that obtained in absence of the matrix; under these conditions the absolute detection limit is 0.6 ng of F

No loss of fluoride was found to occur in the extraction. The absolute reciprocal sensitivity is the same whether extraction is used or not, 0.03 ng of fluoride per μl of final test solution giving an absorbance of 0.01, but the relative reciprocal sensitivity is improved to $1.6\times10^{-7}M$ fluoride in the original sample for an absorbance of 0.01. There is thus a 20-fold enhancement in sensitivity when the extraction method is used.

If necessary the relative reciprocal sensitivity can be further improved in two ways. First, the phase-volume ratio during the preconcentration can be further increased (*e.g.*, $V_{aq}:V_o = 20$ or 40); we have proved that the recovery for pure solutions is still 100%. Secondly, the analyte volume placed in the furnace can be increased to 20 or 40 μl. This has also been tested and the results show that this procedure is accurate and precise. Thus the enhancement of sensitivity can be further increased to $2\times10^{-8}M$ fluoride for 0.01 absorbance.

As an absorbance of 0.01 is about three times the standard deviation of the blank signal, the detection limit is also $2\times10^{-8}M$. The same results can be obtained by using $10^{-3}M$ TPSbDH in pentyl acetate.

Interference of cations. Figure 1 shows that in most cases there is strong interference by higher concentrations of cations when direct analysis is used, but these interference effects are decreased by the extraction method. To show the improvement achieved by using extraction we use the same scale on the interferent concentration axis in both cases. That is, for the direct analysis (without extraction) these are the real concentrations in the initial aqueous phase, but for the analysis by means of extraction the numbers on the scale are ten times the concentration in the initial solution because for any interferents extracted there would be a tenfold concentration.

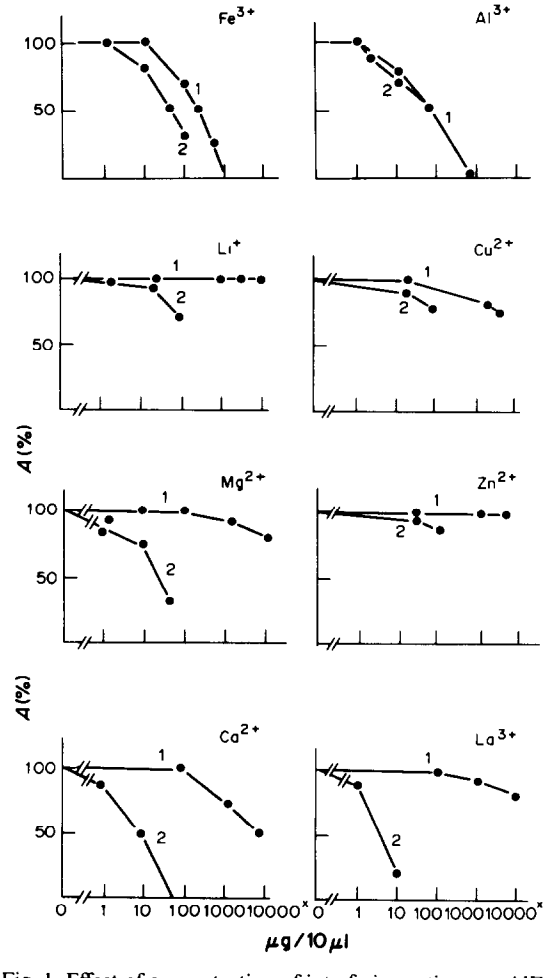

Fig. 1. Effect of concentration of interfering cations on AlF MA signals for 10 ng of F^- per μl: 1, extraction with TPSbDH and back-extraction with $Ba(OH)_2$; 2, without extraction, determination in presence of interferents.

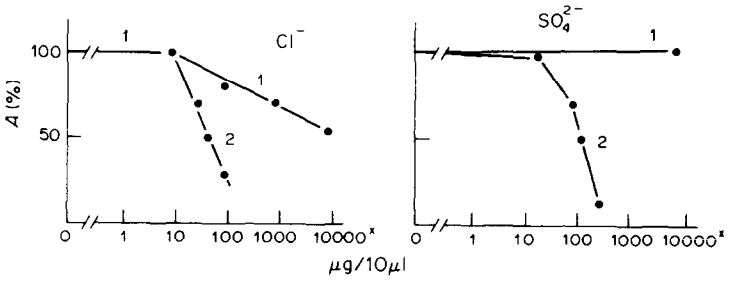

Fig. 2 Effect of concentration of some interfering anions on AlF MA signals; conditions as for Fig 1

The reasons for the depressive effects are very complicated. The effects can occur in the plasma and in the liquid and solid phases. In the plasma the interference of a metal M depends on the dissociation energies of the molecules MF and AlF. In the liquid and solid phases substances may be formed which can cause loss of fluoride by complexation *etc.*

The strong influence of Ca, Mg, and La can be explained as due to the plasma effects. The smaller influence of Zn and Cu confirms this opinion, because the stability of their fluorides in the gas phase is very low.

The influence of Fe^{3+} in the direct determination (without extraction) is due to complex formation between Fe^{3+} and F^- ions and its effect on the thermal decomposition in the furnace. A similar situation exists for large excesses of Al^{3+}, because the buffering action of $Ba(OH)_2$ on the thermal decomposition is diminished. Also large amounts of Al can be volatilized only slowly, so the equilibrium $Al + F \rightleftharpoons AlF$ is not shifted to the right. The extraction mode is also influenced by Al^{3+} and again by fluoride complex formation. In this case $10^{-2}M$ TPSbDH in MIBK should be used.

The relatively small influence of Li^+ in the direct determination without extraction is not clear, because the dissociation energy of LiF (6.0 eV) is high. Perhaps in this case there is fractionated evaporation of the easily volatile lithium salt, but this is only an assumption.

From the curves in Fig. 1 it is possible to calculate the detection limits for fluoride in the presence of various metal ions. For this purpose we used the values of the reciprocal sensitivity for 0.01 absorbance because we estimated experimentally that with our equipment this absorbance is generally about 3 times the standard deviation of the blank. From this value it is possible to calculate the improvement factors. The results are shown in Table 3, which shows that in most cases improvement factors of 2–3 orders of magnitude are achieved. We can distinguish two groups of elements: (1) Li^+, Cu^{2+}, Zn^{2+}, Fe^{3+}, Al^{3+} and (2) Mg^{2+}, Ca^{2+}, La^{2+}. The better improvement factors of the latter group are due to the interference of these elements being much stronger in the direct determination without extraction.

Interference of anions. Figure 2 shows the effect of chloride and sulphate, which both interfere strongly in the direct determination but for different reasons. Chloride interferes in the plasma, by the exchange reaction

$$AlF + Cl \rightleftharpoons AlCl + F$$

as a result of which the AlF concentration is decreased in the presence of higher amounts of chloride.

Sulphate influences the procedure in the liquid and solid phase by volatilization of the more easy volatile HF by pyrohydrolysis reactions. Besides this, it is impossible to use barium hydroxide as matrix modifier; only sodium hydroxide can be used, but this gives poorer performance than barium hydroxide. In both cases extraction gives improvement. Chloride is also extracted and back-extracted and thus still influences the plasma composition, but the extraction of fluoride is better than that of chloride and the concentration of TPSbDH used limits the amount of chloride that can be extracted. No evidence was found that sulphate is extracted. The analytical possibilities of both procedures are indicated in Table 3.

Conclusions

The combination of determination of traces of fluoride by MAS of AlF with fluoride separation from the matrix by extraction with TPSbDH solution is very useful for improvement of the sensitivity and also of the accuracy.

REFERENCES

1. K. Dittrich, B. Ya. Spivakov, V. M. Shkinev and G. A. Vorobeva, *Talanta*, 1984, **31**, 341.
2. *Idem, ibid.*, 1984, **31**, 39.
3. K. Chiba, K. Tsunoda, H. Haraguchi and K. Fuwa, *Anal. Chem.*, 1980, **52**, 1582.
4. H. Chermette, C. Martelet, D. Sandino, M. Benmalek and J. Tousset, *Anal. Chim. Acta*, 1972, **59**, 373.
5. H. Chermette, C. Martelet, D. Sandino and J. Tousset, *Anal. Chem*, 1972, **44**, 857
6. K. Dittrich, *Anal. Chim Acta*, 1979, **111**, 123.
7. K. Dittrich and P. Meister, *ibid.*, 1980, **121**, 205.
8. K. Dittrich and P. Vorberg, *ibid.*, 1982, **140**, 237.
9. K. Dittrich, B. Vorberg, J. Funk and V. Beyer, *Spectrochim. Acta*, 1984, **39B**, 349
10. K. Dittrich and B. Vorberg, *Chem. Analit. (Warsaw)*, 1983, **28**, 539.
11. K. Tsunoda, K. Fujiwara and K. Fuwa, *Anal. Chem.*, 1977, **49**, 2035.
12. K. Tsunoda, H. Chiba, H. Haraguchi and K. Fuwa, *ibid.*, 1979, **51**, 2059.
13. G. K. Schweitzer and S. W. McCarthy, *J. Inorg. Nucl. Chem.*, 1965, **27**, 191.
14. H. Chermette, C. Martelet, D. Sandino and J. Tousset, *ibid.*, 1972, **34**, 1627.
15. M. Benmalek, H. Chermette, C. Martelet, D. Sandino and J. Tousset, *ibid.*, 1974, **36**, 1359.

Talanta, Vol. 32, No. 11, pp 1023–1026, 1985
Printed in Great Britain

0039-9140/85 $3.00 + 0.00
Pergamon Press Ltd

DETERMINATION OF CARBONATE ALKALINITY AND APPARENT DISSOCIATION CONSTANTS IN A MULTIPROTOLYTIC SYSTEM

ZVI-HAI BURBEA and DIDIO HAIMOVITS
Department of Nephrology, Soroka Medical Center, Beer-Sheva, Israel

and

SAM BEN-YAAKOV*
Department of Electrical and Computer Engineering, Ben-Gurion University of the Negev, Beer-Sheva, Israel

(*Received* 22 *August* 1984. *Revised* 10 *June* 1985. *Accepted* 2 *August* 1985)

Summary—A method for analysing the carbonate system in a multicomponent solultion is presented, which does not need knowledge of the total composition of the system. It is based on two titrations with acid, starting at the same pH, one of the original solution and the other after removal of carbonate species as carbon dioxide and restoration of the pH to the value for the original solution by addition of carbonate-free base. The differential titration curve, obtained by subtracting one titration curve from the other, is associated with the carbonate system. A procedure is proposed for calculating from the differential titration curve the apparent first and second dissociation constants of carbonic acid, total CO_2 and the carbonate alkalinity at the original pH of the solution.

It is well recognized that the carbonate system plays a major role in natural waters and biological fluids as well as in many industrial processes. Consequently, there is often a need to characterize it in various solutions of complex ionic composition. Since the apparent dissociation constants[1] of carbonic acid, which are usually applied in such cases, are dependent on the ionic strength and composition of the medium,[2] there is the additional problem of determining the constants in the test solution. This problem can be approached by a general purpose strategy in which an attempt is made to determine all the components of protolytic species by an acid–base titration,[3–5] but difficulties can arise because of the large number of unknowns to be determined and possible overlap of reaction equilibria. Although statistical analyses have been suggested to improve matters,[6,7] this approach is futile when the solution contains other species which exhibit protolytic behaviour over the same pH range as the carbonate system. For example, a high phosphate concentration would severely interfere in any attempt to determine the components of the carbonate system from an acid–base titration.

In the present investigation we explored the possibility of analysing the carbonate system, in a multiprotolytic system, by separating the titration response of the carbonate system from that of other protolytes present. This was accomplished by means of the difference between acid–base titration curves obtained with and without the carbonate system present. The titration curve for the carbonate-free solution was obtained by driving off carbon dioxide from the original solution at low pH and titrating the modified sample. It can be shown that the differential titration curve is a function of only the carbonate system and hence can be used to determine the components and apparent constants of this system. The suggested approach was applied to study of the carbonate system and total alkalinity in the urine of healthy adults, to improve characterization of the mechanism of hydrogen-ion secretion by the kidney and the sources of high pCO_2 differentials between the blood and urine.

THEORETICAL CONSIDERATIONS

The total charge held by the ions in a complex solution can be divided into two parts: the ionic charge of the protolytic species (QP), and the charge of the non-protolytic species (QN).[8] The term "protolytic species" means those components that can interact with H^+ (or OH^-) over the pH-range of interest. This definition is akin to the definition of "alkalinity" suggested recently,[9] except that it is more loosely defined.

The charge held by the protolytic species (which is assumed here to be negative to conform with the concept of "alkalinity") at any stage during an acid titration, $(QP)_t$, can be related to the initial value $(QP)_0$ by:

$$(QP)_t = (QP)_0 - V_t N_a$$

$$= \sum_i (TC)_i V_0 B_i(pH_t, K'_{1_i}, K'_{2_i} \ldots K'_{j_i}) + ([OH^-] - [H^+])(V_0 + V_t) \quad (1)$$

*To whom all correspondence should be addressed.

where $(TC)_i$ is the total concentration of the ith component, V_0 the initial volume of solution, N_a the normality of the titrant acid, V_t the volume of acid added by stage t in the titration, pH_t the pH at stage t, K'_j the jth apparent dissociation constant of component i, and B_i relates the total charge of component i to $(TC)_i$. For the carbonate system:[1]

$$(TC)_{CO_2} = [H_2CO_3^*] + [HCO_3] + [CO_3^{2-}] \quad (2)$$

where

$$[H_2CO_3^*] = [CO_2(aq)] + [H_2CO_3] \quad (3)$$

The function B for the carbonate system can be written explicitly in the form:

$$B_{CO_2} = \frac{\{H^+\}K'_1 + 2K'_1K'_2}{\{H^+\}^2 + \{H^+\}K_1 + K_1K_2} \quad (4)$$

where $\{H^+\}$ is the activity of H^+ as measured by a glass electrode, and K_1 and K_2 are the apparent first and second dissociation constants of carbonic acid. In this case, the carbonate alkalinity,[1] (CA), at a given pH is related to $(TC)_{CO_2}$ by

$$(CA) = (TC)_{CO_2} B_{CO_2} \quad (5)$$

If the titration with acid is continued to a pH at which carbonic acid is virtually completely undissociated, *e.g.*, $pH < pK'_1 - 2$, and carbon dioxide is then stripped off and the pH restored to that of the solution *before* the titration, by addition of base of normality N_b, the (QP) of the restored solution, $(QP)_R$, will be

$$(QP)_R = (QP)_0 - V_aN_a + V_bN_b \quad (6)$$

where V_a and V_b are the total volumes of added acid and base, respectively. Hence, (QP) during acid titration of the carbonate-free solution, $(QP)'_t$, will be:

$$(QP)'_t = (QP)_0 - V_aN_a + N_bV_b - V'_tN_a \quad (7)$$

where V'_t is the volume of acid added by stage t in the second titration. By subtracting $(QP)'_t$ from $(QP)_t$ at points of equal pH along the titration curves we obtain

$$\begin{aligned}(QP)_t - (QP)'_t &= N_aV_a - N_bV_b - N_a(V_t - V'_t) \\ &= (TC)_{CO_2} V_0B_{CO_2} + ([OH^-] - [H^+]) \\ &\quad \times (V_t - V_a - B_b - V'_t) \quad (8)\end{aligned}$$

The last term in equation (8) is negligibly small since the two factors are small, the first because titrations are usually done within the range in which $[H^+]$ and $[OH^-]$ are small compared to (QP), and the second because N_a and N_b can be made high enough for the volume difference to be only a small fraction of the total volume. The equation can thus be rewritten in the form:

$$\frac{N_aV_a - N_bV_b - N_a(V_t - V'_t)}{V_0} = (TC)_{CO_2} \frac{\{H^+\}K'_1 + 2K'_1K'_2}{\{H^+\}^2 + \{H^+\}K'_1 + K'_1K'_2} = z \quad (9)$$

Following an approach suggested earlier,[10] this equation can be rewritten in a linear form:

$$y = m + kx \quad (10)$$

where

$$\begin{aligned}x &= z(K'_2 + \{H^+\})/(2K'_2 + \{H^+\}) \\ y &= z(K_2 + \{H^+\})/(2K'_2 + \{H^+\}) \\ m &= (TC)_{CO_2} K'_1 \\ k &= -K'_1\end{aligned}$$

The equation can be solved for m and k by an iterative least-squares fitting procedure in which K'_2 is incremented by trial and error until a best fit is obtained.[10,11] The K'_2 that gives the best fit, together with the $(TC)_{CO_2}$ calculated from the resulting m and k, will constitute a complete characterization of the carbonate system in the original complex solution.

It should be emphasised that the analytical and computational procedure given above for the determination of K'_1, K'_2 and $(TC)_{CO_2}$ implicitly assumes that the apparent constants of all the protolytic species stay constant during the whole procedure. The error introduced by this assumption should be negligible if the dilution during titration is small (*i.e.*, if $V_a \ll V_0$ and $V_b \ll V_0$ and if there is no appreciable change in the ionic strength due to the addition of acid and base and the elimination of CO_2 from the solution.

The foregoing analysis also assumes that $(TC)_{CO_2}$ during any given titration is kept constant, *i.e.*, that there is no appreciable exchange of CO_2 between the solution and the overlying gas phase. This could prove to be a problem if $(TC)_{CO_2}$ is large enough to cause a high p_{CO_2} build-up at low pH. In such cases the approach given by Edmond[12] might be adopted, in which the titration is done in a completely sealed flask with a bellows or other means of allowing addition of acid during the titration. We have found, however, that if the stirring is slow the rate of CO_2 exchange does not constitute a problem.

The second titration, after CO_2 has been stripped off, can be done by back-titration with sodium hydroxide or by the method selected by us, *viz.* restoring the pH by addition of alkali, followed by titration with acid. The latter method was chosen for two practical reasons: one is that it does not require a second motor-driven burette and the other is that a burette used for dispensing alkali requires a guard tube to eliminate contamination with atmospheric carbon dioxide. However, the method introduces an additional source of uncertainty. Another point that should be made is the practical problem which might arise when attempting to subtract $(QP)'_t$ from $(QP)_t$ to obtain the differential titration curve. Since the titrations are usually done by adding equal increments of acid, a pH-value on the second titration curve that is identical with that at a particular titration point on the first curve will not coincide with a titration point, so direct subtraction of V'_t from V_t is impossible. The

problem can be overcome either by performing a titration in fixed pH increments, *i.e.*, with variable increments of acid, or by fitting a polynomial to the titration curve and recalculating the volume increments for the equi-pH points. The latter approach was applied here since the titration system[13] delivers equal increments of titration acid.

EXPERIMENTAL

Instrumentation

The microcomputer-based titration system was similar to the assembly described earlier.[13]

Solutions

The test solution was artificial urine[14] of ionic strength 0.165*M* and total phosphate concentration 0.015*M*. The salts were dissolved in 0.1*M* hydrochloric acid to prevent precipitation of calcium sulphate. The pH was then raised to about 7 by neutralization with sodium hydroxide while air was bubbled through the solution to equilibrate it with atmospheric carbon dioxide.

Titration and computation

The first titration was done with 1*M* hydrochloric acid to pH 2.5, the CO_2 was stripped by passage of nitrogen, the pH was restored to not less than the original value (but not more than 0.2 pH units higher) by addition of 5*M* sodium hydroxide, and the second titration was also done with 1*M* hydrochloric acid to about pH 2.5. The titration curves were fitted to a high-order polynomial of the form

$$V_t = \sum_{j=0}^{P} A_j(\mathrm{pH}_t)^j \qquad (11)$$

where P is the order of the polynomial. Usually a 7th order polynomial was found to fit the complete titration curve well. By use of these experimental polynomials, the differential titration curve was calculated by evaluating $(V_t - V_t')$ for equally spaced pH values. The differential titration curve was then used in the iterative least-squares fitting procedure[11,13] to derive $K_1'K_2'$ and $(TC)_{CO_2}$ for the original solution. All calculations were done by computer programs written in BASIC and run on a microcomputer system which comprised a Commodore CBM 3032, a printer, a dual disc-driver model 3040, a cassette deck, and a Textronic model 4662 x-y plotter. The system is compatible with the magnetic recording formats of the microcomputer-based titrator.[13] It should be emphasised that the mention of specific hardware models is only for information and does not constitute an endorsement or recommendation of specific brands.

RESULTS AND DISCUSSION

A typical set of results, including the titration curves for the original solution and the CO_2-free solution, and the differential titration curve, is exemplified in Fig. 1. The solid lines connecting the points of the first and second titration curves are for the 7th degree polynomial used. Fitting the polynomial to the complete titration curve, as in Fig. 1, is not really necessary, since the points below pH 5 add little to the regression line [(equation 10)] from which K_1' and K_2' are derived. Hence, it would suffice to perform the fitting over a limited range from the original pH (pH_0) to about pH 5. This considerably eases the task of choosing the polynomial since this portion of the titration curve does not include a sharp inflection and hence a lower-degree polynomial will suffice.

The shape of the differential titration curve (Fig. 1, DIF) is sigmoid and independent of pH below a certain critical value (~ 5), as a direct consequence of the fact that the two titration curves, for the original and CO_2-free solution, are identical in the pH range where the carbon dioxide is virtually all present as undissociated H_2CO_3 and dissolved CO_2 [CO_2 (aq)]. In this pH range, the buffering is controlled by the other protolytic species and not by the carbonate

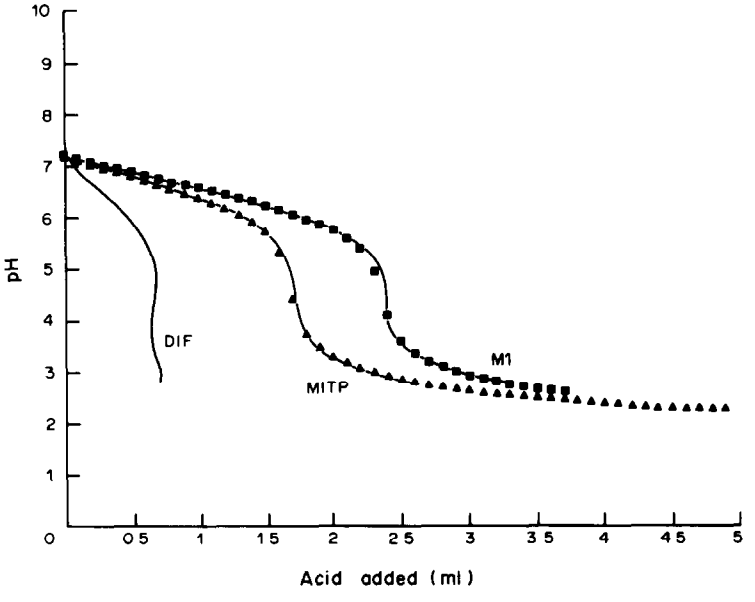

Fig. 1. Acid titration curves for original artificial urine before (M1) and after (MITP) driving off CO_2, and the difference between the two curves (DIF).

Table 1. Titration results for artificial urine sample

pH_0*	Ionic strength, M	pH_t†	Carbonate alkalinity, *meq/l.*	$(TC)_{CO_2}$, *m*M	pK'_1	pK'_2	R^2§
7.65	0.165	7.75	16.4	16.5	6 25	9.59	0.99992

*Initial pH of sample.
†Initial pH of sample in second titration
§Correlation coefficient of least-squares fitting.

system, in either titration. This conclusion can be arrived at mathematically by noticing that for $pH < pK'_1 - 2$, *i.e.*, when $B_{CO_2} \rightarrow 0$, equation (5), the differential titration curve, equation (8), is reduced to

$$N_a V_a - N_b V_b - N_a(V_t - V'_t) = 0 \qquad (12)$$

By application of the iterative procedure for the best fit of the data to the straight line of equation (10), K'_2 was guessed and $(TC)_{CO_2}$ calculated from the slope and intercept of the line (Table 1). The criterion chosen for the goodness of fit was the correlation coefficient, which exhibits a maximum for the best K'_2, as discussed by Sass and Ben-Yaakov.[10]

It should be emphasised that a precondition for accurate K'_1 and/or K'_2 determination is that the titration curves used in the curve fitting include points with pH values which are numerically close (say within one unit) to the pK' of interest. Points with pH values too far from the pertinent pK' are insensitive to that dissociation constant and hence cannot be used to obtain a valid value for it. Consequently, the K'_2 values obtained here may have an appreciable uncertainty. However, since the value of pH_0 was at least 2 units smaller than pK'_2 the effect of K'_2 on the analysis was small and hence high accuracy was not essential in its determination in this case.

The carbonate alkalinity of the original solution can be calculated from pH_0 and the derived values of $(TC)_{CO_2}$, pK'_1 and pK'_2,[1] or by an acid–base balance [which is based on the fact that $(V_t - V'_t)$ at pH below, say, 4 is directly related to the carbonate alkalinity in the original solution, *i.e.*, the contribution of the carbonate system to (QP) at pH_0]. Carbonate alkalinity in the original sample can be directly calculated from equation (12) for pH values below pH 4.5, if the solution pH is restored to pH_0 by the base. If the restored pH differs from pH_0, the volume of base V_b required to reach the original pH_0 of the solution can be calculated from the polynomial fitting [equation (11)] to the second titration. It should be emphasised that the methods suggested here for calculaing the carbonate alkalinity in the original solution constitute, in fact, a hitherto novel approach to measuring a parameter (carbonate alkalinity) which could not have been estimated for a multiprotolytic system by published methods. Carbonate alkalinity estimation by the Gran or modified Gran methods[9,10,12,15] or by end-point titration[16,17] cannot be used for a multiprotolytic system, especially if the ionic composition of the solution is unknown. Similarly, no other published method is available for the determination of pK'_1 and pK'_2 of one species in a multipyrolytic system such as the one studied here.

The proposed method for estimating carbonate alkalinity and the apparent dissociation constants of carbonic acid in solutions of unknown ionic composition is limited, of course, to cases in which carbon dioxide is the sole protolytic gas present when the pH is lowered to below pH 4.5. This is not a severe limitation, however, especially in studying biological solutions, as ammonia is completely protonated at low pH. The method can be applied, for example, to urine, for better understanding of the relationships between $(TC)_{CO_2}$ and p_{CO_2} and to help resolve pending questions concerning the significance of high p_{CO_2} differentials between blood and urine.[18]

Acknowledgement—I should like to thank Dr R. A. Chalmers for his critical review of the manuscript, which helped to sort out some confusing inconsistencies.

REFERENCES

1. G. Skirrow, in *Chemical Ocenaography*, J. P. Riley and G. Skirrow (eds.), Vol. II, Academic Press, London, 1975.
2. S. Ben-Yaakov and M. B. Goldhaber, *Deep Sea Res.*, 1973, **20,** 87.
3. A. Sabatini, A. Vacca and P. Gans, *Talanta*, 1974, **21,** 53.
4. E. Gordon, *J. Phys. Chem.*, 1979, **83,** 1365.
5. *Idem, Anal. Chem.*, 1982, **54,** 1595.
6. M. Schartz and I. Gelb, *ibid.*, 1978, **50,** 1571.
7. A. Braibanti, F. Dallavalle, G. Mori and B. Veroni, *Talanta*, 1982, **29,** 725.
8. S. Ben-Yaakov, *Limnol. Oceanog.*, 1973, **18,** 80.
9. F. Pearson, *J. Water Pollut. Control. Fed.*, 1981, **53,** 1243.
10. E. Sass and S. Ben-Yaakov, *Mar. Chem.*, 1977, **5,** 183.
11. S. Ben-Yaakov and Y. Lorch, *ibid.*, 1983, **13,** 293.
12. J. M. Edmond, *Deep Sea Res.*, 1970, **17,** 737.
13. S. Ben-Yaakov, R. Raviv, H. Guterman, A. Dayan and B. Lazar, *Talanta*, 1982, **29,** 267.
14. K. J. Isselbacher, R. D Adams, E. Braunwald, R. G. Petersdorf and J. D Wilson, Appendix: *Laboratory Findings with Clinical Importance*, in: *Harrison's Principles of Internal Medicine*, 9th Ed., McGraw-Hill, Kogagusha, 1980.
15. G. Gran, *Analyst*, 1952, **77,** 661.
16. D. H. Anderson and R. J. Robinson, *Ind. Eng. Chem., Anal. Ed.*, 1946, **18,** 767.
17. C. H. Culberson, R. M. Pytkowicz and J. E. Hawley, *J. Mar. Res.*, 1970, **28,** 15.
18. J. Malnic, *Am. J. Physiol.*, 1980, **239,** F307.

Talanta, Vol 32, No 11, pp 1027 1033, 1985
Printed in Great Britain

0039-9140/85 $3.00 + 0.00
Pergamon Press Ltd

PREPARATION OF A MERCURY FILM ELECTRODE MODIFIED BY TRI-n-OCTYLPHOSPHINE OXIDE AND THE ELECTROCHEMICAL PROPERTIES OF THIS ELECTRODE

JIŘÍ LEXA
Chemical Laboratories, Central Research Institute, Škoda Works, 316 00 Pilsen, Czechoslovakia

KAREL ŠTULÍK
Department of Analytical Chemistry, Charles University, Albertov 2030, 128 40 Prague 2, Czechoslovakia

(*Received* 12 *April* 1985. *Accepted* 19 *June* 1985)

Summary—Mercury film electrodes have been prepared on silver metal and silver-coated glassy-carbon supports and have been modified by a film of tri-n-octylphosphine oxide (TOPO) in a poly(vinyl chloride) matrix. The electrodes have been characterized in detail and the effects of the modifying film parameters on their electrochemical properties have been studied. It has been shown that these electrodes permit selective and sensitive determinations of many metals. The most important parameters are the thickness of the modifying film, the modifier-to-matrix ratio in the modifying film and the base electrolyte composition. Data concerning the reactions of a number of metal ions on the modified electrode are given.

Chemically modified electrodes (CMEs) have been studied intensively and show great promise for various fields of chemistry and technology (see, for example, some recent reviews[1–5]). From the point of view of analytical chemistry, CMEs can be useful in two ways: (1) when the modifier catalyses the electrochemical reaction of the substance to be determined and thus improves the sensitivity of determination, and (2) when the modifier interacts selectively with a particular component in the test solution (*e.g.*, through ion-exchange, adsorption or liquid extraction), thus improving the selectivity of determination and sometimes also the sensitivity (preliminary accumulation of the substance on the electrode followed by electrochemical stripping). Electrodes can be modified either by very thin films of covalently bonded or adsorbed modifiers, or by thick polymeric films containing a modifier.

A number of recent publications[6–15] have outlined possible applications of CMEs in practical inorganic analysis. Normally solid electrodes are modified; only Lubert *et al.*[15] have attempted modification of a hanging mercury drop electrode.

In the present work we have studied the preparation of a CME suitable for a wide range of applications in inorganic trace analysis. We have chosen a mercury film electrode (MFE) as it is advantageous in electrochemical stripping analysis.[16] Tri-n-octylphosphine oxide (TOPO) has been selected as the modifier; it has been widely employed in selective liquid–liquid extraction procedures for many elements.[17,18] TOPO was earlier used to modify glassy-carbon electrodes,[13–15] permitting a sensitive and selective determination of uranyl ions; the method has been applied to sea-water analysis.[14] A drawback of this electrode, which is simply prepared by the evaporation of the solvent from a TOPO solution placed on the surface of a glassy-carbon electrode, is the poor mechanical stability of the modifying film, which must be prepared anew before each determination. Therefore, we have used an inert poly(vinyl chloride) (PVC) matrix in the preparation of our electrode.

In our study of the electrochemical properties of our CME we assumed that the selective properties of the modifying film could be estimated to a certain extent from the values of the extraction ratios for liquid–liquid extraction. Of course, the actual performance of the electrode will depend mainly on the thickness and structure of the modifying film, which together determine the electrical resistance of the film, the rate of transport of the electroactive substance toward the MFE surface and possibly also affect the kinetics of the charge-transfer reaction.

EXPERIMENTAL

Apparatus

A PA-2 polarograph (Laboratorní Přístroje, Czechoslovakia) was used, supplemented with an adapter of our own construction[19] for potentiometric and galvanostatic stripping measurements, and a model 4103 x–y plotter (Laboratorní Přístroje). The measurements were made with a three-electrode circuit consisting of the working stationary disk MFE modified by a TOPO film (TOPO-MFE), a silver–silver chloride reference electrode (1*M* sodium chloride, with a potential of −0.01 V *vs.* SCE) and a platinum counter-electrode immersed in the base electrolyte and separated from the working space by a porous glass plug (Corning, U.S.A.). The electrolysis vessel, permitting introduction and removal of the test solution through a single tube by pressure variation, has been described elsewhere.[20]

Small solution volumes were measured with Eppendorf micropipettes. The electrical resistance of the modifying film was measured by an RCL bridge (Metra, Czechoslovakia) at frequencies of 800–1000 Hz. In cyclic voltammetric measurements, the solution was deaerated by passage of pure argon; in the other measurements the solution was not

deaerated. All measurements were made at laboratory temperature (20 ± 2°) and the potential values were referred to the silver–silver chloride electrode. For polishing the electrode surface, 0, 3/0 and 5/0 emery papers (SIA, Switzerland) and a 1-μm alumina emulsion (Struers Scientific Instruments, Denmark) were used.

Reagents

The tri-n-octylphosphine oxide used as the modifier was obtained from Fluka, Switzerland. A highly pure PVC was prepared in the Institute of Macromolecular Chemistry, Czechoslovak Academy of Sciences, Prague and had the following parameters: m.w., 1.51×10^5; initiator (LiCl) residue, 11.0 mmole/g of PVC, sulphate ash, 0.07%; viscosity, 2.341 cP; specific volume, 4300 ml/kg. The modifier solution containing TOPO and 10% w/w PVC was always prepared immediately before use, by dissolving 20 mg of TOPO in 9.50 ml of tetrahydrofuran (THF, pure, unstabilized, from VEB Laborchemie Apolda, GDR) and adding 0.50 ml of 4-mg/ml PVC solution in THF.

For preparation of the 1-mg/ml metal stock solutions, 99.9% pure metals (Bi, Cu, Sb, Sn, In, Cd, Zn), and *p.a.* metal chlorides (Cr, Tl), arsenic(III) oxide, ammonium molybdate and uranyl nitrate were used. The metals were dissolved in dilute nitric (Bi, Cu, Cd) or hydrochloric (In and Zn) acid or concentrated sulphuric acid (Sb and Sn). Arsenic(III) oxide was dissolved in sodium hydroxide solution and acidified with sulphuric acid. Thallium(I) chloride was converted into the sulphate by evaporation with concentrated sulphuric acid. The other salts were dissolved in water. All other chemicals were of *p.a.* purity and were not further purified.

Preparation of the modified electrodes (TOPO-MFE)

In experiments with various polymers, the best results were obtained with a high molecular-weight PVC and thus this material was used for the electrode preparation. As mercury films deposited electrolytically on glassy carbon have poor mechanical stability and sometimes also show poor reproducibility,[16,21] silver was used, on the basis of preliminary experiments, for making the MFE. Two procedures have been developed for preparing the CME, differing in the preparation of the mercury film—mechanical (Procedure A) and electrolytic (Procedure B).

Procedure A. The surface of the electrode material (99.9% pure silver as a 5-mm diameter disk, in a PTFE insulating mantle) was polished with the emery papers and alumina emulsion and cleaned by a 2-min immersion in 5–10% solution of potassium hydroxide in ethanol, placed in an ultrasonic bath. The electrode was then rinsed with water and dried in a stream of warm air, and about 5 mg of mercury was evenly spread over the surface. The electrode was set aside for 24 hr and then the excess of mercury was wiped off with dry filter paper. To the mercury film thus formed, a 10-μl volume of $5 \times 10^{-3}M$ TOPO solution in THF, containing 0.193 g of PVC per litre, was applied. The solvent was allowed to evaporate at room temperature and then the modifying film was heated to 70° under an infrared lamp and kept at that temperature for 3 min. The hot electrode was immersed in distilled water, in which it was then stored. This procedure ensures homogeneity of the film and rapid and uniform hydration of the TOPO.

Procedure B. The surface of the electrode material, a 3-mm diameter glassy-carbon disk (GC 20 from Tokai Electrode Mfg., Japan) in a PTFE insulating mantle, was polished and cleaned in the same way as the silver electrode in Procedure A. The carbon surface was then electrolytically plated with silver from a $10^{-3}M$ silver solution in $0.1M$ ammonia/$3 \times 10^{-3}M$ potassium cyanide medium at a potential of −1.00 V (electrolytic current, $I_e = 80$ μA) for 20 min The electrode was rinsed with water, transferred to a $5 \times 10^{-3}M$ mercuric chloride solution in $0.1M$ hydrochloric acid, and mercury was electrolytically deposited on the silver film at a potential of −0.50 V ($I_e = 350$ μA), for 5–10 min The electrode was rinsed with water and dried with warm air, and the modifying film was formed in the same way as in Procedure A, except that only a 5 μl portion of the TOPO/PVC solution was used.

RESULTS AND DISCUSSION

The results of cyclic voltammetric and galvanostatic stripping measurements indicate that electrodes prepared by either procedure exhibit a good sensitivity and reproducibility. However, as electrolytic deposition of the silver and mercury films is better defined, though tedious, than the mechanical preparation of the mercury film, only electrodes prepared by Procedure B were used in the study of the electrochemical properties of the TOPO-MFE.

An electrode prepared by Procedure B can be schematically depicted as shown in Fig. 1. Approximate thicknesses of the silver and mercury films on the carbon support were calculated from the charges passed during their electrolytic preparation (with a correction for the background current, caused primarily by the reduction of oxygen) and the thickness of the TOPO film was estimated from the amount of TOPO deposited on the electrode, and its density (approximately 0.9 g/cm^3). With a 20-min electrolysis for the silver film and an 8-min electrolysis for the mercury, the approximate thicknesses were $l_{Ag} = 0.9$ μm, $l_{Hg} = 1.7$ μm and $l_{TOPO} = 1.6$ μm.

Interaction of metal ions with TOPO is based on the formation of TOPO solvates of metal salts. In the presence of dilute acids it can then be assumed that solvates of the type, $\{[R_3POH(H_2O)_n]^+ A^-\}$, are formed, A^- being the acid anion. Therefore, the metal ion can be back-extracted from TOPO into the aqueous phase by a suitable mineral acid. The H^+ and A^- ions have apparently high mobilities in the TOPO film and ensure a high electrical conductance of the film. For reproducible functioning of the TOPO-MFE it is thus necessary to immerse the electrode for some time in a solution of a dilute acid before the measurement, to remove (*i.e.*, back-extract) any metal ions that remained in the film from the previous measurement cycle and to stabilize the distribution of the H^+ and A^- ions in the TOPO film.

The electrochemical properties of the TOPO-MFE depend on the parameters of the given electrode reaction, and also on the thickness and structure of the TOPO film, its electrical conductance, the value

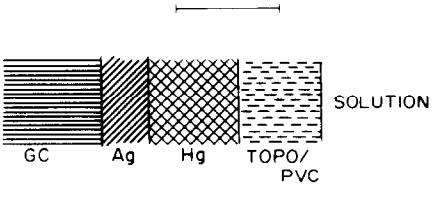

Fig. 1. A cross-section through a TOPO-MFE prepared by Procedure B

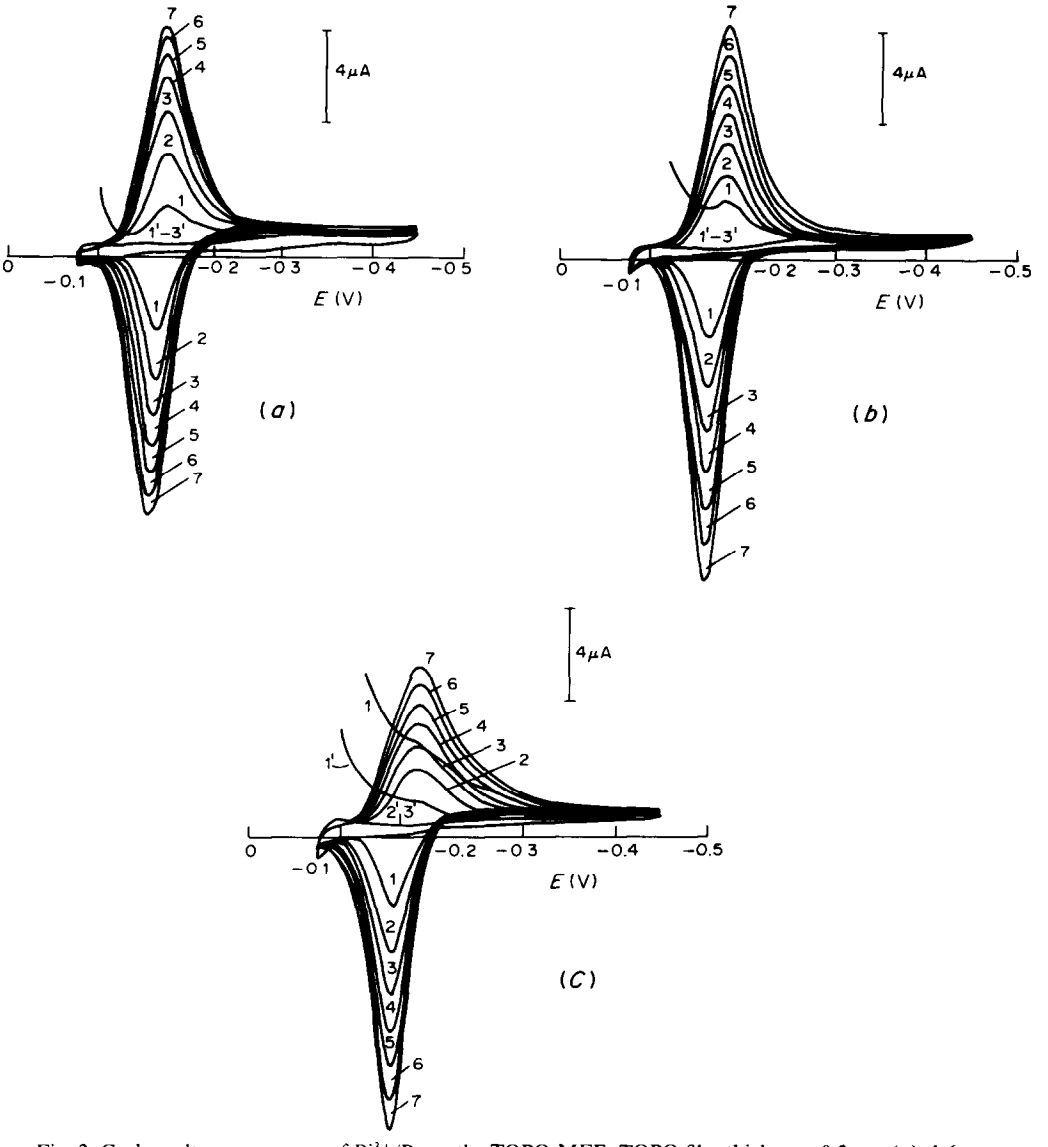

Fig. 2. Cyclic voltamperograms of Bi^{3+}/Bi on the TOPO-MFE. TOPO film thickness: 0.3 μm (*a*), 1.6 μm (*b*) and 3.2 μm (*c*). For the experimental conditions see the text. 1′, 2′, 3′: the three successive cycles in pure base electrolyte; 1–7: seven successive cycles in the solution containing bismuth.

of the distribution constant for the partitioning of the electroactive substance between TOPO and an aqueous solution, and the rates of the extraction interaction and the transport of the extracted substance through the TOPO film towards the mercury surface. As these physicochemical parameters influence one another and are subject to certain changes as a function of time and the conditions under which the measurements are made, the study of the electrochemical properties of the TOPO-MFE is rather complicated. Another complication is the interaction of TOPO with mercury ions, with the formation of relatively stable solvates, as illustrated by the extraction distribution ratios.[22] It can be assumed by analogy with copper[23] that the solvates of mercurous salts are more stable than those of mercuric salts; hence "an intermediate phase" of a mercurous salt solvate may be formed between the TOPO and the mercury phases, especially on polarization to positive potentials.

To study the electrochemical properties of the TOPO-MFE, the Bi^{3+}/Bi system was chosen, with 0.5*M* hydrochloric acid as the base electrolyte, because the reduction of Bi^{3+} on a mercury electrode is virtually reversible in hydrochloric acid medium, and Bi^{3+} is extracted into the TOPO film, as demonstrated by preliminary experiments.

First, the effect of the TOPO film thickness on the rate of Bi^{3+} transport through the film and on the film electrical conductance was studied. Cyclic voltammetry was used to study the transport of Bi^{3+} and its electrode reaction. The solution was deaerated with argon outside the electrolysis cell and then aspirated into the cell, to avoid extraction of bismuth

Table 1. The concentrations of bismuth in the TOPO film, the distribution ratios ($q = c_{TOPO}/c_{aq}$), and the apparent diffusion coefficients of the bismuth solvate in the TOPO film, obtained from the individual voltammetric cycles (see Fig. 2)

	Film thickness 0.3 μm (Fig. 2*a*)			Film thickness 1.6 μm (Fig. 2*b*)			Film thickness 3.2 μm (Fig. 2*c*)		
Cycle	c_{TOPO}, *mole/ml*	*q*	D_{app}, cm^2/sec	c_{TOPO}, *mole/ml*	*q*	D_{app}, cm^2/sec	c_{TOPO}, *mole/ml*	*q*	D_{app}, cm^2/sec
1	2.5×10^{-5}	1000	7×10^{-11}	1.7×10^{-6}	70	5×10^{-9}	0	0	—
2	7.1×10^{-5}	3000	1×10^{-10}	1.2×10^{-5}	500	3×10^{-9}	3.7×10^{-6}	150	2×10^{-8}
3	1.0×10^{-4}	4400	1×10^{-10}	1.8×10^{-5}	750	2×10^{-9}	6.4×10^{-6}	270	1×10^{-8}
4	1.5×10^{-4}	6000	9×10^{-11}	2.2×10^{-5}	900	3×10^{-9}	9.4×10^{-6}	400	8×10^{-9}
5	1.6×10^{-4}	6800	9×10^{-11}	2.7×10^{-5}	1100	3×10^{-9}	1.2×10^{-5}	500	7×10^{-9}
6	1.8×10^{-4}	7300	9×10^{-11}	3.1×10^{-5}	1300	3×10^{-9}	1.5×10^{-5}	630	6×10^{-9}
7	1.9×10^{-4}	7900	9×10^{-11}	3.9×10^{-5}	1600	2×10^{-9}	1.7×10^{-5}	700	7×10^{-9}

into the TOPO film before the actual measurement. Prior to the first measurement, the TOPO-MFE was immersed in 3*M* sulphuric acid for 15 min and was then activated by three cycles of direct current anodic-stripping voltammetry (DCASV) as follows: Bi^{3+} was accumulated in the TOPO film for 80 sec from a stirred solution of 0.5*M* hydrochloric acid containing 1 μg of Bi^{3+} per ml, with the TOPO-MFE disconnected from the potentiostat. The solution was then replaced by 0.5*M* hydrochloric acid not containing bismuth and pre-electrolysis of bismuth from the TOPO film into the mercury film was performed for 40 sec at a potential of −0.300 V, followed by a stripping step at a potential scan-rate of 10 mV/sec. Before the next DCASV cycle, the TOPO-MFE was regenerated by immersion in a stirred solution of 3*M* sulphuric acid for 80 sec.

After the third DCASV cycle, the electrode was regenerated by immersion for 200 sec in stirred 3*M* sulphuric acid. In the measurement itself, the TOPO-MFE was cyclicly polarized, at a potential scan-rate of 5 mV/sec, from −0.075 to −0.450 V. The first three cycles were performed in 0.5*M* hydrochloric acid not containing bismuth, then the solution was exchanged, without regeneration of the TOPO-MFE, for 0.5*M* hydrochloric acid containing 5 μg of Bi^{3+} per ml, and seven successive cycles were performed. The cyclic voltamperograms for TOPO-MFEs with TOPO film thicknesses of *ca.* 0.3, 1.6 and 3.2 μm are given in Fig. 2, plots *a*, *b* and *c*, respectively.

It can be seen from the voltamperograms that the reduction of Bi^{3+} is reversible with the thinnest TOPO film and that the rate of the charge-transfer reaction decreases with increasing film thickness. The electrode reaction rate also decreases somewhat with increasing number of measuring cycles, the decrease being greatest with the thinnest TOPO film [the values of the differences between the potentials of the cathodic and anodic peaks, ΔE_p, for the first and the seventh cycle are *ca.* 15 and 20 mV for film (*a*), 20 and 25 mV for film (*b*) and 30 and 30 mV for film (*c*)]. These effects are apparently connected with changes in the structure of the TOPO–Hg interface, caused by increasing concentration of the bismuth solvate in the TOPO film and possibly by the formation of mercurous ion solvate at more positive potentials. The anodic peaks are higher than the corresponding cathodic ones, in agreement with the theory for cases when the reduced form of the depolarizer is readily soluble in mercury.[24] The character of the voltamperograms was not affected by varying the scan-reversal potential from −0.450 to −1.0 V. Owing to the complex character of the overall process at the TOPO-MFE, no unambiguous dependence of the peak current on the potential scan-rate can be obtained.

Assuming that virtually all the Bi^{3+} ions present in the TOPO film undergo electrode reaction during one potential scan and that virtually all the bismuth atoms present in the mercury film are reoxidized during the reverse scan, the amount of Bi^{3+} present in the TOPO film can be calculated from the electrical charge passed, from which the Bi^{3+} concentration in the TOPO film can be obtained. Apparent diffusion coefficients (D_{app}) of Bi^{3+} ions in the TOPO film can then be estimated from the equation for the peak current, and a concentration distribution ratio of bismuth between the TOPO film and the aqueous phase can be roughly estimated (though extraction equilibrium is not attained during the seven measuring cycles). The results are given in Table 1.

It can be seen that the highest distribution ratios are obtained with the thinnest film, and that the apparent diffusion coefficients decrease with increasing TOPO film thickness. An important role is probably played here by the potential gradient across the TOPO film, which is much greater for the thinnest film, and strongly affects the transport of the solvate. Of course, the numerical values given in Table 1 are only very approximate, because of the non-equilibrium state at the solution–TOPO interface and the very small thickness of the TOPO film (a departure from the conditions of a linear semi-infinite diffusion). Nevertheless, they still yield useful information on the electrode behaviour. The values of the distribution ratios for macroscopic extraction are lower than those found for the TOPO-MFE, but the results described in our next paper[25] for the determination of bismuth in copper alloys confirm the values given in Table 1; the selectivity for bismuth with respect to copper is much better than that predicted from the values of the macroscopic distribution ratios.[17,18]

The electrical resistance of the TOPO/PVC film

increases with increasing PVC content. The weight ratio, PVC:TOPO = 1:10, was selected as a compromise ensuring a sufficient mechanical stability of the film, with a sufficiently low electrical resistance, which is *ca.* 300–500Ω in 0.5*M* hydrochloric acid medium. However, the electrical resistance of the film also depends on the composition of the base electrolyte, on the time for which the TOPO-MFE is immersed in a particular solution and, mainly, on the previous use of the electrode and the procedure used for its regeneration. In most cases the electrode exhibits a certain "memory effect" which must be eliminated by careful pretreatment before the measurement (see above).

The thickness of the TOPO/PVC film also affects the rate of attainment of a constant electrode activity and its maintenance during subsequent measurements. As the criterion of the electrode activity, the slope of the calibration curve is used in this paper. Calibration curves for differential pulse anodic-stripping voltammetric (DPASV) determination of bismuth are given in Fig. 3, for TOPO film thicknesses of *ca.* 0.3, 1.6 and 3.2 μm. The determination was done as follows: bismuth was accumulated for 80 sec in the TOPO film from 0.5*M* hydrochloric acid with a given concentration of Bi^{3+}, with the TOPO-MFE disconnected from the potentiostat. Then the solution was replaced by bismuth-free 0.5*M* hydrochloric acid and pre-electrolysis of Bi^{3+} from the TOPO film into the mercury film was performed at −0.300 V for 40 sec. The stripping was done at a potential scan-rate of 5 mV/sec, a pulse amplitude of −50 mV and a frequency of 1 pulse/sec. The TOPO-MFE was regenerated after each determination by

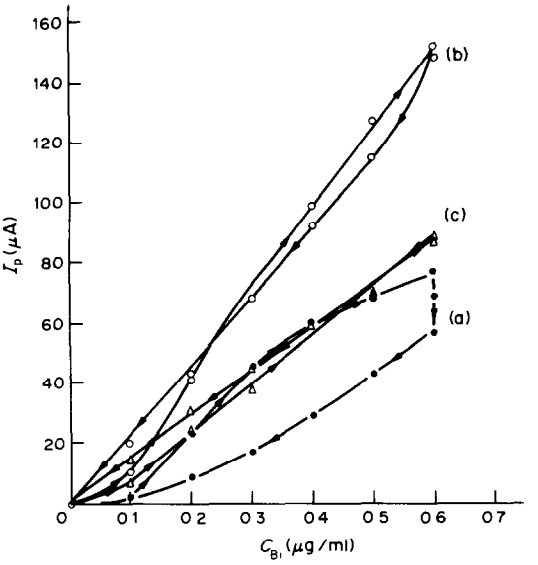

Fig. 3. The effect of the TOPO film thickness on the reproducibility of the TOPO-MFE activity in the determination of bismuth by DPASV. TOPO film thickness: 0.3 μm (*a*), 1.6 μm (*b*) and 3.2 μm (*c*). For the experimental conditions see the text.

immersion in stirred 3*M* sulphuric acid for 80 sec. The bismuth concentration was first gradually increased up to 0.6 μg/ml and then decreased again in steps of the same magnitude.

It can be seen from Fig. 3 that the electrode sensitivity is determined by two opposing factors, the TOPO film extraction capacity and the rate of depolarizer transport through the TOPO film. With thin films the TOPO-MFE activity decreases rapidly, per-

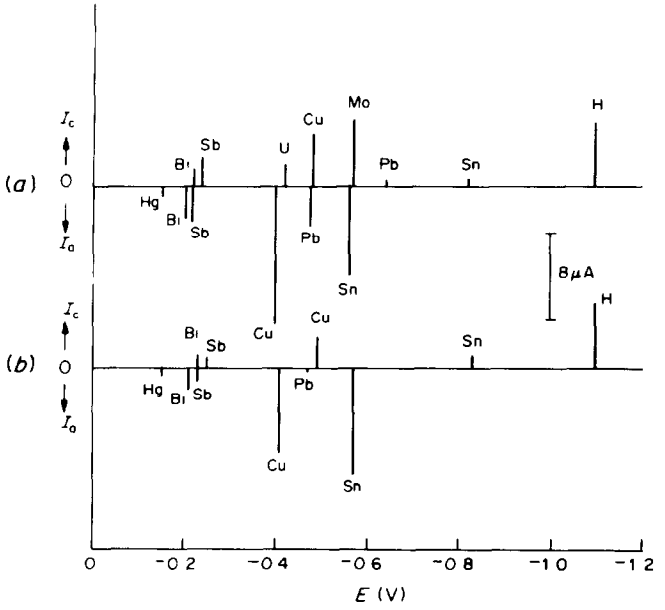

Fig. 4. Cyclic voltammetry of some ions in 1*M* hydrochloric acid. For the experimental conditions see the text. c_M(μg/mol): Cr^{3+} (5), As^{3+} (5), Pb^{2+} (5), Sb^{3+} (0.05), Cd^{2+} (5), Tl^{+} (5), Cu^{2+} (1), Ti^{4+} (5), Bi^{3+} (0.05), In^{3+} (5), Mo^{6+} (0.5), UO_2^{2+} (0.5) and Sn^{4+} (0.5); (*a*) without base electrolyte exchange, (*b*) after replacement of the test solution by pure base electrolyte.

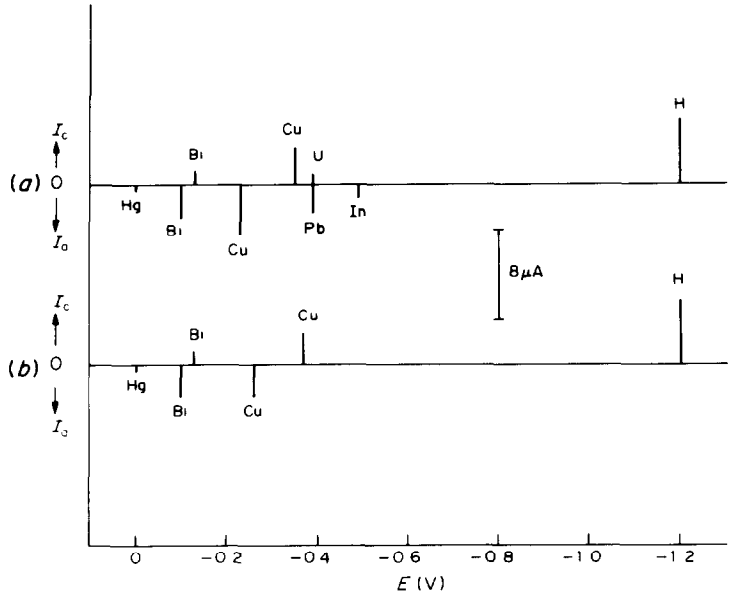

Fig. 5. Cyclic voltammetry of some ions in 0.1 *M* hydrochloric acid. For the other experimental conditions see the text and caption to Fig. 4.

haps owing to reduction of the TOPO film extraction capacity by diffusion of mercury solvates from the Hg-TOPO interface into the bulk of the TOPO film. Thick films exhibit a virtually constant but low activity. Therefore, the film thickness, 1.6 μm, is an optimal compromise under the given conditions.

Further, the behaviour of some other ions at the TOPO-MFE was studied by cyclic voltammetry. The formation of a TOPO solvate of a salt of the given element (and thus extraction of the element into the TOPO film) is indicated by the appearance of peaks on the cyclic voltamperogram after replacement of a solution containing the test element by a pure base electrolyte. Three base electrolytes were tested, 1 *M* and 0.1 *M* hydrochloric acid and 0.1 *M* sodium acetate 0.1 *M* acetic acid buffer (pH 4.6). The test element concentrations varied from 0.05 to 5 μg/ml, depending on the degree of extraction into the TOPO film and the sensitivity of electrochemical measurement.

The following procedure was used. (1) The elements were accumulated in the TOPO film for 10 min, with

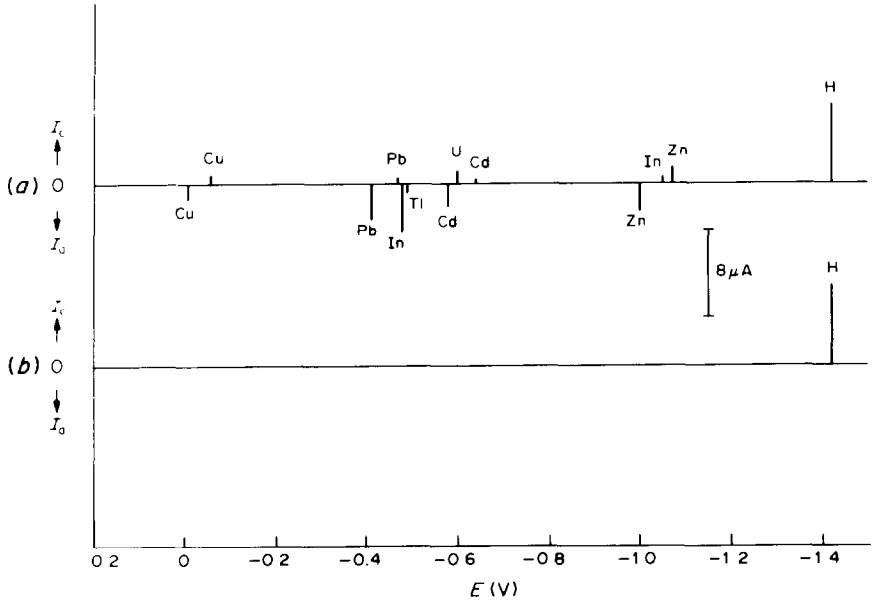

Fig. 6. Cyclic voltammetry of some ions in 0.1 *M* sodium acetate 0.1 *M* acetic acid, pH 4.6. For the experimental conditions see the text. c_M (μg/ml): Pb^{2+} (5), Cd^{2+} (5), Zn^{2+} (5), Co^{2+} (5), Tl^{+} (5), In^{3+} (5), Cu^{2+} (1) and UO_2^{2+} (0.5); (*a*) without base electrolyte exchange, (*b*) after replacement of the test solution by pure base electrolyte.

the TOPO-MFE disconnected from the potentiostat and with passage of argon through the solution. (2) The actual measurement was first performed on the base electrolyte containing the test element and then, for the elements that are extracted into the TOPO film, in the pure base electrolyte after solution exchange. Three potential cycles were applied, from -0.200 V to the potential of H^+ reduction (at which the sum of the electrolytic and capacitive currents attained a value of 8 μA), at a scan-rate of 10 mV/sec. The reverse scan ended at the potential for anodic dissolution of mercury. Before the first and after the last measurement, the TOPO–MFE activity was tested by DCASV of Bi^{3+} (1 μg/ml) in 0.5*M* hydrochloric acid. The electrode was regenerated after each measurement, for 200 sec in 3*M* sulphuric acid, by application of three potential cycles at a scan-rate of 10 mV/sec, ending at the potential of anodic dissolution of mercury.

The results are summarized in Figs. 4–6, where the positions of the segments correspond to the peak potentials and their lengths to the peak currents.

Conclusion

The CME described is generally applicable to selective electrochemical analyses and the properties of the electrode can be suitably modified by varying the experimental conditions (solution composition, experimental technique, thickness and composition of the modifying film). A more detailed discussion of the problems of selectivity and an example of a practical application are given in our next paper.[25]

REFERENCES

1. J. Zak and T. Kuwana, *J. Electroanal. Chem. Interfacial Electrochem.*, 1983, **150,** 645.
2. R. W. Murray, *Phil. Trans. Roy. Soc. London*, 1981, **302,** 253.
3. J. Weber and L. Kavan, *Chem. Listy*, 1980, **74,** 803.
4. R. W. Murray, in *Electroanalytical Chemistry*, Vol. 13, A. J. Bard (ed.), pp. 191–368. Dekker, New York, 1984.
5. K. Štulík and V. Pacáková, in J. Zýka (ed.), *New Trends in Analytical Chemistry*, Vol. 3, SNTL, Prague, in the press.
6. G. T. Cheek and R. F. Nelson, *Anal. Lett.*, 1978, **11,** 393.
7. N. Oyama and F. C. Anson, *J. Am. Chem. Soc.*, 1979, **101,** 3450.
8. J. A. Cox and M. Majda, *Anal. Chim. Acta*, 1980, **118,** 271.
9. J. A. Cox and P. J. Kulesza, *ibid.*, 1983, **154,** 71.
10. *Idem, J. Electroanal. Chem. Interfacial Electrochem.*, 1983, **159,** 337.
11. I. Rubinstein and A. J. Bard, *J. Am. Chem. Soc.*, 1980, **102,** 6641.
12. J. J. Kulys, N. K. Čenas, G.-J. S. Švirmickiene and V. P. Švirmickiene, *Anal. Chim. Acta*, 1982, **138,** 19.
13. K. Izutsu, T. Nakamura, T. Takizawa and H. Hanawa, *ibid.*, 1983, **149,** 147.
14. K. Izutsu, T. Nakamura and T. Ando, *ibid.*, 1983, **152,** 285.
15. K. H. Lubert, M. Schnurrbusch and A. Thomas, *ibid.*, 1982, **144,** 123.
16. F. Vydra, K. Štulík and E. Juláková, *Electrochemical Stripping Analysis*, Horwood, Chichester, 1976.
17. Y. Marcus and A. S. Kertes, *Ion Exchange and Solvent Extraction of Metal Complexes*, Wiley–Interscience, London, 1969.
18. J. C. White and W. J. Ross, *U.S. At. Energy Comm., Rept.*, NAS-NS-3102, Oak Ridge, 1961.
19. J. Lexa, *Chem. Listy*, 1985, **79,** 85.
20. J. Lexa and K. Štulík, *Talanta*, 1983, **30,** 845.
21. M. Štulíková, *J. Electroanal. Chem. Interfacial Electrochem.*, 1973, **48,** 33.
22. T. Ishimori, K. Kimura, T. Fujino and H. Murakami, *J. At. Energy Soc. Japan*, 1962, **4,** 117.
23. I. Janoušek, *Ph.D. Thesis*, Charles University, Prague, 1980.
24. Z. Galus, *Fundamentals of Electrochemical Analysis*, p. 428, Horwood, Chichester, 1976.
25. J. Lexa and K. Štulík, *Talanta*, 1985, **32,** in press

Talanta, Vol. 32, No. 11, pp. 1035–1039, 1985
Printed in Great Britain.

0039-9140/85 $3.00 + 0.00

GRAPHITE-FURNACE AAS WITH ULTRASONIC NEBULIZATION

RAINER WENNRICH, UTE BONITZ, HAGEN BRAUER,
KNUT NIEBERGALL and KLAUS DITTRICH
Karl-Marx-Universität Leipzig, Sektion Chemie, WB Analytik, DDR-7010 Leipzig, Talstrasse 35, GDR

(*Received* 6 *November* 1984. *Revised* 28 *May* 1985. *Accepted* 15 *June* 1985)

Summary—A technique combining ultrasonic nebulization of solutions and graphite-furnace atomic-absorption spectrometry is described. The analytical possibilities of two different techniques are shown. In one the nebulized samples are continuously introduced into a graphite tube operated at constant temperature, and in the other deposited on the inner wall of the graphite tube and heated discontinuously. The method chosen influences the absorption values for several elements. The sensitivity for determination by continuous sampling lies between the values for the normal electrothermal AAS injection technique and flame AAS. Higher sensitivities are obtained with the deposition technique.

Atomic-absorption spectrometry with electrothermal atomization is done mainly by introduction of a small volume of sample solution into a graphite or metal tube atomizer, where it is successively dried, volatilized and atomized by means of a rapid increase in temperature. The first results on work with a constant-temperature furnace were published by L'vov.[1] The sample was introduced from a carbon rod arc into a tube already heated to the working temperature, so that there was thermal equilibrium in the absorption system. The advantage of using a constant-temperature furnace has been demonstrated with various sampling techniques.[2-4] Use of a constant-temperature graphite-tube system with continuous sample introduction was first described by Woodriff and Ramelow.[5,6] Murphy *et al.*[7] later described the use of two different flameless atomizers with continuous sampling for atomic-fluorescence measurements, reporting detection limits of 0.3 pg/ml (Zn), 0.03 ng/ml (Cu) and 1 ng/ml (Bi),when a heated vertical graphite tube was used, with photon counting. These excellent results were confirmed by Molnar and Winefordner,[8] who used a vitreous-carbon furnace with continuous sample introduction. Matousek[9] showed that introduction of a sample aerosol into a heated graphite tube can combine the high sensitivity of electrothermal AAS with the higher precision of flame atomization systems. A pneumatic nebulizer and a droplet separator were used. The sample aerosol was led by a special tube into the furnace, heated to a temperature at which the solvent was evaporated from the aerosol droplets and the resulting solid particles were deposited as a thin layer on a large area of the graphite furnace wall. The graphite tube was then heated to the atomization temperature by various programmes. This technique ensures that no sample soaks into the graphite as it does in the conventional method of injection of a liquid sample. Hence the "chromatographic" effects which can accompany evaporation of solvent from samples soaked into the tube, cannot arise.

This aerosol deposition technique has also been used in the FASTAC system (Instrumentation Laboratory, Inc.). Sotera *et al.*[10] measured the concentration of Bi, Pb, Te and Tl in nickel alloys with the FASTAC system, and a comparison with results obtained by normal electrothermal AAS did not show any differences caused by change in the sampling method. Chamsaz *et al.*[11] reported that the detection limits obtainable with the aerosol deposition technique were in the ng/ml range and up to three orders of magnitude better than those for continuous aerosol introduction into a furnace at atomization temperature. Jenke and Woodriff[12] showed the analytical possibilities of combining use of a long-tube (350 mm) graphite furnace operated at constant temperature, with various pneumatic nebulizers and a desolvation system.

Pneumatic nebulizers are characterized by low efficiency of nebulization and high consumption of solution. We therefore decided to test the possibilities of combining graphite-furnace AAS with ultrasonic nebulization. The advantages of ultrasonic nebulization over pneumatic nebulization have already been demonstrated for ICP–AES,[13,14] and include the smaller and more uniform particle size and the lower carrier-gas flow rate needed to produce an aerosol with greater number density. Use of this technique for continuous sample introduction for electrothermal AAS should give longer residence time and higher concentration of the particles in the hot furnace than pneumatic nebulization would, so the atomization efficiency ought to be better. Furthermore, the trapping on the graphite surface should be more efficient with lower gas flow-rates and smaller particle size.

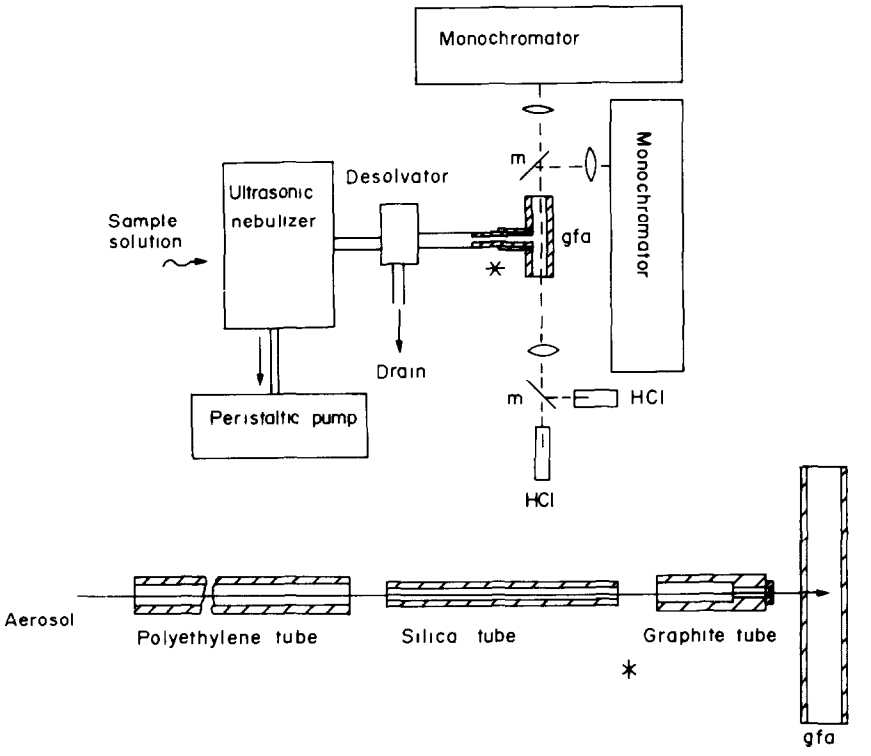

Fig. 1. Block diagram of the atomic-absorption device with the aerosol inlet system consisting of a polyethylene tube (length = 250 mm, bore 5 mm), silica tube (length 60 mm, bore 3.5 mm), graphite tube (length 30 mm, bore 5 mm and 3.5 mm), hole in graphite furnace 5 mm diameter.

EXPERIMENTAL

Equipment

A dual-channel atomic-absorption spectrometer with two monochromators (VEB Carl Zeiss Jena, G.D.R.) and a modified Beckman 1268 graphite furnace were used with a laboratory-built lock-in amplifier and a Kompensograph E recorder (Siemens AG, F.R.G.) (see Fig. 1). For comparison, flame AAS experiments were done with Zeiss AAS-1 and AAS-3 atomic-absorption spectrometers.

Atomizer

The graphite tube (RWO 255) used in our work on laser-AAS[15-17] was connected to a second RWO graphite tube (30 mm long, 10 mm outer diameter and 5 mm bore) which acted as the aerosol inlet. The sample-inlet hole of the Beckman 1268 graphite tube was enlarged to 5 mm. The aerosol inlet tube was connected by a silica tube (50 mm long, 3 mm bore) and a polypropylene tube (5 mm bore) to the desolvation system (see below and Fig. 1). The graphite furnace could be heated to 2850 K. The temperature inside the furnace could not be measured during atomization of the aerosol, so the temperature *vs* applied voltage calibration was done with an optical pyrometer

The lifetimes of normal graphite tubes were between 60 and 80 atomization cycles for continuous supply of aerosol into the hot tube and between 120 and 150 atomization cycles in the deposition technique. These relatively short lifetimes are caused by the high load of NO_2 from the samples vaporized

Nebulizer

The sample solutions were nebulized with an ultrasonic device. A special sample chamber made from either PTFE or poly(methyl methacrylate) (Fig. 2) was fitted with a medical inhaler (USI-50, VEB TUR, Dresden, G.D.R.) operating at 2.64 MHz. The sample solution was deposited with a 1-ml pipette through the sample insertion hole onto the membrane It is also possible to add the sample with a capillary operated by a peristaltic pump.

The aerosol was transported from the ultrasonic nebulizer to the desolvation chamber. Larger droplets were separated from the aerosol stream by a baffle and returned to the membrane for further nebulization. When measurements

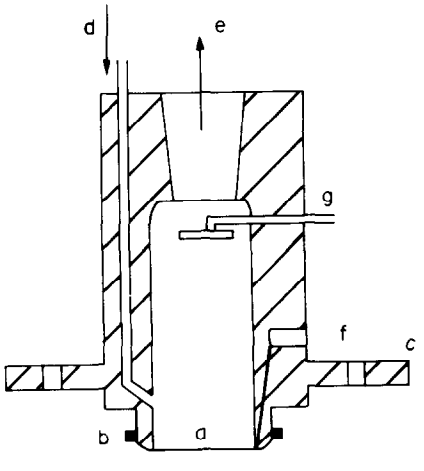

Fig. 2. Sample chamber for ultrasonic nebulization with a, membrane, b, O-ring, c, ground plate, d, argon inlet, e, conical joint for sample dosage and aerosol path to the desolvation unit, f, hole for suction, g, baffle plate with hole for dosage by peristaltic pump.

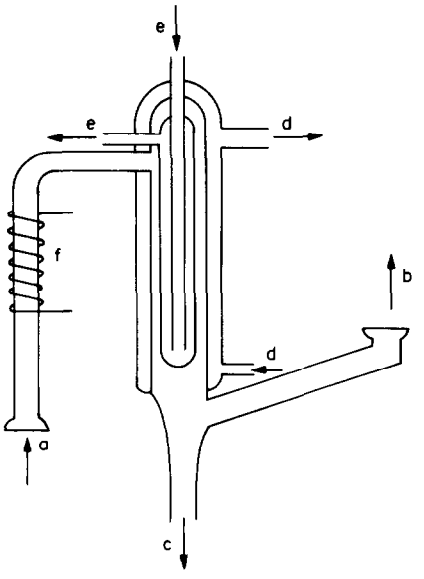

Fig. 3. Desolvation unit with a, aerosol inlet, b, outlet, c, drain, d, outer cooling jacket, e, inner cooling jacket, f, resistance heating.

had been made, the surplus sample solution and the wash solution used to cleanse the nebulizer were sucked off by peristaltic pump. Therefore three holes (0.3 mm) were drilled in the bottom of the nebulizer directly above the membrane and connected to the pump by polypropylene tubes. It was thus possible to measure the volume of sample nebulized. To give a constant nebulization rate over the test period of 90 sec, 2 ml of solution were added to the sample chamber.

Desolvation system

The use of sample volumes greater than 100 μl in a graphite furnace is problematic. In a cold tube this amount of solution will spread over a large area of the tube wall and result in non-uniform atomization. The capacity of the graphite tube may also be exceeded. The direct addition of sample solution into a graphite tube heated to the atomization temperature leads to the decomposition of the aqueous solution and the formation of hydrogen, which then burns at the ends of the furnace (water-gas reaction) The aerosol from the nebulizer was therefore introduced by passage through a tube heated to 800 K to evaporate the solvent, and then through a condenser to remove the solvent vapour from the carrier-gas (Fig. 3). By comparing drainage and uptake volumes it was estimated that 90–95% of the solvent was removed by the condenser.

To determine the efficiency of the system the drain solution was analysed. An arsenic solution (500 ng/ml) was passed through the ultrasonic nebulizer, and arsenic in the condensate was measured by the hydride-generation AAS method and found to be 20–25 ng/ml, which means a desolvation efficiency of approx. 95%.

Solutions

Stock solutions (metal concentration 1 mg/ml) in 1 *M* nitric acid were made from analytical-grade reagents [$AgNO_3$, $Fe(NO_3)_3$]. Stock solutions of aluminium, gallium, indium and manganese (1 mg/ml) were prepared by dissolving the metals and adding nitric acid to give the same concentration of nitrate as in the silver and iron solutions. The stock solutions were diluted with 0.1 *M* nitric acid. For convenience the elements were examined in pairs (Ag–In, Ga–Mn, Al–Fe).

Procedures

The sample solution (2 ml) containing a pair of elements at various concentrations was placed in the nebulizer chamber. The aerosol was transported through the desolvation system and the inlet tube into the graphite furnace by the argon transport gas. Two sampling techniques were tested. In continuous sampling the desolvated aerosol was introduced into a graphite tube already heated to atomization temperature and the atomic absorption signals were measured simultaneously and continuously. In the deposition technique the desolvated aerosol was fed into the "cold" tube for a predetermined time, than the flow was stopped and the normal heating cycle applied to the tube.

RESULTS AND DISCUSSION

Continuous sample introduction

The absorbance values in electrothermal atomic-absorption with continuous sampling are influenced by the tube temperature and the flow-rate of the aerosol transport gas. The efficiency of atomization of the aerosol particles increases with atomizer temperature, but at higher atomizer temperatures the residence time of the particles inside the furnace is reduced by the greater gas expansion. The residence time and atomization efficiency are also reduced by higher gas flow-rates.[18] On the other hand an increase in gas flow-rate raises the solution uptake in the nebulizer and therefore the number of particles inside the atomizer. The influence of gas flow-rate on solution uptake was tested over the range 2.5–14 ml/sec, and the highest uptake was found with 8–10 ml/sec argon flow. At this flow-rate the uptake was 1.7 times that at 2.5 ml/sec. To obtain both high uptake and relatively long residence time we worked with a gas flow-rate of 4 ml/sec. Under these conditions 0.5 ml (standard deviation 0.1 ml) of the 2 ml of sample

Table 1. Comparison of the sensitivities for several elements with different continuous sampling techniques in AAS

		Electrothermal AAS with ultrasonic nebulization		
Element	Wavelength, *nm*	Reciprocal sensitivity (abs = 0.01), *ng/ml*	Linear range, *ng/ml*	C_2H_2–air flame* reciprocal sensitivity, (abs = 0.01), *ng/ml*
Ag	328.1	22	20–600	140
Ga	294.4	40	50–3000	450
In	303.9	41	50–1200	1150
Mn	279.5	10	5–200	100
Al	309.3	190	200–8000	2300
Fe	248.3	70	70–2000	450

*Measured with AAS-1.

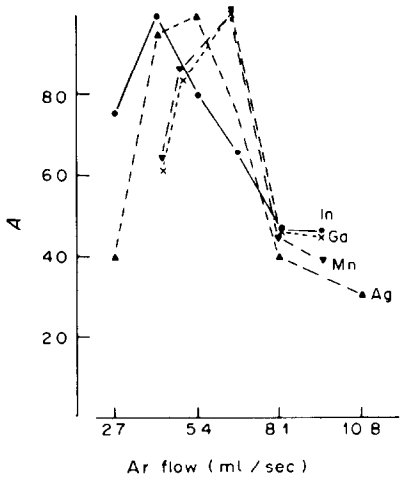

Fig. 4. Influence of the transport-gas flow-rate on the relative absorbance values in deposition technique.

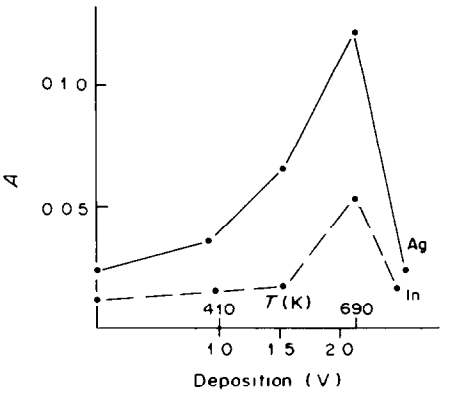

Fig. 5. Influence of the furnace temperature in the deposition step on the absorbance of Ag and In.

solution was nebulized in 90 sec. The actual uptake was measured in all determinations.

The results obtained by continuous sample introduction are listed in Table 1 along with the reciprocal sensitivities obtained in flame AAS. The electrothermal technique combined with continuous sampling gives better results than flame AAS for each element tested, as expected. The relative standard deviation at an absorbance of 0.1 was 3.8% for manganese and 4.6% for gallium for 10 analyses, the actual uptake rate of solution in the nebulizer being taken into account.

Aerosol-deposition method

As expected, the detection limits of the continuous flow technique do not compare favourably with those achieved in normal electrothermal AAS (Tables 1 and 2).

The benefits of the discrete sampling technique of normal electrothermal AAS lie mainly in the long residence times of the particles inside the furnace, caused by the use of gas-stop in the atomization step, but discrete sampling is limited to small solution volumes. We tested the possibility of depositing larger amounts of sample on the wall of the graphite tube by use of aerosol introduction, to increase the sensitivity. The efficiency of the deposition on the furnace wall depends on both the gas flow-rate and the deposition temperature.[9,11]

Effect of the gas flow-rate. In pneumatic nebulization the linear velocity of the aerosol particles before deposition on the graphite tube wall varies between 5 and 30 m/sec. The flow-rates are much lower in ultrasonic than in pneumatic nebulization. The gas flow varied between 2.7 and 10.8 ml/sec (see Fig. 4). In our experiments the aerosol passed through the graphite inlet tube (with an internal diameter of 2.5 mm) before entering the graphite furnace. This means that the linear velocity of the aerosol varied between 0.5 and 2.8 m/sec.

The results of monitoring the relative absorbance as a function of the gas flow-rate for deposition in a cold graphite tube are shown in Fig. 4. The flow of the purge-gas was temporarily interrupted during the atomization step. At flow-rates above 7 ml/sec the efficiency of deposition of the particles on the graphite wall decreased for the elements tested. The difference in behaviour of the elements has not yet been interpreted. Not only the composition and the structure of the desolvated aerosol particles but also the mechanism of binding the particles to the carbon surface are not clear.

Effect of the deposition temperature. Chamsaz *et al.*[11] varied the deposition temperature in pneumatic nebulization and obtained maximum absorbance for Ca, Cd, Mg, Mo at between 420 and 470 K. They expected that at above 470 K a decrease in absorbance could be caused by the gas expansion away from the heated graphite surface acting as an aerodynamic barrier to particle deposition. The results of our experiments are shown in Fig. 5. We found maximum

Table 2. Comparison of the analytical results obtained by different electrothermal techniques

		Ultrasonic nebulization with aerosol deposition			Discrete sampling (10 μl)	
Element	Wavelength, nm	Reciprocal sensitivity (abs = 0.01), ng/ml	pg*	Linear range, ng/ml	Reciprocal sensitivity, ng/ml	pg
Ag	328.1	0.04	13	0.04–2	0.9	9
Ga	294.4	12	4080	12–500	3.5	35
In	303.9	4	1100	4–50	4.5	45
Mn	279.5	0.8	272	0.8–30	0.2	2

*Values taking into account the sample volume nebulized.

absorbance at 690 K for Ag and In at a gas flow-rate of 5.5 ml/sec. The differences from the values reported by Chamsaz *et al.* could be due to the lower gas flow-rate and the smaller particle size in our work.

Analytical results. The results obtained with the aerosol deposition technique are summarized in Table 2. In all cases tested the linear working range was wider for deposition than that for the discrete sampling technique. The absolute sensitivity of the determination was nearly the same in both the discrete-sampling and deposition techniques only for silver. In all other cases the absolute detection limits were up to 100 times worse in deposition. That means we had a high loss of material in deposition of gallium, indium and manganese. The reason for the differences in deposition are not clear up to now. We assume that the deposition of silver is based on a combination of reduction of the silver salts by carbon and the adsorption of metallic silver on the graphite surface. Formation of silver carbide seems impossible and it is not known to exist.[19,20] Gallium, indium and manganese were deposited as oxides on the graphite surface. The nitrates nebulized were decomposed inside the desolvation unit, forming the oxides.[20] In the injection technique the same oxides were formed in the graphite furnace during the heating cycle.

The concentration sensitivity was calculated from the absolute sensitivity values. The concentration sensitivity for silver is much better in the deposition technique. We obtained the same values for indium in both techniques. The concentration sensitivities for manganese and gallium were worse in the deposition technique.

Comparison of the ultrasonic nebulization techniques. A comparison of the analytical results for Ag, Ga, In, Mn in the two techniques of sampling by ultrasonic nebulization—continuous sampling and deposition—show deposition to give better concentration sensitivities (Tables 1 and 2). Because of the distinctly shorter residence time of the particles inside the graphite tube when the continuous sampling technique is used. The large difference in the sensitivity for the determination of Ag from those for determination of Ga, In, Mn we also attribute to the differences in adsorption of the elements on the graphite surface.

CONCLUSIONS

The results presented show that ultrasonic nebulization combined with continuous sampling into a constant-temperature graphite furnace has potential for some special analytical applications, *e.g.*, for the determination of trace elements in flowing solutions, or in reaction vessels with discrete sampling of volumes between 0.1 and 1 ml. The necessary sample volume is smaller in ultrasonic than in pneumatic nebulization, because of the higher efficiency. The technique gives better detection limits and sensitivities but poorer reproducibility than flame AAS. The combination of ultrasonic nebulization with the aerosol deposition technique in electrothermal AAS with normal graphite materials generally gives poorer sensitivity and absolute detection limits than those for discrete sampling and conventional electrothermal AAS, but can be advantageous for certain elements such as silver.

REFERENCES

1. B. V. L'vov, *Spectrochim. Acta* 1961, **17,** 761.
2. *Idem, ibid.*, 1978, **33B,** 153.
3. C. L. Chakrabarti, H. A. Hamed, C. C. Wan, W. C. Li, P. C. Bertels, D. C. Gregoire and S. Lee, *Anal. Chem.*, 1980, **52,** 167.
4. W. Slavin and D. C. Manning, *Spectrochim. Acta*, 1982, **37B,** 955.
5. R. Woodriff and G. Ramelow, *ibid.*, 1968, **23B,** 665.
6. R. Woodriff, *Appl. Spectrosc.*, 1968, **22,** 207.
7. M. K. Murphy, S. A. Clyburn and C. Veillon, *Anal. Chem.*, 1973, **45,** 1468.
8. C. J. Molnar and J. D. Winefordner, *ibid.*, 1974, **46,** 1419.
9. J. P. Matousek, *Talanta*, 1977, **24,** 315.
10. J. J. Sotera, L. C. Christiano, M. K. Conley and H. L. Kahn, *Anal. Chem.*, 1983, **55,** 204.
11. M. Chamsaz, B. L. Sharp and T. S. West, *Talanta*, 1980, **27,** 867.
12. D. R. Jenke and R. Woodriff, *Appl. Spectrosc.*, 1982, **36,** 657.
13. S. S. Berman, J. W. McLaren and S. N. Willie, *Anal. Chem.*, 1980, **52,** 488.
14. K. W. Olson, W. J. Haas, Jr. and V. A. Fassel, *ibid.*, 1977, **49,** 632.
15. K. Dittrich and R. Wennrich, *Spectrochim. Acta*, 1980, **35B,** 731.
16. R. Wennrich and K. Dittrich, *ibid.*, 1982, **37B,** 913.
17. R. Wennrich, K. Dittrich and U. Bonitz, *ibid.*, 1984, **39B,** 657.
18. W. M. G. T. van den Broek and L. de Galan, *Anal. Chem.*, 1977, **49,** 2176.
19. *CRC Handbook of Chemistry and Physics*, 64th Ed., CRC Press, Cleveland, 1983.
20. *Comprehensive Inorganic Chemistry*, Vols. 1 and 3, Pergamon Press, Oxford, 1973.

Talanta, Vol 32, No 11, pp 1041 1045, 1985
Printed in Great Britain

0039-9140/85 $3.00 + 0.00
Pergamon Press Ltd

FLUORIMETRIC DETERMINATION OF BERYLLIUM WITH PYRIDOXAL-5-PHOSPHATE

A. PETIDIER, S. RUBIO, A. GOMEZ-HENS and M. VALCARCEL
Department of Analytical Chemistry, Faculty of Sciences, University of Córdoba, Córdoba, Spain

(*Received* 5 *June* 1985. *Accepted* 14 *June* 1985)

Summary—A simple, rapid and selective method for the determination of beryllium with pyridoxal-5-phosphate has been developed. The system is only fluorescent (λ_{ex} 360, λ_{em} 460 nm) in the presence of a nitrogenous base such as ammonia, ethylenediamine or pyridine, owing to the possible formation of a ternary complex. The calibration graph is linear over the range 8–60 ng/ml. The high selectivity of the method permits the determination of beryllium in various types of alloys.

On account of the wide industrial use of beryllium and its compounds, and to study its toxic effect more deeply, more accurate and selective methods for the determination of small amounts of this element are needed. No specific reagent for it is known so far. Separations to be used will depend on whether it is present in micro or macro amounts in the sample, as well as on the concentration of interfering elements present and the potential interference with the determinative method chosen. The fluorimetric method using morin is subject to many interferences, has been extensively studied, and is the most important method for the determination of submicrogram quantities of beryllium in air,[1,2] urine,[3] bones and other biological materials,[4,5] in which complete recovery of beryllium present may not be an absolute necessity.[6]

The determination of beryllium in alloys on which small amounts of it confer special properties, is very important. Industrial applications of these alloys are numerous and widespread. The copper-base alloys are extensively used in springs of all kinds,[7] especially in electric contacts, as well as in the diaphragms of pressure-sensitive instruments, thanks to their fatigue resistance. They are also used in the manufacture of sparkless tools for use in different industries[8] and in the manufacture of dyes, for pressing plastics, and for deep-drawing metals. Thanks to their high electrical and thermal conductivity, in addition to their hardness, these alloys are also suitable for electrodes and other components for resistance-welding work. Beryllium is used as a minor alloying agent in aluminium-base alloys, retarding oxidation of the melt.[9] It is also used as an alloying agent in nickel to produce a high-strength alloy resistant to corrosion and wear.

The most common procedures for the elimination of interferences in these kinds of sample are precipitation, extraction, electrolysis and ion-exchange, but are tedious and time-consuming. For example precipitation and extraction generally need to be repeated several times to ensure complete separation.

A simple, rapid and highly selective fluorimetric method for determination of beryllium in the most common alloys is described in this work.

EXPERIMENTAL

Reagents

Standard beryllium solution (1 μg/ml). Freshly prepared by appropriate dilution of a stock solution made by dissolving beryllium nitrate (Merck extra pure) in 0.05*M* nitric acid and standardized gravimetrically by precipitation with ammonia.[10]

Pyridoxal-5-phosphate. 0.01*M* solution in 0.01*M* hydrochloric acid. All common reagents and solvents used were of analytical-reagent grade.

Apparatus

A Perkin-Elmer fluorescence spectrophotometer, model MPF-43A, with 1-cm quartz cells and a xenon source was used. The cell compartment of the spectrofluorimeter was kept at a constant temperature of 25° by circulating water through it. The instrumental sensitivity was set at 0.3, and the excitation and emission slits were set to give a 5-nm spectral bandpass. A set of fluorescent polymer samples was used daily to adjust the spectrofluorimeter to compensate for changes in source intensity.

Procedure

To a solution containing 0.2–1.5 μg of beryllium add 0.25 ml of 0.01*M* pyridoxal-5-phosphate and 4 ml of 2*M* ammonia–ammonium chloride buffer solution (pH 9.8). Dilute to 25 ml with distilled water and measure the intensity of the fluorescence at 460 nm, with excitation at 360 nm, against a reagent blank containing no beryllium. Prepare a calibration graph in the same way.

RESULTS AND DISCUSSION

Spectral characteristics

Beryllium reacts with pyridoxal (Py) or pyridoxal-5-phosphate (PyP) in ammoniacal medium, yielding complexes which exhibit intense blue fluorescence. The spectral characteristics of both complexes are analogous but the fluorescence intensity of the Be–PyP complex is twice that of the Be–Py complex. Hence, the former was chosen for the determination. The excitation spectrum of this complex shows two

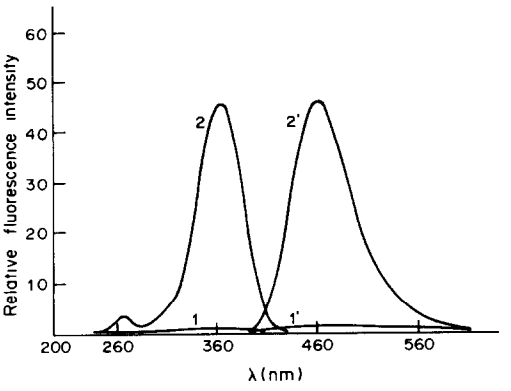

Fig. 1. Uncorrected excitation and emission spectra of PyP (1,1') and the Be–PyP system (2,2'). [Be(II)] = 100 ng/ml, [PyP] = $6 \times 10^{-5}M$, [NH_4Cl/NH_3] = 0.1M.

bands with maxima at 265 and 360 nm (λ_{em} 460 nm), whilst the emission spectrum displays one band with its maximum at 460 nm (λ_{ex} 360 nm) (Fig. 1). The complex forms immediately and the fluorescence intensity remains stable for at least 4 hr.

The fluorescence of the Be–PyP system is only developed when a nitrogenous base, *e.g.*, ammonia, ethylenediamine or pyridine, is present in the solution. At equal concentrations of these bases, the fluorescence of the complex is most intense with ammonia. In sodium or potassium hydroxide solution or in non-nitrogenous buffer solutions (borate, phosphate and carbonate), the system does not emit fluorescence. This fact could be attributed to the possible formation of a ternary complex with the nitrogenous base.

Optimization

The system was optimized by changing each variable in turn whilst the others were kept constant. Figure 2 shows the effect of the different variables.

Figure 2A shows the optimum pH range is 9.5–10.0. An ammonia–ammonium chloride buffer solution of pH 9.8 is therefore used to adjust the pH. Figure 2B shows that the fluorescence of the complex is only developed when the ammonia concentration is about twenty times that of the reagent, and Fig. 2C shows that about a 30-fold molar ratio of the pyridoxal-5-phosphate to beryllium is necessary to obtain the maximum signal.

Temperatures above 35° have a very significant negative effect (Fig. 2D). The effect in the range 20–35° is also negative, but much less pronounced.

To study the effect of ionic strength, three salts (KCl, KNO_3 and $NaClO_4$) were tested at different concentrations, but had only a slight effect on the fluorescent system.

Several organic solvents with different dielectric constants (dimethylformamide > ethanol > acetone > dioxan) and in different concentrations (0–80%) were examined, to determine the effect of the dielectric constant on the fluorescence intensity of the complex. For all these solvents, decrease in the dielectric constant results in a decrease in the fluorescence of the complex.

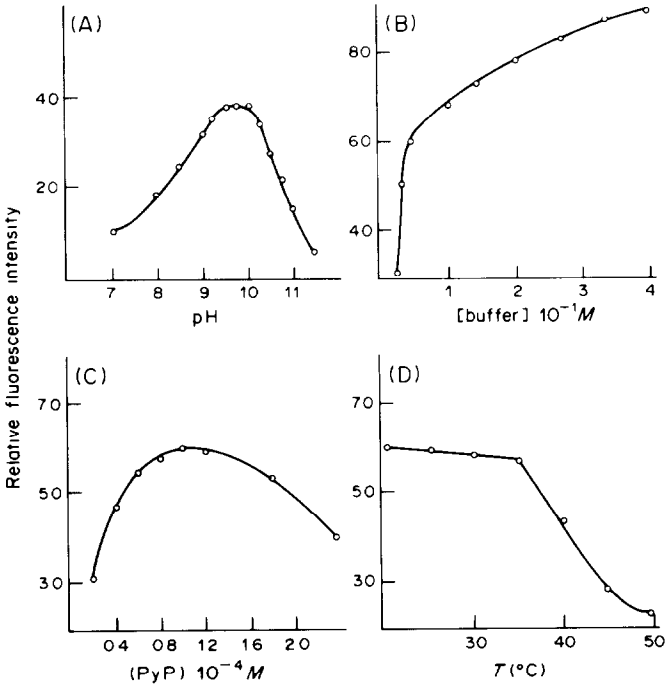

Fig. 2. Influence of (A) pH, (B) buffer concentration, (C) PyP concentration, (D) temperature, on the Be–PyP system.

Table 1. Tolerance limits in the determination of beryllium at the 30 ng/ml level

Tolerance ratio, ion: Be^{2+} w/w	Ion added
400	Al^{3+}*, Cu^{2+}*, Ni^{2+}*
100	Ba^{2+}, Cd^{2+}, Hg^{2+}, Mg^{2+}, Sr^{2+}, Ca^{2+}, Sn^{2+}, Tl^{+}, Zn^{2+}, Pt^{4+}, MoO_4^{2-}, WO_4^{2-}, VO_3^{-}, SeO_3^{2-}, CrO_4^{2-}, AsO_4^{3-}, UO_2^{2+}, Co^{2+}*, Fe^{3+}*, Pb^{2+}*, Cl^{-}, F^{-}, Br^{-}, I^{-}, NO_3^{-}, CO_3^{2-}, PO_4^{3-}, SO_4^{2-}, CN^{-}
10	Mn^{2+}, Sb^{3+}, Ti^{4+}, Sn^{4+}

*In the presence of 0.6 ml of 0.01*M* EDTA.

The maximum fluorescence intensity is obtained when beryllium and the reagent are mixed before the buffer solution is added.

Nature of the fluorescent product

The stoichiometry of the Be(II)–PyP system was evaluated by the molar-ratio and continuous-variations methods in the presence of a constant excess of ammonia. The ratio found in both cases was 2:1. In the Be–3-amino-5-sulphosalicylate complex, a stoichiometry in which the beryllium:ligand ratio is greater than 1:1 has also been found.[11] The Be–ammonia and PyP–ammonia ratios were evaluated by the molar-ratio method, by keeping the PyP and Be concentrations, respectively, constant and high. In both cases, there is a linear increase in the fluorescence intensity as the ammonia concentration increases and the maximum fluorescent signal is only obtained in the presence of a large excess of ammonia. However, it should be emphasized that the slope changes at a Be–ammonia ratio of 1:10 and at a PyP–ammonia ratio of 1:20. If ethylenediamine is used instead of ammonia, the change in slope occurs at a Be–ethylenediamine ratio of 1:5. Although these results are not logical according to the co-ordination number of Be(II), these values are surprisingly consistent if it is taken into account that ethylenediamine can act as a bidentate ligand.

A study of the retention of the complex on an anion-exchange resin showed it to be anionic in nature, but no conclusions about its structure have yet been reached.

Characteristics of the method

There is a linear relationship between the fluorescence intensity and the beryllium concentration between 8 and 60 ng/ml in the final solution. The detection limit, as defined by IUPAC[12] ($K = 3$; $n = 11$) is 7 ng/ml. The precision of the method was studied at several beryllium concentrations. Relative standard deviations of 9.3, 2.0, 2.0 and 1.5% were found for 10, 20, 40 and 60 ng/ml, respectively. These values are satisfactory, considering the low concentrations determined.

Interferences

To find possible analytical applications of the Be–PyP complex, the effect of different foreign ions was examined. The tolerance limits are listed in Table 1. Most of these ions do not cause interference when present in up to 100-fold ratio to beryllium. A 400-fold weight ratio to beryllium was tested for the ions of the metals which form the matrix of the alloys to be analysed [Cu(II), Al(III) and Ni(II)]. The selectivity is very good and the method is adequate for the determination of beryllium in copper-base, aluminium-base and nickel-base alloys. Only Cr(III) interferes at 1:1 weight ratio to beryllium, but its oxidation to Cr(VI) permits the direct determination

Table 2. Empirical determination of beryllium in simulated typical alloys

Alloy	Composition, % Be	Co	Ni	Ag	Uses	Be found, %
Copper-base	4.00				Master alloy	4.00 ± 0.06
	1.90	0.24			Electrical terminals, springs	2.05 ± 0.05
	1.70	0.24			Welder bars	1.62 ± 0.03
	0.50	2.50			Good electrical conductors	0.50 ± 0.03
	0.40	1.60		0.95	Bearings	0.41 ± 0.04
	0.40		1.50		Welding equipment	0.43 ± 0.05
	2.10	0.50			Casting alloys	2.30 ± 0.03
	2.40		1.10		Casting alloys	2.54 ± 0.07
Aluminium-base	5.00				Master alloy	4.93 ± 0.08
	0.20				Aircraft sheet	0.27 ± 0.05
Nickel-base	1.80				Springs	1.87 ± 0.06
	2.70				Castings	2.70 ± 0.07

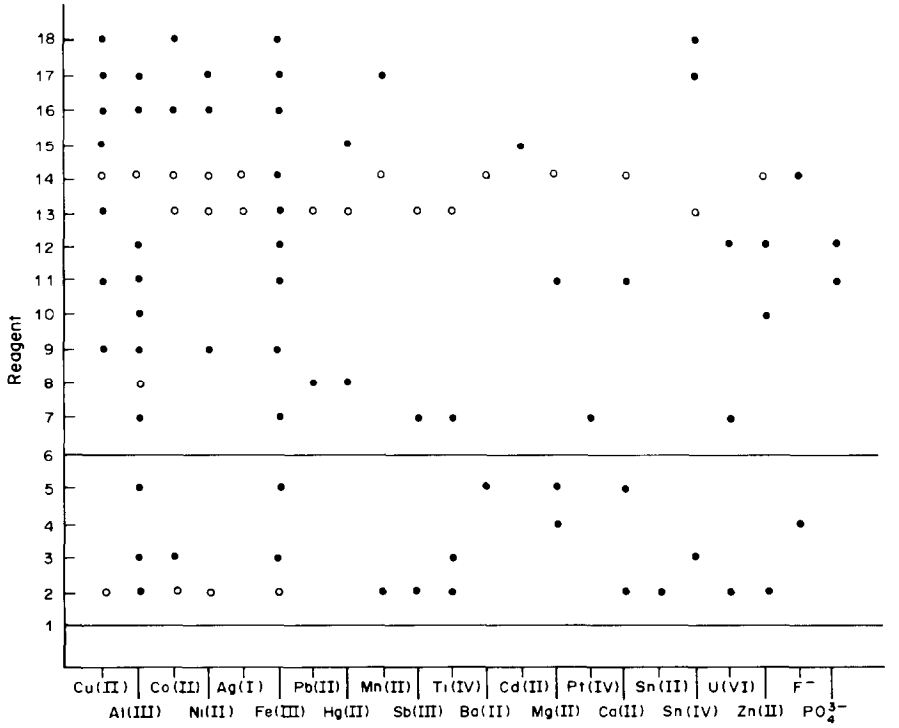

Fig. 3. Comparative selectivity of the fluorimetric methods for Be(II): ● ions which interfere at the same level as Be(II); ○ ions which interfere at the same level as Be(II) but can be masked, thus increasing tolerance ratio; ——— the selectivity of these methods is low and cannot be increased by masking, owing to quenching problems. Reagent. (1) salicylideneaniline;[13] (2) morin,[14] (3) 2-hydroxy-3-naphthoic acid;[15] (4) 4-[bis(carboxymethyl)aminomethyl]-3-hydroxy-2-naphthoic acid;[16], (5) tetracycline,[17] (6) 2-salicylideneamino-3,5-xylene arsonic acid;[18] (7) 2-ethyl-5-hydroxy-3-methylchromone;[19] (8) 2-salicylideneaminobenzene arsonic acid;[20] (9) 2-ethyl-5-hydroxy-7-methoxy-isoflavone;[21] (10) 1-hydroxy-2-carboxyanthraquinone,[22] (11) 3-hydroxy-2-naphthoic acid;[23] (12) 3-amino-5-sulphosalicylic acid,[11], (13) arsenazo (III);[24] (14) 2,2′-(pyridyl)phenol,[25] (15) dibenzoylmethane and pyridine;[26], (16) 4-hydroxy-3-(2-hydroxysalicylideneamino)benzene sulphonic acid;[27] (17) 5-methoxy-2-(salicylideneamino)phenol;[28] (18) 2-(salicylideneamino)benzoic acid.[29]

of beryllium in the presence of 100-fold amounts of chromium.

Applications

The method has been used to determine beryllium in several alloys of industrial interest, without prior separation from the matrix. As standard samples of beryllium in copper-base, aluminium-base and nickel-base alloys were not available, several synthetic ones were prepared.[6]

The samples, containing a total metal-ion concentration of 100 μg/ml. were treated in the same way as the standards, but with 0.6 ml of 0.01*M* EDTA added to each. Table 2 shows the composition of the simulated alloys, their most important industrial applications, and the results obtained in the determination of beryllium. The accuracy of these results proves the validity of the method for these types of sample.

Comparison with other methods

A comparison of the selectivity of this fluorimetric method with that of the fluorimetric procedures described in the literature[11,13-29] is shown in Fig. 3. Only those ions interfering when present at the same level as beryllium have been considered. None of the earlier procedures is more selective than the proposed method. Aluminium and iron (III) generally pose the most serious interferences and, furthermore, are difficult to remove by masking. Only two fluorimetric methods have been applied to the determination of beryllium in alloys. Sill *et al.*[30] determine beryllium in aluminium-alloys and copper-alloys with morin. Resolution of the first type of sample involves repetitive extraction with acetylacetone and chloroform. That of the second type of sample needs a mixture of sodium hydroxide, anhydrous sodium perchlorate, DPTA and triethanolamine as complexing solution, and incubation for 20 min. Furthermore, the temperature must be carefully controlled (a 1 ° change in the working temperature may change the fluorescence by as much as 5 or 6%), and the presence of copper may cause air-oxidation of the morin and hence low results[2] (an alkaline stannite reducing solution is recommended to prevent this oxidation).

Beryllium has also been determined in copper-alloys by Deguchi *et al.*[27] Interfering metals (Cu, Fe, Ni, Co, *etc.*) must be removed by electrolysis at a

mercury cathode. Excess of Al or residual Cu, Fe, Ni, Co, must be removed by extraction into chloroform with 8-hydroxyquinoline.

A comparative study of sensitivity indicates that 60% of the fluorimetric methods reported so far allow determination of beryllium concentrations below 10 ng/ml, morin and 2-salicylideneamino-3,5-xylene arsonic acid being the most sensitive reagents.

The method proposed here is rapid (only EDTA is needed to remove interferences and the complex formation is instantaneous), selective (the main interferences in the other fluorimetric methods are tolerated at higher concentrations) and simple (only a reagent and buffer are needed to develop the fluorescence).

REFERENCES

1. J. Walkley, *Am Ind. Hygiene Assoc. J.*, 1959, **20,** 241.
2. C. W. Sill and C. P. Willis, *Anal. Chem.*, 1959, **31,** 598.
3. S. R. Desai and K. K. Sudhalatha, *Talanta*, 1967, **14,** 1346.
4. R. G. Smith, A. J. Boyle, W. G. Fredrick and B. Zak, *Anal. Chem.*, 1952, **24,** 406.
5. T. Y. Toribara and P. S. Chen, Jr., *ibid.*, 1952, **24,** 539.
6. B. R. F. Kjellgren, C. W. Schwenzfeier, Jr. and E. S. Melick, *in Treatise on Analytical Chemistry*, 1st Ed., Part II, Vol. 6, I. M. Kolthoff and P. J. Elving (eds.), pp. 1–67. Wiley-Interscience, New York, 1964,
7. N. W. Bass, in *The Metal Beryllium*, D. W. White, Jr. and J. E. Burke, (eds), chapter II-C. American Society for Metals, Cleveland, Ohio, 1955.
8. G. C. Darwin and J. H. Buddery, *Beryllium*, Chapter 10. Academic Press, New York, 1960.
9. M. C. Udy, H. L. Shaw and F. W. Boulger, *Nucleonics*, 1953, **11,** 52.
10. L. Erdey, *Gravimetric Analysis*, Part 2, p. 618. Pergamon Press, Oxford, 1965.
11. N. M. Alykov and A. I. Cherkesov, *Zh. Analit. Khim.*, 1976, **31,** 1104.
12. G. L. Long and J. D. Winefordner, *Anal. Chem.*, 1983, **55,** 712A.
13. V. S. Efimychev, *Tr. Khim. i Khim. Tekhnol Gorkii*, 1962, No. 1, 126; *Anal. Abstr.*, 1964, **11,** 1218.
14. M. H. Fletcher, *Anal. Chem.*, 1965, **37,** 550.
15. G. F. Kirkbright, T. S. West and C. Woodward, *ibid.*, 1965, **37,** 137.
16. B. Buděšínský and T. S. West, *Anal. Chim. Acta*, 1968, **42,** 455.
17. N. Takio, N. Hideo and Y. Teruyo, *Bunseki Kagaku*, 1969, **18,** 1068.
18. Z. Holzbecher and K. Volka, *Collection. Czech. Chem. Commun.*, 1970, **35,** 2925.
19. T. Ito and A. Murata, *Bunseki Kagaku*, 1971, **20,** 335.
20. Sh. T. Talipov, A. T. Tashkhodzhaev, L. E. Zel'tser and Kh. Khikmatov, *Zh. Analit. Khim.*, 1973, **28,** 807.
21. A. Murata, M. Tominaga and T. Suzuki, *Bunseki Kagaku*, 1974, **23,** 1349.
22. F. Capitán, F. Salinas and L. M. Franquelo, *Anal Lett.*, 1975, **8,** 753.
23. K. Kasiura, *Chem Analit Warsaw*, 1975, **20,** 389.
24. S. B. Savvin, R. K. Chernova and L. M. Kudryavtseva, *Zh. Analit. Khim.*, 1976, **31,** 269.
25. L. Kábrt and Z. Holzbecher, *Collection. Czech. Chem. Commun.*, 1976, **41,** 540.
26. S. B. Meshkova, S. F. Potapova, L. I. Kononenko and N. S. Poluektov, *Zh. Analit. Khim.*, 1977, **32,** 1529.
27. M. Deguchi, K. Nanba, K. Morishige and I. Okumura, *Bunseki Kagaku*, 1980, **29,** 91.
28. K. Morishige, *Kinki Daigaku Rikogakubu Kenkiu Hokoku*, 1981, **16,** 265.
29. *Idem, ibid.*, 1982, **17,** 411.
30. C. W. Sill, C. P. Willis and J. K. Flygare, Jr., *Anal. Chem.*, 1961, **33,** 1671

Talanta, Vol. 32, No 11, pp 1047–1050, 1985
Printed in Great Britain.

0039-9140/85 $3.00 + 0.00

SEPARATION AND DETERMINATION OF ALUMINIUM BY SINGLE-COLUMN ION-CHROMATOGRAPHY

NANCY E. FORTIER and JAMES S. FRITZ*
Ames Laboratory and Department of Chemistry, Iowa State University, Ames, Iowa 50011, U.S.A.

(*Received* 13 *March* 1985. *Accepted* 30 *April* 1985)

Summary—A quick, reliable method for the determination of Al(III) in the presence of other metal ions is presented. A chromatographic system consisting of a low-capacity cation-exchange column, an eluent of diprotonated *p*-phenylenediamine, and a conductivity detector was used to measure the retention times for various cations. During the course of this work, it was found that Al(III) was eluted later than most bivalent metal ions but earlier than other tervalent metal ions. Therefore the concentration of eluent was adjusted so that an early sharp peak was obtained for Al(III) and the bivalent metal ions were eluted as a group. Through analysis of an NBS standard, as well as of solutions containing Al(III) and other metal ions, the method was shown to be precise, accurate and rapid for determination of Al(III) without interference from common bivalent metal ions.

Although a vast quantity of research has been done on use of chromatography to separate and determine bivalent and rare-earth metal ions, relatively little work has been done on developing a chromatographic method for the determination of aluminium. Classical chromatographic methods generally used gravity eluent flow and required collection of effluent fractions from the column. These fractions then had to be analysed by AAS,[1-3] EDTA titration[4-6] or absorbance measurements after removal of interfering substances.[7] Maslowska and Pietek[8] separated the *p*-hydroxybenzoate complexes of aluminium, iron(III) and cerium(III) on an ion-exchange column, using low pressure and a spectrophotometric detector.

Modern ion-chromatography has been shown to be useful for separating univalent,[9] bivalent[9,10] and rare-earth metal cations.[10] However, with the exception of the rare earths, tervalent metal ions, such as Al(III), have posed a problem in ion-chromatography. A brief note[11] described the separation of aluminium and iron(III) by cation-chromatography, with Tiron as the colour-forming reagent for post-column reaction and spectrophotometric detection.

In the present research, the elution of metal cations from a cation-exchange column of low capacity is studied. The eluent contains the diprotonated cation of either *N*-phenylethylenediamine or *p*-phenylenediamine, and conductivity detection is employed. The original objective was to study how the retention times of various cations change with the type of eluent used. However, aluminium was found to be eluted later than most bivalent metal ions and well before other tervalent metal ions. This forms the basis of a selective and convenient ion-exchange method for determining aluminium.

*Author for correspondence.

EXPERIMENTAL

Apparatus

The instrument used consists of a model AA-94 Eldex dual-channel pump, a model 1116 Eldex column-heater equipped with a 50-μl sample loop, a model No. 269-004 Wescan catex column (capacity 0.03 meq/g, 12–16 μm particle-size, 5% cross-linked, sulphonated polystyrene–divinylbenzene gel, 25 cm length, 2 mm bore.), a model 213A Wescan conductivity detector, and a Curken strip-chart recorder.

Eluents

Reagent-grade *p*-phenylenediamine and perchloric acid were used without further purification. The *N*-phenylethylenediamine was used both as received and after distillation under reduced pressure. The eluent solutions were prepared by dissolving the amine in perchloric acid and diluting with demineralized water, then filtered through a 0.45-μm membrane and degassed. The pH of the eluents was adjusted to 3 with perchloric acid. The purpose of the pH adjustment was to ensure complete protonation of the diamines used, as well as to maintain a constant pH so that the relative strengths of the diamines as eluents could be compared. Once prepared, the eluents were immediately stored under a helium atmosphere and protected from light to prevent decomposition.

Sample solutions

The Al(III) standard stock solution was prepared by dissolving 0.4707 g of Alcoa Research Laboratories standard aluminium wire SCI-A in about 25 ml of concentrated hydrochloric acid with heating, then diluting accurately to 1 litre with demineralized water. The Al(III) solutions used for the calibration curve were prepared by diluting aliquots of this stock solution.

The stock solution of NBS Standard Sample 94a, a zinc-base alloy (see Table 1), was prepared by dissolving the

Table 1. Composition (%) of National Bureau of Standards Standard Sample 94a, Zinc-Base Alloy (Die-Casting)

Al	3.90
Cu	1.08
Mg	0.042
Mn	0.015
Fe	0.015
Pb	0.006
Ni	0.005
Sn	0.005
Cd	0.002

bulk of a 0.5305 g sample in perchloric acid and demineralized water with heating. When effervescence ceased a black residue remained, which went into solution on addition of a small amount of concentrated nitric acid. The solution was accurately diluted to 1 litre with demineralized water to yield a solution with an aluminium concentration of 0.767m*M*.

Other metal ion solutions were prepared by using reagent-grade salts, concentrated perchloric acid and demineralized water. The pH of all metal ion solutions was adjusted with perchloric acid to approximately 3 merely to prevent hydrolysis

RESULTS AND DISCUSSION

Since protonated ethylenediamine had been shown to be an adequate eluent for cation-chromatography,[9,10] it was surmised that other amines might also be useful. The first one tested was *N*-phenylethylenediammonium perchlorate. While at first this appeared to be satisfactory, it was soon noted that the retention times obtained with it were not reproducible. Further experimentation showed that something in the eluent, either an impurity or a decomposition product, was gradually occupying exchange sites on the column. As time passed, the capacity of the column was reduced and retention times were drastically shortened. Figure 1 shows how the retention times for an Al(III) solution changed as more and more eluent was pumped through the column. Attempts to prevent this phenomenon by purifying the amine through distillation under vacuum and slowing the rate of decomposition by keeping the eluent under helium and protected from light were unsuccessful; retention times continued to decrease with elapsed time. Although an injection of nitric acid effectively seemed to remove the species that was occupying the column sites and produced retention times with their initial values, the trend of decreasing retention times with increasing elapsed time merely began again as soon as the nitric acid was eluted. Therefore this eluent was abandoned.

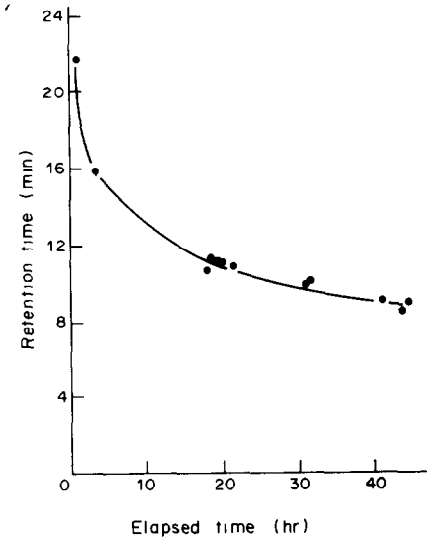

Fig. 1. Plot of the retention time of Al(III) peak *vs.* time elapsed since column equilibration was achieved. Conditions: eluent, 0.994 m*M* *N*-phenylethylenediamine, pH 3.1; temperature, 26 ; flow-rate, 1.02 ml/min.

An eluent prepared by mixing *p*-phenylenediamine and perchloric acid in 1:2 molar ratio worked well. Its absolute conductivity was never measured, but was easily electronically backed-off. At a flow-rate of 1 ml/min, the column back-pressure was about 1200 psig. The retention times given in Table 2 were found to be very reproducible. Occasionally nitric acid was injected as a precautionary measure to prevent any long-term build-up of strongly retained species on the column, although this treatment may have been superfluous. Retention times (t') of ions were unaffected by this treatment.

It has been shown[10] that a plot of log t' *vs.* log [eluent] should be linear with a slope of $-y/2$, y being the charge on the analyte ion. Bivalent metal ions should give a slope of -1, and tervalent metal ions a slope of -1.5. This relationship was shown to hold within experimental error for the bivalent and tervalent ions studied here.

Aluminium determination

To obtain a sharp, early peak for Al(III), it was necessary to increase the concentration of *p*-phenylenediamine; 8.23m*M* was used. At this concentration, the bivalent metal ions were eluted quickly as a group and did not interfere with the Al(III) peak.

Table 2. Retention times for bivalent and tervalent metal ions: temperature 27 , flow-rate 1 ml/min; [*p*-phenylenediamine] 1.99m*M* for bivalent and 6.04m*M* for tervalent ions; retention time of the unretained peak, t_0, 0.44 min

Cation	*t*, *min**	rsd, %
Mg(II)	1.63	0 0
Mn(II)	2.02	1.8
Zn(II)	2.06	0 0
Co(II)	2.17	1.7
Ca(II)	2.83	1.3
Sr(II)	3.92	2.4
Al(III)	8.6	1.9
Lu(III)	22.3	1 3
Tm(III)	23.0	2.2

*Average of at least three runs.

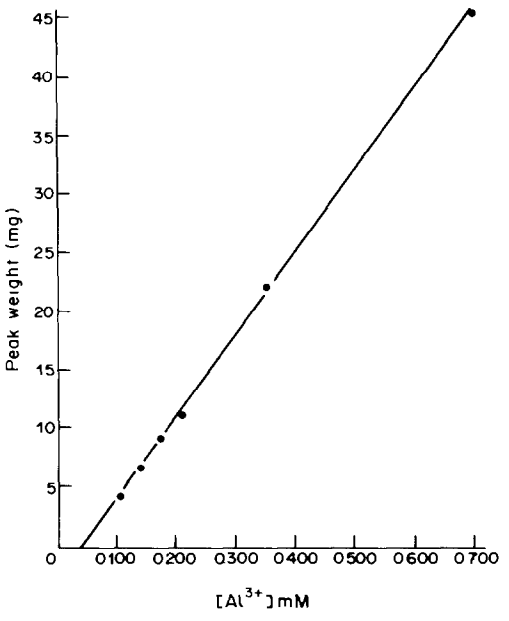

Fig 2. Calibration plot for aluminium standard solutions. Conditions. eluent, 8.23m*M* *p*-phenylenediamine, pH 3.0; temperature, 27°; flow-rate, 0.97 ml/min. Correlation coefficient 0.9996.

Therefore, a study was undertaken to see whether the determination of Al(III) was possible with protonated *p*-phenylenediamine as eluent. All solutions were injected under the following conditions: eluent 8.23m*M* *p*-phenylenediamine, pH 3.00; temperature 27 ; flow-rate 0.97 ml/min. Since an electronic integrator was not available, a calibration curve was prepared by cutting out and weighing the peaks, and plotting peak weight *vs.* concentration of the Al(III) standard solutions. Six different concentrations from 0.1 to 0.7m*M* gave a linear plot (Fig. 2).

To see whether the amount of aluminium in a solution could be accurately determined when other metal ions were present, injections were made of the solution of NBS Standard Sample 94a. To keep the peak for aluminium within the span of the recorder chart, the stock solution was diluted by a factor of two. However, a representative Al(III) peak could not be obtained, owing to the presence of a large negative peak caused by the excess of acid needed to dissolve the alloy. The pH of the undiluted stock solution was found to be only 0.95, whereas the pH of the Al(III) standard solutions ranged from 2.45 to 3.29. Therefore the pH of a 50.0-ml aliquot of the stock solution was adjusted to 2.57 with concentrated ammonia solution and the solution was diluted to 100.0 ml (final pH 2.94). Injections of this solution gave peaks with areas which could be easily measured (Fig. 3).

Injections were also made of two other solutions containing Al(III): Al(III) in presence of a 114-fold molar ratio of uranium(VI), and in a solution containing six other metal ions in the following molar ratios to aluminium: Ca(II) 12-fold, Mg(II), Zn(II), Sr(II) each 13-fold, Co(II) and Mn(II) each 14-fold.

Table 3. Results for aluminium determination

Solution	[Al], m*M* Taken	Found*	rsd, %
NBS Standard Sample 94a zinc-base alloy, 0.2653 g/l.	0.383	0.389	6.1
Al(III) in 19.80 m*M* UO_2^{2+}	0.173	0.173	6.4
Al(III) in a solution of 3.44 m*M*, Ca(II) 3.77 m*M*, Mg(II) 3.77 m*M*, Zn(II) 3.77 m*M*, Sr(II) 4.10 m*M*, Co(II) 4.10 m*M*, Mn(II)	0.286	0.261	3.6

*Average of at least three runs.

The results tabulated in Table 3 show that the chromatographic method described is capable of

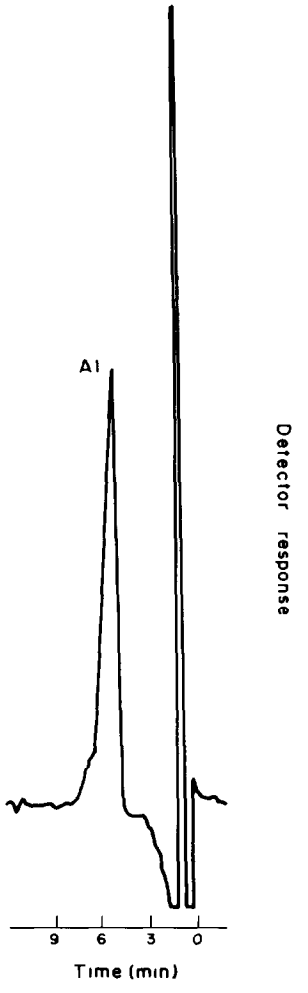

Fig. 3 Solution of NBS Standard Sample 94a, 0.383 m*M* in Al(III), pH 2.94. Conditions: eluent, 8.23m*M* *p*-phenylenediamine, pH 3.0; temperature, 27 flow-rate, 0.97 ml/min

giving quantitative results for aluminium, even in samples containing several other metal ions. Because of the comparatively low precision, it is best to replicate analyses, and use the mean value.

Acknowledgements—The authors wish to thank G. J. Sevenich for his advice and technical assistance. Ames Laboratory is operated for the U.S. Department of Energy under Contract No. W-7405-ENG-85. This work was supported by the Director of Energy Research, Office of Basic Energy Sciences.

REFERENCES

1. K. Brajter and E. Olbrych-Śleszyńska, *Talanta*, 1983, **30**, 355.
2. R. J. Phillips and J. S. Fritz, *Anal. Chim. Acta*, 1982, **139**, 237.
3. K. G. Varshney, S. Agrawal and K. Varshney, *J. Liq. Chromatog.*, 1983, **6**, 1535.
4. S. A. Nabi, R. A. Rao and A. R. Siddiqui, *Z. Anal. Chem.*, 1982, **311**, 503.
5. K. G. Varshney, S. Agrawal, K. Varshney and A. Premedas, *Talanta*, 1983, **30**, 955.
6. K. G. Varshney, A. A. Khan and S. S. Varshney, *Indian J. Chem.*, 1982, **21A**, 398.
7. R. N. Sen Sarma and M. K. Majumdar, *J. Indian Chem. Soc.*, 1982, **59**, 790.
8. J. Maslowska and W. Pietek, *Chromatographia*, 1983, **17**, 693.
9. J. S. Fritz, D. T. Gjerde and R. M. Becker, *Anal. Chem.*, 1980, **52**, 1519.
10. G. J. Sevenich and J. S. Fritz, *ibid.*, 1983, **55**, 12.
11. Dionex Corporation, *Application Note 42*, 1983.

Talanta, Vol 32, No 11, pp. 1051–1054, 1985
Printed in Great Britain.

0039-9140/85 $3.00 + 0.00

DETERMINATION OF THALLIUM IN BISMUTH BY DIFFERENTIAL PULSE ANODIC-STRIPPING VOLTAMMETRY WITHOUT PRELIMINARY SEPARATION

ALEKSANDER CISZEWSKI
Institute of General Chemistry, Technical University of Poznań, 60-965 Poznań, Poland

(*Received* 8 *January* 1985. *Revised* 29 *March* 1985. *Accepted* 24 *May* 1985)

Summary—The determination of trace levels of thallium in bismuth and bismuth salts by differential pulse anodic-stripping voltammetry has been made possible by using a surfactant as an electrochemical masking agent, in addition to a complexing agent. In 0.2*M* EDTA at pH 4.5 as supporting electrolyte in the absence of surfactant, bismuth at concentrations below $10^{-4}M$ does not interfere. When the electrolyte also contains tetrabutylammonium ions at 0.01*M* concentration, bismuth can be tolerated at concentrations up 0.05*M*, and the height of the thallium peak is unaffected. It is thus possible to determine 1 n*M* Tl(I) in the presence of 0.05*M* Bi(III), *i.e.*, Tl at the 1×10^{-6}% level in bismuth. The precision of the determination and the recovery are satisfactory. Neither an 800-fold ratio of Cu(II) nor a 10^7-fold ratio of Pb(II) to Tl(I) interferes in the determination. Other cations such as Zn^{2+}, Cd^{2+}, In^{3+}, Hg^{2+}, Fe^{3+}, Sb^{3+} and Sn^{4+} in 10^4-fold molar ratio to Tl(I) have no effect on the determination. Thallium has been determined in bismuth metal and in bismuth nitrate of various degrees of purity.

Differential pulse anodic-stripping voltammetry (DPASV) has become an important electroanalytical technique, especially for trace analysis, because of its high sensitivity and specifity, but its use is sometimes difficult or even impossible, *e.g.*, in determination of a trace concentration in the presence of a very large excess of another component (especially of an ion which can be reduced to form an amalgam at a potential less negative than that for reduction of the ion of interest). Interferences can be eliminated by a preliminary separation, but this results in poorer precision and accuracy, and prolongs the determination. Suppression of the electrochemical activity of the matrix elements by introduction of a surfactant, known as "electrochemical masking", is an effective way of avoiding the separation.

There are a few promising examples of the use of electrochemical masking in d.c. polarography[1-4] and stripping analysis.[5-10]

The objective of this study was to apply electrochemical masking to determination of thallium, as Tl(I), in the presence of a very large excess of bismuth by DPASV, without preliminary separation. In most solutions bismuth gives a wave at more positive potentials than thallium does, and the well separated half-wave potentials allow determination of both metals in the same test solution, but when bismuth is the matrix element and present in relatively very large amounts, direct determination of thallium is impossible. To solve this problem both a complexing agent (EDTA) and a surface-active agent (tetrabutylammonium ions) were added to the test solution.

EXPERIMENTAL

Apparatus

A Telpod (Poland) pulse polarograph model PP-04 was used. Voltamperograms were displayed on an Endim (GDR) 620.02 XY-recorder. A classical three-electrode system was employed: a Kemula hanging mercury-drop electrode (Kemula Equipment E 69, Radiometer, Copenhagen) as working electrode, a platinum wire as auxiliary electrode and an SCE as reference. The surface area of the hanging mercury drop was 2.1 mm^2. The differential pulse amplitude was 100 mV and scan-rate 11.1 mV/sec. During the deposition step the solutions were stirred. All potentials reported are referred to the SCE.

Reagents

Merck tetrabutylammonium chloride (TBAC) and EDTA (disodium salt) were used. Standard solutions of thallium and bismuth ($10^{-2}M$) were prepared by dissolving the metals in nitric acid. Solutions with concentrations below $10^{-3}M$ were prepared just before use. Water was doubly distilled in a quartz still. The background electrolyte was 0.2*M* EDTA, pH 4.5 ± 0.1, adjusted with purified potassium hydroxide solution. Before measurement all solutions were brought to 20 ± 0.5 in a thermostat.

Procedure

If not stated otherwise, nitrogen was passed for 10 min through 25 ml of the solution to be studied, then a mercury drop was formed at the capillary tip, stirring was begun, nitrogen was passed above the solution, and the solution was electrolysed for a predetermined time at −0.700 V. Stirring was then stopped, and after 20 sec the potential was scanned from −0.700 V to positive potentials and the stripping peak for thallium was recorded.

RESULTS AND DISCUSSION

An EDTA solution (0.2*M*, pH 4.5 ± 0.1) was chosen as background electrolyte to avoid coincidence of

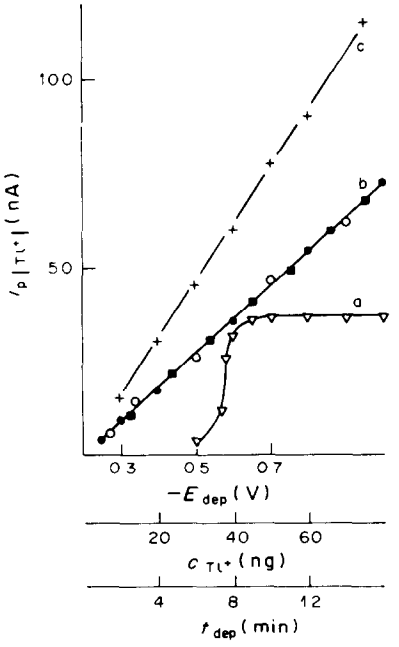

Fig. 1. Dependence of differential pulse anodic stripping peak current for thallium on the deposition potential (*a*), the thallium concentration (*b*) and the deposition time (*c*). Concentration of thallium: (*a*) $1 \times 10^{-8}M$; (*c*) $3 \times 10^{-8}M$. Deposition potential (*b*, *c*): -0.700 V *vs.* SCE. Deposition time (*a*, *b*): 15 min. Background electrolyte: (○) 0.2*M* EDTA, pH 4.5 ± 0.1; (+ ▽●) 0.2*M* EDTA, pH 4.5 ± 0.1, 0.01*M* TBAC; (■) 0.2*M* EDTA, pH 4.5 ± 0.1, 0.01*M* TBAC, 0.01*M* Bi(III). Differential-pulse amplitude 100 mV, scan-rate 11.1 mV/sec.

the stripping peaks for lead and thallium, which occur at similar potentials in various base electrolytes. Figure 1 shows that the proposed medium allows satisfactory determination of thallium at concentrations of about $10^{-9}M$. A deposition potential of -0.700 V was chosen as optimal. The stripping peak is located at -0.48 V, with peak-width 105 mV. A linear relation of peak-current to thallium concentration was found over the range 1×10^{-9}–$1 \times 10^{-7}M$. The plot of peak-current *vs.* deposition period is linear for periods ranging from 1 to 15 min, with a slope of 8 nA/min for $3 \times 10^{-8}M$ thallium, and passes through the origin.

Determination of thallium in the presence of bismuth depends on the bismuth concentration. Under the conditions examined, bismuth gives a stripping peak at -0.13 V. From the values of $E_{p(Tl)}$ and $E_{p(Bi)}$ there should be a high separation factor in the determination of thallium in the presence of bismuth. However, the peak-current of bismuth depends on the original deposition potential. When a deposition potential of -0.700 V is used, the peak-current of bismuth at -0.13 V is very small (Fig. 2, curve *a*). It is found that determination of $1 \times 10^{-8}M$ thallium is possible even in presence of $10^{-4}M$ bismuth. When the concentration ratio of bismuth to thallium is greater than about 10^4, however, there is increasing interference as the ratio increases; the voltammetric curves show only the currents for reduction and oxidation of bismuth, the peak-current for thallium being "swamped", as shown for 0.05*M* bismuth by curve *a* in Fig. 3. This suggests that it would be difficult to determine thallium in the presence of

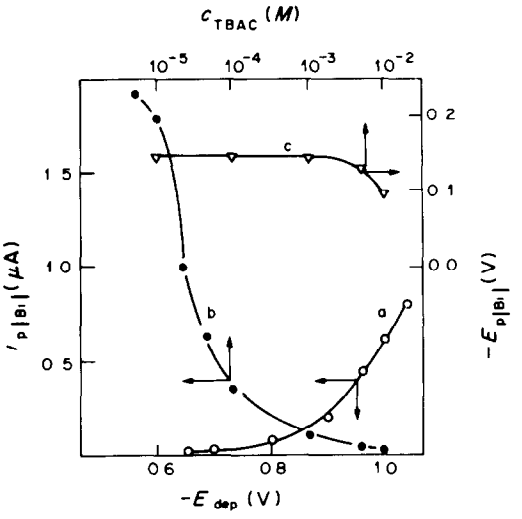

Fig. 2. Variation in the size of the bismuth peak in absence (*a*) and presence (*b*, *c*) of TBAC. (*a*) Peak current *vs.* deposition potential, (*b*) peak current *vs.* [TBAC], (*c*) peak potential *vs.* [TBAC]. Concentration of Bi(III): (*a*) $1 \times 10^{-7}M$; (*b*, *c*) 0.025*M*. Deposition potential (*b*, *c*): -0.700 V *vs.* SCE. Deposition time: (*a*) 300 sec; (*b*, *c*) 100 sec. Background electrolyte: 0.2*M* EDTA, 0.01*M* TBAC, pH 4.5 ± 0.1. Differential pulse amplitude 100 mV, scan-rate 11.1 mV/sec.

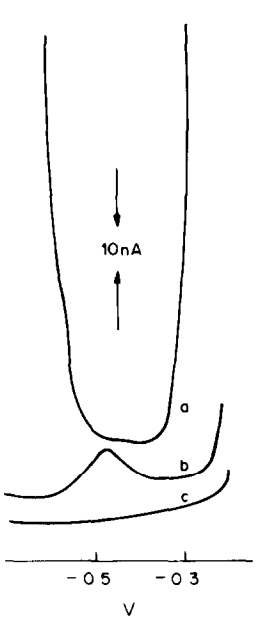

Fig. 3. Differential pulse anodic stripping voltammperograms: (*a*) 0.05*M* Bi(III) + $2 \times 10^{-9}M$ Tl(I); (*b*) 0.05*M* Bi(III) + $2 \times 10^{-9}M$ Tl(I) + 0.01*M* TBAC; (*c*) 0.05*M* Bi(III) + 0.01*M* TBAC. Deposition potential. -0.700 V *vs.* SCE. Deposition time: 15 min. Background electrolyte: 0.2*M* EDTA, pH 4.5 ± 0.1. Differential pulse amplitude 100 mV, scan-rate 11.1 mV/sec

substantially larger amounts of bismuth, and impossible to determine traces of thallium in samples where the matrix is bismuth.

An attempt was therefore made to suppress the electrochemical activity of the matrix element by addition of tetrabutylammonium chloride (TBAC) to act as a surfactant in the solution. The influence of TBAC concentration on the stripping peak-current of bismuth is shown in Fig. 2. The results indicate that a concentration of 0.01*M* TBAC is sufficient to suppress the bismuth peak almost completely. The stripping peak-current for 0.05*M* bismuth in the presence of TBAC is almost the same as that for $10^{-7}M$ bismuth in the absence of TBAC; in contrast, 0.01*M* TBAC has no effect on the thallium peak. Figure 4 shows the differential pulse polarograms for $5 \times 10^{-5}M$ bismuth in the absence (curve *a*) and presence (curve *b*) of TBAC; these curves show the polarographic reduction of Bi(III) at the dropping mercury electrode, and correspond to the deposition step in DPASV measurements. It is obvious that the presence of TBAC virtually completely suppresses the deposition of bismuth during the DPASV procedure, and makes possible the determination of traces of thallium in a bismuth matrix. An illustration of this is presented in Fig. 3, curve *b*, where the amount of thallium corresponds to a level of 5×10^{-6}% in a bismuth matrix.

Results showing the precision and recovery are given in Table 1 and indicate the absence of a systematic error. The method has been tested by determining the thallium content of bismuth metal and of bismuth nitrate of various degrees of purity (Table 2).

Table 1. Accuracy and precision of the determination of thallium in the presence of bismuth and TBAC*

Series	Added Bi, *mg*	Added Tl, *ng*	Tl found, *ng*	Std. devn., *ng*	Relative std. devn., %
I	300	20	19	3	15
II	200	80	79	10	12
III	100	408	410	27	7

*Seven measurements.

Table 2. Thallium content of bismuth matrices

Bismuth matrix	Grade	Sample weight, *g*	Thallium content, *μg/g*
$Bi(NO_3)_3 \cdot 5H_2O$	Reagent	0.485	1.20 (1.22*)
$Bi(NO_3)_3 \cdot 5H_2O$	A.R.	0.485	0.13
Bi	Reagent	0.200	0.75 (0.73*)
Bi	A.R.	0.200	0.06

*Spectrophotometric determination.[12]

Assuming that 5 ng of Tl(I) can be determined by use of a 15-min deposition time and that the amount of bismuth present should not exceed 0.3 g, the lower limit of determination is about 1×10^{-6}% of thallium in metallic bismuth and about 7×10^{-7}% in bismuth salts.

Experiments show that a 10^4-fold molar ratio of Zn^{2+}, Cd^{2+}, In^{3+}, Fe^{3+}, Sb^{3+}, Sn^{4+} and Hg^{2+} to Tl(I) has no effect on the determination of $1 \times 10^{-8}M$ Tl(I). The only serious interference is from Cu^{2+}, for which the reduction potential is −0.27 V. Though the anodic stripping peak of copper is quite far from the thallium peak ($E_{p(Cu)}$−0.26 V), a sufficient concentration of copper substantially increases the background current, thus causing interference. In the presence of 0.01*M* TBAC an 800-fold ratio of copper to thallium can be tolerated.

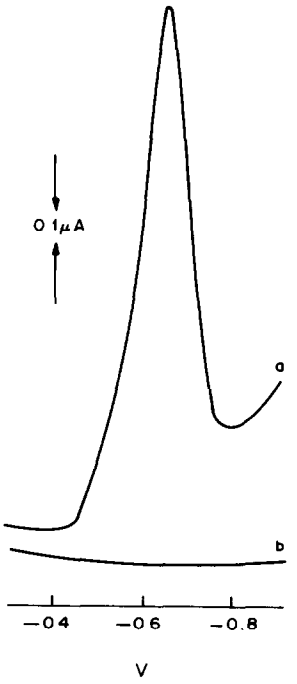

Fig. 4. Differential pulse polarograms for $5 \times 10^{-5}M$ Bi(III): (*a*) 0.2*M* EDTA, pH 4.5 ± 0.1; (*b*) 0.2*M* EDTA, pH 4.5 ± 0.1, 0.01*M* TBAC. Conditions: pulse amplitude 50 mV, scan-rate 2 mV/sec, drop-time 2 sec.

Procedures

Determination of thallium in metallic bismuth. Weigh out about 0.3 g of the bismuth, dissolve it in a few ml of semiconductor-grade nitric acid, than evaporate the excess of acid. Add 0.25 ml of 1*M* tetrabutylammonium chloride and 20 ml of 0.25*M* EDTA. Adjust the pH to 4.5 ± 0.1, by dropwise addition of 10% potassium hydroxide solution, transfer the solution to a 25-ml standard flask and make up to the mark with water. Transfer the solution into the electrochemical cell and pass purified nitrogen or argon through it for 15 min. Perform the electrolytic deposition in stirred solution at −0.700 V *vs.* SCE for 5–15 min, depending on the expected thallium content. After the deposition, switch off the stirrer, wait for 20 sec, then record the voltamperogram from −0.700 to 0 V *vs.* SCE. Repeat the measurement cycle twice more on the same solution, with a new mercury drop each time. Estimate the thallium by the standard-addition method, by making three successive addition of a known volume of thallium (I) standard solution to the same solution, repeating the measurement cycle each time, beginning from the deposition stage. From the linear plot of peak height *vs.* amount of thallium standard added,

read the amount of thallium in the sample. The standard thallium solution must be sufficiently concentrated for the volume added to be accurately measurable (within say 1%) but also to cause negligible change (say $<2\%$) in the total volume.

Determination of thallium in bismuth salts. Weigh out an amount of salt equivalent to about 0.3 g of bismuth, dissolve it in 20 ml of 0.25*M* EDTA, add 0.25 ml of 1*M* tetrabutylammonium chloride, adjust to pH 4.5 ± 0.1 by dropwise addition of 10% potassium hydroxide solution, and dilute to volume in a 25-ml standard flask. Transfer the solution into the electrochemical cell and determine thallium as above.

Acknowledgements—The investigations described in this paper were performed as part of the research programme MR-I-32 The author thanks Dr Z. Łukaszewski for many helpful comments and much encouragement provided in the preparation of this paper.

REFERENCES

1. T. Fujinaga and K. Isutsu, *Bunseki Kagaku*, 1961, **10**, 63.
2. J Kuta, *Z. Anal. Chem.*, 1966, **216**, 243.
3. E. Jacobsen and G. Tandberg, *Anal. Chim. Acta*, 1969, **47**, 285.
4. Z. Łukaszewski, *Talanta*, 1977, **24**, 603.
5. W. Kemula and S. Głodowski, *Roczniki Chem.*, 1962, **36**, 1203.
6. R. Neeb and I. Kiehnast, *Naturwissenschaften*, 1970, **57**, 37
7. P. Sagberg and W. Lund, *Talanta*, 1982, **29**, 460
8. J. Hernandez Mendez, R. Carabias Martinez and M. E. Gonzalez Lopez, *Anal. Chim Acta*, 1982, **138**, 47.
9. J. Georges, *ibid.*, 1981, **127**, 233.
10. Z. Łukaszewski, M. K. Pawlak and A. Ciszewski, *Talanta*, 1980, **27**, 181.
11. A. Ciszewski and Z. Łukaszewski, *ibid.*, 1983, **30**, 873.
12. Z Gregorowicz, J. Ciba and B. Kowalczyk, *ibid*, 1981, **28**, 805.

Talanta, Vol 32, No 11, pp 1055 1057, 1985
Printed in Great Britain

0039-9140/85 $3 00 + 0 00
Pergamon Press Ltd

SHORT COMMUNICATIONS

EXTRACTION OF ARSENIC(III) FROM CHLORIDE–IODIDE SOLUTIONS BY DIPHENYL(2-PYRIDYL)METHANE AND BENZENE

M. EJAZ and E. SIDDIQUE

Department of Chemical Engineering, College of Engineering, King Abdulaziz University, P.O. Box 9027, Jeddah, Saudi Arabia

and

SUHAIL AHMED

Pakistan Institute of Nuclear Science and Technology, Nilore, Rawalpindi, Pakistan

(*Received* 1 *December* 1983 *Revised* 22 *April* 1985. *Accepted* 9 *August* 1985)

Summary—The variation of the partition coefficient of arsenic(III) between chloride–iodide solutions and diphenyl(2-pyridyl)methane in benzene has been studied. The effect of the concentration of hydrochloric acid and iodide in the aqueous phase has been assessed. The partition coefficients are maximal for concentrated acid solutions which are 0.02–0.1 *M* in potassium iodide. Slope-analysis studies were used to elucidate the composition of the extracted species. Polymerization of the solvent species tends to decrease the distribution coefficients of arsenic with increasing concentration of diphenyl(2-pyridyl)methane, especially with trace concentrations of the element. Arsenic can be selectively separated from copper, cobalt, nickel, iron, chromium and antimony, which are usually associated with it in various ores.

Earlier investigations[1–5] have shown that arsenic can be extracted as a chloro-complex by conventional solvents and Lewis-base extractants, but the distribution coefficients are too low for complete extraction in a single step. In an attempt to find a better system, we studied[6] the extraction from chloride–thiocyanate medium with 0.1 *M* diphenyl(2-pyridyl)methane (DPPM) in benzene, but quantitative extraction still needed several equilibration steps. In the present study we examined the use of the weakly basic iodide ion for complexation. The results show that a highly selective and quantitative extraction can be achieved in a single equilibration step from 9 *M* hydrochloric acid/0.02–1 *M* potassium iodide medium with 0.01 *M* DPPM in benzene. Under the experimental conditions for the extraction, several metal ions which are known to form anionic chloride complexes at this acidity are very poorly extracted. They can be removed almost completely from the organic phase in two or three scrub stages, which will not affect the recovery of arsenic, because of its very high extraction coefficients.

EXPERIMENTAL

Reagents and tracers

DPPM was obtained commercially (Aldrich) and used without further purification. Its characteristics have been reported elsewhere.[7] Hydrochloric acid solutions were prepared either from BDH volumetric solution ampoules or from the Merck "*pro analysi*" grade acid, and standardized if necessary. Potassium iodide solutions were prepared from the analytical grade salt and demineralized doubly distilled water, and were kept in dark bottles.

Arsenic-76 ($t_{1/2}$ 26.3 hr) and other tracers used were obtained by neutron irradiation of the pure metals or their oxides in the PARR-1 research reactor of the Pakistan Institute of Technology or obtained from the Radiochemical Centre, Amersham. Some were separated from the parents without a carrier.

Apparatus

The radiochemical purity of the tracers was checked by gamma spectrometry with a 30-cm^3 Ge(Li) detector in conjunction with a Nuclear Data model ND-4410 computerized analyser system. γ-Ray count-rates were determined with a Nuclear Chicago single-channel analyser, model-872, coupled with a 7.5 × 7.5 cm thallium-doped sodium iodide well-type γ-ray scintillation counter. Solid β-emitting samples were assayed with an end-window Geiger assembly equipped with a G.E.C. tube, type EHM/2/S.

Determination of distribution coefficients

Extractions were done at room temperature (23 ± 3°) in 20-ml glass vials: 1 ml of mineral acid containing ^{76}As or other element (activity ~ 10^4 counts . sec^{-1} . ml^{-1}) was put in the vial and potassium iodide solution was added to adjust the iodide concentration to the required level. The aqueous phase was then shaken for 5 min with an equal volume of organic phase (usually 0.1 or 0.01 *M* DPPM in benzene) the phases were separated, and the activities measured. The concentration of arsenic in the original aqueous phase was $< 10^{-5}$ *M*. The organic phases were not pre-equilibrated with the aqueous phase except in solvent-effect studies.

RESULTS AND DISCUSSION

DPPM has been found to behave as a solvating reagent[6] and it is thought it also acts as a base[7] and forms cations in acid solutions. The stability of its ion-association complexes is rather poor. Accord-

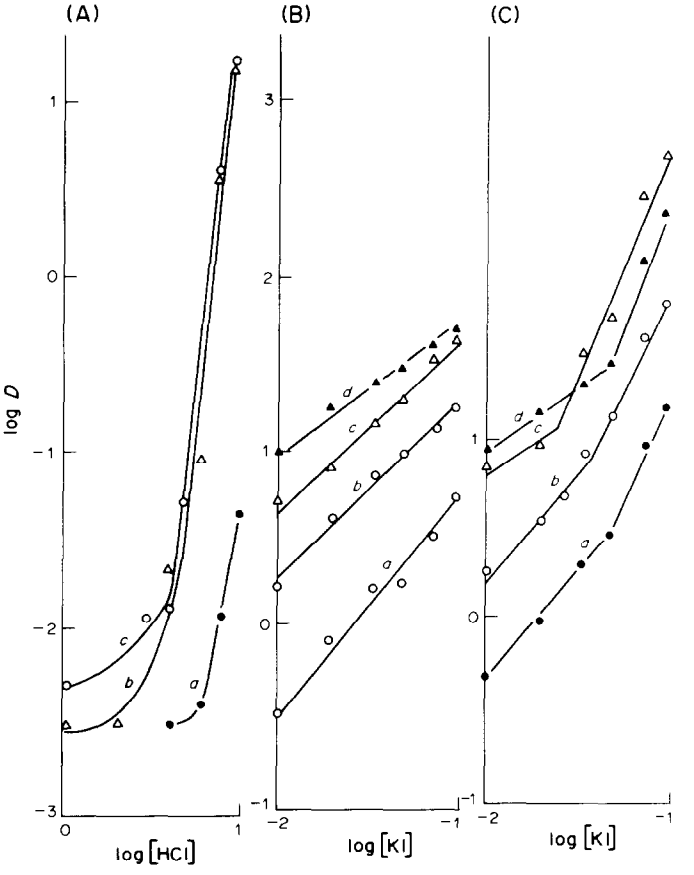

Fig. 1. (A) Distribution coefficients of arsenic(III) for *a*, extraction from hydrochloric acid by 0.1*M* DPPM; *b*, organic phase 0.1*M* DPPM, aqueous phase 0.02*M* KI in hydrochloric acid; *c*, organic phase 0.01*M* DPPM, aqueous phase 0.02*M* KI in hydrochloric acid. (B) Effect of the concentration of potassium iodide on the extraction of arsenic by 0.01*M* DPPM/benzene: [HCl]: *a*, 7*M*; *b*, 8*M*; *c*, 9*M*; *d*, 10*M*. (C) Effect of the concentration of potassium iodide on the extraction of arsenic by 0.01*M* DPPM/benzene: [HCl]: *a*, 7*M*; *b*, 8*M*; *c*, 9*M*; *d*, 10*M*.

ingly the extraction of tracer arsenic with DPPM (0.1*M*) from hydrochloric acid (Fig. 1A,*a*) unlike that with aliphatic amines and quaternary ammonium salts,[9] is almost negligible. This is evidently because of the relatively low pk_{BH^+} value of DPPM. The increase in extraction with increase in hydrochloric acid concentration could be due to the increased formation of extractable chloride complexes of the type $AsCl_4^-$ and/or the salting-out effect of the acid. The extraction of the element from 0.02*M* potassium iodide in hydrochloric acid was then investigated in line with some of our previous investigations.[10,11] The results are presented in Fig. 1A,*b*. The extraction from dilute acid solutions, like that in the absence of iodide, is very poor, but there is a very large increase with increasing acid concentration. Previous investigation[12] has shown that in the presence of trace concentrations of metals, this extractant has a tendency to polymerize, especially in concentrated hydrochloric acid, and hence the extraction sometimes decreases[12] with increasing reagent concentration. We therefore examined the effect of using 0.01*M* DPPM instead of 0.1*M* and found little change in the distribution data (Fig. 1A,*c*).

Figures 1B and 1C show the effect of iodide on the extraction of tracer arsenic from different concentrations of hydrochloric acid by 0.1*M* and 0.01*M* DPPM in benzene, respectively. The *D* values are higher at high iodide concentrations when 0.01*M* DPPM is used. The slope of the lines (Fig. 1C) is close to unity for [KI] < 0.05*M*, indicating the involvement of one iodide ion per complex anion formed.

These results led us to investigate the solvent effect. In every case the organic phase was pre-equilibrated with the corresponding aqueous phase. These studies were made with 0.1*M* potassium iodide at four concentrations of hydrochloric acid (7, 8, 9 and 10*M*). The results are presented in Fig. 2. In all cases, curves were obtained with maxima at around 0.01*M* DPPM. These curves also indicate that 9*M* hydrochloric acid is the optimal concentration for maximum extraction of tracer arsenic. We attribute the decrease in extraction at higher DPPM concentrations to polymerization of protonated DPPM and

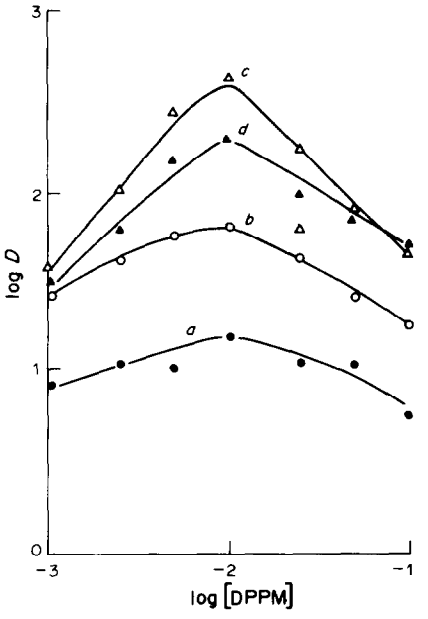

Fig. 2. The effect of the concentration of DPPM on the distribution coefficient of arsenic from different concentrations of hydrochloric acid: [HCl]: *a*, 7*M*; *b*, 8*M*; *c*, 9*M*; *d*, 10*M*.

formation of iodide ion-association complexes with it.

Although this work was devoted mainly to tracer studies, an attempt was made to elucidate the composition of the extractable species by loading-ratio data. For this purpose we used a solution of arsenious oxide in 0.1*M* potassium iodide/9*M* hydrochloric acid medium and extracted it with 0.01*M* DPPM in benzene. It was found that the organic phase was saturated at an arsenic concentration of around 0.75 g/l., which confirms a 1:1 DPPM:arsenic ratio.

Comparison with our previous work[6] shows that this system is much better than the corresponding thiocyanate system, where the maximum *D* value was only around 4. In the present case it is almost two orders of magnitude higher and a single equilibration is sufficient for quantitative extraction.

To study the selectivity, we investigated the partition behaviour of several other elements under the conditions optimal for extraction of arsenic, *i.e.*, 0.1*M* DPPM/benzene, and 0.1*M* potassium iodide in 9*M* hydrochloric acid. The results are shown in Table 1. It is seen that the extraction of arsenic is very selective. Selenium and mercury are two common toxic elements which are co-extracted and the method can be used for their preconcentration. The very high distribution ratios for arsenic also ensure its extraction from large volumes of aqueous phase. Thus under optimum conditions arsenic is more than 99% extracted when the ratio of the organic to aqueous phase volume is 1:20.

Table 1. Distribution coefficients and separation factors [with respect to As(III)] for extraction from 0.1*M* KI in 9*M* HCl with 0.01*M* DPPM in benzene

Species	Concentration, *M*	Distribution coefficient, *D*	Separation factor
As(III)	10^{-5}	441	—
Na^+	10^{-4}	0.0	$>10^4$
K^+	10^{-4}	0.0	$>10^4$
Cs^+	10^{-6}	0.0	$>10^4$
Br^-	10^{-4}	0.01	$\sim 10^4$
Co^{2+}	10^{-4}	0 0	$>10^4$
Ni^{2+}	10^{-3}	0 03	$\sim 10^4$
Cu^{2+}	10^{-5}	0.15	$>10^3$
Zn^{2+}	10^{-4}	0.02	$\sim 10^4$
Cd^{2+}	10^{-3}	0 70	6.3×10^2
Hg(II)	10^{-3}	99	4 47
Ba^{2+}	10^{-6}	0 01	$\sim 10^4$
Sr^{2+}	10^{-5}	0.01	$\sim 10^4$
Fe(III)	10^{-5}	0.22	$\sim 10^3$
Au(III)	10^{-4}	6.10	72
Sc^{3+}	10^{-4}	0.01	$\sim 10^4$
Eu^{3+}	10^{-4}	0 0	$>10^4$
Ce^{3+}	10^{-5}	0 01	$\sim 10^4$
Cr^{3+}	*C.F.	0.0	$>10^4$
Se(IV)	10^{-4}	32	13
Sn(IV)	10^{-4}	0.01	$\sim 10^4$
Hf(IV)	10^{-4}	0.01	$\sim 10^4$
Ru(IV)	10^{-5}	2.80	157
Sb(V)	10^{-5}	0.49	9×10^2
Cr(VI)	*C.F.	0.0	$>10^4$
Mo(VI)	10^{-5}	12	35
Tc(VII)	*C.F.	25	17

*C.F. = Carrier-free.

REFERENCES

1. G. O. Brink, P. Kafalas, R. A. Sharp, E. L. Weiss and J. W. Irvine, *J. Am. Chem. Soc.*, 1957, **79**, 1303.
2. W. Fischer and W. Harre, *Angew. Chem.*, 1954, **66**, 165.
3. H. C. Beard and L. A. Lyerly, *Anal. Chem.*, 1961, **33**, 1781.
4. V. A. Orlova, B. Ya. Spivakov, N. A. Sharova and T. M. Malyutina, *Zh. Analit. Khim.*, 1977, **32**, 1591.
5. E. S. Donaldson, *Talanta*, 1977, **24**, 105.
6. M. Ejaz, S. M. Hasany and Z. Umar, *Sepn. Sci. Technol.*, 1979, **14**, 431.
7. M. Ejaz, M. Iqbal, S. A. Chaudhri and Zamiruddin, *J. Radioanal. Chem.*, 1978, **42**, 335.
8. M. Ejaz, Shamus-ud-Zuha, S. Ahmad, M. S. Chaudhary and M. Rashid, *Mikrochim. Acta*, 1980, **I**, 7.
9. Y. Marcus and A. S. Kertes, *Ion Exchange and Solvent Extraction of Metal Complexes*, p. 961. Wiley, New York, 1969.
10. M. Ejaz, *Anal. Chem.*, 1978, **50**, 740.
11. M. Ejaz, M. A. Qureshi and Shamus-ud-Zuha, *Sepn. Sci. Technol.*, 1981, **16**, 291.
12. M. Ejaz, S. M. Hasany and I. Hanif, *J. Less-Common Metals*, 1981, **77**, 157.

Talanta, Vol 32, No 11, pp. 1058–1060, 1985
Printed in Great Britain

0039-9140/85 $3.00 + 0.00
Pergamon Press Ltd

SPECTROPHOTOMETRIC DETERMINATION OF LEAD WITH 1-(2-PYRIDYLAZO)-2-NAPHTHOL AND NON-IONIC SURFACTANTS

APPLICATION TO ACETIC ACID EXTRACTS OF CERAMIC ENAMELS

J. MEDINA ESCRICHE, M. LLOBAT ESTELLES and A. SEVILLANO CABEZA
Department of Analytical Chemistry, Faculty of Chemical Sciences, Valencia University, Burjasot, Valencia, Spain

(*Received* 24 *November* 1984. *Revised* 24 *May* 1985 *Accepted* 14 *June* 1985)

Summary—The Pb–PAN system in the presence of non-ionic surfactants (polyoxyethylene nonylphenols) has been studied spectrophotometrically. The optimum conditions for Pb determination are pH 9 ($Na_2B_4O_7$–$HClO_4$), 5% surfactant and measurement at 555 nm. The system obeys the Lambert Beer law over the Pb concentration range 1.3–4.5 ppm; the molar absorptivity is 2.02×10^4 l.mole^{-1}.cm^{-1} at 555 nm. The relative standard deviation is 0.9% and the limit of detection 0.12 ppm. Lead can be determined in acetic acid extracts of ceramic enamels by extraction with sodium diethyldithiocarbamate into carbon tetrachloride and stripping with 4*M* hydrochloric acid to remove interferent species. The results obtained are in agreement with those obtained by a standard AAS method.

PAN is widely used as a colorimetric reagent for metals. Its metal complexes are generally only slightly soluble in water, so extraction methods are generally used. An alternative is to use surfactants as solubilizing agents,[1,2] *e.g.*, Triton X-100 in determination of Co, Ni, Mn and Zn and of NEMOL K1030 for determination of Cd.[3–7] A methanolic medium has been used for determination of Pb with PAN.[8]

EXPERIMENTAL

Reagents

Stock solution (1000 μg/ml) of lead nitrate.
Stock $5 \times 10^{-3}M$ solution of *o*-PAN in methanol.
Stock 25% solution of Nemol K1030 (Masso-Carol) with hydrophile–lipophile balance 15.1.

Procedure

Stand 2 g of sample in 50 ml of 4% v/v acetic acid for 24 hr at room temperature, then filter into a 100-ml standard flask and dilute to volume with 4% v/v acetic acid. To 20 ml of this solution add 5 ml of 20% sodium citrate solution, 20 ml of 2.5*M* ammonia/2.5*M* ammonium chloride buffer, 5 ml of 0.5% sodium diethyldithiocarbamate solution and 10 ml of carbon tetrachloride, shake the mixture for 5 min, then separate the phases, shake the organic phase with 10 ml of 1*M* ammonia/1*M* ammonium chloride solution for 5 min, and discard the aqueous phase. Then strip the lead by shaking the organic phase with 10 ml of 4*M* hydrochloric acid for 5 min and separate the phases. Dilute the aqueous phase to volume in a 25-ml standard flask with demineralized water. Neutralize a suitable volume of this solution with sodium hydroxide solution, add 5 ml of 25% Nemol K1030 solution, 5 ml of $5 \times 10^{-3}M$ PAN and 10 ml of 4*M* ammonia/4*M* ammonium chloride buffer, and dilute to the mark in a 25-ml standard flask with demineralized water. Measure the absorbance at 555 nm (in 2-cm cells) against a reagent blank prepared in the same way.

RESULTS AND DISCUSSION

Pb–Nemol K1030–PAN system

Influence of pH. The spectra of Pb–PAN solutions in presence of Nemol K1030 at different acidities, ionic strength 0.1*M* and temperature 25°, measured against reagent blanks (Fig. 1) show an absorption band with a maximum at 555 nm, increasing in intensity with pH, to a maximum at pH 10–11 (Fig. 2). At pH < 9 the absorbance at 555 nm is stable for at least 30 min, but at higher pH the absorbance,

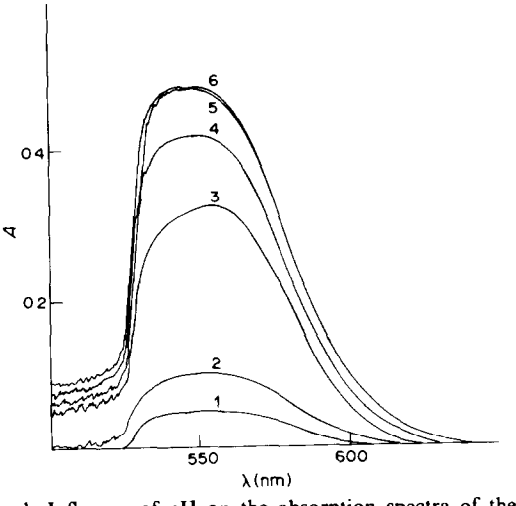

Fig. 1. Influence of pH on the absorption spectra of the Pb–Nemol K1030–PAN complex. pH: 1, 5.9; 2, 6.7; 3, 8.2; 4, 9.3; 5, 10.2; 6, 10.7; Pb (II) 2 ppm, Nemol K1030 5%, PAN $10^{-5}M$.

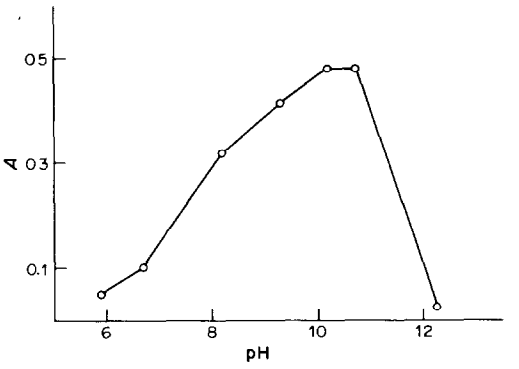

Fig. 2. Absorbance *vs.* pH for Pb–Nemol K1030-PAN at 555 nm. Reference reagent blank.

though higher, decreases slowly with time (Fig. 3). A pH of 9 is therefore chosen as the optimum working pH.

Influence of surfactant concentration. A final surfactant concentration lower than 2% does not prevent appearance of a precipitate in a 2-ppm lead solution with $10^{-3}M$ PAN at pH 9, but higher surfactant concentrations give red solutions. The presence of 2–5% Nemol K1030 makes the absorbance of Pb–PAN solutions and PAN blanks stable for at least 30 min and 5% surfactant concentration is chosen as the most suitable.

Influence of PAN concentration. Varying the PAN concentration with a fixed concentration of lead ($10^{-5}M$) and of Nemol K1030 (5%) at pH 9 shows that a [PAN]/[Pb] ratio of at least 100 is needed to produce an absorbance that is practically independent of the PAN concentration.

Analytical characteristics. The system obeys the Lambert–Beer law over the lead concentration range 1.3–4.5 ppm; the molar absorptivity is 2.02×10^4 $1.\text{mole}^{-1}.\text{cm}^{-1}$ at 555 nm. The relative standard deviation (s_r) of the absorbance for 10 independent tests is 0.9% and the limit of detection (c_L) is 0.12 ppm Pb (c_L is defined[9] as the concentration giving a signal equal to three times the standard deviation of the blank signal).

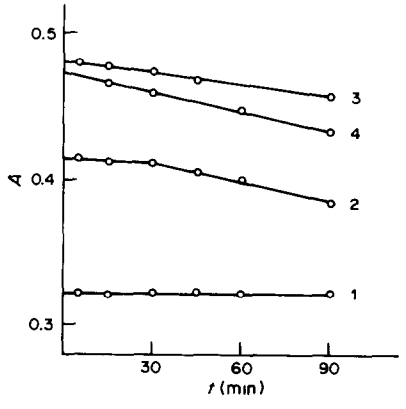

Fig. 3. Stability as a function of pH for Pb–Nemol K1030–PAN solutions, pH: 1, 8.2; 2, 9.3; 3, 10.2; 4, 10.7.

Table 1. Influence of Cd on determination of Pb in presence of NH_4^+/NH_3 buffer solution

	Absorbance at 555 nm		
Pb (*ppm*)	Cd absent	1 ppm Cd	2 ppm Cd
0.55	0.051	0.049	0.054
1 09	0.120	0 118	0.125
2.19	0 227	0.225	0 237
3 28	0.350	0 339	0.354
4.37	0.460	0.448	0 466

Elimination of interferents. The selectivity of the method is improved by extraction with sodium diethyldithiocarbamate and carbon tetrachloride[7] and scrubbing with ammonia buffer to remove interferences. The lead is then quantitatively stripped with 10 ml of $4M$ hydrochloric acid. Lead can be determined in the presence of 1–2 ppm cadmium in $4M$ ammonia buffer (Table 1).

Precision and limit of detection. Analysis of six independent solutions containing 20 ppm each of cadmium, lead and zinc showed that the relative standard deviation of the lead determination is 1.3%, which compares favourably with the corresponding values of 2% and 1.1% obtained for AAS measurement at 217 and 283.3 nm, respectively (for 10 ppm of lead).

Determination of Pb(II) in acetic acid extracts of ceramic enamels

Five industrial samples of ceramic enamels of different composition, supplied by Ferroenamel Española were analysed in triplicate by the proposed method and the results are shown in Table 2.

The values obtained were generally within 5% of those obtained by application of the standard AAS method[10] to the initial acetic acid solutions.

A t-test[11–13] shows that the method has no systematic error and does not need a blank correction.

Table 2. Pb contents of acetic acid extracts of ceramic enamels obtained by the proposed method and by AAS

	Pb, *ppm*			
	AAS		Proposed method	
Sample	X_i	$\bar{X}_i$	X_i	$\bar{X}_i$
1	49.5 49.3 49.5	49.4	51.9 51.5 51.3	51.6
2	11.2 11.1 11.5	11.3	14.4 14.4 14.6	14.5
3	16.1 15.6 16.6	16.1	16.6 17.2 16.8	16.9
4	8.4 8.3 8.4	8.4	8.5 8.8 8.8	8.7
5	27.6 27.3 28.2	27.7	26.2 26.0 26.9	26.4

Table 3. Cd contents of acetic acid extracts of ceramic enamels, obtained by the proposed method and by AAS

	Cd, *ppm*			
	AAS		Proposed method	
Sample	X_i	$\bar{X}_i$	X_i	$\bar{X}_i$
1	36.0 36.5 35.0	35.8	35.0 35.5 35.6	35.4
2	14.1 14.0 14.1	14.1	14.6 14.2 13.7	14.2
3	—		—	
4	6.0 6.3 6.1	6.1	6.5 6.3 6.5	6.4
5	9.4 9.5 9.2	9.4	9.2 9.4 9.1	9.2

Cadmium can also be determined in the 4*M* hydrochloric acid solution obtained in stripping the lead. An aliquot of this solution is neutralized with sodium hydroxide solution, then 2.5 ml of 0.25*M* sodium citrate, 2 ml of 25% Nemol K1030 solution, 2.5 ml of 10^{-3} *M* PAN and 10 ml of borate–perchloric acid buffer solution are added and the solution is diluted to the mark in a 25-ml standard flask with demineralized water.[7] The absorbance is measured at 555 nm and 25° against a PAN blank prepared under identical conditions. Comparison of the results (Table 3) with those obtained by AAS shows a difference of less than 5% and a *t*-test shows there is no systematic error and that a blank correction is not needed.

Acknowledgements—The authors thank Ferroenamel Española, Almazora, Castellón, Spain for collaboration and the supply of the ceramic enamels used in the work.

REFERENCES

1. K. Ueno, in *MTP Intern. Rev. Sci. Phys Chem. Ser. One: Anal. Chem.*, 1973, **13**, 43.
2. W. L. Hinzer, in *Solution Chemistry of Surfactants*, K. L. Mittal (ed.), Vol. 1, pp. 79–127. Plenum Press, New York, 1979.
3. H. Watanabe, *Talanta*, 1974, **21**, 295.
4. Q. Wanbin and Q. Keting, *Fenxi Huaxue*, 1981, **9**, 696, *Chem. Abstr.*, 1982, **97**, 103465.
5. K. Goto, S. Taguchi and Y. Fukue, *Talanta*, 1977, **24**, 752.
6. H. Watanabe, *Bunseki Kagaku*, 1974, **23**, 396; *Chem. Abstr.*, 1974, **81**, 32939.
7. J. Medina Escriche, M. Llobat Estelles and F. Bosch Reig, *Talanta*, 1983, **30**, 915.
8. D. Negoui, A. Kriza and L. Baldue, *Anal. Univ. Bucuresti Ser. Stiint. Nat.*, 1964, **13**, 165.
9. IUPAC, *Compendium of Analytical Nomenclature*, Pergamon Press, Oxford, 1978.
10. ASTM C 738-76.
11. J. Mandel and F. J. Linning, *Anal. Chem.*, 1957, **29**, 743.
12. Comisariat à l'Energie Atomique, *Statistique appliqueé a l'exploitation de mesures*, Masson, Paris, 1978.
13. M. de la Guardia, A. Salvador and V. Berenguer, *An Quim.*, 1981, **77**, 129.

Talanta, Vol 32, No 11, pp. 1061–1063, 1985
Printed in Great Britain

0039-9140/85 $3.00 + 0.00
Pergamon Press Ltd

SIMULTANEOUS DETERMINATION OF LEAD AND THALLIUM BY POTENTIOMETRIC STRIPPING

S. JAYA, T. PRASADA RAO and G. PRABHAKARA RAO
Central Electrochemical Research Institute, Karaikudi-623006, India

(*Received* 15 *March* 1985. *Accepted* 14 *June* 1985)

Summary—A potentiometric stripping analysis procedure has been developed for the simultaneous determination of lead and thallium in chloroacetate–chloride medium. This procedure allows the determination of lead or thallium concentrations as low as 10 ng/ml. The method is precise, and applicable to the determination of lead and thallium in sea-water.

The toxicity of lead and its compounds[1] has resulted in a voluminous literature on its electroanalytical determination in a variety of environmental samples, either by itself or in combination with other heavy metals.[2] The determination of lead by anodic stripping voltammetry (ASV)[3,4] or differential pulse ASV[5] with the hanging mercury drop electrode (HMDE) suffers no problems in presence of copper, zinc and cadmium but encounters serious interference from thallium. ASV procedures have also been reported by other authors.[6,7] For determination of lead and thallium in admixtures most authors have resorted to addition of EDTA.[3,5] Potentiometric stripping analysis, developed by Jagner,[8] offers a simple, rapid and reliable way of determining lead in sea-water, in presence of copper, zinc and cadmium, but so far no attempt has been made to use it to determine thallium or thallium and lead in mixtures.[9,10] This paper reports the determination of lead and thallium in concentration ratios ranging from 1:100 to 100:1.

EXPERIMENTAL

Reagents

The following solutions were prepared with BDH analytical-grade reagents and conductivity water: lead, 0.1*M*; thallium(I), 0.01*M*, mercury(II), 0.01*M*; sodium chloride, 5*M*; chloroacetic acid, 2.0*M*.

Apparatus

A Wenking Model 75 M potentiostat and potential scan generator were used, with a three-electrode cell assembly: a normal calomel reference electrode (NCE), platinum foil counter-electrode and a glassy-carbon (Tokai & Co., Japan, 3 mm diameter) working electrode. The recordings were made on a Digilog XY-2000 recorder.

Procedure

Transfer a suitable known volume (up to 45 ml) of the sample solution containing lead and/or thallium (concentration of each $\leqslant 2$ μg/ml) into a 50-ml standard flask. Add 2.5 ml of 2.0*M* chloroacetic acid, and 0.5 ml each of 5*M* sodium chloride and 10 $^{-3}$*M* mercury(II) and dilute to volume with conductivity water. Transfer the solution into the electrochemical cell. Plate for 4 min at -1.1 V *vs* NCE with stirring. At the end of the deposition period, switch off the applied potential and record the open-circuit potential as a function of time. Prepare a calibration graph for 0.01–2 μg/ml lead or thallium by the same procedure.

Determination of lead and thallium in sea-water

To aliquots of sea-water ($\leqslant$45 ml) add 2.5 ml of 2.0*M* chloroacetic acid and make up to 50 ml. Determine lead and thallium by the procedure described above and/or by the standard-addition technique.

RESULTS AND DISCUSSION

Preliminary studies on the chemical stripping profiles of 5×10^{-7}*M* lead and thallium in a variety of supporting electrolytes showed that the lead and thallium signals are not resolved in acetate, nitrate or carbonate medium. On the other hand, these signals are well resolved in neutral or weakly acidic complexing media.

Effect of supporting electrolyte

The determination of 5×10^{-7}*M* lead and thallium with mercury(II) as the chemical stripping agent was studied in different supporting electrolytes. The results are represented in Table 1, from which it is clear that the stripping signal for thallium is maximal in sodium chloride medium, but the resolution of the thallium signal from the background or the lead signal was not good. Of all the supporting electrolytes studied, 0.1*M* chloroacetic acid–0.5*M* sodium chloride gave the maximum signal for lead and thallium with sufficient resolution. Hence this mixture was chosen as supporting electrolyte for further studies.

Oxidant concentration

As mercury(II) is used for both *in situ* formation of the mercury film and oxidation of the deposited lead and thallium in the chemical stripping step, the effect of varying its concentration between 10^{-6} and 10^{-4}*M* in the determination of 100 ng/ml concentations of thallium and lead was examined. The presence of at least 2.5×10^{-6}*M* mercury(II) was found essential for obtaining maximum sensitivity, and mercury(II) con-

Table 1. Effect of supporting electrolyte [concentration of Pb(II) or Tl(I) = $5 \times 10^{-7}M$, $E_d = -1.1$ V *vs.* NCE, $t_d = 4$ min]

Supporting electrolyte		Stripping time, *sec* Pb	Tl
Acetate buffer	(0.25*M*)	Not resolved	Not resolved
Na_2CO_3	(0.1*M*)	Not resolved	Not resolved
KNO_3	(0.1*M*)	Not resolved	Not resolved
NaCl	(0.25*M*)	8.0 (Not resolved)	5.50 (Not resolved)
Chloroacetic acid buffer	(0.1*M*)	9.4	2.50
Acetate + chloride	(0.025*M*) + (0.25*M*)	4.7	2.35
HCl	(0.1*M*)	7.0	2.35
Citrate	(0.1*M*)	3.6	2.50
Tetramethyl ammonium bromide	(0.1*M*)	5 6	1.80
Chloroacetic acid + sodium chloride	(0.1*M*) + (0 5*M*)	14.2	3.20

centrations up to $2 \times 10^{-5}M$ had no effect on the stripping signals thus obtained. Higher concentrations decreased the stripping signals, however, presumably because the stripping was faster. Hence $10^{-5}M$ mercury(II) was used in further studies.

Deposition potential

The potential of deposition was varied from -1.1 to -0.6 V *vs.* NCE with plating for 4 min for the preconcentration of lead and thallium from a solution containing each at 100 ng/ml concentration. The stripping signal was maximum for both lead and thallium at a deposition potential of -1.05 V.

Sodium chloride concentration

Figure 1 shows that under the other conditions selected, increase in the sodium chloride concentration has no effect on the stripping signal of thallium, but the stripping signal of lead increases with sodium chloride concentration up to 0.4*M* but remains unaltered on further increase in sodium chloride concentration up to 1.0*M*.

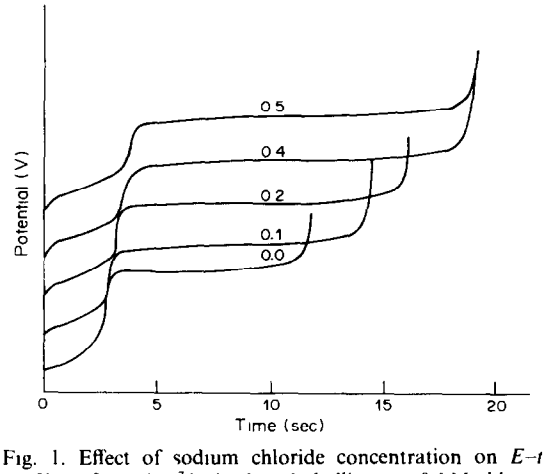

Fig. 1. Effect of sodium chloride concentration on *E–t* profiles of $5 \times 10^{-7}M$ lead and thallium in 0.1*M* chloroacetate buffer (pH 2.5) and 0–0.5*M* sodium chloride, concentration of Hg(II) = $10^{-5}M$, total volume = 50 ml, deposition potential (E_d) = -1.1 V *vs.* NCE; time of deposition (t_d) = 4 min.

Deposition time

The deposition times at -1.1 V were varied from 2 to 16 min. The results are shown in Table 2, from which it is clear that the magnitude of the stripping signal is directly proportional to the plating time. This suggests that the detection limit could be lowered to < 10 ng/ml by increasing the time of deposition.

Calibration data

The calibration graphs obtained by the recommended procedure are linear over the range 5×10^{-8}–$10^{-5}M$ for lead or thallium and pass through the origin. The coefficient of variation for 10 replicate determinations of 0.1 μg/ml lead and thallium were found to be 2 and 1.2% respectively.

Analysis of synthetic mixtures

Table 3 presents the results of analysis of various mixtures of lead and thallium in ratios ranging from 100:1 to 1:100. From the recoveries it is clear that the procedure is suitable for the simultaneous determination of lead and thallium in widely differing concentration ratios.

Table 2. Variation of deposition time (concentration of Pb^{2+} or $Tl^+ = 5 \times 10^{-7}M$, $E_d = -1.1$ V *vs.* NCE, 0.1*M* chloroacetic acid + 0.5*M* NaCl)

Plating time, *min*	Stripping time, *sec* Pb	Tl
2	7.1	1.60
4	14.2	3.2
8	28.4	6.4
16	56.0	12.7

Table 3. Analysis of synthetic mixtures and sea-water samples

Aliquot taken, *ml*	Amount added, *ng/ml*		Amount found, *ng/ml*	
	Pb	Tl	Pb	Tl
Synthetic mixtures				
50	20	20	20	20.4
50	2000	20	1980	19.8
50	20	2000	20	2020
Sea-water				
20	—	—	—	—
45	—	—	—	—
20	20	20	20	19.8
40	100	10	99	10
40	1000	10	995	10

Analysis of sea-water

Sea-water samples collected from the Bay of Bengal were analysed by the procedure described. The results, and the recoveries obtained on addition of known amounts of lead and thallium to the sea-water, are given in Table 3. The recoveries are quantitative.

Conclusions

Unlike other stripping voltammetric techniques, the procedure described here allows the simultaneous determination of lead and thallium, without mutual interference, over a wide range of ratios. The chloroacetate–chloride medium gives a fourfold enhancement in sensitivity for lead, relative to the PSA procedures which use acetate–chloride[8] or 0.01*M* hydrochloric acid[11] as supporting electrolytes. The method is suitable for sea-water analysis.

Acknowledgements—The authors wish to express their gratitude to Prof. K. I. Vasu, Director, Central Electrochemical Research Institute, Karaikudi, for his keen interest in the work and kind permission to publish these results.

REFERENCES

1. E. Berman, *Toxic Metals and Their Analysis*, Heyden, London, 1980.
2. F. Vydra, K. Štulík and E. Juláková, *Electrochemical Stripping Analysis*, Horwood, Chichester, 1976.
3. R. G. Dhaneswar and L. R. Zarparkar, *Analyst*, 1980, **105**, 386.
4. G. E. Bately and T. M. Florence, *J. Electroanal. Chem.*, 1975, **61**, 205.
5. L. K. Hoeflich, R. J. Gale and M. L. Good, *Anal. Chem.*, 1983, **55**, 1591.
6. D. K. Roe and J. E. A. Toni, *ibid.*, 1965, **37**, 1503.
7. W. R. Matson and D. K. Roe, *ibid.*, 1965, **37**, 1594.
8. D. Jagner and A. Granete, *Anal. Chim. Acta*, 1976, **83**, 19.
9. D. Jagner, *Analyst*, 1982, **107**, 593.
10. S. Jaya and T. P. Rao, *Rev. Anal. Chem.*, 1982, **6**, 343.
11. D. Jagner, *Anal. Chem.*, 1978, **50**, 1924.

Talanta, Vol 32, No 11, pp 1064–1066, 1985
Printed in Great Britain

0039-9140/85 $3.00 + 0.00
Pergamon Press Ltd

STUDIES ON DETERMINATION OF FLUORIDE IN ZINC AND LEAD CONCENTRATES BY USING A FLUORIDE ION-SELECTIVE ELECTRODE

S. C. S. RAJAN*, L. M. BHANDARI† and B. R. L. ROW§
Hindustan Zinc Limited, Visakhapatuam-530015, India

(*Received* 8 *June* 1984. *Revised* 18 *September* 1984. *Accepted* 14 *June* 1985)

Summary—A modification of the potentiometric determination of fluoride has been developed, which allows use of aqueous fluoride standards in analysis of lead or zinc concentrates, instead of the need to use matrix-matching or standard additions.

Determination of fluoride in zinc concentrates is important since fluoride can cause problems in the electrolytic production of high-purity zinc with aluminium cathodes.[1] Work was taken up in our laboratories some years ago to develop a procedure for the determination of fluoride in zinc concentrates by use of a fluoride ion-selective electrode, and preliminary results were presented.[2] The work also included determination of fluoride in lead concentrates, since Hindustan Zinc Limited treats these for recovery of lead. The procedure consisted of fusion of the concentrates with sodium hydroxide, extraction of the melt with water, adjustment of the extract to pH 8–9, filtration and measurement of fluoride in the filtrate. The working standards contained similar quantities of sodium hydroxide and acid. Almost immediately afterwards, a paper appeared on the determination of fluoride in zinc concentrate, by use of an ion-selective electrode.[3] The authors, after extensive study of various procedures for decomposition of the sample, also finally recommended fusion with alkali but preferred a single-point standard-addition technique to deal with matrix interference. However, it had earlier been found that the matrix interference could be avoided by neutralizing the alkaline extract to pH 8–9 and then filtering,[4] so it seemed to us possible to use aqueous standards for measurement of fluoride in the sample solution and not to need the single-point standard-addition calibration.

EXPERIMENTAL

Apparatus

An Orion model 407 A ion-meter, 901 ion-analyser, 9409 fluoride electrode and 9001 reference electrode were used.

Reagents

Analytical grade materials were used whenever possible.

Stock fluoride solution, 1000 ppm. Prepared by dissolving 2.210 g of dried sodium fluoride in distilled water and diluting to volume in a 1-litre standard flask. Lower concentrations were prepared by serial dilution.

Buffers.[5] A 1*M* citrate buffer was made by dissolving 294 g of sodium citrate and 20.2 g of potassium nitrate in 800 ml of water, adjusting the pH to 5.0–5.5 with hydrochloric acid (1 + 1) and diluting to 1 litre. A 0.2*M* citrate buffer[5] was similarly made with 58.8 g of sodium citrate and 20.2 g of potassium nitrate.

TISAB.[4] A total ionic strength adjustment buffer was made by adding 58 ml of glacial acetic acid to 12 g of sodium citrate dissolved in 300 ml of water, adjusting the pH to 5.0–5.5 with 25% sodium hydroxide solution and diluting to 1 litre with distilled water.

Procedure

To a 1-g sample in a 100-ml nickel crucible add as nearly as possible (*i.e.*, within 1 pellet) 5 g of sodium hydroxide pellets, put the crucible in a cold electric furnace, and switch on the power. When the temperature has reached 500°, maintain that temperature for 30 min. Occasionally remove the crucible and swirl its contents to ensure uniform dispersion. When the fusion is completed, cool the crucible, add about 30 ml of distilled water, and warm the crucible gently to facilitate dissolution of the cake. Adjust the pH to 8–9 with glacial acetic acid, taking care to avoid development of neutral or acidic conditions during the process. Cool to room temperature, filter through a Whatman No. 41 paper into a 100-ml standard flask, washing the residue and paper with distilled water, and finally dilute to volume. Prepare a blank solution in the same way.

Mix a suitable aliquot (*e.g.*, 25 ml) of this sample solution with an exactly equal volume of buffer. The pH of the buffered sample should be 5.4–5.6. Measure the fluoride content potentiometrically with a fluoride-sensitive electrode, calibrated with standard fluoride solutions (1–10 ppm) mixed in exactly 1:1 ratio with the buffer used. Apply a correction for the fluoride content of the blank, measured in the same way.

RESULTS AND DISCUSSION

The results obtained for three zinc-concentrate and two lead-concentrate samples by the procedure above are presented in Table 1. As no standard samples were available, the accuracy of the method was checked by determining the recovery of standard additions of fluoride.

One of our main concerns was to see whether calibration with pure aqueous standards would give

*Author for correspondence.
†Process Laboratory, Zinc Smelter, Udaipur.
§Regional Office, Hyderabad.

Table 1. Analysis of lead and zinc concentrates by the proposed method and results for the recovery of added fluoride

Sample	F^-, $\mu g/g$ Added	F^-, $\mu g/g$ Found	Relative standard deviation, %	Value for 95% confidence, $\mu g/g$	Recovery, %
Lead Concentrate 1	—	298*	3.5	293 ± 11	—
	200	480	—		93
	300	600	—		102
Lead Concentrate 2	—	150*	6.0	150 ± 10	—
	100	240	—		90
Zinc Concentrate 1	—	275*	2.0	275 ± 6	—
	200	460	—		93
	300	580	—		101
Zinc Concentrate 2	—	178*	2.9	178 ± 6	—
	200	370	—		96
	200	360	—		90

*Average of six replicate analyses.

accurate measurement of fluoride in sample solutions prepared by the procedure described. To do this, fluoride standards were prepared, each by adding 5 g of sodium hydroxide to a suitable volume of a standard solution, diluting to about 30 ml, adjusting to pH 8–9 with glacial acetic acid, and diluting to volume in a 100-ml standard flask. These standards were then mixed in 1:1 ratio with 1*M* citrate buffer and measured potentiometrically for fluoride content. A similar range of purely aqueous standards was prepared, mixed in 1:1 ratio with the buffer and measured.

Comparison of the two sets of results showed that the sodium hydroxide and glacial acetic acid used produced between them an apparent increase of 0.15–0.20 μg/ml in the fluoride concentration. Hence purely aqueous standards can be used for calibration, provided a correction is applied for the reagent blank.

As reported by McQuaker and Gurney,[4] adjustment of the test solution to pH 8–9 and filtration removes most of the interference from matrix elements such as aluminium, iron, silicon, calcium and magnesium. Except for iron, which is usually present at around 5–9% level, these elements occur only at low levels in the concentrates of interest. Since these concentrates contain zinc (*ca.* 50%) or lead (*ca.* 60%) as the major elements, the filtrates were analysed for these two elements by AAS. The zinc and lead values found were in the ranges 40–80 and 5–7 μg/ml respectively, indicating that more than 98% of the zinc and 99% of the lead remained in the residue.

Table 2. Fluoride standards prepared with sodium hydroxide and acetic acid*

F^-, $\mu g/ml$ Taken	F^-, $\mu g/ml$ Found†
1.0	1.18 ± 0.03
2.0	2.18 ± 0.03
4.0	4.17 ± 0.03
5.0	5.13 ± 0.03

*1*M* citric acid buffer used
†Mean ± standard deviation (3 replicates)

Three buffers (1*M* citrate–0.2*M* nitrate, 0.2*M* citrate–0.2*M* nitrate, and TISAB) were tried, and all gave similar results. The 0.2*M* citrate buffer will obviously contain less fluoride than the 1*M* citrate buffer and hence be more suitable for low-level fluoride measurements. The fluoride content of TISAB will depend on the relative fluoride content of the individual buffer components. For those used in the work described, we found 0.5 μg/g in the sodium citrate and 4 μg/g in the sodium hydroxide, and <0.02 μg/ml in the 0.2*M* citrate buffer, 0.08 μg/ml in the 1*M* citrate buffer and 0.05 μg/ml in the TISAB.

We modified the procedure of McQuaker and Gurney[4] by using solid sodium hydroxide for the sample decomposition, instead of adding sodium hydroxide solution and evaporating the water (which takes rather a long time). We found that the pellets weighed about 0.2 g each, and the maximum error in weighing the 5 g was about ±0.2 g. If the sodium hydroxide used contains say 5 μg of fluoride per g, the error introduced by weighing the pellets should not exceed 0.01 ppm fluoride in the value obtained. We also preferred acetic acid to hydrochloric for the pH adjustment, because the buffering action of the acetate system gave better control in preventing formation of acidic or neutral conditions during the adjustment.

The Willard and Winter distillation technique with perchloric acid was also tested and good recoveries of fluoride were obtained. About 400 ml of distillate was found to be sufficient for quantitative recovery from a 1-g sample.

Acknowledgements—The authors thank Shri K. S. Bolia for assistance in the investigations.

REFERENCES

1. R. M. Farmer, Anode pre-conditioning and other changes in Cominco's electrolytic zinc operations, AIME Symposium on Electrometallurgy, 2 December 1968.

2. S. C. S. Rajan, L. M. Bhandari and B. R. L. Row, paper presented at Indian Science Congress, Calcutta, 1980.
3. D. S. Russell, H. B. Macpherson and V. P. Clancy, *Talanta*, 1980, **27**, 403.
4. N. R. McQuaker and H. Gurney, *Anal. Chem.*, 1977, **49**, 53
5. B. L Ingram, *ibid.*, 1970, **42**, 1825.

Talanta, Vol 32, No 11, pp 1067–1068, 1985
Printed in Great Britain

0039-9140/85 $3.00 + 0.00
Pergamon Press Ltd

N-CHLOROPHTHALIMIDE AS A NEW OXIDANT FOR DIRECT TITRATIONS IN AQUEOUS ACETIC ACID MEDIUM

N. JAYASREE and P. INDRASENAN*
Department of Chemistry, University of Kerala, Trivandrum-695034, India

(*Received* 16 *April* 1984. *Revised* 27 *May* 1985. *Accepted* 5 *June* 1985)

Summary—A stable new oxidimetric titrant, *N*-chlorophthalimide in anhydrous acetic acid, is proposed for direct titrations of a variety of simple and complex reductants such as As(III), Sb(III), Fe(II), ferrocyanide, iodide, ascorbic acid, hydroquinone, hydrazine, phenylhydrazine, benzhydrazide, isonicotinic acid hydrazide, semicarbazide, thiourea, aniline, phenol, oxine and its metal complexes, and anthranilic acid and its metal complexes.

In continuation of our work on organic oxidimetric titrants for use in non-aqueous or partially aqueous media,[1-5] we introduce *N*-chlorophthalimide (NCP). Solutions of NCP in anhydrous acetic acid are more stable than those of dibromamine-T,[1] chlorbromamine-T,[2] dihalohydantoins[3-5] and dichloramine-T.[6] The solid compound is also stable for at least three months. Here we report on the application of NCP as an oxidimetric titrant for direct titrations of 31 reductants in aqueous acetic acid medium.

EXPERIMENTAL

Reagents

N-Chlorophthalimide. NCP was prepared by chlorination of phthalimide by the method given in the literature.[7] It is practically insoluble in water, but soluble in acetic acid (19.1 g/kg at 32°) and common organic solvents. An approximately 0.1*N* (0.05*M*) solution was prepared by dissolving 9 g of dry NCP in 1 litre of anhydrous acetic acid. This solution is sensitive to light and heat so was kept in an amber-coloured bottle. The solution was fairly stable, its strength remaining unchanged for the first 4 days and then decreasing by 0.1% per day. For accurate work, daily standardization by the iodometric method used for the haloamides[1,5] is recommended.

Reductants. The reductants used were of analytical-reagent grade. Standard solutions (~0.1*N*) of the 17 common reductants (Table 1) were prepared in appropriate solvents as described earlier.[1,5] The oxinates of Mg^{2+}, Al^{3+}, Mn^{2+}, Fe^{3+}, Co^{2+}, Ni^{2+}, Cu^{2+}, Zn^{2+} and Cd^{2+} (Table 2) were prepared by standard methods.[8,9] Standard solutions (~0.1*N*) of these complexes were prepared in 2*M* hydrochloric acid. These reductant solutions were also analysed by standard methods.[9,10]

Procedures

Direct potentiometric titrations. The apparatus and procedure described earlier[3,4] were used. The reaction mixture in the titration cell was diluted to 50 ml with water and acetic acid to give 50% v/v aqueous acetic acid medium. Addition of potassium bromide (0.5 g) was found to be essential for all the reductants except iodide. For Sb(III) and hydrazine, addition of 2 ml of 2*M* hydrochloric acid was also needed. For Fe^{2+}, 2 ml of 2*M* hydrochloric acid and 2 ml of orthophosphoric acid were required. For thiourea, addition of 0.5 g of sodium acetate was found to be essential. Near the equivalence point the solution was stirred for 30 sec after each addition of the titrant (0.1 ml) to ensure a steady potential. The equivalence points were located as reported earlier,[4,6] and the titrations continued until there was no significant change in potential on further addition of titrant.

Direct visual titrations. The reductant solution was prepared in the same way as for the corresponding potentiometric titration and the indicator was added. A blank titration was done in each case but no blank correction was found necessary.

RESULTS AND DISCUSSION

The results of the titrations are given in Tables 1 (common reductants) and 2 (metal oxinates and anthranilates). NCP undergoes reduction according to the equation

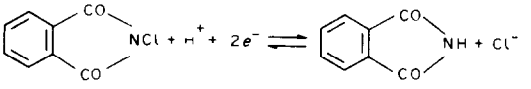

The reduction product was identified as phthalimide. The conditional redox potential in 50% v/v aqueous acetic acid was found to be +0.996 V at 32°.

The potential break in the potentiometric titrations is sharp and in the range 100–400 mV. The visual end-points are also very sharp. Quinoline Yellow was found the most suitable indicator for all but the Fe^{2+}, ferrocyanide, hydroquinone and metal oxinate titrations, for which amaranth was better. Either of these indicators is suitable for most of the titrations.

All the reductants react as reported earlier.[1-6] Except for the iodide titration, bromide must be added to increase the rate of reaction, and the rate of potential equilibration in the potentiometric titrations. Presumably bromine is formed and acts as a more reactive intermediate. For thiourea, the oxidation is still very slow, however, and sodium acetate must also be added.

*Author for correspondence.

Table 1. Titrimetric determination of some common reductants with *N*-chlorophthalimide

Reductants	*n**	Potentiometric titrations: Range studied, *mmole*	Standard deviation, *μmole*	Reduction found,† %	Visual titrations: Range studied, *mmole*	Standard deviation, *μmole*	Reductant found,† %
As(III)	2	0.15–0.30	2.4	100.3	0.49–0.95	2.5	99.9
Sb(III)	2	0.14–0.30	2.8	100.3	0.50–0.97	1.6	100.0
Fe(II)	1	0.29–0.49	1.9	99.8	1 01–1.93	1.3	100.1
Ferrocyanide	1	0.27–0.47	2.4	99.9	0 98–1.87	2.1	100.0
Iodide	1	0.29–0.60	2.9	99.9		unsuccessful	
Ascorbic acid	2	0.15–0.30	2.5	100.1	0.49–0.94	2.6	100.1
Hydroquinone	2	0.12–0.21	2.3	100.1	0.41–0.79	2.0	100.0
Hydrazine	4	0.07–0.13	2.5	99.9	0.22–0.43	0.1	100.0
Phenylhydrazine	4	0.07–0.15	2.3	100.1	0.24–0.47	1.0	100.0
Benzhydrazide	4	0.05–0.13	2.2	99.8	0.23–0.45	2.1	100.0
Isonicotinic acid hydrazide	4	0.07–0.12	2.9	100.1	0.21–0.41	1.7	100.1
Semicarbazide	4	0.07–0.13	1.7	100.2	0.25–0.49	1.6	100.0
Thiourea	8	0.03–0.08	2.8	100.1	0.13–0.26	2.0	100.0
Aniline	6	0.04–0.10	1.5	100.0	0.14–0.29	2.1	99.9
Phenol	6	0.04–0.10	2.8	99.9	0.15–0.29	1.2	100.0
Oxine	4	0.07–0.14	2.4	100.1	0.26–0.50	1.8	99.9
Anthranilic acid	6	0.03–0.09	2.6	100.0	0.21–0.41	6.7	100.0

*Equivalents of NCP per mole of reductant.
†Average of ten replicates.

Table 2. Titrimetric determination of some metal oxinates and anthranilates with *N*-chlorophthalimide

Reductants	*n**	Direct potentiometric titrations: Range studied, *mmole*	Standard deviation, *μmole*	Reductant found,† %	Direct visual titrations: Range studied, *mmole*	Standard deviation, *μmole*	Reductant found,† %
$Mg(C_9H_6ON)_2 \cdot 2H_2O$	8	0.02–0.07	2.3	99.8	0.12–0.24	1.2	100.0
$Al(C_9H_6ON)_3$	12	0.02–0.04	1.3	100.2	0.08–0.16	1.5	100.0
$Mn(C_9H_6ON)_2 \cdot 2H_2O$	8	0.02–0.07	0.1	100.4	0.13–0.26	1.5	100.0
$Fe(C_9H_6ON)_3$	12	0.02–0.04	2.2	99.9		unsuccessful	
$Co(C_9H_6ON)_2 \cdot 2H_2O$	8	0.02–0.05	2.7	100.0	0.11–0.23	2.0	100.1
$Ni(C_9H_6ON)_2 \cdot 2H_2O$	8	0.02–0.06	2.7	99.9	0.09–0.18	1.3	99.9
$Cu(C_9H_6ON)_2 \cdot 2H_2O$	8	0.03–0.06	2.9	100.0	0.11–0.22	2.0	100.0
$Zn(C_9H_6ON)_2 \cdot 2H_2O$	8	0.03–0.08	1.5	100.3	0.10–0.21	0.1	100.0
$Cd(C_9H_6ON)_2 \cdot 2H_2O$	8	0.02–0.06	2.5	100.2	0.10–0.20	0 1	100.0
$Mn(C_7H_{14}O_2N)_2$	12	0.02–0.06	2.6	100.1	0.07–0.15	0 1	100.0
$Ni(C_7H_{14}O_2N)_2$	12	0.02–0.06	3.1	99.9	0.07–0.15	0 1	100.0
$Cu(C_7H_{14}O_2N)_2$	12	0.02–0.05	3.8	99.9	0.07–0.25	1 7	100.0
$Zn(C_7H_{14}O_2N)_2$	12	0.02–0.05	2.9	99.8	0.09–0.19	1.9	100.0
$Cd(C_7H_{14}O_2N)_2$	12	0.02–0.06	3.7	99.9	0.07–0.16	1.8	99 9

*Equivalents of NCP per mole of reductant.
†Average of ten replicates.

The main advantages of NCP over the similar oxidants reported earlier[1–6] are its greater stability and the more rapid equilibration in potentiometric titrations.

Acknowledgement—We are thankful to the authorities of the University of Kerala for awarding a research fellowship to one of us (N.J).

REFERENCES

1. C G. R Nair and P Indrasenan, *Talanta*, 1976, **23**, 239.
2. K. D Mahilamony and P. Indrasenan, *ibid.*, 1981, **28**, 627.
3. M. P. Radhamma and P. Indrasenan, *ibid.*, 1983, **30**, 49.
4. P. Indrasenan and M. P. Radhamma, *Indian J. Chem.*, 1983, **22A**, 729.
5. M. P. Radhamma and P. Indrasenan, *J. Indian Chem. Soc.*, 1984, **61**, 464
6. T. J. Jacob and C. G. R. Nair, *Talanta*, 1972, **19**, 347
7. E. H. Rodd (ed.), *Chemistry of Carbon Compounds*, Vol. IIIB, Elsevier, Amsterdam, 1956.
8. C Duval, *Inorganic Thermogravimetric Analysis*, 2nd Ed , Elsevier, Amsterdam, 1963.
9. A. I Vogel, *A Text Book of Quantitative Inorganic Analysis*, 3rd Ed., Longmans, London, 1964.
10. I. M. Kolthoff, R. Belcher, V. A. Stenger and G. Matsuyama, *Volumetric Analysis*, Vol. III, Interscience, New York, 1957.

Talanta, Vol 32, No 11, pp 1069 1071, 1985
Printed in Great Britain

0039-9140 85 53 00 + 0 00
Pergamon Press Ltd

USE OF NMR FOR QUANTITATIVE ANALYSIS OF PHARMACEUTICALS

J. K. KWAKYE
Department of Pharmaceutical Chemistry, University of Science and Technology, Kumasi, Ghana

(*Received* 11 *February* 1985. *Revised* 13 *May* 1985. *Accepted* 3 *June* 1985)

Summary—Many pharmaceutical preparations have been assayed successfully by the use of NMR. The method utilizes measurement of the area under selected signals of both test and standard samples by means of electronic integrators. The NMR method is simpler and faster than official methods of analysis although less precise.

Nuclear magnetic resonance spectrometry is a technique particularly suited to quantitative measurement, but the pharmaceutical applications were not appreciated until Hollis[1] successfully analysed aspirin, phenacetin and caffeine mixtures (APC) by NMR spectrometry. The impact of the technique on pharmaceutical analysis is shown by the number of articles that have appeared in the literature over the past twenty years. The present paper reports the successful analytical application of NMR to twelve pharmaceutical preparations.

The method involves the addition of an internal standard to the sample and subsequent extraction with a solvent. The appropriate analytical peaks are integrated after the NMR spectrum has been recorded. The weight (W_t) of a component in the sample is then calculated from:

$$W_t = \frac{E_T I_T W_s}{E_s I_s}$$

where E_T and E_s are the NMR "equivalent weights" of sample and standard, I_T and I_s are the integrals of the selected sample and standard peaks and W_s is the weight of standard taken.

The internal standards employed and the "equivalent weights" are listed in Table 1. In addition to the NMR method, the official[2] methods of analysis were also applied for comparison.

EXPERIMENTAL

Apparatus

A Perkin-Elmer NMR spectrometer model R12B operating at 60 MHz, with a probe temperature of 37 ± 1° and integration accuracy of 99.88 ± 0.03% was used for the NMR assays.

Assay of tablets

The average weight of 20 tablets was obtained, the tablets were powdered and a known weight of the powder (equivalent to the weight of active ingredient stated in Table 2) was suspended in the appropriate solvent together with the internal standard. The mixture was allowed to stand for at least 5 min with occasional shaking to ensure complete dissolution, then either centrifuged or filtered through a cotton wool plug saturated with the solvent. The NMR spectrum of the clear supernatant layer or the filtrate was recorded and the analytical regions (see Tables 1 and 2) were integrated at least five times.

Assay of suspensions

A sufficient quantity of the suspension, equivalent to the required weight of active ingredient, was mixed with the internal standard and the solvent, and the mixture was stirred for about 10 min. The analysis was completed as for tablets.

Assay of capsules

The contents of 10 capsules were weighed together and a weight equivalent to a sufficient quantity of active ingredient was suspended in the appropriate solvent together with the internal standard and the mixture was occasionally shaken during the next 5 min, then analysed as for tablets.

Ultraviolet assays

"Orudis" capsules. The contents of 10 capsules were weighed, and a weight of powder equivalent to 50 mg of ketoprofen was shaken with 50 ml of methanol. The suspension was then filtered into a 200-ml standard flask and made up to volume with methanol. Five ml of the solution were diluted to 100 ml with methanol and the absorbance of this solution at 253 nm was measured (1-cm cell). The absorbance of standard ketoprofen solution in methanol was used for calculation.

Table 1. Internal standards employed for analysis of pharmaceuticals

Compound	Analytical group	Resonance position (δ), *ppm*	Equivalent weight
Maleic acid	CH=CH	6.35	58.04
3,4-Dimethoxybenzoic acid	$2(OCH_3)$	3.80	30.36
3-Acetobenzothiophene	$COCH_3$	2.6	58.72
Vanillin	CHO	9.8	152.16

Table 2. Summary of conditions for NMR assays

Formulation	Active ingredient, average weight used, *mg*	Equivalent weight, E_T	Sample analytical group	Resonance position (δ), *ppm*	Internal standard, average weight used, *mg*	Solvent	Volume, *ml*
Panadol	Paracetamol 210	50.4	$NCOCH_3$	2.01	3,4-Dimethoxybenzoic acid, 190	1:3 $CDCl_3$/DMSO,	1.2
Brufen tablets	Ibuprofen 45	34.4	$CH(CH_3)_2$	0.5–4.0	3-Acetobenzothiophene, 45	CCl_4	2
Brufen suspension							
Ephedrine HCl (46.0)	—	40.3	Aromatic peak	Aromatic position	Maleic acid, 42	D_2O	0.5
Pseudo-ephedrine HCl (50.0)							
Butazolidine	Phenylbutazone 38	34.2	$(CH_2)_3CH_3$	0.8–2.4	3-Acetobenzothiophene, 58	$CDCl_3$	0.7
Alka tablets							
Orudis capsules	Ketoprofen 23	84.8	CCH_3	1.4–1.6	3-Acetobenzothiophene, 65	$CDCl_3$	1
Tanderil tablets	Oxyphenbutazone 80	36.0	$(CH_2)_3CH_3$	0.8–2.2	3-Acetobenzothiophene, 60	$CDCl_3$	1
Indocid capsules	Indomethacin 25	119.3	CCH_3	2.38	Vanillin, 64	$CDCl_3$	0.5
Naprosyn tablets	Naproxen 120	57.6	OCH_3 & CH	3.5–4.15	3-Acetobenzothiophene, 90	$CDCl_3$	2
Benoral tablets	Benorylate 120	52.2	$COCH_3$ & $NOCH_3$	2–2.3	Maleic acid, 120	3:1 DMSO(d_6)/$CDCl_3$	2
Benoral suspension							

"Brufen" suspension and tablets. A weight of suspension or powdered tablets, equivalent to about 25 mg of ibuprofen, was stirred with 25 ml of methanol for 10 min. The mixture was then filtered. The filtrate was accurately diluted to 100 ml with methanol and 5 ml of the resulting solution were further diluted with methanol to 100 ml. The absorbance of the final solution was measured at 222 nm (1-cm cell). The absorbance of a standard ibuprofen solution in methanol was used for calculation.

"Naprosyn" tablets. A weight of powdered tablets, equivalent to about 20 mg of naproxen, was stirred with 30 ml of methanol for 10 min and the mixture was then filtered. The filtrate was accurately diluted with methanol to 100 ml, and 5 ml of this solution were further diluted with methanol to 50 ml. The absorbance of the final solution was measured at 273 nm (1-cm cell). The absorbance of a standard naproxen solution in methanol was employed in the calculation.

"Benoral" tablets and suspension. A quantity of the powdered tablets or the suspension, equivalent to 20 mg of benorylate, was stirred with 30 ml of hot methanol for 5 min. The mixture was filtered if necessary and accurately diluted with methanol to 100 ml; 5 ml of this solution were further diluted with methanol to 200 ml. The absorbance of the resulting solution was measured at 240 nm (1-cm cell) The absorbance of standard benorylate solution in methanol was used in the calculation.

RESULTS

The summary of results in Table 3 shows that the NMR and official methods have comparable accuracy except for "Benoral" suspension for which the NMR method gave much higher results.

The NMR method was generally simpler than the official methods other than ultraviolet spectrophotometry. The maximum time required for a single NMR analysis was 40 min, including sample preparation. The NMR method was less precise than other methods (Table 3).

Peak height measurement was found much less accurate and precise than peak area measurement. In assay of "Panadol" peak height measurement gave an error of -10.7% (coefficient of variation 5.2%), the corresponding figures for peak area measurement being $+0.8\%$ (2.5%).

DISCUSSION

The NMR method is simple, fast and readily used for routine analysis. Concentrations of about 10% are generally required for good NMR spectra,[3] but since the volume of solvent required is only about 0.5–2 ml, only a small amount of sample is needed. The NMR spectrum often reveals the presence of impurities, provided these are present in significant concentration ($> \sim 2\%$), and also any decomposition of the compound under investigation (by the appearance of extra peaks). It is often possible to identify the impurities, and NMR quantitative analysis is then a useful check on the quality of the sample. The most obvious drawback is the poor precision. Since most of the published work[4] on NMR quantitative analysis claims low standard deviations, the high values ob-

Table 3. Results for commercial products

Formulation	Active ingredient	Average % of the labelled strength		Coefficient of variation, %	
		NMR	Official	NMR	Official
Panadol	Paracetamol	100.8	101.2	2.5	0.7
Brufen tablets	Ibuprofen	99.7	99.0*	1.9	0.7
Brufen suspension		101.0	100.5*	1.8	
Ephedrine·HCl		100.9	100.0	1.0	0.0
Pseudo-ephedrine·HCl		100.4	—	2.3	—
Butazolidine Alka tablets	Phenylbutazone	102.3	100.9	0.8	0.6
Orudis capsules	Ketoprofen	97.1	97.6*	1.7	1.1
Tanderil tablets	Oxyphenbutazone	97.3	98.5	1.3	0.7
Indocid capsules	Indomethacin	104.6	100.9	2.6	0.7
Naproxyn tablets	Naproxen	97.4	100.2*	1.9	0.5
Benoral tablets	Benorylate	101.4	100.5*	4.8	0.8
Benoral suspension		110.4	99.6*	5.7	0.7

*Ultraviolet spectrophotometry (unofficial method).

tained in this work may be due to non-instrumental factors.

Peak height measurements give erroneous results because they are proportional to the number of protons only when the peak width are the same.[5]

Another problem is possible interference by excipients. For the samples tested here, there was no clear case where excipient resonance peaks interfered with the analytical peaks, though the high value for "Benoral" suspension might be attributable to this type of interference.

The coefficients of variation obtained for the two benorylate products are very high and the method is therefore not recommended for this compound.

REFERENCES

1. D. P. Hollis, *Anal. Chem.*, 1963, **35**, 1682.
2. *British Pharmacopoeia*, The Pharmaceutical Press, London, 1975.
3. R. T. Parfitt, in *Practical Pharmaceutical Chemistry*, Part II, 3rd Ed., A. H. Beckett and J. B. Stanlake (eds.), p. 367. Athlone Press, London, 1976.
4. D. M. Rackham, *Talanta*, 1976, **23**, 269.
5. F. Kasler, *Quantitative Analysis by NMR Spectroscopy*, Academic Press, London, 1973.

Talanta, Vol 32, No 11, pp 1072–1073, 1985
Printed in Great Britain

0039-9140/85 $3.00 + 0.00

SPECTROPHOTOMETRIC DETERMINATION OF TRACE AMOUNTS OF THALLIUM WITH 7-(4,5-DIMETHYLTHIAZOLYL-2-AZO)-8-HYDROXYQUINOLINE-5-SULPHONIC ACID

GAO JIALONG, GU GANG, LIU XILIN and CHEN TONGYUE[1]*
Department of Chemistry, Lanzhou University, Gansu and [1]Department of Metallurgy, Shanghai University of Technology, 149, Yanchang Road, Shanghai, People's Republic of China

(*Received* 30 *January* 1984. *Revised* 11 *April* 1985. *Accepted* 18 *May* 1985)

Summary—A new reagent, 7-(4,5-dimethylthiazolyl-2-azo)-8-hydroxyquinoline-5-sulphonic acid, has been examined to evaluate its usefulness as a spectrophotometric reagent for thallium(III). A purple-red complex is formed in aqueous solution at pH 4–5 in the presence of cetylpyridinium chloride and the stoichimetric ratio is 1:2 (Tl:reagent). The apparent stability constant is 1.5×10^{11}. The effect of diverse ions has been studied and a method for determining trace amounts of thallium is proposed

So far the most important spectrophotometric methods for the determination of thallium in a variety of materials have been based on precipitation of the complex anion TlX_4^- (X is Cl^- or Br^-) by addition of the large cations of various triphenylmethane dyes and extraction of the ion-pair into a suitable organic solvent.[1–3] It would be much more convenient if the extraction could be omitted and water-soluble coloured species used for the determination. The heterocyclic azo dye, 7-(4,5-dimethylthiazolyl-2-azo)-8-hydroxquinoline-5-sulphonic acid (DMTAOx) has been synthesized and found to react with thallium(III) to form an intensely purple-red complex at pH 4–5 in the presence of the cationic surfactant, cetylpyridinium chloride. The molar absorptivity is 1.3×10^5 l.mole^{-1}.cm^{-1} at 560 nm.

EXPERIMENTAL

Reagents

All solutions were prepared with analytical-grade chemicals and demineralized distilled water unless otherwise mentioned

Cetylpyridinium chloride (CPC) 0.2% solution.

Buffer solution, 2M, pH 4.7. Dissolve 133.3 g of sodium acetate trihydrate in demineralized distilled water, add 59.5 ml of glacial acetic acid and dilute to 1 litre.

Standard thallium solution. Prepare a stock solution by dissolving 0.1305 g of thallium nitrate in 20 ml of 0.5*M* hydrochloric acid plus a few drops of 30% hydrogen peroxide, evaporate the mixture to dryness on a steam-bath, take up the residue in 10 ml of 1*M* hydrochloric acid and dilute to volume with water in a 100-ml standard flask to give a 1000 mg/ml thallium(III) solution. Prepare the working solution by appropriate dilution of the stock solution with 0.1*M* hydrochloric acid.

Synthesis of DMTAOx.[4] Dissolve 4.2 g (0.02 mole) of 4,5-dimethyl-2-aminothiazole hydrobromide in 30 ml of 3.5*M* hydrochloric acid, cool the solution in ice-water, slowly add (with stirring) 4.4 ml of 5*M* sodium nitrate (0.022 mole) and continue to stir for 1–2 hr, keeping this azo salt solution at 0°. Dissolve 4.5 g of 8-hydroxyquinoline-5-sulphonic acid and 10.6 g of anhydrous sodium carbonate in 100 ml of water and add this solution to the azo salt solution dropwise with constant stirring during a period of 1 hr, keeping the temperature at 0–5° throughout. Continue to stir for 2 hr more, keep the mixture in the refrigerator overnight, then filter off the crude product and recrystallize it twice from ethanol. The pure product is a dark purple crystalline material, m.p. 170–172°. Found: C 46.8%, H 3.7%, N 16.0%; $C_{14}H_{12}N_3O_4S_2$ requires C 46.2%, H 3.3%, N 15.4%.

Ethanolic DMTAOx reagent solution, 0.02%

Procedure

Transfer up to 10 ml of sample solution containing 1–10 μg of thallium into a 25-ml standard flask, add 2.5 ml of buffer solution, 2 ml of cetylpyridinium chloride solution and 1 ml of DMTAOx solution, dilute to the mark with water and measure the absorbance at 560 nm against a reagent blank.

RESULTS AND DISCUSSION

Absorption spectra

The absorption spectra of the purple-red thallium complex and of DMTAOx itself in aqueous medium are shown in Fig. 1. The complex has an absorption

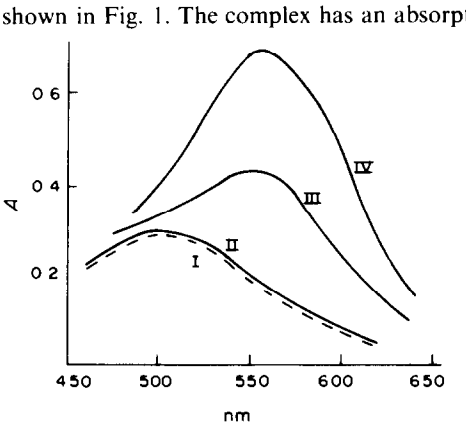

Fig. 1.

*Author for correspondence

Table 1. Determination of thallium in some samples

Sample	Thallium, μg	
	Added	Found
Synthetic No. 1	10.0	9.9
Synthetic No. 2	10.0	9.9
Aluminium alloy	10.0	9.6
Bauxite	10.0	9.5

maximum at 560 nm and an apparent molar absorptivity of 1.3×10^5 l.mole^{-1}.cm^{-1} at this wavelength. The spectral interference of the reagent can be eliminated by measurement against a reagent blank, and the sensitivity is considerably increased by the presence of the cationic surfactant. The CPC has a sensitizing effect on the coloured compound, but does not appear to form a definite complex with it.

Optimal conditions for formation of the complex

The effect of pH on the absorbance of the complex was examined over the range from 1 to 7. The absorbance was found to be maximal and constant at pH 4–5 and to decrease sharply to very low values at pH 3.8. Hence pH 4.7 was selected for use.

It was found that 0.5 ml of 0.02% DMTAOx solution is enough to complex 10 μg of thallium, so 1 ml was chosen for general use. The cationic surfactant CPC gave maximum enhancement of the colour when present at concentrations in the range 1×10^{-4}–$7 \times 10^{-3}M$. In this work, the CPC concentration in the 25 ml of final solution was fixed at $4.8 \times 10^{-3}M$.

The colour development is complete in 10 min at room temperature and the colour is stable for at least 2 hr.

Composition of the complex

The stoichiometric ratio of thallium to DMTAOx in the complex was found to be 1:2 by the Bent and French[5] and continuous-variations[6] methods. By the equilibrium-shift method[7] the apparent stability constant was found to be 1.5×10^{11}.

The effect of various cations and anions on the determination of 10 μg of thallium was examined. A change of ±2% in absorbance was set as the tolerance limit. The tolerance limits can be summarized as follows: Ca^{2+} (1 mg); Al^{3+} (1 mg); Cr^{3+} (1 mg); Ga^{3+} (20 μg); In (20 μg); Co^{2+} (20 μg); Co^{3+} (20 μg); Ni^{2+} (20 μg); Zn^{2+} (50 μg in the presence of $4 \times 10^{-5}M$ tartrate); Cu^{2+} (50 μg in the presence of $4 \times 10^{-5}M$ tartrate); Fe^{3+} (50 μg in the presence of $4 \times 10^{-5}M$ fluoride); F^-, tartrate, Cl^-, NO_3^-, SO_4^{2-} and citrate do not interfere.

Determination of thallium in samples

A 0.5–1.0 g sample is decomposed in a 250-ml beaker with 15 ml of concentrated hydrochloric acid and 10 ml of concentrated nitric acid, then the solution is evaporated almost to dryness, the residue is taken up with 50 ml of water, insoluble material is filtered off and washed, and the filtrate is evaporated to dryness after addition of 5 ml of 1*M* hydrobromic acid (containing three drops of saturated bromine water per 100 ml), this acid addition and evaporation being repeated twice more. The residue is then dissolved in 15 ml of 1*M* hydrochloric acid and extracted with two 15-ml volumes of diethyl ether.[3] The organic solvent is evaporated from the combined extracts and the residue is transferred to a 25-ml standard flask. Then 1 ml of 1*M* ammonium fluoride and 1 ml of 1*M* sodium tartrate are added and the general procedure is applied.

Table 1 shows some results for analysis of two synthetic sample solutions containing (1) 10 mg of iron and 10 μg of thallium; (2) 60 mg of aluminium oxide 10 mg of iron, 5 mg of calcium oxide, 3 mg of magnesium oxide, 2 mg of silica and 10 μg of thallium. The separation and determination were done as mentioned above. Results are also shown for 10 μg of thallium added to an alloy and to bauxite (both originally containing no thallium).

REFERENCES

1. Z. Marczenko, H. Kałowska and M. Mojski, *Talanta*, 1974, **21**, 93.
2. A. T. Pilipenko and Hguen Mong Shin, *Zh. Analyt. Khim.*, 1968, **23**, 934.
3. Rock and Mineral Compilation Section, *Analysis of Rocks and Minerals*, Geology Publication Co., Beijing, 1974.
4. Liu Xilin, Gu Gang, Chen Tongyue and Gao Jialong, *Fenxi Huaxue*, 1983, **11**, 40.
5. H. E. Bent and C. L. French, *J. Am. Chem. Soc.*, 1941, **63**, 568.
6. A. E. Lazarev and V. E. Lazareva, *Zavodsk. Lab.*, 1975, **41**, 534.

Talanta, Vol. 32, No 11, pp 1074–1075, 1985
Printed in Great Britain

0039-9140/85 $3.00 + 0.00
Pergamon Press Ltd

ANALYTICAL PROPERTIES OF 2-OXIMINODIMEDONE DITHIOSEMICARBAZONE

F. SALINAS, J. C. JIMENEZ SANCHEZ and J. M. LEMUS GALLEGO
Department of Analytical Chemistry, Faculty of Sciences, University of Extremadura, 06071 Badajoz, Spain

(*Received* 7 *January* 1985. *Accepted* 4 *April* 1985)

Summary—The synthesis and analytical properties of 2-oximinodimedone dithiosemicarbazone are described.

Thiosemicarbazones have been widely used for spectrophotometric determination of inorganic ions and their analytical applications have been reviewed.[1-3] Monothiosemicarbazones with an electron-donating group in the α-position and α-dithiosemicarbazones have been studied the most. In recent years, some β-dithiosemicarbazones have been studied as analytical reagents. In this paper, the analytical properties of 2-oximinodimedone dithiosemicarbazone [5,5-dimethyl-1,2,3-cyclohexanetrione-2-oxime-1,3-dithiosemicarbazone (ODDT)] are presented.

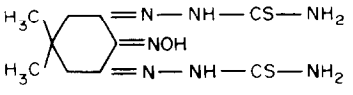

The synthesis of ODDT is based on that of 2-oximinodimedone by reaction of sodium nitrite with dimedone,[4] and subsequent condensation with thiosemicarbazide.

EXPERIMENTAL

Synthesis of ODDT

Dimedone (2 g) was dissolved in a solution of 10 g of sodium hydroxide in 30 ml of water and 30 ml of ethanol; 0.986 g of sodium nitrite was then added, the solution was cooled in a freezing mixture, and stirred while 41 ml hydrochloric acid (1 + 1) were slowly added. To this solution were added 2.6 g of thiosemicarbazide dissolved in 100 ml of water and 200 ml of ethanol, followed by sodium acetate until the pH was 5. The solution was stored for 2 or 3 days in the refrigerator and the solvent was then removed at 30° under reduced pressure. Yellow crystals separated and were washed with ethanol and water (m.p. 182–4°; yield 50–70%). Elemental analysis gave 38.3% C, 5.5% H, 30.9% N and 20.3% S, $C_{10}H_{17}N_5OS_2$ requires 38.1% C, 5.4% H, 31.1% N and 20.3% S

Reactions with cations and anions

The samples were prepared in 25-ml standard flasks with 50–200 μg of the ion, 5 ml of 0.1% solution of ODDT in dimethylformamide, 5 ml of buffer solution, and dilution to volume with distilled water. The spectrum in the region 350–700 nm was recorded, with a reagent blank as reference. The stoichiometries of the reactions were investigated by Job's method and the molar ratio method.

RESULTS AND DISCUSSION

Solubility

The solubility of ODDT in several solvents at room temperature was determined by Wittemberger's method.[5] ODDT is very soluble in dimethylformamide (192 g/l.), ethanol (10.1 g/l.), ethyl acetate (13.0 g/l.), methyl isobutyl ketone (9.2 g/l.) and 3-methyl-1-butanol (9 g/l.) and sparingly soluble in water, chloroform, carbon tetrachloride and cyclohexane.

Stability

A dilute aqueous solution of ODDT ($6 \times 10^{-5} M$) at pH > 2 is reasonably stable and a $3 \times 10^{-3} M$ solution is stable for 2 days if made in dimethylformamide and for a week if made in ethanol or 3-methyl-1-butanol.

Spectral characteristics

The infrared spectrum was obtained (KBr discs) and the bands (cm^{-1}) were assigned to the stretching vibrations of —NH— (3320), —OH, —C=N— (3140–3200) and C=S (1100).

The NMR spectrum was obtained in DMSO-d_6 with tetramethylsilane as internal reference. The peaks (δ, ppm) were assigned as follows: 1.05 (—CH protons), 3.75 (—CH_2— protons), 8.05–8.40 (—NH—, —NH_2 protons) and 11.3 (=N—OH proton).

The ultraviolet absorption spectra for the reagent in water, ethanol, 3-methyl-1-butanol, methyl isobutyl ketone, ethyl acetate and dimethylformamide media showed similar maxima between 310 and 330 nm. The ultraviolet absorption spectra at various pH values are shown in Fig. 1.

Ionization constants

The ionization constants were determined by the Stenström and Goldsmith method[6] at 20° and ionic strength 0.1. The average results obtained were: $pK_1 = 7.5$ (oxime group) and $pK_2 = pK_3 = 11.5$ (C=S group thione-thiol tautomerism).[7] The pK values

Table 1. Characteristics of ODDT compounds

Ion	Medium	λ_{max}, nm	ε, $l.mole^{-1}.cm^{-1}$	Stoichiometry (ODDT:ion)	Colour
Cu(II)	pH < 2	380	8.6×10^3		Yellow
Ni(II)	pH 5.5–7.5	380	7.2×10^3	2:1	Orange
Co(II)	pH 0–2	380	1.0×10^4	3:1	Orange
Fe(II)	HCl 0.6–5*M*	565	9.8×10^3	3:1	Violet
Fe(III)	HCl 1–6*M*	565	9.8×10^3	3.5:1*	Violet
Mn(II)	pH ~ 9	435	5.9×10^3		Brown
V(V)	pH < 2	390	4.4×10^3		Yellow
Pd(II)	pH < 2	380	4.9×10^3		Yellow
Cr(VI)	$HClO_4$ 0.4–1*M*	490	5.6×10^3	3:2	Orange
IO_3^-	$HClO_4$ 1–2*M*	390	3.0×10^4	3:1	Yellow
BrO_3^-	$HClO_4$ 0.75–2*M*	390	3.1×10^4	3:1	Yellow

*0.5 for reduction to Fe(II) which then forms the 3:1 complex.

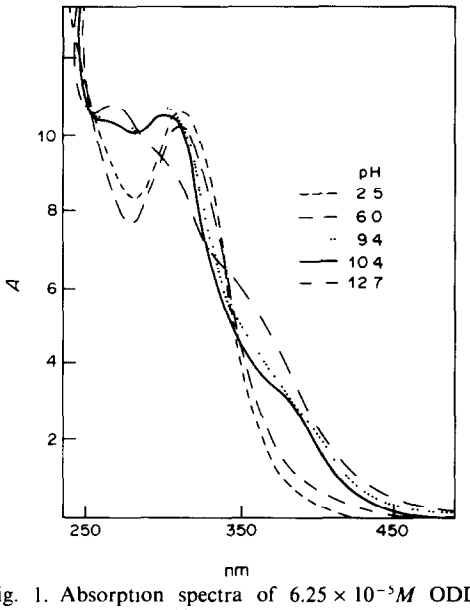

Fig. 1. Absorption spectra of $6.25 \times 10^{-5}M$ ODDT at different pH values.

Table 2. Extraction of ODDT compounds

Ion	Extractant
Cu(II)	EA*, MB*†
Ni(II)	MIKB, MB, EA, CHL
Co(II)	MB, MIBK,* EA*
Fe(II and III)	MB, MIBK,* EA*
Mn(II)	MB, EA, MIBK
V(V)	MIBK, MB*, EA*†
Pd(II)	MB, EA, MIBK
Cr(VI)	MB†
IO_3^-	MB, CHL, MIBK†
BrO_3^-	MB, CHL, EA, MIBK†

EA, ethyl acetate
MB, 3-methyl-3-butanol
MIBK, methyl isobutyl ketone
CHL, chloroform
*With $KClO_4$ present
†Partial extraction.

were also measured potentiometrically, $pK_1 = 7.7$, $pK_2 = 10.4$ and $pK_3 = 11.8$.

Qualitative tests

The reactions of ODDT with 54 inorganic ions were tested at different pH values. ODDT reacts with Fe(II and III) to give a violet colour, Co(II), Ni(II) and Cr(VI) to give an orange colour, Mn(II) brown, and V(V), Cu(II), BrO_3^- and IO_3^-, yellow. The most important results are summarized in Table 1. These are chelating reactions, *e.g.*, with Ni(II), Co(II) and Fe(II), and redox reactions, *e.g.*, with Cr(VI), IO_3^- and BrO_3^-, which involve a two-electron mechanism in acordance with the general redox behaviour of bisthiosemicarbazones.[8,9] The stoichiometry of the Fe(II)–ODDT complex is 1:3 metal:ligand. If we start with Fe(III), this ion is reduced by the reagent, to give the same complex as Fe(II).

Various organic solvents were tested as extractants for the ODDT compounds. The results are summarized in Table 2.

The stability, solubility in various solvents, absence of absorption in the visible region, and the results compiled in Tables 1 and 2 provide a basis for judging the potential analytical utility of ODDT as a chromogenic reagent, especially for the spectrophotometric determination of Fe(II), Co(II), Cr(VI), IO_3^- and BrO_3^-, which will be the subject of further work.

REFERENCES

1. R. B. Singh, B. S. Garg and R. P. Singh, *Talanta*, 1978, **25**, 619.
2. J. M. Cano Pavón, *Microchem. J.*, 1981, **26**, 155.
3. J. M. Cano Pavón, D. Pérez Bendito and M. Valcárcel, *Quim. Anal.*, 1982, **1**, 118
4. J. Hass, *J. Chem. Soc.*, 1907, **91**, 1437.
5. W. Wittemberger, *Chemische Laboratoriumstechnik*, 4th Ed., p. 101. Springer, Vienna, 1950.
6. W. Stenström and N. Goldsmith, *J. Phys. Chem.* 1926, **30**, 1683.
7. B. A. Gingras, R. S. Somorjai and C. H. Bayley, *Can. J. Chem.*, 1961, **39**, 973.
8. M. Román Ceba, J. A. Muñoz Leyva and J. J. Berzas Nevado, *Analyst*, 1978, **103**, 963.
9. K. H. Reddy and D. V. Reddy, *Analyst*, 1983, **108**, 1247.

Talanta, Vol 32, No 11, pp 1077–1081, 1985
Printed in Great Britain

0039-9140/85 $3.00 + 0.00
Pergamon Press Ltd

ANALYTICAL DATA

A COMPARATIVE STUDY OF SOME HYDROXYANTHRAQUINONES AS ACID–BASE INDICATORS

J. BARBOSA, E. BOSCH and R. CARRERA
Department of Analytical Chemistry, University of Barcelona, Barcelona, Spain

(*Received* 12 *March* 1984. *Revised* 20 *February* 1985. *Accepted* 14 *June* 1985)

Summary—Alizarin, Alizarin S, quinizarin and quinalizarin have been compared as acid–base indicators with Bromocresol Green and Methyl Orange as reference indicators. The chromaticity co-ordinates, complementary chromaticity co-ordinates, pK_a values, transition pH-range, pH of maximum colour change, optimum concentration for titrations and the quality of colour change were determined. The results show all four to be good indicators with a colour change quality similar to that of Bromocresol Green.

Reilley *et al.*[1] have developed a complementary chromaticity system and used it to describe indicator transitions. They devised an original system of indices to express the colour quality, but took into account only the limiting colours of the indicators, and did not consider the sharpness of the colour transition. The system therefore gives no criterion for choosing the most suitable indicator concentration. However, the complementary co-ordinates are physical constants for each coloured species, and can be employed for determination of equilibrium constants.[2,3]

The transition sharpness has been considered by Buchar and co-workers.[4,5] They proposed a method, called "Specific Colour Discrimination" (SCD), based on a plot of the number of colour discrimination steps *vs.* pH, which permits the evaluation of the sharpness and sensitivity of the indicator colour change. The SCD values were obtained from transmittance data and thus were a function of light-path length and concentration, and if the SCD values are applied to description of a chemical indicator transition the results are dependent on the experimental conditions of the measurement and not completely representative of the colour changes observed in analytical applications.

To deduce a suitable concentration of an indicator for a titration, Kotrlý and Vytřas[6,7] defined the index of colour-change perceptibility of acid–base indicators as the ratio $\Delta pH/\Delta E$, where ΔE is the total difference between two colours, and correlated this index with the indicator concentration.

In the work described in this paper, determination of the optimal concentration of some indicator solutions was attempted by the Kotrlý and Vytřas method,[7] but the CIELAB co-ordinates were used to calculate the index of colour-change perceptibility. The sensitivity of the indicators, in terms of SCD values, has been evaluated as a measure of the colour-transition quality of the indicators. The sharpness of the transitions has been shown to be a measure of the rapidity of the colour changes. pK_a values of the indicators were determined spectrophotometrically,[2,8] and the values obtained compared with the pH corresponding to the maximum change of colour.

Hydroxyanthraquinones have been widely used as dyes, chelating compounds and acid–base indicators, but few pK_a values and indicator transition ranges have been published. For this study the indicators chosen were 1,2-dihydroxyanthraquinone-3-sulphonic acid (Alizarin S), 1,2-dihydroxyanthraquinone (Alizarin); 1,4-dihydroxyanthraquinone (quinizarin), and 1,2,5,8-tetrahydroxyanthraquinone (quinalizarin). Their chromatic parameters can be used to characterize them as indicators and dyes. Bromocresol Green and Methyl Orange were chosen as reference indicators because of their wide use as neutralization indicators.

EXPERIMENTAL

Apparatus

A Beckman Acta M-VII spectrophotometer with 1, 5 and 10-cm cells, a Radiometer PHM64 pH-meter with glass/calomel electrodes, and a Rockwell AIM-65 20 K RAM microcomputer were used.

Reagents

Alizarin S (Merck A.R.) aqueous solution, 1×10^{-3}M.
Alizarin (Koch-Light analytical grade) solution in ethanol 1×10^{-4}M.
Quinizarin (Merck 98%) solution in ethanol, 3×10^{-6}M.
Quinalizarin (Merck A.R.) solution, in ethanol, 1×10^{-5}M.
Bromocresol Green (Merck A.C.S) aqueous solution, 2×10^{-5}M.

Methyl Orange (Merck A.C.S) aqueous solution, 3×10^{-5}M.

Buffers covering the pH range 2.0–13.0 were prepared at 0.1*M* constant ionic strength.[9]

Procedure and computation method

Approximately $10^{-5}M$ indicator solutions were prepared at 0.1*M* ionic strength by dilution of the stock solutions with suitable buffers. The transmittance (in the visible range) and the pH (at intervals of approximately 0.2) over the colour-change pH range were measured.

To evaluate the chromaticity data, the weighted ordinate method, $\Delta\lambda = 10$ nm, recommended by Kotrlý and Vytřas was used with the coefficients given by Judd.[11] A linear computer program written in BASIC was developed to compute the chromaticity co-ordinates.

The same procedure, after transformation of the transmittances into absorbances, was used to obtain the complementary chromaticity co-ordinates, Q_x, Q_y, and the colour concentration, *J*.

The acid dissociation constants were determined by the method of Reilley and Smith[2] from the complementary chromaticity co-ordinates of several points within the transition range, and also spectrophotometrically by a standard procedure described by Albert and Serjeant.[8]

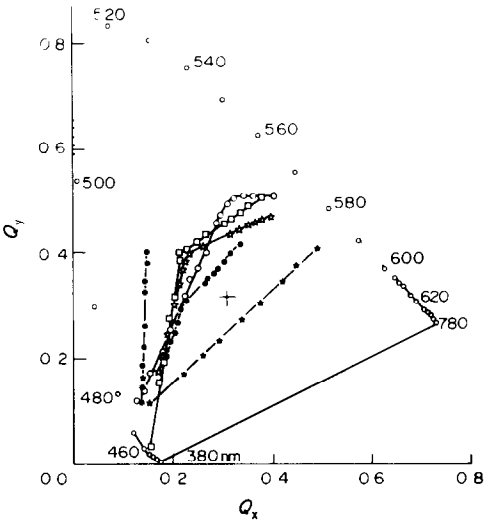

Fig. 2. Colour points of indicators in the complementary chromaticity diagram. Symbols as in Fig. 1.

RESULTS AND DISCUSSION

The colour sequence within the pH range of colour change of indicators, under specified conditions, can be described by the chromaticity co-ordinates *x*, *y* and the relative luminance *Y*. The indicator transition can also be described by means of the complementary chromaticity co-ordinates, which are physical constants, and the quantity *J*, called the "colour concentration", which is dependent on the experimental conditions. These parameters have been determined at different pH values for each indicator. The results obtained are plotted in Figs. 1 and 2. Coloured solutions of different concentrations show different colour points on the *x*, *y* diagram but coincident colour points on the Q_x, Q_y complementary chromaticity diagram.

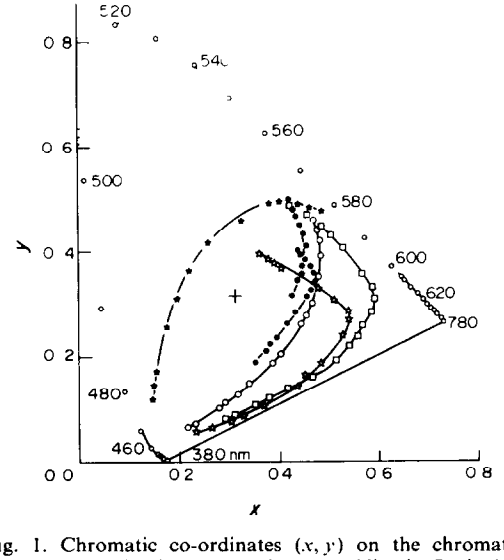

Fig. 1. Chromatic co-ordinates (*x*, *y*) on the chromatic diagram at optimal concentrations: □ Alizarin S, ☆ Alizarin, ○ quinizarin, ● quinalizarin, ★ Bromocresol Green, ✱ Methyl Orange.

The complementary points Q_x, Q_y at any pH value within the colour-change pH range of the indicators lie on a straight line denoting mixtures of the two pure coloured species of the indicator.[3] The hydroxyanthraquinones studied give two linear segments on the complementary chromaticity diagram. This indicates the presence of two different equilibria, each involving a particular colour change. Only one of them can be applied in acid–base titrations in aqueous medium because only one occurs in the pH-range realizable in aqueous solution and, at the same time, shows a good colour-change quality.

The quality of the colour change at the titration end-point depends on the distance between the colour points before and after the transition, but the locations of the points in the diagram are also very important.[1]

For analytical purposes, the most suitable transition of hydroxyanthraquinones occurs between the yellow and red forms, as shown in Figs. 1 and 2. On the complementary chromaticity diagram the segments corresponding to the transitions of the hydroxyanthraquinones studied show a similar orientation. This allows us to establish the sequence of decreasing colour-change quality as quinizarin > Alizarin S > Alizarin > quinalizarin. However, no information about the ideal concentration for use of the indicators is realizable from the complementary chromaticity data.

The pK_a values were determined by the Reilley and Smith method[2] from Q_x, Q_y or Q_z data. To obtain the best results the coordinate which shows the greatest variation within the pH range of the colour change should be used. The advantage of the method in the case of the hydroxyanthraquinones is that it allows use of the colour-point co-ordinates of the singly-

Table 1. Comparative pK_a values of the indicators

	Chromatic method		Standard method		
	pK_1	pK_2	pK_1	pK_2	Reference
Alizarin S	5.72 ± 0.02	10.98 ± 0.02	5.69 ± 0.02	10.98 ± 0.02	This work
			6.72 ± 0.09	9.35 ± 0.05	13
			5.49	10.85	14
Alizarin	7.51 ± 0.07	11.64 ± 0.05	7.36 ± 0.05	11.57 ± 0.05	This work
			8.76 ± 0.08	10.22 ± 0.03	13
			7.45 ± 0.08	11.80 ± 0.08	15
Quinalizarin	5.30 ± 0.05	9.16 ± 0.034	5.28 ± 0.04	9.28 ± 0.03	This work
			5.25 ± 0.09	9.32 ± 0.15	16
Quinizarin	9.35 ± 0.05	11.78 ± 0.12	9.26 ± 0.04	11.79 ± 0.07	This work
			9.21 ± 0.07	11.74 ± 0.04	13
			9.90 ± 0.08	11.18 ± 0.08	15
Bromocresol Green	4.61 ± 0.03		4.60 ± 0.03		This work
			4.66		17
Methyl Orange	3.35 ± 0.04		3.44 ± 0.03		This work
			3.46		17

charged form, which appears only in a very restricted pH range. The results obtained are given in Table 1, and agreed with those obtained by a standard spectrophotometric method.[3] Comparison of our values with those found in the literature (also given in Table 1) is difficult since the few available data are discordant.

To obtain the optimal concentration of the indicators for titration, the Kotrlý and Vytřas[7] method was used. These authors point out that the transition curve for the colour change can be divided into small segments related to changes in a suitable variable, such as pH, which allows expression of the particular change per unit ΔE; ΔE is the total difference between two colours. Thus the ratio $\Delta pH/\Delta E$, called the index of colour-change perceptibility and showing the pH change corresponding to a preselected amount of colour variation, can be correlated with the effect of indicator concentration.

In this work, the colour difference between the two colours, ΔE, was calculated by means of the 1976 CIE ($L^*a^*b^*$) system, which can be applied with advantage.[12]

The chromatic co-ordinates L^*, a^* and b^* were calculated with the equations:

$$L^* = 116(Y/Y_n)^{1/3} - 16$$

$$a^* = 500[(X/X_n)^{1/3} - (Y/Y_n)^{1/3}]$$

$$b^* = 200[(Y/Y_n)^{1/3} - (Z/Z_n)^{1/3}]$$

where $X_n = 98$, $Y_n = 100$ and $Z_n = 118$ are the colour stimuli of a normal individual for white in the 1931 CIE recommendation for light source C, and X, Y and Z are the tristimuli obtained for the indicator solution at a particular pH. The colour co-ordinates a^* and b^* for each indicator transition are given in Fig. 3.

The chromatic difference between two colours is given by

$$\Delta E = [(\Delta L^*)^2 + (\Delta a^*)^2 + (\Delta b^*)^2]^{1/2}$$

where ΔL^*, Δa^*, Δb^* are calculated from the L^*, a^* b^* co-ordinates at the appropriate pH values.

The relation $\Delta pH/\Delta E$ is plotted *vs.* log c, where c is the ratio of the indicator concentration used for calculation of the particular chromaticity transition to the experimental value of the indicator concentration, c_0. The plot of $\Delta pH/\Delta E$ *vs.* log c is given in Fig. 4 and the minimum on the curve obtained shows the optimum concentration of the indicator for the particular titration. The results, referred to 1-cm path-length, are given in Table 2.

The plot of ΔE *vs.* pH (Fig. 5), where ΔE is the difference between any colour point and the colour point of the acid form of the indicator, allows determination of the sensitivity of the colour change of each indicator in terms of the specific colour discrimination (SCD) values ($\Delta E/\Delta pH$ = SCD value).[5] These values refer to the optimum concentration of the indicator solutions and are plotted in

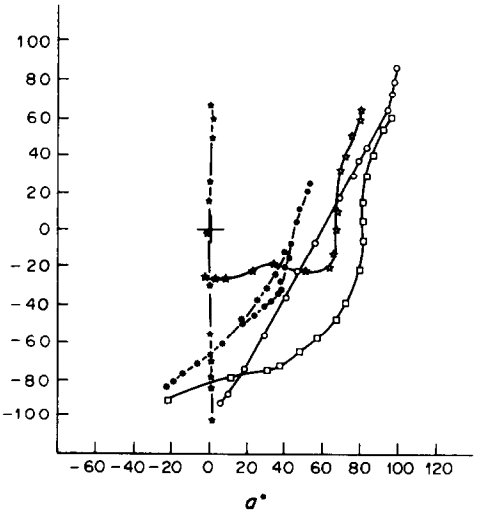

Fig. 3. Chromatic co-ordinates a^* and b^* of the indicator solutions at optimal concentrations. Symbols as in Fig. 1.

Table 2. Colour changes of the indicators

	pH_{mcc}	SCD	$pH_{1/2(SCD)}$	$pH_{mcc} - pK$	pH interval	Optimum concentration, M
Alizarin S	5.20	121	0.75	−0.49	4.6–5.9	6×10^{-4}
Alizarin	6.75	97	0.55	−0.39	6.3–7.4	6×10^{-4}
Quinalizarin	5.12	54	0.53	−0.16	4.7–5.8	1×10^{-4}
Quinizarin	9.03	129	0.88	−0.32	8.3–10.0	2×10^{-4}
Bromocresol Green	4.30	135	1.05	−0.30	3.6–5.2	1×10^{-4}
Methyl Orange	3.67	67	1.20	+0.23	2.4–4.5	3×10^{-4}

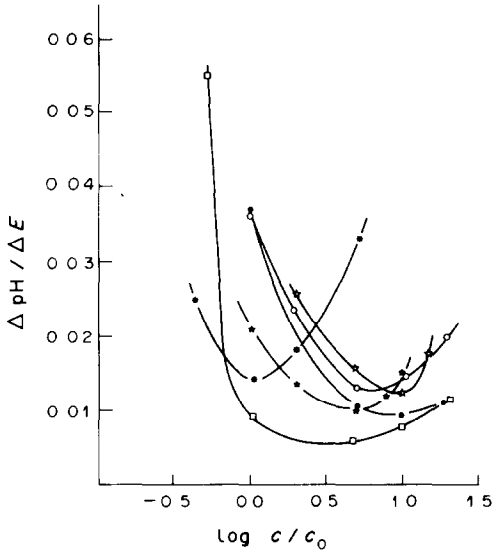

Fig. 4. Dependence of the colour-change perceptibility index, $\Delta pH/\Delta E$, on the relative indicator concentration: □ Alizarin S ($c_0 = 1 \times 10^{-4} M$), ☆ Alizarin ($c_0 = 6 \times 10^{-5} M$), ○ quinizarin ($c_0 = 3 \times 10^{-5} M$, ● quinalizarin ($c_0 = 1 \times 10^{-5} M$), ★ Bromocresol Green ($c_0 = 2 \times 10^{-5} M$), ∗ Methyl Orange ($c_0 = 3 \times 10^{-5} M$)

Fig. 6 and given in Table 2, in which only the useful transitions of the hydroxyanthraquinones are shown. According to these results the colour change sensitivity decreases in the following order: Bromocresol Green > quinizarin > Alizarin S > Alizarin > Methyl Orange > quinalizarin.

The half-bandwidth values ($pH_{1/2\,SCD}$) from Fig. 6 and given in Table 2, define the sharpness of the indicator colour change.[5]

It is convenient, in routine use of an indicator, to know its whole pH range of colour change, which is given by the base-width of the SCD peak. The experimental transition intervals differ from case to case and are usually not symmetrical about the pK_a value, because often one of the two colours is more easily perceptible in presence of the other than *vice versa*. Thus to predict whether an indicator will be suitable for use in a particular titration, the pK and pH of maximum colour change (pH_{mcc}) should be evaluated. These values are shown in Table 2 for each indicator tested.

Evaluation of the colour-change quality of these indicators at optimal concentration, taking into account all the considerations above, shows that Bromocresol Green, quinizarin and Alizarin S are very

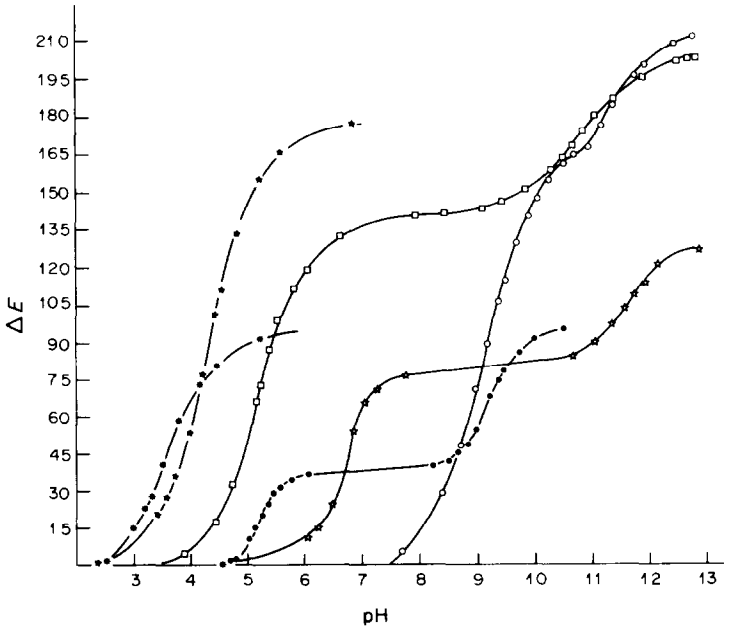

Fig. 5. Change in the chromatic difference values, ΔE, with the pH. Symbols and concentrations as in Fig. 1.

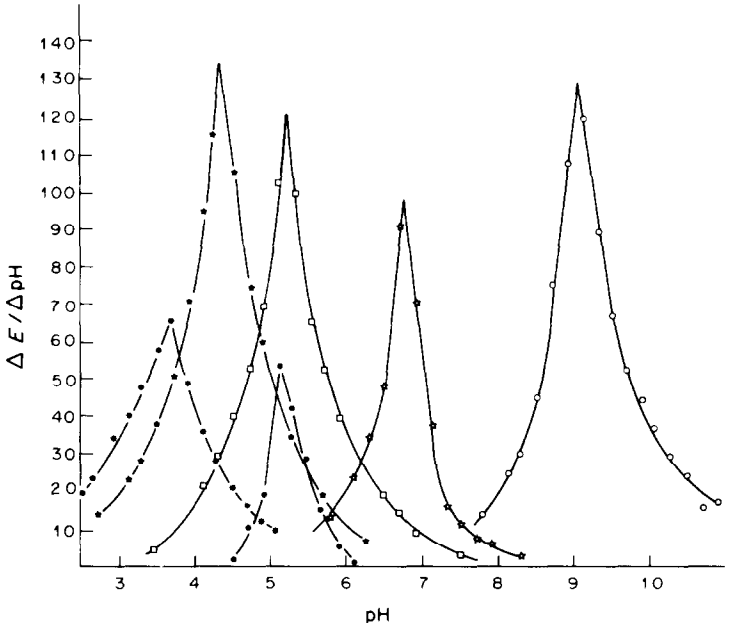

Fig. 6. Change in SCD values with pH. Symbols and concentrations as in Fig. 1.

good indicators which show equivalent colour-change quality. Alizarin is also a good indicator but with slightly lower colour-change quality, whereas Methyl Orange and quinalizarin have similar colour-change quality that is remarkably lower than that of the other indicators mentioned. These results are in agreement with the visual observations.

REFERENCES

1. C. Reilley, H. Flaschka, S. Laurent and B. Laurent, *Anal. Chem.*, 1960, **32**, 1218.
2. C. Reilley and E. Smith, *ibid.*, 1960, **32**, 1233.
3. H. Flaschka, *Talanta*, 1961, **8**, 342.
4. V. M. Bhuchar, V. P. Kukreja and S. R. Das, *Anal. Chem.*, 1971, **43**, 1847.
5. V M. Bhuchar and A. K. Agrawal, *Analyst*, 1982, **107**, 1439.
6. K. Vytřas, *Chem. Zvesti*, 1974, **28**, 252.
7. S. Kotrlý and K. Vytřas, in *Essays on Analytical Chemistry*, E. Wänninen (ed.), pp. 259–280. Pergamon Press, Oxford, 1977.
8. A. Albert and E. P. Serjeant, *The Determination of Ionization Constants*, Chapman and Hall, London, 1962.
9. V. Cerdà and C. Mongay, *An. Quim.*, 1980, **76**, 154.
10. S. Kotrlý and K. Vytřas, *Talanta*, 1971, **28**, 253.
11. D. B. Judd, *Measurement and Specification of Color*, in *Analytical Absorption Spectroscopy*, M. G. Mellon (ed.), Wiley, New York, 1953.
12. F. W. Billmeyer Jr. and M. Saltzmann, *Principles of Color Technology*, 2nd Ed., Wiley, New York, 1981.
13. R. M. Issa, M. S. El-Ezaby and A. H. Zewail, *Z. Phys. Chem. Leipzig*, 1970, **244**, 155.
14. H. E. Zittel and T. M. Florence, *Anal. Chem.*, 1967, **39**, 320.
15. H. Guillet and J. Ch. Parıaud, *Bull. Soc Chim. France*, 1966, 2624.
16. R. M. Issa and A. H. Zewail, *U.A.R. J. Chem.*, 1971, **14**, 471.
17. L. Meites, *Handbook of Analytical Chemistry*, McGraw-Hill, New York, 1963.

Talanta, Vol. 32, No 11, p 1082, 1985
Printed in Great Britain

0039-9140/85 $3 00 + 0.00
Pergamon Press Ltd

DETERMINATION OF THE PROTONATION CONSTANT OF CHLORAMINE-B

M. SUBHASHINI, M. S. SUBRAMANIAN and V. R. S. RAO
Department of Chemistry, Indian Institute of Technology, Madras 600 036, India

(*Received* 20 *March* 1985. *Accepted* 2 *August* 1985)

Summary—The protonation constant of chloramine-B has been determined at pH <3.3 by an ion-exchange method. The value found is 61 ± 5.

Organic haloamines, particularly chloramine-T (CAT) and chloramine-B (CAB) are powerful oxidants, but their behaviour in very strong acid medium is sometimes different from that in weakly acid medium. Strong acid medium is expected to yield a protonated species. The formation of such species $C_6H_5SO_2\overset{+}{N}H_2Cl$ from CAB was noticed in our earlier studies on conductivity measurements of aqueous solutions of CAB.[1] We have now determined the equilibrium constant for the reaction by an ion-exchange technique based on selective determination of the species RNHCl, $R\overset{+}{N}H_2Cl$ and H^+ present in equilibrium, by passage of the sample through a cation-resin column in the Na^+ and H^+ forms.

EXPERIMENTAL

Reagents

Chloramine-B solution (0.1*M*) was standardized by the iodometric method[2] and diluted to $1 \times 10^{-3}M$. All reagents used were of analytical grade.

Dowex 50 × 8 Na^+ form was used for the cation-exchange studies

Procedure

Approximately 8 g of Dowex 50 × 8 (sodium form) was soaked in distilled water for some time, then transferred to a 1 5-cm glass tube (with a stopcock at the bottom) to make a column 25 cm in length above a plug of glass wool. A similar column was converted into the hydrogen form by passage of 10 ml of 2*M* hydrochloric acid and washed free from excess of acid. A 10-ml portion of 0.001*M* CAB, adjusted to pH <3.3, was passed through one of the columns and another through the second column, followed by two 10-ml portions of water. The eluates from the columns were analysed for CAB and H^+ by iodometry and alkalimetry respectively

RESULTS AND DISCUSSION

It was known from our earlier studies that RNHCl formation is maximal at pH 3.3. When an aqueous solution of CAB adjusted to pH 3.3 was passed through the cation-exchange resin (Na^+ form), all CAB was eluted quantitatively, but when the same mixture at pH 3.3 was passed through the resin column in H^+ form, CAB was completely held on the resin owing to the formation of $R\overset{+}{N}H_2Cl$ by reaction with the H^+ of the resin. However, at pH <3.3, aqueous CAB solution contains both RNHCl and $R\overset{+}{N}H_2Cl$. When such a mixture is passed through the Na^+ form column, the eluate will contain only the RNHCl, as $R\overset{+}{N}H_2Cl$ will be held on the resin. Let this amount of RNHCl be *b* μmoles. If a total of *a* μmoles of CAB was taken, then (*a* − *b*) μmoles of $R\overset{+}{N}H_2Cl$ must have been present. When CAB mixture at the same pH is passed through the H^+ form of the resin, the $R\overset{+}{N}H_2Cl$ will displace H^+ from the resin, but the RNHCl present will also be held on the resin by combining with the H^+ in it. So the eluate contains H^+ displaced by $R\overset{+}{N}H_2Cl$ and free H^+ from the original sample. Let the total H^+ thus eluted from the resin be *c* μmoles. The H^+ displaced by $R\overset{+}{N}H_2Cl$ is equivalent to the amount of $R\overset{+}{N}H_2Cl$ and hence the free H^+ is obtained by subtracting this amount (*a* − *b*) from *c*. The experiment is repeated at various pH values. The results are presented in Table 1. The value found (61) is comparable with that found for CAT (100).[3]

Table 1. Protonation constant of CAB (amount used 9.05 μmoles)

pH	RNHCl, μmoles	$R\overset{+}{N}H_2Cl$, μmoles	Total H^+, μmoles	Free H^+, μmoles	K^*
2.21	3.52	5.53	33.08	27.55	57
2.21	3.52	5.53	30.32	24.79	63
2.21	3.77	5.28	30.32	25.04	56
2.60	5.53	3.52	13.23	9.71	66
2.60	5.53	3.52	13.78	10.26	62
2.40	5.03	4.02	18.34	14.32	56
2.40	4.77	4.27	18.34	14.07	64
1.95	1.51	7.54	91.2	83.7	60

*Mean 65, standard deviation 4.

REFERENCES

1. V R. S. Rao, M. S. Subramanian and M. Subhashini, submitted to *Current Science*
2. A. I. Vogel, *A Textbook of Quantitative Inorganic Analysis*, 2nd Ed., p. 376. Longmans, London, 1951
3. S. S. Narayanan and V. R. S. Rao, *Radiochim. Acta*, 1983, **32**, 211.

Talanta, Vol. 32, No. 11, pp. 1083–1087, 1985
Printed in Great Britain

0039-9140/85 $3.00 + 0.00
Pergamon Press Ltd

ANNOTATIONS

PRECONCENTRATION AND PRESEPARATION BY ELECTRO-DEPOSITION OF TRACES OF METALS

ROMAN E. SIODA*
Industrial Chemistry Institute, Warszawa, ul. Rydygiera 8, 01-793, Poland

(*Received* 29 *November* 1983. *Revised* 19 *June* 1985. *Accepted* 2 *August* 1985)

Summary—Several theoretical ideas on metal electro-deposition on inert solid electrodes, from solutions of trace metal ion concentrations, are formulated. The results may be of importance in the application of electro-depositions as analytical preconcentration and preseparation methods.

Inert solid electrodes, especially those without a mercury film, are often discussed in connection with electro-deposition of metals from their solutions at trace concentrations,[1] usually starting from the concept of a formal monolayer of deposit. The term "formal monolayer" means coverage of the whole immersed electrode surface by a close-packed single layer of atoms or molecules. For a metal, the amount in the monolayer can be calculated from the atomic radius and the electrode surface area.[2] The number of moles (n_m) of metal deposited to produce a formal monolayer on an electrode surface area S_e (cm^2) is

$$n_m = S_e/\eta \quad (1)$$

where η (cm^2/mole) is the molar monolayer area, *i.e.*, the monolayer area occupied by one mole of metal.[3] This is a rather simplistic approach, however, as it ignores the fact that because of surface roughness the total surface area will be larger than the nominal area calculated from the linear dimensions of the electrode, and also assumes that deposition will take place uniformly to produce a complete monolayer before *any* deposition can occur on top of already deposited material. Nevertheless the concept is attractive because of its simplicity and amenability to simple mathematical treatment, especially in formulation of the kinetics of an electro-deposition process. In trace-analysis electrolyses, an equilibrium is usually reached, after a long electrolysis time, between the numbers of moles of metal deposited and remaining in solution,[4] since the rate of deposition and the rate of dissolution (chemical or electrochemical) must eventually become equal. The equilibrium concentration in solution is dependent on the extent of coverage of the electrode surface,[5,6] the applied potential and the chemical composition of the solution. Stirring rate and temperature also play a role.

*Present address: c/o Professor D. J. Curran, Department of Chemistry, University of Massachusetts, Amherst, MA 01003, U.S.A

The situation in which a formal monolayer cannot be produced because there is not sufficient metal in the initial solution, has been discussed by Anderson and Sioda.[6] Production of a formal monolayer followed by further deposition has also been discussed,[3] and can be described as follows. The time, t_f (sec), needed to produce a formal monolayer on the electrode, assuming 100% instantaneous reduction, is

$$t_f = 1/\eta N \quad (2)$$

where N is the molar flux of metal ion to the electrode surface (mole.cm^{-2}.sec^{-1}), given by

$$N = k_1 c \quad (3)$$

k_1 being a specific rate constant of deposition (cm/sec), and c the concentration of metal ion in solution (mole/cm^3). The time, t_d (sec), needed to dissolve a formal monolayer is

$$t_d = 1/\eta k_2 \quad (4)$$

where k_2 is a specific rate of dissolution (mole.cm^{-2}.sec^{-1}). At equilibrium, $t_f = t_d$, so the equilibrium concentration of the metal-ion in solution, c_e, is

$$c_e = k_2/k_1 \quad (5)$$

As said above, the concept of a formal monolayer is ideal, and the mechanism of metal deposition is complex and dependent on various experimental conditions. To avoid the resultant difficulties in finding mathematical models, Brainina *et al.*[7] define an "activity", a (mole/cm^3), of a metal deposit, as a simple exponential function of the electric charge, q (C), transferred at the electrode in discharging the ions:

$$a = a_\infty(1 - \exp[-\gamma q]) \quad (6)$$

where a_∞ is the maximal "activity", obtained after transfer of a sufficiently large charge, and γ (C^{-1}) is a constant; a_∞ usually corresponds to complete coverage of the electrode surface area by deposit.[7]

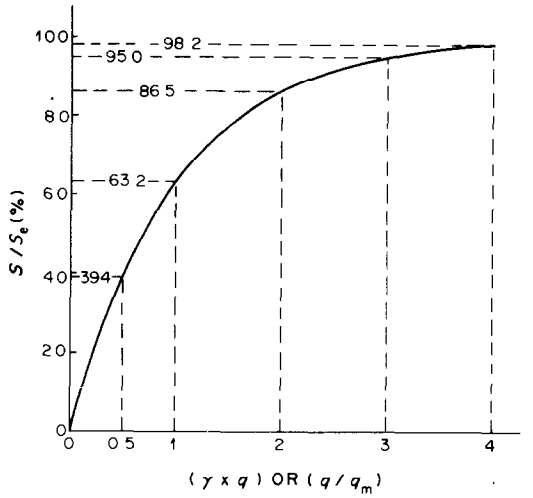

Fig 1. Dependence of the relative electrode area occupied by deposit, S/S_e, on the product of γ and charge, calculated according to equation (7). See also equation (22).

If the electrode potential is recorded as a function of time during electro-deposition at constant current, it asymptotically reaches a constant value corresponding to the electrode surface being fully covered, and the amount of charge transferred up to the start of the levelling-off of potential can be used to determine γ.[7]

An alternative approach, due to Rogers and Stehney,[8] is to consider the fraction of the electrode surface area that will be covered by deposit on transfer of charge q. This is equivalent to equation (6) rewritten as:

$$S/S_e = 1 - \exp[-\gamma q] \tag{7}$$

where S is the area occupied by the deposit, S_e the total area and γ is an experimental constant as in equation (6).

The magnitude of γ can be estimated as follows. When q is small (Fig. 1), S is steeply increasing and at large q asymptotically approaches S_e. At the start of electro-deposition, when most of the electrode is free of deposit, atoms will deposit mainly on the free surface. Thus, for small q we can write

$$dS/dq = \eta/nF \tag{8}$$

where n is the number of electrons transferred per metal ion discharged, and F is the Faraday constant. Equation (8) shows that at the beginning of the electro-deposition the growth of the monolayer is a linear function of time

Differentiation of equation (7), and adoption of the limit $\gamma q \to 0$ gives:

$$dS/dq = \gamma S_e \tag{9}$$

and γ can be obtained from equations (8) and (9):

$$\gamma = \eta/nFS_e \tag{10}$$

Thus, if the growth of the electrode area occupied by deposit in formation of the first monolayer is described by equation (7), γ can be calculated from η and S_e.

Consider, for example, the electrolysis of copper(II) at a 0.2-cm diameter graphite disk electrode. For copper,[9] $\eta = 3.4 \times 10^8$ cm^2/mole, for copper(II) $n = 2$, for the electrode $S_e = 0.0314$ cm^2, so equation (10) gives $\gamma = 5.7 \times 10^4$ C^{-1}. This calculated value can be compared with an experimental one, $\gamma = 2 \times 10^4$ C^{-1}, obtained by electro-deposition of Ni or Ag on a graphite disk electrode.[1] Ni and Ag have molar monolayer areas similar to that for Cu: $\eta = 4.4 \times 10^8$ cm^2/mole for Ag and 3.2×10^8 for Ni.[9] Thus, the agreement between the measured and theoretically calculated values of γ seems satisfactory.

When γ is calculated from equation (10), S_e should denote the actual physical surface area of the electrode. For a well-polished graphite electrode, S_e can be approximated by the geometrical surface area, but for more accurate calculation, the surface roughness factor of graphite should also be used. In the case cited, this should improve the agreement between the γ values.

Effect of analyte concentration

It has been observed that for electro-deposition from very dilute solutions (μg/ml and especially ng/ml concentrations) the half-reaction time increases markedly with decrease in the initial concentration of metal ion,[10] in contrast to the behaviour for the intermediate concentration range, 100 μg/ml or more, for which the specific rate constant of an electro-deposition reaction is independent of concentration.[11] This increase in half-reaction time with decrease in metal ion concentration at trace level can be explained by assuming simultaneous electro-deposition and chemical and/or electrochemical dissolution of the deposit.

Suppose that the test solution initially contains enough metal ion to produce several (*e.g.*, 20) formal monolayers of deposit. Once the deposit completely covers the electrode, the kinetics of the electro-deposition reaction can be described by

$$dc/dt = -\sigma(k_1 c - k_2) \tag{11}$$

where $\sigma = S_e/V$ is a constant given by the electrode area and solution volume (V), k_1 and k_2 being defined as earlier [equations (3)–(5)]. Integration for the initial condition $c = c_0$ at $t = 0$ leads to

$$c = (k_2/k_1) + (c_0 - k_2/k_1)\exp[-\sigma k_1 t] \tag{12}$$

or, from equation (5),

$$c = c_e + (c_0 - c_e)\exp[-\sigma k_1 t] \tag{13}$$

From equation (13) we obtain:

$$t_{1/2}(\sigma k_1) = -\ln[(c_0 - 2c_e)/2(c_0 - c_e)] \tag{14}$$

where $t_{1/2}$ is the half-reaction time, *i.e.*, the time required to decrease by half the initial concentration of the metal ion in solution. Analysis of equation (14)

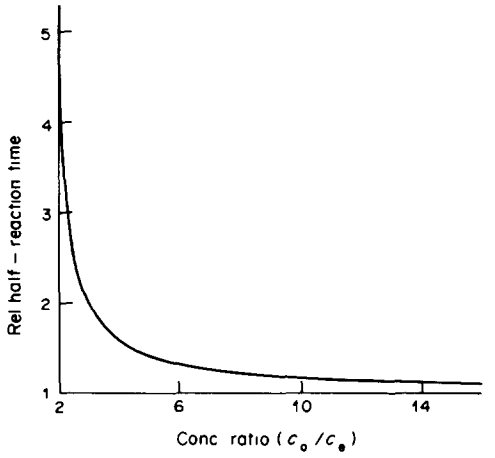

Fig. 2. Dependence of the relative half-reaction time, $t_{1/2}/t^*_{1/2}$, on the ratio of the initial and equilibrium metal-ion solution concentrations, calculated according to equations (14) and (15).

shows that for $c_0 \gg c_e$

$$t^*_{1/2}(\sigma k_1) = \ln 2 \qquad (15)$$

i.e., the half-reaction time, $t^*_{1/2}$, is like that for a first-order reaction with rate constant σk_1. When c_0 is not all that much greater than $2c_e$, $t_{1/2}$ will exceed $t^*_{1/2}$ from equation (15) by an amount that is the greater, the smaller the difference between c_0 and $2c_e$, as shown in Fig. 2. At the limit $c_0 = 2c_e$, $t_{1/2}$ becomes infinite. However when $c_0/c_e \geqq 30$, $t_{1/2}$ will differ by less than 5% from $t^*_{1/2}$. This increase in $t_{1/2}$ with decrease in c_0 is equivalent to a decrease in the specific rate-constants of electro-deposition reactions as c_0 is decreased.

This dependence of $t_{1/2}$ on concentration implies that if c_0 is high enough, a metal deposit several atomic layers in thickness is formed shortly after the start of electro-deposition, but the remaining bulk metal ion concentration will become sufficiently low for k_2, and consequently c_e calculated from equation (5), not to depend on it in any significant way. In this approximation, the dissolution reaction rate is assumed to be practically independent of the bulk metal ion concentration, as long as the latter is low in comparison with the metal ion concentration near the dissolving surface. The dissolution rate is, however, dependent on the solution mixing rate.

Dissolution of metal in an initially metal-free solution

In some electroanalytical measurements, it is expedient to deposit metal from one solution, and dissolve it in another.[12,13] A similar situation arises when an active metal electrode or a metal deposited on an indifferent solid electrode is placed in a conductive solution initially devoid of the metal ion, and an electric potential is applied. It is interesting to calculate the equilibrium metal-ion concentrations in solution when a *protective cathodic potential* is applied to the electrode. This equilibrium follows from an interplay of the kinetic laws of deposit formation and dissolution, and in practice can be several orders of magnitude higher than the true Nernstian equilibrium value for the applied cathodic potential.

For example, a copper foil electrode was placed in 0.1 *M* sodium sulphate acidified to pH 3.2 with nitric acid, then charged to a negative potential by a constant cathodic current of approx. 30 mA/cm^2; after 5 hr of electrolysis, the copper concentration in the solution was found to be 1.75 μM.[14]

To solve the problem mathematically, let us start again and integrate equation (11), using the initial condition $c_0 = 0$ at $t = 0$. The application of a *cathodic potential* means that the rate constant of deposition, k_1, in equation (11) will not be zero. The solution obtained is

$$c = (k_2/k_1)(1 - \exp[-\sigma k_1 t] \qquad (16)$$

or, from (5),

$$c = c_e(1 - \exp[-\sigma k_1 t]) \qquad (17)$$

As shown by equation (17), when a cathodic potential is applied, the metal from the deposit or the active electrode will dissolve and produce the equilibrium concentration c_e of its ions in solution after prolonged electrolysis ($t \to \infty$). The equilibrium concentration thus obtained should be the same as that after prolonged electrolysis of a solution initially containing the metal ion, as discussed above. The two kinetic curves, leading to the same c_e, are shown in Fig. 3 and demonstrate that the equilibrium is established much faster if the solution is initially devoid of the metal ion.

Charges needed for a formal monolayer and for "full" electrode coverage

The charge q_m (C), required to produce a formal monolayer, can be calculated from equation (1) by

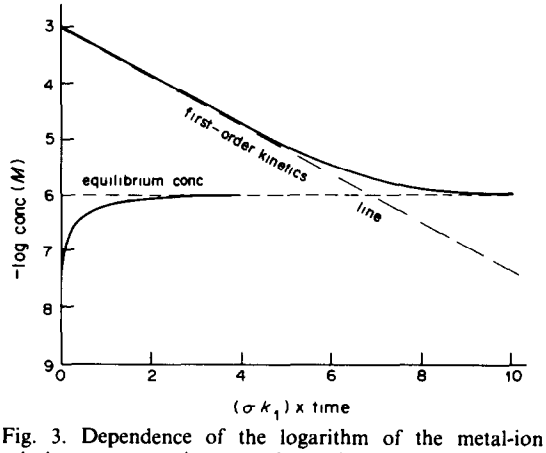

Fig. 3. Dependence of the logarithm of the metal-ion solution concentration on $\sigma k_1 t$, calculated according to equations (13) (upper curve) and (17) (lower curve). The equilibrium concentration, c_e, is 1.0 μM, and the initial concentrations are 1.0 m*M* (upper curve) and 0 (lower curve).

multiplying it by nF, where n is the number of electrons transferred per metal ion discharged:

$$q_m = nFS_e/\eta \quad (18)$$

Taking a more realistic view of deposit growth, *e.g.*, as given by equation (7), and assuming "full" coverage to mean $S/S_e \geqq 0.95$, we obtain from this condition and equation (7)

$$(\gamma q_s) \geqq 3 \quad (19)$$

where q_s is the theoretical charge required to cover at least 95% of the electrode area with deposit. Substituting γ from equation (10) into inequality (19), we obtain:

$$q_s \geqq 3nFS_e/\eta \quad (20)$$

Hence q_m and q_s differ by at least a factor of 3:

$$q_s \geqq 3q_m \quad (21)$$

Thus, according to equation (7), the electrode is practically fully covered when enough metal ion has been discharged from solution to produce at least 3 formal monolayers of deposit. As parts of the deposit may redissolve during the electro-deposition process, the measured charge can be even higher. Hence according to equations (7), (10), and (18), the maximum fraction of electrode area that can be expected to be covered by deposit will be 0.63 ($= 1 - e^{-1}$) for transfer of charge q_m, 0.86 ($= 1 - e^{-2}$), for $2q_m$ *etc.*, as shown in Fig. 1. Equation (7) is then transformed into the more intelligible equation.

$$S = S_e(1 - \exp[-q/q_m]) \quad (22)$$

where q/q_m is the number of formal monolayer charges transferred.

It is believed that this theoretical approach will help in planning and executing analytical electrodepositions with a higher experimental reliability, accuracy, and precision. The related analytical methods of electrolytic preconcentration and preseparation are certainly worthy of further experimental and theoretical exploration, and application in numerous fields of trace analysis.

Acknowledgement—The author is grateful to Mr. Wiesław Otwinowski, M Sc., of the Institute of Precision Mechanics, Warsaw, for the AAS analytical determinations

REFERENCES

1. Kh. Z. Brainina and E. Ya Neiman, *Solid-Phase Reactions in Electroanalytical Chemistry*, Khimiya, Moscow, 1982.
2. M. Haissinsky, *Nuclear Chemistry and Its Applications*, Chapter 20 Addison-Wesley, New York, 1964.
3. R E. Sioda, *Anal. Lett.*, 1983, **16**, 739.
4. F Joliot, *J Chim Phys.*, 1930, **27**, 119
5. C Haenny and P Reymond, *Helv. Chim. Acta*, 1954, **37**, 2067.
6. J. L. Anderson and R. E. Sioda, *Talanta*, 1983, **30**, 627.
7. Kh. Z Brainina, N K. Kiva and V. B. Belyavskaya, *Elektrokhimiya*, 1965, **1**, 311.
8. L. B. Rogers and A. F. Stehney, *J. Electrochem. Soc.*, 1949, **95**, 25.
9. R. E. Sioda, unpublished results.
10. K. Jørstad and B. Salbu, *Anal. Chem.*, 1980, **52**, 672
11. J. J. Lingane, *J. Am. Chem. Soc.*, 1945, **67**, 1916.
12. A. Hu, R. E. Dessy and A. Granéli, *Anal. Chem.*, 1983, **55**, 320.
13. E. B. Buchanan, Jr. and D. D Soleta, *Talanta*, 1982, **29**, 207.
14. R. E. Sioda, *ibid.*, 1984, **31**, 135.
15. *Idem*, *Monatsh. Chem.*, 1985, **116**, 49.

APPENDIX

Earlier experimental work,[14] which formed part of the basis for this paper, has been repeated.

The electrodes were copper foil laminated on one side with plastic, (geometrical surface area: A, 12.0 ± 0.1; B, 14.0 ± 0.1 cm^2). A 0.10*M* sodium sulphate solution acidified with nitric acid to pH 2.0 was used as electrolyte. The rate of copper dissolution in the electrolyte, without application of external electric potential, was measured in the first experiment with electrode A, with magnetic stirring at two different speeds (not measured). In the second experiment the rate of dissolution was measured for electrode B cathodically polarized with a current density of 8.0 mA/cm^2 (average current 0.11 ± 0.01 A), a platinum wire anode being used. Aliquots of solution were removed at intervals and analysed for copper by AAS

The results are presented in Fig. 4. Line 1A shows that dissolution was fastest in the first half-hour, because of rapid dissolution of the oxide coating initially present on the copper surface.[15] Line 1B shows that the rate of dissolution increases with stirring rate. From the slopes of lines 1A and 1B the specific dissolution rate (k_2) of the copper foil was calculated.

For experiment 1A it was

$$1.50 \pm 0.11 \times 10^{-11} \text{ mole.cm}^{-2}.\text{sec}^{-1}$$

(90% confidence interval), and for 1B

$$4.2 \pm 0.2 \times 10^{-11} \text{ mole.cm}^{-2}.\text{sec}^{-1}.$$

These values are two orders of magnitude lower than those reported earlier,[14] which had been obtained by weighing the foil after each dissolution period. Investigation of

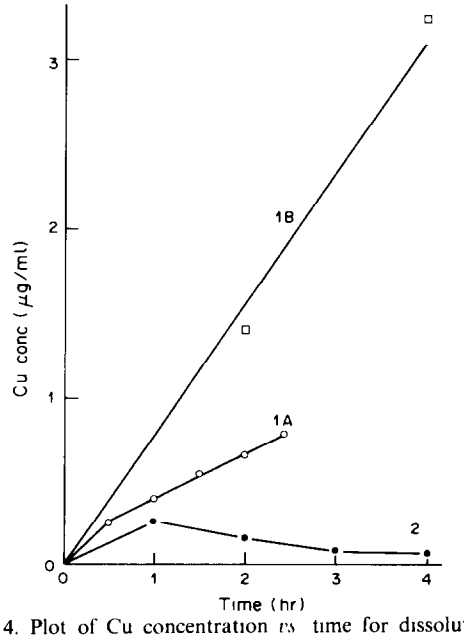

Fig. 4. Plot of Cu concentration *vs* time for dissolution of copper foils in 0.10*M* sodium sulphate acidified to pH 2.0 with nitric acid. Lines 1A and 1B correspond to dissolution without applied external potential, and line 2 to dissolution with a protective, cathodic current of density 8.0 mA/cm^2 applied.

this anomaly showed that part of the lamination bond had also dissolved, leading in the earlier work to erroneously high values for the amount of copper dissolved.

Line 2 in Fig. 4 shows initial dissolution (again of the surface oxide) followed by decrease and then stabilization of the copper concentration at around 64 ng/ml, which is believed to be the equilibrium concentration for the conditions used. It is not much different, taking into consideration the low precision of the determinations, from the previously reported value of 110 ng/ml.[14] Also, different cathodic current densities were used in the two experiments, 34 mA/cm^2 originally, and 8 mA/cm^2 in the present one; the ratios of the electrode geometrical surface area to solution volume were similar, however.

Talanta, Vol. 32, No. 11, pp 1088–1091, 1985
Printed in Great Britain

0039-9140/85 $3.00 + 0.00
Pergamon Press Ltd

VALIDATION OF ACCURACY BY INTERLABORATORY PROGRAMME

R. SUTARNO and HENRY F. STEGER
Mineral Sciences Laboratories, Canada Centre for Mineral and Energy Technology, 555 Booth Street, Ottawa, Ontario, Canada

(*Received* 22 *March* 1985. *Accepted* 18 *May* 1985)

Summary—A statistical design is proposed for assessing the accuracy of an analytical method by its application to a certified reference material in an interlaboratory programme. The validation of accuracy is based on the difference between the certified value and the overall mean of the test programme and is linked to the concept that below a certain limit this difference has no practical significance. It is shown that a certified reference material cannot be used to detect bias in a method if the bias is smaller than the confidence interval of the certified value.

Certified reference materials (CRMs) are widely applied to ensure the reliability of analytical data by use in the calibration of instruments or standardization of reagents and in validation of the accuracy of analytical methods. Nevertheless, there are no general guidelines for relating the uncertainty of the certified value of the reference material to the effectiveness of its uses. Recently, however, Sutarno and Steger[1] proposed an experimental design for validation of the accuracy of an analytical method by analysis of a CRM, in which the uncertainties in the CRM certified values and in the method are taken into account. This procedure requires that the CRM be analysed by the same analyst 10 times, either in a single batch of determinations or in smaller batches over a period of time. The accuracy of the method is validated if the difference between the certified value for the CRM and the mean value obtained by the method is not statistically significant. The significance is based on the magnitude of the uncertainty in the certified value of the reference material, so the better characterized the reference material, *i.e.*, the less the uncertainty in the certified values, the more rigorous is the validation of the accuracy, or the lower the level at which bias in the method can be detected.

From time to time there arise occasions when the analyst is required to validate the accuracy of a method (*i.e.*, to detect bias) to a degree that is not attainable by comparison with the statistical significance of the uncertainty in the certified values for the CRMs available. This paper presents an alternative statistical design for such validation by applying the analytical method to a CRM in an interlaboratory programme.

The proposed test procedure is also applicable to the validation of the "long-term" accuracy of a method by one analyst if at least 10 batches of at least two replicate determinations each are done, each batch at a different time. The results then constitute a multi-data set (*i.e.*, a quasi-interlaboratory programme) in which the variance of the overall mean has a between-periods component. If more than one analyst participates, however, the variance of the overall mean has both between-periods and between-analysts (*i.e.*, between-laboratories) components, but these are inseparable and appear simply as the between-periods variance.

The proposed statistical design has been submitted by the Canadian Certified Reference Materials Project to the Council Committee on Reference Materials (REMCO) of the International Organization for Standardization for inclusion in ISO/REMCO Guide 33 "The Use of Certified Reference Materials".

UNCERTAINTY OF CRMs

The effect of the mode of certification on the type of statistical parameters available and on the estimation of the uncertainty in the certified value, A_c, of the CRM was discussed in the preceding paper.[1] For a reference material certified by an interlaboratory programme, the estimate of the precision of A_c is expressed as σ_c^2, the variance of A_c, or alternatively as a confidence interval (usually 95%). The magnitude of σ_c is estimated from

$$\sigma_c^2 = (S_{Lc}^2 + S_{rc}^2/n_c)/N_c \quad (1)$$

if more than one method was used, or

$$\sigma_c^2 = (\sigma_{Lc}^2 + \sigma_{rc}^2/n_c)/N_c \quad (2)$$

if all participating laboratories used the same method; here, N_c = number of laboratories (excluding those giving results subsequently decided to be outliers) that participated in the certification of the reference material, n_c = average number of replicate determinations per laboratory, S_{Lc} and

σ_{Lc} = between-laboratories standard deviations, S_{rc} and σ_{rc} = within-laboratory standard deviations.

For a reference material certified by use of a "definitive" method by one laboratory, $\sigma_{Lc} = 0$ (by definition) and σ_c^2 becomes

$$\sigma_c^2 = \sigma_{rc}^2/n_c. \quad (3)$$

For convenience, S_{Lc} and σ_{Lc} will both be denoted hereafter by σ_L, and S_{rc} and σ_{rc} by σ_w.

VALIDATION OF ANALYTICAL METHODS

The concept of the use of CRMs to validate the accuracy of an analytical method by interlaboratory programme is based on three premises. First, that the certified value of an element in a CRM is the best estimate of the true value. Second, that the analytical method is validated if the overall results of the test programme differ from the corresponding true values for the CRM by no more than can be accounted for by statistical fluctuation. Third, that the accuracy of the analytical method is also validated even if the difference between the overall mean value $\bar{X}$ for the test programme and A_c of the CRM is statistically significant but is of such magnitude that it is negligible for practical purposes. The last premise is necessary because the probability of detecting a statistically significant difference between $\bar{X}$ and A_c increases with increasing number of laboratories participating in the programme and/or increasing degree of replication.

GENERAL PROCEDURES FOR INTERLABORATORY PROGRAMMES

A physical and documentary validation of the CRM[1] should be performed before use of the CRM in an interlaboratory programme. Subdivision of a unit of the CRM, before distribution, must be done with care to avoid introducing any additional significant error, either systematic or random.

The organization, physical execution and statistical analysis of the results of such an interlaboratory programme are outside the realm of this paper. Details are available from many sources, but ISO/REMCO Guide 35[2] or document ISO 5725[3] are recommended. The statistical parameters calculated are:

$\bar{X}$ = the overall mean (excluding outliers) of the test programme results

$V[\bar{X}]$ = variance of $\bar{X}$

σ_{Lm} = between-laboratories standard deviation of the measurement procedure, estimated by S_{Lm}

σ_m = within-laboratory standard deviation of the measurement procedure, estimated by S_m

The number of laboratories and of replicate determinations

The number of laboratories, k, and the number of replicate determinations, n, of the test interlaboratory programme should ideally be selected according to the tolerable difference, λ, between A_c and $\bar{X}$ at the significance levels α and β. The parameter α is the probability of concluding that A_c and $\bar{X}$ are statistically significantly different when in fact they are not; β is the probability of concluding that A_c and $\bar{X}$ are not statistically significantly different when in fact they are. In practice, however, k and n are seldom decided upon in this way, and indeed there are no firm guidelines for choosing them. One recommendation[4] is that k and n should be at least 8 and 2, respectively. All laboratories should perform the same number of replicate determinations.

The overall mean of the results of the interlaboratory programme represents the best estimate of the value of that characteristic of the CRM by the measurement procedure. The accuracy of the measurement procedure is defined as the agreement between $\bar{X}$ and A_c. The bias of the measurement procedure, δ, is

$$\delta = A_c - \bar{X} \quad (4)$$

and the variance of the bias is

$$V[\delta] = V[\bar{X}] + \sigma_C^2 \quad (5)$$

$$V[\delta] = \left(\sigma_{Lm}^2 + \frac{\sigma_m^2}{n}\right)\Big/k + \sigma_C^2. \quad (6)$$

Theoretically, the measurement procedure is free of bias if $\delta = 0$. In practice, however, $\delta \neq 0$ but the statistical significance of δ depends on the magnitude

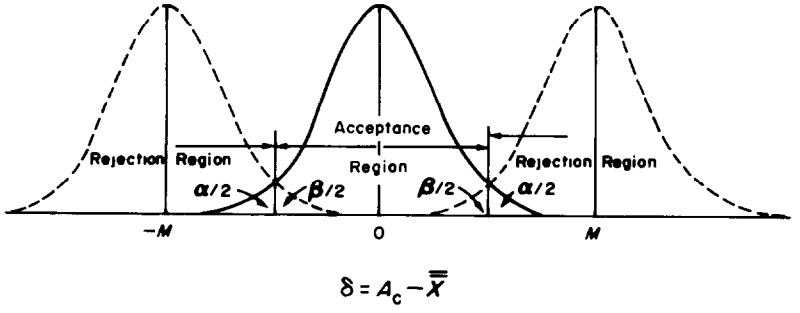

Fig. 1. Frequency distribution of $\delta = A_c - \bar{X}$.

of $V[\delta]$. The larger k and/or n, the smaller will be $V[\delta]$ and the higher the likelihood that δ is statistically significant. In other words, increasing k and/or n increases the chance of being able to detect smaller measurement bias. If k and/or n are large enough, values of δ may be obtained that are statistically but not practically significant, and it is necessary to invoke a parameter, λ, which is the minimum value of 2δ which can be assumed to be practical significance.

To clarify the concept of λ, let us consider the frequency distribution of $\delta = A_c - \bar{X}$.

The null hypothesis is that the measurement procedure is unbiased. In that case the distribution of δ has a mean of zero and variance $V[\delta]$. Figure 1 shows that even if the hypothesis is correct, there is a chance α that the measurement procedure will be rejected as being biased. For $\alpha = 0.05$, the acceptance criterion is

$$|A_c - \bar{X}| \leq 2(V[\delta])^{1/2} \quad (7)$$

The alternative possibility is that the measurement procedure is in fact biased by an amount M. In this case the frequency distribution of δ has a mean of M (or $-M$) and the same variance (Fig. 1, broken lines), and the chance that the measurement procedure is accepted as free from bias is β. For $\beta = 0.05$, the value of M will be

$$M = 4(V[\delta])^{1/2} \quad (8)$$

M is the minimum value of bias in the measurement procedure that can be detected from the interlaboratory results at the probability levels $\alpha = 0.05$ and $\beta = 0.05$.

For a given characteristic of a CRM, M decreases as $V[\bar{X}]$ decreases (*i.e.*, as n and k increase); the minimum occurs at $V[\bar{X}] = 0$:

$$M_{min} = 4\sigma_C \quad (9)$$

The right-hand side of equation (9) is approximately the width of the 95% confidence interval of A_c. In other words, a CRM cannot be used to detect bias in a measurement procedure if it less than the confidence interval of the estimate of A_c.

Sometimes the value of M_{min} for a characteristic of a CRM is so small that it is practically insignificant. In this case, the measurement procedure can be accepted as practically free of bias if M is less than the critical value λ:

$$\lambda \geq M_{min}$$

$$> 4(V[\delta])^{1/2} \quad (10)$$

i.e.,

$$\lambda > 4\left[\sigma_C^2 + \left(\frac{\sigma_{Lm}^2 + \sigma_m^2/n}{k}\right)\right]^{1/2} \quad (11)$$

On the assumption that the analytical method being tested for accuracy is as precise as the method(s) used to certify the reference material, σ_{Lm} and σ_m can be replaced by σ_L and σ_W for the reference material, and a series of combinations of k and n can be computed for use in setting up a test programme.

Table 1. Certification and test programme statistical parameters

Statistical parameters	SCH-1	CCU-1
(A) *Certificate values*		
Element	Fe (total)	Ag
A_c	60.75%	139 μg/g
σ_W	0.09%	2.1 μg/g
σ_L	0.20%	7.5 μg/g
σ_C	0.0017%	1.9 μg/g
(B) *Interlaboratory programme*		
$\bar{X}$	60.67%	145.2 μg/g
S_m	0.10%	1.12 μg/g
σ_{Lm}	0.06%	1.12 μg/g
k	34	10
N	111	20
$n = N/k$	3.26	2

Assessment of accuracy

The accuracy of the measurement procedure is checked by comparing the overall mean of the interlaboratory program, $\bar{X}$, with the certified value of the CRM, A_c by:

$$|A_c - \bar{X}| \leq 2\sqrt{\sigma_C^2 + \sigma_D^2} \quad (12)$$

where σ_C^2 is the uncertainty associated with the CRM and is given by equations (1)–(3), and σ_D^2 is the uncertainty associated with the overall mean of the interlaboratory comparison for the measurement procedure, and is given by

$$\sigma_D^2 = (S_{LM}^2 + S_m^2 n)/k \quad (13)$$

Two decisions are then possible.

(1) If equation (12) is satisfied, the measurement procedure is accepted to be as accurate as those used to certify the CRM. There is only a 5% chance (or less) that the procedure is, in fact, biased by an amount λ or greater.

(2) If equation (12) is not satisfied, $|A_c - \bar{X}|$ is statistically significant but if $|A_c - \bar{X}| \leq \lambda/2$ the measurement procedure is sufficiently accurate for the intended purpose, whereas if $|A_c - \bar{X}| > \lambda/2$ the measurement procedure is not sufficiently accurate for the intended purpose.

EXAMPLES OF THE USE OF CRMs

(1) A CRM, SCH-1,[5] was used for assessing by interlaboratory comparison the accuracy of a method to determine total iron (ISO/TC 102/SC2 N768E).

Table 2. Results for CRM CCU-1

Trial	Ag, μg/g	Trial	Ag, μg/g
1	147, 145	6	143, 145
2	144, 143	7	147, 148
3	147, 149	8	141, 143
4	144, 143	9	147, 146
5	145, 147	10	145, 144

The pertinent statistical parameters are reported in Table 1.

Test for accuracy

$$|A_c - \bar{\bar{X}}| = 60.75 - 60.67 = 0.08\%\ \text{Fe}$$

$$\sigma_C^2 = V[A_c] = 0.0017$$

$$\sigma_D^2 = [S_{Lm}^2 + S_m^2/n]/k = 0.0002$$

$$2\sqrt{\sigma_C^2 + \sigma_D^2} = 0.087\%\ \text{Fe}$$

$|A_c - \bar{\bar{X}}| < 2\sqrt{\sigma_C^2 + \sigma_D^2}$: the method is sufficiently accurate and shows no bias.

(2) A certified copper concentrate, CCU-1,[6] was used to assess the long-term accuracy of a combined fire-assay/atomic-absorption procedure for silver determination, the same analyst analysing duplicate test portions once each month over a period of 10 months. The results are reported in Table 2; the estimated statistical parameters are summarized in Table 1.

Test for accuracy

$$|A_c - \bar{\bar{X}}| = 6.2\ \mu\text{g/g Ag}$$

$$\sigma_C^2 = V[A_c] = 1.9$$

$$\sigma_D^2 = [S_{Lm}^2 + S_m^2/n]/k = 0.188$$

$|A_c - \bar{\bar{X}}| > 2\sqrt{\sigma_C^2 + \sigma_D^2}$: the bias of the method is statistically significant.

The method may still be acceptable with respect to accuracy since

$$|A_c - \bar{\bar{X}}| \leqslant \lambda/2$$

so $\lambda = 2 \times 6.2 = 12.4\ \mu$g/g Ag if the analyst accepts that the bias is not practically significant.

By comparison, if the results for CCU-1 are treated by the procedure of Sutarno and Steger[1] as representing a quasi "single-shot" investigation, the mean value, $\bar{X}$, would of course be the same as $\bar{\bar{X}}$. The criterion for validation of accuracy would then be

$$|A_c - \bar{X}| \leqslant 2\sigma_L \leqslant 15.0\ \mu\text{g/g}$$

and since $|A_c - \bar{X}| = 6.2\ \mu$g/g Ag, the bias of the method is assessed as statistically insignificant.

The two types of accuracy tests performed for CCU-1 illustrate the greater power of the inter-laboratory programme procedure for detecting bias in an analytical method, and this is therefore the recommended procedure whenever the higher cost in terms of time and expense of such a programme warranted by the ultimate purpose of the method.

REFERENCES

1. R. Sutarno and H. F. Steger, *Talanta*, 1985, **32**, 439.
2. ISO/REMCO Guide 35-1984(e), *Certification of Reference Materials—General and Statistical Principles.*
3. ISO 5725-1981(E), in *ISO Standards Handbook 3*, Geneva, 1981.
4. K. A. Brownlee, *Statistical Theory and Methodology in Science and Engineering*, Wiley, New York, 1960.
5. H. F. Steger, W. S. Bowman, R. Sutarno and G. M. Faye, *CANMET Rept.*, 75-168(TR), Energy, Mines and Resources, Canada, Ottawa, 1975.
6. G. H. Faye, W. S. Bowman and R. Sutarno, *CANMET Rept.*, 79-16, Energy, Mines and Resources, Canada, Ottawa, 1979.

Talanta, Vol. 32, No. 12, pp. 1093–1096, 1985
Printed in Great Britain.

0039-9140/85 $3.00 + 0.00

SEPARATION OF *TRANS*-1,2-CYCLOHEXANEDIAMINETETRA-ACETIC ACID CHELATES OF BISMUTH(III), IRON(III) AND COPPER(II) BY REVERSED-PHASE PAIRED-ION CHROMATOGRAPHY

SADANOBU INOUE,* NAOKI HASHIMOTO, SUWARU HOSHI and MUTSUYA MATSUBARA
Department of Environmental Engineering, Kitami Institute of Technology, Kitami-shi, 090 Japan

(*Received* 16 *October* 1984. *Revised* 10 *June* 1985. *Accepted* 29 *August* 1985)

Summary—*Trans*-1,2-cyclohexanediaminetetra-acetic acid (DCTA) chelates of bismuth(III), iron(III) and copper(II) have been separated by two techniques using reversed-phase paired-ion chromatography. In one, the chelates in aqueous solution were separated within 20 min on a 6.0 × 300 mm ERC-ODS column with $10^{-2}M$ tetrabutylammonium ion (TBA^+) in methanol–water mixture (45:55 v/v) as eluent. In the other, the metal ions in aqueous solution were separated within 10 min by direct injection into an ERC-ODS column with $10^{-2}M$ $TBA^+/10^{-3}M$ DCTA in methanol–water mixture (40:60 v/v) as eluent.

There has been considerable interest in the use of high-pressure liquid chromatography (HPLC) to separate and determine metal ions as complexes with various chelating agents such as dithiocarbamates,[1-11] acetylacetone,[12] dithizone,[13,14] 1,10-phenanthroline,[15,16] and 4-(2-pyridylazo)-resorcinol.[17,18] A few reports on the separation of metal chelates of polyaminocarboxylic acids have appeared.[19,20] Jones *et al.*[20] reported the HPLC separation of Cu_2(EGTA), $Cu(NTA)^-$, $Cu(EDTA)^{2-}$ and $Cu(CDTA)^{2-}$, with detection by atomic-absorption spectrometry. Hirowatari *et al.*[19] reported separation of EDTA chelates by reversed-phase paired-ion chromatography.

Recently, HPLC separation and determination of metal ions by direct injection into an eluent containing a chelating agent was reported.[6,8]

In the present paper, separation of the DCTA chelates of bismuth(III), iron(III) and copper(II) by reversed-phase paired-ion chromatography, by two techniques, is described. Although ligands containing sulphur, such as dithiocarbamate, dithizone, *etc.*, are easily oxidized by air, oxidation of DCTA by air is insignificant. The sodium salt of DCTA is easily soluble in water and reacts with bismuth(III), iron(III) and copper(II) to form stable water-soluble chelates which have a charge of −1 for the bismuth(III) and iron(III) chelates, and −2 for the copper(II) chelate. These chelates form ion-association species with the tetrabutylammonium ion (TBA^+). In addition, all three species have useful absorption bands in the ultraviolet region of the spectrum, and the elution behaviour can be unambiguously established by the use of an ultraviolet detector. These properties make DCTA well suited for the separation of bismuth(III), iron(III) and copper(II) by reversed-phase paired-ion HPLC by either of the techniques described below.

EXPERIMENTAL

Reagents

All chemicals used were of analytical-reagent grade.

Standard bismuth(III) solution. Made by dissolving 1.96 g of bismuth (99.999% pure) in about 10 ml of concentrated nitric acid and diluting to 250 ml with $0.8M$ nitric acid.

Standard iron(III) solution. Made by dissolving 4.52 g of ferric ammonium sulphate 12-hydrate in 125 ml of $0.1M$ sulphuric acid and diluting to 250 ml with water.

Standard copper(II) solution. Made by dissolving 2.34 g of cupric sulphate pentahydrate in 125 ml of $0.01M$ sulphuric acid and diluting to 250 ml with water.

These standard solutions were standardized by titration with EDTA solution.

Standard DCTA solution, 0.005M. Made by dissolving 1.8218 g of DCTA (Dojindo, Kumamoto) and 0.4 g of sodium hydroxide in water and diluting to 1000 ml.

Acetate buffer solution, pH 5.0. Made by mixing $0.1M$ acetic acid and $0.1M$ sodium acetate in appropriate proportions.

Apparatus

A Hitachi model 635A HPLC instrument with a wavelength-tunable effluent-monitor set at 254 nm was used. An ERC-ODS column (6.0 × 300 mm, Erma Optical Works) was employed.

Procedures

Method A. Aliquots of the standard metal solutions containing up to 470, 63 and 357 μg of bismuth(III), iron(III) and copper(II), respectively, were pipetted into a 25-ml standard flask, then 5.0 ml of DCTA solution and 2.5 ml of acetate buffer solution were added and the mixture was diluted to volume with water and mixed. A 25-μl portion of this sample solution was injected by microsyringe into the HPLC column. A $0.01M$ solution of tetrabutylammonium bromide (TBA^+Br^-) in methanol–water mixture (45:55 v/v) was used as eluent, at a flow-rate of 1.0 ml/min. The chelates in the eluate were detected by spectrophotometry at 254 nm.

*To whom correspondence should be addressed.

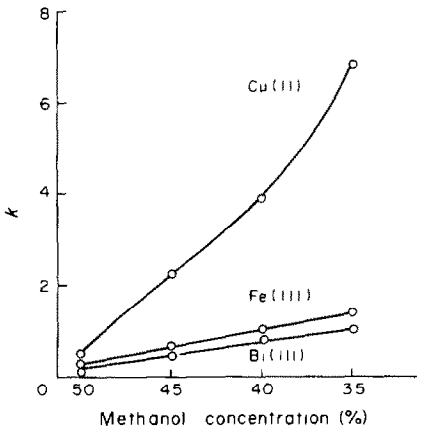

Fig. 1. Relation between k' and methanol concentration in the eluent. Column ERC-ODS; flow-rate 1.0 ml/min; eluent methanol–water ($10^{-2}M$ TBA^+Br^-).

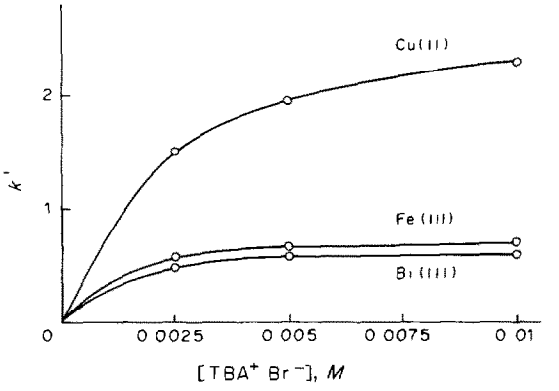

Fig. 2. Relation between k' and tetrabutylammonium bromide concentration in the eluent. Column ERC-ODS; flow-rate 1.0 ml/min; eluent methanol–water 45:55 v/v (TBA^+Br^-).

Method B. Aliquots of the standard metal solutions containing up to 470, 42 and 143 μg of bismuth(III), iron(III) and copper(II), respectively, were pipetted into a 25-ml standard flask, and 5.0 ml of $0.005M$ potassium sodium tartrate (to prevent hydrolysis of the metal ions) and then 2.5 ml of acetate buffer solution were added and mixture was diluted to volume with water and mixed. A 25-μl portion of this solution was injected by microsyringe into the column. A $10^{-2}M$ $TBA^+/10^{-3}M$ DCTA solution in methanol–water mixture (40:60 v/v) was used as eluent at a flow-rate of 1.0 ml/min, and the chelates were detected as in method A.

RESULTS AND DISCUSSION

The DCTA chelates of bismuth(III), iron(III) and copper(II) in aqueous solution have absorption maxima at 267, 260 and 268 nm, respectively. In this study, the chelates in the eluate were all detected at 254 nm although the sensitivity is higher at 268 nm.

Separation of the metal chelates

The effect of methanol content in the eluent on retention behaviour was studied, and the results are shown in Fig. 1. The retention increased as the aqueous component in the eluent increased, which is consistent with theory. The optimum composition of the eluent was 45:55 v/v methanol–water. At lower methanol content, the retention continued to increase, but the peaks were broad and the retention volumes too large for practical work, particularly for the copper(II) chelate. Figure 1 shows that the capacity factor, k', for copper(II) increases remarkably with decrease in methanol content, compared with the values for bismuth(III) and iron(III). This may be attributed to the difference in charge of the chelates, -2 for the copper(II) chelate, and -1 for the other two chelates. The effect of the TBA^+Br^- concentration on the elution behaviour of the chelates is shown in Fig. 2. As might be expected, the k' value for the copper(II) chelate increased with increasing concentration of the ion-pairing reagent, but the values for the bismuth(III) and iron(III) chelates were almost constant at TBA^+ concentrations higher than $2.5 \times 10^{-3}M$. Good resolution could be obtained with $0.01M$ TBA^+Br^- as the pairing reagent, as shown in Fig. 3, but the free DCTA and nitrate ion in the sample solution gave peaks which overlapped the peak for the iron(III) chelate. It was impossible to improve the resolution of these peaks by decreasing the methanol content of the eluent. The retention volumes were 9.2 ml for bismuth(III), 9.8 ml for iron(III) and 19.0 ml for copper(II). The coefficients of variation of peak height were 1.3% for bismuth(III), 1.8% for iron(III) and 3.0% for copper(II) for 12 measurements with 15.7 μg of bismuth(III), 2.1 μg of iron(III) and 11.9 μg of copper(II) per ml of sample solution. The elution order is the same as that observed for the metal–EDTA chelates by Hirowatari *et al.*[19] with $10^{-2}M$ ammonium dihydrogen phosphate and $10^{-2}M$ TBA^+Br^- (pH 3) in 1:9 v/v acetonitrile–water mixture as eluent, and a similar stationary phase. The amounts of bismuth(III) and copper(II) can be determined from the peak heights. The calibration graphs were linear up to 18.8 μg for bismuth(III) and 14.3 μg for copper(II) per ml of sample solution. The detection limits were 37 ng for bismuth(III) and 24 ng for copper(II) in an injected volume of 25 μl of chelate solution (signal to noise ratio 5:1).

Separation of metal ions with DCTA/TBA^+Br^- eluent

To simplify the separation of the metal ions, an attempt was made to eliminate the need for a separate complexation step. Inclusion of the DCTA and TBA^+Br^- in the eluent should permit direct injection of the metal-ion sample solution, with complexation and ion-pair formation taking place on the column. The conditions used for separation of the injected chelate mixture were tried but found unsuitable. The optimum composition of the eluent medium was found to be 40:60 v/v methanol–water mixture. The separation of bismuth(III), iron(III) and copper(II) thus obtained is shown in Fig. 4. It is necessary to add

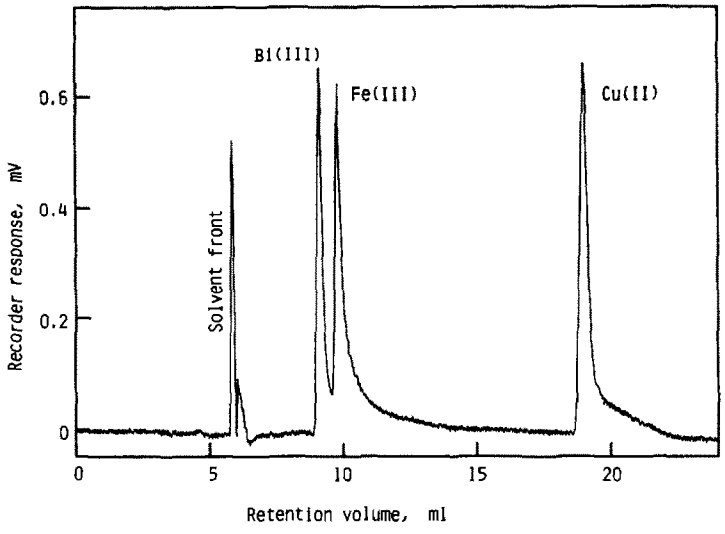

Fig. 3. Chromatogram of DCTA chelates of Bi(III), Fe(III) and Cu(II). Metal-ion concentrations in aqueous solution (μg/ml): Bi(III) 15.7, Fe(III) 2.1, Cu(II) 11.9. Eluent methanol–water 45:55 v/v ($10^{-2}M$ TBA^+Br^-).

potassium sodium tartrate (to give an overall $10^{-3}M$ concentration) to avoid hydrolysis of the metal ions in the sample solution. The tartrate is easily displaced from the metal–tartrate complexes by the DCTA in the eluent. However, the tartrate absorbs slightly at 254 nm and separation of the free tartrate ion and the DCTA chelate of iron(III) is difficult. The k' values of the DCTA chelates in the direct-injection method were 0.15 for bismuth(III), 0.32 for iron(III) and 0.56 for copper(II), whereas with injection of the preformed chelates the k' values were 0.55 for bismuth(III), 0.69 for iron(III) and 2.21 for copper(II). The addition of tartrate to the sample solution had no effect on the k' values in the direct-injection method, so the peaks shown in Fig. 4 are not due to mixed tartrate/DCTA complexes or simple tartrate chelates. The fact that the k' values are smaller in the direct-injection method may be due to the TBA^+ pairing with the DCTA and preventing full formation of the metal–DCTA complexes. The analysis time is shorter for the direct-injection method and the peaks, particularly for the copper(II) chelate, are much sharper than those obtained by the chelate-injection method. However, if the packing in the column is soaked for a long time in eluent containing DCTA, the separation capability of the column falls significantly. Therefore, the use of DCTA in the eluent requires somewhat more care in rinsing the column.

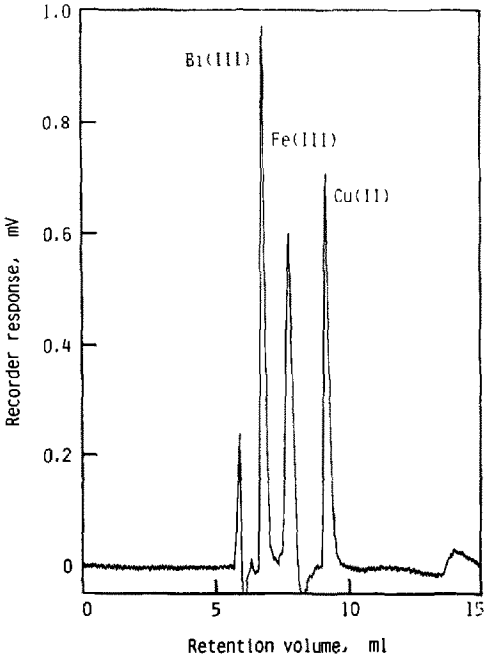

Fig. 4. Chromatogram of DCTA chelates of Bi(III), Fe(III) and Cu(II) formed in the column. Metal-ion concentrations in aqueous solution (μg/ml): Bi(III) 18.8, Fe(III) 1.7, Cu(II) 5.7. Eluent methanol–water 40:60 v/v ($10^{-3}M$ DCTA, $10^{-2}M$ TBA^+Br^-).

REFERENCES

1. G. Schwedt, *Chromatographia*, 1979, **12**, 289.
2. *Idem, ibid.*, 1978, **11**, 145.
3. A. M. Bond and G. G. Wallace, *Anal. Chem.*, 1984, **56**, 2085.
4. *Idem, ibid.*, 1983, **55**, 718.
5. *Idem, ibid.*, 1982, **54**, 1706.
6. *Idem, ibid.*, 1981, **53**, 1209.
7. N. Häring and K. Ballschmiter, *Talanta*, 1980, **27**, 873.
8. R. M. Smith and L. E. Yankey, *Analyst*, 1982, **107**, 744.
9. E. B. Edward-Inatami, *J. Chromatog.*, 1983, **256**, 253.
10. G. Drasch, L. von Mayer and G. Kauert, *Z. Anal. Chem.*, 1982, **311**, 695.
11. J. Lehotay, O. Liška, E. Brandšteterová and G. Guiochon, *J. Chromatog.*, 1979, **172**, 379.
12. J. F. K. Huber, J. C. Kraak and H. Veening, *Anal. Chem.*, 1972, **44**, 1554.

13. M. Lohmuller, P. Heizmann and K. Ballschmiter, *J. Chromatog.*, 1977, **137**, 165.
14. J. W. O'Laughlin and T. P. O'Brien, *Anal. Lett.*, 1978, **11**, 829.
15. J. W. O'Laughlin, *Anal. Chem.*, 1982, **54**, 178.
16. J. W. O'Laughlin and R. S. Hanson, *ibid.*, 1980, **52**, 2263.
17. D. A. Roston, *ibid.*, 1984, **56**, 241.
18. H. Hoshino, T. Yotsuyanagi and K. Aomura, *Bunseki Kagaku*, 1978, **27**, 315.
19. K. Hirowatari, Y. Koumura, K. Kumamoto, K. Hattori and S. Aoshima, *ibid.*, 1981, **30**, 534.
20. D. R. Jones IV and S. E. Manahan, *Anal. Chem.*, 1976, **48**, 502.

Talanta, Vol. 32, No. 12, pp. 1097–1100, 1985
Printed in Great Britain.

0039-9140/85 $3.00 + 0.00

SIGNAL-TO-NOISE OPTIMIZATION IN POLARIMETRY

EDWARD S. YEUNG
Department of Chemistry and Ames Laboratory, Iowa State University, Ames, Iowa 50011, U.S.A.

(*Received* 12 *June* 1985. *Accepted* 23 *August* 1985)

Summary—The signal-to-noise ratio of a polarimeter is considered for cases which include flicker noise. It is found that using good quality polarizers is essential for detecting small rotations. A high-intensity light-source is also desirable, provided that the intensity can be stabilized. The predicted detectability of 2.8×10^{-7} degree with current instruments agrees with previously published experimental results.

The measurement of small amounts of rotation in the polarization plane of light has many applications. Since optical rotation is an inherent characteristic of chiral molecules, many of which are biologically active, polarimetry has been used to study sugars in urine,[1,2] cholesterol in blood,[3] and the structures of components of fossil fuels.[4] Polarimetry has also been used to measure absorption indirectly.[5] In the study of atoms, polarization spectroscopy[6] has been shown to possess good sensitivity.[7] A more fundamental application is the detection of small anisotropies due to weak neutral currents.[8] Yet another application is in Raman-induced Kerr-effect spectroscopy.[9] In each case, it is clear that the more sensitive the polarization detector, the more useful the technique.

In the existing literature, there is some confusion as to how best to optimize the signal-to-noise ratio (S/N) for measurements of polarization rotation. One report indicates that low-quality polarizers are sufficient for obtaining good results.[10] Another report[1] finds that the quality of the polarizers is the key to high sensitivity. Some experimental arrangements call for a small offset from maximum extinction,[11] but others depend on working at the point of maximum extinction.[1] The problem is that S/N has only been considered either in the shot-noise limit[10] or in the flicker-noise limit,[12] but not in the intermediate region typical of many experiments. Furthermore, there is disagreement between equation (24) of Ref. 10 and equation (13) of Ref. 12. It is apparent that a detailed analysis of the signal-to-noise ratio for each type of experimental arrangement is needed to allow proper optimization of the measurements. The results of such an analysis are presented in this paper.

MODEL

The signal obtained from a polarimeter can be derived by using the Jones matrix formalism.[10] Essentially, we are measuring the intensity of the light transmitted through a pair of "crossed" polarizers aligned along the x-axis and y-axis, respectively. Ignoring any attenuation in the polarizing element due to absorption or natural reflection, there is still a non-ideal behaviour, characterized by a parameter k,[10] which causes transmission even if the polarizers are perfectly crossed. The extinction ratio, defined as the fraction of light transmitted with the crossed alignment, is

$$\varepsilon \simeq |k_x|^2 + |k_y|^2 \tag{1}$$

For the purpose of understanding the optimization, we can set $k_x = k_y = k$. If I_0 is the intensity of light of the correct polarization that enters the first polarizer, then the intensity of light transmitted, I_T is given by

$$I_T = I_0 \{2|k|^2 \cos^2(\theta + \chi) + (1 + |k|^4) \sin^2(\theta + \chi)\} \tag{2}$$

where θ denotes the offset of the second polarizer from the crossed position, and χ denotes the amount of rotation caused by the sample, placed between the polarizers. In equation (2) we neglect any depolarization due to circular dichroism in the sample. A more convenient form is obtained by combining equations (1) and (2):

$$I_T = I_0 \{\varepsilon \cos^2(\theta + \chi) + [1 + (\varepsilon/2)^2] \sin^2(\theta + \chi)\} \tag{3}$$

The signal S due to the presence of the sample is readily identified as

$$S = I_0 [f(\theta, \chi) - f(\theta, 0)] \tag{4}$$

where f is the functional relationship inside the braces in equation (3). If modulation is used in conjunction with a lock-in amplifier,[1] the output is proportional to

$$S' = I_0 \{[f(\theta + \Delta, \chi) - f(\theta - \Delta, \chi)] - [f(\theta + \Delta, 0) - f(\theta - \Delta, 0)]\} \tag{5}$$

where Δ is the extent of modulation. For $\theta = 0$ and small rotations χ in the sample, we can see that equation (4) gives a signal proportional to the square of the rotation, whereas equation (5) gives a signal directly proportional to the rotation.

A complete account of the noise in a given experiment is usually very difficult. We can, however, sort out different types of noise according to their functional behaviour. Shot noise is simply $\sqrt{I}$, if I is in units of number of photons observed during the time of data-acquisition. Flicker noise, (or proportional noise, including certain amplifier noise, laser intensity fluctuations and beam misalignment variations) is given by AI, where A is a fractional constant that depends on the experiment. Other types of noise from the electronics may show no intensity-dependence, and can be characterized by a parameter B. So, the total noise N is given by

$$N = \sqrt{I + A^2I^2 + B^2} \tag{6}$$

In equation (6), we have merely classified noise into three types, according to its dependence on I. The actual behaviour of noise can be quite complicated. However, equation (6) is sufficient for a semi-quantitative understanding of signal-to-noise ratios in experimental design. The combination of the three types of noise in equation (6) is based on a previous treatment[13] which showed that

$$N_{AB} = (N_A^2 + N_B^2 + 2CN_AN_B)^{1/2} \tag{7}$$

where N_{AB} is the combined noise from two sources, N_A and N_B, and C is a correlation coefficient that ranges from zero to unity depending on the relation between the sources of noise. Here, we chose $C = 0$ to provide an estimate of the combined noise in the general case when they are not correlated. In situations where the sources of noise are correlated (*e.g.*, errors in photon counting at high intensities), we must use $C = 1$ to show the worst-case behaviour. Equation (7) then reduces to a linear sum, and the noise sources can no longer be distinguished in equation (6).

Explicitly, I is the signal (number of photons) obtained without the sample rotation χ. For equation (4) and (5), we then have

$$I = I_0 f(\theta, 0) \tag{8}$$

We note that by using a lock-in amplifier, we can optimize A and B in equation (5) by providing measurements at a frequency that can be selected. However, A is never completely eliminated, even with the best double-beam arrangement with modulation. For small modulation (Δ) and small signals (χ), equation (5) reduces to $S' = 4I_0\Delta\chi\cos\theta$. We should therefore always work with zero offset of the second polarizer from the crossed position ($\theta = 0$), since S' is then maximized and I and thus N is minimized. When modulation is used, instabilities in the modulation depth will also contribute to the total flicker noise.

RESULTS AND DISCUSSION

On the basis of equations (4), (6) and (8), we can calculate the signal-to-noise (S/N) ratio for various combinations of θ, χ, I_0, A and B. For typical experiments, the constant electronic noise B can be eliminated from consideration. For example, we can increase the gain of the phototube to obtain a signal that makes the contribution from B negligible. In all cases S/N increases with χ. To make useful comparisons, we can determine the S/N per degree of rotation by the sample (χ) as χ becomes infinitely small. The reciprocal of the numerical result then gives the sample rotation needed to produce $S/N = 1$.

It has already been shown in previous work[10] that if $A = 0$, *i.e.*, in the shot-noise limit, the maximum value for S/N is independent of ε for $\varepsilon < 10^{-3}$. The optimum angle θ, however, depends on ε, and varies from 9.07° for $\varepsilon = 6.5 \times 10^{-4}$ to 0.18° for $\varepsilon = 10^{-10}$. With $A \neq 0$, the situation is quite different. This is because for 500-nm light, the shot noise for a 1-μW light-beam is only about 1 part in 10^6 in 1 sec. This is substantially smaller than the fractional flicker noise in most light-sources. To maintain good detection in polarization rotation, we need to keep the light flux reaching the phototube as small as possible, so that the total flicker noise can be reduced. For the more stable laser sources, a fractional flicker noise of $A = 10^{-3}$ is typical. This implies that we should try to approach 0.4 pW of power at the phototube while maintaining as high a power level as possible at the sample. Even with intensity stabilization and/or double-beam optics, A is rarely below 10^{-4}. An excellent set of polarizers at the crossed alignment is thus needed.

To put things in more quantitative terms, we have plotted in Fig. 1 the dependence of θ_{opt}, the offset angle at which S/N is optimized, as a function of the flicker-noise parameter, A, in equation (6). A value of $\varepsilon = 10^{-6}$ is chosen because this is typical of good commercial polarizers. The light intensity, I_0, chosen is 5 μW, a power level that can easily be achieved. The B term, as discussed earlier, has been neglected. Figure 1 is obtained by numerical simulation. Briefly, for a given set of conditions, S/N is determined from equations (4), (6) and (8) for a range of θ values, and θ_{opt} is determined by comparison. Figure 1 shows that A affects θ_{opt} substantially. When the flicker noise is large, we should work with the polarizers nearly in crossed alignment, even though that is not the case

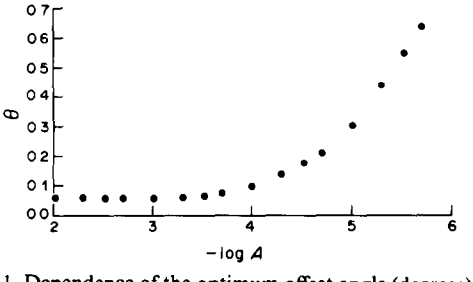

Fig. 1. Dependence of the optimum offset angle (degrees) on the flicker noise: $\varepsilon = 10^{-6}$, $I_0 = 5\,\mu$W.

for the shot-noise limit.[10] Only when A is quite small can we gradually approach the same θ_{opt} as in the shot-noise limit, and only when A is quite large can we use equation (11) of Ref. 12. For higher laser powers, A will be even more dominant in consideration of S/N, and θ_{opt} remains small until A becomes substantially smaller than the values shown in Fig. 1. In either case, even though θ_{opt} does not change much at large A values, S/N at θ_{opt} changes substantially. It can easily be seen that for large values of A, the optimum S/N is roughly inversely proportional to A.

For a given A, the main effect of varying ε is to change the intercept in Fig. 1. For example, the minimum for θ_{opt} when $\varepsilon = 6.5 \times 10^{-4}$ is 1.47°. This is because for such a set of polarizers, moving 1.47° away from the crossed alignment does not substantially change the transmitted light intensity. It is thus possible to increase the signal without introducing additional noise by moving away from extinction. However, the optimized S/N does improve with better polarizers, in contrast to the case for the shot-noise limit. A quantitative picture of this relationship is shown in Fig. 2, which is constructed by fixing A at 0.01 and I_0 at 5 mW. It is clear that within the range shown, there is a linear dependence of log θ on log ε, with a slope of -0.510. For comparison, at the shot-noise limit, the slope should be -0.250. The fact that the values differ by a factor of 2 is accidental. This slope naturally changes gradually from the shot-noise limit when $A = 0$ to larger negative values when A increases. Figure 2 again shows that we should work more closely to crossed alignment than is suggested by considering only shot-noise. The difference between the value of -0.510 here and that of -0.500 in Ref. 12 is significant. In the intermediate region, when both shot noise and flicker noise contribute, equation (11) in Ref. 12 is not strictly valid.

The S/N values from these calculations can be used to estimate detectabilities in polarimeters with a given set of ε, I_0 and A values. Some representative situations are shown in Table 1. For a light-source with significant flicker noise ($A = 10^{-2}$), substantial improvements can be made by using high-quality polarizers. For a stable light-source or one with double-beam compensation ($A = 10^{-4}$), however, the advantage of high-quality polarizers will become significant only if a high light-intensity is available. Conversely, a high-intensity light-source is not required unless the polarizers are of high quality and the source intensity is stable. The best experimental detectability[5] obtained in our laboratory for $\varepsilon = 10^{-10}$ and $I_0 = 5$ mW is 1.3×10^{-6} degree. There, the inherently noisy cw laser is effectively stabilized by polarization modulation,[1] which effectively provides double-beam compensation, to a level approaching $A = 10^{-4}$. Considering that ε is degraded somewhat owing to the presence of an additional liquid cell between the polarizers, the agreement with the predicted value of 2.8×10^{-7} degrees (from the second entry in the last row in Table 1) is excellent. It is interesting to note that the optimal S/N is predicted for $\theta = 1.6 \times 10^{-3}$ degrees, which is an insignificant offset from the crossed alignment, given the mechanical rigidity of typical optical mounts. For exactly crossed alignment, however, the S/N drops from 3610 to 340. This implies that finely adjustable rotational stages are desirable in polarimeters. Table 1 also shows that additional gains in S/N are possible by further stabilization of the intensity of the laser.

Table 1. Optimized S/N values per millidegree of sample rotation in polarimeters

	I_0		
	5 μW	5 mW	50 mW
$\varepsilon = 10^{-6}$			
$A = 10^{-2}$	1.75	1.75	1.75
$A = 10^{-4}$	87.5	174	176
$\varepsilon = 10^{-10}$			
$A = 10^{-2}$	92	190	190
$A = 10^{-4}$	124	3610	9200

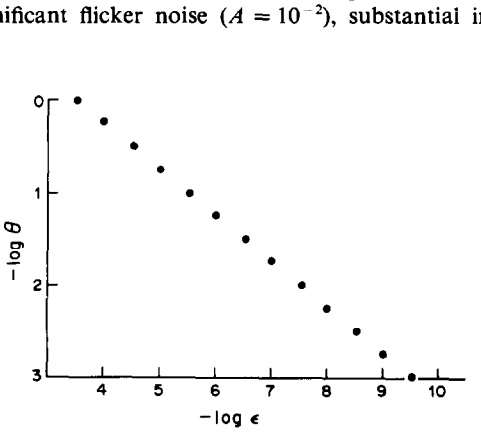

Fig. 2. Dependence of the optimum offset angle (degrees) on the extinction ratio of the polarizers: $A = 10^{-2}$, $I_0 = 5$ mW.

In summary, we can see that the inclusion of even small amounts of flicker noise when considering S/N in polarimeters leads to results very different from those obtained when only shot-noise is included.[10] Neglecting shot-noise[12] is also not appropriate for typical experimental conditions. Optimization is possible by using high-quality polarizers in conjunction with moderate light-intensities and intensity stabilization.

Acknowledgements—The author thanks Donald R. Bobbitt for helpful discussions concerning this topic. This research was partially supported by the U.S. Department of Energy, Office of Basic Energy Sciences, Division of Chemical Sciences, through the Ames Laboratory, Iowa State University, under contract No. W-7405-eng-82.

REFERENCES

1. E. S. Yeung, L. E. Steenhoek, S. D. Woodruff and J. C. Kuo, *Anal. Chem.*, 1981, **52**, 1399.
2. J. C. Kuo and E. S. Yeung, *J. Chromatog.*, 1981, **223**, 321.

3. *Idem, ibid.*, 1982, **229,** 293.
4. D. R. Bobbitt, B. H. Reitsma, A. Rougvie, E. S. Yeung, T. Aida, Y. Chen, B. F. Smith, T. G. Squires and C. G. Venier, *Fuel*, 1985, **64,** 114.
5. D. R. Bobbitt and E. S. Yeung, *Anal. Chem.*, 1985, **57,** 271.
6. R. Teets, R. Feinberg, T. W. Hänsch and A. L. Schawlow, *Phys. Rev. Lett.*, 1976, **37,** 683.
7. W. G. Tong and E. S. Yeung, *Anal. Chem.*, 1985, **57,** 70.
8. T. P. Emons, J. M. Reeves and E. N. Fortson, *Phys. Rev. Lett.*, 1983, **51,** 2089.
9. D. Heiman, R. W. Hellwarth, M. D. Levenson and G. Martin, *Phys. Rev. Lett.*, 1976, **36,** 189.
10. J. J. Kankare and R. Stephens, *Talanta*, 1984, **31,** 689.
11. H. W. Schrotter, in *Nonlinear Raman Spectroscopy and Its Chemical Applications*, W. Keifer and D. A. Long (eds.), pp. 603–611. Reidel, New York, 1982.
12. C. E. Wieman, in *Laser-based Ultrasensitive Spectroscopy and Detection, V*, R. A. Keller, (ed.), *Proc. SPIE*, 1983, **426,** 76.
13. C. Th. J. Alkemade, W. Snelleman, G. D. Boutilier, B. D. Pollard, J. D. Winefordner, T. L. Chester and N. Omenetto, *Spectrochim. Acta*, 1978, **33B,** 383.

Talanta, Vol. 32, No. 12, pp. 1101–1104, 1985
Printed in Great Britain.

0039-9140/85 $3.00 + 0.00

ELECTROCHEMICAL MASKING OF LARGE AMOUNTS OF COPPER IN DPASV AND THE DETERMINATION OF THALLIUM IN THE PRESENCE OF A LARGE EXCESS OF COPPER

A. CISZEWSKI and Z. ŁUKASZEWSKI*
Institute of General Chemistry, Technical University of Poznań, 60-965 Poznań, Poland

(*Received* 25 *March* 1985. *Accepted* 14 *August* 1985)

Summary—The influence of the following surfactants on the peak of copper in 0.2*M* EDTA at pH 4.5 was investigated: polyoxyethylated alkylphenols having an average of 3 and 9.5 ethylene oxide units; polyoxyethylene alcohols having 4 and 7 ethylene oxide units; poly(ethylene glycols) having M.W. 4000, 9000 and 20000; hexadecyltributylphosphonium bromide (HDTBPB), tetraphenylphosphonium bromide (TPPB), *N,N,N,N′,N′,N*-hexamethylhexamethylenediammonium bromide (HMB), benzyl(di-isobutylphenoxyethoxy)dimethylammonium chloride (Hyamine 1622), hexadecyltrimethylammonium bromide (HDTMAB), hexadecyldimethylbenzylammonium chloride (HDDMBAC) and tetrabutylammonium chloride (TBAC). HDDMBAC, as well as all the substances examined which contained an ethylene oxide chain, completely suppressed the copper peak. HDTBPB and TPPB partially suppressed the peak, whereas HDTMAB, HMB and Hyamine 1622 enhanced it. TBAC was without effect. In 0.2*M* EDTA at pH 4.5 containing TBAC at 0.01*M* concentration and 10 ppm of Rokafenol N-3, Cu(II), Pb(II) and Bi(III) can be tolerated at concentrations of up to 0.05*M*, the height of the thallium peak being unaffected. The precision of the determination (3–10%) and the recovery are satisfactory. A 10^3-fold ratio of Fe(III) to Tl(I) does not interfere with the determination.

Because copper is relatively noble compared to most metals, it is deposited along with the others at the deposition stage of all stripping methods. Usually, small amounts of deposited copper do not influence the determination of other metals, but the formation of intermetallic compounds of copper with zinc and cadmium seriously affects the determination of these metals.[1–6] The most severe hindrance to the determination of metal ions in stripping methods is the presence of a high concentration of copper, which makes determination impossible because of the large background current produced by the reduction of copper(II) to the metal, while the other metals are already being oxidized. Similar difficulties connected with the presence of a high concentration of bismuth(III), which has a similar position in the electrochemical series, have been overcome by means of "electrochemical masking" with tetrabutylammonium chloride and a strongly complexing base electrolyte.[7] The simultaneous use of surfactant action and the complexing properties of the base electrolyte leads to the best results. It is possible in this way to determine thallium in the presence of lead[8] or of cadmium,[9] as well as lead in the presence of cadmium,[9] without any prior separation.

Of these elements usually determined by stripping methods, only thallium is not affected by the surfactant. This is because of the small value of the ionic potential (the ionic charge divided by the ionic radius) of thallium(I). Such a situation offers the possibility of eliminating the influence of all other metals on the determination of thallium by stripping methods, and of developing a highly selective or even specific method for the determination of thallium.

The aims of this work were (*i*) to find the conditions for "electrochemical masking" of high concentrations of copper(II); (*ii*) to select conditions for the determination of thallium in the presence of a large excess of copper(II), and simultaneously to maintain those conditions necessary for the determination of thallium in the presence of large amounts of other metals, specifically lead and bismuth, *i.e.*, to take the next step towards developing a specific method for the determination of thallium.

The search for the most effective surfactant covered ethoxyalkylphenols and ethoxyalcohols having different numbers of ethylene oxide units, poly(ethylene glycols) having different molecular weights (but >2000 since PEGs with lower molecular weight are ineffective[10]), as well as a group of ammonium salts and phosphonium salts having different degrees of symmetry. The anionic surfactants are not good for such purposes,[11] and were therefore not examined.

The investigations were done with an EDTA solution at pH 4.5 as the base electrolyte, since this is necessary for the determination of thallium in the presence of excesses of lead, bismuth and cadmium.

*Author for correspondence.

EXPERIMENTAL

Apparatus

A Telpod (Poland) pulse polarograph model PP-04, designed by Kowalski *et al.*, was used. Voltamperograms were displayed on an Endim (GDR) 620.02 XY-recorder. The differential pulse amplitude was 100 or 50 mV and the scan-rate 11.1 mV/sec. Radiometer controlled-temperature Kemula electrode equipment was used. The surface area of the hanging mercury drop was 2.1 mm^2.

Reagents

The non-ionic surfactants Triton X-100 (Merck), Rokafenol N-3, Rokanol KO-4 and Rokanol K-7 (Rokita), poly(ethyleneglycols) of M.W. 4000, 9000 and 20000 (Fluka), and the cationic surfactants *N,N,N,N',N',N'*-hexamethylhexamethylenediammonium bromide (HMB) (Fluka), benzyl(di-isobutylphenoxyethoxy)dimethylammonium chloride (Hyamine 1622) (Serva), hexadecyltrimethylammonium bromide (HDTMAB), (Merck), tetrabutylammonium chloride (TBAC) (Fluka), hexadecyldimethylbenzylammonium chloride (HDDMBAC) (Fluka), hexadecyltributylphosphonium bromide (HDTBPB) (Fluka) and tetraphenylphosphonium bromide (TPPB) (Merck), were used without additional purification.

The supporting electrolyte was 0.2*M* EDTA, prepared from the analytical grade reagent, with the pH adjusted to 4.5 ± 0.1 with electrolytically purified potassium hydroxide solution. The standard solutions of Tl(I), Cu(II), Pb(II) and Bi(III) were prepared by dissolving the purest metals available. Solutions with concentrations below 1 m*M* were prepared just before measurement. All solutions were prepared in water triply distilled in quartz apparatus.

Procedure

The solutions examined were deaerated by passage of purified nitrogen and were brought to $20 \pm 0.2°$ before measurement. In all the experiments preconcentration was done at a potential of -0.700 V *vs.* SCE for 300 or 600 sec, with the solution stirred. The voltamperograms were recorded after a 30-sec quiescent period.

RESULTS AND DISCUSSION

The influence of seven non-ionic and seven cationic surfactants on the stripping peak for $10^{-5}M$ copper in 0.2*M* EDTA at pH 4.5 was investigated by adding increasing concentrations of surfactant. Concentrations of non-ionic surfactants are expressed in parts per million because the commercial materials are polydisperse technical products. Concentrations of the cationic surfactants can be expressed as molarities because they are pure chemical compounds. Because the cationic surfactants are more soluble than the non-ionic surfactants in water they could be investigated at high concentrations. The results relating to the non-ionic surfactants are given in Table 1, and for cationic surfactants in Table 2.

All the non-ionic surfactants suppress the copper peak to much the same extent, and shift it in the anodic direction. Rokafenol N-3 shows the most pronounced effect of this group of surfactants and can completely suppress the copper peak.

In contrast, the cationic surfactants exert widely differing suppressive effects, as can be seen from Table 2: only HDDMBAC strongly suppresses the copper peak, whereas both phosphonium salts (HDTBPB and TPPB) have little effect, in spite of the great differences in structure of these substances. Symmetrical TBAC has virtually no influence on the copper peak, and the remaining quaternary ammonium salts (HMB, Hyamine 1622 and HDTMAB) enhance the peak, especially HDTMAB.

It seems that the enhancement of the peak is attributable not to a greater amount of copper being deposited, but rather to the greater polarographic reversibility in the presence of surfactant (*i.e.*, there is an acceleration of the electrode process). Additional evidence for this explanation is provided by the shift of the peak in the cathodic direction in the presence of the surfactants in question. A similar effect of increase in peak height in the presence of surfactant has been observed for In(III) and Sn(IV) in the presence of long-chain amines and ammonium salts.[12]

It is very interesting to compare the action of HDTMAB, HDDMBAB and Hyamine 1622 on the copper peak. The chemical structures of the first two

Table 1. The effect of non-ionic surfactants on the relative peak height (i_p^x) and peak potential (E_p) of copper in 0.2*M* EDTA at pH 4.5

Surfactant		Surfactant concentration, *ppm*						
		0.01	0.05	0.10	0.50	1.00	5.00	10.0
Rokafenol N-3	i_p^x	0.98	0.81	0.60	0.30	0.20	0	0
	$-E_p$	0.22	0.20	0.17	0.13	0.08	—	—
Triton X-100	i_p^x	0.86	0.73	0.53	0.14	0.10	0.05	0.01
	$-E_p$	0.22	0.21	0.20	0.17	0.14	0.10	0.09
Rokanol KO-4	i_p^x	0.90	0.60	0.43	0.20	0.11	0.06	0
	$-E_p$	0.21	0.20	0.19	0.13	0.12	0.11	—
Rokanol K-7	i_p^x	1.00	1.00	0.60	0.43	0.12	0.03	0
	$-E_p$	0.22	0.22	0.20	0.17	0.10	0.05	—
PEG 4000	i_p^x	0.90	0.69	0.42	0.22	0.16	0.09	0.02
	$-E_p$	0.22	0.20	0.18	0.17	0.15	0.13	0.12
PEG 9000	i_p^x	0.92	0.70	0.44	0.26	0.15	0.07	0.04
	$-E_p$	0.22	0.21	0.19	0.16	0.15	0.14	0.13
PEG 20000	i_p^x	0.94	0.74	0.50	0.28	0.18	0.10	0.05
	$-E_p$	0.22	0.20	0.18	0.16	0.15	0.14	0.13

The concentration of copper was 10μM; deposition potential -0.700 V *vs.* SCE; deposition time 300 sec; differential-pulse amplitude 100 mV.

Table 2. The effect of cationic surfactants on the relative peak height (i_p^x) and peak potential (E_p) of copper in 0.2*M* EDTA at pH 4.5

Surfactant		Surfactant concentration, μM						
		1.00	5.00	10.0	50.0	100	500	1000
HDTBPB	i_p^x	0.85	0.33	0.42	0.58	0.65	0.78	0.82
	$-E_p$	0.15	0.12	0.12	0.13	0.14	0.14	0.14
TPPB	i_p^x	1.00	1.00	0.88	0.82	0.75	0.65	0.51
	$-E_p$	0.22	0.22	0.21	0.21	0.20	0.19	0.18
HDDMBAC	i_p^x	0.41	0.13	0.08	0.07	0.06	0.04	0.02
	$-E_p$	0.20	0.20	0.20	0.19	0.19	0.18	0.18
HMB	i_p^x	1.00	1.00	1.08	1.16	1.17	1.20	1.37
	$-E_p$	0.22	0.22	0.23	0.24	0.25	0.26	0.27
Hyamine 1622	i_p^x	1.08	1.25	1.28	1.96	2.36	2.92	2.17
	$-E_p$	0.22	0.20	0.19	0.15	0.17	0.18	0.19
HDTMAB	i_p^x	2.00	3.43	3.94	2.36	3.29	3.61	4.01
	$-E_p$	0.20	0.17	0.18	0.22	0.22	0.23	0.24
TBAC	i_p^x	1.00	1.00	1.00	1.00	1.00	0.99	0.99
	$-E_p$	0.22	0.22	0.22	0.22	0.22	0.22	0.22

Concentration of copper, deposition potential and time, and the differential-pulse amplitude as for Table 1.

differ solely in the substitution of a methyl group in HDTMAB by a benzyl group in HDDMBAB, but this difference results in peak enhancement by HDTMAB and total suppression by HDDMBAB. Both HDDMBAB and Hyamine 1622 contain an *N*,*N*-dimethyl-*N*-benzyl unit, but the hexadecyl group in HDDMBAB is replaced by the di-isobutylphenoxyethoxy group in Hyamine 1622: the latter gives rise to peak enhancement for copper, though not so marked as that with HDTMAB.

It is worth noting the differing effects of these surfactants on the stripping peaks for other metal ions. TBAC suppresses the peaks of lead and bismuth[7,8] but has almost no effect on the copper peak. Such differentiation is very valuable from the analytical point of view because it offers the possibility of finding selective "electrochemical masking" agents.

Complete suppression of the copper peak can thus be achieved by adding any one of the seven non-ionic surfactants or HDDMBAC. The next step was to determine the maximum concentration of copper(II) which could be totally masked to permit the determination of thallium. When 0.2*M* EDTA at pH 4.5 containing 10 ppm of Rokafenol N-3 (the best of the investigated surfactants) and TBAC at the 0.01*M* level (to suppress the peaks from lead and bismuth) was used as supporting electrolyte and the concentration of thallium was kept constant at 25n*M* (100 ng in the sample volume used) and the concentration of copper was varied within the range 0.5–50m*M*, in all the voltamperograms only the thallium peak was visible and both its height and potential remained unchanged. Thus, it is easy to determine 25n*M* thallium in the presence of 0.05*M* copper.

An example of the "electrochemical masking" of a large excess of copper and the determination of thallium in this way is seen in Fig. 1. In the presence of a small excess of copper the determination of thallium is possible without masking (curve *a*), but the large copper peak does dominate the voltamperogram. The addition of 10 ppm of Rokafenol N-3 completely suppressses this peak, resulting in

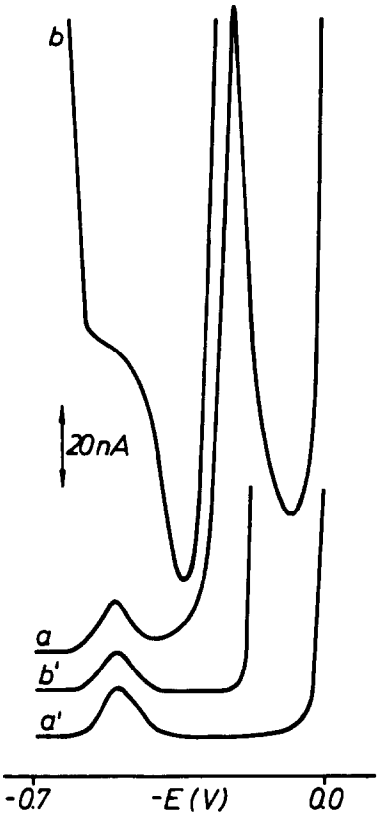

Fig. 1. Differential pulse anodic-stripping voltamperograms for (*a*) 10n*M* Tl(I) + 100n*M* Cu(II); (*a'*) as for *a* + 10 ppm Rokafenol N-3; (*b*) 10n*M* Tl(I) + 5m*M* Cu(II); (*b'*) as for *b* + 10 ppm Rokafenol N-3. Base electrolyte 0.2*M* EDTA + 10 mM TBAC at pH 4.5. Deposition potential −0.700 V *vs.* SCE; deposition time 600 sec; differential-pulse amplitude 50 mV.

Table 3. The determination of thallium in the presence of large amounts of copper, lead and bismuth

Series	Number of tests	Added Cu, *mg*	Pb, *mg*	Bi, *mg*	Tl, *ng*	Tl found, *ng*	Std. devn., *ng*	Rel. std. devn., %
I	5	20	—	—	20	19	1.9	9
II	3	40	—	—	20	19	0.6	3
III	5	20	—	—	100	101	7.9	8
IV	5	20	—	—	200	202	7.6	4
V	3	40	40	40	20	22	2.0	10

Base electrolyte 0.2*M* EDTA + 10m*M* TBAC + 10 ppm Rokafenol N-3 at pH 4.5. Differential-pulse amplitude 50 mV; deposition potential and time as for Table 1. Significance level 95%.

curve *a'*. In the presence of large excess of copper, a very high background current is observed, which makes the determination of thallium impossible (curve *b*). The addition of 10 ppm of Rokafenol N-3 still masks the copper without changing the thallium peak (curve *b'*).

The precision and recovery for the determination of thallium in the presence of a large excess of copper were next examined: the results are given in Table 3. Table 3 also gives results which illustrate the possibility of determining traces of thallium in the presence of high concentrations of lead, bismuth and copper. As can be seen, the precision for the determination of thallium in the presence of a 10^6-fold ratio of copper is typical for such voltammetric measurements and the recovery is good. Also, the combined presence of Pb(II), Bi(III) and Cu(II) in very great excess [2×10^6 ratio to Tl(I)] does not affect the determination of thallium in the supporting electrolyte used.

Unfortunately, the addition of Rokafenol N-3, or of any of the other ethoxy compounds, makes the determination of thallium in the presence of Fe(III) worse. The ratio of Fe(III) to Tl(I) should not exceed 10^3. Such a limit does not hinder the determination of thallium in materials of high purity, in which there should not be more than 30 ppm of iron; however, in analytical and reagent grade chemicals this limit will be an obstacle to the use of this method.

Acknowledgement—This work was supported by Research Program MR-I-32, and the paper was presented at Euroanalysis V, Cracow, 1984.

REFERENCES

1. M. S. Shuman and G. P. Woodward, *Anal. Chem.*, 1976, **48**, 1479.
2. P. Ostapczuk and Z. Kublik, *J. Electroanal. Chem.*, 1977, **83**, 1.
3. J. A. Wise, D. A. Roston and W. R. Heineman, *Anal. Chim. Acta*, 1983, **154**, 95.
4. B. W. Woodget and K. R. Franklin, *Analyst*, 1981, **106**, 1017.
5. G. Schulze and W. Frenzel, *Z. Anal. Chem.*, 1983, **314**, 459.
6. W. Frenzel, *Doctoral Thesis*, Technical University of Berlin, 1984.
7. A. Ciszewski, *Talanta*, 1985, In press.
8. A. Ciszewski and Z. Łukaszewski, *ibid.*, 1983, **30**, 873.
9. Z. Łukaszewski, M. K. Pawlak and A. Ciszewski, *ibid.*, 1980, **27**, 181.
10. Z. Łukaszewski, *ibid.*, 1977, **24**, 603.
11. J. Opydo, *Doctoral Thesis*, Technical University of Poznań, 1982.
12. A. Ciszewski and Z. Łukaszewski, *Anal. Chim. Acta*, 1983, **146**, 51.

Talanta, Vol. 32, No. 12, pp. 1105–1112, 1985
Printed in Great Britain

0039-9140/85 $3.00 + 0.00
Pergamon Press Ltd

NEW CHELATING SORBENTS FOR NOBLE METALS

G. V. MYASOEDOVA, I. I. ANTOKOL'SKAYA and S. B. SAVVIN
V. I. Institute of Geochemistry and Analytical Chemistry, USSR Academy of Sciences, Moscow, USSR

(*Received* 2 *May* 1984. *Revised* 25 *March* 1985. *Accepted* 14 *August* 1985)

Summary—The properties of the new chelate-forming "POLYORGS" sorbents for concentration of noble metals are discussed. POLYORGS are made from different polymeric matrices (polystyrene, copolymers of styrene with divinylbenzene, fibrous materials). They contain heterocyclic amine and amidoxime groups, and are selective for noble metals. Some methods of noble metal determination after preliminary concentration of POLYORGS sorbents are given.

The determination of noble metals in various materials usually requires their preconcentration and often their separation from other elements. Several methods are available for this purpose. The sorption methods are widely used and are the most effective.[1] The selectivity of the sorbents used is dependent on the complex-forming groups they contain. As the noble metals have a greater tendency than other metals to form complexes, the complex-forming sorbents are particularly useful in this respect.[2,3] Many types of selective sorbents are available, but those based on polymeric organic matrices have some interesting properties.[4] Table 1 lists some chelating sorbents which are important for preconcentration and separation of noble metals. These sorbents are based on various polymeric matrices, and have different functional groups. They may be used in the form of beads, powder or fibres.

The high selectivity of these sorbents for the noble metals is mainly achieved by the use of nitrogen and sulphur as donor atoms (Table 1), but the sorbents which do not contain sulphur atoms are the most selective in the presence of Cu, Ni, Co, *etc.* The chelating sorbents containing nitrogen-heterocycle groups are highly selective for noble metals.[4] Additional selectivity with respect to base metals is secured by varying the acidity.

The efficiency of sorbents for analytical purposes depends on their kinetic characteristics, convenience of application, and ease of combination with determination methods.[2]

This paper describes the properties of some new chelating sorbents (POLYORGS*) which are important for selective concentration of noble metals, and gives examples of applications.

PROPERTIES OF POLYORGS

POLYORGS are obtained by the introduction of complexing functional groups into linear polystyrene, macroporous styrene–divinylbenzene copolymers, poly(vinyl alcohol) and polyacrylonitrile fibres, and other matrices.

Some characteristics of the sorbents are given in Table 2. POLYORGS have high capacity for noble metals, are stable in highly acid and alkaline solutions, and can be used for sorption over a wide range of acidity and temperature. Either batch or column methods can be used. The complete preconcentration of a group of noble metals (including rhodium and iridium takes 1–2 hr (Table 3).

POLYORGS are highly selective for noble metals in the presence of non-noble metals (Table 4). The most interesting are POLYORGS IV, V and VI. Preconcentration is complete in presence of copper(II) up to a concentration of at least 50 g/l., nickel(II) and cobalt(II) up to 100 g/l., and iron(III) up to 10–20 g/l. POLYORGS V has the highest selectivity, especially in the presence of iron(III). These base metals are only very slightly sorbed [copper, nickel and cobalt 0.02%, iron(III) 2%], so they have practically no influence on the subsequent determination of the noble metals. Other base metals (Al, Ca, Mg, *etc.*) are not sorbed at all from highly acidic media.

Their high sorption capacity and selectivity allow POLYORGS to be used for preconcentration of noble metals from solutions of complex composition, *e.g.*, the solutions obtained after opening out of rocks, ores, minerals and alloys, or industrial process solutions, *etc.*

The sorption is usually done in 1–3*M* hydrochloric acid medium under static conditions. Sulphate and formate solutions are especially difficult to analyse, however, and need preliminary treatment before the sorption step;[39,40] for large solid samples it is necessary to make a preliminary fusion with copper–nickel alloy or lead or nickel sulphide, followed by dissolution and selective sorption of noble metals by POLYORGS sorbents.[36,38,41-43]

POLYORGS are especially useful for group separation and concentration of noble metals for subsequent determination by selective physical methods, such as a kinetic, spectrophotometric method,[44]

*Trade-mark.

Table 1. Chelate sorbents for preconcentration and separation of noble metals

Sorbent	Structure of chelate group	Polymeric matrix	Metals sorbed	References
Polynitroxaminazo	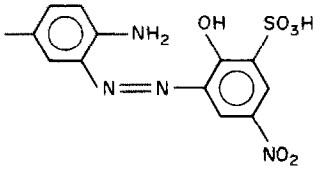	Polystyrene	Au, Pd	5
Polythioxine	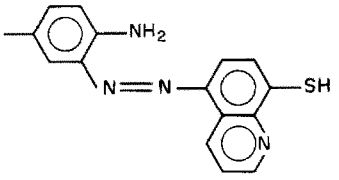	Polystyrene	Pt, Pd, Rh Ir, Ru, Os, Au, Ag	6,7
Polystyrene-azorhodanine	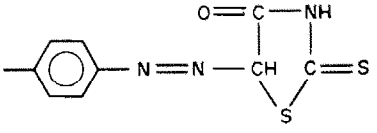	Polystyrene	Pt, Pd, Rh, Ir, Ru, Au	8
POLYORGS II	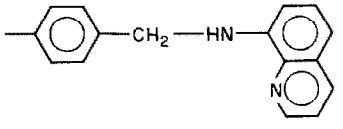	Macroporous copolymer of styrene–DVB	Pt, Pd, Au	9
Mtilon T	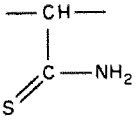	Copolymer of cellulose–acrylonitrile	Pt, Pd, Rh, Ir, Ru, Au, Ag, Hg	10–12
PVA-fibres with thioamide groups	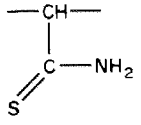	Copolymer of PVA–acrylonitrile	Pd, Pt, Rh, Ir	13–15
SRAFION NMRR	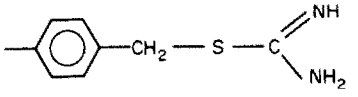	Copolymer of styrene–DVB	Pt, Pd, Ir, Rh, Ru, Os, Au, Ag	16–21
Sorbent with formazan groups	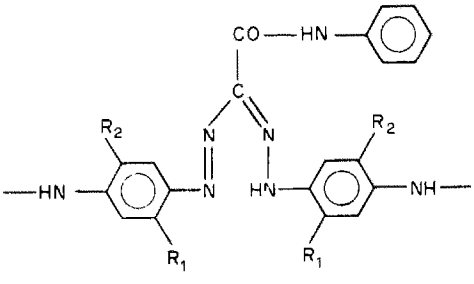	Macroporous styrene–DVB, cellulose, saccharose methacrylate	Pt, Pd, Rh, Ir, Ru, Au, Ag	22–24
Sorbent with isonitrosoacetamide groups	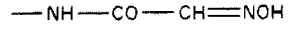	Styrene–DVB, polycondensate of *m*-aminophenol with formaldehyde	Pd, Ag	25
Guanidine sorbent	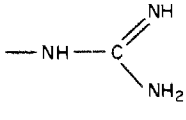	Styrene–DVB	Pt, Pd	26
GMA–EDMA–IDA/	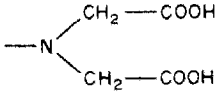	Glycidyl methacrylate–ethylene dimethacrylate	Pt, Pd, Rh, Ir	27–29

Table 1. *Continued*

Sorbent	Structure of chelate group	Polymeric matrix	Metals sorbed	References
Polystyrene–DMABR	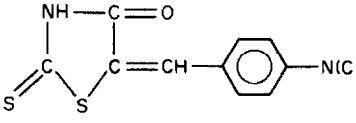	Macroporous styrene–DVB	Ag	30
Polyhydroxamic sorbent	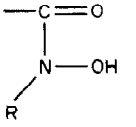	Copolymer acrylonitrile–ethylacrylate–DVB	Au, Ag	31

atomic-absorption,[45] neutron-activation,[36] X-ray fluorescence[46] and atomic-emission spectrometry.[47] The sorbent can be destroyed by ashing at 450–500°,[39,48] or heating with perchloric–sulphuric–nitric acid mixture[38] to recover the elements sorbed. Dry ashing is convenient before emission spectrometry.[39,49] Table 5 gives examples of applications to various types of sample, and some procedures are outlined below.

POLYORGS IV

Determination of noble metals in rocks, ores and other products

Method 1. A 50–100 g sample is mixed with nickel oxide, sulphur and fluxes (sodium carbonate, borax, silica) and heated in a glassy carbon crucible at 1000–1050° for 1 hr. The composition of the mixture varies according to the type of sample (Table 6). The nickel sulphide produced is separated from the slag, which contains small amounts of platinum metals and requires remelting. The nickel sulphide obtained (15–20 g) is accurately weighed, then crushed and ground, and a 5-g portion is weighed into a 150–200 ml beaker, then 50 ml of concentrated hydrochloric acid are gradually added and the mixture is boiled until the sample is completely dissolved. All the base metals and some palladium pass into solution. The solution is evaporated almost to dryness, then 20 ml of *aqua regia* are added and the mixture is boiled for 30 min. The solution is evaporated, 20 ml of hydrochloric acid are added and the solution is again evaporated; this step is repeated. The residue is taken up in 100 ml of 1*M* hydrochloric acid, then 0.2 g of ground POLYORGS IV is added and the mixture is boiled gently for 2 hr. After cooling, the sorbent is filtered off and washed with 1*M* hydrochloric acid, then water, until all nickel salts are removed. The filter and sorbent are put into a beaker, 8–9 ml of a 1:1:1 v/v mixture of concentrated perchloric, sulphuric and nitric acids are added, the beaker is covered, and the mixture is boiled until the organic material is completely decomposed. The acids are then evaporated and the residue is heated with 10 ml of *aqua regia* for 10–15 min. The acids are then evaporated and 10 ml of concentrated hydrochloric acid are added and then evaporated (this step being repeated). The residue is dissolved in 1 ml of 2*M* hydrochloric acid, and 0.3, 0.1 and 0.5 ml portions are transferred into separate 50-ml for catalytic determination of Pd, Rh and Ir respectively.[38]

Method 2. A 3–10 g sample is heated in a Teflon beaker with six times its weight of ammonium bifluoride on a sand-bath until practically all the silicon present has been removed as SiF_4 (or H_2SiF_6). Then 25 ml of concentrated hydrofluoric acid are added to the residue and the remainder of the silicon removed. The residue is treated with two 10-ml portions of concentrated nitric, two or three 20-ml portions of *aqua regia* and finally two or three times with 20-ml portions of concentrated hydrochloric acid, with evaporation almost to dryness after each addition of acid.

The final residue is taken up in 100 ml of 2*M* hydrochloric acid with heating, and the solution is filtered. The filtrate is reserved. The residue and filter are ashed in a muffle, and the residue is fused with four times its weight of barium peroxide at 900° for 2 hr. The cooled melt is leached with hot water, and made 2*M* in hydrochloric acid. The filtrate is added to this solution and the mixture made up to volume in a 250-ml standard flask. About 0.25 g of group sorbent (200 mesh) is added to this solution, and the mixture is gently boiled for 2 hr (with addition of hot water to maintain the volume). The sorbent is filtered off on a filter paper and washed with 50 ml of 2*M* hydrochloric acid and then water.

For atomic-absorption determination the sorbent is dried on a filter, than transferred into a test-tube, and water is added to give a total volume of 5 ml. The mixture is homogenized and a 20–50 μl portion of the suspension (depending on the content of noble metals) is injected into a graphite furnace atomizer and Pd, Pt, Rh and Ir are determined under the conditions given in Table 7.

Determination of noble metals in sulphate solutions

Osmium and ruthenium. The sulphate solution is evaporated to a small volume, 50–100 ml of 1*M* hydrochloric acid are added, and the mixture is boiled for 1 min. Then 100 mg of ground sorbent are added and gentle boiling is continued for 2 hr, extensive evaporation of the solution being avoided. For spectral determination 0.075 g of spectral-grade graphite is added and the solution is filtered with a paper filter. The filter plus sorbent and graphite is placed in a crucible, 0.4 ml of 0.3% sodium sulphate solution is added, then the mixture is dried on a hot-plate and ashed in a muffle furnace at 500° for 20 min. Ruthenium and osmium are determined in the residue spectrographically.[39]

Concentration of platinum, palladium, rhodium, iridium and gold. The sulphate solution is evaporated to small volume, 5 ml of *aqua regia* are added, the beaker is covered, and the solution kept boiling for 1 hr. Then 50 ml of 1*M* hydrochloric acid are added and the mixture is boiled for 1 min. The rest of the procedure is the same as for determination of Os and Ru. Pt, Pd, Rh, Ir and Au are determined in the residue by, for example, atomic-emission spectrometry.

A stock standard solution containing (μg/ml) Pt 0.6, Pd 1.6, and Rh, Ir, Ru, Os, Au 0.4 each, is prepared, and to make the calibration standards 0.1, 0.2, 0.5, 1.0, 2.0, 5.0 and 10.0 ml portions of it are each mixed with 2 ml of *aqua regia* and the mixtures are evaporated to 0.2–0.3 ml, this acid treatment and evaporation being repeated 3 times. Then 2 ml of concentrated hydrochloric acid are added to each solution and evaporated almost to dryness. The resi-

Table 2. Properties of POLYORGS chelate sorbents

Sorbent	Structure of chelate-forming groups	Polymeric matrix characteristics of sorbents	Metals sorbed	Sorption capacity, *mg/g**							References
				Pt	Pd	Rh	Ir	Ru	Au	Ag	
POLYORGS IV	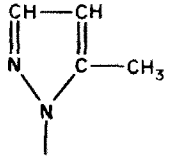	macroporous, copolymer styrene–DVB, faint yellow	Pt, Pd, Rh, Ir, Ru, Os, Au, Ag	100	100	30	30	30	660	263	32–35
POLYORGS V	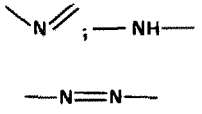	polystyrene, powder, dark red	Pt, Pd, Rh, Ir, Ru, Au, Ag	—	18.4	12.5	12.5	—	340	107	36
POLYORGS VI	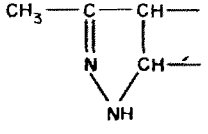	PVA fibres, dark brown	Pt, Pd, Rh, Ir, Ru, Os, Au, Ag	25	48	—	30	—	219	80	37
POLYORGS VII	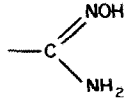	fibres faint yellow	Pt, Pd, Rh, Ir, Ru, Au, Ag	188	130	—	45	—	144	148	—
POLYORGS X	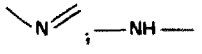	fibres, black	Pt, Pd, Rh, Ir, Ru, Os, Au, Ag	362	108	—	90	—	300	140	—
POLYORGS XI	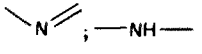	macroporous copolymer, beads, white	Pt, Pd, Rh, Ir, Au	200	170	150	280	—	990	—	—

*From 1–2 mg/ml metal solution in 2*M* hydrochloric acid at 20°.

Table 3. Conditions for noble-metal concentration with POLYORGS sorbents

Sorbent	Acidity	Duration of sorption, *hr*	Temperature, °C	Method of concentration
POLYORGS IV	1–3*M* HCl, 0.5–1*M* HNO_3	2.0	20, 100	batch
POLYORGS V	1–3*M* HCl 0.5–1*M* HNO_3	2.0	100	batch
POLYORGS VI	1–3*M* HCl, H_2SO_4 0.5–1*M* HNO_3	1.0	20, 100	batch
POLYORGS VII	0.1–6*M* HCl 0.5–3*M* HNO_3	1.0–2.0	20, 100	batch, column
POLYORGS X	1–3*M* HCl 0.5–1*M* HNO_3	1.0	20	batch, column
POLYORGS XI	pH 7–3*M* HCl	1.0–2.0	20	batch, column

Table 4. Noble-metal sorption in the presence of non-noble metals (concentration of metals, *μg/ml*: Pt 0.024; Pd 0.072; Rh, Ir, Ru and Au 0.016)

Macrocomponent		Sorption, %														
		POLYORGS IV				POLYORGS V					POLYORGS VI					
Metal	Concentration, *g/l.*	Pt	Pd	Rh	Ir	Pt	Pd	Rh	Ir	Ru	Pt	Pd	Rh	Ir	Ru	Au
Cu(II)	10	100	100	100	100	100	100	100	100	100	96	94	95	98	95	100
	25	100	100	92	100	100	100	100	99	100	90	84	84	95	85	99
	50	100	100	80	100	98	100	98	98	95	81	66	68	89	69	98
	90	97	94	68	94	—	93	84	97	96	—	—	—	—	—	—
Ni(II) or Co(II)	10	100	100	—	—	100	100	100	100	100	100	100	100	100	100	100
	25	100	100	100	100	100	100	100	100	100	98	95	90	100	100	100
	50	100	100	100	100	100	100	100	100	100	93	87	73	100	100	100
	100	100	100	100	98	100	97	100	100	100	—	—	—	—	—	—
	150	100	—	—	—	100	85	100	100	100	—	—	—	—	—	—
Fe(III)	10	72	84	—	84	100	100	98	100	95	100	100	100	98	100	98
	25	58	68	—	64	80	100	97	100	—	95	88	88	98	99	93
	50	37	50	—	40	—	99	100	95	95	—	—	—	—	—	—
	100	—	—	—	—	40	99	100	95	95	—	—	—	—	—	—
	200	—	—	—	—	40	99	100	83	85	—	—	—	—	—	—

dues are each dissolved in 100 ml of 2*M* hydrochloric acid, then 0.1 g of sorbent is added and the mixtures are boiled for 2 hr. After the sorption, 0.075 g of spectral-grade graphite (grain size 0.126 mm) is added and filtration and ashing are performed for Os and Ru determination. The standards are then used for the spectrographic calibration. The analytical-line wavelengths used (nm) are Pt 265.84; Pd 306.53, 302.79; Rh 339.68, 343.49; Ir 266.48, 322.98; Ru 342.83; Au 267.59; Os 305.86, 301.80.

Determination of platinum and palladium in industrial products

A 1-g sample is heated with 20 ml of concentrated nitric acid at 50–60° until reaction ceases, then 60 ml of concentrated hydrochloric acid are added and the mixture is heated at 50–60° for 2–3 hr until dissolution is complete. The solution is evaporated to dryness. The residue is thrice treated by addition of 6*M* hydrochloric acid and evaporation. The resulting residue is dissolved in 30 ml of 1.5*M* hydrochloric acid, the solution is filtered through a paper filter, and the filter is washed with warm 1.5*M* hydrochloric acid. The filtrate is cooled, then diluted to 100 ml with 1.5*M* hydrochloric acid, 6 g of sorbent are added and the mixture is stirred magnetically for 3 hr. The sorbent is then filtered off on filter paper and washed with 1.5*M* hydrochloric acid and hot water.

For X-ray fluorescence determination of Pt and Pd the sorbent is dried together with the filter at ~100°, transferred into a porcelain crucible and thoroughly mixed with 6 g of ammonium molybdate. The crucible is then heated in a muffle furnace at 500° for 3 hr. The crucible is cooled, 2 g of sodium tetraborate are added and the mixture is heated for 3 min, transferred into a mould and pressed under a pressure of 2 tons/cm^2. Then Pt and Pd are determined by X-ray fluorescence.[46]

POLYORGS V

Determination of palladium and iridium in ferrous material

The sample is dissolved in *aqua regia*. The solution, containing not more then 100 g of iron(III) per litre, is evaporated almost to dryness then treated twice by addition of 5 ml of concentrated hydrochloric acid and evaporation almost to dryness. The residue is dissolved in 100 ml of 2*M* hydrochloric acid and boiled gently for 2 hr together with 0.10 g of sorbent, evaporation being avoided.

For spectral determination 0.075 g of spectral graphite is added to the solution, then the sorbent and graphite are filtered off, and washed with 2*M* hydrochloric acid and water. The filter and its contents are put into a crucible, dried on a hot-plate together with 0.4 ml of 0.3% sodium sulphate solution and ashed in a muffle at 500° for 20 min. Pd and Ir are determined in the residue by atomic-emission spectrometry.[36,47]

Table 5. Application of chelate-forming POLYORGS sorbents for the analysis of various products

Sorbent	Metals determined	Sample and noble metal content, g/t		Method of determination	References
POLYORGS IV	Pd, Pt, Ir	Rocks	10^{-3}–1.4	Kinetic method	38
	Pt, Pd, Rh, Ir, Ru	Solutions, ores and other products	down to 10^{-3} 0.04–100	Emission spectrometry Atomic-absorption spectrometry	39–42 43
	Ir	Solutions	0.02–20	Kinetic method, spectrophotometry	44
	Pt, Pd, Rh, Ir	Ores	0.02–10	Atomic-absorption spectrometry	45
	Pt, Pd	Industrial products	3×10^5	X-Ray fluorescence spectrometry	46
POLYORGS V	Pt, Pd, Rh, Ir, Ru, Au	Ores	4×10^{-4}–100	Emission spectrometry, atomic-absorption spectrometry	36
	Pd, Ir	Ferrous products	0.04–15	Emission spectrometry	47
POLYORGS VI	Pt, Pd, Rh, Ir, Ru, Au	Ores and other products	2×10^{-3}–15	Emission spectrometry	42, 48
		Solutions	down to 10^{-3}	Atomic-absorption spectrometry	48, 50
		Copper products	0.6–100		
	Rh	Ores and other products	$5–50 \times 10^{-3}$	Polarography	51
POLYORGS VII	Pt, Pd, Rh, Ir	Industrial products	0.1–3	Emission spectrometry	—
POLYORGS X	Pt, Pd, Rh, Ir, Ru, Au	Ores	4×10^{-4}–100	Emission spectrometry	—
POLYORGS XI	Pt, Pd, Rh	Industrial products	up to 9×10^5	X-Ray fluorescence spectrometry	—

The content of noble metals in solutions is given in g/l.

Table 6. Flux composition for nickel sulphide collection of platinum metals

Component	Sandstone*	Talc, chlorite, serpentine, carbonate rocks with sulphide inclusion†	Talc, chlorite, serpentine, carbonate rocks of breccia type with sulphide admixture†	Peridotite†
Sodium carbonate, *g*	120	70	70	80
Borax, *g*	60	35	35	30
Glass, *g*	30	35	35	60
Nickel oxide, *g*	20	15	15	20–25
Sulphur, *g*	7	0–6	0–6	0

*100-g sample.
†50-g sample.

Table 7. Conditions for atomic-absorption determination of noble metals in sorbent suspension

Element	Wavelength, *nm*	Ashing temperature* (stage II), °C	Atomization	
			Temperature, °C	Time, *sec*
Pd	247.6	1200	2400	7
Pt	265.9	1400	2600	9
Rh	343.5	1400	2600	9
Ir	264.0	1600	2700	10

*Drying at 100°C for 50 sec; ashing (stage I), heating at 400°C for 30 sec; ashing (stage II), heating for 40 sec at temperature stated.

POLYORGS VI

Determination of noble metals in ores and other products

A 3-g sample is dissolved in 50–70 ml of *aqua regia*. The solution is evaporated almost to dryness, then 100–150 ml of hot water are added and the solution is heated for 30 min on a boiling water-bath, then filtered, and the filtrate is reserved. The residue is dried together with the filter and ashed at 500°, and the product is treated with 10–15 ml of *aqua regia*, then 3–5 ml of concentrated hydrofluoric acid are added and the solution is evaporated almost to dryness. The residue is dissolved in 10 ml of *aqua regia*, the solution is added to the reserved filtrate and the mixture is diluted to volume in a 100-ml standard flask with 6*M* hydrochloric acid.

An aliquot of this solution is evaporated, then 2–5 ml of concentrated hydrochloric acid are added and the acids are evaporated. The residue is dissolved in 50–150 ml of 2*M* hydrochloric acid and 0.2–0.3 g of sorbent is added, and the mixture is boiled for 1 hr. The sorbent is then filtered off, washed with 2*M* hydrochloric acid and ashed. The noble metals are determined in the residue by atomic-emission or atomic-absorption spectrometry.[49]

Determination of noble metals in sulphate solutions

A 200-ml portion of the solution, containing micro-amounts of noble metals, is placed in a 300-ml beaker. Then 40 ml of concentrated hydrochloric acid are added and the beaker is placed in an autoclave together with 80 ml of water. The autoclave is tightly closed and heated in an oven for 30–60 min at 190 ± 10°. The autoclave is then cooled. The solution is transferred into a 400-ml beaker, and diluted to 250 ml with 2*M* hydrochloric acid, 0.3–0.4 g of sorbent is added and the mixture is boiled for 1 hr. The sorbent is filtered off and ashed, and the noble metals are determined in the residue by, for example, atomic-emission spectrometry.[37,50]

Determination of noble metals in formate solutions

An aliquot of solution, containing 2–5 μg of noble metals and up to 10 g/l. of copper, iron(III), nickel and other elements, is placed in a porcelain crucible and evaporated almost to dryness. The crucible is put in a muffle and the temperature gradually increased to 450°, and kept at that for 30 min. The crucible is cooled, and the residue dissolved in 5–10 ml of *aqua regia*, with heating for 20 min. The solution is transferred into a 200-ml beaker. evaporated almost to dryness, and again evaporated after addition of 2–5 ml of concentrated hydrochloric acid. The treatment with hydrochloric acid is repeated. The salts are dissolved in 50–100 ml of 2*M* hydrochloric acid, 0.2–0.3 g of the sorbent is added and the mixture is kept boiling for 1 hr. The sorbent is filtered off, washed and ashed, and the noble metals are determined in the residue by, for example, atomic-emission spectrometry.[37,50]

Determination of rhodium in ores and other products with separation from platinum and palladium

A 5–10 g sample is thoroughly mixed with a ground mixture of 10–12 g of lead oxide, 15 g of sodium carbonate, 4 g of borax, 1–2 g of glass and 0.5–1 g of reductant (*e.g.*, flour). The mixture is covered with sodium carbonate and borax in a chamotte crucible, and fused in an electric muffle at 1150° for 60 min. The alloy is cleared from slag and cupelled at 900–1000° for 30–40 min. A lead bead weighing 0.1–0.2 g is obtained and is dissolved in 40 ml of nitric acid (1 + 1) with heating for 30–40 min. The solution is evaporated to 10 ml, then 20 ml of concentrated hydrochloric acid are added and the solution is evaporated almost to dryness. The residue is twice treated by addition of 5 ml of concentrated hydrochloric acid and evaporation. Then 200 ml of 1*M* hydrochloric acid and 0.1–0.3 g of the sorbent are added and the mixture is stirred for 30 min at 20–25° (for separation of Pt and Pd). The sorbent is filtered off on filter paper and washed with 20 ml of 1*M* hydrochloric acid. Then another 0.2 g of the sorbent is added to the filtrate and the mixture boiled for 2 hr, strong evaporation being avoided. The solution is decanted, then 100 ml of hot 1*M* hydrochloric acid are added to the sorbent and the mixture is boiled for 2–3 min. The sorbent is filtered off, and washed with 200 ml of hot 1*M* hydrochloric acid. The filter and sorbent are put in a crucible, and dried and carbonized on a hot-plate. The crucible is then heated in a muffle at 700° for 30 min.

For polarographic determination of Rh the residue is alloyed, the product is dissolved, sodium chloride and thiosemicarbazide are added, and Rh is determined by polarography at 0.9 V.[51]

REFERENCES

1. G. V. Myasoedova and G. I. Malofeeva, *Zh. Analit. Khim.*, 1979, **34**, 1624.
2. G. V. Myasoedova and S. B. Savvin, *Khelatoobrazuyushchie sorbenti*, Nauka, Moscow, 1984.
3. Yu. A. Zolotov, O. M. Petrukhin, G. I. Malofeeva, E. V. Marcheva, O. A. Shiryaeva, V. A. Shestakov,
4. G. V. Myasoedova and S. B. Savvin, *Zh. Analit. Khim.*, 1982, **37**, 499.
5. Yu. M. Dedkov, O. P. Eliseeva, A. N. Ermakov, S. B. Savvin and M. G. Slotinteva, *ibid.*, 1972, **27**, 726.
6. G. V. Myasoedova, O. P. Shvoeva, L. I. Bol'shakova, M. A. Tsirul, Yu. A. Bankovskii and S. B. Savvin, in *Organicheskie reagenti v analiticheskoe khimii*, Tes. Dokl. Kiev, Naukova Dumka, 1975, **1**, 116.
7. S. B. Savvin, I. I. Antokol'skaya, G. V. Myasoedova, L. I. Bol'shakova and O. P. Shvoeva, *J. Chromatog.*, 1974, **102**, 287.
8. N. N. Basargin, Y. G. Rozovskii, V. M. Zharova, V. A. Volchenkova, A. I. Mikhaelyan, V. V. Gorshkov and Zh. Oyuum, in *Organicheskie reagenty i khelatnie sorbenti v analize mineralnikh ob'ektov*, p. 82. Nauka, Moscow, 1980.
9. G. V. Myasoedova, I. I. Antokol'skaya, L. I. Bol'shakova, O. P. Shvoeva and S. B. Savvin, *Zh. Analit. Khim.*, 1974, **29**, 2104.
10. V. A. Orobinskaya, N. E. Chulkova, R. M. Nazarenko, G. A. Dmitrieva, V. P. Ivanova, I. G. Shepet'ko, Z. A. Rogovin and M. O. Lishevskaya, in *Analiz i tekhnologiya blagorodnikh metallov*, p. 90. Metallurgiya, Moscow, 1971.
11. F. I. Danilova, V. A. Orobinskaya, V. S. Parfenova, R. F. Propistsova and S. B. Savvin, *Zh. Analit. Khim.*, 1974, **29**, 2150.
12. F. I. Danilova, V. A. Orobinskaya, V. S. Parfenova, R. M. Nazarenko, V. G. Khitrov and G. E. Belousov, *ibid.*, 1974, **29**, 2142.
13. S. A. Simanova, L. S. Bobritskaya, Yu. N. Kukushkin and I. Ya. Kalontarov, *Zh. Prikl. Khim.*, 1981, **54**, 514.
14. S. A. Simanova, Yu. N. Kukushkin, I. Ya. Kalontarov, V. N. Maksimova and L. G. Mel'gunova, *ibid.*, 1977, **50**, 519.
15. S. A. Simanova, L. S. Bobritskaya, Yu. N. Kukushkin, I. Ya. Kalontarov, R. M. Marupov and Ya. Asrarov, *ibid.*, 1981, **54**, 764.
16. G. Koster and G. Schmuckler, *Anal. Chim. Acta*, 1967, **38**, 179.
17. R. A. Nadkarni and G. H. Morrison, *Anal. Chem.*, 1974, **46**, 232.
18. A. Warshawsky and S. Ehrlich-Rogozinski, *Microchem. J.*, 1977, **22**, 362.
19. R. A. Nadkarni and G. H. Morrison, *J. Radioanal. Chem.*, 1977, **38**, 435.
20. *Idem*, *Anal. Chem.*, 1978, **50**, 294.
21. A. Warshawsky, M. M. B. Fieberg, P. Mihalik, T. G. Murphy and Y. B. Ras, *Sepn. Purif. Methods*, 1980, **9**, 209.

22. M. Grote and A. Kettrup, *Z. Anal. Chem.*, 1979, **295,** 366.
23. *Idem, ibid.*, 1980, **300,** 280.
24. *Idem, ibid.*, 1982, **310,** 369.
25. V. Sýkora and F. Dubský, *Collection Czech. Chem. Commun.*, 1972, **37,** 33, 1504.
26. A. Gulko, H. Feigenbaum and G. Schmuckler, *Anal. Chim. Acta*, 1972, **59,** 397.
27. Yu. N. Kukushkin, J. Kálal, M. I. Benes, J. Štamberg, F. Švec, E. Kalalova, S. A. Simanova and L. G. Mel'gunova, *Izv. Vussh. Uchebn. Zaved. Khim. i Khim. Tekhnol.*, 1977, **20,** 513.
28. E. Kalalová, V. Beiglova, J. Kálal and F. Švec, *Angew. Makromol. Chem.*, 1978, **72,** 143.
29. F. Švec, J. Kálal, E. Kalalová and L. Jandová, *23rd Microsympos. Select. Polym. Sorbents, Prague*, 1982, M26.
30. M. Griesbach and K. H. Lieser, *Z. Anal. Chem.*, 1980, **302,** 109, 181, 184.
31. F. Vernon and Wan Md Zin, *Anal. Chim. Acta*, 1981, **123,** 309.
32. I. I. Antokol'skaya, G. V. Myasoedova, L. I. Bol'shakova, M. G. Ezernitskaya, M. P. Volynets, A. V. Karyakin and S. B. Savvin, *Zh. Analit. Khim.*, 1976, **31,** 742.
33. G. V. Myasoedova, I. I. Antokol'skaya, O. P. Shvoeva, L. I. Bol'shakova and S. B. Savvin, *Talanta*, 1977, **23,** 866.
34. O. P. Shvoeva, G. V. Myasoedova and S. B. Savvin, *Zh. Analit. Khim.*, 1976, **31,** 2158.
35. G. V. Myasoedva, I. I. Antokol'skaya and S. B. Savvin, *23rd Microsympos. Select. Polym. Sorbents, Prague*, 1982, M51.
36. G. V. Myasoedova, I. I. Antokol'skaya, L. I. Bol'shakova, F. I. Danilova, I. A. Fedotova, E. B. Varshal, E. E. Rakovskii and S. B. Savvin, *Zh. Analit. Khim.*, 1982, **37,** 1837.
37. G. V. Myasoedova, I. I. Antokol'skaya, L. V. Emets, E. Ya. Danilova, E. A. Naumenko, F. I. Danilova, I. A. Fedotova, V. I. Seraya, R. Ya. Mushii, L. A. Volf and S. B. Savvin, *ibid.*, 1982, **37,** 1574.
38. I. Yu. Davydova, A. P. Kuznetsov, I. I. Antokol'skaya, N. N. Nikol'skaya and Z. A. Ezhkova, *ibid.*, 1979, **34,** 1145.
39. F. I. Danilova, I. A. Fedotova, I. A. Rozdukhova, G. V. Myasoedova and I. I. Antokol'skaya, *ibid.*, 1978, **33,** 2191.
40. L. I. Pavlenko, I. A. Popova, E. V. Marcheva, G. V. Myasoedova and G. I. Malofeeva, *ibid.*, 1980, **35,** 717.
41. F. I. Danilova, I. A. Fedotova and R. M. Nazarenko, *Zavodsk. Lab.*, 1983, **48,** 9.
42. F. I. Danilova, I. A. Fedotova, G. V. Myasoedova, I. I. Antokol'skaya, S. B. Savvin, R. M. Nazarenko, E. Ya. Danilova, L. V. Emets and E. A. Naumenko, in *Metody vydeleniya i opredeleniya blagorodnikh elementov*, p. 77. GEOCHI AN SSSR, 1981.
43. A. N. Savel'eva and N. P. Khairulina, *Zh. Analit. Khim.*, 1974, **33,** 1380.
44. I. V. Kubrakova, I. I. Antokol'skaya, G. M. Varshal and G. V. Myasoedova, in *Metody vydeleniya i opredeleniya blagorodnikh elementov*, p. 14. GEOCHI AN SSSR, 1981.
45. I. V. Kubrakova, G. M. Varshal, E. M. Sedykh, G. V. Myasoedova, I. I Antokol'skaya and T. P. Shemarykina, *Zh. Analit. Khim.*, 1983, **38,** 2205.
46. G. A. Dmitrieva, S. V. Kubarev, D. B. Grinblat, G. A. Moiseeva, I. I. Antokol'skaya, F. I. Danilova and G. V. Myasoedova, in *Metody vydeleniya i opredeleniya, blagorodnikh elementov*, p. 51. GEOCHI AN SSSR, 1981.
47. F. I. Danilova, G. V. Myasoedova, I. A. Fedotova, I. I. Antokol'skaya, L. I. Bolshakova and S. B. Savvin, *ibid.*, p. 80.
48. G. V. Myasoedova, I. I. Antokol'skaya, F. I. Danilova, I. A. Fedotova, V. P. Grińkov, N. V. Ustinova, E. A. Naumenko, E. Ya. Danilova and S. B. Savvin, *Zh. Analit. Khim.*, 1982, **37,** 1578.
49. F. I. Danilova, I. A. Fedotova, N. V. Ustinova, G. V. Myasoedova, I. I. Antokol'skaya, S. B. Savvin, I. I. Tarasova, A. P. Kuznetsov, S. P. Nosova, E. Ya. Danilova, E. A. Naumenko, L. V. Emets, in *Metody vydeleniya i opredeleniya blagorodnikh elementov*, p. 67. GEOCHI AN SSSR, 1981.
50. F. I. Danilova, V. P. Grin'kov, I. A. Fedotova, N. V. Ustinova, G. V. Myasoedova, I. I. Antokol'skaya, S. B. Savvin, L. V. Emets, E. Ya. Danilova and E. A. Naumenko, *ibid.*, p. 73.
51. L. N. Vasil'eva, Z. L. Yustus, G. V. Myasoedova, I. I. Antokol'skaya and N. A. Ezerskaya, *ibid.*, p. 33

Talanta, Vol. 32, No. 12, pp 1113–1117, 1985
Printed in Great Britain

0039-9140/85 $3.00 + 0.00
Pergamon Press Ltd

GLYCOPYRRONIUM-SELECTIVE ELECTRODES

SHOU-ZHOU YAO* and GIANG-HUA LIU
New Material Research Institute, Department of Chemical Engineering, Hunan University, Changsha, People's Republic of China

(*Received* 18 *September* 1984. *Accepted* 12 *August* 1985)

Summary—Liquid-membrane and PVC-membrane glycopyrronium-selective electrodes have been developed. They are based on the ion-pair complexes of glycopyrronium with dicyclohexylnaphthalenesulphonate, di-isopentylnaphthalenesulphonate, di-isobutylnaphthalenesulphonate and tetraphenylborate. Their response is nearly Nernstian over the pH-range 4–8, and the detection limits range from $10^{-6}M$ to $10^{-5}M$. For the liquid-membrane electrodes, with homologous membrane solvents, the response slopes are linearly related to the inverse of the dielectric constant of the membrane solvent, according to the formula $S = C_0 - C_1/\varepsilon$. A similar relation exists between the slopes for both types of electrode and the dielectric constants of mixed-solvent backgrounds. The electrodes can be used in the potentiometric determination of glycopyrrolate.

Glycopyrronium bromide, 3-(cyclopentylhydroxyphenylacetyl)oxy-1,1-dimethylpyrrolidinium bromide, or glycopyrrolate, is a quaternary ammonium anticholinergic drug that causes side-effects, and is used in the treatment of gastric and duodenal ulcers, to relieve spasm of the lower gastrointestinal tract and as a pre-anaesthetic drying agent. The U.S. Pharmacopeia[1] recommends determination of this substance by non-aqueous titration and extractive spectrophotometry, but these methods suffer from lack of specificity and sensitivity, and are rather inaccurate.

The development of ion-selective electrodes for drugs, based on ion-pair systems, in this laboratory[2–6] and others,[7,8] has resulted in a wide variety of simple and economical analyses. Martin and Freiser[9] have suggested dinonylnapthalenesulphonates as electroactive materials for coated-wire ion-selective electrodes, and these seem promising for the determination of drugs.

Many authors have studied the effects of various parameters on electrode selectivity and detection limits[10–12] but there has been little work on the relationship between electrode slopes and the dielectric constant of the membrane solvent.

This paper describes the preparation and properties of ion-selective electrodes based on the ion-pair complexes of the glycopyrronium ion with dicyclohexylnaphthalenesulphonate (GDCHNS), di-isopentylnaphthalenesulphonate (GDPNS), di-isobutylnaphthalenesulphonate (GDBNS), and tetraphenylborate (GTPB).

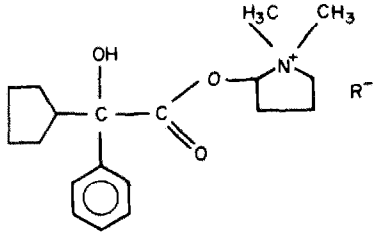

GDCHNS: $R^- = (C_6H_{11})_2C_{10}H_5SO_3^-$
GDPNS: $R^- = (C_5H_{11})_2C_{10}H_5SO_3^-$
GDBNS: $R^- = (C_4H_9)_2C_{10}H_5SO_3^-$
GTPB: $R^- = (C_6H_5)_4B^-$.

EXPERIMENTAL

Apparatus

Potentiometric measurements were made with a model UJ-24 precision d.c. potentiometer (Shanghai Electronic Instrument) and a model PHS-2 precision pH-meter (Shanghai Analytical Instrument) connected in series to indicate potential compensation, the glycopyrronium-selective electrode, and an SCE connected to the sample solution by a $1M$ sodium nitrate bridge. The pH measurements were made with a glass electrode and an SCE. All measurements were done in stirred solutions.

Dielectric constant measurements for membrane solvents were made with a model CC-6 capacitance-meter (Changzhou Electronic Instrument) at constant temperature (25°).

Infrared spectra were recorded on a Carl Zeiss Specord IR-75 spectrophotometer (KBr pellets).

The study of the membrane solvent effect was done at constant temperature (25°) and under constant measuring conditions. The same electrode barrel and porous membrane were used. The whole electrode assembly was washed thoroughly with acetone and ethanol and dried, before every new organic phase was tested.

The background effect was studied at a lower constant temperature (20°) so as to reduce the possible evaporation of organic solvents such as methanol.

Reagents

All chemical reagents used were of analytical-reagent or chemically pure grade. Doubly distilled water was used throughout. Solutions (10^{-7}–$10^{-1}M$) of glycopyrronium bromide were prepared by serial dilution. The purity of the glycopyrronium bromide was >99.0%. Sodium tetraphenylborate solution, $0.01M$ was prepared and standardized by potentiometric titration with standard $0.01M$ silver nitrate, with use of a silver/silver sulphide electrode in conjunction with a double-junction SCE.

*Author for correspondence.

Synthesis of sodium sulphonates

To make the dicyclohexylnaphthalenesulphonate mix together 71 ml of cyclohexanol and 42 g of naphthalene, add dropwise 89 g of concentrated sulphuric acid at 20–25° over 30 min, add dropwise 158 g of 24% fuming sulphuric acid at a temperature below 25° over 1 hr, and continue stirring the mixture for 1 hr. Warm to 50° over 1.5 hr, continue the reaction at 50–55° for 5 hr, then at 55° for 2 hr. Allow the mixture to stand for 8 hr. Discard the lower layer, then wash the upper layer three times with water, add 250 ml of water heated to 35–40°, mix and neutralize to pH 8–10 with 20% sodium hydroxide solution. Heat to boiling, filter, and evaporate the filtrate to precipitate the sulphonate. Recrystallize the crude product from water four times. Recrystallize twice from 1:4 v/v cyclohexanol–ethanol mixture, then recrystallize twice more from water. Dry the crystals at 105°. Elemental analysis gave S 8.14%, C 66.8% (theoretical values: S 8.13%, C 67.0%). The melting point was 197.5–200°, and the infrared spectrum had bands at (cm^{-1}) 2920, 2845; 1440 (CH_2 stretching; deformation), 1240–1140, 1070–1040 (S=O stretching), 1630–1580, 1500 (naphthalene ring C=C stretching), 3050 (naphthalene CH stretching).

Sodium di-isopentylnaphthalenesulphonate and sodium di-isobutylnaphthalenesulphonate can be synthesized in a similar manner, starting from 3-methylbutan-1-ol and 2-methylpropan-1-ol respectively, the reaction being done at lower temperature (40–45°) and ethanol used for recrystallization instead of cyclohexanol–ethanol. The infrared bands (in cm^{-1}) of sodium di-isopentylnaphthalenesulphonate were at 2940, 2850; 1450 (CH_3 stretching; deformation), 1389, 1368 (isopropyl stretching), 2910, 2850; 1450, 740 (CH_2 stretching; deformation), 1250–1140, 1070–1030 (S=O stretching), 1670–1580, 1495 (naphthalene ring C=C stretching), 3030 (naphthalene CH stretching).

Preparation of the ion-pair complexes

GDCHHS was prepared by mixing 40 ml of 0.01*M* glycopyrronium bromide and 50 ml of 0.01*M* sodium dicyclohexylnaphthalenesulphonate, and leaving the mixture overnight. The precipitate was filtered off on a porosity-4 sintered-glass crucible, washed several times with distilled water and dried at 80°. Glycopyrronium di-isopentylnaphthalenesulphonate, glycopyrronium di-isobutylnaphthalenesulphonate and glycopyrronium tetraphenylborate were prepared similarly.

Preparation of the liquid-membrane electrode

The poly(vinylidene fluoride) microporous membrane was prepared essentially as before.[4,5] One part of poly(vinylidene fluoride) powder was dissolved, with gentle heating, in 18 parts of dimethylformamide and 1 part of dibutyl phthalate. The dimethylformamide was evaporated at 80° from the mixture placed in a flat Petri dish. The dibutyl phthalate was washed out by soaking the membrane overnight in ethanol, which was then evaporated from the membrane at 50°. The microporous membrane thus obtained was opalescent and 0.1–0.2 mm thick. A polytetrafluoroethylene electrode barrel was used as the electrode assembly, with the microporous membrane separating the liquid-membrane ion-exchanger from the sample solutions. The liquid membrane was prepared by making a 0.5m*M* solution of the ion-pair complex in each of the various organic solvents. A double-junction SCE containing a solution that was 0.01*M* in both potassium chloride and glycopyrrolate was used as internal reference electrode.

Preparation of the PVC membrane electrode

The PVC membrane electrode was prepared as previously.[2,3] After addition of 0.34 ml of a 1m*M* solution of ion-pair complex in dibutyl phthalate (or other ester used as plasticizer) to 3 ml of 5% solution of PVC in tetrahydrofuran–cyclohexanone mixture (2:1 v/v), the tetrahydrofuran and cyclohexanone were slowly evaporated at room temperature from the mixture placed in a flat 30-mm Petri-dish. The membrane thus obtained was glued to a PVC tube with tetrahydrofuran. A 0.01*M* potassium chloride–0.01*M* glycopyrrolate solution was placed inside the tube as the internal reference solution. An Ag/AgCl electrode was used as internal reference electrode.

RESULTS AND DISCUSSION

Electroactive material effect

PVC membrane glycopyrronium-selective electrodes with various ion-pair complexes as electroactive materials were evaluated in order to compare their function. The results obtained are shown in Table 1. The glycopyrronium dialkylnaphthalenesulphonate electrode with electroactive material of higher molecular weight has a longer linear range and a greater response slope. However, the differences between the electroactive materials tested are small compared with the solvent effects described below.

Liquid-membrane solvent effect

The response of the glycopyrronium-selective liquid-membrane sensors was measured for different liquid exchangers dissolved in several solvents, to test the effect of solvent dielectric constant on the electrode slope. The results for thirteen solvents are shown in Table 2. For organic solvents from a homologous series, the slope, S, increases with increasing dielectric constant, according to the regression equation:

$$S = C_0 - C_1/\varepsilon$$

Values of C_0 and C_1 for phthalic esters and n-alcohols are given in Table 3. Figure 1 shows the slope of S

Table 1. Characteristics of glycopyrronium-selective electrodes with various electroactive materials*

Electroactive material	Slope, *mV/log* C	Linearity range, M	Detection limit, M
GDCHNS	57.5	6.3×10^{-2}–1.3×10^{-5}	6.3×10^{-6}
GDPNS	56.0	6.3×10^{-2}–2.0×10^{-5}	8.0×10^{-6}
GDBNS	55.0	6.3×10^{-2}–4.0×10^{-5}	1.0×10^{-5}
GTPB	56.0	6.3×10^{-2}–1.6×10^{-5}	6.3×10^{-6}

*With dibutyl phthalate as plasticizer–solvent. Slope values given here and in Tables 2–5 are average values of five successive measurements with individual electrodes (standard deviations 0.5–1.0 mV/log *C*).

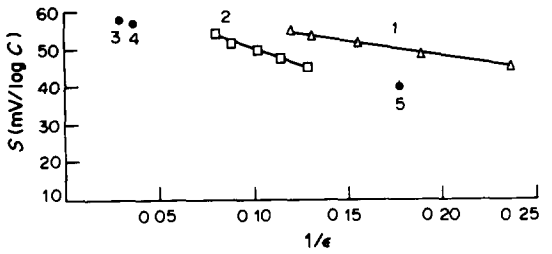

Fig. 1. Plots of S *vs.* $1/\varepsilon$ for liquid-membrane glycopyrronium dicyclohexylnaphthalenesulphonate electrodes with various membrane solvents (25°): 1, phthalic esters; 2, n-alcohols; 3, nitrobenzene; 4, *o*-nitrotoluene; 5, chlorobenzene.

vs. $1/\varepsilon$ for glycopyrronium dicylcohexylnaphthalenesulphonate electrodes.

Background effect

The responses of the liquid-membrane and the PVC-membrane glycopyrronium dicyclohexylnaphthalenesulphonate electrodes were tested for a series of background solvents with differing dielectric constants. The results are shown in Table 4. For a given mixed-solvent system, the slope increases with increasing dielectric constant and it can be related linearly to $-1/\varepsilon$. For the methanol–water and ethanol–water systems, the regression equation for the liquid membrane electrodes was $S = 76 - (1.9 \times 10^3)/\varepsilon$ and for the PVC membrane electrodes $S = 77 - (1.6 \times 10^3)/\varepsilon$.

For the propan-2-ol–water system, the regression equation for the liquid-membrane electrode was $S = 70 - (1.25 \times 10^3)/\varepsilon$.

Concentration of electroactive material

At concentrations of 5×10^{-4}–$5 \times 10^{-3} M$ of glycopyrronium dicyclohexylnaphthalenesulphonate, in dibutyl phthalate as PVC membrane plasticizer and solvent, the electrode had a Nernstian response and gave constant and stable potential readings.

Table 2. Effect of solvent and liquid exchanger on the slopes of liquid-membrane glycopyrronium-selective electrodes (25°)

Solvent	Dielectric constant	Slope, *mV/log*			
		GDCHNS	GDPNS	GDBNS	GTPB
Nitrobenzene	34.8	57.5	56	55	56
o-Nitrotoluene	26.65	57	55.5	54	55.5
Chlorobenzene	5.62	40	39	37	37.5
Dimethyl phthalate	8.32	55	54	52.5	53.5
Diethyl phthalate	7.70	53.5	53	51	52
Dibutyl phthalate	6.44	51	50	50	50.5
Di-iso-octyl phthalate	5.29	48	48	47	48
Didecyl phthalate	4.33	45	45	44	45
n-Hexanol	12.5	54	54	53.5	53
n-Heptanol	11.35	52	52.5	52.5	52
n-Octanol	9.35	50	50.5	50	50
n-Nonanol	8.79	47.5	48	47	47
n-Decanol	7.77	45	45.5	44	43

Table 3. Results of regression analysis for S *vs.* $1/\varepsilon$ relation for liquid-membrane glycopyrronium-selective electrodes

Electrode	Phthalic esters			n-Alcohols		
	C_0	C_1	R^*	C_0	C_1	R^*
GDCHNS	64.7	85.7	0.996	67.7	175.1	0.982
GDPNS	62.8	77.3	0.992	67.3	168.0	0.983
GDPNS	60.8	71.9	0.998	69.2	192.6	0.982
GTPB	63.0	79.3	0.999	69.3	197.5	0.972

Correlation coefficient.

Table 4. Effect of background solvents on response slope of glycopyrronium dicyclohexylnaphthalenesulphonate electrodes (20°)

Background, methanol, %	Slope, a/b^*	ε	Background, ethanol, %	Slope, a/b^*	ε	Background, propan-2-ol, %	Slope, a^*	ε
30	49/54	66.0	10	52/56	74.6	10	53	73.1
50	42/48	56.5	30	48/51	62.6	30	49	58.4
70	33/37	41.5	50	39/44	50.4	50	40	43.7
90	21/27	32.4	70	28/36	39.1	70	28	29.6
			90	12/22	29.0	90	10	20.9

*a and b denote the electrode response slopes for the liquid-membrane electrode (membrane solvent–nitrobenzene) and the PVC membrane electrode (plasticizer solvent–dibutyl phthalate) respectively.

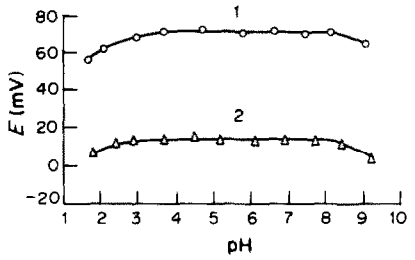

Fig. 2. Effect of pH on the potential of the PVC-membrane glycopyrronium-selective electrode: 1, $1 \times 10^{-2}M$; 2, $1 \times 10^{-3}M$.

For the liquid ion-exchanger in nitrobenzene, the slope reached a maximum at concentrations of 1×10^{-4}–$1 \times 10^{-3}M$.

Effect of pH

The effect of pH on electrode potentials was studied in glycopyrronium bromide solutions in which the pH was varied by addition of hydrochloric acid and/or sodium hydroxide solution from a 10-μl syringe. At pH values between 4 and 8 no significant effect on membrane potentials was observed (Fig. 2.). Above pH 8, formation of glycopyrronium base caused the potentials to become more negative, and at pH values below 3.5–4, the electrodes began to respond to hydrogen ions.

Influence of plasticizers on the PVC-membrane electrode function

Various plasticizers were tested, as reported in Table 5. Dibutyl phthalate as plasticizer-solvent was found to result in the best electrode function.

Selectivity

When glycopyrrolate is determined by titration in a non-aqueous medium, many other basic substances interfere with the determination, and these must be removed beforehand. The effects of some of these substances and other common compounds on the response of the glycopyrronium dicyclohexylnaphthalenesulphonate electrode were examined. The results obtained (Table 6) indicate that cinchonine, quinine, propranolol, dibazole, diphenhydramine, imidazole, berberine, tetrahydropalmatine, chlorpheniramine and tetrabutylammonium are likely to cause interferences, but no significant interferences were caused by other substances tested. The order of selectivity for inorganic cations is: $K^+ > Na^+$; $Cd^{2+} > Ba^{2+} > Ca^{2+} > Mg^{2+}$.

The selectivity coefficients are, in the main, similar for the electrodes with GDCHNS, GDPNS, GDBNS and GTPB as electroactive materials. This indicates that the electrode selectivity depends primarily on the

Table 5. Response characteristics of PVC-membrane glycopyrronium-selective electrodes with different plasticizer–solvents

Plasticizer-solvent	Slope, *mV/log* C	Linearity range, M	Detection limit, M
Dimethyl phthalate	50	6.3×10^{-2}–1.0×10^{-4}	1.0×10^{-5}
Diethyl phthalate	52	6.3×10^{-2}–3.2×10^{-5}	8.0×10^{-6}
Dibutyl phtahlate	56	6.3×10^{-2}–1.3×10^{-5}	6.3×10^{-6}
Di-iso-octyl phthalate	55	6.3×10^{-2}–1.6×10^{-5}	6.3×10^{-6}
Didecyl phthalate	53	6.3×10^{-2}–2.5×10^{-5}	8.0×10^{-6}

Table 6. Selectivity coefficients for the glycopyrronium-selective electrode*

Interferent	K_{ij}	Interferent	K_{ij}
Tetramethylammonium bromide†	1.6×10^{-2}	Propranolol§	0.20
Moroxydine§	4.8×10^{-3}	Ammonium chloride‡	1.4×10^{-4}
Potassium chloride‡	1.3×10^{-3}	Calcium chloride‡	3.4×10^{-3}
Tris(hydroxymethyl)aminomethane†	8.8×10^{-4}	Thiamine†	2.9×10^{-2}
		Theophylline†	9.2×10^{-3}
Sodium chloride‡	6.1×10^{-4}	Magnesium chloride‡	1.3×10^{-3}
Barium chloride‡	1.6×10^{-4}	Atropine†	4.2×10^{-2}
Caffeine†	7.5×10^{-4}	Quinine§	0.50
Dibazole§	2.50	Ammonium tranexamate†	6.4×10^{-4}
Dopamine§	1.5×10^{-2}	Tetraethylammonium bromide†	0.11
Procaine†	0.12	Colchicine†	1.4×10^{-3}
Triethanolamine†	1.0×10^{-3}	Sodium benzoate§	2.1×10^{-4}
Piperazine§	2.5×10^{-4}	Leucine§	1.1×10^{-3}
Diphenhydramine†	6.6	Chlorpheniramine†	3.6
Imidazole†	0.92	Cinchonine†	1.4
Tetrahydropalmatine†	1.0	Berberine†	1.9×10^{2}
Glucose (1%)†	No interference	Tetrabutylammonium bromide†	4.0
Cadmium chloride‡	2.9×10^{-4}		

*Glucopyrronium dicyclohexylnaphthalenesulphate PVC membrane electrode with dibutyl phthalate as plasticizer–solvent.
†Separate solution method ($C_i = C_j = 1mM$).
§Separate solution method ($C_i = 1mM$, $C_j = 10mM$).
‡Mixed solution method ($C_i = 10mM$).

Table 7. Determination of glycopyrrolate

Direct potentiometry			Potentiometric titration			Non-aqueous titration		
Taken, *mg*	Found, *mg*	Recovery, %	Taken, *mg*	Found, *mg*	Recovery, %	Taken, *mg*	Found, *mg*	Recovery, %
18.4	17.8	96.7	8.8	8.9	101.1	510.4	507.3	99.4
67.2	66.1	98.4	11.2	11.0	98.2	501.2	497.4	99.2
108.0	104.8	97.0	12.5	12.4	99.2	490.7	491.4	100.1
14.1	13.9	98.6	16.1	15.9	98.8	505.5	511.3	101.1
16.1	15.9	98.8	19.3	18.9	97.9	520.7	517.3	99.3
5.5	5.6	101.8	25.4	25.0	98.4	522.8	529.2	101.2
157.8	155.0	98.5	29.8	29.5	99.0			
39.0	38.8	99.5	36.2	35.8	98.9			

nature of the interfering ions rather than on the ion-pair complexes used as electro-active materials.

Determination of glycopyrrolate

Results obtained from direct potentiometric determination of glycopyrrolate are given in Table 7. The average recovery is 98.7%, and the standard deviation 1.2%. The results obtained from potentiometric titration of glycopyrrolate with sodium tetraphenylborate show an average recovery of 98.9% and a mean standard deviation of 1.0%. These results are in good agreement with results obtained by the non-aqueous method.[1]

Acknowledgement—This work was supported by the Science Fund of the Chinese Academy of Sciences.

REFERENCES

1. *US Pharmacopoeia, XX*, p. 356. American Pharmaceutical Association, Washington, D.C., 1980.
2. S. Z. Yao and Y. Q. Tong, *Acta Pharm. Sinica*, 1984, **19**, 455.
3. S. Z. Yao, G. L. Shen and S. M. Qiu, *ibid.*, 1983, **18**, 874.
4. S. Z. Yao, X. M. Xu and G. L. Shen, *ibid.*, 1983, **18**, 612.
5. S. Z. Yao, G. L. Shen and Q. L. Dei, *Kexue Tongbao*, 1983, **28**, 1312.
6. S. Z. Yao and G. L. Shen, *ibid.*, 1983, **28**, 988.
7. G. H. Fricke, *Anal. Chem.*, 1980, **52**, 259R.
8. M. E. Meyerhoff and Y. M. Fraticelli, *ibid.*, 1982, **54**, 27R.
9. C. R. Martin and H. Freiser, *ibid.*, 1980, **52**, 1772.
10. W. E. Morf, *The Principles of Ion-selective Electrodes and of Membrane Transport*. Vol. 2, Elsevier, Amsterdam, 1981.
11. R. P. Buck, *Anal. Chim. Acta*, 1974, **73**, 321.
12. J. Koryta, *ibid.*, 1977, **111**, 1; 1982, **139**, 1.

Talanta, Vol. 32, No. 12, pp. 1119–1124, 1985
Printed in Great Britain.

0039-9140/85 $3.00 + 0.00

RAPID AND SELECTIVE CHELATOMETRIC TITRATION OF ALUMINIUM IN NON-FERROUS ALLOYS

ZHOU NAN*
Shanghai Research Institute of Materials, The Ministry of Machine Building Industry, Shanghai, People's Republic of China

and

GU YUAN-XIANG, LU ZHI-REN and CHEN WEI-YONG
The Third Factory of Shanghai Reagent Chemicals, Shanghai, People's Republic of China

(*Received* 4 *April* 1984. *Revised* 30 *July* 1985. *Accepted* 8 *August* 1985)

Summary—A rapid chelatometric method for the determination of Al (4–20%) in magnesium, copper and chromium–aluminium–iron alloys is proposed. HEDTA is used as titrant and Zn solution as back-titrant, with hydrazidazol as indicator. Mn(II), Cu(II), Cd, Zn, Pb, Co(II), Ni, Hg(II), Fe(III), Bi, Cr(III), Sb(III), Ce(III), La, Sn(IV), Ti(IV), Zr and Mo(VI) do not interfere. High selectivity is achieved by a combination of group separation, masking and interference correction. The coefficient of variation varies from 0.2 to 1%.

Chelatometric titration of aluminium has attracted much attention but many cations interfere, so the general practice is to titrate with EDTA all the metals present that can be complexed at the pH used, then add fluoride to decompose the Al–EDTA chelate, and titrate the liberated EDTA, as suggested by Sajó.[1] Even this method is selective only in the absence of Mn(II),[2] Bi, and cations forming EDTA complexes which can be decomposed by fluoride.[3] The selectivity may be improved by a suitable choice of titrant and masking conditions.

In this paper, HEDTA, *N*-(2-hydroxyethyl)-ethylenediamine-*N*,*N*′,*N*′-triacetic acid is proposed as the titrant and hydrazidazol[4] as the indicator, for determination of Al(III), free from interferences caused by Mn(II), Cu(II), Pb(II), Zn, Cd, Ni, Co(II), Hg(II), Bi, Fe(III), Cr(III), Ce(III), La, Sb(III), Sn(IV), Ti(IV), Zr and Mo(VI). It has been successfully applied to the determination of Al (4–20%) in different kinds of non-ferrous alloys, especially those containing Mn, La, Ce, Zr and Mo.

EXPERIMENTAL

Reagents

Analytical-reagent grade chemicals were used unless otherwise specified.

Ascorbic acid solution, 5%. Freshly prepared before use.
1,10-Phenanthroline solution in ethanol, 0.1%.
Monochloroacetic acid solution, 8%.
Naphthyl Red solution in ethanol, 0.05%.
Hydrazidazol solution in acetone, 0.05%.
Sulphosalicylic acid solution, 40%.
Metanil Yellow solution, 0.1%.
Cresol Red solution in 50% aqueous ethanol, 0.1%.
Hexamine solutions, 30% and 15%. Freshly prepared before use.
Sodium diethyldithiocarbamate solutions. Freshly prepared and filtered before use. Solution A, 20 g of sodium diethyldithiocarbamate dissolved in water, filtered and diluted to 150 ml; solution B, 15%, similarly prepared.
*Disodium hydrogen phosphate solution, 0.005*M.
Wash solution. To 100 ml of water add 5 or 6 drops of 8% monochloroacetic acid solution and mix.
Aluminium standard solution. Transfer 1.000 g of aluminium (purity ≧ 99.9%) into a 400-ml Teflon beaker and add 10 ml of 20% sodium hydroxide solution in portions. When the violent reaction has subsided, warm till dissolution is complete. Dilute with 60 ml of water. Pour the solution into a 600-ml beaker containing 250 ml of concentrated hydrochloric acid, while stirring with a Teflon rod, and rinse in with 10 ml of concentrated hydrochloric acid. Transfer the solution quantitatively to a 1-litre standard flask, dilute to volume and mix (1 ml of this solution contains 1.000 mg of aluminium).
*Zn standard solution, 0.02*M. Prepared as described earlier.[4]
HEDTA standard solution. Prepared and compared with the zinc solution as previously reported.[4] Calculate the conversion factor f for the zinc and HEDTA solutions from $f = A/B$, where A ml of HEDTA solution react with B ml of zinc solution. Standardize the HEDTA solution as follows. Pipette 10.00 ml of standard aluminium solution into a 400-ml Teflon beaker. Add 10 ml of water and adjust to pH 1 by dropwise addition of saturated sodium bicarbonate solution. Add 5 ml of ascorbic acid solution and 2 drops of 1,10-phenanthroline solution and (from a burette) 30 ml of HEDTA solution and stir thoroughly with a Teflon rod. Add 10 ml of ethylene glycol, 1 drop of Naphthyl Red solution, and saturated sodium bicarbonate solution dropwise till the red colour disappears. Add 10 ml of 30% hexamine solution, 2 or 3 drops of hydrazidazol solution, and standard zinc solution dropwise from a burette till a distinct blue colour appears. Then titrate with HEDTA to an abrupt colour change to bright red. Complete the standardization by adding 4 ml of hexamine solution and titrating again with HEDTA, and repeating this step until there is no further colour change. Then 1 ml of HEDTA is

*To whom correspondence and requests of reprints should be sent. Present address: 999 Dong Chang Zhi Lu, Shanghai, People's Republic of China.

equivalent to t mg of aluminium: $t = M(V_1 - fV_2)$, where M = mg of Al taken, V_1 = total volume of HEDTA solution used (ml) and V_2 = volume of zinc solution used (ml), and f = the conversion factor as defined above.

Procedures

Determination of Al in magnesium alloys. Transfer a 0.2-g sample into a 250-ml beaker. Add 10 ml of hydrochloric acid (1 + 1) in small portions. When the violent reaction has subsided add a few drops of hydrogen peroxide. Warm till dissolution is complete, then boil gently to destroy excess of hydrogen peroxide. Add 5 ml of 70% perchloric acid and evaporate till dense white fumes appear. Cool to room temperature. Add 50 ml of water, 2 drops of Metanil Yellow solution and saturated sodium bicarbonate solution dropwise till the red colour disappears. Then add 3.0 ml of hydrochloric acid (1 + 1), 10 ml of monochloroacetic acid solution and 20 ml of freshly made sodium diethyldithiocarbamate solution B with vigorous stirring. Let stand for a few minutes, then filter off the precipitate on a filter paper of fine porosity. Wash 3 or 4 times with wash solution, collecting the filtrate and washings in a 500-ml beaker. Acidify the solution to pH 1 with hydrochloric acid (1 + 1). Evaporate the solution to 35 ml, cool to room temperature, transfer to a 50-ml standard flask, dilute to volume and mix. Pipette 20 ml of this solution into a 400-ml Teflon beaker and titrate it by the procedure for standardization of the HEDTA solution with aluminium, starting at the addition of solution, and adding 30 ml of ethanol after the ethylene glycol; after adding the hydrazidazol solution and then zinc solution till a blue colour appears, add 3 ml of zinc solution in excess and 2 ml of disodium hydrogen phosphate solution, and stir vigorously for 30 sec. Add another 2 drops of hydrazidazol solution and complete the titration as described in the standardization procedure. Record the total volumes of HEDTA and zinc solutions used (ml) as V_3 and V_4 respectively.

Transfer a second 20-ml portion of the test solution into another 400-ml Teflon beaker. Stirring with a Teflon rod after each addition, add 5 ml of ascorbic acid solution, 2 drops of 1,10-phenanthroline solution, 2.0 ml of HEDTA solution (from a burette) and saturated sodium bicarbonate solution to adjust the pH to 1–2. After 5 min add 5.0 ml of standard zinc solution from another burette, 5 ml of sulphosalicylic acid solution, 25 ml of water, 30 ml of ethanol, 2 or 3 drops of hydrazidazol solution and sodium bicarbonate solution until a purple colour appears. Then add 4 ml of 15% hexamine solution and 2 ml of disodium hydrogen phosphate solution, and stir vigorously for 30 sec. Add 2 drops of hydrazidazol solution, titrate with HEDTA, then add 2 ml of hexamine solution and titrate again, repeating this step until the colour of the indicator remains unchanged on addition of hexamine. Record the total volumes of HEDTA and zinc solutions used (ml), as V_5 and V_6 respectively. Calculate the percentage of Al from

$$\%\text{Al} = 250t\,[(V_3 - fV_4) - (V_5 - fV_6)]/G$$

where G = the sample weight (mg) in the aliquot taken for titration and t = the Al titre (mg/ml) of the HEDTA standard solution.

Note. This procedure may be simplified in the following case. For samples containing neither Ce nor La omit the addition of disodium hydrogen phosphate in both titrations. For samples containing no Zr omit the second titration, since $V = fV_6$, and calculate the percentage of Al from the simplified equation in the next section.

Determination of Al in copper alloys. Transfer a 0.2-g sample into a 250-ml beaker. Add 5 ml of concentrated hydrochloric acid and a few drops of hydrogen peroxide. Warm till dissolution is complete. Add 10 ml of water and boil gently to destroy excess of hydrogen peroxide. Cool to room temperature. Add 40 ml of water, 3 or 4 drops of Metanil Yellow solution and sodium bicarbonate solution dropwise till the appearance of a violet colour. Then add 3.0 ml of hydrochloric acid (1 + 1), 10 ml of monochloroacetic acid solution, and 30 ml of sodium diethyldithiocarbamate solution A with vigorous stirring. Filter off and wash the precipitate, then acidify and evaporate the filtrate to 35 ml, cool it, dilute to 50 ml in a standard flask, then titrate a 20-ml portion as described for magnesium alloys, omitting the phosphate treatment and second titration. Calculate the percentage of aluminium from

$$\%\text{Al} = 250t\,(V_3 - V_4 f)/G$$

Determination of Al in iron–chromium–aluminium alloys. Transfer a 0.2-g sample into a 250-ml beaker. Add 5 ml of concentrated hydrochloric acid and a few drops of hydrogen peroxide. Warm till dissolution is complete Add 10 ml of 70% perchloric acid and heat till fumes appear, to oxidize Cr(III) to Cr(IV). Then remove Cr(IV) by adding concentrated hydrochloric acid intermittently, 1 or 2 drops each time, until chromyl chloride ceases to be evolved. Then add two 0.1-g portions of sodium chloride to expel the residual Cr(IV). Cool to room temperature and add 10 ml of water and 1 ml of concentrated hydrochloric acid to dissolve the soluble perchlorates. Add 2 drops of Cresol Red solution and sodium bicarbonate solution until the red colour disappears. Beginning at the addition of hydrochloric acid, monochloroacetic acid and sodium diethyldithiocarbamate, continue the determination as for magnesium alloys.

RESULTS AND DISCUSSION

Choice of indicator

Xylenol Orange, though widely used, is unsuitable since it forms a robust complex with Mn(II).[5] Hydrazidazol, a highly selective metallochromic indicator, was chosen because it has been successfully used for titration of zinc in the presence of Mn(II) in aqueous alcoholic medium.[4] It would also seem applicable for back-titration with zinc in the presence of aluminium under the same conditions.

Choice of titrant

The interference of Mn(II) is extremely difficult to eliminate because of the stability of its complexes of EDTA type. Hence it is attractive to titrate the aluminium selectively in the presence of Mn(II). Excess of EDTA can be added, and back-titrated with Bi(III) at pH 3.5,[6] but chloride, Fe(III), Zr, Sn(IV), *etc.* interfere. An alternative is use of triethylenetetraminehexa-acetic acid (TTHA) as titrant and Cu(II) as back-titrant,[7] but Mn(II) hinders the chelation of aluminium by TTHA, which otherwise takes place instantaneously. It is necessary to wait 15–20 min before the back-titration. A further drawback is that the TTHA must be added in only moderate excess, or the strongly coloured Cu–TTHA produced obscures the colour change at the end-point. Hence a more selective titrant is desirable. It should give a large enough conditional stability constant ($> 10^8$) for its aluminium complex, with as low a constant as possible for the Mn(II) complex, and a high constant for the complex of the metal chosen for the back-titration.

The relevant data for six complexones are summarized in Table 1. The values refer to aqueous

Table 1. Formation constants of some complexonates of Al(III), Zn(II) and Mn(II)[8]

Complexonate		log K_{ML}	pH 6 log K'_{ML}	log K'_{AlL} − log K'_{MnL}	log K'_{ZnL} − log K'_{MnL}	log K'_{ZnZ} − log K'_{AlL}
EDTA	Al	16.1	11.3	2.1	2.5	0.4
	Zn	16.5	11.7			
	Mn	14.0	9.2			
NTA	Al	9.5	5.7	1.0	2.2	1.2
	Zn	10.7	6.9			
	Mn	8.5	4.7			
HEDTA	Al	14.4	10.5	3.7	3.8	0.1
	Zn	14.5	10.6			
	Mn	10.7	6.8			
DCTA	Al	17.6	11.4	0.8	1.9	1.1
	Zn	18.7	12.5			
	Mn	16.8	10.6			
DTPA	Al	18.5	11.2	3.0	2.5	−0.5
	Zn	18.0	10.7			
	Mn	15.5	8.2			
EGTA	Al	13.9	7.4	1.6	0.6	−1.0
	Zn	12.9	6.4			
	Mn	12.3	5.8			

medium, but the effect of a fixed alcohol content should be essentially the same for all chelates, so the differences between the conditional constants should not be substantially changed. HEDTA seems the titrant of choice for aluminium.

Search for an auxiliary agent

It would be more convenient to have the aluminium solution at room temperature than heated for the HEDTA titration but the reaction is not quantitative,[9] so use of an auxiliary agent to assist in removing the aquation sheath from aluminium aquo-complexes at room temperature was investigated, and ethylene glycol found useful. It is not known whether a mixed complex is formed, or there is a successive displacement system.

To prevent the formation of inert polynuclear aluminium hydroxo-complexes, HEDTA in excess, ethylene glycol and ethanol should be added successively at pH ≦ 1 and sodium bicarbonate solution used for the rough adjustment of pH, indicated by the colour change of Naphthyl Red. The precise control of pH is as previously reported.[4] Generally two repetitions of the hexamine addition suffice.

The amount of ethylene glycol required for quantitative determination of aluminium was found to be 10–20 ml, as shown in Table 2. As the final volume of the titrated solution may vary from 100 to 150 ml and the optimum concentration of ethanol is 20–40%,[4] 10 ml of ethylene glycol and 30 ml of ethanol are specified in the procedure.

Table 2. Effect of ethylene glycol on the titration of 10 mg of Al(III)

Ethylene glycol added, *ml*	Al found, *mg*
5	9.69
8	9.88
10	10.02
20	10.05

Effect of Mn(II)

The manganese content of the alloys investigated did not exceed 3%. Accordingly aluminium was titrated by the proposed method in the presence and absence of 3 mg of Mn(II) and the latter was found not to interfere. This non-interference results not from complete non-chelation of Mn(II) by the excess of HEDTA, but rather from quantitative displacement of any chelated Mn(II) by the zinc added later, owing to the considerable difference between the conditional formation constants of their HEDTA chelates (Table 1).

Effect of La(III) and Ce(III)

In a weakly acidic medium both La(III) and

Table 3. Titration of La(III) or Ce(III) with HEDTA at pH 6 and room temperature

Cation	Added, *mg*	Net volume of 0.02*M* HEDTA used, *ml* Theoretical	Experimental	Titrated, %
La	11	3.96	0.50*	13
	4	1.44	1.00†	70
	3	1.08	0.80†	74
Ce	11	3.93	0.80*	20
	5.8	2.07	1.30†	63

*Add 1 ml of 0.02*M* Zn(II) and titrate with HEDTA.
†Add excess of HEDTA first and back-titrate with Zn(II).

Table 4. Effect of Na_2HPO_4 on titration of Al(III)

0.005*M* Na_2HPO_4 added, *ml*	Total net volume of 0.02*M* HEDTA used, *ml*		
0	0.00*	8.80†	19.65§
1	0.03*	8.80†	19.60§
2	0.03*	8.85†	19.65§
3	0.05*	8.85†	19.60§
4	0.15*	8.65†	19.35§
5	0.25*		
6	0.45*		

*No Al(III) present.
†Al(III) taken, 8.80 mg.
§Al(III) taken, 19.60 mg.

Ce(III) can be quantitatively titrated with EDTA,[10] or HEDTA,[11] but we have found that their consumption of HEDTA, as indicated by hydrazidazol, is less than stoichiometric, especially in the presence of Zn(II). This may be due to the selectivity of the indicator and the fact that the Zn(II) chelate is rather stronger than the La(III) and Ce(III) complexes. Hence there is a partial displacement reaction between Zn(II) and these complexes, and as hydrazidazol indicates only the Zn(II) titration endpoint La(III) and Ce(III) are incompletely co-titrated, as shown in Table 3.

For complete elimination of their interference the "push–pull" effect of phosphate and zinc (first reported by Přibil and Veselý[12]) can be used:

$$Zn^{2+} + ML^- + HPO_4^{2-} \rightarrow MPO_4 + ZnL^{2-} + H^+$$

where M is La(III) or Ce(III) and L^{4-} is the completely deprotonated anion of HEDTA.

The effect on titrated aluminium solutions was studied by adding 1 ml of 0.02*M* zinc and various volumes of 0.005*M* disodium hydrogen phosphate and titrating again with HEDTA. The total net volumes of 0.02*M* HEDTA consumed for three amounts of aluminium are summarized in Table 4.

Addition of $\leq$3 ml of 0.005*M* disodium hydrogen phosphate to the titrated aluminium solution evidently has no disturbing effect. Its effect on preventing interference by La(III) or Ce(III) was examined by titrating aluminium solutions containing one of these species, then adding 2 ml of 0.005*M* disodium hydrogen phosphate and different amounts of zinc, stirring vigorously for 30 sec and titrating again with HEDTA. The results are shown in Table 5.

Table 5. Release-reaction with 6 mg of La(III) or Ce(III) by 2 ml of 0.005*M* Na_2HPO_4

0.02*M* Zn(II) added, *ml*	Total net volume of 0.02*M* HEDTA used after phosphate treatment, *ml*	
	La(III)	Ce(III)
0	0.40	0.45
1	0.20	0.25
2	0.00	0.05
3	0.00	0.00
4	0.00	0.00

Hence 2 ml of 0.005*M* disodium hydrogen phosphate solution in the presence of 3 ml of 0.02*M* zinc suffice to prevent completely interference from 6 mg of La(III) or Ce(III). This amount was chosen for study because it corresponds to the maximum content (6%) of La or Ce in the alloys currently used in China. (*Note*: owing to its adsorption on the phosphate precipitate, more indicator should be added after the release reaction.)

Synthetic mixtures were titrated by this technique, with the results shown in Table 6, which confirm the efficacy of the method.

Correction for interference by zirconium

Under the specified conditions Zr(IV) and Al(III) are quantitatively co-titrated. A correction must therefore be made by selective titration of Zr(IV) after masking of the aluminium. Sulphosalicylic acid was tried as masking agent for this purpose. It was found that though 2.0–2.5 g of sulphosalicylic acid would efficiently mask up to 20 mg of Al(III), low recoveries of Zr(IV) were obtained (because the zirconium is also partially masked). However, if excess of HEDTA is added at pH 1–2 and the solution allowed to stand for 5 min at room temperature to allow complete complexation of the zirconium, and then the sulphosalicylic acid is added, the aluminium is masked but not the zirconium. The titration is completed by adding an excess of zinc solution and back-titrating the surplus with HEDTA. The net consumption of HEDTA then corresponds to the amount of zirconium present, and if it is zero then zirconium is absent. If Zr(IV), La(III) and Ce(III) are all present, the releasing technique with phosphate should be incorporated.

Group separation of some interfering cations

Under the specified conditions Bi, Cd, Cu(II), Hg(II), Fe(III), Ni, Pb, Sn(IV), V(IV) and Zn would interfere by reaction with HEDTA. Also Sb(III, V) would cause trouble by hydrolysis, and Mo(IV) by forming a coloured complex with the sulphosalicylic acid added in the method of correction for zirconium. In our opinion these species are best removed as a group by precipitation with sodium diethyldithiocarbamate, followed by destruction of the ex-

Table 6. Titration of Al(III) in synthetic samples by the phosphate technique

Cations added, *mg*	Net volume of 0.02*M* HEDTA used, *ml*		Al, *mg*	
	Without phosphate	With phosphate	Taken	Found
—	8.65	8.60	4.75	4.68
	8.83	8.80	4.80	4.75
	9.20	9.20	5.00	4.96
	18.53	18.50	10.00	9.98
	36.70	36.77	19.75	19.84
	36.90	36.85	20.00	19.89
La 6	18.65	18.40	10.00	9.93
	27.80	27.50	15.00	14.84
Ce 6	9.25	8.85	4.80	4.78
	9.60	9.16	5.00	4.94
La 3, Ce 3	10.50	10.00	5.40	5.40
Ce 6, Mn 3	9.42	9.12	5.00	4.92
	10.60	10.20	5.40	5.50
Ce 6, Ti 0.1	11.35	10.95	6.00	5.94*

*Ti(IV) masked with 5 ml of 0.02% *N*-benzoyl-*N*-phenylhydroxylamine solution in ethanol.

cess of precipitant in the filtrate by acidification and heating.

A clean-cut separation can be obtained with 3–4 g of the precipitant. To prevent precipitation of hydrous aluminium oxide the pH must be kept below 3. Hence the pH of the acidified sample solution is first brought to *ca.* 2 with sodium bicarbonate, either Cresol Red or Metanil Yellow being used as indicator (both are adsorbed on the precipitate, so colourless filtrates are always obtained), and a maximum final pH of 3 is ensured by adding 3 ml of 6*M* hydrochloric acid to protonate all the diethyldithiocarbamate added, followed by monochloroacetic acid, which has maximum buffer capacity at pH 2.86. For the same reason the wash solution is acidified to pH < 3 with monochloroacetic acid.

Ti(IV) has been reported to be neither precipitated[13] nor extracted[14] as its diethyldithiocarbamate but it was later shown that a yellow titanium diethyldithiocarbamate is precipitated at pH 1–6 and is extractable at pH 2.[15] Our experiments have confirmed this finding. Analysis of mixtures of standard solutions of Al(III) and Ti(IV) by the procedure for iron–chromium–aluminium alloys gave quantitative results for aluminium.

Table 7. Effects of other cations and ligands on the titration of 10.00 mg of Al

Species	Added, *mg*	Al found, *mg*
Ca(II)	10	10.03
Cr(III)	2.5	10.06
	12	9.95*
Mg(II)	100	10.05
Ti(IV)	1.0	8.47†
SiO_4^{4-}	2.5	10.03
PO_4^{3-}	0.1	10.03
WO_4^{2-}	10	9.95
Sodium sulphate	850	10.00
Monochloroacetic acid	400	10.02

*Volatilized as chromyl chloride before titration.
†Aluminium taken, 8.50 mg.

The effects of various cations and ligands were studied and the results obtained are summarized in Table 7.

Applications

The special features of the method may be summarized as follows:

(1) use of a selective titrant and a selective metallochromic indicator;

(2) use of an alcoholic aqueous medium;

(3) use of a displacement technique to eliminate the interference from La(III) and Ce(III);

(4) a correction for Zr(IV) present;

(5) a simple separation of several cationic species as a group by precipitation with sodium diethyldithiocarbamate.

Use of these techniques in combination greatly enhances the selectivity for titration of Al(III) so that almost all the cations commonly accompanying aluminium do not interfere. This is a decided advantage and has been confirmed by the results for analysis of some synthetic and industrial samples, shown in Tables 8 and 9. Up to 12 mg of Al can be titrated accurately and reproducibly if 30 ml of 0.02*M* HEDTA are added as specified in the procedure, but the amount of Al may be increased to 20 mg if 45 ml of 0.02*M* HEDTA are used. The general procedure is both versatile and flexible. Simplifications are possible in the absence of certain interferents.

Table 8. Determination of Al in some synthetic samples by the proposed method

Composition of the synthetic sample, *mg*	Al, *mg*	
	Taken	Found
Mg 170, Ce 12, Mn 5, Zn 2.8, Zr 2, Si 0.5, Fe 0.2, Cu 0.2, Ni 0.1, Be 0.04	20.00	19.87
	18.00	17.85
Cu 160, Ni 13, Fe 13, Mn 5	8.80	8.85
Cu 107, Zn 40, Fe 13, Mn 5, Pb 2, Bi 0.02 Sb 0.2, As 0.2, Sn 0.4, P 0.2, Be 0.03	20.00	20.03

Table 9. Determination of Al in some non-ferrous alloys

Sample	Composition	Al found, %	
		Proposed method	Other values
Al bronze, SRM	Cu 86.83, Fe 2.29, Sn 0.03, Ni 0.38, Mn 0.88, Si 0.11, As 0.01, P 0.01, Sb 0.003	9.30	9.32*
Cast copper alloy	Cu 67.50, Fe 2.18, Mn 2.04, Pb 0.65, Sn 0.72	6.44	6.42*
Fe–Cr–Al alloy	Cr 60.04, Mo 4.52, Ti 0.17, La + Ce 2.24	14.57	14.52†

*Certified value.
†ASTM E 120-75.

Conclusion

The method is rapid, and the standard deviation has been found to be 0.04 mg ($n = 11$), the coefficient of variation ranging from 0.2 to 1%. Owing to its versatility and flexibility this new method should find many practical applications.

Acknowledgements—Grateful thanks are due to all members of the Directorate of SRIM for encouragement in this work and for permission to publish this paper.

REFERENCES

1. I. Sajó, *Magy. Kem. Foly.*, 1954, **60**, 268.
2. V. N. Tikhonov, *Zh. Analit. Khim.*, 1980, **35**, 448.
3. V. N. Tikhonov and V. A. Budnichenko, *ibid.*, 1974, **29**, 868.
4. Zhou Nan, Lu Zhi-ren and Gu Yuan-xiang, *Talanta*, 1983, **30**, 851.
5. R. Přibil, *Applied Complexometry*, p. 362. Pergamon Press, Oxford, 1982.
6. H. Kirihara, N. Arisaka, G. Nakagawa and K. Kodama, *Bunseki Kagaku*, 1976, **25**, 397.
7. R. Přibil and V. Veselý, *Talanta*, 1971, **18**, 395.
8. J. Inczédy, *Analytical Applications of Complex Equilibria*, pp. 335–353. Horwood, Chichester, 1976.
9. D. H. Wilkins, *Anal. Chim. Acta*, 1960, **23**, 309.
10. S. J. Lyle and M. M. Rahman, *Talanta*, 1963, **10**, 1177.
11. A. K. Gupta and J. E. Powell, *ibid.*, 1964, **11**, 1339.
12. R. Přibil and V. Veselý, *Chemist-Analyst*, 1960, **54**, 100.
13. H. Malissa and F. F. Miller, *Mikrochem. Mikrochim. Acta*, 1952, **40**, 63.
14. H. Bode, *Z. Anal. Chem.*, 1955, **144**, 165.
15. R. C. Rooney, *Anal. Chim. Acta*, 1958, **19**, 428.

Talanta, Vol. 32, No. 12, pp. 1125–1128, 1985
Printed in Great Britain.

0039-9140/85 $3.00 + 0.00

CHELATOMETRIC TITRATION OF BISMUTH WITH HEDTA

ZHOU NAN*
Shanghai Research Institute of Materials, The Ministry of Machine Building Industry, Shanghai, People's Republic of China

and

YU REN-QING, YAO XU-ZHANG and LU ZHI-REN
The Third Factory of Shanghai Reagent Chemicals, Shanghai, People's Republic of China

(*Received* 28 *March* 1985. *Accepted* 8 *August* 1985)

Summary—A new chelatometric method for the determination of Bi in bismuth-base alloys, low-melting alloys and reagent-grade bismuth salts is proposed. It is based on the chelation of Bi(III) with HEDTA, which is added in substoichiometric amount in perchloric acid medium to eliminate the interfering side-reactions of olation and oxolation, followed by pH adjustment and titration at pH 2 with Semi-Xylenol Orange as indicator. It is more selective than the classical EDTA method, and the accuracy and precision are enhanced. The coefficient of variation was found to be ~0.1%.

When present as a major constituent of a sample, bismuth is commonly and conveniently determined chelatometrically, usually with EDTA. Other complexones might serve the purpose as well or even better, however, *e.g.*, bismuth is chelated more strongly at pH <1.8 by NTA than by EDTA.[1] We propose titration with Semi-Xylenol Orange as indicator and *N*-(2-hydroxyethyl)ethylenediamine-*N*,*N*′,*N*′-triacetic acid (HEDTA), as titrant, added substoichiometrically before the pH adjustment for the titration proper. The method is more selective, accurate and precise than earlier methods.

EXPERIMENTAL

Reagents

Analytical-reagent grade chemicals were used whenever possible.

Ascorbic acid solution, 4%. Freshly prepared before use.

Sodium acetate (anhydrous) solution, 10%.

Cresol Red. A 0.1% solution in ethanol.

Semi-Xylenol Orange. A 0.1% solution of the chromatographically-pure chemical in 50% ethanol.

*Bismuth standard solution, 0.02*M. Dissolve 4.660 g of bismuth oxide (99.99% purity) in 6 ml of concentrated perchloric acid by heating. Cool, add 200 ml of 1% v/v perchloric acid, mix, transfer to a 1-litre standard flask, and dilute to volume with 0.1% perchloric acid.

HEDTA standard solution. Dissolve 11.13 g of anhydrous HEDTA in 700 ml of water by warming. Cool to room temperature. Transfer to a 2-litre standard flask, dilute to volume and mix. Standardize as follows. Pipette 25.00 ml of HEDTA solution into a 250-ml beaker, add 5 ml of ascorbic acid solution and 2 drops of Semi-Xylenol Orange solution, and titrate with the standard bismuth solution to the appearance of a red colour, and add 2–3 ml in excess. Back-titrate with the HEDTA solution to the colour change from red to yellow. Calculate the titre T of the HEDTA as mg of Bi per ml, from:

$$T = 0.02 \times 209.0 \times V_1/V_2$$

where V_1 = ml of bismuth standard solution used and V_2 = ml of HEDTA solution used.

Procedures

Analysis of bismuth salts. Transfer an appropriate amount of sample, weighed to the nearest 0.1 mg, into a 250-ml beaker. Add 3 ml of concentrated perchloric acid and heat to strong fumes. Cool, and add from a burette (with stirring) an amount of HEDTA solution *ca.* 2–5 ml less than the total volume needed, as estimated from the approximate composition of the sample. Thoroughly rinse the cover and inner wall of the beaker. Add successively 10 ml of sodium acetate solution, 1 drop of Cresol Red solution and saturated bicarbonate solution dropwise until the red colour of the indicator becomes paler. Add 5 ml of ascorbic acid solution and then bicarbonate solution dropwise until a pale yellow colour appears. Add 2 drops of Semi-Xylenol Orange solution and titrate with HEDTA to the colour change from red to yellow. Calculate the bismuth content from Bi = 100 TV/G%, where G is the sample weight (mg) taken for titration; V is the total volume of titrant used (ml), T is the HEDTA titre for bismuth.

Analysis of alloys (containing no In or Ga). Transfer 0.2–0.25 g of sample, weighed to the nearest 0.1 mg, into a 250-ml beaker. Add 10 ml of concentrated hydrobromic acid and 1 ml of bromine. Warm till dissolution is complete, then add 10 ml of concentrated perchloric acid. Heat to expel completely any volatile bromides and decompose any insoluble bromides. Evaporate the resulting clear solution to 2–3 ml. Cool to room temperature, then complete the titration as described above.

RESULTS AND DISCUSSION

Choice of metallochromic indicator

Catechol Violet has been reported[2] to be the most reliable indicator for the titration of bismuth and the most convenient to use.[3] In an acidified solution the

*To whom correspondence and requests for reprints should be sent. Present address: 999 Dong Chang Zhi Lu, Shanghai, People's Republic of China.

appearance of its blue binuclear Bi-chelate also functions as a narrow-range acid–base indicator[4] to indicate the proper pH for the titration. Xylenol Orange, however, is more sensitive, as shown by Wänninen.[5] The combined use of both also gives satisfactory results,[6] However, Semi-Xylenol Orange is reported to be much more sensitive,[7] and was chosen for this work. A specimen of chromatographic purity recently prepared by us was used.

Choice of medium

As reported earlier[8,9] the least hydrolysable salt of bismuth is its perchlorate, which does not hydrolyse even in a weakly acid solution.[10] Kodama has also pointed out[11] that BiO^+ is stable in perchloric acid medium. This medium was accordingly chosen in order to reduce the unfavourable effects of the side-reaction of bismuth with hydroxide ions.

For the same reason the standard bismuth solution was prepared by dissolving bismuth oxide in an appropriate amount of perchloric acid. Bismuth nitrate dissolved in 6% acetic acid/10% potassium iodide medium has also been reported to be stable,[12] but the presence of iodide might often interfere in practical applications.

Choice of titrant

The formation constant of the Bi–HEDTA chelate log K_f is reported[13] to be $10^{21\,8}$. Hence its conditional formation constant, log K_f' at pH 2 would be 9.8 after correction for log $\alpha_{HEDTA(H)} = 12.0$.[14] This provides a sound theoretical basis for titration of bismuth with HEDTA at this pH, which seems to be optimal since at pH >3 inaccurate results would be obtained.[15]

The use of HEDTA as titrant has the following advantages: (1) it makes the titration more selective; (2) it is very soluble not only in water but also in strong acids, so is especially suitable for the substoichiometric addition technique in strongly acidic medium (*vide infra*); (3) the pH of its standard solution is 2.0–2.5, which is very close to that required for the titration. In contrast, if the disodium salt of EDTA is used as titrant, its solution must be acidified, as pointed out by Kragten,[15] and this acidification often caused the precipitation of some EDTA as the free acid.

Anhydrous HEDTA is preferred because the hygroscopic dihydrate cannot be weighed accurately.

Choice of pH indicator

Methyl Green, Methyl Violet, Malachite Green and Cresol Red were tried and the last was found to be the most suitable.

The substoichiometric addition technique

At pH 1–2 the predominant bismuth species found in solution are BiO^+ and $Bi(OH)^{2+}$.[16] Simple neutralization to this pH would, no matter how efficient the stirring, create a non-equilibrium situation caused by concentration gradients between the reagent and the solution, and localized conditions could momentarily cause too high a pH and the formation of polynuclear complexes such as $Bi_6O_6^{6-}$ and $Bi_6(OH)_{12}^{6-}$,[17] owing to olation and oxolation. These are inert charged species and may persist even after the solution has been mixed thoroughly enough to be thought homogeneous, even though the final conditions do not lead to any penetration into the region of polynuclear hydroxo-complexation in the pH–pM′ diagram.[15] In such cases low results will always be obtained.

From the following equation derived by Kragten[15]

$$\log \alpha_{(poly)} = \left(\frac{q}{p}\right) \mathrm{pH} + \frac{\log \beta_{q,p}^{OH} + \log p}{p} + \frac{p-1}{p} \log [M']$$

the α-coefficient for formation of polynuclear hydroxo-complexes of a multivalent cation, $\alpha_{(poly)}$, increases with increasing pH or [M′] or both. At a fixed pH it increases only as the conditional metal–ion concentration [M′] increases. In order to make negligible the interferences caused by such side-reactions the maximum amount of bismuth to be titrated has been limited to 15,[3] 30,[18] 50,[19] or 80 mg,[20] and the sample weight of low-melting alloys taken for titration specified as 0.1 g.[21,22] Such limitations would, owing to the relative high atomic weight of Bi, make the analytical results inaccurate and imprecise. This is a serious drawback in the analysis of samples with relatively high Bi content.

Therefore another approach, termed substoichiometric addition, was developed by us. It is a variant of direct titration. In a medium of sufficient acidity, in which neither olation nor oxolation of the titrand cation takes place, an appropriate amount of HEDTA, the titrant, is first added. During the subsequent careful pH adjustment to the required value for the titration the complexing action of HEDTA on Bi(III) competes with that of olation and oxolation. In this way [M′] can be markedly decreased and hence $\alpha_{(poly)}$ effectively reduced to a negligible value. It is interesting that in this novel technique the titrant itself serves both for determination and as a masking agent to eliminate olation and oxolation.

This technique has proved to give reliable results and has been successfully used for assaying reagent-grade chemicals with relatively high bismuth content. It was recently adopted as the standard method for this purpose, approved by the Ministry of Chemical Industry, People's Republic of China.

pH adjustment and dilution

For the pH adjustment sodium hydroxide and ammonia would be unsuitable since with either it is impossible to avoid penetration into the region of polynuclear hydroxo-complexation in the pH–pM′ diagram. Hence sodium bicarbonate, as the saturated solution but not as the solid, is used in the presence

of sodium acetate. Kragten[15] has pointed out that the presence of anions of weak acids and bases has a large influence on the shape of the neutralization line in the pH–pM′ diagram. In this respect the use of sodium bicarbonate can be strongly recommended because in acidic medium the bicarbonate anion is converted into carbon dioxide and water. Its use has also proved very satisfactory for pH adjustment of the Al–HEDTA system in order to avoid the formation of inert aluminium species, as reported in another paper of this series.[23]

It should be noted that acidified water should always be used for dilution of acid solutions of a multivalent cation.[15] Accordingly the standard bismuth solution was prepared by a two-step dilution with perchloric acid solutions with successively lower concentrations.

Effect of diverse ions and ligands

The relevant conditional formation constants of a number of HEDTA and EDTA complexes at pH 2 are summarized in Table 1 for comparison. Theoretically speaking, it is quite evident that on the whole the proposed titration system would be more selective.

The effects of some ions and ligands were studied and the results obtained are shown in Table 2. As the method was intended for analysis of low-melting alloys, the amounts of metals studied correspond to their levels in such alloys. No attempt was made to determine tolerance limits, but it should be noted that for V(V) or V(IV) the tolerance limit is 1 mg (otherwise a red chelate is formed with the SXO). Obviously many ionic species, especially those commonly accompanying bismuth, do not interfere. It should be noted that at pH 2 aluminium exerts no interfering action in the proposed system, whereas it does if EDTA is used as the titrant.[25] Zirconium and indium(III) are quantitatively co-titrated, and for samples containing these the Přibil and Veselý method[26] can be applied. The hydrolysis of Ti(IV), Ga(III), Sb(III), Sb(V) and Sn(IV) also causes trouble. Antimony and tin can be previously removed by volatilization as the bromides. This approach ensures no loss of Bi and seems to be preferable to those needing filtration[26,27] or solvent extraction.

The standard deviation for determination of 120 mg of bismuth was found to be 0.16 mg ($n = 12$) and the coefficient of variation to vary from 0.09 to 0.13%, depending on amount of bismuth.

Applications

The proposed method has been satisfactorily used to determine bismuth in various chemicals and nonferrous alloys. Some results are shown in Table 3.

Table 1. Conditional formation constants of some HEDTA and EDTA chelates at pH 2

Cation	log K_f*		log K'_f at pH 2	
	HEDTA	EDTA	HEDTA	EDTA
Al(III)	14.4	16.1	2.4	2.4
Cd(II)	13.0	16.5	1.0	2.8
Ce(III)	14.2	16.0	2.2	2.3
Co(II)	14.4	16.3	2.4	2.6
Cu(II)	17.4	18.8	5.4	5.1
Fe(III)	19.8	25.1	7.8	11.4
Fe(II)	12.2	14.3	0.2	0.6
Ga(III)	16.9	20.3	4.9	6.6
Hg(II)	20.1	21.8	8.1	8.1
In(III)	17.2†	25.0	5.2	11.3
La(III)	13.5	15.5	1.5	1.8
Lu(III)	15.9	19.8	3.9	6.1
Ni(II)	17.0	18.6	5.0	4.9
Pb(II)	15.5	18.0	3.5	4.3
Zn(II)	14.5	16.5	2.5	2.8

*Inczédy.[24]
†Cheng *et al.*[13]

Table 2. Effects of some ions and ligands on the titration of 120.0 mg of Bi(III)

Species tested	Added, *mg*	Bi found, *mg*
Al(III)	8	120.0
Cd(II)	100	120.1
Co(II)	1	120.2
Cr(III)	2	120.1
Cu(II)	5	119.8
Fe(III)	5	120.1
Hg(II)	30	120.2*
In(III)	11.5	141.0
Mo(VI)	8	120.0
Ni(II)	2	120.1
Pb(II)	120	120.2
Te(VI)	7.5	120.0
V(V)	1	120.2
Zn(II)	25	120.0
Zr(IV)	9	140.8
NaCl	35	119.8
Chloroacetic acid	500	119.8
Thiourea	500	119.9
Ethylene glycol	10†	120.0
Diethylene glycol	10†	119.8

*With 0.3 g of thiourea present and ascorbic acid absent.
†Volume added, ml.

Table 3. Determination of Bi in some chemicals and nonferrous alloys

Sample	Bi found, %	
	Proposed method	Other method†
Bismuth-base alloy 359A	83.2*	83.1
Low-melting alloy 231	48.5	48.4
325	49.7	49.7
326	48.9	48.8
329	48.9	49.1
Bismuth nitrate	42.6	42.5
Bismuth sulphate	58.6	58.5
Bismuth oxycarbonate	79.9*	79.9
Bismuth oxynitrate	71.0*	70.9

*Sample weight 0.2 g.
†By controlled-potential electrolysis.

Acknowledgement—Grateful thanks are due to all members of the Directorate of SRIM for encouragement in this work and permission to publish this paper.

REFERENCES

1. J. Vandegans, E. Merciny and G. Duyckaerts, *Anal. Chim. Acta*, 1974, **72,** 391.
2. G. Gattow and D. Schott, *Z. Anal. Chem.*, 1962, **188,** 10.
3. A. I. Busev, V. G. Tiptsova and V. M. Ivanov, *Analytical Chemistry of Rare Elements*, pp. 344–345. Mir, Moscow, 1981.
4. R. A. Chalmers and F. I. Miller, *Analyst*, 1971, **96,** 97.
5. E. Wänninen, in *Indicators*, E. Bishop (ed.), p. 425. Pergamon Press, Oxford, 1972.
6. Zhou Nan, *Hauxue Shiji*, 1979, 273.
7. K. Sonoda, M. Otomo and K. Kodama, *Bunseki Kagaku*, 1978, **27,** 429.
8. W. Rathje, *Angew. Chem.*, 1938, **51,** 256.
9. W. P. Thistlethwaite, *Analyst*, 1952, **77,** 48.
10. J. Doležal, P. Povondra and Z. Šulcek, *Decomposition Techniques in Inorganic Analysis*, p. 71. Iliffe, London, 1966.
11. S. Kodama, *Bunseki Kagaku*, 1955, **4,** 447.
12. E. V. Vikhareva and G. I. Savel'eva, *Zh. Analit. Khim.*, 1984, **39,** 1130.
13. K. L. Cheng, K. Ueno and T. Imamura, *CRC Handbook of Organic Analytical Reagents*, p. 215. CRC Press, Cleveland, 1982.
14. A. Ringbom, *Complexation in Analytical Chemistry*, p. 351. Interscience, New York, 1963.
15. J. Kragten, *Talanta*, 1977, **24,** 483.
16. L. Erdey, *Gravimetric Analysis*, Part 2, p. 117. Pergamon Press, Oxford, 1965.
17. G. Gattow and D. Schott, *Z. Anal. Chem.*, 1962, **188,** 81.
18. G. Schwarzenbach, *Die Komplexometrische Titration*, 5th Ed., p. 241. Ferdinand Enke, Stuttgart, 1965.
19. M. Malát, V. Suk and O. Ryba, *Chem. Listy*, 1954, **48,** 203.
20. F. J. Welcher, *The Analytical Uses of Ethylenediaminetetraacetic Acid*, p. 207. Van Nostrand, New York, 1958.
21. R. Přibil, *Chemist-Analyst*, 1959, **48,** 87.
22. L. I. Sedina, *Zh. Analit. Khim.*, 1960, **15,** 595.
23. Zhou Nan, Lu Zhi-Ren and Gu Yuan-Xiang, *Talanta*, 1985, **32,** 1119.
24. J. Inczédy, *Analytical Applications of Complex Equilibria*, pp. 345–346. Horwood, Chichester, 1976.
25. G. Schwarzenbach, *op. cit.*, p. 154.
26. R. Přibil and V. Veselý, *Chemist-Analyst*, 1965, **54,** 12.
27. W. Szczepaniak and M. Ren, *Talanta*, 1984, **31,** 212.

Talanta, Vol. 32, No. 12, pp. 1129–1132, 1985
Printed in Great Britain.

0039-9140/85 $3.00 + 0.00

CHELATOMETRIC TITRATION OF TIN IN NON-FERROUS ALLOYS WITH HEDTA

ZHOU NAN*
Shanghai Research Institute of Materials, The Ministry of Machine Building Industry, Shanghai, People's Republic of China

and

YU REN-QING, YAO XU-ZHANG and LU ZHI-REN
The Third Factory of Shanghai Reagent Chemicals, Shanghai, People's Republic of China

(*Received* 28 *March* 1985. *Accepted* 8 *August* 1985)

Summary—A new titrimetric method for determination of tin (⩾4%) in aluminium alloys, tin- and lead-base alloys, solders, white bearing alloys, special bronzes and silver brazing alloys is proposed. HEDTA, Semi-Xylenol Orange and bismuth perchlorate are used as titrant, indicator and back-titrant respectively. Measures are taken to overcome the hydrolysis of Sn(IV). Monochloroacetic acid and ethylene glycol are added as auxiliary agents. The standard deviation of this method was found to be 0.2 mg and its coefficient of variation to vary from 0.25 to 2%, according to amount of tin. A novel method of sample decomposition and a modified method for separating Sn(IV) are also suggested.

The redox titration of tin in non-ferrous alloys, though commonly used, seems somewhat inconvenient, since atmospheric oxygen must be rigorously excluded if accurate results are to be obtained. Moreover, the titration should be done at below a certain temperature in order to prevent the side-reactions caused by the reductant used for the prereduction of Sn(IV). Therefore a chelatometric finish should be preferable. The main difficulty encountered is the hydrolysis of Sn(IV). This side-reaction is very pronounced and takes place even at 1*M* hydrogen-ion concentration,[1] thus exerting a very unfavourable effect. To overcome this a new method is proposed in this paper, in which HEDTA, Semi-Xylenol Orange and bismuth perchlorate are suggested as titrant, indicator and back-titrant respectively. Monochloroacetic acid and ethylene glycol are introduced as auxiliary agents. It has been successfully applied to the determination of tin (⩾4%) in different kinds of non-ferrous alloys.

EXPERIMENTAL

Reagents

Analytical-reagent grade chemicals were used unless otherwise specified.

Monochloroacetic acid solution, 9%.

Ascorbic acid solution, 4%. Freshly prepared before use.

Saturated sodium bicarbonate solution.

Aluminium nitrate nonahydrate solution, 4%.

Semi-Xylenol Orange solution. In 50% ethanol, 0.1%.[2]

Cresol Red solution. In ethanol, 0.1%.

N-Benzoyl-N-phenylhydroxylamine solution. In glacial acetic acid, 4%.

Wash solution. Pour 25 ml of sulphuric acid (1 + 1) into 475 ml of water, mix and saturate with *N*-benzoyl-*N*-phenylhydroxylamine.

Tin standard solution. Dissolve 1.0000 g of tin (99.99% pure) in 10–15 ml of concentrated sulphuric acid and 5 ml of concentrated nitric acid, and heat to strong fumes. Cool, add with stirring 5 ml of water, then 100 ml of hydrochloric acid (1 + 3). Transfer to a 500-ml standard flask, dilute to volume with the same acid and mix: 1 ml of this solution contains 2.0 mg of Sn(IV).

Bismuth standard solution. Use 9.703 g of bismuth nitrate pentahydrate instead of bismuth oxide, and prepare as previously described.[2]

HEDTA standard solution. Prepare and compare with the Bi standard bismuth solution as previously described.[2] Calculate the concentration ratio f of these two solutions from $f = A/B$, where A is the total volume of HEDTA solution used (ml) and B that of the standard bismuth solution consumed. Then standardize the HEDTA solution as follows. Into a 250-ml beaker pipette 25.00 ml of the standard tin solution (see note). Add 5 ml of sulphuric acid (1 + 1) and heat to strong fumes. Cool, add successively, with thorough stirring, 5.0 ml of monochloroacetic acid solution, 45 ml of HEDTA solution dropwise from a burette, 10 ml of ethylene glycol and 1 drop of Cresol Red solution. Then add dropwise saturated sodium bicarbonate solution till the red colour of the indicator becomes paler, then 5 ml of ascorbic acid solution, and continue the dropwise addition of sodium bicarbonate solution to the appearance of a pale yellow colour. Let stand for 2 min. Add 2 drops of Semi-Xylenol Orange solution and titrate with standard bismuth solution till a red colour appears. Let stand for 1 min then back-titrate with HEDTA solution to an abrupt colour change from red to yellow. Calculate the titre T of the HEDTA as mg of Sn per ml, from $T = 2V_3/(V_1 - V_2 f)$ where V_1, V_2 and V_3 are the volumes of HEDTA, Bi and Sn solutions used, respectively.

Note. It would be preferable to standardize against an SRM having composition close to that of the sample to be analysed.

Procedures

(*a*) *Determination of Sn in tin-base alloys.* Transfer 0.1 g

*To whom correspondence should be sent. Present address: 999 Dong Chang Zhi Lu, Shanghai, People's Republic of China.

of the sample, weighed to the nearest 0.1 mg, into a 400-ml beaker. Add 5 ml of sulphuric acid (1 + 1) and warm till dissolution is complete. Add 2 or 3 drops of concentrated nitric acid if necessary. Heat to strong fumes, and let fume for 1–2 min. Cool to room temperature and add 5.0 ml of monochloroacetic acid solution. Then continue the titration as described for standardization of the HEDTA solution. Calculate the percentage of Sn from: % Sn = $100T(V_1 - fV_2)/G$ where G is the sample weight (mg) taken for titration.

(*b*) *Determination of Sn in solders, white bearing alloys and lead-base alloys.* Transfer 0.25 g of the sample, weighed to the nearest 0.1 mg, into a dry 50-ml standard flask. Add 10 ml of concentrated hydrochloric acid and 2 or 3 drops of concentrated nitric acid. Immerse the flask in a water-bath at *ca.* 50° until dissolution of the sample is complete, adding a further 1 or 2 drops of nitric acid if necessary. Cool to room temperature, dilute to volume with water, and mix. Filter into a dry beaker through a paper of fine porosity. Pipette 20 ml of the filtrate into a 400-ml beaker, add 5 ml of sulphuric acid (1 + 1) and heat to strong fumes, and let fume for 1–2 min. Cool to room temperature, then complete the titration as described in the preceding paragraph.

(*c*) *Determination of Sn in aluminium alloys.* Transfer 0.2 g of the sample, weighed to the nearest 0.1 mg, into a 250-ml beaker. Add 7 ml of sulphuric acid (1 + 1), then 8 ml of hydrochloric acid (1 + 1). When the violent reaction has subsided, add a few drops of 30% hydrogen peroxide and warm till dissolution is complete. Then boil gently to destroy excess of hydrogen peroxide. Add 75 ml of water and cool to room temperature. Add dropwise, with constant stirring, 12 ml of *N*-benzoyl-*N*-phenylhydroxylamine solution. Let stand for 10 min, filter through a paper of fine porosity, and wash the filter and the beaker thrice with the wash solution. Transfer the filter paper and the precipitate into the original beaker. Add 4 ml of sulphuric acid (1 + 1), 1 ml of 72% perchloric acid and stir thoroughly to disintegrate the paper. Then add an appropriate amount of concentrated nitric acid, mix thoroughly and heat to destroy the filter paper and decompose the organic matter, finally heating to strong fumes for 1–2 min. Cool to room temperature. Then add 5 ml of monochloroacetic acid solution and complete the titration as above.

(*d*) *Determination of Sn in silver brazing alloys.* Transfer 0.25 g of the sample, weighed to the nearest 0.1 mg, into a 250-ml beaker. Add 5 ml of sulphuric acid (1 + 1) and then concentrated acid dropwise and warm till dissolution is complete. Then heat to strong fumes, letting fume for 1–2 min. Cool to room temperature, add 50 ml of hydrochloric acid (1 + 19) and stir vigorously for 1 min. Wash the cover and the inner wall of the beaker with water. Let stand for 5 min, then filter off the silver chloride on a paper of fine porosity. Wash the paper and the beaker with hydrochloric acid (1 + 19) several times. The total volume of washings should be *ca.* 30 ml. Then continue the precipitation with *N*-benzoyl-*N*-phenylhydroxylamine and the subsequent titration as described in the preceding paragraph.

RESULTS AND DISCUSSION

Measures taken to overcome the hydrolysis of Sn(IV)

The strong tendency of Sn(IV) to hydrolyse is the main difficulty encountered. To overcome this the following measures were taken: (1) HEDTA was chosen as titrant since it may be added to a strongly acidic medium, as previously reported;[2] (2) pH 2 was chosen for the back-titration of excess of HEDTA instead of pH 5–6, at which the conditional formation constant of the Sn–HEDTA chelate would be greatly lowered as the result of increasing $\alpha_{Sn(OH)}$ with increasing pH; (3) auxiliary agents were introduced to aid in suppressing the unfavourable effect of hydrolysis.

Choice of back-titrant and metallochromic indicator

Sn(IV) has generally been determined by back-titration because of its ready hydrolysis. Thorium nitrate has been used[1,3–6] at pH 2 as the back-titrant for this purpose, but it is expensive, radioactive and subject to interference by sulphate. Obviously bismuth perchlorate would be a better choice. Its solution is quite stable.[2] Although Xylenol Orange[3,5–7] has been widely used as a metallochromic indicator, Semi-Xylenol Orange was chosen instead since it is more sensitive.

Neutralizing agent, pH indicator and buffer

In principle the pH conditions for back-titrating excess of HEDTA with bismuth are the same as those for titrating bismuth with HEDTA.[2] Accordingly the same neutralizing agent and pH indicator were used. It seemed preferable to conduct the titration in sulphuric acid medium since its pK_2 value is about 2.0, and the bisulphate/sulphate system constitutes a buffer of the required pH.

Search for auxiliary agents

Chloride ion has been used as an auxiliary agent, at a concentration of 1*M*.[8] Preliminary experiments showed that monochloroacetic acid serves the same purpose, and 0.5 g of it is tolerable in the Bi–HEDTA titration system.[2] Its optimum amount as an auxiliary agent for titrating $\leqslant$0.1 g of Sn(IV) was found to be 0.45–0.5 g. Ethylene glycol was also tried, since it has been successfully used in the Al–HEDTA titration system.[9] Detailed study revealed that when both monochloroacetic acid and ethylene glycol are present the consumption of HEDTA by a fixed amount of Sn(IV) is somewhat greater than that in the presence of either auxiliary agent alone, *i.e.*, the hydrolysis of Sn(IV) is more effectively suppressed. The use of both is therefore recommended.

The use of 5–15 ml of ethylene glycol was found to give almost identical results, and use of 10 ml of ethylene glycol is specified in the procedures. It should be noted that 10 ml of dimethylsulphoxide may be used in place of ethylene glycol (see Table 1).

Effects of diverse ions and ligands

Generally speaking, bivalent and lanthanide cations do not interfere since the titration is conducted at too low a pH. The effects of various ions and ligands were studied and the results are summarized in Table 1. The metals were studied at levels corresponding to the composition of the alloys for which the method is intended.

Bi(III), In(III), Ga(III), Zr(IV) and Ti(IV) will interfere, as they are quantitatively co-titrated, and their prior separation is necessary.

Table 1. Effects of some ions and ligands on the titration of Sn(IV)

Ion or ligand added, *mg*	Sn, *mg* Taken	Found
Dimethylsulphoxide, 10*	50.74	50.6
Diethylene glycol, 5*	50.46	40.0
Cu(II), 13	20.20	20.16
Fe(III), 2.5	20.20	20.25
Al(III), 10	20.20	20.25
Mo(VI), 8	20.20	20.16
Sb(III), 2.5	9.60	9.51
13	20.20	20.27
PO_4^{3-}, 0.3	11.02	11.02†
0.45	11.02	11.09†
0.45	49.30	49.41†
Cu(II), 13; Fe(III), 2.5	20.20	20.26
Cu(II), 13; Pb(II), 10; Sb(III), 13	20.20	20.16

*Added (ml) in place of ethylene glycol.
†Five ml of 4% aluminium nitrate solution added before back-titration.

Sample decomposition

It is rather difficult to decompose samples containing both tin and lead. Attack with nitric acid results in the precipitation of metastannic acid which is heavily contaminated because of its strong adsorptive powers. Also, as soon as it appears, it coats the sample surface, and decomposition ceases or becomes very slow. The use of *aqua regia* was considered unsuitable in this case.[10] The combined use of nitric acid and tartaric acid has also some demerits.[10] Moreover, tartaric acid itself interferes in the titration. Attack with glacial acetic acid and hydrogen peroxide[11] also proved to be ineffective. At least 25 ml of 9*M* hydrochloric acid or 150 ml of nitric acid (1 + 1) together with 4 ml of concentrated hydrochloric acid may be used, as suggested by Cohen,[10] but our tests failed to confirm the efficacy of these treatments. The methods recommended by ASTM[12,13] would be inadequate, as the use of 20 ml of concentrated sulphuric acid makes the pH adjustment rather difficult. Fusion with pyrosulphate[14] seems inconvenient. Therefore decomposition of the samples chosen deserved further study. In our opinion the key to complete decomposition lies in effective prevention of the formation of insoluble deposits. Accordingly hydrochloric acid should be added in large excess to complex both Sn(IV) and Pb(II) as anionic species.

Table 2. Effect of hydrochloric acid and total hydrogen-ion concentration on the precipitation of 46.43 mg of Sn(IV)

[HCl], *M*	$[H_2SO_4]$, *M*	Total $[H^+]$, *M*	Sn found, *mg*
0.18	0.36	0.6	46.4
0.24	0.45	0.7	46.4
0.55	0.45	1.0	46.5
0.12	0.84	1.0	46.5
0.18	2.16	2.3	46.4
0.24	2.88	3.1	46.3
0.16	3.42	3.6	46.4
0.18	4.86	4.0	45.3

*Note that at concentrations $\geqslant 1M$, the second dissociation step of sulphuric acid takes place to only a negligible extent.

On the other hand, only a small amount of nitric acid is needed. The proposed method ensures that the samples are decomposed smoothly and effectively at *ca.* 50°, at which there is no loss of tin by volatilization. The decomposition is done in a standard flask for convenience. The dilution to volume gives a preliminary separation of lead as the chloride with no loss of tin.

Preliminary separation of Sn(IV)

For samples containing Ag, Al or Cu as the main constituent a preliminary separation is indispensable. Silver can be readily removed as the chloride from a sulphuric acid medium without loss of Sn(IV). Sn(IV) may be separated from Al(III) and Cu(II) by selective precipitation with *N*-benzoyl-*N*-phenylhydroxylamine. The method originally suggested by Ryan[15] took 4 hr for complete precipitation with an ethanolic solution of the precipitant, at 0°. We have greatly improved it. Glacial acetic acid was chosen as the solvent for the precipitant. Preliminary experiments revealed that the precipitation can be done at room temperature, and is complete within 10 min. It was also found that 400 mg of precipitant is enough for separation of up to 60 mg of tin.

The precipitate formed is a hexaco-ordinated mixed-ligand chelate, $SnCl_2L_2$, as independently found by different authors.[16,17] Therefore the presence of chloride is absolutely necessary, but it should never be added in excess, since it would then compete for Sn(IV) to form anionic complexes, thus exerting an antagonistic effect. Hence the optimal concentration

Table 3. Determination of tin in some synthetic samples by the proposed method

Composition of the sample, *mg*	Sn, *mg* Taken	Found
Sb 13, Pb 11.4, Cu5	81.8	81.8 (a)
Al 188, Cu 6, Ni 3, Mg 2.4, Mn 1.5, Fe 1.5, Si 1.4	46.2	46.3 (c)
	12.00	12.10 (c)
Pb 200, Sb 40, Cu 7.5, Fe 0.25, Bi 0.25	10.10*	10.28 (b)
	43.4	43.4 (b)
	45.4	45.3 (b)
Pb 125, Cu 3.75, Sb 37.5	50.5	50.6 (b)

(a), (b) and (c) refer to the procedure (see text).
*40-ml aliquot of the sample solution taken.

Table 4. Determination of tin in some non-ferrous alloys

Sample	Composition, %	Sn found, %	
		Proposed method	Other methods
SRM 610*	Sb 10.77, Cu 5.97, As 0.12	82.7	82.6 (a)
611*	Sb 10.56, Cu 5.93, Pb 0.53	83.0	82.9 (a)
615*	Sb 11.95, Cu 2.66, Pb 10.28	74.9	75.0 (a)
612A*	Pb 72.8, Sb 14.07, Cd 1.24, Cu 1.68, Ni 0.71, As 0.61	8.95	8.84 (a)
616*	Pb 84.1, Sb 10.42, As 0.35	4.81	4.82 (a)
Pb alloy	Pb 82.95, Sb 12.42	4.12	4.18 (c)
	Pb 58.04, Sb 0.1	41.1	41.3 (c)
Sn alloy	Pb 28.4, Sb 4.52	66.9	67.1 (c)
	Pb 33.15, Ag 2.37	63.8	64.0 (c)
	Sb 10.24, Pb 0.16	89.5	89.2 (c)
Al alloy	Al (remainder)	15.59	15.65 (b)
Bronze	Cu 71.16, Pb 19.3, Fe 0.03, Ni 0.93, Zn 0.02, Ag 0.002	8.31	8.32 (a)
Ag alloy	Ag 49.98, Cu 20.28, Zn 21.45	7.76	7.85 (b)
	Ag 43.90, Cu 20.93, Zn 27.78, Ni 1.83	5.54	5.49 (b)
	Ag 37.86, Cu 27.92, Zn 29.33, Ni 1.26	3.61	3.57 (b)

(a) Certified value; (b) by controlled potential electrolysis; (c) Okell's method.[18]
*Supplied by SRIM, the best-known supplier of SRIMs in China.

of hydrochloric acid was sought and found to be 0.12–0.55*M* (Table 2). To enhance the selectivity, sulphuric acid was added to increase the total acidity. Tests showed that the total hydrogen-ion concentration can be varied from 0.6 to 4*M* without disturbing the recovery of tin, as shown in Table 2. A concentration of 1.0*M* may be chosen for general purposes, but must be raised to 2.3*M* if bismuth is present, to prevent the simultaneous precipitation of BiOCl. Zr(IV), Ti(IV), Nb(V), nitrate and phosphate interfere, however.

Applications

The proposed method has been validated by analysing some synthetic samples (Table 3) and checked by analysis of a few SRM samples (Table 4). Its standard deviation was found to be 0.2 mg of tin ($n = 15$) and the coefficient of variation to vary from 0.25 to 2%. It has been successfully applied to determination of the tin content ($\geqslant 4\%$) of tin- and lead-base alloys, solders, white-metal bearing alloys, aluminium alloys, special bronzes and silver brazing alloys.

Acknowledgements—Grateful thanks are due to all members of SRIM's Directorate for encouragement in this work and for permission to publish this paper.

REFERENCES

1. J. Kragten, *Talanta*, 1975, **22**, 505.
2. Zhou Nan, Yu Ren-Qing, Yao Xu-Zhang and Lu Zhi-Ren, *Talanta*, 1985, **31**, 1125.
3. J. Kinnunen and B. Wennerstrand, *Chemist-Analyst*, 1957, **46**, 92.
4. M. Furuya and M. Tajiri, *Bunseki Kagaku*, 1963, **12**, 59.
5. K. Ueno, *ibid.*, 1965, **14**, 962.
6. C. M. Dozinel, *Modern Methods of Analysis of Copper and its Alloys*, 2nd Ed., p. 111. Elsevier, Amsterdam, 1963.
7. M. Dixon, P. J. Heinle, D. E. Humlicek and R. L. Miller, *Chemist-Analyst*, 1962, **51**, 42.
8. J. Kragten, *Talanta*, 1977, **24**, 483.
9. Zhou Nan, Gu Yuan-Xiang and Lu Zhi-Ren, *Talanta*, 1985, **31**, 1119.
10. A. Cohen, *Rationelle Metallanalyse*, pp. 192–195. Birkhäuser, Basel, 1948.
11. E. G. Brown, *Analyst*, 1954, **79**, 50.
12. ASTM, *1978 Annual Book of ASTM Standards*, Part 12, p. 183. ASTM, Philadelphia, 1978.
13. *Idem, op. cit.*, p. 266.
14. J. Hillebrand, G. E. F. Lundell, H. A. Bright and J. I. Hoffman, *Applied Inorganic Analysis*, 2nd Ed., pp. 274–288. Wiley, New York, 1953.
15. D. E. Ryan, *Can. J. Chem.*, 1953, **31**, 9.
16. Zhou Nan, *Huaxue Shiji*, 1979, **1**, 85.
17. K. Das Mrinal and M. R. Ghosh, *Indian J. Chem.*, 1975, **13**, 515.
18. F. L. Okell, *Analyst*, 1935, **10**, 803.

Talanta, Vol. 32, No. 12, pp. 1133–1139, 1985
Printed in Great Britain

0039-9140/85 $3.00 + 0.00

CALCULATION OF EQUILIBRIUM CONSTANTS FROM MULTIWAVELENGTH SPECTROSCOPIC DATA—III

MODEL-FREE ANALYSIS OF SPECTROPHOTOMETRIC AND ESR TITRATIONS

HARALD GAMPP, MARCEL MAEDER, CHARLES J. MEYER and ANDREAS D. ZUBERBÜHLER
Institute of Inorganic Chemistry, University of Basel, CH-4056 Basel, Switzerland

(*Received* 17 *May* 1985. *Accepted* 5 *August* 1985)

Summary—Factor analysis of spectroscopic data is a well-known tool for the determination of the number of independent absorbing species in a series of mixtures. It has also been used for the reduction of the data-set in the calculation of equilibrium constants from multiwavelength data. The paper presents a new application of this powerful technique. In a completely model-free treatment, data from spectrophotometric or other spectroscopic titrations are subjected to repetitive abstract factor analysis. By starting with only the first two spectra, and introducing the additional measurements one by one, the number of significant eigenvalues is obtained as a function of the progressing titration. On repetition of the process from the opposite end and judicious combination of the results, the formation and dissociation of individual "species" can be obtained. After association of actual stoichiometries with these purely abstract "species" by chemical reasoning, it may be possible to arrive at a semiquantitative description and reasonable estimates for the equilibrium constants. This method is most successful for the detection of minor species which would go unnoticed in any visual inspection of spectrophotometric titration curves.

Factor analysis (FA) is a powerful tool with rapidly growing application to chemistry.[1–3] Predominantly, it serves for the determination of the number of factors or linearly independent components in a given set of data;[4–7] this specific application is also known as principal components analysis. Equally interesting is its use for the reduction of large matrices of raw data to smaller ones. Factor analysis of this second type includes the reduction of GC/MS/IR libraries,[8] analysis of multicomponent fluorescent mixtures,[9] and the calculation of equilibrium or rate constants from multiwavelength spectrophotometric[10–13] or ESR[14–16] data. Finally, some algorithms have been derived for the estimation of the component spectra by making use of the non-negativity of both the species spectra and their concentrations.[17–21]

In the course of our own research on the calculation of equilibrium constants from spectroscopic titration data[22–27] we have routinely used factor analysis for data reduction. This has made it possible to use desk-top computers to treat systems of 30–60 spectra obtained at 20–30 wavelengths. In parts I and II of the series we have discussed the mathematical details[26] and the performance of our program SPECFIT,[27] which makes the numerical treatment of spectroscopic data as straightforward and almost as simple as the analysis of potentiometric titration curves.

Here, we discuss a third and new application of factor analysis, which we wish to call *evolving factor analysis*. This application is related to the first possibility discussed above, *i.e.*, to the determination of independent components in a given data matrix. Its goal is more ambitious, however, in aiming at a completely model-free analysis of spectroscopic titrations. It will yield a picture closely related to species distribution curves and, with the aid of some chemical reasoning, should also give reasonable estimates of the actual equilibrium constants.

EVOLVING FACTOR ANALYSIS (EFA)

Suppose we have a series of M spectra of mixtures containing S different absorbing species, measured at W wavelengths, and arranged into an $M \times W$ data matrix $\mathbf{Y}$. For $M, W > S$, and linear independence of all species spectra and concentration profiles, S can be obtained through factor analysis and is equal to the number of significant eigenvalues of the second-moment matrix $\mathbf{M} = \mathbf{Y}^t\mathbf{Y}$. The decision about whether an eigenvalue is significant or not is in some cases very difficult to reach and has been discussed in great detail.[4–7]

If, in addition, the measurements are obtained by titration of one original solution or by an analogous experiment, then the (unknown) concentrations of all species vary according to a single parameter, *e.g.*, pH or the total ligand concentration. As a consequence, there is some definite order in the whole set of spectra. Traditional factor analysis makes no use of

this additional information; its result is completely independent of the order of the rows and columns of the data matrix **Y**.

In our new approach, factor analysis is successively applied to the sets of the first two, the first 3, 4 ... M spectra and the eigenvalues of the corresponding second-moment matrices $\mathbf{M}_i = \mathbf{Y}_i^t\mathbf{Y}_i$ are calculated in turn ($i = 2,3 \ldots M$). $\mathbf{Y}_i$ is the submatrix of **Y** containing only the first i spectra or rows of **Y**. Thus, as new absorbing species start to become significant, new factors (eigenvalues) evolve, and in *evolving factor analysis* (EFA) these are plotted as a function of the progressing titration. Because the eigenvalues span several orders of magnitude, the actual values are not suitable for graphical representation and the logarithms are used instead.

Not only do EFA plots show the number of eigenvalues significantly greater than zero and thus the number of different species in the subset $\mathbf{Y}_i$, but it also appears that the values of the eigenvalues are somehow correlated to the concentrations of the species. Naturally, a given eigenvalue (and even more so its logarithm) does not in any way directly correspond to a given complex or its concentration. The actual values are strongly dependent on the dissimilarity of the spectra of the various species and on the differences between their concentration profiles. Nevertheless, there is some correlation between concentration and magnitude of the eigenvalue. If at any stage of the titration a new linearly independent species is formed, a new eigenvalue will start to appear as a significant positive value, and with increasing concentration the eigenvalue will increase as well. If, however, the freshly added measurement contains only a new mixture of the previous species, no additional factor will be calculated, although all the old eigenvalues will continue to grow slowly. Of course, the number of significant eigenvectors (*i.e.*, the number of species detected) cannot at any time exceed the number of spectra included.

The performance of the procedure and its use in a model-free analysis of spectroscopic data will be described for three systems of increasing complexity. Calculations were done with a Hewlett-Packard HP 9835. The algorithm of evolving factor analysis was incorporated into the appropriate part (factor analysis) of SPECFIT.[27] All the experimental data were taken from systems described in the literature.[14,22,23]

As a well-studied and relatively simple test system, we chose the complexation of Cu^{2+} by 3,7-diazanonane diamide (DANA, L).[14,28,29] As shown in Fig. 1 and in accordance with the literature, three complexes are formed in aqueous solution. These are CuL^{2+}, $CuLH^{+}_{-1}$ and $CuLH_{-2}$, with log $K^{Cu}_{CuL} = 12.06$, log $K^{H}_{CuL} = 7.05$, log $K^{H}_{CuLH_{-1}} = 8.41$. The species distribution is shown in Fig. 1a. The corresponding result of EFA (Fig. 1b) shows the appearance of the new factors 2, 3 and 4 at around pH 2, 7 and 8. No further factors are observed up to pH 12, which indicates an overall number of four absorbing species in the complete data set. In the present case, chemical reasoning easily leads to association of factors 2, 3 and 4 with the formation of CuL^{2+} (pH 2.5), $CuLH^{+}_{-1}$ (pH 7) and $CuLH_{-2}$ (pH 8). By using these rough estimates and the ligand protonation constants for DANA,[29] log $K^{H}_{LH_2} = 6.55$ and log $K^{H}_{LH} = 8.40$, we directly arrive at log $K^{Cu}_{CuL} = 11.95$, log $K^{H}_{CuL} = 7$ and log $K^{H}_{CuLH_{-1}} = 8$ for the conditions used in the actual ESR experiment ($c_L = c_{Cu} = 0.01M$).[14] These values compare very nicely with the result of the non-linear least-squares calculation, and the results of EFA both clearly suggest a chemical model for the complexation and yield stability constants suitable to serve as initial estimates for a non-linear least-squares treatment.

We have already mentioned that neither the magnitude of an eigenvalue nor its logarithm are direct measures of a concentration, and in fact, all absorbing species have some effect on all the eigenvalues. This is seen in Fig. 1b at around pH 8, where $CuLH^{+}_{-1}$ and $CuLH_{-2}$ are not only responsible for the introduction of factors 3 and 4, respectively, but also have an influence on factors 1 and 2.

Nevertheless, with the necessary precautions, the argument can be carried further and it is possible to arrive at a picture closely resembling a set of species distribution curves through a completely model-free analysis, as shown in Fig. 2, again for Cu^{2+}/DANA. To achieve this, EFA has to be repeated from the opposite end of the measurement, starting with the last 2, 3 ... spectra of the data set, obtained, for example, at the highest pH-values. Now, the appearance of a new factor with progressing analysis corresponds to the appearance of a new species with decreasing pH or its disappearance with increasing pH. Thus, while the first (forward) calculation yielded information only about the formation of species, the backward procedure gives their decay, and superposition of the forward and backward information (Fig. 2a) should give a picture analogous to the actual species-distribution curves. The problem now obviously consists of making the right connection between a formation curve and the corresponding decay curve. The switching from a curve of formation (--- in Fig. 2a) to a curve of decay (. . .) at a crossover may look somewhat arbitrary at first glance. In the normal case this switching is straightforward however. The ith forward eigenvalue has to be connected with the curve of the $(S + 1 - i)$th backward eigenvalue (S = number of species, $i = 2, \ldots, S - 1$). As an example, forward curve no. 2 has to be connected with backward curve no. 3, *** at pH 8 in Fig. 2b. This procedure may be erroneous in special cases, *e.g.*, with double maxima in the concentration profile,[30] but in the present case (compare Fig. 1a with Fig. 2b) it gives plots which are surprisingly similar to the real species distribution curves, reproducing all essential features such as concentration maxima, onset of appreciable formation and range of species coexistence. Obviously, the connected plots of the ei-

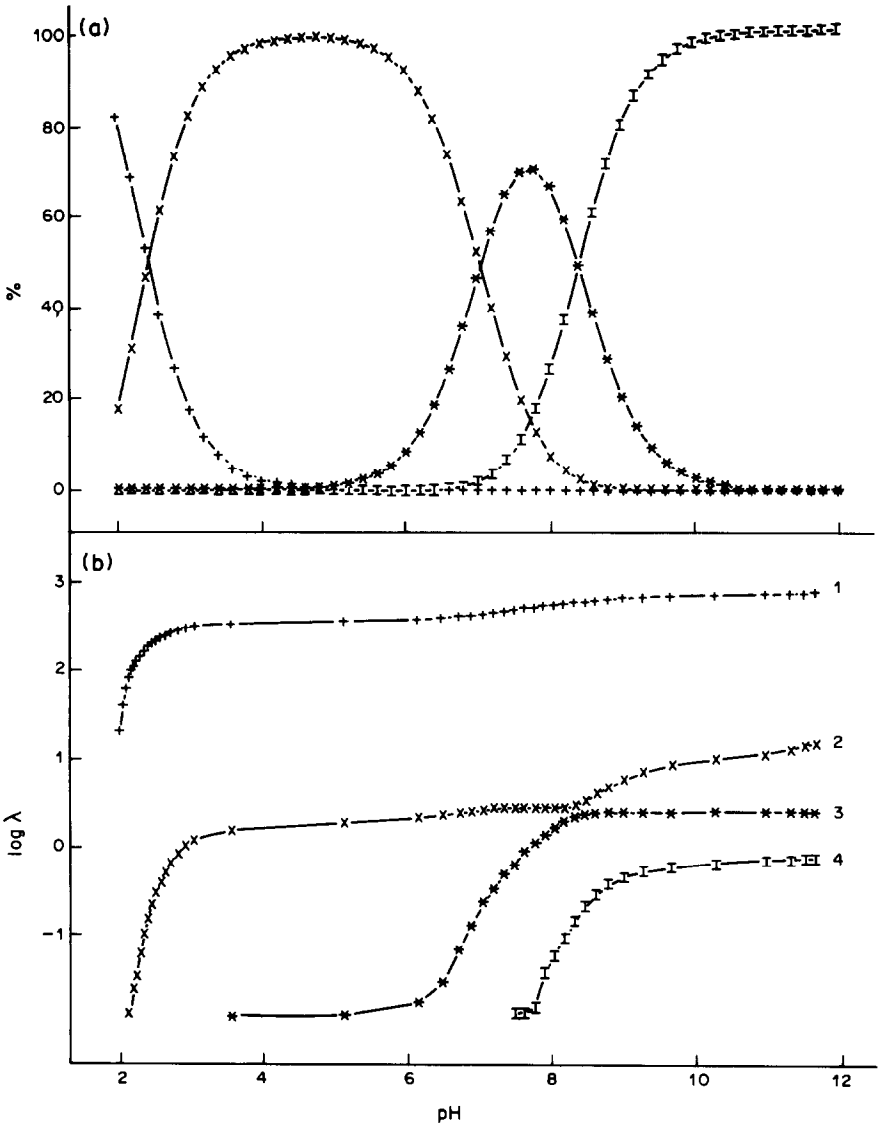

Fig. 1. Complexation of Cu^{2+} by 3,7-diazanonane diamide. ESR data taken from ref. 14; $c_L = c_{Cu} = 0.01M$. (*a*) Species distribution curves based on log $K^H_{LH_2} = 6.55$, log $K^H_{LH} = 8.40$, log $K^{Cu}_{CuL} = 12.06$, log $K^H_{CuL} = 7.05$ and log $K^H_{CuLH_{-1}} = 8.41$. + = Cu^{2+}, × = CuL^{2+}, * = $CuLH^+_{-1}$, I = $CuLH_{-2}$. (*b*) Results from EFA, increasing pH only.

genvalues (Fig. 2b) do not sum to 100% as is the case for the species distribution curves (Fig. 1a). Note also that in Fig. 2 the plot of the most significant (first) eigenvalue has been omitted since its existence simply indicates the presence of an absorbing species, but carries no useful information with regard to the formation or decay of an individual complex. This is generally true and the two systems which are discussed subsequently are treated in the same way.

The complexation of Cu^{2+} by DANA has been studied by potentiometry,[29] spectrophotometry,[28] and ESR;[14] all the species are well defined, and there can be no doubt about the correct chemical model describing all the data within experimental error, even without factor analysis. This is not the case for the Cu^{2+} complexes of 4,7,10-triazatridecanedioic acid.[23] With this ligand, four species, *viz.* Cu^{2+}, $CuLH_2^{2+}$, $CuLH^+$ and CuL may again be expected, but $CuLH_2^{2+}$ is not significant according to potentiometric titrations.[23] Also, visual inspection of the spectrophotometric data would not disclose the presence of four species at any individual wavelength. This is not surprising, since all species are formed between pH 2 and 4, with about 60% $CuLH^+$ and roughly equal amounts of the other three species at around pH 3. $CuLH_2^{2+}$ reaches its maximum concentration of 17% at the nearby pH of 2.8 (*cf.* Fig. 3a).

Our model-free evolving factor analysis, Fig. 3b, gives a picture which is almost as detailed as the one obtained through the complete least-squares analysis

of the multiwavelength spectrophotometric data. The formation and decay of four absorbing species in the pH range 2–4 is demonstrated beyond any doubt. The curves "corresponding" to Cu^{2+} and to CuL would, after appropriate normalization, be practically identical with the actual species distribution curves shown in Fig. 3a. Visual inspection of Fig. 3b indicates the formation of complexes at pH 2.5, 2.7 and 3.5. This leads to estimates of log $K^{Cu}_{CuLH_2} = 5.8$, log $K^{H}_{CuLH_2} = 2.7$ and log $K^{H}_{CuLH} = 3.5$ which again can be used as input for the non-linear least-squares treatment yielding log $K^{Cu}_{CuLH_2} = 5.27$, log $K^{H}_{CuLH_2} = 2.37$ and log $K^{H}_{CuLH} = 3.73$.[23] Thus, in this not quite trivial system, evolving factor analysis (*i*) clearly rules out the model suggested by potentiometry, (*ii*), unequivocally establishes the presence of four absorbing species at low pH (and the absence of any additional equilibria in basic solution), (*iii*), strongly suggests a model of complexation to be used in the non-linear least-squares treatment and (*iv*) provides reasonable estimates of all equilibrium constants from which the final values can be obtained unproblematically in just a few iterative cycles with programs such as SPECFIT.[27]

The third system to be discussed concerns the complexation of Cu^{2+} by glycine ethylamide. By combination of spectrophotometric data from solutions containing 0.25 and 0.5 mole of Cu^{2+} per mole of ligand, the following seven absorbing species have been established: Cu^{2+}, CuL^{2+}, $CuLH^{+}_{-1}$, $CuLH_{-2}$,

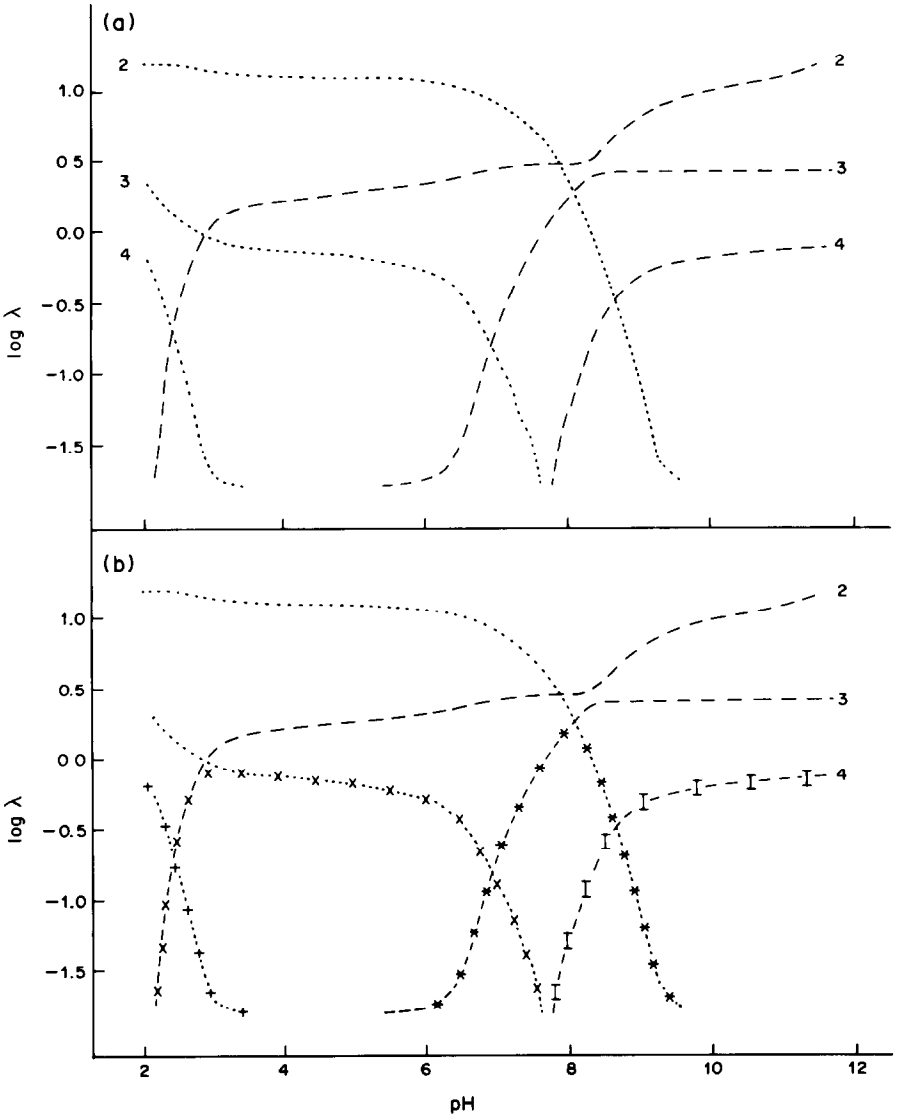

Fig. 2. Complexation of Cu^{2+} by 3,7-diazanonane diamide. Superposition of results from forward (---) and backward (· · · · ·) EFA. (*a*) Plot of evolving factors 2–4. (*b*) Abstract "species distribution curves" obtained by connecting *i*th forward eigenvalue with $(S + 1 - i)$th "backward eigenvalue" $(i = 2 \ldots S - 1)$. Signs correspond to species in Fig. 1 (*a*): + = Cu^{2+}, × = CuL^{2+}, * = $CuLH^{+}_{-1}$, I = $CuLH_{-2}$.

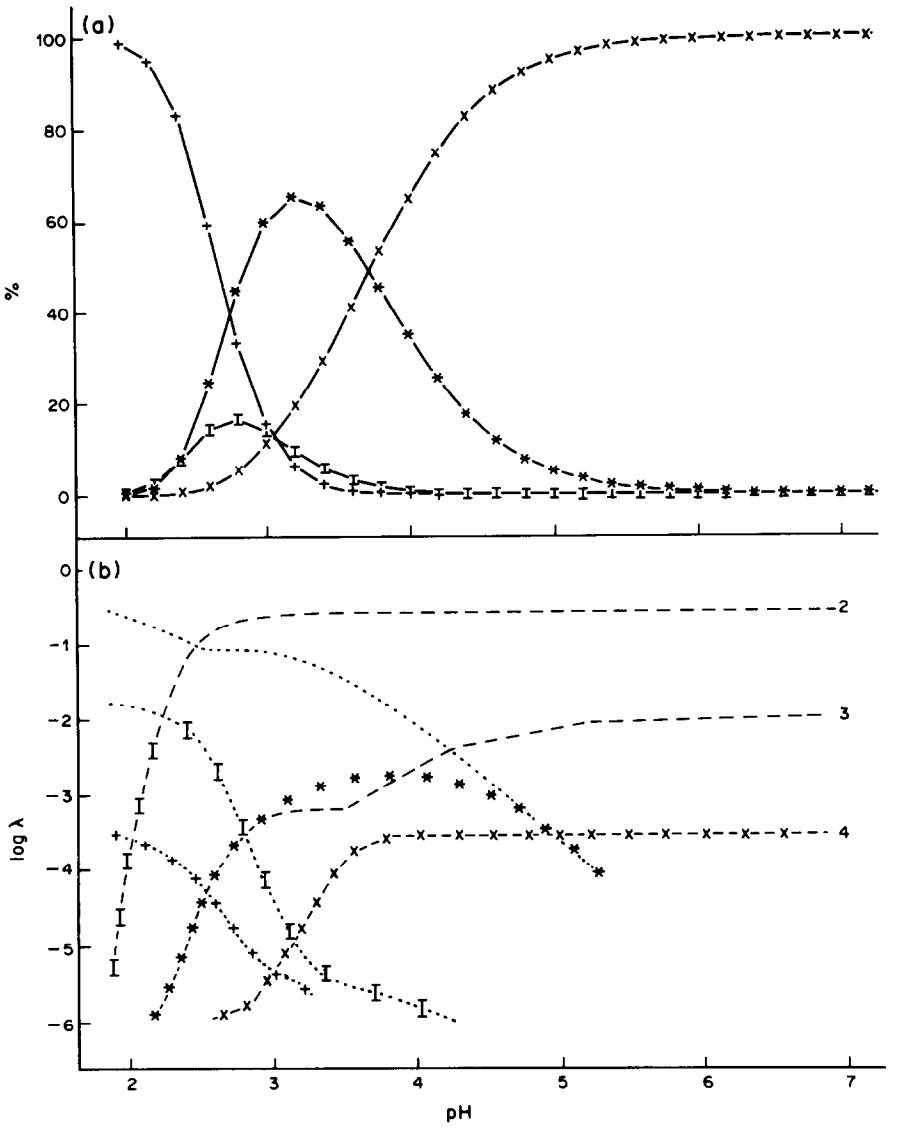

Fig. 3. Complexation of Cu^{2+} by 4,7,10-triazatridecanedioic acid. Data as in ref. 23. $c_L = 0.004M$, $c_{Cu} = 0.0036M$. (*a*) Species distribution curves based on log $K^H_{LH_5} = 2.97$, log $K^H_{LH_4} = 3.55$, log $K^H_{LH_3} = 4.40$, log $K^H_{LH_2} = 9.31$, log $K^H_{LH} = 9.99$, log $K^{Cu}_{CuLH2} = 5.27$, log $K^H_{CuLH} = 3.73$ and log $K^H_{CuLH_2} = 2.37$. + = Cu^{2+}, × = CuL, * = $CuLH^+$, I = $CuLH_2^{2+}$. (*b*) Abstract "species distribution curves" obtained as described for Fig. 2(*b*).

CuL_2^{2+}, $CuL_2H^+_{-1}$ and CuL_2H_{-2}.[22] On the other hand, no more than five significant eigenvectors were needed to represent the complete set of data from a single titration within 1.3×10^{-4} absorbance units, *i.e.*, within experimental uncertainty. Classical principal components analysis or FA would thus have suggested a model with five rather than seven absorbing species.

This system was specifically chosen in order to test the limits of the EFA method. The results are indicated in Fig. 4.

Obviously, EFA at a fixed point of the analysis cannot reveal more factors than the classical FA, which is in fact identical with the last calculation of both forward and backward EFA. Nevertheless we propose to show that even in this quite tricky system the EFA method gives a rather detailed picture, which, unlike that from FA, can be used to estimate the number of absorbing species correctly and even to obtain (very rough) guesses for the equilibrium constants after association of actual species concentrations with the rise and fall of the appropriate eigenvalues.

The following facts may be noted. (*i*) Some important features of the species distribution curves are again nicely reproduced, *e.g.*, the presence of free metal ion, starting at below pH 6 (+); the range of presence of CuL^{2+} (×), CuL_2^{2+} (*) and of $CuL_2H^+_{-1}$

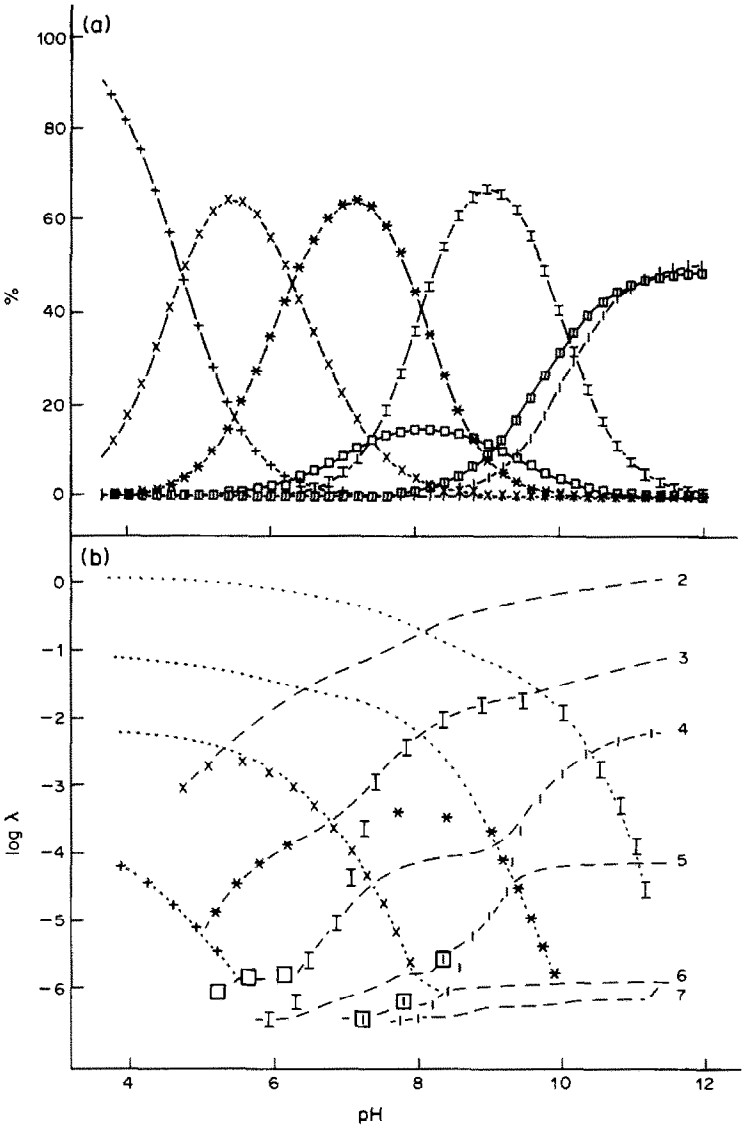

Fig. 4. Complexation of Cu^{2+} by glycine ethylamide. Data as in ref. 22. $c_L = 0.0113m$, $c_{Cu} = 0.0054M$. (*a*) Species distribution curves based on $\log K^{H}_{LH} = 8.19$, $\log K^{L}_{CuL} = 5.50$, $\log K^{L}_{CuL_2} = 4.36$, $\log K^{H}_{CuL} = 7.40$, $\log K^{H}_{CuLH_{-1}} = 9.10$, $\log K^{H}_{CuL_2} = 8.09$, $\log K^{H}_{CuL_2H_{-1}} = 10.23$. $+ = Cu^{2+}$, $\times = CuL^{2+}$, $* = CuL_2^{2+}$, $\square = CuLH^{+}_{-1}$, $\mathrm{I} = CuL_2H^{+}_{-1}$ $\boxplus = CuLH_{-2}$, $| = CuL_2H_{-2}$. (*b*) Abstract "species distribution curves" obtained by appropriate connection of forward and backward eigenvalues.

(I); the formation of new species at pH 5 ($CuLH^{+}_{-1}$, □), 6 ($CuL_2H^{+}_{-1}$, I), 7 ($CuLH_{-2}$, ⊞) and 7.5 (CuL_2H_{-2}, |). (*ii*) Even more distinctly than for the systems discussed before, the successive eigenvectors are now influenced by several complexes, making the construction of "species-distribution curves" critical and in some cases ambiguous. Switching from one factor to another is often necessary, if some direct resemblance to the correct curves is to be maintained. The disappearance of Cu^{2+} (+) and connection of the backward and forward EFA curves to abstract "species distributions" for CuL^{2+} (×) as well as CuL_2^{2+} (*) are straightforward even in this example. Extensive crossovers would be necessary to obtain continuous curves for the other species. This is indicated in Fig. 4b for $CuL_2H^{+}_{-1}$ (I) and for CuL_2H_{-2} (|). The curves are not shown for $CuLH^{+}_{-1}$ (□) and $CuLH_{-2}$ (⊞), to avoid making the picture given too confused to understand. Note, however, that even these last species make themselves noticeable by the addition of a new factor at pH values which are surprisingly close to those where significant amounts are formed according to the species distribution curves, Fig. 4a. Again, to avoid an overcrowded figure, the two least significant eigenvalues have been left out for the backward EFA. (*iii*) Factors 6 and 7

are not significant by themselves according to error analysis. Nevertheless, the formation of two additional species $CuLH_{-2}$ (□) and $Cu_2L_2H_{-2}$ (|) is reflected by their influence on factors 5 and even 4 between pH 8 and 10. Most specifically, the stepwise increase of factor 5 would indeed be sufficient for the formation of additional complexes to be deduced. Thus, by using evolving factor analysis, it is possible to gain information on the formation of absorbing species not only from the total number of significant factors in a given data-set, but also from the actual eigenvalues as a function of the progressing titration. Obviously, EFA is not a cure-all for the problems of analysis of spectrophotometric titrations. Like any other method, it has its limits with respect to the detection of minor species and the complexity of systems that can be analysed unambiguously. However, it is rewarding to note that the limits of this completely abstract and model-free approach do not seem to be any more restricted than those for a complete least-squares analysis.

CONCLUSIONS

Evolving factor analysis represents a new and promising approach to completely model-free analysis of equilibrium systems studied by spectroscopic titration. The information that can be obtained is much more than that available through classical factor analysis, which gives just the result of the last calculation of EFA. A glance at, *e.g.*, Fig. 1b, shows that there is much more valuable information in the whole plot than just the last set of eigenvalues, *i.e.*, the four numbers at pH 12. Of course, EFA is not intended to replace a rigorous non-linear least-squares treatment, and should be used in combination with other methods of analysing spectrophotometric data. Pictures which are remarkably close to the actual species-distribution curves can be obtained even for systems of non-trivial complexity. Evolving factor analysis should be extremely helpful at the stage of model selection, and for obtaining reasonable estimates of the equilibrium constants which are needed for the calculation of the final parameters. EFA is a completely abstract interpretation of spectrophotometric data. Necessarily, association of actual species with the "distribution curves" thus obtained can only be achieved through sound chemical reasoning.

Acknowledgements—Support by the Swiss National Science Foundation (Grant No. 2.021–0.83) is gratefully acknowledged.

REFERENCES

1. B. R. Kowalski, *Anal. Chem.*, 1980, **52,** 112R.
2. I. E. Frank and B. R. Kowalski, *ibid.*, 1982, **54,** 232R.
3. M. F. Delaney, *ibid.*, 1984, **56,** 261R.
4. Z. Z. Hugus and A. A. El-Awady, *J. Phys. Chem.*, 1971, **75,** 2954.
5. S. Wold, *Technometrics*, 1978, **20,** 397.
6. R. N. Cochran and F. H. Horne, *Anal. Chem.*, 1977, 49, 846.
7. E. R. Malinowsky, *ibid.*, 1977, **49,** 606; 1977, **49,** 612.
8. S. S. Williams, R. B. Lam and T. L. Isenhour, *ibid.*, 1983, **55,** 1117.
9. W. Lindberg, J-A. Persson and S. Wold, *ibid.*, 1983, **55,** 643.
10. J. J. Kankare, *ibid.*, 1970, **42,** 1322.
11. E. A. Sylvestre, W. H. Lawton and M. S. Maggio, *Technometrics*, 1974, **16,** 353.
12. M. Maeder and H. Gampp, *Anal. Chim. Acta*, 1980, **122,** 303.
13. M. Maeder and S. Fallab, *Chimia*, 1984, **38,** 269.
14. H. Gampp, *Inorg. Chem.*, 1984, **23,** 1553.
15. *Idem, ibid.*, 1984, **23,** 3645.
16. *Idem, Helv. Chim. Acta*, 1984, **67,** 2164.
17. N. Ohta, *Anal. Chem.*, 1973, **45,** 553.
18. W. H. Lawton and E. A. Sylvestre, *Technometrics*, 1971, **13,** 617.
19. I. M. Warner, G. D. Christian, E. R. Davidson and B. J. Callis, *Anal. Chem.*, 1977, **49,** 564.
20. D. W. Osten and B. R. Kowalski, *ibid.*, 1984, **56,** 991.
21. A. Meister, *Anal. Chim. Acta*, 1984, **161,** 149.
22. M. Briellmann and A. D. Zuberbühler, *Helv. Chim. Acta*, 1982, **65,** 46.
23. H. Gampp, D. Haspra, M. Maeder and A. D. Zuberbühler, *Inorg. Chem.*, 1984, **23,** 3724.
24. K. P. Balakrishnan, Th. A. Kaden, L. Siegfried and A. D. Zuberbühler, *Helv. Chim. Acta*, 1984, **67,** 1060.
25. D. Küry, P. Sandmeier and A. D. Zuberbühler, to be published.
26. H. Gampp, M. Maeder, C. J. Meyer and A. D. Zuberbühler, *Talanta*, 1985, **32,** 95.
27. *Idem, ibid.*, 1985, **32,** 257.
28. A. D. Zuberbühler and Th.A. Kaden, *ibid.*, 1979, **26,** 1111.
29. Th.A. Kaden and A. D. Zuberbühler, *Helv. Chim. Acta*, 1974, **57,** 286.
30. I. Nagypál, M. T. Beck and A. D. Zuberbühler, *Talanta*, 1983, **30,** 593.

Talanta, Vol. 32, No. 12, pp. 1141–1144, 1985
Printed in Great Britain.

0039-9140/85 $3.00 + 0.00

EXTRACTION CHROMATOGRAPHY OF PALLADIUM AND PLATINUM COMPLEXES WITH NITROSO-R-SALT

A. FLIEGER and S. PRZESZLAKOWSKI
Department of Inorganic and Analytical Chemistry, Medical School, 20-081 Lublin, Poland

(*Received* 21 *February* 1985. *Accepted* 2 *August* 1985)

Summary—The retention of palladium and platinum complexes with nitroso-R-salt on silica gel treated with Aliquat 336 has been investigated. The complexation of platinum with nitroso-R-salt (NRS) requires heating of H_2PtCl_6 with an excess of NRS at 100°. The affinity of the complexes for an Aliquat 336 stationary phase increases in the following order: $PdCl_4^{2-} \sim$ Pt–NRS $< PtCl_6^{2-} \ll$ Pd–NRS. The complexes of palladium and platinum can be separated by column chromatography on silica treated with Aliquat 336 and eluted with 0.25*M* perchloric acid (Pt) and 1*M* perchloric acid (Pd).

Although ion-exchange chromatography has been used successfully for the separation of noble metals from other metals and from each other, and many cation- and anion-exchange procedures have been described,[1–5] their use in analytical practice is often limited by incomplete elution (two bands are often formed for the same metal ion, especially for platinum) owing to hydrolysis or reduction, or sorption of two different complexes. Extraction chromatography is a promising separation method for noble metals, and several procedures have been described which utilize as stationary phases tri-n-octylphosphine oxide,[6] tributyl phosphate[7,8] or liquid anion-exchangers[9–11] for column separations. In these chromatographic systems, platinum is always more strongly retained than palladium. The elution of the strongly retained metals [especially of platinum and iridium(IV)] requires concentrated hydrochloric acid and/or nitric acid, both in extraction chromatography and in anion-exchange chromatography.

Ziegler *et al.*[12,13] found that the anionic metal complexes formed with sulphonated chelating reagents can be extracted into organic solvents after reaction of the sulphonate groups of the reagent with alkylammonium cations. Conventional anion-exchangers modified with sulphonated chelating reagents appear to be useful for separation of some metal-ion mixtures.[14–17]

It has also been found that ion-pairs consisting of a large alkylammonium cation and an anion of a sulphonated chelating reagent loaded on silica gel can be used as sorbents for the separation of metal-ion mixtures or for the concentration of some metal ions from very dilute aqueous solutions by extraction chromatography.[18–22]

EXPERIMENTAL

All chromatographic separations were done at room temperature (21 ± 2°).

Reagents

Aliquat 336 (General Mills Chemicals, Inc.) was purified to remove iron.

Silica gel 40, 0.063–0.2 mm (Merck), was purified from iron by repeated washing with dilute hydrochloric acid, and then three times with doubly distilled water to remove the acid.

All other reagents were of analytical grade.

Procedure

Silica gel was impregnated with 0.3*M* Aliquat 336 solution in chloroform. Some experiments were also done with silica treated with a mixture of Aliquat 336 and nitroso-R-salt in chloroform. The procedures for preparation of the sorbents and the column packing have been described previously.[9,19] Mixed solutions of $PdCl_2$ and H_2PtCl_6 in 0.1*M* perchloric acid or solutions of palladium and platinum complexes in 0.1*M* perchloric acid were introduced into the column. The complexation of $PdCl_2$ and H_2PtCl_6 with NRS (mole ratio of NRS to metal varied from 6:1 to 10:1) in 0.1*M* perchloric acid was done at room temperature, or by heating for 2 min at 60° or for 5 min at 100°. Glass columns, 160 × 10 mm, packed with 5 or 8 g of the coated silica gel, were used. The column height was 9 or 12 cm, the dead volume 0.4 ml, the mobile-phase volume 4.5 ml (when the column was packed with 8 g of the sorbent). Two-step elution with dilute perchloric acid under hydrostatic pressure was usually used. Palladium and platinum were determined in individual fractions by AAS, with a single-beam Pye-Unicam SP 192 atomic-absorption spectrometer. Calibration graphs were prepared with standard solutions of Pd and Pt (containing NRS when complexes of both metals with NRS were being examined).

RESULTS AND DISCUSSION

Nitroso-R-salt is most commonly used as a reagent for spectrophotometric determination of cobalt, although coloured complexes are also formed with other heavy metals. For spectrophotometric determination of palladium, brief heating at 60° of the palladium solution with excess of reagent is recommended. The red palladium complex with two[23,24] or three[25] molecules of NRS is then formed. Platinum complexes with NRS have not been described before.

An anion-exchanger modified with NRS has been successfully used for chromatographic separation of some metal-ion mixtures.[26,27] Nitroso-R-salt can be extracted from aqueous solution into a solution of Aliquat 336 or trioctylamine hydrochloride in chloro-

form or benzene, to form an ion-association complex with two alkylammonium cations.[28,29]

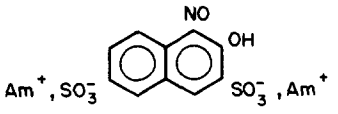

Silica gel coated with a mixture of Aliquat 336 and NRS has been used for separation of metal-ion mixtures and for preconcentration of traces of cobalt from aqueous solutions before its spectrophotometric determination.[19]

Preliminary qualitative attempts to complex platinum with NRS, performed analogously to the complexation of palladium, gave negative results, but heating of H_2PtCl_6 with an excess of NRS at 100° for 5 min resulted in the yellow colour of the free reagent solution changing to orange.

Several unsuccessful attempts were made to separate the chloride complexes of palladium and platinum on columns packed with silica coated with a mixture of Aliquat 336 and NRS, with perchloric acid as eluent. The failure results from incomplete complexation with NRS of the inert chloride complexes of both metals, and strong retention of the chloride complexes, especially of $PtCl_6^{2-}$.

Further experiments were done with silica treated with Aliquat 336, to separate complexes of palladium and platinum with NRS previously prepared in aqueous solution. Perchloric acid solutions were chosen as eluents because the perchlorate anion has low complexing ability and a strong affinity for alkylammonium cations, which should decrease the concentrations of acid required for elution of the metal complexes. Aliquat 336 (methyltricaprylammonium chloride), unlike tertiary amines,[31,32] cannot be introduced into the inner sphere of platinum complexes, so the extraction should be mainly an anion-exchange process.

The yellow complex of palladium with NRS was found to be very strongly retained; 1*M* perchloric acid is required for elution. Platinum is completely eluted with 0.25*M* perchloric acid, which simultaneously elutes nitroso-R-salt from the stationary phase. The shape of the platinum band depends on the conditions used for complexation of the two metals (see Table 1). When an unheated mixture of palladium and platinum with NRS is introduced onto the column, platinum forms two bands (the first yellow-orange, the second almost colourless), and the metals are well separated. A mixture of Pd–Pt and NRS heated for 2 min at 60°, again gives two platinum bands, but not so sharply separated. In chromatography of the chloride complexes of palladium and platinum (without addition of NRS) in analogous experimental conditions, both metals were readily eluted with 0.25*M* perchloric acid, but without separation. Usually palladium is eluted before platinum, when the chloride complexes of the two metals are separated by anion-exchange chromatography or by extraction chromatography. However, under the conditions used for complexation of the two metals with NRS (room temperature or 2-min heating at 60°), it appears that palladium forms a stable complex that is very strongly retained whereas platinum(IV) is only partially complexed with NRS to give an orange-yellow complex, and part of the platinum remains as $PtCl_6^{2-}$. Both platinum complexes are readily eluted with 0.25*M* perchloric acid. The very low retention of the yellow complex may be due to formation of an inner complex, but this supposition requires confirmation by other methods.

Since palladium forms complexes with two or three molecules of nitroso-R-salt, the extraction process for palladium can be described by the anion-exchange reactions:

$$Pd(NRS)_2^{4-} + \overline{4R_4N^+, Cl^-} \rightleftharpoons \overline{(R_4N^+)_4, Pd(NRS)_2^{4-}} + 4Cl^-$$

$$Pd(NRS)_3^{6-} + \overline{6R_4N^+, Cl^-} \rightleftharpoons \overline{(R_4N^+)_6, Pd(NRS)_3^{6-}} + 6Cl^-$$

Table 1. Retention volumes for platinum(IV) and palladium(II) in column extraction chromatography on silica impregnated with 0.3*M* Aliquat 336 in chloroform, with perchloric acid solutions as eluents

Conditions used for preparation of metal complexes	Retention volume, *ml*			
	Eluent 0.25*M* $HClO_4$			Eluent 1*M* $HClO_4$
	Pt (yellow band)	Pt (colourless)	Pd	Pd (red band)
No NRS added (250 μg of Pt, 200 μg of Pd)	—	10	8	—
NRS added, without heating (1250 μg of Pt, 125 μg of Pd; [NRS]:[Me] = 6:1)	7	14	—	8
NRS added, heating at 60° (1250 μg of Pt and 125 μg of Pd, [NRS]:[Me] = 8:1)	8	11	—	6
NRS added, heating at 100° (1250 μg of Pt, 50 μg of Pd, [NRS]:[Me] = 6:1)	10	—	—	6

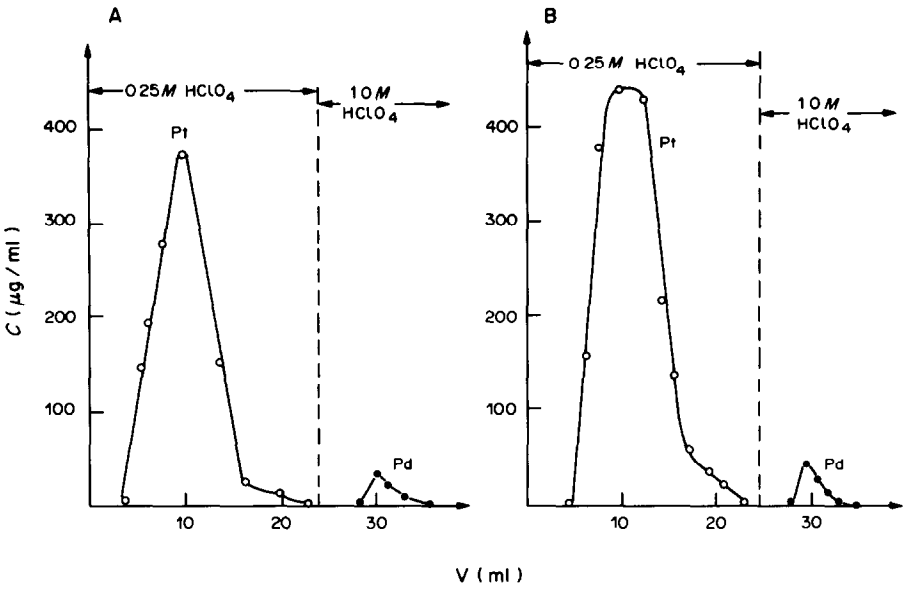

Fig. 1. Chromatograms of mixtures of platinum and palladium complexes with NRS, on silica treated with Aliquat 336. [NRS]:[Me] = 8:1. Complexes formed by heating for 5 min at 100°. Column heights 9 cm, mean flow-rates 0.4 ml/min. A—1250 μg of Pt and 50 μg of Pd; B—2000 μg of Pt and 50 μg of Pd.

Similar ion-pairs are probably formed with the platinum complexes; however, the platinum chloro-complex is also sorbed:

$$\overline{2R_4N^+, Cl^-} + 2PtCl_6^{2-} \rightleftharpoons \overline{(R_4N^+)_2, PtCl_6^{2-}} + 2Cl^-$$

The palladium and platinum complexes with NRS, and also the $PtCl_6^{2-}$ anions are displaced from the stationary phase by perchlorate ions.

The affinity of Aliquat 336 for these complexes increases in the order

$$Pt(NRS)_n^{2n-} \sim PdCl_4^{2-} < PtCl_6^{2-} \ll Pd(NRS)_m^{2m-}.$$

The formation of double bands from platinum can be eliminated by using more drastic conditions of complexation. After heating for 5 min at 100° most of the $PtCl_6^{2-}$ anions do form complexes with NRS; the platinum then forms only a single band. The relatively high retention volume, 10 ml, was probably caused by the large amounts of platinum introduced onto the column.

It should be noted that, independent of the conditions used for forming the complexes, the separation is very sharp and the metals can be eluted with relatively dilute solutions of perchloric acid. The much stronger affinity of Aliquat 336 for the palladium complex with NRS can be utilized for the separation of macro amounts of platinum from small amounts of palladium, or for concentration of traces of palladium from aqueous solutions.

Acknowledgements—This work was supported by the Institute of Chemistry of the Maria Curie-Skłodowska University in Lublin (Grant No. MR.I.14.B1-29). Thanks are due to Professor Edward Soczewiński for his interest in this work.

REFERENCES

1. F. E. Beamish, *The Analytical Chemistry of the Noble Metals*, Pergamon Press, Oxford, 1966.
2. F. E. Beamish and J. C. Van Loon, *Recent Advances in the Analytical Chemistry of the Noble Metals*, Pergamon Press, Oxford, 1972.
3. V. Sykora and F. Dubsky, *Sb. Vys. Školy Chem.-Technol. v Praze, Anal. Chem.*, 1974, **W10**, 113.
4. G. I. Ginzburg, N. A. Yezeroskaya, I. V. Prokofeeva, N. F. Fedorenko, V. I. Shlenskaya and N. K. Belskii, *Analiticheskaya khimiya platinovikh metallov*, Nauka, Moscow, 1972.
5. R. Dybczyński and E. Sterlińska, *J. Chromatog.*, 1974, **102**, 263.
6. E. Cerrai and C. Testa, *Energia Nucl. (Milan)*, 1961, **8**, 510.
7. I. Akaza, T. Kiba and T. Kiba, *Bull. Chem. Soc. Japan*, 1970, **43**, 2063.
8. C. Polandt and T. W. Steele, *Talanta*, 1972, **19**, 839.
9. S. Przeszlakowski and A. Flieger, *ibid.*, 1979, **26**, 1125.
10. *Idem, ibid.*, 1981, **28**, 557.
11. A. Flieger and S. Przeszlakowski, *ibid.*, 1982, **29**, 946.
12. M. Ziegler and O. Glemser, *Angew. Chem.*, 1956, **68**, 620.
13. M. Ziegler, O. Glemser and N. Petri, *Z. Anal. Chem.*, 1956, **153**, 415.
14. W. Kemula and K. Brajter, *Chem. Anal. (Warsaw)*, 1970, **15**, 331.
15. K. Brajter, *ibid.*, 1973, **18**, 125.
16. *Idem, J. Chromatog.*, 1974, **102**, 385.
17. K. S. Lee, W. Lee and D. W. Lee, *Anal. Chem.*, 1978, **50**, 255.
18. S. Przeszlakowski, E. Soczewiński, R. Kocjan, J. Gawecki and Z. Michno, *Polish Patent*, P-219538, Nov. 1979.
19. S. Przeszlakowski and R. Kocjan, *Chromatographia*, 1982, **15**, 717.
20. *Idem, ibid.*, 1983, **17**, 266.
21. *Idem, Abstracts of Euroanalysis V*, Cracow, 1984, p. 216.

22. S. Przeszlakowski and H. Wydra, *Talanta*, 1984, **31**, 401.
23. M. Bobtelsky and B. Mayer, *Anal. Chim. Acta*, 1956, **15**, 164.
24. S. P. Sangel and A. K. Dey, *Z. Anal. Chem.*, 1964, **202**, 15.
25. F. E. Beamish, *Talanta*, 1965, **12**, 743.
26. K. Brajter and E. Dąbek-Złotorzyńska, *ibid.*, 1980, **27**, 19.
27. *Idem*, *Abstracts of Euroanalysis V*, Cracow 1984, p. 199.
28. S. Przeszlakowski and K. Wydra, *Chromatographia*, 1981, **14**, 685.
29. S. Przeszlakowski, R. Kocjan and E. Habrat, *Chem. Anal. (Warsaw)*, 1982, **27**, 73.
30. A. S. Kertes, Y. Marcus and E. Yanir, *Equilibrium Constants of Liquid–Liquid Distribution Reactions, Part 2: Alkylammonium Salts Extractants*, Butterworths, London, 1974.
31. L. M. Gindin, *Izv. Sib. Otd. Akad. Nauk SSR, Ser. Khim. Nauk*, 1967, **6**, 36.
32. L. M. Gindin, *Ekstraktsionny processy i ikh primenene*, p. 57. Nauka, Moscow, 1984.

Talanta, Vol. 32, No. 12, pp. 1145–1150, 1985
Printed in Great Britain.

0039-9140/85 $3.00 + 0.00

POLAROGRAPHIC CATALYTIC NICKEL PREWAVE INDUCED BY SOME CYSTEINE-CONTAINING DIPEPTIDES

F. G. BĂNICĂ
Department of Analytical Chemistry, Bucharest Polytechnic, Spl. Independenţei 313, Bucharest, Romania

(*Received* 19 *November* 1984. *Revised* 1 *June* 1985. *Accepted* 19 *June* 1985)

Summary—The catalytic nickel prewave produced by Cys–Gly, Cys–Tyr and Cys–Phe was studied in acetate buffer at pH 4–6.5. These peptides are more active than cysteine, especially the last two. The catalytic activity is depressed by decrease of pH owing to protonation of the catalyst. However, Cys–Phe and Cys–Tyr are still active at pH < 5, in contrast to Cys–Gly and Cys. This difference is accounted for by the interaction of the aromatic ring with the electrode surface at potentials more positive than the potential of zero-charge. This effect enhances the surface concentration of the catalyst in the case of Cys–Phe or Cys–Tyr. At pH < 5, a catalyst concentration $\leqslant 10^{-5}M$ and large excess of nickel, the current is controlled by the rate of accumulation of catalyst in the adsorbed state. Under these conditions the reducible complex is a 1:1 Ni^{2+}-catalyst chelate. The catalytic wave recorded at pH 4.8 allows the determination of Cys–Phe or Cys–Tyr (10^{-6}–$10^{-4}M$) in the presence of the constituent amino-acids.

Since the establishment of the mechanism of the catalytic polarographic prewave of nickel or cobalt,[1] the catalytic activity of cysteine and some related compounds has been investigated by several authors. Kůta,[2] and Zielinski and Kůta,[3] studied the catalytic prewave of nickel and cobalt, respectively, in the presence of cysteine or cystine. As shown by Căluşaru and Voicu[4,5] selenocysteine behaves analogously in the potential range for the metal-ion prewave, although it does not give a catalytic hydrogen wave of Brdička type. Kolthoff *et al.*[6] described the behaviour of cysteine and several cysteine-like compounds in an attempt to gain more information about the composition of the complex responsible for the appearance of the prewave. It was found that both amino- and carboxylate-groups can act as one of the coordination sites, the other being the thiol group. Recently, López Fonseca and Arredondo[7] showed that even methionine exhibits catalytic activity in the reduction of nickel ion. However, it is not quite clear whether the cation is bound to sulphur or to another group, as in the case of the nickel prewave produced by other amino-acids.[8]

The catalytic prewaves of nickel or cobalt have usually been studied in alkaline media, which are also typical for the Brdička catalytic hydrogen wave.[9] Detailed studies on the catalytic nickel prewave in slightly acidic media have been made for the Ni–selenocystine[10] and Ni–cysteine systems, in both normal[11] and heavy[12] water. Under these conditions the protonation of the catalyst competes with the formation of the reducible complex.

The study of the catalytic properties of oligopeptides is also interesting, from two points of view. First, it is possible to gain some information which is useful in the interpretation of the catalytic properties of large protein molecules. Secondly, some sensitive methods for peptide determination can be based on their catalytic properties. Recent studies in this field were mainly directed toward the investigation of glutathione[13–15] and several dipeptides[16] as catalysts for hydrogen-ion reduction in presence of cobalt or nickel ions. Some preliminary data on the catalytic nickel prewave produced by cysteinyl-dipeptides have also been published.[17,18]

The aim of this work was to study the catalytic nickel prewave produced in acetate buffer by the following compounds: cysteinyl-glycine (Cys–Gly), cysteinyl-phenylalanine (Cys–Phe) and cysteinyl-tyrosine (Cys–Tyr). Since the peptides were in oxidized form, cystine (Cys) was chosen as reference compound.

EXPERIMENTAL

The peptides (Serva), cystine (Merck), cobalt-free nickel chloride (Riedel de Haën), and the other chemicals were analytical-grade materials.

Direct current polarographic measurements were made with an LP 7e polarograph (Czechoslovakia) in combination with a Radelkis OH 814/1 strip-chart recorder at a scan-speed of 100 or 200 mV/min. The characteristics of the dropping-mercury electrode were: drop-time, 5.69 sec, flow-rate, 1.40 mg/sec measured in 0.1*M* sodium acetate at 0 V *vs.* SCE and 64-cm mercury height. The two-electrode cell had an SCE as anode and was kept at 25 ± 0.1°. Pure nitrogen was used to expel oxygen from test-solutions. The pH-values were measured with a glass electrode standardized against NBS standard buffers.

RESULTS

Catalytic nickel prewave produced by peptides

Typical polarograms showing the catalytic prewaves of nickel are presented in Fig. 1. The prewave

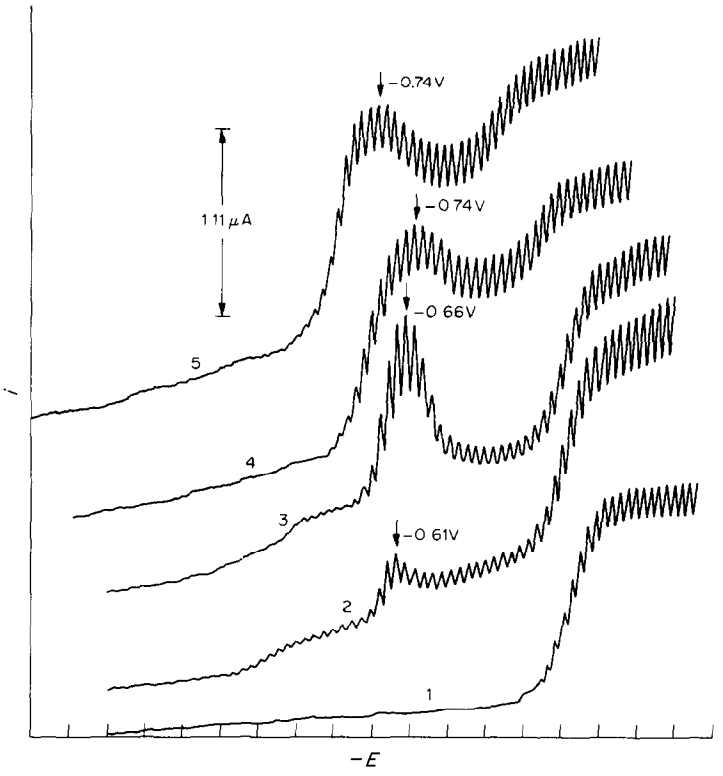

Fig. 1. Catalytic nickel prewave in acetate buffer (pH 5.66). (1) $[CH_3COONa] + [NaClO_4] = 0.1M$; CH_3COOH, $2 \times 10^{-3}M$; $NiCl_2$, $2 \times 10^{-4}M$. (2–4) as for (1), $+10^{-4}M$ catalyst. (2) Cys; (3) Cys–Gly; (4) Cys–Tyr; (5) Cys–Phe. Start potential, 0 V.

has a maximum and its height increases according to the peptide used, in the sequence Cys < Cys–Gly < Cys–Tyr ⩽ Cys–Phe. The potential of the maximum is more negative with Cys–Phe and Cys–Tyr than Cys–Gly or Cys.

The prewave is preceded by the first reduction-wave of the disulphide bond. This wave is inhibited by nickel ion, probably in the same way as in the system Co–cystamine.[19] The inhibition is much stronger with Cys–Phe and Cys–Tyr than Cys–Gly and is hardly observable for Cys.

It must be stressed that the prewave produced by Cys appears on the rising part of the second wave of disulphide reduction, but the peptides are reduced almost entirely in the first step. Thus, in the potential range for the nickel prewave the peptides are present in reduced form on the surface of the electrode, whereas Cys is only partly reduced. Accordingly, the base-line for the nickel prewave is represented by the reduction current of the disulphide. Owing to the inhibitory effect mentioned above, the current recorded in the absence of nickel ion cannot be considered as the background. Consequently, the base-line is obtained by linear extrapolation of the current preceding the rising part of the nickel prewave.

Effect of pH

The effect of pH was investigated in the range 4–6.5 at constant ionic strength ($[CH_3COONa] + [NaClO_4] = 0.1M$). As shown in Fig. 2, the nickel prewave is very sensitive to pH. At pH 6 the catalytic current produced by peptides (curves 1–3) is almost equal to the nickel diffusion current. The nickel prewave produced by Cys (curve 4) is lower and practically vanishes at pH < 5.5. Conversely, the peptides exhibit a significant catalytic activity even at lower pH-values, especially Cys–Phe and Cys–Tyr.

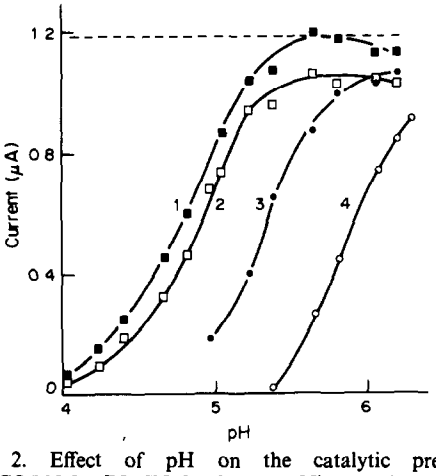

Fig. 2. Effect of pH on the catalytic prewave. $[CH_3COONa] + [NaClO_4] = 0.1M$; $NiCl_2$, $2 \times 10^{-4}M$; catalyst, $10^{-4}M$; CH_3COOH, $2 \times 10^{-3}M$ (for pH > 5) or $1.8 \times 10^{-2}M$ (for pH < 5). (1) Cys–Phe; (2) Cys–Tyr; (3) Cys–Gly; (4) Cys. Dashed line: the nickel diffusion current in the absence of the catalyst.

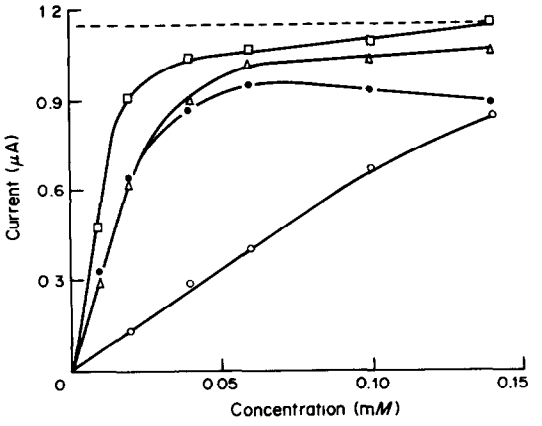

Fig. 3. Effect of the catalyst concentration at pH = 6.13. CH_3COONa, 0.097M; CH_3COOH, $3.7 \times 10^{-3}M$; $NiCl_2$, $2 \times 10^{-4}M$. (○) Cys; (●) Cys–Gly; (△) Cys–Tyr; (□) Cys–Phe. Dashed line: the nickel diffusion current in the absence of the catalyst.

That is why the effect of the other parameters was further investigated in two different pH ranges, namely, ~6 and ~5.

Another effect of a decrease in pH is the slight displacement of the current-maximum towards more positive potentials, and simultaneous narrowing of the maximum.

Effect of catalyst concentration

Figure 3 presents the influence of the peptide concentration at pH 6.13. The catalytic current produced by the peptides increases sharply, reaching a limit at a peptide/Ni^{2+} ratio of about 0.25. At this pH there are no essential differences between the catalytic activities of the peptides, whereas Cys exhibits a much lower activity.

At pH 4.8 Cys–Phe gives rise to the nickel prewave even at $10^{-6}M$ concentration if the Ni^{2+} concentration is increased to $10^{-3}M$ (Fig. 4). Curve 2 in this figure shows a linear dependence of the catalytic current on peptide concentration below $10^{-5}M$. Cys–Tyr behaves similarly, but Cys–Gly is much less active in this pH range.

Effect of Ni^{2+} concentration

At pH about 6 and with $10^{-4}M$ catalyst the catalytic current produced by peptides is practically equal to the nickel diffusion current and linearly dependent on the Ni^{2+} concentration. Conversely, the catalytic current induced by Cys always remains lower than the nickel diffusion current and the ratio of these two currents (i_{cat}/i_{diff}) decreases as the Ni^{2+} concentration increases.

At lower pH-values and/or peptide concentrations the catalytic current is much lower than the diffusion current. Under these conditions the catalytic current varies linearly with the Ni^{2+} concentration. For example, at pH 4.8, $10^{-5}M$ Cys–Tyr and 10^{-4}–$2 \times 10^{-3}M$ Ni^{2+} the relationship is:

$$\bar{i} = 3.8 \times 10^2 c_{Ni} \qquad (1)$$

where $\bar{i}$ is expressed in μA, and c_{Ni} in molarity.

Effect of the height of the mercury reservoir (h) *and determination of current–time* (i–t) *curves for a single drop*

The effect of h was investigated for two special cases: (1) at pH 6.2, $10^{-4}M$ peptide and $2 \times 10^{-4}M$ nickel chloride; (2) pH 4.8, $10^{-5}M$ peptide and $10^{-3}M$ nickel chloride. In the first case the maximum current is a linear function of $h^{1/2}$ (Table 1). Although the nickel prewave current produced by peptides is about 80% of the nickel diffusion current, the wave is not completely diffusion-controlled. The catalytic wave produced by Cys represents about 40% of the diffusion current and shows a marked kinetic charac-

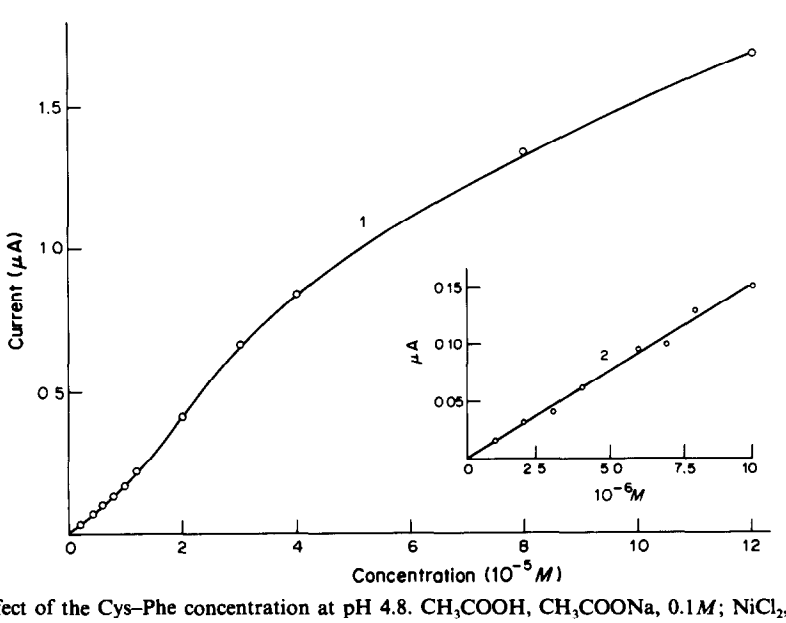

Fig. 4. Effect of the Cys–Phe concentration at pH 4.8. CH_3COOH, CH_3COONa, 0.1M; $NiCl_2$, $10^{-3}M$.

Table 1. The parameters of the $\bar{i}$ *vs.* $h^{1/2}$ straight lines [0.095M CH_3COONa, $3 \times 10^{-3}M$ CH_3COOH (pH 6.20), $10^{-4}M$ catalyst, $2 \times 10^{-4}M$ $NiCl_2$; h had 6 values ranging between 34 and 84 cm; the confidence interval for the intercept is given for $\alpha = 0.1$]

Catalyst	Intercept, μA	Slope, $\mu A/cm^{1/2}$
Cys–Phe	0.182 ± 0.075	0.132
Cys–Gly	0.202 ± 0.12	0.104
Cys–Tyr	0.439 ± 0.10	0.094
Cys	0.544 ± 0.16	0.025

ter. In the second case, only Cys–Phe and Cys–Tyr were studied. The maximum current is a linear function of h, with slope -0.43 for Cys–Phe and -0.45 for Cys–Tyr. The i–t curves were recorded under the same conditions at various potentials. For the rising part of the wave the slope of a $\log i$ *vs.* $\log t$ plot varies between 1 and 1.1. In the range of the minimum current (-0.72 V) the slope is 0.90.

Effect of the constituent amino-acids

At pH 6.2 the nickel prewave produced by Cys ($10^{-4}M$) is not influenced by tyrosine or phenylalanine, even in threefold excess. Consequently, no mixed complexes of Ni^{2+} with cysteine and the other amino-acids are involved in the electrode process. However, some interference by the constituent amino-acids in the Ni^{2+} reduction catalysed by peptides was observed at pH 4.8 and high Ni^{2+} concentration. In Fig. 5 the catalytic current produced by Cys–Tyr is plotted as a fraction of the value measured in the absence of the amino-acid. Tyrosine (curve 1) produces only a slight increase of the catalytic current (about 5%). This value remains unchanged until a 50-fold excess is present. The effect of cysteine (curve 2) is rather different: there is no interference below $5 \times 10^{-5}M$ and a marked increase of the catalytic current at higher concentrations. The current represents 105% of the initial value at $10^{-4}M$ cysteine concentration (10-fold excess) and 110% at about $2 \times 10^{-4}M$. Analogous effects were observed in the case of Cys–Phe and can be attributed to the residual catalytic activity of the amino-acids at pH < 5.

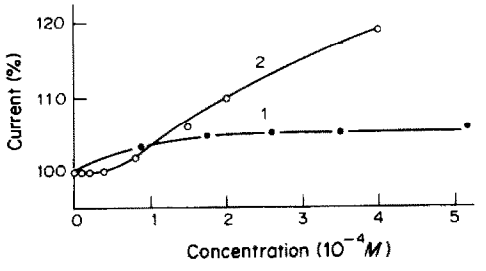

Fig. 5. Effect of the constituent amino-acids on the catalytic prewave produced by Cys–Tyr at pH 4.8. CH_3COOH, CH_3COONa, 0.1M; $NiCl_2$, $10^{-3}M$; Cys–Tyr, $10^{-5}M$. (1) Tyrosine; (2) cysteine.

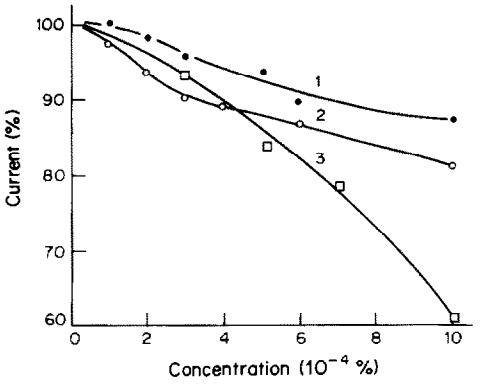

Fig. 6. Effect of surface-active compounds on the catalytic prewave at pH 4.8. CH_3COOH, CH_3COONa, 0.1M; $NiCl_2$, $10^{-3}M$; Cys–Phe, $10^{-5}M$. (1) Ovalbumin; (2) gelatin; (3) Triton X-100.

Effect of surface-active compounds

Figure 6 shows the influence of two protein compounds (ovalbumin, curve 1, and gelatin, curve 2) and of the non-ionic detergent Triton X-100 (curve 3). The current is given as a fraction of the value measured in the absence of the surfactant.

Although gelatin and ovalbumin decrease the catalytic current at low concentrations, their effect tends toward a limit, the current being approximately 90% of the initial value when the surfactant concentration is 10^{-3}%. Conversely, Triton X-100 produces a monotonic decrease in the catalytic current.

DISCUSSION

The catalytic reduction of Ni^{2+} in the presence of cysteinyl dipeptides occurs basically in the same way as in the presence of cysteine itself.[11] The main difference is the higher catalytic activity of peptides. The following steps of the reaction mechanism are the most important.

1. Diffusion of the catalyst (in oxidized form) toward the electrode surface.
2. Adsorption of the catalyst and reduction of the disulphide bond.
3. Reaction of the catalyst (in reduced form) with Ni^{2+} to give the complex reducible in the potential range of the catalytic nickel prewave.
4. Reduction of Ni^{2+} in this complex, followed by release of the catalyst molecule, which can bind another Ni ion.

Steps 3 and 4 are repeated until the drop falls, giving the electrode process its catalytic character.

For a quantitative approach to the mechanism of the electrode process we shall confine ourselves to the following conditions: pH < 5, peptide concentration $\leqslant 10^{-5}M$ and large excess of Ni^{2+} (1–$2 \times 10^{-3}M$). These conditions are interesting from an analytical point of view (*i.e.*, for the determination of peptides in presence of cysteine). The main peculiarity of the

nickel prewave recorded under these conditions is that the catalytic current is much lower than the diffusion current.

Obviously, step 3 occurs with the reactants in the adsorbed state, as previously proved by drop-time *vs.* potential curves.[11] The inhibitory effect of the surface-active compounds in the systems studied here leads to the same conclusion. On the other hand, the effect of h and the slope of the log i *vs.* log t plots point to the accumulation of the catalyst on the surface during the drop-life. Accordingly, the surface concentration of the catalyst in reduced form, Γ_c, will be given by the Koryta equation:[20]

$$\Gamma_c = 2 \times 7.36 \times 10^{-4} c_c D_c^{1/2} t^{1/2} \quad (2)$$

where c_c and D_c signify the bulk concentration and the diffusion coefficient of the oxidized form, respectively, and the factor 2 is introduced because two catalyst molecules are formed by the reduction of one disulphide molecule.

It is well known that the Koryta equation refers to diffusion-controlled adsorption. In the case of the disulphide the concentration gradient is produced by electrochemical reduction. If the reduced form remains in the adsorbed state, then equation (2) holds in the range of the disulphide diffusion current. As already shown, this condition is fulfilled in the potential range of the nickel prewave produced by dipeptides.

The reducible complex is formed by the reaction of nickel ions with the ionized catalyst molecules. The concentration of nickel at the electrode-solution boundary, c_{Ni}°, can be expressed by the following relation derived from the Ilkovič equation:

$$c_{Ni}^{\circ} = c_{Ni}[1 - (i/i_d)] \quad (3)$$

where c_{Ni} is the bulk-concentration of nickel ion, i the instantaneous catalytic current and i_d the diffusion current of Ni^{2+}. Under the conditions stated, $i \ll i_d$ and to a first approximation $c_{Ni}^{\circ} = c_{Ni}$.

The concentration of catalyst in the ionized state, Γ_L, is determined by the pH. However, the influence of this parameter is more complicated. It affects not only the catalytic current but also the width of the wave and the potential of the maximum. These effects can be accounted for by the relationship between the surface activity of the catalyst and its degree of protonation, and are connected with the shape of the catalytic wave. This topic will be dealt with in another paper. The present treatment is restricted to constant pH, and consequently of constant potential for the maximum on the wave. Assuming that protonation of the catalyst in the adsorbed state is an equilibrium

$$qH^+ + L \rightleftharpoons H_qL \quad (4)$$

with formation constant β, the concentration of the ionized form is given by

$$\Gamma_L = K\Gamma_c \quad (5)$$

where $K = 1/(1 + \beta c_{H^+}^q)$ is constant at a given pH. The charge of the catalyst in ionized form is omitted for simplicity.

If the reaction rate of the complex formation is

$$v = k\Gamma_L^p (c_{Ni}^{\circ})^r \quad (6)$$

where k is the rate constant, then the instantaneous current is given by:

$$i = nFv\,(0.85 m^{2/3} t^{2/3}) \quad (7)$$

where the expression in parenthesis represents the instantaneous drop-area at time t,[20] m is the mercury flow-rate, n the number of electrons involved in the charge-transfer reaction and F the Faraday constant. If $n = 2$, then

$$i = 1.7(14.72 \times 10^{-4} D_c^{1/2})^p FkK^p m^{2/3} \times t^{[(2/3)+(p/2)]} c_c^p c_{Ni}^r \quad (8)$$

and the mean current is

$$\bar{i} = \frac{10}{10 + 3p} (14.72 \times 10^{-4} D_c^{1/2})^p FkK^p m^{2/3} \times t_1^{(4+3p)/6} c_c^p c_{Ni}^r \quad (9)$$

t_1 being the drop-time. Denoting the product of the constant factors by Q and taking into account the well-known relationships between h and m or t_1, we have:

$$\bar{i} = Qh^{p/2} c_c^p c_{Ni}^r \quad (10)$$

or

$$\log \bar{i} = \log Q - \frac{p}{2} \log h + p \log c_c + r \log c_{Ni} \quad (11)$$

As shown in the experimental part, under the above-mentioned conditions $\bar{i}$ is a linear function of the nickel or catalyst concentration. Consequently, it follows immediately that $p = 1$ and $r = 1$. According to equations (8) and (10), the instantaneous current must be proportional to $t^{7/6}$ and the mean current to $1/h^{1/2}$. The experimental results agree satisfactorily with these conclusions, proving the validity of the model based on assumption of negligible concentration polarization.

At higher i/i_d values the overall reaction rate is partly determined by the diffusion of Ni^{2+}, as is demonstrated by the data in Table 1. This change in the reaction mechanism accounts for the shape of curve 1 in Fig. 4 as well as for the trend of the catalytic current toward a limit with increase in pH (Fig. 2) or catalyst concentration (Fig. 3).

These results show that in the range of the catalytic nickel prewave a 1:1 Ni^{2+}–catalyst complex is reduced. The same combining ratio was found for the reducible complex in the Co–thiopyrimidine system.[21] The complexing properties of the functional groups in the peptide molecule[22] as well as the striking analogy with the behaviour of free cysteine suggest that the nickel ion is bound to the $-NH_2$ and $-SH$ groups of the cysteine residue. The same conclusion is supported by the lack of noticeable effects of Tyr or Phe on the nickel prewave produced by cysteine.

The catalytic activity depends not only on the complexing capacity of the catalyst but also on its surface activity. This last is determined by two factors: (1) the hydrophobic properties of the molecule and (2) the interaction of the π-electrons from the side-chain of the second amino-acid with the electrode surface.[23] The latter effect accounts for the catalytic activity of Cys–Phe and Cys–Tyr being higher than that of Cys or Cys–Gly, whereas only the first factor is operative in the case of Cys–Gly.

The behaviour of the cysteinyl-peptides studied in this work may be considered as characteristic of this class of compounds. Consequently, it can be presumed that the cysteinyl-peptides are generally more active than cysteine itself in the catalytic reduction of Ni^{2+}, and the catalytic activity is strongly enhanced by the aromatic side-chains.

ANALYTICAL APPLICATIONS

The catalytic nickel prewave produced by cysteinyl-peptides permits their polarographic determination at very low concentrations (10^{6}–$10^{-4}M$). If the sample also contains the constituent amino-acids, it is recommended to use $10^{-3}M$ nickel solution in acetate buffer (0.1M CH_3COOH, CH_3COONa) as supporting electrolyte. The calibration graph for Cys–Phe or Cys–Tyr is linear at peptide concentrations below $10^{-5}M$. For example, for 5 standard solutions of Cys–Phe for the regression equation $\bar{i} = a + bc$, a was $7 \times 10^{-4}\,\mu$A (standard deviation $1.2 \times 10^{-3}\,\mu$A), b was $1.605 \times 10^{4}\,\mu$A. l. mole^{-1}, correlation coefficient, 0.9998; standard deviation of $\bar{i}$, 1.14×10^{-3}. The limit of determination calculated by the method of Currie[24] was $1.1 \times 10^{-6}M$.

The determination limit can be improved by using a higher pH, but the interference of cysteine is then also enhanced. At pH = 4.8, a moderate excess of cysteine (ten fold) or a large excess of phenylalanine or tyrosine (fiftyfold) does not introduce an error (positive) >5%.

The nickel prewave is influenced by surfactants, and their effect must always be taken into account. The standard-additions method is recommended for surfactant-containing samples.

Acknowledgements—The author is indebted to Dr. J. Kadleček, who kindly provided the peptides used in this work, and to Dr. A. Căluşaru for helpful discussion.

REFERENCES

1. H. B. Mark, Jr. and C. N. Reilley, *J. Electroanal. Chem.*, 1962, **4**, 189.
2. J. Kůta, *Z. Anal. Chem.*, 1966, **216**, 243.
3. M. Zielinski and J. Kůta, *Collection Czech. Chem. Commun.*, 1969, **34**, 2523.
4. A. Căluşaru and V. Voicu, *J. Electroanal. Chem.*, 1969, **20**, 463.
5. *Idem, ibid.*, 1971, **32**, 427.
6. I. M. Kolthoff, P. Mader and S. E. Khalafalla, *ibid.*, 1968, **18**, 315.
7. J. M. López Fonseca and M. C. Arredondo, *Analyst*, 1982, **107**, 903.
8. *Idem, An. Quim.*, 1982, **78**, 108.
9. A. Căluşaru, *J. Electroanal. Chem.*, 1967, **15**, 269.
10. A. Căluşaru and V. Voicu, *J. Electroanal. Chem.*, 1973, **43**, 257.
11. F. G. Bănică and A. Căluşaru, *ibid.*, 1983, **145**, 389.
12. *Idem, ibid.*, 1983, **158**, 47.
13. B. Jezowska-Trzebiatowska, M. Jaruga-Baranowska, M. Ostern and H. Kozlowski, *Polish J. Chem.*, 1981, **55**, 2477.
14. M. I. Ostern and M. Jaruga-Baranowska, *Electrochim. Acta*, 1983, **29**, 1173.
15. F. G. Bănică and E. Diacu, *First Int. Symp. Kinetics in Anal. Chem., Córdoba, 1983*, Poster I 13.
16. J. Kadleček and V. Kalous, *J. Electroanal. Chem.*, 1979, **105**, 225.
17. F. G. Bănică, *9th Int. Symp. Microchem. Techn. Trace Analysis, Amsterdam, 1983*, Poster III-29.
18. *Idem, J. Electroanal. Chem.*, 1984, **171**, 351.
19. P. Mader and I. M. Kolthoff, *Anal. Chem.*, 1969, **41**, 932.
20. J. Heyrovský and J. Kůta, *Principles of Polarography*, p. 304. Czechoslovak Academy of Sciences, Prague, 1965.
21. J. M. López Fonseca, P. Sanz Pedrero and C. Gonzalez Posa, *J. Chim. Phys.*, 1980, **77**, 9.
22. H. C. Freeman, in G. L. Eichhorn (ed.), *Inorganic Biochemistry*, Elsevier, Amsterdam, 1975, (Russian transl., Mir, Moscow, 1978, Vol. 1, p. 151).
23. A. N. Frumkin and B. B. Damaskin, in *Modern Aspects of Electrochemistry*, J. O'M. Bockris and B. E. Conway (eds.), Vol. 3, p. 164. Butterworths, London, 1964.
24. L. A. Currie, *Anal. Chem.*, 1968, **40**, 586.

Talanta, Vol. 32, No. 12, pp. 1151–1152, 1985
Printed in Great Britain.

0039-9140/85 $3.00 + 0.00

SHORT COMMUNICATIONS

A POLAROGRAPHIC STUDY OF SOME COMPLEXES OF Tl(I) WITH POLYOXA MACROCYCLIC LIGANDS

MOHAMED MAGDI KHALIL
Assiut University, Faculty of Science, Chemistry Department, Assiut, Egypt

ION TĂNASE and CONSTANTIN LUCA*
Polytechnical Institute of Bucharest, Faculty of Chemical Technology, Department of Analytical Chemistry, Splaiul Independentei 202, 79611-Bucharest, Romania

(*Received* 23 *October* 1984. *Revised* 8 *August* 1985. *Accepted* 29 *August* 1985)

Summary—The log β_1 values at 25° for the reaction in aqueous solution of Tl(I) with 15-crown-5, benzo-15-crown-5, 18-crown-6 and dicyclohexyl-18-crown-6 (isomer *cis-syn-cis*) have been determined by d.c. and a.c. polarographic measurements.

The influence of the complexing capacity of some biological macrocyclic compounds on transport mechanisms in living organisms is now well understood. Studies made during the last few years have aimed at synthesizing such macrocycles or equivalent compounds. In 1967, Pedersen[1-4] synthesized the first "planar" macrocycles, the cyclic polyethers ("crown ethers"), which have outstanding ability to complex some metal cations, particularly those of the alkali and alkaline-earth metals. Dietrich *et al.*[5,6] later synthesized a new macrocycle, diazo-1,10-hexaoxa-4,7,13,16,21,24-dicyclo-[8.8.8]-hexacosane, abbreviated to [2.2.2], and during the following years others synthesized dicycles of the same type, particularly the [2.1.1], [2.2.1], [3.2.2] and [3.3.3] compounds. The inner cavities of these dicycles have different sizes, which allows them to form stable complexes with a large number of metal cations; all these complexes have 1:1 stoichiometry and are soluble in water and (when coupled with a suitable counter-ion) in many organic solvents. The metal cation occupies the central cavity of the macrocycle.

Ligands of this type play an important role in electrochemistry, partly because they allow dissolution of many inorganic salts in various organic media, and partly because, from a theoretical point of view, study of the electrochemical behaviour of the complexes formed is an interesting way of analysing the redox mechanisms which take place at the mercury electrode.

Together with potentiometry, cyclic voltammetry and coulometry,[7-11] polarography is a very useful means of studying the electrochemical behaviour of these macrocyclic compounds and the stability of the compounds formed with various metal cations. Work in this line was initiated by Koryta and co-workers[12-14] with crown ethers, and by Peter and co-workers[15-19] with dicyclic cryptand compounds.

The aim of this work was to obtain d.c. and a.c. polarographic data for complexation with crown ethers (15-crown-5, benzo-15-crown-5, 18-crown-6, dicyclohexyl-18-crown-6: see Fig. 1) in aqueous media.

EXPERIMENTAL

The polarographic measurements were made with a PRG-3 Tacussel polarograph and a three-electrode cell provided with a thermostatic jacket. The capillary used had $m = 1.152$ mg/sec, $t = 4.15$ sec, in 0.1*M* nitric acid at -0.200 V relative to an SCE, with a 60-cm mercury head. All measurements were made at $25 \pm 0.1°$, and the potentials were determined relative to an SCE connected to the working cell through a 0.1*M* nitric acid bridge.

All reagents used were of analytical-grade purity, and the water used was distilled four times. The supporting electrolyte was 0.1*M* nitric acid. Before polarography, solutions were deaerated by passage of purified argon for 10 min.

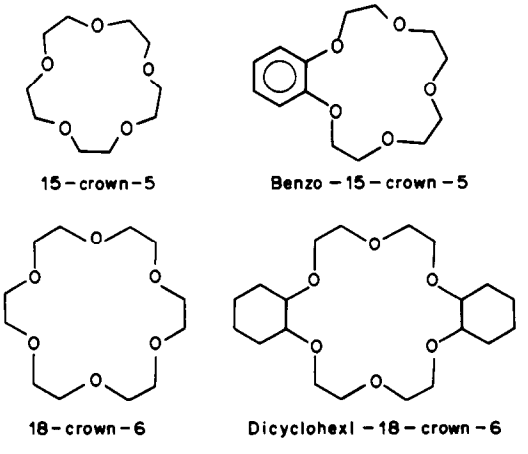

Fig. 1

*To whom correspondence should be addressed.

RESULTS AND DISCUSSION

Addition of the crown polyether to thallium(I) solution in 0.1*M* nitric acid shifts the d.c. half-wave potentials ($E_{1/2}$) and a.c. peak potentials (E_p) for the reduction of the complex ion towards more negative values. The reduction waves for the complexes are reversible and diffusion-controlled. Logarithmic analysis of the d.c. and a.c. polarograms shows a linear relationship of $\log[i/(i_d - i)]$ and E_{dc}, and of $\log(i_p/i)^{1/2} + [(i_p - i)/i]^{1/2}$ and E_p, respectively, with slopes corresponding to a reversible reduction involving the transfer of a single electron.

The variation of the half-wave potential as a function of the logarithm of the ligand concentration was linear for all four polyethers, showing that a single complex is formed in solution; the slopes of the straight lines suggest that a 1:1 complex is formed.

To estimate the stability constants of these complexes we used the relation

$$E^c_{1/2} - E_{1/2} = \frac{RT}{2nF} \ln \frac{D_{M^{n+}}}{D_{ML^{n+}}} + \frac{RT}{nF} \ln \beta_1[L] \quad (1)$$

where $E^c_{1/2}$ is the half-wave potential corresponding to the reduction wave of the complex, $E_{1/2}$ is the half-wave potential corresponding to the reduction wave of uncomplexed thallium(I), $D_{M^{n+}}$ and $D_{ML^{n+}}$ are the diffusion constants for the free metal ion and the complex, β_1 is the stability constant of the complex, and the other symbols have their usual significance. The relation in this form[20-22] is only valid when a single complex species is formed and its stability is high.

Bond[23,24] and others[25-28] have shown that, for reversible electrode reactions, a.c. polarographic measurements may be used with good accuracy to obtain information on the nature and stability of a complexed ion which is electroactive at the dropping mercury electrode.

For a reversible electrode reaction monitored by a.c. polarography, the peak potential E_p is equal to the reversible d.c. half-wave potential $E_{1/2}$ and therefore to estimate the stability constant we can use equation (1), which can be written as

$$\exp\left[-\frac{nFE_{1/2}}{2.303RT}\right] - 1 = \beta_1[L] \quad (2)$$

if we assume that $D_{M^{n+}} \approx D_{ML^{n+}}$.

The values of the stability constants found for the complexes formed by thallium(I) with 15-crown-5, benzo-15-crown-5, 18-crown-6 and dicyclohexyl-18-crown-6 are given in Table 1.

Table 1. The log β_1 values at 25° for the reaction in aqueous solution of Tl(I) with 15-crown-5, benzo-15-crown-5, 18-crown-6 and dicyclohexyl-18-crown-6

Crown ether	Method	
	d.c. polarography	a.c. polarography
15-Crown-5	2.63 ± 0.09	2.72 ± 0.04
Benzo-15-crown-5	2.27 ± 0.07	2.30 ± 0.07
18-Crown-6	2.98 ± 0.05	3.06 ± 0.04
Dicyclohexyl-18-crown-6	3.20 ± 0.20	3.18 ± 0.20

REFERENCES

1. C. J. Pedersen, *J. Am. Chem. Soc.*, 1967, **89,** 2495.
2. *Idem, ibid.*, 1967, **89,** 7017.
3. *Idem, ibid.*, 1970, **92,** 386.
4. *Idem, ibid.*, 1970, **92,** 391.
5. B. Dietrich, J. M. Lehn and J. P. Sauvage, *Tetrahedron Lett.*, 1969, **34,** 2885.
6. *Idem, ibid.*, 1969, **34,** 2889.
7. J. J. Christensen, D. J. Eatough and R. M. Izatt, *Chem. Revs.*, 1974, **74,** 351.
8. J. M. Kolthoff, *Anal. Chem.*, 1979, **51,** 1R.
9. J. Massaux, J. F. Desreux, C. Delchambre and G. Duyckaerts, *Inorg. Chem.*, 1980, **19,** 1893.
10. J. Koryta and M. Gross, in *Topics in Bioelectrochemistry and Bioenergetics*, Vol. 3, p. 93. G. Milazzo (ed.), Wiley, New York, 1980.
11. E. Blasius and K. P. Janzen, in *Topics in Current Chemistry*, Vol. 98, p. 184. Springer-Verlag, Berlin, 1981.
12. J. Koryta and M. L. Mittal, *J. Electroanal. Chem.*, 1972, **36,** 14.
13. K. Angelis, M. Březina and J. Koryta, *ibid.*, 1973, **45,** 504.
14. Zh. Malysheva, J. Koryta and M. Březina, *Collection Czech. Chem. Commun.*, 1975. **40,** 2415.
15. F. Peter and M. Gross, *ibid.*, 1974, **53,** 307.
16. J. P. Gisselbrecht, F. Peter and M. Gross, *ibid.*, 1976, **74,** 315.
17. F. Peter, J. P. Gisselbrecht and M. Gross, *ibid.*, 1978, **86,** 115.
18. C. Boudon, F. Peter and M. Gross, *ibid.*, 1981, **117,** 65.
19. G. Ritzler, F. Peter and M. Gross, *ibid.*, 1981, **117,** 53.
20. J. Heyrovský and D. Ilkovič, *Collection Czech. Chem. Commun.*, 1935, **7,** 198.
21. M. von Stackelberg and H. Freyhold, *Z. Electrochem.*, 1940, **46,** 120.
22. J. J. Lingane, *Chem. Revs.*, 1941, **29,** 1.
23. A. M. Bond, *J. Electroanal. Chem.*, 1969, **20,** 109.
24. *Idem, ibid.*, 1970, **28,** 433.
25. S. L. Gupta and M. K. Chatterjee, *ibid.*, 1964, **8,** 245.
26. *Idem, Rev. Polarog. Kyoto*, 1967, **14,** 198.
27. *Idem, Indian J Chem.*, 1966, **4,** 22.

Talanta, Vol. 32, No. 12, pp. 1153–1155, 1985
Printed in Great Britain.

0039-9140/85 $3.00 + 0.00

SPECTROFLUORIMETRIC ASSAY OF TETRACYCLINE AND ANHYDROTETRACYCLINE IN COMBINATION

M. ABDEL-HADY ELSAYED, M. H. BARARY and H. MAHGOUB
Department of Pharmaceutical Analytical Chemistry, Faculty of Pharmacy, University of Alexandria, Alexandria, Egypt

(*Received* 19 *March* 1984. *Revised* 5 *August* 1985. *Accepted* 23 *August* 1985)

Summary—Spectrofluorimetric methods are described for the assay of tetracycline (TC) and anhydrotetracycline (ATC) in combination, without prior separation. The interference from ATC in the TC assay has been corrected for by forming the aluminium complexes of both drugs and measuring the difference in fluorescence at 475 and 418 nm, with excitation at 393 nm. Similarly, measurement of the fluorescence of the magnesium complexes at 525 and 470 nm (excitation at 440 nm) nullifies TC interference in the ATC assay.

Microbiological,[1–3] spectrophotometric[4] and fluorimetric[7–9] methods have been used for assay of tetracyclines. Compared with the fluorimetric methods, the microbiological methods lack specificity and the spectrophotometric methods are less sensitive. Fluorimetric determination of tetracyclines has been based on formation of the aluminium[8] or magnesium[10] complexes, but there is mutual interference when tetracycline (TC) and anhydrotetracline are both present. ATC is a degradation product of TC and a limit for it is a compendial requirement.[2] The present work describes a mathematical method for eliminating the effect of the intereference.

EXPERIMENTAL

Apparatus

A Perkin–Elmer 650-10S fluorescence spectrometer was used, with a 1 × 1 cm cross-section quartz cuvette. The spectral band-width was 10 nm for both excitation and emission. Before measurement of each batch of samples, the instrument was standardized with quinine sulphate solution (0.05 mg/l.) in 0.1*M* sulphuric acid to give a scale reading of 80% with excitation at 350 nm and emission measurement at 455 nm.

Reagents

*Aluminium chloride solution, 0.75*M.

*Magnesium sulphate solution, 0.75*M.

Sørensen's citrate buffer, pH 6.0. Made by mixing 59.5 ml of 0.1*M* disodium citrate (21.0 g of citric acid monohydrate dissolved in 200 ml of 1*M* sodium hydroxide and made up to 1 litre) with 40.5 ml of 0.1*M* sodium hydroxide, the pH being checked by pH-meter and adjusted if necessary.

Standard solutions of TC and ATC. Made by dissolving 100 mg of tetracycline hydrochloride (Lederle) or 20.0 mg of anhydrotetracycline hydrochloride (prepared according to Simmons *et al.*[11]) and diluting to volume with water in a 100-ml standard flask.

Calibration graphs

For TC. Transfer 0.50, 1.00, 1.50, 2.00 and 2.50 ml portions of standard TC solution into 100-ml standard flasks, dilute to volume with water and mix. Add 5.00 ml of pH-6 buffer to 5.00 ml of each dilution, followed by 2.50 ml of aluminium chloride solution. Let stand for 15 min at room temperature (25°), then measure the fluorescence at 475 (F_{475}) and 418 nm (F_{418}) with excitation at 393 nm. Prepare and measure a blank solution in the same way. Plot F_{475} and $F_{475} - F_{418}$ *vs.* concentration.

For ATC. Transfer 1.00, 2.00 . . . 6.00, 7.00 ml portions of ATC into 100-ml standard flasks and dilute to volume with water. For each standard transfer a 5.00-ml portion into a 25-ml conical flask (initially dry) containing 5.00 ml of pH 6 buffer, and add 2.50 ml of magnesium sulphate solution. Let stand for 15 min at room temperature (~20°), then measure the fluorescence at 525 (F_{525}) and 470 nm (F_{470}) with excitation at 440 nm. Apply corrections for a blank similarly prepared. Plot $F_{525} - F_{470}$ *vs.* concentration.

RESULTS AND DISCUSSION

The methods described were tested as follows.

Determination of TC in the presence of ATC

To prepare mixtures of known composition, standard TC solution was accurately diluted tenfold with water, and 0.50, 1.00, 1.50, 2.00, 2.50, 3.00 ml portions were mixed with 1.00-ml portions of standard ATC solution and diluted accurately to 100 ml. Five-ml portions of each solution were then treated and measured as described. Commercial capsules were also assayed for TC and ATC. The contents of 20 "Tetracid" capsules (Cid Laboratories, Egypt) were mixed and an amount equivalent to 100 mg of TC hydrochloride was transferred to a 100-ml standard flask, and shaken with about 40 ml of water for 3 min to ensure complete dissolution. The solution was then made up to volume with water and filtered; 10.00 ml of filtrate were diluted to volume in a 100-ml standard flask and this solution was analysed as above. The results are given in Table 1.

Determination of ATC in the presence of TC

Standard TC solution was accurately diluted fourfold with water and 2.00-ml portions were mixed with 1.00, 2.00, . . . 6.00, 7.00 ml portions of standard ATC solution and diluted to 100 ml accurately with water. The procedure for ATC calibration graphs was then

Table 1. Fluorometric determination of TC in presence of ATC, in a laboratory-made mixture and in "Tetracid" capsules with added ATC, by the ΔF method

Ratio TC/ATC	Recovery, %	
	Laboratory-made mixture*	"Tetracid" capsules with added ATC*
1/4	99.8	105.2
1/2	101.5	105.8
1/1.30	100.8	105.2
1/1.00	99.8	106.1
1/0.80	100.1	106.3
1/0.67	99.8	105.4
Mean	100.3	105.7
C.V., %	0.7	0.5

*Each mixture contained 0.08 mg of ATC and 0.02–0.12 mg of TC per 100 ml of solution. The recovery for the capsule analysis is based on the nominal TC content of the capsules.

applied to 5-ml portions of these solutions. The results are given in Table 2.

Fluorescence characteristics

Addition of aluminium to TC and ATC in Sørensen buffer at pH 6 gives the corresponding

Table 2. Fluorometric determination of ATC in presence of TC by the ΔF method

Ratio ATC/TC	Recovery, %
1/2.50	100.0
1/1.25	101.0
1/0.83	100.7
1/0.63	99.9
1/0.50	100.4
1/0.42	101.1
1/0.36	100.3
Mean	100.5
C.V., %	0.5

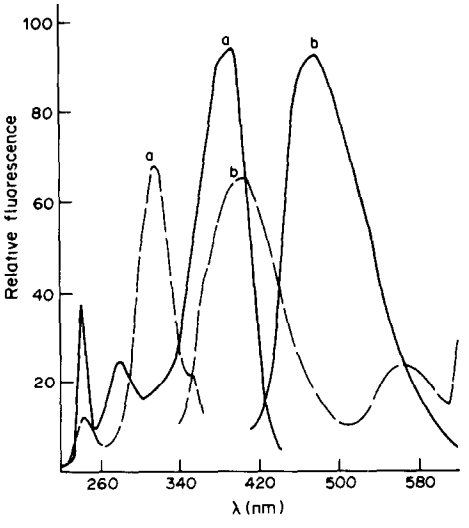

Fig. 1. Fluorescence excitation (a) and emission (b) spectra for 1.2 μg/ml solutions of TC–Al (——) and ATC–Al (– – –). Emission spectra for excitation at 393 nm for TC–Al and 320 nm for ATC–Al.

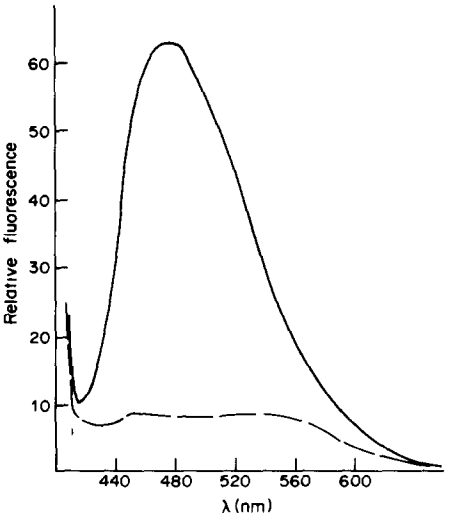

Fig. 2. Fluorescence emission spectra for 1.2 μg/ml solutions of TC–Al(——) and ATC–Al (– – –) (λ_{ex} = 393 nm).

TC–Al and ATC–Al fluorophores, which have different excitation and emission maxima (Fig. 1). Excitation of both fluorophores at 393 nm gives an emission maximum at 475 nm for TC–Al but almost constant background emission at 418 and 475 nm for ATC–Al (Fig. 2).

Addition of magnesium instead of aluminium changes the excitation and emission spectra (Fig. 3). Excitation of both fluorophores at 440 nm gives a maximum at 525 nm for ATC–Mg and almost constant fluorescence in the 470–540 nm region from TC–Mg (Fig. 4).

Assay for TC

The difference in the fluorescence spectra of TC–Al and ATC–Al allows determination of TC without

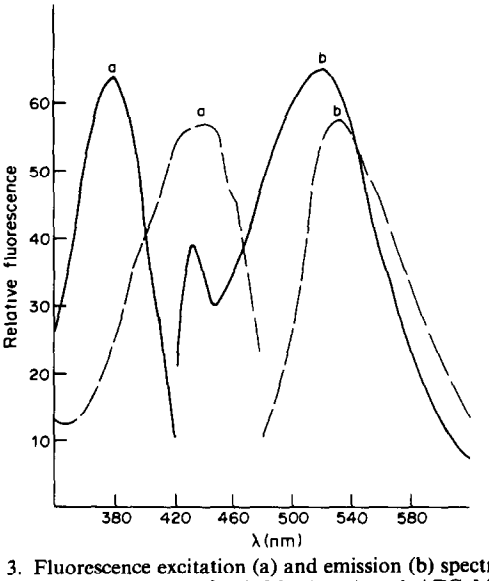

Fig. 3. Fluorescence excitation (a) and emission (b) spectra for 1.2 μg/ml solutions of TC–Mg (——) and ATC–Mg (– – –). Emission spectra for excitation at 380 nm for TC–Mg and 440 nm for ACT–Mg.

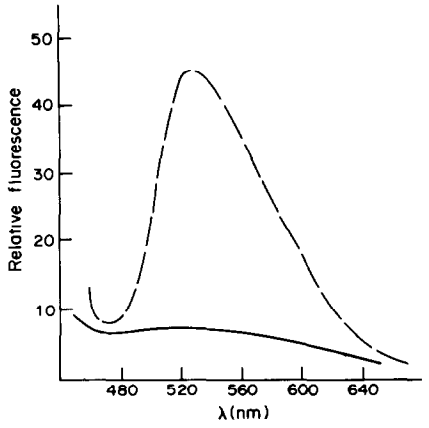

Fig. 4. Fluorescence emission spectra for 1.2 μg/ml solutions of TC–Mg (——), and ATC–Mg (– – –) (λ_{ex} = 440 nm).

interference from ATC. The fluorescence intensity at 475 nm (F_{475}) (λ_{ex} 393 nm) is the sum of that for TC–Al alone (F_{max}) and that for the fluorescence background of ATC–Al (F_B) (Fig. 2), and the fluorescence intensity at 418 nm (F_{418}) of the same solution (λ_{em} still 393 nm) is again the sum of the two fluorescence intensities, F_{min} for TC–Al and F_B for ATC–Al. The difference, $\Delta F = F_{475} - F_{418}$, is clearly equal to $F_{max} - F_{min}$ for TC–Al.

Calibration graphs for TC in the absence of ATC can be prepared by plotting ΔF for the TC–Al fluorophore *vs.* [TC], a linear relationship being obtained. The method is also valid for the determination of TC alone or in the presence of ATC, as confirmed by the results in Table 1.

Assay for ATC

The ΔF method is again applied, with measurement of fluorescence intensity of ATC–Mg at 525 and 470 nm (λ_{ex} 440 nm). A linear relationship is obtained over the concentration range 0.8–0.48 μg/ml in the final solutions. The validity of the method is confirmed by the results in Table 2.

The proposed ΔF methods may find wide application, especially in the spectrofluorimetric assay of the pure drugs or pharmaceutical multi-component formulations containing excipients or diverse components which give linear or no background interference (since correction methods can be applied for linear background). Moreover the high sensitivity makes the methods suitable for biological fluid analysis, after an initial extraction step.[9,10]

REFERENCES

1. D. C. Grove and W. A. Randall, *Assay Methods for Antibiotics*, Medical Encyclopedia, New York, 1955.
2. *U.S. Pharmacopoeia*, 20th Rev., p. 780, U.S. Pharmacopeial Convention, Rockville, Md., 1980.
3. *British Pharmacopoeia*, p. 448. HMSO, London, 1980.
4. O. Hrdy and H. Beyrodtová, *Cesk. Farm.*, 1974, **23**, 122.
5. A. M. Wahbi and S. Ebel, *Anal. Chim. Acta*, 1974, **70**, 57.
6. A. F. Zak, G. I. Loseva, L. P. Snezhnova, V. M. Shatrova, T. I. Navolotskaya and L. M. Yakobson, *Antibiotiki*, 1975, **20**, 685.
7. A. I. Cherkesov and T. V. Alykova, *Zh. Analit. Khim*, 1973, **28**, 377.
8. D. Hall, *J. Pharm. Pharmacol.*, 1976, **28**, 420.
9. R. G. Kelly, L. M. Peets and K. D. Hoyt, *Anal. Biochem.*, 1969, **28**, 222.
10. H. Poiger and Ch. Schlatter, *Analyst*, 1976, **101**, 808.
11. D. L. Simmons, H. S. L. Woo, C. M. Koorengevel and P. Seers, *J. Pharm. Sci.*, 1966, **55**, 1313.

Talanta, Vol. 32, No. 12, pp. 1156–1158, 1985
Printed in Great Britain

0039-9140/85 $3.00 + 0.00

EXTRACTIVE SPECTROPHOTOMETRIC AND FLUORIMETRIC DETERMINATION OF BORON WITH 2,2,4-TRIMETHYL-1,3-PENTANEDIAOL AND CARMINIC ACID

J. AZNAREZ, A. FERRER, J. M. RABADAN and L. MARCO
Department of Analytical Chemistry, Faculty of Sciences, University of Zaragoza, Spain

(*Received* 29 *March* 1985. *Accepted* 22 *August* 1985)

Summary—Boric acid at μg/ml or ng/ml level can be extracted from 1–6*M* hydrochloric acid into 2,2,4-trimethyl-1,3-pentanediol solution in chloroform and thus separated from many ions which interfere in the usual spectrophotometric methods. The boron is determined directly in the organic phase without back-extraction into water, by adding a solution of carminic acid in a mixture of sulphuric and glacial acetic acids (1 + 2 v/v) and measuring the absorbance at 549 nm. The molar absorptivity is 2.58×10^4 l.mole^{-1}.cm^{-1} and Beer's law is valid for the 0.05–0.4 μg/ml boron range. In the fluorimetric method, 509 or 547 nm can be used as the excitation wavelength and 567 nm for emission measurement, giving a linear response in the 8–120 ng/ml boron range. Both methods have been applied to determination of boron in plants and natural waters with good precision and accuracy.

Determination of boron (as boric acid) at μg/ml or ng/ml levels is of great interest in several fields of research and technical control, involving a wide range of sample types, *e.g.*, in agriculture,[1] ores in geochemistry,[2] boron-steels in metallurgy,[3] the nuclear industry.[4] Most methods for the determination are spectrophotometric, using curcumin,[5,6] carminic acid[7] or azomethine-H.[8] By molecular fluorescence photometry, boron can be determined with thoron,[9] morin[10] or dibenzoylmethane.[6] The fluorimetric methods show the greatest sensitivity, allowing the determination of nanograms of boron. However, all the methods have poor selectivity and precision. It is usually necessary to separate the boric acid by distillation of methyl borate, ion-exchange or solvent extraction. In addition, there are problems of contamination by boron from laboratory glassware and of corrosive working media such as concentrated sulphuric acid.

The separation of boric acid by extraction with 1,3-diols[11–13] is highly selective and provides a preconcentration method which eliminates numerous interferences.[14] In this paper, 2,2,4-trimethyl-1,3-pentanediol (TMPD) in chloroform has been used for the extraction. This 1,3-diol extracts the boron more efficiently and over a wider range of acidity—from 1 to 7*M* hydrochloric acid—than do other 1,3-diols. The boron can be determined directly in the organic phase either photometrically or fluorimetrically with carminic acid.

EXPERIMENTAL

Apparatus

A Pye-Unicam SP 8–100 spectrophotometer was used with 1-cm silica cells. Fluorescence measurements were made with a Shimadzu RF-510 spectrofluorimeter. Teflon and platinum containers were used where possible, to avoid contamination from boron in glassware.

Reagents

Stock boric acid solution, boron 1.000 μg/ml. Dissolve 2.860 g of dried boric acid in 500 ml of doubly distilled water, and dilute as required just before use. Store the solutions in polyethylene bottles.

Extractant. A 1% 2,2,4-trimethyl-1,3-pentanediol solution in chloroform, prepared just before use.

Carminic acid solution (0.073%) in glacial acetic acid. The solution is usable for a week.

Carminic acid solution (0.0073%). Dilute the 0.073% solution tenfold with glacial acetic acid just before use.

Sulphuric/acetic acid mixture (1:2 v/v). Prepare on the day of use.

Spectrophotometric procedure

Transfer an aqueous sample solution containing up to 40 μg of boron (as boric acid) into a 100-ml separating funnel, add enough concentrated hydrochloric acid to give a concentration of 6*M*, then add 10 ml of extractant and shake the mixture mechanically for 5 min. Leave the phases to separate. To 1 ml of the extract add 1 ml of 0.073% carminic acid solution and 5 ml of sulphuric/acetic acid mixture. Heat in a thermostatic bath at 75 ± 3° for 10 min. Let cool to room temperature and dilute to volume with sulphuric/acetic acid mixture in a 10-ml standard flask. After 2 hr measure the absorbance at 549 nm against a reagent blank

Fluorimetric procedure

Take a sample volume containing up to 5 μg of boron (as boric acid). Extract with TMPD in chloroform and develop the boric acid–carminic acid compound as before, but with the 0.0073% carminic acid solution. Measure the fluorescence at 567 nm with excitation at 547 or 509 nm. Prepare a calibration graph from standard boron solutions covering the range 10–100 ng/ml for the boron concentration in the solution finally measured.

RESULTS AND DISCUSSION

Extraction of boric acid

A single extraction of 20 μg of boron by the procedure given was 97.5 ± 0.8% complete (10 determinations) from 1–6*M* hydrochloric acid with an

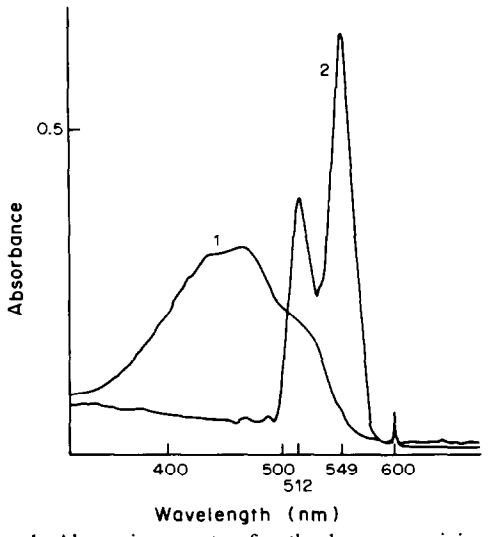

Fig. 1. Absorption spectra for the boron–carminic acid system. Curve 1, reagent only, *i.e.*, $1.5 \times 10^{-4}M$ carminic acid in mixed sulphuric and acetic acids, 1:2 v/v. Curve 2, reagent plus boron at 270 ng/ml in the final solution.

aqueous/organic volume ratio of 3:1. Equilibrium was reached in <5 min, with mechanical shaking. The boric acid was determined by stripping the extracted phase and using the azomethine-H method. Boric acid could also be extracted from 1–2.5*M* sulphuric acid, but in the presence of alkaline-earth metals low results were obtained, owing to adsorption of boric acid by the precipitate formed.

TMPD concentrations higher than 1% facilitate extraction of the boron, but darkening of the solution by charring of the TMPD then causes difficulties at the measurement stage.

Large amounts of iron can be eliminated by prior extraction with methyl isobutyl ketone, without loss of boric acid.

Spectrophotometric characteristics

The absorption spectrum of the boric acid–carminic acid complex in a mixture of sulphuric and glacial acetic acids exhibited maxima at 512 and 549 nm (Fig. 1), when measured against a reagent blank solution.

The absorbance at 549 nm remained constant for 3 hr. A reagent blank solution showed an absorption maximum at 468 nm when measured against pure solvent, and an absorbance of about 0.08 units at 549 nm due to the reagent, so it was necessary to use a reagent blank solution as reference. At 549 nm Beer's law was obeyed over the range 0.05–0.4 μg/ml boron in the final solution measured (5–40 μg of boron in the original sample). The molar absorptivity relative to boron was 2.58×10^4 l.mole^{-1}.cm^{-1} at 549 nm. The relative standard deviation for ten determinations of 30 μg of boron was 2.1%.

Table 2. Determination of boron in plant samples

Sample	Boron content, *ppm* (FAIC)*	Boron found, *ppm*	Relative standard deviation, %
Hevea	55.8	55.0	2.7
Eucalyptus	34.1	31.9	2.7
Codia discolor	25.0	25.8	3.0
Orange	40.0	39.1	2.0
Olive	17.9	17.0	1.7
Cotton	24.8	23.5	1.9

*FAIC: Foliar Analysis Inter-Institutes Committee; results quoted as ±5%.

Interference studies

The effect of the ions most frequently present in plant ash and natural waters, on the determination of 30 μg of boron, is shown in Table 1.

The interference of fluoride can be eliminated by addition of 0.05*M* aluminium chloride solution to give an aluminium concentration twice that required to mask the fluoride.

Spectrofluorimetric characteristics

The excitation spectra of carminic acid and of the boric acid–carminic acid complex in the mixed acid are shown in Fig. 2.

When the emission was recorded at 567 nm (and 5 nm band-width); the excitation spectrum of the complex showed maxima at 337, 469, 509 and 547 nm. The relative fluorescence intensity at 567 nm varied linearly with boron concentration from 8 to 120 ng/ml in the final solution. The best sensitivity was obtained by using excitation at 547 nm (with 10 nm spectral band-width). The detection limit for boron (taken as twice the standard deviation of the fluorescence intensity of a blank solution) was

Table 1. Effect of other ions on the spectrophotometric determinations of 30 μg of boron and on the fluorimetric determination of 5 μg of boron

Ion	Maximum concentration tested without giving interference, M	
	Spectrophotometry	Spectrofluorimetry
Cl^-	7.5	7.5
SO_4^{2-}	2.5	2.5
Na^+, K^+, NH_4^+, Mg^{2+}, Cd^{2+}, Ca^{2+}, NO_3^-	0.15	0.15
Cu^{2+}, Ba^{2+}, MoO_4^{2-}, NO_2^-	0.1	0.05
Mn^{2+}, Sr^{2+}, Pb^{2+}, Cr^{3+}, Ni^{2+}, Zn^{2+}, Al^{3+}, Fe^{2+}, Fe^{3+}	0.05	0.02
F^-	0.01*	0.01*

*Masked with aluminium

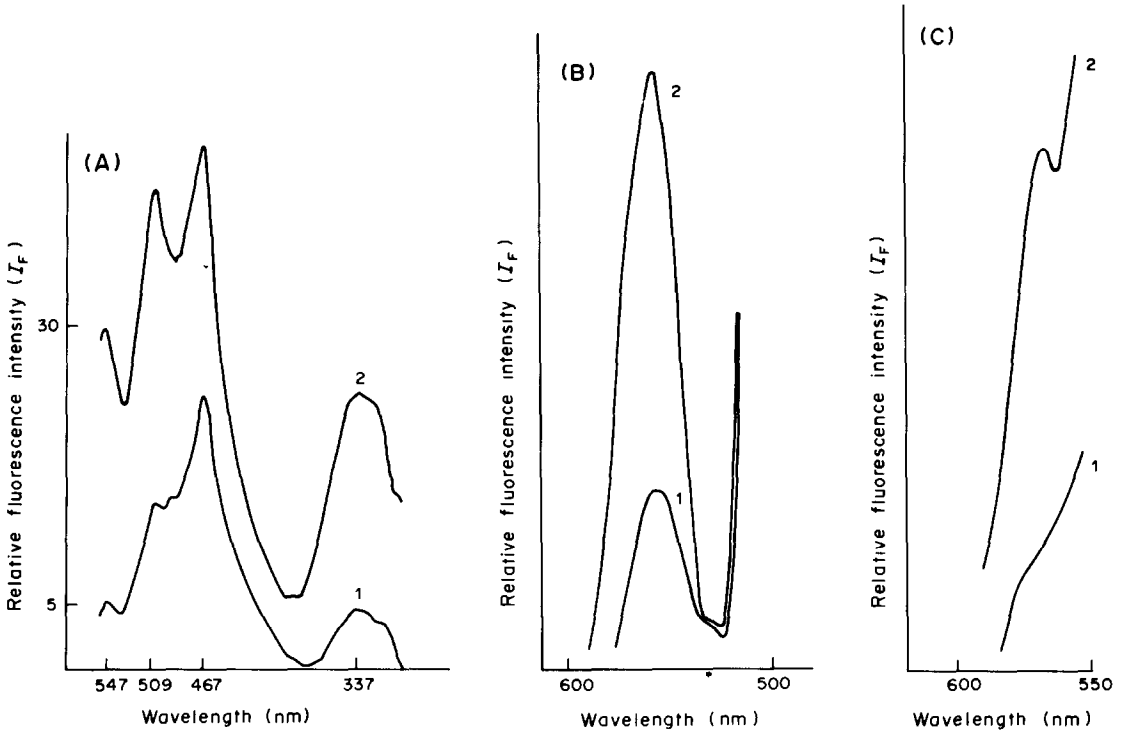

Fig. 2. Fluorescence spectra for the boron–carminic acid system. A, Excitation spectra (emission measured at 567 nm). B, Emission spectra (excitation at 509 nm). C, Emission spectra (excitation at 547 nm). In each case, curve 1 is for reagent only, *i.e.*, $1.5 \times 10^{-5} M$ carminic acid in mixed sulphuric and acetic acids, 1:2 v/v, and curve 2 is for reagent plus boron at 25 ng/ml in the final solution.

Table 3. Fluorimetric determination of boron in natural waters

Sample	Boron found, $\mu g/ml$	Relative standard deviation, %
River water A (Ebro)	0.14	3.0
River water B (Ebro)	0.19	3.0
River water C (Ebro)	0.21	3.0
Urban drinking water (Zaragoza)	0.10	3.5
Well water A	0.35	2.0
Well water (near to a paper mill)	0.96	2.5

3 ng/ml. The precision for 5 μg of boron was 3.8% (ten replicates). The tolerance for other ions in the fluorimetric determination of 50 ng/ml boron is summarized in Table 1.

Applications

Results for the determination of boron in plant samples by the spectrophotometric method are shown in Table 2. Plant samples were ashed and dissolved as indicated elsewhere.[12]

The plant samples had been analysed by the Foliar Analysis Inter-Institutes Committee and were kindly supplied by M. Pinta (Office de la Recherche Scientifique et Technique Outre-Mer). The standard addition method was used to check for loss of boron during ashing, dissolution in $6M$ hydrochloric acid and extraction with TMPD.

The fluorimetric method has been applied to determination of boron in natural water, as shown in Table 3.

REFERENCES

1. J. Bonner and J. E. Varner, *Plant Biochemistry*, Academic Press, New York, 1975.
2. C. T. Walker, *Geochemistry of Boron*, Halsted Press, New York, 1975.
3. E. M. Donaldson, *Talanta*, 1981, **28**, 825.
4. D. D. Siemer, *Anal. Chem.*, 1982, **54**, 1321.
5. American Public Health Association, American Water Works Association and Water Pollution Control Federation, *Standard Methods for the Examination of Water and Waste-water*", 14th Ed., p. 287. Washington DC, 1975.
6. J. Aznárez, A. Bonilla and J. C. Vidal, *Analyst*, 1983, **108**, 368.
7. K. Polyák, A. Halász and G. Szabó, *Agrokem. Talajtan*, 1975, **24**, 151.
8. S. K. Gupta and J. W. B. Stewart, *Schweiz. Landwirtsch. Forsch.*, 1975, **14**, 153.
9. M. Marcantonatos, A. Marcantonatos and D. Monnier, *Helv. Chim. Acta*, 1965, **48**, 194.
10. M. Marcantonatos, G. Gamba and D. Monnier, *ibid.*, 1969, **52**, 538.
11. J. Aznárez and A. Bonilla, *An. Quim*, 1978, **74**, 756.
12. J. Aznárez, A. Bonilla and M. A. Belarra, *Rev. Acad. Cien. Zaragoza*, 1978, **33**, 141.
13. T. Korenaga, S. Motomizu and K. Tôei, *Analyst*, 1980, **105**, 955.
14. J. Aznárez and J. M. Mir, *Analyst*, 1985, **110**, 61.

Talanta, Vol. 32, No. 12, pp. 1159–1160, 1985
Printed in Great Britain.

0039-9140/85 $3.00 + 0.00

MINIPOL, A DESK-COMPUTER PROGRAM FOR REFINEMENT OF PROTONATION CONSTANTS FROM DIFFERENTIAL-PULSE POLAROGRAPHIC DATA

V. CERDÁ* and R. FORTEZA
Department of Analytical Chemistry, Faculty of Sciences, University of Palma de Mallorca, Spain

(*Received* 28 *January* 1985. *Accepted* 22 *August* 1985)

Summary—The program MINIPOL, designed to run on a desk-computer with 32 kbytes of memory, can calculate the optimum values of overall protonation constants and molar intensities of up to 8 species with composition H_rL_p, from differential-pulse polarographic data.

Potentiometry and spectrophotometry are the most widely used techniques for determination of protonation constants.[1] Potentiometry is usually considered to be the more precise, but it cannot be used for the study of sparingly soluble substances or for those with low or high pK_a values. Sometimes these problems can be resolved by using spectrophotometry, but only if the spectra are suitable.

In a previous paper we described the differential-pulse polarographic determination of the protonation constants of diprotic acids,[2] and have applied it to the determination of the overlapping pK values of maleinimide dioxime (MIDO) by several polarographic techniques.[3]

As an aid in the application of differential-pulse polarography to pK determinations, we have modified the program MINISPEF, written by Gaizer and Puskás.[4] MINISPEF uses a non-linear least-squares procedure to calculate optimum values of overall protonation constants and molar absorptivities of up to 8 species of the form H_rL_p, from spectrophotometric data. Our modification allows differential-pulse polarographic data to be used to find protonation constants and molar current.

THE PROGRAM

By analogy to the definition of molar absorptivity ($\varepsilon = A/bC$) for any given wavelength, we can define a molar current (ν) in differential-pulse polarography as $\nu = i/KC$, where i is the current for a given potential, C the concentration and K a coefficient that includes several polarographic constants (the diffusion coefficient, capillary constant, σ, ΔE, *etc.*). The value of ν is independent of certain experimental parameters.[5]

In MINIPOL the logarithms of the overall protonation constants and the molar currents are treated as unknown parameters, and the values which give the minimum of the non-weighted sum of the squares of the residuals (U) of the measured (i_{meas}) and calculated (i_{calc}) currents are calculated, together with the probable errors:

$$U = \sum_i (i_{meas,i} - i_{calc,i})^2$$

$$= \sum_i (i_{meas,i} - \sum_j \nu_j \beta_j^H [L]^{p_j} [H^+]^{r_j} K_j)^2$$

Program description

First, the experimental data are read in and prepared for the subsequent calculations, followed by the stoichiometric coefficients and the starting values of the parameters, with their increments. The part of the program that deals with the search for and refinement of parameters is identical with the same part of MINISPEF.

We have tried to keep the same meaning for the variables and arrays of MINISPEF, but some small changes have had to be introduced. Some variables have been fixed (W = 1, N4 = 2, X1 = 1, X2 = 1, M = 1), but the meanings of some arrays are slightly different – E( ) intensities, Q1( ) = 0, $\nu_M = 0$ (its increment, $T_M = 0$).

Use of the program

The program was developed on a Hewlett-Packard HP-85 desk-computer with 32 kbytes of memory, but with no matrix-handling software (difference from MINISPEF and MINIPOT[6]). The program can treat a maximum of 80 experimental points measured at one reduction potential, and a maximum of 8 simultaneous equilibria can be considered. Consequently, the maximum number of parameters is 17, because the last parameter is always the molar current for L. First the $\log\beta$ values, and then the ν values must be fed in.

MINIPOL is used in the same way as MINISPEF[4] and MINIPOT,[6] so full details are not given here. Like MINISPEF and MINIPOT, MINIPOL allows the simultaneous refinement of a maximum of only

*Author for correspondence.

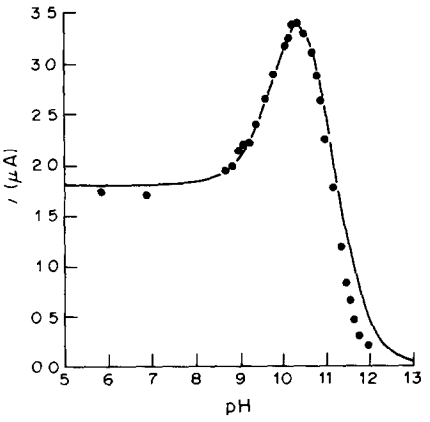

Fig. 1. Acid–base differential-pulse amperometric titration of $3.729 \times 10^{-5}M$ MIDO at -1275 mV. Experimental data. Solid line calculated from values found by MINIPOL: $pK_1 = 10.03 \pm 0.07$, $pK_2 = 11.03 \pm 0.03$, $i_0 = 1.80 \pm 0.04$ μA, $i_1 = 4.86 \pm 0.25$ μA, $i_2 = 0$ μA, $U = 0.012$ μA^2, $s = 0.042$ μA.

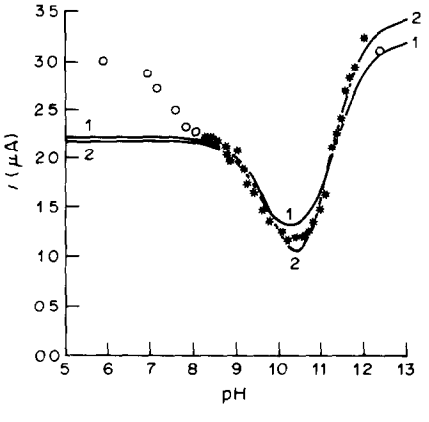

Fig. 2. Acid–base differential-pulse amperometric titration of $3.729 \times 10^{-5}M$ MIDO at -1480 mV. Curve 1: calculated from unrefined values.[2] Curve 2: calculated from values found by MINIPOL. Experimental points marked o were not used for calculations.

four arbitrarily chosen parameters, and when log β and v values are refined simultaneously, the serial numbers of the v values must always precede those of the log β values, and in both cases must be put in order of increasing error values.

Copies of the program are available from the authors on request.

RESULTS

Our experience with MINIPOL has been very favourable. Its convergence is reliable, even if four parameters are refined simultaneously.

We have tested MINIPOL by refining the pK and v values of MIDO obtained previously.[2] Figure 1 shows reasonable coincidence between the curve calculated from the refined pK values (solid line) and the experimental data.

Curve 1 of Fig. 2 was calculated from the data obtained from the linear least-squares method, *i.e.*, $pK_1 = 9.59$, $pK_2 = 11.78$, $v_0 = 5.98 \times 10^4$, $v_1 = 2.50 \times 10^4$, $v_2 = 8.64 \times 10^4$ $U = 2.82\,\mu A^2$, $s = 0.36$ μA). When these data were used as starting values in MINIPOL, the refined values ($pK_1 = 10.05 \pm 0.04$, $pK_2 = 11.09 \pm 0.04$, $v_0 = 5.84 \times 10^4$, $v_1 = 1.07 \times 10^3$, $v_2 = 9.28 \times 10^4$, $U = 0.24$ μA^2, $s = 0.10$ μA) were obtained. From these, curve 2 was calculated, and this agrees better than curve 1 with the experimental points.

The averaged values of pK_1 and pK_2 obtained by polarography agree with those obtained by potentiometric[7] ($pK_1 = 10.09$, $pK_2 = 11.19$) and spectrophotometric[8] ($pK_1 = 10.15$, $pK_2 = 11.19$) techniques. Polarography gives lower precision, however, both in the averaged values and in the results of individual titrations (higher values of U and s). These poorer results are mainly caused by the inherently lower precision of polarographic measurements and by the overlapping reduction mechanisms. This is a major difference between polarography and the other two techniques. While the behaviour of compounds in potentiometry and spectrophotometry depends only on equilibrium considerations, polarographic behaviour also depends on the reduction mechanism, which can change with pH. Thus, the pH-dependence of the final and intermediate products of the reduction mechanism must be taken into account.

Nevertheless, in spite of these difficulties and the lower precision of the results, differential-pulse polarography is possibly a valid alternative when pK values of an electroactive compound cannot be determined by potentiometric or spectrophotometric techniques.

REFERENCES

1. F. C. Rossotti and H. Rossotti, *The Determination of Stability Constants*, McGraw-Hill, New York, 1961.
2. R. Forteza and V. Cerdá, *J. Electroanal. Chem.*, 1984, **179**, 83.
3. *Idem*, *Bull. Soc. Chim. France*, 1984, I-97.
4. F. Gaizer and A. Puskás, *Talanta*, 1981, **28**, 925.
5. A. M. Bond, *Modern Polarographic Methods in Analytical Chemistry*, Dekker, New York, 1980.
6. F. Gaizer and A. Puskás, *Talanta*, 1981, **28**, 565.
7. M. L. Albelda, V. Cerdá, R. Pardo and P. Sánchez-Batanero, *Quim. Anal.*, 1983, I-218.
8. M. L. Albelda, V. Cerdá and C. Mongay, *Bull. Soc. Chim. France*, 1982, I-19.

Talanta, Vol. 32, No. 12, pp. 1161–1162, 1985
Printed in Great Britain.

0039-9140/85 $3.00 + 0.00

DETERMINATION OF THALLIUM(III) BY USE OF A MERCURY REDUCTOR

S. N. DINDI and N. V. V. S. N. M. SARMA
Department of Inorganic and Analytical Chemistry, Andhra University, Waltair, India

(*Received* 12 *March* 1985. *Accepted* 9 *August* 1985)

Summary—A convenient method has been developed for the determination of thallium(III) by using a mercury reductor. Thallium(III) is reduced to thallium(I) in 0.5–4*N* hydrochloric or sulphuric acid medium and the determination is completed by oxidative titration with potassium bromate. The method is extended to analysis of thallium(III)–thallium(I) and thallium(III)–iron(III) mixtures.

Among various metal and metal–amalgam reductors, the mercury reductor is one of the most convenient and its use in the determination of iron(III),[1,2] vanadium(V),[3,4] uranium(VI),[5,6] antimony(V),[7] hexacyanoferrate(III),[2,8] molybdenum(VI)[9] *etc.*, is well known. All these applications are based on the low redox potential of the mercury(I)/mercury couple in acid media. We have now developed a convenient method for the determination of thallium(III) by use of a mercury reductor. The method allows determination of both thallium(III) and thallium(I) in a mixture, by titration of thallium(I) in one aliquot with potassium bromate,[10] and of total thallium in a second aliquot after reduction of the thallium(III) in a mercury reductor. Preliminary studies have shown that iron(II) obtained by reducing iron(III) in a mercury reductor[1] can satisfactorily be titrated with sodium vanadate without interference from thallium(I). Moreover, it has been reported[10] that a mixture of thallium(I) and iron(II) can be titrated with potassium bromate to a visual end-point. On the basis of these observations the method has been extended to allow determination of thallium(III) and iron(III) in a mixture.

EXPERIMENTAL

Reagents

Thallium(III) solutions, 0.025–0.05*M* were prepared by dissolving thallium(III) hydroxide[11] in the desired acid and were standardized.[11,12] Thallium(I) solutions (0.025–0.05*M*) in water were prepared from thallium(I) chloride or sulphate and standardized.[13] Approximately 0.05*M* sodium vanadate and 0.1*M* ferric chloride solutions were prepared and standardized.[14,15] A 0.00833*M* potassium bromate was also prepared and standardized. All other reagents used were of analytical reagent grade.

Determination of thallium(III)

To an aliquot of thallium(III) solution placed in a mercury reductor,[1] enough sulphuric and hydrochloric acids are added to give an overall sulphuric acid concentration of 0.5–4*M* and a chloride ion concentration of 0.05–0.2*M* on dilution to about 100 ml. [Chloride ion is added to precipitate mercury(I) as Hg_2Cl_2.] A rapid stream of carbon dioxide is passed into the solution for about 5 min to displace the air present, then the reductor is stoppered immediately and shaken vigorously for about 5 min. The supernatant solution in the reductor is first decanted into a 250-ml beaker and then filtered into a 500-ml Buchner flask through a G4 filter. The reductor is washed four times (each time with about 20 ml of water and swirling for about 5 sec) and the washings are filtered. Finally, the beaker and filter disc are washed twice with 20-ml portions of water and the washings filtered. The hydrochloric acid concentration of the combined filtrate and washings is adjusted to about 1.5*M*, and the solution is titrated with standard potassium bromate solution[10,13] (Methyl Orange as indicator).

The same determination can also be done in 0.5–4*M* hydrochloric acid medium, without using sulphuric acid, by the same procedure. The determination can also be accomplished in 0.5–4*M* perchloric acid provided there is enough chloride present to remove mercury(I) as mercury(I) chloride.

Precision and accuracy. Solutions containing known amounts of thallium(III) were analysed ten times according to the above procedure. Averages and relative standard deviations were: 131.4 mg, 0.2% (131.3 mg taken) in sulphuric acid medium; 98.9 mg, 0.2% (98.8 mg taken) in hydrochloric acid medium.

Interferences. Titanium, iron, vanadium, uranium, antimony, osmium and iridium interfere in this determination. Phosphate and acetate do not interfere up to an overall concentration of 0.08 and 0.25*M* respectively in the reductor. Any other ions which are either reduced by mercury or oxidized by potassium bromate will interfere.

Determination of thallium(III) and thallium(I) in a mixture

An aliquot of the mixture is taken, enough hydrochloric acid is added to give a concentration of about 1.5*M* on dilution to 100 ml and the thallium(I) is titrated directly with standard potassium bromate solution. This gives the thallium(I) concentration in the mixture. Another aliquot of the same size is taken and, after reduction of thallium(III) to thallium(I), titrated with potassium bromate. The difference between the two titrations gives the thallium(III) content. Some typical results obtained in sulphuric and hydrochloric acid media are shown in Table 1.

Determination of thallium(III) and iron(III) in a mixture

An aliquot of the mixture is placed in the mercury reductor and enough water and concentrated hydrochloric acid are added to give a total volume of about 100 ml of 2*M* hydrochloric acid. A rapid stream of carbon dioxide is passed into the reductor for about 5 min, then the reductor is stoppered and shaken thoroughly for about 5 min. The supernatant solution in the reductor is decanted into a

Table 1. Determination of thallium(III) and thallium(I) in a mixture

	Thallium(III), *mg*		Thallium(I), *mg*	
Medium	Taken	Found	Taken	Found
H_2SO_4	133.1	133.3	42.6	42.8
	78.8	78.8	61.7	61.7
	45.0	44.5	100.2	99.7
HCl	41.9	41.7	38.2	38.2
	53.0	53.2	52.1	51.9
	77.0	76.8	41.4	41.1

Table 2. Determination of thallium(III) and iron(III) in a mixture

Iron(III), *mg*		Thallium(III), *mg*	
Taken	Found	Taken	Found
27.8	27.9	47.8	47.7
30.7	30.4	44.8	44.9
14.0	14.1	74.6	74.9
41.9	41.9	24.9	24.6
33.5	33.3	39.8	40.0
22.3	22.1	59.7	59.7

250-ml beaker and then filtered into a 500-ml conical flask through a Whatman No. 42 filter paper.

The mass in the reductor is washed with five 20-ml portions of 0.5*M* hydrochloric acid, each time with swirling for about 5 sec. Each washing is decanted into the beaker and filtered into the conical flask. The acidity of the solution is adjusted to about 1.5*M* with hydrochloric acid, 5 ml of syrupy phosphoric acid and 3 drops of barium diphenylamine indicator are added and the solution is titrated with standard sodium vanadate. This titration gives the concentration of iron(III).

The procedure is repeated with an identical aliquot of the mixture, but the final solution is titrated with standard potassium bromate[10] solution, after addition of 5 ml of syrupy phosphoric acid, 5 ml of 0.2% copper(II) sulphate solution and 3 drops of Methyl Orange indicator. The bromate titration volume corresponds to thallium(III) plus iron(III). Some representative results are shown in Table 2.

Acknowledgements—We are grateful to Prof. L. S. A. Dikshitulu of our department for his valuable suggestions and to the UGC, New Delhi, for financial assistance.

REFERENCES

1. L. W. McCay and W. T. Anderson, *J. Am. Chem. Soc.*, 1921, **43**, 2372.
2. F. Burriel-Marti, F. L. Conde and S. E. Taccheo, *Anal. Chim. Acta*, 1953, **9**, 293.
3. L. W. McCay and W. T. Anderson, *J. Am. Chem. Soc.*, 1922, **44**, 1018.
4. L. S. A. Dikshitulu and D. Satyanarayana, *Indian J. Chem.*, 1974, **12**, 180.
5. E. R. Caley and L. B. Rogers, *J. Am. Chem. Soc.*, 1946, **68**, 2202.
6. L. S. A. Dikshitulu and D. Satyanarayana, *Z. Anal. Chem.*, 1974, **271**, 366.
7. L. W. McCay, *Ind. Eng. Chem., Anal. Ed.*, 1933, **5**, 1.
8. L. S. A. Dikshitulu and D. Satyanarayana, *Indian J. Chem.*, 1976, **14A**, 142.
9. N. H. Furman and W. M. Murray, Jr., *J. Am. Chem. Soc.*, 1936, **58**, 1689.
10. S. R. Sagi, K. A. Rao and M. S. P. Rao, *Indian J. Chem.*, 1983, **22A**, 95.
11. S. R. Sagi and K. V. Ramana, *Talanta*, 1969, **16**, 1217.
12. I. M. Kolthoff and R. Belcher, *Volumetric Analysis*, Vol. III, p. 370. Interscience, New York, 1957.
13. S. R. Sagi, G. S. P. Raju, K. A. Rao and M. S. P. Rao, *Talanta*, 1982, **29**, 413.
14. G. Gopala Rao and L. S. A. Dikshitulu, *Talanta*, 1963, **10**, 295.
15. A. I. Vogel, *A Text Book of Quantitative Inorganic Analysis*, 3rd Ed., p. 287. ELBS and Longmans, London, 1968.

Talanta, Vol. 32, No. 12, pp. 1163–1166, 1985
Printed in Great Britain.

0039-9140/85 $3.00 + 0.00

SYNTHESIS AND ANALYTICAL PROPERTIES OF THE POLYMERIZED SURFACTANT PPOSA*

KUN-YUAN LIU and RU-QIN YU
Department of Chemistry and Chemical Engineering, Hunan University, Changsha, People's Republic of China

(*Received* 1 *April* 1985. *Accepted* 9 *August* 1985)

Summary—A new low-polymer surfactant, poly(propylene oxide)-α-stearyldimethylammonium chloride (PPOSA) has been synthesized. It contains a polyglycol main chain and quaternary ammonium branched chains. Investigation of the surface-active properties of PPOSA showed that as a sensitizing and solubilizing reagent for spectrophotometric analysis it possesses some of the characteristics of both cationic and non-ionic surfactants. The surfactant shows a sensitizing effect superior or equal to that of classical surfactants commonly used in analytical chemistry. Use of PPOSA leads to development of some excellent micellar spectrophotometric procedures for determining trace metals.

During recent years, mixed surfactants of various kinds have been used to improve micellar spectrophotometric analysis.[1-4] Typical mixed pairs include: cationic/non-ionic, cationic/anionic, anionic/non-ionic and amphoteric/non-ionic surfactants. These mixed systems have not only the properties of the individual surfactants, but also some new properties not possessed by the individual surfactants. Polymerized ionic surfactants have also been used in improved micellar spectrophotometric procedures.[5] In the work described in this paper, a low-polymer surfactant, poly(propylene oxide)-α-alkyldimethylammonium chloride, was synthesized by the polymerization of epichlorhydrin and subsequent quaternization with various trialkylamines. Of the surfactants tested, poly(propylene oxide)-α-stearyldimethylammonium chloride (abbreviated to PPOSA) was found to be the most promising for micellar spectrophotometry and was studied in more detail.

EXPERIMENTAL

Reagents

Epichlorhydrin (Shanghai). Stearylamine (Koch-Light). Dibromogallein (BG, prepared as described by Antonovich *et al.*[6]), 5×10^{-4} *M* solution in 50% aqueous ethanol. Chromazurol S (CAS; B.D.H.), 0.05% solution. Xylenol Orange solution (XO; Shanghai), 5×10^{-4} *M*. Solutions of Mo(VI), W(VI), Be(II) and La(III) (5×10^{-4} *M*) were prepared by standard procedures with analytical-grade or specially pure reagents.

Synthesis of PPOSA

Stearyldimethylamine (m.p. 52–53°) was synthesized by methylation of stearylamine with formaldehyde in formic acid. Epichlorhydrin (15.7 ml, 0.1 mole) in benzene (50 ml) was heated to boiling and 17.8 g (0.06 mole) of stearyldimethylamine were added. The mixture was refluxed for 7 hr, then the benzene was evaporated to leave an orange residue. This crude product was purified by recrystallization from acetone. The white product was dried for 3 hr at below 50° under reduced pressure. The yield was about 70%. Poly(propylene oxide)-α-alkyldimethylammonium chlorides substituted with other alkyl groups such as CH_3, C_3H_7, C_8H_{17}, $C_{12}H_{25}$, *etc.*, were synthesized in a similar way, but were difficult to purify and less efficient as micellar modifying agents for spectrophotometry.

RESULTS AND DISCUSSION

Composition and properties of PPOSA

From the elemental analysis and molecular weight of PPOSA (Table 1), it is postulated that the surfactant has the structure I, similar to that proposed in the patent literature.[7-9] The infrared spectrum has peaks at 722, 1105, 1471, 2850, 2925 and 3350 cm^{-1}, which confirms the postulated structure.

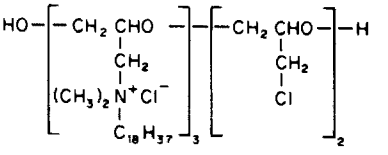

(I)

PPOSA is soluble in water, ethanol, hot acetone and ethyl acetate. It is more soluble in water than are the commonly used cationic surfactants, such as STAC (stearyltrimethylammonium chloride) and CTAB (cetyltrimethylammonium bromide) and can be used as an aqueous solution without precipitation even after long-term storage at relatively low temperatures. PPOSA softens at 70°, turns yellow at 210° and gradually to brown at above 210°, and then blackens. These phenomena are similar to those observed with STAC.[10]

A plot of surface tension σ of the aqueous solution of PPOSA *vs.* concentration c gives a curve with two plateaux at the concentration ranges $0.63–1.5 \times 10^{-4}$ *M* and $> 1.66 \times 10^{-4}$ *M* (Fig. 1), respectively. This phenomenon has not been observed

*Taken from the M.Sc. thesis of K.Y. Liu, Hunan University, 1984.

Table 1. Characterization of PPOSA

	Molecular weight	C, %	H, %	N, %	Cl_{total}, %	Cl_{ionic}, %
Found	1300–1400	63.3	11.3	3.4*	12.9	7.8
Calculated†	1371.3	65.63	11.38	3.06	12.93	7.76

*3.4% by combustion chromatography and 3.1% by gravimetry with tetraphenylborate.
†For structure I.

with common surfactants, but has been found with surfactants similar to PPOSA [synthesized with epichlorhydrin and the tertiary amines $C_{14}H_{29}N(CH_3)_2$ or $C_{16}H_{33}N(CH_3)_2$]. A similar curve was observed for an aqueous solution of polyglycol-20000 mixed with CTAB. A plot of the surface tension of this solution *vs.* concentration of the surfactant mixture also has two plateaux. The points of inflexion correspond to the critical micellar concentrations of the two surfactants in the mixture (Fig. 2). Thus it appears that in the PPOSA molecules, the alkyl oxide moiety and the quaternary ammonium nitrogen attached by a long-chain alkyl group keep their own characteristic features to some extent; this was the intention in the synthetic design of the surfactant. Thus, PPOSA should show the characteristic properties of both cationic and non-ionic surfactants as a sensitizing and solubilizing agent in spectrophotometric analysis.

PPOSA as a micellar modifying agent in spectrophotometry of trace metal ions

Some typical systems in spectrophotometric analysis were chosen to test the micellar modifying effect of PPOSA. These were Mo(VI)–BG, W(VI)–BG, Be(II)–CAS and La(III)–XO.

The Mo(VI)–BG system. The use of PPOSA in combination with some non-ionic surfactants makes the micellar system more reproducible and a lower detection limit for Mo(VI) can be obtained. The colour development was optimized by using a modified simplex method,[11] with the concentrations of hydrochloric acid, BG, PPOSA and Triton X-100 as variable factors and the molar absorptivity ε as the objective function. The optimum procedure found is as follows. To a solution containing less than 10 μg of Mo(VI), add 0.7 ml of 5*M* hydrochloric acid, 0.9 ml each of 5×10^{-4}*M* BG and 0.2% PPOSA solutions, and 0.5 ml of 0.2% Triton X-100 solution. Dilute the solution to 10 ml. After 40 min measure the absorbance at 642 nm against a reagent blank.

The absorbance of the Mo(VI) complex becomes constant within 30 min and remains stable for at least 5 hr. The molar absorptivity is 1.25×10^5 $l.mole^{-1}.cm^{-1}$ at λ_{max} (642 nm). This value is 1.2 times the value obtained without addition of Triton X-100 (1.08×10^5) and 5 times the value obtained without addition of any surfactant (2.5×10^4). PPOSA helps to eliminate the spectral overlap with the reagent that occurs with Mo(VI)–BG, because PPOSA markedly decreases the absorbance of the excess of BG present, and causes the spectrum of the Mo(VI)–BG complex to exhibit a large wavelength shift (from 580 to 642 nm). Beer's law is observed up to 1 μg/ml Mo(VI). The molar ratio method was applied to the ternary system Mo/BG/PPOSA, by keeping the concentration of one component constant and varying those of the other two. In all cases the diagrams obtained showed the stoichiometry to be 1:2:1 (Mo:BG:PPOSA).

In Table 2, the PPOSA system is compared with other micellar Mo(VI)–BG systems reported in the literature.[12]

The Mo(VI)–BG system improved by PPOSA and Triton X-100 is fairly selective. Among more than thirty ions tested, only Ge(IV) and W(VI) showed significant interference that was difficult to eliminate. The effects of Mo(VI), Cr(VI), V(V) and Fe(III) can be eliminated by addition of ascorbic acid, and Sb(III) and Sn(IV) can be masked with EDTA. A

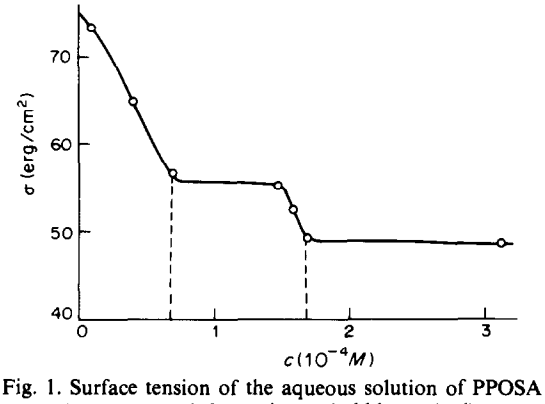

Fig. 1. Surface tension of the aqueous solution of PPOSA (temperature 10°, maximum bubble method).

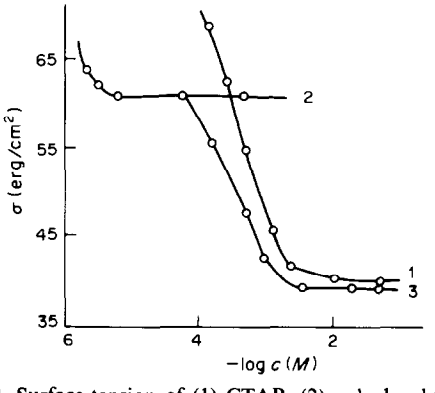

Fig. 2. Surface-tension of (1) CTAB, (2) polyglycol-20000 and (3) their mixed solution (molar ratio 1:1.5).

Table 2. Comparison of spectral parameters for micellar improved Mo(VI)–BG systems

Surfactant	Used alone		Mixed with Triton X-100	
	λ_{max}, nm	ε, 10^4 l.mole^{-1}.cm^{-1}	λ_{max}, nm	ε, 10^4 l.mole^{-1}.cm^{-1}
DTAC	635	8.97	635	9.98
DBAC	645	4.08	635	6.36
TPC	630	6.29	630	6.55
Zeph	650	5.87	645	6.41
CTAB	640	12.0	640	11.3
CPC	630	7.21	635	6.93
CPB	635	6.83	635	7.77
STAC	635	9.88	635	7.92
DDMAA	635	8.86	635	7.98
PPOSA	642	10.8	642	12.5

*DTAC—dodecyltrimethylammonium chloride, DBAC—dodecylbenzyldimethylammonium chloride, TPC—tetradecylpyridinium chloride, Zeph—zephiramine, CPC(B)—cetylpyridinium chloride(bromide), DDMAA—*N*-dodecyldimethylaminoacetic acid.

binary mixture of Mo(VI) and W(VI) can be analysed by applying linear regression to multiwavelength data (details of the proposed method will be published elsewhere).

The W(VI)–BG system. This system was studied as for the Mo(VI)–BG system. The optimized experimental procedure is as follows. To a solution containing less than 20 μg of W(VI), add 1.3 ml of 5*M* hydrochloric acid, 0.8 ml of 1×10^{-3}*M* BG, 1.5 ml each of 0.2% PPOSA and 0.1% Triton X-100 solutions, and dilute to 10 ml. Heat the solution for 20 min at 50°. Cool and after 40 min, measure the absorbance at 618 nm against a reagent blank. The colour is stable for at least 5 hr. The molar absorptivity is 9.8×10^4 l.mole^{-1}.cm^{-1} at λ_{max} (618 nm), which is greater than the values obtained by using other surfactants, such as CTAB.[12] Beer's law is observed for 0.01–2 μg/ml W(VI). The composition of the complex is again 1:2:1 (W:BG:PPOSA). The effect of foreign ions on the determination of W(VI) is nearly the same as on that of Mo(VI), with Mo(VI) interfering seriously.

The Be(II)–CAS system. The reaction of Be(II), CAS and PPOSA is rather slow at room temperature, so it is necessary to heat the solution for full colour development. Five factors (pH, CAS and PPOSA concentrations, reaction temperature and time) were chosen as parameters in optimization of the colour development, with an orthogonal experimental design technique. The optimized procedure is as follows. A solution containing less than 2 μg of Be(II) is mixed with the reagent solutions and hexamine–HCl buffer (pH 4.6) to give 25 ml of a solution that is 3.3×10^{-5}*M* in CAS and 1.5×10^{-4}*M* in PPOSA. The solution is heated at 75° for 20 min. After cooling, the absorbance is measured at 628 nm against a reagent blank. The colour is quite stable and the molar absorptivity is 9.10×10^4 l.mole^{-1}.cm^{-1} at λ_{max} (628 nm), which is greater than the values obtained with other surfactants under the same conditions. Beer's law is obeyed for 0.004–0.08 μg/ml Be(II).

The composition of the complex is 1:2:2 (Be:CAS:PPOSA). The CAS used for complex composition studies was purified as described by Langmyhr *et al.*[13]

Miscellaneous systems. At pH 5.5–6.5, PPOSA reacts with La(III)–XO to form a blue complex, with molar absorptivity 1.39×10^5 l.mole^{-1}.cm^{-1}, which is greater than that obtained by using other common surfactants, such as CPB (1.02×10^5)[14] and near to that obtained by using poly(4-vinyl-*N*-dodecylpyridine)bromide (1.58×10^5).[5] The proposed procedure is as follows. To a solution containing less than 12 μg of La(III), add 0.5 ml of 5×10^{-5}*M* XO, 2 ml of pH 6.0 acetate buffer and 1.2 ml of 0.2% PPOSA, then dilute to 10 ml. After 10 min, measure the absorbance at 618 nm against a reagent blank.

The spectrophotometric characteristics of some other PPOSA micellar systems such as Ni(II)–XO, Bi(III)–Semi-Xylenol Orange, and Al(III)–Pyrocatechol Violet are also superior or equal to those obtained with surfactants commonly used in analytical chemistry. Thus, PPOSA is a promising new surfactant for the micellar spectrophotometric analysis of trace elements.

Acknowledgement—This research was supported by the Science Foundation, Academia Sinica, PRC.

REFERENCES

1. T. P. Rao and T. V. Ramakrishna, *Talanta*, 1980, **27**, 439.
2. Y. X. Zheng and Ch. Y. Li, *Fenxi Huaxue*, 1980, **8**, 404.
3. H. Watanabe, *Talanta*, 1974, **21**, 295.
4. H. M. Shi, G. Zh. Zhang and J. H. Li, *Gaodeng Xuexiao Huaxue Xuebao*, 1984, **5**, 163.
5. Y. Yamashoji, T. Matsushita and T. Shono, *Bunseki Kagaku*, 1981, **30**, 215, 407.
6. V. P. Antonovich, G. I. Ibragmov, E. M. Nevskaya, E. I. Shelikhina and M. A. Chernyshova, *Zh. Analit. Khim.*, 1979, **34**, 81.
7. G. B. Walker and C. M. Cambre, *U.S. Pat.*, 1,059, 117, 1964.
8. L. H. Boch and A. L. Houk, *U.S. Pat.*, 2,454,547, 1948.
9. E. Domba, *U.S. Pat.*, 3,989,636, 1976.

10. R. A. Reck, H. J. Hardwood and A. W. Ralston, *J. Org. Chem.*, 1947, **12**, 517.
11. M. L. Xu, *Fenxi Huaxue*, 1984, **12**, 151.
12. H. X. Shen, *Huaxue Shiji*, 1981, **3**, 205; 1982, **4**, 79.
13. F. J. Langmyhr and K. S. Klausen, *Anal. Chim. Acta*, 1963, **29**, 150.
14. M. Otomo and Y. Wakamatsu, *Bunseki Kagaku*, 1968, **17**, 764.

Talanta, Vol 32, No. 12, p. i, 1985
Pergamon Press Ltd. Printed in Great Britain

PAPERS RECEIVED

Copper(II) complexes of cyclic tetra-azatetra-acetic acids—unusual features and possible analytical applications: RITA DELGADO, J. J. R. FRAUSTO DA SILVA and CANDIDA T. A. VAZ. (6 September 1985)
The application of potentiometric analysis with ion-selective electrodes in analysis of ceramic raw materials: FENG GANG. (10 September 1985)
Behaviour of some dialkyl-lead and trialkyl-lead compounds in the hydride generation procedure and determination with a non-dispersive atomic-fluorescence detector: A. D'ULIVO, R. FUOCO and P. PAPOFF. (10 September 1985)
Analytical applications of synchronous fluorescence spectroscopy: S. RUBIO, A. GOMEZ-HENS and M. VALCARCEL. (13 September 1985)
Spectrophotometric determination of indium in nickel alloy and zinc ores with 1-(2-pyridylmethylideneamine)-3-(salicylideneamine)thiourea: DANIEL ROSALES, ISABEL MILLAN and JOSE L. GOMEZ ARIZA. (12 September 1985)
Determination of silver, antimony, bismuth, copper, cadmium and indium in ores, concentrates and related materials by atomic-absorption spectrophotometry after methyl isobutyl ketone extraction as iodides: ELSIE M. DONALDSON and MOHUI WANG. (17 September 1985)
Aggregation of meso-tetra(*p*-sulphonatophenyl)porphine and its Cu(II) and Zn(II) complexes in aqueous solution: A. CORSINI and O. HERRMANN. (17 September 1985)
A new spectrophotometric method of evaluation of stepwise stability constants for Mo–MNT (1:4) chelate: ANIL K. CHAKRABARTI. (18 September 1985)
Determination of tartaric and malic acids in grape juices by potentiometric titration: O. E. S. GODINHO, N. E. DE SOUZA, L. M. ALEIXO and A. U. IVASKA. (19 September 1985)
Salicylaldehyde and 3-hydroxybenzaldehyde phthalazinohydrazones as analytical reagents: M. CALLEJON, M. CENTENO, M. A. BELLO and A. GUIRAUM. (5 August 1985)
Quantitative separation of iron from some liquid appetite stimulants and iron preparations on zirconium(IV) arsenophosphate columns: K. G. VARSHNEY, KANAK VARSHNEY, SANJAY AGARWAL and S. M. MAHESHWARI. (20 September 1985)
A data-quality assurance program in industrial analytical chemistry: LANCELOT A. FERNANDO. (3 April 1985)
Uptake of copper, zinc, cadmium and lead by acrylonitrile–carbon composite: A. M. ABDALLAH, S. M. HASSAN, M. A. DIAB and Y. A. AGGOUR. (24 September 1985)
Indane-1,2,3-trione monothiosemicarbazone: A new chromogenic reagent for the rapid spectrophotometric determination of copper and palladium: K. HUSSAIN REDDY, K. GIRIDHARA REDDY and D. VENKATA REDDY. (24 September 1985)
Trace measurements of heavy rare-earths by adsorptive stripping voltammetry: JOSEPH WANG and JAVAD M. ZADEII. (25 September 1985)
NMR Method of assay for Gentamicin C: J. K. KWAKYE. (25 September 1985)
Binding properties of aminopolycarboxylato ligands bound on cellulose: M. C. GENNARO, E. MENTASTI and C. SARZANINI. (25 September 1985)
Solvent extraction of zinc with 5,7-dichloro-2-methyl-8-hydroxyquinoline into chloroform: A. IZQUIERDO, R. COMPAÑO and E. BARS. (25 September 1985)
A spectrophotometric study on the stability of molybdenum(V)–thiocyanate complex, in acidic media: SALAH M. SULTAN, S. A. AL-TAMRAH, I. Z. AL-ZAMIL and A. M. AZIZ-AL-RAHMAN. (26 September 1985)
Determination of Pb in high-purity Al and Al-alloys by direct solid ETA-AAS: Enhancement in solution by matrix modification: NADHUM A. N. AWAD and FADHIL JASIM. (26 September 1985)
Galvanic stripping analysis of ultra-trace amounts of lead in sea-water: S. JAYA, T. PRASADA RAO and G. PRABHAKARA RAO. (27 September 1985)
Mechanism of influence of added salts in the separation of light lanthanides in the P215–HCl system by extraction chromatography: LINGYING LI, ZIFEN SU and HAIYAN LONG. (27 September 1985)
Adsorption of metals on activated carbon from aqueous solutions at pH 1–13: HIDEKO KOSHIMA and HIROSHI ONISHI. (30 September 1985)
Extraction and spectrophotometric determination of titanium(IV) with alizarin and fluoride: R. LOPEZ NUNEZ, M. CALLEJON MOCHON and A. GUIRAUM PEREZ. (1 October 1985)
Potentiometric determination of fluorine in silicate rocks with an ion-selective electrode and novel decomplexing agent: G. CALDERONI. (1 October 1985)
A simple sample cell positioner for reducing imprecision due to placement of test-tube shaped sample cells: J. D. INGLE, JR. (2 October 1985)
The role of the auxiliary electrode in electrochemical detectors for microprobe chromatography: SAM A. MCCLINTOCK. (3 October 1985)
Electrochemical behaviour of arsenic on the mercury drop electrode: Determination of micro amounts of arsenic in natural samples by cathodic stripping voltammetry: G. GILLAIN, R. MACHIROUX and P. PITTANCE (4 October 1985)

Talanta, Vol. 32, No. 11, p. i, 1985
Pergamon Press Ltd Printed in Great Britain

PAPERS RECEIVED

Measurement of acidity constants of benzothiadiazines by solvent extraction with a membrane phase separator: ANJUM S. KHAN and FREDRICK F. CANTWELL. (6 August 1985)

Evaluation of colour-change quality and applicability of indicators in anhydrous acetic acid medium: J. BARBOSA, E. BOSCH and L. GARCIA-PUIGNOU. (6 August 1985)

Spectrophotometric methods for the evaluation of acidity constants—II: Numerical methods for two overlapping equilibria: A. G. ASUERO, J. L. JIMENEZ-TRILLO and M. J. NAVAS. (6 August 1985)

The influence of optical design on the signal to noise characteristics of polarimeters: JOUKO J. KANKARE and ROGER STEPHENS. (12 August 1985)

Preconcentration of microgram amounts of lead for oscillopolarographic determination using co-precipitation with calcium oxalate: SENFANG ZHENG and XIAORU MO. (13 August 1985)

Polarographic study of the co-ordinated system Cd(II)–oxalate–nitrate: G. RUIZ-CABRERA, G PASTOR-PINTO, J. C RODRIGUEZ-PLACERES and A. AREVALO. (13 August 1985)

Development and application of organic reagents for analysis—VII: Extraction–fluorimetric determination of perchlorate ions with 2,6-di-*p*-tolyl-4-phenylpyrylium chloride: KENICHIRO NAKASHIMA, SHOKO TOMIYOSHI, SHIN'ICHI NAKATSUJI and SHUZO AKIYAMA. (15 August 1985)

Bismuth(V) and bismuth(III) content of sodium bismuthate and determination of bismuth(V): K. M. INANI, P. D. SHARMA and Y. K. GUPTA. (20 August 1985)

pH-metric determination of sulphate ion: BÉLA NOSZÁL and MÁRIA JUHÁSZ. (20 August 1985)

Design of software for thermal titrations: RICHARD C. GRAHAM. (21 August 1985)

Fluorescence of the zinc–morin complex, enhanced by the use of a non-ionic surfactant: F. HERNANDEZ HERNANDEZ, J MEDINA ESCRICHE and M. T. GASCO ANDREU. (27 August 1985)

The high-order stability constants of quadrivalent and sexivalent uranium complexes at high temperatures: KUNIHIKO TAKEDA, HATSUKI ONIZUKA, HIROHISA YAMASHITA, MITSUNAGA SASAKI and NAOKI MIYATA. (27 August 1985)

Studies of atomization from a graphite platform in graphite-furnace atomic-absorption spectrometry: C. L. CHAKRABARTI, S. B. CHANG, P. W. THONG, T. J. HUSTON and SHAOLE WU. (27 August 1985)

Adsorptive stripping voltammetry of Methylene Blue: SHUNITZ TANAKA, TEIJI KAKIZAKI and HITOSHI YOSHIDA (29 August 1985)

Determining gold in water by batch extraction with an anion-exchanger: JOHN B. MCHUGH. (29 August 1985)

Spectrophotometric and spectrofluorometric determination of zinc and cadmium with 2,2′-pyridil-bis(2-quinolylhydrazone): KEVIN J. WEST and RONALD T. PFLAUM. (20 August 1985)

A simple gravimetric determination of tungsten in tungsten-bearing ores and minerals: ANIL K. CHAKRABARTI. (30 August 1985)

Spectrophotometric determination of clofibrate: Y. K. AGRAWAL and D. R. PATEL. (30 August 1985)

Indirect determination of nitrite in water by atomic-absorption spectrophotometry: XU BO-XING, XU TONG-MING, SHEN MING-NENG and FANG YU-ZHI. (30 August 1985)

Flow-injection determination of ergonovine maleate with amperometric detection at the Kel-F/graphite composite electrode: F. BELAL and J. L. ANDERSON. (2 September 1985)

Determination of chromate and cyanide by anion-exchange with lead iodate—analysis of mixtures with thiocyanate and halides: KRISHNA K. VERMA, PRAMILA TYAGI and MARY GRACE PUSHPA EKKA. (2 September 1985)

Ultramicro flow cell using a capillary tube and optical fibre for semiconductor laser fluorimetry: YUJI KAWABATA, TOTARO IMASAKA and NOBUHIKO ISHIBASHI. (2 September 1985)

Comparison of four digestion methods for the determination of selenium in bovine liver by hydride generation and atomic-absorption spectrometry in a flow system: JEAN PETTERSSON, LENA HANSSON and ÅKE OLIN. (3 September 1985)

Talanta, Vol. 32, No. 9, p. i, 1985
Pergamon Press Ltd. Printed in Great Britain

PAPERS RECEIVED

Simultaneous two and three component determination in multi-component mixtures by extraction-spectrophotometry and thermochromism of ion-association complexes: TADAO SAKAI and NORIKO OHNO. (29 May 1985)
Polarographic reduction of acids in pyridine: The cause of difference in half-wave potentials with various supporting electrolytes: MASASHI HOJO, MASAHIRO AKITA, KAZUKIYO NISHIKAWA and YOSHIHIKO IMAI. (29 May 1985)
Determination of microgram amounts of ascorbic acid by titration with hexa-amminecobalt(III) tricarbonatocobaltate as redox titrant and interference study of metalloids and carbohydrates: TARIK A. K. NASSER, GEORGE Y. MATTI and BAHJAT A. SAEED. (29 May 1985)
Spectrophotometric methods for the evaluation of acidity constants—I: Numerical methods for single equilibria: A. G. ASUERO, M. J. NAVAS and J. L. JIMENEZ-TRILLO. (31 May 1985)
Determination of silicon in urine by direct-current argon-plasma emission spectrometry: MIGUEL RODRIGUEZ and JOSEPH SNEDDON. (31 May 1985)
Spectrophotometric determination of some pharmaceutically-important thione-containing compounds: M. K. SHARAF EL-DIN, F. BELAL and S. M. HASSAN. (3 June 1985)
Bacterial bioluminescence assays of diagnostic heart and liver enzymes: α-Hydroxybutyrate and sorbitol dehydrogenases: A. M. KUUSINEN, T. N.-E. LÖVGREN and R. P. RAUNIO. (3 June 1985)
Simultaneous extraction and determination of copper(II) and nickel(II) with 2,4-dihydroxyacetophenone thiosemicarbazone: A. VARADA REDDY and Y. KRISHNA REDDY. (3 June 1985)
An exploratory study of the indirect fluorimetric determination of dioxouranium(VI) by energy transfer and measurement of fluorescent emission by europium(III): SAMUEL J. LYLE and NIDAL A. ZA'TAR. (4 June 1985)
Sensitive spectrophotometric determination of rhodium(III) and platinum(IV) with 2-methyl-1,4-naphthoquinone monoxime: KAMINI SHRAVAH and S. K. SINDHWANI. (4 June 1985)
Fluorimetric determination of beryllium with pyridoxal-5-phosphate: A. PETIDIER, S. RUBIO, A. GOMEZ-HENS and M. VALCARCEL. (5 June 1985)
Spectrophotometric determination of benzothiadiazines in dosage forms: F. BELAL, M. RIZK, F. A. IBRAHIEM and M. K. SHARAF-ELDIN. (5 June 1985)
Polarographic determination of trace amounts of thorium: ZAOFAN ZHAO, XIAOHUA CAI, PEIBIAO LI and HANDONG YANG. (10 June 1985)
A polarographic method for the simultaneous estimation of bismuth and molybdenum in catalyst samples: R. S. THAKUR, K. M. PARIDA, J. R. RAO and S. B. RAO. (11 June 1985)
A further insight into the mechanism of metal biosorption by examining chitin E.P.R. spectra: M. TSEZOS and S. MATTAR. (11 June 1985)
Indirect spectrophotometric methods for the determination of antibiotics with iodine or periodate, using metol and sulphanilamide: C. S. P. SASTRY, T. E. DIVAKAR and U. VIPLAVA PRASAD. (12 June 1985)
Signal-to-noise optimization in polarimetry: EDWARD S. YEUNG. (12 June 1985)
Thermometric titration of dodecyl sulphate ion with metal–phenanthroline complex: TOSHIAKI HATTORI and HITOSHI YOSHIDA. (13 June 1985)
Interaction of phenothiazines with nitroso-R salt and extractive spectrophotometric determination of phenothiazine drugs: JAYARAMA, M. VIOLET D'SOUZA, H. S. YATHIRAJAN and RANGASWAMY. (13 June 1985)
Simultaneous spectrophotometric determination of *o*-Cresol Red, Semi-Xylenol Orange and Xylenol Orange: S. KICIAK and H. GONTARZ. (14 JUNE 1985)

Talanta, Vol. 32, No. 8A, p. i, 1985
Pergamon Press Ltd. Printed in Great Britain

PAPERS RECEIVED

Evaluation and improvement of the resolution of voltammetric measurements: The chromatographic approach: JOSEPH WANG, DEN-BAI LUO and BASSAM FREIHA. (1 May 1985)
Characteristics of ion-pair extraction/flow-injection analysis for the determination of nitrate and other inorganic anions: MICHIO ZENKI, SHOICHIRO TANAKA and JAMES E. DINUNZIO. (2 May 1985)
Arsenic determination with graphite cloth ribbon in graphite-furnace atomic-absorption spectrometry: ETSURO IWAMOTO, CHAN-HUAN CHUNG, MANABU YAMAMOTO and YUROKU YAMAMOTO. (3 May 1985)
Phosphorescence characteristics of acetophenone, benzopheneone, *p*-aminobenzophene and Michler's ketone in various environments: G. SCHARF and J. D. WINEFORDNER. (7 May 1985)
The application of simplex optimization to flow-injection analysis: E. A. JONES. (8 May 1985)
Action de l'acide citrique sur l'anhydride acétique et la pyridine; Détermination du mécanisme réactionnel et de la structure du composé obtenu: D. BAYLOCQ, C. MAJCHERCZYK and F. PELLERIN. (9 May 1985)
Mise en évidence de deux nouveaux indicateurs acide-base dans l'acide acétique anhydre: M. SARBAR, S. M. GOLABI and M. H. POURNAGHI-AZAR. (9 May 1985)
Identification and determination of the major ions in kidney stones by the ring-oven technique: AYTEKIN TEMIZER, SEDEF KOT and MEHMET BAKKALOĞLU. (9 May 1985)
Determination of submicrogram quantities of iron(II) by a kinetic spectrophotometric method: S. J. RAO, G. S. REDDY and Y. K. REDDY. (9 May 1985)
Influence of the nature of organic phase emulsions on the sensitivity of atomic-absorption determinations: M. T. VIDAL and M. DE LA GUARDIA. (9 May 1985)
Studies on fluorescein—III: The acid strengths of fluorescein as shown by potentiometric titration: HARVEY DIEHL, NAOMI HORCHAK-MORRIS, ALTA J. HEFLEY, LINDA F. MUNSON and RICHARD MARKUSZEWSKI. (10 May 1985)
Studies on fluorescein—IV: Notes on obtaining acid dissociation constants from the titration curves of dibasic acids: HARVEY DIEHL. (10 May 1985)
Determination of trace levels of calcium in steels by using carbon-furnace atomic-absorption and atomic-emission spectrometry: JOSE ALVARADO, FRANCISCO CAMPOS and JOHN M. OTTAWAY. (14 May 1985)
Kinetic determination of manganese traces in different materials by its catalytic effect on the Methylene Green–periodate reaction: M. HERNANDEZ CORDOBA, P. VINAS and C. SANCHEZ-PEDREÑO. (14 May 1985)
Simultaneous determination of ascorbic acid and sulphite in soft drinks by flow-injection analysis: F. LAZARO, M. D. LUQUE DE CASTRO and M. VALCARCEL. (14 May 1985)
***N*-*m*-Tolyl-*p*-methoxybenzohydroxamic acid (TMBHA): A new reagent for the solvent extraction of copper(II):** A. B. ZADE and S. B. GHOLSE. (15 May 1985)
Comments on the paper by Hassan, Iskander and Nashed: MANNAM KRISHNAMURTHY and U. MURALIKRISHNA. (16 May 1985)
Calculation of equilibrium constants from multiwavelength spectroscopic data—III: Model-free analysis of spectrophotometric and ESR titrations: HARALD GAMPP, MARCEL MAEDER, CHARLES J. MEYER and ANDREAS D. ZUBERBÜHLER. (17 May 1985)
Effect of temperature on hydride generation and decomposition for the group Vb elements, and estimation of kinetic stability of gaseous bismuth hydride by an atomic-absorption method: KATSUYUKI FUJITA and TAKEO TAKADA. (20 May 1985)
Flow-injection analysis with multidetection as a useful technique for metal speciation: J. RUZ, A. RIOS, M. D. LUQUE DE CASTRO and M. VALCARCEL. (21 May 1985)
Liquid-state copper(II) ion-selective electrode containing a complex of Cu(II) with salicylaniline: KRZYSZTOF REN. (21 May 1985)
Selective complexometric determination of palladium with thiosulphate as masking agent: SARALA RAOOT and K. N. RAOOT. (21 May 1985)
Spectrophotometric determination of cadmium(II) in high sensitivity conditions with 2-(5-chloro-2-pyridylazo)-5-dimethylaminophenol: M. VILLARREAL, L. PORTA, E. MARCHEVSKY and R. OLSINA. (22 May 1985)
Determination of tungsten in rocks and minerals by chelate-extraction and atomic-absorption spectrometry: N. K. ROY and A. K. DAS. (22 May 1985)
The distribution of elements between polyether-type polyurethane foam, cyclic polyethers and hydrofluoric acid solution: R. CALETKA, R. HAUSBECK and V. KRIVAN. (23 May 1985)
Zinc trace determination: A synchronous derivative fluorimetric approach: F. GARCIA SANCHEZ and M. HERNANDEZ LOPEZ. (27 May 1985)
Sample-pretreatment procedure for routine liquid chromatographic assay of serum cortisol: M. PERLA COLOMBINI, ROBERTA CURINI, ALDO LAGANA, MAURO ROTATORI and GIULIANA VINCI. (27 May 1985)
Studies on fluorescein—V: The fluorescence of fluorescein as a function of pH: HARVEY DIEHL and RICHARD MARKUSZEWSKI. (28 May 1985)
The determination of gold in geological samples: A critical review: S. O. FARWELL and C. T. KAGEL. (29 May 1985)
Analysis of variance in determinations of equivalence volume and of ionic product of water in potentiometric titrations: ANTONIO BRAIBANTI, CLAUDIO BRUSCHI, EMILIA FISICARO and MARZIA PASQUALI. (29 May 1985)

Talanta, Vol. 32, No. 7, p. i, 1985
Pergamon Press Ltd. Printed in Great Britain

PAPERS RECEIVED

Studies on the multibasic fluorescence system of rare earth metals—I: The Eu–TTA–phenanthroline–surfactant system: YANG JINGHE, ZHU GUIYUN, ZUE JIANHUA and ZHANG XINYONG. (27 March 1985)
Studies on the multibasic fluorescence system of rare earth metals—II: The Tb–EDTA–salicylic acid–surfactant system: ZHU GUIYUN, YANG JINGHE, LEI JINGFANG and ZHANG HUI. (27 March 1985)
Simultaneous determination of cadmium and tellurium in electro-deposited cadmium telluride thin films by polarography: ANDRZEJ DARKOWSKI and MICHAEL COCIVERA. (29 March 1985)
Analytical applications of copper(II) and copper(I) in acetonitrile: Potentiometric and spectrophotometric determination of amines through dithiocarbamate formation: B. C. VERMA, D. K. SHARMA, ANILA SOOD, NEELAM SHARMA, USHA SHARMA and H. S. SIDHU. (11 April 1985)
Gravimetric determination of nickel with cyclohexylidine-ammonium 2-aminocyclohexylidine-1-cyclohexene-1-dithiocarboxylate: H. PARHAM and A. SAFAVI. (11 April 1985)
Preparation of a mercury film electrode modified by tri-n-octylphosphine oxide, and the electrochemical properties of this electrode: JIŘÍ LEXA and KAREL ŠTULÍK. (12 April 1985)
Determination of bismuth by electrochemical stripping analysis: Elimination of interferences by using a mercury film electrode modified by tri-n-octylphosphine oxide: application to copper alloys: JIŘÍ LEXA and KAREL ŠTULÍK. (12 April 1985)
Enhanced sensitivity in the AAS determination of sub-microgram quantities of gallium in high-purity aluminium and aluminium alloys by direct solid sampling: NADHOM A. N. AWAD and FADHIL JASIM. (15 April 1985)
Investigation of adsorption behaviour of mercury on microamounts of manganese dioxide from aqueous solutions: SYED MOOSA HASANY and MUNAWAR HUSSAIN CHAUDHARY. (16 April 1985)
Ultrasonic studies for the micro-estimation of zinc as diethyldithiocarbamate: SUNITA PRADHAN, B. K. MAHESHWARI and R. L. YADAV. (16 April 1985)
Gravimetric determination of bismuth and lead by precipitation of the $[(C_4H_9)_4N]_3[Bi(SCN)_6]$ and $[(C_4H_9)_4N]$ $[Pb(SCN)_3]$ ion-pairs. J. HERNANDEZ-MENDEZ A. ALONSO-MATEOS, E. J. MARTIN MATEOS and C. GARCIA DE MARIA. (17 April 1985)
Atomic-absorption spectrophotometric determination of tin by hydride generation in non-aqueous medium after extraction: JOSE AZNAREZ, JOSE M. RABADAN, ANGEL FERRER and PILAR CIPRES. (19 April 1985)
Flow-injection analysis with the iron-induced perbromate–iodide reaction: Spectrophotometric determination of iron: T. D. YERIAN, T. P. HADJIIOANNOU and G. D. CHRISTIAN. (23 April 1985)
Electrometric studies on 2-(*p*-sulphophenylazo)-1,8-dihydroxynaphthalene-3,6-disulphonate (SPADNS) and samarium(III), germanium(III) and yttrium(III) complexes at the d.m.e.: T. C. SHARMA, S. C. SHARMA and K. S. BHANDARI. (23 April 1985)
Spectrophotometric studies on 2-(*p*-sulphophenylazo)-1,8-dihydroxynaphthalene-3,6-disulphonate (SPADNS) and Sm(III) and Gd(III): S. C. SHARMA, K. S. BHANDARI and T. C. SHARMA. (23 April 1985)
Dissociation of 5-fluoro- and 3,5-dinitrosalicylic acids in water–methanol mixtures at 25°: G. POULIAS, N. PAPADOPOULOS and D. JANNAKOUDAKIS. (25 April 1985)
Spectrophotometric determination of chloride in Pt–Al_2O_3/SiO_2 catalysts with $Hg(SCN)_2$–Fe^{3+} reagent: V. J. KOSHI and V. N. GARG. (25 April 1985)
Silver–gelatin method for determination of inorganic peroxides in alkaline solution: T. PAL, A. GANGULY and D. S. MAITY. (29 April 1985)
Speciation by flow-injection analysis: M. D. LUQUE DE CASTRO. (30 April 1985)
Extraction–spectrophotometric determination of titanium(IV) with Malachite Green and *p*-chloromandelic acid, with application to steels: SHIGEYA SATO and SUMIO UCHIKAWA. (30 April 1985)
Separation of nitroimidazoles by reversed-phase high-pressure liquid chromatography: BISHOP B. SITHOLE and ROBERT D. GUY. (30 April 1985)

Talanta Vol. 32, No. 6, p i, 1985
Pergamon Press Ltd Printed in Great Britain

PAPERS RECEIVED

Study of pH and substrate effects on room-temperature phosphorimetry of some indolecarboxylic acids: MARTA ANDINO, J. J. AARON and J. D. WINEFORDNER. (5 March 1985)
Determination of silver, bismuth, cadmium, copper, iron, nickel and zinc in lead- and tin-base solders and white-metal bearing alloys by atomic-absorption spectrophotometry: C. CHOW. (5 March 1985)
Dye–surfactant interactions: A mini-review: M. E. DIAZ GARCIA and A. SANZ-MEDEL. (5 March 1985)
Structure–photodegradation study of 2,3,7,8-tetrachlorodibenzo-*p*-dioxin: JOSEPH B. ADDISON. (20 February 1985)
Properties and analytical application of a new membrane electrode sensitive to molybdenum(VI): L. K. SHPIGUN, E. N. ABANINA, Z. A. GALLAI and N. M. SHEINA. (14 November 1984)
A rapid method for determining tin and molybdenum in geological samples by flame atomic-absorption spectroscopy: ERIC P. WELSCH. (7 March 1985)
Determination of pK_a values of 2,2′-bipyridyl analogues and stability constants of their copper(I) and copper(II) complexes: Relationship to antimycoplasmal activity: H.-D. GAISSER, H. VAN DER GOOT and H. TIMMERMAN. (7 March 1985)
Analysis of sweeps: The cuprous-sulphide collecting system: SILVE KALLMANN. (7 March 1985)
Non-aqueous titrimetric determination of sulphadimidine sodium and sulphadiazine sodium in injections: SOBHI A. SOLIMAN, SAIED BELAL and MONA BEDIAR. (11 March 1985)
Detection and determination of L-cysteine hydrochloride: N. KRISHNA MURTY, V. JAGANNADHA RAO and G. VASUDEVA PRASAD. (12 March 1985)
Determination of thallium(III) alone and in mixtures, by using a mercury reductor: S. N. DINDI and N.V.V.S.N.M. SARMA. (12 March 1985)
Solvent effect on the liquid–liquid partition coefficients of copper(II) chelates with some β-diketones: HISANORI IMURA and NOBUO SUZUKI. (7 December 1984)
Photometric determination of potassium by extraction of DB18C6-K^+-Bromothymol Blue: ZHANG FAN, LIAO JI, CHEN XIUYU and ZHANG NIN. (14 March 1985)
Complexometric determination of Cu(II) and Ni(II) in mixtures by using 2-thio-orotic acid and EDTA: MADHULIKA SHRIVASTAVA and G. S. PANDEY. (14 March 1985)
Potentiometric stripping analysis of lead and thallium: S. JAYA, T. PRASADA RAO and G. PRABHAKARA RAO. (15 March 1985)
Solvent extraction of Cu(II) with *N*-nitroso-*N*-cyclohexylhydroxylamine into methyl isobutyl ketone: Determination of Cu(II) by AAS in river water samples: G. RAURET, L. PINEDA and R. COMPAÑO. (18 March 1985)
Determination of the equilibrium constant (by ion-exchange method) for the formation of $C_6H_5SO_2\overset{+}{N}H_2Cl$ from chloramine-B: M. SUBHASHINI, M. S. SUBRAMANIAN and V. R. S. RAO. (20 March 1985)
The limitations of the thiocyanate spectrophotometric determination of WO_3: JOSE INACIO MARTINS. (20 March 1985)
The fluorescence of X-rays as a quick method to determine WO_3: JOSE INACIO MARTINS. (20 March 1985)
Determination of total phosphorus in water by photochemical decomposition with UV-irradiation: LIU ZAIYOU and WU LIMIN. (20 March 1985)
The application of an ion-selective electrode sensitive to Bi^{3+} cations for the investigation of bismuth complexes with citric and malic acids: WALENTY SZCZEPANIAK and MARIA REN. (20 March 1985)
Analytical applications of emulsions: Determination of lead in gasoline by AA spectrophotometry: E. CARDARELLI, M. CIFANI, M. MECOZZI and G. SECHI. (21 March 1985)
Determination of sodium fluorescein in sea markers by UV spectrophotometry: E. CARDARELLI, M. CIFANI and M. MECOZZI. (21 March 1985)
Extraction of silver, gold and palladium with a polythiolether foam: A. S. KHAN and A. CHOW. (22 March 1985)
Validation of accuracy by interlaboratory program: R. SUTARNO and H. F. STEGER. (22 March 1985)
Separation and determination of aluminium by single-column ion-chromatography: NANCY E. FORTIER and JAMES S. FRITZ. (13 March 1985)
A selective spectrophotometric method for the determination of copper by using the ferron complex of copper(II): S. P. ARYA, J. L. MALLA and VEENA SLATHIA. (25 March 1985)
Methyl isobutyl ketone extraction of iodide complexes from sulphuric acid—potassium iodide media: ELSIE M. DONALDSON and MOHUI WANG. (25 March 1985)
"Electrochemical masking" of large amounts of copper in DPASV and the determination of thallium in the presence of a large excess of copper: ALEKSANDER CISZEWSKI and ZENON ŁUKASZEWSKI. (25 March 1985)
Spectrophotometric determination of titanium with tannin–thioglycollic acid and its application to titanium-treated steels, ferrous and non-ferrous alloys: SAMARESH BANERJEE. (28 March 1985)
Chelatometric titration of bismuth with HEDTA: ZHOU NAN, YU REN-QING, YAO XU-ZHANG and LU ZHI-REN. (28 March 1985)
Chelatometric titration of tin with HEDTA in non-ferrous alloys: ZHOU NAN, YU REN-QING, YAO ZU-ZHANG and LU ZHI-REN. (28 March 1985)
The chemical destruction of the anti-tumour pharmaceuticals 6-mercaptopurine, 6-thioguanine and melphalane and monitoring of its effectiveness by UV spectrophotometry, differential pulse polarography and differential pulse voltammetry: JIŘÍ BAREK, ANTONÍN BERKA and JIŘÍ ZIMA. (29 March 1985)
Extraction-spectrophotometric and fluorimetric determination of boron with 2,2,4-trimethyl-1,3-pentanediol and carminic acid: J. AZNAREZ, A. FERRER, J. M. RABADAN and L. MARCO. (29 March 1985)
Synthesis and analytical properties of polymerized surfactant PPOSA: KUN-YUAN LIU and RU-QIN YU. (1 April 1985)
Polarographic studies on substituted azo-dyes—I: T. C. SHARMA, K. S. BHANDARI and S. C. SHARMA. (1 April 1985)
A study on an electroanalytical method of determination of vinca alkaloids used in cancer chemotherapy: AYTEKIN TEMIZER. (1 April 1985)
A direct method for the spectrophotometric estimation of vanadium(V): R. K. BISWAS, M. N. ISLAM and N. GOSWAMI. (2 April 1985)

Talanta, Vol. 32, No. 5, p i, 1985
Pergamon Press Ltd Printed in Great Britain

PAPERS RECEIVED

Electrochemical detection of purine bases and nucleosides in high-pressure liquid chromatography: ANNA MARIA GHE, GIUSEPPE CHIAVARI and JOANIS EVGENIDIS. (18 February 1985)
Effect of a graphite lid for a cup furnace on enhancement of absorption sensitivity in atomic-absorption spectrometry: KUNIO TAKADA. (18 February 1985)
Comparative studies of combined ion-exchange solvent extraction (CIESE) technique using organic and inorganic ion-exchangers: C. R. BHATTACHARYYA. (18 February 1985)
Determination of palladium with thiocyanate and Rhodamine B by a solvent-extraction method: I. LOPEZ GARCIA, J. MARTINEZ AVILES and M. HERNANDEZ CORDOBA. (19 February 1985)
Determination of activities of asparaginase, RNA-ase and some other hydrolases by microcalorimetry: M. V. REKHARSKY, A. ZH. SKYA, S. V. LOPATNEV, YU. B. SLOZHENIKINA, A. M. EGOROV and G. L. GALCHENKO. (19 February 1985)
Extraction chromatography of palladium and platinum complexes with nitroso-R-salt: A. FLIEGER and S. PRZESZLAKOWSKI. (21 February 1985)
Properties of low-capacity macroporous anion-exchangers and their use with high pH eluents for the determination of weak acids in urine: ANJUM S. KHAN and FREDERICK F. CANTWELL. (22 February 1985)
Potential use of ascorbic acid as a complexing reagent for rare earths in their separation and preconcentration from geological materials for neutron-activation analysis: N. R. DAS. (22 February 1985)
Selective complexometric determination of bismuth with mercaptans as masking agents and its estimation in alloys: SARALA RAOOT and K. N. RAOOT. (22 February 1985)
The extraction of Zn(II), Cd(II) and Pb(II) from hydrochloric acid solutions by Amberlite LA-2 hydrochloride dissolved in 1,2-dichloroethane: WIESŁAWA ZABORSKA and MACIEJ LESZKO. (26 February 1985)
Dissociation constants, reactions and study of some metal chelates of 3-phenyl- and 3-cyclohexyl-2-mercaptopropenoic and 3-phenyl-2-mercaptopropanoic acids: A. IZQUIERDO and N. GARRIGA. (1 March 1985)
Use of *p*-chloranilic acid for the colorimetric determination of some antimalarials: M. S. MAHROUS, M. ABDEL SALAM, A. S. ISSA and M. ABDEL-HAMID. (1 March 1985)
Determination of phenothiazines by charge-transfer complex formation with chloranilic acid: M. RIZK, N. A. ZAKHARI, F. IBRAHIM and M. I. WALASH. (1 March 1985)
Three-wavelength spectrophotometry for determination of trace copper in presence of iron and other ions: LU MIN-GANG, HUANGFU LI-XIA and YIN FANG. (4 March 1985)
Electrothermal atomic-absorption spectroscopic analysis of lake waters for Mn, Fe, Pb and Cd: STUART J. NAGOURNEY, MERRILL H. HEIT and DONALD C. BOGEN. (4 March 1985)
Potentiometric study of the system lead(II)–cysteine in aqueous medium: H. GUTIERREZ, R. PARDO, E. BARRADO and P. SANCHEZ BATANERO. (4 March 1985)

Talanta, Vol. 32, No. 4, p. i, 1985
Pergamon Press Ltd. Printed in Great Britain

PAPERS RECEIVED

Voltammetric determination of the stabilizer additives Acardite II, Centralite I and diphenylamine in propellants: ARNE BERGENS, KENT LUNDSTRÖM and JAN ASPLUND. (15 January 1985)
Spectrophotometric determination of iridium(IV) with propionyl promazine phosphate: B. KESHAVAN and P. NAGARAJA. (15 January 1985)
An ion-selective electrode study of aqueous magnesium phthalate and terphthalate solutions: NAZIK A. FARID, AHMED M. WASFI, MOHIE M. BAHR, HASSAN M. ABD ELBARY and MOSTAFA M. EMARA. (15 January 1985)
Atomic-absorption spectrometric determination of trace metals in zirconium and zircaloy by discrete-sample nebulization: DANIEL A. BATISTONI, LIGIA H. ERLIJMAN and MARIA I. FUERTES. (3 January 1985)
Etude analytique du Goodrite 3114, antioxydant des polyoléfines; comportement vis à vis des agents de stérilisation: F. PELLERIN, C. MAJCHERCZYK and D. BAYLOCQ. (18 January 1985)
Specific kinetic determination of 2,4-dinitrotoluene: SAEEDUZZAFAR QURESHI, SEEMA HAQUE and PUSHKIN M. QURESHI. (18 January 1985)
Stability constants of some thorium complexes in aqueous solutions: P. H. TEDESCO, V. B. DE RUMI and A. PIRO. (3 January 1985)
Multiparametric curve fitting—IX: Simultaneous regression estimation of complex stoichiometry and stability constants: JOSEF HAVEL and MILAN MELOUN. (22 January 1985)
Modification of a packed-column gas-chromatograph/mass spectrometer: YULIN L. TAN and JOHN F. QUANCI. (23 January 1985)
Electroanalytical and thermoanalytical methodology: A unified approach: KRISHNAN RAJESHWAR. (24 January 1985)
Spectrophotometric determination of metronidazole in suspensions: S. B. MAHATO, T. K. DAS and S. K. MOITRA (25 January 1985)
MINIPOL, a desk-computer program for refinement of protonation constants from differential pulse polarographic data: V. CERDA and R. FORTEZA. (28 January 1985)
Determination of certain phenothiazine drugs with diazotized *p*-nitroaniline: S. R. EL-SHABOURI. (30 January 1985)
Spectrophotometric study of palladium(II) with some thio- and dithiodiacids: JORDI COELLO BONILLA, SANTIAGO HERNANDEZ CASSOU and HORTENSIA ITURRIAGA MARTINEZ. (30 January 1985)
Spectrophotometric study of palladium(II) with thiodipropanoic acid, based on the formation of ternary complexes with chloride: SANTIAGO HERNANDEZ CASSOU and HORTENSIA ITURRIAGA MARTINEZ. (30 January 1985)
Selective separation of metal ions with chelate-forming resins prepared by modification of conventional anion-exchangers with SPADNS and Orange II: KRYSTYNA BRAJTER and EWA DABEK-ZŁOTORZYNSKA. (30 January 1985)
Determination of sub-mg/ml levels of mercury in water by electrolytic deposition–flameless atomic-absorption spectrophotometry: XU BO-XING, XU TONG-MING, SHEN MING-NENG and FANG YU-ZHI. (31 January 1985)
Effect of cyclodextrin cavity size on sensitized room-temperature biacetyl phosphorescence: FRANK J. DE LUCCIA and L. J. CLINE LOVE. (8 January 1985)
Adsorption of mono- and bivalent metal nitrates on hydrous lead dioxide: Adsorption behaviour of potassium, copper(II), zinc(II), cadmium(II) and nitrate ions: HIROAKI KAWANO, YOSHIKAZU NAKAI, TOSHIO MATSUDA and TOYOSHI NAGAI. (31 January 1985)
Rapid extractive–spectrophotometric method for the determination of tin in canned foods with 5,7-dichloro-8-quinolinol: A. M. GUTIERREZ, C. PEREZ-CONDE, M. P. REBOLLAR and L. M. POLO DIEZ. (1 February 1985)
Elimination of the effect of interferences caused by iron and aluminium in the determination of cadmium by flame atomic-absorption spectrometry with use of some signal-levelling agents: A. B. EL-SAYED, N. E. AMIN, E. M. NOUR, S. H. ABD EL-HALIM and M. F. EL-SHAHAT. (4 February 1985)
A fluorescent reagent for various reducing agents: HARVEY W. YUROW. (7 January 1985)
A new type of Zeeman-effect atomic-absorption spectrophotometer: JING SHI-LIAN, LI SHAO-YUAN, WANG RONG-RONG, MA YI-ZAI, YU CHU-MING, YAN YAN, ZHANG DONG-HUA, SUN JINA and ZHANG ZHONG-MING. (6 February 1985)
Multiparametric curve fitting—X. A structural classification of multicomponent spectra-analysing programs and their diagnostics for equilibrium model determination: MILAN MELOUN, MILAN JAVŮREK and JOSEF HAVEL. (6 February 1985)
Multiparametric curve fitting—XI: A critical comparison of linear *A*–pH transformations for pK_a, ε_L and ε_{LH} determination: MILAN MELOUN and MILAN JAVŮREK. (6 February 1985)
CONSEL, a least-squares program for estimating stability constants from polarographic data: J. A. SANTABELLA, C. BLANCO, F. ARCE and J. CASADO. (6 February 1985)
A theoretical and experimental study of the waveform in potentiometric stripping analysis with a rotated mercury film electrode: The reversible case: BOY HØYER and LARS KRYGER. (7 February 1985)
***N*-Phenyl-*N'*-acetylthiourea: A specific reagent for determination of osmium(VI) spectrophotometrically:** D. K. DAS. (8 February 1985)
NMR quantitative analysis of pharmaceuticals: J. K. KWAKYE. (11 February 1985)
Extractive fluorimetric determination of ultratraces of lead with cryptand 2.2.2 and eosin: D. BLANCO GOMIS, E. FUENTE ALONSO and A. SANZ-MEDEL. (11 February 1985)
Determination of aromatic amines in FD&C Yellow No. 5 by the diazotization and coupling procedure followed by reversed-phase high-performance liquid chromatographic analysis: JOHN E. BAILEY, JR and CATHERINE J. BAILEY. (1 February 1985)
Application of the calcium–calcichrome colour reaction to the spectrophotometric determination of microamounts of calcium in plants: QIU XING-CHU, ZHANG YU-SHENG and ZHU YING-QUAN. (30 January 1985)
Analytical reactions of hydroxypyridines: RAGHUBIR SINGH SINDU, ANAND KUMAR SHARMA, KRISHNA BIHARI PANDEYA and MOHAN KATYAL. (13 February 1985)

Talanta, Vol. 32, No 3, p i, 1985
Pergamon Press Ltd Printed in Great Britain

PAPERS RECEIVED

Acid–base and chelatometric phototitrations with photosensors and photomembrane sensors: TSUTOMU MATSUO, YOSHITAKA MASUDA and EIICHI SEKIDO. (13 December 1984)
Determination of trace organic dicarboxylic acids and amines by ion-chromatography: SASWATI P. BAG (20 November 1984)
Determination of aluminium in natural and waste waters by atomic-absorption spectrophotometry and fluorimetry: F. HERNANDEZ HERNANDEZ, J. MEDINA ESCRICHE and J. V. MARTIN PRATS. (14 December 1984)
Silica-bound complexing agents: Some aspects of synthesis, stability and pore size: JOHN R. JEZOREK, KATHLEEN H. FALTYNSKI, LARRY G. BLACKBURN, PEGGY J. HENDERSON and H. DARLENE MEDINA (21 November 1984)
Colorimetric determination of piperazine with *p*-benzoquinone: ABDEL-AZIZ M. WAHBI, MOHAMMAD A. ABOUNASSIF and E. A. GAD-KARIEM. (17 December 1984)
Reflections on the modified simplex—I: D. BETTERIDGE, A. G. HOWARD and A. P. WADE. (17 December 1984)
Reflections on the modified simplex—II: D. BETTERIDGE, A. G. HOWARD and A. P. WADE. (17 December 1984)
Electroanalytical study of psychotropic drugs containing the 1,4-diazepine-2-thione group: Determination in urine by differential pulse polarography: M. A. FERNANDEZ-ARCINIEGA, L. HERNANDEZ and A. G. FOGG. (19 December 1984)
Liquid chromatographic separation of metals by on-column chelation with 4-(2-pyridylazo)resorcinol: JAMES E. DINUNZIO, ROBERT W. YOST and EMORY K. HUTCHISON. (21 November 1984)
Thermometric titration study of polyol–borate complexes in aqueous medium: ROBERTO ARUGA. (19 December 1984)
Measurement of pH by glass electrode in aqueous dioxan solutions: R. A. NASH, V. L. YU and S. F. SUN. (10 December 1984)
Multielement preconcentration of trace metals with *meso*-tetra(*p*-sulphonatophenyl)porphine: A. CORSINI, R. DIFRUSCIA and O. HERRMANN. (4 January 1984)
Diazotized anthranilic acid as a chromogenic reagent for traces of acetylacetone in aqueous solution: S. A. RAHIM, B. B. IBRAHEEM and W. A. BASHIR. (21 December 1984)
Nafronyl ion-selective membrane electrodes and their use in pharmaceutical analysis: MARIANA S. IONESCU, VERONICA BADEA, G. E. BAIULESCU and V. V. COŞOFREŢ. (21 December 1984)
Spectrophotometric and titrimetric determination of catecholamines: FATMA BASYONI SALEM. (21 December 1984)
Characterization and elimination of the interfering effects of foreign species in the atomic-absorption determination of manganese: M. M. EL-DEFRAWY, A. M. ABDALLAH, M. A. MOSTAFA and M. A. AKL. (7 January 1985)
Heterogeneous and homogeneous nucleation of cupric hydroxide: STEVEN A. SCHUBERT and NANCY J. STONE (7 January 1985)
Analytical properties of 2-oximinodimedone dithiosemicarbazone: F. SALINAS, J. C. JIMÉNEZ SANCHEZ and J. M. LEMUS GALLEGO. (7 January 1985)
Analytical investigations of cephalosoporins—Part 15: Polarographical comparison of two 3-[(aminocarbonyl)oxymethyl] substituted cephalosporins and the determination of cefoxitin in pharmaceutical formulations: F. I. SENGÜN, I. FEDAI, B. AKSU, A. KESTEK and Y. ALPER. (8 January 1985)
Determination of thallium in bismuth by differential-pulse anodic-stripping voltammetry without preliminary separation: ALEKSANDER CISZEWSKI. (8 January 1985)
Reactions of metal ions and their clusters in the gas phase in laser-ionization Fourier-transform mass spectrometers: BEN S. FREISER. (8 January 1985)
Extraction of uranium by supported liquid membranes containing mobile carrier: KENICHI AKIBA and HIROYUKI HASHIMOTO. (8 January 1985)
Effect of stirring on the ion-pair extraction of copper(II)- and zinc(II)-4,7-diphenyl-1,10-phenanthroline complexes: HITOSHI WATARAI. (3 December 1984)
Liquid–liquid extraction of univalent class B metal ions by the thiacrown compound 13,14-(4′-picrylamino)-1,4,8,11-tetrathiacyclopentadecane: EIICHI SEKIDO, KENJI CHAYAMA and MOTOHO MUROI. (7 December 1984)
Enhancement of sensitivity of ion-exchanger absorptiometry by using a thick ion-exchanger layer: KAZUHISA YOSHIMURA and HIROHIKO WAKI. (9 January 1985)
Spectrophotometric determination of cobalt in iron-, cobalt-, and nickel-base alloys: B V. RAO, V. G. RADHA MENON and K. C. SAROJAM. (10 January 1985)
Determination by GFAA of ultratrace quantities of organotins in sea water, using enhancement methods: E. J. PARKS, W. R. BLAIR and F. E. BRINCKMAN. (31 December 1984)
Utility of 2,3-dichloro-5,6-dicyano-*p*-benzoquinone in the assay of codeine, emetine and pilocarpine: MOHAMED E. ABDEL-HAMID, MOHAMED ABDEL-SALEM, MOHAMED S. MAHROUS and MAGDI M. ABDEL-KHALEK. (11 January 1985)

Talanta, Vol 32, No. 1, p. i, 1985
Pergamon Press Ltd Printed in Great Britain

PAPERS RECEIVED

Comparison of chelating agents immobilized on glass with Chelex 100 for trace Cu(II) removal and preconcentration: DAVID K. RYAN and JAMES H. WEBER. (27 August 1984)
Separation of DCTA chelates of bismuth(III), iron(III) and copper(II) by reversed-phase, paired-ion chromatography: SADANOBU INOUE, NAOKI HASHIMOTO, SUWARU HOSHI and MUTSUYA MATSUBARA. (16 October 1984)
Extraction and preconcentration of selenium from aqueous solutions and determination in water and hair samples by atomic-absorption spectrophotometry: MUHAMMAD EJAZ and M. A. QURESHI. (16 October 1984)
A new numerical method of potentiometric titration end-point detection: Use of rational spline functions: KRZYSZTOF REN and ANNA REN-KURC. (16 October 1984)
Extraction and direct spectrophotometric determination of cobalt with isonitrosothiocamphor: P. K. PARIA and S. K. MAJUMDAR. (16 October 1984)
The complexation of "crowned" 4-(2,4-dinitrophenylazo)phenol with alkali and alkaline-earth metal ions, and its application: KENICHIRO NAKASHIMA, SHIN'ICHI NAKATSUJI, SHUZO AKIYAMA, TAKAHIRO KANEDA and SOICHI MISUMI. (16 October 1984)
A gravimetric procedure for the determination of wet precipitated sulphur, dissolved sulphur, soluble sulphides and hydrogen sulphide: DODDABALLAPUR K. PADMA. (18 October 1984)
Non-dispersive atomic-fluorescence spectrometry of lead with use of hydride generation: A. D'ULIVO and P. PAPOFF. (18 October 1984)
The quantitative characterization and computational elimination of interferent effects in flame atomic-absorption spectrometry: A. KECHOTYCKI, M. KRUPIŃSKI and L. PSZONICKI. (18 October 1984)
Fabrication and evaluation of a graphite (Ag_2S–AgI) electrode: P. RIYAZUDDIN and SYED MD. YOUSUF HUSSAINY. (19 October 1984)
Polarographic behaviour of 3,5-dimethyl-4-(2′-nitrobenzeneazo)isoxazole and 3,5-dimethyl-4-(4′-nitrobenzeneazo)isoxazole: K. RAM and S. BRAHMAJI RAO. (22 October 1984)
The oxidation of iodide to iodate for the polarographic determination of total iodine in sea-water: KAZUFUMI TAKAYANAGI and GEORGE T. F. WONG. (22 October 1984)
Extraction equilibria of some complex combinations with macrocyclic ligands: CONSTANTIN LUCA and MOHAMED MAGDI KHALIL. (23 October 1984)
A polarographic study of some complexes of Tl(I) with polyoxa macrocyclic ligands: MOHAMED MAGDI KHALIL, ION TANASE and CONSTANTIN LUCA. (23 October 1984)
Extractive spectrophotometric determination of organophosphorus pesticides in plant materials as molybdenum blue by using a new reagent: PRATIMA VERMA and V. K. GUPTA. (23 October 1984)
Atomic-absorption spectrophotometric investigation and determination of palladium: M. A. MOSTAFA and M. A. KABIL. (24 October 1984)
Continuous spectrophotometric determination of trace amounts of cadmium and zinc in waste water with 4-(2-pyridylazo)-resorcinol and mixed ionic and non-ionic surfactants: WEN-BIN QI and LI-ZHONG ZHU. (25 October 1984)
Stability constant determination by using linear scan and cyclic voltamperograms: H. M. KILLA. (25 October 1984)
Thermodynamics of formation of magnesium(II), calcium(II), strontium(II) and barium(II) complexes with 2,2′-bipyridyl and 1,10-phenanthroline, at different ionic strengths in aqueous solution: SANTI CAPONE, ALESSANDRO DE ROBERTIS, CONCETTA DE STEFANO and ROSARIO SCARCELLA. (26 October 1984)
Molecular absorption spectrometry (MAS) by electrothermal evaporation in a graphite furnace—XIII: Determination of traces of fluoride by MAS of AlF after liquid–liquid extraction of fluoride with triphenylantimony dihydroxide: K. DITTRICH, V. M. SHKINEV and B. YA. SPIVAKOV. (29 October 1984)
A model of atom formation by the tungsten ribbon furnace in atomic-absorption spectrometry: SUSUMU NAKAMURA. (30 October 1984)
Analytical investigations of cephalosporins—IV: Application of Ellman's reagent for the determination of some selected cephalosporins and their pharmaceutical formulations: F. INCI SENGÜN and KÖCSAL ULAS. (31 October 1984)
Studies on ternary solvent systems of acetonitrile/water/chloroform and 1-propanol/water/cyclohexane, for providing organic phases in solvent mixtures of acetonitrile/water and 1-propanol/water: T. HORI and T. FUJINAGA. (12 October 1984)
Adduct formation in oxinates of certain metals: KASHINATH S. BHATKI. (10 October 1984)
Determination of bismuth by flame atomic-absorption spectrophotometry after separation by adsorption of its 2-mercaptobenzothiazole complex on microcrystalline naphthalene: KOICHI ISHIDA, BAL KRISHAN PURI, MASATADA SATAKE and MOOL CHAND MEHR. (2 November 1984)
Titrimetric determination of isomeric diaminoanisoles, -benzoic acids and -toluenes with bromine: D. AMIN and B. SHABA. (6 November 1984)
Solvent extraction of molybdenum(VI) with 3-phenyl-3-methyl-2-mercaptopropenoic acid in the presence of pyridine: A. IZQUIERDO and L. GARCIA PUIGNOU. (6 November 1984)
Spectrophotometric and second derivative spectrophotometric determination of mercury in organomercurials by means of benzyl 2-pyridylketone 2-quinolylhydrazone: J. MEDINILLA, F. ALES and F. GARCIA SANCHEZ. (6 November 1984)
Graphite-furnace AAS with sampling by ultrasonic nebulization: RAINER WENNRICH, UTE BONITZ, HAGEN BRAUER, KNUT NIEBERGALL and KLAUS DITTRICH. (6 November 1984)
Determination of sulphur in organic compounds by mineralizations with molten alkali-metal hydroxides and gravimetric determination: J. V. GIMENO ADELANTADO and F. BOSCH REIG. (7 November 1984)

Talanta Vol. 32, No. 10, pp i–ii, 1985
Pergamon Press Ltd Printed in Great Britain

PAPERS RECEIVED

Determination of the complex stability constants from the titration curve by the maximum likelihood principle: TADEUSZ HOFMAN and MAŁGORZATA KRZYZANOWSKA. (25 June 1985)

Separation of iron from a mixture of cations by use of dibutyl ether–benzene mixture as liquid membrane: M. A. BEG and M. S. KIDWAI. (25 June 1985)

Direct complexometric fluorotitration of aluminium(III) with EDTA by use of fibre-optics light guides: OTTO S. WOLFBEIS and BERNHARD P. H. SCAFFAR. (27 June 1985)

Matrix modification: The use of protein-free filtrates in the determination of metals in blood by flame atomic fluorescence and emission spectrometry: E. J. EKANEM, C. L. R. BARNARD, J. M. OTTAWAY and G. S. FELL. (27 June 1985)

Simultaneous determination of light rare-earths in monazite sand by densitometry on thin-layer chromatograms: HSU ZHANG-FA, JIA XI-PIN and HU CHAO-SHENG. (27 June 1985)

Evaluation of filter papers as substrates for solid-surface room-temperature fluorimetry and photochemical fluorimetry: JOËLLE FIDANZA and JEAN-JACQUES AARON. (4 July 1985)

Trace metal determination by second harmonic alternating current anodic stripping voltammetry: CLINIO LOCATELLI, FRANCESCO FAGIOLI, CORRADO BIGHI and TIBOR GARAI. (4 July 1985)

Polycrystalline and monocrystalline antimony, iridium and palladium as electrode material for pH-sensing electrodes: EITA KINOSHITA, FOLKE INGMAN, GUNNAR EDWALL, SIGVARD THULIN and STANISŁAW GŁAB.

Multiparametric curve fitting—XI: POLET, computer program for estimation of formation constants and stoichiometric indices from normalized potentiometric data: JOSEF HAVEL and MILAN MELOUN. (9 July 1985)

Analytical applications of absorption spectroelectrochemistry at grazing incidence: JULIAN TYSON. (12 July 1985)

Sample pretreatment in the trace determination of drugs in biological fluids: ANIL C. MEHTA. (12 July 1985)

Least-squares processing of literature data for better approximation of stability constants: L. VINCZE and S. PAPP. (12 July 1985)

Analyse de mélanges complexes sur le couplage "Chromatographie en phase gazeuse/spectrométrie infrarouge par transformée de fourier" équipé de colonnes capillaires: G. MERLOT, B. LACROIX, M. T. ROMON, J. P. HUVENNE and G. FLEURY. (12 July 1985)

Etude de la formation des complexes en solution aqueuse—I: Méthods protométrique informatisée de détermination des concentrations des ions libres en solution (méthode CILS) et d'estimation des constantes de stabilité des complexes: Choix critique des modalités d'application de la méthode à partir d'un exemple simulé: ROBERT FOURNAISE and CHRISTIAN PETITFAUX. (12 July 1985)

Determination and speciation of mercury in a dental work-place by cold vapour atomic-absorption spectrometry and gas–liquid chromatography: M. AKIF SEÇKIN, SEZER AYGÜN and O. YAVUZ ATAMAN. (22 July 1985)

Complexation of hydroxydeoxybenzoins with common cations in aqueous ethanol: V. K. SHARMA and N. R. BANNERJEE. (24 July 1985)

Selective kinetic fluorimetric determination of copper at the ng/ml level: M. C. GUTIERREZ, A. GOMEZ-HENS and M. VALCARCEL. (24 July 1985)

A FORTH package for computer-controlled flow-injection analysis: F. T. M. DOHMEN and P. C. THIJSSEN. (24 July 1985)

Determination of acidity constants of *p*-(imidazol-1-yl)phenyl in the ground and excited singlet states: P. PHANIRAJ, MANNAM KRISHNAMURTHY and SHEN K. DOGRA. (24 July 1985)

Selective spectrophotometric determination of trace amounts of iron(III) by extraction of the mixed-ligand iron–NTA–purpurin complex: F. CAPITAN, A. ARREBOLA RAMIREZ and C. JIMENEZ LINARES. (24 July 1985)

Correction factors for the glass electrode in aqueous *N,N*-dimethylformamide: GUSTAVO GONZALEZ, DANIEL ROSALES, JOSE L. GOMEZ ARIZA and ALFONSO GUIRAUM PEREZ. (24 July 1985)

Ligand-exchange chromatography: Determination of phenols in human urine: LUIGI CAMPANELLA, ENRICO CARDARELLI, TOMMASO FERRI and BIANCA MARIA PETRONIO. (24 July 1985)

Determination of DBP and MBP in organic phases by ion-chromatography: S. G. CHEN and S. J. WANG. (25 July 1985)

Rapid and accurate isotopic measurements on boron in boric acid and boron carbide: NICOLAS L. DUCHATEAU, A. VERBRUGGEN, F. HENDRICKX and P. DE BIEVRE. (25 July 1985)

Interferences by bivalent metal ions in the determination of selenium by hydride generation and atomic-absorption spectrometry: A discussion of the reduction of the metal ions to the claimed metallic state by sodium borohydride: RAGNAR BYE. (25 July 1985)

Spectrophotometric and high-order derivative spectrophotometric determination of mercury(II) with PAN in aqueous medium: R. L. SHARMA and H. B. SINGH. (25 July 1985)

Analytical applications of dithiocarbamates: A review: A. K. SHARMA, V. K. SRIVASTAVA and N. K. KAUSHIK. (25 July 1985)

Analytical properties of di-(2-pyridyl)ketone guanylhydrazone: V. KAVLENTIS, G. VASILIKIOTIS and TH. KOUIMTZIS. (25 July 1985)

Extraction of molybdenum and tungsten with polyurethane foam and with cyclic polyethers: R. CALETKA, R. HAUSBECK and V. KRIVAN. (25 July 1985)

Study of the mixed-metal lanthanum–magnesium–purpurin complex: Spectrophotometric determination of lanthanum: A. ARREBOLA RAMIREZ, F. ALES BARRERO and M. ROMAN CEBA. (25 July 1985)

Determination of chromium in waste water and soil by spectrophotometry: A study on the colour system of Cr(VI)–*o*-NO_2-PF–CTMAB: WEN-BIN QI and LI-ZHONG ZHU. (29 July 1985)

Preconcentration of cobalt with *N*-(dithiocarboxy)sarcosine and Amberlite XAD-4 resin: YUKIO SAKAI and NAOKO MORI. (29 July 1985)

The application of direct current plasma spectrometry to the study of the fractionation of iron and phosphorus in surface waters: I. T. URASA and A. M. O'REILLY. (31 July 1985)

Spectrophotometric determination of Cu^+ and Ag^+ in solution: DIP SINGH GILL, MANDEEP SINGH BAKSHI and BALBIR SINGH BABHORIA. (31 July 1985)
Polarographic examination of active components of *Artemisia maritima*: ASHA BEGERHOTTA and N. R. BANNERJEE. (31 July 1985)
The separation and preconcentration of the rare-earth elements and yttrium from geological materials by multi-acid ion exchange: J. G. CROCK, F. E. LICHTE, G. O. RIDDLE and C. L. BEECH. (31 July 1985)
Extraction-photometric determination of lead with a diazacrown ether dye: YUKIO SAKAI, NAOKO KAWANO, HIROSHI NAKAMURA and MAKOTO TAKAGI. (2 August 1985)
Determination of several trace elements in silicate rock standards by an XRF method with background and matrix corrections: J. PASCUAL. (2 August 1985)
The determination of lanthanides in uranium products by direct-coupled plasma emission spectroscopy: FRANCES FLAVELLE and ALAN D. WESTLAND. (5 August 1985)
Differential pulse polarography of nickel(II) complexes with imidazole and related compounds: A. M. Y. JABER. (5 August 1985)

Talanta, Vol. 32, No. 2, pp. i–ii, 1985
Pergamon Press Ltd. Printed in Great Britain

PAPERS RECEIVED

Topographical method for the design of new ligands: SUSUMU TAKAMOTO. (15 October 1984)
Application of some colorimetric methods for the spectrophotometric determination of phenylbutazone and oxyphenbutazone: A. S. ISSA, Y. A. BELTAGY, M. GABR KASSEM and H. S. DAABEES. (13 November 1984)
Reactions of nitrogen bases with nickel(II) chelates of di-*o*-tolylcarbazone and di-*o*-tolylthiocarbazone: KUMAR S. MATH and T. SURESH. (29 October 1984)
A new reagent for determining trace selenium by gas chromatography: 1,4-Dibromo-2,3-diaminonaphthalene: ZHENG OUYANG, PEI-YI XU, GUAN-LANG XIONG and YUE LIU. (14 November 1984)
Determination of the degree of substitution of sodium carboxymethylcellulose, by potentiometric titration and use of the extended Henderson–Hasselbalch equation and the simplex method for the evaluation: INGRID AGGERYD and ÅKE OLIN. (14 November 1984)
A note on the application of significance tests on the *R*-factor ratio to the selection of species in complex-formation equilibria: MARIUSZ JASKÓLSKI and LECHOSŁAW ŁOMOZIK. (15 November 1984)
The use of glass electrodes for the determination of formation constants—II: Simulation of titration data: PETER M. MAY, KEVIN MURRAY and DAVID R. WILLIAMS. (16 November 1984)
Solvent extraction–spectrophotometric determination of titanium with 5,5′-methylenedisalicylohydroxamic acid (MEDSHA) in ores and steels: F. CAPITAN, M. SANCHEZ, D. GAZQUEZ and L. F. CAPITAN-VALLVEY. (16 November 1984)
Use of thiosemicarbazide as masking agent for the direct determination of bismuth in copper by atomic-absorption spectrometry with hydride generation: TAKEO TAKADA and KATSUYUKI FUJITA. (19 November 1984)
Polarographic catalytic nickel prewave induced by some cysteine-containing dipeptides: F. G. BĂNICĂ. (19 November 1984)
Application of ion-association complex of cobalt tetrathiocyanate with neotetrazolium chloride in spectrophotometric determination of cobalt(II): A. K. SINGH, D. KUMAR and M. KATYAL. (19 November 1984)
Synthesis and physicochemical properties of chemically stable tin(IV) borate as a tool for the quantitative separations of Dy^{3+}–Nd^{3+}, Er^{3+}–Nd^{3+}, Ni^{2+}–Nd^{3+}, Ni^{2+}–Pb^{2+} and Mg^{2+}–Pb^{2+}: P. S. THIND and J. S. GANDHI. (20 November 1984)
Colorimetric determination of two fenamates in capsule dosage form: MOHAMED S. MAHROUS, MAGDI M. ABDEL-KHALEK and MOHAMED E. ABDEL-HAMID. (20 November 1984)
Use of some metal ions for the volumetric determination of some antipyretic antirheumatic drugs: A. S. ISSA, Y. A. BELTAGE, M. GABR KASSEM and H. G. DAABEES. (20 November 1984)
Multiparametric curve fitting—VIII: Reliability of dissociation constants estimated by absorbance–pH curve analysis: MILAN MELOUN and MILAN JAVŮREK. (20 November 1984)
Photometric determination of cobalt by means of photochemically generated *anti*-2-furaldehyde 2-pyridylhydrazone: F. GARCIA SANCHEZ and M. HERNANDEZ LOPEZ. (20 November 1984)
Comments on the paper by Gómez-Neito, Luque de Castro, Martin and Valcárcel: JOSEPH T. VANDERSLICE and GARY R. BEECHER. (21 November 1984)
Extraction of metals by di(2-ethylhexyl)phosphoric acid: S. N. BHATTACHARYYA and K. M. GANGULY. (21 November 1984)
Separation of silver from zinc, cadmium, copper, nickel and other elements by cation-exchange chromatography in nitric acid, with a macroporous resin: F. W. E. STRELOW. (23 November 1984)
Iridium in sea-water: JAMES FRESCO, HERBERT V. WEISS, RICHARD B. PHILLIPS and RONALD A. ASKELAND. (26 November 1984)
Spectrophotometric determination of lead with 1-(2-pyridylazo)-2-naphthol and non-ionic surfactants: Application to acetic acid extracts of ceramic enamels: J. MEDINA ESCRICHE, M. LLOBAT ESTELLES and A. SEVILLANO CABEZA. (27 November 1984)
Extraction chromatographic separation of selenium(IV) and tellurium(IV) from each other and associated elements with trioctylphosphine oxide: R. B. HEDDUR and S. M. KHOPKAR. (27 November 1984)
Spectrophotometric determination of chromium(III,VI) with synergic colorimetric effect of zinc: GUO-ZHEN FANG and JI-KUEN LUO. (28 November 1984)
Towards a donor–acceptor model of physical and chemical adsorption—I. Amorphous surface sorption/adsorption: The adsorption of polynitroaromatics and their anionic complexes on amorphous sodium hydroxide pellets: SAEEDUZZAFAR QURESHI, SEEMA HAQUE and PUSHKIN M. QURESHI. (28 November 1984)
Size fractionation techniques for the determination of elements associated with particulate or colloidal material in natural fresh waters: B. SALBU, H. E. BJØRNSTAD, N. S. LINDSTROM, E. LYDERSEN, E. M. BREVIK, J. P. RAMBAEK and P. E. PAUS. (3 December 1984)
Removal of iron interferences with solvent extraction for geochemical analysis by atomic-absorption spectrophotometry: LIYI ZHOU, T. T. CHAO and R. F. SANZOLONE. (3 December 1984)
Potentiometric determination of sodium in aqueous ethanolic solutions: C. J. COETZEE. (16 October 1984)
Properties and analytical application of a thallium(I) ion-selective electrode: C. J. COETZEE. (16 October 1984)
Methyliminodiacetic acid bound to cellulose in the preconcentration and determination of trace metal cations: M. C. GENNARO, C. SARZANINI, E. MENTASTI and C. BAIOCCHI. (4 December 1984)
Luminescence probe studies of ionomers—II. Steady-state measurements from sulphonated polyethylene and Teflon membranes: MARILY N. SZENTIRMAY, NELSON E. PRIETO and CHARLES R. MARTIN. (5 December 1984)
Determination of metals by second harmonic alternating current voltammetry with a semistationary mercury electrode: C. LOCATELLI, F. FAGIOLI, T. GARAI and C. BIGHI. (6 December 1984)
A new preconcentration method with a PVC membrane containing 7-(1-vinyl-3,3,6,6-tetramethylhexyl-8-quinolinol for the determination of copper in water by X-ray fluorescence analysis: T. YAMADA, E. YAMADA, K. NISHIYAMA, J. KATO and M. SATO. (6 December 1984)
Preparation and gas chromatographic characterization of some crown ether stationary phases: DENNIS D. FINE, HARRY L. GEARHEART, II and HORACIO A. MOTTOLA. (6 December 1984)

Specific nanogram detection of 2,4-dinitrophenylhydrazene with piperidine and sodium hydroxide in dimethyl sulphoxide: SAEEDUZZAFAR QURESHI, AHSAN SAEED and PUSHKIN M. QURESHI. (7 December 1984)
Analysis of anions by capillary solid-state spot-tests: ALI MOHAMMAD and NAIM FATIMA. (11 December 1984)
Micro determination of oxprenolol and metoprolol with ammonium metavanadate: SAEED AHMAD, R. D. SHARMA and I. C. SHUKLA. (11 December 1984)
Comparative studies of combined ion-exchange solvent extraction (CIESE) paper chromatographic separation of metal ions: C. R. BHATTACHARYYA. (11 December 1984)

SUBJECT INDEX

Talanta

The International Journal of Pure and Applied Analytical Chemistry

The illustration of a Greek balance from one of the Hope Vases is reproduced here by kind permission of Cambridge University Press

Annual Subscription Rates (1985)

US$330.00 (2-yr rate US$627.00)—For libraries, government laboratories, research establishments, manufacturing houses and other multiple-reader institutions. Price includes postage and insurance. Published monthly, 1 volume per annum.

Specially Reduced Rate for Individuals

In the interests of maximizing the dissemination of the research results published in this important international journal we have established a two-tier price structure. Any individual, whose institution takes out a library subscription, may purchase a second or additional subscriptions for personal use at the much reduced rate of US$75.00 per annum.

Microform Subscriptions and Back Issues

Back issues of all previously published volumes are available in the regular editions and on microfilm and microfiche. Current subscriptions are available on microfiche simultaneously with the paper edition and on microfilm on completion of the annual index at the end of the subscription year.

Publishing Office

Pergamon Press Ltd, Hennock Road, Marsh Barton, Exeter, Devon EX2 8RP, England (*Tel.* Exeter (0392) 51558; *Telex* 42749).

Subscription Enquiries and Advertising Offices

North America: Pergamon Press Inc., Maxwell House, Fairview Park, Elmsford, NY 10523, U.S.A.
Rest of the World: Pergamon Press Ltd, Headington Hill Hall, Oxford OX3 0BW, England (*Tel.* Oxford (0865) 64881).

Talanta, Vol. 32, No. 7, p. ii, 1985
Pergamon Press Ltd. Printed in Great Britain

PUBLICATIONS RECEIVED

Ionization Potentials: Some Variations, Implications and Applications: L. H. AHRENS, Pergamon Press, Oxford, 1983. Pages xi + 104. $29.50.

This little book is divided almost evenly between a summary and analysis of ionization energy data and a discussion of the application of this information to the understanding of periodic trends in the properties of electropositive elements and their simple compounds. For the general chemist the early chapters will probably be the most useful, as a source of information, familiar and unfamiliar, on ionization energies and their variation across the Periodic Table. The later chapters reflect the author's geochemical background and will be of interest mainly, although not exclusively, to the crystal chemist. The approach is resolutely empirical and quantum mechanics is determinedly eschewed throughout the book. Most of the references quoted are pre-1960, and many pre-1940: while these are often classical papers of undiminished value, it is surely a little misleading to imply, however indirectly, that understanding of the covalent band has not progressed since Coulson's book appeared in 1952? A chapter on "The stability of metal-organic complexes" proves to deal with compounds of metals with organic bases, and not with molecules containing metal–carbon bonds.

Within these limitations, the book contains a good deal of useful information, and could be a valuable source of material for elementary courses in crystal chemistry.

G. P. MCQUILLAN

Trends in Analytical Chemistry, Reference Edition, Vol. 2: P. T. SHEPHERD (editor), Elsevier, Amsterdam. Pages iv + 285. US$92.25. Dfl. 240.00.

This volume meets the publishers' objectives for a topical monthly digest of current developments in analytical chemistry. The coverage of the material is wide and ranges through biotechnology, computing, and analytical chemistry based largely on biological systems.

As would be expected, computer applications in analytical chemistry are much in evidence and six of the articles deal with the preparation of data-bases. One paper of interest deals with the preparation of a data-base for polarography. It has always been a problem that in the polarographic literature much of the data is incomplete and retrieval of data has been very time-consuming. With renewed interest in polarography a data-base would prove invaluable. It is a pity, however, that the article on modern methods of polarography deals only with the basic principles. Analytical chemists unfamiliar with the technique would require some indication of the range of application of these techniques.

One criticism might be that some of the articles tend to emphasise basic principles of well established and proven techniques, whereas there is a lack of fuller discussion on modern techniques. For example, the article on forensic microscopy is largely limited to optical microscopy, with only a brief mention of electron microscopy and electron-probe analysis, both of which merit a fuller discussion.

The inclusion of articles on sampling, sample preparation and storage of samples for trace analysis is most welcome. These articles should be studied by all analytical chemists involved in trace analysis.

This volume and others in the series should prove most useful to analytical chemists wishing to obtain an overview of analytical trends, particularly in biological applications.

J. TOWLER

Talanta, Vol. 32, No. 12, pp. ii–iv, 1985
Pergamon Press Ltd. Printed in Great Britain

PUBLICATIONS RECEIVED

Mutagenicity Testing in Environmental Pollution Control: F. K. ZIMMERMANN and R. E. TAYLOR-MAYER (Editors), Horwood, Chichester, 1985. Pages 195. £27.50.

Mutagenicity, and the related concept of carcinogenicity, of chemicals present in the environment is of importance to all, and is a subject which can provoke considerable emotion. This book provides a very useful introduction to methods of testing for mutagenicity, the applications of such tests to particular environmental problems, and the relationship between mutagenicity and carcinogenicity. The first part is devoted to introducing the types of test available, the effects of mutagens on genetic material and the problems of devising meaningful test batteries. Assessment of genetic risk to humans is very difficult and the authors are careful to point out that a positively identified mutagen may not necessarily be a carcinogen but that it should be given further study. This section is helpful in that those with little background in genetics or microbiology can continue to the later chapters with an understanding of the strengths and limitations of the tests. Some very useful experimental detail is included.

A wide range of environmental situations is covered from food and drink to the problems associated with paper mill effluents, and an alarming number of potential mutagens are identified. River and marine pollution are considered along with mutagenic contamination of agricultural land. The book closes with a comparison between risk assessment associated with ionizing radiation and with chemical mutagens, clearly demonstrating the disagreements which inevitably occur when toxicity to the human population and standards of protection are being considered.

Mutagenicity is a difficult subject to cover but this book is both readable and informative; it should be of interest to scientists in a wide variety of disciplines. It is a book that could usefully be read by any who work with potentially mutagenic chemicals or effluents, to alert them to the difficulties of assessing risk and to the wide variety of compounds which have been demonstrated to have mutagenic activity.

JAYNE A. MATTHEWS

Dictionary of Chemistry and Chemical Technology: German/English: H. GROSS (Editor in Chief), Elsevier, Amsterdam and VEB Verlag Technik, East Berlin, 1984, Pages 633. US $105.75. Dfl 275.00

I earlier welcomed the English/German half of this dictionary (*Talanta*, March 1985) and wondered then if we might find "unbedruckt" which there was given as "not printed on", in this volume, suggesting that the E/G volume was a reversal or translation of the G/E volume: the word does not appear (though "unbenetzbar = non-wettable" does), so there is a degree of independence between the two volumes, although prepared by the same editor and team.

There is again a noticeable emphasis on terms from chemical engineering and paper technology, but the coverage in other fields is also very wide. However, I am aware of gaps: trade names of German products such as Plexiglas = Perspex, Eternit = asbestos cement, seem to be absent, and also many important acronyms such as MAK = TLV, EG = EEC, though some for chemical compounds such as PVA and PTFE are included. The reader will have to refer to *Wörterbuch der Abkürzungen* (Duden, 1979) for others

One feature which struck me quickly was the use of spellings atypical of modern (West?) German usage: here you will find Akrylsäure, Kadmium and Kalzium, while Duden confirms that in technical usage the English-type spellings and Acrylsäure are preferable. Similarly, Azetat and Azetylen displace the more easily recognizable forms. On the plus side I would commend the incorporation of older trivial German names such as Weinsäure and Milchsäure *etc.*, and that the latter is not just translated as lactic acid, but also given the systematic name hydroxypropionic acid. Many compound names are accompanied by formulae, and natural products often by the Latin names of the plants or micro-organisms from which they have been obtained.

To sum up, an impressive collection of words related to Chemistry and Chemical Technology which will be of great assistance to struggling translators, provided somebody else is paying for it. But odd that "Eprouvette = test-tube" is missing from a chemical dictionary...

IAIN L. MARR

HPLC in Nucleic Acid Research: PHYLLIS R. BROWN (Editor) Dekker, New York, 1984. Pages 424. $59.75 (U.S.A. and Canada); $71.50 or SFr. 164 (elsewhere).

Professor Brown and fifteen of her past and present students have produced an authoritative text on the use of high-performance liquid chromatography (HPLC) in nucleic acid research. The book is divided into three parts. The first provides a general introduction to nucleic acids, including accounts of their biosynthesis, physiological functions, structure, properties, and catabolism. The second part of the book comprises seven chapters which consider the methodological aspects of HPLC analysis of nucleic acids, nucleosides and nucleotides. Topics covered include sample preparation, fundamental aspects of chromatography, detection systems, mobile phases and microbore columns. Generally the various chapters in this section are complementary but one of the sections of Chapter 5 (Peak Identification) overlaps with parts of the chapter on Detection Systems. The majority of the book is dedicated to reviewing the applications of HPLC in the analysis of nucleic acids, nucleotides, cyclic nucleotides, oligonucleotides, nucleosides, nucleotide coenzymes, pyrimidine (*e.g.*, fluorouracil) and purine antimetabolite drugs (e.g., 6-mercaptopurine), and certain central nervous system drugs (theophylline). There is also a chapter devoted to the use of HPLC in enzyme assays and this is exemplified by assays for enzymes which are involved in purine and pyrimidine metabolic pathways.

The chapter by Nakano (Central Nervous System Drugs) discusses HPLC analysis for the drug theophylline. Although the author points out the advantages of HPLC analysis, the advantages of other techniques such as enzyme immunoassay

for the routine clinical analysis of blood serum for this antiasthmatic drug are ignored. The impact of HPLC techniques is growing and this well prepared and well illustrated monograph will be a valuable source of information for chromatographers.

L. J. KRICKA

Organic Trace Analysis: KLAUS BEYERMANN. Ellis Horwood, Chichester, 1984. Pages 365. £35.00.

Working on Mrs. Beaton's macro-scale, take a barrel full of procedures, a cupboard full of techniques together with a sack full of tips and tricks related to all the samples of the market place, and then hope you have a supremely orderly and experienced cook to put it all together: this is the recipe for a book attempting to cover the enormously wide field of Organic Trace Analysis. It is a tribute to Klaus Beyermann's expertise and skill that he has combined successfully all the ingredients into a readable and informative book from which the reader can, without difficulty, retrieve all manner of useful facts relevant to his current problems. The readability also owes much to the competent translation editing.

The headings of chapters are rather predictable: General Aspects; Sampling; Sample Treatment; Separation and Concentration; Determination, and a final chapter to give flavour; Special Topics. But the list of sub-headings in the Contents reveals the true breadth and serves to guide the reader quickly to sections of particular interest. All sections are well supplied with references (almost half from 1980–1982) while numerous examples are listed very concisely in the Tables. There are also plenty of illustrations particularly of all those little gadgets which trace- and micro-analysts delight in making to get round awkward problems.

So, you may ask, are there no criticisms? no stones left in the plums of this rich pudding? I find the oft-repeated numerical analysis of the literature e.g. "Separation: 37% by GC, 32% by solvent extraction, 16% by HPLC . . ." "Determination: 37% by GC, 14% by MS . . ." just gets a little tiring and not to be very helpful. It is much harder to find what is NOT included, but I do feel that an English language version (the original is "Organische Spurenanalyse") should include mention of British legislation (e.g. pp. 21 and 84) as well as German and American: this one does not. The layout and setting are of a high standard (but a very few misprints are to be found: p. 143 "Table 5.3, p. *135*"; p. 146, 8 lines up, "gas *chromatographic* analysis"; p. 175, Fig. 5.12 "Zeit" = "*Time*"; p. 179, Fig. 5.17, "block *heater*"; p. 188, Fig. 5.23, "*Fluram*" are worth correcting).

This really is a fine piece of very thorough work, and I would like to echo Professor Beyermann's closing wish "that this volume will help to stimulate interest . . . in this vast . . . field". I am sure it will.

IAIN L. MARR

Analysis of Neuropeptides by Liquid Chromatography and Mass Spectrometry: D. M. DESIDERIO, Elsevier, Amsterdam, 1984. Pages xviii + 236. $63.50, Dfl. 165.

This book is aimed at newcomers to the field of peptide research. In the introductory chapter the author presents a complex account of the objectives and philosophy of the book and explains that the book has been written to function as an interface between techniques and research areas.

There is a chapter devoted to neuropeptides which provides a useful general account of peptides (*e.g.*, peptide synthesis, distribution, degradation). In common with other chapters in the book, this is in the form of a review of the literature and there are copious references to review articles on specific aspects of neuropeptides. The author pays particular attention (Chapter 3, Biochemical Sampling Techniques) to the experimental factors which must be considered in both the collection and analysis of specimens containing peptides (*e.g.*, time factor, post-translational modifications, neuropeptidase activity) and stresses the importance of carefully controlling experimental conditions if meaningful analytical results are to be obtained.

Five of the eight chapters are devoted to analytical techniques (HPLC, RIA, MS) and the two chapters devoted to mass spectrometry (Chapters 6 and 7) constitute nearly half of the book. Various types of mass spectrometry are described and reviewed, including electron ionization, chemical ionization, field desorption, fast-atom bombardment, collision-activated dissociation, ^{252}Cf plasma desorption, and Fourier-transform mass spectrometry.

In the final chapter various recent developments in both HPLC and mass spectrometry are considered, in particular the prospects for the on-line combination of liquid chromatography and mass spectrometry.

The layout and presentation of this camera-ready copy book are excellent but the author's style may not appeal to all readers. Newcomers as well as established workers in peptide research will find this book a useful and concise source of information.

L. J. KRICKA

Biological Reference Materials: WAYNE R. WOLF (editor), Wiley–Interscience, New York, 1984. Pages xv + 425. £69.40.

This book plunges the reader into the world of oyster tissues, kale, orchard leaves, stabilized wine and copepod (a small aquatic crustacean). It is the proceedings of a symposium on biological reference materials (RMs) held at the 10th Annual Meeting of the Federation of Analytical Chemistry and Spectroscopic Societies in Philadelphia in 1983.

The papers, all of which were refereed, are collected under six headings; Certified Materials Available or in Preparation, Homogeneous and Well-Characterized Materials, Quality Control Materials for Nutrient Analysis, Environmental Specimen Banking, Open Discussion, and an Appendix which is a reprinting of NBS Special Publication Number 635 (Reference Materials for Organic Nutrient Content).

The first chapter (H. J. M. Bowen) details the production of the kale reference material. In 1964 a large quantity of kale leaves was harvested, dried and ground to produce 91 kg of a kale leaf powder. This has subsequently been characterized for over 60 elements, of which 42 have been determined repeatedly and often by several techniques (Table 6, p. 14). The remaining chapters in the first section cover reference materials produced or under development by various bodies, including the National Bureau of Standards (NBS), the International Atomic Energy Agency (IAEA), the Community Bureau of

Reference (BCR), and the Marine Analytical Chemistry Standards Program (MACSP) of the National Research Council of Canada.

Parts two and three describe a number of materials intended as agricultural reference materials (*e.g.*, beef muscle, maize) or foodstuff reference materials (*e.g.* milk powder). For example, Wolf and Ihnat (Chapter 10) outline the production and testing of a total daily diet reference material (TDD-1) prepared from a balanced selection of commonly consumed foods. Two of the chapters in Part three deal specifically with quality assurance and quality control materials in the context of food analysis. (Chapters 13 and 14). Elkins (Chapter 13) outlines a programme, organized by the National Food Processors Association, which is intended to improve the quality of analytical results produced by food analysis laboratories. A series of tables show the interlaboratory variability for a number of analytes (lead, arsenic, iron, thiamin, fat, ascorbic acid, *etc.*). For dehydrated samples the interlaboratory variability is good (*e.g.*, thiamin, coefficient of variation = 6%) but for other types of sample, such as raw uncooked products, the interlaboratory variability is very large (*e.g.*, ascorbic acid in green beans, coefficient of variation = 49%).

Part four of this book comprises papers describing aspects of the American and German environmental specimen banking programmes. Environmental specimen banking is undertaken to provide "fossilized" specimens for retrospective analysis in studies of the contamination of the environment by man-made chemicals and their metabolites. It is estimated that at least 60,000 man-made chemicals enter the environment each year and the banking programmes are aiming to provide specimens of different types of material (blood, soil, carp, grass, *etc.*) which will be useful for environmental monitoring and surveillance. Stoeppler (Chapter 16) outlines the progress which has been made in characterizing the content and stability of different environmental specimens selected for the German programme, and draws attention to the need for international collaboration in this important analytical area.

The record of the open discussion on needs and uses for biological reference materials (Part five, Chapter 17) is of dubious value. In my opinion the inclusion of discussions represents a poor return of the effort expended in their recording and transcription and does not add to the usefulness of a proceedings volume.

This book provides a useful overview of current activities in the production and testing of reference materials and will be of interest to a broad spectrum of analytical chemists.

L. KRICKA

Room Temperature Phosphorimetry for Chemical Analysis: TUAN VO-DINH, Wiley/Interscience, New York, 1984. Pages xviii + 304. £47.50.

Though any differences in the examination of phosphorescent radiation from substances frozen in transparent glasses or adsorbed on substrates at room temperature may have only a minor physical significance, this modest change in sample handling has made available to the analytical chemist a new and powerful technique. In the past decade or so the pioneering work of Winefordner and others has established the technique as a reliable and sensitive method of analysis for a wide range of compounds. The present book surveys the progress which has been made during this period and despite the wordy nature of some of the early material gives an excellent introduction to the subject.

After outlining the photophysical principles involved, the author describes typical instrumentation and sample preparation techniques. There follow sections dealing with the problems associated with the technique and with the type of spectra produced by organic compounds. Special methods, such as time-resolved spectroscopy, are discussed, and the remainder of the book is devoted to the application of room-temperature phosphorimetry to analytical chemistry, particularly in conjunction with chromatographic methods. Theoretical models of the emission process in various media are examined and the principles governing the quantitative aspects of the method developed. Examples of the determination of single compounds, or analysis of complex mixtures, in the fields of pharmaceutical chemistry, air pollution and the fuel industry are included.

J. R. MAJER

Modern Chromatographic Analysis of the Vitamins: A. P. DE LEENHEER, W. E. LAMBERT and M. G. M. DE RUYTER (Editors), Dekker, New York, 1985. Pages ix + 556. $85.00 (U.S.A. and Canada), $102.00 or SFr. 255 (elsewhere).

This book provides a practical approach to the determination of vitamins in various media such as biological fluids, pharmaceuticals, foods, and animal feeds, by use of TLC, HPLC, GC, and GC–MS. The first part of the book covers the lipid-soluble vitamins A, D, E, and K, and the second part includes the water-soluble vitamins B, C, and the related compounds such as folic and nicotinic acids. In all there are 12 articles, each written by experts in the respective fields. For each group of vitamins thorough explanation of theory for each technique is presented with the sample preparation step prior to chromatography. The detailed discussion on techniques, coupled with the numerous tables (experimental conditions) and figures (chromatographic traces), provides sufficient information for the experienced analyst to be able to set up a particular assay without immediate need for recourse to the original literature. For the more serious-minded, ample references are provided. The coverage in most of the reviews is up to 1983. In addition, the information on metabolism and biochemical functions of the vitamins is a bonus for a biochemically oriented worker. To have all this information in a single volume is very convenient for the practising chromatographer. Furthermore, a detailed subject index makes it easier to trace the required topic. The book is relatively free from errors, except on p. 80 where there are a couple of misprints. Overall the book is well presented and the format is easy to follow. It should make a useful and timely addition to the libraries of laboratories engaged in vitamin analysis.

ANIL C. MEHTA

Talanta, Vol 32, No. 12, p. III, 1985
Pergamon Press Ltd. Printed in Great Britain

PHARMACIA PRIZE 1983–1984

Presentation of the Pharmacia Prize for 1983–1984 to Dr. Irwin Morris Jr. (centre) and Dr. Randle Collard (right) by Dr. Eric Schinage of Pharmacia Inc., for their paper "GC/MS determination of incidental PcBs in complex chlorinated hydrocarbon process and waste streams", judged to be the best contributed to *Talanta* from an industrial laboratory in 1983–1984. (See *Talanta*, 1983, **30**, 811.)

Talanta, Vol. 32, No. 8A, p. III, 1985
Pergamon Press Ltd. Printed in Great Britain

THE RONALD BELCHER MEMORIAL AWARD

The Publisher of *Talanta* is instituting a Ronald Belcher Memorial Award in commemoration of the late Professor Belcher's outstanding contributions to analytical chemistry, international relations and understanding, his interest in student welfare, and continued association with *Talanta* from his conception of the journal in 1957 right up to his death. The award will take the form of a travel grant of US $1000 to enable a young analytical scientist to undertake travel abroad and will be made in alternate years, starting in 1986. Candidates may be of either sex and any nationality, but must be under 30 years of age at the time of application. Applications may be sent by the candidates themselves, or on their behalf by a responsible senior (*e.g.*, Head of Department, research supervisor), and must be submitted by the end of the year preceding the award. They must include a brief curriculum vitae, a short statement of the purpose of travel and the places to be visited, a testimonial of ability, and a recommendation from a senior research worker.

Applications for the first award, in 1986, should be sent to either

Dr. R. A. Chalmers
Department of Chemistry
University of Aberdeen
Old Aberdeen, Scotland

or

Professor J. D. Winefordner
Department of Chemistry
University of Florida
Gainesville, Florida 32611, U.S.A.

to arrive before 31 December 1985.

Talanta, Vol. 32, No. 8A, p. iii, 1985
Pergamon Press Ltd. Printed in Great Britain

PUBLICATIONS RECEIVED

Pharmaceutical Mass Spectra: R. E. ARDREY, A. R. ALLAN, T. S. BAL, J. R. JOYCE and A. C. MOFFAT, The Pharmaceutical Press, London, 1985. £50. Pages 681.

This book contains a very basic compilation of over 1100 spectra of drugs, metabolites and other compounds of pharmaceutical interest. All spectra were obtained by using magnetic sector instruments with electron energy 70 eV, accelerating voltage 4 V, trap current 100 μA and a source temperature between 100 and 240°C.

The spectra are arranged in alphabetical order of compound name. Unfortunately, each spectrum is identified by only a single compound name, together with its nominal molecular weight. A structural formula for each compound would have been a useful addition. The spectra are well spaced out with no more than two per page and a listing of peak values, expressed as percentage of base peak, is given under each spectrum. These lists appear to be photographic reproductions of computer output to a dot-matrix printer. Indeed this book appears to be just that, the raw data from a computer file, without the full advantages of interactive search facilities. However, manual searching of the data can be achieved by using a molecular weight index, an eight-peak index and the alphabetical index.

No interpretations of the mass spectra have been made and there is no reference to any literature sources that would aid such interpretation. There is not a single chemical formula in the book. I feel these omissions will disappoint some readers. However, to have included such details would have meant a more expensive and even heavier book.

To have all these spectra in a single volume is very convenient for the practising analyst and it will make a valuable contribution to the arsenal of reference books.

P. J. Cox

Statistics for Analytical Chemistry: J. C. MILLER and J. N. MILLER, Horwood, Chichester, 1984. Hardback: £18.50. Softback: £7.95. Pages 202.

This is not the first account of statistics for physical sciences, nor even the first for analytical chemists: Youden (1951), Doerffel (1966) and Eckschlager (1969) have all written for the market. The present authors—a wife and husband team who are respectively statistician and analytical chemist—have followed these two older examples by showing what statistics has to offer and when it can be used to advantage. Statisticians have to accept that analytical chemists don't want proofs of theorems, but can sometimes be persuaded to employ statistical tests, *e.g.*, when the performance of a method or the quality of a product has to be assessed.

What makes this book different—and quite fascinating to read—is the large number of worked examples based on experimental results published in the last few years in the *Analyst*. There is a rumour that this exercise led occasionally to statistically justified conclusions at odds with those presented in the original published papers. Perhaps that is the best recommendation that this book can get—we all ought to be making use of it and viewing our results more critically with its help. Strongly recommended.

IAIN L. MARR

Therapeutic Drug Monitoring and Toxicology by Liquid Chromatography: S. H. Y. WONG (Editor), Dekker, New York, 1985, $107.50. Pages 520.

Over the last seven years, HPLC has come to dominate the quantitative determination of drugs, because of its ability to provide sensitive and specific methods with a minimum of work-up. This is effectively demonstrated in this collection of review articles of the applications of HPLC in the clinical laboratory, with particular emphasis on its role in therapeutical drug monitoring (TDM).

The articles start with a useful review of the reasons and justification for TDM and of the methods (including HPLC) which can be employed. This comparison with alternative techniques such as immunoassay also appears in other sections and is a useful reminder that HPLC is not the only sensitive and selective assay method although its specificity often means that it is displacing some of the other methods.

The remainder of the book is divided into two main sections, first the practice of HPLC, with articles on sampling techniques, computer control, LC–MS and fluorescence and electrochemical detection methods. The second section is a series of reviews by different authors on the application of HPLC to the major classes of drugs, including anti-asthmatics (principally theophylline, for which 56 alternative methods of extraction and separation are listed), antibiotics, anti-depressants, anticonvulsants, antihypertensives, and anti-arythmics. The final two chapters consider the medico-legal aspects of clinical chemistry and survey the determination of groups of drugs which were not reviewed earlier.

Overall the book is well presented and would be useful reading for anyone entering the field or as a reference guide to existing methods for the clinical chemist. The coverage in most of the reviews is up to 1981/82 with occasional references from 1983. The cost is, however, likely to preclude individual purchase.

ROGER M. SMITH

Talanta, Vol. 32, No. 5, p. III, 1985
Pergamon Press Ltd. Printed in Great Britain

THE PHARMACIA PRIZE

Pharmacia AB (Uppsala, Sweden) and the Editorial Board and Publisher of *Talanta* take great pleasure in announcing that the Pharmacia Prize for 1983–1984 (for the paper published in *Talanta* that was judged to be the best contributed from an industrial laboratory) has been awarded to Dr. Randle S. Collard and Dr. Morris M. Irwin, Jr., Dow Chemical USA, for their paper "GC/MS determination of incidental PCBs in complex chlorinated-hydrocarbon process and waste streams" (*Talanta*, 1983, **30**, 811).

Talanta, Vol. 32, No. 3, p. III, 1985
Pergamon Press Ltd Printed in Great Britain

TALANTA ADVISORY BOARD

The Publisher and Editorial Board of *Talanta* welcome Professor S. R. Crouch and Dr K.-H. Koch as members of the Advisory Board.

STANLEY R. CROUCH is Professor of Chemistry at Michigan State University. He was born in California and attended Stanford University from 1958 to 1963. He received his M.S. degree in Chemistry from Stanford in 1963. His graduate studies were done at the University of Illinois under Professor Howard V. Malmstadt, and he received his Ph.D. degree in 1967. He became Assistant Professor of Chemistry at Michigan State University in 1968, Associate Professor in 1972, and Professor in 1977. He was an Alfred P. Sloan Foundation Fellow from 1973 to 1975. His research interests are in analytical atomic and molecular spectroscopy, laser spectroscopy, continuous flow and flow-injection methods, reaction-rate methods in analytical chemistry, fast kinetics, clinical chemistry, liquid chromatography, computers in chemistry, and chemical instrumentation. He has authored or co-authored numerous publications in these areas and has co-authored several textbooks in the "Electronics for Scientists" field with Professors H. V. Malmstadt and C. G. Enke. The latest of these is "Electronics and Instrumentation for Scientists", Benjamin/Cummings, 1981. Professors Malmstadt, Enke and Crouch are instructors in the American Chemical Society short course Electronics for Laboratory Instrumentation and have produced an audio version of this course.

K.-H. KOCH

DR. KARL-HEINZ KOCH, born in 1929 in Dortmund (F.R. Germany), studied chemistry from 1950 to 1957 at the universities of Cologne, Graz (Austria), Münster and Aix-la-Chapelle, where he received his Doctor's degree. Then he began his career in the iron and steel industry. Since 1966 he has been chief of the chemical laboratories of the Hoesch Stahl AG in Dortmund. His fields of activity and interest are atomic-emission, atomic-absorption and X-ray fluorescence spectrometry, the chemical analysis of iron and steel, ferroalloys and non-ferrous metals, water and waste water, and the surface analysis of steel products, besides the chemical and technological investigation of fuels and lubricants. Furthermore he deals with questions of sampling and sample preparation techniques, quality assurance, standardization, reference materials, and laboratory organization. He is author or co-author of about 120 publications. Since 1978 he has been the chairman of the chemists' committee of the Verein Deutscher Eisenhüttenleute (VDEh), and from 1978 to 1984 he was a member of the board of the Analytical Group of the Gesellschaft Deutscher Chemiker (GDCh). Since 1978 he has also been a member (since 1982 the vice-chairman) of the Advisory Board of the "Institut für Spektrochemie und angewandte Spektroskopie" in Dortmund. Finally it should be mentioned that he has been co-editor of the journal *Chemie für Labor und Betrieb* since 1982, and since 1984 a member of the Editorial Board of *Steel Research* (*Archiv für das Eisenhüttenwesen*), the internationally well-known metallurgical journal of Verlag Stahleisen in Düsseldorf.

Talanta, Vol. 32, No. 2, p. III, 1985
Pergamon Press Ltd. Printed in Great Britain

TALANTA ADVISORY BOARD

Daniel Jagner was born in Borås, Sweden in 1940 and graduated in Chemistry and Mathematics at the University of Göteborg, Sweden in 1971. After his dissertation in 1971 he was appointed docent at this University. During 1973–75 he was visiting professor in Analytical Chemistry at Åarhus University, Denmark and subsequently he held a position as senior research fellow, financed by the Swedish Natural Research Council, at the University of Göteborg. In 1983 he was appointed professor in Technical Analytical Chemistry at the University of Lund, Sweden. His research interests cover potentiometric and photometric titration procedures with special reference to automated determination of major sea-water constituents. During recent years he has concentrated on electroanalytical stripping techniques for trace element determination and speciation with emphasis on computerized automation. He is co-author of the monograph "Computer Calculations of Titration Procedures" and co-editor of the monographs "The Changing Chemistry of the Oceans" and "Marine Electrochemistry".

Talanta, Vol. 32, No. 11, pp iii–iv, 1985
Pergamon Press Ltd Printed in Great Britain

PUBLICATIONS RECEIVED

Glass Capillary Chromatography in Clinical Medicine and Pharmacology: H. JAEGER (Editor), Dekker, New York, 1985 Pages XI + 640. $99.75 (U.S.A. and Canada); $119.50, SFr. 299 (elsewhere).

The aim in this book is to bridge an apparent gap between texts directed at the specialist in GC and those written at an introductory teaching level. For the purpose, some 40 authors contribute to 30 chapters which are divided almost equally between Clinical Medicine (Part I) and Pharmacology (Part II). However, Part I also includes underlying chromatographic theory, instrumentation and general practical matters relating to quantitative analysis. These aspects are followed by chapters on applications to amino-acids, sugars, steroids, hormones, fatty acids, phospholipid hydrolysates, bile acids and to "profiling" in metabolic disorders. The study of 5-hydroxytryptamine and its metabolites by direct coupling of GC capillary columns to a mass spectrometer is also described. Other examples of the use of these combined techniques are presented in Part II which, however, is largely devoted to the analysis of specified pharmaceutical substances by glass capillary chromatography and it is difficult to see any underlying plan regarding choice of compound. Of somewhat greater generality are the chapters on GC studies of metabolism of drugs, and families of substances, such as nucleosides and peptide antibiotics. Technique-related contributions deal with use of internal standards and with capillary methods in pharmacokinetic studies.

The advantages (higher resolution and chemical inertness) of capillary GC over packed column GC are emphasised, as is the use of fused silica in place of glass, making reference to the latter in the title possibly misleading. Structural weaknesses, particularly in Part II, and overlap of textual material mark the work as the product of a "committee". Nevertheless, each chapter is generally well planned and documented and the general aim has been achieved; the book demonstrates clearly a wide range of applications in the disciplines concerned.

S. J. LYLE

Quantitative Column Liquid Chromatography: S. T. BALKE, Elsevier, Amsterdam, 1984. Pages xiv + 300. $63.50, Dfl. 165.

With the proliferation of microcomputer-assisted chromatography instrumentation there has been a parallel increase in the use of numerical techniques for treating LC data. These methods are not limited to the direct determination of concentration, but are also used to select and control the instrumental operating conditions. This book examines the background and reviews the application of these techniques to assist the potential user in the selection of an appropriate method.

Following the introductory section, concerned with terminology and the organization of liquid chromatography by method, Chapter 2 provides a summary of chemometric developments. Linear and non-linear regression techniques are extensively discussed, including the use of the Simplex for optimization. Unfortunately, factor analysis and pattern recognition receive much less attention. Chapter 3 is concerned with fractionation and separation. Peak shape and measures of resolution are examined, and the section concludes with the selection of mobile phase components and gradient elution.

Photometric measurements form the basis for the main types of detector employed in LC and quantitative methods of assessing detector performance are considered in the fourth chapter. The less common intrinsic-viscosity detector and low-angle light-scattering detector are briefly mentioned. In Chapter 5 calibration for small molecules and polymers is discussed and the final chapter is devoted to "resolution correction". This latter section is concerned with curve fitting and deconvolution, the book finishing with a Fortran program using the Simplex search procedure to fit a Gaussian shape to an experimental chromatogram.

The book is not a mathematical text nor is it a collection of computer programs for chromatographers. It is a useful addition to the chromatography library and will be appreciated by those requiring a guide to the applications of numerical analysis.

M. ADAMS

Ion-Pair Chromatography: M. T. W. HEARN (Editor), Dekker, New York, 1985. Pages IX + 294. $65.00 (U.S A. and Canada); $78.00, SFr. 195 (elsewhere).

In recent years the phenomenon of ion-pair formation has had a considerable impact on the development of reversed-phase liquid–liquid chromatographic separations of large organic ions. The volume under consideration deals with background theory and applications in several fields. A useful introduction written around acids and bases is provided by M. T. W. Hearn; it is followed by a chapter on theory (W. R. Melander and C. Horváth) and another on thermodynamics and extrathermodynamics (*e.g.*, the Hammett relationship) of functional groups (E. Tomlinson and C. M. Riley). The remaining three chapters cover applications to pharmaceutical products (R. F. Adams), amino-acids, peptides and proteins (M. T. W. Hearn) and nucleic acid derivatives (P. A. Perrone and P. R. Brown). The authors of the first three chapters dealing with general background and theory are all well-known for their contributions to their respective topics. A balanced account of theoretical aspects, including various models put forward to describe IPC, is provided in easily assimilated form and is complemented by the chapter on thermodynamic and related properties. The chapters on applications clearly bring out the utility of IPC in the areas surveyed.

Much information is provided, often in tabular form, in this monograph; each chapter is well documented and references are as up-to-date as can be expected. It can be recommended as a source-book on introductory theory and applications of the technique in the fields covered.

S. J. LYLE

Spurenelementbestimmung durch Neutronenaktivierung: G. PFREPPER, W. GORNER und S. NIESE, Akademische Verlagsgesellschaft Geest & Portig, Leipzig, 1981 Pages 260. Price 65 Marks (DDR).

Das vorliegende Buch, als Band 6 der Reihe "Moderne Spurenanalytik" konzipiert, stellt keine oberflächliche Einführung dar, sondern gibt einen gründlichen Überblick über die typischen sowie ausgefalleneren Anwendungsmöglichkeiten der Neutronenaktivierungsanalyse in der Spurenanalyse. Die kernphysikalischen Grundlagen der Aktivierung, die Kernstrahlungsmessung und radiochemische Trennverfahren werden in dem Umfang besprochen, wie es zum Verständnis notwendig ist. Das letzte Drittel des Buches beschäftigt sich mit der Anwendung der NAA in Geo- und Biowissenschaften, beim Umweltschutz, bei der Analyse von Halbleitermaterialien und Metallen. Die Rolle der NAA für Archäologie, forensische Analytik und die Analyse von organischen Produkten wird nur kurz gestreift. Doch sind hier wie auch in allen anderen Kapiteln ausreichend Literaturzitate angeführt. Von den vielen Zitaten des Buches stammen allerdings nur drei aus den Jahren nach 1977. Dies kann jedoch toleriert werden, da die Entwicklung der NAA einen gewissen Abschluß erreicht hat und die Fortschritte bei Computern und Reinstgermanium-Detektoren keine umwälzenden Neuerungen brachten. Die Tabelle im Anhang enthält für fast alle Elemente die wichtigsten Kernreaktionen in der NAA einschließlich der Reaktionsquerschnitte, Resonanzintegrale usw. Außerdem sind für die gebildeten Radionuklide auch die Zerfalldaten nebst Gammaenergien nach dem Stand von 1974 aufgeführt.

Das Buch eignet sich besonders für Analytiker, die zur Spurenanalyse neben anderen Methoden eventuell die NAA benutzen wollen. Selbst die Radiochemiker unter ihnen werden darin viele Anwendungen und Beispiele finden. Fast noch wichtiger sind die Hinweise der Autoren auf solche Probleme, die sich mit der NAA nicht lösen lassen. Verschwiegen werden auch nicht die bei speziellen Nukliden oder Matrices manchmal erforderlichen sehr langen Bestrahlungs- oder Abklingzeiten, die ein wochenlanges Warten auf das Analysenergebnis nach sich ziehen.

E. BLASIUS

Technique and Applications of Thin Layer Chromatography: J. C. TOUCHSTONE and J. SHERMA (Editors), Wiley, New York, 1985. £88.65. Pages XIV + 395.

This publication is a record of the papers presented at the Third Biennial Symposium on thin-layer chromatography (TLC) held at Parsippany, New Jersey in December 1982. Of the 28 contributions, about 12 are primarily concerned with technique and the remainder with applications covering, mainly, natural product and biological samples. One of the papers of general interest extols the virtues of the use of lasers for detection purposes and another presents a systematic approach to mobile-phase design and optimization. The latter topic is probably of great interest to many would-be users bewildered by the apparent complexity of solvent systems recommended for TLC separations. Unfortunately, this particular exposition is marred by poor presentation and use of worked numerical examples irreconcilable with the tabulated source data. Other useful contributions to technique deal with rotating disc TLC, bonded phases for reversed-phase work and spectral analysis of TLC bands.

The diversity of the range of contributions gives this book a structureless character and the reader needs to forage for information, helped a little by the contents list and short index. On the whole, it seems grossly overpriced for what it offers.

S J. LYLE

Mass Spectrometry of Large Molecules: S. FACCHETTI (Editor) Elsevier, Amsterdam, 1985. Pages xii + 322. Dfl. 230, $85.25.

This book is one of a series devoted to courses and educational seminars held at the Joint Research Centre, Ispra Establishment, Italy, as part of its education and training programme and is published for the Commission of the European Communities, Directorate-General Information Market and Innovation. The text consists of seventeen lectures which formed part of a course taking place on 5–9 September 1983.

While the technique of mass spectrometry has been outstandingly successful in the analysis of compounds of low and medium molecular weight, it is only recently that increases in mass resolution and developments in sample introduction and ionization have made it possible to extend its application to compounds of low volatility and high molecular weight. For this reason, the collation of material about the newer methods of mass spectrometry and the identification of large molecules of biological origin is particulary timely. The advances in instrumentation over the past two decades are reviewed in the second and third lectures, while the subject of inlet systems suitable for substances of high molecular weight is discussed separately. The applications of these new techniques to the analysis of substances of biochemical and medical significance, such as peptides or bile acids, is described in a number of succeeding lectures. There are also detailed examinations of the role of fast-atom bombardment, negative-ion studies and pyrolysis in the structural investigation of large molecules. Since the methods used in the elucidation of the structures of natural polymers can be applied with equal success to the study of synthetic polymers, the mass spectrometric analysis of the latter class of compounds is also discussed briefly.

J. R. MAJER

Talanta, Vol. 32, No. 7, pp. iii–iv, 1985
Pergamon Press Ltd. Printed in Great Britain

NOTICES

THE FOURTH INTERNATIONAL SYMPOSIUM ON BIOLUMINESCENCE AND CHEMILUMINESCENCE

8–10 SEPTEMBER 1986, FREIBURG, WEST GERMANY

Further information is available from Priv. Doz. Dr. J. Schölmerich, Department of Internal Medicine, University of Freiburg, 7800 Freiburg, West Germany.

4TH INTERNATIONAL WORKSHOP ON TRACE ELEMENT ANALYTICAL CHEMISTRY IN MEDICINE AND BIOLOGY

21–23 APRIL 1986

The "Fourth International Workshop on Trace Element Analytical Chemistry in Medicine and Biology" will be held at the Gesellschaft für Strahlen- und Umweltforschung Neuherberg.

It will be the continuation of the well known biennial series of this special type of meeting. A major aim of these meetings is to bring together experts highly experienced in the analytical and biomedical field. We believe that free and effective exchange of views between the analytical specialists on the one hand and biomedical specialists (users of analytical data) on the other is only guaranteed by joint discussion of definite problems. It is hoped that the 4th Workshop will lead again to a productive scientific dialogue between these two groups as far as biomedical applications of trace element analytical research is concerned. The international and multi-disclipinary character of the Workshop should provide a good working forum for all those interested in the subject.

Further information from:

Gesellschaft für Strahlen-und Umweltforschung mbH.
Institut für Angewandte Physik
Physikalisch-Technische Abteilung
Dr. Peter Schramel
Ingolstädter Landstrasse 1
D-8042 Neuherberg
Federal Republic of Germany

Following the Workshop, the "Second International Symposium on Biological Reference Materials" will be organized on 24 and 25 April 1986, by W. R. Wolf with kind support of the GSF.

The aim of this symposium will be to bring together efforts in the study of certified and non-certified biological reference materials useful in the improvement of analytical methods, with special emphasis on the measurement system of nutrient analysis.

For more information please contact Dr. W. R. Wolf, Beltsville Human Nutrition Research Center, Beltsville, Maryland 20705, USA.

37TH PITTSBURGH CONFERENCE ON ANALYTICAL CHEMISTRY AND APPLIED SPECTROSCOPY

ATLANTIC CITY, NEW JERSEY, U.S.A.
10–14 MARCH 1986

The technical programme of the 1986 Pittsburgh Conference will consist of about 30 symposia and 900 contributed papers, supplemented by poster sessions. Authors wishing to present papers at the conference should submit four copies of a 500-word abstract (in single-spaced typing) by 2 August 1985 for assessment by the Program Committee; the abstract and a self-addressed envelope should be sent to Mrs. Alma Johnson, Program Secretary, 12 Federal Drive, Suite 322, Pittsburgh, PA 15235, U.S.A. The abstract must list all the authors (and full addresses for their places of work) and indicate which author is to present the paper. One author must sign the abstract to certify that the paper has not been and will not be published or presented prior to the 1986 Pittsburgh Conference. Papers are requested in the categories listed below, and the appropriate number should be entered in boxes 6 and 7 on the abstract form (the format of which is reproduced below):

01. Air Pollution
02. Atomic Absorption Spectroscopy
03. Automated Analysis—
    a. Laboratory b. Plant
04. Biochemical Analysis
05. Biomedical Pharmaceutical
06. Classical Chemical Analysis
07. Clinical Chemistry
08. Computer Applications
09. Countercurrent Chromatography
10. Electrochemistry
11. Emission Spectroscopy
12. Fluorescence-Luminescence
13. Food Analysis
14. Forensic and Drug Analysis
15. Gas Chromatography—
    a. Applications b. Instrumentation c. Theory
16. Gel Permeation Chromatography
17. General Analysis
18. Industrial Hygiene
19. Infrared Spectroscopy
    a. Applications b. Instrumentation c. Theory
20. Ion Chromatography
21. Laboratory Robotics
22. Liquid Chromatography—
    a. Applications b. Instrumentation c. Theory
23. Mass Spectrometry
24. New Instrumentation
25. New Instrument Concepts
26. Nuclear Magnetic Resonance Spectroscopy
27. Particle Size Analysis
28. Pesticide Analysis
29. Plasma Emission Spectroscopy—
    a. ICP b. DCP
30. Polymer Analysis
31. Process Stream Analysis
32. Raman Spectroscopy
33. Selective Ion Electrodes
34. Surface Analysis—
    a. Auger b. ESCA c. SIMS d. Other
35. Thermal Analysis
36. Thin Layer Chromatography
37. Toxicological Analysis
38. Trace Analysis
39. UV-VIS Spectrophotometry
40. Water Pollution
41. X-Ray Diffraction/Fluorescence Spectroscopy
42. Other (Please Specify)

ABSTRACT FORM

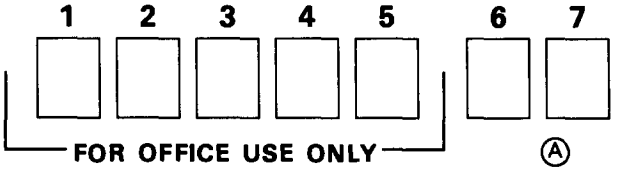

Ⓑ TITLE

Ⓒ AUTHORS, ADDRESS & PHONE/TELEX NUMBERS:

Ⓔ Start Abstract Here: →

Ⓓ SIGNATURE: _____ DATE _____

Material has not and shall not be published/presented prior to the 1986 Pittsburgh Conference

Talanta Vol 32, No. 6, pp iii–iv, 1985
Pergamon Press Ltd Printed in Great Britain

PUBLICATIONS RECEIVED

The Design and Application of Process Analyzer Systems: PAUL E. MIX, Wiley, New York, 1984. Pages xiii + 312. £56.25.

Following a brief examination of the general requirements of process analysers, the author describes the operation and particular requirements of selected types of analyser. The techniques covered include pH and conductivity measurement, moisture and corrosion monitoring, gas and liquid analysis, photometric analysis (ultraviolet, infrared and visible regions of the spectrum, refractometry and light-scattering), automatic titration, density measurement, octane number determination, and gas and liquid chromatography. In addition there are sections on training, maintenance, troubleshooting and documentation. The book will be of less use in Europe, since it refers only to U.S. safety practices, not all of which are accepted in Europe. European users require Certificates of Approval in accordance with the particular standards. U.S. users often accept equipment built in accordance with the requirements of the standards. In addition, though some metric units are used, the interspersion of foot/pound/Fahrenheit units makes life uncomfortable for the reader. As some compensation, the author does distinguish between ppm by volume and ppm by weight and is to be complimented on it; ppm units should never be used (but usually are) without specification of whether v/v, w/v, or w/w ratios are meant. There is also a glossary describing the terminology used, useful lists of names and addresses (mostly of U.S. manufacturers) and of trademarks, some nomographic data charts, and data tables.

On the debit side, it has to be said that coverage of the topics is not always complete, and that the editing and proof-reading could have been better. Reference is made to some effects of deposition on critical surfaces, but there is no mention of the effect of deposition of wax in systems handling crude oil. The section on aluminium oxide hygrometers fails to mention that the resistance of the sensor is temperature-dependent, and that manufacturers therefore make use of the capacitance; to be fair, it should be added that the sensor *is* defined in the text as being a capacitor. In Fig. 5.6 a pressure gauge should be shown downstream from the pressure regulator. Figure 8.6 shows restriction orifices installed to reduce pressure and thus protect pressure-sensitive devices; this is a cheap method but not wise practice in the system shown. Perhaps the greatest fault, however, lies in the sweeping chemical generalizations made in certain places. The section on pH and buffers is a good example—the reader needs to know already much more about buffers and titration curves than is given in the text, if he is not to make some rather poor choices of buffer, for instance. The statement that the zero potential of the measuring and reference electrodes is at pH 7.0 conveyed nothing to at least one reader.

To sum up: provided the reader already has adequate background knowledge or knows his way round the literature, the book contains many ideas and gives much information that will be useful to him. It was certainly written with enthusiasm.

D. J. HUSKINS

Analytical Pyrolysis: K. J. VOORHEES (editor), Butterworths, London, 1984, Pages 486. £35.00.

The material presented in this book is based on a series of 15 invited lectures given at the Fifth International Symposium on Analytical Pyrolysis held in Vail, Colorado. It is interesting that pyrolysis, which is one of the oldest analytical techniques, and often used in early structure determinations, should still be in a rapid state of development today. The impact of modern instrumentation and data processing has obviated the inherent disadvantages, such as the difficulties of accurate temperature control and the intervention of surface catalytic effects. Identification of pyrolysis products, which tend to consist of highly complex mixtures, was originally, however, one of the most severe problems. In this book the authors recommend the use of mass spectrometry and gas chromatography, or a combination of the two, and Fourier transform infrared spectrometry for the solution of this problem. The combination of pyrolysis and instrumental analysis is suggested for the study of a wide range of materials, including fossil fuels, polymers, geological specimens and food products. It is not always clear that the subjects described have been approached from a critical point of view: there is, for example, no mention of the many drawbacks of Curie-point pyrolysis and the fingerprinting of copolymers is presented as a novel technique, whereas in fact it was in use over 20 years ago. Finally, however, if one were to believe the claims made for the pyrolysis–FT–IR technique, there would be no need to consider the application of any other method to the problems outlined in this book, or indeed to any analytical problems.

J. R. MAJER

Analytical Spectroscopy: W. S. LYON (editor), Elsevier, Amsterdam, 1984. Pages xiv + 394. US$75.00. Dfl. 195.000

This book constitutes Volume 19 of the series entitled Analytical Chemistry Symposia and is an account of the Proceedings of the 26th Conference on Analytical Chemistry in Energy Technology, held at Knoxville, TN in October, 1983. There are 64 contributions collected together under five separate headings dealing with what is described in the Preface as "relatively hot fields of analytical chemistry"; Half of the papers are devoted to the use of lasers in chemical analysis and to mass spectrometry, mostly with conventional instruments and well-established techniques. A further third describes the applications of inductively-coupled plasma emission spectrometry, activation analysis, gamma and X-ray spectroscopy, to problems encountered in the energy industry. The remaining 16 papers have miscellaneous topics mostly concerned with the instrumental determination of uranium and other relevant elements, gases and aerosols. One of the more interesting of these topics is the use of supercritical fluids, such as liquid carbon dioxide, as mobile phases in chromatography.

J. R. MAJER

Modern Trends in Analytical Chemistry: E. PUNGOR and G. E. VERESS (editors), Elsevier, Amsterdam, 1984. Pages xiv + 432 (part A) and viii + 195 (Part B). US$134.50. Dfl. 350.00

The material presented here is a record of the two halves of the Scientific Symposium held at Matrafured, Hungary, 17–22 October 1982 and constitutes Volume 18 of the Analytical Chemistry Symposia Series. Part A consists of a collection of 25 lectures and discussions devoted to the topic of Electrochemical Detection in Flow Analysis. Four of these were Plenary lectures, reviewing the use of and problems associated with amperometric and potentiometric detectors in flow systems.

Part B comprises accounts of 10 lectures and discussions collected under the general heading of Pattern Recognition in Analytical Chemistry. The material presented is representative of the growing interest in computer-based analytical chemistry. The most significant aspect of this interest is the demand for analytical instrumentation having artificial intelligence, in particular, spectrometers capable of pattern recognition. The problems of pattern recognition in mass spectrometry and absorption spectrophotometry are discussed and the application of the concept in other types of automatic chemical analysis is given some attention.

J. R. MAJER

Computer Chromatography, Vol. 1: R. E. KAISER and A. J. RACKSTRAW, Hüthig Verlag, Heidelberg, 1983. Pages viii + 171. DM 54; US$25.

This slim volume marks the start of a series concerned with the application of microcomputers to the collection and analysis of chromatographic data. GLC, HPLC and HPTLC methods are discussed. As a result of the authors' own experience of computer-assisted chromatography they suggest a number of new procedures for validating chromatographic results, principally in qualitative analysis, *i.e.*, means of ensuring correct peak identification, along with techniques relevant to quantitative analysis. The book contains as an appendix a list of equipment and programs, with suppliers, which the authors have used in their work. As stated from time to time in the text, certain of the authors' views on chromatography are somewhat contentious. Some of the procedures which they advocate would not be feasible without the use of a computer.

The authors favour using relatively small dedicated computers because this allows the individual user to implement data-manipulation procedures specially designed for the problem in hand, which would not be easy to do with a more powerful central computer serving the needs of several chromatographs simultaneously. A detailed listing of a sample program for peak profile calculation is provided in an appendix, and here and there in the text program fragments are set out to indicate the way in which data may be stored and manipulated. It is unfortunate that the data-storage code (p. 38) is not wholly compatible with the data-retrieval code (p. 40)—how was the number of data points written to disc?

The authors have attempted to present the material in a logical manner and the book provides a thought-provoking introduction to the treatment of chromatographic data with a small computer. This volume merits the attention of those engaged in analytical chromatography.

R. A. HOWIE

Data Handling in Science and Technology, Vol. 1: Microprocessor Programming and Applications for Scientists and Engineers: RICHARD R. SMARDZEWSKI, Elsevier, Amsterdam, 1984. Pages xiv + 354. US$37.75. Dfl. 98.00.

This well written book commences with a lucid description of machine-code programming for the 6502 processor. It begins with an excellent review of the fundamental concepts and continues with a cleverly selected set of sample programs which serve to consolidate the reader's grasp of the various instructions and address modes of the 6502. This section of the book is written specifically for the Rockwell AIM 65 and it is regrettable that the sample programs are not always directly transferable to other machines which use the 6502 processor, *e.g.*, Apple, BBC. Nevertheless, practical experience with the programs should go a long way to dispel any fears of the mysticism associated with machine code which the reader may have.

The later sections of the book contain information relating to the problems of interfacing microcomputers to experiments. The accounts of analogue to digital and digital to analogue conversions, stepper-motor control and the diagrams of circuits for use in these and other applications will be of value to experienced and novice programmers alike. Similarly useful are the sections describing some of the more common data-communications interfaces such as RS232 and IEE-488, and also the operation of the 6522 versatile interface adaptor.

This book is highly recommended on two counts. First, for the novice programmer, it constitutes an excellent primer on the subject of machine code for the 6502 processor. Second, for the more experienced user, it provides a valuable source of data and ideas relating to the development of practical applications of microcomputers in instrumentation.

R. A. HOWIE

Talanta, Vol. 32, No. 4, pp. iii–iv, 1985

PUBLICATIONS RECEIVED

A Manual of Chemical and Biological Methods for Seawater Analysis: T. R. PARSONS, Y. MAITA and C. M. LALLI, Pergamon Press, Oxford, 1984. Hardback $19.50, £12.25; Flexiback $8.95, £5.50. Pages xiv + 173.

It is pertinent to ask for whom this book has been written: it is a manual of selected, well-tried methods, each described in detail, aimed at biologists, environmentalists and engineers, as well as students. However, in view of the problems peculiar to the analysis of sea-water, I would suggest that it could be valuable to any analytical chemist not already well versed in this speciality. Then, it would be instructive to make a comparison with the very fine *Methods of Seawater Analysis* by Grasshoff, which presents many more determinations and alternative methods, and discusses the background to each in much more detail, but the important difference is in the accuracy which each book presents as the norm to be aimed at. Grasshoff is writing for oceanographers for whom small differences in composition between areas, depths or seasons are important: scrupulous attention to detail becomes an overriding consideration in such investigations. Parsons, who collaborated with the late J. D. H. Strickland in *A Practical Handbook of Seawater Analysis*, has here collaborated with a new team in writing for a wider audience of scientists who will expect to find small natural variations and will want to correlate significant differences with other observations on populations, growth rates, behaviour and so on. Accordingly, the prime consideration is to avoid serious errors, and to this end the reader is guided safely through the pitfalls of contamination and loss in trace analysis, but is not burdened with an insistence on parts-per-thousand precision in all measurements.

Some thirty determinations are described, covering nutrients, organics, particulates, pigments, gases and bacteria. This is a book for use in the field station, even in the field itself (or rather, the open sea). I would still recommend that readers consult Grasshoff before planning a survey, to gain a fuller understanding of why certain parameters are important and of how the methods work, but for much routine use and undergraduate teaching, this book will prove very valuable and is to be welcomed warmly.

IAIN L. MARR

Methods of Protein Analysis: ISTVÁN KERESE (editor), Horwood, Chichester, and Akadémiai Kiadó, Budapest, 1984. £39.50. Pages VIII + 371.

Progress in fundamental science is often the result of the need to know more about particular phenomena, both natural and man-made; to know "what causes change" and often to measure how much of "what" causes how much damage. This can only be possible by progress in the relevant fields of analysis. Progress in industrial chemical and biochemical applications of science can only come if the methods for the evaluation of the systems are well established and understood. Economic evaluation may be the dominant factor in deciding whether or not an industrial process should be used, but as the editor of this volume states "It may not be the protein-analyst who through his work directly saves from want the large number of people suffering from protein-starvation, as this is essentially a question of economic investment, but protein-analysis is indispensable when establishing the economic trends".

This pragmatic philosophy has influenced the selection of the methods discussed in the book. The methods are generally those which can be used in the average laboratory and are not those employed "only in the leading institutes specializing in research on the structures of proteins". The chapter dealing with general laboratory methods is not concerned with reference methods but with analyses connected with various fields of everyday application, and the problems associated with obtaining a representative sample, from say an agricultural feed such as hay, are well discussed. The preparation of the material and its characterization are discussed in an exceedingly practical manner. This chapter—in common with others in this volume—is well referenced and gives the reader a feeling of obtaining information from a well practised analyst.

Other chapters deal with techniques and methods, for example that on electrophoretic methods includes a brief but relevant review of the various methods available and a detailed discussion on polyacrylamide gel electrophoresis which is very good. Other chapters deal with chromatography and are very well presented. Obviously in a book of such size, detailed descriptions of individual applications cannot be presented, but since there are over 1000 references, there is ample information presented.

The book is well presented, timely and good value—easy to recommend for those interested in protein analysis.

L. S. BARK

Quality Measuring Instruments in On-line Process Analysis: D. J. HUSKINS, Horwood, Chichester, 1982. £40.00. Pages 455.

This is the second in a series of books by the author and it illustrates his wide practical knowledge of the subject. As a handbook it is really a valuable reference work for those in the particular field but it also offers much to the designers of automatic instruments. This volume deals with instruments which measure some quality of the material being processed or monitored, for example density, viscosity, surface tension, colour, calorific value, octane rating, pH, salt content *etc.* The author clearly sets out the principles of the methods of measurement and then provides a very comprehensive description of the instrumentation available. Many instrument companies are represented in the pages and the author should be congratulated on the wide spread of instruments that he has included. Whilst much of the book seems to centre on the petroleum industry this should not deter readers from referring to it or purchasing it. A comprehensive table of contents allows the reader easy access to the particular material of interest. It is aptly illustrated with numerous diagrams and is a valuable addition to the library shelves.

P. STOCKWELL

Topics in Forensic and Analytical Toxicology (Proceedings of the Annual European Meeting of the International Association of Forensic Toxicologists, Münich, 21–25 August 1983): R. A. A. MAES (editor), Elsevier, Amsterdam, 1984. $57.75, Dfl. 150.00. Pages x + 214.

The number of compounds capable of causing toxic effects has multiplied many times in the past few decades; so have analytical techniques, tests and toxicology-related literature. *Topics in Forensic and Analytical Toxicology* gathers the proceedings of the 1983 European Meeting of the International Association of Forensic Toxicologists. It is a rather heterogeneous collection of papers. A number of generalities related to drug interferences with car-driving capacity precede a paper on embryotoxicity of toxic oils and a presentation of data on deaths involving propoxyphene that occurred at a particular British hospital in the period 1975–1982. Apart from a case-record on tetrahydrofuran poisoning a number of isolated papers deal with analytical procedures: the extraction of alkaline drugs from tissues, the determination of benzodiazepines; beta-blockers, alkaloids and their metabolites, antidepressants and illicit drugs. HPLC and mass spectrometry are the methods of choice in the majority of instances.

The book also offers a series of papers of more general toxicological interest. Modern trends in chemical analysis of addictive drugs are briefly described. The pros and cons of the EMIT-St system are discussed in this respect. Another interesting paper covers the principles, characteristics and practical application of head-space gas chromatography. A multiple toxicological screening programme, applicable in a simple laboratory setting and aimed at yielding the initial clues as to the intoxicating drug, is presented. One of the more interesting papers (by R. Ludweig) scrutinizes the generation and application of toxicological data and so illustrates the lack of sufficient control of such data and the need of more co-ordination of research and documentation in this area. Absence of the latter has led to the generation and multiplication of incorrect information regarding poisoning and its treatment.

A small part of the book is dedicated to clinical toxicology in third world countries: its emergence, its problems and the political strategies to be followed. Finally, round-table discussion on quality control, documentation and post-graduate education in forensic toxicology conclude this volume.

In general, despite its containing some interesting papers, the book would have benefited from more scrutiny as to the originality of some of the contributed material, as well as from more systematic organization and linguistic editing.

M. VERLINDEN

AnalaR Standards for Laboratory Chemicals, 8th Ed., D. J. BUCKNELL (editor), BDH Chemicals, Poole, 1984. Pages XXVIII + 897. £24.00.

This edition of this classical handbook has been produced to mark the fiftieth anniversary of the production of the first edition, and it continues the success of its illustrious predecessors. The format is the same as in previous editions, with detailed practical descriptions of the test methods used, followed by the monographs for the chemicals in the AnalaR range and ending with the appendices listing reagent, indicator and standard solutions. As would be expected, the techniques used have been expanded to include such newer methods as plasma emission and HPLC, the number of chemicals included has been increased (by 70), and many of the older chemicals are now re-issued with tighter specifications and test methods to suit.

The binding is solid, in heavy duty plastic covers which should withstand the ravages of the laboratory bench, where it will undoubtedly spend much of its time, and in the reviewer's opinion it is a book which no chemical laboratory library should be without.

R. C. ROONEY

Handbook of Automated Analysis: WILLIAM A. COAKLEY, Dekker, New York, 1981. Pages xii + 144. S Fr. 55.00.

This book is best described as an extension to the operator's manual for a Technicon Autoanalyzer, and in the reviewer's opinion should be given away with those instruments rather than offered for sale under its present title. At the very least it should have a subtitle which would warn an intending purchaser that the author is so convinced an admirer of Technicon equipment that he cannot conceive of any alternative method of automated analysis.

This having been said, there is no doubt that as an adjunct to the equipment it is very useful. Much of the hyperbole will grate on other readers besides me, and many of us will find the humour childish, but if practical advice on setting up a new Autoanalyser method is needed, this book will provide much of it.

The author is all too obviously an enthusiast for his apparatus, and he is happily oblivious to the idea that any product bearing the Technicon name could be in any way less than perfect, but he is equally obviously extremely experienced in the practical uses of it, and the book is a veritable goldmine of hints and tips which will repay study by any user.

The book is unlikely to last very long in the working laboratory environment for which it is intended, since it is a plastic-spiral bound production with very little paper between the plastic spiral and the edge of the page; perhaps the price could be adjusted to render it a disposable item.

R. C. ROONEY

Petroanalysis '81: CRUMP (editor), Wiley/Institute of Petroleum, London, 1983. £36.00.

This book comprises the papers presented at the symposium organized by the Analysis Sub-Committee of the Institute of Petroleum in October 1981, and the breadth of subjects covered reflects the importance of that symposium. Out of the 37 papers presented it would be invidious to single out individuals for praise or criticism; the general standard of the contents is excellent.

As a book, it is a little more difficult to predict an audience at which it is aimed, since the subjects covered range from a philosophical consideration by Professor Bark on the relationship between the educators of new analytical chemists and their potential industrial employers, to descriptions of analytical techniques in a wide variety of fields and using totally different techniques. From this point of view I regard it as a book for the library shelves rather than the individual's bookcase, but there can be few chemists connected with the petroleum industry who would not find it profitable to read the contents list to see what is of interest in their own field.

From the practical viewpoint, I was disappointed to see a book of this technical quality produced by direct photographic reproduction of the author's typescript. It has led to a very piecemeal appearance, with type faces, sizes and legibility varying from paper to paper, and it has not even managed to completely eliminate typographical errors. Overall, however, it is a book to recommend heartily.

R. C. ROONEY

Talanta, Vol. 32, No. 3, pp. iii–iv, 1985
Pergamon Press Ltd. Printed in Great Britain

PUBLICATIONS RECEIVED

Emanation Thermal Analysis and Other Radiometric Emanation Methods: V. BALEK AND J. TÖLGYESSY, (**Comprehensive Analytical Chemistry,** Vol. XII, **Thermal Analysis,** Part C), Elsevier, Amsterdam, 1984. Pages 304. $80.75; Dfl 190.00.

The emanation method, as one of the radiochemical methods, has been known for more than half a century. During the last two decades the emanation method has successfully been developed in both the theoretical and instrumental aspects. The method is more and more applied in nuclear technology (especially the behaviour of inert gases in irradiated nuclear fuel) and in the study of solids (mainly in such areas as the chemistry of solids, physical chemistry, polymer chemistry, mineralogy, metallurgy, ceramics). Radioisotopes of inert gases have become widely used as universal indicators in analytical chemistry, for the analysis of gases, liquids and solids.

The monograph has eight chapters. The first gives a brief description of the history of the method and the place of this method among other thermodynamic methods.

Chapter 2 gives the main characteristics of the radioisotopes of inert gases applied as radioactive tracers, and describes the diffusion of inert gases into a solid, the inclusion of inert gases in the preparation of the sample or in phase transfer, as well as the irradiation of sample surfaces by accelerated ions of inert gases.

Chapters 3 and 4 give a detailed analysis of the problems in the theory of inert gas separation from a solid. Chapter 5 is devoted to the methods of determination of the separated inert gases, and gives schemes of apparatus, measuring equipment and some practical recommendations. The possibilities and limitations of application of emanation methods, as well as some of the most important applications, are given in Chapter 6. Chapters 7 and 8 deal with the application of radiometric emanation methods in various analytical techniques and several technological processes.

A brief account of the modern state and perspectives of radiometric emanation methods is given in conclusion.

The book is undoubtedly interesting for radiochemists, analytical chemists and technologists who use radioactive indicators; it will also serve to speed further the use of radiometric emanation methods.

B. F. MYASOEDOV
S. S. RODIN

Thermophysical Properties of Solids: Their Measurement and Theoretical Thermal Analysis. JAROSLAV ŠESTÁK, (**Comprehensive Analytical Chemistry,** Vol. XII, **Thermal Analysis,** Part D), Elsevier, Amsterdam, 1984. Pages XIX + 440, $115.50. Dfl 270.00.

Dr Šesták is well known and highly respected internationally for his intensive theoretical studies on the thermal behaviour of materials and, arising from that, the theory of thermal analysis. Although a number of the publications by him and his co-workers have appeared in English, many more, including a recent book, have been published only in Czech and are, therefore, not as well known as they ought to be. Both the author and the publishers are thus to be congratulated for providing this English text, which is essentially an update of an earlier Czechoslovak volume and gives a succinct but thorough account of the findings of many years' work. The abstruse mathematics necessarily involved in a theoretical physical treatment of thermal behaviour is off-putting to many, and yet some understanding of the findings of such a theoretical study is essential to all those involved in what are often regarded as the empirical methods of thermal analysis. In this volume the author has done a great service by keeping the mathematics and advanced physics to the essential minimum and by explaining in words the premises, the operations and the results of the rigorous treatment, thus making the subject comprehensible to the majority. After an introductory chapter that outlines the content of succeeding chapters and correlates the various aspects, subsequent chapters deal with sample characterization from the theoretical viewpoint and the ability of materials to yield information (a subject still too little understood by many), uses of an inter-relationships between thermoanalytical techniques, heat exchange and temperature, various thermodynamic aspects (classical and modern), including the thermodynamics of phase equilibria, the theory of phase transitions, kinetics in relation to heterogeneous reactions, non-isothermal conditions and glass formation, the theory of calorimetry and differential thermal analysis (DTA), measurement of thermal properties, the mathematics of the analysis of curves and the use of computer techniques. An Appendix with 16 valuable tables of data and an excellent index are provided. As to the relevance of all this to analytical chemistry, it is well to remember that techniques such as thermogravimetry and DTA with evolved-gas analysis facilities have a definite place in analytical studies and that such techniques cannot be used to their full advantage without knowledge of the underlying theory and principles. This book, which, unlike many theoretical treatises, is readable (even humorous in parts) and understandable, is therefore a "must" for all those involved in any way in thermal analysis and can be thoroughly recommended to all those who want to know about the basics of the subject.

R. C. MACKENZIE

New Approaches in Liquid Chromatography: Proceedings of the 2nd Annual American–Eastern European Symposium on Advances in Liquid Chromatography, Szeged, Hungary, June 16–18, 1982: H. KALÁSZ (editor), Analytical Chemistry Symposia Series, Vol. 16, Elsevier, Amsterdam 1984. Pages X + 291. U.S. $67.25; Dfl. 175.00.

The contributions to these proceedings are presented under the following headings, with the numbers of papers in parentheses: High Performance Liquid Chromatography (4), Displacement Chromatography (2), Optimisation Possibilities in Liquid Column Chromatography (3), Thin-Layer Chromatography (2), Analysis of Amino Acids (4) and Analytical and

Preparative Separation of Peptides and Proteins (6). The majority of the papers deal with problems in biochemical, pharmaceutical and medical contexts. To the reviewer, the "new approaches" reference in the title would suggest technique and instrumental innovation, whereas developments and applications would convey a more accurate impression of the contents. On the whole, the papers are well-documented and the editor has put together an easily readable text containing clear diagrams and figures. However, the work remains a record of the proceedings of a conference, with the usual attendant weaknesses of imbalance in structure and content and some variable presentation of textual material. The book should be of interest to readers working in the fields indicated above, and deserves to find its way into science libraries, but it is unlikely to tempt the individual purchaser.

S. J. LYLE

Dictionary of Chemistry and Chemical Technology—English/German. H. GROSS (Editor in Chief), Elsevier, Amsterdam, 1984. Pages 714. £65.00; Dfl. 275.00. Jointly published with VEB Verlag Technik, East Berlin.

Here is half a new dictionary—I am already excited because I am so often infuriated by the inadequacies of older dictionaries, technical and general. So what does it offer? The sleeve says "ca. 55.000 entries covering Chemistry (Inorganic, Organic, Physical, Analytical, Industrial), Chemical Engineering, Materials Science, Paper, Leather, Agriculture, Mineral and Petroleum Technology, Metallurgy, and more". And there is more besides: chemicals are listed by systematic and trivial names and the formulae are supplied. Many of the more unusual words have explanations to set the context And yet more, because numerous compound words or combinations are also listed, from simple Red lead (Bleimennige, Pb_3O_4) to Lurgi high-pressure gasification process (Lurgi-Druckvergasungsverfahren) and so on. All of this contributes significantly to make this dictionary much more reliable for the serious translator, and a good deal more helpful for the struggling do-it-yourself linguist. Of course, no dictionary can ever be complete, and I find gaps here in oilfield technology, for example, where the widely-used American slang is largely absent, and in environmental analysis. Some more acronyms ought to have been included: GLC is, but AAS, HPLC and TLV are not.

There are indications that this is the reverse version of an original German/English dictionary, which is also available (I look forward to seeing this other half). How else might "not printed on" (unbedruckt) appear in an English dictionary? But to sum up: the team of scientists, technologists and linguists at the Technical University of Dresden deserve high praise for their efforts in producing this dictionary. Only another lexicographer, and perhaps the regular technical translator, can really appreciate what they have achieved, though any user will reap the rewards of their labours. How much better this is than the soulless computer-produced one-word-for-one-word compilations which are cluttering our reference shelves.

IAIN L. MARR

Chromatography and Mass Spectrometry in Nutrition Science and Food Safety: A. FRIGERIO and H. MILON (eds.), Elsevier, Amsterdam, 1984. Pages xi + 305. $113.50; Dfl 295.00. Proceedings of an International Symposium, Montreux, June, 1983.

By their very nature, foods are extremely complex substances, and their complexity seems to increase in proportion to the power of the current methodology. High-resolution gas chromatography, we are told, has resolved over 500 compounds in the volatiles from coffee, while chromatograms of volatiles from papaya and carrot seem to have more peaks than spaces. The large number of peaks is something of an embarrassment because we feel we ought to try to identify them all: some chapters here deal with the identification of some extraordinary sulphur heterocyclic compounds, based on an analysis of their mass spectra. At the same time, the excellent sensitivity of modern equipment makes possible the detection of pesticides at extremely low levels (4 papers on this topic). For less volatile and less stable compounds, HPLC is favoured, and can now be combined with mass spectrometry, a powerful combination in food science (2 papers). An unusual topic is the racemization of amino-acids, studied by GLC with a chiral stationary phase (1 paper). The advantages of high-temperature capillary GC over conventional packed-column techniques are clearly demonstrated in the analysis of individual triglycerides in chocolate fats (1 paper). Isotope ratio measurements by mass spectrometry to follow the metabolism of labelled compounds with stable isotopes ^{13}C and ^{15}N are now becoming almost routine: this elegant technique of nutrition science is dealt with in 4 papers. Of the 27 contributions, only five mention safety in their titles, so the balance is firmly on the side of nutrition science, with a good deal of very interesting, though rather specialized, reading. The book is set direct from typescript, which is well set out and clearly legible except for one paper produced on a computer dot-matrix printer. This selection of papers gives a good impression of what can be done in the field of food analysis: I cannot help wondering whether the gap between the possible and the practical is widening rather than narrowing as the specialist techniques become ever more highly developed.

IAIN L. MARR

Talanta, Vol. 32, No. 2, pp. iii–iv, 1985
Pergamon Press Ltd. Printed in Great Britain

PUBLICATIONS RECEIVED

Chemical Methods in Gas Chromatography: V. G. BEREZKIN, Elsevier, Amsterdam, 1983. Pages x + 314. US$73.25; Dfl.190.00.

Volume 24 of the series "Journal of Chromatography Library" is a heterogeneous collection of information about the application of chemical methods to gas chromatography. The most familiar applications are those detailed in the first chapter, which deals with derivatization methods and the conversion of non-volatile species into compounds sufficiently volatile to pass through a gas chromatography column. Less widely used, and as a result less familiar, are the analytical techniques based on kinetic methods in which isomers are distinguished by their differential rates of reaction with a common reagent, or catalyst concentrations determined from measurements of the rates of catalysed reactions. Short succeeding chapters are devoted to pyrolysis gas chromatography with the pyrogram used as a fingerprint, and to the carbon skeleton method in which catalytic reduction is used to eliminate functional groups and convert sample components into recognizable hydrocarbons. Other chemical methods reviewed in the book include those in which reactions between components of a mixture with a substrate alter the volatility of some of the components or establish secondary chemical equilibria in the liquid phase, both methods resulting in differential changes in retention volumes. These concepts are used not only in procedures for separation and identification based on specific interactions between solvent and solute or the subtraction of two chromatograms, but also for functional group and trace analysis and the determination of elemental composition.

Although this book has a formidable collection of references and will be useful for the practising analyst, it is extremely wordy and full of unnecessarily long generalizations in the introduction to each chapter. It would have been improved by intelligent editing.

J. R. MAJER

Chemical Sensors: T. SEIYAMA, K. FUEKI, J. SHIOKAWA and S. SUZUKI (editors), Elsevier, Amsterdam, 1983. Pages xiv + 775. US$144.50; Dfl.375.00.

This book, Volume 17 of the Analytical Chemistry Symposia Series, contains a collection of 11 plenary lectures and 121 contributed papers given at an international meeting held in Fukuoka, Japan, 19–22 September 1983 under the auspices of the Electrochemical Society of Japan. The term "chemical sensor" is not one which will be immediately familiar to all analytical chemists. This is due to the generality or vagueness of the concept, which can refer to all physicochemical systems giving responses to specific compounds or classes of compounds. Thus the analyst working with ion-selective electrodes might be surprised to know that he is using "chemical sensors", or that his work has anything in common with those using combustible gas detectors. With such a wide coverage this book must be addressed not to researchers in particular disciplines, but to those involved in the design of monitoring and control systems, to whom the detection rather than the nature of the detector is important.

The first section is devoted to semiconductor detectors of oxidizable gases and vapours. These devices, usually based on heated films of doped zinc or tin oxides, have been available for many years but suffer from defects such as non-linearity of response. The papers in this section describe investigations into the mechanism of their action and the improvement of their performance.

There follows a series of contributions describing potentiometric detectors, *i.e.*, those in which a gas reacts with a solid electrolyte and produces a potential at a suitable electrode. A well-known example of this type is the oxygen detector based on a high temperature electrolyte such as zirconium oxide. Individual papers outline attempts to reduce the operating temperature of the electrolyte and to increase the rate of interaction of gaseous oxygen with the electrolyte by using catalysts. The principle is extended to the detection of other gases, such as sulphur dioxide and carbon dioxide.

The requirements of air-conditioning systems for humidity control have prompted the design of many devices capable of measuring atmospheric moisture, while remaining unresponsive to condensation films. The papers collected in Section C describe some of these devices, most of them based on heated layers of metallic oxides. The concentration of water vapour in atmospheres diffusing into these layers is determined by changes in electrical properties, such as conductance, capacity, or more simply resistance.

The response of microelectronic devices to small concentrations of foreign gases in their environment is discussed in further papers which describe detectors for hydrogen and hydrogen sulphide. Microionic systems are also dealt with and some papers include descriptions of probes in which the electrical conductance of layers is modified by the presence of gaseous oxygen and ammonia. A feature of this type of sensor is said to be the capacity for micro miniaturization.

Problems associated with the transfer of use of the chemical sensors based on ion-selective microelectronic systems from the gaseous to the liquid phase are reviewed in Section E. The application of ion-selective devices as biochemical sensors or chromatographic detectors is also given some attention.

A further collection of papers under the heading of biosensors is devoted largely to the utilization, in clinical situations, of many of the systems already described as chemical detectors. Measurements of gases, such as oxygen and carbon dioxide in blood, have been achieved and chemical detectors responding to more complex biochemical substances, such as glucose, are also reported.

The final section is a heterogeneous group of papers announcing new detectors and methods. Probably the most significant contribution in this section is that discussing the local combination of chemical sensors and microprocessors. Many of the defects of the sensors such as non-linearity, interference or sensitivity to variations of supply voltage may be obviated by modification of the output signals by the microprocessor before transfer to the main control system.

In all sections the plenary lectures provide useful historical reviews and perspectives.

J. R. MAJER

Advances in Chromatography, Vols. 22 and 23: J. C. GIDDINGS, E. GRUSHKA, J. CASES and P. R. BROWN (editors), Dekker, New York, Volume 22, 1983, pages xvi + 323 SFr.148; Volume 23, 1984, xvi + 249, SFr.140.

These volumes have the same breadth of interest and are in the same format as the others in the series. They consist of lengthy reviews of diverse topics and are pitched at the researcher. They are too broadly based and expensive to be attractive to the individual purchaser, but are a good buy for the library. Volume 22 is biased slightly towards biochemical applications and Vol. 23 towards new techniques, such as laser spectroscopic methods in LC (E. Young) and Chromatopyrography (J. C-A Hu).

Talanta, Vol. 32, No. 1, pp iii–iv, 1985
Pergamon Press Ltd. Printed in Great Britain

PUBLICATIONS RECEIVED

Principles of Quantitative X-Ray Fluorescence Analysis: R. TERTIAN and F. CLAISSE, Heyden, London, 1982. Pages xviii + 385. £30.00.

There exists in general a significant gap—though perhaps not as much as a gulf—between most theoreticians and most practising analytical chemists. Indeed, my guess would be that most analysts with only a minute or two to flip through the pages of this book would be frightened by the pages of equations and put it down again, commenting "A practical analyst just goes into the lab and does the analysis, finding a convenient standard which experience tells him will, with a bit of luck, give him nearly the right answer." What Tertian and Claisse are telling us is that it is not only possible to calculate what the corrections in the calculations should be, but also very much more practical, in these days of dedicated computers on every instrument, than it was say 20 years ago (when I remember a colleague spending a week converting intensities into concentrations for a four-component alloy). I should point out that both authors have published very practical methods based, *e.g.*, on dilution techniques, so they are sympathetic to the traditional approach. But they go further: "Adaptability, i.e. achieving a judicious balance of theoretical and practical considerations, is the keynote for quantitative X-ray fluorescence analysis" is how they sum up one of the chapters. Their message is to take advantage of the great computing power we now have, together with our experience in semi-empirical chemical approaches, to solve difficult analytical problems efficiently and accurately.

The text is clear and to the point: in particular I like the brief discussion concluding each chapter and putting the contents in perspective, and also the inclusion of practical details to illustrate the methods described. This is a comprehensive discourse on all aspects of X-ray fluorescence analysis with X-ray tube sources—the special problems of dealing with portable isotope sources, for example, are not considered. So, dear reader, pick up this book again and peruse at first beyond the equations, then go back and overhaul your current methods with the help of the theoretical appraisal given by Tertian and Claisse. Definitely recommended.

IAIN MARR

Instrumental Lipid Chromatography: N. A. PARRIS, 2nd Ed., Elsevier, Amsterdam, 1984. Pages xiv + 432. US$86.50; Dfl.225.00

In this revised edition of the practical manual first published as Vol. 5 of the Journal of Chromotography Library in 1976, the layout and chapter headings remain essentially unchanged. However, a chapter on bonded-phase chromatography and another on the uses of microcomputers and computational techniques have been added; in addition, considerably more space is devoted to ion-pair chromatography than hitherto. While the chapter on bonded phases provides a brief, useful but somewhat dated introduction to this important area of development, that on microcomputer applications is disappointing and barely touches upon recent important practical developments relating to selection of optimum operating conditions and chromatogram resolution.

The text and useful appendices have been expanded by just over 100 pages, SI units introduced, and references updated but usually only to around 1981. While those in possession of copies of the earlier edition are unlikely to find it worthwhile exchanging the old for the new, the revision undoubtedly extends the useful life of this good introductory manual and it can be recommended to those about to establish LC in their laboratories.

S. J. LYLE

Microcolumn High-Performance Liquid Chromatography; P. KUCERA (editor), Elsevier, Amsterdam, 1984. Pages xvi + 302. US$63.50; Dfl.265.00.

Over the past five or six years microbore HPLC has evolved from a laboratory curiosity to a practical technique capable of use in routine analysis. Several manufacturers currently offer conversion kits for their conventional instrumentation and others complete custom-built instruments. The monograph under consideration gives an account of developments mainly over a period of about five years from 1978. Use of packed and open tubular columns of 1 mm internal diameter or less are considered; problems arising from the scale of operation and solutions to them are offered, relating to column preparation, sample introduction and detection systems. Applications are also considered. The book is divided into eight chapters written by "experts". The first, by G. Guiochon and H. Colin, provides an introduction and general survey. It is followed by chapters dealing with design of microbore columns (P. Kucera), theory and practice of high-speed microbore HPLC (R. A. Hartwick and D. D. Dezaro), special analytical techniques (P. Kucera and G. Manius), chemical derivatization (P. Kucera and R. A. Hartwick), columns of capillary dimensions (M. Novotny) and micro LC/MS coupling (J. Henion).

This is the first monograph on microcolumn HPLC and the subject is generally given a good fundamental and practical treatment. The text is well-documented and contains clear diagrams. However, each chapter would appear to have been written as a self-contained unit; consequently, the lack of cross-references has given rise to unnecessary repeitition. This weakness notwithstanding, the monograph can be recommended as a convenient starting point for any analyst who needs to become familiar with the current state of the art in microbore HPLC.

S. J. LYLE

Analysis Using Glass Electrodes: PETER W. LINDER, RALPH G. TORRINGTON and DAVID R. WILLIAMS, Open University Press, Milton Keynes, 1984. Pages 148 + xii. £20.00.

As would be assumed from the title, this book gives a very thorough description of the concept of pH, the development of the glass electrode, and of its use for making pH measurements. The design and construction of electrodes is described, and detailed recommendations are given for use and maintenance. The problem of definition of the pH scale is explained: the UK single-standard approach is compared and contrasted with the multi-standard approach adopted in the USA and many other countries. Methods for determination of hydrogen-ion concentrations (as opposed to activities) are then discussed. These methods require the use of computer programs for least-squares solution of the many mass-balance equations involved. Four such programs, MAGEC, ACBA, MINIPOT and LIGEZ, are reproduced. The unexpected part of this book is the excellent chapter on speciation, a subject which is very much inter-related with $[H^+]$ determination. The nature of speciation calculations is explained, with emphasis on the need for meticulously determined formation constants for use in these calculations. Applications of speciation studies in medicine, industry, oceanic and atmospheric chemistry, environmental problems, and bioavailability of metals are discussed.

MARY MASSON

Applications of Piezoelectric Quartz Crystal Microbalances: C. LU and A. W. CZANDERNA (editors), Elsevier, Amsterdam, 1984. Pages xiv + 394. US$100.00; Dfl.260.00.

Progress in weighing—once the very basis of classical chemical analysis—resulted, through a lengthy period of development, in devices of a high level of sophistication and perfection. Even today, the reliability of mass determination can hardly be surpassed by that of any other analytical measuring principle. Despite the rapid development made in instrumental analysis methods, mass determinations have been and still are the foundation of most analytical procedures; as a rule, however, these determinations are now confined to weighing of the mass of the initial samples. Thus, even micro- and ultramicrobalances—once the pride of the analyst—have now become routine equipment. A special position in terms of operation and application is occupied by piezoelectric quartz crystal microbalances, justifying, even now, the compilation of a monograph.

The editors, C. Lu and A. W. Czanderna, have, together with nine other authors, collected all that is worth knowing about the history, theory, operation and applications of the quartz crystal microbalance (QCM) methods, describing it in 10 chapters. The expression "balance" applies to the QCM only in a wider sense. Its operation is a relative determination of mass in the microgram and nanogram range, measured by means of the frequency change of a piezoelectric quartz crystal as a function of mass surface density loaded onto the crystal.

In addition to the theoretical and methodical principles treated by Czanderna and Lu in chapters 1 (18 pages, 46 references) and 2 (43 pages, 46 references), the analyst will be especially interested in the chapter "Applications of QCM in Analytical Chemistry" by G. G. Guilbault, describing some selective and sensitive detectors for gas chromatography and liquid chromatography, for water, SO_2, NH_3, H_2S, HCl, CO, Hg, organophosphorus compounds and pesticides, and aromatic hydrocarbons, and discussing, among others, some commercially available equipment (30 pages, 71 references). Further fields of specific analytical relevance are included in the chapters on "Applications for Thin Film Deposition Process Control" by H. K. Pulker and J. P. Decosterd, dealing with, *e.g.*, vapour deposition, sputtering and ion plating (61 pages, 73 references), "Simultaneous Measurement of Mass and Temperature" by E. C. van Ballegooijen (45 pages, 50 references), "Application in Surface Science" by L. L. Levenson (23 pages, 94 references), "Plasma-Assisted Etching Studies and Applications" by J. W. Coburn (29 pages, 30 references), "Application to Space System Contamination Studies" by A. P. M. Glassford (70 pages, 23 references) and "Applications in Aerosol Mass Measurement" by M. H. Hop (38 pages, 59 references).

As is quite frequently found in books written in joint authorship, there is some overlap between chapters, and this should have been avoided, if only to produce a lower price for this otherwise thoroughly compiled book. Owing to the highly specialized subject, only a relatively small group of analysts is addressed, but they (like the reviewer) will not be disappointed by the information/price ratio.

The book will evoke great interest in general, within the fields of research and technical science, and beyond the confines of analytical chemistry.

GÜNTHER TÖLG

Fourier Transform NMR Spectroscopy: DEREK SHAW, 2nd Ed., Elsevier, Amsterdam, 1984. Pages xii + 304. US$75.00; Dfl.195.00.

In the last few years the ingenuity and inventiveness of NMR spectroscopists have resulted in the appearance of a huge range of pulse techniques, usually designated by impenetrably cryptic acronyms. The publication of this book could, therefore, scarcely have come at a more appropriate time, for it is an astonishingly comprehensive survey of virtually every aspect of Fourier-transform NMR spectroscopy. Apart from some excellent but necessarily limited review articles in periodicals, it is without rivals in both the range and detail of subject matter and will be indispensable in providing the understanding necessary for productive application of the very many new techniques becoming commercially available.

Though the mathematical treatment is not, by chemist's standards, unapproachable, neither is it entirely accessible. However, for those unprepared or unwilling to follow all of the mathematical reasoning, there still remains the possibility of real insight and genuine understanding. The formal treatment is accessible to non-specialists and the very readable text is complemented by numerous helpful diagrams and sample spectra.

It is regrettable that the quality of production of the volume is such that these diagrams and figures are often rather cramped and lack clarity, especially in the depiction of spectra. Density of printing in the text is variable, an effect most noticeable in the reproduction of mathematical expressions and symbols. This, together with a fair number of misprints, can make for unnecessary difficulties, *e.g.*, pages 15 and 17, bar missing from γ symbol; page 149, four misprints, *etc.*

However, these are small points in relation to an excellent and timely book which is further enhanced by the value of the author's very considerable practical experience.

D. G. WILLIAMSON

Talanta Vol 32, No. 1, pp. *III–VI*, 1985
Pergamon Press Ltd Printed in Great Britain

TALANTA ADVISORY BOARD

The Editorial Board and the Publisher of *Talanta* take pleasure in welcoming the following new members of the Advisory Board of the journal.

P. W. J. M. BOUMANS	D. JAGNER	J. MATOUSEK
R. G. COOKS	R. KELLNER	M. NOVOTNY
T. FUJINAGA	L. KRYGER	WANG ERKANG

Professor Fujinaga is retiring as the Regional Editor for Japan, and that position will be taken over by Professor T. Hori, of the University of Kyoto, who is also welcomed to the editorial team. The Editorial Board and the Publisher also wish to record their sincere thanks for the help given by

P. W. CARR	D. KLOCKOW	J. RŮŽIČKA
C. L. CHAKRABARTI	SHU-CHUAN LIANG	P. E. A. SENISE
O. H. J. CHRISTIE	R. J. MAGEE	L. E. SMYTHE
P. N. KELIHER	H. M. ORTNER	T. S. WEST

who retire from the Advisory Board. They are particularly grateful to Professor T. S. West, who has been associated with *Talanta* from its foundation.

P. W. J. M. BOUMANS

DR. P. W. J. M. BOUMANS studied chemistry and physics at the University of Amsterdam, where he obtained his doctor's degree cum laude in 1961 with a thesis: "Some fundamental aspects of spectrochemical analysis using the d.c. carbon arc". During 1961–68, he was concerned with research and education at the University of Amsterdam, where he wrote a book *Theory of Spectrochemical Excitation*, a chapter on "Excitation of Spectra" and a series of research papers on atomic emission spectroscopy. In 1968 he joined Philips Research Laboratories in Eindhoven, where he is now Chief Scientist, responsible for research in atomic spectroscopy. His prime interests are in the development and advancement of the methodology of emission spectroscopy. Since 1970 these interests have centred on inductively coupled plasmas (ICP). In this field, he has published important articles on ICP optimization, detection limits, line selection, and spectral interferences, including a two-volume tabulation Line Coincidence Tables for ICP Atomic Emission Spectroscopy (1980), which has recently gone into its second (revised) edition. Main topics of his present research are high-resolution ICP spectroscopy and automated sequential ICP analysis. A book *Analysis by Inductively Coupled Plasma Atomic Emission Spectrometry*, edited by Dr. Boumans and for a substantial part also co-authored by him, will appear in 1985. Since 1972, Dr. Boumans has been Editor of *Spectrochimica Acta*, Part B, *Atomic Spectroscopy*, and became Editor-in-Chief of this journal in 1979. Recently, Pergamon Press dedicated to Dr. Boumans an honour issue acknowledging his 25th anniversary in atomic spectroscopy. This issue was published on the occasion of the 23rd Colloquium Spectroscopicum Internationale (CSI), held in Amsterdam in 1983 for which Dr. Boumans was Scientific Affairs Chairman. Dr. Boumans also serves on the Editorial Boards of *Progress in Analytical Atomic Spectroscopy*, *ICP Information Newsletter*, *Analysis* and *Trends in Analytical Chemistry*. He has served on the Board of *Reports on Analytical Atomic Spectroscopy* since 1973.

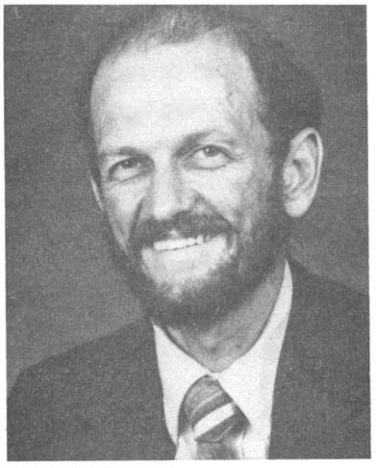

R. G. COOKS

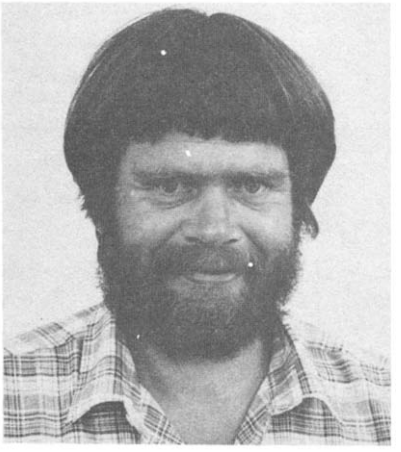

L. KRYGER

PROFESSOR R. GRAHAM COOKS was born in South Africa and educated at Cambridge, England, and entered the U.S. through Kansas. His early training was in natural products organic chemistry with Prof. Frank L. Warren (University of Natal) and in mechanistic organic chemistry with Prof. Peter Sykes (Cambridge). While at Cambridge he worked with Dr. John Bowie and later with Dr. Dudley Williams, on the physical basis of organic mass spectrometry. Review articles on rearrangement reactions and on the kinetics and energetics of fragmentations culminated these efforts. Professor Cooks spent two years on the faculty at Kansas State University, where he developed an interest in kilovolt energy ion/molecule interactions. These interests fitted with those of Dr. John Beynon and Dr. Richard Caprioli with whom he was associated at Purdue for a number of years. The text *Metastable Ions* is a monument to this collaboration. His current research interests lie in the areas of instrument development, surface analysis and ion-scattering (angle-resolved mass-spectrometry). The first of these subjects is focused on MS/MS where he has done pioneering work and where current emphasis is on the hybrid magnet/quadrupole instrument. The focus of the work of his laboratories on surface analysis is the identification of organic and organometallic molecules in complex materials by use of ion and laser beam methods (SIMS and LD). The angle-resolved studies are designed to further enhance the information obtained from mass spectrometry by utilizing a new information domain. Industrial–academic relations, particularly the promotion of joint research through personnel exchange, have been a focal point for his efforts since 1978, when he organized an ACS symposium on the subject. Exchanges for as little as a week have catalysed successful joint research programmes with several industrial laboratories. His interests in instrument development and in the applications of MS/MS to work on natural products, pharmaceuticals and fuels have facilitated these interactions. With Prof. Don Hunt, Prof. Jon Amy, Dr. Karl Wood and Dr. Rich Kondrat, he has developed a short course on MS/MS. He has collaborated on several books and served on a number of advisory panels related to mass spectrometry and analytical instrumentation.

DR. LARS KRYGER graduated in 1971 from Aarhus University, Denmark, with a Master's Degree in Chemistry and Physics. For two years, during his early career, he taught science in Tanzania. In 1975 he obtained his Ph.D. in analytical chemistry at Aarhus University, and after a year of post-doctoral studies at Purdue University, Indiana, he was appointed lecturer at Aarhus University. Since then he has been responsible for establishing analytical chemistry as a research and teaching field in the Chemistry Department of this institution. For a few years after graduation, he worked in the field of inorganic structural analysis, using X-ray diffraction methods. His current research interests are concerned with developments and applications of electrochemical techniques for trace analysis and with applications of microcomputers. In addition, he is interested in pattern recognition and related methods for interpretation of analytical data. In 1981, he received the *Talanta* Louis Gordon Memorial Award for a review on this topic.

T. HORI

R. KELLNER

PROFESSOR TOSHITAKA HORI was born in 1946 in Shiga Prefecture, Japan. After graduating from Kyoto University, he proceeded to the graduate course of the same university and earned a Ph.D. in 1977 under the direction of Professor Taitiro Fujinaga. In this course, he studied heteropoly acid chemistry for the determination of phosphate and other related ions and in 1980 was granted a Research Progress Prize by the Japan Society for Analytical Chemistry. In parallel with his studies, he worked as an assistant at Kyoto University, with Professor Fujinaga, on developing new methods for trace analysis applicable to environmental chemistry. One of the results, concerned with the circulation of trace components in natural waters, was published in a book entitled *Environmental Chemistry on Lake Biwa*. In 1980, after promotion to Associate Professor in the College of Liberal Arts & Sciences, Kyoto University, he started to study the solution chemistry of multicomponent solvent mixtures for selective extraction and separation. Besides his researches at Kyoto University, in 1978 he worked as a research associate with Professor Henryfreiser, University of Arizona, on solvent extraction of mixed-ligand chelates of lanthanides. Since 1980, he has served the Japan Society for Analytical Chemistry as a member of the Editorial Board of *Bunseki Kagaku*.

PROFESSOR ROBERT KELLNER was born in Vienna in 1945, and in 1971 gained his Ph.D. from the Technical University of Vienna, where he has been first Assistant Professor (1970) and since 1977 Associate Professor in the Institute of Analytical Chemistry. Since 1973 he has been secretary of the Austrian Society for Microchemistry and Analytical Chemistry, and since 1975 the secretary of the Working Party on Analytical Chemistry, of the Federation of European Chemical Societies. His research activities are in the fields of surface analysis of polymers, metal-chelate analysis, and coupling of gas chromatography and Fourier-transform infrared spectroscopy. He is very actively involved in teaching, and has published 60 papers and also 4 booklets for his undergraduate analytical chemistry courses.

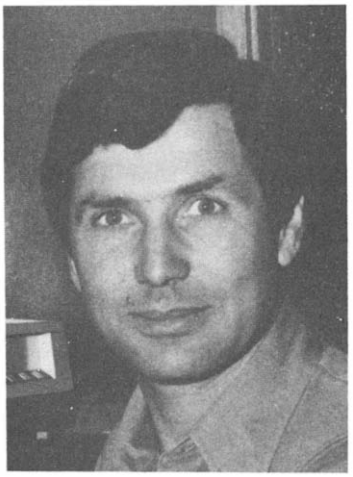

J. MATOUSEK

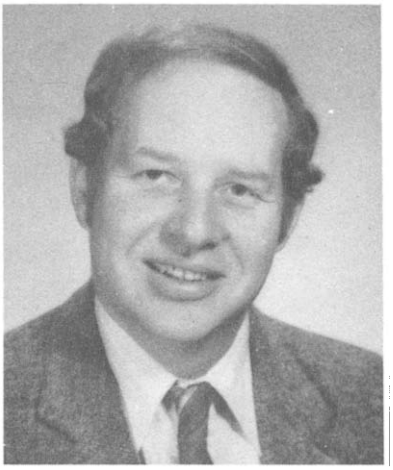

M. NOVOTNY

DR. JAROSLAV MATOUSEK was born in 1938 in Czechoslovakia and in 1962 received the degree of Ing. Analytical Chemistry from the Technical University, Prague, and in 1969 the degree of C.Sc. Analytical

Chemistry from the same institution. In 1978 he gained a Ph.D. from the University of New South Wales, where he was first a Lecturer from 1974, and is now Senior Lecturer. He has also worked with Dr. L. de Galen at the University of Technology, Delft. His research interests lie mainly in analytical atomic spectroscopy, especially electrothermal AAS, and microwave-induced plasmas. He has published some 35 papers in these fields. He is now an Australian citizen and is still waiting for his C.Sc. degree certificate.

MILOS NOVOTNY was born in 1942 in Czechoslovakia. He was educated at the University of Brno and received the Doctorate in Natural Sciences (Biochemistry) in 1965. His postdoctoral experience has included fellowships at the Institute of Analytical Chemistry, Czechoslovak Academy of Sciences, Brno, the Royal Karolinska Institute, Stockholm, and the University of Houston. In 1971, he joined Indiana University as Assistant Professor of Chemistry, and was promoted to full professor in 1978. In 1980, he was a "Visiting Scientist" at the Max Planck Institute for Biology, Tübingen. His main scientific interests are the fundamentals, analytical aspects, and various applications of separation methods. He has published over 150 original scientific papers, a book *Analytical Chemistry of Polycyclic Aromatic Compounds*, and two recently edited volumes on capillary chromatographic methods. His current research interests include both gas and liquid chromatography and their combinations with spectroscopic methods. He is among the pioneers of microcolumn liquid chromatography and capillary supercritical fluid chromatography. Current research is strongly focused on improvements in detection techniques. Professor Novotny has served on several advisory boards for U.S. Government laboratories and the National Academy of Sciences. He has been a member of the Editorial Boards of the *Journal of Chromatography*, *Chemical Instrumentation and Analysis*, and *Journal of High-Resolution Chromatography* and is on the Editorial Advisory Board of *Chromatographia*. Professor Novotny was the Chairman of the 1980 Gordon Conference on Analytical Chemistry and the U.S. Coordinator of the 1983 U.S.–Japan Joint Seminar on "Microcolumn Separation Techniques and their Ancillary Methods". He received the 1983 James B. Himes Award of the Chicago Chromatography Discussion Group, and the 1984 M.S. Tswett Award in Chromatography.

WANG ERKANG

PROFESSOR WANG ERKANG was born near Shanghai in 1933, and graduated with the equivalent of a B.Sc. from Shanghai University in 1952. From 1955 to 1959 he studied under Professor Heyrovský in Prague and received the degree of C.Sc. in Chemistry from the Polarographic Institute of the Czechoslovak Academy of Sciences, Prague. He was a Research Assistant at Changchun Institute of Applied Chemistry, Academia Sinica, from 1952 to 1955, became Research Associate in 1959, Head of the Electroanalytical Chemistry Laboratory in 1975, Associate Professor in 1978, and Professor in 1982 (and concurrently Professor at the Chinese Scientific and Technical University in Hefei and its graduate school in Beijing). His research interests are in analytical chemistry, electroanalytical chemistry and environmental analysis. He is a member of the Editorial Boards of several Chinese journals: *Acta Chimica Sinica*, *Fenxi Huaxue*, *Journal of Physical Test and Chemical Analysis* (*Chemical Edition*), *Journal of Metallurgical Analysis*, *Journal of Applied Chemistry*, *Collected Papers of the Changchun Institute of Applied Chemistry*, and *Analytical Chemistry Laboratory*. He has published about 160 papers and has translated several books into Chinese.

LIST OF CONTENTS

JANUARY

FEBRUARY

MARCH

APRIL

MAY

JUNE

JULY

AUGUST (A)

Henry Freiser Honour Issue

SEPTEMBER

OCTOBER

NOVEMBER

DECEMBER

Talanta, Vol. 32, No 11, p. v, 1985
Pergamon Press Ltd. Printed in Great Britain

ERRATA

In the paper by B. R. Smith *et al.*, *Talanta*, 1984, **31**, 955, in Table 2 the units in the caption should be $\mu g/g$, not mg/g, and Table 3 should read as follows.

Table 3. Comparison of experimental and literature value for fluoride ($\mu g/g$)

Enamel	Dentin
$X_F = 487 \pm 219$	$X_F = 770 \pm 311$
$X_{NF} = 323 \pm 93$	$X_{NF} = 753 \pm 262$
$X_t = 442 \pm 206$	$X_t = 769 \pm 295$
Previous work*	
12.5 ± 9.52 (5)	71.9 ± 39.4 (5)
32–1247 (15)	200–8000 (15,16)
32–1247 (17)	175.6 (13)
293 ± 34 (18)	
130.27 (6)	
79.5 ± 6.04 (19)	
248.0 ± 20.0 (14)	
104.6 (13)	

F = fluoridated source; NF = non-fluoridated source; t = total of all samples; results expressed as mean + standard deviation or as range.
*References in brackets.

In the paper by D. Rosales *et al.*, *Talanta*, 1985, **32**, 467, on page 467, right-hand column, line 4, the percentage of carbon found should be 56.9, not 52.9, and on page 472, the first equation in the left-hand column should be

$$\phi_N = \frac{[AB_N]}{A} = \frac{\beta_N b^N}{1 + \beta_1 b + \beta_2 b^2 + \ldots + \beta_N b^N}$$

Talanta, Vol. 32, No 11, p. v, 1985
Pergamon Press Ltd. Printed in Great Britain

ERRATA

In the paper by B. R. Smith *et al.*, *Talanta*, 1984, **31**, 955, in Table 2 the units in the caption should be $\mu g/g$, not mg/g, and Table 3 should read as follows.

Table 3. Comparison of experimental and literature value for fluoride ($\mu g/g$)

Enamel	Dentin
$X_F = 487 \pm 219$	$X_F = 770 \pm 311$
$X_{NF} = 323 \pm 93$	$X_{NF} = 753 \pm 262$
$X_t = 442 \pm 206$	$X_t = 769 \pm 295$
Previous work*	
12.5 ± 9.52 (5)	71.9 ± 39.4 (5)
32–1247 (15)	200–8000 (15,16)
32–1247 (17)	175.6 (13)
293 ± 34 (18)	
130.27 (6)	
79.5 ± 6.04 (19)	
248.0 ± 20.0 (14)	
104.6 (13)	

F = fluoridated source; NF = non-fluoridated source; t = total of all samples; results expressed as mean + standard deviation or as range.
*References in brackets.

In the paper by D. Rosales *et al.*, *Talanta*, 1985, **32**, 467, on page 467, right-hand column, line 4, the percentage of carbon found should be 56.9, not 52.9, and on page 472, the first equation in the left-hand column should be

$$\phi_N = \frac{[AB_N]}{A} = \frac{\beta_N b^N}{1 + \beta_1 b + \beta_2 b^2 + \ldots + \beta_N b^N}$$

Talanta, Vol. 32, No. 8A, p. v, 1985
Pergamon Press Ltd. Printed in Great Britain

NOTICE

SECOND INTERNATIONAL SYMPOSIUM ON DRUG ANALYSIS

CATHOLIC UNIVERSITY OF LOUVAIN-EN-WOLUVE, BRUSSELS
27–30 MAY 1986

Topics

1. Fundamental Aspects of Drug Analysis.
2. Quality control of Natural and Synthetic Raw Materials.
3. Analysis of Pharmaceutical Preparations.
4. Determination of Drugs in Biological Media.
5. Automation in Drug Analysis.

Programme

Plenary and keynote lectures will be given by invited speakers. Oral presentations will be limited. Preference will be given to poster presentations. Panel discussions will be organized.

Languages

The official languages of the conference are English, French and Dutch.

For further information please contact:

Scientific secretariat: Mrs. C. VAN KERCHOVE, rue Stévinstraat 137, B-1040 Brussels, Belgium
Tel. (02)230 26 85–ext. 33
Administrative secretariat: Mrs. F. REY, Chaussée de Waterloo 1375, B-1180 Brussels, Belgium
Tel. (02)375 16 48

Talanta, Vol. 32, No 6, p. v, 1985
Pergamon Press Ltd. Printed in Great Britain

NOTICE

MTAA-7

MODERN TRENDS IN ACTIVATION ANALYSIS

CALL FOR PAPERS

To commemorate the 50th anniversary of the first publication in the field of activation analysis by G. Hevesy and H. Levi of the Niels Bohr Institute in Denmark, the 7th International Conference on Modern Trends in Activation Analysis will be held in Copenhagen, 23–27 June 1986.

This Conference deals with all aspects of contemporary activation analysis, and scientists from every field where nuclear activation analysis is contributing to scientific or technical progress are invited to attend.

Authors wishing to present a paper at the MTAA-7 Conference must submit three (3) copies of a one-page abstract for evaluation by the Programme Committee no later than 30 June 1985.
Further information is available from:

Dr. K. Heydorn,
General Chairman MTAA-7,
Risø National Laboratory,
Postbox 49,
DK-4000 Roskilde,
DENMARK

Talanta, Vol 32, No 3, p. v, 1985
Pergamon Press Ltd. Printed in Great Britain.

ERRATA

In the paper by Elsie M. Donaldson, *Talanta*, 1984, **31**, 997, the following corrections are needed.
Page 1002, last column, Table 1, the results listed under "Ge found, $\mu g/g$", should be as follows: 4.3_6, 6.3_0, $12._6$, $22._3$, $41._9$, $102._8$, $200._0$.
Page 1002, last column, Table 2, the results listed under "Ge found after addition, $\mu g/g$", should be as follows: 3.1_6, $40._8$, $101._3$, 4.4_6, $42._1$, $101._8$, 2.4_0, $40._4$, $101._0$, 2.4_6, $40._5$, $101._0$, 1.9_6, $39._9$, $99._8$, 6.2_6, $43._6$, $104._0$, 9.2_6, $47._4$, $108._0$, 6.1_6, $43._8$, $105._0$.
Page 1003, Table 4, for "Mean (standard deviation)" read

Mean	2.38	2.40	25.9
Standard deviation	0.06	0.08	0.15

In the paper by O. P. Bhargava and M. Gmitro, *Talanta*, 1984, **31**, 301, the calculation formula on p. 302 is incorrect, and should read:

$$\%\mathrm{P} = \frac{\mu\text{g of phosphorus} \times 0.005}{\text{sample weight (g)} \times \text{sample aliquot (ml)}}$$

Talanta, Vol. 32, No. 3, p. V, 1985
Pergamon Press Ltd. Printed in Great Britain

THE LOUIS GORDON MEMORIAL AWARD

The Editorial Board and Publisher of *Talanta* take great pleasure in announcing that the Louis Gordon Memorial Award for 1984 (for the paper judged to be the best written of those appearing in *Talanta* during the year) will be made to Dr Lilly Gustafsson, of the University of Uppsala, Sweden, for her paper "Interferences in the determination of total nitrogen in natural waters by photo-oxidation to nitrate–nitrite mixture" (*Talanta*, 1984, **31**, 979)

Talanta, Vol. 32, No. 2, p. V, 1985
Pergamon Press Ltd. Printed in Great Britain

LOUIS GORDON MEMORIAL AWARD

Presentation of the Louis Gordon Memorial Award for 1983 to Professor J. M. Ottaway (left) and Dr. J. Marshall (centre) by Dr. R. A. Chalmers. (See *Talanta*, 1983, **30**, 571.)

Talanta, Vol. 32, No. 12, pp. v–vi, 1985
Pergamon Press Ltd. Printed in Great Britain

NOTICES

THE SILVER JUBILEE EASTERN ANALYTICAL SYMPOSIUM

6–10 OCTOBER 1986

New York Hilton Hotel, New York

A limited number of oral and poster presentations on new developments in Analytical Chemistry will be accepted for the Silver Jubilee Eastern Analytical Symposium. These contributed presentations will be grouped into several sessions to complement the invited technical sessions at this, the celebration of the twenty-fifth annual EAS. Prospective authors should submit a 50–100 word abstract on the proposed presentation before the deadline (15 February 1986) indicating preference for oral or poster format, to Concetta M. Paralusz, EAS Program Chairman, Permacel/Avery International, P.O. Box 671, New Brunswick, NJ 08903. Tel. (201)524-5633. Care should be exercised in considering the title and authors of the proposed presentation; if the presentation is accepted, both title and authors will be considered final and not subject to change. Authors of accepted presentations will receive forms for submission of a 200–300 word abstract which will appear in the final programme. The Silver Jubilee EAS will be moving to a new home at the New York Hilton Hotel, the finest convention site in the New York City area.

For details contact:
Dr. S. David Klein
EAS Publicity
642 Cranbury Cross Road
North Brunswick, NJ 08902, U.S.A.
Tel. (201) 846–1582

IInd INTERNATIONAL SYMPOSIUM ON QUANTITATIVE LUMINESCENCE SPECTROMETRY IN BIOMEDICAL SCIENCES

State University of Ghent, Faculty of Pharmaceutical Sciences, May 1987

Details from Dr. W. Baeyens, Symposium Chairman, State University of Ghent, Laboratory of Pharmaceutical Chemistry and Drug Quality Control, Harelbekestraat 72, B-9000-Ghent, Belgium.

KINETICS IN ANALYTICAL CHEMISTRY

SECOND INTERNATIONAL SYMPOSIUM

PREVEZA, GREECE, 9–12 SEPTEMBER 1986

The scope and aims of the conference will intend to reflect the rapid development and increasing importance of kinetic methods of analysis during recent years.

The scientific programme will include catalytic methods (including enzyme catalyzed applications) differential reaction rate methods, and any aspect of kinetic nature with impact on analytical methodology.

The symposium will consist of five plenary lectures, contributed papers, and posters.

Details may be obtained from:
Prof. N. Evmirides
Laboratory of Analytical Chem., Chemistry Dept.
Univ. of Ioannina
Ioannina, Greece

6th INTERNATIONAL CONFERENCE ON FOURIER TRANSFORM SPECTROSCOPY

VIENNA, AUSTRIA, 24–24 AUGUST 1987

The 6th International Conference on Fourier Transform Spectroscopy is to be held in the historic city of Vienna (Austria) in 1987, exactly one century after Michelson proposed that his interferometer could be used for spectroscopy. The conference will cover new developments in Fourier Transform Spectroscopy in the infrared, visible and ultraviolet spectral ranges, as well as theoretical and experimental aspects and applications.

For further information please contact:
INTERCONVENTION,
P.O. Box 80, A-1107 Vienna, Austria
Tel.: (222) 57 63 05, 57 62 88
Telex: 11 12 10.

ATOMSPEKTROSKOPIE: IXth CANAS

NEUBRANDENBURG, DDR, 15–19 SEPTEMBER 1986

This conference on analytical atomic spectroscopy is organized by the Chemical Section of Karl-Marx University, Leipzig and the Chemical Society of the German Democratic Republic as the 9th in the series held in the USSR, Czechoslovakia, DDR, Hungary, Bulgaria and Poland. Details are obtainable from:

Dr. K. Dittrich
Sektion Chemie
Karl-Marx-Universität Leipzig
7010 Leipzig
Talstraße 35
D.D.R.

Talanta, Vol. 32, No. 1, pp. v–vi, 1985
Pergamon Press Ltd. Printed in Great Britain

NOTICES

AMSTERDAM SUMMER SCHOOL ON HPLC

UNIVERSITY OF AMSTERDAM, 17–21 JUNE 1985

This international course will provide a coherent survey of high-performance liquid chromatography as an analytical and preparative technique. Fundamental aspects of theory and instrumentation will be treated in main lectures and seminars by leading international experts in the field. The course includes practical experiments in order to illustrate the potential of the technique. The Summer School will be organized by Prof. H. Poppe and Dr. J. C. Kraak's group working on separation. The official language will be English.

Information and registration through the Municipal Congress Bureau, Oudezijds Achterburgwal 199, 1012 DK Amsterdam, The Netherlands.
Telephone: (0)20–552.3458/59.

COLLOQUIUM SPECTROSCOPICUM INTERNATIONALE XXIV

15–21 SEPTEMBER 1985, GARMISCH-PARTENKIRCHEN, FEDERAL REPUBLIC OF GERMANY

The meeting place will be the "Kongresshaus", a modern congress centre built in the traditional Alpine style and offering all facilities for the formal and informal contents of an international conference. It is situated in the middle of the town at the edge of a beautiful park and within easy walking distance of all places of interest in Garmisch-Partenkirchen. The CSI XXIV is held under the auspices of the "Gesellschaft Deutscher Chemiker" (GDCh) and the "Deutsche Bunsen-Gesellschaft für Physikalische Chemie" and sponsored by the International Union of Pure and Applied Chemistry (IUPAC). The scientific programme will consist of only two kinds of presentation, *i.e.*, invited lectures and posters. There will be about 60 invited lectures summarizing the present state-of-the-art in a specific field and showing new perspectives. The invited lectures will be delivered in three parallel morning sessions. The posters will be shown in the afternoons. We expect about 400 posters which will be grouped thematically in symposia introduced by a coordinator and, after the usual viewing time, thoroughly discussed. By these means, we hope to make the poster show attractive and efficient. Subjects of special interest will be dealt with in panel and round table discussions.

The conference fees will be about
DM 450 for full participants
DM 100 for accompanying persons
DM 100 for students
Information from:
Gesellschaft Deutscher Chemiker
Abteilung Tagungsorganisation
Postfach 900440
D-6000 Frankfurt am Main 90
Bundesrepublik Deutschland

SECOND INTERNATIONAL SYMPOSIUM HELD UNDER THE AEGIS OF IUPAC ON ANALYTICAL CHEMISTRY IN THE EXPLORATION, MINING AND PROCESSING OF MATERIALS

PRETORIA, 15–19 APRIL 1985

Analytical chemistry is vital to the mining and minerals industry. To meet the ever-increasing demands made in the quest for better quality and the more economical exploitation of mineral resources, sophisticated analytical techniques must be constantly developed or existing methods improved. The need for regular and formal exchange of knowledge has resulted in South Africa, with its many mining interests and rich and varied mineral deposits, hosting the second Symposium as a sequel to the first highly successful one held in Johannesburg in 1976. The objective is to highlight the importance of analytical chemistry in the production of materials from the initial stages of exploration and assessment of ores to the beneficiation and, finally, to the refined product. The aim is to bring together from all over the world scientists specializing in the various fields of analytical chemistry to exchange information, to discuss progress in the analytical sciences and to explore future developments. The Symposium should, therefore, be of interest to anyone working in the fields relating to the determination of the quality of materials, *i.e.*, analytical chemists, mineral physicists, metallurgists, geologists, chemical and mining engineers.

All correspondence related to the Symposium should be addressed to:

The Symposium Secretariat S.328
CSIR
Box 395
PRETORIA
0001 South Africa
Tel: (012) 86-9211 x 4412 (Mrs Meyer)
x 2077 (Mrs Rhodes)
International + 271286-9211
Telex 3-21312 SA

All correspondence, as well as enquiries, with regard to accommodation and/or post-symposium tours, should be addressed to:

The Manager (for attention: Mr J. Erasmus)
Publicity and Travel Department
South African Transport Services
Box 1111
JOHANNESBURG
2000 South Africa
Telephone: National (011) 834-2566
International + 2711 834-2506

AUTHOR INDEX